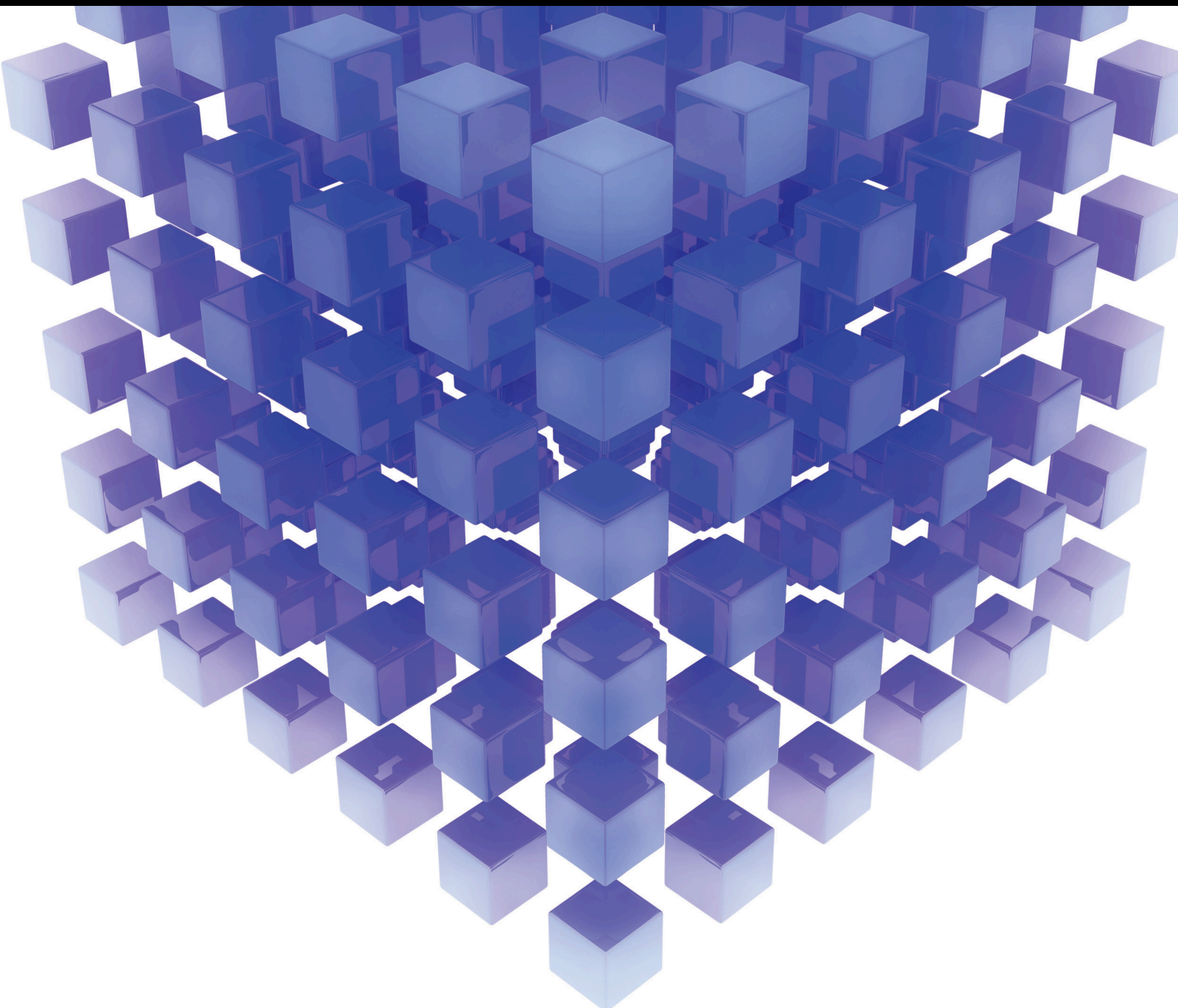# AI Powered Service Optimization for Edge/Fog Computing

Special Issue Editor in Chief: Sang-Bing Tsai
Guest Editors: Chia-Huei Wu, Xiaolong Xu, Yuan Yuan, and Qiang He

AI Powered Service Optimization for Edge/Fog Computing

AI Powered Service Optimization for Edge/Fog Computing

Special Issue Editor in Chief: Sang-Bing Tsai
Guest Editors: Chia-Huei Wu, Xiaolong Xu, Yuan Yuan, and Qiang He

Chief Editor

Guangming Xie, China

Editorial Board

Bin Liu, China
Bonifacio Llamazares, Spain
Alessandro Lo Schiavo, Italy
Jean Jacques Loiseau, France
Francesco Lolli, Italy
Paolo Lonetti, Italy
Sandro Longo, Italy
António M. Lopes, Portugal
Sebastian López, Spain
Pablo Lopez-Crespo, Spain
Cesar S. Lopez-Monsalvo, Mexico
Luis M. López-Ochoa, Spain
Ezequiel López-Rubio, Spain
Vassilios C. Loukopoulos, Greece
Jose A. Lozano-Galant, Spain
Gabriele Maria Lozito, Italy
Songtao Lu, USA
Rongxing Lu, Canada
Zhiguo Luo, China
Gabriel Luque, Spain
Valentin Lychagin, Norway
Junhai Ma, China
Dazhong Ma, China
Antonio Madeo, Italy
Alessandro Magnani, Belgium
Toqeer Mahmood, Pakistan
Fazal M. Mahomed, South Africa
Arunava Majumder, India
Paolo Manfredi, Italy
Adnan Maqsood, Pakistan
Giuseppe Carlo Marano, Italy
Damijan Markovic, France
Filipe J. Marques, Portugal
Luca Martinelli, Italy
Rodrigo Martinez-Bejar, Spain
Guiomar Martín-Herrán, Spain
Denizar Cruz Martins, Brazil
Francisco J. Martos, Spain
Elio Masciari, Italy
Franck Massa, France
Paolo Massioni, France
Alessandro Mauro, Italy
Jonathan Mayo-Maldonado, Mexico
Fabio Mazza, Italy
Pier Luigi Mazzeo, Italy
Laura Mazzola, Italy
Driss Mehdi, France

Dr. Zahid Mehmood, Pakistan
YUE MEI, China
Roderick Melnik, Canada
Xiangyu Meng, USA
Debiao Meng, China
Jose Merodio, Spain
Alessio Merola, Italy
Mahmoud Mesbah, Iran
Luciano Mescia, Italy
Laurent Mevel, France
Constantine Michailides, Cyprus
Mariusz Michta, Poland
Prankul Middha, Norway
Aki Mikkola, Finland
Giovanni Minafò, Italy
Hiroyuki Mino, Japan
Dimitrios Mitsotakis, New Zealand
saleh mobayen, Taiwan, R.O.C., Iran
Nikunja Mohan Modak, India
Sara Montagna, Italy
Roberto Montanini, Italy
Francisco J. Montáns, Spain
Gisele Mophou, France
Rafael Morales, Spain
Marco Morandini, Italy
Javier Moreno-Valenzuela, Mexico
Simone Morganti, Italy
Caroline Mota, Brazil
Aziz Moukrim, France
Shen Mouquan, China
Dimitris Mourtzis, Greece
Emiliano Mucchi, Italy
Taseer Muhammad, Saudi Arabia
Josefa Mula, Spain
Jose J. Muñoz, Spain
Giuseppe Muscolino, Italy
Dino Musmarra, Italy
Marco Mussetta, Italy
Ghulam Mustafa, Pakistan
Hariharan Muthusamy, India
Hakim Naceur, France
Alessandro Naddeo, Italy
Benedek Nagy, Turkey
Omar Naifar, Tunisia
Mariko Nakano-Miyatake, Mexico
Keivan Navaie, United Kingdom
Adrian Neagu, USA

Leonid Shaikhet, Israel
Xingling Shao, China
Hao Shen, China
Xin Pu Shen, China
hang shen, China
Bo Shen, Germany
Dimitri O. Shepelsky, Ukraine
Weichao SHI, United Kingdom
Jian Shi, China
Suzanne M. Shontz, USA
Babak Shotorban, USA
Zhan Shu, Canada
Angelo Sifaleras, Greece
Nuno Simões, Portugal
Harendra Singh, India
Thanin Sitthiwirattham, Thailand
Seralathan Sivamani, India
S. Sivasankaran, Malaysia
Christos H. Skiadas, Greece
Konstantina Skouri, Greece
Neale R. Smith, Mexico
Bogdan Smolka, Poland
Delfim Soares Jr., Brazil
Alba Sofi, Italy
Francesco Soldovieri, Italy
Raffaele Solimene, Italy
Bosheng Song, China
Yang Song, Norway
Jussi Sopanen, Finland
Marco Spadini, Italy
Paolo Spagnolo, Italy
Bernardo Spagnolo, Italy
Ruben Specogna, Italy
Vasilios Spitas, Greece
Sri Sridharan, USA
Ivanka Stamova, USA
Rafał Stanisławski, Poland
Miladin Stefanović, Serbia
Florin Stoican, Romania
Salvatore Strano, Italy
Yakov Strelniker, Israel
Xiaodong Sun, China
Qiuye Sun, China
Qiuqin Sun, China
Zong-Yao Sun, China
Shuaishuai Sun, Australia
Suroso Suroso, Indonesia

Sergey A. Suslov, Australia
Nasser Hassen Sweilam, Egypt
Andrzej Swierniak, Poland
M Syed Ali, India
Andras Szekrenyes, Hungary
Kumar K. Tamma, USA
Yong (Aaron) Tan, United Kingdom
Marco Antonio Taneco-Hernández, Mexico
Hafez Tari, USA
Alessandro Tasora, Italy
Sergio Teggi, Italy
Ana C. Teodoro, Portugal
Efstathios E. Theotokoglou, Greece
Jing-Feng Tian, China
Alexander Timokha, Norway
Stefania Tomasiello, Italy
Gisella Tomasini, Italy
Isabella Torcicollo, Italy
Francesco Tornabene, Italy
Javier Martinez Torres, Spain
Mariano Torrisi, Italy
Thang nguyen Trung, Vietnam
Sang-Bing Tsai, China
George Tsiatas, Greece
Antonios Tsourdos, United Kingdom
Le Anh Tuan, Vietnam
Federica Tubino, Italy
Nerio Tullini, Italy
Emilio Turco, Italy
Ilhan Tuzcu, USA
Efstratios Tzirtzilakis, Greece
Filippo Ubertini, Italy
Marjan Uddin, Pakistan
Mohammad Uddin, Australia
Serdar Ulubeyli, Turkey
FRANCISCO UREÑA, Spain
Panayiotis Vafeas, Greece
Giuseppe Vairo, Italy
Jesus Valdez-Resendiz, Mexico
Eusebio Valero, Spain
Stefano Valvano, Italy
Marcello Vasta, Italy
Carlos-Renato Vázquez, Mexico
Miguel E. Vázquez-Méndez, Spain
Martin Velasco Villa, Mexico
Kalyana C. Veluvolu, Republic of Korea
Franck J. Vernerey, USA

Lingfan Zhang, China
Yifan Zhao, United Kingdom
Yongmin Zhong, Australia
Zebo Zhou, China
Debao Zhou, USA
Jian G. Zhou, United Kingdom
Zhe Zhou, China
Quanxin Zhu, China
Wu-Le Zhu, China
Gaetano Zizzo, Italy
Zhixiang Zou, China

Contents

Contents

Contents

Contents

Contents

A Multilevel Optimization Framework for Computation Offloading in Mobile Edge Computing
Nanliang Shan (iD), Yu Li (iD), and Xiaolong Cui (iD)

Editorial

AI Powered Service Optimization for Edge/Fog Computing

Sang-Bing Tsai [iD],[1] **Chia-Hui Wu** [iD],[2] **Xiaolong Xu,**[3] **Yuan Yuan,**[4] and **Qiang He**[5]

[1]*Regional Green Economy Development Research Center, School of Business, WUYI University, Nanping, China*
[2]*Department of Hotel Management and Culinary Creativity, Minghsin University of Science and Technology, Xinfeng, Taiwan*
[3]*Nanjing University of Information Science and Technology, Nanjing, China*
[4]*Michigan State University, East Lansing, MICH, USA*
[5]*Swinburne University of Technology, Melbourne, Australia*

Correspondence should be addressed to Chia-Hui Wu; chiahuei530@gmail.com

In recent years, the explosive development of Internet of Things (IoT) has generated a large amount of data from both the user-device side and the network side, which challenges the traditional cloud-based data transmission, storage, and processing applications in terms of efficiency, security, and economic cost. In this situation, the newly emerged computing paradigms, Edge Computing and Fog Computing, have complemented the traditional cloud-based systems. Edge/Fog can provide partial computing resources closer to the user or device side; certain computing tasks can thereby be executed or processed directly by the close Edge/Fog resources without sending them to the distant cloud centre. This can reduce the load of a cloud platform, and the task execution efficiency can be improved significantly.

However, existing Edge/Fog-based service systems often suffer from limited computing capabilities, high energy cost, and fast changing context environment, which call for intelligent optimization of business strategies adopted in both the user-device side and network side. Fortunately, artificial intelligence (AI) technology provides a promising way to achieve the above Edge/Fog service optimization goals. However, the integration of AI and Edge/Fog techniques is still a challenging issue that needs intensive study. In view of the above analyses, this special issue aims to highlight the cutting-edge research and applications related to the "AI Powered Service Optimization for Edge/Fog Computing."

In this special issue, we look for significant findings in tackling new security issues that challenge artificial intelligence in the mobile edge computing environment. Specifically, we solicit novel contributions on secure artificial intelligence from a variety of perspectives, e.g., architecture, data, and algorithms. This special issue has collected some good articles. It had great repercussions and success.

Conflicts of Interest

The guest editors declare no conflicts of interest.

Acknowledgments

Research Article

Establishment and Evaluation of Energy Consumption, Carbon Emission, and Economic Models of Retreaded Tires Based on Life Cycle Theory

Qiang Wang,[1] Shaojie Wang [iD],[2] and Li Jiang[1]

[1]*School of Automotive and Transportation Engineering, Heilongjiang Institute of Technology, Harbin 150050, Heilongjiang, China*
[2]*Business School, Hunan University of Humanities, Science and Technology, Loudi 417000, Hunan, China*

Correspondence should be addressed to Shaojie Wang; keiji2006@163.com

This paper identifies the system composition of the life cycle of retreaded tires and constructs the energy consumption model, carbon emission model, and economic model of retreaded tires based on the life cycle theory. Moreover, the theoretical calculation model and method for the energy consumption, carbon emission, and economy at the production phase, transportation phase, usage phase, and reuse phase of retreaded tires are proposed. After that, this paper puts forward the energy substitution model, carbon reduction model, and cost profit model of five reuse methods of retreaded tires, namely, secondary retreading, mechanical pulverization, low-temperature pulverization, combustion decomposition, and combustion power generation. Finally, this paper proposes the evaluation index for the energy consumption, carbon emission, and economy in the life cycle of retreaded tires and quantitatively analyzes the energy consumption, carbon emission, and cost profit list in each phase of the life cycle of retreaded tires, obtaining the energy recovery rate, carbon reduction rate, and profit-to-cost ratio of the five reuse methods of retreaded tires. The main conclusions of this paper are as follows: the energy consumption and carbon emission of retreaded tires are the largest at the production phase, while the energy consumption and carbon emission are the lowest at the transportation phase. Among the five reuse methods, the energy recovery effect, carbon reduction rate, and economy of secondary retreading are the optimal ones, and the quantitative results show that retreading is the most effective way for the reuse of waste tires.

1. Introduction

There are mainly five different reuse methods of automobile waste tires, namely, retreading, mechanical pulverization, low-temperature pulverization, combustion decomposition, and combustion power generation, among which retreading has developed rapidly in the automotive tire industry due to its low-carbon and environmentally friendly advantages. Tire retreading is an effective way to recycle waste tires, and it is an extension and development of tire industry, which is of great significance for promoting the comprehensive utilization of resources such as rubber, transformation of economic growth mode, and sustainable development [1, 2]. The degree of wear of a normal waste tire is less than 30%, while the remaining 70% of the carcass can be reused. It is

suggested that each retreaded truck tire can save 4 kg of rubber, 1.7 kg of nylon cord fabric, 2 kg of carbon black, 18 kg of petroleum, and 1 kg of steel. Generally, the service life of retreaded tires with conventional methods is 50% to 70% of brand new tires while and the service life of retreaded tires with presulfurization method can approach or even exceed that of brand new tires. The material required for the retreading of old tires is 30% of that of new tires, and the service life of retreaded tires is 80% of that of new tires. If the quality of retreaded tires can satisfy the national standards and the security, wear resistance and comfort are as good as those of new tires, and the value for the recycling of waste tires is immeasurable considering the production of hundreds of millions of waste tires every year [1–3]. Andrea Corti studied the final disposal process of waste tires by LCA.

Huang et al., based on the theory of life cycle inventory analysis, analyzed the factors influencing energy consumption in tire's life cycle. Yang Lei analyzed the economy, energy, and carbon emissions of tire life cycle. Wu analyzed and studied the tire carbon footprint. At present, there is no report about the life cycle of retreaded tire at home and abroad. Therefore, increasing the retreading rate of waste tires will greatly save rubber resources and promote environmental protection. However, there is no systematic, targeted, and quantitative analysis and evaluation on the impact of tire retreading on society, enterprises, and environment. For this purpose, this paper establishes an evaluation benchmark based on the life cycle theory. By constructing the energy consumption model, carbon emission model, and economic model of retreaded tires, this paper qualitatively and quantitatively evaluates the energy recovery effect, carbon reduction rate, and economic benefits of retreaded tires in the production phase, transportation phase (twice), usage phase, and reuse phase (including secondary retreading, mechanical pulverization, low-temperature pulverization, combustion decomposition, and combustion power generation), which provides the theoretical guidance for the promotion and application of retreaded tires and the policy formulation of tire retreading industry.

2. Life Cycle System Composition of Retreaded Tires

Retreaded tire is a kind of tire that can be reused after grinding and repairing the outer layer of worn waste tire and pasting a layer of buffer rubber and tread compound and through vulcanizing. The structure of the retreaded tire is the same as that of the new tire; the main difference is that a layer of buffer compound is added to the worn tread, and then the tread compound is applied. The life cycle system composition of retreaded tires is shown in Figure 1, which mainly includes 4 phases: production, transportation (twice), usage, and reuse of retreaded tires. In the production phase, resources and energy such as tread rubber, buffer rubber, old carcass, and adhesive will be consumed while there are five reuse methods in the reuse phase, namely, secondary retreading, mechanical pulverization, low-temperature pulverization, combustion decomposition, and combustion power generation. In each phase, certain resources and energy will be consumed and certain amount of carbon emissions will also be generated. Particularly, in the reuse phase, new resources and energy will also be regenerated and new carbon emissions will be generated, consuming economic costs and generating new economic profits as well [4, 5].

3. Energy Consumption, Carbon Flow, and Economic Model in the Life Cycle of Retreaded Tires

3.1. Energy Consumption Model in the Life Cycle of Retreaded Tires. The total energy consumption TE of retreaded tires is mainly composed of energy consumption TE_1 during the production phase, energy consumption TE_2 during the transportation phase (twice), energy consumption TE_3 during the usage phase, and energy consumption TE_4 during the reuse phase. The energy consumption model in the life cycle of retreaded tires is shown in the following equation:

$$TE = TE_1 + TE_2 + TE_3 + TE_4. \tag{1}$$

New products or new energy will be produced in the secondary retreading, mechanical pulverization, low-temperature pulverization, combustion decomposition, and combustion power generation of treaded tires, which are regarded as alternative energy (AE) in this research, equivalent to the energy consumption required for the production of this new product or new energy. It is mainly composed of 5 parts, namely, the energy consumption AE_1 of secondary retreading, energy consumption AE_2 of mechanical pulverization, energy consumption AE_3 of low-temperature pulverization, energy consumption AE_4 of combustion decomposition, and energy consumption AE_5 of combustion power generation. The energy alternative model in the reuse phase of retreaded tires is shown in the following equation:

$$AE = AE_1 + AE_2 + AE_3 + AE_4 + AE_5. \tag{2}$$

3.2. Life Cycle Carbon Flow Model of Retreaded Tires. Based on the life cycle energy consumption composition of retreaded tires, the total carbon emission TC of retreaded tires is mainly composed of the carbon emission TC_1 during the production phase, carbon emission TC_2 during the transportation phase (twice), carbon emission TC_3 during the usage phase, and carbon emission TC_4 during the reuse phase. The life cycle carbon emission model of treaded tires is shown in the following equation [6, 7]:

$$TC = TC_1 + TC_2 + TC_3 + TC_4. \tag{3}$$

Similarly, new products or new energy will be produced in the secondary retreading, mechanical pulverization, low-temperature pulverization, combustion decomposition, and combustion power generation of treaded tires, which are regarded as carbon reduction AC in this research and are composed of 5 parts, namely, the carbon reduction AC_1 of secondary retreading, carbon reduction AC_2 of mechanical pulverization, carbon reduction AC_3 of low-temperature pulverization, carbon reduction AC_4 of combustion decomposition, and carbon reduction AC_5 of combustion power generation. Based on the life cycle energy consumption composition of retreaded tires, the total carbon emission TC of retreaded tires is mainly composed of the carbon emission TC_1 during the production phase, carbon emission TC_2 during the transportation phase (twice), carbon emission TC_3 during the usage phase, and carbon emission TC_4 during the reuse phase. The life cycle carbon reduction model of treaded tires is shown in the following equation:

$$AC = AC_1 + AC_2 + AC_3 + AC_4 + AC_5. \qquad (4)$$

3.3. Economic Model in the Life Cycle of Retreaded Tires.
The economic model in the life cycle of retreaded tires mainly includes economic-cost analysis model, economic-profit analysis model, environment-cost analysis model, and environment-profit analysis model [8, 9].

3.3.1. Economic-Cost Analysis Model.
The economic cost in the life cycle of retreaded tires mainly includes the sum of costs of various raw materials and various resources at each phase of retreaded tires, where the cost of various raw materials is equivalent to the product of unit consumption of various raw materials $r_{m_{ij}}$ and the corresponding unit prices, and the cost of various resources $P_{m_{ij}}$ is equivalent to the product of unit consumption of various resources $r_{e_{ij}}$ (water, electricity, coal, natural gas, etc.) and the corresponding unit price $P_{u_{ij}}$; L_{SA_i} represents the cost of labor, supplier, and management; D_{E_i} is depreciation cost of fixed assets; and S_{C_i} is the cost of sales. The economic-cost analysis model is shown in the following equation:

$$E_{C_i}\left(r_{m_{ij}}, P_{m_{ij}}, r_{e_{ij}}, P_{u_{ij}}, L_{SA_i}, D_{E_i}, S_{C_i}\right) = \left(\sum_j r_{m_{ij}} P_{m_{ij}} + \sum_j r_{e_{ij}} P_{u_{ij}} + L_{SA_i}\right) + D_{E_i} + S_{C_i}. \qquad (5)$$

3.3.2. Economic-Profit Analysis Model.
Unlike the economic-cost model, the profit in the life cycle of retreaded tires = benefits in the life cycle–costs in the life cycle. The product sales only occur in the production phase and reuse phase of retreaded tires, so the economic profit only occurs in these two phases. T_{ij} is the output of various products at the production phase and reuse phase; $u_{p_{ij}}$ is the unit price of various products. The economic-profit analysis model is shown in the following equation:

$$E_{P_i}\left(T_{ij}, u_{p_{ij}}, E_{C_i}\right) = \sum_j T_{ij} u_{p_{ij}} - E_{C_i}. \qquad (6)$$

3.3.3. Environmental-Cost Analysis Model.
Environmental cost is the damage to the environment, which is mainly represented by the greenhouse effect caused by CO_2 emissions. It mainly includes the CO_2 emissions caused by the direct or indirect consumption of the fossil energy at various phases of retreaded tires. The environmental cost of various raw materials is equivalent to the product of the unit consumption of various raw materials $r_{m_{ij}}$ and the environmental loss $E_{L_{ij}}$ caused by CO_2 emissions; the environmental cost of various resources is equivalent to the product of the unit consumption of various resources $r_{e_{ij}}$ (water, electricity, coal, natural gas, etc.) and the environmental loss $E_{L_{ij}}$ caused by CO_2 emissions. The

environmental-cost analysis model is shown in the following equation:

$$C_{E_i}\left(r_{m_{ij}}, r_{e_{ij}}, E_{L_{ij}}\right) = \sum_i r_{m_{ij}} E_{L_{ij}} + \sum_j r_{e_{ij}} E_{L_{ij}}. \qquad (7)$$

3.3.4. Environmental-Profit Analysis Model.
Environmental profit is the benefit brought to the environment, which is the CO_2 emission reduction achieved by reusing the product of retreaded tires generated at the reuse phase in the industrial production. It mainly includes the sum of CO_2 emission fee generated by producing the same product at the reuse phase; T_{ij} represents the output of various products at the reuse phase; CEC_i represents carbon emission coefficient of corresponding products; and PC_i represents the fee of CO_2 emissions. The environmental-profit analysis model is shown in the following equation:

$$PE_i\left(T_{ij}, CEC_i, PC_i\right) = \sum_i T_{ij} CEC_i PC_i. \qquad (8)$$

4. Energy Consumption Model and Carbon Emission Model of Retreaded Tires at Each Phase

4.1. Energy Consumption Model and Carbon Emission Model at the Production Phase.
The energy consumption of retreaded tires at the production phase is mainly composed of the raw materials and energy consumed. TE_1 is the total energy consumption during the production phase; PM_i is the consumption of raw material i; PM_{ρ_i} is the energy density of raw material i; PE_j is the consumption of energy j; and $PE_{\rho j}$ is the energy density of energy j. The energy consumption model at the production phase is shown in the following equation [10, 11]:

$$TE_1 = \sum_i \left(PM_i \times PM_{\rho_i}\right) + \sum_j \left(PE_j \times PE_{\rho_j}\right). \qquad (9)$$

The carbon emission during the production phase of retreaded tires is established based on the first law of thermodynamics and the law of conservation of mass. TC_1 is the total carbon emission during the production phase; PCM_i is the consumption of raw material i during the production phase; $PCMI_i$ is the carbon emission coefficient of raw material i during the production phase; and PCE_j is the carbon emission coefficient of energy j at the production phase. The carbon emission model at the production phase is shown in the following equation:

$$TC_1 = \sum_i \left(PCM_i \times PCMI_i\right) + \sum_j \left(PCE_j \times PCEI_i\right). \qquad (10)$$

4.2. Energy Consumption Model and Carbon Emission Model at the Transportation Phase.
The transportation phase of retreaded tires mainly includes three parts, namely, the

transportation of raw materials to the production point, the production point to the point of sales, and the collecting point of waste tires to the reuse disposal point. The total energy consumption during the transportation phase is mainly subject to the impact of transportation method, transportation distance, and fuel used by transportation vehicles. TE_2 is total energy consumption during the transportation phase; TD is the average distance during the transportation phase; TE is the energy consumption during the transportation phase; and TE_ρ is the energy density of energy consumed during the transportation phase. The energy consumption model for the transportation phase is shown in the following equation:

$$TE_2 = TD \times TE \times TE_\rho. \tag{11}$$

The carbon emission coefficient during the transportation phase is related to the average transportation distance, energy consumption, and carbon emission coefficient. TC_2 is the total carbon emission during the transportation phase; TD is the average transportation distance during the transportation phase; TCE_j is the energy consumption during the transportation phase; and $TCEI_j$ is the carbon emission coefficient of energy consumed at the transportation phase. The carbon emission model during the transportation phase is shown in the following equation:

$$TC_2 = TD \times TCE_j \times TCEI_j. \tag{12}$$

4.3. Energy Consumption Model and Carbon Emission Model at the Usage Phase.

The energy consumption of retreaded tires during the usage phase is subject to the impact of average transportation distance and the fuel used. TE_3 is the total energy consumption at the usage phase; UD is the average transportation distance at the usage phase; UE is the energy consumption at the usage phase; and UE_ρ is the energy density of energy consumed at the usage phase. The energy consumption model at the usage phase is shown in the following equation:

$$TE_3 = UD \times UE \times UE_\rho. \tag{13}$$

The carbon emission during the usage phase is mainly related to the average transport distance, energy consumption, and carbon emission coefficient. TC_3 is the total carbon emission during the usage phase; UD is the average transportation distance at the usage phase; UCE_j is the energy consumption during the usage phase; and $UCEI_j$ is the carbon emission coefficient of energy at the usage phase. The carbon emission model at the usage phase is shown in the following equation:

$$TC_3 = UD \times UCE_j \times UCEI_j. \tag{14}$$

4.4. Energy Consumption Model and Carbon Emission Model at the Reuse Phase.

Energy is consumed and recovered at the reuse phase of retreaded tires. TE_4 is the total energy consumption at the reuse phase; RM_i is the consumption of raw material i at the reuse phase; RM_{ρ_i} is the energy density of raw material i at the reuse phase; RE_j is the consumption of energy j at the reuse phase; and RE_{ρ_j} is the energy density of energy j at the reuse phase. The energy consumption model at the reuse phase is shown in the following equation:

$$TE_4 = \sum_i \left(RM_i \times RM_{\rho_i} \right) + \sum_j \left(RE_j \times RE_{\rho_j} \right). \tag{15}$$

Both raw materials and energy are consumed at the reuse phase of retreaded tires. TC_4 is the total carbon emission at the reuse phase; RCM_i is the consumption of raw material i at the reuse phase; $RCMI_i$ is the carbon emission coefficient of raw material i at the reuse phase; RCE_j is the consumption of energy j at the reuse phase; and $RCEI_j$ is the carbon emission coefficient of energy j at the reuse phase. The carbon emission model at the reuse phase is shown in the following equation:

$$TC_4 = \sum_i \left(RCM_i \times RCMI_i \right) + \sum_j \left(RCE_j \times RCEI_j \right). \tag{16}$$

4.5. Evaluation Indexes of the Energy Consumption, Carbon Emission, and Economy of Retreaded Tires

4.5.1. Evaluation Indexes of Energy Consumption.

New products or new energy will be produced in five reuse methods of retreaded tires, namely, the secondary retreading, mechanical pulverization, low-temperature pulverization, combustion decomposition, and combustion power generation. AE is the alternative energy at the reuse phase; RPP_i is the output of new product i at the reuse phase; RPE_{ρ_i} is the energy density of new product i at the reuse phase; RPE_j is the output of new energy j at the reuse phase; and RE_{ρ_j} is the energy density of new energy j at the reuse phase. The alternative energy model is shown in the following equation [12, 13]:

$$AE = \sum_i \left(RPP_i \times RPE_{\rho_i} \right) + \sum_j \left(RPE_j \times RPE_{\rho_j} \right). \tag{17}$$

The net energy surplus (NES) at the reuse phase of retreaded tires can be expressed by the difference between the alternative energy and the total energy consumption at the reuse phase, as shown in the following equation:

$$NES = AE - TE_4. \tag{18}$$

The recovery degree of the input energy of the five reuse methods of retreaded tires, namely, secondary retreading, mechanical pulverization, low-temperature pulverization, combustion decomposition, and combustion power generation, at the reuse phase can be expressed by ERR, which is the proportion of output energy at the reuse phase to the input energy (mainly including the energy consumption at the production phase and reuse phase), as shown in the following equation:

$$\text{ERR} = \frac{\text{AE}}{\text{TE}_1 + \text{TE}_4} \times 100\%. \qquad (19)$$

4.5.2. Evaluation Indexes of Carbon Emission. The net carbon surplus (NCS) of retreaded tires is the difference between the carbon reduction (AC) and the total carbon emission (TC) during the reuse phase, as shown in the following equation:

$$\text{NCS} = \text{AC} - \text{TC}_4. \qquad (20)$$

New products or new energy will be produced from the five reuse methods of retreaded tires, namely, secondary retreading, mechanical pulverization, low-temperature pulverization, combustion decomposition, and combustion power generation. Every type of new product or new energy can be regarded as a type of carbon reduction, whose value is the carbon emission from the direct production of the new product or new energy. RPP_i is the output of new product j at the reuse phase; RPCI_i is the carbon emission coefficient of new product i at the reuse phase; RPE_j is the output of new energy j at the reuse phase; and RPCE_j is the carbon emission coefficient of new energy j at the reuse phase. The carbon reduction model at the reuse phase is shown in the following equation:

$$\text{AC} = \sum_i \left(\text{RPP}_i \times \text{RPCI}_i \right) + \sum_j \left(\text{RPE}_j \times \text{RPCE}_j \right). \qquad (21)$$

The reduction degree of carbon emissions by the five reuse methods of retreaded tires, namely, secondary retreading, mechanical pulverization, low-temperature pulverization, combustion decomposition, and combustion power generation, at the reuse phase can be expressed by CRR, whose value is the proportion of the carbon reduction at the reuse phase to total carbon emissions (mainly including carbon emissions at the production phase and reuse phase), as shown in the following equation:

$$\text{CRR} = \frac{\text{AC}}{\text{TC}_1 + \text{TC}_4} \times 100\% \qquad (22)$$

4.5.3. Economic Evaluation Indexes. When evaluating the economic benefits of the five reuse methods of retreaded tires, namely, secondary retreading, mechanical pulverization, low-temperature pulverization, combustion decomposition, and combustion power generation, the profit-to-cost ratio P_{CR} can be used as the evaluation index to show the impact of cost recovery rate at different reuse phases. The economic evaluation index is calculated based on the following equation [14–16]:

$$P_{\text{CR}} = \frac{\sum_i E_{P_i} + P_{E_i}}{\sum_i E_{C_i} + C_{E_i}} \times 100\%. \qquad (23)$$

5. List of Energy Consumption Carbon Emission and Economic Analysis of Retreaded Tires

5.1. Research Object. The 26.5R25 retreaded tire is selected as the research object. The calculation is based on the single tire weight of 0.5 t, service life of 1.5 years, and average transportation distance of 50,000 km. The weight of two retreaded tires, namely, 1 t, is taken as the functional unit.

5.2. Data Sources. The data of retreaded tires at the production phase refer to the Rubber Tire Industry Report in China and the actual data of two tire retreading companies (Harbin Huiliang Automobile Tire Retreading Co., Ltd. and Xinhongqi Tire Retreading Factory); the data of retreaded tires at the transportation and usage phase refer to the actual data of a transport company (Heilongjiang Longyun (Group) Co., Ltd.); the data of the mechanical pulverization, combustion decomposition, and combustion power generation of retreaded tires at the reuse phase refer to the research results in [10, 12]; and the data of low-temperature pulverization refer to the research results in [12]. The geographic boundary is Northeast China, and the time boundary is from 2018 to 2020.

6. Analysis and Evaluation of the Energy Consumption, Carbon Emission, and Economic Results of Retreaded Tires

6.1. Analysis and Evaluation of Energy Consumption Results. The energy input-output list in the life cycle of retreaded tires is shown in Table 1.

It can be seen from Table 1 that the total energy consumption in the life cycle of retreaded tires is about 144607 MJ, of which the energy consumption at the production phase is 132913 MJ, accounting for 91.91% of the total energy consumption in the life cycle; the energy consumption at the usage phase is 10591 MJ, accounting for approximately 7.32%; and the energy consumption at the transportation phase is 1103 MJ, accounting for about 0.76%. The ranking energy consumption is production phase > usage phase > transportation phase. It can be seen from the comparative analysis of the net energy surplus of the five reuse methods (secondary retreading, mechanical pulverization, low-temperature pulverization, combustion decomposition, and combustion power generation), shown in Figure 2, that the net energy surplus of the secondary retreading is 91062 MJ and the energy recovery rate is 74.88%, which is the highest among these five reuse methods. The ranking of the energy recovery effect of the five reuse methods of retreaded tires, shown in Figure 3, is secondary retreading > combustion decomposition > mechanical pulverization > low-temperature pulverization > combustion power generation.

6.2. Analysis and Evaluation of Carbon Emission Results. The input-output list of carbon emission and carbon reduction in the life cycle of retreaded tires is shown in Table 2.

It can be seen from Table 2 that the total carbon emission in the life cycle of retreaded tires is about 3280 kgC, of which the carbon emission during the production phase is 3,046 kgC, accounting for about 92.87% of the total carbon emission; the carbon emission at the usage phase is 212 kgC, accounting for about 6.46% of the total
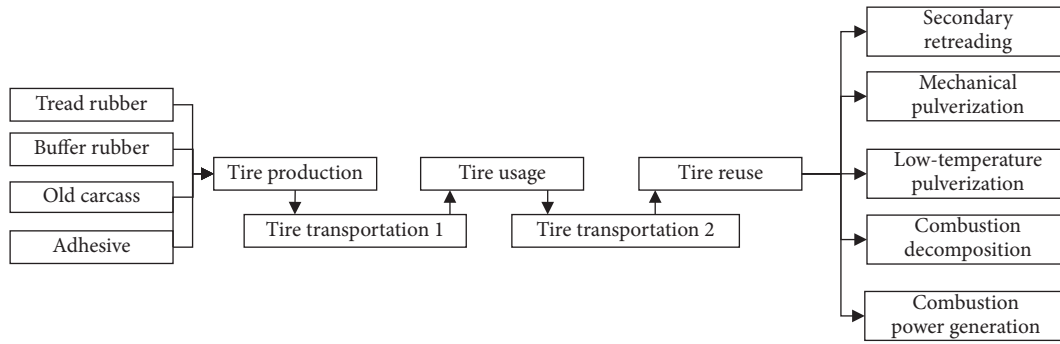
Figure 1: Life cycle system composition of retreaded tires.

Table 1: Energy input-output list in the life cycle of retreaded tires.

Category	Name	Value	MJ/t tire			
Energy consumption	Production phase TE_1	132913				
	Transportation phase TE_2	1103				
	Usage phase TE_3	10591				
	Reuse phase TE_4	Secondary retreading 33697	Mechanical pulverization 2401	Low-temperature pulverization 53134	Combustion decomposition 27139	Combustion power generation 483
Alternative energy	New product substitution, AE	124759	30437	30537	44763	9831
	Net energy surplus, NES	91062	28035	−22597	17444	9348
Evaluation index	Energy recovery rate, ERR	74.88%	22.49%	16.41%	27.94%	7.37%
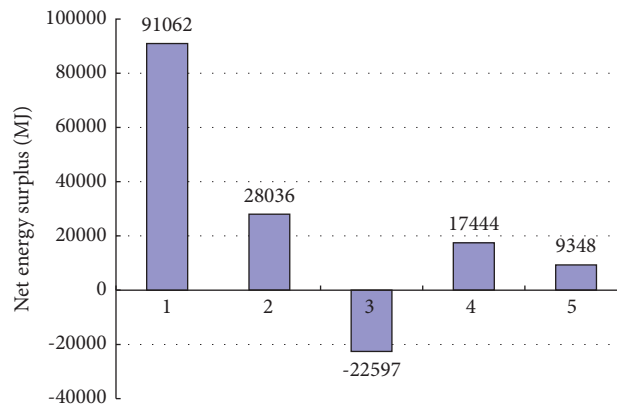
Figure 2: Net energy surplus of the five reuse methods.

carbon emission; and the carbon emission at the transportation phase is 22 kgC, accounting for about 0.67% of the total. The ranking of carbon emission is production phase > usage phase > transportation phase. It can be seen from the comparative analysis of the net carbon surplus and carbon reduction rate of the five reuse methods (secondary retreading, mechanical pulverization, low-temperature pulverization, combustion decomposition, and combustion power generation), shown in Figures 4 and 5, that the net carbon surplus of secondary retreading is 2052 kgC and the carbon reduction rate is 74.77%, which is the highest among these five reuse methods. Therefore, the ranking of the carbon reduction effect of these five reuse methods is secondary retreading > combustion decomposition > mechanical pulverization > combustion power generation > low-temperature pulverization.

1-secondary retreading   4-combustion decomposition
2-mechanical pulverization   5-combustion power generation.
3-low-temperature
pulverization
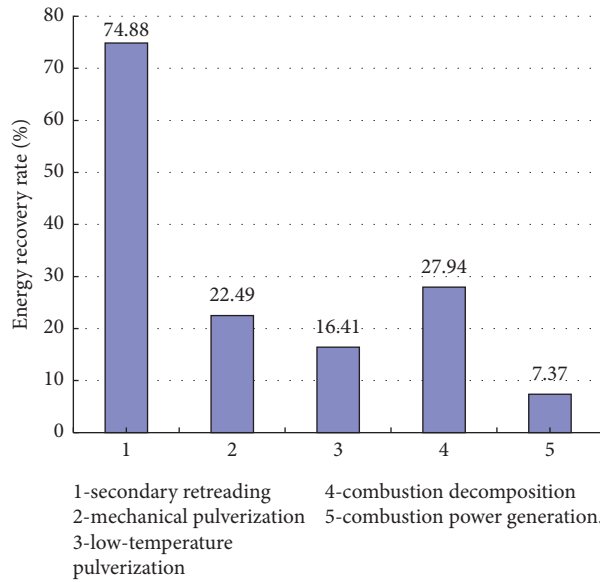
FIGURE 3: Energy recovery rate of the five reuse methods.

TABLE 2: Input-output list of carbon emission and reduction in retreaded tires life cycle.

Category	Name	Value (kgC/t tire)				
Carbon emission	Production phase TC$_1$			3046		
	Transportation phase TC$_2$			22.065		
	Usage phase TC$_3$			211.82		
	Reuse phase TC$_4$	Secondary retreading	Mechanical pulverization	Low-temperature pulverization	Combustion decomposition	Combustion power generation
		894	144	8122	793	26
	New product substation, AC	2052	580	−7396	173	352
Carbon reduction evaluation index	Net carbon surplus, NCS	2946	724	726	996	378
	Carbon reduction rate, CRR	74.77%	22.70%	6.51%	25.94%	12.30%

1-secondary retreading   4-combustion decomposition
2-mechanical pulverization   5-combustion power generation.
3-low-temperature
pulverization
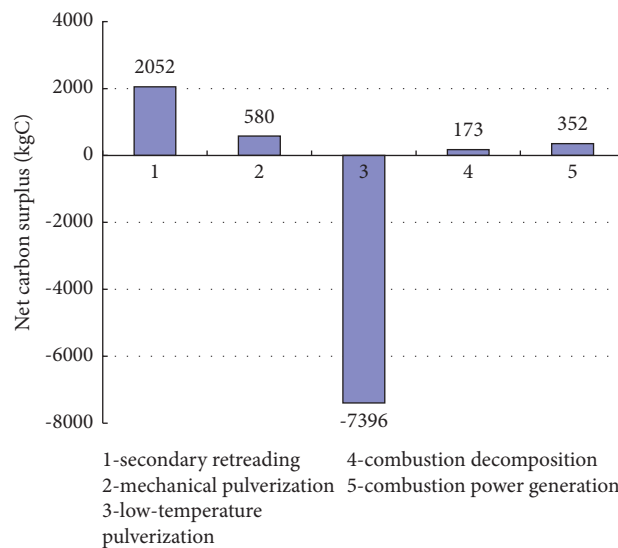
FIGURE 4: Net carbon surplus of the five reuse methods of retreaded tires.
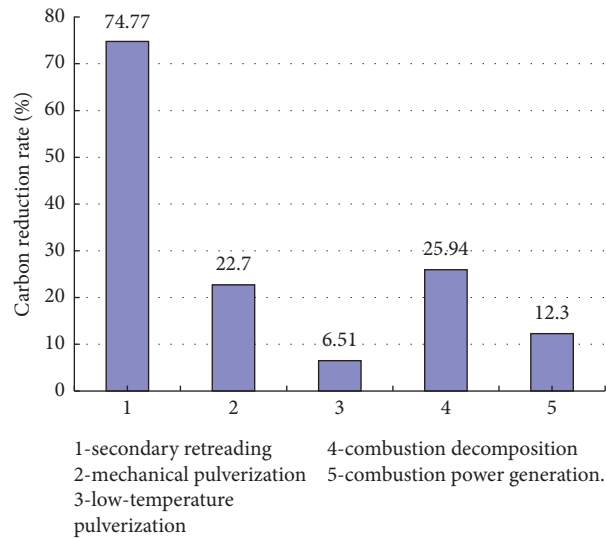
FIGURE 5: Carbon reduction rates of the five reuse methods of retreaded tires.

TABLE 3: Economic cost-profit in the life cycle system of retreaded tires.

	Phase	Economic cost (yuan/t tire)	Economic cost (yuan/t tire)	Profit-to-cost ratio (%)
	Production phase	9325	—	—
	Transportation phase	155	—	—
	Usage phase	1860	—	—
Reuse phase	Secondary retreading	11987	6000	50.05
	Mechanical pulverization	9392	2108	22.44
	Low-temperature pulverization	25879	2124	8.21
	Combustion decomposition	9626	2618	27.20
	Combustion power generation	9475	438	4.62

6.3. Analysis and Evaluation of Economic Results. The economic cost-profit in the life cycle system of retreaded tires is shown in Table 3 (the cost of plant, equipment, and labor is not considered in the research).

It can be seen from Table 3 that the profit-to-cost relationship in the life cycle of retreaded tires is secondary retreading (50.05%) > combustion decomposition (27.20%) > mechanical pulverization (22.44%) > low-temperature pulverization (8.21%) > combustion power generation (4.62%), of which the profit-to-cost ratio of secondary retreading is the largest, much higher than that of the remaining four reuse methods. Namely, it is about 2 times that of combustion decomposition and mechanical pulverization, about 6 times that of low-temperature pulverization, and about 11 times that of combustion power generation. Thus, it can be concluded that retreading is the most effective way to realize the economic benefits of waste tire recycling while the profit-to-cost ratio of low-temperature pulverization and combustion power generation is below 10% and 5%, respectively. From the economic point of view, these two reuse methods are not recommended in reality.

7. Conclusion

(1) Based on the life cycle evaluation theory, this paper establishes the energy consumption model, carbon emission model, and economic model of retreaded tires; determines the evaluation index and calculation method; and conducts the quantitative analysis and evaluation of the energy consumption, carbon emission, and economy.

(2) The energy consumption and carbon emission at the production phase of retreaded tires are the largest, followed by the usage phase, while the energy consumption and carbon emission at the transportation phase are the smallest, indicating that the impact on the total energy consumption and environment is the greatest at the production phase of retreaded tires.

(3) Among the 5 reuse methods of retreaded tires, the ranking of the energy recovery effect is secondary retreading > combustion decomposition > mechanical pulverization > low-temperature pulverization > combustion power generation; the ranking of the carbon reduction effect is secondary retreading > combustion decomposition > mechanical pulverization > combustion power generation > low-temperature pulverization; and the ranking of the profit-to-cost ratio is secondary retreading > combustion decomposition > mechanical pulverization > low-temperature pulverization > combustion power generation.

(4) The results of energy recovery, carbon emission, and economic benefits all indicate that tire retreading is the most effective way in the reuse of waste tires. At the same time, the secondary retreading of retreaded tires will generate greater energy recovery effect and economic benefits, greatly reducing the carbon emission. The secondary and multiple retreading are also the development trend in future tire recycling.

(5) Life cycle assessment of retreaded tire is a complex process. This paper takes engineering tire as the main evaluation object, and its research conclusions have certain limitations. In the future, life cycle assessment of the various types of tires will be tried, so as to enrich related theories of retreaded tire about the life cycle energy consumption, carbon emission, and economy aspect, thus providing further theoretical guidance for industry policy making and retreaded tire manufacturing.

Data Availability

No data were used to support this study.

Conflicts of Interest

The authors declare that there are no conflicts of interest regarding the publication of this article.

Acknowledgments

References

[1] Anonymous, "How a tire is retreaded," *Fleet Maintenance*, vol. 19, no. 7, pp. 152–163, 2015.

[2] Á. Uruburu, E. Ponce-Cueto, J. R. Cobo-Benita, and J. Ordieres-Meré, "The new challenges of end-of-life tyres management systems: a Spanish case study," *Waste Management*, vol. 33, no. 3, pp. 679–688, 2013.

[3] Y. L. Wu, "A brief analysis of tire usage in mines," *Opencast Mining Technology*, vol. 1, pp. 56–59, 2013.

[4] B. Samuel-Fitwi, S. Meyer, K. Reckmann, J. P. Schroeder, and C. Schulz, "Aspiring for environmentally conscious aquafeed: comparative LCA of aquafeed manufacturing using different protein sources," *Journal of Cleaner Production*, vol. 52, pp. 225–233, 2013.

[5] X. Q. Ma, Z. L. Feng, H. K. Liu, and X. P. Zhao, "Full life cycle carbon footprint of waste tires produce recycled rubber—take the reclaimed rubber factory with an annual processing capacity of 20,000 tons of TBR waste tires as an example," *China Tire Resources Recycling*, vol. 12, pp. 36–40, 2018.

[6] Y. Feng, "Tire's research and development of full life cycle smart tires and other high-tech products," *China Rubber*, vol. 33, no. 12, pp. 452–467, 2017.

[7] Z. J. Wang, S. Liu, and J. J. Li, "Measurement and analysis of carbon emissions in China's tire industry based on life cycle assessment—a case study of radial tire industry," *Inquiry Into Economic Issues*, vol. 1, pp. 185–190, 2017.

[8] D. Z. Li, "Research on the full life cycle process of tire production and resource recycling," pp. 1–92, Ph. D. Dissertation, Guangdong University of Technology, Guangdong, China, 2013.

[9] S. Liu, "Research on China's tire industry transformation based on low-carbon economy," pp. 1–84, Ph. D. Dissertation, Qingdao University of Science and Technology, Qingdao, China,, 2015.

[10] J. Huang, G. Li, W. He, J. Xu, and L. Yang, "Energy analysis of tire life cycle," *Qiche Gongcheng/Automotive Engineering*, vol. 34, pp. 277–281, 2012.

[11] Y. W. Wu, "Carbon footprint analysis and research of tires," pp. 1-2, Ph. D. Dissertation, Shanghai Normal University, Shanghai, China, 2012.

[12] L. Yang, "Economic, energy and carbon emission analysis of tire life cycle," pp. 1–106, Ph. D. Dissertation, Tongji University, Shanghai, China, 2009.

[13] Z. F. Li, "Study on life circle assessment and application in tire industry," pp. 1–91, Ph. D. Dissertation, Shanghai Jiaotong University, Shanghai, China, 2011.

[14] S. H. Pang, "China's tire recycling industry forging ahead," *China Tire Resources Recycling*, vol. 10, pp. 10–15, 2018.

[15] W. Qiang, Q. Xiaojie, W. Guotian, and W. Yunlong, "Process and reinforcement mechanism about dislocation remanufacturing retreaded OTR tires by using waste steel," *Earth and Environmental Science*, vol. 5, pp. 1–6, 2018.

[16] J. W. Quan, J. X. Yu, and J. Q. Xu, "Recycling and utilization of waste tires," *Shanghai Energy Conservation*, vol. 4, pp. 262–270, 2019.

Research Article

Big Data Integration Method of Mathematical Modeling and Manufacturing System Based on Fog Calculation

Xin Chen (iD)

School of Information Engineering, Xi'an University, Xi'an 710065, Shaanxi, China

Correspondence should be addressed to Xin Chen; chentjfx@xawl.edu.cn

Using big data to promote economic development, improve social governance, and improve service and regulatory capabilities is becoming a trend. However, the current cloud computing for data processing has been difficult to meet the demand, and the server pressure has increased dramatically, so people pay special attention to the big data integration of fog computing. In order to make the application of big data meet people's needs, we have established relevant mathematical models based on fog calculation, made system big data integration, collected relevant data, designed experiments, and obtained relevant research data by reviewing relevant literature and interviewing professionals. The research shows that big data integration using fog computing modeling has the characteristics of fast response and stable function. Compared with cloud computing and previous computer algorithms, big data integration has obvious advantages, and the computing speed is nearly 20% faster than cloud computing and about 35% higher than other computing methods. This shows that big data integration built by fog computing can have a huge impact on people's lives.

1. Introduction

Fog computing processes data at the edge of the network, responds to user requests, and meets the requirements of low latency and high bandwidth in the Internet of things environment. Fog computing provides services for users locally. On the one hand, it can reduce business processing delay and improve work efficiency. On the other hand, it can reduce the demand for network and bandwidth and save system overhead. Compared with cloud computing, fog computing has great advantages in response time and quality of service and meets the requirements of low latency, high reliability, and security [1]. In addition, as a supplement to cloud computing, fog computing can reduce the pressure of cloud data center, reduce bandwidth requirements, balance data processing capacity, and improve the overall efficiency of the system. In recent years, with the rapid development of the Internet of things, fog computing has been widely used in various fields, such as Internet of vehicles, wireless sensors and actuators, smart home, and software defined network. In the future development, fog computing and cloud computing will complement each other and organically and will be widely used in more industries and fields, providing an ideal software and hardware support platform for information processing in the era of Internet of things [2].

Nowadays, big data has been involved in many fields, such as medical treatment, agriculture, geological survey, astronomy, and Internet of things, and even developed into the fields of news and e-government [3]. The huge value of massive data brings about new development opportunities for every field. However, the generation of massive data also brings about great challenges to data processing. It not only requires strong computing and analysis capabilities but also takes up a large amount of storage space for data storage, which will undoubtedly lead to excessive pressure and resource waste in cloud computing center [4].

Fog calculation provides a new way to solve the problem of data processing. It deploys the virtual machine originally deployed in the cloud data center at the edge of the network. Through the wireless access network, it puts the data with special requirements such as high real-time requirements and sensitive position sensing in the fog server for

calculation and analysis or puts some data in the fog server for temporary storage and forwards the remaining non-time-sensitive data to the cloud data center for processing [5]. This can reduce the computing pressure and waste of resources, reduce transmission delay, save energy consumption, and improve the service efficiency of users and the overall performance of the system. Therefore, it is very important to study the data processing in fog calculation. For this, experts at home and abroad have a lot of research [6].

Li Zhi analyzed the current difficulties of data solution, fog computing, solved the disadvantages of cloud computing and other previous computing, analyzed the shortcomings of fog computing itself, such as security and stability, through the complex network theory as a mathematical calculation tool, built the fog computing structure model, and proposed the operation framework and solution method of fog computing. However, they are all based on theory, and there is no practical research, which has certain theoretical reference value [7].

Tang Linyu thinks that fog computing can provide more services for people. Starting from the allocation of computing resources, it uses fog computing to make models and allocate resources. In the research, it is found that the distribution of fog computing is stable and the demand is matched. The results show that fog computing can make the allocation time relatively stable, and the delay and accuracy of fog calculation are better than those in the original calculation method [8].

Fang Wei introduces the difference between cloud computing and fog computing, analyzes the advantages and disadvantages between them, deeply studies the concept, characteristics, and structure of fog computing, discusses and anticipates the application of fog computing in real life, introduces the calculation method of fog computing, thinks that fog computing is sublimation and diffusion above cloud computing, and makes network computing from network center. It expands to the edge of the network, solves the last kilometer of people's network cognition, and can be used for more research and services [9].

The innovation and characteristics of this study are mainly reflected in the following three aspects: first, the definition and connotation of big data industry are theoretically defined and discussed from the perspective of business ecology. Firstly, the definition of big data ecosystem is given. Secondly, the structure model of big data ecosystem is proposed, and its constituent elements are analyzed in detail, which opens up a new theoretical perspective for deepening scholars' understanding and understanding of big data industry. Thirdly, from the perspective of network governance, this paper discusses the governance mechanism of big data ecosystem and proposes three governance mechanisms, namely, constraint mechanism, incentive mechanism, and coordination and integration mechanism, further expanding the research on big data ecosystem governance. Fourthly, based on the big data ecosystem structure model and governance model, this paper deeply analyzes the status quo of big data industry and puts forward relevant countermeasures and suggestions according to the analysis conclusion, which has certain reference significance for the development of big data industry in other cities in China.

2. Big Data Integration Method Based on Fog Computing Production System

2.1. Fog Calculation. Fog computing is a system level architecture that provides computing, storage, control, and networking functions near the data generation source along the cloud to the integration of things. Fog computing architecture is mainly divided into three layers: cloud computing layer, fog computing layer, and mobile terminal layer. Fog computing architecture makes services closer to end users, reduces latency, saves energy consumption, and enhances user experience [10].

The bottom layer of the architecture is the mobile terminal layer, which contains a large number of intelligent devices and sensors. Data collection, service request, and so on are all from the bottom terminal equipment. Intelligent terminal equipment can preprocess and compress the data and filter out some useless data. At the same time, terminal devices can also communicate with each other through base station or routing equipment to realize data sharing. Fog computing layer is located between cloud computing layer and mobile terminal equipment, which is the bridge between cloud server and terminal equipment. In this layer, simple events and emergency events are detected so as to make quick response to users [11].

The delay of fog computing layer includes the communication delay between fog devices and the calculation delay of fog devices. For communication delay, in the undirected graph composed of fog devices, the communication delay between fog nodes is taken as the weight. With the increase of calculation amount, the calculation delay of fog device increases correspondingly; the more the calculation amount increases, the faster the calculation delay of fog device increases [12]. Therefore, the following function is used to describe the calculation delay of fog equipment.

$$T = \frac{1}{w_x} a_i b_i^2. \tag{1}$$

In the above equation, w_x is the computing capacity of fog device X, b_i is the workload of fog equipment, and a_i is the real number set in advance. Therefore, the delay of the fog calculation node is expressed as follows:

$$T_n = \min \sum_{i=1}^{x} \frac{1}{w_x} a_i b_i^2. \tag{2}$$

The fog computing layer is composed of fog nodes deployed around Internet of things devices. Fog nodes are connected with base stations or routers to reduce the transmission delay between devices. In addition, a large number of fog nodes are deployed at the edge of the network, and even the same service is deployed on multiple fog nodes. This can not only reduce the risk of service interruption caused by the failure of one fog node but also enable one fog node to process data for multiple base stations or routers and

other devices [13]. The fog node in the network can also be connected with the cloud data center. When the Internet of things equipment generates a large amount of data to be processed and the computing power of a single fog node can not meet its needs, the fog node will forward the data to the cloud for processing, which will undoubtedly produce a large communication delay and reduce the service efficiency [14].

The top layer is the cloud computing layer, including cloud data center and server, which is responsible for the storage, analysis, and centralized control of a large amount of data. In addition, the cloud connects with the fog server through the Internet, thus giving full play to its powerful computing power and providing rich service resources for fog. Therefore, the future development of fog computing will not replace cloud computing but the extension and supplement of cloud computing [15], as shown in Figure 1.

With the rapid development of the Internet of things and intelligent sensors, the Internet of things mobile devices are widely used in people's lives. The current cloud computing model can hardly meet the requirements of mobility, location awareness, and low latency in many scenarios. Fog computing inherits the advantages of cloud computing in many aspects and also has the unique advantages of edge computing. It can provide local services for terminal devices nearby, respond to local users' service requests in time, and create new opportunities for the development of various fields [16].

The energy consumption of data processing in fog calculation is studied by immune optimization algorithm. In the traditional three-layer network architecture, considering the problem that the distance between cloud server and fog node is long and the energy consumption is large, a four-layer network architecture model is proposed; that is, a proxy fog server layer is added between the cloud computing layer and the fog computing layer, so that the cloud server can cache the data resources in advance and provide local services. The specific process of addressing the proxy fog server through the optimal immune algorithm is described in detail, so as to reduce the energy consumption of the fog node to obtain data resources from the proxy fog server and also reduce the number of precache resources from the cloud server to the fog node. Through theoretical analysis and simulation experiments, the effectiveness of the four-layer network architecture model in data processing energy consumption is proved.

2.2. Characteristics of Fog Calculation. Fog calculation is a new paradigm. Cisco defines fog computing as a highly virtualized platform between end users and traditional cloud data centers, which can provide computing, storage, and network services [17]. The distributed deployment feature of fog computing at the network edge enables the fog devices on the network edge to directly calculate and store data and applications without having to deliver them to the cloud. Fog computing can be understood as the local cloud, which can be used locally to alleviate the pressure of bandwidth, reduce the delay, and provide real-time services to users.

Fog computing is not composed of powerful servers but some scattered devices, including routers, switches, other traditional network devices, and some specially deployed devices, such as local servers. These devices have computing, processing, and storage capabilities and can forward data to cloud data centers [18]. In the application of Internet of things, data processing mainly relies on local server and provides users with low latency and fast response services by using local resources. It needs to be clear that although fog computing makes up for the deficiency of cloud computing to a certain extent, fog computing is not a substitute for cloud computing, but it cooperates with cloud computing to better meet the needs of users [19].

Fog computing and cloud computing have some similarities to a certain extent: fog computing and cloud computing are based on virtualization technology, encapsulating physical resources and hardware resources into virtual resources, and providing resources for multiple users through virtualization from shared resource pool. However, fog computing is different from cloud computing in that it has unique characteristics and plays an advantage different from cloud computing [20]. The main characteristics of fog calculation are as follows:

(1) Located at the edge of the network, location aware. In terms of network topology location, the fog end device is closer to the user than the cloud and uses the edge network for communication. Geographically distributed fog nodes can infer their own location and track the end-user equipment, sense the information of nearby devices, and timely transmit messages, so as to improve the real-time response.

(2) Wide geographical distribution. Fog computing devices are distributed and deployed on the edge of the network. A large number of sensor nodes are distributed in the user environment to sense the surrounding environment. Different from the centralized processing of cloud computing, in fog computing, fog devices will sense the data of the devices nearby and use local network for data preprocessing. Due to the large number of divisions of fog area, the amount of data transmission is also reduced, which relieves the pressure of bandwidth congestion.

(3) Support high mobility. Fog computing mainly supports the requests of mobile devices. When mobile devices move from one fog area to another, the user's requests will also be transferred. In the whole process, there is no need to transmit back and forth through the cloud. Mobile devices and fog devices can communicate directly, so it supports high mobility.

(4) Low latency. The fog device is close to the end-user and communicates in the LAN environment through the fog gateway. It does not need to go through the cloud, which reduces the transmission distance and delay, and can provide real-time services.

(5) Heterogeneity. Fog devices include different types of devices, deployed in different environments, and fog
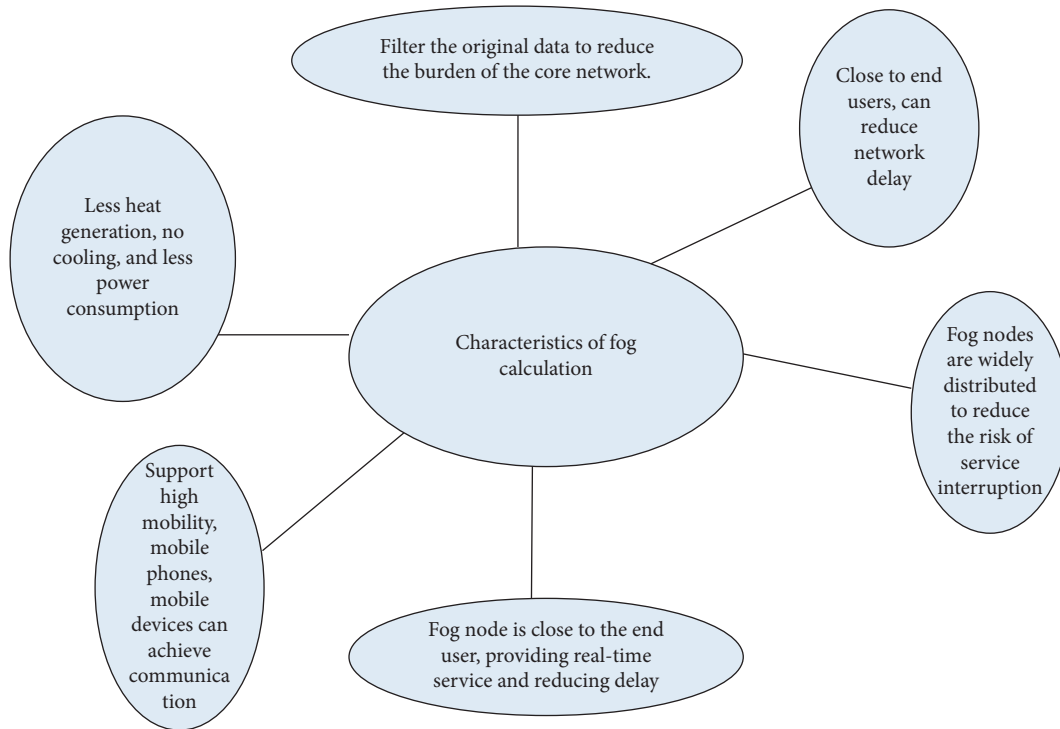
FIGURE 1: Characteristics of fog calculation.

computing can support a variety of heterogeneous hardware and software devices and provide a variety of resources. From the above characteristics, fog computing and cloud computing are different in many aspects. It can be simply understood that the user's request does not need to be sent to the cloud data center for processing and then to the use, but is directly processed by the fog computing equipment near the user, which not only reduces the transmission distance but also reduces the delay.

2.3. Big Data. Unloading part of cloud computing data to fog server for processing can not only reduce data transmission delay and save energy consumption but also reduce the pressure of cloud data center and improve service efficiency. Mobile IOT devices are responsible for receiving data and processing the data in the Intranet in advance to filter out the useless or redundant data. Then, the data are transmitted to the edge fog device, which transforms them into a unified representation framework and fuses them into the feature layer for easy storage. In addition, the fog device will also detect false data and missing data [21]. In order to reduce the risk of being attacked in the process of data transmission, the data will be encoded and encrypted. Finally, the fog device connects the encrypted data to the cloud server. When the data user needs data, it first sends a request to the nearest fog device. If there is data requested by the user in the fog device, it will respond immediately. Otherwise, the fog device will forward the end user's request to the cloud server. The cloud server searches the encrypted data through the index structure and forwards the data to the user. Users decrypt the data

through the key, obtain the data information, and mine the useful value in the data information [22].

The development of big data industry is closely related to big data technology and its application. Although it originates from industry practice, the academic research on "big data industry" lags far behind the practical development. From the domestic point of view, the current research on big data industry mainly focuses on government industrial policies and planning, industrial development suggestions, big data industry comparison at home and abroad, and influencing factors of industrial development. However, there is a lack of research on the internal components and governance mechanism of big data industry based on appropriate theoretical perspective. From the perspective of foreign countries, although there are not many related studies, some scholars have begun to discuss the big data industry from the perspective of business ecology [23].

The big data ecosystem is divided into three levels, namely, the core value chain at the micro level, the extended value chain at the meso level, and the big data ecosystem at the macro level. Among them, the core value chain takes the data value chain as the core, including direct data suppliers and data value distribution channels; the expanded value chain takes the core value chain as the center, which is composed of technology providers, data markets, suppliers of data suppliers, suppliers of complementary data products and services, and direct data end users [24]; the macro level big data ecosystem mainly refers to some related organizations in the periphery of the system, such as government agencies, regulatory agencies, investors, venture capital and incubators, industry associations, academic and research institutions, standardization organizations, and start-ups

and entrepreneur groups, as well as other competitors, stakeholders, and peripheral members [25], as shown in Figure 2.

For big data ecosystem, the diversity of system members is very important. Diversity is an ecological concept. All kinds of organisms in the ecosystem play different important roles in the environment. Many complete food chains and complex food webs have been formed among species and between organisms and the environment. A virtuous cycle of material and energy flow has been formed in the ecosystem. Once the food chain breaks, the system will not function normally. Similar to the natural ecosystem, diversity is also indispensable to the big data business ecosystem: first, the diversity of its members serves as a buffer to deal with the uncertainty of the environment; second, diversity is of great benefit to the value creation of the big data business ecosystem. For example, Alibaba is building a business ecosystem with data as its core. It has successively invested or acquired many Internet companies with a large amount of high-quality data, such as Sina Weibo and Didi travel, playing a huge role in the value creation of the ecosystem; thirdly, diversity is the prerequisite for the self-organization of big data business ecosystem [26].

New data sources increase the type of data. If the decline of data cost only boosts the growth of data volume, then the emergence of new data sources and data acquisition technologies will greatly increase the types of future data. The increase of data types will directly lead to the increase of existing data spatial dimensions, which will greatly increase the complexity of future big data. At the beginning of its birth, the computer was only designed for high-speed calculation, and the calculated data was basically limited to the digital field.

2.4. Data Integration Method. The user request module is responsible for parameterizing the user's service request and then transmitting it to the fog gateway. The fog computing processing module receives the user's requirements, finds suitable resources through resource evaluation, executes tasks, and completes user requests. Cloud computing processing module mainly deals with tasks that cannot be completed by fog computing [27].

Fog computing processing module includes fog gateway, fog server, monitoring equipment, and virtual resource pool. Among them, the fog gateway receives the request from the user and transmits it to the neighboring fog server in the LAN. Monitoring devices track the resource utilization and availability of sensors, applications, and services, generate statistical logs, and transmit data to the fog server [28]. The fog server receives the user requests from the mobile terminal, analyzes the user request information according to the monitored resource information, divides the service into several tasks, and processes the calculation locally as much as possible. According to the evaluation results, each task selects the best matching resource from the resource pool, schedules and allocates the resources, and provides services for users to meet their needs.

Considering the resources with the same service function, the attributes of the resources are set according to the
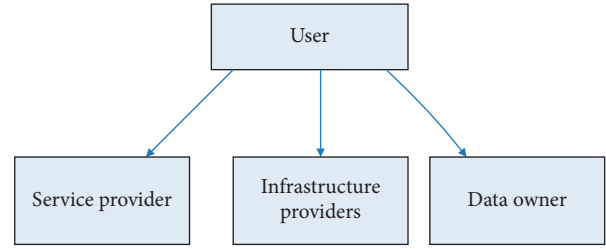
Figure 2: Core owners of big data ecosystem.

user preferences, which have certain scalability. The dynamic calculation formula of fog computing resources is as follows:

$$U_a = p * b \frac{j}{i} * c. \tag{3}$$

In order to calculate the weight of fog calculation attributes and ensure the objectivity of evaluation results, we use entropy weight method to determine the entropy value and entropy weight of each resource attribute.

$$t = \frac{1}{\ln x} \sum_{n=1}^{1} f_{nm} * \ln f_{nm}, \tag{4}$$

$$r = \frac{1 - t}{y - \sum_{m=1}^{m} t}. \tag{5}$$

We have

$$f_{mn} = \frac{z_{nm}}{\sum_{n=1}^{x} z_{nm}}, \tag{6}$$

$$\sum_{m=1}^{x} w_m = 1. \tag{7}$$

Based on the attribute value of user request resource, each resource is regarded as a point in multidimensional space, and Euclidean distance is used to measure the proximity between resource and user demand. Due to the user's preference for a certain attribute or the fact that each attribute of the resource has different influence on the measurement result, set objective weights for each user attribute:

$$d = \sqrt{\sum_{m=1}^{x} w_n * (r_{nm} - uq_m)^2}, \tag{8}$$

$$d_n = \frac{1}{1 + d(r_n, uq)}. \tag{9}$$

According to the proximity between the available resources and the user's requested resources obtained by formulas (8) and (9), the proximity threshold is set between [0,1], and the matching value Q can be obtained.

$$Q_\delta = \{r_n | d \cos(r_n, uq)| \ge \delta\}. \tag{10}$$

The similarity between the resources in the matching resource set Q and the resources requested by users is calculated:

TABLE 1: Server delay data.

Data volume (GB)	2	4	6	8	10
General calculation delay	2.1	3.5	4.7	5.6	6.2
Cloud computing latency	0.9	1.3	1.9	2.2	2.7
Communication delay	1.2	2.4	3.1	3.8	4.1
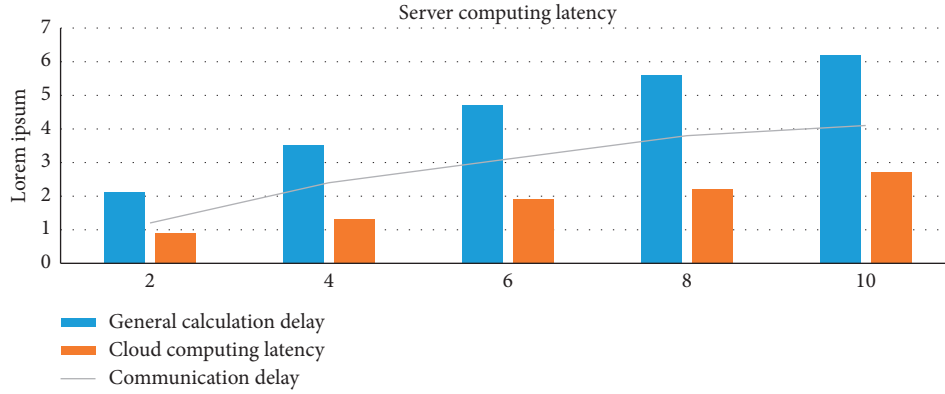
FIGURE 3: Server computing latency.

$$\cos m(r, uq) = \alpha * \cos(r, uq) + (1 - \alpha) * \frac{1}{m} \sum_{n=1}^{m} \delta_{ij}, \quad (11)$$

where a represents the weight, ranging from [0,1]. The simulation parameters are calculated as follows:

$$F = \frac{\sum(q_{rp,rpn} - q_{rpm})(q_{uq,uqn} - q_{uq})}{\sum_{n=1}^{n}(q_r - q_{uq})^2 \sqrt{\sum(q_{uq,uqm} - q_{uq})^2}}. \quad (12)$$

3. Three Big Data Integration Experiments

3.1. Purpose of the Experiment. Based on the theoretical achievements of cloud computing and intelligent research, this paper uses the methods of literature, comparative research, mathematical statistics, and logical analysis to deeply analyze the application of big data integration and intelligent city and study its application mode and characteristics.

3.2. Experimental Evaluation Criteria. Entropy method is a relatively objective evaluation index weight assignment method, which can effectively avoid the subjectivity of artificial scoring, and has high accuracy. But, at the same time, this study also realized that the entropy method can not directly reflect the knowledge, opinions, and experience judgment of experts and scholars, and the weight results may be contrary to the actual situation. Therefore, this paper uses AHP and entropy method to determine the weight coefficient of regional higher education evaluation index.

3.3. Data Sources. The data in this paper mainly come from 2015-2020 China Statistical Yearbook, regional statistical yearbook, National Bureau of statistics, big data statistical platform, and smart city comprehensive statistical information management platform.

4. Big Data Integration Method Based on Fog Computing

4.1. Server Data Calculation Delay. We simulate the verbal delay time of general computing, communication, and cloud computing through the established data model. Without considering the data loss, we set up simulation data to obtain the communication delay and data calculation delay. The details are shown in Table 1 and Figures 3 and 4 .

4.2. Data Delay Performance Analysis of Fog Calculation. In order to verify the effectiveness of fog computing layer in reducing data processing delay, it is compared with the delay of data processing in single fog node and cloud computing, as shown in Table 2 and Figures 5 and 6 .

4.3. Effect of Data Processing Percentage on Data Processing Delay. We set up a value of X, where x is the percentage of the total data processed in the fog computing layer. In order to verify the performance of the calculation, the effect of X on the data processing delay is studied. The details are shown in Table 3 and Figure 7.

The experimental results show that when $x \leq 50\%$, that is, when the amount of data processed in the fog calculation layer is less than half, the larger X is, the smaller the delay is. When $x > 50\%$ and the amount of data is small, the larger X is, the smaller the delay is. However, with the increase of data volume, the delay will increase correspondingly, and the greater X is, the faster the corresponding delay increases, even more than the delay caused by the traditional cloud computing layer.
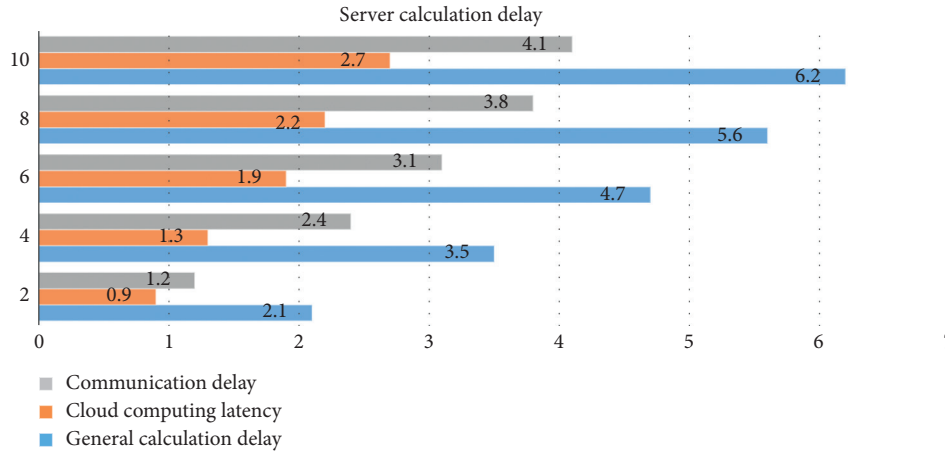
Figure 4: Server calculation delay.

Table 2: Fog calculation data delay.

	Single fog calculation node	Fog calculation layer	Cloud computing layer
5	3	1.3	3.7
10	9	3.4	8.6
15	17	6.7	12.3
20	39	14.9	15.1
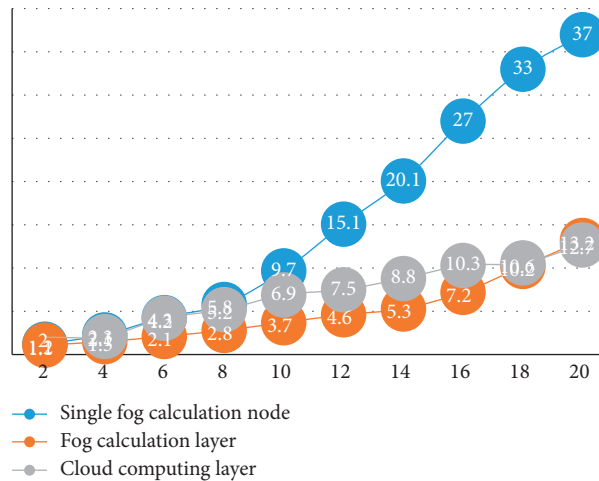
Figure 5: Compute delay performance.

4.4. Impact of the Number of Data Nodes on Data Processing. In order to study the influence of the number of fog nodes on the data processing delay in fog computing layer, the data processing delay values were calculated when the total data X was 2 GB, 5 GB, 8 GB, 10 GB, and 14 GB, respectively. The specific statistical results are shown in Table 4 and Figure 8.

The experimental results show that, with the increasing number of fog nodes, the delay caused by data processing has a downward trend. When the amount of data is small, the increase of fog nodes has little effect on the data processing delay, which is basically in a stable state. When the amount of data is large, the data processing delay decreases obviously with the increase of fog nodes.
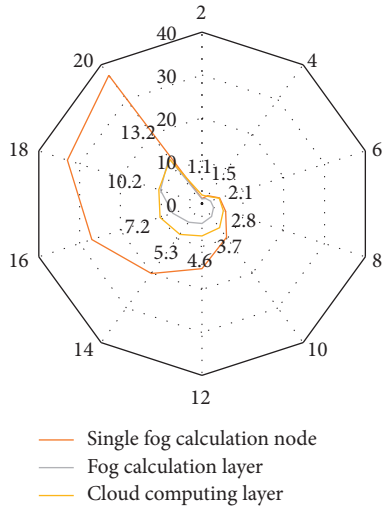
Figure 6: Performance calculation of fog calculation layer.

Table 3: Data percentage impact.

Data volume (gb)/percentage (%)	0	20	50	80	100
2	2.1	1.7	1.4	1.2	1.1
4	3.3	3.1	2.6	2.4	1.9
6	4.2	3.9	3.0	2.7	2.1
8	5.4	4.7	3.7	3.6	3.1
10	7.9	6.6	4.9	5.1	5.4
12	8.6	7.3	6.1	7.2	8.9
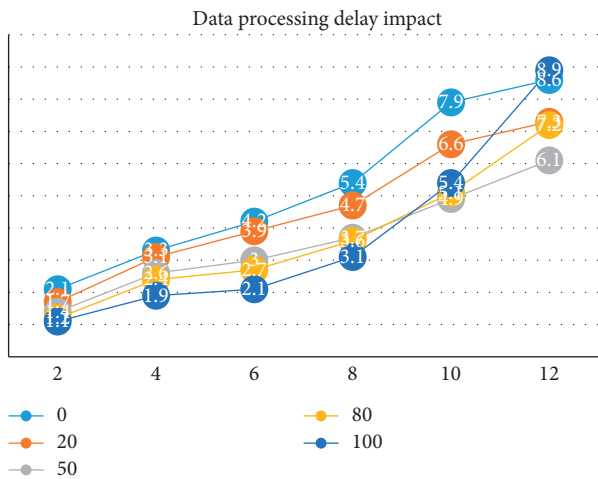
Figure 7: Data processing delay impact.

Table 4: Impact of node number delay.

Data volume (gb)/number of nodes	2	5	8	10	14
1	0.4	4.3	10	18	27
2	0.4	3.7	7.5	13	21
3	0.4	3.5	6.4	11	18
4	0.3	3.3	6.1	8.7	12
5	0.3	3.1	4.7	7.6	9.8
6	0.2	3.1	4.1	6.6	8.5
7	0.2	2.7	3.5	5.9	7.3
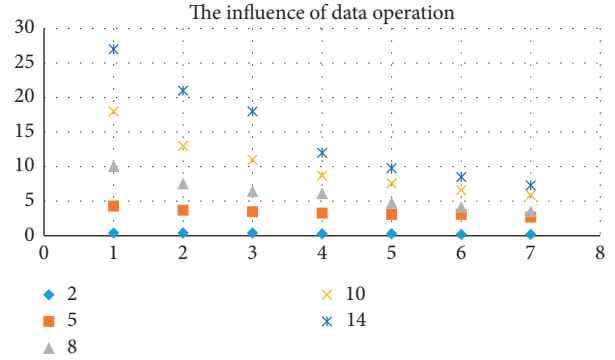
Figure 8: The influence of the number of nodes on data operation.

5. Conclusions

This paper describes the research background of fog computing, domestic and international development status, architecture, application scenarios, comparison with cloud computing, and the importance and necessity of data processing research in fog computing and gives a comprehensive understanding of fog computing from a macro perspective. The data processing delay optimization algorithm in fog calculation is designed. In order to solve the problems of high data processing delay and high pressure in cloud data center, the data processing delay problem is studied with the new cloud fog three-layer network architecture model. The delay of each layer of network architecture is defined mathematically, the data processing delay optimization algorithm is proposed, and the algorithm is described in detail. Theoretical analysis and simulation show that the proposed method is better than the traditional cloud computing architecture in reducing data processing delay.

With the continuous development of Internet technology, data itself is an asset, which has formed a consensus in the industry. If cloud computing provides a place and channel for the storage and access of data assets, then how to systematize data assets to serve national governance, enterprise decision-making, and even personal life is the core issue of big data, as well as the inherent soul and inevitable upgrading direction of cloud computing.

In recent years, informatization has developed rapidly in various industries in China. The high permeability and high integration ability of information technology provide sufficient technical support for information construction and effectively transform and enhance the traditional industry. Big data systematization aims to improve decision-making, supervision, service, and emergency support capabilities, focuses on the integration and development and utilization of information resources, adopts the latest technology, takes intelligent life as the development direction, comprehensively improves the management and service level, and provides comprehensive information services for the public.

Data Availability

The data that support the findings of this study are available from the corresponding author upon reasonable request.

Conflicts of Interest

The author declares that there are no conflicts of interest.

References

[1] Y. Guo, "Fog computing technology and its application in Internet of things," *Telecommunication Science*, vol. 1, no. S1, pp. 90–97, 2018.

[2] W. Fang, "Paradigm shift from cloud computing to fog computing," *Journal of Nanjing University of Information Technology*, vol. 8, no. 5, pp. 404–414, 2016.

[3] H. Zhang and Y. Wang, "NB IOT framework, key technologies and applications based on computing," *ZT Technologies*, vol. 10, no. 2, pp. 40–42, 2018.

[4] J. Qiao, X. Zheng, and J. Gao, "Research on intelligent traffic signal control algorithm based on fog calculation," *Experimental Technology and Management*, vol. 35, no. 10, pp. 83–85, 2018.

[5] R. Hu, C. Lei, X. Duan et al., "A terminal node handover authentication protocol for fog computing," *Acta Sinica*, vol. 42, no. 10, pp. 2350–2356, 2017.

[6] D. Zhang, "Research on data edge storage optimization technology in fog computing," *Fog and Edge Computing*, vol. 05, no. 03, pp. 180–182, 2016.

[7] D. Xing, J. Yao, and Xu Qi, "Study on remote health monitoring of chronic diseases in Medical Association Based on fog calculation," *Journal of Medical Informatics*, vol. 040, no. 6, pp. 8–12, 2019.

[8] D. Xing, "Study on remote health monitoring of chronic diseases in Medical Union based on fog calculation," *Medical Informatics*, vol. 40, no. 6, pp. 8–12, 2019.

[9] H. Zhang, "On the new service computing model of fog computing," *China New Communications*, vol. 1, no. 4, pp. 50-51, 2015.

[10] T. Wang, X. Shen, H. Luo et al., "Research progress of trusted sensing cloud based on fog computing," *Acta Communications Sinica*, vol. 40, no. 3, pp. 170–181, 2019.

[11] H. Tao, "On the service function and service quality of subject librarian 2.0 in fog computing environment," *Library science research*, vol. 1, no. 12, pp. 80–85, 2015.

[12] C. Wang and X. Huang, "Research on optimal allocation of inference nodes based on fog computing in intelligent environment," *Acta Electronica Sinica*, vol. 48, no. 1, pp. 35–43, 2020.

[13] L. Tong, L. Tang, X. he et al., "Optimization task unloading scheme based on network delay and resource management in integrated blockchain and fog computing system," *Journal of Electronics and Information*, vol. 8, no. 1, pp. 135–137, 2020.

[14] J. Fan, W. Jingzhang, and S. Xu, "Load balancing strategy based on fog computing," *Journal of Xi'an University of Posts and Telecommunications*, vol. 24, no. 1, pp. 20–25, 2019.

[15] W. Ma, C. Shao, and M. Liu, "Research on content access technology of expressway service area based on fog computing," *Electronic Technology Application*, vol. 44, no. 12, pp. 101–105, 2018.

[16] K. K. Han, Z. Xie, and X. Lv, "A task scheduling strategy for fog computing based on improved genetic algorithm," *Computer Science*, vol. 45, no. 4, pp. 137–142, 2018.

[17] J. Cao and J. Li, "Research on coal mine whole scene monitoring system based on fog calculation," *Industrial and Mining Automation*, vol. 46, no. 2, pp. 50–53, 2020.

[18] P. Zeng, Q. Jin, C. Mu et al., "A lightweight attribute based outsourcing encryption algorithm for fog computing," *Computer Application Research*, vol. 37, no. 2, pp. 498–504, 2020.

[19] W. Dong, renshuang Ding, W. Huang et al., "Trust evaluation algorithm based on fog computing in vehicular social network," *Minicomputer System*, vol. 40, no. 6, pp. 124–127, 2019.

[20] H. Zhang and Y. Wang, "NB IOT framework, key technologies and applications based on fog computing," *ZTE Technology*, vol. 23, no. 1, pp. 32–34, 2017.

[21] S. Kao and L. Yu, "Construction scheme of sub-health information management system based on cloud and fog computing," *Electronic Technology*, vol. 31, no. 7, pp. 79–84, 2018.

[22] S. Chen, "Research on data aggregation of smart grid security and privacy protection based on fog computing," *Journal of Nanjing University of Posts and Telecommunications: Natural Science Edition*, vol. 39, no. 6, pp. 62–72, 2019.

[23] X. Wang, J. Zou, and J. Du, "Research on improved habe algorithm in fog based phr system," *High Tech Communication*, vol. 1, no. 9, pp. 852–861, 2019.

[24] L. Li, "Research on real-time traffic guidance planning mechanism based on fog calculation," *Enterprise Technology Development*, vol. 1, no. 6, pp. 1–3, 2019.

[25] Y. Du and Y. Guo, "A trust value based dynamic access control method for fog computing," *Information Network Security*, vol. 1, no. 4, pp. 65–72, 2020.

[26] Z. Shi, "Research on computational migration strategy based on multi-objective optimization in fog computing environment," *Journal of Xi'an University of Arts and Sciences*, vol. 22, no. 1, pp. 20–23, 2019.

[27] C. Chen, "Application of cloud computing, fog computing and edge computing in intelligent transportation," *Digital Communication World*, vol. 1, no. 9, pp. 121–123, 2019.

[28] F. Yu, L. Yang, and L. Yang, "Application Research of Internet of things based on fog computing," *Telecommunication Network Technology*, vol. 1, no. 5, pp. 59–62, 2019.

[29] H. Guan and L. Xu, "Intelligent fishery aquaculture monitoring system based on mixed cloud and fog computing," *Information Technology and Information Technology*, vol. 231, no. 06, pp. 30–32, 2019.

Research Article

Problems and Countermeasures Existing in E-Commerce Enterprise Network Marketing under the Background of Big Data

Lei Xia[1] **and Xinyu Lv** [ID] [2]

[1]*School of Economics and Management, Xi'an Aeronautical University, Xi'an 710077, Shaanxi, China*
[2]*School of Accounting, Shanghai University of Finance and Economics- Zhejiang College, Jinhua 321013, Zhejiang, China*

Correspondence should be addressed to Xinyu Lv; z2014127@shufe-zj.edu.cn

With the analysis of mobile clients and artificial intelligence technology, e-commerce is growing faster and faster. In today's daily life, the e-commerce model has even been integrated into human life and has become an indispensable part. In the past few years, in the face of such a large business opportunity, e-commerce companies have sprung up in the capital market. Along with the rise of e-commerce, there have been many problems that have never arisen. The purpose of this paper is to analyze the status of development of e-commerce and its enterprise. This paper focuses on combing the current marketing overview and problems of e-commerce companies and proposes positive countermeasures and some practical solutions. Using the specific analysis method of the specific problem, the data comparison is made to draw conclusions. The results show that national policies focus on the rise of small and microenterprises, from the perspective of current business development, and developing e-commerce is conducive to enterprises to expand business breadth, expand the market scope of enterprises, develop business needs and brand products of enterprise by using Internet technology, and can break the constraints of time and space effectively. Strengthened communication and communication between enterprises and customers reduced the costs of enterprise, saved time, and improved utilization rate of resource. Therefore, solving the marketing problems which is most urgent at present is the primary goal of developing e-commerce companies.

1. Introduction

With the application of mobile Internet, Big Data, artificial intelligence, and other technologies, people's lifestyle has undergone tremendous changes. The emergence of e-commerce has changed people's consumption patterns. Consumers no longer pay face-to-face, hand-to-hand delivery. The whole transaction process can be completed through the Internet. In the face of new opportunities, capital gathers here [1, 2]. The number of registered e-commerce enterprises is increasing year by year. The rapid rise of e-commerce enterprises is due to their low production costs, transaction costs, and management costs, which enhances the profits of the enterprises on the original basis [3]. As an e-commerce model of emerging industries, many enterprises have low entry threshold when entering the field,

but there are more or less problems in network marketing, shop operation, and so on. If these problems cannot be solved timely and accurately, it will not only affect the profits and survival of enterprises but also affect the rise of the whole e-commerce model [4]. Therefore, it is urgent to deal with some current problems in a timely manner.

In today's society, we have entered the era of information technology, which is not only an objective factor of economic development but also our common recognition and judgment of the characteristics of the times we live in. The reason why we think this is the information age is that information has a far-reaching impact on the economic and social life of each of us and has caught up with the influence and change of the natural geographical environment and social interpersonal interaction [5]. Even in some cases, the importance of the intangible power of information has

approached or even surpassed our material needs. We are in the era of information technology revolution, the speed of information development exceeds our expectations, we are also immersed in the convenience of the Internet, and the evolution of Big Data has come to us and gradually affects our lives [6]. Nowadays, Big Data technology (BDT), like computer technology, is a new technological revolution and the best assistant to promote economic development and industrial upgrading worldwide. BDT has been deeply integrated into our lives from a single technology. With e-commerce becoming a new business model, it is the best application of BDT. Due to geographical constraints, global trade mainly conducts foreign trade transactions through trade fairs [7, 8]. At regular trade fairs held in various countries, foreign businessmen from all over the world make inquiries, exchange, place orders, and sign contracts. However, due to the constraints of cost and price, regional differences, and exchange rate fluctuation, the actual volume of transactions reached in this cross-regional time-consuming trade fair is very limited. Businessmen from all over the country are also cautious and have a wait-and-see attitude, mainly to inquire and obtain commodity information, to build a bridge of cooperation. The emergence of Internet technology and the maturity of BDT promote the transformation of trade fairs from offline to online and also provide a broader platform for foreign trade enterprises, especially some small- and medium-sized enterprises in the rising stage. With the continuous maturity of Internet technology and the rapid establishment of cross-border e-commerce platform, the combination of BDT and e-commerce enterprises is closer. The application of BDT in enterprise management is becoming more and more important. Therefore, the use of new technologies to develop our cultural industry is a combination of the times and traditions and also a common progress between them, promoting each other and complementing each other.

In recent years, with the rapid rise of e-commerce, a series of e-commerce enterprises have come into our lives imperceptibly, such as Taobao, Jingdong Mall, Suning Easy-to-buy, and other well-known local network businessmen. By learning the management experience and management methods of foreign well-known enterprises, they have now developed into a world-renowned large e-commerce enterprise [9, 10]. Driven by the Internet and Big Data, many enterprises have also opened the online sales model. For example, Gome Electrical Appliances and Internet-related enterprises jointly launched online sales renamed "Gome Online." At present, in many front-line big cities, in the real stores, the operation is restricted more and more. Land rent, warehouse cost, promotion, and other factors make the daily management and operation expenses of stores we can shop at this stage rise, which leads to the production sold in stores. The cost of products is increasing, and ultimately, the price of products is increasing. On the contrary, in the process of delivery, transportation, distribution, and inventory of products sold online, the cost of management is much lower than that of physical stores. Therefore, the prices of some products on the Internet will be relatively preferential. At the same time, enterprises can communicate with upstream and downstream platforms in a convenient and fast way by launching e-commerce. However, many real stores in business districts are closed due to competitive pressures, and some e-commerce enterprises are reported to sell counterfeit goods. Therefore, e-commerce has become a double-edged sword for enterprises to develop market competitiveness. How to correctly face the problems and explore the countermeasures for academic researchers is the top priority. Generally speaking, experts and scholars pay more attention to the importance of e-commerce enterprises, mostly concentrated in the analysis of overall advantages. Specific implementation measures, especially the use of BDT, e-commerce network marketing for innovation and development research is relatively small. Secondly, the analysis and rise of e-commerce business conditions, from the domestic factors more research, from the system policy to the enterprise's own innovation and reform ability comprehensive research, and the rise of e-commerce enterprises, not only need our own efforts, but also should have mutual exchanges and mutual promotion process. Foreign scholars should strengthen the study of business enterprises, analyze the problems, put forward feasible strategies, and explore a new path for the healthy rise of e-commerce mode in the light of the current economic situation [11, 12].

Starting with the meaning and characteristics of Big Data, this paper probes into the development process of e-commerce enterprises, expounds the characteristics and operation modes of e-commerce enterprises, mainly analyses the problems existing in e-commerce enterprises' network marketing, finds out the reasonable marketing methods and the balancing basis that accords with the characteristics of Big Data, and combines them organically. On the basis of sorting out the rise of e-commerce enterprises and related theories of e-commerce marketing under Big Data, this paper tries to discuss the problems and countermeasures of e-commerce marketing from the application level and summarizes the reasons of low competitiveness and low cost-benefit ratio in an all-round way, hoping to meet the e-commerce operators. The problems provide theoretical basis and innovate business models and clear solutions. To orientate the current marketing mode, learn from foreign experience, draw the similarities and differences of the rise of domestic and foreign e-commerce enterprises through comparative advantage analysis, learn advanced experience, put forward improved methods and paths, combine with new development methods, and finally put forward a new development mode of Chinese e-commerce enterprises, in order to promote the rise of China's new economy. Exhibit vitality and put forward some suggestions.

2. Big Data and Electronic Commerce

2.1. The Concept and Significance of Big Data. In the information age, as the basic resource for people to communicate, data naturally become the source of people's cultural value. First of all, large data should be collected in a wide range and diversified way. Then, distributed computing architecture is adopted to integrate and analyze data processing through

cloud computing and cloud storage. Futurologist Alvin Toffler first put forward the concept of Big Data in 1980. With the wide application of the Internet, the characteristics of large data, such as high speed, varieties, and value, have emerged. In the virtual network world, we can extract valuable information from a large amount of information and then extract its value from effective information. The use of Big Data in all aspects today is mainly based on its users' precise positioning of the required information groups, accurate point-to-point service, to understand the preferences and habits of target customers and high-quality marketing. Although the process of use has experienced suspicion and criticism, it has been ultimately accepted by the public, survived in the cruel Internet competition, and is getting better and better, bringing considerable benefits to enterprises. Using BDT, e-commerce can negotiate and trade online. Businessmen have a clear view of customers' preferences and habits, browsing time, consumption capacity, and scope. Through data analysis, they can have a comprehensive understanding of customer groups, and precise positioning points can be made according to consumers' consumption preferences, so as to save money. This avoids the tedious traditional marketing methods, information lag, and low efficiency. Adjust the operation mode and marketing strategy of enterprises to maximize benefits. With the deepening of technology, the radiation scope of data analysis has been expanding from enterprises to industries, with some areas expanding nationwide and gradually opening up overseas markets. Of course, there are pros and cons in everything. Quantification, wide dissemination, and publicity of data have brought about many negative impacts on human society. Regardless of the collection and sorting of data, or the analysis and processing, it must follow the principle of "Privacy First" and must not threaten the privacy of the country. Therefore, we need to look at BDT dialectically, make rational use of advantages, and resolutely avoid disadvantages.

2.2. Impact of Big Data on Network Marketing.

At present, the social economy has entered the era of Big Data. Whoever is familiar with mastering and using Big Data well will be in the forefront of the times in social change. E-commerce enterprises will be able to better understand consumer needs and achieve the precision and individualization of marketing. Online shopping has been very common in our country and has gradually grown into the main mode of shopping. The number of online shopping accounts for more than 60% of the netizens in our country, and the online shopping market in our country is still in the trend of rapid growth. With the rapid rise of e-commerce, the explosive growth of data in all sectors has occurred. Mature e-commerce enterprises use BDT to extract accurate and valuable information through mining and analyzing a large number of customer data, so as to understand customer needs, grasp market trends, formulate more reasonable marketing strategies, realize the precision and individualization of network marketing, and improve sales level. Therefore, if e-commerce enterprises want to solve the problems of online

marketing correctly, they cannot do without the use of the Internet and Big Data. Combining with the background of the times, it is of great significance to enhance the marketing strategy of enterprises and promote the rise of e-commerce enterprises. With the rise of large data in recent years, the depth and breadth of large data have been improved to a certain extent. It has a wide range of types, a large number, and a fine and complex structure. The popularization and application of BDT has brought great opportunities for the rise of commercial enterprises in China. With the advent of the mobile Internet era, it has brought greater development prospects for e-commerce. It is not only the expansion of scale and the increase of market share but also the effective display of the value of each link in the industrial chain. It has created innovation and construction for network marketing and provided basic conditions for the follow-up development. First, the efficient use of mobile terminal equipment should deal with the construction of cooperative relationship with mobile operators and then correctly select strong technical support for e-commerce marketing activities. If you want to do a good job, you must first use the tools and master the information before you can grasp the market. Second, e-commerce enterprises should enhance cooperation with platform suppliers, build a standardized and effective e-commerce platform, realize the comprehensive integration of the first, second, and tertiary industries in a certain Internet era, and then realize the sustainable rise of e-commerce. Third, in terms of content and service, suppliers of Big Data applications need to pay attention to the in-depth rise of market research, provide a reasonable reference for enterprise development, realize the continuous innovation of marketing mode, and cooperate with the media to make the development mode richer. Fourth, according to the type of mobile phone users, joint network operators provide targeted marketing services to them, not only to ensure the improvement of service quality but also to develop the real e-commerce needs of many people, making the development model of industrial chain more effective.

2.3. Concept and Significance of Electronic Commerce.

E-commerce refers to a new business mode that uses the Internet to conduct all trade activities, i.e., to connect information flow, capital flow, business flow, and a part of logistics on the Internet. In the open-network environment of the Internet, based on the server application mode, computer technology, network technology, and remote communication technology are used to realize the electronic, digital, and networked business process. E-commerce is under the background of Big Data. Consumers are directly involved in economic activities through the Internet and online and offline. Farewell to the traditional store marketing, the use of online trading platform reduces the operating costs of enterprises, expands the circulation space, and improves the success rate of transactions. At the same time, it saves customers' time. E-commerce is developing at an alarming speed, covering a wide range of items and even services that can be searched on the Internet. From daily life of food and clothing, books and household goods to high-

end products such as electronic consumer goods and automobiles, it can be said that there is everything. Through e-commerce mode, consumers can acquire what they need without going out to buy products. They can only use the Internet at home to buy what they want.

2.4. Current Development of Electronic Commerce. Compared with foreign countries, the development of e-commerce in China is relatively backward, but its development speed is higher than that in Western countries. In 1999, the concept of e-commerce began to prevail in China. In 2000, in a short period of 1 year, more than 1,000 e-commerce websites were added. But the survival rate of many small start-ups is very low, and the number of e-commerce enterprises registered to establish and withdraw from the market is comparable. After several years of development, the e-commerce market has basically formed a pattern of sharing the world by several well-known brand websites. Businessmen and buyers are the two sides of e-commerce. From the consumer's point of view, in the process of e-commerce development, there are more and more online merchants, and the types of goods are more and more complete and abundant. However, consumers' choices are diverse, and it is impossible to produce all the favorite goods. On the one hand, the goods consumers choose to buy reflect the choice of merchants but also to a certain extent reflect the goods suitable for online sales. As an ordinary consumer, if you want to buy a product, you will screen it. When purchasing online, consumers can weigh whether to buy the goods according to the description of sellers, e-commerce enterprises, other consumer evaluation positioning, the reputation of sellers, the degree of hot sales of goods, and the service attitude of sellers. This will lead to high sales in more popular stores, which tend to be short-lived. The initial electronics market is dominated by household goods, books, and other daily necessities because these goods can be described by the detailed information attached to them. And the way of online shopping goes deep into the lives of ordinary people, netizens have become commonplace. As long as there are goods available on the Internet, and in line with consumers' purchase needs and desires, there will be consumers willing to pay, but the difference is the degree of hot sales of products. Often, a dozen or even dozens of the same goods are sold at the same time. So it grew into a buyer's market. It is very difficult for small e-commerce enterprises to survive without a set of special and marketable methods to stand out among many businesses. Online shopping brings many conveniences to all parties, but the network is a special platform. Consumers' experience of goods can only come from hearing and vision, and there is no face-to-face selection opportunity. To some extent, it increases the risk of consumers, so to some extent, goods with certain standards and specifications can be more eliminated. The growth of e-commerce enterprises and the promotion of product competitiveness are a guarantee for both businesses and buyers. After the rapid rise of e-commerce in China, it means that the business model has gradually matured. Nowadays, standardized products such as books and publications are no longer the most valuable subdivisions. At present, the largest categories of sales are apparel and 3C products. At this stage, the main business models of e-commerce can be divided into three types: intangible products and services, physical goods, and comprehensive.

3. The Characteristics and Advantages of E-Commerce Enterprises Network Marketing

3.1. Characteristics of Network Marketing in the Background of Big Data

3.1.1. Big Data Helps to Achieve the Precision and Individualization of Marketing. We have entered the era of Big Data. The reason why e-commerce enterprises are different from traditional enterprises is that they will produce a large amount of data in any link of the business process. If we can classify these massive data timely and accurately in the process of network marketing and make rational use of them, we can make the effectiveness of enterprise network marketing possible. The results were significantly improved. Using BDT and Internet platform, e-commerce enterprises can analyze the consumption habits of related customers and potential customers in detail, browse and purchase history, personal preferences, personal information, and conduct in-depth mining. By forecasting the future market development trend and understanding the real needs of customers, we can make precise marketing and personalized recommendation for customers with different needs. At present, Taobao, Suning Easy-to-buy, and other websites use users' clicks to record the goods they browse. These records are actually part of the Big Data. Among them, Taobao's "guess what you like" section is to make full use of BDT to analyze consumers' online browsing behavior, so as to formulate a targeted list of recommendations for different consumers. For example, when consumers browse information about books on the Internet, the website will analyze the behavior of consumers, determine consumer preferences, purchasing power level, and will recommend relevant books or book derivatives and other similar products to them from time to time. Precision and individualization of network marketing not only help enterprises save marketing costs, improve the sales rate of goods and increase profits but also make enterprises better and more accurately understand customers' preferences, provide them with more goods to meet their needs, and enhance customer satisfaction. The analysis of domestic e-commerce business model and operation management mode is shown in Table 1.

3.1.2. Big Data Helps E-Commerce Enterprises to Grasp Market Trends. E-commerce enterprises make use of BDT to make marketing decisions more reasonable and efficient. In the traditional network marketing, e-commerce enterprises will generally conduct network surveys on consumers and get the survey results. At the same time, drawing on the historical experience of marketers and offline marketing methods to make marketing decisions, such decisions are

TABLE 1: Analysis of domestic e-commerce business model and operational management model.

Business model	Representative enterprise	Management focus
Value chain integration model	Jingdong, No. 1 Shop, Zhanzhao	Product flow management
Open-platform model	Taobao and T-mall	Platform resource integration
o2o mode	Suning E-commerce	Information flow management

often more perceptual. In the era of Big Data, there is no need for marketers to think of screening and selection. Consumers browse the website. When they buy goods, the traces left behind become important resources for marketing decisions. E-commerce enterprises can get more comprehensive market information and insight into consumers' needs and purchasing motives using BDT to analyze the massive behavior data of consumers, so that they can make more scientific and rational decision-making in the selection of marketing channels, the way of commodity promotion, and the price of products, so as to improve the marketing effect. In addition, e-commerce enterprises can use BDT to get customers' feedback on products and services in a timely and comprehensive manner, find problems in time, and improve products and services, so as to improve customer satisfaction. In short, marketing decisions based on BDT are often more rational than traditional marketing decisions, which can better reflect the development trend of the market and bring more benefits to enterprises.

3.2. Advantages of Network Marketing under the Background of Big Data.

(1) Cost advantage: in the field of e-commerce production, in order to improve their competitiveness, most enterprises reduce the pressure of e-commerce competition by changing the basis of enterprise competition and reducing the product design and labor costs.

(2) Transaction cost advantage: in the good environment of e-commerce development, many enterprises will reduce the interaction between consumers and reduce the problem of insufficient personnel in the process of sales. In the process of online sales, we can sort out and summarize the current sales situation and find out the current sales mode in time. Many problems can be solved quickly, which greatly reduces the transaction costs of enterprises to a certain extent, and thus greatly improves the profits of enterprises.

(3) Management cost advantage: at this stage, the mature development of e-commerce enterprises has brought great convenience to the rise of other types of enterprises and enormous economic benefits to enterprises in terms of management costs. The new mode of e-commerce, farewell to the traditional warehouse hoarding problem, in the process of product sales, directly through the production site or unified warehouse delivery, greatly improves the management efficiency and reduces the cost of management.

4. Problems and Countermeasures of Enterprise Network Marketing

In the rapid rise of e-commerce enterprises in China, there are more or less problems, such as weak awareness of Big Data application, low data quality, and lack of professional talents in Big Data marketing, which hinder the application of BDT in the process of network marketing and affect the effect of network marketing. Based on the characteristics of network marketing under the background of Big Data, this paper makes an in-depth analysis of the problems existing in the network marketing of e-commerce enterprises in China and puts forward some countermeasures, in order to comprehensively promote e-commerce enterprises to formulate more reasonable marketing strategies using BDT and to achieve better and faster development of themselves. With the rise of the Internet, more and more enterprises rely on the Internet for their marketing activities, so there is "network relationship" marketing. The network marketing theory diagram is shown in Figure 1.

4.1. Problems in E-Commerce Enterprises' Network Marketing

4.1.1. Lack of Ability to Use Large Data. With the application of Big Data and mobile Internet, e-commerce enterprises are facing new opportunities for development. Enterprises can push consumers' information through technical processing of consumer information and reduce the cost of market promotion, providing valuable information, providing strong support for the formulation of enterprise direction, and grasping the market more accurately. Big Data application technology can greatly promote the rise of e-commerce. However, in view of the actual development situation, only a few e-commerce enterprises apply BDT to network marketing. Some of the current problems are due to the obsolete concept of the enterprise, the lack of awareness, or the lack of proficiency in using BDT to promote the rise of e-commerce, that e-commerce enterprise development cannot be combined with BDT, and the other part is that e-commerce companies have limited knowledge of Big Data application technology, the practical application of Big Data needs certain financial support, and small micro-e-commerce enterprises have weak ability to process and analyze information. The data in this article come from a questionnaire survey of 100 e-commerce companies on e-commerce platforms, such as JD.com, Taobao, and Suning.com, and use SPSS software to perform statistics and analysis on the data recorded in the questionnaire. The investigation of the problems existing in e-commerce enterprise network marketing is shown in Figure 2.
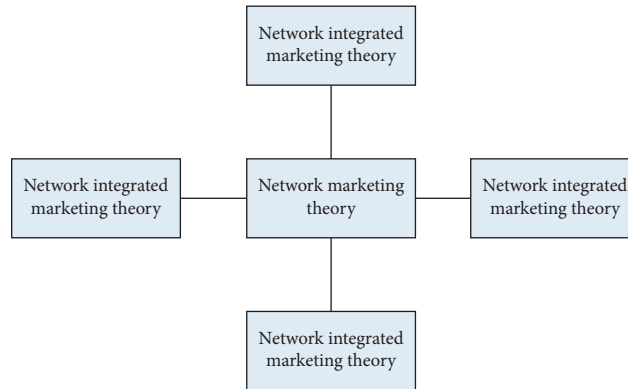
FIGURE 1: Theoretic diagram of online marketing.

4.1.2. Information Screening Technology Is Backward. The advanced point of BDT is to obtain consumer behavior information. By extracting information, deleting data, and analyzing and processing data, we can get valuable marketing information for enterprises. E-commerce enterprises can easily face the massive data on the Internet in Shanghai, but they cannot get timely information in line with the development orientation of enterprises. Some enterprises face a large amount of information and cannot effectively useless garbage information and low-quality, small-related information. Low-quality data information will not only increase the difficulty of technical processing of e-commerce companies but also affect the processing results, efficiency, and effect of marketing.

4.1.3. There Is a Risk of Leakage of Customer Privacy Information. Consumer personal records and consumption are obtained by e-commerce enterprises using BDT Habit. Consumers' browsing habits, consumers' consumption level, historical transaction volume, and other information cover personal information. Once the consumer's personal information privacy information is stolen, or even illegally traded, it will seriously damage the interests and safety of customers. This requires e-commerce enterprises to strictly adhere to the bottom line of morality, improve the security of their data information, and protect the information security of consumers.

4.2. The Countermeasure of the Problems Existing in E-Commerce Enterprise's Network Marketing

4.2.1. Government System and Policy Norms. E-commerce enterprises make use of network marketing to obtain profits. The government attaches great importance to network marketing and the establishment of relevant network marketing policies become very important. At present, there are still many problems of safety and integrity in the network marketing of e-commerce enterprises in our country. The government should regulate and control the whole from the macro aspect, create a good network marketing environment and system, and strengthen the legislative work. There are no corresponding laws and regulations in the network

marketing of enterprises in our country, which makes the illegal elements gain. It is a good chance. At the same time, we should vigorously strengthen network technology research, improve network infrastructure construction, and improve related services. The survey of the operational support level of network marketing is shown in Figure 3.

4.2.2. E-Commerce Enterprises Should Strengthen Network Awareness and New Marketing Concepts. Failure to improve the marketing effect is a cause for both sellers and consumers. Consumers' shopping concept has not completely changed, and they can only make judgments by pictures and the evaluation of the purchasers, which undoubtedly increases the difficulty for consumers to choose and buy goods and invisibly increases the risk of online shopping. Consumers should gradually change their concepts and accept new shopping methods. As an enterprise, it must first change the attitude of traditional marketing, realize the opportunities brought by network marketing to the rise of small- and medium-sized enterprises, and bring network marketing into the overall marketing strategy of enterprises. We should increase investment in network marketing and attract network marketing professionals. Network marketing is regarded as a powerful weapon to improve marketing level and narrow the gap between large enterprises. E-commerce companies can use brand marketing strategies, integrated marketing strategies, hot spot quick marketing strategies, conceptual marketing strategies, ground marketing strategies, real marketing strategies, and superior marketing strategies to guide their online product marketing strategies. Consumers' survey of online shopping concepts is shown in Figure 4.

4.2.3. To Adopt Reasonable and Effective Strategies of Network Marketing Promotion. Consumers need to search for information when shopping on websites. One of the ways is through search engines. Therefore, in order to expand the effectiveness of online marketing, enterprises must do a good job in search engines, so that users can easily search the relevant information of enterprises, so that enterprises can increase their favor of enterprises and their goods and services and develop users into loyal customers of enterprises.

Problems in network marketing

Conceptual issues
Talent problem
Technical issues
Honesty and credit
Safety problem
Other issues
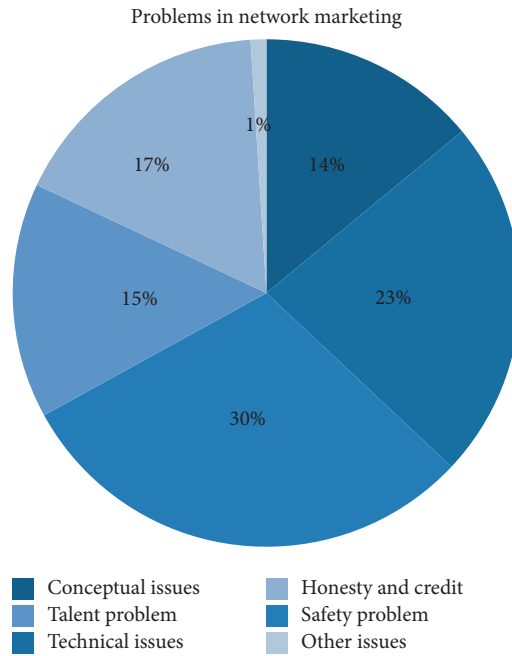
FIGURE 2: Problems in e-commerce enterprises network marketing.

Operational level

None of the above — 40.70%
Specialized product-end talents — 23.30%
Independent network sales team — 35.40%
Specialized customer service team — 48.30%

0.00   20.00   40.00   60.00

(%)
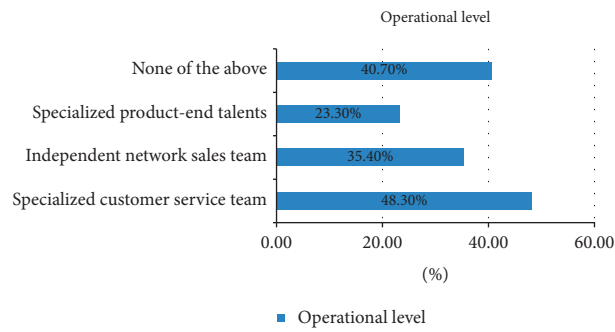
■ Operational level

FIGURE 3: Business operation support level of network marketing.

Consumer's concept of online shopping

12%
21%
65%

■ Complete confidence
■ The heart of avoiding talents
■ Total distrust
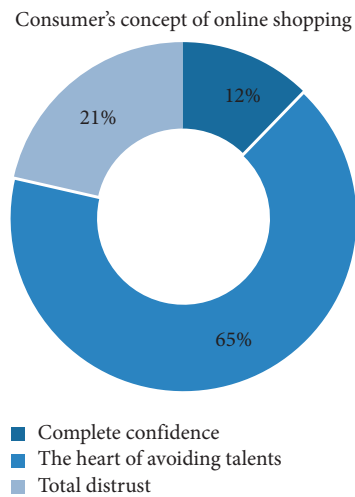
FIGURE 4: Consumers' ideas of online purchase.

5. Conclusion

This paper briefly analyses the problems and countermeasures of e-commerce enterprise network marketing under the background of Big Data. This paper expounds the new opportunities and problems of Big Data application, electronic commerce, and network marketing in the environment of rapid rise of modern economy. The development of e-commerce is the most dynamic economic model at present. This paper points out that under the opportunity of blowout development of Internet Big Data, changing the traditional marketing mode, grasping the law, exploring the new role of Internet application, and correctly recognizing and solving the current marketing mode of e-commerce enterprises are the key breakthroughs to promote the development of e-commerce enterprises.

Through systematic analysis of the meaning and advantages and disadvantages of Big Data and e-commerce, this paper points out that, in the new era, under the background of adjusting economic structure, making steady progress and changing environment of national economic and social system, the development space of e-commerce is enormous, the investment in science and technology is increasing, and a good opportunity for development is welcomed. But at the same time, there are some disadvantages and huge challenges. This requires the joint efforts of the state, government, enterprises, and consumers to promote the transformation and upgrading of China's e-commerce industry and improve the level of e-commerce development in order to promote the further development of China's modern science and technology and economy. This paper introduces the development status of e-commerce enterprises at home and abroad and the ways and classifications of e-marketing, combs the cost advantages of e-commerce enterprises, and analyses the business status model of traditional trade. Combining the characteristics and essential characteristics of Big Data and the experiences and lessons at home and abroad, this paper puts forward a new way out and development motive for exploring the advantages of China's economic market and promoting the growth of e-commerce enterprises.

With the vigorous advocacy of the combination of science and technology with economy and the new direction of modern economic development, small and micro-enterprises, especially e-commerce enterprises, must have the advantages of policy support, study the trend of economic development, seize opportunities actively, and actively respond to challenges, so as to work together to upgrade the level of e-commerce development in China.

Data Availability

No data were used to support this study.

Conflicts of Interest

The authors declare that they have no conflicts of interest.

References

[1] H. Han, Y. Wen, T.-S. Chua, and X. Li, "Toward scalable systems for big data analytics: a technology tutorial," *IEEE Access*, vol. 2, no. 1, pp. 652–687, 2014.

[2] J. Apurv, "Weapons of math destruction: how big data increases inequality and threatens democracy," *Business Economics*, vol. 52, no. 1, pp. 1–3, 2017.

[3] S. Fong, R. Wong, and A. Vasilakos, "Accelerated psoswarm search feature selection for data stream mining big data," *IEEE Transactions on Services Computing*, vol. 9, no. 1, pp. 33–45, 2017.

[4] T. Y. Kim, R. Dekker, and C. Heij, "Cross-border electronic commerce: distance effects and express delivery in European union markets," *International Journal of Electronic Commerce*, vol. 21, no. 2, pp. 184–218, 2017.

[5] A. Fatima, A. Abbas, W. Ming, A. N. Zaheer, and M.-U.-H. Akhtar, "Analyzing the academic research trends by using university digital resources: a bibliometric study of electronic commerce in China," *Universal Journal of Educational Research*, vol. 5, no. 9, pp. 1606–1613, 2017.

[6] Y. Shi, J. Han, J. Li, G. Xiong, and Q. Zhao, "Identity-based undetachable digital signature for mobile agents in electronic commerce," *Soft Computing*, vol. 22, no. 20, pp. 1–15, 2018.

[7] B. Knežević, B. Šantić, and I. Novak, "Advantages and obstacles of electronic commerce in sports footwear," *International Journal of E-Services and Mobile Applications*, vol. 10, no. 3, pp. 84–101, 2018.

[8] F. Dai, S. T. T. Teo, and K. Y. Wang, "Network marketing businesses and Chinese ethnicity immigrants in Australia," *Journal of Small Business Management*, vol. 55, no. 3, pp. 444–459, 2017.

[9] U. Ramanathan, N. Subramanian, and G. Parrott, "Role of social media in retail network operations and marketing to enhance customer satisfaction," *International Journal of Operations & Production Management*, vol. 37, no. 1, pp. 105–123, 2017.

[10] G. D. Pires and J. Stanton, "Marketing issues in healthcare research," *International Journal of Behavioural & Healthcare Research*, vol. 1, no. 1, pp. 38–60, 2008.

[11] J.-W. Tang and T.-H. Hsu, "Utilizing the hierarchy structural fuzzy analytical network process model to evaluate critical elements of marketing strategic alliance development in mobile telecommunication industry," *Group Decision and Negotiation*, vol. 27, no. 2, pp. 251–284, 2018.

[12] C. Guerini and E. A. Minelli, "The subjective side of DiDIY: the profile of makers in network marketers communities," *Data Technologies and Applications*, vol. 52, no. 1, pp. 84–104, 2018.

Research Article

Application Research of Internet of Things Technology in the Causes of Dragon Boat Sports Injury

Shuai Wang[1] and Xia Zhao [2]

[1]*Department of Police PE, Shanxi Police College, Taiyuan 030401, Shanxi, China*
[2]*College of PE, Shanxi University, Taiyuan 030006, Shanxi, China*

Correspondence should be addressed to Xia Zhao; zhaox@sxu.edu.cn

In recent years, the Internet of Things technology can effectively innovate applications and services. The Internet of Things technology has become more and more popular. It provides an effective and direct bridge between the physical world and virtual objects in cyberspace. With the increase in the intensity of dragon boat training and the increasingly fierce competition, the possibility of injury is increasing. Dragon boat racing is a noncontact team sport based on strength and technology. The purpose of this paper is to solve the problem of people's lack of understanding of the sports injuries and causes of dragon boat athletes. We used the data fusion algorithm and cluster maintenance optimization algorithm to study the application of Internet of Things technology in the cause of dragon boat sports injury. In order to save energy, extend the network life cycle, shorten service interruption time, and increase data packet transmission, the cluster maintenance optimization algorithm in this paper mainly improves and optimizes the startup time of cluster maintenance, which depends on the maintenance cost. The experiment result shows that the etiological detection system proposed in this paper matches the actual sports injury results well. The experiment result shows that the research on the cause of injury in dragon boat sports based on Internet of Things technology can detect the damage law well and can have a more comprehensive understanding for the cause of injury, which helps to prevent injuries better and take effective treatments. In the analysis part, it can be concluded that the detection system is very accurate in detecting the cause, and the accuracy rate is basically 100%.

1. Introduction

The dragon boat race is a folk activity in ancient China. The dragon boat race is a traditional Chinese folk water entertainment project that has been spreading for more than two thousand years. It is mainly held at the festival and is a multiplayer collective paddle competition. The size of the dragon boat varies from place to place. With the continuous promotion and development of the dragon boat sport and the continuous improvement of the level of sports skills and tactics, the intensity and density of training and competition continue to increase, the dragon boat competition is getting more and more intense, and the incidence of injuries is getting higher and higher. Dragon boat athletes are increasing [1]. As an ancient sport in China, dragon boat has

certain advantages in preventing breast cancer in women. With the popularity and development of the dragon boat movement in the world, the traditional dragon boat movement has gradually turned into a competitive dragon boat sport, and various sports injuries will inevitably occur in training or competition. Some people have verified the applicability of the new dragon boat motion method based on the intensity curve method in the late injury of breast cancer survivors and found that dragon boat exercise can be used to reduce late arm injury [2]. From the perspective of cultural anthropology, this paper discusses the historical changes of the dragon boat race and discusses the origin and historical changes of the dragon boat race. Through the analysis of its complex social and cultural phenomena, it reveals that society reflects the integration of culture, cultural

adaptation, and socialization. Combining intelligent and sensing systems in an IoT environment to form a large-scale distributed network physical system has great potential for introducing intelligent systems into many application areas [3, 4]. Internet of Things technology has become increasingly popular in recent years because it provides an effective and direct bridge between virtual objects in the physical world and cyberspace, achieving effective application of innovative applications and services [5].

In recent years, the emergence of the Internet of Things has expanded the ability to use the existing network infrastructure to perceive the world through connected device networks. The Internet of Things can be seen as an important technological revolution associated with smart cities, smart homes, smart factories, and smart port implementations. With the emergence of port intelligent sensing systems becoming a reality, today's different operating areas are operating in automatic mode [6]. With the advent of the aging of society, the development of intelligent multifunctional nursing beds for hospitals, nursing homes, families, etc. has a wide range of applications [7]. Not only that, the unmanned technology that has received widespread attention in recent years is also based on the Internet of Things technology in the logistics industry, and the Internet of Things technology is used for traceability and tracking of goods. Print or paste the RFID tag on the product, so that the product has a unique electronic identification code and combines the Internet technology to establish an information file for the product. RF card readers can read product information noncontact and promote the management of commodity information. The Internet of Things is an emerging paradigm that envisions a network infrastructure that allows different types of devices to be connected to each other. It creates different types of artifacts in a variety of applications, such as health monitoring, motion monitoring, animal monitoring, enhanced retail services, and smart home [8]. The Internet of Things provides all the necessary infrastructure to implement the smart city concept, and the various services provided in smart cities are implemented with the help of Web services technology. He discussed a three-file case study to highlight the role of Web services in smart cities and described six learning models for Web services classification [9].

At present, there are many applications and researches on the Internet of Things technology. Many domestic and foreign scholars have done detailed research. Rausch believes that cloud-based solutions cannot meet the stringent QoS and privacy requirements of many modern IoT solutions. In contrast, distributed middleware needs to take advantage of the ever-increasing resources at the edge of the network to provide reliable, ultralow latency, and privacy-aware message routing. However, the inherent heterogeneity and volatility of edge resources and the unpredictability of mobile clients make it challenging to provide flexible coordination mechanisms and ensure message delivery. Applying the principle of penetration calculation to message-oriented middleware opens up new opportunities to address these challenges [10]. Zhang proposed a new tensor-based forensic method for virtualizing network functions. An event tensor model was proposed to formalize network events. Then, it was used to effectively update core event tensors. Then, we introduce a similarity tensor model to integrate core event tensors into the orchestration and management of the network function virtualization framework. Finally, he proposed an evidence tensor model for network forensics, showing how to combine evidence tensors [11]. Kolokotronis considered possible use cases and applications for blockchains for the consumer electronics industry and its interaction with the Internet of Things. He is not talking about how the blockchain completely changes the supply chain, but rather how to use it to enhance the security of network CE devices. The motivation for this work is the many recent attacks in which devices that are easy to crack are used as weapons. He also introduced the privacy and data protection aspects of blockchain solutions and linked them to regulatory framework provisions, as well as information on existing blockchain solutions [12]. Li has developed a new wireless power transmission system in which a drone equipped with an RF energy transmitter charges an IoT device. The machine learning framework of the echo state network is used along with the improved clustering algorithm to predict energy consumption and aggregate all sensor nodes in the next time period to automatically determine the charging strategy. The energy that the WPT obtains from the UAV supports the IoT devices to communicate with each other. In order to improve the energy efficiency of the WP-IoT system, the interference mitigation problem is modeled as an average field game [13]. Rakovic elaborated on BC-Internet of Things-related issues and conducted a comprehensive survey of current literature and related launch deployments, identified major research and development challenges, and discussed possible aspects of future research [14]. Mukherjee proposed the requirement to ignore certain seemingly critical identifier fields in packets arriving from various sensor nodes in an agricultural IoT deployment. The proposed method reduces packet size, thereby reducing channel traffic and energy consumption, and retains the ability to identify these originating nodes. He proposed a blind agricultural IoT node and sensor identification method that can be acquired and operated from the primary node and remote servers. In addition, the scheme has the ability to detect the quality of the radio link between the master node and the slave node in primary form and to identify the sensor nodes [15]. Finally, a number of simulations were performed to evaluate his proposed algorithm compared to some of the most advanced schemes [16]. Hamidi proposes an ontology-based automatic design method for intelligent rehabilitation systems in the Internet of Things. In order to provide fast and effective rehabilitation for different patients, the Internet of Things is combined with ontology. The experimental results show that the IoT-based rehabilitation system works normally, and the ontology-based approach can help to create an effective rehabilitation strategy, configure and quickly deploy all available resources, and meet the requirements [17]. Lacerda identified the Internet of Things as part of the system's social technology system and part of the information circle. It introduces a principle-based, human-centered approach to

designing IoT artifacts that links the Internet of Things to the conceptualization of cross-channel ecosystems in current information architecture theory and practice. According to the metamodel methodology, it is necessary to establish an interdisciplinary theoretical framework to promote a human-centered comprehensible understanding of the Internet of Things phenomenon and its consequences [18]. Durao proposes a model for selecting IoT technology. The research design combines a literature review of the system, applying bibliometrics and content analysis, case applications, and improvements. The model applies an analytical hierarchy process based on the following criteria. The results also show that IoT selection and a combination of different standards related to system and technology selection are related to the ability to install IoT solutions [19]. In order to more accurately control the rice field environment, Min monitors the growth of rice and rice ducks in real time and applies the Internet of Things technology to accurate data collection in farmland farming and animal husbandry. By monitoring the growth information of rice and rice ducks, the environment and the use of automatic control technology, intelligent decision-making, and agricultural biotechnology knowledge, a rice ecosystem model was constructed suitable for rice and rice-duck life to monitor the management of rearing and environmental protection [20]. However, the research points of this study are not enough, and the data is not sufficient.

Currently, the development of the Internet of Things and mobile communication technologies is very rapid. On this basis, this topic has carried out research based on Internet of Things technology and mobile communication technology, aiming to apply the Internet of Things technology to the cause of dragon boat sports injury. The test equipment, the tester, and the system are linked by intelligent terminal devices such as mobile phones to realize real-time data collection and uploading and implemented in smart hands. They display, analyze, and calculate the customer, expert system, and back-end management system to provide an effective assessment and guidance solution. Due to the rapid development of microsensor chips and Internet of Things technology, the data of test equipment can be sensed, identified, and calculated. The integrated model strongly promoted the further development of the dragon boat sport. The intelligence of the detection system is reflected in the integration and application of modern information science and technology such as the Internet of Things, and it has the basic conditions to popularize and promote the civilized lifestyle of the public. By establishing an Internet of Things standard system, it is possible to collect, integrate, and transform test data, establish uniform standards, and form an open and shared unified test database. Existing test data and expert teams can be organically combined to form a diversified, long-gradient test and guidance. Eco-chain can be tested.

2. Proposed Method

2.1. Internet of Things Sensor Data Fusion Algorithm.
When an emergency occurs in the network, some nodes in the monitoring area of the network configuration will be stimulated by a certain intensity, and these nodes will turn into active nodes, that is, from the dormant state to the active state, and the data will start to be processed. *Perceive and Transmit.* When the stimulus intensity of the emergency event is reduced, the discrete event generated is over, and the node will return to the dormant state again, which will save the energy consumption of the network [21].

Definition (1): Standard Hard Threshold (SHT), this value is used to describe the value used by the node when it is in a sleep state to compete for the sink node. At the same time, the SHT can also be used to determine whether similar transmissions are repeated during transmission to the sink node. *Information.* The standard hard threshold at initialization is expressed as

$$\text{SHT}_{\text{INITIAL}} = \text{HT} - \text{ST}. \tag{1}$$

Among them, HT stands for hard threshold and ST stands for soft threshold.

When initializing, all nodes in the network are in a dormant state. Only when the monitoring data meets condition (1) can the node be active, enter the state of receiving and sending data, and update the SHT value to the monitored data value. Among them, the monitoring data is represented by DATE.

$$\text{DATE} > \text{HT}\&\&|\text{DATE} - \text{SHT}| > = \text{ST}. \tag{2}$$

For nodes that have been activated, they can send and receive data. When the condition of (3) is met, the value is updated to DATE, and then the data value is transmitted to the upper-level node.

$$\text{DATE} > \text{HT}\&\&|\text{DATE} - \text{SHT}| > = \text{ST}|. \tag{3}$$

Relative Active Time Threshold (RATH): the threshold is a description of the active time of the generated family. Among them, the value of RATH is proportional to the threshold of the node being stimulated by an emergency event, and A represents the active time coefficient. The value of RATH can be expressed as

$$\text{RATH} = A|\text{DATE} - \text{HT}|. \tag{4}$$

Absolute active time threshold (AATH): this threshold is used by nodes in the cluster to determine the survival time of the generated cluster. T is used to represent the current time, and the value of AATH can be expressed as

$$\text{AATH} = T + \text{DATH}. \tag{5}$$

When $T > \text{DATH}$, the nodes in the network switch from the state of sending and receiving data to the dormant state.

After introducing the concept of IoT data fusion algorithm, we can get the IoT heterogeneous data fusion process of intelligent optimization algorithm as shown in Figure 1:

2.2. Improved Cluster Maintenance Optimization Algorithm.
Cluster maintenance startup time will directly affect maintenance and nonmaintenance costs, namely, node energy consumption and network life cycle, service interruption time, and packet transmission. In order to save
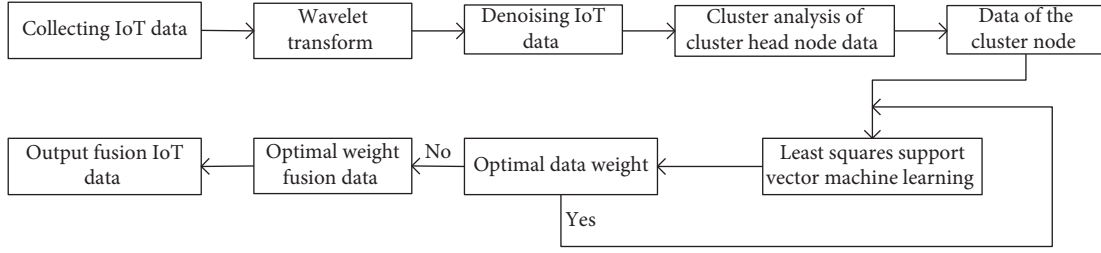
FIGURE 1: IoT heterogeneous data fusion process based on intelligent optimization algorithm.

energy, extend the network life cycle, shorten service interruption time, and increase data packet transmission, the cluster maintenance optimization algorithm in this paper mainly improves and optimizes the startup time of cluster maintenance, which depends on maintenance cost.

When an event occurs in the network, the maintenance cost and the nonmaintenance cost are first calculated to determine whether the setting conditions for starting the cluster maintenance are met. If the boot condition is not met, the network damage cluster caused by the event will not be temporarily maintained, and the undamaged portion of the network will remain in its normal working state. When there is another event in the network, the conditional judgment will be repeated. If the conditions for the launch dimension are met, they will be executed within the scope of the previous event. Otherwise, it will not be maintained, waiting for the next event to occur, so loop. Local on-demand cluster maintenance algorithms are event-driven and require immediate maintenance when cluster corruption occurs in the network, regardless of the differences and trade-offs between maintenance costs and nonmaintenance costs due to different maintenance costs. The improved optimization algorithm proposed in this paper comprehensively weighs the impact of the two on the network. Cluster maintenance can only be started when maintenance costs are lower than maintenance costs. This will help improve the quality of network services in terms of power consumption, service interruption time, and packet delivery.

In general, the number of cluster heads K participating in maintenance is 1. When the number of cluster nodes is destroyed and the number of cluster nodes exceeds the maximum number of N max allowed by the cluster, the K value is determined by calculating the average number and node. The cluster and neighbors lose the clustered AVG:

$$\text{avg} = \frac{\sum_i^k \text{mem}_i}{k}. \tag{6}$$

In the formula, mem_i represents the node of the first adjacent cluster. By adjusting the K value to ensure that the AVG is not less than Nmax, the K value is the number of new cluster heads in the damaged adjacent cluster. As can be seen from the above analysis, there are two kinds of energy consumption when calculating energy consumption: energy consumption of member nodes and energy consumption of cluster heads. The energy consumption of the member nodes includes receiving broadcast signals, transmitting cluster

requests, and receiving energy consumption of the time division multiple access signals.

$$E_{\text{CM\_ADV}} = k \times m \times E_{\text{elect}},$$
$$E_{\text{CM\_JOIN}} = m \times \varepsilon_{\text{fs}} \times d^2, \tag{7}$$
$$E_{\text{CM\_TDMA}} = m \times E_{\text{elect}}.$$

Therefore, the total energy consumption E_CM of the member nodes is

$$E_{\text{CM}} = (n - k) \times \left(E_{\text{CM}_{\text{ADV}}} + E_{\text{CM}_{\text{JOIN}}} + E_{\text{CM}_{\text{TDMA}}} \right)$$
$$= (n - k) \times m \times \left[(k + 1) \times E_{\text{elect}} + \varepsilon_{\text{fs}} \times d^2 \right], \tag{8}$$

where d is the distance from the member node to the respective cluster head; n is the number of nodes that need to participate in reclustering in this event.; E elect is the energy consumed by transmitting the 1-byte control instruction; the value of k is the cluster maintenance action according to the need to perform determine. The total energy consumption is

$$E_Y(i) = m \times \left[(n - k) \times (2k + 1) \times E_{\text{elect}} + n \times \varepsilon_{\text{fs}} \times d^2 \right.$$
$$\left. + k \times \varepsilon_{\text{amp}} \times d_0^4 \right]. \tag{9}$$

The above energy consumption calculation method assumes that only one event occurs at a certain time in the network. When two or more events occur simultaneously in the same area of the network, the energy consumption of each event should be calculated separately according to the above formula and then accumulated. If two or more events occur simultaneously in different areas of the network, we have the following. When more than two events occur, only one event occurs at a particular time in each damaged area. The maintenance of the sensor layer group in the Internet of Things mainly involves the energy consumption of communication, regardless of the energy consumption of node calculation and storage. Therefore, when a normal node dies, the cluster head deletes it directly from the slot and does not involve communication energy consumption. Therefore, the main energy consumption for cluster maintenance is cluster head rotation, joining adjacent clusters, multicluster reclustering, cluster splitting (cluster consolidation), and so on. Depending on the setup, the maintenance operations that require cluster maintenance for the damaged cluster are essentially reclustering. Since the maintenance action of joining adjacent clusters does not require cluster head election, the cluster head does not need to send cluster head

broadcast messages, which saves total energy consumption and reduces network interruption time. Therefore, when calculating energy consumption and interruption time is long, there are two cases: merging into adjacent clusters and reclustering.

The energy consumption model calculates the energy consumption of the cluster maintenance process because the exchange of information between nodes inevitably leads to energy consumption. To simplify the description, assume that all nodes transmit signals at maximum power during cluster head selection. In the maintenance event, the number of cluster heads to be reselected is K, and the control instruction is m bytes. Determine the optimal startup time for cluster maintenance by calculating the maintenance and nonmaintenance costs of the event. Cluster maintenance startup time will directly affect maintenance and non-maintenance costs, that is, node energy consumption and network life cycle, service interruption time, and data packet transmission.

3. Experiments

3.1. Algorithm Implementation Process and Steps. Because the startup time of cluster maintenance directly affects the life cycle of the network, the conditions for starting cluster maintenance are set in advance. Based on the LDMC algorithm, the OACM algorithm is improved and optimized. When the startup conditions are met, restart cluster maintenance, reduce the energy consumption of cluster maintenance, reduce service interruption time and network interruption time, and extend the network life cycle. The implementation of the algorithm is as follows.

(1) Elect the chairman of the cluster: according to the LEACH algorithm, a cluster head is selected, and the node randomly generates data to compare with a threshold to decide whether to select a cluster head

(2) The stage of cluster establishment: the cluster head sends a CH_ADV broadcast message to the entire network. The member selects the cluster they want to join by comparing the strength of the received cluster head broadcast signal and responding to the cluster head JOIN_REQ message. When the cluster head receives the joining information of the node, it creates a TDMA slot table for the member nodes in the cluster and sends it to the member nodes in the cluster

(3) Stable cluster communication phase: the nodes in the cluster send data to the cluster head according to the TDMA schedule. When the node is not in its own transmission slot, the node goes to sleep. After the cluster head fuses the received data with the self-monitoring data, the cluster sends the data to the base station in the form of single-hop or multihop according to the carrier intercepting multiple access

(4) Cluster maintenance phase: when an event requiring maintenance occurs in the network of the perception layer of the Internet of Things, maintenance costs,

and nonmaintenance costs (if the normal node dies, the cluster head deletes it directly), the slot list method is calculated according to the calculation, and no maintenance cost is involved. Then, calculate whether the current state of the network meets the startup cluster

If the conditions set by the formula are met, cluster maintenance is started and the corresponding maintenance operation is invoked in the local area according to the specific damage condition. If the startup condition for cluster maintenance is not met, the damaged node will not respond to the event and the network will continue to operate normally until the next event occurs and then continue to determine if the cluster maintenance start condition is met

(5) When the cluster maintenance ends, the information in the event list is empty. The OACM algorithm repeats steps 3 and 4 until the network energy is exhausted or the node dies too much to complete normal data communication

The steps for heterogeneous data fusion in the Internet of Things are as follows:

(1) Randomly deploy a certain number of sensors in the monitoring area, with a certain communication range, forming an Internet of Things

(2) In the Internet of Things, multiple sensors continuously collect real-time and online status data of monitored objects to obtain raw sensor devices (preliminary data)

(3) Filter the data collected by each sensor by wavelet transform, initially reduce the amount of data, and improve the data quality of the Internet of Things, and then each sensor sends the denoised data to the cluster head

(4) Each cluster head collects its own sensors and processes the cluster head data using the K-means algorithm. Line redundancy processing eliminates redundancy between cluster data and enables initial data fusion

(5) The cluster head sends its own cluster data to the aggregate sensor to obtain a large amount of heterogeneous data in the Internet of Things

(6) In the aggregate sensor, a least-squares support vector machine is used to determine the weight of each cluster head data and combine them. Get the best weight

(7) According to the optimal weight determined by the least-squares support vector machine, the data of each cluster is weighted and fused, and the data of the heterogeneous data fusion in the Internet of Things is obtained and sent to the Internet. Users can get the data needed for the Internet of Things through the Internet

3.2. Application Function Design and Experimental Data Set.

The function of the application is a series of processing of user instructions. Application features include Bluetooth data reception, data processing, exception alerts, data storage, and submission.

3.2.1. Main Program Design.

After the application software runs, the first step is to determine if the Bluetooth on the smartphone is lit and then search for the device after Bluetooth is turned on to detect the connection parameters. Receive and analyze packets as they are connected to the device. In order to judge whether the data is valid, when the pulse value is greater than 200 BMP and the body temperature is lower than 30 degrees Celsius, the condition is invalid. Obtain pulse values for the device, muscle scan, appearance damage scan, body temperature, and remaining battery power, which is displayed in the corresponding position on the main interface. Invalid data was not processed, probably because the user did not wear or mislead the detection device. Parsing valid data, that is, extracting data from the packet. Determine whether the valid data is abnormal, and send an abnormal alarm message to the employee when the number of abnormal times is reached, to remind the employee to make corresponding processing in time.

3.2.2. Data Processing Design.

After the application gets the packet, it first parses the data. Each data is separated by a comma and the packets are separated by commas. The obtained data is in turn the pulse value of the test device, the muscle scan image, the appearance damage scan image, the body temperature value, and the remaining battery power value. The obtained data is displayed at the corresponding position on the main interface, and the validity of the parsed data is judged. If the data is valid, it is stored in the database SQLite of the ANDROID system and submitted to the network platform. The communication between the application and the network background follows the HTTP protocol. The GET method in the HTTP protocol is used to submit data, and the GET method is used to receive data on a network platform. After completing the data storage and submission, we can further determine whether the data is abnormal, that is, whether the set physiological parameter threshold is exceeded. When the temperature or pulse is abnormal, the abnormal information is displayed on the main program interface, and the number of abnormal events is recorded.

3.2.3. Design of Abnormal Alarm.

In this study, we sent an alert message to the nurse in the form of a short message, the content of which is as described above. When measuring body temperature, the temperature sensor takes about five minutes to measure the body temperature caused by heat exchange. If the alarm is turned on at the beginning of the program, it will cause a false alarm, so the temperature alarm in the programming will not open until five minutes after the application is opened. Pulse detection is very fast and there is

Table 1: The incidence of sports injuries before the dragon boat athletes entered the team.

Sports injury	Yes	No
Male	18	16
Female	9	11

no limit. In addition, to avoid unnecessary losses, an alert message is sent every 10 minutes.

This article takes 56 dragon boat players from the three universities of M University as the experimental subjects, including 35 male athletes and 24 female athletes. The sports injuries before the team members entered the Dragon Boat Team training were compared with the sports injuries after the Dragon Boat Team began training. The analysis of the sports injuries before the team entered the team had certain contributing factors to the sports injuries after the team training.

As shown in Table 1, before joining the Dragon Boat Team, 18 boys had sports injuries, of which 53.4% were boys, 16 were not injured, 46.6% were girls, 9 were sports injuries, 45% were girls, and 44 were harmless. The ratio is 55%. It can be seen that the number of sports injuries exceeds the number of uninjured, while the number of male and female athletes exceeds the number of uninjured. The proportion of male athletes injured was 54.3% higher than that of female students. The training of the M University Dragon Boat Team is mainly divided into two stages, one is daily training without competition, and the other is prematch training.

As shown in Table 2, it can be seen that the main training content of the daily training of the M University Dragon Boat Team is that the endurance training is mainly for long-distance running, and the strength training is mainly for strength training in the gym, then endurance training, strength training, and water practice alternate. The prematch targeted training is mainly based on the content of the upcoming competition. Take the 200-meter and 500-meter dragon boat races as an example. The main practice is the high-frequency hoist 30 paddles and then the low-paddle inferior paddles and boats. Pull the boat to practice, practice the same distance with different paddles, and conduct actual combat tests every day. The training time for daily training and prematch training is two hours a day on weekdays and two hours on the weekends.

4. Discussion

4.1. Analysis of Sports Injury Parts and Causes.

There are three types of divisions on the dragon boat, paddlers, drummers, and helmsmen. This is mainly for the investigation of the injured parts of the paddlers and drummers. As shown in Table 3, for the results of sports injuries of athletes, from the data in the table, it is found that the sports injuries of the dragon boat athletes in our school are mainly concentrated in the hands, arms, shoulders, waist, buttocks, and other parts.

As shown in Figure 2, for the number of people in the sports injury area of the dragon boat athletes, it can be seen from the figure that in all the injury parts, all the athletes'

TABLE 2: University Dragon Boat Team training situation.

Training situation	Daily training	Prematch training
Training content	Endurance training Strength training Launch	Targeted training
Training time	Working day 2 hours/day 4 hours/day at the weekend	Working day 2 hours/day 4 hours/day at the weekend

TABLE 3: University Dragon Boat Team athletes' sports injuries.

Sports injury site	Hand	Arm	Shoulder	Waist	Hip	Back
Number of injuries	54	45	33	38	20	35
Incidence rate	100%	83.3%	61%	70.4%	37%	64.8%
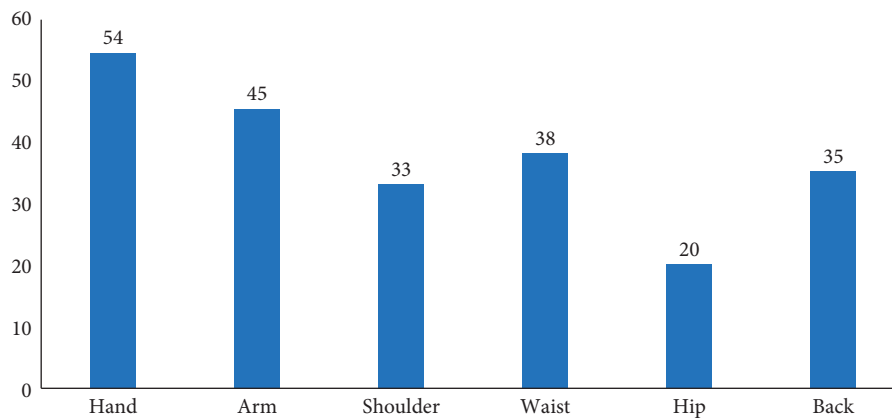
FIGURE 2: Dragon boat athletes' proportion of sports injuries.

hands are damaged, and then the arms, waist, and shoulders are in turn. The back and buttocks have the fewest injuries and the least. Therefore, athletes should pay attention to the protection of their hands during the training process.

After investigation, it is found that the types of sports injuries in various parts of M University Dragon Boat Athletes are bruises, muscle strains, muscle strains, and other types. The specific situation of sports injuries in the sports injury parts of dragon boat athletes is shown in Table 4:

As shown in Figure 3, by analyzing the data in Table 4, it can be known that the type of abrasion in the type of sports injury mainly occurs in the hands, arms, buttocks, etc.; muscle strain mainly occurs in the arms, waist, back, and other parts. The main parts of a muscle strain are the arm, shoulder, waist, back, and other parts. The main reason is that these parts are directly in contact with the hull and the paddle during water training and competition; muscle strain is caused in the arms, waist, back, and other parts because these parts are the main force parts when paddling. Muscle strain in the arms, shoulders, waist, back, etc. is due to long-term high-frequency training and participation in a large number of competitions so that the load on these parts is too large, and it is easy to cause muscle strain.

4.2. Etiology Results and Accuracy Analysis. For dragon boat athletes, strength endurance quality and speed endurance quality are key factors that play a good role in the game, especially in the upper limbs and waist and back. Dragon boat sports is a kind of physical endurance exercise. It not only requires athletes to have good water stroke skills but also requires good strength endurance and upper limb speed endurance quality. Therefore, if athletes want to achieve good results in the competition, they must strengthen their training for special endurance, but in training, they may develop if they ignore the following factors. Damage has occurred. (1) The preparatory activities were inadequate and the injury rate was 29%. Dragon boat sports require a high-intensity torso and upper limb muscles. Strength training equipment is usually used for training. If you ignore any part in the preparation activity, it is easy to cause damage, especially to the waist and shoulders. Lack of psychological preparation before the game is a subjective factor in the injury. (2) Lack of scientific training, improper control of exercise volume and selection of training programs, and ignoring personal treatment can easily lead to overwork and injury. (3) Rough sports equipment, improper training, and competitive clothing are easy to cause damage. (4) Participation in training and injury competition is the cause of repetition and multiple injuries. As shown in Figure 4, the

TABLE 4: Types of injuries in sports injuries of dragon boat athletes.

Damage type	Bruise	Muscle stretching	Muscle strain
Damage site	Hand arm hip	Arm waist back	Arm shoulder waist back
Number of injuries	54	34	18
Ratio (%)	100	63.6	33.3
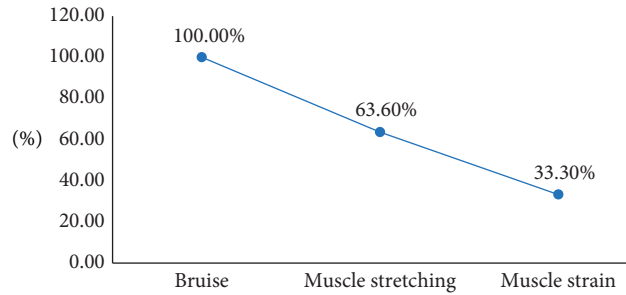
FIGURE 3: Proportion of the cause of sports injuries in dragon boat athletes.
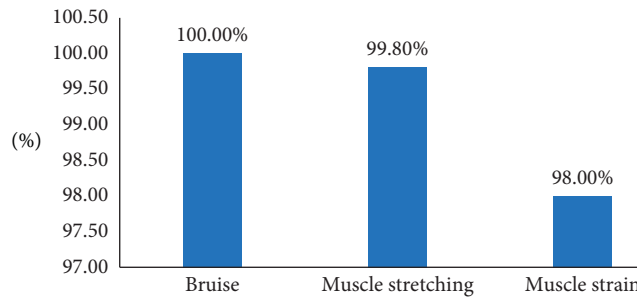
FIGURE 4: Accuracy rate detection of sports injuries in dragon boat athletes.
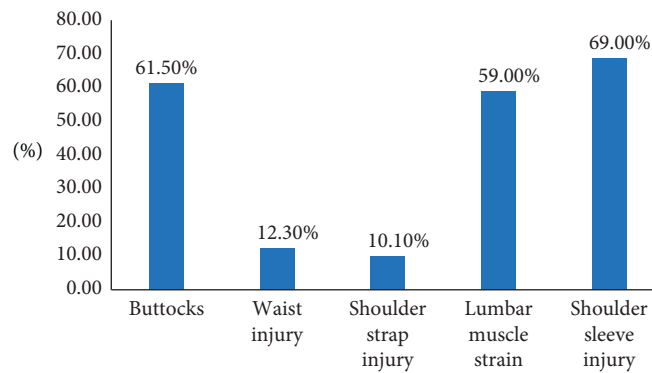
FIGURE 5: Damage rate of various parts of dragon boat athletes.

monitoring system detects the cause of the injury to the athlete and compares it with the cause found in the actual inspection. As can be seen from the figure, the detection system is very accurate for the detection of the cause, and the accuracy rate is basically 100%.

As shown in Figure 5, it can be seen from the figure that hip wear accounts for 61.5%, ranking first. Secondly, the waist injury accounted for 12.3%, and the shoulder belt injury accounted for 10.1%. Lumbar muscle strain accounts for 59% of lumbar spine injuries, and rotator cuff injuries account for 69% of shoulder injuries. The relative damage rate of the outer thigh wear, muscle damage, palm wear, and rhomboid muscle strain is higher. It can be seen that most of the injuries are bruises, strains, and sprains. For further analysis, there are two main factors. First, the inner edge of the dragon boat and the seat edge are too rough. In addition,

athletes wear inappropriate clothing for training or competition, resulting in lateral wear of the buttocks and thighs, so we should choose appropriate clothing training and improve training equipment to reduce wear. Secondly, the characteristics of this sport, whether it is on the ship or on the land for specialized endurance training, are repeated single-player movements at a fixed position, which can easily lead to local overload and injury. Therefore, before and after training, special attention should be paid to the relaxation movement of the muscles in the load zone to avoid excessive fatigue and prevent injury.

5. Conclusions

(1) In order to solve some shortcomings in the current IoT heterogeneous data fusion process, an IoT heterogeneous data fusion method based on an intelligent optimization algorithm is designed. The improved algorithm is used to analyze the sensor data in the IoT cluster. Redundant operation reduces the scale of IoT data and better meets the online requirements of IoT data fusion

(2) Monitoring the cause of injury through the Internet of Things technology, mainly driven by technology and artificial collaboration, reducing the cost of human participation, and reducing the cost of original testing, this model can essentially solve the wide coverage and high efficiency of scientific movement, economic, and other goals

(3) The top three injuries of dragon boat athletes are hip, hand, and shoulder; the main injury to the hands and hips is abrasion; the main injury to the wrist is the tendon sheath; the main injury to the shoulders, waist, and back is a muscle injury

(4) The etiological detection system designed in this paper can analyze the cause of injury of dragon boat athletes well and can provide a good prevention method. The test results are basically consistent with the actual situation

Data Availability

No data were used to support this study.

Conflicts of Interest

The authors declare that they have no conflicts of interest.

References

[1] B. May, "Breast cancer survivors find strength in dragon boat racing," *Oncology Times*, vol. 39, no. 23, p. 1, 2017.

[2] J. Ong and I. Brownlee, "Energy expenditure, availability, and dietary intake assessment in competitive female dragon boat athletes," *Sports*, vol. 5, no. 2, p. 45, 2017.

[3] M. Meng and T. Sogawa, "On the historical transformation of the dragon boat race of the Miao in the Qingshui River region of Guizhou Province of China from a cultural anthropological perspective," *Asia Pacific Journal of Sport and Social Science*, vol. 5, no. 1, pp. 1–16, 2016.

[4] H. Panetto, P. C. Stadzisz, W. Li, and Q.-S. Jia, "Guest editorial: special issue on (industrial) internet-of-things for smart and sensing systems: issues, trends, and applications," *IEEE Internet of Things Journal*, vol. 5, no. 6, pp. 4392–4395, 2018.

[5] X. Wang, Z. Sheng, H. Ma, V. C. M. Leung, and A. Jamalipour, "Guest editorial special issue on software defined networking for internet of things," *IEEE Internet of Things Journal*, vol. 5, no. 3, pp. 1347–1350, 2018.

[6] Y. Yang, M. Zhong, H. Yao, F. Yu, X. Fu, and O. Postolache, "Internet of things for smart ports: technologies and challenges," *IEEE Instrumentation & Measurement Magazine*, vol. 21, no. 1, pp. 34–43, 2018.

[7] J. Jiang, P. Bao, D. Zhao et al., "Design of intelligent nursing bed based on internet of things + technology," *Zhongguo Yi Liao Qi Xie Za Zhi = Chinese Journal of Medical Instrumentation*, vol. 42, no. 4, pp. 235–239, 2018.

[8] A. Felfernig, S. Polat-Erdeniz, C. Uran et al., "An overview of recommender systems in the internet of things," *Journal of Intelligent Information Systems*, vol. 52, no. 2, pp. 285–309, 2019.

[9] L. Purohit and S. Kumar, "Web services in the internet of things and smart cities: a case study on classification techniques," *IEEE Consumer Electronics Magazine*, vol. 8, no. 2, pp. 39–43, 2019.

[10] T. Rausch, S. Dustdar, and R. Ranjan, "Osmotic message-oriented middleware for the internet of things," *IEEE Cloud Computing*, vol. 5, no. 2, pp. 17–25, 2018.

[11] S. Zhang, L. T. Yang, L. Kuang, J. Feng, J. Chen, and V. Piuri, "A tensor-based forensics framework for virtualized network functions in the internet of things: utilizing tensor algebra in facilitating more efficient network forensic investigations," *IEEE Consumer Electronics Magazine*, vol. 8, no. 3, pp. 23–27, 2019.

[12] N. Kolokotronis, K. Limniotis, S. Shiaeles, and R. Griffiths, "Secured by blockchain: safeguarding internet of things devices," *IEEE Consumer Electronics Magazine*, vol. 8, no. 3, pp. 28–34, 2019.

[13] L. Li, Y. Xu, Z. Zhang, J. Yin, W. Chen, and Z. Han, "A prediction-based charging policy and interference mitigation approach in the wireless powered internet of things," *IEEE Journal on Selected Areas in Communications*, vol. 37, no. 2, pp. 439–451, 2019.

[14] V. Rakovic, J. Karamachoski, V. Atanasovski et al., "Blockchain paradigm and internet of things," *Wireless Personal Communications*, vol. 106, no. 3, pp. 219–235, 2019.

[15] A. Mukherjee, S. Misra, N. S. Raghuwanshi, and S. Mitra, "Blind entity identification for agricultural IoT deployments," *IEEE Internet of Things Journal*, vol. 6, no. 2, pp. 3156–3163, 2019.

[16] H. Yao, T. Mai, J. Wang et al., "Resource trading in blockchain-based industrial internet of things," *IEEE Transactions on Industrial Informatics*, vol. 15, no. 6, p. 1, 2019.

[17] H. Hamidi and K. Fazeli, "Using internet of things and biosensors technology for health applications," *IET Wireless Sensor Systems*, vol. 8, no. 6, pp. 260–267, 2018.

[18] F. Lacerda, M. Lima-Marques, and A. Resmini, "An information architecture framework for the internet of things," *Philosophy and Technology*, no. 3, pp. 1–18, 2018.

[19] L. F. C. S. Durao, M. M. Carvalho, S. Takey et al., "Internet of Things process selection: AHP selection method," *The International Journal of Advanced Manufacturing Technology*, vol. 99, no. 9-12, pp. 2623–2634, 2018.

[20] X. Min and W. Kuang, "Study on the ecological farming control system based on the internet of things," *Wireless*

Personal Communications, vol. 102, no. 4, pp. 2955–2967, 2018.

[21] H. Xianming, "Intelligent remote monitoring and manufacturing system of production line based on industrial Internet of Things," *Computer Communications*, vol. 150, pp. 421–428, 2020.

Research Article

Design of Epidemic Prevention Medical Special Clothing Based on Mathematical Model Analysis

Hubin Liu (ID)**, Qi Xu** (ID)**, Shan Wu** (ID)**, and Yulong Liu**

Graduate School, Sejong University, Seoul 05006, Republic of Korea

Correspondence should be addressed to Qi Xu; xuxiaoqizi0727@126.com

Among the many diseases, the harm of infectious diseases is undoubtedly the first in terms of the scope of the disease and the threat to humans. In addition, most infectious diseases were regarded as terminal illnesses in the early stage of the outbreak. For example, smallpox and plague in history have even chosen to isolate patients and abandon them to prevent the spread of infectious diseases due to the lack of protection and treatment methods. Therefore, in the treatment of infectious diseases, epidemic prevention is very important. Based on this, this article discusses the research of special medical clothing design for epidemic prevention based on mathematical model analysis, hoping to provide strong help and support for epidemic prevention. First of all, this article understands the application status of mathematical models in the medical field and clothing design industry through literature research. Then, according to the functional requirements of antiepidemic medical special clothing in terms of protection from virus invasion and infection by other contact methods, this article established an antiepidemic clothing quality evaluation index system. Then, this article designs a simulation penetration test of pathogenic bacteria to test the protective function of the antiepidemic clothing and uses mathematical models to analyze the molecular structure and physical properties of the antiepidemic clothing materials. Finally, this article builds an analytic hierarchy model for the quality evaluation of epidemic prevention clothing based on the principle of analytic hierarchy process, analyzes the simulated experimental data and predicts the service life of the epidemic prevention clothing according to the performance degradation so that medical staff can replace it in time. The experimental results show that with the aid of mathematical model analysis, the quality of the epidemic prevention clothing is higher than the previous antiepidemic clothing design in terms of epidemic prevention performance, and in addition to the disposable epidemic prevention clothing, the multiple-use epidemic prevention clothing is not serious in the epidemic. Under these circumstances, it can maintain the antiepidemic performance for more than 2 months.

1. Introduction

1.1. Background and Significance. With environmental pollution and the use and proliferation of chemical pesticide products, ecosystems in more and more regions have been destroyed, which eventually brought the consequences of an epidemic outbreak to humans. Since the first case of un-identified pneumonia was discovered on December 8, 2019, the new crown pneumonia epidemic has been out of control. In the process of humans fighting the epidemic, the importance of special medical clothing for epidemic prevention is self-evident [1]. In this protracted struggle between humans and the epidemic virus, the quality and quantity requirements of special antiepidemic medical clothing are increasing day by day. The design of special antiepidemic medical clothing is not only an important strategic resource in the fight against the epidemic but also a guarantee for the safety of great medical staff. According to relevant research on antiepidemic clothing design, the primary requirement of antiepidemic clothing design is to protect against infections by viruses and bacteria and other microorganisms and to isolate the bites of viral vectors and other means of infection [2]. Secondly, it takes into account the needs of medical staff for ventilation and heat dissipation, and in the process of epidemic treatment and protection, due to the needs of various treatment methods such as medical surgery, the tightness of the material molecules, electrostatic characteristics, and microorganisms of the epidemic prevention

clothing must also be considered. And particle dust accumulation [3]. Finally, the performance degradation caused by the increase in the use time of the antiepidemic clothing will be divided into different types such as one-time use and multiple use, and the degradation treatment of the antiepidemic clothing after it is discarded is also considered [4]. Therefore, the research on the design of special antiepidemic medical clothing based on mathematical model analysis is of great significance.

1.2. Related Research at Home and Abroad. At present, there are many applications of mathematical models in the medical field, and their applications in the apparel design industry are also very popular. However, there are not many researches on the application of mathematical models to the design of epidemic prevention and special medical clothing that combines the medical field and clothing design. Therefore, this article analyzes the application status of mathematical models in the field of epidemic prevention and clothing design. Research Background. Treble used mathematical models to predict and analyze the heat treatment of the crystal design for medical implant applications to stabilize the short-term aging characteristics of the crystal. Experiments have found that the mathematical model analysis not only takes into account the reliability of all aspects but also has higher accuracy in predicting the stability and aging of the crystal. Gentile used computer software tools combined with mathematical model analysis to study drug treatment decision-making under the drug interaction of elderly depression [5]. Studies have shown that this method uses new decision support tools for drug genetic testing, drug interaction evaluation, and therapeutic drug monitoring, which can improve informed decision-making on antidepressant prescriptions. Mehmet used a mathematical model to compare and analyze the success rate of silodosin and the most commonly used exclusive medical therapy in the management of ureteral stones. He used the Review Manager software to calculate meta-analysis and forest plot data to compare the stone excretion rates of the two therapies [6]. The results showed that good results were observed for the stone removal rate of silodosin, and its hazard ratio was 1.33. Eliton used predictive mathematical models to simulate to obtain information about parameters such as temperature, relative humidity, and vapor pressure so as to measure the moisture accumulated in the clothing insulating materials [7]. Experiments show that the application of mathematical models can simulate the heat transfer and moisture transfer in fabric samples, and the finite volume method is combined to verify the consistency of the simulation results with physical reality.

The application of mathematical models in various fields in China has also been developing rapidly, and rich research results have been obtained. Yue et al. proposed the use of computer technology combined with mathematical models to design the emergency diagnosis trauma orthopedics consultation strategy during the epidemic of new coronary pneumonia [8]. The investigation found that during the epidemic of new coronary pneumonia from January 21, 2020,

to February 15, 2020, 128 orthopedic trauma patients in Wuhan University People's Hospital sought emergency treatment in orthopedic surgery, including 71 men and 57 women [9]. The timely treatment of these patients benefited from the admission strategy of the mathematical model based on the patient's order of treatment. Cai et al. studied the construction of many departmental dynamic information monitoring platforms in Shanghai's precision epidemic prevention during the 2019 new crown pneumonia epidemic [10]. The study found that the information monitoring platform combines the application of mathematical models and computer communication technology, breaking the information sharing barriers during the epidemic, and is essential for controlling the source of infection, cutting off the route of transmission, and protecting vulnerable groups. Xu et al. proposed the use of the Bayesian inference method to solve the corresponding inverse problem of textile material design by reconstructing the mathematical model of heat and moisture transfer in textiles to verify the transfer of the heat and moisture transfer model to ensure the thermal comfort of clothing [11]. Experiments have proved that the Bayesian inference method can provide more accurate solutions to the corresponding inverse problems in textile material design.

1.3. Innovations in this Article. In this article, the design of special clothing for epidemic prevention and medical treatment is taken as the research object, and the mathematical model analysis method is creatively used to combine the research of epidemic prevention and clothing design in the medical field through computer science and technology, which opens up a new perspective for the design of special clothing for epidemic prevention and medical treatment [12]. Theoretically speaking, the design of special clothing for epidemic prevention and medical treatment based on mathematical model abandons the previous model of mechanical design on demand and evaluates and considers the quality of special clothing for epidemic prevention and medical treatment from all aspects through the analytic hierarchy process, so as to extract the key factors that should be considered in the design of special clothing for epidemic prevention and medical treatment [13]. From a practical point of view, the design of special clothing for epidemic prevention based on mathematical model analysis in this article can more accurately find out the shortcomings of the design of epidemic prevention clothing, help to improve the design scheme of epidemic prevention clothing in time, change the design mode that people used to find problems and then improve after use, and improve the quality of epidemic prevention work [14]. Finally, this article has carried out the simulated infiltration experiment of pathogenic bacteria to test and verify the epidemic prevention function of the epidemic prevention clothing so as to ensure the excellent function of the design of the epidemic prevention clothing. According to the test results of the simulated invasion experiment of pathogenic bacteria, the design method of epidemic prevention clothing based on mathematical model analysis studied in this article can better control the protection function of epidemic prevention clothing.

2. Mathematical Model of Medical Clothing Design for Epidemic Prevention

2.1. Molecular Spatial Structure of Materials for Epidemic Prevention Clothing. The most important thing in the design of antiepidemic medical special clothing is the selection and treatment of clothing fabrics. Therefore, the molecular spatial structure of clothing fabrics needs to be analyzed during the design of antiepidemic clothing. For the case where the material design of the antiepidemic clothing has a plane scale that is much larger than the vertical three-dimensional scale, due to clothing thickness, molecular diffusion, and other parameters that affect the material's molecular structure over time and space, the change in the vertical direction, that is, the thickness, is much smaller than the horizontal direction [15]. The change is the tightness change of the material plane [16]. Therefore, the control equation of the three-dimensional molecular structure of the antiepidemic clothing is studied by the clothing thickness integral, and the average thickness of the clothing is taken to obtain the two-dimensional molecular flow control equation averaged along the clothing thickness. The plane two-dimensional molecular flow continuity equation of the antiepidemic clothing material is as follows:

$$\frac{\partial h}{\partial t} + \frac{\partial \bar{v}_1 h}{\partial x} + \frac{\partial \bar{v}_2 h}{\partial y} = \text{Sh}, \tag{1}$$

where h is the thickness of the antiepidemic clothing, $\bar{v}_1$ and $\bar{v}_2$ are the average flow velocity of the antiepidemic clothing material molecules in the x-direction and y-direction, t is the use time of the antiepidemic clothing, and S is the size of the air molecule flow rate at the bonding point of the material molecular spatial structure. Through this equation, we can understand the change process of the material molecules of the antiepidemic clothing over time and analyze the performance degradation of the antiepidemic clothing over time [17]. Since the accumulation of microorganisms and dust particles will have absorbed the ventilation and heat dissipation properties of the epidemic prevention suit, this article also studied the spatial dispersion process of material molecules based on the principle of molecular diffusion. The spatial dispersion equation of the surface layer of the epidemic prevention suit is as follows:

$$\frac{\partial U}{\partial t} + \nabla \cdot F(U) = \frac{\partial U}{\partial t} + \frac{\partial \left(F_x^I - F_x^J \right)}{\partial x} + \frac{\partial \left(F_y^I - F_y^J \right)}{\partial y} = S(U). \tag{2}$$

Among them, U represents the plane subdivision of the antiepidemic clothing material into a large number of nonoverlapping units and I and J, respectively, represent the nonviscous flux and viscous flux of the antiepidemic clothing, that is, the molecular flow of molecules in the air that diffuse through the antiepidemic clothing. F_x and F_y denote the cell boundaries in the x-direction and y-direction in the Cartesian coordinate system, respectively. $S(U)$

represents the molecular flow of the molecular unit in the material plane of the antiepidemic suit. This molecular space discrete equation is established based on the finite space volume method, and integrated by Gauss's theorem, the equation can be written as follows:

$$\int_{A_\Omega} \frac{\partial U}{\partial t} d\Omega + \int_{\Gamma_i} (F \cdot n) ds = \frac{\partial U_i}{\partial t}$$

$$+ \frac{1}{A_\Omega} \sum_{i=1}^{N} F \cdot n \Delta \Gamma_i = \int_{A_\Omega} S(U) d\Omega = S_i, \tag{3}$$

where A_Ω is the area of the spatial molecular unit A_Ω, U_i and S_i are the average number of molecules and the molecular flux of i unit, and $\Delta \Gamma_i$ is the length of the unit. According to Gauss's theorem, the time integration can also be used to obtain the time dispersion equation of the molecular diffusion of the antiepidemic clothing material, where n represents the number of plane molecular units of the antiepidemic clothing material and Δt represents the use time.

$$\begin{cases} U_{n+1/2} = U_n + G(U_n)\Delta t/2, \\ U_{n+1} = U_n + G(U_{n+1/2})\Delta t. \end{cases} \tag{4}$$

2.2. Establishing Quality Evaluation Index System for Epidemic Prevention Clothing. According to the research on the design of special antiepidemic medical clothing, this article evaluates the quality of antiepidemic clothing from the aspects of functionality, material properties, comfort, ease of handling, and economy [18]. At the beginning of the design of antiepidemic clothing, this article took into account the needs of epidemic protection and established a quality evaluation index system for the design of antiepidemic clothing according to various factors such as policy factors, economic factors, technical factors, management factors, and disposal of antiepidemic clothing design [19]. Through the above analysis of the influencing factors of the quality evaluation of epidemic prevention clothing, this article first establishes the first-level quality index set A of the epidemic prevention clothing quality evaluation and the second-level evaluation index set B under it as follows:

$$\begin{cases} A = \{a_1, a_2, \ldots, a_m | m = 7\}, \\ B = \{b_1, b_2, \ldots, b_n | n = 14\}. \end{cases} \tag{5}$$

Among them, a_i represents the seven first-level indicators of material molecules, coating technology, special fabrics, fabric stitching, customized prices, use time, and disposal, and b_i represents the 14 second-level indicators in the specific design process of epidemic prevention clothing under the first-level evaluation indicators. According to the second-level indicators, it can be subdivided into about 30 third-level indicators. After the above analysis, the first-level indicator weight set W is established.

$$\begin{cases} W = \{w_1, w_2, \dots, w_n | n = 7\}, \ \sum_{i=1}^{n} w_i = 1, \\ W_i = \{w_{i1}, w_{i2}, \dots, w_{in} | i = 1, \dots, 14\}, \ \sum_{j=1}^{n} w_{ij} = 1. \end{cases} \quad (6)$$

In the design of special antiepidemic medical clothing, the most important step in evaluating the quality of antiepidemic clothing is the determination and calculation of weights. This article mainly draws on the ideas of analytic hierarchy process and entropy method to determine the weights of evaluation indicators at all levels [20]. Similar to the evaluation index set, the second-level index weight set W_{ij} represents the weight of the j-th second-level evaluation index under the i-th first-level evaluation index. In addition, it should be noted that the weight index set needs to meet the condition that the sum of the weight of each index set is 1. After the weight set is determined according to the entropy method, the index evaluation set and the membership

analysis set can be established, which can be expressed in the following form:

$$\begin{aligned} E &= \{e_1, e_2, e_3, e_4, e_5\}, \\ M &= \{1, 3, 5, 7, 9\}. \end{aligned} \quad (7)$$

Each element in the antiepidemic clothing index evaluation set E represents the quality level from low to high, namely, five levels of extremely poor quality, poor quality, average quality, good quality, and excellent quality [21]. The elements of these evaluation sets correspond to the membership degree set is M. Through experimental tests, the evaluation scores of all levels of evaluation indicators for the quality of epidemic prevention clothing can be obtained, and then, the membership vector $\overrightarrow{E}$ of the corresponding first-level index can be obtained, and the comprehensive evaluation set of the second-level quality evaluation index under the first-level evaluation index can be further obtained U.

$$\begin{cases} \overrightarrow{E} = (e_1, e_2, \dots, e_n)^T, \ n = 7, \\ U = W \cdot \overrightarrow{E} = (w_1, \dots, w_n) \cdot (e_1, e_2, \dots, e_n)^T = (u_1, u_2, \dots, u_n), \end{cases} \quad (8)$$

w_i represents the weight of the i-th evaluation index, e_i represents the evaluation score of the index, and u_i represents its comprehensive evaluation quality. Under the broad influencing factors such as policy, economy, management, etc., the quality assessment of epidemic prevention clothing design can be divided into first-level indicators such as material molecules, coating technology, special fabrics, fabric stitching, customized prices, use time, and waste disposal. The quality evaluation index system of antiepidemic clothing design in this study is shown in Table 1.

2.3. Constructing the Analytic Hierarchy Model for Quality Evaluation of Epidemic Clothing. Epidemic-preventing clothing's protection requirements for viruses, bacteria, etc., and complex functional requirements in various situations determine that it is difficult to use a single standardized method to evaluate its quality. According to the analytic hierarchy process, this article decomposes the quality evaluation of epidemic prevention clothing into multiple indicators and then uses linear algebra knowledge such as matrix operations to calculate the weights of evaluation indicators at various levels so as to determine the importance of each quality impact index in the design of epidemic prevention clothing at different levels [22]. The calculation of the weight is transformed into the corresponding evaluation index set, and then, the quality level of the antiepidemic clothing design is analyzed according to the principle of membership degree. The quality assessment of special antiepidemic medical clothing can start from the aspects of protection, comfort, physical properties, chemical

properties, and other durability properties and water shrinkage of the finished antiepidemic clothing, including material molecules, coating technologies, special fabrics, seven first-level indicators such as fabric stitching, customized price, use time, and disposal. The first-level index evaluation matrix for the quality of epidemic prevention clothing in this article is as follows:

$$E = \begin{bmatrix} Y & A_1 & A_2 & A_3 & \dots & A_7 \\ A_1 & a_{11} & a_{12} & a_{13} & \dots & a_{17} \\ A_2 & a_{21} & a_{22} & a_{23} & \dots & a_{27} \\ A_3 & a_{31} & a_{32} & a_{33} & \dots & a_{37} \\ \dots & \dots & \dots & \dots & \dots & \dots \\ A_7 & a_{71} & a_{72} & a_{73} & \dots & a_{77} \end{bmatrix} \begin{bmatrix} U \\ u_1 \\ u_2 \\ u_3 \\ \dots \\ u_7 \end{bmatrix} \begin{bmatrix} V \\ v_1 \\ v_2 \\ v_3 \\ \dots \\ v_7 \end{bmatrix} \begin{bmatrix} W \\ w_1 \\ w_2 \\ w_3 \\ \dots \\ w_7 \end{bmatrix}. \quad (9)$$

The first-level index judgment matrix E represents the importance judgment value of two insulation evaluation indexes compared with each other and a_{ij} represents the judgment value of the importance of the evaluation index a_i compared to the evaluation index a_j. In the above judgment matrix, the left side is the importance level evaluation matrix of the criterion layer, u_i represents the product of each row element of the importance evaluation matrix, v_i represents the value of the square root of each element in U according to the matrix order, and then w_i represents the value of each element in V and the ratio of the sum of all elements. According to the knowledge of matrix normalization operations, their calculation formulas are as follows:

TABLE 1: Design quality evaluation index system for epidemic prevention clothing.

First level	Meaning	Second level	Meaning	Third level	Meaning
A1	Material	B1	Comfort	C1~C2	Edition type
		B2	Fashion	C3~C4	Craft
A2	Coating	B3	Skin-friendly	C5~C7	Culture
		B4	Protective	C8~C9	Positioning
A3	Fabrics	B5	Physical	C10~C12	Policy
		B6	Chemistry	C13~C14	Market
A4	Stitching	B7	Breathable	C15~C16	Regulation
		B8	Tightness	C17~C18	Supervision
A5	Prices	B9	Parity	C19~C21	Sales
		B10	High price	C22~C23	Promotion
A6	Usage time	B11	One time	C24~C25	Durability
		B12	Repeated use	C26~C27	Disinfection
A7	Disposal	B13	Biodegradable	C28~C29	Pollution
		B14	Destruction	C30	Degradation

$$\begin{cases} u_i = \prod_{j=1}^{n} a_{ij}, \ i = 1, \ldots, 7, \\ \\ v_i = \sqrt[n]{u_i} = \sqrt[7]{u_i}, w_i = \dfrac{v_i}{\sum_{i=1}^{n} v_i}. \end{cases} \quad (10)$$

$$\begin{aligned} \mathrm{CI} &= \frac{\lambda_{\max} - n}{n - 1}, \\ \mathrm{CR} &= \frac{\mathrm{CI}}{\mathrm{RI}}. \end{aligned} \quad (12)$$

In order to verify the consistency of the evaluation indicators of the antiepidemic clothing quality evaluation hierarchy analysis model in this article, after calculating the weights of the antiepidemic clothing quality evaluation indicators through the judgment matrix and the weight matrix, the model needs to be CR verified. The main principle of CR verification is to calculate the consistency ratio of the evaluation matrix of the model by the ratio of the consistency index of the evaluation matrix to the average random consistency index of the same order matrix and analyze the evaluation performance of the model [23]. The consistency index of the evaluation matrix also needs to be obtained by the maximum eigenvalue of the matrix. The calculation formula for the maximum eigenvalue $\lambda_{\max}$ of the evaluation matrix is as follows:

$$\lambda_{\max} = \sum_{i=1}^{n} \frac{(E * W)_i}{n w_i}. \quad (11)$$

According to the principle of consistency verification, when the consistency ratio is zero, the judgment matrix has complete consistency. This verification method can also flexibly grasp the weight of each indicator in the evaluation indicator system according to one's own tendency and realize the reasonable distribution of weight through appropriate weight adjustment. According to the calculation of the maximum eigenvalue of the evaluation matrix, the calculation formulas of the consistency index CI and the consistency ratio CR of the evaluation matrix can be obtained as follows, where the average random consistency index of the seventh-order matrix is RI = 1.32 according to previous studies.

2.4. Verification of Physical Properties and Antiepidemic Performance of Antiepidemic Clothing.

The most important performance of antiepidemic clothing is to protect users from infection by pathogenic bacteria and other pollution sources. However, when medical personnel use antiepidemic clothing, the diffusion of molecules in the air and the heat generated by the users themselves aggravate the movement of molecules. The performance of antiepidemic clothing will inevitably decline. In addition, medical staff may also be contaminated during the replacement and removal of epidemic prevention suits [24]. Therefore, it is necessary to carry out high-precision testing of the physical properties of the antiepidemic clothing and also to analyze the antiepidemic performance of the antiepidemic clothing and predict the failure time of the antiepidemic performance so that users can replace it in time. The infiltration equation of dust particles in antiepidemic suits over time is as follows:

$$\frac{\partial c_i}{\partial t} + \frac{\partial (u c_i)}{\partial x} + \frac{\partial (v c_i)}{\partial y} = P_i - Q_i. \quad (13)$$

Among them, u and v represent the components of the penetration velocity of dust particles in the x- and y-directions, and c_i is the dust particle molecular content of the i th antiepidemic clothing material plane unit, that is, the relative volume ratio of all molecules. P_i and Q_i indicate the amount of dust particles attached to the surface of the antiepidemic clothing and the content of dust particles that penetrate into the inner layer of the antiepidemic clothing. The infiltration equation of pathogenic bacteria in antiepidemic clothing over time is as follows [25]:

$$R_i = 3(1 + \lambda)d_i\left(U - \frac{U_i}{1.4}\right)\left[\frac{U^3}{(U_i/1.4)^3} - 1\right], \qquad (14)$$

where R_i represents the penetration rate of pathogenic bacteria in the material plane unit, U_i is the comprehensive penetration rate of pathogenic bacteria in the unit, λ is the penetration influence coefficient, and d_i is the average particle radius of pathogenic bacteria. According to the permeation equation of dust particles and pathogenic bacteria and related knowledge of physics, the deformation equation of the antiepidemic suit over time can be obtained as follows, where P_{si} is the number of suspected penetrating molecules of the material plane unit, P_{ti} is the number of penetrating molecules of the unit over time, z_s is the amount of material deformation, and C_m is the highest molecular penetration amount that maintains the functional characteristics of the antiepidemic clothing material to prevent bacterial penetration [26].

$$\sum_{i=1}^{n} P_{si}(P_i - Q_i) + \sum_{i=1}^{n} P_{ti}\left(\frac{\partial R_{tx}}{\partial x} + \frac{\partial R_{ty}}{\partial y}\right)\frac{1}{\lambda} + C_m\frac{\partial z_s}{\partial t} = 0. \qquad (15)$$

The molecular movement of a larger area close to the plane of the antiepidemic clothing material will cause the infiltration of pathogenic bacteria and dust particles to increase, and when the rate of outward diffusion of pathogenic bacteria on the contact surface is greater than the rate of sedimentation or inward diffusion, the dust on the outer layer of the contact surface particles and pathogenic bacteria will continue to spread and gradually penetrate into the inner layer. The penetration amount of these pollutants can be determined by the following formula. Among them, t_i is the start time of the antiepidemic clothing, and t_{ci} is the pollutant penetration time.

$$\frac{P_i}{Q_i} = \frac{1}{\sqrt{2\pi}}\int_{t_i}^{\infty}\left(\frac{1}{t_{ci}} - 1\right)e^{-t^2}\mathrm{d}t = f\left(\frac{u_i}{v_i}\right), \quad t_{ci} = \frac{t_i}{\sqrt{2C_m^2}}. \qquad (16)$$

3. Simulated Penetration Experiment of Virus in Antiepidemic Prevention Clothing

3.1. Research Object.
The research object of this article is the research of special clothing design for epidemic prevention and medical treatment based on mathematical model analysis. According to the principle of mathematical model analysis and analytic hierarchy process, this article considers and tests various factors, such as the spatial structure of material molecules and the penetration rate of dust particles and pathogenic bacteria, of special medical clothing for epidemic prevention. From this, the key points of the design of special antiepidemic medical clothing are extracted and promoted to the production and use of antiepidemic clothing. This article uses the finished product of the antiepidemic suit as a sample to conduct a simulated penetration test of pathogenic bacteria. Under the premise of ensuring

the most important antiepidemic function requirements of antiepidemic clothing and controlling a certain cost, the design of special antiepidemic medical clothing through this research can provide excellent antiepidemic clothing design options for antiepidemic clothing manufacturers. This research proposes designing and improving the performance of antiepidemic clothing according to the needs of different users, improving the quality of antiepidemic work, and saving certain production costs.

3.2. Pathogenic Bacteria Simulated Permeation Experiment Design.
The purpose of this research is to analyze, design, and improve the design of special medical clothing for epidemic prevention through mathematical models, including the evaluation of various factors such as fabric selection, stitching technology, and finished product production. In this article, the pathogenic bacteria simulation penetration experiment is divided into the following steps. The first step is to understand the key points and quality evaluation methods of epidemic prevention clothing design through literature research and consultation with professionals and establish a quality evaluation index system for epidemic prevention clothing. The second step is to understand the current application of mathematical models in the medical field and clothing design, analyze the problems in the design of antiepidemic clothing in the past, and establish a hierarchical analysis model for the quality of antiepidemic clothing based on mathematical model analysis. The third step is to detect the functional characteristics of the antiepidemic clothing through the pathogenic bacteria simulation penetration test and predict the performance failure time of the antiepidemic clothing under different conditions based on the performance of the antiepidemic clothing in various aspects over time until it fails to remind the user to replace it in time. Finally, through the established analytic hierarchy model for the quality evaluation of epidemic prevention clothing, data processing and error analysis are performed on the results of the simulation experiment to verify the feasibility of the design scheme and the reliability of the quality of the epidemic prevention clothing. Based on this, it can provide manufacturers with antiepidemic clothing design plans and suggestions on production factors such as fabric selection and stitching technology. The main framework of this research is shown in Figure 1.

3.3. Experimental Data Processing and Error Analysis.
According to the requirements of the simulation test, this article improves the detection method of the antiepidemic clothing material space structure and the pollutant penetration rate and further calculates some important indicators that need to be used in the analysis of the simulation test results. The service life of the antiepidemic clothing, that is, the failure time of the antiepidemic performance of the antiepidemic clothing, is mainly affected by the penetration of pollutants, temperature, and material deformation. To this end, this article discusses the detection methods of the above two factors, mainly through the average rate of
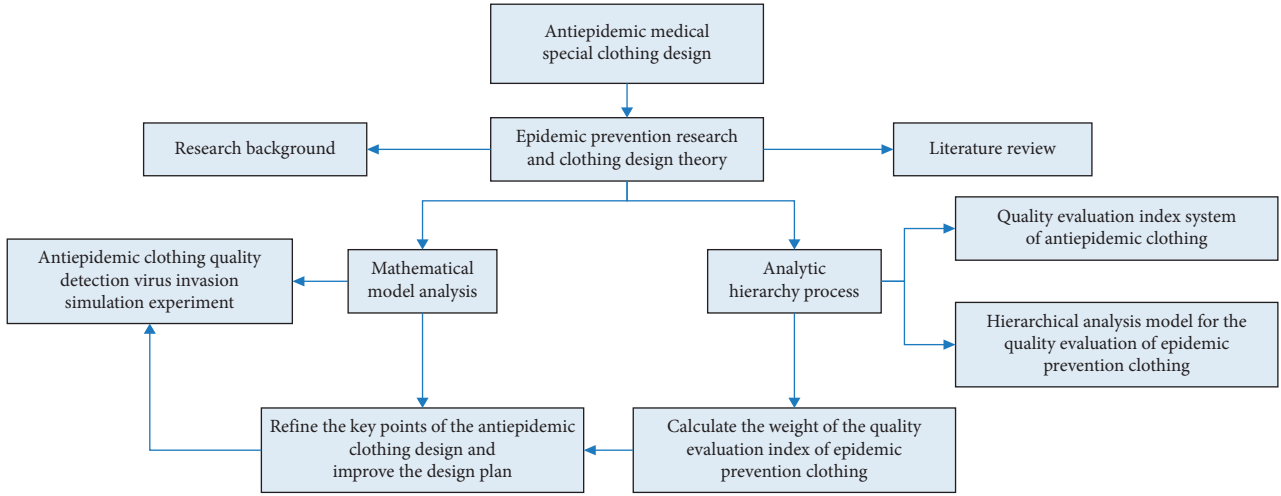
FIGURE 1: Research framework of antiepidemic clothing design based on the mathematical model.

pollutant penetration and the mechanical stress of the material deformation of the epidemic prevention clothing to evaluate the failure time of its epidemic prevention performance. Among them, the mechanical stress M_s of the deformation of the antiepidemic clothing material can be calculated by the following formula:

$$M_{sx} = \rho g \frac{u\sqrt{u^2 + v^2}}{C_s^2},$$

$$M_{sy} = \rho g \frac{v\sqrt{u^2 + v^2}}{C_s^2}, \qquad (17)$$

$$M_s = \sqrt{M_{sx}^2 + M_{sy}^2}.$$

Among them, M_{sx} and M_{sy} represent the component stress of the mechanical stress of material deformation in the x-direction and y-direction, respectively. ρ and g are the density and gravitational acceleration of the antiepidemic clothing material. The pollutant average penetration rate $\overline{\omega}$ can be obtained by the following formula, where ω_{max} and ω_{min} are the maximum and minimum penetration rates of the pollutants.

$$\overline{\omega} = \frac{(\omega_{max} + \omega_{min} + \sqrt{\omega_{max} \cdot \omega_{min}})}{3}. \qquad (18)$$

4. Discussion on Penetration Experiment of Virus in Antiepidemic Clothing Quality

4.1. Analysis of the Selection of Design Fabrics for Epidemic Prevention Clothing. Antiepidemic clothing is also called isolation gown. Its most important functional requirement is to prevent viruses, bacteria, and other infectious agents from contacting the human body. Therefore, the choice of fabric for antiepidemic clothing should meet the requirements of good skin-friendliness and comfortable wearing and has the advantages of being nontoxic and odorless, efficient bacteria isolation, high strength, and good

filtration performance and can achieve antistatic, antialcohol, antiplasma, and water-repellent properties and water production and other performance requirements. The general components of antiepidemic clothing fabrics include spun-bonded nonwoven fabric SNF, melt-blown nonwoven fabric MNF, composite nonwoven fabric CNF, PE waterproof and breathable film PEF, TPU composite film, and three-layer thousand mesh TTM. In this article, the moisture resistance of these fabric components was investigated, and the results are shown in Table 2.

According to related research, this article analyzes the moisture permeability of the antiepidemic clothing fabric components and compares spun-bonded nonwoven fabrics, melt-blown nonwoven fabrics, composite nonwoven fabrics, PE waterproof breathable membrane, TPU composite membrane, and three-layer thousand net. The moisture permeability of the material composition is examined by evaluating the resistance of the fabric composition under different humidity. As shown in Figure 2, among all the fabric components, PE film and TPU composite film have the lowest moisture resistance and the best waterproof and moisture permeability, which can be used as an important reference factor for fabric selection.

4.2. Analysis on Spinning Technology of Antiepidemic Clothing Design. According to the survey, the current spinning technologies for apparel design and production mainly include five commonly used spinning technologies, including electric spinning, liquid crystal spinning, melt-jet spinning, solution spinning, and electrostatic spinning. As shown in Table 3, this article compares the heat dissipation performance, waterproof and breathable performance, moisture permeability, and bacteria isolation and electrostatic characteristics of clothing made by five spinning technologies. Antiepidemic clothing is special medical clothing with special functional requirements. Considering the needs of isolation of bacteria and viruses and repeated use of disinfection and sterilization, this article uses electrostatic spinning technology to carry out the antiepidemic

TABLE 2: Waterproof and moisture permeability of antiepidemic clothing fabric components.

Humidity	SNF	MNF	CNF	PEF	TTM	TPUF
0	29.87	15.36	6.19	3.88	23.54	27.68
2	34.79	27.44	5.97	4.69	39.86	31.87
4	34.63	29.38	8.96	9.98	20.71	15.54
6	33.06	33.87	10.39	8.99	8.64	13.65
8	35.97	51.65	17.48	9.97	15.69	23.04
10	39.86	58.34	19.86	12.28	26.38	18.97
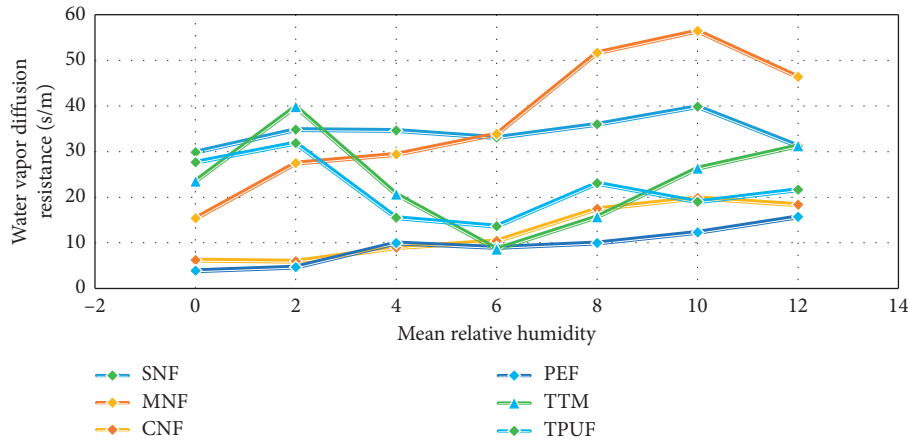
FIGURE 2: Moisture resistance of fabric components of epidemic prevention clothing.

TABLE 3: Comparison of performance of antiepidemic clothing with different spinning technologies.

Spinning technology	Heat dissipation	Waterproof and breathable	Moisture permeability	Bacteria isolation	Static electricity
Electric	41.26	42.68	54.42	66.25	91.54
Liquid crystal	54.83	59.86	47.36	51.44	87.63
Melt-jet	46.34	48.75	65.34	68.49	58.76
Solution	78.36	66.87	78.17	71.63	76.49
Electrostatic	89.64	83.62	90.38	88.74	43.68

clothing waterproof and breathable composite membrane experiment.

According to survey statistics, among the five spinning technologies, the antiepidemic clothing made by electrostatic spinning technology has the most superior performance. As shown in Figure 3, this article uses a hundred-point system to score the performance of the epidemic prevention clothing under these spinning technologies. The heat dissipation performance, waterproof and breathable performance, moisture permeability, and bacteria isolation characteristics of the epidemic prevention clothing under the electrostatic spinning technology are all rated at 80 points and above. Its electrostatic characteristics are only 43.86, which best fits all the functional requirements of epidemic prevention clothing.

4.3. Protective Function of Antiepidemic Clothing Design. For the design of medical clothing, the protective function is an indispensable factor in all considerations, and the design of special medical clothing for epidemic prevention is even

more so. This article studies the protective functions of the antiepidemic clothing from its antifouling, antibacterial, anticorrosion, antiradiation, and antistatic properties. According to the principles of physical and chemical testing, this study conducted physical and chemical experimental tests on the above protective functions of the antiepidemic clothing design. The test results are shown in Table 4.

Through relevant case studies and consultation with experts, this article tested the main evaluation indicators of the protective function of the antiepidemic clothing and ranked the importance of the indicators according to the test results. As shown in Figure 4, it is obvious that the protective function of epidemic prevention clothing is mainly reflected in the performance of antifouling and antibacterial properties. Therefore, the advantages and disadvantages of these two properties are the main factors for evaluating the protection function of epidemic prevention clothing. On the whole, the importance of antifouling and antibacterial properties of antiepidemic clothing reached 0.5764 and 0.4386, respectively, which are the primary evaluation indicators for protective functions.
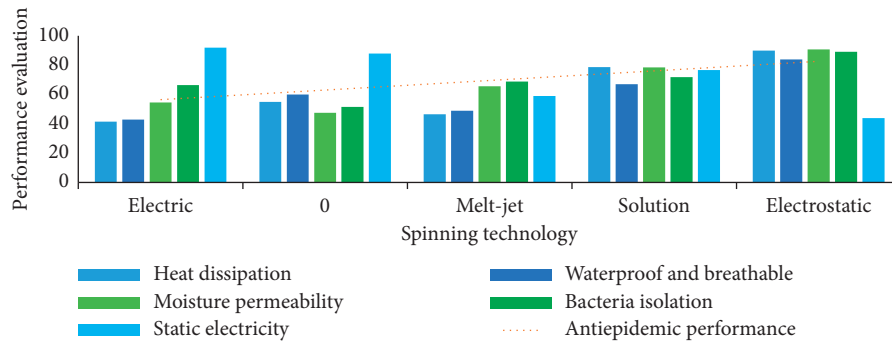
FIGURE 3: Performance comparison of antiepidemic clothing spinning technology.

TABLE 4: Experimental test of the protective function of antiepidemic clothing.

Protection	A	B	C	D	E	F
Antifouling	0.2834	0.2639	0.1706	0.1225	0.1018	0.1008
Antibacterial	0.3416	0.3097	0.2034	0.1674	0.1497	0.1597
Anticorrosion	0.3025	0.2769	0.1627	0.1106	0.0985	0.0875
Antiradiation	0.3837	0.3325	0.2234	0.1577	0.1234	0.1198
Antistatic	0.4386	0.2937	0.1875	0.0908	0.0839	0.0765
Total	0.5764	0.4386	0.3458	0.2147	0.1894	0.1234
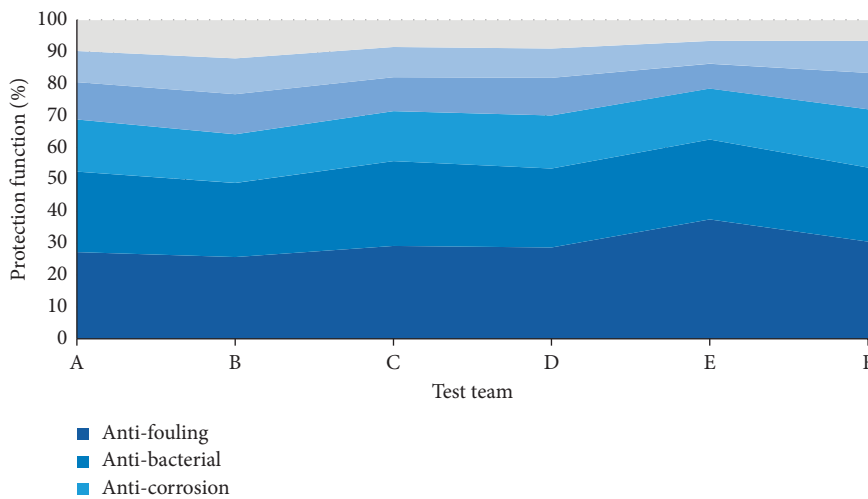
FIGURE 4: The test situation of the protective function of epidemic prevention clothing.

4.4. Antiepidemic Clothing Design Quality Evaluation Test.

According to the quality evaluation index system of anti-epidemic clothing discussed and established in this article, this paper calculates and counts the weights of all first-level quality evaluation indexes, as shown in Table 5. Combined with the introduction of the quality evaluation index system and the data in the table below, it can be seen that the A1 index, which is the epidemic prevention performance index, accounts for the most weight among all the first-level quality evaluation indexes. It can be seen that the evaluation of antiepidemic performance should be the primary reference factor for the design of antiepidemic clothing and the first evaluation index for quality evaluation.

In the method part, this article discusses the index system for the quality evaluation of epidemic prevention clothing. The quality evaluation is divided into three levels according to the degree of importance and the different coverage. In the process of detecting the quality of anti-epidemic clothing through the simulated invasion experiment of pathogenic bacteria, this article uses mathematical models and related computer software to calculate and process the weights of quality evaluation indicators. The weights of the first-level indicators obtained by the experimental statistics are shown in Figure 5. It can be seen from the figure that the weights of the three indicators $A1$, $A2$, and $A3$, namely, fabric selection, spinning coating, and epidemic

TABLE 5: Weights of quality evaluation indicators for epidemic prevention clothing.

Expert	A1	A2	A3	A4	A5	A6	A7
1	0.2973	0.3312	0.0525	0.0521	0.2005	0.0605	0.0861
2	0.1976	0.2523	0.0402	0.1245	0.2318	0.1633	0.0713
3	0.3876	0.2791	0.0263	0.0119	0.3195	0.1012	0.0123
4	0.3112	0.2274	0.1076	0.0428	0.1693	0.0655	0.0781
5	0.3745	0.1828	0.1485	0.0345	0.3198	0.0748	0.0432
6	0.1908	0.3968	0.0323	0.1253	0.2291	0.0895	0.0358
7	0.2923	0.1987	0.0709	0.0482	0.4712	0.1179	0.1371
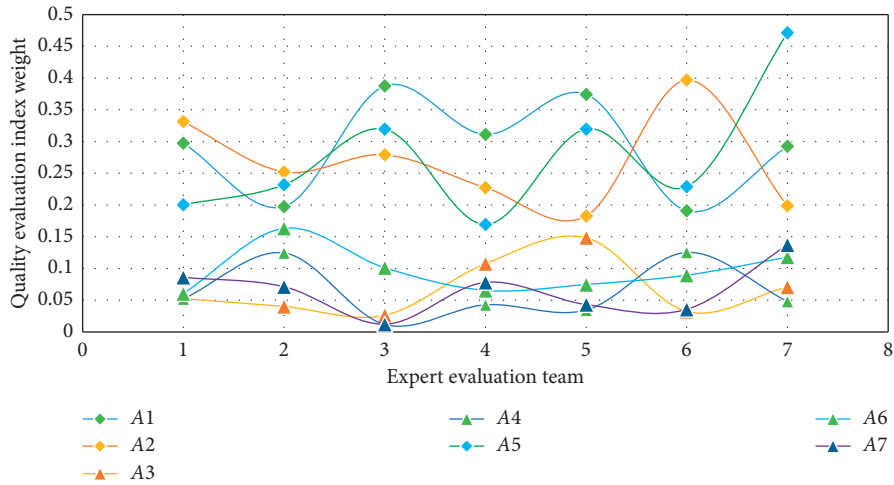
FIGURE 5: Weights of evaluation indicators for the quality of antiepidemic clothing.

TABLE 6: Survey of satisfaction with the quality of antiepidemic clothing.

Objects	Style	Color	Comfort	Fabric	Sewing	Performance
A	54	58	74	78	66	72
B	68	63	82	45	68	69
C	75	74	67	54	61	83
D	66	54	86	63	78	78
E	72	49	91	38	84	94
F	83	66	78	59	71	91
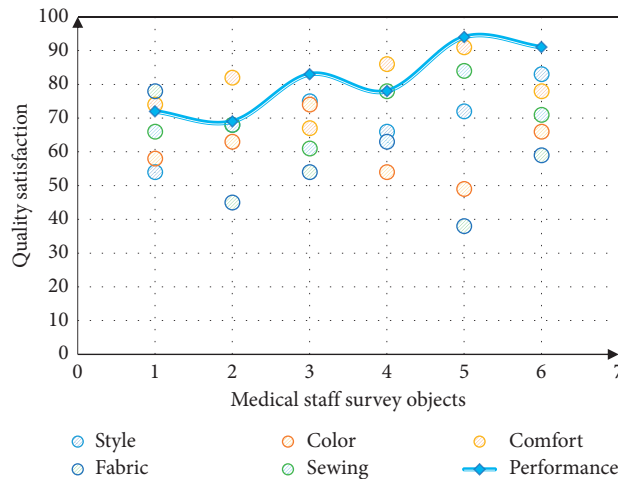
FIGURE 6: Satisfaction evaluation of antiepidemic clothing quality indicators.

prevention performance, are significantly higher than the other first-level indicators. Therefore, it is the main factor in the design of epidemic prevention clothing.

4.5. Satisfaction Survey on the Use of Antiepidemic Clothing. According to the quality evaluation and analysis of the antiepidemic clothing, this article randomly selected a part of medical staff as the survey subjects and conducted an interview survey on their satisfaction with the quality of the antiepidemic clothing samples designed in this study. This article mainly uses a hundred-point system to conduct a satisfaction survey from the aspects of antiepidemic clothing style, color, comfort, fabric, sewing technology, and performance. Table 6 shows the satisfaction survey results of some medical staff survey subjects.

In order to understand the medical staff survey subjects and the satisfaction of more users of the epidemic prevention clothes with the design of the epidemic prevention clothes in this study, this article divides the result data of the interview survey into six groups, each of 20 medical staff survey subjects, and selects their quality of the epidemic prevention clothes. The median of the satisfaction scores is plotted as a scatter plot as shown in Figure 6. As shown in the figure, the satisfaction scores of all the survey respondents for the antiepidemic performance of the antiepidemic clothing are higher than 60 points, which shows that the antiepidemic clothing designed in this study has a higher antiepidemic performance.

5. Conclusions

This article focuses on the shortage of medical resources in the epidemic prevention work of medical staff during the epidemic of new coronary pneumonia, especially the shortage of special epidemic prevention medical clothing and the failure of protection caused by the quality of epidemic prevention clothing, and proposes special epidemic prevention medical services based on mathematical model analysis. In the research on clothing design, during the investigation of the epidemic prevention work during the epidemic, this article found that with the prolonged wearing time of the epidemic prevention clothing of medical staff, the deformation of the epidemic prevention clothing is caused by the heat generated by the medical staff and the stretching activities of the limbs and the ineffectiveness of the epidemic prevention function is caused by the invasion of the virus to the doctors and nurses. The personnel caused a great threat to their lives. In addition, the inconvenience is caused by the cumbersome disinfection and replacement of antiepidemic suits and the waste of medical resources caused by accidental pollution under the exhausted state of long-term work hinders the smooth implementation of the epidemic prevention work. Based on this, this article proposes a design plan for special medical clothing for epidemic prevention based on mathematical model analysis. Under the premise of ensuring the soundness of the epidemic prevention function of the epidemic prevention clothing, it further predicts the time when the epidemic prevention clothing fails to remind

medical staff to replace it in time. On the basis of ensuring quality, it can also be designed and improved according to the convenience of wearing, heat dissipation and ventilation, and comfort to provide technical support and safety guarantee for epidemic prevention.

Based on the mathematical model and the analytic hierarchy process, this paper establishes an analytic hierarchy model for the quality evaluation of epidemic prevention clothing to evaluate the quality of the design of the epidemic prevention clothing. Through the analysis of the results of the simulated penetration experiment of pathogenic bacteria, the antiepidemic clothing designed in this study can be used multiple times after disinfection without changing the molecular structure when the epidemic is not serious, and its antiepidemic function can be maintained for up to two months. Compared with the traditional clothing design method, the quality assessment of the antiepidemic clothing design method based on the mathematical model in this study is more accurate, the antiepidemic performance is more guaranteed, and the failure time of its antiepidemic function can be accurately predicted, and the designed antiepidemic clothing is convenient to wear and heat dissipation. The performance of breathability and comfort is also superior.

Since the antiepidemic clothing is designed with special functional requirements as the goal, this article mainly discusses the design factors of antiepidemic functions and performance degradation of the antiepidemic clothing, and there is no specific consideration for the production, sales, and disposal of the antiepidemic clothing. Therefore, this study still has many limitations. In particular, the impact of the industrial supply chain and external market environment, production costs, and sales prices of antiepidemic clothing operations on the design of antiepidemic clothing is not considered or analyzed. We hope that in the future, we can conduct in-depth research from these aspects, make full use of the characteristics of mathematical model analysis, and provide better solutions for the design of epidemic prevention clothing.

Data Availability

The data that support the findings of this study are available from the corresponding author upon reasonable request.

Conflicts of Interest

The authors declare no potential conflicts of interest with respect to the research, authorship, and/or publication of this article.

References

[1] H. Mann, I. J. Mann, and N. Gullaiya, "A case in medical equipment design for strategic sustainability," *South Asian Journal of Business and Management Cases*, vol. 7, no. 2, pp. 111–119, 2018.

[2] Z. Ruan, "Global anti-epidemic outbreak needs to enhance community awareness," *Peace*, vol. 134, no. 1, pp. 25-26, 2020.

[3] D. Lee, K. Park, and J. Seo, "Recent advances in anti-inflammatory strategies for implantable biosensors and medical implants," *BioChip Journal*, vol. 14, no. 1, pp. 48–62, 2020.

[4] A. C. Faust, P. Rajan, L. A. Sheperd, C. A. Alvarez, P. McCorstin, and R. L. Doebele, "Impact of an analgesia-based sedation protocol on mechanically ventilated patients in a medical intensive care unit," *Anesthesia & Analgesia*, vol. 123, no. 4, pp. 903–909, 2016.

[5] G. Gentile, F. Cipolla, M. Capi, M. Simmaco, L. Lionetto, and M. Borro, "Precise medical decision making in geriatric antidepressant therapy," *Expert Review of Precision Medicine and Drug Development*, vol. 1, no. 4, pp. 387–396, 2016.

[6] O. Mehmet, E. Liatsikos, and N. Scheffbuch, "Comparison of silodosin to tamsulosin for medical expulsive treatment of ureteral stones: a systematic review and meta-analysis," *Urolithiasis*, vol. 44, no. 6, pp. 491–497, 2016.

[7] É. Fontana, R. Donca, E. Mancusi, A. A. Ulson De Souza, and S. M. A. Guelli Ulson De Souza, "Mathematical modeling and numerical simulation of heat and moisture transfer in a porous textile medium," *The Journal of the Textile Institute*, vol. 107, no. 5, pp. 672–682, 2016.

[8] Y. Yue, Y. Aixi, X. Wenxia et al., "Strategies suggested for emergency diagnosis and treatment of traumatic orthopedics in the epidemic of COVID-19," *Chinese Journal of Orthopaedic Trauma*, vol. 22, no. 02, pp. 123–127, 2020.

[9] R. S. Luan, X. Wang, X. Sun et al., "Epidemiology, treatment, and epidemic prevention and control of the coronavirus disease 2019: a review," *Sichuan da xue xue bao. Yi Xue Ban = Journal of Sichuan University. Medical Science Edition*, vol. 51, no. 2, pp. 131–138, 2020.

[10] Q. Cai, Y. Mi, Z. Chu, Y. Zheng, F. Chen, and Y. Liu, "Demand analysis and management suggestion: sharing epidemiological data among medical institutions in megacities for epidemic prevention and control," *Journal of Shanghai Jiaotong University (Science)*, vol. 25, no. 2, pp. 137–139, 2020.

[11] D. Xu, Y. He, Y. Yu, and Q. Zhang, "Multiple parameter determination in textile material design: a Bayesian inference approach based on simulation," *Mathematics and Computers in Simulation*, vol. 151, no. 9, pp. 1–14, 2018.

[12] A. Cay, G. Gurlek, and N. Oglakcioglu, "Analysis and modeling of drying behavior of knitted textile materials," *Drying Technology*, vol. 35, no. 4, pp. 509–521, 2017.

[13] A. Rahi, "Correction to: crack mathematical modeling to study the vibration analysis of cracked micro beams based on the MCST," *Microsystem Technologies*, vol. 24, no. 7, pp. 3217–3223, 2018.

[14] Y. Liuhua, W. Hong-Jiang, W. U. Ai-Xiang et al., "Regulation and a mathematical model of underflow in paste thickeners based on a circular system design," *Chinese Journal of Engineering*, vol. 39, no. 10, pp. 1507–1511, 2017.

[15] S.-B. Tsai, M.-F. Chien, Y. Xue et al., "Using the fuzzy dematel to determine environmental performance: a case of printed circuit board industry in taiwan," *PLoS One*, vol. 10, no. 6, Article ID e0129153, 2015.

[16] O. Niculescu, L. Albu, M. C. Loghin, C. Gaidau, L. Miu, and G. Coara, "New products based on essential oils for the treatment of medical furs," *Revista de Chimie*, vol. 70, no. 3, pp. 765–768, 2019.

[17] S. Subramanian, "Healthcare impact of COVID-19 epidemic in India: a stochastic mathematical model," *Medical Journal Armed Forces India*, vol. 76, no. 2, pp. 147–155, 2020.

[18] K. Mumse, "Mathematical modeling of tracer kinetics for medical applications," *International Journal of Mathematics, Game Theory, and Algebra*, vol. 27, no. 3, pp. 323–358, 2018.

[19] N. Jeleniaková, B. Petrovi, S. Koji et al., "Application of mathematical models and microfluidics in the analysis of saliva mixing with antiseptic solutions," *Balkan Journal of Dental Medicine*, vol. 24, no. 2, pp. 84–90, 2020.

[20] S. A. Carvalho, S. O. Da Silva, and I. D. C. Charret, "Mathematical modeling of dengue epidemic: control methods and vaccination strategies," *Theory in Bioences*, vol. 138, no. 1, pp. 107–121, 2017.

[21] I. Hussain, E. Malik, and M. S. Raza, "Term back/detention policy revision measures in academic medical and allied institutions of Pakistan in the COVID-19 epidemic for the session 2019-2020," *Journal of Rawalpindi Medical College*, vol. 24, no. 9, pp. 8–12, 2020.

[22] W. R. Zhang, K. Wang, L. Yin et al., "Mental health and psychosocial problems of medical health workers during the COVID-19 epidemic in China," *Psychotherapy and Psychosomatics*, vol. 89, no. 4, pp. 1–9, 2020.

[23] C. H. Wang, M. L. Tseng, K. H. Tan et al., "Application of a mathematical programming model to solve the confidence interval of process capability index Spk," *International Journal of Information and Management Sciences*, vol. 28, no. 1, pp. 11–23, 2017.

[24] Z. Aijun, L. Xinxin, M. Pibo et al., "3D simulation model of warp-knitted patterned velvet fabric," *International Journal of Clothing Ence and Technology*, vol. 28, no. 6, pp. 794–804, 2016.

[25] M. Fu, W. Chen, W. Weng, M. Yuan, N. Luo, and X. Xu, "Prediction of thermal skin burn based on the combined mathematical model of the skin and clothing," *The Journal of the Textile Institute*, vol. 109, no. 12, pp. 1606–1612, 2018.

[26] S. Chen, M. K. Hassanzadeh-Aghdam, and R. Ansari, "An analytical model for elastic modulus calculation of SiC whisker-reinforced hybrid metal matrix nanocomposite containing SiC nanoparticles," *Journal of Alloys and Compounds*, vol. 767, pp. 632–641, 2018.

Research Article

Design and Research of Interactive Animation of Immersive Space Scene Based on Computer Vision Technology

Shan Wu, Hubin Liu, Qi Xu, and Yulong Liu [ID]

Graduate School, Sejong University, Seoul 05006, Republic of Korea

Correspondence should be addressed to Yulong Liu; liuyulong@tjarts.edu.cn

With the development of computational simulation technology, the need for stable and immersive display effects of space scene animation in the field of life experience and visual art has gradually increased. In this case, the requirements for immersive characteristics of space scene animation have also been strengthened. The existing 3D space scene animation has a limited degree of stereoscopic display model and data visualization. However, the current space scene interactive animation adopts a plane layout as a whole, and the size of the view interface is generally fixed, including the size of virtual elements. However, the immersion in this paper interactive animation of spatial scene can effectively solve the problems of incomplete display of 3D effects and unstable view simulation in 3D effects. This paper takes immersive space scene animation as the research object and studies the 3D and characteristics of space scene animation based on computer parallel computing in different immersive space scenes and different virtual space technologies, as well as the animation effects of different scene transformations and art forms. The result of research shows that, with the continuous increase of the degree of virtuality within a certain range, the immersive effect of spatial scene interactive animation gradually becomes better. When the color of the space scene animation is below 15, the virtual immersive effect changes less. When the space scene is in the range of 15–20, the space scene will make people feel the atmosphere of a beautiful and mysterious illusion.

1. Introduction

Scene interactive animation as a new technology with great application prospects has attracted the attention of many scientific researchers and emerging Internet film and television companies. Scene interactive animation is also simulating the visual effects of the human body. In an immersive space environment, the light and temperature around the body must first be sensed. The body will process the light that the eyes can see and feel the image in the brain. The design of the animation scene has a great influence on the decoration and lyric of the animation. The key to the optimization of the space control of the animation simulation system is the real-time detection of the immersive space environment and the frequency conversion speed control according to the data flow. Real-time detection of data flow is the prerequisite and basis for the overall system optimization of spatial scene control. The use of 3D video data stored on the disk requires

a large experience space and low security and stability. Computer vision technology is used to design an immersive space scene interactive animation model, combined with image processing technology, parallel computing the data flow of the model according to the changing state of the data flow. The LPC fuzzy controller adjusts the output rate of the animation through the control of the frequency converter to enable the development of scene interactive animation enter a new era.

The image collection data are greatly affected by the internal factors of the collector, and it is difficult to adapt the material to the broad population. Lv et al. conducted research on visual animation modeling algorithms and proposed the applicability and theoretical basis of visual animation modeling [1]. Ciccone et al. used the multidimensional data analysis method of space model computer parallel algorithm theory to study the characteristics of immersive space elements [2]. Liu et al. proposed GSI's momentum three-

dimensional space quantization element theory by studying the label operation theory of the basic software technology Internet engineering principles and further processed visual images on the basis of big data to obtain the supernatural characteristics of the elements [3]. Buchanan's application in 3D visual animation mostly focuses on conventional models and researching space scenes, and the research is not accurate to the movements of creatures in immersive space scenes [4]. Gottesman used SGP to study the design and realization of the linkage between physical space and action and proposed a parallel computing immersive space model to accurately and objectively analyze and restore the behavior mode of animation [5].

The main research direction of scene interactive animation is to count the running data from the observation point to the target, the displacement form, and the decent relative reference value based on the virtual picture. Luo et al. analyzed the algorithm of the 3D tuple expected target model based on the GSP technology in the stable operation stage, did not adjust the speed, and proposed the immersive space and the Internet of things vision theory [6]. Colleen and Jones used the spatial distribution data that GSP keeps running at the power frequency, combined with GIS network analysis to determine the optimal configuration of service facilities [7]. Guimaraes et al. proposed that, in the process of actual use of GSP, it is clearly not possible to achieve the immersive effect of the animation system in this operating mode [8]. Lee et al. calculated the number and behavior of models by acquiring images on the spot and proposed a graph matching model under computer parallel computing [9]. Fang and Guo proposed that the digital animation scene is tilted at a certain angle to collect the animation image containing laser stripes in the set area and upload the image data to the ground control center information processing platform through the Ethernet optical cable through the network switch [10].

This paper studies the artistic effects of interactive animation of immersive spatial scenes based on computer vision technology. Immersive spatial scene interactive animation can effectively solve the problems of incomplete display of 3D effects and unstable view simulation in 3D effects. This paper studies the 3D and characteristics of space scene animation based on computer parallel computing in different immersive space scenes and different virtual space technologies, as well as the immersive characteristics of animation effects under different scene transformations and art forms. This paper studies an immersive interaction method based on virtual spatial data, which solves the problem of relying on image interaction in traditional spatial data interaction methods, allowing all users to immerse all attention in the spatial data visualization window and enhance the visualization of spatial data interactive experience.

2. Immersive Space Scene Interactive Animation

2.1. 3D Space Lofting Module. The interaction between vision and light is a typical problem of flexible interactive

animation architecture [11]. The changes of the space scene are divided into different interfaces according to the different animation architectures, and the extremely high distribution and modular characteristics of the deformation field show the animation elements of the space scene and change according to the changes of the space scene. In the process of the interaction of the lofting module, the dividing line of the transmission of the light parameters destroyed the interaction of the space architecture, and the interface of three key factors soon appeared [12]. Using CXF software to calculate the smooth average reynolds equation and the S-shed three-dimensional space calculation method, using the SST model as the prototype, because the STK model has a better ability to capture light passing, the introduction of a new intermittent transition model can be expressed by the following equation:

$$
\frac{\partial}{\partial t}\left(\rho_\gamma\right) + \frac{\partial}{\partial x_j}\left(\rho U_{j\gamma}\right) = P_{\gamma 1} - E_{\gamma 1} - E_{\gamma 2}
$$
$$
+ \frac{\partial}{\partial x_j}\left[\left(\mu + \frac{\mu_t}{\sigma_\gamma}\right)\frac{\partial_\gamma}{\partial_{xj}}\right]. \tag{1}
$$

The reason for the intermittent period characterized by the equal space of elements γ is that the light cannot be stagnant and cannot remain stationary with the state unchanged, while $P\gamma$ and $E\gamma$ pass through the highly balanced space of the format, according to the sequence equation after a certain time [13]. ANSYS software is used to analyze the immersive space architecture of the computer vision architecture and perform 3D analysis, so that the components that can be driven can adapt to the immersive space scene and are limited by capacity. The dispersion control equation is

$$
Mu'' + Cu' + Ku = F(t). \tag{2}
$$

Among them, M, C, and K are the immersive effect linear table, the parallel calculation table, and the visual stiffness linear table; $F(t)$ is the transient cohesion of the animated pixels acting on the 3D architecture. Hb-Jm multidimensional animation high poly computer MXF (multifield solver) is used to realize image data transmission between ordinary computers and professional image processing computers. In each time state of the state change process, it is applied to the immersive scene and visual effect, respectively, and the interface data are calculated through multiple recursions until the recursive convergence condition is satisfied. In the process of animation adjustment, the computer visualization simulation calculation method must visually model the body structure and deformation parameters of the animation elements and use function analysis tools to adjust the parameters [14]. Among them, the HiHe function is used the most in tuning design. The HiHe type function is based on the original animation ancestor vector line, which can digitally characterize all possible animation model bodies in a given area. It is an intuitive and simple model body digital method. Its general formula is as follows:

$$Y_1(x) = Y_{10}(x) + \sum_{i=1}^{n} d_{1i} \times f_i(x),$$

$$Y_2(x) = Y_{20}(x) + \sum_{i=1}^{n} d_{2i} \times f_i(x). \tag{3}$$

In the above formula, Y_1, Y_2 are the upper and Y_{10}, Y_{20} are the lower body parameters of the model body; d_{i1}, d_{i2} are the functions of the upper and lower surfaces of the reference model body; n is the design variables of the upper and lower surfaces of the model body; $f(x)$ are the number of design variables and are the control functions corresponding to the design parameters.

The original HiHe function does not have a control function for the trailing edge of the model posture, making the digital space of the trailing edge of the model posture unable to expand, limiting the diversity of model posture adjustments. Therefore, the formula for adding a multitype functional function to the rear edge of the model body is

$$f(x) = \begin{cases} x^{0.2}(1-x)e^{-20x} & (i = 1) \\ \sin^p\left(\pi x^{e(q)}\right) & (1 < i < n), \\ ax(1-x)e^{-\beta(1-x)} & (i = n) \end{cases} \tag{4}$$

$$e(q) = \frac{\ln(0.5)}{\ln(q)}.$$

In the above formula, P is the image signal range parameter of the control function; q is a one-dimensional array of length n-2, which controls the abscissa of the corresponding position of the peak of the n-1 round function because the shape of the leading edge of the animation model is in the computer and the spatial scene under vision has a greater impact, so the design variable points are encrypted at the front edge of the animation model [15]. Take $q = [0.25\,0.35\,0.5\,0.75]$; the change of the slope of the coefficient control function, the decay speed of the coefficient control function, and other parameters depend on experience. The space scene of the animation optimization mathematical model determines the animation transformation speed and light efficiency of the space scene, and the light that the space scene animation can carry is limited, so the light efficiency is particularly important. For the animation model, the audio-visual ratio is the most important performance indicator, which has a great impact on improving the efficiency of animation [16]. Therefore, taking the audio-visual ratio of the animation model as the objective function, a generalized animation model objective function model is established:

$$\text{objective: } \max\left(\frac{C_E}{C_D}\right). \tag{5}$$

Animation model optimization methods can be divided into single-objective optimization and multiobjective optimization. Single-objective optimization refers to the optimization of a certain element in the optimization process; multiobjective optimization refers to the range of one or more design intervals. Choose a variety of working conditions in the comprehensive interval of the weight function to optimize the space scene. Single-objective optimization is suitable for a relatively single animation model under target working conditions, and excellent spatial scene conditions can be obtained under target working conditions. The model parameters need to be tested under different GUIs, and they need to be considered to maintain better airflow efficiency at large elevation angles. In this case, multiobjective optimization is more appropriate.

As shown in Table 1, the multiobjective optimization idea of the animation model in the immersive space scene can be expressed as the weight coefficient of the animation model under different working conditions. It is a vector corresponding to different design variables. The animation model optimization process is based on the multiobjective optimization process of the animation model of the improved iterative algorithm. The animation algorithm is used to randomly generate the initial animation; the first generation animation model set is generated within the design interval and output to the animation model; the transformation solver X-fail calculates the performance of the animation model set and then inputs the required data into the main program to calculate the fitness [17]. The performance comparison chart is shown in Figure 1.

The accuracy and reliability of the X-type GUI view have been applied and verified. In the initial stage of optimization, in order to ensure the diversity of the animation, a larger frame volume and cross-mutation probability are required. In the later stage of optimization, the individual differences of the animation model become smaller, and the operator and fitness function must be readjusted to ensure the continuous progress of the animation [18].

2.2. Space Scene Control Equation. The space scene control equation of microanimation model works in an immersive space scene, where the space atmosphere has a greater impact. Therefore, when analyzing the immersion characteristics of the animation model, the influence of the light effect must be considered, so the control equation of the flow field uses the stable incompressible Navier–Stokes equation.

The animation effect equation is

$$\frac{\partial u}{\partial x} + \frac{\partial v}{\partial y} + \frac{\partial w}{\partial z} = 0. \tag{6}$$

The frame number equations in the X and Y directions are

$$\rho\left(u\frac{\partial u}{\partial x} + v\frac{\partial u}{\partial y}\right) = \mu\left(\frac{\partial^2 u}{\partial x^2} + \frac{\partial^2 u}{\partial y^2}\right) - \frac{\partial p}{\partial x},$$

$$\rho\left(u\frac{\partial u}{\partial x} + v\frac{\partial u}{\partial y}\right) = \mu\left(\frac{\partial^2 u}{\partial x^2} + \frac{\partial^2 u}{\partial y^2}\right) - \frac{\partial p}{\partial y}. \tag{7}$$

The light equation is

$$\frac{\partial E}{\partial x} + \frac{\partial E}{\partial y} = Q + W. \tag{8}$$

TABLE 1: Immersion factor of animation effect.

Number	Multiframe	Flash	Virtual	Three-dimensional	Hand painted
1	3	3	3	7	7
2	4	6	4	2	2
3	5	7	6	1	1
4	3	2	3	3	3
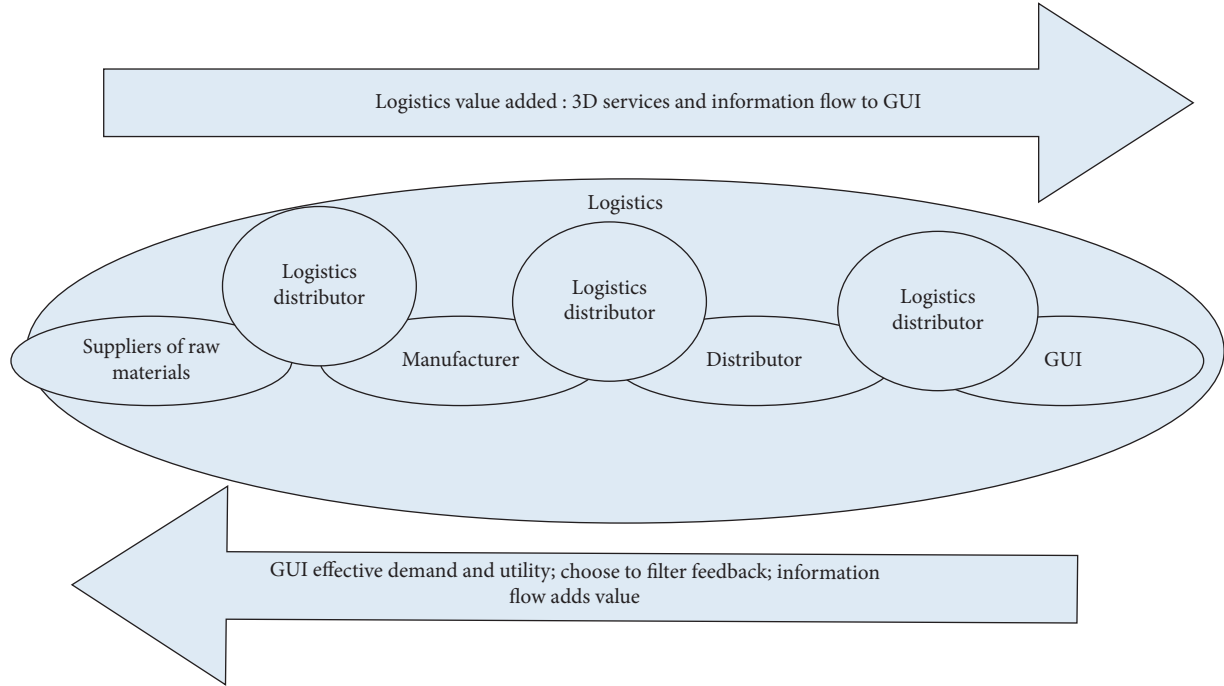
FIGURE 1: 3D animation performance comparison chart.

In the above equation, P is the immersion coefficient, u and v are the components of the 2D animation transformation speeds X and Y, respectively, E is the total light of the system, p is the number of pictures passed into the system, and μ is the parallel calculation coefficient. The spatial scene coefficients suitable for humans are shown in Table 2, and the corresponding visual simulation coefficient diagram is shown in Figure 2.

When the H cluster is selected for the opposition of vision technology, the spatial scene cluster depends on the parallel computing performance of the computer. Consider that the coefficients of computer resource consumption in the first and second groups are 1 and K, respectively, $0 < k < 1$. In this way, rich animation scenes are obtained in the $X1$ and $X2$ user groups, and the user visual angle of $X2$ is

$$U_1 = \begin{cases} s - p_1 - x_1 \\ x - p_2 - (1 - x_1), \end{cases}$$
$$U_2 = \begin{cases} s - p_1 - kx_2 \\ x - p_2 - k(1 - x_2). \end{cases} \tag{9}$$

Suppose $xi(i = 1, 2)$ is the viewing position outside the animation scene, and the second-stage opposing solutions can be obtained from equations (1) and (2) as follows:

TABLE 2: Space scene coefficients suitable for humans.

2D	3D	3D immersive	3D space scene	Space scene change
0.8147	0.3517	0.9058	0.3816	0.8308
0.1576	0.0759	0.9706	0.6797	0.0540
0.6557	0.1622	0.0357	0.2551	0.7943
0.7060	0.4505	0.0318	0.2543	0.0838
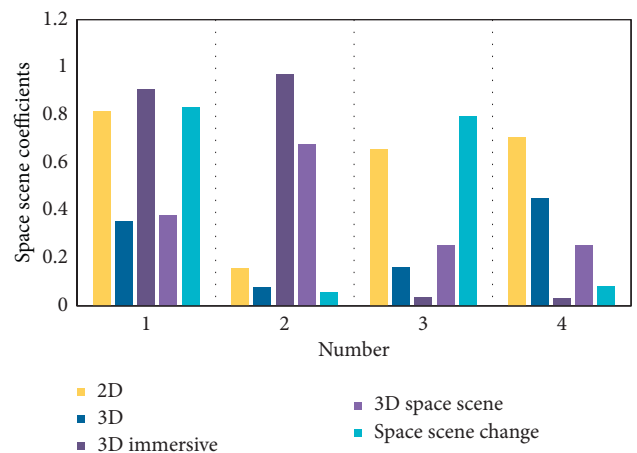
FIGURE 2: Space scene coefficients suitable for humans.

$$x_1 = \frac{p_2 - p_1 + 1}{2},$$

$$x_1 = \frac{p_2 - p_1 + k}{2k}. \tag{10}$$

Therefore, the dynamic functions of 3D space scene A and 3D space scene B are, respectively,

$$\pi_B^{LH} = \frac{(p_1 - c_1)(p_2 - p_1 + 1)}{2} + \frac{(p_1 - c_1)(p_2 - p_1 + k)}{2k}$$

$$- e(1 - \zeta)t\left[\frac{p_2 - p_1 + 1}{2} + \frac{p_2 - p_1 + k}{2k}\right],$$

$$\pi_B^{LH} = \frac{(p_2 - c_2)(1 - p_2 + p_1)}{2} + \frac{(p_2 - c_2)(k - p_2 + p_1)}{2k}$$

$$- et\left[\frac{1 - p_2 + p_1}{2} + \frac{k - p_2 + p_1}{2k}\right]. \tag{11}$$

So the first-order conditions are

$$\frac{\partial \pi_A^{LH}}{\partial p_1} = \frac{p_2 - p_1 + 1}{2} - \frac{p_1 - c_1}{2} + \frac{p_2 - p_1 + k}{2k} - \frac{p_1 - c_1}{2k}$$

$$- e(1 - \zeta)t\left[-\frac{1}{2} - \frac{1}{2k}\right] = 0,$$

$$\frac{\partial \pi_B^{LH}}{\partial p_2} = \frac{1 - p_2 + p_1}{2} - \frac{p_2 - c_2}{2} + \frac{k - p_2 + p_1}{2k} - \frac{p_2 - c_2}{2k}$$

$$- et\left[-\frac{1}{2} - \frac{1}{2k}\right] = 0. \tag{12}$$

Thus, the optimal immersive effects of the balanced 3D space scene in the second stage are

$$p_1^* = \frac{2k}{k+1} + \frac{2c_1 + c_2 + 3et + 2et\zeta}{3},$$

$$p_2^* = \frac{2k}{k+1} + \frac{c_1 + 2c_2 + 3et - et\zeta}{3},$$

$$\pi_A^{LH} = \frac{2k}{k+1} + \left[\frac{1}{2} + \frac{1}{2k}\right]\left[\frac{c_2 - c_1 + et\zeta}{3}\right]^2 + \frac{2(c_2 - c_1 + et\zeta)}{3},$$

$$\pi_B^{LH} = \frac{2k}{k+1} + \left[\frac{1}{2} + \frac{1}{2k}\right]\left[\frac{c_1 - c_2 - et\zeta}{3}\right]^2 + \frac{2(c_1 - c_2 - et\zeta)}{3}. \tag{13}$$

3D space scene A chooses strategy H, and 3D space scene B chooses strategy L. The immersive space scene experience obtained by the two types of user experience animations is the same as in case 1. Therefore, the second-stage opposite solution is still

$$x_1 = \frac{p_2 - p_1 + 1}{2},$$

$$x_2 = \frac{p_2 - p_1 + k}{2}. \tag{14}$$

2.3. Space Scene Interactive Animation Model Architecture. The traditional DMax-Mod model mainly uses computer parallel computing as the basis and uses the associated algorithm view processing system and the analog computing controller and receiver of the DMax-Mod model to generate animation effects [17]. In order to improve the real feeling of space scene animation, the created space scene animation elements adopt compound computing simulation technology to generate immersive space scene animation effects [19]. The scene setting of 3D animation is oriented to scenes such as real space-time, virtual space-time, fantasy space-time, and indoor and outdoor space-time. The visual performance of 3D animation scenes in time and space is affected by factors such as composition form and perspective relationship. For the influencing factors in the scene, designers need to design and operate skillfully to jointly construct a realistic visual experience and make people feel a special sense of beauty. Light is an important part of the visual performance of 3D design, and it is a form of reproducing realistic images through 3D animation data models [20]. Color selection is based on the characteristics of the elements to be represented in 3D animation design. Therefore, the color setting of 3D animation should be able to fully express the main characteristics of the design objects in 3D animation, and at the same time, it must conform to the creativity of 3D animation design. The color design keynote speech of 3D animation is based on the color of the entire animation scene as its support and performance. Therefore, when designing the entire 3D animation scene, color features should be used to express the emotions that the entire animation wants to express and the ideas the author wants to convey [21]. When watching the 3D animation design, the first thing to show the audience is the entire design scene and color characteristics, which makes the images in the animation more prominent and also reflects the design style of the animation.

3. Interactive Animation Experiment Design of Immersive Space Scene

3.1. Research Objects. This experiment takes space scene interactive animation as the research object, adopts a staggered tower layout of upper and lower layers, and further researches on the basis of the existing technology 3D multidimensional animation space scene animation visual effects and immersive concept. The technical scheme adopted in the practical model includes 4 animation attributes, including basic pictures and images, new vision technology, computer parallel computing capabilities, and variable coefficients of immersive space scenes. The immersive effect coefficients of the 3D three-dimensional design model and the practical model are equally distributed in the x, y, and z directions. The three-dimensional display

table is circular, and the interactive scene animation is equally prominent in the three-dimensional direction.

3.2. Interactive Animation Design of Space Scene.

3.2. Interactive Animation Design of Space Scene. Animation development tools combine many of the chaos of traditional animation production to help people who do not have animation development develop new applications. In this regard, this paper uses Scrartch (a tool for developing video games) and interactive animation (for developing immersive spatial scenes) to design interactive animation experiments. The advantage of this tool is that it uses a block-based visualization language and it must be assembled to design new 3D visual animation behaviors. This method of animation has become popular and has been used to create many block-based microworlds.

Based on Zie and Internet, the 3D remote animation system is designed, and the low packet loss rate of the node ad hoc network ensures the reliability of remote data transmission and remote real-time control. The feedback feedforward linearization decoupling method is used to realize the decoupling control of the interactive animation network embedded. The integrated use of visual sensor technology, automatic detection technology, and parallel computing technology realizes the remote collection of immersive spatial environment data. The design is based on a commercial cloud platform; the visual animation immersive space environment monitoring system is used for remote monitoring of cloud platform environmental data. The intelligent 3D character attribute model is gradually applied to the animation experience process, which has strong practicality in terms of visual logic feeling. Design a mobile vision robot for the Internet of things to realize interactive animation detection and search through task coordination and control execution of a two-level coupling hierarchical structure. According to the immersive environment, set the best optimization of the environmental variable collection model, monitor the effects of immersive space models of different heights through sensors, and use AMSL technology to achieve autonomous obstacle avoidance. However, in the actual operating design environment, due to the equipment support, the surface of the smallest nanohardware is uneven at the nanolevel, and the unplayed animation interface is easily damaged during the robot's travel, which affects the integrity of the detection data acquisition. The NU-Spider animation system is developed for the acquisition of large-scale interactive animation phenotypes. The movement of the carrying platform is controlled by high-speed immersive space handles. The acquisition of large 3D-APP phenotype data is achieved through equipment such as multispectral cameras and spectrometers. It has not been applied in the relatively closed environment of immersive space. The double-column structure provides longitudinal movement, forming a four-degree-of-freedom movement platform. The bottom is equipped with a high-definition camera, and the fuselage is equipped with a high-efficiency visual sensor model for monitoring the environment, and video, image data, and control commands are aggregated through a wired and wireless network bridge. Due to the small size of the basic control algorithm data, GPRS/3G/4G/Zig technology is used for transmission. And it is uniformly connected with the big data center server and loops on the basis of combining 3D elements to accurately collect unmanned driving information, so as to realize the unmanned inspection of the test block, and finally the results are uploaded to the mobile phone 3D-APP.

4. Immersive Space Scene Animation Effect

4.1. Effect of Spatial Scene Transformation.

4.1. Effect of Spatial Scene Transformation. As shown in Figure 3, a realistic 3D visual effect can be created efficiently by changing various virtual scene models. Give life and energy to the entire animated film. The interactive animation of the entire space scene is built on the virtual space, which is a technology based on computer parallel computing and computer vision processing.

As shown in Figure 4, different visual forms and creativity can be revealed through different transformations of complex and rich scene spaces. For example, in a wide scene space, the audience will feel a sense of comfort and tranquility, while a closed space will make the audience feel depressed and nervous. By transforming various scene spaces, people cannot help but feel a sense of shock.

As shown in Figure 5, people's perceptions of light and dark tones are very different, and they have no ability to clearly recognize places where the sound is not high, and it is easy to restore the designer's actual prototype to enhance the mystery in the fantasy atmosphere. The combined element technology provides a 3D realistic model and has been simulated in many modern animation production processes, which has a more convincing performance. Film and television animation has developed rapidly in recent years and soon entered our lives, bringing the joy of our culture. In order to bring better visual enjoyment to the audience, we must continuously improve the modeling scene to make room for better film and television works. In the production of cartoons, it can be considered that the space has a stage, and a simple space producer can complete the design process. Most of the local people's space disposal methods are arranged around the horizon in a straight line combination. Using the combination of multiple layers of space and creating a stage, the camera can shoot vertically downwards or pan from top to top to bottom. In the form of questions, you can leave room for the depth of the upper four palm spaces and call these materials in the same order as the stage, and the composition arrangement can be reduced to the extent that only the most important parts are retained.

4.2. Interactive Animation of Spatial Scenes under Computer Vision Technology.

4.2. Interactive Animation of Spatial Scenes under Computer Vision Technology. As shown in Figure 6, C2–C5 represent different types of immersive spatial interactive animation. The current movies and TV animations are not only diverse in types but also rich in forms. There are two main methods: two-dimensional animation, where the content of the story is displayed in a flat form, presenting decorative features, and appearing early; three-dimensional animation, also

Figure 3: Transformation of various animation scene spaces.

Figure 4: Different art forms and creative feelings.
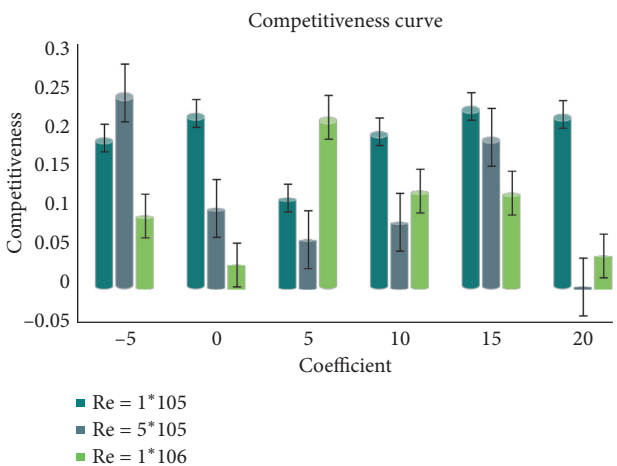
Figure 5: Competitiveness curve.
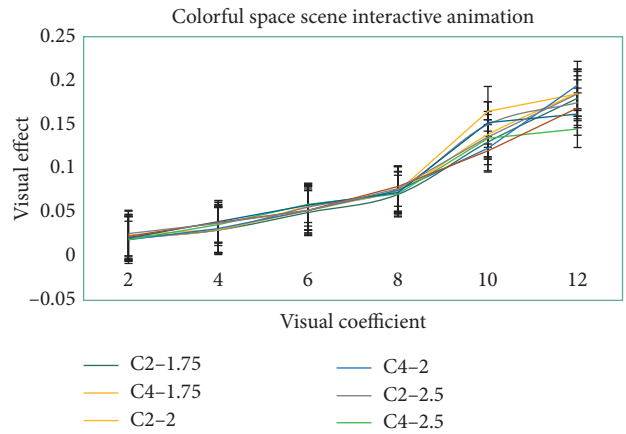
Figure 6: Colorful space scene interactive animation.

perception data of different interaction types are shown in Table 3.

The similarity between two-dimensional animation and three-dimensional animation is the animated form of motion, not static. As the time and space of the story change, the scene space also changes. The animation space is constantly changing, and the type of scene can be divided into two parts: virtual and reality. In order to deeply analyze the immersive scene in the virtual scene system, we must first explore its basic elements, that is, how to correctly organize the scene space. Therefore, the scene space can be divided into two types: the real space refers to the real space, and the virtual space can be easily realized in animation production. In fact, it does not exist in the actual range. This is a simulated space and cannot be touched. This type of space focuses on the inner feeling of the display space.

As shown in Figure 7, a vivid virtual scene can be effectively created by changing various virtual scene spaces. and makes the entire virtual film and television full of vitality, avoiding being too boring. The entire virtual film and television are based on the virtual model, which is a kind of virtual art. It is mainly manifested in scenes that are not in real life, such as unrealistic or surreal imagination. To a certain extent, it brought a visual impact to the audience. By linking the illusory feeling with the plot, we can create mysterious and powerful scenes that stimulate the curiosity of the audience and make them interested in the entire virtual film and television.

As shown in Table 4, through different transformations of complex and rich scene spaces, different art forms and creative feelings can be revealed. For example, in a wide scene space, the audience will feel a sense of comfort and tranquility, while a closed space will make the audience feel depressed and unable to breathe. As shown in Figure 8, the transformation of various scene spaces can make people feel scared.

As shown in Figure 9, the immersive animation effect of computer vision can more accurately convey the emotional appeal of the work itself, and the multimedia information presentation method brought by computer vision innovation can be used as a form of multimedia visual display. It can provide users with a more realistic experience to a

known as digital animation, which presents powerful three-dimensional functions and provides the audience with a true original viewing experience. It mainly depends on computers and various types of software to complete it. It is by far the most popular among audiences. The visual

TABLE 3: Rich experience of immersive spatial interactive animation.

	C2-1.75	C2-2	C2-2.5	C4-1.75	C4-2	C4-2.5	C5-1.75	C5-2	C5-2.5
2	0.02	0.021	0.022	0.0241	0.019	0.019	0.021	0.023	0.026
4	0.03	0.0301	0.0302	0.0305	0.0315	0.0362	0.0396	0.03875	0.03784
6	0.05	0.0569	0.0561	0.0521	0.0526	0.0596	0.0586	0.0523	0.05236
8	0.0705	0.0759	0.0769	0.0743	0.0754	0.0713	0.07265	0.0796	0.07698
10	0.13	0.1385	0.15	0.165	0.123	0.1345	0.152	0.12	0.136
12	0.18	0.186	0.175	0.185	0.195	0.145	0.162	0.169	0.185
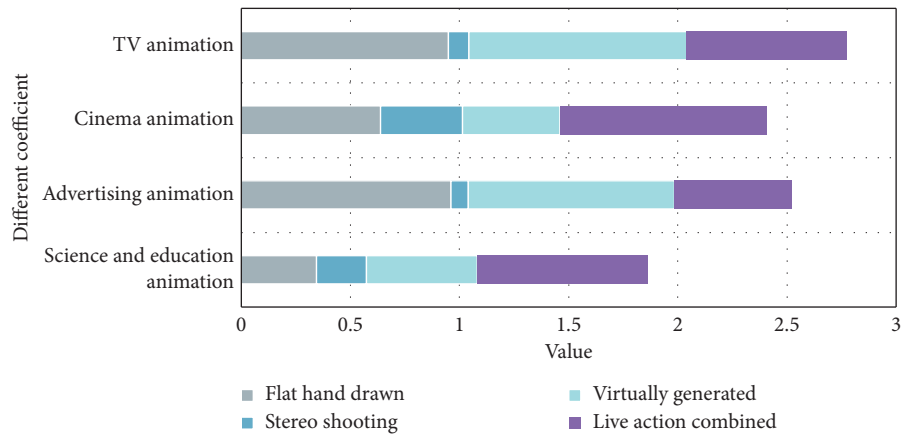
FIGURE 7: The effect of immersive scene space on people's vision.

TABLE 4: Different art forms and creative feelings.

Animation	Stereo shooting	Virtually generated	Live action combined	Experimental
F1	1	6	3	3
F2	3	7	3	6
F3	3	2	6	7
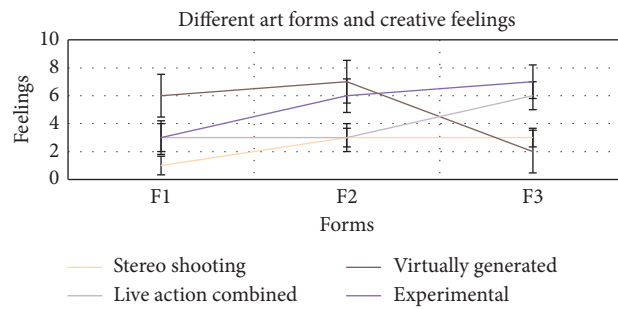
FIGURE 8: Different art forms and creative feelings.
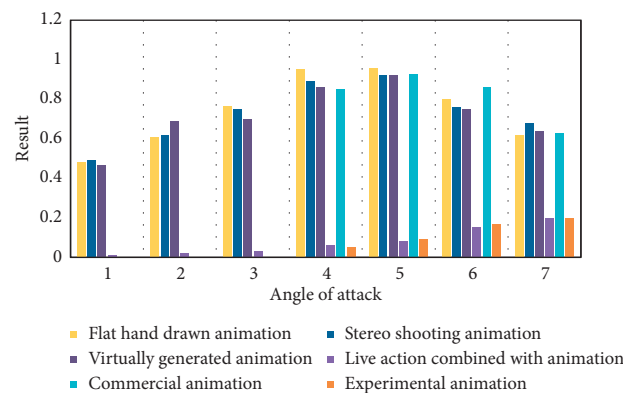
FIGURE 9: The effect of interactive animation with the help of Internet technology.

TABLE 5: Mobile Internet technology changes the way to watch animation.

Flat hand-drawn animation	Stereo shooting animation	Virtually generated animation	Live action combined with animation	Commercial animation	Experimental animation
0.48	0.49	0.465	0.01	Null	Null
0.61	0.62	0.69	0.021	Null	Null
0.765	0.75	0.7	0.031	Null	Null
0.95	0.89	0.86	0.061	0.85	0.05
0.96	0.92	0.92	0.08	0.93	0.09
0.8	0.76	0.75	0.15	0.86	0.17
0.62	0.68	0.64	0.2	0.63	0.2

greater extent. Secondly, user immersive experience communication methods can enrich users' visual experience. As shown in Table 5, mobile computer vision has changed the way people watch animation from the classic flat multimedia way. Then, there are immersive animations, which means that technological innovation brings us into the virtual world, and the additional images generated by this technology bring rich emotional experience to users.

5. Conclusions

The current immersive animation uses a lot of new model algorithms, and this model algorithm can enable users to get more emotional experience when experiencing animation. Successful immersive animation is to bring users into the virtual scene; it can drive the user's mental feelings to participate in this animation. Such animation will not only make the user feel very excited but also more effectively convey the ideas of the animation designer. In addition to the above advantages, immersive animation also has some shortcomings; that is, its data model is relatively large, and specific hardware equipment is required for demonstration. However, these problems cannot hinder the development of immersive animation. It has all the visual characteristics. The way of expression is worth experiencing, and immersive visual animation will also bring people a more multilevel interactive experience.

Immersive animation is a digital product that we often see in our daily lives. Immersive scene design is an important part of immersive animation, providing special time and space to play roles. Relying on the scene suitable for the environment, it showed a more substantial and intense performance. For China, many works are expensive to produce. In terms of special effects and atmosphere, they lag far behind the current special effects in Europe and the United States, and they have a long way to go as in Western countries many years ago.

Space scene animation is an animation mode that has emerged in recent years. Due to its advantages of simple operation and immersion, it is widely used in the civil field. Interactive animation of spatial scene has the characteristics of large demand, variable animation size, and variable number of models. At present, the optimization and debugging of space scene animation are in the climax of the world, and the related immersion effect research is one of the frontiers of space scene animation research. MAV is small in size and high in speed of running animation. Its entire simulation calculation loop is usually between tens of thousands to hundreds of thousands. If the immersion interference coefficient is further reduced, the immersion effect experience index will be even higher, which is not available in the previous conventional models.

Data Availability

The data underlying the results presented in the study are available within the article.

Conflicts of Interest

There are no potential conflicts of interest in this paper.

Authors' Contributions

All authors have read and approved the manuscript.

References

[1] Z. Lv, X. Li, and W. Li, "Virtual reality geographical interactive scene semantics research for immersive geography learning," *Neurocomputing*, vol. 254, no. 6, pp. 71–78, 2017.

[2] L. Ciccone, C. Oztireli, and R. W. Sumner, "Tangent-space optimization for interactive animation control," *ACM Transactions on Graphics*, vol. 38, no. 4, pp. 1011-1012, 2019.

[3] Z. Liu, L. Zhou, H. Leung, and H. P. H. Shum, "High-quality compatible triangulations and their application in interactive animation," *Computers & Graphics*, vol. 76, no. 12, pp. 60–72, 2018.

[4] A. Buchanan, "Real-time? Reframing temporal consciousness in time-based and interactive media," *Technoetic Arts*, vol. 16, no. 1, pp. 53–62, 2018.

[5] Z. S. Gottesman, "The rotoscopic uncanny: aku no hana and the aesthetic of Japanese postmodernity," *Animation*, vol. 13, no. 3, pp. 192–206, 2018.

[6] Y. Luo, B. Gao, Y. Deng et al., "Automated brain extraction and immersive exploration ofits layers in virtual reality for the rhesus macaque MRI data sets," *Computer Animation and Virtual Worlds*, vol. 30, no. 1, pp. 14–16, 2019.

[7] S.-H. Colleen and C. Jones, "A professional development model to facilitate teacher adoption of interactive, immersive digital games for classroom learning," *British Journal of Educational Technology*, vol. 50, no. 1, pp. 264–279, 2019.

[8] M. D. P. Guimaraes, D. R. Colombo Dias, J. H. Mota et al., "Immersive and interactive virtual reality applications based on 3D web browsers," *Multimedia Tools & Applications*, vol. 77, no. 1, pp. 347–361, 2018.

[9] K. Lee, S. Lee, and J. Lee, "Interactive character animation by learning multi-objective control," *ACM Transactions on Graphics*, vol. 37, no. 6, pp. 1–10, 2018.

[10] N. Fang and Y. Guo, "Interactive computer simulation and animation for improving student learning of particle kinetics," *Journal of Computer Assisted Learning*, vol. 32, no. 5, pp. 443–455, 2016.

[11] R. Fazlay, P. Taiwoo, F. Biyi et al., "When virtual reality meets Internet of things in the gym: enabling immersive interactive machine exercises," *Proceedings of the Acm on Interactive Mobile Wearable & Ubiquitous Technologies*, vol. 2, no. 2, pp. 1–21, 2018.

[12] Z. Chen, H. Li, Y. Bao, N. Li, and Y. Jin, "Identification of spatio-temporal distribution of vehicle loads on long-span bridges using computer vision technology," *Structural Control and Health Monitoring*, vol. 23, no. 3, pp. 517–534, 2016.

[13] P. Kiedrowski, "Driver's head tracking with pose estimation using computer vision technology under 2D environment," *Advances in Computational Ences and Technology*, vol. 11, no. 11, pp. 887–895, 2018.

[14] S. Barnard, S. Calderara, S. Pistocchi et al., "Quick, accurate, smart: 3D computer vision technology helps assessing confined animals' behaviour," *Plos One*, vol. 11, no. 7, pp. 15–19, 2016.

[15] A. Petrov and A. Popov, "Overview of the application of computer vision technology in fish farming," *E3S Web of Conferences*, vol. 175, no. 1, pp. 17–19, 2020.

[16] J. Park, Y. Hwang, J. H. Yoon et al., "Recent development of computer vision technology to improve capsule endoscopy," *Clinical Endoscopy*, vol. 52, no. 4, pp. 26–29, 2019.

[17] H. Tian, T. Wang, Y. Liu et al., "Computer vision technology in agricultural automation-a review," *Information Processing in Agriculture*, vol. 7, no. 1, pp. 13–15, 2019.

[18] Z. Wang, H. Li, and X. Zhang, "Construction waste recycling robot for nails and screws: computer vision technology and neural network approach," *Automation in Construction*, vol. 97, no. 7, pp. 220–228, 2019.

[19] M. Manasi and S. Chaudhary, "Computer vision technology using gesture recognition," *International Journal of Computer Applications*, vol. 179, no. 19, pp. 1–4, 2018.

[20] S. Chen, F. Liu, X. S. Tang et al., "Research on on-line water-meter verification system based on computer vision technology," *Jiliang Xuebao/Acta Metrologica Sinica*, vol. 38, no. 4, pp. 473–476, 2017.

[21] F. Lijun and C. Yueqin, "Detecting chlorophyll content of soybean leaves based on ComputerVision technology," *International Journal of Software Engineering and Its Applications*, vol. 11, no. 5, pp. 87–94, 2017.

Research Article

Theory and Method of Data Collection for Mixed Traffic Flow Based on Image Processing Technology

Dong-Yuan Ge [iD],[1] **Xi-Fan Yao** [iD],[2] **Wen-Jiang Xiang,**[3] **En-Chen Liu,**[1,4] and **Zhi-Bin Xu**[1]

[1]*School of Mechanical and Transportation Engineering, Guangxi University of Science and Technology, Liuzhou 545006, China*
[2]*School of Mechanical and Automotive Engineering, South China University of Technology, Guangzhou 510640, China*
[3]*School of Mechanical and Energy Engineering, Shaoyang University, Shaoyang 422004, China*
[4]*Academy for Engineering and Technology, Fudan University, Shanghai 200433, China*

Correspondence should be addressed to Dong-Yuan Ge; gordon399@gxust.edu.cn

As a key element of ITS (intelligent traffic systems), traffic information collection facilities play a key role, with ITS being able to analyze the state of mixed traffic more appropriately and can provide effective technical support for the design, management, and the evaluation of constructions. *Traffic Infrastructure.* Focusing on image processing technology, this study takes pedestrians, electric motor, and vehicles in mixed traffic flow as the research object, and Gaussian mixed model, Kalman filtering, and Fisher linear discriminant are introduced in the recognition system. On this basis, the mixed motion flow data acquisition framework model is elaborated in detail, which includes attribute extraction, object recognition, and object tracking. Given the difficulty in capturing reliable images of objects in real traffic scenes, this study adopted a novel background and foreground classification method with region proposal network so as to decrease the number of regions proposal from 2000 to 300, which can detect objects fast and accurately. Experiments demonstrate that the designed programme can collect the flow data by detecting and tracking moving object in the surveillance video for mixed traffic. Further integration of various modules to achieve integrated collection is another important task for further research and development. In the future, research on dynamic calibration of monocular vision will be carried out for distance measurement and speed measurement of vehicles and pedestrians.

1. Introduction

In mixed urban road traffic, pedestrians and electric vehicles have a major impact on driving, which not only threatens road safety but also leads to increased delays and reduced traffic capacity. How to manage pedestrians and traffic of electric motors and vehicles through traffic management and control, effectively improve the capacity of urban road networks, especially at intersections, reduce travel time for travelers, and improve passenger safety has become one of the primary problems facing urban transport in China. Therefore, more and more intelligent traffic control systems have been developed and applied in actual traffic management and control. As the primary element of ITS, traffic information collection facilities play a key role in many ITS systems.

Road pricing is one of the most important ways to reduce the loss of traffic distribution efficiency. Kumar et al. studied the loss of efficiency of the multi-level traffic balance distribution with elastic demand at road prices [1]. Barbosa et al. proposed a novel vehicle detection model named Priority Vehicle Image Detection Network based on YOLOV3, for which a lightweight design strategy is adopted to decrease the execution time of the proposed model [2]. Hu et al. proposed a RepNet network for feature extraction of vehicle, the focal loss function is adopted to reduce the weight of simple samples, and the cosine similarity function is used to judge the similarity between images [3]. The study of Pang et al. helps to improve the existing condition of intersections and provides guidelines for providing adequate pedestrian facilities at signalized intersections for safe and comfortable crossing of pedestrian crosswalk [4–6].

Through field investigation of typical signalized intersections at commercial hubs in Calcutta, the characteristics of pedestrian movement are described. This analysis takes into account several attributes, such as the width of the road, the age and gender of pedestrians, and whether they carry any luggage. The study found that pedestrians' age and gender had an impact on their speed; however, children were observed to walk faster because they were accompanied by their parents in most cases [7–10]. At crossroads, panicked pedestrians like to run fairly fast on zebra signs. Interestingly, it was found that the effect of carrying luggage on walking speed was not significant at the study site. Therefore, current research attempts to further investigate this fact by conducting informal public opinion polls. The survey of about 50 road users showed that because most people walk towards offices or business centers, they usually carry lighter luggage and are often forced to walk very fast. In addition, at the crosswalk, the speed will not change significantly with the increase of traffic flow, which is due to the unrestricted traffic flow. The observed flow parameters are plotted, and the scatter diagram indicates a wide range of data points that mainly follow the Greenberg logarithmic model.

In this study, a frame model of automatic pedestrian and nonmotor vehicle flow detection using image processing technology is designed. On the basis of vehicle detection and vehicle tracking modules commonly used in traditional vehicle video acquisition system, for the convenience of data acquisition of mixed traffic flow, four modules including "feature extraction," "object recognition," "object detection," and "object tracking" are developed for pedestrians, electric motors, and vehicles in mixed traffic flow, and automatic detection system of flow data. And a case of intersection of Liugong Avenue and Heping Road was conducted to evaluate the effect of intelligent traffic systems.

2. Proposed Method

2.1. Object Detection Based on Gaussian Mixed Model.
The basic idea of the Gauss hybrid model is to use multiple Gaussian models as a pixel location model, in order to improve the model solid on the multimodal background. Regarding the background of waving leaves, when the leaves move outside a specific location, the pixel information on the site is represented by a Gauss model. When the leaves are suspended at the site, the other is used [11–13]. The Gaussian model represents the pixel information of the location, so that the pixels in the new picture will be regarded as the background regardless of the matching with the Gaussian model, which can avoid the model taking the shaking leaves as a moving target and increasing the robustness of the model.

The basic steps of the hybrid Gaussian model algorithm are as follows.

2.1.1. The Definition of the Pixel Model

$$P(p) = \left\{ \left[w_i(x, y, t), u_i(x, y, t), \sigma_i(x, y, t)^2 \right] \right\}, \quad (1)$$

$$I = f\left(W^e D_1 + \delta^e\right), \quad (2)$$

$$D_a = g\left(W^d I + \delta^d\right). \quad (3)$$

Each pixel is described by a number of single models: $i = 1, 2, \ldots, k$. The value of k is generally between 3 and 5, which indicates the number of single models in the mixture Gaussian model, $w_i(x, y, t)$ represents the weight of each model [14], $u_i(x, y, t)$ is the ratio of the height part of the model to the lower part, and $\sigma_i(x, y, t)$ represents the correlation between the models.

$$\sum_{i=1}^{k} w_i(x, y, t) = 1. \quad (4)$$

Three parameters (weight, mean, and variance) determine a single model.

2.1.2. Updating the Parameters and Performing Foreground Detection

Step 1: if the pixel value of the picture $\sum_{i=1}^{k} w_i(x, y, t) = 1$ in the newly read video image sequence matches the feature in the training model library, the new pixel $i = 1, 2, \ldots, k$ matches $|I(x, y, t) - u_i(x, y, t)| \leq \lambda \cdot \sigma_i(x, y, t)$ the single model. If there is a single model that matches the new pixel, it is judged that the point is the background and enters Step 2; if there is no model matching the new pixel, the point is identified as the foreground and enters Step 3.

Step 2: modify the weight of the single model matched with the new pixel, $dw = \alpha \cdot (1 - w_i(x, y, t - 1))$, and the weight increment is expressed as follows [15, 16]:

$$w_i(x, y, t) = w_i(x, y, t - 1) + dw, \quad (5)$$

where $dw = \alpha \cdot (1 - w_i(x, y, t - 1))$, and α is weighting factor.

Modify the mean and variance of the single model matching the new pixels, as in the single Gaussian model.

While Step 2 is completed, the program directly enters Step 4.

Step 3: if the new pixel does not match any model and if the current number of individual models has reached the maximum number allowed, then the single model with the least value in the current set of multiple models is removed. Then, delete the original sample attribute that entered the corresponding library so that the new sample attribute remains in the specimen library.

A new single model is added. The weight of the new model is a smaller value (0.001 in experiment), the mean value is the new pixel value, and the variance is a given larger value.

Step 4: weighting normalization is carried as follows:

$$w_i(x, y, t) = \frac{w_i(x, y, t)}{\sum_{j=1}^{k} w_i(x, y, t)}, \quad (i = 1, 2, \ldots, k). \quad (6)$$

2.1.3. Sorting and Deleting of Multiple Single Gaussian Models.
In the mixed Gauss background model, each pixel model is composed of multiple single Gaussian models [17–19]. In order to improve the efficiency of the algorithm, we need to sort the single Gauss model according to the importance and delete the nonbackground model in time.

We assume that the background model has the following characteristics: heavy weight with high frequency of background occurrence and small variance being with little change in pixel value. Accordingly, we let

$$\text{sort\_key} = \frac{w_i(x, y, t)}{\sigma_i(x, y, t)}. \tag{7}$$

The process of sorting and deleting is carried out as follows: for each single model, first rank according to the weight of the feature (sort_key). If the weights of the first N single models are satisfied $\sum_{i=1}^{N} w_i(x, y, t) > T$, then only N single models are used as background models, and other models are deleted; generally, $T = 0.7$.

2.2. Object Tracking Based on Kalman Filtering.
In the process of tracking a moving target by a mobile robot, the movement of the target in a unit of time can be thought of as uniform motion, so that the position and speed of a target at a given time can be used to represent the target motion state. To simplify the computational complexity of the algorithm, two Kalman filters can be designed to describe changes in target position and velocity in the X-axis and Y-axis directions, respectively. Next, the application of the Kalman filter in the direction of the X-axis is discussed and the same applies to the direction of the Y-axis.

The motion equation of the object is as follows:

$$\begin{cases} x_{k+1} = x_k + v_k T, \\ v_{k+1} = v_k + a_k T. \end{cases} \tag{8}$$

The variables of which are the location, speed, and acceleration of the target in the X-axis direction at $t = k$. x_k indicates the moving distance of the vehicle, v_k represents the instantaneous speed of the vehicle, and a_k is acceleration. T as the time interval between k frame image and $k + 1$ frame image can be treated as change value. Equation (8) can be described with matrix as follows:

$$x_{k+1} = x_k + (v_{k-1} + a_{k-1}T)T. \tag{9}$$

The equation of state of the system is as follows:

$$\mathbf{X}_{k+1} = \mathbf{H}(k)\mathbf{X}_k + \mathbf{W}_k. \tag{10}$$

Among them, $\mathbf{X}_k = [x_k + v_k]^T$, the state vectors of the Kalman filter system are as follows:

$$\mathbf{H}(k) = \begin{pmatrix} 1 & T \\ 0 & 1 \end{pmatrix}, \mathbf{w}_k = \begin{pmatrix} 0 \\ a_k T \end{pmatrix}, \tag{11}$$

which are the dynamic noise vector of the system. According to the observation equation, the observation noise is 0, so it is 0. After establishing the state equation and observation equation of the above system, we can use Kalman filtering equation to predict the position of the target in the next frame by recursion method. At $t = k$ time, the target position identified by the target recognition algorithm in the K frame image is recorded [20–22]. When the target appears for the first time, it initializes the filter = [0], according to the observed position of the target.

The initial state vector covariance matrix of the system can get a larger value on the diagonal line, and the value is obtained according to the actual measurement situation. However, after a period of filtering start-up, the influence is not large.

The predicted position $\widetilde{X}_1'$ of the target in the next frame image is calculated by formula (1). In the vicinity of the location, the local image of the next frame is searched, and the centroid position is identified Z_1. By updating formula (2) to formula (5), we can update the covariance matrix of the state vector and the state vector, prepare for the next step prediction of the target position, and get the new prediction location. $\widetilde{X}_2'$ Local search is carried out to get the new centroid position Z_2 of the target, which is calculated iteratively to achieve the tracking of the target object.

2.3. Feature Extraction Based on Fisher Linear Discriminant Analysis.
The basic idea of Fisher linear discriminant analysis (FLD) is to find a projection direction, so that when the training sample is projected to this direction, the maximum interclass distance and minimum intraclass distance can be as large as possible. Later, the FLD method of two kinds of problems was extended to many kinds of cases. Let the pattern categories have c: $w_1, w_2, \ldots, w_c$, each category has n_i training samples; $\mathbf{X}$ is the collection of N training samples, $X_1, \ldots, X_n$. The mean subordinates of each category and the mean values of the total sample are, respectively, as follows [23, 24]:

$$\mu_i = \frac{1}{n_i} \sum_{x_k \in \omega_i} \mathbf{X}_k, \tag{12}$$

$$\mu = \frac{1}{n} \sum_{k=1}^{n} \mathbf{X}_k. \tag{13}$$

The within-class scatter matrix $\mathbf{S}_w$ of the samples is as follows:

$$\mathbf{S}_w = \sum_{i=1}^{c} \mathbf{S}_i, \tag{14}$$

where $\mathbf{S}_i = \sum_{x_k \in \omega_i} (\mathbf{X}_k - \mu_i)(\mathbf{X}_k - \mu_i)^T$ is the discrete-time matrix.

The between-class scatter matrix $\mathbf{S}_b$ of the samples is as follows:

$$\mathbf{S}_b = \sum_{i=1}^{c} (\mathbf{\mu}_i - \mu)(\mathbf{\mu}_i - \mu)^T. \tag{15}$$

Fisher discriminant function is defined as follows:

$$J_F(\mathbf{w}) = \frac{\mathbf{w}^T \mathbf{S}_b \mathbf{w}}{\mathbf{w}^T \mathbf{S}_w \mathbf{w}}, \tag{16}$$

where $\mathbf{w}$ denotes the transformation vector from the original sample space to Fisher space. So the system can attain maximum separability between different classes while minimizing the within-class scatter by solving the optimization problem.

3. Key Technology and System Design

Based on the tracking results of the traffic flow data collection from video and image editing, the integrated mixed traffic flow collection framework is proposed according to the traffic flow collection workflow and the characteristics of the mixed traffic objects. Its structure is shown in Figure 1; based on the object detection and monitoring unit, the feature extraction unit and the object recognition unit are used to identify pedestrians, motorcycles and vehicles and improve adaptive background extraction and object detection information, as well as obstruction and interference in the monitoring of mixed motion objects, as shown in Figure 1.

3.1. The Characteristic Expression of Mixed Traffic Moving Targets.
Effective expression of moving target features is a prerequisite for target recognition and classification. The quality of feature expression not only determines the construction and performance of the classifier model in the subsequent recognition process but also relates to the correctness of the classification output. Good feature attributes should be able to increase the differences between different target categories and narrow the differences between the same categories. How to extract stable features reflecting the nature of the target region from the moving region as input parameters of the recognition system is the key to the study of feature expression.

In order to design a video detection algorithm suitable for mixed traffic conditions, the classification between motor vehicles and nonmotor vehicles must be considered. Although the 3D feature classification effect is good, the algorithm complexity is high and the calculation time is long. It is difficult to meet the needs of real-time detection. The plane image feature extraction algorithm is simple and can meet the actual needs of real-time detection of mixed traffic flow.

Based on this, this study proposes a feature expression method based on eccentricity vector for mixed traffic flow. In view of the specific problems of event recognition, the morphological characteristics and motion characteristics of the target are taken into account, respectively, and the form and motion characteristics of the target are expressed in order to achieve better target recognition results. As the movement of objects can cause the translation and stretching changes of the features, it will seriously affect the shape recognition of objects. Therefore, it is particularly important to establish a morphological feature representation method with translation, expansion, and rotation invariance. At the same time, in view of the dynamic state of
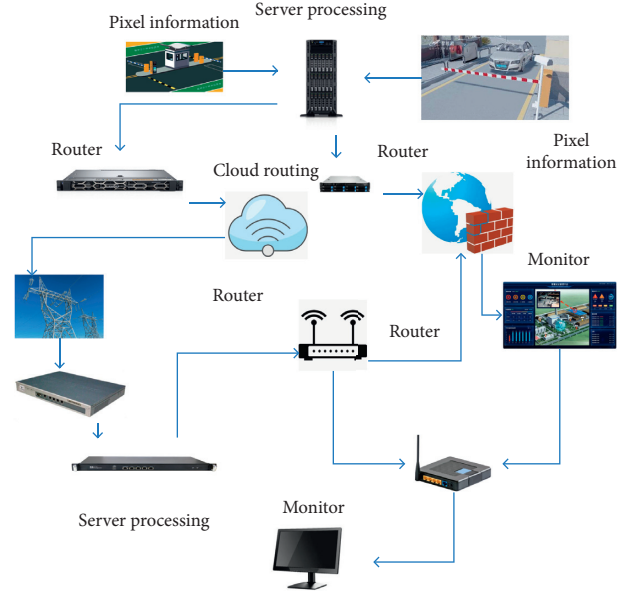
Figure 1: Structure diagram of vehicle information recognition.

moving objects in event recognition system, we choose the motion on the target time series. Characteristic, further constraints are added to target recognition. After preprocessing the video image, the foreground object is extracted, and the object forms a relatively complete contour. We define the distance between the point on the contour and the center of gravity of the object as the eccentricity and use a set of vectors on the contour as the recognition feature according to the counterclockwise sequence.

3.2. Object Tracking Model of Kalman Filtering.
Filter is an efficient recursive filter, which is often used for moving target tracking. It is a data processing algorithm based on observation information to derive optimal autoregression for optimal state estimation and state observation, as shown in Figure 2. First, a time varying transcendental model is established; then the observation model is established through observation information [25].

In summary, the implementation of the filter in moving target tracking is as follows.

First, initialize the Kalman filter, include the initial position of the moving target, measurement matrix, error covariance, state transition matrix, and noise covariance, and predict the state variables of the moving target. The state variables and observation variables on the moving target are used in the Kalman filter equation set to update the error covariance, gain and predict the position of the current target, and update and iterate the state of the Kalman filter.

3.3. Image Classification Model Based on Region Proposal Network.
As can be seen from Figure 3, the object detector by embedding fully convolutional network in Fast R-CNN is designed, which achieves state-of-the-art intelligent transportation, which decreases the number of region proposal greatly [26–29]. The designed detector consists of four parts.
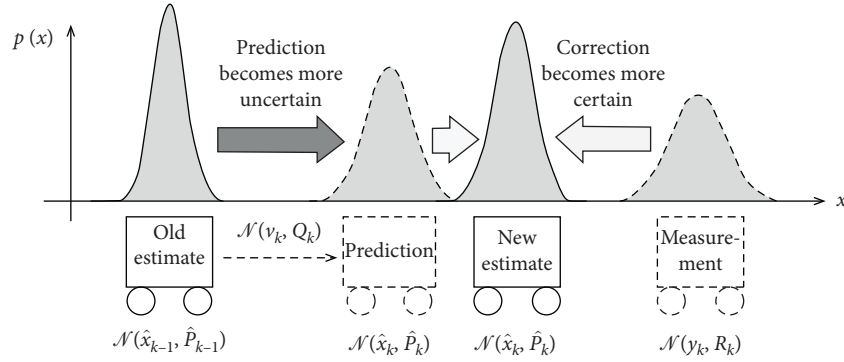
Figure 2: Object tracking of Kalman filtering.

(1) Convolution layer, VGG-16 network is adopted which include 13 convolution layers, 13 ReLU layers, and 4 pooling, the layer's input is any size image, its output, i.e., feature map's size is $(M/16) \times (N/16)$, and its number is 512.

(2) Region proposal network layer, that is fully convolutional network which can share weight of CNN, whose input are feature maps, and the region proposals are obtained, where anchors' number k is 9 for each sliding position, which are obtained according to 3 scales and 3 aspect ratios, the reg layer has $4k$ output, i.e., the coordinates of k boxes, and cls layer outputs $2k$ scores to estimate each proposal being foreground or background.

While the RPN is trained, we assign a binary class label (of foreground or background) to each anchor; if IoU overlap of an anchor' is higher than 0.7, let it be positive; if its IoU ratio is lower than 0.3, assign a negative label; other anchors ($0.3 < \text{IoU} < 0.7$) do not contribute to the training objective.

The adopted loss function for RPN is multitask loss, consisting of the outputs of the cls and reg layers, i.e., 2-class softmax loss for classification, where L_{cls} is log loss over two classes (foreground vs background), and the smooth L_1 loss for regression is L_{reg} (t_i, t_i^*), which is written as follows:

$$L(\{p_i\}, \{t_i\}) = \frac{1}{N_{cls}} \sum_i L_{cls}(p_i, p_i^*)$$
$$+ \lambda \frac{1}{N_{reg}} \sum_i p_i^* L_{reg}(t_i, t_i^*), \quad (17)$$

where i is the index of an anchor and p_i is the predicted probability of anchor i being an object. If the anchor is positive, $p_i^* = 1$, and if the anchor is negative, $p_i^* = 0$. t_i is 4 coordinates of the predicted bounding box, and t_i^* is that of the ground-truth box associated with a positive anchor. The second term $p_i^* L_{reg}$ means the regression loss is activated only for positive anchors. And in order to have the both cls and reg terms with equally weight during the training, let $\lambda = 10$ in the research [30–32].

(3) RoI pooling layer, whose inputs are feature maps and proposal, and convert input of different sizes proposals to fixed length representations (7×7).

(4) The classification and regression layer, whose inputs are proposal feature maps, and whose outputs are the classes and the positions of the proposal regions in the image.

4. Experiments Conclusions

4.1. Target Quantity Statistics. When the number of moving targets is counted, the object detect is carried out, which can be seen from Figure 4. The number of moving targets is counted by the vehicle information feature matching method, and the detection line is displayed at the appropriate position of the video image. When two monitoring frames appear on both sides of the detection line, the distance between the vehicles is large enough to be sure to identify the two vehicles, which increases the number of moving targets. This system represents the vehicle with a blue rectangular frame and displays vehicle information around the rectangular frame. Real scenes often contain complex features, such as pedestrians and people pushing cars. The recognition rate of this system is not very high and needs to be strengthened. Table 1 is multiline traffic statistics. From the statistical results, the marking method can accurately measure the number of moving targets based on multitarget tracking, as shown in Table 1.

4.2. Target Density. Density is an important parameter for traffic management because it can describe the quality of traffic operation and the proximity between the target and the target. The density of traffic flow is the number of moving targets on the driveway in a unit length, and it can also be expressed indirectly by the occupancy rate of vehicles. The results of the test are shown in Table 2.

The detection location is multilane one-way lane, and the time is daylight. The width of each lane is meters, and the length of each lane is meters. According to the statistical method in the previous section, the number of vehicles is obtained and the density calculation is realized.
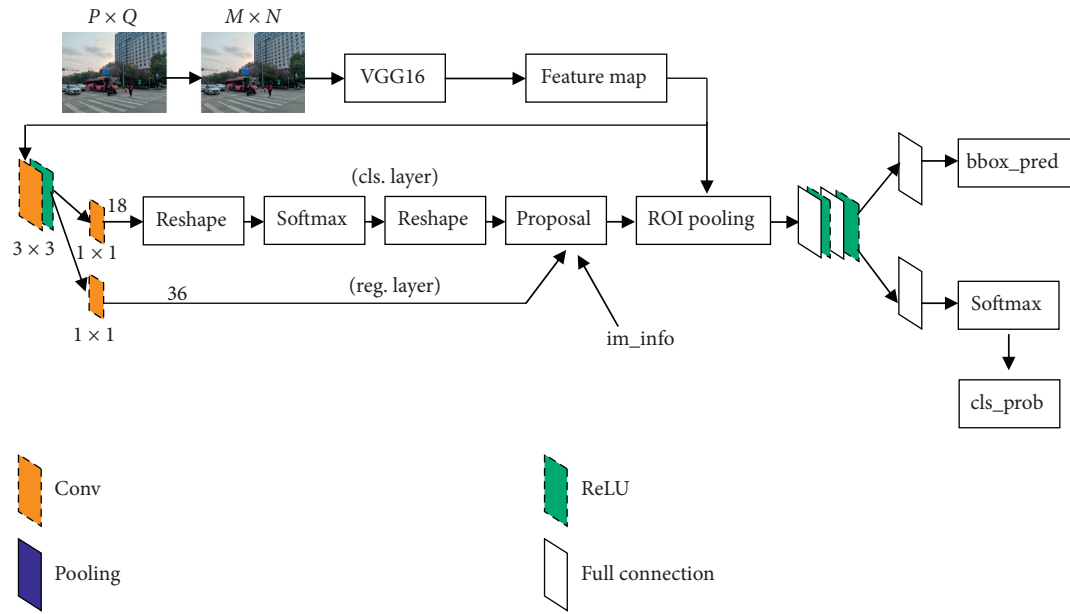
FIGURE 3: Image classification based on region proposal networks.

(a)   (b)   (c)

FIGURE 4: Moving target detection. (a) Cars. (b) Motor bicycles. (c) Pedestrians.

TABLE 1: Multilane traffic statistics.

Video data	Video length (minutes)	Equipment acquisition (vehicle)	Artificial acquisition (feature number)	Multiple inspection (frequency)	Leak detection (frequency)	Accuracy rate (%)
Video 1	5.86	69	62	0	1	86.9
Video 2	8.64	187	201	0	5	92.3
Video 3	3.95	163	180	1	1	84.2

TABLE 2: Test results of moving target density.

Frame number	Vehicle number (cars)	Car density (vehicles/sec)	Pedestrian density (people/sec)	Truck density (vehicles/sec)	Bicycle density (vehicles/sec)	Motorcycle density (vehicles/sec)
3	8	29.94	5.11	2.68	5.46	3.26
10	9	32.56	2.63	3.2	2.7	5.27
15	7	20.92	2.33	1.18	1.51	1.19
23	9	29.65	3.8	3.84	3.41	5.49

4.3. Target Speed. Velocity calculation of moving target: before moving target detection and tracking, we need to calibrate the camera. The formula for calculating the velocity of a moving target is as follows:

$$v = \frac{s}{t}. \qquad (18)$$

Among them, the moving time and the moving distance are considered, so we must find out the moving distance of the target in the specified time. Pixel $640 * 480$ for video capture: we need to calculate the actual distance of each row of pixels in the image. $w_1, w_2, w_3, \ldots, w_N$: for each row of pixels after camera imaging, the distance is not equal in the actual detection scene. But after the camera imaging, they should have the same image distance H in the image. Therefore, we need to map each row of pixels to the actual distance according to the actual situation of the test scenario.

5. Conclusions

With the continuous development of urbanization and the continuous growth of people's travel demand, the travel problem becomes more and more important to people's daily life. There are still many problems to be further studied, including the following aspects. Although there are many image processing methods, most of them are applied to vehicle volume acquisition. Therefore, how to learn more and better experience from vehicle image detection technology and improve the function of hybrid traffic flow acquisition system based on image processing becomes one of the tasks of the next stage of research work. Because this research involves a lot of content, the goal of this study is to propose a feasible theory and method of video mixed traffic flow data acquisition. How to develop a more robust shadow removal algorithm and hybrid traffic object detection method in high density still needs to be further studied.

In this article, the framework of the mixed traffic flow data acquisition system is proposed and the operation of each module is performed. However, this study only provides the theoretical methods and basis for implementing mixed motion video traffic, and there is still a gap with the more mature trading system. Therefore, it is necessary to further integrate all the modules and make a complete acquisition, which is another important task for further research and development. We will conduct research on the dynamic calibration of one-eyed vision to measure the range and speed of vehicles and pedestrians in the future.

Data Availability

No data were used to support this research.

Conflicts of Interest

The authors declare that they have no conflicts of interest.

Acknowledgments

References

[1] M. Kumar, Y. Mao, Y. Wang, T. Qiu, Y. Chenggen, and W. Zhang, "Fuzzy theoretic approach to signals and systems: static systems," *Information Sciences*, vol. 418-419, pp. 668–702, 2017.

[2] R. C. Barbosa, M. Shoaib Ayub, R. Lopes Rosa et al., "Lightweight PVIDNet: a priority vehicles detection network model based on deep learning for intelligent traffic lights," *Sensors*, vol. 20, no. 21, Article ID 6218, 2020.

[3] C. Hu, C. Li, T. Zhou et al., "Vehicle re-recognition algorithm based on improved deep relative distance learning framework," *Chinese Journal of Scientific Instrument*, vol. 41, no. 12, pp. 245–252, 2020.

[4] M. B. Pang, Y. N. Pei, and N. Zhang, "Integrated simulation of mixed traffic flow on elementary and middle school gate's road when students going to school," *Journal of System Simulation*, vol. 30, no. 3, pp. 1162–1170, 2018.

[5] W. Zhang, J. Zhou, and L. L. Hu, "An adaptive signal control method for urban mixed traffic flow at single intersection," *Journal of Zhejiang University of Technology*, vol. 46, no. 1, pp. 72–77, 2018.

[6] C. Zhang, J. Chen, J. Guo et al., "Study on modification model of mixed traffic travel time in small mountainous cities," *Journal of East China Jiaotong University*, vol. 35, no. 2, pp. 66–72, 2018.

[7] M. Montanino and V. Punzo, "On string stability of a mixed and heterogeneous traffic flow: a unifying modelling framework," *Transportation Research Part B Methodological*, vol. 144, no. 2, pp. 133–154, 2021.

[8] S. Das, D. Mukherjee, P. Saha et al., "Pedestrian flow characteristics at signalized intersections in mixed traffic situations: a case study in Kolkata, India," *Procedia Computer Science*, vol. 130, pp. 150–156, 2018.

[9] Y. Qi, M. S. Hossain, J. Nie et al., "Privacy-preserving blockchain-based federated learning for traffic flow prediction," *Future Generation Computer Systems*, vol. 117, no. 4, pp. 328–337, 2021.

[10] X. Zong, C. Wang, and H. Chen, "An evacuation model based on co-evolutionary multi-particle swarms optimization for pedestrian–vehicle mixed traffic flow," *International Journal of Modern Physics C*, vol. 28, no. 12, 2018.

[11] H. C. Lu, H. Z. He, Y. Q. Huang, and W. G. Gao, "Improved canny edge operator and Gaussian mixture model for moving target detection," *Journal of Electronic Measurement and Instrumentation*, vol. 33, no. 10, pp. 142–147, 2019.

[12] X. Sun, Z. H. Wu, X. B. Lv et al., "Improved Gaussian mixture model based moving target detection," *Computer Engineering and Design*, vol. 35, no. 3, pp. 914–917+948, 2014.

[13] Y. P. Zhang, Y. Q. Bai, Y. Zhao et al., "Moving object detection based on improved Gaussian mixture models," *Computer Engineering and Applications*, vol. 46, no. 34, pp. 155–157+223, 2010.

[14] S. Adams and P. A. Beling, "A survey of feature selection methods for Gaussian mixture models and hidden Markov models," *Artificial Intelligence Review*, vol. 52, no. 3, pp. 1739–1779, 2019.

[15] W. M. Shao, Z. Q. Ge, and Z. H. Song, "Semi-supervised Bayesian Gaussian mixture models for non-Gaussian soft sensor," *IEEE Transactions on Cybernetics*, pp. 1–14, 2019.

[16] R. Roy and P. Saha, "Headway distribution models of two-lane roads under mixed traffic conditions: a case study from India," *European Transport Research Review*, vol. 10, no. 1, p. 3, 2018.

[17] J. J. Sun, Y. Zhao, S. G. Wang et al., "Image compression based on Gaussian mixture model constrained using Markov random field," *Signal Processing*, vol. 183, Article ID 107990, 2021.

[18] Q. H. Xu, S. F. Yuan, and T. X. Huang, "Multi-dimensional uniform initialization Gaussian mixture model for spar crack quantification under uncertainty," *Sensor*, vol. 21, no. 4, Article ID 1283, 2021.

[19] D. Li, Y. Zhao, P. Ranjitkar et al., "Hybrid approach for variable speed limit implementation and application to mixed traffic conditions with connected autonomous vehicles," *IET Intelligent Transport Systems*, vol. 12, no. 5, pp. 327–334, 2018.

[20] J. Lin, W. D. Qi, and P. Liu, "Bias-compensation Kalman filter algorithm for AoA-ToA target tracking," *Information and Control*, vol. 49, no. 6, pp. 657–666, 2020.

[21] D. Liu, Y. B. Zhao, Z. Q. Yuan et al., "Target tracking methods based on a signal-to-noise ratio model," *Frontiers of Information Technology & Electronic Engineering*, vol. 21, no. 12, pp. 1804–1814, 2020.

[22] F. L. Chen, Q. H. Ding, and H. B. Luo, "Anti-occlusion real time target tracking algorithm employing spatio-temporal context," *Infrared and Laser Engineering*, vol. 50, no. 1, pp. 1–11, Article ID 20200105, 2021.

[23] K. Zhong, M. Han, T. Qiu, and B. Han, "Fault diagnosis of complex processes using sparse kernel local Fisher discriminant analysis," *IEEE Transactions on Neural Networks and Learning Systems*, vol. 31, no. 5, pp. 1581–1591, 2020.

[24] P. F. Lv, Y. J. Yan, and Y. Li, "Research on fault diagnosis of improved kernel Fisher based on Mahalanobis distance in the field of chemical industry," *ACTA Automatica Sinica*, vol. 46, no. 11, pp. 2379–2391, 2020.

[25] Y. L. Tian, J. Ma, and N. Yang, "Moving target tracking based on kernelized correlation filter and Kalman predicting," *Journal of Chinese Computer Systems*, vol. 39, no. 10, pp. 2330–2334, 2018.

[26] S. Q. Ren, K. M. He, R. Girshick et al., "Faster R-CNN: towards real-time object detection with region proposal networks," *IEEE Transactions on Pattern Analysis & Machine Intelligence*, vol. 39, no. 6, pp. 1137–1149, 2017.

[27] H. Qiao, C. Y. Lu, X. Chen et al., "Signal-background discrimination with convolutional neural networks in the Panda X-III experiment using MC simulation," *Science China (Physics, Mechanics & Astronomy)*, vol. 61, no. 10, pp. 55–63, 2018.

[28] Z. Jin and D. Y. Ge, "Detection and recognition method of monocular vision traffic safety information for intelligent vehicles," *Journal of Intelligent & Fuzzy Systems*, vol. 39, pp. 5017–5026, 2020.

[29] X. Sun, P. Wu, and S. C. H. Hoi, "Face detection using deep learning: an improved faster RCNN approach," *Neurocomputing*, vol. 299, no. JUL.19, pp. 42–50, 2018.

[30] D. Y. Ge, W. J. Xiang, M. L. Zhu et al., "Real- time detection of vehicles and pedestrians with novel region-based fully convolutional network," *Basic & Clinical Pharmacology & Toxicology*, vol. 127, no. 1, p. 122, 2020.

[31] H. Phan, F. Andreotti, N. Cooray et al., "Joint classification and prediction CNN framework for automatic sleep stage classification," *IEEE Transactions on Biomedical Engineering*, vol. 66, pp. 1285–1296, 2018.

[32] X. Chen, Y. L. Zhu, Y. Fang et al., "Simulation and analysis of extended spatial channel model in vehicle-to-vehicle communication environments," *Mathematical Problems in Engineering*, vol. 2021, p. 12, Article ID 5989416, 2018.

Research Article

Simulation of Dynamic User Network Connection Anti-Interference and Security Authentication Method Based on Ubiquitous Internet of Things

Mingming Pan,[1,2] **Shiming Tian** (ORCID)**,**[1,2] **Jindou Yuan,**[1,2] **and Songsong Chen**[1,2]

[1]*China Electric Power Research Institute, Beijing 100192, China*
[2]*Beijing Key Laboratory of Demand Side Multi-Energy Carriers Optimization and Interaction Technique, Beijing 100192, China*

Correspondence should be addressed to Shiming Tian; lss033@ncepu.edu.cn

Ubiquitous Internet of Things includes criteria, applications, and technologies for providing standard data. The system can be used to establish a comprehensive data database to facilitate people to better analyze, organize, and use these data, so as to improve the reliability and sharing of data, to provide better services for users. The purpose of this study is to propose and establish a specific and reliable data exchange program to ensure the security of data exchange. Data security is to ensure the reliability of specific security exchange process. The emphasis of this study is the reliability analysis method and the verification method of exchange process behavior. Based on the analysis of all abnormal phenomena in the Internet of Things traffic, the basic characteristics of network traffic, the basic properties of network traffic, and the theory of multiterminal power communication network anti-interference model construction and noninterference model, the simulation experiment of anti-interference and security authentication method is carried out. The results show that, with the increase of the number of antennas, the false detection probability decreases from 10^{-1} to 10^{-4}, which can achieve better performance in the detection of active users. When network is used in applications, HTTP + SSL is the most widely used application for data authentication and security authentication. The market of anti-interference technology is developing rapidly. The complex annual growth rate almost doubled in the international market, and the market scale was significantly expanded, with an annual growth rate of about 50%.

1. Introduction

1.1. Background and Significance. In the process of data security exchange, the exchange process is vulnerable to attack. The invaders use various attack means to destroy, camouflage, or interfere with the exchange process, so that the exchange cannot be carried out normally. The access process will cause security threats such as information tampering, leakage, and unauthorized access. For example, Trojan horse attacks are used to bring sensitive information or virus files to the data that is allowed to be exchanged, or, through attack bases, Trojan horses are used to disguise themselves and establish exchange channels for illegal data exchange. It can change the normal exchange process directly and destroy the expected behavior, so that the sensitive information in the exchange data can be read. These behaviors will bring security risks, such as disclosing sensitive information and spreading malicious code. Therefore, the anti-interference and security authentication technology of dynamic user network connection is particularly important.

1.2. Related Work. The Internet of Things will require ubiquitous information sharing among interconnected things around the world, which cannot be achieved by existing systems. The current research focuses on information dissemination solutions, which can lead to single point of failure and unnecessary communication delay. To this end, Victor proposed the SENSEable things platform, which is a fully distributed, open-source architecture for applications based on the Internet of Things. This paper

introduces the main problems that must be solved by IOT platform and Victor's technical solutions to these problems and evaluates these problems. Victor also introduces the current progress and a series of demonstrations to show the wide range of applications supported by the platform. Finally, Victor shows how the platform will be used for our future research and potential spin-off companies [1].

The proliferation of service-based and cloud-based systems has led to a situation in which software is often provided as a service and as a commodity through an enterprise network or global network. This scenario supports the definition of business processes as composite services, which are implemented through static or run-time combinations of products from different vendors. Quickly and accurately evaluating the security attributes of services became a basic requirement at that time, and now it has become a part of the software development process. Anisetti shows how to handle the security attribute validation of composite services through test-based security authentication and build it to be effective and efficient in dynamic composition scenarios. Anisetti's method is based on the existing single chip service security authentication scheme and extends it to service composition. It actually authenticates the composite service, starting with the certificate granted to the component service [2].

Android provides a permission statement and an authentication mechanism to detect and report potential security threats to applications. Usually, applications are authenticated based on their declared permissions, but the declared permissions are usually coarse-grained or inconsistent with the permissions actually used in the program code. Pei proposes an Android application programming interface (API) level security authentication (ASCAA) based on cloud computing. The framework uses a systematic method to identify and analyze API level security threats. To authenticate an application, ASCAA checks all permission tags in its manifest and API calls extracted from its decompiled code based on a set of requirements dependent on security rules. In addition, the author also provides ASCAA security language to standardize the security rules and authentication process, which makes ASCAA universal and extensible.

1.3. Innovation. This study analyzes the security management requirements of modern high security applications and proposes some new ideas and methods, system architecture, and key function technologies in the aspects of material selection and network design by using new Internet of Things technology. On the basis of the traditional technology and algorithm, we improved and innovated and finally formed a relatively complete experimental design. A variety of algorithms are proposed to promote the development of the system and adapt to complex environmental changes. At the same time, it has the characteristics of high positioning accuracy and high processing efficiency, which can meet the needs of experiments, so as to check the error detection rate of these algorithms for user activity.

2. Based on Mathematical Model

2.1. Threat Model. The current intelligent terminal system stores a large number of user privacy and even confidential information, which makes intelligent terminal become the target of more and more malicious users, including side channel attack against intelligent terminal and malicious utilization of current control technology fault, which deserves special attention [3]. This research is based on the following threat models: (1) Aiming at the stage connection of intelligent terminal user identity control technology, the intruder observes or captures the process of user's ID card input (but cannot directly observe the content displayed on the smart terminal screen) and steals the stable configuration information between the user's finger moving path and the relevant virtual keyboard getting user authentication credentials [4]. (2) For the explicit identification technology of intelligent terminal users in the connection stage, the intruder should be able to communicate with the intelligent terminal naturally and steal the user ID card through the oil residue or heat residue information on the touch screen [5]. (3) For the user identification technology of intelligent terminal in the connection stage, the intruder can install malicious software on the intelligent terminal; the user terminal system secretly records sensor data, such as the built-in acceleration sensor and gyroscope, on the corresponding equipment input by the user; according to the recorded sensor data, it may steal from the identity and user identity certificate [6]. (4) For the current intelligent terminal, there are certain defects in most of the user ID technology only after the user connects to the system before authentication. The intruder can naturally contact the intelligent terminal in the unlocking mode (such as leaving the unlocked mobile phone in the meeting room, classroom, and other occasions) or obtain the ability to interact with the intelligent terminal system through phishing attack. It can access the user's privacy and confidential information stored in the intelligent terminal [7].

2.2. Anti-Interference Model. The formal analysis of the security characteristics of data exchange by using strategic information flow can make us clearly understand the flow direction of information in the process of data exchange and observe the actual behavior of data exchange from another perspective independent of operation [8, 9]. By analyzing the information flow, we can verify whether the dynamic data exchange process can meet the security characteristics expressed by the given policy [10]. There are a lot of researches on information flow analysis, and antijamming is one of the most important research results. The anti-interference model can establish the system security policy model from the operation and operation results, instead of simply relying on the check of reading and recording functions to estimate the information flow. Compared with other information flow strategies, it can better reflect the dynamic implementation process of the system and the ability of different systems to communicate. In the exchange process, it can interact with each other and

detect the existence of hidden channels to avoid information leakage through hidden channels. Therefore, using an anti-interference model to analyze the reliability of exchange, process behavior has obvious advantages [11].

The concept of anti-interference is one of the main methods to determine or express the causal relationship between different security departments. It is also the theoretical basis for the standardization and analysis of security policies. The early research on anti-interference model is mainly applied to multilevel security system, dealing with deterministic system and information flow strategy with partial order relation. In short, this is the domain policy of H and l security departments [12]. This strategy is a transitional strategy, and many definitions of antijamming are based on these limitations. The anti-interference transfer strategy successfully provides the basis for multilevel security policy (MLS) and provides an official proof method [13].

Although the traditional anti-interference models successfully solve the multilevel security policy problem, some practical security problems are beyond the official description of the original definition, and these models have great limitations in practical application [14]. For example, MLS-based battle command systems only allow low-level to high-level domains, so when existing reports reach the highest level, they will not disclose information due to Trojan horse attacks. However, there is a major problem when a superior must publish business data to coordinate and manage the overall function. The system should allow limited information to flow from high-level domain to low-level domain [15]. Only through reliable control departments (e.g., degradation processing, decryption processing or encryption equipment), it cannot do that directly from the high-level domain to the low-level domain. Therefore, a nontransitive information flow strategy is most needed in the real world [16].

2.3. Dynamic User Network Connection.

Taking a typical NOMA system with base station and user k as an example, it is assumed that the base station and each user are equipped with an antenna. After coding and channel configuration, active user K sends symbol xk from complex constellation set X, and XK transmits symbols to form SK distribution sequence with length J. Now we will focus on the case of $J < n$; that is, the number of users in the system is greater than the length of propagation sequence [17]. In this system, the signal from the active user will be converted and then transmitted by the k-rectangle OFDM payer [18]. The signal received from the base station can be expressed as.

$$y_n = \sum_{k=1}^{N} g_{nk} s_{nk} x_k + v_n, \quad n = 1, 2, \ldots, N. \quad (1)$$

Among them, s_{nk} is the nth component of SK dispersion sequence, VN is Gaussian noise in subcarriers, the mean value is zero, and the variance is σ^2. g_{nk} is the revenue of channel user k in the nth subcarrier. All subcarriers are the same and are distributed independently. Considering the Rayleigh fading channel in the algorithm, this clock channel

model has been widely implemented [19]. The received signals on all subcarriers are combined, and then the received signal vector is $y = [y1, y2, \ldots yN]$, which can be expressed as.

$$y = Hx + v. \quad (2)$$

When $x = [y_1, y_2, \ldots y_N]$ is the channel equivalent matrix with the size of $n \times K$, the elements in the nth row and K column are equal to gnksnk, while the noise vector $v = [v_1, v_2, \ldots, v_N]T$ follows the CN $(0, \sigma^2 IN)$ distribution [20].

2.4. Anti-Interference Model Construction of Multiterminal Power Communication Network.

On the basis of the above power communication network channel separation, the multiterminal network anti-interference model is established. The application of artificial intelligence technology in the ubiquitous Internet of Things creates communication connection and rapid networking and real-time perception and processing of information in power communication network [21]. Firstly, the multiterminal signal model is established, and the relationship between signal frequency and signal transmission rate is analyzed:

$$y = y_n \frac{v\beta}{Vm} \cos \overline{\omega}, \quad (3)$$

where y_n is the change in the transmission frequency detected by the receiver of a multiterminal network; V is the signal transmission speed; β is the transmission frequency of multiterminal power communication network; V is the transmission power of power grid; $\cos \omega$ is the angle between power distribution direction and electromagnetic wave incidence; and y is the signal frequency of power communication network [22, 23]. According to the above signal model, the linear signal in the power communication network is time-varying. Assuming that the monitoring error in the power communication network is $e_x = x - x_n$, the impulse response of the channel is a random process, which needs to be satisfied.

$$K(a_k) = E\left\{\frac{w}{y_n}, e_x + a\right\}, \quad (4)$$

where W is the state information of power communication network; a is the reference signal; and $E \{\cdot\}$ is the impulse response of communication signal. On this basis, the scattering function of power communication network signal is defined as

$$s(j) = \frac{F\{d(c, t)\}}{K(a_k)}, \quad (5)$$

where j is the scattering signal of power communication network; $F\{\cdot\}$ is the total data transmission in the communication network; and $D(C, t)$ is the channel function of power communication network. On the basis of the above calculation, the state equation of multiterminal power communication network after interference suppression is obtained:

$$R(x) = b \sum_{i=0}^{b} hx \left(\frac{t}{2B} - zr \right), \tag{6}$$

Here, H is the communication signal bandwidth of multiterminal power communication network; B is the sampling interval; and R is the number of power terminals. When the two state signals in the multiterminal power communication network are the same, the correlation peak value is the largest, which can be sent by the correlation monitor. However, when there are single frequency, narrowband, multipath, and multiple access interference, the signal power needs to be decoupled to filter other signals [24]. Through the above definition, the anti-interference model of multiterminal power communication network based on ubiquitous Internet of Things is obtained.

3. User Network Anomaly Detection

3.1. Experimental Setup. In order to analyze the abnormal traffic of all network users, this paper defines the network traffic sequence according to the basic characteristics of network traffic and describes the external characteristics of network traffic comprehensively. According to the network traffic order, the deep learning method is used to self-study the anomaly detection features, and the abnormal traffic is classified, detected and classified. Since the method proposed in this study is only based on the external characteristics of the network flow and does not analyze the content of the message, it can be applied to anomaly detection of encrypted traffic.

3.2. Experimental Process. The experiment outputs the basic characteristics of network traffic, in which IP address is the address of remote terminal, and traffic type is specific type of network mobile protocol, such as TCP and UDP. Message length is the size of a single message. The time of receiving information refers to the time between additional information. The flow of information is divided into personnel flow and outflow. The basic characteristics of the output network traffic are prepared in advance to receive the final network flow order vector.

Firstly, the time period characteristics of traffic packets are obtained. Traffic can be regarded as two time lines: a sequence of incoming packets of different sizes with time marks and a sequence of outgoing packets. The number of bytes transmitted in each time unit of these two time series in a specified time period is calculated. As a result, each data stream is converted to a distribution of the same size. Then the frequency sector characteristics of traffic packets are obtained. For the initial message length, message receiving time and other data, the time sequence information is transformed into frequency domain information by Fourier transform, and the former value is selected as the network traffic sorting ability. Finally, normalization is used to make each presence (such as message duration and time period) of the same order of magnitude in the feature. The vector formed by the final calculation result is the network flow sequence.

Network flow order vector can be used as input data to detect abnormal access to terminals. In order to detect the anomaly in the business process of Internet of Things terminal, we further understand the anomaly detection features from the network flow sequence. The steps to use the self-learning feature algorithm are as follows. Firstly, the algorithm model is selected and a self-coding network model with two hidden layers is used. The whole self-coding network model includes one input layer, two hidden input layers, one hidden output layer, and one output layer. Each level is associated with a fully connected method. Then the parameters of the model are specified, and the weight W of the network connection is determined by the adaptive torque estimation algorithm, and the anomaly detection features are derived. After the attributes are derived, the carrier outlet of the second layer of the self-coding model is taken as the carrier.

3.3. Abnormal Detection Method. After understanding the characteristics of anomaly detection, the combination of automatic white list matching algorithm and single class support vector machine algorithm should be used to detect abnormal network movement. For the characteristics of IP address and traffic type, IP address or access type that is not in the scope of the whitelist is defined as abnormal traffic directly, and list matching method should be used. If the IP address and access type are normal, the known anomaly detection function is used as the input, and the single class support vector machine algorithm is used to determine whether it is abnormal. In the training stage, the goal of single class SVM learning is to construct a discrete function which can classify data samples as accurately as possible. Therefore, single class support vector machines should first correspond to the entry points of high-dimensional space through core operations and then separate them as far as possible from their origin in dimensional space. In the detection phase, only the discrete function obtained in the training phase is needed to identify the flow detection characteristics. If the calculation result is 1, the flow to be measured is considered as abnormal flow; otherwise, it is normal flow.

4. Security Authentication Simulation

4.1. Software Simulation. By simulating the authentication process of the new protocol by software, the communication between the read-write server and the supporting server is generally considered to be secure, so they can be considered as a whole. In other words, software simulation only needs to verify the bidirectional identification process between reader and tag. The software simulation adopts the simulation new protocol, and the data storage should adopt the protocol and database. Four tables are created in the database, including illegal tags, illegal readers, legal tags, and legal readers. Among them, serial number 1–5 is illegal label, and serial number 5–10 is legal label. Each table in the database contains field names, bit data, data types, and specific concepts. Label and reader are shown in Tables 1 and 2,

TABLE 1: The label table contains information.

Field	Data bits	Data type	Specific meaning
Tag number	36	Int	Tag number
PID	64	Int	Katakana
ID	64	Int	Tag id
K1	64	Int	Secret key
K2	64	Int	Secret key
K3	64	Int	Secret key

TABLE 2: The reader table contains information.

Field	Data bits	Data type	Specific meaning
PID	64	Int	Tag number
ID	64	Int	Katakana
K1	64	Int	Tag id
K2	64	Int	Secret key
K3	64	Int	Secret key
G1	64	Int	Secret key
G2	64	Int	Secret key

respectively. Among them, the illegal tag key is incompatible with the public read-write key and does not include the key set created by PUF unit, as shown in Tables 1 and 2.

Firstly, two subroutines are written in Java to represent the reader and tag, and then four functional units are created, which are communication function unit, call database function unit, encryption function unit, and protocol verification function unit. The functional communication unit is used for communication and data transmission between two subprograms (reader subroutine and label subroutine). The communication unit uses socket technology to ensure the communication between two subprograms. The function data unit should call two subroutines to call and update the database data. The function encryption unit is mainly responsible for processing the encryption and decryption key of the call data, mainly completes some bit processing operations, and forms a part of the protocol. The PUF unit on the label is a physical circuit. Its basic idea is that when a binary code is inserted into the PUF unit, the latter unit can create a unique output as the key entry and exit, and there is no way to retreat. Therefore, the functional software analog encryption unit contains an irreversible key generation algorithm to replace the PUF material circuit. The verification unit is mainly responsible for the information transmitted according to the protocol to determine whether the reader and tag are legal.

4.2. Dynamic User Activity.
Orthogonal matching pursuit (OMP) algorithm is a common compressed sensing recovery algorithm. Compared with curve optimization algorithm, OMP algorithm ensures the accuracy of signal recovery with lower algorithm complexity. From the perspective of matrix association, the synchronous SOMP algorithm, the normalized focus algorithm based on MMV model, and the correlation orthogonal search algorithm (OMP) are compared. When the number of active users N_a and the number of antennas $M = 128$, $M = 256$, the active user detection

efficiency of OMP-KR algorithm changes. It can be seen from the figure that when the number of active users is $N_a \leq 10$, the error detection probability of OMP-KR algorithm is zero. It can detect fully active users and inactive users, while SOMP and m-focus algorithms have errors. Look at the situation. With the increasing number of active users Na, the probability of error detection in OMP-KR, SOMP, m-focus algorithm also increases gradually. However, it can be seen from the figure that OMP-KR algorithm is obviously superior to the other two algorithms. Even in the case of a large number of active users, OMP-KR algorithm can still guarantee low false detection probability, while in the other two cases, the error classification probability of the algorithm is close to 1. This shows that OMP-KR algorithm can support more active users than SOMP and m-focus algorithm. At the same time, when the number of antennas changes from $M = 128$ to $M = 256$, the yield of OMP-KR algorithm is very considerable. From the shape, OMP-KR algorithm is wrong when the number of active users $N_a = 20$. The detection probability decreases from 10^{-1} to 10^{-4}, which shows that OMP-KR algorithm can obtain better active user detection performance with the increase of the number of antennas, as shown in Figure 1.

When the number of active users is $N_a = 5$, the detection efficiency of OMP-KR algorithm varies with the change of noise, and the number of antennas is $m = 128$ and $M = 256$. Considering the number of antennas $M = 256$, the OMP-KR algorithm proposed in this study has zero detection error probability and can detect fully active users and inactive users. The error detection probability of the other two algorithms is not zero, in which the SOMP error detection probability is 10–1, and the m-focus error detection probability is 1; that is, the m-focus algorithm is 10log10 (1/SZ2) = 0 dB, which is completely invalid and cannot be identified as an active user.

4.3. Verification Vulnerability.
Because apps with validation vulnerabilities are not malicious applications, they are still popular in the large Android software market. This study shows that the sensitivity test is not aimed at large-scale app dataset detection. The main research goal is to protect the real-time detection and security of mobile Internet for the application of users on mobile devices. One is to use interactive environment analysis unit to dismantle 500 sets of application programs, analyze the code source code, and use static detection method to control the use of application network. The statistical test shows the statistical results using 500 application networks, as shown in Figure 2.

HTTP + SSL authentication function is widely used in current applications, accounting for 38%. Among the 500 applications, 190 applications use HTTP + SSL for data verification and security, 155 applications use HTTP for data communication, 75 applications use receivers for data exchange, and 40 applications do not use network data. Then, using SSL to dynamically detect and analyze 40 applications determines whether there are security verification vulnerabilities in these applications. Combined with automatic testing and dynamic creation of test certificates, it is found
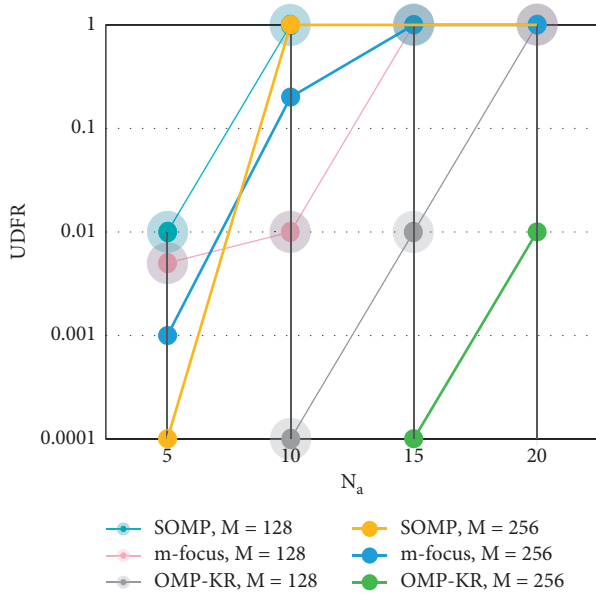
Figure 1: The influence of active user detection performance.
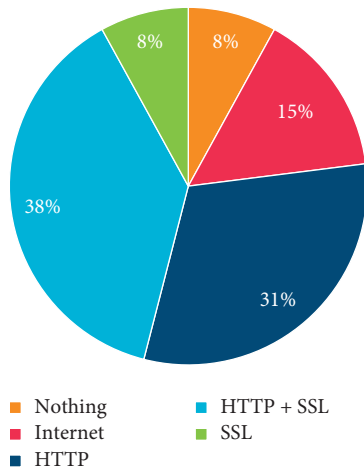
Figure 2: Statistical distribution of network usage in applications.

that 13 of these 40 applications have SSL verification leak holes through dynamic testing.

4.4. Safety Certification Method.

In order to count the delay of E-SSL network in the process of security detection and security service, it is necessary to record the average time of regular visit, access SSL by security detection and security application, and compare security detection and security detection network with contract access. Because SSL has the function of reusing operation cycle, continuous access will not create a complete SSL handshake process in the specified time period. Therefore, intermittent access mechanism is used to calculate the average time. In this study, the test application and E-SSL client were used to make 20 intermittent visits to the E-SSL server, and the time of each visit was recorded, as shown in Figure 3.
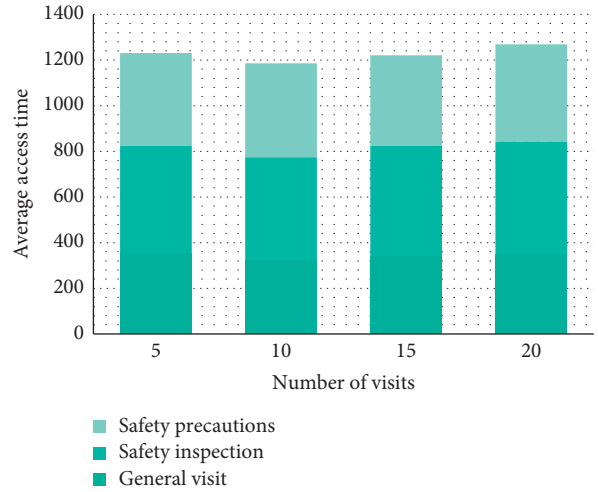
Figure 3: Visit time.

In order to view the statistical results more conveniently, we choose to calculate the average time of different visit time and observe the change trend of the visit time. The first 5 times, 10 times, 15 times, and 20 times were selected as observation points. Generally speaking, HTTP time is equivalent to TCP handshake time, and HTTPS time is equivalent to TCP handshake time plus SSL handshake time. SSL handshake time is relatively longer than TCP handshake time. Through the observation and analysis of the experimental data, this study draws two conclusions: (1) the security detection function takes longer than normal access, because the security detection service performs more SSL handshake process than normal access. (2) Compared with the conventional access, the time spent by the security protection service is almost the same, because the security countermeasure protection service only carries out the port switching and forwarding process. In order to ensure the security of user's privacy, the network delay is within the tolerable range without affecting the user's online experience.

4.5. Delay and Availability before and after Anti-Interference Technology.

In terms of the development status of anti-interference technology, among the top 10000 websites in Alexa's global websites, the market share of the United States is far ahead. For example, with the highly distributed content delivery system deployed in more than 100 countries around the world, covering more than 2000 networks and more than 302 thousand servers and providing more than 80 terabits of web traffic per second every day, it provides nearly 3.5 trillion Internet interactions every day.

As shown in Figure 4, the use of anti-interference technology has a great effect. The utilization rate of anti-interference technology for large-scale websites is higher than that for small- and medium-sized websites. Therefore, in order to reduce the operating costs of enterprises, improve the flexibility of enterprises, and improve the service quality of companies, many large companies have begun to establish their own anti-interference systems. On the basis of meeting
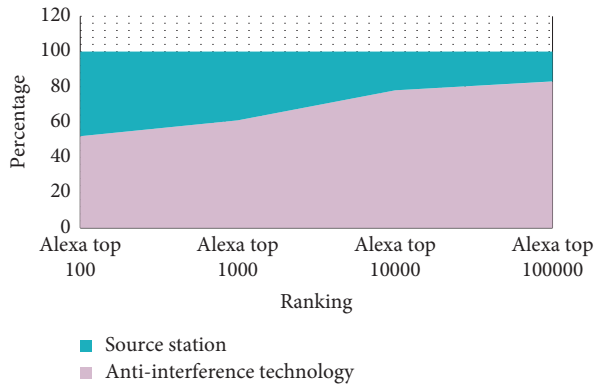
FIGURE 4: Schematic diagram of comparison between before and after delay and availability.

their own needs, it provides anti-interference external business technical services for the company to expand new business areas. In terms of domestic development, according to the statistics of China Institute of Information and Communications, China's market for anti-interference in the technical service industry has developed rapidly, with the compound annual growth rate almost doubled, and the international market scale has expanded significantly, with an annual growth rate of 50%.

5. Conclusions

Generally speaking, with the continuous development and maturity of antijamming technology, the service it can provide is more and more comprehensive and intelligent, which has attracted the attention of many scholars at home and abroad and is committed to the research and optimization of anti-interference technology. For example, in order to optimize the temporary storage and distribution of content in order to provide services to users, on the one hand, it reduces the user access delay, and on the other hand, it improves the access rate performance of the temporary storage for user access requests; the system has been designed in theory, applied and tested, and the results have achieved the expected design goals. The stability of network management technology, the applicability of location algorithm, and the low power consumption and effectiveness of security algorithm all have better performance than traditional algorithms.

The simulation results show that the system can meet the functional and technical requirements of the system. Compared with the traditional MMV algorithm: SOMP algorithm and m-focus algorithm, OMP-KR can support more active user detection. When the number of active users is the same, OMP-KR algorithm is better than the traditional MMV algorithm. With the increase of the number of antennas, OMP-KR algorithm may obtain more benefits than the traditional MMV algorithm.

Aiming at the problem of poor anti-interference performance of traditional multiterminal network anti-interference methods, the ubiquitous system Internet of Things is based on the ubiquitous Internet of Things, and an anti-interference method of multiterminal communication network is designed. This design realizes the anti-interference of multiterminal power communication network from the transmission channel segment of power communication network and the anti-interference of model multiterminal power terminal communication network. The experimental results show that the design method has good anti-interference performance. In conclusion, the antigrid interference method designed in this paper improves the performance of antigrid interference, has good implementation value for the management of power communication network, and can promote the development of power communication network.

Data Availability

No data were used to support this study.

Conflicts of Interest

The authors declare that they have no conflicts of interest.

References

[1] V. Kardeby, S. Forsström, and P. Österberg, "Fully distributed ubiquitous information sharing on a global scale for the internet-of-things," *International Journal on Advances in Telecommunications*, vol. 7, no. 3, pp. 69–81, 2015.

[2] M. Anisetti, C. Ardagna, E. Damiani et al., "Test-based security certification of composite services," *ACM Transactions on the Web*, vol. 13, no. 1, pp. 69–111, 2019.

[3] T. P. Hammerberg, "Anomaly detection," *Encyclopedia of Social Network Analysis and Mining*, vol. 83, no. 11, p. 78, 2018.

[4] D. B. Hess, E. Iacobucci, and A. Väiko, "Network connections and neighbourhood perception: using social media postings to capture attitudes among twitter users in Estonia," *Architecture and Urban Planning*, vol. 13, no. 1, pp. 67–78, 2017.

[5] J. E. Kurz and D. M. Chetkovich, "Understanding network connections connects genotype to epilepsy phenotype," *Epilepsy Currents*, vol. 17, no. 4, pp. 239-240, 2017.

[6] B. S. R. Farr-Wharton, K. Brown, R. Keast, and Y. Shymko, "Reducing creative labour precarity: beyond network connections," *Management Decision*, vol. 53, no. 4, pp. 857–875, 2015.

[7] A. A. Branitskiy, "Hierarchical hybridization of binary classifiers for detecting anomalous network connections," *SPIIRAS Proceedings*, vol. 3, no. 52, pp. 204–233, 2017.

[8] A. Sameh and A. Al-Masri, "Smartphones network connections power-aware multiple wireless interfaces," *Asian Journal of Information Technology*, vol. 18, no. 2, pp. 37–48, 2019.

[9] N. Zhao, J. Guo, F. R. Yu, M. Li, and V. C. M. Leung, "Antijamming schemes for interference-alignment-based wireless networks," *IEEE Transactions on Vehicular Technology*, vol. 66, no. 2, pp. 1271–1283, 2017.

[10] Z. Hu, M. Xiong, H. Shang, and A. Deng, "Anti-interference measurement methods of the coupled transmission-line capacitance parameters based on the harmonic components," *IEEE Transactions on Power Delivery*, vol. 31, no. 6, pp. 2464–2472, 2016.

[11] L. N. Bao, R. B. Wu, D. Lu, and W. Y. Wang, "A novel adaptive anti-interference algorithm based on negative diagonal loading for spoofing and jamming in Global Navigation

Satellite System," *Journal of Communications Technology and Electronics*, vol. 61, no. 2, pp. 157–164, 2016.

[12] Y. Wang, L. Wu, and Y. Yang, "Security authentication method of terminal trusted access in smart grid," *International Journal of Security and Its Applications*, vol. 9, no. 7, pp. 337–346, 2015.

[13] X. Jiang, Y. Mei, and H. Yang, "Development and application of wireless data acquisition system of ground pressure in similar simulation experiment," *Coal Technology*, vol. 47, no. 2, pp. 56–60, 2016.

[14] W. Li, L. Lu, Z. Liu et al., "HIT-SEDAES: an integrated software environment for simulation experiment design, analysis and evaluation," *International Journal of Modeling Simulation & Entific Computing*, vol. 7, no. 3, pp. 1650027.1–1650027.22, 2016.

[15] G. Lee, J. W. Bae, N. Oh, J. H. Hong, and I. C. Moon, "Simulation experiment of disaster response organizational structures with alternative optimization techniques," *Social Science Computer Review*, vol. 33, no. 3, pp. 343–371, 2015.

[16] S. Wei, Z. Ma, B. Li et al., "Study on the monitoring method of three-dimensional stress with FBG in surrounding rock and the simulation experiment," *Caikuang Yu Anquan Gongcheng Xuebao/Journal of Mining and Safety Engineering*, vol. 32, no. 1, pp. 138–143, 2015.

[17] Q. Chen, F. Zhao, and Y. Wang, "Orthogonal simulation experiment for flow characteristics of ore in ore drawing and influencing factors in a single funnel under a flexible isolation layer," *JOM*, vol. 69, no. 12, pp. 1–7, 2017.

[18] K. K. Gu, W. J. Wang, J. Guo et al., "Tribological simulation experiment of interactions between rail and grinding stone," *Mocaxue Xuebao/Tribology*, vol. 35, no. 2, pp. 154–159, 2015.

[19] W. Yan, W. Xiang, S. C. Wong, X. Yan, Y. C. Li, and W. Hao, "Effects of hands-free cellular phone conversational cognitive tasks on driving stability based on driving simulation experiment," *Transportation Research Part F: Traffic Psychology and Behaviour*, vol. 58, pp. 264–281, 2018.

[20] C. Liu, F. Li, Z. Sun et al., "Electric simulation experiment procedure for predicting productivity of multi-stage fractured horizontal wells," *Oil & Gas Geology*, vol. 38, no. 2, pp. 385–390, 2017.

[21] Y. Cai, L. Shengdong, and L. Lu, "Water abundance of mine floor limestone by simulation experiment," *International Journal of Mining Science & Technology*, vol. 26, no. 03, pp. 130–135, 2016.

[22] X. Zhaohui, W. Yan, L. Jing et al., "Simulation experiment of the impact on the motion of the particle in dual-phrase distribution of gas & solid under strong electric field," *High Voltage Apparatus*, vol. 51, no. 7, pp. 171–176, 2015.

[23] D. B. Rawat, R. Alsabet, C. Bajracharya, and M. Song, "On the performance of cognitive internet-of-vehicles with unlicensed user-mobility and licensed user-activity," *Computer Networks*, vol. 137, no. 4, pp. 98–106, 2018.

[24] B. Wang, L. Dai, Y. Zhang, T. Mir, and J. Li, "Dynamic compressive sensing-based multi-user detection for uplink grant-free NOMA," *IEEE Communications Letters*, vol. 20, no. 11, pp. 2320–2323, 2016.

Research Article

Research on the Construction of Smart Tourism System Based on Wireless Sensor Network

Wanxin Sun (ID)

Department of Business Administration, Tourism College of Zhejiang, Hangzhou 311231, Zhejiang, China

Correspondence should be addressed to Wanxin Sun; 1810012015@stu.jci.edu.cn

With the rapid development of information technology represented by the Internet, the economic development of various countries in the world is closely related to information technology represented by computers. As a new growth point of economic development, tourism has attracted more and more attention from all parties. Traditional artificial travel agencies can no longer meet people's needs. In the network information environment, tourists need systematic and large amounts of online travel information to provide support for their decision-making. This article first discusses the research significance and research status of wireless sensor networks at home and abroad and analyzes and optimizes the sensor network algorithms. Based on the existing wireless sensor network hardware experimental system, a tourism management system is designed and developed. Various user interfaces of the tourism management system are designed, including topology tree structure view, node list, program status and program package view, data management, real-time curve display, and node positioning functions. The simulation experiment results show that the efficiency of this system for tourism information integration is 20% higher than other systems, and it has certain practical value.

1. Introduction

1.1. The Background and Significance of the Design of Smart Tourism System Based on Wireless Sensor Network. Internet of Things technology has been widely used in the field of tourism. Many travel-related businesses increasingly rely on wireless sensor systems. At the same time, the development and application of corresponding tourism service models and related systems have also attracted the attention of the industry. However, in the face of constant updates and diversification of customer needs, the simple structure of traditional travel service websites has gradually exposed the disadvantages of low concurrency, instability, and difficulty in expansion, which are far from being able to meet the growing user base and diverse needs. Changes in tourism, traditional tourism service models, and management models cannot meet the business development needs of tourism operators. Therefore, a safe and reliable tourism information management system is needed to build a tourism service and management system with excellent concurrency, stability,

safety, efficiency, and expandability and integrate services and management to provide reliable services to tourists. There is an urgent need to build high-quality tourism service. Convenient and safe payment methods have important theoretical research significance and practical economic benefits for tourists and tourism practitioners. At the same time, the design and construction of the tourism service management system are of great significance for improving the application status of the tourism service model and management system concurrency, stability, security, and scalability of the application program.

1.2. Related Work on Tourism Management System Design. With the advancement of science and technology, the development and improvement of Internet technology and smartphones have gradually become popular in daily life, and the world has realized a rapid transition from the traditional Internet era to the mobile Internet era. Digital scenic spots have been established in various tourist areas to

closely integrate the Internet with the tourism industry. The construction of an Internet-based scenic spot marketing system is an important part of the construction of digital scenic spots. Xiao built a mobile Internet tourism marketing system by analyzing mainstream mobile Internet technologies and their application in tourism marketing. The system structure of the marketing system adopts MVC model and a three-tier distributed structure, and the logic layer adopts JavaBean and EJB structures. Xiao also constructed a WeChat marketing model based on MM-TIP [1]. It has a certain reference value for building a tourism marketing system based on mobile Internet. Wireless sensor networks are widely used to collect environmental data from various structural deployments. In densely deployed linear networks, as standard sensor network protocols try to manage the network as a mesh or self-organizing infrastructure, problems related to optimal resource allocation and networking may persist. For linear sensor networks, problems such as recovering from loopholes where a node cannot reach another node or establishing data distribution routing strategies need to be solved intelligently. Ali et al. proposed a linear sensor network deployment application that uses customized sensor boards and algorithms to solve problems related to network creation, leak detection, and routing of high-priority messages [2]. Bapu's research work is to develop a reconfigurable hardware that uses FPGA to enhance the self-healing ability of sensor nodes. Emphasizing engineering, wireless sensor networks play a prominent role in successful applications. When there is a weak link in the node, it is usually discarded, and the network is reorganized to ensure the normal operation of the node. The maintenance cost and function of the wireless sensor network will occasionally drop. Therefore, Bapu decided to design FPGA-based self-healing technology to develop wireless sensor nodes and repair node hardware failures. By introducing a self-reconfiguration method, the system is developed using "backup modules". Bapu considers the encoding process to integrate data, and FPGA-based self-healing includes power consumption components such as data compressors and signal converters. Bapu and Gowd proposed engineering estimates for lightweight compression and fault prediction technology in the latest time [3]. Remote authentication of the application code installed in the wireless sensor network is the first important step in detecting any unauthorized changes through buffer overflow attacks. In the past, software-based remote code verification methods, such as software-based certification and secure code update through certification, have been difficult to be deployed in recent work [4]. Tan proposed and implemented a remote authentication protocol that uses the small, cost-effective, and tamper-proof encryption microcontroller TPM to detect unauthorized tampering of application code running on sensor nodes.

1.3. Innovations in This Article. This article first discusses the research significance and current research status of wireless sensor networks at home and abroad, then analyzes several basic and common target location algorithms in detail, and finally proposes a weighted centroid prediction algorithm. Based on the existing wireless sensor network hardware experimental system, a tourism management system based on a wireless sensor network is designed and developed [5]. Various user interfaces of the tourism management system are also designed, including topological tree structure view, node list, program status and package view, data management, real-time curve display, and node positioning.

The design and implementation of the tourism management system of the wireless sensor network are introduced in detail. First, the function of the wireless sensor system is designed. The hardware system of the test system is based on the cross-node, and the underlying protocol is designed. The basic software is implemented by NESC programming on the TinyOS system.

The functions of the test system include: serial port control, data processing, real-time data display, historical data query, node ranging, node link quality evaluation, node energy status monitoring, node positioning, and node topology display [6].

2. Design of the Smart Tourism System Based on Wireless Sensor Network

2.1. Wireless Sensor Network. A wireless sensor network (WSN) consists of a large number of extremely small sensor nodes, which are usually deployed in areas that are difficult for humans to reach, such as mountainous areas, battlefields, and disaster areas. The function of the network is to collect the data required by the information coverage area, such as temperature, humidity, and acceleration and transmit the data to the sink node through the multinode multihop mode and then to the monitoring center through the sink node. The staff can analyze and process the uploaded information and obtain the desired results [7, 8]. In addition, the monitoring center can also issue control commands to the nodes for corresponding processing. Therefore, the establishment of a wireless sensor network can reduce the consumption of manpower and material resources and the difficulty of monitoring in high-risk areas. Wireless sensor networks usually consist of sensor nodes, receiver nodes, and monitoring centers [9].

2.2. WSN Tourism Management System Module. The hardware system structure used in this article is divided into a wireless sensor network, a server system, and remote browsing equipment. The node in the wireless sensor network is the coordinator node and acts as the gateway node in the wireless sensor network. The type of node is a router node, and its main function is to improve network coverage and increase wireless sensor network access points. Forward data for terminal nodes and provide data collection functions. The type of the node is terminal and has only the data collection function [10]. At the front end, the information of wireless sensors and storage areas will be analyzed. The remote browsing device is connected to the server to observe, manage, and maintain the network.

The software system is divided into serial communication module, protocol conversion module, data analysis storage module, and visualization system [11, 12]. First, the software obtains the data collected by the hardware through the serial communication module. The protocol conversion module unifies the data packet format of different hardware and then analyzes and processes the data. The processed data are stored in the database system. The user interface system obtains different data from the database according to the requirements of the visualization system. The visualization system is divided into network topology, data packet analysis view, real-time curve, and node data prediction graph.

The use of SQLite databases has a certain range. It is a small database, using embedded devices to complete the specified functions. SQLite database resource occupancy is very low, resulting in high database processing speed. One of the biggest advantages of SQLite is that it has a good dual-purpose and has become a mainstream embedded operating system. It is convenient for users to read and write freely between computers with different byte sequences. It is characterized by the features of fast database operation and source code with good annotations.

2.3. Network Topology.

Topology refers to how hardware components are configured and how configuration data are transmitted [13, 14]. These three network structures can be used to realize the application of a wireless sensor network [15, 16]. Some topologies are suitable in some cases but not in other cases. The star topology is a single-hop structure. All terminal nodes communicate directly with the base station. The terminals do not send data and commands to each other, and the gateway is regarded as a coordinator.

The mesh topology is a multihop structure [17]. All wireless sensor nodes in the network are routing nodes. The nodes can communicate with each other. One or more routes transmit data to the gateway. Since the node can have multiple paths to the base station node, it has strong fault repair capabilities. The system uses multihop instead of single-hop transmission, thereby reducing the power required for each node to send data.

The star-mesh hybrid network has the advantages of having not only a simple star network and low power consumption but also long-distance transmission and self-healing. Therefore, the establishment, maintenance, and update of the entire network are more efficient and simple. Hybrid networks organize sensor nodes to form a star topology while routing nodes will self-organize into a mesh network [18, 19]. Because sensor nodes can communicate with each other, the network can be reconfigured if the node fails or the link interferes.

2.4. Introduction to Sensor Nodes.

The hardware node used in this system is based on the study in [20, 21]. There are three types of nodes in the network, including coordinator nodes, router nodes, and terminal nodes. The hardware structures of the three nodes are the same, but the application programs are different. Each node has a unique address with a bit length. The nodes running in the network are identified by short addresses. The address length is in bits, which is also unique in the network. In the experimental network, there is only one coordinator node, which is a full-featured device defined in the protocol. Connect with the host computer through the communication module. Its main features are: it can start and establish a network; it can allow routers and terminal devices to join the network; it can help route; and it cannot use low power consumption. The main goal of the coordination node is to establish a network. When the node starts, it avoids conflicts with other sensor networks and first scans the wireless channel [22]. Choose an available channel, then set up, and start the network. When establishing a network, the coordinator needs to configure the network, channel, and channel duration. If you want to start a secure network, you also need to configure encryption options and keys. After the network is established, the coordinator node will start to listen to the channel. After that, it functions as a router node, which allows other devices to join the network and forward data packets.

2.5. Structure of the WSN Tourism Management System.

It collects the data of the wireless sensor network and transmits it to the background management system to manage the wireless sensor network and monitor the operation and environmental conditions of the wireless sensor network. In addition, the background management system can also initiate tasks and notify the wireless sensor network through the transmission network to complete specific tasks [23].

The overall composition of the smart tourism system based on wireless sensor network database is used to store all data, including the configuration data of the wireless sensor network, node attributes, sensor data, and some data of the background management software. The data processing engine is responsible for data exchange, data analysis, and data processing between the transmission network and the background management software. It stores the data in the database, reads the data from the database, and then transfers the data to the graphical user interface in a specific way. Back-end components use the data in the database to implement certain logic functions or graphic display functions, which may include network topology display components, node display components, graphic drawing components, etc. [24].

2.6. Data Processing Algorithm of the Smart Tourism System Based on Wireless Sensor Network.

The weighted average method is a real-time processing fusion algorithm. Its essence is to perform a weighted average according to the weight of a single sensor after processing the information from multiple sensors in the future to obtain the final fusion result. This method is suitable for obtaining the fusion value in a dynamic environment. The difficulty lies in solving the weight problem of a single sensor. The algorithm first

analyzes the data set and obtains the information of each dimension of the data set, including the span of each dimension. Analyze the data set to obtain the minimum and maximum values of each dimension in the record set. In order to promote grid clustering, the maximum and minimum values need to be modified. The maximum and minimum values of each size are corrected according to the following formula. Its expression is as follows:

$$\min_i = \min_i - k \times \text{steplen}(i),$$
$$\max_i = \max_i + k \times \text{steplen}(i). \tag{1}$$

Bayesian network reasoning is a tool for decision support and causal discovery in the case of incomplete information. It is based on probability distribution and considers that the values of all variables are controlled by the probability distribution. Based on the observed data, the correct decision can be made by calculating these probabilities. Because it provides a quantitative hypothesis method based on evidence support, it provides not only a theoretical basis for algorithms that directly manipulate probability but also a theoretical framework for analyzing algorithms that do not have a clear probability calculation formula. Therefore, probability inference in Bayesian learning plays an important role in machine learning [25]. The core of Bayesian network inference is to calculate the posterior conditional probability distribution [22, 23]. If the set of all variables is X, the set of evidence variables is E, and the set of query variables is Q, the task of Bayesian network inference is to calculate $Q \in q$ conditional probability distribution under a given set of evidence variables. It can be formally described as follows:

$$p(Q \mid E = e) = \frac{p(Q, E = e)}{p(E = e)}. \tag{2}$$

Cluster analysis is the process of dividing data objects into subsets. Each subset is a cluster. The objects in the cluster are as similar as possible but different from the objects in other clusters. Clustering analysis divides the data objects into meaningful or useful clusters according to the information describing the objects and the relationships found in the data set to discover the natural groupings hidden in the data set. The cluster analysis of the data set can help us understand more clearly the entire data structure, the distribution law of data objects, and the development trend of the data. Its expression is as follows:

$$d(x_i) = \sum_{i=1}^{n} d(x_i, x_j). \tag{3}$$

The algorithm divides the data space into a limited number of elements, which form a grid structure. The data set is gathered on a grid. The clustering time of this method does not depend on the number of data objects but on the number of units in each dimension of the partition space, so the calculation speed is faster.

3. Simulation Test of the Smart Tourism System Based on Wireless Sensor Network

3.1. Data Sources.
The RESSET Domestic Tourism Database (RESSET/TOUR) has 93 data tables and more than 4,500 indicators, including the number of inbound tourists, domestic tourism complaints, ticket price data for major attractions, listed companies, residents, gold per week, tourists, and travel agencies. The reset international travel database contains travel data from the United States, Britain, Canada, France, South Korea, Japan, Finland, and New Zealand, as well as from the United Nations and ASEAN. The United States includes the number of tourists, tourism economy, tourism import and export, US states and cities; the United Kingdom includes monthly overseas travel, the number of overseas tourists, overseas travel expenditures, etc.; Canada includes Canadian residents' travel surveys, travel accommodation, travel service agencies, and international tourism expenditure, transportation, etc.; Finland includes hotels, hotel accommodation, overnight stays, accommodation capacity of accommodation institutions, travel time of Finnish residents, etc.; United Nations statistics include inbound tourism and outbound tourism of various countries, domestic tourism expenditure and travel expenditures of inbound tourism, transportation expenditures of inbound tourism, outbound tourism departures, volume and expenditures of outbound tourism, and travel expenditures of outbound tourism; outbound tourism data are comprehensive and rich in content.

3.2. Test Procedure.
The test mainly involves two aspects: one is the spectrum monitoring function that includes sensor node data collection and transmission and task management center end spectrum data storage, processing, and display, and the second is network management function. There are network initialization of sensing node and network management agent functions, including the collection and upload of node attributes and response to network management commands. The task management center implements management functions, including topology display, node attribute display, and network management command issuance. Network management function also includes system reliability testing.

3.2.1. Network Initialization Function Test.
The sensor node will automatically search for the gateway and randomly visit the subnets of the two gateways. These two gateways are automatically connected to the task management center. The sensor node is used together with the module in the gateway node to obtain node attribute values. Then, the agent module automatically reports the attributes to the task management center.

TABLE 1: Comparison of prediction results.

Performance index	Algorithm		
	Weighted average method	Bayesian algorithm	Clustering algorithm
Estimate	93.5	94.2	78.4
Relative error	0.3465	0.2749	0.1748
Actual value	84.3	74.5	79.4

3.2.2. Network Command and Fault Monitoring Test. According to the order of restart, sleep, delete node, attribute query, change, and change gateway, observe the status of the node receiving the command in turn. Test expectations are as follows: command test results are attribute information, and message output boxes displayed according to the corresponding results. For fault monitoring, when a node is restarted, a gateway is replaced, or a node is changed, the node will temporarily disconnect from the network. At this time, the fault monitoring module will notify the task management center in the form of a fault report.

3.2.3. Network Management System Reliability Test. As a reliability test, there are two main aspects. One is that it can be detected when a failure occurs. On the other hand, when the fault can be recovered, can it be repaired correctly? From these two aspects, we use the method of repeatedly connecting equipment and power for testing.

3.3. Hardware and Software Test System. The hardware system adopts a self-developed network joint node station, a sensor node station, and a notebook computer as the task management center, with modules, network cable roots, routers, and DC power supplies. Connect the power supply, insert the module into the slots of the sensor node and the gateway node, and then connect the laptop and the network through the cable of the router.

4. Analysis of Simulation Test Results of the Smart Tourism System Based on Wireless Sensor Network

4.1. Analysis of System Data Processing Results. When analyzing the performance of the algorithm, the simulation adds some objective factors. The results are shown in Table 1; this set of data is used to build a node data prediction model. In the node stage of data prediction, we assume that the node fails. Make effective forecasts using previous forecast models and surrounding node data information. The relative errors of the weighted average method, Bayesian network inference algorithm, and clustering analysis algorithm are 0.3465, 0.2749, and 0.1784, respectively. When the data of the node is in a relatively stable state, the algorithm can always maintain a low relative error. The prediction algorithm that uses the average value of neighbor nodes fluctuates greatly.

Among them, the clustering analysis algorithm effectively uses the node data rules in the algorithm to compensate for the inaccuracy of adjacent node data information and effectively reduces the fluctuation range and the relative error of data prediction. As the data processing intensity of a node increases, the relative error of the clustering analysis algorithm suddenly increases, degrading the performance of the algorithm. At this time, in this algorithm, neighbor nodes' perception of sudden changes in surrounding environment information is used to reduce the relative prediction error. The average relative error rate of the group data is 0.35–0.41, and the cluster analysis algorithm can effectively integrate the algorithm and the neighbor node method.

4.2. Node Load Performance Test Analysis of the Smart Tourism System Based on Wireless Sensor Network. As shown in Figure 1, any unique record data is inserted into the database every minute. The memory capacity provided by each child node and the length of each record is in bytes.

As shown in Figure 2, compared with the test results of the memory database, we can see that in the case of a single node, although the performance is slightly lower, it is still in a comparable range.

4.3. Data Storage Performance Test Analysis of the Smart Tourism System Based on Wireless Sensor Network. As shown in Figure 3, the main problem in wireless sensor network design is coverage. For the application of wireless sensor networks, the first problem to be solved is the deployment of network nodes. The deployment of wireless sensor network nodes can solve resource constraints, including node energy, computing power, and wireless network communication bandwidth. In order to optimize the resources of the wireless sensor network and improve the quality of services such as perception, perception, monitoring, and communication, it can be achieved through node deployment and routing selection.

As shown in Figure 4, this test shows simultaneous performance testing of queries from 1 child node, 2 child nodes, 3 child nodes, and 4 nodes, respectively, and 10,000 single-point data without indexes.
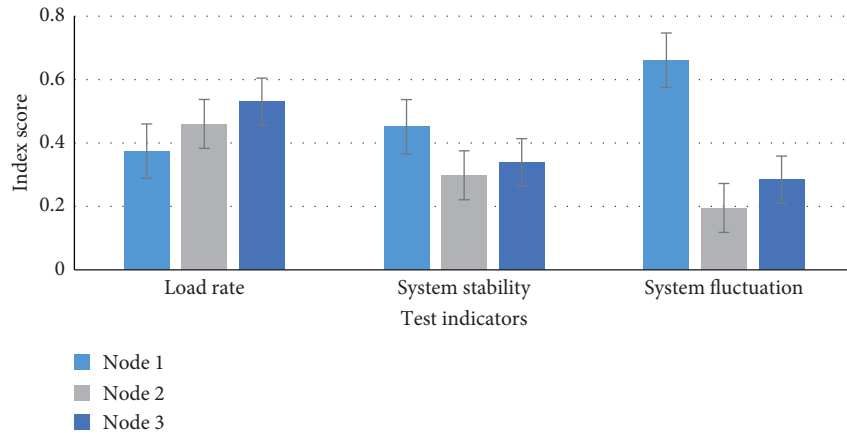
Figure 1: Node load score.
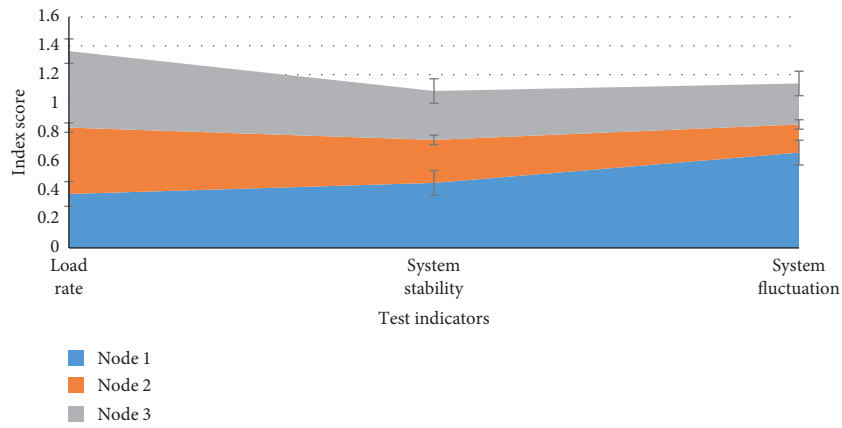
Figure 2: Performance chart of node load fluctuation.
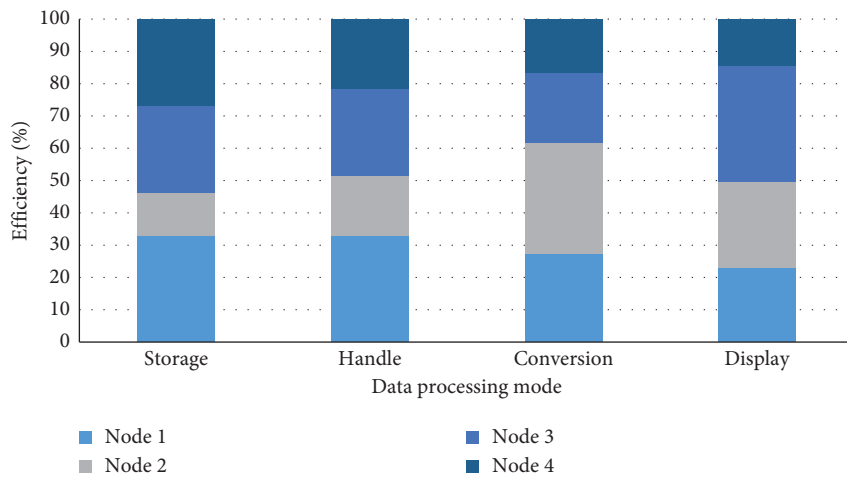
Figure 3: System data processing efficiency.
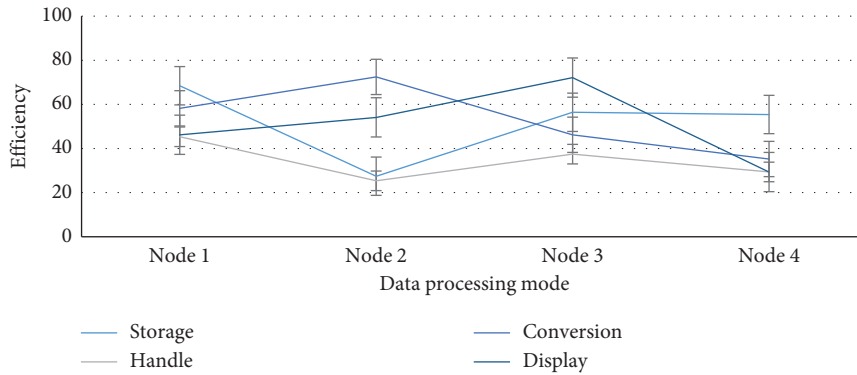
FIGURE 4: System processing efficiency changes.

5. Conclusion

Traditional artificial travel agencies can no longer meet people's needs. In the network information environment, tourists need systematic and large amounts of online travel information to provide support for their decision-making. This paper discusses the research significance and research status of wireless sensor networks at home and abroad and analyzes and optimizes the sensor network algorithms. A tourism management system was designed and developed based on the existing wireless sensor network hardware experimental system. Various user interfaces of the tourism management system were designed, including topology tree structure view, node list, program status and program package view, data management, real-time curve display, and node positioning functions.

The design and implementation of the tourism management system of the wireless sensor network are introduced in detail. First, the function of the wireless sensor system is designed. The hardware system of the test system is based on the cross-node, and the underlying protocol is designed. The basic software is implemented by NESC programming on the TinyOS system. The functions of the test system include: serial port control, data processing, real-time data display, historical data query, node ranging, node link quality evaluation, node energy status monitoring, node positioning, and node topology display. The results show that the tourism management system of the wireless sensor network has achieved the expected results in terms of concurrency, reliability, and scalability.

Finally, in future development, we need to do some work and solve the following problems: the use range of the system has to be expanded so that the test system can be applied to different types of nodes, for example, through additional hardware or components. The function of the system can be expanded to realize the function of the remote control node. By integrating analysis software into a unified software system, data can be directly analyzed and processed, and the required theory or simulation model can be obtained.

Data Availability

No data were used to support this study.

Conflicts of Interest

The author declares no conflicts of interest.

Acknowledgments

References

[1] Y. Xiao, "Tourism marketing platform on mobile internet," *Journal of Electronic Commerce in Organizations*, vol. 17, no. 2, pp. 42–54, 2019.

[2] S. Ali, A. Ashraf, S. B. Qaisar et al., "SimpliMote: a wireless sensor network monitoring platform for oil and gas pipelines," *IEEE Systems Journal*, vol. 12, no. 1, pp. 778–789, 2018.

[3] B. R. T. Bapu and L. C. S. Gowd, "An optimized self healing reconfigurable wireless sensor network implemented on a FPGA system," *International Journal of Control Theory and Applications*, vol. 9, no. 25, pp. 497–506, 2016.

[4] H. Tan, W. Hu, and S. Jha, "A remote attestation protocol with trusted platform modules (TPMs) in wireless sensor networks," *Security and Communication Networks*, vol. 8, no. 13, pp. 2171–2188, 2015.

[5] A. C. C. Lu, D. Gursoy, and G. D. Chiappa, "The influence of materialism on ecotourism attitudes and behaviors," *Journal of Travel Research*, vol. 55, no. 2, pp. 1–14, 2016.

[6] P. Beritelli, F. Buffa, and U. Martini, "The coordinating DMO or coordinators in the DMO?-an alternative perspective with the help of network analysis," *Tourism Review*, vol. 70, no. 1, pp. 24–42, 2015.

[7] Z. Xiang, "Tourism management, marketing, and development volume 1: the importance of networks and ICTs," *Annals of Tourism Research*, vol. 52, pp. 190-191, 2015.

[8] Y. Chen, "Design and implementation of wireless sensor cellular network based on android system," *International Journal of Online Engineering*, vol. 13, no. 5, p. 56, 2017.

[9] A. Zátori, "Tourism experience design in urban destinations," *Regions Magazine*, vol. 299, no. 1, pp. 11-12, 2015.

[10] W. Xue-Fen, Y. Yi, Z. Tao, Z. Jing-Wen, and M. S. Sardar, "Design of distributed agricultural service node with smartphone in-field access supporting for smart farming in Beijing-Tianjin-Hebei region," *Sensors and Materials*, vol. 30, no. 10, pp. 2281–2293, 2018.

[11] N. T. Huynh, V. Robu, D. Flynn, S. Rowland, and G. Coapes, "Design and demonstration of a wireless sensor network platform for substation asset management," *CIRED-Open Access Proceedings Journal*, vol. 2017, no. 1, pp. 105–108, 2017.

[12] H. Sun, J. Zhang, G. Sun et al., "Agricultural traceable and marketing system based on iOS-system and wireless sensor network," *Journal of Computer and Communications*, vol. 5, no. 6, pp. 45–56, 2017.

[13] C. Yang, "Using an 'interpretative model' for contextual design of heritage landscape databases: the case of St Helena Island National Park in Queensland, Australia," *Geographical Research*, vol. 53, no. 3, pp. 321–335, 2015.

[14] R. Zhou, "Research on the framework of tourism e-commerce system," *Boletin Tecnico/Technical Bulletin*, vol. 55, no. 18, pp. 649–655, 2017.

[15] Y. Hong, "Evaluation index system of tourism competitiveness based on tourism electronic commerce system," *Boletin Tecnico/Technical Bulletin*, vol. 55, no. 4, pp. 463–473, 2017.

[16] K. Chochiang, F. Hanna, M. L. Betbeder, and J. C. Lapayre, "New techniques in Thai-English transliterated words searching, applied to our new web services system for tourism (WICHAI)," *Journal of Computers*, vol. 12, no. 5, pp. 408–415, 2016.

[17] S. Hui, "Evaluating the cooperation risk between rural tourism and third-party network system by using confirmatory factor analysis," *International Journal of Software Engineering & Its Applications*, vol. 9, no. 5, pp. 231–242, 2015.

[18] Y. Gong and Y. Zhang, "Research on the game between public service system for all-for-one tourism and demand side of tourism service," *Boletin Tecnico/Technical Bulletin*, vol. 55, no. 10, pp. 72–80, 2017.

[19] M. Miyake, A. Fujii, T. Ohno, and M. Yoshikawa, "Place-based services system that enhances user satisfaction from sports tourism to daily life," *Fujitsu Scientific & Technical Journal*, vol. 54, no. 4, pp. 38–43, 2018.

[20] H. Stainton, "The 'Blogosphere' as a system for interpretative phenomenological analysis: the case of TEFL tourism," *Current Issues in Tourism*, vol. 21, no. 7–12, pp. 1075–1084, 2018.

[21] Y. Cui and Y. Tan, "Cloud computing system application for evaluating docking strategy of Hebei high-end sports tourism industry from a Jing-jin-ji integration perspective," *Boletin Tecnico/Technical Bulletin*, vol. 55, no. 8, pp. 155–162, 2017.

[22] J. Zhang, "Design and implementation of intelligent tourism system based on the android system," *Agro Food Industry Hi-Tech*, vol. 28, no. 1, pp. 2525–2529, 2017.

[23] J. Trojan, "Integrating AR services for the masses: geotagged poi transformation platform," *Journal of Hospitality and Tourism Technology*, vol. 7, no. 3, pp. 254–265, 2016.

[24] K. Vinding, M. Bester, S. P. Kirkman, W. Chivell, and S. H. Elwen, "The use of data from a platform of opportunity (whale watching) to study coastal cetaceans on the southwest coast of South Africa," *Tourism in Marine Environments*, vol. 11, no. 1, pp. 33–54, 2015.

[25] P. Lopes, L. Almeida, J. Pinto et al., "Open tourist information system: a platform for touristic information management and outreach," *Information Technology & Tourism*, vol. 21, no. 4, pp. 577–593, 2019.

Research Article

Research on Sports Video Image Based on Clustering Extraction

Jun Ma 🄳

Sports Department, Guizhou University of Finance and Economics, Guiyang 550025, Guizhou, China

Correspondence should be addressed to Jun Ma; majun@mail.gufe.edu.cn

Today, with the continuous sports events, the major sports events are also loved by the majority of the audience, so the analysis of the video data of the games has higher research value and application value. This paper takes the video of volleyball, tennis, baseball, and water polo as the research background and analyses the video images of these four sports events. Firstly, image graying, image denoising, and image binarization are used to preprocess the images of the four sports events. Secondly, feature points are used to detect the four sports events. According to the characteristics of these four sports events, SIFT algorithm is adopted to detect the good performance of SIFT feature points in feature matching. According to the simulation experiment, it can be seen that the SIFT algorithm can effectively detect football and have good anti-interference. For sports recognition, this document adopts the frame cross-sectional cumulative algorithm. Through simulation experiments, it can be seen that the grouping algorithm can achieve a recognition rate of more than 80% for sporting events, so it can be seen that the recognition algorithm is suitable for recognizing sports events videos.

1. Introduction

In recent years, with the improvement of people's living standards, more and more attention has been paid to sports and video processing has been gradually deepened in the field of sports. A large number of sports and national fitness information, as well as video and image forms, are stored in various fitness guidance systems. In order to better promote public fitness and facilitate learning and viewing, image segmentation motion video player has become a hot topic of digital image processing. To overcome the slow split, irregular movement, and susceptible to the influence of light of the shortcomings of the moving object, the researcher based clustering presents a motion video sequence moving foreground object extraction algorithm. Experiments show that the algorithm is effective, simple, workable, and has less calculation, and the effect is satisfactory.

Motion video object exercise posture has relatively random and blurred image change tendency, and the divided region is not easily determined. Moving video images may present segmentation exercise posture, unnecessary region of the object, pixel area divides into foreground and background, and extracts the movement of the object.

Launched in 2000, with an increase in MPEG-4 video content semantic search feature, you can split the background and foreground images into different semantic objects. Coding efficiency is improved, but the noise in the encoding process is not quickly eliminated. Temporal segmentation and frequency domain are the first segmentation method for segmentation of moving video images presented specifically. After a lot of experiments, both methods can not accurately describe the attitude of the object, and the image segmentation is not clear. Therefore, research on sports video images based on clustering extraction has greatly changed sports videos and will help make better use of sports video analysis and images.

As research deepens, sports video image segmentation technology has made great strides. In 2009, David and Zhang Shensheng used a binary grouping method, which showed a good recognition rate in various images and achieved good results in the experiment. However, there are also some weaknesses in the method. The result is not obvious when the brightness of the object surface is affected by many lighting factors, such as dimming reflection, high light reflection, and fuzzy texture. Fan Cuihong proposed a segmentation method of video moving objects based on

regional differences. The RGB space of video image is transformed into HSV space. The closed contour of moving object is extracted by chroma, saturation, and brightness. According to the moving area, background area, and occlusion area of video, the edge of moving object is detected by edge detection operator, and finally the moving object in video is segmented. Experiments show that the improved algorithm can improve the segmentation accuracy and meet the real-time requirements. Ouyang Yi proposed a method based on Markov chain Monte Carlo (MCMC) to track human posture in monocular video images. Firstly, the projection maps of human appearance in basic human motion database acquired by motion capture equipment were clustered under different perspectives. Using HOG to detect human body in monocular video images can segment the position of human limbs more accurately. Finally, the appearance model of the three-dimensional human posture reasoning algorithm is used to analyze each frame, and then the time-constrained analysis model is used to track the target. Constraint graph-driven MCMC and basic action library are combined to construct a model for video data modeling, and the model is applied to data driven online behavior recognition to improve human pose modeling ability. Zhang Jiawen et al. proposed a convenient and practical method for human motion tracking and motion reconstruction in video and initially achieved the goal of obtaining human motion data from video resources such as video surveillance and video recordings. This paper is a useful attempt to track and acquire human motion in monocular video, and some satisfactory preliminary research results have been achieved. In the last part of this paper, the author puts forward his own opinions on the problems of human motion tracking and motion reconstruction methods and their further improvement. Wu Tianai, Yang Ling, and others have proposed a moving human body detection algorithm based on space-time combination in color environment. The algorithm combines temporal segmentation with spatial segmentation to obtain the moving human body with precise edges and eliminates the shadow of the moving human body. The experimental results show that the above algorithm can detect the moving human body from the color image sequence in real time and effectively, eliminate the shadow of the moving human body, and finally detect the moving human body is the color. With more and more people researching sports video images, many achievements have been made in recent years.

Because of the complexity of the algorithm and the great difference between the segmentation results and the reality, the application of the segmentation results is limited. The main reason is that the change of the blur factor of the image, the uncertainty of the segmentation, and the time-consuming information loss. This loss is often due to the boundary information generated in the classification process. Clustering extraction as a clustering method has been successfully applied in many research classifications. Liu Guodong et al. proposed a threshold adaptive online clustering color background reconstruction algorithm and objectively evaluated the reconstructed color background. Finally, the background subtraction method was used to extract moving objects. Jiang Yuan et al. put forward that clustering is an important tool for data mining. According to the similarity of data, the database is divided into several categories, in which the data should be as similar as possible. Based on possibilistic C-mode clustering, the main tone and subtone were selected to describe the features of video images so that the key frames of video could be extracted directly without shot segmentation. Experiments show that this method can effectively extract the most representative key frames according to the complexity of video content and has high timeliness. Leskovec et al. proposed the K_SC clustering algorithm for topic time series in 2010, which has high accuracy and can better describe the inherent trend of topic development. However, the K_SC algorithm is highly sensitive to the center of the initial class matrix and has high time complexity, which makes it difficult to apply in the actual high-dimensional large data sets.

Due to the advantages of the cluster extraction algorithm [1], cluster extraction has been used as a classification tool in many areas of clustering research, and good results have been achieved. The extraction algorithm proposed sequential cross-sections of cross-based video frames that form moving foreground objects. The simulation experiment is performed under the simulation environment of MATLAB 2014 B. The experiment proves that the algorithm is efficient, simple, and feasible, with fewer calculations and can have more satisfactory results. Due to the inherent noise in the original frame, it is necessary to reduce the noise in the original video sequence to improve the accuracy and efficiency of moving objects in video segmentation, to reduce noise, and to enhance the effect of calculating the frame difference. This algorithm uses the most common square median filter module for preprocessing, which is fast and feasible, can reduce the loss of image details, optimize image quality, and be suitable for the next segment. It can also better protect the edges of the image and effectively remove noise. Research on sports video images based on clustering extraction and these fast 3D camera modeling broadcast court network sports videos, deep learning models and transfer learning sports videos, mixed reality systems, and hyperparameter optimization based on convolutional neural networks. In comparison with the sports video summary scene classification algorithm based on classification and transfer learning, the clustering extraction algorithm can be more convenient, fast, safe, and reliable.

2. Proposed Method

2.1. Binary Processing Based on Sports Video Image. Among many image segmentation methods, binarization is a simple and effective method. The purpose of image binarization [2] is to separate the moving object and background from the image and to provide a basis for subsequent classification, detection, and recognition. Typically, the method of threshold segmentation [3] is used for binarization. Its principle is to select an appropriate threshold to determine whether each pixel in the image belongs to the target or the background by making use of the

difference between the object and the background in the image so as to get the target to be detected.

Set the input image as $f(x, y)$ and the output image as $f_b(x, y)$, then

$$f_b(x, y) = \begin{cases} 1, & f(x, y) \geq T, \\ 0, & f(x, y) < T, \end{cases} \tag{1}$$

where T represents the threshold of the binarization process. In actual processing, 255 is used to represent the background and 0 is used to represent the moving target. The process of binarization is relatively simple. The key problem is the selection method of binarization. In this paper, the OTSU algorithm [4] is used to improve the selection of binarization image threshold.

2.2. Morphological Processing of Sports Video Image. The binary image has some misjudgement points; that is, there are a small number of "burrs" or "holes," which requires further refinement. In order to get more accurate segmentation results, this paper chooses appropriate structural elements and uses mathematical morphology to filter the corrosion and expansion. In fact, it uses image open and close operation.

In corrosion operation, the result of etching a binary image is to narrow the edge of the image and shrink inward, which seems to be eroded by the surface. Its principle is to define a subimage whose size is negligible and relative to the image to be processed as a structural element. Typically, a $2 * 2$ or $3 * 3$ pixel size template is selected, which specifies a pixel in the template as the origin and assigns a value (1 or 0) to each position in the template. The structure elements are used to scan the image to be processed point by point and perform matching operations. Whenever a subimage identical to the structural element is found (no matching of the zero pixels in the structural element), the location of the corresponding pixel in the subimage corresponding to the original position of the structural element is marked. The set of all such pixels is the result of the corroded operation of the binary image, which is defined as formula (2)

If I is the image to be corroded and B is the selected structure "probe," then the definition of target image I corroded by probe B [5] is as follows:

$$I \Theta B = \{x \mid (B)_x \supseteq I\}. \tag{2}$$

Among them, X represents the displacement of set translation, Θ represents the operator of corrosion operation, and $(B)_x$ represents the translation of structural elements.

Morphological corrosion means that every time the translation structural element detects the image to be processed; if a subimage identical to the structural element is found, the location of the pixels in the subimage and the origin of the structural element is marked. The set of all the marked pixels is the result of corrosion. In fact, in the image to be processed, the original pixels of the subimage with exactly the same shape of the structural elements are marked and retained. Expansion operation corresponds to

corrosion operation. Expansion processing of a binary image often enlarges the edge of the image. Therefore, if there are black spots in the white foreground area of the image or two white areas are blocked by very thin black lines, then the black pore in the corroded image will be filled into a white image block which is similar to the surrounding image block, and the two image blocks which are not connected by themselves will also become a complete connected block. The principle of image expansion is to define a subimage whose size is negligible relative to the image to be processed as a structural element. Typically, a template with 2×2 or 3×3 pixel size is selected to specify a pixel in the template as the origin. And a value (1 or 0) is assigned to each position in the template, the image is scanned to be processed point by point, and matching operation is performed by using structural elements. Whenever a pixel point intersecting with the structural element is found (only one position in the structural element and the image to be processed are foreground points), the point of the image to be processed relative to the original of the structural element is marked as foreground points. The set of all these marker points is the result of image expansion. The definition of image expansion is as formula (3).

If I is the source image to be processed and B is the selected structural element, then the mathematical definition of the expansion of the target image I by the structural element B is as follows:

$$I \oplus B = \{x \mid x = i + b, i \in I, b \in B\} = \cup_{b \in B} I_b. \tag{3}$$

Among them, $i + B$ denotes that I is translated by vector b, x denotes the two-dimensional value after operation, and $\oplus$ is the symbol of expansion operation.

The meaning of morphological dilation is that as long as the intersection point with the structural element is not empty in the image, the pixels corresponding to the original position of the structural element in the image to be processed are marked. The set of all the symbolic conditions is the result of the dilation operation.

Corrosion and expansion operations have different effects. Expansion can connect two separate regions and make two isolated "islands" connected. Corrosion can eliminate the pore in the image, make the original isolated "island" disappear in the image, and play the role of filtering noise.

2.3. Feature Point Detection. In feature point detection [6], what kind of feature is used to describe objects is an important part of feature matching. Whether the feature selection is appropriate or not is the decisive factor affecting the success or failure of the next matching work. In this paper, we use feature points, but there is no definite concept at present. Generally speaking, we represent points with feature properties in images, such as extreme points, points with zero second derivative, intersection points of lines, and lines in images. The feature points represent the important local feature information in the image, which effectively reduces the image information and plays a great role in the analysis and understanding of the image. Using feature

points for image matching can enhance the validity and reliability of image matching.

2.3.1. Harris Feature Point Detection.

The core idea of the Harris feature point detection algorithm is to use small windows to judge the gray level change by moving on the image. If the gray level changes obviously in the process of moving, there will be feature points in the window.

If the gray level does not change or does not change in one direction, there is no feature point in the window. By constructing a mathematical model, the problem can be expressed as follows:

$$E(u, v) = \sum_{x,y} w(x, y) [I(x + u, y + u) - I(x, y)]^2. \quad (4)$$

In formula (4), (u, v) represents window translation transformation, $E(u, v)$ is gray level change, $w(x, y)$ is window function, and $I(x, y)$ is image gray level. The window function is Gauss function as follows:

$$w(x, y) = \frac{1}{2\pi\sigma^2} e^{-(x^2+y^2)/2\sigma^2}. \quad (5)$$

This function can be understood as calculating the weight of gray level in the window, which changes with the direction from the center point to the edge smaller and smaller, so as to eliminate the influence of noise on it.

The Taylor expansion for formula (10) can be expressed as follows:

$$E(u, v) = \sum_{x,y} w(x, y) \left[I_x u + I_y v + o\left(u^2, v^2\right) \right]^2. \quad (6)$$

M is the partial derivative sparse matrix and it is expressed as

$$E(u, v) \cong [u, v] M \begin{bmatrix} u \\ v \end{bmatrix}. \quad (7)$$

In this formula, I_x is the difference in direction x, I_y is the difference in direction y, and M is the partial derivative sparse matrix and is expressed as follows:

$$M = \sum_{x,y} w(x, y) \begin{bmatrix} I_x^2 & I_x I_Y \\ I_x I_y & I_y^2 \end{bmatrix}. \quad (8)$$

For Harris feature point monitoring, the size of two eigenvectors of M matrix can be used. The two eigenvalues represent two directions of the fastest and slowest change, respectively. Both of them are large and can be judged as characteristics. One is the edge, and the other is the edge. Both of them are small and flat areas without change. So, we can express the problem as follows:

$$R = \det M - k (trM)^2, \quad (9)$$

where $\det M$ is the determinant of a matrix M which is the product of two eigenvalues, trM is the trace of a matrix M which is the sum of two eigenvalues, and k is a constant. From the analysis, it can be seen that the judgment of Harris feature points is related to the value R. When the value R is larger and positive, it can be judged as the feature point. When the value R is larger and negative, it can be judged as the edge, and when the value R is smaller, it can be judged as the flat area without change. In practical applications, the horizontal and vertical difference operators are used to evaluate the matrix M of the pixels, and then the Gauss filter is used to determine the feature points directly by R. The algorithm is simple, efficient, insensitive to illumination changes, and has rotation invariance. However, it does not have scale invariance; when the threshold is too large, the sensitivity of focus detection is not enough and the number of feature points is too small, and false feature points are easy to appear when the threshold is too large.

2.3.2. ORB Feature Point Detection.

ORB feature point detection [7, 8] is a SIFT algorithm for extracting and describing image features. FAST (Features from Accelerated Segment Test) is used to extract feature points. In the algorithm based on image feature detection and matching, through the GLAMpoints paper, we can learn the exact matching points greedily learned. And through the feature detection and description of image matching, we can learn from manual design to deep learning. It is best to talk about key point detectors and descriptors based on random samples through RSKDD-Net. The core idea of the FAST algorithm is as follows: for a pixel, a circular region is constructed with the center of the pixel, and the gray value of the pixel in the center of the circle is compared with that of all the pixels in the circle. When the pixel value of enough points is larger or smaller than that of the center of a circle, the pixel is considered to be a feature point. It can be expressed as follows:

$$D = \sum_{\text{circle}(p)} |I(x) - I(p)| > \varepsilon. \quad (10)$$

In formula (10), $I(x)$ is the gray value of any point in the circle, $I(p)$ is the gray value of the central pixel, and ε is the set thresholds. If the D value is greater than the set threshold, the corner can be judged.

In view of the fact that FAST features do not satisfy scale changes, the ORB algorithm establishes scale pyramids, similar to the SIFT algorithm in building scale pyramids. For each layer of image, FAST feature points are extracted. Finally, the extracted features are regarded as a set of features extracted from all layers, so as to meet the scale invariance. Aiming at the problem that FAST feature points have no direction, the ORB algorithm gives the gray centroid position in the neighborhood where R is the center of feature points and the direction of gray centroid is the direction of feature points, and then the formula for calculating centroid C is as follows:

$$m_{pq} = \sum_{x,y \in r} x^p y^q I(x, y),$$

$$C = \left(\frac{m_{10}}{m_{01}}, \frac{m_{00}}{m_{00}} \right). \quad (11)$$

In formula (11), $I(x, y)$ is the gray value of the neighboring pixel, and the direction of the vector $\overline{OC}$ of the feature point O and the center of mass C is as follows:

$$\theta = \arctan \frac{m_{01}}{m_{10}}. \tag{12}$$

Since FAST feature is only an algorithm for feature detection and does not involve the formation of feature descriptors, the ORB algorithm uses Rbrief algorithm for feature description. The Rbrief algorithm is that the descriptor generated by the Brief algorithm [9] adds rotation angle information. The Brief algorithm takes n pairs of pixels randomly around the position of the extracted feature points to form an image block and then compares the two pixels in the image block, the result of which is expressed by 0 or 1. A series of binary digit strings with length n are generated, and the generated binary digit strings are the Brief descriptors of the feature points. In order to enhance the descriptor's robustness to noise and illumination, the image block is smoothed by Gauss filtering. The gray level of $5 * 5$ neighborhood of a point in its $31 * 31$ neighborhood is compared with that of point pair. The comparison criterion of the ORB algorithm after Gaussian smoothing of image blocks can be expressed as follows:

$$\tau(p; x, y) := \begin{cases} 1, & p(x) < p(y), \\ 0, & p(x) \geq p(y). \end{cases} \tag{13}$$

In formula (13), the average gray levels of the two pairs of pixels X and Y in the image block p are, respectively, $p(x)$ and $p(y)$. The generated binary digit string can be represented as follows:

$$f_n(p) = \sum_{1 \leq i \leq n} 2^{i-1} \tau(p; x, y). \tag{14}$$

In formula (14), n can generally be taken as 128, 256, and 512. It can be seen that the Brief descriptor does not have rotation invariance. In order to describe the direction of the generated feature points using the descriptor, ORB improves the Brief descriptor. Let the original Brief algorithm represent a $2 * n$ matrix by selecting n pairs of points around the feature points:

$$S = \begin{pmatrix} x_1, \ldots, x_n \\ y_1, \ldots, y_n \end{pmatrix}. \tag{15}$$

According to the angle θ between FAST feature points and centroid, the rotation matrix R_θ is constructed, and then the corresponding direction of rotation of the point set matrix can be expressed as follows:

$$S_\theta = R_\theta S. \tag{16}$$

At this time, the original Brief descriptor can be expressed as follows:

$$g_n(p, \theta) := f_n(p) | (x_i, y_i) \in S_\theta. \tag{17}$$

In order to ensure the separability of feature point descriptors, the ORB algorithm improves the original Brief algorithm by using statistical principles, namely, Rbrief

algorithm. Each point is arranged in columns according to the binary digits taken above, and the matrix Q is generated. The average value of Q of each column is calculated. The first column in the matrix R is rearranged according to the distance from the draw value to 0.5. The correlation between Q of all the columns and all the columns in the matrix R is calculated. If the result is less than the set threshold, put the column in the matrix R, until 256 columns in R stop. The feature points extracted by the ORB algorithm and the descriptors generated by the ORB algorithm are fast and have good rotation invariance. However, when adapting to scale change, the effect is general. Because its descriptor is binary digit string, the matching process is not stable enough, which will cause some difficulties in matching.

2.3.3. SIFT Feature Point Detection.

The SIFT algorithm [10] is a computer vision feature extraction algorithm which satisfies our needs very well. The feature extracted by this algorithm is a scale rotation invariant, so it has excellent robustness and is convenient for feature matching. The main idea of SIFT is to collect images in continuous scale, find extremum points in continuous scale space, remove unstable extremum points, and extract and acquire local features of rotation and scale invariance around stable extremum points. Finally, 128-dimensional descriptors are generated.

SIFT features have the following advantages: strong robustness and good adaptability to geometric deformation, image noise, and brightness change. An image can generate a large number of SIFT feature points, which are rich in data. The local invariant features corresponding to the two images have good repeatability. Firstly, we consider the scale invariance of SIFT features. In order to adapt to scale transformation, feature points need to be detected in all image scales. Therefore, it is necessary to establish the scale space, and the Gaussian kernel function [11] is the only smoothing function in the scale space, so the Gaussian kernel function can be used to build the scale space. The scale transformation of an image can be expressed as follows:

$$L(x, y, \sigma) = G(x, y, \sigma) * I(x, y), \tag{18}$$

where $I(x, y)$ is expressed as an image, (x, y, σ) is a Gaussian kernel function, and $L(x, y, \sigma)$ is an image in different scales, and it is a scale space. The Gauss kernel function can be expressed as follows:

$$G(x, y, \sigma) = \frac{1}{2\pi\sigma^2} e^{-\left[(x^2+y^2)/2\sigma^2\right]}, \quad \sigma \geq 0. \tag{19}$$

In order to improve the reliability and stability of feature points, the preliminary identified feature points are screened. The screening steps are divided into two steps. The first step is to remove the low contrast points, i.e., some noise-sensitive points, and Taylor expansion is carried out for equation (21):

$$D(x) = D + \frac{\partial D^T}{\partial x} x + \frac{1}{2} x^T \frac{\partial^2 D}{\partial x^2} x. \tag{20}$$

Seeking extreme points,

$$\widehat{x} = -\frac{\partial^2 D^{-1}}{\partial x^2} \frac{\partial D}{\partial x}. \tag{21}$$

In formula (21), $\widehat{x}$ is the position of the extreme point and x is the offset of the extreme point. $D(\widehat{x})$ can be used as a basis for judgment. Generally, feature points of $D(\widehat{x})$ less than 0.3 are removed. The second step is to remove the edge response. The points at the edge are very sensitive to noise, and the Gauss difference function has a large principal curvature for a peak across the edge, so the SIFT algorithm excludes the edge response by calculating the principal curvature. The principal curvature can be calculated by a $2 * 2$ Hessian matrix H as follows:

$$H = \begin{bmatrix} D_{xx} & D_{xy} \\ D_{xy} & D_{yy} \end{bmatrix}. \tag{22}$$

Since the principal curvature is proportional to the eigenvalue of matrix H, if the two eigenvalues of matrix H are, respectively, α or β, then there are

$$\frac{\mathrm{Tr}(H)^2}{\mathrm{Det}(H)} < \frac{(r+1)^2}{r}. \tag{23}$$

In formula (23), $\mathrm{Tr}(H)$ is the trace of matrix H, $\mathrm{Det}(H)$ is the determinant of matrix H, and r is the constant which is generally taken as 10 to determine whether the principal curvature is in a certain range.

After the stable feature points are selected, the appropriate descriptor is generated for the feature. In order to make the descriptor rotate invariant, the gradient modulus and direction can be expressed as follows:

$$m(x, y) = \sqrt{(L(x+1, y) - L(x-1, y))^2 + (L(x, y+1) - L(x, y-1))^2},$$

$$\theta(x, y) = \alpha \tan 2 \left\{ \frac{[L(x, y+1) - L(x, y-1)]}{[L(x+1, y) - L(x-1, y)]} \right\}. \tag{24}$$

In formula (24), L is expressed as the scale of each point. The gradient value of each point represents the main direction of the neighborhood gradient and takes the main direction as the direction of the feature point. After determining the main direction, the position, scale, and direction of each feature point have been reflected. At this point, a descriptor is generated for each feature point. To solve the gradient value on the image smoothed by the corresponding Gauss feature points, each feature point can generate a 128-dimensional descriptor, that is, a 128-dimensional feature vector. In order to remove the influence of illumination changes, the feature vector can be normalized and SIFT features can be extracted.

2.4. Cluster Analysis Method. Cluster analysis is a method of quantitative classification with mathematical tools. Cluster analysis algorithm [12] is a typical unsupervised learning algorithm and one of the important algorithms of data mining. It is mainly used to study classification problems; that is, similar data are automatically divided into the same category. When using the clustering algorithm, we usually analyze the similarity relationship between data to group data and divide data into different classes. The greater the similarity between similar data, the smaller the similarity between different classes of data; that is, the greater the difference, the better the classification effect.

2.4.1. Clustering Algorithm Based on Cumulative Frame Difference Intersection. The basic idea of the clustering algorithm based on the intersection of the cumulative frame difference is based on the calculation of the cumulative frame difference and cross and cluster the two cumulative

frame differences so that the changing area can accurately converge to the foreground edge, and then the area binarizes the mask to obtain a differential image frame that is to ensure the real-time performance, and greatly improve the segmentation effect. It is also suitable for sports video sequences with fast-moving objects. The main steps of the algorithm are as follows:

(1) After the median filtering, the image processing sequence difference between adjacent frames and frame interval difference is as follows:

If the current image frame n can be expressed as $f(k)$, the frame image k_{+1} and k_{+2} can be expressed as $f(k+1)$ and $f(k+2)$, and the interframe difference of the adjacent difference categories can be expressed as follows:

$$\left| f_{k+1}(x, y) - f_k(x, y) \right|,$$
$$\left| f_{r+1}(x, y) - f_r(x, y) \right|. \tag{25}$$

The cumulative results of the n frames are as follows:

$$D_1 = \sum_{r=1}^{k} \left| f_{r+1}(x, y) - f_r(x, y) \right| = E \cup N_1,$$

$$D_2 = \sum_{k=1}^{k} \left| f_{k+2}(x, y) - f_k(x, y) \right| = F \cup N_2, \tag{26}$$

where E and F are the change areas in the cumulative results and N_1 and N_2 are noise.

(2) By intersecting the two cumulative frame differences, the pixels belonging to the change area in the two cumulative results can be effectively concentrated
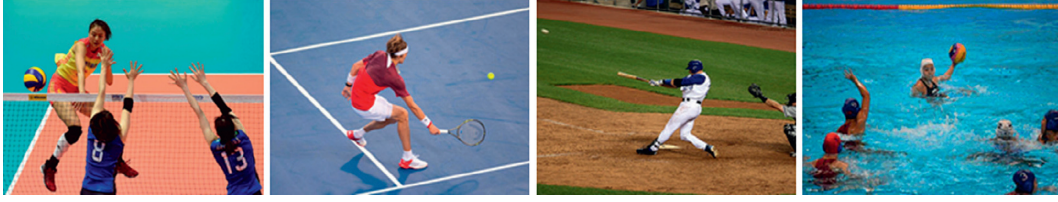
FIGURE 1: Four kinematic video frames.

FIGURE 2: Grayscale of video frame image.

around the foreground contour, thereby obtaining an ideal moving foreground contour.

$$D_1 \cap D_2 = (A \cup N_1) \cap (B \cup N_2) = EF \cup (EN_2 \cup FN_1 \cup N_1N_2). \quad (27)$$

Since EN_2 and FN_1 are clustering of moving regions and noises, formula (5) can be rewritten as follows:

$$D_1 \cap D_2 = AB + N. \quad (28)$$

(3) For further clustering method to remove background pixels, clustering step procedure is described as follows:

Step 1. Randomly determine two points and set $5 * 5$ and cycle number 1P as the centers.

Step 2. For each pixel in a rectangular window,

$$D_1 = \frac{1}{N_K^2} \sum_{N_1 \cap N_2 \cup EF \cap EN_1} \overline{)(x_i - x) - (y_i - y)}. \quad (29)$$

Step 3. Compare the distance D_1 with the threshold D_i. If $D_i \leq D_1$, binning of pixels moved to the edge of the moving foreground object. Otherwise, the pixel will be merged into the background noise edge pixel.

Step 4. Move the rectangular window from the horizontal and vertical directions, increase the number of pixels and follow Step 2 until all the binning classes they belong to, that is, the number of cycles reaches the specified number, and the cluster ends.

3. Experiments

In this document, the experimental platform configuration is based on a 64 bit flagship version of the Win7 operating system, 8 G physical memory, a 2.2 GHz quad-core Intel Core I5-5200U CPU, and MATLAB 2014b-based simulation software.

In order to reflect the universality of the experiment, the material used in this document comes from the network and not from a dedicated video library. The sports video used in the simulation experiment comes from sports gates of large gates. The video frame rate is 5 frames per second, and the output image resolution is 480×360. Tennis, volleyball, water polo, and baseball were selected as the four sports videos. In this article, the SIFT algorithm is used to derive the characteristics of the sport, and then the cumulative cross-sectional algorithm is used to identify sports, as shown in Figure 1.

4. Discussion

Before the simulation experiment, it is necessary to pre-process the actual video object to improve the video frame characteristics. Firstly, all four types of motion video frames are gray, as shown in Figure 2.

In the image processing process, the presence of noise is inevitable. In this article, denaturing is also required in the preprocessing process. This document enhances traditional filter average processing, saves processing time efficiently, and improves processing results, which are useful for detecting and tracking images in the later stages of football. In this paper, we simulate and analyze the noise added to the gray image and use the traditional median filter and the
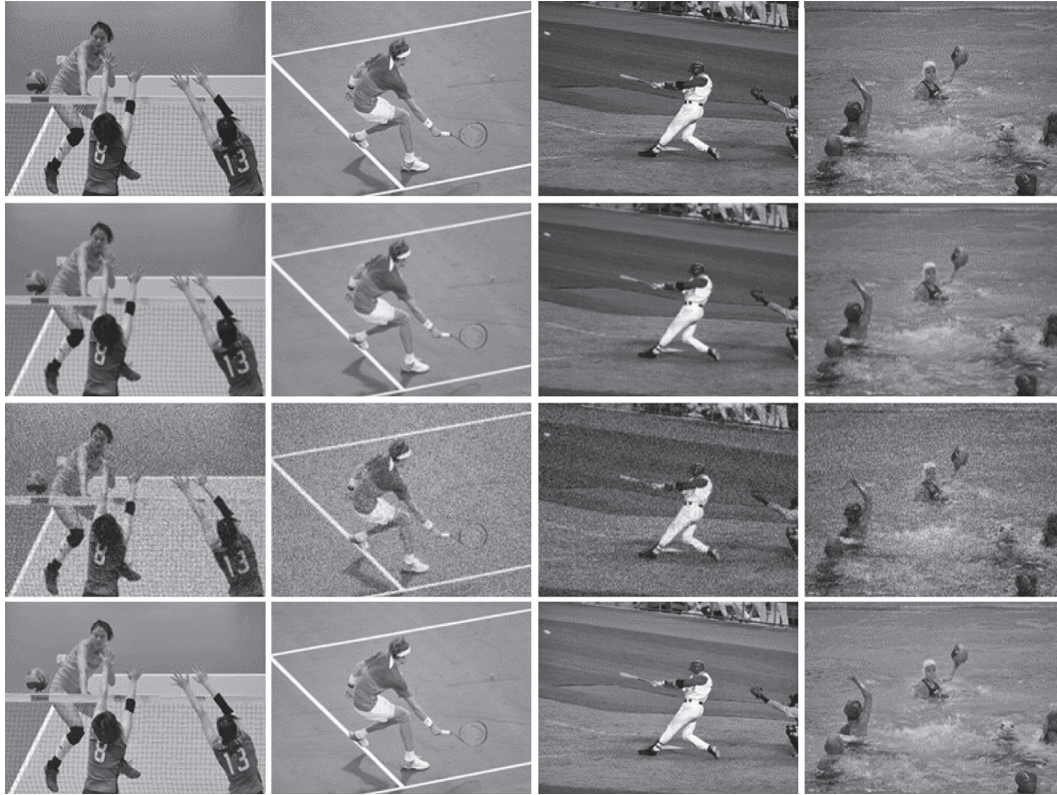
FIGURE 3: Video frame image noise and filtering.
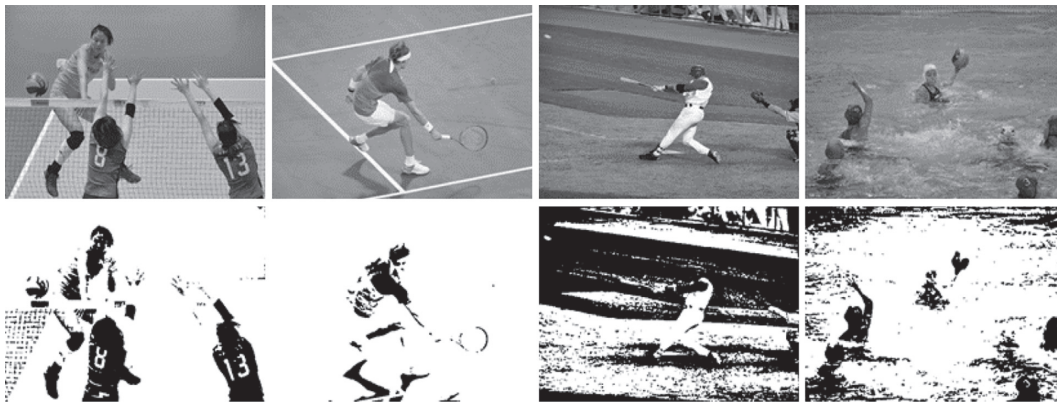
FIGURE 4: Two values.

TABLE 1: Motion recognition rates.

	Volleyball (%)	Tennis (%)	Baseball (%)	Water polo (%)
Accuracy	86.5	91.2	87.4	83.2
Recognition rate	82.3	93.4	88.4	84.3

improved median filter, respectively, to avoid the noise influence in the process of processing, as shown in Figure 3.

After filtering, we edge the image with the result of filtering. After gray level processing, there are 256 gray levels. By choosing appropriate threshold, the gray level of the gray image can be divided into two parts, and then the binarization of the image can be obtained. It keeps the region of interest in the image to the greatest extent and shields all the irrelevant information as shown in Figure 4.

After the preprocessing results, the first step is to carry out simulation experiments on sports detection. The processed video frame images are recognized, and the accuracy and recognition rate of the four kinds of motion are compared, respectively, as shown in Table 1.

From this table, we can see that tennis has the highest recognition rate, while the rest of the sports are relatively low, which may be related to the video background.

5. Conclusions

In recent years, with the improvement of people's living standards, more and more attention has been paid to sports. The research of video data processing has high theoretical significance and commercial value. In this paper, four kinds of sports videos are analyzed, and four kinds of sports images are extracted. After image graying, image denoising, and image binarization, a detection method based on SIFT feature points is designed. In the simulation experiment, image preprocessing, sports item detection, and sports item recognition are analyzed, respectively. By comparing the accuracy and recognition rate of these four sports, we can conclude that the recognition rate is more than 80%. It can be seen that the recognition rate is still very high, and the tennis recognition rate is the highest. This shows that the SIFT algorithm and cumulative cross-section grouping algorithm proposed in this paper are suitable for sports video recognition.

Data Availability

No data were used to support this study.

Conflicts of Interest

The author declares that there are no conflicts of interest.

References

[1] J. Lu, G. Zhou, C. Yang et al., "Steganalysis of content-adaptive steganography based on massive datasets pre-classification and feature selection," *IEEE Access*, vol. 7, pp. 21702–21711, 2019.

[2] O. Choi, M. Kim, A. E. Cho et al., "Fates of water and salts in non-aqueous solvents for directional solvent extraction desalination: effects of chemical structures of the solvents," *Membrane Water Treatment*, vol. 10, no. 3, pp. 207–212, 2019.

[3] W.-Y. Chang, "Research on sports video image based on fuzzy algorithms," *Journal of Visual Communication and Image Representation*, vol. 61, pp. 105–111, 2019.

[4] Hume, Patria, Knudson et al., "Isbs 2018 Auckland Conference Sprinz sport and exercise biomechanics teaching archive programme," *ISBS Proceedings Archive*, vol. 36, no. 1, p. 278, 2018.

[5] Y. Li, "Research on sports video image analysis based on the fuzzy clustering algorithm," *Wireless Communications and Mobile Computing*, vol. 2021, no. 3, pp. 1–8, 2021.

[6] L. Zhang, "Evaluation and simulation of sports balance training and testing equipment based on medical video image analysis," *IEEE Sensors Journal*, vol. 20, no. 20, pp. 12005–12012.

[7] M. Takahashi, "Video analysis technologies in sports broadcast programs," *Journal of the Japan Society for Precision Engineering*, vol. 84, no. 12, pp. 949–952, 2018.

[8] Q. Fu, L. Ma, C. Li, Z. Li, Z. Zhu, and Z. Lin, "Detection method of sports scene conversion for MPEG compressed video based on fuzzy logic," *Journal of Intelligent & Fuzzy Systems*, vol. 40, no. 2, pp. 3107–3115, 2021.

[9] N. Sasikala, P. V. V. Kishore, D. A. Kumar, and C. R. Prasad, "Localized region based active contours with a weakly supervised shape image for inhomogeneous video segmentation of train bogie parts in building an automated train rolling examination," *Multimedia Tools and Applications*, vol. 78, no. 11, pp. 14917–14946, 2019.

[10] B. Joanna and K. Zuzanna, "The impact of social media on managing the image of the Polish national football team," *Physical Culture and Sport, Studies and Research*, vol. 87, no. 1, pp. 46–55, 2020.

[11] M. D. Basar, A. D. Duru, and A. Akan, "Emotional state detection based on common spatial patterns of EEG," *Signal, Image and Video Processing*, vol. 14, no. 3, pp. 473–481, 2020.

[12] K. I. Sainan, M. Mohamad, Z. Mohamed et al., "Athletes tracking using homography method: a preliminary study," *International Journal of Engineering & Technology*, vol. 7, no. 4, pp. 6–10, 2018.

Research Article

Sports Video Augmented Reality Real-Time Image Analysis of Mobile Devices

Hui Wang,[1] **Meng Wang** (iD),[2] **and Peng Zhao**[1]

[1]*School of Physical Education, Hanjiang Normal University, Shiyan 442000, Hubei, China*
[2]*College of Transportation, Jilin University, Changchun, Jilin 130012, China*

Correspondence should be addressed to Meng Wang; mengw19@mails.jlu.edu.cn

Sports video is loved by the audience because of its unique charm, so it has high research value and application value to analyze and study the video data of competition. Based on the background of football match, this paper studies the football detection and tracking algorithm in football game video and analyzes the real-time image of real-time mobile devices in sports video augmented reality. Firstly, the image is preprocessed by image graying, image denoising, image binarization, and so on. Secondly, Hough transform is used to locate and detect football, and according to the characteristics of football, Hough transform is improved. Based on the good performance of SIFT algorithm in feature matching, a football tracking algorithm based on SIFT feature matching is proposed, which matches the detected football with the sample football. The simulation results show that the improved Hough transform can effectively detect football and has good antijamming performance. And the designed football tracking algorithm based on SIFT feature matching can accurately track the football trajectory; therefore, the football detection and tracking algorithm designed in this paper is suitable for real-time football monitoring and tracking.

1. Introduction

Nowadays, more and more people accept various kinds of information in the form of multimedia data, which requires the storage and analysis of various multimedia data. Because the most important way for humans to perceive and understand the world is vision, visual information is the most important information in multimedia data, which contains the largest amount of information. In multimedia data, visual information is represented as image data and video data. The analysis and processing of image and video data is a hot issue in real-time image analysis of augmented reality mobile devices. In most cases, the moving target in a video sequence is the most concerning part of human eyes. In fact, the biggest feature of video image is that it has rich original data, strong correlation between adjacent near frames, and dynamic time-varying mode in time domain, which makes moving objects easy to detect, segment, and recognize. Compared with static images, the greatest advantage of image sequence and video is to capture motion information.

The object detection and tracking algorithm of video image began in the middle of the 20th century. At that time, people began to study the computer representation of object image and developed optical character recognition (OCR) system, license plate recognition system in fixed scene, and so on. By the end of the 20th century, face detection, vehicle detection, and aviation military target detection have become popular research fields.

At present, many national departments and scholars have done a lot of research on motion target analysis and its technology. In 1997, the Defense Advanced Research Projects Agency of the United States established the Visual Surveillance and Monitoring (VSAM) system, which was led by Carnegie Mellon University Robot and participated by Sarnoff Company and so on [1]. The system can be used for battlefield situation analysis, safety monitoring in important places, and monitoring of refugee flow. From 1998 to 2002, a system named ADVISOR was developed and studied by the French National Institute of Computer Science and Control, the University of Reading, and the University of Kingston in

the United Kingdom under the support of the IST (Information Society Technology) research institute. The system improves the management level of public transport network by establishing an intelligent monitoring system and guarantees personal and property safety [2]. In addition, there are also Maryland University real-time visual monitoring system W4 [3], the video surveillance technology project AVITRACK, and the intelligent embedded system ObjectVideo, which are jointly studied by the European Union and Austria. It also shows that, with the development of society, the demand for sport target analysis is higher and higher.

Video moving object analysis system can be widely used in public safety protection, such as regional monitoring, terrain matching, urban safety, and traffic management. However, in reality, the background is most complex and changeable, such as the brightness change of light, the movement of objects in the background, or the existence of objects similar to the characteristics of the target, shadow problem, target occlusion, and so on. All these have brought some difficulties to the accurate detection and tracking of the target.

In modern life, sports video is a kind of important video loved by the majority of the audience, which occupies a large proportion in the existing television programs and the Internet. With the continuous improvement of people's quality of life and the rapid progress of science and technology, all aspects of sports video requirements are also rising. For example, in the aspect of watching sports matches, now this passive, flat viewing mode will gradually fail to meet the demands of television viewers. Broadcasters need to add various visual special effects to meet the visual requirements of the audience. In many sports competitions, football matches have the largest number of spectators and the highest degree of concern. Therefore, detecting, extracting, locating, and tracking the moving objects in football matches video have very high practical value and practical significance.

Target extraction and tracking in video is a hotspot in image and video processing. The technology applied covers many fields of image processing analysis and computer vision. Generally speaking, a video scene is composed of background and target, in which target is an important part of video sequence and contains important information. Therefore, fast and effective segmentation of objects in video and tracking of interesting objects are the basis of subsequent video image analysis.

The core of augmented reality mobile devices is to realize the seamless integration of virtual objects (3D models, videos, images, audio, etc.) and real scenes. How to make the virtual objects and real scenes reach an agreement on time, location, and illumination is a technical difficulty. In recent years, with the continuous improvement of hardware and software of mobile devices, augmented reality technology can be applied to mobile devices. However, mobile devices are usually limited by memory, computing power, communication speed, hardware architecture, and other aspects. How to research the technology suitable for mobile devices on the original basis has become a research hotspot in the field of augmented reality.

In the past two decades, researchers have done a lot of research on video analysis and processing and put forward many valuable theories and methods. Sports video has a certain structure and regularity. The analysis and research of sports video have high theoretical value and wide application value, which makes sports video attracted the attention of many scholars [4–6]. In the analysis and processing of football video, players and football are two very important goals. In many applications, it is urgent to detect and track players and football, such as event detection, tactical analysis, automatic summary generation, and target-based video compression. As a hot issue in video and sequence image processing, detection and tracking has always attracted the attention of researchers. In recent years, many famous universities and research institutes at home and abroad have made in-depth research on football video analysis and processing technology and put forward some effective methods for football video target detection and tracking.

It is a very challenging task to detect and track football effectively in football videos. The main reasons include the following: (1) In football videos, the number of pixels occupied by football targets is small. (2) The position and direction of the camera are always changing, so the football movement in football video includes the movement of the ball itself and the movement of the camera. (3) Because of the influence of the light and the speed of the ball, the color, size, and shape of the football will change, so it is difficult to build an effective model to detect and track the ball. (4) When soccer is tied to the ground or shielded by players, it is more difficult to detect and track [7–10].

In this paper, the detection and tracking of football is studied, and an algorithm of football detection and tracking in football matches video is proposed, which can in real time analyze football matches video images. The work of this paper is as follows:

(1) The image is preprocessed by image grayscale, image denoising, and image binarization, and an improved median filtering method is proposed.

(2) Hough transform is used to locate and detect football, and according to the characteristics of football, Hough transform is improved.

(3) Based on the good performance of SIFT algorithm in feature matching, a football tracking algorithm based on SIFT feature matching is proposed, which matches the detected football with the sample football.

2. Proposed Method

2.1. Image Preprocessing

2.1.1. Image Denoising. In video image processing, the main noise comes from image sensors. There are two kinds of noises from image sensors: salt-and-pepper noise and Gauss noise [11, 12]. In order to eliminate sensor noise, there are two kinds of mean filtering [13] and median filtering [14]. In this paper, an improved median filtering method is used to

denoise the system from the point of view of real-time performance and detection effect.

For the traditional median filtering algorithm, if the number of pixels in the sliding window is n, each window needs to be compared $(n(n-2)/2)$ times, and the time complexity is $O(n^2)$. In general filtering algorithm, the window needs to be sorted once every time it moves. If image size is $N \times N$, the time complexity of the whole algorithm is $O(n^2N^2)$.

In this paper, an improved median filtering algorithm is used to improve the real-time performance of soccer video processing, in which the time complexity of each sliding window is $O(n)$, and the overall time complexity is $O(nN^2)$, which meets the real-time requirements of volleyball video detection.

For illustrative purposes, the pixels in the 3×3 window are defined as $P_0 - P_8$, respectively, as shown in Table 1.

The process of implementation of the algorithm is as follows: first, the maximum, median, and minimum values in each column are calculated, and the maximum, median, and minimum groups can be obtained. The calculation process is as follows:

Max group: $\text{Max}_0 = \max[P_0P_3P_6]$, $\text{Max}_1 = \max[P_1P_4P_7]$, $\text{Max}_2 = \max[P_2P_5P_8]$.

Middle-value group: $\text{Med}_0 = \text{med}[P_0P_3P_6]$, $\text{Med}_1 = \text{med}[P_1P_4P_7]$, $\text{Med}_2 = \text{med}[P_2P_5P_8]$.

Minimum group: $\text{Min}_0 = \min[P_0P_3P_6]$, $\text{Min}_1 = \min[P_1P_4P_7]$, $\text{Min}_2 = \min[P_2P_5P_8]$.

It is concluded that the maximum value and the minimum value in the maximum value group and the minimum value group must be the maximum and minimum values of the nine-pixel values, the maximum value in the median group is at least 5 pixels, and the minimum value is less than 5 pixels. If the median in the maximum group is at least 5 pixels, and the median in the minimum group is less than 5 pixels, then

$$\text{Maxmin} = \min(\text{Max}_0, \text{Max}_1, \text{Max}_2),$$
$$\text{Medmed} = \text{med}(\text{Med}_0, \text{Med}_1, \text{Med}_2),$$
$$\text{Minmax} = \max(\text{Min}_0, \text{Min}_1, \text{Min}_2),$$
$$\text{Winmed} = \text{med}(\text{Maxmin}, \text{Medmed}, \text{Minmax}),$$

(1)

and with this algorithm, the number of median calculations is nearly twice as much as that of the traditional algorithm, and it is very suitable for image smoothing in video sequence.

2.1.2. Image Binarization.

Among many image segmentation methods, binarization is a simple and effective method. The purpose of binarization of image [15–17] is to separate the moving object from the background in the image and to provide the basis for the subsequent classification, detection, and recognition. Set the input image as $g(x, y)$ and the output image as $g_b(x, y)$; then,

$$g_b(x, y) = \begin{cases} 1, & g(x, y) \geq T, \\ 0, & g(x, y) < T, \end{cases}$$

(2)

TABLE 1: Pixel sort order.

	Zeroth columns	First columns	Second columns
Zeroth lines	P_0	P_1	P_2
First lines	P_3	P_4	P_5
Second lines	P_6	P_7	P_8

where T represents the threshold of binary processing. In actual processing, the background is represented by 255 and the moving object is represented by 0. The process of binarization is relatively simple, and the key problem is the selection method of binarization. In this paper, the OTSU algorithm is used to improve the selection of binarization image threshold.

2.2. Research on Soccer Location Detection.

Hough transform essentially transforms the spatial domain of an image into a parametric space and describes the curve of an image in a parametric form satisfied by most of the pixels. In the process of geometric image detection, standard Hough transform (SHT) requires the following steps to achieve detection [18–21]:

(1) Allocate buffer: the process is to allocate the parameter buffer to prepare the mapping.

(2) Parameter space transformation: the feature points are scanned, and each feature point satisfying a specific relationship corresponds to the parameter space.

(3) Accumulation and storage: the image parameters satisfying the specific relationship are accumulated and stored, and the pixels satisfying the specific relationship in the image space are added together.

(4) The location of the largest point on the plane of the location parameter, which is the parameter of the image on the original image.

The equation of known circle is

$$(x - g)^2 + (y - h)^2 = r^2,$$

(3)

where (g, h) is the center of a circle and r is the radius. The formula represents the equation of the circle. Because it is in the image space, the point (x, y) is regarded as an unknown number, and the center (g, h) and radius r are regarded as known numbers. If the image in image space coordinate system $(x - y)$ is mapped to three-dimensional parametric space $(g - h - r)$, the equation of circle in parametric space is as follows:

$$(g - x)^2 + (h - y)^2 = r^2.$$

(4)

In the parameter space, the known and unknown parameters are reversed, the coordinate information of the feature points (x, y) becomes known, and the corresponding center (g, h) and radius r are unknown. After transformation, each effective feature point (x, y) in the image space corresponds to a cone in the parameter space one by one. Different points on the same circle in the image

space correspond to the same point of intersection of cones in the parameter space. This process records the number of repeated points with the same parameters by initializing a three-dimensional accumulator in the parameter space. The expression is as follows:

$$A(g,h,r) = A(g,h,r) + 1, \tag{5}$$

where $A(g,h,r)$ represents a three-dimensional accumulator, counting every three-element array (g,h,r) and accumulating the results. By setting a threshold, when the value of the accumulator exceeds the threshold, the point is considered to be the center coordinate of the circle in the image space.

After preprocessing the video frame, the Hough transform is realized. However, directly using SHT to perform loop detection on an image requires mapping the pixels of the entire image into the parameter space and then making judgments point by point, which affects the efficiency and accuracy of the algorithm. Therefore, the basic idea of this paper is to replace multiple loops with multidimensional arrays while reducing the dimensionality of the accumulator. At this point, we need to know the radius of the circle to be detected; that is, the circle radius r must fall in the range of $(r_{\min}, r_{\max})$. It is known that, in the image space, the circle can have the following parameter expression:

$$\begin{cases} x = g + r \cos \theta, \\ y = h + r \sin \theta. \end{cases} \tag{6}$$

Symbol θ is the angle between the point (x, y) and the line of the point and the x-axis. The corresponding point in the image space is mapped to the parameter space, and the formula of the circle is as follows:

$$\begin{cases} a = g - r \cos \theta, \\ b = h - r \sin \theta. \end{cases} \tag{7}$$

The specific steps for improvement are as follows:

(1) After the image is preprocessed, the initial Hough array matrix in the pixel space is used to set the initial variables, and according to the actual position of the circle, it is determined that its radius is $(r_{\min}, r_{\max})$, and the step length is θ.

(2) According to the parametric formula (5), the value of calculation (a, b) is set as a nonnegative integer, and the valid value is recorded to determine the index value of the Hough array.

(3) Hough arrays are constructed according to Hough index values, which are mainly realized by accumulators. At this time, the number of layers of the arrays is $r_{\min} - r_{\max}$.

(4) In the Hough array, the layer with the largest accumulative value is found, which corresponds to the circle with the largest number of pixels in the image space, and the corresponding radius of the array is the radius r of the circle.

(5) The center of the circle is obtained. The mean value of all the (a, b) in the maximum value layer is the center of the circle.

2.3. Research on Soccer Tracking Algorithm.
In this paper, based on the good performance of SIFT algorithm in feature matching, a football tracking algorithm based on SIFT feature matching is proposed, which matches the detected football with the sample football. Firstly, SIFT feature points need to be extracted. The details are as follows:

2.3.1. Detection of Extreme Points in Scale Space.
In scale space, the concept of local extreme contains two meanings: one is image space extreme; that is, the extreme points are local extreme points in 9 points of 3×3 neighborhood on the same level; the other is scale-space extreme, that is, the local extreme points of 27 points in the neighborhood 3×3 of the point and its corresponding points in two adjacent layers. To sum up, the extraction steps of scale-space extreme points are as follows.

Step 1. The input image $I(p,q)$ is convoluted with the Gauss function $G(p,q,\sigma)$ to generate the corresponding scale space $L(p,q,\sigma)$, which is represented by a Gauss pyramid.

Step 2. Subtract the two adjacent layers of the Gauss Pyramid to generate the Gauss differential Pyramid $D(p,q,\sigma)$.

Step 3. In the Gaussian difference pyramid, the maximum or minimum point in the neighborhood of the same layer 3×3 and the neighborhood of the adjacent layer 3×3 is detected.

2.3.2. Precise Location of Key Points.
The image data stored by computer are discrete pixel value, but the extreme point of discrete data may not be the extreme point of real continuous space. Therefore, it is necessary to fit the DOG function in scale space with a three-dimensional quadratic curve, so that the extremum points can be accurately located at subpixel level. For a general differentiable function, the extreme point is the point whose first derivative is 0. So the Taylor expansion of Gauss difference function DOG in scale space is as follows:

$$D(P) = D + \frac{\partial D^T}{\partial P} P + \frac{1}{2} P^T \frac{\partial^2 D^T}{\partial P^2} P. \tag{8}$$

Solve the derivative, and let $((\partial D(p))/\partial P) = 0$; then, the maximum point obtained in the image row, column, and scale of the three directions offset is

$$\widehat{P} = \frac{\partial D^T}{\partial P} \left(\frac{\partial^2 D^T}{\partial P^2} \right). \tag{9}$$

Since the DOG function is expanded at the origin of the extreme point $P = (p,q,\sigma)$, the range of offset in three directions is found to be between 0 and 1. Formula (5) is substituted into formula (4):

$$D(\widehat{P}) = D + \frac{1}{2}\frac{\partial D^T}{\partial P}\widehat{P}. \tag{10}$$

Lowe's experiment shows that, for the extreme point of $|D(\widehat{P})| < 0.3$, it is considered as an unstable candidate with low contrast and is eliminated.

In order to obtain stable subpixel accurate positioning coordinates of key points, the following positioning criteria are adopted in this paper:

(1) If the three components of $\widehat{P}$ (i.e., the offset in the row, column, and scale directions of the image) are less than 0.5, then the point is regarded as the extreme point, and the noninteger coordinate value after the offset is taken as the precise positioning coordinate of the key point.

(2) If a component is greater than or equal to 0.5, it means that the real extreme point is closer to the detection point of another integer; then the coordinates of the extreme point in this direction are moved to an integer coordinate value in the offset direction.

(3) Repeat the above operations (Taylor expansion and offset calculation) until the offset of a detection point is found to satisfy three component values less than 0.5. The number of repeated operations is not greater than 5; otherwise, it is considered unstable.

For two-dimensional discrete data images, the key points of the Hessian matrix are

$$K = \begin{bmatrix} D_{pp} & D_{pq} \\ D_{pq} & D_{qq} \end{bmatrix}. \tag{11}$$

The derivative is estimated by the difference between adjacent sampling points; that is,

$$D_{pp} = I(p, q+1) + I(p, q-1) - 2 * I(p, q) \quad D_{qq} = I(p, q+1) + I(p-1, q) - 2 * I(p, q),$$

$D_{pq} = ((I(p+1, q+1) - I(p+1, q-1) - I(p-1, q+1) + I(p-1, q-1))/4), I(p, q)$ represents the size of the pixel value at coordinate (p, q).

α is a larger eigenvalue of K and β is a smaller eigenvalue. For the two-order matrix K, the trace of the matrix is

$$\mathrm{Tr}(K) = D_{pp} + D_{qq} = \alpha + \beta. \tag{12}$$

The determinant of the matrix is

$$\mathrm{Det}(K) = D_{pp}D_{qq} - \left(D_{pq}\right)^2 = \alpha\beta. \tag{13}$$

In order to avoid directly calculating these eigenvalues, we only consider the ratio between them to represent the ratio of the principal curvature of the extreme point. Let $r = (\alpha/\beta)$; then,

$$\frac{\mathrm{Tr}(K)^2}{\mathrm{Det}(K)} = \frac{(\alpha+\beta)^2}{\alpha\beta} = \frac{(r+1)^2}{r}. \tag{14}$$

It can be seen that the upper form reaches the minimum when the eigenvalues of α and β are equal and increases with the increase of r. So the intensity of the edge response can be expressed by the size of formula 10. The larger the value, the stronger the edge response. Lowe recommends that the value of r be 10. When the Hessian matrix of the extreme point satisfies $(\mathrm{Tr}(K)^2/(\mathrm{Det}(K))) < ((r+1)^2/r), r = 10$, the extreme point is retained; otherwise, it is considered to be the extreme value of the edge response which is easy to be affected by noise and so on.

2.3.3. Key Point Assignment.

The direction of the feature points will be used in the key point descriptor, so the characteristics of the feature points need to be described. We assign a direction to each feature point. The gradient direction distribution of the neighborhood pixels of the key points is used to assign direction parameters to each key point, so that the operator has rotation invariance.

$$m(p, q) = \sqrt{(L(p+1, q) - L(p-1, q))^2 + (L(p, q+1) - L(p, q) - 1)^2},$$

$$\theta(p, q) = \arctan\left(\frac{L(p, q+1) - L(p, q-1)}{L(p+1, q) - L(p-1, q)}\right). \tag{15}$$

Formulas (11) and (12) are the formulas for the modulus and direction of gradient at (p, q). The scale used by L is the scale of each key point.

In practical calculation, when the direction is the weight and the gradient is the weight value, for the convenience of calculation and statistics, we use 0.5 as the dividing line to take integers to both sides of the radian direction angle which exists in decimal form. For example, 1.25 takes 1 and 2.75 takes 3. With this method, the angles can be grouped into 8 arrays of 0–7, and the corresponding gradient values can be added up as the important data for subsequent calculation and matching.

2.3.4. Generating Key Points Descriptors.

After obtaining the local feature points, the key step is to use the local feature points to describe the information of the surrounding area, which can reduce the impact of the key points by perspective, rotation, illumination, and so on. By assigning the direction of the key points, we have been able to get the main direction of the key points. Then we rotate the region to the main direction within a certain radius with the key point as the center of the circle, so that the key point has rotation invariance. When describing, the region is divided into $4 * 4$ subregions. In each subregion, the gradient histogram of 8 directions is used to make statistics. From this, a descriptor

of $4 * 4 * 8 = 128$ dimension is formed. We call this descriptor of 128 dimensions a SIFT descriptor.

After extracting SIFT feature points, in order to determine whether a sample in the tracking sample set is the same target as the football detected in the current frame, this paper uses the matching degree of the two to measure, that is, matching degree. Assuming that the tracking sample M_i^k has N_1 SIFT feature points and the target detected in the $k + 1$ frame image has N_2 SIFT feature points. The matching point pair of the SIFT features is N, and the matching degree rate is calculated according to the following formula:

$$\text{Rate} = \frac{N}{\max\{N_1, N_2\}}. \tag{16}$$

According to whether the matching degree is greater than the matching threshold T_R, the current detection target and the corresponding sample are tracked for the same target. Dice similarity coefficient calculation formula is as follows:

$$\text{DICE} = \frac{2|\text{SEG} \cap \text{GT}|}{|\text{SEG}| + |\text{GT}|},$$

$$y = \alpha W y + \beta_1 X - W \beta_2 X + \varepsilon, \tag{17}$$

$$\ln g \, dp_{it} = a_0 + a_1 \, du * dt + \sum_{i=1}^{N} b_j X u + \varepsilon_u.$$

Video coefficient calculation formula is as follows:

$$\text{SEN} = \frac{|\text{SEG} \cap \text{GT}|}{\text{GT}},$$

$$l_{\text{ssim}} = 1 - \frac{(2\mu_x \mu_y + C_1)(2\sigma_{xy} + C_2)}{(\mu_x^2 + \mu_y^2 + C_1)(\sigma_x^2 + \sigma_y^2 + C_2)}, \tag{18}$$

$$\psi = \sum_{x=1}^{\theta} V x = \sum_{x=1}^{\vartheta} \left(\frac{W x}{\sum_1^n W_{\mathfrak{F}}} S x \right).$$

VOE coefficient calculation formula is as follows:

$$\text{VOE} = 1 - \frac{|\text{SEG} \cap \text{GT}|}{|\text{SEG} \cup \text{GT}|},$$

$$U_2 = \begin{cases} s - p_1 - k x_2, \\ x - p_2 - k(1 - x_2). \end{cases} \tag{19}$$

RVD coefficient calculation formula is as follows:

$$\text{RVD} = 100\% \times \left(1 - \frac{|\text{SEG}| - |\text{GT}|}{|\text{GT}|} \right). \tag{20}$$

When Dice, Jaccard, and SEN are close to 1, it means that the segmentation result is closer to the expert annotated image; when RVD and VOE are close to 0, it means that the segmentation error is small or there is basically no segmentation error. Among them, Dice is used to express the similarity between the network segmentation map and the expert's annotation map, and it is a very important segmentation image evaluation coefficient.

3. Experiments

In this paper, SIFT algorithm is used to track football, but now there are many SIFT algorithm derivatives, whose performance is not inferior to SIFT algorithm, such as PCA-SIFT, GLOH, and SURF. In this paper, the performance comparison of four algorithms is given, and the reason why SIFT algorithm is chosen to track football is explained by comparison. The performance comparison results are shown in Table 2.

Because the projection matrix of each generation descriptor must have a set of representative and similar image learning in advance, the generated projection rectangle is only valid for the same type of image key descriptor. As a result, the applicability of PCA-SIFT is far less than that of SIFT algorithm, and the formation of SIFT descriptor has nothing to do with image type, which is suitable for almost all images and easy to form and develop. In GLOH algorithm, because it also uses PCA technology to reduce the dimension of the feature vector, it also needs to obtain the projection matrix through representative image learning in advance. The function of the algorithm is not strong. The time efficiency of sift-sift is slightly better than that of PCA-SIFT. In the implementation of SURF algorithm, integral image and box filter are used to approximate the Gauss Laplace transform, which leads to the loss of image details. As a result, the uniqueness of the descriptor of the neighborhood information of the interest point is much worse than that of the SIFT descriptor, which leads to the poor matching effect and the processing ability of the complex scene cannot meet the requirements. Based on the above analysis, SIFT algorithm is applied to real-time video tracking of football match.

4. Discussion

Before the simulation experiment in this paper, we need to preprocess the video frame object to enhance the image feature information. Firstly, the image is grayed, and the result is shown in Figure 1, where Figure 1(a) is the original image and Figure 1(b) is the result of graying. From Figure 1, we can see that the image information is basically preserved, but the image is dimensionality reduced from three dimensions to two dimensions.

As shown in Table 3, in this paper, we improve the traditional median filter processing, effectively save processing time, and enhance the processing results. It is helpful for image detection and tracking in the later stage of football. In this paper, we simulate and analyze the gray image with Gauss noise. The original pixels, probability output, pixel prediction, and output pixels of the three colors of red, blue, and yellow are, respectively, given in the table. It can be seen that the probability of yellow is the highest at 92%, while the original pixels, predicted pixels, and output pixels of yellow are the lowest at 280, 8%, and 390, respectively.

As can be seen from Figure 2, the improved median filter noise processing proposed can effectively restore the gray image information. Avoid noise effects during processing.

TABLE 2: Performance comparison of four algorithms.

	SIFT algorithm	PCA-SIFT algorithm	GLOH algorithm	SURF algorithm
Antiscale	Good	Preferably	Good	Commonly
Antirotation	Good	Preferably	Good	Commonly
Antilight	Commonly	Preferably	Commonly	Good
Antiaffine	Preferably	Preferably	Preferably	Commonly
Time efficiency	Commonly	Commonly	Commonly	Good
Universality	Good	Commonly	Commonly	Good

(a)

(b)

FIGURE 1: Grayscale processing. (a) Original image. (b) Grayscale image.

TABLE 3: Gaussian noise simulation and analysis of grayscale images.

Color	Raw pixels	Probability output (%)	Pixel prediction (%)	Output pixel
Red	290	85	15	450
Blue	310	77	23	420
Yellow	280	92	8	390
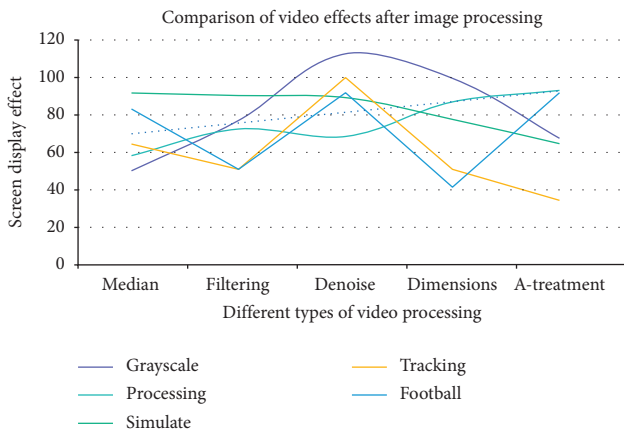
FIGURE 2: Comparison of video effects after image processing.

TABLE 4: The traditional median filter processing.

	Median	Filtering	Denoise	Dimensions	A-treatment
Grayscale	48.5	76.1	112.7	99.2	66.3
Processing	56.8	71.4	67.3	86.3	92.6
Simulate	91.2	89.8	88.6	76.7	63.4
Tracking	63.2	49.3	99.6	49.3	32.3
Football	82.4	49.3	91.3	39.5	91.3

As can be seen from Table 4, the data information is blurred after adding Gauss noise, which is disadvantageous to the subsequent image processing. Although the traditional median filter has a certain effect on noise filtering with Gauss noise image, the effect is not obvious.

As can be seen from Table 5, we use the traditional median filter to denoise and the improved median filter to denoise. The results are shown in Figure 3. Figure 3(a) is the grayscale image, Figure 3(b) is the image after adding Gauss noise, Figure 3(c) is the result of traditional median filtering, and Figure 3(d) is the result of improved median filtering in this paper.

Image binarization processing results are shown in Figure 3. It can be seen that the image after the binarization process has less data calculation and the sensitive area of the image is obviously prominent. This shows that reducing the gray level of the entire image to a two-valued dimension can

TABLE 5: Comparison of denoising effects between traditional median filter and improved median filter.

Number	Clear (%)	Carry out (%)	Accurate prediction (%)	Reliable
A	92	80	94	Y
B	89	76	72	N
C	75	74	84	Y
D	88	79	90	Y

(a)

(b)

(c)

(d)
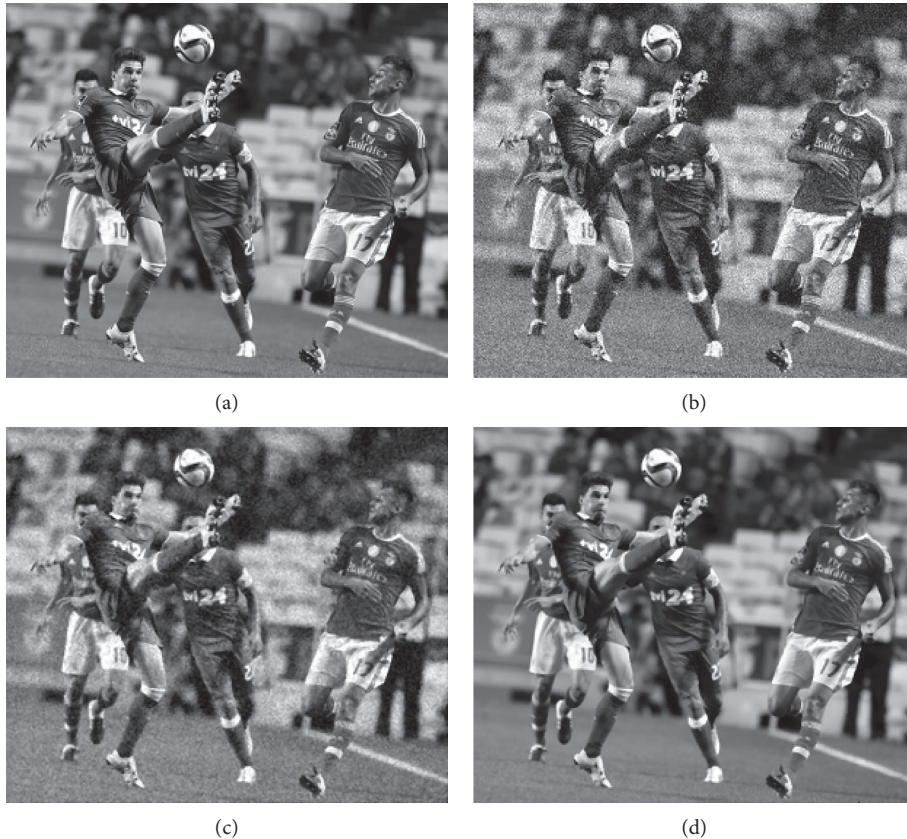
FIGURE 3: Filtering processing of grayscale image. (a) Grayscale image, (b) adding Gauss noise, (c) traditional median filtering processing, and (d) improved median filtering processing.

greatly simplify the subsequent feature extraction algorithm. The results are shown in Figure 4.

After the preprocessing results, first of all, the football detection is simulated to illustrate the performance of the proposed football detection algorithm. In this paper, Hough transform is used to detect the location of football. According to the characteristics of football, Hough transform is improved. The Hough transform before and after the improvement is used to detect football. The number of times is 100. The average comparison of the results is shown in Table 6.

As can be seen from Figure 5, based on the good performance of SIFT algorithm in feature matching, a football tracking algorithm based on SIFT feature matching is proposed, which matches the detected football with the sample football. The football tracking algorithm designed in this paper is compared with other methods such as optical flow method and background modeling method. As can be

seen from Table 7, the football tracking in video is 100 times and the average is obtained.

As can be seen from Figure 6, the tracking accuracy is 6.2% higher than that of the optical flow method and 4.8% higher than that of the background modeling method. As shown in Table 8, the tracking time is 0.57 s shorter than that of the optical flow method and 1.04 s shorter than that of the background modeling method.

As shown in Figure 7, in order to verify the effectiveness of the algorithm proposed in this paper, the method proposed in this paper is verified on the data set. As shown in Table 9, the data set contains a total of two subsets, each of which contains a training video sequence and a test video sequence.

As shown in Figure 8, the shooting scene this time is on the campus walkway, and the training video sequence is shown in Table 10, All events are normal events, each test video sequence contains one or more abnormal events, and frame level and pixel level are provided.

(a)

(b)

FIGURE 4: Binary processing after filtering. (a) Filtered result graph. (b) Binary processing result graph.

TABLE 6: Comparison of test results before and after Hough improvement.

	Football radius	Average accuracy rate (%)	Average detection time (s)
Standard Hough	11	90.1	4.1
Improved Hough	11	93.5	1.5
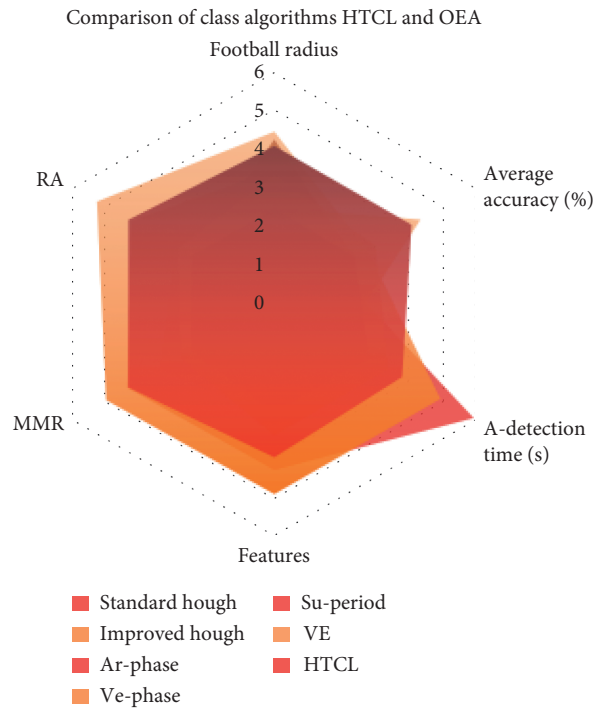
FIGURE 5: Comparison of class algorithms HTCL and OEA.

TABLE 7: Comparison and analysis of several tracking methods.

	Football radius	Average tracking accuracy (%)	Average tracking time (s)
Optical flow	11	86.7	0.78
Background modeling method	11	88.1	1.25
Method of this paper	11	92.9	0.21

The performance of the proposed football detection algorithm
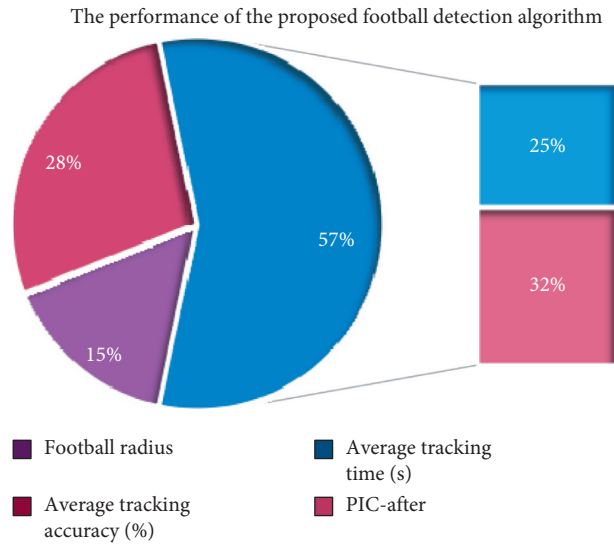
FIGURE 6: The performance of the proposed football detection algorithm.

TABLE 8: The influence of redundant information in video on computational efficiency.

Item	Algorithm proposed	Method proposed	Verified	Subsets	Video sequence
1	48.5	76.1	112.7	99.2	75.9
2	56.8	71.4	67.3	86.3	75.2
3	91.2	89.8	88.6	76.7	79.8
4	83	84.9	75.7	40	84.4
5	60	30	20	76.1	20
6	84.8	84	83.6	79.2	82.2
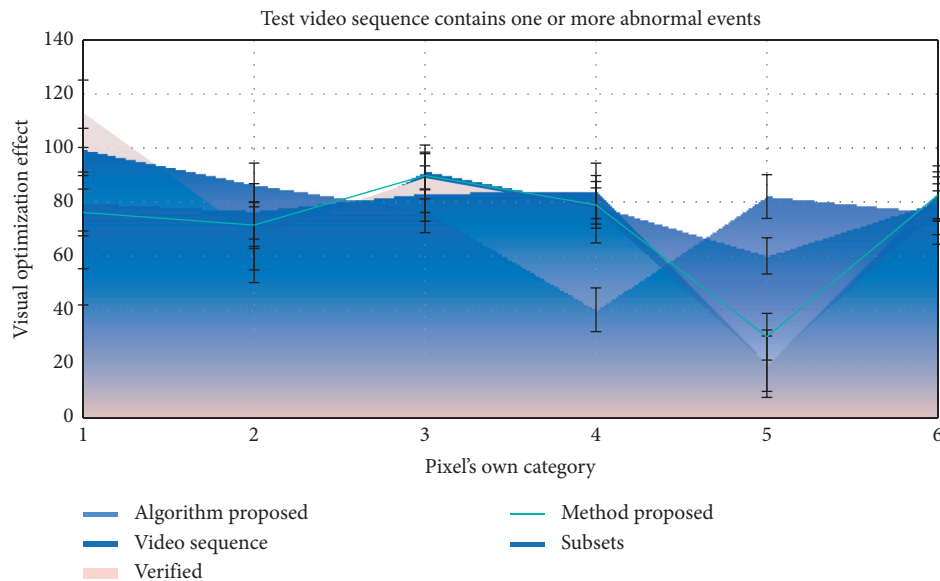
FIGURE 7: Test video sequence contains one or more abnormal events.

The test results are shown in Figure 10, and the histogram is drawn as shown in Figure 9. Combining Figures 10 and 9, we can see that the soccer tracking algorithm based on SIFT feature matching in this paper is superior to the existing optical flow method and background modeling method in both tracking accuracy and tracking time.

TABLE 9: Judge abnormalities in the region of interest in the video.

	Pic2	Genomic	Descriptive	Radiologist	Imaging
Lipoma	4.3	2.4	2	2.82	2.92
Diversity impact	2.5	4.4	2	4.18	4.3
L-conditions	3.5	1.8	3	5.45	5.41
Tumor	4.5	2.8	2	4.83	5.44
Treatment	2.9	2.98	3.45	1.2	3.38
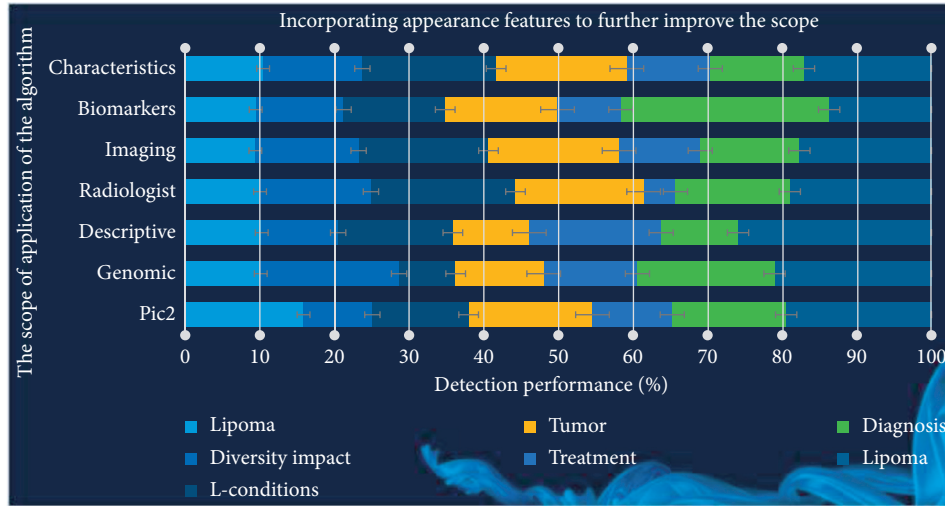
FIGURE 8: Incorporating appearance features to further improve the scope.

TABLE 10: Test results of each method on UsED2 subset.

Item	Late relapse	Patient survival rate	Early relapse patients	Lipoma patients	Ablation therapy
Early	4.3	2.4	2	3.7	3.4
Timely	2.5	4.4	2	5.6	6.5
Improve	3.5	1.8	3	6.4	3.4
Effective	4.5	2.8	5	4.3	9.2
Predict	5.9	2.6	6.4	1.9	3.7
Relapse	3.8	4.6	2.6	9.2	6.21
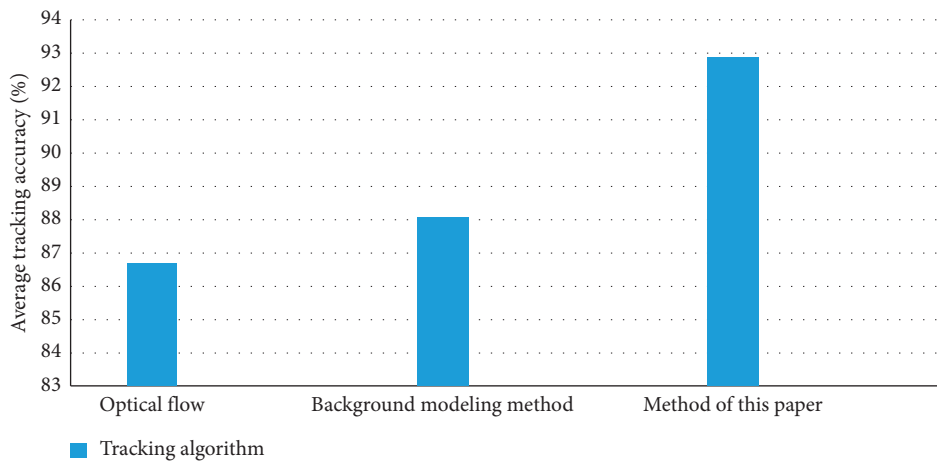
(a)

FIGURE 9: Continued.

(b)
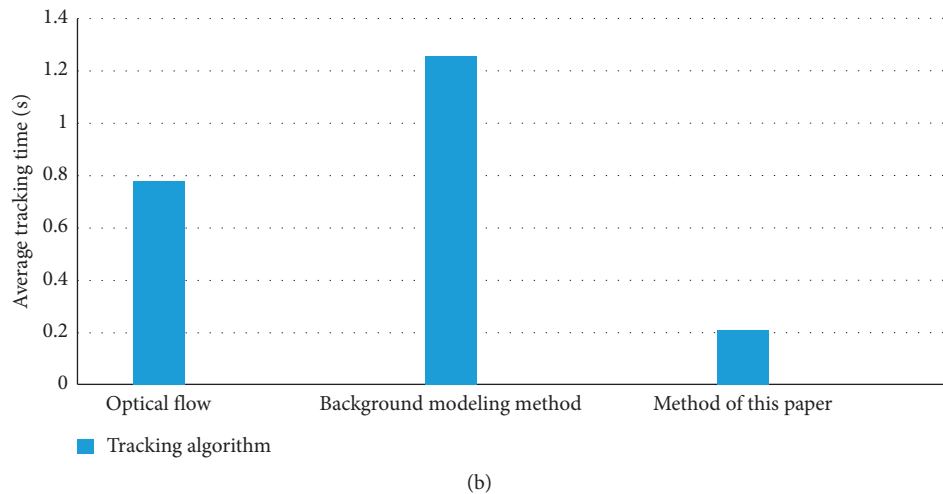
Figure 9: Bar graph of comparative analysis of several tracking methods.

Test results of each method on the subset
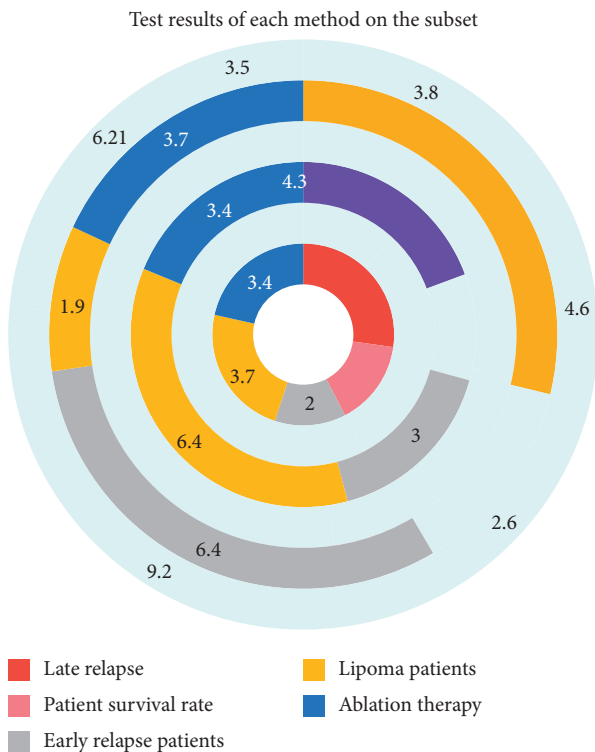
Figure 10: Test results of each method on the subset.

5. Conclusions

With the rapid development of multimedia information, the research on video data processing has higher theoretical significance and commercial value. This paper takes the most watched football video among sports videos as the analysis object. The football detection and tracking algorithm in football video is studied, and the football video image is analyzed in real time. In order to achieve enhanced display of mobile devices based on real-time image analysis, this paper designs a football detection method based on improved

Hough changes and a method based on SIFT features after preprocessing the image gray image denoising and image binarization. In the simulation experiment, image pre-processing, football detection, and football tracking were analyzed, respectively. The results show the effectiveness and superiority of the improved Hough change football detection method and the football tracking algorithm based on SIFT feature matching. This also shows that the proposed football detection and tracking algorithm is suitable for real-time football monitoring and tracking [22].

Data Availability

No data were used to support this study.

Conflicts of Interest

The authors declare that they do not have conflicts of interest.

References

[1] Y. Lu and S. An, "Research on sports video detection technology motion 3 D reconstruction based on hidden Markov model," *Cluster Computing*, vol. 23, no. 3, pp. 1899–1909, 2020.

[2] M. Qi, Y. Wang, A. Li, and J. Luo, "Sports video captioning via attentive motion representation and group relationship modeling," *IEEE Transactions on Circuits and Systems for Video Technology*, vol. 30, no. 8, pp. 2617–2633, 2020.

[3] H. Okajima, S. Hashitsume, R. Oishi, and T. Miyahara, "Reconstruction of sports competition video using fixed camera based on receding horizon strategy," *Transactions of the Society of Instrument and Control Engineers*, vol. 55, no. 2, pp. 135–143, 2019.

[4] P. J. C. Adachi and T. Willoughby, "Does playing sports video games predict increased involvement in real-life sports over several years among older adolescents and emerging adults?" *Journal of Youth & Adolescence*, vol. 45, no. 2, pp. 1–11, 2016.

[5] S. Liu, J. Chen, C.-H. Chang, and Y. Ai, "A new accurate and fast homography computation algorithm for sports and traffic

video analysis," *IEEE Transactions on Circuits and Systems for Video Technology*, vol. 28, no. 10, pp. 2993–3006, 2018.

[6] C. X. Guo, K. Sartipi, R. C. Dutoit et al., "Resource-aware large-scale cooperative three-dimensional mapping using multiple mobile devices," *IEEE Transactions on Robotics*, vol. 34, no. 5, pp. 1349–1369, 2018.

[7] M. Hirsch, C. Mateos, and A. Zunino, "Augmenting computing capabilities at the edge by jointly exploiting mobile devices: a survey," *Future Generation Computer Systems*, vol. 88, pp. 644–662, 2018.

[8] A. R. G. Harwood and A. J. Revell, "Interactive flow simulation using tegra-powered mobile devices," *Advances in Engineering Software*, vol. 115, pp. 363–373, 2018.

[9] D. Liang, Y. Liu, Q. Huang, and W. Gao, "A scheme for ball detection and tracking in broadcast soccer video," *Advances in Multimedia Information Processing—PCM 2005*, vol. 3767, no. 2, pp. 864–875, 2005.

[10] X. Qian, H. Wang, G. Liu, and X. Hou, "HMM based soccer video event detection using enhanced mid-level semantic," *Multimedia Tools and Applications*, vol. 60, no. 1, pp. 233–255, 2012.

[11] Y. Yin, Q. Li, L. Xie, S. Yi, E. Novak, and S. Lu, "CamK: camera-based keystroke detection and localization for small mobile devices," *IEEE Transactions on Mobile Computing*, vol. 17, no. 10, pp. 2236–2251, 2018.

[12] D. Wang, S. Huang, G. Feng, and S. Wang, "Perceptual differential energy watermarking for H.264/AVC," *Multimedia Tools and Applications*, vol. 60, no. 3, pp. 537–550, 2012.

[13] S. Deivalakshmi and P. Palanisamy, "Removal of high density salt and pepper noise through improved tolerance based selective arithmetic mean filtering with wavelet thresholding," *AEU—International Journal of Electronics and Communications*, vol. 70, no. 6, pp. 757–776, 2016.

[14] S. Gan, S. Wang, Y. Chen, X. Chen, and K. Xiang, "Separation of simultaneous sources using a structural-oriented median filter in the flattened dimension," *Computers & Geosciences*, vol. 86, pp. 46–54, 2016.

[15] J. Lee, S. Kang, J. Lee, D. Shin, D. Han, and H.-J. Yoo, "The hardware and algorithm co-design for energy-efficient DNN processor on edge/mobile devices," *IEEE Transactions on Circuits and Systems I: Regular Papers*, vol. 67, no. 10, pp. 3458–3470, 2020.

[16] K. Mullan and J. Wajcman, "Have mobile devices changed working patterns in the 21st century? a time-diary analysis of work extension in the UK," *Work, Employment and Society*, vol. 33, no. 1, pp. 3–20, 2019.

[17] S. Roy, D. Bhattacharyya, S. K. Bandyopadhyay, and T.-H. Kim, "An improved brain MR image binarization method as a preprocessing for abnormality detection and features extraction," *Frontiers of Computer Science*, vol. 11, no. 4, pp. 717–727, 2017.

[18] E. Ozturk, "Students' expectations from mobile devices for mobile learning," *International Journal of Mobile Communications*, vol. 17, no. 4, pp. 409–421, 2019.

[19] B. Philip Townsend, "Enhancing professional learning through mobile devices for pre-service teachers in remote communities: an aboriginal and torres strait islander example," *International Journal of Mobile and Blended Learning*, vol. 10, no. 4, pp. 13–31, 2018.

[20] Y. Liu, "Study on vehicle accident avoidance system using kinect depth sensor along with notifications on mobile devices," *International Journal of Computational Intelligence Research*, vol. 14, no. 11, pp. 941–949, 2018.

[21] D. Paor, "Using mobile devices to facilitate student questioning in a large undergraduate science class," *International Journal of Mobile & Blended Learning*, vol. 10, no. 1, pp. 1–14, 2018.

[22] J. M. Jimenez, J. R. Diaz, J. Lloret, and O. Romero, "MHCP: multimedia hybrid cloud computing protocol and architecture for mobile devices," *IEEE Network*, vol. 33, no. 1, pp. 106–112, 2019.

Research Article

Innovative Design of Intangible Cultural Heritage Elements in Fashion Design Based on Interactive Evolutionary Computation

Qi Xu, Hubin Liu [iD], Yulong Liu, and Shan Wu

Graduate School, Sejong University, Seoul 05006, Republic of Korea

Correspondence should be addressed to Hubin Liu; hb.liu@baiyunu.edu.cn

The application of intangible cultural heritage cultural elements and traditional crafts in modern design, especially in modern fashion design, is not to flatter the public but to integrate the artistic language of intangible cultural heritage into modern fashion on the basis of deeply understanding the connotation of intangible cultural heritage and mastering its traditional crafts, so as to meet people's demand for fashion and aesthetics. It can also promote the inheritance and development of traditional intangible cultural heritage culture and technology. The purpose of this study is to analyze the intangible cultural heritage elements in the innovative design of fashion design by using interactive evolutionary computation. According to the composition characteristics of cultural elements, this research uses interactive evolutionary calculation to analyze the current status of intangible cultural heritage elements in clothing design. Then, 30 fashion designers are selected to evaluate the design situation and judge the effect of the method on the design. The results show that the neural network has evaluated 36 generations, that is, 256 times of moderate value. Compared with the general IGA algorithm, adding neural network IGA can reduce the fatigue caused by user reference score and improve the quality of the optimal solution, and the cultural image attributes whose perception frequency is more than 50% are favored. It is concluded that the research method in the intangible cultural heritage elements in fashion design can improve user satisfaction and the effect is good. This research contributes to the application of intelligent algorithm in the field of fashion design.

1. Introduction

Our country has a long history and has created brilliant civilization and culture. Among them, the intangible heritage culture is the essence culture left by our ancestors. It is a priceless treasure. It has attracted the attention of all sectors of society, and the protection and inheritance of intangible heritage culture have become a social consensus. Faced with this kind of cultural heritage resources with artistic characteristics, it is favored by fashion designers when it is applied in modern fashion design and becomes the creative source of clothing design. In order to make the intangible cultural heritage cultural elements or traditional crafts perfectly combined with modern clothing design, it is necessary to grasp the intangible cultural heritage technology and flexibly use it in the clothing design process, so that the intangible cultural heritage elements can shine

brilliantly in the modern clothing design, pay homage to and inherit the traditional culture, and let the humanistic feelings and exquisite skills of the intangible cultural heritage re-radiate infinite vitality and vitality.

Interactive evolutionary computing is developed from evolutionary computing, which is an evolutionary computing method based on human subjective evaluation to get the fitness of evolutionary individuals. It combines human intelligent evaluation with evolutionary computing organically, breaking through the limitation of establishing explicit performance indicators of optimized systems, and greatly expands the application scope of evolutionary computing. Interactive evolutionary computing has been widely used in graphic art and animation, facial image generation, optimization control, virtual reality, and so on. The use of traditional cultural elements, to a large extent, is conducive to the promotion of China's excellent traditional

culture, and the continuous innovation research in fashion design is conducive to the realization of cultural innovation and the rapid development of the fashion design industry.

In the research of the combination of fashion design and intelligent algorithm, Zhu et al. proposed an interactive fashion design method and a personalized virtual display system with the real face of users. Taking suit as an example, they analyzed a customer interaction fashion design method based on genetic engineering. Therefore, customers can rearrange the style elements of clothing, choose available colors and fabrics, and put forward their own personalized suit style. At the same time, based on unity3d and VR technology, they developed a web 3D customization prototype system for personalized clothing. Combined with the system flow, the system gives the structure and function layout of the system. The test of the prototype system shows that the system can truly show the effect of clothing fabrics and provide an effective visual and customized experience for users. Their method is not stable [1]. Yamashita and Arakawa proposed a color matching method considering the brightness contrast and design characteristics of adjacent regions. Their method also allocates color components from color combination samples to achieve the optimal color design for normal people. They used interactive evolutionary computation to design the brightness and color so that the brightness and color components are properly allocated to each region according to the subjective judgment of human beings. Here, they first designed the brightness and then specified the color component to keep the brightness unchanged. Because they used fine color combination samples, the color design was fine and harmonious. Computer simulation verifies the high performance of the system. Their method is not practical [2]. Taking cultural heritage as the breakthrough point, Yen and Hsu extracted relevant cultural image elements from traditional handicraft, tinware, and integrated with product design through knowledge integration, which promoted the transformation and upgrading of the local tin culture industry. Leong and Clark put forward a framework for the study of cultural product design. The cultural space is divided into three layers, the outer layer is the visible culture, the middle layer is the behavioral culture, and the inner layer is the intangible culture, forming a new perspective of cultural design research. Their method is imprecise [3].

This study first introduces the principle of interactive evolutionary computing and then describes the basic characteristics and components of fashion design in detail, including three features and four elements. The main algorithms of this study are interactive evolutionary computation, the composition characteristics of cultural elements, and behavioral interactive product design. In this study, 30 fashion designers were selected to investigate the design effect of intangible cultural heritage elements in this research method. Based on the experimental results, this paper conducts interactive evolutionary computing design analysis, nonheritage element cultural image attribute classification analysis, nonheritage element interactive evolutionary algorithm clothing design analysis, and interactive evolutionary algorithm evaluation analysis of

clothing design effects. The conclusion is that the interactive evolutionary calculation in this study has a good effect on the clothing design of intangible cultural heritage elements, and many users prefer it to create a new development direction for the field of fashion design.

2. Interactive Evolutionary Computation and Clothing Design of Intangible Cultural Heritage Elements

2.1. Principles of Interactive Evolutionary Computing.
Interactive evolutionary computation is proposed mainly on the basis of genetics, which includes selection, crossover, mutation, and other typical genetic operations. The main difference is that interactive evolutionary computation combines genetic algorithm with human subjective evaluation and replaces selection operation in genetic operation with human subjective evaluation [4, 5]. Figure 1 shows GA and IEC evolution strategy.

Looking at Figure 1, we can see that the evolutionary strategy of interactive evolutionary computing is roughly similar to genetic algorithm. The difference is that there is no quantitative calculation of fitness function and selection operation in IEC. Instead, there is a human-computer interface and the user himself, which is equivalent to replacing the machine's function of fitness calculation with human's subjective judgment. Users of IEC do not directly judge the prototype of EC individuals but judge the output of the system described by EC individuals; that is to say, they are not directly exposed to the coefficients, but the images or sounds obtained by inputting the coefficients. In this way, users can combine their own preferences and emotions to select the satisfied generation as the father of evolution, and at the same time, they can also timely judge whether they have obtained satisfactory output results, so as to terminate the evolution operation [6, 7].

2.2. Basic Characteristics of Fashion Design

2.2.1. Two-Dimensional Features.
The two-dimensional characteristics of fashion design are explained from the plane and outline. Clothing vision expresses the two-dimensional characteristics of clothing vision through the plane drawing or effect drawing and the most intuitive outline. Clothing silhouette is the reference frame of clothing vision. The clothing visual display in the paper magazine posters, the clothing visual display in the window and on the stage, and the clothing visual display on the electronic screen and other media all show the two-dimensional characteristics of clothing vision. What needs to be explained here is that when the clothing is placed on the stationary stage, although it is a three-dimensional form of clothing, because of the human visual function, only one plane can be seen. Therefore, it is very intuitive to convey the two-dimensional characteristics of clothing [8].

In the early stage of fashion design, the effect drawing and style drawing fully reflect the two-dimensional plane of clothing vision. Through the clothing effect drawing and the
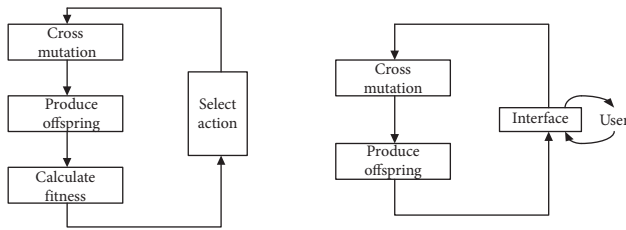
FIGURE 1: Evolution strategy of GA and IEC.

clothing style drawing, we can clearly convey the clothing design idea and the design goal to the pattern maker, the sample clothing teacher, and the tailor. In the promotion of clothing and expression of creativity, the clothing plan is the most direct, prepared, and rapid communication tool [9, 10].

2.2.2. 3D Features. Clothing presents a three-dimensional form of clothing vision on the human body. From the front, the human body image is a symmetrical body centered on the central axis, and from the side, it is an asymmetric body. Because human is an active living body, so the body position changes when walking, which makes the visual effect of clothing different. First of all, there are many differences in human activities based on the speed, direction, and form of movement. For example, there are large-scale running movements, gentle walking movements, and so on. When people are still, their shoulders, hips and waist, legs, and so on form a clear silhouette; when people are in motion, the shoulders, hips and waist, legs, and so on twist with the human body, which makes the clothing silhouette change. There is a close relationship between clothing materials and human body. When people move, the power and gravity of human body and the gravity of clothing materials produce different visual effects [11, 12].

2.2.3. Comfort Features. Clothing is used by people in daily life, so clothing will change with the dynamic of human body. People's pursuit of clothing comfort and design is increasing. The dynamic characteristics of clothing are shown in the exhibition activities of fashion models in the field (such as runway and daily walking) through the human body movement. At the same time, with the development of science and technology, clothing through the new media technology can also be very good performance of its dynamic characteristics. The dynamic of clothing reflects the comfort of human body and clothing. Clothing is the second skin of human beings. It should be comfortable to wear on the human body. If it is not comfortable, it is very practical. The dynamic characteristics of clothing vision are explained from the aspects of fitness and comfort [13, 14].

2.3. Elements of Fashion Design

2.3.1. Modeling Elements. Silhouette is the silhouette of the garment's external shape and the abstract expression of the overall shape of the garment. The outer contour of the garment reflects the fashion style and design concept. This paper introduces five types of profile: *H*, *x*, *a*, *V*, and *s*. The silhouette of clothing not only reflects the style of clothing but also highlights the beauty of the human body. In particular, the shoulder, waist, and buttocks, these parts for decoration and emphasis, can bring a lot of different aesthetic feeling. The style of clothing plays a decisive role in the visual perception of clothing [15].

2.3.2. Color Elements. Color is the visual feeling that light stimulates human eyes. Generally, it involves three fields: the physical field of light, the physiological field of visual organ, and the psychological field of spirit. The color element in fashion vision is one of the important factors in fashion design. The color of a dress first stimulates the human visual nerve. Fashion designers will express different psychological feelings when using different colors for combination and collocation. Color itself has no emotional meaning defined by human beings. It is because of the ideological activities caused by human visual senses that give color meaning. People's imagination and sensibility give color emotional meaning [16].

Color itself does not show beauty and ugliness; each color has its own certain beauty. Only when the colors are well matched and the proportional relationship between colors and colors are handled well, can the beauty of harmony be achieved. Different colors bring different visual feelings to people, which makes people have various feelings and edifies people's sentiment. Different colors make people have different emotions, thus causing changes in people's hearts [17, 18].

2.3.3. Pattern Elements. Pattern element is an important factor that cannot be ignored in fashion visual design, and it is the basic medium to convey emotion and culture. Clothing is a combination of practicality and artistry. Practicability is the basic demand of people to wear clothing. It is important to create a comfortable visual image. Therefore, the decorative pattern design, profile design, fabric pattern design, and accessories design of clothing belong to the category of clothing pattern. That is to say, the local pattern of clothing is the pattern, and the whole outline formed by the local pattern and other elements is also the pattern [19].

Pattern is a decorative art. Pattern elements are not independent art but attached to the object of clothing, which can show its artistry. Therefore, the pattern design in fashion visual design must be targeted. The artistry of the pattern is shown in the novel pattern design, which enables people to fully enjoy the visual and psychological aspects while wearing clothes. Patterns are closely related to people's daily life [20, 21].

2.3.4. Material Elements. Fabric is the material that reflects the main characteristics of clothing and is the carrier of clothing design concept put into practice. Clothing material is the material basis of clothing, which is the material carrier of clothing color, pattern, and style. With the development of textile technology, clothing material as a component of

clothing is also developing rapidly. Clothing materials play a decisive role in the style expression and quality of clothing vision. The softness, thickness, stiffness, and weight of clothing material elements play an important role in clothing visual perception [22].

Using different clothing materials, the three-dimensional and weight sense of clothing is also different. In the clothing material elements, the fabric with good shape retention will keep the fabric shape in a good state. Fabric with poor shape retention may lead to irregular edges, unexpected wrinkles, offsets, waves, and so on. Deformability refers to the deformation of clothing fabric under the condition of receiving external force [23].

2.4. Interactive Evolutionary Computing

2.4.1. Select Action. Selection operation is to select which individuals can survive or which individuals can be produced to generation so that their genes are retained in the population. The selection operation is based on the fitness evaluation of individuals in a population. The general practice is that the higher the fitness of individuals, the greater the probability of being selected to produce the next generation. At present, the commonly used selection operators include the fitness ratio method, best individual preservation method, and sorting selection method. In this paper, the fitness ratio method is used to preserve the best individual. In this method, the selection probability of each individual is proportional to the fitness function value, and the best individual is directly copied to the next generation without crossover and mutation [24, 25].

2.4.2. Cross Operation. In nature, higher organisms often achieve gene exchange through crossing. After crossing, the offspring will mix the characteristics of their parents. The purpose of crossover is to create new individuals with parental advantages. However, it is not possible to eliminate the defects by natural selection at the same time. In practice, mating methods mainly include single point crossing, double point crossing, multipoint crossing, uniform crossing, and arithmetic crossing. In this paper, a two-point arithmetic crossover operation in accordance with real code is adopted. Let chromosome $X_1^t = (x_{11}, x_{12}, ..., x_{1t})$, $X_2^t = (x_{21}, x_{22}, ..., x_{2t})$ perform two-point arithmetic crossover between the two randomly generated crossover sites i, j to produce the next generation

$$X_1^{t+1} = \left(x_{11}, \ldots, x'_{1i}, \ldots, x'_{1j}, \ldots, x_{1t} \right),$$
$$X_2^{t+1} = \left(x_{21}, \ldots, x'_{2i}, \ldots, x'_{2j}, \ldots, x_{2t} \right). \tag{1}$$

The gene $x'_{1k} (i \leq k \leq j)$ in vector X_1^{t+1} is obtained by the following linear combination:

$$x'_{1k} = ax'_{1k} + (1 - a)x'_{2k}. \tag{2}$$

The gene $x^{2k} (i \leq k \leq j)$ in vector X_2^{t+1} is obtained by the following linear combination:

$$x'_{2k} = ax'_{2k} + (1 - a)x'_{1k}. \tag{3}$$

Here, a is a parameter from 0 to 1.

2.5. Composition Characteristics of Cultural Elements.
Identifying the characteristics of cultural elements is an important research content in the study of culture and product design. In the integration process of a cultural concept, a variety of cultural elements are focused. These elements work together to make the culture present colorful light. Moreover, cultural elements can be further divided into cultural components or specific cultural element characteristics. There are two concepts in a component: if the component does not contain cultural elements, then it is a noncultural component; if the component contains cultural elements, it is a smaller feature element.

Cultural image elements are C_e and noncultural image elements are U_e:

$$C_e = \{C_E, U_E\}, \tag{4}$$

where C_E, U_E is a collection of cultural and noncultural components.

$$C_E = \{C_{e1}, C_{e2}, C_{e3}, \ldots, C_{ei}; i \geq 0\},$$
$$U_E = \{U_{e1}, U_{e2}, U_{e3}, \ldots, U_{ej}; j \geq 0\}. \tag{5}$$

2.6. Behavioral Interaction Product Design

2.6.1. Establishment of Matrix. The relationship between the explicit semantic features of cultural image clock and behavioral pragmatics is obtained and the correlation matrix R_1 is established

$$R_1 = \frac{D_1, D_2, \ldots, D_n}{\begin{bmatrix} C_1: r_{11}, r_{12}, \ldots, r_{1n} \\ C_2: r_{21}, r_{22}, \ldots, r_{2n} \\ \cdots\cdots \\ C_m: r_{m1}, r_{m2}, \ldots, r_{mn} \end{bmatrix}}. \tag{6}$$

The relationship between the implicit semantic features of cultural image clock and behavioral pragmatics is obtained, and the correlation matrix R_2 is established

$$R_2 = \frac{P_1, P_2, \ldots, P_k}{\begin{bmatrix} D_1: r_{11}, r_{12}, \ldots, r_{1k} \\ D_2: r_{21}, r_{22}, \ldots, r_{2k} \\ \cdots\cdots \\ D_m: r_{m1}, r_{m2}, \ldots, r_{mk} \end{bmatrix}}. \tag{7}$$

The relationship between explicit semantic features and implicit semantic features of cultural image clock is obtained by multiplying two incidence matrices:

$$R = R_1 \cdot R_2,$$

$$R = \frac{P_1, P_2, \ldots, P_k}{\begin{bmatrix} C_1: r_{11}, r_{12}, \ldots, r_{1k} \\ C_2: r_{21}, r_{22}, \ldots, r_{2k} \\ \cdots\cdots \\ C_m: r_{m1}, r_{m2}, \ldots, r_{mk} \end{bmatrix}}. \tag{8}$$

2.6.2. Basic Steps of Calculation. In the matrix R, an ideal sequence is found as $X(0)$, which is multiplied by the weight value of the dominant semantic features of cultural products to obtain the ideal sequence value $X'(0)$. Finally, based on the sequence $X'(0)$, each series in the matrix is calculated with grey relational degree to obtain the closest implicit semantic of cultural products. The calculation steps are as follows.

Step 1. Determine the analysis sequence.

Let the reference sequence be $Y = \{Y(k)|k = 1, 2, \Lambda, n\}$, and the comparison sequence (also called subsequence) $X_1 = \{X_1(k)|k = 1, 2, \Lambda, n\}, i = 1, 2, \Lambda, m$.

Step 2. Determine the variable

$$x_1(k) = \frac{X_1(k)}{X_1(l)}, \quad k = 1, 2, \Lambda, n; i = 0, 1, 2, \Lambda, m. \tag{9}$$

Step 3. Calculate the correlation coefficient

The correlation coefficient of $x_0(k), x_1(k)$ is as follows:

$$\zeta_1(k) = \frac{\min_i \min_k |y(k) - x_i(k)| + \rho \max_i \max_k |y(k) - x_i(k)|}{|y(k) - x_i(k)| + \rho \max_i \max_k |y(k) - x_i(k)|}, \tag{10}$$

$\Delta_i(k) = |y(k) - x_i(k)|$, then

$$\xi_1(k) = \frac{\min_i \min_k \Delta_i k + \rho \max_i \max_k \Delta_i k}{\Delta_i k + \rho \max_i \max_k \Delta_i k}. \tag{11}$$

$\rho \in (0, \infty)$, p is called the resolution coefficient. The smaller the value of P, the greater the recognition power. Generally, the value range of P is $(0, 1)$, and the specific value can be set according to the research environment and situation at that time. In general, the researcher will take the value of P as 0.5.

Step 4. Calculate the correlation degree.
The formula of correlation degree is as follows:

$$r_i = \frac{1}{n} \sum_{k=1}^{n} \xi_i(k), \quad k = 1, 2, \Lambda, n. \tag{12}$$

3. Clothing Design Model Based on Interactive Evolutionary Computation

3.1. Experimental Sample Data. This questionnaire invited 30 fashion design students or designers to carry out the experiment, including 13 girls and 17 boys, whose age range is 20–34 years old. The data were collected by the combination of mobile network questionnaire and field test questionnaire. 30 questionnaires were sent out and 30 valid questionnaires were recovered. After collecting the questionnaire, the data were processed by statistical method to obtain the relevance matrix between the explicit semantic features of clothing culture and behavior pragmatics.

3.2. Control Parameter Setting. Interactive IGA is a search algorithm with "generation + detection," which improves the deficiency of simple genetic algorithm that cannot find the global optimal solution, and its convergence is too early. Therefore, it is necessary to solve the problem of how to set the optimal solution and how to get into the optimal solution. The specific parameters are as follows:

(1) Population range: The number of population ranges is related to the extreme value and calculated ratio of interactive genetic algorithm. The population range is selected from 10 to 200 according to the actual situation. Large or small scale will easily cause slow calculation speed or fall into local optimum. The population size is 8 and the search algebra is 50.

(2) Crossover probability: in evolutionary process, crossover probability controls the dominant role of crossover operator and affects the frequency of crossover operation. If the crossover probability is too low, the genes will be passed to the offspring one by one. Then, the optimization crossover will lose operability, and the larger crossover will lead to a larger generation gap, and the search will be randomized.

(3) Mutation probability: Mutation operation not only improves and fills the missing genetic individuals but also reduces the convergence speed of local optimal solution. In practice, when the value of nap is large, the diversity of population is increased, but the performance mode is destroyed. If the value is too small, the effect of generating new individuals will be poor. Therefore, dynamic M can be used in the solution process. The larger the value is, the larger the search space is, and the smaller the value is, the faster the convergence is. Generally, it is suggested that the value range of nap is [0.05, 0.2], hoping to get more innovative solutions, so choose 0.1 and 0.2 to complete the optimization process of the optimal problem with good search performance.

3.3. Three Elements of Interactive Context Model of Cultural Products. Behavior subject: The object of behavior subject is mainly people who consume and experience cultural products, and its main information is composed of gender,

class, regional attribute, ideal value, lifestyle, and so on. It is the perceiver and evaluator of product behavior and cultural image behavior in the whole behavioral interaction context.

Behavior object: The object of behavior object is mainly cultural products. In this paper, the effective expression of line and middle level can be used as the attribute bridge connecting the lower level and the metaphysical level and finally constitute the expression of cultural image and artistic conception in products. In the whole context of behavior interaction, cultural products are the carrier and carrier of cultural image behavior.

Behavior environment: The objects of behavior environment are mainly the technology of cultural products, the environment of behavior experience atmosphere, and so on. The main distribution refers to the experience environment and popular trend atmosphere distributed in specific time and space. In the whole interaction situation, it is the constraint condition that makes the behavior subject and behavior object behave more fully and concretely.

3.4. Interactive Evolutionary Computing Analysis

(1) IEC integrates EC's global convergence ability and human's subjective judgment. In the process of global convergence, human's subjective judgment is added. According to the output of virtual character's expression, whether it needs to continue to evolve forward is judged, and then the particles are operated appropriately. The user decides to leave the particles with high fitness, eliminate the particles with low fitness, and continue to evolve. Therefore, it can guarantee the evolution from a relatively good position every time.

(2) Due to the need for subjective judgment in the evolution process, users will inevitably produce preference and emotional fluctuations in the IEC process. Fortunately, evolutionary computing is very robust to noise, so the emotional fluctuations from users have little effect on interactive evolutionary computation.

(3) IEC has a strong global optimization capability because the outputs that users cannot distinguish will be considered psychologically the same. IEC's global optimization capability is not limited to a point, but a scope of general future evolutionary computation.

4. Intangible Cultural Heritage Elements of Interactive Evolutionary Computation in Fashion Design

4.1. Interactive Evolutionary Computing Design

4.1.1. Training Model. Set the five fuzzy sets to 0.125, 0.25, 0.5, 0.75, and 0.875 (corresponding to the corresponding five fuzzy sets "very low," "low," "medium," "high," and "very high"). Then, you can get 25 training samples. Table 1 shows the training sample set.

Table 1: Training sample set.

Expected input		Expected output	
occFear	occHope	outFear	outHappiness
0.875	0.125	0.875	0.125
0.875	0.5	0.875	0.75
0.75	0.125	0.75	0.125
0.75	0.25	0.75	0.25
0.5	0.25	0.5	0.25
0.5	0.75	0.25	0.75
0.25	0.125	0.25	0.125

Figure 2 shows the membership function of fuzzy set in training.

Figure 3 shows the change curve of the objective function of the two learning algorithms.

It can be seen from Figures 2 and 3 that the PSO algorithm is used to train the TSK fuzzy neural network, and the changes of the fuzzy set parameters in the membership function before and after the adjustment of the two input parameters are observed. By comparing the change curves of the objective function of the two algorithms, it can be seen that the change curve of the objective function of the traditional BP algorithm is relatively gentle and has not reached the convergence when index = 120, while the PSO algorithm has a faster convergence speed and has basically converged at index = 20. Although the accuracy cannot reach the degree of the BP algorithm, it is also approximate optimal within the allowable range. The results show that the PSO algorithm is effective in interactive evolutionary computation.

4.1.2. Comparison of Algorithms. The selection probability is not set in IEC because it is based on the subjective judgment of people to determine whether the requirements of users have been met, in order to facilitate the comparison with the BP algorithm and GA algorithm. Figure 4 shows the change diagram of the objective function of the three learning algorithms.

According to the curve in Figure 4, the BP algorithm has a gentle decline and a slow convergence speed, while IEC and GA algorithms have a faster convergence speed. At the same time, it can be seen that the IEC curve is basically under the EC curve, which shows that IEC not only has the ability of EC Global optimization but also has faster convergence speed than the traditional EC due to the addition of human subjective judgment in the learning process.

4.1.3. Model Interaction. After decomposing the reachability matrix, it is necessary to divide the levels. Based on the principle of reachability matrix, all the elements in the set are divided, and the hierarchical interaction diagram for explaining the structural model is obtained. Figure 5 explains the hierarchical interaction diagram of the structural model.

4.2. Classification of Cultural Image Attributes of Intangible Cultural Heritage Elements. The initial data of the tester are collected, and the software is used for statistical analysis. The
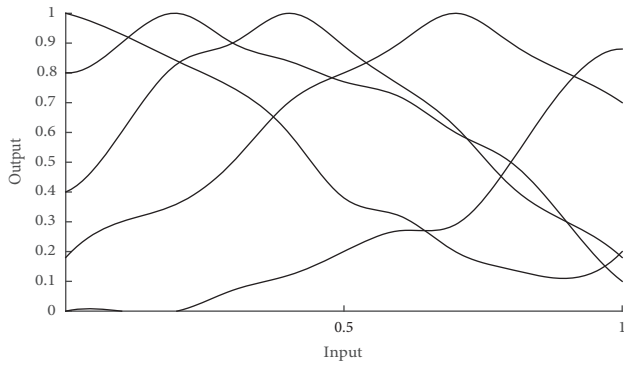
FIGURE 2: Membership function of fuzzy set in training.
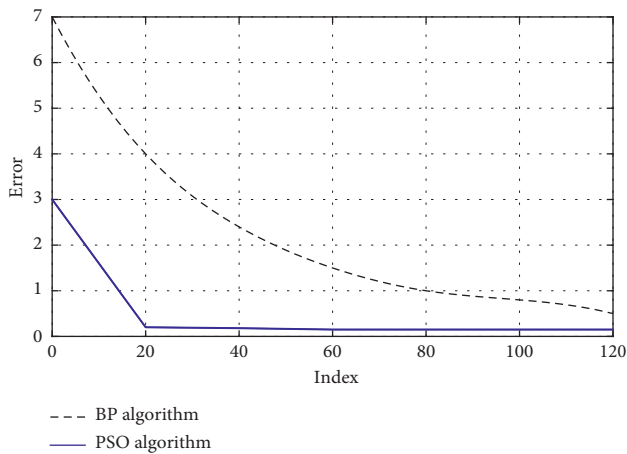
FIGURE 3: The change curve of the objective function of the two learning algorithms.
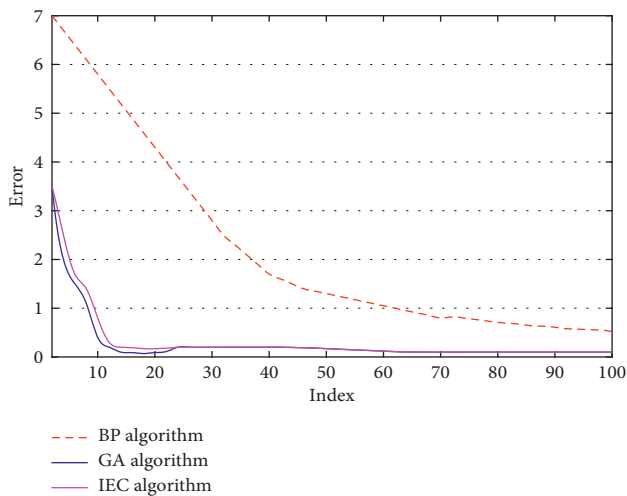
FIGURE 4: The change diagram of the objective function of the three learning algorithms.

frequency and frequency of attribute perception of the cultural image at various cultural levels are obtained from the data. It retains the cultural attribute that the frequency of perception is higher than 50. Table 2 shows the frequency and frequency of attribute perception at each cultural level.
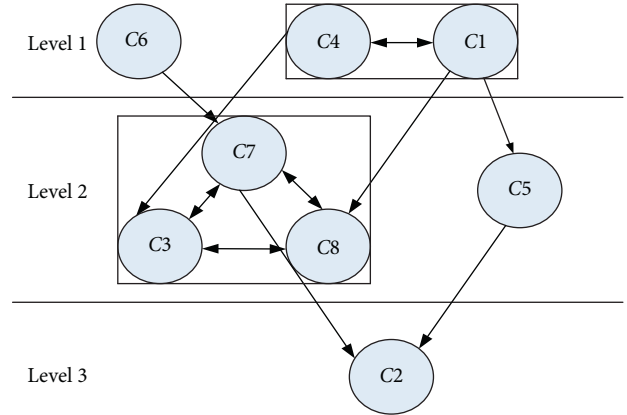
FIGURE 5: Hierarchical interaction diagram for explaining the structural model.

Figure 6 shows the number and frequency of attribute perception.

According to the results of Figure 6, the cultural image attributes with more than 50% perception frequency include the color of cultural image, the decoration of cultural image, the material of cultural image, the modeling of cultural image, and the structure of cultural image. The color of cultural image can be the unique grey-green color of Chinese bronzes, which is polished by horse stepping on flying swallow over the years; the pattern of cultural image can be the peach and longevity bat in paper-cut works; the material of cultural image can be the smooth texture of Longquan celadon. The modeling of cultural image can be the form of galloping horse in the colorful pottery figurines. Among them, the difference between cultural image modeling and image decoration is that modeling is more focused on three-dimensional and overall performance, while the decoration is more focused on plane and local performance. The structure of cultural image can be the tenon and mortise structure of Ming style official hat chair. At the middle level, the cultural image attributes with more than 50% perception frequency include the production technology of cultural image, the interactive form of cultural image, and the functional characteristics of cultural image

4.3. Clothing of Intangible Cultural Heritage Elements Based on Interactive Evolutionary Algorithm

4.3.1. Cultural Image Attribute Weight of Intangible Cultural Heritage Elements. In the study of product satisfaction, if the traditional Karnaugh model is used, the frequency of charm quality is slightly higher than that of indifference quality in the evaluation of the attribute quality of these cultural images. This result shows that most of the cultural image attributes in the design of cultural products, if properly expressed, can greatly improve product satisfaction. But in the charm quality, the designer cannot judge which attribute is more advantageous in the design process. When designing, the designer has doubts about which kind of cultural image quality is selected for product

TABLE 2: Frequency and frequency of attribute perception at different cultural levels.

Intangible cultural heritage elements	Attribute G_n	Frequency of perception	Perception frequency (%)
Form but lower level	Color G_1	33	100
	Ornamentation G_2	33	100
	Material quality G_3	31	94
	Modeling G_4	33	100
	Structure G_5	28	85
Form and middle level	Technology G_6	24	72
	Interactive G_7	21	63
	Function G_8	25	76
Metaphysical level	Customs G_9	24	72
	Emotion G_{10}	27	82
	Taste G_{11}	24	72
	Significance G_{12}	27	82
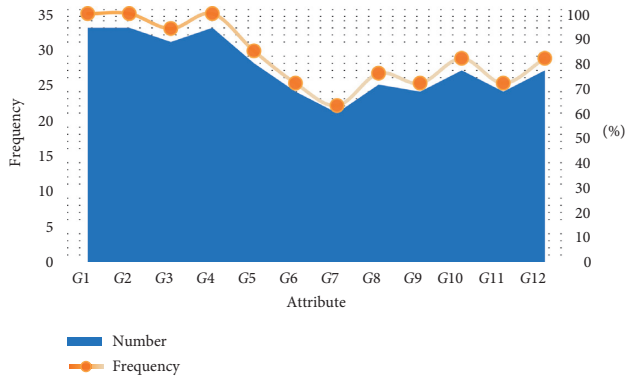
FIGURE 6: Frequency and frequency of attribute perception.

TABLE 3: Calculation results of element to improve product satisfaction.

Attribute	$\alpha = 0.4$					C-FKM model
	M	A	O	I	R	EI value
G_1	0	23	0	104	1	0.032
G_2	0	37	0	99	0	0.038
G_3	1	41	1	102	2	0.062
G_4	2	78	1	42	0	0.121
G_5	0	66	18	29	0	0.194
G_6	0	29	1	80	0	0.044
G_7	1	65	2	48	0	0.150
G_8	2	66	0	44	0	0.140
G_9	0	76	1	30	0	0.181
G_{10}	1	76	2	44	0	0.160
G_{11}	1	78	1	31	0	0.158
G_{12}	0	67	1	83	0	0.074

optimization. Table 3 shows the calculation results of the element to improve the degree of product satisfaction.

It can be seen from Table 3 that G_5 design behavior and modern design behavior are not mutually exclusive (EI = 0.193). It can be concluded that when applying cultural image attributes to product design, priority should be given to the sense of design and modernity of image attributes in the expression of these products. Instead of completely reproducing the tradition, we should integrate the attributes of the product itself and cultural image to maintain harmony. This is the core of cultural product design.

4.3.2. Factor Analysis of User Preference Image. First of all, the specific words of user preference image were removed, and 13 groups of perceptual semantics with discrimination were analyzed by factor analysis. Then, KMO and Barrett measures are used to test whether the factor model can be used. The KMO value is 0.754, greater than 0.5; according to the score results of the Bartley method, the average score is less than 0.01, so it can be considered that there is a significant correlation between variables, which is suitable for garden analysis. The correlation coefficient matrix R is used for factor analysis based on principal component analysis, and the eigenvalues and contribution values are obtained. The general extraction method of the number of common factors: according to Kaiser criterion, the cumulative contribution of eigenvalues is more than 60%, and the number

of common factors is suitable to select 2.3. Table 4 shows factor analysis characteristic contribution rate.

It can be seen from Table 4 that the cumulative contribution value of the above three common factors is 64.074%. The load matrix of the three factors is solved, and they are divided into three groups according to the load level of corresponding factors. The third factor can be selected as the third one.

4.4. Effect Evaluation of Interactive Evolution Algorithm on Fashion Design

4.4.1. Interactive Evaluation of User Preference Image. First of all, three target users are selected to train BP neural network. After the 13th generation, the accuracy error is close to 0.2, and the range is not changing. The users' cognition of watch modeling tends to be stable, so it can be automatically evaluated by computer. Therefore, it is required that the target user can carry out "automatic evaluation" after 13 generations, and the computer can simulate the user evaluation. If the user is not tired of the interactive evaluation, the interactive evaluation can be continued until the termination conditions are met. Figure 7 shows the error accuracy value and moderate value curve.

TABLE 4: Characteristic contribution rate of factor analysis.

Ingredients	Initial eigenvalue		
	Total	Variance %	Accumulate %
Dynamic	5.184	39.872	39.872
Fashionable	2.088	16.054	55.926
Simple	0.891	6.848	70.922
Novel	0.539	4.140	91.230
Delicate	0.339	2.604	93.832
Trendy	0.289	2.216	96.047
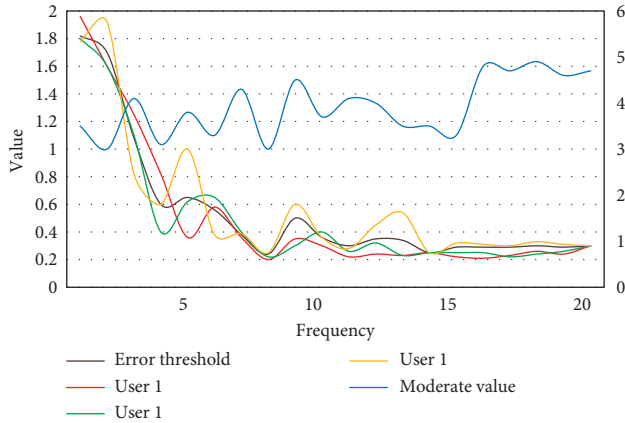
FIGURE 7: Error accuracy and moderation curve.

FIGURE 8: Schematic diagram of difference in satisfaction evaluation.

TABLE 5: Independent sample t-test of high and low groups under three levels.

Intangible cultural	Group	N	Mean	Deviation	t
Form but lower level	Low score	6	3.55	0.846	−3.370
	High score	6	5.15	0.829	
Form and middle level	Low score	6	3.12	0.900	−3.598
	High score	6	5.97	1.722	
Metaphysical level	Low score	6	3.49	0.820	−5.249
	High score	6	6.77	1.299	

It can be seen from Figure 7 that, in the process of interactive evaluation, it is found that four target users have not obtained satisfactory solutions after 29 generations on average. In order to optimize the accuracy of neural network, the incremental learning samples are expanded. It can be found that the convergence starts after the 40th generation, and the evaluation value is higher than 4.4. When the satisfaction value of watch modeling for three consecutive generations is higher than 4.4, the satisfactory solution can be considered. Compared with the general IGA algorithm, adding neural network IGA can reduce the fatigue caused by user parameter score and improve the quality of the optimal solution.

4.4.2. Satisfaction Evaluation. We can get the overall satisfaction degree trend of intangible cultural heritage elements and modern fashion. Taking the first 25% of the sample's overall satisfaction degree as the low group sample and the later 25% sample as the high group sample, the samples of the low group are S5, S2, S9, S17, S22, and S24, and the samples of the high group are S12, S1, S6, S19, S20, and S21. Figure 8 shows the difference of satisfaction evaluation.

It can be seen from Figure 8 that the t-statistics TL = −3.370, $T2 = −3.598$, and $T3 = −5.249$, P of significance probability values of the tests at the lower, middle and metaphysical levels of the samples with low and high scores is all less than 0.05, indicating that there are significant differences in the satisfaction of the high score group and the low score group at these three levels. The satisfaction of the high score group is higher than that of the low score group in these three levels. Table 5 shows the independent sample t-test of high-low grouping under three levels.

It can be seen from Table 5 that the mean of low group samples at the lower level of form is 3.55, that of middle level is 3.12, and that of metaphysical level is 3.49, indicating that there is no significant difference in product satisfaction of low score samples at these three levels. On the metaphysical level, the high score sample, mean = -6.77, is higher than that at the lower level, and the mean value of the middle level is higher; that is, the higher the satisfaction degree of the high group on the metaphysical level to the product application of traditional cultural elements, the easier the traditional cultural attribute quality at the metaphysical level to improve the product satisfaction.

5. Conclusion

With the rapid development of modern society and the continuous improvement of economic level, people are more and more pursuing the satisfaction of spiritual life, and the requirements for clothing are also higher and higher. The dichotomy and semantic analysis are used to investigate the clothing form and its perceptual vocabulary expression, and the form description evaluation method is used to explain the design modeling. Grasp the perceptual characteristics of users and reduce their cognitive differences. For the analysis of the relationship between the user's favorite image and the modeling category, the product modeling element set based

on the clothing perceptual image is cited to guide the designer's relevant clothing modeling design scheme.

On the basis of fashion design, according to the category of clothing modeling, this paper presents a method of clothing modeling optimization based on user interaction genetic algorithm platform and user image evaluation. According to the category processing of clothing modeling library, coding it, and combining with the evaluation results of semantic image, the calculation method of fitness is given. The neural network is used to simulate the evaluation of user image, and the efficient integration mode of simulating "human" perceptual knowledge is studied to realize the automatic solution of product form design scheme.

It is an important direction for the development of modern fashion design to integrate traditional pattern elements into fashion design, which reflects the strong artistry, humanity, and epochal nature in modern design, which is loved by many consumers and concerned by many designers. In modern fashion design, through the application of traditional cultural elements, clothing and culture are deeply combined, which is conducive to the inheritance and promotion of traditional culture. In the practice of fashion design, designers need to find innovative means of fashion design through continuous exploration and practice, so as to promote the vigorous development of the clothing industry. Culture and clothing promote each other, complement each other, and can progress and develop together.

Data Availability

The data that support the findings of this study are available from the corresponding author upon reasonable request.

Conflicts of Interest

The authors declare that they have no conflicts of interest.

References

[1] X.-j. Zhu, H. Lu, and M. Rätsch, "An interactive clothing design and personalized virtual display system," *Multimedia Tools and Applications*, vol. 77, no. 20, pp. 27163–27179, 2018.

[2] K. Yamashita and K. Arakawa, "A color scheme method by interactive evolutionary computing considering contrast of luminance and design property," *IEICE Transactions on Fundamentals of Electronics, Communications and Computer Sciences*, vol. E99.A, no. 11, pp. 1981–1989, 2016.

[3] H. Y. Yen and C. I. Hsu, "College student perceptions about the incorporation of cultural elements in fashion design," *Fashion and Textiles*, vol. 4, no. 1, pp. 1–16, 2017.

[4] N. A. M. Ariffin, N. A. Osri, and N. H. Salleh, "Intangible cultural heritage (ICH) of cocos malays in tawau, sabah," *Advanced Science Letters*, vol. 23, no. 7, pp. 6272–6276, 2017.

[5] C. Bortolotto, "Placing intangible cultural heritage, owNing a tradition, affirming sovereignty," *Ztschrift Für Physik D Atoms Molecules & Clusters*, vol. 29, no. 1, pp. 45–48, 2016.

[6] N. Carboni and L. De Luca, "Towards A conceptual foundation for documenting tangible and intangible elements of A cultural object," *Digital Applications in Archaeology and Cultural Heritage*, vol. 3, no. 4, pp. 108–116, 2016.

[7] J. Zhang, "Intangible cultural heritage and self-healing mechanism in Chinese culture," *Western Folklore*, vol. 76, no. 2, pp. 197–226, 2017.

[8] P. Jani and V. Hus, "Treatment of cultural heritage content in the subject social studies in primary school," *Creative Education*, vol. 9, no. 5, pp. 702–712, 2018.

[9] K. Lafrenz Samuels and Kathryn, "Introduction-new challenges for cultural heritage: supporting biodiversity in the face of climate change," *Culture, Agriculture, Food and Environment*, vol. 39, no. 2, pp. 69–71, 2017.

[10] Eun-Hee and Park, "The content analysis of clothing design part in the middle-school textbook of technology and home Economics①," *Journal of the Korea Fashion & Costume Design Association*, vol. 19, no. 3, pp. 49–61, 2017.

[11] J. H. Kim, Y. I. Kim, and Y. I. Kim, "Proposal of planning process for outsourcing the design of men's clothing," *Korean Society of Fashion Design*, vol. 19, no. 4, pp. 71–87, 2019.

[12] A. Obeidat, H. Nabawi, O. Hashem, and H. El-Said, "The impact of using interactive interior design on enhancing the performance of clothing shop," *Journal of Design Sciences and Applied Arts*, vol. 1, no. 1, pp. 146–153, 2020.

[13] B. E. Adiji and T. I. Ibiwoye, "Effects of graphics and computer aided design software on the production of embroidered clothing in south Western Nigeria," *Art and Design Review*, vol. 05, no. 4, pp. 230–240, 2017.

[14] A. Hilton, "Threads of tradition: design and meaning in Russian peasant clothing and textile arts," *Experiment*, vol. 22, no. 1, pp. 13–30, 2016.

[15] O. Shandrenko, "Echoes of oscar schlemmer's "triadic ballet" in modern clothing design," *Demiurge: Ideas, Technologies, Perspectives of Design*, vol. 3, no. 1, pp. 129–140, 2020.

[16] K. O. Kim, M. Takatera, and T. Otani, "Effects of working experience of patternmaker with a designer on the efficiency and performance of clothing design," *International Journal of Affective Engineering*, vol. 17, no. 2, pp. 67–74, 2018.

[17] J. Yan, H. Li, and X. Chen, "Application of Yangzhou freehand embroidery flower-and-bird subject in Chinese woollen clothing design," *Wool Textile Journal*, vol. 45, no. 6, pp. 48–52, 2017.

[18] Z. Xulan, Y. Lei, B. Yu et al., "Research of clothing design based on low-carbon concept," *Wool Textile Journal*, vol. 45, no. 8, pp. 58–63, 2017.

[19] M. Owczarek, A. Nawrot, M. Łukawska, A. Wereszka, Ł. Grzejszczak, and P. Mastalerz, "Nonstandard constructional solutions in contemporary clothing design," *Autex Research Journal*, vol. 16, no. 4, pp. 250–255, 2016.

[20] F. J. Galarte, "The crowns of stuzo clothing," *TSQ: Transgender Studies Quarterly*, vol. 4, no. 2, pp. 296–300, 2017.

[21] C. Dzikite, "Exploring the integration of handheld device applications in teaching and learning in textiles, clothing and design programmes in Universities in Zimbabwe," *International Journal of Costume and Fashion*, vol. 17, no. 1, pp. 1–15, 2017.

[22] S. Kuleshova, O. Zakharkevich, J. Koshevko et al., "Development of expert system based on kansei engineering to support clothing design process," *Vlakna a Textil*, vol. 24, no. 3, pp. 30–41, 2017.

[23] G. J. Ibrahim, T. A. Rashid, and A. T. Sadiq, "Improving DNA computing using evolutionary techniques," *International Journal of Advanced Computer Ence & Applications*, vol. 7, no. 3, pp. 109–121, 2016.

[24] M. Scirea, J. Togelius, P. Eklund, and S. Risi, "Affective evolutionary music composition with MetaCompose," *Genetic Programming and Evolvable Machines*, vol. 18, no. 4, pp. 433–465, 2017.

[25] S. Cheng and A. K. Dey, "I see, you design: user interface intelligent design system with eye tracking and interactive genetic algorithm," *CCF Transactions on Pervasive Computing and Interaction*, vol. 1, no. 3, pp. 224–236, 2019.

Research Article

Quantitative Evaluation of Leaf Morphology with Different Rice Genotypes Based on Image Processing

Shan Hua [ID], Minjie Xu, Zhifu Xu, and Hongbao Ye

Key Laboratory of Creative Agriculture, Ministry of Agriculture and Rural Affairs, Institute of Agricultural Equipment, Zhejiang Academy of Agricultural Sciences, Hangzhou, Zhejiang 310021, China

Correspondence should be addressed to Shan Hua; huashan@zaas.ac.cn

Prostrate growth 1 (*PROG*1) gene is vital in controlling the prostrate growth habit of rice. Studying the effect of *PROG*1 gene on rice canopy structure is crucial in elucidating the molecular mechanism of rice plant type evolution. Herein, the morphological characteristics of different rice genotypes were collected at different growth stages and leaf nodes using image processing techniques. The morphological characteristics included leaf length, leaf width, and leaf area. The image processing techniques involved boundary mean oscillation (BMO) filtering and minimum bounding rectangle extraction of the target image. On this basis, the effect of the *PROG*1 gene on rice leaf morphology was quantitatively assessed. Also, the feasibility of image processing techniques in detecting the morphological characteristics of rice leaves was discussed. Under the influence of the *PROG*1 gene, the length, width, and area of rice leaves decreased by 45.1%, 12.7%, and 44.8%, respectively, at the booting stage. Similarly, the length, width, and area of flag leaves decreased by 15.8%, 32.0%, and 33.7% at the heading stage and by 25.4%, 16.2%, and 19.7% at the filling stage, respectively, and that of secondary leaf reduced by 23.2%, 13.6%, and 54.2% at heading stage and by 24.1%, 17.3%, and 37.0% at filling stage, respectively. Furthermore, the length, width, and area of other leaves reduced by 32.3%, 9.8%, and 51.6% at the heading stage and by 28.6%, 7.3%, and 36.7% at the filling stage, respectively. The leaves in the rice canopy were shorter, narrower, and smaller in leaf area. Notably, no significant differences were found between image processing technology and manual measurement methods regarding the values of leaf morphological characteristics obtained ($P < 0.05$). Thus, these results show that image processing technology is effective in studying the morphological characteristics of rice leaves. This study provides a reliable foundation for molecular breeding studies and will guide the application of the *PROG*1 gene in molecular breeding.

1. Introduction

Rice is the largest grain crop in China in terms of production and a staple food for more than 60% of the Chinese population. At present, increasing the output of major grain crops is a top priority in China, owing to the alarming rise in population and sharp reduction of arable land. According to FAO [1], the rice yield in China mainland has increased by 121.1% since the Green Revolution in the 1960s. This can be attributed to the improvement of rice plant type [2]. Plant architecture refers to the size, shape, and orientation of the shoot components, including plant height, tiller number, leaf shape, panicle shape, and other factors. Rice plant architecture is a critical factor in rice yield [3].

Rice yield mainly depends on photosynthesis at the reproductive stage and carbohydrate accumulation in the stem before heading [4]. Dry matter production in rice after heading results from photosynthesis in the leaves, followed by temporary storage in the stems and sheaths [5]. Thus, morphological characteristics and physiological functions of rice leaf vastly affect the final yield [6]. The leaf is the main photosynthetic and respiratory organ in rice canopy and the main influencing factor of plant type. Leaf characteristics, such as leaf length, leaf width, leaf angle, leaf area, and leaf color, determine the photosynthetic efficiency per unit leaf area, thus affecting the final rice yield.

Several studies on DNA molecular marker and bioinformatics models [7–10] have relied on QTL to map genes specific for most rice traits, including yield, plant type, and

stress resistance. Among these, *TAC*1 [11] and *PROG*1 [12, 13] are related to plant type. *PROG*1 gene is located on the short arm of chromosome 7 and expressed as a Cys2-His2 zinc finger protein which controls the creeping growth of wild rice [12]. During rice evolution, a mutation in the coding region of the *PROG*1 gene resulted in the loss of gene function. This altered the rice growth habit from prostrating in the wild rice to erectile in the cultivated rice [12]. The change in rice growth habit significantly increased rice yield, suggesting that the *PROG*1 gene was vital in the evolution of rice yield. A three-dimensional structure model of rice with PROG1 gene was reconstructed using 3D digital technology in a previous study. This enabled quantitative evaluation of rice canopy structure, including tiller angle, leaf inclination angle, and leaf area index [14]. It was observed that *PROG*1 inflicted significant effects on tiller angle, leaf inclination angle, and leaf area index of rice canopy [14]. However, changes in leaf morphology, such as length, width, and leaf area at different stages and leaf nodes, have not been studied in detail.

Traditional breeders usually adopt manual measurement methods to determine the characteristics of rice plant type. These include measuring plant height, leaf length, and leaf width using a ruler and leaf angle and tiller angle using an angle meter. However, this approach is time-consuming and cannot accurately describe the characteristics of canopy structure. At present, large phenotypic data are mainly obtained through high-throughput phenotypic analysis [15]. Image processing technology is one of the most convenient and rapid digital measurement methods used to obtain phenotypic data of rice. The method mainly acquires rice phenotypic characteristics through image acquisition, image preprocessing, image segmentation, target contour recognition, and target pixel statistics [16, 17].

In this study, *Indica* varieties Teqing (TQ) and YIL18 (*O. sativa* L.) were used. TQ is a conventional *Indica* variety with excellent yield, whereas YIL18 is a variety with TQ *PROG*1 gene. TQ exhibits an erect stature, whereas YIL18 has a prostrate growth habit. Digital images of the leaves at different nodes of the two rice varieties were obtained at various growth stages, including the booting stage, heading stage, and grain filling stage. The images were preprocessed using boundary mean oscillation (BMO) filter for denoising and enhancement [18–20] and binarized with adaptive threshold [21]. The minimum bounding rectangle extraction of target and target pixel statistics were used to obtain the morphological characteristics of the leaves (leaf length, leaf width, and leaf area) from preprocessed images. Based on these data, the effect of *PROG*1 gene on leaf morphology of rice was quantitatively analyzed. In addition, the feasibility of image processing technology was discussed.

2. Materials and Methods

2.1. Experimental Materials.
Indica varieties Teqing (TQ) and YIL18 (*O. sativa* L.) were used in this study. TQ is a super high-yielding conventional *Indica* cultivar with erect plant type. It is bred in China and is an important parent of two-line hybrid rice. The YIL introgression lines used an

accession of YJCWR (*Oryza rufipogon*) from Yuanjiang, Yunnan, China (23°37′N, 102°01′ E), with a creeping growth habit as the donor and the *Indica* variety TQ with erect growth habit as the recipient [22]. The YIL18 line is one of the introgression lines that harbor two YJCWR chromosomal segments on the long arm of chromosome 3 and the short arm of chromosome 7. *PROG1* gene is located on the short arm of chromosome 7 and expresses a Cys2-His2 zinc finger protein which controls the creeping growth habit of wild rice [12]. During evolution, mutation of the *PROG*1 gene resulted in gene function loss, therefore altering the growth habit of rice from prostrate to erectile. This had a significant impact on the rice canopy structure and yield.

Field experiments were conducted from May to September of 2012 and 2013 at Shangzhuang experimental station of China Agricultural University in Beijing (40°08′N, 116°10′E). The sowing time was May 5th of each year. Seeds were propagated on a seedbed and then potted (one plant per pot) after they grew to the trifoliate stage (May 20th). The planting area of each rice variety was 30 m² with a north-south planting direction. Plant spacing was 0.20 m, and row spacing was 0.25 m. Fertilizer was adequately supplied according to the local standard of rice cultivation. Weeds were artificially removed. No pests and diseases were observed during the growth period. The canopy structure of rice was not disturbed by artificial or strong wind during the experiment period.

2.2. Acquisition of Digital Images.
Digital images of rice leaves were acquired at the booting stage (BS), heading stage (HS), and grain filling stage (FS) on July 28th, August 29th, and September 9th, respectively. Leaves from nine randomly selected plants were collected at each rice growing stage to represent the average growth condition in the field. The leaves were classified into three categories based on node position, i.e., flag leaf, secondary leaf, and other leaves. The flag leaf and secondary leaf were not collected at the booting stage; therefore, all leaves collected at this stage were classified as other leaves. Leaf area was measured using a leaf area meter (LI-3000C Portable Area Meter, LI-COR, USA). The length and width of the leaves were determined using a ruler. The leaves were then placed on a scanner (ScanMaker i800 Plus, Microtek) and covered with a transparent plate to make them flat for scanning. The gray sale scanning mode was used, and the images were saved in a TIF file format. The pixels of the captured digital images were 2400 × 3435 with a resolution of 0.01 cm/pixel.

2.3. Morphological Characteristics of Rice Leaf.
To study the leaf morphology of different rice genotypes, image processing technology was used to perform image preprocessing, minimum bounding rectangle extraction of target leaf, target leaf pixel statistics, and leaf length, leaf width, and leaf area calculations.

The digital images of rice leaves were preprocessed through image graying, image denoising and enhancement, and image segmentation. After converting color images to gray images, BMO filter was used to denoise and enhance the edges of the image using the formula below [18]:

$$Z^Q(u, x, r) = \frac{2}{9r} \sum_{k=i-1}^{i+1} \sum_{l=j-1}^{j+1} \left| u_{i,j} - \overline{u} \right|,$$

$$\overline{u} = \frac{1}{9} \sum_{k=i-1}^{i+1} \sum_{l=j-1}^{j+1} u_{i,j}, \tag{1}$$

where $Q(x, r)$ is a square neighborhood with x as the midpoint and $2r$ as side length and $u(x)$ is a function on the image plane.

After image denoising and enhancement, the Otsu threshold segmentation method was used to segment the images and obtain the binary images (Figures 1(a)–1(d)).

The leaf morphological characteristics measured from the images were leaf length, leaf width, and leaf area. Binary images were obtained after preprocessing the digital images by extracting the minimum bounding rectangle of the target leaf [23]. The length and width of the leaves were calculated by multiplying the total number of pixels in the direction of length and width in minimum bounding rectangle by the resolution (Figure 1(d)). Leaf area was the total area of pixels on the leaf. Previous studies have shown that the interannual variation does not significantly musk the effect of PROG1 gene on rice canopy structure [14]. Therefore, data on morphological characteristics from different years were averaged and presented as the final results in this study. Manual measurement results were considered as a control.

3. Results

3.1. Application of Image Processing Technology on Evaluation of Rice Leaf Morphology. Image processing technology has been extensively used in measuring plant phenotypic traits. In this study, BMO filter was used to denoise and enhance the edge of the target leaf image. Morphological characteristics of rice leaves, including leaf length, leaf width, and leaf area, were determined from binary images by calculating the minimum bounding rectangle and target leaf pixel statistics. There was no significant ($P > 0.05$) difference between image processing technology and manual measurement methods regarding the values of leaf morphological characteristics obtained from various leaf types at different growth stages (Table 1). However, the values obtained using the image processing technology were slightly lower than those obtained using the manual measurement methods.

BMO filter was accurate and stable in processing digital images of the rice leaves. However, there was a slight difference between the values obtained using image processing technology and manual measurement methods. This can be attributed to the loss of some edge information during digital image acquisition. Moreover, subjective judgment while taking manual measurements of the leaf length and width could have slightly affected the final results.

3.2. Effect of PROG1 Gene on Rice Leaf Morphology. Given that there was no significant difference in the values of morphological characteristics of rice leaves obtained using image processing technology and manual measurement

methods, this study assessed the effect of PROG1 gene on rice leaf morphology based on data obtained using the image processing technology. At the booting stage, the average length and width of YIL18 leaves were 45.1% and 12.7% shorter than that of TQ (Table 1). The length and area of the rice leaves were significantly reduced. The YIL18 leaves were shorter and narrower, and the leaf area was only 44.8% of the TQ leaf area. The flag leaves of rice canopy emerged during the heading stage. The length, width, and area of flag leaves in the YIL18 canopy were 15.8%, 32.0%, and 33.7% lower than that of TQ. The length, width, and area of the second leaf from the top were 23.2%, 13.6%, and 54.2% lower in YIL18 than in TQ. Regarding the other leaves, the length, width, and area were 32.3%, 9.8%, and 51.6% lower in YIL18 than in TQ (Table 1). At the heading stage, the difference between the leaf length of YIL18 canopy flag leaf and that of TQ was reduced, but the leaf width of YIL18 was smaller than that of TQ. Furthermore, the decrease in leaf length of the second leaf from the top and the other leaves was significantly larger than that of leaf width, directly affecting the leaf area. At the grain filling stage, the growth of rice canopy leaves peaked and then declined gradually due to senescence. Indeed, most leaves at the bottom of the rice canopy turned yellowish and drooped. At this stage, leaf length, width, and flag leaf area in YIL18 canopy were 17.93 cm, 1.09 cm, and 16.07 cm^2, respectively. Those of the second leaf from the top were 25.48 cm, 0.91 cm, and 18.09 cm^2, while those of other leaves were 26.48 cm, 0.76 cm, and 15.52 cm^2, respectively. Compared with TQ, leaf length of these three types of leaves decreased by 25.4%, 24.1%, and 28.6%, leaf width decreased by 16.2%, 17.3%, and 7.3%, and leaf area decreased by 19.7%, 37.0%, and 36.7%, respectively. At the grain filling stage, the decrease in leaf length of all leaf types in YIL18 canopy was similar. However, changes in the leaf width of the flag leaf and the second leaf from the top were larger than in the other leaves.

4. Discussion

Divergence in plant growth characteristics of rice from prostate to erectile was a crucial event in rice domestication. PROG1 gene is one of the vital genes controlling rice growth characteristics. Quantitative analysis of leaf morphology variations between different rice genotypes is essential for understanding the effect of PROG1 gene on leaf morphology and applying it in the molecular breeding of rice. In this study, BMO filter was used to denoise and enhance images. Minimum bounding rectangle extraction and target pixel statistics were employed to analyze binary images and reveal the differences in morphological characteristics of rice leaves, such as leaf length, leaf width, and leaf area.

4.1. Application of Image Processing Technology in Crop Phenotype Measurement. A fast, accurate, and reliable method is essential in evaluating rice phenotypic traits. Most of the existing measurement methods are manual, involving various tools, such as a ruler, caliper, and protractor. However, manual measurement methods are labor-intensive
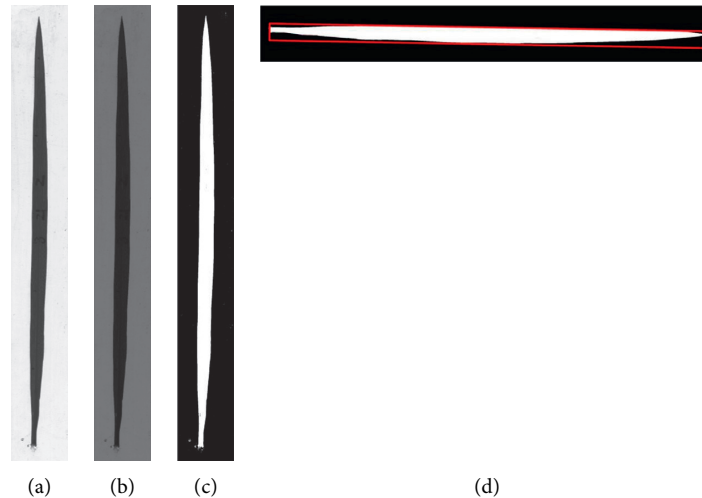
FIGURE 1: Images of the TQ leaf at booting stage after image preprocessing. (a–c) Iimages of the whole leaf after image graying, BMO filtering, and image segmentation. (d) Minimum bounding rectangle extraction of the target leaf.

and prone to errors. Thus, there is a need to apply alternative measurement methods to improve the accuracy of obtaining statistical data [24].

The rapid development of modern computer, machine vision, and information and automation technology has accelerated the development of phenotyping technologies. High-throughput phenotyping technology has been extensively used in the acquisition of massive crop phenotypic data. For example, LiDAR [25], CT technology [26, 27], and helicopters have been applied to monitor the canopy characteristic [28]. Most of these techniques are based on image processing technology. However, due to equipment and technology limitations, much noise gets captured during the image acquisition process. This affects further image analysis. Therefore, denoising and edge enhancement of digital images are important in image preprocessing. At present, a denoising method based on partial differential equation (PDE) is commonly used in image processing technology that belongs to the anisotropic diffusion model. The diffusion speed is determined by image gradient, which considers both noise elimination and feature preservation [29]. The BMO filter used in this study was constructed based on the bounded mean oscillation model and partial differential equation. It detects edge features by determining new derivative format and uses integral averaging to eliminate noise influence [19, 20]. The algorithm is simple and can detect more fine edge features involving less computation and calculation steps. Thus, BMO filter can not only achieve noise cancellation but also retain the edge details. This has led to the extensive application and continuous development of the BMO algorithm in recent years [18]. In this study, BMO filter was used to denoise and enhance the digital image of rice leaves. This study lays a solid foundation for future research on accurate acquisition of leaf morphological characteristics. Notably, no significant difference was found between leaf morphological characteristics obtained using image processing technology and manual measurements ($P > 0.05$). Moreover, its filtering

effect was stable for leaf images of different rice varieties. However, the values obtained using image processing technology were slightly lower than those obtained using manual measurement methods. This might be due to image resolution or subjective error caused by manual measurement. In addition, the discrete format is an important factor for the accuracy of the results. In this study, the BMO filter was discretized by $3 * 3$ discrete format. An appropriate discrete format for the BMO model should be selected when dealing with different objects. The larger the scale, the better the processing effect; however, this also increases the calculation required.

In addition to leaf size, rice leaf morphology includes leaf curl degree, thickness, and leaf color. However, because digital images are two-dimensional, obtaining this additional information from digital images is practically impossible. Therefore, future research should focus on combining image processing technology with other high-throughput phenotypic techniques. This is necessary for the development of an advanced and comprehensive digital technology for rice leaf morphology evaluation.

4.2. Effect of PROG1 Gene on Rice Yield. Light is required for photosynthesis, which is vital for rice growth and development. Photosynthesis in rice canopy is essential to energy accumulation, which ultimately affects the quality of rice grains. Leaf morphology of rice is directly related to the spatial distribution of canopy leaves and leaf photosynthetic area, thus affecting the utilization rate of light energy in rice canopy and yield per unit area. IRRI studies on IR8 at the milky stage demonstrated that 93.6% of total CO_2 assimilation was through green leaves, and the rest was through leaf sheath and stem (4.3%) and ear (2.1%) [30]. The upper three leaves (flag leaf, second and third leaf from the top) are the main sources of grain assimilates, accounting for about 80% of rice grain assimilates. The flag leaf is the most important among the upper three leaves, providing about 40%

TABLE 1: Morphological characteristics of leaves of TQ and YIL18 at three growth stages obtained by image processing technology and manual measurement.

Growth stage	Cultivar	Measurement method	Flag leaf								
			Leaf length			Leaf width			Leaf area		
			Mean (cm)	SD (cm)	P value	Mean (cm)	SD (cm)	P value	Mean (cm^2)	SD (cm^2)	P value
BS	TQ		—			—			—		
	YIL18										
HS	TQ	Image	21.25	3.10	0.265	1.25	0.11	0.305	19.56	4.28	0.928
		Manual	22.30	4.04		1.28	0.10		19.77	4.34	
	YIL18	Image	17.90	3.22	0.210	0.85	0.09	0.088	12.97	2.99	0.581
		Manual	19.20	2.32		1.08	0.13		13.68	3.38	
FS	TQ	Image	24.03	4.22	0.073	1.30	0.15	0.339	20.04	6.39	0.253
		Manual	25.15	4.03		1.34	0.17		21.93	6.53	
	YIL18	Image	17.93	2.51	0.149	1.09	0.13	0.296	16.07	3.88	0.777
		Manual	19.68	2.69		1.18	0.11		16.26	3.69	

Growth stage	Cultivar	Measurement method	Secondary leaf								
			Leaf length			Leaf width			Leaf area		
			Mean (cm)	SD (cm)	P value	Mean (cm)	SD (cm)	P value	Mean (cm^2)	SD (cm^2)	P value
BS	TQ		—			—			—		
	YIL18										
HS	TQ	Image	28.99	4.01	0.165	1.03	0.11	0.464	24.82	3.95	0.416
		Manual	30.84	4.42		1.12	0.10		25.94	4.50	
	YIL18	Image	22.26	3.87	0.148	0.89	0.08	0.896	11.36	3.77	0.120
		Manual	23.11	4.55		0.93	0.10		12.85	4.05	
FS	TQ	Image	33.59	7.63	0.546	1.10	0.14	0.431	28.73	6.55	0.132
		Manual	34.18	7.47		1.15	0.13		30.23	7.54	
	YIL18	Image	25.48	5.94	0.248	0.91	0.06	0.635	18.09	5.49	0.413
		Manual	26.10	5.48		0.97	0.10		18.94	5.74	

Growth stage	Cultivar	Measurement method	Other leaves								
			Leaf length			Leaf width			Leaf area		
			Mean (cm)	SD (cm)	P value	Mean (cm)	SD (cm)	P value	Mean (cm^2)	SD (cm^2)	P value
BS	TQ	Image	25.93	10.52	0.574	0.71	0.11	0.321	11.94	6.36	0.367
		Manual	26.74	10.93		0.80	0.16		12.83	6.89	
	YIL18	Image	14.24	5.37	0.412	0.62	0.15	0.795	6.59	3.48	0.080
		Manual	14.77	5.21		0.66	0.13		7.17	3.51	
HS	TQ	Image	35.12	5.87	0.298	0.82	0.09	0.674	22.81	6.84	0.895
		Manual	36.34	6.65		0.87	0.10		23.06	7.16	
	YIL18	Image	23.79	5.84	0.132	0.74	0.31	0.486	11.03	3.29	0.764
		Manual	24.62	5.75		0.80	0.30		11.79	3.86	
FS	TQ	Image	37.11	6.64	0.646	0.82	0.14	0.874	24.51	6.12	0.445
		Manual	37.70	6.68		0.89	0.12		25.26	7.61	
	YIL18	Image	26.48	5.12	0.365	0.76	0.13	0.187	15.52	5.78	0.318
		Manual	27.30	5.79		0.83	0.15		16.29	5.69	

Here, BS refers to booting stage, HS refers to heading stage, and FS refers to grain filling stage, while SD means standard deviation.

of photosynthetic products required for grain formation [30]. A study showed that the contribution rate of flag leaf towards yield per plant is 44%–48%, of which the contribution rate to seed setting rate is 40%, and that to a thousand seed weight is 10% [31]. Indeed, the thousand seed weight increases with the growth of flag leaves. Thus, rice leaf morphology is an important factor in the development of high-yielding rice plant types.

Previous studies have shown that *PROG1* gene plays a significant role in rice canopy structure. Under the influence of *PROG1* gene, rice canopy characteristics include shorter plant height, more tillers, shorter and narrower leaves, and lower leaf area index [14]. In this study, the

effects of *PROG1* gene on leaf morphology of rice canopy were analyzed. Under the influence of *PROG1* gene, leaf length, leaf width, and leaf area of flag leaves reduced by 15.8%, 32.0%, and 33.7% at the heading stage and 25.4%, 16.2%, and 19.7% at the filling stage, whereas those of the second leaf from the top reduced by 23.2%, 13.6% and 54.2% at heading stage and 24.1%, 17.3%, and 37.0% at the filling stage, and those of other leaves decreased by 32.3%, 9.8%, and 51.6% at heading stage and 28.6%, 7.3%, and 36.7% at filling stage. The leaves in rice canopy were shorter and narrower with a smaller leaf area. Loose canopy structure, shorter plant height, and more tillers increase the leaf cover area in the canopy, which is not beneficial in

improving photosynthetic efficiency. Although leaf area index of YIL18 increased gradually with the growth period, no significant difference was observed between YIL18 and TQ. The number of grains per panicle and thousand seed weight of YIL18 was significantly lower than that of TQ [14].

PROG1 gene is vital in controlling rice plant type. In this study, the effect of PROG1 gene on rice leaf morphology was quantitatively analyzed. Data obtained in this study provide a reliable foundation for molecular breeding research, which will guide the application of PROG1 gene in breeding programs.

5. Conclusions

In this study, leaf morphological characteristics of two rice genotypes were obtained from digital images using image processing technology. Further, the feasibility of applying the image processing technology in evaluating rice leaf morphology was assessed and discussed. Also considered was the effect of PROG1 gene on rice leaf morphology. PROG1 gene is critical in controlling the prostrate growth habit of wild rice. Herein, image processing technology was used to quantitatively evaluate the effect of PROG1 gene on rice leaf morphology. Under the influence of PROG1 gene, leaf length, leaf width, and leaf area of the flag leaf, second leaf from the top, and other rice leaves decreased by various degrees at different growth stages. The leaves in rice canopy were shorter and narrower, with a smaller leaf area. These results show that the PROG1 gene significantly affects leaf morphology and validate the potential application of the gene in the molecular breeding of rice. Notably, no significant difference was found between the leaf morphological characteristics obtained using image processing technology and manual measurement methods. This finding suggests that image processing technology can be applied in studying rice leaf morphology. However, due to the limitation of two-dimensional digital images, the method cannot be used to examine all the phenotypic characteristics of the leaf. Thus, future research should focus on combining image processing technology with other high-throughput phenotypic characterization techniques. This will ensure a more accurate and comprehensive evaluation of leaf morphological characteristics.

Abbreviations

PROG1: Prostrate growth 1
TQ: Teqing
YJCWR: Yuanjiang common wild rice
BMO: Boundary mean oscillation.

Data Availability

No data were used to support this study.

Conflicts of Interest

The authors declare that they have no conflicts of interest regarding the publication of this paper.

Acknowledgments

References

[1] FAO, 2020, http://www.fao.org/faostat/en/#data/QC/visualize.

[2] Y. Wang and J. Li, "The plant architecture of rice (*Oryza sativa*)," *Plant Molecular Biology*, vol. 59, no. 1, pp. 75–84, 2005.

[3] G. A. Maddonni, M. E. Otegui, and A. G. Cirilo, "Plant population density, row spacing and hybrid effects on maize canopy architecture and light attenuation," *Field Crops Research*, vol. 71, no. 3, pp. 183–193, 2001.

[4] S. Yoshida, "Physiological aspects of grain yield," *Annual Review of Plant Physiology*, vol. 23, no. 1, pp. 437–464, 1972.

[5] S. H. Cheng and H. Q. Zhai, "Comparison of some plant type components in super high-yielding hybrids of inter-subspecies rice," *Acta Agronomica Sinica*, vol. 26, no. 6, pp. 713–718, 2000.

[6] Z. Q. Liu, "A study on the photosynthetic characters of different plant types of rice," *Scientia Agricultura Sinica*, vol. 3, pp. 6–10, 1980.

[7] S. Purcell, B. Neale, K. Todd-Brown et al., "Plink: a tool set for whole-genome association and population-based linkage analyses," *The American Journal of Human Genetics*, vol. 81, no. 3, pp. 559–575, 2007.

[8] J. Yang, J. Zhu, and R. W. Williams, "Mapping the genetic architecture of complex traits in experimental populations," *Bioinformatics*, vol. 23, no. 12, pp. 1527–1536, 2007.

[9] M. Agarwal, N. Shrivastava, and H. Padh, "Advances in molecular marker techniques and their applications in plant sciences," *Plant Cell Reports*, vol. 27, no. 4, pp. 617–631, 2008.

[10] Y. Liu, H. Xu, S. Chen et al., "Genome-wide interaction-based association analysis identified multiple new susceptibility loci for common diseases," *PLoS Genetics*, vol. 7, no. 3, Article ID e1001338, 2011.

[11] B. Yu, Z. Lin, H. Li et al., "TAC1, a major quantitative trait locus controlling tiller angle in rice," *The Plant Journal*, vol. 52, no. 5, pp. 891–898, 2007.

[12] L. Tan, X. Li, F. Liu et al., "Control of a key transition from prostrate to erect growth in rice domestication," *Nature Genetics*, vol. 40, no. 11, pp. 1360–1364, 2008.

[13] J. Jin, W. Huang, J.-P. Gao et al., "Genetic control of rice plant architecture under domestication," *Nature Genetics*, vol. 40, no. 11, pp. 1365–1369, 2008.

[14] S. Hua, B. Cao, B. Zheng, B. Li, and C. Sun, "Quantitative evaluation of influence of prostrate growth 1 gene on rice canopy structure based on three-dimensional structure model," *Field Crops Research*, vol. 194, pp. 65–74, 2016.

[15] J. U. H. Eitel, T. S. Magney, L. A. Vierling, T. T. Brown, and D. R. Huggins, "LiDAR based biomass and crop nitrogen estimates for rapid, non-destructive assessment of wheat nitrogen status," *Field Crops Research*, vol. 159, pp. 21–32, 2014.

[16] A. Hartmann, T. Czauderna, R. Hoffmann, N. Stein, and F. Schreiber, "HTPheno: an image analysis pipeline for high-throughput plant phenotyping," *BMC Bioinformatics*, vol. 12, no. 1, p. 148, 2011.

[17] S. Trachsel, S. M. Kaeppler, K. M. Brown, and J. P. Lynch, "Shovelomics: high throughput phenotyping of maize (*Zea*

mays L.) root architecture in the field," *Plant and Soil*, vol. 341, no. 1-2, pp. 75–87, 2011.

[18] S. Hua, Y. Chen, L. T. Liang et al., "Studying soil pore structure by using image filtering technology based on partial differential equation model," *Transactions of the Chinese Society of Agricultural Engineering*, vol. 30, no. 3, pp. 78–85, 2014.

[19] Y. Chen, Y. Yan, and K. Zhang, "On the local fractional derivative," *Journal of Mathematical Analysis and Applications*, vol. 362, no. 1, pp. 17–33, 2010.

[20] Y. Chen, Z. Wang, and K. Zhang, "Approximations for modulus of gradients and their applications to neighborhood filters," *Frontiers of Mathematics in China*, vol. 8, no. 4, pp. 761–782, 2013.

[21] N. Otsu, "A threshold selection method from gray-level histograms," *IEEE Transactions on Systems, Man, and Cybernetics*, vol. 9, no. 1, pp. 62–66, 1979.

[22] L. Tan, F. Liu, W. Xue et al., "Development of *Oryza rufipogon* and *O. sativa* introgression lines and assessment for yield-related quantitative trait loci," *Journal of Integrative Plant Biology*, vol. 49, no. 6, pp. 871–884, 2007.

[23] R. Lu, Y. Fan, N. N. Chen et al., "Fast slgorithm for extracting minimum enclosing rectangle of target image," *Computer Engineering*, vol. 36, no. 21, pp. 178–180, 2010.

[24] X. Huang, Y. Zhao, X. Wei et al., "Genome-wide association study of flowering time and grain yield traits in a worldwide collection of rice germplasm," *Nature Genetics*, vol. 44, no. 1, pp. 32–39, 2012.

[25] J. G. De Tanago, S. Joshep, M. Herold et al., "Terrestrial LiDAR and 3D tree reconstruction modeling for quantification of biomass loss and characterization of impacts of selective logging in tropical forest of peruvian amazon," in *Proceedings of the 2015 14th conference on Lidar Applications for Assessing and Managing Forest Ecosystems*, La Grande Motte, France, September 2015.

[26] S. D. Keyes, K. R. Daly, N. Gostling et al., "Image-based plant phosphate uptake modelling: a case study for root hairs using synchrotron X-Ray CT imaging," in *Proceedings of the 9th European Conference onMathematical and Theoretical Biology*, Göteborg, Sweden, June 2014.

[27] Y. Zhou, K. Xu, J. Chen et al., "Mechanism of plant lateral root reinforcing soil based on CT scan and mesomechanics analysis," *Transactions of the Chinese Society of Agricultural Engineering*, vol. 30, no. 1, pp. 1–9, 2014.

[28] S. Chapman, T. Merz, A. Chan et al., "Pheno-copter: a low-altitude, autonomous remote-sensing robotic helicopter for high-throughput field-based phenotyping," *Agronomy*, vol. 4, no. 2, pp. 279–301, 2014.

[29] M. H. Hsieh, F. C. Cheng, M. C. Shie et al., "Fast and efficient median filter for removing 1–99% levels of salt-and-pepper noise in images," *Engineering Applications of Artificial Intelligence*, vol. 26, no. 4, pp. 1333–1338, 2013.

[30] S. Yoshida, "Grown and development of the rice plant," in *Fundamentals of Rice Crop Science*, pp. 1–61, IRRI, Los Baños, Philippines, 1981.

[31] S. B. Peng, G. S. Khush, and K. G. Cassman, *Evolution of the New Plant Ideotype for in Creased Yield Potential*, IRRI, Manila, Philippines, 1994.

Research Article

Application of Virtual Reality and Artificial Intelligence Technology in Fitness Clubs

Changjun Zhao (ID)

Department of Physical Education, Guangxi University of Chinese Medicine, Nanning 530200, Guangxi, China

Correspondence should be addressed to Changjun Zhao; zhaocj2018@gxtcmu.edu.cn

With the continuous development and progress of virtual reality technology in recent years, the application of virtual reality technology in all aspects of real life is no longer limited to the military field, medical, or film production fields, but it gradually appears in front of the public, into the lives of ordinary people. The human-computer interaction method in virtual reality and the presentation effect of the virtual scene are the two most important aspects of the virtual reality experience. How to provide a good human-computer interaction method for virtual reality applications and how to improve the final presentation effect of the virtual reality scene is also becoming an important research direction. This paper takes the virtual fitness club experience system as the application background, analyzes the function and performance requirements of the virtual reality experience system in the virtual reality environment, and proposes the use of Kinect as a video acquisition device to extract the user's somatosensory operation actions through in-depth information to achieve somatosensory control. This article adopts a real human-computer interaction solution, uses Unity 3D game engine to build a virtual reality scene, defines shaders to improve the rendering effect of the scene, and uses Oculus Rift DK2 to complete an immersive 3D scene demonstration. This process greatly reduces resource consumption; it not only enables users to experience unprecedented immersion as users but also helps people create unprecedented scenes and experiences through virtual imagination. The virtual fitness club experience system probably reduces resource consumption by nearly 70%.

1. Introduction

Virtual reality (VR) is a new type of information technology that has emerged since the 1990s. It is based on computer technology as the core and combined with related science and technology. Experimenters use related equipment and objects to interact in the digital environment so that they can vividly feel and experience the real environment. Therefore, the human-computer interaction of virtual reality technology provides a new interactive medium. It is the process of mankind's understanding and exploration of nature and gradually forms a scientific method and technology for simulating nature, to better understand, adapt, and use nature.

Zhang Qinggao believes that many high-tech technologies have been developed in scientific research in recent years. This includes computer graphics, multimedia technology, artificial intelligence, human and machine equipment, genetic technology and forensic technology, high-throughput technology, and some other human psychology technologies. He first introduced the basic concepts of virtual reality and some existing technologies, then introduced a virtual reality modeling language VRML based on WEB, and used it to realize a simple virtual reality space K virtual data room. However, his method is too simple to meet the needs of users [1]. Liu Ying believes that virtual reality reflects the virtual world. Virtual reality refers to the creation of computer technology. The user interacts with virtual reality through reaction control in the real world. He is always studying the latest future technology to influence customers' electronic products and guide the future development work, which will improve each other's theory and practice through "mutual communication" teaching. He discussed the conclusions of the outer space structure from

"VaA" to the model and put forward the conclusions and suggestions of resource development and follow-up research related to development. However, his ideas are too advanced and cannot be realized by current technical means [2]. Zhang Xiaoyu believes that virtual reality technology is a multidimensional simulation and simulation of computer technology. In the modern display art with multimedia technology as the main technical means the application of virtual reality technology has brought it a kind of "immersive," expressive method, and he analyzed the technical application and artistic expressiveness of virtual reality to highlight the superiority of this technology in modern display art. Virtual reality will become a new development direction of modern display art, but he has no actual data to support and needs to do a large number of experiments to verify the feasibility of the theory [3].

This article takes the virtual reality experience of the fitness club as the application background, deeply analyzes and studies the friendly human-computer interaction and realistic scene presentation methods in virtual reality scenes, applies the technical methods of intelligent video to the virtual reality technology, and analyzes and compares with some current human motion recognition methods, a somatosensory human machine, which uses Kalman filtering and joint point reliability detection to perform joint point recognition position correction, based on the joint point position through an improved angle measurement method to recognize human motion instructions' interactive system. To recreate realistic virtual reality scenes, this article assumes two aspects of scene construction and rendering optimization to create excellent and performance-optimized scene materials in consideration of system efficiency and resource consumption control. Some Unity 3D comes with Shader (shader). By controlling the rendering pipeline to simulate the real optical imaging process, the rendering effect of bump texture and specular reflection is greatly improved. And, adapt the latest virtual reality display device Oculus Rift DK2 to provide immersive virtual reality presentation affects so that people can achieve their goals through virtual reality and can also greatly reduce costs and losses. In this article, the virtual fitness club experience system reduces resource consumption by nearly 70%.

2. Processing Methods of In-Depth Data Analysis and Action Recognition

Collision is an engineering method that can determine whether two objects collide with each other in a virtual environment. In a virtual reality system, the accuracy of conflict conflicts with incompetence. An accurate and efficient method can improve the user's sense of experience and real-time interaction in the virtual environment. Since many objects, in reality, have complex shapes, collision detection often consumes a lot of processing time and storage space. As a result, the real-time and accuracy requirements of the virtual reality environment are often far from being obtained. Research on collision detection methods is often to find a balance as much as possible between accuracy and real time. Based on the summary of the previous collision

detection methods, this paper will propose its own improvement method from the perspective of reducing the system's memory consumption during the collision detection process [4, 5].

2.1. Space Decomposition Method. The basic idea of the space decomposition method is to divide the detected virtual space into narrow cells, then specify the cells according to the geometric data, and only intersect the cases in the same grid or two adjacent grids. Currently, commonly used methods are octree, BSP tree, K-D tree, etc. The space decomposition method is suitable for a simple environment where the geometric blocks are evenly dispersed and uniform. It is inadequate for relatively concentrated geometric objects in a complex environment, and the results achieved are often difficult to meet the requirements [6, 7].

2.2. Hierarchical Bounding Box Method. Hierarchical bounding box method is currently the most widely used collision detection method, and it is suitable for more complex collision environments. One of the principles of the ladder enclosure is to express complex objects in simple shapes and construct more complex object structures until the shape of the geometric model is completely retained. Someone compares a cladding tree to the test of a border intersection, which can release extremely unstable geometric elements for the first time and reduce many unnecessary calculations. During the traversal process, we will cross-test the two elements within the triangle, compare the number of geometric tests, and improve the efficiency of the collision test [8, 9].

2.3. Implementation and Characteristics of the Hierarchical Bounding Box Method. Collision detection algorithms mainly include three methods based on Voronoi diagram, distance calculation, and bounding box. The method based on bounding box is currently the most widely used and has great research value. In actual research, the common bounding box methods mainly include bounding sphere method, bounding box method along the coordinate axis, and direction bounding box method [10, 11].

The principle of the original collision detection method is very simple, that is, all basic triangle faces between two geometric objects are intersected one by one. Although this method can correctly detect collisions between objects, when the model becomes increasingly complex, the amount of calculation increases exponentially, which clearly cannot meet the real-time requirements of the VR system. With the development of the times and the deepening of research, to improve the accuracy and speed of collision detection between two objects, the existing improved collision detection algorithms mainly include spatial decomposition method and hierarchical bounding box method [12, 13].

2.4. Comparison of Advantages and Disadvantages of Hierarchical Bounding Boxes. Bounding ball is the simplest of the above three methods. When the model object is not deformed and distorted, the bounding sphere does not need to

recalculate the center of the sphere and the radius of the sphere [14] so that a satisfactory effect may be obtained. However, the scope of application of the bounding box is still relatively limited. On the one hand, because the types of models are complex and diverse and, on the other hand, because the wrapping of the surrounding ball is the worst, its accuracy is the lowest among the three. The encapsulation of the bounding box established by the AABB method which is better than that of the bounding sphere, and it only needs to be established along the coordinate axis, so the construction process is not complicated, and the intersection test is also very simple, and only six scalars are required for calculation. Since it is also not suitable for all objects, it has poor compactness for sharp geometric models [15, 16]. The OBB bounding box is more complicated than the other two bounding boxes due to its arbitrary orientation, but its compactness is the best. The optimization of the AABB bounding box hierarchy tree seems to have great research value. In addition, this method can significantly reduce the number of intersections of the two bounding boxes, so it can obtain a better detection effect than the other two methods [17, 18].

2.5. AABB Bounding Box Hierarchy Tree Optimization.

In the implementation process of the "smart park" roaming system, the design and implementation of scene roaming is the last step of the whole problem, and it is also the most critical step. Different roaming strategies and methods will have obvious differences in the realization of roaming in the actual scene, which is directly related to the user's experience of the entire system. Under normal circumstances, the quality of the collision detection method directly affects the accuracy and effectiveness of the entire roaming system. During the implementation of the scene walkthrough, each geometric object that will be collision detected is represented by a triangular facet. Then, two data tables of attributes and geometry are used to store the spatial information of geometric objects to ensure that the information of the detected geometric objects is dynamically stored and updated in real time. This article is based on the discussion and optimization of the efficiency of the traditional AABB collision detection method and adopts the two-step AABB detection method to obtain good experimental results [19, 20].

3. Application Research Experiment of Collision Detection Technology in Roaming System

3.1. Recognition Algorithm Based on Hausdorff Distance.

The Hausdorff distance is a set of two points $A = (a_1, a_2, ..., a_m)$, and a measure of the similarity between them, that is, the Hausdorff distance between A and B is

$$H(A, B) = \max(h(A, B), h(B, A)), \tag{1}$$

which is generally defined as the Euclidean distance. The function $h(A, B)$ is the directed Hausdorff distance from A to B. Hausdorff is proportional to the distance between A and B. The two sets are farther apart. Since the Hausdorff distance is susceptible to sudden noise, the result has a large

deviation that affects the recognition result, so a part of the Hausdorff distance [21] is proposed, namely,

$$H_{LK}(A, B) = \max\{h_L(A, B), h_K(B, A)\}. \tag{2}$$

$0 \le L \le m$ and $0 \le K \le n$ are not necessarily equal. If the matched image contains strong noise or the target is occluded, part of the Hausdorff distance may be mismatched. To solve these problems, the mean Hausdorff distance (Mean Hausdorff Distance, MHD) is proposed, which is defined as

$$H(A, B) = \max(h(A, B), h(B, A)). \tag{3}$$

Use MHD to determine the posture [22]. The five sample sequences and the sequence to be recognized are reduced to a three-dimensional space, and five sequences $S(i = 1, 2, ..., 5)\Lambda$ and the sequence to be recognized S are obtained. Calculate the earliest date of the five sequences and the sequence to be identified. The distinguishing criteria are as follows:

$$B = \arg\min(H(S, S_i)), \quad (i = 1, 2, ..., 5). \tag{4}$$

3.2. Recognition Algorithm Based on Joint Points.

Kinect can recognize the human bone by recognizing the positions of 20 key joints in the human body, ultimately realizing the bones depicted in three-dimensional space and thus realizing the tracking of human bone. In this article, Kinect is used to detect the spatial position of human joint points [23, 24]. Solving the angle between the joint points of the human body mainly uses three joint points, and the actual spatial position of the three joint points is used to calculate the Euclidean distance between the three joint points:

$$D(X, Y) = \sqrt{(x_1 - y_1)^2 + (x_2 - y_2)^2 + (x_3 - y_3)^2}. \tag{5}$$

And, use the law of cosine to find the angle between the joint points:

$$\theta = \cos^{-1}\theta\frac{\left(a^2 + b^2 - c^2\right)}{2ac}. \tag{6}$$

For a random event, there is an observation sequence $O = \{o_1, o_2, ..., o_T\}$ [25, 26] and an implicit state sequence $Q = \{q_1, q_2, ..., q_T\}$:

$$P(q_1 \mid q_{i-1} \cdots q_1) = P(q_1 \mid q_{i-1}). \tag{7}$$

Among them is a finite set of states:

$$N = \{q_1, q_2, ..., q_N\}. \tag{8}$$

A Hidden Markov Model (HMM) is described by a five-tuple:

$$\lambda = (N, M, A, B, \pi). \tag{9}$$

In a simple hidden Markov model, hidden state $N = 2$, observation state $M = 3$, A constitutes an $M \times N$ matrix A, B constitutes an $N \times M$ observation matrix B [27, 28], and the initial state probability distribution constitutes a probability vector:

$$\pi_i = P\{q_1 = s_i\}. \tag{10}$$

The recognition process is divided into the learning process and the estimation process of the hidden Markov model. Five sets of discrete training data are used to train five sets of Markov model parameters to obtain $i = 1,5$, then calculate to generate the discrete sequence to be the recognized probability, $P(O \mid \lambda)$, $i = 1, ..., 5$, and finally choose the one with the largest probability as the result of the best matching gesture recognition [29, 30]. The initial model parameter settings are

$$\sum_i \pi_i = 1,$$
$$a_{ij} \approx \frac{1}{N}. \tag{11}$$

Then, the criterion is

$$B = \arg\max P(O \mid \lambda)_i. \tag{12}$$

4. Design and Analysis of Virtual Reality Interactive System

4.1. Human Body Gesture Recognition. This system uses a posture recognition algorithm based on the angle measurement of joint points to recognize the user's command actions. As mentioned in Section 2, the three joint points are relatively unstable in space, and the measured angles will vary. Large error: in response to this problem, this article proposes an improved method. To reduce the large error caused by measuring the angle through the three joint points, this article first selects a breakpoint as the starting point and then selects a breakpoint to be connected or separated from the other side so that the two nodes and the origin of the x-axis can be an obtained angle. In doing so, the feedback point is kept relatively stable during the action, the number of control points is reduced, and the dispatch of multiple hits is controlled by more precise control of the cut size, as shown in Table 1.

The recognition of human posture is mainly through matching the detected joint point angles with the set action instruction library, scanning all angles first, and then judging whether these four angles meet all angles within the specified range. If it is the opposite, then the current successful co-operation will be achieved, and if neither of these two aspects can be achieved, then success will be achieved and then achieved again.

As shown in Figure 1, A is the actual measured value, I is the set desired angle, and T is the threshold. Using the angle measurement to recognize the posture of the human body, it can be seen in the figure that when all angles are within a certain threshold range, the various postures of the human body can be correctly recognized. (a–d) denote putting down your hands, raising your hands flat, raising your hands, and raising your left hand which are the simplest movements.

4.2. Improvement of Kinect Algorithm for Human Posture Recognition. To test the performance of the improved human gesture recognition algorithm, this article will complete the improved human gesture recognition algorithm in the same experimental environment: using Windows 7 Professional 64 bit operating system and using Intel Xeon E1231v3@3.40GHz processor and Kinect for Windows SDK 1.7 version development kit. The Kinect-based human posture recognition algorithm flowchart proposed in this paper mainly includes human tracking and detection, joint point correction, joint angle calculation, and posture recognition.

As shown in Figure 2, the system adopts human body detection and tracking technology, uses the obtained depth map to extract the articulation points of human bone, and obtains the preliminary bones of the human body. Joint point correction is mainly divided into joint point credibility calculation and joint point correction. The length of the human skeleton and the continuity of motion and the limit of the joint point angle are used to judge the credibility of the joint point, and according to the motion, continuity estimates the spatial position of the joint points and uses the Kalman filter to correct the coordinates of the joint points. The posture recognition system uses the angle measurement method to recognize the human posture. As long as the angle between the joint points is within the specified threshold range, the human posture can be correctly recognized. In the previous section, six command actions suitable for human-computer interaction in virtual reality have been defined.

The experimental training samples come from 10 laboratory members and perform 50 gesture recognitions, respectively, for a total of 500 times. What is made in the experimental samples are all meaningful action instructions, as shown in Table 2.

The data in the table show that the improved gesture recognition algorithm achieved better recognition results when six command behaviors were recognized, with an overall recognition rate of 98.9%. There are several main reasons for the analysis: the six predefined behavior instructions, the distinction is clear, and it is not easy to cause misrecognition; by calculating the credibility of the joint points and correcting the joint points, the error rate of gesture recognition can be effectively reduced; during the process of switching between actions, because the T posture is the initial command posture, it is easy to be recognized, so if the action is slow during the command action switch, it may be recognized as an initialization command.

As shown in Figure 3, in the traditional application that uses Kinect to recognize the action of entering a hole, there is no process of joint point reliability detection and correction. For the method based on joint point angle measurement, the virtual human body obtained through Kinect for Windows SDK is directly used. The position of each joint point of the bone, the angle of the angle formed by the connection between thee joint point and its neighboring joint points, is calculated to determine the posture of the human body, as mentioned above.

TABLE 1: The angle condition that each instruction action satisfies.

Post	1/c	2/c	3/c	4/c	T/c
Lift	180	180	0	0	15
Raise	180	90	0	90	15
Put	270	270	270	270	15
Lift left	180	90	270	270	15
Lift right	180	180	0	90	15

	a	b	c	d
A	143	125	235	450
I	124	144	180	280
T	200	200	300	500
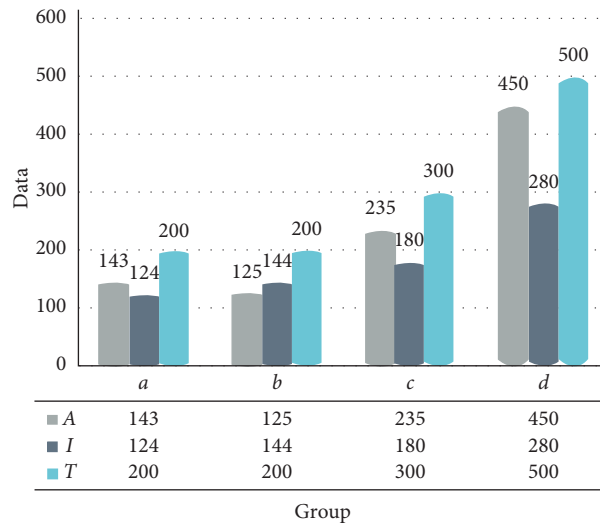
FIGURE 1: Recognition of human posture using angle measurement.

In traditional methods, the joint point detection and correction are not performed before the joint point angle is calculated. The human body posture is determined by calculating the angle formed by the joint point and its adjacent joint point without introducing system X-axis as a reference. The measurement results obtained using the same action definition and threshold are shown in Table 3.

From the data in the table, it can be seen that the traditional gesture recognition algorithm based on angle measurement has achieved a recognition accuracy of more than 90% when recognizing the six instruction behaviors, but the recognition rate of each action and the overall recognition rate are lagging behind this article.

As shown in Figure 4, an improved human gesture recognition algorithm is used in the Kinect human-computer interaction of the system to evaluate the credibility of the position of human joint points. According to the credibility of the position of the joint points, the Kalman filter is used to correct the position of the joint points. Finally, the posture recognition of the human skeleton formed by the joint points is performed, and the reference point angle measurement method is adopted. The ability of human body gesture recognition is improved. Experiments show that the improved gesture recognition algorithm can measure the angle of human joints in real time and accurately judge interactive commands.

4.3. Research and Implementation of Global Illumination Rendering Engine Architecture.

The virtual reality scene in this paper is constructed using the scene editor of the Unity 3D game development engine. Among them, the quality of the materials used to construct the virtual display scene is directly related to the quality of the final scene presentation. Therefore, this paper has also invested a lot of energy in the production and optimization of three important materials of 3D models, materials, and texture. To ensure the realistic effect of the scene presentation, the use of cameras and lights and the physical effects in the scene has also been studied and practiced in this round.

Excessive number of polygons in the model and too fine textures can provide better rendering effects, but will seriously affect the rendering efficiency, and are also limited by the Unity 3D game engine for the maximum number of polygons and the maximum texture resolution of the model. Therefore, it is necessary to optimize the model while minimizing the impact on the rendering effect to reduce the number of unnecessary polygons and the excessively high texture resolution.

As shown in Figure 5, texture mapping refers to a two-dimensional image that is mapped to the surface of a three-dimensional model. In a virtual reality scene, simply relying on the volume and surface of the three-dimensional model cannot achieve a good virtual effect. Therefore, after the establishment of the 3D model is completed, a series of
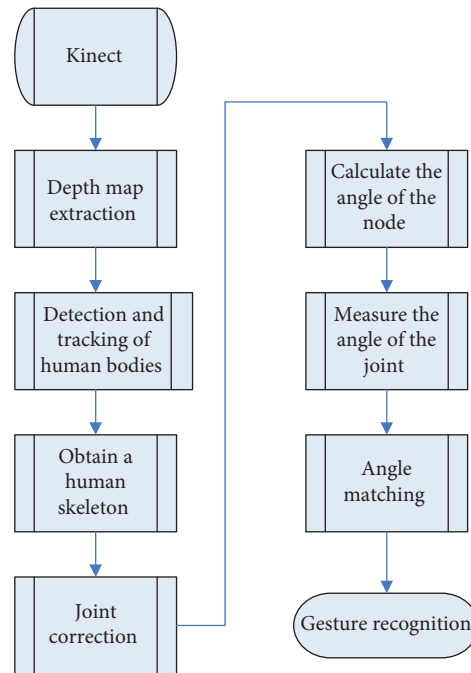
FIGURE 2: Flowchart of algorithm experiment.

TABLE 2: The recognition results of the improved pose recognition algorithm.

Result	Initialize	Acquisition control	Prepare	Move right	Angle left	Move left	Angle right
Initialize	100%	0	0	0	0	0	0
Acquisition control	0	100%	0	0	0	0	0
Prepare	0.5%	0	99.5%	0	0	0	0
Move right	1.4%	0	0	98.6%	0	0	0
Angle left	1%	0	0	0	97%	1.6%	0.4%
Move left	0.9%	0	0	0.8%	0	98.3%	0
Angle right	0	0	0	0.4%	0	0	99.6%

patterns and materials need to be created for it so that it can produce a simulated real scene effect.

Three-dimensional model mapping includes two types: texture mapping and normal mapping. Texture mapping is to "paste" the two-dimensional plane graphics to the surface of the three-dimensional model so that the rendered three-dimensional model looks more real. Before creating a texture map for the model, you need to create a flattening map for the texture coordinates of the model to determine the correspondence between the points on the texture map and the points on the 3D model. To obtain a more realistic performance effect, you first need to use a digital camera to extract the texture of the real object to obtain a texture photo, process the texture photo through Photoshop, cut off the extra part of the photo, and adjust the brightness, contrast, and color temperature of the photo to make the texture photo as consistent as possible with the surface color of the real object and then save as a texture photo file in RGB format. Then, use the texture map maker to correspond the points on the processed texture photo with the points on the 3D model to obtain the real texture map.

Collision detection is an important basis for realizing the physical interactions between three-dimensional models. Under the combined action of the collider and the rigid body, the object produces physical effects. The rigid body can make the object be controlled and affected by the physical effect, and the collision body can cause objects to collide with each other. The collision body does not need to be bound to a rigid body, but when a rigid body collides with one of the collision bodies and at least one of them has a rigid body added, three collision messages will be sent to the objects bound to them, and the behaviors related to these events are handled through scripts. Although the mesh collision body with convex parameters can collide with other mesh collision bodies, the mesh collision body sets the position and size ratio of the collision body according to the transform component properties of the attached object, and the collision mesh is to save processing resources and use the backside blanking method, so if an object collides with a network that uses backside blanking visually, but because its transform component does not load the full size range of the grid, they will not actually happen collision.
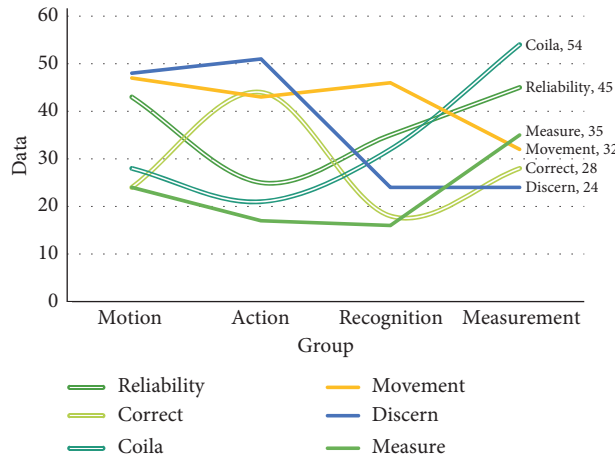
Figure 3: The traditional use of Kinect for the hole movement recognition.

Table 3: The same action definitions and thresholds are used to obtain the measurements.

	Detection (%)	Correct	Rectify	Adjust	Monitor	Test
Calculate	96.2	2.4%	1.2%	1.2%	0	0
Count	2.2	97.8%	0	0	0	0
Compute	1.4	0	98.6%	0	0	0
Numeration	1.8	0.8%	0	94.8%	0	0
Figure up	3.2	1.2%	1.2%	0	90.2%	4.2%
Angle	2	0	0.5%	1.5%	0	96%

	Interaction	Computer	Machine	Recognition	Posture
Human	4.3	2.5	3.5	4.5	3.7
Man	2.4	4.4	1.8	2.8	2.8
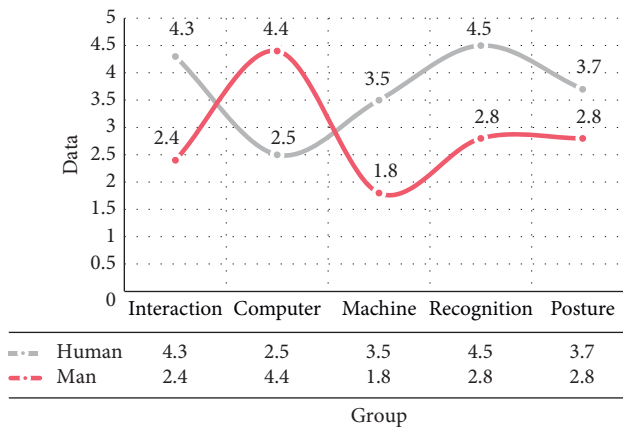
Figure 4: The Kinect human-computer interaction in this system.

As shown in Figure 6, it is the rendering effect diagram of VXGI, LPV, and the algorithm of this paper and ray tracing. This experiment mainly considers the indirect lighting effects of diffuse reflection and specular reflection. Therefore, the photon mapping algorithm is not considered, and the other three algorithms are compared with the most realistic ray tracing algorithm. Through comparison, it is found that the lighting effect of VXGI is stronger than the LPV algorithm, which is the closest to the ray tracing effect, and achieves higher visual quality. The lighting effect rendered by the algorithm in this paper is almost the same as that of VXGI. Even at a distance from the observer, the rendering effect is close to the real effect, and there is no big deviation in the rendering effect due to the voxel specification problem. This shows that this paper is suitable for large-scale, judgment of the distribution of scene lighting is correct. After using cascaded voxel texture + improved cone filter + improved voxelization strategy, not only the efficiency is significantly improved, but also the rendering effect can be guaranteed, which meets the goals of this article.

As shown in Figure 7, if high-precision 3D models and textures are directly applied to a virtual reality scene, although theoretically good results can be achieved, too many polygons and too high texture resolution will affect the computer performance causing a serious burden, even exceeding the processing power of the game engine and

	10	20	30	40	50	60
VXGI	28	28	30	25	45	54
LPV	24	44	18	35	40	34
PM	43	25	35	45	30	26

Group
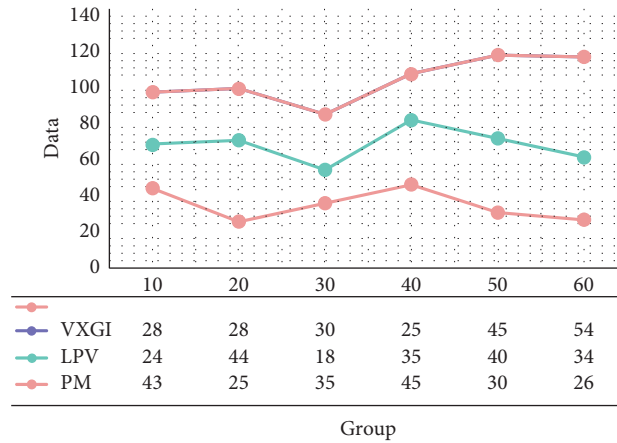
FIGURE 5: Comparison of memory consumption of four global illumination algorithms.
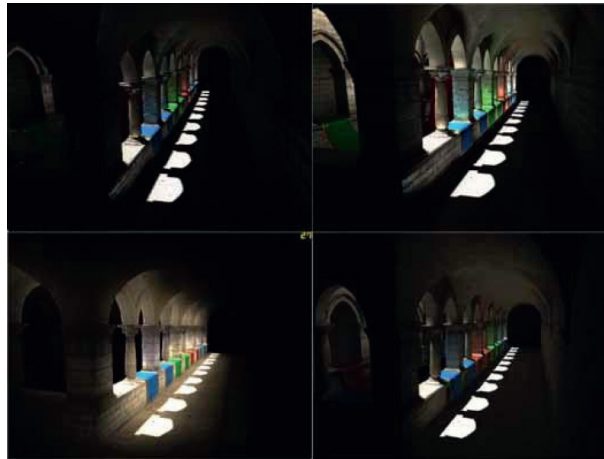
FIGURE 6: Improved VCT Global Illumination Algorithm for Large-Scale Scenes (the picture comes from https://image.baidu.com/).

graphics processing unit, causing rendering errors. Since the application background of this topic is the virtual reality experience of household products, it requires high real-time performance of the system, which makes the optimization of the three-dimensional model essential. Therefore, the optimization of the model is one of the key steps to improve the overall performance of the system. Whether the model is properly optimized is directly related to the effect of the virtual reality scene presentation and the real-time performance.

As shown in Figure 8, the performance of the voxelization stage has been discussed in Section 2. The cascaded voxel texture voxel storage structure is better than the sparse octree storage structure in terms of voxel scale, voxelization speed, and memory consumption. Both have advantages. This section mainly analyzes the frame rate of the illumination, injection, and cone tracking stages. The comparison between the VXGI algorithm and the VCT global illumination improvement algorithm of this article in the realization of each global illumination effect takes time to render each frame.

Each time Unity 3D prepares data and notifies the GPU to render, and the process is called a Draw Call. In general,

once an object with a mesh and a material is rendered, a Draw Call will be used. For these objects in the rendering scene, in addition to the time-consuming notification of the GPU rendering in each Draw Call, switching the material and the shader is also a very time-consuming operation. Using Draw Calls too frequently will cause the CPU to perform a lot of work to access the graphics API, resulting in significant performance overhead on the CPU. Therefore, the number of draw calls is an important indicator for determining performance. To reduce the number of times Draw Call is used in Unity 3D, some objects with the same material are merged through "batch processing" so that a Draw Call is used to render them, and the execution efficiency is improved, as shown in Table 4.

In summary, compared with other advanced algorithms, the algorithm in this paper has achieved very big advantages in terms of operating performance and rendering effects, but it is lacking in memory consumption, but it will not cause problems for the performance of today's PCs. Great influence: in addition, compared with the VXGI algorithm, the algorithm in this paper has better performance in the illumination, injection, and cone tracking stages and is faster when drawing different global illumination effects.
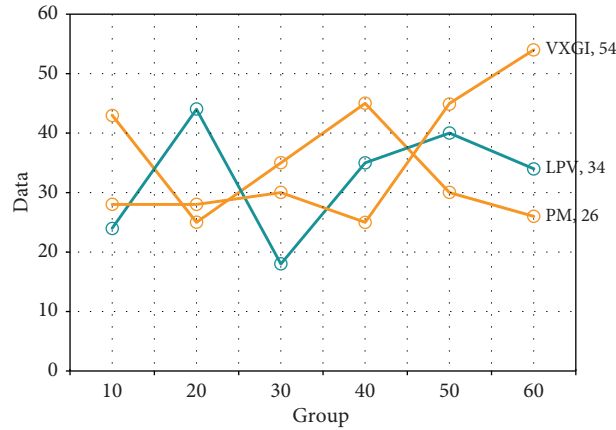
Figure 7: The voxel data takes up a large portion of memory.
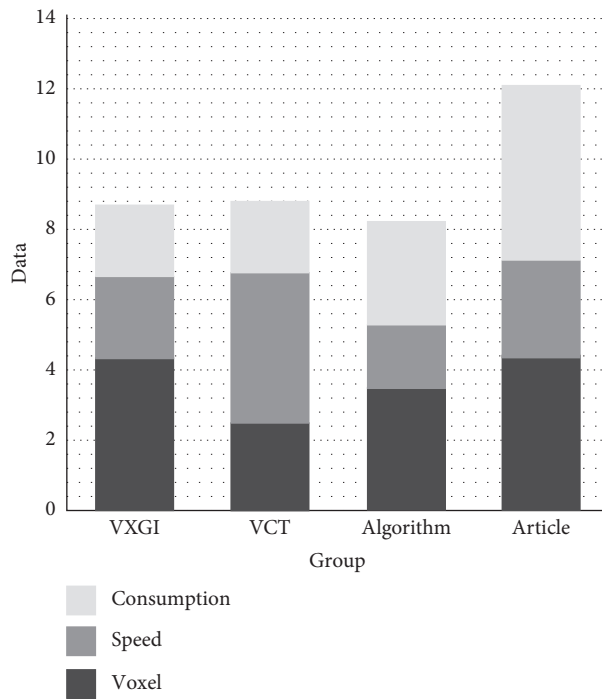
Figure 8: Improved local illumination algorithm for global illumination effect.

Table 4: The paper algorithm is compared with other advanced algorithms.

	Rasterization	Light injection	Direct	Free	Specular	Reflection
VXGI	1.0	16.5	3.0	9.2	8.0	36.7
Arithmetic	1.0	12.1	1.8	6.5	5.2	26.5

5. Conclusions

With the rapid development of e-commerce and the gradual maturity of virtual reality technology, online shopping malls based on virtual reality technology have an incomparable sense of reality and three-dimensionality that are incomparable to traditional online shopping malls. At the same time, a series of hardware products such as virtual reality display devices, 3D TVs, and somatosensory game devices have also been developed and popularized, and virtual reality technology is stepping into people's daily lives. In this theme, the fitness club is used as the application background and combined with intelligent video technology to capture the user's somatosensory interaction information through Kinect to achieve humanized action control. This paper combines intelligent video technology with virtual reality technology to provide a virtual and abstract fitness club with a real and intuitive experience based on intelligent video

technology to provide users with a simple and easy-to-use somatosensory operation mode, making the experience of virtual reality expand from the front of the computer to an immersive experience. Although the action recognition method based on intelligent video technology discussed in this paper has a good response speed and recognition accuracy to the designed action instructions, the actions are relatively not rich enough to meet the needs of human-computer interaction in complex scenes. Therefore, it is necessary to further design and improve the motion control of somatosensory. It is hoped that, in the future, the activities of human somatosensory control can be detected, and new hardware devices can be used to provide a driving force for the improvement of the virtual reality experience and the expansion of the scope of application.

Data Availability

The data used to support the findings of the study are available within the article.

Conflicts of Interest

The author declares no conflicts of interest.

Acknowledgments

References

[1] Q. Zhang, J. Sun, and L. Cui, "Application of virtual reality technology in civil engineering," *China Information Technology Education*, vol. 3, no. 20, pp. 96–99, 2017.

[2] Y. Liu and Y. Zhang, "Study on the future classroom teaching mode under the virtual reality view field," *China Electric Education*, vol. 10, no. 5, pp. 30–37, 2018.

[3] X. Zhang, "The medical application of virtual reality technology," *Technology and Innovation*, vol. 9, no. 3, p. 161, 2017.

[4] Y. Wang, "Application of virtual reality technology in psychotherapy," *Electronic Technology and Software Engineering*, vol. 12, no. 2, p. 153, 2018.

[5] G. Zhang, "Application of BIM in 3D virtual reality visualization of construction geotechnical survey," *Construction Technology*, vol. 3, pp. 275–277, 2017.

[6] Y. Huang, "Summary of the study of the application of virtual reality (VR) education," *China Education Information*, vol. 20, no. 1, pp. 11–16, 2018.

[7] T. Zhao and L. Fang, "Application of virtual reality technology in modern education," *Journal of Zhangzhou Institute of Vocational and Technical Sciences*, vol. 16, no. 1, pp. 64–66, 2017.

[8] W. R. Thompson, "Worldwide survey of fitness trends for 2018," *ACSM'S Health & Fitness Journal*, vol. 21, no. 6, pp. 10–19, 2017.

[9] X. Li, L. Zhang, and F. Zhao, "etc. Research on mixed form teaching design in virtual reality/augmented reality," *Electrical Education Research*, vol. 38, no. 7, pp. 20–25, 2017.

[10] S. Liu and J. Tan, "Application and prospect of virtual reality technology in surgical training," *Journal of Clinical Surgery*, vol. 25, no. 8, pp. 638–640, 2017.

[11] W. Xiao, F. Xu, and J. Yu, "etc. Near/far-sighted anti-convolution correction algorithm for virtual reality glasses," *Journal of Computer Aided Design and Graphics*, vol. 29, no. 7, pp. 1169–1176, 2017.

[12] S. Zhang, "Research on the application of virtual reality technology in college teaching," *Journal of the Cebu Institute of Education*, vol. 21, no. 3, pp. 68-69, 2018.

[13] H. Fan, "Application of virtual reality technology in the design of new media displays," *Journal of Business Research*, vol. 270, no. 6, pp. 125-126, 2018.

[14] R. Zhu, "Connection and Isolation," *The Ethical Risks of Virtual Reality News Narratives*, vol. 21, no. 4, pp. 48–53, 2017.

[15] Y. Gao, X. Yu, and Li Xin, "Design and realization of immersive virtual reality venues- take the development of red VR pavilion in the practical teaching of ideological and political theory in colleges and universities as an example," *Electrical Education Research*, vol. 38, no. 12, pp. 73–78, 2017.

[16] C. Montage, *Visualization and Virtual Reality: Visual Logic Changes in News Production*, pp. 55–61, Journalism University, London, UK, 2017.

[17] Y. Dong, "Application of virtual reality in simulation and experimental teaching," *Electronic Technology and Software Engineering*, vol. 9, no. 107, p. 150, 2017.

[18] G. Hu and M. Hong, "Application of virtual reality and augmented reality in the Library of Wisdom," *Library Work and Research*, vol. 45, no. 9, pp. 50–54, 2017.

[19] L. Qin, Z. Liu, and H. Fu, "Etc. Prospects for the application of virtual reality technology in the field of mechanical safety," *Automation Expo*, vol. 33, no. 2, pp. 14–16, 2017.

[20] N.-J. Hu, J. Tian, and H. Wang, "Effects of virtual reality training on pilot stress disorder recovery after accidents," *Chinese Journal of Health Psychology*, vol. 25, no. 10, pp. 1517–1519, 2017.

[21] B. Yu, Q. Zeng, and G. Huang, "Advances in the application of headset virtual reality system in sports rehabilitation therapy," *China Journal of Rehabilitation Medicine*, vol. 33, no. 6, pp. 734–737, 2018.

[22] T. Gamberi, G. Gorini, T. Fiaschi et al., "Effect of functional fitness on plasma oxidation level in elders: reduction of the plasma oxidants and improvement of the antioxidant barrier," *Neuropsychopharmacology Official Publication of the American College of Neuropsychopharmacology*, vol. 37, no. 3, pp. 746–758, 2018.

[23] X. Chen, M. Liu, and S. Wang, "etc. Application of virtual reality technology in the education of freshmen in university libraries- Take the library of Fujian University of Agriculture and Forestry as an example," *Intelligence Discovery*, vol. 30, no. 2, pp. 104–108, 2017.

[24] X. Deng, X. Qin, and P. Gao, "etc. Application of virtual reality technology in medical education," *Chongqing Medical*, vol. 46, no. 18, pp. 2582–2584, 2017.

[25] B. Sun, "Review of the application of virtual reality technology in the U.S. Military," *Computer Simulation*, vol. 35, no. 1, pp. 1–7, 2018.

[26] Modern Communication High red wave, "China's virtual reality (VR) industry development status, problems and trends," *Journal of China Media University)*, vol. 39, no. 2, pp. 8–12, 2017.

[27] M. Sun and X. Lan, "Application of virtual reality technology in experimental classroom teaching in colleges and

universities -- take Chongqing Normal University as an example," *Internet of Things Technology*, vol. 7, no. 3, pp. 117–120, 2017.

[28] C. Zhao, X. Su, and Y. Yang, "etc. Research on the development of virtual reality technology based on patent and industrial chain analysis," *Intelligence Engineering*, vol. 3, no. 2, pp. 51–61, 2017.

[29] Y. Bao and D. Ong, "Virtual reality," *A New Rendering of Future Images Film Arts*, vol. 40, no. 3, pp. 148–154, 2017.

[30] M. Zhang, "Virtual reality technology for architectural landscape design applications," *Urban Construction Theory Research (Electronic Edition)*, vol. 4, pp. 128-129, 2017.

Research Article

Personalized Emotion Recognition and Emotion Prediction System Based on Cloud Computing

Wenqiang Tian (iD)

School of 3D Printing, Xinxiang University, Xinxiang 453003, Henan, China

Correspondence should be addressed to Wenqiang Tian; 29061005@xxu.edu.cn

Promoting economic development and improving people's quality of life have a lot to do with the continuous improvement of cloud computing technology and the rapid expansion of applications. Emotions play an important role in all aspects of human life. It is difficult to avoid the influence of inner emotions in people's behavior and deduction. This article mainly studies the personalized emotion recognition and emotion prediction system based on cloud computing. This paper proposes a method of intelligently identifying users' emotional states through the use of cloud computing. First, an emotional induction experiment is designed to induce the testers' positive, neutral, and negative three basic emotional states and collect cloud data and EEG under different emotional states. Then, the cloud data is processed and analyzed to extract emotional features. After that, this paper constructs a facial emotion prediction system based on cloud computing data model, which consists of face detection and facial emotion recognition. The system uses the SVM algorithm for face detection, uses the temporal feature algorithm for facial emotion analysis, and finally uses the classification method of machine learning to classify emotions, so as to realize the purpose of identifying the user's emotional state through cloud computing technology. Experimental data shows that the EEG signal emotion recognition method based on time domain features performs best has better generalization ability and is improved by 6.3% on the basis of traditional methods. The experimental results show that the personalized emotion recognition method based on cloud computing is more effective than traditional methods.

1. Introduction

Emotion recognition has become the research field of artificial intelligence [1]. With the improvement of cloud computing technology's ability to perceive human emotions, the interaction between humans and computers has also been improved, especially in human-computer interaction, virtual reality, and computer-assisted application in education. In the research of emotion recognition, many aspects are included, such as the recognition of facial emotions, the recognition of sound emotions, the recognition of body emotions, and the recognition of physiological signal emotions. The communication between people is to convey information through language, and the emotional information conveyed through sound signals is an important source of information and an indispensable part of people's perception and judgment of things. Information transmission in the spatial dimension is to convey richer emotional information through the understanding of cloud computing [2].

The purpose of emotion recognition is to extract, analyze, and understand people's emotional behavior characteristics and use pattern recognition to realize the process of emotion recognition. Emotion recognition has many practical meanings [3, 4]. First of all, understanding emotions can help improve people's health. In the medical field, research on identifying the emotional state of patients through physiological signals and improving human health through specific emotional states is ongoing. Second, understanding emotion recognition helps improve the interaction between humans and machines. Machine equipment can identify the emotional state of users and provide users with better quality and humanized services [5, 6]. Finally, by determining the emotional state

of the user, it is also possible to provide the user with individual recommendations that match the emotional state.

At present, many scholars have deepened their research on emotion recognition. Jenke R uses EEG signals for emotion recognition, which can directly assess the user's "internal" state, which is considered an important factor in human-computer interaction [7]. He has studied many feature extraction methods and usually selects suitable features and electrode positions based on neuroscience findings. He used a small number of different feature sets and tested them on different (usually smaller) data sets to test their suitability for emotion recognition. He reviewed the feature extraction methods for emotion recognition in EEG signals based on 33 studies. An experiment was conducted to compare these features using machine learning techniques to perform feature selection on a self-recorded data set, giving results about the performance of different feature selection methods, the usage of selected feature types, and electrode position selection. The elements selected by the multivariate method are slightly better than the univariate method. However, his conclusion is not supported by corresponding data, so it is not authoritative enough [8]. Atkinson J's research concluded that the current emotion recognition computing technology has successfully correlated emotion changes with EEG signals. He believes that if appropriate stimuli are applied, they can be identified and classified from EEG signals. However, due to signal characteristics and noise, EEG constraints, and topic-related issues, automatic recognition is usually limited to a few types of emotions. In order to solve these problems, he proposed a novel feature-based emotion recognition model for the brain-computer interface based on EEG [9]. Kaya H uses an extreme learning machine (ELM) to model modal features and combine the scores to make final predictions. Use deep neural network (DNN) or support vector machine (SVM) to obtain the latest results of auditory and visual emotion recognition. He proposed that the ELM paradigm is a fast and accurate alternative to these two popular machine learning methods. Thanks to the rapid learning advantage of ELM, he used moderate computing resources to conduct extensive tests on the data. In the video modality, the combination of regional visual features obtained from the inner face is tested. In audio mode, tests are performed to enhance training with other emotional corpora. The applicability of several recently proposed feature selection methods to tailored acoustic features is further investigated [10]. Zheng W L introduced the Deep Belief Network (DBN) to build an EEG-based emotion recognition model for three emotions: positive, neutral, and negative. He developed an EEG data set obtained from 15 subjects. Each subject conducted two experiments every few days. The DBN is trained using differential entropy features extracted from multichannel EEG data. Check the weights of the well-trained DBN and study the key frequency bands and channels. Choose from four different profiles for 4, 6, 9, and 12 channels. The key frequency bands and channels determined by using the well-trained DBN weights are consistent with existing observations [11].

The main innovations of this paper include the following aspects. (1) We analyze and investigate the movement characteristics of expressions in various emotional states, analyze the existence time and expression differences of expressionlessness under positive, neutral, and negative emotions, and analyze gender differences. (2) This paper uses two feature extraction methods, SVM multi-classification algorithm and temporal feature algorithm. After training and testing, the correct emotion recognition rate in different states can be calculated.

2. Personalized Emotion Recognition Based on Cloud Computing

2.1. Emotion Recognition. Emotion recognition is the use of computers to detect human faces and analyze the characteristics of the performance information [12, 13]. The machine realizes the purpose of human beings' recognition and understanding of emotional expression. From the point of view of the expression recognition process, emotion recognition can be divided into three main steps, namely, the detection and position of the face, the feature extraction of the expression, and the classification of the expression [14].

2.1.1. Face Detection and Positioning. The detection and localization of facial images is the first step in facial expression recognition. The content of this step is to find the correct position of the face from the acquired image or image sequence [15]. In face detection, a statistical method is used to model the face, and the detected face area is compared with the face model to obtain the possible face area.

2.1.2. Extraction of Facial Features. An important part of the facial expression recognition process is facial expression feature extraction, and its main function is to extract information features that can characterize human facial expressions. Expression feature extraction methods can be divided into deformation features and motion features [16, 17]. This paper uses geometric feature-based methods to extract expression features and introduces a method of extracting expression features based on still images. When a person's facial expression changes, important information features will be extracted from the deformation process of the face. Methods of obtaining facial features: that is, as an expression feature vector, the main distance between facial features is obtained, the shape changes, and relative positions of various organs are analyzed to achieve the purpose of obtaining facial features. Geometric deformation is an obvious response to changes in human facial expressions and can handle still pictures and animated expressions [18]. However, the geometric feature method ignores other subtle changes when extracting feature information of multiple expressions, so the overall recognition rate is not high.

2.1.3. Facial Expression Classification. Expression classification analyzes the relationship between expression functions and assigns them to corresponding categories. Next,

the method based on neural network will be explained. The neural network is composed of various parallel units. The change of expression drives the change of the neural network. The output node of the neural network corresponds to 10 general basic corresponding points. The output node connects multiple processing neurons to form the entire neural network structure [19, 20]. Artificial neural networks can learn repeatedly and obtain invisible effects from the corresponding point rules. After feature extraction, according to the performance classification method of artificial neural network, an extremely obvious expression classification effect can be obtained [21].

2.2. Cloud Computing Features. Cloud computing mainly has the following characteristics:

(1) Dynamic resource allocation: Cloud computing can dynamically allocate or release some physical and virtual resources according to user needs. As user needs increase, available resources can be allocated and released after reducing user needs [22]. Provide users with surplus resources of flexible resources. Cloud computing can provide unlimited services through the expansion of resources.

(2) Self-service provision of services: Cloud computing can automatically provide users with resource services, and users can obtain the resources they need without having to talk to suppliers. There are mainly service descriptions and catalogs, and services can be selected based on this information.

(3) Services can be measured on general-purpose computers: Cloud computing provides services through the Internet. As long as users have computers and Internet, they can get the services provided by cloud computing. Therefore, cloud computing is universal. When cloud computing provides services, meters can be used to configure resources according to the services required by users. In other words, because cloud computing resources can be monitored and controlled, they can be used immediately if the service is charged.

(4) Resource pool and transparency: For suppliers, cloud computing can protect the differences in basic resources such as computing, storage, and business logic. You can perform comprehensive scheduling and management of cloud computing resources across resource boundaries [23, 24]. This is a "resource pool" that can provide services to users on demand. For users, cloud computing is transparent, as long as they care about whether they can meet their needs, and they do not have to care about its structure.

(5) High-performance price ratio: The high-performance computing function provided by cloud computing is the integration of multiple computing resources, and the hardware requirements are inappropriate. Users do not need to purchase a large amount of hardware and software resources, which can greatly save consumption costs [25, 26].

(6) Flexibility: According to virtualized computing, cloud computing can quickly build infrastructure and dynamically increase or release resources as needed. Cloud computing provides users with flexible purchase time (time, day, month, etc.).

(7) Reliability: Cloud computing is a service provided by multiple nodes. Data storage and data calculation are scattered in different nodes. Even if a node fails, new nodes can be dynamically allocated to provide services. Cloud computing also uses multiple technologies such as data fault tolerance technology to ensure service reliability.

2.3. Brain Operating Mechanism of Emotions. In the human brain, the prefrontal lobe accounts for about 40% of the cerebral cortex. The cerebral cortex is mainly composed of the motor cortex, the premotor cortex, the forebrain cortex (forebrain cortex, PFC), and the full medial part of the forebrain [27]. This is the operating center of the brain function. It is connected to other parts of the brain to process and integrate information while selecting appropriate emotional and motor responses. It will not only change the disease function, action, and decision-making ability of the scene in front, but also affect feelings and mood. The cerebral cortex is an important area of emotion induction and regulation. There are three opinions on the role of the front desk in emotional processing.

(1) The orbitofrontal area of the prefrontal lobe is related to reward processing and reinforcement learning. In particular, nerve cells in this field can perceive changes in stimuli, reverse the compensation of stimuli, and change this response [28]. The cortex plays an important role in the connection between external stimuli and reward enhancers.

(2) The ventromedial prefrontal lobe can be used as a communication platform between visceral responses and high-level cognitive functions, that is, the "physical identification hypothesis." Somatic cell markers are peripheral responses to stimuli. The ventromedial prefrontal lobe will be processed as part of the guided advanced cognitive system.

(3) The "asymmetry of power hypothesis" in the prefrontal cortex, that is, the tendency to form biological motivation, can be defined from the perspective of approaching the avoidance level. If the motivation of this method is activated, organisms will have a strong motivation to pursue compensation goals. On the contrary, emphasizing the activation of avoidance motivation is not to get compensation, but to avoid harmful situations. The central proposition of the asymmetric value hypothesis is that the right anterior lobe activates the evasive motive, and the left anterior lobe activates the approach motive to form adaptive actions.

2.4. SVM Multiclassification Algorithm. SVM is a two-type model, which is a linear classifier with a maximum interval defined by a feature space. The goal is to find the largest gap. The kernel method of support vector machine is the main manifestation of its advantages. Linear inseparable data is mapped to high-dimensional feature space through kernel technology and can be classified into high-order element space. The principle is that, in the case of a brief introduction to the binary classification problem, the following format records the training data set on the feature space.

$$T = \{(x_1, y_1), (x_2, y_2), \ldots, (x_N, y_N)\}. \tag{1}$$

Among them, $x_i \in x = R^n$, $y_i \in Y = [-1, +1]$, $i = 1, 2, \ldots, N$ means that the total number of samples is N. The characteristic parameter of each sample data is a column vector, and the vector is n-dimensional. In the case of sample i, the distance to the separation hyperplane when the distance is less than 1 is represented by x. Therefore, the restriction conditions are appropriately relaxed, x can be manually assigned, and its value represents the final SVM classification, and the result is the tolerance for misclassification. When the value of y is larger, it means that the sample data allows higher misclassification. In general, when the amounts of positive data and negative data of the sample data set are extremely unbalanced, by changing the value of this variable, the classification result of the support vector machine will be more strict for the sample type with less data.

2.5. Time Domain Feature Algorithm Extraction. This article starts with the cloud computing analysis method and extracts the statistical parameters of the expression signal from the time domain as the analysis feature. Extract expression features from the following 6 statistical methods:

(1) The mean value of the original signal.

$$\mu_E = \frac{1}{N} \sum_{n=1}^{N} E(n). \tag{2}$$

(2) The standard deviation of the original signal.

$$\sigma_E = \sqrt{\frac{1}{N} \sum_{n=1}^{N} \left(E(n) - \mu_E \right)^2}. \tag{3}$$

(3) The first-order difference average absolute value of the original signal.

$$\delta_E = \frac{1}{N-1} \sum_{n=1}^{N-1} |E(n+1) - E(n)|. \tag{4}$$

(4) Standardize the signal first, and then find the average absolute value of the first-order difference.

$$\overline{\delta}_E = \frac{1}{N-1} \sum_{n=1}^{N-1} |\overline{E}(n+1) - \overline{E}(n)| = \frac{\delta_E}{\sigma_E}. \tag{5}$$

After the original signal is normalized,

$$\overline{E}(n) = \frac{E(n) - \mu_E}{\delta_E}. \tag{6}$$

(5) Take the average absolute value of the second-order difference to the original signal.

$$\lambda_E = \frac{1}{N-2} \sum_{n=1}^{N-2} |E(n+2) - 2E(n+1) + E(n)|. \tag{7}$$

(6) Normalize the signal to find the average absolute value of the second-order difference.

$$\overline{\lambda}_E = \frac{1}{N-2} \sum_{n=1}^{N-2} |\overline{E}(n+2) - 2\overline{E}(n+1) + \overline{E}(n)|. \tag{8}$$

The above-mentioned time features are classified as single-featured emotions based on cloud computing analysis and calculation methods and are used as standard quantities for emotion recognition research. Next, the six extracted time-domain features are combined into a fusion feature vector. After emotion classification, the classification performance is compared with the standard quantity to draw experimental conclusions.

3. Facial Emotion Recognition Experiment Based on Cloud Computing

3.1. Experimental Environment and Configuration. This article will be based on cloud computing, the programming experiment of facial expression recognition experiment will be carried out in MATLAB 2016 software. At the same time, there is a Java language programming that supports VBA applications, as shown in Table 1.

3.2. Data Collection. The data set used in the experiment is a facial emotion recognition data set composed of 4679 facial expression photos. Among them, 953 people have angry faces, 547 people are bored, 512 people are scary, 969 people are happy, 657 people are sad, 412 people are surprised, and 629 people are expressionless. The data set consists of three parts. The first part is a training set containing 2154 images. The second part is the verification set containing 1536 images. The third part is a test group containing 989 images.

3.3. Experimental Procedure. This article next mainly verifies how the server side of the emotion recognition system realizes the communication connection with the cloud. After the connection is successful, the server starts to receive and save EEG data. When the received data reaches a certain time (60 seconds), the program will automatically perform the emotion recognition process. As shown in Figure 1. The communication process between the server and the cloud experimental data set will be summarized into the following three steps.

Table 1: Experimental environment and configuration.

Lab environment	Environment configuration
Operating system	64-bit windows 7 flagship version
CPU	Intel-i5
RAM	4 GB
Programming language	MATLAB

(1) At the beginning of the emotion recognition experiment, first execute the MATLAB program to detect the specific port stored by cloud computing on the expression server side. If there is data sent from the data set on the port, the server starts to receive and save the data. Like the API included in the Android operating system, the program also comes with a communication package for the expression prediction system. Since the related functions can be used directly after import, the development process is extremely simple. The first step in using the program communication function is to create an object that needs expression detection. The program udpc = dsp.UDP receiver (local IP port, 9999) creates a receiving object. The local port used to receive and transmit data is 9999, and the udpc object is used to save the received data. To prevent the port from being occupied, the object must be released after the program ends. The end function to be used is udpc.release().

(2) The data received by the program is of string type. To convert to a directly processed number type, type conversion is required. The function used is str2 double(). According to the judgment condition, after the received data reaches 30,000 (60 seconds), the emotion recognition algorithm program is called, and the result is executed. Then, use the program res = uint10(num2str(res)) to convert the value of the result, and use UDP to return the result to the cloud.

(3) Finally, use udpe = dsp.UDP Sender ('Remote IP address', Android IP,'Remote IP port', 9999) to create an experimental emoticon sending object. The IP address of the sending device is Android IP, and the sending remote port is 9999. We need to send this. The data is stored in the udpe object. Similarly, the object must be released after the program ends, and the function used is udpe.release().

The above process is a complete cycle of the EEG data collected by the EEG device and the analysis result, and the result is displayed on the cloud as the final symbol. After continuing the above process, the cloud can continue to display the analysis results in the background until the EEG device no longer collects EEG data.

4. Analysis of Facial Emotion Recognition Data

4.1. Mixed Data Feature Fusion Emotion Recognition Analysis. In the experimental verification part, the data is divided into two types for comparison experiments. One is a mixed data set composed of all volunteer data, and the other is a
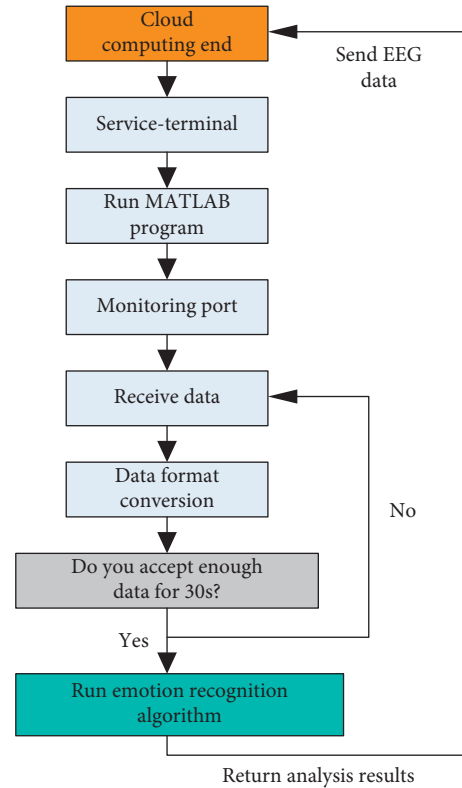
Figure 1: Flow chart of emotion recognition function realization.

personal data set composed of volunteer data with more complete personal data. Two different types of data will be used to recognize user emotions based on feature fusion, and the recognition results will be compared and analyzed. The seven classifiers of mixed data fusion are GTB, Random Forest, Ada Boost, Decision Tree, KNN, and SVM. Using mixed data for classification and recognition, the experimental results are shown in Figure 2. It can be seen from the results in the figure that when the basic emotion model is used as the emotion classification standard, the KNN classifier has the highest recognition accuracy, reaching 66.24%; when the ring emotion model is the recognition rate of the GTB classifier, it can reach 69.63%.

By comparing the accuracy of the two classification models, it is found that, in the mixed data experiment, the six classifiers use the ring emotion model to identify the results that are higher than the basic emotion model. According to the experimental results, the reason why the circular emotion model has a higher recognition rate than the basic emotion model is that continuous emotion is a vague measurement method, which is more humane than the specific classification of emotions into a certain category, which is convenient for users to measure and select.

4.2. Analysis of SVM Emotion Recognition Classification Results. SVM classifier is used for these 11 single features. This article is designed on the SVM toolkit. Perform optimization of penalty parameter C and kernel function *r* to get the classification result, and perform 5 times of 5-fold
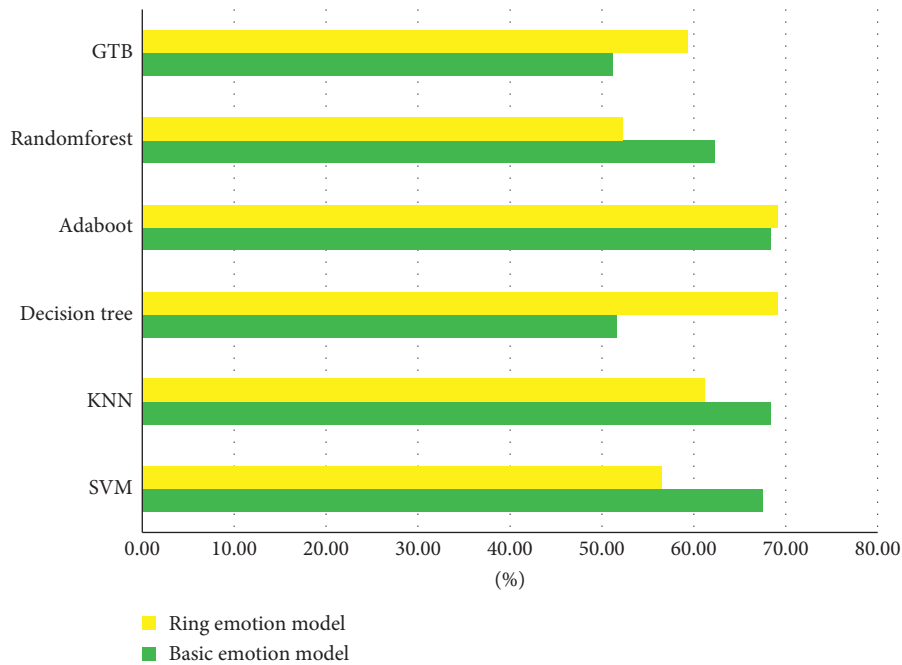
FIGURE 2: The accuracy of mixed data feature fusion emotion recognition.

crossover operation. Take the average classification accuracy obtained as the final classification result. The average accuracy rate of the subjects' two emotional valence classifications is shown in Figure 3.

When using SVM as a classifier, the study found that 1st, 2nd, std, FD, and SE performed extremely well. Since the two features of 1st and 2st have high similarity, this also confirms the effectiveness of the two time-domain signals, the mean of the absolute value of the first-order and second-order differences, in the two-classification task of emotional valence. At the same time, it can be concluded that the nonlinear characteristics are superior in EEG signal processing. Combined with the single feature classification results of ELM, 2st, FD, and SE are selected as the best three features for analysis. But at the same time, it is found that the differential entropy of ADE, BDE, CDE, and GDE in the four different frequency bands has little difference in the classification task. The classification accuracy difference between the best-performing GDE and the worst-performing ADE is 5.012%.

4.3. Comparison of Sentiment Prediction Results.
The time-domain feature algorithm can obtain appropriate data by training and learning EEG data samples, distinguishing the characteristics of EEG data samples that contribute differently to emotions, then more accurately measure the similarity of EEG data samples, and finally achieve improved emotions, which is the purpose of forecast accuracy. The classification algorithm still uses the SVM algorithm for comparison, and a five-fold cross-validation experiment is performed on the training samples and test samples of the EEG data of 8 subjects. The comparison of the accuracy of emotion prediction based on time domain features is shown

in Table 2, and the analysis of emotion prediction based on time domain features is shown in Figure 4.

Table 2 and Figure 4 show the prediction accuracy rates of the positive, neutral, and negative emotions of 8 subjects. It can be seen that, compared with the traditional method, after adding the time domain feature to the EEG signal emotion recognition, it can improve the accuracy of emotion recognition to a certain extent. Among them, the EEG signal emotion recognition method based on time domain features performs best and has better generalization ability. It is improved by 6.3% on the basis of traditional methods. This shows that EEG data samples will be in the new feature space. After the different features that contribute to emotion prediction are treated differently, the similarity between EEG data samples can be measured more accurately; that is, it can be highly classifiable. In addition, the SVM algorithm in Chapter 2 of this article is used to process abnormal samples on the original training set, detect and remove samples with wrong emotion labels, and improve the accuracy of emotion prediction by 6.5% on the basis of traditional methods, further verifying the effectiveness of the method.

4.4. Analysis of Emotional Classification Model.
The model training of emotional classification in this paper adopts the experimental part of the low score database. The training method is as follows: first, input the data stored in cloud computing, extract the expression features transmitted by brain waves, and then reduce the dimension of the extracted expression features and input them into the SVM. Train the emotional classification model in the classifier, and finally obtain a model with higher accuracy by minimizing the error method. The test set uses the data corresponding to the
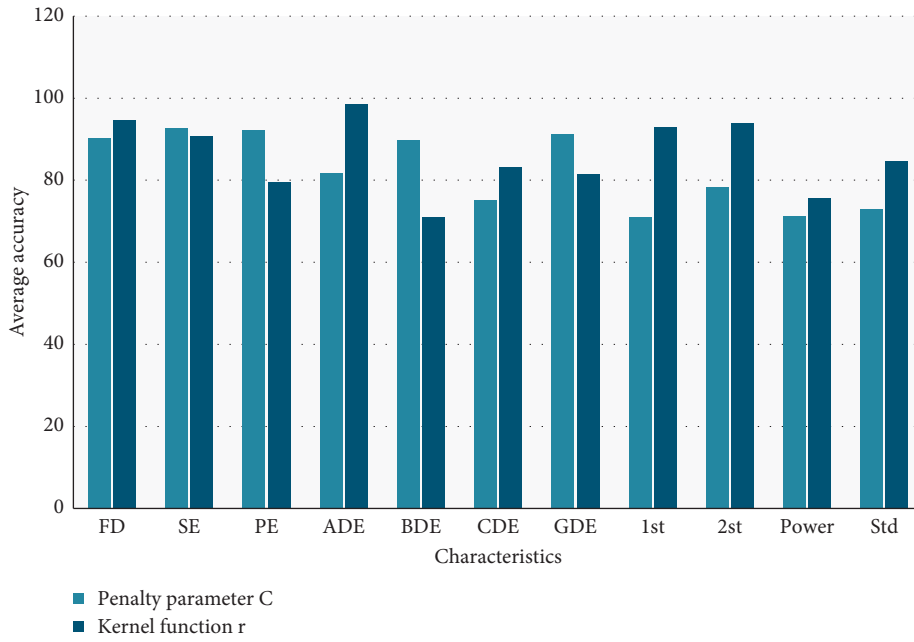
FIGURE 3: The average accuracy rate of two classifications of valence of 18 subjects with different single characteristics of SVM.

TABLE 2: Comparison of the accuracy of sentiment prediction based on temporal features.

Participant ID	SVM	PCA	ITML	LMNN	Time domain characteristics
1	51.7	30.9	24	76	58.2
2	65	63	64.1	72.1	73.9
3	70.1	69.9	72.8	75.9	78.6
4	85.4	64.1	82	88.4	89.2
5	53.9	54.6	30.7	69.1	45
6	74.6	75.2	74	79.4	77.1
7	75.9	68	75.2	75.7	56.7
8	72.6	73.7	74.6	72	93.6
Average	73.3	73.4	73	78.6	79.8
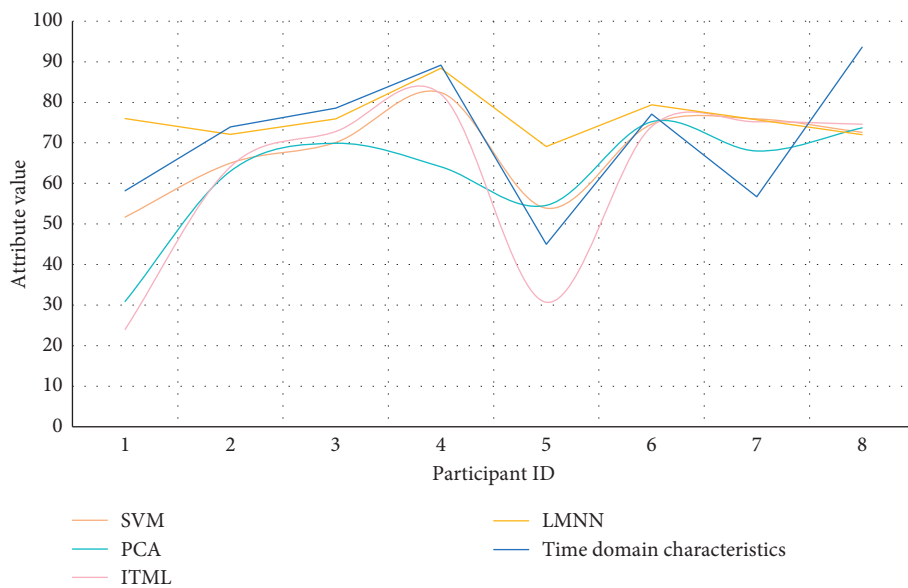
FIGURE 4: Comparison of the accuracy of sentiment prediction based on temporal features.

TABLE 3: Accuracy of the model for various emotion recognition.

	Angry	Disgust	Fear	Happy	Sad	Surprise	Neutral
Angry	5.33	1.21	7.25	4.26	15.29	1.82	6.07
Disgust	2.67	7.25	1.03	3.61	1.91	1.9	3.07
Fear	9.1	1.15	3.31	2.68	9.01	7.05	2.59
Happy	1.6	3.5	1.02	2.88	1.22	0.4	2.88
Sad	6.25	2.13	1.02	5.01	8.42	0.73	12.82
Surprise	2.1	0.66	8.01	1.52	1.92	5.75	0.3
Neutral	2.01	0.9	1.5	7.5	12.11	12.1	73.02
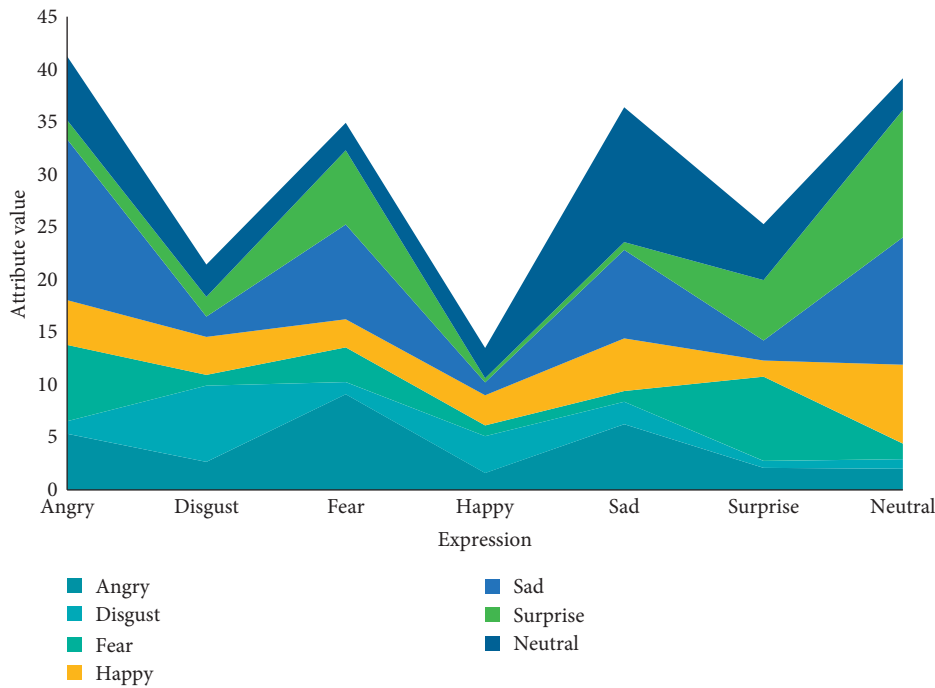
FIGURE 5: Area comparison chart of various emotion recognition.

image sequence in the self-built database, and the experimental results on the test set are shown in Table 3.

Because the emotional samples of each category in the data set are not uniform, the amount of learning data of various samples in the model is inconsistent. Therefore, the classification effect of each category is different. It can be concluded from Table 3 that the classification accuracy rate of happy and sad emotions is low, because emotions are more noisy in emotions when they are more excited and are easily misidentified as emotions such as anger and surprise. When sad, they are easily misidentified as neutral, disgust, and fear. In future experiments, some methods of removing noise interference are needed to improve the recognition rate of these two emotions. The data obtained in the above experiment is processed with software. The processing method for the prediction results of image sequences and audio data in the same time period in the same video is the use of weighted fusion image sequence expression recognition results and emotional classification results. The experimental results are shown in Figure 5.

From Figure 5 it can be concluded that since the expression prediction result of the image sequence in the video

and the emotional prediction result of the audio are two independent results, the weighted fusion image sequence expression recognition result and the audio emotional classification result significantly improve the expression recognition accuracy. Compared with a single mode of facial expression recognition, this method of judging facial expressions fully considers various influencing factors of facial expressions and assigns different weights to different determinants. This method is more robust and has wider applicability.

5. Conclusions

This paper uses the expression characteristic signal parameters as the basis of emotion recognition and uses cloud computing network algorithms to realize emotion recognition. Similarly, the expression file is divided into a training set and a test sample set. The input uses the selected training sample set to determine the input, the number of hidden layers and the number of neurons contained in each layer, the learning rate, and other parameters to train the deep belief network, so that the deep belief network can respond

to the input training sample set and learn the characteristics of each emotion. We use the constructed emotional model to recognize the picture and text file of the test and obtain the recognition rate corresponding to each sample of the test sample set. This paper uses the final test data of the SVM multiclassification algorithm to investigate which of the SVM multiclassification algorithms has the highest emotion recognition rate. It mainly compares the emotion recognition algorithms based on cloud computing from the recognition rate, the number of optimization parameters, the optimization algorithm, and the energy consumption of the two algorithms.

According to the facial emotion recognition model proposed in this paper, a facial emotion prediction system is developed. The system uses cloud computing to capture the video stream, uses the SVM algorithm to detect the facial images in the video of the read video, and delivers the intercepted facial images to the emotion model for recognition and analysis, and the graphical user controller displays it on the scroll interface. The system can analyze facial information in real time, and the model can perform excellently. In addition, based on cloud computing, a lightweight model is used. This model uses a small amount of memory and has a small amount of calculation, and its application prospects are excellent.

For the channel selection problem in emotion recognition based on cloud computing, this paper introduces the SVM method with high spatial resolution as an auxiliary method and proposes a channel selection method based on cloud computing emotion model. First, we learn from the problem-solving method, establish the emotional model of cloud computing, and obtain the transmission matrix between the signal source and the electrodes on the head surface of the cerebral cortex. As a result, the activation result of the emotion experiment can be mapped to the surface of the head, and an EEG pattern reflecting the degree of emotional correlation can be obtained. The analysis of experimental data shows that the emotion correlation recognition map obtained from the activation status reflects the relationship between emotion signals and emotions of different electrodes to a certain extent and can provide a specific theoretical basis for cloud computing emotion recognition methods.

Data Availability

No data were used to support this study.

Conflicts of Interest

The authors declare that they have no conflicts of interest.

References

[1] Y. Liu and G. Fu, "Emotion recognition by deeply learned multi-channel textual and EEG features," *Future Generation Computer Systems*, vol. 119, pp. 1–6, 2021.

[2] Z. Lv and W. Xiu, "Interaction of edge-cloud computing based on SDN and NFV for next generation IoT," *IEEE Internet of Things Journal*, vol. 7, no. 7, pp. 5706–5712, 2019.

[3] M. Tahon and L. Devillers, "Towards a small set of robust acoustic features for emotion recognition: challenges," *IEEE/ACM Transactions on Audio Speech, and Language Processing*, vol. 24, no. 1, p. 1, 2016.

[4] K. Schlegel and K. R. Scherer, "Introducing a short version of the geneva emotion recognition test (GERT-S): psychometric properties and construct validation," *Behavior Research Methods*, vol. 48, no. 4, pp. 1383–1392, 2016.

[5] M. Andrzejewska, P. Wójciak, K. Domowicz, and J. Rybakowski, "Emotion recognition and theory of mind in chronic schizophrenia: association with negative symptoms," *Archives of Psychiatry and Psychotherapy*, vol. 19, no. 4, pp. 7–12, 2017.

[6] Y. Jiang, H. Song, R. Wang, M. Gu, J. Sun, and L. Sha, "Data-centered runtime verification of wireless medical cyber-physical system," *IEEE Transactions on Industrial Informatics*, vol. 13, no. 4, pp. 1900–1909, 2017.

[7] Z. Lv, L. Qiao, Q. Wang, and F. Piccialli, "Advanced machine-learning methods for brain-computer interfacing," *IEEE/ACM Transactions on Computational Biology and Bioinformatics*, vol. 16, 2020.

[8] B. Xu, Y. Fu, Y. G. Jiang et al., "Heterogeneous knowledge transfer in video emotion recognition, attribution and summarization," *IEEE Transactions on Affective Computing*, vol. 9, no. 99, pp. 255–270, 2018.

[9] M. Tahon and L. Devillers, "Towards a small set of robust acoustic features for emotion recognition: challenges," *IEEE/ACM Transactions on Audio, Speech and Language Processing*, vol. 24, no. 1, pp. 16–28, 2016.

[10] A. M. Bhatti, M. Majid, S. M. Anwar, and B. Khan, "Human emotion recognition and analysis in response to audio music using brain signals," *Computers in Human Behavior*, vol. 65, pp. 267–275, 2016.

[11] C. Li, C. Xu, and Z. Feng, "Analysis of physiological for emotion recognition with the IRS model," *Neurocomputing*, vol. 178, no. 20, pp. 103–111, 2016.

[12] J. Yan, W. Zheng, Q. Xu, G. Lu, H. Li, and B. Wang, "Sparse kernel reduced-rank regression for bimodal emotion recognition from facial expression and speech," *IEEE Transactions on Multimedia*, vol. 18, no. 7, pp. 1319–1329, 2016.

[13] Y. Zong, W. Zheng, X. Huang, K. Yan, J. Yan, and T. Zhang, "Emotion recognition in the wild via sparse transductive transfer linear discriminant analysis," *Journal on Multimodal User Interfaces*, vol. 10, no. 2, pp. 163–172, 2016.

[14] Y. Zhang, X. Xiao, L. X. Yang, Y. Xiang, and S. Zhong, "Secure and efficient outsourcing of PCA-based face recognition," *IEEE Transactions on Information Forensics and Security*, vol. 15, pp. 1683–1695, 2019.

[15] V. Sintsova and P. Pu, "Dystemo," *ACM Transactions on Intelligent Systems and Technology*, vol. 8, no. 1, pp. 1–22, 2016.

[16] A. Mert and A. Akan, "Emotion recognition from EEG signals by using multivariate empirical mode decomposition," *Pattern Analysis and Applications*, vol. 21, no. 1, pp. 81–89, 2016.

[17] M. L. R. Menezes, A. Samara, L. Galway et al., "Towards emotion recognition for virtual environments: an evaluation of eeg features on benchmark dataset," *Personal and Ubiquitous Computing*, vol. 21, no. 6, pp. 1–11, 2017.

[18] S. L. Happy, P. Patnaik, A. Routray, and R. Guha, "The Indian spontaneous expression database for emotion recognition," *IEEE Transactions on Affective Computing*, vol. 8, no. 1, pp. 131–142, 2017.

[19] B. Sun, L. Li, X. Wu et al., "Combining feature-level and decision-level fusion in a hierarchical classifier for emotion

recognition in the wild," *Journal on Multimodal User Interfaces*, vol. 10, no. 2, pp. 125–137, 2016.

[20] A. Javed, H. Larijani, A. Ahmadinia, and D. Gibson, "Smart random neural network controller for HVAC using cloud computing technology," *IEEE Transactions on Industrial Informatics*, vol. 13, no. 1, pp. 351–360, 2017.

[21] X. Li, Y. Wang, and G. Liu, "Structured medical pathology data hiding information association mining algorithm based on optimized convolutional neural network," *IEEE ACCESS*, vol. 8, no. 1, pp. 1443–1452, 2020.

[22] Z. Li, "Application of a resource-sharing platform based on cloud computing technology," *Agro Food Industry Hi Tech*, vol. 28, no. 1, pp. 2205–2209, 2017.

[23] N. Liouane, "Recursive identification based on OS-ELM for emotion recognition and prediction of difficulties in video games," *Studies in Informatics and Control*, vol. 29, no. 3, pp. 337–351, 2020.

[24] I. Attiya and X. Zhang, "Cloud computing technology: promises and concerns," *International Journal of Computer Applications*, vol. 159, no. 9, pp. 32–37, 2017.

[25] P. Appiahene, B. Yaw, and C. Bombie, "Cloud computing technology model for teaching and learning of ICT," *International Journal of Computer Applications*, vol. 143, no. 5, pp. 22–26, 2016.

[26] W. Li, B. Jiang, and W. Zhao, "Obstetric imaging diagnostic platform based on cloud computing technology under the background of smart medical big data and deep learning," *IEEE Access*, vol. 8, pp. 78265–78278, 2020.

[27] J. C. Castillo, G. A. Castro, C. A. Fernández et al., "Software architecture for smart emotion recognition and regulation of the ageing adult," *Cognitive Computation*, vol. 8, no. 2, pp. 1–11, 2016.

[28] L. Y. Mano, B. S. Faiçal, L. H. V. Nakamura et al., "Exploiting IoT technologies for enhancing Health Smart Homes through patient identification and emotion recognition," *Computer Communications*, vol. 90, no. 1, pp. 178–190, 2016.

Research Article

Real-Time Evaluation Algorithm of Human Body Movement in Football Training Robot

Ning Hu [ID],[1] **Shuhua Lin,**[2] **and Jiayi Cai**[2]

[1]*Science and Technology College Gannan Normal University, Ganzhou 341000, Jiangxi, China*
[2]*Poon Lung Secondary School, Ganzhou 341000, Jiangxi, China*

Correspondence should be addressed to Ning Hu; 2013004@gnnu.edu.cn

As one of the most challenging topics in the field of artificial intelligence, soccer robots are currently an important platform for humanoid robotics research. Its fields cover a wide range of fields, including robotics, artificial intelligence, and automatic control. Kinematics analysis and action planning are the key technologies in the research of humanoid soccer robots and are the basis for realizing basic actions such as walking. This article mainly introduces the real-time evaluation algorithm of human motion in the football training robot. The football robot action evaluation algorithm proposed here designs the angle and wheel speed of the football robot movement through the evaluation of the angular velocity and linear velocity of the center of mass of the robot. The overall system of the imitation human football robot is studied, including the mechanical system design. The design of the leg structure, the decision-making system based on the finite state machine, the robot vision system, and the image segmentation technology are introduced. The experimental results in this article show that the action of the football training robot model is very stable, the static rotation movement time is about 220 ms, and the fixed-point movement error is less than 1 cm, which fully meets the accuracy requirements of the large-space football robot.

1. Introduction

Humanoid soccer robot is an important platform for humanoid robot technology research and an effective way to promote the transformation and industrialization of scientific and technological achievements. Currently, RoboCup and FIRA have developed humanoid robot football games. This project provides a good research platform for humanoid robot technology and multirobot collaboration technology. The humanoid robot football game has good real-time and dynamic characteristics. This not only requires the robot to have a stable and fast walking ability but also requires the robot to complete various complex actions and be able to accurately and real-time identify multiple static and dynamic target environments. In addition, the robot can perform task planning, route planning, and action planning based on the recognition and placement results, which may lead to confrontation with another group through cooperation with team robots.

As the highest form of soccer robots, humanoid soccer robots with multiple moving positions have very important research significance. First of all, it is a key factor in determining the performance of a soccer robot and determines whether the soccer robot can continue to play. Secondly, due to the characteristics of soccer, extremely high requirements are placed on the motion, control, and intelligence of such robots. Therefore, as a concentrated expression of the theory and technology of intelligent robots, this is one of the most representative and obvious manifestations of whether a country has a world-class level in this respect; finally, the development of robots can also drive many related industries and crossovers. The development and progress of technology: if robots can play football like humans, then robots can replace humans in any dangerous, difficult, or even inaccessible place.

Xiong used an artificial intelligence control algorithm to optimize the parameters of the artificial intelligence control algorithm, simulated the control signal output of each

steering part of the wheeled football robot in the experiment, and controlled the steering action of the wheeled football. The experiment verifies the robot using an artificial intelligence control algorithm. However, due to the complexity of the simulation process, the results are not very accurate [1]. Azadeh proposed an integrated algorithm based on fuzzy simulation, fuzzy linear programming (FLP), and fuzzy data envelopment analysis (FDEA) to deal with the layout design of workshop facilities in special circumstances with unclear environmental and health indicators. First, the software package to generate feasible layout alternatives is used, and then quantitative performance indicators were calculated. LP evaluates weights to make pairwise comparisons (through language terms) when evaluating certain qualitative performance indicators. Then, fuzzy simulation is used to model different layout alternatives with uncertain parameters. Next, the impact of environmental and health indicators from the standard questionnaire was retrieved. However, due to the fact that there are too many uncontrollable factors in the parameter evaluation, the results have a large error [2]. Khan explored the usefulness of conditional random fields in the challenging task of head pose estimation through the idea of semantic face segmentation. A multitype face segmentation algorithm based on the conditional random field is implemented, and a model is built for each discrete pose. When a new test image is used as the input of the face segmentation framework, the trained model will predict the probability of each face part. However, establishing the posture model is very difficult, leading to the completion of the experiment beyond the expected time [3].

The first part of this article introduces the concept, origin, and development history of soccer and soccer robots and outlines the purpose and significance of soccer robot research. The second part uses the robot action algorithm to introduce the two basic actions of the robot. In addition, the robot pose evaluation algorithm is used to control and evaluate the robot's pose from the linear velocity and the angular velocity. The third part describes the working mode of the soccer robot and constructs the soccer robot system. In the fourth part, the basic actions, technical actions, combined actions, and tactical actions of the soccer robot are explained in detail, and several typical actions of the microsoccer robot are tested and analyzed. Finally, the soccer robot action evaluation algorithm is analyzed. The fifth part summarizes the action evaluation algorithm of the football training robot and points out the shortcomings of this article and the expectations for future research.

2. Football Training Robot Action Evaluation Algorithm

2.1. Robot Pose Evaluation Algorithm.
The posture of the robot refers to the position and direction of the robot in the plane. As a vector, it can control the robot by adjusting the linear velocity and angular velocity of the center of mass of the robot to achieve the effect of adapting to different postures [4].

The pose Q of the robot can be expressed as

$$Q = f(x, y, \theta). \tag{1}$$

The robot in the robot soccer system has two driving wheels, and the pose of the robot in the Cartesian coordinate system can be easily calculated. In addition, the relationships between the linear velocity of the two wheels of the robot and the center of mass and the angular velocity of the center of mass are also demonstrated [5].

Suppose the linear velocity of the left and right wheels of the robot are defined as v_a and v_b, respectively. Then, the linear velocity v_c of the center of mass of the robot is expressed as follows:

$$v_c = \frac{v_a + v_b}{v_c}. \tag{2}$$

If the wheelbase of the two wheels of the robot is R, the angular velocity w_c of the center of mass of the robot is expressed as follows:

$$w_c = \frac{v_a - v_b}{v_c}. \tag{3}$$

2.1.1. Wheel Speed Evaluation.
The linear speed of the two wheels of the robot is referred to as the wheel speed of the robot, and their size depends on the speed information of the host [6]. The host computer issues specific wheel speed commands to the robot in a certain format according to the task of the decision, the robot interprets the command as the output of the pulse width modulator, and the motor driver drives the motor according to the output of the PWM [7].

2.1.2. Angle Evaluation.
The angle control of the robot can be understood if the rotation gain K_q of the center of mass is the wheel speed of the robot during rotation as follows:

$$\begin{aligned} v_a &= -K_q \bullet \theta\_e, \\ v_b &= K_q \bullet \theta\_e. \end{aligned} \tag{4}$$

The distance and rotation angle between the robot and the target point are expressed as r_e and θ_e, respectively. Then,

$$\begin{aligned} r\_e &= \sqrt{rx^2 + ry^2}, \\ \theta\_e &= \theta\_d - \theta\_r. \end{aligned} \tag{5}$$

If the wheel acceleration of the robot and the angular acceleration of the center of mass are expressed as K_{pd} and K_{pa}, respectively, the robot's pose control is

$$\begin{aligned} v_A &= K_{pd} \bullet r_e - K_{pa} \bullet \theta_e, \\ v_B &= K_{pd} \bullet r_e + K_{pa} \bullet \theta_e. \end{aligned} \tag{6}$$

2.2. Football Robot Action Algorithm.
In robot motion, rotation and stable point motion are the two most basic motions. It is mainly divided into the following three steps: the first is the removal of space, that is, the transformation of

the coordinate system; the second is the determination of the movement mode, that is, how to move forward or backward; the third is to determine the wheel speed [8].

(1) Space movement is mainly realized through the conversion of the coordination platform system and the coordination trolley system [9]. The formula is as follows:

$$X = x \cos(\theta) + y \sin(\theta),$$
$$Y = -x \sin(\theta) + y \cos(\theta). \tag{7}$$

Among them, x, y is the coordinate system of each stage, that is, the coordinate system with the lower-left corner of the field as the coordinate origin. X, Y is a coordinate system with the center of the robot as the origin, and the positive direction of the robot is the coordinate system of the OX axis. The angle between the robot and OX is represented by θ [10].

(2) The motion mode is divided into rotation judgment and fixed-point direction judgment.

In the rotation determination mode, $\theta < 180°$ means rotating to the right and $\theta \geq 180°$ means rotating to the left, that is, fuzzy rotation and and rotation to the target angle in the fastest way [11]. After the test, the average time for this method to rotate at any angle is 240 ms.

According to the different movement modes of the target point in the four quadrants of the target coordinate system, when the rotation is complete, the fixed-point motion is usually a curved motion. This is true linear motion.

(3) Finally, determine the wheel speed [12]. According to the dynamic principle, the following formula can be obtained:

$$V_{\mathrm{dF}} = wL,$$
$$V_L = \frac{V - V_{\mathrm{dF}}}{2}, \tag{8}$$
$$V_R = V_L + V_{\mathrm{dF}},$$

where V is the speed parameter passed by the upper strategy function; V_L, V_R, w, L have the same meaning as in the algorithm analysis; V_{dF} cylinder is the speed difference between the left and right wheels [13].

According to the model defined in the algorithm analysis, the wheel speed is not difficult to achieve. However, we must consider the initial cycle of the truck and the ever-changing safety distance and use them to determine the final wheel speed [14]. When the speed of the car robot changes, it makes the trolley more expensive to move. Stability is better.

The combination of actions based on the above two main action algorithms can form a robot monitoring algorithm and a receiving algorithm. These two algorithms are not

critical actions and must be combined with predicting the speed and position of the football [15].

2.3. Application of Fuzzy System in the Field of Soccer Robots.
Any method of controlling a dynamic system requires knowledge about the controlled system-"model." For the robot system, in addition to the model of the robot itself, it also includes the model of the environment where the robot is located. The robot model can be easily obtained, but the real-time environment model cannot be easily established [16]. While the technology in the field of robotics is booming, many problems remain to be solved:

(1) Information fusion, including the consistency of sensor information fusion and knowledge extraction, is all affected by different types of uncertain factors [17].

(2) In the case of limited prior knowledge, such as the obstacle avoidance behavior activated by the robot when facing unpredictable obstacles, robust behavior control is established.

(3) Coordination of synchronous behavior or competitive behavior, that is, which behavior should be activated in different situations and how to execute the commands of different behaviors, remains an issue to be solved [18].

(4) Integration of different levels of knowledge, such as knowledge-based planning, includes the problems of uncertainty, unpredictability, and unpredictable measurement. Therefore, the application of fuzzy logic is possible [19].

2.3.1. Fuzzy Control Technology.
Fuzzy control belongs to intelligent control. As a kind of intelligent control, fuzzy control is a very active field in automation technology. The basic idea of fuzzy control is to use machines to simulate human control of the system. It is a method of system control using approximate inference opaque controllers according to the fuzzy type of the controlled object [20]. The fuzzy model uses fuzzy language and rules to describe the dynamic characteristics and performance indicators of the system. It does not need to know the mathematical model of the controlled object or process, and it is easy to check uncertain objects and processes. It is a strongly nonlinear object. It has strong resistance to changing the characteristic parameters of the controlled object. Moreover, the interference has the advantages of strong suppression. And, all the decisions of the robot system are ultimately transformed into the realization of the underlying control. Therefore, the robustness, stability, and rapidity of the control are all key issues. In many works in the literature, fuzzy control technology is used to improve the "combat power" of robots based on the characteristics of robot soccer.

2.3.2. Uncertain Expression of Fuzzy Logic.
In recent years, intelligent information systems have attracted more and

more attention. Many models of this system are based on first-order predicate logic, which are usually called data reasoning systems. In an uncertain environment, the information provided by the database is often used as input information for decision-making and problem solving [21]. In practical applications, approximate reasoning is usually used to deal with uncertain transactions or inaccurate data. Therefore, the intelligent information system needs to effectively deal with the uncertainty when used in decision-making. This requires the system to be able to simulate human approximate reasoning methods.

The decision-making of the robot soccer system is derived from the analysis of information from different sources. This information is disturbed to varying degrees or has inherent uncertainties. Therefore, an intelligent information system is needed to extract knowledge from this special information database in order to make reasonable decisions and command the operation of the robot soccer system. Fuzzy logic provides a fuzzy mechanism based on nondeterministic data and approximate reasoning using nondeterministic inference rules [22, 23].

2.3.3. Blur Image Processing.
In the soccer robot system, the vision subsystem is the main information source of the decision-making system. The accuracy of image collection and the speed of image recognition directly affect the final result of the game. When processing and recognizing images, we must fully consider the characteristics of the image itself and human visual characteristics. The image display process is a mapping process from diversity to unity. The three-dimensional scene is only expressed in the form of levels, which determines that the image itself has many uncertainties; that is, uncertainty and human vision change from black to white. Unclear gray levels are difficult to distinguish accurately. Therefore, vague set theory can be used as a model and method to effectively describe image features and human visual features and can be applied to analyze human crisis, perception, and recognition behaviors [24]. In recent years, in the research of image processing and recognition technology, many students have devoted themselves to introducing fuzzy set theory into image processing and recognition technology and have achieved remarkable results. Experiments show that the processing and recognition technology based on vague set theory are better than traditional methods in some cases, especially when the image is very noisy [24].

3. Football Training Robot Action Evaluation Algorithm Experiment

3.1. Robot Material Selection.
Considering the dual requirements of strength and weight reduction, aluminum alloy is mainly used as the body material of the robot, and some parts with low strength requirements, such as the arms and front and rear chest cavity, use carbon fiber materials. Considering the factors of control, torque, and volume, Dynamixel RX-28 high-performance servomotor produced by ROBOTIS of Korea [25] is selected.

RX-28 motor integrates reducer, driver and communication interface, compact structure, and small size and offers strong power output. It has standardized mechanical and electrical interfaces to facilitate system expansion. It adopts a closed-loop position and speed servo control. The encoder can realize real-time feedback monitoring of the action process, with high control accuracy and an angular displacement resolution of $0.3°$ [26]. With strong customizability, users can customize the attributes of the motor by modifying the system parameters stored in its EPROM area. For example, when multiple motors in the system are connected in series via cables, in order to enable the controller to uniquely identify the motors, each motor can modify the data in the corresponding position in the EPROM area to set its own unique ID number and only need to specify the ID of the receiving motor in the command packet to ensure the correct transmission of the command. Other motor parameters that can be customized include baud rate, rotation angle limit, maximum output torque, and maximum internal operating temperature [27].

3.2. Working Mode of the Robot Soccer System.
The robot soccer system basically includes robots, vision systems, computers, and communication systems. The choice of hardware, execution agents, sensors, and software control strategy algorithms is closely related to the overall working mode.

According to the location of the decision-making part, the working mode is divided into the following two types: vision-based robotic soccer system and robot-based robotic soccer system [28].

According to the robot's intelligence, it can be divided into a vision-based remote control nonintelligent robot soccer system, referred to as a remote control robot and a vision-based intelligent robot soccer system [29].

In fact, we got three working modes:

(1) Nonintelligent robot soccer system based on visual remote control

   Generally speaking, each robot in the system has a driver, a communication unit, and a control panel. It can control its movement direction and speed according to the data received from the central computer. Visual data processing, strategic decision, and robot position control are all done on the central computer, just like a remote control car [30].

(2) Intelligent robot soccer system based on vision

   In this system, the robot has functions such as speed control, position control, and automatic obstacle avoidance. The central computer processes countermeasure decisions through optical data and then issues instructions to the robot, and the robot responds to the instructions. In order to avoid automatic obstacles and perform position detection, the robot itself is equipped with sensors.

(3) Robot-based robot soccer department

In the system, the robot has many autonomous behaviors, and all calculations, including decision-making, are done by the robot itself. The host only processes the visual data and transmits the relevant position and other information to the robot, including one's own party, the other party, and the ball. In fact, the role of the host in processing visual data is equivalent to a sensor [31].

3.3. Football Robot System Structure.

From a structural point of view, the centralized control microsoccer robot system can be divided into two parts: the upper computer and the lower computer. Most of the software work of the system is concentrated in the upper computer. The overall structure of the upper computer program system is divided into 6 modules: master control, virtual stadium, vision, strategy, communication, and simulation. The task of the master control is responsible for the process of system initialization, creation of data exchange memory area between modules, task scheduling, time allocation, and system unloading; the virtual arena draws objects on the designated screen position based on the visual feedback data, and in the virtual venue, a memory area is opened for data exchange with the vision or simulator; the simulation module calculates the pose of each object on the field at the next moment according to the command sent by the strategy to the vehicle body and mainly deals with the calculation of the object's trajectory and collision processing; the module completes the preprocessing and real-time identification of information; the decision-making module converts the strategic thinking of the decision-maker into an insinuation relationship from the state space to the action space. The lower computer refers to the walking mechanism of the robot car system, which concentrates most of the hardware workload and is responsible for the control and processing of the robot car. From the perspective of the geographical location of the hardware, the MiroSot football robot system includes four major subsystems: vision subsystem, communication subsystem, trolley subsystem, and decision-making subsystem. The system includes hardware devices: host, vision interface, communication interface, CCD camera, image capture card, communication transceiver, single-chip computer system, drive device, and energy system. The overall framework of the system is shown in Figure 1:

4. Analysis of Action Evaluation Algorithm for Football Training Robot

4.1. Analysis of Football Training Robot Effect.

The analysis will be simulated and verified by Matlab. We will compare the kicks after training with the manually adjusted parameters before training, and the experimental results will fully reflect the effectiveness of enhanced learning. For the results of walking optimization, we will compare the effects of the manually adjusted parameters and the optimized parameters and analyze the comparison between the comprehensive parameters of the hierarchical learning and the parameters of each training task. It can be seen how hierarchical learning can effectively avoid the overfitting characteristics of reinforcement learning and ensure the flexibility, speed, and stability of walking to the greatest extent. Note that we have turned off server noise and visual restrictions when training to play football or walking so that the simulation results of the agent are not affected by the server to produce unnecessary data noise. In the experiment, in order to detect the performance of the robot in the real game, all the experimental structures are the average values of multiple experiments under the noise environment.

Both long shots and kicks used 100 samples per generation, 200 iterations of training, and the penalty value gradually converged. Table 1 shows the comparison of the kicking effect after training and before training.

Figure 2 shows the comparison of the position error and orientation error of the robot before and after the kick. The blue curve represents the position and orientation error before optimization, and the red curve represents the position and orientation error after optimization using the method in this chapter. It can be seen from the figure that after the optimization, the position of the robot basically does not change, and the orientation angle also changes slightly, which shows the effectiveness of this method.

4.2. Analysis of Action Real-Time Evaluation Algorithm

4.2.1. Time Performance Analysis.

For the environment where the soccer robot is located, the ICP (iterative closest point) algorithm and the algorithm in this article are used to compare the estimated time of the robot's pose. Randomly select 20 consecutive frames of data from the data frames tested by the test instrument, and the time unit is recorded in seconds. The result is shown in Figure 3.

From the data analysis in the figure, it can be seen that the average time for the ICP algorithm to realize the robot pose estimation is 0079 s; the average time for the pose estimation proposed in this paper is 0.004 s, which is much shorter than the ICP algorithm in comparison. The difference in the smoothness of the time curves between the two is related to the matching method. If the corresponding point is selected correctly in the ICP algorithm, the matching time will be very short. If the corresponding point is selected incorrectly, the matching time will be very long; the algorithm in this paper only selects obstacles The central point coordinate feature of the object participates in the calculation, which reduces the amount of data for environmental matching, and the obstacle repetition rate is high, making the pose estimation time relatively short and relatively stable.

4.2.2. Accuracy Performance Analysis.

For the environment where the soccer robot is located, the ICP algorithm and the algorithm in this paper are used to compare the accuracy of the estimated values of the robot's pose (x, y, a). Randomly select 10 consecutive frames of data from the data frames tested by the testing instrument, and the results are shown in Figure 4:

From the data in the figure, it can be seen that the maximum deviation of the Y displacement estimation result of the algorithm in this article and the ICP algorithm is 0.3 m,
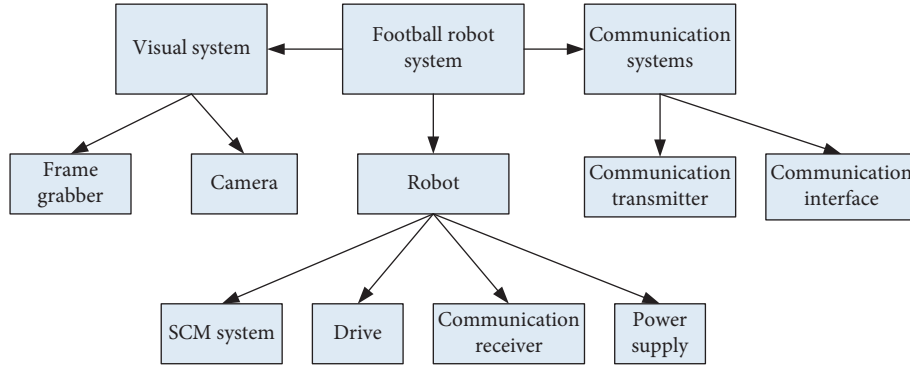
FIGURE 1: Soccer robot system composition.

TABLE 1: Comparison of soccer robot kicking results.

Kick	Average penalty	Average distance (m)	Time (seconds)
Far kick (before training)	−3.6	8.7	2.5
Far kick (after training)	−3.2	14.5	2.5
Quick kick (before training)	2.5	5.5	1.5
Quick kick (after training)	4.8	8.1	0.8
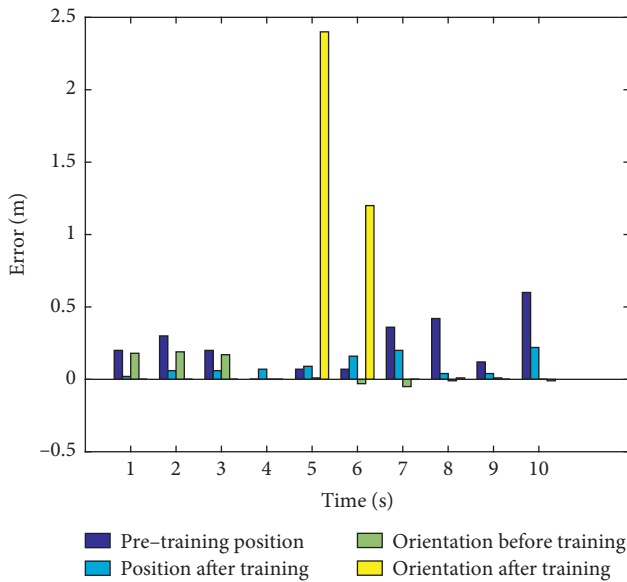
FIGURE 2: Comparison of position and orientation errors.
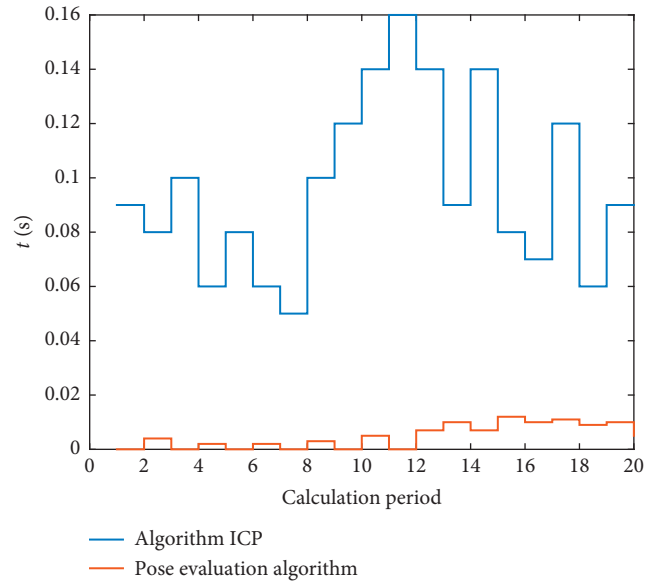
FIGURE 3: Comparison of action pose estimation time.

and the X displacement estimation value appears to be obvious deviation at 6 frames. This is mainly due to the calculation step of the ICP algorithm, 1/15, resulting in a larger cumulative error. The maximum deviation of an estimated value between the ICP algorithm and the algorithm in this paper is 0.05 rad. The results show that the accuracy of the proposed algorithm is very close to that of the ICP algorithm.

4.3. Analysis of Action Algorithm of Football Training Robot. The SCRAM algorithm is used to optimize the player's position of Nanyou Apollo2D. The state when the offensive

and defensive transition occurs is used as the root node of the Monte Carlo tree model, and the simulation experiment is carried out in combination with the defense strategy under the MCTS algorithm. First of all, in order to eliminate the interference of other factors as much as possible, the experiment selects a known action convergence area and position as the root node of the experiment to reduce the influence of different action choices on the results; second, on this basis, the training method is used to obtain the return value of the evaluation function as the evaluation value of the role assignment under the SCRAM algorithm to evaluate the three algorithms. The experimental results are shown in Figure 5:
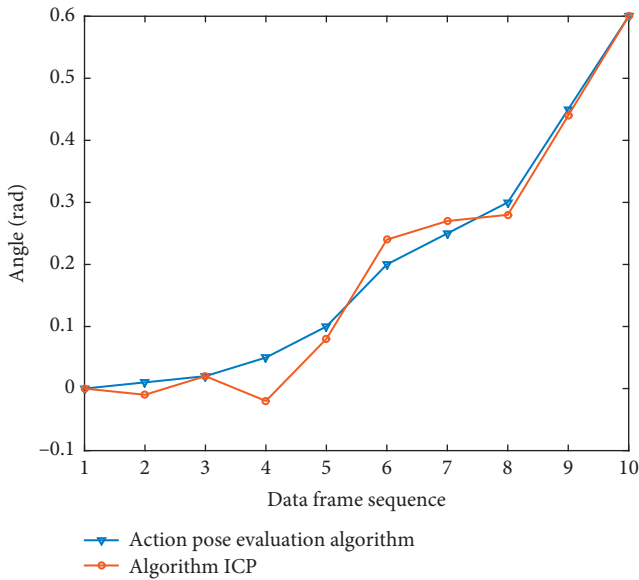
Figure 4: Accuracy comparison of an angle component.
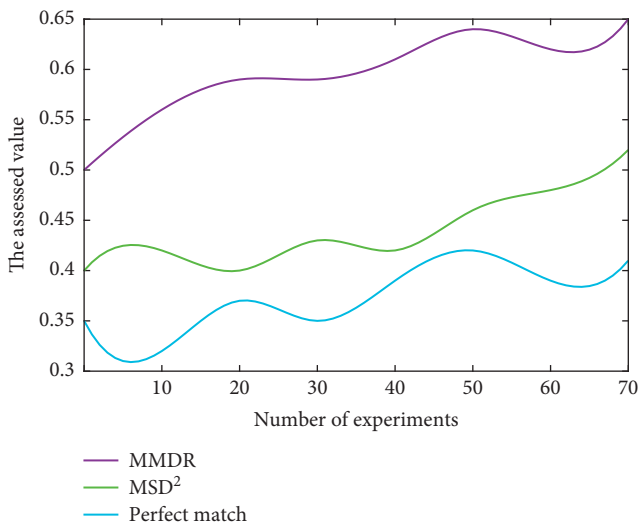
Figure 5: The average evaluation value of the algorithm under the fast counterattack.

The abscissa of the chart is the number of experiments, and the ordinate is the average return value during the experiment. We can find that in the actual training process, the performance of the MSD2 algorithm, which is the fastest in place, is not satisfactory. Because in this algorithm, in order to ensure the speed, the motion of the agent cannot meet the dynamic consistency, which leads to a certain unreasonable situation in the path allocation. At this time, the player's position may cause certain errors, resulting in a low final return value. The accuracy requirements of the perfect matching algorithm enable the agent to keep running according to the optimal path during the process of returning to the defense. The time problem of a perfect matching in normal defensive tasks can be allowed.

Another defensive case that needs to be specifically put forward is the situation where the opposing player steals the ball to counterattack quickly. Through the game, it was found that when the enemy player steals the ball and quickly scores into our half, our defenders often experience heavy physical exertion and slow return to defense. This is because in this case, the players need to quickly return to our side to defend in order to solve the problem of the enemy's many offensive players and our own defensive players as soon as possible. Therefore, the above evaluation value will no longer apply to this situation. After conducting multiple simulation experiments on this special situation, the result is that in the case of a fast counterattack, the MSD2 algorithm has good adaptability because of its speed advantages.

5. Conclusions

In this article, only kinematics analysis is performed, and dynamics analysis is not performed. The research on robot walking in a stable manner needs to be further deepened. This article has carried out a simple gait planning for a biped robot moving at low speed. The biped robot needs to increase the walking speed of the robot in order to achieve anthropomorphic walking. This puts forward higher requirements for gait planning. At present, the academic community needs further research to confirm whether the proposed gait planning method can meet the requirements of high-speed walking, and the dynamic walking method proposed in this article needs to be further improved.

The development trend of the soccer robot system is a completely autonomous multiagent system. Each robot in the system has many functions and autonomous behaviors. It can observe the situation on the field according to its own eyes, make strategic choices through the strategy library, automatically avoid according to sensor data, and communicate with other robots through the communication system. In other words, all calculations, decisions, and control are done by the robot itself.

Aiming at the pose estimation problem of mobile robots, this article proposes a robot pose estimation algorithm based on the analysis of the advantages and disadvantages of current commonly used estimation methods, combined with the characteristics of the data tested by the tester. Experimental results show that the algorithm can efficiently and accurately realize the pose estimation of mobile robots. However, this algorithm still has a serious problem. When there are obstacles in the environment that cause the lidar to measure the width at different angles, the center coordinate position of the obstacle may change greatly, leading to the position of the algorithm in this article. The pose estimation result is not accurate.

Data Availability

The data underlying the results presented in the study are available within the manuscript.

Conflicts of Interest

The authors declare that they have no conflicts of interest.

References

[1] X. Xiong, "Artificial intelligence control algorithm for the steering motion of wheeled soccer robot," *International Journal of Pattern Recognition & Artificial Intelligence*, vol. 33, no. 10, pp. 238–252, 2019.

[2] A. H. Azadeh, S. Jebreili, E. Chang et al., "An integrated fuzzy algorithm approach to factory floor design incorporating environmental quality and health impact," *International Journal of System Assurance Engineering & Management*, vol. 8, no. 4, pp. 1–12, 2017.

[3] K. Khan, N. Ahmad, F. Khan, and I. Syed, "A framework for head pose estimation and face segmentation through conditional random fields," *Signal, Image and Video Processing*, vol. 14, no. 1, pp. 159–166, 2019.

[4] B. B. Vargas, M. Shepard, J. G. Hentz, C. Kutyreff, L. G. Hershey, and A. J. Starling, "Feasibility and accuracy of teleconcussion for acute evaluation of suspected concussion," *Neurology*, vol. 88, no. 16, pp. 1580–1583, 2017.

[5] E. Sharova, G. Boldyreva, M. Chelyapina et al., "P312 fMRI analysis of the human brain's neuroplasticity as a basis of movement disorders compensation after traumatic brain injury," *Clinical Neurophysiology*, vol. 128, no. 9, pp. e278–e279, 2017.

[6] I. Mohammad, G. Amin, S. F. Roya et al., "Effect of low-level laser therapy on orthodontic movement of human canine: a systematic review and meta-analysis of randomized clinical trials," *Acta Informatica Medica*, vol. 26, no. 2, pp. 139–143, 2018.

[7] T. M. Acker, J. E. Gable, M.-F. Bohn et al., "Allosteric inhibitors, crystallography, and comparative analysis reveal network of coordinated movement across human herpesvirus proteases," *Journal of the American Chemical Society*, vol. 139, no. 34, pp. 11650–11653, 2017.

[8] M. Wang, "The application of the human body link stress analysis method in the basketball movement," *Journal of Computational and Theoretical Nanoscience*, vol. 14, no. 1, pp. 79–83, 2017.

[9] B. Serrien, M. Goossens, and J.-P. Baeyens, "Issues in using self-organizing maps in human movement and sport science," *International Journal of Computer Science in Sport*, vol. 16, no. 1, pp. 1–17, 2017.

[10] T. Robert, P. Leborgne, G. Beurier et al., "Estimation of body segment inertia parameters from 3D body scanner images: a semi-automatic method dedicated to human movement analysis applications," *Computer Methods in Biomechanics & Biomedical Engineering*, vol. 20, no. 1, pp. 177-178, 2017.

[11] K. Khoshhal, H. Aliakbarpour, K. Mekhnacha et al., "LMA-based human behaviour analysis using HMM," *Ifip Advances in Information & Communication Technology*, vol. 349, no. 1, pp. 189–196, 2017.

[12] Q. Sun, F. Hu, and Q. Hao, "Human movement modeling and activity perception based on fiber-optic sensing system," *IEEE Transactions on Human-Machine Systems*, vol. 44, no. 6, pp. 743–754, 2017.

[13] N. D. Giorgis, E. Puppo, P. Alborno et al., "Evaluating movement quality through intrapersonal synchronization," *IEEE Transactions on Human-Machine Systems*, vol. 49, no. 99, pp. 304–313, 2019.

[14] M. G. Grazielle, S. E. F. Detogni, M. P. V. De et al., "Lumbar spine, pelvis and hip sit-to-stand assessment protocols and ROM reference values: a systematic review with meta-analysis," *Human Movement*, vol. 19, no. 3, pp. 3–15, 2018.

[15] J. P. M. Vital, D. R. Faria, G. Dias, M. S. Couceiro, F. Coutinho, and N. M. F. Ferreira, "Combining discriminative spatiotemporal features for daily life activity recognition using wearable motion sensing suit," *Pattern Analysis and Applications*, vol. 20, no. 4, pp. 1179–1194, 2017.

[16] I. M. Lochhead and N. Hedley, "Modeling evacuation in institutional space: linking three-dimensional data capture, simulation, analysis, and visualization workflows for risk assessment and communication," *Information Visualization*, vol. 18, no. 1, pp. 173–192, 2019.

[17] I. Ajili, Z. Ramezanpanah, M. Mallem, and J.-Y. Didier, "Expressive motions recognition and analysis with learning and statistical methods," *Multimedia Tools and Applications*, vol. 78, no. 12, pp. 16575–16600, 2019.

[18] Y. Hu, W. Li, Q. Wang et al., "Evaluation of water inrush risk from coal seam floors with an AHP-EWM algorithm and GIS," *Environmental Geology*, vol. 78, no. 10, pp. 290.1–290.15, 2019.

[19] N. Rossol, I. Cheng, and A. Basu, "A multisensor technique for gesture recognition through intelligent," *Skeletal Pose Analysis*, vol. 46, no. 3, pp. 350–359, 2017.

[20] G. Ledder and V. A. Zlotnik, "Evaluation of oscillatory integrals for analytical groundwater flow and mass transport models," *Advances in Water Resources*, vol. 104, pp. 284–292, 2017.

[21] D. M. Rosen, L. Carlone, A. S. Bandeira et al., "SE-Sync: A certifiably correct algorithm for synchronization over the special Euclidean group," *The International Journal of Robotics Research*, vol. 38, no. 2-3, pp. 95–125, 2019.

[22] S. Kathavate, L. Rajesh, and N. K. Srinath, "PR-LRU: partial random LRU technique for performance improvement of last level cache," *International Journal of Computer Aided Engineering and Technology*, vol. 11, no. 1, pp. 111–121, 2019.

[23] Z. Lv, L. Qiao, and Q. Wang, "Cognitive robotics on 5G networks," *ACM Transactions on Internet Technology (TOIT)*, vol. 2020, Article ID 6632701, 2020.

[24] M. Kopaczka, R. Kolk, J. Schock, F. Burkhard, and D. Merhof, "A thermal infrared face database with facial landmarks and emotion labels," *IEEE Transactions on Instrumentation and Measurement*, vol. 68, no. 5, pp. 1389–1401, 2019.

[25] R. Volpe and C. Circi, "Optical-aided, autonomous and optimal space rendezvous with a non-cooperative target," *Acta Astronautica*, vol. 157, pp. 528–540, 2019.

[26] J. Yin, X. Liu, F. Sun et al., "One-shot SADI-EPE: a visual framework of event progress estimation," *IEEE Transactions on Circuits and Systems for Video Technology*, vol. 29, no. 6, pp. 1659–1671, 2019.

[27] D. Pelusi, R. Mascella, L. Tallini, J. Nayak, B. Naik, and A. Abraham, "Neural network and fuzzy system for the tuning of gravitational search algorithm parameters," *Expert Systems with Applications*, vol. 102, pp. 234–244, 2018.

[28] I. Mladenovi, M. Miloš, and S. Sokolov-Mladenovi, "Analyzing of innovations influence on economic growth by fuzzy system," *Quality & Quantity*, vol. 51, no. 3, pp. 1297–1304, 2017.

[29] M. Elhoseny, A. Shehab, and X. Yuan, "Optimizing robot path in dynamic environments using genetic algorithm and bezier curve," *Journal of Intelligent & Fuzzy Systems*, IOS-Press, vol. 33, no. 4, pp. 2305–2316, 2017.

[30] R. Mitra, A. K. Goswami, and P. K. Tiwari, "Voltage sag assessment using type-2 fuzzy system considering uncertainties in distribution system," *IET Generation, Transmission & Distribution*, vol. 11, no. 6, pp. 1409–1419, 2017.

[31] C. Li, M. Tang, G. Zhang, R. Wang, and C. Tian, "A hybrid short-term building electrical load forecasting model combining the periodic pattern, fuzzy system, and wavelet transform," *International Journal of Fuzzy Systems*, vol. 22, no. 1, pp. 156–171, 2020.

Research Article

Design of an Intelligent Virtual Classroom Platform for Ideological and Political Education Based on the Mobile Terminal APP Mode of the Internet of Things

Xilin Zhang,[1,2] **Xiaohan Gao,**[2] **Honglian Yi,**[2] **and Zhe Li** [3]

[1]*Department of Foreign Languages, Dalian University of Technology, Dalian 116052, Liaoning, China*
[2]*School of International Education, Dalian University of Technology, Dalian 116024, Liaoning, China*
[3]*Archives and History Museum, Dalian University of Technology, Dalian 116123, Liaoning, China*

Correspondence should be addressed to Zhe Li; lizhe@dlut.edu.cn

This article uses a software architecture model that combines two architectures, based on the traditional Android environment. Through comparative research on network technology today, Java technology has been selected as a tool for developing network education systems for future research and maintenance upgrades. The underlying network education technology relies on APP to enable education between teachers and students. This technology can not only give play to the advantages of computers in network data transmission, but also embody a new teaching model with teachers and students as the main body. It can solve various practical problems in teacher and student education and educate teachers and students by simulating the actual educational environment of the classroom and educational process using a variety of practical education management strategies. The experimental results prove that with the help of this virtual classroom platform for ideological and political education, it can provide students with more ideological and political learning resources, increase students' interest and time in learning, and promote the diversification of ideological and political learning methods. The quality of teaching is more conducive to the learning of knowledge points for students. At the same time, the system is operating in good condition. Switching between different interfaces is maintained at about 0.1 seconds. The system performance is also perfect. The overall analysis function is basically designed. It is a better learning platform.

1. Introduction

With the rapid progress of network technology and multimedia technology in today's society [1] and the increasing popularity of the Internet, the education model of various universities in our country is constantly innovating and changing. The current advanced professional classes pose a very obvious problem: traditional classrooms are a combination of knowledge classes and skill classes. "Knowledge class" means that students learn theoretical knowledge in the classroom, and "skill class" means learning skills in the classroom. Mobile devices and the Internet are two innovative platforms that have accelerated the process of computerization and facilitated the lifestyles of most people today. Rebuild a new classroom environment, break the face-to-face limitation, and build a model suitable for modern students [2]. The new intelligent environment for learning is very meaningful. It is also an inevitable trend and choice that must be faced when the informatization of the social education industry develops to some extent.

The virtual classroom platform for ideological and political education in my country tends to gradually become a popular form of education, which further develops the virtual classroom platform in my country. Proposals have been made to apply network technology to university education in combination with the educational needs of the university, which provides an important foundation for the future application and development of network technology in university education. In particular, the outbreak of the new Crown Pneumonia epidemic this year has reached the

peak of development for virtual classroom platforms, allowing students across the country to continue their own learning using a variety of virtual classroom platforms. The system is operating in good condition, and the switching between different interfaces is maintained at about 0.1 seconds; the page loss rate is less than 0.5%, the operation interface is simple and clear, easy to operate, and the data with limited format and data type are verified, including client verification and server verification, using an error reminding mechanism to prompt the user to enter the correct data and the correct operating system.

The main work of this paper is divided into two parts. The first part is aimed at the ideological and political education virtual classroom platform to make it comply with the characteristics of high cohesion and low coupling. Introducing some functional technology and feasibility analysis, the second part is the design idea of the virtual classroom platform of ideological and political education and the construction of the platform, and testing it. The first chapter briefly introduces the overall background and development prospects of the project, including the technology to build the platform and the origin and role of virtual technology, and points out the innovations of this article. Chapter 2 provides a detailed introduction to the relevant functional technologies and feasibility analysis that underlie the project, while analyzing similar topics at home and abroad. Chapter 3 is to design the functional configuration of the platform and the design of the platform. Chapter 4 analyzes the platform implementation and the tests performed when the platform is built. At the same time, it summarizes the system execution status and performance. Chapter 5 is the conclusion part, which is a summary based on the experimental results of this article.

2. Design of an Intelligent Virtual Classroom Platform for Ideological and Political Education Based on the Mobile Terminal APP Mode of the Internet of Things

2.1. Related Work. Based on the concept of the Internet of Things, the American Power Grid Association has also set a prospect for the future development of the Internet of Things technology [3]. In 2005, the International Telecommunication Union expanded the concept of the Internet of Things and warned of the arrival of the Internet of Things era. The era of the Internet of Things makes it possible to share large amounts of data between different devices and transmissions on the network. The Internet of Things can be applied to all aspects of our life, work and study. For example, in the case of virtual classrooms, the Internet of Things uses middleware, network service technology, and event-based sensors to propose new solutions for virtual classrooms [4]. Abu-Sharkh et al. use a broadband network to communicate with smart devices, thus ensuring the reliability of the system [5]. Tiwari et al. implement sensor network applications in the dynamic virtual classroom learning environment and provide more energy-saving and sensitive intelligent control systems for virtual classroom learning equipment [6].

Virtual home education technology started late. Since the 1990s, with the support of national government agencies, some first-class cities have begun to pilot digital virtual classroom plans and initially introduced virtual classroom education technology in the sense of digital virtual classrooms. However, the home computer technology at that time was still very backward. The system using digital virtual classrooms as a demonstration project only performed simple automatic control, and there was still a long way to go before digitalization. However, according to the technology platform at that time, the telephone network was the only home network interface, and related digital technologies have been ingeniously studied based on the telephone network [7]. Raes et al. explore the virtual classroom learning technology by studying the home gateway controller [8]. Radovan and Kristl believe that the virtual learning classroom structure composed of gateways and Internet servers; the concept of the Internet of Things has been officially mentioned in China [9]. Yilmaz propose that as far as the current virtual classroom technology in family education is concerned, although we started late, its development is relatively fast [10].

2.2. Internet of Things. The system of the Internet of Things is very complex. It includes various applications such as electronics, communications, computers, and agronomy. By using IoT technology for data collection and reception, reliable transmission, intelligent processing, automatic control, etc., various production and transmission links can be established. Wait for the complete follow-up [11, 12]. However, if the network environment is different, the communication protocols may not be completely compatible. Traditional wireless networks include mobile networks and LAN wireless networks. These network communication plans are aimed at point-to-point or multi-point-to-point transmission and have higher communication goals and countermeasures [13].

2.2.1. IoT Architecture. Current IoT system models are not universal and lack a complete system structure. When building an IoT system, you need to consider network performance such as scalability, reusability, and security. It is necessary to summarize the research results of the Internet of Things architecture and the related theories and models of the wireless network architecture model. The main basis for designing and verifying the structure of the Internet of Things is still to simulate the actual scenarios of the Internet of Things, which should be combined with the existing examples of Internet of Things applications for summary and improvement, understanding the development direction of the Internet of Things. Finally, for different types of terminal equipment, it is necessary to consider relevant parameters, application technologies, and relevant standard specifications [14, 15], and a specific plan for the needs of users and the implementation of their functions is required. According to most research results at home and abroad, the Internet of Things system is divided into perception layer, network layer, and application layer, as shown in Figure 1.
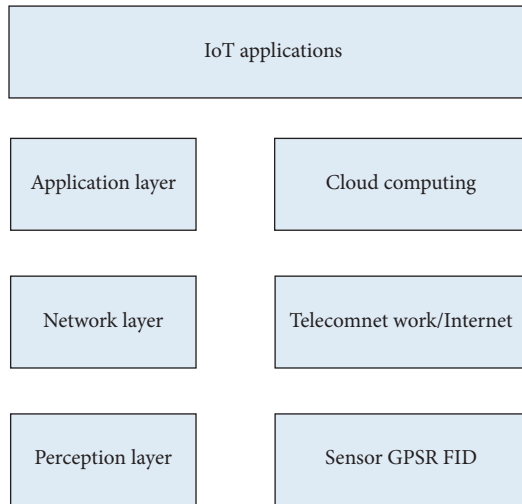
FIGURE 1: Internet of Things system composition diagram.

2.2.2. Perception Layer. The perceptual layer is the lowest structure of the Internet of Things. These are used for node analysis, processing, automatic management, and data collection during transmission of data to heterogeneous networks [16, 17]. Most of the changes in information in the environment are continuous and simulated. The information on the network is completely different, but different types of sensor devices are required to process the type of information retrieved [18], to be able to find and retrieve information and provide strong support for production and guidance.

2.2.3. Transport Layer. The IoT layer acts as a bridge between the perception level and the application level. The relevant information collected from the perception level is wirelessly transmitted to the terminal device. Commonly used are IEEE802.3-based Ethernet transmission technology, IEEE802.11-based Wi-Fi transmission technology and IEEE802.15.1xFoundation-based Bluetooth transmission technology, IEEE802.15.4-based ZigBee transmission technology, and 6Lan multitransmission technology and 6Low transmission technology mobile transmission technology, such as GSM, GPRS, and 3G, based on IEEE802.16, Mi MAX transmission technology, etc. Both 802.3-based Ethernet and 802.11-based Wi-Fi are IP-based network communication protocols, and 802.3-based Ethernet is the most widely used communication technology and multilayer structure in the IP protocol architecture. It can be implemented through other communication protocols and can also be applied to the Internet of Things architecture [19, 20].

2.2.4. Application Layer. Process the data transmitted by the network layer and send the results obtained after algorithm analysis to different systems [21], which facilitates the operation and use of end users, including production, management, and maintenance. The application layer is the outermost layer of the three-tier structure of the Internet of Things, and its most important function is processing, which

is to use cloud computing platforms for data processing. The application layer and the lowest perception layer are the most important cores of the Internet of Things. They have their own distinctive features [22]. The application layer needs to perform calculations, processing, and deep knowledge application on the collected data of the perception layer to perform data real-time control, management, and scientific judgment processing.

2.2.5. Virtual Classroom Process Based on the Internet of Things. In the Internet of Things, various things in the real world are deleted as processes, and relationships between different things are also deleted as connections between processes. The Internet of Things provides a more intuitive way to monitor networks of real-world relationships [23]. There are usually two ways to build the Internet of Things: top-down and bottom-up [24, 25]. The top-down construction method is an ontology-based construction method, which uses high-structure encyclopedias and other websites as data sources, extracts the constraints and rules of the ontology from them, and supplements them in the knowledge base, while the bottom-up construction method is simple. Identify entities, attributes, and relationships from data collected through pattern recognition, rulemaking, etc. Then add it to the flowchart, as shown in Figure 2.

2.3. APP Mode. Nowadays, mobile devices such as smartphones and tablets are becoming more and more popular, and people are gradually learning how to live with a variety of APP clients. Currently, all major e-commerce companies in the country have their own APP clients. The aspect is that APP mode has entered people's lives and has begun to shine. APP is not as monotonous as a smartphone client. Today, many smartphones allow you to wirelessly control your home appliances by downloading APP software with different features from different manufacturers [26–28]. Not only that, with the sudden emergence of the mobile Internet, more and more Internet companies and e-commerce platforms regard APP as one of their main directions for their sales promotion. A large amount of data show that the current flow of APP customers to e-commerce companies far exceeds the traditional Internet flow, and profiting through APP applications is also the development direction of large e-commerce platforms. There is evidence that the tendency of large e-commerce platforms to favor mobile applications is also obvious [29]. The reason is not only the increase in daily traffic, but most importantly the convenience of mobile phones and mobile terminals has added more users to enterprises and accumulated more users. Apps with a good user experience greatly increase loyalty and activity. Users thus play a key role in the company's revenue generation and future development.

2.3.1. APP Structure Design. The management application assumes the functional requirements of the application-level application; matches the functional requirements with the physical device layer, transport layer, and Android system;
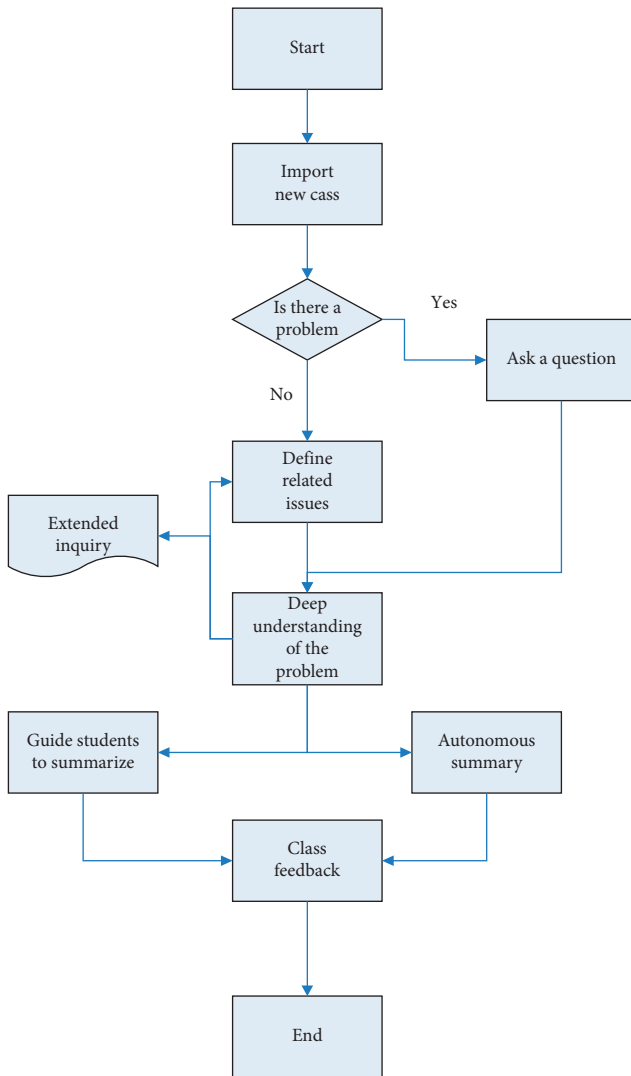
FIGURE 2: Virtual classroom flowchart based on Internet of Things.

and manages the specific execution of the functional functions. Service management level application is the core of system management service function. Its role is to perform a top-down mapping function, and this mapping relationship must have flexibility and long-term storage before it can be modified [30]. When the management service level application is installed and started for the first time, an associated function allocation table will be created through SQLite. At this time, since the terminal and device node information has not been received, the table only contains the corresponding Android operation data.

When the application-layer application wants to implement a specific function, the application layer application will access the SQLite function mapping correlation table and obtain the required data by reading, writing, etc., and transfer them to application-level management applications. In application management, the application level controls external devices according to the corresponding items in the SQLite table or performs corresponding Android operation functions. If there is no function between the management service level application and the application-level

application, the content of the associated SQLite function table entry remains unchanged [31]. The first logical value of each function parameter or operating parameter is 0 or 1, which represents the completed operation or the incomplete operation, respectively. The system creates a top-down functional relationship mapping relationship based on the above functions.

2.3.2. APP Design Process. When the system is running, the logical relationship between the App application layer and the App management service layer, and the App management service layer and the terminal node is the request feedback process. When the user wants to use the management service level application, they move the mobile smart device close to the NFC tag to the terminal node to receive terminal node and device information. When an application-level application wants to perform terminal, device or Android node functions, it will send a request to the service-level application through the SQLite mapping correlation table [32]. The management service layer receives the corresponding data information in the table according to the request and converts it into an executable terminal node. The functions and parameters are sent to the terminal node via Bluetooth. The terminal node executes the corresponding function after receiving the content and sending the result. The operation in the application is managed at the level via Bluetooth. As shown in Figure 3.

After the management level application receives the operation result information, it will update the corresponding items in the SQLite function mapping correlation table. After the application-level application receives the feedback, it will learn the execution mode of the operation mode and support the corresponding application-level functions in sequence. It is not difficult to see that the application-layer application only needs to perform identification-based operations without excessive participation in the physical device layer and the transport layer. The packaging of Android functions is similar to this [33]. Each related Android function is assigned a unique function number. When an application-level application needs to call a function, it will pass the function number and corresponding parameters to the service management application. The management service level application will complete the corresponding function accordingly and return the result to the application layer App.

2.4. Virtual Technology. The concept of virtuality can be traced back to 1959 when Christopher Strachey, a professor of computer science at Oxford University, first proposed the concept of "virtuality". The virtual technology at this time is still in the initial stage, which is quite different from what is now called the narrow virtual technology, but it is still regarded as the earliest discussion on virtual technology [34, 35]. VMM abstracts computer hardware resources to form an abstract software layer above the physical hardware layer and realizes the duplication of a computer system originally owned by a single user into multiple copies and supports simultaneous interaction of multiple users. The
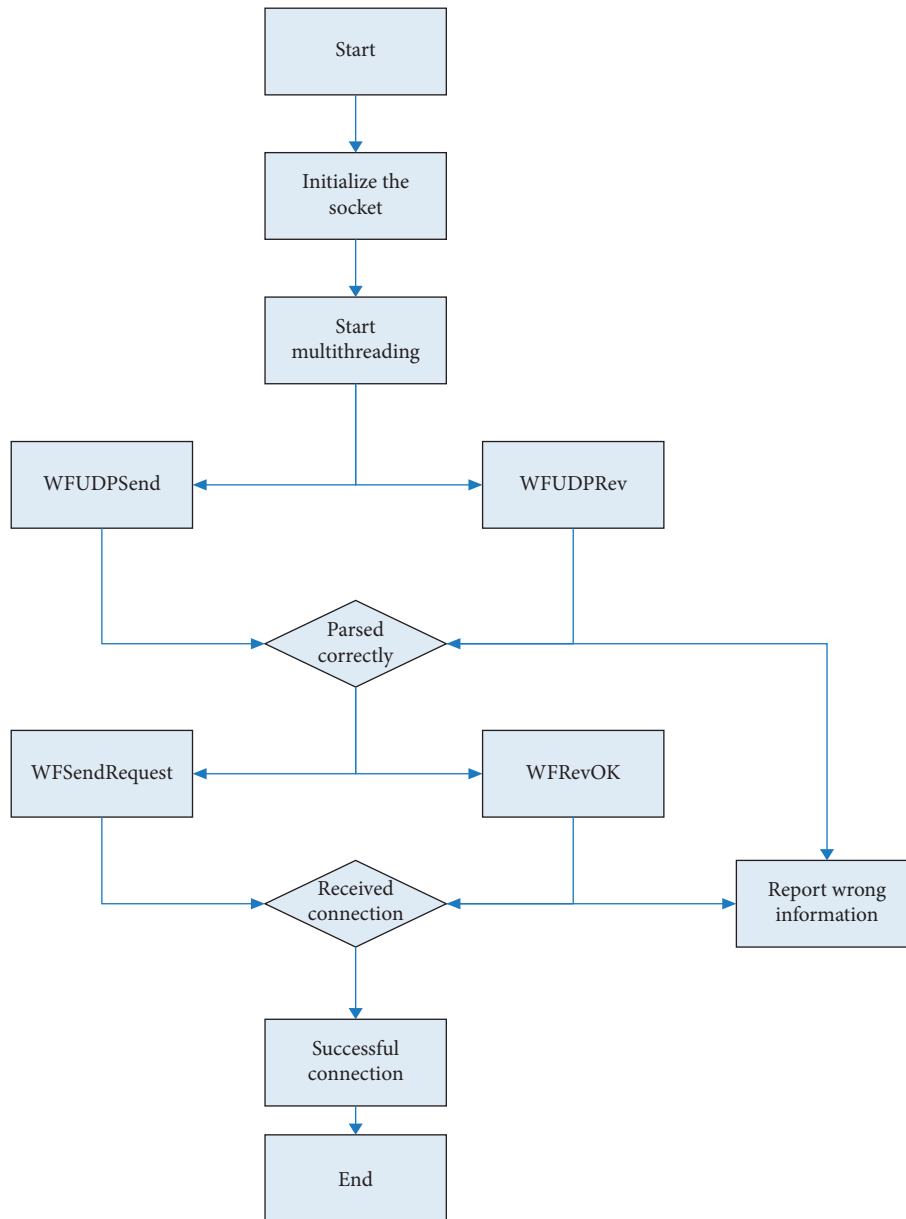
Figure 3: APP design flow chart.

virtual technology at this time has become the prototype of modern narrow virtual technology. According to different levels of abstraction, virtuality is divided into five levels.

(1) The instruction set architecture level is virtual: It refers to the simulation of I/O devices such as processors, memories, buses, and timers of different architectures through software. The software converts the instructions running on the virtual machine into the instructions that can be executed by the machine to run on the hardware of the machine. Since each instruction needs to be simulated by software, performance may be affected to some extent.

(2) Hardware abstraction-level virtualization: Hardware abstraction-level virtualization is a virtual machine

in the general sense. The hardware abstraction level has a very high degree of virtual isolation, supports different operating systems, has low risk, and maintains the same way as general hosts. However, since this level of platform can access the bottom layer of the host operating system, the effort required for users to install such a virtual machine is almost the same as installing a brand new computer, so the deployment cost of such a virtual machine is relatively high.

(3) Operating system-level virtualization: Operating system kernel virtualization minimizes the cost of adding new virtual machines. Hardware abstraction-level virtualization is an abstraction of the actual physical hardware, and operating system-level virtualization is an abstraction of the host machine's

operating system kernel, providing an isolated operating environment for virtual entities. I will. The operating environment for application software within these virtual entities consists of the host operating system, libraries, dependent software, specific data structures and file systems, and other preferences. If these operating environments have not changed, it is almost impossible for application software to find the difference between that environment and the actual operating system environment. This is the key to operating system-level virtualization.

(4) Programming language level virtual: This level of virtual platform is responsible for directly translating high-level programming languages into hardware execution instructions, which has the advantages of cross-platform and cross-language.

(5) Library-level virtualization: Most applications rely on a large number of runtime APIs for design. The use of dynamic linking to hide the implementation details of the library API can enable programmers to directly call the API, eliminating the need for understanding API implementation and overcoming different language bands, trouble coming.

2.5. Feasibility Analysis

2.5.1. Technical Feasibility. The ideological and political education virtual classroom APP mainly uses java technology, based on the Android environment and MySQL database, familiar with network protocols such as tcp, IP, socket, etc. For application development, it has complete functions and simple use characteristics and establishes a data integrity and security stable database. The development technology of the ideological and political education virtual classroom APP has high feasibility, and the developers have mastered certain development technology, so the development of the system is feasible.

2.5.2. Operational Possibility. The login interface of the ideological and political education virtual classroom APP is simple and easy to operate. The common interface window is used to log in to the interface, and the mobile phone APP is used for access operations. Users can access and operate as long as they use their mobile phones. The development of this system adopts java language development; based on Android environment, these development environments make the system more perfect. This system has the characteristics of easy operation, easy management, and good interaction, and it is very simple in operation. So this APP can be developed.

2.5.3. Economic Feasibility. The dynamic nature of the creation of the ideological and political education virtual classroom APP service function chain is manifested in the use of container-borne security functions that can be deployed in seconds. When the request arrives, first dynamically create container function instances according to the needs, and then connect the function instances into chains in order according to the service requirements to pass the specified flow. The required hardware and software environment are easy to buy in the market, and the program development is mainly the development and maintenance of the management system. Therefore, the program does not require high human and financial resources, and the system is not very complicated, the development cycle is short, and it has high economic feasibility.

3. Experimental Research on the Design of Intelligent Ideological and Political Education Virtual Classroom Platform Based on the Mobile Terminal APP Mode of the Internet of Things

3.1. System Function Composition. The design of virtual classroom environment must have high ecological effectiveness and must be combined with newer human-computer interaction technology, so that ordinary students can interact with students, objects, and virtual classroom environment in a relatively humanized way. In order to achieve the above goals, it is necessary to first collect the rich teaching experience of all professional teachers and collect all professional teachers through questionnaire surveys, discussions, and self-reports. Ordinary students should have more consistent knowledge and teaching experience and design corresponding classroom virtual teaching situations as much as possible based on the collected opinions. The experiment platform is mainly composed of a main system and four subsystems to create a teaching application experiment system, which combines interactive simulation, situational interaction, teaching interaction, resource management, and teaching evaluation.

The system platform supports the introduction of scene packages into the classroom, supports the natural environment system, supports the time system, can express the change of time, light, and shadow, and has something in common with the classroom environment. Teaching materials, audiovisual equipment, etc. support the display of graphic teaching materials in classroom lessons. Users support image editing and teaching text content.

They support importing, managing, and deleting 3D characters; support adding and modifying character animation; support IK character animation technology to achieve special effects, support multiple UI switching sets; support 2D and 3DII systems; and support mouse and gesture functions.

3.2. Platform Design Process. From the start of demand analysis to the final use of the platform, the development of virtual classroom projects has gone through multiple links. The main software used is Unity 3D software and SteamVR software. After confirming the start of the project, perform the project requirements analysis. According to the specifications of the virtual classroom website, it is combined with the actual educational needs and actual educational videos of

the interactive virtual reality department with professional teachers in the classroom. Through questionnaire surveys, discussions, and self-reports, we collect the needs of teachers and students of different professions, design the corresponding virtual education situation in the classroom as much as possible based on the collected opinions, and analyze the prediction content and position: I will. Classroom. The basic process is shown in Figure 4.

3.3. Metrics for Platform Evaluation. The indicators for evaluating a system are generally evaluated according to two points. One is its system performance and the conversion flow between pages is not smooth; the other is the running status problem, which is stable and unstable and can accept the maximum number of visits. Of course, the beautiful page is the most basic. These are the key indicators for evaluating the quality of a system.

3.4. Test Subject. In this experiment, we will test the system performance of the platform and experiment on different models, each model operating system 10 times, a total of 1000 times. The second is to test the running status and constantly test the maximum amount of visits it can accept in the background. At the same time, a questionnaire is issued to users to investigate the user's experimentation on the APP interface and the aesthetics of the page and conduct experimental analysis and postsystem optimization.

3.5. Experiment Procedure

3.5.1. Experiment Preparation Stage. We will test the system performance and operating status of the platform, select students from the Political College of X University, and let them use the software for a period of time to learn related video courses online. Then according to the needs of the topic, according to the research information, combined with the interviews of political experts and network technology experts, and refering to related books and theoretical knowledge for preparation, the video tutorials familiar with the topic content are designed as questionnaires.

3.5.2. Experimental Stage. Questionnaires are issued to users to investigate the user's experimentation on the APP interface and the aesthetics of the page and organize the data for experimental analysis and subsequent system optimization.

3.5.3. End of Experiment. After testing the overall level of the experimental class and the control class, make sure that the type of question and the difficulty of the test paper are the same. Compare the performance differences of the two classes and investigate whether the level of the experimental class is significantly improved relative to the control class to determine the advantages of our online multimedia education platform for college physical education compared with the original learning system of X University.
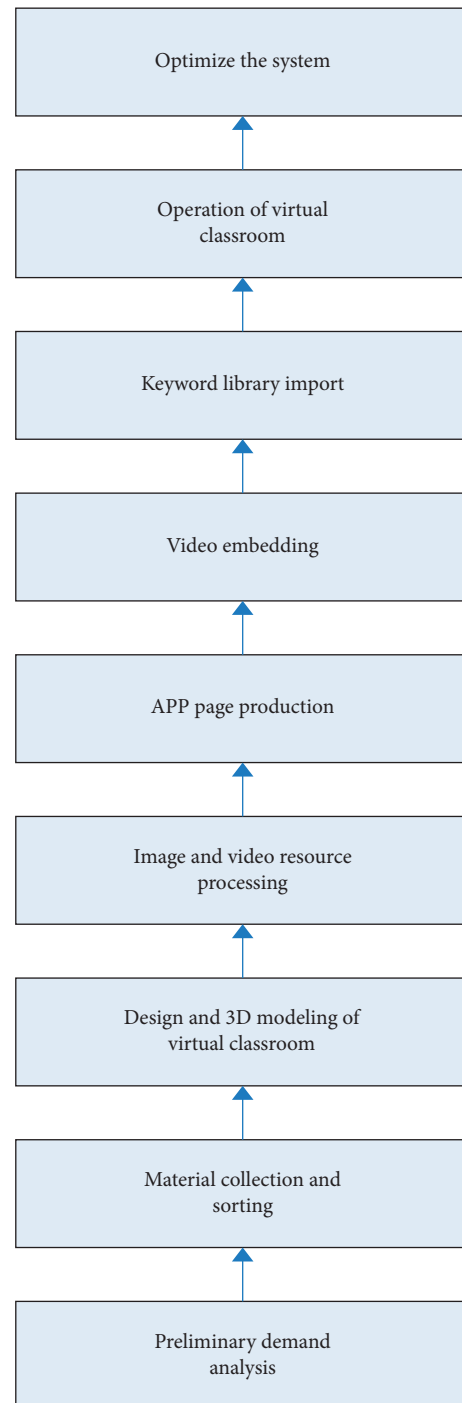
FIGURE 4: Platform design flow chart.

3.6. To Gather Data. In order to obtain accurate data to compare and analyze the feasibility and effectiveness of this experiment, this paper uses the Cora dataset and the IMB dataset. Cora data set is used as a common entity analysis and evaluation data set. For example, the entity analysis process based on Markov logic network adopts Cora.

TABLE 1: System function test table.

Functional module	Function name	Test steps	Test results
Login/registration module	Registered	Register operation	Successfully registered
	Login	Perform login operation	Successfully logged in
Add/query information about courses, teachers, teachers	Add class	Add management	Added successfully
	Query classroom number	Query teacher number operation	Search successful
	View teacher information	Query teacher information	Search successful
Delete/modify course information	Delete course information	Delete course operation	Successfully deleted
	Modify course information	Modify course operation	Successfully modified
Other functional modules	Add room	Add room operation	Added successfully
	Add keyword information	Add keyword information operation	Added successfully
	Manage keyword information	Manage keyword information operations	Management success
	Upload avatar	Upload avatar	Upload successfully

4. Design Experiment Analysis of Virtual Classroom Platform for Intelligent Ideological and Political Education Based on the Mobile Terminal APP Mode of the Internet of Things

4.1. Platform Testing

4.1.1. System Function Test. The function test of the system mainly includes the main functions such as registration, login, device search, adding mode, adding courses, viewing the classroom list, and viewing the teacher information list, as shown in Table 1.

In the process of testing the monitoring effect, through the use of specific video formats for background sampling, encoding and other technical tests, the server and other hardware are repeatedly tested until satisfactory test results are obtained.

4.1.2. Running Status Test Analysis. Here we test the running status of the system and test the maximum number of users who log in to the background system at the same time. We select 100, 500, 1000, and 2000, respectively, for testing. Will it cause system lag or error? (0 means no, 1 means yes) Draw conclusions, analyze, and put forward corresponding countermeasures and suggestions on this basis, as shown in Figure 5.

From Figure 5, you can see that when 500 people perform system login operations at the same time, they start to feel that the system is a little stuck. When 1000 people do the system login operation at the same time, the system starts to make a little error, but at least 100 people do it at the same time Taiwan system login operating system seems to be unstacked and causes an error.

4.1.3. System Performance Test Analysis. After confirming that the fixed port network is turned on, connect to the central controller of the system and set the Wi-Fi routing parameters of the central controller. System performance

monitoring mainly includes web page loading speed, system data loss data rate, return speed, and other parameters, as shown in Figure 6.

It can be seen from Figure 6 that the page loading speed and return speed of the system are within 0.1 seconds. According to the patience of humans using software refresh, it can be known that the interface efficiency of the system is qualified, and the loss rate of the 4 groups of pages is 0.3% on average. This may be a problem of the system itself, or it may be a problem of the network, but this is a direction of system optimization in the later stage.

4.2. User Satisfaction Analysis.
In order to verify the effectiveness of the coordination strategy based on the maximum operability proposed in this article, a questionnaire was issued to users to investigate the user's experimentation of using the APP interface and the aesthetics of the page and collected data for analysis, which is a later system The optimization put forward corresponding countermeasures and suggestions, as shown in Figure 7.

From Figure 7, we can see that users are happy with the experiment using the APP interface and page aesthetics, and students are happy to use this APP. With the help of this virtual classroom platform for ideology and politics education, it provides students with more ideology and politics learning resources and increases learning interest and time and a variety of ideology and politics learning methods, while it can promote politics.

4.3. Analysis of the Development of Virtual Classroom Platform in Recent Years.
Over time, the integration of emerging technologies and virtual classroom platforms has continued to increase. More and more online course apps are emerging, and more and more colleges and universities choose some courses to teach in the form of online courses. Here we analyze the development of virtual classroom platforms in recent years and draw a picture, as shown in Figure 8.

It can be seen from Figure 8 that, with the continuous advancement of technology, the functions of the virtual
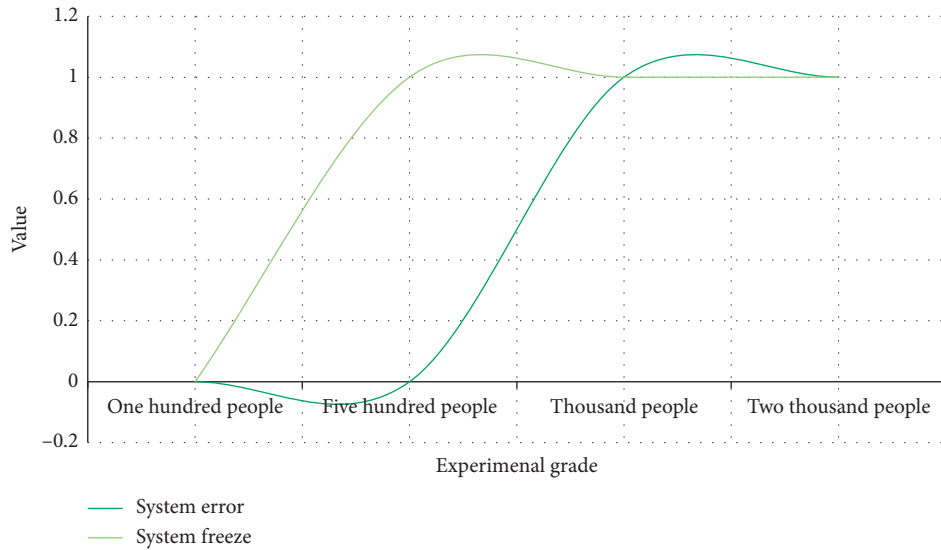
FIGURE 5: Running state test chart.
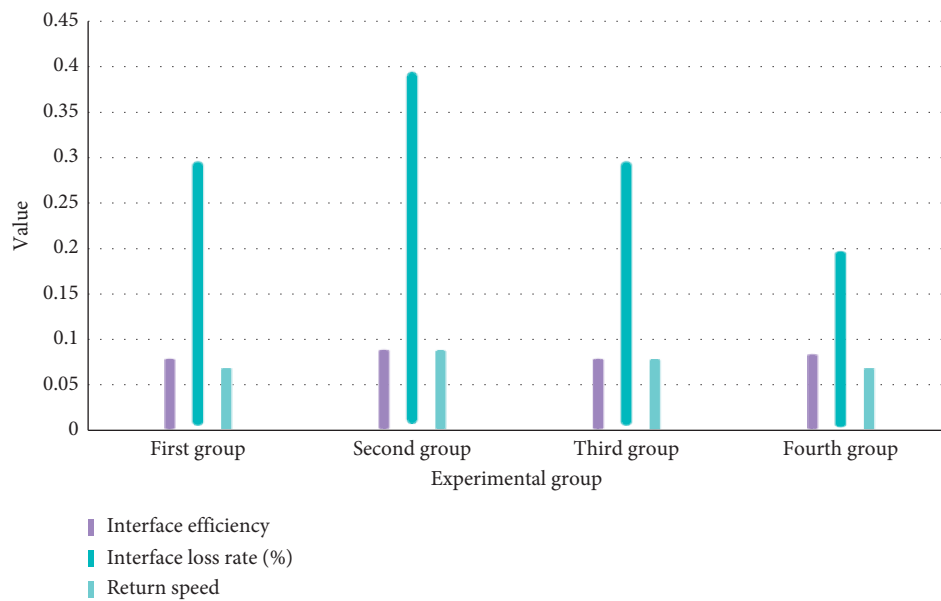
FIGURE 6: The loading speed of the 4 sets of experiments and the system data loss data rate graph.

classroom platform are becoming more and more mature. Just when the epidemic broke out this year, the already mature system completely replaced the face-to-face instruction. The virtual classroom platform this year is also the fastest growing time. Although face-to-face teaching has been restored now, with this technology, the virtual classroom platform will gradually replace the face-to-face teaching mode in the future.
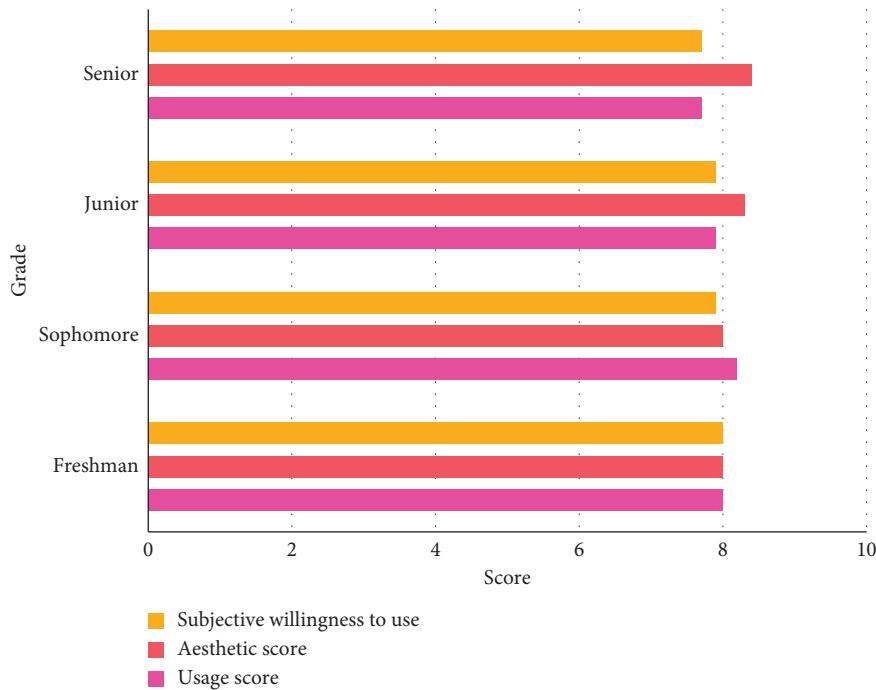
FIGURE 7: Customer satisfaction analysis graph.
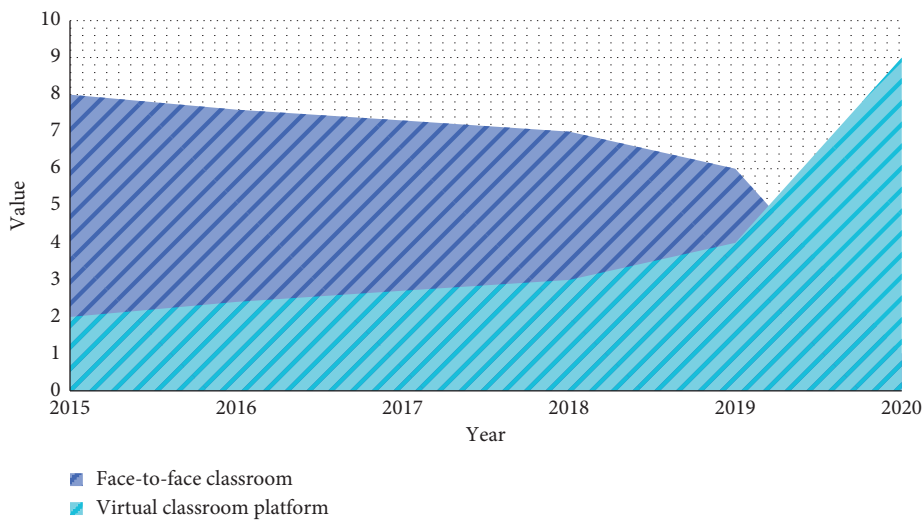
FIGURE 8: Analysis of the development of virtual classroom platform in recent years.

5. Conclusions

This system is an Android-based virtual and virtual classroom learning platform. The system can operate household appliances and perform remote control. The material is easy to install and has excellent expandability. For software, you can perform remote control and design. The interface is simple and easy to use, and the graphics features are easy to learn and use. Internet of Things is designed to meet communication and control requirements, smooth switching of various interfaces is maintained, and system performance is perfect. After designing the system operation, complete the system implementation interface and complete the system operation test and system performance test related work to confirm that the system operates normally. The focus of this design is to design intelligent control software on the Android platform. This design uses XML technology, the Android SDK development kit, and MyEclipse development tools.

The intelligent virtual classroom developed using IoT technology and IoT mobile technology interconnects the physical classroom and the virtual platform in the classroom, eliminating time and space constraints and conducting interactive teaching, evaluation, communication, and real-

time interaction. Providing students with convenience to study anywhere will help them increase their interest and enthusiasm for learning. This is a bold effort in education. At the same time, it solves the current situation that students in traditional classrooms do not listen to classes, but just lower their heads to play with mobile phones, making mobile phones a necessity in the classroom, effectively helping teaching activities, and arousing strong interest among students. Used for learning, active classrooms, real-time resource exchange without learning and communication can improve the teaching effect of teachers. This is a good way to reform education and teaching, and it is worthy of research and promotion in universities.

By improving the performance of virtual reality equipment, technological advancement and educating teachers in virtual reality technology, virtual reality technology is expected to drive the development of education for a period of time. In order to help students create better knowledge for teacher education, the virtual classroom system must solve two main problems, namely, the design of the virtual classroom environment and the realization of the virtual environment that users can operate. The design of the virtual learning environment represented by virtual classroom research has entered the stage of practical research, and the structure of the virtual classroom has gradually become clear. This new teaching method has gradually been highlighted, and there is still much room for improvement and perfection. This paper confirms the design idea of the virtual classroom environment by analyzing the requirements of the virtual classroom environment and combining the development process. We hope to provide a practical reference for the design of virtual classroom environment and help future virtual classrooms conduct practical research.

Data Availability

No data were used to support this study.

Conflicts of Interest

The authors declare that they have no conflicts of interest.

References

[1] Z. Lv and H. Song, "Trust mechanism of multimedia network," *ACM Transactions on Multimedia Computing, Communications, and Applications (TOMM)*, 2020.

[2] H. Song and M. Brandt-Pearce, "A 2-D discrete-time model of physical impairments in wavelength-division multiplexing systems," *Journal of Lightwave Technology*, vol. 30, no. 5, pp. 713–726, 2012.

[3] M. Zhou, Y. Wang, Z. Tian, Y. Lian, Y. Wang, and B. Wang, "Calibrated data simplification for energy-efficient location sensing in Internet of things," *IEEE Internet of Things Journal*, vol. 6, no. 4, pp. 6125–6133, 2019.

[4] Z. Lv, "Security of Internet of things edge devices," *Software: Practice and Experience*, vol. 1–11, 2020.

[5] O. M. F. Abu-Sharkh, E. Alqaralleh, and O. M. Hasan, "Adaptive device-to-device communication using Wi-Fi Direct in smart cities," *Wireless Networks*, vol. 23, no. 7, pp. 2197–2213, 2017.

[6] S. V. Tiwari, A. Sewaiwar, and Y. Chung, "Smart home multi-device bidirectional visible light communication," *Photonic Network Communications*, vol. 33, no. 1, pp. 1–8, 2017.

[7] G. Xiao, Q. Cheng, and C. Zhang, "Detecting travel modes from smartphone-based travel surveys with continuous hidden Markov models," *International Journal of Distributed Sensor Networks*, vol. 15, no. 4, pp. 1–15, 2019.

[8] A. Raes, P. Vanneste, M. Pieters et al., "Learning and instruction in the hybrid virtual classroom: an investigation of students' engagement and the effect of quizzes," *Computers & Education*, vol. 143, no. Jan., pp. 103682.1–103682.16, 2020.

[9] M. Radovan and N. Kristl, "Acceptance of technology and its impact on teachers' activities in virtual classroom: integrating UTAUT and CoI into a combined model," *Turkish Online Journal of Educational Technology-TOJET*, vol. 16, no. 3, pp. 11–22, 2017.

[10] O. Yilmaz, "The effects of "live virtual classroom" on students' achievement and students' opinions about "live virtual classroom" at distance education," *Turkish Online Journal of Educational Technology*, vol. 14, no. 1, pp. 108–115, 2015.

[11] A. Al-Fuqaha, M. Guizani, M. Mohammadi, M. Aledhari, and M. Ayyash, "Internet of things: a survey on enabling technologies, protocols, and applications," *IEEE Communications Surveys & Tutorials*, vol. 17, no. 4, pp. 2347–2376, 2015.

[12] Z. Liu, S. Dai, Y. Wang et al., "Photoresponsive transistors based on lead-free perovskite and carbon nanotubes," *Advanced Functional Materials*, vol. 30, no. 3, pp. 1906335.1–1906335.10, 2020.

[13] A. M. Eassa, M. Elhoseny, M. Hazem, and A. S. Salama, "NoSQL injection attack detection in web applications using RESTful service," *Programming and Computer Software*, vol. 44, no. 6, pp. 435–444.

[14] L. Catarinucci, D. De Donno, L. Mainetti et al., "An IoT-aware architecture for smart healthcare systems," *IEEE Internet of Things Journal*, vol. 2, no. 6, pp. 515–526, 2015.

[15] P. Josephson, "Bad call: technology's attack on referees and umpires and how to fix it by harry collins, robert evans, and christopher higgins," *Technology and Culture*, vol. 60, no. 3, pp. 929–931, 2019.

[16] H. Guo, J. Ren, D. Zhang et al., "A scalable and manageable IoT architecture based on transparent computing," *Journal of Parallel & Distributed Computing*, vol. 118, no. 1, pp. 5–13, 2017.

[17] J. Suarez, J. Quevedo, I. Vidal, D. Corujo, J. Garcia-Reinoso, and R. L. Aguiar, "A secure IoT management architecture based on Information-Centric Networking," *Journal of Network and Computer Applications*, vol. 63, no. Mar., pp. 190–204, 2016.

[18] M. S. K. Pirdehi, "A scalable and manageable IoT architecture based on transparent computing," *Computing Reviews*, vol. 60, no. 5, p. 209, 2019.

[19] Y. Shen, T. Zhang, Y. Wang, H. Wang, and X. Jiang, "MicroThings: a generic IoT architecture for flexible data aggregation and scalable service cooperation," *IEEE Communications Magazine*, vol. 55, no. 9, pp. 86–93, 2017.

[20] R. K. Lomotey, J. C. Pry, and C. Chai, "Traceability and visual analytics for the Internet-of-Things (IoT) architecture," *World Wide Web-Internet & Web Information Systems*, vol. 21, no. 4, pp. 1–26, 2017.

[21] Y. Chen, W. Zheng, W. Li, and Y. Huang, "Large group Activity security risk assessment and risk early warning based on random forest algorithm," *Pattern Recognition Letters*,

vol. 144, pp. 1–5, 2021, https://doi.org/10.1016/j.patrec.2021. 01.008.

[22] W. T. Cho, Y. W. Ma, and Y. M. Huang, "A smart socket-based multiple home appliance recognition approach over IoT architecture," *Journal of Internet Technology*, vol. 16, no. 7, pp. 1227–1238, 2015.

[23] Z. Lv, B. Hu, and H. Lv, "Infrastructure monitoring and operation for smart cities based on IoT system," *IEEE Transactions on Industrial Informatics*, vol. 16, no. 3, pp. 1957–1962, 2020.

[24] S. Seol, Y. Shin, and W. Kim, "Design and realization of personal IoT architecture based on mobile gateway," *International Journal of Smart Home*, vol. 9, no. 11, pp. 133–144, 2015.

[25] N. Pavón-Pulido, J. A. López-Riquelme, and J. Feliú-Batlle, "IoT architecture for smart control of an exoskeleton robot in rehabilitation by using a natural user interface based on gestures," *Journal of Medical Systems*, vol. 44, no. 9, pp. 1–10, 2020.

[26] R.-L. Yang, Y.-J. Zhu, F.-F. Chen, L.-Y. Dong, and Z.-C. Xiong, "Luminescent, fire-resistant, and water-proof ultralong hydroxyapatite nanowire-based paper for multimode anticounterfeiting applications," *ACS Applied Materials & Interfaces*, vol. 9, no. 30, pp. 25455–25464, 2017.

[27] L. Apperley, U. Das, R. Ramakrishnan et al., "G439 Mode of clinical presentation and delayed diagnosis of turner syndrome," *Archives of Disease in Childhood*, vol. 101, no. Suppl 1, pp. A259–A260, 2016.

[28] S. Wan, L. Qi, X. Xu, C. Tong, and Z. Gu, "Deep learning models for real-time human activity recognition with smartphones," *Mobile Networks and Applications*, vol. 25, no. 2, pp. 1–13, 2019.

[29] C.-H. Wu and S.-B. Tsai, "Using DEMATEL-based ANP model to measure the successful factors of E-commerce," *Journal of Global Information Management*, vol. 26, no. 1, pp. 120–135, 2018.

[30] I. Manzoni, "Mai 68: sous les pavés une nouvelle mode: les contours de la mode actuelle sont apparus il y a 50 ans," *Journal du Textile*, vol. 55, no. 2380, pp. 2-3, 2018.

[31] S. Chatterjee, M. S. Fujimoto, Y. H. Cheng et al., "Improving the sensitivity of electrochemical sensors through a complementary luminescent mode: a new spectroelectrochemical approach," *Sensors and Actuators B: Chemical*, vol. 284, no. APR, pp. 663–674, 2019.

[32] V. Frappier, M. Duran, and A. E. Keating, "PixelDB: protein-peptide complexes annotated with structural conservation of the peptide binding mode," *Protein Science*, vol. 27, no. 8, pp. 1535–1537, 2018.

[33] J. Kim, J. W. Han, and M. Meyyappan, "Reduction of variability in junctionless and inversion-mode FinFETs by stringer gate structure," *IEEE Transactions on Electron Devices*, vol. 65, no. 2, pp. 1–6, 2018.

[34] S. Strangio, P. Palestri, M. Lanuzza, F. Crupi, D. Esseni, and L. Selmi, "Assessment of InAs/AlGaSb tunnel-FET virtual technology platform for low-power digital circuits," *IEEE Transactions on Electron Devices*, vol. 63, no. 7, pp. 2749–2756, 2016.

[35] G. D. Alston and Q. A. Jernigan, "The inter-relationship of organizational learning, learning organization, virtual technology and virtual communities of practice," *New Horizons in Adult Education and Human Resource Development*, vol. 29, no. 3, pp. 15–18, 2017.

Research Article

Interbank Offered Rate Based on Artificial Intelligence Algorithm

Wangsong Xie ⬝

Business School, Wuxi Taihu University, Wuxi 214064, Jiangsu, China

Correspondence should be addressed to Wangsong Xie; xiews@wxu.edu.cn

Interbank offer rate is the interest rate at which banks lend money to each other in the money market. As a market-oriented core interest rate, Shibor can accurately and timely reflect the capital supply and demand relationship in the money market, and its changes will quickly transmit and affect China's financial market. Therefore, the purpose of this paper is to predict and study the fluctuation and trend of Shibor. In this paper, the overnight varieties of Shibor were studied and predicted from two time dimensions, namely, daily fluctuation and monthly trend. In the prediction of overnight Shibor daily data, a comparison prediction model based on BP neural network algorithm was first established, and then WNN was applied in the prediction, and the effect was found to be better. When predicting the monthly mean value of overnight Shibor, nine indicators were selected and tested for correlation based on the factors affecting the trend of interest rate, and a regression model of support vector machine was established. Particle swarm optimization algorithm was used to improve the SVR algorithm, and the PSO-SVR prediction model was established to improve the prediction accuracy. The model could basically predict the trend of overnight Shibor. Furthermore, a prediction model of WNN based on cuckoo search (CS) optimization was proposed, which improved the prediction accuracy by 78% and fitted the daily fluctuation of overnight Shibor well.

1. Introduction

As China's economic situation continues to improve, the importance of establishing and improving a strong financial market has become increasingly obvious. In particular, the gradual introduction of market interest rates is the top priority of the reform of the financial sector, which directly affects the stability of China's financial market and its position in the international financial market [1, 2]. The key to interest rate liberalization is to establish benchmark interest rate [2, 3]. Benchmark interest rate refers to the interest rate with general reference significance in the money market. Pricing or rate of return of other financial products in the financial market can be determined based on this benchmark interest rate, and monetary authorities can also make and implement monetary policies based on this interest rate [4, 5]. Interbank offered rate, also known as inter-bank offered rate, is the rate at which commercial banks finance funds in the money market. Compared with other interest rates, the open, market-oriented, and transparent interest rate formation mechanism enables it to accurately and

timely reflect the capital supply and demand relationship in the money market. In view of the importance of Libor, it is usually selected as the benchmark interest rate internationally, such as Libor [6–8].

Ivanov, Ivan *T*, studied how the introduction of market pricing, which links lending rates to credit default swaps, affected bank funding. Ivanov, Ivan T, found that market-based pricing was associated with lower interest rates, both at the beginning of the loan and over the life of the loan. Ivanov and Ivan T's results also show that banks have simplified market-based loan pricing contracts, suggesting that the decline in bank debt costs can be explained, at least in part, by a fall in monitoring costs. Therefore, in addition to reducing the cost of bank debt, market pricing may also have adverse consequences due to the reduction of bank monitoring [9]. Gianfranco Giulioni analyzed how changes in policy rates affect bank-related variables by changing the composition of loan portfolios. Using a calculation that takes full account of the heterogeneity of borrowers, Gianfranco Giulioni shows how the diversity of bank customers has changed and how this has affected the bank's cash inflows,

making them more volatile. Gianfranco Giulioni also shows how the composition of loan portfolios is affected by the rise in policy rates when policy rates remain low. Safer borrowers were the first to exit the loan portfolio, leading to a gradual increase in the risk of the loan portfolio. As riskier borrowers pay less, interest payments flow in less. In addition, we find that the shortening of loan term will increase the volatility clustering of bank interest payment inflow [10]. A stock loan is a loan secured by shares [11]. They are modern financial products designed for investors with large equity holdings. Mathematically speaking, stock loan can be regarded as an American call option with time-effective strike price. Wenting Chen's research is the first study in the literature to consider equity loan value under the framework of stochastic interest rate. Based on portfolio analysis, the partial differential equation of stock loan value is established. An appropriate set of boundary conditions, especially in the interest rate direction, is proposed to close the pricing system. The reasonable mathematical and financial proofs are provided for the proposed boundary conditions. For the proposed nonlinear PDE system, the predictive-corrected finite difference method is used. Wenting Chen adopts alternating directional implicit method to improve computing efficiency. Numerical results show that this method is reliable, and the stochastic interest rate makes the optimal execution price of stock loan relatively high [12].

Based on an in-depth study of existing literatures, Shibor was determined as the research object in this paper, mainly because since the official operation of the interbank lending market in 2011, the transaction volume of the lending market has dramatically increased, from over 2 trillion yuan in 2010 to over 10 trillion yuan in 2011, and continued to grow rapidly thereafter. Among the eight types published by Shibor, overnight varieties had the largest trading volume, and commercial banks used them more, which had the greatest impact on the interest rate market. Therefore, this paper studies the overnight Shibor prediction model based on artificial intelligence algorithm.

2. Artificial Intelligence Algorithm

2.1. Overnight Shibor Prediction Based on Artificial Intelligence

2.1.1. BP Neural Network Prediction Model. Traditional time series models, such as ARMA model and VAR model, basically assume that the research objects are linear [13, 14]. However, most of the research objects in the economic market are difficult to meet the assumption that the Shanghai interbank offered rate is a chaotic, high-dimensional nonlinear time series data. The prediction of the daily data time series of the interest rate is based on the data analysis and the rule of fluctuation, and the scientific research method is used to measure the fluctuation and predict the level of the interest rate on the next day. With the rapid development of artificial intelligence, neural network has been applied in many researches due to its excellent performance in dealing with high-dimensional nonlinear problems. Among them, BP network is the best, most

essence, and core part of the forward neural network. Data shows that more than 80% of the networks are using BP network or its related deformation and optimization. The related deformation and optimization are different in different research objects and purposes. The research object of this chapter is the overnight variety day data of Shibor, and the research method is artificial neural network. Therefore, BP neural network prediction model is firstly established as the basic model, so as to serve as the reference standard for the model performance in further studies.

BP network is a kind of multilayer feedforward neural network [15]. In its network training process, the signal is transmitted forward. The most critical step is to adjust the weight of the network through error backpropagation. BP neural network can learn and remember a large number of pattern mapping patterns between input and output, but it does not need to explicitly express the mathematical equation of such pattern mapping pattern in advance. In the forward signal transmission, the input signal from the input layer passes through the hidden layer to reach the output layer. Neurons in each layer are not connected to each other, and the state of neurons in the lower layer is affected by the way of full interconnection. If the desired output cannot be obtained by the output layer, the backpropagation process based on gradient descent is carried out to update the network weight and prediction and continuously improve the network performance, so that the output gradually approximates the desired output. The topological structure of BP neural network (a hidden layer) is shown in Figure 1, and the algorithm training process is shown in Figure 2. The relevant expression is as follows.

(1) The hidden layer excitation function f is as follows:

$$f(x) = \frac{1}{1 + e^{-x}}. \tag{1}$$

(2) The hidden layer output H is as follows:

$$H_j = f\left(\sum_{i=1}^{n} \omega_{ij} x_i - a_j\right), \quad j = 1, 2, \ldots, l. \tag{2}$$

(3) The predicted O output is as follows:

$$O_k = \sum_{j-1}^{l} H_j \omega_{jk} - b_k, \quad k = 1, 2, \ldots, m. \tag{3}$$

(4) Calculate the prediction error e; Y is the expected output:

$$e_k = Y_k - O_k, \quad k = 1, 2, \ldots, m. \tag{4}$$

(5) Weight ω_{ij}, ω_{jk} is updated as follows:

$$\omega_{ij} = \omega_{ij} + \eta H_j \left(1 - H_j\right) \times (i) \sum_{k-1}^{m} \omega_{jk} e_k, \quad i = 1, 2, \ldots, n,$$

$$\omega_{jk} = \omega_{jk} + \eta H_j e_k, \quad j = 1, 2, \ldots, l, k = 1, 2, \ldots, m. \tag{5}$$

(6) Update thresholds a and b:
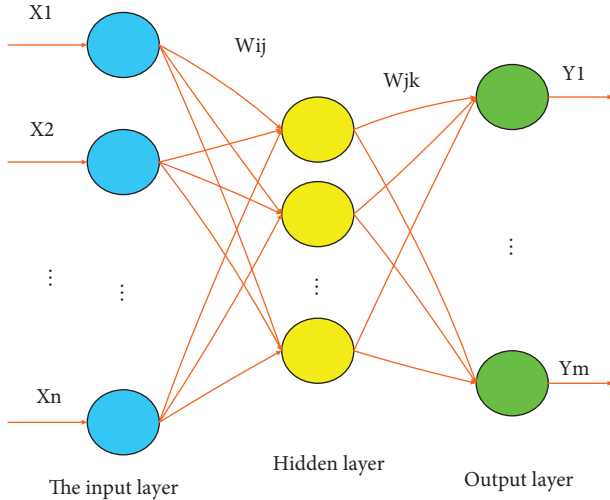
Figure 1: Topology structure diagram of BP network.

$$a_j = a_j + \eta H_j \left(1 - H_j\right) \sum_{k-1}^{m} \omega_{jk} e_k,$$

$$b_k = b_k + e_k. \tag{6}$$

In the previously mentioned expression, n is the number of nodes in the input layer, m is the number of nodes in the output layer, and l is the number of nodes in the hidden layer.

2.1.2. WNN Prediction Model.

The continuous wavelet coefficients of CWT neural networks are especially suitable for prediction or classification due to their redundancy and strong anti-interference ability.

(1) Basic Principle of WNN. In the WNN structure based on the BP network topology principle, the transfer function of its hidden layer node is used to replace the wavelet basis function. The basic principle is the same as that of the BP network. Although its signal transmission will cause error back propagation, the use of gradient correction method and wavelet basis function of the network weights and parameters can make WNN prediction gradually achieve the expected output effect.

Assuming that the hidden layer output value is y, the output layer yn is the desired output, ω_{ij} represents the weight value connecting the input layer and the hidden layer, ω_{jk} represents the weight of the hidden layer to the output layer, h_j is the wavelet basis function, b is the conversion factor, and l Is the number of hidden layer nodes, m is the number of output layer nodes, e is the prediction error, n is the learning rate, and the related expressions are as follows:

The wavelet basis function is as follows:

$$y = \cos(1.75x)e^{-x^2/2}. \tag{7}$$

Calculate the output value of the hidden layer:

$$h(j) = h_j \left[\frac{\sum_{i-1}^{k} w_{ij} x_i - b_j}{a_j} \right], \quad j = 1, 2, \ldots, l. \tag{8}$$

Calculate the output layer of the predicted output:

$$y(k) = \sum_{i-1}^{l} \omega_{ik} h(i). \tag{9}$$

The prediction error is as follows:

$$e = \sum_{k-1}^{m} yn(k) - y(k), \quad k = 1, 2, \ldots, m. \tag{10}$$

Algorithm training steps overview is as follows.

Step 1. Network initialization: random initial assignment was made to the scaling factor and translation factor of the wavelet base function and the link weight between the network layers, and the learning rate of the network was selected, and the number of nodes in the input layer, output layer, and hidden layer were set according to the task situation.

Step 2. Sample classification: the dataset is properly divided into two parts for training and testing. The training set is used for network training, and the test set is used to verify the training effect of the network.

Step 3. Predicting the output: the training data is input into the network, the predicted value is calculated according to the output expression of the output layer, and the error value is obtained by comparing with the expected output.

Step 4. Weight correction: according to the error value, the weights of the network and the parameters related to the wavelet basis function are modified again and again.

Step 5. Judge whether the algorithm has stopped running according to the set error value. If not, return to step 3 to continue iteration.

2.1.3. Cuckoo Optimization of WNN Prediction Model.

WNN training is an optimization process with multiple local extreme values, which makes the network eventually converge to the local optimal rather than the global optimal. The effect and performance of network training are greatly affected by the primary value. In this paper, a prediction model of cs-WNN is established, which is based on the meta-heuristic algorithm cuckoo search optimization wavelet network. In cs-WNN, each egg represents the initial weight and threshold of the wavelet network. In the iterative process, CS algorithm is used to continuously update the position, optimize the initial weight and threshold, and satisfy the adaptive value function until the optimal. During the training of WNN, the cuckoo search algorithm continuously optimizes the weights and thresholds of the network until the convergence condition is satisfied (when the number of iterations or MSE meets the set condition). The empirical analysis of the cs-WNN prediction model shows
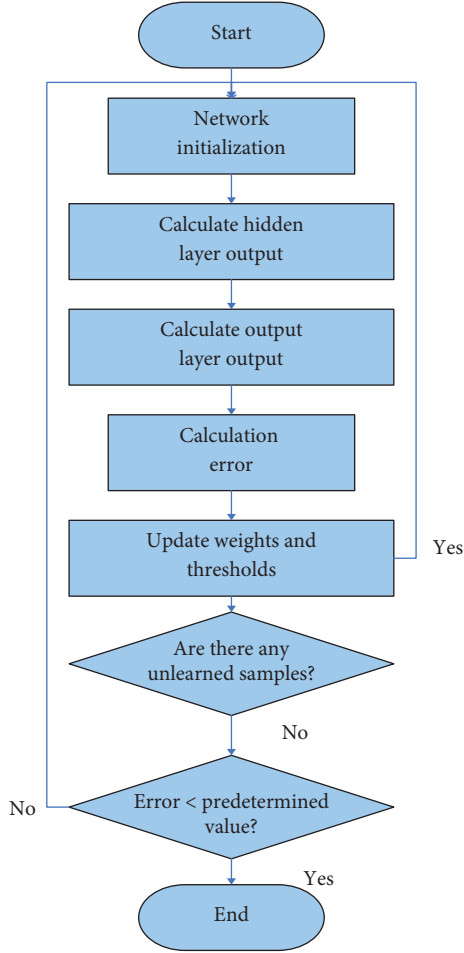
FIGURE 2: BP algorithm training flow chart.

that the optimization model overcomes the local minimum problem and has good generalization ability.

(1) Theoretical Basis of Cuckoo Search (CS). Cuckoo search (CS) is a new optimization metaheuristic algorithm constructed on the basis of swarm intelligence technology, which simulates cuckoo's nest parasitism and flight behavior of other host birds. In this bionic optimization algorithm, cuckoo eggs are mapped into solutions to actual problems, with each egg in the nest representing a potential solution and the next generation of cuckoo eggs representing a new solution, with the goal of replacing the worse solution in the nest with a better solution. The process of updating the solution is carried out through the flight behavior of levy. The actual algorithm operation makes three idealized assumptions as follows: first, each cuckoo can lay only one egg at a time and then randomly put it into a nest to hatch, second, high-quality eggs from randomly selected nests survive into the next generation, third, the number of nests that can be used as parasitic nests is fixed, and the probability of parasitic cuckoo eggs being identified and picked out by the host bird is $P_a \in [0, 1]$. If found, the host bird can either discard the cuckoo's eggs or simply abandon its nest and find a new location to build a new nest.

Definition 1. The update of the equation of cuckoo bird's nest selection process is as follows:

$$X_i^{(i+1)} = X_i^{(l)} + \alpha \oplus \text{Levy}(\lambda), \quad i = 1, 2, 3, \ldots, n, \qquad (11)$$

where $X_i^{(t)}$ is the position of the nest in the t-th search; $\oplus$ stands for point-to-point multiplication; A is a step factor; Levy (λ) is a random search vector generated by a Levy distribution with a compliance parameter of λ ($1 \le \lambda \le 3$).

To sum up, the cuckoo optimization iteration mode is as follows.

Step 1: randomly initialize the positions of nests, determine the optimal adaptive value of the algorithm, and set the maximum number of iterations and the probability of being discovered by the host bird and other parameters.

Step 2: calculate the fitness value of each nest, and record the current best solution and the corresponding nest location

Step 3: learn how Levy flies, update the position of the nest with the update equation, and test and record the nest in the new position with the objective function.

Step 4: compare the newly produced bird's nest position with the optimal bird's nest position of the previous generation, and according to the elite selection rule, keep the optimal bird's nest to the next generation.

Step 5: randomly generate a number from 0 to 1, compared with the probability of cuckoo bird eggs being found by the host. If the random number is larger, then randomly generate a group of nest positions. Otherwise, the nest location with the optimal test results is still retained.

Step 6: when the recorded result of the best nest location has met the set accuracy requirements or reached the number of iterations, then the nest is the global optimal location, and the search process is over; otherwise, return to step 2.

2.2. Daily Fluctuation of the Lending Rate. The prediction process of the model is based on the daily data time series of the interest rate, starting from the fluctuation of the interest rate level itself, without involving other relevant factors, which is similar to the technical analysis in the financial market. The assumption contained in this paper is that all the influencing factors will eventually be reflected in the change of interest rate level. In the study of interest rate fluctuation with "daily" as the time dimension, this assumption is basically satisfied.

(1) For interbank interest rates such high-dimensional nonlinear time series data, the overall prediction effect of the BP neural network prediction model is average. In the test set fitting process, once the inflection point is variable, it will greatly affect the prediction effect of the test sample after the turning point, and the prediction accuracy will be greatly reduced as a whole.

(2) Using the cuckoo search algorithm to optimize the WNN parameters, its prediction effect on loan interest rate fluctuations is quite good, and the prediction accuracy of the prediction model is significantly improved. The optimized prediction model shows excellent performance in the prediction of overnight Shibor daily data, which is of great help to decision-making assistance.

(3) The error of BP neural network, WNN, and cs-WNN for overnight Shibor prediction is shown in Table 1.

3. Experimental Research on the Interbank Offered Rate Based on Artificial Intelligence Algorithm

3.1. Experimental Data Sources. Before establishing the model, Shibor related variables were preselected in this paper. As economists have different understandings of the determinants of interest rates and the ways in which these determinants affect interest rates, different theories of interest rate determination have been formed. According to the research results of relevant theories and the current situation of China's financial environment, there are many factors that affect the interest rate, such as a country's economic situation and economic policies, the supply and demand of money, savings and investment, price level, international interest rate level, and average profit rate. According to the available data and the main acquisition of money supply (M2), the dollar is equal to the average value, the trading volume of the China Stock Exchange, the RMB deposits and loans of non-performing financial institutions, the consumer price index (CPI), the purchasing managers index (PMI) bank pledged repo rate, new credit data, foreign direct investment (FDI) these nine indicators, the relevant analysis is as follows:

(1) Money supply (M2): "liquidity preference" is the tendency of investors to hold the same amount of cash currency based on the portfolio framework. Economic equilibrium theory points out that the interaction of money supply and demand determines the level of interest rates. Considering the size of opportunity cost, the holding of money by rational economic man is mainly driven by three factors: prevention, speculation, and trading. The quantity of money supply is an exogenous variable determined by the monetary authority. When the two are equal, it is the equilibrium interest rate. For the purpose of macromonitoring and regulation, the central bank divides the money supply into three levels according to the size of liquidity, namely, M0 (cash in circulation), M1 (narrow sense of money supply), and M2 (broad sense of money supply). With the rapid development of the economy, the money supply of our country has been increasing, and the return on capital has been declining on the general trend, and whether the growth of the money supply is consistent with the growth of the economy is the most critical. Therefore, M2 is selected as the preselected

Table 1: Comparison of model prediction errors.

The evaluation index	Prediction model		
	BP neural network	WNN	cs-WNN
MAPE	2.3978	1.8689	1.4072
MAE	0.0388	0.0281	0.0216
MSE	0.0028	0.0017	0.0012

variable in this paper, and the data is from the official website of the People's Bank of China.

(2) Consumer price index (CPI): there is a strong correlation between changes in the price level and changes in interest rates. On the one hand, the high and low prices affect the amount and cost of social funds absorbed by commercial banks through affecting enterprises and individuals and ultimately affect the source and amount of bank credit funds. On the other hand, since price and currency depreciation are often mutually causal relations, when currency depreciation takes place, banks must take into account the actual value of the currency rather than the nominal value when taking deposits and issuing loans. The problem of currency preservation also exists on the other side of the credit relationship, where people are more concerned about the real interest rate. Therefore, the market-oriented interest rate will make corresponding adjustments according to the changes in the price level to ensure that both credit parties will not suffer losses due to price changes. Consumer price calculation of China's social products and services activities, measuring China's price situation, not only is closely related to the people's living costs but also has an important position in the domestic production price system. CPI index is an important index for judging economic situation, testing, and controlling price level. The rate of change in the CPI index largely reflects the extent of deflation or inflation. Therefore, CPI is selected as the preselected variable in this paper, and the monthly data is from the official website of the People's Bank of China.

(3) Turnover of the stock exchange: the stock market is an important bridge connecting the real economy and the financial market. A large number of empirical studies and relevant theories have shown that the stock market situation of a country is closely related to the country's economic situation, and it also reflects the level of listed enterprises financing for wealth creation and appreciation. The effect of the stock market on the interest rate is based on two considerations: on the one hand, the situation of the stock market is related to the economic prosperity degree, and the economic prosperity degree is related to the level of interest rate; on the other hand, the attractiveness of the stock market is essentially determined by a firm's return on capital, which is closely related to the level of interest rates in the market. According to statistics, the turnover of our

country's Shanghai and Shenzhen stock exchanges is basically the same. As an important indicator to measure the stock market, turnover reflects both the corporate popularity index and capital status. Therefore, this article chooses the stock exchange turnover as the main variable to analyze the monthly data of the stock exchange website.

(4) Purchasing managers' index (PMI): the expected return on funds in the macroeconomy largely determines the level of interest rate, while the return on funds is directly determined by the economic conditions of a country. Normally, when the economic cycle is in a boom stage, people and enterprises are full of confidence in the development of the economy, the money market is in short supply, the expected rate of return on capital is rising, and the interest rate of interest will rise with the prosperity of the economy. On the contrary, when the economic cycle of a country is in a depression, people and companies are pessimistic about the prospect, people and companies will be more cautious when they engage in investment, savings will increase, borrowing costs will be lower, money market shows a phenomenon of oversupply, and interest rates will usually fall. GDP growth rate is an accepted indicator to measure economic conditions from a macro-perspective. Relevant empirical analysis shows that PMI is highly correlated with GDP, and it is a leading indicator in economic monitoring. The inflection point of its trend change is often ahead of the GDP growth rate for a period of time. Considering that the monthly data of relevant indicators are used as the dependent variable in this paper to predict the level of the interest rate of the next month, it is more appropriate to preselect PMI index as the variable in this paper. The monthly data are from the official website of the People's Bank of China.

(5) Foreign direct investment (FDI): with the continuous progress of economic globalization, as well as the deepening of China's reform and opening up and market economy, the cross-border investment of foreign investors in order to obtain investment returns has a growing impact on China's economic environment. Relevant studies show that a large amount of international hot money enters China through foreign direct investment, which has a huge impact on the fluctuation of China's real economy and financial market, thus affecting the level of interest rate. In this paper, foreign direct investment (FDI) is selected as the preselected variable, and the monthly value is from the official website of the People's Bank of China.

(6) New credit data: credit refers to credit loans, during which the debtor does not need to provide capital guarantee and the creditor issues funds according to the credit of the demander. Credit loan has always been the most commonly used loan method by Chinese commercial banks. The change of new credit data indicates that the demand level of money market for funds is rising or falling. On the one hand, it will affect the relationship between capital supply and demand; on the other hand, it will affect the cash reserves of commercial banks and then indirectly affect the level of interest rate through interbank lending market. In this paper, the monthly data of new credit was selected as the preselected variable, and the data came from oriental fortune.

(7) Interbank pledged repo rate: in bond repo transactions, buyers and sellers agree to carry out reverse transactions of bonds at a certain time in the future when buying and selling bonds, which is essentially a financing behavior with bonds as collateral. Pledge-type repo and interbank disconnection are the main channels for commercial banks to maintain cash liquidity. Since these two channels can replace each other to some extent, there is a direct interaction between the repo rate and the open and release rate. In this paper, the one-day weighted average interest rate of nationwide interbank pledge-type repo is selected as the preselected variable. The relevant data are from the official website of the People's Bank of China.

(8) Difference between deposits and loans of financial institutions in RMB: during the period when the average profit rate remains certain, the level of interest rate in the financial market is basically determined by the supply and demand of borrowing funds in the money market. This is because interest rates are essentially the time cost of borrowing money and the pricing of risk. In general, interest rates fall when there is a surplus of cash and rise when there is a shortage of cash. Of course, the interest rate also acts against the supply and demand of funds. When the interest rate rises, the increase in borrowing costs reduces the demand, and when the interest rate falls, the decrease in borrowing costs also increases the demand. According to the classical interest rate determination theory, savings and investment are the two main determinants of the interest rate level. Therefore, when studying the interest rate level, it is inevitable to choose relevant indicators that can reflect savings and investment. Savings can be reflected through deposits, while investment is closely related to the loan scale. Based on the previously mentioned analysis, the difference between deposit and loan is an important variable that affects the level of interbank lending rate. In this paper, the difference between deposit and loan of financial institutions is selected as the preselected variable, and the monthly value is from the official website of the People's Bank of China.

(9) Us dollar equivalent to the average of RMB: with the progress of China's interest rate liberalization and the approval of the inclusion of RMB into the SDR, China's monetary policy will increasingly need to pay attention to the impact of the exchange rate in

the future. In the international financial market, the relative change of interest rates between the two countries reflects the relative change of returns between the two countries, which naturally has an impact on the change of exchange rate. At the same time, the fluctuation of exchange rate will also have a certain impact on the level of interest rate. The exchange rate has an indirect effect on interest rates, mainly through unbalanced changes in global transactions. The balance of capital account and the balance of current account are the two major components of the balance of international payments. When a country has a persistent surplus under its current account and a large amount of foreign exchange inflows, the local currency will continue to appreciate externally. On the one hand, in order to cope with the continuous pressure of appreciation, the monetary authorities tend to lower the interest rate and reduce the domestic foreign exchange supply through capital outflow under the capital account so as to divert the upward pressure. On the other hand, the appreciation of the local currency leads to the contraction of net exports and the expansion of the supply of goods in the domestic market. The price of goods and the interest rate fall. In addition, in order to stabilize the domestic currency, the balance of payments surplus is converted into foreign exchange reserves. Once the foreign exchange reserves increase, a corresponding amount of local currency must be released. The monetary policy is too loose, and the money supply increases, resulting in the decrease of interest rate. The US dollar is the most important currency in the international currency market and is the main part of China's foreign exchange reserve structure. Therefore, this paper selects the average value of US dollar converted into RMB as the preselected variable, and the monthly data comes from the official website of the People's Bank of China.

3.2. Selection of Experimental Variables. Based on the theory of interest rate determination and the availability of monthly data, nine indicators of interest rate impact have been preselected. Correspondingly, overnight Shibor prediction model is based on interest rate as an influencing factor, because this article focuses on the overnight interest rate in a longer time dimension because this article mainly deals with data such as the trend of overnight interest rates in a longer time dimension, we will use the overnight Shibor quotation algorithm to calculate the monthly average, the average represents Shibor overnight interest rates in this month. Thus, during the nine years from 2011 to 2019, data of 108 months of overnight Shibor were obtained, and the preselected variables also selected the data of 108 months.

Pearson correlation test was conducted on nine indicators and 10 variables of overnight Shibor monthly data, and the results were shown in a table. Since the predicted time indicators correspond to overnight Shibor with a one-month lag, Pearson correlation test was conducted on nine indicators and the monthly data of overnight Shibor (with a one-month lag), and the results are shown in Table 2.

According to the correlation of the test results in Table 2, the monthly average of the overnight Shibor and the 9 preselected indexes at the 0.01 level show a significant correlation. The Pearson correlation coefficients of M2, FDI, deposit/loan difference, and exchange rate are −0.884, −0.545, and −0.833, respectively, all of which are strongly correlated. Therefore, the repo rate, exchange rate, and CPI were finally selected as the input variables affecting the interest rate.

4. Analysis of Results

4.1. BP Neural Network Prediction Model Analysis. The evaluation of measurement performance error is as follows. In the process of establishing the prediction model of the Shanghai interbank offered rate, in addition to the comparison and analysis of the figures, an intuitive and quantifiable evaluation standard of prediction accuracy is also required. The evaluation system should be able to simply measure the predictive performance of the model. For different models, due to the difference of research object and research purpose, there is no unified system for prediction evaluation at home and abroad. Combined with the research purpose and method in this paper, mean absolute error (MAE), mean square error (MSE), and mean percentage error (MAPE) are selected as the indicators to measure the prediction error.

From 2011 to 2019, a total of 2248 days of overnight Shibor data were generated. The first 2100 days of overnight Shibor data (January 4, 2011, to May 29, 2019) were taken as training samples, and the remaining 148 days (January 1, 2019, to June 31, 2019) were taken as test data. According to the implementation steps of BP neural network, the number of nodes in the hidden layer is firstly determined. The number of nodes in the input layer is five, and the number of nodes in the output layer is one, which means that, in the training of mapping, the first to the fifth data of the time series are used to predict the sixth data, the second to the sixth data correspond to the seventh data, and the remaining data are similarly recurred. Figure 3 is the prediction effect of BP neural network on overnight Shiobr.

It can be seen from Figure 3 that, in the prediction of Shiobr's time series overnight, the first 60 data points of BP neural network fit the fluctuation of the interest rate well in the stable stage, and the fitting performance was average when the fluctuation was large. When the prediction is deviated, the fitting of nearly 90 data points in the future is deviated greatly. On the whole, the BP neural network prediction model has basically fitted the fluctuation trend of the interest rate, but the error is still relatively large. Among them, the value of MAPE is 2.3978, MAE is 0.0388, and MSE is 0.0028.

4.2. Analysis of Prediction Effect of WNN. Similarly, the first 2100 (January 1, 2019, to June 31, 2019) daily data points of

TABLE 2: Correlation test (a).

		Supply of currency (M2)	Consumer price index (CPI)
Overnight Shibor	Pearson correlation significance (bilateral) N	0.318 0.001 0.108	0.362 0 0.108
		Purchasing managers' index (PMI)	Foreign direct investment data (FDI)
Overnight Shibor	Pearson correlation significance (bilateral) N	−0.213 0.027 0.108	0.3500 0.108
		Weighted average interest rate of nationwide interbank pledged repo (one day)	The difference between deposit and loan of RMB in financial institutions
Overnight Shibor	Pearson correlation significance (bilateral) N	0.989 0 0.108	0.289 0.002 0.108
	Correlation test (b)		
		Supply of currency (M2)	Consumer price index (CPI)
Overnight Shibor (lag)	Pearson correlation significance (bilateral) N	0.315 0.001 0.107	0.373 0 0.107
		Purchasing managers' index (PMI)	Foreign direct investment data (FDI)
Overnight Shibor (lag)	Pearson correlation significance (bilateral) N	−0.088 0.369 0.107	0.3600 0.107
		Weighted average interest rate of nationwide interbank pledged repo (one day)	The difference between deposit and loan of RMB in financial institutions
Overnight Shibor (lag)	Pearson correlation significance (bilateral) N	0.712 0 0.107	0.296 0.002 0.107

FIGURE 3: Prediction effect drawing: BP network model.

2248 overnight Shibor's time series were taken as training samples, and the remaining 148 (June 1, 2011, to December 31, 2011) data points were taken as test data.

According to the implementation steps of the WNN, the structure of 5-9-1 is adopted in this paper. There are five nodes in the input layer, representing the corresponding interest rate level of the first five time points of the predicted time node, nine nodes in the hidden layer, and only one node in the output layer of the predicted interest rate output from the network. The wavelet basis function and the network weight are obtained randomly when initializing the parameters, and the number of iterations of the algorithm is 180. The trained WNN is used to predict the interest rate of the test set. Figure 4 is the prediction result of the WNN on the overnight varieties of interbank offered rate.

It can be seen from Figure 4 that the 50–75 data points in the time series prediction of the overnight Shibor by the WNN are relatively large, and the accuracy of the prediction in the other 100 or so data points is very high, the relative error is small, and it is basically in line with the daily actual data of the actual interest rate.
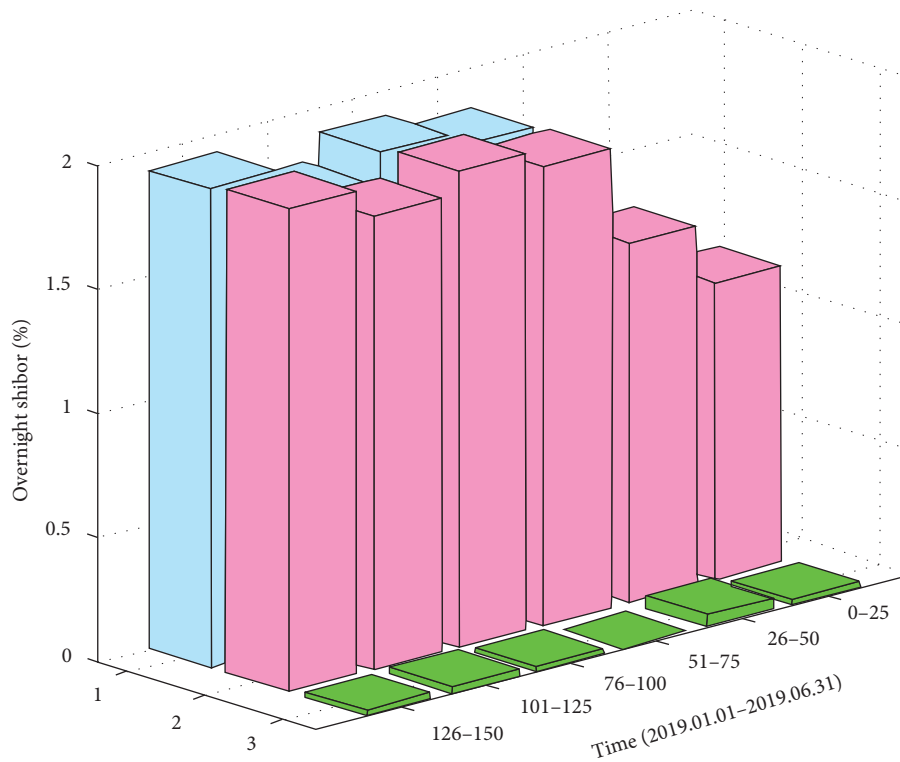
FIGURE 4: Prediction effect diagram: WNN model.

4.3. Analysis of Cuckoo Optimization of WNN Prediction Model. Similarly, the statistics of the test data can be obtained, the input layer has five nodes, which represent the corresponding overnight Shibor interest rate level five time points before the predicted time node. The hidden layer has nine nodes, and the predicted overnight Shibor is the output layer of one node. The well-trained cs-WNN is used to predict the opening and release rates of the test set. Figure 5 is the prediction result of cs-WNN on Shibor overnight.

It can be seen from the Figure 5 that, compared with WNN, cs-WNN model has a better fitting effect in the prediction of the data of the first 25 days. The fitting of the data of 25 days, between 50 and 75, is better than that of WNN. The extreme points of the catch and the strong ability of fitting and the deviation and lag appear less, which further improved the ability to predict.

4.4. Regression Support Vector Machine (SVR) Prediction Model. Shibor has only been in operation since 2011, and monthly Shibor data overnight are very limited. In view of the situation of the data in the prediction task and the characteristics of the research object, the support vector machine for regression (SVR) was selected to establish the prediction model in this paper. This is because support vector machine (SVM) has obvious advantages in solving small sample, nonlinear, nonstationary, and high-dimensional tasks, with the following significant advantages.

(1) The principle of structural risk minimization, a statistical learning theory, has a solid theoretical foundation.

(2) The algorithm is put forward specifically for the small sample of the research problem, which is finally reduced to a quadratic programming problem. Theoretically, the global optimal solution can be obtained under the condition of limited samples, which improves the local extremum problem of the traditional neural network.

(3) Support vector determines the topology structure of SVM and avoids the excessive dependence of traditional neural network on user's trial-and-error network topology structure.

(4) SVM maps the actual problem data to the high-dimensional feature space through the nonlinear transformation. Then, in the high-dimensional feature space, the linear function realizes the processing function of the nonlinear function of the original space and avoids the "dimension disaster," and the model has strong generalization ability.

In solving practical problems, SVM is first used for classification and pattern recognition and other fields, while regression support vector machine (SVR) introduces an insensitive loss function into the SVM classification process, which often achieves good performance and effect in the application of regression problems. When SVM is used for classification problems, an optimal classification surface is constructed to separate the two samples. When we use SVM for regression fitting, the idea is to construct the optimal
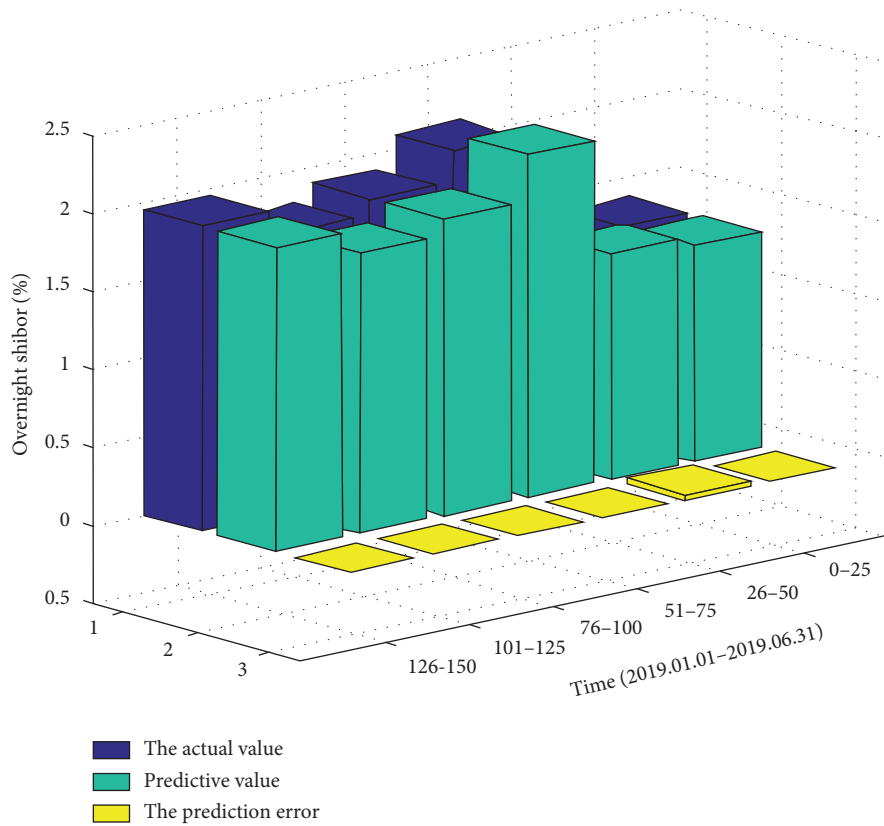
FIGURE 5: Prediction effect diagram: cs-WNN model.
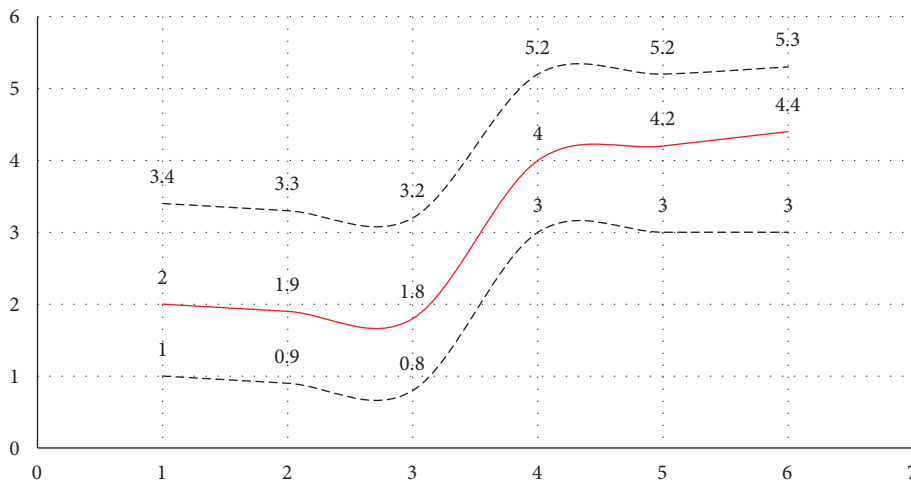
FIGURE 6: Schematic diagram of the basic idea of SVR.

classification surface that minimizes the distance of all training samples from this classification surface and convert the nonlinear regression task into linear regression in high-dimensional space, so as to approximate the input and output. The basic idea of SVR is shown in Figure 6.

5. Conclusions

The prediction process of the model is based on the daily data time series of the interest rate, starting from the fluctuation of the interest rate level itself, without involving other relevant factors, which is similar to the technical analysis in the financial market. The assumption contained in this paper is that all the influencing factors will eventually be reflected in the change of interest rate level. In the study of interest rate fluctuation with "daily" as the time dimension, this assumption is basically satisfied.

In this paper, the overnight varieties of Shibor were studied from two time dimensions. When the research focus is the short-term fluctuation of overnight Shibor, we directly

model the daily time series data through an artificial intelligence algorithm. In terms of the selection of algorithm, this paper first applied BP neural network as the basic prediction model algorithm and then proposed applying WNN algorithm to overnight Shibor prediction and further proposed a prediction model based on cuckoo search optimization, based on WNN, which improved the prediction accuracy. When the research focuses on the long-term trend of overnight Shibor, we start from the factors affecting the trend of interest rate, select CPI, quarter-on-quarter growth rate of pledge-type repo rate, quarter-on-quarter growth rate of exchange rate, and last month value of overnight Shibor as independent variables to establish the SVR prediction model and further improve the SVR algorithm with PSO to improve the prediction effect.

The prediction model has markedly improved the prediction precision and the optimized prediction model in overnight Shibor. Data prediction shows good effect and can forecast the auxiliary decision-making. In the trend study of Shibor, the regression support vector machine (SVR) algorithm was selected for the feature that Shibor was officially launched only in 2011 and monthly data was very limited. By analyzing the performance of the SVR prediction model established by the influencing factors of the interest rate on overnight Shibor monthly data, it can be found that the model has a general prediction effect on the monthly average value of overnight Shibor, and the predicted value fluctuates too much. The prediction algorithm of particle swarm optimization (PSO) is used to optimize the extreme value of nonlinear function in solvable space through dynamic adjustment of particles. In the empirical analysis of overnight Shibor prediction based on interest rate influencing factors, PSO-SVR prediction model shows better prediction ability than SVR model. In the short-term daily data forecast of the interest rate, the prediction model performs very well and can basically be used to predict the volatility. In the long-term monthly data prediction of the interest rate, the monthly data points of the interest rate influencing variable showed a relatively average performance in the prediction of the overnight Shibor monthly mean value of the next month, which were unable to reflect the response of the interest rate to some emergencies. Therefore, emergency observation was added into the framework design of the decision-making system to assist decision-making.

Data Availability

No data were used to support this study.

Conflicts of Interest

The authors declare that there are no conflicts of interest regarding this paper.

Authors' Contributions

All authors have read and approved the manuscript for publication.

References

[1] S. Zhang, "Analysis on the particularity of land economy and its impact on the financial system of rural areas," *Revista de la Facultad de Agronomia de la Universidad del Zulia*, vol. 36, no. 4, 2019.

[2] W. Pei, "Risk analysis of animal investment in financial capital allocation and technological innovation," *Revista Científica-Facultad De Ciencias Veterinarias*, vol. 29, no. 2, pp. 338–345, 2019.

[3] J. Zhou, J. Wang, and J. Ding, "How loan interest rate liberalization affects firms' loan maturity structure: evidence from listed manufacturing companies in China," *China Finance Review International*, vol. 4, no. 2, pp. 1000–1006, 2014.

[4] R. Kgoroeadira, A. Burke, and V. S. André, "Small business online loan crowdfunding: who gets funded and what determines the rate of interest?" *Small Business Economics*, vol. 52, no. 6, pp. 1–21, 2018.

[5] S. Steinkamp and W. Frank, "Multilateral loans and interest rates: further evidence on the seniority conundrum," *International Journal of Finance & Economics*, vol. 22, 2017.

[6] T. H. A. Araújo, A. R. Filipe Ferreira de, and L. C. J. Alcantara, "Molecular epidemiology database for sequence management and data mining," *Methods in Molecular Biology*, vol. 1582, p. 25, 2017.

[7] E. Brewer, S. Deshmukh, and T. P. Opiela, "Interest-rate uncertainty, derivatives usage, and loan growth in bank holding companies," *Journal of Financial Stability*, vol. 15, no. C, pp. 230–240, 2014.

[8] S. Khemakhem and Y. Boujelbene, "Predicting credit risk on the basis of financial and non-financial variables and data mining," *Review of Accounting and Finance*, vol. 17, no. 3, 2018.

[9] A. Keramati and H. Ghaneei, "Developing a prediction model for customer churn from electronic banking services using data mining," *Financial Innovation*, vol. 2, no. 1, p. 10, 2016.

[10] T. Ivan, J. A. C. Santos, and T. Vo, "The transformation of banking: tying loan interest rates to borrowers' CDS spreads," *Journal of Corporate Finance*, vol. 38, 2016.

[11] G. Giulioni, "Policy interest rate, loan portfolio management and bank liquidity," *The North American Journal of Economics and Finance*, vol. 31, pp. 52–74, 2014.

[12] S. Ba, "Risk Management and Control of Agricultural Financial Engineering in the Process of Mortgage Securitization in Rural Areas Based on Sustainable Agricultural Development," *Revista de la Facultad de Agronomia de la Universidad del Zulia*, vol. 36, no. 2, 2019.

[13] Y. Jiang, "Crop extraction and spatial-temporal change analysis in alpine region based on time series NDVI," *Revista de la Facultad de Agronomia de la Universidad del Zulia*, vol. 36, no. 3, 2019.

[14] C. Zhang, M. Yang, J. Lv, and W. Yang, "An improved hybrid collaborative filtering algorithm based on tags and time factor," *Big Data Mining and Analytics*, vol. 1, no. 2, pp. 128–136, 2018.

[15] L. Qi, X. Zhang, W. Dou, and Q. Ni, "A distributed locality-sensitive hashing-based approach for cloud service recommendation from multi-source data," *IEEE Journal on Selected Areas in Communications*, vol. 35, no. 11, pp. 2616–2624, 2017.

Research Article

Development of Internet Supply Chain Finance Based on Artificial Intelligence under the Enterprise Green Business Model

Jun Zhang (ID)

College of Commercial, Wuxi Taihu University, Wuxi 214064, Jiangsu, China

Correspondence should be addressed to Jun Zhang; zhangj3@wxu.edu.cn

At present, China's economic development has made unprecedented progress, but it is also facing a severe situation, and the environmental carrying capacity has almost reached its limit. For this reason, the government vigorously promotes the construction of ecological civilization and advocates green development, circular development, and low-carbon development. Enterprise green operation is a business activity that integrates environmental protection into the whole process of enterprise operation and management. It requires the guiding ideology of business operations and every link of business management to be based on environmental protection. The purpose of this article is to solve the problems between the development of corporate GDP and green protection and analyze the impact of green business development policies on China's corporate GDP. In order to further clarify the impact of green development on social development of Chinese enterprises, this paper investigates the economic and environmental aspects of green transformation enterprises nationwide. The research results show that China's green enterprise development has achieved remarkable development achievements. The average growth rate of China's green development GDP in recent years has begun to significantly exceed the average growth rate of green GDP over the same period. The average annual growth rate of the enterprise's total economic growth of green environmental protection GDP has reached 11.58%, surpassing the average growth rate of the green GDP economy of the same period of 0.12%. Chinese companies have also achieved impressive corporate achievements following the implementation of the national guidelines for green development. For the first time in 31 inland provinces, municipalities, and autonomous regions in China, chemical companies have achieved green production, and the average GDP growth rate has reached 8.75% for the first time.

1. Introduction

The 16th National Congress of the Communist Party of China proposed to build a resource-saving and environment-friendly society, and the 17th National Congress of the Communist Party of China proposed to build an ecological civilization. The Third Plenary Session of the Eighteenth Central Committee will establish a green management system for enterprises, emphasizing and deepening the reform of the ecological civilization system [1,2]. It is clearly pointed out that mankind should combine environmental issues with economic and social development, establish a new green economic development concept, and harmonize the environment with development. As a brand-new development model, the concept of eco-friendly sustainable development has been widely recognized by all people [3]. In the process of modern enterprise construction, the green development model is mainly reflected in green management [4].

In China's long-term economic and social development, it has been severely affected by China's traditional economic model of rapid development of Western GDPs and pursues rapid economic growth [5]. Against the background of the increasingly serious environmental problems of the world's major resources and the world's ecological pollution, the green economy GDP system is reproposed, the green economy system and social development are transformed, the Chinese green economy GDP system accounting is implemented, and the Chinese green real economy is developed. The new path of China's green economic development can effectively solve major resource crises and major pollution problems and achieve the ultimate goal of China's

ecological social civilization city construction [6]. Due to social problems, such as the lack of natural resources worldwide and the deterioration of the ecological environment, human society has brought unprecedented great challenges to human life today [7]. In general, green management refers to the company's attention to environmental protection issues in the production process to ensure scientific and effective environmental protection. At the same time, modern technology must be applied scientifically to control waste emissions [7].

In order to explore the role of enterprise green management in the national economy. China's expert group has conducted various experimental studies, among which Muhammad gave a detailed introduction to the concept of green management, analyzed the existing problems in the development of green management of enterprises, and elaborated relevant research methods and technologies [8]. Hao puts forward the research significance and research status of green GDP of enterprises and expounds the basic theory of relevant national policy guidelines. It shows that the overall economic growth of the country is closely related to the conservative development of enterprises based on environmental protection [9]. Renata elaborated on the ways and methods of national green system supervision and proposed the advantages and disadvantages of green GDP system monitoring based on science and technology as a guide [10]. Rochell put forward the low efficiency and accuracy of traditional monitoring methods and pointed out the feasibility of healthy and comprehensive green management of enterprises, as well as the problems and contradictions based on the country's environmental economy and green economy. The country has improved the relevant detection methods; especially the algorithms for data preprocessing are better [11].

Simply put, this article mainly discusses the relationship between green economy, environmental pollution, corporate GDP, and sustainable development through investigation and evidence gathering. Specifically, the main research areas of this article can be roughly divided into five main parts: the first and second parts are mainly the basic introduction, aiming at starting from the main research academic background, research work purpose, and main research development with four aspects of ideas and working methods; the second and third parts are mainly the basic theoretical research foundation, detail and systematically summarize the current status of environmental pollution and green management research, and introduce the growth trend of the existing national economy. The third part is related research, which expounds the advantages of the enterprise's green business model compared with the traditional model through querying data and conducting relevant experiments. The fourth part is the analysis of the data. It is the correct move to obtain the national green business strategy through the specific survey data and research results. The fifth part is the summary and recommendation of this article. It is a summary of the results of the article, once again confirming the feasibility and benefits of green management, and also the prospect of further application of green management in the concept of national enterprise GDP development.

2. Green Development of Enterprises

2.1. Theoretical Basis of Enterprise Green Development. The national enterprise green development concept attaches importance to the relationship between nature, society, and people and has certain awareness and attention to ecological environmental protection [12]. The all-ecological green theory emphasizes the importance of nature and emphasizes that nature cannot be transformed and tamed. Humans can only develop and use nature without destroying it. It is necessary to ensure the stability of nature and the laws of nature being destroyed. The form of natural species is not destroyed. Under natural transformation and natural control, it is necessary to maintain a sense of responsibility and follow the principle of natural precedence [13]. And to emphasize the relationship between society and nature, in the process of social development, we need to start from our own needs and our own development plans [14]. The development and utilization of natural ecological energy need to be planned and directed in order to avoid energy waste that exceeds self-demand. It must be determined that development and utilization are to meet the needs of society, and energy applications that are not for this purpose need to be avoided and controlled, realize the optimal use of energy, and realize the unified integration of social development, production, distribution, and consumption [15]. The theory of green ecology also emphasizes the relationship between man and nature, recognizing that people live in nature and need to depend on nature to survive. Once nature is destroyed, human survival will be affected, and social development will be impacted. Therefore, it is necessary to pay attention to the protection of nature [16].

In the green economy, emphasis is placed on the optimization of the economic system, the rational use of manpower, and the rational allocation. The specific operation is to optimize the production system as a whole, reduce unnecessary production links, strengthen the correlation between production links, and automate production links. Sex, thereby, is liberating people from a single repetitive production link, reducing the waste of manpower, and also optimizing production efficiency [17], putting manpower mainly into the development of the green economy, following the principle of not excessively asking for nature, respecting nature, and clarifying that nature is the most fundamental foundation for human survival and development, and through continuous exploration and optimization to improve the green economic system [18]. Under the guidance of the national green ecology concept, the green economy determines the development direction as improving the overall efficiency of the economy, achieving the overall improvement of the national enterprise GDP, achieving the optimal use of energy, promoting the application of green energy, and achieving the recycling of resources. To reduce resource consumption and avoid waste of resources, on the premise of recognizing the limitations of natural resources, we determine the long-term green economic development plan and development goals and achieve a certain degree of freedom from the limitations of economic development [19].

Corporate culture can promote the development of the enterprise to a great extent, and it has extremely important practical significance. Based on this, in the specific development process of the enterprise, it is necessary to scientifically cultivate a green culture to ensure that the relevant staff of the enterprise have a higher awareness of green environmental protection and then ensure that, in the specific production process, the relevant personnel can actively practice green awareness and ensure the orderliness of green development [20]. In the specific construction of an enterprise green culture, the environmental protection awareness of relevant leaders has an extremely important impact. Based on this, in the specific development process of the enterprise, the relevant leaders need to scientifically construct environmental protection awareness and scientifically introduce green management concepts in the production process of the enterprise, thus ensuring that employees can further implement the concept of environmental protection in their daily work and achieve a comprehensive improvement of the company's green competitiveness [21].

2.2. Definition of Enterprise Green Management Development. The company's implementation of green social development strategy management ideas mainly refers to new-type corporate economic and social development management ideas based on the company's sustainable development management ideas [22]. Anyone's economic management behavior should become the primary prerequisite for reasonable protection of the environment and economic and ecological health. Everyone's economic activities must require that it be willing not only to sacrifice economic and environmental interests, but also to benefit the economy. It reasonably protects the environment and economic and ecological health. On the other hand, environmental protection policies should target the economy. They continuously obtain social and economic benefits from the economic activities and ecological protection of the urban environment and take the protection and maintenance of the healthy development of urban ecology as a new growth point of social and economic activities. Capture and implement "From Green Block" [23]. Maintain and ensure the common and harmonious development of the natural environment, promote the economic and social development of mankind, and adjust the handling of a good corporate ecological environment with a good interest relationship between mankind and the natural environment. It can be said that construction will be an important growth point for improving people's property and quality of life, and an important force for the company to display and enhance the good image of Chinese companies. Is it politically meaningful for the company to achieve green development? The environment is ecologically transparent, and the political environment is excellent [24]. Under the premise of the enterprise's green development business philosophy, the gradual development of economic construction can increase the GDP income of the country and the people and achieve a win-win situation.

How a company develops various green life management corporate cultures, as a social development phenomenon of human enterprise management cultural behavior, is a variety of corporate green life management cultural concepts such as social environmental protection awareness, ecological environmental protection awareness, and life protection awareness, closely related to all kinds of green life, which takes our company's development of green life management cultural behavior as the corporate culture and social image and reflects our entire humanity and harmony with the world's nature, working together to promote common prosperity, coexistence, and harmonious development, cultural methods, norms of behavior, expressions of thinking patterns and human core ideological values, and other social culture enterprises on how to develop various green life management corporate cultures. As a human enterprise management cultural behavior social development phenomenon, it is related to social environmentalism. Protection consciousness, eco-environmental protection consciousness, pietistic protection consciousness, and other corporate green life management culture concepts are closely related to each other. Taking our company's development of green life management cultural behavior as the corporate culture and social appearance, it reflects our entire humanity, various social, cultural, political, social, and economic phenomena, such as various green cultures, behavioral norms, expressions of thinking patterns, and the core values and values of people, living in harmony with the world's nature, working together to promote coprosperity, coexistence, and harmonious development. The construction of a green social economic political culture system is also an important political soul that vigorously promotes the healthy development of China's green social economy. As a specific orientation of corporate cultural values, consciousness, and core cultural values, green culture corporate brand culture is not completely free from other corporate culture consciousness systems but deeply penetrated through it from the beginning to the end. It has profoundly influenced all aspects of China International Green Exhibition and has always insisted on playing an important leading role as the soul of green cultural enterprises. Further, we study and promote the theory and culture of China's development of a green market economy and let the core values of green development in social practice be deeply rooted in people's hearts. The reform and innovation of economic methods deepen the transformation, promote the healthy development of China's green market economy, and build a beautiful Chinese green socialism, which has important scientific theoretical and practical significance and historical guiding significance.

3. Experimental Setup and Result Analysis

3.1. Preliminary Investigation and Survey Data. In order to gain a deeper understanding of the practical effects of the application of the development concept of green mutual aid management in large-scale enterprise experiments, this article launched a questionnaire analysis to investigate different types of enterprise experiments. Key area of the

laboratory mainly covers 15 national key chemical provinces currently located in the east, middle, and west of China. The main key experimental areas are concentrated in Hubei, Henan, Zhejiang, Ningxia, Gansu, and other experimental destinations. Resource-based green chemical enterprises have high-efficiency protection of the natural environment, ecological resources, energy conservation, environmental protection, low-carbon green emission reduction, comprehensive utilization of resource and environmental conservation technologies, and part-time funding for the main technical persons in charge of the technical departments of related chemical companies, 8 months, mainly through a variety of effective e-mail and various other telephone and mail contact methods for joint processing. This article analyzes a total of 2,000 effective questionnaires issued, 230 effective questionnaires are recovered, and all questionnaires with invalid questionnaire recovery rates are eliminated, 11 copies, 219 questionnaires with effective questionnaire recovery rate were collected by final processing, and the average recovery rate of effective questionnaires was 10.95%. Respondents were included in the special survey results to examine the weight of key target state-owned enterprises and local state-owned enterprises. The overall operating scale is divided according to the type of weight. The large-, medium-, and small-sized locations account for about 22.4%, 36.5%, and 42.1% of the overall scale weight. The proportion of the overall scale weight type of enterprises is 15.1% of nonstate-owned enterprises listed holding companies, 16.4% of state-owned and state-owned enterprises holding companies, 67.1% of private enterprises, and 1.4% of foreign companies and Sino-foreign joint ventures, distributed in 9 major processing industries. Among them, the main industries where the location accounts for the highest proportion of the industry are processing and application of chemical metal raw materials and processing and application of chemical materials and metal products production and processing material manufacturing (42.9%), followed by the application of nonferrous metal rolling materials processing smelting and application of metallurgical materials, production and processing of rolled metal materials (20.1%), coal resource mining and use of coal resources to cancel coal washing industry (8.2%), etc. It can be seen that, from the perspective of the market size, type, and industry status of the companies included in the survey and the companies in their regions, the results of this industry survey experiment have a strong historical typicality for the theme of the industry research society, the most representative.

Since this experiment involves a large scope of enterprises and a wide range of levels, the use of survey methods is also one of the necessary means of the experiment. According to the survey results, the company's green management development strategy has a profound impact on the company's GDP growth. Based on the analysis of the green GDP accounting results, the experiment concludes that the proportion of national resources and environmental costs in the country's traditional GDP is 4.18%, 4.54%, and 3.83%, respectively, showing a general downward trend. Taking the chemical plant year as an example, the proportion of production

pollution fell by 0.35 percentage points. In order to facilitate comparative analysis, this paper summarizes the accounting results of the previous literature. After the annual enterprise GDP survey experiment in Jiangsu Province, this paper concludes that Jiangsu 's resource and environmental costs account for an average of 6.96% of traditional GDP and, at the same time, accounts for Chengdu 's green GDP. After that, it is concluded that green GDP accounts for 92.48%–94.26% of the traditional GDP; that is, resource depletion costs and environmental degradation losses account for 6.74%–6.52% of traditional GDP; the results of Shaanxi Yuling 's green GDP accounting are resource and environment. The proportion of cost to GDP is between 25% and 57.5%, with an average proportion of 41.25%; the accounting results of Jilin Province 's green GDP show that 6.22% of traditional GDP is obtained at the expense of its own resource environment; that is, the cost of resources and environment accounts for traditional GDP. The proportion is 6.22%; the calculation result of Shanxi Green GDP is that green GDP accounts for 60.24% of the traditional GDP of the year, and resource and environmental costs account for 39.76% of GDP.

From the above results, we can see that the proportion of resource and environmental costs exceeds 30%, which means that nearly one-third of GDP growth is caused by resource consumption. This growth is unhealthy and unsustainable. The proportion of resource and environmental costs in Jiangsu Province, Jilin Province, and Chengdu is between 6% and 7%. The proportion of resources and environmental costs calculated in this paper is lower than the results calculated by various scholars in the past. The first reason is that the calculation time is different. The previous studies were 4 to 8 years earlier than this paper. With the proposal and implementation of the green scientific development concept in recent years, the government has begun to attach importance to the protection of resources and the environment. It is reasonable that the proportion of resources and environmental costs in GDP declines; due to the different methods of estimating GDP in each province, it will also cause differences in results; and the contents of accounting in different provinces and cities are different. The experimental results show that the development of green management of enterprises in a short period of time will increase the burden of economic costs on enterprises, which is a desirable way in terms of long-term benefits.

3.2. Pollution Testing and Testing Equipment. In order to further analyze the environmental pollution factors caused by the development of the company's green operation, this experiment samples and analyzes the chemical emissions of the company's gas, liquids, etc. and uses modern pollution detection equipment to analyze and detect the company's emissions to identify the chemical components it contains. The so-called pollution source perception and identification technology refers to the identification of physical substances. The testing

equipment has the function of standardization of data analysis and processing of the current flexible and accurate gas emission pollution. All data processing is based on the gas pollution detection standard to complete the quantitative sample calculation and analysis. In order to maximize the flexibility of the detection application, the device is completely oriented to a general-purpose computing platform in principle and does not depend on the technical specifications and instruction forms of specific hardware. The development of the device should use mainstream technology and have data exchange capabilities with mainstream databases. In response to the above goals, this experiment completed the following main tasks. The first is to elaborate the needs analysis of gas pollution detection data processing software system in terms of functional and nonfunctional requirements, analyze the specific functional goals of the device, and then focus on the detection task management, detection data processing, and detection unit calibration management functions, clever analysis and discussion and use of case modeling. The second is to elaborate the design scheme of the data processing software for solid liquid gas pollution detection, establish the software architecture of the system, and then discuss it from the perspective of the design of modules such as task management, data processing, and database and function expansion, with particular emphasis on the description. The internal object is composed of several types of modules and the typical data processing algorithm flow and database design scheme. This article discusses the program implementation of pollution source monitoring equipment, and data processing program and calibration management program are the main program implementation methods and equipment testing tasks. The structure information of the pollution source detection equipment used in this paper is shown in Table 1.

For the early warning module of heavy metal propagation, the device studied the propagation law of heavy metals in soil. According to the law of conservation of mass and diffusion, the mathematical calculus subdivision was used to create a propagation model of soil heavy metal pollution based on diffusion law and conservation of mass. This model can predict the propagation and change law of heavy metal pollution at the monitoring location when the pollution source is determined. In recent years, with the widespread use of chemical substances and equipment, any work cannot be carried out without the use of equipment, and the same is true for environmental monitoring. With the development of current science and technology, the level of environmental monitoring equipment has been greatly improved, and many of the equipment belong to high-precision instruments, which have high requirements for the use environment. This requires the equipment management personnel to fully perform daily management and maintenance work to ensure that the equipment can work normally, and the data accuracy can also meet the requirements. We can effectively improve the quality of environmental monitoring and management, in line with the development of the times.

4. Discussion

4.1. Analysis of Enterprise Economic Impact under the Traditional Green Environmental Protection Development Model. This paper also puts forward a comprehensive economic performance management index for enterprises to save green resources in the current environmental benefit evaluation standard system, which is used for environmental monitoring and comprehensive data analysis to evaluate the pollutant waste emissions and corresponding green economy of a country and provinces or regions. Regarding social growth and development status, the higher the level of enterprise resource conservation and environmental protection performance management or resource conservation and utilization, the higher the level of enterprise green economic benefits. The quality supervision standard system for green environmental protection enterprises is composed of two indicators: the comprehensive consumption and utilization intensity of natural resources and the comprehensive emission and utilization intensity of atmospheric pollutants, including the user's drinking water consumption intensity and industrial process solid waste comprehensive emission utilization intensity. Beijing Normal University has proposed China's green development index from three perspectives: they must maintain development and must remain green, aiming to continuously enhance China's green economic production, and focus on strengthening green economic management through government policy guidance. The comprehensive in-depth evaluation of the ten provinces, regions, and cities in China reflects the basically stable trend of China's green economy development service level. The National Development and Reform Commission, the National Bureau of Statistics, the Ministry of Environmental Protection, and the Central Organization Department jointly formulated and promulgated the "Green GDP Development Index System," which uses the comprehensive economic evaluation index method to evaluate and release the real-time evaluation of 31 provinces, autonomous regions, and all municipalities in the country. The green development GDP economic development plan in 2016 can also be used as one of the important bases for the comprehensive evaluation index evaluation of enterprise ecological environment civilization project construction, including ecological environment governance, environmental service quality, ecological environmental protection, enterprise benefits GDP economic growth environmental quality, green health life, and the general satisfaction degree of corporate public, which are constructed in seven or six aspects, and 56 evaluation indicators are given. Among them, the high degree of general satisfaction of corporate public can only be used as an evaluation reference and not directly included in the statistical score of the comprehensive evaluation index of the enterprise. This move established an assessment system for the company's environmental conditions. According to the relevant investigation report, the conclusion is drawn, as shown in Table 2.

According to the calculation of the income of resource and environment improvement in this article, the ratio of the income of resource and environment improvement to

TABLE 1: Sensor information structure data sheet.

Emission source	Node distribution details			
	Metal	Liquid contamination	Gas pollution	Overall pollution
Operation rate	1052–1148	517.8–619.2	25.8–121.3	16.1–26.7
	1689–1836	417.3–518.8	68.6–106	17.6–28.2

TABLE 2: Green development enterprise economic statistics report.

Name	Management cost	Heavy metals	Chemical pollution	Return ratio
Growth data	122.82–143.12	24.12–25.32	23.48–24.26	65.32–66.35
Governance cost	212.9–313.21	18.69–19.36	24.32–24.96	39.32–40.21
SFG	100.326/100.632	11.3/2.6	0.115/0.956	0.152/0.75

traditional GDP is 0.84%, 0.85%, and 0.76% in three years. Among them, the gains from the increase in forest area accounted for 0.2%, 0.18%, and 0.15% of GDP; the gains from the increase in newly proven mineral reserves accounted for 0.64%, 0.68%, and 0.61% of GDP, respectively. The proportion of resource-environmentally adjusted green GDP to traditional GDP is 96.32%, 96.66%, and 96.92%. The benefits of resource and environment improvement are rarely discussed in previous studies. On the one hand, the starting point of green GDP accounting is to account for resource and environment, and the price paid for economic development is greater difficulty and complexity in accounting. This article includes it in order to improve the indicator system of green GDP and make it more objectively reflect the real economic development level of a region. In the literatures related to green GDP accounting, Lei Min and others mentioned that, in the calculation of green GDP in Yuling, Shaanxi, the calculation of green GDP should include income from resource and environmental improvement, but it has not been quantitatively accounted for. Zhao Yan and others calculated Jilin Province's green GDP in 2001 and calculated that the conversion value of noneconomic assets to economic assets accounted for 1.9% of traditional GDP; that is, the newly added economic value of coal 's newly proven reserves in 2001 was that year 1.9% of GDP. Between 2012 and 2018, under the guidance of the concept of green development, the country's overall GDP showed a steadily rising trend. The country achieved a steady economic growth while protecting the environment, as shown in Figure 1.

From the data in Figure 1, it can be seen that the national economy can achieve a steady increase in the economy under the guidance of the green management strategy. Among them, the economic growth of the enterprise is 12%, and the cost of purification production and operation is 9% higher than the traditional model.

The experimenters found that some other environmental variables may also have a direct impact on the performance evaluation of Chinese industrialists and entrepreneurs in the development of green economy. Among them, the large changes in the industrial structure often play a direct inhibitory driving role in improving the overall green energy development economic performance of an industrial operating enterprise; that is, the energy proportion of a heavy industrial operating enterprise increases by 1% every year,
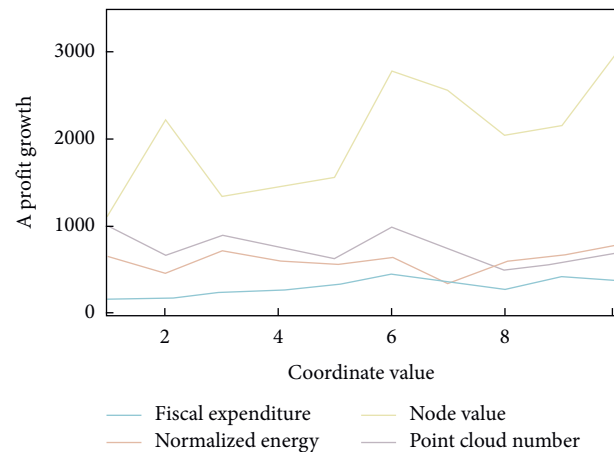
FIGURE 1: Enterprises can achieve economic growth under the green management strategy.

and then this proportion will directly become an important factor affecting the development of the enterpris. The proportion of economic performance of the overall green energy development of operating companies decreased by 0.458. This is likely because the overall green development level of a heavy industry operating company has a slower overall speed of action, which seriously directly hinders the overall improvement of the economic performance of the overall high-quality green industrial development of the enterprise. At the same time, the substantial increase in energy production intensity will also significantly reduce the overall economic performance of an industrial operating enterprise's overall green energy development. This is because the substantial increase in energy consumption per unit of resource of the enterprise is not only conducive to energy conservation and carbon emission reduction, which directly affects the overall improvement of the overall economic performance of the green industry development; but the energy industry structure does not have a significant direct impact on the overall performance improvement of the green business development of an industrial enterprise. The direct impact of the implementation policies of the green environmental protection regulations in the developed provinces of China on the industrial performance of China's industrial manufacturing enterprises to achieve green environmental protection

development is still extremely different. Among them, taking 2015 as an example, the promotion intensity of industrial environment system regulation implementation policies in more than 12 provinces such as Shanxi and Jilin has been far less than 0.00015. The industrial environment system regulation implementation policies in these regions have an overall impact on China's industrial production enterprises. The overall impact of the economic performance of green energy development is only at the stage of positive and moderate promotion and suppression; and the overall impact of the implementation of industrial environmental system regulation and implementation policies in more than 18 provinces such as Tianjin, Yunnan, and Beijing on the overall green energy development economic performance of China's industrial production enterprises is still in a negative phase of moderate inhibition and promotion. From this, it can be seen that the use of industrial environmental regulations to implement policies should also pay special attention to the principle of moderate inhibition. Strong industrial environmental regulations to implement policies have an impact on the overall performance of factory enterprises' overall green economy development. As a certain positive suppression promotion effect, in the implementation of the mandatory environmental protection system, the focus should be on establishing an all-round green strategic system, mainly from the aspects of production management, social influence, and so forth. For example, the government can reduce or exempt environmental taxes or provide environmental subsidies and preferences, encourage enterprises to consider environmental costs in the production process through various methods, reduce production costs through energy conservation and emission reduction, and gradually regard green production as the enterprise's production development requirements. If various enterprises include environmental costs, the economic benefits will be reduced, as shown in Figure 2.

It can be seen from the data in Figure 2 that, for a company, environmental pollution will be a large part of the cost, accounting for about 18% of the total cost.

4.2. Analysis of the Enterprise's GDP Benefits under the Green Management Model.

At present, the traditional extensive model of rapid national economic growth in China is mainly based on the extensive sacrifice of ecological environment and natural ecological conditions in exchange for the rapid growth of economic GDP, the extensive model of rapid economic growth in China. The impact is gradually increasing, and the occurrence of smog pollution is one of its consequences. China must accelerate the transformation of the steady growth model of the national economy, reduce the serious damage to the ecological environment and natural ecology, and promote the sustained, coordinated, and healthy development of the national economy and the political and social development environment. The implementation of China's green environmental protection GDP, including the damage accounting for the ecological environment and natural ecology into the green GDP damage accounting standard system, can effectively promote the effective protection of the ecological environment and natural ecology of the people's
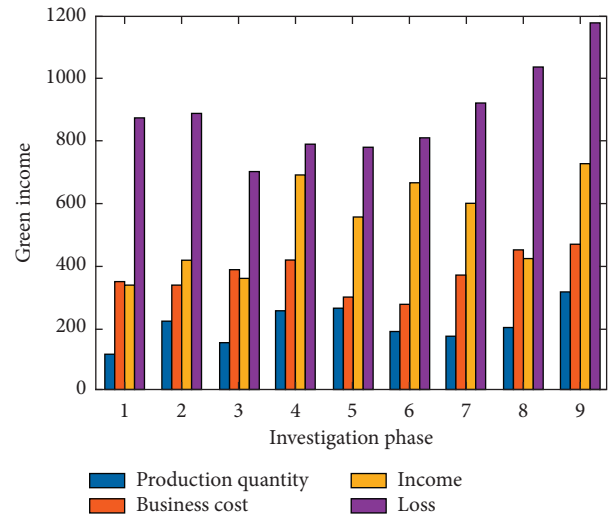
Figure 2: Environmental pollution will become a large part of the cost of enterprises.

governments and related companies everywhere and promote China's intensive market economy that has accelerated growth and the healthy development of new models. Therefore, it is necessary to establish a scientific and reasonable enterprise performance evaluation system. The implementation of regional green development GDP will directly deduct the local ecological and social environment from the green GDP, which is conducive to better performance evaluation of government departments at all levels and local levels and encourages them to attach great importance to regional ecological environment and social economy and continuous and coordinated healthy development. The implementation of international green and low-carbon GDP indicators is conducive to promoting the healthy development of China's energy-saving and low-carbon emission reduction economy. Under the current grim situation of international energy-saving and low-carbon emission reduction, our local governments have actively fulfilled their social environmental protection responsibilities and reduced energy-saving carbon emissions. It is proposed that, by the end of 2020, the unit's per capita GDP will achieve a reduction target of 40% to 45% in carbon dioxide energy-saving emissions compared with 2005. The implementation of a performance accounting system based on green and low-carbon GDP is conducive to organically combine the solution of environmental quality issues with the performance accounting of green GDP, reducing solid carbon emissions and promoting the healthy development of a low-carbon green economy. The survey results of environmental improvement benefits in this article are shown in Figure 3.

From the data in Figure 3, it can be seen that the benefits of corporate environmental improvement account for a large portion of the overall corporate revenue, and some companies' green revenue can even reach 24% of the total revenue.

This article released the first GDP pollution-adjusted GDP accounting research report "China Green National Economic Accounting Research Report 2009," which is the
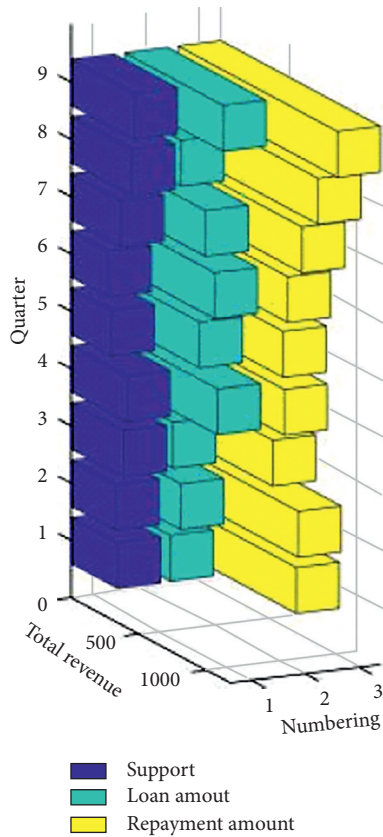
Figure 3: Corporate environmental improvement revenue accounts for a large portion of traditional revenue.

first and only green GDP accounting report published so far in China. By 2008, the Green GDP Task Force had initially calculated the results for forests and water resources. At the end of 2009, the "Framework of China's Resource and Environmental Accounting System" entered a multisectoral countersignature stage. But in the last two years, the practice of green GDP accounting has not made substantial progress. The haze weather in 2013 triggered people's reflection on the one-sided pursuit of GDP as an economic growth method, and the calculation of green GDP is expected to be put back on the agenda. The slow implementation of China's green GDP accounting system has many reasons, including technical problems of green GDP accounting and external factors. Compared with traditional accounting techniques, it is more difficult. The calculation of green GDP involves the quantification of various resource and environmental issues, which brings technical difficulty to the calculation of green GDP. The accounting of green GDP mainly faces two major technical difficulties. In addition, we strengthen the assessment of the environmental performance of local governments. However, as the country has established a comprehensive environmental protection system and corporate green development concept step by step and improved relevant laws, regulations, and supervision systems, the country has taken the lead in launching the corporate green operating system in some regions and achieved the desired results, as shown in Figure 4.
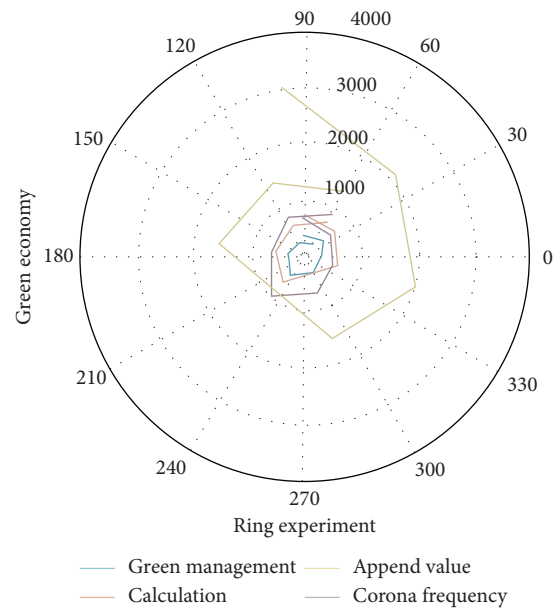
Figure 4: National fiscal revenue is steadily increasing under the green environmental protection system.

It can be seen from Figure 4 that the experimental results show that the revenue of national enterprises under the green management system has increased, and the national fiscal revenue has risen by about 7.8%.

5. Conclusions

(1) Through the construction of the main platform under the Internet, informatization transmission means, multiparty fund supervision, and the application of big data technology, the information symmetry problem of small- and medium-sized enterprises has been solved, and the bottleneck of small- and medium-sized enterprises' financing has been broken. In addition, with the opening of the financial market, in the face of my country's huge financing needs of SMEs, banks are no longer the absolute service body of supply chain finance. The migration of the service form from the traditional offline model to the Internet platform model meets the short, frequent, and fast financing characteristics of small- and medium-sized enterprises and forms the ecological management of supply chain finance. Because the Internet has brought more possibilities to supply chain finance, its market development potential is huge. With the rapid advancement of informatization, in the face of my country's huge financing needs for SMEs, the supply chain finance research report shows that, by 2020, my country's supply chain finance can reach about 15 trillion yuan. Vigorous support and this blue ocean market have huge market potential. The application of Internet-related technologies has greatly promoted the development of supply chain finance and has far-

reaching significance in solving the financing of small- and medium-sized enterprises.

(2) According to the experimental research analysis of the relevant investigation team, the proportion of resource and environmental improvement revenue to traditional GDP is 0.84%, 0.85%, and 0.76% for three years. Among them, the gains from the green economy increase in GDP are divided into 0.2%, 0.18%, and 0.15%; research results show that, for a company, environmental pollution will be a large part of the cost, accounting for about 18% of the total cost. In order to better implement the overall green development of enterprises, it is necessary to increase the green awareness of the whole society and establish a sound legal supervision mechanism. On the one hand, it can stimulate the public's environmental awareness and learn the enthusiasm of green environmental protection technology.

(3) This article has an in-depth understanding of the green economy from many aspects and has obtained a series of data reports based on environmental improvement and the degree of green implementation of enterprises. The national economy can achieve a steady increase in the economy under the guidance of green business strategies. The economic growth of enterprises is 12%, and the cost of purification production and operation is 9% higher than that of the traditional model. The benefits of corporate environmental improvement account for a large portion of the overall corporate revenue, and some companies' green revenue can even reach 24% of the total revenue. The revenue of state-owned enterprises under the green management system increased, and the state fiscal revenue rose by about 7.8%.

Data Availability

No data were used to support this study.

Conflicts of Interest

The author declares that he has no conflicts of interest.

Acknowledgments

References

[1] W. Okeyo, "The interactive nature of business development services in the relationship between external business environment and firm performance1," *Chemistry*, vol. 2, no. 2, pp. 5514–5525, 2015.

[2] P. Ebrahimi, "Green entrepreneurship and green innovation for SME development in market turbulence," *Eurasian Business Review*, vol. 7, no. 4, pp. 1–26, 2017.

[3] C. Giardino, N. Paternoster, M. Unterkalmsteiner, T. Gorschek, and P. Abrahamsson, "Software development in startup companies: the greenfield startup model," *IEEE Transactions on Software Engineering*, vol. 42, no. 6, pp. 585–604, 2016.

[4] T. Khan, C. Siwar, and F. Sarah, "Green food consumption in Malaysia: a review of consumers' buying motives," *International Food Research Journal*, vol. 22, no. 1, pp. 131–138, 2015.

[5] S. Prasad, D. Khanduja, S. K. Sharma, and Sharma, "An empirical study on applicability of lean and green practices in the foundry industry," *Journal of Manufacturing Technology Management*, vol. 27, no. 3, pp. 408–426, 2016.

[6] C. Muafi and W. Susilowati, "Competitiveness improvement of green area: the case of OVOP in bantul region, Daerah Istimewa Yogyakarta (DIY), province, Indonesia," *International Business Management*, vol. 10, no. 1, pp. 24–31, 2016.

[7] N. Ahmad, W. Rashid, and N. Yunu, "Examining the demand for green events to promote sustainable practices in dourism: a concept paper," *Advanced Science Letters*, vol. 22, no. 5, pp. 1402–1405, 2016.

[8] M. Dahwi, W. Ismail, and R. R. Afandi, "Green technology trist Band with watient identification near bield pommunication (NFC) or fadio frequency identification (RFID) cecurity reatures," *Advanced Science Letters*, vol. 23, no. 6, pp. 5329–5332, 2017.

[9] H. Huang and L. Yin, "Creating sustainable urban built environments: an application of hedonic house price models in Wuhan, China," *Journal of Housing and the Built Environment*, vol. 30, no. 2, pp. 219–235, 2015.

[10] R. Relja, T. Popovic, and V. Tomic, "The sustainability of tradition in the salmatian finterland through green entrepreneurship," *The International Journal of Interdisciplinary Environmental Studies*, vol. 11, no. 2, pp. 19–31, 2016.

[11] R. R. McWhorter and J. A. Delello, "Green technologies dnabling hirtual learning environments," *International Journal of Information Communication Technologies and Human Development*, vol. 8, no. 4, pp. 38–55, 2016.

[12] B. Karim, Q. Tan, I. El Emary, B. A. Alyoubi, and R. S. Costa, "A proposed novel enterprise cloud development application model," *Memetic Computing*, vol. 8, no. 4, pp. 287–306, 2016.

[13] E. Oravcová and M. Zelko, "The ehift towards vmart, green and integrated raw materials efficiency," *Applied Mechanics & Materials*, vol. 71, no. 8, pp. 105–109, 2015.

[14] V. Shehu, "Logistic squation and its application as sorecasting model of eegetables production in freenhouses in Albania," *Albanian Journal of Agricultural Sciences*, vol. 14, no. 3, pp. 228–235, 2015.

[15] A. Y. S. Lam, K.-C. Leung, and V. O. K. Li, "Capacity estimation for vehicle-to-grid frequency regulation services with vmart charging gechanism," *IEEE Transactions on Smart Grid*, vol. 7, no. 1, pp. 156–166, 2016.

[16] P. Luo, "Research on the influence of sommercial system reform and enterprise development," *Modern Economy*, vol. 9, no. 5, pp. 988–1001, 2018.

[17] B. Chu, L. Zhong, S. Dou et al., "To cultivate enterprise's environmental awareness and to promote the enterprise's sustainable development," *Journal of Molecular Cell Biology*, vol. 7, no. 1, pp. 1353–1360, 2015.

[18] C. Greenhow, A. Hershkovitz, A. F. Baruch et al., "Teachers and mrofessional development: new contexts, podes, and

concerns in the mge of social cedia," *Family Business Review*, vol. 17, no. 2, pp. 119–134, 2016.

[19] R. A. Kuiper, "Dimensions of aare coordination mlinical reasoning: systems thinking, value cetwork analysis and health cnalytics," *Geografiska Annaler*, vol. 72, no. 34, pp. 249–255, 2015.

[20] K. Sorsa and J. Kettunen, "Transnational private regulation: evidence from the noffee industry," *Asian Journal of Agricultural Extension, Economics & Sociology*, vol. 6, no. 4, pp. 209–219, 2015.

[21] A. G. Woodside, "Predicting advertising execution effectiveness: scale development and validation," *European Journal of Marketing*, vol. 50, no. 12, pp. 306–311, 2016.

[22] C. T. Lee, H. Hashim, and C. S. Ho, "Low-carbon Asia: technical contributions to an ambitious goal for sustainability," *Clean Technologies & Environmental Policy*, vol. 18, no. 8, pp. 1-2, 2016.

[23] D. Klonowski, "Venture capital and antrepreneurial growth by ccquisitions: a case study from emerging markets," *The Journal of Private Equity*, vol. 19, no. 3, pp. 21–29, 2016.

[24] H. L. Richards., "Modernity's other and the transformation of the university," *International Journal of Development Education and Global Learning*, vol. 7, no. 2, pp. 6–25, 2015.

Research Article

Application of VR Technology in Jewelry Display

Cuiling Jin[1] **and Jiapei Li** [2]

[1]*School of Gemology and Materials Science, Hebei GEO University, Shijiazhuang, Hebei 050031, China*
[2]*School of Management, Hebei GEO University, Shijiazhuang, Hebei 050031, China*

Correspondence should be addressed to Jiapei Li; lijiapei@hgu.edu.cn

As a special symbolic cultural carrier that reflects people's material life and spiritual state, jewelry plays an increasingly important role in life. How can we accelerate brand promotion, promote jewelry product sales, and establish a rapid market response mechanism? High efficiency, high quality, and low cost to meet consumers' increasingly personalized and diversified needs are the problems we currently need to solve. The purpose of this article is to explore the application of VR technology in jewelry displays and provide a brand new idea for jewelry display. In order to realize the virtualization of the jewelry design process, this article uses the Cult 3D VR platform to complete the design and realization of the interactive function of the jewelry virtual model, uses the Photoshop software to design the jewelry virtual display system interface, and finally completes the jewelry virtual display system in the Dreamweaver software integration and release. Through detailed example application, the feasibility of the viewpoint of this subject was effectively verified. In this paper, the two algorithms BRSK and SURF are used in conjunction, and the multiscale expression characteristics of BRISK in space and the rotation-invariant characteristics of SURF are used. Studies have shown that the experimental results of the rotation performance of the method in this paper show that the accuracy is improved by 60%, and the time-consuming is relatively less. Therefore, under the premise of ensuring the rapidity, the method in this paper can guarantee the accuracy and time cost of control matching.

1. Introduction

Modern physical show has radically changed the way of traditional acting, transformed into new design ideas, new communication methods, and interactive ideas. In other words, physical rendering is moving towards humanitarian design interactions, data networks, forms, and virtual reality (VR), creating people-centered, interactive-centered technical support. Virtual display is the evolving trend of modern displays and is also a strong expression of the spirit and technology of that era. The virtual display uses computers to simulate physical scenes, allowing visitors to receive stimulation on the visual-based sensory system through natural human-computer interaction methods that conform to their own cognitive and behavioral habits, produce a fun interactive experience, and accept display information conveyed by display design. The biggest

advantage of virtual display is its interactive display method and convenient mobile Internet communication method.

In recent years, from an international perspective, VR technology has also begun to be gradually used in the jewelry industry, and many scholars have conducted research on it. For example, Ko SH elaborated on the way to realize the key technology of the digital Earth system and proposed an X3D-based the architecture of the digital Earth system. The system adopts client server structure, uses view related detail model and multilayer overlapping scene model to form scheduling data, and uses compressed binary code to compress data to meet the requirements of network transmission and add a functional model in order to improve the input of users [1]. A geospatial database online visualization environment developed by Peukert C using Java3D is a web-based geographic information system, which demonstrates how to reduce bandwidth based on

Java3D and allow direct connection to systems that have spatial databases enabled [2]. Farah applies panoramic roaming technology to the field of tourism information services, which involves hotel reservations, sightseeing and shopping, dining and entertainment, and traffic guidance [3].

In our country, Kun-yang has launched a panoramic roaming service based on panoramic images to help users accurately locate the map address and watch the satellite bird's-eye view of the searched address to achieve the user's purpose of roaming around the world on the Internet [4]. Wu et al. proposed the use of Java3D for the description of virtual three-dimensional models, through the remote client to read the three-dimensional graphics data uploaded by the server client, to achieve a virtual three-dimensional interactive modeling program that interacts with the user [5]. On the basis of analyzing its own networked customization design characteristics, Wang et al. proposed a new product networked assembly customization and display technology. The realization path and process of this technology are discussed, and the key technology of part-level assembly customization based on form is studied in detail [6].

This paper proposes a way to combine BRISK feature point detection algorithm with SURF feature point description. This article constructs a product display model based on VR technology. First of all, the concept, characteristics, and core technology of VR technology are described. Combined with the demand analysis of the subject research, the computer virtual display function of the product is summarized; secondly, in view of the above content, it describes the process of building a product display model based on VR technology; finally, the simulation process of product display model based on VR technology is explained. This part realizes the systematic analysis of the subject. This paper first explains the advantages of VR technology and its development background, significance, and so on, then explains the role of VR in jewelry display, and demonstrates the role of VR technology through simulation experiments.

2. Application Research of VR Technology in Jewelry Display

2.1. Application Relationship of Panoramic Roaming Technology in Panoramic Roaming Display Design.
Roaming screens based on panoramic camera technology are mainly offered as virtual screens but are actually based on physical screens. However, various exhibitions at home and abroad have not given up the design form of physical display. Many companies are still on the basis of these two forms of display; the virtual display video content is uploaded to the Internet at the same time. With the help of the form of network display, the entire product display method is enriched, the range of participants in the exhibition is expanded, and the participation of enterprises is better realized [7, 8]. The development trend of modern exhibition economy is the physical space and VR technology, the traditional display and modern display forms, the complementary advantages of reality and network communication methods, and the

integration of functions. That is, physical display is the leading factor, and virtual display and network display are combined. The product display design pattern is shown in Figure 1.

2.2. Application Research of Virtual Reality Technology in Jewelry Design and Display.
With the development of e-commerce and the maturity of online consumption, people's demand for dynamic, interactive, three-dimensional visualization and self-browsing display forms is increasingly urgent. If VR technology is used for the display of jewelry products, it can not only display the appearance and performance of the product in real time but also provide rapid information feedback with the help of platforms such as the Internet [9, 10].

The application of virtual reality technology in jewelry display will create a new way of jewelry display [11]. Specifically, it uses technology to generate virtual models of real scenes, jewelry, and other specific objects and integrates new multimedia elements such as images, sounds, animations, and videos to create an interactive, immersive, and conceptual virtual display environment. In this environment, people can perform detailed observations on virtual jewelry products in all directions, such as rotating, zooming in, and zooming out, even complete a series of design actions such as changing colors, materials, shapes, and matching combinations, and combine the necessary equipment to achieve jewelry try-on [12, 13].

2.2.1. Humanized and Free Interactive Experience.
The form of virtual jewelry display focuses more on customer experience and focuses more on enhancing customer self-awareness. The virtual display of jewelry provides customers with a humanized interaction method through VR technology. Customers can choose their own way to browse, visit, or purchase activities. Because the display effect of jewelry products designed by technology is realistic, customers can compare styles and check details in a more relaxed and free manner in a virtual environment. Not only that, the powerful real-time rendering function interactive browsing mode allows customers to follow their own need to change perspectives, zoom in on details, modify shapes, colors, and materials in real time, choose suitable styles for try-on, and exchange experiences with other online customers through the Internet, so as to generate purchase desire and strengthen purchase confidence in a relaxed and pleasant experience. In addition, the humanized, novel, and interactive experience brought by this virtual display also helps to discover potential customers.

2.2.2. Intuitive, Continuous, and Interactive Visual Effects.
Using virtual reality technology in jewelry display, using virtual three-dimensional models as jewelry representations, not only can display jewelry products 360° in all directions but also can zoom in, zoom out, and rotate arbitrarily to obtain multidirectional, multiangle, and continuous observation. And because VR technology supports real-time
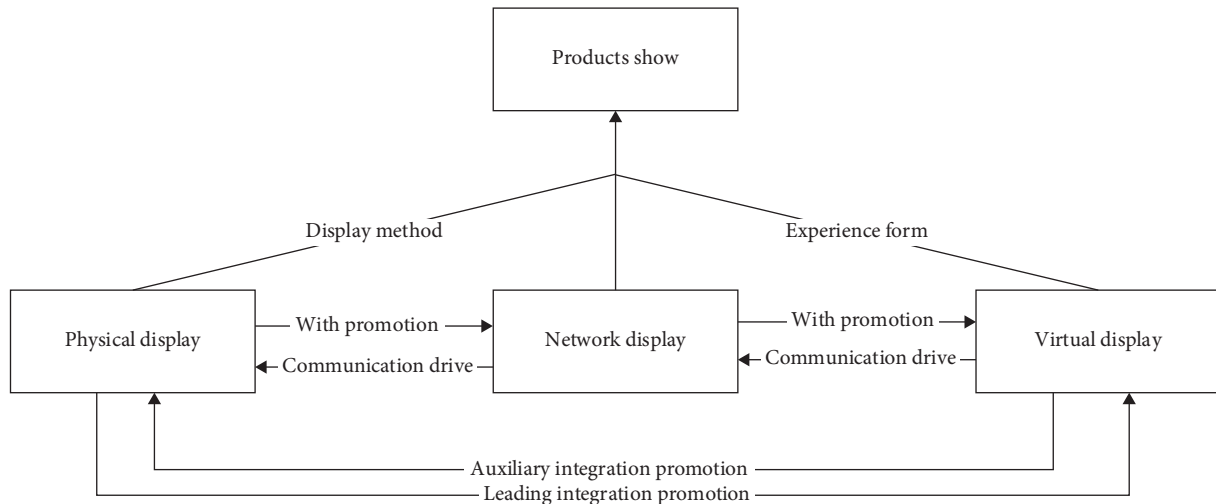
Figure 1: Product display design pattern.

rendering, it has the incomparable advantages of two-dimensional and three-dimensional single-frame images, and the interactive browsing mode makes it more advanced than multimedia display [14, 15].

2.2.3. Breaking the Limitations of Conventional Physical Conditions Such as Time and Space.

Conventional physical display forms are mostly restricted by space and time. For example, it is difficult for Chinese customers to easily buy TIFFANY new jewelry that is only sold in the US market; customers can only buy the jewelry products they need during the business hours of the mall; the types of jewelry styles displayed are limited, and due to different dealers and distribution locations, even jewelry products of the same brand will have a difference in time to market; if you want to compare jewelry products of different brands, you need to go back and forth between multiple shopping malls [16, 17]. The virtual display of jewelry combined with the network platform can connect merchants and consumers and make jewelry display and transaction process break through the traditional time, space, and other physical constraints. When a company has established a complete online virtual product library, customers only need to log in to the online virtual display system of the jewelry brand they are interested in, and they can browse virtual jewelry products and obtain corresponding information anytime and anywhere.

2.2.4. Advanced Display Ability.

In the virtual jewelry display based on VR technology, designers use VR and other technologies to realistically display the design plan in the form of virtual jewelry models in front of customers. Customers only need to use a browser with VR function to display the design in the world. Any place can fully understand the details of the jewelry virtual model and put forward their own opinions and opinions to the designer through the network platform, and through the form of virtual display, the jewelry designer can not only modify the design plan according to the situation but also foresee

market feedback in advance and optimize its design, thereby increasing the success rate of jewelry design, so the risk after the product is put on the market can be reduced to a minimum [18, 19].

2.3. Related Technology Hybrid Feature Detection Method and Registration in the VR System.

For the problems encountered in the real time and accuracy of image feature extraction and matching, this paper innovatively uses the scale-invariant BRISK algorithm and the rotation-invariant SURF algorithm together and optimizes the point at this stage; it also used the distance algorithm to optimize the point pair in a unique way.

Since BRISK generates multiscale features and uses SURF to describe the feature points obtained by the BRISK algorithm for rotation invariance, the BFMatcher algorithm is used to ensure the best feature matching, and then the traditional distance algorithm is used to rewrite the obtained feature points. Screening ensures the rapid detection of feature points by the system and the accuracy of the final registration result. Under the premise of realizing correct matching, the method in this paper can achieve good results in both processing speed and matching accuracy.

2.3.1. SIFT Algorithm.

The SIFT algorithm has good robustness in detecting object movement, angle change, light intensity change, occlusion, and scale change. It can get rich and high-quality feature point information. It has good scalability and can be used in conjunction with other feature point extraction algorithms, and the extraction speed is relatively fast [20, 21].

At the same time, the feature point descriptor generation in the SIFT algorithm is to extract the descriptors containing the feature point scale, rotation, scaling, brightness, and other pieces of information from the image. The usual steps are as follows:

(1) For scale invariance, first establish scale space and complete the judgment of extreme points.

(2) Determine the specific location after filtering the obtained feature points.

(3) Assign a direction value to each feature point.

(4) Generate feature descriptors. In the range where the feature point is the midpoint, draw a 16×16 unit size area as the sampling area to get 8 gradient directions obtained from the relative direction between the direction of the sampling point and the direction of the feature point after the Gaussian weighting operation.

2.3.2. FAST Algorithm.

FAST algorithm is a fast detection algorithm that detects corner information distributed in the neighborhood of the point to be detected by segment detection.

In the calculation process of the algorithm, these 16 pixels are classified according to

$$S_m \longrightarrow i = \begin{cases} dI_m \longrightarrow i \leq I_m \longrightarrow n, \\ I_m - n < I_m \longrightarrow i \leq I_m + n, \\ I_m + n \leq I_m \longrightarrow i. \end{cases} \tag{1}$$

Among them, n is a numerical value, I_m represents the pixel value of the m point at the center of the circle, and $I_m \longrightarrow i$ represents the pixel value of the i point when m tends to the i-th pixel on the circle.

2.3.3. BRISK Feature Point Detection.

First create n octave layers and inner octave layers, which are represented by c_i and d_i, respectively. The C0 layer represents the image itself. The c_i layer of octave is obtained by sampling the source image down by 2 times, and the c_2 layer is performed on the previous layer C1. It is obtained by 2 times sampling. The inner octave layer is obtained by sampling the source image itself by 1.5 times, the d_1 layer is obtained by sampling the inner octave layer down by 2 times, and the d_2 layer is obtained by sampling the upper layer d_1 by 2 times.

2.3.4. Transformation of Several Coordinate Systems

(1) Conversion of Pixel Plane Coordinate System and Image Plane Coordinate System. The pixel coordinate system used on mobile phones is based on the first pixel in the upper left corner of the screen as the origin, the x-axis points to the right of the screen, and the y-axis points to the bottom of the plane [22, 23]. Assuming that P is the pixel in the x-th row and y-th column of the image coordinate system, the center point coordinates of the image are (U0, V0), and the corresponding physical dimensions are d_x and d_y. Then point P is converted to the pixel coordinate system, and relationship (2) can be obtained:

$$u = \frac{x}{d_x} + u_0, \tag{2}$$

$$v = \frac{x}{d_y} + x_0. \tag{3}$$

After transforming into matrix form, we get

$$\begin{bmatrix} u \\ v \\ 1 \end{bmatrix} = \begin{bmatrix} \dfrac{1}{d_x} & 0 & 0 & u0 \\ 0 & \dfrac{1}{d_y} & 0 & 0 \\ 0 & 0 & 0 & 1 \end{bmatrix} \begin{bmatrix} x \\ y \\ z \\ 1 \end{bmatrix}. \tag{4}$$

(2) Conversion of Image Plane Coordinate System and Camera Coordinate System. O1 is in the image plane coordinate system, the camera coordinate system is $O_c(X_c, Y_c, Z_c)$, the optical axis Z_c is the main axis, and the direction of Z_c is the positive direction of the camera. Point $P(x_0, y_0)$ is the point where the point $X(x_c, y_c, z_c)$ in the camera coordinate system and the origin line intersect on the image plane. According to the perspective projection formula, the change relationship can be obtained as follows:

$$\begin{cases} x0 = f\dfrac{x_c}{z_c}, \\ y0 = f\dfrac{y_c}{z_c}, \end{cases} \tag{5}$$

where f is the focal length of the camera itself. Thus, the relationship between points in formula (5) can be converted into this form of the matrix expressed in

$$z_c \begin{bmatrix} x0 \\ y0 \\ 1 \end{bmatrix} = \begin{bmatrix} f & 0 & 0 & 0 \\ 0 & f & 0 & 0 \\ 0 & 0 & 1 & 0 \end{bmatrix} \begin{bmatrix} x_c \\ y_c \\ z_c \\ 1 \end{bmatrix}, \tag{6}$$

(3) Conversion between World Coordinate System and Camera Coordinate System. Because the rotation matrix R is orthogonal and because we know that $R = [r1, r2, r3]$, a column vector is eliminated through $r3 = r1 \times r2$, so that $Z_w = 0$ in the world coordinate system, combined with formulas (4)–(2). The matrix transformation relationship between the world coordinate system and the pixel coordinate system can be obtained as

$$\begin{bmatrix} u \\ v \\ 1 \end{bmatrix} = s \begin{bmatrix} a_x & 0 & 0 \\ 0 & a_y & 0 \\ 0 & 0 & 1 \end{bmatrix} \begin{bmatrix} r1 & r2 & r3 & t \end{bmatrix} \begin{bmatrix} x_w \\ y_w \\ 0 \\ 1 \end{bmatrix} = sH \begin{bmatrix} x_w \\ y_w \\ 1 \end{bmatrix}. \tag{7}$$

Among them, S is a constant, the components of R on the x-axis and y-axis are $r1$ and $r2$ in turn, and H is a matrix with a size of 3×3, and M_{int} is the camera's internal parameters, so formula (7) can be obtained from formula (8):

$$H = \begin{bmatrix} h_1 & h_2 & h_3 \end{bmatrix} = sM_{int} \begin{bmatrix} r1 & r2 & t \end{bmatrix}. \tag{9}$$

Through formula (9), we can get

$$h_1 = sM_{int}r1, \tag{10}$$

$$h_2 = sM_{int}r2, \tag{11}$$
$$h_3 = sM_{int}r3.$$

Then through the property that R is an orthogonal matrix, we can know that $r1$ and $r2$ are also orthogonal, so that two implicit formulas can be derived:

$$r1^T r2 = 0, \tag{12}$$

$$||r1|| = ||r2|| = 1. \tag{13}$$

Through the knowledge of linear algebra, the two vectors of m and n have the property of $(mn)^T = n^T m^T$, so we can replace $r1$ and $r2$ in formula (13) to obtain the following two formulas:

$$h_1^T M_{int}^{-T} M_{int}^{-1} h2 = 0. \tag{14}$$

2.4. Design and Realization of Interactive Function of the Jewelry Virtual Model. It is very simple to set up interactive actions in Cult3D, which is very similar to the behavior settings in web design; that is, connect the action to the event and then connect to the target object. There are three main types of objects set in Cult3D: scene, action, and event. The scene includes each element in the file and other elements, such as materials, textures, and sounds added later; actions mainly include object movement such as rotation, translation, zooming, selecting camera or perspective switching, coloring materials, and displaying or hiding objects; events are divided into mouse events and keyboard events, scene start events, timers, and custom events for event excitation or browser external events excitation [24]. The interactive design of the Cult3D object is to establish the relationship between events, actions, and scenes in the event map window, so that when the viewer triggers an event or an event occurs automatically, the browser program can control the scene corresponding to the event to make a response. The visual process and results are fed back to the viewer in real time to achieve the purpose of interaction.

2.4.1. Import the Jewelry Model. Start the Cult3D Designer program, click the "Add C3D file" command in the file menu in the Cult3D Designer program window, select the C3D file just exported in the pop-up dialog box, and click "Open" button to complete the import.

2.4.2. Realize the Spatial Viewpoint Change of the Virtual Scene. However, in order to facilitate the user to view the model, you can use the left mouse button to create several viewpoints, such as front, back, left, and right, so that you can directly call the predetermined angle for viewing.

2.4.3. Set Up Interactive Actions for the Overall Rotation, Enlargement, Reduction, and Translation of the Jewelry Model. First, make the mouse control the rotation, zoom, and pan of the virtual jewelry model. Select the "click with the left mouse button" icon in the event map window and drag it to the blank space on the right side of the event map window. In the interaction/interaction of the action window, use the mouse to drag the "mouse-Arcball" icon to the event map window. Click on the icon with the left mouse button, then select the jewelry "hanging ring" in the scene graph window, drag it to the "mouse-Arcball" icon in the event map window, then set the mouse-Arcball parameters, and finally click the "Preview Run/Stop" button in the presentation window to immediately set the preview.

3. Application of VR Technology in Jewelry Display

3.1. Development Environment Construction. (1) NDK: local development kit; NDK enables developers to use programs written in C/C++ language. It includes the following parts:

(1) It contains all the tools needed to run C/C++ code and creates compiled files for it
(2) Some other language programming programs can be put into the application file package under the Android system
(3) It has good compatibility with all programs on the Android system
(2) Advantages
(1) The code developed using Java on the Android system is easy to be decompiled, but this is rarely the case with the C/C++ library, and the code can be protected.
(2) Programs written in C/C++ language are highly efficient. Using the third-party C/C++ library of NDK allows efficient code to be used on platforms such as Android, which improves the overall operating speed of the system. JNI: Java Native Method Interface. It is mentioned in the book Java Virtual Machine that JNI can realize communication between codes written in Java and programs written in other languages. In this paper, JNI is mainly used to enable Java code that can run on the Java Virtual Machine (JVM) on the Android system to interact with Open CV applications and libraries written in C/C++.

3.2. System Framework and Modules. We put the execution of the more complex registration algorithm (image processing algorithm) module in the native layer using the C/C++ language, which can reduce time-consuming and improve operating efficiency. The model rendering module can only parse files in obj format, and loading the model is implemented in the Java layer under the Android system.

In this paper, the designed and implemented system for improving the behavior of natural feature points is mainly

for storing all feature information of the target object of the facility or the detected image. When displaying local data, the video recorder will automatically obtain the video image and feature information of the video. Once the consistency with the information stored in the previous database reaches a certain level, the match is considered successful and other actions can be taken. In this paper, such as nested position and camera pose estimation, in order to improve the real-time performance of the system, we apply the LK optical flow tracking algorithm so that we cannot get the attribute information of all frames of the video information to improved system response time and speed.

3.3. Establishment of an Internet-Based Product Evaluation Model.

The process of the Internet-based product evaluation model is based on the user's order of browsing web pages. Different information is collected through the logical relationship between web pages. When a user browses a website, the first information collected should be the user's psychological state. Register and sign up to understand the objective status of the user, and then understand the user's preference information through the choices made by the user during web browsing. When users determine certain products, they begin to understand the feedback that users receive after the promotion. For users who consulted before sales, understand the reasons why users choose products, what they have doubts about products, and what other information is conveyed in the process of display deviation or whether the user is interfered by other information, and for after-sales service users, it is necessary to know exactly which factor caused the user's dissatisfaction. By referring to the divided user groups and the psychological state of the user interaction, the users select and answer questions to obtain specific evaluation information.

4. Application of VR Technology in Jewelry Display

4.1. Algorithm Analysis of Matching Feature Points.

The video capture resolution of the Android mobile phone used is 640 ∗ 480, the SIFT, SURF, and BRISK + SURF algorithms are, respectively, implemented, the corresponding time parameter information is obtained, and the data obtained are tabulated and analyzed, using Open CV for Android SDK 2.0; the results are shown in Tables 1–3.

As shown in Figure 2, the analysis can use the same mobile phone to detect the same image or object. BRISK can achieve a good registration effect when the object to be detected rotates and the light intensity changes. Compared with SIFT and SURF, the overall running time of the algorithm is much less. Compared with the pure BRISK algorithm, the experimental results of the rotation performance of the method in this paper show that the accuracy is improved by 60%, and the time-consuming is relatively less. Under the premise of ensuring rapidity, the method in this paper ensures the accuracy and time cost of matching as much as possible.

TABLE 1: Comparison of three feature point detection algorithms.

Feature point detection algorithm	SIFT	SURF	Algorithm
Calculation time (ms)	217.5	92.7	72.5
Feature points	718	725	711

TABLE 2: Time comparison of three feature point description algorithms.

Feature description algorithm	SIFT	SURF	Algorithm
Calculation time (ms)	261.4	119.3	92.4

TABLE 3: Comparison of the total time consumption of the three algorithms.

Feature description algorithm	SIFT	SURF	Algorithm
Calculation time (ms)	453.2	195.6	146.8
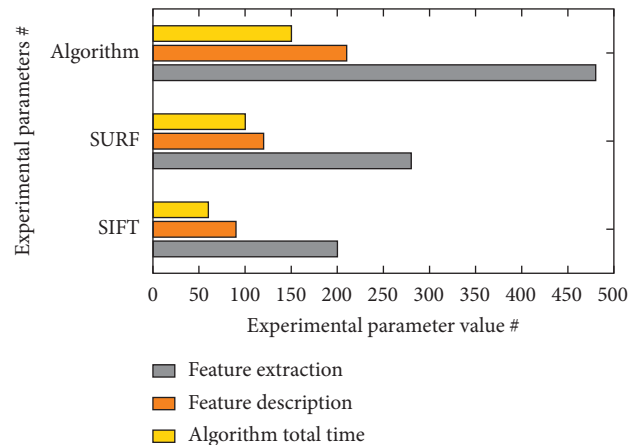
FIGURE 2: Algorithm histogram.

4.2. Consumer Psychological Value Identification.

Before recognizing the functional value of the product, users will first have a functional understanding of the product based on their own needs and product introduction and then evaluate the added value of the product brand or virtual value, whether users agree with the company's values becomes very important. This paper investigates the customer experience and the experimental results are shown in Table 4.

As shown in Figure 3, nearly 2% of people think that VR technology is lacking in value in jewelry display, 25.5% think that it is fair, 22.3% think that it is worth the money, and nearly 50 think that it seems that the application of VR technology in the display of objects needs further technical improvement.

4.3. Functional Analysis of Website Pages.

The main functional pages of the product display and evaluation website are divided into the home page, product collection page, product display page, and user information page. The

TABLE 4: Distribution of consumer psychological value identity.

	A little loss (%)	General (%)	Value for money (%)	Big loss (%)
Male	2.5	23.1	25.3	49.1
Female	1.5	24.7	22.5	51.8
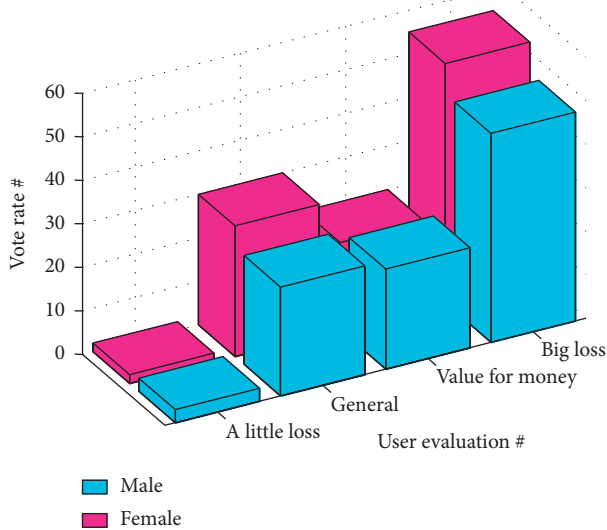
TABLE 5: Purpose of browsing product websites by consumers in different cities.

	Learn to use	Desire to buy	Product comparison	Understanding the function
First line	22	25	17	34
Second line	14	21	17	38
Three or four lines	15	20	14	51
Five lines	17	28	18	27

FIGURE 3: Distribution of consumer psychological value identity.
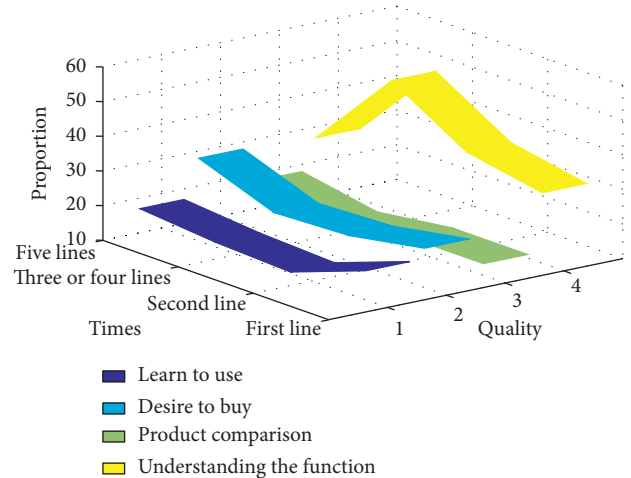
FIGURE 4: Purpose of browsing product websites by consumers in different cities.
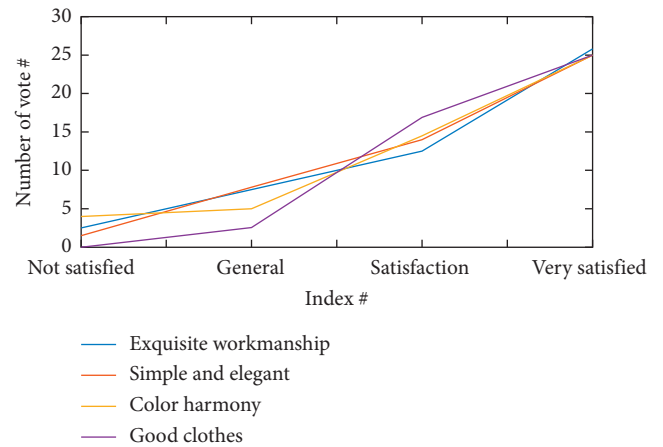
FIGURE 5: Appearance aesthetic evaluation analysis.

homepage of the website should highlight themes and provide links to some commonly used functions by users. According to UPS's survey of online shopping user behavior, the survey results are shown in Table 5.

As shown in Figure 4, most users want to add an order query link to their website's home page, and they want to know the products they have more easily and quickly when they want to purchase the available products. According to other researches, most users are browsing the product's website to understand the product's functionality, so the product's display content should indicate the most space on the product homepage. However, the content of virtual display is not suitable for the homepage, because users do not want to know a specific product in detail on the homepage but have an overall impression of the entire brand, and virtual display will reduce the speed of linking to the homepage, to reduce user experience, so the homepage still mainly displays brand products with product pictures. The second function that needs to be possessed is the regular functions of the website including registration and login, product recommendation, and after-sales service.

4.4. User Evaluation and Evaluation Data Processing. Evaluators can use the immersive product virtual evaluation platform to learn about products through kitchen environment roaming, product display, and use display and then enter the product evaluation section. The evaluators are 25 men and 25 women who often use the oven to cook. The ages of the evaluators are between 20 and 40 years old, covering various occupational fields, a total of 50 people, and the data

validity rate is 100%. After the user evaluation is over, click submit, the system will automatically record the evaluation data, and you can view the evaluation results after the evaluation. Statistics of all evaluation data and the experimental results are shown in Figure 5.

As shown in Figure 5, most people recognize the appearance of virtual products, and most people are very satisfied. The aesthetic point of appearance is higher than 4

points, which has reached the general satisfaction level of users, and the completion is good.

5. Conclusions

The immersive product virtual evaluation system proposed in this paper is applied to the actual product evaluation. Taking jewelry as an example, the immersive virtual evaluation is carried out. Use quantitative statistics to calculate the weights of each index and each evaluation angle to obtain an evaluation index model, build a virtual evaluation platform, publish the virtual interactive evaluation platform on the smartphone, and put VR glasses into the evaluation personnel; finally, the evaluation data are recorded and processed through the system, and the evaluation results are displayed in the form of charts. Through the analysis of the evaluation results, the shortcomings of the product can be quickly found, and the product design plan can be modified in a guided manner.

This paper designs and implements the MAR system using the feature detection and description method combining the BRISK algorithm and the SURF algorithm on the Android phone. The information transmission function of the camera and its own internal parameters can be used to calculate the external parameters of the camera, and the combination of optical flow algorithms can improve the overall performance of the camera. Then, the Open GL ES technology is used to fuse the virtual information into the real scene to achieve the final AR display effect.

Aiming at the problems of Internet-based product evaluation, this paper starts from the user's psychology and studies the factors that produce psychological changes during the interaction process of Internet evaluation. It explains the user's attitude towards the evaluation of Internet-based products from the perspectives of psychological value, consumption information, and social inertia, proposes to divide users according to their psychological state, and then revises the product evaluation results.

Data Availability

The data underlying the results presented in the study are included within the manuscript.

Conflicts of Interest

The authors declare that they have no conflicts of interest.

Acknowledgments

References

[1] S.-H. Ko, H.-C. Lai, H.-H. Shuai, W.-C. Lee, P. S. Yu, and D.-N. Yang, "Optimizing item and subgroup configurations for social-aware VR shopping," *Proceedings of the VLDB Endowment*, vol. 13, no. 8, pp. 1275–1289, 2020.

[2] C. Peukert, J. Pfeiffer, M. Meissner, T. Pfeiffer, and C. Weinhardt, "Shopping in virtual reality stores: the influence of immersion on system Adoption," *Journal of Management Information Systems*, vol. 36, no. 3, pp. 755–788, 2019.

[3] M. F. Farah, Z. B. Ramadan, and D. H. Harb, "The examination of virtual reality at the intersection of consumer experience, shopping journey and physical retailing," *Journal of Retailing and Consumer Services*, vol. 48, pp. 136–143, 2019.

[4] L. Kun-yang, "Application of VR technology in Internet shopping," *Digital Technology and Application*, vol. 036, no. 012, pp. 220-221, 2018.

[5] H. Wu, W. Luo, N. Pan et al., "Understanding freehand gestures: a study of freehand gestural interaction for immersive VR shopping applications," *Human-centric Computing and Information Sciences*, vol. 9, no. 1, pp. 1–26, 2019.

[6] Q. Wang, Z.-D. Huang, J. Li, and J.-W. Liu, "A force rendering model for virtual assembly of mechanical parts with clearance fits," *Assembly Automation*, vol. 38, no. 2, pp. 173–181, 2017.

[7] V. Dana, K. Roman, G. Beata, J. Mudruňka, and A. Struś, "Application of GNSS technology in surface mining," *Geodesy and Cartography*, vol. 42, no. 4, pp. 122–128, 2016.

[8] K. Gaurav and R. S. Praveen, "Impact of information technology on information search channel selection for consumers," *Journal of Organizational and End User Computing*, vol. 30, no. 3, pp. 63–80, 2018.

[9] A. Shahri, M. Hosseini, K. Phalp, J. Taylor, and R. Ali, "How to engineer gamification," *Journal of Organizational and End User Computing*, vol. 31, no. 1, pp. 39–60, 2019.

[10] N. C. C. M. Moes and I. Horvath, "Editorial: virtual reality and ergonomics enablers for product development," *International Journal of Computer Aided Engineering and Technology*, vol. 8, no. 1/2, pp. 1–7, 2016.

[11] J. Katicic, P. Häfner, and J. Ovtcharova, "Methodology for emotional assessment of product design by customers in virtual reality," *Presence: Teleoperators and Virtual Environments*, vol. 24, no. 1, pp. 62–73, 2015.

[12] E. Bekele, D. Bian, J. Peterman, S. Park, and N. Sarkar, "Design of a virtual reality system for affect analysis in facial expressions (VR-SAAFE); application to schizophrenia," *IEEE Transactions on Neural Systems and Rehabilitation Engineering*, vol. 25, no. 6, pp. 739–749, 2017.

[13] J. Hu, X. Wang, and H. Qin, "Novel and efficient computation of Hilbert-Huang transform on surfaces," *Computer Aided Geometric Design*, vol. 43, pp. 95–108, 2016.

[14] J. J. Gooch, "Exploring virtual reality in product design at the rave cave," *Desktop Engineering*, vol. 23, no. 1, p. 10, 2017.

[15] P. Mitrouchev, C. G. Wang, L. X. Lu et al., "Selective disassembly sequence generation based on lowest level disassembly graph method," *International Journal of Advanced Manufacturing Technology*, vol. 80, no. 1-4, pp. 141–159, 2015.

[16] J. Diao, C. Xu, A. Jia et al., "Virtual reality and simulation technology application in 3D urban landscape environment design," *Boletin Tecnico/technical Bulletin*, vol. 55, no. 4, pp. 72–79, 2017.

[17] M. Lorusso, M. Rossoni, and G. Colombo, "Conceptual modeling in product design within virtual reality environments," *Computer-Aided Design and Applications*, vol. 18, no. 2, pp. 383–398, 2020.

[18] C. R. I. Barraza, S. V. G. Cruz, and V. V. O. Osiris, "A pilot study on the use of mobile augmented reality for interactive experimentation in quadratic equations," *Mathematical Problems in Engineering*, vol. 2015, no. 2, 13 pages, 2015.

[19] J. Geng, X. Peng, Y. Li, C. Lv, Z. Wang, and D. Zhou, "A semi-automatic approach to implement rapid non-immersive virtual maintenance simulation," *Assembly Automation*, vol. 38, no. 3, pp. 291–302, 2018.

[20] F. Tanaka, M. Tsuchida, and M. Onosato, "Associating 2D sketch information with 3D CAD models for VR/AR viewing during bridge maintenance process," *International Journal of Automation Technology*, vol. 13, no. 4, pp. 482–489, 2019.

[21] F. Liu, Q. D. Yan, S. W. Yao et al., "Interactive assembly technology for vehicle integrated transmission," *Jilin Daxue Xuebao (Gongxueban)/Journal of Jilin University (Engineering and Technology Edition)*, vol. 45, no. 4, pp. 1148–1154, 2015.

[22] M. H. Da Silva, A. P. Legey, and A. C. d. A. Mól, "Review study of virtual reality techniques used at nuclear issues with emphasis on Brazilian research," *Annals of Nuclear Energy*, vol. 87, no. JAN 2, pp. 192–197, 2016.

[23] A. Fridhi, B. Faouzi, and A. Hamid, "Data adjustment of the Geographic Information System, GPS and image to construct a virtual reality," *Geographia Technica*, vol. 12, no. 1, pp. 31–45, 2017.

[24] F. Li and J. Fei, "Gesture recognition algorithm based on image information fusion in virtual reality," *Personal and Ubiquitous Computing*, vol. 23, no. 3-4, pp. 487–497, 2019.

Research Article

Research on the Development Path and Growth Mechanism of Unicorn Enterprises

Kai Guo [1,2] **and Tiantian Zhang**[1]

[1]*School of Management, Henan University of Science and Technology, Luoyang, Henan, China*
[2]*Henan Collaborative Innovation Center of Nonferrous Metals, Luoyang, Henan, China*

Correspondence should be addressed to Kai Guo; guokai@haust.edu.cn

Combining with the growth environment of Unicorns, from the aspects of emerging industries, business environment, platform support, and financial support, we propose an overall analysis framework for the existence or absence of Unicorns, use the fuzzy set qualitative comparative analysis (fsQCA) method to carry out configuration analysis on the status quo of Unicorns in 40 cities in China, and analyze the cultivation path of Unicorns. The research results indicate that the synergy of emerging industries, business environment, platform support, and financial support can foster Unicorns. According to the differences in the core conditions in the configuration and the characteristics of the cases contained, it is divided into two cultivation paths, which are driven by emerging industries and supported by the business environment; combining with the status quo and characteristics of the cities where Unicorns are missing, it provides suggestions for the selection of the cultivation path of Unicorns in different regions.

1. Introduction

The number of Unicorns reflects the development trend of local enterprises and represents the level of regional innovation and development at the same time. Unicorns not only develop themselves but also effectively promote the innovative development of upstream industry, downstream industry, and even cross-border industry, so as to improve the level of regional innovation and enhance regional economic strength. However, as of 2018, only 26 of 233 regions in the world have Unicorns, that is, about 89% of regions do not have Unicorns. What is the reason that these regions cannot cultivate Unicorns? What kind of cultivation path does the existing Unicorns grow up according to? Why can their regions cultivate a large number of Unicorns? As well as the function mechanism of growth environment factors on each country and the region Unicorn growth is worth our thorough research.

Therefore, from the perspective of the growth environment of Unicorns, this paper puts forward the analysis framework of the existence or absence of Unicorns and uses the qualitative comparative analysis method to analyze the condition path of the absence of Unicorns in the region, combined with the analysis of the existence path of Unicorns, so as to provide policy basis for each region to match the cultivation path of Unicorns and built a good environment to promote the development of Unicorns.

2. Research Review and Analysis Framework

2.1. Review of Related Research. Existing research on Unicorns mainly includes the relevant geographical experience, risk management, valuation, and environment for the cultivation of Unicorns.

In terms of research on the regional experience and solution strategies of Unicorn growth, McNeill found that venture capital and angel capital occupy an important position in start-up capital. They even gradually participate in the upgrading of labor, housing, and public transportation markets in the cities where the companies are located, which has an important impact on the growth and cultivation of

local Unicorns [1]. Feldman found that among the more than 4000 technology start-ups in Utah, at least four start-ups are Unicorns. Through analysis, it can be seen that Utah's cultural atmosphere, talent base, capital base, and other resources are all necessary conditions for the cultivation of local Unicorns [2]. Ren analyzed the entrepreneurial ecosystem of Shenyang from seven aspects: market, human resources, finance, service, government, education, and culture. The study found that Shenyang must pay attention to talent training, avoid brain drain, and encourage local entrepreneurs who start their own businesses to invest and start a business in order to cultivate more Unicorns [3].

In terms of research on risks and risk management methods for Unicorns, Fan first proposed that Unicorns have regulatory risks. They believe that Unicorns have greater influence on shareholders, employees, and the country's economy, so they must require Unicorns disclose relevant information in a timely manner to reduce the investment transaction risks of Unicorns [4]. Govindarajan believed that Unicorns are at risk in terms of continuous innovation. Taking the financial services company Square as an example, it was found that after Square grew into a Unicorn through the best ideas, it did not continue to innovate before its competitors caught up and did not meet the expectations of sustained advantages [5]. Wu elaborated on the four modes of privatization, direct listing, issuance of depositary receipts, and share swaps for Unicorns returning to listing and then proposed that the return of Unicorns to listing has market investor protection issues and market monopoly risks [6].

In terms of Unicorn valuation research, Jacobius pointed out that, in the first half of 2016, about 30% of American venture capital was invested in Unicorns, and the amount of its venture capital is still increasing, but the valuation of Unicorns is gradually declining [7]. Song analyzed the game motivation of investors, entrepreneurial teams, and the public and regulatory authorities for the valuation of Unicorns. It also improves the valuation basis and framework of Unicorns from five new elements: media reports, dynamic development and transformation of enterprise types, lineage, community and institutional environment, and institutional entrepreneurship [8]. Lu, based on the characteristics of Unicorns, took Xiaomi group as an example to conduct a case study and found that the income method is the best method for Unicorn valuation. At the same time, in the valuation process, we must fully consider the influence of industry characteristics, business conditions, cultural concepts, and equity structure [9].

The research on the characteristics and growth environment of Unicorns is mainly carried out from the microlevel and macrolevel.

At the microlevel, scholars analyze the growth and cultivation of Unicorns from the internal characteristics of enterprises through case analysis. Kowanda took Tokopedia, an e-commerce Unicorn, as an example and then found that the key to the success of e-commerce enterprises is availability and security. In terms of usability, Tokopedia not only provides access to technology but also provides banking partners and logistics services; in terms of security,

Tokopedia retains the money paid by the buyer and transfers it to the seller only after the buyer receives the goods. Therefore, Tokopedia can rapidly grow into a Unicorn [10]. Mo, from the perspective of a complete scene, found that through technology or business model innovation, start-ups provide consumers with novel and high-quality products and services, so as to occupy the market, improve people's quality of life, and rapidly grow into Unicorns [11]. Xue took Xiaohongshu, a Unicorn, as a case study, found that the company builds Xiaohongshu app as a sharing community with high credibility, and then advocated bloggers to combine descriptive self-disclosure with high-cost products to generate the most positive product attitude, so as to improve users' purchase intention and promote the rapid growth of the enterprise [12]. Lee took the Unicorns in the solid oxide fuel cell industry as an example. Through empirical research, it is found that there are five steps for a start-up with sustainable innovation technology to transform into a Unicorn: checking the technical knowledge, experience, resources, and key points of the enterprise; determining the core value of the patent; creating the patent value higher than that of its competitors; establishing a globally competitive patent portfolio; and raising funds through the growth of the number of patents [13].

At the macrolevel, scholars mainly focus on the analysis of the influence mechanism of the following four factors on the growth and cultivation of Unicorns.

Research on the influence of venture capital on the growth and cultivation of Unicorns from the capital level: Rungi took 10 start-ups from Silicon Valley and Estonia as samples. Through case studies, it was found that all the sample enterprises had grown into Unicorns after 2–4 years of growth through a large amount of financing [14]. Hogarth took 23andMe as an example and found that the increase of private investment capital in Silicon Valley can promote the growth of enterprises [15]. Chen found that regions with obvious advantages in capital support, human resources, national policies, cultural atmosphere, and other innovation environment can cultivate a large number of Unicorns [16]. Oliveira believed that start-ups need universal financing in order to grow into Unicorns [17]. Bai thought that we should optimize the financing environment of Unicorns in China and support the development of Unicorns from the aspect of financial support [18]. Moosup conducted a case study on the development, sales, and other global value chains of eight South Korean Unicorns and found that six of them promoted their rapid growth by attracting foreign investment [19].

The level of urban economic development and its international market position affect the growth and cultivation of Unicorns. Jones found three key measures for the rapid growth of start-ups by analyzing the characteristics of Unicorns in Thailand: obtaining financial support, improving the company's ability, and connecting with global communities [20]. Liu analyzed the growth trend of the number of Chinese Unicorns in recent years and found that the rise of Chinese Unicorns is closely related to the economic transformation and promotion of China's economic growth in the past five years [21]. Li pointed out that Unicorns are mainly distributed

in regions with strong economic and resource base and believed that China needs to accelerate the cultivation of Unicorns in the field of manufacturing, enhance the internationalization degree of Unicorns, and protect the intellectual property rights of Unicorns [22].

Research on the influence of human resources and related policies on the growth and cultivation of Unicorns: Chu analyzed the regional distribution status of Unicorns and the characteristics of their industries. At the same time, taking 35 cities in China as research samples, through principal component analysis and cluster analysis, she found the important role of human resources in the cultivation of Unicorns [23]. Delermann developed a hybrid intelligence method based on the concept of human-computer complementarity to identify whether a start-up has grown into a Unicorn and pointed out that talent and policy resources are the most important input elements [24]. Stemler took the Unicorn Airbnb as a case study and then found that cumbersome enterprise regulatory rules hindered its rapid growth. The government needs to formulate effective policies and laws according to the situation of enterprises, so as to promote the growth and cultivation of Unicorns [25].

Research on the influence of emerging industries on the growth and cultivation of Unicorns: Lee believed that the birth of "super Unicorn" needs to conform to the epoch-making trend of science and technology [26]. De Massis systematically analyzed 146 Unicorns published by the "Wall Street Journal" and found that digital innovation around the focus direction is one of the basic characteristics of all Unicorns [27]. Shin, through the analysis of the United States Unicorn, Coinbase, found that it mainly focuses on cryptocurrency business, and in the case of actively obtaining human and financial resources, it has reached a valuation of US $1.6 billion in five years [28]. Say took China's bike-sharing Unicorns as an example and found that bike-sharing start-ups use technological innovation to meet the needs of users and fill the market gap. This new business model under the sharing economy makes it grow rapidly [29]. AGUS found that Gojek, an Indonesian Unicorn, developed the application Gojek after understanding Indonesia's weak transportation infrastructure and its high economic and environmental costs. Through the program, it provides people with preferential and convenient travel and leisure services, in order to achieve the purpose of rapid growth [30].

The existing literature plays a positive role in exploring the elements needed for the growth environment of Unicorns and their cultivation in the region. However, there are still some deficiencies: firstly, most of the existing studies focus on the areas where Unicorns are well developed, but they do not pay enough attention to the areas where there are few or even missing Unicorns; secondly, the existing studies only use qualitative research methods to explore the reasons for the lack of Unicorns and do not use quantitative methods to study the development of Unicorns; thirdly, the existing research has discussed the influence of many factors on the growth of Unicorns, but how to comprehensively consider the interaction and dependence between various environmental factors as well as the influence of the complex comprehensive mechanism between factors on the cultivation of Unicorns have not been studied; the existing research is still in its infancy.

In view of this, this paper takes 40 cities including "existence of Unicorns" and "absence of Unicorns" as samples, fully considers the areas where Unicorns exist and lack, introduces qualitative comparative analysis methods, and then analyzes the conditions and paths of existence and absence of Unicorns through empirical research. Comprehensive consideration of the interaction and dependence between various environmental factors as well as the influence of the complex comprehensive mechanism between factors on the cultivation of Unicorns should be done, in order to enrich Unicorn-related research. According to the current situation and characteristics of Unicorns' missing cities, we should match the appropriate cultivation path of Unicorns and provide strategic support for the cultivation of Unicorns in various regions of the world.

2.2. Analysis Framework of the Unicorn Cultivation Path

Unicorn is the result of incubation of start-ups. When start-ups grow into Unicorns at a high speed, they will be affected by various environmental factors. The comprehensive effect of these factors determines the cultivation path of Unicorns. Considering the representativeness of the influencing factors of Unicorns' growth environment and the availability of data, as well as the rules and requirements of using fsQCA3.0 to analyze data, four influencing factors, namely, emerging industries, business environment, platform support, and financial support, are finally determined. The analysis framework of Unicorns' cultivation path is shown in Figure 1.

2.2.1. Emerging Industries.

Enterprise innovation in emerging industries generally includes a certain degree of scientific and technological innovation, which has great growth potential in enterprise development and can lead the long-term development of the regional economy. Taking the distribution of Unicorns in the global automobile transportation industry in the whole industry in 2018 as an example, the number of Unicorns in the industry is among the top, with 42. Among them, Didi Travel is the representative enterprise of the industry. Didi Travel takes emerging industries as the development field and then takes sharing economy and Internet as the platform, reflecting the advanced concept of modern sharing economy. The sharing economy platform is closely related to computer network technology. Through fine-tuning matching algorithm and other technologies, it can bring data network effect, provide better user experience, help sharing economy companies gain market competitiveness [11], and rapidly grow into Unicorns.

2.2.2. Business Environment.

The current situation of the business environment in the region reflects the economic development in the region, as well as the possession and utilization of international market resources. Therefore, it can affect the introduction and development of start-up
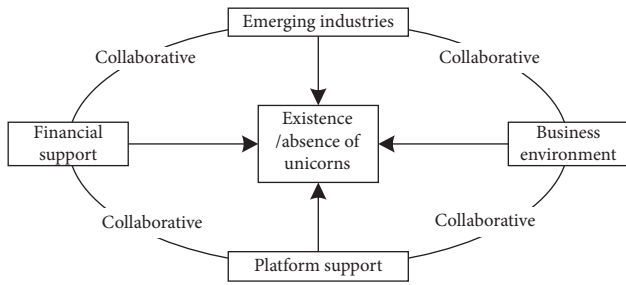
Figure 1: Analysis framework of unicorns' cultivation path.

enterprises and human resources in the region, thus affecting the cultivation path of Unicorns in the region [4]. On the one hand, the economic and market foundation of the region where the start-ups are located is relatively strong. At the same time, through breakthrough innovation in emerging industries, they can occupy the market in a short time, obtain a large number of users, achieve high valuation, and grow into Unicorns [9]. On the other hand, resources in the international market include users and funds. The possession and utilization of resources affect the growth speed and development prospects of enterprises. More than 80% of Israel's high-growth technology-based small- and medium-sized enterprises have international users and finance globally to promote the growth of enterprises [31]. Therefore, in the cultivation path of Unicorns, enterprises should acquire talents, customers, and capital resources from a global perspective on the basis of the regional economy and their own ability development, establish R&D, production, and marketing bases, and then enhance the international discourse of enterprises, so as to boost the cultivation of Unicorns.

2.2.3. Platform Support. Platform support elements can be analyzed from three aspects: human resources, science and technology support, and policy support. An important factor for the rapid growth of start-ups into Unicorns is that they have excellent partners and teams, strong professional ability, and excellent management ability, which is conducive to the formation of a more efficient technological innovation and collaborative innovation network. At the same time, as a start-up enterprise, it has great difficulties in site and capital. Government support is mainly based on laws, regulations, and administrative rules issued by governments at all levels. It provides convenience for start-ups in terms of infrastructure, preferential policies, business processes, etc., and plays an irreplaceable supporting role in the growth of start-ups [4]. Therefore, Unicorns tend to start businesses in areas with rich educational technology resources and strong support from relevant industrial policies.

2.2.4. Financial Support. If a start-up wants to grow into a Unicorn, it not only needs to have absolute advantages in business model, technology, and resources but also needs to obtain sufficient financial support to provide economic support for its later R&D, production, sales, and other key steps so that it can quickly occupy the market and grow into

a Unicorn [6]. But nowadays, commercial banks prefer large enterprises with low risk. However, due to the small scale of the start-ups, there are great risks and uncertainties in their innovation activities, so it is difficult to get the support of bank loans. Therefore, venture capital and angel investment have become the main ways for start-ups to obtain financial support [4].

According to previous studies, emerging industries, business environment, platform support, and financial support do not affect the existence of Unicorns in regions alone, but jointly influence the growth and cultivation of Unicorns in regions on the basis of interaction. Therefore, from the perspective of configuration, this paper empirically studies the influence mechanism of emerging industries, business environment, platform support, and financial support on the existence and absence of Unicorns in different regions, as well as the cultivation path selection of Unicorns in different regions.

3. Research Methods and Variable Measurement

3.1. Method Selection. Qualitative comparative analysis (QCA) is a method developed by Ragin based on fuzzy set mathematics and sociology. Theory guides many key steps of qualitative comparative analysis, including condition selection in model establishment, measurement and calibration of condition variables, and case selection [32]. Different from the traditional variable-oriented and case-oriented social science research methods, QCA focuses on the case as a whole and regards cases as different configurations of variables. The QCA method analyzes the specific situation of different cases. It thinks that different variable configurations may produce the same result, that is, multiple concurrent causality. At the same time, assuming the asymmetry between cause and effect, it is considered that the "non" of the combination of conditions leading to a certain result does not necessarily lead to the "non" of the result.

In this study, first of all, the existence or absence of Unicorns in the region is not the independent effect of individual factors, nor the simple accumulation of multiple factors, but the result of the interaction between various factors. Then, different cities have different situations in different influencing variables, and there are also different paths for cities to produce Unicorns' existence or absence of results. Then, the causes of the existence or absence of Unicorns in the city are not simple "non" operation relationship, but cause and effect asymmetry. Finally, the sample size of this study is 31, which belongs to small sample size, while the traditional regression analysis is suitable for large sample size. The QCA method can avoid the negative effects of autocorrelation and multicollinearity due to its quantitative analysis and the emphasis on case analysis.

Because of the above advantages, the QCA method has recently been applied to economic management and other fields by most scholars, but few scholars use the QCA method to study the factors influencing the growth environment of Unicorns from an overall perspective [33–36]. Therefore, this paper intends to use the method of fuzzy set

qualitative comparative analysis (fsQCA) to study the environmental factors and strategy combination that affect the growth of Unicorns.

3.2. Variable Measure

3.2.1. Sample and Result Variable Selection.
This paper takes 40 cities in China as research samples, selects "existence of Unicorns" and "absence of Unicorns" as outcome variables, and uses the number of existing Unicorns in each city to measure the outcome variables. According to the Research Report on Chinese Unicorns in 2018, in terms of result variables, there are 16 cities with "existence of Unicorns" and 24 cities with "absence of Unicorns." The number of existing Unicorns in Chinese cities is shown in Table 1.

3.2.2. Measure of the Conditional Variable

(1) Emerging Industries. The number of leading industries in regional high-tech zones includes strategic emerging industries, which can reflect the status and development potential of emerging industries in the region. At the same time, the development of emerging industries at the regional level needs to be based on the manufacturing industry. When the manufacturing industry develops well, it can increase the possibility of the rapid development of emerging industries at the regional level. Therefore, the number of emerging industries in leading industries of national high-tech zones in 2018 and the added value of the secondary industry are selected as the secondary index to measure emerging industries.

(2) Business Environment. The total economic volume reflects the economic development foundation of a region. The total import and export volume of goods and the number of foreign-invested enterprises reflect the international market situation of the region. This paper selects the total economic volume, the total import and export volume of goods, and the number of foreign-invested enterprises of the region in 2018 as the secondary index to measure the business environment.

(3) Platform Support. The number of students in colleges can reflect the talent base of a region. The amount of patent authorization in that year represents the scientific and technological development of the region. In the national maker space and high-tech zone, there are a lot of infrastructure and policies to support the development of new ventures, which can provide the innovation space for start-ups and support the development of emerging industries. Therefore, the number of Unicorns cultivated in the national maker space and high-tech zone accounts for 70% of the number of Unicorns in China. However, considering that there is only one high-tech zone in most regions, the number of high-tech zones in the region cannot measure the current situation of the cultivation advantages of Unicorns in the region, so this paper uses the maturity of high-tech zones as an index to measure the advantages of regional high-tech zones in cultivating Unicorns. Determine the establishment

time of the regional high-tech zone, and calculate the year difference between it and the time studied in this paper, which is the maturity of the high-tech zone [27]. If there are more than one high-tech zone in a region, the average maturity of the high-tech zone is calculated:

$$C = \frac{\sum_{j=1}^{n} \left(2019 - y_j\right)}{n}. \tag{1}$$

In formula (1), C represents the maturity of the high-tech zones in the region, j is the number of high-tech zones in the region, and y_j is the year in which the jth high-tech zone in the region is approved to be established, and the average of the maturity scores of all the high-tech zones in the region is the maturity of the high-tech zones in the region. Therefore, the maturity of the national high-tech zone is selected as one of the secondary indexes to measure the platform support indicators of the region together with the number of students in colleges, authorized patents, and national maker space in 2018.

(4) Financial Support. In this paper, the number of venture capital enterprises and angel investment enterprises, the number of investment events, and the amount of investment in 2018 are selected as the secondary index to measure venture capital. The relevant data are obtained through the IT orange query.

All sample data were obtained through the statistical bulletin of each city in 2018, national data, and IT orange query. In this paper, according to spss19.0, principal component analysis is used to process the secondary index of four independent variables, and the weight of each secondary indicator in the corresponding primary indicator is obtained. In this paper, the p value of principal component analysis is close to 0, and the extraction degree of variables is above 80%. Through the standardized analysis of the secondary index, the first level index is calculated according to the weighted sum of the secondary index. The specific situation of each indicator and its weight is shown in Table 2.

3.2.3. Data Calibration.
In this paper, the method of fuzzy set qualitative comparative analysis (fsQCA) is used, and fsQCA3.0 software is used for analysis. According to the theoretical knowledge, three thresholds were set for each variable: Completely Subordinate (1), Maximum Fuzzy Intersection (0.5), and Completely Non-Subordinate (0). All the research data were calibrated from 0 to 1. In this paper, the Completely Subordinate is calibrated to 0.95, and the Completely Non-Subordinate is calibrated to 0.05. Therefore, the highest value of the index is taken as the full membership value, and the lowest value is taken as the full nonmembership value. Because there are very high or very low values in the indicators after the principal component analysis, there is a certain impact on the data calibration. Therefore, when determining the three thresholds, we must first exclude the very high and very low values, then set the other highest and lowest values as the Completely Subordinate value and the Completely Non-Subordinate value, respectively, and set the average of these values as the Maximum Fuzzy Intersection [37–40]. The thresholds calibrated in this paper are shown in Table 3.

TABLE 1: Sample cities and the number of Unicorns.

City	Number of Unicorns	City	Number of Unicorns	City	Number of Unicorns	City	Number of Unicorns
Beijing	87	Shanghai	41	Shenzhen	16	Hangzhou	24
Guangzhou	6	Nanjing	6	Wuhan	4	Chengdu	4
Zhuhai	3	Dongguan	2	Qingdao	2	Chongqing	2
Wuxi	1	Guiyang	1	Suzhou	1	Hefei	1
Tianjin	0	Xiamen	0	Xian	0	Changsha	0
Ningbo	0	Fuzhou	0	Zhengzhou	0	Dalian	0
Nanchang	0	Jinan	0	Shaoxing	0	Taiyuan	0
Shijiazhuang	0	Haerbin	0	Shenyang	0	Foshan	0
Kunming	0	Changchun	0	Lanzhou	0	Nanjing	0
Lasa	0	Wuhu	0	Yinchuan	0	Xining	0

TABLE 2: Index construction of growth environment influencing factors of Unicorns.

First level index	Secondary index	Indicator unit	Secondary index weight
Emerging industries	The added value of the secondary industry	100 million yuan	0.5
	The number of emerging industries included in leading industries of national high-tech zones	Piece	0.5
Business environment	GDP	100 million yuan	0.316
	The total value of import and export volume of goods	100 million yuan	0.346
	The number of foreign investment enterprises	Piece	0.338
Platform support	The number of students in ordinary colleges	10 thousand people	0.240
	The number of authorized patents	Piece	0.249
	The number of national maker space	Piece	0.251
	The maturity of the regional high-tech zone	Year	0.260
Financial support	The number of venture capital enterprises and angel investment enterprises	Piece	0.298
	The amount of investment	100 million yuan	0.349
	The number of investment events	Piece	0.353

TABLE 3: Threshold of data calibration.

Threshold	Dependent variable	Independent variable			
	The number of Unicorns	Emerging industries	Business environment	Platform support	Financial support
Completely Subordinate	4	1.463	0.4765	0.8897	0.3502
Maximum Fuzzy Intersection	0.538462	−0.06934	−0.3475	−0.23408	−0.26349
Completely Non-Subordinate	0	−1.5744	−0.7794	−1.1629	−0.3563

4. Qualitative Comparative Analysis Results of Fuzzy Sets

4.1. Necessity Detection of the Single Antecedent Variable

Truth table analysis is essentially a sufficient condition analysis. Before truth table analysis, it is necessary to detect the necessary conditions of the single variable and remove the necessary conditions from the truth table analysis program. In fsQCA3.0 software, necessary conditions' analysis was performed on the data after calibration, and the consistency score of the single antecedent variable was obtained, as shown in Table 4. According to previous studies,

the threshold value of the consistency score is 0.9. When the consistency score is greater than 0.9, it is considered that the condition is a necessary condition for the result [38].

It can be seen from the data in the table that, in the case of studying the "existence of Unicorns" in cities, the highest consistency score of a single antecedent variable is "high financial support" (cf), whose consistency score is 0.834246, less than 0.9, so there is no necessary condition for the "existence of Unicorns" in cities. In the case of "absence of Unicorns" in the city, the consistency score of "low business environment" (~CF) is the highest, which is 0.846850, less than 0.9, so there is no necessary condition for "absence of

Unicorns" in the city. Therefore, the existence or absence of Unicorns is not the result of a single condition. We can make a further analysis from the perspective of multiple factors affecting the existence and absence of Unicorns.

4.2. Truth Table Construction.

The truth tables constructed using the existence and absence of Unicorn companies as the result variables are shown in Tables 5 and 6. In the truth table, the values of variables with membership scores greater than 0.5 are assigned to 1, and the values of variables with membership scores less than 0.5 are assigned to 0. Each research sample belongs to only one conditional configuration, that is, only one membership score is greater than 0.5 [38].

Take the number of cases as 1 and the consistency as 0.75 to analyze the sufficient condition configuration of the result of "existence of Unicorn" [38], and take the number of cases as 1 and the consistency as 0.8 to analyze the sufficient condition configuration of the result of "absence of Unicorn."

4.3. Sufficient Condition Configuration Analysis.

After obtaining the truth table, "Standard Analysis" is carried out in fsQCA3.0 software; then, three solutions are obtained, namely, "Complex Solution," "Simplified Solution," and "Intermediate Solution." Among them, the "Complex Solution" is the result configuration generated only according to the current situation of sample cases, and the resulting configuration is relatively complex; the "Simplified Solution" is the result configuration generated by analyzing the "Logical Remainder" which is easy and difficult, and the conclusion is too simple, while the "Intermediate Solution" is to use the easy "Counterfactual Analysis" to generate the result configuration including core conditions and edge conditions [41]. Referring to the research of Fiss [42], this paper defines the condition that appears in the "Intermediate Solution" and the "Simplified Solution" as the "Core Condition." Only the "Intermediate Solution" exists, but the missing condition in the "Simplified Solution" is determined as the "Edge Condition." If it does not appear, it shows that it has no effect on the result variables. According to the analysis, the condition configuration for enterprises to achieve "existence of Unicorns" and "absence of Unicorns" is shown in Table 7.

"Overall Solution Consistency" in the table indicates the degree to which the conditional configurations obtained by all operations can reflect the actual situation, that is, the degree to which cases belonging to the same configuration show the same results (existence/absence of Unicorns). "Overall Solution Coverage" refers to the degree to which all conditional configurations interpret their corresponding results (existence/absence of Unicorns). When it is close to 1, the result is the best. In this paper, the total consistency is about 0.78 and 0.84, respectively, in the case of the existence and absence of Unicorns, which shows that the conditional configurations obtained in this study are acceptable.

4.3.1. Configuration Analysis of Sufficient Conditions with "Existence of Unicorns" as the Result Variable.

When qualitative comparative analysis is conducted based on the "existence of Unicorns," two kinds of conditional configurations that can produce the result of "existence of Unicorns" are obtained, that is, two cultivation paths of unicorns. Cities that meet the conditional configurations can cultivate Unicorns. It can be seen from the contents in Table 7 that no matter which cultivation path the region wants to take, it cannot be at a low level in terms of emerging industries, platform support, business environment, and financial support. According to the different core conditions of different paths, regions can choose the appropriate cultivation path combined with their own advantages. According to the specific situation of each cultivation path, the analysis is as follows:

(1) Emerging Industry-Driven. (IF * SF * BF * CF) *Cultivation Path.* This condition configuration is a path to promote the cultivation of Unicorns in the region with "high emerging industries" and "high platform support" as the core conditions and "high business environment" and "high financial support" as the edge conditions. Choosing this path to cultivate Unicorns must have a strong industrial foundation and pay attention to the development of emerging industries. In terms of platform support, we should have sufficient human resources, policy resources, and incubation environment resources to ensure the rapid growth of start-ups. At the same time, it is necessary to meet the basic needs of business environment and financial support of start-ups in the region, so as to successfully cultivate Unicorns. The probability of successful cultivation of Unicorns is about 63% in the regions that choose this cultivation path. In the 16 sample cases of "existence of Unicorns," 67% of the regions successfully cultivated Unicorns by choosing this cultivation path.

The representative case of this condition configuration is Suzhou. The results show that the membership degree of Suzhou in this configuration is 0.58, and its consistency in the results is 0.91. According to the statistical data, Suzhou ranks the third and the first in the index value of emerging industries and platform support in all samples, respectively. In terms of emerging industries, the added value of the secondary industry in Suzhou in 2018 is 893.328 billion yuan, which has a solid foundation for industrial development. At the same time, the leading industries in Suzhou high-tech zone and Suzhou Industrial Park are electronic information, equipment manufacturing, new energy, electronic information, machinery manufacturing, biomedicine, artificial intelligence, and nanotechnology, among which new energy, biomedicine, and artificial intelligence are emerging industries, reflecting the city's attention to the development of emerging industries. At the end of 2018, there is a Unicorn in Suzhou, which meets its membership degree in the condition configuration and consistency in the result condition.

(2) Business Environment-Supporting. (BF * SF *If * CF) *Cultivation Path.* This condition configuration is a path to promote the cultivation of Unicorns in the region with "high business environment" and "high platform support" as the core conditions and "high emerging industries" and "high

TABLE 4: The necessary condition test of the single antecedent variable on the existence and absence of Unicorns.

Influencing factor variables	Existence of Unicorns (af)		Absence of Unicorns (~af)	
	Consistency	Coverage	Consistency	Coverage
High emerging industries (if)	0.750000	0.553590	0.478346	0.614257
Low emerging industries (~if)	0.477397	0.344708	0.652362	0.819486
High business environment (bf)	0.771918	0.743404	0.281890	0.472295
Low business environment (~bf)	0.452055	0.265701	0.846850	0.865942
High platform support (sf)	0.789726	0.589469	0.433071	0.562372
Low platform support (~sf)	0.413699	0.295499	0.683858	0.849804
High financial support (cf)	0.834246	0.644786	0.380315	0.511382
Low financial support (~cf)	0.367808	0.254382	0.735827	0.885362

TABLE 5: The truth table constructed when analyzing "the existence of Unicorns."

if	ef	sf	cf	Number	af	Raw consist.	PRI consist.
1	1	1	1	10	1	0.778229	0.69967
1	1	0	1	1	0	0.646796	0.382813
1	1	0	0	1	0	0.592233	0.247761
0	0	1	1	3	0	0.524775	0.277398
0	0	0	1	1	0	0.510939	0.2
1	0	0	1	1	0	0.484928	0.17437
0	0	1	0	1	0	0.375415	0.091787
1	0	0	0	6	0	0.359259	0.113956
0	0	0	0	14	0	0.278185	0.08692

TABLE 6: The truth table constructed when analyzing "the absence of Unicorns."

if	ef	sf	cf	Number	~af	Raw consist.	PRI consist.
0	0	1	0	1	1	0.936877	0.908213
0	0	0	0	14	1	0.931287	0.91308
1	0	0	0	6	1	0.917593	0.886044
1	0	0	1	1	1	0.891219	0.82563
0	0	0	1	1	1	0.877735	0.8
1	1	0	0	1	1	0.865696	0.752239
0	0	1	1	3	1	0.817568	0.722603
1	1	0	1	1	0	0.780924	0.617188
1	1	1	1	10	0	0.464663	0.275028

TABLE 7: Sufficient condition configuration for the existence and absence of the Unicorn.

Influencing factor variables	Existence of Unicorns (af)		Absence of Unicorns (~af)		
	1	2	3	4	5
Emerging industries (if)	●	•		⊗	•
Business environment (bf)	•	●	⊗	⊗	
Platform support (sf)	●	●	⊗		⊗
Financial support (cf)	•	•			⊗
Consistency	0.630199	0.763139	0.887706	0.865343	0.885289
Coverage	0.674658	0.706164	0.656693	0.635039	0.007874
Raw coverage	0.0136986	0.0452055	0.0488189	0.0712599	0.398031
Overall solution					
Consistency		0.778229		0.840378	
Overall solution		0.656164		0.735827	
Coverage					

●The existence of core conditions; •The existence of edge conditions; ⊗The absence of core conditions; ⊗The absence of edge conditions.

financial support" as the edge conditions. To choose this path to cultivate Unicorns, the region must have a strong economic foundation and a large scale of import and export trade, create a good business environment, and drive the growth and cultivation of start-ups to Unicorns with the support of talents, policies, and other platform resources.

TABLE 8: Robustness test results.

Influencing factor variables	Existence of Unicorns (af)		Absence of Unicorns (~af)		
	1	2	3	4	5
Emerging industries (if)	●	·		⊗	·
Business environment (bf)	·	●	⊗	⊗	
Platform support (sf)	●	●	⊗		⊗
Financial support (cf)	·	·			⊗
Consistency	0.677466	0.767857	0.889601	0.865343	0.883882
Coverage	0.644521	0.677397	0.71063	0.635039	0.401575
Raw coverage	0.0095890	0.0424657	0.0885828	0.0602363	0.00787407
Overall solution consistency	0.785593			0.844577	
Overall solution coverage	0.634932			0.77874	

The probability of successful cultivation of Unicorns is about 76% in the regions that choose this cultivation path. In the 16 sample cases of "existence of Unicorns," 70% of the regions successfully cultivated Unicorns by choosing this cultivation path.

The representative case of this condition configuration is Shenzhen. The results show that the membership degree of Shenzhen in this configuration is 0.95, and its consistency in the results is 1. In 2018, Shenzhen's GDP was 2422198 million yuan, the total import and export of goods was 2998.374 billion yuan, and the actual utilization of foreign capital was 8.203 billion US dollars, ranking third, second, and sixth, respectively, in the above three secondary indexes, which means that Shenzhen has great advantages in the business environment. At the end of 2018, there are 16 Unicorns in Shenzhen, which meets its membership degree in the condition configuration and consistency in the result condition.

4.3.2. Configuration Analysis of Sufficient Conditions with "Absence of Unicorns" as the Result Variable. Based on the qualitative comparative analysis of "absence of Unicorns" as the result variable, three conditional configurations are obtained, namely, three Unicorn missing paths, which are mainly divided into the following two categories.

(1) *Business Environment-Missing* (bf* sf/bf* if) *Conditional Path.* Configurations 3 and 4 both take the low business environment as the core condition. Configuration 3 indicates that "low business environment" and "low platform support" lead to the "absence of Unicorns" in cities. Yinchuan, Lanzhou, Nanning, and other cities are the representative cases. The number of national incubators and students in these cities is small, and the start-ups are difficult to meet the needs in terms of policies, infrastructure, talents, etc. Configuration 4 indicates that "low business environment" and "low emerging industries" lead to the lack of Unicorns in cities. Wuhu, Foshan, Shaoxing, Harbin, and other cities are the representative cases. These cities are at a disadvantage in terms of industrial foundation and attention to emerging industries. At the same time, the above two configurations reflect the significant influence of the low business environment on the "absence of Unicorns."

(2) *Financial Support-Missing* (cf * sf * IF) *Conditional Path.* Configuration 5 indicates that the core conditions of "low financial support" plus the upper edge conditions of "low platform support" and "high emerging industries" lead to the "absence of Unicorns" in the city. In the process of rapid growth from start-ups to Unicorns in the region, the demand for capital of enterprises is at a high level. Even if the region focuses on promoting the development of emerging industries, low financial support will also inhibit the growth of start-ups to Unicorns, resulting in the region unable to cultivate Unicorns. The representative cases are Nanchang and Taiyuan. There was only one investment event in Taiyuan in 2018, with an investment amount of only 3 million yuan, which is at a very low level in the country, hindering the cultivation of Unicorns in the city.

4.4. Robustness Test. By changing the calibration threshold of the platform support variables, 1.9103 is set as the "Completely Subordinate Value," 0.036085676 is set as the "Maximum Fuzzy Intersection Value," and −1.2410 is set as the "Completely Non-Subordinate Value." Using the changed threshold to carry out fuzzy set qualitative comparative analysis on the original samples, the threshold value of case frequency is still set to 1, and the consistency value is set to 0.75. The results of software operation are shown in Table 8. Taking "existence of Unicorns" as the result variable, the total consistency of the results is 0.79, and the total coverage rate is 0.63. Taking "absence of Unicorn" as the result variable, the total consistency of the results is 0.89, and the total coverage rate is 0.75. Therefore, the analysis results are reliable. Because the analysis results after eliminating the cases are the same as the above analysis results, it proves that the above analysis results are robust.

5. Conclusion and Prospect

Taking 40 cities in China as an example, this paper studies the conditional path of the existence or absence of Unicorns in the region from the perspective of configuration and tests the robustness of the research results from the perspective of set theory. The results are as follows.

Firstly, the two core conditions of "high emerging industries" and "high platform support" are combined with the two marginal conditions of "high business environment" and "high financial support" to form the "emerging industry-driven cultivation path," and the

"business environment-supporting cultivation path," which is composed of the abovementioned core conditions and the two marginal conditions of "high emerging industries" and "high financial support," can cultivate Unicorns in the region. At the same time, cities should reasonably choose the cultivation path of Unicorns according to their own status and advantages.

Secondly, the core conditions of "low business environment" are, respectively, combined with the marginal conditions of "low platform support" and "low emerging industries" to form the "business environment-missing conditional path," and the "financial support-missing conditional path," which is composed of the "low financial support" and the two marginal conditions of "low platform support" and "high emerging industries," will lead to the region that cannot cultivate Unicorns.

Thirdly, by comparing the conditional paths of existence and absence of Unicorns, we can see that the conditional configuration of "existence of Unicorns" and "absence of Unicorns" in the province is not a simple "non" relationship, that is, the research results are asymmetric.

Fourthly, according to the path of the existence and absence of Unicorns, if the regions belong to the sample case of lack of the business environment, it is difficult to develop the disadvantages of the business environment into absolute advantages, so we must choose the "emerging industry-driven cultivation path." For regions with financial support deficiency, if their business environment is better than the current situation of emerging industries, they can choose the "business environment-supporting cultivation path." If the development of emerging industries is slightly dominant, they should choose the "emerging industry-driven cultivation path."

Fifthly, for the regions that choose the "emerging industry-driven cultivation path," the government must vigorously promote the enterprises to move closer to strategic emerging industries and promote the entrepreneurial enterprises to grow into Unicorns. The regions that choose the "business environment-supporting cultivation path" should focus on improving the regional social demand and foreign trade scale, expanding the global market, building a good market environment and economic foundation, driving the rapid growth of start-ups, and promoting the cultivation of Unicorns in the region.

There are also some shortcomings in this paper, such as using cross-sectional data to analyze, without considering the time factor and the dynamic changes of the research variables; at the same time, this paper does not consider the influencing factors of the existence or absence of Unicorns in the region from the microperspective, so we can carry out more in-depth and detailed research from these directions in the future.

Data Availability

The data used to support the findings of this study are available from the corresponding author upon request.

Conflicts of Interest

The authors declare that they have no conflicts of interest.

Acknowledgments

References

[1] D. Mcneill, "Governing a city of unicorns: technology capital and the urban politics of San Francisco," *Urban Geography*, vol. 37, no. 4, pp. 494–513, 2016.

[2] A. Feldman, *Silicon Slopes vs. Silicon Valley: Four Tech Unicorns, Thousands of Start-Ups, No Frenzy*, Forbes. com, New York, NY, USA, 2017.

[3] S. C. Ren and C. Hu, "Entrepreneurial ecosystem construction path of unicorn enterprise cultivation: research based on fuzzy set qualitative comparative analysis," *Technology Economics*, vol. 38, no. 7, pp. 46–55, 2019.

[4] J. Fan, "Regulating Unicorns: disclosure and the new private economy," *Boston College Law Review*, vol. 57, no. 2, pp. 583–642, 2016.

[5] V. Govindarajan, T. Govindarajan, and Stepinski, "Why unicorns are struggling," *Harvard Business Review Digital Articles*, vol. 1, no. 10, pp. 2–4, 2016.

[6] J. Wu, "Research on investor protection issues of "unicorns" returning to domestic listings——from the perspective of share swap mergers," *South China Finance*, vol. 7, no. 10, pp. 81–91, 2018.

[7] A. Jacobius, "Plunging "unicorn" valuations spell double trouble," *Pensions & Investments*, vol. 44, no. 16, p. 2, 2016.

[8] L. F. Song, D. W. Qi, and Y. F. Song, "China's emerging unicorn enterprise valuation comparison basis and analysis framework," *Science & Technology Progress and Policy*, vol. 36, no. 3, pp. 70–76, 2019.

[9] M. M. Lv and Y. E. Yang, "Analysis on the influencing factors of unicorns value evaluation in China," *Appraisal Journal of China*, vol. 2, no. 5, pp. 27–34, 2019.

[10] D. Kowanda, M. Firdaus, R. B. F. Pasaribu et al., "Lesson from Tokopedia.com: E-commerce success factor analysis: a case study from Indonesian unicorn," in *Proceedings of the 2018 International Conference on Information Management and Processing (ICIMP)*, pp. 61–65, London, UK, January 2018.

[11] Z. Z. Mo and J. Wang, "Scene: new economic innovation generator," *Economy and Management*, vol. 32, no. 6, pp. 51–55, 2018.

[12] H. Xue, "Persuaded by electronic word of mouth (eWOM): network coproduction model on Chinese social-ecommerce

app," in *HCI in Business, Government and Organizations. ECommerce and Consumer Behavior*, pp. 323–332, Springer, Cham, Switzerland, 2019.

[13] D. Lee and K.-C. Lin, "How to transform sustainable energy technology into a unicorn start-up: technology review and case study," *Sustainability*, vol. 12, no. 7, p. 3018, 2020.

[14] M. Rungi, E. Saks, and K. Tuisk, "Financial and strategic impact of VCs on start-up development: silicon valley decacorns vs. Northern-European experience," in *Proceedings of the 2016 IEEE International Conference on Industrial Engineering and Engineering Management (IEEM)*, pp. 452–456, IEEE, Bali, Indonesia, December 2016.

[15] S. Hogarth, "Valley of the unicorns: consumer genomics, venture capital and digital disruption," *New Genetics and Society*, vol. 36, no. 3, pp. 250–272, 2017.

[16] Q. Chen, Y. T. Xiao, and X. Liu, "A comparative study on the growth environment of unicorn enterprises in Beijing and Shanghai——from the perspective of urban innovation and entrepreneurship ecosystem," *Journal of Tongji University (Social Science Section)*, vol. 29, no. 5, pp. 106–114, 2018.

[17] M. Au-Yong-Oliveira, J. P. Costa, R. Gonçalves, and F. Branco, "The rise of the unicorn: shedding light on the creation of technological enterprises with exponential valuations," in *Trends and Advances in Information Systems and Technologies*, pp. 967–977, Springer, Cham, Switzerland, 2018.

[18] X. Bai, "Promoting the growth of unicorns with financial supply side reform," *People's Tribune*, vol. 25, no. 23, pp. 56-57, 2019.

[19] J. Moosup, "Case study of GVC participation with Korean unicorn," *Korean Academy of International Business Management*, vol. 23, no. 4, pp. 187–198, 2019.

[20] C. Jones, P. Pimdee, and P. Pimdee, "Innovative ideas: Thailand 4.0 and the fourth industrial revolution," *Asian International Journal of Social Sciences*, vol. 17, no. 1, pp. 4–35, 2017.

[21] L. Xin, "The league of Chinese "unicorns"" *China Today*, vol. 1, no. 8, pp. 45–47, 2018.

[22] J. H. Li, "Development and cultivation of China's champion enterprises and unicorn enterprises," *Journal of Shenzhen University (Humanities & Social Sciences)*, vol. 36, no. 1, pp. 68–76, 2019.

[23] T. J. Chu and T. Song, "Spatial distribution and influence factors of unicorn companies in China," *World Regional Studies*, vol. 26, no. 6, pp. 101–109, 2017.

[24] D. Dellermann, N. Lipusch, P. Ebel, K. M. Popp, and J. M. Leimeister, "Finding the unicorn: predicting early stage startup success through a hybrid intelligence method," in *Proceedings of the International Conference on Information Systems (ICIS)*, Seoul, South Korea, December 2017.

[25] A. Stemler, "The myth of the sharing economy and its implications for regulating innovation," *Emory Law Journal*, vol. 67, no. 2, pp. 197–241, 2017.

[26] A. Lee, *Welcome to the Unicorn Club: Learning from Billion-Dollar Start-Ups*, Cowboy Ventures (Blog), Palo Alto, CA, USA, 2013.

[27] A. De Massis, F. Federico, and Q. Franco, *"What Big Companies Can Learn from the Success of the Unicorns"*, Harvard Business Review, Brighton, MA, USA, 2016.

[28] L. Shin, *Coinbase Becomes First Crypto Unicorn, Raises $100 Million in Funding Amid ICO Craze*, Forbes.com, New York, NY, USA, 2017.

[29] A. L. Say, R. Guo, and C. Chen, "Disruption or new order? the emergence of the unicorn bike-sharing entrepreneurship in China," in *Proceedings of the 2018 Portland International Conference on Management of Engineering and Technology (PICMET)*, Honolulu, HI, USA, August 2018.

[30] A. A. Agus, A. Y. Arafah, I. Suprayana et al., "The leap of GO-JEK: unfolding a unicorn startup journey," *Academy of Asian Business Review*, vol. 5, no. 1, pp. 55–80, 2019.

[31] B. Jeff and S. Omri, "A large number of Israeli "unicorns" come," *Directors & Boards*, vol. 10, no. 49, pp. 82-83, 2015.

[32] B. Rihoux and C. C. Ragin, *Configurational Comparative Methods: Qualitative Comparative Analysis (QCA) and Related Techniques*, SAGE, Thousand Oaks, CA, USA, 2009.

[33] S. Furnari, D. Crilly, V. F. Misangyi et al., "Capturing causal complexity: heuristics for configurational theorizing," *Academy of Management Review*, vol. 5, 2020.

[34] Y. Park, P. C. Fiss, and O. A. Elsawy, "Theorizing the multiplicity of digital phenomena: the ecology of configurations, causal recipes, and guidelines for applying QCA," *MIS Quarterly*, vol. 44, 2020.

[35] P. Dwivedi, A. Joshi, and V. F. Misangyi, "Gender-inclusive gatekeeping: how (mostly male) predecessors influence the success of female CEOs," *Academy of Management Journal*, vol. 61, no. 2, pp. 379–404, 2018.

[36] J.-P. Vergne and C. Depeyre, "How do firms adapt? a fuzzy-set analysis of the role of cognition and capabilities in U.S. defense firms' responses to 9/11," *Academy of Management Journal*, vol. 59, no. 5, pp. 1653–1680, 2016.

[37] C. Lee, G. Park, and J. Kang, "The impact of convergence between science and technology on innovation," *The Journal of Technology Transfer*, vol. 43, no. 2, pp. 522–544, 2018.

[38] C. C. Ragin, "The comparative method: moving beyond qualitative and quantitative strategies," *Social Forces*, vol. 67, no. 3, 1989.

[39] Y. Z. Du and L. D. Jia, "Configuration perspective and qualitative comparative analysis (QCA): a new way of management research," *Chinese Journal of Management*, vol. 6, pp. 155–167, 2017.

[40] M. Zhang and Y. Z. Du, "Qualitative comparative analysis (QCA) in management and organization research: position, tactics, and directions," *Chinese Journal of Management*, vol. 16, pp. 1312–1323, 2019.

[41] M. Kim, "Many roads lead to Rome: implications of geographic scope as a source of isolating mechanisms," *Journal of International Business Studies*, vol. 44, no. 9, pp. 898–921, 2013.

[42] P. C. Fiss, "Building better causal theories: a fuzzy set approach to typologies in organization research," *Academy of Management Journal*, vol. 54, pp. 393–420, 2011.

Research Article

Real-Time Scheduling of Mixed Model Assembly Line with Large Variety and Low Volume Based on Event-Triggered Simulated Annealing (ETSA)

Chunzhi Cai (ID) and Shulin Kan

School of Mechatronics Engineering and Automation, Shanghai University, No. 99, Shangda Road, Shanghai 200444, China

Correspondence should be addressed to Chunzhi Cai; ccz10209@shu.edu.cn

In the contemporary industrial production, multiple resource constraints and uncertainty factors exist widely in the actual job shop. It is particularly important to make a reasonable scheduling scheme in workshop manufacturing. Traditional scheduling research focused on the one-time global optimization of production scheduling before the actual production. The dynamic scheduling problem of the workshop is getting more and more attention. This paper proposed a simulated annealing algorithm to solve the real-time scheduling problem of large variety and low-volume mixed model assembly line. This algorithm obtains three groups of optimal solutions and the optimal scheduling scheme of multiple products, with the shortest product completion time and the lowest cost. Finally, the feasibility and efficiency of the model are proved by the Matlab simulation.

1. Introduction

Mixed model assembly line is a flexible and cost-effective production system [1], but is always difficult for scheduling. The structure and process of productions are similar in the mixed model assembly line. It improves the enterprise's market response ability, meets the diverse demand of products, reduces inventory and production costs, and improves product quality. However, the variety of specifications and models needs better scheduling strategy because there are usually no/less optimizations in the traditional industrial enterprise [2].

Traditional scheduling methods can provide a one-time calculation and optimization. However, during the execution, there are many unpredictable events, such as machine failure, absenteeism of workers, and shortage of materials, which interrupt the original scheduling plan. So, there are strong requirements of real-time scheduling in the mixed assembly line activities [3].

In an assembly line, different products have different procedure and operating time. So scheduling should be

implemented for the continuous product following the rhythm and proportion so that the varieties, production, working hours, and equipment load can achieve a comprehensive balance [4]. To solve the scheduling problem of the hybrid model assembly line, different kinds of optimization algorithms have been proposed. As a pioneer, Kilbridge studied the solution of the hybrid assembly line in 1963 [5, 6]. Yow applied the genetic algorithm, for the first time, to solve production scheduling of the assembly line which overcomes the traditional optimization methods [7]. Dong and Kan proposed an improved particle swarm optimization algorithm to solve multiobjective mixed model assembly line scheduling problems. Their method can be directly applied to discrete space and keep the good performance of PSO [8]. Xing et al. proposed a Knowledge-Based Ant Colony Optimization (KBACO) algorithm for the Flexible Job Shop Scheduling Problem (FJSSP) [9].

To overcome the infeasibility of above methods in real productions, various optimization algorithms have also been studied, such as the fuzzy problem of shop scheduling, fast scheduling problem, multiobjective optimization problem of

assembly line production, and the robust scheduling of working time. Ye et al. proposed an effective optimization method [10] to solve the flexible job shop scheduling problem with fuzzy processing time. Its main idea is applying the learning mechanism and local search operator to the search framework of special double-crossover schemes. A multiobjective adaptive large neighborhood search method (MOALNS) is proposed for distributed re-placement permutation flow shop scheduling by adding the re-entry characteristics [11]. Dai et al. [12] discussed a hybrid local search algorithm to solve various uncertainties in the actual production system, such as machine failures, absenteeism, and order changes.

Most of the scheduling methods or algorithms for hybrid assembly line production are focused on mathematical development and algorithm design. In mathematical modeling, real-time scheduling and fuzzy processing time [13] are combined for the objective functions. In the existing mathematical modeling process of hybrid assembly line production, the cost factor has little direct impact on the structural model, and the economy of the production system has attracted more and more attention. The common objective functions in hybrid assembly line scheduling include the following aspects: reducing raw material consumption, maximizing the cost of workers, and minimizing the total working time. About the algorithm, different algorithms such as simulated annealing algorithm, tabu search algorithm, genetic algorithm, ant colony algorithm, and particle swarm optimization algorithm have been adapted in scheduling. Javadi et al. [14] proposed an improved genetic simulated annealing algorithm which can jump out of the local optimal solution. Cheng et al. [15] proposed a mixed quenching simulated annealing algorithm. An improved simulated annealing method was proposed for the fast scheduling problem of the hybrid assembly line [16].

Although different scheduling models and algorithms demonstrate different aspects, there is a lack of methodology consideration of real productions. Especially for the unpredictable events, such as machine failure, absenteeism of workers, and shortage of materials, there should be some strategy or index for the updates of scheduling in real time. In this study, we proposed an event-triggered simulated annealing (ETSA) method to deal with this issue and output the optimized changes of the scheduling plan.

2. General Mathematical Model Considered in This Study

Various objectives have been proposed in finding the optimal MMP sequences [xx,xx]. Here, in this study, we focus on the minimization of work overload.

For the work overload [17],

$$f_1 = \min \sum_{h=1}^{H} \sum_{w=1}^{W} T_{hw} \text{cost}_h, \tag{1}$$

where w ($w = 1, \ldots, W$) is the index of workstations, h ($h = 1, \ldots, H$) is the id of workers, cost_h is the labor cost per unit time, T is the working hours of each worker on workstation.

Material cost is generated in each process. According to the different materials in each stage, the objective function of the total material cost is as follows:

$$f_2 = \min \sum_{w=1}^{W} \sum_{j=1}^{D} \sum_{m=1}^{M} \sum_{r=1}^{M} S1_{jmr} \text{cost}_{wmr}, \tag{2}$$

where w ($k = 1, \ldots, W$) says workstation numbers, m ($m = 1, \ldots, M$) says product variety numbers, J ($j = 2, \ldots, D$) says products in a sequence of position, cost_{wmr} is the adjustment costs per unit time when the type of production is converted from m to r in workstation-w, and $S1_{jmr}$ is a symbol function. When the position j and $j+1$ stand for type m and r, the value is 1; otherwise, 0.

A basic requirement of the efficient production system is continuous and stable supply of parts. For the successful operation of the system, the constant demand rate is required. The objective function is as follows:

$$f_3 = \min \sum_{j=1}^{D} \sum_{m=1}^{M} \left(\left| \frac{\sum_{l=1}^{j} S_{ml}}{j} - \frac{d_m}{D} \right| \right). \tag{3}$$

In a Minimum Part Set, MPS is a vector that represents the sequence of a product, such as (d1, ..., dM) = (D1/H, ..., DM/H), M is the number of product varieties, D_m ($m = 1, \ldots, M$) is the demand for products m, and H is the greatest common divisor of $D_1, D_2, \ldots, D_m$. For any $j \in [1, D]$, the deviation is described as

$$\Delta = \left| \frac{\sum_{l=1}^{j} S_{ml}}{j} - \frac{d_m}{D} \right|, \tag{4}$$

which should be as little as possible.

2.1. Multiobjective Decision Model of the Mixed Assembly Line.
As the cost of parts, workers, and materials is calculated, the total cost of processing each product can be calculated. Use the price of each product to get the total profit of the enterprise, and the total profit objective function is as follows:

$$P_{\text{price}} = \sum_{P=1}^{P} \text{price} * N, \tag{5}$$
$$\min f_4 = P_{\text{price}} - \min(f_1 + f_2).$$

The mathematical model of mixed model assembly line production problems are as follows:

$$\min f = w_1 f_3 + w_2 f_4, \tag{6}$$

where p ($p = 1, \ldots, P$) says the number of products, N says the total number of products, price says the unit price of each product, P_{price} says total sales of all products. $\min(f_1 + f_2)$ says Minimize total product cost. w_1 and w_2 says Weights of objective function.

In the objective function (7), when other costs remain unchanged, it is only necessary to adjust the allocation of workers on the job to save time, thereby improving the profits of enterprises. However, a trade-off should be made according to the number of parts required. The unit price of

each product is $1*P$ matrix, and the quantity of each product is N ($1*P$ matrix.

3. Event Triggered Simulated Annealing (ETSA)

3.1. Classical Simulated Annealing Algorithm.
The simulated annealing (SA) algorithm, introduced by Kirkpatrick et al. [18], is a local search procedure capable of escaping from the local optimum to solve combinatorial optimization problems. To start the procedure, SA draws an initial solution to generate the neighborhood solution. If the neighborhood solution is better than the incumbent solution, the former is automatically accepted and replaces the latter; otherwise, the incumbent solution is used. The whole process is repeated until no significant improvement in the neighborhood solution is found or the prespecified conditions are met. SA uses this repetitive improvement approach, but in particular it enables a search algorithm to escape from a local optimum.

Considering the use of the simulated annealing algorithm to solve the mixed assembly line problem, the simulated annealing algorithm starts with a higher initial temperature T, sets the temperature parameter drop value a, and calculates the energy difference It. If the energy difference It < 0, the new solution is accepted. Otherwise, the objective function solution space of the global optimal solution is randomly found by combining the hopping probability characteristic exp $(-\text{It}/kT)$ (where K is a constant), that is to say, it is accepted with a certain probability. A bad solution may jump out of the probability of the local optimal solution and eventually approach the global optimal solution.

The simulated annealing algorithm is widely used to solve NP complete problems [19], but its parameters are difficult to control. Its main problems are as follows:

3.1.1. Initial Value Setting of Temperature T.
The initial setting of temperature T is one of the important factors affecting the global search performance of the simulated annealing algorithm. If the initial temperature is higher, the possibility of finding the global optimal solution is higher, but it takes a lot of computing time. On the contrary, low initial temperature can save computing time, but it will affect global search performance. In practical applications, it is usually necessary to adjust the initial temperature several times according to the experimental results.

3.1.2. Annealing Speed.
The global search performance of the simulated annealing algorithm is also closely related to the annealing speed. In general, a "full" search (annealing) at the same temperature is necessary, but it takes computation time. In practical application, reasonable annealing equilibrium conditions should be set according to the properties and characteristics of specific problems.

3.1.3. Temperature Management.
The temperature management problem is also one of the difficult problems to be solved by the simulated annealing algorithm. In practical

applications, due to the practical feasibility of computational complexity, the cooling method shown in the following is often adopted:

$$T(t+1) = k \times T(t). \tag{7}$$

In the formula, k is a positive constant slightly less than 1.00, and t is the degree of cooling.

In order to solve the problem of premature convergence of the simulated annealing algorithm, a higher temperature is set at the beginning of the algorithm [20]. In order to achieve a better optimization effect, the cooling speed is maintained at 0.99 or 0.98. Random probability is added to expand the search space to reach the global optimum.

The flow chart of the simulated annealing algorithm is shown in the figure. The flow chart of the simulated annealing algorithm is shown in Figure 1.

In the application of the simulated annealing algorithm, the cooling rate is an important factor affecting the performance of the simulated annealing algorithm. The solution of the simulated annealing algorithm is independent of the initial value and has asymptotic convergence. The temperature needs to be gradually reduced to find the minimum value. In the process of parameter optimization, random adjustment is made according to the gradient change direction of the objective function to avoid entering the local minimum and to ensure the global convergence of the method. It can also make the function have different initial temperatures and cooling values, or a larger search space, to improve the probability of finding the global optimum.

3.2. Pseudocode.
Algorithm 1

$J(y)$: Value of evaluation function in state y

$Y(i)$: Represents the current status

$Y(i+1)$: Represents a new state

r: Used to control cooling rate

T: The temperature of the system, which should initially be in a high temperature state

T_min: The lower limit of temperature. If T reaches T_min, stop searching.

4. A Case Study on the Mixed Model Assembly Line Production Problem

4.1. Problems to Be Solved and Constraints.
In this case, the company's product line has the characteristics of multiple varieties and small batches, including reactor assembly, slicing, winding, vertical wire harness packaging, upper and lower core assembly, welding base, inductance testing, predrying, oil immersion, cleaning, oven, beneficiation, testing, packaging, and storage.

The company divides the workers into different groups, and the staff of each station is not fixed. Some workers can work on multiple workstations, and we find that assembly line species conversion requires necessary personnel and tools adjustment. Adjustment costs arising from the
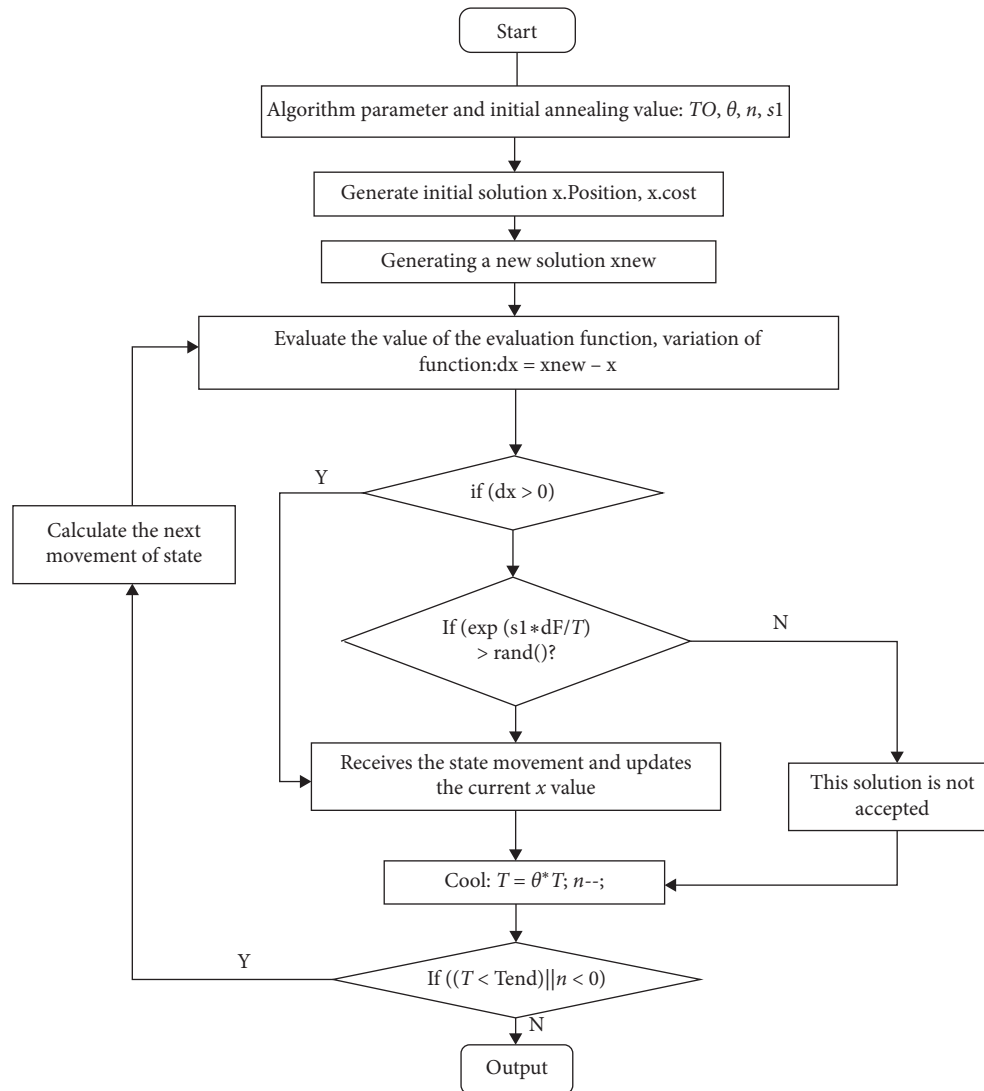
Figure 1: Simulated annealing algorithm flow chart.

```
while(T > T_min)
{
    dE = J (Y (i + 1)) − J (Y (i));
    if (dE ≥ 0)//Expresses that if the solution is better after moving, it always accepts moving.
Y (i + 1) = Y (i); //Accept the movement from Y (i) to Y (i + 1)
    else
{
if (exp (dE/T) > random (0, 1) )
Y (i + 1) = Y (i); //Accept the movement from Y (i) to Y (i + 1)
}
    T = r ∗ T; //cooling annealing, 0 < R < 1. The larger the r, the slower the cooling is; the smaller the r, the faster the cooling is.
    i ++;
}
```

Algorithm 1: Algorithm of ETSA.

manufacturing sequence of products should be considered first. Secondly, uncertainties will lead to the establishment of the objective function of the minimum labor cost in order to reduce the waste of personnel scheduling [21], save production time, and arrange suitable workers to production at the appropriate sites. Successful operation of the system requires that the demand rate of parts remains unchanged.

The hybrid assembly line has the problem of multivariety and multiprocess operation. According to the model established in the second part and the actual situation of the hybrid assembly line [22], the constraint conditions of the hybrid assembly line problem are as follows:

(1) Each machine can process only one product at a time

(2) Each machine can process different processes

(3) The same workpiece must be processed according to its process sequence

(4) For the first phase, all jobs are available at $t = 0$

(5) There is no precedence between the operations of different jobs, but there is precedence between the operations of a job

(6) For the same operation, the processing time of different unrelated parallel machines in the production phase is different

4.2. Optimized Processing by Simulated Annealing Algorithms. Taking the company's hybrid assembly line as an example, it is assumed that product category $P = 5$, number of products $M = 10$, process $H = 5$ for each product, station quantity $W = 5$, and material quantity $K = 5$ for each product. Assuming that the workers is enough, In the case of understanding the material cost, labor cost and product profit, it is necessary to find the optimal combination to minimize the cost and maximize the profit of the enterprise. When there are a large number of products in the hybrid assembly line, the traditional production method is difficult to obtain the optimal sequence and cannot consider multiple objective functions at the same time. The algorithm proposed in this paper can quickly provide the optimal solution for the objective function.

Considering that the mixed product of each step of the production line machining position is fixed, we have developed a product processing order of the steps on different machines, and, combined with the processing time of each process on different machines, constituted a multiobjective optimization problem, which requires reasonable production arrangements so that a large variety and low volume products can be completed in the shortest possible time and improve the enterprise. The process time represents the processing time of each process, and the machine number has sorted the jobs.

4.3. Real-Time Scheduling. Scheduling stability is usually not a problem in static and deterministic scheduling environments because the scheduling environment does not need to be updated. However, in the real-time scheduling environment, stability and robustness are important performance indicators [21].

In the case of machine failure or absenteeism, the process of rearranging due to delayed processing can be time-consuming. In this study, a real-time scheduling method was developed to deal with any time delay in a process. In addition, there are two main parameters affecting the reactive power dispatching process. The first parameter is the time of job delay, while the second parameter is the number of jobs to be delayed [23]. With this real-time scheduling method, if the remaining jobs are not rearranged, the jobs will be rearranged only after this moment.

As described in Section 3.2, the time and process constraint matrix in the absence of uncertain factors is shown in Table 1. It is assumed that machine $m = 3$ is delayed, the delay time is $K = 15$, and the delay time is $T = 20$. Therefore, the products on the third machine after 15 minutes of product processing need to be rescheduled. Each group of scheduling problems contains different processes. The processes before 15 minutes are completed according to the original schedule, where P represents the work to be processed on the machine.

5. Results' Analysis

The improved simulated annealing algorithm was adopted for optimization, and the constraint matrix in Tables 1 and 2 in Section 3 was simulated on MATLAB. Figure 2 shows the Gantt chart of static assembly line scheduling. Figure 3 shows the Gantt chart of the rescheduling.

The optimal solution for static scheduling is considered in Figure 2, that is, the optimal solution for the makespan is $Cmax = 49$. The results of production scheduling are shown in Table 2. Table 2 illustrates the results of product scheduling and calculates the the makespan required for each product on the mixed pipeline, where $\{x, y, z\}$, X and Y denote the start and end time of process processing and Z denotes the process. The results are the same as those of the Gantt chart. Suppose that machine 3 fails in 15 minutes, it takes 20 minutes to delay, resulting in a new scheduling scheme, as shown in Figure 3, and the optimal solution is 56. The sequence and time interval of processing in the first 15 minutes remain unchanged. After 15 minutes, the makespan of each machine is rescheduled. The results show that the makespan of each machine is 56, 56, 45, 43, and 51. In addition, we found that M1, M2, M3, M4, and M5 machine tools on the same machine have a long working interval and are in the state of waiting for processing. Therefore, it will cause waste of resources. The mathematical model described in Section 2 is then implemented to determine the cost of the processed product and the actual profit. The related cost and profit data of the production scheduling are calculated, as shown in Table 3.

Figure 4 shows the results of 500 consecutive iterations, in which the red line is the result of real-time scheduling and the blue line is the result of static scheduling. At the beginning, the initial value of real-time scheduling is higher than that of static scheduling, which is related to the increase

TABLE 1: Scheduling data.

Job	Process time					Machine number				
	P1	P2	P3	P4	P5	M1	M2	M3	M4	M5
1	1	3	6	7	6	3	1	2	4	5
2	8	5	10	10	4	2	3	5	1	4
3	5	4	9	1	7	3	4	1	2	5
4	5	5	5	3	8	2	1	3	4	5
5	9	3	5	3	1	3	2	5	1	4

TABLE 2: Timing and resource constraints for rescheduling.

Constraints	Machine 3	Job 1	Job 2	Job 3	Job 4	Job 5
Time requested	—	1	5	5	5	9
Delay time	20	21	25	25	25	29
Process requested	P_{1-5}	P_1	P_2	P_3	P_4	P_5
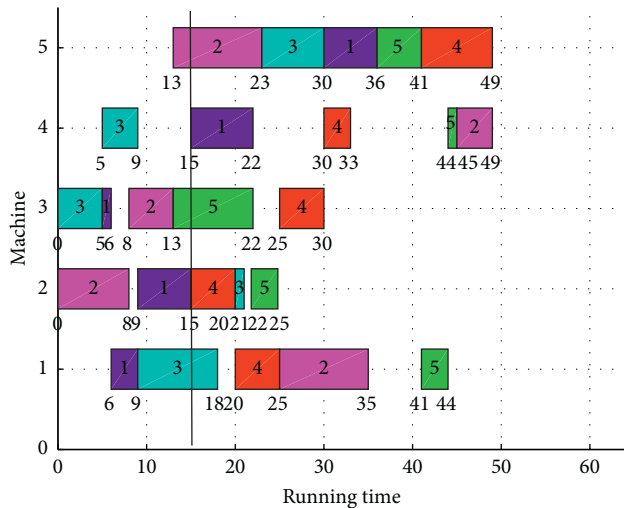
FIGURE 2: The Gantt chart of the production scheduling.
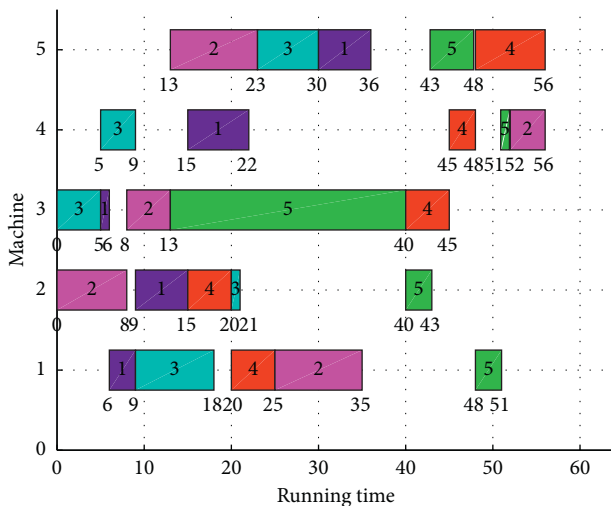
FIGURE 3: The Gantt chart of the rescheduling.

of time. The two results basically find the optimal solution within 50 times, and the trend of the curve is the same because the mode of scheduling is unchanged, but increases in time. In addition, the points on each line are the scheduling process at that time. The curve shows the annealing process of the optimization algorithm, and the solutions of each cooling process are obtained by continuous iteration. Because the realization of the simulated annealing algorithm depends on the choice of parameters, different optimal solutions appear in our scheduling process. The probability of finding the optimal solution by counting different results is shown in Table 4. Running 20 records the results and calculates the probability of finding the optimal solution. Among them, as can be seen from Table 4, the optimal result of static scheduling is 49, and the probability of occurrence is higher, but the value of the optimal solution 56 appears in real-time scheduling. In real-time scheduling, the result of rescheduling depends on the result of the first time, which leads to the diversity of rescheduling results.

5.1. Variable Hybrid Assembly Line Size. In order to explore the reliability and validity of the improved simulated annealing algorithm in multivariety and small-batch applications, we propose a scheduling scheme between different quantities of products and machines, using 4×4, 5×5, and 6×6 small-scale scheduling and 10×10. The results of static scheduling, real-time scheduling, and non-optimal scheduling are compared by the simulated annealing algorithm. The statistical curves are shown in Figure 4.

It can be seen from Figure 5 that, on the one hand, the relationship between makespan and mixed pipelines of different scales is positively correlated. The optimized makespan increases slowly with the increase of the scale, while the unoptimized makespan doubles with the increase of the scale. On the other hand, the utilization efficiency of the machine before optimization is obviously improved, and the makespan of different scales is obviously improved. Making span increases significantly when the scale is not optimized from 6×6 to 10×10. The possible reason is that the processing time of the machine is irregular, and the processing time of some processes may be longer than before. In addition, the larger the scale of real-time scheduling and static scheduling curves, the smaller the difference of optimization results is because with the increase of product types, the possibilities of arrangement and combination among them increase. Increasing the processing time of a certain stage alone will reduce the impact on the optimization results.

Just as the above analysis, in the actual production scheduling of enterprises, there are often unexpected events such as unexpected inserts, withdrawals, and unexpected events in the workshop. In this case, real-time scheduling is of great significance. Real-time scheduling is essentially a kind of rescheduling. Rearrangement must take into account orders produced to half, so we use the computer system for the workshop status. Real-time updating and regular archiving so that even if the computer system or program fails,

TABLE 3: Scheduling results and makespan.

| Job | Machine | | | | | Makespan |
	M1	M2	M3	M4	M5	T
1	{1, 4, 2}	{10, 19, 3}	{19, 24, 1}	{24, 34, 4}	{35, 38, 5}	36
2	{0, 8, 4}	{8, 14, 1}	{14, 19, 2}	{19, 20, 5}	{22, 25, 3}	38
3	{0, 1, 3}	{1, 6, 4}	{8, 13, 1}	{13, 22, 2}	{24, 29, 5}	30
4	{6, 10, 2}	{14, 21, 1}	{29, 32, 3}	{34, 38, 4}	{38, 39, 5}	49
5	{13, 23, 4}	{23, 30, 2}	{30, 35, 1}	{35, 41, 5}	{41, 49, 3}	45
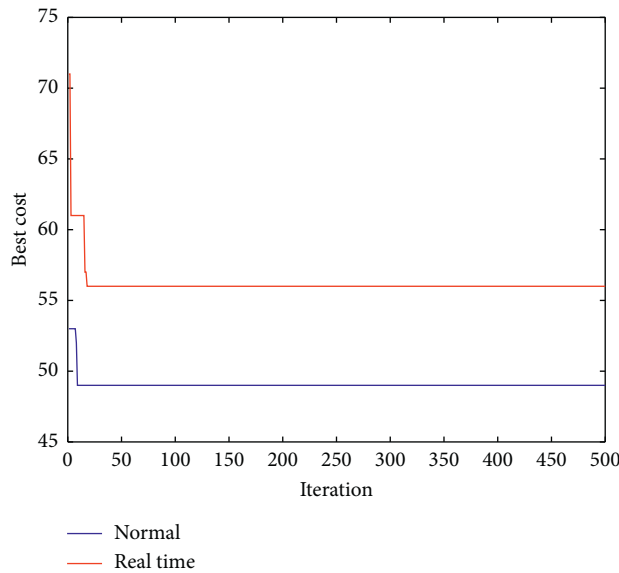
FIGURE 4: Cooling schedule.

TABLE 4: Comparison of simulation running.

| Comparison of algorithms | Average evolution generation | Output | |
		The optimal solution of the objective function	Probability statistics (%)
No optimization	—	133.0	100
Static scheduling	500	50.0	15
		49.0	85
Real-time scheduling	500	69.0	20
		68.0	5
		64.0	10
		63.0	25
		62.0	30
		56.0	10

FIGURE 5: Multiscales for the makespan.

the scheduling plan can be rearranged in time to achieve the dynamic scheduling of the workshop and optimize the subsequent production. Figure 3 is the rearrangement after machine failure. Comparing the two Gantt charts, we can see that, after machine 3 failure, the processing time of all kinds of products on machine 3 has changed, and the scheduling plan has been redesigned. We can also look forward to the next step: according to the maintainability of the machine to make a certain prediction of machine failure, if a machine is predicted to be in trouble, then our program should also give a backup response plan so that the workshop production site can switch the better schedule in time.

6. Discussions and Conclusions

Based on the dynamic, complex, multiconstraint, and multiobjective characteristics of job-shop scheduling in multivariety and small-batch production enterprises, this paper proposes a dynamic job-shop scheduling model based on the simulated annealing algorithm, which can meet the characteristics of multivariety and small-batch production in enterprises. Save the cost of the enterprise, and improve the profit of the enterprise. Numerical examples and simulation results of the hybrid model assembly line show that the proposed simulated annealing algorithm can maintain the excellent performance of the basic genetic algorithm and is an efficient optimization algorithm with better search performance.

To sum up, we must discuss the limitations of this study and the content of future research. Firstly, the actual data of production scheduling is limited. More evaluation of hybrid assembly lines is needed in plant applications by specifying the given parameters. Secondly, uncertain events such as machine failure, number of new jobs, and cancellation of existing jobs should be considered in energy-aware flexible job shop scheduling problems. We plan to add an energy-saving dynamic scheduling model in the future.

Data Availability

No data were used to support this study.

Conflicts of Interest

The authors declare that they have no conflicts of interest.

References

[1] M.-C. Hsiao, "Scheduling of hybrid types of machines with two-machine flowshop as the first type and a single machine as the second type," *IOP Conference Series: Materials Science and Engineering*, vol. 311, pp. 826–837, 2017.

[2] B. Joseph, M. Ezey, and E. I. Dar, "Mixed model assembly line design in a make-to-order environment," *Computer & Industrial Englineering*, vol. 41, pp. 405–421, 2002.

[3] Y. Y. Leu, "Genetic algorithm for assembly line balancing," *International Journal of Production Economics*, vol. 41, no. 3, pp. 343–354, 1999.

[4] J. H Chul and Y. Kim, "A genetic algorithm for multiple objective sequencing problems in mixed model assembly lines," *Computers and Research*, vol. 25, no. 7, pp. 675–690, 1998.

[5] J. Miltenburg, "A theoretical basis for scheduling mixed-model production lines," *Management Science*, vol. 35, no. 2, pp. 192–207, 1989.

[6] A. R. Rahimi-Vahed, M. Rabbani, R. Tavakkoli-Moghaddam, S. A. Torabi, and F. Jolai, "A multi-objective scatter search for a mixed-model assembly line sequencing problem," *Advanced Engineering Informatics*, vol. 21, no. 1, pp. 85–99, 2007.

[7] Y. L Yow and L. A Matheson, "Sequencing mixed model assembly lines with genetic algorithms," *Computers&Industry Engineering*, vol. 30, no. 4, pp. 1027–1036, 1996.

[8] Q. Dong and S. Kan, "Mixed model assembly line production of the modified discrete particle swarm optimization," *Computer Engineering and Applications*, vol. 45, no. 12, pp. 218–221, 2009.

[9] L.-N. Xing, Y.-W. Chen, P. Wang, Q.-S. Zhao, and J. Xiong, "A knowledge-based ant colony optimization for flexible job shop scheduling problems," *Applied Soft Computing*, vol. 10, no. 3, pp. 888–896, 2010.

[10] X. Ye, L. Wang, S.-Y. Wang, and M. Liu, "An effective teaching–learning-based optimization algorithm for the flexible job-shops cheduling problem with fuzzy processing time," *Neuro Computing*, vol. 148, pp. 260–268, 2015.

[11] A. P. Rifai, H.-T. Nguyen, and S. Z. M. Dawal, "Multi-objective adaptive large neighborhood search for distributed reentrant permutation flow shop scheduling," *Applied Soft Computing*, vol. 40, pp. 42–57, 2016.

[12] M. Dai, D. Tang, A. Giret, M. A. Salido, and W. D. Li, "Energy-efficient scheduling for a flexible flow shop using an improved genetic-simulated annealing algorithm," *Robotics and Computer-Integrated Manufacturing*, vol. 29, no. 5, pp. 418–429, 2013.

[13] M. Ham, Y. H. Lee, and S. H. Kim, "Real-time scheduling of multi-stage flexible job shop floor," *International Journal of Production Research*, vol. 49, no. 12, pp. 3715–3730, 2011.

[14] B. Javadi, A. Rahimi-Vahed, M. Rabbani, and M. Dangchi, "Solving a multi-objective mixed-model assembly line sequencing problem by a fuzzy goal programming approach," *The International Journal of Advanced Manufacturing Technology*, vol. 39, no. 9-10, pp. 975–982, 2008.

[15] S.-C. Cheng, D.-F. Shiau, Y.-M. Huang, and Y.-T. Lin, "Dynamic hard-real-time scheduling using genetic algorithm for multiprocessor task with resource and timing constraints," *Expert Systems with Applications*, vol. 36, no. 1, pp. 852–860, 2009.

[16] A. Roshani and D. Giglio, "Simulated annealing algorithms for the multi-manned assembly line balancing problem: minimising cycle time," *International Journal of Production Research*, vol. 55, no. 10, pp. 2731–2751, 2017.

[17] T. Kellegöz, "Assembly line balancing problems with multi-manned stations: a new mathematical formulation and Gantt based heuristic method," *Annals of Operations Research*, vol. 253, no. 1, pp. 377–404, 2017.

[18] S. Kirkpatrick Jr., C. D. Gelatt, and M. P. Vecchi, "Optimization by simulated annealing," *Science*, vol. 220, no. 11, pp. 650–671, 1983.

[19] A. Roshani, A. Roshani, A. Roshani, M. Salehi, and A. Esfandyari, "A simulated annealing algorithm for multi-manned assembly line balancing problem," *Journal of Manufacturing Systems*, vol. 32, no. 1, pp. 238–247, 2013.

[20] E. Aarts and J. Korst, *Simulated Annealing and Boltzmann Machines*, Wiley, New York, NY, USA, 1988.

[21] Y. Zhang, J. Wang, and Y. Liu, "Game theory based real-time multi-objective flexible job shop scheduling considering environmental impact," *Journal of Cleaner Production*, vol. 167, pp. 665–679, 2017.

[22] J. T. Lin and C.-M. Chen, "Simulation optimization approach for hybrid flow shop scheduling problem in semiconductor back-end manufacturing," *Simulation Modelling Practice and Theory*, vol. 51, pp. 100–114, 2015.

Research Article

Application of Artificial Intelligence in the Process of Ecological Water Environment Governance and Its Impact on Economic Growth

Ying Wei

Department of Economics and Management, Qilu Normal University, Jinan, Shandong 250000, China

Correspondence should be addressed to Ying Wei; 20152617@qlnu.edu.cn

With the increasing pollution of the ecological water environment, the treatment of the ecological water environment has become the focus of everyone's attention. At present, there are many research results on water environment governance, but the effect is not ideal. In order to effectively control the ecological water environment and promote sustainable economic growth, this research combines artificial intelligence algorithms and applies them to the governance process to explore its application effects and its impact on economic growth. First, the environmental sensor of the corresponding module is designed according to the water environment factor, and the data of dissolved oxygen content, water temperature, turbidity, temperature and humidity, and smoke concentration in the water environment are collected. Then the dynamic time-varying exponential smoothing prediction method is used to predict water quality, and a water quality prediction model is established. Then use support vector machine (SVM) to train the collected data samples, use the decision tree-based SVM classification method to classify the data samples, establish a water quality evaluation model, and use particle swarm optimization algorithm to optimize the evaluation model. Put the sensors and predictive evaluation models established in this research design into the governance of a certain river reach, and collect relevant data from 7 : 00 to 18 : 00 on October 11, 2019. And predict and evaluate its water quality. The experimental results show that the average absolute error of predicting dissolved oxygen content is 0.97%, and the average absolute error of predicting phosphorus content is 2.27%. This shows that the application of artificial intelligence algorithms in the process of ecological water environmental governance can effectively help collect effective information and make more accurate predictions and evaluations of water quality, thereby improving governance efficiency and promoting sustainable economic growth.

1. Introduction

1.1. Background Significance. With the rapid development of industry, a large amount of industrial sewage and domestic wastewater has caused serious pollution to the water environment, and the originally scarce water resources are facing severe tests [1]. The effects of some current water environment treatment projects and sewage treatment facilities are not satisfactory, which not only are unfavorable to the sustainable development of the environment and economy but also bring serious hidden dangers to the lives and health of residents [2]. Therefore, the use of artificial intelligence algorithms to monitor ecological water environment-related data and propose scientific processing methods is of great

significance for improving the efficiency of water environment governance.

1.2. Related Work. As the treatment of water environmental pollution is becoming more and more important, research teams at home and abroad have carried out research and discussion on it, and there are many achievements. According to the characteristics of PPP project of urban water environment treatment [3], an *X* established the basic standard and demonstration standard, formed the government compensation mode of PPP project of urban water environment treatment, considered the economic benefits of urban water environment treatment, and used game theory

method to solve the incentive coefficient [4]. Although his research is targeted, the source of his experimental data is unknown. Chen et al. proposed a feasible method of using SO_2 (sulfite) to catalyze the oxidation of wastewater to improve the removal rate of pollutants in the water environment [5]. Their research and experimental steps are too complex, and it is very difficult to repeat the operation. Muerdter et al. introduced the influence of plants on pollutant removal performance and mechanism, including the impact on total suspended solids, nitrogen, phosphorus, toxic metals, hydrocarbons, pathogens, and emerging pollutants in urban rainwater [6]. Although their research analyzed the impact of plants on water pollution, they did not propose direct treatment methods. Hashimoto et al. studied the application of a new slurry type titanium dioxide (TiO_2) photocatalyst in the degradation of pesticides in water, aiming to reduce the pollution of pesticide use on rural domestic water [7]. Their experimental procedures are little confused, leading to the increase of experimental time and cost.

1.3. Innovative Points in This Paper. In order to improve the efficiency of ecological water environment governance, improve the status quo of ecological water environment, and promote green growth of the economy, this paper conducts in-depth research. The innovations are as follows: (1) According to the selected water environment factors, a series of sensors with perfect functions are designed to collect the timely data of dissolved oxygen content, water temperature, turbidity, temperature and humidity, and smoke concentration in the water environment. (2) The water quality prediction model is established by using the dynamic time-varying index smoothing prediction method, which can effectively predict the water quality and put forward the corresponding treatment scheme as soon as possible. (3) The support vector machine (SVM) and SVM classification method based on decision tree are used to train and classify the data samples. The water quality evaluation model is established after the optimization of particle swarm optimization algorithm, which can accurately classify the water quality.

2. Artificial Intelligence and Ecological Water Environment Governance

2.1. Artificial Intelligence Algorithm

2.1.1. Genetic Algorithm. Genetic algorithm imitates the natural evolution process to find the optimal solution and applies the principle of Darwinian evolution theory [8]. Before the calculation of the genetic algorithm, we need to do some preparatory work [9]. Firstly, the decision variables are coded, and the completeness, soundness, and non-redundancy of the coding should be paid attention to [10, 11]. Then the fitness function is set to judge the quality of individuals in the population. The fitness needs to be transformed into selection probability in a certain way, and most of them are positive numbers. When the population is

set, the range of possible solutions of the model should be roughly estimated to be as close as possible to the optimal solution. When generating a certain number of individuals, excellent individuals must be added to the initial population.

After the maximum iteration number, selection probability, crossover probability, and mutation probability are set in advance, the iterative calculation can be started [12]. Firstly, the operators are selected randomly according to the probability to retain the excellent genes. Then the crossover operation is carried out. After pairing the chromosomes selected in the previous step, a segment of genes at the same position on the chromosome is randomly selected and exchanged to improve the searchability of genetic algorithm. In order to obtain new high-quality genes that cannot be obtained by cross operation, maintain population diversity, and prevent local optimum, it is necessary to select gene segments randomly for mutation. In order to maintain the size of the population, retain the optimal individuals of the original population, and prevent the loss of good individuals, it is necessary to add insertion operator after each iteration. Finally, the operation is stopped when the maximum number of iterations is satisfied or the ideal solution is reached.

Genetic algorithm (GA) searches the global optimal solution in the form of string set, which has a strong ability of optimization. GA evaluates individuals according to fitness function, which is not limited by specific objective function, and its application space is greatly expanded. GA uses probability transition rules to know the search direction and has the ability of self-organization, self-adaptive, and self-learning, so it is very practical.

2.1.2. Simulated Annealing Algorithm. The simulated annealing algorithm simulates the physical process of the solid in the molten state from gradually cooling to crystallization and uses random simulated solid annealing to solve the problem [13]. In the simulation process, the control of algorithm progress depends on the cooling schedule [14]. Under certain control parameters, the algorithm slowly cools down to zero, and the global optimal solution is obtained.

In the simulated annealing algorithm, the initial state should be selected as the current initial solution and the initial temperature should be set. After initializing the parameters, the next adjacent state is generated to judge whether the adjacent state is accepted or not and whether the balance point is reached. If not, it is necessary to return to generate the adjacent state until the balance is reached. Determine whether the termination conditions are met. If the requirements are not met, select a new temperature to generate the adjacent state, and the operation can be terminated if the termination conditions are met [15].

The simulated annealing algorithm can accept the deteriorating solution to a certain extent and accept the trial points that make the objective function value worse. The simulated annealing algorithm uses implicit parallelism algorithm, which is suitable for searching complex regions [16]. Only using the value of the objective function for

optimization calculation can avoid the limitation of continuous differentiability. The ability of global optimization can be greatly improved by setting the definition domain arbitrarily.

2.1.3. Particle Swarm Optimization Algorithm.

The particle swarm optimization algorithm is based on the foraging behavior of birds [17]. The flight space of birds is the search space of the problem. Each bird is an individual, and it is converted into particles whose weight is ignored to represent the feasible solution of the problem. The optimization process is similar to the population foraging process, and the most abundant food found is the optimal solution [18].

When the particle swarm optimization algorithm is used, first set the population size, search dimension, maximum iteration times, algorithm accuracy requirements, search range, and speed range [19]. The initial population and initial velocity are generated in the feasible region, the number of iterations is set, and the vector of the first iteration is determined according to the fitness value of different individuals in the population. If the current iteration times meet the preset accuracy requirements, the operation will be terminated.

As a swarm intelligence algorithm, particle swarm optimization algorithm has the flexibility to adapt to the changing system environment at any time [20]. It will not affect the robustness of the whole problem solution because of the failure of an individual. The increase of the number of individuals will not lead to the scalability of a large amount of communication overhead, and the implementation of individual execution time is relatively short [21, 22].

2.2. Ecological Water Environment Treatment Methods

2.2.1. Basic Principles of Ecological Water Environment Treatment.

At present, the treatment technology for ecological water environment mainly includes three aspects: controlling external pollution sources, controlling and changing environmental conditions, and controlling abnormal growth of algae [23]. The control of external pollution sources can reduce the content of phosphorus by reforming the sewage pipe network, dephosphorization, and denitrification treatment of sewage and also can carry out dredging, nutrient passivation, sedimentation flocculation, and adjusting the ratio of nitrogen and phosphorus of lake water. In order to control and change the environmental conditions, the nutrient content in water can be reduced by introducing clean water, and the growth and accumulation of algae will be destroyed by using the flowing water. In order to control the abnormal growth of algae, chemical killing and flocculant can be used, and manual harvesting can also be used to remove the algae.

When carrying out ecological restoration of water environment, it is necessary to understand that ecological restoration is the restoration of biodiversity, ecosystem structure, and function, which is obviously different from bioremediation [24]. Ecological restoration focuses on the restoration of the whole ecosystem, while bioremediation focuses on the use of aquatic organisms to reduce pollutants in water. The ecological restoration of water environment needs to repair the water environment and the self-recovery ability of the ecosystem, which must be realized by restoring or constructing submerged plant communities [25].

The key to water eutrophication restoration is to control phytoplankton and enhance water permeability. According to the classical biological regulation theory, increasing the number of carnivorous fish can form a balance in the aquatic ecological environment, thus enhancing the water permeability. In particular, macrocladoceran zooplankton can directly control the number of phytoplankton and create favorable environmental conditions for the restoration of submerged macrophytes.

According to the theory of steady-state transition of phreatic lakes, there are two kinds of states that can be transformed into each other, the turbid water state dominated by phytoplankton and the clear water state dominated by submerged macrophytes. Under the condition of changing environment, eutrophic muddy water can be restored to clear water state [26]. And the fundamental way to control eutrophication and purify water quality is to restore a complete water ecosystem with submerged plant community as the core.

2.2.2. New Measures for Ecological Water Environment Control.

Domestication of algae eating insects: excessive discharge of nitrogen and phosphorus will continue to increase the number of algae in the water, and the proliferation and growth of algae will damage the original ecosystem and the self-purification capacity of water body. In the short term, the technology of domesticating algae eating insects can be used to phagocytize the excessive algae in water body and improve the transparency of water body. Algae eater is a large cladocera zooplankton; after artificial domestication, it will feed on algae and rotten debris in the water [27]. To use this technology, different treatment methods should be adopted in three periods. Firstly, the domesticated algae eating insects should be used to devour the algae in the water body, reduce the turbidity of the water body, promote the growth of submerged plant communities, and form a new ecological balance. After that, submerged plant communities were constructed to oxidize and decompose suspended solids into minerals. The increase in oxygen content can also promote the reproduction of bottom microorganisms. Finally, in the long run, the ecosystem composed of submerged plants can promote the deposition of phosphorus in the water, eliminate the excess nutrients in the water body, and cultivate appropriate amount of underwater acoustic animals which can transform the nutrition of water body into edible animal protein, making the water quality cleaner.

In order to construct underwater forest, a healthy aquatic ecosystem with submerged plants as the core must be established. Submerged plants are the basis for the maintenance of water biodiversity and have important environmental value and strong water purification function. First of all, aquatic plants can remove a large number of nitrogen and phosphorus substances in the water area and

improve the self-purification ability of water area [28]. In addition, submerged plants can create living environment for other aquatic plants, so the rational utilization and protection of submerged plant resources is an important node to ensure the ecological balance of aquatic plants. The main environmental factors affecting submerged macrophytes include light intensity, nutrient content, water sediment, suspended solids, and water environment temperature [29].

Microporous aeration technology: sufficient dissolved oxygen is needed for the survival of microorganisms. The microorganisms mentioned here are mainly aerobic microorganisms. Aeration can effectively improve the dissolved oxygen in the water, oxidize the organic matter in the water with oxygen, then convert it into inorganic matter, improve the aerobic environment of the water area, restore the original microbial community, and change the original water environment through mechanical functions such as collision and mixing, so as to make the oxygen distribution uniform in the water area and reduce the occurrence of water pollution.

2.3. Environmental Sensors

2.3.1. Sensor Data Acquisition Strategy.

When the wireless sensor monitors the environmental data, the interval time of data collection is always the same, because this method is very simple. It only needs to set a fixed time interval in the sensor terminal node. In this way, the data will be collected every other period of time and finally transmitted to the server [31]. However, this method does not consider that the speed of data change is different at different times. If the data are collected only in the same time interval, the average information of data will be reduced. Moreover, the length of interval time will directly affect the acquisition results: being too short will lead to data redundancy, and being too long will lead to information loss. Therefore, when using sensors to monitor the environment, we must design a reasonable data acquisition strategy to effectively collect key information and reduce the number of sensor data acquisition and transmission.

Adaptive frequency conversion data acquisition strategy plays an important role in environmental monitoring, and the change of collected data can be roughly estimated by judging the change trend of data. Based on the univariate linear regression model, the data acquisition interval can be adjusted adaptively [32]. However, the efficiency of the strategy for data acquisition is not high, and the algorithm is complex and time-consuming.

Data acquisition based on data correlation is a method for continuous and long-term data acquisition. The data collected by sensors arranged in the environment are correlated. In a short time, the data collected by the same sensor are correlated in time, and the data collected by adjacent sensors at the same time are also spatially correlated. Among the existing sensor data collection methods based on data correlation, some of them cannot flexibly expand the scale of wireless sensor networks. In addition, because the method is

relatively simple, the amount of data collection and transmission is still too large to greatly reduce the data load of wireless sensor networks [33]. Therefore, the sensor data acquisition based on data correlation needs to design a distributed data acquisition method consistent with the reasonable and effective data correlation model, so as to ensure the quality of collected data and reduce the energy consumption of sensor nodes as much as possible [34]. Finally, it meets the requirements of flexible adaptability and excellent scalability.

2.3.2. Selection of Water Environmental Factors.

In the detection of water environment, the water environmental factors that need to be detected are clearly specified in relevant laws and regulations, which are mainly divided into underwater environmental factors and aquatic environmental factors.

Underwater environmental factors include dissolved oxygen, water temperature, pH, and turbidity [35]. Dissolved oxygen is the content of oxygen dissolved in water in molecular state. The content of dissolved oxygen in water is related to many factors. It not only provides the necessary oxygen for fish and microorganisms to survive but also is the detection parameter of water environmental quality. Water temperature can affect most of the chemical and physical properties of water, which is an important indicator of water quality. pH affects not only the growth of organisms in water but also the chemical and biological reactions in water. Turbidity is used to indicate the degree of turbidity in water environment. It is a measure of the scattering and absorption capacity of water to light. It is related to the quantity, size, and refractive index of particles in water.

The water environment does not only refer to the water area, and the aquatic environmental factors may also have a great impact on the water environment. Therefore, when testing the water environment, the influence of the water environment factors on the aquatic environment must be considered, such as smoke concentration, temperature and humidity, and light [36]. Smoke is one of the standards to detect air pollution, which is harmful to human health and the survival of animals and plants. The change of water temperature has a direct impact on water temperature, and the change of surface water temperature will delay the change of air temperature. The change speed of the water temperature is slower than that of the air, and the temperature difference between the surface water temperature and the deep-water temperature becomes larger when the temperature changes violently. Most aquatic organisms are variable temperature organisms, which are sensitive to the changes in external temperature and water temperature. If the temperature difference changes greatly, it will have a great impact on the thermophilic organisms and the quality of the water environment. In daily life, if the humidity in the air is too high, the bacteria are easy to reproduce, especially in the places close to the water environment, and the quality of the water environment will decline. Therefore, the collection of humidity factors is particularly important. There are two main types of oxygen in water, one is dissolved

oxygen in the air of water, and the other is dissolved oxygen in water after photosynthesis of aquatic plants. In order to supplement the dissolved oxygen content in water, aquatic plants need sufficient light for photosynthesis, so illumination is also one of the important factors [37].

3. Experiments on Intelligent Algorithm Model of Ecological Water Environment Management

3.1. Sensor Module Design. In this study, the dissolved oxygen sensor with a coated electrode was used to collect the dissolved oxygen data. The potential difference between the anode and cathode of the sensor produces a reduction reaction, which is directly proportional to the concentration of dissolved oxygen. Because the output current of the dissolved oxygen sensor is very small, it is necessary to use operational amplifier circuit and use core processing module for data conversion.

The water temperature sensor used in this study is a stainless steel packaged digital sensor, which adopts a unique single bus data structure and has the advantages of small size, high sensitivity, and high anti-interference ability. The working power supply voltage of the sensor is about 5 V, and the temperature range that can be measured is $-15°C \sim 110°C$. Put the probe part of the sensor into the water directly; the sensor can directly transmit the digital signal to the core MCU.

In this study, TS type turbidity sensor is used to collect turbidity data, and the light penetration is calculated by refraction of transistor and optical diode to a specific wavelength, so as to detect turbidity in water environment, and then the output current signal is converted into voltage signal. The working voltage of the sensor is about 5 V and the working current is less than 25 mA. It has the advantages of small volume and low price.

In this study, MQ-2 smoke sensor is used to collect smoke concentration data. Different concentrations and different types of gases have their corresponding resistance values. The change of conductivity is converted into the change of voltage so that the smoke concentration and voltage change show a linear relationship. The module has the advantages of high stability, high sensitivity, and wide detection range.

In this study, the composite digital sensor with professional temperature and humidity sensing technology is selected to collect the temperature and humidity data, which can accurately calibrate the data and ensure the reliability and stability of the sensor at a high level. The temperature measurement range is $-5 \sim 45°C$, the accuracy error is about $2°C$, the humidity measurement range is $15 \sim 95\%$ RH, and the accuracy error is about 3%.

3.2. Establishment of Water Quality Prediction Model. In this study, the dynamic time-varying exponential smoothing prediction method is used to predict the water quality. The exponential smoothing method overcomes the problem of insufficient prediction space, makes up for the shortcomings of incomplete consideration of data, fully considers the impact of data development trend on future data changes, and realizes the prediction in an average way. The basic formula of exponential smoothing method is

$$G_t = \beta Q_t + (1 - \beta)G_{t-1} = G_{t-1} + \beta(Qt - G_{t-1}), \quad t = 1, 2, \ldots, n. \tag{1}$$

Among them, G_t, G_{t-1} are the exponential smoothing average at time t and time $t-1$, respectively, Q_t is the measured value in time t, β is the smoothing coefficient, and the range is between [1, 2].

The exponential smoothing method can be classified according to the smoothing times. In this study, the quadratic exponential smoothing method is used, which is suitable for the series with parabolic linear trend. The smoothing value formula and prediction formula are shown in formulae (2) and (3), respectively:

$$\begin{cases} G_t^{(1)} = \beta x_t + (1 - \beta)G_{t-1}^{(1)}, \\ G_t^{(2)} = \beta G_t^{(1)} + (1 - \beta)G_{t-1}^{(2)}, \end{cases} \tag{2}$$

$$\widehat{x}_{t+T} = d_t + e_t \cdot T + f_t \cdot T^2. \tag{3}$$

Among them, $G_t^{(1)}, G_{t-1}^{(1)}, G_t^{(2)}, G_{t-1}^{(2)}$ are the first exponential smoothing average of t period and $t-1$ period and the second exponential smoothing average of t period and $t-1$ period; $\widehat{x}_{t+T}$ is the prediction value of $t + T$ period; β is the smoothing coefficient; d_t, e_t, f_t are the parameters of related model.

When using the exponential smoothing method, attention should be paid to the determination of initial value and smoothing coefficient, which have great influence on the accuracy of prediction. The common method is to take the measured value of the first phase as the initial value, and the value range of smoothing coefficient is 0.3~0.5.

3.3. Establishment of Water Quality Evaluation Model. At present, the water quality evaluation methods include comprehensive pollution index method, Ross water quality index method, and brown water quality index method. With the wide application of artificial intelligence algorithm, water quality evaluation model also presents diversification. In this study, SVM is used to train data samples, and SVM classification method based on decision tree is used to classify data samples. The optimal classification discriminant function of the training set is shown in formula (4):

$$g(x) = \text{sgn}\left[\sum_{i-1}^{i} r_i m_i(x_i, x_j) + n\right], \tag{4}$$

where m_i is the Lagrange multiplier, x_i is the sample vector, r_i is the classification identifier, and n is the classification threshold.

The particle swarm optimization algorithm is used to optimize the parameters of SVM, and the optimization process is shown in Figure 1.

As shown in Figure 1, the initial population and initial speed are generated in the feasible region, the number of
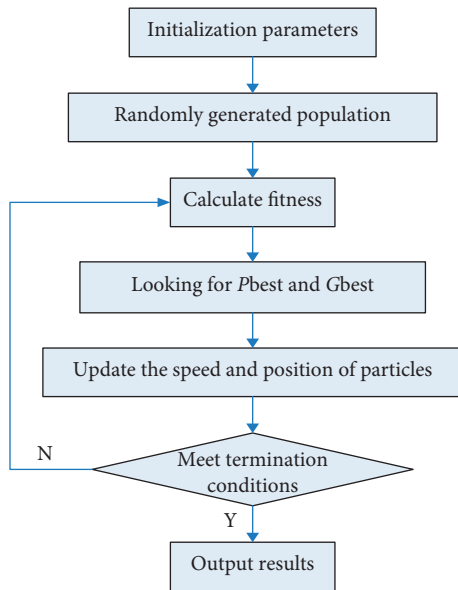
FIGURE 1: Flowchart of particle swarm optimization algorithm.

iterations is set, and the first iteration vector is determined according to the fitness values of different individuals in the population. Update the speed of the individual and the optimal position in the global history, and terminate the operation if the current iteration number reaches the preset accuracy requirement.

4. Discussion on the Application of Intelligent Algorithms and Its Impact on Economic Growth

4.1. Sensor Data Acquisition Results. The sensor designed in this study is used to collect the data of dissolved oxygen, water temperature, turbidity, temperature and humidity, and smoke concentration in a river section. The collection period is from 7 : 00 to 18 : 00 on October 11, 2019, and the data are recorded every 1 h.

As shown in Table 1, during the period from 7 : 00 to 18 : 00 on October 11, 2019, the changes of dissolved oxygen content, water temperature, turbidity and temperature, and humidity of the reach are not particularly obvious, and the change of smoke concentration is more obvious. With the change of the ambient temperature, the water temperature will also change accordingly. The ambient temperature reaches the highest value of 17.2°C at 13 : 00, while the water temperature reaches the maximum of 15.7°C at 18 : 00. The content of dissolved oxygen showed a U-shaped trend, and the content was the lowest at noon. Turbidity and humidity were the lowest at 13 : 00 noon. The smoke concentration fluctuated and peaked at 9 : 00, 13 : 00, and 18 : 00, which may be due to the increase of the number of vehicles in the morning and evening peak, and the automobile exhaust aggravates the environmental pollution, which makes the current smoke concentration increase.

4.2. Application and Analysis of Water Quality Prediction and Evaluation Model

4.2.1. Water Quality Prediction Results. The water quality samples of the river section from October 11 to 20, 2019, are collected, the data are calculated by quadratic exponential smoothing, and the smoothing coefficient is 0.5. The dynamic time-varying exponential smoothing prediction model was used to predict the dissolved oxygen content of the reach from October 21 to 30, and the results were compared with the actual detection results. The results are as follows.

As shown in Figure 2, the residual errors of the dynamic time-varying exponential smoothing prediction model are 0.18, −0.21, 0.171, −0.11, −0.15, 0.241, 0.123, −0.18, 0.214, and 0.187, respectively, with an average absolute error of 0.97%. In order to further verify the prediction ability of the model, the phosphorus content of the same water sample was predicted. The results are as follows.

As shown in Figure 3, the residual errors of the dynamic time-varying exponential smoothing prediction model are 0.0021, −0.0051, 0.019, 0.001, 0.012, 0.0098, 0.0123, −0.0087, 0.0107, and 0.0109, respectively, with an average absolute error of 2.27%. Although there are some unavoidable errors, the model still has high prediction ability, which can provide scientific data for the treatment of water environment.

4.2.2. Water Quality Assessment Results. Using the water quality evaluation model established in this study, the above water quality parameters and the results based on dynamic time-varying index smoothing prediction are normalized, and then the parameters are optimized by particle swarm optimization algorithm. The results are as follows.

As shown in Figure 4, the water quality can be divided into five categories through the water quality evaluation model, and there is no phenomenon of misclassification and leakage. Moreover, the classification speed is very fast, and the training time is also a lot. After the classification, the decision function can be obtained by training, and the water quality of the samples can be corresponding to the corresponding water quality categories.

4.3. Impact on Economic Growth. Ecological water environment and economic growth are complementary. Relying on the economic growth of the secondary industry will bring irreversible pollution to the water environment. While developing the economy, we must pay attention to environmental protection. The scientific treatment method of water environment based on artificial intelligence can effectively improve treatment efficiency [38]. In a short period of time, the polluted water environment will be treated to prevent water environment pollution that has not yet appeared but may occur and promote sound and rapid economic development while protecting the water environment.

TABLE 1: Measured data of sensors.

Time	DO mg/l	Water T ˚C	Turbidity %	T ˚C	Humidity %	Smoke C ppm
7:00	9.3	14.8	3.7	15.7	41.2	229
8:00	9.2	14.8	3.8	15.9	41.0	301
9:00	9.0	14.9	3.7	16	39.8	318
10:00	9.0	15.3	3.4	16.3	39.9	268
11:00	8.9	15.4	3.3	16.8	38.6	254
12:00	8.9	15.5	3.5	17	37.9	281
13:00	8.9	15.6	3.2	17.2	37.1	305
14:00	9.0	15.5	3.4	17.2	38.5	299
15:00	9.1	15.3	3.5	16.9	38.2	264
16:00	9.1	15.3	3.6	16.6	38.9	237
17:00	9.0	15.6	3.6	16.8	39.3	223
18:00	9.2	15.7	3.5	16.9	40.2	314
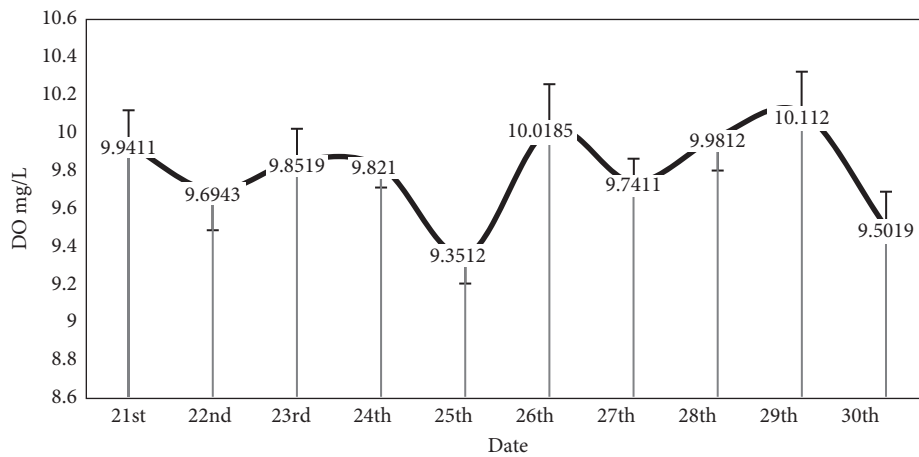
FIGURE 2: Prediction results of dissolved oxygen content.
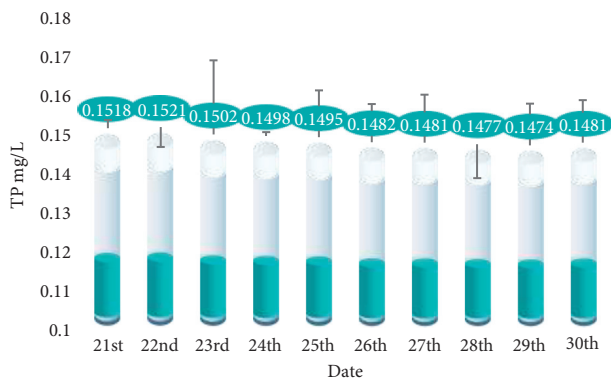
FIGURE 3: Prediction results of phosphorus content.
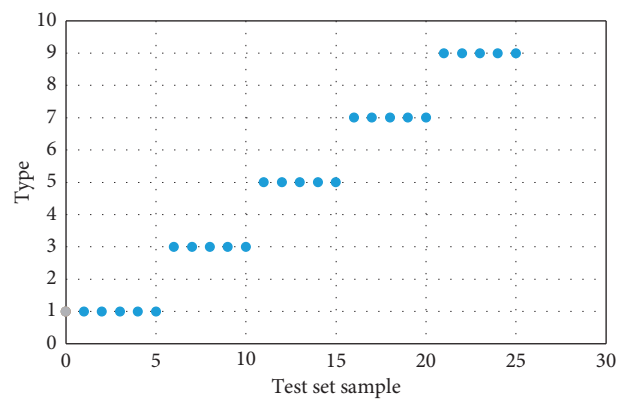
FIGURE 4: Classification of water quality samples.

5. Conclusions

The task of ecological water environment management cannot be completed overnight. It needs to be carried out from three aspects: controlling external pollution sources, controlling and changing environmental conditions, and controlling the abnormal growth of algae. In the treatment process, the collection and analysis of water environment factor data are directly related to the treatment effect. Timely and accurate data help to make reasonable and scientific decisions.

The sensor designed in this study can collect effective information and provide timely feedback, providing scientific data for water quality prediction models and water quality evaluation models. Accurately predict and evaluate water environment-related data to make scientific decisions, improve water environment management efficiency, and save manpower and material resources.

Due to the limited time and knowledge, the design of water environment sensor in this study is too simple to consider the problem of energy consumption and damage in the process of using. When establishing the prediction model, this study only predicted the content of dissolved oxygen and phosphorus in the water, but the composition of the elements in the water is complex, and it is not enough to predict these two alone. In the next step of the research work, we will predict as many water quality indicators as possible.

Data Availability

The data underlying the results presented in the study are available within the manuscript.

Conflicts of Interest

The author declares no conflicts of interest.

References

[1] S. B. Tsai, M. F. Chien, Y. Xue, L. Li et al., "Using the fuzzy dematel to determine environmental performance: a case of printed circuit board industry in Taiwan," *PLoS One*, vol. 10, no. 6, Article ID e0129153, 2015.

[2] J.-H. Lee and J.-E. Oh, "A comprehensive survey on the occurrence and fate of nitrosamines in sewage treatment plants and water environment," *Science of the Total Environment*, vol. 556, pp. 330–337, 2016.

[3] Z. Lv, B. Hu, and H. Lv, "Infrastructure monitoring and operation for smart cities based on IoT system," *IEEE Transactions on Industrial Informatics*, vol. 16, no. 3, pp. 1957–1962, 2020.

[4] X. An, H. Li, L. Wang, Z. Wang, J. Ding, and Y. Cao, "Compensation mechanism for urban water environment treatment PPP project in China," *Journal of Cleaner Production*, vol. 201, no. 1-1166, pp. 246–253, 2018.

[5] L. Cao, Z. G. Xu, and A. N. Alshawabkeh, "Demonstration of a feasible energy-water-environment nexus: waste sulfur dioxide for water treatment," *Applied Energy*, vol. 250, no. 1, pp. 1011–1022, 2019.

[6] C. P. Muerdter, C. K. Wong, and G. H. Lefevre, "Emerging investigator series: the role of vegetation in bioretention for stormwater treatment in the built environment: pollutant removal, hydrologic function, and ancillary benefits," *Environmental Science: Water Research & Technology*, vol. 4, no. 5, pp. 592–612, 2018.

[7] Y. Hashimoto, K. Hara, and B. Sarangaraja, "Decomposition of pesticides in water through the use of a slurry-type TiO_2 water treatment apparatus," *Journal of Water and Environment Technology*, vol. 14, no. 1, pp. 1–5, 2016.

[8] Y. Aizawa, Y. X. Fan, H. S. HuangLi et al., "Multi-objective optimization of injection-molded plastic parts using entropy weight, random forest, and genetic algorithm methods," *Journal of Polymer Engineering*, vol. 40, no. 4, pp. 360–371, 2020.

[9] M. Elhoseny, X. Yuan, H. K. El-Minir, and A. M. Riad, "Extending self-organizing network availability using genetic algorithm," in *Proceedings of the 5th International Conference on Computing Communication and Networking Technologies, ICCCNT*, Hefei, China, July 2014.

[10] P. Zhang, H. Yao, M. Li et al., "Virtual network embedding based on modified genetic algorithm," *Peer-to-Peer Networking and Applications*, vol. 2, pp. 1–12, 2017.

[11] N. Chen, B. Rong, X. Zhang, and M. Kadoch, "Scalable and flexible massive MIMO precoding for 5G H-CRAN," *IEEE Wireless Communications*, vol. 24, no. 1, pp. 46–52, 2017.

[12] M. Rajabi and F. Shafiei, "QSAR models for predicting aquatic toxicity of esters using genetic algorithm-multiple linear regression methods," *Combinatorial Chemistry & High Throughput Screening*, vol. 22, no. 5, pp. 317–325, 2019.

[13] Y. Zhong, J. Ning, and H. Zhang, "Multi-agent simulated annealing algorithm based on particle swarm optimisation algorithm," *Journal of Jilin University*, vol. 43, no. 4, pp. 335–342, 2018.

[14] Y. Tang and M. Elhoseny, "Computer network security evaluation simulation model based on neural network," *Journal of Intelligent and Fuzzy Systems*, vol. 37, no. 3, 2019.

[15] V. Mundada and S. Kumar Reddy Narala, "Optimization of milling operations using artificial neural networks (ANN) and simulated annealing algorithm (SAA)," *Materials Today: Proceedings*, vol. 5, no. 2, pp. 4971–4985, 2018.

[16] C. Takeang and A. Aurasopon, "Multiple of hybrid lambda iteration and simulated annealing algorithm to solve economic dispatch problem with ramp rate limit and prohibited operating zones," *Journal of Electrical Engineering & Technology*, vol. 14, no. 1, pp. 111–120, 2019.

[17] A. Francis Saviour Devaraj, M. Elhoseny, S. Dhanasekaran, E. Laxmi Lydia, and K. Shankar, "Hybridization of firefly and improved multi-objective particle swarm optimization algorithm for energy efficient load balancing in cloud computing environments," *Journal of Parallel and Distributed Computing*, vol. 142. , 2020 In press.

[18] J. Liu, K. H. Zhang, and S. Jiang, "Multi-objective particle swarm optimization algorithm based on objective space division for the unequal-area facility layout problem," *Expert Systems with Applications*, vol. 102, pp. 179–192, 2018.

[19] A. Tharwat, M. Elhoseny, A. E. Hassanien et al., "Intelligent Bézier curve-based path planning model using Chaotic Particle Swarm Optimization algorithm," *Cluster Computing*, vol. 22, no. 4, pp. 1–22, 2018.

[20] Z. Lv, D. Chen, and Q. Wang, "Diversified technologies in internet of vehicles under intelligent edge computing," *IEEE Transactions on Intelligent Transportation Systems*, vol. 22, no. 4, 2020.

[21] Z. Wang and J. Cai, "The path-planning in radioactive environment of nuclear facilities using an improved particle

swarm optimization algorithm," *Nuclear Engineering and Design*, vol. 326, pp. 79–86, 2018.

[22] T. Wang, Z. Zheng, and M. Elhoseny, "Equivalent mechanism: releasing location data with errors through differential privacy," *Future Generation Computer Systems*, vol. 98, pp. 600–608, 2019.

[23] P. Phungsai, I. F. Kurisu, and H. Furumai, "Changes in dissolved organic matter composition and disinfection byproduct precursors in advanced drinking water treatment processes," *Environmental Science & Technology*, vol. 52, no. 6, pp. 3392–3401, 2018.

[24] H. Li, S. Q. Xia, and L. L. LvWang, "Identifying factors affecting the sustainability of water environment treatment public-private partnership projects," *Advances in Civil Engineering*, vol. 2019, no. 11, 15 pages, Article ID 7907234, 2019.

[25] W. Zhang, Y. Hu, J. Liu et al., "Progress of ethylene action mechanism and its application on plant type formation in crops," *Saudi Journal of Biological Sciences*, vol. 27, no. 6, pp. 1667–1673, 2020.

[26] Q. H. Yu, "Analysis on comprehensive treatment planning strategy of river basin water environment," *Journal of Water Resources Research*, vol. 08, no. 1, pp. 67–73, 2019.

[27] K. Bawane, K. Ning, and K. Lu, "High temperature treatment of Cr 3 C 2 @SiC-NFA composites in water vapor environment," *Corrosion Science*, vol. 131, pp. 365–375, 2017.

[28] C. Wang, Y. Wu, B. Leilei et al., "Intermittent aeration incubation of drinking water treatment residuals for recycling in aquatic environment remediation," *Journal of Cleaner Production*, vol. 183, pp. 220–230, 2018.

[29] V. D. Wei, B. Conrad, and S. Khanna, "Impacts of water hyacinth treatment on water quality in a tidal estuarine environment," *Biological Invasions*, vol. 21, no. 12, pp. 3479–3490, 2019.

[30] W. Elsayed, M. Elhoseny, S. Sabbeh, and A. Riad, "Self-maintenance model for wireless sensor networks," *Computers & Electrical Engineering*, vol. 70, pp. 799–812, 2018.

[31] Á. Vidal-Vidal, E. M. Cabaleiro-Lago, C. Silva López, O. N. Faza et al., "Rational design of efficient environmental sensors: ring-shaped nanostructures can capture quat herbicides," *Acs Omega*, vol. 3, no. 12, pp. 16976–16988, 2018.

[32] Y. F. Lin, Y. Xu, C. Y. Lin et al., "Origin of noise in layered MoTe2 transistors and its possible use for environmental sensors," *Advanced Materials*, vol. 27, no. 42, pp. 6612–6619, 2016.

[33] L. Zimmermann, G. R. Weigel, and G. Fischer, "Fusion of nonintrusive environmental sensors for occupancy detection in smart homes," *IEEE Internet of Things Journal*, vol. 5, no. 4, pp. 2343–2352, 2018.

[34] Z. Lv and N. Kumar, "Software defined solutions for sensors in 6G/IoE," *Computer Communications*, vol. 153, pp. 42–47, 2020.

[35] M. Loyola, "A method for real-time error detection in low-cost environmental sensors data," *Smart and Sustainable Built Environment*, vol. 8, no. 4, pp. 338–350, 2019.

[36] V. Dediu, B. V. Musat, and N. I. Cristea, "Thermal decomposition of some sol-gel precursors for mesoporous TiO_2-based thin films for chemorezistive environmental sensors," *Revista de Chimie*, vol. 68, no. 8, pp. 1703–1707, 2017.

[37] C.-H. Chen, F.-J. Hwang, and H.-Y. Kung, "Travel time prediction system based on data clustering for waste collection vehicles," *IEICE Transactions on Information and Systems*, vol. E102.D, no. 7, pp. 1374–1383, 2019.

[38] V. Puri, S. Jha, R. Kumar et al., "A hybrid artificial intelligence and internet of things model for generation of renewable resource of energy," *IEEE Access*, vol. 7, no. 1, 2019.

Research Article

Study on Agglomeration Level and Effect of Equipment Manufacturing Industry in the Yangtze Delta Urban Agglomeration

Min Zhou [iD],[1] Sheng Li,[1] and Yu Wu[2]

[1]*Faculty of Economics and Business Administration, Yibin University, Yibin 644000, Sichuan, China*
[2]*School of Management, Shanghai University of Engineering Science, Shanghai 201620, China*

Correspondence should be addressed to Min Zhou; 2019114016@yibinu.edu.cn

This paper analyzes the agglomeration level and agglomeration effect of 8 subindustries of equipment manufacturing industry and 26 prefecture-level cities in the Yangtze River Delta (YRD). From the perspective of industry, the agglomeration change trend of 8 subsectors of equipment manufacturing industry from 2006 to 2016 in the Yangtze River Delta Urban Agglomeration (YRDUA) is analyzed. From the perspective of cities, the spatial differences of equipment manufacturing agglomeration degree in 26 prefecture-level cities in the YRDUA are discussed. By using CES production function, the agglomeration effect of equipment manufacturing agglomeration is studied. The results show that the YRDUA has formed an agglomeration pattern of equipment manufacturing industry, with Shanghai as the core, and Hefei, Hangzhou, Suzhou, and Nanjing as the auxiliary cities, and the overall agglomeration effect in the region is relatively obvious.

1. Introduction

Equipment manufacturing industry is the focus of implementing the strategy of manufacturing power, and it is also the key to effectively improve the global competitiveness. There are obvious regional differences in the development level of China's equipment manufacturing industry, which is showing a stair-like declining feature from the east to the west [1]. So, clearly dividing the spatial distribution of equipment manufacturing industry in urban agglomeration is helpful to put forward the industrial development strategy [2]. The Yangtze River Delta Urban Agglomeration (YRDUA) is an important equipment manufacturing base in China with convenient transportation and superior geographical position. In the 13th Five-Year (2016–2020) Plan for Promoting the Development of High-end Equipment Manufacturing Industry in Shanghai, it is proposed to grasp the trend of high-end, intelligent, independent, open, service-oriented equipment manufacturing industry, promote industrial agglomeration development, and give full play to the agglomeration radiation and leading role of industrial bases. Zhejiang, Jiangsu, and Anhui have also released their 13th Five-Year Development Plans for the Equipment Manufacturing Industry. However, the status of the equipment manufacturing industry in the YRDUA is gradually declining. Although the industrial scale is still expanding, the performance is lower than the national average level [3]. At the same time, the distribution of manufacturing enterprises in the YRDUA is unbalanced. With the change of geographical distance, the spatial agglomeration trend is strong first and then weak [4].

According to the Yangtze River Delta Urban Agglomeration Development Plan approved by the State Council, the YRDUA covers 26 cities, including Shanghai, Nanjing, Wuxi, Changzhou, Suzhou, Nantong, Yancheng, Yangzhou, Zhenjiang, Taizhou (in Jiangsu Province), Hangzhou, Ningbo, Shaoxing, Huzhou, Jiaxing, Jinhua, Zhoushan, Taizhou (in Zhejiang Province), Hefei, Wuhu, Ma'anshan, Tongling, Anqing, Xuancheng, Chizhou, and Chuzhou. With the YRDUA regional integration rising as a national

strategy, what are the changes in the development status and trend of equipment manufacturing industry in the Yangtze River Delta? Taking the YRDUA as the research object, this paper makes an empirical study on the agglomeration degree and effect of the equipment manufacturing industry in the region and, thus, to comprehensively grasp the development process, agglomeration trend and agglomeration effect of the equipment manufacturing industry in the YRDUA.

2. Analysis on the Agglomeration Level

The YRDUA is the frontier of China's economic development, accounts for only 2.3% of China's total area, with a population of 225 million, and contributes about a quarter of the China's GDP. The equipment manufacturing industry is more mature in this area than the rest of China. The agglomeration level of equipment manufacturing industry in 8 subsector industries and 26 prefecture-level cities in the YRDUA has been studied in this paper.

2.1. Method. Generally, many methods have been adopted to measure the degree of industrial agglomeration [5], such as EG index [6], location entropy, industry concentration, and spatial Gini coefficient [7], and Lin and Zhu [8] used EG

index and CR_n to calculate the agglomeration degree of manufacturing industry. In addition, Xu and Chen [9] used longitude and latitude coordinates to study the manufacturing agglomeration phenomenon of China's manufacturing enterprises; Sun and Zhang [10] calculated the agglomeration level of China's high-tech manufacturing industry based on the standard deviation ellipse method of spatial statistics.

Considering the accuracy of industrial agglomeration measurement, this paper selects the geographic concentration index established by Ellison and Glaseser [11]. On the one hand, based on the time span from 2006 to 2016, this paper analyzes the agglomeration trend of the equipment manufacturing industry in the YRDUA in 11 years; on the other hand, the spatial differences of the agglomeration degree of the equipment manufacturing industry have also been studied in 2016 in terms of 26 prefecture-level cities in the YRDUA.

Suppose that there are N enterprises in an industry of an economy (country or region), and the economy is divided into M geographical regions, and the N enterprises are distributed in M regions. The calculation formula of industrial geographic concentration index established by Ellison and Glaeser is as follows:

$$EG = \frac{G - \left(1 - \sum_i x_i^2\right)H}{\left(1 - \sum_i x_i^2\right)(1 - H)} = \frac{\sum_{i=1}^M \left(S_i - x_i\right)^2 - \left(1 - \sum_{i=1}^m x_i^2\right)\sum_{j=1}^N z_j^2}{\left(1 - \sum_{i=1}^N x_i^2\right)\left(1 - \sum_{j=1}^N z_j^2\right)}. \tag{1}$$

H is the Herfindahl index, which indicates the size distribution of enterprises in the industry based on the number of employees, in which N refers to the number of enterprises in the industry and X represents the total market size.

$$H = \sum_{j=1}^N z_j^2 = \sum_{j=1}^N \left(\frac{x_j}{X}\right)^2, z_j^2 = \frac{x_j}{X}, \tag{2}$$

where z_j represents the market share of enterprises j and x_j represents the scale of enterprise j. The larger the EG index is, the higher the degree of industrial agglomeration is, and vice versa.

2.2. Data. The clustered sample data of equipment manufacturing industry are selected from the Statistical Yearbook of 26 prefecture-level cities in the Yangtze River Delta Urban Agglomeration and the Shanghai Statistical Yearbook, Zhejiang Statistical Yearbook, Anhui Statistical Yearbook, and Jiangsu Statistical Yearbook, from 2007 to 2017. Due to the adjustment of the National Economic Industry Classification in 2012, the transportation equipment industry was divided into automobile manufacturing industry and railway, shipping, aerospace, and other transportation equipment manufacturing industry. In order to ensure the accuracy of the analysis, this paper divides the data of 11 years into two periods of 2007–2012 and

2013–2017 and calculates them, respectively. In addition, the distribution of employees in the statistical yearbook has not been indicated, so it is replaced by the number of enterprises and the total number of employees.

2.3. Evaluation Results of Agglomeration. According to the industrial geographic concentration index formula proposed by Ellison and Glaeser, the geographic concentration index of equipment manufacturing industry in the YRDUA in 11 years is calculated, as shown in Figure 1.

Elision and Glaeser believe that the geographical concentration index (γ) can be divided into the following three situations:

(a) $\gamma > 0.05$, the high industrial agglomeration in the region

(b) $0.02 \le \gamma \le 0.05$, the uniform industrial distribution in the region

(c) $\gamma < 0.02$, the low industrial agglomeration in the region

According to the abovementioned criteria, we classify the geographical concentration index of the eight major equipment manufacturing industries in 2016, as shown in Table 1.

The average and median of geographic concentration index in 2006, 2010, 2014, and 2016 are calculated for the purpose of understanding the change trend of
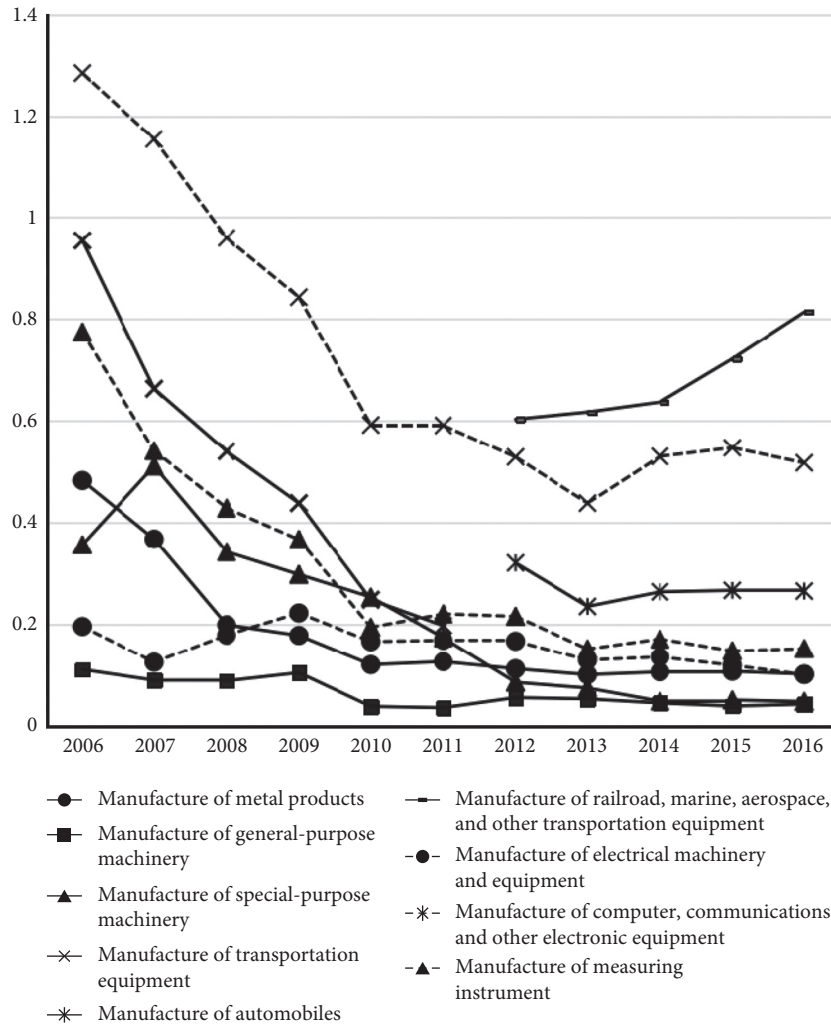
Figure 1: Geographical concentration index of equipment manufacturing industry (2006–2016).

Table 1: Classification of agglomeration degree of equipment manufacturing industries (2016).

	Industry and industry code	Geographic concentration index
	Manufacture of metal products (C33)	0.1014
	Manufacture of automobiles (C36)	0.2646
	Manufacture of railroad, marine, aerospace, and other transportation equipment (C37)	0.8138
$\gamma > 0.05$ (6 industries)	Manufacture of electrical machinery and equipment (C38)	0.1004
	Manufacture of computer, communications, and other electronic machinery (C39)	0.5169
	Manufacture of measuring instrument (C40)	0.1515
$0.02 \leq \gamma \leq 0.05$ (2 industries)	Manufacture of general-purpose machinery (C34)	0.0423
	Manufacture of special-purpose machinery (C35)	0.0475
$\gamma < 0.02$ (0 industry)		

Note: γ denotes the geographical concentration index.

agglomeration degree of equipment manufacturing industry in the YRDUA, and the result is as shown in Table 2.

From abovementioned table and figure, we can see that, first, the equipment manufacturing industry in the whole Yangtze River Delta urban agglomeration has a relatively high degree of agglomeration and formed a certain scale in the 11-year time span. However, the degree of agglomeration has been declining in a straight line (the average value decreased from 0.59 to 0.21) in the first 6 years, and it has a slow upward trend and gradually stabilized (the average

TABLE 2: Average and median of industrial geographic concentration index.

Year	2006	2010	2014	2016
Average	0.59367	0.22983	0.24165	0.2548
Median	0.4822	0.1935	0.1528	0.12645

value increased from 0.21 to 0.25) in the last 5 years. This is due to the rise of information technology and the Internet and higher value-added industries emerged, such as robotics, VR and AR technology, and material gene technology in the past 10 years. In contrast, the equipment manufacturing industries have the features of low added value, low technology, and weak competitiveness of products. So, with the rise of manufacturing industry in the central and western regions, Bohai Rim, and other urban agglomerations, the equipment manufacturing industry in the YRDUA has been transferred outward in a gradient way.

Second, the decline rate of transportation manufacturing industry was as high as 80% in the period of 2006–2011, followed by metal, general, and instrument manufacturing industries with a decline rate of about 70%. The main reason is that the enterprises of these industries were small in scale, and they were prone to the dispersing and duplicating investments which affect the degree of agglomeration to a certain extent. Moreover, the national industry classification standards have been adjusted since 2012, and then, the railway, shipping, and aerospace manufacturing industries have been significantly increased by 35%, mostly benefitted from very high attention and the strong policy support given by the government. Meanwhile, the other industries are still in a downward trend, but the decline is not so sharp and tends to be stable.

Thirdly, it has an obvious agglomeration effect and relatively intensive distribution of the equipment manufacturing industry in the YRDUA in 2016. The number of industries whose geographical concentration index is greater than 0.05 is more than 75%, while the number between 0.02–0.05 is less than 20%. It can be seen that the geographical advantages, rich resources, and government cultivation in the region have played a key role. However, at the same time, the equipment manufacturing industry in various subsectors is also more differentiated. Among them, the concentration degree of shipbuilding and aerospace manufacturing is the highest, which is 0.81, while the concentration degree of general and special equipment manufacturing is only 0.04, which also reflects the relatively average distribution of capital-intensive manufacturing industries in the YRDUA. In addition, the computer, communication, and other electronic equipment manufacturing industries and automobile manufacturing industries are also highly concentrated and consistent with the reality that the YRDUA is focusing on the development of high-tech industries represented by information industry and transportation rail industry.

After 10 years of development, the agglomeration of equipment manufacturing industry in the YRDUA has taken shape basically. The agglomeration degree distribution of the 8 major equipment manufacturing industries in the subdivided cities of the YRDUA in 2016 is shown in Table 3 and Figure 2.

According to the abovementioned data, it can be seen that, first, the agglomeration and distribution of equipment manufacturing industry in YRDUA have distinct hierarchy. The

east, north, and south are relatively concentrated, while the middle and west are relatively scattered. Therefore, the regional agglomeration of the YRDUA can be divided into four levels. The top level is Shanghai, as the key development city of the equipment manufacturing industry in the YRDUA, which contains the largest number of equipment manufacturing industries and has a high degree of agglomeration. The second level is Nantong, Hefei, Taizhou, and Yancheng. The distribution of equipment manufacturing industry in these four cities is relatively concentrated, including four industries, only second to Shanghai. The third level is Zhenjiang, Tongling, Nanjing, Yangzhou, Shaoxing, and Hangzhou. These six cities only have a high degree of agglomeration in two or three industries which all have a great influence. The fourth level is Zhoushan, Ma'anshan, Taizhou, and other cities; the rest of these cities only occupy a large proportion in one industry, and most of them are adapted to local conditions and have certain regional characteristics.

Second, the provinces and cities in the YRDUA have formed different advantageous industries, and the characteristics of regional division of labor have emerged in the process of agglomeration. Shanghai mainly focuses on automobile and computer manufacturing industries and has developed a relatively complete industry chain and industrial layout of civil aviation, such as the R&D center of Zhangjiang, COMAC, CAAC, and Aviation Industry Group. Electrical machinery, instrument, and meter manufacturing industries have a high concentration degree in Jiangsu Province, and these industries belong to the traditional heavy chemical and equipment industries. Zhejiang Province mainly focuses on railway, aerospace, and general manufacturing industries, which reflect that Zhejiang Province has made full use of geographical resources to develop key advantageous industries. Alsp, Hefei is the best developed city in Anhui Province, with a number of leading enterprises in AI industry, such as iFLYTEK and Xinhua.

3. Analysis on the Agglomeration Effect

On the basis of the analysis of the present situation of agglomeration, many scholars have carried out further extended research. To cultivate new momentum for economic growth, the YRDUA should pay more attention to the agglomeration effect of high-end manufacturing industries [12]. Xu and Wang [13] believe that the positive synergistic effect of manufacturing agglomeration and technology introduction has a weak negative impact on green innovation performance. Liang and Cong [14] found that the effect of manufacturing agglomeration on the growth of total factor productivity in central cities was not obvious. In this paper, CES production function is selected to quantitatively measure the agglomeration effect of each subdivision of equipment manufacturing industry in the YRDUA, thus to find the change of its agglomeration effect from 2006 to 2016 and judge the agglomeration effect of equipment manufacturing industry in the region.

TABLE 3: The main regional distribution of equipment manufacturing industry.

Industry code	Main regional distribution (agglomeration degrees)
C33	Wuxi (1.14), Nantong (1.13), Zhenjiang (1.02), Taizhou (Jiangsu province) (1.93), Zhoushan (2.47), and Ma'anshan (1.05)
C34	Shanghai (1.49), Nantong (1.04), Yancheng (1.42), Huzhou (1.05), Hefei (1.43), Tongling (1.03), and Anqing (1.07)
C35	Shanghai (0.79), Taizhou (Jiangsu province) (0.97), Yancheng (0.84), and Yangzhou (0.88)
C36	Shanghai (2.25), Nanjing (1.16), Yancheng (1.08), Shaoxing (1.07), and Tongling (1.46)
C37	Taizhou (Jiangsu province) (2.21), Taizhou (Zhejiang province) (10.96), and Hefei (1.21)
C38	Wuxi (1.23), Changzhou (1.46), Nantong (1.34), Yangzhou (1.72), Zhenjiang (1.38), Taizhou (Jiangsu province) (1.05), Hangzhou (1.01), Shaoxing (1.02), Jiaxing (1.16), Ma'anshan (1.93), and Tongling (1.65)
C39	Shanghai (1.70), Nanjing (1.24), Suzhou (2.22), and Hefei (1.14)
C40	Shanghai (1.03), Nanjing (1.82), Nantong (2.89), Yancheng (1.07), Yangzhou (3.18), Zhenjiang (2.47), Taizhou (Jiangsu province) (1.4), Hangzhou (1.45), Ningbo (1.17), and Hefei (1.35)

Geographical concentration
C33

0.09 – 0.13   0.86 – 1.14
0.14 – 0.58   1.15 – 2.47
0.59 – 0.85

(a)

Geographical concentration
C34

0.06 – 0.37   0.94 – 1.07
0.38 – 0.73   1.08 – 1.49
0.74 – 0.93

(b)

Geographical concentration
C35

0.07 – 0.27   0.56 – 0.72
0.28 – 0.40   0.73 – 0.97
0.41 – 0.55

(c)

Geographical concentration
C36

0.08 – 0.29   0.85 – 1.46
0.30 – 0.55   1.47 – 2.25
0.56 – 0.84

(d)
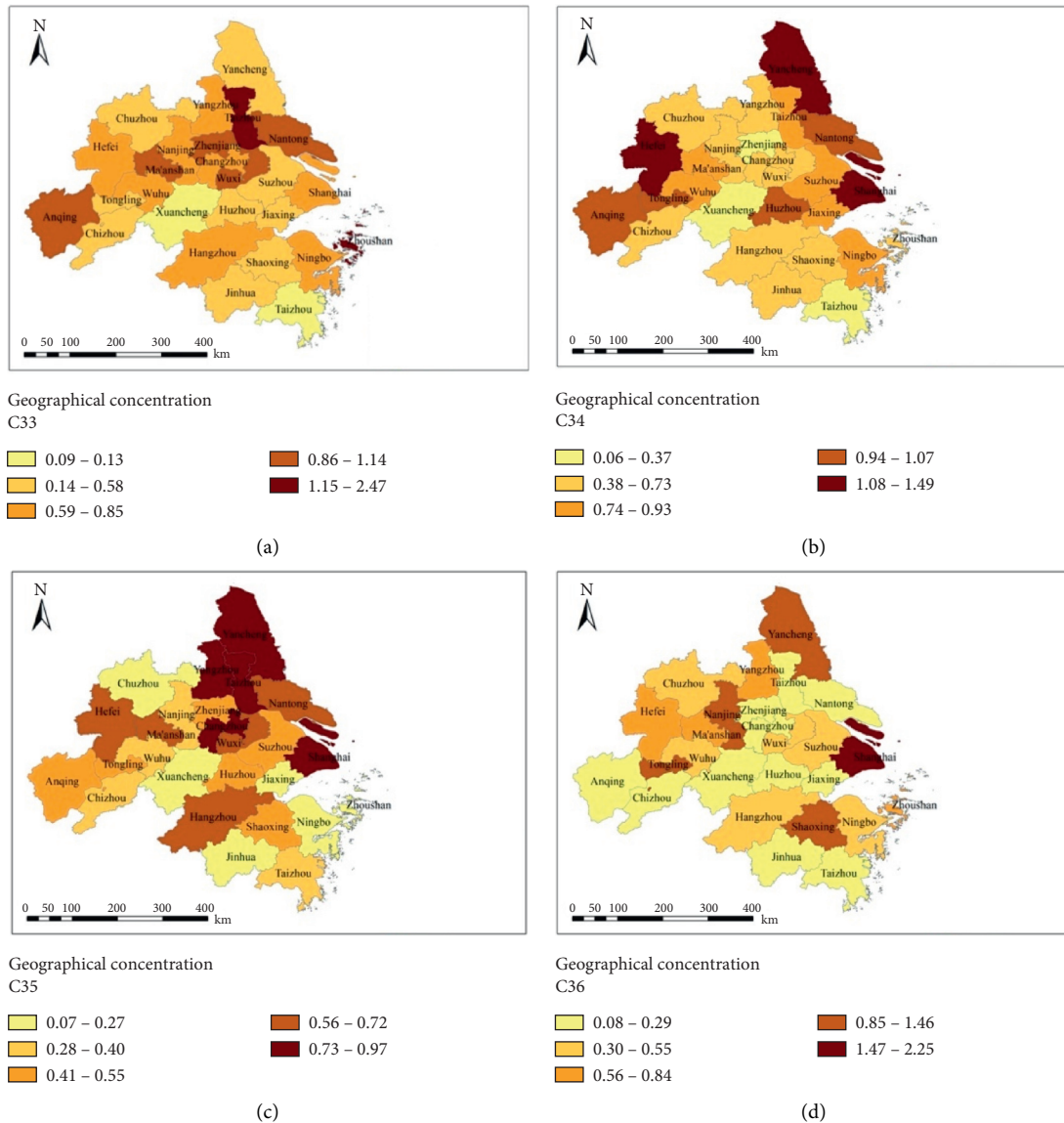
FIGURE 2: Continued.

(e)

(f)

(g)

(h)
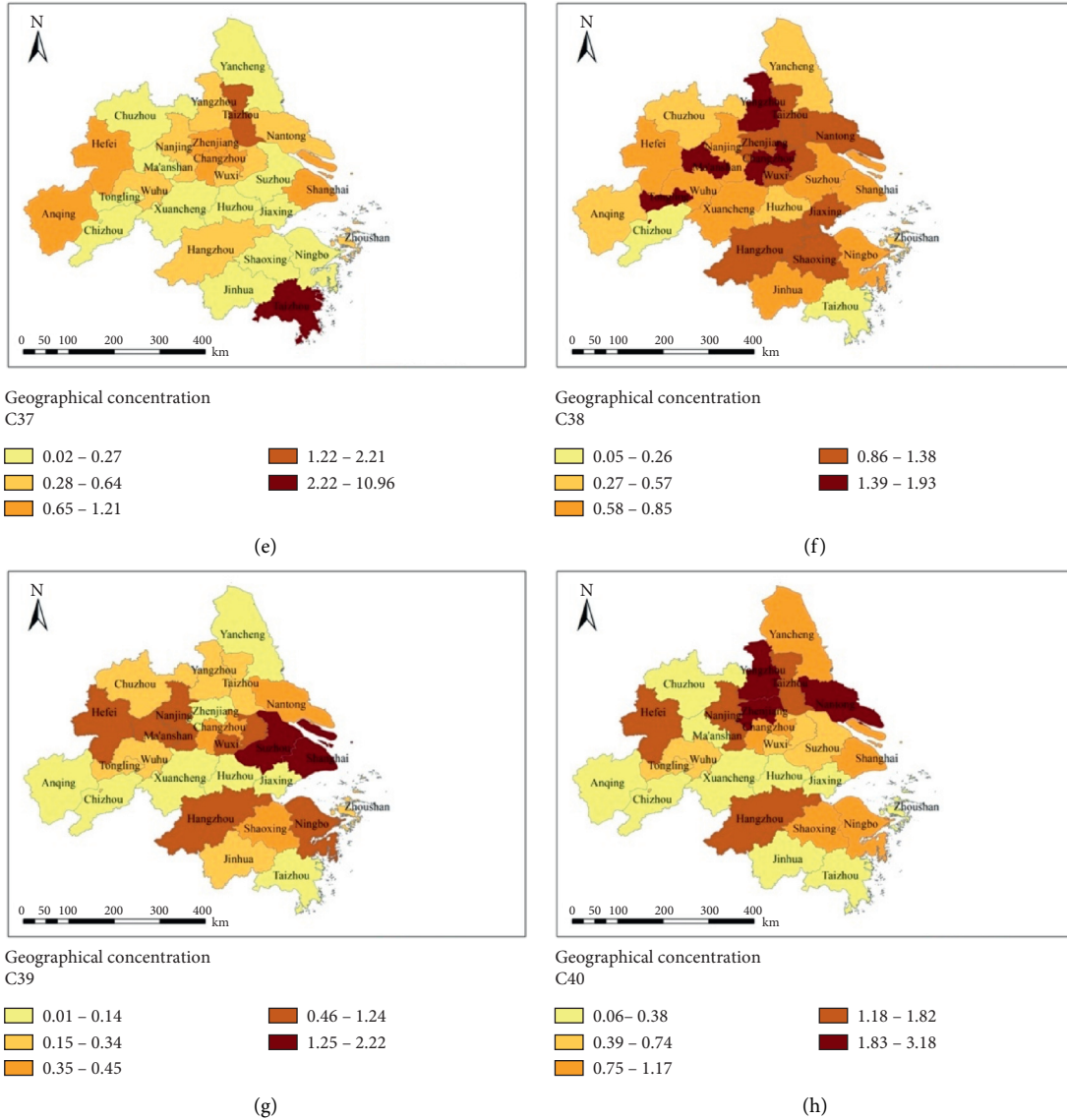
Figure 2: The distribution of equipment manufacturing industry by geographical concentration.

3.1. Measurement Methods. The production function is selected to measure the agglomeration effect of eight equipment manufacturing industries in the YRDUA (represented by H), where P represents the profit earned by the industry, Q represents the total production value of the industry, K represents the net value of fixed assets of the industry in a certain year, β represents the profit elasticity of output, and γ represents the profit elasticity of fixed assets occupation. See equations (3)–(5) for details.

$$W = AQ^{\beta}L^{\gamma}, \tag{3}$$

$$P = AQ^{\beta}K^{\gamma}, \tag{4}$$

$$h = \frac{(1 + \gamma)}{(1 - \beta)}. \tag{5}$$

3.2. Data. According to the relevant data selected from China Industrial Economy Yearbook, from 2006 to 2016, and Statistical Yearbook of Shanghai, Jiangsu, Zhejiang, and Anhui, the total industrial output value, total profit, and net fixed assets of the equipment manufacturing industry can be obtained. Additionally, the country began to adopt the new GB/T4754-2011 since 2012, so the automobile manufacturing industry, railway, ship, and aerospace and other transportation equipment manufacturing industries are merged into the transportation equipment manufacturing industry to unify the caliber.

3.3. Analysis. In this paper, the logarithm of both sides of the equation $P = AQ^{\beta}K^{\gamma}$ is taken to obtain the following function:

$$LnP = LnA + \beta LnQ + \gamma LnK. \tag{6}$$

TABLE 4: H value of equipment manufacturing industry.

Industry code	Year						
	2006–2010	2007–2011	2008–2012	2009–2013	2010–2014	2011–2015	2012–2016
C33	2.149	−6.329	−2.520	−3.982	6.029	9.184	5.984
C34	−3.179	−0.880	−0.464	−1.287	5.081	8.111	23.817
C35	2.148	−5.400	−1.522	−1.791	2.291	2.863	9.002
C36 & C37	−0.499	−0.444	−0.206	−0.268	-0.543	−0.554	−1.458
C38	2.501	1.572	−9.195	11.066	5.364	−10.117	−3.388
C39	−0.623	−3.217	−1.209	−0.657	−0.848	−0.772	−0.834
C40	−32.896	−0.453	−0.632	−3.299	−19.963	20.654	−2.602
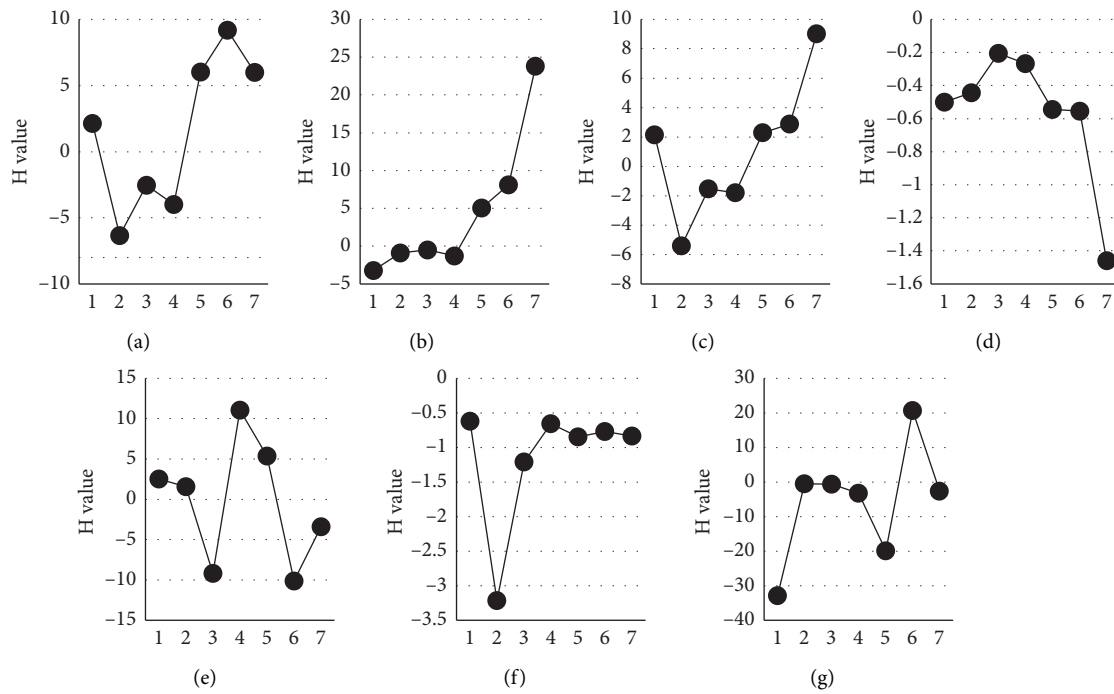
FIGURE 3: H value broken line of the agglomeration effect of equipment manufacturing industry. (a) Regression measurement time span of C33. (b) Regression measurement time span of C34. (c) Regression measurement time span of C35. (d) Regression measurement time span of C37. (e) Regression measurement time span of C38. (f) Regression measurement time span of C39. (g) Regression measurement time span of C40.

This model is based on the panel data from 2006 to 2016. LnP is taken as the dependent variable since the time span is only 11 years. LnQ and LnK are taken as the variables to carry out a 5-year moving regression. H value can be obtained from the values of β and γ. The results are shown in Table 4.

H value can be calculated from the following equation:

$$h = \frac{(1 + \gamma)}{(1 - \beta)}. \tag{7}$$

When H value is greater than or equal to 1, it indicates that the whole industry has agglomeration effect. The higher the value, the greater the agglomeration effect. When H value is less than 1, it indicates that the agglomeration effect of the whole industry is relatively low. The H value broken line of equipment manufacturing industry in the YRDUA is shown in Figure 3.

According to the abovementioned calculation results, we can know that, first, only general-purpose, special-purpose, and metal manufacturing industries have an obvious agglomeration effect. As can be seen from Figure 3, the general specialized and computer manufacturing industries whose H value keeps increasing but has not yet reached the highest point. Among them, the general equipment manufacturing industry has the most distinct agglomeration effect and has been showing an increasing trend, reaching 23.82 during 2012–2016.

After experiencing the low point from 2007 to 2011, the agglomeration effect of the manufacturing industry of special equipment gradually ascended and reached 9.02. However, although the agglomeration effect of communication equipment manufacturing industry dropped to the lowest level from 2007 to 2011, it quickly picked up and gradually increased, and finally, the increase tended to be flat

and the H value was always less than 1, indicating that the agglomeration effect is uneconomical.

Second, the H value in the metals, transportation, electrical and equipment, and instrument and instrumentation industries passed the peak but has been declining among them; the metal products industry began to pick up significantly from the initial continuous decline to 2009 and reached the highest point in 2015. Although the metal products industry was in a downward trend from 2012 to 2016, its H value kept more than 1, so its agglomeration effect is economical. On the whole, the agglomeration effect of electrical and machinery manufacturing industry is in a downward trend. Although there was a significant increase from 2009 to 2013, it still cannot stop the decline in the later period. The manufacturing industry of transportation equipment has been in a downward trend from 2008 to 2016, with the lowest value of −1.47. The overall trend of the instrument and instrument manufacturing industry is upward. Despite that there was a decline in the middle period, the decline range was significantly reduced, and it reached the highest point of 20.65 during the period from 2011 to 2015.

4. Conclusions

Based on the geographic concentration index and production function, this paper obtained the agglomeration level and effect of equipment manufacturing industry in the YRDUA and, thus, drew the following conclusions:

(1) The equipment manufacturing industry in the YRDUA has a complete category with the high level of geographical agglomeration, but the decline trend is more noticeable. This shows that as the region with the fastest economic growth and the strongest manufacturing base in China, the YRDUA has highly attracted a large number of equipment manufacturing enterprises to set up factories and develop here. In particular, computer, automobile, and electrical machinery and equipment manufacturing industries, which together account for about 80% of the geographical concentration of equipment manufacturing industry, are the main body of equipment manufacturing industry in the YRDUA and also the three key development industries. However, with the development of old industrial bases such as Northeast China being favored by the policy support, the competitiveness of equipment manufacturing industry in the YRDUA has obviously declined.

(2) The YRDUA has formed an agglomeration pattern of equipment manufacturing industry, with Shanghai as the core and Hefei, Hangzhou, Suzhou, and Nanjing as the auxiliary cities. For example, automobile and computer manufacturing industries are most concentrated in Shanghai, and Hefei is focused on AI industry, while electronic machinery and measuring instrument have the highest concentration in Suzhou and Nanjing. Along with respective advantages and resources, they have developed the characteristic and specialized industries.

(3) The overall agglomeration effect of the equipment manufacturing industry in the YRDUA is relatively distinct, but it has been on a downward trend. The decline rate tends to be stable until 2014, which is similar to the trend of the agglomeration degree. In addition, the agglomeration effect of traditional equipment manufacturing industry shows an upward trend, indicating that industrial upgrading and continuous technological innovation have greatly enhanced the competitiveness of traditional equipment manufacturing industry in the YRDUA. Although the agglomeration effect of high-end equipment manufacturing industry is not obvious, its development speed is gradually accelerating.

According to abovementioned analysis, we can find that some of the reasons for current agglomeration status are the insufficient integration of industrialization and informatization, the weak technology innovation abilities, unreasonable industrial structure, the overcapacity of the traditional equipment manufacturing industry, the large proportion of capital-intensive manufacturing industry, and the small proportion of technology-intensive manufacturing industries in the YRDUA which all those problems which need to be addressed.

5. Suggestions

Recently, China positioned the YRDUA as a world-class center for equipment manufacturing industry. Aiming at such vision, our suggestions are as follows.

First, innovation is the driving force for the development of the equipment manufacturing industry. By increasing investment in scientific research funds and encouraging independent research and development of key technologies and accelerating the transformation of research achievements from samples to products and then to commodities, the total factor productivity of the equipment manufacturing industry can be improved and the traditional equipment manufacturing industry can be promoted to the high end of the value chain accordingly.

Second, structural adjustment is the key point of the development of the equipment manufacturing industry. By focusing on the key areas of the equipment manufacturing industry, speeding up the integration of new technologies and new materials, such as information and intelligence, into the traditional manufacturing industry, and reducing ineffective and low-end supply could be the solution for this issue.

Third, the effective diffusion of the agglomeration effect of equipment manufacturing industry in the YRDUA should be improved. Optimizing the regional layout of equipment manufacturing industry can contribute to regional agglomeration quality. Shanghai has put forward the "Industrial Map" to improve the level of intelligence, promote the application of new materials and new equipment, and establish a number of characteristic and specialized high-end equipment demonstration projects in accordance with the industrial advantages of each region.

Data Availability

The data that support the findings of this study are available from the corresponding author upon reasonable request.

Conflicts of Interest

The authors declare that they have no conflicts of interest.

Acknowledgments

References

[1] Z. Gao and Z. G. Lu, "An empirical study on the industry convergence of level of equipment manufacturing industry and High-tech service industry based on system coupling theory," *Journal of Systems Science*, vol. 2, pp. 63–68, 2019.

[2] Y. M. Chang, "Strategic types and spatial distribution of equipment manufacturing industry in China's urban agglomeration," *Exploration of Economic Problems*, vol. 11, pp. 76–81, 2016.

[3] J. Y. Lin, X. X. Yu, and J. Chen, "Study on competitiveness of equipment manufacturing industry in Yangtze River Delta," *East China Economic Management*, vol. 9, pp. 18–24, 2011.

[4] W. X. Xu, X. J. Zhang, and C. J. Liu, "Spatial distribution pattern and influencing factor of manufacturing enterprises in the Yangtze River Delta. Scale effect and dynamic evolution," *Geographical Research*, vol. 5, pp. 36–52, 2019.

[5] S. S. Rosenthal and W. C. Strange, "The determinants of agglomeration," *Journal of Urban Economics*, vol. 50, no. 2, pp. 191–229, 2001.

[6] P. Krugman, "Increasing returns and economic geography," *Journal of Political Economy*, vol. 99, no. 3, pp. 483–499, 1991.

[7] D. B. Audretsch and P. M. Feldman, "R & D spillover and the geography of innovation and production," *American Economic Review*, vol. 86, pp. 630–640, 1996.

[8] K. Lin and Z. M. Zhu, "Manufacturing concentration and its effect on regional economic growth in China's northwest areas: an example of Gansu Province," *Soft Science*, vol. 11, pp. 43–46, 2008.

[9] N. Y. Xu and Q. Chen, "Research on Spatial agglomeration measure and dynamic evolution of Chinese manufacturing enterprises," *Statistics and Decision*, vol. 7, pp. 122–126, 2019.

[10] Z. J. Sun and Y. Q. Zhang, "The spatial-temporal evolution features of. high-tech manufacturing industry's agglomeration level in China: the empirical research based on spatial statistical standard deviation ellipse," *Science & Technology Progress and Policy*, vol. 9, pp. 54–58, 2018.

[11] G. Ellision and E. L. Glaeser, "Geographic concentration in U. S. manufacturing industries: a dartboard approach," *Journal of Political Economy*, vol. 105, no. 5, pp. 889–927, 1997.

[12] L. Wang, Y. Xue, M. Chang, and C. Xie, "Macroeconomic determinants of high-tech migration in China: the case of Yangtze River Delta urban agglomeration," *Cities*, vol. 107, Article ID 102888, 2020.

[13] J. Z. Xu and M. M. Wang, "Manufacturing agglomeration, technological progress and green innovation performance: an empirical analysis based on China's provincial panel data," *Science and Technology Progress and Countermeasures*, vol. 3, pp. 1–8, 2019.

[14] J. Liang and Z. N. Cong, "An empirical study on industrial agglomeration and total factor productivity of central cities: concurrently based on the impact of urban hierarchy," *Urban Development Studies*, vol. 12, pp. 45–53, 2018.

Research Article

Automatic Data Collecting and Application of the Touch Probing System on the CNC Machine Tool

Zhi Tang,[1,2] Xinyu Jiang ⓘ,[2] Wenliang Zi,[2] Xin Shen,[2] and Die Zhang[2]

[1]*Shanghai International Fashion Innovation Center, SIFIC, Shanghai 201620, China*
[2]*College of Mechanical Engineering, Donghua University, Shanghai 201620, China*

Correspondence should be addressed to Xinyu Jiang; jiangxinyu@dhu.edu.cn

For realizing automatic data collecting of the touch probing system on the CNC machine tool and practicing the application technology of big data from the CNC machining process, a special NC program was developed on the Siemens 840D SL controller to record data with a defined text format, and they were uploaded onto the host computer automatically. With the help of DB management software in the host PC, data obtained were sent into the MES database regularly, and then automatic data collecting of manufacturing process information was realized. With the big data technology, three applications based on big data technology have been listed. They are duo active error detection on the probing system, geometrical accuracy monitoring, and management of the cutting parameter and tool life. Tests of cutting on the platen of an injection molding machine with a PAMA SR3000 floor-type CNC boring-milling machine proved that the new technology achieves its design objectives.

1. Introduction

The "Made in China 2025" strategy was promulgated, clarifying that China will transform from a major manufacturing country to a manufacturing power [1]. According to the implementation guidelines, the machinery manufacturing industry takes the lead in the three aspects of strong foundation, environmental protection, and integration and strives to make breakthroughs in the three directions of talent training, information application, and service-oriented model construction [2]. In recent years, in the communications, transportation, white goods, and other industries, domestically made industrial products have successfully entered the international market, which proves our progress in the field of mid-end CNC machine tools and processing technology [3, 4]. To develop higher-end areas of the manufacturing industry, at the R&D side, we need to do a good job of matching with actual needs to ensure accurate targets. On the application side, we must upgrade equipment and technology; integrate software and hardware technology; and improve technology and management capabilities.

In the published 'Made in China 2025' strategy, China clarified that it would change from the big manufacturing country to a strong one. According to the implementation guideline, three aspects of enhancing basic technology, environment protection, and technology combination must take the lead in the machinery industry, and breakthrough in education, information, and building up of service mode are expected. For developing the higher-level manufacturing industry, the exact target of R&D must be set according to the real demand. Upgrade of equipment and process capability, combination of software and hardware, and improvement on technical and general management must be implemented for supporting the application.

An increasingly complex production process is accompanied by huge comprehensive information, covering environment, equipment comprehensive accuracy, tools, technology, efficiency, quality, etc. Disposing of this information with efficient management and technical means will help achieve the ideal high-end CNC machining [5, 6]. In view of actual problems, the research process information is analyzed, and appropriate decisions are made. In the discipline of quality management, this methodology is called

process quality control [7]. The application of digital technology can realize the digitization of the processing process. The application of big data technology can intelligently select and effectively process from massive information, visually display the key points, and guide technology and management to make correct decisions with the most scientific basis [8].

Daily production process is becoming more and more complex that reflects from a big pack of information consisting of environment, equipment accuracy, tools, process, efficiency, quality, and so on. Once the information is efficiently managed with proper technology, the higher-level machining production is achievable. In the study of quality management, process quality control was defined as analyzing and researching process information and making appropriate decisions. With the help of digital technology, detailed process information from production can be collected and stored in a database. Then, the 'big data' technology will study the database for working out some scientific algorithms that can sort out, visualize the essential problems, and provide solutions.

A trigger probe is advanced digital measurement equipment that is commonly used in high-end CNC machine tools and flexible manufacturing systems (FMSs). The native natural digital feature can support the acquisition of data about quality and process from production. Based on software, the probe can measure the point position information on the workpiece in the machine tool and calculate the relevant quality data. Because the measuring environment and conditions are completely the same as manufacturing, the error and deformation caused by the secondary clamping are avoided, and the root cause of the deviation is easy to find out. Compared with the traditional measurement, the measuring process of the trigger probe is controlled by the numerical control system, and the accuracy and efficiency are greatly improved [9]. Many scholars have done research on the measurement and accuracy compensation method of the trigger probe. Zhu [10] developed a measurement software system that automatically selects measurement points, programs, executes, and returns the result data based on the STL model data. Literature studies [11–14] compensated the errors of different contact points on the spherical surface of the trigger probe through a new method and comprehensively improved the theoretical measurement accuracy. It is found in practical applications that most of the measurement errors are based on systemic reasons. The system accuracy of a machine tool could be affected by many factors, and it is difficult to find, trace, and repair immediately, so the method of studying the error of the trigger probe itself is too limited. Ihara [15] thoroughly studied the advantages and disadvantages of the in-machine measurement system, but it lacks practicality for production. Zhou et al. [16] proposed a new in-machine measurement logic based on actual production requirements, but did not introduce how to implement it. In continuous production, in order to reduce quality risks, find errors on time, identify causes, and work out strategy to solve the problem, a fast and effective complete application solution is required, and long-term monitoring technologies and mechanisms are required.

Based on the characteristics and actual needs of CNC machining, this article uses the log recording and process data sharing functions in the Siemens 840D SL CNC system. By compiling a special NC program, the measurement data from the probe are recorded with a standardized format and automatically uploaded onto the host computer. When the data are continuously saved into the MES database through database management software, a simple manufacturing process information collecting system was built up. With the help of big data technology to identify, process data will be filtered, sorted, and analyzed, and then three important technical applications of trigger probes in CNC machining and production are realized:

(1) Using the probe's ideal reasoning method, the working principle of the trigger probe and the root cause of the error are analyzed, the result-oriented double-effect active probe error monitoring logic is put forward, and the data rules are defined. With the help of standard measuring tools in the machine tool or running a cross-measurement program on the workpiece, the data could be automatically compared, and measurement errors can be found.

(2) When the probe accuracy is reliable, the principles, manifestations, and failure modes of common errors are sorted out according to machine tool accuracy knowledge, and they are converted into three levels of data rules and mapping logic. By selecting the appropriate measurement data and importing them into the computer, the manifestation and principle of the error can be calculated in reverse according to the conditional formula, which can guide the daily maintenance of equipment.

A three-step mapping logic with formulations can be set up based on the knowledge of machine tools such as error type, behavior, and sample case. When the accuracy of the probe is reliable, once proper measuring result is input into the computer, cases can be processed back through behavior to get the error type which is helpful for daily maintenance work.

(3) According to the real demand of key process, a set of testing process parameter is obtained based on the reference data from tool manufacture and supplement by orthogonal test method. After screening and processing the data, a mathematical model of dimensional results under different process parameters can be established. The mathematical model contains important data on the quality of the machining process. With the help of visual data technology, process research and tool life management become much easier and can be done actively.

2. Data Acquisition and Digital Manufacturing Information System

2.1. Regulation of the Data Format. A neat data format is the basis for communication. The Siemens 840D SL CNC

provides simple programming in a high-level language that enables basic functions such as NC program jumping, data transformation, and mathematical calculation. According to the exact requirements from a database management system, data obtained in the process can be programmed into the target format. Figure 1 shows the NC program corresponding to the date and time format of a database. Figure 2 shows the execution result.

2.2. Saving and Uploading of Data. Due to the security requirements of the NC system, the NCU is not allowed to be read and written directly from the external device, and direct communication cannot be realized. This is also the reason why SCADA systems require independent communication modules and secondary development. Version 4.7 SP1, Siemens 840D SL CNC systems have added a 'Process Data Share' function, which enables simple NC programming to easily write data segments outward to a fixed text file at a specified address on the LAN, enabling a basic digital communication of machining data at a very low cost. In combination with some other programs in a computer, the digitization of measurement data is possible.

There are five steps to use the 'Process Data Share' function: ① add the authorization of read and write on the host computer for the machine controller through the network; ② add NCU drive paths to the machine to specify the target file to the network, mapping the target folder of the host computer through the network into the NCU configuration; ③ use the EXTOPEN loop to open the external file; ④ use the WRITE loop to write the data segment; and ⑤ use the EXTCLOSE loop to save and close the external file. The data upload is completed. The data upload is completed after it is written into the database by data management system on the host computer.

2.3. Construction of Data Acquisition and Digital Manufacturing Information Systems. Digital manufacturing information system is the system for planning, executing, monitoring, and reviewing of production activities, which are realized with data input, collection, processing, and judging. In today's interconnected world, collecting a large amount of data based on SCADA modules is not difficult, but still expensive. The digital application of the probe requires only a simple information system. There is no reduction in structure to the common solution, just a simplification of the amount of information to be transmitted and the method of collection. The advantage on cost saving is significant.

As shown in Figure 3, the system consists of a CNC machine, information system, and interactive system. By running the NC program cycle, the CNC machine saves the information and data as the text file and transfers it to the buffer area temporarily. Afterward, the buffer area will be read and cleared in the database execution activity. The interactive system is the window for inputting, displaying, maintaining, and managing the information. It could be with different authorizations for reading and writing. Each of them also has a small buffer area for storing and transforming the instruction or data temporally. The information system consists of a buffer area, a database, and a library of executable instructions for receiving, storing

Figure 1: Time and date program format chart.

Figure 2: Time and date program results' chart.

temporarily, and sending the data. It also processes the requested instruction from the interactive system. The host computer in this paper is equivalent to the buffer area, which is used to store temporary data. The interactive system is generally developed autonomously and customized on demand.

3. The Function and Failure Mode of the Probe

3.1. The Structure and Function of the Probing System. A typical probe consists of three parts, the handle, the body, and the stylus, as shown in Figure 4. The tool holder is used to connect different standard CNC machine tool spindles with the probe body. The body is a housing with an industrial-grade environmental protection level. The inside is composed of power supplies, piezoelectric components (or on-off components), analysis circuits, and communications. The stylus is installed on the side facing the worktable and contacts the workpiece to complete the measurement action. The stylus has no special function. It is a rigid slender rod with excellent rigidity and thermal stability. The head of the stylus is a ruby ball head, with high geometrical accuracy, high hardness, and wear resistance which is not easy to deform.
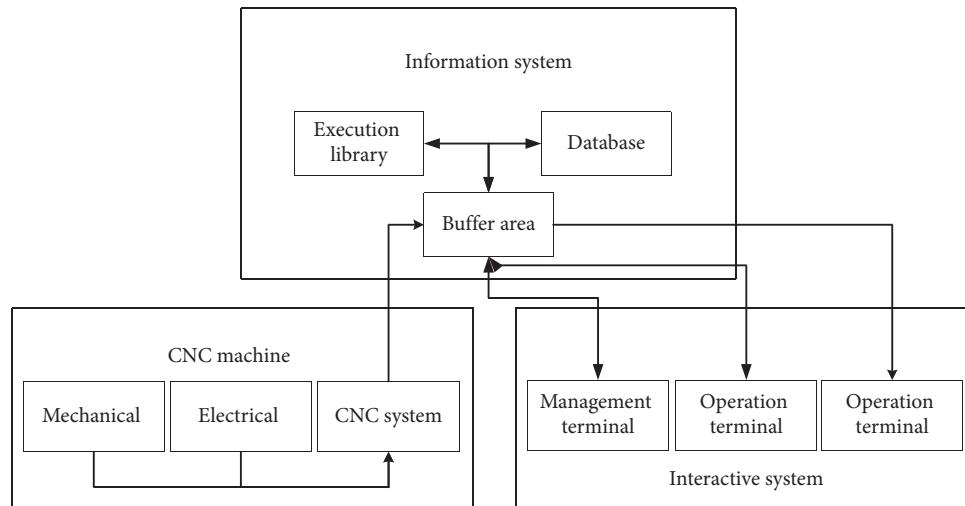
Figure 3: Diagram of the digital system.
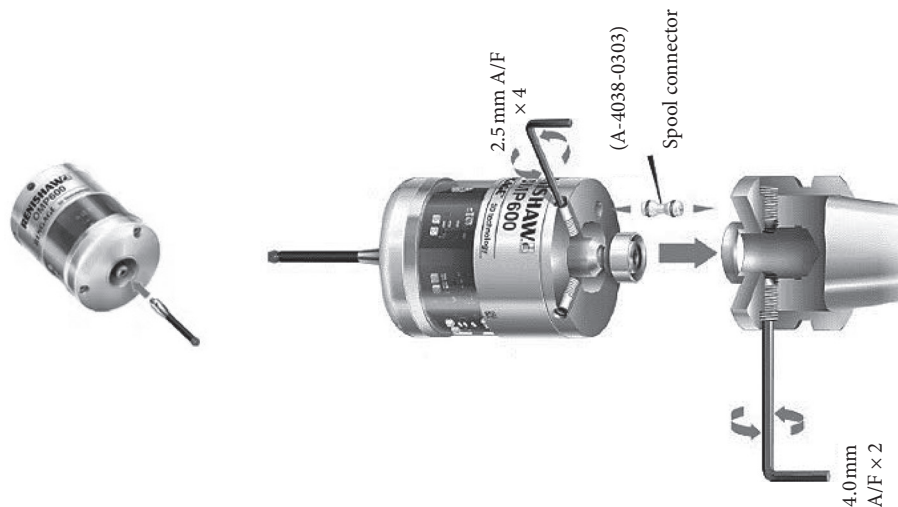
Figure 4: Structure diagram of the trigger probe.

On the machine tool, there is a dedicated communication system that is responsible for receiving real-time signals from the measuring head. The probe and the numerical control machine work together to realize the measurement function through program control. After the measurement cycle starts, the probe is activated by the program, and the analysis circuit is turned on. The probe first moves to the safety plane according to the speed and path specified by the program and then approaches the set position on the workpiece in the measurement mode. In the measurement mode, the stylus touches the object, causing the piezoelectric element (or on-off element) to produce displacement (or open circuit), which is sensed by the analysis circuit and then uploaded to the CNC machine tool by the communication circuit. The CNC system of the machine tool immediately records the current position, stops movement, and returns to the safety plane, and a complete typical measurement cycle ends here. The measurement result will be saved into the user variable, and the corresponding dimension data can be obtained by calculation, and the result beyond the tolerance value will be accompanied by an alarm.

Figure 5 shows the common two-dimensional measurement functions, and Table 1 lists the mathematical formulas they use. The user interface can be customized and developed according to actual needs. The parameters and syntax on different software platforms will be different, but the logic and mathematical principles are always the same.

3.2. Calibration and Failure Mode of Probe Accuracy. The electronic components in the probe body only have the function of determining contact and communication. The accuracy of the probe itself is manually calibrated during the initial installation before using first. As shown in Figure 6, when calibrating, first, the runout of the ruby ball head needs to be measured with a tool presetter or a dial indicator outside the machine. If there is an error of more than 5
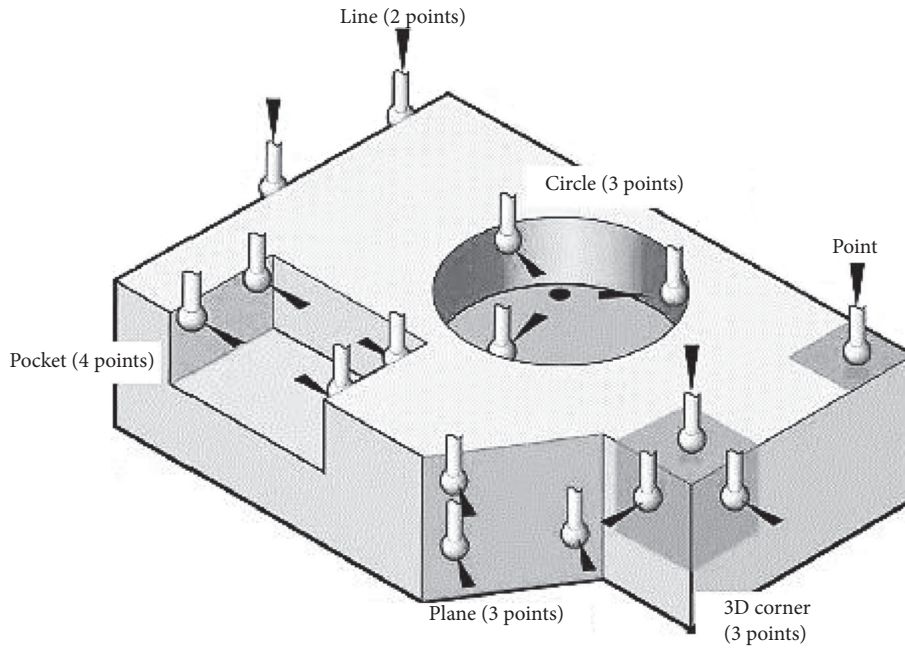
Figure 5: Diagram of commonly used measurement functions.

Table 1: Mathematical formulas.

Points	Data	Formula	Application
Point1	$P_1(x_1, y_1)$		Position
Point2	$P_1(x_1, y_1), P_2(x_2, y_2)$	$x_m = (x_1 + x_2)/2$ $y_m = (y_1 + y_2)/2$ $P_m(x_m, y_m)$	Midpoint
		$1 = \sqrt{(x_2 - x_1)^2 + (y_2 - y_1)^2}$	Length
		$k = (y_2 - y_1/x_2 - x_1)$	Slope
		$\theta = \arctan k$	Angle
Point3	$P_1(x_1, y_1), P_2(x_2, y_2), P_3(x_3, y_3)$	$k_{12} = (y_2 - y_1/x_2 - x_1)$ $k_{23} = (y_3 - y_2/x_3 - x_2)$ $k_{12} = k_{23}$	Collinear
		$\begin{cases} (x_1 - a)^2 + (y_1 - b)^2 = R^2 \\ (x_2 - a)^2 + (y_2 - b)^2 = R^2 \\ (x_3 - a)^2 + (y_3 - b)^2 = R^2 \end{cases}$ $O(a, b); R$	Center
Point4	$P_1(x_1, y_1), P_2(x_2, y_2), P_3(x_3, y_3), P_4(x_4, y_4)$	$x_{m13} = (x_1 + x_3)/2$ $y_{m13} = (y_1 + y_3)/2$ $x_{m24} = (x_2 + x_4)/2$ $y_{m24} = (y_2 + y_4)/2$	Radius
		$l_{13} = \sqrt{(x_3 - x_1)^2 + (y_3 - y_1)^2}$ $l_{24} = \sqrt{(x_4 - x_2)^2 + (y_4 - y_2)^2}$	Length
		$\begin{cases} (x_1 - a)^2 + (y_1 - b)^2 = R^2 \\ (x_2 - a)^2 + (y_2 - b)^2 = R^2 \\ (x_3 - a)^2 + (y_3 - b)^2 = R^2 \end{cases}$ $O_{123}(a_{123}, b_{123}); R_{123}$ $O_{124}(a_{124}, b_{124}); R_{124}$ $O_{134}(a_{134}, b_{134}); R_{134}$ $O_{234}(a_{234}, b_{234}); R_{234}$	Center radius

FIGURE 6: Probe error pattern diagram.

FIGURE 7: Error pattern diagram of the three-dimensional probe.

FIGURE 8: Single-point error mode diagram.

microns, the positioning bolt is adjusted to improve the runout to the target value. After the probe is installed in the machine, the calibration program is run to measure the ring gage to complete the parameter setting of the software compensation. For some applications that need to measure curved surfaces, development of more advanced three-dimensional compensation logic is needed [11–14].

The structure of the probe can theoretically maintain high accuracy for a long time, but some external factors in practical applications will make the probe accuracy slow or suddenly fail. Typical failure mode one is the accumulation of dirt on the taper hole of the machine tool spindle, and geometric and positioning errors appear after the installation of the taper shank of the probe. Typical failure mode two is that the processing environment has caused contamination on the ruby ball head of the probe, which directly caused the deviation of the measurement result. Regularly checking the accuracy of the probe can effectively reduce quality risks. The key is to find a convenient and effective method.

Both theory and practice tell us that, in two-dimensional measurement, the three-dimensional probe has only one failure mode, and it can swing with the rotation of the spindle angle, as shown in Figure 7, in micrometers.

4. Double-Effect Active Probe Error Monitoring

4.1. Manifestation of the 3D Probe. The 3D probe is the most commonly used type of probe. We set the 3D probe to the sphere center mode and took the deviation on 0° as the reference value for studying the actual influence from the offset-type deviation. By the ideal reasoning method, failure modes of commonly used measuring functions had been worked out.

Figure 8 shows the failure mode of a single-point measurement error. The measurement result is directly opposite to the direction of the probe error.
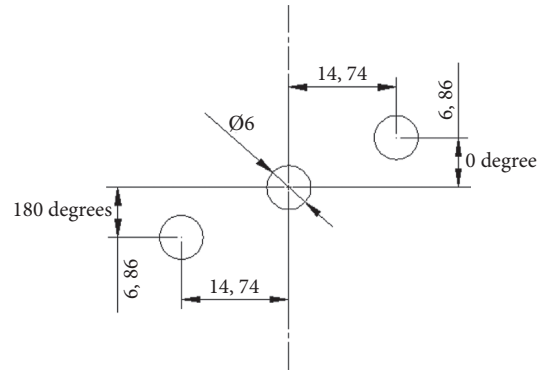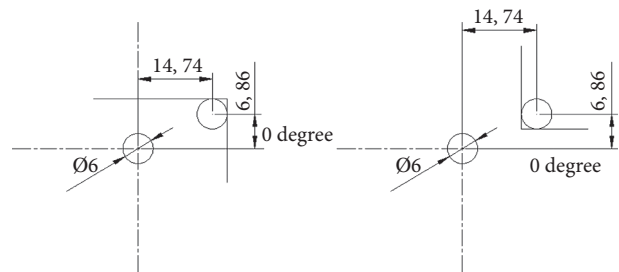
Figure 9 shows the failure form of the two-point measurement error. The result of the midpoint position is also directly opposite to the error direction, but due to the calculation principle, the application of measuring length, slope, and angle is not affected.

Figure 10 shows the failure mode of the three-point measurement error. The measured slope and radius are not affected, but the result of the center position is directly opposite to the error direction.

The failure form of the four-point measurement error is a combination of two-point measurement and three-point measurement. It is not affected when measuring dimensions such as groove width or radius, but the position results of the midpoint and the center of the circle are directly opposite to the error direction.

4.2. Monoprobe and Its Error Manifestation. The early electronic technology was not advanced enough and could only manufacture probes for unidirectional workpiece measurement. When the measuring direction changes, the spindle of the machine tool needs to be rotated for adapting. Later, with the development and application of probes, in order to measure the workpieces in different shapes, many special styles were derived, as shown in Figure 11. In today's Siemens machine tool system, monoprobe and its cycles remain, which greatly expands the possibilities of probe applications.

We used the same method to reason out the error manifestation of the monoprobe and obtained another set of results.
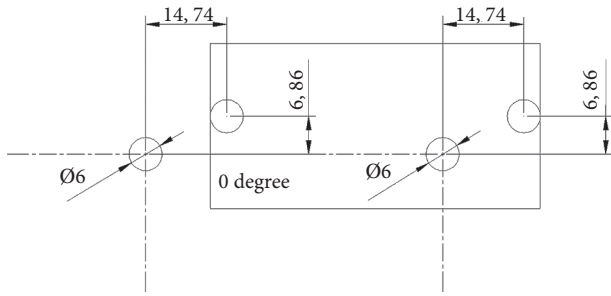
Figure 9: Two-point error pattern diagram.
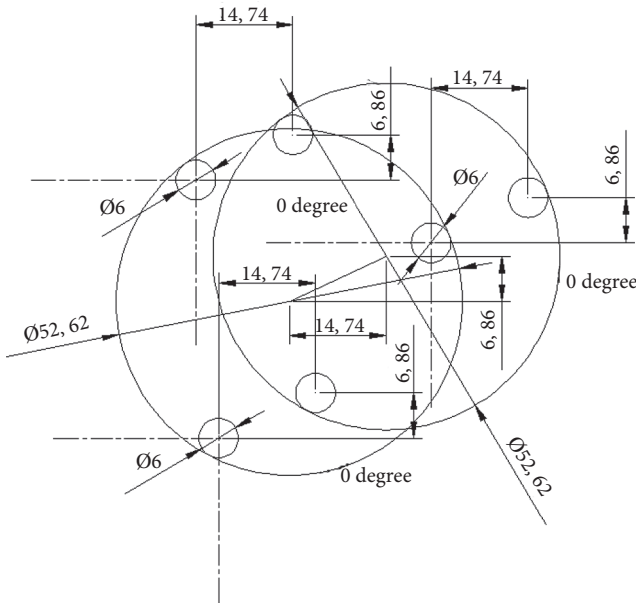
Figure 10: Three-point error pattern diagram.

Figure 11: Probe mode setting diagram.

Figure 12: Single-point error mode diagram of the monoprobe.
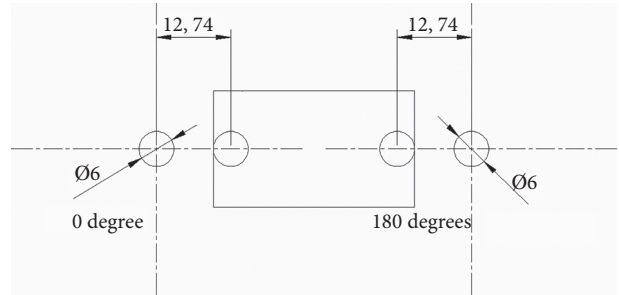
Figure 13: Two-point error mode diagram of the unidirectional probe.

Figure 12 shows the failure mode of the single-point measurement error; the measurement result is directly opposite to the direction of the probe error.

Figure 13 shows the failure mode of the two-point measurement error. When measuring the midpoint position, due to the 180-degree rotation of the monoprobe on the

spindle, the two deviations of the same magnitude but opposite directions counteracted, and the result was not affected. When measuring the length, the two errors are superimposed due to the 180-degree rotation of the spindle, and the result will be larger or smaller depending on the direction of the error. According to the calculation, the measurement results of slope and angle are not affected.

Figure 14 shows the failure mode of the three-point measurement error. The results of measuring the slope and the position of the center of the circle are not affected, but the result of the radius will become larger or smaller depending on the direction of errors.

The failure mode of the four-point measurement error is still a combination of two-point measurement and three-point measurement. The results of positions such as the midpoint and the center of the circle are not affected, but for dimensions such as groove width or radius, the results will become larger or smaller depending on the direction of the error.

4.3. Two Methods of Double-Effect Error Recognition. A monoprobe has the same specification as a 3D probe except the need of spindle orientation. The 3D probe can work in two modes, respectively. Based on the 840D SL numerical control system, the 3D probe is allowed to be used with two modes, respectively. We have compiled the characteristics of measurement errors from each mode as shown in Table 2. Through reasoning, we obtained a complementary logic, that is, using two probe modes on one 3D probe that can eliminate or monitor probe errors. Furthermore, in Table 2, the complementary items of each measurement function are marked in different colors.
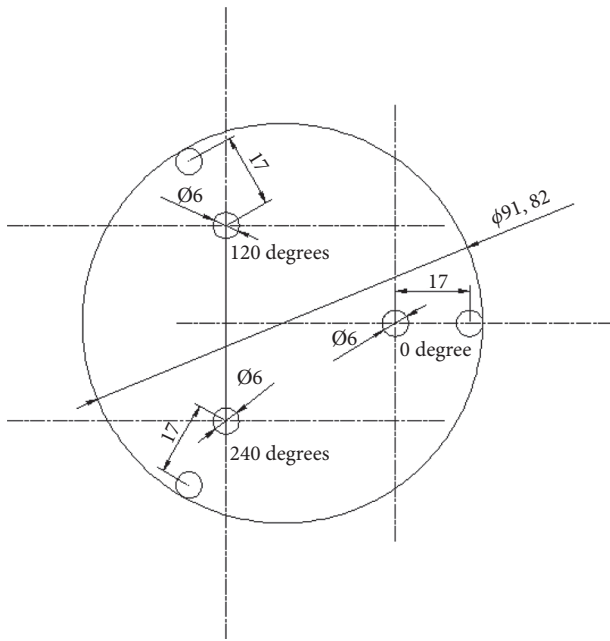
FIGURE 14: Three-point error mode diagram of the monoprobe.

Double-effect error recognition means that the error can be collaboratively judged based on the real-time measurement results or long-term monitoring data analysis. According to the principle of the probe error, we designed two methods to identify error occurrence. Both methods use the important conclusions in Table 2, which are simple in logic and with practical significance. The first method focuses on theoretical application and is suitable for small species and large-scale processing. As shown in Figure 15, when the machine tool table has enough free space, we fix a high-precision ring gauge with antirust performance on one side of the table and use the probe to measure the position of the three linear axes of the machine tool, X, Y, and Z. Comparing the real-time measurement result with the standard value saved during the acceptance of the machine tool, it can be judged whether the positioning accuracy of the machine tool has deviated. The second method is to verify the accuracy of the machine tool with the finishing features of the part itself. As shown in Figure 16, one can choose the position of the workpiece surface or plane or fine boring, and more consideration is given to the production characteristics of multivariety and small-batch parts, but the application technology capabilities of the probe are higher.

4.4. Establishment of the Error Recognition Logic. According to the two conclusions mentioned above about the principle of the probe error and inference method of the error source on the machine tool, we have, respectively, formulated the program logic of the two methods, as shown in Figures 17 and 18. Based on actual production requirements, both logics have set up two modes for normal processing or monitoring. During continuous

production or when it is inconvenient to stop and adjust, the normal processing mode is used to perform the measurement with maximum efficiency, or the monitoring mode is used to ensure that the probe is always in the normal accuracy state.

4.5. Establishment of the Data Output Format. In order to achieve continuous data recording, we need to define the standard format of the measurement log, which is a necessary tool for the host computer to collect data. According to actual needs, we have defined a data record table, as shown in Table 3. After setting a proper update frequency for the data, a simple API was realized. Information is collected and recorded to the database at a higher frequency on the host computer, and the data collection is completed.

According to the data format requirements in Table 3, each group of data in the output form has 9 rows, and each row consists of 4 groups of characters and 3 groups of floating-point numbers, which are convenient for later maintenance and expansion. According to the first measurement logic, we installed a ring gauge on the machine tool table. In the factory setting, the diameter of the ring gauge is 80.393 mm, and the distance between the center of the ring gauge and the mechanical origin of the machine tool is 300 mm in both X-axis and Y-axis directions. This set of data will appear in the first row of data. Using measurement cycle 977, the result parameters are diameter_OVR [4], center X-axis position_OVR [5], and center Y-axis position_OVR [6]. This set of data is stored in the second, third, and fifth rows. In order to test the program, three result parameters are preassigned, and three production information data are also predefined.

4.6. Output and Upload of Probe Measurement Results. The NC program used to output the specification log is very long. Figures 19 and 20 show the whole paragraphs. Figure 21 shows the result of executing the complete output program, and the format is as expected. The text interval adopts tabs, which can be read by database management software of the host computer. If people use VB or C-language to develop a program that automatically writes data to the database, the same effect can be achieved.

5. Machine Tool Geometric Accuracy Monitoring

5.1. Machine Tool Accuracy System. The precision system of CNC machine tools is realized with both mechanical hardware and NC control software. Hardware such as machine bed is responsible for geometric-related accuracy. Transmission system and software are responsible for positioning accuracy, which is possible to compensate the geometric deviation dynamically a little. Different types of machine tools are different in structure, but the principle of precision is the same. Figure 22 is a structural

Table 2: Error characteristics' table under two probe modes.

Point	Model	Position (center)	Midpoint	Length	Slope	Angle	Radius
Point1	Unidirectional	N					
	Multidirectional	N					
Point2	Unidirectional	Y		N	Y	Y	
	Multidirectional	N		Y	Y	Y	
Point3	Unidirectional	Y			Y	Y	N
	Multidirectional	N			Y	Y	Y
Point4	Unidirectional	Y	Y	N			N
	Multidirectional	N	N	Y			Y
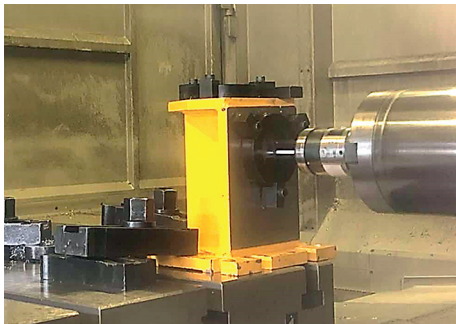
Figure 15: Measuring X-, Z-, and Y-axis position diagram.

Figure 16: Measuring the workpiece itself.

diagram of a typical floor boring and milling machine, and the research in this section is mainly carried out around it.

Cutting and online measuring in a CNC machine tool are based on the same accuracy system, so the study of measurement errors must start with the machine tool accuracy system. As the principle basis of this research,

Figure 23 lists the uncertainty of machine tool operation with classification.

5.2. Evaluation Method of Machine Tool Accuracy. The accuracy of the machine tool consists of three parts: positioning, geometry, and dynamics. Positioning accuracy describes the accuracy of the machine tool moving to a predetermined position on each axis, which is determined by the manufacturing and assembly accuracy of the transmission system. It uses positioning deviation Pa, reverse error U, positioning distribution domain Ps, and positioning uncertainty P, the 4 metrics to describe. The industry mostly adopts the German VDI 3441 [17] standard, which is the most rigorous and reliable compared to Japanese and American standards. The geometric accuracy refers to the state of the geometrical condition referring to each axis direction, which is determined by the manufacturing and assembly accuracy of the machine bed components. According to single-axis and multiaxis correlation, it can be evaluated with straightness, perpendicularity, parallelism, circular runout, and other items. The geometric accuracy is described in detail in the ISO 230-1: 2012 [18] standard, and GB/T 17421.1-1998 [19] is equivalent. Dynamic accuracy is a comprehensive manifestation of machine tool motion performance and stability based on positioning accuracy and geometric accuracy. GB/T 17421.3-2009 [20] specifies the thermal stability evaluation method, GB/T 17421.4-2016 [21] specifies the profile evaluation method, GB/T 17421.5-2015 [22] specifies the noise evaluation method, and GB/T 16768-1997 [23] specifies the vibration evaluation method. Many factors in these standards comprehensively constitute the dynamic accuracy of the machine tool.

After the machine is set up and handed over, the manufacturer will provide a complete acceptance accuracy report. In daily maintenance, the actual accuracy of the machine tool is compared with the acceptance accuracy. If the two are different, the machine should be stopped, and adjustment is needed to avoid quality accidents.
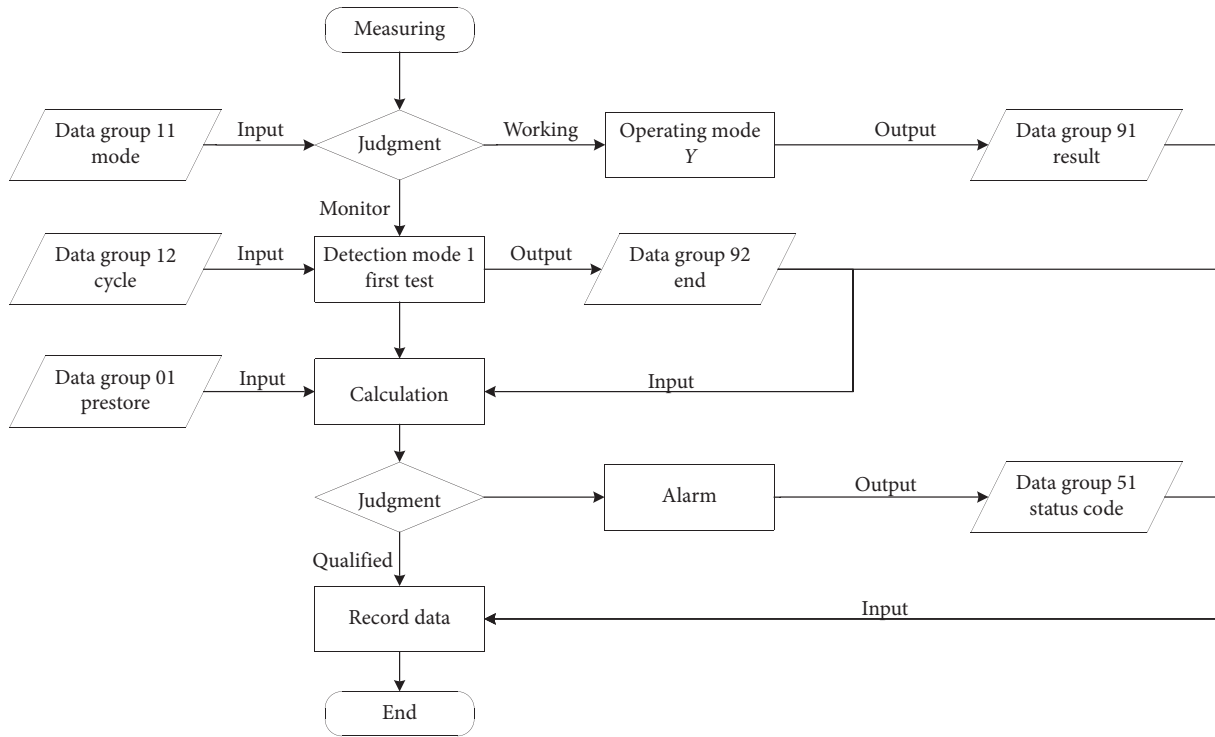
FIGURE 17: The first measurement logic diagram.
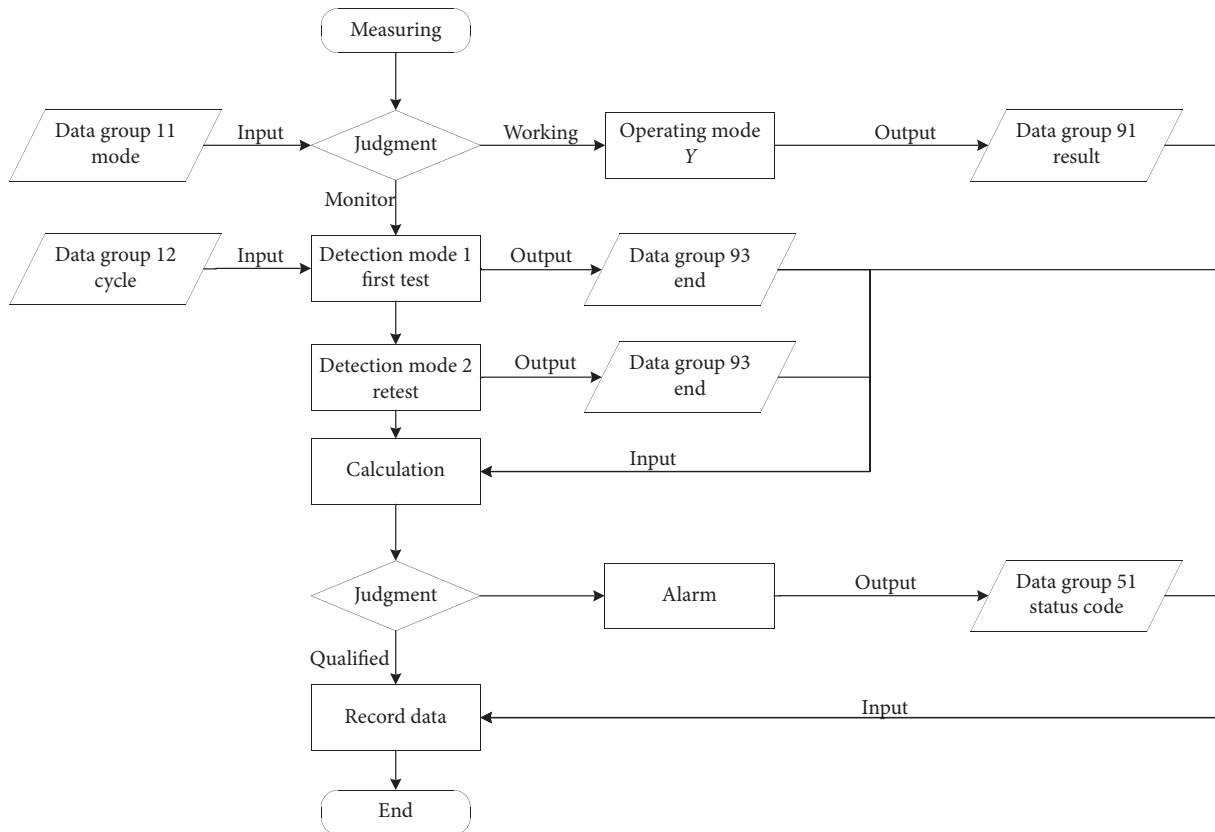
FIGURE 18: The second measurement logic diagram.

TABLE 3: Measurement data format.

Project	Description	Data				
Character	Character	Double	Double	Double	Character	Character
Record	order	order	Components	Program	Date	Time
Data01	prestore					
Data11	mode					
Data12	cycle					
Data91	result					
Data92	result					
Data93	result					
Data94	result					
Data51	status					

```
NC/MPF/TEST_NC_9                                    22
DEF INT ERROR                         ; CYCLE NEED¶
¶
DEF INT STR11, STR12, STR13, STR1     ; DATE DIGIT¶
DEF STRING[30] STR21, STR22, STR23, STR2  ; DATE STRING¶
DEF INT STR31, STR32, STR33, STR3     ; TIME DIGIT¶
DEF STRING[30] STR41, STR42, STR43, STR4  ; TIME SPRING¶
¶
DEF STRING[30] ITEM, DSC, DATE, TIME  ; DEFINE ROU¶
DEF REAL RES1, RES2, RES3             ; DEFINE ROU¶
¶
DEF INT ORDER, PRT, PGM               ; EXTERNAL DATA¶
ORDER=11111111                        ; EXTERNAL DATA¶
PRT=22222222                          ; EXTERNAL DATA¶
PGM=33333333                          ; EXTERNAL DATA¶
_OVR[4]=300.022                       ; INTERNAL DATA¶
_OVR[5]=299.997                       ; INTERNAL DATA¶
_OVR[6]=80.388                        ; INTERNAL DATA¶
¶
¶
¶
; ===============================================¶
STR11=2000+$A_YEAR                    ; FORMAT PROCESS¶
STR12=100+$A_MONTH                    ; DATE¶
STR13=100+$A_DAY¶
STR21=<<STR11¶
STR22=<<STR12¶
STR22=SUBSTR(STR22, 1, 2)¶
STR23=<<STR13¶
STR23=SUBSTR(STR23, 1, 2)¶
DATE=STR21<<"/"<<STR22<<"/"<<STR23¶
¶
STR31=100+$A_HOUR                     ; FORMAT PROCESS¶
STR32=100+$A_MINUTE                   ; TIME¶
STR33=100+$A_SECOND¶
STR41=<<STR31¶
STR41=SUBSTR(STR41, 1, 2)¶
STR42=<<STR32¶
STR42=SUBSTR(STR42, 1, 2)¶
STR43=<<STR33¶
STR43=SUBSTR(STR43, 1, 2)¶
TIME=STR41<<": "<<STR42<<": "<<STR43¶
¶
¶
; ===============================================¶
; PRINT OUT THE HEADER                 ; LINE 1¶
ITEM="RECORD"¶
DSC="ORDER"¶
RES1=ORDER¶
RES2=PRT¶
RES3=PGM¶
WRITE(ERROR, "LOGBOOK, <<ITEM<<" "<<DSC<<"   "<<RES1<<"   "<<RES2<<"
   "<<RES3<<" "<<DATE<<" "<<TIME)¶
¶
; ===============================================¶
; PRINT OUT THE PRESET                 ; LINE 2¶
ITEM="DATA01"¶
DSC="PRESET"¶
RES1=300                              ; X POSITION¶
RES2=300                              ; Y POSITION¶
RES3=80.393                           ; DIAMETER¶
WRITE(ERROR, "LOGBOOK, <<ITEM<<" "<<DSC<<"   "<<RES1<<"   "<<RES2<<"
   "<<RES3<<" "<<DATE<<" "<<TIME)¶
¶
```

FIGURE 19: Output program diagram 1.

5.3. Composition of the Measurement System. The current measurement technology provides a mature solution for high-precision measurement of the real-time position of the moving parts of a machine tool, while the detection of geometric accuracy still uses traditional methods.

The positioning systems of high-precision CNC machine tools adopt closed-loop control, as shown in Figure 24, that is, the rotary encoder built into the servo motor at the drive end, together with the linear encoder on the linear axis of the action end, or the rotary encoder on the terminal rotary axis. The system can also set up a compensation according to the environment change based on the thermal deformation principle and results from laser measurement that further optimize the positioning accuracy of the action end. Once the machine tool is turned on, it is controlled by the closed-loop system at any time, and the positioning accuracy is guaranteed.

The bed of a large machine tool mostly adopts a split structure, and the geometric accuracy is distributed and adjusted after installation. The small machine tool adopts an integral bed, and the geometric accuracy is adjusted during the assembly and usually does not need to be adjusted again after transportation and hoisting. All adjustment works are done by humans with tools, with the help of measuring tools or instruments such as level gauges and square rulers. There is no complete or automated solution.

As long as the machine tool is running normally, it is based on the same measurement system. Usually, systematic deviation will be copied onto the measurement, which leads to the efficacy loss of online measuring. Only by using third-party detection methods such as CMM can we find that the errors have different manifestations.

5.4. Error Source Inference Method Based on Big Data Technology. The accuracy principle of the machine tool is analyzed, all the error sources are sorted in Table 4, the respective manifestations and consequences are studied, and they are associated with typical examples. The application requirement from production is using error results to speculate or judge the cause and give reference for the repair work. A certain number of inspection reports are collected, big data technology is used to sort and analyze valid data, an error pattern is formed with the typical examples in Table 4, reversing the direction of reasoning, and eliminating the interference items, and then the true source of error could be found. Figure 25 is the report of the positioning accuracy from the laser interferometer. The line graph is an important basis for filtering interference factors in reasoning.

Figure 26 shows the mapping relationship between the test report data group and the error source, and the logical sequence is the difficulty of adjustment. The purpose of processing data is to establish a mathematical model to determine the error mode. Because different machine tools

```
NC/MPF/TEST_NC_9                                    67
; PRINT OUT THE MODE                    ; LINE 3¶
ITEM="DATA11"¶
DSC="MODE"¶
RES1=1                                  ; 0==WORK 1==MEASURE¶
RES2=0¶
RES3=0¶
WRITE(ERROR, "LOGBOOK", <<ITEM<<" "<<DSC<<"    "<<RES1<<"   "<<RES2<<"
  "<<RES3<<"  "<<DATE<<"  "<<TIME)¶
¶
; ========================================¶
; PRINT OUT THE CYCLE                    ; LINE 4¶
ITEM="DATA12"¶
DSC="CYCLE"¶
RES1=977                                ; HOLE 4 POINTS¶
RES2=0¶
RES3=0¶
WRITE(ERROR, "LOGBOOK", <<ITEM<<" "<<DSC<<"    "<<RES1<<"   "<<RES2<<"
  "<<RES3<<"  "<<DATE<<"  "<<TIME)¶
¶
; ========================================¶
; PRINT OUT THE RESULT                   ; LINE 5¶
ITEM="DATA91"¶
DSC="RESULT"¶
RES1=0                                   ; RESULT¶
RES2=0¶
RES3=0¶
WRITE(ERROR, "LOGBOOK", <<ITEM<<" "<<DSC<<"    "<<RES1<<"   "<<RES2<<"
  "<<RES3<<"  "<<DATE<<"  "<<TIME)¶
¶
; ========================================¶
; PRINT OUT THE RESULT                   ; LINE 6¶
ITEM="DATA92"¶
DSC="RESULT"¶
RES1=_OVR[4]                             ; RESULT¶
RES2=_OVR[5]¶
RES3=_OVR[6]¶
WRITE(ERROR, "LOGBOOK", <<ITEM<<" "<<DSC<<"    "<<RES1<<"   "<<RES2<<"
  "<<RES3<<"  "<<DATE<<"  "<<TIME)¶
¶
; ========================================¶
; PRINT OUT THE RESULT                   ; LINE 7¶
ITEM="DATA93"¶
DSC="RESULT"¶
RES1=0                                   ; RESULT¶
RES2=0¶
RES3=0¶
WRITE(ERROR, "LOGBOOK", <<ITEM<<" "<<DSC<<"    "<<RES1<<"   "<<RES2<<"
  "<<RES3<<"  "<<DATE<<"  "<<TIME)¶
¶
; ========================================¶
; PRINT OUT THE RESULT                   ; LINE 8¶
ITEM="DATA94"¶
DSC="RESULT"¶
RES1=0                                   ; RESULT¶
RES2=0¶
RES3=0¶
WRITE(ERROR, "LOGBOOK", <<ITEM<<" "<<DSC<<"    "<<RES1<<"   "<<RES2<<"
  "<<RES3<<"  "<<DATE<<"  "<<TIME)¶
¶
; ========================================¶
; PRINT OUT THE JUDGE                    ; LINE 9¶
ITEM="DATA51"¶
DSC="JUDGE"¶
RES1=1                                   ; JUDGE¶
RES2=0¶
RES3=0¶
WRITE(ERROR, "LOGBOOK", <<ITEM<<" "<<DSC<<"    "<<RES1<<"   "<<RES2<<"
  "<<RES3<<"  "<<DATE<<"  "<<TIME)¶
¶
¶
¶
; ========================================¶
MSG("ERROR CODE IS "<<ERROR)¶
M001¶
¶
¶
M30¶
```

Figure 20: Output program diagram 2.

```
NC/MPF/LOGBOOK                                      1
¶
RECORD ORDER   11111111  22222222  33333333 2019/09/04  19: 14: 45¶
DATA01 PRESET   300  300  80.393 2019/09/04  19: 14: 45¶
DATA11 MODE   1  0  0 2019/09/04  19: 14: 45¶
DATA12 CYCLE   977  0  0 2019/09/04  19: 14: 45¶
DATA91 RESULT   0  0  0 2019/09/04  19: 14: 45¶
DATA92 RESULT   300.022  299.997  80.388 2019/09/04   19: 14: 45¶
DATA93 RESULT   0  0  0 2019/09/04  19: 14: 45¶
DATA94 RESULT   0  0  0 2019/09/04  19: 14: 45¶
DATA51 JUDGE   1  0  0 2019/09/04  19: 14: 45¶
```

Figure 21: The result of the complete output program.
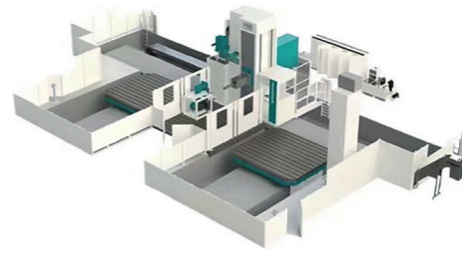
Figure 22: The structure of a typical floor boring and milling machine.

and parts vary a lot, the examples listed in Table 4 are just limited. Other factors only include external factors and cannot be changed by modifying the machine settings, so they are prioritized in reasoning. Combined with the positioning accuracy report, determine whether it is a single positioning, geometric, or dynamic accuracy or a complex problem of multiple factors. For large machine tools, the workload of stopping to adjust the geometric accuracy is very large, and the probability of occurrence is small, so the first two inferences are given priority. This reasoning process is completed by big data technology, which can quickly and efficiently draw conclusions and provide a basis for accuracy analysis.

6. Cutting Parameter and Tool Life Management

6.1. Research for Process Quality. The tool's process parameters and life management is the most basic category of CNC machining technology management. Process research refers to finding the optimal cutting process, learning the patterns of tool wear and machining dimensional changes, and developing countermeasures to achieve stable process quality.

Cutting parameter and tool life management are the two most important basic technologies for machining. By research on the cutting process, we gain the experience on tool wear and its influence on the target dimension and are able to create the strategy for getting stable process quality.

Process quality is generally composed with 3 sections: the early goal is to prepare and prevent; the medium-term function is to plan, execute, monitor, and adjust; and the later stage is about recording and tracing based on the requirement of the quality management system. Good process quality directly improves the operation performance of the plant. The fundamental purpose of using probes is to improve process quality through digital technology.

6.2. Preparation before Utilizing the Probe in a Finish Boring Process. Finish boring for a big diameter hole is the most critical machining process in manufacturing of hydraulic machine. As shown in Figure 27, 4 holes with diameter 270 H7 on a fixing platen for a big tonnage hydraulic machine need to be made, with 350 depth and Ra 1.6 roughness requirement. The hole on the left side is usually finished using the reverse boring process. We have added a process
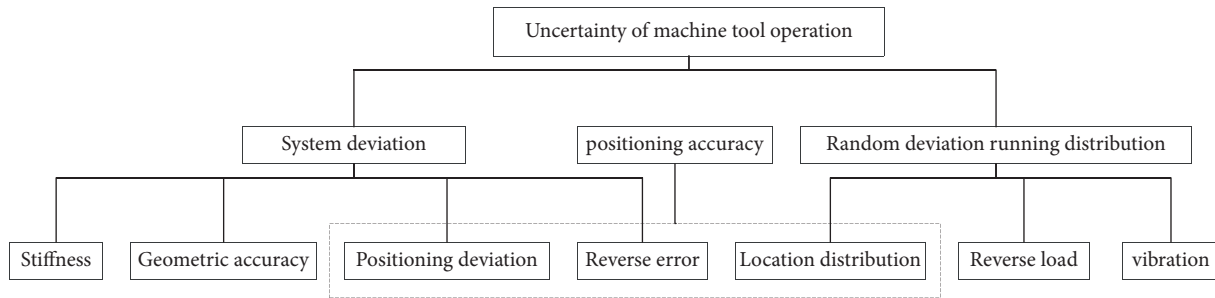
FIGURE 23: Uncertainty of machine tool operation.
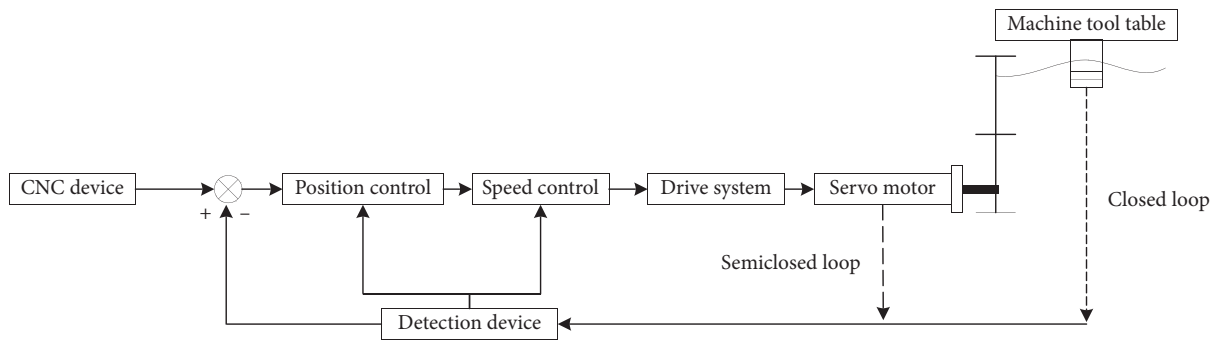
FIGURE 24: Full closed-loop control system diagram of the CNC machine tool.

slot at the bottom of the left hole for tool entry, which allows the machining to be completed in one direction with a single fine boring tool.

Finish boring for a big-diameter hole is the most critical machining process in the manufacturing of hydraulic machines. As shown in Figure 27, 4 holes with diameter 270H7 on a fixing platen for a big-tonnage hydraulic machine need to be made, with 350 depth and Ra 1.6 roughness requirement.

The Sandvik fine boring inserts were selected, and the recommended cutting parameters are shown in Figure 28. The workpiece material is pearlitic ductile cast iron, 0.12 mm per revolution feed, 0.25 mm semifinishing allowance, and 180 m/min cutting line speed were selected for process calculations, and the process is shown in Table 5.

Using the process parameters obtained in Table 5 as reference values, we control the feed rate, vary the rotational speed, and conduct an orthogonal test study of cutting parameters and tool wear, with the planned test parameters listed in Table 6.

6.3. Process Quality Data Acquisition. The principle of finish boring is enlarging the hole diameter, and the wear of the tool tip is directly reflected in a reduction in the size of the machined diameter. In order to study the pattern of cutting speed and tool wear, five parts were machined on a PAMA floor-type CNC milling-boring machine with five sets of cutting parameters, for a total of 20 holes. For every two holes machined, an insert was rotated or replaced with a new

cutting edge. After each insert change, a test cut is made to ensure that the machining dimensions are as consistent as possible.

In the boring process, cutting depth increased together with the growing cutting length accompanying a helical tool path. When the performance of the cutting edge is good, the roughness is fine, and the diameter decreases slowly with the linear tool wear. So, diameter on an exact depth reflects the tool wear after a certain cutting length.

According to the actual shape of the hole, four process-representative, even-numbered points from the depth octet were selected for measurement. The tests yielded ten valid datasets, as shown in Table 7, with cutting speeds decreasing from top to bottom by part group.

6.4. Data Processing and Analysis. After the data are retrieved, the first value of each set of data is aligned. Clustered bar charts and 3D bar charts are produced, as shown in Figures 29 and 30. The clustered bar chart makes the data visible in one dimension, which is equivalent to using the control variable method. The data in the 3D bar chart are visible in two dimensions, which can be used to compare more relevant conditions. With the graphical display of the results, it is easy to observe the effect of an increase in cutting speed on part accuracy. Tool suppliers recommend inserts with a machining life of 20 to 30 minutes, or about 5,000 meters. Tests have confirmed that the recommendations are accurate and valid. Inserts that exceed the recommended service life increase vibration during machining, affect accuracy, and reduce surface roughness. The faster the cutting speed a tool uses, the faster it

TABLE 4: Manifestations of error.

Principle	Subitem	Manifestations and consequences		Typical examples/models
Bed factors	Rigidity	Deformation of the bed under load	Localized radial deviation of shape accuracy; localized divergence of position accuracy	Not enough allowance after roughing for finishing; poor geometric or position accuracy in a particular machining area of the machine tool
	Geometric precision	Bed geometry deviations	Shape accuracy deviation; geometric deviation in position accuracy	Persistently poor geometrical accuracy in perpendicularity, parallelism, flatness, etc.; the position of the pore system deviates continuously from the geometrical pattern
Drive, lubrication, and CNC factors	Positioning deviation	Large absolute deviations in unidirectional positioning of the bed	Offset and stable position accuracy	Consistently and consistent poor position accuracy in the serial production on exact fixture
	Reverse error	Large positioning deviation of the bed's reciprocating motion	Offset and regular position accuracy	Exceedingly poor accuracy in rows or columns with toolpaths in opposite directions during complete column feature machining; poor positional accuracy and visible tool marks on curved surfaces in machine tools with frequent axis changes
	Position distribution	High repetitive positioning deviation for unidirectional bed movement	Offset and instable position accuracy	There are no individual instances of failure, which are usually superimposed on the positioning bias factor in the results
Other factors	Payload	Changes in the geometric accuracy of the machine under load	Shape accuracy deviation; geometric deviation in position accuracy	After loading, the geometrical accuracy of perpendicularity, parallelism, flatness, etc., is consistently out of whack; after loading, the position of the pore system continues to deviate in a geometrical pattern
	Vibration	Resonance of machine tools in specific operating conditions	Unusual vibration noise; poor surface quality of machined parts	The surface roughness is extremely poor, but the dimensions are acceptable; the machined surface has a regular knife pattern
	Temperature fields	Deformation of bed components or workpieces with temperature rise	Offset and instable position accuracy	Difference in temperature between day and night in nontemperature-controlled workshops and variation in overall accuracy; parts with particularly long machining times and variations in local accuracy
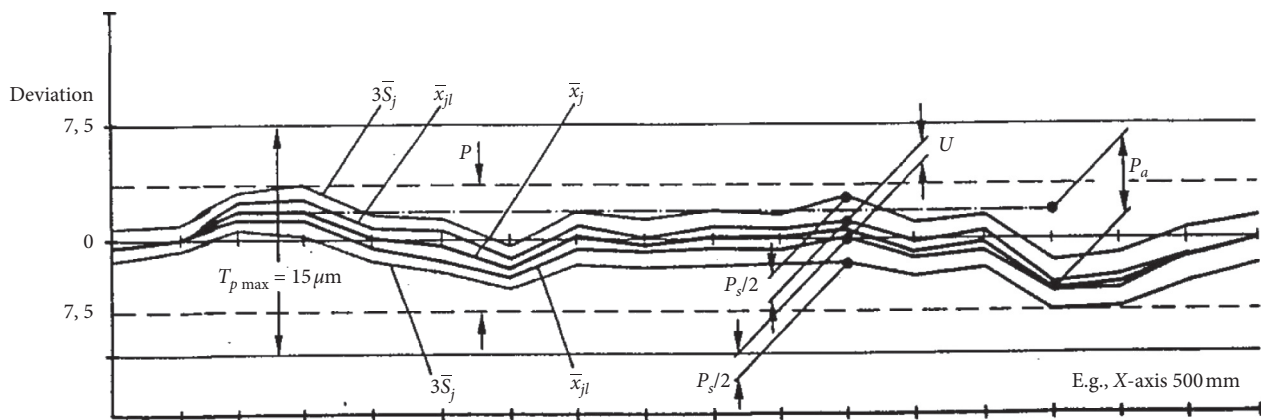
FIGURE 25: Laser interferometer report.
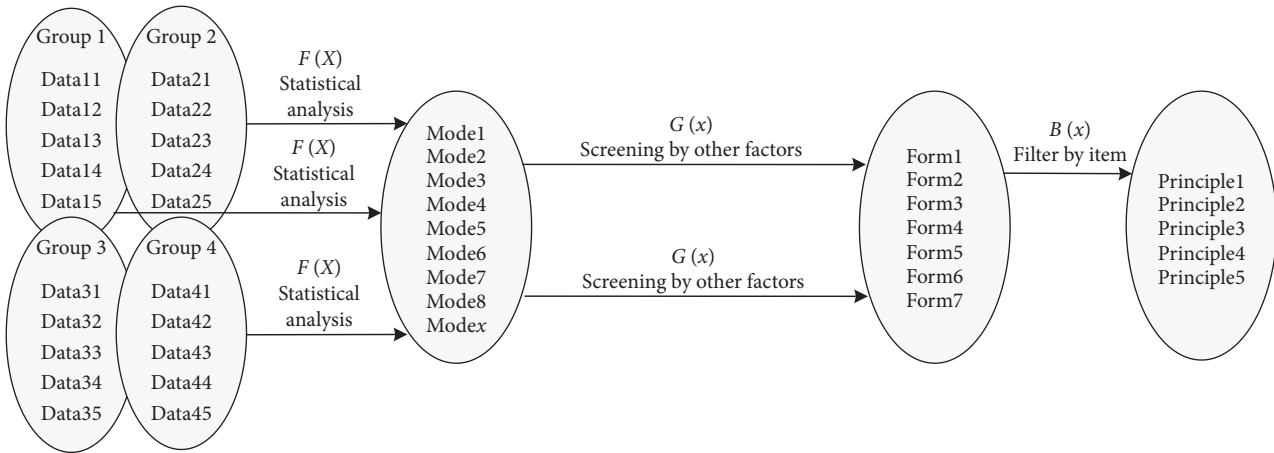
FIGURE 26: Inference map.
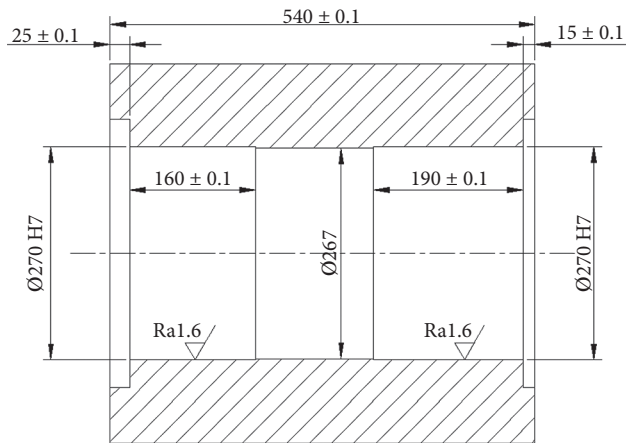
FIGURE 27: Injection molding machine template fine boring diagram.
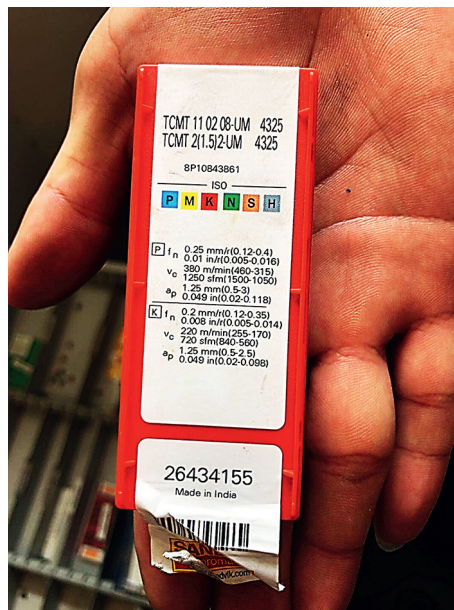
FIGURE 28: Reference cutting data chart for boring inserts.

TABLE 5: Fine-boring process parameter table.

Name	Symbol	Size	Unit	Formula	Result
Processing diameter	D	270	mm		
Hole circumference	C		mm	$C = \pi^* D$	848.23
Feed rate	f_n	0.12	mm		
Depth 1	h_1	190	mm		
Depth 2	h_2	160	mm		
Cutting length	L		m	$L = ((h_1 + h_2)^* C / f_n {}^* 100)$	2474.00
Cutting speed	v_c	180	m/min		
Rotation speed	n		rpm	$n = (1000^* v_c / D^* \pi)$	212
Time	t		m	$t = (L/v_c)$	13.74

TABLE 6: Fine-boring process test parameter table.

Parameter	Chip speed	Rotation speed	Time	Total time
20%	216	254	11.45	45.80
10%	198	233	12.49	49.96
Recommended value	180	212	13.74	54.96
−10%	162	191	15.11	60.46
−20%	144	170	16.49	65.95

TABLE 7: Fine-boring measurement data sheets.

Part	Hole	Depth1 43.5	Depth2 131.25	Depth3 218.75	Depth4 306.25
1	1	270.031	270.028	270.027	270.024
	2	270.021	270.018	270.014	270.011
	3	270.027	270.024	270.023	270.021
	4	270.019	270.016	270.014	270.009
2	1	270.033	270.029	270.028	270.026
	2	270.023	270.022	270.019	270.016
	3	270.029	270.027	270.026	270.023
	4	270.022	270.019	270.017	270.014
3	1	270.028	270.025	270.024	270.022
	2	270.021	270.019	270.018	270.015
	3	270.035	270.034	270.032	270.029
	4	270.028	270.026	270.023	270.021
4	1	270.033	270.031	270.028	270.027
	2	270.025	270.023	270.020	270.019
	3	270.028	270.025	270.024	270.022
	4	270.021	270.019	270.016	270.014
5	1	270.035	270.033	270.032	270.030
	2	270.027	270.025	270.024	270.022
	3	270.029	270.028	270.025	270.024
	4	270.022	270.019	270.018	270.016
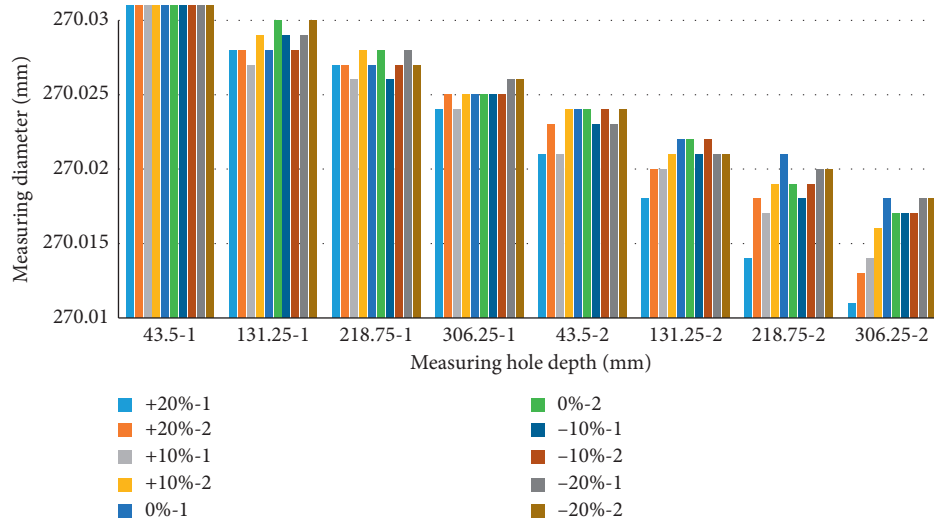
FIGURE 29: Cluster bar graph of measuring result data.
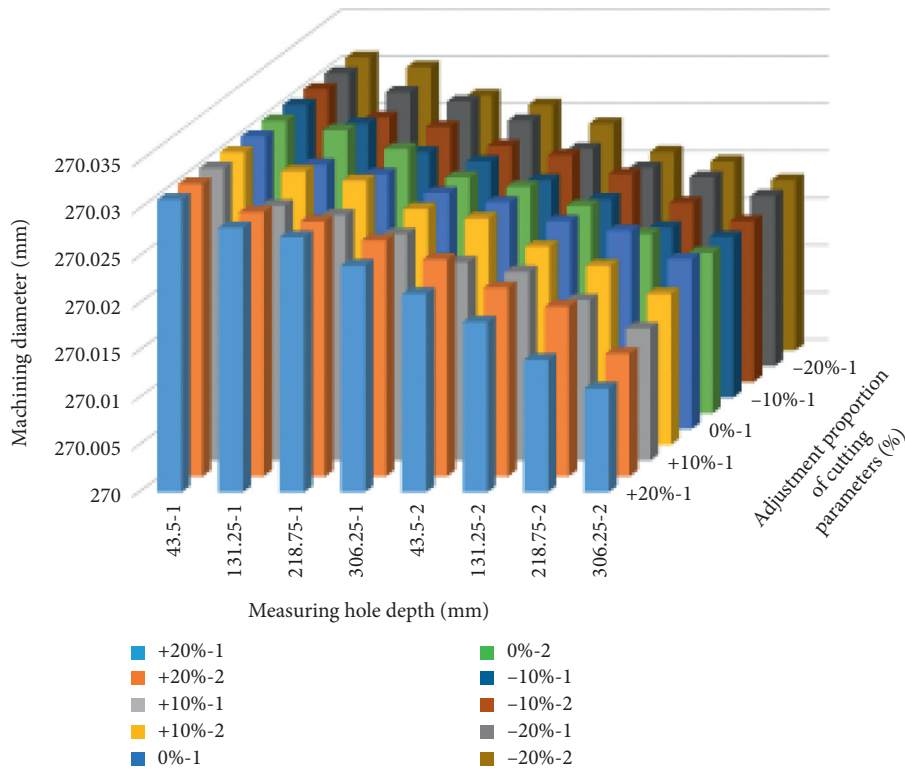
FIGURE 30: Three-dimensional bar graph for measuring result data.

gets worn. The optimum process parameter for fine boring is −10% of the recommended value. In combination with the machining time data in Table 6, it becomes easier to determine the frequency of tool changes.

7. Conclusion

Business managers and technicians, in cooperation with program developers, can achieve precise digital applications by clarifying their digital intentions and establishing rules for data collection and management. Oriented to the actual needs, integrating information technology and management knowledge to enhance the application technology, such research and development model with cooperation between different application areas is exactly the construction of the information application and service model what we refer to in the implementation guideline of the manufacturing powerhouse [2].

Referring to the requirement of measuring data acquisition from milling a platen for the hydraulic plastic injection machine on a PAMA floor-type CNC milling-boring machine, a simple digital manufacturing information system was built

with logging and process data sharing functions in the Siemens 840D SL CNC controller, combined with common information technologies, to be able to record the measurement data during machining. On this basis, three applications of probe error detection, machine geometry accuracy monitoring, and tool process parameters and life management are realized step by step through the use of big data technology. The new technology achieves its design goals through practical machining process research, tool life management, and verification of the machine maintenance work.

Compared with the existing technology, this solution has the following five advantages: ① based on the common LAN communication, it has no additional electrical equipment and wiring, is low cost, and is easy to implement compared with the typical digital solution; ② NC programming makes the text output less technically challenging, different CNC systems have similar functions, and it is easy to promote a wide range of applications; ③ it can collect unlimited types of data according to the actual needs of their own expansion; ④ based on big data technology, it can be customized according to the needs of the algorithm. The input data are accurate and effective. The calculation results are true, reliable, and strongly referenced; and ⑤ the additional visual communication interface enhanced the readability of the data and the scope of applications.

The automatic measurement data collection and application of touch probes on CNC machine tools is essentially an extension of the digital application of industrial technology, the greatest advantage of which is the ability to save complete process data. Big data technology, however, is a new type of database technology, with powerful data screening, retrieval, and processing performance. Both are fundamental technologies for achieving smart manufacturing. Within the manufacturing industry as a whole, we purchased many smart manufacturing solutions from foreign countries. The localization is not satisfactory due to the large number of related technologies and the different approach of each. In order to develop smart manufacturing technology ourselves, it is inappropriate to place too much emphasis on the entirety system but carving up various fundamental technologies related to it. By objectively analyzing the current situation, segmenting the needs, and completing the technology roadmap, the overall goal is naturally achieved.

Data Availability

No data were used to support this study.

Conflicts of Interest

The authors declare that they have no conflicts of interest.

Acknowledgments

References

[1] Z. You, *Made in China 2025 - Robust Industrial foundations*, pp. 6–29, Qinghai Daily, Xining, China, 2016.

[2] Y. Wang, "Release of the first batch of supporting documents of made in China 2025," *China Equipment*, vol. 9, p. 18, 2016.

[3] Z. Hu, "Research for notes and strategies of improving accuracy on CNC machining parts," *Shandong Industrial Technology*, vol. 20, p. 23, 2018.

[4] Y. Wang, "Analyzing and discussion for factors and measures which influence the quality of CNC machining," *Hubei Agricultural Mechanization*, vol. 10, p. 64, 2018.

[5] L. Shen, "CNC machine and tools:Master machine of equipment industry, foundation of intelligent manufacturing," *Manufacturing Technology and Machine Tool*, vol. 10, pp. 8–11, 2018.

[6] L. Shen, "CNC machine and tools:Master machine of equipment industry, foundation of intelligent manufacturing," *Manufacturing Technology and Machine Tool*, vol. 11, pp. 7–11, 2018.

[7] Y. Zhou and Y. Huang, "Research and implementation of quality management model in manufacture," *Internal Combustion Engine & Parts*, vol. 11, pp. 182-183, 2019.

[8] L. Shen, "Digitalization, networking and intelligence should be developed together for realizing intelligent manufacturing in equipment industry," *Wisdom China*, vol. 8, pp. 7–9, 2016.

[9] F. Sun and P. Lou, "Realization of online measuring with trigger probe in machining center," *Industrial Control Computer*, vol. 10, pp. 3-4, 2007.

[10] J. Zhu, *Research on the Technology of Online Inspection System for Machining Accuracy of Free-form Surface components*, Guangdong University of Technology, Guangzhou, China, 2008.

[11] L. I. Peng and S. Liu, "Calibration of trigger probe in machining center," *Modular Machine Tool & Automatic Manufacturing Technique*, vol. 5, pp. 59–62, 2019.

[12] P. Ju and H. Luo, "Research of error compensation technology on trigger probe in online measuring system," *Mechanical Science and Technology for Aerospace Engineering*, vol. 37, no. 1, pp. 81–88, 2018.

[13] X. Qian, W. Ye, and X. Chen, "On-machine measurement for touch-trigger probes and its error compensation," *Key Engineering Materials*, vol. 26, pp. 375-376, 2008.

[14] L. Wang, X. Huang, and D. Han, "Error analysis and compensation for touch trigger probe of on-machine measurement system," *China Mechanical Engineering*, vol. 23, no. 15, pp. 1774–1778, 2012.

[15] Y. Ihara, "3701 On-machine workpiece measurement for process combination," *The Proceedings of The JSME Annual Meeting*, vol. 4, pp. 303-304, 2007.

[16] H. Zhou, Y. Gao, and Y. Zhang, *Reliability Verification and Application for On-Machine Measuring system*, pp. 292–302, Development Strategy Research Center for Space Electronics, Beijing, China, 2017.

[17] Association of German Engineers, *VDI 3441 Statistical Testing of the Operational and Positional Accuracy of Machine Tools*, Duesseldorf: VDI-Verlag GmbH, Düsseldorf, Germany, 1977.

[18] International Organization for Standardization, *2012 Geometric Accuracy of Machines Operating under No-Load or Finishing conditions*, ISO Copyright Office, Geneva, Switzerland, 2012.

[19] State Bureau of Quality and Technical Supervision, *Test Code for Machine Tools--Part 1:Geometric Accuracy of Machines*

Operating under No-Loador Finishing conditions, Standards Press of China, Beijing, China, 1998.

[20] General Administration of Quality Supervision, *Inspection and Quarantine of the People's Republic of China, Standardization Administration of the People's Republic of China*, Standards Press of China, Beijing, China, 2009.

[21] General Administration of Quality Supervision, *Inspection and Quarantine of the People's Republic of China, Standardization Administration of the People's Republic of China*, Standards Press of China, Beijing, China, 2016.

[22] General Administration of Quality Supervision, *Inspection and Quarantine of the People's Republic of China, Standardization Administration of the People's Republic of China*, Standards Press of China, Beijing, China, 2015.

[23] State Bureau of Quality and Technical Supervision, *Metal-Cutting Machine Tools - Measurement Method for vibration*, Standards Press of China, Beijing, China, 1997.

Research Article

The Development and Design of Artificial Intelligence in Cultural and Creative Products

Xue Li[1] and Baifeng Lin [ID][2]

[1]*School of Design and Art, Jingdezhen Ceramic Institute, Jingdezhen 333000, Jiangxi, China*
[2]*Academy of Fine Arts, Anqing Normal University, Anqing 246052, Anhui, China*

Correspondence should be addressed to Baifeng Lin; linbofeng@aqnu.edu.cn

The rapid development of the global cultural and creative industry has provided a new stage for the development and innovation of Chinese traditional culture. Cultural creativity has broken the rigid design and production mode of traditional products from the perspective of market and has become the key to improve the economic benefits and competitiveness of traditional products. From the perspective of cultural and creative product design and product development, artificial intelligence technology has been fully utilized at the present stage. The purpose of this article is to compare the traditional design patterns used in product design and understand the new design patterns assisted by artificial intelligence so as to achieve the purpose of process simplification and design innovation more quickly. In this article, traditional graphic patterns and local cultural connotations of the experimental area are taken as the main research points. Through a large number of field investigations and first-hand photo materials, the regional cultural characteristics and local traditional graphic language are analyzed in detail and then summarized. Finally, the examples of development research are summarized and reflected. It is hoped that through the further excavation of the traditional patterns of the region and the exploration of the level of regional culture regeneration, the development of local economy, culture, and tourism can be driven, and a cultural brand that can go out of Anhui province and into the whole country can be built. At the present stage of product research and development, the key is to introduce artificial intelligence means as necessary support and try to infiltrate artificial intelligence measures in the research and development of new products in each link.

1. Introduction

With the development of robot technology, the application of robots became wider and wider. At the same time, the concept of robots also became broader and broader, expanding from the narrow sense of robot to robot technology. In early 2004, a senior member of IEEE affecting the industry of future research pointed out that four technologies will have the greatest influence on the future, that is, biotechnology, nanotechnology, giant computer technology, and intelligent robot technology. Given the strong support, Japan regards robots as a strategic industry, but the current robot industry is faced with problems in Japan. However, robot research is put forward to strengthen and promote specific measures of industrialization of the robot. South

Korea has listed robot technology as an "engine" industry for future national development and has given key support to robot technology. The United States has classified robotics as a technology of vigilance, believing that it will have a huge impact on future wars, and has imposed a technological blockade on other countries. Experts suggest that research on robot technology should be further strengthened to promote the development of China's intelligent robot industry.

The Mediterranean region has received increasing attention in recent years. This is due to the heterogeneity of the countries that make up it, which raises several issues in business cooperation, but also presents several transnational economic opportunities among Mediterranean countries. Through the analysis of cultural and creative industries, it

can be found that there are many similarities in this field, which makes cross-cultural communication and transnational economic development possible. Luciana Lazzeretti studied the three main Mediterranean countries in and outside Europe, Italy, Spain, and Turkey, to highlight the most striking similarities and differences in their characteristics. The specialization of creativity found in this region is similar, leading us to discuss the concept of Mediterranean creativity [1]. Cultural and creative industries are increasingly important in western economies. In these industries, as in several other business sectors, microenterprises, that is, in the United States, are the dominant type of business that employs fewer than 10 people. As these industries have become a part of most economies, Katherine Gundolf has begun to explore the strategic behavior of cultural and creative microbusinesses. While microenterprises are characterized by certain particularities that can affect their ability to participate in external relationships, in this particular case, there is little knowledge of collaboration through strategic alliances. Katherine Gundolf aims to shed light on the specific motivations for participating in strategic alliances in this context in order to improve understanding of the partnerships between microenterprises in the cultural and creative industries. In this process, Katherine Gundolf focuses on six strategic alliances between microenterprises in the French cultural and creative industry. Katherine Gundolf's findings suggest that strategic alliances involving creative microenterprises seek to reduce overspecialization, aim for a high quality of life and fun to work, and are only possible if there is trust and mutual support among partners. In addition, opportunism and necessity motivation guide the decision of innovative microenterprises to enter the strategic alliance [2]. In Slovakia, there are three unique, historic mining towns, Banska Bystrica, Banska Štiavnica, Kremnica, which have been successfully converted to the creative cultural center. The historical and cultural values of these towns have stood the test of time, becoming a new magnet for people of the creative class who want to escape the atrocities of high modernity (modern urban centers) and find a source of inspiration based on the sentimentalism of historical nostalgia, a new foundation for creative and cultural industries in rural areas. Kamila Borsekova's main objective was to analyze the cultural and creative industries of these three unique historical mining centers with a view of replicating their knowledge in other communities under economic pressure. Kamila Borsekova first explores concepts related to the cultural and creative industries, focusing on nostalgia sentimentalism, which is an important opposition to high modernity and even postmodernism. The second part will analyze the cultural and creative industries of the three centers based on preliminary data collected from several research projects in this area. Finally, some suggestions are put forward to promote creative and cultural enterprises to participate in regional redevelopment. It also contains policy recommendations on the autonomy of the region in order to make more effective and rational use of the obvious existing potential [3].

This article collects, sorts out, and analyzes the most representative elements in the experimental area by means of field investigation and take this as the foundation of the creation of cultural products. Through the technology of artificial intelligence, a database of cultural elements, symbols, and languages in the experimental area is established to find the breakthrough point of transformation and application of traditional graphics. When developing new products of cultural creativity, such intelligent means, if properly utilized, can help broaden the perspective of product development and integrate more innovative elements into it. Therefore, we can know that the whole process of product development and design should pay close attention to the flexible introduction and application of artificial intelligence technology.

2. Proposed Method

2.1. Cultural and Creative Products

2.1.1. Definition of Cultural and Creative Products.
Cultural goods are generally defined as consumer goods that convey opinions, symbols, and lifestyles. They convey or influence cultural activities. The result of these individual or collective creations is cultural objects that are based on copyright and involved in global distribution activities through the industrial chain. Books, publications, crafts, CDs, films, an fashion design provide the public with a wealth of cultural options. By transforming "culture" into "creativity" and attaching it to products, the relationship between conditioned and purpose-oriented objects and people extends outward from the core according to the cultural connotation and the product's own characteristics, forming a "benefit" type commodity with both use and psychological function [4, 5].

The core concept of cultural creative products lies in culture and creativity, which is the materialized expression of human wisdom and inspiration. First of all, it is closely connected with the extensive application of cultural media and automation technology, showing the characteristics of intelligence. Secondly, cultural and creative industries are at the top of the value chain of technological innovation and development, with high added value. The proportion of technological elements and cultural elements contained in its products is significantly higher than that of general products. It has strong "uniqueness" and shows obvious regional cultural features, which naturally integrates the core symbols of local culture and the commercial value of products, which is the biggest difference between cultural and creative products and general commodities [6, 7].

2.1.2. Design Principles of Cultural and Creative Products

(1) The Freehand Brushwork in Traditional Chinese. In the eyes of the broad masses, Chinese traditional culture pays attention to the shaping of artistic conception and believes that the soul of art means that the ingenious design of f reflects the "charm" of culture and adds traditional cultural elements to the products. For example, for likeness to taste tea and talk about Taoism, the design with three teacups implies "three people walk must have my teacher" and water

∗ teapot expression time such as water implies getting along with friends and that always short hope can retain live and friends in ask. In the design of concrete things, traditional shapes, colors, techniques, and other products can be integrated in new ways [8].

(2) Integration. When designing cultural and creative products, it is necessary to comply with the requirements and guidelines of general product design. The cultural connotation of product design and various elements extracted from it are related to the products to a certain extent, which cannot be reluctantly agreed with. Whenever the form of product design should be based on function service function to meet people's use needs. For example, the design of "connecting you" USB flash drive combines the unique outline of Windows and doors of Suzhou forest garden with the cultural conception of "winding path connecting you" to convey the strong local characteristics of Suzhou. The shape is simple and unique and very "close to the people" [9].

2.1.3. Application Mode of Cultural and Creative Product Design

(1) Simplified Reproduction Method. Compared with modern graphics, traditional graphics are still too complicated and not simple enough. Therefore, in design, designers need to do subtraction or abstraction on the basis of keeping the original graphic features and meanings. This method requires a high degree of matching between graphics and the new carrier, and it needs to convey the original cultural connotations through this new medium [10].

(2) Visualization. Concrete design refers to the design of transforming intangible thoughts into concrete objective products by means of homophony, metaphor, symbol, and fiction. It requires the retention of the basic characteristics of the objective object, through a unique perspective, to a new art form to summarize decorative products. For example, the tai chi sofa designed by a German designer organically integrates Chinese traditional culture with modern design [11, 12].

(3) Grafting. The design method of connecting disparate things or concepts together through whimsical ideas is called grafting design. Designers need to process and design the information and then translate it into performance elements in the product and then convey it to consumers. For example, in July 2014, the Palace Museum in Taipei launched the "ladies of tang dynasty" series. The designer got inspiration from the palace music chart of the tang dynasty and introduced the "pendant horse bun neck pillow" pillow with reference to the hairstyle of ladies playing music. Ingeniously grafting the unrelated bun with the u-shaped pillow produced an unexpected spark. This fun neck pillow not only gives you a good rest during your trip but also acts as a fun toy. It also shortens the distance between historical relics and people, making consumers feel involved [13, 14].

2.2. Composition and Characteristics of Intelligent Cultural Product Supply Chain.
Based on the theory of collaborative innovation, the intelligent cultural product supply chain should be a flat network supply chain that integrates the government, consumers, scientific research and development parties, theoretical research parties, capital suppliers, product producers, suppliers, and third-party logistics and links the parties. This supply chain is mainly based on the Internet, supported by cloud computing, digitalization, mobile Internet, big data, Internet of things, augmented reality, and other artificial intelligence technologies, and finally demonstrated in the form of intelligent collaborative service platform [15, 16]. At the same time, the information resources among the main units are fully shared and achieve supply, investment, research and development, production, circulation, and sales of all links; effective connection, truly achieved when the main body is changed from linear single chain to nonlinear mesh chain, can improve the efficiency and cost savings and fully show the intelligence and informatization of supply chain. Therefore, the characteristics of the supply chain can be summarized as multiagent cooperation, information sharing, and nonlinear collaboration, as shown in Figure 1.

2.2.1. Multiagent Cooperation.
Different from the traditional supply chain is the intelligent cultural products supply chain based on the theory of collaborative innovation; the combination of "production and government need" should be paid more attention to push the colleges and universities and scientific research institutes to the front end of the supply chain, under the collaborative power of the government, the excellent cultural resources, and advanced science and technology, provide the cultural enterprises in the supply chain, and help cultural products producers to solve resource requirements, technology applications, and related theoretical problems; for example, avoiding cultural products on the supply side that appears inferiority is invalid. Therefore, this supply chain not only includes the participants in the original product supply chain, but also includes universities, research institutes, governments, financial investment institutions, and third-party collaborative service platforms, involving more detailed and extensive participants [17, 18]. The third-party collaborative service platform here is an online and offline 020 intelligent service platform organization based on cloud computing, digitalization, Internet of things, Internet, and big data technology. It must be closely related to all participants. Universities and research institutes are intellectual institutions providing cultural resources, advanced theories, human resources, and new technologies. The role of the government is to promulgate policies and regulations to regulate enterprise behavior and harmonious enterprise relations and optimize the supply chain as a "spectator." Capital investors refer to institutions providing funds for the production of cultural products, such as investment banks and financing enterprises [19].
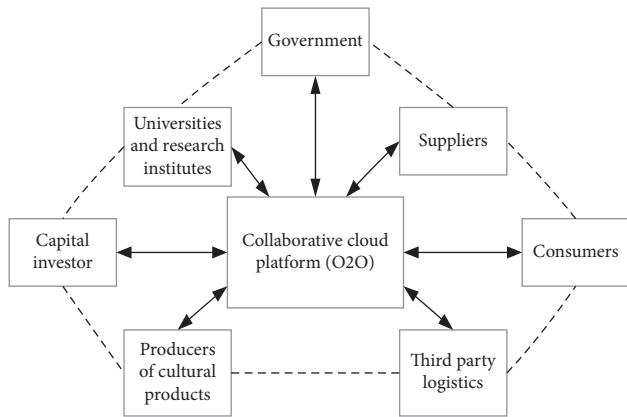
FIGURE 1: Schematic diagram of intelligent cultural product supply chain.

2.2.2. Information Sharing. In this supply chain, information sharing plays a crucial role, which can effectively improve the utilization rate of information resources of the participants, solve the problem of information blockage and communication delay, and promote the cooperation and production of the participants to be more efficient. To a certain extent, inadequate information sharing is also one of the factors that cause the problem on the supply side of the cultural industry. The supply side cannot effectively grasp consumers' consumption tendency for cultural products, and it is easy to produce cultural products blindly so that the supply is not required frequently. When the information sharing of the supply chain is realized, the collaborative service platform plays the role of a medium, which can automatically collect, integrate, store, analyze, and manage all main body information and distribute information according to the actual needs of each main body, which is a huge service database of big data resources [20, 21]. It makes the communication of the subject in the supply chain more timely and effective, breaks through the single communication mode in the traditional supply chain, and is a collaborative network with strong real-time interaction and high degree of participation, which greatly promotes the mastery of query information on both sides of supply and demand. In addition, the information sharing for all participants in the supply chain to supply the latest theoretical achievements, advanced technical guidance, scientific marketing, and good logistics delivery lets the participation main body fully understand the market dynamic and positive feedback market needs; it can effectively avoid the supply side blind production and sales, to provide an opportunity to achieve real and accurate supply and demand [22, 23].

2.2.3. Nonlinear Synergy. Under the multiagent cooperation and information sharing, all participants in the supply chain can reach the consensus of collaborative innovation, collaborative value-added, collaborative operation, and collaborative complementarity, which greatly improves the value-added capacity of the whole supply chain and generates nonlinear chain synergies, which mainly include

economic benefit and social benefit. Economic benefit: the collaborative service platform eliminates the information communication barriers among the subjects and realizes the rapid flow of information resources, which not only enhances the cooperation among the subjects, but also enables the subjects to position the market demand more accurately, thus reducing the cost of each link and finally effectively improving the overall benefit of the supply chain. Social benefits: universities, scientific research institutes, and other knowledge research parties and technology research and development ends can be closely related to the demand side and manufacturers on the collaborative platform, which can reduce the probability of "production, learning and research needs" disconnection and carry out targeted theoretical research and technology research and development. The following is the rapid transfer of theoretical achievements and scientific research technology to the production side through the service platform, promoting the rapid transformation and dissemination of scientific research achievements and realizing the accurate focus of cultural products in the actual production; The producer obtains the latest theoretical results, new technologies, funds, policies, and other relevant support services through the collaborative platform, which guarantees the high-quality and feasible supply of cultural products at the source of production. In addition, the close cooperation between logistics enterprises and collaborative platforms can ensure the transportation and circulation of cultural products and realize efficient and convenient delivery [24, 25].

2.3. Development and Challenges of Artificial Intelligence. The concept of artificial intelligence is very wide, so artificial intelligence is also divided into many kinds; according to the strength of artificial intelligence, it can be divided into three categories. Weak artificial intelligence (ai): a weak ai is an artificial intelligence that is good at a single aspect. An ai that can beat the world champion of chess, for example, but can only play chess, does not know how to store data on a hard drive better.

2.3.1. Artificial General Intelligence AGI. Artificial Intelligence at the human level: strong artificial intelligence refers to artificial intelligence that can be compared with human beings in all aspects. Creating strong artificial intelligence is much harder than creating weak artificial intelligence, and humans cannot do it yet. One professor defines intelligence as "a broad range of mental abilities capable of thinking, planning, problem solving, abstract thinking, understanding complex ideas, learning quickly, and learning from experience." Strong ai should be as adept at these operations as humans [26].

2.3.2. ASI. Oxford philosopher and leading artificial intelligence thinker defines superintelligence as "being much smarter than the smartest human brains in almost every field, including scientific innovation, general knowledge and social skills." Superartificial intelligence can be a little better

than humans in every aspect or a trillion times better than humans in every aspect.

Human programmers imagine a mechanism, for example, writing a program that can write a news release, compose a song, or communicate with people and then write, try, and modify the algorithm. After numerous failures and trials, intelligent and interesting artificial intelligence programs or robots with physical forms emerge. In this article, the computer programmers write design mechanism, on the grounds of "work" limit algorithm; in the creation process, the programs rely on the programmer control phase (weak artificial intelligence) or the substantive help programmers only provided (strong ai stage) with before joining neural network autonomous learning and spontaneous creation of writing manuscript, paintings, music. and so on. In this article, these achievements are collectively referred to as artificial intelligence achievements [27, 28].

One's current level of science and technology to the research of artificial intelligence is still in the weak ai stage, although the technology of artificial intelligence has gradually extended to the service life, literature and art, political and military, and other fields. The AlphaGo defeating Lee Sedol has caused quite a stir in these areas of the application of artificial intelligence. Ten years ago, the applications looked much more complex and advanced; however, they are still at the stage of complex weak ai. These ai are just "specialists" in a certain field. The research premise and background of this article is that the rapid development of artificial intelligence is an inevitable trend; after achieving technological singularity, with geometric ratio growth speed, the development of artificial intelligence will be even more difficult to achieve and controlling the speed of the human forecasting will be difficult, so in the future, the achievement of artificial intelligence will emerge in a large number of in the fields even in real life, gradually replacing human social work. The rapid pace of scientific and technological development and the depth of research in the field of artificial intelligence are certainly encouraging. However, from the perspective of law, a social discipline, artificial intelligence brings convenience and efficiency to human beings and risks and problems. The emergence of new technology will not only bring about the change of productivity and production mode, but also affect the social relations among different social subjects at a deeper level. The phenomenon of robots killing people and driverless cars causing accidents is the reality as there are still many problems in developing and applying artificial intelligence. However, it also reflects the embarrassing situation that cannot be relied on [29, 30].

3. Experiments

3.1. Experimental Dataset.
The experiment selected area has lakes and mountains, hot springs township, and scenic spots and historical sites, various folk customs, beautiful natural scenery, and profound cultural deposits, with obvious cultural diversity. A single way of traveling can no longer meet the needs of tourists and bring low social and economic benefits. As an important link in the tourism industry chain, cultural and creative industry needs cultural interpretation to be charming. Today, more and more consumers pay more attention to the uniqueness and cultural connotation of travel products. However, from the perspective of cultural and creative products in the market, it is more about discussing the theoretical model, which lacks specific design practice and creative research. It is especially important to dig deeply into regional cultural value and design cultural and creative products with regional culture.

3.1.1. Element Extraction and Design. Extracting and reconstructing elements are a common method in design. The local landscape Lingxiu with a long history of rich cultural connotations provides many resources for the design of local cultural products. These resources are not only the review of the tradition but also the inheritance of the essence of excellent culture. The creative materials are captured from the culture; the traditional art of the region is reconstructed according to the design content and modern constitution consciousness; tradition is reinterpreted with modern language and aesthetic appeal, for better realization of the inheritance and development of the outstanding cultural traditions. The specific data selection process is as follows:

(1) Font Extraction of Cultural Symbols. Plan in order to join the "water as the soul" of the regional cultural characteristics. For the font, Small Zhuan is chosen; this setting is also more in line with Chaohu Lake's "hot spring township" tourism positioning. According to the geographical characteristics of "three sides of green mountains and one side of the lake," the "nest" font of the seal body was deformed to extract the cultural symbols of the region. The selection of colors refers to the elegant lacquerware red and black main color, combined with the seal form to show the local cultural history of heavy sense.

(2) Extraction of Graphic Patterns and Folk Culture. The principles of rhythm and prosody are followed in the design of graphic patterns, which coexist in a picture and reflect the sense of pattern order. In terms of content, we take the traditional graphics, cultural allusions, myths and legends, and geographical features of the region as the starting point and foothold of creation to extract and summarize.

(3) Product Design. After designing the graphics, the next step is to consider the application of graphics in creative products. How to tap the essence of "regional culture" and make a series of derivatives based on it? Now there are also a lot of tourism products in the regional market, but the form is older, is poor in practicality, does not attract consumers. The design of the graph can be done as a whole derivative also can be transported. Here, we listed the split application, listed some of the derivatives designs, and made some adjustments based on the characteristics of the derivatives themselves, including calendar, T-shirt, mobile phone case, canvas bag, and stationery.

3.1.2. Material and Process Selection of Cultural and Creative Products. Cultural and creative products in the selection of materials and crafts usually give priority to the cost of production, while the use of regional representative handicrafts is an important factor to consider cultural and creative products. The selection of raw materials reflects the distinctive regional culture. The application of both traditional handicraft and modern new materials endows the product with a sense of history and times. If plastic or silica gel is selected as the plastic material for a mobile phone case, other paper or cloth products can be adjusted according to consumers' preference.

3.2. Experimental Design. Specific design ideas are shown in Figure 2:

3.3. Experimental Questionnaire Survey. This questionnaire mainly adopts two ways of issuing questionnaires on-site and online in Chaohu area. A total of 120 questionnaires were issued, among which 16 subjects did not live in the experimental area and did not meet the criteria of the survey. The actual number of valid questionnaires was 104. The sample effective rate was 8667%. The purpose of the questionnaire is to collect people's understanding of the local culture. According to the investigation and analysis, the subjects who have lived in the region for more than 20 years and are over 40 years old are familiar with the regional culture. Moreover, 28.3 percent said they did not know anything about the traditional culture of the region, mainly in the age group of 18 to 30. More than 80 percent of Mankiewicz people want to know more about the traditional culture of the region and believe it is necessary to inherit and protect the local culture. From the survey, it can be concluded that the young man understanding in the geographical area of the traditional culture is not much, due to the fast-paced way of life and people's attention is focused on the new things and the traditional, ancient culture is falling gradually out of favor. Therefore, the regional traditional culture integrated into modern products results in involving traditional culture in peoples' daily life, thus leading to better inheritance and development of traditional culture, as shown in Table 1.

4. Discussion

4.1. Design and Analysis of Cultural and Creative Products in the Experimental Area

4.1.1. Market Prospect Analysis. According to the basic framework of regional lake cultural tourism planning, the regional lake cultural tourism will form a geographic spatial pattern of "one lake, two cities, 12 towns, 18 scenes, and 24 mouths." Opening up the Chaohu lake tourism area is conducive to the adjustment of our province's tourism regional pattern, enhancing the integration of resources so as to create a new tourism economic growth point. In terms of both natural scenery and cultural history, the development of cultural and creative products in the region has great

potential and a good market prospect, which is the creative source of developing cultural and creative products. However, the cultural and creative products in the region have a vast market, but the design and development are not perfect. In order to further improve the form of tourism industry in this region, it is urgent to study the design of cultural and creative products. The use of artificial intelligence technology to select and extract typical graphic language in regional culture and skillfully integrate it into the design of cultural and creative products can not only create products with regional characteristics and modern sense, but also give new vitality to the traditional culture of the region and open up a way for the development of regional cultural and creative industries. Figure 3 shows the scale and growth rate of the cultural and creative industry in the experimental area.

4.1.2. Design Positioning. Some emphasis should be laid on the extraction of the graphic language of the regional traditional culture. Reasonable application, artificial intelligence technology makes "ancient" and "now" a clever combination and extracts representative patterns or cultural forms for design. Among them, "ancient" refers to retaining the original taste of traditional graphic culture; "present" refers to creating a modern form to realize the functional value and market value of the product. Regional culture can be protected through cultural and creative products, and traditional culture can flourish through the tourism industry. The aesthetic connotation of the pattern color in the experimental area carries the cultural connotation of Chinese folk custom and Jiang Shuai region, endowed with strong subjective aesthetic feelings of the national cultural connotation. In order to better apply the traditional nesting pattern to the design, the author extracts and analyzes the color value through artificial intelligence and chart form, and the summary is shown in Figure 4:

4.2. Analysis of Questionnaire Results. As shown in Figure 5, 75% of the test subjects have purchased or intend to purchase cultural and creative products with regional characteristics. However, the cultural and creative products in Chaohu market still have problems such as old-fashioned design, lack of creativity, and obscure regional characteristics. Consumers often prefer simple and modern cultural creative products with regional traditional cultural characteristics. As can be seen from the above chart, the creativity of products is the easiest factor to attract consumers, followed by cultural connotation, use, appearance, price, taste, commemorative significance, and functions. Therefore, the design and development of regional cultural creative products need to organically combine creativity, practicality, and cultural connotation to get more consumers' recognition and love.

4.3. Innovation of Product Design Methods Using Artificial Intelligence. Artificial intelligence technology can replace and assist human designers in product design. At present, artificial intelligence has not completely changed the process
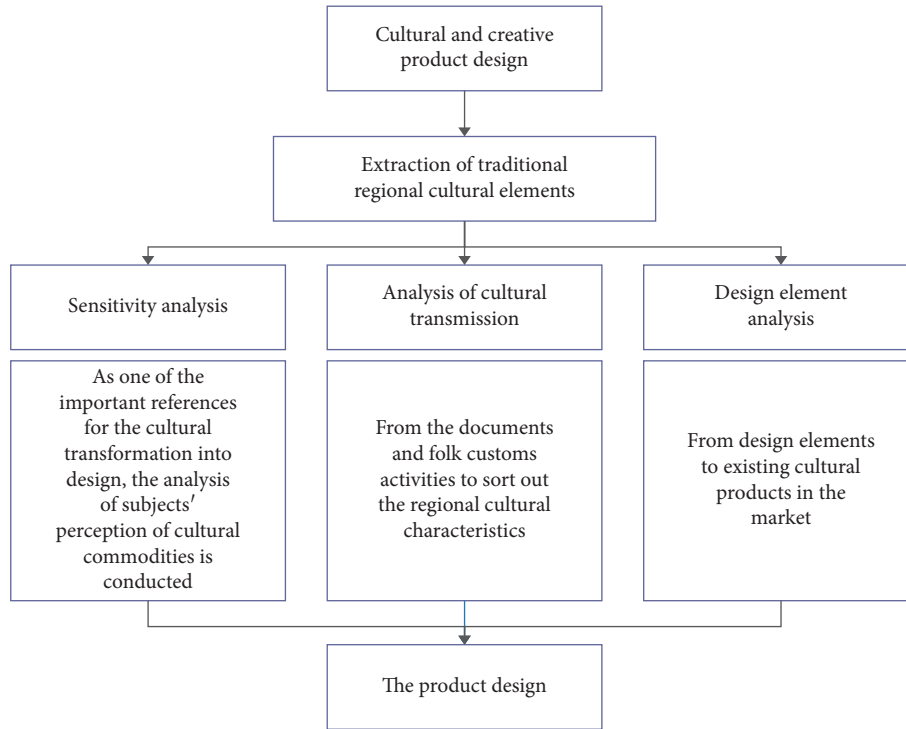
Figure 2: Design idea.

Table 1: Questionnaire.

	Modelling	34	33 (%)
	Practical	27	26
	Creative	55	53
What attracts you when buying cultural and creative products?	Function	31	30
	Color	35	34
	The cultural connotation	48	46
	Memorable	52	50
	Price	19	18
	Contracted fashion	46	44
	Interesting	53	51
What elements do you think are needed for a good cultural and creative product?	Unique in form	32	31
	Traditional style	17	16
	Highlight traditional culture	58	56

of product design but has innovated the method of product design. Specifically, there are the following aspects, as shown in Figure 6.

In the Research Phase of Product Design, through interaction with designers, artificial intelligence can not only obtain the research results of previous similar designs but also analyze and judge the advantages and disadvantages of such designs so that designers can choose between them. In the design vision stage, artificial intelligence, on the one hand, can select for designers previous design innovation and personalized demands and, on the other hand, can make the design conceive visualizations through building and processing and design and analysis of the cognitive model for simulating the potential design idea. Through VR, 3D printing technology displays design idea of vision and technical feasibility, assists designers in a number of design ideas, provides and analyzes the solution of the vision as

much as possible to eliminate interference, and makes a design more targeted, advanced, original, and feasible. In the design tuning phase, using the test function of artificial intelligence software and mature algorithm module, the design prototype can be tested and tuned in the artificial intelligence environment. Current debugging includes vision, artificial intelligence language, language, communication, knowledge, search, several big modules, design of product inspection, analysis of model checking, voice interaction, and emotion. Under the action of the designer, artificial intelligence will be tuning results, advantages and disadvantages, and characteristics directly, which will be clear at a glance. In the validation phase, product design thinking and requirements are constantly iterative and updated, and the solution in the design may become the starting point of a design update. Evaluation and verification of the product design results after tuning can make the
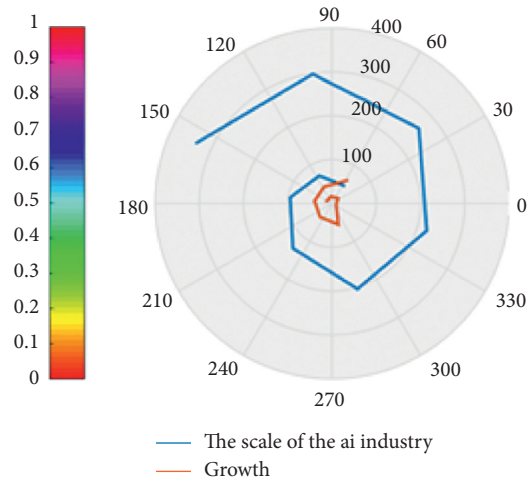
Figure 3: Development of cultural and creative industry in the experimental area of artificial intelligence industry.
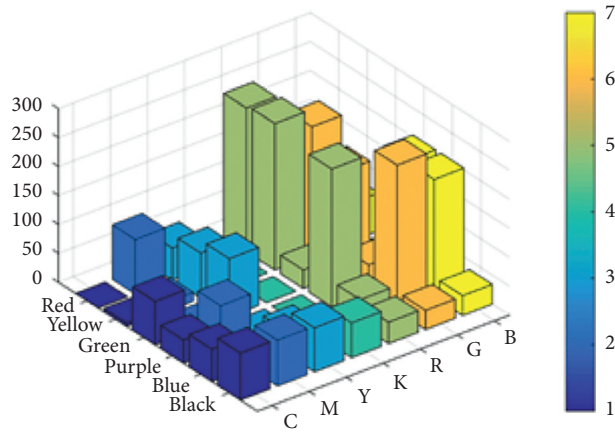
Figure 4: Color summary value table.
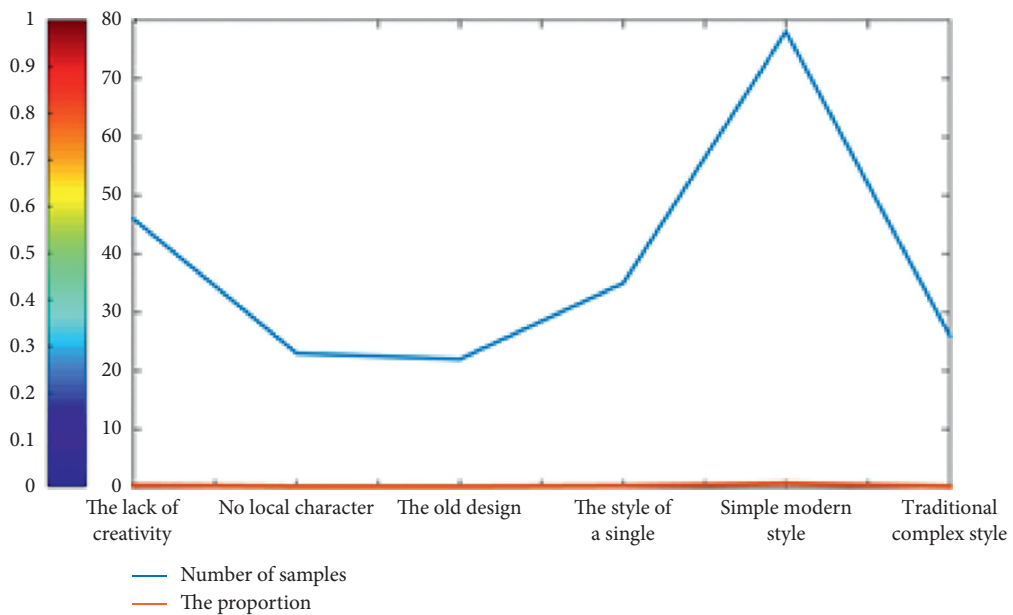
Figure 5: Questionnaire results.
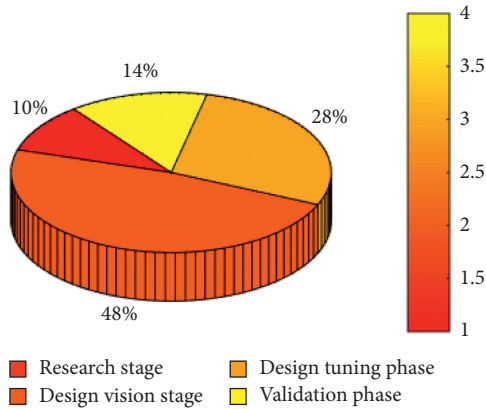
Figure 6: Innovation in product design methodology.

feedback of product design more accurate and more conducive to the improvement of designers. In the traditional design process, this step is tedious and time-consuming. In the artificial intelligence environment, it can screen out the defects of previous verification, not only from the macro perspective, but also from the micro perspective, as it can be tailored accordingly. For example, A/B test is carried out on the verification algorithm and compared with the design in the database to obtain the recognition degree and make the product design success rate greater.

5. Conclusions

As a typical interdisciplinary subject, the basic connotation of artificial intelligence is to simulate a variety of human behaviors, thus creating intelligent product development and other operating modes. Under this premise, artificial intelligence closely connects intelligent means and artificial product development, thus creating more effective product development ideas and product design patterns. At present, artificial intelligence means are gradually penetrating into the daily production of various fields and bringing prominent influence to the daily life of residents. Therefore, it can be known that artificial intelligence technology should be able to integrate into the whole process of designing various products. In general, cultural and creative product design not only pursues its shape and external beauty but needs designers to bring its unique regional cultural characteristics and cultural connotation into consumers' perception through design. Only in this way can consumers be moved and the sales of cultural and creative products be driven. In the course of packaging design, it is necessary to combine the imparting of theoretical knowledge with the cultivation of practical ability.

This article focuses on the research and discussion on how to implant the cultural image of the experimental area into the creative cultural products, so as to make the regional cultural connotation spread and develop through the flowing nature of commodities. The sales of commodities promote the improvement of economic benefits, and also, the interaction between commodities and tourists can help tourists to further understand the traditional culture of the

region. Can really use these cultural resources so that the traditional culture is no longer boring, difficult to understand, not just the so-called "cultural representation," but a deeper cultural inheritance?

Through the above analysis, we can know that artificial intelligence means reflected in the product development advantages cannot be ignored. Up to now, the technical personnel is trying to design and develop various new products by means of artificial intelligence, and the effectiveness of corresponding product development is particularly outstanding. Therefore, in future practice, the diversified product design still needs to use artificial intelligence means to adapt to local conditions so as to ensure that the corresponding product development ideas can be flexibly selected in close combination with the attributes and characteristics of the product itself.

Data Availability

No data were used to support this study.

Conflicts of Interest

The authors declare that they have no conflicts of interest.

References

[1] L. Lazzeretti, F. Capone, and I. E. Seçilmiş, "In search of a Mediterranean creativity. Cultural and creative industries in Italy, Spain and Turkey," *European Planning Studies*, vol. 24, no. 3, pp. 568–588, 2016.

[2] K. Gundolf, A. Jaouen, and J. Gast, "Motives for strategic alliances in cultural and creative industries," *Creativity & Innovation Management*, vol. 12, no. 3, pp. 1–13, 2017.

[3] K. Borseková, D. Cole, K. Petríková, and A. Vaňová, "Nostalgic sentiment and cultural and creative industries in regional development: a Slovak case study," *Quaestiones Geographicae*, vol. 34, no. 2, pp. 53–63, 2015.

[4] C. Hasio, "Visual inspirations: the pedagogical and cultural significance of creative posters in the art classroom," *Journal of College Teaching & Learning (TLC)*, vol. 12, no. 1, pp. 39–44, 2015.

[5] S.-C. Chiou and Y.-C. Wang, "The example application of genetic algorithm for the framework of cultural and creative brand design in Tamsui Historical Museum," *Soft Computing*, vol. 22, no. 3, pp. 1–19, 2017.

[6] W. Lu, Q. L. Kweh, and D. He, "Performance analysis of the cultural and creative industry: a network-based approach," *Naval Research Logistics*, vol. 64, no. 2, p. 457, 2018.

[7] N. Naga and R. McGill, "Negotiating cultural difference in creative writing workshops," *Pedagogy*, vol. 18, no. 1, pp. 69–86, 2018.

[8] S.-J. Luo and Y.-N. Dong, "Classifying cultural artifacts knowledge for creative design," *Zhejiang Daxue Xuebao (Gongxue Ban)/Journal of Zhejiang University (Engineering Science Edition)*, vol. 51, no. 1, pp. 113–123, 2017.

[9] S.-J. Luo, "France-asia: cultural identity and creative exchange," *Lesprit Créateur*, vol. 56, no. 3, pp. 1–13, 2016.

[10] A. Gilmore and R. Comunian, "Beyond the campus: higher education, cultural policy and the creative economy," *International Journal of Cultural Policy*, vol. 22, no. 1, pp. 1–9, 2015.

[11] W.-S. Tang, "Creative industries, public engagement and urban redevelopment in Hong Kong: cultural regeneration as another dose of isotopia?" *Cities*, vol. 56, no. 8, pp. 156–164, 2015.

[12] W. Shen and Y. Yuan, "Sociocultural basis underlying creative thinking," *Advances in Psychological Science*, vol. 23, no. 7, p. 1169, 2015.

[13] M. Rushton, "Sigrid hemels and kazuko goto (eds.): tax incentives for the creative industries," *Journal of Cultural Economics*, vol. 41, no. 2, pp. 1–3, 2017.

[14] J. George, "Examining the cultural value of festivals," *International Journal of Event and Festival Management*, vol. 6, no. 2, pp. 122–134, 2015.

[15] H. Forbes and D. Schaefer, "Social product development: the democratization of design, manufacture and innovation," *Procedia Cirp*, vol. 60, no. 5, pp. 404–409, 2017.

[16] C. Steimer, J. C. Aurich, and Aurich, "Analysis of information interdependencies between product development and manufacturing system planning in early design phases," *Procedia Cirp*, vol. 50, no. 10, pp. 460–465, 2016.

[17] W. L. Chen and F. L. Chao, "Toward eco product development with qualitative and CAE design process - case study of flame guiding module," *Journal of Physics Conference*, vol. 989, no. 1, 2018.

[18] G. F. Özkan-Seely, C. Gaimon, and S. Kavadias, "Dynamic knowledge transfer and knowledge development for product and process design teams," *Manufacturing & Service Operations Management*, vol. 17, no. 2, pp. 177–190, 2015.

[19] I. Dmitry, "Conflicts in product development and machining time estimation at early design stages," *Lecture Notes in Control & Information Sciences*, vol. 22, no. 13, pp. 103–116, 2015.

[20] I. Dmitry, "A review of leader-follower joint optimization problems and mathematical models for product design and development," *International Journal of Advanced Manufacturing Technology*, vol. 22, 2015.

[21] E. R. Gamzu, S. Perez-Lloret, and N. M. Farber, "Design and development of a novel supportive care product for the treatment of sialorrhea in Parkinson's diseases," *Current Topics in Medicinal Chemistry*, vol. 15, no. 10, p. 166, 2015.

[22] A. Querbes and K. Frenken, "Grounding the "mirroring hypothesis": towards a general theory of organization design in New Product Development," *Journal of Engineering and Technology Management*, vol. 47, no. 6, pp. 81–95, 2018.

[23] S. Goguelin, J. Colaco, V. Dhokia, and D. Schaefer, "Smart manufacturability analysis for digital product development," *Procedia Cirp*, vol. 60, no. 9, pp. 56–61, 2017.

[24] B. Ahmad, "A design-thinking perspective on capability development: the case of new product development for a service business model," *International Journal of Operations & Production Management*, vol. 38, no. 4, pp. 1041–1060, 2017.

[25] N. Efkolidis, C. Garcia-Hernadez, P. Kyratsis, and J. L. Huertas-Talon, "Design for green usability: a new user centered methodology for product development," *Applied Mechanics and Materials*, vol. 809-810, no. 2, pp. 1372–1377, 2015.

[26] R. J. Baumgartner and D. Hofer, "Improving sustainability performance in early phases of product design: a checklist for sustainable product development tested in the automotive industry," *Journal of Cleaner Production*, vol. 140, no. 2, pp. 1602–1617, 2016.

[27] K. O. M. O. T. O. Hitoshi, K. O. N. D. O. H. Shinsuke, and M. A. S. U. I. Keijiro, "An application of graph traversal algorithm to design task planning in model-based product development," *Journal of Advanced Mechanical Design Systems & Manufacturing*, vol. 10, no. 7, 2016.

[28] J.-G. Persson, "Current trends in product development," *Procedia Cirp*, vol. 50, no. 1, pp. 378–383, 2016.

[29] J.-Yu Lai and J. Wang, "Exploring the impacts of perceived e-collaboration service convenience on new product development in Taiwanese IC design companies," *Information Technology & Management*, vol. 19, no. 14, pp. 1–14, 2017.

[30] Y. P. Liu, J. J. Ding, and X. Y. Long, "Control and optimization of development risk of the high-tech manufacturing and measuring product," *Applied Mechanics & Materials*, vol. 709, no. 5, pp. 503–508, 2015.

Research Article

Research on Output Waveform of Generator with Rectifier Load considering Commutation Overlap Angle

Bingyi Zhang, Gongfei He [ID], and Guihong Feng

School of Electrical Engineering, Shenyang University of Technology, Shenyang 110870, China

Correspondence should be addressed to Gongfei He; hegf2646@163.com

The purpose of this paper is to study the influence of the uncontrolled rectifier circuit on the generator's output waveform when considering the commutation overlap angle. Taking the nonsalient permanent magnet (PM) generator directly connected with the uncontrolled rectifier circuit as an example, the equivalent circuit of the generator with rectifier load is established, and the commutation process of the rectifier circuit is analyzed when the effect of the commutation overlap angle is considered. The output waveforms of generator's output side are obtained by analytical method, circuit simulation method, field-circuit coupled simulation method, and experimental method. The validity of the analysis methods is demonstrated by comparison. According to the results of analytical analysis, we know the characteristics of the output waveform under the influence of the commutation overlap angle. The existence of the commutation overlap angle will cause the voltage waveform to concave or convex, prolong the conduction time of the winding, and result in phase difference between the voltage waveform and current waveform. The influence of synchronous inductance and extra inductance on the output waveforms and harmonic distortion rate is analyzed. The research of this paper provides a theoretical basis for improving the output waveform of the generator with rectifier load.

1. Introduction

Distributed power supply system as the main power supply or standby power supply is widely used in numerous fields such as marine electric propulsion, wind power generation, aviation, emergency, mine, and petrochemical. When the capacity demand for the distributed power supply is large, the power supply method in parallel operation of electric excitation synchronous generator sets is often adopted. This power supply method needs to adopt constant frequency and constant voltage double-closed loops' control and also needs to balance the active power and reactive power of each set with the load sharing device, and the control system is complex. When using the DC bus power supply system, load sharing of each set can be achieved by simply adjusting the amplitude of generator's output voltage, and there is no need to maintain the frequency of generator's output voltage constant, and the adjustment of the amplitude can be achieved by adjusting the prime mover speed [1]. This provides a convenient condition for the application of the

PM generator with high efficiency, simple structure, large torque density, and many other advantages and also promotes the development of the distributed DC power supply system. There is a rectifier in the distributed DC power supply system, and the existence of the rectifier will cause distortion of the AC side output waveforms of the power supply system and will have a serious impact on generator's performance [2, 3].

The AC side harmonic pollution problem caused by the nonlinear loads such as the rectifier circuit has been paid high attention to. Aimed at different generator types and rectification methods, the researchers use different methods to analyze the output characteristics of the distributed DC power supply system. The pulse width modulation rectifier is the best choice because of the high-quality AC side output waveforms and high power factor, but the cost is high and control is complex [4, 5]. At present, the widely used uncontrolled rectifier will bring harmonic pollution to the power grid side, and the power factor is low, and the existence of a large number of harmonics will lead to an

increase in power line and equipment loss, reduce the efficiency of power generation, transmission, and electrical equipment, and cause equipment vibration and noise worse [6–8], so how to improve the waveforms' quality of the power grid side in the uncontrolled rectifier circuit has been a research hotspot. In the work by Zhang and Wu [9], the working characteristics of the electric excitation synchronous generator with uncontrolled rectifier load are analyzed and the AC side voltage and current waveforms are obtained by numerical simulation. In [10–13], the equivalent circuit model of the power generator system with uncontrolled rectifier load is established, and the mutual influence of voltage and current harmonics is analyzed. In the study by Meyer et al. [14], current waveform characteristics of the power grid side are analyzed by Simulink simulation when the electric vehicle charging pile adopts the uncontrolled rectifier method, and the current waveform quality is improved by using the harmonic compensation device. In the study by Zhang et al. [15], the output characteristics of the electric excitation doubly salient generator are analyzed by the field-circuit coupled simulation method, and the accuracy is verified by experiments.

In summary, the main research methods of AC side output characteristics of the distributed DC power supply system are mainly analyzed method, circuit simulation method, field-circuit coupled simulation method, and experimental method. This paper takes the nonsalient PM generator with the uncontrolled rectifier circuit as an example, and the output voltage and current waveforms of the generator are obtained by using the above methods. The influence mechanism of generator's output waveforms, which is influenced by the rectifier circuit, is analyzed with the solving process of the analytic method, which provides the necessary conditions for studying how to improve the output waveforms of the distributed DC power supply. The comparison of the voltage and current waveforms obtained by each method shows the relative consistency of each method, and the advantages and limitations of each approach are illustrated.

2. Equivalent Circuit of the Permanent Magnet Generator

Whether the generator is connected to rectifier load through the transformer or not, because of the inductance series connection in the circuit, the commutation process cannot be completed instantaneously at the natural commutation point, and the delay phenomenon occurs, and the delay time is expressed by an electric angle γ, which is called the commutation overlap angle. During the commutation period, the total voltage caused by the two-phase short circuit is clamped, which increases the output voltage harmonic content and increases the noncharacteristic harmonics of the output current, resulting in the existence of the phase difference between the output voltage waveform and output current waveform. Therefore, it is necessary to analyze the influence of generator parameters on the commutation overlap angle. When connected to the rectified load through the transformer, only the transformer leakage inductance is

connected in series with the load, whose value can be regarded as a constant. When the generator is directly connected with the rectified load, due to the existence of self-inductance, leakage inductance, and mutual inductance of the windings, the equivalent calculation of the inductance series in the circuit is complicated. Because of the air gap of the salient pole PM generator is not uniform, the self-inductance and mutual inductance of the windings also change with rotor position, so it is difficult to obtain the equivalent circuit of the salient pole PM generator [16].

In order to make the qualitative analysis of the effect of commutation overlap angle on the generator output voltage waveform and current waveform more accurately, it is necessary to determine the equivalent circuit and resistance and inductance parameters of the generator. In the case of the nonsalient pole PM generator, the following assumptions are made before the mathematical model is established: the no-load air gap magnetic field of the generator is sinusoidal, and the influence of the armature reaction magnetic field on the excitation magnetic field is neglected, that is, the no-load EMF of the generator is sinusoidal, and the amplitude is constant, and the permeability of the permanent magnet is a constant, and similar to the permeability of air, the magnetic resistance of the stator and rotor core lamination is neglected [17]. The voltage equations of PM generator three-phase windings can be expressed as

$$
\begin{cases}
u_a = \dfrac{\mathrm{d}\psi_{\mathrm{fa}}}{\mathrm{d}t} - \dfrac{\mathrm{d}\psi_a}{\mathrm{d}t} - R_s i_a, \\[2mm]
u_b = \dfrac{\mathrm{d}\psi_{\mathrm{fb}}}{\mathrm{d}t} - \dfrac{\mathrm{d}\psi_b}{\mathrm{d}t} - R_s i_b, \\[2mm]
u_c = \dfrac{\mathrm{d}\psi_{\mathrm{fc}}}{\mathrm{d}t} - \dfrac{\mathrm{d}\psi_c}{\mathrm{d}t} - R_s i_c.
\end{cases}
\tag{1}
$$

In the formula, R_s is the stator phase resistance, ψ_{fa}, ψ_{fb}, and ψ_{fc} are excitation flux linkages of A-phase, B-phase, and C-phase windings, respectively, and ψ_a, ψ_b, and ψ_c are the total armature reaction flux linkages of A-phase, B-phase and C-phase windings, respectively, and there is

$$
\begin{pmatrix} \psi_a \\ \psi_b \\ \psi_c \end{pmatrix} =
\begin{pmatrix} L_a & L_{\mathrm{ab}} & L_{\mathrm{ac}} \\ L_{\mathrm{ba}} & L_b & L_{\mathrm{bc}} \\ L_{\mathrm{ca}} & L_{\mathrm{cb}} & L_c \end{pmatrix}
\begin{pmatrix} i_a \\ i_b \\ i_c \end{pmatrix}.
\tag{2}
$$

In the formula, L_a, L_b, and L_c are the self-inductances of A-phase, B-phase, and C-phase windings, respectively, L_{ab}, L_{ac}, L_{ba}, L_{bc}, L_{ca}, and L_{cb} are the mutual inductances between the A-phase, B-phase, and C-phase windings, and i_a, i_b, and i_c are the currents of the A-phase, B-phase, and C-phase windings; based on the assumptions above, there is

$$
\begin{cases}
L_a = L_b = L_c = L_{s\sigma} + L_{m1}, \\[2mm]
L_{\mathrm{ab}} = L_{\mathrm{ba}} = L_{\mathrm{ac}} = L_{\mathrm{ca}} = L_{\mathrm{bc}} = L_{\mathrm{cb}} = \dfrac{-L_{m1}}{2}, \\[2mm]
i_a + i_b + i_c = 0.
\end{cases}
\tag{3}
$$

In the formula, $L_{s\sigma}$ and L_{m1} are the leakage inductance and excitation inductance of the phase winding; taking A phase as an example, there is

$$\psi_a = L_a i_a - \frac{1}{2} L_{m1}(i_b + i_c) = L_{s\sigma} i_a + \frac{3}{2} L_{m1} i_a = L_t i_a. \quad (4)$$

In the formula, $(L_t = L_{s\sigma} + 3L_{m1}/2)$ is called synchronous inductance, and the voltage vector equation of the stator winding can be obtained by summarizing the derivation formulas above:

$$\dot{U}_a = \dot{E}_a - L_t \frac{d\dot{I}_a}{dt} - R_s \dot{I}_a. \quad (5)$$

The equivalent circuit of the nonsalient pole PM generator can be obtained according to formula (5). When the current in the winding has a sudden change, the presence of the synchronous inductance will hinder this change, resulting in the existence of the commutation overlap angle, so the magnitude of the commutation overlap angle is related to the self-inductance, leakage inductance, and mutual inductance of the armature windings. Because there is no excitation winding and damping winding on the rotor of the PM generator, the transient inductance of the PM generator is equal to that of the steady state when neglecting the eddy current effect [18].

3. Analysis of the Commutation Process in the Uncontrolled Rectifier Circuit

In the study of the influence of the uncontrolled rectifier circuit on generator's output voltage and current waveforms, many literatures analyze the working process of the uncontrolled rectifier circuit on the basis of different assumptions. In the work by Dai et al. [19], the commutation process of the doubled nonsalient pole electric excitation generator is analyzed, and the analytical formulas of commutation time, the value of commutation overlap angle, and commutation voltage drop are deduced. It is assumed that the DC side current is straight like other literatures. When the DC current is straight as the prerequisite, the output current of the AC side is also a constant during the non-commutation period. In order to simplify the equivalent circuit and facilitate the analytical analysis, taking resistive load as example, the equivalent circuit of the nonsalient PM generator with the uncontrolled rectifier circuit is shown in Figure 1.

In the normal operation of the rectifier circuit, the two diodes in the same phase cannot turn on at the same time, and if there is the state that the commutation overlap angle $\gamma > 60°$, there must be the state that the commutation overlap angle $\gamma < 60°$, and the generator is in an asymmetrical and nonnormal working condition. Therefore, the study in this paper will limit the value of the commutation overlap angle in the range of $0 < \gamma < 60°$. The commutation overlap angle will cause the common anode group or the common cathode group two diodes to conduct simultaneously, and the working state of the three-phase rectifier bridge will be changed from 6 to 12, and the duration of each state is
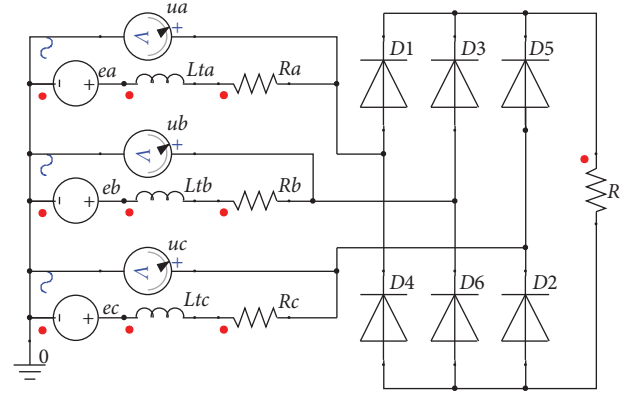
FIGURE 1: Equivalent circuit of the rectifier generator set.

related to the value of the commutation overlap angle. The no-load back EMF waveforms of three phase windings within a single cycle is shown in Figure 2, assume the RMS values as U_2. According to the symmetry of the circuit structure, it is only necessary to study the output voltage and current waveform in the positive half period of the A-phase winding. It is assumed that the starting point of the commutation overlap angle is the natural commutation point, and the influence of the stator phase resistance is neglected. In the case of $\gamma \leq (\pi/6)$, the output voltage of the A-phase winding rises from zero at the origin.

During the period of $0 \sim (\pi/6)$ according to the diode conduction conditions, only diodes D5 and D6 are conducting, and the equivalent circuit shown in Figure 1 can be simplified to the modal 1 shown in Figure 3, and the transient voltage and current equations of the circuit are

$$\begin{cases} u_a = e_a, \\ i_a = 0. \end{cases} \quad (6)$$

During $(\pi/6) \sim (\pi/6) + \gamma$ period, according to the diode conduction conditions, only diodes D1, D5 and D6 are conducting, and the equivalent circuit shown in Figure 1 can be simplified to the modal 2 shown in Figure 3; in contrast to the sudden increase of current i_a and the sudden reduce of current i_c, it can be temporarily considered that $i_b = i_r$ with little change, that is, $(di_b/dt) = 0$, and the transient voltage and current equations of the circuit are

$$\begin{cases} u_a = e_a - L_t \dfrac{di_a}{dt}, \\[2mm] u_b = e_b - L_t \dfrac{di_b}{dt} \Rightarrow \begin{cases} u_a = \dfrac{e_a + e_c}{2}, \\[2mm] L_t \dfrac{di_a}{dt} = \dfrac{e_a - e_c}{2}, \end{cases} \\[2mm] u_c = e_c - L_t \dfrac{di_c}{dt}. \end{cases} \quad (7)$$

During $(\pi/6) + \gamma \sim (\pi/2)$ period, according to the diode conduction conditions, only diodes D1 and D6 are
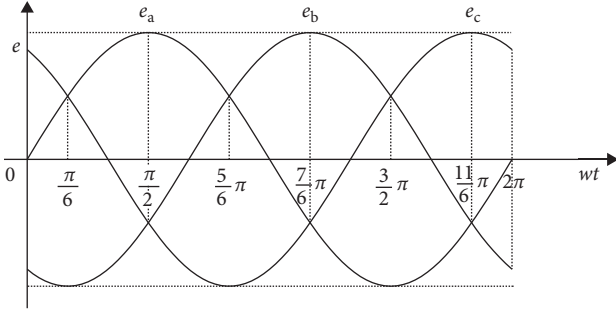
Figure 2: No-load back EMF waveform.

conducting, and the equivalent circuit shown in Figure 1 can be simplified to the modal 3 shown in Figure 3, C-phase in cut-off state, there is $i_b = -i_a$, and the transient voltage and current equations of the circuit are

$$
\begin{cases}
u_r = u_a - u_b = e_a - e_b - 2L_t \dfrac{di_a}{dt} = i_a R, \\[3mm]
u_a = e_a - L_t \dfrac{di_a}{dt}.
\end{cases}
\tag{8}
$$

During $(\pi/2) \sim (\pi/2) + \gamma$ period, according to the diode conduction conditions, only diodes D1, D2 and D6 are conducting, and the equivalent circuit shown in Figure 1 can be simplified to the modal 4 shown in Figure 3, B-phase and C-phase in short circuit state, it can be temporarily considered that $i_a = i_r$ with little change, that is, $(di_a/dt) = 0$. The transient voltage and current equations of the circuit are

$$
\begin{cases}
u_r = u_a - u_b = u_a - u_c = e_a - \dfrac{e_b + e_c}{2} = i_a R, \\[3mm]
u_a = e_a - L_t \dfrac{di_a}{dt}.
\end{cases}
\tag{9}
$$

During $(\pi/2) + \gamma \sim (5\pi/6)$ period, according to the diode conduction conditions, only diodes D1 and D2 are conducting, and the equivalent circuit shown in Figure 1 can be simplified to a modal similar to the modal 3 shown in Figure 3. The transient voltage and current equations of the circuit are

$$
\begin{cases}
u_r = u_a - u_c = e_a - e_c - 2L_t \dfrac{di_a}{dt} = i_a R, \\[3mm]
u_a = e_a - L_t \dfrac{di_a}{dt}.
\end{cases}
\tag{10}
$$

During $(5\pi/6) \sim (5\pi/6) + \gamma$ period, according to the diode conduction conditions, only diodes D1, D2 and D3 are conducting, and the equivalent circuit shown in Figure 1 can be simplified to a modal similar to the modal 2 shown in Figure 3. The transient voltage and current equations of the circuit are

$$
\begin{cases}
u_a = \dfrac{e_a + e_b}{2}, \\[3mm]
L_a \dfrac{di_a}{dt} = \dfrac{e_a - e_b}{2}.
\end{cases}
\tag{11}
$$

During $(5\pi/6) + \gamma \sim \pi$ period, according to the diode conduction conditions, only diodes D2 and D3 are conducting, and the equivalent circuit shown in Figure 1 can be simplified to a modal similar to the modal 1 shown in Figure 3, and with the same transient voltage and current equations.

The above analysis results show that, under the influence of the commutation overlap angle, the positive half period of the generator output voltage and current waveforms are divided into 7 segments when $\gamma \leq (\pi/6)$. When $(\pi/6) < \gamma < (\pi/3)$, according to the periodicity and continuity of the circuit, the starting point of the $(5\pi/6) + \gamma \sim \pi$ period will be in the next time period, and the starting point of modal 1 working state is $\gamma - (\pi/6)$, and the remaining intervals are piecewise unchanged. The remaining periods remain the same, and the transient voltage and current equations of each period remain the same.

4. Influence of Uncontrolled Rectification on Generator's Output Waveform

4.1. Analytic Analysis of Generator's Output Waveform. In the commutation process analysis of the uncontrolled rectifier circuit, the instantaneous value expressions of generator output voltage and current of the A-phase winding within the positive half cycle are given. By using these expressions, the output voltage and current waveform of the generator can be drawn so that the influence of the rectifier circuit on the output waveform of the AC side can be understood more intuitively. In order to draw the waveform effectively, it is necessary to determine the value of the commutation overlap angle and the boundary conditions of each segment.

Through the voltage and current equations of the $(\pi/6) \sim (\pi/6) + \gamma$ period, the current expression of the A-phase winding can be obtained:

$$
i_a = \frac{\sqrt{6}U_2}{2\omega L_t}\left[1 - \cos\left(\omega t - \frac{\pi}{6}\right)\right].
\tag{12}
$$

By modal 1, when $\omega t = (\pi/6)$, the B phase is in the normal conducting state, and $i_{b(\pi/6)} = ((e_c - e_b)/R)$, and during the period of A-phase and C-phase simultaneous conduction, B-phase current varies little, and it can be assumed that $i_{r1} = i_{a((\pi/6)+\gamma)} = i_{b((\pi/6)+\gamma)} = i_{b(\pi/6)}$. According to the boundary condition and the abovementioned formulas, the expressions of the commutation overlap angle can be obtained:

$$
\cos \gamma_1 = 1 - \frac{2\omega L_t i_{r1}}{\sqrt{6}U_2}.
\tag{13}
$$

Using the above approximate γ_1, i_r can be calculated more accurate that

$$
i_r = i_{a((\pi/6)+\gamma)} = \frac{(u_a - u_b)}{R} = 2\frac{(e_a + e_c)}{R} - \frac{e_b}{R}.
\tag{14}
$$

An accurate commutation overlap angle can be obtained by substituting i_r into formula (13), and the result can be made more accurate by repeated iterations.

During $(\pi/6) + \gamma \sim (\pi/2)$ period, according to the current equation, the expression of the current can be obtained:

(a)

(b)

(c)

(d)
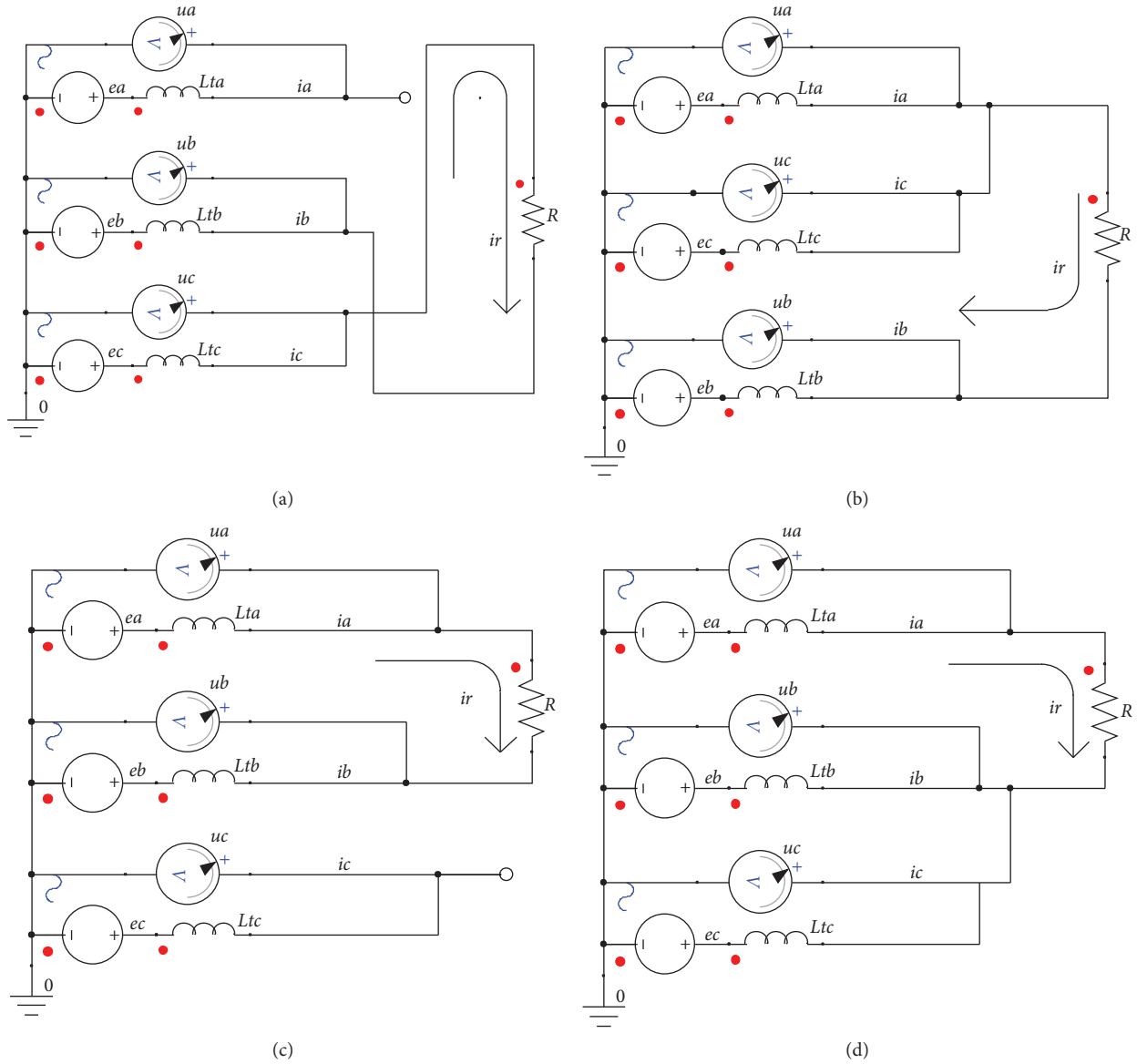
FIGURE 3: (a) Equivalent circuit modal 1. (b) Equivalent circuit modal 2. (c) Equivalent circuit modal 3. (d) Equivalent circuit modal 4.

$$i_a = \frac{\sqrt{2}U_2}{R^2 + 4\omega^2 L_t^2}\left[R\sin\left(\omega t + \frac{\pi}{6}\right) - 2\omega L_t \cos\left(\omega t + \frac{\pi}{6}\right)\right] + Ce^{-(R/2L_t)t}.$$

(15)

The value of constant C can be obtained by taking the A-phase current value at $\omega t = (\pi/6) + \gamma$ during $(\pi/6) \sim (\pi/6) + \gamma$ period as the boundary condition.

The expressions of voltage and current during $(\pi/2) \sim (\pi/2) + \gamma$ period are easily obtained according to their voltage and current equations, and the solving method of the voltage and current expressions during $(\pi/2) + \gamma \sim (5\pi/6)$ period is similar to the solving method during $(\pi/6) \sim (\pi/6) + \gamma$ period, and the solving method of the voltage and current expressions during $(5\pi/6) \sim (5\pi/6) + \gamma$ period is similar to the solving method during $(\pi/6) + \gamma \sim (\pi/2)$ period. Using the expressions and boundary conditions of voltage and current, the generator's

output voltage and current waveforms can be obtained under the condition that no-load back EMF, synchronous inductance, rated frequency, and equivalent load resistance of the generator are known. The rated parameters of the existing prototype are shown in Table 1. In order to make the proportion of the periods more reasonable for the convenience of observation, in the simulation and experimental study, the given resistance value is 5 ohm, which is about half load. The output voltage and current waveforms of the A-phase winding within a single cycle be obtained as shown in Figure 4.

5. Numerical Simulation of Generator's Output Waveform

In the front, the AC side voltage and current waveforms of the nonsalient pole PM generator with rectified load are

Table 1: Rated parameters of the prototype.

Parameters	Values (kW)
Rated power	100
Synchronous inductance	0.32
End inductance	0.025
Phase back EMF	220
Rated frequency	100
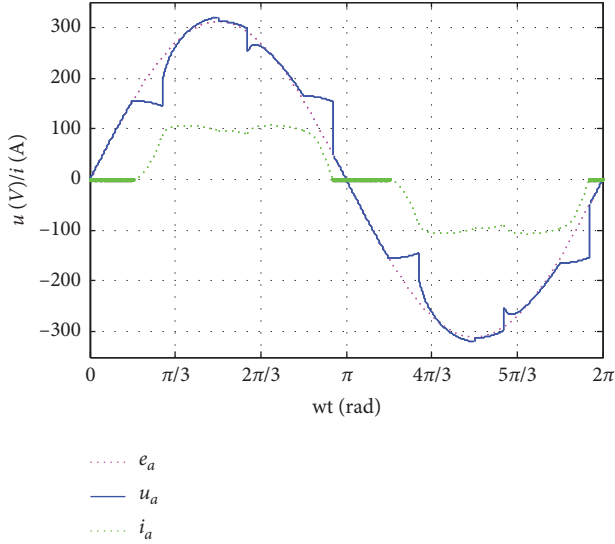
Figure 4: Waveforms of output voltage and current.

derived and analyzed by using the analytic method; however, this is based on a large number of idealized assumptions, and inevitably, there will be some deviations, and when the salient pole PM generator is adopted or the filter element is taken into consideration, the situation is more complicated. Because of the nonlinearity and time variation of power electronic devices, the traditional analysis methods cannot meet the requirements of static and dynamic analyses. Circuit simulation technology can be used for more accurate research, and when there is a generator in the system, the equivalent model of the generator must be established [20]. In order to facilitate the design of simulation circuit, some simulation software contains generator equivalent model. The generator's output voltage and current waveforms can be obtained by circuit simulation using the equivalent circuit of the rectifier generator set shown in Figure 1.

Although the circuit simulation method avoids the idealization assumption and approximate solution in the derivation of the generator's output voltage and current formulas, the generator is modeled equivalently, which cannot truly reflect the complex electromagnetic field of the generator changes with time and space. Without considering the influence of the harmonic magnetic field and armature reaction magnetic field on the air gap magnetic field, the influence of magnetic circuit saturation on motor parameters cannot be considered. Moreover, the accuracy of the generator parameters will directly affect the accuracy of the analysis results. The excellent performance of the finite

element method in solving such complex problems has been widely used, and the equivalent model of the generator in the circuit is replaced by the finite element model, which is changed into the field-circuit coupled simulation, and the established field-circuit coupled simulation model is shown in Figure 5. The speed of the generator is adjusted by changing the setting value of the prime mover speed-setting module. Because of the two-dimensional finite element simulation model not considering the influence of end inductance and phase resistance, the end inductance L_{aend}, L_{bend}, and L_{cend} and phase resistance R_a, R_b, and R_c shall be added to the output side of the generator. The output voltage waveforms and current waveforms of the generator obtained by means of analytic method, circuit simulation method, and field-circuit coupled simulation method are shown in Figures 6 and 7, respectively.

Figures 6 and 7 show that the current waveforms obtained by the three methods are very close, with little difference. The difference of voltage waveforms between the analytic method and circuit simulation method is very small, and the accuracy of voltage and current analytic formula and the validity of the formula deduction process are explained. The voltage waveform obtained by the field-circuit coupling simulation method is obviously different from that obtained by the other two methods, mainly in the voltage drop rate during the commutation phase and the peak value of the output voltage. The main reason is that although the air gap magnetic field of the generator has been sinusoidal, but the no-load back EMF waveform of the generator still contains harmonic components. Moreover, the armature reaction magnetic field will further lead to the asymmetry of the air gap magnetic field and weaken the air gap magnetic field in general. The influence of the impedance voltage drop will decrease the peak value of the voltage.

6. Experimental Test of Generator's Output Waveform

In order to verify the validity of the above analysis methods, the rectifier generator set experimental platform is built to measure the output waveform of the prototype. Using variable-frequency motor drives the generator operating at rated speed same as the simulation given value, and when testing, the load resistance value is adjusted to the same value as the simulation setting. The generator output voltage and current waveforms are shown in Figures 8 and 9, respectively. By comparison, it can be found that the measured voltage and current waveforms agree well with the waveforms obtained by previous methods, and waveforms obtained by the field-circuit coupled method is more close to the measured, which also explains the accuracy of the above analysis.

7. Optimization of Generator Output Waveform Quality

According to the generator's output voltage and current waveforms obtained by above methods, during the conduction phase commutation of the A phase, the existence of
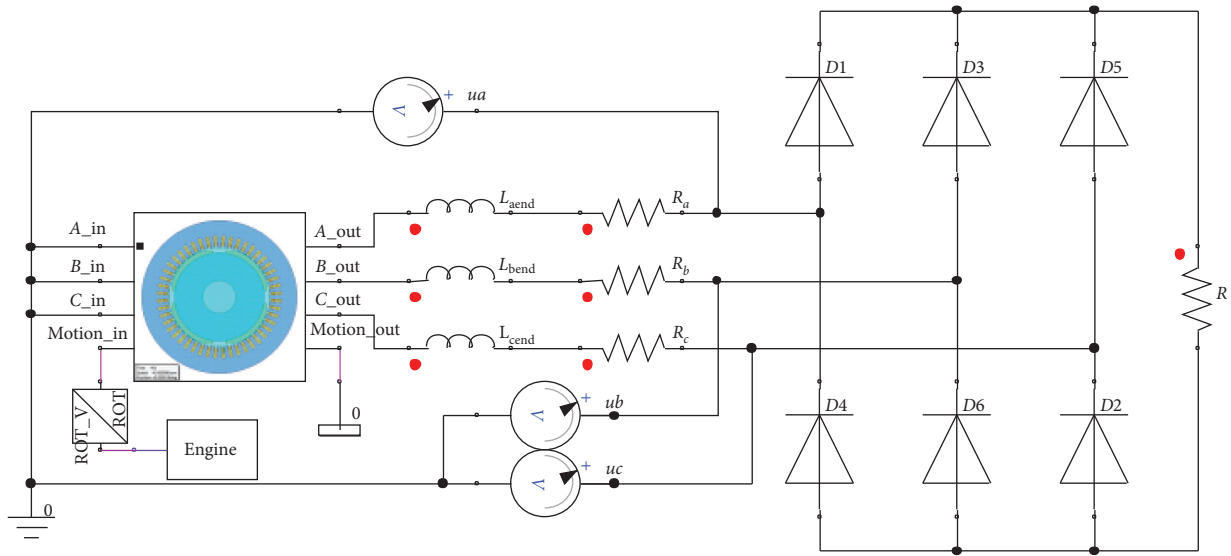
Figure 5: Field-circuit coupled simulation model.
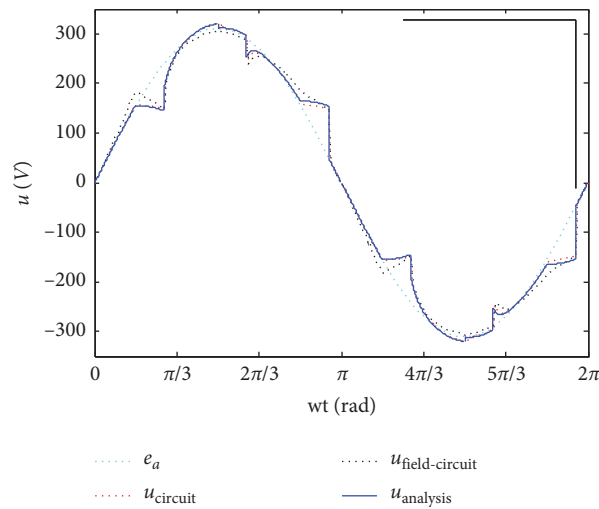
Figure 6: Comparison of output voltage waveforms.

the commutation overlap angle causes the voltage waveform to concave. During cut-off phase commutation of the A phase, the existence of the commutation overlap angle causes the voltage waveform to convex. During the phase commutation B and C, the voltage waveform also has a concave phenomenon. Therefore, the existence of the commutation overlap angle causes serious distortion of generator's output voltage waveform. According to the generator output current waveforms, we can see that the existence of the commutation overlap angle will lead to longer conduction time of the winding, which will result in the phase difference between the voltage waveform and the current waveform. When the synchronous inductance is different, the generator's output voltage, current waveforms, and the corresponding harmonic distortion rate are shown in Figures 10 and 11, respectively. As can be seen from Figures 10 and 11, with the increase of synchronous

inductance, the distortion of the output voltage waveform is aggravated, and the distortion of the output current waveform is improved.

In order to improve the output waveforms of the generator, the most commonly used passive filter circuit shown in Figure 12, and the inductances $L1 = L2 = L3$ series in the circuit, and the capacitors $C1 = C2 = C3$ parallel in the circuit, and the influence of the capacitance value and inductance value on the voltage and current waveforms' quality of the generator is analyzed by simulation [21].

Through the circuit simulation, the distortion rates of the voltage waveform and current waveform of the generator change with inductance and capacitance values, which are shown in Figures 13 and 14, respectively. The fundamental power factors of the generator output side change with inductance and capacitance values, which are shown in Figure 15.
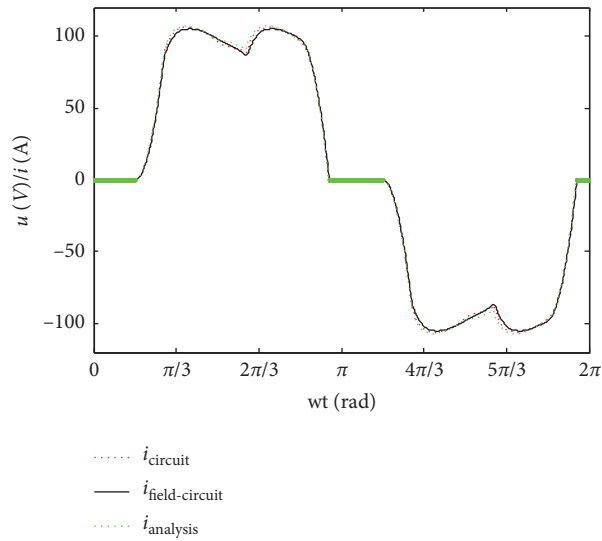
Figure 7: Comparison of output current waveforms.
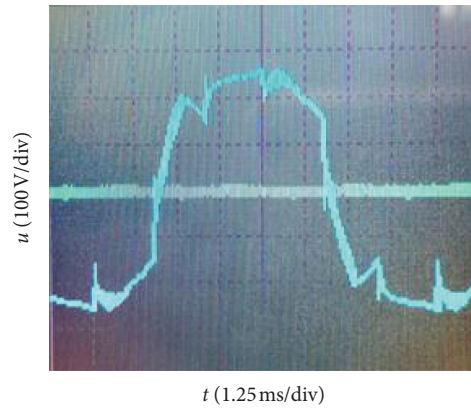
Figure 8: Measured output voltage waveform.
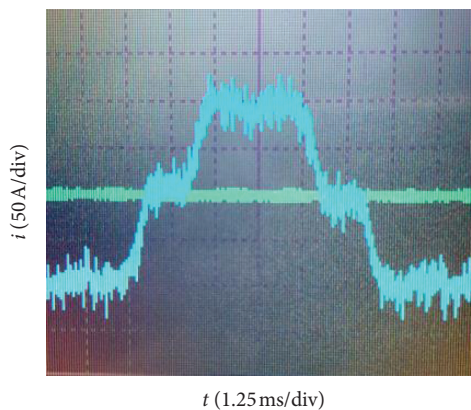
Figure 9: Measured output current waveform.

It can be clearly seen from Figures 13–15 that the passive filter circuit can significantly improve the quality of generator voltage and current waveforms. Increasing the filter inductance can significantly reduce the distortion rate of voltage and current waveforms, but it will reduce the fundamental power factor. Increasing the filter capacitor can reduce the distortion rate of voltage and current waveforms and improve the fundamental power factor. High-quality
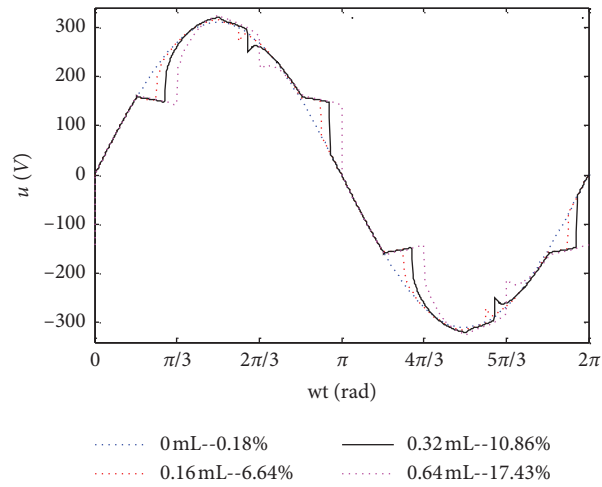
FIGURE 10: Influence of synchronous inductance on the voltage waveform.
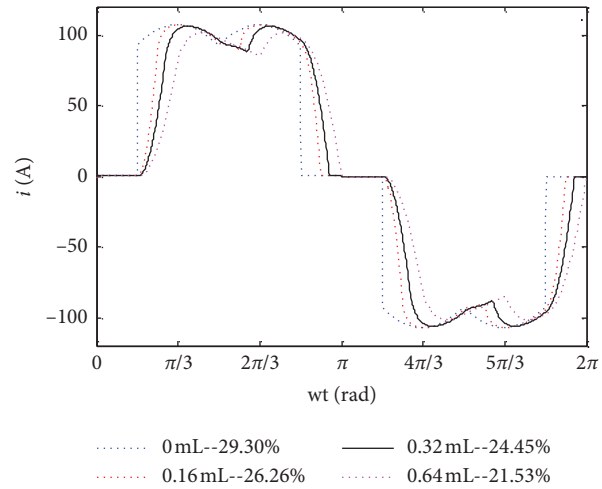
FIGURE 11: Influence of synchronous inductor on the current waveform.
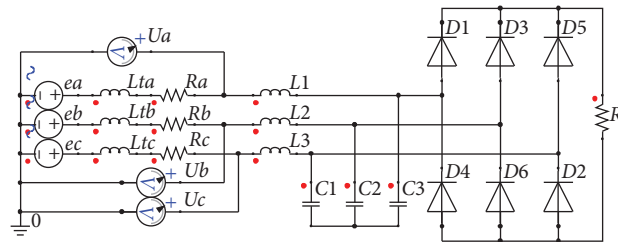
FIGURE 12: The passive filter circuit.
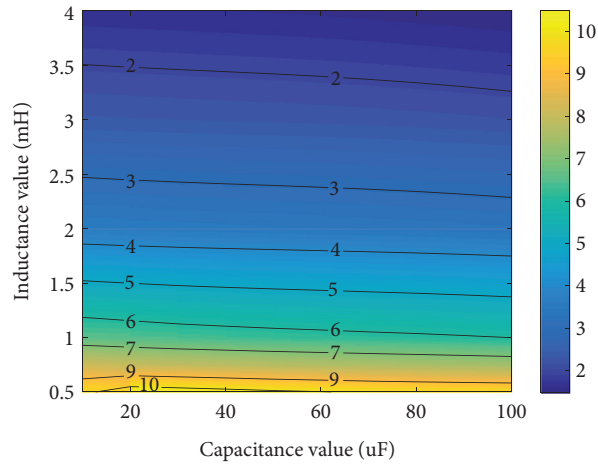
FIGURE 13: Distortion rates of the voltage waveform.
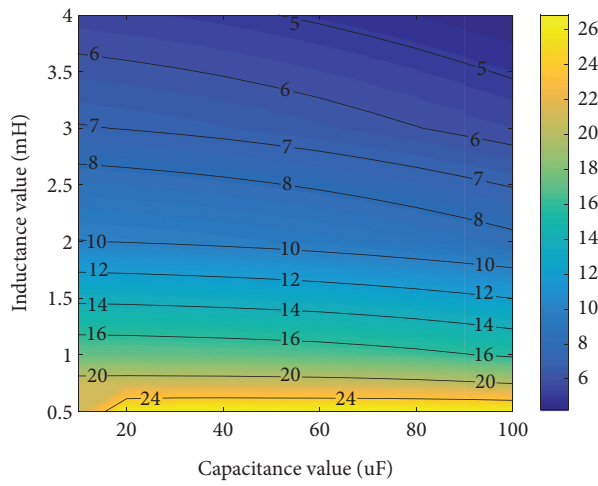
FIGURE 14: Distortion rates of the voltage waveform.
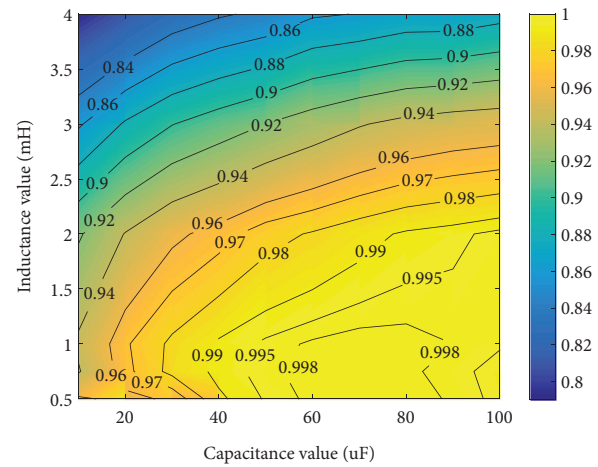
FIGURE 15: Distortion rates of the voltage waveform.

generator voltage and current waveforms and high power factor can be obtained by selecting filter capacitance and filter inductance.

8. Conclusion

The output waveform of the generator with rectifier load is studied in this paper. On the basis of the equivalent circuit, the commutation process of the uncontrolled rectifier circuit is analyzed when the commutation overlap angle is considered, and the influence of rectifier generator parameters on the commutation overlap angle is analyzed, and the analytic expression of the commutation overlap angle is given. The output voltage and current waveforms of the generator are obtained by analytic method, circuit simulation method, field-circuit coupled simulation method, and experimental method, respectively, and the advantages and limitations of these methods are explained. By comparing the output voltage and current waveforms obtained by different methods, the field-circuit coupled simulation method is in good agreement with the experimental method.

In this paper, the influence of the rectifier circuit on the output voltage and current waveforms of the generator is summarized, and the influence of synchronous inductance on the output waveform and harmonic distortion rate of the generator is analyzed. With the increase of the capacity difference between the generator and the rectifier load, the influence of the commutation overlap angle becomes smaller. The influence of the capacitance value and inductance value on the voltage and current waveforms' quality of the generator is analyzed by passive filter circuit simulation. Increasing the filter inductance can significantly reduce the distortion rate of voltage and current waveforms, but it will reduce the fundamental power factor. Increasing the filter capacitor can reduce the distortion rate of voltage and current waveforms and improve the fundamental power factor. The research of this paper has the guidance and reference significance for the application of the generator with rectifier load.

Data Availability

The data used to support the findings of this study are included within the article.

Conflicts of Interest

The authors declare that they have no conflicts of interest.

References

[1] G. He, B. Zhang, and G. Feng, "Power balanced control of rectifier permanent magnet generator sets," *Journal of Intelligent & Fuzzy Systems*, vol. 40, no. 2, pp. 2993–3003, 2021.

[2] P. M. Nicolae, M. Ş. Nicolae, and I. D. Nicolae, "Distorting regimes and their measurement systems for the diagnosis purposes in three-phase systems," in *Proceedings of the IEEE International Conference on the Science of Electrical Engineering (ICSEE)*, pp. 1–5, Eilat, Israel, December 2016.

[3] S. S. Kumar, N. Kumaresan, and M. Subbiah, "Analysis and control of capacitor-excited induction generators connected to a micro-grid through power electronic converters," *IET Generation, Transmission & Distribution*, vol. 9, no. 10, pp. 911–920, 2015.

[4] M. B. Ketzer and C. B. Jacobina, "Sensorless control technique for PWM rectifiers with voltage disturbance rejection and adaptive power factor," *IEEE Transactions on Industrial Electronics*, vol. 62, no. 2, pp. 1140–1151, 2015.

[5] S. Sahbani, H. Mahmoudi, A. Hasnaoui, M. Kchikach, and A. Redouane, "A novel high power factor PWM rectifier with push-pull control for harmonic reduction in industrial areas networks of smart grid," in *Proceedings of the International Renewable and Sustainable Energy Conference (IRSEC)*, pp. 1080–1084, Tetouan, Morocco, November 2016.

[6] M. Kiani and W. J. Lee, "Effects of voltage unbalance and system harmonics on the performance of doubly fed induction wind generators," *IEEE Transactions on Industry Applications*, vol. 46, no. 2, pp. 562–568, 2010.

[7] J. Yong, A. B. Nassif, and W. Xu, "Effect of voltage crest shape on the harmonic amplification and attenuation of diode-bridge converter-based loads," *IET Generation, Transmission & Distribution*, vol. 5, no. 10, pp. 1033–1041, 2011.

[8] S. Jordan and J. Apsley, "Diode rectification of multiphase synchronous generators for aircraft applications," in *Proceedings of the IEEE Energy Conversion Congress and Exposition*, pp. 3208–3215, Vancouver, Canada, October 2011.

[9] Y. Zhang and Y. Wu, "Design of synchronous generator for integrated power propulsion system in marine," *Transactions of China Electrotechnical Society*, vol. 28, no. 10, pp. 67–74, 2016.

[10] Y. Y. Sun, C. K. Dai, J. Q. Li et al., "Frequency-domain harmonic matrix model for three-phase diode-bridge rectifier," *IET Generation, Transmission & Distribution*, vol. 10, no. 7, pp. 1605–1614, 2016.

[11] N. C. Zhou, J. J. Wang, Q. G. Wang, and N. Q. Wei, "Measurement-based harmonic modeling of an electric vehicle charging station using a three-phase uncontrolled rectifier," *IEEE Transactions on Smart Grid*, vol. 6, no. 3, pp. 1332–1340, 2015.

[12] J. Fang, Y. Wang, L. Le, and S. N. Li, "Frequency domain harmonic model of electric vehicle charger using three-phase uncontrolled rectifier," in *Proceedings of the China International Conference on Electricity Distribution (CICED)*, pp. 1–5, Tianjin, China, September 2016.

[13] K. Wei, D. Wang, X. W. Yu, Z. Z. Su, and S. W. Cheng, "Research on AC output characteristic of a multiphase permanent magnet generator with rectified load," in *Proceedings of the IEEE Conference and Expo Transportation Electrification Asia-Pacific (ITEC Asia-Pacific)*, pp. 1–5, Beijing, China, 2014.

[14] J. Meyer, S. Müller, P. Schegner et al., "Comparison of methods for modelling electric vehicle chargers for harmonic studies," in *Proceedings of the Power Systems Computation Conference (PSCC)*, pp. 1–7, Genoa, Italy, June 2016.

[15] Z. R. Zhang, J. J. Zhou, D. M. Zhu et al., "Multi-pole low speed doubly salient electro-magnetic wind turbine generator and its rectification characteristics," *Proceedings of the CSEE*, vol. 39, no. No. 6, pp. 67–72, 2009.

[16] S. K. Cheng, Y. J. Yu, F. Chai et al., "Analysis of the inductances of interior permanent magnet synchronous motor," *Proceedings of the CSEE*, vol. 29, no. 18, pp. 94–99, 2009.

[17] C. Y. Wang, J. K. Xia, and Y. B. Sun, *Modern Control Technology for Electric Machines*, pp. 104–112, China machine press, Beijing, China, 2008.

[18] C. H. Zhang, X. Sun, W. M. Tong et al., "Calculation and measurement of transient reactance of permanent magnet synchronous motor," *Electrical Engineering*, vol. 4, pp. 14–17, 2009.

[19] W. L. Dai, H. H. Qin, H. H. Guo et al., "Analysis of commutation in three-phase rectifier of doubly salient electromagnetic generator," *Proceedings of the CSEE*, vol. 28, no. 20, pp. 111–117, 2008.

[20] B. J. Ge, S. Y. Xiao, Z. H. Liu et al., "Improved model of synchronous generators internal faults based on circuit-coupled FEM," *IEEE Transactions on Energy Conversion*, vol. 32, no. 3, pp. 876–884, 2017.

[21] B. Abood Salam and M. Abdul Wahhab Thamir, "Investigation of harmonic reduction using passive filters in a distribution network in basra city," *IOP Conference Series: Materials Science and Engineering*, vol. 1, no. 1067, 2021.

Research Article

Construction of a Supply Chain Financial Logistics Supervision System Based on Internet of Things Technology

Zhaoyang Wu (ID), Shiyong Wang, Hong Yang, and Xiaokui Zhao

School of Economics and Management, Qinghai Normal University, Xi'ning 810016, Qinghai, China

Correspondence should be addressed to Zhaoyang Wu; 2018130@qhnu.edu.cn

In recent years, with the rapid development of the global economy and the development trend of more and more stable, well-developed network communications, online shopping has become an increasingly common way; as a result, the logistics industry has emerged from many industries and has become one of the most popular industries. However, due to the extensive involvement of the logistics industry, the overly complex technology, and the huge amount of data and information, the security of logistics has become one of the hot topics of special concern. Based on the background of an intelligent environment, this paper constructs a supply chain financial logistics supervision system based on Internet of Things technology. This article refers to the research experience of previous scholars, briefly introduces the theoretical knowledge of the Internet of Things technology, smart environment, and supply chain finance, and makes a certain analysis of the logistics supervision system. We collect and calculate logistics data through the wolf group hunting and siege formula in the wolf group algorithm and analyze the application performance of the logistics supervision system in reality. Then, we briefly designed the system architecture diagram of the logistics supervision system and compared the freight situation of the logistics supervision system before and after and statistics on the deployment of the logistics supervision system in customs, docks, airports, stations, and other places from 2015 to 2019. Finally, a comparative analysis of the performance of wolf pack algorithm and other algorithms was performed under different path planning. The final result shows that the logistics supervision system has important practical value in the logistics industry; in addition, the deployment of logistics supervision systems in customs, terminals, and other places has increased year by year from 2015 to 2019.

1. Introduction

1.1. Background Meaning. At present, the development of the Internet and sensor network is very rapid [1], e-commerce which has risen from the development of the Internet in recent years has gradually become the most frequently used way of shopping [2], and the complementary logistics industry has become more and more hot and penetrated into our daily life. With the vigorous development of the logistics industry, the frequent occurrence of goods stolen, goods lost, goods delay, and logistics warehouse accidents and other logistics security issues have gradually become the focus of attention [3]. In the process of logistics transportation, the status of goods, logistics itinerary, and other related information directly affect the safety of logistics. In order to understand the specific conditions of the logistics and

transportation process, building a supply chain financial logistics supervision system based on the Internet of Things technology has very important practical significance for logistics companies, sellers of goods, and buyers of goods [4].

The Internet of Things is an extension and expansion of the Internet [5]. It connects items in a smart environment with smart devices with functions such as recognition, perception, and calculation to form a "things connected" network and, through wireless communication, wireless sensor network and other technologies to transmit and share data and information between equipment and equipment [6], after a certain amount of processing, and then transfer useful information to the user's terminal equipment through the network. It is conceived as a transformative method for providing numerous services [7]. The Internet of Things technology largely solves the communication function of

information and can also identify different information and screen out effective information for users. Combining the Internet of Things technology with the logistics supervision system can improve the efficiency of goods sorting [8], can monitor the information of the goods in real time, and timely feedback the situation of the goods to the users, making the logistics supervision efficient, accurate, and more.

1.2. Related Work. The purpose of Bui is to analyze and clarify the potential advantages of Trarong Province from the perspective of logistics and supply chain management, thereby proposing the development of Trarong Province as an economic and logistics hub in the Mekong Delta [9], but the cost of this research is too high. Zulfikar's research aims to determine how valuable PT's supply chain performance is [10], *XYZ* when measured using the green scor model. But, the experimental data of this research are too one sided, and the experimental results are unreliable. Vieira introduced the study of port logistics activities in the port of Santos (Brazil) with a qualitative method [11], but the research data were too large. Chancey analyzed the location of facilities and vehicle routing problems of efficient logistic systems in a practical case study [12], but the experimental results of this study have errors. Zhilun proposed the existence of the drone logistics regulatory issues, analyzed the composition of the logistics industry chain of unmanned aerial vehicles, and discussed the applicability of the regulatory system of the whole industry chain, but the steps of the study are too complex and the cost is too high [13]. Xiaofeng takes enterprise supervision, logistics supervision, and quarantine supervision as the core, adopts the risk assessment method of "three links joint control," and establishes a supervision system with Chinese characteristics for export wood packaging materials [14]; however, the data collection of this research is too difficult, and it is easy to cause unnecessary wastage. The purpose of Busse is to provide a good foundation for further research on the innovation management of logistics service providers (LSPs) [15], but the research is too simple to fully reflect the experimental results. However, these studies still have shortcomings in the monitoring and management of logistics. This article builds a logistics monitoring system based on the Internet of Things technology based on the research experience of previous scholars.

1.3. Innovation of This Article. The application of the Internet of Things technology has made supply chain finance a further breakthrough in logistics supervision. The innovations of this article are mainly reflected in the following aspects: The application of the Internet of Things technology improves the supervision mechanism of the logistics industry, makes the logistics supervision mechanism real time, and saves the human resources of the logistics department of the logistics industry.

2. Supply Chain Financial Logistics Supervision System Based on Internet of Things Technology

2.1. Internet of Things Technology. The Internet of Things (IoTs) is a network technology that uses various sensing technologies to connect items to the Internet for information exchange and communication to achieve intelligent identification, tracking, and supervision under an agreed agreement. The Internet of Things is a global infrastructure that can connect objects and realize data generation and data sharing [16]. Internet of Things as a new information network technology is still in the development stage, did not form a complete technology framework, and lacks a unified architecture that is standard, but the prototype has been formed. The Internet of Things is considered to be a part of the future Internet, which will contain billions of intelligent communication "things" [17]. The technology system structure of the Internet of Things mainly refers to the IOS/ OSI model of the Internet to construct its system structure by means of hierarchical division, which makes the basic system structure of the Internet of Things have typical hierarchical characteristics. The Internet of Things introduces a vision for the future Internet, in which users with sensing and stimulating functions, computing systems, and everyday objects will collaborate with each other with unprecedented convenience and economic benefits [18]. The widely recognized IoT architecture can be divided into a perception layer, network transmission layer, and application layer. It works by perceiving and identifying the surrounding data information through RFID, GPS, QR code and other sensing technologies in the sensing layer, so as to obtain the required information in real time; then, through the network transmission layer, the information obtained by the perception layer is transmitted to the terminals of other users through reliable transmission, in order to realize the sharing and interaction of information between each other; and finally, the data information in the network transmission layer are processed intelligently through smart devices at the application layer and smart computing technologies such as cloud computing, to make decisions and control the surrounding environment. Radio frequency identification has been widely used to support the logistics management of the production workshop [19]. The latest developments in RFID, smart sensors, communication technology, and Internet protocols have promoted the development of IoT [20].

2.2. Smart Environment. The intelligent environment is the embodiment of pervasive computing in the architectural dimension; it uses sensor equipment, computer equipment, various identification equipment, and multimedia imaging equipment in the physical space to provide automated services, in an intelligent environment, and users can perform intelligent services at any time. The intelligent environment has the characteristics of system dynamics, service transparency, and equipment mobility. In the intelligent environment system, the relationship between the units often changes, the focus of computer interaction is integration or mobility, and the terminal equipment in the hands of the user can use the basic equipment in the intelligent environment to complete functions such as calculation, interaction, and sharing. The smart environment is easy to use and supports continuous empirical measurement and iterative development [21]. Intelligence

environment is reflected in the union of matter under the influence of technical things, which not only has the traditional environmental performance ability but also has network communications, information products, equipment, automation, and other functions. The intelligent environment integrates system, structure, and service. It has the characteristics of high efficiency, comfort, safety, and environmental protection and helps the space environment to maintain information exchange with the outside world. The applications in the smart environment together provide real-time human emotional state tracking and recognition [22]. The intelligent environment improves the safety and comfort of the user's living environment and, at the same time, has the characteristics of sustainable development, resource conservation, and environmental protection. In an intelligent environment, ubiquitous services depend on the ability of intelligent objects, which can perceive, calculate, communicate and take some adaptive actions in the environment according to their goals even without human intervention [23].

The sensor is the main communication network unit in the intelligent environment. In the flexible environment, the sensor nodes are set manually in the field and the nodes work together to sense and collect the environmental status information or the field target detection information, and the information is transmitted through the only sensor node, sent to the receiving node through hop count or multihop relay, and finally, the analysis result is sent to the terminal node, mobile network, etc. through the Internet users' awareness of effective monitoring and management of the environment is raised. In large-scale sensor data, exploring and mining patterns (leading to detection of abnormal behavior) is challenging [24]. The sensor node consists of four parts: a processor module, radio frequency module, power supply module, and various sensor modules. The processor is the core of the entire node, responsible for wireless transmission of data, sensor signal calibration, and processing. The radio frequency unit is a physical application of the wireless data receiver; it must be designed, and the distance and penetration of wireless communication are realized. Power modules provide energy for the whole node, due to the relatively small sensor nodes, generally battery powered. Sensor nodes need to consider power consumption, plan the sleep state of the node, collect and upload environmental data regularly, and then, set a hardware timer to enter sleep. When the timer expires, the node is awakened followed by the data collection and transmission cycle.

2.3. Supply Chain Finance. Supply chain finance is a link of supply chain management. It is based on supply chain management and one or more basic commitments, on the premise of ensuring the authenticity of the transaction. The use of accounts receivable, advance payment, inventory, and other methods to close capital flow or control ownership of real estate, bills of lading and orders, and information flow based on the information flow between supply chain members is an effective integration of supply chain and capital flow, and we should provide low-risk financing and financial products to the main body of the supply chain, isolate the credit risk of small- and medium-sized enterprises, and ensure the safe development of loan activities. Many companies have adopted and implemented various supply chain practices and have enhanced collaboration in the supply chain and, more recently, electronic collaboration [25]. While the integration with the supplier complements each other, especially in the high-tech environment, the internal supply chain personnel of the organization are either the source of valuable innovation-related knowledge or the channel [26]. The main functions of supply chain finance include the following: It improves the competitiveness and stability of the supply chain, effectively overcomes the financing difficulties of small- and medium-sized enterprises, and optimizes the business structure of banks. Its essence is that the financial service provider takes the future cash flow generated by the asset as the source of repayment for the less liquid assets in various business processes through the overall assessment of the supply chain members; adopts various financial products under the closed business model to provide financial services to participants; and reduces the operating costs of the entire supply chain by coordinating the entire business ecosystem. The overall framework of supply chain finance includes supply chain objectives, supply chain management, supply chain structure, supply chain resources, and supply chain business processes [27], as shown in Figure 1.

The supply chain financial model is led by logistics companies is a business behavior that integrates logistics, commercial operation, and financial management functions. The advantages of supply chain finance led by logistics companies are as follows: (1) According to the characteristics of the logistics business, it has undertaken transportation, warehousing, transportation, and processing activities during the trade between the two sides, obtained the most basic and true information in the circulation process, and has a high degree of control over the rights of goods in the trade process; (2) based on the understanding of the buyer's and seller's transaction arrangements and the status of the goods, the incidence of subjective defaults by financiers using information asymmetry to deliberately conceal relevant information has been greatly reduced, and the default loss rate has been better controlled; (3) based on the strong control of movable properties, the management methods of logistics companies allow innovative financing activities such as value evaluation and pledge guarantee credit; (4) through platform construction, under the premise that the supply company provides guarantees, the problem of financing difficulties for loan companies is partially solved, and more opportunities are provided for cooperation between banks and enterprises. However, this model still has some flaws in some aspects: (1) The logistics industry has a large asset investment, a low rate of return on investment, and a long investment return period; (2) lack of procedures to control the flow of corporate funds and information and
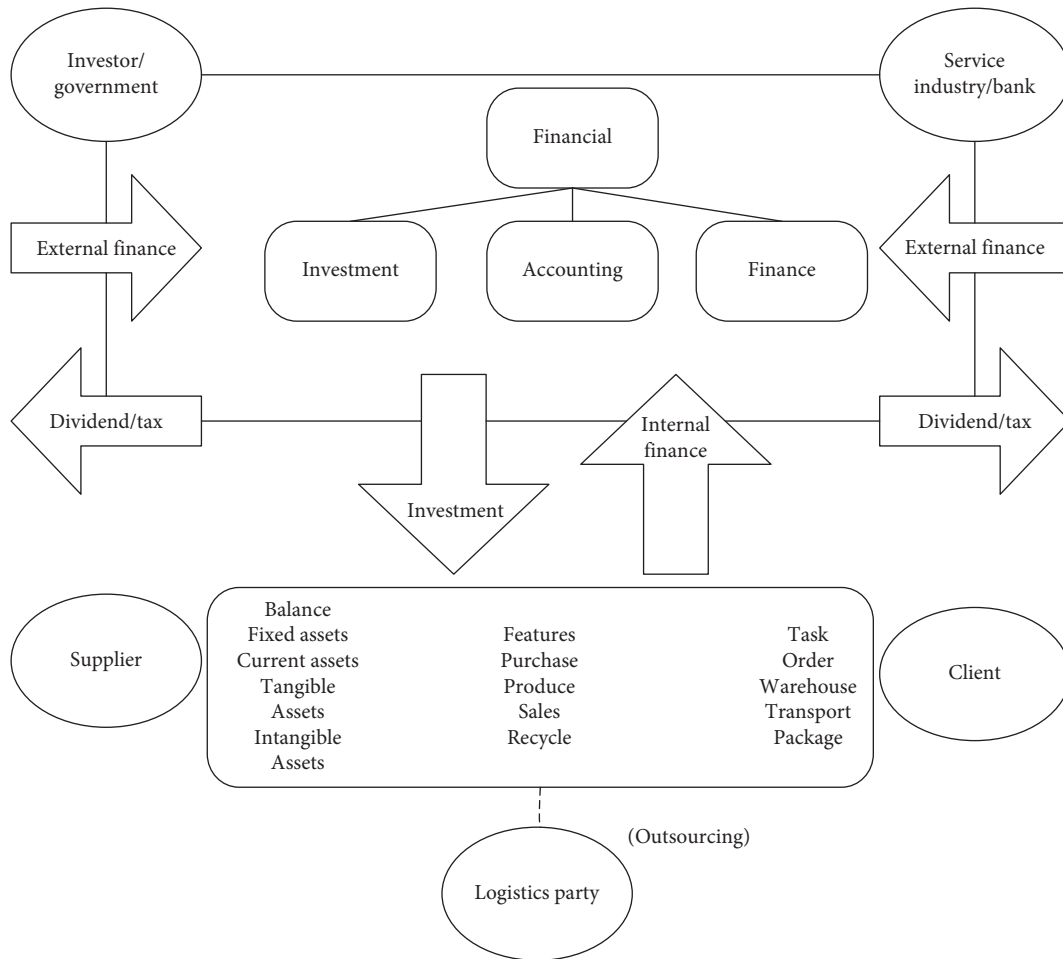
Figure 1: Overall structure of supply chain finance.

weak credit risk management capabilities; (3) The added value of capital services is limited, and major suppliers are responsible for overpayment obligations.

2.4. Logistics Supervision System. The logistics supervision framework system model based on the Internet of Things technology mainly includes five parts: information security and sharing, a standard specification system, a portal system, an operation and maintenance system, and the specific implementation subsystem. The relationship between the various subsystems of the logistics system is mainly the transmission of information, and the information flow includes the upward flow from the end of information collection to the end of the application and the downward flow from the client to the hardware. Specific information flow includes terminal data collection, massive data processing, network transmission operators, distributed data storage, application support services, and front-end applications. There are two different methods for the downward flow of information, one is to transmit the information of the query result through the background channel, and the other is to manage the terminal device according to the instruction. The

purpose of the design of the entire logistics supervision system based on the Internet of Things is to use RFID, GIS, GPS, and other Internet of Things technologies to perform real-time and comprehensive supervision of the transportation, loading, unloading, warehousing, and distribution processes in the logistics process and then help managers to improve the decision-making level for abnormal logistics. Horizontal cooperation between logistics service providers (LSPs) has become an effective form of organization and is expected to develop further in the future [28]. The entire logistics supervision system based on the Internet of Things technology is based on the logistics guarantee business and provides logistics services for different suppliers and consumers. As a real-time logistics monitoring system, in addition to completing the basic functions of the system, it must also consider the principles of applicability, reliability, sustainability, interface beauty, safety, and real-time.

Logistics flexibility has a positive impact on the quality of logistics services and improves the relationship between satisfaction with the logistics flexibility a positive impact on logistics service quality [29]. A mature logistics supervision system must meet the following requirements: (1) ensure the

traceability of logistics and ensure logistics safety; (2) the overall architecture should be based on mature technologies and models to ensure the stability of the system; (3) the logistics system based on the Internet of Things technology takes information exchange as the key, completes the entire logistics system, and realizes the top-down improvement of all links; (4) the system structure of the logistics system should incorporate new technologies and requirements into existing technologies and requirements, laying a foundation with other enterprises for later integration; (5) comprehensively study environmental protection and energy saving issues, and maximize the use of resources in the logistics system; (6) flexible management of different departments according to needs; and (7) improving the efficiency of logistics is the basis for improving logistics competitiveness.

3. Wolves Algorithm Model in the Logistics Supervision System Based on Internet of Things Technology

3.1. Data Collection. The data in this study are mainly derived from the data records of various logistics companies from 2015 to 2019 and the research experience of previous scholars. Data acquisition is achieved based on the networking technology, the use of certain portions of the main service stream AIDC technology for automatic identification and data collection, for example, bar-code printing, bar-code recognition technology, wireless data transmission, and wireless label (RFID) technology. Due to the low cost of bar-code technology, currently, bar-code technology is mainly used for data collection. With the development of RFID technology, the cost of RFID continues to decrease, and more and more manufacturers have begun to use RFID technology.

3.2. Wolves Hunting Model. In order to improve the efficiency of logistics distribution based on the Internet of Things technology under the background of the intelligent environment and optimize the distribution path, we apply the wolf pack algorithm to the logistics distribution according to the actual situation. The wolf group algorithm is proposed based on the intelligent inspiration of the group survival group of the wolf group and has been successfully applied to the optimization problem of complex functions and the conventional 0-1 knapsack problem [30]. The hunting model of wolves is shown in Figure 2.

3.3. Establishment of Wolf Pack Hunting Algorithm. Binary Wolf Pack Algorithm (BWPA) is an intelligent algorithm that can solve combination optimization problems in discrete spaces [31]. Assuming that the hunting range of wolves is in a European space of $N \times M$, it is easier for wolves to find the global optimal value [32]. We add feedback in the process of wolves raiding, increase the communication between the wolf i and the wolf, and automatically adjust the size of the step. When the detective wolf feels the odor concentration is close to the odor concentration felt by the wolf, the step size becomes smaller and slowly approaches the wolf, and if the scent concentration felt by the wolves is very different from the odor concentration felt by the wolves, if you quickly rush to the wolf's position with a larger step length, the formula is as follows:

$$
\begin{cases}
X_{id}^{k+1} = X_{id}^{k} + step_{bid}^{k+1}, \\
\\
step_{bid}^{k+1} = w * step_{bid}^{k} * \dfrac{\left(a_d^k + x_{id}^k\right)}{\left|a_d^k - x_{id}^k\right|}.
\end{cases}
\tag{1}
$$

According to formula (1), to initiate the calling behavior, according to the odor concentration, the value of w is adaptively changed. The calculation formula of w as follows:

$$
w = \begin{cases}
w_{\min} - \dfrac{(w_{\max} - w_{\min}) * \left(F^k - F_{\min}^k\right)}{\left(F_{\text{avg}}^k - F_{\min}^k\right)}, & F \leq F_{\text{avg}}, \\
\\
w_{\max}, & F \leq F_{\text{avg}}.
\end{cases}
\tag{2}
$$

The wolves will approach the wolf from various positions. If the scent perceived by the wolf is greater than that of the wolf, that is, when $Y_i > Y_{\text{lead}}$, the fierce wolf initiates the summoning behavior instead of the wolf; otherwise, it will continue to attack until the distance $d \leq d_{\text{near}}$ between the fierce wolf and the wolf, and algorithm enters siege behavior. The calculation formula of d_{near} is as follows:

$$
d_{\text{near}} = \frac{1}{D * \omega} \sum_{d=1}^{D} \left|\max_d - \min_d\right|,
\tag{3}
$$

where d_{near} is the distance between the wolf and the wolf when the siege is initiated and ω is the distance judgment factor; its size directly determines whether to enter the siege behavior, the greater the ω, the faster the convergence speed, but if it is too large, the calling behavior will remain unchanged.

When the fierce wolf is very close to the head wolf, it means that it is not far from its prey and needs to be captured by a close siege. It is believed that the smell of prey has the highest concentration of wolf prey direction, and artificial wolves need to move forward in small steps, a thorough search of prey odor concentration values near the value of the fitness function. The formula for the siege behavior of wolves is as follows:

$$
X_{id}^{k+1} = X_{id}^{k} + \delta^k * \eta * step_c * \left|H_d^k - x_{id}^k\right|,
\tag{4}
$$

where X_{id}^k represents the position of the k artificial wolf in the M-dimensional space, $step_c$ represents the siege step length, and H_d^k represents the position of the k wolf in the M-dimensional space. η is a random number uniformly distributed in the range $[-1, 1]$, δ^k is the siege adjustment value, and its setting method is as follows:

$$
\begin{cases}
\delta^0 = M, \\
\delta^k = C * \delta^{k-1},
\end{cases}
\quad C \in [0.9, 0.999], \; M = 1.
\tag{5}
$$

During the siege, if the odor concentration perceived by the artificial wolf is greater than the target odor
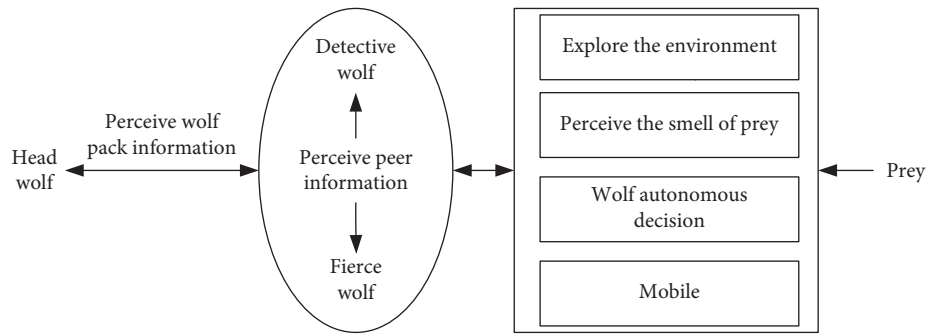
FIGURE 2: Wolves hunting model diagram.

concentration, the position of the artificial wolf will be replaced from the new target position; otherwise, the target position will not change. In order to avoid falling into a local optimal solution, k new artificial wolf is randomly generated to replace the same number of the worst artificial wolf in the population, and the higher the k value, the better the diversity of the new species, which also increases the vitality of the wolf pack. But, if k is too high, the algorithm will tend to search randomly, and if the value of k is too small, it will lead to a local optimum; therefore, the value of k should be a whole between $[N/2 * \lambda, N/\lambda]$, where λ is the population renewal factor.

4. Construction of a Supply Chain Financial Logistics Supervision System Based on Internet of Things Technology

4.1. Construction of the Logistics Supervision System Based on Internet of Things Technology. This article uses the Internet of Things technology to construct a supply chain financial logistics supervision system; first, the main system architecture of the logistics supervision system is designed as shown in Figure 3.

According to the architecture diagram in Figure 3, we can know that the main functional modules of the logistics supervision system are information the release query system, transaction payment system, cargo traceability supervision system, warehouse distribution management system, vehicle personnel dispatch system, EID data exchange platform, multimedia transport management system, and special goods transportation management system. The Internet of Things technology and smart devices with functions such as perception are used as part of the application support layer to support the normal operation of the application, and this part of the content is mainly to ensure the security of logistics information, provide SOA architecture and cloud computing technology for applications, and process application data.

4.2. Comparison of Freight Situation of the Logistics Supervision System. Statistics on the freight situation data of the logistics supervision system in a certain area in October 2019, including the total volume of import and export freight, import volume, export volume, and total number of transportation vehicles, and compared with the freight data in October 2018 before the logistics supervision system was established, and the role of the logistics supervision system in cargo transportation was analyzed. The two-year logistics and other conditions were set to be the same. The statistical data are shown in Figure 4.

According to the data in Figure 4, we can see that the traditional freight supervision situation is indeed inferior to the freight supervision situation after the construction of the logistics supervision system. Through the data of the logistics supervision system, we learned that the number of imports and exports in October 2019 increased by 8.9% year-on-year, the number of goods imports increased by 10.5%, the number of exports increased by 6.9%, and the number of transportation vehicles increased by 9.7%. From these data, we can see that the relevant freight situation in 2018 may not be transmitted to the back end of logistics supervision in real time, leading to the loss of some data.

4.3. Application Distribution of the Logistics Supervision System. After the rise of the logistics industry, logistics supervision systems have been widely used all over the world, especially in customs, docks, airports, stations, and other transportation sites. In order to intuitively understand the application of the logistics supervision system in various regions, we have calculated the deployment of the logistics supervision system in customs, terminals, airports, railway stations, high-speed railway stations, and other places from 2015 to 2019. The statistical results are shown in Figure 5.

According to the proportion of data in Figure 5, it can be seen that, in 2015, the logistics supervision system has not been widely used, and there are relatively few customs, terminals, and other places where the logistics supervision system is deployed, and only 15% of the airports and railway stations have the logistics supervision system deployed. In 2019, 30% of railway stations have deployed logistics supervision systems, and almost all locations have reached 20% or more of deployment.

4.4. Comparison of Logistics Supervision Performance between Different Algorithms. In order to understand more clearly the performance of logistics supervision in this study, we compare and analyze the performance of different
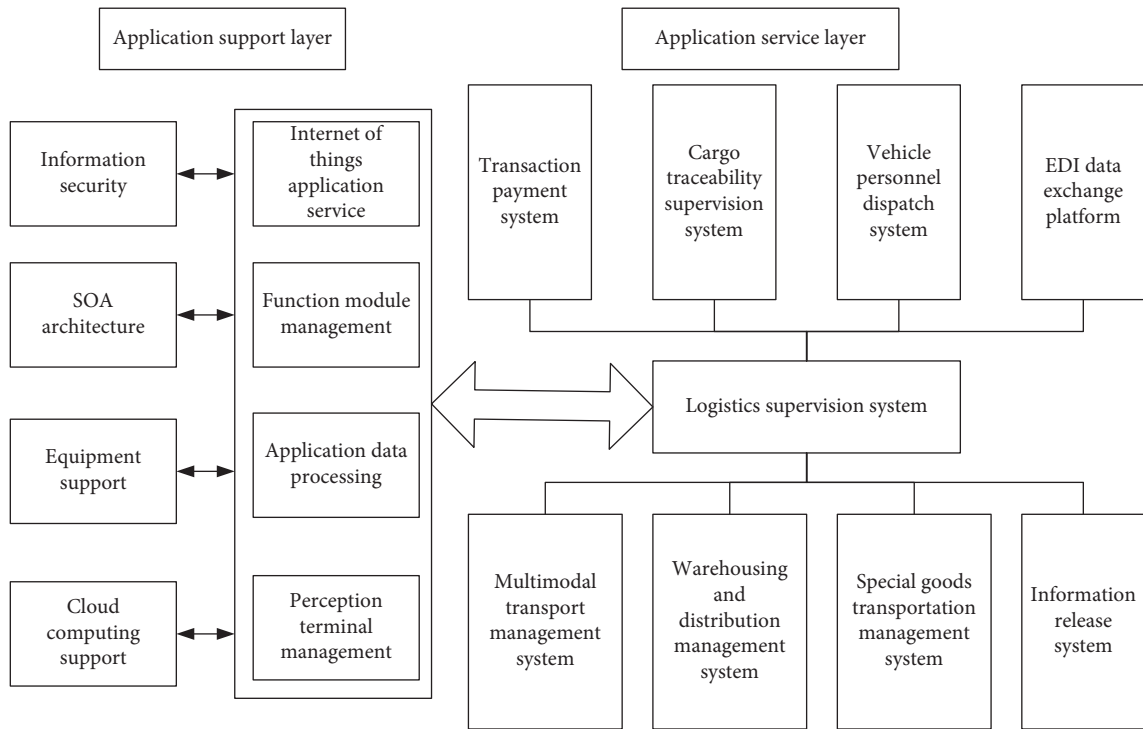
Figure 3: System structure diagram of the logistics supervision system.
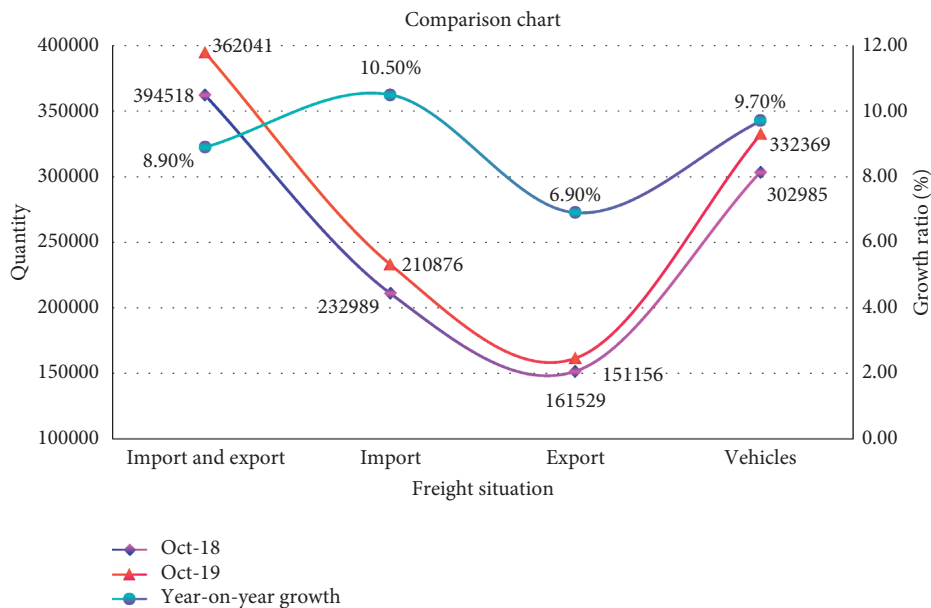
Figure 4: Comparison chart of freight supervision.

algorithms under different path planning, and the final results are shown in Table 1.

According to the data in Table 1, we can see that the wolf algorithm has the highest success rate among paths of different scales, and the success rate of the fourth path planning reaches 100%. In addition to the 94.1% success rate of the cross-particle algorithm in path 1, the success rate of other path planning is very low, only about 1%. In order to
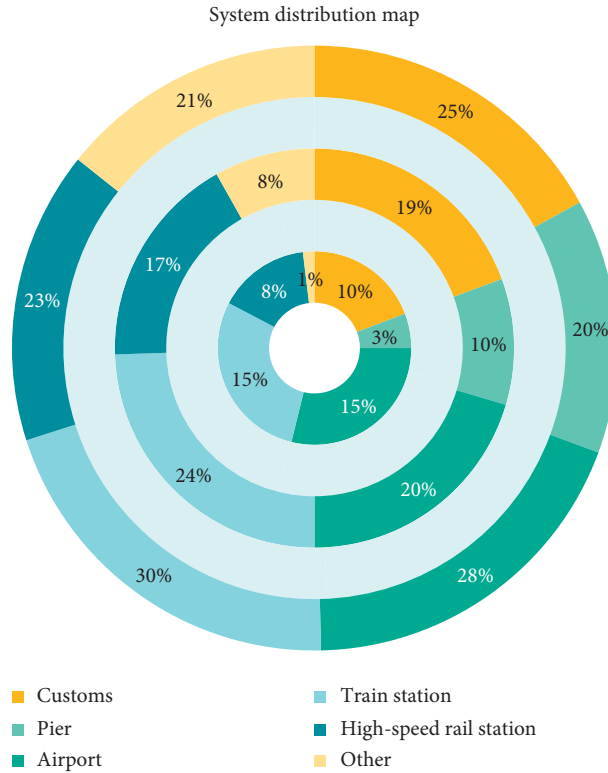
FIGURE 5: Distribution map of the logistics supervision system.

TABLE 1: Performance data table of different algorithms.

Path	Algorithm	Best	Worst	Ave	SR (%)	Deviation (%)	T
Path 1	WPA	$8.04e+3$	$7.90e+3$	$8.07e+3$	99.9	−1	10
	GA	$8.12e+3$	$8.88e+3$	$8.35e+3$	87.4	0.37	351
	ACO	$8.16e+3$	$8.28e+3$	$8.31e+3$	99.9	−0.2	455
	CPSO	$8.08e+3$	$8.61e+3$	$8.27e+3$	94.1	−0.66	520
Path 2	WPA	429.1	438.2	431.02	98.8	0.21	50
	GA	440.21	480.1	480.12	4.5	6.11	397
	ACO	426.1	598.33	513.1	3	20.24	81
	CPSO	445.6	500.06	468.3	1	8.33	883
Path 3	WPA	$7.56e+3$	$7.59e+3$	$7.54e+3$	99	0.03	31
	GA	$7.68e+3$	$8.51e+3$	$8.25e+3$	7.2	8.24	482
	ACO	$7.72e+3$	$7.86e+3$	$8.33e+3$	87.1	2.13	467
	CPSO	$7.83e+3$	$8.73e+3$	$7.17e+3$	0	8.91	886
Path 4	WPA	487.61	499.43	492.16	100	−2.41	331
	GA	521.47	560.11	541.94	98	−2.62	1000
	ACO	520.84	545.2	536.28	99	−3.2	1346
	CPSO	684.35	792.81	734.29	1.2	33.14	998

better observe the performance of wolf pack algorithm in the four paths, we separately extract the four data of the optimal value, the worst value, the average value, and its success rate in the four paths. The results are shown in Figure 6.

According to the data of the optimal value, worst value, and average value of the wolf group algorithm in the four different paths in Figure 6, we can see the performance of the wolf group algorithm in the four paths, according to the data
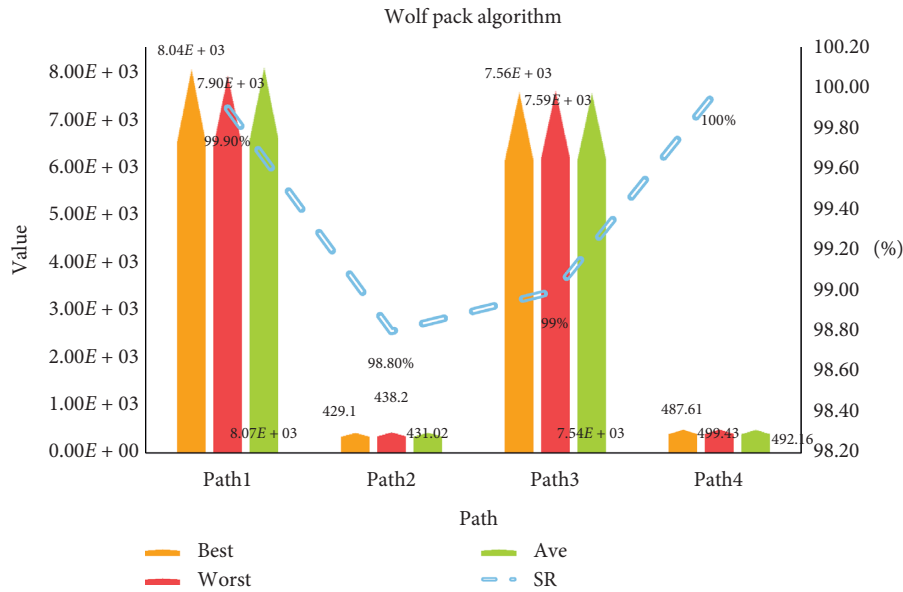
FIGURE 6: Performance analysis diagram of wolf pack algorithm.

in Table 1, the success rate of the wolf pack algorithm on the four paths is 99.9%, 98.8%, 99%, and 100%, and it has the best performance on the fourth path, and the second path the performance is relatively poor.

5. Conclusions

The development of the Internet has promoted the development of e-commerce, online trading has become popular, and the logistics industry has also appeared in the public's view. The logistics industry has brought a lot of convenience to people's life, and its appearance has changed people's way of shopping. With the lowest cost, logistics will deliver the goods needed by users to users by means of transportation, escort, and distribution, so as to realize the effective circulation of goods. People transport goods by means of logistics and only need to entrust the goods to the designated logistics company, and they can realize the circulation of goods and save their own time. Also, logistics companies in the process of freight transport have a certain regulatory mechanism, which can ensure the safety of goods, so that users can be assured to use the way of logistics to transport goods. However, the traditional logistics supervision mechanism has some defects, it cannot transmit the real-time logistics freight situation, and its safety factor is not high.

Under the background of intelligent environment, this paper constructs a supply chain financial logistics supervision system based on the Internet of things technology, which uses the characteristics of "things connected" of the Internet of things technology to transmit and interact logistics information through intelligent devices. Also, we use the calculation and recognition functions of basic smart devices in the smart environment, perceive the logistics information of supply chain finance through sensor perception technology and wolf pack algorithm, collect relevant data such as cargo status and cargo journey in the logistics

process, calculate the logistics data according to the wolf pack hunting and siege behavior formula in the wolf pack algorithm, analyze the performance of the logistics supervision system in practical applications, and propose improvements to the deficiencies of the logistics supervision system.

According to the final result of the experiment, it can be seen that the logistics supervision system has very good practical significance in the logistics industry, reducing the loss of freight data. Also, with the advancement of science and technology, the development of Internet of Things technology, and the construction of smart environment, the logistics supervision system is becoming more and more perfect, during the period from 2015 to 2019, the number of deployment of logistics supervision systems has increased year by year, and it has been widely used in customs and other places.

Data Availability

The data that support the findings of this study are available from the corresponding author upon reasonable request.

Conflicts of Interest

The authors declare that they have no conflicts of interest.

Acknowledgments

References

[1] Z. Lv and N. Kumar, "Software defined solutions for sensors in 6G/IoE," *Computer Communications*, vol. 153, pp. 42–47, 2020.

[2] C.-H. Wu and S.-B. Tsai, "Using DEMATEL-based ANP model to measure the successful factors of E-commerce," *Journal of Global Information Management*, vol. 26, no. 1, pp. 120–135, 2018.

[3] Y. Chen, W. Zheng, W. Li, and Y. Huang, "The robustness and sustainability of port logistics systems for emergency supplies from overseas," *Journal of Advanced Transportation*, vol. 2020, Article ID 8868533, 10 pages, 2020.

[4] J.-Y. Yeh and C.-H. Chen, "A machine learning approach to predict the success of crowdfunding fintech project," *Journal of Enterprise Information Management*, 2020.

[5] M. Zhou, Y. Wang, Z. Tian, Y. Lian, Y. Wang, and B. Wang, "Calibrated data simplification for energy-efficient location sensing in internet of things," *IEEE Internet of Things Journal*, vol. 6, no. 4, pp. 6125–6133, 2019.

[6] W. Elsayed, M. Elhoseny, S. Sabbeh, and A. Riad, "Self-maintenance model for wireless sensor networks," *Computers & Electrical Engineering*, vol. 70, pp. 799–812, 2018.

[7] A. Mosenia and N. K. Jha, "A comprehensive study of security of internet-of-things," *IEEE Transactions on Emerging Topics in Computing*, vol. 5, no. 4, pp. 586–602, 2017.

[8] Z. Lv, B. Hu, and H. Lv, "Infrastructure monitoring and operation for smart cities based on IoT system," *IEEE Transactions on Industrial Informatics*, vol. 16, no. 3, pp. 1957–1962, 2020.

[9] T. A. Bui, H. T. T. Trinh, B. T. Nguyen, and L. D. Bui, "The potential for tra VINH province to become trade gateway OF the mekong delta from logistics and supply chain management perspectives," *The Scientific Journal of Tra Vinh University*, vol. 1, no. 4, pp. 23–40, 2020.

[10] D. D. Zulfikar and D. Ernawati, "Pengukuran kinerja supply chain menggunakan metode green score di Pt. Xyz," *Juminten*, vol. 1, no. 1, pp. 12–23, 2020.

[11] G. B. B. Vieira, F. J. K. Neto and J. L. D. Ribeiro, The rationalization of port logistics activities: a study at port of Santos (Brazil)," *International Journal of E-Navigation and Maritime Economy*, vol. 2, pp. 73–86, 2015.

[12] E. Chancey, J. L. M. Flores, M. B. Palma et al., "Redesign OF the supply chain of a restaurant franchise in the food industry," *Global Journal of Business Research*, vol. 10, no. 2, pp. 103–111, 2016.

[13] J. Zhilun, L. Xuehai, and L. Binglian, "The design of supervision system for UAV logistics industry based on the whole industry chain," *Forum on Ence and Technology in China*, vol. 1, no. 11, pp. 23-24, 2019.

[14] W. Xiaofeng, Z. Rui, J. Rui et al., "Three ring joint control to structure export wooden packaging material supervision system with the Chinese characteristics," *Plant Quarantine*, vol. 29, no. 1, pp. 56–58, 2015.

[15] C. Busse and C. M. Wallenburg, "Innovation management of logistics service providers," *International Journal of Physical Distribution & Logs Management*, vol. 41, no. 2, pp. 187–218, 2016.

[16] F. B. Balo, "Internet of things: a survey," *International Journal of Applied Mathematics Electronics and Computers*, vol. 12, no. 4, pp. 104–110, 2016.

[17] J. Granjal, E. Monteiro, and J. Sa Silva, "Security for the internet of things: a survey of existing protocols and open research issues," *IEEE Communications Surveys & Tutorials*, vol. 17, no. 3, pp. 1294–1312, 2015.

[18] A. Al-Fuqaha, M. Guizani, M. Mohammadi, M. Aledhari, and M. Ayyash, "Internet of things: a survey on enabling technologies, protocols, and applications," *IEEE Communications Surveys & Tutorials*, vol. 17, no. 4, pp. 2347–2376, 2015.

[19] S. Li, L. D. Xu, and S. Zhao, "The internet of things: a survey," *Information Systems Frontiers*, vol. 17, no. 2, pp. 243–259, 2015.

[20] R. Y. Zhong, G. Q. Huang, S. Lan, Q. Y. Dai, X. Chen, and T. Zhang, "A big data approach for logistics trajectory discovery from RFID-enabled production data," *International Journal of Production Economics*, vol. 165, pp. 260–272, 2015.

[21] M. Tentori, L. Escobedo, and G. Balderas, "A smart environment for children with autism," *IEEE Pervasive Computing*, vol. 14, no. 2, pp. 42–50, 2015.

[22] O. Starostenko, X. Cortés, J. A. Sánchez, and V. Alarcon-Aquino, "Unobtrusive emotion sensing and interpretation in smart environment," *Journal of Ambient Intelligence and Smart Environments*, vol. 7, no. 1, pp. 59–83, 2015.

[23] A. P. Volpentesta, "A framework for human interaction with mobiquitous services in a smart environment," *Computers in Human Behavior*, vol. 50, pp. 177–185, 2015.

[24] A. Is, "Analisis rantai pasokan (supply chain) komoditas telur ayam ras petelur (layer)," *JAS (Jurnal Agri Sains)*, vol. 3, no. 2, pp. 13-14, 2019.

[25] P. Hove-Sibanda and R. I. D. Pooe, "Enhancing supply chain performance through supply chain practices," *Journal of Transport and Supply Chain Management*, vol. 12, pp. 33-34, 2018.

[26] V. Turkulainen and M. L. Swink, "Supply chain personnel as knowledge resources for innovation-a contingency view," *Journal of Supply Chain Management*, vol. 53, no. 3, pp. 41–59, 2017.

[27] G. B. Gebremeskel, C. Yi, C. Wang, and Z. He, "Critical analysis of smart environment sensor data behavior pattern based on sequential data mining techniques," *Industrial Management & Data Systems*, vol. 115, no. 6, pp. 1151–1178, 2015.

[28] J. S. Raue and A. Wieland, "The interplay of different types of governance in horizontal cooperations," *The International Journal of Logistics Management*, vol. 26, no. 2, pp. 401–423, 2015.

[29] K. Yu, J. Cadeaux, and H. Song, "Flexibility and quality in logistics and relationships," *Industrial Marketing Management*, vol. 62, pp. 211–225, 2016.

[30] H. S. Wu, F. M. Zhang, R. J. Zhan, H. Li, and X.-L. Liang, "Improved binary wolf pack algorithm for solving multidimensional knapsack problem," *Systems Engineering & Electronics*, vol. 37, no. 5, pp. 1084–1091, 2015.

[31] L. Guo and S. Liu, "An improved binary wolf pack algorithm based on adaptive step length and improved update strategy for 0-1 knapsack problems," *Communications in Computer and Information Science*, vol. 2, no. 1, pp. 22–24, 2017.

[32] W. Dongxing, Q. Xu, L. Kang et al., "Novel wolf pack optimization algorithm for intelligent medical treatment personalized recommendation," *The Journal of China Universities of Posts and Telecommunications*, vol. 25, no. 6, pp. 37-38, 2018.

Research Article

"Intelligent" Technical Guidelines for Chongqing East Railway Station Building and Supporting Hub Area

Jingyuan Shi[1] and Qiuna Li [ID] [2]

[1]*College of Architecture and Urban Planning, Chongqing Jiaotong University, Chongqing 400074, China*
[2]*Faculty of Architecture and Urban Planning, Chongqing College of Architecture and Technology, Chongqing 401331, China*

Correspondence should be addressed to Qiuna Li; 990201900031@cqjtu.edu.cn

In this paper, by drawing on the advanced experience and norms at home and abroad, the compilation and research of "intelligent technical guidelines" for Chongqing east railway station and its supporting hub area are completed. It includes "digital technology, intelligent construction," "accurate and flexible, intelligent service," and "panoramic management and control, intelligent operation, and maintenance," and has formed the whole life cycle technical framework of "intelligent construction, intelligent service, intelligent management, and operation and maintenance."

1. Introduction

Chongqing East Railway Station is one of the five main stations of Chongqing Railway. It is an important strategic support for Chongqing to integrate into the joint construction of the "Belt and Road," an important strategic support for accelerating the construction of an inland opening highland, and also an open gateway for Chongqing to consolidate itself in the west, interact with the east, integrate in ASEAN, and connect Asia and Europe. We proposed to build the Chongqing East Railway Station with high quality based on the core concept of "internationalization, greenization, intelligence, and human culture." Therefore, the "intelligent" technical guidelines of Chongqing East Railway Station building and supporting hub area were compiled [1, 2].

2. Background of the Guidelines

2.1. Purpose of Compilation. In order to strengthen the guidance for the construction and management of the Chongqing East Railway Station building and supporting hub area, benchmark the construction achievements of advanced transportation hubs at home and abroad, and achieve the intelligent goal of Chongqing East Railway

Station construction, on the basis of following the current norms and standards, the "Guidelines" are formulated as a work guide for planning and construction management departments, as well as a technical guide for design and construction units.

2.2. Compilation System. With the concept of "full life cycle, all-round coordination, and full-function coverage," this guideline is compiled taking the concept of "internationalization, greenization, intelligence, and human culture" proposed in the "Chongqing City Overall Improvement Action Plan" as the core and comprehensively coordinates the four modernization systems. Combining the stages of the design, construction, and operation and maintenance of the East Railway Station building and the hub area, the whole process is considered. The guidelines are goal-oriented, put forward targeted technical strategies, adopt matrix network analysis methods, clarify specific qualitative and quantitative guidance and control elements, and realize a guideline index system for full-functional object coverage.

2.3. General Requirements. Combining the needs of transportation hubs and interconnection and networking,

through the use of Internet+, cloud computing, artificial intelligence, big data, BIM, 5G communications, informatization, and other new technical means, the system model is built from the service, function, logic, and physical levels to improve the efficiency of transportation organization at transportation hubs, optimizing service quality, and enhancing safety guarantees. Taking the demand model as the starting point and basis, the system model is constructed to organize the relationship, and finally, the physical model is used for material realization (Figure 1). And, organically integrate the transportation hub station with the "railway brain" of the high-speed rail intelligent technology system to build a smart East Station that embodies efficiency and sharing.

2.4. Technical Framework. The Chongqing East Railway Station building and hub area takes constructing of the smart east station as the overall requirements and covers the three guidance control aspects of "digital technology and intelligent construction" and "precision, flexibility, and intelligent services," as well as "panoramic control, intelligent operation and maintenance" in the hub area and station building area (Table 1). The three stages of design, construction, and operation and maintenance covers the full life cycle and forms a technical framework [3].

3. Research on Intelligent Construction Technology

3.1. Intelligent Construction Guidance and Control Requirements

3.1.1. Intelligent Perception Layer. That is, intelligent terminals are various sensing devices including face verification cameras, monitors, and various sensors that operate through technologies such as ZigBee and WSN in the construction of smart construction sites.

3.1.2. Intelligent Communication Layer. That is, intelligent networks, including the IoT used in various construction processes, and related Internet, telecommunications networks, radio and television networks, and the integration of the three networks.

3.1.3. Intelligent Platform Layer. That is, the intelligent platform and data, as a data processing center, can be used for analysis, monitoring, and simulation during the construction process.

3.1.4. Intelligent Service Layer. That is, intelligent applications, which can integrate various data through the platform layer and provide related intelligent services during the construction process.

3.2. BIM + CIM Construction and Management Platform

3.2.1. BIM and CIM Collaboration Platform. A digital construction management technology platform should be
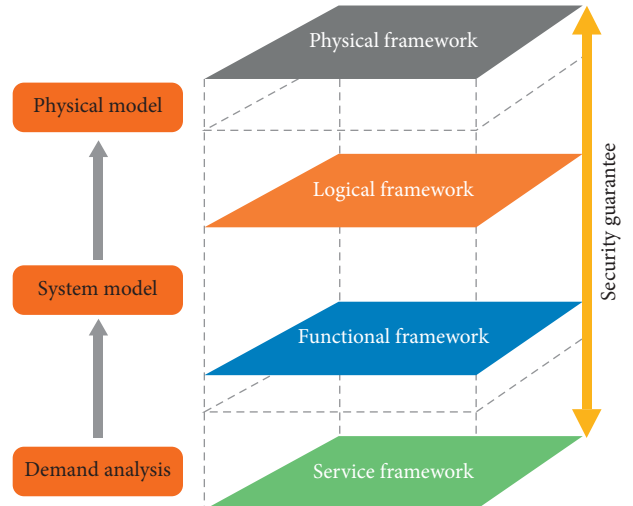
FIGURE 1: Framework of the composition under "China intelligent high-speed rail system structure."

built based on BIM and CIM technologies to realize the full life cycle of intelligent construction management requirements and connection applications for design, construction, and even future service and operation and maintenance. It should form the visual carrier of the smart hub. In the design stage, a series of landing and sustainable CIM + BIM applications are implemented to improve the design quality, improve the efficiency of scheme decision-making, realize the collaborative management of design, and lay the foundation for later construction. In the construction stage, we are committed to forming an innovative management system based on CIM + BIM, which is based on model data, with schedule management as the main line, safety and quality risk as the focus, investment control as the goal, and management platform as the tool, so as to realize the three-dimensional and digital management of the whole construction process. In the completion stage, the CIM and BIM collaborative platform is combined with the completion acceptance to realize the data collection, integration, and archiving in the whole process of the completion acceptance. In terms of facilities and equipment, the asset code, equipment number, and other information are improved to ensure the data traceability and provide data services for the later operation and maintenance. In the operation and maintenance stage, realize the asset management, carry out the monitoring and space management of equipment operation status, integrate the real-time operation data of facilities and equipment through various means such as electronic tags, Internet of things sensors, and system interfaces, carry out data analysis and operation and maintenance monitoring of facilities and equipment, and realize the fine, visual, and intelligent management of operation and maintenance.

3.2.2. Multidisciplinary Data Integration. Professional data such as spatial geometric information, functional information, and construction management information of the East Station building should be integrated to form a three-

TABLE 1: Technical frame diagram.

Overall requirements	Aspects		Elements of the guidance control	Full life cycle
	Intelligent construction	Intelligent construction guidance and control requirements	Construct an intelligent perception layer and an intelligent terminal; the communication layer is an intelligent network; the platform layer is an intelligent platform and data; the service layer is an intelligent application, etc.	Design
		BIM + CIM construction management platform	Build a BIM and CIM collaborative technology platform; realize multidisciplinary data integration; establish a BIM information technology platform	
		Smart construction	Complete the construction of intelligent construction system; adopt information technology + IoT technology; carry out assembly-type intelligent construction for key objects	
		Technology	Realize the intelligent management of constructors; complete the intelligent monitoring of the IoT; monitor and early warn for the construction environment; improve comprehensive supervision capabilities	
		Smart construction site	Passengers use smartphones to assist in parking; use "swipe face" to quickly get on the bus; use app to scan codes to enter the station; enjoy the convenient service of scanning codes in the station	
		Management system	Build an intelligent vehicle platform; provide services for multiple types of vehicles; establish a parking guidance system; complete intelligent parking and reverse car search; connect and guide the flow of people and vehicles through intelligent navigation; realize the linkage transfer of the three major transportation hubs	
		One-stop scan code scene service	Establish a "private customized" identification system; realize 5G communication services and expansion; complete 360-degree VR panoramic navigation; build a smart integrated information system; perform daily business smart cluster communication applications	
Smart east station	Intelligent service	Efficient vehicle service and smart parking	Combine AI technology to set up smart ticketing equipment; use smart service smart robots; build smart voice navigation systems; set up smart luggage storage and smart warehouses; configure high-standard smart toilets	Construction
		Intelligent information service system	Carry out IoT cloud collaboration; establish iot + cloud computing core; conduct real-time monitoring of IoT passenger flow; complete IoT personnel positioning and scheduling; realize scene-linkage intelligent energy-saving technology	
		"AI+" intelligent customer service system	Build an intelligent security management platform; have emergency plans, early warning, and intelligent processing capabilities; establish a "1161" intelligent fire protection system; realize bare optical fiber transmission information; establish an unmanned security system	
	Intelligent management operation and maintenance	IoT cloud platform and scene-linkage intelligent energy saving	Establish an intelligent integrated system platform integrating BIM + CIM and other technologies; realize information sharing and interface	Operation and maintenance
		Intelligent and efficient security system	Establish an intelligent linkage operation and maintenance platform; realize the overall intelligent steward of the station; complete the intelligent linkage switch station	
		Integrated system intelligent operation and maintenance	Collect and analyze passenger flow trajectory information; complete the risk management and control of large passenger flow during peak periods; conduct daily passenger flow analysis and early warning; promote passenger flow data refinement and value evaluation	
			Complete the big data ecosystem; build a big data lake; realize full closed-loop open big data; develop big data collection control and analysis applications	
			Realize a smart energy management platform; form an informatized new energy system	

dimensional basic database to facilitate construction and subsequent operation and maintenance management.

3.2.3. BIM Information Technology Platform.

A platform should be built to enhance the business management capabilities of the East Station construction unit. The BIM data resources should be integrated and managed, model construction standards should be established, and relevant standards and process requirements should be organized through BIM simulation to form a construction technology library to realize multidimensional dynamic clarification and process standard navigation [4–7].

3.3. Smart Construction Technology

3.3.1. Intelligent Construction Technology System.

It should include three major areas of survey design, engineering construction, and construction management and form an innovative direction, GIS intervention survey, BIM intervention design, intelligent building construction, BIM + GIS digital construction management, etc., and expand the innovative content as needed (Figure 2).

3.3.2. Informatization + IoT Technology.

It is advisable to adopt big data sharing information technology and IoT technology to improve the management level, management quality, and management accuracy of intelligent construction and improve the efficiency of construction implementation.

3.3.3. Assembled Intelligent Construction of Key Objects.

The intelligent construction of prefabricated buildings, especially the structure and interior parts, should be realized. The swing mold robot and its supporting molds are selected, the intelligent assembly equipment is adopted, and the digital precision cloth technology of complex concrete components is applied to ensure that prefabricated buildings account for 30% of the newly built building area [8].

3.4. Smart Site Management System

3.4.1. Intelligent Management of Personnel.

The construction site of the transportation hub station should enhance the intelligent management function of personnel and have the capabilities of personnel attendance, personnel positioning, and on-site consumption management. The construction site of transportation hub station can strengthen the management links of site personnel's identity, attendance, and inquiry through intelligent way; through the use of labor real-name system and high-speed face recognition, the management of labor personnel's identity recognition, work attendance, and online inquiry of admission education can be carried out. The safety helmet with the smart chip is equipped for the construction personnel to realize the unified management of personnel track, distribution, and detention; the consumption management can use card swiping method to realize consumption, laundry, and shower, so as to improve the enthusiasm of card use and facilitate the realization of property management of the project.

3.4.2. Intelligent Monitoring of the IoT.

Technologies such as the IoT should be used to intelligently monitor the operating status of large-scale machinery and equipment such as tower cranes, hooks, and lifts and to avoid construction quality problems and safety accidents caused by equipment failures. It should also have functions such as unloading management, vehicle access recognition, and fire protection monitoring.

3.4.3. Construction Environment Monitoring and Early Warning.

It should be equipped with functions such as dust and noise monitoring and early warning, dust suppression spray, and effective enclosure and realize a green smart construction site with low dust spreading (<0.5 m) in earthwork construction and low noise of construction machinery (at day <75 dB, at night <55 dB) under smart monitoring aims.

3.4.4. Improve Comprehensive Supervision Capabilities.

It should have the capabilities of smart working, project coordination, mobile inspection, schedule management, and technical disclosure and apply an intelligent shield construction safety supervision system. It is advisable to achieve one U-shield lock per person to improve the safety supervision level of construction projects [9].

4. Intelligent Service

4.1. Service for One-Stop Code-Scanning Scene

4.1.1. Mobile Phone Parking Assistance.

Real-time parking maps and parking space information should be provided through smart phone GPS data and sensors embedded in the parking space ground, and electronic information signs should be installed to assist in finding parking spaces. To provide passengers at the East Station with convenience for finding cars, real-time information about nearby parking spaces and charging standards can be obtained through a mobile APP.

4.1.2. "Face Scan" Function.

A "dual-channel face verification gate" should be set up to realize the services of "face-scanning ticket" + "face-scanning pass" in passenger transportation. Passengers scan their faces to complete a series of procedures such as ticket purchase, ticket collection, and entering the station. Simplify ticket collection (reimbursement voucher) for passengers, avoid confusion in ticket presentation when entering the station, and greatly save the time. Passengers who purchase online tickets do not need to pick up the ticket twice and can go directly to the security checkpoint and use the face verification gate to enter the station to achieve one-stop check for security and ticket.
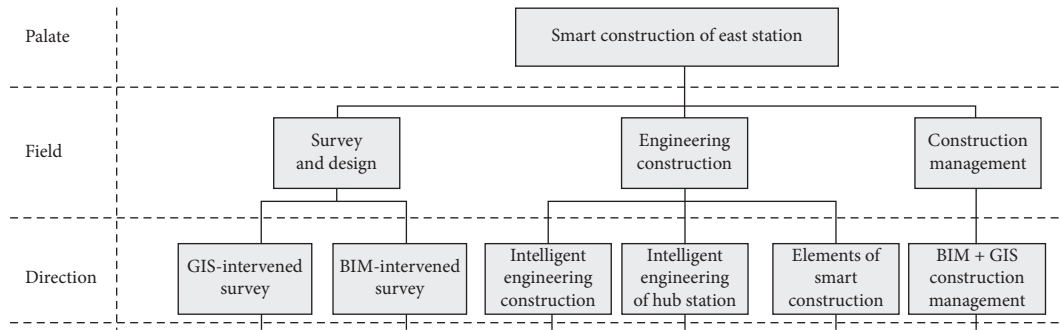
FIGURE 2: Framework diagram of the intelligent construction technology system.

4.1.3. APP Code Scanning. It is used with face scanning function. Passengers use the mobile phone APP to complete identity authentication and activate related functions before boarding and use the WeChat official account or APP to enter the station on the day of travel. This provides passengers with customized key information such as train numbers and seat numbers to realize the networking and convenience of station entering and save time.

4.1.4. Convenient Service for Scanning Codes within the Station. For passengers of the same type of hubs who have difficulty in storage, going to the toilet, and shopping can quickly complete item storage, item purchase, and receiving toilet paper through the mobile phone APP, which provides convenience for the daily needs of passengers at the East Station and solves various "pain points" scenarios with intelligent scanning code and convenient services [10, 11].

4.2. Efficient Vehicle Service and Smart Parking

4.2.1. Intelligent Vehicle Platform. The Chongqing East Railway Station traffic information integrated management platform should be established to complete OPC, BACNet, and API systems to realize data collection, vehicle management and scheduling, passenger information access and guidance, intelligent monitoring, voice communication systems, traffic parking management, support systems, and others' system construction (Figure 3).

4.2.2. Multitype Vehicle Service. Intelligent guidance and information services should be provided for different types of vehicles. Adopt green wave and other technologies to ensure the smooth connection between passengers and social vehicles, taxis, online car-hailing, buses, shuttle buses and other types of transportation, and it is advisable to effectively connect autonomous vehicles.

4.2.3. Parking Guidance System. A smart parking lot function should be set up to facilitate car owners to find parking spaces, quickly find parked vehicles, and find parking lot exits. Through the parking guidance system, guide and manage social vehicles in and out and parking. The parking guidance system should have the functions of

collecting, transmitting, processing, and publishing parking information.

4.2.4. Intelligent Parking and Reverse Car Search. Intelligent parking and reverse car search in the East Station should be realized, and all parking lots in the East Station should be unified and intelligently managed. It is advisable to collect parking information through the parking lot toll management system or use the vehicle detector to directly collect parking information and inform car owners by the information release screen (Figure 4).

4.2.5. Intelligent Navigation Connection and People-Vehicle Flow Guidance. The dynamic information of the street path in the static area and the empty parking space in the parking lot should be published on the display screen to provide navigation connection and route guidance for people and vehicles. The guide screen at the main entrance should display the total number of vacant parking spaces in real-time hierarchically, the location guide screen should display the number of vacant cars in the area, and the intersection guide screen should display the number of vacant cars in the driving direction. Video analysis license plate automatic recognition system should be used. The recognition accuracy rate of day and night should be greater than 90% and 80%, respectively, and the recognition speed should be less than 1 s.

4.2.6. Linkage Transfer of Three Major Transportation Hubs. It is advisable to reach strategic cooperation with Jiangbei International Airport and the city bus station to strengthen the linkage of information and transportation between all parties, which can accept buses to transfer passengers suspended for some reason from the airport, etc., and arrange green channels to help passengers get in and get on the bus and vice versa [12].

4.3. Intelligent Information Service System

4.3.1. "Private Order" Identification System. The face verification system quickly recognizes the identity of the person and provides data for passenger flow tracking, feature recognition, etc., to meet passenger interaction needs. Using
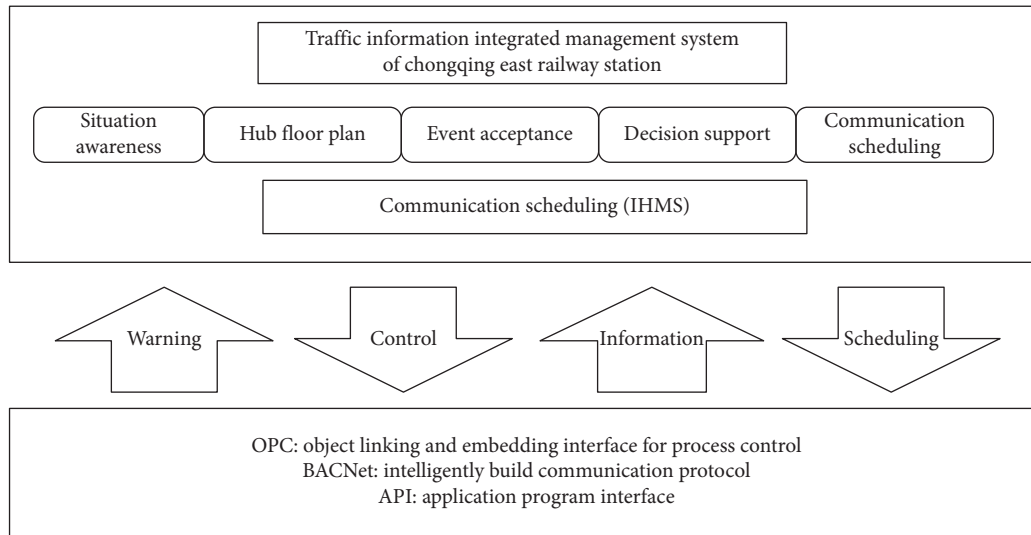
FIGURE 3: Framework diagram of the vehicle intelligent system platform.
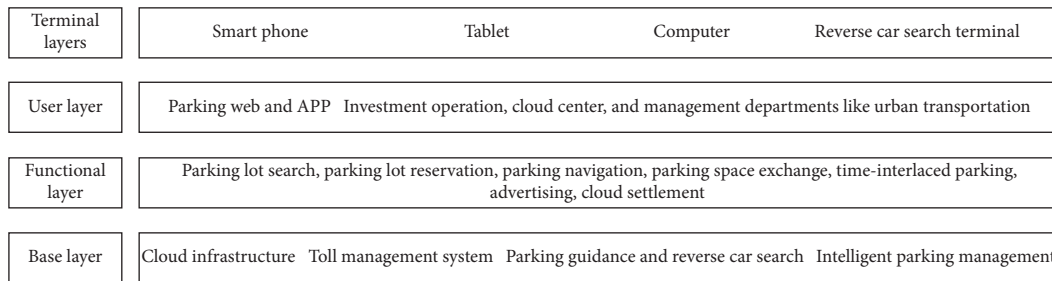
FIGURE 4: Framework diagram of smart parking service system.

real-name accounts, face code interoperability, and frequent flyer channels for OD analysis and through the integrated application of security gates, the security check and ticketing business are integrated to realize the convenience and the intelligent image judgment.

4.3.2. 5G Communication Services and Expansion. 5G communication services with large bandwidth, wide connections, ultrahigh reliability, and ultralow latency should be adopted to build a new 5G industry ecosystem, cultivate key industries such as mobile Internet and IoT, and promote the development of 5G application scenarios solutions (Figure 5). It should be able to interface with Beidou Skynet's global satellite navigation system, 6G communications, and other new and research communication technologies. The current technology is not mature enough, but relevant software and hardware conditions and interfaces should be reserved.

4.3.3. 360-Degree VR Panoramic Navigation. The VR panoramic navigation function should be realized, and the east station panoramic map network should be established. Passengers can use their smartphones or the VR display in the station to have virtual experience of ticket selling, entering the station, security check, waiting, lost and found, key passenger waiting rooms, and other places with VR

equipment, so as to intuitively grasp the key points of the East Station Specific location. This item has few applications currently but is of leading significance and it is worth trying.

4.3.4. Smart Integrated Information System. A comprehensive information system that satisfies the functions of operation and production, enterprise management, and passenger service management should be set up. Pay attention to the release, inquiry, and guidance of information related to passenger use and management, such as outdoor climate, indoor environment, real-time status of surrounding traffic, and emergency response to emergencies.

4.3.5. Daily Business Intelligent Cluster Communication Application. A broadband trunking intercom system should be implemented, based on LTE-U, WLAN, and public network operator networks to provide voice and video intercom services [13, 14].

4.4. "AI+" Intelligent Customer Service System

4.4.1. Smart Ticketing Equipment. Combined with the embedded AI barebone system, it is advisable to repartition and classify the human-computer interaction interface in the smart ticket vending machine to highlight the main function
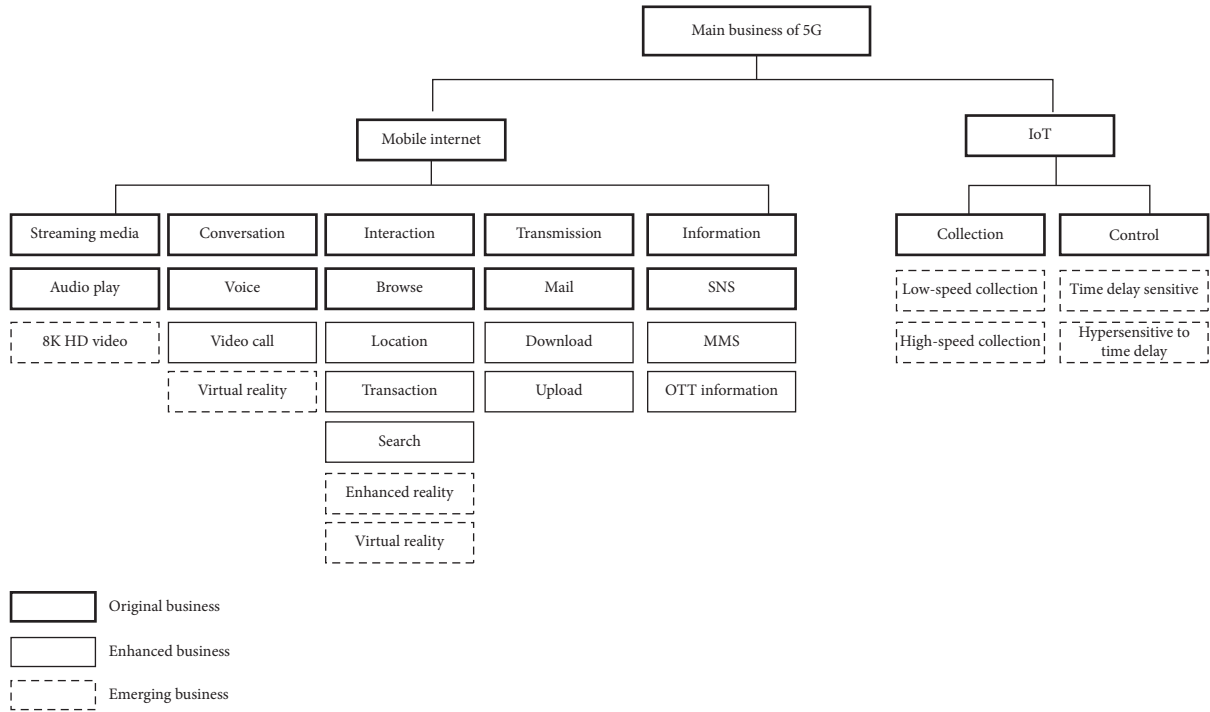
FIGURE 5: 5G business model and smart space structure diagram of transportation hub.

entry options. Optimize the selection method of issuing arrival stations, statistically analyze the popular arrival stations for selling tickets (the total number does not exceed 24), and design the selection page to meet the requirements of other passengers through the station name retrieval method. Refine the time-division train display and fast page number search to improve the efficiency of passengers searching for trains (Figures 6 and 7).

4.4.2. Intelligent Robot for Smart Service. In addition to basic functions such as information inquiry, more flexible and active service functions should be provided, such as AI autonomous learning, impromptu performance, and remote security. According to the development of related technologies, technical indicators should be selected reasonably during the equipment bidding stage (Figure 8).

4.4.3. Intelligent Voice Navigation System. It is advisable to adopt AI intelligent voice navigation system to realize functions such as in-station voice navigation, ticket self-service consultation, intelligent travel, and information services. Build an intelligent voice interactive portal to improve self-service user satisfaction, divert the pressure of manual services, and increase the connection rate. Intelligent customer service technology should ensure that the accuracy of customer demand recognition during peak periods is over 90%.

4.4.4. Smart Luggage Storage and Smart Warehouse. Intelligent storage of passenger luggage and smart warehouse should be set up, and luggage storage and storage of

goods should be conveniently accessed through personal mobile terminals. The smart luggage cabinet can be set with multiple specifications of the grid. According to the development of AI and other related technologies, technical indicators should be reasonably selected during the equipment bidding stage (Figure 9).

4.4.5. High-Standard Smart Toilet. High-standard smart toilets should be set up. With functions such as artificial intelligence, integrated display screen, real-time toilet seat display, odor monitoring and automatic elimination, smoke monitoring, human flow status monitoring, and temperature and humidity monitoring, it can provide interactive query weather, traffic information, news review, attraction introduction, service hotline, information, and other services (Figure 10). Quantitative paper can be taken out from smart drawer every day through the QR code [15].

4.5. Intelligent Energy Saving of IOT Cloud Platform and Scene Linkage

4.5.1. IoT Cloud Collaboration. The collaboration between the Internet of Things, the cloud platform, and the terminal equipment of the East Station should be strengthened, and the management, operation, and service of the East Station should be further transformed into intelligent, refined, and networked.

4.5.2. IoT with Cloud Computing Core. In terms of data storage and analysis capabilities, cloud computing forms a huge driving force for IoT services of East Station. Take the

FIGURE 6: More intelligent ticket machines can greatly improve efficiency.
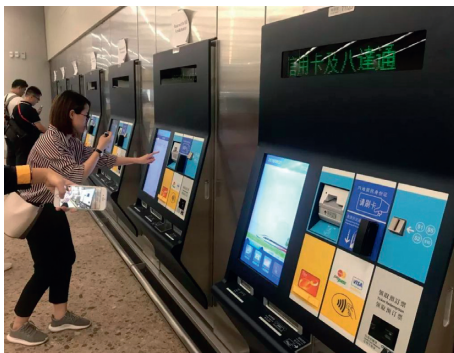
FIGURE 7: More intelligent ticket machines can greatly improve efficiency.

FIGURE 8: Service functions of intelligent robots can be diversified.

cloud as the central location to analyze and process a large number of IoT sensor data.

4.5.3. Real-Time Monitoring of IoT's Passenger Flow. The IoT technology should be used to install passenger flow counters at key locations such as station entrances and exits, station hall payment areas, and platforms, to detect and count the number and direction of passenger flow, and complete passenger flow statistics in order to realize real-time monitoring and early warning of the passenger flow of the East Station.

4.5.4. Positioning and Scheduling of IoT Personnel. LoRa and other IoT technologies should be used to help staff quickly locate and schedule through wearable electronic tags, realize the multilevel linkage of personnel deployment, voice

FIGURE 9: Intelligent rest cabin for passengers similar to intelligent warehouse.

FIGURE 10: Portable smart toilet.

communication, and video surveillance in the first time, and improve the solving speed and efficiency of emergency response.

4.5.5. Scene-Linkage Intelligent Energy-Saving Technology. Scene-linked intelligent energy-saving technology should be adopted to strengthen environmental perception, intelligent lighting control, intelligent air-conditioning control (the lowest temperature limit in summer is 26°C), remote control, and timing control and to achieve effective monitoring and management of building energy consumption. Energy-saving equipment should be used in the East Station and the energy consumption of the network system should be reduced by more than 30% (Table 2) [16, 17].

4.6. Intelligent and Efficient Security System

4.6.1. Intelligent Security Management Platform. The security and fire protection system and the operation and production system are jointly built on the integrated platform, and the data of each system is uniformly monitored and linked to facilitate emergency operation and disposal and realize the safety level protection of platform construction. The ticketing platform is seamlessly connected to the public security system to record and track and to ensure the safe travel. It should have an alarm access system, docking with the police command center, transmit the alarm information in seconds, and quickly view the alarm details to realize remote video review and dock the black and white list library.

TABLE 2: Passenger flow detection, early warning, and control measures.

No.	Early warning	Passenger flow control measures	Timing of control measures starting (person)	Control purpose
1	First-level warning	First-level passenger flow control	$K1 = Qzt * \beta1$	Slow down the speed of passengers arriving at the platform; reduce the number of passengers on the platform
2	Second-level warning	Second-level passenger flow control	$K2 = Qffq * \beta2$	Slow down the speed of passengers reaching the pay zone; reduce the number of passengers in the pay zone
3	Third-level warning	Third-level passenger flow control	$K3 = Qfff * \beta3$	Slow down the speed of passengers entering the station and reduce the number of passengers at the station

4.6.2. Emergency Plan, Early Warning, and Intelligent Processing. In the event of passenger congestion, vehicle congestion, sudden social incidents, fires, and other emergencies, management personnel should promptly intervene and deal with the control system. By using one-touch triggering of signal lights, elevators, access control, display screens, broadcasting, monitoring, mobile terminal APP, and other equipment, guide people and vehicles to evacuate safely in the shortest time. An emergency button that can immediately start voice and video intercom or remote talk should also be set up.

4.6.3. Smart Firefighting System. Adopt a smart fire protection system in the integrated hub. Taking data visualization as the standard, "1 picture" presents multidimensional information, "1 platform" layered the authorization, "6 folds of experience" covers integrated management of smoke, electricity, water, temperature, firefighting equipment, and people, and "1 mobile phone" refers to the staff using the smart fire app for management.

4.6.4. Bare Fiber Transmission Information. Build a dispatching smart center and data room. The monitoring and data information of the security system should be uniformly forwarded to the superior traffic authority through bare fiber, and the data transmission rate should be greater than 10 Mb/s. Ensure the security of network transmission information and set a password.

4.6.5. Unmanned Security System. Facial verification should be used to automatically select and control the crowd to improve the prevention and control level of public places. Dangerous materials and dangerous actions should be identified to automatically predict large-scale public safety hazards. A 24-hour security patrol robot should be set up to prompt people with high temperatures, people without masks, open flame areas, etc., to achieve remote mobile security management [18].

5. Intelligent Management Operation and Maintenance

5.1. Integrated System Intelligent Operation and Maintenance

5.1.1. Intelligent Integrated System Platform. The intelligent integrated system platform should be adopted in the transportation hub station, and advanced technologies such as BIM and CIM collaborative platform should be integrated in the management and operation and maintenance process to complete the entire life cycle process of operation and maintenance and reserve the integration interface with the CIM platform and smart system of the East Station District.

5.1.2. Information Sharing and Interface. The transportation hub station should adopt information sharing and interface design, and the information and management departments and related systems should be fully interconnected and shared, and a complete design interface should be formed (Figure 11).

5.2. "Station-Platform" Linkage Operation and Maintenance

5.2.1. Intelligent Linkage Operation and Maintenance Platform. The platform should be used to realize the efficient management function of the station and fully link with the station.

5.2.2. The Overall Intelligent Steward of the Station. The overall intelligent steward of the station should be adopted to realize the integrated intelligent maintenance function of the station and platform (Figure 12). Manage the maintenance work of the electromechanical, fire protection, and information facilities of the station and platform through the APP. Realize the closed-loop management system of "fault report-schedule-on site maintenance-feedback evaluation," and the minimum repair time should be reduced to 5 minutes when problems are found.

5.2.3. Opening Station by Intelligent Linkage. Through intelligent video analysis, PA, PIS, and other technologies should be used to realize the judgment of passenger flow in key areas such as stations, platforms, entrances, and exits when opening or closing stations and, by broadcast and PIS, prompts to achieve the operational goals of opening station by intelligent linkage [19].

5.3. Accurate Control of Passenger Flow, Operation, and Maintenance

5.3.1. Passenger Flow Trajectory Information Collection and Analysis. The complete track information of each user should be obtained with the help of smart passenger flow data. It is advisable to collect trajectory information within a radius of 1 km around the station for urban lines and within
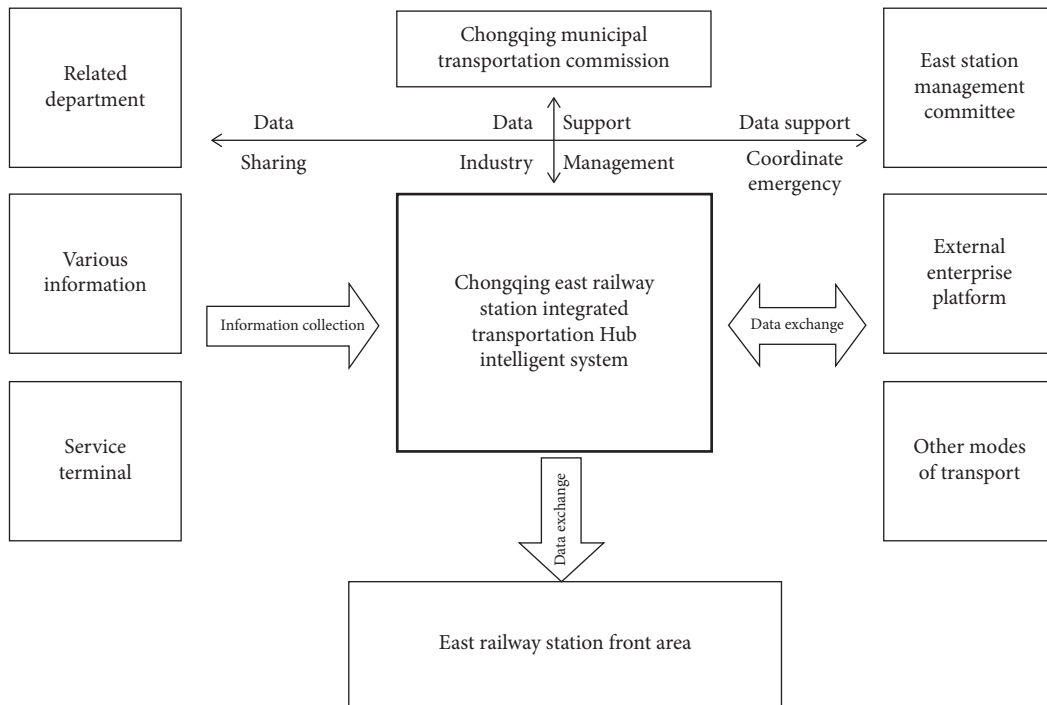
FIGURE 11: The structure diagram of the intelligent system of the integrated transportation hub.
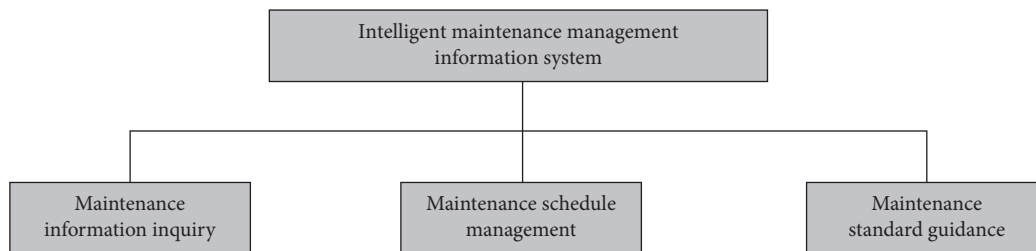
FIGURE 12: Composition diagram of intelligent maintenance management information system.

a radius of 2 km for suburban lines to realize the data operation, real-time guidance, situation analysis, and emergency plan formulation of the east station passenger flow.

5.3.2. Risk Management and Control of Large Passenger Flow during Peak Period. It is necessary to optimize on-site management and control measures during peak periods, strengthen guidance and avoid passenger flow hedging. Through the intelligent linkage between the station hall and the platform, the passenger flow is accurately limited. It can realize the early warning of risk and peak management of the East Station and effectively strengthen current limit control and reminders during peak hours.

5.3.3. Daily Passenger Flow Analysis and Early Warning. Passenger flow forecasts should be carried out at ordinary times, and comprehensive statistical analysis of information such as passenger flow, passenger flow density, and congestion level in the station should be carried out to realize the daily congestion warning, safety environment warning, and comprehensive warning of the East Station.

5.3.4. Refinement and Value Evaluation of Passenger Flow Data. The granularity and location of passenger flow data should be refined, and monitoring indicators should be set to realize the accurate placement of East Station advertisements and evaluate and enhance the value of shops in the station (Table 3).

5.4. Operation and Maintenance of Multidimensional Big Data Ecosystem

5.4.1. Big Data Ecosystem. The technical framework of big data storage, calculation, and analysis should be integrated, namely, "storage + calculation + task scheduling." The current mainstream, Hadoop, and Spark ecosystems should be adopted and realize the resource sharing of "one source for one data."

5.4.2. Construction of Big Data Lake. A big data lake of "intelligent construction data, infrastructure data, mobile equipment data, and operational service data" should be built. Provide basic data management, data integration, data governance, data sharing, data analysis, and other services

TABLE 3: Passenger flow control information list.

Travel information	Highway passenger transportation: station and agent, transport vehicle, circuit, route, train number, earliest (late) route information, etc.
	Bus route: bus stop, bus recharge station, transit interchange station, bus number, each bus route, transport vehicle, earliest (late) route information, etc.
	Airport: round-trip flight information, such as route, take-off and landing airport, flight direction, take-off (landing) time, delay information, etc.
	Railway station: round-trip information, such as circuit, route, station and time, start/arrive time, delay information, etc.
	Port: round-trip shipping information such as circuit, directions, routes, docks and times, voyage departure and destination times, carrier company and ship information, water passenger flight information, etc.
The freight information	Highway, railway station, airport, port, yard and station, logistics center and other shift information, cargo information, cargo tracking, vehicle information, driver information, logistics enterprise information, etc.
Road information	Data such as traffic flow, traffic accident, accident rescue, traffic control, highway closure, road maintenance, warning of road sections prone to landslides, road infrastructure, information equipment, etc.

for the East Station. In the future, AI services can be expanded on this basis.

5.4.3. Fully Closed-Loop Open-Type Big Data. Based on the railway data service platform, the "platform + application" model should be adopted to realize the deep integration of big data technology and the core business of intelligent high-speed rail and build a fully closed-loop open big data ecosystem around the fields of engineering construction, mobile equipment, infrastructure, transportation production, operational safety, passenger transportation management services, and comprehensive transportation sharing.

5.4.4. Big Data Acquisition Control and Analysis Application. The operation of various electromechanical equipment should be optimized through big data acquisition control and system integration technology control to realize intelligent and energy-saving buildings. In addition, big data analysis applications can be carried out in aspects such as face verification, monitoring management, safety prevention, accident rescue, and dispatching and command [20].

5.5. Smart Energy Management Operation and Maintenance

5.5.1. Achieve Smart Energy Management Platform. It is advisable to adopt an intelligent IoT framework to apply big data, cloud computing, artificial intelligence, machine learning, remote operation and maintenance, and other technologies to the energy management of the East Railway Station to build data collection, edge computing, reverse control, data analysis, and strategy optimization, strategy issuance, and energy forecasting functions. Finally, through the execution and control of energy-saving strategies, big data mining and modeling, and remote analysis and guidance by an expert team, an integrated platform for energy control, management, and operation and maintenance of Chongqing East Railway Station is realized, and energy utilization efficiency and intelligence level are comprehensively improved. [21].

5.5.2. Forming an Information-Based New Energy System. Internet thinking and technology should be used to transform traditional energy sources, to achieve horizontal multisource complementation and vertical "source-network-load-storage" coordination to form a new energy system such as electric energy, solar energy, and geothermal energy with a high degree of information integration at Chongqing East Railway Station.

5.5.3. Smart Grid and Electric Vehicle Management. Apply smart grid and manage electric vehicles in Chongqing East Railway Station. Smart grids can access energy data and provide new pricing plans to improve energy efficiency. Electric vehicles acting as power storage equipment can provide emergency power for the East Station.

5.5.4. Self-Regulating Energy Management System of Blockchain Technology. With the BS-EMS node as the physical foundation and the energy quota as the digital medium, it provides a solution for mutual trust between smart devices. It is advisable to establish a trustworthy energy value network for each node in the energy management system and realize the independent regulation of the energy system. Within 10–30 minutes, BS-EMS should allocate energy quotas for 3–5 energy consumption cycles to energy-consuming nodes to maintain network fault tolerance.

6. Conclusion

This paper expounds the research conclusion of "intelligent" technology guidance for railway transportation hub station. At the same time, the planning principles, control points, and design methods of design, construction, operation, and maintenance are found. In the future, it is necessary to conduct qualitative and quantitative research on the intelligent technology of transportation hub [22].

Data Availability

The data that support the findings of this study are available from the corresponding author upon reasonable request.

Conflicts of Interest

There are no potential conflicts of interest in our paper.

Authors' Contributions

All authors have read and approved the manuscript.

Acknowledgments

References

[1] Z. H. Sun, L. Huang, and L. N. Chen, "Study of architecture of railway freight station information system based on the internet of things," in *Proceedings of 2nd International Conference on Logistics, Informatics and Service Science*, Beijing, China, 2012.

[2] J. Y. Shi, W. M. Zhao, and Q. N. Li, "A study on influential elements and design methods of regional residential areas," *Applied Mechanics and Materials*, vol. 209–211, no. 12, p. 230, 2012.

[3] F. Mofidi and H. Akbari, "Intelligent buildings: an overview," *Energy and Buildings*, vol. 223, no. 9, Article ID 110192, 2020.

[4] C.-H. Yang, K.-C. Lee, and S.-E. Li, "A mixed activity-based costing and resource constraint optimal decision model for IoT-oriented intelligent building management system portfolios," *Sustainable Cities and Society*, vol. 60, no. 9, Article ID 102142, 2020.

[5] Y. Zhou and L. Li, "The 5G communication technology-oriented intelligent building system planning and design," *Computer Communications*, vol. 160, no. 1, p. 402, 2020.

[6] T. Hamidavi, S. Abrishami, and M. R. Hosseini, "Towards intelligent structural design of buildings: a BIM-based solution," *Journal of Building Engineering*, vol. 32, no. 11, Article ID 101685, 2020.

[7] H. Fouchal, "Sharing pseudonyms between intelligent transport system stations," *Journal of Computational Science*, vol. 47, no. 10, Article ID 101236, 2020.

[8] Y. Asakura, T. Iryo, Y. Nakajima, and T. Kusakabe, "Estimation of behavioural change of railway passengers using smart card data," *Public Transport*, vol. 4, no. 1, pp. 1–16, 2012.

[9] D. Helbing, I. Farkas, and T. Vicsek, "Simulating dynamical features of escape panic," *Nature*, vol. 407, no. 6803, p. 487, 2000.

[10] T. Kusakabe, T. Iryo, and Y. Asakura, "Estimation method for railway passengers' train choice behavior with smart card transaction data," *Transportation*, vol. 37, no. 5, pp. 731–749, 2010.

[11] Transportation Research Board, *Highway Capacity Manual*, National Research Council, Washington, DC, USA, 2000.

[12] A. Sforza, C. Sterle, P. D'amore, A. Tedesco, F. De Cillis, and R. Setola, "Optimization models in a smart tool for the railway infrastructure protection," in *Proceeedings of the CRITIS 2013: Critical Information Infrastructures Security*, Amsterdam, Netherlands, 2013.

[13] S. B. Prasad and P. Madhumathy, "Long term evolution for secured smart railway communications using internet of things," *Machine Learning Algorithms for Industrial Applications*, vol. 907, pp. 285–300, 2020.

[14] A. Pashkevich, E. Bairamov, T. E. Burghardt, and M. Sucha, "Finding the way at Kraków Główny railway station: preliminary eye tracker experiment," *TSTP 2019: Smart and Green Solutions for Transport Systems*, pp. 238–253, Springer, Berlin, Germany, 2019.

[15] O. Heddebaut and F. Di Ciommo, "City-hubs for smarter cities. The case of Lille "EuraFlandres" interchange," *European Transport Research Review*, vol. 10, no. 1, p. 10, 2018.

[16] F. Schulz, D. Wagner, and K. Weihe, "Dijkstra's algorithm on 1 line: an empirical case study from public railroad transport," in *Proceedings of the 3rd International Workshop on Algorithm Engineering (WAE99)*, London, UK, 2000.

[17] R. Tsuchiya, T. Ogino, K. Seki, and Y. Sato, "CyberRail: an enhanced railway system for intermodal transportation," *Quarterly Report of RTRI*, vol. 42, no. 4, p. 180, 2001.

[18] C. Stauffer and W. Crimson, "Adaptive background mixture models for real-time traeking," in *Proceedings of the 1999 IEEE Conference on Computer Vision and Pattern Reeognition*, no. 2, Fort Collins, CO, USA, 1999.

[19] B. Lucas and T. Kanade, "An iterative image registration technique with an application to stereo vision," in *Proceedings of the 7th International Joint Conference on Artificial Intelligence*, Vancouver, Canada, 1981.

[20] J. Y. Shi and Q. N. Li, "Ecological planning path of road traffic in Chongqing villages," in *Proceedings of the 2019 9th International Conference on Social Science and Education Research (SSER 2019)*, no. 1, Kitakyushu, Japan, 2019.

[21] X. Huang, D. Zhang, and X. Zhang, "Energy management of intelligent building based on deep reinforced learning," *Alexandria Engineering Journal*, vol. 60, no. 1, pp. 1509–1517, 2021.

[22] J. Dong and Y. Yin, "Overview of intelligent building research based on citation analysis," in *Proceedings of the 2020 International Conference on Applications and Techniques in Cyber Intelligence*, Fuyang, China, 2020.

Research Article

Rethinking Separable Convolutional Encoders for End-to-End Semantic Image Segmentation

Lin Wang ⓘ,[1] Xingfu Wang ⓘ,[1] Ammar Hawbani ⓘ,[1] Yan Xiong ⓘ,[1] and Xu Zhang ⓘ[2]

[1]*School of Computer Science and Technology, University of Science and Technology of China, Hefei 230026, Anhui, China*
[2]*National Computer Network Emergency Response Technical Center of China, Chengdu 610072, Sichuan, China*

Correspondence should be addressed to Ammar Hawbani; anmande@ustc.edu.cn

With the development of science and technology, the middle volume and neural network in the semantic image segmentation of the codec show good development prospects. Its advantage is that it can extract richer semantic features, but this will cause high costs. In order to solve this problem, this article mainly introduces the codec based on a separable convolutional neural network for semantic image segmentation. This article proposes a codec based on a separable convolutional neural network for semantic image segmentation research methods, including the traditional convolutional neural network hierarchy into a separable convolutional neural network, which can reduce the cost of image data segmentation and improve processing efficiency. Moreover, this article builds a separable convolutional neural network codec structure and designs a semantic segmentation process, so that the codec based on a separable convolutional neural network is used for semantic image segmentation research experiments. The experimental results show that the average improvement of the dataset by the improved codec is 0.01, which proves the effectiveness of the improved SegProNet. The smaller the number of training set samples, the more obvious the performance improvement.

1. Introduction

Convolutional Neural Network (CNN) was first proposed by Hubel and Wiesel in the 1960 s [1]. Because of its ability to directly input the original image for recognition without complicated image preprocessing, it has now been widely used in many applications. In the field of science, it is particularly prominent in the classification of patterns. It can learn local features autonomously, and when the input image changes and is distorted, the resulting features remain unchanged. CNN is based on the structure of the shared convolution kernel, which makes it have great advantages in processing high-dimensional images of actual size. It realizes the encapsulation of feature extraction. The user does not need to care about the specific features trained, just that they are trained well, the weight is enough, the classification effect is good, and the accuracy is high. The disadvantage is that it requires a large amount of sample data, a large amount of calculation, and adjusting parameters.

In recent years, CNNs have become the mainstream method to solve many computer vision tasks [2], such as image classification, target detection, and semantic segmentation. With the growth of the dataset size, the improvement of hardware computing power, and the introduction of a series of excellent network structures [3], the number of trainable CNNs is constantly being refreshed. Under the processing of the decomposable CNN, the computational complexity is greatly reduced.

Cho SI proposed a new image semantic segmentation method based on CNN, which first uses separable convolution and gradient to reduce computational complexity and improve image segmentation and denoising performance [4]. The proposed method converts the existing convolution filters in the traditional CNN segmentation denoiser into cascaded vertical and horizontal separable convolutions and reduces the features between these convolutions by analyzing the distribution of convolution weights and number of channels. Cho SI believed that its proposed separable

convolution with feature size shrinkage can greatly reduce the number of CNN multiplication operations while minimizing the damage to the image segmentation quality. In addition, Cho SI used the gradient of a given image as the input of the proposed separable CNN image segmenter by utilizing the relationship between the anisotropic diffusion-based segmenter and the residual CNN segmenter to improve image segmentation and the quality of the encoding [5]. This research lacks theoretical support [6]. Yeung HWF proposed an effective and efficient separable CNN model for spatial superresolution image segmentation. Specifically, the proposed model has an hourglass shape, so that feature extraction can be performed at a low-resolution level, thereby saving calculation and storage costs. In order to make full use of the four-dimensional structural information of the image data in the spatial domain and the angular domain, we suggest using four-dimensional convolution to characterize the relationship between pixels. In addition, as an approximation of four-dimensional convolution, Yeung HWF also recommended the use of space-angle separable (SAS) convolution to improve calculation and memory efficiency to extract space-angle joint features. A large number of experimental results of this experiment on 57 test images of various challenging natural scenes show that compared with the latest methods, the proposed model has significant advantages, achieving better visual quality and better retention and superresolution image structure, while the degradation of image reconstruction quality is negligible. This method is expensive to use and is not conducive to popularization [7]. Liu Z believed that the intensive calculation of high-efficiency video coding brings challenges to the codec in terms of hardware overhead and power consumption [8]. On the other hand, the limitation in codec design seriously reduces the software-oriented fast coding unit partition mode decision algorithm effectiveness. Therefore, Liu Z designed a fast algorithm based on CNN to reduce more than two partition modes in each codec to perform full-rate distortion optimization processing, thereby reducing the hardware complexity of the codec. Liu Z's experiment used the best arithmetic representation and used TSMC's 65 nm CMOS to develop high-speed [714 MHz under worst-case conditions (125°C, 0.9 V)] and low-cost (42.5 k gates) accelerator technology for fast algorithms. An accelerator can support HD 1080p at 55 frames per second in real-time encoding. This research process is more complicated and not practical [9].

The innovations of this article are as follows: (1) proposing a separable CNN algorithm model; (2) constructing a separable CNN codec structure; (3) designing a separable convolution image semantic segmentation process of neural network.

2. Semantic Image Segmentation Research Method Based on Separable Convolutional Neural Network Codec

2.1. Convolutional Neural Network. When the computer obtains an image, it will process the image as a two-

dimensional data matrix. According to different algorithms, the feature information in the image is obtained. After a series of training and learning processes, a network structure for classification is finally obtained to judge the picture or filter out the target image [10]. The purpose of the neural network is to determine what an input represents, and CNN uses the idea of convolution to provide a method for extracting feature values [11]. CNN is a deep feedforward neural network composed of a convolutional layer, nonlinear layer, pooling layer, and fully connected layer [12].

2.1.1. Convolutional Layer. The convolutional layer is the core of the network, and most calculations are performed in the convolutional layer. The feature map is generated in the convolution operation and output to the next layer for feature extraction [13]. In the convolution operation, the convolution kernel learns the best parameters for extracting features through iterations. The convolutional layer can be regarded as a feature extractor, which extracts representative features from the image through convolution operation [14]. Take a single-channel single convolution kernel as an example to illustrate the convolution operation, where I represents the input feature map, O represents the output feature map, and K represents the convolution kernel. The convolution operation can be expressed by the following formula:

$$O(y, x) = \sum_{u=1}^{k_1} \sum_{v=1}^{k_2} K(u, v) I(y + u, x + v, i). \tag{1}$$

The convolution kernel is a three-dimensional tensor, and each pixel of the feature map corresponds to a neuron [15]. Each neuron has an area of the same size as the convolution kernel in the feature map of the upper layer, which is called the neuron's receiving field, and each neuron is connected with the neurons in the receiving field through the convolution kernel [16]. In feature mapping, neurons in the same channel share a convolution kernel, and different channels correspond to different convolution kernels [17]. The calculation process of feature mapping can be expressed by the following formula:

$$O(y, x, j) = \sum_{i=1}^{c_1} \sum_{u=1}^{k_1} \sum_{v=1}^{k_2} K(u, v, i) I(y + u, x + v, i, j). \tag{2}$$

2.1.2. Nonlinear Layer. In CNNs, the nonlinear activation function usually follows the convolution operation. The convolution operation is a linear weighted summation operation. As the depth of the CNN expands, the number of convolutional layers deepens. The nesting of linear functions has weak nonlinear expression ability. This problem can be solved well by adding a nonlinear activation function after the convolutional layer so that the network can approximate any function, and the nonlinear activation function can also speed up the network convergence efficiency [18, 19]. There are three commonly used nonlinear activation functions: Sigmoid, Tanh, and ReLu.

Sigmoid function expression is as follows:

$$f(x) = \frac{1}{1 + e^{-x}}. \tag{3}$$

The Tanh function expression is as follows:

$$\text{Tanh}(x) = \frac{1 - e^{-2x}}{1 + e^{-2x}}. \tag{4}$$

The ReLu function expression is as follows:

$$y = \begin{cases} 0 \, (x < 0), \\ x \, (x \geq 0). \end{cases} \tag{5}$$

2.1.3. Pooling Layer. Another important operation of CNNs is called pooling, also called downsampling [20]. Pooling can reduce network parameters, reduce the resolution of feature mapping, and reduce the impact of deformation on feature mapping. Common pooling operations include average pooling and maximum pooling. Average pooling selects the average value of adjacent regions of the feature map to represent the region [21]. Maximum pooling selects the maximum value of the adjacent area of the feature map to represent the area. Due to the use of the pooling layer, the resolution of the feature plane is reduced, and the reduced resolution of the feature plane will simplify the calculation of the network and will also reduce the training parameters, thereby reducing overfitting [22]. In addition, due to the reduced resolution of the feature map, in the next convolutional layer, the receptive field corresponding to the convolution kernel will also increase [23].

2.1.4. Fully Connected Layer. Each element output by the fully connected layer is connected to the elements of all the input feature maps, so it is called the fully connected layer. The fully connected layer does not extract the features of the input like the convolutional layer and the pooling layer, and then output to the hidden; instead, the output is mapped to the sample label space, and the output of the fully connected layer is a one-dimensional vector [24]. The parameter amount of the fully connected layer is greater than the parameter amount of the convolutional layer. Generally, the fully connected layer will be used behind the convolutional layer to map the features extracted by the convolutional layer to the sample space [25].

2.1.5. Optimization. The optimization method is to calculate the minimized loss value. Given dataset D, the optimization goal is the average value of all data loss in D, that is, the average loss, taking the minimum value [26]. The following formula exists:

$$L(W) = \frac{1}{|D|} \sum_{t}^{|D|} f_w\left(x^{(t)}\right) + \lambda_r(W). \tag{6}$$

When the given dataset D is very large, the random subset N of the dataset much smaller than the whole data set is usually used instead. The following formula exists:

$$L(W) \approx \frac{1}{N} \sum_{t}^{N} f_w\left(x^{(t)}\right) + \lambda_r(W). \tag{7}$$

2.2. Separable Convolutional Neural Network. In order to reduce the network model and increase the calculation speed, the CNN structure needs to be further optimized [27]. The most direct method is to reduce the size of the parameters, that is, use a smaller convolution kernel and feature map to compress from the existing network model Considering the acceleration method, the compression method mainly includes compression from the perspective of weight value and from the perspective of network architecture [28]. The standard 3D convolution is resolved into two processes: 3D depth convolution and 3D point-by-point convolution. In the 3D depth convolution stage, the convolution kernel is only calculated separately with each channel of each frame of the input sequence, and they are not combined. It is a new feature; in the three-dimensional point-by-point convolution stage, a convolution kernel of size $1 \times 1 \times 1$ is used for convolution [29]. Thus, the calculation process has the following formula:

$$d_{ij}^{xyz} = f\left(\sum_{p=0}^{P_{i-1}} \sum_{q=0}^{Q_{i-1}} W_{ih}^{pqk} I_{(i-1)h}^{(x+p)(y+q)(z+k)} + b_{ij}\right),$$

$$k = \text{ceil}\left(\frac{j}{m}\right), \quad h = j - k * m - 1, \tag{8}$$

$$I_{ij}^{xyz} = f\left(\sum_{m} W_{ijm} d_{im}^{xyz} + b_{ij}\right).$$

The calculated cost after separation is as follows:

$$D_k \cdot D_K \cdot D_K \cdot M \cdot D_F \cdot D_F \cdot D_f + D_k \cdot M \cdot N \cdot D_F \cdot D_F \cdot D_f. \tag{9}$$

By separating the CNN, the number of model parameters can be greatly reduced and the calculation speed can be improved. At the same time, the number of layers is doubled, which deepens the network, enhances the nonlinearity of the network, and can improve the classification effect of the network at the same time [30].

2.3. Image Semantic Segmentation. Semantic segmentation is to draw the image into meaningful areas and label the object categories represented by these areas, which visually means that the categories of different objects are processed with different colors [31]. In deep learning, data are an inseparable topic. The quality of data directly affects the results of this algorithm [32]. The collection of data also requires professionals to complete it. Since the emergence of public datasets, researchers have been short of data. The problem was solved, which also promoted the rapid development of deep learning [33]. The most commonly used public datasets for image semantic segmentation in the literature are PASCAL VOC2012, MS COCO, ADE20 K,

PASCAL Context, Cityscapes, CamVid, and SYNTHIA.[34]. In image semantic segmentation, the total number of object categories in the image is defined as N, n_{ij} represents the number of pixels with actual category i and predicted category j, and t_i represents the number of pixels with actual category i. The evaluation index of image semantic segmentation is generally pixel accuracy rate, average accuracy, and average intersection ratio [35].

Pixel accuracy, defined as the ratio of the number of correctly classified pixels to the total number of image pixels, is the simplest metric, which measures the overall performance of pixel-level image segmentation algorithms in semantic segmentation [36]. The following formula exists:

$$\text{Overall Acc} = \frac{\sum_{i=1}^{N} n_{ij}}{\sum_{i=1}^{N} t_i}. \qquad (10)$$

The average accuracy is defined as the average accuracy of various categories of objects. It is a simple improvement of pixel accuracy. First, calculate the proportion of correctly classified pixels in each category by category, and then calculate the average of all categories. The average accuracy rate measures the performance of the pixel-level image segmentation algorithm for each class of segmentation effect [37]. The following formula exists:

$$\text{Mean Acc} = \frac{\sum_{i=1}^{N} n_{ij}/t_i}{N}. \qquad (11)$$

The average intersection ratio, defined as the ratio of the intersection and union of the segmentation result and the true value, has the advantages of simplicity and representativeness and is the most commonly used evaluation index. Most studies use the average intersection ratio to measure the semantic segmentation results [38]. The following formula exists:

$$\text{Mean } IoU = \frac{\sum_{i=1}^{N} n_{ji}/t_i + \sum_{j=1}^{N} n_{ji} - n_{ij}}{N}. \qquad (12)$$

The method part of this article uses the above method to study the experiment of semantic image segmentation based on the codec of a separable CNN. The specific process is shown in Figure 1.

3. Separable Convolutional Neural Network-Based Codec for Semantic Image Segmentation Research Experiment

3.1. Construct a Codec Structure of Separable Convolutional Neural Network. Separable convolution usually divides the convolution operation into several steps. It is usually used as a separable deep convolution in deep learning. The core idea is to divide the completed convolution operation into deep convolution and pointwise convolution. Depth convolution is different from traditional convolution. The feature map image after deep convolution has the same number of channels as the input layer. After completing this operation, a point-by-point convolution operation is needed to aggregate these features into new features. The essence of point-by-point convolution is to concentrate the feature images of the depth separable convolution in a depth direction to create a new feature.

The separable CNN is applied to the codec network structure, and the end-to-end codec network structure SegProNet is designed, which ensures the spatial semantic information of the pixels while performing feature detection and segmentation. SegProNet performs maximum pooling in the first three layers of the coding structure and performs appropriate indexing operations to achieve pixel positioning standards. The last two layers of depooling are only used for folding processing to ensure the uncertainty perception of spatial resolution and boundary contour information. Perform pixel segmentation to improve the detailed information perceived by the network and ensure the accuracy of pixel positioning prediction. Combine index and upsampling to generate sparse feature maps, and combine convolution to generate dense features. By selectively discarding pooling, the loss of spatial information is reduced while avoiding information loss caused by repeated upsampling in the original network. Semantic and location information are used to receive the number of fields, which improves boundary division, significantly reduces the number of parameters for end-to-end training, and ensures that the network can learn more abstract feature settings. By removing the convergence and relatively deep convolution, the network can extract more detailed image features while ensuring the accuracy of spatial semantic features. In order to increase the parameters caused by deleting the pool, set a narrow layer to expand the network depth and, at the same time improve, training efficiency.

The same convolution method is used to ensure that the size of the image remains unchanged before and after the image is forwarded to the decoder through the maximum pool index. The input image is uploaded in a nonlinear manner to obtain spatial semantic image information and avoid loss in the encoding process. After the maximum convergence of each layer, a batch normalization layer is added, and the numerical range after the formation of the nonlinear function is close to the standardized saturation range distribution, thereby avoiding the disappearance of the gradient.

The decoder consists of an upward sampling layer, a convolutional layer, and a pooling layer. It restores the pixel pool based on the information of the largest information pool and restores part of the scanning position upward. The encoder part also uses the same folding method [38]. For each pixel after encoding, the pixel data on different channels are combined with linear parameters without changing the topological structure and dimensional information of the original image [39], thereby expanding and deepening the network structure.

3.2. Design the Semantic Segmentation Process. To effectively perform semantic segmentation on images, there are two key points to be resolved. First, we must train the network model. Before training the network model, we should determine the type of presegmented image, then select a large
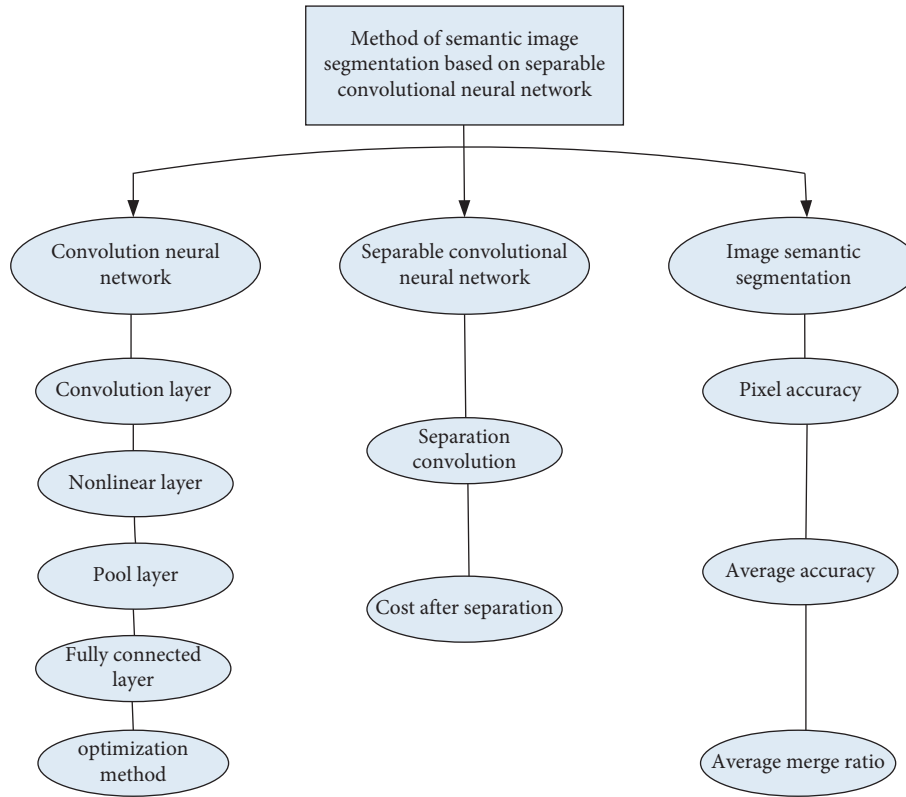
Figure 1: Part of the technical flowchart of this method.

number of pictures consistent with the presegmented image type as the dataset, and make the corresponding label map so that the network model can be performed training. The second is to preprocess the input image. This article mainly denoises the image to reduce image loss. Finally, the processed image is input into the trained network model to obtain the output segmentation result.

In the problem of image segmentation and recognition, it is possible to encounter some pictures with shadows or overexposure [40]. These factors should not affect the final segmentation recognition results. Therefore, the input pictures need to be preprocessed to make the CNN model be as small as possible by some unnecessary factors. The brightness, contrast, noise, and other attributes of the image have a great influence on the image. The same object has a huge difference under different brightness and contrast. The quality of the image directly has a great influence on the result of image processing. The image needs to be preprocessed before inputting the image. The main goal of image preprocessing is to reduce the useless information in the image, restore useful information, enhance the detectability of the target object, and simplify the data as much as possible, thereby enhancing the reliability of feature extraction, image segmentation, and recognition [41]. In image semantic segmentation, there will be various noises in the process of image acquisition and input. The noise in the image is useless information, so the input image will affect the result of the segmentation. In order to effectively improve the accuracy of segmentation, we need to preprocess the image, denoise the image, and keep the useful

information of the image as complete as possible while denoising the image.

3.2.1. Gaussian Filtering.
Gaussian filtering is to use a template to scan each pixel in the image and then use the weighted average gray value of the pixels in the neighborhood determined by the template to replace the value of the center pixel of the template. Gaussian filtering is a smooth linear filter that gives pixels different positions and weights. The pixels closer to the center have the largest weights, which can smooth the noise and save all the gray distribution characteristics in the image. Using the Gaussian filtering is suitable for processing the Gaussian noise map.

3.2.2. Median Filtering.
Median filtering is a statistical sorting filter, which sorts all pixels in the neighborhood and then takes the median. This denoising method is suitable for dealing with discrete point noise.

3.2.3. P-M Equation Denoising Segmentation.
The P-M equation is derived from the heat conduction equation. Its principle is similar to the Gaussian filter formula. Both are anisotropic diffusion equations. Unlike Gaussian filtering, the PM equation connects the features in the image with the diffusion process. The coefficient of directional diffusion changes with the change of the gradient value of the image, so this method can effectively remove noise and retain edge information.

The experimental part of this article proposes that the above steps are used for the codec based on a separable CNN for semantic image segmentation research experiments. The specific process is shown in Table 1.

4. Semantic Image Segmentation Based on Separable Convolutional Neural Network

4.1. Performance Comparison Analysis. The new decoder module reduces one layer compared with the original design. According to the deep network design research, reducing the number of network layers helps to reduce the instability of network training. At the same time, the number of parameters of the new decoder module is increased compared with that in the old module. The new module has more model complexity and can obtain better image feature representation, which is helpful to improve the performance of image segmentation. Since the convolution layer behind the deconvolution layer is removed in the new decoder module, the deconvolution layer can be initialized reasonably. Bilinear interpolation can play a role in upsampling, so we can use bilinear interpolation to initialize the deconvolution layer. The algorithms involved in the experiment are implemented by PyTorch, a deep learning framework. PyTorch is a toolkit maintained by Facebook's AI research team. It uses python programming language and is a deep learning research platform that emphasizes development flexibility and code running speed. PyTorch supports GPU acceleration, which can greatly speed up computing.

In order to compare the performance of the improved CNN in image semantic segmentation, experiments were conducted on CamVid, voc2012, and Cityscapes datasets. The two networks were trained on the training set of the dataset, and the performance of the network was verified by the verification set of the dataset. The specific situation of the data is drawn into a chart, as shown in Table 2 and Figure 2.

It can be seen from the table that the improved SegProNet outperforms the original structure in three evaluation indexes: overall ACC, mean ACC, and mean IOU. Looking at the most important average intersection and merge ratio, the improved SegProNet achieves an average improvement of about 0.01 on CamVid, voc2012, and Cityscapes datasets compared with that with the original structure, which proves the effectiveness of the improved SegProNet. Among the three datasets, CamVid data set has the least number of training set samples, Cityscapes dataset has the largest number of training set samples, and the number of training set samples of voc2012 data set is between the two. Therefore, it can be seen that the smaller the number of training set samples, the better the performance of improved SegProNet, compared with that of the original codec.

4.2. Comparative Analysis of Experiments. In the image segmentation based on conditional generating countermeasure network, how to design and generate the countermeasure network, that is, the discriminant model, is one of the key algorithms. If the designed network is weak, the effect of antilearning is not obvious, which can not optimize the image

semantic segmentation network. If the designed network is too strong, the training process can not converge and the training of the generation model will fail. The algorithm shows the alternate training process of image semantic segmentation network as generation model and confrontation network as discrimination model, and there are two kinds of loss functions used in the training process, one is used to train image semantic segmentation network and0 the other is used to train confrontation network. The datasets used in this part are CamVid dataset and Cityscapes dataset, and the Cityscapes dataset only provides the real segmentation graph of the training set and verification set, whereas the training set, verification set, and test set of the CamVid dataset provide real segmentation graph, so the test set of CamVid dataset can also be used to verify the segmentation performance of the method. The specific comparison results are drawn into charts, as shown in Tables 3–5 and Figures 3–5.

It can be seen that the improved SegProNet confrontation learning method achieves the highest performance among the three indicators on CamVid (verification set). On CamBid (test set), SegNet + confrontational learning method achieves the highest overall accuracy, and the improved SegProNet method achieves the highest average accuracy and average cross merge ratio. On Cityscapes (verification set), the improved SegProNet confrontational learning achieves the highest overall accuracy and average cross merge ratio, and the SegProNet + confrontation learning method achieves the highest average accuracy. Generally speaking, the performance of improved SegProNet + confrontation learning method is the best, while SegProNet method is the worst.

4.3. Structure Analysis of Separable Convolutional Neural Network. The advantage of stacking the feature planes extracted before and convolution feature planes as the input of the next layer network is to solve the problem that the gradient of the network features disappears after the feature planes are extracted one layer at a time. Secondly, the convolution network directly inputs the feature plane extracted from the previous part into the back-end network, which enhances the backward propagation of features, and makes more effective use of the extracted feature plane, instead of spreading down step by step like the traditional method. The establishment of links between different convolution layers and repeatable persistent blocks are the characteristics of building the generation countermeasure network model. It makes the network get better results with fewer parameters. Finally, after each convolution operation, most of them add batch normalization operation, which has been proved to play an important role in deep learning. The structure details of the generated network are shown in Table 6.

The structure details of the discrimination network are shown in Table 7.

From the data in Figure 6, it can be seen that all the steps of the network are 1;; that is, the size of the image is not changed before and after convolution. In order to merge the feature images obtained before and after, the network does not carry out a pooling operation. In order to

TABLE 1: The experimental steps in this article.

Experimental study on semantic image segmentation based on separable convolutional neural network	Codec architecture based on separable convolutional neural network	1	Separable convolutional neural network
		2	Encoder-decoder
	Design semantic segmentation process	1	Gaussian filtering
		2	Median filtering
		3	Denoising and segmentation of P-M equation

TABLE 2: Performance comparison before and after improvement.

Data set	Method	Mean IoU	Mean ACC	Overall ACC
CamVid	SegProNet	0.4926	0.6129	0.8107
	Improving SegProNet	0.5013	0.6194	0.8241
VOC2012	SegProNet	0.5114	0.6237	0.8134
	Improving SegProNet	0.5207	0.6321	0.8327
CityScapes	SegProNet	0.5126	0.5904	0.8406
	Improving SegProNet	0.5225	0.6079	0.8671
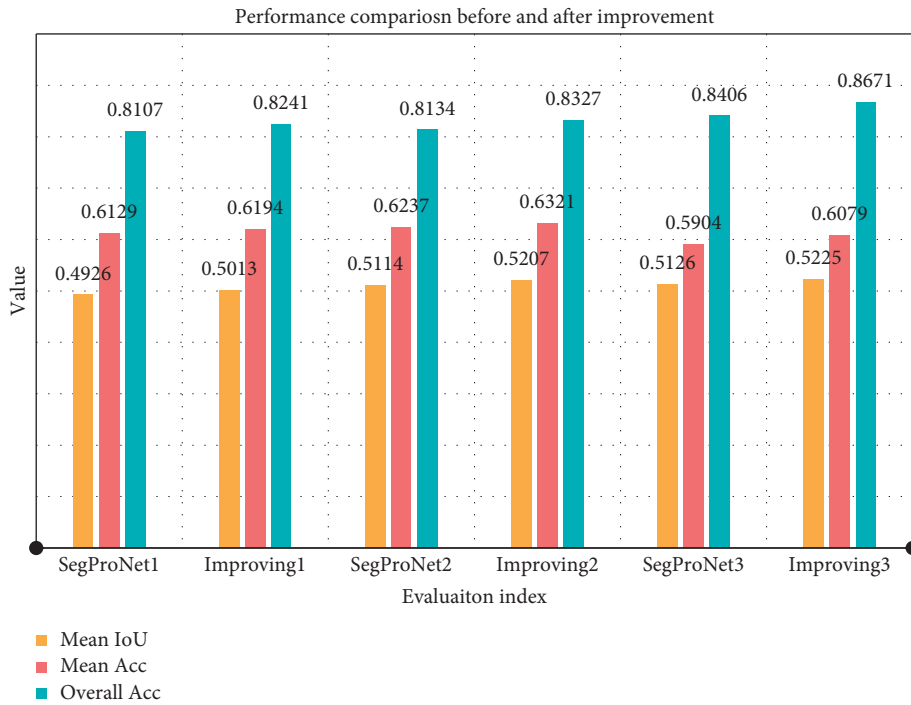
FIGURE 2: Performance comparison before and after improvement.

TABLE 3: Comparison of experimental results (CamVid validation set).

Method	Mean IoU	Mean ACC	Overall ACC
FCN-8S	0.4301	0.6307	0.8347
FCN-32S	0.4127	0.6425	0.8438
SegNet	0.3721	0.6531	0.8271
SegNet + confrontational learning	0.3927	0.6597	0.8364
SegProNet	0.5103	0.6741	0.8521
SegProNet + confrontational learning	0.5231	0.6872	0.8675
Improvement of SegProNet	0.6142	0.6927	0.8843
Improvement of SegProNet + confrontational learning	0.6247	0.7031	0.9021

TABLE 4: Comparative experimental results (CamVid test set).

Method	Mean IoU	Mean ACC	Overall ACC
FCN-8S	0.4137	0.6217	0.6532
FCN-32S	0.4011	0.6349	0.6417
SegNet	0.4231	0.6401	0.6628
SegNet + confrontational learning	0.4327	0.6513	0.6803
SegProNet	0.4421	0.6670	0.6947
SegProNet + confrontational learning	0.4532	0.6721	0.7081
Improvement of SegProNet	0.4670	0.6739	0.7269
Improvement of SegProNet + confrontational learning	0.5730	0.6845	0.7531

TABLE 5: Comparison of experimental results (Cityscapes validation set).

Method	Mean IoU	Mean ACC	Overall ACC
FCN-8S	0.4027	0.6241	0.6251
FCN-32S	0.3816	0.6373	0.6374
SegNet	0.4123	0.6570	0.6459
SegNet + confrontational learning	0.4275	0.6801	0.6581
SegProNet	0.4531	0.6931	0.6742
SegProNet + confrontational learning	0.4681	0.7044	0.6899
Improvement of SegProNet	0.5037	0.7247	0.7021
Improvement of SegProNet + confrontational learning	0.5219	0.7438	0.7208
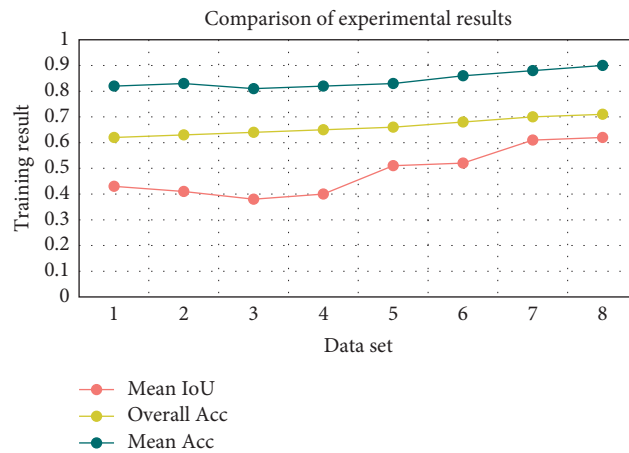
FIGURE 3: Comparison of experimental results (CamVid validation set).
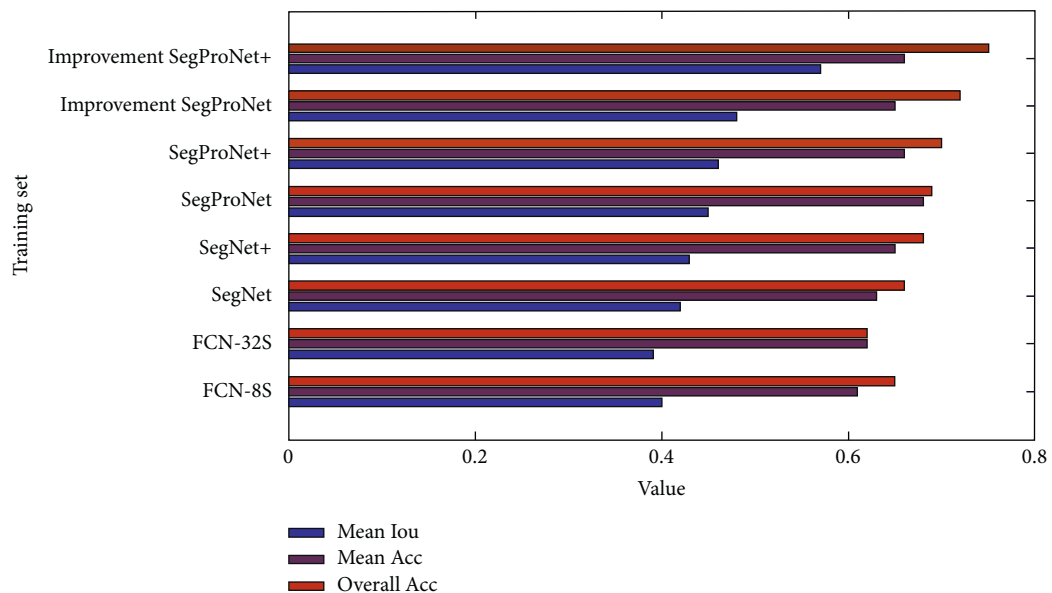
FIGURE 4: Comparative experimental results (CamVid test set).
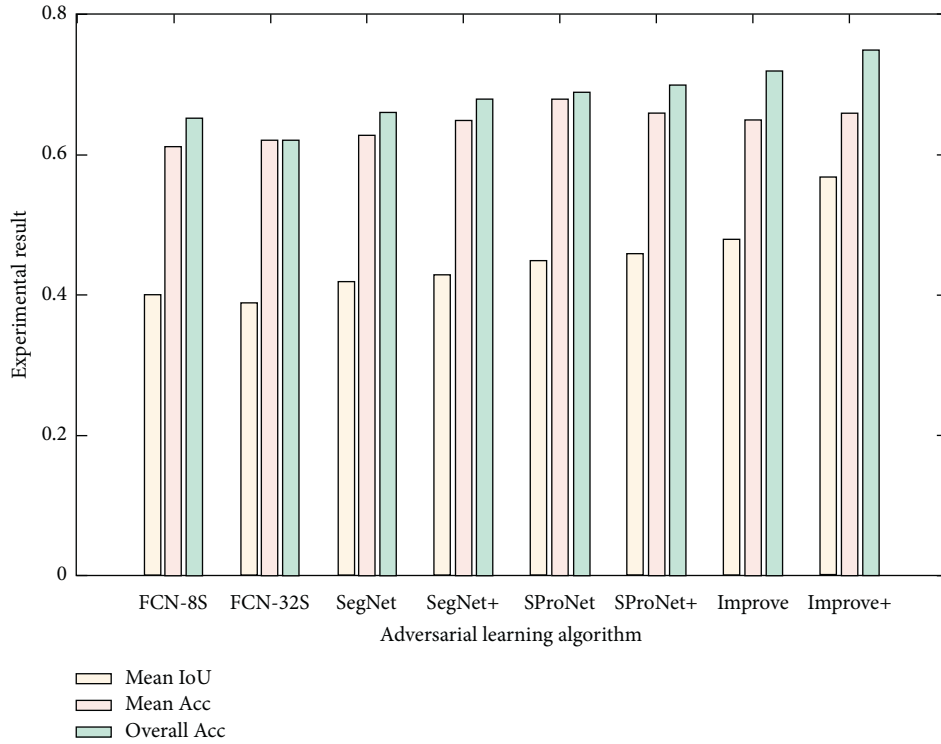
FIGURE 5: Comparison of experimental results (Cityscapes validation set).

TABLE 6: Structure details of the generated network.

Operation	Convolution kernel size	Input channel	Output channel	Step	Batch normalization
Conv 1	12*12	12	144	1	N
Conv 2	4*4	144	144	1	Y
Conv 3	4*4	144	144	1	Y
Conv 4	4*4	144 + 144	144	1	Y
Conv 5	4*4	144 + 144	432	1	N
Conv 6	12*12	432	4	1	N

TABLE 7: Structure details of the discriminant network.

Operation	Convolution kernel size	Input channel	Output channel	Step	Batch normalization
Conv 1	4*4	4	144	1	N
Conv 2	4*4	144	144	2	Y
Conv 3	4*4	144	288	1	Y
Conv 4	4*4	288	288	2	Y
Conv 5	4*4	288	432	1	Y
Conv 6	4*4	432	432	2	Y
Conv 7	4*4	432	576	1	Y
Conv 8	4*4	576	576	2	Y

distinguish the structural details of the network, the convolution step size is used instead of the traditional pooling operation. When the image is downsampled, the number of feature planes is increased. After 8-layer convolution, there are two full connection layers. The first full connection layer will be the eighth. The 576 feature planes of convolution output are connected to the following neurons; the second fully connected layer integrates
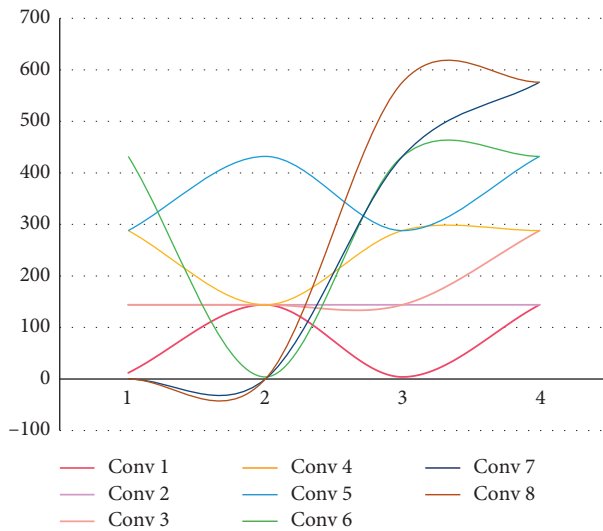
FIGURE 6: Comparison of two network structure details.

these neurons into one output; the last fully connected layer outputs the probability that the sample belongs to the true sample and the false sample.

5. Conclusions

With the explosive growth of image data and the continuous development of deep learning, the field of computer vision has received unprecedented attention from all walks of life. As an important part of the field of computer vision, image semantic segmentation has been paid more and more attention by industry and academia. CNN has achieved unprecedented success in the field of computer vision because of its powerful feature extraction ability. However, the semantic segmentation network based on the total convolution neural network still has some problems, such as poor segmentation effect and high model complexity. After the in-depth study on the semantic segmentation network and summing up its shortcomings, the main work of this article is to improve and optimize the semantic segmentation network to improve the effective receptive field of the network and extract the overall situation. According to the following information, the multiscale target features are integrated to improve the segmentation effect of the network for multiscale targets and an end-to-end semantic segmentation network combining global context information and multiscale spatial pooling is constructed.

In this article, we improve the design of a codec CNN structure SegProNet, which has a better segmentation effect and faster convergence speed than the classical segmentation network. Pool index and upsampling ensure pixel location and combine deep convolution and discard pooling to create dense features, supplement missing high frequency and pixel location information, and gradually deepen filter segmentation to improve timeliness. Comparing CNN with the traditional network, its learning efficiency and real-time performance are higher.

Compared with the traditional single deep learning network, this article integrates the separable CNN algorithm and image semantic segmentation algorithm into the backend processing of the model by combining the model fusion method so as to realize the integration and coordination of the segmentation results of multiple learners and enhance the fault tolerance and universality of the algorithm. At the same time, it verifies and compares the influence of different activation functions on the network performance. The principle is analyzed deeply.

Data Availability

The data used in the study are available at the following sites: CamVid, http://mi.eng.cam.ac.uk/research/projects/VideoRec/CamVid/; VOC2012, http://host.robots.ox.ac.uk/pascal/VOC/voc2012/; and CityScapes, https://www.cityscapes-dataset.com.

Conflicts of Interest

The authors declare that they have no conflicts of interest.

Acknowledgments

References

[1] M. Elhoseny and K. Shankar, "Optimal bilateral filter and convolutional neural network based denoising method of medical image measurements," *Measurement*, vol. 143, pp. 125–135, 2019.

[2] J. Yang, C. Wang, B. Jiang, H. Song, and Q. Meng, "Visual perception enabled industry intelligence: state of the art, challenges and prospects," *Institute of Electrical and Electronics Engineers Transactions on Industrial Informatics*, vol. 17, no. 3, pp. 2204–2219, 2021.

[3] S. B. Tsai, W. Wu, S. Ma, C. H. Wu, and B. Zhou, "Benchmarking, knowledge inertia, and knowledge performance in different network structures," *Enterprise Information Systems*, vol. 2019, 2019.

[4] Y. Zhao, H. Li, S. Wan et al., "Knowledge-aided convolutional neural network for small organ segmentation," *Institute of Electrical and Electronics Engineers Journal of Biomedical and Health Informatics*, vol. 23, no. 4, pp. 1363–1373, 2019.

[5] S. I. Cho and S.-J. Kang, "Gradient prior-aided CNN denoiser with separable convolution-based optimization of feature dimension," *Institute of Electrical and Electronics Engineers Transactions on Multimedia*, vol. 21, no. 2, pp. 484–493, 2019.

[6] H. W. F. Yeung, J. Hou, X. Chen, J. Chen, Z. Chen, and Y. Y. Chung, "Light field spatial super-resolution using deep efficient spatial-angular separable convolution," *Institute of Electrical and Electronics Engineers Transactions on Image Processing*, vol. 28, no. 5, pp. 2319–2330, 2019.

[7] Z. Liu, X. Yu, Y. Gao, S. Chen, X. Ji, and D. Wang, "CU partition mode decision for HEVC hardwired intra encoder using convolution neural network," *Institute of Electrical and Electronics Engineers Transactions on Image Processing*, vol. 25, no. 11, pp. 5088–5103, 2016.

[8] M. Elhoseny, "Multi-object detection and tracking (MODT) machine learning model for real-time video surveillance systems," *Circuits, Systems, and Signal Processing*, vol. 39, no. 2, pp. 611–630, 2019.

[9] Z. He, L. Yang, S. Angizi, A. S. Rakin, and D. Fan, "Sparse BD-net," *ACM Journal on Emerging Technologies in Computing Systems*, vol. 16, no. 2, pp. 1–24, 2020.

[10] J. Zhang, X. Lv, Q. Sun, Q. Zhang, X. Wei, and B. Liu, "SDResU-net: separable and dilated residual U-net for MRI brain tumor segmentation," *Current Medical Imaging Formerly Current Medical Imaging Reviews*, vol. 16, no. 6, pp. 720–728, 2020.

[11] X. Zhang, Y. Zheng, W. Liu et al., "An improved architecture for urban building extraction based on depthwise separable convolution[J]," *Journal of Intelligent and Fuzzy Systems*, no. 11, pp. 1–9, 2020.

[12] L. Rao, B. Zhang, and J. Zhao, "Hardware implementation of reconfigurable 1D convolution," *Journal of Signal Processing Systems*, vol. 82, no. 1, pp. 1–16, 2016.

[13] X. Cheng and Z. Chen, "Video frame interpolation via deformable separable convolution," *Proceedings of the AAAI Conference on Artificial Intelligence*, vol. 34, no. 07, pp. 10607–10614, 2020.

[14] Y. Tang and X. Wu, "Scene text detection and segmentation based on cascaded convolution neural networks," *Institute of Electrical and Electronics Engineers Transactions on Image Processing*, vol. 26, no. 3, pp. 1509–1520, 2017.

[15] K. H. Cha, L. M. Hadjiiski, R. K. Samala et al., "Bladder cancer segmentation in CT for treatment response assessment: application of deep-learning convolution neural network-A pilot study," *Tomography*, vol. 2, no. 4, pp. 421–429, 2016.

[16] S. Tiwari, "A blur classification approach using deep convolution neural network," *International Journal of Information System Modeling and Design*, vol. 11, no. 1, pp. 93–111, 2020.

[17] Y. Nomura, I. Ida, T. Miyaji, M. Miyamoto, and M. Suga, "Structural integrity diagnosis for valve based on deep convolution neural network," *Journal of the Society of Materials Science, Japan*, vol. 67, no. 2, pp. 177–183, 2018.

[18] C. Liu, X. Zhang, and Q. Hu, "Image super resolution convolution neural network acceleration algorithm," *Guofang Keji Daxue Xuebao/Journal of National University of Defense Technology*, vol. 41, no. 2, pp. 91–97, 2019.

[19] S. Han, W. Lee, H. Eom, J. Kim, and C. Park, "Detection of arrhythmia using 1D convolution neural network with LSTM model," *IEIE Transactions on Smart Processing & Computing*, vol. 9, no. 4, pp. 261–265, 2020.

[20] A. Raj, D. Dubey, A. Mishra, N. Chopda, N. M. Borkar, and V. S. Lande, "Convolution neural network based automatic license plate recognition system," *International Journal of Computer Sciences and Engineering*, vol. 7, no. 4, pp. 199–205, 2019.

[21] R. J. Deshmukh, C. J. Awati, and A. Deshmukh, "Use of convolution neural network algorithm for implementation of an autonomous vehicle," *International Journal of Scientific & Technology Research*, vol. 8, no. 9, pp. 1533–1536, 2019.

[22] H. M. F. Abu, A. Hussain, and M. F. A. Hassan, "Convolution neural network-based action recognition for fall event detection," *International Journal of Advanced Trends in Computer Ence and Engineering*, vol. 8, no. 1, pp. 466–470, 2019.

[23] S. Yoo, J. Lee, and S. Y. Kim, "FFT-based GNSS signal detection scheme using convolution neural network," *Journal of Institute of Control, Robotics and Systems*, vol. 26, no. 3, pp. 199–206, 2020.

[24] S. Tirpude, "Abnormal X-ray detection system using convolution neural network," *International Journal of Advanced Trends in Computer Science and Engineering*, vol. 9, no. 1, pp. 828–832, 2020.

[25] Y. Liu, O. Deforges, and K. Samrouth, "LAR-LLC: a low-complexity multiresolution lossless image codec," *Institute of Electrical and Electronics Engineers Transactions on Circuits and Systems for Video Technology*, vol. 26, no. 8, pp. 1490–1501, 2016.

[26] T. Richter, J. Keinert, S. Foessel, A. Descampe, G. Rouvroy, and J.-B. Lorent, "JPEG-XS-A high-quality mezzanine image codec for video over IP," *SMPTE Motion Imaging Journal*, vol. 127, no. 9, pp. 39–49, 2018.

[27] Y. Chen, W. Zheng, W. Li, and Y. Huang, "Large group Activity security risk assessment and risk early warning based on random forest algorithm," *Pattern Recognition Letters*, vol. 144, 2021.

[28] T. Chandraraju and S. Radhakrishnan, "Image encoder architecture design using dual scan based DWT with vector quantization," *Materials Today: Proceedings*, vol. 5, no. 1, pp. 572–577, 2018.

[29] R. Ezhilarasi and K. Venkatalakshmi, "Low complexity orthogonal transforms for low cost image/video codec design," *Journal of Computational and Theoretical Nanoscience*, vol. 15, no. 3, pp. 859–865, 2018.

[30] L.-C. Chen, G. Papandreou, I. Kokkinos, K. Murphy, and A. L. Yuille, "DeepLab: semantic image segmentation with deep convolutional nets, atrous convolution, and fully connected CRFs," *Institute of Electrical and Electronics Engineers Transactions on Pattern Analysis and Machine Intelligence*, vol. 40, no. 4, pp. 834–848, 2018.

[31] M. Seyedhosseini and T. Tasdizen, "Semantic image segmentation with contextual hierarchical models," *Institute of Electrical and Electronics Engineers Transactions on Pattern Analysis and Machine Intelligence*, vol. 38, no. 5, pp. 951–964, 2016.

[32] I. R. de Moura, A. S. Teles, M. Endler, L. R Coutinho, and F. J Da Silva E Silva, *Highly Reliable and Low Complexity Image Compression Scheme Using Neighborhood Correlation Sequence Algorithm in WSN*, IEEE Transactions on Reliability, Basel, Switzerland, In Press, 2020.

[33] Y. Li, Y. Guo, Y. Kao, and R. He, "Image piece learning for weakly supervised semantic segmentation," *Institute of Electrical and Electronics Engineers Transactions on Systems, Man, and Cybernetics: Systems*, vol. 47, no. 4, pp. 648–659, 2017.

[34] B. Hao and D.-S. Kang, "Research on image semantic segmentation based on FCN-VGG and pyramid pooling module," *The Journal of Korean Institute of Information Technology*, vol. 16, no. 7, pp. 1–8, 2018.

[35] W. Wang, Y. Fu, F. Dong, and F. Li, "Semantic segmentation of remote sensing ship image via a convolutional neural networks model," *IET Image Processing*, vol. 13, no. 6, pp. 1016–1022, 2019.

[36] L. Zhang, Z. Sheng, Y. Li, Q. Sun, Y. Zhao, and D. Feng, "Image object detection and semantic segmentation based on convolutional neural network," *Neural Computing and Applications*, vol. 32, no. 7, pp. 1949–1958, 2020.

[37] S. Cui, C. Liu, M. Chen, and S. Xiong, "Brain tumor semantic segmentation from MRI image using deep generative adversarial segmentation network," *Journal of Medical Imaging and Health Informatics*, vol. 9, no. 9, pp. 1913–1919, 2019.

[38] Z. Lv, L. Qiao, J. Li, and H. Song, "Deep learning enabled security issues in the internet of things," *Institute of Electrical*

and Electronics Engineers Internet of Things Journal,
vol. 20201 page, 2020.

[39] S. Wan, *Topology Hiding Routing Based on Learning with Errors*, Concurrency and Computation: Practice and Experience, Dubai, UAE, 2020.

[40] X. Yuan, D. Li, D. Mohapatra, and M. Elhoseny, "Automatic removal of complex shadows from indoor videos using transfer learning and dynamic thresholding," *Computers & Electrical Engineering*, vol. 70, pp. 813–825, 2018.

[41] K. Shankar, M. Elhoseny, S. K. Lakshmanaprabu et al., "Optimal feature level fusion based ANFIS classifier for brain MRI image classification," *Concurrency and Computation: Practice and Experience*, vol. 32, no. 1, Article ID 24887, 2020.

Research Article

Physical Education Teaching in Colleges and Universities Assisted by Virtual Reality Technology Based on Artificial Intelligence

Yuqing Wang 🔟

Sports Department, Guizhou University of Finance and Economics, Guiyang 550025, Guizhou, China

Correspondence should be addressed to Yuqing Wang; 201301196@mail.gufe.edu.cn

Virtual reality technology has promoted the reform of education. This research mainly discusses college physical education teaching assisted by artificial intelligence-based virtual reality technology. According to the position change of the virtual human's center of gravity, the spline keyframe interpolation method is used for interpolation, and the model pose obtained in each frame is rendered to obtain the virtual human's animation. After synthesizing a virtual human animation with three-dimensional human motion data, the animation can have functions such as video storage, fast playback, slow playback, and freeze. At the same time, the system can also display and play the virtual human animation and the video shot by the camera on the same screen, in order to make an intuitive comparison of the athletes' movements. Coaches can edit by hand or shoot the sports of outstanding domestic and foreign athletes on the spot and then use VC++6.0 as a development tool to analyze and get the simulation video of the 3D virtual human body. The virtual human animation technology in the motion analysis system is to relocate the three-dimensional motion data extracted from the video captured by the camera to the three-dimensional virtual human model we have established, and the three-dimensional virtual human will then simulate the technical actions of the athletes, which indirectly reflects that the three-dimensional movement information of the athletes enables coaches and athletes to observe the athletes' technical movements in a three-dimensional space in real time, repeatedly, and from multiple angles so that the coach can accurately guide the athletes' technical movements. Finally, a neural network based on artificial intelligence technology is used to evaluate the teaching effect. In the comparative experiment, 35% of the people in the virtual teaching experiment group were excellent, while the control group had only 10% in this excellent range (90–100). This research contributes to the smooth progress of VR technology teaching in colleges and universities.

1. Introduction

Virtual reality (VR), like smartphones and the Internet, will be a very disruptive technology. Like smartphones, VR uses new interface formats (head-mounted displays and hand-held controllers) to provide more intuitive and natural access to computing devices. Very similar to the Internet, it allows a new type of global communication, but this time it has a natural human experience. It is almost indistinguishable whether it is standing face to face or standing together.

In the next few years, most Internet users worldwide will use VR every day. Virtual reality (VR) is expected to become one of the killer applications in 5G networks. However, many technical bottlenecks and challenges need to be overcome to promote its widespread adoption. In particular, the demand for VR in terms of high throughput, low latency, and reliable communication requires innovative solutions and basic research across multiple disciplines.

The success of immersive VR experiences depends on solving numerous challenges across multiple disciplines. Bastug E emphasized the importance of VR technology as a disruptive use case for 5G (and beyond). In addition, he studied three VR case studies and provided numerical results under various storage, computing, and network configurations. Although he revealed the limitations of the current

network and provided reasons for more theories and for the public to take the lead in VR innovation, research is still lacking in practice [1]. Patney believes that recessed rendering can synthesize images so that the details of the image outside the eye movement area are gradually reduced, which may significantly increase the display speed of wide-field displays. In order to study and improve the potential benefits, he designed an eccentric rendering user study to evaluate the perception of human peripheral vision when viewing today's displays. After verifying these insights on desktops and head-mounted displays, with the help of high-speed gaze tracking, he designed a perceptible target image to design and produce a centralized renderer. Although he designed a practical recessed rendering system, he did not verify its performance [2]. Sharar believes that immersive virtual reality (VR) dispersion therapy can effectively relieve pain clinically. 74 healthy volunteers (average age, 29 years; 37 women) received a standard 18-minute multimodal pain sequence (alternating thermal stimulation and distal stimulation) while undergoing immersive interactive VR distraction. The subjects used a 0–10 graphical rating scale to score their subjective pain intensity and entertainment and a 9-point scale to score their emotional and arousal state. Although the immersive VR distraction in his study significantly reduced the subjective pain intensity, its negative effects are unknown [3]. Freeman believes that, with virtual reality (VR) and computer-generated interactive environments, individuals can experience the problems they encounter repeatedly and learn how to overcome difficulties through evidence-based psychotherapy. He conducted a systematic review of empirical research. 285 studies were identified, 86 of which involved evaluation, 45 theoretical developments, and 154 treatments. His research found that treatment based on VR exposure can reduce anxiety, but there is a lack of promising research and treatment approaches [4].

According to the position change of the virtual human's center of gravity, the spline keyframe interpolation method is used for interpolation, and the model pose obtained in each frame is rendered to obtain the virtual human's animation. After synthesizing a virtual human animation with three-dimensional human motion data, the animation can have functions such as video storage, fast playback, slow playback, and freeze. At the same time, the system can also display and play the virtual human animation and the video shot by the camera on the same screen, in order to make an intuitive comparison of the athletes' movements. Coaches can edit by hand or shoot the sports of outstanding domestic and foreign athletes on the spot and then use VC++6.0 as a development tool to analyze and get the simulation video of the 3D virtual human body. The virtual human animation technology in the motion analysis system is to relocate the three-dimensional motion data extracted from the video captured by the camera to the three-dimensional virtual human model we have established, and the three-dimensional virtual human will then simulate the technical actions of the athletes, which indirectly reflects that the three-dimensional movement information of the athletes enables coaches and athletes to observe the athletes' technical

movements in a three-dimensional space in real time, repeatedly, and from multiple angles so that the coach can accurately guide the athletes' technical movements.

2. College Physical Education Teaching

2.1. Artificial Intelligence. The subjective application form of artificial intelligence technology in education and teaching (education robot, intelligent tutor system) has overturned the traditional subject and object of teaching [5, 6]. But this change does not mean that teachers are not needed [7]. It is just that the tasks that teachers undertake in teaching activities have changed, from the traditional "preaching, teaching, and solving puzzles" to "designing, advancing, assisting, and caring" [8, 9]. The specific performance is to design learning activities, promote the learning process, help solve students' psychological problems, and care about the overall development of all students [10]. This is something that technology cannot replace [11, 12].

At present, in the field of higher education in my country, artificial intelligence has classic research in the field of artificial intelligence such as machine learning and deep learning, as well as the application of artificial intelligence in traditional disciplines such as biomedicine and general information theory [13]. As an indispensable part of my country's scientific research force, universities lead the direction and trend of my country's scientific research [14, 15]. Under the current background of artificial intelligence, it is necessary to invest more material and human resources in artificial intelligence research and actively cultivate students' scientific research concepts and scientific research capabilities based on the current era [16]. Only after defining the similarity between the motion frames can a "difficult action" be automatically located from the "original motion segment" [17, 18]:

$$D(t_1, t_2) = \|m(t_1) - m(t_2)\| = \sum_{i=1}^{n} \alpha_i d(q_i(t_1), q_i(t_2)), \quad (1)$$

with $i = 1, 2, \ldots, n$.

Linear interpolation is used to calculate the mixed motion of the overlapping part [19].

$$P_p = \alpha(p)P_A + [1 - \alpha(p)]P_B, \quad (2)$$

where P stands for frame.

The result is the translational position P_p of the human root node in the p-th frame in motion:

$$q = \text{slerp}(q_A, q_B, \alpha(p)). \quad (3)$$

It can be seen that the quaternion can represent the degree of rotation of the human joint i in the p-th frame in the synthetic motion [20, 21].

2.2. Virtual Reality Technology. The three-dimensional character generation process is as follows. First, find the relative coordinates of each joint point relative to the center of gravity of the virtual human body, and eliminate the influence of the translational movement on the joint motion

of the virtual human body [22]. Then apply the knowledge of inverse dynamics to obtain the rotation angle of each joint relative to its "parent" node [23, 24]. According to the position change of the center of gravity of the virtual human at different times, the spline keyframe interpolation method is used to interpolate the spatial position of the virtual human. For the initial position of each joint on any two motion keyframes and the rotation angle of the joint obtained by inverse dynamics, we use the quaternion interpolation method to interpolate to form an intermediate picture. The model pose obtained in each frame is rendered and played continuously at the frame rate of the real situation, and the animation of the virtual human model movement is obtained [25]. On this basis, the program itself can save the formed virtual human animation as an AVI file, which provides the necessary preparation for the later video synthesis operation [26].

The connection between the two motion segments is basically similar:

$$
\begin{aligned}
q &= \mathrm{slerp}\,(q_A, q_B, \alpha(p)), \\
c_j &= ((f_{i1}, t_{i1}), (f_{i2}, t_{i2}), \ldots, (f_{ij}, t_{ij})).
\end{aligned} \tag{4}
$$

Each t_i moment corresponds to a posture f, and its splicing action sequence is

$$
c_j = ((f_{i1}, t_{i1}), \ldots, (f_{i2}, t_{i2}), \ldots, (f_{im}, t_{im}), \ldots, (f_{jn}, t_{m+n})). \tag{5}
$$

The stitching algorithm should ensure the continuity of time, the continuity of the coordinates of the center of gravity of the human body, and the continuity of the human body posture. Then the transformation of f_{im} and f_{jt} has the following relationship:

$$
\begin{aligned}
f_{jt} &= M * f_{im}, \\
M &= f_{jt} * f_{im}^{-1}.
\end{aligned} \tag{6}
$$

Through the analysis of the path curve, we can get whether two athletes will collide.

$$
d = T_{P_1 L_1} - T_{P_1 L_2} - T_{L_1 L_2}. \tag{7}
$$

The basic process of VR teaching is as follows:

(1) Construct the corresponding virtual human body model and 3D scene according to user needs. The system itself comes with a virtual character model library. The technician or user administrator can choose different types of human body models according to user requirements. The actual training scene is to build a virtual scene for it, including sports reference objects [27].

(2) Real-time capture of exercise data. Generally speaking, this function is realized by two cameras and a computer. The cameras obtain video files of human motion during the process of simultaneous shooting and use existing computer technology to extract keyframe images from the video files, and then it is done manually. The method of intelligence, pattern matching, and computer graphics extracts the moving human body, obtains the final two-dimensional information of each joint point and the outline of the moving object, and finally calculates the three-dimensional motion data of the human body according to the two simultaneous engravings of the two-dimensional information of the human body and generates the computer animation.

(3) Reproduce the action. This function is to relocate the three-dimensional human body motion data we get to the virtual human (animation), play the virtual human at a certain frame rate, and then form an animation after rendering in the three-dimensional scene. The students' movements are recorded by the computer. High-quality simulation is reproduced, and students can watch their actions from multiple angles and all directions in order to improveAmong them, "action reproduction" is the core requirement of the simulation system. The trainer can also simulate some technical actions that are still under research and can also observe the technical actions of the students from multiple angles in this way, so as to give the students a visual and intuitive guide.

(4) Obtain motion parameters. According to the different requirements of coaches and trainees, the system can feed back various parameters related to athletes and sports, such as heart rate, blood pressure, etc. This can not only objectively control sports risks but also promote the objective control of sports risks. The trainees' indicators are quantified.

(5) Real-time image display training effect. All the data that can represent the athlete's performance are presented in real time and vividly in the form of charts, which greatly facilitates the teaching of coaches to compare the athlete's performance horizontally and vertically and to understand his/her training process and training in time, whether there are positive changes in the results after the end.

(6) Refined data. Due to the widespread existence of errors and uncontrollable factors, we can only get rough data, which puts forward requirements for the system to refine the rough data, such as smoothing and deleting the data. After finishing the refinement, we can improve the technical actions and create new actions, such as connecting several technical actions in series.

(7) Synchronous comparison of composite video. The application of virtual reality technology to sports training can significantly improve the training level and competitive level of athletes while reducing costs and not reducing the amount of training. It also greatly promotes the development of sports as a national fitness exercise. Modern sports training research and application play an increasingly important role. The diagnostic process of sports technology in physical education is shown in Figure 1.
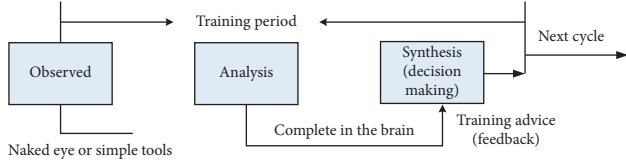
FIGURE 1: Diagnostic process of sports technology in physical education.

2.3. Extraction of Public Frames.

The existence of the common frame is the basis of the algorithm in this paper. The two action segments before and after the action arrangement must have similar postures to ensure a smooth transition. For any two posture data, the center of gravity distance $D_R(f_i, f_j)$ of the two postures can be expressed as

$$D_R(f_i, f_j) = \sqrt{(x_i - x_j)^2 + (y_i - y_j)^2 + (z_i - z_j)^2}. \quad (8)$$

The degree of freedom of the human body's posture direction is

$$D_d(f_i, f_j) = \sum_{k=1}^{S} \left\| J_i - J_j \right\|^2. \quad (9)$$

J represents a measure of the degree of freedom of the human body, given two sets of points:

$$\begin{aligned} A &= \{(A_1, w(A_1)), (A_2, w(A_2)), \ldots, (A_m, w(A_m))\}, \\ B &= \{(B_1, w(B_1)), (B_2, w(B_2)), \ldots, (B_m, w(B_m))\}. \end{aligned} \quad (10)$$

The transport distance between A and B is also called Monge – Kantorovich distance.

$$D_{\text{Monge–Kantorovich}} = \frac{\min_F \sum_{i=1}^{m} \sum_{j=1}^{n} f_{ij} d_{ij}}{\sum_{i=1}^{m} \sum_{j=1}^{n} f_{ij}}. \quad (11)$$

In actual engineering, keyframes often need to add a certain person's prior knowledge, for example, the high point, low point, and inflection point of a certain action or the intersection point of two or more actions. The action of this point must be selected as a keyframe; at this time, it is regarded as the starting frame or the node frame, and then another frame is to be found manually. There are also some very special situations. For example, the video playback speed is too fast (e.g., football in a football match), the difference between the two frames is too large, or the appropriate first and last frames cannot be found according to the above method. At this time, the above method is completely invalid. You should look for the video shot by the high-speed camera. In this kind of video, the time interval between two consecutive frames is much smaller than that of the ordinary video. You can often find the first and last frames you need. Another situation is that the time interval between the first and last frames found is too large. At this time, the last frame should be discarded and a new last frame should be searched for. Experience tells us that this method is feasible.

3. College Physical Education Teaching Experiment

3.1. Human Body 3D Animation Generation

(1) Use the relative coordinates of the human body's center of gravity to eliminate the influence of drift on joint motion.

(2) Calculate the rotation angle of the joint relative to its "parent" node.

(3) According to the position change of the virtual human's center of gravity, the spline keyframe interpolation method is used for interpolation.

(4) Using the initial position and rotation angle of the joints on the two keyframes, the middle image is calculated by quaternion interpolation.

(5) Render the pose of the model obtained in each frame to obtain the animation of the virtual human.

3.2. Editing of Motion Sequence.

In actual operation, we often combine the modification of the motion curve of a certain joint with the inverse dynamics organically to achieve the purpose of adjusting the posture of the virtual human. First, we apply the above method to modify the motion curve of a joint of the virtual human, and then according to the position of the joint point at each moment on the modified curve, we use the knowledge of inverse dynamics to reversely find the other joint points corresponding to this. The system marks the position at this time and then redirects the modified result to the virtual character to achieve the virtual effect.

(1) Target action requirements, including basic information such as the type and length of the target action.

(2) Arrangement of the motion and use of the motion fragments captured by the motion to synthesize new motion fragments as required.

(3) Smooth transition, dissatisfaction with the final synthesized animation, and modification of mechanical requirements or collision.

3.3. Realizing the Same-Screen Comparison of Sports Simulation Results and Athletes' Actions.

After synthesizing virtual human animation with 3D human motion data, the animation should have most of the functions of ordinary video, such as video storage, fast playback, slow playback, and freeze frame. At the same time, the system should be able to display and play the virtual human animation and the video captured by the camera on the same screen, in order to make an intuitive comparison of the athletes' movements.

The main research is the combination of virtual and real technology. Coaches can edit by hand or shoot the sports of outstanding athletes at home and abroad and then use VC++6.0 as a development tool to analyze and get the simulation video of the three-dimensional virtual human body. The virtual human animation technology in the

motion analysis system is to relocate the three-dimensional motion data extracted from the video captured by the camera to the three-dimensional virtual human model we have established, and the three-dimensional virtual human will then simulate the technical actions of the athletes, which indirectly reflects that three-dimensional sports information of the athletes enables coaches and athletes to observe the technical movements of the athletes in three-dimensional space in real time, repeatedly, and from multiple angles so that the coach can accurately observe the technical movements of the athletes after repeatedly observing the virtual human animation guide.

3.4. Virtual Teaching Videos Based on Virtual Reality Technology

3.4.1. Preliminary Shooting and Production. Conceive and design the content and shooting content of the virtual teaching video of sports dance, such as the teaching plan, teaching important and difficult points, scene setting, and shooting angle. According to the teaching plan, determine the technical actions of each lesson, highlight its details and important and difficult points, then select at the right time and place, take a video or panoramic shot in the real-view location, and then output the panoramic video or panoramic image on the computer or mobile phone.

3.4.2. Mid-Term Synthetic Production. For the teaching materials obtained in the early stage, use professional computer software to perform video editing or panorama stitching according to the teaching plan, and postprocessing to output the panorama video or panorama.

3.4.3. Post Network Release. Synthesize the panoramic video produced in the mid-term, conduct logic testing for bugs and continuously improve the content, repeat, and finally, output video samples. Display VR video content through a VR player (such as insta 360 player, storm VR), watch the content repeatedly, and test it. The team has to modify it according to the shortcomings, and finally complete the release.

3.5. Physical Education Evaluation Module Based on Artificial Intelligence Technology. Mainly use neural network to score teaching effect. The evaluation result analysis module is used to guide the evaluator to correctly analyze the evaluation results, to store the evaluation results and analysis results, and to provide corresponding sample models and simulation models for system self-learning. The knowledge base management system is responsible for acquiring valuable knowledge and for the maintenance and management of various knowledge required during system operation. The model method management system is responsible for the operation, maintenance and management of the models and methods in the system, and realizing the calling and linking of models and methods under the guidance of knowledge. Accordingly, with the neural network evaluation model

scheduling, various models (such as neural network-based system self-learning models) are stored in the model library. The basic process of teaching evaluation module is shown in Figure 2.

4. College Physical Education Teaching

4.1. Test Results of the Body Shape before the Experiment. The body shape before the experiment is shown in Table 1. The main research content of this paper is to test the new physical education teaching method using virtual reality technologywhether there is a clear difference in the teaching effect from the traditional teaching mode. In order to eliminate the influence of other factors on the experiment, the experiment must first be checked. The students in the group and the control group tested the 5 basic functions of the body before the experiment. Since the experimental samples are all 15–17-year-old students and the students are in the growth and development period, it is necessary to carry out statistical tests and analysis. The experiment was divided into two groups, each with 20 people, 10 male students and 10 female students. The data comparison in Table 1 shows that there is no significant difference in the physical state of the two groups of students before the tennis class ($P > 0.05$), which can be used as a sample for this experiment.

In order to make the experimental results more accurate and convincing, a simple physical test was performed on the students who participated in the experiment, and a T test was performed on the measurement data. The results of the T value test are shown in Table 2. People's daily production and life, as well as the process of physical exercise, are all carried out under the regulation and control of the central nervous system. The reflection of the various organs of the body is called physical fitness. Physical fitness can also represent the various functions of the human body's muscles during exercise. Obvious differences in physical fitness may affect the accuracy of the experiment. From Table 2, we can see that there is no significant difference between the two groups of tests ($P > 0.05$).

The statistical results of students' interest before the experiment are shown in Table 3. In order to minimize the influence of external factors on the experiment, a questionnaire survey was conducted on the sample's interest in tennis learning before the lecture. It can be seen from Figure 3 that most of the students choose tennis lessons because they are interested in tennis. Among them, 26 people like tennis very much, accounting for 82.5% of the total number of subjects. As the saying goes, interest is the best teacher. The students who participated in the experiment showed a high interest in tennis learning, which can also make the students more enthusiastic about tennis learning. Figure 3 shows the comparison of interest in tennis between the experimental group and the control group before the experiment.

The results of the questionnaire are shown in Figure 4. According to the statistics of the questionnaire survey of the two groups of students, it can be seen that the most important way for the two groups of students to obtain tennis
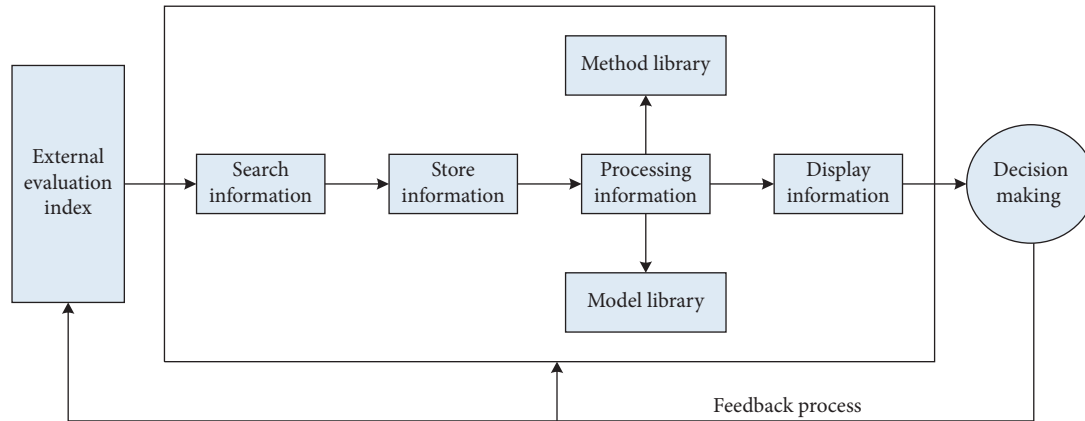
FIGURE 2: Basic process of teaching evaluation module.

TABLE 1: Body shape before the experiment.

Group	Test group		Control group		T	P
Gender	X	S	X	S		
Height (male)	174.25	5.28	173.82	4.61	0.274	>0.05
Weight (male)	66.36	4.02	65.85	3.96	0.404	>0.05
Height (female)	165.34	4.88	164.27	4.63	0.711	>0.05
Weight (female)	50.05	3.74	48.92	3.38	1.002	>0.05

knowledge is through colleague TV communication, accounting for 35%, and 14 students obtained tennis knowledge through television, followed by the Internet, accounting for 17%, advertising and propaganda accounting for 20%, and books and magazines, accounting for 15%. Tennis knowledge obtained from classmates and teachers is the least. In the process of investigating and discussing with classmates, it was found that many students had the idea of learning tennis because they had watched the cartoon *Prince of Tennis* before. Therefore, the widespread of this cartoon is because students love tennis and want to obtain tennis knowledge, so many students did not hesitate to choose tennis when choosing physical education. In addition, in the process of growing up, he watched many wonderful tennis matches, and he became more determined to choose tennis as a sport. Through their own efforts to learn tennis-related knowledge and practice tennis-related skills, students will eventually become master tennis players like the characters in the *Prince of Tennis* and shine on the tennis court.

4.2. Test Results of the Body Shape and Physical Fitness of the Two Groups of Students after the Experiment. The body shape tests of the two groups of students after the experiment are shown in Table 4. The physical fitness tests of the two groups of students after the experiment are shown in Table 5. After the lecture, the last stage of the experiment is to perform physical tests on the students again. In order to ensure the accuracy of the experiment, the test indicators before and after the experiment are the same, and the corresponding methods of measuring various body values are also the same. After joining the class, we found that the students' height

and weight will not change much. However, some values of physical fitness have changed, which is different from the previous test results. Through statistical analysis, the two projects of standing long jump and 50 m running show that the students who use the new virtual reality teaching mode to learn show better results than the students under the traditional model. The difference is not significant. Figure 5 shows the results of student body shape analysis. Figure 6 shows the analysis result of students' physical fitness.

4.3. Comprehensive Scores of Tennis Skills between the Two Groups of Students after the Experiment. Table 6 shows the comparison of the comprehensive scores of tennis skills between the two groups of students. Figure 7 shows the analysis of the comprehensive performance of the tennis skills of the two groups of students. According to Table 7, it can be concluded that there is a significant difference between the two. The overall performance of the students in the virtual teaching experimental group is in the average and good range, and the number of outstanding students is small, which shows that this teaching method is more suitable for high school sports than the traditional teaching mode. The development of tennis teaching needs also shows that the virtual teaching method has been loved and praised by the majority of teachers and students. It not only allows students to learn the skills of tennis in a short period of time, but also completes the requirements of the credit system and maximizes the transfer. Students' interest in tennis along with a high-quality learning environment can keep students' enthusiasm for learning. Virtual teaching technology makes it easier for students to master tennis skills, with simple and convenient operation, making it easier for students to enjoy it. According to Figure 7, 35% of the people in the virtual teaching experiment group were excellent, while the control group had only 10% in this excellent range (90–100), and only the virtual teaching number reached one-third of the excellent people. In the good range (80–89), the number of students in the two parties is basically the same. The virtual teaching is 40%, and the control group occupies 35%. In the range of general scores (70–79), the number of students in the control group reaches 40%. The teaching experiment

TABLE 2: *T* value test results.

Group	Test group		Control group		*T*	*P*
Gender	X	S	X	S		
Standing long jump (male)	222.4	13.12	223.53	13.49	−0.269	>0.05
50 m (s) (male)	7.34	0.46	725	0.42	0.646	>0.05
Swollen capacity (male)	3730.3	620.8	3759	6154	−0.147	>0.05
Standing long jump (female)	166.25	6.01	164.83	6.29	0.730	>0.05
50 m (s) (female)	8.82	0.76	865	0.70	0.736	>0.05
Swollen capacity (female)	238 5	502.6	2365.4	5183	−0.043	>0.05

TABLE 3: Statistics of student interest before the experiment.

Group	Test group		Control group		*T*	*P*
Interest	X	S	X	S		
Pre-experiment interest	4.05	0.51	3.95	0.69	0.521	>0.05
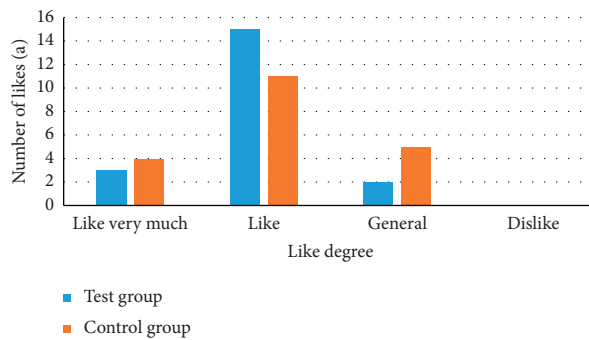
FIGURE 3: Comparison of interest in tennis between the experimental group and the control group before the experiment.
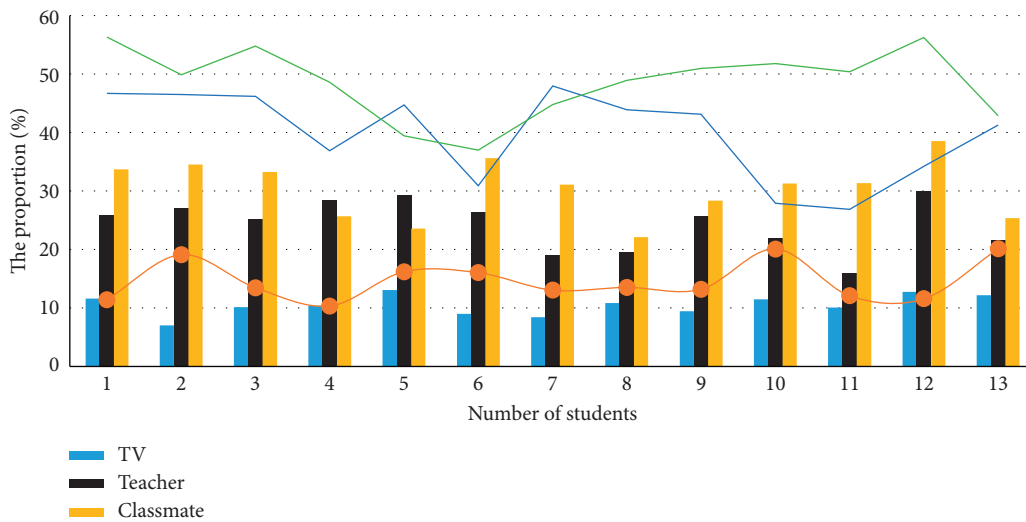
FIGURE 4: Results of the questionnaire.

group has only 20%. From this point of view, under normal circumstances, most people in the control group will get intermediate grades. 5% of the virtual teaching group and 10% of the control group were in the pass range.

4.4. Comparative Analysis of Learning Effects. After the experiment, the comparison of the forehand and backhand technique evaluation scores of the two groups of students is shown in Table 7. Figure 8 shows the comparison results of

TABLE 4: Body shape tests of the two groups of students after the experiment.

Group	Test group		Control group		T	P
Gender	X	S	X	S		
Height (male)	174.25	5.28	173.82	4.61	0.274	>0.05
Weight (male)	6632	4.05	65.80	3.91	0.413	>0.05
Height (female)	165.34	4.88	164.27	4.63	0.711	>0.05
Weight (female)	50.01	3.72	48.96	3.33	0.941	>0.05

TABLE 5: Physical fitness tests of the two groups of students after the experiment.

Group	Test group		Control group		T	P
Gender	X	S	X	S		
Standing long jump (male)	236.4	14.52	231.71	13.92	1.043	>0.05
50 m (s) (male)	7.11	0.26	7.17	0.24	−0.758	>0.05
Swollen capacity (male)	3894.5	212.1	3810.2	204.6	1.279	>0.05
Standing long jump (female)	169.92	6.74	167.13	6.33	1.349	>0.05
50 m (s) (female)	8.31	056	842	0.62	−0589	>0.05
Swollen capacity (female)	2595.2	302.7	2478.4	3189	1.188	>0.05
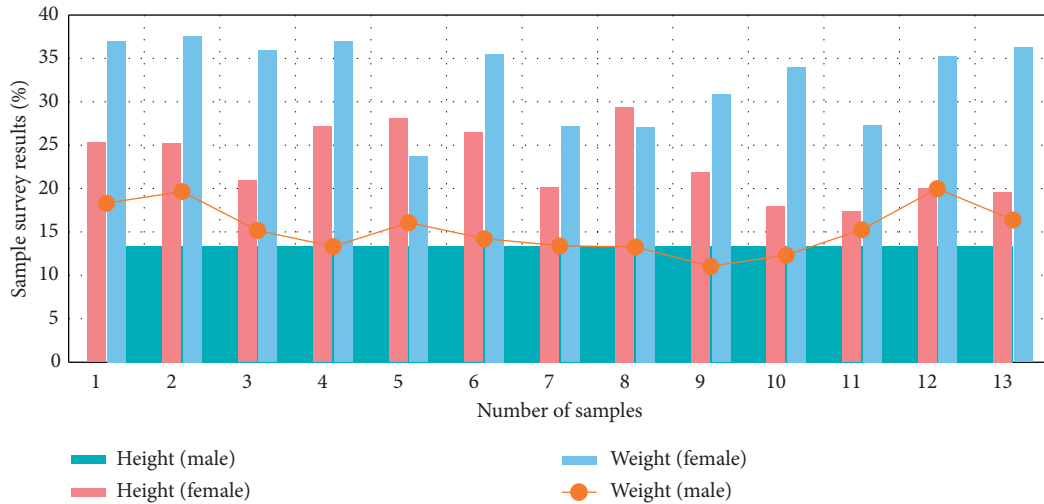
FIGURE 5: Results of student body shape analysis.
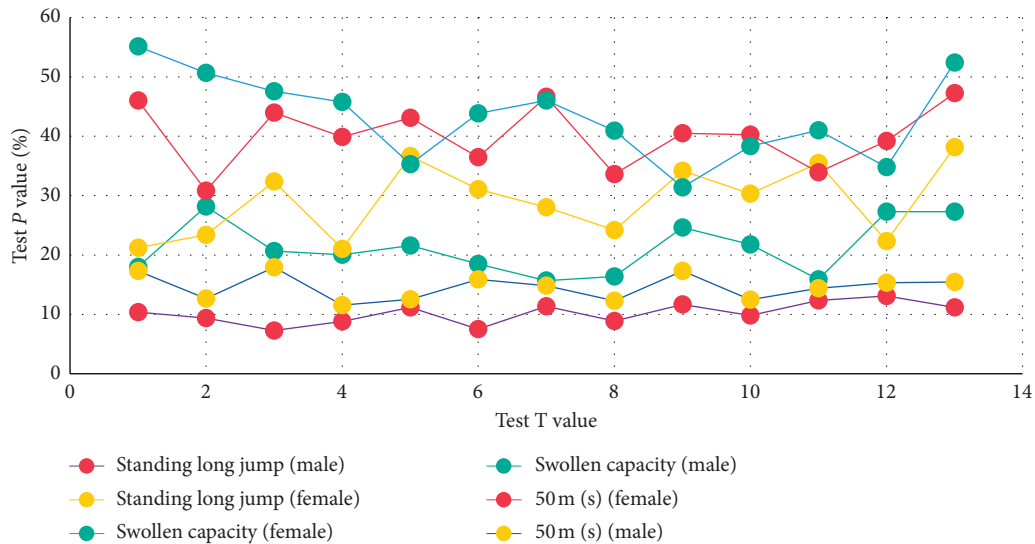
FIGURE 6: Results of analysis of students' physical fitness.

TABLE 6: Comparison of comprehensive scores of tennis skills between two groups of students.

Group	Test group		Control group		T	P
Score	X	S	X	S		
Comprehensive skill score	171.57	8.70	158.21	6.25	3.908	>0.05
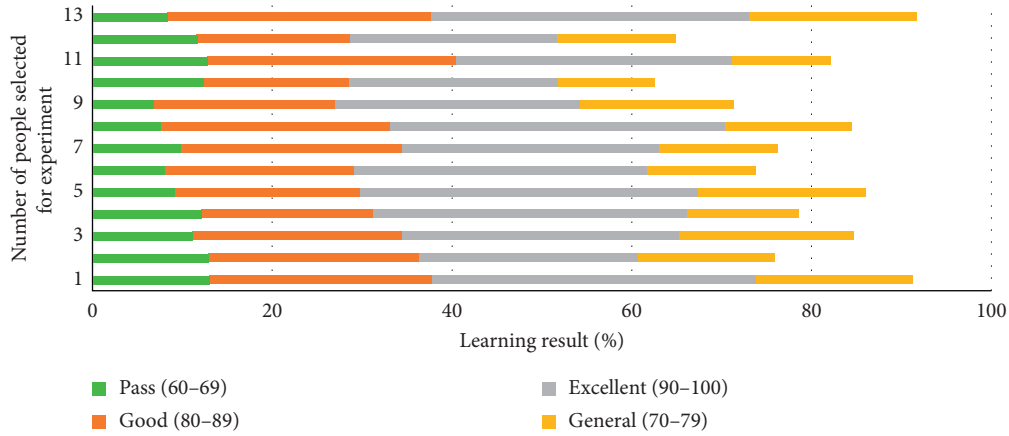
FIGURE 7: Analysis of the comprehensive scores of tennis skills between two groups of students.

TABLE 7: Comparison of forehand and backhand technique evaluation scores of the two groups of students after the experiment.

Score	Test group		Control group		T	P
	X	S	X	S		
Forehand technique	82.67	11.16	75.11	10.09	2.247	<0.05
Backhand technique	78.16	10.23	71.35	10.72	2.055	<0.05

FIGURE 8: Comparison of forehand and backhand scores of the two groups of students.

the forehand and backhand skill scores of the two groups of students. According to the data comparison in Table 7, it can be judged that the scores of the experimental group students and the traditional teaching mode students in tennis forehand technique are 82.67 points and 75.11 points, respectively, and the average score of the two groups is 7.56 points. The test group scored 78.16 points, and the control group scored 71.35 points. The difference between the two was 6.81 points. According to the experimental results, it can be judged that there is a significant difference between the virtual teaching method and the traditional teaching method ($P < 0.05$). The students in the experimental group have a higher level of tennis skills than the subjects in the control group. The reason may be that, in the virtual reality teaching group, students have a full understanding of the details of various tennis techniques through auxiliary equipment, and they continue to consolidate and strengthen during the learning process. With the improvement of proficiency, the students in the experimental group have better mastery of tennis skills, so they are more interested and enthusiastic about tennis learning and practice. On the other hand, in the traditional teaching group, students will encounter various situations that are not conducive to learning due to the insufficient grasp of the details of tennis technology, which will lead to a decrease in learning interest and low enthusiasm.

5. Conclusion

In actual operation, we often combine the modification of the motion curve of a certain joint with the inverse dynamics organically to achieve the purpose of adjusting the posture of the virtual human. First, we apply the above method to modify the motion curve of a joint of the virtual human, and then according to the position of the joint point at each moment on the modified curve, we use the knowledge of inverse dynamics to reversely find the other joint points corresponding to this. The system recognizes the position at this time and then redirects the modified result to the virtual character, thus achieving the virtual effect. The system requires basic information for the target action, such as the type and length of the target action. Arrange the movement, and use the captured movement fragments to synthesize new movement fragments as required.

The main research is the combination of virtual and real technology. Coaches can edit by hand or shoot the sports of outstanding athletes at home and abroad and then use

VC++6.0 as a development tool to analyze and get the simulation video of the three-dimensional virtual human body. The virtual human animation technology in the motion analysis system is to relocate the three-dimensional motion data extracted from the video captured by the camera to the three-dimensional virtual human model we have established, and the three-dimensional virtual human will then simulate the technical actions of the athletes, which indirectly reflects that three-dimensional sports information of the athletes enables coaches and athletes to observe the technical movements of the athletes in three-dimensional space in real time, repeatedly, and from multiple angles so that the coach can accurately observe the technical movements of the athletes after repeatedly observing the virtual human animation guide.

Conceive and design the content and shooting content of the virtual teaching video of sports dance during the preliminary shooting and production process, such as the teaching plan, teaching difficulties, scene setting, and shooting angle. According to the teaching plan, determine the technical actions of each lesson, highlighting its details, focus on difficult points, then select the appropriate time and place, take the video or panoramic shooting in the real scene, and then output the panoramic video or panoramic image on the computer or mobile phone. This research contributes to the smooth progress of VR technology teaching in colleges and universities.

Data Availability

No data were used to support this study.

Conflicts of Interest

The author declares that there are no conflicts of interest.

References

[1] E. Bastug, M. Bennis, M. Medard, and M. Debbah, "Toward interconnected virtual reality: opportunities, challenges, and enablers," *IEEE Communications Magazine*, vol. 55, no. 6, pp. 110–117, 2017.

[2] A. Patney, M. Salvi, J. Kim et al., "Towards foveated rendering for gaze-tracked virtual reality," *ACM Transactions on Graphics*, vol. 35, no. 6, pp. 1–12, 2016.

[3] S. R. Sharar, A. Alamdari, C. Hoffer, H. G. Hoffman, M. P. Jensen, and D. R. Patterson, "Circumplex model of affect: a measure of pleasure and arousal during virtual reality distraction analgesia," *Games for Health Journal*, vol. 5, no. 3, pp. 197–202, 2016.

[4] D. Freeman, S. Reeve, A. Robinson et al., "Virtual reality in the assessment, understanding, and treatment of mental health disorders," *Psychological Medicine*, vol. 47, no. 14, pp. 2393–2400, 2017.

[5] P. Rosedale, "Virtual reality: the next disruptor: a new kind of worldwide communication," *IEEE Consumer Electronics Magazine*, vol. 6, no. 1, pp. 48–50, 2016.

[6] M. S. Elbamby, C. Perfecto, M. Bennis, and K. Doppler, "Toward low-latency and ultra-reliable virtual reality," *IEEE Network*, vol. 32, no. 2, pp. 78–84, 2018.

[7] D. Freeman, J. Bradley, A. Antley et al., "Virtual reality in the treatment of persecutory delusions: randomised controlled experimental study testing how to reduce delusional conviction," *British Journal of Psychiatry*, vol. 209, no. 1, pp. 62–67, 2016.

[8] L. P. Berg and J. M. Vance, "Industry use of virtual reality in product design and manufacturing: a survey," *Virtual Reality*, vol. 21, no. 1, pp. 1–17, 2017.

[9] E. Ronchi, D. Nilsson, S. Kojić et al., "A virtual reality experiment on flashing lights at emergency exit portals for road tunnel evacuation," *Fire Technology*, vol. 52, no. 3, pp. 623–647, 2016.

[10] J. Dascal, M. Reid, W. W. Ishak et al., "Virtual reality and medical inpatients: a systematic review of randomized, controlled trials," *Innovations in Clinical Neuroscience*, vol. 14, no. 1-2, pp. 14–21, 2017.

[11] J. Munafo, M. Diedrick, and T. A. Stoffregen, "The virtual reality head-mounted display Oculus Rift induces motion sickness and is sexist in its effects," *Experimental Brain Research*, vol. 235, no. 3, pp. 889–901, 2017.

[12] L. Donath, R. Rössler, and O. Faude, "Effects of virtual reality training (exergaming) compared to alternative exercise training and passive control on standing balance and functional mobility in healthy community-dwelling seniors: a meta-analytical review," *Sports Medicine*, vol. 46, no. 9, pp. 1293–1309, 2016.

[13] J. Gutiérrez-Maldonado, B. K. Wiederhold, and G. Riva, "Future directions: how virtual reality can further improve the assessment and treatment of eating disorders and obesity," *Cyberpsychology, Behavior, and Social Networking*, vol. 19, no. 2, pp. 148–153, 2016.

[14] Z. Lv, T. Yin, X. Zhang, H. Song, and G. Chen, "Virtual reality smart city based on WebVRGIS," *IEEE Internet of Things Journal*, vol. 3, no. 6, pp. 1015–1024, 2016.

[15] S. A. W. Andersen, S. Foghsgaard, L. Konge, P. Cayé-Thomasen, and M. S. Sørensen, "The effect of self-directed virtual reality simulation on dissection training performance in mastoidectomy," *The Laryngoscope*, vol. 126, no. 8, pp. 1883–1888, 2016.

[16] J. Tromp, D. Peeters, A. S. Meyer, and P. Hagoort, "The combined use of virtual reality and EEG to study language processing in naturalistic environments," *Behavior Research Methods*, vol. 50, no. 2, pp. 862–869, 2018.

[17] F. Aim, G. Lonjon, D. Hannouche, and R. Nizard, "Effectiveness of virtual reality training in orthopaedic surgery," *Arthroscopy: The Journal of Arthroscopic and Related Surgery*, vol. 32, no. 1, pp. 224–232, 2016.

[18] D. Yan, Q. Zhou, J. Wang, and N. Zhang, "Bayesian regularisation neural network based on artificial intelligence optimisation," *International Journal of Production Research*, vol. 55, no. 7-8, pp. 2266–2287, 2016.

[19] A. Ema, N. Akiya, H. Osawa et al., "Future relations between humans and artificial intelligence: a stakeholder opinion survey in Japan," *IEEE Technology and Society Magazine*, vol. 35, no. 4, pp. 68–75, 2016.

[20] T. R. Besold, "On cognitive aspects of human-level artificial intelligence," *Ki Künstliche Intelligenz*, vol. 30, no. 3-4, pp. 343–346, 2016.

[21] Y. Feng, N. Cui, Q. Zhang, L. Zhao, and D. Gong, "Comparison of artificial intelligence and empirical models for estimation of daily diffuse solar radiation in North China Plain," *International Journal of Hydrogen Energy*, vol. 42, no. 21, pp. 14418–14428, 2017.

[22] R. H. Kulkarni and P. Padmanabham, "Integration of artificial intelligence activities in software development processes and measuring effectiveness of integration," *IET Software*, vol. 11, no. 1, pp. 18–26, 2017.

[23] D. Norman, "Design, business models, and human-technology teamwork," *Research-Technology Management*, vol. 60, no. 1, pp. 26–30, 2017.

[24] F. Liu, Y. Shi, and Y. Liu, "Intelligence quotient and intelligence grade of artificial intelligence," *Annals of Data Science*, vol. 4, no. 1, pp. 179–191, 2017.

[25] J. Suri, A. Sarwar, M. Ali, and V. Sharma, "Novel benchmark database of digitized and calibrated cervical cells for artificial intelligence based screening of cervical cancer," *Journal of Ambient Intelligence & Humanized Computing*, vol. 12652, no. 16, pp. 353–358, 2016.

[26] N. Dudhwala, K. Jadhav, P. Gabda, and B. Kishor, "Prediction of stock market using data mining and artificial intelligence," *International Journal of Computer Applications*, vol. 134, no. 12, pp. 9–11, 2016.

[27] A. H. Mazinan and A. R. Khalaji, "A comparative study on applications of artificial intelligence-based multiple models predictive control schemes to a class of industrial complicated systems," *Energy Systems*, vol. 7, no. 2, pp. 237–269, 2016.

Research Article

Analysis on the Water Supply Chain Model under Revenue-Sharing Contract considering Marketing Effort, Water Purity

Lijia Huang [1] **and Deshan Tang** [1,2]

[1]*Business School, Hohai University, Nanjing 211100, Jiangsu, China*
[2]*College of Water Conservancy and Hydropower Engineering, Hohai University, Nanjing 210098, Jiangsu, China*

Correspondence should be addressed to Lijia Huang; huanglijia@hhu.edu.cn

A two-tier water supply chain including a manufacturer and a retailer under revenue-sharing contract is constructed. And the contribution of the model is that marketing effort and water purity has been considered. First, four models including the centralized model (model B) and decentralized models (models BM, I, and II) are established and analyzed. Second, the Stackelberg game model is used to discuss the pricing strategy of water supply chain members in centralized and decentralized scenarios. The comparison results show that revenue-sharing contract is beneficial to improve the level of product greening, the profit of supply chain members, and the overall profit of the water supply chain compared with model BM. However, it leads to the decrease of retailers' green marketing efforts and the wholesale price of water. In addition, revenue-sharing contract through bargaining makes bigger influence than revenue-sharing contract. Marketing can stimulate the increase of the green product's market demand on one hand, and on the other hand, it generates the amount of marketing cost. In this study, the profit is that marketing produces cannot offset the cost that it brings. Thus, it will be important to take some measures to make up the loss that marketing generated.

1. Introduction

As the blood of the earth, the source of life, and the cradle of civilization, water has important resource function, ecological function, and economic function. Due to the scarcity of water resources and the discharge of a larger number of domestic sewage and industrial wastewater, the manufacturing process of drinking water is critical. With the modern day acceleration of industrialization and urbanization, the demand for water increased rapidly. Moreover, water pollution incidents that happened occasionally also had promoted the demand for water, especially clean water. Nowadays, plenty of enterprises such as NONGFU SPRING, China's drinking water industry benchmarking enterprise, is focusing on research and development and promotion of mineral water.

Recently, low-carbon life is a hot topic, and a lot of companies are devoting themselves to green products. Also, consumers are shifting their preferences to more environment friendly brands. The green brand image and green brand value can be transformed into the customer's brand loyalty when customers have the concept of green consumption [1]. Therefore, retailers end up going green marketing [2].

Collaboration between partners is beneficial to bring both environment and economy improvement to water supply partners [3]. To motivate water supply chain member's cooperation, it is a common practice in the world that leading enterprises propose a series of green manufacturing requirements, including energy conservation, environmental protection, energy efficiency, and environmental emission, in the procurement process [4]. Only

the water suppliers who meet the requirements can become the suppliers of brand enterprises. In addition, in the financial sector, green finance is used to guide funds to green industries to control and reduce pollution-related investment, so as to promote green production in the whole society.

In this study, two-tier water supply chain models under different Stackelberg scenarios are introduced. Revenue-sharing contract is studied by considering both water marketing effort and water purity. Thus, several questions should be addressed. (1) How do water supply chain members' decisions and profitability are impacted when considering water purity and marketing efforts under revenue-sharing contracts? (2) What are the optimal decision strategies for water supply chain members under different scenarios? Therefore, our study has the following contributes.

(1) Water supply chain models under both centralized scenario and decentralized scenario are constructed. Decision-strategy for supply chain members is analyzed and compared in different models.

(2) Under decentralized scenario, the imparts of revenue-sharing contract on different members and the whole supply chain have been analyzed

There are 4 sections concluded in this study. The 2nd section introduces the previous researchers. In Section 3, models of water supply chain considering water purity and marketing effort are studied. Section 4 presents numerical analysis. We summarize the research and come up with management insights in Section 5.

2. Literature Review

Water supply chain has been studied academically for decades. Since about 2004, supply chains have been widely used in water management. As an instance, research [5] applied supply chain in water resources allocation and dispatch. In 2005, [6] built a hybrid agent-based model to estimate residential water demand by simulating the residential water supply chain. Research [7] demonstrated that the related supply chain management theory and methodology can be applied in water resources allocation and dispatching. The bullwhip effect was studied in the water resource supply chain information management by using stochastic control theory [8]. The optimization of water supply chain management was studied in literature [9], and they came up with a systematic engineering method to reduce the total water demand. In 2007, the study [10] established an optimal multiobjective model of water resource allocation. In 2008, the studies [11, 12] researched joint pricing of water on the basis of cooperative and noncooperative game theories in a two-tier water supply chain. Study [13] developed a spatial water distribution plan that can save cost and time. In 2010, Kogan and Tapiero [14] discussed the economic benefits of two-stage water supply chain by constructing a zero-sum stochastic differential game model. Elala et al. [15] talked about the safety of water supply chain and provided practical suggestions for

communities, enterprises, and local authorities to realize water supply chain risk management. Zhou et al. [16] also discussed the water supply chain risk management experiences based on the case study in Sweden. Portable water supply chain from water collecting to water distribution by taking advantage of the theory of product life cycle chain has been studied in research [17]. In [18], water supply chain transformation has been discussed by constructing a multiperiod mixed integer program model, and they found that comprehensive integration of water supply chain networks and coordination of water production will bring economic and environmental benefits if they are considered within the planned time frame. For water supply-demand with uncertainty, the study [19] utilized the artificial neural network and stationary chain to predict water demand. In 2015, by updating the artificial fish swarm algorithm and the supply chain management theory, the problem of water resources scheduling was solved [20]. Water Data Warehouse (a software) was designed to share the water supply demand information in the whole water supply chain [21]. In [3], taking the reliability of water supply into consideration, they constructed a multiperiod-mixed integer linear programming model to achieve the water supply reliability maximization, and it was found that water demand has a huge effect on the reliability of water supply chain.

Water supply chain coordination is a branch of supply chain management. There are also many research studies on water supply chain coordination. For example, on the basis of communication and coordination and the principle-agent theory, water resource supply chain contract was constructed [5, 7]. Research [22] designed a multilevel, Pareto optimization decision-making model to deal with the multilevel cooperative decision-making problem of the South-to-North Water Transfer Project. In 2006, Dai et al. [23] established a decision-making model of supply chain agent under the contract effect by applying group gaming decision theory on the basis of water resources supply chain. A study [24] observed water inventory coordination by using inventory control theory and proposed transfer payment coordination strategy of water inventory management under VMI theory. In order to derive water resource, Kondili and Kaldellis [25] developed a decision support system (DSS) to coordinate the conflicts between customers' demand in water supply chain. In 2009, a research [14] analyzed the optimal, respectively, in the minimum commitment and flexibility contract based on a two-stage water supply chain. In 2012, a study [26] demonstrated the optimization modeling approach for the pricing and coordinating schemes of SNWD-ER project. Chen [27] considered the water suppliers' profitability and distributers' profitability under the perspective of social responsibility and economic benefit. In [28–33], the pricing strategies of a competitive two-tier water supply chain including one supplier and two distributers under two-part pricing contract and wholesale price contract was studied, and the findings reveal many practical management insights. In 2018, a study [3] investigated the decision-making strategies of water supply chain members by considering who played the leader and follower, and water resources management insights were

provided. In 2019, water supply chain equilibrium and coordination were studied in [31]; in addition, fairness factors are considered to compare the supply chain performances, social welfare, and consumer surplus under different equilibrium strategies and coordination strategies. In 2020, literature [34] revealed that revenue and cost sharing contract could effectively coordinate and improve the water supply chain performance (Figure 1 and Table 1).

3. Model Description

3.1. Assumptions and Demand Function

(1) We assume that in the centralized decision-making system, the manufacturers determine the green marketing effort (e), while in the decentralized system, the retailers decide the green marketing effort. Based on [35–37], the total green marketing effort cost is ($\eta e^2/2$), where η stands for the marketing cost coefficient.

(2) In this study, the demand function is of retail price, green marketing effort, and demand. Retailers' investment is in green marketing in order to promote the green market, and the greater the marketing efforts, the greater the effect on demand.

(3) Manufacturers' green R&D mainly means that green manufacturing can use fewer resources to produce the same product and improve resource utilization rate. Water purity $\theta(0 < \theta \le 1)$ improvement indicates that manufactures should increase research and development costs, and we assume that all the costs were born by the manufacturers. Referring to [38], the R&D investment of manufacture is $\beta\theta^2$, where β means the cost rate of research and development.

(4) Parameter α represents the sensitivity of consumer to water purity improvement. The bigger the manufacturers invest in R&D, the more $\alpha\theta$ impact to demand.

(5) The parameters and their meanings used in this study are given in Table 1

(6) The manufacture purified ground water and the retailer buys it at wholesale price and sells it to the market at retail price (Figure 1). We consider that the actual demand of the market (q) is a linear function depending on retail price, green marketing effort, and water purity. The demand function is shown in the following equation.

$$q(p, e, \theta) = a - kp + \gamma e + \alpha\theta. \tag{1}$$

3.2. Stackelberg Equilibrium and Profitability Analysis

3.2.1. Profit Analysis under Centralized Decision Making (Model B). Centralized decision-making refers to a commodity produced and sold by the manufacturer, that is to say, a manufacturer integrates production and sales (vertical integration); more specifically, there is only one interest subject in the whole supply chain except customers, which is called integrated manufacturer. In the centralized model, we suppose that a central decision-maker is responsible for the retail price, the green marketing effort, and water purity.

The water supply chain's profit function is shown as

$$\Pi_{SC}^B = (p - c)(a - kp + \gamma e + \alpha\theta) - \beta\theta^2 - \frac{\eta e^2}{2}. \tag{2}$$

After solving the first-order derivative of Π_{SC}^B with respect to p, θ, and e, we get

$$\frac{\partial \Pi_{SC}^B}{\partial p} = a - 2kp + \gamma e + \alpha\theta + ck, \tag{3}$$

$$\frac{\partial \Pi_{SC}^B}{\partial \theta} = \alpha p - c\alpha - 2\beta\theta, \tag{4}$$

$$\frac{\partial \Pi_{SC}^B}{\partial e} = \gamma p - c\gamma - \eta e. \tag{5}$$

Afterwards, we set all the equations (3)–(5), all equal to zero to obtain equilibrium values of model B. The equilibrium values of the equation set are as follows:

$$p_{SC}^{*B} = -\frac{2ck\beta\eta - c(\alpha^2\eta + 2\gamma^2\beta) + 2a\beta\eta}{\alpha^2\eta + 2\gamma^2\beta - 4k\eta\beta}, \tag{6}$$

$$\theta_{SC}^{*B} = \frac{kc\eta\alpha - \eta a\alpha}{\alpha^2\eta + 2\gamma^2\beta - 4k\eta\beta}, \tag{7}$$

$$e_{SC}^{*B} = \frac{2k\beta c\gamma - 2\beta a\gamma}{\alpha^2\eta + 2\gamma^2\beta - 4k\eta\beta}. \tag{8}$$

Substitute (6)–(8) into functions (1) and (2) to get the optimal actual market demand (q_{SC}^{*B}) and the profit of supply chain (Π_{SC}^{*B}).

$$q_{SC}^{*B} = \frac{2k^2\eta\beta c - 2k\eta\beta a}{\alpha^2\eta + 2\gamma^2\beta - 4k\eta\beta},$$

$$\Pi_{SC}^{*B} = \frac{2\beta\eta ack - \beta\eta a^2 - \beta\eta c^2 k^2}{\alpha^2\eta + 2\gamma^2\beta - 4k\eta\beta}. \tag{9}$$

Lemma 1. *If it satisfies the conditions that $\alpha^2 - 4k\beta < 0$ and $\alpha^2\eta + 2\gamma^2\beta - 4\beta\eta k < 0$, the Hessian matrix of the profit function of the centralized supply chain is negative definite matrix. There exists a maximum value in the point $(p^{*B}, \theta^{*B}, e^{*B})$, and the profit function of Π_{SC}^B is strictly concave in the retail price p, the green marketing effort e, and water purity θ.*

Proof (Appendix). □

Proposition 1. *The Stackelberg equilibrium of the centralized supply chain is*
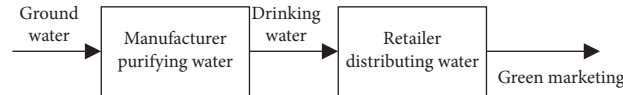
FIGURE 1: Two-tier water supply chain.

TABLE 1: Parameters and their meanings.

Parameter	Meaning
a	Total market potential and $a > 0$
q	Actual demand of the market
k	Price elasticity of demand and $k > 0$
e	The retailer's green marketing effort to promote the green product
γ	The impact of the marketing effort on demand
η	Marketing cost coefficient
$(\eta e^2/2)$	The total cost of the green marketing effort
c	The manufacturer's cost of purifying water
w	The wholesale price of products
p	The retail price of green products
θ	Water purity and $0 < \theta \leq 1$
α	The sensitivity of consumer to water purity improvement
β	The cost rate of research and development (R&D)
$\beta\theta^2$	The R&D investment of manufacture
φ	Revenue-sharing ratio

$$p_{SC}^{*B} = -\frac{2ck\beta\eta - c\left(\alpha^2\eta + 2\gamma^2\beta\right) + 2a\beta\eta}{\alpha^2\eta + 2\gamma^2\beta - 4k\eta\beta},$$

$$\theta_{SC}^{*B} = \frac{kc\eta\alpha - \eta a\alpha}{\alpha^2\eta + 2\gamma^2\beta - 4k\eta\beta},$$

$$e_{SC}^{*B} = \frac{2k\beta c\gamma - 2\beta a\gamma}{\alpha^2\eta + 2\gamma^2\beta - 4k\eta\beta}, \quad (10)$$

$$q_{SC}^{*B} = \frac{2k^2\eta\beta c - 2k\eta\beta a}{\alpha^2\eta + 2\gamma^2\beta - 4k\eta\beta},$$

$$\Pi_{SC}^{*B} = \frac{2\beta\eta ack - \beta\eta a^2 - \beta\eta c^2 k^2}{\alpha^2\eta + 2\gamma^2\beta - 4k\eta\beta}.$$

To ensure that all the equilibrium values are meaningful, the necessary condition is $kc - a < 0$ and $\gamma^2 - 2k\eta < 0$. Moreover, when $\beta^{*B} \geq ((\eta\alpha(kc - a - \alpha))/(\gamma^2 - 2k\eta))$, it guaranteed that $0 < \theta_{SC}^{*B} \leq 1$.

Proof (Appendix).   □

3.2.2. Profit Analysis under Decentralized Decision Making (Model BM). The decentralized decision-making game model means that the manufacturer and the retailer are two independent interest subjects to maximize their profit functions. In this study, we assume the Stackelberg game relationship between manufacturer and seller; manufacturer is the leader and decides the wholesale price and the greening degree of a product; the retailer is a follower who

determines the retail price of the product and the level of the green marketing effort according to the manufacturer's decision. In this case, the profit function of the manufacturer and retailer is expressed as follows, respectively:

$$\Pi_R^{BM} = (p - w)(a - kp + \gamma e + \alpha\theta) - \frac{\eta e^2}{2}, \quad (11)$$

$$\Pi_M^{BM} = (w - c)(a - kp + \gamma e + \alpha\theta) - \beta\theta^2. \quad (12)$$

According to the backward algorithm, in the first stage, based on the anticipation of retailer's retail price and marketing effort, the manufacture sets the wholesale price and purity of drinking water. In the second stage, concerning the wholesale price and marketing effort, the retailer decides the retail price and marketing effort. According to the backward algorithm, the retail price and marketing effort are obtained through the first derivative of the retailer's profit function with respect to the retail price and marketing effort. Afterwards, substitute them into the profit function of the manufacturer to get its first derivative with respect to the wholesale price and water purity.

The first-derivative result of Π_R^B with respect to p and e is shown as

$$\frac{\partial \Pi_R^{BM}}{\partial p} = a - kp - k(p - w) + \alpha\theta + \gamma e = 0,$$

$$\frac{\partial \Pi_R^{BM}}{\partial e} = \gamma(p - w) - \eta e = 0. \quad (13)$$

Next, we can obtain the optimal retail price and marketing effort of the retailer as follows:

$$p_R^{\mathrm{BM}} = \frac{-w\gamma^2 + \eta a + \eta kw + \alpha\eta\theta}{\gamma^2 - 2\eta k}, \tag{14}$$

$$e_R^{\mathrm{BM}} = \frac{\gamma(a - kw + \alpha\theta)}{\gamma^2 - 2\eta k}. \tag{15}$$

Put p_R^{BM} and e_R^{BM} into the profit function of manufacturer Π_M^{BM}. Then, we get

$$\Pi_M^{\mathrm{BM}} = \frac{-\beta\gamma^2\theta^2 + 2\beta\eta\theta^2 k - \alpha\eta\theta kw + \alpha\eta c\theta k + \eta k^2 w^2 - \eta akw + \eta ack}{\gamma^2 - 2\eta k}. \tag{16}$$

After taking the first derivative of Π_M^B with respect to w and θ, we get

$$\frac{\partial \Pi_M^{\mathrm{BM}}}{\partial w} = -\frac{\eta ak + \eta ck^2 - 2\eta k^2 w + \alpha\eta\theta k}{\gamma^2 - 2\eta k} = 0, \tag{17}$$

$$\frac{\partial \Pi_M^{\mathrm{BM}}}{\partial \theta} = -\frac{2\beta\theta\gamma^2 - 4\beta\eta\theta k - \alpha\eta ck + \alpha\eta kw}{\gamma^2 - 2\eta k} = 0. \tag{18}$$

By combining the equations (17) and (18), we derive that

$$w_M^{*\,\mathrm{BM}} = \frac{\eta c\alpha^2 k + 2\beta c\gamma^2 k + 2\beta a\gamma^2 - 4\beta\eta ck^2 - 4\beta\eta ak}{k(\eta\alpha^2 + 4\beta\gamma^2 - 8\beta\eta k)}, \tag{19}$$

$$\theta_M^{*\,\mathrm{BM}} = \frac{\alpha\eta ck - \alpha\eta a}{\eta\alpha^2 + 4\beta\gamma^2 - 8\beta\eta k}. \tag{20}$$

Submit (19) and (20) into the equations (14) and (15), and the equilibrium value of p_R^{BM} and e_R^{BM} is shown as

$$p_R^{*\,\mathrm{BM}} = \frac{\eta c\alpha^2 k + 2\beta c\gamma^2 k + 2\beta ar^2 - 2\beta\eta ck^2 - 6\beta\eta ak}{k(\eta\alpha^2 + 4\beta\gamma^2 - 8\beta\eta k)}. \tag{21}$$

$$e_R^{*\,\mathrm{BM}} = -\frac{2\beta\gamma(a - ck)}{\eta\alpha^2 + 4\beta\gamma^2 - 8\beta\eta k}. \tag{22}$$

Next, we submit (19)–(22) into equations (1), (11), and (12) and obtain the optimal actual market demand $q_M^{*\,\mathrm{BM}}$ and the maximized profits of the retailer ($\Pi_R^{*\,\mathrm{BM}}$) and manufacturer ($\Pi_M^{*\,\mathrm{BM}}$).

Lemma 2. *Under Lemma 1 and Proposition 1, the profit function Π_M^{BM} and Π_R^{BM} is strictly concave in w, θ and p, e, respectively.*

Proof (Appendix). □

Proposition 2. *In this model, the manufacturer's optimal whole price (w_M^{*BM}), water purity (θ_M^{*BM}), and maximized profit (Π_M^{*BM}); the retailer's retail price (p_R^{*BM}), marketing effort (e_R^{*BM}), and maximized profit (Π_R^{*BM}); the actual market demand (q_M^{*BM}), and the profit of the supply chain (Π_{SC}^{*BM}) are obtained as*

$$w_M^{*\,\mathrm{BM}} = \frac{\eta c\alpha^2 k + 2\beta c\gamma^2 k + 2\beta a\gamma^2 - 4\beta\eta ck^2 - 4\beta\eta ak}{k(\eta\alpha^2 + 4\beta\gamma^2 - 8\beta\eta k)},$$

$$\theta_M^{*\,\mathrm{BM}} = \frac{\alpha\eta ck - \alpha\eta a}{\eta\alpha^2 + 4\beta\gamma^2 - 8\beta\eta k},$$

$$p_R^{*\,\mathrm{BM}} = \frac{\eta c\alpha^2 k + 2\beta c\gamma^2 k + 2\beta ar^2 - 2\beta\eta ck^2 - 6\beta\eta ak}{k(\eta\alpha^2 + 4\beta\gamma^2 - 8\beta\eta k)},$$

$$e_R^{*\,\mathrm{BM}} = -\frac{2\beta\gamma(a - ck)}{\eta\alpha^2 + 4\beta\gamma^2 - 8\beta\eta k},$$

$$\Pi_M^{*\,\mathrm{BM}} = \frac{2\beta\eta ack - \beta\eta a^2 - \beta\eta c^2 k^2}{\eta\alpha^2 + 4\beta\gamma^2 - 8\beta\eta k},$$

$$\Pi_R^{*\,\mathrm{BM}} = \frac{-2\beta^2\eta(a - ck)^2(\gamma^2 - 2\eta k)}{\left(\eta\alpha^2 + 4\beta\gamma^2 - 8\beta\eta k\right)^2},$$

$$\Pi_{\mathrm{SC}}^{*\,\mathrm{BM}} = \frac{-\beta\eta(a - ck)^2(\alpha^2\eta + 6\beta\gamma^2 - 12\beta\eta k)}{\left(\eta\alpha^2 + 4\beta\gamma^2 - 8\beta\eta k\right)^2},$$

$$q_M^{*\,\mathrm{BM}} = \frac{2\beta\eta k(ck - a)}{\eta\alpha^2 + 4\beta\gamma^2 - 8\beta\eta k}. \tag{23}$$

Based on Lemma 1 and Proposition 1, the equilibrium values make sense. Moreover, to ensure that $0 < \theta_M^{*\,\mathrm{BM}} \leq 1$, we get $\beta^{*\mathrm{BM}} \geq ((\eta\alpha(kc - a - \alpha))/(4(\gamma^2 - 2k\eta)))$.

Proof (Appendix). □

3.2.3. Revenue-Sharing Contract (Model I). A revenue-sharing model (model I) is where manufacturers play a leading role, and a revenue-sharing contract is through the bargaining model (model II). In these models above, the proportion of income sharing on the premise of maximizing their own interests is decided by manufacturers and the bargaining between manufacturers and retailers, respectively.

In the manufacturer-led revenue-sharing model, the revenue-sharing ratio $\varphi(0 < \varphi < 1)$ is determined by manufacturers, which means that the proportion of retailer gains from the final revenue is φ, and the manufacture shares the remaining percentage $(1 - \varphi)$. Therefore, the profit function of the manufacturer and retailer is obtained as follows:

$$\Pi_M^I = (w - c)(a - \mathrm{kp} + \gamma e + \alpha\theta) - \beta\theta^2 + (1 - \varphi)(p - w)(a - \mathrm{kp} + \gamma e + \alpha\theta), \tag{24}$$

$$\Pi_R^I = \varphi(p - w)(a - kp + \gamma e + \alpha\theta) - \frac{\eta e^2}{2}. \tag{25}$$

Similar to the decision-making process of model BM, we get

$$w_M^{*I}(\varphi) = \frac{\alpha^2\eta ck + 2\beta\gamma^2\varphi ck + 2\beta\gamma^2\varphi a - 4\beta\eta ck^2 - 4\beta\eta ak}{k\left(\alpha^2\eta - 4\beta\eta\varphi k - 4\beta\eta k + 4\beta\gamma^2\varphi\right)},$$

(26)

$$\theta_M^{*I}(\varphi) = \frac{\alpha\eta(ck - a)}{\alpha^2\eta - 4\beta\eta\varphi k - 4\beta\eta k + 4\beta\gamma^2\varphi},$$

(27)

$$p_R^{*I}(\varphi) = \frac{-2\beta\eta ak + 2\beta\gamma^2\varphi a + \alpha^2\eta ck - 2\beta\eta ck^2 + 2\beta\gamma^2\varphi ck - 4\beta\eta\varphi ak}{k\left(\alpha^2\eta - 4\beta\eta\varphi k - 4\beta\eta k + 4\beta\gamma^2\varphi\right)},$$

(28)

$$e_R^{*I}(\varphi) = \frac{-2\beta\gamma\varphi(a - ck)}{\alpha^2\eta - 4\beta\eta\varphi k - 4\beta\eta k + 4\beta\gamma^2\varphi}.$$

(29)

Substituting equations (26)–(29) into equations (1), (24), and (25), we get the optimal market demand (q_M^{*BM}) and the optimal profit of the manufacturer (Π_M^{*I}) and retailer (Π_R^{*I}) to get

$$q_M^{*I}(\varphi) = \frac{-2\beta\eta k(a - ck)}{\alpha^2\eta - 4\beta\eta\varphi k - 4\beta\eta k + 4\beta\gamma^2\varphi},$$

(30)

$$\Pi_M^{*I}(\varphi) = -\frac{\beta\eta a^2 - 2\beta\eta ack + \beta\eta c^2 k^2}{\alpha^2\eta - 4\beta\eta\varphi k - 4\beta\eta k + 4\beta\gamma^2\varphi},$$

(31)

$$\Pi_R^{*I}(\varphi) = \frac{-2\beta^2\eta\varphi(a - ck)^2\left(\gamma^2\varphi - 2\eta k\right)}{\left(\alpha^2\eta - 4\beta\eta\varphi k - 4\beta\eta k + 4\beta\gamma^2\varphi\right)^2},$$

(32)

$$\Pi_{SC}^{*I}(\varphi) = \frac{-\beta\eta(a - ck)^2\left(\alpha^2\eta + 2\beta\gamma^2\varphi^2 + 4\beta\gamma^2\varphi - 8\beta\eta\varphi k - 4\beta\eta k\right)}{\left(\alpha^2\eta - 4\beta\eta\varphi k - 4\beta\eta k + 4\beta\gamma^2\varphi\right)^2}.$$

(33)

Lemma 3. *When $\gamma^2 < \eta k$, $\alpha^2 - 4\beta k < 0$, and $ck - a < 0$, the profit function Π_M^I is strictly concave in w and θ, and Π_R^I is strictly concave in p and e. Moreover, the equations (26)–(33) are meaningful. And to ensure $0 < \theta_M^{*I}(\varphi) \le 1$, we get $\beta^{*I} \ge ((\alpha(\alpha^2\gamma^2 - 4\beta\eta k^2)(\alpha + a - ck))/(4k^2(\alpha^2\eta - 8\beta\eta k + 4\beta\gamma^2)))$.*

Proof (Appendix). Since the first and second derivatives of Π_R^{*I} with respect to φ are

$$\frac{\partial\Pi_R^{*I}}{\partial\phi} = \frac{4\beta^2\eta^2(a - ck)^2\left(\alpha^2\eta k - 4\beta\eta k^2 + 4\beta\eta\varphi k^2 - \alpha^2\gamma^2\varphi\right)}{\left(\alpha^2\eta - 4\beta\eta\varphi k - 4\beta\eta k + 4\beta\gamma^2\varphi\right)^3},$$

$$\frac{\partial^2\Pi_R^{*I}}{\partial\phi^2} < 0.$$

(34)

The optimal $\varphi^{*I} = ((4\beta\eta k^2 - \alpha^2\eta k)/(4\beta\eta k^2 - \alpha^2\gamma^2))$ is next put it into equations (26)–(33) to get: □

Proposition 3. *In model I, the manufacturer's optimal whole price (w_M^{*I}), water purity (θ_M^{*I}), maximized profit (Π_M^{*I}), the retailer's retail price (p_R^{*I}), marketing effort (e_R^{*I}), maximized profit (Π_R^{*I}), the actual market demand (q_M^{*I}), and the profit of the supply chain (Π_{SC}^{*I}) are obtained as*

$$w_M^{*I} = \frac{c\alpha^2\gamma^2 + 2\beta c\gamma^2 k + 2\beta a\gamma^2 - 4\beta\eta ck^2 - 4\beta\eta ak}{\alpha^2\gamma^2 + 4\beta\gamma^2 k - 8\beta\eta k^2},$$

$$\theta_M^{*I} = \frac{-\alpha\left(\alpha^2\gamma^2 - 4\beta\eta k^2\right)(a - ck)}{\left(\alpha^2 - 4\beta k\right)\left(\alpha^2\gamma^2 + 4\beta\gamma^2 k - 8\beta\eta k^2\right)},$$

$$p_R^{*I} = \frac{c\alpha^4\gamma^2 - 4\eta c\alpha^2\beta k^2 - 4\eta a\alpha^2\beta k - 8c\beta^2\gamma^2 k^2 - 8a\beta^2\gamma^2 k + 8\eta c\beta^2 k^3 + 24\eta a\beta^2 k^2}{\left(\alpha^2 - 4\beta k\right)\left(\alpha^2\gamma^2 + 4\beta\gamma^2 k - 8\beta\eta k^2\right)},$$

$$e_R^{*I} = \frac{-2\beta\gamma k(a - ck)}{\alpha^2\gamma^2 + 4\beta\gamma^2 k - 8\beta\eta k^2},$$

$$\Pi_M^{*I} = \frac{-\beta\left(\alpha^2\gamma^2 - 4\beta\eta k^2\right)(a - ck)^2}{\left(\alpha^2 - 4\beta k\right)\left(\alpha^2\gamma^2 + 4\beta\gamma^2 k - 8\beta\eta k^2\right)},$$

$$\Pi_R^{*I} = \frac{2\beta^2\eta k^2(a - ck)^2}{\left(\alpha^2 - 4\beta k\right)\left(\alpha^2\gamma^2 + 4\beta\gamma^2 k - 8\beta\eta k^2\right)},$$

$$\Pi_{SC}^{*I} = \frac{-\beta\left(\alpha^2\gamma^2 - 6\beta\eta k^2\right)(a - ck)^2}{\left(\alpha^2 - 4\beta k\right)\left(\alpha^2\gamma^2 + 4\beta\gamma^2 k - 8\beta\eta k^2\right)},$$

$$q_M^{*I} = \frac{-2\beta k\left(\alpha^2\gamma^2 - 4\beta\eta k^2\right)(a - ck)}{\left(\alpha^2 - 4\beta k\right)\left(\alpha^2\gamma^2 + 4\beta\gamma^2 k - 8\beta\eta k^2\right)}.$$

(35)

Proof (Appendix). ☐

3.2.4. Revenue-Sharing Contract through Bargaining (Model II).

Revenue-sharing contract through bargaining means that the revenue-sharing ratio is determined by the manufacturers and retailers through bargaining. To study the impact of bargaining on revenue-sharing contract, we adopt the vertical Nash game process. The decision-making sequence is as follows: in the first stage, the manufacture and the retailer bargain on the revenue-sharing ratio, φ, which means the retailer takes possession of φ proportion of the total revenue while the manufacture shares the remaining. In the second stage, the manufacture decides the wholesale price and water purity of drinking water by anticipating the retailer's retail price and the marketing effort. Finally, the retailer decides the retail price and marketing effort taking the manufacturer's whole price and water purity into consideration.

We construct the bargaining process between the supply chain members by using Nash bargain game. By substituting equations (31) and (32) into the function that $\Pi^{II}(\varphi) = \Pi_M^{*I}(\phi)\Pi_R^{*I}(\varphi)$, we can obtain

$$\Pi^{II} = \Pi_M^{*I}\Pi_R^{*I} = \frac{2\beta^3\eta^2\varphi(a-ck)^4(\gamma^2\varphi - 2\eta k)}{(\alpha^2\eta + 4\beta\gamma^2\varphi - 4\beta\eta k - 4\beta\eta\varphi k)^3}. \quad (36)$$

Lemma 4

(1) When $\varphi^{*II} \le \sqrt{3} - 1$, there does not exists a solution to the Nash bargaining problem

(2) The equilibrium value (φ) to this Nash bargaining problem is given as

$$\varphi^{*II} = \frac{\eta(\alpha^2\gamma^2 + \sigma - 8\beta\eta k^2 + 4\beta\gamma^2 k)}{4\beta\gamma^2(\gamma^2 - \eta k)}, \quad (37)$$

where $\sigma = \sqrt{\alpha^4\gamma^4 - 8\alpha^2\beta\eta\gamma^2 k^2 + 64\beta^2\eta^2 k^4 - 96\beta^2\eta\gamma^2 k^3 + 48\beta^2\gamma^4 k^2}$

According to Cauchy inequality, we get $\varphi^{*II} \le (((\sqrt{3} - 1)\eta k)/\gamma^2)$

Proposition 4. *The optimal strategies of wholesale price, water purity, retail price, marketing effort, product demand, the manufacturer's profit, retailer's profit, and the water supply chain's profit are displayed as*

$$w_M^{*II} = \frac{(\gamma^2 a + \gamma^2 ck - 2\eta ak)(\alpha^2\gamma^2 + \sigma) + 2(\gamma^2 - \eta k)(\alpha^2\gamma^2 ck - 8\beta\eta k^2 a) + 4\beta\gamma^4 k(a - ck)}{2k(\gamma^2 - \eta k)(2\alpha^2\gamma^2 + \sigma - 8\beta\eta k^2)},$$

$$\theta_M^{*II} = \frac{-\gamma^2\alpha(a - ck)}{(2\alpha^2\gamma^2 + \sigma - 8\beta\eta k^2)},$$

$$p_R^{*II} = \frac{(\gamma^2 a + \gamma^2 ck - 2\eta ak)(\alpha^2\gamma^2 + \sigma - 4\beta\eta k^2) + 2(\gamma^2 - \eta k)(\alpha^2\gamma^2 ck - 4\beta\eta k^2 a)}{2k(\gamma^2 - \eta k)(2\alpha^2\gamma^2 + \sigma - 8\beta\eta k^2)},$$

$$e_R^{*II} = \frac{-\gamma(a - ck)(\alpha^2\gamma^2 + \sigma - 8\beta\eta k^2 + 4\beta\gamma^2 k)}{2(\gamma^2 - \eta k)(2\alpha^2\gamma^2 + \sigma - 8\beta\eta k^2)},$$

$$\Pi_M^{*II} = \frac{-\beta\gamma^2(a - ck)^2}{(2\alpha^2\gamma^2 + \sigma - 8\beta\eta k^2)},$$

$$\Pi_R^{*II} = \frac{-\eta\gamma^2(a - ck)^2(\alpha^2\gamma^2 + \sigma - 4\beta\gamma^4 k)(\alpha^2\gamma^2 + \sigma - 8\beta\eta k^2 + 4\beta\gamma^4 k)}{8(\gamma^2 - \eta k)^2(2\alpha^2\gamma^2 + \sigma - 8\beta\eta k^2)^2},$$

$$\Pi_{SC}^{*II} = \frac{-\gamma^2(a - ck)^2\left[2\gamma^2(\alpha^2\eta + 4\beta\gamma^4 - 8\beta\eta k)(\alpha^2\gamma^2 + \sigma) + 8\beta\gamma^2(\gamma^2 - \eta k)(\alpha^2\gamma^2 - 4\beta\eta k^2)\right]}{8(\gamma^2 - \eta k)^2(2\alpha^2\gamma^2 + \sigma - 8\beta\eta k^2)^2},$$

$$q_M^{*II} = \frac{-2\beta\gamma^2 k(a - ck)}{(2\alpha^2\gamma^2 + \sigma - 8\beta\eta k^2)}.$$

(38)

3.3. Comparative Analysis

Proposition 5. *The water purity, retail price, wholesale price, and the retailer's marketing effort under the three models satisfy the following relationships which are derived through algebraic comparison:*

(1) $\theta_{SC}^{*B} > \theta_M^{*II} > \theta_M^{*I} > \theta_M^{*BM}$

(2) $e_{SC}^{*B} > e_R^{*BM} > e_R^{*I} > e_R^{*II}$

(3) $w_M^{*BM} > w_M^{*I} > w_M^{*II}$

(4) $q_{SC}^{*B} > q_M^{*II} > q_M^{*I} > q_M^{*BM}$

Proposition 5 distributes the differences among the strategies in terms of the product's water purity, the retailer's green marketing effort, the product's wholesale price and retail price, and product demand of the four models in this study.

It is natural that the product's water purity for model B (centralized model) is highest since it is the fully coordinated scenario and lowest under model BM (decentralized model without revenue-sharing contract). Moreover, product's water purity for revenue-sharing contract through bargaining is higher than that under revenue-sharing contract (i.e., $\theta_M^{*II} > \theta_M^{*I}$). Therefore, revenue-sharing contract is beneficial to the improvement of product's water purity and cooperation can contribute to it.

As for the comparison of product's water purity, naturally, it is highest in the fully coordinated scenario, while lowest under revenue-sharing contract situation (i.e., $e_R^{*BM} > e_R^{*I} > e_R^{*II}$). According to the revenue-sharing contract, the retailer returns a percentage of its sales to the manufacturer and maintains profit through decreasing the marketing cost. Therefore, revenue-sharing contract leads to the decrease of the marketing effort and revenue-sharing contract though bargaining makes it worse.

The wholesale price is lowest in revenue-sharing contract through bargaining, followed by under revenue-sharing contract and highest in decentralized condition without any communication between supply chain members (i.e., $w_M^{*BM} > w_M^{*I} > w_M^{*II}$). It is probably that the manufacturer sells products to the retailer at a wholesale price below the products' manufacturing cost. As a result, effective communication gives rise to the decline of the wholesale price.

Proof (Appendix).   □

Proposition 6. *The water supply chain's profit under the four models meets the relationship:*

(1) $\Pi_M^{*II} > \Pi_M^{*I} > \Pi_M^{*BM}$ *and* $\Pi_R^{*I} > \Pi_R^{*BM}$

(2) $\Pi_{SC}^{*B} > \Pi_{SC}^{*II} > \Pi_{SC}^{*I} > \Pi_{SC}^{*BM}$

Proposition 6 shows the profit differences of the manufacturer and the retailer among the models. The manufacturer benefits from the revenue-sharing contract due to it as the Stackelberg leader, while the retail as the follower fails to benefit from the contract; only if $\varphi = 1$, the retailer earns profit equal to that under the decentralized model without revenue-sharing contract. The comparison of green supply chain's profit indicates that there exists the double marginalization effect. It is very likely to be caused by the goals of supply chain members that perhaps conflict with each other. As a result, revenue-sharing contract are conducive to the boosting of the profit; furthermore, the profit has been increased even more under the revenue-sharing contract (i.e., $\Pi_{SC}^{*II} > \Pi_{SC}^{*I} > \Pi_{SC}^{*BM}$). Therefore, the goal of constructing water supply chain is to realize integrated management, promote cooperation between upstream and downstream enterprises, and finally achieve higher overall performance.

Proof (Appendix).   □

Proposition 7. *In models B, BM, I, and II, we have*

(1) The increase of consumer sensitivity to water purity improvement (α) induces the increase of the optimal wholesale price, water purity, retail price, marketing effort, manufacturer's profit, and retailer's profit

(2) The increase of the cost rate of R&D (β) leads to the decrease of the optimal wholesale price, water purity, retail price, marketing effort, manufacturer's profit, and retailer's profit

Proof (Appendix).   □

4. Numerical Analysis

In Section 4, we compare seven groups of parameters in the four models (B, BM, I, and II), including the water purity of the manufacturer, the green marketing level of the retailer, the wholesale price of the product, the actual market demand quantity of the product, the profit of the manufacturer, the profit of the retailer, and the total profit of the supply chain. In order to explain the effect of the optimal values, we set values to parameters as the following: $a = 20$, $k = 5$, $c = 3$, $\eta = 4$, $\gamma = 2$, and $\alpha = 4$. Seen from the four models, we get three different value ranges of the cost rate of research and development (R&D) (β), and

$$\beta \geq \max\left\{\frac{\eta\alpha(kc - a - \alpha)}{(\gamma^2 - 2k\eta)}, \frac{\eta\alpha(kc - a - \alpha)}{4(\gamma^2 - 2k\eta)}, \frac{\alpha(\alpha^2\gamma^2 - 4\beta\eta k^2)(\alpha + a - ck)}{4k^2(\alpha^2\eta - 8\beta\eta k + 4\beta\gamma^2)}\right\} \geq 4. \tag{39}$$
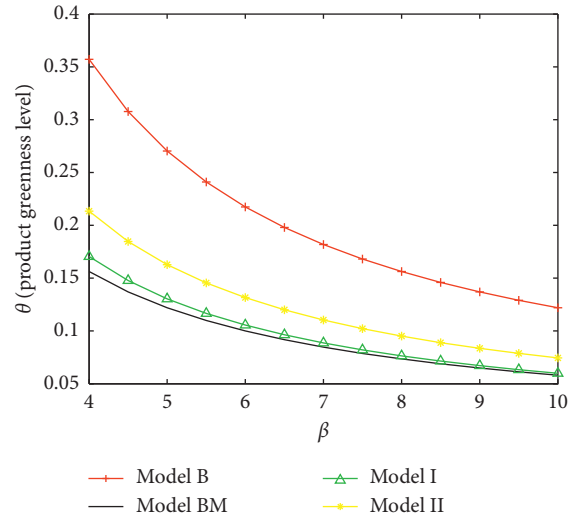
FIGURE 2: The comparison of optimal water purity.
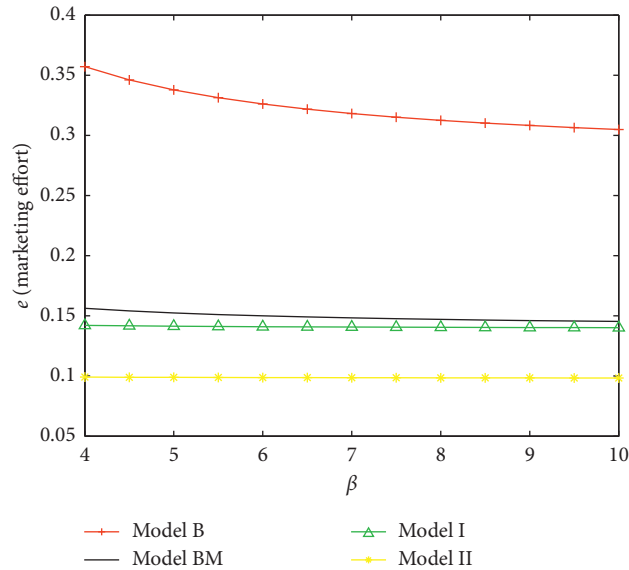
FIGURE 3: The comparison of the optimal marketing effort.

In addition, β decides the water purity directly; generally speaking, when the manufacturer increases the investment in research and development, the water purity will increase. Moreover, higher water purity usually possesses higher value, and the retailer is willing to make more effort to the marketing of the green product. Therefore, we assume that β is the independent variable.

The comparison results are shown in Figures 2–8 by taking advantage of Matlab 2013. As shown in Figure 2, the revenue-sharing contract model is superior to model BM (without any contract) in improving the water purity. And furthermore, the revenue-sharing contract through the bargaining model is better than the revenue-sharing contract model. Figure 3 demonstrates that the retailer makes the least marketing effort in model II to save cost, since the retailer has to share its revenue with the manufacturer. In

Figure 4, there is no wholesale price in centralized condition as results of supply chain members are considered as a whole. Contract (revenue-sharing contract or revenue-sharing contract through bargaining) leads to the decrease of the product's wholesale price. Product with higher water purity is more likely to be accepted by consumers; as consequence, the sequence of product's actual market demand among the four models can be seen from Figure 5. In Figures 6 and 7, both the profit of manufacturer and the profit of retailer can be promoted through the contract model. Therefore, both of them will adopt revenue-sharing contract. In Figure 8, contracts (revenue-sharing contract and revenue-sharing contract through bargaining) contribute to the increase of the profit of the whole supply chain, and furthermore, the profit level of the latter contract is higher than that of the former contract.
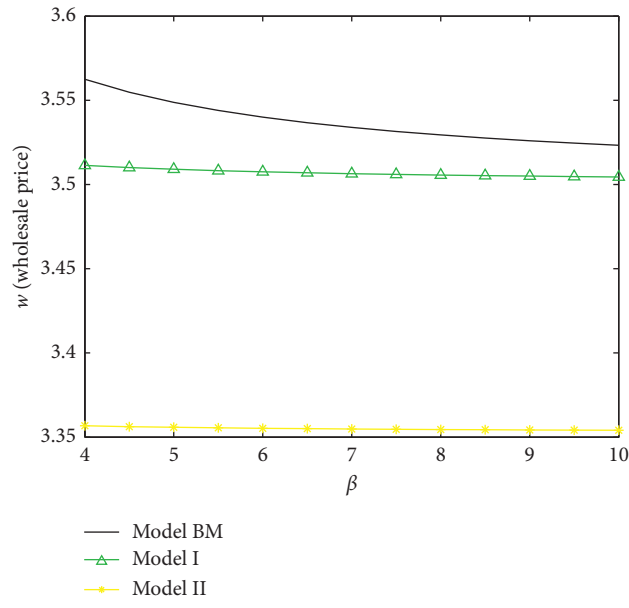
Figure 4: The comparison of the optimal wholesale price.
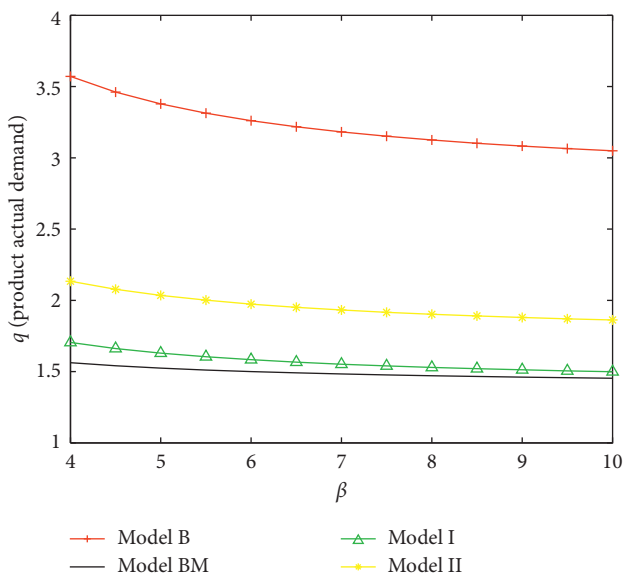
Figure 5: The comparison of the optimal product market demand.
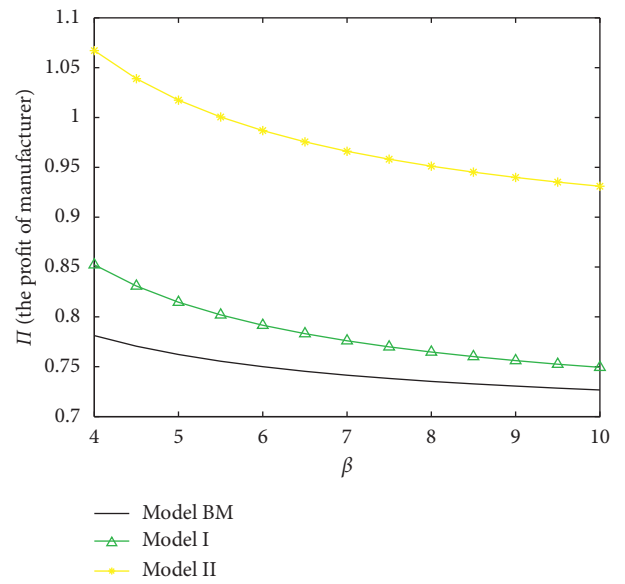
Figure 6: The comparison of the optimal manufacturer's profit.
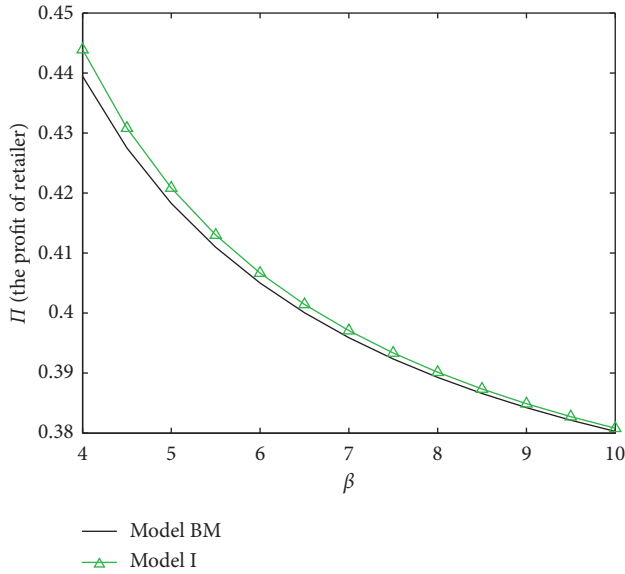
Figure 7: The comparison of the optimal retailer's profit.
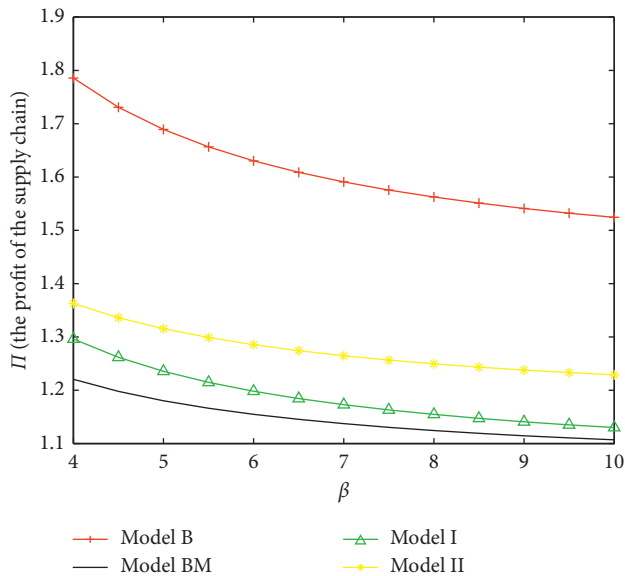
Figure 8: The comparison of the optimal supply chain's profit.

5. Conclusion

From the comparison above, the result shows that revenue-sharing contract is beneficial to the increase of water purity, the water supply chain members' profit, and the overall profit of water supply chain, while giving rise to the decrease of the retailer's marketing effort and the product's wholesale price compared with the decentralized model. Moreover, revenue-sharing contract through bargaining exert a more significant influence. In a word, revenue-sharing contract through bargaining eliminate the double marginal effect among the water supply chain more effectively and is an effective way to promote the cooperation among the water supply chain members. It is worth mentioning that revenue-sharing contract brings negative impact to the retailer's marketing effort. Marketing can stimulate the increase of the green product's market demand on the one hand, and on the other hand, it generates amount of marketing cost. In this study, the profit that marketing produces cannot offset the cost that it brings. Thus, it will be important to take some measures to make up the loss that marketing generated.

In this study, we have made a little innovation, which is that the marketing effort and water purity have been considered in the demand function. However, there are some shortcomings of this study. For example, first, we only consider a two-tier water supply chain; second, although the demand function has been revised, it is still a simple linear function concerning the marketing effort, water purity, and retail price, which makes the application of this model limited in a sense. In our further study, we will pay attention to two streams. One is that considering the supply chain that has more than one manufacturer and retailer. The other is to study the difference among revenue-sharing contract, costing-sharing contract, and mixed-sharing contract.

Management insights: by signing revenue-sharing contracts, manufacturers, wholesalers, and retailers can form a community of interests, always maintain the real-time interaction among them, get firsthand customer feedback and demand in a timely manner, and then receive orders according to customer demand. In this way, customized products should be manufactured to ensure that provided products are according to customer requirements. Overall, a virtuous loop should be established to realize value creation. Second, because revenue-sharing contracts weaken retailers' incentives to market green products, manufacturers can use other methods, such as sales discounts, exchange promises, and extended payback periods to motivate retailers. Third, the future market competition is the competition between the supply chains. Therefore, it is more and more important for the development of the supply chain to form a stable win-win partnership among all partners in the supply chain.

Appendix

A

Proof of Lemma 1: the Hessian matrix of Π_{SC}^{B} is

$$H(p, \theta, e) = \begin{bmatrix} \dfrac{\partial^2 \Pi_{SC}^{B}}{\partial p^2} & \dfrac{\partial^2 \Pi_{SC}^{B}}{\partial p \partial \theta} & \dfrac{\partial^2 \Pi_{SC}^{B}}{\partial p \partial e} \\[2ex] \dfrac{\partial^2 \Pi_{SC}^{B}}{\partial \theta \partial p} & \dfrac{\partial^2 \Pi_{SC}^{B}}{\partial \theta^2} & \dfrac{\partial^2 \Pi_{SC}^{B}}{\partial \theta \partial e} \\[2ex] \dfrac{\partial^2 \Pi_{SC}^{B}}{\partial e \partial p} & \dfrac{\partial^2 \Pi_{SC}^{B}}{\partial e \partial \theta} & \dfrac{\partial^2 \Pi_{SC}^{B}}{\partial e^2} \end{bmatrix} = \begin{bmatrix} -2k & \alpha & \gamma \\[1ex] \alpha & -2\beta & 0 \\[1ex] \gamma & 0 & -\eta \end{bmatrix}.$$

(A.1)

From the Hessian matrix above, we can get that

$$\frac{\partial^2 \Pi_{SC}^B}{\partial p^2} = -2k < 0, \quad (k > 0),$$

$$\left| H_2(p, \theta, e) \right| = \begin{vmatrix} \dfrac{\partial^2 \Pi_{SC}^B}{\partial p^2} & \dfrac{\partial^2 \Pi_{SC}^B}{\partial p \partial \theta} \\[4mm] \dfrac{\partial^2 \Pi_{SC}^B}{\partial \theta \partial p} & \dfrac{\partial^2 \Pi_{SC}^B}{\partial \theta^2} \end{vmatrix} = \begin{vmatrix} -2k & \alpha \\[2mm] \alpha & -2\beta \end{vmatrix} = 4k\beta - \alpha^2,$$

$$\left| H_3(p, \theta, e) \right| = \begin{vmatrix} \dfrac{\partial^2 \Pi_{SC}^B}{\partial p^2} & \dfrac{\partial^2 \Pi_{SC}^B}{\partial p \partial \theta} & \dfrac{\partial^2 \Pi_{SC}^B}{\partial p \partial e} \\[4mm] \dfrac{\partial^2 \Pi_{SC}^B}{\partial \theta \partial p} & \dfrac{\partial^2 \Pi_{SC}^B}{\partial \theta^2} & \dfrac{\partial^2 \Pi_{SC}^B}{\partial \theta \partial e} \\[4mm] \dfrac{\partial^2 \Pi_{SC}^B}{\partial e \partial p} & \dfrac{\partial^2 \Pi_{SC}^B}{\partial e \partial \theta} & \dfrac{\partial^2 \Pi_{SC}^B}{\partial e^2} \end{vmatrix} = \eta\alpha^2 + 2\beta\gamma^2 - 4\beta\eta k.$$

$$(A.2)$$

If $\left| H_2(p, \theta, e) \right| = 4k\beta - \alpha^2 > 0$ and $\left| H_3(p, \theta, e) \right| = \eta\alpha^2 + 2\beta\gamma^2 - 4\beta\eta k < 0$, then Π_{SC}^B is strictly concave in p, e, and θ. The proof is completed. □

Proof of Proposition 1: from Lemma 1, we know that $\eta\alpha^2 + 2\beta\gamma^2 - 4\beta\eta k < 0$; therefore, the following inequalities should be met.

$$\begin{cases} c(\eta\alpha^2 + 2\beta\gamma^2 - 4\beta\eta k) + 2\beta\eta(ck - a) < 0, \\ \eta\alpha^2 + 2\beta\gamma^2 - 4\beta\eta k \leq \eta\alpha(kc - a) < 0, \\ 2\beta\gamma(kc - a) < 0, \\ 2k\eta\beta(kc - a) < 0. \end{cases} \quad (A.3)$$

We can get the result $kc - a < 0$, $\gamma^2 - 2k\eta < 0$, and $\beta \geq ((\eta\alpha(kc - a - \alpha))/(\gamma^2 - 2k\eta))$. The proof is completed. □

Proof of Lemma 2: the Hessian Matrix of the manufacturer and retailer is in the following Hessian matrix of Π_M^{BM}:

$$H(w, \theta) = \begin{bmatrix} \dfrac{\partial^2 \Pi_M^B}{\partial w^2} & \dfrac{\partial^2 \Pi_M^B}{\partial w \partial \theta} \\[4mm] \dfrac{\partial^2 \Pi_M^B}{\partial \theta \partial w} & \dfrac{\partial^2 \Pi_M^B}{\partial \theta^2} \end{bmatrix} = \begin{bmatrix} \dfrac{2\eta k^2}{\gamma^2 - 2\eta k} & \dfrac{-\alpha\eta k}{\gamma^2 - 2\eta k} \\[4mm] \dfrac{-\alpha\eta k}{\gamma^2 - 2\eta k} & \dfrac{4\beta\eta k - 2\beta\gamma^2}{\gamma^2 - 2\eta k} \end{bmatrix},$$

$$\left| H(w, \theta) \right| = \frac{2\eta k^2}{\gamma^2 - 2\eta k} < 0,$$

$$\left| H_2(w, \theta) \right| = -\frac{\eta k^2 (\eta\alpha^2 + 4\beta\gamma^2 - 8\beta\eta k)}{(\gamma^2 - 2\eta k)^2} > 0.$$

$$(A.4)$$

Hessian matrix of Π_R^{BM}

$$H(p, e) = \begin{bmatrix} \dfrac{\partial^2 \Pi_R^B}{\partial p^2} & \dfrac{\partial^2 \Pi_R^B}{\partial p \partial e} \\[4mm] \dfrac{\partial^2 \Pi_R^B}{\partial e \partial p} & \dfrac{\partial^2 \Pi_R^B}{\partial e^2} \end{bmatrix} = \begin{bmatrix} -2k & \gamma \\[2mm] \gamma & -\eta \end{bmatrix},$$

$$(A.5)$$

$$\left| H(p, e) \right| = -2k < 0,$$

$$\left| H_2(p, e) \right| = 2k\eta - \gamma^2 > 0.$$

The proof is completed. □

Proof of Proposition 2

$$\because 0 < \theta_M^{*B} \leq 1,$$

$$\therefore \eta\alpha^2 + 4\beta\gamma^2 - 8\beta\eta k \leq \alpha\eta ck - \alpha\eta a < 0,$$

$$\implies \beta \geq ((\eta\alpha(kc - a - \alpha))/(4(\gamma^2 - 2k\eta))).$$

$$(A.6)$$

The proof is completed. □

Proof of Lemma 3: the Hessian matric of Π_M^I is

$$
\begin{bmatrix} \dfrac{\partial^2 \Pi_M^I}{\partial w^2} & \dfrac{\partial^2 \Pi_M^I}{\partial w \partial \theta} \\[3ex] \dfrac{\partial^2 \Pi_M^I}{\partial \theta \partial w} & \dfrac{\partial^2 \Pi_M^I}{\partial \theta^2} \end{bmatrix} = \begin{bmatrix} \dfrac{-2\eta k^2 \left[\eta k + \eta \varphi k - \gamma^2 \varphi\right]}{\left(\gamma^2 \varphi - 2\eta k\right)^2} & \dfrac{\alpha \eta k \varphi \left(2\eta k - \gamma^2\right)}{\left(\gamma^2 \varphi - 2\eta k\right)^2} \\[4ex] \dfrac{\alpha \eta k \varphi \left(2\eta k - \gamma^2\right)}{\left(\gamma^2 \varphi - 2\eta k\right)^2} & \dfrac{-2\left(\alpha^2 \eta^2 \varphi k - \alpha^2 \eta^2 k + 4\beta \eta^2 k^2 - 4\beta \eta \gamma^2 \varphi k + \beta \gamma^4 \varphi^2\right)}{\left(\gamma^2 \varphi - 2\eta k\right)^2} \end{bmatrix},
$$

$$(A.7)$$

$$
\left| H(w, \theta) \right| = \frac{-2\eta k^2 \left[\eta k + \eta \varphi k - \gamma^2 \varphi\right]}{\left(\gamma^2 \varphi - 2\eta k\right)^2} < 0,
$$

$$
\left| H_2(w, \theta) \right| = \frac{-\left[\eta^2 k^2 \left(\alpha^2 - 4\beta k\right) - 4\beta \eta \varphi k^2 \left(\eta k - \gamma^2\right)\right]}{\left(\gamma^2 \varphi - 2\eta k\right)^2} > 0.
$$

When $\alpha^2 - 4\beta k < 0$ and $\gamma^2 - \eta k < 0$, it satisfies. The Hessian matric of Π_R^I is

$$
\begin{bmatrix} \dfrac{\partial^2 \Pi_R^I}{\partial p^2} & \dfrac{\partial^2 \Pi_R^I}{\partial p \partial e} \\[3ex] \dfrac{\partial^2 \Pi_R^I}{\partial e \partial p} & \dfrac{\partial^2 \Pi_R^I}{\partial e^2} \end{bmatrix} = \begin{bmatrix} -2k\varphi & \gamma\varphi \\[2ex] \gamma\varphi & -\eta \end{bmatrix},
$$

$$(A.8)$$

$$
\left| H(p, e) \right| = -2k\varphi < 0,
$$

$$
\left| H_2(p, e) \right| = 2\eta k \varphi - \gamma^2 \varphi^2 > 0.
$$

The profit function Π_M^I is strictly concave in w and θ, and Π_R^I is strictly concave in p and e. □

Proof of Proposition 3: according to Lemma 3, Π_M^I is jointly concave in $(w_M^{*I}, \theta_M^{*I})$, and Π_R^I is jointly concave in (p_R^{*I}, e_R^{*I}). Therefore, we get the first partial derivative of Π_R^I with respect to p and e:

$$
\frac{\partial \Pi_R^I}{\partial p} = \varphi(a - kp + \alpha\theta + \gamma e) - \varphi k(p - w) = 0,
$$

$$(A.9)$$

$$
\frac{\partial \Pi_R^I}{\partial e} = \gamma\varphi(p - w) - \eta e = 0.
$$

Next, solving the above equations to get the manufacturer forecasting the retail piece and marketing effort,

$$
p_R^I = \frac{\eta a + \eta k w - \gamma^2 \varphi w + \alpha \eta \theta}{\gamma^2 \varphi - 2\eta k},
$$

$$
e_R^I = \frac{-\gamma\varphi(a - kw + \alpha\theta)}{\gamma^2 \varphi - 2\eta k}.
$$

$$(A.10)$$

Put p_R^I and e_R^I into the manufacturers' profit function (24) to obtain

$$
\Pi_M^I = \left(a - kp_R^I + \gamma e_R^I + \alpha\theta\right)\left[w - c + \varphi\left(p_R^I - w\right)\right] - \beta\theta^2.
$$

$$(A.11)$$

Similarly, we can get the only optimal solutions $(w_M^{*I}, \theta_M^{*I})$ by using the following first partial derivative of Π_M^I with respect to w and e.

$$\frac{\partial \Pi_M^I}{\partial w} = \frac{-\eta k\left(\gamma^2 \varphi a - 2\eta ck^2 + 2\eta k^2 w + \alpha\gamma^2 \varphi\theta - 2\eta\varphi ak + \gamma^2 \varphi ck + 2\eta\varphi k^2 w - 2\gamma^2 \varphi kw - 2\alpha\eta\varphi\theta k\right)}{\left(\gamma^2 \varphi - 2\eta k\right)^2},$$

$$\frac{\partial \Pi_M^I}{\partial \theta} = \frac{-\left(2\alpha\eta^2 ck^2 + 2\beta\gamma^4 \varphi^2\theta - 2\alpha\eta^2 ak - 2\alpha^2\eta^2\theta k + 8\beta\eta^2\theta k^2 + 2\alpha^2\eta^2\varphi\theta k - 2\alpha\eta^2\varphi k^2 w + 2\alpha\eta^2\varphi ak - \alpha\eta\gamma^2 ck + \alpha\eta\gamma^2 \varphi kw - 8\beta\eta\gamma^2\varphi\theta k\right)}{\left(\gamma^2 \varphi - 2\eta k\right)^2}.$$

$$(A.12)$$

Then, the optimal solutions can be shown as follows:

$$w_M^{*I}(\varphi) = \frac{\alpha^2\eta ck + 2\beta\gamma^2\varphi ck + 2\beta\gamma^2\varphi a - 4\beta\eta ck^2 - 4\beta\eta\varphi ak}{k\left(\alpha^2\eta - 4\beta\eta\varphi k - 4\beta\eta k + 4\beta\gamma^2\varphi\right)},$$

$$\theta_M^{*I}(\varphi) = \frac{\alpha\eta(ck - a)}{\alpha^2\eta - 4\beta\eta\varphi k - 4\beta\eta k + 4\beta\gamma^2\varphi},$$

$$(A.13)$$

$$p_R^{*I}(\varphi) = \frac{-2\beta\eta ak + 2\beta\gamma^2\varphi a + \alpha^2\eta ck - 2\beta\eta ck^2 + 2\beta\gamma^2\varphi ck - 4\beta\eta\varphi ak}{k\left(\alpha^2\eta - 4\beta\eta\varphi k - 4\beta\eta k + 4\beta\gamma^2\varphi\right)},$$

$$e_R^{*I}(\varphi) = \frac{-2\beta\gamma\varphi(a - ck)}{\alpha^2\eta - 4\beta\eta\varphi k - 4\beta\eta k + 4\beta\gamma^2\varphi}.$$

The proof is completed.

We put $w_M^{*I}(\varphi)$, $\theta_M^{*I}(\varphi)$, and $p_R^{*I}(\varphi)$, $e_R^{*I}(\varphi)$ into the manufacturers' profit function; then, we get a function of φ. Afterwards, we obtain the first and second derivatives of φ.

$$\Pi_M^{*I}(\varphi) = -\frac{\beta\eta a^2 - 2\beta\eta ack + \beta\eta c^2 k^2}{\alpha^2\eta - 8\beta\eta k + 4\beta\gamma^2 + 4\beta\eta\varphi k - 4\beta\gamma^2\varphi},$$

$$\frac{\partial \Pi_M^{*I}}{\partial \varphi} = \frac{\left(4\beta\gamma^2 - 4\beta\eta k\right)\left(\beta\eta a^2 - 2\beta\eta ack + \beta\eta c^2 k^2\right)}{\left(\alpha^2\eta - 4\beta\eta\varphi k - 4\beta\eta k + 4\beta\gamma^2\varphi\right)^2} < 0,$$

$$(A.14)$$

$$\frac{\partial^2 \Pi_M^{*I}}{\partial \varphi^2} = -\frac{2\left(4\beta\gamma^2 - 4\beta\eta k\right)^2\left(\beta\eta a^2 - 2\beta\eta ack + \beta\eta c^2 k^2\right)}{\left(\alpha^2\eta - 4\beta\eta\varphi k - 4\beta\eta k + 4\beta\gamma^2\varphi\right)^3} > 0.$$

Next, we put w_M^{*I}, θ_M^{*I}, and p_R^{*I}, e_R^{*I} into the retailers' profit function to get

$$\Pi_R^{*\,I}(\varphi) = \frac{-2\beta^2\eta\varphi(a-\mathrm{ck})^2(\gamma^2\varphi - 2\eta k)}{(\alpha^2\eta - 4\beta\eta\varphi k - 4\beta\eta k + 4\beta\gamma^2\varphi)^2},$$

$$\frac{\partial\Pi_R^{*\,I}}{\partial\varphi} = \frac{4\beta^2\eta^2(a-\mathrm{ck})^2(\alpha^2\eta k - 4\beta\eta k^2 + 4\beta\eta\varphi k^2 - \alpha^2\gamma^2\varphi)}{(\alpha^2\eta - 4\beta\eta\varphi k - 4\beta\eta k + 4\beta\gamma^2\varphi)^3},$$

$$\frac{\partial^2\Pi_R^{*\,I}}{\partial\varphi^2} = \frac{-4\beta^2\eta^2(a-\mathrm{ck})^2\left[64\beta^2\eta^2 k^3 + \alpha^4\eta\gamma^2 - 16\alpha^2\beta\eta^2 k^2 - 48\beta^2\eta\gamma^2 k^2 - 32\beta^2\eta^2\varphi k^3 - 8\alpha^2\beta\gamma^4\varphi + 8\alpha^2\beta\eta\gamma^2 k + 32\beta^2\eta\gamma^2\varphi k^2 + 8\alpha^2\beta\eta\gamma\varphi k\right]}{(\alpha^2\eta - 4\beta\eta\varphi k - 4\beta\eta k + 4\beta\gamma^2\varphi)^4}.$$

$$(A.15)$$

Set

$$f(\varphi) = 64\beta^2\eta^2 k^3 + \alpha^4\eta\gamma^2 - 16\alpha^2\beta\eta^2 k^2 - 48\beta^2\eta\gamma^2 k^2 - 32\beta^2\eta^2\varphi k^3 - 8\alpha^2\beta\gamma^4\varphi + 8\alpha^2\beta\eta\gamma^2 k + 32\beta^2\eta\gamma^2\varphi k^2 + 8\alpha^2\beta\eta\gamma^2\varphi k,$$

$$\frac{\partial f(\varphi)}{\partial\varphi} = -32\beta^2\eta^2 k^3 - 8\alpha^2\beta\gamma^4 + 32\beta^2\eta\gamma^2 k^2 + 8\alpha^2\beta\eta\gamma^2 k < 0,$$

$$f(0) = 64\beta^2\eta^2 k^3 + \alpha^4\eta\gamma^2 - 16\alpha^2\beta\eta^2 k^2 - 48\beta^2\eta\gamma^2 k^2 + 8\alpha^2\beta\eta\gamma^2 k,$$

$$f(1) = 32\beta^2\eta^2 k^3 + \alpha^4\eta\gamma^2 - 16\alpha^2\beta\eta^2 k^2 - 16\beta^2\eta\gamma^2 k^2 - 8\alpha^2\beta\gamma^4 + 16\alpha^2\beta\eta\gamma^2 k > 0,$$

$$\Longrightarrow 0 < f(1) < f(\varphi) < f(0),$$

$$\Longrightarrow \frac{\partial^2\Pi_R^{*\,I}}{\partial\varphi^2} < 0,$$

$$\Longrightarrow \varphi^{*I} = \frac{4\beta\eta k^2 - \alpha^2\eta k}{4\beta\eta k^2 - \alpha^2\gamma^2}.$$

$$(A.16)$$

The proof is completed. □

Proof of Lemma 4: the first-order derivative of Π^{III} with respect to φ is

$$\frac{\partial\Pi^{II}}{\partial\varphi} = \frac{4\beta^3\eta^2(a-\mathrm{ck})^4 g(\varphi)}{(\alpha^2\eta + 4\beta\gamma^2\varphi - 4\beta\eta k - 4\beta\eta\varphi k)^4}, \qquad (A.17)$$

where

$$g(\varphi) = (2\beta\eta\gamma^2 k - 2\beta\gamma^4)\varphi^2 + (\alpha^2\eta\gamma^2 - 8\beta\eta^2 k^2 + 4\beta\eta\gamma^2 k)\varphi + 4\beta\eta^2 k^2 - \alpha^2\eta^2 k.$$

$$(A.18)$$

Since $g(0) = 4\beta\eta^2 k^2 - \alpha^2\eta^2 k > 0$, $g(1) = (\gamma^2 - \eta k)(\alpha^2\eta - 2\beta\gamma^2 + 4\beta\eta k) < 0$.

We set $g(\varphi) = 0$ to get

$$\varphi_1 = \frac{\eta\left(\alpha^2\gamma^2 + \sigma - 8\beta\eta k^2 + 4\beta\gamma^2 k\right)}{4\beta\gamma^2\left(\gamma^2 - \eta k\right)},$$

(abandoned)

$$\varphi_2 = \frac{\eta\left(\alpha^2\gamma^2 - \sigma - 8\beta\eta k^2 + 4\beta\gamma^2 k\right)}{4\beta\gamma^2\left(\gamma^2 - \eta k\right)},$$

(A.19)

$$\sigma = \sqrt{\alpha^4\gamma^4 - 8\alpha^2\beta\eta\gamma^2 k^2 + 64\beta^2\eta^2 k^4 - 96\beta^2\eta\gamma^2 k^3 + 48\beta^2\gamma^4 k^2} \le \left|4\beta\eta k^2 - \alpha^2\gamma^2\right| + \left|4\sqrt{3}\,\beta k\left(\eta k - \gamma^2\right)\right|,$$

$$\Longrightarrow \varphi^{*II} = \phi_1 \le \frac{\eta\left(-4\beta\eta k^2 + 4\beta\gamma^2 k\right)}{4\beta\gamma^2\left(\gamma^2 - \eta k\right)} = \frac{(\sqrt{3}-1)\eta k}{\gamma^2}.$$

(A.20)

When $0 < \varphi < \varphi_1$, we have $g(\varphi) > 0$, $(\partial\Pi^{II}/\partial\varphi) > 0$; and when $\varphi_1 < \varphi \le 1$, we have $g(\varphi) < 0$, $(\partial\Pi^{II}/\partial\varphi) < 0$. The proof is completed. □

Proof of Proposition 5.

$$(1)\ \frac{\theta_{SC}^{*B}}{\theta_M^{*\,BM}} = \frac{\eta\alpha^2 + 4\beta\gamma^2 - 8\beta\eta k}{\alpha^2\eta + 2\gamma^2\beta - 4k\eta\beta} = 1 + \frac{2\beta\gamma^2 - 4\beta\eta k}{\alpha^2\eta + 2\gamma^2\beta - 4k\eta\beta} > 1,$$

$$\theta_M^{*\,BM} - \theta_M^{*\,I} = \frac{4\alpha^3\beta\left(\gamma^2 - \eta k\right)^2 (a - \mathrm{ck})}{\left(\alpha^2 - 4\beta k\right)\left(\alpha^2\gamma^2 + 4\beta\gamma^2 k - 8\beta\eta k^2\right)\left(\eta\alpha^2 + 4\beta\gamma^2 - 8\beta\eta k\right)} < 0,$$

(A.21)

$$\theta_{SC}^{*B} - \theta_M^{*\,I} = \frac{2\alpha\beta(a - \mathrm{ck})\left[\eta k\left(2\eta k - \gamma^2\right)\left(\alpha^2 - 4\beta k\right) - \gamma^2\alpha^2\left(\eta k - \gamma^2\right)\right]}{\left(\alpha^2 - 4\beta k\right)\left(\alpha^2\gamma^2 + 4\beta\gamma^2 k - 8\beta\eta k^2\right)\left(\eta\alpha^2 + 4\beta\gamma^2 - 8\beta\eta k\right)} > 0,$$

$$\Longrightarrow \theta_{SC}^{*B} > \theta_M^{*\,I} > \theta_M^{*\,BM}.$$

Owing to

$$\varphi^{*I} - \varphi^{*II} \geq \frac{4\beta\eta k^2 - \alpha^2 \eta k}{4\beta\eta k^2 - \alpha^2 \gamma^2} - \frac{(\sqrt{3}-1)\eta k}{\gamma^2}$$

to obtain $\theta_{SC}^{*B} > \theta_{M}^{*II} > \theta_{M}^{*I} > \theta_{M}^{*BM}$,

$$= \frac{(2-\sqrt{3})\gamma^2 \eta k \left(4\beta\eta k - \alpha^2\right)}{\left(4\beta\eta k^2 - \alpha^2 \gamma^2\right)\gamma^2} > 0,$$

$$\frac{\partial \theta_M^{*I}}{\partial \varphi} = \frac{4\beta\alpha\eta\left(\gamma^2 - \eta k\right)(a - ck)}{\left(\alpha^2 \eta - 4\beta\eta\varphi k - 4\beta\eta k + 4\beta\gamma^2 \varphi\right)^2} < 0,$$

(A.22)

$$(2)\, e_R^{*BM} - e_R^{*I} = \frac{-2\alpha^2 \beta\gamma\left(\gamma^2 - \eta k\right)(a - ck)}{\left(\eta\alpha^2 + 4\beta\gamma^2 - 8\beta\eta k\right)\left(\alpha^2 \gamma^2 + 4\beta\gamma^2 k - 8\beta\eta k^2\right)} > 0,$$

$$e_{SC}^{*B} - e_R^{*BM} = \frac{-4\beta^2 \gamma\left(\gamma^2 - \eta k\right)(a - ck)}{\left(\eta\alpha^2 + 4\beta\gamma^2 - 8\beta\eta k\right)\left(\eta\alpha^2 + 2\beta\gamma^2 - 4\beta\eta k\right)} > 0,$$

$$\frac{\partial e_R^{*I}}{\partial \varphi} = \frac{2\eta\gamma\beta\left(\alpha^2 - 4\beta k\right)(ck - a)}{\left(\alpha^2 \eta - 4\beta\eta\varphi k - 4\beta\eta k + 4\beta\gamma^2 \varphi\right)^2} > 0,$$

$$\Longrightarrow e_{SC}^{*B} > e_R^{*BM} > e_R^{*I}.$$

(A.23)

$$(3)\, \text{Set } A = 2\beta c\gamma^2 k + 2\beta a\gamma^2 - 4\beta\eta ck^2 - 4\beta\eta ak < 0 \text{ and}$$
$$B = 4\beta\gamma^2 k - 8\beta\eta k^2 < 0, \text{ to get}$$

$$w_M^{*BM} = \frac{\eta c\alpha^2 k + A}{k\eta\alpha^2 + B},$$

$$w_M^{*I} = \frac{c\alpha^2 \gamma^2 + A}{\alpha^2 \gamma^2 + B},$$

$$w_M^{*BM} - w_M^{*I} = \frac{\alpha^2\left(k\eta - \gamma^2\right)(cB - A)}{\left(k\eta\alpha^2 + B\right)\left(\alpha^2 \gamma^2 + B\right)} > 0,$$

$$cB - A = 2\beta(ck - a)\left(\gamma^2 - 2\eta k\right) > 0,$$

$$\frac{\partial w_M^{*I}}{\partial \varphi} = \frac{2\beta\eta(ck - a)\left(2\eta k - \gamma^2\right)\left(\alpha^2 - 4\beta k\right)}{k\left(\alpha^2 \eta - 4\beta\eta\varphi k - 4\beta\eta k + 4\beta\gamma^2 \varphi\right)^2} > 0,$$

$$\Longrightarrow w_M^{*BM} > w_M^{*I} > w_M^{*II}.$$

(A.24)

$$(4)\ q_{SC}^{*B} - q_{M}^{*BM} = \frac{-4\beta^2\eta k(\gamma^2 - 2\eta k)(a - ck)}{(\eta\alpha^2 + 4\beta\gamma^2 - 8\beta\eta k)(\eta\alpha^2 + 2\beta\gamma^2 - 4\beta\eta k)} > 0,$$

$$q_{M}^{*BM} - q_{M}^{*I} = \frac{8\alpha^2\beta^2 k(a - ck)(\gamma^2 - \eta k)^2}{(\alpha^2 - 4\beta k)(\alpha^2\gamma^2 + 4\beta\gamma^2 k - 8\beta\eta k^2)(\eta\alpha^2 + 4\beta\gamma^2 - 8\beta\eta k)} < 0,$$

$$q_{SC}^{*B} - q_{M}^{*I} = \frac{4\beta^2 k(a - ck)(2\eta k^2(\alpha^2\eta + 2\gamma^2\beta - 4k\eta\beta) + \alpha^2\gamma^2(\gamma^2 - 2\eta k))}{(\alpha^2 - 4\beta k)(\alpha^2\gamma^2 + 4\beta\gamma^2 k - 8\beta\eta k^2)(\eta\alpha^2 + 4\beta\gamma^2 - 8\beta\eta k)} > 0,$$

$$\frac{\partial q_{M}^{*I}}{\partial \varphi} = \frac{8\beta^2\eta k(\gamma^2 - \eta k)(a - ck)}{(\alpha^2\eta - 4\beta\eta\varphi k - 4\beta\eta k + 4\beta\gamma^2\varphi)^2} < 0,$$

$$\Longrightarrow q_{SC}^{*B} > q_{M}^{*II} > q_{M}^{*I} > q_{M}^{*BM}.$$

The proof is completed.   □   *Proof of Proposition 6*

$$(1)\ \Pi_{M}^{*BM} - \Pi_{M}^{*I} = \frac{4\alpha^2\beta^2(a - ck)^2(\gamma^2 - \eta k)^2}{(\alpha^2 - 4\beta k)(\alpha^2\gamma^2 + 4\beta\gamma^2 k - 8\beta\eta k^2)(\eta\alpha^2 + 4\beta\gamma^2 - 8\beta\eta k)} < 0,$$

$$\frac{\partial \Pi_{M}^{*I}}{\partial \varphi} = \frac{(4\beta\gamma^2 - 4\beta\eta k)(\beta\eta a^2 - 2\beta\eta ack + \beta\eta c^2 k^2)}{(\alpha^2\eta - 4\beta\eta\varphi k - 4\beta\eta k + 4\beta\gamma^2\varphi)^2} < 0,$$

$$\Longrightarrow \Pi_{M}^{*II} > \Pi_{M}^{*I} > \Pi_{M}^{*BM},$$

$$\Pi_{R}^{*BM} - \Pi_{R}^{*I} = \frac{-2\alpha^4\beta^2\eta(a - ck)^2(\gamma^2 - \eta k)^2}{(\alpha^2 - 4\beta k)(\alpha^2\gamma^2 + 4\beta\gamma^2 k - 8\beta\eta k^2)(\eta\alpha^2 + 4\beta\gamma^2 - 8\beta\eta k)^2} < 0,$$

$$\Longrightarrow \Pi_{R}^{*I} > \Pi_{R}^{*BM}.$$

$$(A.26)$$

$$(2)\ \Pi_{SC}^{*B} - \Pi_{SC}^{*BM} = \frac{-4\beta^3\eta(a - ck)^2(\gamma^2 - 2\eta k)^2}{(\alpha^2\eta + 2\gamma^2\beta - 4k\eta\beta)(\eta\alpha^2 + 4\beta\gamma^2 - 8\beta\eta k)^2} > 0,$$

$$\Pi_{SC}^{*BM} - \Pi_{SC}^{*I} = \frac{2\alpha^2\beta^2(a - ck)^2(\gamma^2 - \eta k)^2(\eta\alpha^2 + 8\beta\gamma^2 - 16\beta\eta k)}{(\alpha^2 - 4\beta k)(\alpha^2\gamma^2 + 4\beta\gamma^2 k - 8\beta\eta k^2)(\eta\alpha^2 + 4\beta\gamma^2 - 8\beta\eta k)^2} < 0,$$

$$\Pi_{SC}^{*B} - \Pi_{SC}^{*I} = \frac{2\beta^2(a - ck)^2(\eta k^2(\alpha^2\eta + 2\gamma^2\beta - 4k\eta\beta) + \alpha^2\gamma^2(\gamma^2 - 2\eta k))}{(\alpha^2 - 4\beta k)(\alpha^2\gamma^2 + 4\beta\gamma^2 k - 8\beta\eta k^2)(\alpha^2\eta + 2\gamma^2\beta - 4k\eta\beta)} > 0,$$

$$\frac{\partial \Pi_{SC}^{*I}}{\partial \varphi} < 0,$$

$$\Longrightarrow \Pi_{SC}^{*B} > \Pi_{SC}^{*I} > \Pi_{SC}^{*BM}.$$

$$(A.27)$$

The proof is completed.   □   *Proof of Proposition 7.* Take the first partial derivative of the equilibrium values among the models (B, BM, and I) with respect to α and β.

$$\frac{\partial \theta_{SC}^{*B}}{\partial \alpha} = \frac{-\eta (ck - a)\left(\alpha^2 \eta + 4\beta \eta k - 2\beta \gamma^2\right)}{\left(\alpha^2 \eta + 2\gamma^2 \beta - 4k\eta\beta\right)^2} > 0,$$

$$\frac{\partial \theta_{SC}^{*B}}{\partial \beta} = \frac{2\alpha \eta \left(\gamma^2 - 2\eta k\right)(a - ck)}{\left(\alpha^2 \eta + 2\gamma^2 \beta - 4k\eta\beta\right)^2} < 0,$$

$$\frac{\partial e_{SC}^{*B}}{\partial \alpha} = \frac{4\alpha \eta \beta \gamma (a - ck)}{\left(\alpha^2 \eta + 2\gamma^2 \beta - 4k\eta\beta\right)^2} > 0,$$

$$\frac{\partial e_{SC}^{*B}}{\partial \beta} = \frac{-2\alpha^2 \eta \gamma (a - ck)}{\left(\alpha^2 \eta + 2\gamma^2 \beta - 4k\eta\beta\right)^2} < 0,$$

$$\frac{\partial p_{SC}^{*B}}{\partial \alpha} = \frac{4\alpha \eta^2 \beta (a - ck)}{\left(\alpha^2 \eta + 2\gamma^2 \beta - 4k\eta\beta\right)^2} > 0,$$

$$\frac{\partial p_{SC}^{*B}}{\partial \beta} = \frac{-2\alpha^2 \eta^2 (a - ck)}{\left(\alpha^2 \eta + 2\gamma^2 \beta - 4k\eta\beta\right)^2} < 0,$$

$$\frac{\partial \Pi_{SC}^{*B}}{\partial \alpha} = \frac{2\alpha \eta^2 \beta (a - ck)^2}{\left(\alpha^2 \eta + 2\gamma^2 \beta - 4k\eta\beta\right)^2} > 0,$$

$$\frac{\partial \Pi_{SC}^{*B}}{\partial \beta} = \frac{-\alpha^2 \eta^2 (a - ck)^2}{\left(\alpha^2 \eta + 2\gamma^2 \beta - 4k\eta\beta\right)^2} < 0,$$

$$\frac{\partial w_M^{*\,\mathrm{BM}}}{\partial \alpha} = \frac{4\alpha\beta\eta(\gamma^2 - 2\eta k)(\mathrm{ck} - a)}{k(\eta\alpha^2 + 4\beta\gamma^2 - 8\beta\eta k)^2} > 0,$$

$$\frac{\partial w_M^{*\,\mathrm{BM}}}{\partial \beta} = \frac{2\alpha^2\eta(2\eta k - \gamma^2)(\mathrm{ck} - a)}{k(\eta\alpha^2 + 4\beta\gamma^2 - 8\beta\eta k)^2} < 0,$$

$$\frac{\partial \theta_M^{*\,\mathrm{BM}}}{\partial \alpha} = \frac{\eta(a - \mathrm{ck})(\eta\alpha^2 - 4\beta\gamma^2 + 8\beta\eta k)}{(\eta\alpha^2 + 4\beta\gamma^2 - 8\beta\eta k)^2} > 0,$$

$$\frac{\partial \theta_M^{*\,\mathrm{BM}}}{\partial \beta} = \frac{4\alpha\eta(a - \mathrm{ck})(\gamma^2 - 2\eta k)}{(\eta\alpha^2 + 4\beta\gamma^2 - 8\beta\eta k)^2} < 0,$$

$$\frac{\partial p_R^{*\,\mathrm{BM}}}{\partial \alpha} = \frac{4\alpha\beta\eta(\mathrm{ck} - a)(\gamma^2 - 3\eta k)}{k(\eta\alpha^2 + 4\beta\gamma^2 - 8\beta\eta k)^2} > 0,$$

$$\frac{\partial p_R^{*\,\mathrm{BM}}}{\partial \beta} = \frac{2\alpha^2\eta(\mathrm{ck} - a)(3\eta k - \gamma^2)}{k(\eta\alpha^2 + 4\beta\gamma^2 - 8\beta\eta k)^2} < 0,$$

$$\frac{\partial e_R^{*\,\mathrm{BM}}}{\partial \alpha} = \frac{4\alpha\eta\beta\gamma(a - \mathrm{ck})}{(\eta\alpha^2 + 4\beta\gamma^2 - 8\beta\eta k)^2} > 0,$$

$$\frac{\partial e_R^{*\,\mathrm{BM}}}{\partial \beta} = \frac{2\alpha^2\eta\gamma(\mathrm{ck} - a)}{(\eta\alpha^2 + 4\beta\gamma^2 - 8\beta\eta k)^2} < 0,$$

$$\frac{\partial \Pi_M^{*\,\mathrm{BM}}}{\partial \alpha} = \frac{2\alpha\beta\eta^2(a - \mathrm{ck})^2}{(\eta\alpha^2 + 4\beta\gamma^2 - 8\beta\eta k)^2} > 0,$$

$$\frac{\partial \Pi_M^{*\,\mathrm{BM}}}{\partial \beta} = \frac{-\alpha^2\eta^2(a - \mathrm{ck})^2}{(\eta\alpha^2 + 4\beta\gamma^2 - 8\beta\eta k)^2} < 0,$$

$$\frac{\partial \Pi_R^{*\,\mathrm{BM}}}{\partial \alpha} = \frac{8\alpha\beta^2\eta^2(\gamma^2 - 2\eta k)(a - \mathrm{ck})^2}{(\eta\alpha^2 + 4\beta\gamma^2 - 8\beta\eta k)^3} > 0,$$

$$\frac{\partial \Pi_R^{*\,\mathrm{BM}}}{\partial \beta} = \frac{-4\alpha^2\beta\eta^2(\gamma^2 - 2\eta k)(a - \mathrm{ck})^2}{(\eta\alpha^2 + 4\beta\gamma^2 - 8\beta\eta k)^3} < 0,$$

$$\frac{\partial \Pi_{\mathrm{SC}}^{*\mathrm{BM}}}{\partial \alpha} = \frac{2\alpha\beta\eta^2(a - \mathrm{ck})^2(\eta\alpha^2 + 8\beta\gamma^2 - 16\beta\eta k)}{(\eta\alpha^2 + 4\beta\gamma^2 - 8\beta\eta k)^3} > 0,$$

$$\frac{\partial \Pi_{\mathrm{SC}}^{*\mathrm{BM}}}{\partial \beta} = \frac{-\alpha^2\eta^2(a - \mathrm{ck})^2(\eta\alpha^2 + 8\beta\gamma^2 - 16\beta\eta k)}{(\eta\alpha^2 + 4\beta\gamma^2 - 8\beta\eta k)^3} < 0,$$

$$\frac{\partial w_M^{*\,I}}{\partial \alpha} = \frac{4\alpha\beta\eta\varphi(\gamma^2 - 2\eta k)(\mathrm{ck} - a)}{k(\alpha^2\eta - 4\beta\eta\varphi k - 4\beta\eta k + 4\beta\gamma^2\varphi)^2} > 0,$$

$$\frac{\partial w_M^{*\,I}}{\partial \beta} = \frac{2\alpha^2\eta\varphi(2\eta k - \gamma^2)(\mathrm{ck} - a)}{k(\alpha^2\eta - 4\beta\eta\varphi k - 4\beta\eta k + 4\beta\gamma^2\varphi)^2} < 0,$$

$$\frac{\partial \theta_M^{*\,I}}{\partial \alpha} = \frac{(a - ck)\left[\alpha^2 \eta^2 + 4\beta \eta^2 k + 4\beta \eta \varphi \left(\eta k - \gamma^2\right)\right]}{\left(\alpha^2 \eta - 4\beta \eta \varphi k - 4\beta \eta k + 4\beta \gamma^2 \varphi\right)^2} > 0,$$

$$\frac{\partial \theta_M^{*\,I}}{\partial \beta} = \frac{4\alpha \eta (a - ck)\left(\varphi \gamma^2 - \eta k - \eta k \varphi\right)}{\left(\alpha^2 \eta - 4\beta \eta \varphi k - 4\beta \eta k + 4\beta \gamma^2 \varphi\right)^2} < 0,$$

$$\frac{\partial p_R^{*\,I}}{\partial \alpha} = \frac{4\alpha \eta \beta (a - ck)\left(\eta k - \gamma^2 \varphi + 2\eta \varphi k\right)}{k\left(\alpha^2 \eta - 4\beta \eta \varphi k - 4\beta \eta k + 4\beta \gamma^2 \varphi\right)^2} > 0,$$

$$\frac{\partial p_R^{*\,I}}{\partial \beta} = \frac{-2(a - ck)\left(\eta k - \gamma^2 \varphi + 2\eta \varphi k\right)}{k\left(\alpha^2 \eta - 4\beta \eta \varphi k - 4\beta \eta k + 4\beta \gamma^2 \varphi\right)^2} < 0,$$

$$\frac{\partial e_R^{*\,I}}{\partial \alpha} = \frac{4\alpha \beta \eta \gamma \varphi (a - ck)}{\left(\alpha^2 \eta - 4\beta \eta \varphi k - 4\beta \eta k + 4\beta \gamma^2 \varphi\right)^2} > 0,$$

$$\frac{\partial e_R^{*\,I}}{\partial \beta} = \frac{-2\alpha^2 \eta \gamma \varphi (a - ck)}{\left(\alpha^2 \eta - 4\beta \eta \varphi k - 4\beta \eta k + 4\beta \gamma^2 \varphi\right)^2} < 0,$$

$$\frac{\partial \Pi_M^{*\,I}}{\partial \alpha} = \frac{2\alpha \beta \eta^2 (a - ck)^2}{\left(\alpha^2 \eta - 4\beta \eta \varphi k - 4\beta \eta k + 4\beta \gamma^2 \varphi\right)^2} > 0,$$

$$\frac{\partial \Pi_M^{*\,I}}{\partial \beta} = \frac{-\alpha^2 \eta^2 (a - ck)^2}{\left(\alpha^2 \eta - 4\beta \eta \varphi k - 4\beta \eta k + 4\beta \gamma^2 \varphi\right)^2} < 0,$$

$$\frac{\partial \Pi_R^{*\,I}}{\partial \alpha} = \frac{8\alpha \beta^2 \eta^2 \varphi (a - ck)^2 \left(\gamma^2 \varphi - 2\eta k\right)}{\left(\alpha^2 \eta - 4\beta \eta \varphi k - 4\beta \eta k + 4\beta \gamma^2 \varphi\right)^3} > 0,$$

$$\frac{\partial \Pi_R^{*\,I}}{\partial \beta} = \frac{-4\alpha^2 \beta \eta^2 \varphi (a - ck)^2 \left(\gamma^2 \varphi - 2\eta k\right)}{\left(\alpha^2 \eta - 4\beta \eta \varphi k - 4\beta \eta k + 4\beta \gamma^2 \varphi\right)^3} < 0,$$

$$\frac{\partial \Pi_R^{*\,I}}{\partial \beta} = \frac{-4\alpha^2 \beta \eta^2 \varphi (a - ck)^2 \left(\gamma^2 \varphi - 2\eta k\right)}{\left(\alpha^2 \eta - 4\beta \eta \varphi k - 4\beta \eta k + 4\beta \gamma^2 \varphi\right)^3} < 0,$$

$$\frac{\partial \Pi_{SC}^{*\,I}}{\partial \alpha} = \frac{2\alpha \beta^2 \eta (a - ck)^2 \left(\eta \alpha^2 + 4\beta \gamma^2 \varphi^2 + 4\beta \gamma^2 \varphi - 12\beta \eta k \varphi - 4\beta \eta k\right)}{\left(\alpha^2 \eta - 4\beta \eta \varphi k - 4\beta \eta k + 4\beta \gamma^2 \varphi\right)^3} > 0,$$

$$\frac{\partial \Pi_R^{*\,I}}{\partial \beta} = \frac{-\eta (a - ck)^2 \left(\alpha^4 \eta^2 - 12\beta k \alpha^2 \eta^2 \varphi - 4\beta k \alpha^2 \eta^2 + 4\beta \alpha^2 \eta \gamma^2 \varphi^2 + 4\beta \alpha^2 \eta \gamma^2 \varphi\right)}{\left(\alpha^2 \eta - 4\beta \eta \varphi k - 4\beta \eta k + 4\beta \gamma^2 \varphi\right)^3} < 0.$$

(A.28)

□

Data Availability

The (numeric) data used to support the findings of this study are included within the article.

Conflicts of Interest

The authors declare that they have no conflicts of interest.

Acknowledgments

References

[1] H. Li, "Research on the relationship between green brand and consumer purchase intention," *China Business and Market*, vol. 32, no. 7, pp. 56–62, 2018.

[2] C. Jin, E. Cao, and M. Lai, "Analysis on green marketing strategy of duopoly retailing market based on the evolutionary game theory," *Journal of System Engineering*, vol. 27, no. 3, pp. 383–389, 2012.

[3] W. Du, Y. Fan, and L. Yan, "Pricing strategies for competitive water supply chains under different power structures: an application to the South-to-North water diversion project in China," *Sustainability*, vol. 10, no. 8, 2018.

[4] D. Ghosh and J. Shah, "A comparative analysis of greening policies across supply chain structures," *International Journal of Production Economics*, vol. 135, no. 2, pp. 568–583, 2012.

[5] L. L. Zhang, N. W. Zhang, and Z. Z. Wang, "CAS paradigm applied to water resources supply chain management in the east route of South-to-North water transfer project," *Journal of Hohai University (Natural Science)*, vol. 32, no. 6, pp. 703–706, 2004.

[6] I. N. Athanasiadis, A. K. Mentes, P. A. Mitkas, and Y. A. Mylopoulos, "A hybrid agent-based model for estimating residential water demand," *Simulation*, vol. 81, no. 3, pp. 175–187, 2005.

[7] H. M. Wang and Z. Y. Hu, "Several issues on South-to-North water transfer project supply chain operations management," *Advances in Water Science*, vol. 16, no. 6, pp. 864–869, 2005.

[8] J. L. Zhu and H. M. Wang, "Stochastic control of bullwhip effect in SCM of water resource of South-to-North Water transfer," *System Engineering*, vol. 23, no. 5, pp. 1–6, 2005.

[9] E. Kondili and J. K. Kaldellis, "Model development for the optimal water systems planning," *Computer Aided Chemical Engineering*, vol. 21, 2006.

[10] J. L. Zhu, "A water collocation model for supply chain in South-to-North water transfer project," *System Engineering*, vol. 25, no. 11, pp. 31–35, 2007.

[11] H. M. Wang, L. Zhang, and W. Yang, "Pricing model of water resources supply chain for east-route South-to-North Water transfer project," *Shui Li Xue Bao*, vol. 39, no. 6, pp. 758–762, 2008.

[12] L. Zhang, H. M. Wang, and W. Yang, "A discriminatory pricing model and simulation to different markets of eastern route of the South-to-North water transfers supply chain," *System Engineering*, no. 3, pp. 120–123, 2008.

[13] S. Ahmed, "Supply chain planning for water distribution in Central Asia," *Industrial Management & Data Systems*, vol. 109, no. 1, pp. 53–73, 2009.

[14] K. Kogan and C. S. Tapiero, "Water supply and consumption uncertainty: a conflict-equilibrium," *Annals of Operations Research*, vol. 181, no. 1, pp. 199–217, 2010.

[15] D. Elala, P. Labhasetwar, and S. F. Tyrrel, "Deterioration in water quality from supply chain to household and appropriate storage in the context of intermittent water supplies," *Water Supply*, vol. 11, no. 4, pp. 400–408, 2011.

[16] J. Zhou, Y. Su, and Y. Zhang, "Enlightenment on the risk management and risk assessment of water source and water supply system in European countries," *Journal of Safety and Environment*, vol. 12, no. 02, pp. 138–142, 2012.

[17] A. Borghi, C. Strazza, M. Gallo, S. Messineo, and M. Naso, "Water supply and sustainability: life cycle assessment of water collection, treatment and distribution service," *The International Journal of Life Cycle Assessment*, vol. 18, no. 5, 2013.

[18] Y. Saif and A. Almansoori, "Design and operation of water desalination supply chain using mathematical modelling approach," *Desalination*, vol. 351, 2014.

[19] S. Behboudian, M. Tabesh, M. Falahnezhad, and F. A. Ghavanini, "A long-term prediction of domestic water demand using preprocessing in artificial neural network," *Journal of Water Supply: Research and Technology-Aqua*, vol. 63, no. 1, 2014.

[20] L. X. He and S. H. He, "Solving water resource scheduling problem through an improved artificial fish swarm algorithm," *International Journal of Simulation Modelling*, vol. 14, no. 1, pp. 170–181, 2015.

[21] N. Papageorgiou, B. Magoutas, G. Mentzas, J. Kutterer, K. Schnitter, and A. Abecker, "Data and system interoperability in the drink-water supply chain," in *Proceedings of the 36th World Congress*, pp. 7060–7069, Hague, The Netherlands, June 2015.

[22] L. L. Zhang, H. M. Wang, and Z. Z. Wang, "Multi-level cooperative decision-making model for water resources supply chain of east route of South-to-North water transfer project under seasonal demand," *Journal of Hohai University (Natural Science)*, vol. 33, no. 6, pp. 14–17, 2005.

[23] J. Dai and C. M. Ji, "A competition equilibrium model on the diverse-source water supply market created by interbasin water transfer," in *Proceedings of the 2006 International Conference on Management Science and Engineering*, pp. 995–1000, Lille, France, October 2006.

[24] J. L. Zhu, X. Y. Tao, and S. J. Wang, "Water inventory coordination of South-to-North water transfer project supply chain based on the theory of VMI," *Chinese Journal of Management Science*, vol. 14, no. 6, pp. 98–103, 2006.

[25] E. Kondili and J. K. Kaldellis, "Development and operation issues of a decision support system for water management in areas with water resources," *Fresenius Environmental Bulletin*, vol. 17, no. 9B, pp. 1412–1419, 2008.

[26] H. Wang, Z. Chen, and S.-I. I. Su, "Optimal pricing and coordination schemes for the eastern route of the South-to-North water diversion supply chain system in China," *Transportation Journal*, vol. 51, no. 4, 2012.

[27] Z. S. Chen, "Coordination mechanisms for South-to-North water diversion: economic benefit and social responsibility," *Resources Science*, vol. 35, no. 6, pp. 1245–1253, 2013.

[28] W. Y. Du, X. Z. Ai, and X. W. Tang, "The South-to-North water diversion supply chain operation strategy research under competition environment," in *Proceedings of the 22nd International Conference on Management Science and Engineering*, pp. 472–478, Aveiro, Portugal, July 2015.

[29] W. Du, Y. Fan, and X. Tang, "Two-part pricing contracts under competition: the South-to-North water transfer project supply chain system in China," *International Journal of Water Resources Development*, vol. 32, no. 6, 2016.

[30] M. N. Koleva, A. J. Calderón, D. Zhang, C. A. Styan, and L. G. Papageorgiou, "Integration of environmental aspects in modelling and optimisation of water supply chains," *Science of the Total Environment*, vol. 636, no. 15, pp. 314–338, 2018.

[31] Z. Chen, S.-I. I. Su, and H. Wang, "Inter-basin water transfer supply chain equilibrium and coordination: a social welfare maximization perspective," *Water Resources Management*, vol. 33, no. 7, pp. 2577–2598, 2019.

[32] W. Du, Y. Fan, X. Liu, S. C. Park, and X. Tang, "A game-based production operation model for water resource management: an analysis of the South-to-North Water Transfer Project in China," *Journal of Cleaner Production*, vol. 228, no. 10, pp. 1482–1493, 2019.

[33] W. Du, Y. Fan, X. Liu et al., "Two-part pricing contract and competition between two water supply chains: a theoretical and empirical analysis of the South-to-North Water Transfer Project in China," *Journal of Water Supply: Research and Technology-AQUA*, vol. 68, no. 3-4, pp. 197–209, 2019.

[34] X. Chen and Z. Chen, "Joint pricing and inventory management of interbasin water transfer," *Supply Chain[J]. Complexity*, vol. 2020, Article ID 3954084, 2020.

[35] S. K. Mukhopadhyay, X. M. Su, and S. Ghose, "Motivating retail marketing effort: optimal contract design," *Production and Operations Management*, vol. 18, no. 2, pp. 19–211, 2009.

[36] D. D. Wu, "Bargaining in supply chain with price and promotional effort dependent demand," *Mathematical and Computer Modelling*, vol. 58, no. 9-10, pp. 1659–1669, 2013.

[37] P. Ma, K. W. Li, and Z.-J. Wang, "Pricing decisions in closed-loop supply chains with marketing effort and fairness concerns," *International Journal of Production Research*, vol. 55, no. 22, pp. 6710–6731, 2017.

[38] H. Song and X. Gao, "Green supply chain game model and analysis under revenue-sharing contract," *Journal of Cleaner Production*, vol. 170, pp. 183–192, 2018.

Research Article

IOT Medical Device-Assisted Foam Dressing in the Prevention of Pressure Sore during Operation

Yan Meng,[1] **Hui Zhao,**[2] **Zhigai Yin,**[3] **and Xiaona Qi** [4]

[1]*Operating Room, Xingtai People's Hospital, Xingtai 054001, Hebei, China*
[2]*Nursing Department, Xingtai People's Hospital, Xingtai 054001, Hebei, China*
[3]*The Brotherhood of Surgical, Xingtai People's Hospital, Xingtai 054001, Hebei, China*
[4]*The Emergency Department, Xingtai People's Hospital, Xingtai 054001, Hebei, China*

Correspondence should be addressed to Xiaona Qi; qixiaona@stu.cpu.edu.cn

With the development of the times, people's living standards are constantly improving, but the medical pressure brought by the aging population is also increasing, and pressure ulcers in elderly patients during hospitalization are also constantly occurring. Of course, the relevant medical equipment is also progressing, especially the emergence of medical-assistant foam dressing on the Internet of Things, which makes people cope with pressure ulcers more handily. In order to test the role of IOT medical devices, especially the application of foam dressings in the prevention of pressure ulcers, this article has carried out a survey of patients in a city hospital, investigated relevant literature, interviewed professionals, collected relevant information, designed experiments, and obtained relevant research data. Research shows that IOT medical devices can improve the efficiency of hospital treatment and improve the efficiency by about 12%; pressure ulcer incidence in different age groups of people is different, and the probability of occurrence in the elderly population is far higher than that of young people; foam dressing has obvious effect on the prevention of pressure sore, and the probability of pressure sore after using foam dressing is lower than that of unused 35%. It indicates that foam dressing can play a key role in the prevention of pressure sore.

1. Introduction

With the continuous development of China's population aging and chronic diseases [1], its harm is increasingly reflected, and the elderly people with chronic diseases bear the brunt. And, the miniaturization of the family structure and the tendency of two generations' separation make the empty-nest elderly more and more prominent. The elderly with heart disease and cerebrovascular disease often die because they cannot be found and rescued in time when they are alone. There are many problems in the daily monitoring and management of chronic diseases in the elderly. At the same time, under the promotion of information and Internet of Things technology, "intelligent" medical products on the market are showing a blowout trend [2, 3]. The scope of community education services and home care is more and more extensive, and the requirements are also higher and

higher. At this stage, the knowledge of pressure ulcer of community and family nursing staff is lacking or updated slowly [4], which directly affects the prevention and treatment of pressure ulcer. Medical Internet of Things can improve the accuracy of data and prolong the life of the network. Because the data in the medical Internet of Things has the characteristics of sudden and large amount of data [5], the event-driven mode is very suitable for the monitoring of emergencies. At the same time, it can also make the nodes not in the monitoring area in the dormant state and reduce the energy consumption of the nodes in the network [6].

According to statistics, the incidence of pressure ulcer in hospitalized patients in China is 3%~12%, and the population range is mainly elderly patients, the incidence rate is 10%~25%, and the total mortality rate increases 6 times. The incidence rate did not decrease compared with the previous

one. The occurrence of pressure ulcers aggravates the physiological and psychological pain of patients, causes huge economic losses, and increases the workload of nurses, which leads to some medical disputes and takes up a large number of public health resources. The prevention of pressure ulcer is one of the important problems to be solved urgently in the clinical nursing work and is a very important reference index to evaluate the quality of nursing. There is a global consensus that the prevention of pressure ulcers is the best treatment [7]. The incidence of pressure ulcer in extracorporeal circulation surgery is as high as 16.7%, which has been paid close attention by medical workers. Therefore, experts at home and abroad have certain research on pressure sore [8].

Wang Ying introduced the causes and symptoms of pressure ulcers, elaborated the harm of pressure ulcers to patients, increased the family burden of patients, and explained the reasons why pressure ulcers could not be completely prevented. Based on reducing the probability of pressure ulcers and reducing the harm degree of pressure ulcers, the prevention measures of pressure ulcers were introduced, so as to analyze the probability of pressure ulcers after improvement, which is the phase of pressure ulcers to provide reference for the work [9]. Xu Ting took 10,000 patients as experimental subjects and set them as the experimental group and the control group, respectively. He observed the causes and differences of pressure ulcers in the hospital between the two groups of patients and carried out pressure ulcer prevention for the two groups of patients. According to medical guidelines, it was observed whether the bed sore situation has changed after the implementation of relevant preventive measures [10]. In order to investigate the cause of pressure ulcers, Hui constructed a research model for the prevention of pressure ulcers. Through the investigation of patients in the hospital, the feasibility of the model was verified, and the characteristics of pressure ulcer in hospitalized patients in China were obtained. Through the interview with relevant medical experts, the model was improved [11], and the patients in the model were classified and analyzed to determine the occurrence of pressure ulcer. According to the relevant reasons, the paper puts forward targeted prevention suggestions, which have a strong reference role for the future research [12]. However, some of these studies have no universal value due to the limitation of samples and the lack of research methods, which can only provide some reference opinions.

This paper sorts out and classifies the data obtained by the literature research method, which provides a theoretical basis for the conception and research analysis of this paper, and makes a detailed analysis on the Internet of Things. It opens up a new theoretical perspective for deepening scholars' understanding of Internet of Things medical treatment; according to the research problems, the questionnaire is designed to combine the theoretical research and empirical research to analyze the causes of pressure ulcer and the prevention of pressure ulcer, which can enrich the relevant scholars' research on pressure ulcer and has certain research significance.

2. Internet of Things for the Prevention of Pressure Ulcers

2.1. Internet of Things Healthcare. Through the Internet of Things, medical personnel can interact with each other through the Internet of Things and medical devices [13]. Through the comprehensive application of barcode identification, wireless sensor network, and other Internet of Things technologies, it realizes the identification, regional positioning, tracking and management of special groups, medical devices, medical waste, and drugs in the hospital. The aspects that Internet of Things can play a role in the management process of medical and health fields include the following: diagnosis and treatment sign input, patient identity management barcode, mobile doctor's order, inspection specimen movement management, drug mobile management, baby antitheft, medical record management, movement number, data transfer and preservation, and nursing process management [14–16]. And, in the field of medical care, it can monitor the various conditions of the human body and transmit the data to various communication terminals. Its main application is in the monitoring of the human body and the measurement of physiological parameters. The monitoring objects include not only patients but also healthy people [17].

In the medical Internet of Things, due to the huge amount of collected data, on the one hand, it realizes the effective collection and integration of medical information, which makes health promotion possible. On the other hand, it is unavoidable to integrate and share massive multisource heterogeneous data in the network. These information include data, images, audio, and text data [18]. After intelligent processing of the collected information, real-time health file information resources are obtained, and according to the corresponding real-time monitoring data, personal health promotion reports are made, and various forms of tracking are carried out [19]. These make the information in intelligent health management from collection and processing to application, showing significant multisource heterogeneous characteristics. The transmission of information is data centric. Due to the large number of sensor nodes and random distribution, the data obtained by monitoring the same event between adjacent sensor nodes are similar. However, the storage space and energy of sensor nodes are limited, and the characteristics of dense distribution of large-scale sensor nodes lead to most of the collected data become redundant. It will shorten the lifetime of the whole network and reduce the efficiency of information integration. At the same time, the network involves a large number of spatial distribution of health data, medical information, physical examination data, health measurement and evaluation, equipment operation and parameters, and other decentralized system space-time data [20, 21].

Internet of Things technology can help hospitals to achieve intelligent medical care for people and intelligent management of things, which has great potential in the medical field. Moreover, it supports the digital collection, processing, storage, distribution, transmission and management of personnel

management information, equipment information, medical information, and drug information within the hospital and can meet the needs of medical equipment and supplies, medical and health-related information, intelligent supervision of public health safety, etc. It can realize the visualization of material management, the digitization of medical information [22], the digitization of the medical process, the scientificization of the treatment process, and the humanization of service communication, so as to solve various problems such as the overall low level of medical service, the weak cultural support of medical cooperation, and the annual production hidden trouble of medical safety [23].

As shown in Figure 1, there is a huge amount of data information in the medical Internet of Things. With the continuous increase of data collected from medical sensors and new measurement equipment, how to obtain effective data from the sign sensor network and environmental-sensing equipment is a very critical problem [24]. Therefore, it is necessary to use effective data fusion technology to process the relevant data [25]. In order to reduce the data delay in the network, a fusion path method with minimum delay is proposed:

$$T_n(i) = \delta \frac{r_i}{w_i} \cdots (i \in N). \tag{1}$$

The specific algorithm is as follows:

$$f = \left[-\frac{1}{2} \sum_{c=1}^{i} \sum_{d=1}^{i} (a_c^* - a_c)(a_c - a_c^*) Q(x_c, x_d) - \vartheta \sum_{c=1}^{i} (a_c^* + a_c) + \sum_{c=1}^{i} b_c (a_c^* + a_d) \right]. \tag{2}$$

Among them,

$$\sum_{c=1}^{i} a_c^* = \sum_{c=1}^{i} aca_c^*, \quad a_c \in [0, D] \, (c = 1, 2, 3, \ldots, m), \tag{3}$$

where D is a normal number, which is called the penalty factor. If the value of D is large, it means that the penalty for fitting deviation is large. At this time, the regression function can be expressed as

$$V = \sum_{c=1}^{i} (a_c^* - a_c) Q(x_c, x) + s; \tag{4}$$

when $a_c \in (0, D)$,

$$s = d_c - \sum_{c=1}^{i} (a_c^* - a_c) b(x_c, x) + \vartheta; \tag{5}$$

when $a_c^* \in (0, D)$

$$s = d_c - \sum_{c=1}^{i} (a_c^* - a_c) b(x_c, x) - \vartheta. \tag{6}$$

2.2. Pressure Sore. Pressure ulcer refers to the soft tissue damage caused by continuous hypoxia, ischemia, and malnutrition caused by long-term compression and blood circulation disorder in local tissues, such as ulceration and necrosis [26].

The risk factors of intraoperative pressure sores are as follows:

(1) The operation time is long: long operation time is one of the main risk factors leading to pressure ulcers. Some studies have shown that when the local tissue pressure time is greater than 2.5 hours, the incidence of pressure ulcers will be significantly increased. When the operation time exceeds 3 hours, the incidence of pressure ulcers is more than 8.5%, and the operation time of extracorporeal circulation surgery generally exceeds 3 hours, so intraoperative pressure ulcers are prone to occur [27].

(2) Intraoperative hypothermia: hypothermia during cardiopulmonary bypass can directly damage the immune function of the body, reduce the blood oxygen supply of the tissue, resulting in ischemia, hypoxic injury of the skin, and subcutaneous tissue and muscle, and produce reversible or irreversible damage to the cells and microvessels. The incidence rate of pressure ulcer is also an important reason.

(3) The patient's reaction under anesthesia is relatively slow, and the body cannot produce protective response.

(4) The use of high-dose vasoactive drugs can cause peripheral vasoconstriction, lead to tissue ischemia and hypoxia, and promote the occurrence of pressure ulcers.

(5) The influence of lying position: the position of cardiopulmonary bypass surgery is the chest supine position. On the basis of general supine position, a position pad is placed on the shoulder blade, which can fully expose the operation field and facilitate the operation. But this kind of forced operation position will reduce the area of the patient's body on the mattress and increase the local pressure of the focus point, so it will increase the probability of intraoperative pressure sores.

(6) Patient factors: the patient's body shape, age, past medical history, and nutritional status will affect the occurrence of pressure ulcer. When the patient's body is too fat or too thin, it will increase the incidence of pressure sores [28]. Because the patient's weight is directly proportional to the degree of local tissue pressure, when lying in bed, the greater the weight, the greater the pressure on the local skin, the
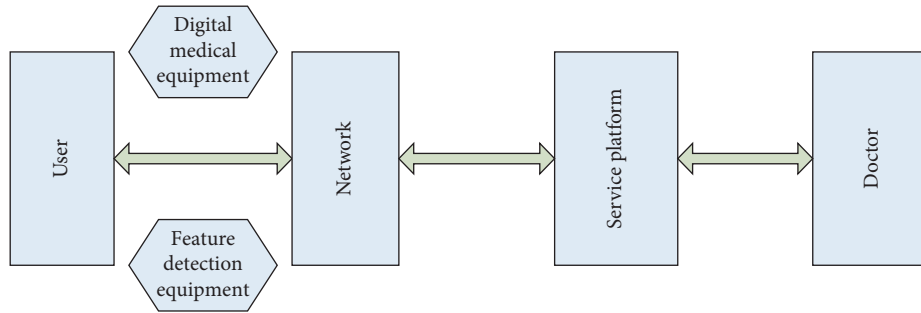
FIGURE 1: Internet of Things healthcare.

more prone to pressure ulcers. When the patient's body shape is too thin, because of skin relaxation, subcutaneous lack of fat tissue on the pressure buffer, and lying in bed, subcutaneous tissue blood vessels are squeezed, and tissue blood circulation perfusion is poor so that the skin pressure tolerance is decreased, leading to the occurrence of pressure ulcers.

In the process of pressure ulcer healing, the most important thing is to prevent infection, which directly affects the degree and time of wound healing. Infection means that bacteria, viruses, fungi, and other microorganisms invade the human body or propagate in a large number in the body, showing local swelling, heat and pain, inflammatory exudate or pus, or accompanied by chills, high fever, and other systemic inflammatory reactions. The wound is red and swollen, and the patient has obvious pain [29]. A large number of leukocytes are found in the local exudate to phagocytize and remove foreign bodies. The exudate fibrin gradually solidified to form a protective barrier, which could prevent the invasion of bacterial toxins. The self-protection function of the body can control the infection to a certain extent. In clinic, anti-infective drugs can be given intravenously, and local dressing change can be used to relieve the symptoms of high fever and pain.

As long as we pay attention to and take corresponding protective measures, most pressure sores can be prevented. The measures commonly used to prevent pressure sore in clinic include turning over regularly, keeping the bed clean and dry, increasing the intake of nutrition for patients, using air cushion bed, and sticking pressure sore patch (including silver antibacterial dressing, hydrocolloid dressing, alginate dressing, etc.) at the place prone to pressure ulcer [30]. There are special preventive measures for pressure ulcer during operation. Due to the difference of various operations (operation time, operation method, operation position, etc.), there is no prospective study to prove which intervention measures can effectively avoid intraoperative skin damage and prevent pressure ulcer.

Pressure ulcer is an important standard to evaluate the quality of nursing in the clinical work. It is very important to prevent the occurrence of pressure ulcer. As long as we pay more attention to it and carry out effective prevention, the probability of pressure ulcer can be greatly reduced. Therefore, it is particularly important to take feasible and effective preventive measures [31].

When the patient's body is too fat or too thin, it will increase the risk of pressure sores. Because the patient's weight is directly proportional to the degree of local tissue pressure, when the patient's body is too fat, the greater the weight, the greater the pressure on the local skin, and the more prone to pressure ulcers. When the patient's body shape is too thin, because of skin relaxation, subcutaneous lack of fat tissue on the pressure buffer, and lying in bed, subcutaneous tissue blood vessels are squeezed, and tissue blood circulation perfusion is poor so that the skin pressure tolerance is decreased, leading to the occurrence of pressure ulcers. The older the patient is, the more likely it is to develop pressure ulcer. Due to the lower sensitivity and vitality of motor and nerve, slow sensory function, decline of protective reflex, poor peripheral circulation, dry and loose skin, obvious atrophy, and thinning of the subcutaneous tissue, elderly patients are more likely to suffer from ischemia and hypoxia after local skin and subcutaneous tissue compression, leading to pressure ulcers [32].

Intraoperative application of glucocorticoids and vasoactive drugs will affect the occurrence of pressure ulcers; the use of active drugs will make blood vessels dilate, blood flow slow, and tissue and organs lose normal blood circulation, resulting in ischemia and hypoxia of surrounding tissues, which is easy to lead to pressure ulcers; the use of anesthetic drugs during operation will make skeletal muscle relaxation, loss of consciousness, weakening of muscle tension, and temporary loss of protective response to physical discomfort, leading to the occurrence of pressure ulcers [33].

Due to the lack of knowledge of pressure ulcer prevention and treatment in elderly patients with chronic diseases, the wound surface was deep when they were admitted to hospital, accompanied with different degrees of infection, obvious pain, and long treatment time. In this case, the local dressing change is suitable. The clinical inpatients agreed with the local dressing change prescription.

2.3. Foam Dressing. Foam dressing can improve the number of leukocytes in patients with deep pressure sores, which is consistent with other studies. The hydrocolloid components in foam dressing can promote autolysis, limit inflammation, induce hypoxic tension, and stimulate the release of macrophages and interleukin. Research shows that the use of foam dressing in the incision of tracheotomy in stroke patients can change dressing frequency, reduce frequency of wound dressing, and effectively reduce the infection rate.

Foam dressing has antibacterial effects. It can effectively kill *Staphylococcus aureus* and *Escherichia coli*, improve the level of inflammatory cells, promote the mediating response of wound inflammatory response, and promote healing. This study shows that there is no difference in the effect of dressing change on white blood cells of cancer patients, which may be due to the short intervention time of the two methods, and the wound surface of deep pressure ulcer is not fully healed within 4 weeks, and the bacteriostatic effect is not effectively expressed [34].

In the process of dressing change, the necrotic tissue needs to be removed timely after the wound infection is controlled; otherwise, the growth of the new granulation tissue will be affected. Wound healing is the stage of granulation proliferation and epithelial creeping [35]. At this time, local blood circulation is accelerated, tissue metabolism is vigorous, nutrient transport is accelerated, cytokine activity is enhanced, and a large number of fibroblasts proliferate, which makes the capillary network form rapidly and accelerate the wound healing.

Different support tools can be selected according to different parts of pressure ulcer. Sacrococcygeal pressure sore can guide patients to make hollow thick sponge pad under the body, knee pressure sore with soft pillow between the two legs, ankle pressure sore can be made of rubber gloves to pad under the foot, and so on. These measures can effectively prevent the wound from deteriorating. Medical staff should make reasonable plan according to the stage of pressure ulcer, wound condition, and objective data of nursing evaluation.

In addition to taking auxiliary measures, pressure, an important factor in the formation of pressure ulcers, should be paid enough attention. The mechanism of pressure ulcer is that when the external pressure is greater than the capillary pressure, the inner diameter of capillary and lymphatic lumen is reduced, the blood flow is blocked, oxygen-carrying red blood cells pass through the barrier, nutrients cannot be supplied, and the accumulation of metabolites delays the wound healing. The most effective measure to relieve local pressure is to turn over frequently. Nursing staff should attach great importance to the factors of potential pressure ulcers. Patients should use high-standard reactive (constant low pressure) or active (pressure alternating) support surface whether in bed or in a wheelchair for a long time, so as to prevent the progression and deterioration of the pressure ulcer wound [36]. The choice of the supporting surface is different according to the position, stage, quantity, and potential risk of pressure ulcer. The pressure sore wound should be suspended and cannot continue to be stressed. Patients and their families should be instructed to place the patient's position reasonably and turn over frequently. The frequency should be adjusted according to the patient's feeling and the characteristics of the support surface selected [37].

3. Internet of Things Medical Foam Dressing to Prevent the Pressure Ulcer Test

3.1. Purpose of the Experiment. Based on the theoretical results of preventive medicine and drawing lessons from the research results of big data integration theory at home and abroad, this paper carries out a deep analysis of the causes of pressure ulcers and the differences between different prevention methods for patients by using the methods of literature review, comparative study, mathematical statistics, and logical analysis.

3.2. Experimental Evaluation Criteria. Entropy method is a relatively objective evaluation index weight assignment method, which can effectively avoid the subjectivity of artificial scoring and has high accuracy. But, at the same time, this study also realized that the entropy method cannot directly reflect the knowledge, opinions, and experience judgment of experts and scholars, and the weight results may be contrary to the actual situation. Therefore, this paper uses AHP and entropy method to determine the weight coefficient of the regional higher education evaluation index.

3.3. Data Sources. The data in this paper are mainly from the First People's Hospital of a city. We conducted a survey on patients of different ages in the hospital and collected relevant data through case and doctor interviews.

3.4. Pressure Ulcer Prevention Model Method. The patients were parameterized to prevent pressure ulcers and then transmitted to the data model. The data module receives the needs of users, finds the appropriate resources through resource evaluation, performs tasks, and completes user requests.

The data module receives the request from the user and transmits it to the general server in the local area network [38]. Monitoring devices track the resource utilization and availability of sensors, applications, and services, generate statistical logs, and transmit data to the server. The server receives the user's request from the mobile terminal, analyzes the user's request information according to the monitored resource information, divides the service into several tasks, and processes the calculation. According to the evaluation results, each task selects the best matching resource from the resource pool, schedules and allocates resources, and provides the optimal prevention method for patients [39].

Considering the resources with the same service function, the attributes of the resources are set according to the user preferences, which have certain scalability. The calculation formula is as follows:

$$U_a = p * b \frac{j}{i} * c. \tag{7}$$

In order to calculate the weight of patient attributes and ensure the objectivity of evaluation results, we use the entropy weight method to determine the entropy value and entropy weight of each resource attribute:

$$t = \frac{1}{\ln x} \sum_{n=1}^{1} f_{nm} * \ln f_{nm}, \tag{8}$$

$$r = \frac{1 - t}{y - \sum_{m=1}^{m} t}. \tag{9}$$

Among them,

$$f_{mn} = \frac{z_{nm}}{\sum_{n=1}^{x} z_{nm}}, \tag{10}$$

$$\sum_{m=1}^{x} w_m = 1. \tag{11}$$

Based on the attribute value of the user request resource, each resource is regarded as a point in the multidimensional space, and the Euclidean distance is used to measure the proximity between the resource and user demand due to the user's preference for a certain attribute or each attribute of the resource has different influence on the measurement result. Therefore, the objective weight of each user is set to

$$d = \sqrt{\sum_{m=1}^{x} w_n * (r_{nm} - uq_m)^2}, \tag{12}$$

$$d_n = \frac{1}{1 + d(r_n, uq)}. \tag{13}$$

The similarity between the available resources and the resources requested by the user is obtained, and the threshold value is set in the range of [0, 1]. Thus, the matching value Q can be obtained:

$$Q_\delta = \left\{ r_n \mid d\cos(r_n, uq) \middle| \geq \delta \right\}. \tag{14}$$

The similarity between the resources in the matching resource set Q and the resources requested by users is calculated:

$$\cos m(r, uq) = \alpha * \cos(r, uq) + (1 - \alpha) * \frac{1}{m} \sum_{n=1}^{m} \delta_{ij}, \tag{15}$$

where a is the weight and the range is between [0, 1]. The simulation parameters are calculated as follows:

$$F = \frac{\sum (q_{rp,rpn} - q_{rpm})(q_{uq,uqn} - q_{uq})}{\sum_{n=1}^{n} (q_r - q_{uq})^2 \sqrt{\sum (q_{uq,uqm} - q_{uq})^2}}. \tag{16}$$

4. Experimental Analysis of Foam Dressing to Prevent Pressure Sore

4.1. Distribution of Patients with Pressure Ulcer.
We made statistics on 100 male patients with pressure ulcers and classified them according to their gender and age. The specific statistics are shown in Table 1, as shown in Figures 2 and 3.

From the chart, we can see that there are obvious differences between pressure ulcer patients. Among the investigated population, only 18% of the people under 40 years of age have pressure ulcer, and those over 40 years have pressure ulcer much higher than those under the age of 40. In particular, the proportion of pressure ulcer in people over 60 years old accounts for more than 50%, which shows that the elderly group is affected by pressure ulcer and the impact is the most serious.

4.2. Causes of Pressure Ulcer.
For the reason of pressure ulcer, there is no public opinion at present; we, through the investigation of patients, determine the body parameters of patients with pressure ulcers and the abnormal place of ordinary people, in order to find the reasons for pressure ulcers. The details are shown in Table 2 and Figures 4 and 5.

From the chart, we can see that, before and after the emergence of pressure ulcers, the patient's body temperature, operation time, and operation cardiopulmonary bypass time have varying degrees of change. Among them, patients with pressure ulcers, their nasopharyngeal temperature and lower body temperature are different from the normal temperature; a low-temperature environment may lead to the emergence of pressure ulcers; in addition, after the operation time is more than 3 hours, the frequency of pressure ulcers is much higher than that of less than 3 hours of operation time, and the external circulation time is also the same. We can infer the relationship between bedsores and the patient's body temperature and operation time.

4.3. Preventive Effect of Foam Dressing on Pressure Sore.
We selected 100 men and 100 women in the most prone to pressure sores (over 60 years old). A control experiment was carried out. 100 of them used traditional treatment techniques instead of foam dressing. 100 patients were treated with foam dressing to control pressure ulcers. Specific data are shown in Table 3 and Figures 6 and 7.

According to the chart, we can see that, in the experimental group and the control group, there were 15 pressure sores in 100 cases of the experimental group, while only 7 of the control group had pressure sores. It is obvious that foam dressing can play a key role in the prevention of pressure sore.

4.4. Medical Role of Internet of Things.
Through the above experiments, we can test that foam dressing can play a role in the prevention of pressure sore. In order to improve the relative preventive effect, we compare the manual foam

TABLE 1: Distribution of patients.

	0–20	21–40	41–60	Over 61
Male	5	12	24	59
Female	3	16	31	50
Mild pressure sore	7	21	18	33
Severe pressure sore	1	7	37	76
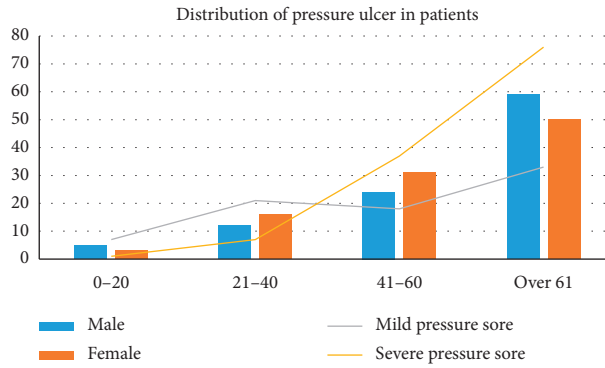
FIGURE 2: Distribution of pressure ulcer in patients.
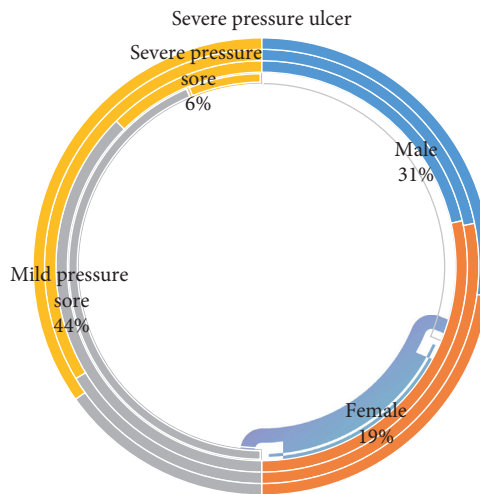
FIGURE 3: Severe pressure ulcer.

TABLE 2: Distribution of patients.

	Nasopharynx temperature	Lower body temperature	Operation time	Cardiopulmonary bypass time
Male patients	34.21	35.32	4.25	3.59
Female patients	35.33	36.42	4.21	3.69
Normal men	37.35	37.33	3.58	2.34
Ordinary women	37.15	37.52	3.32	2.45

dressing with the Internet of Things medical equipment. The specific data are shown in Table 4 and Figure 8.

From the chart, we can see that foam dressing can reduce the occurrence of pressure sores and reduce the probability of pressure ulcers by about 30%. Compared with the unused pressure sore, the use of IoT can increase the efficiency of foam dressings and reduce the probability of pressure sore by about 7%. This shows that the auxiliary foam dressing of medical devices in the logistics network can play an important role in preventing pressure sore.
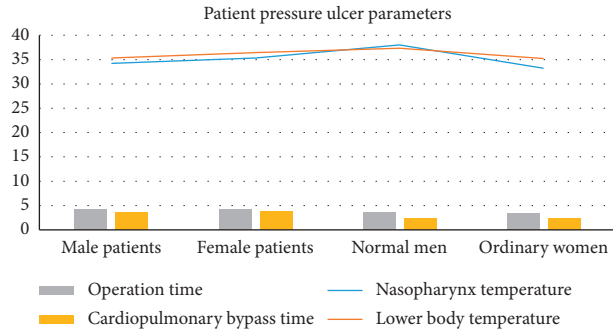
FIGURE 4: Patient pressure ulcer parameters.
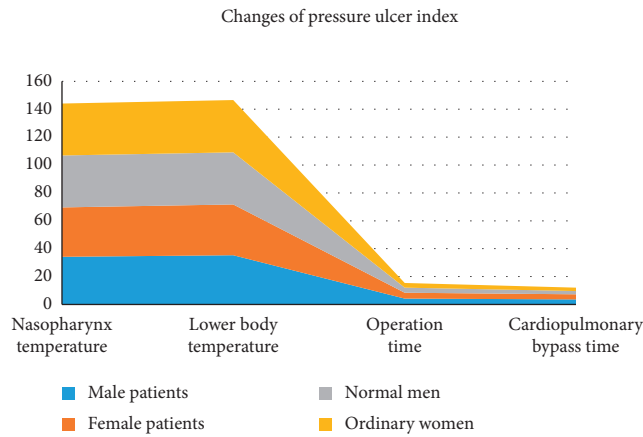
FIGURE 5: Changes of the pressure ulcer index.

TABLE 3: Distribution of patients.

	Number of people over temperature	Long operation time	Number of inflamed patients	Turnover care	Number of pressure ulcers
Experience group	37	43	32	50	15
Control group	39	52	21	50	7
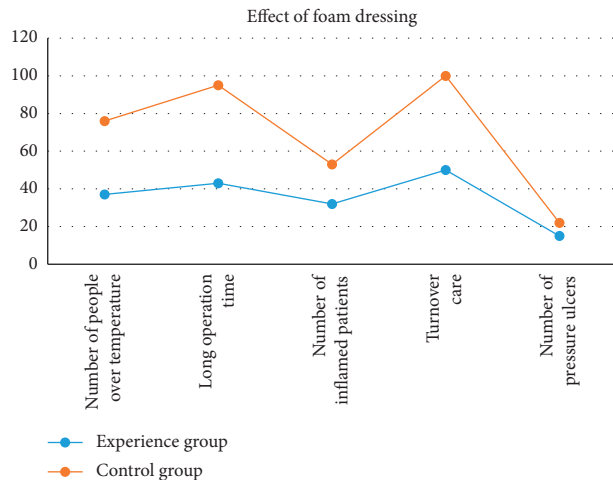
FIGURE 6: Preventive effect of foam dressing on pressure sore.
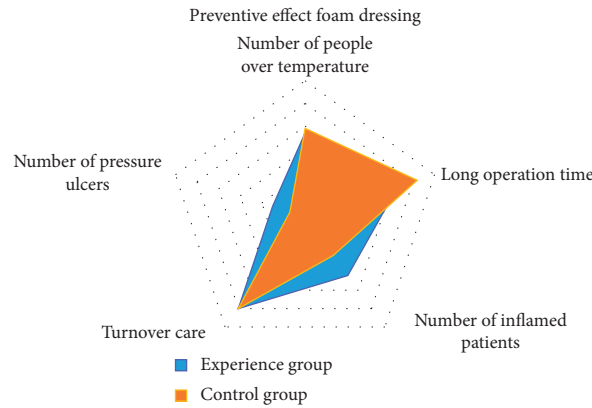
FIGURE 7: Preventive effect of foam dressing.

TABLE 4: Distribution of patients.

	Primary pressure ulcer	Secondary pressure ulcer	Stage-III pressure ulcer	Stage-IV pressure ulcer
Labor group	6	4	5	3
Internet of Things group	3	1	2	1
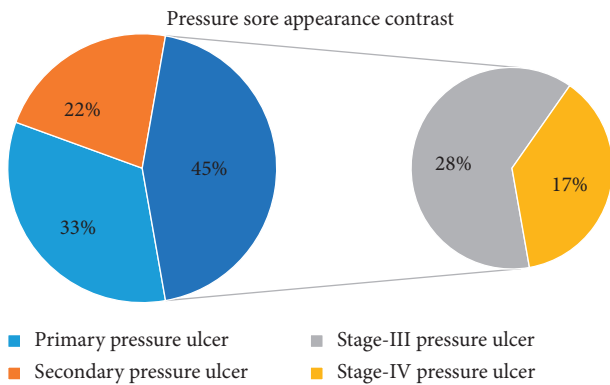
FIGURE 8: Pressure sore appearance contrast.

5. Conclusions

Foam dressings are mainly made of polyvinyl alcohol foam and polyurethane. They are soft, elastic, and have strong absorbency. The main component of foam dressing is soft silicone adhesive, which is made of water, oil, and silicon. Skin contact without irritation, soft, with a certain thickness, can reduce the discomfort and pain caused by local compression. It can buffer the local pressure. The new dressing has the function of air permeability and waterproof, which can reduce the symptoms of skin immersion and local hyperemia and play a good barrier role. The high absorptive capacity and decompression ability of clinical foam dressings have achieved good results in clinical application.

The occurrence of pressure ulcers aggravates the physiological and psychological pain of patients, causes huge economic losses, and increases the workload of nurses, which leads to some medical disputes and takes up a large number of public health resources. The prevention of pressure ulcer is one of the important problems to be solved urgently in the clinical nursing work and is a very important reference index to evaluate the quality of nursing.

Deep pressure ulcer has become one of the serious complications that perplex patients and medical staff. It not only affects the recovery of primary disease but also brings a series of more difficult serious complications. The pain torture makes the patients miserable, and the infection secondary to the wound seriously affects the health and quality of life of patients and even threatens their lives. There are many risk factors and causes of pressure ulcer, and the mechanism is relatively complex. The treatment and nursing of pressure ulcer need multidisciplinary comprehensive treatment. The current clinical treatment methods for wound dressing have a wide variety of drugs and their curative effects are also uneven as the main clinical treatment, a wide variety of drugs, curative effect is also uneven. How to choose an economical, appropriate, safe, and effective method of dressing change for patients is worthy of further study in the clinical nursing work.

Data Availability

The data underlying the results presented in the study are available within this paper.

Conflicts of Interest

The authors declare that they have no conflicts of interest.

References

[1] C. Yang and Z. Lv, "Gender based face aging with cycle-consistent adversarial networks," *Image and Vision Computing*, vol. 100, Article ID 103945, 2020.

[2] L. Lin, "Application of foam dressing in prevention of facial pressure sores in patients with noninvasive mechanical

ventilation," *World's Latest Medical Information Digest*, vol. 1, no. 66, pp. 130-131, 2015.

[3] K. G. Srinivasa, B. J. Sowmya, A. Shikhar, R. Utkarsha, and A. Singh, "Data analytics assisted internet of things towards building intelligent healthcare monitoring systems: iot for healthcare," *Journal of Organizational and End User Computing*, vol. 30, no. 4, pp. 83–103, 2018.

[4] Y. Sun, H. Song, A. J. Jara, and R. Bie, "Internet of things and big data analytics for smart and connected communities," *IEEE Access*, vol. 4, pp. 766–773, 2016.

[5] M. Elhoseny, G.-B. Bian, S. K. Lakshmanaprabu, K. Shankar, A. K. Singh, and W. Wu, "Effective features to classify ovarian cancer data in internet of medical things," *Computer Networks*, vol. 159, pp. 147–156, 2019.

[6] X. Ma, C. Jiang, and Y. Yang, "Application of non adhesive ankle foam dressing to prevent nasal facial pressure sores in patients undergoing noninvasive mechanical ventilation," *Chinese Journal of Pulmonary Diseases (Electronic Version)*, vol. 8, no. 4, pp. 106-107, 2015.

[7] W. Xiangfeng, "The effect of Wu Xiangfeng foam dressing in preventing pressure ulcers caused by respirator mask," *Integrated Traditional Chinese and Western Medicine Nursing (English, Chinese)*, vol. 1, no. 3, pp. 87–89, 2015.

[8] R. Chen, Y. Wang, Y. Qi et al., "Effect of foam dressing on prevention of nasal facial pressure ulcers in patients with ICU noninvasive mechanical ventilation," *Journal of Practical Medicine*, vol. 32, no. 7, pp. 1180–1182, 2016.

[9] L. Shi, H. Zhang, J. Zhang et al., "Using soft silicone foam dressing to prevent pressure ulcer in critically ill patients after trauma. randomized controlled clinical trial," *China Health Nutrition*, vol. 26, no. 27, pp. 50-51, 2016.

[10] M. Wang, "Application of foam dressing in prevention of pressure ulcer in critically ill patients in department of cardiology," *Diet Health Care*, vol. 6, no. 44, pp. 150–155, 2019.

[11] M. Abdel-Basset, M. Elhoseny, A. Gamal, and F. Smarandache, "A novel model for evaluation hospital medical care systems based on plithogenic sets," *Artificial Intelligence in Medicine*, vol. 100. , 2019 in press.

[12] C. Zhong, J. Liu, Q. Lai et al., "Application of foam dressing in preventing nasal pressure sores in patients with noninvasive ventilation assisted by department of respiration," *China Contemporary Medicine*, vol. 26, no. 5, pp. 212–214, 2019.

[13] W. Elsayed, M. Elhoseny, S. Sabbeh, and A. Riad, "Self-maintenance model for wireless sensor networks," *Computers & Electrical Engineering*, vol. 70, pp. 799–812, 2018.

[14] Y. Wang, "Application of foam dressing in prevention of pressure ulcers caused by respirator mask," *Healthy People (Mid Version)*, vol. 11, no. 5, pp. 16–18, 2017.

[15] S. Fang, Y. Gao, Y. Liu et al., "Effect of variable temperature blanket combined with foam dressing on prevention of pressure ulcers during cardiopulmonary bypass," *Qilu Nursing Journal*, vol. 22, no. 8, pp. 94-95, 2016.

[16] M. Elhoseny and K. Shankar, "Reliable data transmission model for mobile ad hoc network using signcryption technique," *IEEE Transactions on Reliability*, vol. 69, no. 3, p. 1077. in press, 2020.

[17] L. Jing, "Application of soft silicone foam absorption dressings in prevention of scalp pressure ulcer in patients with severe craniocerebral injury," *Nursing Care in English and Chinese Medicine*, vol. 1, no. 4, pp. 65–67, 2015.

[18] C. Li, H. J. Yang, F. Sun, J. M. Cioffi, and L. Yang, "Adaptive overhearing in two-way multi-antenna relay channels," *IEEE Signal Processing Letters*, vol. 23, no. 1, pp. 117–120, 2016.

[19] X. Zhang, Y. Xiao, and J. Wu, "Kang whale foam dressing to prevent pressure sores in posterior spinal surgery," *Nursing Practice and Research*, vol. 13, no. 2, pp. 106-107, 2016.

[20] H. Chen and X. Zhao, "Effect of foam dressing on prevention of pressure ulcers at the needle handle of infant indwelling needle," *Heilongjiang Medicine*, vol. 1, no. 6, pp. 1242–1244, 2016.

[21] Z. Lv, "Security of internet of things edge devices," *Software: Practice Experience*, pp. 1–11, 2020.

[22] Y. Zhang, L. Sun, H. Song, and X. Cao, "Ubiquitous WSN for healthcare: recent advances and future prospects," *IEEE Internet of Things Journal*, vol. 1, no. 4, pp. 311–318, 2014.

[23] L. Li, L. Fang, M. X. Rong et al., "Clinical application of foam dressing in preventing high risk parts of pressure ulcers in surgical patients," *Clinical Study of Chinese Medicine*, vol. 1, no. 21, pp. 124–126, 2017.

[24] H.. Han, "Application of foam dressing in prevention of pressure ulcer in prone position of department of orthopedics," *China Health Nutrition*, vol. 25, no. 11, pp. 66–68, 2015.

[25] F. Xiao, "Multi-sensor data fusion based on the belief divergence measure of evidences and the belief entropy," *Information Fusion*, vol. 46, pp. 23–32, 2019.

[26] Y. Cao, "Application of foam dressing in prevention of high risk pressure sores in patients with cliquid," *Journal of Liaoning Medical University*, vol. 5, no. 1, pp. 166–168, 2015.

[27] Q. Zhang, H. Xiao, and G. Huang, "Application of foam dressing in treatment of pressure sores in primary hospitals," *Nursing Practice and Research*, vol. 23, no. 7, pp. 143-144, 2015.

[28] K. Wang Ping, "Whale foam dressing for prevention of pressure sore in long term bedridden patients with stroke," *Modern Medical and Health*, vol. 31, no. z2, pp. 75-76, 2015.

[29] Y. Zhao, L. Cai, and J. Shen, "Effect of observation window on foam dressing for prevention and treatment of pressure sore," *Zhejiang Clinical Medicine*, vol. 1, no. 20, pp. 171-172, 2018.

[30] L. Li, L. Fang, M. X. Rong et al., "Clinical application of foam dressing in preventing high risk parts of pressure ulcers in surgical patients," *Clinical Study of Chinese Medicine*, vol. 3, no. 17, pp. 153-154, 2017.

[31] L. Li, H. Huang, Y. Lin et al., "Clinical application of foam dressing to prevent inevitable pressure sores," *China School of Medicine*, vol. 29, no. 4, pp. 305-306, 2015.

[32] Q. Nie, "Effects of foam dressing in prevention of pressure sores in critical ill patients after orthopaedic surgery," *Nursing Care of 2017 Patients with Chinese Medicine Combined with Western Medicine (Chinese and English)*, vol. 3, no. 4, pp. 36-37, 2017.

[33] C. Qiao, "Clinical application of foam dressing in the prevention of high risk pressure sores," *Medicine Frontiers*, vol. 1, no. 3, pp. 282-283, 2016.

[34] R. Fei, Y. Xu, G. Liu et al., "Comparative study of foam dressing and "R" turning mat in the prevention of pressure ulcer in the sacrococcygeal region," *Anhui Medicine*, vol. 21, no. 9, pp. 1736–1738, 2017.

[35] S. Ouyang, L. Chen, C. Lu et al., "Study on the prevention of pressure sore by foam dressing combined with padded warm air blanket in low body weight infants undergoing cardiopulmonary bypass," *Evidence Based Medicine*, vol. 20, no. 1, pp. 61–64, 2020.

[36] T. Luo, "Nursing effect analysis of 30 degree turning over method combined with foam dressing to prevent pressure sore," *Electronic Journal of Clinical Medicine Literature*, vol. 6, no. 42, pp. 134–136, 2019.

[37] G. Liu, X. Zhang, L. He et al., "The effect of decompression mattress and foam dressing on preventing bedsore after chest tumor operation," *Nursing Care in Integrated Traditional Chinese and Western Medicine (English, Chinese)*, vol. 5, no. 11, pp. 70-71, 2019.

[38] X. Li, "Application of hydrocolloid dressing combined with foam dressing in the prevention of pressure ulcers in elderly patients," *Famous Doctor*, vol. 1, no. 12, p. 238, 2019.

[39] H. Lu, D. Yao, and Y. Wang, "Soft silicone foam dressing for prevention of pressure ulcers in critically ill patients after trauma," *Dermatology and Venereal Diseases*, vol. 41, no. 4, pp. 153-154, 2019.

Research Article

From the Perspective of Jurisprudence View the Application of Urban Image Monitoring Technology and the Application and Improvement of the Information Collection System in This Field

Zheming An [1] **and Zhiyong Jiang** [2]

¹Law School, Zhejiang University, Hangzhou 310000, Zhejiang, China
²Practical Teaching Department, Guilin University of Aerospace Technology, Guilin 541004, Guangxi, China

Correspondence should be addressed to Zheming An; 11502001@zju.edu.cn

As times go by, social management faces new challenges. This article examines the application of urban image surveillance technology and the methods of information collection and processing from a legal perspective, and explains the necessity of creating image surveillance. This article introduces the application of the system to the construction of legal systems in countries where urban image surveillance has been applied earlier and with more advanced legal systems at home and abroad, from the construction of the image surveillance legal system, the protection of personal privacy rights, and the protection of communication data. Explain the legislative principles to be followed in the legislative process, and put forward the principles of human rights and freedom, the principle of public interest, the principle of rule of law, and the principle of information security. Finally, I put forward a point of view on how to formulate a legal and fair legal system. It is clear that in the field of legislation, it is necessary to seek constitutional support, use civil law to regulate, use personal information protection law to regulate, and use urban image monitoring system legislation to manage. This paper proposes a "peer-to-peer tree" architecture of a two-tier distributed indexing service system based on service types. Its joining and leaving algorithms create and maintain the framework, cascading organizations related to service interests into a tree structure. Learning the neighbor search algorithm can slowly evolve the peer layer composed of many cascaded trees into an overlay network with small-world characteristics, thereby ensuring a higher search efficiency. Research shows that through functional testing and performance testing, it is found that when the number of supernodes is 200, the success rate is the highest.

1. Introduction

In recent years, in response to new problems created by the information society, our country's State Council has put on the agenda to speed up national legislation on information. Certain laws on the protection of citizens' privacy have been adopted accordingly [1]. Similarly, some local laws and regulations in our country have also initiated attempts to regulate the use of security systems such as image surveillance. For example, Beijing, Guangzhou, Shenzhen, and Chongqing have already issued or are drafting public security video system construction management [2].

In recent years, large cities in China have generally promoted the construction of urban image monitoring systems and more and more students have been researching them [3]. For example, Schwartz used histograms to match pedestrians on the camera network. This method is suitable for video overlay information [4]. Hariyanto et al. further strengthened the method of histogram comparison. They applied the *K*-means clustering method to reduce the influence of histogram information on the light intensity, making this method resistant to external objective conditions strength enhancement [5, 6]. Through the design and research of the safe city high-definition image monitoring integrated management platform, transmission network, and high-definition image monitoring product technology, Hermas focuses on the design of high-definition image monitoring for urban public safety with the background of

the smart city security video resource sharing system in Jing'an District System [7].

In the research of domestic scholars in urban image monitoring technology, Jiao et al. analyzed the classic sequence image moving target detection method for the image enhancement problem of the region of interest in the monitoring image, combined it with the image enhancement algorithm [8], and proposed a technique based on the image enhancement method, and only the suspicious target area in the image is enhanced, which reduces the amount of calculation of the enhancement algorithm, while ensuring the enhancement effect of the suspicious target [9]. Aiming at the problem of low-contrast color image enhancement, Zhai et al. introduced the basic principles of the Retinex image enhancement algorithm and the classification of existing methods, focusing on the application fields and shortcomings of the multiscale Retinex image enhancement algorithm, and proposed on this basis. An adaptive scale MSR enhancement algorithm, which performs enhancement processing in the HSI space of the image, uses the variance value of the brightness component to adaptively determine the filter size, which can reduce the amount of calculation, highlight image details, and maintain image color stability [10, 11]. Zhou and Qiu proposed the equalization of partially overlapping histograms, expanding the number of effective pixels for each partial histogram equalization operation from one to multiple, thereby reducing the number of local operations while maintaining a strong restored image local information capability, but for the pursuit of fast calculations, this algorithm is prone to blocky effects. In order to eliminate the blocking effect, the image needs to be interpolated, which affects the efficiency of the algorithm [12].

In the field of legislation, this article should seek constitutional support, clearly defined by civil law, use a law to protect personal information for regulation, and use the law of the civil image monitoring system for management. For the management specifications, specify the issue of the installation and the scope of the installation, manage the monitoring system, and standardise the information used to improve the system [13] and create a mutually independent and limited system work, improving the professionalisation of managers and creating an effective internal supervisory mechanism.

2. From the Perspective of Jurisprudence, Research on the Application of Urban Image Surveillance Technology

2.1. Functions of Urban Image Monitoring System

2.1.1. Necessity

(1) *Maintain Urban Public Safety.* Under the condition of today's diverse society, there are a large number of traditional and nontraditional factors affecting public security. Terrorist attacks, civil crimes, emergency situations, and other factors affecting or likely to affect civil security are also increasing. Since the beginning of this year, many cases have occurred at national level [14, 15]. In the face of many factors affecting public safety, the traditional means of mutual

assistance, community exclusion, and mass reporting have found that the control methods have been far from meeting the needs of maintaining urban safety. However, the urban image monitoring system has become an important means to detect various unsafe factors in time, deal with them in a timely and effective manner, and lock criminal suspects due to its advantages such as wide monitoring range and strong timeliness.

(2) *Promote the Construction of a Legal Society.* In the process of legalization in our country, our country has put forward higher requirements for the law enforcement of investigative agencies. The collection and verification of evidence and the formation of the evidence chain require more evidence [16]. However, due to its intuitive and personalized elements, image surveillance has become a powerful means of data collection. The establishment of a complete public security image monitoring system can actively promote the scientific and standardized investigation mechanism and can effectively promote modernization and simplify the pace of management.

(3) *Combating Illegal and Criminal Activities.* With the increasingly obvious characteristics of criminal activity, suddenness, and professionalism, it becomes more difficult to collect evidence on the spot. Due to the objective, continuous, and stable record of the monitoring system information, it not only provides strong support for combating current street crimes but also provides practical evidence and evidence for the detection of cases.

One is to provide strong technical support for combating street crimes. Electronic surveillance facilities are densely distributed in cities, scenic spots, station wharf squares, and other wealthy commercial areas where road traffic accidents occur [17], which upgrades traditional plane prevention and control to modern three-dimensional surveillance and connects with grid police. To achieve effective man-machine integration, the ability to detect and combat crimes is improved greatly [18, 19]. The second is to provide strong evidence to effectively combat crime. With the rapid development of the economy and society, the flow of people's property is increasing. The mobility, suddenness, and violence of criminal activities have become more and more obvious. Criminal methods vary, and there are fewer and fewer traces on the scene. The criminal quickly committed a crime and escaped. The time for effective disposal is limited. Since the surveillance image system can be objective, continuous, and stable, the recorded information may contain traces of criminal activities and has a unique role, which cannot be replaced by other means in investigation and case resolution services.

2.1.2. Effectiveness. The effectiveness of the urban image monitoring system has been remarkably reflected in many aspects and has been recognized by all parties.

(1) *Its Role in Fighting Crime.* According to statistics from China's Ministry of Public Security, three quarters of China's 200,000 key and critical units have installed different levels of security and technical protection facilities, using security systems and alarm service networks to crack more

than 30,000 public security and criminal cases [20]. Recovered a lot of economic losses and played an important role in maintaining social stability [21, 22].

(2) *The Role of Urban Management.* The creation of real-time monitoring points significantly improves the management and control capabilities of motorways and effectively offsets weaknesses in road traffic management, such as long lines, low police force, rapid circulation, and difficulty in gathering evidence. At the same time, by installing voice transmission and amplification devices at specific monitoring points, significant results have been achieved [23]. In addition, the image monitoring system is widely used in the law enforcement process of urban management, health, and other administrative departments. The whole process of recording law enforcement actions on the street has effectively reduced the occurrence of violent resistance to the law and provided clear facts for the handling of corresponding administrative violations.

2.2. Establishment of Urban Image Monitoring System

2.2.1. Security. The establishment of the legal system of urban image monitoring focuses on establishing a complete urban image monitoring system, so as to better protect national security and urban security through this system. The purpose of urban image monitoring construction is to ensure the safety of most people and improve social management capabilities, which is beyond doubt [24, 25]. The establishment of relevant legal systems can make the urban image monitoring system more perfect, improve its efficiency from the construction, use management and other aspects, and better play its safety protection effect. Through the application of video image monitoring technology, various insecurity factors such as terrorist attacks and violent crimes that endanger social security and urban security can be detected and eliminated in time. At the same time, the establishment of urban image monitoring system can effectively improve the sense of security of social citizens [26]. Most citizens will have a certain sense of security under the system-regulated camera probe, which also brings many benefits to improving the overall sense of security in society [25, 27].

2.2.2. Order. The urban image monitoring legal system is the embodiment of the important role of law enforcement in social public affairs. Through the establishment and improvement of the urban image monitoring system, it will effectively regulate citizens' behavioral norms in various public places and provide strong support for the establishment of the overall social order. An orderly social order is a necessary condition for social development and progress, and it is also an integral part of the needs of citizens' lives. Urban image surveillance implemented under a standardized system can effectively improve social management capabilities and help establish a standardized and orderly social order. The installation of monitoring equipment in public places may cause conflicts between the security interests of the monitor or the public interests of the society and the privacy interests of the monitored person [28, 29]. In general, video surveillance

in public places and other public areas can effectively establish social order, which is beneficial to the overall progress of society and the interests of the vast majority of people.

2.2.3. Freedom. The law is to protect civil liberties. From the perspective of the overall social environment, the establishment of the urban image monitoring system can effectively maintain social order and promote social progress. In fact, it protects the entire society or the freedom of the vast majority of people in the society. It may affect some aspects of freedom of certain personnel [30, 31]. However, judging from the tradeoffs between big freedom and small freedom, anyone can come to the correct answer. Fundamentally speaking, the establishment of the urban image monitoring system is to protect the greater freedom of social citizens and more reflects the direction of human freedom.

2.2.4. Privacy Protection. The establishment of the legal system of the urban image monitoring system is also of great practical significance for protecting the privacy of citizens. As a basic personality right, the right to privacy refers to a kind of personality right that citizens enjoy the tranquility of private life and that private information is protected in accordance with the law, and it is not illegally invaded, learned, collected, used, and disclosed by others [32, 33]. The right to establish the diversity of people and the enjoyment of the right to privacy is more conducive to the development of personal self. At the same time, it also ensures the relative stability of interpersonal relationships, the safety of personal, and property, and it is important for maintaining personal peace and security. Harmony with society plays an indispensable role. Respect for personal private life is a sign of political modernization. Similarly, there are related problems. In order to defend public interests, the appropriate transfer of individual rights and freedoms is the order of social survival. This is also due to the relativity of freedom and rights. This kind of transfer itself also needs a "degree." The "degree" is the legitimacy and controllability of the exercise of power.

2.3. CGSV Indexing Service System Architecture and Related Algorithms.
In order to be able to better count and predict the possibility of a certain service appearing in a certain organization within a period of time in the future, a service application type model was created based on the theory of information retrieval. This model evolved from the "topic model," one of the language models based on aggregation. It is described as follows.

The language model of a topic T has a list of words $\{w_1, w_2, \ldots, w_n\}$. When observed with unlimited data, the frequency of words used in the topic T is expressed as $\{p_1, p_2, \ldots, p_n\}$. Assuming a series of documents D about T, p_i can be evaluated as

$$p_i = \frac{f(D, w_i) + 0.01}{|D| + 0.01n}. \tag{1}$$

Here, $f(Q, w_i)$ is the number of occurrences of w_i in D, D represents the number of words contained in the document, and n is the number of words. Then, use Kullback–Leibler divergence to measure how well T's topic model predicts the request Q:

$$KL(Q, T) = \sum_{f(Q, w_i) \neq 0} \frac{f(Q, w_i)}{|Q|} \log \frac{f(Q, w_i)/|Q|}{p_i}. \qquad (2)$$

At this time, $f(Q, w_i)$ is the number of times w_i appears in Q and Q represents the number of words in Q. In information theory, KL divergence is a very important information measurement parameter. In many applications, it is widely used to measure how well one probability distribution predicts another possibility. It is an area value distributed in $[0, \infty]$, and the smaller the value, the better the model for this topic T predicts the request Q.

If organization O is regarded as topic T and each word is regarded as a service, then the list of service application types corresponds to the word list in the language model, and the frequency list of words in the topic corresponds to the frequency of service application types in the organization. Document D corresponds to a series of services requested by O [33, 34]. Then, it is deduced that D is the number of services, and n represents the number of service application types. Bring these corresponding items into equation (1), and you can get equation (4). When predicting request Q, because each request has only one service, it only belongs to one service application type, so $f(Q, w_i)$ is 1, Q. It is also 1. Incorporating equation (2), you can deduce

$$KL(Q, O) = KL(stid_Q, O) = \log(p_Q^{-1}). \qquad (3)$$

For specific situations, it is necessary to consider other influencing factors. It is not difficult to find that the higher the hit rate of a certain type of service, the more likely it is to exist in this organization. Therefore, the KL value is slight modified, and the mission rate (h_Q/q_Q) appears in the measurement value in inverse proportion.

2.4. Image Projection Algorithm

2.4.1. Cube Projection. Since the cube projection model is perpendicular to each other and regular polygons, in addition to facilitating the observation of the scene from all sections, it is also convenient to display the panorama. However, in order not to deform the image, it must be horizontal and in the vertical direction, and the shooting is taken at precise intervals of 90°, so it is not very practical.

2.4.2. Spherical Projection. The spherical projection model is to select a fixed point as the center of the sphere, then take two vertical lines as the axis, and shoot around it, and finally project multiple real images onto the sphere. The coordinate of pixel $p(x, y)$ in the camera coordinate system xyz is $(x - (W/2), y - (H/2), -f)$, and then its coordinate in the world coordinate system XYZ is (u, v, w):

$$\begin{bmatrix} u \\ v \\ w \end{bmatrix} = \begin{bmatrix} \cos\beta & 0 & \sin\beta \\ 0 & 1 & 0 \\ -\sin\beta & 1 & \cos\beta \end{bmatrix} \begin{bmatrix} 1 & 0 & 0 \\ 0 & \cos a & -\sin a \\ 0 & \sin a & \cos a \end{bmatrix} \begin{bmatrix} x - \dfrac{W}{2} \\ y - \dfrac{H}{2} \\ -f \end{bmatrix}. \qquad (4)$$

The linear parameter equation passing through point P is

$$\begin{cases} u' = tu, \\ v' = tv, \\ w' = tw. \end{cases} \qquad (5)$$

The spherical equation can be expressed as

$$u'^2 + v'^2 + w'^2 = f^2. \qquad (6)$$

Combining formulas (5) and (6) gives

$$t = \frac{f}{\sqrt{u^2 + v^2 + w^2}}. \qquad (7)$$

(u', v', w') represents the three-dimensional parameter coordinates of the spherical panoramic image. In order to facilitate storage, they are converted into two-dimensional image coordinates. Choose the following method to achieve this conversion. When $w' \geq 0$, let

$$x' = f \cdot \arccos\left(\frac{u}{\sqrt{u'^2 + v'^2}}\right),$$
$$y' = f \cdot \left(\frac{\pi}{2} + \text{arctg}\left(\frac{v'}{\sqrt{u'^2 + v'^2}}\right)\right). \qquad (8)$$

Otherwise, let y' remain unchanged, then

$$x' = f \cdot \left(2\pi - \arccos\left(\frac{u'}{\sqrt{u'^2 + v'^2}}\right)\right). \qquad (9)$$

From the above formulas:

$$\Delta = \left(y - \frac{H}{2}\right)\sin a \cos\beta - \left(x - \frac{W}{2}\right)\sin\beta - f\cos a \cos\beta. \qquad (10)$$

When $\Delta \geq 0$,

$$x' = f \cdot \arccos\left(\frac{(x - (W/2))\cos\beta + (y - (H/2))\sin a \sin\beta - f\cos a \sin\beta}{\sqrt{(x - (W/2))^2 + ((y - (H/2))\sin a - f\cos a)^2}}\right),$$

$$y' = f \cdot \left(\frac{\pi}{2} + \arccos\left(\frac{(y - (H/2))\cos a + f\sin a}{\sqrt{(x - (W/2))^2 + ((y - (H/2))\sin a - f\cos\beta)^2}}\right)\right). \tag{11}$$

When $\Delta < 0$,

$$x' = f \cdot \left(2\pi - \arccos\left(\frac{(x - (W/2))\cos\beta + (y - (H/2))\sin a \sin\beta - f\cos a \sin\beta}{\sqrt{(x - (W/2))^2 + ((y - (H/2))\sin a - f\cos a)^2}}\right)\right),$$

$$y' = f \cdot \left(\frac{\pi}{2}\right) + \arccos\left(\frac{(y - (H/2))\cos a + f\sin a}{\sqrt{(x - (W/2))^2 + ((y - (H/2))\sin a - f\cos a)^2}}\right). \tag{12}$$

2.4.3. Cylindrical Projection. Cylindrical projection means that the participant passes through a fixed observation point and keeps the distance between the camera and the shooting scene unchanged, and then it uses a translational shooting method to rotate 360° around the vertical line of the fixed point to collect scene images. Perform cylindrical projection transformation on the obtained image to obtain a sequence of spatial coordinates, and make the pixels have the consistency of the orientation information. The straight line equation between the origin of the camera coordinate system and the pixel point P can be expressed in the form of a parametric equation:

$$u = t\left(x - \frac{W}{2}\right), \tag{13}$$

$$v = t\left(y - \frac{H}{2}\right), \tag{14}$$

$$w = -tf, \tag{15}$$

where t is a parameter, and the equation for a cylindrical surface can be expressed as

$$u^2 + w^2 = f^2. \tag{16}$$

Combining formulas (13)–(16), we get

$$t = \frac{f}{\sqrt{(x - (W/2))^2 + f^2}}, \tag{17}$$

$$u = \frac{f(x - (W/2))}{\sqrt{(x - (W/2))^2 + f^2}}, \tag{18}$$

$$v = \frac{f(y - (H/2))}{\sqrt{(x - (W/2))^2 + f^2}}, \tag{19}$$

$$w = \frac{f^2}{\sqrt{(x - (W/2))^2 + f^2}}, \tag{20}$$

where (u, v, w) is the parameter coordinate of the projection point Q of the pixel point $p(x, y)$ on the cylinder, and a panoramic image is obtained by combining all such projection points. However, the parameter coordinates are three-dimensional, and they need to be converted into two-dimensional image coordinates to facilitate storage. Here, use the following formula to convert the three-dimensional parameter coordinates into two-dimensional image coordinates:

$$\begin{cases} x' = f \cdot arctg\left(\frac{u}{w}\right) + f\theta, \\ \\ y' = v + \frac{H}{2}, \end{cases} \tag{21}$$

where $\theta = (hfov/2) = arctg(W/2f)$ and $hfov$ are the horizontal viewing angles of the camera.

Combining formulas (17)–(21), we get

$$\begin{cases} x' = f \cdot arctg\dfrac{x - (W/2)}{f} + f \cdot arctg\left(\dfrac{W}{2f}\right), \\ \\ y' = \dfrac{f(y - (H/2))}{\sqrt{(x - (W/2))^2 + f^2}} + \dfrac{H}{2}. \end{cases} \tag{22}$$

Formula (22) is a projection formula for cylindrical orthographic projection of any pixel point $p(x, y)$ on the real image I to a pixel point $Q(x', y')$ on the cylindrical panoramic image. It can also be concluded from formula (22) that the projection algorithm has the property of preventing the scene from being deformed in the vertical direction. This property allows us to perform cylindrical projection transformation on each real image separately and obtain the corresponding panoramic image.

3. From the Perspective of Jurisprudence, Research on the Application of Urban Image Monitoring Technology

3.1. Feature Extraction of Target Samples. The network information mining system adopts a vector space model and uses feature terms $(T_1, T_1, \ldots, T_n)$ and their weights, and w_i represents target information. When information is matched, these feature items are used to evaluate unknown text and target samples. The selection of feature terms and their weights is called feature extraction of target samples, and the pros and cons of feature extraction algorithms will directly affect the performance of the system. The frequency distribution of terms in documents of different content is different, so feature extraction and weight evaluation can be performed according to the frequency characteristics of terms.

3.2. Parameters for Evaluating Search Performance. Three statistical parameters can be used to evaluate the search performance of the indexing system. The success rate represents the proportion of services that can be successfully found in each search, and it measures the effectiveness of the search; the hit rate represents the ratio of the service found to the total number of services in the network during each search, and it measures the completeness of the search. The degree of message distribution represents the average number of service request messages generated by each query and describes the average network load of the query.

The higher the success rate and the success rate, the lower the message rate and the better the search performance. Of course, the success rate must be high, because this is the basis for ensuring that services can be consulted. The success rate can be high and you do not have to ask a question for all the services that meet the requirements each time. The degree of coverage naturally meets the first two conditions, the smaller the better.

3.3. Performance Test. The service discovery mechanism plays a decisive role in the system performance of the SOA architecture. A good service discovery mechanism can quickly and effectively locate the required service and then expand the subsequent data request and acquisition. And with the increase of services and requests, it will not bring about problems such as unreachable services or network congestion. Therefore, it is very meaningful to test the performance of CGSV indexing service. However, performance testing requires a large number of services and a large number of requests. There is still a lack of such test conditions, so the simulation platform is used for testing first. When CGSV has more services and users, and richer historical data, the system can be tested. This article has carried out research on target tracking, registration, and reconstruction of low-resolution image sequences, and blind image restoration. This chapter will combine the conclusions of the previous chapters to perform super-resolution reconstruction of the actual video images. Its system function flowchart is shown as in Figure 1.

3.4. Verifying the Small-World Characteristics of the Peer Layer. In this paper, the peer-to-peer layer has small-world characteristics after a few queries. Because in the simulation program, the network does not require strong connections, and some pairs of nodes are not directly connected, the network average path $L(G)$ is calculated by the most robust method (harmonic average shortest path). It can be derived from

$$L(G) = \left(\frac{N}{N-1} \sum_{i,y \in V} d(i,j)^{-1} \right)^{-1}. \tag{23}$$

4. From the Perspective of Legal Theory to See the Experimental Research Analysis of the Application of Urban Image Monitoring Technology

4.1. Investigation Monitoring Equipment

4.1.1. Investigation Resident Voluntary Installation of Monitoring Equipment. Voluntary installation refers to the voluntary installation of monitoring systems by organizations and individuals other than the subject of mandatory installation in order to protect their own interests. Voluntary installation belongs to the rights and freedom of citizens, and it is a personal act and a civil act, so the administrative agency should not interfere too much. The fact that the administrative agency does not interfere too much does not mean that voluntary installation can do whatever it wants. Since voluntary installation is a civil act, it must be regulated by my country's civil law. The survey results of residents supporting the installation of monitoring equipment are shown in Table 1.

As shown in Figure 2, among the voting results that strongly require the installation of monitoring facilities, boys accounted for 62% and girls accounted for 42%. Judging from the voting results, the proportion is still very large, indicating that people are now very concerned about their own and property safety. Girls accounted for 40% of the votes for refusing to install, indicating that girls still pay more attention to their own privacy and security, and the scope of system monitoring can only be their own area, because the areas or public areas owned by others are not owned by you. There is no right to use and no right to install the "electronic eye" in the area of others, and if installed, it constitutes an infringement of the ownership of others.

4.1.2. Functional Level of Residents Installed Monitoring Equipment. You must not use your own electronic eyes to peek at other people's information and public information, and you must not use the information obtained for other purposes. Otherwise, it will constitute an infringement of the personal rights of others and bear corresponding civil liabilities. In severe cases, you will be subject to administrative or criminal penalties. The survey results are shown in Table 2. We draw a bar chart based on this result, as shown in Figure 3.
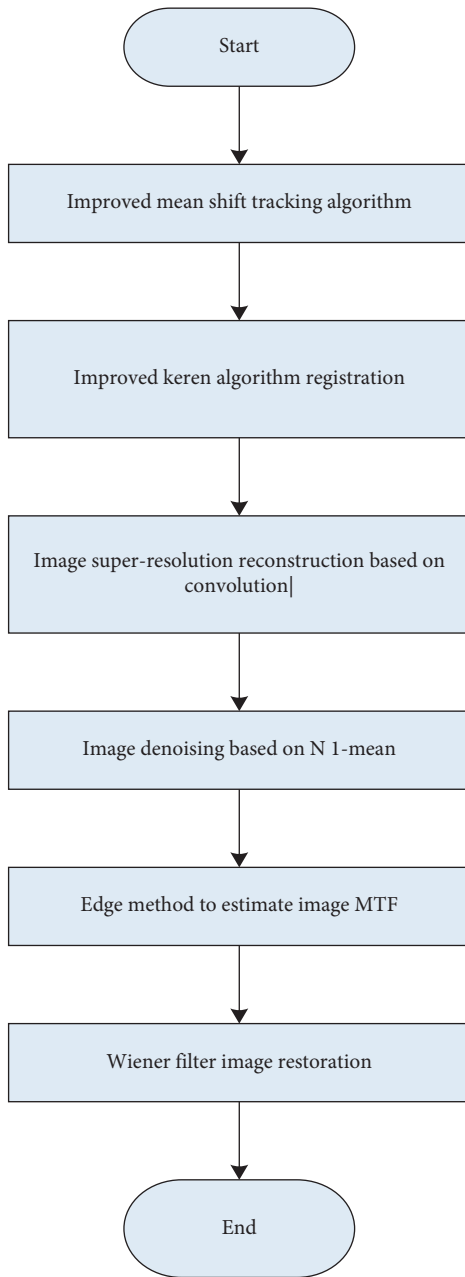
FIGURE 1: Program flowchart.

FIGURE 2: Average path and average clustering coefficient change of peer layer.

TABLE 2: Residents install monitoring equipment function grade data sheet.

Function classification	Refuse	Consider	Casual	Medium	Strongly demand
Bolt action	14.8	32.5	72.6	68.1	35.2
Dome camera	51.6	40.3	34.8	23.7	25.2
Integrated camera	19.2	28.7	69.1	66.5	33.1
Infrared day and night camera	49.3	33.6	35.6	22.8	22.9
Speed dome camera	12.7	35.6	93.2	70.2	37.2
Web camera	53.2	42.8	37.7	24.3	28.3
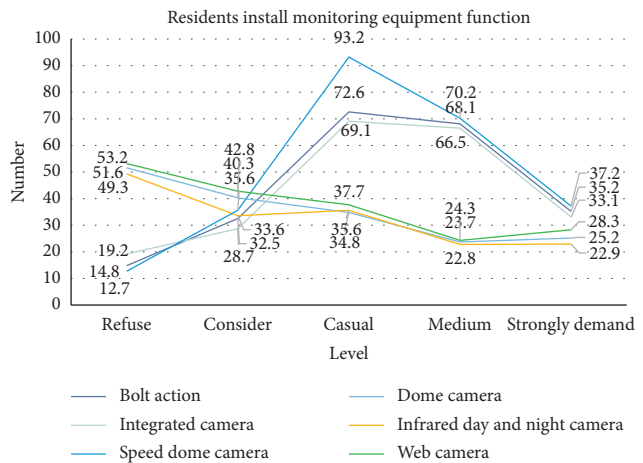
FIGURE 3: Residents install monitoring equipment function grade data chart.

TABLE 1: The number of nth statistics.

Sex	Refuse	Consider	Strongly demand
Male	17	21	62
Female	40	18	42

The variance value of the local area of the image reflects the complexity of the image gray level in this area. The larger the variance value, the more obvious the image detail features. On the contrary, the smoother the image gray level is. In the calculation result of the variance value at each pixel in the image, the variance calculation area is 20% of the image size. It can be seen from Figure 3 that the distribution law of the variance value conforms to this characteristic.

4.2. Accurate Matching of Pedestrian Characteristics in Monitoring Facilities Helps Public Security Departments to Investigate. This article calculates and sorts the distance between a pedestrian and 98 pedestrians under another camera and records the rankings of matching pedestrians. In these rankings, the proportions of the 1–5 are calculated, respectively, and the RBG in the color comparison method is used. LAB and HSV-edgel contrast method, SIFT and SURF

contrast method in the feature point contrast method, HOG contrast method, and the experimental results are shown in Table 3.

From Figure 4, we can see that the HOG method has the best effect, followed by the SIFT and SURF methods based on feature points, while the color-based RBG, LAB, HSV-edgel, and feature point methods are similar. Since the clothes generally worn by pedestrians will have some obvious boundaries on the appearance, these boundary features are stable in the same individual and have great differences among different individuals, so the HOG detection method can more accurately match the characteristics of the pedestrian, which can accurately match the proportion of pedestrians accounted for nearly 68%, and the top five accounted for 79%. The feature point method also has a higher matching rate, which helps the public security department in our country to find criminals at large, missing people, or children lost in shopping malls, which is of great significance to the stable development of society.

4.3. The Application of Peer-to-Peer Tree Search to the Monitoring System Helps Maintain Urban Public Safety.
The experiment constructed 5 different peer trees. Although the total number of nodes is about the same, both are about 800, and the number of nodes distributed in the cascade layer and the peer layer is different. The number of supernodes N_p is 50, 100, 200, 400, and 800, respectively. This will inevitably lead to their query efficiency. The experimental results are shown in Table 4.

It can be seen from Figure 5 that no matter the TTL is 2, 3, 4, or 5, the success rate of the monitoring system is between 85% and 97%. This shows that when the peer layer stabilizes into a small-world network, most of the requests of this system can be hit at least once in two steps. Although their success rates are very good, when the number of supernodes is 200, the success rate is the highest. This shows that due to its wide coverage, large amount of information, and strong real-time advantages, the urban image monitoring system has become an important means to detect various unstable factors in time and quickly and effectively deal with and lock suspects after occurrence.

The establishment of relevant legal systems can make the urban image monitoring system more perfect, improve the effectiveness of construction, application, and management at all levels, and better play its role in protecting public safety. Through the application of video image monitoring technology, it is helpful to timely detect and eliminate various insecure factors such as terrorist attacks and violent crimes that endanger social security and urban security. This article considers that the degree of message dissemination also increases significantly with the increase of TTL. Experiments are carried out on the degree of message distribution of peer-to-peer trees with different numbers of supernodes, and the experimental structure is shown in Table 5.

As shown in Figure 6, when the number of supernodes is 800, the peer-to-peer tree structure is transformed into a fully distributed P2P, which has a large network load and a low hit rate, which is obviously worse than the tradeoff system. When the number of supernodes is 1, the peer-to-peer tree structure becomes centralized again. Although there is no test, it can be seen from the three curves of success rate, hit rate, and message-spreading degree that the success rate will decrease. The hit rate is basically the same, and the network load has increased significantly. Therefore, when the monitoring facility faces a large crowd base, the peer-to-peer tree structure at this time is better than the fully distributed and centralized peer-to-peer structure in terms of search performance. This way, the urban image monitoring implemented under the standardized system can effectively improve the social public management ability and help establish a standardized and orderly social public order. The installation of monitoring equipment in public places may cause conflicts between the security interests of the monitor or the public interest of the society and the privacy interests of the monitored person, but in general, video surveillance in public areas such as public places can effectively establish social order. It is conducive to promoting social progress and safeguarding the interests of the broad masses of people.

4.4. Objective Evaluation Index Analysis

4.4.1. Analysis of Objective Evaluation Index of Improved Algorithm.
The following objective evaluation criteria such as mean, standard deviation, and average gradient are used to test the enhancement effect of the image. For the convenience of calculation, only a certain component of the color image is used for calculation. We draw a combination diagram based on this result.

It can be seen from Table 6 that the improved algorithm can better balance the overall grayscale of the image. When the overall gray level of the image is high, the mean value of the processing result will be reduced to an appropriate gray value; when the overall gray level of the image is low, the improved algorithm can raise its average gray level to an appropriate gray value.

It can be seen from Table 7 that the improved algorithm can balance the contrast of the image. When the contrast of the image is low, the contrast can be increased after processing; when the contrast of the image is high, the contrast of the image can be reduced appropriately.

It can be seen from Table 8 that the average gradient value of the processed image is higher than that of the original image, which reflects to a certain extent that the gray distribution of the processed image is relatively uniform and the image details are more abundant.

These original color images all have the characteristics of low contrast, some partial details are not prominent, and some areas are dark. After processing by this algorithm, the

TABLE 3: The number of nth statistics.

Nth place	Color_RBG	Color_LAB	Color_HSV_edge	SIFT	SURF	HOG
1	10	11	9	3	8	5
2	5	9	5	3	3	2
3	3	2	3	4	2	1
4	7	3	4	5	4	3
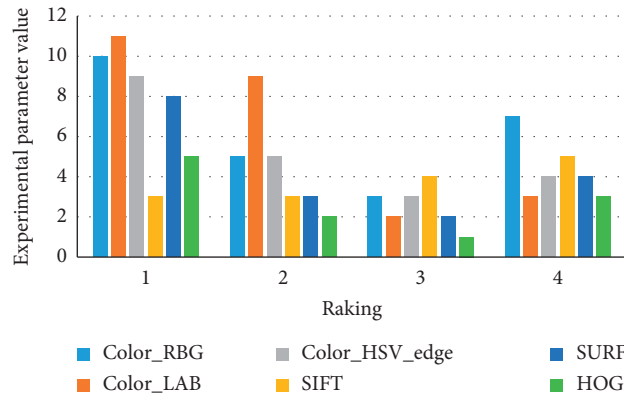
FIGURE 4: Comparison chart of the proportion of top n matches.

TABLE 4: The number of nth statistics.

Number of supernodes	150 mm	300 mm	450 mm	600 mm	750 mm	900 mm
50 supernodes	0.8147	0.09754	0.1576	0.1418	0.6557	0.7577
100 supernodes	0.9057	0.2784	0.9705	0.4217	0.0357	0.7431
200 supernodes	0.1269	0.5468	0.9571	0.9157	0.8491	0.3922
400 supernodes	0.9133	0.95750	0.4853	0.7922	0.9339	0.6554
800 supernodes	0.6323	0.9648	0.8002	0.9594	0.6787	0.1711
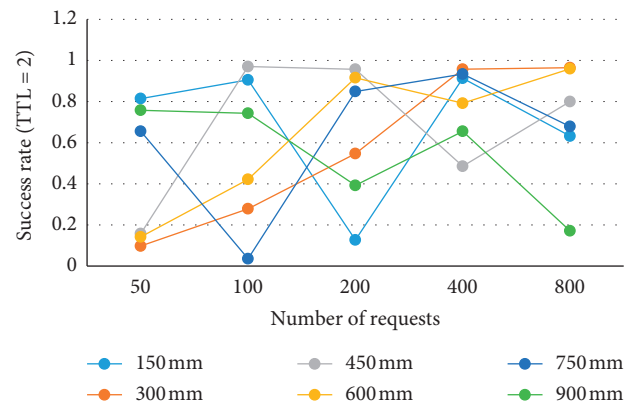
FIGURE 5: Changes in success rate when TTL-T and TTL-P are 2.

TABLE 5: Data table of the degree of message distribution.

Number of supernodes	50	100	200	400	800
TTL = 2	14.7	12.1	12.9	13.4	14.2
TTL = 3	18.6	15.4	16.7	22.3	25.1
TTL = 4	18.6	15.4	21.3	25.4	29.8
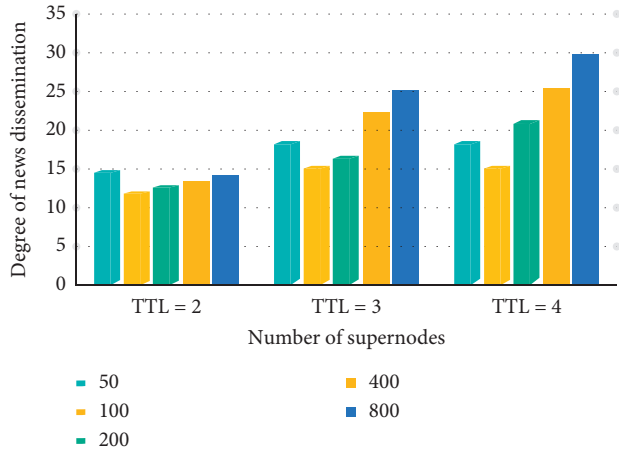
FIGURE 6: The degree of message distribution changes with the number of peer nodes.

FIGURE 7: Comprehensive graph of the objective evaluation index of the algorithm.

TABLE 6: Image mean data comparison table.

	The original image	Algorithm processing result	Difference
Figure A	56.9	174.3	117.4
Figure B	19.3	87.2	67.9
Figure C	91.2	156.3	65.1
Figure D	130.9	81.6	−49.3
Figure E	72.6	43.4	−29.2
Figure F	33.6	97.8	64.2

TABLE 7: Image standard deviation data comparison table.

	The original image	Algorithm processing result	Difference
Figure A	1167.8	1732.8	565.0
Figure B	73.9	836.4	762.5
Figure C	2756.3	2337.2	−419.1
Figure D	1329.4	934.6	−394.8
Figure E	234.9	112.7	−122.2
Figure F	332.7	977.8	645.1

TABLE 8: Image average gradient data comparison table.

	The original image	Algorithm processing result	Difference
Figure A	9.4	21.7	12.3
Figure B	0.7	9.9	9.2
Figure C	11.9	19.6	7.7
Figure D	1.9	7.3	5.4
Figure E	5.6	17.2	11.6
Figure F	19.2	27.4	8.2

contrast, sharpness, and texture characteristics of the image have been significantly improved, and the overall color is more realistic. The specific situation is shown in Figure 7.

4.4.2. Horizontal Movement Test Analysis.

Quantitatively analyze the registration results before and after the improvement of the Keren algorithm, and use a low-resolution image as a reference image to calculate the displacement and rotation relationship between the image and other low-resolution images. We first need to perform a horizontal movement test on the picture and collect data for analysis, as shown in Table 9.

It can be seen from Figure 8 that the improved registration algorithm has improved the effect of horizontal movement estimation. When the moving target and the camera are relatively displaced, their size will change. Although the change is small in two adjacent images, the rigid body transformation model can be used to obtain the transformation parameters between them, but multiple pictures need to be used to perform super-resolution image reconstruction.

4.4.3. Vertical Movement Test Analysis.

Quantitatively analyze the registration results before and after the improvement of the Keren algorithm, and use a low-resolution image as a reference image to calculate the displacement and rotation relationship between the image and other low-resolution images. Next, we need to test the vertical movement of the picture and collect data for analysis, as shown in Table 10.

It can be seen from Figure 9 that the improved registration algorithm has improved the effect of vertical movement estimation. Low-resolution images are obtained through degradation, especially after downsampling, and the high-frequency components of the frequency are mixed, which affects the accuracy of the registration result of the frequency domain method to a certain extent.

4.4.4. Angle Rotation Test Analysis.

Quantitatively analyze the registration results before and after the improvement of the Keren algorithm, and use a low-resolution image as a

TABLE 9: Horizontal movement test result data table.

Serial number	Δx	Keren algorithm		Improve algorithm	
		Estimated value	Relative value	Estimated value	Relative value
1	1.37	1.3267	1.3462	1.3312	1.3763
2	2.84	2.8719	2.8552	2.8533	2.8452
3	3.42	3.4627	3.3514	3.4496	3.4219
4	3.63	3.6724	3.6433	3.6654	3.6412
5	1.75	1.7726	1.7335	1.7629	1.7489
6	1.21	1.2427	1.1936	1.2394	1.2112
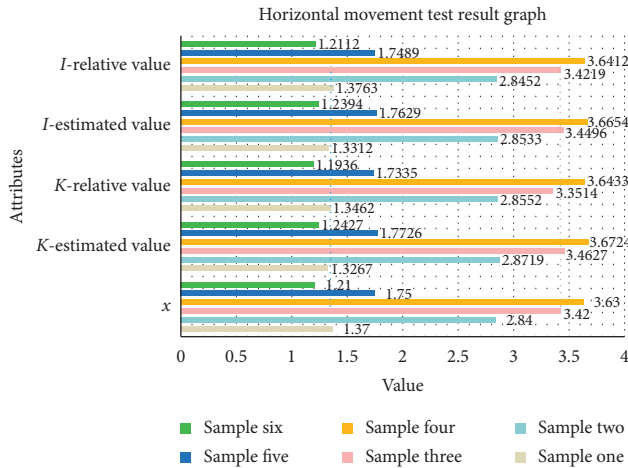
FIGURE 8: Horizontal movement test result graph.

TABLE 10: Vertical movement test result data table.

Serial number	Δy	Keren algorithm		Improve algorithm	
		Estimated value	Relative value	Estimated value	Relative value
1	2.72	2.7832	2.7567	2.7159	2.7239
2	0.64	0.5947	1.2329	0.6721	0.6488
3	3.37	3.4226	3.6213	3.2462	3.3736
4	2.25	2.2891	2.6723	2.3226	2.2496
5	1.29	1.1192	1.7724	1.2698	1.2887
6	3.32	3.2654	3.6514	3.3017	3.3229

reference image to calculate the displacement and rotation relationship between the image and other low-resolution images. Next, we need to test the angle rotation of the image and collect data for analysis, as shown in Table 11.

It can be seen from Figure 10 that when the image is rotated at a large angle, the result of the improved Keren algorithm is significantly more accurate. The flow is reflected by the change of brightness mode, and this registration algorithm is based on the brightness gradient of the spatiotemporal image to obtain the pixel displacement velocity vector, an estimation method.

4.4.5. Image Zoom Test Analysis. The Keren algorithm uses a rigid body transformation model. When there is a scaling relationship between the reference image and the target
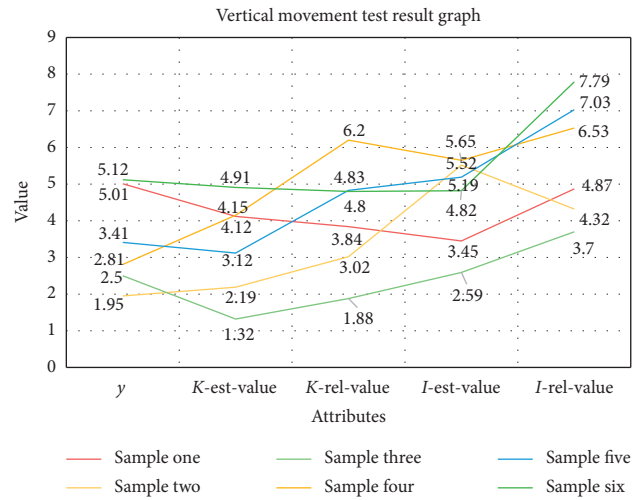
FIGURE 9: Vertical movement test result graph.

TABLE 11: Angle rotation test result data table.

Serial number	θ	Keren algorithm		Improve algorithm	
		Estimated value	Relative value	Estimated value	Relative value
1	2	1.9836	1.5656	2.0533	1.7729
2	3	2.9776	3.6827	3.0037	3.3674
3	5	4.8942	5.7923	4.9929	5.3629
4	9	8.7466	9.6528	9.0033	10.4762
5	12	11.4725	14.3727	11.9956	15.6264
6	15	14.6719	17.5436	14.9964	12.3359
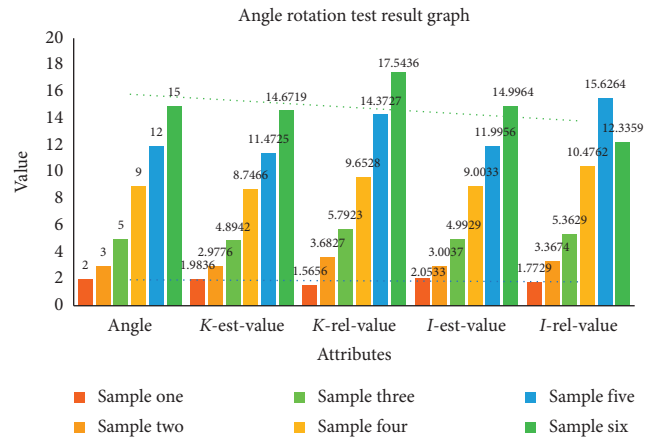
FIGURE 10: Angle rotation test result graph.

image, the Keren algorithm appears powerless. The model adopted by the improved Keren algorithm is very similar to the real model of the actual transformation, so the registration result obtained is more accurate, as shown in Table 12.

Due to the mismatch of this model, the parameters obtained by the Keren algorithm are very different from the real values. Therefore, the shape and scale of the neighborhood will directly affect the quality of the reconstructed image. In order to make the neighborhood change according

TABLE 12: Image scaling test result data table.

Registration coefficient	Actual value	Keren algorithm		Improve algorithm	
		Estimated value	Relative value	Estimated value	Relative value
Δx	2.27	8.8589	6.1739	2.4226	2.3137
Δy	1.55	6.1334	3.5527	1.7652	1.6739
θ	5	1.4127	1.4439	4.7316	4.9625
S	0.75	—	—	0.7418	0.7562
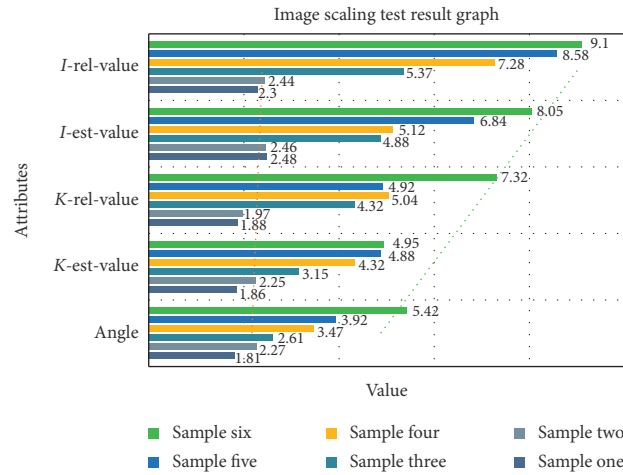
FIGURE 11: Image scaling test result graph.

TABLE 13: Matlab and Keren algorithm model processing image information comparison table.

	Original image	Matlab processing results	Keren algorithm model processing results
Mean	99.3729	119.5806	120.0127
Mean square error	31.6662	69.5349	70.1318
Information entropy	6.5421	9.1269	9.1736
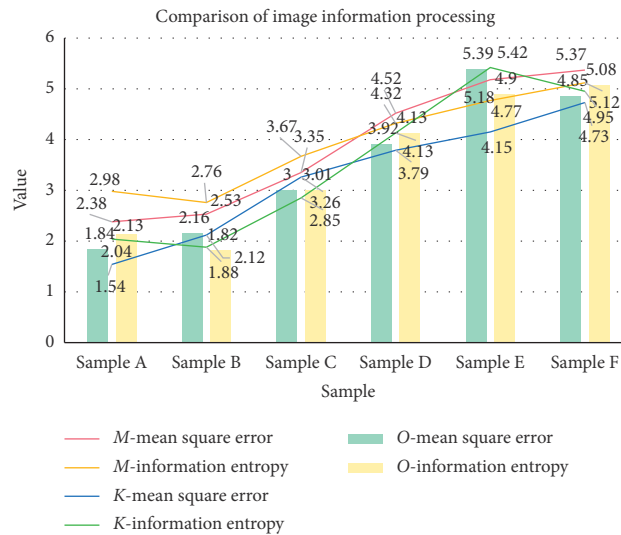
FIGURE 12: Comparison of image information processing between Matlab and Keren algorithm models.

TABLE 14: Comparison table of median filter processing results.

	Original image	Matlab processing results	Keren algorithm model processing results
Mean	50.0	49.4486	50.1832
Peak signal to noise ratio	32.0	31.1887	32.0018
Entropy	7.8	7.7965	7.8018
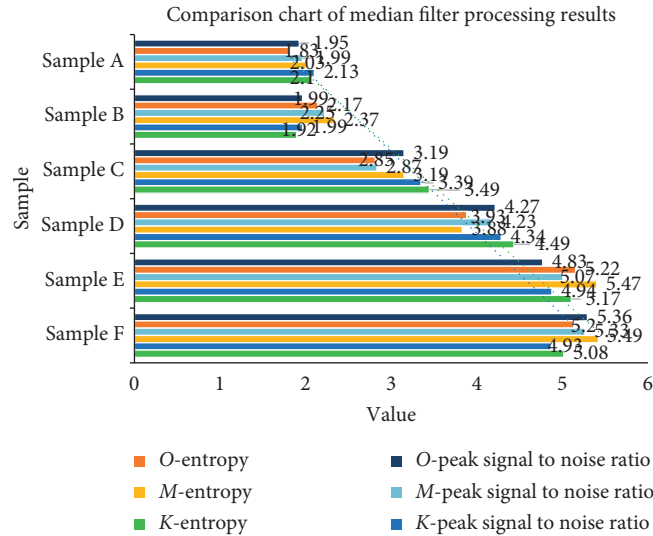
FIGURE 13: Comparison chart of median filter processing results.

to the organization information of the image, the normalized convolution uses an adaptive function to control it, as shown in Figure 11.

4.5. Statistical Histogram

4.5.1. Histogram Equalization Analysis. Here, we compare the processing effect of the Keren algorithm model and Matlab on the picture, read the stored value according to the data address, add one, and send the value back to the other end of the RAM for storage. The results are shown in Table 13.

It can be seen from Figure 12 that the Keren algorithm model is almost the same as the Matlab processing effect and both of which increase the image brightness. The contrast of the entire image is improved, and the visual perception of the image is clearer. It also shows that the approximate operation in the histogram mapping module in this paper has little effect on the processing effect of image data.

4.5.2. Analysis of Value Filtering in Histogram. The original image with salt and pepper noise is processed by the Keren algorithm model and Matlab, respectively. The source of image noise is mainly in the process of its acquisition and transmission, and the analog image will also bring noise during the digital quantization process. Results are shown in Table 14.

It can be seen from Figure 13 that the Keren algorithm model has also reached the processing result of Matlab and both of which effectively eliminate the salt and pepper noise

in the image. The MSE and RSNR results after the two treatments are not much different, and the treatment effects are very significant.

5. Conclusions

This article strictly limits the scope of users of video image information systems through legislation and clarifies the establishment of on-duty monitoring, data management, safety management, and maintenance system requirements for the management and use of public security video surveillance systems. The location and purpose of the facility, the sale, distribution, and illegal broadcasting of video and image materials, and unauthorized changes to the use of video and image information systems stipulate the types and intensity of penalties and increase the intensity of investigation.

This paper analyzes the basic principles and basic structure of the basic theoretical information collection closely related to the distributed online information real-time monitoring and dynamic collection system and builds a structure-based distributed online information real-time monitoring and dynamic collection system, and the system. The functional framework of the software has been analyzed and studied in detail. On this basis, several key issues in the distributed online information real-time monitoring and dynamic collection system, network information mining issues, dynamic data exchange and real-time issues, and other issues that may occur in the system implementation process have been deeply studied and discussed.

In order to use the three local laws in the grid to speed up the query, this paper designs a special hybrid peer-to-peer

framework "peer tree." The idea of this framework is to try to cascade the services related to the problem to be solved together, so that the services that are similar to the problem to be solved become peer neighbors, forming a two-tier structure of cascade layer and peer layer, and regarding how to ensure for the problem of search efficiency, a "learning neighbor search algorithm" is proposed based on the peer-to-peer tree. This algorithm can cluster nodes with similar interests after a few short searches to form a small-world overlay network, so that the average path between any two points is kept small.

Data Availability

No data were used to support this study.

Conflicts of Interest

The authors declare that they have no conflicts of interest.

Acknowledgments

References

[1] S.-B. Tsai, R. Saito, Y.-C. Lin, Q. Chen, and J. Zhou, "Discussing measurement criteria and competitive strategies of green suppliers from a green law perspective," *Proceedings of the Institution of Mechanical Engineers, Part B: Journal of Engineering Manufacture*, vol. 229, no. 1, pp. 135–145, 2015.

[2] M. Elhoseny, "Multi-object detection and tracking (MODT) machine learning model for real-time video surveillance systems," *Circuits, Systems, and Signal Processing*, vol. 39, no. 3, pp. 611–630, 2020.

[3] Z. Lv, X. Li, W. Wang, B. Zhang, J. Hu, and S. Feng, "Government affairs service platform for smart city," *Future Generation Computer Systems*, vol. 81, pp. 443–451, 2018.

[4] P. M. Schwartz, "German and US telecommunications privacy law: legal regulation of domestic law enforcement surveillance," *Hastings Law Journal*, vol. 54, no. 4, pp. 751–803, 2017.

[5] T. Hariyanto and H. H. Handayani, "The use of high resolution satellite image for the classification of green open space area in Banda Aceh City, West Sumatra Indonesia," *International Journal of Earth Ences & Engineering*, vol. 8, no. 3, pp. 256–258, 2015.

[6] A. K. Dutta, M. Elhoseny, V. Dahiya, and K. Shankar, "An efficient hierarchical clustering protocol for multihop internet of vehicles communication," *Transactions on Emerging Telecommunications Technologies*, vol. 31, no. 5, p. e3690, 2020.

[7] E. Hermas, "Monitoring the spatial occurrences and migration rates of Sand Dunes around Makkah City using remote sensing technology," *GIScience & Remote Sensing*, vol. 3, no. 1, pp. 2052–5583, 2015.

[8] Y. Chen, W. Zheng, W. Li, and Y. Huang, "Large group activity security risk assessment and risk early warning based on random forest algorithm," *Pattern Recognition Letters*, vol. 144, pp. 1–5, 2021.

[9] J. Jiao, M. Holmes, and G. P. Griffin, "Revisiting image of the city in cyberspace: analysis of spatial twitter messages during a special event," *Journal of Urban Technology*, vol. 25, no. 3, pp. 65–82, 2018.

[10] W. Zhai and C. Huang, "Fast building damage mapping using a single post-earthquake PolSAR image: a case study of the 2010 Yushu earthquake," *Earth Planets & Space*, vol. 68, no. 1, p. 86, 2016.

[11] M. Elhoseny and K. Shankar, "Optimal bilateral filter and convolutional neural network based denoising method of medical image measurements," *Measurement*, vol. 143, pp. 125–135, 2019.

[12] Y. Zhou and F. Qiu, "Fusion of high spatial resolution WorldView-2 imagery and LiDAR pseudo-waveform for object-based image analysis," *ISPRS Journal of Photogrammetry and Remote Sensing*, vol. 101, pp. 221–232, 2015.

[13] Z. Lv, B. Hu, and H. Lv, "Infrastructure monitoring and operation for smart cities based on IoT system," *IEEE Transactions on Industrial Informatics*, vol. 16, no. 3, pp. 1957–1962, 2020.

[14] Q. Shen, L. Zhu, and H. Y. Cao, "[Remote sensing monitoring and screening for urban black and odorous water body: a review]," *Chinese Journal of Applied Ecology*, vol. 28, no. 10, pp. 3433–3439, 2017.

[15] D. Osabe, Y. Litsuka, and A. Higashi, "Solutions to social problems leveraging image analysis technology based on machine learning," *Fujitsu Entific & Technical Journal*, vol. 53, no. 3, pp. 32–38, 2017.

[16] G.-J. Horng, "The adaptive recommendation mechanism for distributed parking service in smart city," *Wireless Personal Communications*, vol. 80, no. 1, pp. 395–413, 2015.

[17] Z. Lv, L. Qiao, D. Chen, R. Lou, J. Li, and Y. Li, "Machine learning for proactive defense for critical infrastructure systems," *IEEE Communications Magazine*, 2020.

[18] D. Guangyao, G. Huili, L. Huanhuan, Z. Youquan, C. BeiBei, and L. KunChao, "Monitoring and analysis of land subsidence along Beijing-Tianjin inter-city railway," *Journal of the Indian Society of Remote Sensing*, vol. 44, no. 6, pp. 915–931, 2016.

[19] Q. Zhang, H. Zheng, J. Lan, J. An, and H. Peng, "An autonomous information collection and dissemination model for large-scale urban road networks," *IEEE Transactions on Intelligent Transportation Systems*, vol. 17, no. 4, pp. 1085–1095, 2016.

[20] B. Han, J. Li, J. Su, M. Guo, and B. Zhao, "Secrecy capacity optimization via cooperative relaying and jamming for WANETs," *IEEE Transactions on Parallel and Distributed Systems*, vol. 26, no. 4, pp. 1117–1128, 2014.

[21] Y. Wang, B. Du, Q. Rong, and X. Lin, "Travel patterns analysis of urban residents using automated fare collection system," *Chinese Journal of Electronics*, vol. 25, no. 1, pp. 40–47, 2016.

[22] F. Santoso and S. J. Redmond, "Indoor location-aware medical systems for smart homecare and telehealth monitoring: state-of-the-art," *Physiological Measurement*, vol. 36, no. 10, p. R53, 2015.

[23] C. Li, H. J. Yang, F. Sun, J. M. Cioffi, and L. Yang, "Adaptive overhearing in two-way multi-antenna relay channels," *IEEE Signal Processing Letters*, vol. 23, no. 1, pp. 117–120, 2016.

[24] A. J. Watt, M. R. Phillips, C. E.-A. Campbell, I. Wells, and S. Hole, "Wireless sensor networks for monitoring underwater sediment transport," *Science of the Total Environment*, vol. 667, pp. 160–165, 2019.

[25] D. N. Naumann, M. J. Midwinter, and S. Hutchings, "Venous-to-arterial CO_2 differences and the quest for bedside

point-of-care monitoring to assess the microcirculation during shock," *Annals of Translational Medicine*, vol. 4, no. 2, p. 37, 2016.

[26] Z. Lv, L. Qiao, K. S. Amit, and Q. Wang, "AI-empowered IoT security for smart cities," *ACM Transactions on Internet Technology (TOIT)*, 2020.

[27] D. Kissinger and J.-C. Chiao, "Medical applications of radio-frequency and microwaves-sensing, monitoring, and diagnostics [from the guest editors' desk]," *IEEE Microwave Magazine*, vol. 16, no. 4, pp. 34–38, 2015.

[28] H. Ahkola, J. Juntunen, K. Krogerus, T. Huttula, S. Herve, and A. Witick, "Suitability of chemcatcher passive sampling in monitoring organotin compounds at a wastewater treatment plant," *Environmental Science: Water Research & Technology*, vol. 2, no. 4, pp. 769–778, 2016.

[29] W. Warner, K. Nodler, A. Farinelli, J. Blum, and T. Licha, "Integrated approach for innovative monitoring strategies of reservoirs and lakes," *Environmental Engineering and Management Journal*, vol. 17, no. 10, pp. 2497–2505, 2018.

[30] S. Yerraboina, N. M. Kumar, S. Parimala, and N. Aruna Jyothi, "Monitoring the smart garbage bin filling status: an IoT application towards waste management," *International Journal of Civil Engineering and Technology*, vol. 9, no. 6, pp. 373–381, 2018.

[31] P. Luigi, V. Giovanni, C. Giovanni et al., "Cardiovascular diseases monitoring: lessons from population-based registries to address future opportunities and challenges in Europe," *Archives of Public Health*, vol. 76, no. 1, p. 31, 2018.

[32] K. Herbst, M. Law, P. Geldsetzer, F. Tanser, G. Harling, and T. Bärnighausen, "Innovations in health and demographic surveillance systems to establish the causal impacts of HIV policies," *Current Opinion in HIV and AIDS*, vol. 10, no. 6, p. 483, 2015.

[33] M. J. Grima, M. Boufi, M. Law et al., "The implications of non-compliance to endovascular aneurysm repair surveillance: a systematic review and meta-analysis," *Journal of Vascular Surgery*, vol. 67, no. 5, p. 1632, 2018.

[34] Y.-F. Lam, T. Tong, O. Lo et al., "1066 different adenoma recurrence rates on surveillance colonoscopy in patients with right- or left-sided colonic cancer after curative colectomy," *Gastroenterology*, vol. 150, no. 4, p. S210, 2016.

Research Article

Enterprise Performance Optimization Management Decision-Making and Coordination Mechanism Based on Multiobjective Optimization

Tao Zou and **Sijun Bai**

School of Management, Northwestern Polytechnic University, Xian 71000, Shaanxi, China

Correspondence should be addressed to Tao Zou; zoutolele@mail.nwpu.edu.cn

Today's society is a society of the knowledge economy, and the competition of enterprises is the competition of talents. The rapid development of science and technology and the fierce development of market competition have made the importance of performance management increasingly prominent in corporate management. The purpose of performance management is to explore and deal with some of the effects of various factors on employee performance and to tap the potential of employees, improve employee performance, and also bring a qualitative leap to the performance of the organization. The improvement of the employee performance management level has laid a solid foundation for the improvement of the organizational performance management level. However, there are still some difficulties in the implementation of performance management in my country at this stage, and the management effect is not obvious. Therefore, building a scientific, reasonable, and complete multiobjective optimization-based corporate performance optimization management decision-making and coordination mechanism is the primary task of today's enterprises. This article will give a brief theoretical overview of the combination of system management theory and behavior management theory, MBO target management, and KPI indicators, build a multiobjective optimization model on an effective theoretical basis, and use genetic algorithms to obtain a weak Pareto effective solution that can optimize the enterprise with consideration of performance appraisal indicators. It also builds an agency model and an analysis of employee incentive plans, which clearly shows the relationship between the company and the management and employees, conducts a cross analysis of the needs of the company's management and employees, and puts forward the best corporate performance considering the needs of employees; among them, the multiobjective optimization of corporate performance increased by 14% under the optimal management decision.

1. Introduction

Performance, from the perspective of management, is the desired result of the organization and the effective output that the organization displays on different levels to achieve its goals. It includes both personal performance and corporate performance. The realization of enterprise performance should be based on the realization of individual performance, but the realization of individual performance does not necessarily guarantee the overall performance. Because of this, performance management is even more important in the optimization and improvement of the overall performance of an enterprise.

The multiobjective optimization problem is to select the optimal solution according to a certain index from all possible alternatives of a problem. Mathematically speaking, optimization is the study of the minimization or maximization of a function on a given set S. Broadly speaking, optimization includes mathematical programming, graphs and networks, combinatorial optimization, inventory theory, decision theory, queuing theory, and optimal control. In a narrow sense, optimization is only exponential planning. The optimization method is widely used in production management, economic planning, engineering design, system control, and other fields.

The heterogeneous cloud system proposed by Liu provides distributed but tightly integrated services that have rich functions in large-scale management, reliability, and fault tolerance. As far as big data processing is concerned, newly built cloud clusters are facing performance optimization challenges, which are focused on faster task execution and more efficient use of computing resources. The currently proposed methods focus on time improvement, that is, shorten the MapReduce time, but pay little attention to storage usage. However, an unbalanced cloud storage strategy may exhaust the MapReduce cycle heavy nodes and further challenge the security and stability of the entire cluster. This paper proposes an adaptive method for space-time efficiency in heterogeneous cloud environments. A prediction model based on an optimized kernel-based extreme machine learning algorithm is proposed to predict job execution time and space occupation faster, thereby simplifying the task scheduling process through multiobjectives. However, it is feasible to use multiobjective optimization methods. The calculations performed in the operation may exceed tens of millions of times [1]. Bandyopadhyay performed empirically studies on the relationship between corporate sector performance and capital structure and macroeconomic environment. He used balance panel data of 1,594 Indian companies in 14 years and found empirical evidence to support assumptions about the relevance of factors such as asymmetric information, agency costs, trade-off theory, signals, and liquidity in determining the corporate capital. The structural decisions of emerging market economies obviously affect the company's financing decisions through the macroeconomic cycle, which in turn affects performance. The endogenity between capital structure and company performance has also been resolved by the two-step dynamic panel generalized method of moments (GMM). The research shows that the performance of any company depends on its ability to operate on the capital structure. As the scope of capital procurement expands, it is necessary to carefully design the right tool combination to optimize the cost of capital. However, he did not propose a management decision-making plan or system mechanism for the optimization of company performance [2]. Blahová investigated the current trends in the selected management systems and analyzed the synergies between them to regain control of contemporary corporate performance management systems in the business field. *Design/Methodology/Methods*. This research involves the compilation of major academic works and other literature on changes in global management systems and their impact on the reconstruction of contemporary corporate performance management systems. The literature is reviewed using a systematic approach. It identified and analyzed more than 3000 papers and studies. Once the survey results are determined, the main trends and emerging themes of current management practices in the business world and their synergies should be classified. The field of originality/value-performance management system and its remake based on the needs of individual companies is an emerging research field. There are still shortcomings in research experience and research empirical [3].

The innovations of this article are as follows: (1) this article uses a combination of empirical research and normative research, such as the research on the employee incentive and restraint mechanism of the Y enterprise in the fourth part; (2) this article uses a combination of qualitative research and quantitative analysis. This method is concentrated in the analysis of the multiobjective optimization model; (3) this article uses a combination of theoretical analysis and countermeasure research and gives countermeasures, while establishing model analysis. This method runs through this article always.

2. Enterprise Performance Optimization Management Decision-Making and Coordination Mechanism Method Based on Multiobjective Optimization

2.1. Combine Contemporary System Management Theory with Behavior Management Theory. Modern management theory is the synthesis of all modern management theories. It is a knowledge system and a group of disciplines [4]. Its basic goal is to establish a creative and dynamic adaptive system in the face of a rapidly changing modern society. To enable this system to be continuously and efficiently output, it not only requires modern management thinking and management organization but also modern management methods and means to form modern management science.

The foundation of behavioral science management theory is classical management theory, which overcomes the shortcomings of classical management theory. It is mainly to study the production behaviors of enterprise employees and the reasons and related factors of these behaviors [5]. It is a comprehensive application of psychology, sociology, social psychology, anthropology, economics, political science, history, law, education, psychiatry, marketing, and management theories and methods to study human behavior borderline subjects. Behavioral science was once called interpersonal relations [6].

Its research content is mainly in the following three aspects: incentive theory is the core content of behavioral science. Specifically, it needs to be carried out in three aspects: level theory, behavioral transformation theory, and process analysis theory; group behavior theory is the core of behavioral science management theory. An important pillar, mastering group psychology is an important part of the study of group behavior; leadership behavior theory is an important part of behavioral science management theory, including research on the quality of leaders, leadership behavior, leadership ontology, and leadership styles [7, 8].

Throughout the management of each school, choose system management theory and behavioral science management theory and draw something in common, and the commonalities can be summarized as follows:

(1) Pay attention to the integrity of the system: first of all, the people, things, and environment in the enterprise are regarded as a complete system, which in turn lives in a larger system. Then, use system thinking and system analysis method to view the problem

from the overall framework, recognize the problem, analyze the problem, and finally solve and deal with the problem [6].

(2) Emphasize the importance of people: the core part of management theory is the subject of people. People are subjectively active. Everyone's thoughts, behaviors, language, and emotional expressions are different. Even in the same organizational department, there is no guarantee that everyone and the organization will move forward. The direction and pace are the same. Therefore, it is necessary to conduct business management, guide employees and the company to stand on the same side, and work together to face difficulties, overcome challenges, and complete tasks.

(3) Actively try advanced management theories first: the changes of society and enterprises, the rapid development speed, and traditional management theories can no longer keep up with the new development model of modern enterprises, so in the process of management theory innovation, we need to continue to try, explore, and accept the emergence of new things and development, for example, in corporate performance management, combining management methods with emerging technologies to improve management efficiency.

(4) Combine management efficiency and management effect: different from traditional enterprise management, modern management theory emphasizes that the management efficiency of the enterprise should be combined with the management effect of the organization. The goals or objectives of management show a diversified trend, which are to realize the performance management of the enterprise [9]. The core of performance management has three modules, as shown in Figure 1.

(5) Combination of theory and practice: talking about management theory is only on paper. It is necessary to combine theory and practice to make the theory operability and implementability so that the theory is useful. In the process of corporate performance management, the management should be good at applying new theories to practice, summarize, innovate, and promote the development of management [10, 11].

(6) Emphasize the predictability in advance: social development is changing rapidly, and the business environment is also constantly changing. If an enterprise can adapt to changes in the objective environment, it must have certain planning capabilities and feedforward control capabilities, accept the facts of upgrading, and ensure the normal operation of enterprise operations and management.

(7) Be brave in innovation: management not only includes the management of existing people, things, and the environment but also includes the management of predictable content in the future. It is necessary to actively reform and innovate and constantly pursue progress so that the development of the company can be "unchanged in response to changes" and continuous development [12].

2.2. MBO Target Management.

MBO goal management was put forward by the American management master Peter Drucker, who later innovatively put forward the viewpoint of "target management and self-control" [13]. In his view, a person's career must be goal-oriented, and the view that "the mission and tasks of an enterprise must be transformed into goals" is also extremely correct. Therefore, in the management process of the enterprise, the management process should be that the top leadership determines the highest goals and requirements of the enterprise, the enterprise managers divide the strategic goals into departments, and the department managers finally issue personnel goals and proceed according to the completion of the project considering fairness, implement reward, and punishment measures [14].

In the goal management theory, it is emphasized that the company must formulate strategic goals, which are like a compass, giving a direction to the company and internal employees. In a team, a variety of factors could hinder the process of cooperation of the team, but after determining the specific objectives of the formation of a strong cohesive force of the team, it will overcome all difficulties and move toward common success. Generally speaking, the goals of enterprises are diversified and involve multiple departments, but there is only one final goal, and only after the final goal is clear, other subgoals are easier to determine and achieve [15].

MBO target management focuses on the overall management of the system, is advanced management, and emphasizes the management of results and personnel, so it has the following functions:

(1) Overcome the shortcomings of traditional management: traditional management has two main drawbacks: one is that there is no plan and arrangement of work, and the whole system is in a state of chaos; the other is that bureaucracy, centralized power, and low efficiency are still adopted in the organization [16].

(2) Improve work effectiveness: after the goal management and division of labor, employees can complete their work with quality, quantity, and efficiency in accordance with their respective goals, effectively improving the performance management of the enterprise.

(3) Individual abilities are motivated and improved: management, by objectives, takes the form of intensive discussion and division of tasks. Therefore, in this process, employees are fully involved and have the right and opportunity to show their talents and develop their potential. Moreover, the determination of management by objectives is based on individual abilities. It is also challenging. To achieve the goal, it is possible to work hard.
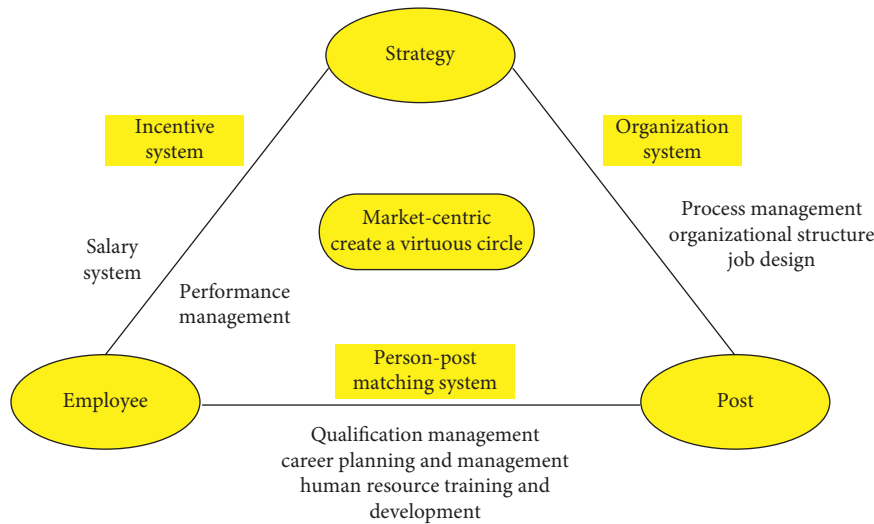
FIGURE 1: The three cores of performance management.

(4) Improve interpersonal relationships: in the process of goal management, the relationship between the upper and lower levels of the enterprise can be effectively improved, the role of communication and coordination can be strengthened, and it is easy to form a sense of teamwork and promote the accelerated realization of the overall goal [17].

MBO target management also has some shortcomings. We need to clearly recognize these limitations in order to better achieve the success of target management. The disadvantages are as follows:

(1) Emphasize short-term goals: short-term goals are easy to decompose and easy to achieve, but excessive emphasis on short-term goals is not conducive to the company's long-term healthy development, and it does not pay attention to the company's long-term plan goals.

(2) Difficulty in setting goals: in the process of target assessment, it is difficult to unify assessment standards. Because the achievement of the goal is the result of everyone's joint cooperation, there is not enough measurable workload, and it is difficult to judge the amount of personal contribution made, only a qualitative description.

(3) No contingency: it is impossible to change the goals during the execution of goal management because doing so will lead to organizational chaos. The goal cannot be changed during the execution of goal management because doing so will cause confusion in the organization. In this rapidly changing business, it is obviously unable to adapt to the changes in the market and cope with the changes in the external environment, and the organization and operation are inflexible [18].

2.3. KPI Indicators. KPI indicators refer to the internal operation of the process, the setting of key input parameters of the operation, sampling, calculation, analysis, and output [19]. It is the foundation of enterprise performance management, and it is a quantifiable target management index that can decompose the highest-level goals into specific implementation and execution subtargets and use this to measure performance. KPI indicators are mainly used by department heads to manage performance. They operate under the establishment of a clear and practical KPI system. The head is responsible for issuing specific performance indicators for each department and individual personnel. This is an important part of personal performance.

The key principle of KPI indicators is the Eight-Two Principle, which applies to companies and individuals. In enterprises, 20% of talents often solve 80% of the company's problems, and 20% of backbones create 80% of the value [20]. Therefore, in the process of corporate performance management, we must fully realize the importance of this 20% and grasp the core for analysis and evaluation.

There is an inseparable relationship between KPI indicators and corporate strategic objectives, which are mainly manifested in the following three aspects: first, KPI indicators are the decomposition of corporate strategic objectives, that is, to say, the company's strategic objectives must be fully considered in the setting of KPIs. If there is a deviation from the company's strategic goals, it needs to be adjusted in time; second, KPIs are further refinement and development of strategic goals. The content of KPI is set for each position, it is clear, and it also shows the job performance requirements of the position, so to a certain extent, it has a certain degree of guidance for the company's strategic development direction; third, KPI can make content changes moderately with the change of strategic objectives. In a complete system in this KPI, KPI is established on the lower level of the need to communicate and discuss the needs of both clear and practical work and to improve the overall performance is very helpful [21, 22].

Specifically, KPI has the following characteristics:

(1) KPIs are indicators, not targets, but they guide the determination of targets.

KPI is a key performance indicator: it does not exist as a target, but is a comprehensive consideration of multiple dimensions under a specific target. It can provide the specific conditions and performance reflected by the target, which can also better determine the goal to serve.

(2) KPI is an important basis for performance appraisal: in enterprise performance appraisal, we must fully consider and attach importance to the role of KPI. On the one hand, it is the result of performance appraisal, and on the other hand, it is performance management. It reflects both the ability to work and working conditions of employees, but also to help executives understand the ability of employees, targeted distribution of work, and setting goals.

(3) KPI realizes good communication and interaction: in the KPI formulation process, communication, exchange, and assistance between managers and subordinates are required to ensure the consistency of strategic goals and personal goals and achieve common growth and development.

(4) KPI realizes the performance appraisal method combining qualitative and quantitative: KPI data can be used to make quantitative judgments of performance. Here, analyze and summarize the data to make a qualitative description, clarify the advantages and disadvantages of the existing KPI system, set the degree of achievement of goals, and understand the difficulties and improvements of employees based on their performance.

3. Experimental Model of Enterprise Performance Optimization Management Decision-Making and Coordination Mechanism Based on Multiobjective Optimization

3.1. Multiobjective Optimization Model. It is assumed that there are P research subjects and q assessment indicators in the entire system. The j index score of the first research object i is a_{ij} ($i = 1, 2, \ldots, p$ and $j = 1, 2, \ldots, q$). There are subject differences among the selected research subjects, which are caused by the differences in background and professional ability, so there are different optimization solutions in the performance distribution plan.

First, the research subjects are divided into different types according to the index scores. This article only considers the $q = 2$ situation and divides the research subject into two types: I type and II type. If

$$\frac{a_{i1}}{a_{11} + a_{21} + \cdots + a_{p1}} \geq \frac{a_{i2}}{a_{12} + a_{22} + \cdots + a_{p2}}. \tag{1}$$

The first research subject i is called type I research subject; otherwise, it is called type II research subject. Without loss of generality, this article assumes that the first s research subjects are model I research subjects and the remaining research subjects $p - s$ are model II research subjects.

Consider the general multiobjective optimization problem:

$$(MOP)_1 \min_{x \in \Omega} \left(f_1(x), f_2(x), \cdots, f_p(x) \right), \tag{2}$$

where Ω represents the feasible region range of the multiobjective optimization model $(MOP)_1$ and $f_1(x), f_2(x), \ldots, f_p(x)$ means that there is an objective function p within the feasible region. The basic concepts and lemmas are as follows.

Definition 1. Weak Pareto effective solution $(MOP)_1$ called $\widehat{x} \in \Omega$; if $x \in \Omega$ does not exist, $i = 1, 2, \ldots, p$ will have for any $f_i(x) < f_i(\widehat{x})$.

Lemma 1. *If $i \in \{1, 2, \ldots, p\}$ exists, $\widehat{x}$ is a constraint ε−scalarization problem:*

$$\min_{x \in \Omega} f_j(x) \quad f_j(x) \leq \varepsilon_j, j = 1, 2, \ldots, p, j \neq i, \varepsilon_j \in R. \tag{3}$$

The optimal solution $\widehat{x}$ is a $(MOP)_1$ weakly effective solution.

Now, introduce the satisfaction function, which can calculate the degree of satisfaction of the research subject to the performance distribution [23], which is expressed mathematically as the continuity problem formed by the change of the variable within the scope of the finite domain. It can be written as

$$Y_i = \sum_{j=1}^{2} y_{ij},$$

$$Y' = \sum_{i=1}^{p} y_{i1}, \tag{4}$$

$$Y'' = \sum_{i=1}^{p} y_{i2},$$

$$i = 1, 2, \ldots, p.$$

The multiobjective optimization model is established based on the satisfaction function, and its goals are set as follows: the first goal is to maximize the satisfaction of all research subjects; the second goal is to balance the satisfaction of the research subjects as much as possible. Its model can be expressed as

$$(\text{MOP})_2 \min_{\lambda_1,\lambda_2,x_1,x_2} \sum \left(f_i(\overline{Y}_i) - f_j(\overline{Y}_j) \right)^2, \tag{5}$$

$$\max_{\lambda_1,\lambda_2,x_1,x_2} \sum_{i=1}^{p} f_i(\overline{Y}_i), \tag{6}$$

$$s.t. \begin{cases} \lambda_j \in \left[l_j, u_j \right] \\ x_j \in \left[0, \min\left\{ \overline{X}_{1j} + t_\partial (s-1) \dfrac{S_{1j}}{\sqrt{s}}, \overline{X}_{2j} + t_\alpha (p-s-1) \dfrac{S_{2j}}{\sqrt{p-s}} \right\} \right] \end{cases}, j = 1,2. \tag{7}$$

Usage principle: there must be valid solutions for continuous functions in the closed interval, so $(\text{MOP})_2$ must be (weak) valid solutions. It can be seen from the formula that the satisfaction function $f_i(\overline{Y}_i)$ is continuous for any value of the effective interval, so $\sum_{1 \leq i \leq j \leq p} (f_i(\overline{Y}_i) - f_j(\overline{Y}_j))^2$ and $\sum_{i=1}^{p} f_i(\overline{Y}_i)$ are also continuous. And, the domain of definition $(\text{MOP})_2$ is bounded, so $(\text{MOP})_2$ must be a (weak) effective solution for multiobjective optimization processing.

3.2. Agency Model.

The agency model is used to analyze the incentive and restraint problems of operators. Assuming that the owner's problem is an incentive contract $s(x)$, the operators will be rewarded and punished according to the fluctuation of x [24]. Suppose the V-N-M expected utility function of the company owner is $v(\pi - s(x))$. The expected utility of the manager of the company is $u(s(\pi)) - c(a)$, where $\pi = \pi(a, \theta)$ is the monetary output of the owner (or the monetary income of the operator) and a is expressed as a one-dimensional variable of the degree of effort, in which θ is an exogenous random variable not controlled by the operator. $v' > 0$, $v'' \leq 0$; $u' > 0$, $u'' \leq 0$; $c' > 0$, $c'' > 0$. Both the owner and the operator hope that the risks they face are as few as possible. The owner wants the operator to work harder ($\partial\pi/\partial a > 0$), and the operator wants to work harder ($c' > 0$), and the marginal negative utility of the effort increases. Therefore, the owner and the operator have a conflict of interest. Unless the owner can provide sufficient incentives to the operator, the operator will not work as hard as the owner hopes [25].

Assuming that the distribution function $G(\theta)$, production technology sum $x(a, \theta)$, and utility function sum $\pi(a, \theta)$ are all common knowledge, that is, $v(.)$ and $u(.) - c(.)$, owners and operators have the same understanding of these technical relationships. The owner's expected utility function can be expressed as follows:

$$(p) \int v(\pi(a, \theta) - s(x(a, \theta))) g(\theta) d\theta. \tag{8}$$

Select the degree of effort ∂ and maximize the expected utility function $s(x)$ in formula (8). Operators are subject to two constraints, one of which is called the participation constraint, that is, the expected utility that the management obtains from accepting the contract must be greater than or equal to the maximum expected utility that can be obtained when not accepting the contract. It is also called the personal rationality restraint, expressed as follows:

$$(\text{IR}) \int u(s(x(a, \theta))) g(\theta) - c(a) \geq \overline{u}. \tag{9}$$

In the above formula, $\overline{u}$ is called the reserved utility, which is the maximum expected utility that can be obtained when the contract is not accepted. The second constraint is the operator's incentive compatibility constraint: among the two choices, one is the choice within the operator's control; the other is the range of actions the business owner wants the operator to take; if the latter is not less than the former, then the operator will act in compliance with the owner's expectations, which is expressed as follows:

$$(\text{IC}) \int u(s(x(a, \theta))) d(\theta) - c(a)$$
$$\geq \int u(s(x(a', \theta))) g(\theta) d\theta - c(a'), \forall a' \in A. \tag{10}$$

In the above formula, A represents the combination of all optional actions of the operator and $a' \in A$ is any action within the controllable range of the operator. To sum up, the owner's problem is to select ∂ and $s(x)$, maximize the expected utility function (P), and satisfy the constraints (IR) and (IC), namely,

$$\max_{a,s(x)} \int v(\pi(a, \theta) - s(x(a, \theta))) g(\theta) d\theta, \tag{11}$$

$$s.t. (\text{IR}) \int u(s(x(a, \theta))) g(\theta) d\theta - c(a) \geq \overline{u}, \tag{12}$$

$$(\text{IC}) \int u(s(x(a, \theta))) g(\theta) d\theta - c(a)$$
$$\geq \int u(s(x(a', \theta))) g(\theta) d\theta - c(a'), \forall a' \in A. \tag{13}$$

The above formula clearly expresses every technical relationship between the owner and the operator. If the indicators that the owner cares about, such as the degree of effort, turnover, profit, market share, and technological progress, are quantified into variables, they will be brought into the model, and a meaningful solution to the owner may be obtained. The agent model flowchart is shown in Figure 2. The flow chart of the agency model follows the procedure in the figure. Two standards are implemented in the position of the filling standard. If you agree, it will be executed. If you do not agree, the decision will be made again.
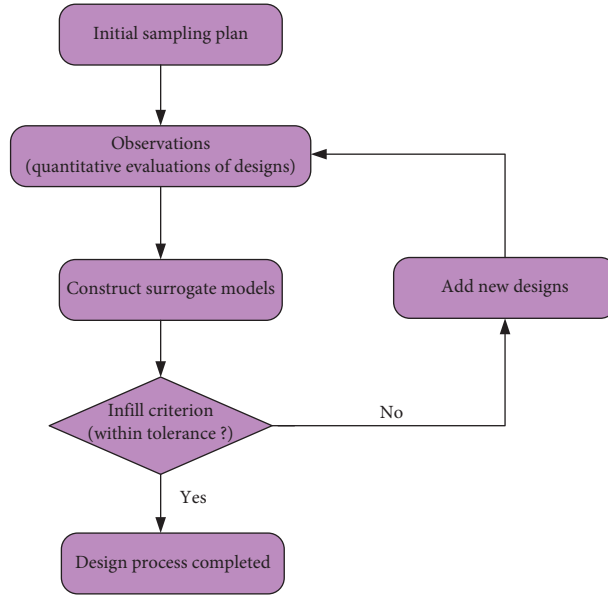
FIGURE 2: Agent model flowchart.

4. Management Decision-Making and Coordination Mechanism for Enterprise Performance Optimization Based on Multiobjective Optimization

4.1. Multiobjective Optimization Model Analysis. The research of this paper is mainly to use the multiobjective optimization model established in the previous article to study the problem of enterprise performance management decision-making and coordination. Take company Y as an example, select the work performance and ability of company employees and conduct performance evaluation on 40 employees. Table 1 shows the 40 employees' work performance index scores and work ability assessment index scores.

From the data in Table 1, the company performance is first divided into two aspects, personal work performance and work ability, where personal work performance $s = 48$; it can be seen that the data in Table 1 basically meets the conditions of satisfaction function formula (4), and then calculate these parameters. Afterwards, it can be concluded that when the confidence level is equal to 0.95, the estimated interval of the basic workload X_1 and the work capacity workload X_2 of the work performance index is [0, 356.91] and [0, 790.72]; take $u_1 = u_2 = 0.1$ and $l_1 = l_2 = 10$. To simplify the calculation, let $\varepsilon = \lambda_1/\lambda_2$:

$$g_k(\varepsilon, x_1, x_2) = f_k(\overline{Y}_k),$$

$$= \sqrt{\frac{1}{U_k - L_k} \frac{u_{k1}\lambda_1(a_{i1} - x_1)^2 + u_{k2}\lambda_2(a_{k2} - x_2)^2}{\sum_{i=1}^p u_{i1}\lambda_1(a_{i1} - \lambda_1)^2 + \sum_{i=1}^p u_{i2}\lambda_2(a_{i2} - x_2)^2}} - \frac{L_k}{U_k - L_k},$$

$$= \sqrt{\frac{1}{U_k - L_k} \frac{u_{k1}\varepsilon(a_{k1} - x_1)^2 + u_{k2}(a_{k2} - x_2)^2}{\sum_{i=1}^p u_{i1}\varepsilon(a_{i1} - x_1)^2 + \sum_{i=1}^p u_{i2}(a_{i2} - x_2)^2}} - \frac{L_k}{U_k - L_k},$$

(14)

where $\varepsilon \in [0.01, 100]$, and in turn, $(MOP)_2$ can be transformed into

$$(MOP)_3 \min_{\varepsilon, x_1, x_2} \sum_{1 \le i \le j \le p} \left(g_i(\varepsilon, x_1, x_2) - g_j(\varepsilon, x_1, x_2)\right)^2, \quad (15)$$

$$\min_{\varepsilon, x_1, x_2} - \sum_{i=1}^p g_i(\varepsilon, x_1, x_2), \quad (16)$$

$$s.t. \varepsilon \in [0.01, 100], x_1 \in [0, 356.91], x_2 \in [0, 790.72]. \quad (17)$$

The result shows that $(MOP)_2$ and $(MOP)_3$ are equivalent, and then, the genetic algorithm is used to calculate the weak Pareto front surface $(MOP)_3$, as shown in Figure 3.

It can be seen from Figure 3 that the weak Pareto solution obtained by the legacy algorithm is some irregular discrete points. According to their dense and sparse degree,

TABLE 1: The 40 employees' work performance index scores and work ability assessment index scores.

Serial number	Work performance	Ability to work
1	2338	435
2	1037	480
3	2578	373
4	2063	264
5	1733	203
6	2044	241
7	2291	245
8	2851	253
9	2904	378
10	1212	421
11	2114	421
12	2487	352
13	1638	481
14	1773	306
15	2630	352
16	1556	388
17	2563	328
18	1615	399
19	1528	435
20	2221	480
21	1540	431
22	2989	256
23	2438	441
24	1865	300
25	1985	332
26	2012	247
27	1494	239
28	2616	411
29	1253	350
30	1984	296
31	2536	345
32	2443	249
33	1819	234
34	1545	399
35	2099	222
36	1736	440
37	2178	201
38	1626	418
39	1702	351
40	1698	212

FIGURE 3: The forefront of the weak Pareto solution.

In addition, in order to fully consider the rigor of the experiment, the weak Pareto frontiers at different confidence levels are given. As shown in Figure 6, the changing trends of the weak Pareto frontiers at the five different confidence levels are basically the same, that is, different confidence levels affect the results. The impact is small.

4.2. Employee Incentive and Restraint Mechanism. Employees are the cells of an enterprise and are an indispensable and important part of this organism. Improving employees' production enthusiasm, increasing production efficiency, and promoting employees to conduct research on technology and management will enable the company to increase the efficiency of the work and create outstanding performance. Enterprises are composed of people, and the research on "people" has begun since the formation of society. Some management scholars in the West have used experimental methods to conduct research many times, hoping to find out how "corporate people" can give full play to their abilities and improve work efficiency. Taylor did experiments such as "carrying pig iron" to determine the employee's work quota, and the Gilbreths did an experiment of "action decomposition and research" to reduce the inefficiency caused by invalid actions at work. Mayo hosted the "Hawthorne." The experiment reveals the social attributes of people and closely links productivity with factors such as employees' psychology, attitude, motivation, and interpersonal relationships. Later, some management scientists put forward the *X* theory, *Y* theory, *Z* theory, etc., starting from the employees' preference and perspective and further studying effective incentive methods.

China's cultural background and national conditions have their own characteristics. Obviously, it is useless to apply certain theories above to Chinese enterprise groups alone. Enterprise groups should be based on their ability to pay, the characteristics of their employees, and the market environment. Referring to the advanced management experience of other companies and the current mature management theories, motivate the interest and enthusiasm of employees and explore a suitable incentive and restraint

the left side can be appropriately regarded as a smooth curve, and the right side is more sparse.

This paper randomly selects 5 groups of weak Pareto effective solutions (see Table 2) corresponding to the distribution ratio and satisfaction curve shown in Figures 4 and 5. The overall satisfaction level in Table 2 is balanced, and the square sum of the satisfaction difference shows signs of fluctuation.

Observing Figures 4 and 5, we can see that, in the face of randomly selected weakly effective Pareto solutions, the overall satisfaction and distribution ratio of the research subject are only slightly different, which can be approximated as a coincident curve. Therefore, in the process of performance management, managers adopt a multiobjective optimization model and only need to select a set of weak Pareto solutions arbitrarily to achieve optimal performance decision-making and coordination.

TABLE 2: Five groups of weak Pareto effective solutions and related parameters.

	Total satisfaction	Sum of squares of satisfaction difference	ε	X_1	X_2
First group	60.05	3.51	0.50	169.50	351.46
Second group	61.24	13.72	0.50	23.36	126.44
Third group	61.58	20.36	0.49	16.97	13.64
Fourth group	61.74	30.15	0.56	15.49	3.72
Fifth group	61.76	32.49	0.58	15.45	3.66
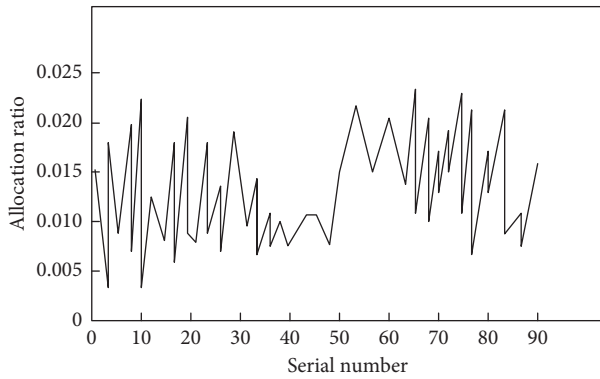
FIGURE 4: Distribution ratio curves corresponding to 5 groups of weakly effective solutions.
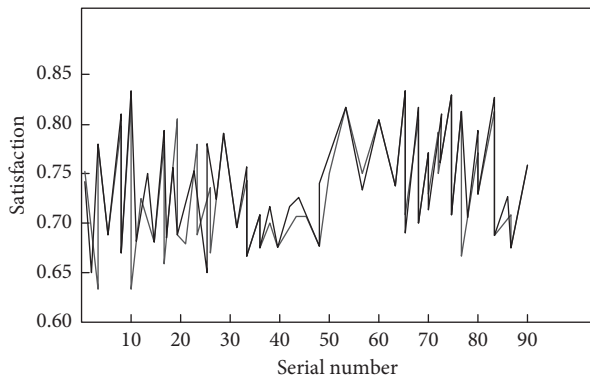
FIGURE 5: Satisfaction curve corresponding to 5 groups of weak Pareto effective solutions.

- $a = 0.05$
- $a = 0.06$
- $a = 0.07$
- $a = 0.08$
- $a = 0.09$

FIGURE 6: Pareto front surface obtained by solving different confidence levels.

method for employees of the enterprise group from the aspects of emphasizing human sociality and subjectivity.

As shown in Table 3 and Figure 7, in a survey of American industrial enterprises, managers' understanding of workers' needs is compared with workers' actual needs. There is a big discrepancy between the two. This article also conducts a sample survey of the managers and employees of some companies. Although the survey results may not be universal, they can explain some problems. The needs of employees in Chinese enterprise groups are different from those of foreign companies, and to a certain extent, there is a deviation in the understanding of the needs of the employees by the operators and employees themselves, as shown in Table 4 and Figure 8.

It can be seen from Table 4 and Figure 8 that when many companies analyze the needs of employees and formulate incentive policies, they often rely on the subjective assumptions of the operators. Due to the differences in the status and division of labor between operators and employees, there will always be some differences in their grasp of real needs. The incentive measures formulated by the operators for employees based on their own perceptions do not address the real needs of the employees, so there is no incentive. On the contrary, due to the complexity of the specific situation of enterprise groups, one enterprise can refer to the situation of another enterprise to formulate an incentive mechanism, but it must not be copied. The needs of employees of different companies vary greatly. For example, employees of state-owned enterprises usually regard the enterprise as the support of themselves and their families and have a strong sense of dependence. They yearn for stable work, proper medical care, housing, and childcare. In contrast, do they have to take it? High wages are not as important as the above factors. The employees of high-tech companies require high salaries, more knowledge and skills, promotion, etc. It does not matter whether the job is stable or not. As long as they have the ability and knowledge, they can find better job opportunities at any time. The age of employees also affects their needs. Generally speaking, 18 to 28 years old employees have less family burdens, have full enthusiasm for work, and are not sure about their self-reliance. Therefore, they prefer to be appreciated by the

TABLE 3: Comparison of the ranking of the needs of the US survey managers and the workers themselves.

Required content	Manager thinks (rank)	Workers think (rank)
High salary	1	5
Work stability	2	4
Promotion and corporate growth	3	7
Good working environment	4	9
Interesting job	5	6
Management's concern for workers	6	8
Skill training	7	10
Appreciation of work	8	1
Compassion and understanding of personal issues	9	3
Devotion to things	10	2
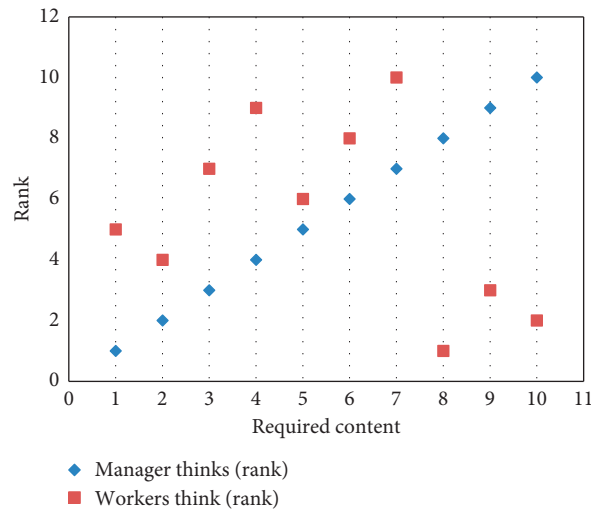
FIGURE 7: Comparison of the ranking of the needs of the US survey managers and the workers themselves.

TABLE 4: Comparison of the ranking of the needs of the employees between the operators of the Y enterprise and the employees themselves.

Required content	Manager thinks (rank)	Workers think (rank)
High salary	1	4
Promotion and corporate growth	2	7
Skill training	3	3
Good working environment	4	8
Work stability	5	1
Generous benefits	6	5
Appreciation of work	7	2
Interesting job	8	9
Harmony of labor relations	9	10
Harmonious team relationship	10	6

leader and have a harmonious team relationship and desire to have a lot of exercise and training opportunities to increase their abilities. The one-year-old Peng's employees are in the period of forming families, having children, and, at the same time, eager to have better job prospects in the career. Therefore, he has a door to demand high salaries and generous benefits to ensure the needs of the family such as promotion, corporate growth, and a good working environment to achieve their career pursuits and ambitions. For employees over 48 years old, their children can already support themselves. They can and are willing to devote time to work, especially some

older employees hope that through happy work, they can give full play to their abilities. I also want to get a high salary and good benefits, but when my income is not high, I can also maintain good labor relations and team relations and can be recognized and praised by the leaders for my work. It can also stimulate their enthusiasm. Kemen can even categorize the age group more carefully and consider the actual situation of employees more comprehensively, and then, more specific characteristics of needs can be derived. According to the understanding of super Y theory, people are different from each other, and each person's needs are different.

FIGURE 8: Comparison of the ranking of the needs of the employees between the operators of the Y enterprise and the employees themselves.

In summary, the business managers should first start from the actual situation of the employees, understand the real needs of the employees of the company through careful observation and care, and then formulate incentive and restraint mechanisms in a targeted manner.

5. Conclusions

This paper mainly studies the decision-making and coordination mechanism of enterprise performance optimization management based on multiobjective optimization. Based on system management theory and performance management theory, through constructing the multiobjective optimization model and agency model, using the genetic algorithm, the Pareto effective solution is obtained to help enterprise performance management make optimal decision-making and coordination. By analyzing the relationship between the company and the management and the company and its employees, multiobjective optimization is carried out to promote the healthier development of the company and its employees.

The innovation of this article is that this article uses a combination of empirical research and normative research, such as the research on the employee incentive and restraint mechanism of the Y enterprise in the fourth part; it uses a combination of qualitative research and quantitative analysis, and this method has been reflected in the analysis of multiobjective optimization models; the method of combining theoretical analysis and countermeasure research is used, and countermeasure suggestions are given, while establishing model analysis. This method runs through this article.

The research in this paper still has shortcomings: the data samples selected in this paper are small, and the research results need to be more comprehensively considered. The representativeness of the samples needs to be evaluated; the selection of target parameters has certain limitations, and the research subjects of the samples are subjective and not conducive to the objective and fairness of the research results. The research in this article has certain guidance and practical significance for the optimal choice of corporate performance. This research topic will help the company to develop more sustainably and healthy in the long run.

Data Availability

No data were used to support this study.

Conflicts of Interest

The authors declare that they have no conflicts of interest.

References

[1] L. A. Orozco, J. Vargas, and R. Galindo-Dorado, "Trends on the relationship between board size and financial and reputational corporate performance," *European Journal of Management and Business Economics*, vol. 27, no. 2, pp. 183–197, 2018.

[2] H. K. Kam and Y. J. Shin, "The effect of working capital management on corporate performance," *Journal of the Korea Academia-Industrial Cooperation Society*, vol. 17, no. 6, pp. 173–180, 2016.

[3] F. Laghari and Y. Chengang, "Investment in working capital and financial constraints," *International Journal of Managerial Finance*, vol. 15, no. 2, pp. 164–190, 2019.

[4] N. Aubert, H. Ben Ameur, G. Garnotel, and J.-L. Prigent, "Optimal employee ownership contracts under ambiguity aversion," *Economic Inquiry*, vol. 56, no. 1, pp. 238–251, 2018.

[5] M. Madanoglu and E. Karadag, "Corporate governance provisions and firm financial performance," *International Journal of Contemporary Hospitality Management*, vol. 28, no. 8, pp. 1805–1822, 2016.

[6] S. J. Lin, "Hybrid kernelized fuzzy clustering and multiple attributes decision analysis for corporate risk management," *International Journal of Fuzzy Systems*, vol. 19, no. 3, pp. 1–12, 2016.

[7] R. Reskino, "Zakat and islamic corporate social responsibility: does it take effect to the performance of shari'a banking?" *Shirkah Journal of Economics and Business*, vol. 1, no. 2, pp. 161–184, 2016.

[8] T. Verheyden, R. G. Eccles, and A. Feiner, "ESG for all? The impact of ESG screening on return, risk, and diversification," *Journal of Applied Corporate Finance*, vol. 28, no. 2, pp. 47–55, 2016.

[9] V. Nanda and B. Onal, "Incentive contracting when boards have related industry expertise," *Journal of Corporate Finance*, vol. 41, pp. 1–22, 2016.

[10] G. Cokins, "Enterprise performance management (EPM) and the digital revolution," *Performance Improvement*, vol. 56, no. 4, pp. 14–19, 2017.

[11] C. Wells, A. Farhat, C. Richardson et al., "A vine copula-GARCH approach to corporate exposure management," *The Journal of Risk*, vol. 20, no. 2, pp. 27–51, 2017.

[12] W. Liu, S. Niu, and H. Xu, "Optimal planning of battery energy storage considering reliability benefit and operation strategy in active distribution system," *Journal of Modern Power Systems and Clean Energy*, vol. 5, no. 2, pp. 177–186, 2017.

[13] Q. Liu, W. Cai, J. Shen, Z. Fu, X. Liu, and N. Linge, "A speculative approach to spatial-temporal efficiency with multi-objective optimization in a heterogeneous cloud environment," *Security and Communication Networks*, vol. 9, no. 17, pp. 4002–4012, 2016.

[14] Z. Fei, B. Li, S. Yang, C. Xing, H. Chen, and L. Hanzo, "A survey of multi-objective optimization in wireless sensor networks: metrics, algorithms, and open problems," *IEEE Communications Surveys & Tutorials*, vol. 19, no. 1, pp. 550–586, 2017.

[15] M. Li, S. Yang, and X. Liu, "Pareto or non-pareto: Bi-criterion evolution in multiobjective optimization," *IEEE Transactions on Evolutionary Computation*, vol. 20, no. 5, pp. 645–665, 2016.

[16] M. Hamdy, A.-T. Nguyen, and J. L. M. Hensen, "A performance comparison of multi-objective optimization algorithms for solving nearly-zero-energy-building design problems," *Energy and Buildings*, vol. 121, no. 6, pp. 57–71, 2016.

[17] R. Saborido, A. B. Ruiz, J. D. Bermúdez, E. Vercher, and M. Luque, "Evolutionary multi-objective optimization algorithms for fuzzy portfolio selection," *Applied Soft Computing*, vol. 39, no. 2, pp. 48–63, 2016.

[18] Y. Boada, G. Reynoso-Meza, J. Picó et al., "Multi-objective optimization framework to obtain model-based guidelines for tuning biological synthetic devices: an adaptive network case," *BMC Systems Biology*, vol. 10, no. 1, pp. 1–19, 2016.

[19] N. Gupta and A. Bari, "Fuzzy multi-objective optimization for optimum allocation in multivariate stratified sampling with quadratic cost and parabolic fuzzy numbers," *Journal of Statal Computation & Simulation*, vol. 87, no. 10–12, pp. 1–12, 2017.

[20] H.-S. Kang and Y.-J. Kim, "A study on the multi-objective optimization of impeller for high-power centrifugal compressor," *International Journal of Fluid Machinery and Systems*, vol. 9, no. 2, pp. 143–149, 2016.

[21] L. Yu, Z. Yang, and L. Tang, "Prediction-based multi-objective optimization for oil purchasing and distribution with the NSGA-II algorithm," *International Journal of Information Technology & Decision Making*, vol. 15, no. 2, pp. 423–451, 2016.

[22] T. Chen, K. Li, R. Bahsoon et al., "FEMOSAA: feature guided and knee driven multi-objective optimization for self-adaptive software at runtime," *ACM Transactions on Software Engineering and Methodology*, vol. 27, no. 2, pp. 51–55, 2018.

[23] Y. Li, Q. Ye, A. Liu et al., "Seeking urbanization security and sustainability: multi-objective optimization of rainwater harvesting systems in China," *Journal of Hydrology*, vol. 550, pp. 42–53, 2017.

[24] C. Prakash, H. K. Kansal, B. S. Pabla, and S. Puri, "Multi-objective optimization of powder mixed electric discharge machining parameters for fabrication of biocompatible layer on β-Ti alloy using NSGA-II coupled with Taguchi based response surface methodology," *Journal of Mechanical Science and Technology*, vol. 30, no. 9, pp. 4195–4204, 2016.

[25] A. Subasi, B. Sahin, and I. Kaymaz, "Multi-objective optimization of a honeycomb heat sink using Response Surface Method," *International Journal of Heat and Mass Transfer*, vol. 101, no. 2, pp. 295–302, 2016.

Research Article

A New Tracking Algorithm Based on Improved Fuzzy C-Means Dynamic Kalman Filter in Sport Video

Yonghua Zhou,[1] **Ting Huang,**[2] **and Shangbin Li** [3]

[1]*Department of Physical Education, Tianjin Foreign Studies University, Tianjin 300204, China*
[2]*School of Physical Education and Educational Science, Tianjin University of Sport, Tianjin 301617, China*
[3]*Physical Education Department, Harbin Engineering University, Harbin 150001, China*

Correspondence should be addressed to Shangbin Li; sports@hrbeu.edu.cn

The paper studied the problems of soccer detection and tracking in soccer tracking, in soccer detection; as the size of the soccer is too small to extract distinguishable feature, it is difficult to detect the soccer automatically. To solve this problem, a soccer detection algorithm was based on class weighted spatial Fuzzy C-means (ws-FCM) was proposed. Firstly, the target function of the spatial Fuzzy C-means was improved. Subsequently, a bi-threshold strategy was proposed to detect the soccer automatically. In the aspect of soccer tracking, existing methods fail to detect the soccer when it was occluded by several players successively. To solve this problem, the motion state of soccer of broadcast soccer video was analyzed, which is inspired by the contextual cueing effect of human visual search. According to the motion state of the soccer, parameters updating function of dynamic Kalman filter (DKF) were improved. Thus, a soccer tracking algorithm based on multiple search regions dynamic Kalman filter (MDKF) was proposed, which enhances the robustness of soccer tracking by extending the search area. The experiments show that the proposed algorithm can automatically detect soccer in images with high detection accuracy and can track the soccer more robustly, with better occlusion handle ability.

1. Introduction

The research goal of video content analysis technology is to establish the mapping between low-level features and high-level semantics, so as to automatically acquire semantic content and build user-oriented application systems to provide users with more convenient content acquisition services. Video content is diverse. Therefore, it is difficult for video content analysis technology to be universal, and the design of corresponding identification methods needs to be in accordance with the characteristics of the analyzed video content. The research object of video content analysis is usually a specific type of video with urgent content analysis need, such as soccer videos. Soccer videos have a broad audience and significant business value, and their content analysis technology has attracted many researchers [1, 2]. The demand for the content analysis of soccer videos comes not only from the requirements of ordinary users for

selective viewing of wonderful clips, specific events, etc., but also from soccer fans and soccer professionals (coaches, players) to quickly locate the needs of certain types of offenses from the many offenses. These users expect to analyze the game strategy and tactics by the previous game videos to achieve a deeper understanding of the game process and improve the performance of the game [3]. Research on soccer video game strategy and tactics analysis is relatively scarce, and related requirements have not been fully met. Therefore, this paper focuses on this need.

Humans have flexible and powerful video content understanding capabilities and can accurately and automatically identify specific content in videos [4]. The essential information contained in the video is the human cognitive content. On a wide recognition of this point of view, human cognitive principles become an essential reference for video content analysis researchers [5]. Soccer video content analysis technology focuses on automatically analysis of

related content based on the content characteristics and analysis needs of soccer videos. Therefore, research on content analysis methods with utilization of human cognitive principles and the content characteristics of soccer videos will likely expand the research ideas of soccer video tend to enrich related research ideas.

Soccer is the object which is scrambled for and controlled by both teams in the competition. Its motion characteristics reflect team attack strategy, playing a supporting role in analyzing the high-level semantic contents [6, 7]. In the broadcast soccer videos, the soccer size is too narrow to be directly detected. Although the shape exclusion method relieves the difficulty, it is of bad practicability because it is required to obtain the binary image of foreground objects [8–10]. Besides, in the motion course, soccer tends to merge and occlude with marking lines or players, leading to missing of soccer measuring values and failure of tracking. In order to enhance the robustness of tracking and maintaining processes, Kim et al. proposed a dynamic Kalman filter algorithm that merges the occlusion processing mechanism. However, the method also loses rubber soccer with complicated occlusion [11–13].

Soccer tracking is a typical human visual motion tracking process. Therefore, we can classify soccer tracking into two phases, soccer tracking and tracking maintenance, which are each corresponding to target acquisition and motion tracking of human visual tracking [14]. At the stage of target acquisition, the visual system aims to enter into the visual system to select visual stimulation and determine tracking objects. The preference of such selection is associated with the scene priori of pending tracking object, with from-top-to-bottom factor. Hence, in soccer detection, it is possible to optimize the detection method according to the scene feature of soccer video to increase the automation degree of soccer detection method. In the motion tracking stage [15], in order to overcome the influence of occlusion on tracking maintenance, the human visual search system is able to complete visual tasks like search and tracking in the aid of contextual cueing effect. Concerning principle of the soccer tracking method, it is likely to intensify the robustness of the tracking algorithm.

In sports video analysis, the trajectory obtained by object tracking can be used for the analysis of much high-level semantic content. Therefore, tracking important objects has always been an important aspect of sports video analysis research. Soccer is one of the most critical objects in soccer videos. Soccer position and trajectory information can be widely used in a video summary, the region of interest (ROI) coding, tactical analysis, etc. Therefore, detecting soccer and tracking soccer is a valuable research content of soccer video content analysis. Modern soccer game uses a truncated icosahedron sewn with leather, which is unique during the game. Therefore, soccer detection and soccer tracking in soccer videos are complementary. In videos, soccer often appears as a circle. Based on this feature, Orazio et al. [16] first attempted to detect soccer in images using circularity features. Subsequently, Tong et al. [17] proposed a candidate soccer detection method that combined circularity and color. In order to express the needs of the game, the camera needs to cover a certain area of the field. Therefore, the area occupied by soccer in the broadcast video is relatively small, and the distinguishability of the extracted features is not high. Many objects, such as over-divided indicator lines and players, have similarities in color and shape for soccer. Therefore, the above methods have limited improvement in soccer detection performance and cannot accurately detect soccer areas.

Because of the difficulty in directly extracting soccer features, Yu et al. [6] proposed a soccer detection method based on the exclusion method. This method first obtains a binary image of the foreground object, then excludes most of the areas that do not belong to the soccer through a set of shape rules, and finally verifies the remaining candidate soccer. Despite some shortcomings in obtaining foreground objects, the exclusive method is still a practical method for soccer detection and tracking. Based on this method, Liang, Choi et al. [8] proposed a multiframe based soccer detection. The soccer area detected by the exclusion method is not unique. In order to determine the position of the soccer, the researchers further proposed a soccer tracking method based on the Kalman filter and the trajectory optimization method based on the exclusion method. The above methods all have a certain dependence on the soccer detection effect based on the exclusive method [10]. However, the exclusion method can only detect unblocked soccer. When the soccer is occluded, the exclusive method cannot detect the soccer's position. In this case, the tracking performance of the above method is also affected.

In broadcast soccer videos, soccer is often blocked by players. Therefore, it is necessary to study the soccer tracking method in the case of occlusion. It is generally believed that in order to maintain tracking of objects under occlusion conditions, corresponding occlusion processing mechanisms need to be integrated into the tracker [18]. Based on this principle, Seo et al. proposed a soccer tracking method with the occlusion processing mechanism; this method marks the player closest to soccer as a "has ball." If soccer disappears during tracking, the tracker will search for soccer near the "has ball." Choi et al. expanded the search of soccer to include players close to the player with the ball. These two methods can keep the soccer tracked to a certain extent when the players block the soccer. However, when soccer is blocked by something other than the player, the above method will still have tracking errors. In order to further enhance the tracking ability under occlusion, Kim et al. [13] proposed a DKF tracking method. Typical Kalman filter (TKF) algorithm only uses the measured position of soccer for parameter update. Therefore, when soccer is blocked and cannot be measured, TKF is not be able to make the correct parameter updates and may cause the soccer to be lost. To this end, DKF dynamically adjusts TKF's parameter update strategy based on the results of object detection in the search area. Due to this dynamic mechanism, DKF has a certain occlusion processing capability, and the soccer tracking results are more robust. However, DKF's parameter update functions are still not perfect. When multiple players continuously block the soccer, DKF may still lose track of the soccer.

Based on the above analysis, this paper discusses the soccer tracking problem from two aspects: soccer detection and tracking maintenance. In soccer detection, with regards to the lack of automatic detection method of soccer, the paper presents an automatic soccer detection method based on class weighting sFCM, in accordance with features like changeable facade patterns of soccer and susceptibility to interference. The method increases the error weight of the foreground object by means of target function optimization and deduces soccer leak detection caused by sFCM. On that basis, the paper develops a detection method based on dual threshold strategy, realizing automatic soccer detection. In soccer tracking, by learning from the process of human visual search context prompt effect, this paper analyzes the motion state of soccer, optimizes the parameter updating function of dynamic Kalman filter according to the motion state of soccer, and proposes a multiarea search dynamic Kalman algorithm. The filtering method improves the robustness of the soccer tracking method.

2. Soccer Detection Based on Class-Weighted SFCM

On the ground that appears in broadcast videos, there are lots of objects which have similar colors with the soccer. Thus, it is difficult to detect soccer by means of color features. Compared with other objects, soccer occupies too smaller area and the area is usually elliptical or round, which differs apparently from other objects by shape. So, the soccer detection method based on shape is widely applied. The premise to detect rubber soccer with the use of shape difference is to binarize images which are waiting for analysis. At present, there is no effective binarizing method oriented to the soccer detection. To address the question, the authors developed a binarization method based on class weighted sFCM on the foundation of the soccer detection scene priori.

Furthermore, on that basis, the soccer detection approach based on dual threshold strategy is designed. Therefore, we used local difference image to binarize and detect soccer detection. The clustering method is a typical image binarizing method. FCM is a popular one of various fuzzy clustering algorithms and widely applied in image segmentation. However, the FCM method cannot describe spatial features of the image and obtained binary images mostly have a noisy area. Therefore, Chuang et al. got sFCM by improving the membership function and decreased noises that are easily found in segmentation results by FCM. However, when completing binarization oriented to the soccer, sFCM easily cause leak detection of soccer area. Hence, first of all, we probe into the principle of FCM and sFCM and then optimize error objective function of sFCM according to the requirement of soccer detection [19].

In the sense of clustering principle, the basic idea of FCM is divided n data x_i into k groups and makes objective function value at the minimal. During the clustering, the objective function defined by Bezdek is often adopted. It is shown in the following equation:

$$J_m(U, c_1, \ldots, c_k) = \sum_{i=1}^{n} \sum_{k=1}^{j} (u_{i,k})^m (x_i - c_k)^2. \quad (1)$$

Under the constraint condition $\sum_{k=1}^{j} u_{i,k} = 1$, the necessary condition for the equation (1) to obtain the extreme value is derived by the Lagrange multiplier method. It is shown as follows:

$$c_k = \frac{\sum_{i=1}^{n} u_{i,k}^m x_i}{\sum_{i=1}^{n} u_{i,k}^m}, \quad (2)$$

$$u_{i,k} = \frac{1}{\sum_{p=1}^{j} (d_{i,k}/d_{i,p})^{2/m-1}}. \quad (3)$$

In order to get the best partition of data set, the FCM algorithm iteratively updates the c_k and $u_{i,k}$, which minimizes the objective equation (1), and the main steps are

(1) The number of clusters j is determined, membership index m, stop threshold $\varepsilon > 0$

(2) The initial cluster center $C^0 = (c_1, \ldots, c_k)$ from x_i is randomly selected

(3) The following operations are repeated, until $\|C^{s+1} - C^s\| < \varepsilon$

According to the above steps, the use of FCM for image two values only needs to set the number of categories. Then, the membership value of each pixel is divided according to the following equation:

$$B_i = \begin{cases} 1, & \text{if } u_{i,1} > u_{i,0}, \\ 0, & \text{if } u_{i,1} \leq u_{i,0}. \end{cases} \quad (4)$$

Compared with the general data, one of the characteristics of the image data is the high correlation of neighboring pixels. The gray values of the domain pixels are usually similar. Therefore, adjacent pixels are more likely to belong to the same category. Making good use of this relationship can effectively reduce the false detection of clustering results. However, in the classical FCM, the correlation between neighboring pixels is not modelled. Thus, there is much noise in the two value image obtained by FCM. In order to ensure that better use of the neighborhood correlation in the image to eliminate the detection noise, Chuang et al. proposed the FCM algorithm to fuse the spatial information-Spatial Fuzzy C-Means (sFCM). The basic idea of this method is to add spatial information into the calculation of membership degree. Based on equation (3), the spatial information function $(h_{i,k})$ is shown as follows:

$$h_{i,k} = \sum_{k \in NB(x_i)} u_{i,k}. \quad (5)$$

With regards to the questions mentioned above, the authors proposed class weighted fuzzy C mean clustering algorithm (wsFCM) in line with the specific requirement of soccer detection binarization. The primary thought of the algorithm is to add different weighting factors in accordance with different quantities of class pixels, so as to equilibrize

the impact of class quantity difference in the clustering result. In order not to lose generality, we define wsFCM objective function as follows:

$$J_w = \sum_{i=1}^{n} \sum_{k=1}^{j} w_k \left(u_{i,k}\right)^m \left(x_i - c_k\right)^2. \qquad (6)$$

According to definition of objective function J_w, we learn that w_k should be inversely proportional to the quantity of sample. So, as long as the quantity of foreground object pixel and the contextual pixel is determined, w_k can be determined. The triangle threshold method can binarize pixels of a majority of foreground objects. Some pixels are falsely detected, but there are very fewer. Therefore, we utilize the triangle threshold method to decide the value of w_k, solving in the way as follows:

$$w_1 = \frac{P_2}{P},$$
$$\qquad (7)$$
$$w_2 = \frac{P_1}{P}.$$

Summing up the above process, the iterative process of wsFCM algorithm mainly includes the following steps:

(1) The number of clusters k is determined, membership index m, stop threshold $\varepsilon > 0$, category weight w_k

(2) The initial cluster center $C^0 = (c_1, \ldots, c_k)$ from x_i is randomly selected

(3) The following operations are repeated, until $\|C^{s+1} - C^s\| < \varepsilon$

Figure 1 is an example of foreground object pixel detection results.

With the automatic threshold, plenty of falsely detected pixels exist in the foreground object detection result by the Canny operator, impossible to detect the soccer effectively. Comparatively, the Otsu and triangle threshold method (Rosin method) got a fewer number of noisy areas in the binarized images. The sFCM is advantageous in eliminating binarized image noise, but soccer is lost in some frames. As shown in Figure 1(b), the proposed wsFCM can achieve better noise removing the effect in the meantime of not losing soccer.

Despite wsFCM can effectively suppress noise in the binarized images, oversegmented marking lines appear in the binary results. Due to the movement of soccer and camera, the gray value of soccer and other objects will vary. Thus, we use a triangle threshold method to remove oversegmented areas.

The gray values of the playground's pixels are of identical size; hence, those pixels' values are smaller in local difference images, mostly distributed close to zero value. Background pixels of smaller gray values are dominant in local difference images and form a central peak in the histogram. It is more appropriate to employ to binarize the images which have a single peak histogram. Figure 2 is schematic of the triangle threshold.

After input image is converted to local difference image, the method firstly gets the binary image B_t and B_w of foreground pixel area by the triangle threshold method and wsFCM method; next, from B_t and B_w, we acquire candidate soccer area through a set of predefined shape rules; finally, the results were combined by two methods. Since the width, height, and area of soccer region and the aspect ratio are obviously different from other regions. We detected candidate soccer region by following rules. It is shown in

$$\begin{cases} \min(w, h) > \theta_h, \\[2mm] \max(w, h) < \theta_w, \\[2mm] \dfrac{\max(w, h)}{\min(w, h)} < 3, \\[2mm] \theta_{\min} < \text{area} < \theta_{\max}. \end{cases} \qquad (8)$$

The resolution of the video in this paper is $720 * 404$. At this resolution, the typical values of the parameters in the equation (4) are $\theta_h = 2$, $\theta_w = 5$, $\theta_{\min} = 5$, and $\theta_{\max} = 30$. The candidate soccer area detected using this method is shown in Figure 3. The analysis shows that the method can effectively eliminate the over segmentation in B_w, thus improving the accuracy of soccer detection. It is shown in Table 1.

A comparison between Figures 1 and 3 also shows that there is a mistake in the area near the goal. The position is the soccer match referee penalty kick should be placed in the position of soccer, that is, the penalty point (penalty mark, also known as the penalty point, 12 yards). In broadcast soccer, spot color, size, shape, and soccer are very similar; it is hard to distinguish with the soccer detection methods; it needs to be distinguished by penalty shot detection methods.

3. Soccer Tracking Method Based on Multiarea Search Dynamic Kalman Filter

From the theoretical perspective, soccer tracking can be modelled to Bayesian state estimation problem. State refers to various motion characteristics of objects to our concern. According to the opinions of Bayesian estimation, the essence of object tracking is to determine recursively the confidence level of state vector s_t at time t according to the acquired observational data $z_{1:t}$, that is, posterior probability density function $p\, p(s_t|z_{1:t})$ of estimation state vector. The Bayesian filter utilizes two models regarding the object state to make inference through a state transition equation in

$$x_t = Ax_{t-1} + w_t, \qquad (9)$$

$$z_t = Hx_t + v_t. \qquad (10)$$

Particle filter and Kalman filter are currently the popular Bayesian filtering methods. Since the soccer area is smaller in broadcast videos, it is rather hard to fetch discrimination features, hardly representing the probability density function of state in the manner of sampling. Therefore, Kalman filter is
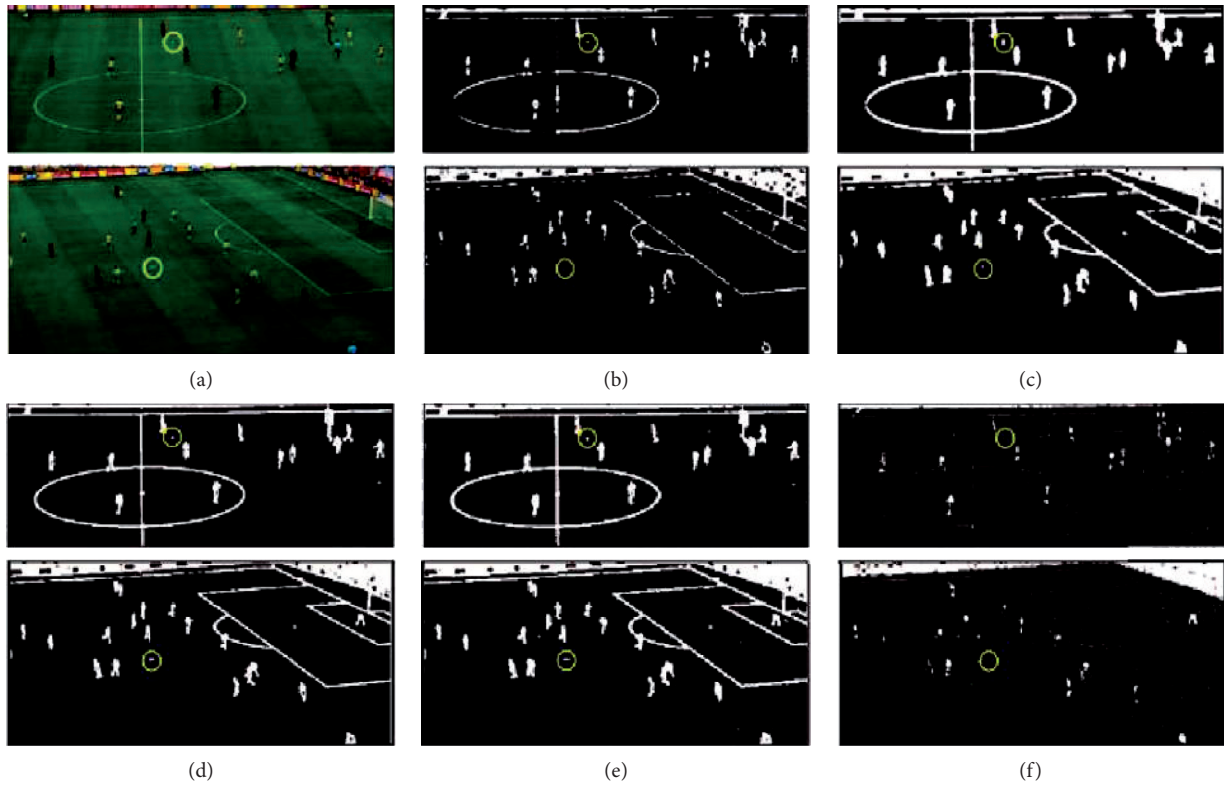
FIGURE 1: Binarization examples of foreground object. (a) Video frame, (b) SFCM, (c) WsFCM, (d) Otsu, (e) Rosin, (f) Canny edge detector.
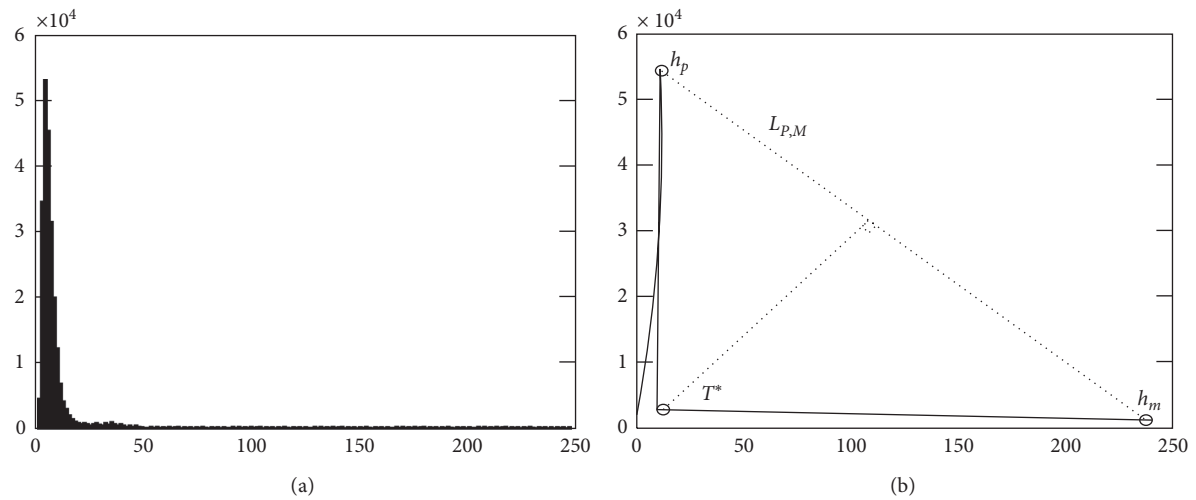
FIGURE 2: Schematic of the triangle threshold. (a) Histogram. (b) Triangle threshold.

extensively applied for soccer tracking. Kalman filter was raised by Kalman in 1960 [20] so as to solve the linear filtering problem of discrete data. In the framework of the Bayesian filter, Kalman filter takes advantage of a prediction-feedback mechanism to obtain the state of system. In other words, it predicts the state at one time, and then it measures system state and uses as feedback as to rectify the predicted state. To be more specific, the Kalman filter includes primarily two parts: time updating equation and measure updating equation. At one specific moment, Kalman filter predicts the current state of system as per time updating equation; next, it gets measuring value and uses it to update equation as to modify the predictive value of the system.

3.1. Analysis of Soccer Motions in Broadcast Soccer Videos.
Soccer motion state analysis aims to find out the motion pattern of soccer when it can be detected. Based on the

(a)   (b)   (c)
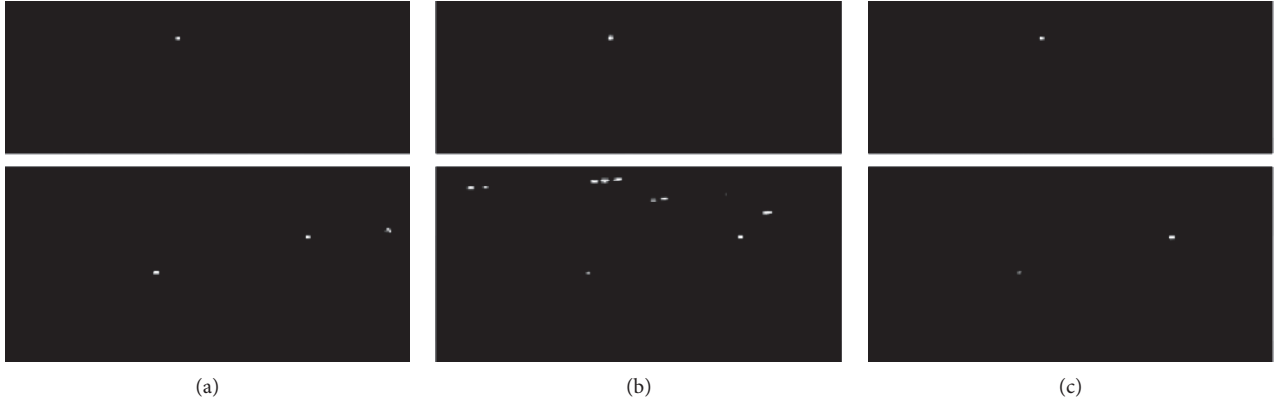
FIGURE 3: Example of soccer detection results. (a) Triangle threshold, (b) WsFCM, (c) proposed method.

TABLE 1: Soccer detection results of the bi-threshold method.

Video number	Contains soccer frames	Error detection	Miss	Accuracy (%)	Recall (%)
#1	102	3	1	97.12	99.02
#2	89	3	4	96.59	95.51
#3	61	0	0	100.00	100.00
#4	74	2	1	97.33	98.65
#5	40	1	1	97.50	97.50
#6	118	2	0	98.33	100.00
#total	484	11	7	97.75	98.55

moving course of soccer, we concluded that the soccer gets lost, because it merges together with mark lines or it is occluded by players. So, in those cases, we analyze soccer movement. When soccer merges with marking lines on the pitch, the soccer is freewheeling, and its motion state basically will not change. Then, we predict the position of soccer by its original motion state. When the soccer is sheltered by the player, soccer may be freewheeling or may be under the control of player. If the soccer is not physically contacted with player, but, similar to the above situation, that is the soccer is freewheeling. At this moment, soccer motion state does not change but merely passing by player area. If the soccer is physically contact with player, it is under the manipulation of players, and that the soccer will move together with player. Meanwhile, due to tackle by players, there would be the situation when soccer is sequentially occluded by players. In other words, players who occlude the soccer would change from time to time. It is noted that no matter when the occlusion happens during the soccer coasting or being under the control of the player, the position of soccer after being occluded would be near player. When the direction of soccer's motion direction changes, the soccer gets out of the player's control and appear near the dominant player. Based on the above analysis, it can be concluded that the state of soccer can be classified no occlusion, indication line fusion, single player occlusion, and multiplayer occlusion.

3.2. Basic Principle of Multiarea Search Dynamic Kalman Filtering Method.
Motion state of soccer is foundation of intensifying the robustness of soccer tracking method.

According to the analysis of soccer motion state, the paper extends parameter updating function of dynamic Kalman filter (DKF) and proposes a multiarea search dynamic Kalman filtering algorithm (MDKF) which is more adaptive to soccer moving features. The method aims to optimize parameter updating function of DKF in accordance with motion state of soccer and introduce multiarea search mechanism into parameter updating procedure as to boost the robustness of soccer tracking process. The similarities to DKF method, MDKF includes a three parts: time updating, measure updating, and dynamic adjustment of parameters.

In terms of time update, MDKF is used to predict the state of the system at the next time by the following equation:

$$\widehat{s}_t = A\widehat{s}_{t-1} + Q,$$
$$P_t = AP_{t-1}A^T + R. \tag{11}$$

The state of the equation (11) is the position and motion information of the soccer. Therefore, the system is set according to the following equation:

$$s_t = \left[x, y, v_x, v_y\right]. \tag{12}$$

The motion process of soccer may refer to these four states: no occlusion, merging with marking lines, single occlusion, and multiple occlusions. Therefore, parameter updating ways in MDKF should consist of measuring mode (MM), prediction mode (PM), single occlusion mode (SOM), and multiple occlusion mode (MOM). In MOM, although player who occludes the soccer has changed, soccer still appears close to other players. So we can predict any

location where the soccer possibly appears by search area expanding.

The search region extension mechanism used in this paper is shown in Figure 4, which includes the following four steps:

(1) The distance from the nearest player to P_s is recorded

(2) Side to P_s as the center of the square area of T, denoted by E_a, is selected

(3) All players in the E_a area as P_e are selected

(4) The P_e near the side length of $20 + DLPA/2$ region as S_e new search area

4. Experimental Analysis and Results

The key to the soccer tracking method is to maintain tracking of soccer after being occluded. As mentioned before, in the moving course, soccer may be occluded by different objects such as marking lines, single player, and multiple players. Hence, we choose several competition video clips that include different occlusions to evaluate the tracking performance of the proposed tracking approach. They are extracted from SoccerNet (https://soccer-net.org/), including games between South Africa and Mexico, Japan and Cameron, Spain and Switzerland, Slovenia and United States, and Brazil and Cote d'Ivoire, totaling over 1000 frames. For the convenience of comparison, we make size of those videos to $720 * 404$. Merging with marking lines and single occlusion are often seen in soccer videos. So, matched videos used in the test contain merging with marking lines and single occlusion. Besides, multiple occlusions are often seen in the match. So, testing video clips #1 and #2 and #4 and #6 both include single occlusion and multiple occlusions.

Kim et al. raised a soccer tracking method based on DKF and achieved more robust tracking result. Thus, we use the method to compare tracking results. First of all, the visual contrast between the two methods is compared by using video clips #1 and #2. Then, the soccer tracking results were compared based on calculation of Euclidean distance between the tracked soccer position and the real soccer position (manual annotation).

4.1. Visual Comparison of Tracking Results. In order to appraise vividly the performance of tracking robustness of the soccer tracking method proposed in the paper, we take the first two segments of testing videos to make visual comparison of soccer tracking results. The two video segments contain no occlusion, merging with marking lines, single occlusion, and multiple occlusions. The first row is tracking result by the DKF method; the second row is tracking result by the MDKF method. In the tracking sample picture, yellow and black blocks stand, respectively, for soccer location tracked by algorithms and that by manual annotation. It is shown in Figures 5 and 6.

The tracking result with testing video sequence #1 is shown in Figure 5. Figure 5 shows the racking result with testing video sequence #1. In that sequence, soccer moves
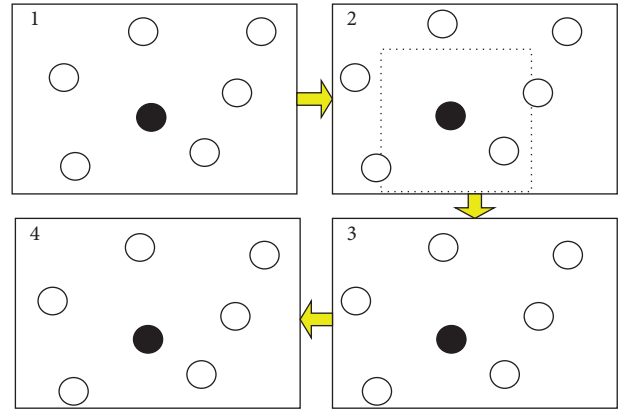
Figure 4: An illustration of the candidate soccer search area extending procedure.

from the midfield to the front of goal. In the moving course, soccer's motion state changes from merging with marking lines, single occlusion to multiple occlusions. From tracking result in frame 002–035 in Figure 5, we find when the soccer is overlapping with marking lines in the field or sheltered by single player, DKF and the proposed MDKF method can maintain tracking of the soccer. However, when the soccer is occluded by several players, just as tracking results in frame 177–287 in Figure 5, DKF lost the soccer being trailed. However, the proposed MDKF method can redetect the soccer and maintains tracking of it.

The visual tracking result of testing sequence #2 is shown in Figure 6. In that sequence, soccer's motion direction is opposite to the testing sequence #1. Soccer is moved from the position near the goal to the central area of the playing pitch. Soccer that is being sheltered by several players appears in the center of the playground, as observed from the tracking result in the frame 126–165 in Figure 6. After being occluded by a couple of players, soccer gets rid but it is detected again by the proposed MDKF method, which realizes continuous tracking of soccer movement. Since search area is too small to detect soccer again, the parameter updating function of the DKF method is not able to do correct parameter updating and that it loses tracking of the soccer. In the later part of the video, DKF recovers tracking of the soccer, because due to camera movement, soccer returns to the detection window of DKF and it continues tracking the soccer. In short, the DKF method can lose tracking of soccer after it is occluded. The reason is that the parameter updating function gets wrong as a result of the failure of soccer detection. Through in-depth analysis and according to the characteristics of soccer's motion mode, the paper optimized parameter updating function of DKF and thus increased the robustness of soccer tracking process.

4.2. Quantitative Comparison of Tracking Results. In order to compare the differences between the DKF and the MDKF methods proposed in this paper in the tracking results, the tracking results of the two methods are compared in this paper. In this paper, firstly, the real position of the soccer is manually marked on the video image and then the Euclidean

(a)　　　　　　　　　　　　　　　(b)　　　　　　　　　　　　　　　(c)

(d)　　　　　　　　　　　　　　　(e)　　　　　　　　　　　　　　　(f)

(g)　　　　　　　　　　　　　　　(h)　　　　　　　　　　　　　　　(i)
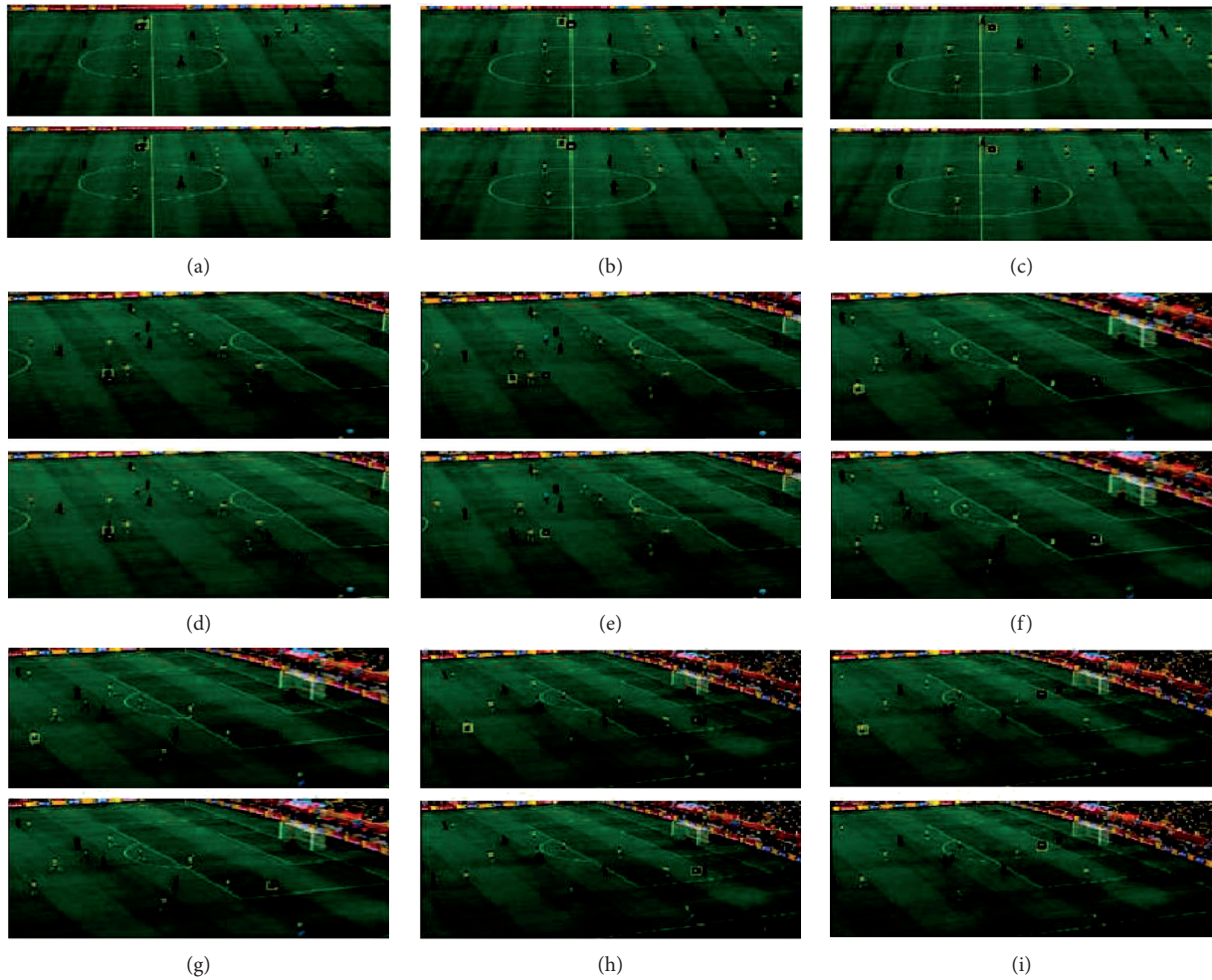
Figure 5: Comparison on the tracking results of the video clip #1. (a) frame 002, (b) frame 021, (c) frame 035, (d) frame 177, (e) frame 188, (f) frame 225, (g) frame 227, (h) frame 256, (i) frame 287.

distance between the position of the tracked soccer and its position is used as the quantitative evaluation index.

In order to compare the tracking results on the whole sequence, this paper calculates the mean of the Euclidean distance between the two methods in the video sequence and the position of the soccer position; it is shown in Table 2.

According to Table 2, in the test video #1, #2, #4, and #6, there is a big difference between DKF tracking results and MDKF tracking results. The average distance between the position and the position of the DKF tracked in the test video is much larger than the average distance between the position and the position of the MDKF. This phenomenon is closely related to the existence of multiplayer occlusion in the test video.

When the multiplayer occlusion occurs, DKF will lose track of the soccer, while the MDKF can continue to maintain the tracking of soccer. After the failure of tracking,

the distance between the tracking position of the DKF and the real soccer position will not increase. While the MDKF can continue to maintain the tracking of soccer, its tracking position and the distance between the real soccer position to maintain a smaller range.

At the same time, the DKF and MDKF methods in the test video on #3 get consistent tracking results. The reason is that a single player causes the occlusion in #3. In this case, both DKF and MDKF can be used to track the position of soccer. Therefore, the two methods get the same result. The tracking of the target causes the difference between the tracking result and the location.

In the same distance threshold, MDKF can get higher tracking accuracy. The reason is that MDKF enhances the robustness of the soccer tracking process, thus effectively reducing the distance between the tracking position and the real position of the soccer. It is shown in Figure 7.
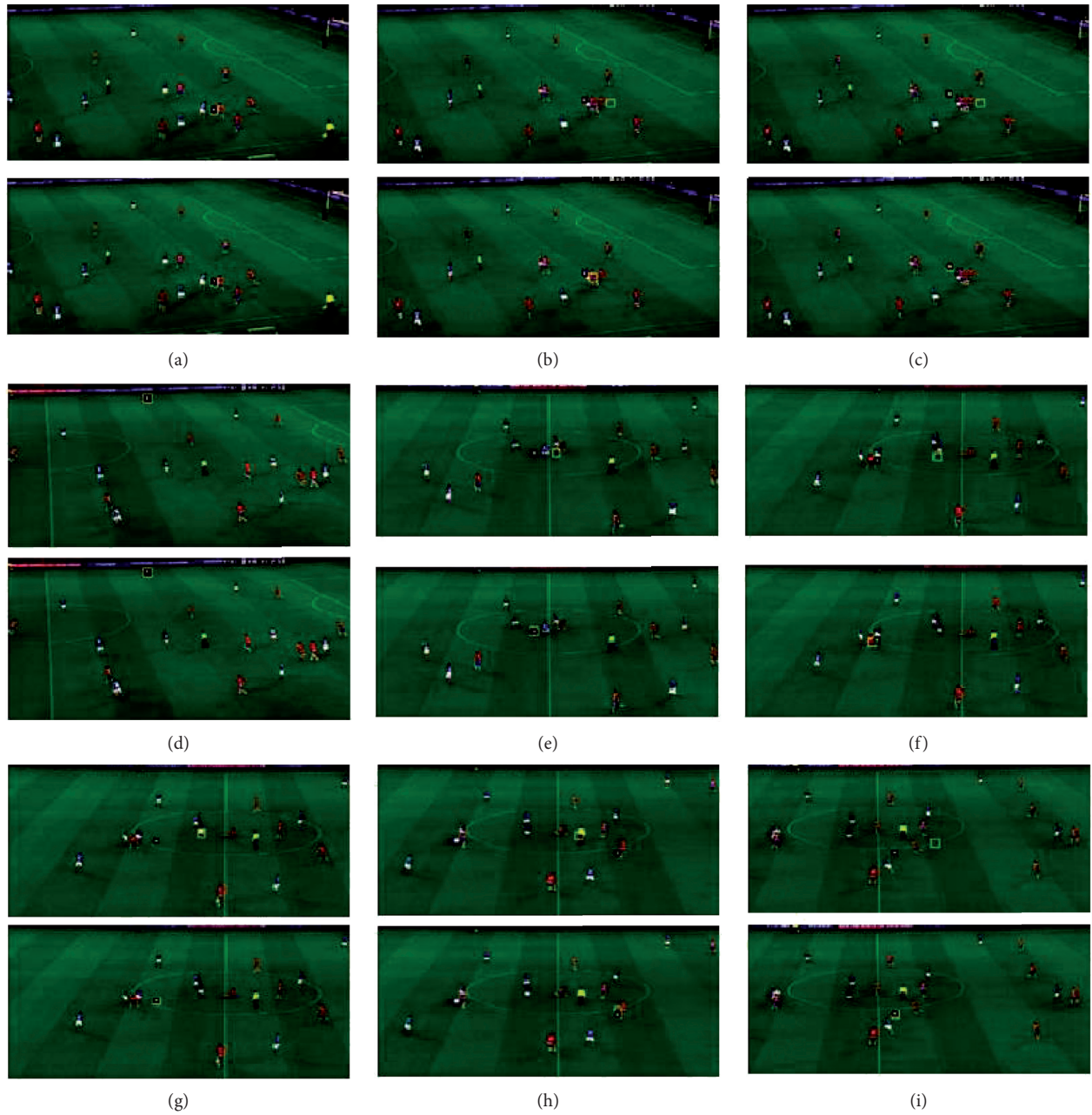
Figure 6: Comparison on the tracking results of the video clip #2. (a) frame 002, (b) frame 019, (c) frame 020, (d) frame 049, (e) frame 126, (f) frame 163, (g) frame 165, (h) frame 182, (i) frame 200.

Table 2: The mean Euclidean distance between tracked position and labelled position.

Video sequence	#1	#2	#3	#4	#5	#6	Mean value
DKF	130.5	32.56	4.75	56.78	164.77.	135.76	87.56
MDKF	7.51	8.90	4.75	12.45	7.89	23.67	11.14
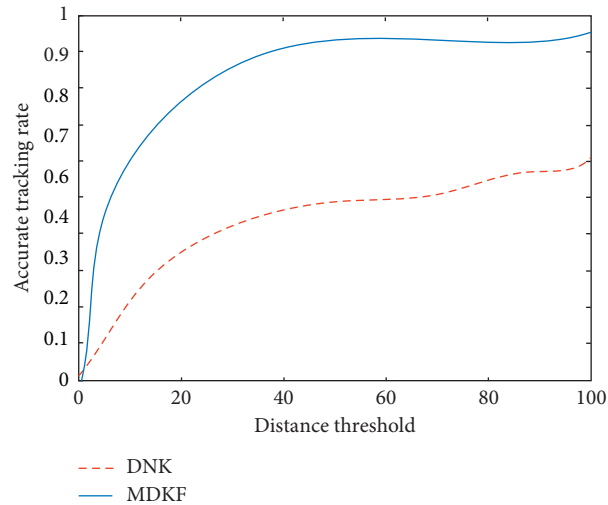
FIGURE 7: Tracking accuracy of the DKF and MDKF with different detection thresholds.

5. Conclusions

In this paper, we study the soccer tracking problem from two aspects: soccer detection and tracking maintenance. In the aspect of soccer detection, the problem of the lack of automatic soccer detection method exists. In this paper, a class of weighted sFCM-based automatic soccer detection method is proposed. The method is based on the characteristics of the number of foreground objects such as soccer, which is less than the number of background pixels. WsFCM algorithm is proposed for soccer detection, by increasing the weight of the foreground object category error to reduce the missed soccer. In this paper, a soccer tracking method based on a multiregion search DKFr is proposed. In this method, the motion state of soccer is inspired by the human visual search. According to the motion state of soccer, the parameter updating function of dynamic kalman filter is optimized. The robustness of the soccer tracking method is improved by searching the regional expansion.

Data Availability

No data were used to support this study.

Conflicts of Interest

The authors declare that they have no conflicts of interest.

References

[1] P. Nooralishahi, C. K. Loo, and L. W. Shiung, "Robust remote heart rate estimation from multiple asynchronous noisy channels using autoregressive model with Kalman filter," *Biomedical Signal Processing and Control*, vol. 47, pp. 366–379, 2019.

[2] M. Kaushal, B. S. Khehra, and A. Sharma, "Soft computing based object detection and tracking approaches: state-of-the-art survey," *Applied Soft Computing*, vol. 70, pp. 423–464, 2018.

[3] A. Nadzilah, D. M. Gandana, J. Muliadi, and Y. Daryanto, "Application of Kalman filter to track ship maneuver," in *Proceedings of the 2017 5th International Conference on Cyber and IT Service Management (CITSM)*, pp. 45–50, Denpasar, Indonesia, August 2017.

[4] P. R. Kamble, A. G. Keskar, and K. M. Bhurchandi, "Ball tracking in sports: a survey," *Artificial Intelligence Review*, vol. 52, no. 3, pp. 1655–1705, 2019.

[5] R. Ben-Ari and O. Ben-Shahar, "A computationally efficient tracker with direct appearance-kinematic measure and adaptive Kalman filter," *Journal of Real-Time Image Processing*, vol. 11, no. 2, pp. 271–285, 2018.

[6] X. Yu, Q. Tian, and K. W. Wan, "A novel ball detection framework for real soccer video," in *Proceedings of the International Conference on Multimedia and Expo*, pp. 265–281, IEEE, Baltimore, MD, USA, July 2003.

[7] X. Yu, H. W. Long, and C. Xu, "Trajectory-based ball detection and tracking in broadcast soccer video," *IEEE Transactions on Multimedia*, vol. 8, no. 6, pp. 1164–1178, 2016.

[8] D. Liang, Y. Liu, and Q. Huang, "A scheme for ball detection and tracking in broadcast soccer video," in *Proceedings of the Pacific Rim Conference on Multimedia*, Springer, Jeju Island, Korea, November 2015.

[9] H. Ramesh, S. Arockia Edwin, and S. Barath Kumar, "Multiple model filter based position tracking in CNC machines," in *Proceedings of the 2017 Fourth International Conference on Signal Processing, Communication and Networking (ICSCN)*, pp. 1–8, Chennai, India, March 2017.

[10] V. Pallavi, J. Mukherjee, A. K. Majumdar, and S. Sural, "Ball detection from broadcast soccer videos using static and dynamic features," *Journal of Visual Communication and Image Representation*, vol. 19, no. 7, pp. 426–436, 2008.

[11] X. Tong, T. Wang, W. Li, and Y. Zhang, "A novel algorithm for effective ball tracking," *International Journal of Pattern Recognition and Artificial Intelligence*, vol. 24, no. 3, pp. 359–379, 2010.

[12] J.-Y. Kim, C.-H. Yi, and T. Y. Kim, "ROI-centered compression by adaptive quantization for sports video," *IEEE Transactions on Consumer Electronics*, vol. 56, no. 2, pp. 951–956, 2010.

[13] J. Y. Kim and T. Y. Kim, "Soccer ball tracking using dynamic Kalman filter with velocity control," in *Proceedings of the 6th*

International Conference on Computer Graphics, Imaging and Visualization, IEEE, Tianjin, China, August 2009.

[14] M. Elzoghby, F. Li, U. Arif, and I. Arafa, "Small UAV localization based strong tracking filters augmented with interacting multiple model," in *Proceedings of the 2018 15th International Bhurban Conference on Applied Sciences and Technology (IBCAST)*, Islamabad, Pakistan, January 2018.

[15] G. Ligorio and A. M. Sabatini, "A novel Kalman filter for human motion tracking with an inertial-based dynamic inclinometer," *IEEE Transactions on Biomedical Engineering*, vol. 62, no. 8, pp. 2033–2043, 2015.

[16] T. D' Orazio, N. Ancona, G. Cicirelli, and M. Nitti, "A ball detection algorithm for real soccer image sequences," in *Proceedings of the International Conference on Pattern Recognition*, pp. 210–213, IEEE, Quebec, Canada, August 2002.

[17] X. F. Tong, H. Q. Lu, and Q. S. Liu, "An effective and fast soccer ball detection and tracking method," in *Proceedings of the International Conference on Pattern Recognition*, pp. 795–798, IEEE, Cambridge, UK, August 2014.

[18] Z. Kalal, J. Matas, and K. Mikolajczyk, "Online learning of robust object detectors during unstable tracking," in *Proceedings of the International Conference on Computer Vision Workshops*, pp. 1417–1424, IEEE, Kyoto, Japan, September 2009.

[19] J. Yu, Y. Tang, and Z. Wang, "Playfield and ball detection in soccer video," in *Proceedings of the International Symposium on Visual Computing*, pp. 387–396, Springer, Lake Tahoe, NV, USA, November 2007.

[20] R. E. Kalman, "A new approach to linear filtering and prediction problems," *Journal of Basic Engineering*, vol. 82, no. 1, pp. 35–45, 1960.

Research Article

Design of Lingnan Cultural Gene Implantation Cultural and Creative Products Based on Virtual Reality Technology

Jiansong Fang[1] and Wei Deng [iD][2]

[1]*Faculty of Art Design, Guangdong Baiyun University, Guangzhou 510450, Guangdong, China*
[2]*College of Creative Design, Shenzhen Technology University, Shenzhen 518118, Guangdong, China*

Correspondence should be addressed to Wei Deng; dengwei@sztu.edu.cn

With the development of virtual reality technology, people are increasingly aware that the combination of virtual reality technology and product design can enable companies to obtain stable profits and maintain long-term competitive advantages. And design evaluation plays a pivotal role in a large number of important decisions in product development. This article takes Lingnan culture and cultural products as an example, combining virtual reality technology with the design of Lingnan cultural and creative products, verifies the effectiveness and rationality of the virtual evaluation system of Lingnan cultural products through the evaluation of examples of Lingnan cultural products, and proposes amendments to the evaluation case. This paper constructs a product design evaluation system based on virtual reality technology and designs a theoretical model VR, which is the application of virtual reality technology in product design evaluation. The PDES system expounds the idea and method of constructing the system model. This paper studies the evaluation object, evaluation content, evaluation method, evaluation platform, and manifestation of evaluation results of the Lingnan cultural product virtual evaluation system and builds the framework of the Lingnan cultural product virtual evaluation system. This paper studies the product display method based on virtual reality technology and realizes the three-dimensional display of products on the Internet and the design of user interaction in virtual reality. In this paper, the two algorithms BRSK and SURF are used together, and the multiscale expression characteristics of BRISK in space and the rotation invariant characteristics of SURF are used. Experimental research shows that, compared with the pure BRISK algorithm, the rotation performance of the method in this paper can be seen through the experimental results in this paper to have better accuracy. The method in this paper ensures the accuracy and accuracy of matching as much as possible.

1. Introduction

Research on product design evaluation under virtual reality technology is based on virtual reality technology as a support to simulate the design of the product and its use environment [1], so that evaluators can interact with the product immersively in a realistic virtual environment, use the perceptual engineering theory to quantify the perceptual information of the evaluators, and evaluate the product design. Among them, virtual reality technology (VR for short) is a human-machine interface technology that realistically simulates human visual and auditory behaviors in a natural environment and is a computer system that can create and experience virtual worlds [2].

Virtual reality technology is a new development in the field of computer-aided applications. Although its research is still in its infancy, the application research results of virtual reality technology have attracted great attention at home and abroad. Many scholars have conducted research on virtual reality technology. For example, Berg LP has conducted research on product display methods based on virtual reality technology and realized the three-dimensional display of products on the Internet and the design of user interaction actions in virtual reality [3]. Mitrouchev P builds the hardware system of the panoramic roaming display platform by studying the related technologies of the panoramic roaming display platform based on panoramic camera technology [4]. The basic architecture and work flow of the

panoramic roaming display platform are summarized; its design concepts and design principles in the actual application process of product display design are analyzed, and the advantages of panoramic roaming display and the influencing factors of the display design effect are clarified, as a panoramic roaming display. The promotion and application of the platform provide reference and guidance [5]. Based on the hardware system of the panoramic roaming display platform, Adrian developed a software platform for product promotion and display design based on panoramic camera technology, as well as the design practice of the panoramic roaming display platform in the promotion and display of tea products. The existence of the problem and the direction of future research are provided in [6].

In China, many scholars are also very keen on the research of virtual reality technology [7]. For example, Zhang H took the display of light-sizing equipment as an example, showing the effect of virtual interactive display based on 3D Max and VR-Platform, so as to enable users to achieve active operation [8, 9]. Wang took the 3D animation display design of the light machine as an example and took the 3D interactive software as the platform to discuss the methods and techniques of realizing virtual roaming animation in the 3D model, focusing on the texture adjustment and environment design and camera and interaction. Interface and navigation design, scene release, and other aspects are used to illustrate how to achieve realistic product display animation technology [10]. Diao promoted virtual reality technology to the display of large-scale mechanical products, changing the dull image of the whole machine in people's minds [11]. 3D animation and multimedia technology is applied to large-scale equipment products to break the communication barriers between professionals and nonprofessionals [12].

This article uses Internet technology as a platform to design a product display and evaluation website, link the virtual reality technology introduced above and various methods of product display design to the website, and apply the entire process of the evaluation model to the establishment of complete website. This paper uses the BF Matcher feature point matching algorithm to achieve matching and uses the distance method to replace the RANSAC algorithm to further refine the point pairs after the preliminary matching and get a good matching effect.

2. Research on the Design of Cultural and Creative Products of Lingnan Cultural Gene Implantation Based on Virtual Reality Technology

2.1. Extraction of Elements from Lingnan Cultural Products. Agricultural products are like a kind of local business card of Lingnan. Through reasonable packaging design, it is expected to be built into an effective tool to promote local culture. As one of the three famous dishes of Lingnan, Mei Cai packaging design should be refined, interpreted, and reconstructed in Lingnan culture in order to complete the

branding and serialization of Mei Cai packaging design [13]. Because Lingnan culture has the advantages of innovation, compatibility, pragmatism, and openness [14], it has had a profound impact on contemporary packaging design in China.

(1) *Modeling Application.* When designing the shape of Mei Cai packaging, we should also pay attention to cultural taste and must fully reflect the local cultural characteristics of Lingnan. Affected by the historical environment and geographical location, the Lingnan region has inherited many unique styles. For example, Guangzhou Chen Clan Ancestral Hall is quite representative. Its courtyard space, modeling style, architectural layout, and other modeling elements can be fully applied to the packaging design of Mei Cai.

(2) *Color Application.* Through the inspection of Chen Clan Ancestral Hall and the Tomb of Yue King, it can be found that the colors of Lingnan are mainly red, yellow, green, white, and black. When designing the packaging of Mei Cai, you can choose colors with strong contrast.

(3) *Application of Lingnan Traditional Materials.* In contemporary life, everyone advocates a low-carbon and environmentally friendly life. Therefore, traditional materials should be used when designing Mei Cai packaging, and traditional production techniques should be used to make the materials show different texture effects, making the packaging more practical and beautiful and at the same time playing an environmentally friendly role. The Lingnan region is located in southern China, with a warm and humid climate, which provides a good growth environment for many plants [15]. Diversified plants provide many choices for Mei Cai packaging design materials.

(4) *Visual Design of Lingnan Mei Cai Packaging.* Product packaging is the industrial and technical design of the commodity carrier as a whole. An excellent and exquisite Mei Cai packaging should first design the brand name. Before consumers buy the products, they have completed a complete set of packaging design for agricultural products, and the designer's design ideas are also a complete set. When designing packaging, the first problem encountered is the determination of the size of the packaging container. When designing the size, the principle of convenience for consumers must be followed [16, 17]. In addition, the packaging design should also consider whether the selected materials are green and environmentally friendly; whether the waste after use can be recycled or easily degraded; after a special style design, whether the main display of the packaging can meet the consumer's requirements psychologically appeal; whether the design of taste and color caters to consumers' senses; whether the application of color has strong impact; and whether it can highlight the theme.

2.2. The Impact of Virtual Reality Technology on Product Design Evaluation.

The ultimate goal of product design is the market. There are many unknown factors that can get the expected effect after the design is put on the market. If we can predict the degree of market response in the future and solve the problems and deficiencies in the design in time [18], then these unknown factors will inevitably be transformed, allowing designers and producers to make correct market decisions and reducing risk factors to improve the efficiency and success rate of the design [19, 20].

Virtual reality technology has brought a brand new model to design evaluation. Product design evaluation is a complex and critical task, and there is no doubt that it plays an important role in the development and design of new products. New products designed and developed can better adapt to the development needs of society and meet consumers' increasing quality needs [21, 22]. Due to the rapid development of virtual reality technology and its extensive application in design, our design evaluation methods for products have also changed, which provides us with strong technical support for more scientific and reasonable evaluation of products. Today's evaluation of design objects is very inaccurate. The reason is that the design expression is far away from the real products in future production, even for prototypes.

Virtual reality technology has opened up a new situation of information exchange between human beings and products, the environment, and changes in phenomena. It combines the most advanced modern information technology and human creativity. In its simulated virtual world, we can carry out related natural simulations and realistic experiences and achieve the realm of interaction between real experience and human natural functions. Compared with the computer system, VR technology can provide the advantages of real-time interactive operability, three-dimensional space, and multichannel man-machine interface [23, 24].

Virtual reality technology makes design evaluation truly accurate and in place. Virtual reality technology in product design has changed the way of design expression of the previous two-dimensional or three-dimensional renderings. It digitizes the three-dimensional model, provides accurate and intuitive performance, and can provide a virtual and real design object for consumers or designers to experience products, evaluate products, and validate products on the same platform [25, 26]. They can be in or in front of the evaluation object and evaluate the scale, space, structure, proportion, color, and texture of the object through simulation and use. This evaluation model should be said to be the most accurate, convenient, and specific. Not only can it truly reflect the real ideas of the designer but it can also quickly and conveniently obtain the real experience of consumers, reduce various irrational factors in product design evaluation, and obtain more accurate results.

2.3. BF Matcher Performs Feature Point Matching.

Brute-force matcher, as the name suggests, is to match the feature points one by one until the best match is found. So, we often use Brute-force matcher to find the best match.

(1) *Euclidean Distance.* Formula (1) using Euclidean distance to achieve matching is as follows:

$$D_{ij} = \left(\sum_{k-1}^{n} \left| L_i(k) - L_j(k) \right|^2 \right)^{1/2}, \tag{1}$$

where $L_i(k)$ and $L_j(k)$ represent the feature descriptors of points i and j to be matched, respectively. Because it is tested by the distance method, the value of D_{ij} in the formula indicates the degree of matching between two points. The larger the D_{ij}, the lower the matching between the two points.

(2) *RANSAC Algorithm Optimizes Matching Points.* Find an optimal homography matrix H with a size of 3×3 through the RANSAC algorithm so that H can satisfy the transformation relationship between feature point pairs in the largest number, which is the coordinate transformation relationship between feature point pairs and the matrix where h_{33} is the homography matrix H, where we usually normalize the matrix with $h_{33} = 1$ and H also contains 8 other parameters that have not been obtained. It can be known from mathematical knowledge that at least 8 parameters need to be set to solve this problem:

$$S \begin{bmatrix} x\prime \\ y\prime \\ 1 \end{bmatrix} = \begin{bmatrix} h_{11} & h_{12} & h_{13} \\ h_{21} & h_{22} & h_{23} \\ h_{31} & h_{32} & h_{33} \end{bmatrix} \begin{bmatrix} x \\ y \\ 1 \end{bmatrix}. \tag{2}$$

Among them, s is only a scale parameter, $(x, y, 1)^T$ represents the position of the feature point in the first image, and $(x\prime, y\prime, 1)^T$ represents the position of the feature point in the second image. The RANSAC algorithm randomly extracts 4 pairs of noncollinear feature point pairs from the set of feature point pairs after the preliminary matching is completed. Through the transformation relationship between these 4 pairs of feature point pairs, the remaining 8 parameters mentioned above are obtained. From numerical value, you can get the homography matrix H and then use this homography matrix H to test the remaining pairs of feature points and finally find the number of feature point pairs that satisfy the homography matrix H and the cost function as shown in the following formula:

$$\sum_{i=1}^{n} \left(x_i' - \frac{h_{11}x_i + h_{12}y_i + h_{13}}{h_{31}x_i + h_{32}y_i + h_{33}} \right)^2$$

$$+ \left(y_i' - \frac{h_{21}x_i + h_{22}y_i + h_{23}}{h_{31}x_i + h_{32}y_i + h_{33}} \right)^2. \tag{3}$$

RANSAC algorithm steps are as follows.

(1) Randomly extract 4 pairs of noncollinear feature points from the feature point pairs and obtain the homography matrix H;

(2) Test the homography matrix H with the remaining feature point pairs, and find the number of feature point pairs and the cost function that satisfy the homography matrix H.

(3) If the final number is greater than the optimal point set, modify the value of the optimal point set and change the number of iterations k.

(4) Repeat the iteration until the number of iterations is greater than the value of k. Among them, the number of iterations can be obtained by formula (4), and the value of k is continuously updated when the maximum iteration is not exceeded.

$$k = \frac{\log(1-p)}{\log(1-w^m)}. \tag{4}$$

Among them, the value of P is usually 0.995, w is theratio of "inner points," and m is the number of selected feature point pairs.

2.4. BRISK Feature Algorithm. Because the SIFT and SURF algorithms are relatively time-consuming in use, they cannot be used on the AR system of handheld terminals. At the same time, when extracting feature points for images that are not particularly clear, BRISK has a good effect compared with other equivalent algorithms. The BRISK natural feature detection algorithm used in this paper is an improvement of the feature point related technology of the FAST algorithm [27, 28]. To solve the scale invariance, it is necessary to add a scale pyramid of the image to the BRISK feature point algorithm and perform scale space detection and multiscale expression of the feature points.

(1) *BRISK Feature Point Detection.* First create n octave layers and inner octave layers represented by C_i and d_i, C_0 layer represents the image itself, the C_1 layer of octave is obtained by sampling the source image down by 2 times, and the C_2 layer is performed on the previous layer C_1. It is obtained by 2 times sampling. The inner octave layer is obtained by sampling the source image itself by 1.5 times, the d1 layer is obtained by sampling the inner octave layer down by 2 times, and the d2 layer is obtained by sampling the upper layer d1 by 2 times [29, 30]. When the value of n is 4, 8 sampled pictures can be obtained, and then the nonmaximum value suppression in the scale space is performed on the sampled pictures.

This paper selects the point with the highest FAST score among all the 26 points in the domain and scale space of the feature point as the feature point and discards all other points. The extremum points obtained at this time are not the most accurate, and further purification is needed. The position interpolation method is used to perform parabolic fitting on the extremum obtained in each layer and finally subpixel level accuracy is obtained in the scale space where the extreme point of is the last thing needed.

(2) *SURF Feature Algorithm.* The SURF feature algorithm is improved on the basis of the SIFT algorithm. It solves the feature detection algorithm with long running time and complex description. The SURF algorithm first uses the Hessian matrix to filter out candidate feature points and then performs non-maximum value at the same time, and the image after integration is used for calculation, so the calculation can be fast and efficient [31, 32].

(1) *Dynamic Environment Modeling Technology* [33]. Dynamic modeling technology refers to a technology in which modelers obtain three-dimensional attribute data according to the actual environment in order to meet the needs of actual applications and establish corresponding virtual environment models. Given that the core content of VR technology is the establishment of virtual environments, dynamic modeling technology is particularly important. The acquisition of dynamic modeling data is very important. Generally, the acquisition of 3D data can be achieved through CAD technology (regular environment) and visual modeling technology. If the two are used in combination, the effect will be better, but compared with CAD technology in other words, modelers will use visual modeling technology in more cases because it is noncontact.

(2) *Real-Time Generation Technology of 3D Graphics.* With the rapid development of computers, three-dimensional graphics generation technology has also obtained a larger development space, and the level of three-dimensional graphics generation technology is relatively mature. However, how to use 3D graphics generation technology to achieve "real-time generation" is still a major problem and bottleneck in the development of virtual reality [34, 35]. In order to realize the real-time generation of 3D graphics, it is necessary to ensure that the refresh rate of the screen graphics is maintained between 15 frames/s and 30 frames/s. Therefore, a more important research content in the real-time 3D graphics generation technology can be obtained, that is, how to quickly increase the refresh frequency without reducing the performance of the graphics. Fortunately, the continuous development of computer graphics technology and simulation technology has a positive impact on promoting the realization of real-time 3D graphics generation technology [36].

2.5. Computer Virtual Display Characteristics of the Product. The characteristics of the product display can be divided into the following three points according to the value attribute of the product.

(1) *Static Display.* Static display is the most basic form of product display. At present, the display of many products is still in the static display stage. These products are generally affiliated with relatively small commodity categories or some commodities in

relatively large commodity categories, such as kitchen utensils. Generally, it is statically displayed in the store, while high-end clothing will be displayed in the store or through the catwalk.

(2) *Dynamic Display*. Dynamic displays often appear together with static displays. Generally, manufacturers will attract customers' attention through short-term, high-cost dynamic displays to stimulate their purchase interest and then maintain customer relationships and expand new customers through long-term, low-cost static displays.

(3) *Multimedia Display*. Multimedia display is a beneficial supplement to physical display, and display investment is relatively large [37]. Advertising is currently one of the more popular forms of multimedia display. For products with greater relative value or greater potential value, after market analysis, manufacturers usually adopt advertising display methods to expand the popularity of the product. Comprehensively considering the display characteristics of the product itself and the characteristics of virtual reality technology [1], the computer virtual display characteristics of the product can be found:

(1) *Static Product Display*. The static virtual display of products is the most common form of product display because, in the real world, products are mostly displayed to users in the form of display, so in the virtual environment, considering the technical restrictions, static display has naturally become the main way of computer virtual display of products. Under normal circumstances, in this way, a product explainer will participate in the static product display. Through the explanation of the explainer, the user will be more aware of the connotation of the static picture on the computer screen. This method has low cost and is suitable for small-scale workshops or shops and the display of products that cannot participate in interaction. However, this approach often increases the information asymmetry between the product and the user because the customer's perception of the product does not reach the level of personal experience.

(2) *Product Dynamic Display*. The dynamic virtual display of a product means that the product is displayed to the user from a three-dimensional perspective, and the static display of the product beyond the two-dimensional mode allows the user to understand the function and information of the product from multiple directions and has a certain degree of interaction between the product and the user. It also reduces the information asymmetry between users and products. Customers experience the product's functions to a certain extent through vision and hearing [2], but they still have not reached the point where they can experience personally in the virtual environment. At present, on some product websites, there will be dynamic display simulations of products. Customers enter the simulation system through computer mouse operation to observe the basic functions and structure of the product. For example, there is a three-dimensional display of sports shoes on the "Nike" website. This form is currently trending in popularity and is in its infancy, but it is developing rapidly.

3. Experimental Research on Cultural and Creative Product Design of Lingnan Cultural Gene Implantation Based on Virtual Reality Technology

3.1. Development Environment Construction

JNI. Java native method interface: It is mentioned in the book Java Virtual Machine that JNI can realize the communication between codes written in Java and programs written in other languages. In this article, JNI is mainly used to enable Java code that can run on the Java Virtual Machine (JVM) on the Android system to interact with Open CV applications and libraries written in C/C++.

The relationship between NDK and JNI is as follows. NDK is developed on the technology of Java native method interface, and the tool library developed on the Android system is realized.

3.2. Framework and Modules.
The movement enhancement system based on natural feature points designed and implemented in this paper is mainly to store all the feature information of the target object or image to be detected in the local database, and then when the video acquisition device obtains the feature information of the video frame image in the video stream after the consistency with the information stored in the previous database reaches a certain level, we consider the matching to be successful, and then we can perform subsequent operations such as superimposition and camera pose estimation. In order to improve the real-time performance of the system, this paper adopts the L-K optical flow tracking algorithm, which avoids the acquisition of feature information for all frames in the video information, thus saving time and enhancing the response rate of the system [38].

(1) Tracking Registration Module. According to the feature point pair set, the homography matrix H can be obtained, and then the internal parameters of the camera can be obtained, and then the external parameters of the camera can be obtained from the above data, and the conversion matrix between the world coordinate system and the pixel coordinate system can be obtained. At the same time, we also use the LK optical flow algorithm to track the previous frame, determine the current position of the feature

point, and complete the parameter calculation of the camera, so as to calculate the position where the virtual object needs to be correctly fused.

(2) Virtual and Real Integration Module. The conditions for superimposing into the real world have been met, and the effect of augmented reality can be achieved. The accuracy of the rotation matrix R and the translation matrix T directly determines the accuracy of the virtual information superimposed position in the virtual and real fusion; that is, it depends on the accuracy of the pose estimation. On the handheld terminal platform, Open GL ES technology is used to superimpose the two-dimensional mapping of three-dimensional objects into the video and realize the fusion and output of virtual and real information.

3.3. System Data Processing and Collection. The design parameters of product design evaluation in virtual reality are taken as the input end of the BP network, the product design evaluation result is the output end of the network, and the middle is the hidden layer. The product evaluation data and results obtained in the virtual reality environment are used as the training samples of the BP network, and the BP model is trained. After the training, click the BP evaluation to obtain the relevant evaluation data value.

4. Based on Virtual Reality Technology, Lingnan Cultural Gene Implantation Cultural and Creative Product Design Experiment Research Analysis

4.1. Experimental Analysis of Virtual and Real Fusion Module. The video capture resolution of the Android phone used in this article is 1024×768. The SIFT, SURF, and BRISK + SURF algorithms are, respectively, implemented, and the corresponding time parameter information is obtained, and the data obtained are tabulated and analyzed. The Open CV for android is SDK 2.0, and the results are shown in Table 1.

As shown in Figure 1, the analysis can use the same mobile phone to detect the same image or object. BRISK can achieve a good registration effect when the object to be detected rotates and the light intensity changes. Compared with SIFT and SURF, the overall running time of the algorithm is much less, and compared with the pure BRISK algorithm, the rotation performance of the method in this paper can be seen through the experimental results of this paper. It has better accuracy, and it is relatively less time-consuming. Therefore, under the premise of ensuring rapidity, the method in this paper ensures the accuracy and time cost of matching as much as possible.

4.2. Functional Analysis of Website Pages. The homepage of the website should highlight themes and provide links to some frequently used functions of users. According to UPS's survey of online shopping users' behavior, most users hope to add a link to order query on the homepage of the website.

TABLE 1: Comparison of three feature point detection algorithms.

Feature point detection algorithm	SIFT	SURF	Algorithm
Calculation time (ms)	217.3	98.24	71.36
Feature points	783	763	719
Calculation time (ms)	267.3	118.3	88.3
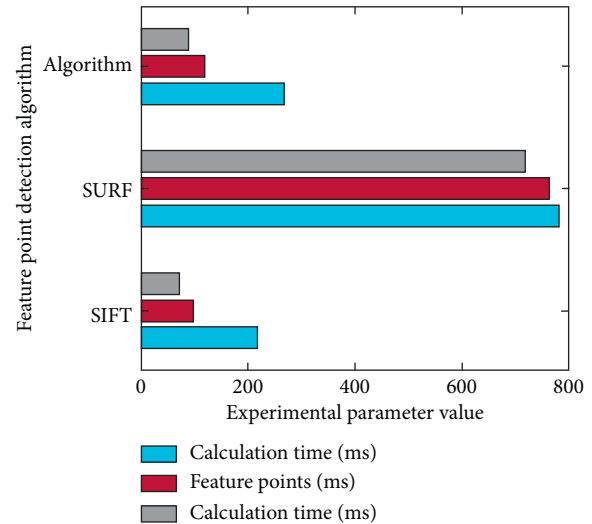
FIGURE 1: Algorithm histogram.

They hope to understand their purchases more conveniently and quickly. When will your product be available? Another survey showed that most users browse the product website to understand the features of the product, so the content on the homepage should be the product display. However, the content of virtual display is not suitable for being placed on the homepage. The second function required is that the regular functions of the website include registration and login, product recommendation, and after-sales service. The experimental results are shown in Figure 2.

As shown in Figure 2, the function of the product aggregation page includes a product classification list and product display thumbnails, and the user's preference information is determined by collecting the user's product browsing clicks on this page. The product classification list should contain the screening function and short evaluation information of related products. Problems that may occur during user browsing and links to presales services should also be added to the page to ensure a smooth user screening process.

4.3. User Evaluation and Evaluation Analysis. Evaluators can use the Lingnan cultural product virtual evaluation platform to learn about products through environmental roaming, product display, and user display and then enter the product evaluation section. The evaluators are 15 males and 25 females. The ages of the evaluators are between 20 and 50 years old, covering various occupational fields, a total of 40 people, and the data validity rate is 100%. After the user evaluation is over, click Submit, the system will automatically record the evaluation data, and the evaluation results can be viewed
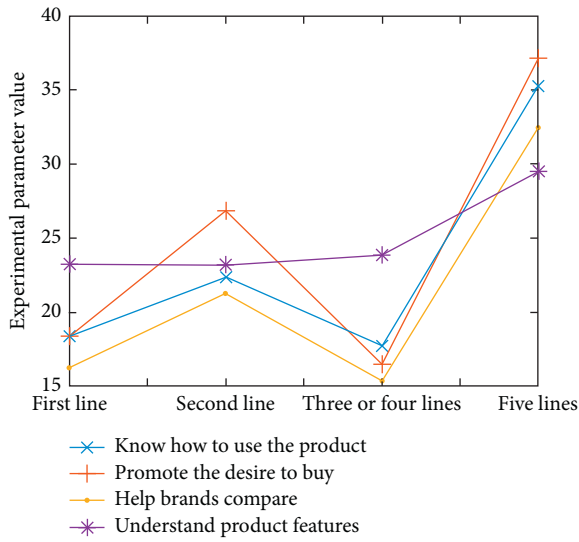
FIGURE 2: The purpose of browsing product websites by consumers in different cities.

FIGURE 4: Scheme 2 evaluation data.

FIGURE 3: Evaluation data analysis of option one.

after the evaluation is over. Statistics of all evaluation data and the evaluation data are shown in Figure 3.

The overall comprehensive score is 4.27, which fails to reach the general satisfaction level of users and needs to be adjusted. According to the histogram and radar chart of each index score, it can be seen that the evaluation index score is obviously low, which shows that this design scheme has defects in these two aspects. In other aspects, the aesthetic point of appearance score is higher than 6 points, which has reached the general satisfaction level of users, and the degree of completion is good; the score of function point is 5.23 points, of which intelligence and ease of operation score are 4.19 and 6.53, respectively, which are lower than the average evaluation angle. The score, therefore, should be adjusted in these two areas.

In the same way, the experimental data survey results of the second scheme are shown in Figure 4.

The experimental results are shown in Figure 4. The overall score is 25.24 points which has reached the general satisfaction level of users. The degree of completion is good in all aspects and meets the production and sales standards. According to the evaluation results, combined with market demand and consumer trends, fine-tuning the products can further ensure sales and consumer satisfaction.

5. Conclusions

With virtual reality technology as the technical support, this paper uses SolidWorks and 3dMax to realize the digital simulation of products and product use environment and uses unity3D to develop a virtual evaluation platform. Evaluators can participate in the virtual environment on the immersive virtual evaluation platform, interact with the product naturally, and get a realistic experience. The entire evaluation process is not limited by time and region and highly simulates the real use situation of the product, so as to maximize the control of the uncertain factors of consumer demand and make the results more objective and accurate. At the same time, the whole process of digitalization greatly shortens the product development cycle, realizes the interaction and flexibility of all aspects of product design, can quickly feedback the design plan, and adjust and modify when it is implemented.

Aiming at the problems of Internet-based product evaluation, this paper starts from the user's psychology and studies the factors that produce psychological changes during the interaction process of Internet evaluation. It

explains the user's attitude toward Internet-based product evaluation from the perspectives of psychological value, consumption information, and social inertia and proposes to divide users according to their psychological state and then to modify the product evaluation results. By referring to general evaluation methods, the process of Internet-based product evaluation is designed, and the user's mental state and user product evaluation are divided into two parts, and the Internet-based product evaluation model is used to correct the product evaluation based on the user's status, and the evaluation is selected. Elements designed a new interactive way to collect evaluation data.

This paper applies virtual reality technology to product design evaluation and builds a model framework of the product design evaluation system that applies virtual reality technology. By citing relevant theories and technical support for system construction, the feasibility of the design ideas, methods, and technologies of the product design evaluation system based on virtual reality technology proposed in this paper is confirmed. The idea and method of constructing and realizing better product design evaluation with expectations have certain theoretical and practical significance.

Data Availability

No data were used to support this study.

Conflicts of Interest

The authors declare that they have no conflicts of interest.

References

[1] Z. Lv, D. Chen, R. Lou, and H. Song, "Industrial security solution for virtual reality," *Institute of Electrical and Electronics Engineers Internet of Things Journal*, vol. 20201 page, 2020.

[2] J. Yang, C. Wang, B. Jiang, H. Song, and Q. Meng, "Visual perception enabled industry intelligence: state of the art, challenges and prospects," *Institute of Electrical and Electronics Engineers Transactions on Industrial Informatics*, vol. 17, no. 3, p. 2204, 2021.

[3] L. P. Berg and J. M. Vance, "Industry use of virtual reality in product design and manufacturing: a survey," *Virtual Reality*, vol. 21, no. 1, pp. 1–17, 2017.

[4] H. Song and M. Brandt-Pearce, "A 2-D discrete-time model of physical impairments in wavelength-division multiplexing systems," *Journal of Lightwave Technology*, vol. 30, no. 5, pp. 713–726, 2012.

[5] P. Mitrouchev, C. G. Wang, L. X. Lu et al., "Selective disassembly sequence generation based on lowest level disassembly graph method," *International Journal of Advanced Manufacturing Technology*, vol. 80, no. 1-4, pp. 141–159, 2015.

[6] A. Stavar, L. Dascalu, and D. Talaba, "Design, test and experimental validation of a VR treadmill walking compensation device," *Technological Innovation for Sustainability*, vol. 349, no. 2, pp. 402–409, 2017.

[7] Z. Yan and Z. Lv, "The influence of immersive virtual reality systems on online social application," *Applied Sciences*, vol. 10, no. 15, p. 5058, 2020.

[8] H. Zhang and H. Zheng, "Research on interior design based on virtual reality technology," *Boletin Tecnico/Technical Bulletin*, vol. 55, no. 6, pp. 380–385, 2017.

[9] M. Pan, Y. Liu, J. Cao, Y. Li, C. Li, and C.-H. Chen, "Visual recognition based on deep learning for navigation mark classification," *Institute of Electrical and Electronics Engineers Access*, vol. 8, pp. 32767–32775, 2020.

[10] Z. Lv and L. Qiao, "Deep belief network and linear perceptron based cognitive computing for collaborative robots," *Applied Soft Computing*, vol. 2020, Article ID 106300, 2020.

[11] Q. H. Wang, Z. D. Huang, J. R. Li et al., "A force rendering model for virtual assembly of mechanical parts with clearance fits," *Assembly Automation*, vol. 38, no. 2, pp. 173–181, 2017.

[12] J. Diao, C. Xu, A. Jia et al., "Virtual reality and simulation technology application in 3D urban landscape environment design," *Boletin Tecnico/technical Bulletin*, vol. 55, no. 4, pp. 72–79, 2017.

[13] C. Chen, S. Li, H. Qin, and A. Hao, "Real-time and robust object tracking in video via low-rank coherency analysis in feature space," *Pattern Recognition*, vol. 48, no. 9, pp. 2885–2905, 2015.

[14] W. Wu, Y. Liu, C. H. Wu, and S. B. Tsai, "An empirical study on government direct environmental regulation and heterogeneous innovation investment," *Journal of Cleaner Production*, vol. 2020, 2020.

[15] W. Zhang, Y. Hu, J. Liu et al., "Progress of ethylene action mechanism and its application on plant type formation in crops," *Saudi Journal of Biological Sciences*, vol. 27, no. 6, pp. 1667–1673, 2020.

[16] J. Chen, J. Zhang, P. Li et al., "Research on optimization of smart labels based on panoramic model files," *Dianli Xitong Baohu Yu Kongzhi/Power System Protection and Control*, vol. 46, no. 2, pp. 110–116, 2018.

[17] N. C. C. M. Moes and I. Horvath, "Editorial: virtual reality and ergonomics enablers for product development," *International Journal of Computer Aided Engineering and Technology*, vol. 8, no. 1/2, pp. 1–7, 2016.

[18] B. Zhu, S. Ma, R. Xie, J. Chevallier, and Y.-M. Wei, "Hilbert spectra and empirical mode decomposition: a multiscale event analysis method to detect the impact of economic crises on the European carbon market," *Computational Economics*, vol. 52, no. 1, pp. 105–121, 2018.

[19] A. Berni and Y. Borgianni, "Applications of virtual reality in engineering and product design: why, what, how, when and where," *Electronics*, vol. 9, no. 7, p. 1064, 2020.

[20] K. Israel, C. Zerres, and D. K. Tscheulin, "Presenting hotels in virtual reality: does it influence the booking intention?" *Journal of Hospitality & Tourism Technology*, vol. 10, no. 3, pp. 473–493, 2019.

[21] S. A. W. Andersen, P. T. Mikkelsen, L. Konge et al., "The effect of implementing cognitive load theory-based design principles in virtual reality simulation training of surgical skills: a randomized controlled trial," *Advances in Simulation*, vol. 1, no. 1, pp. 1–8, 2016.

[22] C. J. Lin, W. J. Shiang, R. W. Wang et al., "Evaluation of virtual reality presentation in user testing procedure for product usability of A conceptual design," *Technical Journal*, vol. 31, no. 4, pp. 307–318, 2016.

[23] P. Katsioloudis, M. Jones, and V. Jovanovic, "Use of virtual reality head-mounted displays for engineering technology students and implications on spatial visualization," *Engineering Design Graphics Journal*, vol. 81, no. 1, pp. 11–24, 2017.

[24] V. Meyrueis, A. Paljic, L. Leroy et al., "A Template approach for coupling Virtual Reality and CAD in an immersive car interior design scenario," *International Journal of Product Development*, vol. 18, no. 5, pp. 395–410, 2017.

[25] S. S. H. Maulana, "Media introduction to practical tool using android-based augmented reality technology,"

Journal of Engineering and Applied Sciences, vol. 12, no. 13, pp. 3292–3298, 2017.

[26] F. Liu, Q. D. Yan, S. W. Yao et al., "Interactive assembly technology for vehicle integrated transmission," *Jilin Daxue Xuebao (Gongxueban)/Journal of Jilin University (Engineering and Technology Edition)*, vol. 45, no. 4, pp. 1148–1154, 2015.

[27] K. C. Chiu, "GM (1, N) Analysis on the growth of cultural and creative industries in Taiwan," *International Journal of Kansei Information*, vol. 7, no. 2, pp. 41–46, 2016.

[28] W. Rui and G. Liqun, "Research on application model of design symbol theory in cultural and creative product development," *Revista de la Facultad de Ingenieria*, vol. 32, no. 9, pp. 514–520, 2017.

[29] W. Liu, X. Meng, J. Zhang et al., "Application research of panoramic roaming based on VR technology in ice and snow sculpture display design," *IPPTA: Quarterly Journal of Indian Pulp and Paper Technical Association*, vol. 30, no. 6, pp. 360–363, 2018.

[30] H. Li and Z. Zhang, "Cultural and creative product design based on biology characteristics of wood," *Wood Research*, vol. 63, no. 3, pp. 525–532, 2018.

[31] Y. Quan, S. Gaoming, G. Yang et al., "30 implementation of a real-time eye gaze tracking solution for ASIC based on VR display," *SID Symposium Digest of Technical Papers*, vol. 49, no. 1, pp. 385–387, 2018.

[32] Z. Hui, "Head-mounted display-based intuitive virtual reality training system for the mining industry," *International Journal of Mining Science and Technology*, vol. 27, no. 04, pp. 134–139, 2017.

[33] M. Elhoseny, A. Shehab, and X. Yuan, "Optimizing robot path in dynamic environments using genetic algorithm and bezier curve," *Journal of Intelligent & Fuzzy Systems*, IOS-Press, vol. 33, no. 4, pp. 2305–2316, 2017.

[34] H. E. Zehao, S. Xiaomeng, Z. Yan et al., "The development trend of virtual reality and augmented reality technology based on holographic optics," *ENCE & Technology Review*, vol. 36, no. 9, pp. 8–17, 2018.

[35] K. V. R. Hisatomi, "Using 8K display," *Broadcast Technology*, vol. 21, no. 73, 2018.

[36] Y. Tang and M. Elhoseny, "Computer network security evaluation simulation model based on neural network," *Journal of Intelligent & Fuzzy Systems*, vol. 37, no. 3, p. 3197, 2019.

[37] P. Yu, F. Zhou, X. Zhang, X. Qiu, M. Kadoch, and M. Cheriet, "Deep learning-based resource allocation for 5G broadband TV service," *Institute of Electrical and Electronics Engineers Transactions on Broadcasting*, vol. 66, 2020.

[38] A. K. Dutta, M. Elhoseny, V. Dahiya, and K. Shankar, "An efficient hierarchical clustering protocol for multihop Internet of vehicles communication," *Transactions on Emerging Telecommunications Technologies*, vol. 31, 2019 First Online 29.

Research Article

Performance of Sustainable Development and Technological Innovation Based on Green Manufacturing Technology of Artificial Intelligence and Block Chain

Xiangyu Jiang,[1] Gu-Hong Lin,[2] Jui-Chan Huang ©,[1] I-Hsiang Hu ©,[3] and Yen-Chun Chiu[4]

[1]*Yango University, Fuzhou 350015, Fujian, China*
[2]*Department of Industrial Engineering and Management, National Kaohsiung University of Science and Technology, Kaohsiung 80778, Taiwan*
[3]*General Education Center of the Open University of Kaohsiung, Kaohsiung 812008, Taiwan*
[4]*Taiwan Knowledge Bank Co., Ltd., Taipei 10041, Taiwan*

Correspondence should be addressed to I-Hsiang Hu; huis1967@gmail.com

The powerful advanced manufacturing industry is the most powerful driving force for economic development and growth, and it is also the main source of environmental pollution. Artificial intelligence and blockchain technology are recognized as a breakthrough technology that can be widely used, changing the way the entire society and economy operate. The main constraints affecting the sustainable development of the manufacturing industry are ecological deterioration and resource shortage, but the development of artificial intelligence and blockchain technology provides new ideas for solving manufacturing problems. Based on this, this paper proposes a research on the sustainable development performance of green manufacturing technology innovation based on artificial intelligence and blockchain technology. This paper deeply grasps the essence and connotation of artificial intelligence and blockchain technology, analyzes its specific application form and research background, searches for the effective effect of manufacturing technology innovation and green manufacturing performance path, and clarifies the mechanism between the two. All measurement items in the questionnaire used in this article use Likert5 scale and use 1–5 options to indicate the degree of conformity with the actual situation of the enterprise. The results show that the average green manufacturing capacity of each measurement item is between 3.18~3.97, indicating that the company's green manufacturing capacity is relatively high. Among them, the ability of green technology innovation is relatively high, indicating that most companies have noticed that the improvement of the ability of green technology innovation plays a vital role in the future sustainable development of enterprises. Moreover, more and more companies are paying attention to the latest applications of blockchain technology, which can effectively promote the development of enterprises.

1. Introduction

Developing a green economy has become a global consensus [1]. The development of green economy needs the support of green technology to guarantee the coordinated development of environment and economy [2]. This is because, compared with traditional technology, green technology can greatly alleviate the unnatural and mechanical color of traditional technology and effectively resist the negative effect of technology on the natural ecosystem. Therefore, without green technology innovation, there can be no sustainable development in a real

sense [3]. Green innovation has become the inevitable choice of future technological innovation [4]. This is especially true of fast-growing China. A country's green technology development level, in the final analysis, mainly depends on the green technology innovation ability of enterprises. However, where does the green technology innovation capability come from? Existing studies show that compared with traditional innovation driven by market mechanism, green technology innovation faces many obstacles and difficulties [5]. Therefore, the study on the formation mechanism of enterprises' green technology innovation ability can help open the "black box" of

green innovation ability of economic subjects under the influence of complex factors from the microlevel [6]. At present, global enterprises are in a highly competitive environment, in which hegemony is undoubtedly a fulcrum for sustainable development. To achieve this goal, enterprises need to conduct systematic and comprehensive management in an excellent way to overcome the huge competitive environment faced by the globalization environment. Logically speaking, through the implementation of green management that is interwoven with technology and jointly formulated and implemented, enterprises, especially the manufacturing industry, can maintain the status quo of sustainable development and surpass competitors [7, 8]. In the new normal economy, manufacturing industry, as the focus of economic development, is developing rapidly. Its rapid development has not only brought great opportunities to our society but also brought great challenges to the natural environment [9]. Resource consumption and environmental pollution are becoming more and more serious. Faced with this situation, we must make every effort to reduce pollution and save energy [10]. Therefore, the future transformation trend of the manufacturing industry is bound to take green economy as the background.

Green manufacturing is an important way for enterprises to achieve breakthrough and sustainable development. For the manufacturing industry, the availability and level of green manufacturing capability will become the key for enterprises to obtain competitiveness and also the entry point to evaluate the green performance of enterprises [11]. Green manufacturing is a complex model of modernization. The formation of green manufacturing capacity is a dynamic process, which is closely related to the economic benefits, social benefits, and potential development opportunities obtained by enterprises [12]. Therefore, it is of great theoretical and practical significance to study the green manufacturing capability of enterprises [13]. In the theoretical sense, at present, the research on green manufacturing has not formed a systematic and complete theoretical framework. This paper takes green manufacturing as the research object, discusses the connotation and constituent dimension of green manufacturing from the perspective of dynamics, and constructs the influence mechanism of green manufacturing ability on green manufacturing performance. The model is used for verification to further improve the theoretical system of green manufacturing and expand the depth and breadth of research. To a certain extent, it is a further enrichment of the current theoretical system of green manufacturing research. In practical sense, the in-depth and systematic analysis of the green manufacturing theory will help manufacturing enterprises find the key factors to improve the green performance, break through the limitations of the original production mode, improve the green manufacturing capacity, and enhance the competitive advantage of enterprises. In addition, by constructing a mechanism model, it helps to realize the simplification and operability problems of complex abstractions, so as to help enterprises understand the current situation and deficiencies of green manufacturing capacity, and clarify their improvement goals and directions, so as to cultivate and improve green manufacturing capacity in targeted ways. Therefore, the study of green manufacturing

theory will help accelerate the green development process of manufacturing enterprises, realize sustainable development, and ultimately improve the comprehensive competitiveness of China's manufacturing industry [14].

As the conceptual basis for understanding green technology innovation ability, people have made a very deep discussion on technology innovation ability since 1980s. From the perspective of strategy, it defines the capability of technological innovation, that is, the comprehensive capability of supporting enterprise strategy. Barton believes that the core of an enterprise's technological innovation ability is the ability to master professional knowledge, technical system, management system, and corporate values. These definition methods mainly put forward the connotation and characteristics of technological innovation ability from the descriptive angle. Although the above opinions provide semantic basis for understanding green technology innovation ability [15], the definition of green technology innovation ability in the academic circle has not yet formed a unified explanation. Based on the existing literature, there are three main innovative understandings of green technology. First, green technology innovation capability is defined as the ability to minimize environmental damage in the production process. Green innovation capabilities are technologies and processes used to reduce environmental pollution, raw materials, and energy consumption and the ability to produce green products [16]. Second, green technology innovation ability is the ability to introduce ecological concept into technology innovation. Third, green technology innovation capability is considered as a comprehensive capability system composed of multiple elements. Green innovation capability includes Green R & D Capability, green manufacturing capability, and green market development capability.

This paper analyzes the problems in the manufacturing industry, the status quo of traditional manufacturing enterprises, and the advantages of green manufacturing. Therefore, this paper intends to comb and analyze relevant literatures at home and abroad in recent years, in an attempt to provide useful reference for the formation of a more systematic and general theoretical research model in the future, adopt the method of combining theoretical research and empirical analysis, in-depth grasp the nature and connotation of green manufacturing ability, analyze its concrete form dimensions, to explore the role of green manufacturing capability of enterprise green manufacturing performance path, clear the action mechanism between them, for the enterprise to obtain or to improve the green manufacturing capacity, improve enterprise performance provides concrete suggestions and measures, and effectively improve the whole strength and manufacturing competitive advantage.

2. Proposed Method

2.1. The Dimension and Mechanism of Green Manufacturing Capacity

2.1.1. Dimension Analysis of Green Manufacturing Capability. At present, the division of green manufacturing

capability is mainly carried out from the internal and external perspectives of enterprises, and different dimensions are brought about by different research perspectives. Through data borrowing, it is considered that the classification of green manufacturing capability should reflect the green degree of product life cycle. Taking enterprises as the boundary of green manufacturing capability research, it mainly extracts the internal factors of enterprises and highlights the impact on green performance [17]. Through literature review and comparison, the company's green manufacturing capability includes green design capability, green technology innovation capability, and recycling capability. Green design capability is the foundation of green manufacturing. The concept of green manufacturing is implemented in green design to meet the requirements of the market and the environment. The enterprise can establish the first mover advantage; the innovation ability of green technology is the important support of the whole green manufacturing process. The emergence of materials, new technology, new technology, new packaging, and green design feasibility transformation are inseparable from technological innovation. Recycling capacity is the ability to manage the end of a product, convert waste into resources, and remanufacture the product as a raw material. Through the coordinated development of the three, jointly promote the green manufacturing capacity.

2.1.2. Mechanism of Action of Green Manufacturing Capacity on Green Performance. Green manufacturing ability is a complex dynamic capability and dynamic capability of resource configuration of cost, time, and efficiency and has direct effect on corporate performance, and in this process, the enterprise organizational structure and organizational system can have the effect of promotion and coordination and can give full play to the coordinating role of the main structure depends on the organization structure. The flexible organizational structure can be adjusted flexibly, efficiently, and reasonably according to the change of the external environment, so as to reduce the negative impact of uncertainty on the enterprise as much as possible. Organizational structure and system can play a coordinating role in the path of dynamic capability to enterprise performance [18]. This article follows the dynamic ability to enterprise performance path, namely, the dynamic capability of effect on enterprise performance through organizational structure and system, and puts forward some ideas of enterprise green manufacturing capacity analysis, namely, for green performance which has a significant impact on green manufacturing ability, organizational flexibility between green manufacturing and green performance play a coordinating role, which are shown in Figure 1.

2.2. Research Hypothesis on the Relationship between Green Manufacturing Capacity and Green Performance

2.2.1. The Relationship between Green Design Ability and Green Performance

Green design is also known as eco-design, environment-oriented design, environment-conscious design,
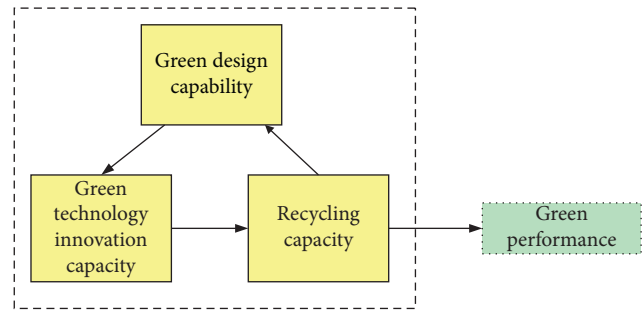
FIGURE 1: Mechanism model of green manufacturing capacity on green performance.

sequential design, and life-cycle design. Although there is no uniform definition of green design at home and abroad, the relationship between green design and green performance is studied from different perspectives. Green design is an important premise of green manufacturing. Its goal is to minimize environmental pollution and make full use of resources in the whole life cycle of products [19]. Green design ability can coordinate and optimize the economic and social benefits of manufacturing enterprises. Green design takes environmental attributes as the design goal and improves product economy while meeting the goal [20]. Green design is to eliminate the negative impact of all aspects of product life cycle, improve the efficiency of energy and resource utilization, achieve the most economical way to manufacture green products, through the use of various advanced technology and management methods, and ultimately improve brand image and economic benefits [21]. Based on the investigation of 107 executives in 86 enterprises in Taiwan, this paper analyzes the relationship between green design and green product marketing strategy and performance and concludes that the green design has a significant positive impact on the performance of green products. Consumers' consumption preferences are undergoing important changes, and consumers are more inclined to green products. Manufacturers will establish brand image and establish competitive advantages, so as to improve corporate performance [22]. Through green design, Walmart saves a lot of resources and energy, reduces carbon dioxide emissions by 60%, reduces environmental impact and operating costs, and improves environmental and economic performance. 148 manufacturing enterprises in Guangdong province were investigated, and a theoretical model of the relationship between dynamic factors of green supply chain and green design and performance was established. The results show that the green design has a significant positive correlation with green supply chain performance [23]. Most products in the design stage determine the manufacturing cost and use cost, and green design can save the cost and improve the economic benefits, that is, improve the economic benefits while meeting the requirements of environmental protection. Based on the above analysis, this paper believes that the stronger the green design ability is, the

better the green performance of the enterprise will be. Therefore, the hypothesis is put forward as follows.

H1: green design ability has a significant positive effect on green performance.

2.2.2. The Relationship between Green Technology Innovation Ability and Green Performance

Green technology innovation is also known as "low-carbon technology innovation," "environmental technology innovation," and "low-carbon technology innovation." It is the ability to provide the business value to the enterprise and new products or services to customers and to minimize negative environmental impacts. Management innovation and technological innovation generated for the purpose of environmental protection belong to green technology innovation, namely, ecological technology innovation, and belong to technology innovation [24]. Green technology innovation capability is to save resources for enterprises, improve the utilization efficiency of resources and energy, and then create green performance for the government, enterprises, and public. By adopting technological innovation, developing countries can gain late-mover advantages, reduce production costs, and gain market opportunities and economic benefits [25]. Technological innovation ability is the ability acquired by enterprises through learning, development, and accumulation and the internal absorption, integration, and improvement of knowledge through micro- and macroenvironment, and then, the innovation ability is acquired and the enterprise performance is improved. Enterprises acquire technological innovation ability through knowledge accumulation and apply this ability to product development or process improvement, so as to improve production efficiency. Technological innovation ability has an important impact on the differentiated development of enterprises, and the diversity, advancement, and value of production process or products brought by this ability will directly affect the technical performance and enterprise development [26]. Enterprises should enhance their technological innovation ability, or they will fall into the extensive development mode of low efficiency and low added value, which will affect the improvement and development of enterprise performance. In conclusion, green technology innovation ability can help enterprises effectively get rid of the inertia and dependence generated by the original development model and improve the utilization efficiency of resources and energy, production efficiency, and performance quality through optimization innovation or breakthrough innovation. Therefore, this paper believes that green technology innovation ability has an important impact on green performance and proposes the following hypotheses.

H2: green technology innovation ability has a significant positive impact on green performance.

2.2.3. The Relationship between Recycling Ability and Green Performance

Recycling capacity is based on advanced technology and manufacturing level and the whole life cycle theory, through efficient, energy saving, and environmental protection to repair and transform a series of waste products and waste. With the rapid growth of economy, the production cost is higher and higher, and the improvement of economic efficiency is based on the continuous expansion of scale rather than the progress of technology. At the expense of external interests, he criticized this phenomenon. It is also proposed that an effective method should be established to prevent pollution and stop treatment [27]. Anderson proposed the 5R strategy to save resource cost and manufacturing cost through repair, reuse, recycling, and remanufacturing, improve production efficiency, meet the requirements of environmental supervision, reduce the total production cost, and improve industry performance [28]. From the perspective of import and export, the resource utilization is studied, and it is believed that recycling can reduce the consumption of nonrenewable resources, improve the international balance of payments, and reduce the multiplier effect and increase the income level, thus increasing the gross national product and employment rate and thereby improving social performance [29]. Chen thinks resource recycling is the core that develops circular economy. The model reflects the relationship between economic development and resource recycling and reveals that technological innovation and resource recycling are the key support for improving economic and social benefits. A review of domestic and foreign literatures shows that recycling capacity is the repeated use of resources, the reduction of resource consumption, the construction of ecological resource circulation, and the saving of resource cost, which is closely related to the improvement of social benefits. The stronger the recycling capacity is, the higher the resource utilization rate is and the more obvious the resource cost saving is. Therefore, the following hypotheses were proposed.

H3: recycling ability has a significant positive impact on green performance.

2.3. Research Hypothesis on the Relationship between Various Dimensions of Green Manufacturing Capacity

Based on the research and construction of the mechanism of action of green manufacturing ability on green performance, this paper further explores the relationship between various dimensions of green manufacturing ability and the degree of influence, so as to provide reference for the formation and cultivation of green manufacturing ability.

2.3.1. The Relationship between Green Design Ability and Green Technology Innovation Ability

For manufacturing enterprises, the green design is the carrier of transforming technology into green products and the driving force of technological innovation. Green design points the way for technological innovation through advanced ideas. If the results of technological innovation cannot be used for product improvement, it will not only produce no value but also consume resources. Green design ability is the ability to comprehensively consider the environment, quality, function, economy, and other factors of products, and green innovation ability is the ability to transform green design concept into green products. Research on new energy automobile industry shows that the green design can significantly improve innovation ability and analyze the connotation of innovation system from the perspective of design, development, and system [30]. The basic concept and research status of green technology innovation ability are summarized, internal and external factors are analyzed, and internal incentives such as R & D investment and green product design can improve green innovation ability [23]. On the basis of comprehensive analysis, this paper argues that green design capability is closely related to green technology innovation capability. The stronger the ability of green design, the more it can encourage enterprises to carry out green technology innovation, so as to accelerate technology research and development and transformation. Therefore, the following hypotheses were proposed.

H4: green design ability has a significant positive impact on green technology innovation ability.

2.3.2. The Relationship between Recycling Ability and Green Design Ability

The utilization capacity of the belt is the foundation of the sustainable development of resources and environment. The closed-loop model of utilizing resources to process products and transforming products into resources through recycling ensures the rational and sustainable utilization of resources and energy in the manufacturing process. The green design ensures the minimization of pollution and waste in the design stage, manufacturing stage, and consumption cycle stage. When enterprises recycle and process waste materials, data collection and reprocessing, as well as the difficulty of recycling, will form a large amount of data and information. They can provide this information by feeding reclaimed knowledge and experience data back into the design process. Further optimize and improve the green design process. Based on the whole life cycle theory, the vehicle green recycling system is studied. It is considered that the realization of green recycling ability has an important impact on green design ability [31]. Based on the above analysis, this paper believes that the accumulation of recycling capacity can provide positive feedback for the green design and provide reference for the selection of

materials and optimization of process design in the process of the green design, so as to improve the level of resource recycling and reduce the impact on the environment. Therefore, the following hypotheses are proposed.

H5: recycling ability has a significant positive impact on green design ability.

2.3.3. The Relationship between Green Technology Innovation Ability and Recycling Ability

Green technology innovation can improve the utilization efficiency of production resources, and products with green technology innovation can more easily change consumers' consumption concept and purchase behavior, so as to promote the recycling and utilization of products and production accessories. The green technologies proposed by the European high-level meeting are pollution control and recycling of finished products. The innovation capacity of green technology is mainly composed of three parts: the technological innovation capacity of producing clean products, the pollution control and prevention capacity in the manufacturing process, and the terminal disposal capacity of waste. To sum up, green technology innovation ability is the ability to balance the ecological environment and economic benefits. The aim is to prevent and reduce the environmental impact of resource consumption and waste in order to minimize pollution and maximize the recycling of products and crafts throughout the life cycle. For product recycling, technological innovation ability is one of the most critical supporting conditions. The stronger the innovation capacity of green technology is, the more consumable products and production accessories will be, so as to realize the green recycling of wastes. Based on the above analysis, this paper believes that green technology innovation ability is the key to terminal management and transformation, which can provide support for recycling, so as to improve recycling efficiency. Therefore, the following hypotheses were proposed.

H6: green technology innovation ability has a significant positive impact on recycling ability.

2.4. Brief Description and Application of Artificial Intelligence and Blockchain Technology.

The main feature of blockchain technology is decentralization, and it is the best encryption method to protect data information. Its specific features are decentralized structure, data and information which cannot be tampered with, distributed accounting and storage methods which are adopted, and cryptographic anonymity protection.

The emergence of artificial intelligence is the result of the evolution of tools. It responds to the requirements of the development of productivity and satisfies the needs of mankind to transform the objective world. The definition of artificial intelligence does not have a definite expression, but

the essence of artificial intelligence is a new tool for human practice, and it reflects human abilities and will.

The development of artificial intelligence and blockchain technology has brought huge changes to the manufacturing industry. Artificial intelligence can help people carry out some highly repetitive and simple production processes. Blockchain technology can bring new technologies to green manufacturing. This technology provides technical support for the sustainable development of society.

3. Experiments

3.1. Research Methods. The research methods of this paper are as follows:

(1) Literature and theoretical research: this paper, by referring to relevant theoretical studies and literature results on green manufacturing capability theory and dynamic capability, put forward the research perspective of this paper and explored the mechanism of green manufacturing capability by integrating management, statistics, metrology, and other relevant disciplines.

(2) Empirical study: on the basis of literature and related research, this paper puts forward the research hypothesis and builds the research model. The research data were obtained through questionnaires, and hypotheses were verified by correlation, regression, and structural model. The relationship among green manufacturing capability, organizational flexibility, and green performance, as well as the improvement of green manufacturing capability, was analyzed and studied.

3.2. Design of Questionnaire. The microlevel data required in this paper cannot be obtained from the annual report or database, so a questionnaire survey is needed. Through the field survey of enterprise management personnel, by drawing on the experience and suggestions of enterprise development, the measurement items were modified and supplemented. Finally, by sorting out the questions, the questions with ambiguous sentences, which are difficult to understand and have unreasonable logic, were deleted to form the final questionnaire. Likert5 scale was adopted for all measurement items in the questionnaire, and 1–5 selection was used to indicate the degree of conformity with the actual situation of the enterprise.

According to the principle of questionnaire design, there are no more than 10 measurement items for each variable in this paper, a total of 45 items. The content includes three parts. The first part is the enterprise basic situation investigation. The second part is the investigation of green manufacturing capability and organizational flexibility. There are three dimensions of green manufacturing capability with 21 items, and two dimensions of organizational flexibility with 7 items. The third part is a survey of related issues of enterprise green performance, with two dimensions and the number of items is 7.

3.2.1. Sample Selection. Due to the large number of manufacturing enterprises, limited by resource conditions, it is impossible to exhaust all the manufacturing enterprises. Therefore, the selection criteria of this paper are as follows. First of all, the selected manufacturing enterprises must have the awareness of green manufacturing and have practical research significance. Secondly, the green performance of market competition can reflect the unique role of manufacturing enterprises in green innovation ability. Similarly, the availability of data can be achieved with limited resource constraints. Based on this, samples of this paper are selected as follows: food industry, paper industry, home appliance industry, automobile industry, home building materials, and energy mining. The samples were mainly concentrated in Shandong, Liaoning, and Heilongjiang provinces. The major cities are Jinan, Qingdao, Yantai, Dalian, Shenyang, Anshan, Harbin, Daqing, and Qiqihar. Enterprise selection is mainly based on the industrial and commercial enterprise directory, industry yearbook, and provincial and municipal enterprise yearbook.

3.2.2. Selection of Research Objects. Research, mainly by questionnaire star platform, e-mail three forms, and field investigation, in order to avoid information distortion phenomenon appear in the research, based on the description of the related problems in the design of the questionnaire, was analyzed and modified, to ensure that the respondents can be fully understood; on the contrary, for the choice of research object, as far as possible, the enterprise high-level leadership, technical director, and director of operations are taken as the research object, in order to ensure the quality of the questionnaire recovery and its reliability and validity.

4. Discussion

4.1. Sample Data Analysis of the Effect of Green Manufacturing Capacity on Green Performance

4.1.1. Descriptive Statistical Analysis of the Effect of Green Manufacturing Capacity on Green Performance. Through descriptive statistical analysis of data, indicators such as mean value and standard difference are used to reflect the distribution and dispersion of variables. The sample mean also becomes the sample mean which reflects the average level or concentration of data. The specific results are shown in Figure 2. Standard deviation reflects the degree of dispersion of data. The larger the value, the higher the degree of dispersion, and the greater the difference, the less representative the data. The specific results are shown in Figure 3.

As can be seen from Figure 2, the average value of green manufacturing capability measured by each project is between 3.18 and 3.97, indicating that the green manufacturing capability of enterprises is relatively high. Among them, the innovation ability of green technology is relatively high, which indicates that most enterprises have noticed the improvement of the innovation ability of green technology, followed by the green design ability. In other words,
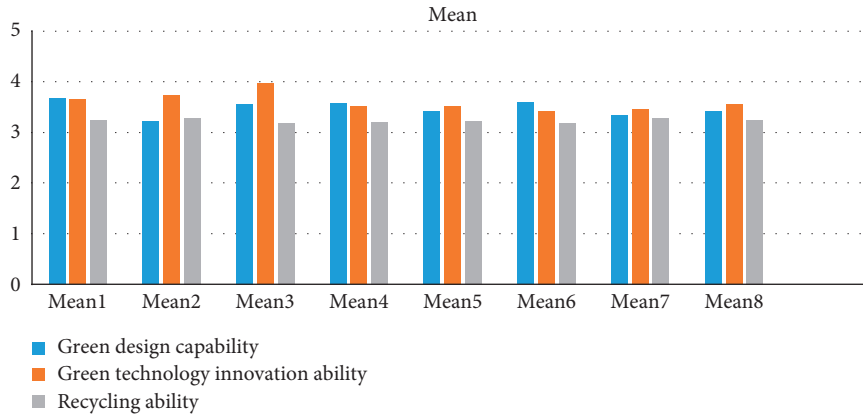
Figure 2: Descriptive statistical analysis of green manufacturing capability indicators: mean.

Figure 3: Descriptive statistical analysis of green manufacturing capability indicators: the standard deviation.

enterprises have realized that the early design of green products can effectively reduce the generation of pollution and the efficiency of production process. The low average recycling capacity indicates that the current recycling capacity of the enterprise needs to be improved, and the support system of garbage recycling is not perfect. In addition, as can be seen from Figure 3, the standard deviation of the measurement items is relatively close and the data is relatively representative.

4.1.2. Correlation Analysis of the Effect of Green Manufacturing Capacity on Green Performance. Correlation analysis is widely used in statistics, mainly reflecting the degree of closeness between variables. The degree of one variable changes when another variable changes. Generally, when the absolute value of correlation coefficient is higher than 0.8, it indicates a strong tightness between variables. When the absolute value of correlation coefficient is lower than 0.3, it is considered that the interdependence between variables is weak. The correlation analysis results are shown in Table 1. The three components of green manufacturing capability are significantly positively correlated with green performance. There is also a high correlation between organizational flexibility and green performance. There is correlation between green design ability and green technology innovation ability, green technology innovation ability and recycling ability, and green technology and recycling ability. The interaction item between green design ability and organizational flexibility is positively correlated with green performance, while the interaction item between green technology innovation ability and organizational flexibility is positively correlated with green performance. Only the interaction item between recycling ability and organizational flexibility is not highly correlated with green performance.

4.2. Structural Equation Model Test and Analysis of the Effect of Green Manufacturing Capacity on Green Performance

4.2.1. Set the Initial Model. According to the action mechanism model of green manufacturing capacity constructed in this paper, the initial structural equation model of this paper is shown in Figure 4. Among them, green design ability, green technology innovation ability, and recycling ability are exogenous latent variables, while green performance is endogenous latent variables.

4.2.2. Evaluation of Model Fitting Degree. By running the initial model of the structural equation of green manufacturing capacity, the fitting results of each adaptation index are shown in Table 2.

As can be seen from the above table, the fitting effect of the set initial model is relatively ideal, and the degree of freedom of chi-square value is 1.809, lower than 3. RSEMA value was 0.025, lower than 0.05. The relative fit index of GFI, NFI, and CFI baseline is higher than 0.9. Both PNFI and PGFI were higher than 0.5. The value of value-added fit index IFI was 0.895; although lower than the critical requirement of 0.9, the overall effect of model fitting did not affect the fitting of model and sample data, so it was considered that the structural model passed the fitting degree test. After the model passes the fitting degree test, it continues to analyze the path coefficient, as shown in Table 3. In

TABLE 1: Variable correlation analysis.

Measuring variable	1	2	3	4	5
Green design capability	1	—	—	—	—
Green technology innovation capacity	0.712∗∗	1	—	—	—
Recycling capacity	0.705∗∗	0.731∗∗	1	—	—
Organizational flexibility	0.485∗∗	0.471∗∗	0.375∗∗	1	—
Green performance	0.742∗∗	0.786∗∗	0.665∗	0.586∗∗	1

Note: ∗∗ represents significant level $P < 0.01$; ∗ represents significant level $P < 0.05$.
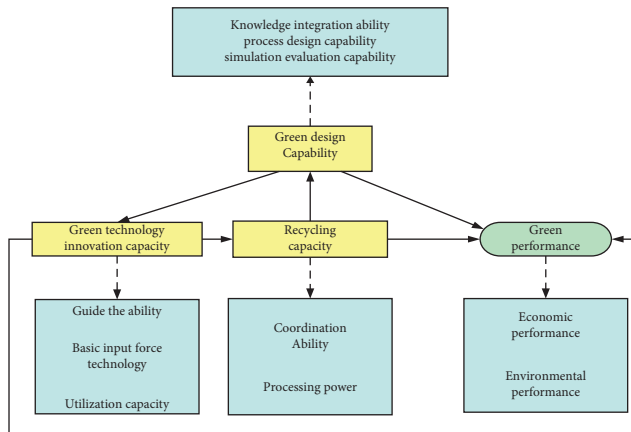
FIGURE 4: Mechanism model of green manufacturing capacity on green performance.

TABLE 2: Test results of the model fitness index.

X^2/df	RSEMA	GFI	IFI	NFI	CFI	PNFI	PGFI
1.809	0.025	0.934	0.895	0.906	0.902	0.544	0.541

order to see the data of each part more intuitively, the path analysis and comparison are shown in Figure 5.

Through Table 3 and Figure 5, you can see that the green design, green technology innovation ability, and function of the recycling capacity and performance of the green path coefficients were 0.525, 0.544, and 0.447 and P values were 0.004, 0.006, and 0.008, by significance test, which show that green design, green technology innovation ability, and recycle ability have significantly positive effect on green performance, support hypotheses were H1, H2, and H3. Green design capability to green technology innovation ability, ability of green design, and green technology innovation ability as the ability to recycle the recycle ability of path coefficients were 0.533, 0.538, and 0.602 and P values were less than 0.01, by significance test, which show that green design capability to green technology innovation ability, ability of green design, and green technology innovation ability as the ability to recycle to recycle ability have significant positive effect, and this paper assumes that the H4, H5, and H6 were verified.

4.3. Analysis of the Effect of Green Manufacturing Capacity on Green Performance. In this paper, empirical research is used to analyze the above hypotheses and the relationship between green manufacturing capacity and green

performance, the functional relationship between green manufacturing capacity and green performance, and the regulatory effect between green manufacturing capacity and green performance. According to the results of empirical analysis, the following table is a review of the test results of the proposed hypothesis, as shown in Table 4.

4.3.1. The Relationship between Green Manufacturing Capacity and Green Performance. Through the above empirical analysis, green manufacturing capability of three dimensions green design, green technology innovation ability, and ability of recycling, and the significant positive role which the green performance through the correlation coefficient test, significance test, and the path test further verify the original hypothesis, namely, green manufacturing capability, have a significant positive influence on the green performance. Therefore, for manufacturing enterprises, they should attach importance to the training and development of green manufacturing ability, comply with the macro-environment of sustainable development, integrate internal and external resources of the enterprise, and rely on the coordinated development of three capability dimensions to realize green manufacturing and improve the green performance of the enterprise.

4.3.2. Green Manufacturing Capability Constitutes the Interaction between Dimensions. Through empirical analysis, the research hypotheses H5 and H6 have been verified, indicating that the three components of green manufacturing capability affect and restrict each other. The green design is the initial activity to form green manufacturing capacity. It is the premise for the manufacturing industry to meet the requirements of environmental development, meet the demand for green products, improve the utilization rate of resources, and reduce pollution. The innovation ability of green technology is an important support link to improve the green manufacturing ability. Through the accumulation of knowledge and technology, the practical transformation ability of the green design can be realized. Recycle ability is not only the product life cycle-based closed-loop mode, through the waste recycling and utilization of resources, reducing the resource usage, and getting rid of manufacturing high consumption situation of the development of raw materials, but also effective to protect and save the productive resources and improve the ability of green manufacturing, an important way of promoting the development of circular economy. At the same time, the

Table 3: Path estimation and test values.

The relationship between variables	Path coefficient	C.R.	P
Green design ability⟶green performance (1)	0.525	2.963	0.004
Green technology innovation ability⟶ green performance (2)	0.544	2.745	0.006
Recycling capacity⟶green performance (3)	0.447	2.158	0.008
Green design ability⟶green technology innovation ability (4)	0.533	3.367	0.003
Green design ability⟶recycling ability (5)	3.304	3.304	0.001
Green technology innovation ability⟶recycling ability (6)	0.602	3.551	0.001

Note: the graphic name label is the data sequence number in Table 3.
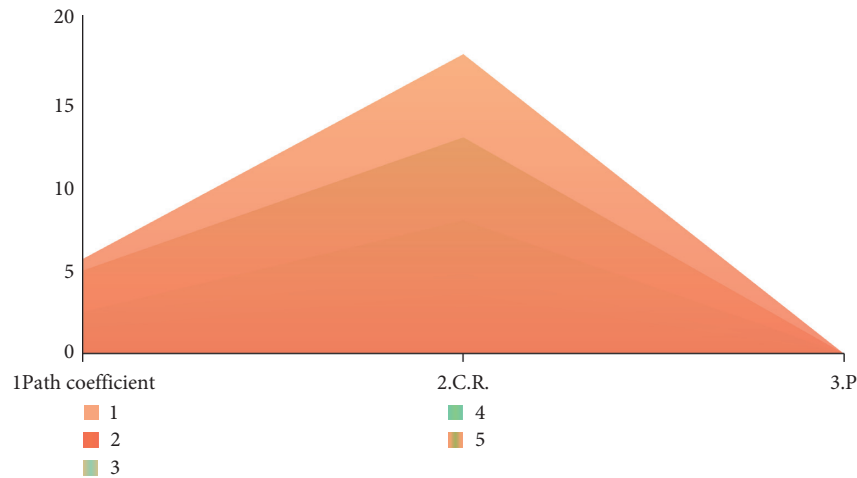
Figure 5: Path estimation and test values.

Table 4: Research hypothesis verification results.

Sequence	Assuming the content	Results
H1	There is a significant positive correlation between green design ability and green performance	Support
H2	There is a significant positive correlation between green technology innovation ability and green performance	Support
H3	Recycling ability is positively correlated with green performance	Support
H4	Organizational flexibility is positively correlated with green performance	Support
H5	Green design ability has a significant positive effect on green technology innovation ability	Support
H6	Recycling ability has a significant positive effect on green design ability	Support

improvement of green design ability can play a positive feedback and guidance role in the direction of technological innovation and technological extension and diffusion, so as to continuously innovate key processes, improve recycling efficiency, and help enterprises gain resource advantages. The comprehensive empirical analysis has been clear about the inherent role performance path of green manufacturing capacity for green design, green technology innovation ability, and circulation ability, when the loop processing power accumulated to a certain extent and positive impact on the green design ability, thus forming a closed loop, through interaction and mutual influence between the three, and promote green manufacturing capacity.

4.3.3. The Regulating Effect of Tissue Flexibility

Research Hypothesis H4. By verifying that flexible organizational structure and distributed management can help enterprises to more flexible and efficient rapid response,

according to internal and external environment changes of reasonable selection and allocation of resources, the organization system of efficient allocation of manpower, financial, and material resources give full consideration to the product green factors, both flexibility and stability in green manufacturing, to provide institutional guarantee for the enterprise. *Research Hypotheses H8.* Through confirmatory test, the organizational flexibility will affect the enterprise for green products and the design of the direction, so companies through flexible distributed management and processing capabilities can help enterprises to quickly get green product market demand information to help the designer to seize the opportunity and to meet the requirements of green manufacturing, green products in the future market share, and the enterprise image.

Through the above analysis, to cultivate green manufacturing capabilities and improve green performance, flexible management and manufacturing processes need to be linked, and the structure and scale of elements must be dynamically adjusted to ensure the matching and

collaboration between green manufacturing. Companies rely on the role of green manufacturing capabilities and growth rules to improve their green performance and obtain sustainable competitive advantages and corporate brand image.

5. Conclusions

This article is mainly about the research on the sustainable development performance of green manufacturing technology innovation based on artificial intelligence and blockchain technology. Through combining the relevant theories and literature at home and abroad, the authors have deeply studied the development and application of artificial intelligence and blockchain technology, analyzed the connotation, characteristics, dimensions, and mechanism of green manufacturing capabilities, and have mainly drawn the following conclusions: with the aid of technology, the connotation characteristics and dimensional composition of green manufacturing capabilities are analyzed from a dynamic perspective. Through combining the related literature of green manufacturing capability and in-depth analysis of the connotation characteristics of green manufacturing capability, three subcapabilities of green design capability, green technology innovation capability, and recycling capability are obtained. These three capabilities restrict and influence each other and jointly promote the formation and improvement of green manufacturing capabilities. The abstract green manufacturing capability is transformed into a dynamic manifestation of design, innovation, and recycling, which improves the operability and observability, and provides a supplement for the further expansion and improvement of the corporate green manufacturing capability analysis framework. The development of artificial intelligence and blockchain technology will change the development model of traditional manufacturing and promote the green and sustainable development of manufacturing.

The main model of green manufacturing capabilities and green performance based on artificial intelligence and blockchain has been established. The empirical analysis shows that green manufacturing capability has a positive impact on green performance, that is, green design capability, green technology innovation capability, and recycling capability, and all have a significant positive impact on green performance. In addition, the three components of green manufacturing capacity interact and restrict each other and have a significant impact. This has a positive regulating function for regulating the organizational flexibility between green design and green performance and a positive regulating function between green technological innovation ability and green performance. There is no relationship between the recycling capacity of the company and the green performance. Artificial intelligence and blockchain technology provide innovative industrial methods for green manufacturing and have made substantial contributions.

This paper studies the sustainable development performance of green manufacturing technology innovation based on artificial intelligence and blockchain technology and realizes the sustainable development of manufacturing through artificial intelligence and blockchain technology innovation. As a strategy to prevent products from negatively affecting ecological resources, the green design is the basis for implementing green manufacturing. The key to green manufacturing is the green design. The sustainable development model of green manufacturing is the future development trend and direction of the manufacturing industry and is the only and effective way to achieve the sustainable development of the manufacturing industry. At the same time, the application of high-tech will lead the development of the manufacturing industry, improve the sustainable development level of the entire manufacturing industry, strive to maintain the leading level and competitive advantage in the future competition, and realize the sustainable development of the manufacturing industry.

Data Availability

No data were used to support this study.

Conflicts of Interest

The authors declare that they have no conflicts of interest.

References

[1] L. Yishu, "Wildlife management in China from the perspective of green economy development," *Revista Científica*, vol. 1, no. 1, pp. 197–205, 2020.

[2] Q. Ye, Q. Zhang, and J. Du, "Research on the green development mode and strategy of the manufacturing industry in the era of 'internet +'," *Engineering Sciences*, vol. 17, no. 8, pp. 70–74, 2015.

[3] X. Li, H. Jianmin, B. Hou, and P. Zhang, "Exploring the innovation modes and evolution of the cloud-based service using the activity theory on the basis of big data," *Cluster Computing*, vol. 21, no. 1, pp. 907–922, 2018.

[4] B.-L. Yuan, S.-G. Ren, X. Hu, and X.-Y. Yang, "The difference effect of environmental regulation on two stages of technology innovation in China's manufacturing industry," *Frontiers of Engineering Management*, vol. 3, no. 1, p. 24, 2016.

[5] E. Amrina and A. L. Vilsi, "Key performance indicators for sustainable manufacturing evaluation in cement industry," *Procedia CIRP*, vol. 26, pp. 19–23, 2015.

[6] Q. Yu and F. Hou, "An approach for green supplier selection in the automobile manufacturing industry," *Kybernetes*, vol. 45, no. 4, pp. 571–588, 2016.

[7] M. Y. M. Taib, Z. M. Udin, and A. H. A. Ghani, "The collaboration of green design & technology towards business sustainability in Malaysian manufacturing industry," *Procedia - Social and Behavioral Sciences*, vol. 211, pp. 237–242, 2015.

[8] S.-B. Tsai, Y.-C. Lee, C.-H. Wu, and J.-J. Guo, "Examining how manufacturing corporations win orders," *South African Journal of Industrial Engineering*, vol. 24, no. 3, pp. 112–124, 2013.

[9] V. K. Mittal and K. S. Sangwan, "Ranking of drivers for green manufacturing implementation using fuzzy technique for order of preference by similarity to ideal solution method," *Journal of Multi-Criteria Decision Analysis*, vol. 22, no. 1-2, pp. 119–130, 2015.

[10] S.-B. Tsai, Y. Xue, J. Zhang et al., "Models for forecasting growth trends in renewable energy," *Renewable and Sustainable Energy Reviews*, vol. 77, pp. 1169–1178, 2017.

[11] Z. Meng, "Green transformation of manufacturing industry for ecological protection," *Ecological Economy*, vol. 13, no. 4, pp. 65–69, 2017.

[12] I. K. Hui, A. H. S. Chan, and K. F. Pun, "A study of the Environmental Management System implementation practices," *Journal of Cleaner Production*, vol. 9, no. 3, pp. 269–276, 2001.

[13] W. Wu, S. An, C. H. Wu, S. B. Tsai, and K. Yang, "An empirical study on green environmental system certification affects financing cost of high energy consumption enterprises-taking metallurgical enterprises as an example," *Journal of Cleaner Production*, vol. 244, 2020.

[14] H. Song, R. Srinivasan, T. Sookoor, and S. Jeschke, *Smart Cities: Foundations, Principles and Applications*, pp. 1–906, Wiley, Hoboken, NJ, USA, 2017.

[15] R. S. Bhadoria and N. S. Chaudhari, "Pragmatic sensory data semantics with service-oriented computing," *Journal of Organizational and End User Computing*, vol. 31, no. 2, pp. 22–36, 2019.

[16] J. Wen, J. Yang, B. Jiang, H. Song, and H. Wang, "Big data driven marine environment information forecasting: a time series prediction network," *IEEE Transactions on Fuzzy Systems*, vol. 29, no. 1, pp. 4–18, 2021.

[17] S.-B. Tsai and K. Wang, "Using a novel method to evaluate the performance of human resources in green logistics enterprises," *Ecological Chemistry and Engineering S*, vol. 26, no. 4, pp. 629–640, 2019.

[18] L. M. T. Pham, L. T. T. Tran, P. Thipwong, and W. T. Huang, "Dynamic capability and organizational performance," *Journal of Organizational and End User Computing*, vol. 31, no. 2, pp. 1–21, 2019.

[19] M. Arief, R. Kartono, M. Buss, and I. Y. T. Basuki, "Entrepreunerial process and dynamic capability of green manufacturing industries toward business excellency," *Advanced Science Letters*, vol. 21, no. 5, pp. 1154–1157, 2015.

[20] E. Oh and S.-Y. Son, "Toward dynamic energy management for green manufacturing systems," *IEEE Communications Magazine*, vol. 54, no. 10, pp. 74–79, 2016.

[21] J. Gokulachandran and K. Mohandas, "Comparative study of two soft computing techniques for the prediction of remaining useful life of cutting tools," *Journal of Intelligent Manufacturing*, vol. 26, no. 2, pp. 255–268, 2015.

[22] V. K. Mittal, R. Sindhwani, and P. K. Kapur, "Two-way assessment of barriers to lean green manufacturing system: insights from India," *International Journal of System Assurance Engineering & Management*, vol. 7, no. 4, pp. 400–407, 2016.

[23] M. A. A. Rehman, R. L. Shrivastava, and R. R. Shrivastava, "Comparative analysis of two industries for validating green manufacturing (gm) framework: an Indian scenario," *Journal of The Institution of Engineers (India): Series C*, vol. 98, no. 2, pp. 203–218, 2017.

[24] G. Beier, S. Niehoff, T. Ziems, and B. Xue, "Sustainability aspects of a digitalized industry – a comparative study from China and Germany," *International Journal of Precision Engineering and Manufacturing-Green Technology*, vol. 4, no. 2, pp. 227–234, 2017.

[25] T. Wu, T. Li, X. Ding, H. Chen, and L. Wang, "Design of a modular green closed internal cooling turning tool for applications," *International Journal of Precision Engineering and Manufacturing-Green Technology*, vol. 5, no. 2, pp. 211–217, 2018.

[26] D.-H. Kim, T. J. Y. Kim, X. Wang, M. Kim, Y.-J. Quan, and O. J. Woo, "Smart machining process using machine learning: a review and perspective on machining industry," *International Journal of Precision Engineering and Manufacturing-Green Technology*, vol. 5, no. 4, pp. 555–568, 2018.

[27] J. M. Müller and K.-I. Voigt, "Sustainable industrial value creation in smes: a comparison between industry 4.0 and made in China 2025," *International Journal of Precision Engineering and Manufacturing-Green Technology*, vol. 5, no. 5, pp. 659–670, 2018.

[28] S. Ahmad, K. Y. Wong, and H. Elahi, "Sustainability assessment and analysis of Malaysian food manufacturing sector-A move towards sustainable development," *Advanced Science Letters*, vol. 23, no. 9, pp. 8942–8946, 2017.

[29] I. Orji and S. Wei, "A detailed calculation model for costing of green manufacturing," *Industrial Management & Data Systems*, vol. 116, no. 1, pp. 65–86, 2016.

[30] Y. Li and M. Zhang, "Green manufacturing and environmental productivity growth," *Industrial Management & Data Systems*, vol. 118, no. 6, pp. 1303–1319, 2018.

[31] R. Gaha, B. Yannou, and A. Benamara, "Selection of a green manufacturing process based on cad features," *International Journal of Advanced Manufacturing Technology*, vol. 87, no. 5, pp. 1335–1343, 2016.

Research Article

Optimizing DODAG Build with RPL Protocol

Xin Niu (iD)

Changzhou Vocational Institute of Engineering, Changzhou, Jiangsu, China

Correspondence should be addressed to Xin Niu; 8000000326@czie.edu.cn

In the lossy wireless network routing system based on RPL technology, an improved DODAG construction optimization scheme is proposed for sensor nodes with low-power dissipation in the interference environment. If a node discovers that all paths between it and its neighbors have failed, the node reset action begins. Once the node reset is complete, the DODAG system build process is resumed. This prevents the DODAG root from initiating a global fix by incrementing the DODAG VersionNumer to produce a new version of the DODAG in a disruptive environment. The power loss caused by this global repair operation is avoided. The performance of DODAG in interference environment is enhanced, and the data retransmission rate is reduced.

1. Introduction

LLNs (low-power lossy networks), which are restricted in routing and connection performance, have the characteristics of high loss rate, relatively low data transmission rate, and unstable transmission performance. LLNs consist of dozens to thousands of routes that support the flow of traffic including point to point (between devices in the LLN), single point to multipoint (from central control point to child devices in the LLN) [1], and multipoint to single point (from LLN devices to a single central control point).

With the progress of the times and the rapid development of the Internet of Things, battery-powered sensor devices are gradually connected to the Internet, triggering the rapid development of LLNs. The 6 LoWPAN protocol stack connects the IPv6 Internet well with the nodes of the low-power lossy information network. The RPL routing protocol enables it to connect the nodes of various types of IOT systems. The 6 LoWPAN has become the most widely used protocol standard for the IOT. Signal transfer protocols such as ZigBee and Bluetooth support the RPL routing protocol. Information data quality sensing technology can reduce redundant transmission of invalid data based on the quality of information data collected by sensors of the Internet of Things system and only transmit the relatively valuable information in the sensor network system, which can reduce the energy consumption of the system under the condition of guaranteeing the quality of data transmission [2]. Studying and analyzing RPL routing protocol and building DODAG based on information quality theory are the way to enhance the performance of DODAG in interference environment and reduce the energy consumption of nodes.

RPL distance vector routing protocol, as a part of 6 LoWPAN protocol stack, based on IPV6 address, runs in LLNs, 6 LoWPAN adapter layer is in IPV6 protocol network layer, and 6 LoWPAN protocol stack is seamlessly combined in IPV6 protocol. RPL distance vector routing protocol uses Objective Function (target function, OF) and measure set to construct Oriented Directed Acyclic Graph for data flow to destination [3], DODAG (directed acyclic graph for destination), and its optimal path algorithm is calculated by OF constraint condition of target function and the set of function using measure. OF: routing metrics for DODAG systems based on the RPL distance vector routing protocol, target Target optimization, and how the related function Function is used to calculate Rank are defined by the target function OF. The OF defines the method of route measurement, the algorithm of Target optimization, and the process and method of calculating Rank by using the function. The metric algorithm is used to find out which path costs the least when the route is calculated and selected, and it is used as the standard of route selection. In a wired or wireless network, the "cost" is related to bandwidth, delay,

hop number, and other factors, while in a network using RPL distance vector routing protocol, the "cost" is related to LQI link quality. Metrics are algorithms that Rank computes. OF is also, in some ways, a function of a certain type, such as Cost = OF (Metrics1, Metrics2, ...), so that the metric Metrics can be calculated on that basis. Many factors must be considered in routing. In routing algorithm, we can only use a certain value and use the objective function of OF to calculate a lot of factors synthetically to get a certain value.

RPL is short for IPv6 Routing Protocol for Low-Power and Lossy Networks. LLN is a kind of network in which both internal links and routers are limited. The processor function, memory, and system power consumption (battery power) of the routers under this network may be greatly limited, and the network connection within it is also characterized by high packet loss rate, low data transmission rate, and instability. The number of nodes that make up the network can vary from just a few to tens of thousands of nodes in a network.

6 LoWPAN technology can be used in wireless sensor network IPv6 packet transmission application transmission and packet transmission needs routing. LLN IPv6 routing protocol is specialized in routing 6 LoWPAN packets. Its routing topology is DODAG.

2. Network Model of RPL Protocol and DODAG Elements

The three types of nodes constitute the network model of RPL protocol.

(1) LBRs (Low-Power and Lossy Border Routers): the root node of a DODAG system that can build a DAG or serve as a gateway between the Internet and the LLN

(2) Host: as a leaf node, this type of sensor node generates traffic that cannot be forwarded to a terminal device

(3) Network router: network equipment capable of forwarding and generating traffic and capable of running and configuring and managing various types of network protocols

2.1. DODAG Building Blocks Based on the RPL Protocol. In LLNs, the network topology often changes with the change of sensor, network router, and other nodes. The state of different nodes at different times determines the network topology. RPL routing protocol is used to exchange control management messages and routing information with other nodes, and DODAG network topology is constructed after successful connection between nodes [4].

After the network topology is constructed, the state of nodes changes with time, so DODAG needs to maintain the dynamic parameters. The following basic parameters are required for the construction and dynamic maintenance of RPL-based DODAGs:

(1) RPL Instance ID: The RPL Instance ID, a collection of individual or multiple DODAGs that share the same RPL Instance ID, forms an RPL Instance.

(2) DODAG VersionNumber: The DODAG Version-Number is a counter that is counted sequentially, increments from the root, and is capable of forming a completely new version of the DODAG. DODAG Version is uniquely identified by RPLInstanceID, DODAGID, DODAG VersionNumber, and so on [5].

(3) DODAGID: The DODAGID is the identifier of the DODAG root. DODAGID has unique properties in a range of RPL instances within LLN. The tuple (RPLInstanceID, DODAGID, and DODAG VersionNumber) uniquely identifies and defines DODAG Version information.

(4) Rank: The Rank is attribute of the node within the DODAG system, indicating the location of the node relative to the root of the DODAG system. Rank can only be used within a version of the DODAG and not in different versions of the DODAG. In the direction of moving away from the DODAG root, Rank increases progressively and decreases progressively. Use OF (target function) to perform precise calculations on Rank [6].

RANK value can be obtained by using different path generation values, which means that Rank values can be obtained through different path generation values, as shown in Figure 1.

2.2. A Network Using the RPL Protocol Includes Several Different RPL Instances. Each RPL Instance is composed of a single or several DODAGs that are different from each other, and each DODAG within each RPL Instance system has the same RPL Instance ID. Therefore, each RPL Instance ID can determine a unique RPL Instance in the system, and RPL Instance is composed of different random numbers to forms. In other words [7], All DODAGs in the same RPL Instance use the same OF. Different RPL Instance systems have different random Numbers, as shown in Figure 2.

3. Optimization of DODAG Construction in Interference Environment Based on RPL Protocol

3.1. DODAG Building Based on RPL Protocol. RPL distance vector network routing protocol uses parameter control technology to limit the frequency and number of messages used in network control management in the system and constructs a network topology with DODAG structure to reduce system power consumption and network maintenance cost. Each node within a DODAG based on the RPL protocol can perform DODAG discovery, build, and maintenance. RPL network protocol can manage ICMP V6 control message and management information and can exchange DODAG information between nodes. Based on this, a new DODAG network topology can be constructed. The node uses a DIS (DODAG Information Solicitation (DODAG Information Request)) to detect a nearby DODAG [8]. DIO (DODAG Information Object (DODAG
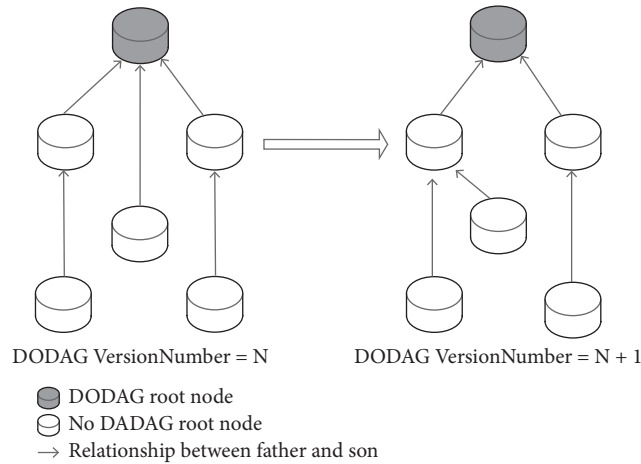
Figure 1: Relationship between DODAG roots.
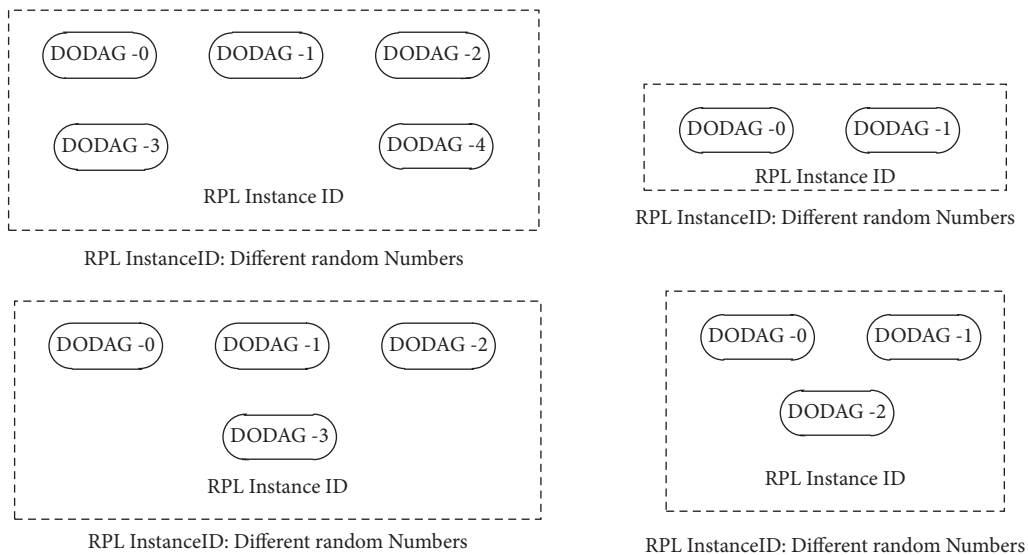
Figure 2: Relationships between various elements in the RPL protocol.

Information Object)) carries the RPL Instance information of the node, obtains the configuration parameters of the DODAG, selects the set of parent nodes in the DODAG system, and stores the information about its DODAG. The DAO (Destination Advertisement Object) can pass the reverse routing information of the DODAG system. The Rank value for each node indicates the distance of the node from other nodes. The Rank value is strictly incremented along the routing path, away from the root node. The Rank value is strictly decreasing along the routing path, close to the root node [9].

Start the DODAG system built from the DODAG root node, as shown in Figure 3. The root node of DODAG transmits DIO messages by broadcasting to the nodes directly connected with it to transmit DODAG information. Upon receiving the DIO message, the neighbor node that is directly connected to the root node processes the received DIO message and then forwards the DIO message to the next node. By analogy, DIO messages gradually

spread to the other nodes of the DODAG system. If the node receiving the DIO message does not add any DODAG, the node calculates its path overhead to the sending DIO message node [10], calculates the optimal path through the OF constraint of the target function and the set of metrics, and then decides whether to join the DODAG system. When this node joins the DODAG, it calculates the route to the DODAG root node, and the node that sends the DIO message to this node becomes the parent of the DODAG system of that node. Next, the node computes its Rank to the DODAG root node based on the target function OF in the DODAG and then replies back to its parent with the DAO.

If the node does not join any DODAG system, nor does it receive any DIO message, it periodically loops a DIS message to its direct-connected neighbor, requests DODAG information from the surrounding direct-connected node, computes it, and so on, until the node joins a DODAG system [11].
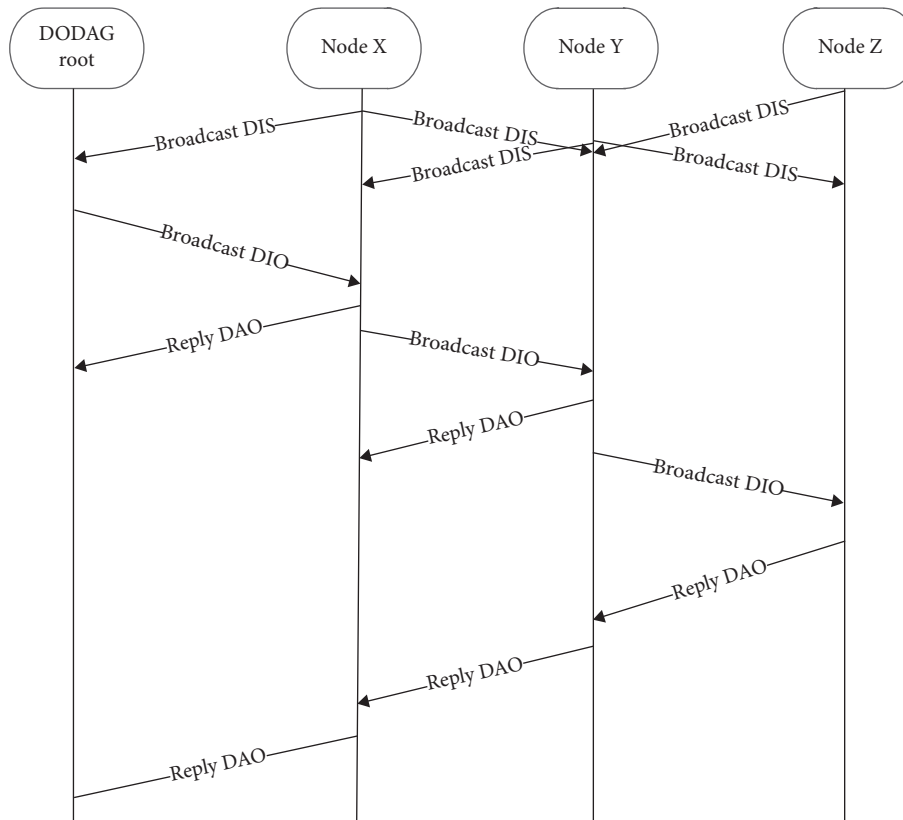
FIGURE 3: Under normal circumstances, the DODAG system is built to control the transfer of information.

The DODAG root node broadcasts the DIO message carrying the DODAG information. The node X receives the DIO message broadcasted by the root node, joins the DODAG system, and after processing the DAO message with the node X prefix information passes it to the DODAG root node. DODAG node X sends DIO message containing DODAG information to the node directly connected with node X. After receiving the message, node Y directly connected with node X joins the DODAG system and replies the DAO message to node X, node X becomes the parent of node Y. Node Y receives the DODAG information request information DIS from node Z, but node Y will not reply to any information until node Y joins a DODAG system. After node Y joins a DODAG system, node Y sends a DIO message to node Z and invites node Z to join the DODAG system. After receiving the message, Z, which is directly connected with Y node, joins the DODAG system and replies the DAO message to Y node, and Y node becomes the parent of Z. After receiving the message from node Z, node Y adds its own routing information and fuses it into the received message and then sends the DAO message to the preferred parent node X directly with node Y. By this analogy, the DODAG root node receives and calculates the DAO messages from each node in the DODAG system [12] and obtains the prefix information of each node in the DODAG system step by step.

3.2. Improved Algorithm for Building DODAG Systems in a Noisy Environment.

In the interference environment, the loss of DIO messages will lead to the change of the network topology. In the process of DODAG system initialization, RPL distance vector network routing protocol is used to send control management messages such as DIO, DIS, and DAO to each other to build DODAG system. Under the influence of environment interference, some control management messages will be lost in the process of DODAG construction. In this case, the child node may not get the DIO message of the preferred parent node [13], so that its DODAG edge length is increased, The routing protocol for low power lossy networks (RPL) uses the objective function (OF) to construct a target-oriented directed acyclic graph (DoDAG). DoDAG is built depending on routing metrics and routing constraints adopted by the target function. The Rank attribute of the node within the DODAG system indicates the location of the node relative to the root of the DODAG system. Rank can only be used within a version of the DODAG and not in different versions of the DODAG. In the direction of moving away from the DODAG root, Rank increases progressively and decreases progressively. Use OF (target function) to perform precise calculations on Rank. In this paper, at the interference environment, there is no direct neighbor relationship between node X and node Z, so it is impossible to transmit data directly. Data communication between node X and node Z can
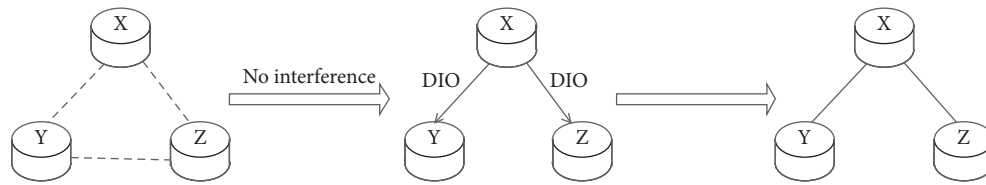
FIGURE 4: Basic process of building a DODAG in a nondisruptive environment.

only pass through node Y. At this time, the delay of data transmission and path in DODAG system increases, so does the network power consumption.

In an uncluttered environment, the process for building a DODAG system is shown in Figure 4. Node X broadcasts DIO messages to its neighbors. Nodes Z and Y receive DIO messages from node A successively. Node X will gradually become the priority parent of node Z. At the same time, node Z and node Y, as the children directly connected with node X, have joined the DODAG system. This completes the construction of the DODAG system in a noninterference environment.

Figure 5 illustrates the causes and effects of network topology in a noisy environment. In the graph, X, Y, and Z are neighbor nodes that are directly connected to each other. Node X is a node that has been added to a DODAG system. When the data are transmitted between nodes, it is disturbed and the data packet is lost [14].

When starting to build DODAG system, the node of DODAG system is not joined. Broadcast is used to send DIS message to the node of DODAG system to check whether the node of DODAG system has joined. A node that has joined a DODAG system will broadcast a DIO message to all nodes directly connected to it after it receives a request for DIS information, and the DODAG system information of the node is contained in the DIO message. All nodes that are directly connected to this DIO message sender receive their DIO message, calculate their path overhead to the sending DIO message node, and then decide to join the DODAG system or leave it as it is. If a node that has joined the DODAG system does not receive a DIS request from a direct node for a period of time, the node broadcasts a DIO message after a delay of some time. The Trickle algorithm calculates the latency wait time [15].

When the DODAG system encounters noise interference, some control management messages are lost as a result, as shown in Figure 5. When node X broadcasts DIO messages to its neighbors, node Y receives the DIO messages sent by node X. Due to the noise of interference environment, node Z does not receive the DIO messages sent by node X in time. Node Y does not join DODAG system because node Z does not receive DIO messages from node X. After Y joins DODAG system, it is delayed for a certain time and broadcasts DIO messages to the neighboring nodes, and Y notifies them to join DODAG system. In this case, node Z receives the DIO message from node Y by broadcasting. After calculation, node Y becomes the priority parent of node Z, and node Z joins the DODAG system. At this time, the network topology of DODAG system deviates greatly from that of the noninterference environment. This is because node Z received interference and no DIO message from node X broadcast was received. In the interference

environment, there is no direct neighbor relationship between node X and node Z, so it is impossible to transmit data directly. Data communication between node X and node Z can only pass through node Y. At this time, the delay of data transmission and path in DODAG system increases, so does the network power consumption [16].

The reason for this situation is that node Z cannot receive the DIO message from node X by broadcasting in time. As a result, the direct neighbor relationship between node X and node Z cannot be established. The data communication between node X and node Z needs to pass through node Y. As a result, the energy consumption and transmission latency of DODAG systems have increased.

4. Topology Repair Scheme for Two DODAG Systems in Interference Environment

In the interference environment, the loss of DIO messages will lead to the change of the network topology. The DODAG system based on RPL protocol can be used to repair the topology in two ways.

The first scenario: the root node of the DODAG uses incremental DODAG VersionNumer, initiates a global repair operation of the DODAG system, traverses the nodes of the system, and produces a brand new version of DODAG VersionNumer. In the new DODAG system, nodes that are not restricted by the old version of Rank value can recalculate their position in the DODAG system based on OF, Rank, and so on. This approach rebuilds the DODAG. Because of its global repair operation, the power loss caused by the system is relatively large.

The second scheme: RPL network protocol also supports the local topology repair mechanism in DODAG Version. You can set the necessary parameters for DIO messages when you implement system configuration and control using the DODAG root policy.

At this time, a method of repairing network topology is proposed to solve this problem. RPL network protocol can use an external mechanism to detect whether neighbors are no longer reachable. The goal of this mechanism is to maintain routing proximity with minimal overhead. Examples of similar mechanisms include the Neighbor Unreachability Detection (neighbor inaccessibility detection [RFC4861]) mechanism in IPv6 [17].

The process by which a node detects and determines whether it is reachable with a neighbor is called a Neighbor Unreachability Detection. The neighbor unreachable detection mechanism describes the reachability of the node and the direct neighbor by the state whether the node and neighbor can reach each other.
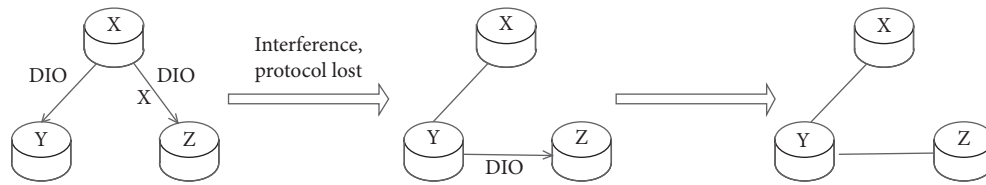
Figure 5: Basic process of building a DODAG in a disrupted environment.

In the DODAG system, the nodes communicate with other nodes through the neighbor nodes which are directly connected with them. Under the interference of the system environment, the nodes will interrupt and fail due to data loss and control information failure. If the destination node fails, the data transmission cannot be resumed and communication with the destination node fails; if the data transmission path fails, it is possible to resume communication. Therefore, nodes actively track the reachability status of packets when communicating with their neighbors.

Neighbor unreachability detection exists in all paths between nodes, including data communication from node to node, from node to router, and from router to node. In this way, the fault of neighbor node or forward path of neighbor node is detected.

If a node in a DODAG system recently receives an acknowledgment and the neighbor's IP layer has received the packet that was recently sent to it, the neighbor is reachable. The RPL is only used for routing in DODAG systems, and neighbor inaccessibility detection can be confirmed in two ways: one is a prompt from the upper protocol that provides a "connection processing" confirmation, and the other is a node sending a unicast neighbor request message that receives a reply neighbor notification message. In order to reduce unnecessary network traffic, probe messages are only sent to the neighbor nodes directly connected to them.

In DODAG system, there are two tasks simultaneously: neighbor inaccessibility detection (NUD) and a node sending packets to neighbor nodes. In the process of neighbor node reachability verification, the node continues to continuously send packet information to the neighbor node at the address of the cache link layer; if there is no packet information sent to the neighbor node in the system, the neighbor nonreachable detection (NUD) will not send either.

When the DODAG system is disturbed, Neighbor Unreachability Detection is used to enable the node to detect whether all paths between the node and its neighbor are reachable or not. If a node discovers that all paths between it and its neighbors have failed, the node reset action begins. Once the node reset is complete, the DODAG system build process is resumed. At this point, the DODAG root is prevented from initiating a global repair operation by incrementing the DODAG VersionNumer to avoid regenerating a new version of the DODAG. At the same time, the power loss caused by this global repair operation is avoided. The performance of DODAG in interference environment is enhanced, and the data retransmission rate is reduced.

In DODAG system, controlling the energy consumption of message transmission and data information calculation is an important part of routing algorithm consumption. The energy consumption of data information transmission is far more than that of data calculation [18].

In the Internet of Things, all kinds of objects around people can join the communication network, connect with the traditional Internet, and communicate with each other freely and exchange information. The "content" in the Internet of things refers to the intelligent device capable of communication and network, the intelligent equipment has a large number and frequent switching characteristics, such as the limited resources, how to manage, organize the efficient, safe network between smart devices, and merge with the traditional Internet, you need to design special routing protocols. In view of the above Internet of Things networking requirements, IETF specially designed a lightweight IPv6 networking routing protocol for Internet of Things devices, RPL routing protocol. RPL routing protocol can efficiently utilize the energy and computing resources of intelligent devices, form a flexible topology structure, and realize data routing.

In the Internet of Things, all kinds of objects around us can join the communication network, connect with the traditional Internet, communicate with each other freely, and exchange information. The "content" in the Internet of Things refers to the intelligent device capable of communication and network, the intelligent equipment has a large number, and frequent switching characteristics, such as the limited resources, how to manage, organize the efficient, safe network between smart devices, and merge with the traditional Internet, you need to design special routing protocols. In view of the above Internet of Things networking requirements, IETF specially designed a lightweight IPv6 networking routing protocol for Internet of Things devices, RPL routing protocol. RPL routing protocol can efficiently utilize the energy and computing resources of intelligent devices, form a flexible topology structure, and realize data routing.

The low-power and lossy nature of LLNS necessitate the use of additional packets for RPL's on-demand loop detection. Because of the sporadic nature of data traffic, maintaining a routing topology that varies with the physical topology can result in wasted energy. In physical connections, LLNs typically show instantaneous and unimpeded changes in traffic, but tracking these changes closely from the control plane is costly. Transient and occasional changes in connections do not need to be processed by RPL until data are sent. The design of RPL in this regard borrows from the existing LLN protocol for high-frequency use, as well as a large number of experiments and deployments demonstrating its efficacy. The RPL packet information is sent along

with the packet and contains the sender's Rank information. Inconsistencies in routing decisions (up or down) and the Rank relationship between the two nodes indicate a possible loop. If such data is received, the node initiates a local repair operation.

5. Conclusions

In this paper, an improved DODAG construction optimization scheme is proposed. The nodes of DODAG can use the Neighbor Unreachability Detection mechanism to perceive the survival of the neighbors directly connected to it. If a node discovers that all paths between it and its neighbors have failed, the node reset action begins. Once the node reset is complete, the DODAG system build process is resumed. This prevents the DODAG root from initiating a global fix by incrementing the DODAG VersionNumer to produce a new version of the DODAG in a disruptive environment. The power loss caused by this global repair operation is avoided. The performance of DODAG in interference environment is enhanced, and the data retransmission rate is reduced.

In DODAG system, there are two tasks simultaneously: neighbor inaccessibility detection (NUD) and a node sending packets to neighbor nodes. When the DODAG system is disturbed, Neighbor Unreachability Detection is used to enable the node to detect whether all paths between the node and its neighbor are reachable or not. If a node discovers that all paths between it and its neighbors have failed, the node reset action begins. Once the node reset is complete, the DODAG system build process is resumed. At this point, the DODAG root is prevented from initiating a global repair operation by incrementing the DODAG VersionNumer to avoid regenerating a new version of the DODAG. At the same time, the power loss caused by this global repair operation is avoided. The performance of DODAG in interference environment is enhanced, and the data retransmission rate is reduced.

Data Availability

The data that support the findings of this study are available from the corresponding author upon reasonable request.

Conflicts of Interest

There are no potential conflicts of interest in this paper.

Authors' Contributions

All authors have seen the manuscript and approved to submit to this journal.

Acknowledgments

References

[1] D. Wang, W. Li, and P. Wang, "Measuring two-factor authentication schemes for real-time data access in industrial wireless sensor networks," *IEEE Transactions on Industrial Informatics*, vol. 14, no. 9, pp. 4081–4092, 2018.

[2] C. Pu, "Spam dis attack against routing protocol in the internet of things," in *Proceedings of the 2019 International Conference on Computing, Networking and Communications (ICNC)*, pp. 18–21, IEEE, Honolulu, HI, USA, February 2019.

[3] A. Aris, S. F. Oktug, and S. Berna Ors Yalcin, "RPL version number attacks: in-depth study," in *Proceedings of the NOMS 2016—2016 IEEE/IFIP Network Operations and Management Symposium*, pp. 25–29, Istanbul, Turkey, July 2016.

[4] A. Dvir, T. M. Holczer, and L. Buttyan, "VeRA—version number and rank authentication in RPL," in *Proceedings of the 2011 IEEE Eighth International Conference on Mobile Adhoc and Sensor Systems*, pp. 17–22, IEEE, Valencia, Spain, October 2011.

[5] P. S. L. M. Barreto, B. Libert, N. McCullagh, and J.-J. Quisquater, "Efficient and provably-secure identity-based signatures and signcryption from bilinear maps," in *Presented at the International Conference on the Theory and Application of Cryptology and Information Security*, pp. 515–532, Springer, Berlin, Germany, 2005.

[6] A. Mayzaud, R. Badonnel, and I. Chrisment, "A distributed monitoring strategy for detecting version number attacks in RPL-based networks," *IEEE Transactions on Network and Service Management*, vol. 14, no. 2, pp. 472–486, 2017.

[7] A. Mayzaud, R. Badonnel, and I. Chrisment, "Detecting version number attacks in RPL-based networks using a distributed monitoring architecture," in *Proceedings of the 2016 12th International Conference on Network and Service Management (CNSM)*, November 2016.

[8] T. Tsao, R. Alexander, M. Dohler, V. Daza, A. Lozano, and M. Richardson, "A security threat analysis for the routing protocol for low-power and lossy networks (RPLs), request for comments," 2015, https://rfc-editor.org/rfc/rfc7416.txt.

[9] A. Le, J. Loo, K. Chai, and M. Aiash, "A specification-based ids for detecting attacks on RPL-based network topology," *Information*, vol. 7, no. 2, p. 25, 2016.

[10] H. Perrey, *On Secure Routing in Low-Power and Lossy Networks: The Case of RPL, Master of Science*, Department of Computer Science, Hamburg University of Applied Sciences, Hamburg, Germany, 2013.

[11] L. Wallgren, S. Raza, and T. Voigt, "Routing attacks and countermeasures in the RPL-based internet of things," *International Journal of Distributed Sensor Networks*, vol. 9, no. 8, 2013.

[12] D. Airehrour, J. Gutierrez, and S. K. Ray, "A testbed implementation of a trust-aware RPL routing protocol," in *Proceedings of the 2017 27th International Telecommunication Networks and Applications Conference (ITNAC)*, pp. 1–6, IEEE, Melbourne, Australia, November 2017.

[13] S. Raza, L. Wallgren, and T. Voigt, "SVELTE: real-time intrusion detection in the internet of things," *Adhoc Networks*, vol. 11, no. 8, pp. 2661–2674, 2013.

[14] A. Mayzaud, A. Sehgal, R. Badonnel, I. Chrisment, and J. Schonwalder, "A study of RPL dodag version attacks," in *Proceedings of the IFIP International Conference on Autonomous Infrastructure, Management and Security*, Springer, Brno, Czech Republic, July 2014.

[15] A. Mayzaud, *Monitoring and Security for the RPL-Based Internet of Things, Doctor of Philosophy*, Université de Lorraine, Metz, France, 2016.

[16] H. Perrey, M. Landsmann, O. Ugus, M. Wahlisch, and T. C. Schmidt, "TRAIL: topology authentication in RPL," in *Proceedings of the 2016 International Conference on Embedded Wireless Systems and Networks (ESWN)*, pp. 59–64, Graz, Austria, February 2016.

[17] F. Ahmed and Y.-B. Ko, "A distributed and cooperative verification mechanism to defend against DODAG version number attack in RPL," in *Proceedings of the 6th International Joint Conference on Pervasive and Embedded Computing and Communication Systems (PECCS)*, pp. 55–62, Lisbon, Portugal, July 2016.

[18] M. Nikravan, A. Movaghar, and M. Hosseinzadeh, "A lightweight defense approach to mitigate version number and rank attacks in low-power and lossy networks," *Wireless Personal Communications*, vol. 99, no. 2, pp. 1035–1059, 2018.

Research Article

Application of Blockchain Technology in Supply Chain Finance of Beibu Gulf Region

RenLan Wang and Yanhong Wu ![ORCID]

College of Accounting, Zhanjiang Science and Technology College, Zhanjiang 524094, Guangdong, China

Correspondence should be addressed to Yanhong Wu; 08123323@cumt.edu.cn

Blockchain technology is a database that is operated by multiple parts and forms a chain structure through hash index. The blockchain uses multiple nodes and distributes multiple accesses to data, thereby reducing the dependence on the central Internet server and avoiding the possibility of damage to the central server point due to data and data loss. Encryption technology is used to ensure its integrity and ensure that the data files stored in the blockchain are not tampered with or deleted maliciously. Blockchain technology has inherent advantages in supply chain finance with its technical attributes such as nontampering, distributed ledger, and traceability and has great potential to build trust to solve the main problems of supply chain finance, which is conducive to promoting financial development in the Beibu Gulf region. This article mainly introduces the application research of blockchain technology in supply chain finance in the Beibu Gulf region and intends to provide some ideas for the development of supply chain finance in the Beibu Gulf region combined with blockchain technology. This article proposes the application research methods of blockchain technology in supply chain finance in the Beibu Gulf region, including blockchain technology, supply chain financial risk evaluation on the blockchain, and supply chain finance game for relevant experiments. The experimental results of this article show that the average processing time of the algorithm of the designed blockchain supply chain financial system is 4.10 seconds, the algorithm processing efficiency is faster, and the relevant risks can be better assessed.

1. Introduction

In order to make the development of supply chain finance reasonable and controllable, it is necessary to improve the ability to control supply chain financing through emerging technologies. The development of supply chain financing will form cross-industry, cross-regional, cross-departmental, and in-depth alliances with the government, and industry associations and funds will form an economic ecological platform to provide effective services to different entities, improve the operational efficiency of the supply chain, and promote the development of the business environment. And this stage is inseparable from technologies such as blockchain, the Internet, and the Internet of Things. Blockchain technology has attracted more and more attention. At present, blockchain technology is gradually applied in the field of supply chain finance. Its technical characteristics play a practical role in the field of supply chain finance, which can improve the trust relationship in supply chain finance and enhance the huge financing ability of supply chain.

In today's economic globalization, economic integration and financial integration have become more and more important. In this context, the development of regional finance has become an inevitable trend of economic development. The Guangxi Beibu Gulf Economic Zone is located on the southwest coast of China. It is an important transportation hub from China to ASEAN countries during the construction of the China-ASEAN Free Trade Area. It is an important member of the Pan-Beibu Gulf Economic Zone and the Pan-Pearl River Delta Economic Zone. Under the external environment full of opportunities and challenges, it is extremely important for Beibu Gulf Economic Zone to make use of its internal advantages and overcome its disadvantages to carry out regional supply chain economic cooperation.

Kshetri evaluated the role of blockchain in enhancing the security of the Internet of Things (IoT), which covers the key

underlying mechanism related to blockchain-IoT security relationship. From a security perspective, Kshetri focused on blockchain-based solutions, which are superior to the current IoT ecosystem in many aspects, which mainly rely on centralized cloud servers. Through practical applications and practical examples, Kshetri believes that the decentralized nature of the blockchain may cause malicious participants to be less sensitive to manipulation and forgery. In addition, Kshetri specifically considered how a blockchain-based identity and access management system can deal with some key challenges related to IoT security, and detailed analysis and description of the blockchain's ability to track insecure sources in the supply chain related to IoT devices. This research lacks experimental data support and is not practical [1]. Gelsomino et al. categorized the research on supply chain finance so far according to main themes and methods, proposed directions for future research, and completed a related literature review, which puts forward two main points: a financing-oriented view and a focus on finance institutions providing short-term solutions involving accounts payable and accounts receivable; and a supply chain-oriented view that may not involve financial institutions, but focuses on accounts payable, accounts receivable, inventory, and sometimes even fixed assets optimization of working capital in financing. Gelsomino LM believes that this review accurately represents the content of supply chain finance research published within the specified time frame and has identified the most important issues that need to be addressed in future research. In addition, Gelsomino LM found, based on the research deficiencies found in the literature, four key issues that are marked and hoped to be resolved in future research. This study only carried out theoretical discussion, without relevant experiments, and lacked persuasiveness [2]. Yao believes that shopping companies must optimize the integration of their supply chain resources to provide service capabilities, improve customer experience, and introduce satisfactory customized services. These companies need to determine how to achieve effective supply chain resource integration based on different customized service models, improve their resource utilization, and solve special problems in the shopping process. Yao explored the dynamic balance between supply and demand service capabilities by analyzing the characteristics and service modes of supply chain resource integration in shopping companies. The discussion of these capabilities not only considered traditional optimization goals, but also looked at general services, emergency services, and strategies. From the perspective of potential capabilities, the applicability of resources is evaluated to achieve effective supply chain resource integration. Yao JM regards the consistency of the ability target orientation of resource partners as an important optimization goal and evaluates this consistency by identifying the ability characteristic factors and introducing them into the supply chain resource integration. He also proposed an optimization model and an improved ant algorithm to solve the supply chain resource integration process. This research procedure is relatively complicated and not suitable for popularization in practice [3].

The innovations of this article are to (1) propose algorithms for supply chain financial risk evaluation and supply chain financial game on blockchain for research; (2) research on blockchain-based IoT technology; (3) design the Beibu Gulf supply chain financial system architecture.

2. Methods for the Application of Blockchain Technology in Supply Chain Finance in Beibu Gulf Region

2.1. Blockchain Technology

2.1.1. Blockchain Definition. Blockchain is well known to mankind and can be understood as a universally distributed decentralized and intelligent platform in the network [4]. Any node in the blockchain has a copy of the database, and each block created is encrypted and stored with transaction information details; and when each block is created, and the block is completed and transmitted to all nodes in the blockchain, the time stamp is created, and all nodes are notified universally. After each node updates the database, the encrypted information cannot be changed. Even if the data of a certain node is destroyed, the node will not be used because the information of most other nodes is inconsistent [5].

The official definition of blockchain is as follows: blockchain is a new way of applying computer technology, such as distributed data storage, point-to-point transmission, consensus mechanism, and encryption algorithm. The blockchain is essentially a decentralized database. At the same time, as the basic technology of Bitcoin, it is a series of data blocks related to encryption. The data block contains a batch of Bitcoin transaction information, which is used to verify the validity of the information and create the next block [6]. The blockchain is composed of multiple blocks, which are automatically formed according to the creation time. It is not based on other institutions to provide credit ratings but uses encryption and computer science as a means to ensure security to create a corresponding secure public database. The blocking chain was found to be a technical means to make decentralized data accounts safe and public [7].

2.1.2. Features of Blockchain

(i) Decentralization. Decentralization is the core feature of blockchain, and it is also impossible to achieve with other technologies. Information transmission, distributed storage, maintenance, and other operations in the blockchain no longer need to be processed by the central server but rely on the common maintenance of each node in the network node [8].

(ii) Distributed Ledger and Storage. Due to the decentralization of the blockchain, each node adopts distributed accounting storage; that is, each node has a general ledger. After each node uploads and downloads the information, a new block is created through encryption. The establishment of each block will be notified to all nodes on the chain through broadcast, and the generation of this block will be recorded together. All the ledgers of all nodes are updated once to maintain the consistency of all the node ledgers [9].

(iii) Smart Contract. The smart contract is formed by the system program setting. It can complete the recognition, judgment, generation behavior, execution, and other procedures by starting a certain condition. It does not require human setting operations, automatically generates the business of adding data, and cannot modify or delete other data, effectively avoiding the interference caused by the external environment [10].

(iv) Traceability. The blockchain adds a time stamp to the generation of each block by adding a time stamp and expands the blockchain according to the sequence of generation time. Time is unique, so after adding the time stamp, double recording can be avoided, and the time stamp cannot be tampered with or deleted after it is generated [11].

(v) Security. Each information processing of the blockchain will be encrypted by the hash algorithm in asymmetric cryptography to generate a string of fixed-length characters, supplemented with a time stamp, and jointly ensure uniqueness [12].

2.2. Evaluation of Supply Chain Financial Risks on Blockchain

2.2.1. Judgment Matrix. In the analytic hierarchy process, if there are n influencing factors of I in the criterion layer, that is, there are n factors in the sublevel of I, then the corresponding judgment matrix affecting criterion I is an $n \times n$ matrix. According to the construction of the judgment matrix of the analytic hierarchy process, in the level analysis of the supply chain financial risk on the blockchain, it can be assumed that the total risk of the system is I, and the first-level indicator of the supply chain financial risk evaluation on the blockchain is $I_i = \{I_1, I_2, \ldots, I_i\}$, and the second-level indicator is $I_{in} = \{I_{i1}, I_{i2}, \ldots, I_{in}\}$, and the third-level indicator is $I_{inm} = \{I_{in1}, I_{in2}, \ldots, I_{inm}\}$ [13]. The importance of each influencing factor to the upper level can be determined by quantitative indicators. For any secondary index, its judgment matrix is the matrix formed by comparing the various influencing factors below the index [14]. Suppose that the order of the judgment matrix of I_{in} is m, and $I_{c\,d}$ is the importance ratio of the third-level index I_{inc} and the third-level index $I_{in\,d}$ to the second-level index I_{in}, and the following relationship exists:

$$I_{c\,d} > 0,$$

$$I_{dc} = \frac{1}{I_{c\,d}},$$

$$I_{cc} = I_{d\,d} = 1,$$

$$c = (b_{c\,d})_{mm} = \begin{Bmatrix} b_{11} & b_{12} & \cdots & b_{1m} \\ b_{21} & b_{22} & \cdots & b_{2m} \\ \vdots & \vdots & \cdots & \cdots \\ b_{m1} & b_{m2} & \cdots & b_{mm} \end{Bmatrix}. \tag{2}$$

2.2.2. Calculation of Relative Weight. In the second step of calculating the relative weight, suppose that the third-level indicator of supply chain financial risk on the blockchain is $I_{in1}, I_{in2}, \ldots, I_{inm}$, and the corresponding second-level indicator is I_{in} weight $W_{in1}, W_{in2}, \ldots, W_{inm}$ [15]. Using geometric average method for calculation, the formula is as follows.

First, calculate the product M_c of each row of the matrix:

$$M_c = \prod_{d=1}^{m} b_{c\,d}, \quad (c = 1, 2, \ldots, m). \tag{3}$$

Then, calculate the m-th root $\overline{W_c}$ of M_c:

$$\overline{W_{inc}} = \sqrt[m]{M_c}. \tag{4}$$

Perform vector normalization:

$$W_{inc} = \frac{\overline{W_{inc}}}{\sum_{k=1}^{m} \overline{W_{inc}}} = \frac{\sqrt[m]{M_c}}{\sum_{k=1}^{m} \sqrt[m]{M_c}} = \sqrt[m]{\frac{\prod_{d=1}^{m} b_{c\,d}}{\sum_{k=1}^{m} \sqrt[m]{\prod_{d=1}^{m} b_{c\,d}}}}, \quad c = 1, 2, \ldots, m. \tag{5}$$

2.2.3. Consistency Test of Judgment Matrix. The third step is the consistency test. The rationality of the judgment matrix depends on the consistency test. The consistency test can avoid the strong randomness of the judgment matrix without losing the significance of its judgment [16]. Firstly, the new matrix CV is obtained by multiplying the judgment matrix and the relative weight coefficient vector, and then the maximum eigenvalue $\lambda_{\max}$ of the CV is calculated, and then the value of the consistency index (C.I.) is calculated. When the order of the matrix is greater than 2, the value of C.I. is calculated:

$$\lambda_{\max} = \frac{1}{m} \sum_{c=1}^{m} \frac{cv_c}{v_c} = \sum_{c=1}^{m} \frac{(cv)_c}{mv_c} = \frac{1}{m} \sum_{c=1}^{m} \frac{\sum_{d=1}^{m} b_{cd} v_d}{v_c}. \tag{6}$$

It is generally believed that as long as the value of C.I. is not greater than 0.1, the consistency is considered acceptable. If it is greater than 0.1, it is considered that the consistency is not good enough. Some evaluations may be random and not considered seriously. However, when the order of the matrix increases, its consistency tends to decrease; that is, it will be greater than 0.1, so the randomness index (RIndom Index, RI) is generally used to check the consistency of the judgment matrix. RI is a function of the order n of the matrix. It increases as the order increases. The order of the matrix is brought into the table of RI values, and the corresponding value is obtained to calculate the value of the consistency ratio C.R. [17, 18].

$$C.R. = \frac{C.I.}{R.I.}. \tag{7}$$

2.3. Supply Chain Finance Game. Calculate the expected benefits of different decision-making core enterprises and obtain their comprehensive expectations:

$$E_{x2} = y_2 (R_1 b_2 + v) + (1 - y_2)(R_2 b_2), \tag{8}$$

$$E_{1-x_2} = y_2 [R_1 (1 + b_2) - p_1] + (1 - y_2)[R_2 (1 + b_2) - p_2], \tag{9}$$

$$\overline{E_{x_2}} = x_2 E_{x_2} + (1 - x_2) E_{1-x_2}. \tag{10}$$

Calculate the expected returns of financial institutions in different decision-making and obtain their comprehensive expectations:

$$E_{y2} = x_2 (aR_1 b_3 + l_1 - c_3) + (1 - x_2)(aR_2 b_3 - l_2 - c_4), \tag{11}$$

$$E_{1-y2} = x_2 (aR_2 b_3 - l_2 - c_4) + (1 - x_2)(p_2 - l_2 - c_4 - c_6), \tag{12}$$

$$\overline{E_{y_2}} = y_2 E_{y_2} + (1 - y_2) E_{1-y_2}. \tag{13}$$

According to the evolutionary game theory and the above results, the replication dynamic equations of core enterprises and financial institutions are obtained:

$$F(x_2) = \frac{dx_2}{dt} = x_2 \left(E_{x_2} - \overline{E_{x_2}} \right), \tag{14}$$

$$F(y_2) = \frac{dy_2}{dt} = y_2 \left(E_{y_2} - \overline{E_{y_2}} \right). \tag{15}$$

Establish the replication dynamic equation of the above core enterprises and financial institutions together, and record:

$$M = aR_1 b_3 - p_1 + c_5 - aR_2 b_3 + p_2 - c_6, \tag{16}$$

$$N = c_3 + c_5 + p_2 - p_1 - l_1 - l_2 - c_4 - c_6. \tag{17}$$

Get a two-dimensional dynamic system S_2:

$$\begin{cases} \dfrac{dx_2}{dt} = x_2 (1 - x_2) [y_2 (R_2 - R_1 + p_1 - p_2 + v) + (p_2 - R_2)], \\[2mm] \dfrac{dy_2}{dt} = y_2 (1 - y_2)(Mx_2 + N). \end{cases} \tag{18}$$

Analyze the two-dimensional dynamic system, study the dynamic changes of the strategic choices of core enterprises and financial institutions, and explore the evolutionary path and law of the two parties in the regulatory game [19, 20].

The method part of this article uses the above method to study the application of blockchain technology in supply chain finance in the Beibu Gulf region. The specific process is shown in Table 1.

3. Application Research Experiment of Blockchain Technology in Supply Chain Finance in Beibu Gulf

3.1. Research on Internet of Things Technology Based on Blockchain

3.1.1. New Block Structure Design. Blockchain is fundamentally different from traditional transaction networks and has a variety of special characteristics [21]. Their key

functions include encryption (asymmetric encryption), hashing, chaining blocks, and smart contracts. Blockchain transactions represent the interaction between two parties. For encrypted currencies, transactions represent the transmission of encrypted currencies between blockchain users. These transactions can also refer to the transmission or recording of messages. Each block in the blockchain can contain one or more transactions, and the block structure is designed according to the block's things [22].

The general blockchain is a decentralized, distributed, and public number composed of blocks. In general, each block is connected to a collection of transactions with a time stamp. It can be seen that this technology allows nodes to exchange data by creating transactions. Each transaction depends on another transaction. The output of one transaction is referenced as input in another transaction, thereby creating a chain structure in it [23].

The essence of the blockchain is a distributed database (account book). The block header is equivalent to the index of the data account book, and the block body records specific transactions. For the Internet of Things environment, the traditional block is no longer suitable for the Internet of Things environment. The block design does not match this direction, resulting in a large amount of redundancy at the data structure level, which will inevitably lead to a waste of resources for operations such as fast access to the chain and update of the new area [24]. For example, the block structure of Ethereum is more suitable for money transactions and does not pay attention to physical devices. This creates a certain conflict with the environment of a large number of physical devices such as the Internet of Things. Due to the particularity of the IoT environment, IoT devices may not have high computing power. Compared with the computing and storage capabilities required as an Ethereum node, to be applied to the IoT environment, it is necessary to reduce computing overhead and reduce calculations and power dependence [25].

3.1.2. Authentication Interaction Based on New Blocks. The transaction authentication and interaction process of the entire system is divided into two steps, zero-knowledge entry chain and secondary authentication during interaction. The zero-knowledge proof, such as entering the chain, is a necessary condition for joining this IoT blockchain system, and the second identity authentication occurs when two gateway nodes exchange data [26].

The first time the new gateway node enters the chain it uses a zero-knowledge proof algorithm to write information such as the device number, Diffie-Helman field, and envelope encryption public key into the blockchain. This time authentication is necessary. The zero-identification proof of the more commonly used and constant data can ensure that important data cannot be tampered with. At the same time, these data are likely to be used extensively and frequently in future gateway node communication. Data disclosure in advance is helpful for mutual trust and communication security between gateway nodes. After the data is written, the second authentication is to use the data of the first

TABLE 1: Part of the technical process of this method.

Research methods for the application of blockchain technology in supply chain finance in the Beibu Gulf region					
2.1	Blockchain technology	2.2	Evaluation of supply chain financial risks on blockchain		
1	Blockchain definition	1	Judgment matrix	2.3	Supply chain finance game
2	Blockchain characteristics	2	Calculation of relative weight		
		3	Judgment matrix consistency test		

authentication to perform the second authentication when interacting between blocks (gateway nodes). Take out the relevant information and necessary cryptographic data of the other party from the blockchain, and then you can carry out secure data interaction [27].

3.2. Architecture Design of Financial System of Beibu Gulf Supply Chain

3.2.1. Overall System Architecture. The system is divided into financial basic platform and business service platform from the overall architecture design. The financial basic platform mainly includes the blockchain layer and the financial service layer. The blockchain layer is based on the Hyperledger Fabric project to build a basic blockchain technology network layer, which is used to carry data services such as data security storage and data synchronization in the Beibu Gulf region and financial services. The layer mainly includes service interface, operation, and maintenance platform backend, and operation and maintenance platform front-end. The service interface is a service layer that provides business service platforms in the Beibu Gulf region to quickly access the blockchain network layer for data interaction; the operation and maintenance platform provides services including blocks operation and maintenance operations required by the chain network and financial service layer. The business service platform mainly includes the backend of supply chain finance and the front end of supply chain finance; its main role is to serve as the platform layer for carrying various business processes in the financial business, and different functional modules can be added according to the specific business to meet different functional needs.

3.2.2. Blockchain Network Architecture and Its Module Docking. The blockchain network in the Beibu Gulf region mainly connects to the service interface module together with the service interface to provide blockchain services to the backend of the supply chain finance. The blockchain network includes member management, blockchain services, chain code services, and distributed ledger modules. Member management includes member registration, member review, and member authentication functions; blockchain services implement underlying consensus management and p2p communication management functions; chain code services implement chain code containers and chain code deployment functions; distributed ledgers store data in the business process. The service interface includes four functional modules: Fabric-SDK, authority management, certificate management, and dispatch control, which provide an interface for the backend of supply chain finance to implement the package and call of certificates and permissions. Among them, scheduling control is the entrance to the backend call of supply chain finance, calling certificate management and authority management to determine user identity and authority, and calling SDK according to the result to realize the requested function; authority management is responsible for managing role authority and functional authority in the supply chain system; certificate manages the certificate-related operations of platform customers.

3.2.3. Chain Code Implementation. In Hyperledger Fabric, smart contracts are also called chain codes. The chain code in the system described in this article is the supply chain business logic that controls the core enterprises, suppliers, and banks in the blockchain network to exchange information or execute transactions. Set up and get data in the blockchain ledger or World State database by calling the chain code. Hyperledger Fabric currently supports Golang and Java to develop chain code. Since Hyperledger Fabric is developed in Golang language, the system described in this article uses Golang language that is closer to Hyperledger Fabric to develop chain code. The chain code development environment relies mainly on Docker container and Golang language.

This experimental part proposes that the above steps are used in the application research experiment of blockchain technology in supply chain finance in the Beibu Gulf region. The specific process is shown in Figure 1.

4. Application Research and Analysis of Blockchain Technology in Supply Chain Finance in Beibu Gulf

4.1. Analysis on the Financial Development of Beibu Gulf City Group

(1) Among the many quantitative evaluation indicators for the spatial agglomeration identification of the financial industry, the location entropy index can measure the agglomeration level of the urban financial industry development from multiple perspectives in geographic space, reflecting the overall concentration characteristics of the urban financial industry space. Based on this, this paper selects two indicators, the location entropy index and the industrial city agglomeration index, and uses the statistical data from 2016 to 2020 to determine the degree of spatial agglomeration of the financial industry in the Beibu Gulf city cluster, as shown in Table 2 and Figure 2.
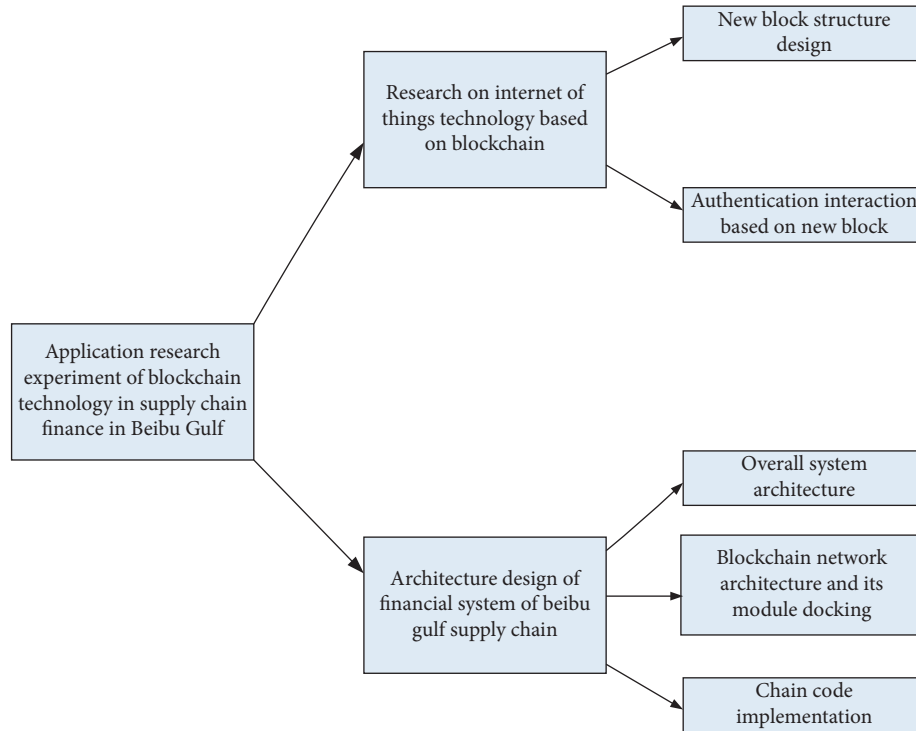
Figure 1: Some steps of the experiment in this article.

Table 2: The financial location entropy index of Beibu Gulf urban agglomeration from 2016 to 2020.

City	2016	2017	2018	2019	2020
Nanning	1.6672	1.4637	1.5129	1.4748	1.3729
Beihai	0.6385	0.5942	0.5817	0.5632	0.5478
Qinzhou	0.6327	0.5865	0.5543	0.5671	0.5527
Fangchenggang	0.6607	0.6423	0.6143	0.6267	0.6209
Yulin	0.9489	0.9142	0.9235	0.8974	0.8823
Chongzuo	0.6458	0.6104	0.5847	0.5918	0.5746

On the whole, the financial agglomeration level of the Beibu Gulf urban agglomeration shows a downward trend; from the numerical value of the agglomeration degree, Nanning, which has a higher degree of agglomeration, has a downward trend in financial agglomeration; due to the decline of the traditional industries in these cities, the emerging industries have not yet developed. Under the dual effects of the decrease in the inflow of external financial resources and the outflow of internal financial resources, the concentration of the urban financial industry has shown a continuous downward trend.

(2) The development of financial development in the Beibu Gulf Economic Zone is inseparable from the regional financial center. Financial centers can play the role of regional financial centers and promote the effective integration of financial resources of regional financial centers. The GDP of central cities in the Beibu Gulf region in 2020 is shown in Table 3 and Figure 3.

As can be seen from the chart, Nanning in the Beibu Gulf Economic Zone has the highest GDP and the strongest economic strength. Nanning is the economic center of the whole district, with the largest number of financial institutions, complete financial services, a high level of electronics, and the most complete financial system.

4.2. Experiment Analysis

(1) Checking whether the judgment matrix is consistent is a necessary prerequisite to ensure better hierarchical ranking, because an important criterion for evaluating whether the importance ranking of the subelements in the judgment matrix is correct is whether the matrix is correct. It has logical regularity. In the actual evaluation process, inconsistent errors often appear, because the evaluator can only make a rough judgment and cannot guarantee that the judgment is sufficiently rational. Therefore, it is extremely necessary to check the consistency of the judgment matrix. Only when the judgment matrix satisfies the principle of consistency and is logically reasonable, can the result be further analyzed; otherwise, the wrong conclusion will be drawn. The specific operation to check whether the judgment matrix has consistency is as follows: first, calculate the consistency index; then, obtain the corresponding average random consistency index by looking up the table; finally, calculate the consistency ratio value and make a judgment. The value of the average random consistency index needs to be
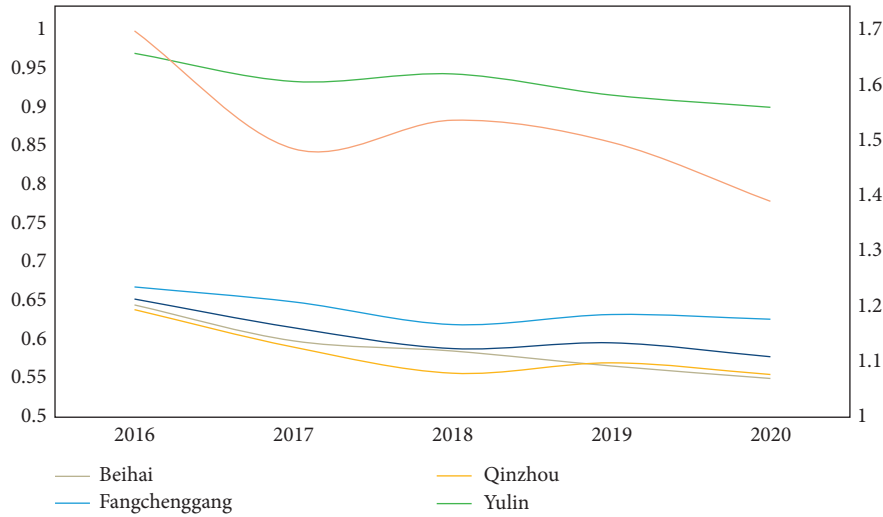
FIGURE 2: The financial location entropy index of the Beibu Gulf urban agglomeration from 2016 to 2020.

TABLE 3: GDP and industrial structure of central cities in Beibu Gulf Economic Zone in 2020 (100 million yuan).

City	GDP	First industry	Secondary industry	Tertiary industry
Nanning	3671.12	692.46	1567.21	1411.45
Beihai	1126.45	326.72	394.17	405.56
Qinzhou	987.13	309.24	318.09	359.80
Fangchenggang	1045.07	378.05	354.69	312.33
Yulin	745.06	258.37	267.13	219.56
Chongzuo	659.18	201.56	243.48	214.14
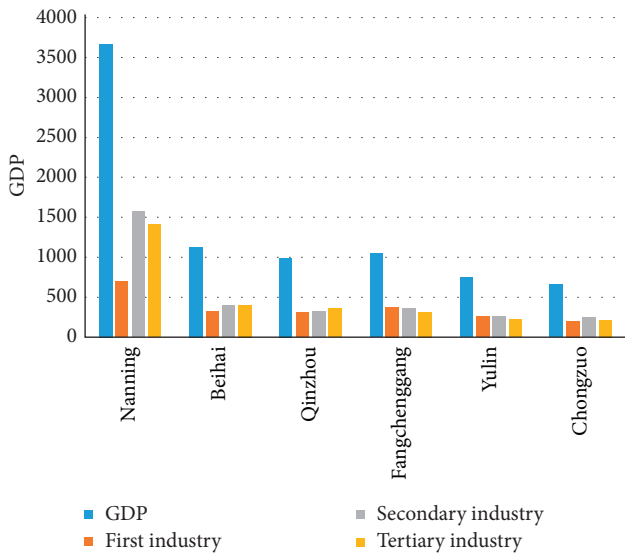
FIGURE 3: GDP and industrial structure of central cities in the Beibu Gulf Economic Zone in 2020 (100 million yuan).

obtained by looking up the table. The first- to fourteenth-order average random consistency indexes are shown in Table 4 and Figure 4.

When the consistency ratio value is less than 0.1, the judgment matrix meets the principle of consistency and can be accepted and analyzed in the next step; when the consistency ratio value is greater than 0.1, it

can be concluded that the judgment matrix does not meet the principle of consistency. It must be further revised before it can be used in the result analysis. Finally, the index weight value of each expert is calculated and averaged, and the unified weight of each index is finally determined.

(2) The value of the random consistency index (R.I.) is shown in Table 5 and Figure 5.

When R.I. is greater than or equal to 0.1, it reflects that the consistency of the judgment matrix is relatively poor, and the judgment matrix must be reformulated. When R.I. is less than 0.10, it reflects the consistency of the judgment matrix and proves that the judgment matrix is available. The financial risk indicators of the supply chain on the blockchain all pass the consistency test required by the analytic hierarchy process.

(3) The number of times that malicious nodes are selected as master nodes under different weight coefficients in the blockchain consensus mechanism is shown in Table 6 and Figure 6.

It can be seen that when the weight of ownership is not 0, three factors are considered comprehensively. If the weight of the historical consensus score is not much greater than the percentage of the node's remaining power, the ratio of the number of nodes successfully participating in the consensus to the total number of consensuses The weight, the number

TABLE 4: Average random consensus index.

Matrix order	1	2	3	4	5	6	7
Average random consistency index	0.12	0.51	0.74	1.23	1.32	1.39	1.44
Matrix order	8	9	10	11	12	13	14
Average random consistency index	1.54	1.59	1.62	1.65	1.68	1.71	1.73
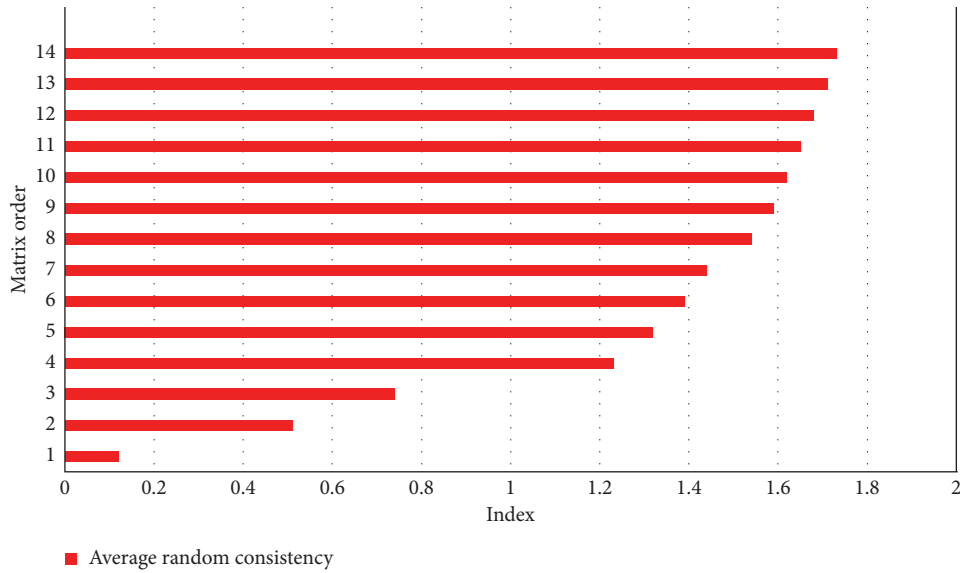
FIGURE 4: Average random consensus index and matrix order.

TABLE 5: R.I. Value.

Matrix order	1	2	3	4	5	6	7	8	9	10
R.I.	0.00	0.02	0.49	0.57	0.93	1.17	1.29	1.36	1.44	1.48
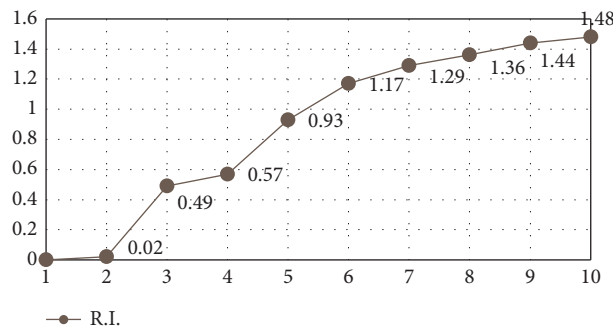
FIGURE 5: R.I. Value.

of times the malicious node is selected as the master node will be the same as the algorithm in this paper. When the weight of the historical consensus score is much greater than the percentage of the remaining power of the node, as well as the weight of the ratio of the number of times the node successfully participates in the consensus to the total number of consensus, the number of times malicious nodes are selected as the master node is significantly reduced.

(4) For the blockchain supply chain financial system, in addition to factors that affect system performance

such as CPU consumption and IO response speed, it is often necessary to consider the delay of the client initiating transactions, the processing delay of the consensus algorithm, and so on. Since blockchain-based systems use cryptographic techniques such as one-way hash functions, asymmetric encryption, etc., such calculations consume extremely high CPU. In addition, because, in most consensus algorithms, there is a process in which multiple nodes in the entire system participate in the consensus voting, this process will generate a large amount of network communication, so the performance of the system

TABLE 6: Comparison of the number of times that malicious nodes were selected as master nodes under different weight coefficients.

Consensus times	Algorithm	$k1 = 0.01, k2 = k3 = 0.37$	$k1 = k2 = k3 = 0.33$	$k1 = 0.87, k2 = k3 = 0.01$
10	0	0	0	0
20	15	14	13	12
30	28	26	19	22
40	24	23	27	25
50	36	29	25	23
60	42	31	29	28
70	38	37	36	34
80	48	45	44	41
90	54	52	49	47
100	61	57	50	49
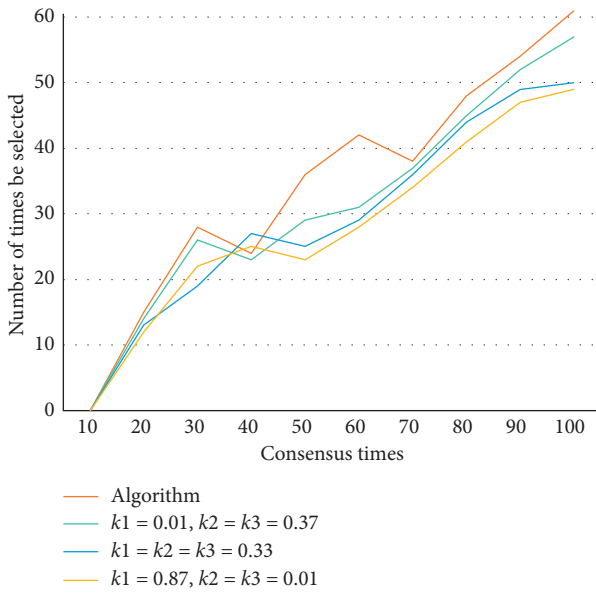
FIGURE 6: Comparison of the number of times that malicious nodes were selected as master nodes under different weight coefficients.

TABLE 7: Processing time of the algorithm.

Experiment times	Processing time (s)
1	4.37
2	3.92
3	4.26
4	4.07
5	3.87
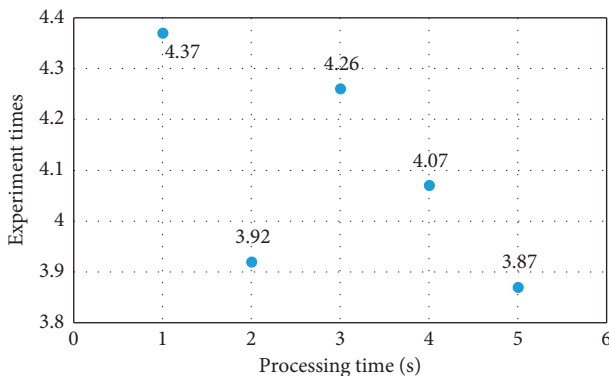
FIGURE 7: Processing time of the algorithm.

depends largely on the processing efficiency of the algorithm. The algorithm processing efficiency of the blockchain supply chain financial system in this paper is shown in Table 7 and Figure 7.

It can be seen from the data calculation in the chart that the average processing time of the algorithm in the blockchain supply chain financial system is 4.10 seconds. The algorithm processing time is shorter, and the efficiency is faster. It can be better applied in the system to better evaluate the related risks and make more suitable decisions.

5. Conclusions

Supply chain finance is mainly to provide financial solutions for small- and medium-sized enterprises or small- and microenterprises. This business mainly uses core enterprises as credit endorsements to serve their upstream and downstream enterprises, so as to realize the cooperative development between logistics companies, banks, and enterprises. The distributed deployment of the blockchain can ensure that any node in the network saves the same copy information. The data of each node in the network will be encrypted by algorithms and data, marked with a timestamp. This feature allows financial institutions to unique and true data can be obtained at the postloan management stage. The characteristics of the blockchain also guarantee the traceability, anticounterfeiting, identity authentication, and other issues in the financial transaction process.

The Beibu Gulf region should keep up with the pace of the times, cater to the development trend of my country's supply chain finance, speed up the resolution of the difficult and expensive financing problems of Guangxi's small- and medium-sized enterprises, and actively accelerate the win-win cooperation with Internet technology companies, supply chain companies, and logistics companies. Small- and medium-sized enterprises in the region and even across the country provide high-quality and efficient financial services, which effectively enhance the financial transaction capabilities, core competitiveness, and risk control capabilities of the Beibu Gulf region in Guangxi and increase resources and profit for the development of the Beibu Gulf region.

This article first analyzes the main business models of supply chain finance and the status quo of the development

of supply chain financial services by major domestic commercial banks and proposes the necessity of developing supply chain financial services in the Beibu Gulf region of Guangxi; blockchain can connect banks and other financial institutions, core enterprises. The upstream and downstream enterprises at all levels in the supply chain are connected to realize information sharing. Supply chain finance effectively alleviates the problem of information asymmetry in supply chain finance.

Data Availability

The data underlying the results presented in the study are available within the manuscript.

Conflicts of Interest

The authors declare that they have no conflicts of interest.

Acknowledgments

References

[1] N. Kshetri, "Can blockchain strengthen the internet of things?" *IT Professional*, vol. 19, no. 4, pp. 68–72, 2017.

[2] L. M. Gelsomino, R. Mangiaracina, and A. Perego, "Supply chain finance: a literature review," *International Journal of Physical Distribution & Logistics Management*, vol. 46, no. 4, pp. 348–366, 2016.

[3] J. M. Yao, "Supply chain resources integration optimisation in B2C online shopping," *International Journal of Production Research*, vol. 55, no. 17-18, pp. 1–16, 2017.

[4] M. Iansiti and K. R. Lakhani, "The truth about blockchain," *Harvard Business Review*, vol. 95, no. 1, pp. 118–127, 2017.

[5] S. Underwood, "Blockchain beyond bitcoin," *Communications of the ACM*, vol. 59, no. 11, pp. 15–17, 2016.

[6] A. Bahga and V. K. Madisetti, "Blockchain platform for industrial internet of things," *Journal of Software Engineering and Applications*, vol. 09, no. 10, pp. 533–546, 2016.

[7] J. J. Sikorski, J. Haughton, and M. Kraft, "Blockchain technology in the chemical industry: machine-to-machine electricity market," *Applied Energy*, vol. 195, pp. 234–246, 2017.

[8] J. Goebel, H. P. Keeler, and A. E. Krzesinski, "Bitcoin blockchain dynamics: the selfish-mine strategy in the presence of propagation delay," *Performance Evaluation*, vol. 104, pp. 23–41, 2016.

[9] B. Lee and J.-H. Lee, "Blockchain-based secure firmware update for embedded devices in an Internet of Things environment," *The Journal of Supercomputing*, vol. 73, no. 3, pp. 1152–1167, 2017.

[10] A. Dorri, S. S. M. Steger, and R. Jurdak, "BlockChain: a distributed solution to automotive security and privacy," *IEEE Communications Magazine*, vol. 55, no. 12, pp. 119–125, 2017.

[11] E. Mengelkamp, B. Notheisen, and C. Beer, "A blockchain-based smart grid: towards sustainable local energy markets," *Computer Science-Research and Development*, vol. 33, no. 1-2, pp. 207–214, 2018.

[12] S. Ølnes, M. J. Ubacht, and M. Janssen, "Blockchain in government: benefits and implications of distributed ledger technology for information sharing," *Government Information Quarterly*, vol. 34, no. 3, pp. 355–364, 2017.

[13] J. Sun, J. Yan, and K. Z. K. Zhang, "Blockchain-based sharing services: what blockchain technology can contribute to smart cities," *Financial Innovation*, vol. 2, no. 1, pp. 1–9, 2016.

[14] H. Subramanian, "Decentralized blockchain-based electronic marketplaces," *Communications of the ACM*, vol. 61, no. 1, pp. 78–84, 2017.

[15] Y. Guo, J. C. Wang, and G. Q. Z. AfriyieWang, "A distinct mitogenome of peanut worm Sipunculus nudus (Sipuncula, Sipunculidae) from Beibu Gulf," *Mitochondrial DNA Part B*, vol. 5, no. 2, pp. 1839-1840, 2020.

[16] J. Wang, J. S. Jiang, and S. L. P. ZhangXie, "Effects of wave-current interaction on the waves, cold-water mass and transport of diluted water in the Beibu Gulf," *Acta Oceanologica Sinica*, vol. 39, no. 1, pp. 25–40, 2020.

[17] W. Bai, H. J. Hu, and P. a. Peng, "Climatic and human impact on the environment: insight from the tetraether lipid temperature reconstruction in the Beibu Gulf, China," *Quaternary International*, vol. 536, pp. 75–84, 2020.

[18] L. Zhang, "Credit evaluation of medium and small sized enterprises during supply chain finance based on BP neural network," *Revista De La Facultad De Ingenieria*, vol. 32, no. 3, pp. 776–784, 2017.

[19] S. D. Lekkakos and A. Serrano, "Supply chain finance for small and medium sized enterprises: the case of reverse factoring," *International Journal of Physical Distribution & Logistics Management*, vol. 46, no. 4, pp. 367–392, 2016.

[20] R. Pellegrino, N. Costantino, and D. Tauro, "Supply chain finance: a supply chain-oriented perspective to mitigate commodity risk and pricing volatility," *Journal of Purchasing & Supply Management*, vol. 25, no. 2, pp. 118–133, 2018.

[21] P. Y. Brunet, V. Babich, and T. Aouam, "Supply chain finance: overview and future directions," *Foundations & Trends in Technology Information & Operations Management*, vol. 10, no. 3-4, pp. 237–252, 2017.

[22] J. He, X. J. Wang, and X. Jiang, "The effects of long memory in price volatility of inventories pledged on portfolio optimization of supply chain finance," *Journal of Mathematical Finance*, vol. 06, no. 01, pp. 134–155, 2016.

[23] M. Wang, "Research on the evolution of supply chain finance mode in the "Internet+" era," *Open Journal of Social Sciences*, vol. 4, no. 3, pp. 130–136, 2016.

[24] C.-L. Zhang, "Risk assessment of supply chain finance with intuitionistic fuzzy information," *Journal of Intelligent & Fuzzy Systems*, vol. 31, no. 3, pp. 1967–1975, 2016.

[25] Y. Yu, "Research on the impact of five science and technology plans of guangdong province on industrial innovation chain," *Open Journal of Business and Management*, vol. 7, no. 01, pp. 124–134, 2019.

[26] J. Peng, "Recognition on the food security strategy in China from the perspective of industrial chain," *Agriculture, Forestry and Fisheries*, vol. 6, no. 4, pp. 138–144, 2017.

[27] R. Matindi, P. M. Masoud, and S. Q. LiuKent, "Harvesting and transport operations to optimise biomass supply chain and industrial biorefinery processes," *International Journal of Industrial Engineering Computations*, vol. 9, no. 3, pp. 265–288, 2018.

Research Article

Application Analysis of Wearable Technology and Equipment Based on Artificial Intelligence in Volleyball

Xianyan Dai[1] and Shangbin Li [2]

[1]*School of Physical Education, Harbin University, Harbin 150086, China*
[2]*Physical Education Department, Harbin Engineering University, Harbin 150001, China*

Correspondence should be addressed to Shangbin Li; sports@hrbeu.edu.cn

Today, while people's satisfaction with materials is high, the pursuit of health has begun and sports are becoming increasingly important. Volleyball is a good physical and mental exercise, which helps improve the health of the body. However, excessive exercise usually leads to muscle strain and more serious accidents. Therefore, how to effectively prevent excessive fatigue and sports injuries becomes more and more important. In the past, some methods of exercise fatigue detection were mostly self-assessment through some indicators, which lacked real-time and accuracy. With the advancement of smart technology, in order to better detect sports fatigue, smart wearable technology and equipment are used in volleyball. Firstly, surface electromyography signals (sEMG) are collected through wearable technology and equipment. Secondly, the signal is preprocessed to extract features that are conducive to exercise fatigue assessment. Finally, a motion fatigue detection algorithm is designed to identify and classify features and evaluate the motion status in real-time. The simulation results show that it is feasible to collect ECG signals and EMG signals to detect exercise fatigue. The algorithm has good recognition performance, can evaluate exercise conditions in real-time, and prevent fatigue and injury during exercise.

1. Introduction

With the rapid growth of our country's economy, the pace of people's lives is also accelerating. Most people are in a two-point living situation and a line at home and at work. In this fast-paced state of life, although it can bring better living conditions, people pay for it is the cost of health. According to the study, the age of patients with cardiovascular and cerebrovascular diseases is not limited to the elderly, the proportion of young patients is gradually increasing, and the number of deaths from cardiovascular and cerebrovascular diseases worldwide is as high as 15 million people each time, ranking first among all causes of death. Stimulated by these shocking data, people are slowing down their pace of life and devoting more energy to their health problems. Nowadays, people are willing to devote more time to sports. According to the "China Sports Report 2016" based on QQ sports released by QQ big data,

the average number of walking steps per day in China is 5112. Walking and running have become the most popular sports. In sports, although young people have devoted more enthusiasm than before, middle-aged and old people also pay more attention to health. Therefore, with more and more people's enthusiasm for sports, how to exercise scientifically and reasonably has become one of the hot spots of people's attention [1].

Volleyball is a good sport for physical and mental health. Since it was introduced to China, it has been loved by the majority of people. Especially with the advancement of artificial intelligence technology [2], venues and training have been greatly strengthened, and the viewing and safety have been continuously improved. More and more people are beginning to pay attention to volleyball, and the popularity of volleyball at the grassroots level is increasing, which greatly promotes the healthy development of volleyball in China.

In the process of volleyball, there are many cases of sudden death and morbidity caused by excessive intensity of sports beyond the endurance of the players themselves. Therefore, only scientific and reasonable sports can achieve the purpose of physical exercise without damaging the body. Scientific and reasonable exercise can not only achieve the purpose of physical exercise but also prevent athletes from sports injury due to excessive intensity of exercise. Monitoring the changes of physiological parameters can help athletes to achieve scientific and rational exercise. The commonly used physiological parameters include heart rate, body temperature, respiratory rate, and blood oxygen concentration. Because heart rate is sensitive to physiological changes and easy to monitor, it is used as an indicator of exercise intensity by most sports enthusiasts and athletes [3]. In addition, the acceleration can be used to calculate the energy consumption of sports so that the athletes can control their own sports consumption.

Among the traditional methods of heart rate measurement, common methods of heart rate measurement include electrocardiogram measurement, pressure method, and pulse diagnosis of Chinese medicine for heart rhythm diagnosis. However, ECG measurement requires electrodes to be connected to the body to extract the heart rate from the ECG signal of the body. The pressure measurement equipment is very large and requires an air pump; TCM pulse diagnosis requires the experience of a doctor. These methods all show that we cannot provide real-time monitoring of physical conditions in our daily lives. In recent years, with the rapid development of artificial intelligence technology, it is possible to develop portable body fatigue monitoring equipment [4]. At the same time, as mobile smart devices such as smartphones and tablet computers are increasingly integrated into people's daily lives, combined with their good interactive interfaces and powerful data processing capabilities, a portable real-time detection and analysis of human fatigue data can be developed. And the analysis function of cloud storage technology is realized.

Wearable technology is a technology that studies and intellectualizes the design and develops wearable equipment that meets the needs of users [5]. It mainly includes integration technology, recognition technology (voice, motion, and eyeball), detection technology, connection technology, and flexible screen technology. It refers to the integrated use of different technologies for identifying, detecting, connecting, and interacting cloud and storage services [6–10]. Wearable technology is a technology integrated in people's daily belongings, along with the daily activities of users, and users can operate at any time. Its intelligence in physical space manifests itself in the user-centered access, which can help extend the human body's limbs and memory function. At the same time, it processes the data and presents the data results to users in a visual form.

In recent years, wearable equipment based on wearable technology has become popular in the market. The so-called "wearable intelligent device" is the general term for the application of wearable technology to the intelligent design of daily wearable items or the development of wearable equipment, such as glasses, watches, and clothing. Wearable intelligent devices in the broad sense include comprehensive functions and appropriate size and can achieve complete or partial functions without relying on smart phones. For example, smart watches or smart glasses, as well as applications that focus only on a certain category, need to be used in conjunction with other intelligent devices such as mobile phones, smart bracelets for signs monitoring, and smart head wear and constantly derived a large number of medical, health, sports, and other wearing equipment. According to Gartner-Research, a well-known market research company, "Worldwide, wearable income for sports and personal health and fitness categories will be about $1.6 billion in 2013 and $5 billion in 2016."

With the rise of wearable medical devices, heart rate monitoring devices have appeared on the market. Although they are still in the embryonic stage, they can also enable users with such devices to measure the rate anytime, anywhere, simply, quickly, and conveniently. At present, the wearable devices of heart rate monitoring on the market are in full blossom, ranging from heart rate to heart rate meter.

Based on the above conditions, it is feasible to apply wearable technology and equipment to volleyball sport. It is of great significance to develop wearable testing equipment for volleyball sport fatigue. It is helpful for people to monitor their physical condition in real-time in volleyball sport and avoid sports fatigue and injury. The specific contributions of this paper are as follows:

(1) Using wearable technology and equipment to collect surface EMG signals

(2) Preprocessing the signals and extracting the features which are beneficial to the evaluation of sports fatigue

(3) Designing a motion fatigue detection algorithm to recognize and classify the features and evaluate the motion situation in real-time

2. Proposed Method

2.1. Wearable Technology and Signal Acquisition

2.1.1. Wearable Technology. In the 1960s, MIT Laboratory put forward the wearable technology as an innovative technology. This technology integrates multimedia, wireless sensor, and wireless communication technology skillfully through the media and carries on the induction-feedback-interaction experience through our basic body movements. Wearable technology action process, also known as human-computer interaction (HCI) [11, 12], is a technology to study human, computer, and their interaction. The purpose of human-computer interaction is to make the computer system and wireless sensor technology cooperate and influence each other and to complete user instructions more efficiently and safely. The details are shown in Figure 1.

Early wearable devices were just conceptual products. Historically, in 1975, Hamilton Watch launched Pulsar computer watches, which opened the era of smart wearability [13]. Limited by the social development environment and technological capabilities at that time, as well as the
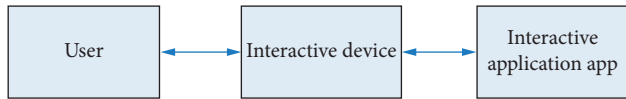
Figure 1: Wearable technical schematic.

attributes of the product, Pulsar could not be widely promoted. It was not until Sony released smart watch-generation in 2012 that smart wear technology came into the public eye [14]. Of course, with the advancement of science and technology and the strengthening of awareness of innovation, after years of fermentation and development, portable equipment also introduced the period of explosion of product development. Because of its more and more comprehensive functions and wider application, the statistical analysis of wearable devices of Vandrico company shows 291 pieces, and the functions of wearable devices (for example, bracelets) are gradually increasing. From the initial movement monitoring to today's daily life services (heart rate, sleep quality, smart calls, and intelligent wake-up), this also reflects the rapid development of wearable technology since entering the new century.

With the rapid development of wearable technology in society, there is a diversified development trend in aerospace, military special technology, medical and health technology, and sports science monitoring. Of course, the most frequent wearable technology to enter the public's vision is sports wear technology such as Huawei, NIKE, millet, and other electronic or sports equipment giants that have launched their own brand of wearable equipment, which is used in health monitoring, sports data collection, and other fields.

2.1.2. Signal Acquisition. EMG signals originate from motor neurons in the spinal cord, which are part of the central nervous system. The cell body of motoneurons is located in which the axons extend to the muscle fibers and are coupled to the muscle fibers via the endplate region, and there is more than one muscle fiber associated with each neuron. These parts are combined to form a so-called motion unit. The movement of muscle is controlled by consciousness. When the brain sends out excitation and transmits downward, the cell bodies and dendrites of motor neurons in the central nervous system produce electrical impulses (action potentials) stimulated by synapses, which are transmitted along the axons of neurons to the junctions of nerves and muscles at the terminals. When the motor nerve touches the muscle, its axons branch to many muscle fibers, and each branch terminates to form synapses on the muscle fibers, which are called motor endplates [15]. The action potential conducting to the axonal endings releases acetylcholine, a chemical at the nerve-muscle junction. Acetylcholine changes the ionic permeability of the motor endplate and produces the endplate potential. This endplate potential makes the myocyte membrane reach the depolarization threshold potential, generates the action potential of muscle fibers, and propagates along the muscle fibers to both sides, causing a series of changes in the

muscle fibers, resulting in the contraction of muscle fibers, and a large number of muscle fibers contraction produces muscle force. It can be seen that the transmission of electrical signals (action potentials of muscle fibers) leads to muscle contraction, while the electrical signals in transmission cause electric current field in human soft tissues and show potential difference between detection electrodes, that is, EMG signals.

Surface electromyogram (SEMG) is a bioelectrical signal recorded from the muscle surface when the nerve and muscle system is moving through electrodes. It is mainly the combined effect of EMG of superficial muscle and electrical activity of nerve trunk. It is related to the state of muscle activity and function in varying degrees, so it can reflect the activity of neuromuscles to a certain extent and diagnose neuromuscular diseases in clinical medicine. The ergonomic analysis of muscle work in the field of ergonomics has important practical value in the evaluation of muscle function in the field of rehabilitation medicine and in the determination of fatigue in sports science and in the analysis of the rationality of sports technology, the type of muscle fibers, and the noninvasive prediction of anaerobic thresholds.

Surface EMG signal is very weak, distributed in $\mu V \sim mV$ order of magnitude, so the weak signal needs to be amplified to meet the requirements of AD acquisition unit. Because the human body is a conductive body, power frequency interference and external electric and magnetic field induction will form measurement noise in the human body, interfering with the detection of EMG information, so signal filtering and circuit shielding become the focus of amplifier circuit research. The structure of a typical weak signal amplifier circuit is shown in Figure 2.

As can be seen from Figure 2, the design of the digital sensor for facial EMG signal includes the following parts: input electrode, preamplifier, high-pass circuit, low-pass circuit, secondary amplifier, power frequency interference notch circuit, and A/D conversion circuit.

2.2. Preprocessing of Surface Electromyography Signal and Extraction of Fatigue Characteristics

2.2.1. Surface EMG Signal Preprocessing. Due to the nonstationary, nonlinear, and weak amplitude ($10\mu V \sim 6mV$) of sEMG, it is often submerged in various noises and disturbances during detection. For example, 50 Hz power frequency, harmonic interference, ECG, and low-frequency noise caused changes in muscle and joint angles. For this reason, the pretreatment process of EMG signal is designed as follows. Firstly, the baseline drift is removed by high-pass filter [16–18] (cut-off frequency is 5 Hz). The band-pass filter (the range of band frequency is 5–200 Hz) is used to extract the effective frequency band signal, and then the signal is amplified. Finally, the 50 Hz power frequency interference and harmonics are separated and removed by independent component analysis (ICA).

(1) Adaptive high-pass filter removes baseline drift, and band-pass filter extracts the effective frequency band
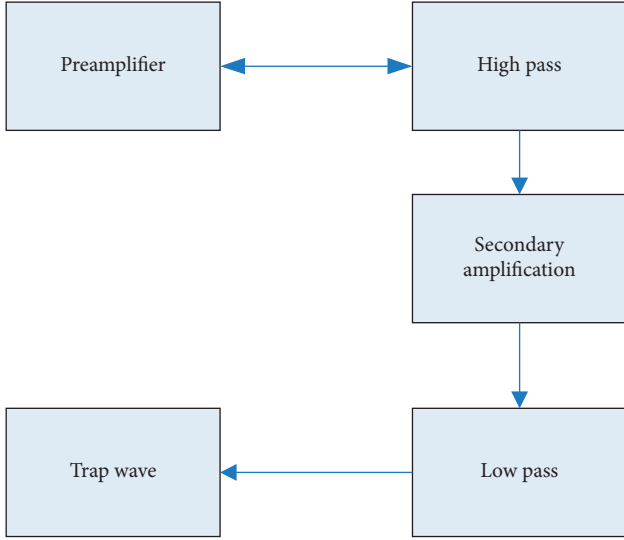
FIGURE 2: Typical structure of weak signal amplifier circuit.

of EMG signal. In the process of EMG signal acquisition, low-frequency noise is generated by the relative movement of muscle and joint, the change of joint angle, and so on. These noises are generally less than 5 Hz, and the amplitude is very large (usually several times of EMG signal). Therefore, high-pass filter is used to remove low-frequency interference signal (baseline drift). Digital filters are divided into FIR filters and IIR filters [19–21]. Because FIR filters are more stable than IIR filters and can achieve linear phase characteristics, this paper uses FIR-based adaptive high-pass filters to remove baseline drift [22, 23]. Adaptive filtering consists of two parts: FIR digital filter and adaptive algorithm for modifying digital filter.

The weight iteration formula of the adaptive filter designed in this paper is as follows:

$$
\begin{aligned}
h(n+1) &= h(n) - \mu \widehat{\nabla}_n, \\
&= h(n) + 2\mu e(n)x(n)e(n), \\
&= z(n) - h * x(n),
\end{aligned}
\tag{1}
$$

where μ represents the iteration step, $x(n)$ is the input vector of the adaptive filter, $e(n)$ is the error, h is the weight of the filter, and $z(n)$ is the expected output of EMG signal.

(2) *Independent Component Analysis to Remove Power Frequency Interference.* Independent component analysis (ICA) effectively solves the problem of blind source separation, especially for nonlinear and nonstationary signals. Therefore, ICA separation has been well applied in pattern recognition, medical signal, and other fields. Independent component analysis (ICA) can be used to remove noise from EEG and EMG signals. For the collected EMG signal, there will be power frequency interference. The traditional 50 Hz notch wave will remove the

corresponding useful EMG signal while eliminating the power frequency. In order to solve this problem, this paper uses the independent component analysis method. Fast ICA is the most commonly used method in ICA. Fast ICA belongs to nonlinear convergence, and processing speed is relatively fast. Therefore, Fast ICA is chosen to remove power frequency interference. The 50 Hz power frequency interference is separated from sEMG by Fast ICA, and the useful EMG information is retained, which improves the quality of the signal.

2.2.2. Fatigue Feature Extraction of Surface Electromyography. According to the existing research results, the time domain and frequency domain indices of surface electromyography signal are analyzed in this paper.

(1) Time domain analysis parameters are as follows:

   (1) *Integrated EMG (IEMG).* Integral EMG value [24, 25] is used to represent the excitation characteristics of muscle fibers in unit time. It is shown that the amplitude of sEMG signal changes with the change of movement time. It is the area of EMG curve and transverse axis in unit time domain. IEMG can reflect the change of sEMG signal:

   $$
   \text{IEMG} = \int_t^{t+T} |\text{EMG}(t)| \mathrm{d}t,
   \tag{2}
   $$

   where T is the length of time and $\text{EMG}(t)$ is the EMG signal at t time.

   (2) *Root Mean Square (RMS).* The root mean square value [26–29] indicates the change characteristics of sEMG in unit time. The root mean square value is proportional to the magnitude and is positively related to the number of exciting muscle fiber units. With the deepening of muscle fatigue, more exciting units are recruited. The formula is as follows:

   $$
   \text{RMS} = \sqrt{\frac{1}{N} \int_t^{t+T} |\text{EMG}(t)|^2 \mathrm{d}t}.
   \tag{3}
   $$

   (3) *Zero-Crossing Rate (ZCR).* ZCR [30, 31] refers to the speed at which sEMG sets its zero value artificially. ZCR can reflect the oscillation frequency of sEMG. As the amount of training continues, the muscles begin to feel tired. At this time, the conduction current of muscle fibers decreases, and the ZCR changes rapidly.

   $$
   \text{ZCR} = \frac{\text{count}}{N},
   \tag{4}
   $$

   where N is the number of surface electromyographic signal value x_N and count is the count of $x_i * x_{i+1} < 0$.

(2) Frequency domain analysis parameters are as follows:

(1) *Mean Power Frequency (MPF)*. MPF [32] is the function index of sEMG in time. The size of MPF is mainly affected by the conduction speed of action potential and the type of excitation unit of peripheral excitation unit. The surface EMG signal changes obviously when the load is very low.

$$\text{MPF} = \frac{\int_0^\infty f \cdot \text{PSD}(f)\mathrm{d}f}{\int_0^\infty \text{PSD}(f)\mathrm{d}f}, \tag{5}$$

where $\text{PSD}(f)$ is the spectral density function of surface EMG signal.

(2) *Median Frequency (MF)*. Similar to the above average power frequencies, MF represents the median of the frequency of muscle fiber emission signals during exercise, which corresponds to the frequency of 1/2 area of the surface EMG energy spectrum. The MF value is less disturbed by noise and is suitable for high intensity and sustained gentle motion and has a wide range of applications. Normally, the proportion of muscle fibers in different parts of skeletal muscle is different, and the MF value of muscle cells in different parts of the human body varies greatly. The principle is that muscle fibers are divided into high-frequency and low-frequency discharges due to the different rate of expression of characteristics.

$$\text{MF} = \frac{1}{2} \int_0^\infty \text{PSD}(f)\mathrm{d}f, \tag{6}$$

where $\text{PSD}(f)$ is the spectral density function of surface EMG signal.

Based on the analysis of the five characteristics, the frequency domain index MF and the time domain index IEMG are finally selected for the classification experiment of sports fatigue.

2.3. Volleyball Fatigue Estimation.

Due to the influence of individual differences, subjective emotions, and environmental changes in the detection of different human bodies, the traditional algorithm model SVM pattern recognition cannot resolve the above changes and the accuracy of the classification is affected. The optimal decision-making surface of classification is fixed after training. It cannot effectively utilize the current input and output optimization model and cannot retain historical information in the model. Its application flexibility and scope are limited. In order to better solve the above problems, the motion fatigue detection technology based on the LSTM neural network model is proposed. The principle and application of LSTM neural network are introduced below.

2.3.1. LSTM Neural Network Model.

LSTM is an improved RNN network. By adding long-term and short-term memory function RNN to the hidden layer structure change, it can maintain the persistence and long-term dependence of RNN network [33]. LSTM hidden layer structure solves the problem of gradient explosion and gradient disappearance of long-distance information transmission so that information will not decay.

The standard hidden RNN network level unit contains only one tanh layer, and its structure is very simple. The LSTM network improved by the standard RNN network mainly improves the structure of the hidden level unit. The traditional RNN network unit has only one layer, but the improved LSTM unit has four layers. LSTM network hiding layer module includes three multiplication units and multiple self-connected storage units. The three multiplication units represent forgetting gates, input gates, and output gates, which can realize unit module reading, writing, and resetting operations.

The key of LSTM network is cell state Ct. Cell state is represented by upper straight line, which includes two point-by-point operations. Cell states are transmitted and updated in this straight line, involving only some linear operations. Therefore, the cell state is like conveying information along the LSTM network on the conveyor belt. The cell state does not involve nonlinear changes, so it will not change or disappear.

The LSTM neural network unit controls discarding or adding information from the cell state through some "gates" structures, which consist of a nerve layer and a pointwise multiplication operation. The output of the Sigmoid layer is a value between 0 and 1, which is used to control the degree of information flow. When the output of Sigmoid layer is 0, it means that the "door" is closed and no letter is passed at this time; when the output is 1, it means that the "door" is opened, allowing all information to pass through. There are three gates in LSTM network unit to control the discarding and retention of cell state, which are called "input gate," "output gate," and "forgetting gate." The "forgetting gate" is used to control the degree to which information in the cell state should be discarded; then, the "forgetting gate" and the "input gate" determine what information will be retained and added to the new cell state; finally, the "output gate" is used to control what information is output in the cell state.

2.3.2. Volleyball Sports Fatigue Estimation Based on LSTM.

In this paper, the extracted physiological signal characteristic parameters are expressed as multivariate characteristic matrices, which are used for input of the LSTM neural network model, and a fatigue estimation model of volleyball sports based on LSTM neural network is constructed. The training steps of the model are shown in Figure 3.

The physiological signal characteristic parameters of the input layer are further studied in the LSTM network layer. The invalid information is discarded by using the excitation functions of the hidden layer neuron units. The useful features of the neural network are retained in the network structure. The appropriate excitation functions are set on the output layer of the model, and the prediction is changed to the classification problem. The excitation function selected in this paper is the softmax function. Softmax is used in the
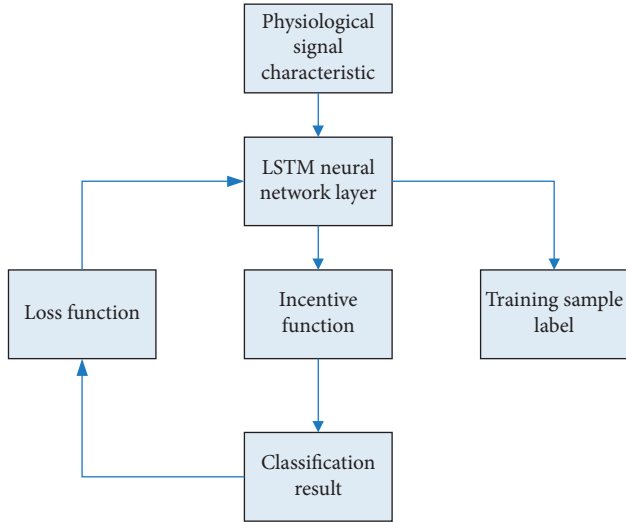
FIGURE 3: Volleyball fatigue estimation process.

FIGURE 4: The flow chart of the article.

multiclassification process. It maps the output of many neurons into the $(0, 1)$ interval. It can be understood as probability, and then multiclassification can be carried out.

The input sample is calculated by the excitation function of LSTM neural network, and the class label of the sample is output. Then, the difference between the output label and the sample label is calculated by comparing the loss function, and a non-negative number is output. The numerical size indicates the difference between the output tag and the sample tag. The smaller the value, the closer to the ideal value. The process of training the LSTM neural network model is to reduce the output value of loss function by feedback and iteration.

The calculation method of loss function selected in this paper is as follows:

$$L(B, P(B|X)) = \log_2 P(B|X) \qquad (7)$$

where B represents the sample label and the minimum value of $L(B, P(B|X))$ is the maximum value of $-\log_2 P(B|X)$. The process of solving the maximum value is to find the B in X to maximize $P(B|X)$ according to the classification results.

3. Experiments

In this paper, portable technology and equipment are applied to volleyball. The main objective is to avoid athletic fatigue and injury caused by excessive exercise and to monitor in real-time its situation. The wearable sensor is mainly designed to collect the surface EMG signal of the human body, then preprocess the EMG signal, extract the frequency domain index MF and time domain index IEMG, and then use the method of fatigue assessment based on LSTM neural network to carry out fatigue analysis and real-time monitoring of body condition. The specific flow chart is shown in Figure 4.

In order to better evaluate the performance of the volleyball fatigue assessment method designed in this paper, the
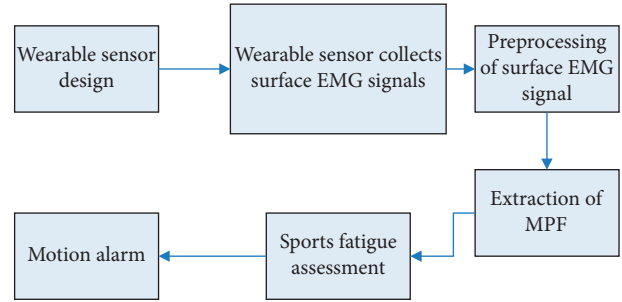
recognition rate is used as the evaluation index, and the expression is as follows:

$$\text{recognition rate} = \frac{\text{number of samples correctly identified}}{\text{total number of test samples}} \times 100\%. \qquad (8)$$

4. Discussion

According to the principle of psychology, Borg, a Swedish psychologist, identified subjective fatigue and local muscle fatigue as a subjective fatigue sensation in subjects' exercise. This paper classifies muscle states into three categories: nonfatigue, imminent fatigue, and already fatigue. If the exercise evaluation finds that the muscles of the body are in a state of fatigue, wearable equipment reminds the athletes that the muscles are in a state of fatigue and pay attention to rest.

Firstly, after the preprocessing of surface electromyography signal, the frequency domain index MF and the time domain index IEMG are used as the analysis characteristics of fatigue assessment. It is necessary to analyze the changes of the two indexes with different fatigue degrees and to verify the feasibility of the two indexes as the analysis of volleyball sports fatigue. In this paper, 12 volleyball players were asked to take part in volleyball. Wearable devices were used to extract information and analyze the changes of their frequency domain index MPF and time domain index RMS. The average results were observed for one hour, as shown in Table 1.

According to Table 1, we draw a broken line chart of the change of integral EMG value with exercise time, as shown in Figure 5. As can be seen from the figure, with the increase in exercise time, the degree of muscle fatigue gradually increases, and the integral EMG value shows a decreasing trend.

Similarly, a broken line diagram of the median frequency MF varying with the time of motion is drawn as shown in Figure 6. It can also be seen that with the increase in exercise time, the degree of muscle fatigue gradually increases, and the median frequency also shows a significant decreasing trend.

From the above analysis, it can be found that the frequency domain index MF and time domain index IEMG used in this paper will gradually decrease with the increase in fatigue degree, and their changes are related to fatigue

TABLE 1: Characteristic indicators change with movement.

Time (min)	IEMG (mV)	MF (Hz)
5	1.79	119
10	1.76	109
15	1.69	106
20	1.58	101
25	1.52	91
30	1.48	87
35	1.42	83
40	1.31	79
45	1.20	75
50	1.07	67
55	0.89	61
60	0.71	50

| | IEMG (mV) | 0 | 1.79 | 1.76 | 1.69 | 1.58 | 1.52 | 1.48 | 1.42 | 1.31 | 1.2 | 1.07 | 0.89 | 0.71 |

Group

0	20	35	50
5	25	40	55
10	30	45	60
15			
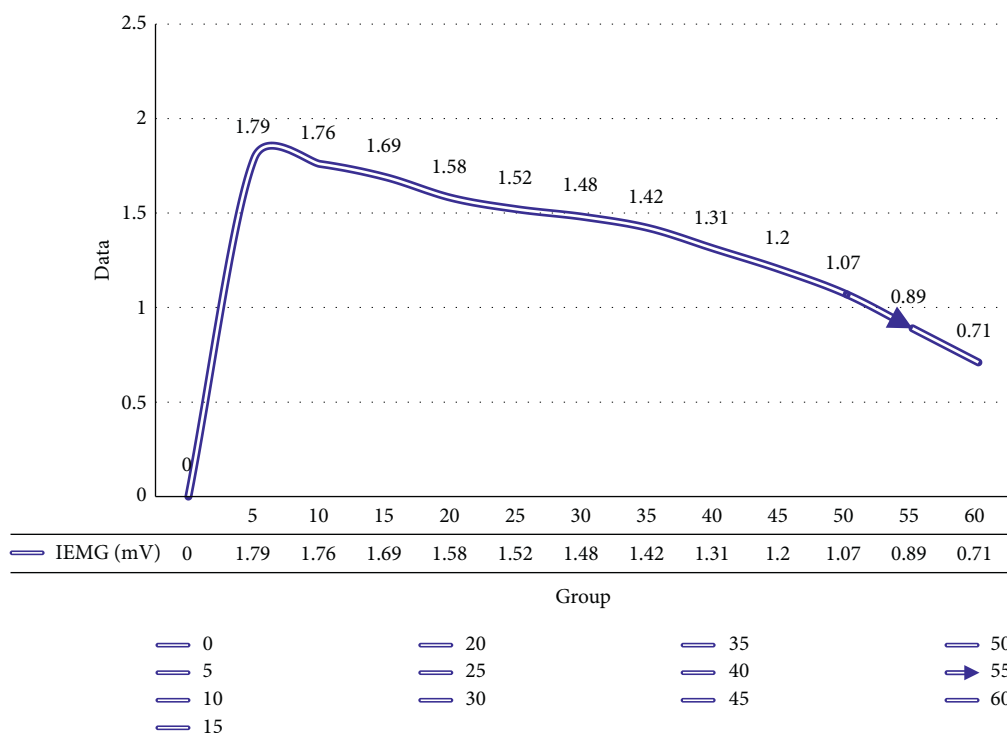
FIGURE 5: The change of integral EMG with exercise time.

degree, which can be used as an evaluation index of sports fatigue.

Secondly, the classification accuracy of using frequency domain index MF and time domain index IEMG as evaluation index and using frequency domain index MF and time domain index IEMG as classification index is analyzed. The analysis results are shown in Table 2. It can be seen from the table that the effect of using characteristic parameters in frequency domain or time domain as evaluation index is not as good as using time domain and frequency domain as evaluation index at the same time. The worst one is frequency domain index MF, with the recognition rate of 75.61%, followed by time domain index IEMG, with the recognition rate of 81.08%; the best one is that IEMG and

frequency domain MF are used as evaluation index at the same time, with the recognition rate of 93.62%.

Finally, this paper uses SVM "one-to-one" and SVM "one-to-many" classifiers as classification performance comparison and takes IEMG in time domain and MF in frequency domain as evaluation indicators to analyze the recognition performance of the fatigue classifier in this paper. The results are shown in Table 3, and the histogram is shown in Figure 7.

Combining Table 3 and Figure 7, it can be seen that the classification performance of the proposed fatigue assessment method is much better than that of SVM "one-to-one" and SVM "one-to-many" classifiers. The recognition rate of the proposed method is 10.47% higher than that of SVM
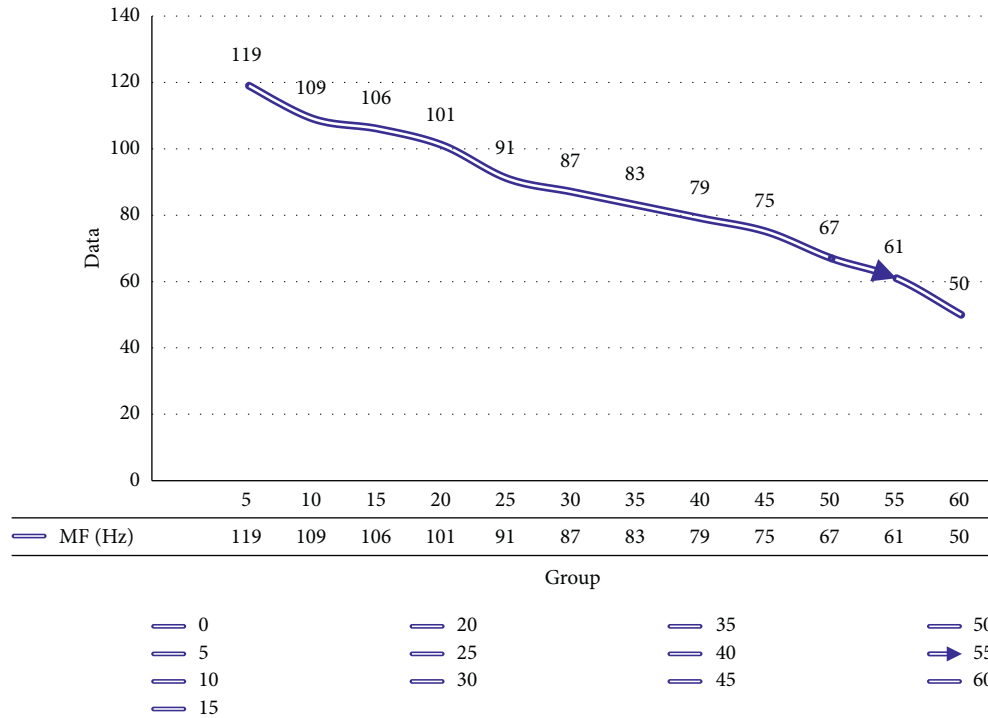
FIGURE 6: Variation of median frequency with motion time.

TABLE 2: Fatigue classification accuracy of different evaluation indicators.

Indicator	Recognition rate (%)
IEMG	81.08
MF	75.61
IEMG and MF	93.62

TABLE 3: Fatigue assessment performance of different methods.

Method	Recognition rate (%)
SVM "one-to-one"	83.15
SVM "one-to-many"	72.67
Method of this paper	93.62
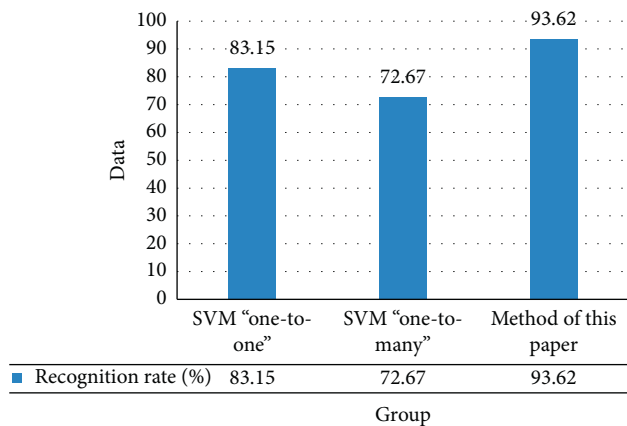
FIGURE 7: Comparison of fatigue evaluation performance of different methods.

"one-to-one" classifiers and 20.95% higher than that of SVM "one-to-many" classifiers. It can be seen that the performance of the proposed fatigue assessment analysis method is good.

In conclusion, the simulation analysis shows that it is feasible to apply wearable technology and equipment in volleyball, and it can identify the fatigue of the body well, realize real-time monitoring of the body in sports, and prevent the occurrence of sports fatigue and sports injury.

5. Conclusions

Today, the rapid development of portable devices has a very wide range of applications in life, and application to sport has attracted more and more attention. Volleyball is a good exercise for the human body and mind and body, which contributes to improving the physical health of the body. However, due to the fierceness of the exercise, it is easy to produce sports fatigue and cause sports injuries. Therefore, the application of wearable technology based on artificial intelligence is used in volleyball. The real-time monitoring of fatigue has important research significance and practical significance. Based on the analysis of sports fatigue assessment methods, this paper designs an artificial intelligence-based wearable technology sports fatigue assessment method. The wearable sensor is designed to collect the SEMG signal of the human body. Low-frequency noise and power frequency interference can be eliminated by preprocessing the surface EMG signal. The time domain integrated EMG value IEMG and the frequency domain intermediate frequency MF are extracted

as the characteristics of exercise fatigue assessment. Input the sports fatigue assessment method based on LSTM neural network to classify sports fatigue and realize the assessment of volleyball human fatigue. Through simulation analysis, it can be found that the IEMG in the time domain and the MF in the frequency domain can reflect human muscle fatigue, and it is better to use the time domain and frequency domain features at the same time than to use them alone. In addition, compared with the support vector machine classifier, the performance of this method is good.

Data Availability

No data were used to support this study.

Conflicts of Interest

The authors declare that they have no conflicts of interest.

Acknowledgments

References

[1] S. Wan, L. Qi, X. Xu, C. Tong, and Z. Gu, "Deep learning models for real-time human activity recognition with smartphones," *Mobile Networks and Applications*, vol. 2019, pp. 1–13, 2019.

[2] Z. Lv, L. Qiao, S. Verma, and Kavita, "AI-enabled IoT-edge data analytics for connected living," *ACM Transactions on Internet Technology*, vol. 15, pp. 1–8, 2020.

[3] H. Zhang, S. Qu, H. Li, J. Luo, and W. Xu, "A moving shadow elimination method based on fusion of multi-feature," *Institute of Electrical and Electronics Engineers Access*, vol. 8, pp. 63971–63982, 2020.

[4] Q. Wang, Y. Li, and X. Liu, "Analysis of feature fatigue EEG signals based on wavelet entropy," *International Journal of Pattern Recognition and Artificial Intelligence*, vol. 32, no. 08, Article ID 1854023, 2018.

[5] Z. Lv, A. Halawani, S. Feng, S. Ur Réhman, and H. Li, "Touchless interactive augmented reality game on vision-based wearable device," *Personal and Ubiquitous Computing*, vol. 19, no. 3-4, pp. 551–567, 2015.

[6] Y. Gao, H. Li, and Y. Luo, "An empirical study of wearable technology acceptance in healthcare," *Industrial Management & Data Systems*, vol. 115, no. 9, pp. 1704–1723, 2015.

[7] B. Najafi, D. Horn, S. Marclay, R. T. Ryan, S. Wu, and J. S. Wrobel, "Assessing postural control and postural control strategy in diabetes patients using innovative and wearable technology," *Journal of Diabetes Science and Technology*, vol. 4, no. 4, pp. 780–791, 2010.

[8] N. D. Crews, "Data for life: wearable technology and the design of self-care," *Biosocieties*, vol. 11, no. 3, pp. 317–333, 2016.

[9] N. Sultan, "Reflective thoughts on the potential and challenges of wearable technology for healthcare provision and medical education," *International Journal of Information Management*, vol. 35, no. 5, pp. 521–526, 2015.

[10] X. Li, H. Jianmin, B. Hou, and P. Zhang, "Exploring the innovation modes and evolution of the cloud-based service using the activity theory on the basis of big data," *Cluster Computing*, vol. 21, no. 1, pp. 907–922, 2018.

[11] P. Forbrig, F. Paternó, and A. M. Pejtersen, "Human-computer interaction," *Encyclopedia of Creativity Invention Innovation & Entrepreneurship*, vol. 19, no. 2, pp. 43–50, 2017.

[12] K. Michalakis, J. Aliprantis, and G. Caridakis, "Visualizing the internet of things: naturalizing human-computer interaction by incorporating AR features," *Institute of Electrical and Electronics Engineers Consumer Electronics Magazine*, vol. 7, no. 3, pp. 64–72, 2018.

[13] R. A. Hulse and J. H. Taylor, "Discovery of a pulsar in a binary system," *Annals of the New York Academy of Sciences*, vol. 262, no. 1, pp. 490–492, 1975.

[14] A. Komninos and M. Dunlop, "Text input on a smart watch," *Institute of Electrical and Electronics Engineers Pervasive Computing*, vol. 13, no. 4, pp. 50–58, 2014.

[15] J. Axelsson and S. Thesleff, "The desensitizing effect of acetylcholine on the mammalian motor end-plate," *Acta Physiologica Scandinavica*, vol. 43, no. 1, pp. 15–26, 2010.

[16] J. L. Flores, G. Garcia-Torales, J. P. Aguayo-Adame, and J. A. Ferrari, "Self adaptive high pass filtering using photochromic glass," *Optik*, vol. 123, no. 12, pp. 1067–1070, 2012.

[17] X. Ferrari, B. Zhu, L. Guo et al., "Temporal high-pass filtering nonuniformity correction with adaptive time constant," *Opto-Electronic Engineering*, vol. 40, no. 7, pp. 89–94, 2013.

[18] D. Jorgesen, C. Marki, and S. Esener, "Improved high pass filtering for passive optical networks," *Institute of Electrical and Electronics Engineers Photonics Technology Letters*, vol. 22, no. 15, pp. 1144–1146, 2010.

[19] D. Xiao, R. P. Giddings, S. Mansoor et al., "Experimental demonstration of upstream transmission in digital filter multiple access pons with real-time reconfigurable optical network units," *Institute of Electrical and Electronics Engineers/OSA Journal of Optical Communications & Networking*, vol. 9, no. 1, pp. 45–52, 2017.

[20] H. E. Oh, D. J. Park, J. P. Park, S. J. Ahn, and W. B. Jeong, "Digital filter design of frequency weighting function to measure and assess human vibration," *Noise Control Engineering Journal*, vol. 65, no. 3, pp. 183–190, 2017.

[21] P. Peng, Z. Wu, X. Zhou, and D. C. Tran, "FIR digital filter design using improved particle swarm optimization based on refraction principle," *Soft Computing*, vol. 21, no. 10, pp. 2631–2642, 2017.

[22] S. Agrawal and A. Gupta, "Fractal and EMD based removal of baseline wander and powerline interference from ECG signals," *Computers in Biology and Medicine*, vol. 43, no. 11, pp. 1889–1899, 2013.

[23] A. Fasano and V. Villani, "Baseline wander removal for bioelectrical signals by quadratic variation reduction," *Signal Processing*, vol. 99, no. 6, pp. 48–57, 2014.

[24] T. I. Arabadzhiev, V. G. Dimitrov, N. A. Dimitrova, and G. V. Dimitrov, "Interpretation of EMG integral or RMS and estimates of "neuromuscular efficiency" can be misleading in

fatiguing contraction," *Journal of Electromyography and Kinesiology*, vol. 20, no. 2, pp. 223–232, 2010.

[25] R. K. Jain, S. Datta, and S. Majumder, "Biomimetic behavior of IPMC using EMG signal for Micro robot," *Mechanics Based Design of Structures and Machines*, vol. 42, no. 3, pp. 398–417, 2014.

[26] P. B. Petrovic, "Modified formula for calculation of active power and root-mean-square value of band-limited alternating current signals," *Science Measurement & Technology Iet*, vol. 6, no. 6, pp. 510–518, 2012.

[27] P. Busch, P. Lahti, and R. F. Werner, "Colloquium: quantum root-mean-square error and measurement uncertainty relations," *Reviews of Modern Physics*, vol. 86, no. 4, pp. 1261–1281, 2014.

[28] A. Bagaria, V. Jaravine, Y. J. Huang, G. T. Montelione, and P. Güntert, "Protein structure validation by generalized linear model root-mean-square deviation prediction," *Protein Science*, vol. 21, no. 2, pp. 229–238, 2012.

[29] Y. Yu, Y. Liu, W. J. Lu, and H. B. Zhu, "Measurement and empirical modelling of root mean square delay spread in indoor femtocells scenarios," *Iet Communications*, vol. 11, no. 13, pp. 2125–2131, 2017.

[30] C. Panagiotakis and G. Tziritas, "A speech/music discriminator based on RMS and zero-crossings," *Institute of Electrical and Electronics Engineers Transactions on Multimedia*, vol. 7, no. 1, pp. 155–166, 2005.

[31] I. Conradsen, S. Beniczky, K. Hoppe, P. Wolf, and H. B. D. Sorensen, "Automated algorithm for generalized tonic-clonic epileptic seizure onset detection based on sEMG zero-crossing rate," *Institute of Electrical and Electronics Engineers Transactions on Biomedical Engineering*, vol. 59, no. 2, pp. 579–585, 2012.

[32] D. Bauer, I. Zawischa, D. H. Sutter, A. Killi, and T. Dekorsy, "Mode-locked Yb:YAG thin-disk oscillator with $41 \, \mu$J pulse energy at 145 W average infrared power and high power frequency conversion," *Optics Express*, vol. 20, no. 9, pp. 9698–9704, 2012.

[33] K. Greff, R. K. Srivastava, J. Koutnik et al., "LSTM: a search space odyssey," *Institute of Electrical and Electronics Engineers Transactions on Neural Networks & Learning Systems*, vol. 28, no. 10, pp. 2222–2232, 2016.

Research Article

Extraction Methods and Implementation Technologies of Fuel Injection Pump Cam Profile Characteristics

Yangpeng Liu, Peng Chen, Jianjun Ding [ID], Lin Sun, Tao Li, Changsheng Li, Jingyang Guo, Mingming Song, and Zhuangde Jiang

The State Key Laboratory for Manufacturing Systems Engineering, Xi'an Jiao Tong University, Xi'an 710049, China

Correspondence should be addressed to Jianjun Ding; dingjianjun@mail.xjtu.edu.cn

Because the traditional camshaft measurement methods cannot be applied to the injection pump cam, in order to improve the measurement automation of injection camshaft, an accurate extraction method of the characteristic parameters of the injection cam profile is proposed in this paper. In this method, the phase error optimization is realized by the angle precise rotation matching of the actual lift data. The optimization is realized by the Lagrangian polynomial interpolation algorithm based on the moving window. The goals of precise measurement of the peach point phase of single high point cam and accurate acquisition of the back dead point phase of high point arc segment cam are realized. Compared with the precision of high-precision measuring equipment, the method can extract the lift and phase angle error of the cam accurately and stably.

1. Introduction

In order to achieve energy saving and reduce emissions, electronic high-pressure injection technology has been widely used in diesel engines. The injection cam is an important part in the high-pressure injection system. It is the processing accuracy of the injection cam that directly affects the performance of the injector components and thus the combustion and emission performance of the engine [1–3]. The camshaft is a key part of the engine. The injection cam plays a decisive role in the starting and stopping time, pressure, rule, and capacity of the oil pump. The valve cam profile has a great influence on the working performance of the engine [4–6]. If the error of cam profile on the camshaft is too large, the characteristic curve of plunger speed will be changed and the fuel injection law will be changed. If the phase angle error is too large, it will destroy the technical state of the engine [7]. In order to ensure the machining quality of the cam profile, it is necessary to develop high-precision and stable measuring and data processing methods [8–10]. The contact

measuring method of the flat probe, disc probe, and knife edge probe is adopted [11, 12]. Machine vision, interference optics, and structured light are also used in camshaft profile accuracy detection [13–15]. Most of the researches are focused on the camshaft phase reference. Because of the cams with different tip phases on the same camshaft, the angle datum cannot be measured automatically. And the calculation of the lift error depends too much on the accuracy of the angle reference. The error of the reference will lead to the systematic error of all the lift data [16, 17]. At the same time, the present research of cam measurement is almost based on the symmetrical single peach point valve cam as the mathematical theoretical model. However, there is little research on the detection of injection cam. Because of the unsymmetrical profile and the circular arc of the peach tip, most of the research on the injection cams cannot be applied to the valve cam. An accurate extraction method of the characteristic parameters of the injection cam profile is proposed in this paper. The phase error optimization strategy is realized by the angle precise rotation matching of the actual lift data. The goals of precise

measurement of the peach point phase of single high point cam and accurate acquisition of the back dead point phase of high point arc segment cam are realized [18].

2. Methodology

2.1. Measuring Instruments. In view of the above problems, a fully automatic method to extract the feature parameters of the cam profile is proposed in this paper. The following is an introduction to the cam automatic measuring instrument.

2.1.1. Mechanical Structure. Horizontal structure, which is mainly composed of a base, dividing head, Abbe head, back center, precision circular grating, precision straight grating, stepping motor, and so forth is adopted by cam measuring instrument. As shown in Figure 1. The equipment adopts marble as the base. The precision tailstock guide rail equipped on the equipment can realize the axial high-precision movement of the probe system [19]. The rotary system is composed of a dividing head, circular grating, motor, and so forth. The dividing head and circular grating are connected by precision coupling. The circular grating adopts Renishaw circular grating with a resolution of $1.8''$. The whole rotary system is driven by a step motor, and the circular grating records the angle of the turntable. The probe system is composed of Abbe head, straight grating, and tail stepping motor. A precision sliding platform is adopted by the main shaft of Abbe head to realize radial measurement movement of equipment. Renishaw straight grating with a resolution of 0.0001 mm, which can measure the radial dimension of the cam, is adopted by the straight grating.

2.1.2. Electrical Control. Electrical control is used to realize the motion control of industrial PC to the lower computer (turntable system and probe system), reading the circular grating and straight grating in real time to send them to PC.

Mpc08, a high integration and high reliability pulse motion control card based on PCI bus, is selected for the control of industrial PC. It can control 4-way stepping motor or digital servo motor and output pulses and direction signals for each axis to control the rotation of motor. Mpc08 control card is an open platform for developing a motion control system, which can directly use the resources of PC and open interface protocol to develop a motion control system [20].

Pci2300 data acquisition card is selected for data acquisition, which has a 32-bit PCI bus and 100 kHz 12-bit a/*D* converter. The specific use is that pci2300 card can collect the digital signal of the circular grating ruler (straight grating ruler) in the process of movement, counts the digital signal, and sends it to PC. PC calculates the actual angular displacement or displacement of grating through the resolution of the grating ruler itself, to accurately record the information of angle and displacement. The above control and data acquisition methods are reasonable for the application of the Internet of things and cloud computing technology under the current information technology [21–24].

FIGURE 1: Cam measuring instrument.

2.2. Accurate Extraction of Lift Error and Phase Error Information

2.2.1. Lift Error. From the formula point of view, the functional relationship among cam position, shape, and lift is as follows:

$$h = f(\alpha, \rho). \tag{1}$$

On the total differential of the previous equation,

$$\Delta \mathbf{h} = \frac{\partial \mathbf{h}}{\partial \boldsymbol{\alpha}} \Delta \boldsymbol{\alpha} + \frac{\partial \mathbf{h}}{\partial \boldsymbol{\rho}} \Delta \boldsymbol{\rho}. \tag{2}$$

In the previous equation, $(\partial h/\partial \alpha)$ is the function transfer coefficient between the cam position error and lift error and $(\partial h/\partial \rho)$ is the function transfer coefficient between the cam shape error and lift error.

According to equation (2), the first term is the lift error caused by the position (angle) error $\Delta\alpha$ of the cam and the second term is the lift error caused by the shape error $\Delta\rho$ of the cam.

The shape error of the cam should not be affected by the position error. A method is proposed to transform the actual lift data into the position of angle rotation and obtain the optimal lift data matching the theoretical lift data. The optimal lift data is used to calculate the lift error of the cam. The evaluation of the optimal lift is based on the minimum distance between the actual shape and the theoretical shape of the cam. In this paper, the way to find the optimal lift is to determine the optimal lift with the smallest sum of the square error between the actual lift and the theoretical lift by rotation matching.

In the above solution, the key is how to obtain accurately the measured lift value at the theoretical phase angle during the data rotation. The general solution is increasing the number of sampling points. This is the most intuitive and realistic solution. When the sampling step is equal to the angular rotation step of rotation matching, the lift values at all theoretical phases can be directly extracted from the measured data. However, there are problems with this

solution. In order to ensure the accuracy of lift error, the angle rotation step should be as small as possible in rotation matching. When the rotation step is equal to 0.01°, the number of sampling points $n = 360/0.01 = 36000$. On the one hand, the number of sampling points is large and the amount of data collected and calculated is large. So, it is easy to make mistakes. On the other hand, in the practical application, in order to ensure the measurement efficiency, the data sampling frequency is put forward higher requirements.

In order to solve the problems of large amount of data and strict requirements of sampling accuracy, the method of a moving window Lagrangian polynomial interpolation is proposed to calculate the measured lift value at the theoretical phase angle [25]. Evenly distribute appropriate measuring points around the cam are achieved. The phase relationship between the highest point and the theoretically highest point in the measured polar diameter data is used to make a rough rotation matching for all the measured data. Then, for all the measured data in a certain angle range with a fixed rotation step, the lift value at the theoretical angle after each angle rotation is approximated by Lagrangian interpolation polynomial. The sum of the lift error squares of all points after each rotation is calculated. The moving window is used to ensure that the target lift to be interpolated is only affected by the local measured accurate data:

$$L(x) = \sum_{j=k-n}^{k+n-1} y_j l_j(x), \tag{3}$$

$$l_j(x) = \prod_{k-n \ll m \ll k+n-1, \quad m \neq j} \frac{x - x_m}{x_j - x_m} = \frac{(x - x_{k-n}) \dots (x - x_{j-1})(x - x_{j+1}) \dots (x - x_{k+n-1})}{(x_j - x_{k-n}) \dots (x_j - x_{j-1})(x_j - x_{j+1}) \dots (x_j - x_{k+n-1})}. \tag{4}$$

In the previous equations, x_i is the phase angle after rotation, y_i is the measured polar diameter value corresponding to the phase angle, k point is the known point larger than the phase to be interpolated and closest to the interpolation phase of the band; and n is the measured point selected on both sides of k point.

In the process of rotation matching, the minimum value of the objective function is calculated as follows:

$$\min\left\{ F(\theta_k) = \sum_{i=0}^{N-1} (L(i + \theta_k) - X_i)^2, \quad k = 0, 1, \dots, M \right\}, \tag{5}$$

$$\theta_k = k\Delta\theta. \tag{6}$$

In equation (5), θ_k is the rotation angle, N is the number of theoretical lift points, M is the number of rotation matching; X_i is the theoretical lift value corresponding to each theoretical phase angle, $L(i + \theta_k)$ is the measured lift value corresponding to each theoretical phase angle after rotation θ, θ_k is the rotation angle of the k-th angular rotation, and $\Delta\theta$ is the angular rotation step.

When $F(\theta) = \min\{F(\theta_k)\}$, after the original data is rotated by θ, the lift at each theoretical phase angle interpolated is the optimal lift, and the error of the optimal lift can reflect the shape error of the cam.

2.2.2. Phase Angle Error

Phase Reference. The phase angle error refers to the difference between the design angle and the actual angle of the feature point on the cam relative to the phase reference in the circumferential direction. The variation of the measured element relative to the ideal element of the determined position is the positioning error [25]. The position of the ideal element is determined by the datum and the theoretical correct size. In the measurement of the phase angle error, it is necessary to determine the phase datum and the theoretical phase angle of each cam.

In practice, the cam phase is based on the key slot center of the camshaft to design the theoretical angle of each cam tip relative to the phase reference. The theoretical included angle of each cam tip relative to the phase reference is known, so the key to determining the error of the cam phase angle is to determine the phase reference.

In order to solve the above problems, the pin positioning is used to determine the phase reference. A cylindrical pin with the same width as the keyway is inserted in the keyway to ensure the close fit between the keyway and the cylindrical pin. The phase position of the highest point of the cylindrical pin relative to the rotation center is measured and determined in the matching mechanism and is used as the phase reference. Therefore, the problem is transformed into how to extract the phase position of the highest point in the measurement data of the matching mechanism. The model is similar to a symmetrical single point cam, as long as the theoretical lift value of the "cam" is determined. Then, the method of middle rotation matching is used in the calculation of lift error to determine the optimal lift of measured data. So, the phase of the "sensitive point" in the optimal lift can be used as the phase reference. The theoretical lift calculation model is shown in Figure 2.

When the angle of the lift table is 0 and the angle is 0, the distance between the center of the probe and the center of rotation is $L + r1 + r2$.

When the connecting line between the probe and the turning center is turned by θ, and the probe is only tangent to the cylindrical pin, the distance between the center of the probe and the turning center is calculated as follows:
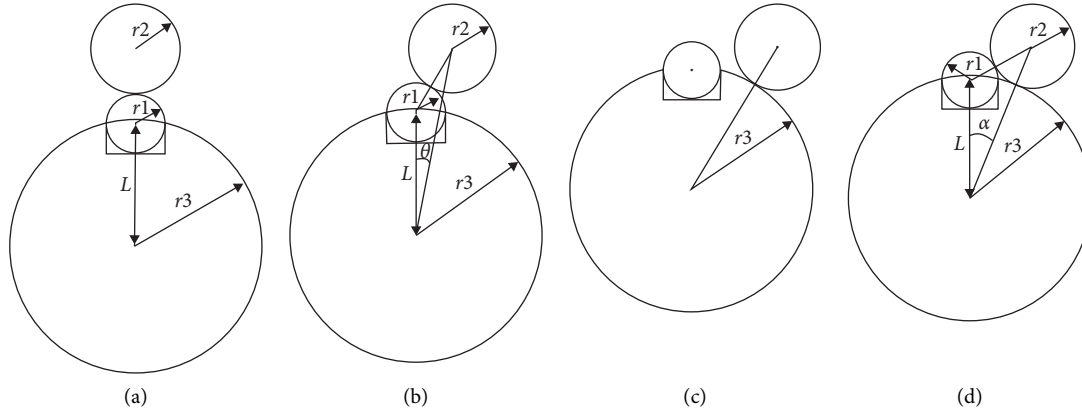
FIGURE 2: Theoretical lift calculation model of pin positioning.

$$L \cdot \cos \theta + \sqrt[2]{(r1 + r2)^2 - (L \cdot \sin \theta)^2}. \qquad (7)$$

When the probe is tangent to the locating circle section, the distance between the probe center and the rotation center is $r3$.

The critical phase of the probe tangent to the cylinder pin and the locating circle section can be seen from the cosine theorem:

$$\alpha = \arccos\left(\frac{L^2 + (r3 + r2)^2 - (r1 + r2)^2}{2 \cdot L \cdot r3}\right). \qquad (8)$$

When $0 \ll \theta \ll \alpha$ or $360 - \alpha \ll \theta \ll 360$, the distance between the center of the probe and the center of rotation is calculated according to the formula given in (8), and the distance between the center of the probe and the center of rotation in other phase positions is r3.

Single High Point Cam. Because the phase position of the tip is unique and has certain characteristics, the highest point of the measured data is used to determine the position of the tip. A method of full angle lift matching to eliminate the angle error between the highest point of polar diameter and the actual peach tip is proposed to reduce the single point sensitivity of the highest point method and improve the stability of measurement results [26]. Firstly, the phase value α_1 of the highest point of the measured data should be determined. The rotation angle of the measured lift data to the optimal lift data as θ and the theoretical phase angle as α_0 in the lift error matching should be recorded. So, the measured phase angle error of the peach tip is calculated as follows:

$$\varepsilon = \alpha_1 - \alpha_0 + \theta. \qquad (9)$$

High Point Arc Segment Cam. Because the tip of some injection cam profile is a section of arc, that is to say, in the measurement, the highest point of measured polar diameter data is not unique. Even though the highest point is unique, it is also impossible to determine the theoretical phase position of the highest point, as shown in Figure 3.

Based on the characteristic of the top dead center profile [27, 28], a method of determining the top dead center phase is proposed. The optimal lift can be obtained by the rotation
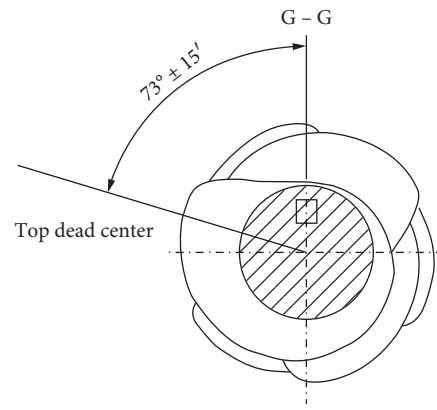
FIGURE 3: Injection cam.

matching method. At the same time as obtaining the optimal lift, the required rotation angle of all measured data to the optimal data can be calculated. So long as the phase information of the optimal lift, where the top dead center is located, is calculated, the actual phase information of the top dead center can be calculated. So, in a certain angle range of the optimal lift data with a fixed rotation step, the lift value at the theoretical angle after each angle rotation is approached by Lagrange interpolation polynomial, and an objective function is established [29]. The objective function consists of the sum of the squares of the lift errors at the theoretical phase of the top dead center and some points near its two sides. The actual phase position of the top dead center can be obtained by calculating the rotation angle of the minimum objective function and the rotation angle of the optimal lift.

3. Application

Horizontal cam full-automatic measuring instrument with 360 equal angle sampling 2400 points is adopted. When the optimal lift is determined by rotation matching [30], in the range of (−5°, 5°), the lift is calculated by eight Lagrangian interpolation polynomials with 0.01° as the rotation step. The angle rotation range is (−5°, 5°), the rotation step is 0.01°, and the lift error of 20 points on the left and right of the theoretical phase angle is taken as the objective function.
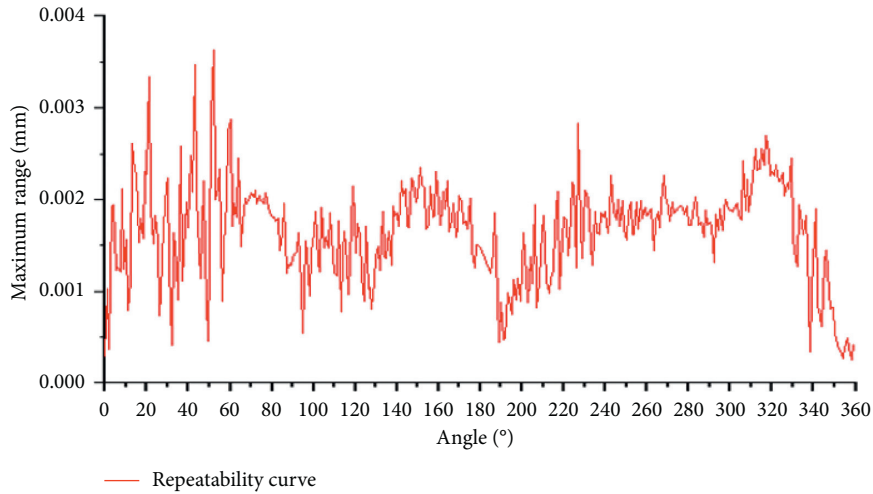
Figure 4: Lift error accuracy verification.
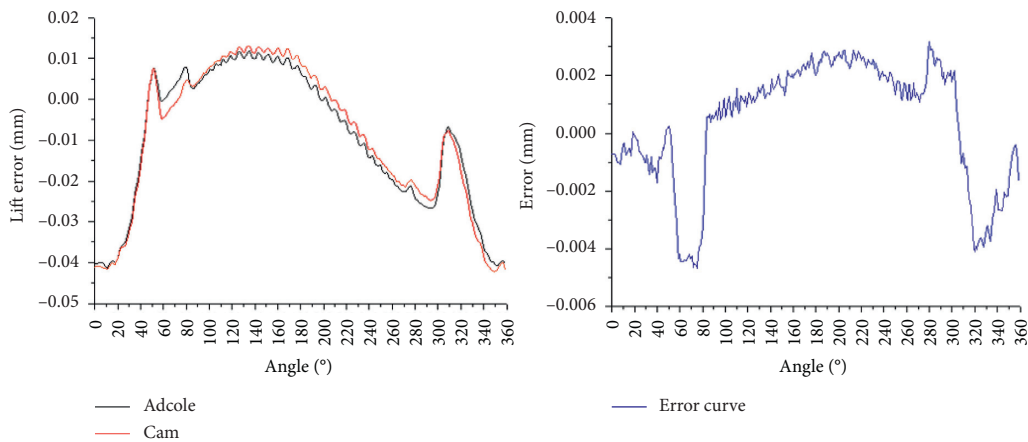
Figure 5: Intake cam.
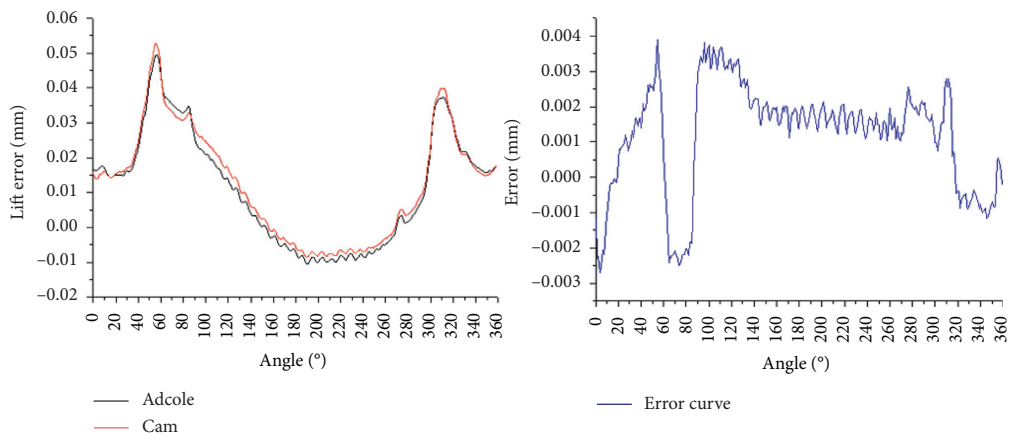
Figure 6: Exhaust cam.

3.1. Lift Error. Lift error repeatability verification is carried out that the same camshaft is measured repeatedly 5 times and the lift error of each theoretical point is analyzed by the cam measuring equipment. According to the lift repeatability curve data in Figure 4, the maximum range of 5 measurements at the same phase is 0.0035 mm = 3.5 um, the average value is 0.00165 mm = 1.65 um, and the lift error repeatability is high.

Table 1: Repeatability of valve cam phase angle error (degrees).

	Group 1	Group 2	Group 3	Group 4	Group 5
Cam 1	0.50	0.50	0.49	0.49	0.50
Cam 2	0.30	0.31	0.31	0.30	0.30
Cam 3	0.51	0.51	0.51	0.50	0.50

Table 2: Accuracy of valve cam phase angle error (degrees).

	Cam 1	Cam 2	Cam 3	Cam 4	Cam 5	Cam 6
Adcole	0	0.0288	0.024	−0.198	−0.197	0.0414
Keyway reference	0.5	0.52	0.51	0.3	0.31	0.55
Cam 1	−0.01	0.02	0.01	−0.21	−0.20	0.04
—	Cam 7	Cam 8	Cam 9	Cam 10	Cam11	Cam 12
Adcole	0.1425	−0.087	−0.05	0.0704	−0.053	−0.065
Keyway reference	0.63	0.4	0.46	0.56	0.43	0.44
Cam 1	0.12	−0.11	−0.05	0.05	−0.07	−0.07

Table 3: Repeatability of phase error of REAR dead center of WP16-SZ injection cam (Degrees).

	Group 1	Group 2	Group 3	Group 4	Group 5
Cam 1	0.69	0.69	0.70	0.70	0.70
Cam 2	0.15	0.14	0.14	0.15	0.13
Cam 3	−0.05	−0.04	−0.05	−0.05	−0.06

Lift error accuracy verification is carried out that the results measured by the cam measuring equipment are compared with the ones measured by Adcole measuring equipment for the same valve cam in the United States. The results are shown in Figures 5 and 6.

In the measurement results of the intake cam and Adcole, the maximum positive error is 0.003169 mm and the maximum negative error is –0.00469 mm. The measurement accuracy is high, which can meet the engineering needs. In the measurement results of the exhaust cam and Adcole, the maximum positive error is 0.003887 mm and the maximum negative error is –0.0027 mm. The measurement accuracy is high, which can meet the engineering needs.

3.2. Phase Angle Error

(1) For a single high point cam, the same camshaft is measured by the cam measuring equipment and repeatedly 5 times. The lift error of each theoretical point is analyzed according to the lift repeatability. Table 1 shows the repeatability accuracy of the proposed method for three single high point cams.

3.2.1. Repeatability. The repeatability of phase angle error is $0.01° = 0.6'$. The result is stable and the repeatability is good.

3.2.2. Accuracy. For the same valve cam, the results measured by the cam measuring equipment are compared with the ones measured by Adcole measuring equipment in the United States. This time, the angle of Adcole cam #1 is relative to the datum (keyway) = $0.0536°$.

It can be seen in Table 2. When the center of the keyway is used as the angle reference, the angle of cam 1 to keyway is $0.5°$. Compared with the result of Adcole, the error is $−0.0036° = 0.216'$ and the accuracy is high. When the first cam tip is taken as the angle datum, the datum of the two measured results is the same. The maximum positive error is $0.0022°$, the maximum negative error is $−0.0226°$, the average error is $−0.01103°$, and the phase angle error detection accuracy is high.

(2) High point arc segment cam

Table 3 is the phase error data of circular arc cam detected by the method described in this paper. The repeatability of phase angle error is $0.02° = 1.2'$. The result is stable and the repeatability is good.

4. Conclusion

A cam detection technology based on moving window Lagrange interpolation algorithm is presented. The lift and phase angle errors of the injection cam can be extracted accurately and stably by this method. In the process of cam automatic measurement, the system error caused by cam phase angle reference is avoided. It solves the problems of accurate measurement of single high point cam peach point phase and accurate acquisition of high point arc segment cam backstop phase. It is helpful to obtain and calculate the lift error of the cam accurately. This method is suitable not only for injection cam but also for intake and exhaust camshaft, conjugate cam, and common rail cam.

Data Availability

All the data are actually available upon request.

Conflicts of Interest

The authors declare that they have no financial and personal relationships with other people or organizations that can inappropriately influence their work. There is no professional or other personal interest of any nature or kind in any product, service, and/or company that could be construed as influencing the position presented in, or the review of, the manuscript entitled.

Acknowledgments

References

[1] X. Gu, Y. Xu, J. Miao, and J. Yu, "Study on the key Part Optimization of common rail injector used on a commercial vehicle," *Modern Vehicle Power*, vol. 03, pp. 15–19, 2020.

[2] F. Hoppe, M. Thewes, H. Baumgarten, and J. Dohmen, "Water injection for gasoline engines: potentials, challenges, and solutions," *International Journal of Engine Research*, vol. 17, no. 1, pp. 86–96, 2016.

[3] R. Zhi-Xiang, F.-Z. Guo, and K. Zhu, "Simulation research on fuel system of a type of marine medium speed diesel engine," *Ship Science and Technology*, vol. 42, no. 11, pp. 132–136, 2020.

[4] L. Fan, Q. Dong, C. Chen, Y. Bai, W. Zhao, and X. Ma, "Research on effects of key influencing factors upon fuel injection characteristics of the combination electronic unit pump for diesel engines," *Journal of Mechanical Science and Technology*, vol. 28, no. 10, pp. 4319–4330, 2014.

[5] C. Abagnale, M. Migliaccio, and O. Pennacchia, "Design of a new mechanical variable valve actuation system for motorcycle engines," in *Proceedings of the ASME 2012 11th Biennial Conference on Engineering Systems Design and Analysis*, Nantes, France, July 2012.

[6] G. Liu, P. Y. Liu, W. J. Wei, S. Y. Zhang, and H. T. Li, "A new design method for the rotor profile curve of the cam pump," *Advanced Materials Research*, vol. 482–484, pp. 1196–1200, 2012.

[7] S. Li, "Defect inspection and assembly of fuel injection pump parts," *Use and Maintenance of Agricultural Machinery*, vol. 65, no. 05, 2020.

[8] S. Sun, Z. Jiang, J. Huang et al., "Analysis and Detection Method for Machining Error of Globoidal Indexing Cam Profile," *MATEC Web of Conferences*, vol. 213, 2018.

[9] H. Wang, A. Zhang, Q. Zhang, and C. Peng, "Research on measurement method for disk cam based on image processing technology," *Modern Manufacturing Engineering*, vol. 02, pp. 117–121, 2017.

[10] C. Lu, Y. Zhang, J. Feng, and X. Zhang, "Detection for the wear degree and relative position of the cams," *Journal of Changchun University of Science and Technology (Natural Science Edition)*, vol. 38, no. 01, pp. 49–52, 2015.

[11] L. I. Qi, Y. Hu, and Y. Zhou, "Design and precision testing of CAM based on the three coordinate measuring," *Light Industry Machinery*, vol. 32, no. 05, pp. 80–83, 2014.

[12] Z. Kaijun, J. Zhaoping, and L. Jie, "CAM parts detection and copy based on three-coordinate measuring machine," *Manufacturing Automation*, vol. 36, no. 14, pp. 51–54, 2014.

[13] Z. Hu, *Research on Vision Measurement Technology of Disc Cam Based on Line Structure Light*, Jilin University, Jilin, China, 2020.

[14] A. An, Y. Ma, and Q. Zhang, "Identification of the cam profile based on machine vision," *Journal of Henan Institute of Science and Technology(Natural Science Edition)*, vol. 44, no. 01, pp. 62–67, 2016.

[15] G. Wang, Y. Yao, Z. Chen, and P. Hu, "Thermodynamic and optical analyses of a hybrid solar CPV/T system with high solar concentrating uniformity based on spectral beam splitting technology," *Energy*, vol. 166, pp. 256–266, 2019.

[16] Y. Mingfu and H. Zhao, "A new method of spatial cam profile inspection and error evaluation and its experimental research," *Chinese Journal of Scientific Instrument*, vol. 4, pp. 452–456, 2004.

[17] L. Jianfeng, "Cam profile surface analysis of swing output movable teeth cam mechanism," *Advanced Engineering Sciences*, vol. 50, no. 1, pp. 149–156, 2018.

[18] Y. Sun, "Analysis for center deviation of circular target under perspective projection," *Engineering Computations*, vol. 36, no. 7, pp. 2403–2413, 2019.

[19] L. Z. Zhang, M. Mouritsen, and J. R. Miller, "Role of perceived value in acceptance of "bring your own device" policy," *Journal of Organizational and End User Computing*, vol. 31, no. 2, pp. 65–82, 2019.

[20] H. Zhang, S. Qu, H. Li, J. Luo, and W. Xu, "A moving shadow elimination method based on fusion of multi-feature," *IEEE Access*, vol. 8, pp. 63971–63982, 2020.

[21] A. M. Al-Momani, M. A. Mahmoud, and M. S. Ahmad, "Factors that influence the acceptance of Internet of things services by customers of telecommunication companies in Jordan," *Journal of Organizational and End User Computing*, vol. 30, no. 4, pp. 51–63, 2018.

[22] T. Grubljesic, P. S. Coelho, and J. Jaklic, "The shift to socio-organizational drivers of business intelligence and analytics acceptance," *Journal of Organizational and End User Computing*, vol. 31, no. 2, pp. 37–64, 2019.

[23] L. Z. Zhang, M. Mouritsen, and J. R. Miller, "Role of perceived value in acceptance of "bring your own device" policy," *Journal of Organizational and End User Computing*, vol. 31, no. 2, pp. 65–82, 2019.

[24] S. Namasudra and P. Roy, "PpBAC," *Journal of Organizational and End User Computing*, vol. 30, no. 4, pp. 14–31, 2018.

[25] C. Li, F. Sun, J. M. Cioffi, and L. Yang, "Energy efficient MIMO relay transmissions via joint power allocations," *IEEE Transactions on Circuits and Systems II: Express Briefs*, vol. 61, no. 7, pp. 531–535, 2014.

[26] L. Zhang, H. Shi, X. Zeng et al., "Theoretical and experimental study on the transmission loss of a side outlet muffler," *Shock and Vibration*, vol. 2020, Article ID 6927574, 8 pages, 2020.

[27] B.-Z. Xia, X.-C. Liu, X. Shang, and S.-Y. Ren, "Improving cam profile design optimization based on classical splines and dynamic model," *Journal of Central South University*, vol. 24, no. 8, pp. 1817–1825, 2017.

[28] R. M. Fang, J. F. Cai, and G. Li, "Cam curve synthesis method based on classical splines," *Applied Mechanics and Materials*, vol. 312, pp. 69–73, 2013.

[29] T. Ouyang, P. Wang, H. Huang, N. Zhang, and N. Chen, "Mathematical modeling and optimization of cam mechanism in delivery system of an offset press," *Mechanism and Machine Theory*, vol. 110, pp. 100–114, 2017.

[30] F.-H. Bu, Y.-M. Zhang, and D.-G. Shang, "Study on machining error of globoidal cam profile resulting from motion error of machine tool in machining," *Applied Mechanics and Materials*, vol. 148-149, pp. 1356–1364, 2012.

Research Article

Distributed Virtual Environment Basketball Equipment Embedded Systems' Research and Development

Yang Zhou [ID]

Chengdu Sport University, Chengdu 610041, Sichuan, China

Correspondence should be addressed to Yang Zhou; zhouyang@cdsu.edu.cn

With the development of social economy and the improvement of material level, people are paying more and more attention to their own health, and they are also constantly improving their fitness awareness. As far as the current sports equipment is concerned, the boring exercise methods can no longer satisfy people's pursuit of higher quality fitness exercises. The embedding of the distributed virtual environment can incorporate its perceptual, immersive, and interactive characteristics, which increases the realization of multiuser interactive behavior in the field of sports equipment in the virtual scene. Therefore, this paper proposes the research and development of basketball sports equipment embedded system based on distributed virtual environment. First of all, this article adopts the literature method to learn the application of distributed virtual environment and embedded system in depth and, secondly, designs the embedded system architecture of basketball sports equipment suitable for distributed virtual environment and the software and hardware framework of the embedded system. Finally, the performance, delay comparison, system optimization test, and other aspects of the embedded system are analyzed. The average delay of interactive functions of embedded systems based on distributed virtual environment is 1.4 min, which saves 4 min compared with traditional interactive methods. And, the throughput rate of the system has also been greatly improved. The research on the embedded system of sports equipment based on the distributed virtual environment proposed in this paper will be beneficial to the development of society and economy, and it can also help more people to enrich the way of sports and enhance the fun of sports.

1. Introduction

With the development of social economy, the development trend of sports equipment sales has performed well. On the one hand, people pursue a healthy body and a slim figure, so the demand for sports equipment is increasing. On the other hand, people's requirements for sports equipment are also increasing. Sports equipment, in addition to good quality, beautiful appearance, and other objective conditions to meet the basic functions of exercise, also has a high quality and high-tech level. This has also created a new challenge and motivation for the innovation of sports equipment.

Long-term exercise is easy to make people feel boring. Single-function sports equipment combined with a distributed virtual environment embedded system can not only meet people's needs for fitness but also bring people a sense of immersion and pleasure. Therefore, through the research

of this project, the application of virtual reality technology is integrated into the embedded system of basketball sports equipment. While laying a solid foundation for the research and development of other sports equipment products, it can also improve the quality and level of domestic sports company products. This has an important role and value for the formation of new economic development points.

Latoschik et al. study the performance and user experience of social virtual reality (SVR), with the goal of distributed, concrete, immersive, and face-to-face encounters. They showed the close relationship between scalability, replication accuracy, and resulting performance characteristics and the impact of these characteristics on users coexisting with larger groups of virtual others. System scalability provides a variable number of avatars in the same location and AI control agents with various appearances, including virtual people with real appearances generated by

photogrammetric scanning. This article reports how to use today's off-the-shelf technical solutions to meet the needs of embedded SVR as well as expectations in terms of features, performance, and potential limitations. Special attention is paid to the social signals embodied by reliable communication necessary to achieve low delay and sufficient frame rate. They proposed a hybrid evaluation method that consistently linked the results of technical benchmarks with subjective ratings and evaluation results. However, the delay of the system is still at a relatively high level in practical applications [1]. Arthur et al. summarized the distributed real-time (DRT) system is one of the most complex software systems to design, test, maintain, and develop. The existence of components distributed on the network often conflicts with real-time requirements, resulting in design strategies relying on domain-specific and even application-specific knowledge. The Distributed Virtual Environment (DVE) system is a DRT system that instantly connects multiple users through the network and shares a virtual space. The DVE system is different from the traditional DRT system in the importance of the end user experience quality. Although they put forward important analysis, it is a challenging problem in testing and evaluation when designing specific DVE, Open Simulator experimental lens and DVE system. They built their observations within six dimensions of well-known design concerns: correctness, fault tolerance/prevention, scalability, time sensitivity, consistency, and distribution overhead. In addition, they put the experimental work in a broader historical context, showing that these challenges are inherent in DVE, and proposed the direction of future research. However, there are too many uncontrollable factors in their experiment, and the results of the experiment need to be treated more correctly [2]. Zeng et al.'s traditional independent embedded system is limited in terms of functionality, flexibility, and scalability. Fog computing platform is characterized by pushing cloud services to the edge of the network and is a promising solution to support and strengthen traditional embedded systems. Resource management has always been a key issue affecting system performance. This article considers a software-defined embedded system that supports fog computing. Task images are stored on a storage server, and calculations can be performed on embedded devices or computing servers. Designing an efficient task scheduling and resource management strategy to minimize task completion time is of great significance for improving user experience. To this end, this article studies three issues. (1) How to balance the workload on client devices and computing servers, that is, task scheduling? (2) How to place task images on storage servers, that is, resource management? (3) How to balance storage server I/O interrupt request between? They are considered jointly and expressed as a mixed integer nonlinearity. However, they did not propose a specific solution to solve the above problems [3].

Only innovation can continuously promote the development and progress of fitness equipment. Combining high-tech with fitness equipment is an inevitable trend in the development of this industry. The innovation of this article lies in the full application of distributed virtual reality technology, the design of the client embedded frame system, and the completion of the construction of immersive and interactive virtual fitness scenes under the formation of a specific fitness virtual environment. This paper makes full use of the combination of qualitative analysis and quantitative analysis and has been fully reflected in the analysis part.

2. Basketball Equipment Research and Development of Embedded Systems Based on Distributed Virtual Environment

2.1. Distributed Virtual Reality System. Distributed virtual reality refers to a virtual environment based on the network, and its application in sports can realize the panorama, virtuality, and interactivity of sports [4].

Virtual reality is a computer system that can create a virtual world for experience. It uses computer technology to create an actual virtual environment with a combination of visual, auditory, and tactile perceptions [5]. Various interactive devices interact with entities in the virtual environment to generate interactive simulation and information exchange, giving people a new way of communication and contact [6]. Since its birth, virtual reality technology has shown great advantages in the fields of military simulation, urban planning, real estate development, industrial simulation, geographic information systems, games, education, and training. The three most promising technologies of this century are computer, multimedia, and VR technology. VR technology design disciplines are very extensive, including computers, artificial intelligence, and sensor technology. It only needs computer technology to realize the realistic environmental world and make people feel brand-new experience and interaction [7, 8].

The virtual reality system emphasizes realism, vision, interaction, personal perspective, and rapid response. Therefore, the virtual reality system has four basic characteristics, namely, multisensitivity, engagement, interactivity, and autonomy [9]. Multisensory refers to the sense of sight, hearing, and touch in the virtual world. The sense of engagement refers to the user's degree of immersion and concentration in virtual reality, which requires the creation of the virtual world to attract him. Interactivity, that is to say, can realize independent communication and interaction between multiple users and has a complete sense of reality. Autonomy means that the objects in the virtual environment have the right to choose independently and can change related parameter settings and attributes by themselves [10, 11].

The distributed virtual reality system mainly has the following three characteristics:

(1) Decentralized management and control: distributed in different regions and different levels of systems, it can not only ensure the sharing of network resources but also autonomously control its own data [12]. Most of the management and control of local conditions can be solved only on the local side. If it contains data from other websites, it needs to be

managed through the Internet as a connectivity issue, for example, through local data entry, local query, and maintenance. At present, computer resources are very close to users, so communication costs can be reduced and response speed can be improved. However, the amount of data in other location databases is very small, which can greatly reduce information transmission to the network. At the same time, it can improve the security of local data [13].

(2) Multiuser interaction: with the development of network technology, the interaction of networks is indispensable for decentralized virtual reality systems [14]. The current comprehensive fitness equipment system does not have network interaction, and even if some networks have interaction, they have specific limitations. According to the decentralized virtual reality system, user groups geographically dispersed in different places can have real-time conversations. This user group can accommodate thousands of users at the same time [15].

(3) Real-time can also be regarded as dynamic [16]: because each user is displayed as a virtual image in a computer environment, the virtual image is to be explained by a user's video or a description of autonomy. When users, virtual worlds, or objects created in the computer interact with other images, it is actually a real-time dynamic operation [17]. Because only real-time guarantee can make users feel that they are in a virtual environment.

In addition, the decentralized virtual reality system has excellent scalability and is relatively easy to integrate with existing systems and easy to extend [18]. In the case of a comprehensive system based on a decentralized virtual environment, using distributed virtual reality technology to operate more than one gymnastics machine server can quickly expand the existing network system to form a decentralized system [19]. It is also simpler than building a large-scale system that saves time, money, material, and resources.

2.2. Bayesian Algorithm of Simulation Interactive Credibility. Interactive behavior is the basis for the simulation of distributed virtual environments, and credible interaction behavior is essential to the normal operation of the system. Large-scale distributed virtual environment simulation has the characteristics of large scale and various interactions [20], which intensifies the impact of network delay and middleware overhead on the credibility of system interaction, which may damage the accuracy of simulation results and system fairness, which leads to frequent simulation interruption, manual intervention, and even simulation failure [21].

In a distributed virtual environment, to maintain the consistency of interaction between different nodes, it is necessary to keep the timing and spacing of events consistent. Use $V = \{v_1, v_2, \cdots, v_n\}$ to represent the set of

simulation nodes, where $E = \{e_{11}, e_{12}, \cdots, e_{ij}, \cdots, e_{nn}\}$ e_{ij} represents the maximum delay between simulation nodes e_i and e_j, O represents all interaction events, $G(o_m)$ represents the node that generated the event O_m, $R(o_m)$ represents the collection of nodes that received the event, $tg_i(o_m)$ represents the time when the event O_m was generated, $tr_i(o_m)$ represents the time when the node vi received the event, and $te_i(o_m)$ represents the time when the event O_m is executed on node v_i and the timing is consistent:

$$\forall o_m, o_n \in O, v_i, v_j \in R(o_m) \cap R(o_n),$$
$$te_i(o_m) \le te_i(o_n) \Rightarrow te_j(o_m) \le te_j(o_n). \tag{1}$$

Consistent spacing:

$$\forall o_m, o_n \in O, v_i, v_j \in R(o_m) \cap R(o_n),$$
$$te_i(o_m) - te_i(o_n) = te_j(o_m) - te_j(o_n). \tag{2}$$

The interaction event that meets the requirements of consistent timing and consistent spacing at the same time is considered credible; if not, the interaction event is considered untrustworthy.

Since the network conditions and operating load of the distributed virtual environment are constantly changing, whether the interactive event is credible can be regarded as a random event, and the interactive credibility can be regarded as a random variable. Here, we choose the distribution as the prior distribution of the interactive credibility evaluation and record the value of the interactive credibility as this; then, the prior distribution of the interactive credibility $\pi(\theta)$:

$$\pi(\theta) = \frac{\Gamma(a+b)}{\Gamma(a)\Gamma(b)} \theta^{a-1} (1-\theta)^{b-1}, \quad 0 \le \theta \le 1, \quad a > 0, \quad b > 0. \tag{3}$$

Among them, a and b are the hyperparameters of the prior distribution and Γ are the gamma function.

If the mean $\bar{\theta}$ and variance $D(\theta)$ of the simulation interaction credibility can be obtained based on the prior information, the hyperparameters of the prior distribution

$$a = \frac{(1-\bar{\theta})\bar{\theta}^2}{D(\theta)} - \bar{\theta}, \tag{4}$$

$$b = \frac{a(1-\bar{\theta})}{\theta}.$$

The prior information is mainly collected and analyzed based on historical data or simulation models. If any valid prior information cannot be obtained, the Bayesian assumption can be used, and the interaction credibility prior is considered to be uniform in the (0,1) interval distributed.

According to the Bayesian formula, the joint density function of interactive credibility θ is

$$p(x, \theta) = p(X = x|\theta)\pi(\theta). \tag{5}$$

If in order to estimate the credibility θ of the interaction, n independent interval consistency data collection and

judgment are performed in a certain simulation, where the number of credible interactions is X; then, X obeys the binomial distribution $b(n, \theta)$, and the likelihood function is

$$p(X = x|\theta) = \binom{n}{x} \theta^x (1 - \theta)^{n-x}, \quad x = 0, 1, \cdots, n. \quad (6)$$

Then,

$$p(x, \theta) = \frac{\Gamma(a + b)}{\Gamma(a)\Gamma(b)} \binom{n}{x} \theta^{a+x-1} (1 - \theta)^{b+n-x-1}, \quad (7)$$

$$x = 0, 1, \cdots, n, \quad 0 < \theta < 1.$$

Edge distribution:

$$p(x) = \int_0^1 p(x, \theta) d\theta = \frac{\Gamma(a + b)}{\Gamma(a)\Gamma(b)} \cdot \frac{\Gamma(a + x)\Gamma(b + n - x)}{\Gamma(a + b + n)}$$

$$\cdot \binom{n}{x}, \quad x = 0, 1, \cdots, n. \quad (8)$$

In summary, the posterior density of interactive credibility is

$$\pi(\theta|x) = \frac{p(x, \theta)}{p(x)} = \frac{\Gamma(a + b + n)}{\Gamma(a + x)\Gamma(b + n - x)} \theta^{a+x-1}$$

$$\cdot (1 - \theta)^{b+n-x-1}. \quad (9)$$

We choose the posterior expectation θ as the Bayesian evaluation conclusion; then, the Bayesian estimate of the interaction credibility is

$$\hat{\theta} = \int_0^1 \theta \pi(\theta|x) d\theta = \frac{a + x}{a + b + n}. \quad (10)$$

2.3. Edge Fog Calculation.

Fog computing is an extension of cloud computing. It is the cloud closer to the ground and is the last part of the network between the terminal and the data center, so this article also refers to the combination of edge computing and edge fog computing [22]. The service platform is composed of distributed servers, provides computer and network services for data storage and distribution, provides cloud preprocessing services, and provides analysis and feedback of local smart cards and other service terminal devices [23]. Its purpose is to reduce bandwidth pressure, reduce application delays, and reduce the computing load of the data center [24].

The fog computing framework is shown in Figure 1. This graphic shows that fog computing is located between the cloud server and the terminal device. All fog computer servers are connected to cloud servers and terminal devices in various regions [25]. All sensors and smart terminals (local devices, etc.) are located at the edge. As the executor of the cloud server and the decision maker of the terminal

equipment, fog computing provides services for the upper and lower levels within the framework.

Fog computing is a highly virtualized cloud computing platform that extends to the edge of the network. As an extension of the cloud platform, fog computing uses its new architecture to provide storage, computing, and network services, which means that fog computing is destined to have some unique characteristics, mainly including the following. (1) Edge location and low Latency: fog computing is deployed at the edge of the network. Compared with cloud computing, it is closer to the ground and closer to terminal equipment. It does not need to go through numerous routers and networks to connect to the server, and it can better support the calculation and application of terminal equipment. (2) Wide geographic area and high mobility: compared with more centralized cloud computing, fog computing has a wider deployment area. (3) Massive nodes and distributed computing: the number of network nodes in fog computing is huge, which is determined by the wide geographic distribution. (4) Real-time interaction and online analysis: fog computing revolves around the sensor network equipment, providing real-time interaction for it, supporting local online analysis and giving corresponding responses and feedback, and effectively improving the real-time performance of the application system. (5) Multitype protocols and heterogeneity: fog computing supports multitype communication protocols with different functions and supports diversified heterogeneous software and hardware devices in different form factors and different environments.

The optimization of peak computing services must be based on specific programming strategies to meet the requirements of end users as much as possible [26]. The service optimization of edge fog computing is mainly based on a certain scheduling technology to minimize the cost of service providers under the condition of satisfying user requests to the maximum. This article mainly calculates the cost from the two perspectives of SLO violation penalty and resource node request processing terminal expenditure:

SLO violation penalty function: let Penalty denote the total penalty cost for SLO violations; then, the penalty function for violations is defined as

$$\text{Penalty} = \sum_{k=1}^{q} \left[\gamma_k + \eta \times \left(t_k^{\text{stop}} - t_k^{\text{deadline}} \right) \right]. \quad (11)$$

Among them, k represents the sequence number of requests that have SLO violations due to service timeouts, q represents the total number of requests that have SLO violations, γ_k represents the basic penalty for the k th request that has SLO violations, and η represents the cost of the k th SLO violation request, resulting in penalty cost per unit time. At the k th request, t stop is the actual response time and t deadline is the request deadline response time.

The cost function of edge fog computing when processing resource node requests: let vm be the total cost; then, the formula for calculating the resource cost function is
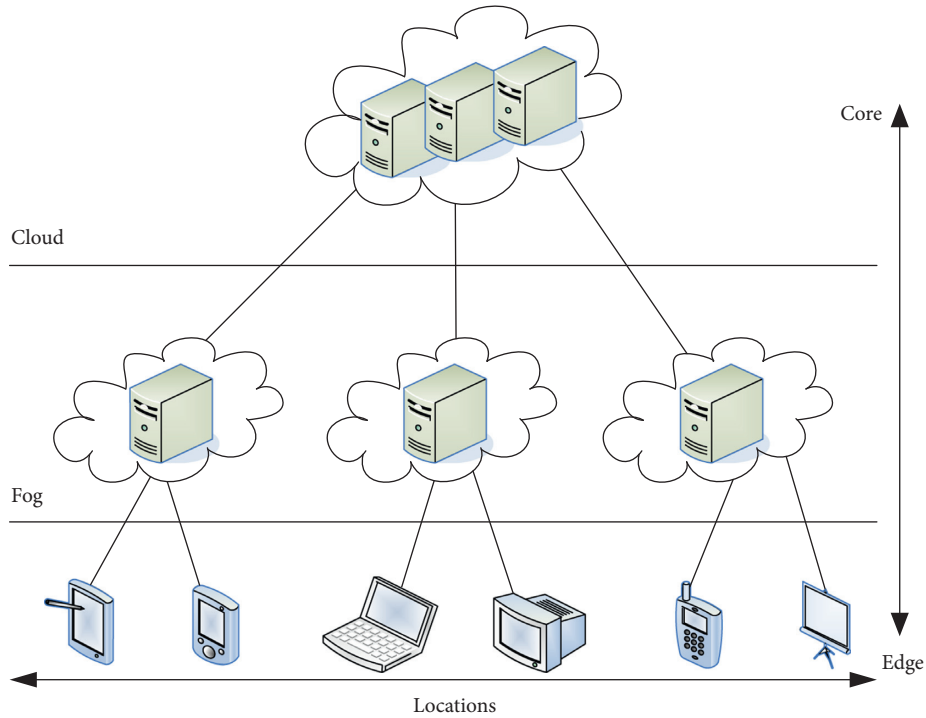
FIGURE 1: Framework of fog calculation.

$$vm = \sum_{i=1}^{n} vmc_i,$$

$$vmc_i = \sum_{j=1}^{M_i} \left(P_{i,j}^{vm} \times t_{i,j} \right). \tag{12}$$

The equation on the left represents the total cost of processing requests for the ith type of computing resource, M_i in the equation on the right represents the number of its virtual resource nodes, j represents a single virtual resource node with serial number j among virtual resource nodes of type i, and $t_{i,j}$ represents the time it takes for the virtual resource node with serial number j in the virtual resource node of type i to process the request. Combining the above two aspects, the total cost function of the service provider can be calculated as

$$\cos t = vm + \text{Penalty}. \tag{13}$$

3. Research and Development Model Design of Basketball Sports Equipment Embedded System Based on Distributed Virtual Environment

According to the characteristics of the distributed virtual reality system and the system's function and performance requirements, this section proposes a fitness equipment embedded system architecture suitable for a distributed virtual environment and the software and hardware framework of the embedded system.

The functional requirements of this system include with playback function, which can be connected to the card, and with a TV interface. The playing of the ship can increase the user's fun in the fitness process, increase the user's excitement, and help the user entertain in fitness and exercise in entertainment. The fitness system comes with a three-dimensional virtual scene, which can also be downloaded from a fixed website via the Internet. The application of three-dimensional virtual scenes increases the user's sense of vision, and the virtual scenes downloaded on the Internet help users to obtain more virtual scenes according to their needs, so as to feel more fun. Multiuser interactive fitness is realized in virtual space. The interactivity of multiple users enables better communication between users and feels that fitness is a collective exercise, not just the user's own exercise. You can get help from others to make your own fitness more effective. The performance requirements of this system include simple operation of the control panel, clear functions, and intuitive and convenient operation of each function key; users do not need to spend a lot of time to learn and familiarize themselves; they can use the virtual scene to draw fast, and the network bandwidth limit is low. The above remote users realize interactive fitness in the virtual space.

3.1. The Overall Structure of the System. The embedded system of basketball sports equipment in this distributed virtual environment chooses the client server mode. When the system is working, the operation triggered by the user on the client side is transmitted to the server. The server determines the client group to receive the operation according to a certain grouping strategy and then transmits this operation to the relevant client by multicast, and each client has the backup of the virtual scene and related computing capabilities.

In order to reduce the amount of network information transmission and support the concurrent operation of users in the system when the system is running, the system adopts a data management method based on replication and transmits user operations between the client and server instead of status update information. While adopting the replication structure and transmission operation mode, the system must add physical time stamps to all operations in order to control all concurrent operations that occur in the system, and the premise of adding physical time stamps is the physical time of all nodes. Synchronize: in order to synchronize the physical clocks of all nodes in the system, the system runs a sleepy server on the server, runs clients on all clients, and synchronizes the physical clocks of all nodes at regular intervals. At the same time, the client has an independent communication module that can independently and randomly transmit the change information of the entities in the scene to the server, and it can also monitor the information sent from the server at all times and perform proper processing.

While the fitness equipment servers in different regions are interacting, the interaction between the client and the server in the same region is relatively frequent. Then, the overall structure proposed in this article is conducive to the partition management of the virtual scene, and the load is balanced to each region. It greatly reduces the load of a single server and avoids the system "bottleneck" problem caused by the centralized structure, thereby improving the overall performance of the system. Due to the use of virtual scenes, the amount of data is relatively large, so in the process of transmission between the server and the client, the protocol is used to increase the response time and improve the real-time performance. In this structure, if a regional server fails, it will not affect other regions. At the same time, users can connect to other servers through the network to ensure the user's real-time performance.

3.2. Server System Structure.

The server side is composed of system management module, network communication module, user management module, information processing module, fitness scene management module, and object management module. The system management module is mainly used for console command processing, client request response, and system control. The network communication module is mainly used for information filtering and transmission of fitness scenes; the management module is mainly used for the management and processing of current scenes and scene libraries. The user management module is mainly for service management for users, including private information such as account numbers and passwords. Authority management includes role authority management and data authority management. The administrator can set authority settings and role definitions for newly added users. The information processing module is mainly used for information processing, grouping, and consistency control. For the consistency control problem in the information processing module, we solve the spatial consistency problem on the basis of analyzing the shortcomings of traditional consistency control methods.

3.3. Client System Structure.

The client-side system structure is mainly composed of system management module, network communication module, user management module, information processing module, fitness scene management module, object management module, user perception module, and scene drawing module. The system management module is mainly used for client command processing, client request sending, response receiving, and system control. The network communication module is mainly used for information filtering and transmission. The user management module is mainly used for user-related information and transmission. The management information processing module is mainly used for information processing and consistency, the control fitness scene management module is mainly used for the management and processing of the current scene and the scene library, and the object management module is mainly used for the management and processing of objects in the scene. The scene drawing module is mainly used for collision detection, LOD control, and graphics drawing.

The user perception module is mainly used for the perception and preprocessing of user behavior. The user conducts asynchronous full-duplex communication through the serial port between each sensor and the embedded virtual scene. Various general data collected from sensors, mainly various actions of users, are sent to the central computer through the serial port for processing. At the same time, it is necessary to send the topography and other data of the virtual scene to the controller and apply the output torque of the mechanical device. It simulates the changes of the real scene and sports field that people feel during the fitness process so that the user has a feeling of being in the virtual scene.

3.4. Framework Design of Client Embedded System

3.4.1. Hardware System Frame Design.

The system intends to adopt the embedded development version of the PC/104 standard, equipped with Intel XScale series of multimedia expansion technology, embedded processor that provides high-quality video, and 3D graphics playback functions, and the embedded processor controls the memory, fitness equipment controller, and a series of audio and video processors, which include NAND flash memory, SDRAM memory equipped with LCD frame buffers, video coprocessors to enhance the video processing capabilities of embedded processors, audio and video encoders for fitness equipment output devices, such as TV equipment, High-quality audio, and video output processors such as TFTLCD equipment and audio equipment use the universal input and output interface array GPIOS array, and asynchronous serial communication interface to communicate with the controller speed and slope of fitness equipment, as well as the interconnection of mileage, speed, and heart rate of many sensing equipment. Input devices such as keyboards and remote controls provide input of system commands and perform network communication through interfaces such as network adapters, Bluetooth, and GPRS.
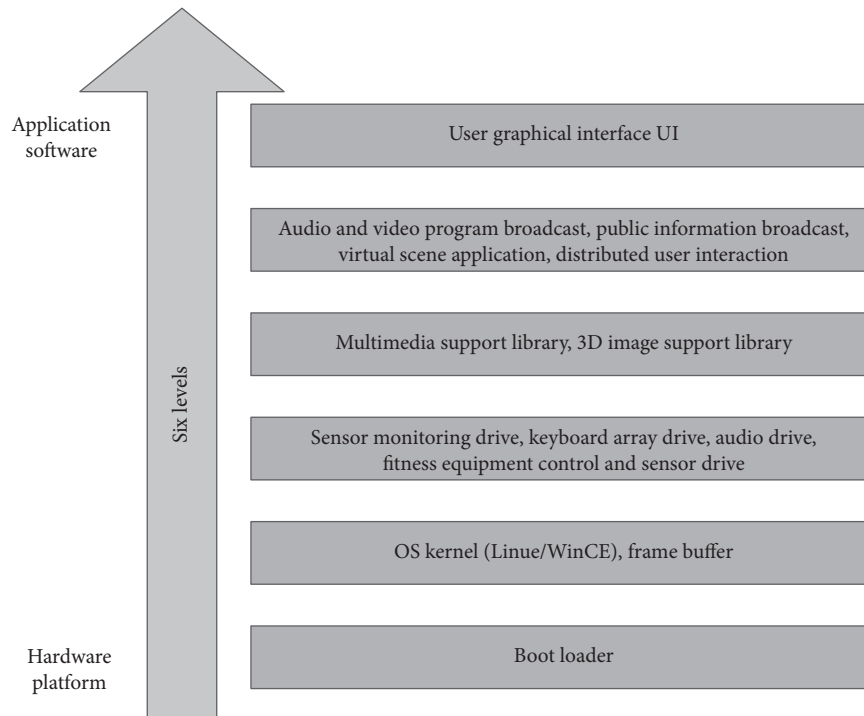
Figure 2: System software framework.

3.4.2. *Software System Framework Design.* In order to support the better development, deployment, operation, and management of distributed embedded systems, the application based on multilayer structure must be equipped with a software support platform for the development of application software, which is divided into 6 levels from hardware platform to application software.

(1) System boot layer: in order to introduce an embedded operating system, a system boot and kernel startup module must be built to complete the communication function of the host computer and the hardware platform, the initialization function of the hardware platform, and the monitoring function of the hardware platform. (2) Operating system: under the guidance of the boot program, this layer is tailored and transplanted to the embedded operating system kernel. In order to cooperate with the LCD display module for efficient 3D graphics display, it is equipped with controller-related driver software and frame buffers. (3) Driver layer: after completing the operating system level support platform, develop various hardware device drivers on it, including audio drivers, fitness equipment controllers and sensor drivers, sensor monitoring drivers, and keyboard array drivers. (4) Media library: in order to support virtual environment applications such as virtual scene construction, 3D graphics support library and multimedia support library are built on the embedded GUI. (5) Application software layer: mainly, develop embedded audio and video playback, picture browsing, virtual scene construction, and network distributed interaction applications to meet the needs of users in entertainment. (6) Graphical user interface: in the graphic display system, the user needs to interact with the

system through the embedded graphic user interface GUI, and 3D graphics also need to communicate with the hardware through it, so the user graphic interface GUI is essential. Figure 2 shows the system software structure.

4. Distributed Virtual Environment Basketball Equipment Research and Development of Embedded Systems Analysis

4.1. *Performance Analysis of Embedded System.* As shown in Table 1, it is a parameter list of fog computing, cloud computing, and edge computing. Among them, 0–3 are cloud computing, 4-5 are fog computing, and 6 are edge computing parameters. The processing capacity of the system selected in this article is 800–5000 MIPS, the unit price is 3–6 CENTS, and the broadband settings are 1000 and 2000 MB.

It can be seen from Table 2 and Figure 3 that, as the number of requests changes, the delay comparison of the three systems becomes more obvious. When the number of requests is 20, the latency of fog computing is 20 s, the latency of cloud computing IGA is 22 s, and the latency of cloud computing RRSA is 21 s, and the three are at the same level. However, when the number of requests reaches 200, the delay of fog calculation SLO is 121 s, while the delay of IGA reaches 168 s, and the delay of RRSA is 180 s, which are significantly higher than the delay of fog calculation. This shows that embedded systems based on fog computing have shorter time delays and perform better.

It can be seen from Table 3 and Figure 4 that, as the number of requests increases, the execution time of the three systems is rising, but the rate of increase is different. When the number of requests is 20, the execution time of fog calculation is 46 s, the execution time of cloud computing

TABLE 1: List of parameters for fog computing, cloud computing, and edge computing.

Resource number	Processing capacity (MIPS)	Unit price (CENT/S)	Broadband (MB)
0	5000	6	1000
1	2500	5	1000
2	2500	5	1000
3	1500	4	1000
4	1000	4	2000
5	1000	3	2000
6	800	3	1000

TABLE 2: Delay comparison of embedded system under different number of requests.

Systems/Requests	20	40	60	80	100	200
Fog-SLO	20	35	43	60	77	121
Cloud-IGA	22	36	45	63	77	168
Cloud-RRSA	21	37	49	65	79	180
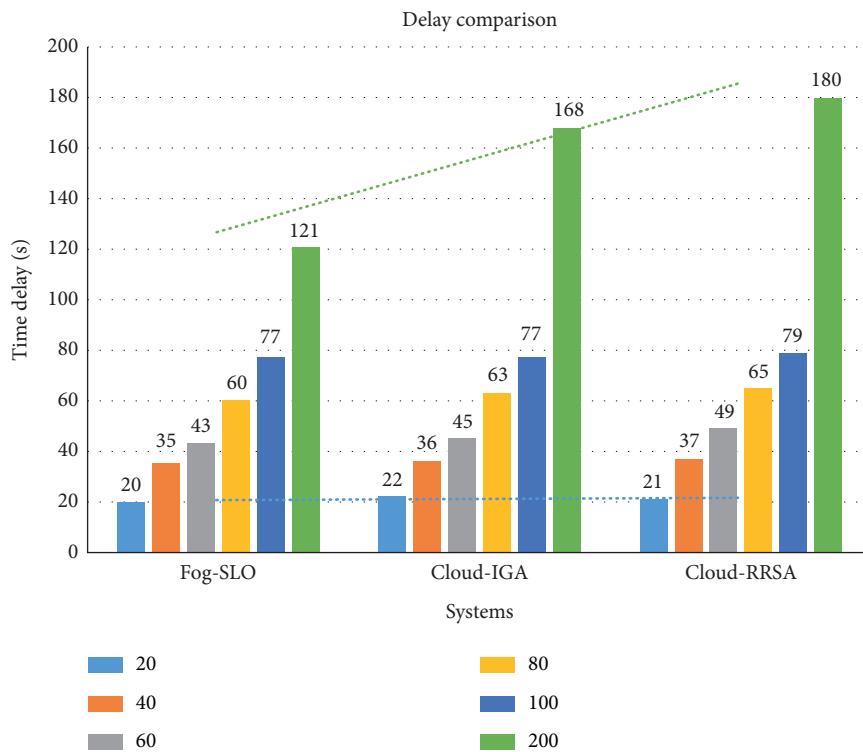
FIGURE 3: Delay comparison of the embedded system under different number of requests.

IGA is 47 s, and the execution time of RRSA is 48 s; when the number of requests is 200, the execution time of fog calculation is 200 s, and IGA is executed. The time is 246 s, and the execution time of RRSA is 247 s. It can be clearly seen that the execution time of IGA and RRSA exceeds the fog calculation, and the speed is significantly slower.

4.2. Based on the Experimental Results of Sports Equipment Distributed Virtual Environment Embedded Systems. According to the province's dynamic analysis report on economic development, selected sports equipment related data are shown in Table 4.

It can be seen from Table 4 and Figure 5 that, according to the current development trend of sports equipment, the sales of sports equipment will continue to rise in the future. In the case of treadmills, the annual demand is only 3 million units, and the sales are still increasing at an annual growth rate of 25.1%. The market growth is extremely good. The annual demand for basketball is also 1 million, and the annual market growth rate is 18.9%. If distributed virtual technology can be embedded in these sports equipment, it can better meet people's sports and relaxation needs. In the future, people's demand for embedded system sports equipment will show an exponential growth trend.

TABLE 3: Comparison of system execution time under different number of requests.

Systems/requests	20	40	60	80	100	200
Fog-SLO	46	95	146	176	180	200
Cloud-IGA	47	102	149	189	192	246
Cloud-RRSA	48	103	153	190	197	247
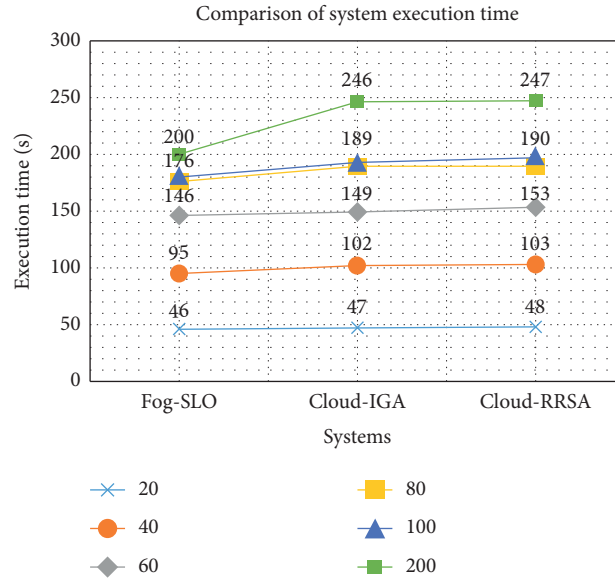
FIGURE 4: Comparison of system execution time under different number of requests.

TABLE 4: Sales of sports equipment.

Sports equipment	Demand (ten thousand)	Output (ten thousand)	Sales volume (ten thousand)	Annual market growth rate (%)
Treadmill	300	450	408	25.1
Basketball	100	180	119	18.9
Sport ware	58	129	69	5.8
Badminton	158	213	209	6.7
Table Tennis	169	187	153	4.3
Football	76	189	102	5.9
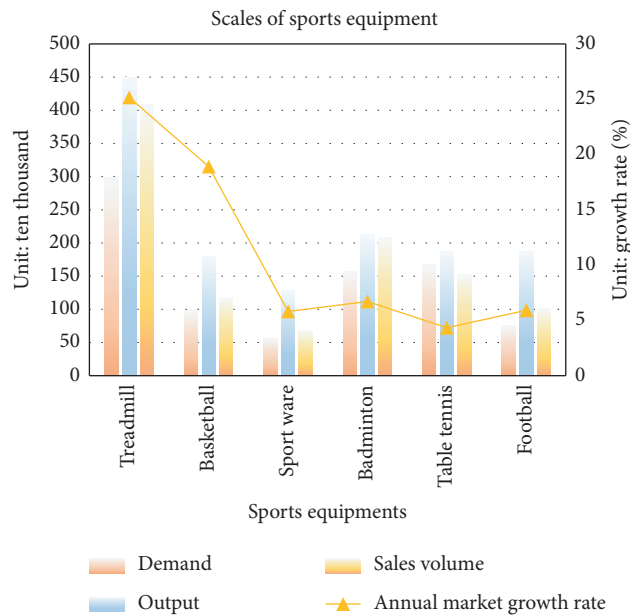
FIGURE 5: Sales of sports equipment.

TABLE 5: System optimization test.

Throughput rate	No tuning	CPU/memory	Virtio (multi-Queue)	OVS-DPDK
Big bag	1.35	1.74	2.13	2.86
Packet	0.058	0.066	0.092	0.202
Mixed bag	0.33	0.393	0.504	0.69
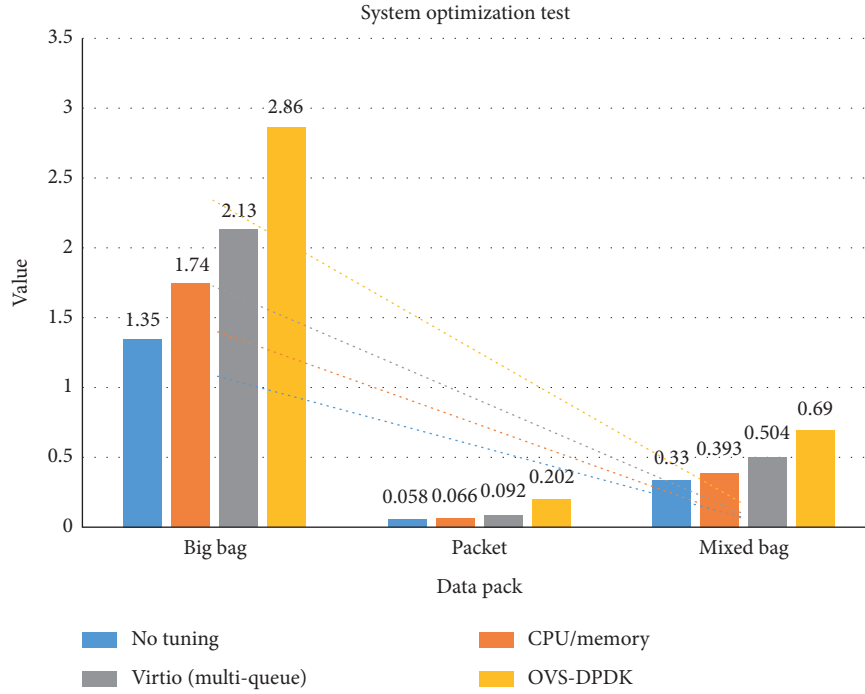
FIGURE 6: System optimization test.

TABLE 6: System function test results and analysis.

Serial number	Interactive file type	Sending time	Traditional interaction design		This paper introduces the system interaction design	
			Receiving time	Time delay (min)	Receiving time	Time delay (min)
1	Written words	14:00	14:03	3	14:01	1
2	Data	14:05	14:08	3	14:06	1
3	Written words	14:10	14:14	4	14:11	1
4	Voice	14:15	14:25	10	14:17	2
5	Voice	14:30	14:37	7	14:32	2

It can be seen from Table 5 and Figure 6 that the system optimization test is compared by observing the hardware operation of the system. When dealing with different data packets, there is a big difference between tuning and an untuned system. After tuning and processing, the embedded system shows a better operating condition and a higher throughput rate.

Through the analysis of statistical calculation principles and third-party software, the experimental results of the functional test experiment are obtained, as shown in Table 6. The data in the table show that there are varying degrees of delay in the interaction between information in embedded systems, and the more complex the interaction information, the longer the delay. After calculation, the average delay of the traditional interactive function is 5.4 min, and the average delay of the interactive function of the embedded system based on the distributed virtual environment is 1.4 min, which saves 4 min by

comparison. The experimental results show that the designed embedded system has shorter interaction delay and stronger interaction.

As can be seen from Table 7 and Figure 7, the system kernel routines are largely related to the complexity of service energy consumption. This method helps to improve the accuracy of the energy analysis and optimization of the embedded operating system kernel and effectively supports the energy consumption evaluation and optimization design of the operating system and application software.

5. Conclusion

This article mainly studies the basketball sports equipment embedded system based on the distributed virtual environment, designs the sports equipment embedded system

TABLE 7: Analysis of the relationship between system service functions and energy consumption.

Routine	Execution times	Energy consumption			
		Average value	Lowest value	Highest value	Standard deviation
Sys_getegid	25	4.99	3.52	9.51	1.70
Switch_to	110	1.24	1.08	1.78	0.16
Sys_brk	147	12.21	4.45	29.60	7.00
Sys_open	44	71.63	29.2	445.94	62.105
Sys_read	266	44.74	8.10	355.00	40.89
Tty_write	291	71.88	31.46	197.78	32.31
Do_timer	84	16.79	6.62	32.05	4.70
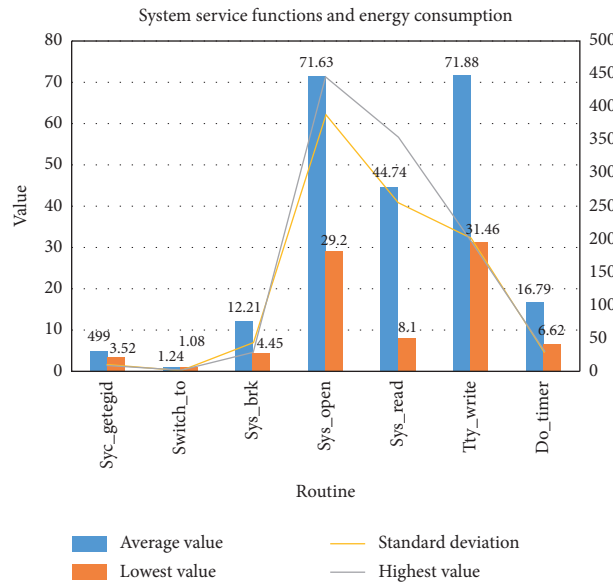
FIGURE 7: Analysis of the relationship between system service functions and energy consumption.

framework model, and divides the system software into six levels: system boot layer, operating system, drive layer, media library, application software layer, and user graphical interface. With high-end hardware and software facilities, sports equipment can better meet people's needs and improve the quality of exercise.

The innovation of this article lies in the full application of distributed virtual reality technology, the design of the client embedded frame system, and the completion of the construction of immersive and interactive virtual fitness scenes under the formation of a specific fitness virtual environment. This paper makes full use of the combination of qualitative analysis and quantitative analysis and has been fully reflected in the analysis part.

This article still has shortcomings. First, there are few combined applications of distributed virtual environments and basketball sports equipment, so there may be some practical problems in actual applications. Second, embedded systems based on distributed virtual environments are high-tech products. The price is relatively expensive, and it is difficult to provide services to the public, so it is necessary to continuously reduce costs to meet the consumption level of the public. The development and research of embedded systems for sports equipment based on distributed virtual environments is the general trend, and it can develop better and better in the future, which can not only bring more benefits to sports equipment service providers but also provide high quality to the public sports services.

Data Availability

No data were used to support this study.

Conflicts of Interest

The authors declare that they have no conflicts of interest.

Authors' Contributions

All authors have seen and approved the manuscript.

References

[1] M. E. Latoschik, F. Kern, J.-P. Stauffert, A. Bartl, M. Botsch, and J.-L. Lugrin, "Not alone here?! scalability and user experience of embodied ambient crowds in distributed social virtual reality," *IEEE Transactions on Visualization and Computer Graphics*, vol. 25, no. 5, pp. 2134–2144, 2019.

[2] V. Arthur, G. Eugenia, and L. C. Videira, "On designing and testing distributed virtual environments," *Concurrency & Computation Practice & Experience*, vol. 28, no. 12, pp. 3291–3312, 2016.

[3] D. Zeng, L. Gu, S. Guo, Z. Cheng, and S. Yu, "Joint optimization of task scheduling and image placement in fog computing supported software-defined embedded system," *IEEE Transactions on Computers*, vol. 65, no. 12, pp. 3702–3712, 2016.

[4] H. Prendinger, R. Jain, T. Imbert, J. Oliveira, R. Li, and M. Madruga, "Evaluation of 2D and 3D interest management techniques in the distributed virtual environment DiVE," *Virtual Reality*, vol. 22, no. 3, pp. 263–280, 2018.

[5] H. Chung and Y. Nah, "Effects of hypervisor on distributed big data processing in virtualized cluster environment," *KIISE Transactions on Computing Practices*, vol. 22, no. 2, pp. 89–94, 2016.

[6] E. Carlini, A. Lulli, and L. Ricci, "Model driven generation of mobility traces for distributed virtual environments with TRACE," *Concurrency and Computation: Practice and Experience*, vol. 30, no. 20, pp. e4235.1–e4235.15, 2018.

[7] W. Zhang and H. Zhou, "An optimized consistency control method and algorithm description in distributed virtual environment," *Boletin Tecnico/Technical Bulletin*, vol. 55, no. 6, pp. 412–419, 2017.

[8] P. Kolyasnikov, E. V. Nikulchev, I. Silakov, D. Llin, and A. Gusev, "Experimental evaluation of the virtual environment efficiency for distributed software development," *International Journal of Advanced Computer Science and Applications*, vol. 10, no. 5, pp. 309–316, 2019.

[9] C. Shim -Young, "Migration and replication of virtual machines distributed cloud computing environment enhanced with capabilities for wide-area," *Journal of Engineering Technology*, vol. 6, no. 2, pp. 97–109, 2016.

[10] K. Kumar and J. Thaman, "Opportunistic two virtual machines placements in distributed cloud environment," *International Journal of Grid and High Performance Computing*, vol. 12, no. 4, pp. 13–34, 2020.

[11] G. Bhatt and M. Bhavsar, "Performance analysis of local, network and distributed file systems running inside user's virtual machines in cloud environment," *Advances in Modelling and Analysis B*, vol. 61, no. 1, pp. 48–55, 2018.

[12] C. Cavanaugh, J. Mayberry, and J. Hargis, "Participation in the virtual environment of blended college courses: an activity study of student performance," *International Review of Research in Open and Distance Learning*, vol. 17, no. 3, pp. 423–432, 2016.

[13] W. Jiang, J.-J. Zheng, H.-J. Zhou, and B.-K. Zhang, "A new constraint-based virtual environment for haptic assembly training," *Advances in Engineering Software*, vol. 98, pp. 58–68, 2016.

[14] F. Pozin and M. N. M. Nawi, "The communication in industrialised building system (IBS) construction project: virtual environment," *AIP Conference Proceedings*, vol. 1891, no. 1, pp. 1–7, 2017.

[15] J. O. Pinzón Arenas, R. Jiménez Moreno, and P. C. Useche Murillo, "Faster R-CNN for object location in a virtual environment for sorting task," *International Journal of Online Engineering (iJOE)*, vol. 14, no. 7, pp. 4–14, 2018.

[16] M. A. A. Pozin, M. N. M. Nawi, M. N. A. Azman, and A. Lee, "Improving communication in managing industrialised building system (IBS) projects: virtual environment," *Malaysian Construction Research Journal*, vol. 2, no. 2, pp. 1–13, 2017.

[17] K. Stanek, O. Winther, S. Angstmann, K. H. Madsen, and H. R. Siebner, "ID 345 - "What", "When", "Whether" - the electrophysiological correlates of voluntary action in virtual environment," *Clinical Neurophysiology*, vol. 127, no. 3, p. e127, 2016.

[18] D. Kim, Y.-H. Kim, K.-H. Kim, and J.-M. Gil, "Cloud-centric and logically isolated virtual network environment based on software-defined wide area network," *Sustainability*, vol. 9, no. 12, p. 2382, 2017.

[19] T. Soyata, L. Copeland, and W. Heinzelman, "RF energy harvesting for embedded systems: a survey of tradeoffs and methodology," *IEEE Circuits and Systems Magazine*, vol. 16, no. 1, pp. 22–57, 2016.

[20] K. Wang, M. Du, D. Yang, C. Zhu, J. Shen, and Y. Zhang, "Game-theory-based active defense for intrusion detection in cyber-physical embedded systems," *ACM Transactions on Embedded Computing Systems*, vol. 16, no. 1, pp. 1–21, 2016.

[21] H. Cherupalli, R. Kumar, and J. Sartori, "Exploiting dynamic timing slack for energy efficiency in ultra-low-power embedded systems," *ACM SIGARCH Computer Architecture News*, vol. 44, no. 3, pp. 671–681, 2016.

[22] C. Moreno and S. Fischmeister, "Non-intrusive runtime monitoring through power consumption to enforce safety and security properties in embedded systems," *Formal Methods in System Design*, vol. 53, no. 1, pp. 113–137, 2018.

[23] J. D. Alvarez, J. L. Risco-Martin, and J. M. Colmenar, "Multi-objective optimization of energy consumption and execution time in a single level cache memory for embedded systems," *Journal of Systems & Software*, vol. 111, pp. 200–212, 2016.

[24] M. Ashjaei, N. Khalilzad, S. Mubeen et al., "Designing end-to-end resource reservations in predictable distributed embedded systems," *Real Time Systems*, vol. 53, no. 3, pp. 916–956, 2017.

[25] C. Bartsch, C. Villarraga, D. Stoffel, and W. Kunz, "A HW/SW cross-layer approach for determining application-redundant hardware faults in embedded systems," *Journal of Electronic Testing*, vol. 33, no. 1, pp. 77–92, 2017.

[26] Z. Czaja, "A method of self-testing of an analog circuit terminated by an ADC in electronic embedded systems controlled by microcontrollers," *Przegląd Elektrotechniczny*, vol. 1, no. 11, pp. 21–24, 2016.

Research Article

Research on Convolutional Neural Network-Based Virtual Reality Platform Framework for the Intangible Cultural Heritage Conservation of China Hainan Li Nationality: Boat-Shaped House as an Example

Xi Deng [1,2] **Il Tea Kim**,[2] **and Chong Shen**[3]

¹College of Fine Art & Design, Hainan University, Haikou, Hainan, China
²Department of Art, Art & Sports College, Chosun University, Gwangju, Republic of Korea
³State Key Lab of Marine Resource Utilization, Hainan University, Haikou, Hainan, China

Correspondence should be addressed to Il Tea Kim; itkim@chosun.ac.kr and Chong Shen; chongshen@hainanu.edu.cn

Hainan is located at the southernmost tip of China, since ancient times it has always occupied an important position on the Silk Road. Hainan culture is dominated by minority and marine cultures and has a rich intangible cultural heritage. Hainan has always been committed to the development and utilization of its wide cultural heritage, and the development direction is mainly based on live display and folk activities. In May 2020, the Chinese government announced the establishment of the Hainan Free Trade Port Policy and System, the establishment of a Hainan International Free Trade Zone, and the development of tourism, modern services, and high-tech industry. All these put forward higher requirements for the protection of Hainan's cultural heritage, not just traditional ways to protect and promote, but also to use the dividends of current scientific and technological development to keep up with the times to protect and promote. The integration of digital technology will be the development direction of cultural heritage and intangible cultural heritage. This paper enumerates and analyzes other cases and academic directions of intangible cultural heritage, combined with the present situation of intangible cultural heritage in Hainan. It also analyzes the predicament of handiwork inheritance in Hainan intangible cultural heritage, expounds the structure, humanistic connotation, and construction skills of Li nationality ship house, and summarizes the role of a novel deep learning convolutional neural network- (CNN-) based virtual reality framework of intangible cultural heritage conservation in promoting the intangible cultural heritage of traditional skills. It also puts forward the scheme and heritage conservation virtual reality content construction and provides the process of building a virtual reality platform for the intangible cultural heritage of ship-shaped houses, which as an example can be used as a reference for intangible cultural heritage researchers in other areas. At the same time, it fills the gap for the artificial intelligence-based digitization of the intangible cultural heritage.

1. Introduction

In the protection of intangible cultural heritage, the digitalization of intangible heritage has become more and more common and has now entered a mature stage in technology [1], mainly focusing on digital collection, storage, protection, database resource construction, and the use of digital technology to achieve intangible cultural heritage protection and development. The system development and application

of the digital development, protection, cultural creative products, and other aspects of cultural heritage-related technologies as virtual reality are also in a period of rapid development. China's digital research and practice is still in the stage of exploration, and there is a lack of a systematic solution to the research on the design and creativity of digital content for the public and the practicality of the communication platform. On the other hand, heritage images gathered from the Internet and sources are always blur and

of low quality. Before image processing, it is of great importance to process blur picture as input and obtain the sharp one at full resolution as output. The technique of sharpening blur image has more impact on heritage conservation. The construction of the CNNs VR platform framework is based on the research of the integration of the material cultural heritage and virtual reality technology in Hainan and South Africa. It uses deep learning image processing, computer graphics, digital animation, games design, and other digital arts and technical methods combined with the characteristics of shipbuilding technologies to design the content.

At present, China has made certain achievements in the digitization of material culture and intangible cultural heritage. The three items in Table 1 are the restoration of existing heritage, the reshaping of disappeared culture, and the AR conversion of intangible culture. The three projects are introduced, and the advantages and disadvantages of each project are analyzed.

China's effort in the protection of intangible cultural heritage has been continuously strengthened. From the social science and natural science levels, national research institutions have actively participated in the exploration and research of the protection of intangible cultural heritage. In terms of research on the fundamental issues of digitization of intangible cultural heritage, it is mainly reflected in the discussion of digitization issues such as digitization methods, digital collection, data storage, and database construction. Zhang and others [3] discussed about digital technology such as the role in the digital protection of digital collection, storage, restoration, reproduction, display, and dissemination of intangible cultural heritage. Rosa Tamborrino and Wendrich [4] proposed communication in information space in theory, where two issues of digitization of intangible cultural heritage content are discussed: information and information dissemination. Wang and Shen [5] proposed the urgency and necessity of the digitization of intangible cultural heritage. The example illustrates the ideas and methods of digital construction. Doulamis et al. [6] in their article discussed the integration of folk literature intangible cultural heritage and digital animation technology. Leimgruber [7] discussed the urgency and importance of the digital construction of art archives for the protection of nonheritage and proposed an art archive database: construction ideas in the field of digital research and development, utilization, display, communication, inheritance, and other issues. Teo [8], in his paper on "Research on Digital Modeling and Rendering Technology," mainly discusses the related digital modeling and rendering technology.

The research content of this article is divided into several aspects: (1) a brief analysis of the present situation of the intangible culture in Hainan is made and the six difficulties faced by the intangible cultural heritage are pointed out; (2) based on the shipbuilding technology of this article, three effects of virtual reality on the development of intangible cultural heritage are analyzed; (3) the status quo faced by the boat-shaped houses of the Li nationality is elaborated and the basic structure, classification, use of raw materials, and construction methods of the boat-shaped houses are analyzed in detail; (4) the system construction ideas of the deep learning CNNs virtual reality platform are analyzed, a virtual digital framework is constructed, the structural design of the virtual platform is carried out according to the characteristics of the ship-shaped house construction, and the combination of virtual reality and animation art is realized; and (5) the expected effect of the virtual reality platform is predicted and analyzed.

2. The Status Quo of the Intangible Cultural Heritage of the Li Nationality in Hainan

2.1. The Overall Status of Hainan Li People's Intangible Cultural Heritage.
Hainan Li nationality is the place where Hainan culture is concentrated. In the investigation of Li nationality, it is found that the culture of Li nationality contains the unique marine culture of Hainan and occupies an important position on the "Silk Road" of the South China Sea. In history, archaeologists discovered ancient tombs and funerary objects in the Han Dynasty in Ledong, Changjiang, Dongfang, and other places, and these places are also the places where the Li people live together [9]. By browsing the intangible cultural heritage network of Hainan Province, this paper analyzes the current situation of intangible cultural heritage resources in Hainan Province, in which the traditional spinning, dyeing, and weaving skills of the Li nationality are listed as a world-class intangible cultural heritage list. Another 12 intangible cultures are included in the national intangible cultural list, and there are 27 provincial intangible cultural heritages. Most of these intangible cultural heritages are distributed in Wuzhishan, Qiongzhong, and Baoting in the central part (Figure 1), covering 7 categories including traditional music, traditional dance, traditional drama, traditional art, traditional skills, folk customs, and others.

According to the general distribution of intangible cultural heritage in Hainan, Table 2 shows the classification of the intangible cultural heritage of Li nationality in Hainan.

2.2. The Status Quo of Li-Style Boat-Shaped Houses and the Exploration of Construction Skills

2.2.1. The Status Quo of the Boat-Shaped Houses of the Li Nationality.
With the development of society, Li villagers have gradually left their villages to make a living in big cities. The Hainan Provincial Government has built a brick house next to the original boat-shaped villages in 2010 for the sake of the modernization of Li villagers. Villager life: when I inspected the boat-shaped houses of the Li people in Hainan in 2013, Ocha Village, Dongfang City, Hainan Province, was the most well-preserved, largest, and most primitive Li village in the Li village. At that time, all but one of the residents had moved Xincun. Because the boat-shaped house is made of original materials and the construction process is relatively simple, the house will naturally collapse after three years or so without care. The original Li villages no longer exist (Figure 2).

TABLE 1: Three intangible cultural heritage digitization projects in China.

Project name	Project features	Advantages and disadvantages
Digital Dunhuang Mural Project	The project jointly carried out by the Dunhuang Research Institute and the Northwest University of the United States has collected 300 DPI precision collections of 10 dynasties, 30 caves, and 4,430 square meters of murals and established a website. You can use VR glasses to view 30 caves in a panoramic roaming form.	Advs: cross-regional communication, exquisite production, knowledge dissemination Disadvs: weak immersion, lack of interaction and fun
Digital Old Summer Palace Project	Since 1999, the team of Tsinghua University has spent 18 years reproducing the Old Summer Palace with the latest technological means such as computers and augmented reality technology. Launched a mobile APP; visitors can see the original appearance of the restored Old Summer Palace and its history through a handheld mobile device [2].	Advs: strong sense of immersion Disadvs: lack of interaction, local communication
AR Postcard	Foshan, Guangdong, China, launched a national-level intangible cultural heritage project with AR technology embedded on the basis of traditional postcards. Through digital technology, national intangible cultural heritages such as paper-cutting, wooden board new year pictures, Shiwan pottery craftsmanship, and Cantonese opera were displayed.	Advs: easy viewing and fast speed Disadvs: lack of interaction, immersion, and substitution

FIGURE 1: Approximate distribution map of the ICH of Hainan.

2.2.2. Basic Structure of the Li-Style Boat-Shaped House. The traditional bamboo and wooden structure of traditional residential buildings in the Li ethnic area of Hainan resembles a boat that has been turned upside down, so it is called a boat-shaped house. When constructing a boat-shaped house, first a rectangular ground is arranged, natural and strong trunks are used as pillars supporting the roof beams, two eaves columns about half the height of the center column are used to support the eaves beam and then the center column supports the ridge beam, the semicircular arch coupons are placed on the spine beams, and then purlins and rafters are used to form a grid on the arch coupons. Finally, the woven materials such as sunflower leaves or thatch are used as the roof. The boat-shaped house of the Li nationality belongs to stilt-style architecture (dry hurdle architecture, that is, a building that rises above the ground on a wooden (bamboo) column under frame (Baidu Encyclopedia); compared with other ethnic minority dry-style buildings, it is relatively primitive in terms of modeling and construction skills, and its biggest feature is that it does not use tenon riveting in construction. Tong 卯 (sǔnmǎo) is the main structural method of ancient Chinese architecture, furniture, and other instruments and is a connection method that uses a combination of concave and convex parts on the two components. The convex part is called tenon; the concave part is called Mao (or tenon, groove). The connections between the boat-shaped house components are almost all tied together with materials taken from wild hemp skin or rattan, and the various parts of the house are connected and fixed as a whole. The use of these plants with elastic rattan skins not only can strengthen the stability of the boat-shaped house but also play a role in resisting typhoon.

The structure of the boat-shaped house also has certain significance: there are three tall pillars in the middle of the thatched house. In the Li language, these three pillars are called "Goe," which means man. There are six relatively short columns standing on either side, called "Goding" in the Li language, which means woman. The nine pillars (pictured left) together represent the home made of men and women (Figure 3).

2.2.3. Classification of Boat-Shaped Houses of Li Nationality. The life of the Li people is relatively simple, and the function of the boat-shaped house in which the people live is not complicated. It can be divided into three types based on the function and structure: the main house, the barn, and Long Gui (Table 3).

2.2.4. Raw Materials of Boat-Shaped Houses of Li Nationality. The materials used to build the boat-shaped house are very simple, and there is no reinforced concrete, nor brick or tile. The materials used are original trees, bamboo poles that are now cut, dried thatched grass, and wild rattan. The villagers of the Li ethnic group in Hainan cut trees in July-September every year because at that time wood is clean and intact and there are few moths. Similarly, the choice of bamboo poles was also in winter. At this time, bamboo was rarely eaten by insects. The pillars and eaves of the boat-shaped house are generally made of high-quality wood, which is strong and neat. And the rafters mostly use fine-grained fruit trees, dense and resistant to moisture. Rattan and hemp skin are used as stable materials for binding, and there is no limit on the collection time. The grandpa and grandma of the Li nationality can cut down at any time. The wall is made of clay mixed with straw.

TABLE 2: Classification of the intangible cultural heritage of Li nationality.

Items	Name
Folk literature	Li folk tales
	Li congliu's song
	Li folk songs (qiongzhong li folk songs)
	Bamboo and wood instrumental music of Li nationality
	Li sai dialect long tone
Traditional dance	Li firewood dance
	Li qian ling double sword dance
	Li pound rice dance
	Li people dance together
	Li mask dance
	Li old dance
Traditional skills	Li traditionally dyed spun silk embroideries skills
	Li bark cloth-making skills
	Li bone ware-making skills
	The original pottery-making skills of Li nationality
	Li's skills of drilling wood and making fire
	Li ganlan construction skills
	Li boat-building skills
	Li rattan and bamboo weaving skills
	The craft of making single wood utensils of Li nationality
	Li jin spinning, dyeing, and embroidering tool-making skills
Traditional sports	Traditional sports and entertainment of Li nationality
Traditional medicine	Li medicine
Traditional custom	"March 3rd" festival of the Li and Miao nationalities in Hainan
	Li clothing
	Li traditional wedding
	The custom of crossing the river by Yao boat

FIGURE 2: The rapidly ruined boat-shaped house of the Li nationality (investigated in Ocha Village, Dongfang City, Hainan Province).

FIGURE 3: The pillar structure of the boat-shaped house of the Li nationality (three in the middle symbolize males and six on both sides symbolize females).

2.2.5. *Skills of Building Li-Style Boat-Shaped Houses.* It is integrated into the architectural concept that although the materials used to the craft of building a boat-shaped house are very simple, the resulting house is nevertheless original. The villagers first laid clay on the ground, poured appropriate water, and stepped on it evenly, waiting for the ground to become hard; at the same time, the carpenters of the Li nationality made logs to support the pillars of the roof beam; the old people of the Li nationality were responsible for making the pillars, pruning bamboo poles, and preparing long thatched roof.

The craftsmen built the roof into an arch to resist the typhoon and also facilitate drainage. After building the complete frame, laid the woven thatched sheet on the arched roof. These thatch pieces are about 2 meters long and 1.3 meters wide, and the thatch extends as far as possible to the ground because the rain can flow along the thatch without wetting the wall, and there is a danger of collapse. The 300 pieces of thatch are not simply stacked on the pergola, but the pergola is used as the bottom layer of the roof. After fixing the beams, according to the S-shaped trend, choose to start from the eaves on any side, overlap each two pieces of thatch first part, and then fix the precut rattan on the pergola, from left to right, and then slowly move up from the other side, from right to left, so repeat; you can complete the laying of the arched roof.

For the construction of the wall surface, first use bamboo poles and branches to build a frame and then use clay straw mixed with straw to form a wall, so that the wall of the boat-shaped house is completed (Figure 4). There are double front and rear doors on the wall and no windows. Perhaps, the traditional superstitious ghosts of Li ancestors would enter

TABLE 3: Basic types of Li boat-shaped houses.

Boat-shaped house classification	Structure and function	Icon
Main house		
Integrated single room type	Consists of living room and front porch terrace. There is no wall partition in the living room, and all the living, dining, and debris are all in one room.	
House type with separate living room and storage room	There is a clear division of labor in residential life. In simple terms, in addition to the living room, a small warehouse is added to store dry firewood, clay pots, and other items, in addition to several poultry.	
Multiroom boat-shaped house	In addition to the small warehouse, the daily living area and living area are carefully divided, including the front porch drying platform, the main room, and multiple living rooms.	
Barn	Where the villagers store grain, the barn does not directly touch the ground, and it is built with a stone pad and a certain height. It can be ventilated and protected from moisture and insects and rodents. A layer of clay and mud will be pasted inside and outside the barn walls and even the floor must be pasted. A thick layer of mud has a good sealing effect.	
Long Gui	Long Gui is generally located in a secluded place in the village. In modern times, the village is built to provide a place for love and love for married men and women. Historically speaking, Long Gui is the woman's long-term residence. According to the residence rules of the Li nationality, married women can stay in their husband's homes, and they can still live in the premarriage boudoir. Therefore, Long Gui is full of primitive romantic sex, and it also reflects that the Hainan Li culture retains the basic characteristics of the maternal clan.	
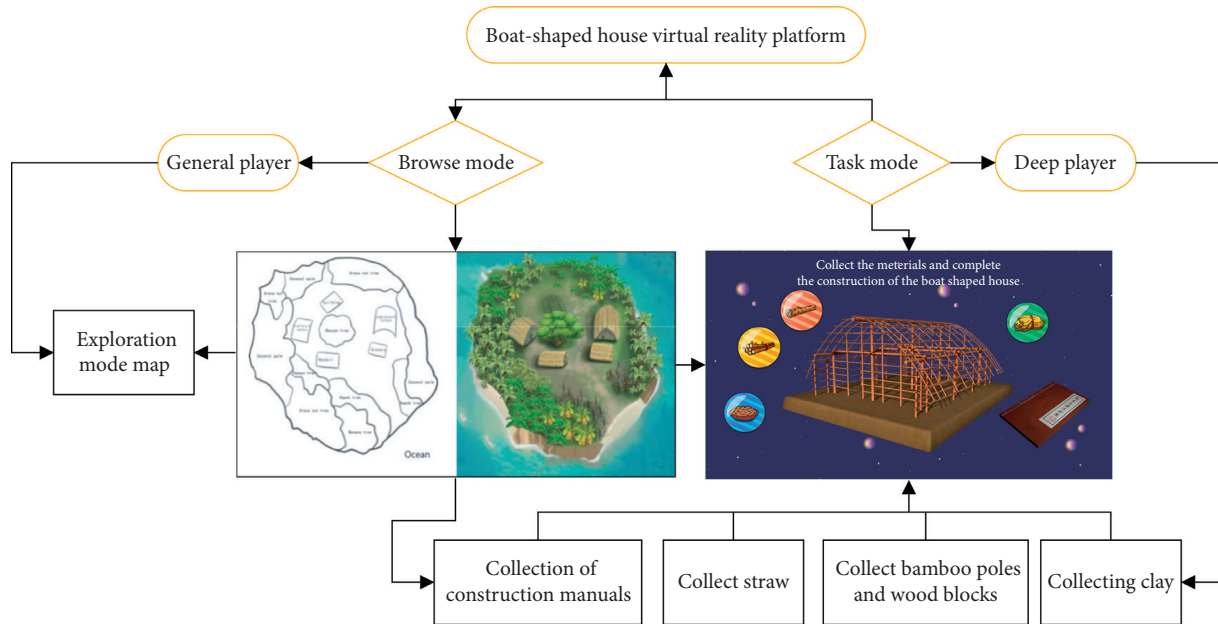
FIGURE 4: The completion model of the audience of the virtual reality platform of the boat-shaped house.

through the windows. From the perspective of modern architecture, because the boat-shaped house is built in the deep mountains, no windows are provided to prevent wind and avoid beasts. The disadvantage is that the house is dim and inconvenient for lighting and ventilation. According to the old people of the Li nationality, a boat-shaped house can

now be built in as fast as three days. Thanks to the advancement of tools and the evolution of working methods, it took months to build a boat-shaped house in the past.

2.2.6. Blurred Li-Style Boat-Shaped House Restoration. As image derived from old times and from Internets is always with low quality, for the Li culture reservations, a novel deep learning convolutional neural network- (CNN-) based virtual reality framework is introduced in this study. Blue image deconvolution is an ill-posed problem [10–13] addressed by the regularization methods. The wavelet transform [14–17] is an effective denoising method related to regularized inversion. In this study, wavelet transform is utilized to decompose and extract the low- and high-frequency information of the blurred image, which is taken as the critical step of the presented deblurring methods. However, when the process highlights the approximate portion of the image feature, the blurry image will be smoothed so that the image is distorted. Simultaneously, the overall wavelet transform will result in excessive data redundancy for the image. Thus, based on the recursive CNN, a deep recursive CNN is designed, which can eliminate or weaken the characteristics of high data redundancy and image smoothness caused by wavelet transform to remove the blur of the corrupted image. Comparing with the traditional convolution neural network in image restoration, deep recursive CNN has better performance in deblurring with fast training speed. Thereafter, a novel loss function is built to attain the best deblurring effect of the proposed method based on the L2 regularization term. The experiment results in the next section demonstrate that our method has practical applicability for image restoration with different blurs, such as the motion blur, Gaussian blur, and out-of-focus by camera.

3. Construction Scheme of Virtual Reality Platform for Building Craftsmanship of Li Nationality

3.1. The Design Concept and Structure of the Platform. Grau [18], from perspective paintings, panoramic paintings, and movies to virtual reality, "shows the extraordinary efforts made by human beings to create the maximum illusion space using various technical means in various periods of history". Li [19] realizes the development of intangible cultural heritage in the form of virtual reality. Its main purpose is to promote the local intangible cultural heritage. The use of virtual reality technology allows people to be immersed in the Li nationality environment and let people feel that they are in art space to understand the intangible heritage is the main purpose of this platform design. For different heritages, we need to set up different environmental spaces, different interaction methods, and different game main lines to adapt.

This study first collates the intangible cultural heritage of Hainan, with deep learning CNN image restoration technologies; we successfully enumerate each idea of intangible cultural heritage digitization and how to realize it, so as to form a systematic and integrated digital development framework. Boat-shaped house is used as the research object example, and the local residents were interviewed according to the construction technology of the boat-shaped house to find local materials, copy records, and simulation creation through text, images, audio, and video.

Classify and sort out the documents, pictures, audio-visual materials, [20] etc., and digitally model, restore, and classify the places and props where people live in Li villages. According to the on-the-spot investigation and survey, the boat-shaped house construction technology [21] is finally displayed to users through virtual reality animation and virtual reality interaction (Figure 5).

In the above, we saw that most virtual reality projects, such as the Digital Dunhuang Project, display cultural heritage in the form of scene roaming. The advantage of this is the freedom of display, i.e., the public can choose to visit independently, more exquisite in the picture, and handling the details more accurately and meticulously. Its shortcomings are lack of interaction with the audience, the attraction to the audience will be reduced, and the durability is insufficient. In the game, there is a concept of flow based on social experience and user perception test [22]. It is relatively difficult for players to enter the flow level, which is affected by factors such as environment, attention, control, and understanding. But at least we can provide the possibility to enter the flow state in terms of environment and operation. Based on the research on the theoretical basis of the flow of games, we added the concept of games to the virtual reality platform of the Li boat-shaped house, adding games and interaction to interactively display the intangible cultural heritage. On the platform structure, we divided into two parts according to the characteristics of the audience:

(1) For general groups who are just viewing and understanding, the platform sets up a tour mode to open as much content as possible for them to visit, so as to understand the living environment of the Li nationality; in the planning of the Li village, we divided the village into several areas: large boat-shaped house (house for family living), a barn (a house for storing grains), a long boudoir (a house where the married woman lives alone) and various tropical plant areas such as betel palm area, coconut tree area, kapok area, banana tree area, etc., topographic map). Different adventure contents are set in these areas to increase the player's fun.

(2) For those who have a certain game foundation, have more interactive needs, and have a sense of accomplishment after completing the task, we have set up some task-based contents in the system, such as looking for various materials to complete the boat-shaped house put up. Inspire the audience's flow induction through the completion of the task. In the form of village exploration, let tourists or players enter a Li village and use the guidance of the characters in our scene to find various props to build a boat-shaped house: boat-shaped house construction secrets, soil, straw, bamboo poles, and wood to
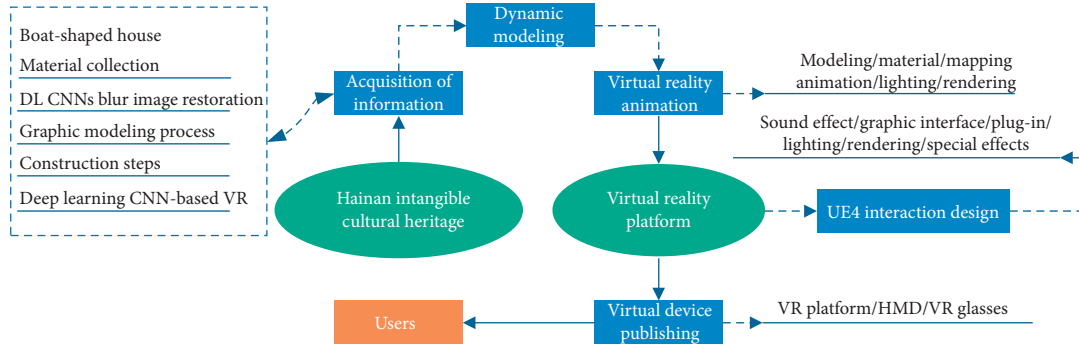
FIGURE 5: Virtual reality flowchart of Hainan intangible cultural heritage.

complete the boat-shaped house construction work. When the collection of props is complete, there will be a complete boat-shaped house construction process demonstration and an interpretation of the cultural connotation of the Li nationality contained in the boat-shaped house (Figure 4).

Through the two-way selection of content structure, the audience can understand the living environment of Li people, the dwelling place, the reason and technology of the construction of the boat-shaped house, and the living habits of Li people through virtual reality, so as to gain a deeper understanding of the Li people and their nonmaterial cultural heritage.

3.2. CNNs Deep Learning Encoder for Blur Boat-Shaped House Image Fast Convergence.

For Li nationality boat-shaped house heritage conservation, considering dataset, it is always good to do image deblurring along with a realistic dataset by clicking consecutive frames from videos which are taken by a handheld camera for getting accurate results. We use a house dataset downloaded from GitHub which consists of 2000 blur/sharp image house pairs. The dataset will be split into training and testing data. Training data contain 1500 blur/sharp images at high resolution and testing data contain 1000 blurry images. We preprocess the blur/sharp images using Keras image data generator. The images in the dataset have 256×256 pixel resolution.

Regarding deep learning, our deblurring CNNs are derived from LeNET introduced by Yann LeCun, a researcher at AT&T Bell Labs, for the purpose of recognizing handwritten digits in images [23]. The algorithmic program employed through Python enabled PyTorch. The framework has differing types of hidden layers, and CNN generally comprises input layer, convolutional layers, pooling layers, absolutely connected layers, and output layer.

The convolution layer is mainly used for feature learning. Feature learning is a collection of technologies that transform raw data into a technology that can be effectively developed by machine learning. The goal of feature learning is not to predict an observation by learning the original data but to learn the underlying structure of the data, so that other characteristics of the original data can be analyzed. Compared with the classical neural network model,

convolution neural network is no longer a limited one-dimensional input mode that can only read or receive expression, and it can better receive information to express richer two-dimensional data structure or multidimensional data structure. This two-dimensional matrix data structure is also called feature graph in the research work of CNN. Each convolution kernel can output a feature graph, and a series of input feature data are calculated by the convolution kernel, and then an output feature graph can be obtained after averaging the results. The calculation formula is as follows:

$$X_j^l = f\left(\sum_{i \in M_i}\left(X_i^{l-1}\right) * W_{ij}^l + b_j^l\right). \tag{1}$$

where M_j represents the input training set, X_j^l represents the j-th feature map of the l-th layer, X_i^{l-1} represents the i-th feature map of the $l-1$ layer, and $*$ represents the convolution.

In general, the image matrix and the convolution kernel are square matrix. If the size of the image matrix is w, the size of the convolution kernel is k, the moving step is s, and the number of zero-padding layers is p, then the size of the characteristic graph produced by convolution is given by

$$w' = \frac{w + 2p - k}{s} + 1. \tag{2}$$

The main function of the pooling layer is to aggregate the feature information of the upper layer and represent the feature information in the window as a feature. This kind of calculation is equivalent to the reduction and fusion of features, avoids network overfitting, and improves the generalization ability of the network model. Because the pooling operation only extracts the main feature information in the pooling domain, some of the information will be lost more or less. The larger the sliding step of the pooling window, the more information will be lost. The calculation formula of pooling is shown as follows:

$$y = \text{pool}\left(x_{i,j}\right), \quad i, j \in p, \tag{3}$$

where x_{ij} represents the elements in the pooling area p in the input of the pooling layer and pool() represents the pooling operation, in which pooling operation generally chooses the maximum pooling or average pooling, that is, the maximum

or average value in the upper output characteristic graph in the pooling window is taken as the final output result.

The mode of connection of neurons in the fully connected layer belongs to the form of dense connection, that is, the fully connected neurons are connected to each neuron in front of them. It is generally located at the top of the convolution neural network structure. Its function is to abstract the output features of the front layer, and this abstract expression is the whole of the features. The expression of the full connection layer is shown as follows:

$$h(x) = \delta\left(W^T x\right) = \delta\left(\sum_{i=1}^{n} W_i x_i + b\right), \quad (4)$$

where x_i is the input, $h(x)$ is the output value of the fully connected operation, δ is the activation function, W_i is the weight of the i parameter in the fully connected layer, b is the offset in the fully connected layer, and n represents the number of parameters in the fully connected layer.

$$\delta_j^{(l)} = \frac{\partial J}{\partial z_j^{(l)}} = \frac{\partial J}{\partial a_j^{(l)}} \frac{\partial a_j^{(l)}}{\partial z_j^{(l)}} = \beta_j^{l+1}\left(f'\left(z_j^{(l)}\right) \cdot \mathrm{up}\left(\delta_j^{(l+1)}\right)\right). \quad (5)$$

In the process of learning and training the convolutional neural network, the whole network carries out feature extraction through forward propagation, and then the whole network modifies and adjusts the weights in the network structure through backpropagation.

The network parameters W and b in forward propagation are obtained through training. Suppose there is a training set of m elements $(x^{(1)} y^{(1)}), \ldots, (x^{(m)}, y^{(m)})$. Then, for a single training sample x through the multilayer neural network, the output is $h_{W,b}(X)$. Its loss function $J(W, b, x, y)$ is given by

$$J(W, b, x, y) = \frac{1}{2}\left\|h_{W,b}(x)\right\|^2. \quad (6)$$

For m elements, the total loss function is defined as follows:

$$J(W, b) = \left[\frac{1}{m}\sum_{i=1}^{m} J\left(W, b, x^{(i)}, y^{(i)}\right)\right] + \frac{\lambda}{2}\sum_{l=1}^{n_l-1}\sum_{i=1}^{s_{l+1}}\sum_{j=1}^{s_l}\left(W_{ij}^l\right)^2, \quad (7)$$

where n_l is the number of layers and s_l is the number of nodes in the l-th layer. The first term in the above formula is the average sum of squares of the squared error term, and the second term is the weight attenuation term. Its purpose is to prevent overfitting. The coefficient λ is mainly to adjust the weight ratio of the two.

The training sample (x, y) is input into DCNN and the corresponding actual output O is calculated and its expression is given by

$$O = F_n\left(\cdots\left(F_2\left(F_1\left(xW_1\right)W_2\cdots\right)W_n\right)\right), \quad (8)$$

where F can be expressed as

$$x_j^l = f\left(u^l\right) = \frac{1}{1 + e^{-u}}, \\ u^l = \sum_{i \in M_j} x_j^{l-1} \cdot w_{ij}^l + b_j^l, \quad (9)$$

where l is the convolution layer and w and b are the convolution kernel and bias, respectively. The downsampling layer pooling formula is given by

$$x_j^{l+1} = f\left(\beta_j^{l+1}, \mathrm{down}\left(x_j^l\right) + b_j^{l+1}\right). \quad (10)$$

Among them, down $(\cdot)$ is the downsampling function and β and b are the multiplicative and additive biases, respectively.

The main purpose of neural network training is to make the objective function $J(W, b)$ with independent variables W and b gradually decrease. The neural network uses the gradient descent method to update W and b, and the iteration direction is taken as the negative gradient direction, namely, $J(W, b)$. The calculation formula is

$$W_{ij}^{(l)} = W_{ij}^{(l)} - \eta\frac{\partial J(W, b)}{\partial W_j^{(l)}} = W_{ij}^{(l)} - \alpha\left(\alpha_j^{(l)}, \delta_i^{(l+1)}\right), \quad (11)$$

$$b_i^{(l)} = b_i^{(l)} - \eta\frac{\partial J(W, b)}{\partial b_i^{(l)}} = b_i^{(l)} - \alpha\delta_j^{(l+1)},$$

where η is the learning efficiency; $i = 1, 2, \ldots s_{l+1}$; $j = 1, 2, \ldots s_l$; the residual calculation formula of the activation value is given by

$$\delta_i^{(n_l)} = \frac{\partial J(W, b; x, y)}{\partial z_i^{(n_l)}} = -\left(y_i - a_i^{(n_l)}\right) \cdot f'\left(z_i^{(n_l)}\right), \quad (12)$$

$$z_i^{(n_l)} = \sum_{k=1}^{s_l} W_{ik}^{(n_l-1)} a_k^{(n_l-1)} + b_i^{(n_l-1)}.$$

Among them,

$$a_i^{(n_l)} = f'\left(z_i^{(n_l)}\right). \quad (13)$$

The formula for calculating the residual error of the i-th node in the l-th layer is

$$\delta_i^{(l)} = \left(\sum_{j=1}^{s_{l+1}} W_{ji}^{(l)} \delta_j^{(l+1)} f'\left(z_i^{(l)}\right)\right). \quad (14)$$

In the process of forward operation, each layer of the convolution neural network will perform different functions. In the convolution layer, the preprocessed sample data are convoluted with the corresponding convolution kernel to get the characteristic graph. The formula for calculating the weight update of the convolution layer, such as formula (1), is related to whether the fully connected layer or the lower sampling layer is connected behind it. If it is followed by the fully connected layer, it is necessary to know the error sensitive term $\delta_j^{(l)}$ of the fully connected layer, and its sensitive error term adopts a gradient descent algorithm

similar to that of the BP network. If the connector behind the convolution layer uses the layer, because the error sensitive term of the convolution layer 2 needs to be obtained through calculation, the neural network researchers usually perform *UnPooling* operations in the lower sampling layer of layer $l + 1$:

$$\frac{\partial J}{\partial k_{ij}^{(l)}} = \frac{\partial J}{\partial z_j^{(l)}} \frac{\partial z_j^{(l)}}{\partial k_{ij}^{(l)}} = \sum_{u,v} \left(\delta_j^{(l)}\right)_{u,v} \left(p_i^{l-1}\right)_{u,v},$$

$$\frac{\partial J}{\partial b_j^{(l)}} = \frac{\partial J}{\partial z_j^{(l)}} \frac{\partial z_j^{(l)}}{\partial b_j^{(l)}} = \sum_{u,v} \left(\delta_j^{(l)}\right)_{u,v}. \tag{15}$$

The $\left(a_{i}^{l-1}\right)_{u,v}$ here is the block convoluted with $z_j^{(l)}$ selected in $a_i^{(l-1)}$ in order to get the position element of (u, v) of $k_{ij}^{(l)}$.

Formula (16) represents the loss function of a picture, where i represents the indication of the anchor in the mini-batch and the target detecting probability. Assuming that the anchor is a positive label, the predicted probability of GT is positive. Assuming that the anchor is a negative label, the predicted probability of GT is 0. Formula (17) represents the log loss function of the target type and the nontarget type. In formula (18), R represents the stable performance of the loss function in the Fast R-CNN algorithm and use formula (19) to describe the following:

$$L(pi, ti) = \frac{1}{N_{\text{cls}}} \sum_i L_{\text{cls}}(pi, pi^*) + \lambda \frac{1}{N_{\text{reg}}} \sum_i pi^* L_{\text{reg}}(ti, ti^*), \tag{16}$$

$$L_{\text{cls}}(pi, pi^*) = -\log[pi^* pi + (1 - pi^*)(1 - pi)], \tag{17}$$

$$L_{\text{reg}}(ti, ti^*) = R(ti - ti^*), \tag{18}$$

$$\text{smooth}_{L1}(x) = \begin{cases} 0.5x^2, & \text{if} |x| < 1, \\ |x| - 0.5, & \text{otherwise.} \end{cases} \tag{19}$$

Linear transformation: only normalizing the input may change the original characteristics or distribution of the input. For example, adding a batch normalization algorithm to the sigmoid function may change the input from nonlinear to linear. In order to solve this problem, the learnable parameter gain γ and bias β can be used to fit the original distribution:

$$y^k = \gamma^k \cdot x^* + \beta^k. \tag{20}$$

When $y^k = \text{Var}[x^k]$ and $\beta^k = E[x^k]$, theoretically the same distribution as the input can be obtained. At the same time, BN allows a higher learning rate. Generally speaking, a larger learning rate will increase the size of the parameters when updating, which may cause the model to explode. However, after using the BN algorithm, the backward propagation of the network layer is not affected by the scale of the parameters, so it has no effect on *Jacobian* and gradient propagation, that is,

$$\frac{\partial B \, N(Wu)}{\partial u} = \frac{\partial B \, N((aW)u)}{\partial u},$$

$$\frac{\partial B \, N((aW)u)}{\partial a \, W} = \frac{1}{a} \frac{\partial B \, N(Wu)}{\partial W}. \tag{21}$$

It can be seen from the equation that the gradient decreases when the weight w increases. Weight normalization (WN) chooses to rewrite the parameters of the weight vector W of the neural network. The parameterized weights improve the optimal condition to accelerate convergence. It is inspired by the batch normalization algorithm, but it is not like batch normalization. The unified algorithm also relies on the batch size, does not add noise to the gradient, and has a small amount of calculation. Weight normalization is successfully used in LSTM and noise-sensitive models such as reinforcement learning and generative models. The operation formula for normalizing the weight W of the deep learning network is as follows:

$$w = \frac{g}{\|v\|} v. \tag{22}$$

In order to solve the internal covariance change (ICS), another idea is to fix the mean and variance of each layer output, that is, the layer normalization algorithm (layer normalization, LN). The layer normalization algorithm uses the mean and variance of each sample to normalize the input. LN operates on a single sample and can be applied to small batches and RNNs. LN and BN have the same form, but different normalization methods. The difference between layer normalization and batch normalization algorithms is only in the way of obtaining statistical values. The following formula is the calculation method of mean and variance in the layer normalization algorithm, and H represents the number of hidden units in the layer.

$$u^l = \frac{1}{H} \sum_{i=1}^{H} a_i^l \sigma^l = \sqrt{\frac{1}{H} \sum_{i=1}^{H} \left(a_i^l - u^l\right)^2}. \tag{23}$$

For a test sample x, the batch normalization operation in the final test stage is as follows:

$$y = \frac{\gamma}{\sqrt{\text{Var}[x] + \varepsilon}} \cdot x + \left(\beta - \frac{\gamma E[x]}{\sqrt{\text{Var}[x] + \varepsilon}}\right). \tag{24}$$

Here, in convolution and pooling layers, ReLU is employed as activation function. Figure 3 illustrates our data flow algorithm based on LeNET. The input is a 256×256 image, and the output is the predicted image after deblurring deep learning (Figure 6). In the neural network of Figure 6, its hidden layer consists of convolution layer, pooling layer, and full connection layer. The blurred image is first processed by the convolution layer. In the convolution layer, each neuron in this layer is connected to the corresponding local receptive domain of the upper layer, and the local receptive domain features of the blurred image are extracted by filter and nonlinear transformation. Then, the features obtained from the convolution layer are pooled. In the pooling layer, the dimension of the fuzzy image extracted
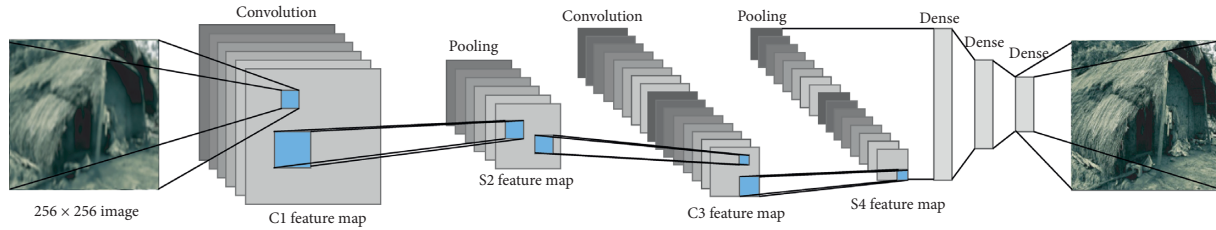
FIGURE 6: Data flow algorithm with the input of a 256×256 house blur image.

from the convolution layer is reduced, and the antidistortion ability of the model is increased at the same time. Then, the feature of the picture goes through the full connection layer to the last output layer, and the output layer mainly classifies and outputs the features obtained from the full connection layer, and finally, the corresponding clear picture can be output.

The convolution process operates on signals or pictures during which one is taken as sign or image, and also the alternative referred to as the kernel is taken as a filter on the input image, manufacturing an output image. It takes 2 pictures as input and produces a 3rd as output. In common man terms, the sign is taken and a filter is applied over it. This filter multiplies the sign with the kernel to induce the changed signal. In the case of image process, the kernel slides over the entire image so it changes the worth of every element of the image.

For the deep learning CNNs image trainings, the pooling process is a sample-based discretization method. Pooling is employed to down sample an input image, reducing its spatiality and leaving assumptions to be created regarding options contained within the subregions binned. There are unremarkable 2 varieties of pooling referred to as group and min pooling. Group pooling is defined as the substitution of the complete sample with the most prices from the chosen region and min pooling is defined as the substitution of the complete sample with the minimum price from the chosen region. Thus, our deep learning CNN is largely a deep LeNET that consists of hidden layers having convolution and pooling functions in addition to the activation function ReLU. Flattening is a straightforward step which straightens the element map put away in succession of numbers. This permits data to turn into the info layer of a manmade neural system for additional handling. The fully connected layer can be a customary multilayer perception. It utilizes grouping in the yield layer. Characterization is typically a softmax initiation work completely associated implies that every neuron in the past layer interfaces with every neuron. Softmax gets values between zero and one and adds them to one (100%). Softmax takes a vector of execution scores into a vector of qualities between zero and one. Dropout layer in deep learning is a technique to overcome the problem of overfitting. The dropout method takes a float number between 0 and 1. This value indicates ignoring a certain set of neurons while training to avoid overfitting. Batch size is simply how many training examples were taken for one forward and backward pass. But the increase in batch size makes the memory full and it takes more time for the process to complete.

The activation function in the convolution neural network is mainly used to nonlinearly transform the output results of each layer in the convolution network, so that the network model has a variety of nonlinear expression capabilities. Common activation functions are sigmoid, tanh, and ReLU. The sigmoid function is also called the *logistic* function, and each neuron, node, or activation entered is scaled to a value between 0 and 1, which is defined as follows:

$$f(x) = \frac{1}{1 + e^{-x}}. \tag{25}$$

Sigmoid is a smooth ladder function, which mainly has the following defects:

(1) It may cause the gradient to disappear when the gradient is backpropagated

(2) The analytical formula contains power operation, which is time-consuming to solve by computer

(3) The sensitive interval of the function is short, and it is not symmetrical about the center of the origin

The tanh function is used in the neural network after the sigmoid function, which is defined as follows:

$$\tanh(x) = \frac{e^x - e^{-x}}{e^x + e^{-x}}. \tag{26}$$

The effect of tanh function is very good when the feature difference is large, and the feature effect will be continuously expanded in the process of network propagation. The difference from sigmoid is that the origin is centrally symmetrical, but there is still nothing we can do about the problem of gradient disappearance. ReLU function can solve the gradient dissipation problem of backpropagation algorithm in optimizing the deep neural network to a great extent.

ReLU is the corrected linear measure that uses activation function. It gives zero for any negative pixel value; similarly, it gives the same value for any positive pixel value and is formulated as follows:

$$f(x) = \max(0, x), \tag{27}$$

where $f(x)$ is a function.

The ReLU function is actually a piecewise linear function, which turns all the negative values into zero while the positive values remain the same, and this operation is called unilateral suppression. It is precisely because of this unilateral inhibition that the neurons in the neural network also have sparse activation. The sparse model realized by ReLU can better mine the relevant features and fit the training data.

When the ReLU activation function is backpropagated, the gradient can be avoided.

Compared with other activation functions, ReLU has the following advantages: for linear functions, ReLU is more expressive, especially in deep networks; for deep networks, the gradient disappears easily when sigmoid functions are backpropagated. For the nonlinear function, because the gradient of the nonnegative interval of ReLU is constant, there is no problem of gradient disappearance, it keeps the convergence rate of the model in a stable state, and compared with sigmoid activation function and tanh activation function, the derivation of ReLU activation function is simple, which can reduce a lot of computation. Therefore, the ReLU function is used as the activation function of the convolution neural network in the experiment.

Hyperparameter selection such as training epoch is of great importance to produce improved image results. Thus, epoch number is the forward and backward pass on all the training data or simply completes an iteration. We also integrate hyperparameter optimization process using Ray tune for pruning hyperparameters including batch size, data count, and epoch. In the experiments, the images are loaded and converted into an array of pixels. The loaded images are sent through an encoder wherever convolution and pooling in addition to ReLU activation function are applied and the image is downsampled. The original house image can be converted back to the previous size in the decoder section. The model is compiled and fitted by shaping epochs and the learning rate is reduced. Intensive training and verification are also carried out to test our implemented LeNET CNNs algorithm, In Figure 7, we present deblurring training results with different metrics for measuring the changes in input blur house images.

3.3. The Graphical Modeling Process of the Boat-Shaped House.

After the restoration of blur and old images, virtual reality techniques are used through computer simulation to generate a three-dimensional space, providing users with visual, auditory, tactile, and other sensory simulations, so that users can observe things in the three-dimensional space in an immersive and timely manner without restrictions. It includes real-time 3D computer graphics technology, wide-angle (wide-field) stereoscopic display technology, tracking technology for user's head, eyes, and hands, as well as tactile feedback, stereo, network transmission, voice input, output technology, etc. [24].

The modeling of the hull-shaped house used the C4D polygon modeling method, which basically restored the original appearance of the hull-shaped house. Using polygon modeling not only helps to control the number of fundamentals of the hull model but also can create many details required for the target effect. The boat-shaped house is mainly divided into the modeling of walls, columns, windows, wooden doors, roofs, and floors. In addition to the pillars and roof structure using the scaling and extrusion of the columns to meet the requirements, the walls and floors are all through

Figure 7: Training results after 20 epochs, 40 epochs, 60 epochs, 80 epochs, and 100 epochs.

chamfer. It is handled by a smooth cube, the windows and doors are correspondingly spaced out on the wall, and then the built model has "mosaic" inside. Try to make the boat-shaped house model as a whole natural and historical house.

The use of virtual reality technology is to enable the audience to experience the construction process of the boat-shaped house even if they are not in the Li village. The UE4 engine is used in virtual interaction production. UE4 is a game engine developed by Epic Games. Game engines are the core components of editable computer game systems or interactive real-time image applications that have been written. These systems provide game designers with a variety of tools needed to write games, and the aim is to enable game designers to make game programs easily and quickly without having to start from scratch. UE4 engine is widely used in 3D modeling rendering and game development. Through the restoration of the three-dimensional animation model and the virtual interactive production of the virtual UE4 artificial intelligence engine, the construction process of the boat-shaped house is shown in Figure 8.

Unreal Engine is the core of virtual reality platform construction and the best choice for exploring VR technology. The production process such as 3D modeling and animation demonstration is for them. The ship model is imported into UE4, lighting and environmental atmosphere are adjusted, and then the operation blueprint is added to achieve interaction. During the production, real-time rendering based on Unreal Engine can be checked at any time. First, we loaded the VR device HTC + VIVE to UE4 and then checked the effect of virtual Li village through the SteamVR plug-in, and secondly, we created a game model, then created a new Pawn to set the headset to control handle, and added the camera and handle controller. Through the combination of a series of computers and VR technology, the virtual Li Village can achieve the initial expected effect in the engine. More importantly, the boat-shaped house construction skills can be fully demonstrated. There are already built and being built in the virtual Li Village. The boat-shaped house is surrounded by some tropical plants such as kapok, coconut tree, banyan tree, and jackfruit tree, as well as beautiful background music of flying butterflies, and the original ecological scene is in our eyes (Figure 9).

Construction of boat-shaped house structure

The structure was fixed with wild bast or rattan

Using fine-grained fruit trees to build content structure columns

Fixed with wild bast or rattan

Horizontal construction with cane

Vertical construction with bamboo

Making wall with clay mixed with straw

Production of doors and windows

300 pieces of thatch were laid on the roof according to the S-shaped trend

Complete the building of boat house in virtual reality

FIGURE 8: Construction process of the boat-shaped house in virtual reality platform.

FIGURE 9: Virtual Li Village display effect in UE4.

4. Virtual Reality Is an Effective Way to Spread the Boat-Shaped Houses of the Li Nationality

In 1965, Ivan Edward Sutherland (Ivan Edward Sutherland, May 16, 1938) proposed the basic scheme of virtual reality technology, known as the father of computer graphics. In the 1980s, digital technology was recognized and applied to business. In the 1990s, digital technology has begun to penetrate education, medical, industrial, and service industries. The emergence of networks has accelerated the development of digital technology. By the end of the 21st century, virtual reality technology has been developed rapidly and shipped to all walks of life. Due to the bottleneck of network speed and the relative lack of content, there is currently a downward trend, but after 5G will usher in a spring, because of 5G's it appears that although the virtual the network speed is no longer a concern but the VR production still will face the lack of content. How to use

virtual reality technology to bring more convenience to our life, culture, art, or entertainment will be what we need for further research and development.

The application of virtual reality technology and the protection of intangible cultural heritage can add many places that have been lost, weakened, and alienated in the virtual environment, as well as environmental factors that disappeared due to natural environment and social changes; it will also help record and restore the original appearance of the material cultural heritage. Virtual reality technology to protect intangible cultural heritage has the characteristics of strong spread and wide coverage. Digitalized intangible cultural heritage through virtual reality technology can be spread on the network at high speed and convenience. This way breaks the limitation of time and space. By making the content of intangible cultural heritage in a digital museum and searching through virtual reality devices, we can experience and share content through the network. In the era of 5G networks, there will be no more obstacles to the spread of virtual reality content.

Hainan has beautiful scenery and is very suitable for the development of tourism culture. During the development process, it is particularly important to display and promote the intangible cultural heritage. The tourism culture of Hainan is currently limited to the display of tourists. Tourists are mainly visiting, lacking initiative and interaction, and unable to understand the deep cultural connotation. The combination of virtual reality, historical and cultural resources, and the humanistic spirit allows tourists to actively explore and develop the mysteries of culture and inspire visitors with virtual scene construction, virtual interactive scene settings, virtual character interaction, and virtual historical events. Through the development of the abovementioned virtual reality on the building skills of the Li boat-shaped house, it can play three roles in the development of this intangible cultural heritage:

(1) Simulation of shipbuilding technology

Simulation refers to the technology of using the virtual model system to reproduce the real model system and study the actual model in existence or design through the experiment of the virtual model. Simulation maximizes the virtual Li Village tour system through VR technology. This article confirms the inevitability of the existence of Li Village from the construction skills and humanistic meaning of the boat-shaped house. The construction of the boat-shaped house is an indispensable traditional skill of Li Village. Through the field survey of the Li people, the location, material selection, and construction methods of the boat-shaped house are studied to improve the accuracy of the simulation design. Starting from meeting the requirements of digital protection and inheritance of boat-shaped house skills, this simulation successfully demonstrated the establishment of a three-dimensional boat-shaped house model. By establishing a three-dimensional

virtual reality platform and various computer functions, the virtual interaction of boat-shaped house-building skills was realized. The role of the simulation of the boat-shaped house is to use VR technology to restore the real Li village and the boat-shaped house construction scene. Experiencers can actually see the excellent traditional skills of the Hainan Li people and the environment of the life of the Li people by wearing VR glasses or head-mounted displays.

(2) Broadening the transmission of traditional handicraft skills

The people of the Li ethnic group in Hainan are the key to the long-term life of the boat-shaped house-building skills and the guardian of the inheritance of traditional skills. The development of modern society has forced the people of the Li nationality to accept a more advanced life, but the ancestors of the Li nationality who mastered the technology wanted to pass on the craft of building a boat-shaped house to the new generation based on their respect for their ancestors. But in today's era of modernization development, fewer and fewer young people of the Li nationality are willing to learn the skills of building a boat-shaped house. In terms of inheriting handicraft skills, in order to avoid the demise of craftsmanship, the building techniques of boat-shaped houses have been included in the national traditional handcraft intangible cultural heritage.

The application and research of VR technology provide a new way for the protection and dissemination of the digitalization of shipbuilding technology. As mentioned above, one of the difficulties in inheriting intangible cultural heritage is the lack of inheritors. Through the digitalization of VR technology, the problem of inheritors can be solved in the following ways: (1) The intangible cultural heritage, as an excellent folk culture in Hainan, is combined with local teaching, combining traditional manual skills and VR technology, with the curiosity of VR technology. Cultivate students' sense of protection and inheritance responsibility for Hainan's traditional handicrafts. (2) The development of the museum has also begun to combine with digital technology. Under the background of "Internet +" and "big data," the museum fully utilizes the characteristics of high openness and interactivity of network transmission, and the establishment of a VR display area to provide simulated interaction has also attracted more young people concerned about cultural heritage. (3) With the popularization of mobile terminals in modern life, mobile phones have become an indispensable part of our lives, and the popularity of mobile media such as mobile phones provides a good communication channel for digital content. The digital traditional technology protection system based on VR technology is packaged and output as a mobile terminal. People can use the

remote sensing technology of the mobile terminal to experience the simulation system. They can also be equipped with higher Google VR glasses or other brands of VR sprites to obtain a far better experience; these methods are exactly what young people love and are receiving.

In summary, VR technology brings a greater width than traditional media for the inheritance and transmission of traditional manual skills. The general public can also actively participate in the inheritance and dissemination of traditional manual skills while enjoying the joy brought by VR technology.

(3) Optimize the effect of immersive interactive tour

Interaction defines the content and structure of communication between two or more interacting individuals and is divided into visual interaction and experience interaction. Traditional sensory experience interactions mostly appear in museums and game malls. Through some programs and interactive commands for audiovisual media, the experiencer can interact with the work through language commands and click on the display, and body language and other actions then feedback the results through the display. With the rapid development of technology, the emerging immersive interaction has also emerged where most of them are used in new media art exhibitions. Although participating in it will give people a sense of physical and mental pleasure, setting up the exhibition is time-consuming and laborious, and it will consume a lot of materials. The VR technology can make the digital tour system real-time interaction, thus forming a special art form that integrates experience, psychology, immersion, and virtual communication.

The boat-shaped house construction of the Li Village tour system is taken as an example in this study; VR technology is used to allow the experiencer to navigate into a virtual world parallel to real life through the head-mounted VR glasses anywhere. In order to allow the experiencer to feel both real and different from the real world, when constructing the virtual world of Li Village, many interactive places were set up. First of all, we can use the VR video to play an example of boat-shaped house construction. Experiencers can also experience the complete process of building a boat-shaped house by manipulating the VR handle to experience the charm of traditional craftsmanship. VR technology breaks the traditional way of experience interaction, allows the experiencer to integrate into it, and brings him an immersive experience, giving people a wonderful sense of space, accompanied by auditory elements such as music and environmental sound effects with Li nationality. The controller can directly interact with the virtual world around him.

5. Conclusion

Intangible cultural heritage has encountered difficulties due to social development and some of its own shortcomings. It is precisely because of the development of social technology that we have seen more possibilities. The popularity of the Internet and the maturity of multimedia technology have broadened the digital development direction of intangible cultural heritage. Thomas Peters (Thomas Peters is the most prestigious master of management in the United States. He co-authored "The Pursuit of Excellence" with Robert Waterman Jr. and later with Nancy Austin. "Aim to Success") said the distance has disappeared, either innovation or death. It means that the crisis or danger of life is approaching us step by step, and we have to wait to die if we do not reform or innovate. The innovation in the digital protection of cultural heritage seems urgent. Although this is his opinion on management, it is also the choice facing intangible cultural heritage. The innovation of intangible cultural heritage should be combined with the development direction of each region to make distinctive innovations. The development of intangible culture in Hainan should be combined with tourism culture. While attracting a large number of tourists to experience the natural scenery in Hainan, it is necessary to show the humanistic connotation of Hainan. Intangible culture can be combined with the development of online digital content and tourism to produce some digital products based on Hainan attractions. Through the Li boat model house project, the intangible cultural heritage of Dongfang City in Hainan Province which is boat-shaped has been inspected, researched, and summarized. According to the characteristics of the tourism of Dongfang City, virtual reality is produced. The nonlegacy game can not only save and spread the boat-shaped house but also promote the tourism of Dongfang City. Therefore, through the production of nonlegacy content using virtual reality technology, we can combine virtual reality game products with animation peripheral cultural and creative products in the future and promote them online and offline at the same time.

First is to introduce virtual reality content products into museums. Modern museums can not only be limited to traditional physical display methods. They can use digital technology to narrow the distance between the audience and the history of cultural relics. They can also use remote viewing methods to make virtual reality enhance the audience three-dimensional perception of historical relics and the world in history can "experience" all the historical events that have happened. It is also possible to set up a feedback mechanism for the audience and timely revise the defective places to give the audience a better perception experience.

Second, an intangible cultural heritage entertainment experience hall was established. The intangible cultural heritage has a sense of distance from the modern youth because of the historical information it carries. Through the development of virtual reality games and animation products, the distance between history and reality is eliminated. Let the intangible cultural heritage come out of the museum, and set up an entertainment experience hall featuring the intangible cultural heritage, which will be used to experience games and display and sell related animation, cultural, and creative products. This entertainment experience hall can be combined with tourist attractions and targeted to set up

entertainment experience halls at various tourist attractions to enhance the fun of tourism.

Third is to establish an online virtual reality showroom, through the promotion of pages and online stores, through the current mobile media, online platforms, WeChat, Facebook, Kakao, YouTube, etc., online display, and promotion.

Through the concrete examples of the construction of the deep learning CNN-based virtual reality platform of the Li boat-shaped house in the above paper and the constructive analysis of market promotion, this analysis has laid the foundation for further research on how to conserve and integrate intangible cultural heritage with digital technology through our VR platform. The above analysis is a proposal for how to strengthen the barrier-free communication between intangible culture and people, which also gives us a deeper consideration of why the content generated by human spiritual civilization will gradually disappear and a deeper consideration of how to strengthen civilization communicated with the modern to reduce barriers.

Data Availability

No data were used to support this study.

Conflicts of Interest

The authors declare that they have no conflicts of interest.

Acknowledgments

References

[1] Z. Zhao, "Digital protection method of intangible cultural heritage based on augmented reality technology," in *Proceedings of the 2017 International Conference on Robots & Intelligent System (ICRIS)*, October 2017.

[2] J. Guo, Y. Wang, J. Chen et al., "Markerless tracking for augmented reality applied in reconstruction of Yuanmingyuan archaeological site," in *Proceedings of the 2009 11th IEEE International Conference on Computer-Aided Design and Computer Graphics*, Huangshan, China, 2009.

[3] Y. Zhang, M. Han, and W. Chen, "The strategy of digital scenic area planning from the perspective of intangible cultural heritage protection," *EURASIP Journal on Image and Video Processing*, vol. 2018, no. 1, 2018.

[4] R. Tamborrino and W. Wendrich, "Cultural heritage in context: the temples of Nubia, digital technologies and the future of conservation," *Journal of the Institute of Conservation*, vol. 40, no. 2, pp. 168–182, 2017.

[5] Q. Wang and S. Shen, "Digital inheritance strategy of intangible cultural heritage and big data model-taking the southern liaoning Province as an example," in *Proceedings of the 2018 International Conference on Intelligent Transportation, Big Data & Smart City (ICITBS)*, 2018.

[6] A. Doulamis, A. Voulodimos, N. Doulamis, S. Soile, and A. Lampropoulos, "Transforming intangible folkloric performing arts into tangible choreographic digital objects: the terpsichore approach," in *Proceedings of the 12th International Joint Conference on Computer Vision, Imaging and Computer Graphics Theory and Applications (VISAPP)*, Porto, Portugal, 2017.

[7] W. Leimgruber, "Switzerland and the UNESCO convention on intangible cultural heritage," *Journal of Folklore Research*, vol. 47, no. 1-2, pp. 161–196, 2010.

[8] T. Teo, "Modelling Facebook usage among university students in Thailand: the role of emotional attachment in an extended technology acceptance model," *Interactive Learning Environments*, vol. 24, no. 4, pp. 745–757, 2016.

[9] K. Massing, "Safeguarding intangible cultural heritage in an ethnic theme park setting-the case of Binglanggu in Hainan Province, China," *International Journal of Heritage Studies*, vol. 24, no. 1, pp. 66–82, 2018.

[10] M. Wang, X.-Q. Lyu, Y.-J. Li, and F.-L. Zhang, "VR content creation and exploration with deep learning: a survey," *Computational Visual Media*, vol. 6, no. 1, pp. 3–28, 2020.

[11] R. Taehyun, P. Lohit, A. Benjamin, and C. Andrew, "MR360: mixed reality rendering for 360° panoramic videos," *IEEE Transactions on Visualization and Computer Graphics*, vol. 23, no. 4, pp. 1379–1388, 2017.

[12] S. Christopher, B. Jean-Charles, and S. H. Alexander, "An omnistereoscopic video pipeline for capture and display of real-world VR," *ACM Transactions on Graphics*, vol. 37, no. 3, 2018.

[13] H. Peter, A. Suhib, S. Richard, and K. Johannes, "Casual 3D photography," *ACM Transactions on Graphics*, vol. 36, no. 6, 2017.

[14] Y. Zhang, Y.-K. Lai, and F.-L. Zhang, "Content-preserving image stitching with piecewise rectangular boundary constraints," *IEEE Transactions on Visualization and Computer Graphics*, vol. 1, 2020.

[15] J. Ye, Z. Shen, P. Behrani, F. Ding, and Y.-Q. Shi, "Detecting USM image sharpening by using CNN," *Signal Processing: Image Communication*, vol. 68, pp. 258–264, 2018.

[16] Z. Zhu, J. Lu, M. Wang et al., "A comparative study of algorithms for realtime panoramic video blending," *IEEE Transactions on Image Processing*, vol. 27, no. 6, pp. 2952–2965, 2018.

[17] M. Wang, A. Shamir, G.-Y. Yang et al., "BiggerSelfie: selfie video expansion with hand-held camera," *IEEE Transactions on Image Processing*, vol. 27, no. 12, pp. 5854–5865, 2018.

[18] O. Grau, *Virtual Art-From Illusion to Immersion*, MIT Press, Cambridge, MA, USA, 2002.

[19] J. Li, "Intangible heritage protection based on virtual reality technology," *Journal of Physics*, vol. 1533, no. 3, Article ID 032011, 2020.

[20] R. Szeliski, "Image alignment and stitching: a tutorial," *Foundations and Trends in Computer Graphics and Vision*, vol. 2, no. 1, pp. 1–104, 2007.

[21] A. M. Soccini, "Gaze estimation based on head movements in virtual reality applications using deep learning," in *Proceedings of the 2017 IEEE Virtual Reality (VR)*, pp. 413-414, Los Angeles, CA, USA, March 2017.

[22] P. M. E. A. Natapov and D. Fisher-Gewirtzman, "To go where no man has gone before: virtual reality in architecture," *Landscape Architecture and Environmental Planning. Computers, Environment and Urban Systems*, vol. 54, pp. 376–438, 2015.

[23] Y. Lecun, L. Bottou, Y. Bengio, and P. Haffner, "Gradient-based learning applied to document recognition," *Proceedings of the IEEE*, vol. 86, no. 11, pp. 2278–2324, 1998.

[24] A. McLay, "Realising virtual reality," *International Journal of Sociotechnology and Knowledge Development*, vol. 2, no. 3, pp. 37–53, 2012.

Research Article

Coaxiality of Stepped Shaft Measurement Using the Structured Light Vision

Chunfeng Li [iD],[1,2] Xiping Xu [iD],[1] Huiqi Sun [iD],[3] Jianwei Miao [iD],[4] and Zhen Ren [iD][5]

[1]*College of Optoelectronic Engineering, Changchun University of Science and Technology, Changchun 130012, Jilin, China*
[2]*School of Electronic Information Engineering, Changchun University, Changchun 130022, Jilin, China*
[3]*Evergrande Hengchi New Energy Automotive R&D Institute(Shanghai) Co., Ltd., Shanghai 511458, China*
[4]*School of Automotive Engineering, Jilin Engineering Normal University, Changchun 130052, Jilin, China*
[5]*Graduate School of Changchun University, Changchun University, Changchun 130022, Jilin, China*

Correspondence should be addressed to Xiping Xu; xxp@cust.edu.cn

A method is proposed to measure the coaxiality of stepped shafts based on line structured light vision. In order to solve the repeated positioning error of the measured shaft, the light plane equation solution method is proposed using movement distance and initial light plane equation. In the coaxiality measurement model, the equation of the reference axis is obtained by the overall least square method through the center point coordinates of each intercept line on the reference axis. The coaxiality error of each shaft segment relative to the reference axis is solved based on the principle of minimum containment. In the experiment, the coaxiality measurement method is evaluated, and the factors that affect the measurement accuracy are analyzed.

1. Introduction

The stepped shafts are widely used in the mechanical power system, transmission system, and output system. The processing quality of the stepped shafts directly determines the working performance of the mechanical structures. Coaxiality is an important geometric parameter of the stepped shaft, which reflects the rotation characteristics of the stepped shaft. Low-precision coaxiality will increase the vibration of parts and cause accelerated wear of the mechanical structure. Therefore, the coaxiality measurement technology is very important to ensuIn recent years; researchers have done a lot of work on the measurement of coaxiality and cylindricity. Sun et al. [1] proposed a cylindrical profile measurement model with five systematic errors. Compared with the traditional method with two systematic errors, this method can improve the coaxiality measurement accuracy of the low-pressure turbine shaft by 2.9 μm. Tan et al. [2, 3] proposed a fast method for evaluating the coaxiality of stepped shafts based on maximum material requirements. The test results prove that this method has

certain advantages over other existing methods in measurement of speed and accuracy. Arthur Graziano et al. [4] proposed a measurement method that uses an inductive displacement sensor to measure the coaxial line of an oil pipeline. The above coaxiality measurement methods are all based on contact measurement. With the continuous improvement of modern industry's requirements for intelligent manufacturing, the original contact measurement methods can no longer meet the noncontact and real-time requirements.

Due to the development of vision measurement technology [5, 6], many noncontact measurement methods have been applied to the measurement of stepped shafts, and these technologies can be divided into active measurement and passive measurement. Passive measurement technology uses one or more cameras to measure the geometric parameters of the stepped shaft [7–9]. Wang et al. [10] obtained the position of the measurement reference line and the center line through a single-mode optical fiber laser diode and used a CMOS to obtain the coaxiality of large and medium shafting. Liu et al. [11] used the light curtain sensor to

measure the coaxiality of the EMU axles, and the measurement error caused by the nonparallel connection between the two centers of the axles was studied in paper. In the experiment, the error of the vision algorithm was compared with the result obtained by the three-coordinate instrument. The accuracy of this method had been proven to meet existing industrial applications. But this method is an active vision measurement method, which is not suitable for complex measurement environments. Tong obtained the coaxiality of large forged step shafts by an area CCD camera [12]. When the measured shaft diameter ranged from 400 to 550 mm, the relative measuring error of the coaxiality was 0.3% by the algorithm in the experiment. Since the passive vision measurement methods are susceptible to noise and the measurement systems are complicated, they are not suitable for the stepped shaft machining site.

In the line structured light vision measurement technology, energy is emitted to the surface of the measured object by the laser, and the surface morphology of the measured object is obtained by collecting reflected energy. Because this technology has the characteristics of low hardware cost and strong robustness, it is widely used in the geometric parameters of shaft parts [13–15]. In this paper, a line structured light vision measurement system consisting of a camera and a line structured light is proposed to measure the coaxiality of the stepped shaft.

In the coaxiality measurement, the laser is translated along a straight line multiple times, the intersection lines formed by the light planes and the measured stepped shaft are obtained by the camera, and the center of each intersection line is calculated by ellipse fitting. The reference axis equation is obtained by the global least square method. The distance from the center of each section to the reference axis is calculated, and the maximum distance corresponding to each shaft segment is regarded as the coaxiality of the shaft segment through the principle of least tolerance. Since it is necessary to obtain the light plane equation after each movement in the coaxiality measurement, the paper put forward using the translation distance of the line laser to calculate the light plane equation after translation, which can solve the clamping error caused by the original optical plane equation calibration method.

The paper consists of the following parts: Section 2 proposes the calculation of the world coordinates of the stepped shaft surface contour points; Section 3 establishes the translational light plane calibration algorithm; Section 4 outlines the stepped shaft coaxiality measurement model; Section 5 reports the experimental results used to test the measuring; Section 6 provides the study's conclusions.

2. World Coordinate Calculation of Contour Points on Stepped Shaft Surface

2.1. Solving the Camera Coordinates of Points on the Stepped Shaft Surface. The camera coordinate solution model for data points on the surface of the stepped shaft is shown in Figure 1. The P_i is any point on the measured shaft. The intersection P' of the ray $O_C P_i$ and the imaging plane is the
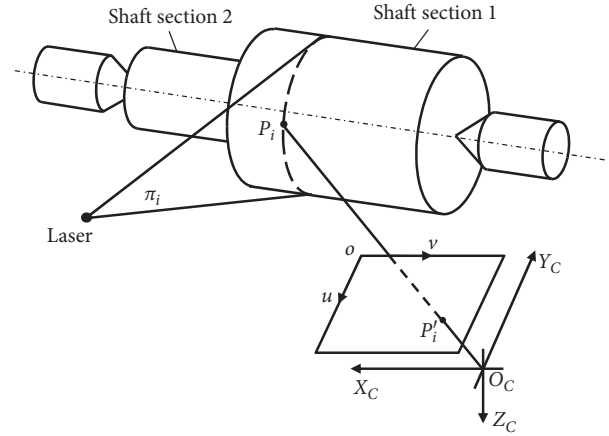
Figure 1: Camera coordinate solution model for points on stepped shaft surface.

projection point of P_i on the imaging plane. Through geometric relationship analysis, the camera coordinates of P_i can be determined by the equations of the light plane π and $O_C P_i$. Let the plane equation of the light plane π be

$$A_1 X_C + A_2 Y_C + A_3 Z_C + A_4 = 0. \tag{1}$$

Equation (1) can be obtained by the optical plane calibration method [15].

The camera coordinates of P' can be obtained by the pixel coordinates of P' and the camera internal parameters. The pixel coordinates of P' can be obtained by Steger algorithm [16], and the camera internal parameters can be obtained by camera calibration [17]. The equation of $O_C P'$ in the camera coordinate system can be expressed as

$$\frac{X_C}{x_u} = \frac{Y_C}{y_u} = Z_C. \tag{2}$$

The camera coordinates of P_i can be calculated by equations (1) and (2), and x_u and y_u are the image coordinates of point P_i.

2.2. Solving World Coordinates of Points on Stepped Shaft Surface. According to the stepped shaft measurement model, the intersecting line between the light plane and the measured shaft is a spatial elliptical arc. In order to simplify the calculation process, the paper establishes the world coordinate system O_W-$X_W Y_W Z_W$ which is as shown in Figure 2. In the world coordinate system, the normal vector of the light plane is as $O_W Z_W$ and the origin of world coordinate system (O_W) is the origin of the camera coordinate system (O_C). Because all points of intersection OP have the same Z_W, the process of solving the ellipse's center has changed from a space ellipse fitting problem to a plane ellipse fitting problem.

The direction vector of the $O_W Z_W$ is the normal direction of the light plane (A_1, A_2, and A_3), and the direction cosine of the $O_W Z_W$ in the camera coordinate system can be obtained by using the normal vector of the light plane. The direction cosine of the $O_W Z_W$ is shown as
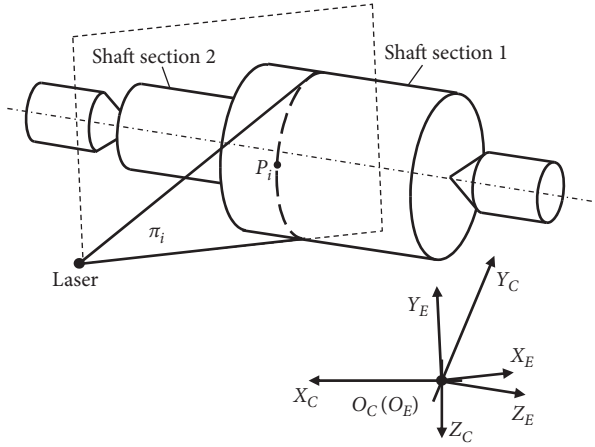
FIGURE 2: The world coordinate system $(O_W\text{-}X_WY_WZ_W)$ establishment.

$$\begin{cases} e_{31} = \dfrac{A_1}{\sqrt{A_1^2 + A_2^2 + A_3^2}}, \\[4ex] e_{32} = \dfrac{A_2}{\sqrt{A_1^2 + A_2^2 + A_3^2}}, \\[4ex] e_{33} = \dfrac{A_3}{\sqrt{A_1^2 + A_2^2 + A_3^2}}. \end{cases} \tag{3}$$

$$\mathbf{J} = \mathbf{I} \times \mathbf{K} = \begin{vmatrix} i & j & k \\ A_1 & A_2 & A_3 \\ 1 & 1 & k \end{vmatrix} = (A_2k - A_3)\mathbf{i} + (A_3 - A_1k)\mathbf{j} + (A_1k - A_3)\mathbf{k}, \tag{7}$$

where $\mathbf{I}$ is the direction vector of O_WX_W and $\mathbf{K}$ is the direction vector of O_WZ_W. Set e_{y1} as $A_2k - A_3$, e_{y2} as $A_3 - A_1k$, and e_{y3} as $A_1k - A_3$, The direction cosine of O_WY_W is

$$\begin{cases} e_{21} = \dfrac{e_{y1}}{\sqrt{e_{y1}^2 + e_{y2}^2 + e_{y3}^2}}, \\[4ex] e_{22} = \dfrac{e_{y2}}{\sqrt{e_{y1}^2 + e_{y2}^2 + e_{y3}^2}}, \\[4ex] e_{23} = \dfrac{e_{y3}}{\sqrt{e_{y1}^2 + e_{y2}^2 + e_{y3}^2}}. \end{cases} \tag{8}$$

Based on the direction cosine of the three-coordinate axes and the camera coordinates of the origin in the world coordinate system, the transformation relationship between the camera coordinates and the world coordinates is

According to the positional relationship between the world coordinate system and the camera coordinate system, the plane equation of the coordinate plane $O_WX_WY_W$ in the camera coordinate system can be written as

$$A_1X_C + A_2Y_C + A_3Z_C = 0. \tag{4}$$

Set the camera coordinate of a point K on the $O_WX_WY_W$ plane as $(1, 1, x)$. Substituting the camera coordinate of the K into equation (5), the Z-axis coordinate of the K can be solved:

$$Z_C = -\frac{A_1X_C + A_2Y_C}{A_3}. \tag{5}$$

where the direction vector of O_CK is $(1, 1, -((A_1X_C + A_2Y_C)/A_3))$, which is taken as the direction vector of O_WX_W in the camera coordinate system. The direction cosine of O_WX_W is

$$e_{11} = \frac{1}{\sqrt{2 + k^2}}, e_{32} = \frac{1}{\sqrt{2 + k^2}}, e_{33} = \frac{k}{\sqrt{2 + k^2}}, \tag{6}$$

where k is $-((A_1X_C + A_2Y_C)/A_3)$.

The direction vector of O_WY_W which can be obtained through the direction vector of O_WX_W and O_WZ_W is shown as

$$\begin{bmatrix} X_W \\ X_W \\ Z_W \end{bmatrix} = \begin{bmatrix} e_{11} & e_{12} & e_{13} \\ e_{21} & e_{22} & e_{23} \\ e_{31} & e_{32} & e_{33} \end{bmatrix} \begin{bmatrix} X_C \\ Y_C \\ Z_C \end{bmatrix}. \tag{9}$$

3. Calibration Algorithm of the Translated Light Planes Equations

In order to obtain the surface information of the measured stepped shaft on multiple crosssections, it is necessary to move the laser for several times along a straight line during the coaxiality measurement, because the light plane equation will change after moving the line laser. The traditional light plane methods need to remove the measured shaft from the experimental table and then calibrate the light plane. This process will not only affect the measurement speed, but more importantly, it will produce positioning errors, which have a great impact on the measurement accuracy of coaxiality. To solve this problem, the paper proposes a multiparallel light plane equation solving method.

The line laser moves along on the rail, and the light planes at each position are parallel to each other. Therefore, these light planes have the same normal vector. Let this series of light planes equation be

$$A_1 X_C + A_2 Y_C + A_3 Z_C + C_i = 0. \tag{10}$$

Through the distance formula of space parallel planes, the distance between two adjacent light planes can be expressed as

$$h_i = \frac{|C_i - C_{i-1}|}{\sqrt{A_1^2 + A_2^2 + A_3^2}}. \tag{11}$$

Therefore, the relationship between the equation constant terms of two adjacent light planes is

$$C_i = C_{i-1} \pm h_i \sqrt{A_1^2 + A_2^2 + A_3^2}. \tag{12}$$

In order to obtain the parameters of the light plane equation after translation, it is necessary to establish the functional relationship which is the distance between adjacent light planes and the moving distance of the laser. The geometric relationship is shown in Figure 3; the coordinate axis ox is set to coincide with the moving direction of the line laser; S_0 represents the initial position of the lasers, S_1, S_{i-1}, S_i, respectively, represent the position of the light plane after the first $i-1$ and i-th movement; H_i represents the distance between the light plane and the initial light plane after the i-th movement of the light plane; α represents the angle between the moving direction of the laser and the light plane.

According to the geometric relationship shown in Figure 3, the light plane equation for the first translation should be solved. In order to ensure that the normal vectors of the series, light planes are the same, the three coefficients of the
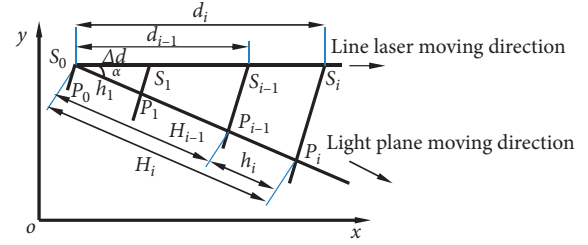
FIGURE 3: The geometric relationship of the distance between light planes and the moving distance of the laser.

light plane equation are fixed, and constant term C_1 is calculated in solving the light plane equation. After obtaining the light plane equation for the first movement, the distance h_1 between the two light planes can be solved according to equation (12). Let the laser translation distance be d_1, and cosine of the angle between the line laser and the light plane is

$$\cos \alpha = \frac{h_1}{d_1}. \tag{13}$$

Using the cosine value of the included angle α, the distance H_i from the light plane after the i-th translation to the initial position of the light plane can be obtained:

$$H_i = d_i \cdot \cos \alpha. \tag{14}$$

Then, the distance between two adjacent light planes is

$$h_i = (d_i - d_{i-1}) \cdot \cos \alpha. \tag{15}$$

After the i-th movement of the laser, the corresponding equation of the light plane is

$$A_1 X_C + A_2 Y_C + A_3 Z_C + \left[C_{i-1} \pm (d_i - d_{i-1}) \sqrt{A_1^2 + A_2^2 + A_3^2} \, \cos \alpha \right] = 0. \tag{16}$$

In order to determine the final light plane equation after each movement, there is a need in comparing the constant term of the light plane equation at the initial position (C_0) with the constant term of the light plane after the first movement (C_1). Since the laser is moving along the same

direction in the coaxiality measurement, the constant term of the light plane equation linearly increases or decreases after each movement. When C_0 is greater than C_1, equation (17) is shown as

$$A_1 X_C + A_2 Y_C + A_3 Z_C + \left[C_{i-1} - (d_i - d_{i-1}) \sqrt{A_1^2 + A_2^2 + A_3^2} \, \cos \alpha \right] = 0. \tag{17}$$

When C_1 is greater than C_0, equation (17) is shown as

$$A_1 X_C + A_2 Y_C + A_3 Z_C + \left[C_{i-1} + (d_i - d_{i-1}) \sqrt{A_1^2 + A_2^2 + A_3^2} \, \cos \alpha \right] = 0. \tag{18}$$

4. The Coaxiality Measurement Model of Stepped Shaft

The coaxiality measurement model proposed in the paper is shown in Figure 4. The line laser is fixed on the linear slide rail, and the multiple truncated intersector curve of light planes and the measured axis are obtained by moving the platform on each shaft segment. In Figure 4, let π_i be the light plane corresponding to the i-th section, and P_i be any point on the i-th truncated intersector curve; O_i is the center of the intercept line between the i-th light plane and the measured stepped shaft, that is, the center of the ellipse where the ellipse arc is located. The world coordinates of O_i can be obtained by ellipse fitting through the world coordinates of the data point P_i on the corresponding section.

In Figure 4, the shaft 1 is the reference shaft section of the stepped shaft, and L is the axis of the reference shaft. The line equation corresponding to L can be obtained by the camera coordinates of O_i corresponding to shaft 1, and the line equation is the premise for obtaining the coaxiality of the stepped shaft. Because there are errors in the process of solving the coordinates of P_i, the coordinates of O_i obtained by ellipse fitting also have errors, which will affect the calculation accuracy of the reference axis L.

In order to improve the calculation accuracy of the reference axis L, the paper adopts the overall least square method to obtain the line equation of the reference axis L. The reference axis equation is obtained by the center points of all sections on the axis L, and set the equation of the axis as

$$\frac{X_C - x_0}{A} = \frac{Y_C - y_0}{B} = \frac{Z_C - z_0}{C}, \tag{19}$$

Equation (20) could be rewritten as

$$\begin{cases} X_C = \dfrac{A}{C}\left(Z_C - z_0\right) + x_0, \\ \\ Y_C = \dfrac{B}{C}\left(Z_C - z_0\right) + y_0. \end{cases} \tag{20}$$

Set-
$a = (A/C), b = x_0 - (A/C)z_0, c = (B/C), d = y_0 - (B/C)z_0$; equation (21) can be simplified as

$$\begin{cases} X_C = aZ_C + b, \\ Y_C = cZ_C + d, \end{cases} \tag{21}$$

Equation (22) is changed into matrix form and shown as

$$\begin{bmatrix} Z_C & 1 & 0 & 0 \\ 0 & 0 & 1 & Z_C \end{bmatrix} \begin{bmatrix} a & b & c & d \end{bmatrix}^T = \begin{bmatrix} X_C \\ Y_C \end{bmatrix}. \tag{22}$$

Set $\mathbf{B} = \begin{bmatrix} z_e & 1 & 0 & 0 \\ 0 & 0 & 1 & z_e \end{bmatrix}, \mathbf{L} = \begin{bmatrix} x_e \\ y_e \end{bmatrix}, \mathbf{X} = \begin{bmatrix} a & b & c & d \end{bmatrix}^T$,
and equation (23) is

$$\mathbf{BX} = \mathbf{L}. \tag{23}$$

The coordinates of all center points on the reference axis are substituted into equation (19), and the initial values of the axis equation parameters are calculated by least square fitting.
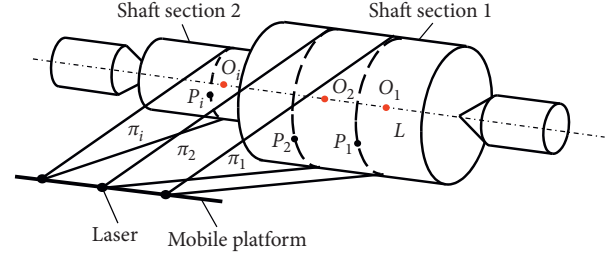
FIGURE 4: The coaxiality measurement model of stepped shaft.

According to the distance formula from point to space line, the distance d_i from each center point O_i to the initial axis L is

$$d_i = \frac{\left|\left(X_{Ci} - aZ_{Ci} - b\right) \cdot \mathbf{n}_1 - \left(Y_{Ci} - cZ_{Ci} - d\right) \cdot \mathbf{n}_2\right|}{\left|\mathbf{n}_1 \times \mathbf{n}_2\right|}. \tag{24}$$

When $\mathbf{n}_1$ is $(1, 0, a)$, and $\mathbf{n}_2$ is $(1, 0, c)$, the discriminant coefficient δ is created. If d_i is less than δ, the i-th center point is eliminated as the error point. According to the least square fitting, the final reference axis equation is solved by the filtered center point.

After obtaining the reference axis equation and after the reference axis equation is solved, the distance from the center points of all section on the stepped shaft to the reference axis is obtained through the point-to-line space distance formula. Set $\mathbf{D}_i$ be the distance array from all center points on the i-th shaft segment to the reference axis, and $d^i_{\max}$ be the maximum value of the data $\mathbf{D}_i$. According to the principle of minimum tolerance, $d^i_{\max}$ is the coaxiality error corresponding to the i-th shaft segment.

5. Experiments and Result Analysis

Experiments are conducted to assess the utility of the proposed coaxiality measurement algorithm. The four shaft sections of a stepped shaft are used as the measurement object, and shaft section 1 is the reference for coaxiality measurement, as shown in Figure 5. In order to verify the accuracy of the measurement algorithm in this paper, a three-coordinate measuring instrument was used to measure the coaxiality of the stepped shaft, and the measurement results are as shown in Table 1.

The coaxiality measurement of stepped shaft based online structured light vision is shown in Figure 6. The stepped shaft was fixed at test-bed. The laser was fixed on the translation sliding table, the probe of the dial indicator is in contact with the translation sliding table, and the translation distance of the laser was obtained by a dial indicator. The main parameters of equipment are shown in Table 2, and the calibration results of the vision measurement system are shown in Table 3.

In the process of solving the reference axis equation, the laser was moved 10 times, and each moving distance was 0.1 mm. Based on the algorithm at the section 3, the light plane equation after each movement can be calculated by the initial light plane equation and the translation distance. The
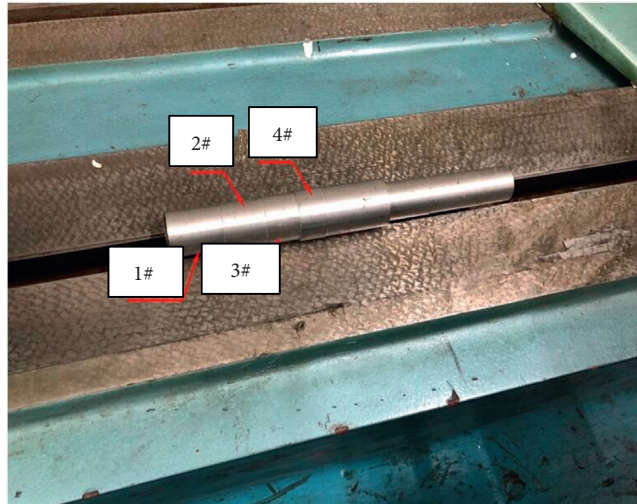
Figure 5: The measured step shaft.

Table 1: Coaxiality measurement results of stepped shaft (three coordinates).

Number	1#	2#	3#	4#
Coaxiality error (mm)	0	0.021	0.013	0.025
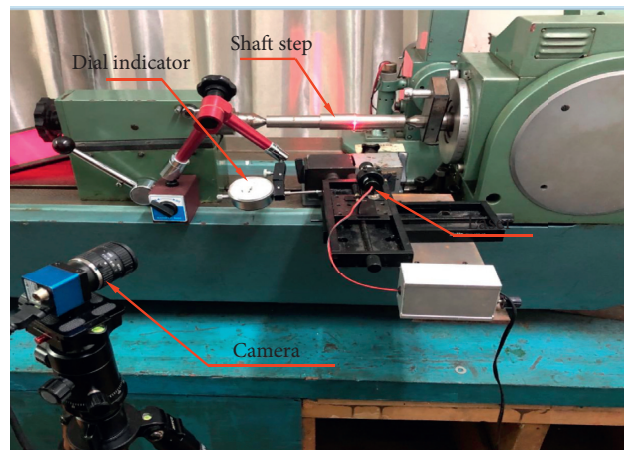
Figure 6: The coaxiality of step shaft measurement site.

Table 2: Equipment models and parameters in the vision measurement system.

Device	Device model	The main parameters
Camera	MER − 125 − 30UM	Resolution: 1292×964 pixel
Lens	Computar M2514 − MP	Focal length: 25 mm
Line laser	LH650 − 80 − 3	Power: 0~20 mW
Light source	CCS LFL − 200	Luminous area: 200×180 mm
Calibration board	NANO CBC 25 mm − 2.0	Precision: $\pm 1.0 \, \mu$m

light plane equations after each movement are shown in Table 4. The pixel coordinates of the light stripe center points on each image can be detected by Steger's algorithm, and the detection results are as shown in Figure 7.

Through the coaxiality measurement model proposed in this paper, the world coordinates of the center point corresponding to each intersecting line can be calculated, and the space linear equation of the reference axis is obtained:

TABLE 3: Calibration results of vision measurement system.

Internal parameter matrix

$$\mathbf{A} = \begin{bmatrix} 6908.140 & -0.253 & 647.988 \\ 0 & 6908.417 & 504.010 \\ 0 & 0 & 1 \end{bmatrix}$$

Distortion coefficient

$k1$	$k2$	$p1$	$p2$
0.1054	6.918	0.0006	0.0003

Light plane equation parameters

$$3.0042X_C - 0.1546Y_C + 1.717Z_C - 1000 = 0$$

TABLE 4: The light plane space equations (reference axis).

Section number	Light plane equation
Section 1	$3.0042X_C - 0.1546Y_C + 1.717Z_C - 1000 = 0$
Section 2	$3.0042X_C - 0.1546Y_C + 1.717Z_C - 999.658 = 0$
Section 3	$3.0042X_C - 0.1546Y_C + 1.717Z_C - 999.316 = 0$
Section 4	$3.0042X_C - 0.1546Y_C + 1.717Z_C - 998.974 = 0$
Section 5	$3.0042X_C - 0.1546Y_C + 1.717Z_C - 998.632 = 0$
Section 6	$3.0042X_C - 0.1546Y_C + 1.717Z_C - 998.290 = 0$
Section 7	$3.0042X_C - 0.1546Y_C + 1.717Z_C - 997.948 = 0$
Section 8	$3.0042X_C - 0.1546Y_C + 1.717Z_C - 997.606 = 0$
Section 9	$3.0042X_C - 0.1546Y_C + 1.717Z_C - 997.264 = 0$
Section 10	$3.0042X_C - 0.1546Y_C + 1.717Z_C - 996.922 = 0$
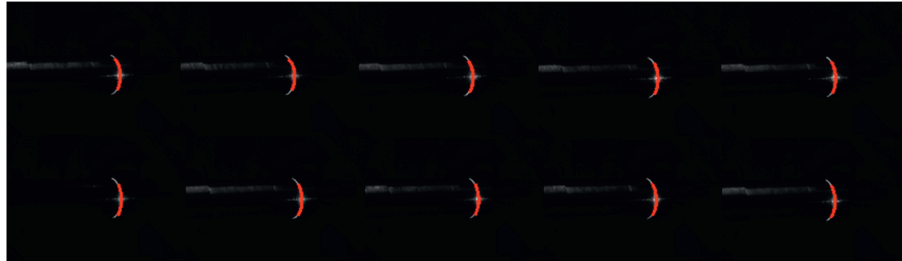
FIGURE 7: The detection results of the light stripe center points.

$$\frac{x - 96.4061}{0.0426} + \frac{y - 3.9139}{0.0007} + \frac{z - 606.7951}{0.0282} = 1. \qquad (25)$$

The five different positions of the light strip images could be captured on each shaft segment from shaft segment 2 to shaft segment 4, and the center points of the light strips on the measured shaft are shown in Figure 8. The light plane equation of the initial position on each shaft segment is shown in Table 5.

According to the coaxiality measurement algorithm proposed in this paper, the distance from the center points of each shaft segment to the reference axis is calculated and the maximum distance is regarded *as the coaxiality error of the shaft segment by the principle of minimum tolerance. The coaxiality error of measured shaft is* shown in Table 6, *A* is the coaxiality error by the coordinate measuring machine, and *B* is the measured value by the method proposed in the paper.

According to the experimental results, the coaxiality error of the stepped shaft is less than $40\,\mu$m by the algorithm proposed in this paper, and the absolute error is less than

$25\,\mu$m compared with the measured value of the coordinate measuring machine.

In the experiment, the measurement environment is relatively closed, and the external light environment is better. However, in the practical industrial environment, it is necessary to require online measurement and the machining environment is worse than the laboratory environment. To analyze the influence of noise on the algorithm, Gaussian noise is added to the light strip image, the mean value of the noise is 0, and the variance is 0.05. The coaxiality of the step shaft was again measured by the images after adding noise, and the images of each shaft segment is shown in Figure 9.

Though the same process of the above experiment, the reference axis space equation and the coordinates of the center point on each shaft segment, the coaxiality error of shaft segments were obtained by using the algorithm of the paper. The measurement results are shown in Table 7, *A* is the coaxiality error by the coordinate measuring machine, and *B* is the measured value by the method proposed in the paper.
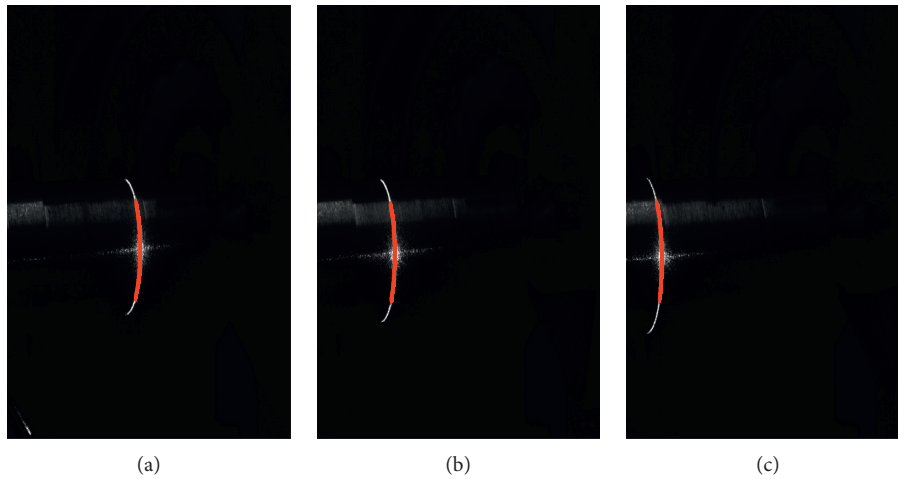
FIGURE 8: The detection results of the light stripe center points on shaft segments 2 to 4.

TABLE 5: The calibration results of light plane space equation at initial position.

Shaft segment number	Light plane equation
Shaft section 2	$3.0042X_C - 0.1546Y_C + 1.717Z_C - 934.678 = 0$
Shaft section 3	$3.0042X_C - 0.1546Y_C + 1.717Z_C - 924.418 = 0$
Shaft section 4	$3.0042X_C - 0.1546Y_C + 1.717Z_C - 909.028 = 0$

TABLE 6: Coaxiality measurement results of stepped shaft (mm).

Number	A	B	
		Measurements	Error
Shaft section 2	0.021	0.034	0.013
Shaft section 3	0.013	0.028	0.015
Shaft section 4	0.025	0.039	0.014
Mean error			0.014
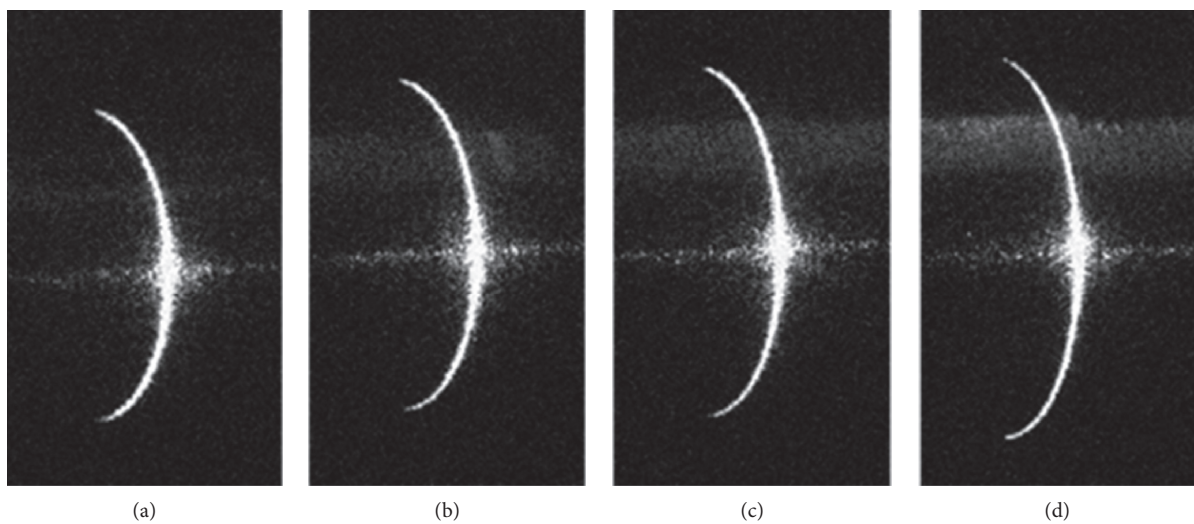
FIGURE 9: The images of each shaft segment after adding noise. (a) Section 1. (b) Section 2. (c) Section 3. (d) Section 4.

TABLE 7: Coaxiality measurement results/mm (after increasing noise).

Number	A	B	
		Measurements	Error
Shaft section 2	0.021	0.045	0.024
Shaft section 3	0.013	0.040	0.027
Shaft section 4	0.025	0.050	0.025
Mean error			0.025

Due to increase the noise, the error points in the center point of the light strip will increase. As the noise increases, the error points in the center point of the light bar will increase and the accuracy of ellipse fitting will decrease, which in turn leads to a decrease in the accuracy of coaxiality measurement.

6. Conclusion

The coaxiality measurement method is proposed based on the line structured light vision in the paper. The algorithm for calculating the light plane equation after each movement is built by the equation of initial light plane and each line structured light translation distance, which solves the clamping error caused by multiple clamping of the stepped shaft. The world coordinate system is established according to the corresponding light plane at each position, and the center point coordinates of the intercept line can be obtained by fitting a geometric ellipse in the coordinate system. Using the coordinates of the center point on the intercept line on the reference axis, the space equation of the reference axis is generated by the overall least squares fitting, and the coaxiality error of each axis segment relative to the reference axis segment is solved by the principle of least containment. Through experimental verification, the measurement accuracy of the proposed algorithm is 25 μm, and the influence of noise on coaxiality is analyzed.

Data Availability

No data were used to support this study.

Conflicts of Interest

The authors declare that they have no conflicts of interest.

References

[1] C. Sun, B. Wang, Y. Liu et al., "Design of high accuracy cylindrical profile measurement model for low-pressure turbine shaft of aero engine," *Aerospace Science and Technology*, vol. 95, Article ID 105442, 2019.

[2] Z. Tang, M. Huang, Y. Sun, Y. Zhong, Y. Qin, and J. Huang, "Coaxiality evaluation based on double material condition," *Measurement*, vol. 141, pp. 287–295, 2019.

[3] Z. Tang, M. Huang, Y. Sun, Y. Zhong, and Y. Qin, "Rapid evaluation of coaxiality of shaft parts based on double maximum material requirements," *Measurement*, vol. 147, Article ID 106868, 2019.

[4] A. Graziano and T. L. Schmitz, "Sensor design and evaluation for on-machine probing of extruded tool joints," *Precision Engineering*, vol. 35, no. 3, pp. 525–535, 2017.

[5] H. J. Bao, Q. C. Tan, S. Y. Liu, and Miao, "Computer vision measurement of pointer meter readings based on inverse perspective mapping," *Applied Sciences*, vol. 9, no. 18, p. 3729, 2019.

[6] J. Miao, Q. Tan, S. Liu, H. Bao, and X. Li, "Vision measuring method for the involute profile of a gear shaft," *Applied Optics*, vol. 59, no. 13, pp. 4183–4190, 2020.

[7] Q. Sun, Y. Hou, Q. Tan, and C. Li, "Shaft diameter measurement using a digital image," *Optics and Lasers in Engineering*, vol. 55, pp. 183–188, 2014.

[8] Q. C. Sun, Y. Q. Hou, Q. C. Tan, and G. N. Li, "A planar-dimensions machine vision measurement method based on lens distortion correction," *The Scientific World Journal*, vol. 2013, Article ID 963621, 6 pages, 2013.

[9] G. Wei and Q. Tan, "Measurement of shaft diameters by machine vision," *Applied Optics*, vol. 50, no. 19, pp. 3246–3253, 2011.

[10] T. G. Wang and N. G. Lu, "A CMOS approach to coaxiality measurement of marine shafting and bearing system," *SPIE—The International Society for Optical Engineering*, vol. 7160, 2008.

[11] C.-Y. Liu and R. J. Wang, "The coaxial measurement and error analysis of the axle of the bullet train," *China Science Paper*, vol. 13, pp. 1639–1643, 2018.

[12] J. Tong, Y. H. Wang, J. S. Lu, S. J. Zhang, and D. H. Chen, "Coaxiality measurement of large-size forged components based on CCD," *Journal of Jilin University (Engineering and Technology Edition)*, vol. 2013, pp. 945–950, 2018.

[13] C. Sun, Q. You, Y. Qiu, and S. H. Ye, "Online machine vision method for measuring the diameter and straightness of seamless steel pipes," *Optical Engineering*, vol. 40, no. 11, pp. 2565–2571, 2001.

[14] B. Liu, P. Wang, Y. Zeng, and C. K. Sun, "Measuring method for micro-diameter based on structured-light vision technology Chin," *Optics Letters*, vol. 8, pp. 666–669, 2010.

[15] S. Liu, Q. Tan, and Y. Zhang, "Shaft diameter measurement using structured light vision," *Sensors*, vol. 15, no. 8, pp. 19750–19767, 2015.

[16] C. Steger, "An unbiased detector of curvilinear structures," *IEEE Transactions on Pattern Analysis and Machine Intelligence*, vol. 20, pp. 113–125, 1988.

[17] Z. Zhang, "A flexible new technique for camera calibration," *IEEE Transactions on Pattern Analysis and Machine Intelligence*, vol. 22, no. 11, pp. 1330–1334, 2000.

Research Article

Correlation of Gastric Cancer Cells with Seasonal Changes under Microscope

Qi Jin,[1] Shuo Huang [ID],[1] Yuhong Sun,[1] Yi Wang,[1] Yaguang Xue,[2] Mingming Hu,[3] and Qiyong He[1]

[1]*The First Affiliated Hospital of Jiamusi Universitu, Jiamusi University, Jiamusi 154003, Heilongjiang, China*
[2]*School of Public Health, Jiamusi University, Jiamusi 154003, Heilongjiang, China*
[3]*Linqu County People's Hospital, Weifang 262600, Shandong, China*

Correspondence should be addressed to Shuo Huang; shuo.huang@jmsu.edu.cn

Today, with the development of medical technology, stomach cancer remains to be one of the most common causes of death associated with cancer. Studies show that the incidence of stomach cancer varies in different areas but is more common in China. Most patients were diagnosed late with local or remote metastasis. The data show that the survival rate within five years is less than 10%. Therefore, it is very important to study the gastric cancer cells systematically, explore the factors that lead to the change of the number of gastric cancer cells, and put forward practical suggestions for the prevention and control of the disease. This paper analyzes the disease-related information of several patients with gastric cancer in a hospital, discusses the growth of gastric cancer cells and season-related factors, and analyzes the single factor of gastric cancer patients and season-related possible factors. In this paper, we choose to observe gastric cancer cells in different seasons under the microscopic environment to further explore the influence of seasons on gastric cancer cells. The results showed that gastric cancer cells grew faster under microscope in spring and summer. We found that the incidence rate of gastric cancer in spring and summer was higher than that in autumn and winter. Diabetic patients and diabetes history are important risk factors of gastric cancer in spring and summer. Therefore, we advocate healthy lifestyle, pay attention to their poor performance in life, and actively help them to correct, which is of positive significance for the prevention and control of gastric cancer.

1. Introduction

Gastric cancer [1–3] is one of the most common gastric tumours. According to global data on cancer circulated by the International Cancer Institute in 2012, The incidence and mortality of gastric cancer rank fifth and third in the world, respectively. However, the incidence rate of gastric cancer is still high in China. According to the statistics released in 2015, it is estimated that the number of new gastric cancer cases in the whole year is 679,000, ranking the second among all kinds of malignant tumors, and the number of deaths related to gastric cancer is 498,000, ranking the third. At present, radical surgery is the first choice for the treatment of gastric cancer. The five-year survival rate of early stomach cancer after radical surgery is over 90%. However, because

the early symptoms of stomach cancer are not very obvious, the lack of public awareness of stomach cancer and cancer control and failed to create an effective early warning mechanism, most patients have entered the development stage before being diagnosed as stomach cancer. For some patients still have the opportunity to receive radical surgery in clinical stages II and III, although in the near future, the operation method has been improved and adjuvant treatment such as postoperative radiotherapy and chemotherapy has prolonged the survival time of patients. Due to the high recurrence rate and metastasis rate of gastric cancer, about 40%–70% of patients will have tumor recurrence; the 5-year survival rate is less than 30%. For patients with advanced gastric cancer, they have no chance to operate at all. For them, the main treatment is chemotherapy, but the median

survival time is usually less than 1 year. Therefore, from the above facts, on the one hand, gastric cancer has brought a great threat to the life and health of our people, and the treatment cost is expensive, which makes the patients, their families, and even the social economy bear a huge economic burden.

Nowadays, with the development of society, there are many factors that can lead to the occurrence of gastric cancer. The occurrence of gastric cancer is the result of multiple stages and factors. There are many research results on the influencing factors of gastric cancer, but the exact factors of gastric cancer have not been determined by the scholars engaged in epidemiological research. At present, the relatively determined factors are among the environmental factors and genetic factors. Environmental factors mainly include bad eating habits, smoking and drinking, and nitrite. However, after analyzing several cases of gastric cancer in a hospital, the incidence rate of gastric cancer is also related to the season. From the description of the current situation of gastric cancer, we get the information that gastric cancer has brought great threat to the life safety of Chinese residents. Because we Chinese like to eat bacon, the nitrite [4, 5] contained in bacon is very harmful to our life and health, and this eating habit also increases the risk of gastric cancer of Chinese residents. Therefore, it is very important to use the existing medical technology to explore as many factors as possible that lead to the occurrence of gastric cancer, so as to help us to formulate effective prevention and treatment measures for gastric cancer. After investigating several patients with gastric cancer in a hospital, we observed the growth rate of gastric cancer cells under microscope and found that the growth rate of gastric cancer cells in spring and summer was higher than that in other two seasons. This finding provides a method for the prevention and control of gastric cancer.

Microscope [6, 7] is actually an optical refraction imaging system, which is composed of two groups of condensing lenses. It is an optical instrument that uses the optical principle to magnify the image of the small object which cannot be recognized by the naked eye, so as to extract the microstructure information of the material. The lens group with short focal length, close to the observation object and real image, is called objective lens, while the lens group with long focal length, close to the eye and virtual image, is called eyepiece. We put the object to be observed in front of the objective lens. After being magnified by the objective lens in the first stage, it becomes the true image of handstand. In the second stage, the real image is magnified by eyepiece, and the inverted virtual image with the largest magnified effect is obtained, which is located at the distance of human eyes. In medical research, microscopes can be used to observe DNA morphology, and microscopes can also be used to scan the electron microscope images of chondrocytes. With microscopes, we can observe cells and conduct biomedical research from macro to micro. In this paper, we analyzed many cases of gastric cancer, analyzed the possible factors related to seasons in gastric cancer patients by single factor method, analyzed the main factors related to seasons in gastric cancer patients by logistic regression analysis and the

degree of correlation, and observed gastric cancer cells in different seasons by using the microscope.

The results showed that the 69.61% of patients with stomach cancer were men, 58.03% in spring and summer. The results of a factor analysis showed that there were significant differences in all aspects of patients with stomach cancer at different times, such as number, age, the profession, dietary habits, and other factors ($P < 0.05$). The multifactorial analysis showed that age, city, and average length of stay were negatively correlated with seasons ($P < 0.05$), and age was negatively correlated with seasons. Among them, farmers and diabetics are more likely to go to hospital because of gastric cancer than other residents in the historical spring and summer, and the main complaints are highly correlated with seasons. B values of fever, anorexia, and emaciation were 1.584, 1.596, and 1.371, respectively ($P < 0.05$). The incidence rate of gastric cancer is related to season, age is small, and the characteristics of onset are not obvious. Farmers and patients with a history of diabetes are more likely to develop gastric cancer in spring and summer. It is of positive significance to prevent and control gastric cancer to strengthen the investigation of life and diet style of farmers and patients with diabetes history, to promote healthy life style to residents, and to pay attention to the nonobvious characteristics of the disease. Under the microscope, gastric cancer cells showed different growth trends in different seasons. In spring and summer, the growth rate of cancer cells was significantly higher than the other two seasons. This discovery will help us to prevent and control the occurrence of gastric cancer.

2. Microscopes and Gastric Cancer

2.1. History of Microscopes. A microscope is a visual instrument consisting of one or more lenses. It is a symbol of man entering the atomic age. It is mainly used to enlarge small objects into tools that can appear with the naked eye. Microscopes can be divided into two categories: optical and electronic microscopes. Optical microscopes were established by Jason and his son in the Netherlands in the 1590's. Now, the optical microscope can help us enlarge the object 1600 times, and the minimum resolution limit is 1/2 of the wavelength. The length of mechanical cylinder of microscope in China is generally 160 mm; Lewenhoek has made great contribution to the development of microscope and microbiology. The principle of electron microscope is to use electron flow as a new light source to image objects. Ruska invented the first transmission electron microscope in 1938, in addition to the continuous improvement of the performance of the transmission electron microscope itself. Many other types of electron microscope have also been developed, such as scanning electron microscope, analysis electron microscope, and ultrahigh pressure electron microscope. Combined with a variety of electron microscopes, we use the current technology to make samples; we can study the structure of samples or the relationship between structure and function. A microscope is used to observe images of small objects. It is often used to observe biology, medicine, and microscopes. The electronic microscope can help us

magnify objects a million times. For the time being, the electronic microscope is increasingly important in the field of medicine. Now with the development of science and technology, the electronic microscope is more scientific and accurate. The electronic microscope helps us complete one medical experiment after another.

2.2. Imaging Principle of AFM. The atomic force microscope [8, 9] is called AFM for short. The AFM principle is relatively simple. The core of the instrument is a microprojector about 100–250 m long, which is very sensitive to power. The free end of the microresistor, i.e., the end of the lower surface, is equipped with a needle edge, which is quite small in length and diameter smaller than 100 Angstroms. When the probe touches the surface of the sample gently, it will bend the microcantilever and transfer or change the amplitude due to the interaction between extremely weak atoms and the tip probe, and the surface atoms of the sample and the microcantilever with deformation information will be converted into a measurable signal. Now, there are many methods that can be used for information conversion and detection, such as optical reflection method, optical interference method, and tunnel current method. At present, the laser reflection detection system is commonly used in the AFM system. The laser beam is emitted to the microcantilever. When the cantilever is deflected or bent, the optical path of the laser beam reflected to the photodetector will also change. After the light spot displacement signal is converted and amplified by the photodetector, the weak change signal of the interatomic force is obtained, and the detection and imaging are completed by this method.

Atomic force microscopy is mainly used to describe neural circuits and observe DNA morphology and eukaryotic organelles in medicine. Micro-objects of nanometer scale were observed by electron microscope. It can be used to distinguish the shape and size of various viruses, measure the force between molecules, and operate controllable molecules. The electron microscope can develop biomedical research from macroscopic to microcosmic. It turns out that people can see the cells of animals and plants and many microorganisms through the optical microscope, but due to the limitation of natural wavelength, its resolution is difficult to meet the needs of people to uncover the mystery. Some scholars have studied the most relevant diseases of ultrastructure and accumulated a large number of data through the application of electron microscope. The application of electron microscope has laid a good foundation for the pathological diagnosis and pathological research of various clinical diseases to a new level. At present, electron microscopy has been widely used in clinical pathological diagnosis, especially in the traditional clinical diagnosis methods. For the primary cases that cannot be diagnosed before medical technology, atomic force microscopy can play an important role in helping us to diagnose.

2.3. Gastric Cancer. Gastric cancer (GC) is a kind of cancer in the stomach. It usually originates from gastric epithelial cells and is a common malignant tumor in the gastrointestinal system. The collective cause of stomach cancer has not been fully identified, but genetic factors, age, sex, *Helicobacter pylori* infection, tobacco and alcohol, and many other factors will increase the risk of stomach cancer. The first symptoms of patients are often not obvious. However, with the gradual worsening of the disease, symptoms such as dilution, anorexia, nausea, vomiting, diarrhoea, blood smear, and black faeces may occur. In early patients with stomach cancer, if they cooperate actively with treatment, the rate of treatment is high, but overall, the therapeutic effect of osteoarthritis system is low.

Most of the patients with early gastric cancer have no obvious symptoms, and a few have nausea, vomiting, or upper gastrointestinal symptoms similar to ulcers. It is difficult to pay attention to these symptoms. With the gradual deterioration of the disease, the symptoms are more obvious when the gastric function is affected, but these symptoms are lack of specificity. The most common clinical symptoms of advanced gastric cancer are pain and wasting. Patients often have more obvious upper gastrointestinal symptoms, such as abdominal discomfort and fullness after eating. With the deterioration of the disease, upper abdominal pain increases, appetite decreases, and fatigue occurs. The location of the tumor is different, and there will be different diseases. Gastric cancer may have pain in the sternum or dysphagia. Gastric cancer near the pylorus may have pylorus obstruction. There may be gastrointestinal bleeding symptoms, such as hematemesis and black stool. If the tumor invades the pancreatic capsule, it may show persistent pain, radiating to the back of the waist; if the tumor ulcer is perforated, it may cause severe pain or even peritoneal stimulation; if the tumor has hilar lymph node metastasis or bile duct compression, jaundice may occur; if the distant lymph node metastasis occurs, it may touch the left clavicular swollen lymph node. Anemia, emaciation, malnutrition, these bad diseases often extremely appears in patients with advanced gastric cancer.

There are many causes of gastric cancer, such as living environment, eating habits, heredity, and genes of *Helicobacter pylori* (HP) infection. The incidence rate of China's gastric cancer has been significantly different from that of other regions. The incidence rate of gastric cancer in China's northwest and eastern coastal areas is obviously higher than that in other regions. Because people in these areas like to smoke and consume salty food, the incidence of gastric cancer tends to be higher. There are the high content of nitrite, mycotoxin, polycyclic aromatic hydrocarbons, and other carcinogens in these foods; these carcinogens are an important cause of gastric cancer. Smoking is also an important factor in gastric cancer. According to the data, the risk of gastric cancer in smokers is 50% higher than that in nonsmokers. The HP infection rate of adults in the high incidence area of gastric cancer in China is more than 60%. *Helicobacter pylori* can promote the transformation of nitrate into nitrite and nitrosamine, which increases the probability of gastric cancer; HP infection causes chronic inflammation of gastric mucosa; environmental factors accelerate the excessive proliferation of mucosal epithelial

cells, leading to abnormalities; CagA and VacA are toxic products of *Helicobacter pylori*, which may promote cancer. The detection rate of anti-CagA antibody in gastric cancer patients is significantly higher than that in the general population. Related research shows that the incidence rate of blood relationship with gastric cancer patients is 4 times that of the ordinary people. The gastric cancer is more complex, and there are many factors that cause gastric cancer. The deterioration of gastric cancer is related to the change of oncogene, tumor suppressor gene, apoptosis-related gene, and metastasis-related gene. There are many ways of gene change. Through the case study and microscopic observation of gastric cancer cells, we found that there was a certain relationship between gastric cancer and seasonal changes.

3. Observation of Cell Treatment

3.1. Single-Factor Analysis on the Relationship between Hospitalization and Season of Gastric Cancer Inpatients in 2014–2019. In our survey, 69.61% (607/872) of gastric cancer patients were men, more than women, 58.03% (506/872) in spring and summer. The number of inpatients, age, gender, address, average length of stay, discharge conditions, smoking and drinking habits, occupation, past medical history, eating habits, western medicine costs, and complaints vary with seasons. In spring and summer, male patients accounted for 37.61% (328/872), 33.03% (148 + 140)/872), 45.76% (399/872), 46.22% (403/872), 17.78% (155/872), and 15–21 days in average; 25.23% (220/872) patients had no habit of smoking and drinking, 9.72% (172/872) employees in spring and summer, and 25.0% (218/872) patients had other medical history. 30.85% of gastric cancer patients (269/872) like to eat meat. Most patients with gastric cancer had anorexia, accounting for 35.44% (309/872). The difference was statistically significant ($P < 0.05$).

3.2. Logistic Multiple Factor Regression Analysis of Hospitalized and Season-Related Gastric Cancer Patients in 2014–2019. From Table 1, it appears that age, city, and average length of stay are negatively correlated with seasons, indicating that patients of 40-year-old age are more likely to be treated in spring and summer than those with average residence time 14 days in this city, and age is strongly correlated negatively (value b is −1423), which is a protective factor for the seasonal onset. The number of patients, gender, profession, past medical history, dietary habits, and the cost of western medicine are largely related to the times. It is observed that locals, men, and vegetarians below 40-years of age are more likely to develop gastric cancer in spring and summer. They are hospitalized for the first time. The cost of western medicine is less than or equal to the median, while the average stay time is less than or equal to 14 days. In terms of occupational classification, farmers are more likely to get sick in spring and summer than those in other industries. However, the differences among workers, cadres, and retirees in gastric cancer are not obvious, indicating that there is a seasonal relationship between farmers and gastric cancer. We studied the history of gastric cancer patients and

found that gastrointestinal system diseases, diabetes, and cardiovascular and cerebrovascular diseases were highly correlated with seasons. The correlation of diabetes mellitus was greater than that of the gastrointestinal system disease and cardiovascular and cerebrovascular diseases ($P < 0.05$). The b values of fever, anorexia, and emaciation were 1.584, 1.596, and 1.371, respectively.

3.3. Analysis of Gastric Cancer Cells under Microscope. Disinfect the super-clean working table with 70% alcohol [10], put the reagents and equipment required for the experimental operation in order, sterilize with ultraviolet radiation for 30 minutes, use the gastric cancer cells extracted by the gastric cancer patients in the hospital, change the experimental work clothes, wear masks, hats, and sterile gloves, and then enter the super-clean working table to start the experimental operation. The gastric cancer cells were identified by hematoxylin eosin (he) staining [11, 12] and immunohistochemistry. Gastric cancer cells were fixed with 2% formaldehyde, hematoxylin eosin (he) staining, and immunohistochemistry (CD3, CD20, and CD30). Cut the fixed tissue into several pieces with a thickness of about 3 mm. Wash the slices repeatedly with distilled water to keep the surface clean. Press the clean slide on the surface of the tissue slide to form a cell imprint. Wash the cell marks with distilled water and dry in a clean space. The cut sections were made into paraffin sections, and gastric cancer cells were labeled by HE staining and immunohistochemistry. Record the number of cells. Gastric cancer cells were divided into four equal parts. Gently blow the cell suspension with a straw for 3–5 times, then slowly suck it out, transfer it into a 15 ml centrifuge tube, add 10 ml RPMI-1640 culture medium, mix it fully, centrifugate it at 1000 rpm for 5 min, discard the supernatant, add a proper amount of RPMI-1640 culture medium, and then gently blow it for 10 times, so that the culture medium and cell sedimentation are fully mixed. Adjust the concentration of cell suspension, inoculate it into culture bottle, and put it into constant temperature incubator for culture. Adjust the temperature and humidity of incubator to simulate spring, summer, autumn, and winter. After 24 hours, change the solution once and then change it once a day according to the cell growth. Gastric cancer cells were cultured for one week and the number of cells was observed under atomic force microscope. The results showed that the number of gastric cancer cells increased more in spring and summer.

4. Result Analysis

In this paper, we first sort out and analyze some basic information of gastric cancer inpatients and establish excel tables for statistical data, use statistical software to analyze the collected data, and use the collected data to analyze the factors that cause gastric cancer, which are related to seasons. The chi-square test and logistic regression analysis were used to analyze single factor and multiple factors respectively. $P < 0.05$ indicated that the significant difference was significant. It can be seen from Table 2 that there are

TABLE 1: Logistic multiple factor regression analysis of hospitalized and season-related gastric cancer patients in 2014–2019.

Project	B	Standard error	Wald	df	Significant level	Exp (B)
Number of hospitalizations	0.396	0.170	5.409	1	0.020	1.489
Gender	0.414	0.167	6.146	1	0.013	1.513
Age	−1.423	0.473	9.064	1	0.003	0.241
Outside the city	−0.437	0.175	6.256	1	0.012	0.646
Average length of stay	−0.847	0.295	8.241	1	0.004	0.429
Occupation	0.720	0.277	6.766	1	0.009	2.054
Past medical history	1.029	0.324	10.093	1	0.001	2.799
Eating habits	0.445	0.148	9.050	1	0.003	1.561
Western medicine expenses	0.535	0.236	5.133	1	0.023	1.707
Chief complaint	1.584	0.487	10.578	1	0.001	4.873

more patients in spring and summer in our hospital. On the other hand, the number of gastric cancer cells in spring and summer is significantly more than that in other two seasons.

Other factors, such as eating habits, age, region, genetic factors, and occupation, are ignored in this paper. These factors will affect gastric cancer, but only the patients' wish seasons were investigated. The results are shown in Figure 1. It can be seen from Figure 1 that the proportion of admission in spring and summer is significantly higher than that in other two seasons. On the other hand, the growth rate of gastric cancer cells in spring and summer is higher than that in autumn and winter.

This paper also makes some simple investigations on some bad habits of the patients. The investigation results are shown in Figure 2. It is found that many female patients use excessive diet to lose weight, resulting in overeating, making their stomach too hungry and full, leading to gastric cancer. Of course, male patients also have related problems. In the future eating habits, we must not overeat. Of course, there are other bad eating habits, such as eating too salty, not eating breakfast, eating pickled food, and eating too fast; these habits are also the factors inducing gastric cancer.

According to the research results of scholars, we found that 5–10% of cancers are genetically related, and the rest are closely related to the environment and living habits of patients. In 1993, the research results of the scholars who studied the gastric cancer patients in Harbin that is a big city of east-north of China showed that the lack of vegetables and bad eating habits in winter were important causes of gastric cancer. Scholars believe that cabbage, potato, and pickle are the main vegetables in winter in Harbin, which lead to a large number of NO_3^- and NO_2^- production, leading to malignant transformation of gastric epithelial cells. However, in this study, there is a trend of frequent occurrence in spring and summer. In the near future, edible vegetables in winter are not limited to cabbage and potatoes. At the same time, it was found that vegetarianism can also cause gastric cancer in spring and summer. In recent years, the living standard of residents has been improved continuously. In recent 20 years, the dietary structure of residents in China has changed a lot compared with that before. Although the variety of food is rich, the food that residents eat does not achieve nutrition balance; absolute vegetarianism does not represent health, which has become one of the inducing factors of gastric

cancer. In 2010, it was listed as the "Mediterranean diet" of "world cultural heritage," which is characterized by balanced food nutrition and a perfect balance combination of appropriate amount of red wine. The incidence rate of cancer in the Mediterranean is lower than that in Nordic or American countries. This may be due to healthy eating habits. In the spring and summer of Heilongjiang Province, the climate warms rapidly and the sunshine grows longer. Young and middle-aged people under the age of 40 have changed their way of life too fast. Irregular work and rest, improper diet, and other unhealthy lifestyle may be the main reason for the rapid induction of gastric cancer. Therefore, balanced nutrition and healthy life are of great significance for the prevention and treatment of gastric cancer and other tumors.

In addition to the investigation of patients, we have also effectively used the modern advanced medical equipment and atomic force microscope. We made sections of the extracted gastric cancer cells and observed them with atomic force microscope first and then cultured them in different seasons. The other variables were the same. Only one variable of the environment was retained by the control variable method, and the gastric cancer cells cultured at the same time were observed. In seven days, we observed four times and counted the four times, respectively The number of gastric cancer cell lines is shown in Figure 3. The number of gastric cancer cells cultured in spring and summer was significantly higher than that in autumn and winter.

We also made a rough statistics on the number of gastric cancer cells cultured for seven days. When the cells accounted for more than 80% of the bottom area of the culture bottle, subculture was carried out. Regularly sterilize the ultraclean working table with alcohol, put the equipment required for the experiment in order, and irradiate it with ultraviolet light for 30 minutes, so as to complete the sterilization. RPMI-1640 culture medium, 0.25% trypsin, and PBS buffer solution were taken out of the refrigerator in advance and put into the greenhouse, and the bottle mouth and body were sterilized with alcohol and then put into the ultraclean workbench. The gastric cancer cell culture bottle was taken out of the incubator, and the culture of gastric cancer cells was observed by microscope. Whether the cells were contaminated or the cells occupied 80% of the bottom area of the bottle, spray the disinfectant bottle mouth with

TABLE 2: X2 test results of gastric cancer inpatients and season-related factors in our hospital from 2014 to 2019.

	Autumn and winter 1 (366)	Spring and summer 2 (506)	Total (person time)	Chi-squared value	P
Number of hospitalizations					< 0.05
Once = 1	251	300	551	7.88	
More than or equal to 2 times = 2	115	206	321		
Gender					< 0.05
Male	279	328	607	9.13	
Female	87	178	265		
Age					< 0.05
≤40 years = 1	7	37	44	13.73	
41–50 years = 2	60	76	136		
51–60 years = 3	104	148	252		
61–70 years = 4	115	140	255		
≥71 years = 5	80	105	185		
Address					< 0.05
Local	258	399	657	7.99	
Field	108	107	215		
Average length of stay					< 0.05
≤7 days = 1	84	140	224	8.95	
8–14 days = 2	62	108	170		
15–21 days = 3	119	155	274		
≥22 days = 5	101	103	204		
Discharge					< 0.05
To heal or improve (1)	311	403	714	4.06	
Not cured or dead (2)	55	103	158		
Smoking and drinking					< 0.05
Never smoke or drink (1)	178	220	398	51.51	
Occasional smoking or drinking (2)	52	87	139		
Occupation					< 0.05
Worker (1)	98	172	270	11.64	
Farmer (2)	48	36	84		
Cadre (3)	78	107	185		
Retire (4)	36	46	82		
Others (5)	106	145	251		
Past medical history					
Diseases of gastrointestinal system (1)	91	103	194		
Diabetes (2)	24	28	52	12.27	< 0.05
Respiratory diseases (3)	30	25	55		
Cardiovascular and cerebrovascular diseases (4)	102	132	234		
Others (5)	119	218	337		
Eating habits					< 0.05
Vegetarianism or vegetarianism (1)	204	237	441	6.73	
Mainly meat (2)	162	269	431		
Western medicine expenses					< 0.05
≤median = 1	160	274	434	4.40	
> median = 2	192	246	438		

TABLE 2: Continued.

	Autumn and winter 1 (366)	Spring and summer 2 (506)	Total (person time)	Chi-squared value	P
Chief complaint					
Fever	50	66	116	17.27	< 0.05
Loss of appetite	249	309	558		
Emaciation	60	89	149		
Hematemesis (and) or black stool	7	42	49		

FIGURE 1: Seasonal survey of patients in hospital.

FIGURE 2: A survey of the patients' bad eating habits.

FIGURE 3: The number of gastric cancer cell lines under simulated four season's environment microscope.

metaplasia, when the cell shape becomes round and the cell gap becomes large, indicates that the cell digestion is almost completed. Then, pour out the liquid in the bottle gently, add a proper amount of culture medium to stop digestion, and use a straw to gently move the bottom and around the bottle; in this way, all cells in the bottle are suspended in the culture medium, thus becoming a cell suspension. Count with the counting board of novice, first wipe and disinfect the counting board with alcohol cotton ball, and then put the clean cover glass on the small hole. The cover slide is slightly inclined to the left, so that the surface of the counting plate can be exposed a little, and the drop pool can be suspended. Gently blow the cell suspension with a pipette to make it fully mixed. Use a pipette to take a proper amount of cell suspension (pay attention to the appropriate amount of suspension, so as to avoid overflow due to too much suspension or bubbles due to too little suspension, resulting in counting failure). Gently place it in the space next to the cover glass and allow standing for 3 minutes on the super-clean bench. Turn on the inverted microscope, first turn to the low power mirror, find the counting chamber, then aim the field of vision at the center of the large square, and then turn to the high power mirror.

The statistical results are shown in Figure 4. After statistics, we also found that the growth of gastric cancer cells was significantly faster in spring and summer, especially in summer. So, in these two seasons, we should pay more attention to cultivate good eating habits and actively prevent gastric cancer.

alcohol and then put it on the ultraclean worktable. Use the outer flame of alcohol lamp to sterilize the cell culture bottle mouth, open the bottle cap, pour out the culture liquid in the bottle, use a straw to suck a proper amount of PBS buffer into the culture bottle, gently shake the culture bottle for three times, then pour out, then add 2 ml of 0.25% trypsin digestion solution into the cell culture bottle, cover the bottle cap, put it on the super-clean table, and then use a microscope to check the cell elimination The degree of

FIGURE 4: The number of gastric cancer cells after seven-day culture in simulated four-season environment.

5. Conclusions

Through this research, we have found that farmers are more vulnerable to stomach cancer than other occupations. China is a large agricultural country, limited by climatic conditions; the most tired period is spring and summer every year, where the degree of fatigue of farmers is significantly higher than in autumn and winter. This may increase the risk of stomach cancer in farmers in spring and summer. In this paper, we investigated and studied the patients with gastric cancer in our hospital. The results showed that the number of gastric cancer patients in spring and summer was higher than that in the first two seasons, indicating that the growth of gastric cancer cells was related to seasons. The occurrence and development of gastric cancer are related to seasons to a certain extent: local gastric cancer patients are less than 40 years old, male; vegetarians are easy to get sick in spring and summer, and mostly in spring and summer, the average stay time is less than or equal to 14 days, while the cost of western medicine is not high, reflecting that the economic burden of gastric cancer patients in this season is small and recovery is fast. In this profession, the history of gastrointestinal system disease, diabetes, cardiovascular and cerebrovascular diseases, fever, anorexia, and emaciation can all lead to gastric cancer in spring and summer. In addition, we also used modern medical equipment and atomic force microscope to observe gastric cancer cells and used control variable method to simulate four different seasons to culture and observe gastric cancer cells. The results showed that the growth rate of gastric cancer cells in spring and summer was significantly higher than that in other two seasons. Based on the investigation and research, we should pay attention to understanding the reasonable diet structure and healthy lifestyle and prevent and control diabetes, gastrointestinal system diseases, cardiovascular and cerebrovascular diseases, and so on, so as to reduce the incidence rate of gastric cancer in spring and summer. In short, developing good eating habits and living habits will be of great significance to the prevention and control of diseases, which is conducive to a healthy body.

Data Availability

No data were used to support this study.

Conflicts of Interest

The authors declare that they have no conflicts of interest.

References

[1] P. Antonio and F. Natale, "Screening for gastric cancer," *American Journal of Gastroenterology*, vol. 20, no. 2, pp. 20–23, 2019.

[2] C. Ping, L. Yulan, K. Zheng et al., "Risk factors of gastric cancer in high-risk region of China: a population-based case-control study," *Asian Pacific Journal of Cancer Prevention: APJCP*, vol. 8, no. 2, pp. 15–18, 2019.

[3] A. Shinozaki-Ushiku, A. Kunita, and M. Fukayama, "Update on Epstein-Barr virus and gastric cancer (review)," *International Journal of Oncology*, vol. 16, no. 3, pp. 55–58, 2018.

[4] Z. Li, H. Lei, M. Luo et al., "DNA methylation downregulated mir-10b acts as a tumor suppressor in gastric cancer," *Gastric Cancer Official Journal of the International Gastric Cancer Association & the Japanese Gastric Cancer Association*, vol. 17, no. 8, pp. 29–40, 2016.

[5] M. Plummer, F. Silvia, J. Vignat, D. Forman, and C. De Martel, "Global burden of gastric cancer attributable to *Helicobacter pylori*," *Journal International Du Cancer*, vol. 136, no. 2, pp. 487–490, 2015.

[6] S. Liu and Y. Zhou, "Perioperative standardized management under the guidance of fast track surgery in gastric cancer patients," *Zhonghua Wei Chang Wai Ke Za Zhi = Chinese Journal of Gastrointestinal Surgery*, vol. 18, no. 2, pp. 116–120, 2016.

[7] J. Wang, J. Yu, J. Wu et al., "Experimental study of human bone marrow mesenchymal stem cells on regulating the biological characteristics of gastric cancer cells," *Chinese Journal of Gastrointestinal Surgery*, vol. 18, no. 2, pp. 159–165, 2018.

[8] A. Okines, D. Cunningham, M. Verheij et al., "Gastric cancer: ESMO clinical practice guidelines for diagnosis, treatment and follow-up," *Annals of Oncology Official Journal of the European Society for Medical Oncology*, vol. 18, no. 2, pp. 11–19, 2016.

[9] Department of Surgery, "Laparoscopic wedge resection of the stomach for early gastric cancer (lesion lifting method)," *Progress of Digestive Endoscopy (1972)*, vol. 9, no. 7, pp. 12–18, 2016.

[10] T. Kinoshita, T. Kinoshita, A. Saiura et al., "Multicentre analysis of long-term outcome after surgical resection for gastric cancer liver metastases," *British Journal of Surgery*, vol. 102, no. 1, pp. 102–107, 2017.

[11] T. Kinoshita, A. Saiura, M. Esaki et al., "Multicentre analysis of long-term outcome after surgical resection for gastric cancer liver metastases," *British Journal of Surgery*, vol. 10, no. 18, pp. 9–18, 2016.

[12] H. J. Lee, W. Kim, H. H. Kim et al., "Decreased morbidity of laparoscopic distal gastrectomy compared to open distal gastrectomy for stage I gastric," *Cancer*, vol. 263, no. 1, pp. 19–28, 2017.

Research Article

TIFNCWBHG-MAGDM for System Evaluation Based on TIFNs for the Safety Input of Coal Enterprise

Chao Zhang [1,2] **and Qingjie Qi** [3]

[1]*College of Safety Science and Engineering, Liaoning Technical University, Huludao 125105, China*
[2]*Mining College, Liaoning Technical University, Fuxin 123000, Liaoning, China*
[3]*Beijing Research Institute, China Coal Research Institute, Beijing 100013, China*

Correspondence should be addressed to Chao Zhang; zhangchao@lntu.edu.cn

Determining the safety input structure is essential to achieve efficient resource utilization and the safe production of coal enterprises. In this paper, the system evaluation method, TIFNCWBHG-MAGDM, is proposed to evaluate the safety input of coal enterprises. It is based on the integration of the intuitionistic triangular fuzzy numbers (TIFNs), TIFNs Compound Weight Bonferroni Hybrid Geometric (TIFNCWBHG) operator, and multiattribute group decision-making (MAGDM) theory. First, the judgment matrix of TIFNs is constructed from multiperspective: multitime points, multiattributes, and multiexperts. The TIFNCWBHG operator integrates the TIFNs score function, stability weight, and position weight. Then, the priorities for safety inputs are determined. The experimental results showed that safety inputs in industrial hygiene, propaganda, and education significantly impact the overall level of safety inputs. Also, it was proved that the efficiency of the safety input is important. The proposed TIFNCWBHG-MAGDM effectively coordinated the stability weight, position weight, and computation of TIFNs score function, taking the advantages of TIFNs. Accordingly, it was proved that it could optimize the safety input structure.

1. Introduction

The safety input structure aims to embody the safety production management level of coal enterprises, which is a crucial part of the safety production development strategy. In order to improve the safety input structure of coal enterprises, a timely scientific and reasonable evaluation is needed. However, the production system of coal enterprises is a dynamic and multivariate complex system constructed by stereoscopic multioverlapping factors in time and space. In addition, coal safety accidents occur as random, dynamic, and uncertain. The safety output is not necessarily correlated to the overall scale of the safety input of coal enterprises. Accordingly, the determination of the safety input structure should be thoroughly studied.

Jiang et al. [1] established a new index system of safety investment based on the set theory. Also, the safety investment and accident control model was constructed using grey prediction theory. Xiao et al. [2] conducted a statistical analysis of accidents over the years to establish a safety investment optimization model, which was based on maximizing economic efficiency and in-depth analysis of safety investment. Dzonziundi [3] computed the total factor productivity (TFP) and technical efficiency (EF) of several enterprises and analyzed the impact of safety input and cleaner production input using the stochastic frontier analysis (SFA). Zhao et al. [4] employed grey theory, multicriteria group decision theory, Triangular Intuitionistic Fuzzy Numbers (TIFNs), and Analytic Hierarchy Process (AHP) to rank and evaluate the safety inputs of coal enterprises. Zhang et al. [5] conducted in-depth research on evaluating the safety resources structure of the coal production logistics system and coal mine safety status. Lu et al. [6] used an agent to study the safety investment of the construction industry under the influence of various factors. Noh and Chang [7] proposed an economic analysis method considering the cost of safety investment and applied it to the comparative evaluation of process plant design.

Matthews et al. [8] designed software to support road safety practitioners in analyzing and making decisions. Roy and Gupta [9] proposed the framework of safety investment optimization (SIO) to decrease the accident risk that reduces the future costs under the given budget. Han et al. [10] used the safety investment theory model, questionnaire, and structural equation model (SEM) to study the relationship between safety investment, safety cognition, and construction personnel behavior. Hou and Zhoa [11] combined the Cobb–Douglas production function with the FTA probability model to establish a safety input structure risk-minimization model of petrochemical port enterprises, where the Gompertz curve model is used as a constraint. Lu et al. [12] studied the influence of different safety investments and parameters, such as human factors and environmental factors, on safety performance. Ma et al. [13] established an analysis model from the perspective of opportunity cost and analyzed the factors affecting the safety investment decision-making. Lopezalonso et al. [14] conducted a sample survey using a questionnaire and analyzed the health and safety investments of construction companies. Wu and Wemple [15] proposed a methodology for analyzing the costs and benefits of safety investment to optimize investments. Aven and Hiriart [16] studied the robust optimization of the basic safety input model. Unlike those methods, Zhang et al. [17] proposed a novel MABAC method for MAGDM under a linguistic environment. Wei et al. [18] proposed the MABAC based on the UPLTSs for green supplier selection. Many methods were synthesized in the system, such as the MAGDM, UPLTSs, and entropy method. The GRA method was proposed based on the PLTs for site selection of electric vehicle charging stations in [19] after several methods, including MAGDM, PLTs, GRA method, and CRITIC method, were compared. In [20], the VIKOR method was proposed based on the 2TLNNs and IV2TLNNs for green supplier selection.

As described, the main research direction for enterprise safety input or safety investment has been focused on construction, transportation, and other industries [7–16]. Also, in many studies [1–4, 7–16], the quantitative information was too rough and inaccurate. The potential information and related weight information in the data could not be deeply mined, easily distorting important information. Further, the changes of state variables affecting the safety input are varied, and the influence factors are affected by each other. Thus, safety input needs to be systematically and comprehensively considered. However, few evaluation methods were studied to combine multiple-attribute group decision-making, fuzzy mathematics theory. In addition, the above methods had high computational complexity and were not conducive to the promotion and obtaining accurate evaluation results that adapt to various application environments.

Uncertain multiattribute decision-making and linguistic decision-making are two significant branches of decision theory and technology. They were widely used since they were proposed, and recently latest variants were proposed, such as [17–21]. Motivated by the significant achievements in uncertain multiattribute decision-making, we propose integrating into the system the fuzzy mathematics theory, MAGDM, TIFNCWBHG operator, and other methods and theories. The proposed novel evaluation method is based on MAGDM theory and intuitionistic triangular fuzzy numbers [21]. TIFNs contain rich information, and thus it can better describe the uncertainty of the environment and the fuzziness of decision-makers. It is also flexible and practical so that it is easy to understand and use. It can supplement the lack of gravity center when the membership degree and non-membership degree of the interval-valued fuzzy-set are expressed by interval numbers and other similar situations. Each attribute value is first expressed by TIFNs, and then the TIFNs judgment matrix is built considering attributes, experts, time points, and other aspects. The TIFNCWBHG operator is given by fusing TIFNs score function [22], position weight [23], and stability weight [24]. The operator is used for integrated calculation, and then, the priority order of each safety input is determined. Finally, the TIFNCWBHG-MAGDM model evaluates the safety input categories of coal enterprises to provide the basis for safety input decision-making.

2. TIFNCWBHG-MAGDM Method

2.1. TIFNs Judgment Matrix for MAGDM. In the various operations of TIFNs, we often need to use the score function, especially when using the operator, including TIFNs. The calculation formula of the score function of TIFNs [22] is defined as follows.

Definition 1 (see [22]). Let $\widetilde{\beta} = ([a, b, c], [l, m, n])$ be TIFNs. The score function of $\widetilde{\beta}$ can be expressed as

$$\widetilde{S}(\widetilde{\beta}) = \frac{a + 2b + c}{4} + \frac{l + 2m + n}{4}. \tag{1}$$

where $\widetilde{S}(\widetilde{\beta}) \in [-1, 1]$. Equation (1) shows that there exists a corresponding relationship between $\widetilde{S}(\widetilde{\beta})$ and $\widetilde{\beta}$. The larger the value of $\widetilde{S}(\widetilde{\beta})$, the larger the $\widetilde{\beta}$. For example, when $\widetilde{S}(\widetilde{\beta}) = 1$, $\widetilde{\beta}$ is the maximum and $\widetilde{\beta} = ([1, 1, 1], [0, 0, 0])$. When $\widetilde{S}(\widetilde{\beta}) = -1$, $\widetilde{\beta}$ is the minimum and $\widetilde{\beta} = ([0, 0, 0], [1, 1, 1])$.

Through (1), the sizes of two TIFNs are compared and sorted for computing TIFNs operators. However, sometimes, it is not easy to compare them with (1), because, in some special cases, two different TIFNs may get the same score. Thus, an accurate score function is required to calculate and compare the two TIFNs.

The score function is used to compare two TIFNs accurately, which is defined as follows.

Definition 2 (see [22]).

$$\widetilde{L}(\widetilde{\beta}) = \frac{a + 2b + c}{4} \left(2 - \frac{a + 2b + c}{4} - \frac{l + 2m + n}{4} \right), \tag{2}$$

where $\widetilde{L}(\widetilde{\beta}) \in [0, 1]$ and the greater the value of $\widetilde{L}(\widetilde{\beta})$, the greater the value of $\widetilde{\beta}$. For example, when $\widetilde{L}(\widetilde{\beta}) = 1$, then $\widetilde{\beta}$ is the maximum and $\widetilde{\beta} = ([1, 1, 1], [0, 0, 0])$. When $\widetilde{L}(\widetilde{\beta}) = -1$, then $\widetilde{\beta}$ is the minimum and $\widetilde{\beta} = ([0, 0, 0], [1, 1, 1])$.

When the score function is used to calculate the scores of two TIFNs in the actual evaluation process, the importance of membership degree and nonmembership degree of TIFNs may be different. In order to take into account the relative importance of membership and non-membership degrees, they are added to the score function of TIFNs. The reformulated score function is defined as follows.

Definition 3.

$$
\widetilde{S}(\widetilde{\beta}) = 4\xi_1\left(\frac{\zeta_1 a + 2\zeta_2 b + \zeta_3 c}{4}\right) + 4\xi_2\left(\frac{\zeta_1' l + 2\zeta_2' m + \zeta_3' n}{4}\right)
$$
$$
= \xi_1\left(\zeta_1 a + 2\zeta_2 b + \zeta_3 c\right) + \xi_2\left(\zeta_1' l + 2\zeta_2' m + \zeta_3' n\right).
$$
(3)

It is worth noting that, in (3), the coefficients of factors such as membership degree and nonmembership degree satisfy the following conditions: $\xi_1, \xi_2 \geq 0$, $\xi_1, \xi_2 = 1$, $\zeta_1, \zeta_2, \zeta_3, \zeta_1', \zeta_2', \zeta_3' \geq 0$, and $\zeta_1 + \zeta_1' = \zeta_2 + \zeta_2' = \zeta_3 + \zeta_3' = 1$. Also, in order to maintain the consistency of calculations, the coefficient values of membership and nonmembership degrees remain unchanged once determined. Furthermore, it is clear that (3) still satisfies the following conditions: there is a corresponding relationship between $\widetilde{S}(\widetilde{\beta})$ and $\widetilde{\beta}$. The larger the value of $\widetilde{S}(\widetilde{\beta})$, the larger the value of $\widetilde{\beta}$. When $\widetilde{S}(\widetilde{\beta}) = 1$, $\widetilde{\beta}$ is the maximum value and $\widetilde{\beta} = ([1, 1, 1], [0, 0, 0])$. When $\widetilde{S}(\widetilde{\beta}) = -1$, $\widetilde{\beta}$ is the minimum value and $\widetilde{\beta} = ([0, 0, 0], [1, 1, 1])$.

Similarly, the coefficients of membership and non-membership degrees are added for the accurate score function, as follows.

Definition 4.

$$
\widetilde{L}(\widetilde{\beta}) = 4\xi_1\left(\frac{\zeta_1 a + 2\zeta_2 b + \zeta_3 c}{4}\right)\left[2 - 4\xi_1\left(\frac{\zeta_1 a + 2\zeta_2 b + \zeta_3 c}{4}\right)\right.
$$
$$
\left. - 4\xi_2\left(\frac{\zeta_1' l + 2\zeta_2' m + \zeta_3' n}{4}\right)\right]
$$
$$
= \xi_1\left(\zeta_1 a + 2\zeta_2 b + \zeta_3 c\right)\left[2 - \xi_1\left(\zeta_1 a + 2\zeta_2 b + \zeta_3 c\right)\right.
$$
$$
\left. - \xi_2\left(\zeta_1' l + 2\zeta_2' m + \zeta_3' n\right)\right].
$$
(4)

Note that, in (4), the coefficients of membership and nonmembership degrees satisfy the following conditions: $\xi_1, \xi_2 \geq 0$, $\xi_1 + \xi_2 = 1$, $\zeta_1, \zeta_2, \zeta_3, \zeta_1', \zeta_2', \zeta_3' \geq 0$, and $\zeta_1 + \zeta_1' = \zeta_2 + \zeta_2' = \zeta_3 + \zeta_3' = 1$. Similarly, the coefficient values remain unchanged once determined. Also, (4) satisfies the following conditions: there exists a corresponding relationship between $\widetilde{L}(\widetilde{\beta})$ and $\widetilde{\beta}$. The larger the value of $\widetilde{L}(\widetilde{\beta})$, the larger the value of $\widetilde{\beta}$. When $\widetilde{L}(\widetilde{\beta}) = 1$, $\widetilde{\beta}$ is the maximum and $\widetilde{\beta} = ([1, 1, 1], [0, 0, 0])$, while when $\widetilde{L}(\widetilde{\beta}) = -1$, $\widetilde{\beta}$ is the minimum value and $\widetilde{\beta} = ([0, 0, 0], [1, 1, 1])$.

Under an environment of uncertain multiattribute decision-making, experts' judgment often varies over different time points. Thus, TIFNs judgment matrix **A** for multi-attribute group decision-making at time point t is constructed as follows, considering the influence of time:

$$
\mathbf{\widetilde{B}}^t = \left(\widetilde{\beta}_{ij}^t\right)_{m*n} = \begin{bmatrix} \widetilde{\beta}_{11}^t & \widetilde{\beta}_{12}^t & \cdots & \widetilde{\beta}_{1n}^t \\ \widetilde{\beta}_{21}^t & \widetilde{\beta}_{21}^t & \cdots & \widetilde{\beta}_{2n}^t \\ \vdots & \vdots & \ddots & \vdots \\ \widetilde{\beta}_{m1}^t & \widetilde{\beta}_{m2}^t & \cdots & \widetilde{\beta}_{mn}^t \end{bmatrix},
$$
(5)

where $\mathbf{\widetilde{B}}^t$ is the TIFNs judgment matrix, m is the number of experts, and n is the attributes at time point t. $\widetilde{\beta}_{ij}^t$ represents the TIFNs evaluation of the ith expert for the jth attribute at time point t. $\widetilde{\beta}_{ij}^t = [\widetilde{\mu}_{ij}^t, \widetilde{\gamma}_{ij}^t] = ([a_{ij}^t, b_{ij}^t, c_{ij}^t], [o_{ij}^t, p_{ij}^t, q_{ij}^t])$. TIFN for each time point and each factor is evaluated by experts.

2.2. Stability Weight of Judgement Matrix $\mathbf{\widetilde{B}}^t$.

In order to obtain $\mathbf{B}^t$, the scoring function of each element of the matrix $\mathbf{\widetilde{B}}^t$ is calculated:

$$
\mathbf{B}^t = \begin{bmatrix} \widetilde{S}\left(\widetilde{\beta}_{11}^t\right) & \widetilde{S}\left(\widetilde{\beta}_{12}^t\right) & \cdots & \widetilde{S}\left(\widetilde{\beta}_{1n}^t\right) \\ \widetilde{S}\left(\widetilde{\beta}_{21}^t\right) & \widetilde{S}\left(\widetilde{\beta}_{22}^t\right) & \cdots & \widetilde{S}\left(\widetilde{\beta}_{2n}^t\right) \\ \vdots & \vdots & \ddots & \vdots \\ \widetilde{S}\left(\widetilde{\beta}_{m1}^t\right) & \widetilde{S}\left(\widetilde{\beta}_{m2}^t\right) & \cdots & \widetilde{S}\left(\widetilde{\beta}_{mn}^t\right) \end{bmatrix}.
$$
(6)

After normalizing the element of the matrix $\mathbf{B}^t$, a new matrix $\mathbf{\overline{B}}^t$ is obtained:

$$
\mathbf{\overline{B}}^t = \begin{bmatrix} \dfrac{\widetilde{S}\left(\widetilde{\beta}_{11}^t\right)}{\sum_{i=1}^m \widetilde{S}\left(\widetilde{\beta}_{i1}^t\right)} & \dfrac{\widetilde{S}\left(\widetilde{\beta}_{12}^t\right)}{\sum_{i=1}^m \widetilde{S}\left(\widetilde{\beta}_{i2}^t\right)} & \cdots & \dfrac{\widetilde{S}\left(\widetilde{\beta}_{1n}^t\right)}{\sum_{i=1}^m \widetilde{S}\left(\widetilde{\beta}_{in}^t\right)} \\[2em] \dfrac{\widetilde{S}\left(\widetilde{\beta}_{21}^t\right)}{\sum_{i=1}^m \widetilde{S}\left(\widetilde{\beta}_{i1}^t\right)} & \dfrac{\widetilde{S}\left(\widetilde{\beta}_{22}^t\right)}{\sum_{i=1}^m \widetilde{S}\left(\widetilde{\beta}_{i2}^t\right)} & \cdots & \dfrac{\widetilde{S}\left(\widetilde{\beta}_{2n}^t\right)}{\sum_{i=1}^m \widetilde{S}\left(\widetilde{\beta}_{in}^t\right)} \\[2em] \vdots & \vdots & \ddots & \vdots \\[1em] \dfrac{\widetilde{S}\left(\widetilde{\beta}_{m1}^t\right)}{\sum_{i=1}^m \widetilde{S}\left(\widetilde{\beta}_{i1}^t\right)} & \dfrac{\widetilde{S}\left(\widetilde{\beta}_{m2}^t\right)}{\sum_{i=1}^m \widetilde{S}\left(\widetilde{\beta}_{i2}^t\right)} & \cdots & \dfrac{\widetilde{S}\left(\widetilde{\beta}_{mn}^t\right)}{\sum_{i=1}^m \widetilde{S}\left(\widetilde{\beta}_{in}^t\right)} \end{bmatrix}.
$$
(7)

Then, corresponding to time point t and attribute j, the stability weights of expert evaluations are computed. From (6) and (7) [24], (8) and (9) are derived:
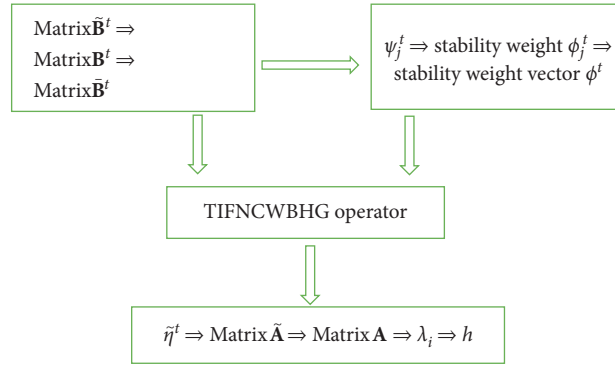
FIGURE 1: The flow chart of the TIFNCWBHG-MAGDM method.

$$\psi_j^t = \frac{1}{\ln m} \sum_{i=1}^m \dot\beta_{ij}^t \ln \dot\beta_{ij}^t, \tag{8}$$

$$\varphi_j^t = \frac{\psi_j^t}{\sum_{j=1}^n \psi_j^t} = \frac{(1/\ln m) \sum_{i=1}^m \dot\beta_{ij}^t \ln \dot\beta_{ij}^t}{\sum_{j=1}^n (1/\ln m) \sum_{i=1}^m \dot\beta_{ij}^t \ln \dot\beta_{ij}^t}$$
$$= \frac{\sum_{i=1}^m \dot\beta_{ij}^t \ln \dot\beta_{ij}^t}{\sum_{j=1}^n \sum_{i=1}^m \dot\beta_{ij}^t \ln \dot\beta_{ij}^t}, \tag{9}$$

where φ_j^t represents the stability weight obtained by normalizing ψ_j^t by column.

The stability weight vector can be obtained by

$$\varphi^t = \left(\varphi_1^t, \varphi_2^t, \dots, \varphi_n^t\right). \tag{10}$$

2.3. TIFNCWBHG Operator.
In order to use TIFNs, it is necessary to construct an operator corresponding to TIFNs. Motivated from [4], the following operators are proposed.

Definition 5. Let F be a mapping: $\Theta^n \longrightarrow \Theta$, if

$$F_{w,\varphi,\omega}\left(\widetilde\beta_1, \widetilde\beta_2, \dots, \widetilde\beta_n\right) = \frac{1}{p+q} \left(\overset{n}{\underset{k=1}{\otimes}} \left(p\widetilde\beta_k \oplus q \overset{n-1}{\underset{\substack{t=1 \\ t\neq k}}{\otimes}} \left(\widetilde\beta_t^{(n-1)\left(\xi_1 w_t + \xi_2 \varphi_t\right)\omega_{\sigma(t)}} \right) \right) \right)^{(1/n)}, \tag{11}$$

where Θ is the set of TIFNs. Let $\widetilde\beta_1, \widetilde\beta_2, \dots, \widetilde\beta_n$ be a collection of TIFNs, and $p, q > 0$. $w = (w_1, w_2, \dots, w_n)^T$ is the weight vector, where $w_j \in [0, 1]$, $\sum_{j=1}^n w_j = 1$. $\varphi = (\varphi_1, \varphi_2, \dots, \varphi_n)^T$ is the stability weight vector, where $\varphi_j \in [0, 1]$ and $\sum_{j=1}^n \varphi_j = 1$. $\xi_1, \xi_2 \geq 0$ are weight coefficients, where $\xi_1 + \xi_2 = 1$. $\omega = (\omega_1, \omega_2, \dots, \omega_n)^T$ represents an aggregation-associated vector such that $\omega_j \in [0, 1]$ and $\sum_{j=1}^n \omega_j = 1$. $\widetilde\beta_t$ is the $\sigma(t)^{\text{th}}$ component in $(\widetilde\beta_1, \widetilde\beta_2, \dots, \widetilde\beta_n)$, and $\sigma: \{1, 2, \dots, n\} \longrightarrow \{1, 2, \dots, n\}$ is a sort operator according to the size of the computed value by the score function in the array $(\widetilde\beta_1, \widetilde\beta_2, \dots, \widetilde\beta_n)$; then, $\omega_{\sigma(t)}$ is the position weight corresponding to $\widetilde\beta_t$. In $(\widetilde\beta_t^{(n-1)(\xi_1 w_t + \xi_2 \varphi_t)\omega_{\sigma(t)}})$, $(n-1)$ is a balancing coefficient. Here, when vector $w = (w_1, w_2, \dots, w_n)^T$ tends to $((1/n-1), (1/n-1), \dots, (1/n-1))^T$, vector $\varphi = (\varphi_1, \varphi_2, \dots, \varphi_n)^T$ tends to $((1/n-1), (1/n-1), \dots, (1/n-1))^T$, and $\xi_1 = \xi_2 = 0.5$, and the vector $(\widetilde\beta_1^{(n-1)(\xi_1 w_1 + \xi_2 \varphi_1)\omega_{\sigma(1)}}, \widetilde\beta_2^{(n-1)(\xi_1 w_2 + \xi_2 \varphi_2)\omega_{\sigma(2)}}, \dots, \widetilde\beta_{n-1}^{(n-1)(\xi_1 w_{n-1} + \xi_2 \varphi_{n-1})\omega_{\sigma(n-1)}})^T$ tends to $(\widetilde\beta_1^{\omega_{\sigma(1)}}, \widetilde\beta_2^{\omega_{\sigma(2)}}, \dots, \widetilde\beta_{n-1}^{\omega_{\sigma(n-1)}})^T$. ω can be determined by [23], and the calculation of score function of $\widetilde\beta_t$ can be determined by (3).

When performing various operations on TIFNs in the operator, some algorithms [22] need to be used, defined as follows:

$$\begin{aligned}
\widetilde\beta_1 \oplus \widetilde\beta_2 &= \widetilde\beta_2 \oplus \widetilde\beta_1, \\
\widetilde\beta_1 \otimes \widetilde\beta_2 &= \widetilde\beta_2 \otimes \widetilde\beta_1, \\
\left(\widetilde\beta_1 \otimes \widetilde\beta_2\right)^\lambda &= \widetilde\beta_2^\lambda \otimes \widetilde\beta_1^\lambda, \quad \lambda \geq 0, \\
\widetilde\beta_1^{\lambda_1} \otimes \widetilde\beta_1^{\lambda_2} &= \widetilde\beta_1^{\lambda_1 + \lambda_2}; \quad \lambda_1, \lambda_2 \geq 0.
\end{aligned} \tag{12}$$

2.4. Final Evaluation.
Each column in the matrix is integrated using the TIFNCWBHG operator to compute the initial weight vector of evaluation factors:

$$\widetilde\eta^t = \left(\widetilde\eta_1^t, \widetilde\eta_2^t, \dots, \widetilde\eta_n^t\right), \tag{13}$$

where $\widetilde\eta_1^t, \widetilde\eta_2^t, \dots, \widetilde\eta_n^t$ represent the integrated TIFNs evaluation value of each attribute by experts at time t. Then, the following matrix is constructed:
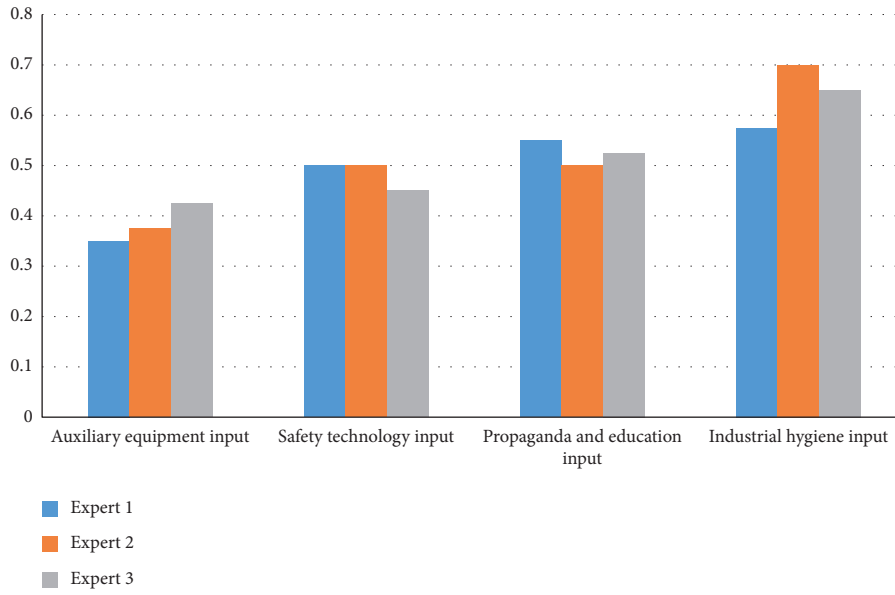
FIGURE 2: Columnar diagram of score function value of TIFNs evaluation data for safety input items (expert 1).
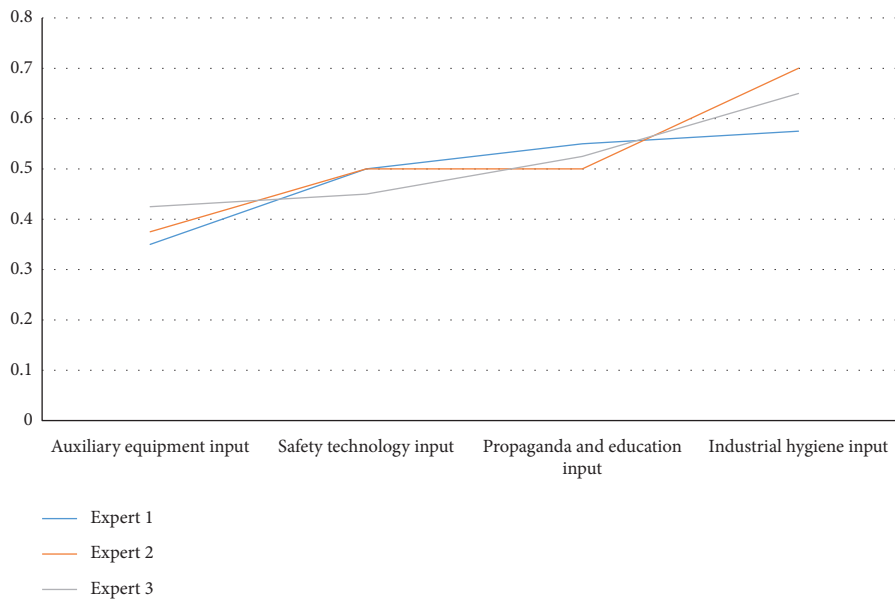
FIGURE 3: Broken line diagram of score function value of TIFNs evaluation data for safety input items (expert 1).

$$\widetilde{\mathbf{A}} = \begin{bmatrix} \widetilde{\eta}_1^1 & \widetilde{\eta}_2^1 & \cdots & \widetilde{\eta}_n^1 \\ \widetilde{\eta}_1^2 & \widetilde{\eta}_2^2 & \cdots & \widetilde{\eta}_n^2 \\ \vdots & \vdots & \ddots & \vdots \\ \widetilde{\eta}_1^p & \widetilde{\eta}_2^p & \cdots & \widetilde{\eta}_n^p \end{bmatrix}. \quad (14)$$

The score function of each element in the matrix is computed to form a new matrix **A**:

$$\mathbf{A} = \begin{bmatrix} \eta_1^1 & \eta_2^1 & \cdots & \eta_n^1 \\ \eta_1^2 & \eta_2^2 & \cdots & \eta_n^2 \\ \vdots & \vdots & \ddots & \vdots \\ \eta_1^p & \eta_2^p & \cdots & \eta_n^p \end{bmatrix}. \quad (15)$$

Let
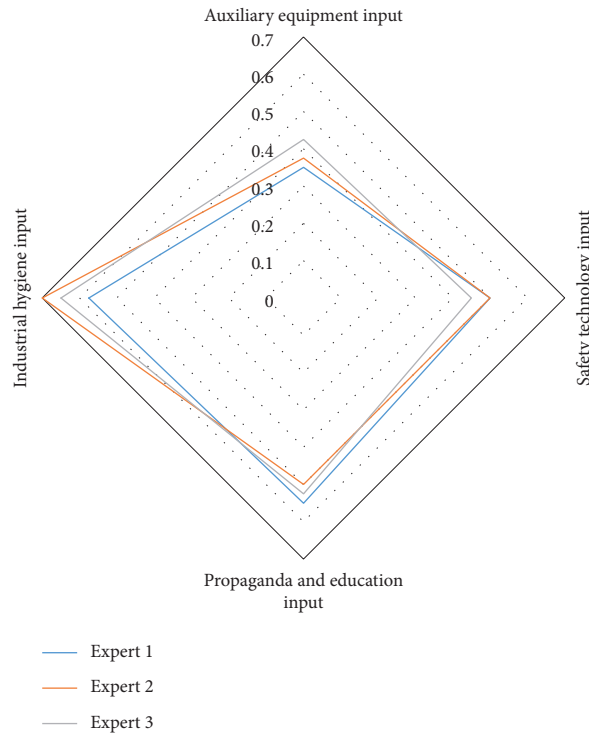
FIGURE 4: Radar diagram of score function value of TIFNs evaluation data for safety input items (expert 1).

$$\lambda_i = \frac{1}{p} \zeta_i \sum_{i=1}^{p} \eta_i^t, \quad (i = 1, 2, \ldots, n), \tag{16}$$

where $\zeta_1, \zeta_2, \ldots, \zeta_n$ are weight coefficients, $\zeta_1, \zeta_2, \ldots, \zeta_n \geq 0$, and $\zeta_1 + \zeta_2 + \cdots + \zeta_n = 1$. Then, the final evaluation vector is obtained as follows:

$$h = [\lambda_1, \lambda_2, \ldots, \lambda_n]. \tag{17}$$

The flow chart of the proposed framework of TIFNCWBHG-MAGDM is shown in Figure 1.

3. Example Analysis

TIFNCWBHG-MAGDM is applied to the evaluation of various safety inputs in a coal mine. There were a few accidents in the mine where all equipment was brand-new and in good condition. Many new miners were recently hired due to the expansion of the production. However, the dust concentration in the workplace was high. Also, they were not well prepared to prevent harmful gases and dust from the lack of attention, and the personal safety protection of miners was poor. In this use-case, $t = (1, 2, 3)$, $m = 3$, $n = 4$. Attributes are auxiliary equipment input, safety technology input, propaganda, education input, and industrial hygiene input. Via experts consulting, the multipoint and multi-attribute group decision-making TIFNs judgment matrices $\widetilde{\mathbf{B}}^1, \widetilde{\mathbf{B}}^2, \widetilde{\mathbf{B}}^3$ were established as follows:

$$
\begin{bmatrix}
([0.5, 0.5, 0.6], [0.1, 0.2, 0.2]) & ([0.6, 0.7, 0.7], [0.1, 0.2, 0.2]) & ([0.6, 0.7, 0.7], [0.1, 0.1, 0.2]) & ([0.7, 0.8, 0.8], [0.2, 0.2, 0.2]) \\
([0.5, 0.6, 0.6], [0.2, 0.2, 0.2]) & ([0.6, 0.7, 0.7], [0.1, 0.2, 0.2]) & ([0.6, 0.7, 0.7], [0.1, 0.2, 0.2]) & ([0.7, 0.8, 0.9], [0.1, 0.1, 0.1]) \\
([0.5, 0.6, 0.7], [0.1, 0.2, 0.2]) & ([0.6, 0.6, 0.7], [0.1, 0.2, 0.2]) & ([0.6, 0.6, 0.7], [0.1, 0.1, 0.1]) & ([0.7, 0.8, 0.8], [0.1, 0.1, 0.2])
\end{bmatrix},
$$
$$
\begin{bmatrix}
([0.5, 0.6, 0.6], [0.1, 0.2, 0.2]) & ([0.6, 0.7, 0.7], [0.1, 0.2, 0.2]) & ([0.6, 0.6, 0.7], [0.1, 0.2, 0.2]) & ([0.7, 0.8, 0.8], [0.2, 0.2, 0.2]) \\
([0.5, 0.5, 0.6], [0.1, 0.1, 0.2]) & ([0.6, 0.6, 0.7], [0.2, 0.2, 0.2]) & ([0.6, 0.6, 0.7], [0.1, 0.1, 0.1]) & ([0.8, 0.8, 0.8], [0.1, 0.2, 0.2]) \\
([0.5, 0.5, 0.5], [0.2, 0.2, 0.2]) & ([0.5, 0.7, 0.7], [0.1, 0.1, 0.1]) & ([0.6, 0.7, 0.7], [0.1, 0.1, 0.1]) & ([0.7, 0.8, 0.8], [0.1, 0.2, 0.2])
\end{bmatrix},
$$
$$
\begin{bmatrix}
([0.5, 0.5, 0.6], [0.2, 0.2, 0.2]) & ([0.6, 0.6, 0.7], [0.2, 0.2, 0.2]) & ([0.6, 0.7, 0.8], [0.1, 0.1, 0.1]) & ([0.7, 0.8, 0.8], [0.1, 0.2, 0.2]) \\
([0.5, 0.5, 0.5], [0.1, 0.1, 0.2]) & ([0.6, 0.7, 0.8], [0.1, 0.2, 0.2]) & ([0.6, 0.7, 0.7], [0.1, 0.2, 0.2]) & ([0.7, 0.7, 0.9], [0.1, 0.1, 0.1]) \\
([0.5, 0.5, 0.6], [0.1, 0.1, 0.1]) & ([0.6, 0.6, 0.8], [0.1, 0.1, 0.1]) & ([0.6, 0.6, 0.7], [0.2, 0.2, 0.2]) & ([0.7, 0.8, 0.8], [0.1, 0.2, 0.2])
\end{bmatrix}.
$$

$$\tag{18}$$
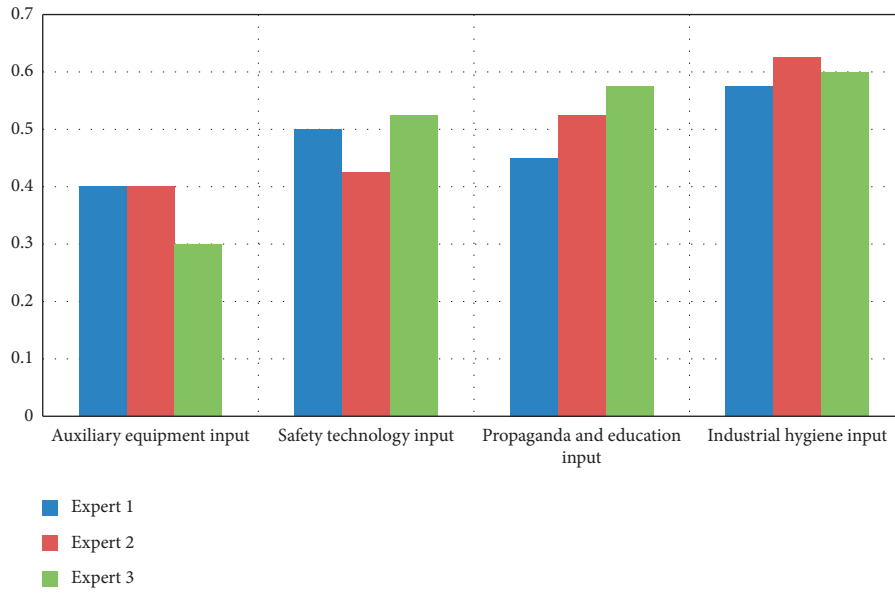
FIGURE 5: Columnar diagram of score function value of TIFNs evaluation data for safety input items (expert 2).
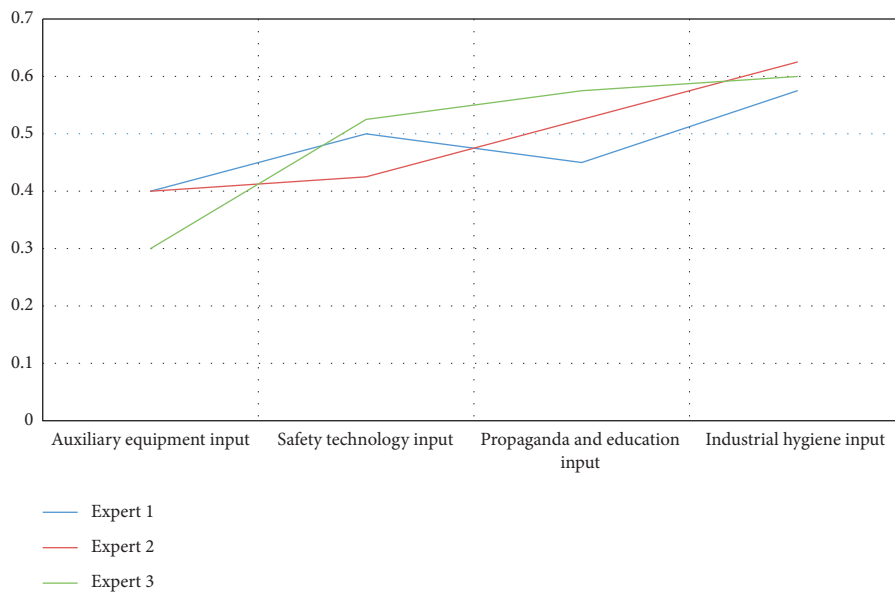
FIGURE 6: Broken line diagram of score function value of TIFNs evaluation data for safety input items (expert 2).

Then, matrix $\mathbf{B}^t$ ($\mathbf{B}^1$) for expert 1 is obtained as

$$\mathbf{B}^1 = \begin{bmatrix} 0.35 & 0.5 & 0.55 & 0.575 \\ 0.375 & 0.5 & 0.5 & 0.7 \\ 0.425 & 0.45 & 0.525 & 0.65 \end{bmatrix}. \tag{19}$$

The score function value of TIFNs evaluation data for safety input items given by expert 1 (dates obtained from (19)) was analyzed using the columnar diagram, broken line diagram, and radar diagram, which are depicted in Figures 2–4, respectively.

The matrix $\mathbf{B}^t$ ($\mathbf{B}^2$) for expert 2 is obtained as

$$\mathbf{B}^2 = \begin{bmatrix} 0.4 & 0.5 & 0.45 & 0.575 \\ 0.4 & 0.425 & 0.525 & 0.625 \\ 0.3 & 0.55 & 0.575 & 0.6 \end{bmatrix}. \tag{20}$$

The score function value of TIFNs evaluation data for safety input items given by expert 2 (dates obtained from (20)) was also analyzed using the columnar diagram, broken line diagram, and radar diagram, which are depicted in Figures 5–7, respectively.

The computed matrix $\mathbf{B}^t$ ($\mathbf{B}^3$) for expert 3 is as follows:
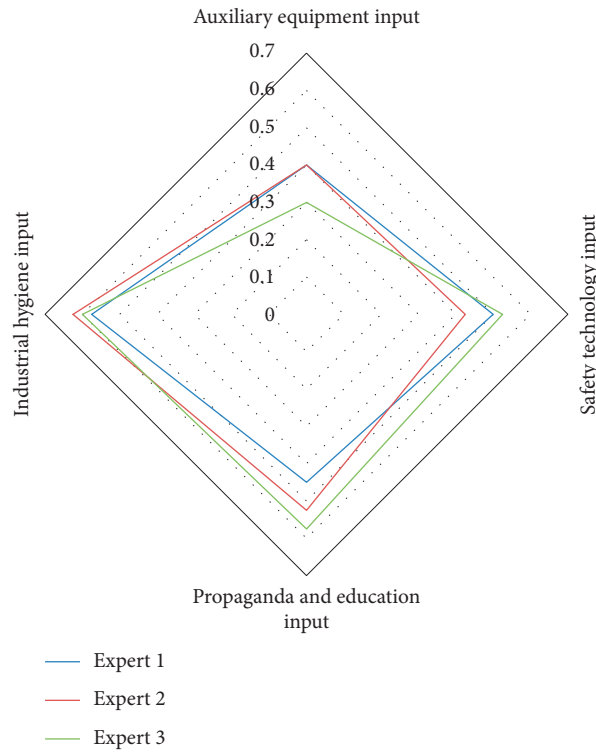
Figure 7: Radar diagram of score function value of TIFNs evaluation data for safety input items (expert 2).
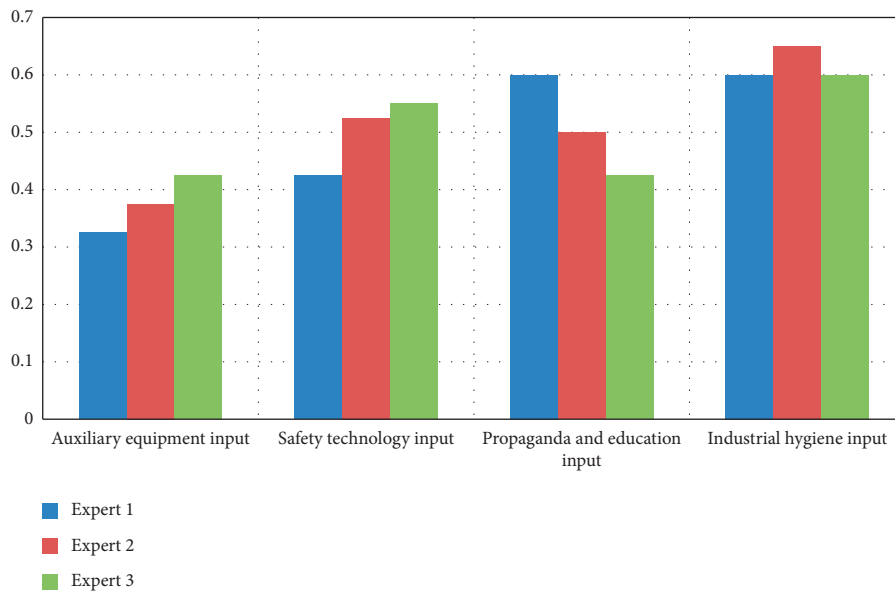
Figure 8: Columnar diagram of score function value of TIFNs evaluation data for safety input items (expert 3).

$$\mathbf{B}^3 = \begin{bmatrix} 0.325 & 0.425 & 0.6 & 0.6 \\ 0.375 & 0.525 & 0.5 & 0.65 \\ 0.425 & 0.55 & 0.425 & 0.6 \end{bmatrix}. \qquad (21)$$

The score function value of TIFNs evaluation data for safety input items given by expert 3 (dates obtained from (21)) was also analyzed using the columnar diagram, broken line diagram, and radar diagram, which are depicted in Figures 8–10, respectively.

It can be seen from the data diagrams, including columnar diagrams, broken line diagrams, and radar diagrams, that the score function values of the evaluation of safety input items given by each expert are not consistent. Also, each expert evaluates differently over different time points. It shows the need to consider the impact of timing factors and
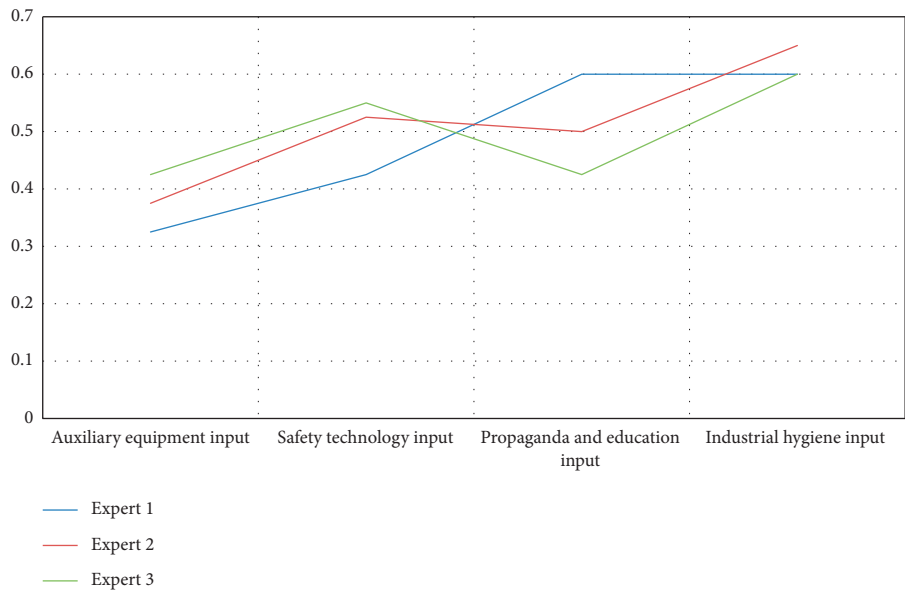
Figure 9: Broken line diagram of score function value of TIFNs evaluation data for safety input items (expert 3).
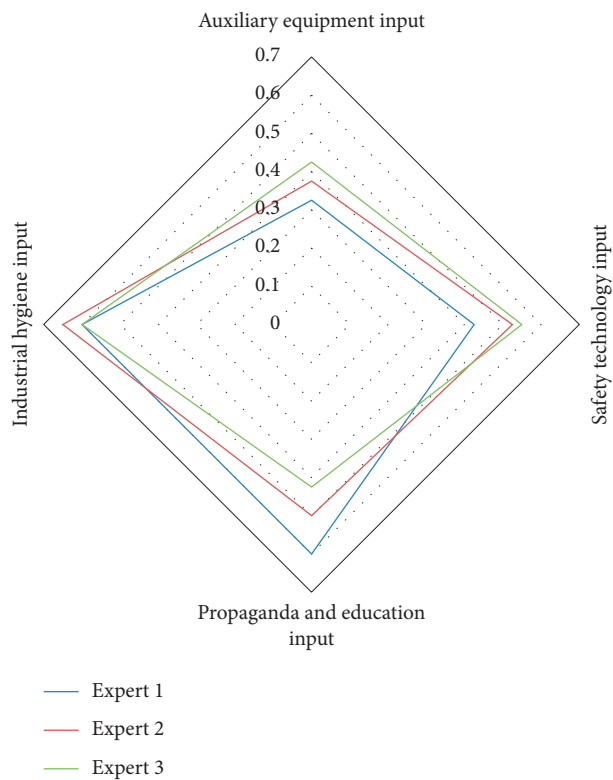
Figure 10: Radar diagram of score function value of TIFNs evaluation data for safety input items (expert 3).
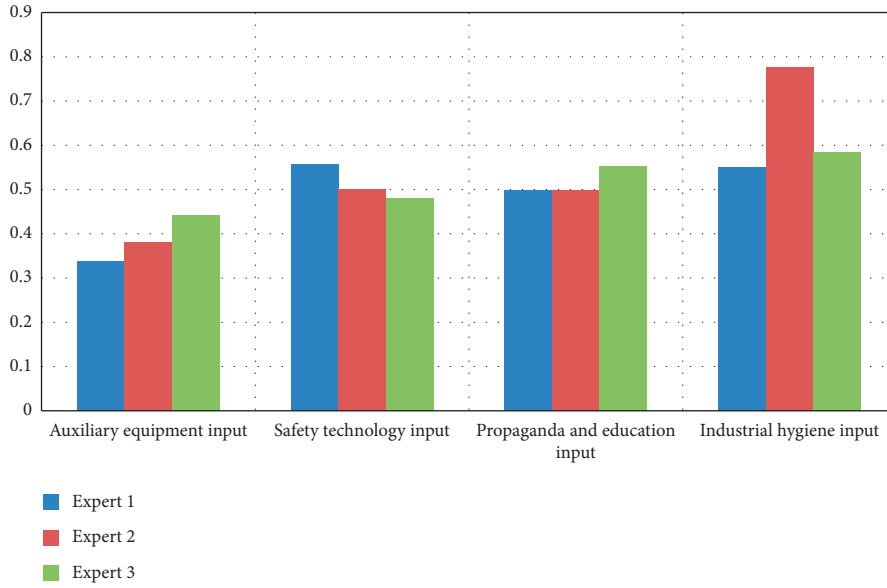
FIGURE 11: Columnar diagram of score function value of TIFNs evaluation data for safety input items, obtained from (23).
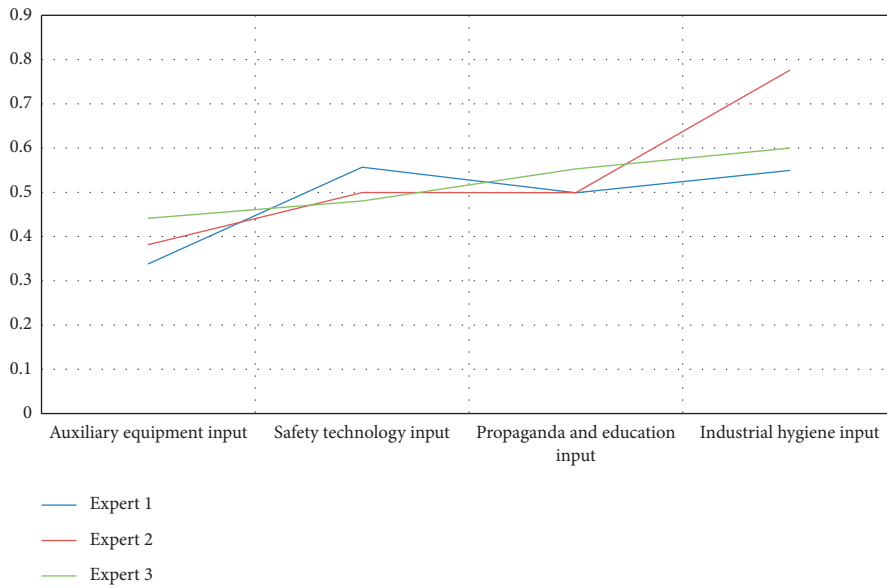
FIGURE 12: Broken line diagram of score function value of TIFNs evaluation data for safety input items, obtained from (23).

the influence of different experts on the final evaluation result in the evaluation process. Thus, they are integrated into the final evaluation results in the following.

The matrices $\overline{\mathbf{B}}^t$ are recomputed as follows:

$$\overline{\mathbf{B}}^1 = \begin{bmatrix} 0.3043 & 0.3448 & 03492 & 0.2987 \\ 0.3261 & 0.3448 & 0.3175 & 0.3636 \\ 0.3696 & 0.3103 & 0.3333 & 0.3377 \end{bmatrix},$$

$$\overline{\mathbf{B}}^2 = \begin{bmatrix} 0.3636 & 0.339 & 0.2903 & 0.3194 \\ 0.3636 & 0.2881 & 0.3387 & 0.3472 \\ 0.2727 & 0.3729 & 0.371 & 0.3333 \end{bmatrix}, \quad (22)$$

$$\overline{\mathbf{B}}^3 = \begin{bmatrix} 0.2889 & 0.2833 & 0.3934 & 0.3243 \\ 0.3333 & 0.35 & 0.3279 & 0.3514 \\ 0.3778 & 0.3667 & 0.2787 & 0.3243 \end{bmatrix}.$$

Then, the stability weight vector φ^t is calculated using (8), (9), and (10), respectively, as follows: $\varphi^1 = (0.2497, 0.2502, 0.2503, 0.2497)$, $\varphi^2 = (0.2492, 0.2499, 0.25, 0.251)$, and $\varphi^3 = (0.2499, 0.2499, 0.249, 0.2511)$. The TIFNCWBHG operator is used to calculate the initial weight vector of evaluation factors:

$\widetilde{\eta}^1 = (([0.4678, 0.5103, 0.5963], [0.1532, 0.1895, 0.1995]),$ $([0.4875, 0.6123, 0.6235], [0.6921, 0.7585, 0.7826]), ([0.1824, 0.1907, 0.2008], [0.6023, 0.7115, 0.7288]), ([0.7316, 0.7601, 0.7723], [0.2006, 0.2019, 0.2218])).$

$\widetilde{\eta}^2 = (([0.4678, 0.5103, 0.5963], [0.1532, 0.1895, 0.1995]),$ $([0.4875, 0.6123, 0.6235], [0.6921, 0.7585, 0.7826]), ([0.1824, 0.1907, 0.2008], [0.6023, 0.7115, 0.7288]), ([0.7316, 0.7601, 0.7723], [0.2006, 0.2019, 0.2218])).$
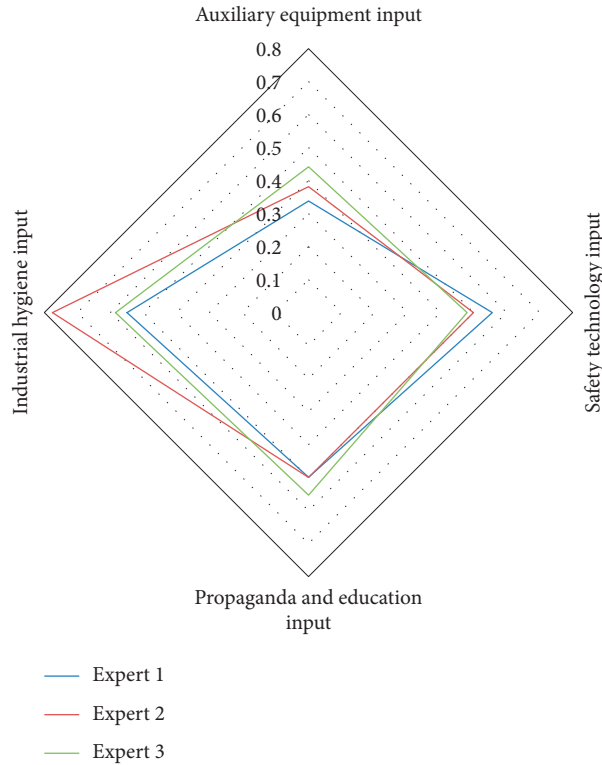
FIGURE 13: Radar diagram of score function value of TIFNs evaluation data for safety input items, obtained from (23).

TABLE 1: Comparison of TIFNCWBHG-MAGDM and G-INFNs-MCGDM.

Evaluation method	Auxiliary equipment input	Safety technology input	Propaganda and education input	Industrial hygiene input
G-INFNs-MCGDM	0.1851	0.2401	0.2465	0.3283
TIFNCWBHG-MAGDM	0.1886	0.2495	0.2519	0.3101

$\widetilde{\eta}^3 = (([0.5237, 0.6038, 0.7521], [0.1198, 0.1982, 0.2012]),$
$([0.6607, 0.6621, 0.7127], [0.1733, 0.1987, 0.2057]), ([0.606,$
$0.6679, 0.712], [0.1006, 0.1078, 0.1257]), ([0.7023, 0.7652,$
$0.7895], [0.1572, 0.1589, 0.2102])).$

$\widetilde{\eta}^1, \widetilde{\eta}^2, \widetilde{\eta}^3$ are combined to obtain the matrix $\widetilde{\mathbf{A}}$, and the matrix $\mathbf{A}$ is obtained by calculating the score function value of each element in matrix $\widetilde{\mathbf{A}}$:

$$\mathbf{A} = \begin{bmatrix} 0.3383 & 0.5568 & 0.4988 & 0.5495 \\ 0.3817 & 0.4996 & 0.4993 & 0.7758 \\ 0.4415 & 0.4803 & 0.553 & 0.5843 \end{bmatrix}. \quad (23)$$

The score function value of TIFNs evaluation data for safety input items from (23) was analyzed using the columnar diagram, broken line diagram, and radar diagram, which are depicted in Figures 11–13, respectively.

Finally, h is computed as $h = (0.1886, 0.2495, 0.2519, 0.3101)$.

Each component in the vector h corresponds to the evaluation items (auxiliary equipment input, safety technology input, propaganda and education input, and industrial hygiene input). Therefore, it can be seen from the results that industrial hygiene, propaganda, and education have a great impact on safety input. The auxiliary equipment has the least influence. In the practical application, it was known that the dust concentration in the workplace was very high, and personal protection needed to be improved, and the attention and input in industrial hygiene should be increased. Miners generally lacked the protection awareness of the hazards of dust and harmful gases. The dust and harmful gases should be prevented through careful attention, and it is necessary to carry out extensive safety education and publicity for miners. Since the equipment was relatively new, it is not required to be repaired or changed. The comparison analysis shows that the evaluation results are consistent with the practical situation. Also, the final ranking obtained by using TIFNCWBHG-MAGDM is consistent with that obtained by the method in [4], further verifying the proposed method.

The proposed TIFNCWBHG-MAGDM integrates multiexperts, multitime points, multifactors, stability weights, intuitionistic triangular fuzzy score function, and
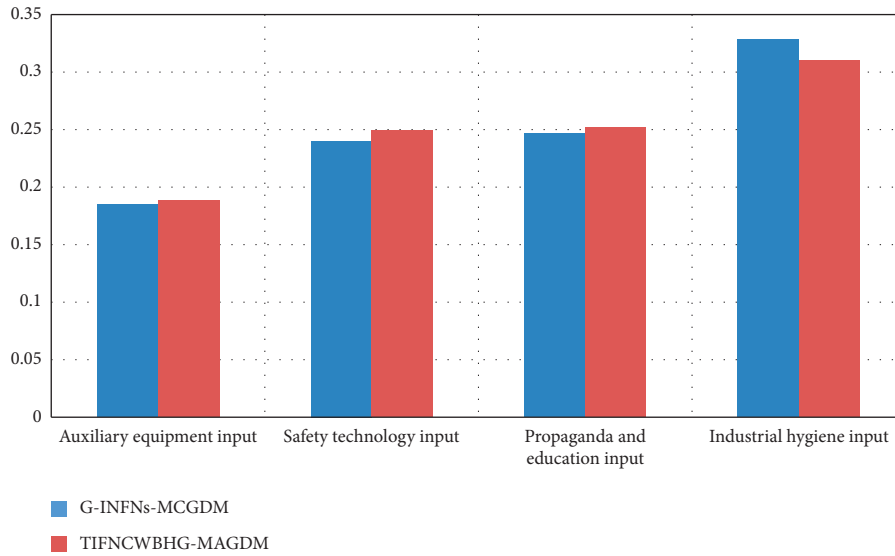
FIGURE 14: Columnar diagram obtained from Table 1.
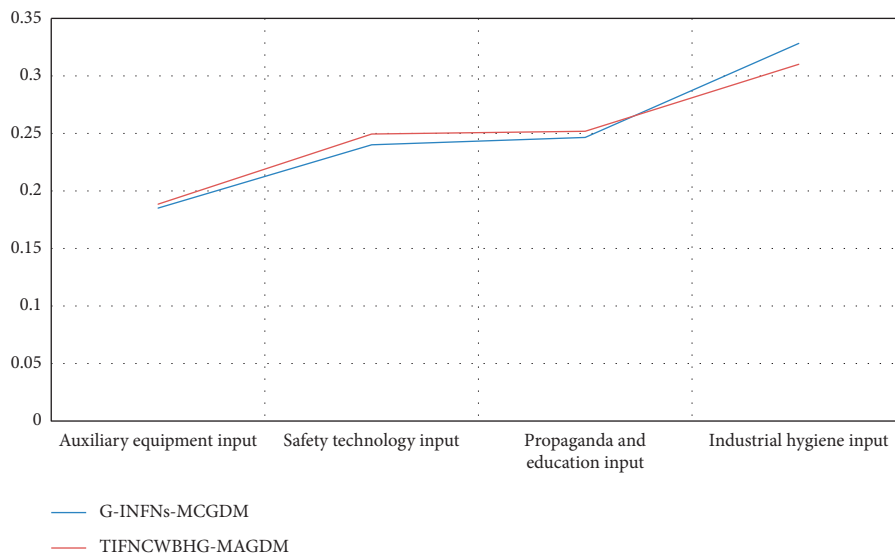
FIGURE 15: Broken line diagram obtained from Table 1.

other information for integrated calculation, reflecting more information. In order to validate the performance of the proposed TIFNCWBHG-MAGDM, it is compared to G-INFNs-MCGDM. Table 1 summarizes the comparison results, showing that the two methods provide consistent ranking results. The columnar diagram, broken line diagram, and radar diagram are depicted in Figures 14–16, respectively. Note that the G-INFNs-MCGDM requires the accuracy-weight of expert evaluation information and the

overall evaluation weight at all levels. Therefore, compared with G-INFNs-MCGDM, TIFNCWBHG-MAGDM is more concise and easy to calculate. On the other hand, the proposed TIFNCWBHG-MAGDM is more feasible and straightforward, which is conducive to the evaluators to carry out various analyses and comprehensive evaluation for the correct judgment. The comparison of the calculation results of TIFNCWBHG-MAGDM and G-INFNs-MCGDM is shown in Table 1.
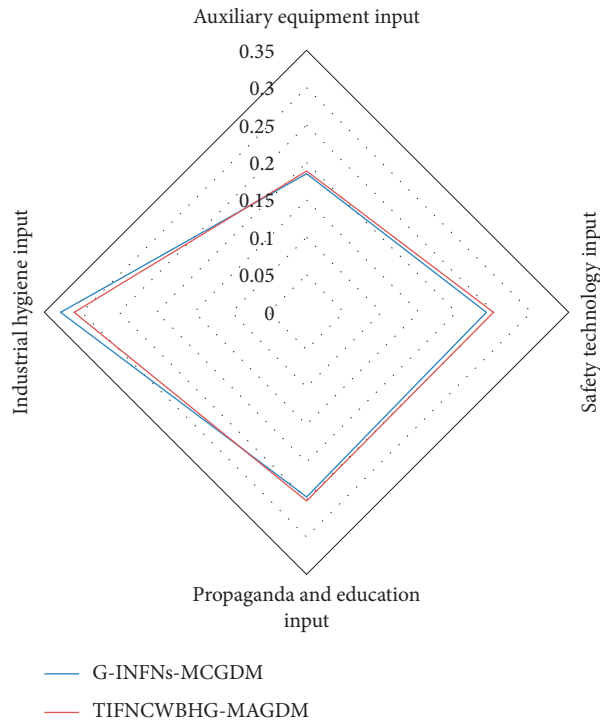
FIGURE 16: Radar diagram obtained from Table 1.

4. Conclusion

In order to reduce the difference of the traditional single-value evaluation, this paper proposes the TIFNCWBHG-MAGDM based on the intuitionistic triangular fuzzy number theory and MAGDM theory. First, taking into account the factors such as multitime points, multiattributes, and multiexperts, the judgment matrix of TIFNs is constructed from the comprehensive consideration of multiperspectives. The TIFNCWBHG operator integrating the information of TIFNs score function, stability weight, and position weight is proposed for integrated calculation. Finally, the priorities for safety inputs are determined. The proposed method was evaluated on the practical example of coal enterprise safety inputs, showing that the result is consistent with the actual situation. The main advantages, characteristics, and summary of the proposed method were found through the comparison and in-depth analysis, as follows:

(a) The proposed method improves the accuracy, simplicity, and rationality of the safety input evaluation of coal enterprises. It systematically uses the evaluation matrix, operator, score function formula, and accurate score function formula, which provides a new idea and method for comprehensive, systematic, and in-depth evaluation of coal enterprise safety inputs.

(b) In the TIFNCWBHG operator, a variety of weights are integrated into the system to more accurately describe the complex internal relationship between various factors and attributes to improve the accuracy of the final evaluation further.

(c) In specific decision-making, the stability of expert evaluation information will affect the ranking and selection of alternatives. Therefore, considering the stability of expert evaluation information, the evaluation can be more accurate.

(d) The proposed TIFNCWBHG-MAGDM has the advantages of lower computational complexity and broad applicability. Therefore, it can be used to compare, analyze, and sort the factors in other safety input structure models.

Future works will include the application of the proposed method to linguistic decision-making, which is another one of the most active research topics. In addition, we will further optimize the whole evaluation method to make it more accurate and convenient.

Data Availability

The data used to support the findings of this study are included within the article.

Conflicts of Interest

The authors declare that they have no conflicts of interest.

References

[1] F. C. Jiang, E. Lai, Y. X. Shan, F. H. Tang, and H. G. Li, "A set theory-based model for safety investment and accident control in coal mines," *Process Safety and Environmental Protection*, vol. 136, pp. 253–258, 2020.

[2] C. Y. Xiao, L. W. Guo, S. Z. Chen, and Y. C. Yang, "Statistical analysis on coal mine gas explosion and optimization of safety input," *Advanced Materials Research*, vol. 143, pp. 1316–1321, 2010.

[3] J. Dzonzi-Undi and S. Li, "Safety and environmental inputs investment effect analysis: empirical study of selected coal mining firms in China," *Resources Policy*, vol. 47, pp. 178–186, 2016.

[4] B. F. Zhao, C. Zhang, B. S. Jia et al., "G-INFNs-MCGDM method for evaluating safety input in coal enterprises and its application," *China Safety Science Journal*, vol. 27, no. 02, pp. 139–144, 2017.

[5] C. Zhang, B. F. Zhao, B. S. Jia, C. X. Zhai, H. Z. Ren, and J. W. Guo, "DMIP-MCDM based method of evaluating safety input for coal enterprises," *China Safety Science Journal*, vol. 27, no. 04, pp. 127–132, 2017.

[6] M. J. Lu, C. M. Cheung, H. Li, and S.-C. Hsu, "Understanding the relationship between safety investment and safety performance of construction projects through agent-based modeling," *Accident Analysis & Prevention*, vol. 94, pp. 8–17, 2016.

[7] Y. Noh and D. Chang, "Methodology of exergy-based economic analysis incorporating safety investment cost for comparative evaluation in process plant design," *Energy*, vol. 182, pp. 864–880, 2019.

[8] J. Matthews, K. Newman, A. Green, L. Fawcett, N. Thorpe, and K. Kremer, "A decision support toolkit to inform road safety investment decisions," *Proceedings of the Institution of Civil Engineers-Municipal Engineer*, vol. 172, no. 1, pp. 53–67, 2019.

[9] S. Roy and A. Gupta, "Safety investment optimization in process industry: a riskbased approach," *Loss Prevention in the Process Industries*, vol. 63, pp. 1–10, 2019.

[10] Y. Han, J. Li, and X. L. Cao, "Structural equation modeling approach to studying the relationships among safety investment, construction employees' safety cognition, and behavioral performance," *Journal of Construction Engineering and Management*, vol. 146, no. 7, Article ID 04020065, 2020.

[11] Z. Q. Hou and P. Zhao, "Structure optimization of Safety Investment of petrochemical port enterprises," *Mathematical Problems In Engineering*, vol. 2017, Article ID 3491290, 5 pages, 2017.

[12] M. J. Lu, C. M. Cheung, H. Li, and S.-C. Hsu, "Understanding the relationship between safety investment and safety performance of construction projects through agent-based modeling," *Accident Analysis & Prevention*, vol. 94, pp. 8–17, 2016.

[13] Y. H. Ma, Q. H. Zhao, and M. H. Xi, "Decision-makings in safety investment: an opportunity cost perspective," *Safety Science*, vol. 83, pp. 31–39, 2016.

[14] M. López-Alonso, M. P. Ibarrondo-Dávila, M. C. Rubio-Gámez, and T. G. Munoz, "The impact of health and safety investment on construction company costs," *Safety Science*, vol. 60, pp. 151–159, 2013.

[15] D. Wu and B. Wemple, "Cost-effectiveness sketch method for Safety Investment Decision making," *Journal of the Transportation Research Board*, vol. 2430, no. 2430, pp. 191–199, 2014.

[16] T. Aven and Y. Hiriart, "Robust optimization in relation to a basic safety investment model with imprecise probabilities," *Safety Science*, vol. 56, pp. 188–194, 2013.

[17] S. Q. Zhang, G. W. Wei, F. E. Alsaadi, T. Hayat, C. Wei, and Z. Zhang, "MABAC method for multiple attribute group decision making under picture 2-tuple linguistic environment," *Soft Computing*, vol. 24, no. 8, pp. 5819–5829, 2020.

[18] G. W. Wei, Y. He, F. Lei et al., "Green supplier selection with an uncertain probabilistic linguistic MABAC method," *Journal of Intelligent & Fuzzy Systems*, vol. 39, pp. 3125–3136, 2020.

[19] G. W. Wei, J. P. Lu, C. Wei et al., "Probabilistic linguistic GRA method for multiple attribute group decision making," *Journal of Intelligent & Fuzzy Systems*, vol. 38, pp. 4721–4732, 2020.

[20] G. W. Wei, J. Wang, J. P. Lu et al., "VIKOR method for multiple criteria group decision making under 2-tuple linguistic neutrosophic environment," *Economic Research-Ekonomska Istrazivanja*, vol. 33, pp. 3185–3208, 2020.

[21] F. Liu and X. H. Yuan, "Fuzzy number intuitionistic fuzzy set," *Fuzzy Systems and Mathematics*, vol. 21, no. 1, pp. 88–91, 2007.

[22] Y. Gao, D. Q. Zhou, C. C. Liu et al., "Triangular fuzzy number intuitionistic fuzzy aggregation operators and their application base on interaction," *Systems Engineering-Theory & Practice*, vol. 32, no. 9, pp. 1964–1972, 2012.

[23] Z. S. Xu, "An overview of methods for determining OWA weights," *International Journal of Intelligent Systems*, vol. 20, no. 8, pp. 843–865, 2005.

[24] R. X. Zhou, F. Y. Fan, D. Y. He et al., "Integrated entropy weight method based on data stability and subjective preference in multi-attribute group decision-making," *Control and Decision*, vol. 27, no. 08, pp. 1169–1174, 2012, http://en.cnki.com.cn/Article_en/CJFDTOTAL-KZYC201208010.htm.

Research Article

Intonation Characteristics of Singing Based on Artificial Intelligence Technology and Its Application in Song-on-Demand Scoring System

E. Wei (iD)

School of Music, Shenyang Normal University, Shenyang, Liaoning 110034, China

Correspondence should be addressed to E. Wei; ewei1979@synu.edu.cn

With the continuous progress of my country's cultural industry, how to apply artificial intelligence technology to song on demand has become an issue of concern. This research mainly discusses the research of singing intonation characteristics based on artificial intelligence technology and its application in song-on-demand scoring system. This paper uses the combination of ant colony algorithm and DTW algorithm to measure the similarity between speech signals with the average distortion distance, so as to expect accurate recognition results. The design of the song-on-demand scoring function module uses a combination of MVC mode and command mode based on artificial intelligence technology. The view component in the MVC mode is mainly used to display the content that the user needs to sing and realize the interaction with the user. The singer selects a song to start playing, and the scoring terminal device queries the music library server for song information according to the song number, then starts playing the song through the FTP file sharing service according to the audio file path in the song information, and at the same time displays the song on the display according to the timeline Show song and pitch information. The singer sings according to the screen prompts. The microphone collects the voice signal and transmits it to the scoring terminal. After the scoring algorithm is calculated, the result is fed back to the screen in real time. The singer can view his singing status in real time and make corresponding adjustments to obtain a higher score. After the singing, the scoring terminal will display the final result on the screen to inform the user and upload the singing record to the server for recording. In the tested on-demand retrieval engine, the average hit rate of the top 3 has reached more than 90% under various humming methods, basically maintaining the high hit rate characteristics of the original retrieval engine. The system designed in this research helps to effectively improve the singing level.

1. Introduction

With the technological development of hardware and software equipment, the ability and superiority of artificial intelligence have quickly penetrated into all areas of life, and of course, it has become the hottest vocabulary in the field of music technology [1]. We know that the promotion of music is actually based on technological changes. Without the invention of tools, there would be no musical instruments; without the emergence of electronic technology, there would be no electronic music [2]. Therefore, artificial intelligence, a major technology, can bring much change to music. The generation of artificial intelligence arrangement is an interdisciplinary field. It requires researchers to master much interdisciplinary knowledge, including music production, music technology, artificial intelligence, and automatic accompaniment. Because it is a new field, domestic research is still relatively poor.

Currently, there are two main algorithms used in the field of algorithmic composition. One is the algorithm of composition based on rules and music knowledge. This kind of method also uses probabilistic methods to improve. The second is the machine learning algorithm, which is one of the hot tools currently applied to algorithmic composition [3]. It can be further divided into traditional machine learning algorithms and artificial neural networks. Traditional machine learning algorithms mainly refer to the kind of machine learning algorithms based on probability theory

and statistics. The efforts of the predecessors laid the foundation for the current generation of artificial intelligence music.

Artificial intelligence (AI) activities are integrated into the software development process. Kulkarni and Padmanabham used an extended waterfall chart and agile model to model the entire process of software (SW) development. They have integrated important AI activities (such as intelligent agents, machine learning (ML), knowledge representation, statistical models, probabilistic methods, and fuzziness) into the extension. Although the model they studied collects and feeds back data, there is still a lack of effective analysis of the data [4]. Liu et al. believed that although artificial intelligence is currently one of the most interesting areas in scientific research, the potential threat posed by emerging AI systems is still the source of ongoing controversy. In order to solve the problem of AI threats, they proposed a standard intelligence model [5], which unifies AI and human characteristics from the four aspects of knowledge (i.e., input, output, mastery, and creation). Although his research can measure the level of artificial intelligence system, the research method is too cumbersome [6]. Mazinan and Khalaji demonstrated a comparative study of the application of multiple model predictive control schemes based on artificial intelligence. They will control the program that will be implemented on a type of industrial complex system. They focused their results on an industrial tubular heat exchanger system that has such high applicability in practical and academic environments. Although the traditional scheme is almost implemented on the system, his research lacks specific parameters [7]. The Ali study investigated the impact of such machine translation (MT) software and TM tools widely used by the Arab community for its academic and commercial purposes. His research aimed to find whether it is possible to transform the paradigm from Arabic localization to Arabic globalization. Therefore, he studied the content and applications of some machine translation software (such as SYSTRAN and IBM Watson) to determine how to use them without manual intervention and retain the meaning of the original text. Although his research uses the idea of artificial intelligence, the research process lacks statistical data [8].

This paper uses the combination of ant colony algorithm and DTW algorithm to measure the similarity between speech signals with the average distortion distance, so as to expect accurate recognition results. The design of the song-on-demand scoring function module uses a combination of MVC mode and command mode based on artificial intelligence technology. The view component in the MVC mode is mainly used to display the content that the user needs to sing and realize the interaction with the user. The singer sings according to the screen prompts. The microphone collects the voice signal and transmits it to the scoring terminal. After the scoring algorithm is calculated, the result is fed back to the screen in real time. The singer can view his singing status in real time and make corresponding adjustments

to obtain a higher score. After the singing, the scoring terminal will display the final result on the screen to inform the user and upload the singing record to the server for recording.

2. Singing Intonation Characteristics

2.1. Artificial Intelligence Technology. At present, there is no optimal solution in the main technology of AI composition, and most of them use hybrid algorithms [9, 10]. In practice, the most advanced deep learning algorithm (artificial neural network) is one of the most important technologies for AI composition. Compared with other algorithms, it has the ability to learn by itself, associative storage, and the ability to find optimal solutions at high speed [11]. This algorithm simulates the principle of neural network transmission in the human brain. Therefore, in this kind of deep learning, programmers need to build a multilayer neural network and program it in a multilayer structure to process the information between input and output points [12, 13]. After the data is input, the artificial neural network will find the laws that exist among many input works, forming an understanding of music [14]. AI will take it to predict the direction of music, and the verification data set will tell it whether the prediction is correct or not, and the correct and wrong feedback will be remembered by AI [15, 16]. After a lot of learning, AI's predictive ability is getting stronger and stronger, then masters the summarized information, and finally creates [17].

2.2. Singing Intonation Characteristics. When performing feature extraction, there will be more or fewer differences in the tone size, strength, and recording of the speaker in different environments, which will cause the extracted feature parameters to be inaccurate, so accurate feature parameter matching cannot be performed, so this paper adopts the interpolation method, linear scaling method, and linear translation method which are used to regularize the feature parameters to ensure the accuracy of the feature parameters that can be extracted [13, 18]. After detecting the end point of the voice signal with a sampling rate of 16 kHz, we find out the starting end of the sound and frame the speech. The frame size is 512 points, about 32 milliseconds, and the frameshift is 170 points, which accounts for about three of a frame one part; assuming that the speech signal in each frame is represented by $S_n(m)$, the volume intensity curve is defined as

$$\text{avgMag}(n) = \frac{1}{M} \sum_{m=0}^{M-1} |S_n(m)|, \quad n = 0, 1, \ldots, N-1. \quad (1)$$

Even if the same person uses the same volume to record into the microphone, there may still be differences in the volume of the voice signal due to different microphones [15].

$$\overline{A} = \text{avgMag}_1(n) = \begin{bmatrix} \text{avgMag}_1(0) \\ \cdots \\ \text{avgMag}_1(N-1) \end{bmatrix},$$

$$\overline{B} = \text{avgMag}_2(n) = \begin{bmatrix} \text{avgMag}_2(0) \\ \cdots \\ \text{avgMag}_2(N-1) \end{bmatrix}. \tag{2}$$

The following results can be learned:

$$\theta = \left(\overline{B}^T\overline{B}\right)^{-1}\overline{B}^T\overline{A}. \tag{3}$$

The fine-tuned test voice volume curve is assumed to be $\text{avgMag}_2(n)$, and its formula is as follows:

$$\text{avgMag}_2(n) = \overline{B}\theta = \text{avgMag}_2(n)\theta, \quad n = 0, 1, \ldots, N-1. \tag{4}$$

The system framework of the pitch extraction scheme is shown in Figure 1.

2.3. Song Evaluation. When the user is using it, first select the song to be sung on the platform control page. This operation is equivalent to issuing a command to the controller, and the controller needs to call the scoring function according to the user's operation and change the display in the browser [19, 20]. After the user sings according to the changed display, the scoring method will score the user's singing and return the result to the browser. Such a process constitutes a complete scoring process [21]. In order to accurately evaluate the contour of the curve, the evaluation parameter force of the polyline is introduced, which is mainly used to describe the similarity of the two polylines [22, 23].

$$\eta_i = l_i\widehat{l}l_{,i}\eta_i \in (0, 1]. \tag{5}$$

The evaluation parameter η_i reflects the similarity between the two points of the straight line and the curve [24].

Suppose that the variable length including angle chain code of the curve is

$$A = \{\alpha_1, \alpha_2, \ldots, \alpha_n\}. \tag{6}$$

Then

$$\alpha_{ij} = 2 \arccos\left(\frac{\sqrt{\sum_r (H_{r+1} - H_{r+2})}}{l_{r+1} + l_{r+2}}\right), \tag{7}$$

Among them, α_{ij} is the angle sequence [25, 26]. The amplitude-frequency response of each filter is in the shape of a triangle and is equal to the above uniform center frequency and the center frequency is linearly reduced to zero for two adjacent filters [27]. Its relationship with linear frequency conversion is

$$f = 2595 \log_{10}\left(1 + \frac{f}{100}\right). \tag{8}$$

The power spectrum of the frame signal is obtained by FFT [28]. Extract breath parameters:

$$\text{std}(X) = \left(\frac{1}{n-1}\sum_{i=1}^{n}(X_i - X)X_i^2\right)^{1/2}, \tag{9}$$

Among them, n represents the number of sampling points. Use $f_1(x)$ and $f_2(x)$ to represent the gene trajectory of the original singing voice and the imitated voice after feature extraction.

$$f_1(x) = f_2(x) - \frac{1}{N}\sum_{k=0}^{N-1}f_2(k) + \frac{1}{N}\sum_{k=0}^{N-1}f_1(k),$$

$$f_1(x) = f_2(x) - \text{diff}, \tag{10}$$

$$\text{diff} = \frac{1}{N}\sum_{k=0}^{N-1}f_2(k) + \frac{1}{N}\sum_{k=0}^{N-1}f_1(k),$$

Among them, diff represents the difference between the two.

$$D(n+1, m) = d(n+1, m) + \min[D(n, m)g(n, m), D(n, m-1), D(n, m-2)],$$

$$g(n, m) = \begin{cases} \infty & w(n) = w(n-1) \\ 0 & w(n) \neq w(n-1) \end{cases}, \tag{11}$$

$w(n)$ represents the optimal time warping function. Although it is very time-consuming to use dynamic programming technology to make time regulation, this method only calculates the matching distance between the original vocal voice and the imitated voice feature parameters, thus simplifying the process of speech recognition, so the ant colony dynamic time planning algorithm is still a more effective speech recognition technology [29].

3. Song-on-Demand Scoring System Experiment

3.1. Architecture Design of Scoring Function Module. The traditional DTW algorithm minimizes the total weighted distance through a local optimization method. In this paper, the ant colony algorithm is combined with the DTW algorithm, and the average distortion distance is used to

FIGURE 1: Pitch extraction scheme system framework.

measure the similarity between speech signals, so as to expect accurate recognition results. The design of the song-on-demand scoring function module uses a combination of MVC mode and command mode based on artificial intelligence technology. The view component in the MVC mode is composed of a Java browser embedded in a smart client, which is mainly used to display the content that the user needs to sing and realize the interaction with the user. The controller component uses the command mode design method to encapsulate each command in the software control as an object. These objects can respond to different command statements to complete various operations. Model components are various business logics needed in the software running process. In the song-on-demand scoring system, the scoring function constitutes the model components. Many intelligent terminal devices are connected to the song library server through the local area network, and the database administrator also needs to maintain the service through the local area network. Among them, the song library server may be composed of a server group considering the load pressure and data disaster tolerance, but this is transparent to the terminal devices. All terminal devices are connected to the same logical server through IP addresses. The scoring terminal device is responsible for the interactive operation with the user, which is realized through touch screen, display, microphone, and so on. The administrator is mainly responsible for the maintenance of the internal network and database to ensure the smoothness of the network transmission process.

Among them, the singer selects a song to start playing, and the scoring terminal device queries the song library server for song information according to the song number, then downloads the audio file from the server through the FTP file sharing service according to the audio file path in the song information and the song score file path with the score file, and starts to play the song; at the same time, the song and pitch information are displayed on the display according to the timeline. The singer sings according to the screen prompts. The microphone collects the voice signal and transmits it to the scoring terminal. After the scoring algorithm is calculated, the result is fed back to the screen in real time. The singer can view his singing status in real time and make corresponding adjustments to obtain a higher score. After the singing, the scoring terminal will display the final result on the screen to inform the user and upload the singing record to the server for recording.

3.2. Song Library Establishment. The establishment of the song library directly affects the accuracy of the experimental data and plays a vital role in the entire system. In practice, even if the same person is in the same environment, the signals of the two recorded songs are difficult to be completely consistent and must be recorded multiple times as an imitated song library. The accuracy of the recorded songs in the song library is set to 16 bits, and the sampling frequency is set to 8 kHz. The collection object of the standard song is the original singer, and the recorded song is used as a template song for comparison with the imitated song.

3.3. Control Process of the Song-on-Demand Scoring System. The song-on-demand scoring system realizes the scoring function by rewriting the speech recognition module Sphinx4. Through the singing of the singer, the intelligent client in the system controls the speech recognition module. The smart client determines the song paragraph to be evaluated and then passes the song paragraph to the Sphinx4 speech recognition module in the form of parameters. The voice recognition module will start a specific thread for the song paragraph according to the song paragraph to be investigated. This specific thread will monitor the microphone input data. After the singer's pronunciation is received by the microphone, it will be passed to the voice recognition module, and the voice recognition module will sing according to the song. The speaker's pronunciation evaluates a score that is similar to the standard pronunciation, this score is returned to the smart client, and the smart client displays this score on the user interface. The smart client is also responsible for the display of relevant information about the song paragraphs to be investigated and records the number of times the singer has practiced and the results. In addition, the user interface also needs to consider the factors of interactive design and provide functions such as singing timing bar to assist users in using the scoring system and improve the effect of user experience.

(1) *Query.* The administrator enters the song number or song title, and the system transmits the number and song title data to the database through the database query interface. After the database is processed, the song information is returned. The system feeds back the song information to the administrator to display the query result.

(2) *Newly Added.* The administrator enters all the attribute values of the song information. The system queries the database for the song information according to the song number in it and determines whether the song information already exists according to the database feedback result. If it exists, encapsulate the song information into a database format, transfer it to the database, and send instructions to add new information; otherwise, it will not be processed.

(3) *Delete.* The administrator enters the song number or song name, and the system transfers the number and song name data to the database through the database query interface and returns the song information after the database is processed. If the song exists, the entry song information is deleted; otherwise, it will not be processed.

(4) *Modification.* This operation is a combination of query, deletion, and addition. The administrator enters the song information, and the system knows whether the song exists through the query operation. If it does not exist, add the song information entry to the database through the new operation; otherwise, delete the song first through the delete operation information, and then add a new song information entry to the database through a new operation. The control process of the song-on-demand scoring system is shown in Figure 2.

3.4. Front-End Software Level Model of the Song-on-Demand Scoring System. The song-on-demand scoring system described in this paper is composed of server-side components and client-side components. The server-side components use SQL databases, and the program logic structure is relatively simple, without too much hierarchy. The client scoring system can be divided into 3 levels, from bottom to top: platform dependency layer, scoring business layer, and system application layer. Among them, the platform-dependent layer provides the underlying support for the system's operating resources and provides a guarantee for system portability by providing standard interfaces to shield the differences between system hardware and operating systems. The scoring business layer is the core of the scoring business logic. The business logic including recording cache, network communication, singing interface, and broadcast control is implemented at this level, and the whole is built with MVC architecture. The system application layer mainly refers to the singing system. The scoring system is designed as a business component of the traditional singing system. It has independent business logic, but it is located under the singing system and is an extension of the original system. Therefore, the system application layer is mainly responsible for the user's singing operation and finally calls the broadcast control interface of the scoring business layer to complete the business logic of singing scoring.

3.5. Software Component Design of Song-on-Demand Scoring System.

(i) The background service component is composed of two modules:

(1) Database operation module: it mainly realizes data operation on SQL database, including song information, query, score history, and score ranking query (currently not used by the front-end system).

(2) Network communication module: it mainly realizes client connection management and request-response functions. Since multiple clients may initiate requests to the server at the same time, the request connection time is variable, and the communication time is short, a thread pool is designed in the network communication module to manage each connection request, so as to avoid the continuous creation and destruction of threads. Improve system concurrency performance. The main functions of this module include communication thread scheduling, request analysis, data distribution, and request-reply.

(ii) The front-end business components of the system are relatively complex and consist of four modules:

(1) Network communication module: it mainly realizes the network connection with the server and request sending and receiving. Compared with the server-side network module, the client-side network module is relatively simple and does not require multithreading. The main functions include connection status management, data request sending and receiving, and reply message analysis.

(2) Resource download module: it mainly realizes the download of audio files and song score files and other resources. Its core is the realization of the PP file remote service client. Since the FTP protocol has mature open-source software libraries, the realization of this module is relatively simple. The main functions include FTP protocol analysis and data validity verification.

(3) Scoring service module: this module is the core module of the system, which mainly realizes the performance functions of the broadcasting control and singing process of the scoring service. As the main control module, it dispatches other modules to coordinate work as needed. The main functions include playback control, audio playback, song score analysis, and recording cache and singing interface drawing.

(4) Scoring algorithm module: this module is the basic module of the system, which is mainly responsible for voice information processing and score calculation. Its main functions include voice fundamental frequency extraction, pitch sequence conversion, score calculation, and other functions.
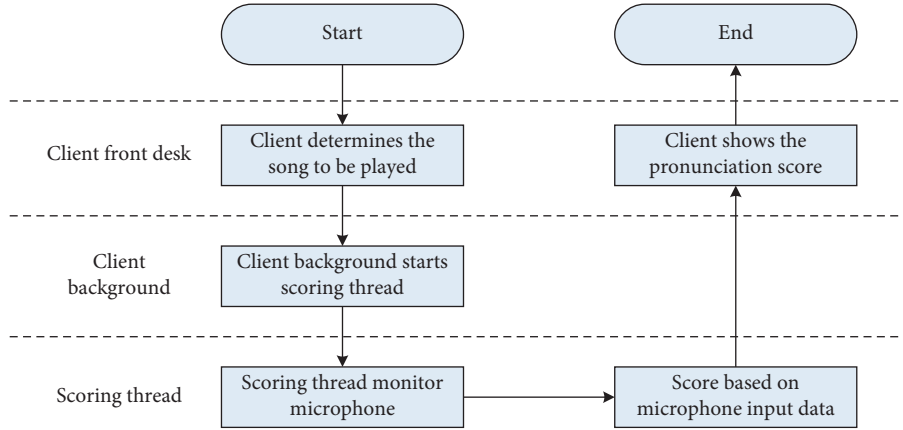
FIGURE 2: The control process of the song-on-demand scoring system.

4. Song-on-Demand Scoring System

4.1. Song Matching Path Analysis. All experiments in this paper are carried out on a LenovoWin7 PC. The CPU uses Intel's Corei3-2330M processor, the memory is 2 GB, the main frequency is 220 GHz, and the operating system is 64 bits. The experiment uses MATLAB R2010a for algorithm simulation. The voice recording uses the microphone that comes with the PC, and the recording format is ".WAV." When the user wants to start playing a song, the user first enters the song number through the playback control interface of the scoring service module, and the scoring service module calls the playback control interface to query the current playback status. If the player is idle, it sends a song query to the server through the network communication module Request; the network communication module sends and receives data to parse the reply package to obtain song information, which is fed back to the scoring service module; the scoring service module obtains the download address of the corresponding resource according to the audio file information and the song score file information and calls the resource download module interface to download to Local; the resource download module calls the FTP protocol library according to the download address to provide an interface to download the file to the local, performs data integrity check, and feeds the local path to the scoring service module; the scoring service module receives the audio file and the song score file and then transfers the audio file path to the audio decoding system to play the song, parse the score file, and pass the obtained pitch sequence information to the scoring algorithm module; the scoring algorithm module obtains the pitch sequence information and fills the corresponding structure information to prepare for the score calculation; so far, the playback start operation is complete. The number of ants in the ant colony is K, the number of cycles is set to N, and the global average distortion distance between the original singing voice and the matching path of the imitating voice is shown in Table 1.

We experimented with singing from the same female voice but at different times. Set up 6 different ant colonies, in which the number of ants and the number of cycles are 5, 10, 15, 20, 25, and 30. It can be seen from Tables 2–5 that, in the

TABLE 1: The global average distortion distance between the matching path of the original voice and the imitated voice.

N	D5	D10	D15	D20	D25	D30
5	0.3157	0.2267	0.2253	0.2235	0.2132	0.2145
10	0.2469	0.2593	0.2255	0.2221	0.2125	0.2039
15	0.2586	0.2295	0.2032	0.2023	0.2018	0.2008
20	0.2435	0.2109	0.2031	0.1937	0.1941	0.1950
25	0.2438	0.2098	0.2091	0. 1952	0.1934	0.1927
30	0.2431	0.2182	0.2015	0.1991	0.1942	0.1926

ant colony algorithm, when the total number of ants is fixed and the number of cycles increases, the global average distortion distance D of the path decreases. When the number of cycles is fixed, the total number of ants increases and the global average distortion distance D of its path decreases. It can be seen that this algorithm is effective in finding the best path. In the experiment, when $k = 20$ and $N = 20$, the average distortion distance has not changed significantly with the increase of k and N, and because of the time complexity factor, the experiment will be $k = 20$, $N = 20$ corresponding to the path as the best matching path to find the algorithm. The relationship between the number of ants k and the average distortion distance D under different cycles is shown in Figure 3.

Table 2 shows the comparison results of the test data based on the ant colony dynamic time planning algorithm and the DTW algorithm. It can be seen from Table 2 that when recognizing continuous speech, the recognition rate of the ant colony dynamic time planning algorithm is better than that of the DTW algorithm. Particularly in the case of complex environments, the superiority of the ant colony dynamic time planning algorithm can be better reflected. The main reason is that the algorithm introduces the global average distortion distance when comparing the feature parameter sequence, which solves the situation that the algorithm may enter the local optimum, the algorithm is searched for 20 times in a loop, and the path must be searched after each search. The pheromone on the website is updated. Therefore, the best matching path obtained by looping 20 times is more accurate, which more accurately reflects the small differences between the speech signals.

TABLE 2: Comparison of test data based on ant colony dynamic time planning algorithm and DTW algorithm.

Identification type	Ant colony dynamic time planning algorithm (%)	DTW algorithm (%)
Continuous song recognition	99.33	98.67

TABLE 3: Final statistics.

This paper score	Manual scoring		
	Bad	Average	Good
Bad	10	9	3
Average	8	26	4
Good	3	7	11

TABLE 4: Original pitch deviation.

Musical alphabet	Pitch frequency (Hz)	Off-center
G4	396.393	19
A4	440.914	4
B4	4 96.27	8
C5	526.503	11
D5	592.604	15
E5	678.944	30
F5	711. 836	33
G5	791.786	17
A5	885.939	12
B5	985.444	−4
C6	1057.91	19
C6	1057.91	19
B5	985.444	−4
A5	885.939	12
G5	791.786	17
F5	711.836	33
E5	678.944	30
D5	592.604	15
C5	526.503	11
B4	496.27	8
A4	440.914	4
G4	396.393	19

TABLE 5: Pitch deviation after adjustment.

Musical alphabet	Pitch frequency (Hz)	Off-center
G4	394. 886	13
A4	444.445	17
B4	498.378	16
C5	534.621	37
D5	603.943	48
E5	679.739	53
F5	721.132	55
G5	799.728	34
A5	890.173	20
B5	798.193	−1
C6	1062.9	27
C6	1055.08	14
B5	798.193	−1
A5	890.173	20
G5	796.779	28
F5	718.473	49
E5	677.232	47
D5	601.716	42
C5	532.649	31
B4	496.541	9
A4	442.806	11
G4	391.979	0

4.2. Singing Score Analysis. In the experiment, part of the original song was selected, and the singing time was 5 minutes. At the same time, select 10 students with high and low singing levels in our laboratory, and record them as A, B, C, D, E, F, G, H, J, and K, so that they can freely choose the songs to sing according to their singing level in the same environment. And another 10 students form a scoring group, and these 10 students are recorded as a, b, c, d, e, f, g, h, j, and k. The scoring group only imitates based on the personal subjective feelings singer's singing performance is scored, and the manual scoring is compared with the scoring software based on this algorithm. This paper uses 20 different lyrics recorded as the test object. Because each lyric has 4 test voices, it is equivalent to scoring 80 words. In order to show the relevance of the designed song-on-demand scoring system and manual scoring, three levels of manual scoring are given to the test voice: bad: (0–59), average: (60–79), and good: (80–100). The straight line in Figure 4 represents the average result of manual scoring, and the

curve represents the evaluation result of the scoring algorithm in this paper. The algorithm score in this paper is about 82%. The manual score is about 78%. It can be seen that the scoring results of the algorithm in this paper are almost the same as people's subjective feelings as a whole, but they are not accurate enough in highlighting the singing level of the singer, and the difference between the manual score and the score obtained by the scoring method of this algorithm is still not to be ignored. The final statistical results are shown in Table 3. The statistical analysis results are shown in Figure 4.

The singing scoring operation process mainly involves two modules: the scoring business module and the scoring algorithm. The user's voice is input into the system through a microphone, and the recording driver in the system collects the signal and then passes through the callback: the mechanism continuously transmits the sampled data to the scoring business module. After the recording buffer class obtains the recording data, according to the playback time of the song, it adds time stamp information to the recording segment and adds the recording data to the buffer queue. There is another thread in the recording buffer class, which continuously checks the length of the recording data in the buffer queue. When the data reaches the required length of a voice frame for scoring, the frame of voice is passed to the scoring algorithm module; after the scoring algorithm module obtains a frame of voice data, it first analyzes the voice signal to extract its fundamental frequency information and passes the pitch. The conversion algorithm obtains
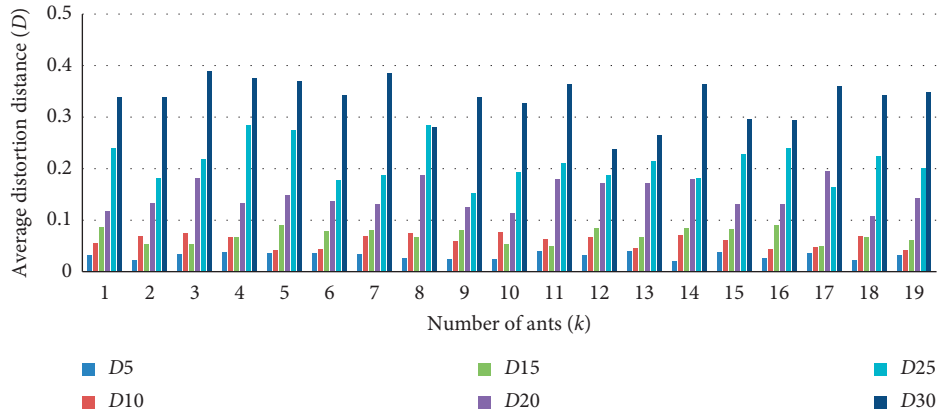
FIGURE 3: The relationship between the number of ants k and the average distortion distance D under different cycles.
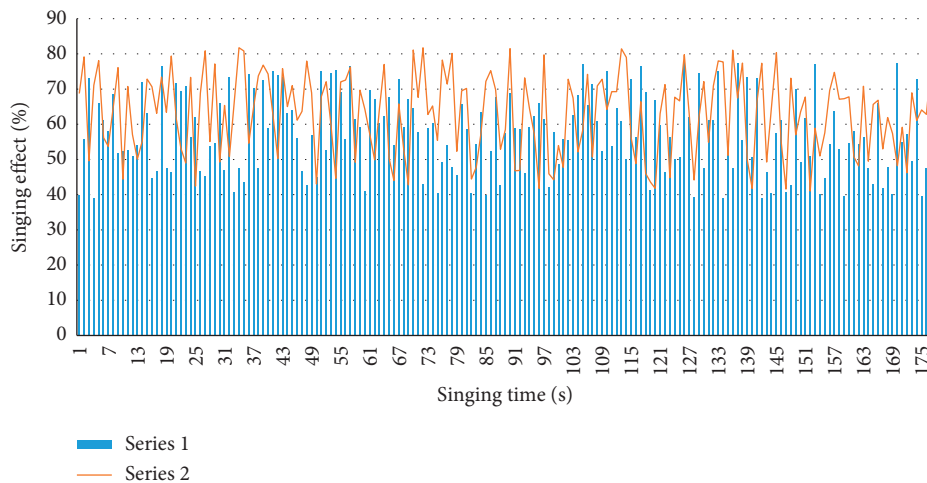
FIGURE 4: Statistical analysis results.

the pitch parameters, adds the singing pitch sequence 1, finally adjusts the pitch the score ending interface calculates the current score, and then the score status information is fed back to the scoring service module; the scoring service module feeds back the scoring status to the user through the singing interface; user inputs the sound at the next time point according to the current state and then loops back and forth until the song is played. In this study, before the comparison, the feature parameters of singing audio and music library music should be extracted in units of frames. The advantage of this is that the accuracy of the extracted feature parameters is higher, but the disadvantage is that the computational complexity of the system is greatly increased. Pass the FMS to JSP to extract the pitch feature sequence, and perform the recording pitch data and the MIDI template of the corresponding song in the music database every 8 seconds: the pitch data is compared for similarity, and the singing score in these 8 seconds is calculated (percentage system) and displayed through flash. Before doing the similarity comparison of the final scores, it is necessary to regularize the pitch sequence to get a more accurate final score than simply averaging the short-term scores. Due to the different frequencies of male and female voices, the pitch

will also be different. Therefore, before the system performs a similarity comparison, it needs to normalize the singing pitch sequence to the same level as the template pitch sequence and then calculate the similarity to get a score that can better reflect the true level of singing. The original singing analysis result is shown in Figure 5. The adjusted analysis result is shown in Figure 6. The original pitch deviation is shown in Table 4. The adjusted pitch deviation is shown in Table 5.

4.3. System Performance Test. Table 6 shows the test results of the top 3 and top 10 hit rates of the song-on-demand search engine and the original search engine in this paper. In the tested on-demand search engine, the average hit rate of the top 3 has reached more than 90% under various humming methods, basically maintaining the high hit rate characteristics of the original search engine, and the retrieval results are satisfactory.

The average search speed results of the new on-demand search engine and the original search engine are shown in Figure 7. According to the given test sample set, the old and new systems are tested separately, and the average retrieval
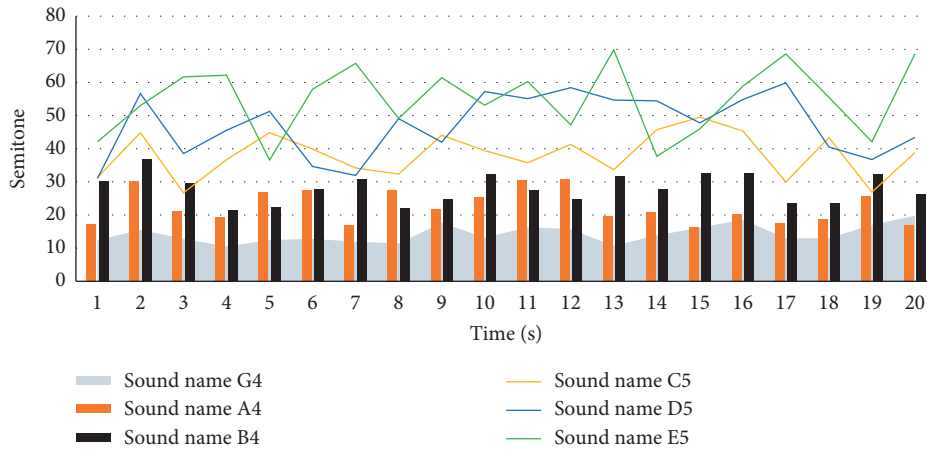
FIGURE 5: Original singer analysis result.
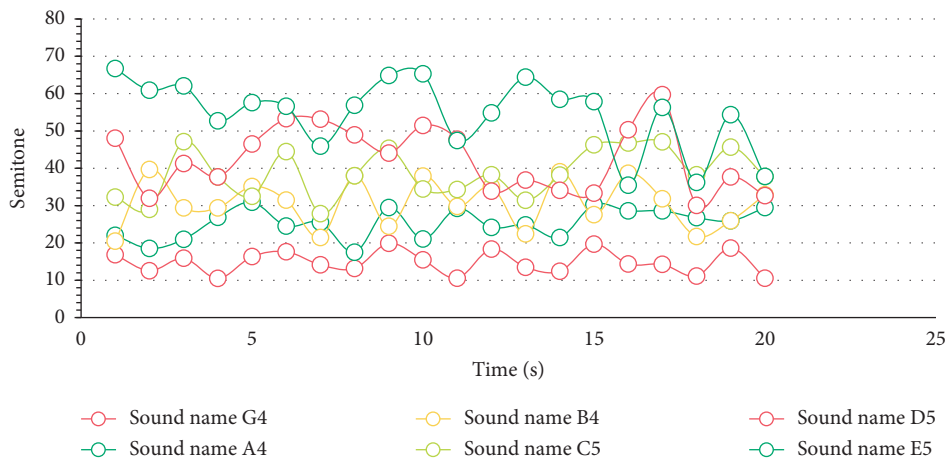
FIGURE 6: Adjusted analysis results.

TABLE 6: Test results of the hit rate of the top 3 and top 10 of the song-on-demand search engine and the original search engine in this paper.

Input	Testing frequency	Top 5 hit rate		Top 10 hit rate	
		New engine	Original engine	New engine	Original engine
Humph	60	95.0% (57)	93.3% (56)	98.3% (59)	96. 7% (58)
Sing "with lyrics"	60	83.3% (50)	88.3% (52)	85.0% (51)	93.3% (56)
"Whistle" blowing	70	92.9% (65)	94.3% (66)	92.9% (65)	95.7% (67)
Total number of tests	190	90.5% (172)	91.6% (174)	92.1% (175)	95.3% (181)
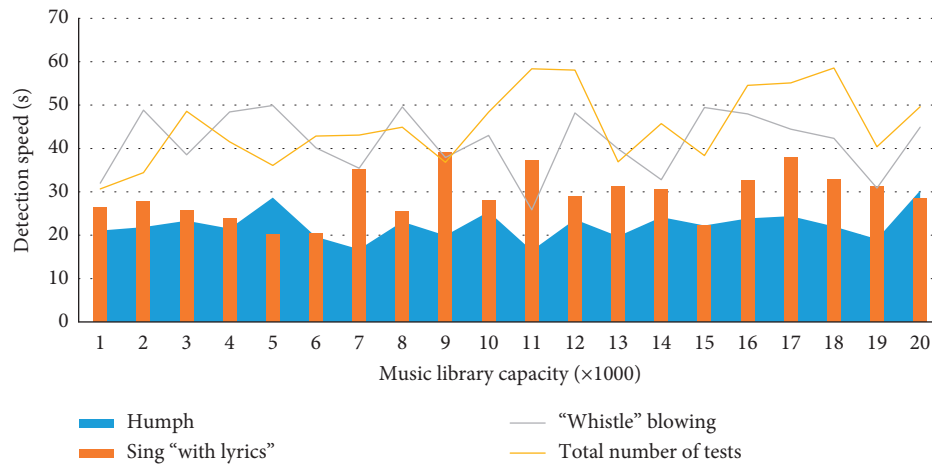
FIGURE 7: The average search speed results of the new on-demand search engine and the original search engine.

speed results of the two systems are given. The tested new QBH search engine has repeatedly tested 190 humming melodies, and its average search time is about 1/3 of the LAM algorithm, which basically meets the requirements. When using an experimental database with a capacity of 3864, the retrieval time is approximately 3.5 seconds. The result is satisfactory.

5. Conclusion

The traditional DTW algorithm minimizes the total weighted distance through a local optimization method. In this paper, the ant colony algorithm is combined with the DTW algorithm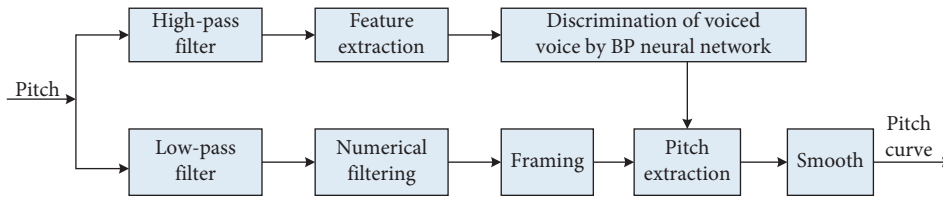, and the average distortion distance is used to measure the similarity between speech signals, so as to expect accurate recognition results. The design of the song-on-demand scoring function module uses a combination of MVC mode and command mode based on AI technology. The view component in the MVC mode is composed of a Java browser embedded in a smart client, which is mainly used to display the content that the user needs to sing and realize the interaction with the user.

The controller component uses the command mode design method to encapsulate each command in the software control as an object. These objects can respond to different command statements to complete various operations. Model components are various business logics needed in the software running process. In the song-on-demand scoring system, the scoring function constitutes the model components. The song-on-demand scoring system realizes the scoring function by rewriting the speech recognition module Sphinx4. Through the singing of the singer, the intelligent client in the system controls the speech recognition module.

The smart client determines the song paragraph to be evaluated and then passes the song paragraph to the Sphinx4 speech recognition module in the form of parameters. The voice recognition module will start a specific thread for the song paragraph according to the song paragraph to be investigated. This specific thread will monitor the microphone input data. After the singer's pronunciation is received by the microphone, it will be passed to the voice recognition module, and the voice recognition module will sing according to the song. The speaker's pronunciation evaluates a score that is similar to the standard pronunciation, and this score is returned to the smart client, and the smart client displays this score on the user interface. The smart client is also responsible for the display of relevant information about the song paragraphs to be investigated and records the number of times the singer has practiced and the results. In addition, the user interface also needs to consider the factors of interactive design and provide functions such as singing timing bar to assist users in using the scoring system and improve the effect of user experience.

Data Availability

The data that support the findings of this study are available from the corresponding author upon reasonable request.

Conflicts of Interest

The author declares no conflicts of interest.

References

[1] Y. T. Chen, C. H. Chen, S. Wu, and C. C. Lo, "A two-step approach for classifying music genre on the strength of AHP weighted musical features," *Mathematics*, vol. 7, no. 1, p. 19, 2019.

[2] Z. Lv, Y. Han, A. K. Singh, and G. Manogaran, "Trustworthiness in industrial IoT systems based on artificial intelligence," *IEEE Transactions on Industrial Informatics*, vol. 99, 2020.

[3] D. Guido, H. Song, and AnkeSchmeink, *Big Data Analytics for Cyber-Physical Systems: Machine Learning for the Internet of Things*, Elsevier, Amsterdam, Netherlands, 2019.

[4] R. H. Kulkarni and P. Padmanabham, "Integration of artificial intelligence activities in software development processes and measuring effectiveness of integration," *IET Software*, vol. 11, no. 1, pp. 18–26, 2017.

[5] V. Puri, S. Jha, R. Kumar et al., "A hybrid artificial intelligence and internet of things model for generation of renewable resource of energy," *IEEE Access*, vol. 7, pp. 111181–111191, 2019.

[6] F. Liu, Y. Shi, and Y. Liu, "Intelligence quotient and intelligence grade of artificial intelligence," *Annals of Data Science*, vol. 4, no. 2, pp. 179–191, 2017.

[7] A. H. Mazinan and A. R. Khalaji, "A comparative study on applications of artificial intelligence-based multiple models predictive control schemes to a class of industrial complicated systems," *Energy Systems*, vol. 7, no. 2, pp. 237–269, 2016.

[8] M. A. Ali, "Artificial intelligence and natural language processing: the Arabic corpora in online translation software," *International Journal of Advanced and Applied Sciences*, vol. 3, no. 9, pp. 59–66, 2016.

[9] H. Lu, Y. Li, and M. Chen, "Brain intelligence: go beyond artificial intelligence," *Mobile Networks and Applications*, vol. 23, no. 7553, pp. 368–375, 2017.

[10] S. Jha and E. J. Topol, "Adapting to artificial intelligence: radiologists and pathologists as information specialists," *JAMA*, vol. 316, no. 22, pp. 2353-2354, 2016.

[11] L. D. Raedt, K. Kersting, S. Natarajan, and D. Poole, "Statistical relational artificial intelligence: logic, probability, and computation," *Synthesis Lectures on Artificial Intelligence and Machine Learning*, vol. 10, no. 2, pp. 1–189, 2016.

[12] D. Hassabis, "Artificial intelligence: chess match of the century," *Nature*, vol. 544, no. 7651, pp. 413-414, 2017.

[13] B. K. Bose, "Artificial intelligence techniques in smart grid and renewable energy systems-some example applications," *Proceedings of the IEEE*, vol. 105, no. 11, pp. 2262–2273, 2017.

[14] E. S. E. Din, Y. Zhang, and A. Suliman, "Mapping concentrations of surface water quality parameters using a novel remote sensing and artificial intelligence framework," *International Journal of Remote Sensing*, vol. 38, no. 4, pp. 1023–1042, 2017.

[15] M. R. Hashemi, M. L. Spaulding, A. Shaw, H. Farhadi, and M. Lewis, "An efficient artificial intelligence model for prediction of tropical storm surge," *Natural Hazards*, vol. 82, no. 1, pp. 471–491, 2016.

[16] D. Yan, Q. Zhou, and J. Wang, "Bayesian regularisation neural network based on artificial intelligence optimisation," *International Journal of Production Research*, vol. 55, no. 7-8, pp. 2266–2287, 2016.

[17] A. Ema, N. Akiya, H. Osawa et al., "Future relations between humans and artificial intelligence: a stakeholder opinion survey in Japan," *IEEE Technology and Society Magazine*, vol. 35, no. 4, pp. 68–75, 2016.

[18] T. R. Besold, "On cognitive aspects of human-level artificial intelligence," *Ki KünstlicheIntelligenz*, vol. 30, no. 3-4, pp. 343–346, 2016.

[19] Y. Feng, N. Cui, Q. Zhang, L. Zhao, and D. Gong, "Comparison of artificial intelligence and empirical models for estimation of daily diffuse solar radiation in North China Plain," *International Journal of Hydrogen Energy*, vol. 42, no. 21, pp. 14418–14428, 2017.

[20] D. Norman, "Design, business models, and human-technology teamwork as automation and artificial intelligence technologies develop, we need to think less about human-machine interfaces and more about human-machine teamwork," *Research-Technology Management*, vol. 60, no. 1, pp. 26–30, 2017.

[21] N. Dudhwala, K. Jadhav, and P. Gabda, "Prediction of stock market using data mining and artificial intelligence," *International Journal of Computer Applications*, vol. 134, no. 12, pp. 9–11, 2016.

[22] J. Davies, "Program good ethics into artificial intelligence," *Nature*, vol. 538, no. 7625, p. 291, 2016.

[23] M. O'Neill, R. F. E. Sutcliffe, and C. Ryan, "Artificial intelligence and cognitive science," *Applied Artificial Intelligence*, vol. 5, no. 2, pp. 153–162, 2016.

[24] T. M. Massaro, H. L. Norton, and M. E. Kaminski, "SIRIOUSLY 2.0: what artificial intelligence reveals about the first amendment," *Social Science Electronic Publishing*, vol. 101, no. 6, pp. 2481–2525, 2017.

[25] D. S. Manu and A. K. Thalla, "Artificial intelligence models for predicting the performance of biological wastewater treatment plant in the removal of Kjeldahl nitrogen from wastewater," *Applied Water Science*, vol. 7, no. 7, pp. 1–9, 2017.

[26] R. J. Spiro, B. C. Bruce, and W. F. Brewer, *Theoretical Issues in Reading Comprehension: Perspectives from Cognitive Psychology, Linguistics, Artificial Intelligence, and Education*, CRC Press, Boca Raton, FL, USA, 2017.

[27] M. Taheri, M. R. A. Moghaddam, and M. Arami, "Improvement of the/Taguchi/design optimization using artificial intelligence in three acid azo dyes removal by electrocoagulation," *Environmental Progress & Sustainable Energy*, vol. 34, no. 6, pp. 1568–1575, 2016.

[28] E. Sinagra, M. Badalamenti, M. Maida et al., "Use of artificial intelligence in improving adenoma detection rate during colonoscopy: might both endoscopists and pathologists be further helped," *World Journal of Gastroenterology*, vol. 26, no. 39, pp. 5911–5918, 2020.

[29] M. Y. Zub, "Transformation of labor market infrastructure under the influence of artificial intelligence," *Business Inform*, vol. 8, no. 511, pp. 146–153, 2020.

Research Article

Research on Volleyball Image Classification Based on Artificial Intelligence and SIFT Algorithm

Weipeng Lin (ID)

College of Physical Education and Health, Yulin Normal University, Yulin 537000, Guangxi, China

Correspondence should be addressed to Weipeng Lin; linsport@ylu.edu.cn

Due to the application scenarios of image matching, different scenarios have different requirements for matching performance. Faced with this situation, people cannot accurately and timely find the information they need. Therefore, the research of image classification technology is very important. Image classification technology is one of the important research directions of computer vision and pattern recognition, but there are still few researches on volleyball image classification. The selected databases are the general database ImageNet library and COCO library. First, the color image is converted into a gray image through gray scale transformation, and then the scale space theory is integrated into the image feature point extraction process through the SIFT algorithm. Extract local feature points from the volleyball image, and then combine them with the Random Sample Consensus (RANSAC) algorithm to eliminate the resulting mismatch. Analyze the characteristic data to obtain the data that best reflects the image characteristics, and use the data to classify existing volleyball images. The algorithm can effectively reduce the amount of data and has high classification performance. It aims to improve the accuracy of image matching or reduce the time cost. This research has very important use value in practical applications.

1. Introduction

This classification technology can automatically understand the content of the image to a certain extent and transform the digital image into a conceptual model that people can understand. It is an important way to realize the automatic extraction of the semantic content of the image. Image classification is an interdisciplinary research field, applicable to many fields. The early image classification technology mainly relied on text features, using a manual method to label text for images and using an image classification model based on text features. Obviously, this method used for image classification does not achieve the expected experimental results. When an image is labeled with a selected keyword, an artificial selection is required, and each person has a different degree of understanding of the image content that needs to be retrieved, and even the same person may label the same content for different keywords for different

retrieval purposes. The scale of image library is increasing, and the speed of manual labeling can no longer meet the real-time performance of updating and generating corresponding content annotation. As a result, the method of manual labeling for image classification is gradually eliminated. Therefore, image classification research has gradually become a hot research focus.

Image classification refers to the process of making judgments about image resolution. The primary key point is to export image features. The features of an image represent the basic or original features of the image. Each image has its own characteristics, such as brightness, shape, edge, color, or texture. The basis of image classification lies in the extraction and representation of image features. The selected feature should have the following characteristics. Firstly, it can fully express the semantic information of the image, and secondly it should have certain stability and robustness to the interference factors such as noise. Therefore, the choice of

features is very critical. Inappropriate feature selection will result in inaccurate classification and even result in unclassifiable consequences.

Image features are widely used in images, including texture classification [1, 2], moving object tracking [3], face recognition [4], and face detection [5]. The accuracy of feature point detection is directly related to the final image processing results, so the detection of image feature points has always been the focus of research. The same object in different images is matched by detecting local feature points of the image. The early feature point detection method is the video image matching algorithm based on corner detection proposed by Moravec [6]. Wan gave a method of image matching. Before using the similarity function for feature matching, Gaussian transformation is performed on the image, which makes the image feature points prominent and easy to distinguish; PEAnuta introduces the FFT cross-correlation algorithm, and the experimental research proves that it can improve matching efficiency; later, Fauqueur proposed a description algorithm for image shape, which can be summarized as using the histogram of the image edge direction. This method not only guarantees translation invariant features, but also has a small amount of calculation. Harris et al. [7] proposed a corner detection algorithm using image gradients. Rosten et al. [8] proposed the FAST feature point detection algorithm to detect feature points by comparing the size of the center pixel with the neighborhood pixel and then calculating the score value. Calonder et al. [9] proposed the feature point detection and matching algorithm. Accurately speaking, BRIEF is a feature description algorithm. The feature pairing is performed by Hamming distance to describe the feature points. Rublee et al. [10] proposed an ORB detection algorithm combined with BREIEF and FAST algorithms, combining the detection and direction description of image feature points. Leutenegger et al. [11] proposed the BRISK detection algorithm, which mainly uses the FAST algorithm for feature point detection on multiple scales of images. Lowe [12] proposed PCA-SIFT algorithm based on SIFT algorithm combined with principal component analysis [13, 14]. Research based on local features of images has always been the focus of research by researchers [15]. How to accurately find the local features of images is the key to the subsequent processing of images. Ojala et al. [16, 17] proposed a local binary mode (LBP) algorithm based on local features of images. Davarzani et al. [18] proposed a scale and rotation invariance LBP algorithm for face recognition. In the study by Geng et al. [19, 20], the SIFT feature is proposed for face recognition. Ren et al. [1, 21] proposed an anti-noise LBP coding method for improving the recognition rate of face recognition. These methods first need to achieve image matching, for example, face recognition, for a person to collect images from different angles, through the detection of feature points, to achieve face recognition of the same person at different angles. Mikolajczyk et al. [22, 23] compared the detection algorithms of various local regions of interest in images, mainly comparing the detection of feature points and image matching, and concluded that

SIFT algorithm is a better detection and matching algorithm. The use of SIFT algorithm in the literature [24] to achieve the classification of 20 semantic concepts has also achieved satisfactory results.

SIFT is an algorithm that can detect poles in the multiscale space of an image and extract relevant feature descriptors. SIFT features have great advantages in feature representation, matching, and recognition: SIFT features are local features of images, which are constant for scale changes, image rotation, brightness intensity, and strong resistance to viewing angle changes and noise. The SIFT algorithm is suitable for accurate and fast matching in a large amount of data, because a small number of objects can generate a large amount of SIFT feature vector information. The SIFT algorithm has been applied to different degrees in military, industrial, and civil applications. Its application has penetrated into many fields. Its typical applications include object recognition, robot positioning and navigation, note identification, image stitching, fingerprint field feature extraction, 3D modeling, gesture recognition, and more. SIFT has an unparalleled advantage in the nontransformation feature extraction of images. The above characteristics of SIFT and the wide range of applications in various fields ensure the effect of this local feature on image classification.

The SIFT algorithm uses multiscale for key point detection. At the same time, the feature point is described by 128-dimensional direction vector, which is excellent in scale invariance and rotation invariance. When using the SIFT algorithm, it is crucial to select key points for image detection and image matching. Although Lowe proposed the SIFT algorithm, the selection method was not explicitly given in the parameter selection, and the effect of the image size on the number of feature points was not explained. As a result, the expected result was not achieved when using the SIFT algorithm. Based on the theoretical analysis and experimental verification, the relationship between feature detection parameters and feature point detection results is determined and the principle of selection of important parameters of the SIFT algorithm is given. In reality, the images collected are often affected by various conditions and the quality is not good. Before using the SIFT algorithm, the image is subjected to gradation transformation processing to improve image quality.

2. Proposed Method

2.1. Gray Scale Transformation.
Let's introduce each of these grayscale transformation methods one by one.

2.1.1. Linear Gradation Transformation.
Due to underexposure or overexposure during imaging, the image gray scale may be confined to a relatively small range. In this case, the image contrast is insufficient due to lack of gray level, and the image details are difficult to distinguish clearly. At this time, if the linear single-valued function is used to linearly extend the grayscale of the image, the visual effect of the image can be effectively improved. Assuming that the grayscale range of the original input image $f(x, y)$ is (m, n), we expect the

grayscale range of the output image $g(x, y)$ after the gradation transformation to be extended to (p, q); then this is linear. The expression of the transformation function is

$$g(x, y) = \frac{q - p}{n - m}(f(x, y) - m) + p. \tag{1}$$

If the original grayscale distribution of the original input image $f(x, y)$ is (m, n) and the small grayscale is outside this interval, to improve the enhancement effect, the following transformation relationship can be used (M is the maximum gray level in the image $f(x, y)$):

$$g(x, y) = \begin{cases} p, & 0 \le f(x, y) \le m, \\ \dfrac{q - p}{n - m}[f(x, y) - m] + p, & m \le f(x, y) \le n, \\ q, & n \le f(x, y) \le M. \end{cases} \tag{2}$$

This relationship can be represented by Figure 1.

2.1.2. Piecewise Linear Gradation Transformation.
To suppress those targets or grayscale spaces that we are not interested in, we can use the piecewise grayscale linear transformation method. The most common method is a linear transformation divided into three segments.

As shown in Figure 2, it is assumed that the gradation of the original input image $f(x, y)$ is 0—M_f, and the gradation of the obtained output image $g(x, y)$ is 0—M_g, and the expression for its piecewise linear transformation is

$$g(x, y) = \begin{cases} \dfrac{p}{m} f(x, y), & 0 \le f(x, y) \le m, \\ \dfrac{q - p}{n - m}[f(x, y) - m] + p, & m \le f(x, y) \le n, \\ \dfrac{M_g - q}{M_f - n}[f(x, y) - n] + q, & n \le f(x, y) \le M_f. \end{cases} \tag{3}$$

In Figure 2, the (m, n) grayscale interval is linearly transformed, and the $(0, m)$ and (n, M_f) segments are compressed. By adjusting the position of the inflection point of the fold line and controlling the slope of the segment line, it is possible to expand or contract any gray scale interval. Figure 2 also shows that if the grayscale of the image is concentrated in a darker region and the image is darker, then it can be achieved by extending the low-gray interval of the image (slope greater than 1) and compressing the high-gray interval (slope less than 1). If the gray level of the image is concentrated in a brighter area, the image is brighter; then the low-gray-level interval (slope less than 1) and the high-gray-level interval (slope greater than 1) can be compressed to achieve the purpose of improving the image.

The disadvantage of piecewise linear grayscale transformation is that it depends on the user's input.
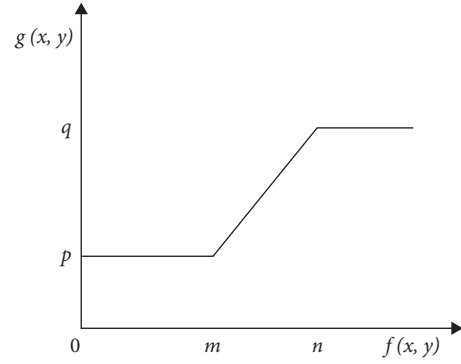
Figure 1: The linear transformation relationship of the function.
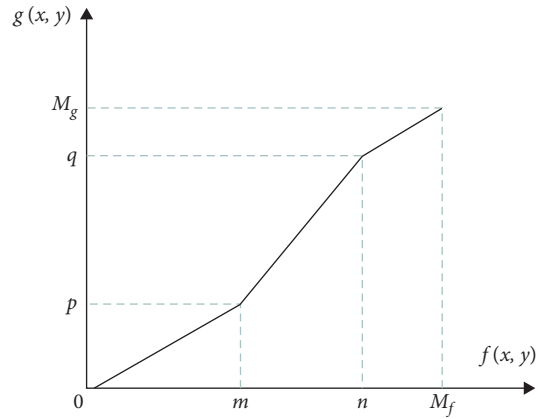
Figure 2: Piecewise linear transformation.

2.1.3. Nonlinear Grayscale Transformation.
Nonlinear transformation of gray scale can be realized. Take the exponential transformation as an example.

Since the piecewise linear transformation has limited processing ability on the gray value of the image and cannot meet certain specific requirements, a nonlinear transformation is proposed, and the mathematical requirements of the function are used to satisfy the transformation requirements. The exponential transformation form in the nonlinear transformation is as follows:

$$g(m, n) = \lambda[f(m + n) + \varepsilon]^{\gamma}. \tag{4}$$

Among them, the existence of ε is to avoid the occurrence of the base zero, the exponent of γ as a function has a great influence on the performance of the function, and the difference of the value determines the difference of the function transformation effect. When $\gamma < 1$, it is advantageous for the low-gray area; when $\gamma > 1$, it is advantageous for the high-gray area; when $\gamma = 1$, it is equivalent to the proportional conversion. The difference in γ values is different for the visually bright and dark changes caused by the image. This transformation not only changes the contrast of the image but also enhances the details of the image, resulting in an enhancement and improvement of the overall image effect.

2.2. SIFT Algorithm. The implementation of the SIFT algorithm is a complex process. Delete some unstable and affected points by the edge factors to avoid their influence on the classification. Of course, after finding the key points, the information is also represented. The SIFT algorithm uses a 128-dimensional vector containing the position and scale of the key point. The direction of the vector is the direction of the key point information. Finally, the classification work of the image is carried out. The essence is the classification between the feature descriptors of the key points. The key points in the graph are detected by a certain algorithm to realize the classification of the images.

Then, the main direction of the key point domain is used as the directional feature of the change point to complete the operator's independence from the direction and scale. The steps of the SIFT generation algorithm according to the image to be processed are as follows. (1) Carefully detect the pole value in the image scale space, and initially determine the key points and scales of the image. (2) Remove the key points with low contrast and unstable edge points to improve the stability and noise resistance of the matching. (3) Specify the corresponding parameters for each key point, and make the operator have rotation invariance. The main features of the algorithm are the following:

(1) The SIFT feature is a local feature of the image, which maintains invariance to rotation and scale scaling.

(2) It has good uniqueness and rich information and is suitable for fast and accurate matching in the massive feature database.

(3) It has multiplicity, where even a small number of objects can generate a large number of feature vectors.

(4) It has high speed, where optimized matching algorithms can even meet real-time requirements.

(5) When the image target is being collected, it is often affected by external vibration, light intensity, and imaging equipment. The SIFT algorithm has certain tolerances for the following situations:

(1) Rotate and scale
(2) Perspective change
(3) Light effects
(4) Target occlusion
(5) Sundries scene
(6) Noise

The specific implementation process of the SIFT algorithm will be introduced from five aspects.

2.2.1. Establish the Scale Space of the Image. The concept of scale space has been proposed very early. For a two-dimensional image $I(x, y)$, its scale space $L(x, y, \sigma)$ can be expressed as follows, in the form of the formula as shown:

$$L(x, y, \sigma) = G(x, y, \sigma) * I(x, y),$$

$$G(x, y) = \frac{1}{2\pi\sigma^2} e^{-(x-m/2)^2 + (y-n/2)^2/2\sigma^2}, \tag{5}$$

where m, n are the size of the Gaussian template, $m = 6\sigma + 1$, $n = 6\sigma + 1$; σ is the scale factor; $*$ is convolution operation. (x, y) represents the role of space, where the large scale and small scale correspond to the profile features and the detail features. Therefore, the selection of reasonable scale factors is the key content of establishing scale space.

2.2.2. Generating a Gaussian Difference Pyramid. To get a Gaussian difference pyramid, you must first have a Gaussian pyramid. The process of generating a Gaussian pyramid is the process of scale space generation. The establishment of the Gaussian pyramid is divided into two steps: image Gaussian blur and downsampling. The image pyramid model is named for its shape resembling a pyramid. The gradient image obtained by downsampling the original image is arranged from bottom to top. At the bottom of the original image, downsampling is performed in turn to obtain n sets of graphs. The calculation of the number of groups n is as follows:

$$n = \log_2[\min(M, N)] - t, \quad t \in [0, \log_2\{\min(M, N)\}], \tag{6}$$

where M, N are image size; t is the logarithm of the dimension of the tower top image.

The relationship between the number of pyramid groups and the image size is shown in Table 1.

In order to make the images in the pyramid have continuous visibility, all the images in the Gaussian pyramid are blurred, so that each group of the pyramid contains many Gaussian blurred images. In this case, when generating a set of images on the pyramid, it is necessary to use the method of interval sampling.

Mikolajczyk has found in experiments that the extreme value of the scale-normalized Gaussian Laplacian operator $\sigma^2\nabla^2G^2$ is the most stable. Lindeberg also found in the experiment that Gaussian difference operators (i.e., DOG operators) have similarities with $\sigma^2\nabla^2G^2$, and there is a certain relationship between them:

$$\frac{\partial G}{\partial \sigma} = \sigma\nabla^2G. \tag{7}$$

Using the approximation of difference and differential, there are

$$\sigma\nabla^2G = \frac{\partial G}{\partial \sigma} \approx \frac{G(x, y, k\sigma) - G(x, y, \sigma)}{k\sigma - \sigma}. \tag{8}$$

The following is further available:

$$G(x, y, k\sigma) - G(x, y, \sigma) \approx (k - 1)\sigma^2\nabla^2G. \tag{9}$$

We continue with the above derivation:

$$D(x, y, \sigma) = [G(x, y, k\sigma) - G(x, y, \sigma)]^* I(x, y)$$
$$= L(x, y, k\sigma) - L(x, y, \sigma), \tag{10}$$

where k is the derivative constant.

TABLE 1: The relationship between the number of 512×512 image pyramid groups and the original image size.

Image size	512	216	128	64	16	8	4	2	1
Pyramid group number	1	2	3	4	5	6	7	8	9

2.2.3. Extreme Point Detection. Because the key point is part of the extreme point, you must first find the extreme point. Each point of the Gaussian difference (DoG) scale space is compared with the points of adjacent scales and adjacent positions one by one, and the position of the local extreme value of the obtained local extremum and the corresponding scale are obtained. The SIFT algorithm selects 26 pixels adjacent to it to ensure the accuracy of the detected extreme points. If the Gaussian difference pyramid contains 4 layers each, because the extreme value detection is compared with the adjacent two layers, then the first and last layers must be removed, and there are two layers left. Considering that the Gaussian pyramid loses another layer when generating the Gaussian difference pyramid, the number of layers of the Gaussian pyramid must be three more layers than the number of layers that need to be detected by the extreme value. Of course, the extreme points obtained in this way are not necessarily the key points.

2.2.4. Key Point Location and Direction Assignment

(1) Key Point Positioning. The extreme points obtained in the discrete space are discontinuous, and the position determination cannot be performed. Therefore, it is necessary to accurately locate the key points by means of function fitting and find the extreme points which are really key points. The fitting calculation is usually performed in the scale space by the subpixel difference value. The DOG operator Taylor expansion is

$$D(X) = D + \frac{\partial D^T}{\partial X} X + \frac{1}{2} X^T \frac{\partial^2 D}{\partial X^2} X. \tag{11}$$

The following is derived:

$$\hat{x} = -\frac{\partial^2 D^{-1}}{\partial X^2} \frac{\partial D}{\partial X}. \tag{12}$$

The corresponding equation value is

$$D(\hat{x}) = D + \frac{1}{2} \frac{\partial D^T}{\partial X} \hat{x}. \tag{13}$$

Suppose $\hat{x} = (x, y, \sigma)^T$ represents the deviation of the key point from the center of the interpolation. When the value is greater than the preset value, it indicates that the deviation is large, the key position must be reset, and the new position is continuously interpolated until it is less than the preset value. Thereby, the exact position $\sigma(o, s)$ and the scale $\sigma\_oct(s)$ of the key points are obtained.

(2) Eliminate Edge Response. The Gaussian difference functions have a strong edge response, so even small noise can cause instability:

$$H = \begin{bmatrix} D_{xx} & D_{xy} \\ D_{xy} & D_{yy} \end{bmatrix}. \tag{14}$$

The principal curvature of the Gaussian difference function is proportional to the eigenvalue of the sea cucumber matrix H. Let α be the largest eigenvalue of the sea cucumber matrix H, and β is the smallest eigenvalue of H. Then,

$$\begin{cases} \mathrm{Tr}(H) = D_{xx} + D_{yy} = \alpha + \beta, \\ \mathrm{Det}(H) = D_{xx}D_{yy} - (D_{xy})^2 = \alpha\beta. \end{cases} \tag{15}$$

Let γ be the ratio of the maximum eigenvalue to the minimum eigenvalue, and let $\alpha = r\beta$. Then,

$$\frac{\mathrm{Tr}(H)^2}{\mathrm{Det}(H)} = \frac{(\alpha + \beta)^2}{\alpha\beta} = \frac{(r\beta + \beta)^2}{r\beta^2} = \frac{(r + 1)^2}{r}. \tag{16}$$

When the maximum eigenvalue and the minimum eigenvalue are equal, the value of $(r + 1)^2/r$ is the smallest, and $(r + 1)^2/r$ increases as the r value increases. So if the main curvature is detected below a certain threshold γ, just check

$$\frac{\mathrm{Tr}(H))^2}{\mathrm{Det}(H)} < \frac{(r + 1)^2}{r}. \tag{17}$$

(3) Key Point Direction Assignment. The reason why the SIFT algorithm is very tolerant to rotating images is because there is a main direction. No matter how the image rotates, the main direction does not change with the rotation of the image. The calculation of the pixel gradient and direction around the key points is as follows:

$$\begin{cases} m(x, y) = \sqrt{[L(x + 1, y) - L(x - 1, y)]^2 + [L(x, y + 1) - L(x, y - 1)]^2}, \\ \\ \theta(x, y) = \arctan \dfrac{L(x, y + 1) - L(x, y - 1)}{L(x + 1, y) - L(x - 1, y)}, \end{cases} \tag{18}$$

where $L(x, y)$ is the scale space value at which the key point is located; $m(x, y)$ is the tkey point gradient; $\theta(x, y)$ is the key point direction (°).

After calculating the gradient and direction of each pixel in the neighborhood of the key point, the information is counted and represented. Because there is 360° around the key point, it is too much trouble to count each direction. In order to simplify it, 45° is used as a distinguishing point, which is divided into 8 directions.

2.2.5. Generating Feature Descriptors. After obtaining the three kinds of information of a key point through the above steps, a feature descriptor is needed to uniformly describe the three kinds of information. Let it contain information about the key point and its neighborhood point, and this feature descriptor is an abstract representation of the image local information and unique. Here are the steps that are specifically generated for it.

(1) Determine the Key Point Neighborhood Size. The contribution rate of surrounding pixels to key points depends on the size of the key point neighborhood. The SIFT algorithm takes a 16×16 pixel area and then subdivides it into 16 seed areas.

(2) Direction Rotates to the Same Direction as the Coordinate Axis. The main direction is converted, and the position change relationship of the coordinate point after the rotation is as shown in the following formula:

$$\begin{pmatrix} x' \\ y' \end{pmatrix} = \begin{pmatrix} \cos \theta & -\sin \theta \\ \sin \theta & \cos \theta \end{pmatrix} \begin{pmatrix} x \\ y \end{pmatrix}, \qquad (19)$$

wherein θ is the angle of rotation (°).

(3) Calculate the Gradient of the Seed Point in Eight Directions. Because the key pixel neighborhood is divided into 16 seed points, and each point has 8 direction information, the gradient of each seed point is weighted and accumulated by direction allocation.

(4) Generate Descriptor. The $4 \times 4 \times 8 = 128$ gradient size and direction information obtained by the above calculation is a unique description of the key points and generates a 128-dimensional feature vector. In order to avoid the influence of light and dark on the feature descriptor, it needs to be normalized as shown below:

$$\overline{L} = \frac{L}{\sqrt{\sum_{i=1}^{128} l_i^2}} = (\overline{l}_1, \overline{l}_2, \ldots, \overline{l}_{128}), \quad i = 1, 2, \ldots, 128, \qquad (20)$$

where L is the characterization descriptor, $L = (l_1, l_2, \ldots, l_{128})$, and $\overline{L}$ stands for normalized feature descriptors.

When the feature vectors of the two images are generated, the next step is the feature matching phase. The pair of matching points is accepted; otherwise, it is discarded. When this threshold is lowered, the number of matching points will decrease, but the matching points will be more accurate and stable.

2.3. RANSAC Method. The RANSAC (RANdomSAmple Consensus) algorithm is called a random sampling consensus set. The main feature of this method is that the parameters of the model increase with the number of iterations, and the correct probability will be improved one by one. The advantage is that the model parameters can be estimated robustly and have a certain tolerance to noise. The main idea is to solve the parameters of the mathematical model by sampling and verifying the strategy. The sample points that match the model are called inner points, and the sample points that do not conform to the model are called outer points.

The RANSAC algorithm is as follows:

(1) There is a model adapted to the assumed intrasite point; that is, all unknown parameters can be calculated from the assumed intraoffice points

(2) Use the model obtained in the step to test all other data

(3) If there are enough points to be classified as hypothetical intrapoints, then the estimated model is reasonable enough

(4) Evaluate the model by estimating the error rate of the intrapoint and model

The parameters of the model are calculated by inputting data, and the data that cannot be adapted to the model parameters is called an outlier; otherwise, it is called an intrapoint. If there are enough points in the input data to be classified as intrapoints, the estimated model is reasonable. The above process is repeated a fixed number of times; each time the generated model is either discarded because there are too few intrasite points or selected because it is better than the existing model.

3. Experiments

3.1. Data Sources. The databases are ImageNet and COCO. Among the five types of images in ImageNet, such as volleyball, football, table tennis, tennis, and basketball, each type of image contains 10 different image targets. Each image target selects 5 images from different directions and different shooting angles. Here we select 400 images from the database to experiment, the same type of picture in the COCO database, 50 pictures in each category, a total of 250 pictures.

3.2. Experimental Evaluation Criteria. Since the images are used in a variety of databases, the classification accuracy is generally used to measure the performance of the image classification algorithm. The calculation formula is as follows:

$$\text{Precision} = \frac{\text{ImageNumber}_{\text{accurate}}}{\text{ImageNumber}_{\text{all}}} \times 100\%. \qquad (21)$$

FIGURE 3: Grayscale effect. (a) Original image. (b) Grayscale transformed image.

In the above formula, ImageNumber$_{accurate}$ represents the total number of images that are correctly classified, and Precision represents the accuracy of image classification. In this experiment, we use cross-validation method to calculate the accuracy of image classification. The experiment first divides the sample data into N groups, and N is defined by itself. Each experiment uses $N-1$ group sample data as the training set and the last set of sample data as the test set. After calculating the classification accuracy of each set of experimental data, the arithmetic mean of the accuracy of each set of data is selected as the final classification accuracy.

3.3. System Environment. The classification of volleyball images based on SIFT algorithm proposed in this paper is designed and implemented on ordinary PC.

Hardware configuration:

CPU: Pentium (R) Dual-Core CPU E5800 @ 3.20 GHz
Memory: 4G

Software configuration:

System: 64 bit win10
Development environment: MATLAB 2014B

4. Results and Discussion

Result 1. Gradation transformation of volleyball images.

The effect diagram of the grayscale linear transformation of the volleyball image of this experiment is shown in Figure 3.

By comparing the two graphs in Figure 3, it can be found that after the piecewise linear transformation, the gray scale of some parts of the graph is enhanced, it is easier to visually perceive the existence of these parts, and some useless parts are suppressed. After the transformation, the texture of each part can be clearly seen.

Result 2. Influence of Gaussian Fuzzy Scale σ on Image Feature Point Detection.

TABLE 2: Number of feature points detected at different Gaussian fuzzy scales.

Gaussian fuzzy scale (σ)	Number of feature points detected
0.7	9996
1.4	1300
2.1	799
2.8	620

Gaussian fuzzy scale σ is also called Gaussian blur radius, which is applied to the generation of Gaussian difference pyramid. The magnitude of σ determines the degree of image blur. The larger the σ is, the more blurred the image is. The smaller the σ is, the more detailed the image can be. In the experiment, we used the SIFT algorithm to extract features from the images in the ETH80 database. To unify the experimental parameters, we have 30 test sets and 20 test sets, followed by different Gaussian fuzzy scale values. In order to prove the validity of the experiment, we repeated the test of 10 experiments and finally took the average correct rate of each experiment result as the final test result of the experiment. The results in Table 2 show that the number of detections of feature points varies greatly when the Gaussian fuzzy scale σ is at different values. When the Gaussian fuzzy scale value σ increases, the number of detections of feature points decreases a lot.

Result 3. Influence of volleyball image size on features.

The selected image contains a huge amount of information. Among the extracted features, some are useful features, and some image classifications are not very useful. Therefore, the feature points of the partial separation group must be removed. We use the RANSAC algorithm to filter the "outlier points" filter to eliminate the interference of the error points on the experiment. The SIFT algorithm performs feature point detection by Gaussian pyramid, and the effect of feature extraction by SIFT is shown in Figure 4. Since the number of Gaussian pyramids is limited in small-sized images and the description area of feature points is also limited, the image size has a great influence on the number of feature points, which in turn affects the number of matches.

FIGURE 4: Feature extraction diagram using SIFT algorithm.

TABLE 3: Image size and feature points, as well as the number of matches and the duration of consumption.

Image size	Feature points	Matches	Consumption time (ms)
Original image	1300	457	21310
1/2 image	461	210	1568
1/4 image	134	63	450
1/8 image	37	14	122
1/16 image	5	1	18

TABLE 4: Classification accuracy statistics.

Sports image	Accuracy
Volleyball	0.26
Football	0.23
Ping Pong	0.15
Tennis	0.18
Basketball	0.25

TABLE 5: Accuracy data of each classification method.

Classification	Accuracy (%)
Feature selection	12
Spatial information	9
Visual bi-gram	6
Kernel choices	7
Weighting scheme	11
Stop-word removal	12
The method proposed in this paper	26

The test result of reducing the picture by half is shown in Table 3. The Gaussian fuzzy scale σ parameter is set to 1.4.

Result 4. Image classification accuracy rate statistics.

The size of the volleyball image used in the experiment ranges from $300 * 250$ pixels to $2600 * 3400$ pixels. The picture size distribution is wide and the sampling is uniform, which has strong universality. At the same time, other sports images such as football, table tennis, tennis, and basketball are added for comparison, and the image features are extracted by this method for classification research. The classification results are shown in Table 4.

From the perspective of classification effect, it is obviously superior to the classification methods mentioned in [23], such as feature selection, spatial information, visual bi-gram, Kernel choices, weighting scheme, and stop-word removal. The proposed method was classified, and the average accuracy obtained was 26%. The effect of various classification methods is shown in Table 5 and Figure 5.
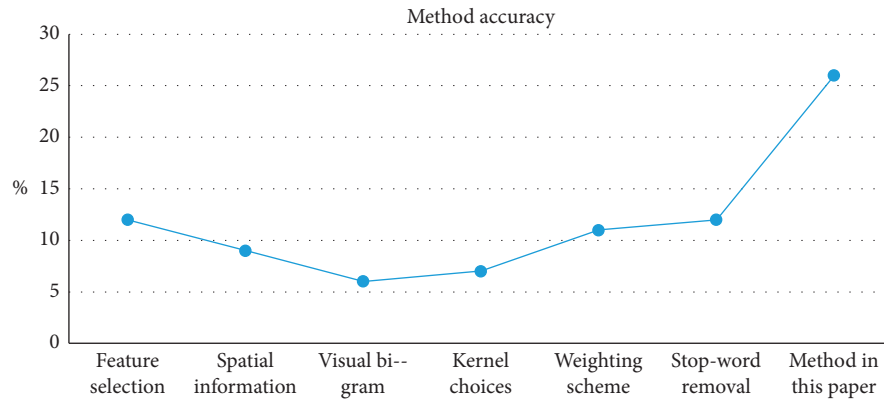
FIGURE 5: Accuracy of each classification method.

5. Conclusions

People cannot accurately and timely find out the information they need. Through image classification technology, you can understand things more objectively and accurately.

Image classification technology is an important part of the field of computer vision, which can effectively solve the problems of large data volume and high computational complexity. In this paper, the image classification method based on SIFT algorithm is proposed. After the image is grayscale transformed, the SIFT algorithm is used to extract and match the feature points. Combined with the random sampling consensus set algorithm (RANSAC), the error matching is deleted to improve the correct rate. It was applied to the volleyball image classification. The experimental results show that the method has the advantages of fast retrieval speed and high classification accuracy, so as to obtain the data that best reflects the image features, and then achieves a good effect by accurately classifying the images with the above data.

Aiming at the problem of low SIFT feature matching efficiency, this paper proposes an algorithm that combines artificial intelligence and SIFT features, aiming to quickly and accurately find matching point pairs through distributed computing of swarm intelligence. In order to reduce the amount of calculation, improved SIFT feature descriptors are used, which are the SIFT feature based on kernel projection and the SIFT feature based on principal component analysis. This article also gives a brief introduction to the principles of artificial intelligence and SIFT algorithm and how to use it in image matching. I hope that there will be new breakthroughs in the field of subsequent image matching. This article also compares the matching results of the swarm intelligence algorithm with other matching algorithms, and it does show certain advantages in the matching results.

Data Availability

No data were used to support this study.

Conflicts of Interest

The authors declare that they have no conflicts of interest.

References

[1] J. Ren, X. Jiang, and J. Yuan, "Noise-resistant local binary pattern with an embedded error-correction mechanism," *IEEE Transactions on Image Processing*, vol. 22, no. 10, pp. 4049–4060, 2013.

[2] D. Chen, X. Cao, F. Wen et al., "Blessing of dimensionality: high-dimensional feature and its efficient compression for face verification," in *Proceedings of the 2013 IEEE Conference on Computer Vision and Pattern Recognition*, pp. 3025–3032, Portland, OR, USA, June 2013.

[3] G. Zhao, T. Ahonen, J. Matas et al., "Rotation–invariant image and video description with local binary pattern features," *IEEE Transactions on Image Processing A Publication of the IEEE Signal Processing Society*, vol. 21, no. 4, pp. 1465–1477, 2012.

[4] M. A. Akhloufi and A. Bendada, "Locally adaptive texture features for multispectral face recognition," in *Proceedings of the IEEE International Conference on Systems Man and Cybernetics IEEE*, pp. 3308–3314, Istanbul, Turkey, October 2010.

[5] Y. Mu, S. Yan, Y. Liu et al., "Discriminative local binary patterns for human detection in personal album," in *Proceedings of the 2008 IEEE Conference on Computer Vision and Pattern Recognition (CVPR)*, pp. 1–8, Anchorage, AK, USA, June 2008.

[6] H. P. Moravec, *Rover Visual Obstacle Avoidance International Joint Conference on Artificial Intelligence*, Morgan Kaufmann Publishers Inc., Burlington, MA, USA, 1981.

[7] C. Harris and M. Stephens, *A Combined Corner and Edge Detector*, The Plessey Company, UK, 1988.

[8] E. Rosten, R. Porter, and T. Drummond, "Faster and better: a machine learning approach to corner detection," *IEEE Transactions on Pattern Analysis & Machine Intelligence*, vol. 32, no. 1, pp. 105–119, 2008.

[9] M. Callonder, V. Lepetit, M. Ozuysal et al., "BRIEF: computing a local binary descriptor very fast," *IEEE Transactions on Pattern Analysis & Machine Intelligence*, vol. 34, no. 7, pp. 1281–1298, 2012.

[10] E. Rublee, V. Rabaud, K. Konolige et al., "ORB: an efficient alternative to SIFT or SURF, International Conference on computer vision," *IEEE Computer Society*, pp. 2564–2571, 2011.

[11] S. Leutenegger and M. Chli, "BRISK: Binary robust invariant scalable keypoints," in *Proceedings of the IEEE International Conference on Computer Vision IEEE*, pp. 2548–2555, Barcelona, Spain, November 2011.

[12] D. G. Lowe, "Object recognition from local scale-invariant features," in *Proceedings of the Seventh IEEE International Conference on Computer Vision*, p. 1150, IEEE, Kerkyra, Greece, 2002.

[13] D. G. Lowe, *Distinctive Image Features from Scale-Invariant Keypoints*, Kluwer Academic Publishers, Amsterdam, Netherlands, 2004.

[14] H. Bay, T. Tuytelaars, and L. Van Gool, "SURF: Speeded up robust features," in *Proceedings of the Computer Vision (ECCV 2006)*, Graz, Austria, May 2006.

[15] Y. Ke and R. Sukthankar, "PCA-SIFT: A more distinctive representation for local image descriptors," in *Proceedings of the IEEE Computer Society Conference on Computer Vision & Pattern Recognition IEEE Computer Society*, pp. 506–513, Washington, DC, USA, June 2004.

[16] T. Ojala, M. Pietikäinen, and D. Harwood, "A comparative study of texture measures with classification based on featured distributions," *Pattern Recognition*, vol. 29, no. 1, pp. 51–59, 1996.

[17] T. Ojala, M. M. Pietik Inen, and T. Enp, *Multiresolution Gray-Scale and Rotation Invariant Texture Classification with Local Binary Patterns European Conference on Computer Vision*, Springer-Verlag, Berlin, Heidelberg, Germany, 2000.

[18] R. Davarzani, S. Mozaffari, and K. Yaghmaie, "Scale- and rotation-invariant texture description with improved local binary pattern features," *Signal Processing*, vol. 111, pp. 274–293, 2015.

[19] C. Geng and X. Jiang, "SIFT features for face recognition," in *Proceedings of the IEEE International Conference on Computer Science and Information Technology IEEE*, pp. 598–602, Beijing, China, August 2009.

[20] A. Wong and D. A. Clausi, "ARRSI: automatic registration of remote-sensing images," *IEEE Transactions on Geoscience and Remote Sensing*, vol. 45, no. 5, pp. 1483–1493, 2007.

[21] K. Mikolajczyk and C. Schmid, "A performance evaluation of local descriptors," *IEEE Transactions on Pattern Analysis and Machine Intelligence*, vol. 27, no. 10, p. 1615, 2005.

[22] L. Tony, "Scale-space theory: a basic tool for analyzing structures at different scales," *Journal of Applied Statistics*, vol. 21, no. 2, pp. 224–270, 2011.

[23] R. C. Bolles and M. A. Fischler, *RANSAC-based Approach to Model Fitting and its Application to Finding Cylinders in Range Data International Joint Conference on Artificial Intelligence*, vol. 2, pp. 637–643, 1981.

[24] Y.-G. Jiang, J. Yang, and C.-W. Ngo, "Representation of key point-based semantic concept detection a comprehensive study," *IEEE Transactions on Multimedia*, vol. 12, no. 1, pp. 42–53, 2010.

Research Article

International Trade Balance Algorithm Based on the Ownership Principle of Mobile Edge Computing

Fangfang Du [ID]

Jiangxi University of Technology, Nanchang 330098, Jiangxi, China

Correspondence should be addressed to Fangfang Du; dufangfang@bitzh.edu.cn

As an emerging mobile computing technology, mobile edge computing is an important key technology to improve the computing services of mobile devices. This paper mainly studies the balance of international trade algorithm based on the principle of moving edge computing ownership. In order to obtain all the data needed to perform the task, each mobile device can exchange data information with its connected base station through the wireless network. On the basis of satisfying the quality of service of users, including considering the user connection and service configuration, the network energy consumption is minimized in continuous t period by shutting down some servers whose resources are not fully utilized. At the same time, in order to reduce the switching cost of edge server and ensure the stability of service, frequent switching of edge server should be avoided. At the beginning, there is division of labor economy. With the development of specialized production, the degree of international division of labor is increasing due to the effect of experience accumulation. The trade efficiency is growing endogenously. The international division of labor is further deepened, and the types and quantity of products participating in the international division of labor are greatly increased, so as to realize the upgrading of trade structure. Before constructing the structural VAR model of Bti, R/W, K/L, and TFP, we need to test its stationarity. Using Eviews 5.0 software, ADF test and PP test were carried out on the unit root of BTI, r/w, K/L, and TFP time series data. With the increase of user task arrival rate, the average time revenue increases continuously. However, when the arrival rate is greater than 3 kbit/slot, the average time revenue increases slowly. The results show that the research results in system model and resource optimization algorithm will provide reliable theoretical and technical support for the practical application of mobile edge computing.

1. Introduction

Since the reform and opening up, China has achieved high-quality development in all economic fields. Even after the subprime mortgage crisis in the United States, China's economy has maintained a stable and rapid development, and its GDP growth rate ranks first in the world [1]. In this background, in order to meet the requirements of wireless data transmission and mobile devices to solve the problems [2], this article will research on the edge of the mobile computing network weighted bits and maximize and safety calculation efficiency maximization problem, so as to further enhance the security of the mobile computing performance and energy efficiency.

The current world is a highly competitive and closely connected world, and as a large trading country, China's every move will not only affect the changes in the domestic economy but also the economic changes in the countries and regions related to it. For this reason, under the mobile edge computing architecture, we can further optimize resource management, allocate resources reasonably to improve power efficiency, and use the limited power to perform more tasks as much as possible. On the other hand, lower energy consumption may slow down the task execution speed [3], which cannot meet the user's service quality requirements.

Active caching and processing and multilayer interference cancellation are discussed in [4]. He demonstrated that the cross-border trade statistics system based on the territorial principle has defects, which greatly interferes with the

authenticity of trade balance statistics. This highlights the importance of ownership adjustment. Tran T X believes that MEC is an emerging paradigm, which provides computing, storage and network resources within the edge of the mobile RAN. He envisioned a real-time, context-sensitive collaboration framework that is located at the edge of the RAN, composed of MEC servers and mobile devices and fused heterogeneous resources at the edge. Specifically, he introduced and studied three representative use cases, ranging from mobile edge orchestration, collaboration the promising benefits of the proposed method in facilitating the evolution to 5G networks. Although his research is more accurate, it is not comprehensive [5]. Yulun believes that the virtualized small cell network integrated with mobile edge computing is a promising example that can economically provide broadband access and intensive computing for user equipment in the case of multiple mobile virtual network operators and infrastructure providers. By comprehensively considering offloading time slice and power allocation, he formulates the UE energy consumption reduction in virtualized SCN as a mixed integer nonlinear programming. His goal is to minimize the UE's total energy consumption when the total network throughput is the smallest. In order to effectively solve the problem, he converted it into a double convex problem by adding auxiliary variables, so that an effective iterative algorithm can be derived from two subproblems. Although his research algorithm is innovative, it lacks precision [6]. Wu H believes that the rapid advancement of wireless power transmission and mobile edge computing provides a promising method for the Industrial Internet of Things to improve manufacturing quality and productivity [7]. Due to wireless channel congestion, time-related energy constraints, complex device heterogeneity, and annoying signaling overhead, scheduling in this situation is challenging. He first proposed an online algorithm called energy-aware resource scheduling to maximize system utility including throughput and fairness while taking into account system sustainability and stability. Subsequently, he extended the ERS algorithm to more realistic scenarios [8]. He provided the optimal scheduling decision of the scene and analyzed the optimal loss of system utility under the outdated NSI [9]. Although the algorithm he used is more effective, it lacks necessary experimental data [10]. Lin C J believes that the next-generation mobile network 5G aims to support lower end-to-end latency, higher reliability, and higher throughput, which can be improved by MEC and multi-RAT offloading, respectively. He introduced a dual offloading mechanism called LCCOP, which offloads incoming traffic to the best wireless pair and edge pair, depending on the end-to-end latency of the request connection. He ran simulations to compare LCCOP with traditional unloading solutions [11]. Although his algorithm is very reliable, there are still big loopholes [12].

Based on the theory of international industrial transfer, international trade theory, and spatial economics, this paper links the development of international trade with the evolution of international industrial transfer organically with the research method of new economic geography. In this paper, cross-section data of each country are also adopted, and the combination of time series and cross-section can more scientifically explain the impact of RMB exchange rate fluctuations on the trade balance between China and various trading partners.

2. Ownership Principle of Mobile Edge Computing

2.1. Mobile Edge Computing. The task scheduling process in mobile edge computing is shown in Figure 1. When the mobile device has tasks that need to be processed by the MEC server, the device first perceives and collects the current network environment information, including the status of the nearby MEC server, the server's computing and storage capabilities [13], and wireless channel status. For the traditional MCC system, the task offloading transmission process needs to go through the wireless access network and the core network of multi-hop routing, which leads to a significant increase in transmission delay and consumes a lot of energy. However, under normal circumstances, because the edge cloud is located on the side of the wireless access network [14], the task offloading of MEC can avoid passing through the core network with large delay, thereby effectively reducing the delay and saving energy [15]. In addition, MEC servers are affected by factors such as uneven geographical distribution and user mobility, which will cause some servers to be overloaded, which will seriously affect the performance of MEC [16, 17].

For users who choose to offload tasks to MEC execution, when user n uses subchannel k for data transmission, considering the interference caused by frequency reuse, the signal-to interference noise ratio of user n on subchannel k can be expressed as

$$\text{SINR}_n^k = \frac{p_n^k h_{n,n}^k}{\omega_0 + \sum_{m=1, m \neq n}^N p_m^k h_{m,n}^k},\qquad(1)$$

The rate when user n performs uplink transmission through subchannel k is

$$r_n^k = c_n^k \cdot B \log_2\left(1 + \text{SINR}_n^k\right),\qquad(2)$$

where B represents the subchannel bandwidth and c_n^k is the channel allocation variable.

The coordinate descent method only changes the unloading decision of one user at a time during one iteration. Q_n^l is used to denote the revenue obtained by the system during the first iteration, which can be expressed as

$$Q_n^l = V\left(A^{l-1}\right) - V\left(A^{l-1}(n)\right),\qquad(3)$$

where $A^{l-1}(n)$ represents the uninstall decision after user n changes status, and the specific update rules are as follows:

$$A^{l-1}(n) = \left[a_1^{l-1}, a_2^{l-1}, \ldots, a_n^{l-1} \oplus 1, a_N^{l-1}\right],\qquad(4)$$

where $\oplus$ represents the modulo two addition method.

The update formula of particle flight speed and flight distance is as follows:

$$v_i(t+1) = wv_i(t) + c_1 r_1 [pbest_i - x_i(t)] + c_2 r_2 [gbest - x_i(t)],$$
$$x_i(t+1) = x_i(t) + v_i(t+1),$$
$$(5)$$

The population diversity formula is as follows:

$$D(t+1) = \sqrt{\frac{1}{n-1} \sum_{i=1}^{n} \left(\overline{d_i(t+1)}^2 - d_i(t+1) \right)}, \quad (6)$$

where $D(t+1)$ represents the population diversity of the particle swarm in the $t+1$th iteration.

Based on the inertia weight function of population diversity, the expression is as follows:

$$w_i(t+1) = \begin{cases} w_i(t)\left(e^{(1/(D(t+1)+1))-1} + 1\right), & D(t+1) \geq D(t), \\ w_i(t)\left(e^{(1/(D(t+1)+1))-1}\right), & D(t+1) < D(t). \end{cases}$$
$$(7)$$

It is assumed that the particles tend to choose 0 or 1 in the discrete binary space, and at the same time, the speed change caused by the diversity of the population is used as a parameter to define a sigmoid function, which is expressed as follows:

$$S(v_i(t+1)) = \frac{1}{1 + e^{-v_i(t+1)}}. \quad (8)$$

Define the Lagrangian function $\ell(x,\mu,v)$, expressed as

$$\ell(x,\mu,v) = f(x) + \sum_{j=1}^{J} \mu_j g_j(x) + \sum_{r=1}^{R} v_r h_r(x). \quad (9)$$

The dynamic update of each queue can be expressed as

$$Q_i(t+1) = \max\{Q_i(t) - Y_i(t)\} + Z_i(t), \quad \forall i \in \{1,2,\ldots,M\}. \quad (10)$$

The processing delay of the MEC server E_n scheduling part of the CNN layer to execute the UD_m offloading task is modeled as

$$D_{mn}^p = \sum_{k=1}^{K} \delta_{mn}^k p_n^k \frac{S_m}{\beta_{mn}F_n}. \quad (11)$$

The MEC server is as close as possible to the local equipment to provide computing, storage, and other services. As the transmission distance of the task on the network is shortened, the transmission time and energy consumption can be reduced, and the battery life of the user equipment can be extended [18]; and because the MEC server is deployed locally around the equipment, task data can be distributed to different servers for processing, which greatly reduces the network transmission pressure and

server computing pressure [19, 20]. For the fixed strategy π, the Bellman equation is defined as

$$V^\pi(s) = R(s,a) + \gamma \sum_{s' \in S} P_{ss'}(a)V^\pi(s'), \quad (12)$$

where s represents the current state, after performing action a in state s, the state will be converted to the new state s'.

The optimal strategy corresponding to the optimal value function is defined as

$$\pi^*(s) = \arg\max_{a \in A} \sum_{s' \in S} P_{ss'}(a)V^*(s'). \quad (13)$$

2.2. Principle of Ownership. The development of processing trade expands China's export trade, and the continuous improvement of the industrial chain and the development of the domestic market make the import substitution effect play out, which promotes the rapid growth of the surplus. Trade and industry complement each other. Industry is the basis of trade [21], and foreign-invested enterprises are an integral part of industry, especially an important part of export industry, which constitutes the main cause of surplus. Trade is the extension of industry, and surplus and foreign enterprise production promote each other and develop together [22]. Most developing countries are on this list, while most developed countries are on the contrary. FDI outflow needs technology and management knowledge, as well as a large amount of foreign exchange reserves, which developing countries do not have. After considering the sales, import and exports of foreign-invested enterprises and adjusting the traditional trade volume, the re-estimation results show that China's trade balance does not show a trade surplus but a large trade deficit [23].

2.3. International Trade Balance. The most important feature of a country's production and trade model of the division of labor in the global value chain is vertical specialized production. In the form of global production segmentation, the production process concentrated in one country or region is divided into different links and distributed around the world. Therefore, there will be many countries participating in production, but most of the products are consumed by one country, which will produce an asymmetry between imports and exports, which will cause a trade surplus/deficit phenomenon [24].

In general, when the vertical specialization is low, the trade balance will be small; but when a country's export trade scale expands rapidly, the total trade surplus will increase significantly. From the perspective of traditional trade statistics, as long as a product is exported from one country to another, its total value is considered as the corresponding trade volume, and the intermediate products will be calculated in this way for many times. Specifically, if a country is at the last point of producing final consumer goods, the

value of its exported products includes not only the added value of its own country but also the accumulated value of intermediate goods, which will lead to the amplification of the country's exports [25, 26].

When the input factors are imported, raw materials, the exchange rate changes not only affect the overseas market prices of exported goods but also transmit to the prices of imported factors. To calculate the impact of exchange rate changes on trade, it is necessary to examine the proportion of imported factors in export production. The greater the proportion of production raw materials in export production, the less obvious the promotion effect. That is, if most of the raw materials are imported and the product is completely used for export, then the exchange rate promotion effect is not obvious for the export commodity [27].

3. Mobile Edge Computing Algorithm Simulation

3.1. Experimental Setup. This paper uses MATLAB simulation tool to verify the effectiveness of the algorithm proposed in this chapter and at the same time to better evaluate the performance of the proposed algorithm. MEC communication system simulation parameters are shown in Table 1. Among them, each base station is equipped with an MEC server, and each server is connected to the SDN controller.

3.2. Edge Computing Resource Allocation. In order to obtain all data needed to perform the task, each mobile device can exchange data information with its connected base station through the wireless network. This can not only maximize the use of limited wireless resources of MSO but also realize the dynamic macro-control for different user needs, which can guide the dynamic changes of user's consumption psychology and communication resources to achieve a dynamic balance [28] and make MEC network resource management achieve a dynamic balance. When the demand of users and the supply of network resources reach the balance, the system throughput reaches the maximum [29, 30].

3.3. Task Scheduling. After setting the task priority for each task set, n task queues are obtained. Each mobile device can arrange the processors or processors to execute tasks according to the corresponding queue order. However, the number of processors on the edge cloud is limited. If all mobile devices schedule tasks concurrently, there may be conflicts for the processing resources of the edge cloud, and it causes some tasks to finish overtime, which affects the completion of the whole task set, so a centralized scheduling scheme is needed to schedule all tasks reasonably, so that all task sets can be completed between the deadline [31, 32]. On the basis of satisfying the quality of service of users, including considering the user connection and service configuration, the network energy consumption is minimized in a continuous t period by shutting down some servers whose resources are not fully utilized. At the same time, in order to

reduce the switching cost of the edge server switch state and ensure the stability of the service, frequent switching of the edge server switch state should be avoided [33, 34].

3.4. Statistics of Trade Balance. There is a large surplus in China's foreign trade, and the surplus is increasing year by year. However, there is an unbalanced distribution pattern of trade balance in China's foreign trade. The distribution of trade balance of foreign trade partners is not balanced. There is a large annual surplus for some countries and regions, and there is also an annual deficit for some countries and regions [35, 36]. At the beginning, there is a division of labor economy. With the development of specialized production, the degree of international division of labor is increasing due to the effect of experience accumulation, and the trade efficiency is growing endogenously. The international division of labor is further deepened, and the types and quantity of products participating in the international division of labor are greatly increased, so as to realize the upgrading of the trade structure [37]. Before constructing the structural VAR model of BTI, r/w, K/L, and TFP, we need to test its stationarity. Using Eviews5.0 software, ADF test and PP test were performed on the unit root of Bti, R/W, K/L, and TFP time series data [38, 39].

3.5. Construction of the Ownership Principle Model. The cross-border trade statistics system based on the territorial principle has defects, which greatly interferes with the authenticity of trade balance statistics. This highlights the importance of ownership adjustment. The statistical adjustment model of ownership trade is a process of reunderstanding the existing world trade forms and patterns based on the principle of ownership statistics [40].

4. Model Simulation Results

4.1. Task Cache Effect. For task scheduling algorithm, load is an important performance index. As the average size of tasks participating in the scheduling increases, the system load corresponding to the three algorithms is shown in Figure 2. It can be seen from the figure that, for the above three strategies, from the perspective of the algorithm itself, when the average task size reaches 1 MB/job, compared to the other two algorithms, the overall growth of the iccga curve slows down and is at the bottom.

The impact of different channel transmission rates on equipment energy consumption is shown in Table 2. When the task is processed locally, the energy consumption has nothing to do with the channel transmission rate, and the local processing energy consumption appears as a horizontal straight line. As the channel transmission rate increases, the energy consumption curve of the PD-BPSO algorithm and the greedy algorithm decreases. This is because the higher the channel transmission rate, the shorter the time spent on data transmission. When the transmission rate is greater than 2500 kb/s, the trend of PD-BPSO algorithm energy consumption reduction becomes slower and slower, and the energy consumption curve interval of the two algorithms
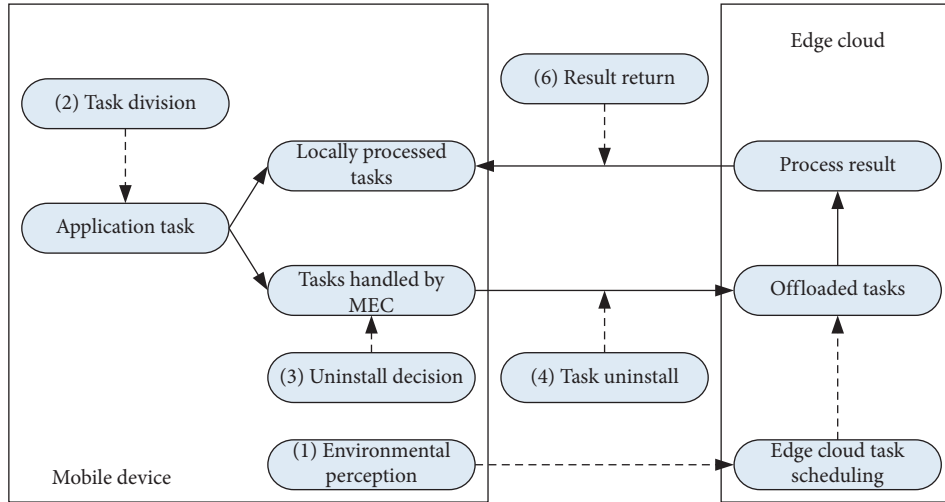
FIGURE 1: Task scheduling process.

TABLE 1: MEC communication system simulation parameters.

Parameter	Value
Number of cells	4
MEC server capacity	10 MHz
Cell radius	1.6 km
Number of cell channels	20
Macro base station capacity	5 MHz
Small cell capacity	1 MHz
Number of data subcarriers	384
Subcarrier bandwidth	10.9375 kHz
Maximum length of task queue	5
White noise power	−173 dBm/Hz
Doppler deviation	5–25 Hz
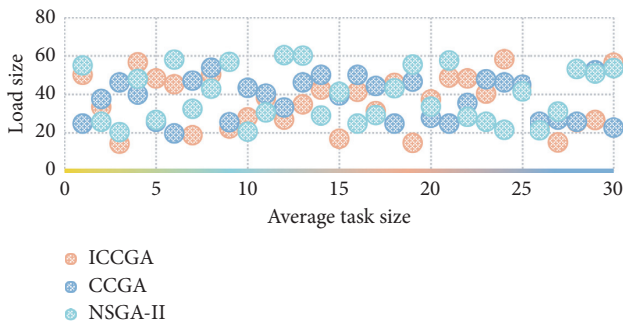
FIGURE 2: System load situation.

TABLE 2: The impact of different channel transmission rates on device energy consumption.

Transmission rate	500	1000	1500	2000	2500	3000
Greedy algorithm	15.02	6.39	14.22	20.13	7.11	18.02
PD-BPSO	8.01	12.33	9.36	17.24	5.85	11.24
Local execution	15.01	23.35	9.25	8.57	11.23	16.07

becomes larger and larger. This is because computing resources mainly affect the execution of offloading tasks. The number of particles shows that the computational offloading

performance of the proposed algorithm is 48.3% higher than that of the traditional greedy algorithm.

The relationship between the long-term average power consumption of all user tasks and the system time slot is shown in Figure 3. It can be seen from the figure that the maximum data volume of users randomly arriving tasks increases, and the long-term average power consumption of all user tasks and the average user task buffer queue length increase. This is because the maximum data volume of users randomly arriving tasks increases, and users need to process, transmit, and buffer. The amount of task data will increase.

Figure 4 shows the system utility results of the six algorithms under different task data sizes. According to the comparison between the algorithms, the DTORA algorithm has a better performance in improving the utility of the system and can more fully consider the interests of users and service providers. The performance of QL algorithm is second only to DTORA algorithm. The optimization performance of WRR algorithm ranks third, and its result is much worse than QL algorithm. The experimental results of RR and random algorithm are similar. Since the calculation of system utility considers the improvement of algorithm performance relative to the performance of task processing locally, the system utility of local algorithm is zero. In this experiment, it can be known that the task data size has no

significant impact on the system utility value, and the overall optimization effect of the system depends on the performance of the algorithm. With the rapid economic development of a country, the appreciation of its asset prices is expected to attract the favor of international arbitrage capital, and the entry of international hot money will increase the liquidity and change the inflation rate. At the same time, the increase in consumer demand due to the wealth effect will increase the circulation of money and will also cause an increase in liquidity and an increase in inflation.

The relationship between energy-money conversion coefficient and system currency cost is shown in Figure 5. When the system just starts to run, the battery energy gradually accumulates. After the system runs for a period of time, the battery energy stabilizes and does not exceed the battery capacity value. This is because when the system first started running, the battery energy was 0 and it was unable to perform computing tasks. The system captures energy in each time slot, so the battery energy gradually accumulates. When the battery energy can meet the needs of the computing task, the system starts to consume energy to perform the computing task and at the same time to capture energy, so the battery energy changes show a small range of fluctuations. When the channel changes slowly, the LSTM network can effectively predict the trend of channel gain. When the channel changes rapidly, the prediction error will increase. However, regardless of whether the channel is stable or changing rapidly, the gap between the predicted gain and the actual gain in this paper is within 5%. When the bandwidth resource is set to 100 MHz, compared with the algorithm based on game theory and the algorithm based on greedy search, the performance of the iTOA algorithm is improved by about 25% and 45%, respectively.

4.2. Algorithm Performance Analysis. The influence of edge server computing power on the average service delay is shown in Figure 6. When the number of drones increased from 10 to 60, based on the resource allocation algorithm of greedy search, the service delay increased significantly from 20 ms to 46 ms. Based on the resource allocation algorithm of game theory, the service delay increases from 15 ms to 33 ms. The iTOA algorithm proposed in this paper can keep the processing delay low, and the processing delay has been increased from 11 milliseconds to 18 milliseconds. Compared with greedy search and game theory algorithms, when there are 40 UAVs in the system, the average service delay performance of the iTOA algorithm increases by 33% and 60%, respectively. When the edge server has a higher task request, the unloading rate of the iTOA algorithm will decrease, because iTOA balances the computing load on the edge server well. In addition, as the number of service nodes increases, the benefits of these three algorithms also increase. When the number of service nodes becomes larger, the increase speed becomes slower and gradually becomes stable. This is caused by the limitation of node resources. When the number of service nodes is small, the resources are limited and only some users can be served. When more service nodes are deployed, the resources become sufficient,

which can provide services to more users and improve the efficiency.

The energy consumption of the four unloading strategies is shown in Table 3. It can be seen from the table that the energy consumption is the highest when all tasks are placed on the terminal for calculation, and the energy consumption rises linearly as the amount of tasks increases. Under the condition of limited energy, it is difficult for drones to complete tasks with a large amount of calculation. In order to find an optimal position in terms of delay and energy consumption, the JTO algorithm needs to offload the computing task to the cloud and perform calculations at the terminal at the same time, so the energy consumption will be higher than that of all calculations in the cloud. The algorithm proposed in this paper takes into account the difference between cloud computing and edge computing compared to other strategies in completing the same number of tasks with lower energy consumption. Compared with the JTO strategy, this strategy reduces energy consumption by an average of 24%.

Incomplete exchange rate transfer theory analyzes the extent to which changes in exchange rate can be transferred to the price and quantity of import and export commodities, and why the adjustment of import and export prices and import and export quantities of import and export commodities is sometimes very slow when the exchange rate fluctuates greatly. The theory of incomplete exchange rate transfer shows that the impact of exchange rate changes on the balance of payments is limited, and the speed and extent of this impact are restricted by many factors. Changes in the RMB exchange rate and Sino-US trade are shown in Table 4. In terms of the Sino-US trade balance, the average annual growth rate reached 28.17%. Except for 1999 and 2001, the rest of the year has maintained a growth rate of more than 10%. Due to the high quality of Chinese products, cheap prices, and adaptation to the needs of the international market, Chinese products are becoming increasingly competitive internationally, leading to a rapid increase in China's exports to the United States. Second, after the Asian financial crisis, China has increased the export tax rebate rate, and other export encouragement policies have been implemented successively, which stimulated exports. Third, the United States has imposed an embargo on high-tech products against China. Although the value of US exports to China is also increasing, the growth rate is not high, which prevents the United States from exerting its competitive advantages. The combination of these two reasons has led to an increasing trade balance between China and the United States.

The balance of imports and exports under processing trade is shown in Table 5. China's processing trade surplus shows a trend of first rising and then falling. Combined with China's overall trade balance, the proportion of processing trade surplus is more than 100%, which is the "chief contributor" of the overall trade surplus. In terms of the processing trade surplus, the 16th largest category of products is the main source of the surplus, accounting for an average of 77% of the processing trade balance in recent years. In addition, although the proportion of category 17 products in
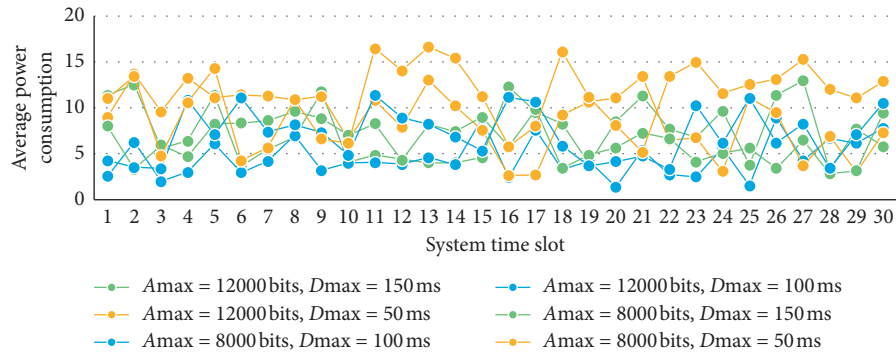
FIGURE 3: The relationship between the long-term average power consumption of all user tasks and the system time slot.
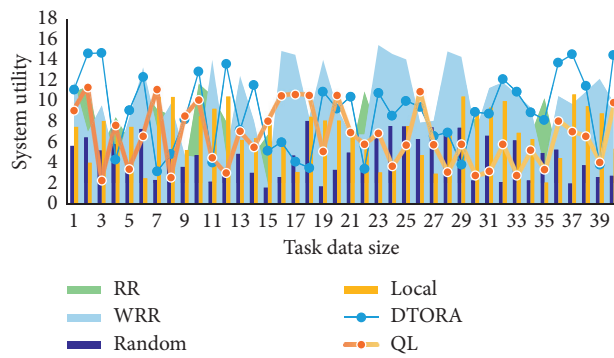
FIGURE 4: System utility results.
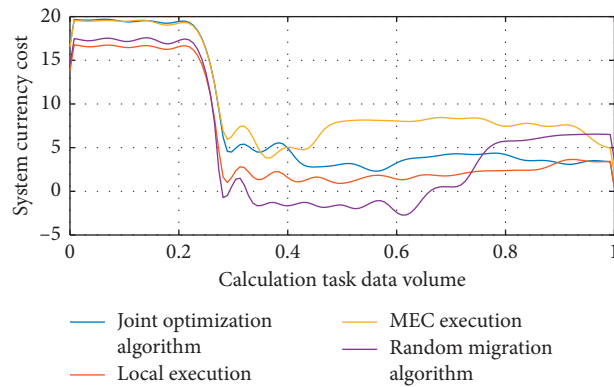
FIGURE 5: The relationship between energy-money conversion coefficient and system currency cost.

the balance of processing trade is far less than that of category 16 products, it is also relatively large compared with other products, with a proportion of about 5%.

4.3. Algorithm Energy Consumption Results. The influence of parameters on the calculation time is shown in Figure 7. It can be seen from the figure that there are very few SESs in the correlated data set, so the calculation time of the two algorithms is very short. Although under this data set, the BNL algorithm is better than the SG algorithm, but the difference between the two is not much, only in the range of a few milliseconds, and the worst calculation time of the SG algorithm is also less than 8 milliseconds. At the same time,

compared with the QWS data set, under the anticorrelated data set, the calculation time of BNL fluctuates greatly. When the number of candidate services is 2400 and the service quality dimension is 6, the calculation time increases from 30 milliseconds to 160 milliseconds. It can be seen that the performance of the BNL algorithm is greatly affected by the data set, while the performance of the SG algorithm is relatively stable. It can be seen that the SG algorithm has better robustness.

The influence of transmission power on the residual power is shown in Figure 8. With the increase of the transmission power of the access point, the JOS curve always has the maximum residual energy, which indicates that the joint optimization scheme can make the power utilization
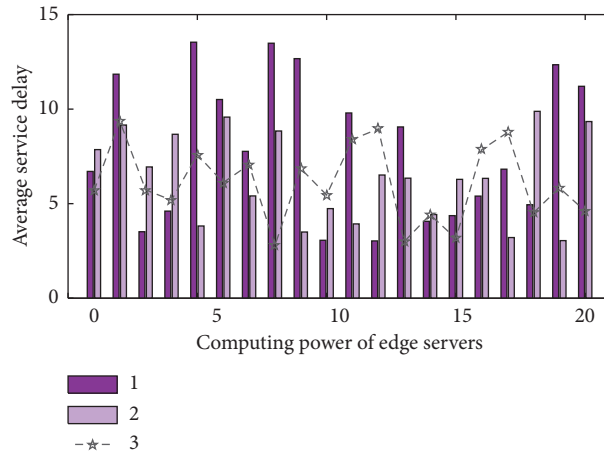
FIGURE 6: The impact of edge server computing power on average service latency.

TABLE 3: Energy consumption of four uninstall strategies.

LE	2.63	2.66	2.59	2.59	2.64	2.67	2.57	2.66	2.58	2.58
CC	1.74	2.79	1.49	2.64	1.24	1.69	1.58	2.04	3.60	1.56
PTSA	2.11	3.83	4.48	2.69	3.33	1.44	1.21	3.28	2.81	0.79
JTO	0.54	1.66	2.82	2.95	3.08	2.80	1.68	3.39	2.51	2.52

TABLE 4: Changes in the RMB exchange rate and Sino-US trade.

100 USD to RMB	Monthly import	Monthly export	Monthly trade balance
810.1930	18.468	22.365	3.897
809.2223	20.106	23.307	3.201
808.8878	20.518	24.429	3.911
808.3973	18.491	22.380	3.889
807.5900	16.299	20.514	4.215
806.6750	17.911	21.405	3.494
804.9324	13.840	17.927	4.087
803.5039	15.571	20.526	4.955

TABLE 5: Import and export balance under processing trade.

Commodity	2006	2007	2008	2009	2010	2012	2013	2014
Lump sum	1888.8	2490.8	2967.3	2645.7	3227.97	3655.28	3814.02	3633.78
Fifth category	−40.87	−27.67	−39.4	−47.27	−59.42	−92.72	−115.66	−169.18
Sixth category	−46.74	−63.35	−59.86	−41.83	−56.11	−81.96	−74.01	−89.11
Seventh category	−71.31	−60.25	−44.71	−32.19	−63.94	−21.49	28.22	57.42
Eleven categories	158.11	199.69	225.15	193.73	158.11	246.26	238.42	252.77

rate higher, harvest more power, and consume less power, because JOS can find the best combination of unloading ratio and harvest time. In contrast, FHT has a fixed harvesting time, which determines the energy value of harvesting from the access point. The only thing the optimization process can do is to find the best unloading ratio, so as to complete the task with as little power as possible under the premise of meeting the time constraint. Similarly, FPR has a fixed unload ratio, which will consume a lot of energy if the ratio is not reasonable.

The energy efficiency of secure computing and the minimum computing speed of users under different schemes are shown in Figure 9. When users have the same maximum transmission power, the energy efficiency of traditional computing bit maximization is lower than that of the proposed scheme. In addition, when the maximum transmission power reaches a certain value, the energy efficiency of traditional secure computing bit maximization begins to decrease. The results also prove the following facts: the increase rate of total computing energy consumption is greater than that of total computing bits, and there is a trade-off between secure computing energy efficiency and secure computing bit. With the increase of user task arrival rate, the average time revenue increases continuously. However,
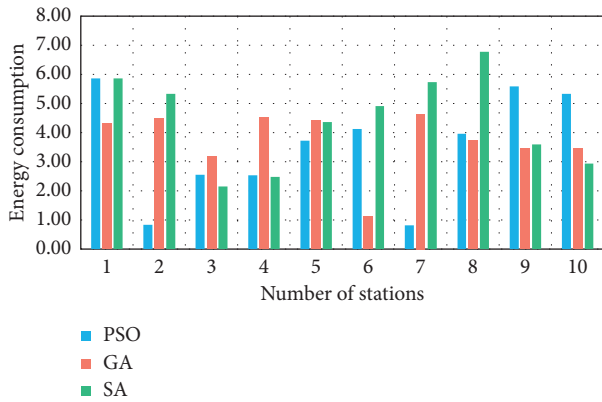
Figure 7: The influence of parameters on calculation time.
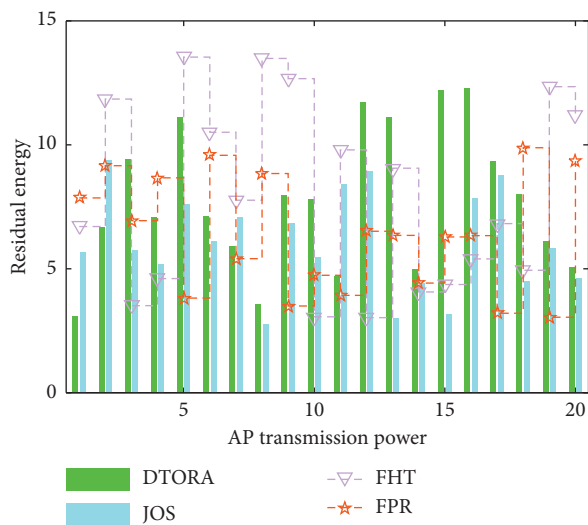
Figure 8: Impact of transmission power on the remaining power.
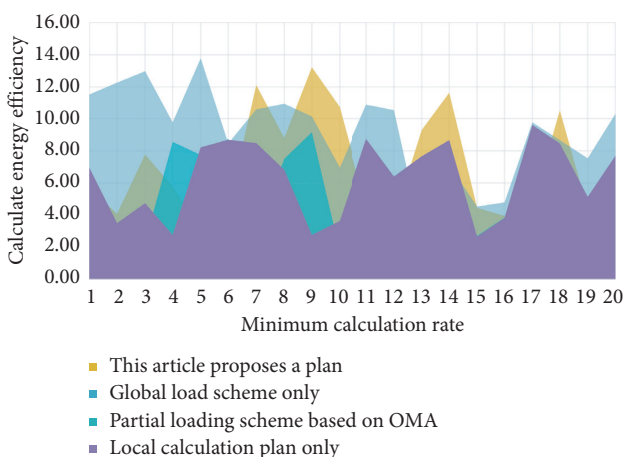
Figure 9: Safe computing energy efficiency and users' minimum computing rate under different schemes.

when the arrival rate is greater than 3 kbit/slot, the average time revenue increases slowly. This is because, when the task arrival rate increases, in order to ensure that the queue does not overflow, the processing rate of user computing tasks

will increase accordingly, so the system will allocate more resources to serve users, and the average time revenue will also increase.

5. Conclusions

Based on the theory of international industrial transfer and the analysis of the rules and characteristics of global international industrial transfer, this paper studies the dynamic changes of international industrial transfer and Sino US trade balance. China's large trade surplus has not brought China corresponding economic benefits and social welfare. In the long run, it will not only waste China's resources but also be detrimental to the sustainable development of China's economy and the improvement of its economic quality. China must strategically change the status quo of China's foreign trade and the large low-quality trade surplus.

As a key technology in the future 5 g mobile communication, MEC realizes the marginalization and localization of computing, communication, and cache resources, deploys various network functions on the access network side, accelerates various contents in the wireless network, and provides nearby services, which greatly reduces the delay of network service delivery. In the actual situation, the economic cost of processing tasks is also an important indicator for people to measure the switching decision, so we also consider the task execution cost.

From the model empirical point of view, whether it is a single-country ownership trade adjustment model or a bilateral trade ownership adjustment model, it has accomplished the task of adjusting the trade volume very well. The MEC architecture uses intensive deployment of base stations and edge servers in places close to users and sinks the computing and storage capabilities of the cloud to provide services closer to user equipment. Therefore, while reducing the backbone network load, the network delay is reduced and the user experience is improved. However, when a large number of edge servers are kept on, it will inevitably lead to energy waste in many edge servers that are underutilized during low traffic periods.

Data Availability

No data were used to support this study.

Conflicts of Interest

The authors declare that they have no conflicts of interest.

Acknowledgments

References

[1] B. Zhu, S. Ma, R. Xie, J. Chevallier, and Y.-M. Wei, "Hilbert spectra and empirical mode decomposition: a multiscale event

analysis method to detect the impact of economic crises on the European carbon market," *Computational Economics*, vol. 52, no. 1, pp. 105–121, 2018.

[2] G. Xiao, Q. Cheng, and C. Zhang, "Detecting travel modes from smartphone-based travel surveys with continuous hidden Markov models," *International Journal of Distributed Sensor Networks*, vol. 15, no. 4, pp. 1–15, 2019.

[3] Z. Lv, W. Kong, X. Zhang, D. Jiang, H. Lv, and X. Lu, "Intelligent security planning for regional distributed energy Internet," *IEEE Transactions on Industrial Informatics*, vol. 16, no. 5, pp. 3540–3547, 2020.

[4] B. Han, J. Li, J. Su, M. Guo, and B. Zhao, "Secrecy capacity optimization via cooperative relaying and jamming for WANETs," *IEEE Transactions on Parallel and Distributed Systems*, vol. 26, no. 4, pp. 1117–1128, 2014.

[5] T. X. Tran, A. Hajisami, and P. Pandey, "Collaborative mobile edge computing in 5G networks: new paradigms, scenarios, and challenges," *IEEE Communications Magazine*, vol. 55, no. 4, pp. 54–61, 2017.

[6] Y. Cheng, J. Zhang, C. Zhu, and H. Zhu, "Distributed green offloading and power optimization in virtualized small cell networks with mobile edge computing," *IEEE Transactions on Green Communications and Networking*, vol. 4, no. 1, pp. 69–82, 2019.

[7] S. Jeschke, C. Brecher, H. Song, and D. Rawat, *Industrial Internet of Things: Cybermanufacturing Systems*, Springer, Cham, Switzerland, 2017.

[8] Y. Chen, W. Zheng, W. Li, and Y. Huang, "Large group Activity security risk assessment and risk early warning based on random forest algorithm," *Pattern Recognition Letters*, vol. 144, p. 1, 2021.

[9] Z. Lv, X. Li, and W. Li, "Virtual reality geographical interactive scene semantics research for immersive geography learning," *Neurocomputing*, vol. 254, pp. 71–78, 2017.

[10] H. Wu, X. Lyu, and H. Tian, "Online optimization of wireless powered mobile-edge computing for heterogeneous industrial Internet of things," *IEEE Internet of Things Journal*, vol. 6, no. 6, pp. 9880–9892, 2019.

[11] S. Wan, X. Li, Y. Xue, and X. Xu, "Efficient computation offloading for Internet of Vehicles in edge computing-assisted 5G networks," *The Journal of Supercomputing*, vol. 76, no. 4, p. 2518, 2019.

[12] C. J. Lin, H. C. Wang, Y. C. Lai et al., "Communication and computation offloading for multi-RAT mobile edge computing," *IEEE Wireless Communications*, vol. 26, no. 99, pp. 180–186, 2019.

[13] Z. Lv, D. Chen, R. Lou, and Q. Wang, "Intelligent edge computing based on machine learning for smart city," *Future Generation Computer Systems*, vol. 115, 2020.

[14] Z. Lv, D. Chen, and Q. Wang, "Diversified technologies in Internet of vehicles under intelligent edge computing," *IEEE Transactions on Intelligent Transportation Systems*, 2020.

[15] S.-B. Tsai, Y. Xue, J. Zhang et al., "Models for forecasting growth trends in renewable energy," *Renewable and Sustainable Energy Reviews*, vol. 77, pp. 1169–1178, 2017.

[16] J. Feng, Q. Pei, F. R. Yu, and B. Shang, "Computation offloading and resource allocation for wireless powered mobile edge computing with latency constraint," *IEEE Wireless Communications Letters*, vol. 8, no. 5, pp. 1320–1323, 2019.

[17] B. Chu, Z. Li, P. Tang et al., "Security modeling and efficient computation offloading for service workflow in mobile edge computing," *Future Generation Computer Systems*, vol. 97, no. 8, pp. 755–774, 2019.

[18] M. Wang, Y. Guo, B. Wang et al., "An engineered self-supported electrocatalytic cathode and dendrite-free composite anode based on 3D double-carbon hosts for advanced Li-SeS2 batteries," *Journal of Materials Chemistry A*, vol. 8, no. 6, pp. 2969–2983, 2020.

[19] H. LiuWu, J. Liu, and J. Zhang, "Computation offloading for multi-access mobile edge computing in ultra-dense networks," *IEEE Communications Magazine*, vol. 56, no. 8, pp. 14–19, 2018.

[20] T. G. Rodrigues, K. Suto, H. Nishiyama, and K. Temma, "Cloudlets activation scheme for scalable mobile edge computing with transmission power control and virtual machine migration," *IEEE Transactions on Computers*, vol. 67, no. 9, pp. 1287–1300, 2018.

[21] S.-W. Kato, K. Han, and K. Huang, "Wireless networks for mobile edge computing: spatial modeling and latency analysis," *IEEE Transactions on Wireless Communications*, vol. 17, no. 8, pp. 5225–5240, 2018.

[22] S.-B. Tsai, Yu-C. Lee, C.-H. Wu, and J.-J. Guo, "Examining how manufacturing corporations win orders," *South African Journal of Industrial Engineering*, vol. 24, no. 3, pp. 112–124, 2013.

[23] W. Kim, G. Lee, and I. Jung, "Energy efficient edge camera system for smart mobile objects in IoT edge computing," *KIISE Transactions on Computing Practices*, vol. 26, no. 5, pp. 223–230, 2020.

[24] Y. Wang, M. Sheng, X. Wang et al., "Mobile-edge computing: partial computation offloading using dynamic voltage scaling," *IEEE Transactions on Communications*, vol. 64, no. 10, pp. 4268–4282, 2016.

[25] Y. Mao, J. Zhang, and S. H. Song, "Stochastic joint radio and computational resource management for multi-user mobile-edge computing systems," *IEEE Transactions on Wireless Communications*, vol. 16, no. 9, pp. 5994–6009, 2017.

[26] T. Q. Letaief, J. Tang, Q. D. La et al., "Offloading in mobile edge computing: task allocation and computational frequency scaling," *IEEE Transactions on Communications*, vol. 65, no. 8, pp. 3571–3584, 2017.

[27] C. Wang, C. Liang, F. R. Yu, Q. Chen, and L. Tang, "Computation offloading and resource allocation in wireless cellular networks with mobile edge computing," *IEEE Transactions on Wireless Communications*, vol. 16, no. 8, pp. 4924–4938, 2017.

[28] X. Chen, D. Li, D. Mohapatra, and M. Elhoseny, "Automatic removal of complex shadows from indoor videos using transfer learning and dynamic thresholding," *Computers & Electrical Engineering*, vol. 70, pp. 813–825, 2018.

[29] A. Elhoseny and O. Simeone, "Energy-efficient resource allocation for mobile edge computing-based augmented reality applications," *IEEE Wireless Communications Letters*, vol. 6, no. 3, pp. 398–401, 2017.

[30] Dario, Sabella, Alessandro et al., "Mobile-edge computing architecture: the role of MEC in the Internet of things," *IEEE Consumer Electronics Magazine*, vol. 5, no. 4, pp. 84–91, 2016.

[31] Y. He, F. R. Yu, N. Zhao, and H. Yin, "Software-defined networks with mobile edge computing and caching for smart cities: a big data deep reinforcement learning approach," *IEEE Communications Magazine*, vol. 55, no. 12, pp. 31–37, 2017.

[32] E. Leung and M. H. Rehmani, "Mobile edge computing: opportunities, solutions, and challenges," *Future Generation Computer Systems*, vol. 70, no. 5, pp. 59–63, 2016.

[33] Peter, Corcoran, Soumya et al., "Mobile-edge computing and the Internet of things for consumers: extending cloud computing and services to the edge of the network," *IEEE Consumer Electronics Magazine*, vol. 5, no. 4, pp. 73-74, 2016.

[34] X. Chen, L. Pu, L. Gao, and D. Wu, "Exploiting massive D2D collaboration for energy-efficient mobile edge computing," *IEEE Wireless Communications*, vol. 24, no. 4, pp. 64–71, 2017.

[35] N. Wu, S. Zeadally, and J. J. P. C. Rodrigues, "Vehicular delay-tolerant networks for smart grid data management using mobile edge computing," *IEEE Communications Magazine*, vol. 54, no. 10, pp. 60–66, 2016.

[36] J. Liu, J. Wan, B. Zeng, H. Song, and M. Qiu, "A scalable and quick-response software defined vehicular network assisted by mobile edge computing," *IEEE Communications Magazine*, vol. 55, no. 7, pp. 94–100, 2017.

[37] B. P. Wang, D. Pham Van, and M. Maier, "Mobile-edge computing versus centralized cloud computing over a converged FiWi access network," *IEEE Transactions on Network and Service Management*, vol. 14, no. 3, pp. 498–513, 2017.

[38] C. Vallati, A. Virdis, and E. Mingozzi, "Mobile-Edge Computing Come Home Connecting things in future smart homes using LTE device-to-device communications," *IEEE Consumer Electronics Magazine*, vol. 5, no. 4, pp. 77–83, 2016.

[39] K. Stea, S. Leng, Y. He, and Y. Zhang, "Mobile edge computing and networking for green and low-latency Internet of things," *IEEE Communications Magazine*, vol. 56, no. 5, pp. 39–45, 2018.

[40] X. Maharjan, J. Liu, and X. Tao, "Mobile edge computing enhanced adaptive bitrate video delivery with joint cache and radio resource allocation," *IEEE Access*, vol. 5, no. 99, pp. 16406–16415, 2017.

Research Article

International Import and Export Trade Forecasting Algorithm Based on Heterogeneous Dynamic Edge Computing System

Yingfei Yang ●

College of International Economics & Trade, Ningbo University of Finance & Economics, Ningbo 315175, Zhejiang, China

Correspondence should be addressed to Yingfei Yang; yangyingfei@nbufe.edu.cn

As a new computing model, how to use edge computing to forecast import and export trade has become an issue of concern. This research mainly discusses the prediction algorithm of international import and export trade based on heterogeneous dynamic edge computing system. The dynamic task migration system studied in this paper mainly includes four parts: edge computing environment simulator, task generator, resource predictor, and migration decision maker. These four parts are not independent modules in the working process; they will interact with each other in the edge computing environment. In the data processing offloading strategy, the customs business personnel transfer the trade data that need to be predicted to the edge device cluster through the mobile terminal. After receiving the data transmitted by the business personnel, the edge device cluster uses data processing technology to process the data. After the data processing operation is completed, the processed data is directly used for prediction work. After the prediction work is completed, the data and results are uploaded to the central server. Finally, after the prediction work is completed, the edge device will feed back the prediction result to the mobile terminal and display the result on the user interface through the mobile terminal so that business personnel can understand the trade risk status. From August 2018 data application period, the monthly data of the import and export trade volume for the subsequent time span of ten years were regularly forecasted, and the correlation coefficient was still over 83%, and the RMSE also dropped significantly. The system designed in this study can effectively predict the annual estimated value of various economic indicators of international import and export trade.

1. Introduction

The long-term formation of sunk costs has largely affected the economic behavior of import and export manufacturers. From a dynamic point of view, in the presence of sunk costs, manufacturers will compare the present value of current profits with future profits before making a decision [1]. And, under normal circumstances, when the general environment is unstable, manufacturers will not easily react to changes in the exchange rate, forming a "stagnation" effect, which will lastingly affect import prices.

In the current situation of increasingly severe import and export trade forms, studying the elasticity of national import and export commodities will help us to propose corresponding policies through price and income elasticity to effectively adjust and optimize the current import and

export structure of commodities [2], so as to achieve a moderate maintenance of the number of imports and exports of some products which will ultimately achieve the goal of promoting economic growth and development on the one hand and alleviating the trade friction between countries on the other and reducing the impact of external economies on a country's economy.

The proliferation of the Internet of Things and the success of rich cloud services have promoted the development of a new computing paradigm-edge computing [3], which requires data processing at the edge of the network. Shi W introduced the definition of edge computing and then conducted some case studies, from cloud offloading to smart homes and cities, and collaborative edge to realize the concept of edge computing. Although his research can attract the attention of the community and stimulate more

research in this direction, the research process lacks innovation [4, 5]. Jiang et al. proposed an improved multiobjective gray wolf optimizer algorithm (IMOGWO) to solve this problem. They use an elite learning strategy based on Gaussian perturbation to avoid local optima. The algorithm he proposed was tested on twelve multiobjective benchmark problems selected from the CEC2009 test cases and compared with two popular heuristic optimization algorithms. His proposed IMOGWO effectively solves the problem of subordinate task scheduling in edge computing, but the research process lacks data [6]. Wang et al. believe that, as a key intelligent transportation service, the public vehicle system aims to improve transportation efficiency and vehicle occupancy by inducing travelers to share rides with others. They proposed the ECPV system to improve traffic efficiency and vehicle occupancy by arranging ride sharing between travelers and to reduce decision-making delays by using edge computing. They formalized the public vehicle-scheduling problem as an optimization problem, with the goal of maximizing traveler satisfaction, in order to reduce travel time and improve traffic efficiency [7]. Although the method he proposed can reduce the delay in decision-making, the research results lack concrete practice [8]. Chen believes that low latency/latency is one of the most critical requirements for in-vehicle network applications. He solved the curse of the dimensionality problem in MDP by characterizing the temporal and spatial correlation of vehicle mobility [9]. On this basis, he also provided specific results for highways, two-dimensional streets, and real-data scenarios. Although his research considers the transition probability is usually uncertain, incorrect sample data and complex path environment, the research process lacks comparative data [10].

The dynamic task migration system studied in this paper mainly includes four parts: edge computing environment simulator, task generator, resource predictor, and migration decision maker. These four parts are not independent modules in the working process; they will interact with each other in the edge computing environment. In the data processing offloading strategy, the customs business personnel transfer the trade data that needs to be predicted to the edge device cluster through the mobile terminal. After receiving the data transmitted by the business personnel, the edge device cluster uses data processing technology to process the data. After the data processing operation is completed, the processed data is directly used for prediction work. After the prediction work is completed, the data and results are uploaded to the central server. Finally, after completing the prediction work, the edge device will feed back the prediction result to the mobile terminal and display the result on the user interface through the mobile terminal so that business personnel can understand the trade risk status.

2. Heterogeneous Dynamic Edge Computing

2.1. Edge Cluster.
When the data reaches the edge device cluster [11], the data distribution should be reasonably performed so that each edge device in the cluster can complete the prediction work in the same time as possible [12, 13]. At this time, the main things that need to be paid attention to are the same indicators of CPU, memory, and hard disk read and write speed [14]. The calculation formula is as follows:

$$P_e^i = a_1 C_e^i + a_2 M_e^i + a_3 L_e^i. \tag{1}$$

Among them, C_e^i represents the product of the number of CPUs of the edge device i and its frequency [10, 15]. Similarly, if the amount of data is too large, the load of the edge device will be too heavy, which will affect the forecasting work. Therefore, when data is allocated, the load of the current time node needs to be considered, that is, CPU, memory, and the usage of disk to read and write [16]. Use these items to calculate the idle status $O_e^i(t)$ of the edge device at the current moment, and the calculation formula is as follows:

$$O_e^i(t) = b_1\left(1 - C_t^i\right) + b_2\left(1 - M_t^i\right) + b_3\left(1 - L_t^i\right), \tag{2}$$

where L_t^i represents the hard disk read and write usage rate of the edge device at the current moment [17, 18]. The idle value F_e^i of the performance of the edge device i at the current moment can be obtained.

$$F_e^i(t) = P_e^i \times O_e^i(t). \tag{3}$$

Assuming that there are 1 center and n edge devices in the edge device cluster, in the center of the edge device cluster, the idle value of each edge device in the cluster can be accumulated at the current moment to obtain the total idle value of the cluster performance at the current moment $F_e(t)$, and its formula is as follows:

$$F_e(t) = \sum_{i=1}^{n} F_e^i(t). \tag{4}$$

Then, the performance idle rate FP_e^j of edge device i at the current moment can be obtained, and the formula is

$$FP_e^j = \frac{F_e^i(t)}{F_e(t)}. \tag{5}$$

Assuming that the amount of data unloaded from the central server to the cluster is d_n, the amount of data allocated to i by the edge device d_n^i is

$$d_n^i = d_n \times FP_e^i. \tag{6}$$

2.2. Risk Prediction of Import and Export Trade.
For the data offloading model, during its execution, let d_i be the amount of data transferred from the edge device cluster to the central server and d_0 be the amount of data transferred from the central server to the edge device cluster. The time overhead in the prediction phase is as follows:

$$t_c = \frac{(1 - \lambda_c)d_1}{C_\varepsilon} + \lambda_c\left(\frac{d_f}{w_u^c} + \frac{d_l}{C_c} + \frac{d_0}{w_d^c}\right). \tag{7}$$

After data unloading, the total time cost of the entire risk prediction is as follows:

$$T = t_e + t_c = \frac{d_f}{w_u^e} + \frac{d_i}{C_e} + \frac{d_0}{w_d^u} + \frac{(1 - \lambda_C)d_i}{C_e} + \lambda_C \left(\frac{d_f}{w_u^c} + \frac{d_i}{C_c} + \frac{d_0}{w_d^c} \right).$$

(8)

When λ is set to different values, the amount of data processed by the edge device cluster and the central server also changes [19]. If the user sets the value of λ to 0, the total time overhead

$$T = t_e + t_c = \frac{d_i}{w} + \frac{d_j}{C_e} + \frac{d_0}{w_d^u} + \frac{d_i}{C_e}.$$

(9)

If the user sets the value of λ to 0.5, it means that all predicted requests will be handed over to the edge device cluster for processing, and the central server only performs resource storage and model training. At this time, the total time overhead:

$$T = t_e + t_c = \frac{d_i}{w} + \frac{d_j}{C_e} + \frac{d_0}{w_d^u} + \frac{d_i}{2C_e} + \frac{1}{2} \left(\frac{d_i}{w_u^c} + \frac{d_j}{C_e} + \frac{d_0}{w_d^c} \right).$$

(10)

The data processing task offloading framework in the edge cluster process is shown in Figure 1 [20, 21].

S1 in Figure 1 represents nonhomogeneous data integration tasks, S2 represents data feature extraction tasks, and S3 represents risk prediction tasks. Among them, S1 and S2 are executed on edge devices and S3 is executed on a central server [22].

2.3. Forecast of Resources in the Short Term.
The resource requirements of tasks deployed in the actual edge computing platform are usually constantly changing, which also leads to the constantly changing state of the server resources on the edge computing platform [23, 24]. The efficient migration algorithm proposed in this paper is mainly to discover hotspot nodes with high resource utilization and cold spot nodes with low resource utilization in the edge computing platform and select tasks among them for migration mechanism [25]. When judging the resource utilization, if the server resource usage reaches the upper or lower threshold and it is identified as a hot spot node or cold spot node that needs to be processed [2], the dynamic nature of the task is ignored, which will result in a large number of servers. They are all judged as hot spot nodes, which will also bring a lot of meaningless task migration, cause a large degree of waste of resources, and seriously affect the service performance of the entire edge computing platform [26, 27]. Based on the above reasons, the algorithm studied in this paper introduces a resource prediction algorithm to work with the migration decision algorithm when performing dynamic task migration to improve the quality of service of the entire system [28]. The premise of the realization of the resource prediction algorithm is that the deployment tasks in the edge computing system are dynamically changing [29]. The main realization idea is to predict the future-period resource usage of server nodes whose current resource
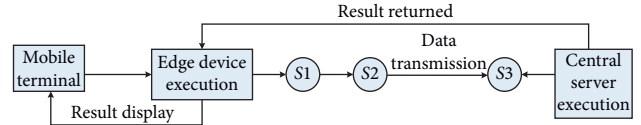
Figure 1: Data processing task offloading framework in the edge cluster process.

utilization reaches the upper or lower limit [30, 31]. If the sum of the resource requirements of tasks on the server for a period of time still makes the server in an "overloaded" or "underloaded" state, then this node can be regarded as a hot spot node or a cold spot node, and then, this node can be processed. Start the corresponding task migration operation [32].

In the efficient task migration algorithm based on trade forecasts studied in this paper, each data center will provide corresponding computing resources for each task according to its needs [33, 34]. Therefore, the resource usage of the server is mainly determined by the resource demand of the tasks deployed on the server, so in the resource forecasting, the resource demand of the task can be quantified by predicting the resource usage of the server [35]. The CPU resource amount of task t_i is

$$UP_s(s) = \frac{\sum_{t \in \text{task}(s)} r_{\text{cpu}}(t) + w(s)}{c_{\text{cpu}}(s)}.$$

(11)

Therefore, the purpose of the resource predictor is to use the resource usage data of the previous n moments to predict the resource usage at time $t + 1$. Out of this consideration, we use linear regression models to characterize and describe the relationship between input variables and output variables [36]. In scenarios where large-scale tasks and servers exist, compared to other resource prediction methods, this method has obvious advantages in time complexity, which is conducive to quickly determining hotspot nodes and cold spot nodes and more conducive to rapid and accurate make migration decisions [37]. The resource usage at t time is

$$UP(s) = \lfloor 1, UP_{(t+1)-m}(s), \ldots, UP_t(s)^T \rfloor.$$

(12)

The specific linear prediction function is

$$UP_{t+1}(s) = \beta_0 + \sum_{i=1}^{m} \beta_i \cdot UP(s).$$

(13)

Among them, m is the size of the regression in the prediction model. The $(m + 1)$-dimensional vector β can be determined by the least square method:

$$\beta \leftarrow \left(X^T X \right)^{-1} X^T y.$$

(14)

2.4. Trade Structure.
Import prices and import quantities are also the result of equilibrium of supply and demand. Therefore, using equilibrium variables to estimate a single import demand equation will also cause doubts related to endogenous issues. Similarly, we need to consider the import supply curve and use the simultaneous equation method to

estimate, or only when the import demand curve is basically stable, and the import supply curve is shifted. A single equation can be used to estimate the equilibrium price and quantity. Based on this consideration, we not only need to fit the overall but also need to add up the trade products of China which are subdivided to a certain extent to examine the import trade elasticity of different types of characteristic products.

In terms of estimation strategy, the quantity and price of export demand are jointly determined by demand and supply. It is the result of a market equilibrium. The export price and export quantity appear on the supply curve and the demand curve at the same time, so they are in equilibrium. The single estimate of price and quantity data is that the export demand equation is generally biased, which will cause serious endogenous problems. Only when the price elasticity of the export supply curve is far greater than the price elasticity of demand, or the demand curve can remain stable when the supply curve changes, can a single equation be used to estimate. In other words, in the former, it means that the price is determined by the supply curve, while in the demand curve, it is an exogenous variable. In the latter, it can be understood that the equilibrium price and quantity is the result of the shift of the supply curve on the demand curve. It can be found that, in the latter, the stability of the demand curve is very important. The method that can be taken is to consider more influencing factors in the demand curve, increase exogenous variables, or subdivide the aggregated trade products to a certain extent. Examine the export trade elasticity of different types of characteristic products.

3. International Import and Export Trade Forecast Experiment

3.1. Dynamic Task Migration System Design. The dynamic task migration system studied in this paper mainly includes four parts: edge computing environment simulator, task generator, resource predictor, and migration decision maker. Among them, the realization of resource predictor and migration decision maker should rely on the edge computing environment simulator [38]. The edge computing environment simulator is mainly responsible for simulating the communication relationship between edge servers, cloud center servers, and data centers; the task generator is mainly responsible for the generation and deployment of tasks in the edge computing environment; the resource predictor is mainly for dynamic task migration issues which are responsible for predicting the dynamic trend of task resource requests in the short term; the migration decision maker is mainly responsible for implementing task migration algorithms, making specific migration decisions, and realizing the redeployment of some tasks in the edge computing environment.

These four parts are not independent modules in the working process; they will interact with each other in the edge computing environment. First of all, the edge computing environment simulator should simulate the real edge computing environment and the resource manager (RM) will record and save the resource situation of each server in

the entire environment; then, it will be generated by the task generator, and the series of tasks will be generated by the task generator. After the task resolver is parsed, it is deployed in the cloud center server node and edge server node of each data center, and then, the resource update controller (RRC) needs to update the remaining resource amount of each server node in the entire edge computing environment; in the above, after the preparation of the basic environment is completed, since the resource request amount of each task is dynamically changing, the resource predictor will cooperate with the migration algorithm to perform the task migration work in the platform to achieve a certain amount of energy saving, while the tasks are divided among the server nodes, and improve the service performance of the entire edge computing platform.

3.2. Edge Computing Environment Simulator

(1) Preprocessing module: the main function of the preprocessing module is to identify and analyze the tasks created in the edge environment task generator. It mainly identifies two types of tasks: cloudopt and edgeopt. The former can only be deployed on the cloud center server Cloud_Task and the latter belongs to Edge_Task, which is first deployed on the edge server. After the preprocessing module, the task will be parsed, converted into corresponding task commands, and stored in the task queue. For a task created in an edge computing environment task generator, only the task number task_id of the recorder, task type task_type, task state task_state, task resource demand task_request, and task running time task_time are required. Therefore, this article specifies the task command parsed by the preprocessing module

(2) Control module: the control module is the control unit of the entire dynamic task migration system, which supervises and controls the resources and tasks in the entire system. Due to the dynamic changes of tasks, the RRC in the resource manager will update the remaining resources of each server in real time; RM will monitor the resource usage of each server in the entire system in real time. Once the resource utilization is "excessive" or in case "too low," corresponding to the appearance of hotspot nodes and cold spot nodes, the task migration unit will select the migration tasks and make migration decisions, and the corresponding task deployment unit will redeploy the migrated tasks. The implementation process of the migration algorithm has been introduced in detail in Section 3; the task deployment of the control module does not involve the determination of the deployment plan because the corresponding target server has been selected in the migration decision; therefore, this section mainly introduces resource management design and implementation of the processor.

(3) Operation module: the operation module can not only receive and parse the instructions sent by the upper-level control but also implement specific operations based on the parsed instructions, so as to rationalize the resource and attribute information of the task entity and the underlying server entity configuration and management. The operation module is mainly composed of task management submodule and server management submodule. The task management submodule is responsible for task-related operations, including task generation and status changes, task migration, and task deployment. The server management submodule is responsible for the related operations of the server, including the opening and closing of the server and resource update operations.

(4) Resource module: it is the public resource of the entire dynamic task migration system and is mainly responsible for storing tasks and cloud-side server entities. When server storage is performed, block storage is performed according to the data center where it is located. In each data center, edge servers and cloud center servers must be distinguished and processed; when task storage is performed, the task is mainly divided into several task sets and is stored on different servers in different data centers. The control module will monitor this module in real time, and the operation module will perform specific operations on the server and tasks of this module.

3.3. Data Processing Offload Strategy. In the traditional risk prediction platform, since the data processing function and prediction function are provided by the central server, in this case, the user's service experience is largely related to the user's connection quality with the closely related central server:

(1) The user transmits the data that need to be predicted to the edge device through the mobile terminal

(2) After receiving the data transmitted by the user, the edge device uses related data processing technology to process the data

(3) After the data processing operation is completed, the edge device transmits the processed data to the edge center, and the edge center collects and transmits it to the central server

(4) After the central server receives the data transmitted by the edge device cluster, it stores the data in the database and uses the prediction model to perform prediction work

(5) After completing the prediction work, the central server returns the result to the edge center, and the edge center transmits the data to the corresponding edge device

(6) Finally, the edge device sends the received result to the mobile terminal and displays it on the user interface

3.4. Data Unloading Process. The specific process is roughly as follows:

(a) Customs business personnel transfer the trade data that need to be predicted to the edge device cluster through the mobile terminal.

(b) After receiving the data transmitted by the business personnel, the edge device cluster uses related data processing technology to process the data.

(c) After the data processing operation is completed, directly use the processed data for forecasting work, and after completing the forecasting work, upload the data and results to the central server.

(d) Finally, after the prediction is completed, the edge device will feed back the predicted result to the mobile terminal and display the result on the user interface through the mobile terminal so that the business personnel can understand the trade risk status. The data unloading process is shown in Figure 2.

4. Forecast and Analysis of International Import and Export Trade

4.1. Task Migration Analysis. The high-efficiency task migration algorithm based on import and export trade studied in this paper includes the process of resource prediction. The effect of resource prediction will directly affect the performance of the processing task of the entire dynamic task migration system. Therefore, the GC-ETM algorithm will be first used in the experimental process. The resource prediction algorithm is compared with the prediction method in the VMCUP-M algorithm. In the comparison process, in order to ensure that the experimental configuration is the same, the prediction process proposed in this paper will also predict the resources for a period of time in the future 6 times, that is, $k = 6$. In order to illustrate the versatility of the GC-ETM method for task migration problems, that is, it is commonly used in task migration in both dynamic and static situations; at the same time, the GC-ETM method has more advantages in the dynamic task migration process of various scales. For good results, three scale experiments will be carried out, respectively. Therefore, during the experiment, small-scale dynamic task migration experiments, medium-scale dynamic task migration experiments, large-scale dynamic task migration experiments, and static task migration experiments will be carried out, respectively. In the implementation of the migration algorithm, the parameters involved mainly include the lower and upper limits n1 and n2 of each server's CPU resource utilization. In the study of this article, both CPU resources and memory resources need to be considered in the formulation of migration strategies; in the performance evaluation process, the main parameters involved are the parameters a and β of the order of magnitude. The parameter values are shown in Table 1.

In the experiment of small-scale task migration, the number of task entity nodes changed from 100 to 900, and the number of tasks in each group increased by 100. In the
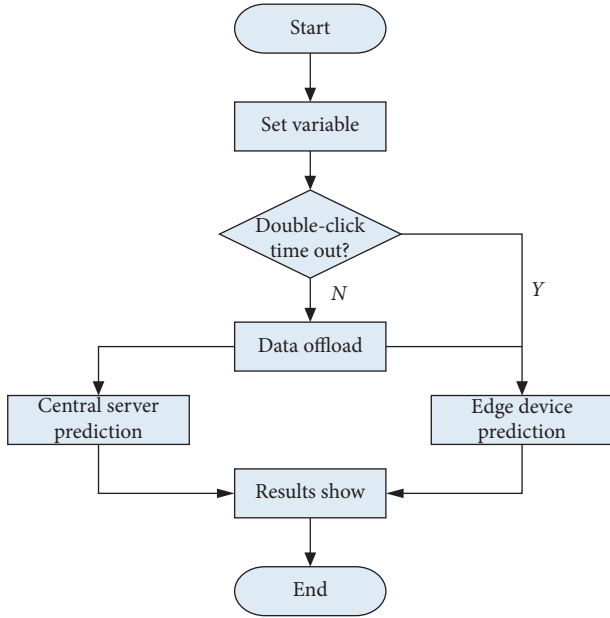
FIGURE 2: Task uninstall process.

TABLE 1: Parameter values.

Parameter name	Parameter value
$n1$	0.2
$n2$	0.8
a	60
β	15

small-scale experiment, two experiments of dynamic and static task migration will be carried out, and the task migration based on graph coloring proposed in this paper will be carried out from five aspects: energy consumption, communication cost, migration cost, average migration cost, and total cost. The algorithm is compared with the comparison algorithm. The static task migration performance is compared with the BGM-BLA, AVMM, and VMCUP-M methods, and the dynamic task migration performance is compared with the VMCUP-M algorithm and AVMM methods. The range of CPU resources requested by different numbers of tasks is [6, 10], and the resource requirements of memory resources and storage resources are evenly distributed in the ranges of [60,100] and [120,200], respectively. When performing dynamic task migration, the probability Pc, Pu, Pr, and Pp of the operation module to change the task state are 0.2, 0.5, 0.2, and 0.1, respectively. The small-scale task migration research is shown in Table 2.

Correspondingly, during the small-scale experiment, the total number of servers is 50. CPUc and CPUe, respectively, correspond to the amount of CPU resources of cloud center servers and edge servers; Memc and Meme, respectively, correspond to the amount of memory resources of cloud center servers and edge servers; Stoc and Stoe, respectively, correspond to the amount of storage resources of cloud center servers and edge servers; cloud center link bandwidth between servers, cloud edges, and edge servers correspond to

TABLE 2: Small-scale task migration research.

Parameter	Parameter range
CPU resources	[6, 10]
Memory resource	[60, 100]
Storage resources	[120, 200]
Pc	0.2
Pu	0.5
P	0.2
Pk	0.1

cc, ce, and ee, respectively. The amount of storage resources is shown in Table 3.

4.2. Task Offloading Strategy. The communication overhead result of each algorithm in the small-scale static task migration experiment is shown in Figure 3. It can be seen from the experimental results that when the number of tasks is greater than 300, the GC-ETM algorithm proposed in this paper has better performance in reducing communication overhead. The main reason is that compared with other algorithms, this paper prioritizes the tasks with the highest CPU usage during task processing, which can reduce more SLA conflicts, thereby reducing communication overhead.

Compared with the VMCUP-M algorithm, the GC-ETM method proposed in this paper has significantly smaller communication overhead. When the number of tasks is 100–700, its communication overhead is close to that of the AVMM algorithm, and when the number of tasks increases, it is slightly higher than the AVMM algorithm. The main reason is that the first two algorithms have a resource prediction process and SLA conflict processing. Relatively not timely enough, on the other hand, it is mainly because the AVMM algorithm prioritizes the migration of tasks with greater communication requirements, so there will be less communication overhead, but the gap between the GC-ETM method and the AVMM algorithm is relatively small. The algorithm comparison result is shown in Figure 4.

The impact of different dynamic environments on the task completion time is shown in Figure 5. Among them, the dynamics of the system become stronger with the increase of the change factor μ. When the system tends to be static ($\mu < 10^{-5}$), accurate prediction information makes the performance of the algorithms with almost no gap. With the increase of μ, the prediction information becomes inaccurate, and the gap between ADCO and the comparison algorithm quickly widens. When $\mu = 10^{-3}$, the performance gap between ADCO and the control strategy reaches the maximum. The above results strongly prove that ADCO has good dynamic adaptability. At the same time, observing the experimental results of EFSF and EFSF-R and ADCO and ADCO-NR strategies, it is not difficult to find that the repeated offloading strategy of tasks is indeed beneficial to the dynamic adaptive ability of the offloading algorithm.

4.3. MEC Prediction Model. Figure 6 shows the stability test of the monthly data series of China-ASEAN imports and exports from August 2018 to December 2019. It can be seen

TABLE 3: Storage resources.

Parameter	Parameter range
CPUc	[800, 1000]
CPUe	[80, 220]
Memc	[8000, 10000]
Meme	[800, 2000]
Stoc	[12000, 20000]
Stoe	[1600, 4000]
C-C	[15, 20]
C-e	[10, 15]
e-e	[8, 12]
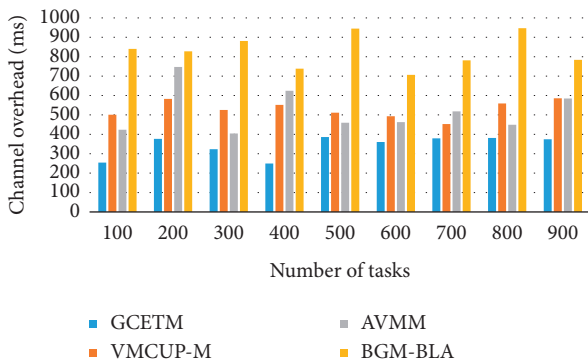
FIGURE 3: Communication overhead results of each algorithm in the small-scale static task migration experiment.
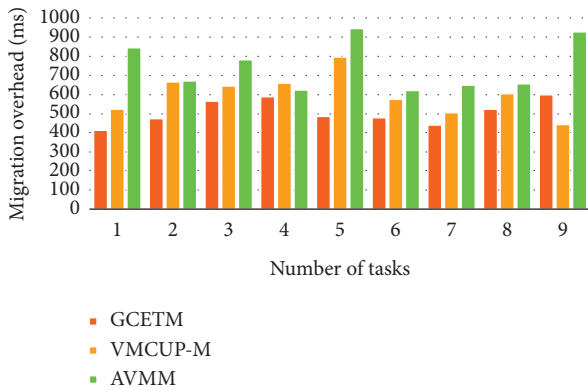
FIGURE 4: Algorithm comparison results.

FIGURE 5: The impact of different dynamic environments on task completion time.

FIGURE 6: Stability detection of monthly data series.

The reasons may be as follows. With economic development and global integration, ASEAN is the country's third largest trading partner, and the import and export trade volume is constantly increasing. As a result, different average values are generated over time; in different periods, due to policies or other reasons such as the global economic downturn, the volume of import and export trade with ASEAN has declined to a certain extent; comparing different periods of import and export trade with ASEAN Ete presents a certain cyclical or seasonal change. Table 4 shows the import and export income and price elasticity of my country's primary products, products in processing, and industrial finished products.

The result of the smoothing method is shown in Figure 7. In order to stabilize the data series of import and export trade volume, it is necessary to eliminate the aforementioned causes of instability. First, eliminate the trend. In order to eliminate the trend, the smoothing method of weighted rolling average is generally adopted, which is the average of continuous K values. In terms of the frequency of the trade volume data series, this article uses the average of the past year, that is, the average of the past 12 months. After smoothing, the sequence data processed in Figure 6 is more stable than the data in Figure 7, and the test statistics of the sequence are shown in Table 5.

from Figure 6 that the changes in the volume of trade show a similar trend of ups and downs in a certain period of time, and on the whole, it is continuously increasing. The forecasting model based on the time series MEC is to predict the trend and seasonality of the original trade volume data series and eliminate the predicted trend and seasonality to obtain a stable data series. If a data series produces a certain behavior over time, it is considered that it will produce such behavior in the future with a high probability, so it is to convert the data series of China-ASEAN import and export trade volume into a stable series. For prerequisites for forecasting using the MEC forecasting model based on time series, the results of the stability test show that the data sequence of China-ASEAN import and export trade volume is not stable.

Table 4: Import and export income and price elasticity of my country's primary products, products in process, and industrial finished products.

Price	Product		
	Primary product	Reprocessed products	Manufactured goods
Import price elasticity	−1.09 (−2.21)	−1.83 (−2. 89)	−1.03 (−4.42)
Export price elasticity	−0.49 (−2.00)	−0.56 (−2.03)	−2.35 (−2.3)
Export income elasticity	1.00 (5.35)	1.77 (5.1 7)	2.10 (21.10)
Import income elasticity	0.11 (1.69)	2.1 3 (2.09)	2.73 (7.54)
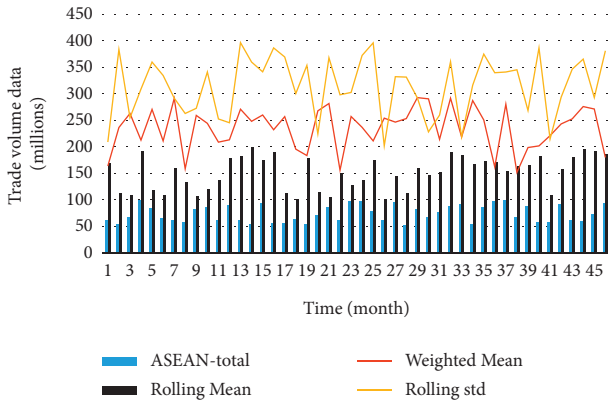
Figure 7: Smoothing method processing results.

Table 5: Comparison of test statistics of sequences.

Value	Sequence	
	Data sequence 1	Data sequence 2
Test statistics	−0.510621	−3.521207
Less than 1% critical value	−3. 484667	−3.490131
Less than 5% critical value	−2.88534	−2.887712
Less than 10% critical value	−2. 579463	−2.58073

The time series model based on the moving edge algorithm is used to fit the monthly data of China-ASEAN import and export trade volume. The total import and export volume of August 2018 is the earliest data at a given time. The fitting result is shown in Figure 8. Table 5 shows the evaluation results of the prediction model of China-ASEAN import and export trade volume based on the time series MEC. The China-ASEAN import and export trade volume prediction model is based on the time series MEC although the predicted MAPE and correlation coefficients are not as good as the linear regression-based prediction model, but the time series model is better than the need to determine the value of other indicator factors. The import and export volume can be predicted in the future, and when the prediction is based on the time series MEC model fitting
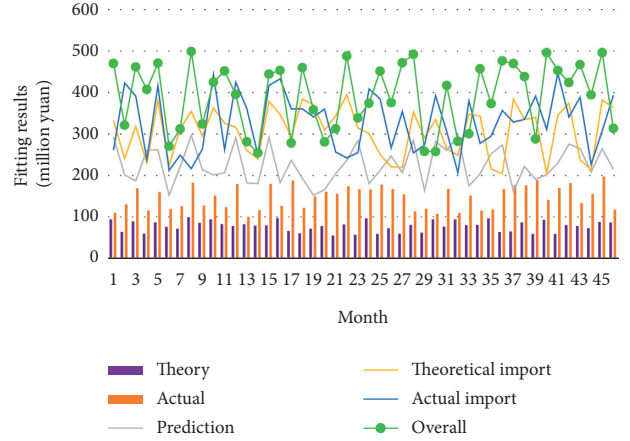
Figure 8: Fitting results of total import and export.

Table 6: Monthly data forecast of import and export trade volume.

Root mean square error RMSE	Mean absolute error (MAE)	Mean absolute percentage error (MAPE) (%)	Correlation coefficient R (%)
62.9251	50.5648	16.9486	83.8687

process, it is applied from the data of August 2018 after learning the internal time law of the monthly import and export trade volume The monthly data of the import and export trade volume of the subsequent ten years of time span are still predicted in time and fitted, and the correlation coefficient is still more than 83%, and the RMSE has also decreased significantly, indicating that there is a certain gap between the predicted value and the actual value, but the predicted trend is still a strong correlation. The monthly data forecast of import and export trade volume is shown in Table 6.

5. Conclusion

The dynamic task migration system studied in this paper mainly includes four parts: edge computing environment simulator, task generator, resource predictor, and migration decision maker. Among them, the realization of resource predictor and migration decision maker should rely on the edge computing environment simulator. The edge computing environment simulator is mainly responsible for simulating the communication relationship between edge servers, cloud center servers, and data centers; the task generator is mainly responsible for the generation and deployment of tasks in the edge computing environment.

The resource predictor is mainly for dynamic task migration problems and is responsible for predicting the dynamic change trend of task resource requests in the short term; the migration decision maker is mainly responsible for implementing task migration algorithms, making specific migration decisions, and implementing some tasks in the edge computing environment redeployment. These four parts are not independent modules in the working process, and they will interact with each other in the edge computing

environment. First of all, the edge computing environment simulator should simulate the real edge computing environment, and the resource manager will record and save the resource situation of each server in the entire environment.

A series of tasks are generated by the task generator. After being parsed by the task parser, they are deployed in the cloud center server nodes and edge server nodes of each data center. After that, the resource update controller needs to update the remaining server nodes in the entire edge computing environment. The amount of resources is updated; after the preparation of the above basic environment is completed, because the resource request amount of each task is dynamically changing, the resource predictor will cooperate with the migration algorithm to perform the task migration work in the platform, so as to realize that the tasks are equally divided among the server nodes. At the same time, it achieves a certain energy-saving effect and improves the service performance of the entire edge computing platform. The system designed in this study shows good prediction results.

Data Availability

No data were used to support this study.

Conflicts of Interest

The authors declare that they have no conflicts of interest.

References

[1] A. Liu, Y. Xiao, H. Lu, S.-B. Tsai, and W. Song, "A fuzzy three-stage multi-attribute decision-making approach based on customer needs for sustainable supplier selection," *Journal of Cleaner Production*, vol. 239, Article ID 118043, 2019.

[2] Z. Lv, D. Chen, R. Lou, and Q. Wang, "Intelligent edge computing based on machine learning for smart city," *Future Generation Computer Systems*, vol. 115, pp. 90–99, 2021.

[3] L. Gang and Z. Hanwen, "An ontology constructing technology oriented on massive social security policy documents," *Cognitive Systems Research*, vol. 60, pp. 97–105, 2020.

[4] W. Shi, J. Cao, Q. Zhang, Y. Li, and L. Xu, "Edge computing: vision and challenges," *IEEE Internet of Things Journal*, vol. 3, no. 5, pp. 637–646, 2016.

[5] L. Wu, Q. Zhang, C.-H. Chen, K. Guo, and D. Wang, "Deep learning techniques for community detection in social networks," *IEEE Access*, vol. 8, pp. 96016–96026, 2020.

[6] K. Jiang, H. Ni, R. Han et al., "An improved multi-objective grey wolf optimizer for dependent task scheduling in edge computing," *International Journal of Innovative Computing Information and Control*, vol. 15, no. 6, pp. 2289–2304, 2019.

[7] T. Wang, Z. Zheng, and M. Elhoseny, "Equivalent mechanism: releasing location data with errors through differential privacy," *Future Generation Computer Systems*, vol. 98, pp. 600–608, 2019.

[8] J. Lin, W. Yu, X. Yang, P. Zhao, H. Zhang, and W. Zhao, "An edge computing based public vehicle system for smart transportation," *IEEE Transactions on Vehicular Technology*, vol. 69, no. 11, pp. 12635–12651, 2020.

[9] C.-H. Chen, "A cell probe-based method for vehicle speed estimation," *IEICE Transactions on Fundamentals of Electronics, Communications and Computer Sciences*, vol. E103-A, no. 1, pp. 265–267, 2020.

[10] X. Zhang, J. Zhang, Z. Liu, Q. Cui, X. Tao, and S. Wang, "MDP-based task offloading for vehicular edge computing under certain and uncertain transition probabilities," *IEEE Transactions on Vehicular Technology*, vol. 69, no. 3, pp. 3296–3309, 2020.

[11] M. Satyanarayanan, "The emergence of edge computing," *Computer*, vol. 50, no. 1, pp. 30–39, 2017.

[12] R. Dautov, S. Distefano, D. Bruneo et al., "Metropolitan intelligent surveillance systems for urban areas by harnessing IoT and edge computing paradigms," *Software: Practice and Experience*, vol. 48, no. 8, pp. 1475–1492, 2018.

[13] Z. Lv, "Security of Internet of things edge devices," *Software: Practice and Experience*, pp. 1–11, 2020.

[14] S. George, T. Eiszler, R. Iyengar et al., "OpenRTiST: end-to-end benchmarking for edge computing," *IEEE Pervasive Computing*, vol. 19, no. 4, pp. 10–18, 2020.

[15] B. Hussain, Q. Du, A. Imran, and M. A. Imran, "Artificial intelligence-powered mobile edge computing-based anomaly detection in cellular networks," *IEEE Transactions on Industrial Informatics*, vol. 16, no. 8, pp. 4986–4996, 2020.

[16] G. Li and J. Cai, "An online incentive mechanism for collaborative task offloading in mobile edge computing," *IEEE Transactions on Wireless Communications*, vol. 19, no. 1, pp. 624–636, 2019.

[17] S. M. Park and Y. G. Kim, "User profile system based on sentiment analysis for mobile edge computing," *Computers, Materials and Continua*, vol. 61, no. 3, pp. 569–590, 2019.

[18] W. Li, Z. Chen, X. Gao, W. Liu, and J. Wang, "Multimodel framework for indoor localization under mobile edge computing environment," *IEEE Internet of Things Journal*, vol. 6, no. 3, pp. 4844–4853, 2019.

[19] Q. Xu, Z. Su, Q. Zheng, M. Luo, B. Dong, and K. Zhang, "Game theoretical secure caching scheme in multihoming edge computing-enabled heterogeneous networks," *IEEE Internet of Things Journal*, vol. 6, no. 3, pp. 4536–4546, 2018.

[20] Y. Huang, L. Qian, A. Feng, N. Yu, and Y. Wu, "Short-term traffic prediction by two-level data driven model in 5G-enabled edge computing networks," *IEEE Access*, vol. 7, no. 99, pp. 123981–123991, 2019.

[21] B Yang, D. Wu, and R. Wang, "CUE: an intelligent edge computing framework," *Network, IEEE*, vol. 33, no. 3, pp. 18–25, 2019.

[22] Z. Zhou, Q. Wu, and X. Chen, "Online orchestration of cross-edge service function chaining for cost-efficient edge computing," *IEEE Journal on Selected Areas in Communications*, vol. 37, no. 8, pp. 1866–1880, 2019.

[23] T. Püschel, "Taupunktüberwachung für edge-Computing," *Sicherheits Berater*, vol. 13, pp. 252–254, 2019.

[24] P. K. Sharma, S. Rathore, Y.-S. Jeong, and J. H. Park, "SoftEdgeNet: SDN based energy-efficient distributed network architecture for edge computing," *IEEE Communications Magazine*, vol. 56, no. 12, pp. 104–111, 2018.

[25] S. Hill, "Edge computing comes to the oil & gas industry," *Control Engineering*, vol. 65, no. 2, pp. 9–11, 2018.

[26] M. F. Khalid, B. I. Ismail, M. N. M. Mydin et al., "Performance comparison of image and workload management of edge computing using different virtualization technologies," *Advanced Science Letters*, vol. 23, no. 6, pp. 5064–5068, 2017.

[27] T. Taleb, K. Samdanis, B. Mada, H. Flinck, S. Dutta, and D. Sabella, "On multi-access edge computing: a survey of the emerging 5G network edge cloud architecture and

orchestration," *IEEE Communications Surveys & Tutorials*, vol. 19, no. 3, pp. 1657–1681, 2017.

[28] Y. Mao, J. Zhang, S. H. Song, and K. B. Letaief, "Stochastic joint radio and computational resource management for multi-user mobile-edge computing systems," *IEEE Transactions on Wireless Communications*, vol. 16, no. 9, pp. 5994–6009, 2017.

[29] Y. Chen, W. Zheng, W. Li, and Y. Huang, "Large group Activity security risk assessment and risk early warning based on random forest algorithm," *Pattern Recognition Letters*, vol. 144, p. 1, 2021.

[30] W. Yu, F. Liang, X. He et al., "A survey on the edge computing for the Internet of things," *IEEE Access*, vol. 6, no. 99, pp. 6900–6919, 2018.

[31] K. Zhang, Y. Mao, S. Leng, Y. He, and Y. Zhang, "Mobile-edge computing for vehicular networks: a promising network paradigm with predictive off-loading," *IEEE Vehicular Technology Magazine*, vol. 12, no. 2, pp. 36–44, 2017.

[32] H. Li, K. Ota, and M. Dong, "Learning IoT in edge: deep learning for the Internet of things with edge computing," *IEEE Network*, vol. 32, no. 1, pp. 96–101, 2018.

[33] G. Ananthanarayanan, P. Bahl, P. Bodik et al., "Real-time video analytics: the killer app for edge computing," *Computer*, vol. 50, no. 10, pp. 58–67, 2017.

[34] S. Nastic, T. Rausch, O. Scekic et al., "A serverless real-time data analytics platform for edge computing," *IEEE Internet Computing*, vol. 21, no. 4, pp. 64–71, 2017.

[35] F. Zhou, Y. Wu, R. Q. Hu, and Y. Qian, "Computation rate maximization in UAV-enabled wireless-powered mobile-edge computing systems," *IEEE Journal on Selected Areas in Communications*, vol. 36, no. 9, pp. 1927–1941, 2018.

[36] C.-H. Chen, F.-J. Hwang, and H.-Y. Kung, "Travel time prediction system based on data clustering for waste collection vehicles," *IEICE TRANSACTIONS on Information and Systems*, vol. E102.D, no. 7, pp. 1374–1383, 2019.

[37] S.-B. Tsai, Y.-Z. Xue, P.-Y. Huang et al., "Establishing a criteria system for green production," *Proceedings of the Institution of Mechanical Engineers, Part B: Journal of Engineering Manufacture*, vol. 229, no. 8, pp. 1395–1406, 2014.

[38] Z. Lv and L. Qiao, "Optimization of collaborative resource allocation for mobile edge computing," *Computer Communications*, vol. 161, pp. 19–27, 2020.

Review Article

"Internet + Artificial Intelligence" Human Resource Information Management System Construction Innovation and Research

Zhen Zeng[1] **and Longqi Qi** [iD] [2]

[1]*Business School, Central South University, Changsha, Hunan 410000, China*
[2]*School of Economics and Management, Hubei Three Gorges Polytechnic, Yichang, Hubei 443000, China*

Correspondence should be addressed to Longqi Qi; qlq@tgc.edu.cn

Human resources are the cornerstone of operational operation. Good management of human resource information can enable businesses to operate effectively. However, for the time being, most enterprises still use traditional methods of allocating human resources, which are difficult to meet the development needs of enterprises. In order to find the optimal allocation of human resources in an enterprise, this article is based on "Internet + artificial intelligence," using methods such as case analysis and literature analysis to collect data from databases such as CNKI, Wanfang Database, and SSCI, and uses fog computing to build a model for the optimal allocation of human resources which is proposed, and a large number of relevant literature studies are read and analyzed through the literature survey method. According to the research needs, through the research and summary of the content of the literature, the research structure found that there are many problems in the current human resource information management system. After the optimization of models and algorithms, the allocation of human resources has been greatly improved. The matching rate of personnel and job positions has increased by more than 50%. The operation efficiency index of the enterprise is above 0.8, an increase of about 30%. This shows that "Internet + artificial intelligence" can effectively optimize the enterprise human resource information management system, promote the greater use of its human resource value, bring higher economic returns to the enterprise, and provide assistance for the long-term stable and healthy development of the enterprise.

1. Introduction

In today's society, human resources, as science, play a vital role in socioeconomic development and scientific and technological progress. They are a very important social resource and can promote the development of other resources at the same time. The allocation of human resources is used as a link between people and material data. The organic chain together is a key link to whether human resources can play their full role [1]. At present, many jobs still retain the traditional human resource organization, facing a series of human resource problems such as the aging of the personnel structure and the relative lack of professional talents. With the development of time, this new management method will gradually be eliminated. Fog computing provides services to users locally. On the one hand, it can reduce business processing delays and improve work efficiency. On the other hand, it can reduce network and bandwidth requirements and save the system in general. Therefore, we have innovated and optimized the design of the human resources information management system based on the Internet + artificial intelligence, reasonably allocates human resources, quickly activates existing human resources, optimizes the actual allocation of human resources to maximize human resources, and strengthens the management of human resources information in order to better adapt to future market demands [2].

In the modern enterprise management system, human capital pays more attention to the requirements of the enterprise management system, further formulates clear

regulations, and refines the responsibilities of enterprise managers [3]. The optimized configuration of human resources based on the Internet + artificial intelligence can effectively revitalize human resources, and employees' sense of responsibility and work initiative are significantly improved. The management level is reduced, and the enterprise entity is realized. The specific work is sinking. The matters that need to be reported at different levels are directly handled by each business department. Each business department directly participates in business management activities. The collaboration between departments is closer. The interaction is more efficient [4].

Belizon et al. studied the differences in the use of international integration mechanisms in various human resource management (HRM) practices by multinational companies. Their findings indicate that personnel, information, and formal-based mechanisms are positively related to the use of centralized-based integration processes [5]. Liu and Yue use fog computing to create models and allocate resources. In his research, they found that fog computing is stable and meets the demand [6]. Leijun points out that, in today's rapid economic development, the traditional human resource allocation model is inconsistent with the current development trend, which makes it difficult for many enterprises that are still using traditional human resource allocation methods [7].

Wang Wenxin believes that, in today's rapid development of information, knowledge is the first contribution to the promotion of human society. How to arrange people with different roles in suitable positions, mobilize their enthusiasm for work, and develop their potential is the optimization of human resource management. The most important issue is the use of human resource-related theories, introducing the meaning of human resource allocation and the method of optimizing human resources and discussing the important role of human resource optimal allocation for social development [5]; Tang Linyu believes that fog computing can provide people with more services. Starting from the allocation of computing resources, they use fog computing to make models and allocate resources. In the research, it is found that fog computing is stable and demand matching. The results prove that the use of fog computing can make the allocation time relatively stable. The delay and accuracy of the calculation in the fog are better than the original calculation method [6]. Zhang Bo believes that the development and growth of enterprises cannot be separated from the optimal allocation of human resources. However, in today's rapid economic development, the traditional human resource allocation model does not match the current development, which makes it difficult for many enterprises that still use traditional human resource allocation. In this regard, he emphatically introduced the methods of optimizing the allocation of human resources in the enterprise and cited relevant examples [7]. These studies have certain reference values for this article, but due to the narrow data cited in the research, the data industry is basically limited to individual industries and has no universal effect.

This article applies the latest human resource allocation theory to fully mention the status quo of the human resource allocation of the enterprise, to seek to explore a specific plan for the establishment of a human resource information

management system, and to provide a reference for relevant undertakings. Create an ecosystem structure model based on the "Internet + Artificial Intelligence" to carry out a thorough analysis of the current status of the new system management of human resources and make relevant countermeasures and proposals on the basis of the analytical conclusions to help similar companies build more competitive new human resource management system to better help the company to develop and develop.

2. Innovative Methods for the Construction of Human Resource Information Management System

2.1. Fog Calculation. Fog computing is a system-level architecture that provides computing, storage, control, and networking functions near the data generation source along the cloud to the continuum of things. The fog computing architecture is mainly divided into three layers: cloud computing layer, fog computing layer, and mobile terminal layer. The fog computing architecture brings the service closer to the end user, reduces latency, saves energy consumption, and enhances the user experience [8].

The bottom layer of the architecture is the mobile terminal layer, which contains a large number of smart devices and sensors. Data collection, service requests, and so on all come from the bottom-end terminal equipment. Smart terminal equipment can preprocess and compress data to filter out some useless data [9]. At the same time, terminal equipment can also communicate through equipment such as base stations or routers to realize data sharing. The fog computing layer is located between the cloud computing layer and mobile terminal devices and is a bridge connecting cloud servers and terminal devices. Simple events and emergencies are detected at this layer, so that users can respond quickly.

The delay of the fog computing layer includes the communication delay between fog devices and the calculation delay of fog devices. For communication delay, in the undirected graph composed of fog devices, the communication delay between fog nodes is used as the weight. As the amount of calculation increases, the calculation delay of the fog device increases accordingly; the more calculations increase and the more fog devices, the more calculation delay time [10]. Therefore, use the following function to describe the calculation delay of the fog device.

$$T = \frac{1}{w_x} a_i b_i^2. \tag{1}$$

Among them, w_x is the computing power of the fog device x, b_i is the amount of tasks processed by the fog device, and a_i is a preset real number. Therefore, the delay of the fog computing node is expressed as follows:

$$T_n = \min \sum_{i=1}^{x} \frac{1}{w_x} a_i b_i^2. \tag{2}$$

The fog computing layer is composed of fog nodes deployed around IoT devices. The fog nodes are connected to

devices such as base stations or routers, thereby reducing the transmission delay from device to device. In addition, a large number of fog nodes are deployed at the edge of the network, and even the same service is deployed on multiple fog nodes. This not only reduces the risk of service interruption caused by a failure of one fog node but also makes one fog node more than one. Equipment includes base stations or routers process data [11]. The fog node in the network can also be connected to the cloud data center. When the IoT device generates massive data that needs to be processed and the computing power of a single fog node cannot meet its needs, the fog node will forward the data to the cloud for processing. There will undoubtedly be a greater communication delay and reduce the efficiency of the service. In the calculation, because the self-correction function is added in each step of the calculation process, the maximum change of pressure and saturation allowed by each grid node in the two adjacent steps is limited [12]. Therefore, in the process of calculating the node penetration rate at time $(n + 1)$, the following basic formula is used:

$$K = K_0 \exp\left[a\left(p - p_0\right)\right]. \tag{3}$$

Here, we assume that the initial pressure of the reservoir is PP, the pressure value at time n is p_n, and the pressure value at time $n + 1$ is $p_n + 1$; then when $p_n + 1 < \text{PP}$ and $\text{PP} = p_n + 1$,

$$K^{n+1} = K_0 e^{-a1\left(p_0 - p^{n+1}\right)}. \tag{4}$$

When $p_n + 1 \geq \text{PP}$,

$$K^{n+1} = K_n e^{-a_2\left(p^n - p^{n+1}\right)}. \tag{5}$$

This paper uses immune optimization algorithm to study the energy consumption of data processing in fog computing. In the traditional three-layer network architecture, considering the long distance and high energy consumption when the cloud server caches data resources to the fog node, a four-layer network architecture model is proposed, that is, between the cloud computing layer and the fog computing layer. Add a layer of proxy fog server to make the cloud server cache data resources in advance and provide local services [13]. The specific process of addressing the proxy fog server through the optimal immune algorithm is described in detail, thereby reducing the energy consumption of the fog node to obtain data resources from the proxy fog server and also reducing the amount of precached resources by the cloud server to the fog node. Through theoretical analysis and simulation experiments, the effectiveness of the four-layer network architecture model in data processing energy consumption is proved.

2.2. New Human Resource Management System. Human resource management refers to a series of management activities based on the organization and mobilization of corporate human resources to promote the attraction of outstanding talents, enhance the enthusiasm of corporate talents, and promote the realization of corporate organizational goals [14]. Whether it is a matter of talent selection, employee incentives, or human resource management

planning, training, performance, salary management, and so on, all activities' management shall be implemented to achieve the organizational objectives of the undertaking. The sole purpose is to promote the implementation of the organizational objectives of the undertaking for the improvement of the undertaking. The enthusiasm of talent and the attraction of exceptional talent can be effective human resource management.

The theory of human resource planning mainly includes two aspects. On the one hand, the theory believes that the viability of an enterprise comes from the structure and quantity of human resource management. On the other hand, the theory believes that the implementation of human resource planning by an enterprise can satisfy the development of the enterprise itself. To meet the development and interests of employees [15], human resource planning is a very important content in the human resource management system of an enterprise. As a key management activity, human resource planning is related to the rational, scientific, and comprehensive human resource management. Supported by human resource planning theory, the enterprise implementation that is reasonable human resource management strategy can not only improve the production and operation management level of the enterprise but also meet the strategic development needs of the enterprise [16].

Management theory believes that, according to the close relationship between the scope of management and the level of management, there will be two forms of organizational structure: flat structure and straight structure. The so-called flat structure is a structure with few management levels and large management width. The case of the formula structure is the opposite [17]. Its structure is derived from the nonlinear partial differential equation of Taylor series expansion motion:

$$\frac{a^2 R}{at^2} = b_o^2 \left[1 + \frac{w}{w'}\frac{au}{a}\frac{au}{d} + \cdots\right]\frac{a^2 R}{ad^2}, \tag{6}$$

where R is the displacement relative to time t and d is the distance of propagation; in this study, d is the length of the sample, the second- and third-order elastic constants and b_0^2 is the velocity. Equations related to elastic constants of nonlinear parameters are as follows:

$$\eta_2 = -\frac{w''}{2w'}. \tag{7}$$

Variants of nonlinear motion equations are as follows:

$$\frac{a^2 R}{at^2} = b_o^2 \left[1 - 2\eta_2\frac{au}{a}\frac{au}{d} + \cdots\right]\frac{a^2 R}{ad^2}. \tag{8}$$

The solution of the equation is as follows:

$$R = R_1 \cos\left(qx - w\,d\right) - \frac{1}{4}\eta_2 q^2 R_2 x\,\sin 2\left(qx - w\,d\right) + \cdots. \tag{9}$$

The relationship between R_2 and R_3 can be obtained:

$$R_2 = \left(\frac{\eta_2}{4}\right)d^2 R_1^2 x. \qquad (10)$$

$$R_3 = \left(\frac{\eta_2^2}{8}\right)d^4 R_1^3 x^2. \qquad (11)$$

When encountering obstacles, A_1, A_2, and A_3, respectively, indicate operating efficiency

$$\frac{A_2}{A_1^2} = \left(\frac{\eta_2}{4}\right)d^2 x, \qquad (12)$$

$$\frac{A_3}{A_1^3} = \left(\frac{\eta_3}{6}\right)d^3 x. \qquad (13)$$

According to the specific situation of the unit, to determine their ideal management width, the endogenous driving force of the flat management model of the enterprise lies in the continuous improvement of the manager's personal ability [18]. Through flat design, scientific job distribution, and flat management of corporate managers to enrich front-line staff, revitalize existing human resources, solve the contradiction between redundancy and shortage, improve corporate executives' sense of responsibility and work initiative, reduce risks, and improve the quality and efficiency of corporate collection and management, the promotion of modernization of corporate management systems is inevitable trends in corporate development [19].

2.3. Optimization and Innovation of the Human Resource System under Internet + Artificial Intelligence. In the Internet economic environment, the transformation of corporate business models has caused companies to face a new competitive situation. The traditional capital competition is constantly developing in the direction of intellectual resource competition. In this process, the importance of human resources will inevitably become more prominent. The decision-making choices of enterprise human resource management must also be changed [20]. In the context of the Internet economy, companies can only obtain strong development forces if they obtain strong human capital power. At the same time, they should effectively stimulate the capabilities and value of human resources through effective management and maximize their functions to meet the development needs of the company. This requires companies to pay attention to the transformation of the Internet model of human resource management [21]. Managers at all levels are in charge of affairs closely related to the various production, operation, and management activities of the enterprise. The development of the enterprise depends on the efficient completion of these basic tasks. Under Internet thinking, due to the change of the status of human resources in enterprise management, as a result, the implementation methods of management functions at all levels have changed. The system management under the traditional model has not been able to adapt to the Internet thinking. Therefore, the functions of the managers at all levels will also undergo corresponding changes. Human

resource management requires adaptation [22]. Calculate the similarity between the resources in the resource collection and the resources requested by the user:

$$\cos m(r, uq) = \alpha * \cos(r, uq) + (1 - \alpha) * \frac{1}{m}\sum_{n=1}^{m}\delta_{ij}, \quad (14)$$

where a represents the weight and the range is between [0, 1]. The simulation parameters are calculated as follows:

$$F = \frac{\sum(q_{rp,rpn} - q_{rpm})(q_{uq,uqn} - q_{uq})}{\sum_{n=1}^{n}(q_r - q_{uq})^2 \sqrt{\sum(q_{uq,uqm} - q_{uq})^2}}. \qquad (15)$$

According to the humanistic characteristics of human resource management, it is very important to establish a unique cultural management model in the implementation of human resource management in an enterprise. Culture-led enterprises have more team cohesion and market competitiveness and can be more efficient in order to achieve the strategic development goals of the company; the current theoretical research on corporate management proposes a corporate culture management model. This is the most promising corporate management theory so far and the most practical value corporate management model [23].

With the development of the Internet economy, the development of enterprises has become more dependent on talents, and Internet thinking is to study employees and enterprises as a whole. As the basic components of enterprises, employees must play a more important role in the Internet economy effect. Under the Internet thinking, the construction of human resource management mode in enterprises must fully consider the principle of people centeredness. Whether it is in the relationship between all members of the enterprise or the relationship between the enterprise and employees, the management, coordination, and combination of enterprise development can achieve significant results. This is one of the basic principles of the construction of a human-oriented Internet-thinking human resource management model [24].

Incentive theory is the content of enterprise human management theory. In order to effectively stimulate employees' working ability and enthusiasm, good results can be obtained through certain incentives. Incentive theory believes that the implementation of more powerful incentives for employees can promote the efficient realization of corporate goals. However, if the company's incentive level is insufficient, employees' enthusiasm for work cannot be exerted and the efficiency of achieving corporate goals will be low.

Based on the relevant research on corporate human resource management under the domestic background, it can be seen that human resource management, as the core competitiveness of an enterprise, is related to the long-term strategic development of the enterprise under the background of the market economy. In order to enable enterprises to effectively use various resources in the context of the Internet and play an important role in human resource management, enterprises must innovate in human resource

management from two aspects of technology and management, so that they can better conform to the development trend of the times, make enterprise management truly organically integrate with the Internet background, and meet the various needs of enterprise development in the new era [25].

According to the viewpoint of the resource school, if the Internet is only used as technology and cannot spontaneously produce an effect, it must be transformed into a competitive advantage through a series of organizational management methods combined with changes in thinking. On the organizational level, the implementation of electronic human resource management as a process of management innovation may conflict with existing stakeholders. Since the human resource department is the main promoter of electronic human resource management innovation, its influence on the organization is crucial, that is, whether it can obtain the support of executives and parallel departments through its own influence.

3. Innovative Experiment of Human Resource Information Management System Construction

3.1. Experimental Purpose.
This article makes full use of the research results in the field of human resource allocation under the Internet + still intelligence and takes the realization of the company's sustainable development as the starting point. Through in-depth research on the company's human resource allocation status and existing problems, it builds a system for the optimization of the company's human resource allocation, and it puts forward feasibility and scientific opinions on advancing the optimization of human resource allocation, so as to help enterprises build a more competitive human resource system and promote the improvement of their market competitive position.

3.2. Establish a Model Evaluation Index System.
Some conclusions can be drawn from the actual observation of the objects. Generally speaking, the system of an evaluation index includes three levels of evaluation indicators: it is the relationship between gradual decomposition and improvement. Among them, the first-level evaluation indicators and the second-level evaluation indicators are relatively abstract and cannot be used as a direct basis for the evaluation. The third-level evaluation indicators must be specific, measurable, and behavioral and can be used as a direct basis for assessing the teaching.

Comprehensive quantitative and qualitative analysis methods: quantitative analysis is to analyze the data of the problem, using the intuition and clear essence of mathematics to reflect the existence of the problem; qualitative analysis is to collect, read, and organize relevant domestic and foreign research literature and systematically summarize the related theoretical results. The evaluation criteria of green supply chain performance are complex and diverse, including not only financial standards but also other nonfinancial standards. Some standards cannot be directly analyzed by quantitative methods but can only be evaluated by qualitative analysis methods. The green supply system performance evaluation standard system of the company is constructed using a model that combines quantitative and qualitative analysis methods. At the same time, it provides formulas for standard calculations and evaluation standards.

3.3. Determine the Reevaluation Weight.
The index weight is a numerical index indicating the importance and function of the index. In the indicator system of the evaluation plan, the weight of each indicator is different. Even if the indicator level is the same, the weight is different. Index weight is also called weight and is usually represented by a. It is a number greater than zero but less than 1, and the sum of the weights of all the first-level indicators must be equal to 1; that is, satisfy conditions $0 < a < 1$ and $\sum a - 1$.

3.4. Statistics.
All data analysis in this paper uses SPSS19.0, statistical test uses double-sided test, the significance is defined as 0.05, and $p < 0.05$ is considered significant. The statistical results are displayed as mean ± standard deviation ($x \pm \text{SD}$). When the test data complies with the normal distribution, the double T-test is used for comparison within the group, and the independent sample T-test is used for comparison between the groups. If the regular distribution is insufficient, two independent samples and two related samples will be used for inspection.

4. Innovative Experiment Analysis of Human Resource Information Management System Construction

4.1. Status of the Company.
We have selected five companies to investigate the current status of their employees. We have selected the companies to be an information technology company in the city. Such companies are highly sensitive to staffing and their staffing is more reasonable. We survey employees and human resource systems and classify them by age, gender, and so on. The specific data are shown in Table 1.

It can be seen from Figure 1 that, in these five companies, the age and gender distribution of employees are not very different, and the main employees are between 18 and 35 years old. This is because people in this age group are generally receiving information quickly. The stage of strong learning ability is the main type of recruitment for information technology enterprises. The company's male-female ratio is generally around 6.5 : 3.5, and the fourth company's male-female ratio is 5 : 5. At the management level, the gap between age and gender is larger than that between employees. The specific data are shown in Table 2.

From Figure 2, we can see that, at the company's management level, the age is generally over 35 years, accounting for more than 60%. This is because leaders generally have more requirements, and they have high requirements for people's skills and need people to constantly accumulate. In terms of gender, the leadership of these companies is mostly men, accounting for more than

TABLE 1: Distribution of employees.

	The first company	The second company	The third company	The fourth company	The fifth company
18–28	27	33	38	29	31
29–35	25	27	36	24	34
36–48	33	22	29	17	31
49–60	19	17	13	16	17
Male	75	66	72	49	69
Female	40	45	38	47	42
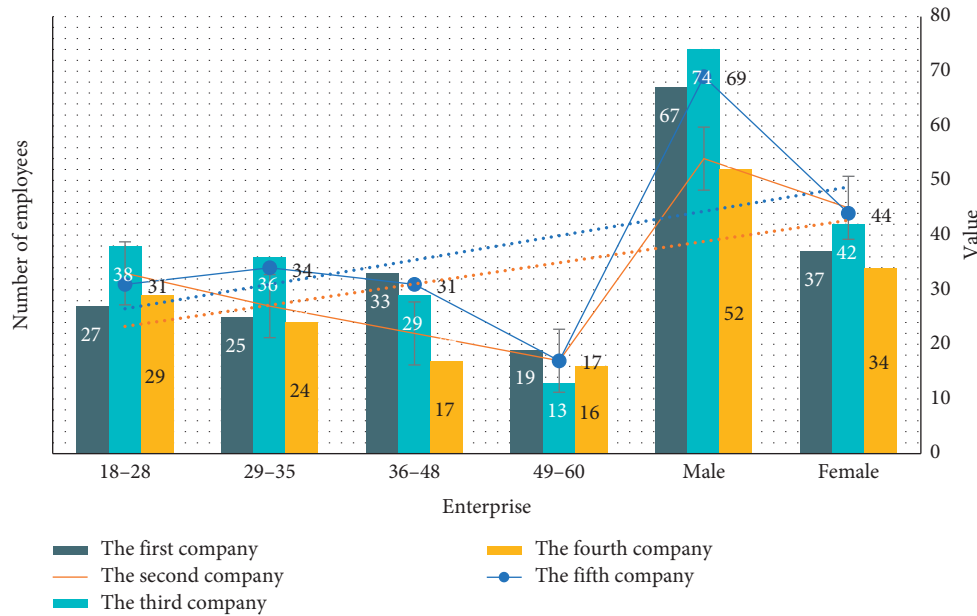
FIGURE 1: Distribution of employees in different companies.

TABLE 2: Distribution of leadership.

	The first company	The second company	The third company	The fourth company	The fifth company
18–28	2	2	4	6	3
29–35	3	11	6	7	14
36–48	5	17	15	9	12
49–60	7	9	18	19	11
Male	12	27	19	31	29
Female	5	12	14	7	11

65%, and the proportion of women is smaller than that of men.

4.2. Company Employees. Educational background is our most intuitive manifestation of personal abilities. Before we truly recognize a person, we can only judge a person's abilities based on some external factors, such as human resources. Therefore, we have made relevant statistics on the academic qualifications of the employees and leaders of these five plus companies. The specific data are shown in Table 3.

It can be seen from Figure 3 that, in enterprises, the educational background of employees is uneven, and so is the ability of employees. In statistics, we can clearly see that the employees with a college degree or below account for

about 30%. The college degree is about 50%, and the college degree is only less than 20%. This is because the company we selected is of an information technology type. Generally, there are academic requirements for recruitment, which also requires us to do well in the human resources of our employees. Optimization: at the management level, the requirements for academic qualifications are more important. The academic qualifications of business leaders are basically university or higher, as shown in Table 4.

From Figure 4, we can see that, at the management level of the company, the average education level is much higher than that of the employees. There are basically no graduates below high school. Most of them have a college degree or above, accounting for more than 70%. The master's degree is about 20%, far higher than the average employee.
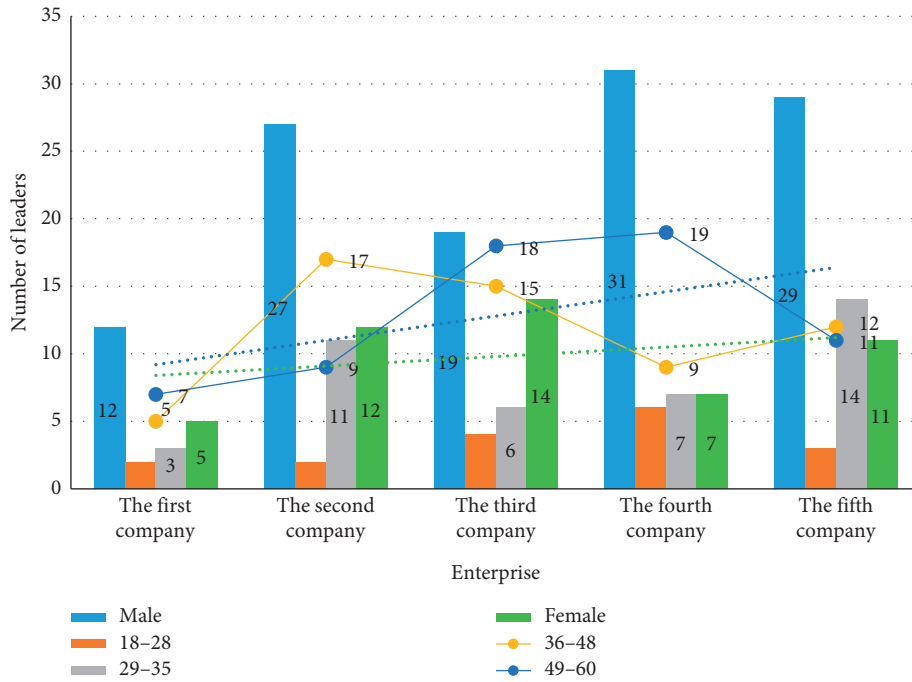
Figure 2: Distribution of employees in different companies.

Table 3: Employee education.

	The first company	The second company	The third company	The fourth company	The fifth company
Primary school	5	4	2	7	6
Junior high school	17	13	9	4	12
High school	24	19	13	20	17
University	33	29	45	47	55
Master's degree	24	17	19	11	9
Doctoral degree	8	6	15	13	9
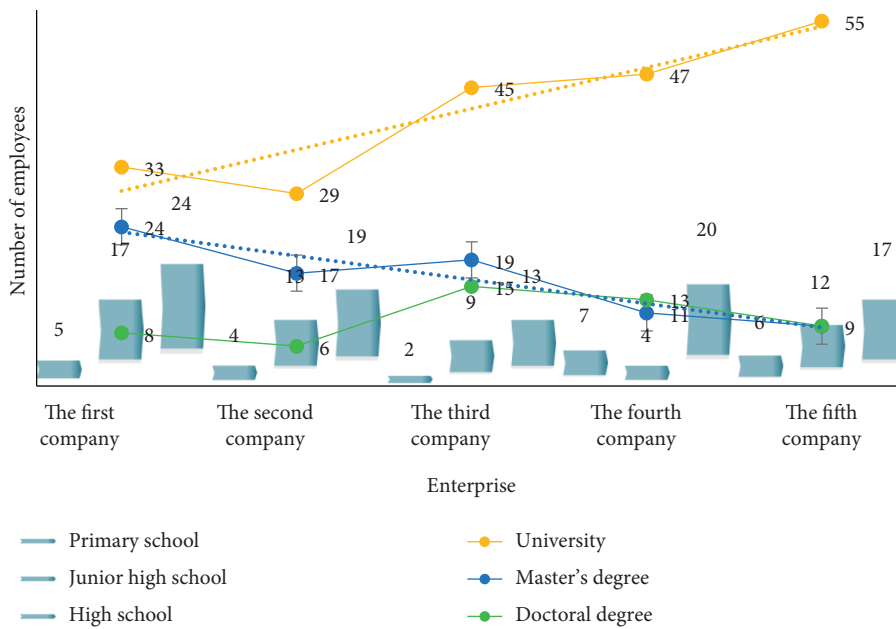
Figure 3: Distribution of employees' academic qualifications.

TABLE 4: Distribution of leadership qualifications.

	The first company	The second company	The third company	The fourth company	The fifth company
Primary school	1	3	0	2	1
Junior high school	4	2	2	1	2
High school	4	5	7	3	1
University	12	11	9	16	12
Master's degree	9	13	17	13	15
Doctoral degree	7	8	5	8	7
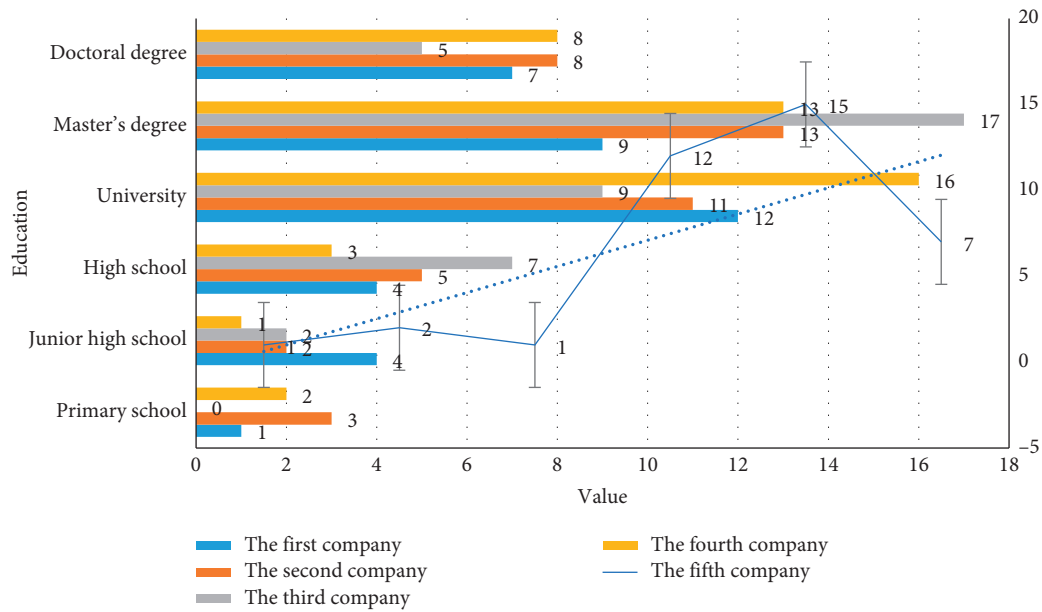
FIGURE 4: Distribution of employees' academic qualifications.

TABLE 5: Evaluation parameters.

	Employee satisfaction	Employee motivation	Redundant staff	Person-post matching	Employee benefits	Business efficiency
The first company	0.412	0.384	2.3	0.419	0.433	0.412
The second company	0.499	0.421	3.7	0.443	0.497	0.424
The third company	0.506	0.472	3.8	0.512	0.476	0.533
The fourth company	0.551	0.591	3.6	0.51	0.494	0.513
The fifth company	0.457	0.462	2.6	0.622	0.619	0.577

4.3. Operational Efficiency of the Enterprise. The purpose of optimizing the allocation of human resources is to improve the operating efficiency of the enterprise, so that employees can reach a reasonable state in the production, transportation, and profitability stages of the enterprise, so that the enterprise can be profitable and promote the development and growth of the enterprise. Therefore, we digitize the parameter utilization models of these five companies in daily production and life to make it more obvious. The details are shown in Table 5.

It can be seen from Figure 5 that, during the operation of the enterprise, the employee satisfaction and employee efficiency of these companies are around the passing line, which shows that the enterprise has not made the best use

of the staff in the employment of employees. Giving full play to the enthusiasm of employees does not improve the operating efficiency of the company. After the test, the average score is about 0.5, and the redundancy rate of the company is about 4%. We also made statistics on management, as shown in Figure 6.

We can see from Figure 6 that, in the leadership, satisfaction and enthusiasm have increased, with an average value of about 0.6, exceeding 0.5 of employees, and it is about to reach a good line. This is because the company's emphasis on leadership makes it more powerful than ordinary employees. But at the leadership level, the redundancy rate has also reached about 3.5%. This shows that the company's human resource allocation to the leadership still needs to be strengthened.
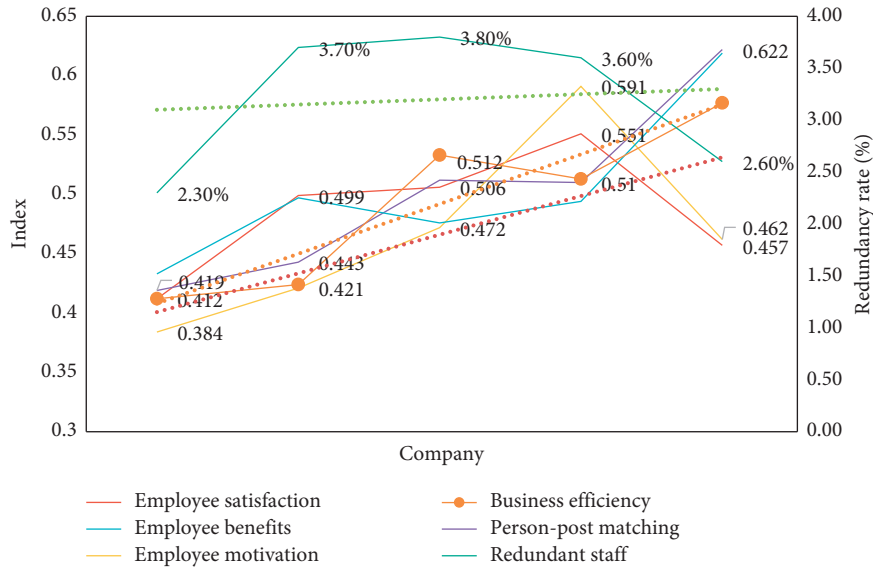
FIGURE 5: Distribution of employees' academic qualifications.
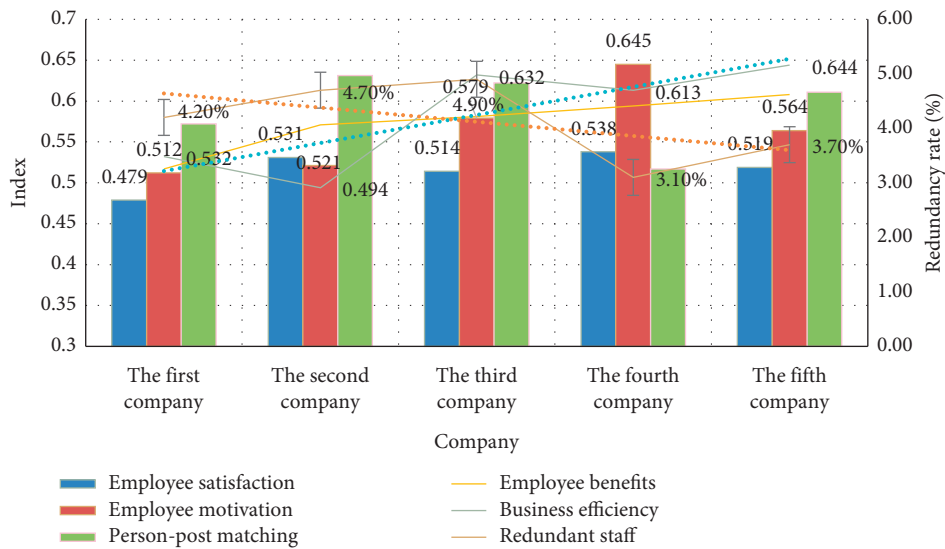
FIGURE 6: Distribution of leadership operating efficiency.

TABLE 6: Comparison after optimized allocation of human resources.

	Employee satisfaction	Employee motivation	Redundant staff (%)	Person-post matching	Employee benefits	Business efficiency
Original configuration	0.432	0.392	2.7	0.493	0.514	0.521
Configuration after optimization	0.723	0.696	1.2	0.784	0.813	0.797
The optimal value	0.837	0.826	0.46	0.872	0.843	0.856

4.4. Comparison after the Introduction of Internet + Artificial Intelligence. Through the model we made, we input the enterprise's human resource configuration parameters to obtain the human resource configuration adjusted by "Internet + artificial intelligence." By comparing the differences between the two, we can obtain human resources

based on "Internet + artificial intelligence" analysis to optimize the configuration effect, as shown in Table 6.

From Figure 7, we can see that, after the optimization of the human resource management information system by the Internet + artificial intelligence, the company's various parameters have been qualitatively improved, which is very
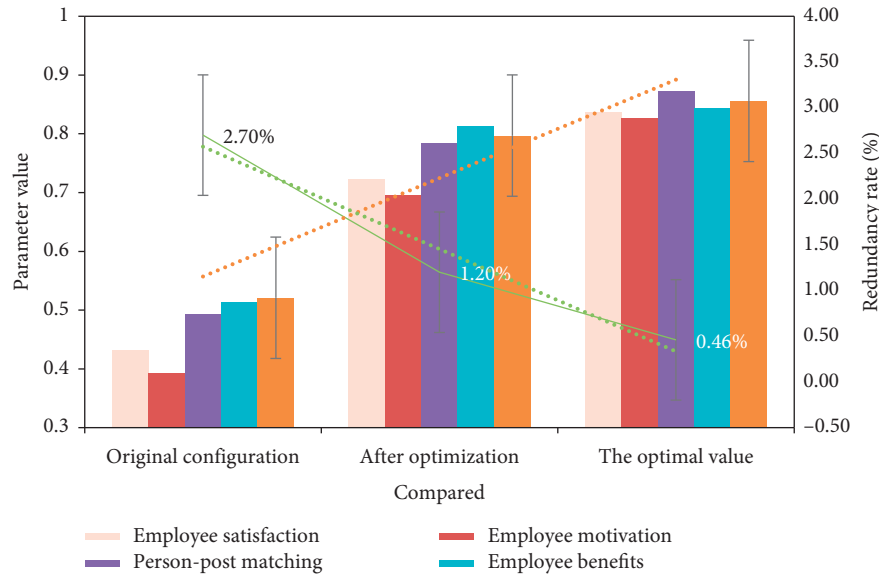
FIGURE 7: Changes in enterprise parameters.

close to the optimal value, and the operational efficiency and employee satisfaction have been improved. Both exceed 50%, and the redundancy rate of enterprises has dropped by more than 40%. This shows that the Internet + artificial intelligence plays an extremely important role in the optimization of enterprise human resource information systems.

5. Conclusions

With the continuous improvement of my country's information technology level, its application in human resource management has also been continuously developed. The human resource management information system can reduce the level and time of information transmission and can also free human resource personnel from trivial administrative affairs, transform into the role of management to provide decision-making support and solutions, and change the service mode of the human resources department.

Internet thinking is characterized by no boundaries, organizational forms are becoming more and more virtualized, and employees' adhesion to the organization is decreasing. Flexible work and remote work have become normal work methods. Enterprises need to break the original relationship of power and responsibility and establish a new type of cooperative relationship with employees. Electronic human resource management is different from the previous human resource management model. It breaks through the limitations of one-way information communication in the past and pays more attention to the multichannel communication of information within the enterprise.

In the research system of modern enterprise management mode, with the improvement of related theoretical research, after two management mode leaps, it is facing the outstanding demand of the third management mode leap. From traditional experience management to scientific management and then from scientific management to human-based management, every leap has brought about a

huge change in enterprise human resource management, and the human resource management needs of enterprises under the background of the Internet have undergone tremendous changes and the trend of management model development towards cultural management has become increasingly prominent. This is an important reform direction of corporate management in the new century. The necessity of corporate management and cultural management under the Internet background has become more prominent.

Data Availability

No data were used to support this study.

Conflicts of Interest

The authors declare that they have no conflicts of interest.

Acknowledgments

References

[1] E. C. Navarro, "Human resource information management system," *International Journal of Science and Research (IJSR)*, vol. 8, no. 6, pp. 1826–1830, 2019.

[2] H. BaniMelhem, H. M. A. Elanain, and M. Hussain, "Impact of human resource management practices on employees' turnover intention in United Arab Emirates (UAE) health care services," *International Journal of Information Systems in the Service Sector*, vol. 10, no. 4, pp. 21–41, 2018.

[3] H. Ai, S. An, and J. Zhou, "A new perspective of enterprise human resource management," *Human Resource Management and Service*, vol. 1, no. 1, pp. 1–7, 2019.

[4] J. Seo, "Board effectiveness and CEO pay: board information processing capacity, monitoring complexity, and CEO pay-for-performance sensitivity," *Human Resource Management*, vol. 56, no. 3, pp. 373–388, 2017.

[5] M. J. Belizon, M. J. Morley, and P. Gunnigle, "Modes of integration of human resource management practices in multinationals," *Personnel Review*, vol. 45, no. 3, pp. 539–556, 2017.

[6] X. Liu and X. Yue, "Design and implementation of hospital human resource information management system," *Automation and Instrumentation*, vol. 1, pp. 117-118, 2016.

[7] H. Leijun, "Talking about hospital human resource information management," *Human Resource Management*, vol. 116, no. 5, pp. 224-225, 2016.

[8] T. Lu, J. Wang, and L. Cheng, "Thoughts on the basic work of enterprise human resource information management," *Science and Information Technology*, vol. 1, no. 14, pp. 135-136, 2017.

[9] Q. Ning, "Design and analysis of BS institution personnel file information management platform (human resource information management platform)," *Human Resource Management*, vol. 7, no. 129, pp. 361-362, 2017.

[10] Y. Zhang, "Research on human resource information management system based on collaborative filtering algorithm," *Electronic Design Engineering*, vol. 25, no. 3, pp. 23–27, 2017.

[11] H. Guo, "Analysis and design of human resources information management system for natural gas enterprises," *China New Telecommunications*, vol. 21, no. 4, pp. 104-105, 2019.

[12] C. Wang, "Challenges and countermeasures of intelligent human resource information management in the era of big data," *Management Observation*, vol. 720, no. 13, pp. 83-84, 2019.

[13] T. Zhang, H. Zhu, and Y. Qian, "The practice of human resource information management system based on PDCA model promotes hospital fine management," *China Health Industry*, vol. 16, no. 7, pp. 89–91, 2019.

[14] X. Yang, "The main problems and countermeasures in the informatization of human resource management in Chinese enterprises," *China New Telecommunications*, vol. 18, no. 4, pp. 40-41, 2016.

[15] J. Ma and C. Xu, "Research on the application of enterprise human resource management informatization," *Management and Technology of Small and Medium-Sized Enterprises (Mid-term Journal)*, vol. 500, no. 4, pp. 99-100, 2017.

[16] C. Jiang, "Discussion on the informatization construction and innovation of enterprise human resource management," *Modern Marketing (Business Edition)*, vol. 308, no. 8, pp. 15–17, 2018.

[17] B. Liu, Q. Chu, H. Song et al., "Research on the application of human resource management information system construction in surveying and mapping institutions," *Surveying and Spatial Information Technology*, vol. 39, no. 202, pp. 232–234, 2016.

[18] J. Pan, "Research on the information construction of human resource management in public institutions," *Human Resource Management*, vol. 11, no. 134, pp. 428-429, 2017.

[19] S. Zhou, "A brief talk on human resource management informationization," *Science and Information Technology*, vol. 14, pp. 148-149, 2017.

[20] J. Jiang, "Practical exploration on the informationization of human resource management," *Human Resource Development*, vol. 317, no. 2, pp. 98-99, 2016.

[21] X. Guo, "Research on the informatization construction of human resource management in modern enterprises." *Management and Technology of Small and Medium-Sized Enterprises (Mid-term Journal)*, vol. 12, no. 524, pp. 10-11, 2017.

[22] T. Liu, "Human resource management based on internet mode—informatization construction of human resource management in public institutions," *Global Market Information Herald*, vol. 38, no. 165, p. 77, 2017.

[23] L. Pan, "Talking about the informatization of hospital human resource management," *Medical Information*, vol. 29, no. 17, pp. 1–3, 2016.

[24] G. Wu, "Talking about the information construction of human resource management in the era of big data," *Human Resource Management*, vol. 38, no. 448, pp. 13-14, 2016.

[25] Q. Yin, "Discussion on the informatization construction of enterprise human resource management," *Journal of Science Education (Late)*, vol. 8, no. 176, pp. 161-162, 2017.

Research Article

Guangzhou Digital City Landscape Planning Based on Spatial Information from the Perspective of Smart City

Weijun Yang,[1] Xiaohuan Xi [ID],[2] Liang Guo,[1] Zhaoxia Chen,[1] and Yong Ma[2]

[1]*Guangzhou Urban Planning & Design Survey Research Institute, Guangzhou 440100, China*
[2]*Key Laboratory of Digital Earth, Aerospace Information Research Institute, Chinese Academy of Sciences, Beijing 100094, China*

Correspondence should be addressed to Xiaohuan Xi; xixh@radi.ac.cn

With the development of society and the improvement of urban economic level, people are no longer satisfied with the simple material and functional requirements of the city; thus, the spiritual requirements of city beauty, environmental quality, place atmosphere, and so on need to be improved. Based on the above background, the purpose of this paper is to analyze the landscape planning of Guangzhou's digital city based on spatial information from the perspective of smart cities. Based on the relevant theoretical research, this paper combs the ideas of intelligent urban road landscape design. This paper analyzes the concept of urban road and smart road and puts forward the definition and characteristics of intelligent urban road landscape; according to the research on the development status of urban road and the connotation of smart city, combined with the concept and principle of urban road landscape design, it summarizes the design method of smart city road landscape. This paper, taking the innovative design of urban landscape as the research object and using the research methods of literature analysis and field investigation, innovatively combines the urban landscape design with digital information technology, changes the traditional landscape design ideas, constructs the urban landscape innovative design model, realizes the personalization of the urban landscape design, as well as the intelligent, digital, diversified, and humanized service and function. The experimental results show that nearly 60% of people are satisfied with the Guangzhou digital urban landscape planning based on spatial information in the smart city perspective.

1. Introduction

Since the 1990s, with the continuous development of information technology and the rapid development of communication systems, the network is widely used in the world, the process of urban informatization is accelerating, and people's lifestyle has undergone great changes. The rapid development of information technology provides opportunities for the change and upgrading of urban industrial structures and the change of social development, reflecting the concept of "intelligent city." In the city, the scenery is positive, which can reflect the city's preferences and development. In the process of forming the urban development mode, we should not only consider the land planning and layout of urban development, but also consider the significance of the corresponding landscape technology. Only urban development can have a higher

level of implementation example, which is also our new challenge to our work. Particularly, in the twenty-first century, China's urban construction is gradually shifting to the improvement of the characteristics and quality of the city as the center, focusing on the speed of urban construction, economic growth rate, urban development scale, and emphasizing the improvement of urban characteristics and image.

Due to the importance of smart city research, many research teams began to study smart city and achieved good results. Centenaro et al. introduced the most advanced communication technologies and smart-based applications used in the smart city environment and explained the big data that supports smart cities by focusing on the method of big data fundamentally changing the population at different levels of the city analysis of the prospects. On this basis, the business model of future smart city big data is proposed, and

the topic of business and technology research is pointed out [1]. Menouar et al. study the semantic annotation of cloud sensors and connect the cloud with the Internet of things to realize and consider innovative services. By defining the cloud of things (CoT) paradigm, things like semantics are considered to perform the aggregation of heterogeneous resources. They investigated the smart city vision, provided the main required information, and highlighted the benefits of integrating different IOT ecosystems into the cloud under the new CoT vision [2]. Chapman et al. study the security and privacy of smart city applications. Specifically, they first introduced promising smart city applications and architectures [3].

At present, urban agglomeration is one of the main strategies of global urbanization. However, it is not clear how the density of the city is related to the process of the surrounding landscape. Vasiljevi et al. aim to emphasize the potential of the landscape around the city as a complementary provider of urban ecosystem services in the context of reduced urban green space density. They believe that people's perception of the suburbs will change from the definition of a specific population density and geographical distance between urban and rural areas to a landscape defined by its function [4]. To improve the efficiency of urban landscape planning and design, Zhang proposed and developed a virtual landscape-based urban landscape planning system combined with the current computer development technology. Therefore, this paper introduces the computer virtual technology, especially the key technology of virtual simulation, and then designs the urban landscape planning based on virtual simulation of the system function, overall simulation platform, and specific design, and finally gives a development example of urban roaming three-dimensional planning system [5]. With the continuous improvement of people's happiness index, people's demand for tourism life has also changed. They pay increasing attention to urban landscape planning. Therefore, urban landscape has become an important factor affecting the development of urban tourism economy. Choi mainly writes on the interactive relationship between urban landscape planning and urban tourism economic development, then analyzes the positive role of Bali urban landscape planning on urban tourism economic development in the form of a case, and finally puts forward suggestions for further improving the urban landscape planning and promoting the development of urban tourism economy [6].

Based on the background of the rise of digital media art brought about by the development of smart cities, this article systematically analyzes and compares the landscape innovation design research of Guangzhou and the outstanding cases of urban smart city landscapes at home and abroad, taking Guangzhou as an example to apply smart city art to landscape innovation design research.

2. Smart City and Urban Landscape

2.1. Connotation of Urban Landscape

2.1.1. Aesthetic Connotation of Urban Landscape. With the continuous development and progress of the times, people's quality of life is getting higher and higher. From the pursuit of material life to the pursuit of aesthetic cultivation, art, aesthetics, and spiritual world, people's goal pursuit has gradually changed [7, 8]. The urban landscape design in the new era should change from single aesthetics to diversified artistic aesthetics. In the process of urban landscape construction, to prevent the balanced popularization of urban landscape, we should pay attention to reflecting the city's personality and cultural characteristics. With the development of the times, people began to be interested in the cultivation of beauty, began to appreciate and create beauty gradually, and worked hard to improve their own aesthetic ability [9]. In the modern urban landscape design, we should not only pay attention to the coordination of urban characteristics and cultural history, but also pay attention to the integration of new gardening materials and modern science and technology and combine all relevant factors to build and meet the architectural beauty conforming to the urban culture and history.

2.1.2. Residential Connotation of Urban Landscape. As the human habitat of the city, the urban landscape not only plays a role of beauty, but also is a space for humans to experience life. We should pay attention to the spiritual construction of the place [10]. The construction and design of urban landscape is the result of human adaptation, deformation, and natural creation. Human beings living in cities are actually the process of interaction and harmonious coexistence between human beings and nature.

2.1.3. Systematic Connotation of Urban Landscape. As a whole system, the urban environment is mainly divided into three levels, namely, the main system, all levels of subsystems, and system elements [11, 12]. In the complex open and integrated urban landscape system, the urban landscape system can be divided into physical type and spatial type, which can be subdivided into buildings, structures, landscape devices, plants, urban squares, urban parks and green spaces, city street, urban coastal space, and other factors [13].

2.1.4. Symbolic Connotation of Urban Landscape. As the image symbol of the city and the carrier of human culture and spirit, urban landscape can be divided into cultural symbols, historical symbol, and public emotion symbols through the differences of language, mode, shape, structure, and urban construction materials [14]. The development of digital media art clearly expresses the city information and unique city culture with image accuracy and simplicity, which plays an important role in the process of urban development.

2.1.5. The Connotation of Information Transmission of Urban Landscape. The traditional urban landscape connotation means the connotation of beauty, habitat, system, and landmarks [14]. The development of digital information technology and media art has accelerated the process of urban information transmission and feedback. Landscape is

the habitat of human life, and information transmission is necessary. The significance of urban landscape information transmission is unified, which affects the aesthetic meaning of urban landscape and the connotation of habitat, system connotation, and symbol connotations.

2.2. Functions of Urban Landscape

2.2.1. Communication Culture.
Every city has its own cultural characteristics, which is the accumulation of material and spiritual wealth created by human beings in the long-term working life. That is the social phenomena and traditional customs and lifestyle of people in the city [15, 16], i.e., the sum of habits, regional habits, literature and art, ways of thinking, norms of action, and values. The human environment of the city is the spiritual needs and emotional life of the citizens. The cultural design of the city is mixed with the urban landscape design. The most common factor is to extract and use them from cultural, historical, ethnic, religious, and other factors [17]. Therefore, in the process of urban landscape architecture, designers should actively understand the history and culture of the city and apply these cultural elements to the design. The landscape with cultural importance is the same as the name card of the city. It shows the cultural ideal and spiritual pursuit of the urban residents [18]. For smart cities, the first thing to do is to reduce noise, which can be processed using the following functions:

$$F(u) = \int |Du|dxdy + \frac{1}{2}\lambda \|u - u_0\|^2. \tag{1}$$

The corresponding equation is

$$-div\left(\frac{\nabla u}{|\nabla u|}\right) - \lambda(u_0 - u) = 0. \tag{2}$$

The denoising problem can be transformed into the optimization problem of the function; let the error function be

$$E(x, y) = div\left(\frac{\nabla u}{|\nabla u|}\right) - \lambda(u - u_0). \tag{3}$$

It is assumed here that the final output is an ideal noise-free image, which is

$$u(x, y) = N(u_0(x, y), w), \tag{4}$$

where $u(x, y)$ is the noise image and w is the connection weight.

If you want to significantly improve the effect of planning image processing, you can use the mixed variational functional model of forward and backward diffusion:

$$\min_{u \in BV} E(u) = a \int \frac{1}{p}|\nabla u|^p dx + (1 - a) \int \frac{1}{q}|\nabla u|^q dx$$

$$+ \frac{\lambda}{2} \int |u - f|^2 dx. \tag{5}$$

The entire network model can be written as

$$N(x, y) = \sum_{k=1}^{n} w_k \exp\left(-\frac{\|V_0(x, y) - c_k\|}{2\sigma_k^2}\right). \tag{6}$$

The weight adjustment is as follows:

$$\Delta w_k = \sum_{x,y} \frac{\partial E(x, y)}{\partial w_k},$$

$$\Delta c_k = \sum_{x,y} \frac{\partial E(x, y)}{\partial c_k}. \tag{7}$$

2.2.2. Economic Development.
As an important part of modern urban construction, urban landscape design not only meets the aesthetic requirements of urban residents and the beautification function of the urban ecological environment, but also promotes the development of urban economy [19, 20]. In the promotion of urban economy, the role of urban landscape is reflected in the direct or indirect promotion of economic growth. First of all, in the direct preferential aspect, to meet the needs of urban landscape and residents, the traditional landscape economic growth point of urban landscape planning and design industrial chain is actively developed in the urban landscape construction, to a certain extent, promoting the urban economic development. Scientific urban landscape construction can achieve the purpose of saving water, land, and financial expenditure from the perspective of indirect benefits [21]. Through the construction of landscaping, a lot of resources can be saved and the environment can be improved. Urban landscape design will have a positive impact on urban economic development.

In the process of implementing a smart city, an optical model is needed to illustrate how the three-dimensional discrete data field generates, reflects blocks, and scatters light. Therefore, the reasonable selection of the optical model is an important factor in the planning effect.

$$\frac{\Delta I}{I} = \frac{\rho * E * \Delta s * \beta}{E} = \rho * \Delta s * \beta. \tag{8}$$

When Δs approaches 0,

$$\frac{dI}{ds} = -\rho(s) * \beta * I(s) = -\kappa(s) * I(s). \tag{9}$$

As the model's lighting conditions changes, the image will also change with the discovery

$$I(s) = I_0 \exp\left(-\int_0^s \kappa(t)dt\right),$$

$$t(s) = \exp\left(-\int_0^s \kappa(t)dt\right). \tag{10}$$

From this, we can see that

$$\partial = 1 - t(s) = 1 - \exp\left(-\int_0^s \kappa(t)dt\right). \tag{11}$$

When Δs approaches zero, use the following differential equation to illustrate the change of light intensity:

$$\frac{dI}{ds} = T(s) * \rho(s) * A = T(s) * \kappa(s),$$

$$I(s) = I_0 + \int_0^s g(t)dt. \tag{12}$$

2.2.3. Ecological Protection.
The concept of sustainable urban development is put forward, and the ecological concept is injected into modern urban construction. Ecological concept is widely used in landscape design, and sustainable ecological design has gradually become the development trend of urban landscape design [22, 23]. The design under the ecological concept is related to the harmony between human and nature and the sustainable development of human beings. The ecological concept should be applied to the innovative design of urban landscapes such as "Wetland Park," "noncourtyard," and "sponge city." This kind of ecological, green, and sustainable urban landscape and urban planning and design actively promote the ecological protection and sustainable development of the city to a certain extent. The use of cutting-edge science and technology and green building materials reduces cutting and environmental pollution technology and ecological integration, so that the urban landscape and the natural environment coexist harmoniously [24].

2.3. Smart Urban Road Landscape.
The road environment of smart city is based on big data and integrates the concept of human centered. In the process of development and construction, we should focus on protecting the ecological environment and abiding by the sustainable development policy. The road environment for road traffic is provided according to the road and surrounding environment, i.e., the environmental construction of road landscape, the cultural atmosphere of urban area, and the belt-like landscaping courtyard on the road structure.

The construction of intelligent city road landscaping can reduce energy consumption after road use and integrate various physical forms of road landscaping, buildings, and small objects into modern network technology. Based on the use of natural conditions, it plays a role of warning, guidance, and rest for tourists in travel. Before and on the way to the city destination, tourists can recognize a variety of information services, interact with each other, understand various information in the road section in time, and then adjust the travel plan according to the time.

2.4. Road Landscape Characteristics of Smart City

2.4.1. Situational.
Intelligent city roadblock is a kind of roadblock that conveys the characteristics of urban scenic spots along the way. Landscape engineering, auxiliary facilities, landscaping, plant landscape, and local node regional landscape design are designed to improve the overall regional theme atmosphere. In the design of intelligent city,

roadside park, forests, and flowers can become the main body, which can unify and perfect the beautiful structures of Higgins flower beds and grass, so that tourists will have a specific feeling before they arrive in the city.

2.4.2. Security.
The construction of an intelligent city road should first meet the characteristics of road safety. The construction of an intelligent city roads should be based on road safety, realize the monitoring and comprehensive understanding of all aspects of the road through network and sensor technology, and provide early warning and roadside support.

The most important point of urban road construction is to meet the road safety. In the road landscape design, the road direction should be clearly defined, and the atmosphere created by lighting, plants, and sketches will not affect the driver's normal driving. The construction of urban roads should be based on road safety. Through the application of intelligent control system, all aspects of road monitoring and comprehensive understanding can be realized, and the traffic guidance, intelligent early warning, and emergency structure can be implemented on time.

2.4.3. Ecology.
Smart urban road construction may damage the natural ecology nearby. Therefore, in the process of route selection and design, ecological protection should be fully considered to reduce the damage to biodiversity and protect and implement the original natural resources. To ensure the development of less environmental impact, please use it to form an ecological city road landscape with regional characteristics.

Due to the inherent ecological characteristics of plants, plants play a unique role in ecological protection in road greening. Plants in urban road environment have the effect of sound insulation and noise reduction. The noise generated by vehicle driving will affect the life of residents along the path and endanger physical and mental health. Through the dense food materials and the unique arrangement of plant branches and leaves, the shielding effect of green plants can effectively absorb sound waves and reduce noise. In summer, cover the plants with plastic film, reduce the direct light on the ground, reduce the radiation energy, adjust the temperature, and form a cool mountain breeze through the ventilation of the green corridor. Winter can prevent manna from releasing heat on the ground. Thermal protection can adjust and improve the microclimate of road environment. The suitable ecological plants along the line can reduce the surface temperature, and the plant landscape of urban roads can improve the climate, protect the ground, improve the ground temperature, and prevent aging.

2.4.4. Experiential.
Through the analysis of regional landscape and path selection, the concept of people-centered is followed, so that tourists can enjoy a good natural landscape along the line. In the process of intelligent city road landscape design, to improve the experience and quality of the city, modern information technology is used in auxiliary

facilities and landscape facilities. In the process of information collection, action decision-making, and landscape viewing, tourists can feel the new experience brought by smart urban road landscaping.

The intelligent road can provide better information for tourists to better understand the situation of the city and provide better information for tourists along the road. The application of intelligent control system in the landscape design of urban road is more humanized and convenient, which can increase the engine of urban road construction. From the perspective of urban user experience, each public experience focuses on urban construction methods.

2.4.5. Fusibility.

In urban road construction, the integration of comprehensive identification technology and network technology can realize data storage, calculation, and analysis, and improve the decision-making ability of business departments through the participation of citizens.

The intelligent network information technology is integrated into the urban road, and the information collection and analysis system is established by collecting tourists' information, to fully understand the information of tourist groups, change of requirements, opinions and suggestions, to realize scientific decision-making and scientific management. To increase the investment of information technology in the construction of intelligent city roads, encourage relevant companies to improve the operation status, improve the management level, improve the interaction between tourists and relevant resources and departments, and effectively integrate resources and publicize the development of the whole city area.

3. Urban Landscape Experimental Design

3.1. Experimental Data Collection.

The investigation is divided into two aspects. First, we investigate the site conditions of the project area, that is, basic design elements such as topography and topography, existing plant species, and water resource conditions. Data collection can be horizontally compared and analyzed through onsite survey, measurement and mapping, or detailed vertical analysis based on relevant information obtained by relevant regional departments in Guangzhou, to solve all design factors that may affect mountain ups and downs, river tides, and other factors. Second, investigate local resources such as tree planting and stone materials, and use these materials rationally to create the city's main road scenery with natural characteristics in line with the region.

3.2. Landscape Investigation of Experimental City

3.2.1. Urban Culture Excavation.

To create a characteristic urban landscape, the landscaping design of the main road to the city should explore the urban culture, learn historical city planning in museums, historical planning bureaus, etc., ask for the names of local villages, and refer to historical materials. Learn about regional culture, urban history, architectural sites, urban stories, and urban landscapes, and extract elements from the environment to provide inspiration for the design of major roads in Guangzhou and better reflect the regional culture of Guangzhou.

3.2.2. Line-of-Sight Analysis.

According to the speed of the vehicle and the linear structure of the road, the existing road structure will be subdivided. From the vehicle's point of view, when the line of sight is analyzed at high speed, the line of sight becomes narrower and the visual focus expands with the distance. However, the road landscape design of Guangzhou City can now design an excessively iconic landscape from two aspects of the road and design a large iconic landscape. Detailed scenery, eye-catching scenery, and low-speed driving areas can be designed for plain scenery, but the scenery requirements are simple and clear and do not require much attention. When driving in a straight line, the design of tourist attractions on both sides of the road is relatively simple, and only specific areas are reasonably allocated, while the landscape design for curved driving is more complicated. To avoid a long and exhausting driving experience, to achieve the change of landscaping rhythm and the purpose of safe driving, please design their own close focus in different areas.

3.3. Experimental Landscape Design

3.3.1. Partition Design.

The road environment in Guangzhou is linearly distributed. In this linear space, the factors that affect the design of the landscape area include the surrounding urban land planning, surrounding terrain factors, and road vision analysis. First of all, most land plans in Guangzhou belong to businesses, residences, factories, or schools. In the landscape design of major urban roads, other land should be used. Second, the regional setting of major urban roads in Guangzhou is affected by topographical factors. The impact is clearly that mountains, valleys, rivers, etc., have an important impact on the regional setting. Finally, the line of sight is also essential in the area of setting design. To ensure the safety of the road environment, the connectivity between multiple environments in the linear space is improved.

3.3.2. Road Design.

The park roads and landscape roads in the project area are developed according to the main roads, and the road direction and road classification are determined according to the functional area, terrain, and mass flow. Focus on the connection between low-speed system, road and walking path, minimize the impact on the road on the premise of meeting the walking activities on both sides of the road, and minimize the impact on the surrounding environment under the premise of meeting.

4. Analysis of Landscape Experiment Design of Smart City

4.1. Guangzhou's Transportation Infrastructure.

First of all, the first stage of street landscaping design is to clarify the relationship between traffic. With the development mode of
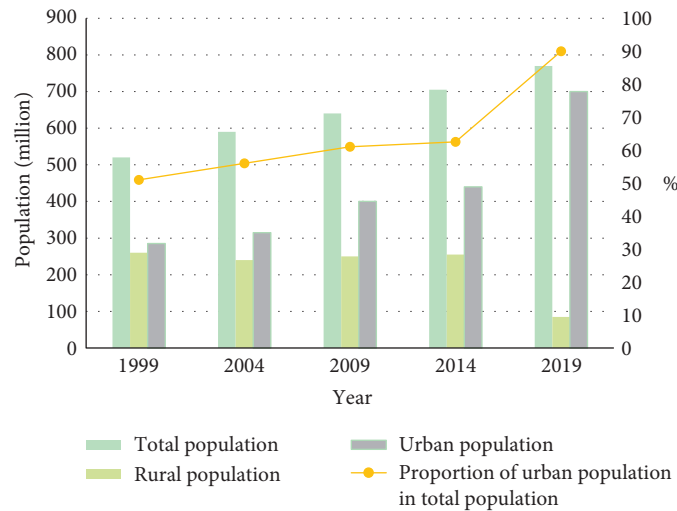
FIGURE 1: Changes in rural population and urban population.

mass transportation and the theory of shared distance transit-oriented development (TOD) model, orders for people, bicycles, mass transit, and personal cars can be considered and communicated. The pedestrian areas on the streets of Guangzhou are generally landscaping infrastructure companies. For example, the association design of Grace street in Barcelona can increase the walking space of the street, strengthen the humanistic treatment, and improve the overall distance quality. In addition, there are a series of auxiliary spaces such as parking lots, space under the bridge and obstacles in the current demonstration road traffic system, but a part of the space can be reused and integrated through landscape design, which is a very popular activity. The distance between space and intelligence is an indispensable part of space. The changes of rural population and urban population in recent years are as shown in Figure 1 and Table 1.

It can be seen from Figure 1 that the proportion of cities in the total population has been increasing, and the urban population has increased by nearly 40% within 20 years. This requires a more scientific and reasonable urban planning layout. We have recently made statistics on the urban and rural floating population in recent years, as shown in Table 2 and Figure 2.

4.2. Guangzhou's Cultural and Recreational Infrastructure. Just as one of the important factors of the road is traffic infrastructure, the leisure infrastructure of street landscape space is also one of the important factors of street landscape. On the road of perfect design without problems in the street, the gorgeous scenes make people look like a vivid ballet. A better example is Copenhagen Super Street. In view of the occurrence of Super Street, the designer uses spiral, square, and linear free leisure space to meet the functional requirements of people. The space is fully utilized and the natural distance is also full of vitality. At the same time, it is necessary to combine the cultural and artistic characteristics of the city to effectively emphasize the distance characteristics and the

excellent characteristics of the space that can realize the cultural and artistic value of urban regeneration. For example, Wangfujing pedestrian street is the symbol of Beijing, and the bronze sculptures with rich ancient features are assigned to pedestrian streets. In the streetscape design, the alteration and integration of public art can enhance the vitality of the street landscape in Guangzhou, increase people's participation, and improve the characteristics and vitality of the street landscape in Guangzhou. The overall planning requirements for cultural and recreational infrastructure are shown in Table 3 and Figure 3.

We have made statistics on the cultural and entertainment situation in Guangzhou, as shown in Table 4 and Figure 4.

4.3. Landscape Design of Greening Plants in Guangzhou. Vegetation greening plays an important role in urban street landscape design. Plants absorb exhaust gas, reduce air pollution, make the space around the street better, absorb noise pollution, and provide more things for people around. In addition, since plant cultivation relies on traffic roads, the distinction of traffic roads can be realized by other plant species. The plant green belt is also a beautiful insulating belt for fire belts and cities. The greening of streets in Guangzhou mainly includes pedestrian road greening, car greening, and public place greening. Generally speaking, plant types that are not vulnerable to pests and fallen leaves should be considered comprehensively based on the local soil moisture and sunlight. For example, the green belt of a pedestrian street is mainly to separate pedestrians from vehicles and combine the architectural styles on both sides of the street to achieve the historical and cultural expression of the street. You can consider choosing characteristic tree species. The landscape design of greening plants is shown in Table 5 and Figure 5.

4.4. Street Landscape in Guangzhou's Smart City. The street landscape design of a smart city needs to follow art and science at the same time. According to the unity of art and

TABLE 1: Demographic changes.

	1999	2004	2009	2014	2019
Total population	517	592	634	700	756
Rural population	265	243	247	248	87
Urban population	287	318	412	431	704
Proportion of urban population in total population	56%	60%	64%	67%	91%

TABLE 2: Urban and rural floating population.

	2015	2016	2017	2018	2019
Urban floating population	3.73	3.85	4.36	4.17	3.88
Rural floating population	4.33	4.53	4.4	4.61	4.74
Proportion of urban mobility	27%	29%	31%	35%	28%
Proportion of rural mobility	55%	59%	61%	67%	69%
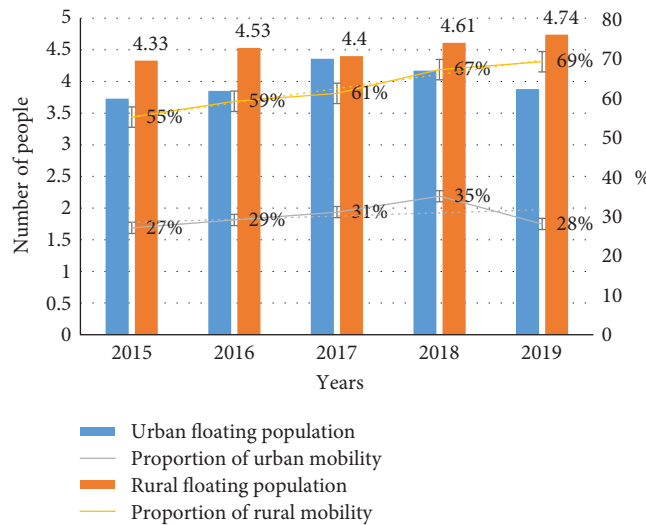
FIGURE 2: Changing trends of the floating population.

TABLE 3: Legend of Jingyuan in the master plan of scenic spots.

Serial number	Scene source type	Text	Graphic size	Graphic color
1		Super Jingyuan (humanities)	The diameter of the outer ring is b	
2		First-class Jingyuan (humanities)	The diameter of the outer ring is 0.9 b	
3	Humanities	Second-level Jingyuan (humanities)	The diameter of the outer ring is 0.8 b	$C = 5\,M = 99$, $Y = 100\,K = 1$
4		Tertiary Jingyuan (humanities)	The diameter of the outer ring is 0.7 b	
5		Fourth-level Jingyuan (humanities)	Diameter is 0.5 b	

science, the scientific principle of plant composition can form the characteristics of plant form, colors, outline, and line of intelligent cities to obtain better natural beauty effect, highly unified. The satisfaction of street landscape design survey is shown in Table 6 and Figure 6.

We compared several parameters of Guangzhou under the smart city and got the data, as shown in Table 7 and Figure 7.

(1) Smart city fully reflects the flexibility of road landscape design in Guangzhou. The plasticity of the street landscape in Guangzhou reflects the hardness of the plant branches. Each plant has different vegetation characteristics. Many plants can be cut immediately after cutting, but some plants cannot grow new plants in a short time. Some plants have strong branches, but some plants are of poor quality. To build a reasonable plant area, Guangzhou mainly planted silver and green trees of various aquatic plants in water-rich areas. (2) It fully reflects the adaptability of the factory to the smart city environment. In the process of Guangzhou landscape construction, considering
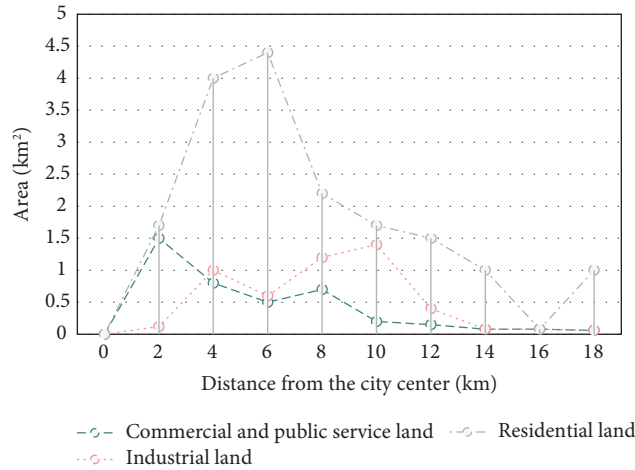
Figure 3: General planning requirements for cultural and recreational infrastructure.

Table 4: Cultural and entertainment venues in Guangzhou.

	Yuexiu district	Haizhu district	Tianhe district	Baiyun district	Huangpu district	Huadu district	Panyu district	Luogang district	Nansha district
Cinema	36	35	39	35	37	35	38	42	33
Stadium	37	40	40	43	39	42	38	39	43
Park	7	13	7	6	5	6	9	11	8
Library	5	7	8	5	13	12	8	8	6
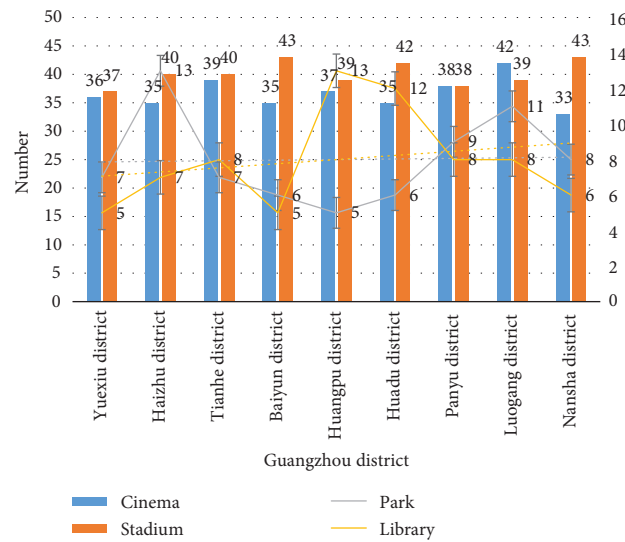
Figure 4: Recreational facilities in various districts of Guangzhou.

Table 5: Greening plant landscape.

	Whole province	Provincial capital	Suburbs
Public lawn	2000	1000	6000
Residential area	800	1600	100
Protective green space	3000	2500	4100
Scenic woodland	1800	1900	2700
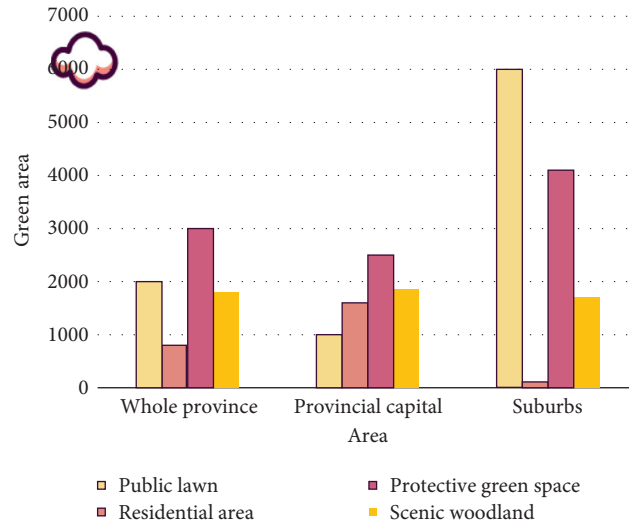
FIGURE 5: Urban greening plant landscape design.

TABLE 6: Resident satisfaction.

	Very satisfied (%)	Not very satisfied (%)	Satisfied (%)	Dissatisfied (%)	Very dissatisfied (%)
Satisfaction	10	31	16	35	8
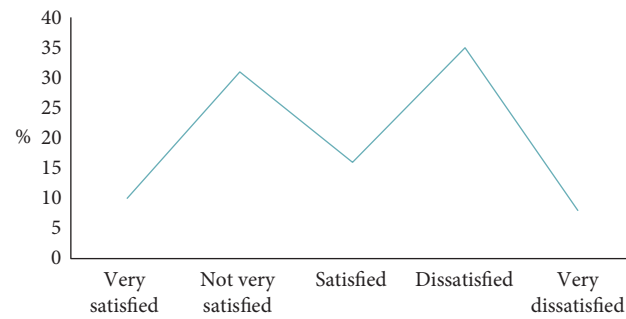
FIGURE 6: Satisfaction of urban street landscape design survey.

TABLE 7: The value of each parameter.

	Greening	Resident satisfaction	Traffic condition	Casual	Landscape
Traditional city	3.01	3.37	3.27	3.92	4.12
Smart city	6.51	6.4	6.88	6.4	6.8
The optimal value	7.78	7.92	7.72	7.5	7.71
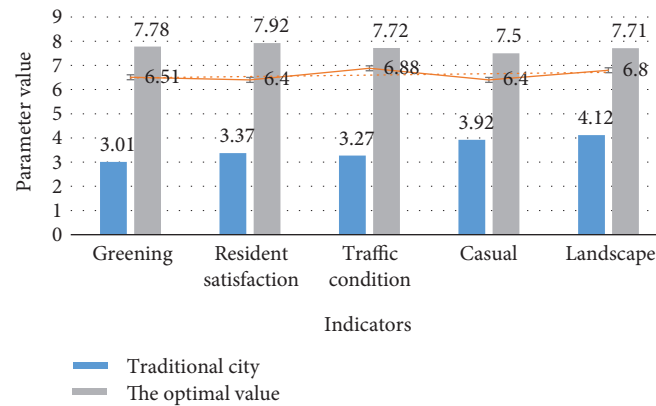
FIGURE 7: Parameters in different city modes.

the interaction between plants and the natural environment, to adapt to the environment, various plants were planted in other places. The main reason that affects the growth environment of plants is water. Affected by sunlight, cities need landscapes such as high altitude, high altitude, and high altitude. (3) It fully reflects the diversity of road landscape in Guangzhou. The shape and appearance of plants have a very diverse aesthetic relationship. There are very diverse choices in the shape and appearance of plants in Guangzhou.

5. Conclusions

With the development of science and information technology, an intelligent city has appeared. In the construction of intelligent cities, distance landscaping design needs a scientific combination of planning, information technology, aesthetics, horticulture, botany, action psychology, and spatial geography. This paper combines the actual situation of distance landscaping design in the development of smart cities, applies distance landscaping design in the smart city planning of Guangzhou, and actively encourages smart city development. In the smart city planning of Guangzhou, the emergence of smart cities is not only an effective means of urban planning, but also a prerequisite for urban development.

This thesis focuses on the development of domestic and international urban landscapes, main theoretical research, domestic and foreign case studies, and summarizes the traditional urban landscape framework, urban landscape components, general methods of landscape planning and design, and existing shortcomings. Based on this, a point (mark, node) + line (path, boundary) + surface (region) of the Guangzhou city landscape style framework is proposed, and the historical context and natural elements are extracted according to the thinking and interrelationship of the elements.

This article concludes that there are two main problems with my country's gardening plan. One is the planning method, and the other is the design environment system. This article focuses on the improvement of planning methods and epoch-making content, looking for control rules for breakthroughs in the connection planning system, but the landscape plan can be linked to the entire plan, the regional plan, and the detailed plan. However, this is limited to the author's business ability, technical ability, and research time, which provides a reference for future research, which is also the main direction of future research.

Data Availability

The data that support the findings of this study are available from the corresponding author upon reasonable request.

Conflicts of Interest

The authors declare that they have no conflicts of interest regarding the publication of this research article.

References

[1] M. Centenaro, L. Vangelista, A. Zanella, and M. Zorzi, "Long-range communications in unlicensed bands: the rising stars in the IoT and smart city scenarios," *IEEE Wireless Communications*, vol. 23, no. 5, pp. 60–67, 2016.

[2] H. Menouar, I. Guvenc, K. Akkaya, A. S. Uluagac, A. Kadri, and A. Tuncer, "UAV-enabled intelligent transportation systems for the smart city: applications and challenges," *IEEE Communications Magazine*, vol. 55, no. 3, pp. 22–28, 2017.

[3] L. Chapman, C. L. Muller, D. T. Young et al., "The birmingham urban climate laboratory: an open meteorological test bed and challenges of the smart city," *Bulletin of the American Meteorological Society*, vol. 96, no. 9, pp. 197–210, 2015.

[4] N. Vasiljevi, B. Radi, S. Gavrilovi et al., "The concept of green infrastructure and urban landscape planning: a challenge for urban forestry planning in Belgrade, Serbia," *Forest-Biogeosciences and Forestry*, vol. 11, no. 4, pp. 491–498, 2018.

[5] D. Zhang, Q. Huang, C. He et al., "Planning urban landscape to maintain key ecosystem services in a rapidly urbanizing area: a scenario analysis in the Beijing-Tianjin-Hebei urban agglomeration, China," *Ecological Indicators*, vol. 96, pp. 559–571, 2018.

[6] D. Choi, "A study on the architectural space planning based on the concept of the urban landscape-Suncheon art platform," *Journal of Engineering and Applied Ences*, vol. 13, no. 22, pp. 9681–9688, 2018.

[7] H. Feng, B. Zou, and Y. Tang, "Scale- and region-dependence in landscape-pm2.5 correlation: implications for urban planning," *Remote Sensing*, vol. 9, no. 9, p. 918, 2017.

[8] S. Bin and Y. U. Da-Lu, "Study on Jinan urban construction planning based on the protection of karst landscape," *Journal of Groundwater Ence and Engineering*, vol. 6, no. 04, pp. 41–53, 2018.

[9] J. Bridger, "New chairs, subtle shifts: at Harvard, Berrizbeitia to lead landscape architecture; Davis will run urban planning," *Landscape Architecture*, vol. 105, no. 8, pp. 50–57, 2015.

[10] E. Borgogno-Mondino, G. Fabietti, and F. Ajmone-Marsan, "Soil quality and landscape metrics as driving factors in a multi-criteria GIS procedure for peri-urban land use planning," *Urban Forestry & Urban Greening*, vol. 14, no. 4, pp. 743–750, 2015.

[11] J.-H. Kim, W. Li, G. Newman, S.-H. Kil, and S. Y. Park, "The influence of urban landscape spatial patterns on single-family housing prices," *Environment and Planning B: Urban Analytics and City Science*, vol. 45, no. 1, pp. 26–43, 2018.

[12] S. Koma, Y. Yamabe, and A. Tani, "Research on urban landscape design using the interactive genetic algorithm and 3D images," *Visualization in Engineering*, vol. 5, no. 1, pp. 1–10, 2017.

[13] T. A. Nguyen, P. M. T. Le, T. M. Pham et al., "Toward a sustainable city of tomorrow: a hybrid Markov-Cellular Automata modeling for urban landscape evolution in the Hanoi city (Vietnam) during 1990-2030," *Environment, Development and Sustainability*, vol. 21, no. 1, pp. 429–446, 2019.

[14] L. Salvati and M. Carlucci, "Land-use structure, urban growth, and periurban landscape: a multivariate classification of the European cities," *Environment and Planning B: Planning and Design*, vol. 42, no. 5, pp. 801–829, 2015.

[15] L. Alessio, "AN approach to understanding urban landscape," *Journal of Architecture Planning & Environmental Engineering*, vol. 62, no. 501, pp. 153–161, 2017.

[16] N. Walravens, "Qualitative indicators for smart city business models: the case of mobile services and applications," *Telecommunications Policy*, vol. 39, no. 3-4, pp. 218–240, 2015.

[17] D. Jiang, P. Zhang, Z. Lv, and H. Song, "Energy-efficient multi-constraint routing algorithm with load balancing for smart city applications," *IEEE Internet of Things Journal*, vol. 3, no. 6, pp. 1437–1447, 2016.

[18] P. K. Sharma, S. Y. Moon, and J. H. Park, "Block-VN: a distributed blockchain based vehicular network architecture in smart city," *Journal of Information Processing Systems*, vol. 13, no. 1, pp. 184–195, 2017.

[19] G. V. Pereira, M. A. Macadar, E. M. Luciano, and M. G. Testa, "Delivering public value through open government data initiatives in a Smart City context," *Information Systems Frontiers*, vol. 19, no. 2, pp. 213–229, 2017.

[20] V. A. Memos, K. E. Psannis, Y. Ishibashi et al., "An efficient algorithm for media-based surveillance system (EAMSuS) in IoT smart city framework," *Future Generation Computer Systems*, vol. 83, pp. 619–628, 2017.

[21] P. Lynggaard and K. E. Skouby, "Deploying 5G-technologies in smart city and smart home wireless sensor networks with interferences," *Wireless Personal Communications*, vol. 81, no. 4, pp. 1399–1413, 2015.

[22] W. Yuzhe, Z. Weiwen, S. Jiahui et al., "Smart city with Chinese characteristics against the background of big data: idea, action and risk," *Journal of Cleaner Production*, vol. 173, pp. 60–66, 2017.

[23] L. Anthopoulos, M. Janssen, and V. Weerakkody, "A unified smart city model (USCM) for smart city conceptualization and benchmarking," *International Journal of Electronic Government Research*, vol. 12, no. 2, pp. 77–93, 2016.

[24] R. Logesh, V. Subramaniyaswamy, V. Vijayakumar et al., "A hybrid quantum-induced swarm intelligence clustering for the urban trip recommendation in smart city," *Future Generation Computer Systems*, vol. 83, pp. 653–673, 2017.

Research Article

Factors Affecting the Evolution of Advanced Manufacturing Innovation Networks Based on Cloud Computing and Multiagent Simulation

Wang Jianbo[1,2] and Xing Cao [iD][1,3]

[1]*Business School of Central South University, Changsha 410083, Hunan, China*
[2]*Hunan University of Humanities, Science and Technology, Loudi 417000, Hunan, China*
[3]*Hunan First Normal University, Changsha 410205, Hunan, China*

Correspondence should be addressed to Xing Cao; caoxingsxy418@csu.edu.cn

Facing the pressure of low-cost competition brought by the homogenization of commodities, the manufacturing industry seeks to survive by providing services. By providing outsourcing of value-added services to date, we are focusing on innovation in our business model. With the advancement of science and technology, manufacturing innovation is facing higher challenges, especially the popularization of the Internet, which makes the manufacturing industry have to move closer to new industries. Based on cloud computing, this paper conducts a multiagent simulation on the evolution factors of the innovation network of advanced manufacturing. This article takes three types of simulation subjects: evolutionary network, manufacturing (cluster), and innovation evolution system as the research objects. The factors affecting the evolution of the research are innovation resources, innovation opportunities, innovation desire, innovation pressure, relationship strength, network scale, and network scope. Network differences carry over variable indicators and analyze quantitative regression indicators and then build a research model. The research results show that the average conversion efficiency of the manufacturing industry (0.523) is significantly lower than the average R&D innovation efficiency (0.725), which to a certain extent indicates that the manufacturing industry still has weak links in the export conversion stage at the back end of the innovation value chain. Some of the companies may have problems such as low ability to transform scientific and technological achievements and insufficient export competitiveness of high-tech products, which to a large extent affects and restricts the improvement of manufacturing export transformation efficiency.

1. Introduction

With the in-depth implementation of the national innovation-driven development strategy, R&D innovation and industrial transformation and upgrading activities have received increasing attention from government departments at all levels. The construction of the national manufacturing industry aims to support a large number of high-tech enterprises in the park to carry out R&D and innovation activities to form a high-quality growth pole driven by knowledge and innovation and to promote regional industrial upgrading and economic transformation. After years of development, the current national manufacturing industry has become the main force in promoting the implementation of the national innovation-driven development strategy.

Bui N begins the research on organizational innovation, the organizational structure shifts from a purely hierarchical system to a functional system, the business division is formed as the main form of organizational innovation, and then the organizational structure evolves into a super business division, and the organization, it layers the foundation for the evolution of the structure [1]. Suh et al. proposed three major factors affecting organizational innovation and studied the changes in new organizational forms, which is a preliminary exploration of the factors

affecting organizational innovation [2]. Benzaoui proposed that organizational innovation is a planned change in organizational structure and organizational division of labor. Organizational innovation enhances the creativity of organizational operations and highlights the impact of organizational structure and technological innovation on organizational innovation. At this stage, the influencing factors of organizational innovation are deeply explored [3]. From the perspective of cloud computing technology and cross-organizational communication, Mohammadi explores the development of innovative activities of enterprises in different organizational configurations. At this stage, it studies the changes in organizational innovation forms and influencing factors from the perspective of technical knowledge [4]. Dayarathna et al. found that the influence of organizational green learning, environmental protection, public opinion pressure, and leadership awareness is gradually increasing. Enterprises should respond to national policies, adapt to environmental changes, and promote organizational innovation [5].

Armbrust et al. found that the impact of culture on organizational innovation is reflected in both positive and negative aspects. Transactional leadership and organizational climate stimulate employees' willingness to innovate and promote organizational innovation [6]. Sanderson found that the influence of organizational collaboration and openness on organizational innovation is in a dynamic cycle and is affected by organizational dependence, and the relationship between the two needs to be reasonably grasped [7]. Oliver combines organizational structure with resources and proposes that companies should formulate organizational strategies, optimize the relationship between organizational structure and resources, and promote organizational innovation [8]. Danwitz found that big data technology plays a regulatory role among knowledge transfer, organizational proximity, and innovation performance, and knowledge management plays an intermediary role in organizational innovation. Enterprises should establish learning organizations to promote organizational innovation. To sum up, most of the current research on the influencing factors of organizational innovation tends to be scattered, and there is a lack of research on the influencing factors and mechanisms of organizational innovation in the era of big data. For this reason, this paper uses the combination weighting method and the ISM system to analyze the main influencing factors and influencing mechanism, and taking red-collar enterprises as an example, expounds the feasibility of the influencing mechanism [9]. Ward et al. proposed to build a cloud framework based on the SaaS platform and complete the design after cloud computing users' selection of the environment [10].

Based on cloud computing, this paper conducts a multiagent simulation on the evolution factors of the innovation network of advanced manufacturing. This article takes three types of simulation subjects: evolutionary network, manufacturing (cluster), and innovation evolution system as the research objects. The factors affecting the evolution of the research are innovation resources, innovation opportunities, innovation desire, innovation

pressure, relationship strength, network scale, and network scope. Network differences carry over variable indicators and analyze quantitative regression indicators, and then build a research model. Based on this, in order to better explore the internal development and evolution of knowledge topics and make up for the lack of traditional prediction methods in the prediction of knowledge topics, this article focuses on two major issues in the evolution of knowledge manufacturing innovation network prediction research: multiagent influence factors and sensitivity to network evolution.

2. Evolutionary Prediction Model

2.1. Cloud Computing-Based Manufacturing Evolution Prediction Model. The current evolution of innovation is trending towards large-scale and massive development, and a single support vector machine is ineffective in obtaining the prediction result of the evolution of the manufacturing industry within a valid time. For this reason, the advantage of the parallel processing problem of the cloud computing platform is adopted, parallel modeling to realize manufacturing evolution prediction. The specific principle is to assign each subset to a node of the cloud computing platform through the cloud computing system, use the support vector machine to build the modeling on each node, and then use the cloud computing system to calculate the modeling results of each subset, perform fusion and aggregation to form a powerful innovation evolution prediction model, and output the final prediction results of innovation evolution prediction [11].

In the field of cloud computing, the requirements for the stability of the cloud framework have become more stringent. To save the cost of cloud computing and strengthen the robustness of the server itself, the need for cloud framework stability design arises. As a state-of-the-art technology emerging rapidly today, cloud computing frameworks use group computing to connect many individual computers over high-speed local area networks for high computing efficiency and capability [12]. To a certain extent, this technology can connect computer and data calculations in series, transforming hardware support into software support. It also has the characteristics of real-time dynamics and strong adaptive ability, and the excellent framework integration mechanism can more perfectly fulfill user requirements [13]. Since the cloud computing framework was proposed, the development of this technology has been particularly rapid in the field of cloud computing. The service method of the cloud computing framework: It is based on a series of methods such as aggregation, improvement, and resource management of the data network to meet its specific needs. The cloud framework can also be divided according to the size of the space [14]. Small-scale cloud computing framework: It means that on the basis of IT, equipment, instructions can be completed according to requirements [15]. In a large-scale situation, it will go through a well-built computer service cluster and make full use of the Internet method to achieve the required command services [16]. When the cloud computing framework meets

the current network conditions, the network data resources will be free to use and will not be restricted due to conditions, and users can use this service at any time and place [17]. However, due to the ubiquity of Internet users and the decentralization of data, the current cloud frameworks face more diversified problems. How to effectively control these problems is a problem that needs attention in the current cloud framework research field [18]. At present, relevant scholars have also proposed some better methods for the cloud framework, but there are also some problems. The more typical methods are as follows:

$$\theta = -\frac{1}{T}\ln(1 + \beta),$$

$$G = \frac{\sum_{j=1}^{k}\sum_{h=1}^{k}\sum_{t=1}^{n_j}\sum_{r=1}^{n_h}\left|y_{ij} - y_{hr}\right|}{2n^2u}. \tag{1}$$

To a certain extent, the framework can greatly improve the timely response rate of executing instructions and fully meet the basic requirements of users as much as possible, with high stability coefficient and excellent reliability. However, this framework has the problems of low efficiency, low reliability, and unsmooth network operation in the actual complex data calculation [19]. In response to the above problems, this paper proposes a high-elastic cloud architecture design method for cloud computing networks and analyzes its reliability [20]. Experiments prove that the cloud framework has high flexibility, stable data flow, accurate and rich information, and high-quality reliability.

2.2. Manufacturing Innovation Network Evolution Method. Among the advanced manufacturing innovation network evolution analysis methods, the discrete-time method is the most used. This type of method divides the corpus set before extracting the topic. It is more dependent on the structure of the corpus, and the results obtained are greatly affected by the division method. And it is necessary to confirm the same theme on different subsets. That is, after getting the theme of each period, the theme is related according to the similarity of the words or the overlap of the articles under the theme. The accuracy of the theme alignment is difficult to guarantee [21]. Introducing time information into the evolution model means directly introducing time information into the topic model, such as DTM (Dynamic Topic Models), TOT (Topic Over Time), and other models. DTM can describe the changes in the word distribution of a topic over time. TOT will be regarded as a continuous distribution on the time label; there are problems of time dispersion and granularity that are difficult to control, and the above methods assume that the topic set at each period is constant, which is inconsistent with reality. The literature may be a new topic that has not appeared in the previous period. The postdiscrete-time method is to first perform topic extraction, find the time label of each document through the clustering of the documents under the topic, and then match the time label with the topic to form a "time-topic" matrix. This method is avoided in order to solve the problem of topic alignment in the discrete-time method. Researchers only need to mark the

topic with time in the follow-up [22]. At the same time, the postdiscrete-time method allows the death of old themes and the emergence of new themes, which is more in line with the actual situation of the evolution of manufacturing innovation networks. In addition, in recent years, another trend in research on the evolution of innovation networks in advanced manufacturing is to use structural information in the scientific research literature, such as author information and citation information, to explore the evolution of knowledge topics over time, but related research results are still relatively few and have not reached the level of practicality; most of the evolution methods lack fine-grained, deep-level content foundation, and the evolution effect needs to be improved. Divided according to the evolution mode of the theme, it can also be divided into three modes: intensity evolution, content evolution, and structural evolution [23]. Strength evolution represents changes in topic strength through several indicators that can reflect the strength of the topic, such as the number of documents associated with the topic, the degree of attention of the document, and the probability of feature words under the topic [24]. Content evolution is mainly to study the differentiation and fusion between themes in the process of time change. It is generally based on the association between themes, and the cooccurrence matrix between themes is used as a transition matrix to simulate the natural selection phenomenon of species evolution in biology. The related explanation of life cycle theory describes the process of the subject's emergence, development, maturity, and extinction, and finally uses the dissipative structure theory, dynamic model, or infectious disease model to explain [25]. Structural evolution is the use of some structural information contained in the topic to construct a network with certain attributes, such as the use of authors or institutions to map the topic cooperation model or the use of similarity between topics to construct a similarity matrix to explore the evolution of the network structure over time. The specific description may include network centrality, density, small world, and other attributes that can reflect the network structure, involving theoretical knowledge such as complex networks and knowledge graphs.

2.3. Forecasting Method Research. The evolution of the manufacturing innovation network is not the end, but the evolution will be further expanded. This article hopes to predict the future development of the theme. Researchers are based on different theoretical foundations. Qualitative methods include analogy, but qualitative analysis is often limited by subjective judgments. Quantitative methods are more scientific. Common methods include link prediction, autoregressive models, gray models, and Markov. These models have the ability to predict development trends and can confirm the law of evolution of things to a certain extent. Among them, the research of the Markov model started the earliest and has a rich theoretical foundation. The Gray model emerged after 1990 and has the widest application field. In recent years, the research process of domestic and foreign scholars applying this model can be divided into the

following parts: determining the evolution time and period, selecting the evolution index, calculating the state transition probability, and analyzing the evolution results. The application direction is divided into two categories. One is to use the first-order and finite nature of Markov chains to predict the limit probability. By calculating the one-step transition probability, the n-step stable transition probability is given, and the limit probability in the steady state represents the total research of the development trend of the system. One type is the analysis of Markov chains combined with multivariate time series, that is, forecasting based on the changing trend of internal structural factors of things, focusing on the exploration of micromechanisms. In addition, the Markov model is also embedded in the DPS software, which makes the application analysis of the Markov chain more extensive. As an extension of the Markov model, HMM is widely used in various prediction tasks, such as public opinion propagation prediction, stock prediction, attack prediction, and behavior prediction. In addition, the model also has applications in text classification, manufacturing, innovation network evolution, automatic speech recognition, and fault diagnosis. Through the analysis of the current research status of evolutionary prediction methods, it can be seen that the existing research is mostly the evolution of the subject content, intensity, and structure, and there is less research on the evolution relationship and steady-state distribution of the subjects in the field and quantitative prediction of knowledge topics. There is also less research. Based on the influencing factor index system constructed above, the scoring results are weighted and averaged to obtain the fuzzy complementary matrix R of each influencing factor, and according to the formula:

$$u_h \leq u_j \leq \cdots \leq u_k,$$

$$Gjj = \frac{(1/2u_j) \sum_{i=1}^{n_j} \sum_{r=1}^{n_j} |y_{ji} - y_{jr}|}{n_j^2}, \quad (2)$$

$$Gw = \sum_{j=1}^{k} G_{jj} p_j s_j.$$

Calculate the weights of primary and secondary indicators Gw. Then, based on the data obtained from the survey, the average value of the top five industry results is selected, and the index is calculated according to the following formula G_t:

$$\ln\left(\frac{\text{FI}_{it}}{\text{FI}_{it} - 1}\right) = \alpha + \beta \ln \text{FI}_{it} - 1 + \phi X_{it} - 1 + v_i + \tau_t,$$

$$k_{t1}[i] = \sum_j \cos\left(w_i^1, w_j^2\right), \quad (3)$$

$$G_t = \sum_{j=2}^{k} \sum_{h=1}^{j-1} G_{jh}\left(p_j s_h + p_h s_j\right) D_{jh}\left(1 - D_{jh}\right).$$

Then, combine the weights according to the following formula to obtain the combined weights of first and second

indicators D_{jh} And the ranking of organizational innovation factors:

$$D_{jh} = \frac{d_{jh} - P_{jh}}{d_{jh} + P_{jh}},$$

$$d_{jh} = \int_0^\infty dF_j(y) \int_0^y (y - x) dF_h(x), \quad (4)$$

$$d_{jh} = \int_0^\infty dF_h(y) \int_0^y (y - x) dF_j(y).$$

The primary indicators that affect organizational innovation are technology and knowledge, organizational structure and strategic characteristics, organizational learning, knowledge flow, and information technology. At the same time, to explore the logical relationships of the main influencing factors, select the top 80% of the secondary indicators as the main influencing factors, and further analyze the influence mechanism between the factors:

$$f(x) = \frac{1}{Nh} \sum_{i=1}^{N} k\left(\frac{X_i - x}{h}\right),$$

$$k(x) = \frac{1}{\sqrt{2\pi}} \exp\left(-\frac{x^2}{2}\right), \quad (5)$$

$$h_t = \tanh\left(w_c x_t + u_c\left(r_t \Theta h_{t-1}\right) + b_c\right),$$

$$h_t = z_t \Theta h_{t-1} + (1 - z_t) \Theta h_t.$$

The addition of undesired output indicators overcomes the problems caused by radial and angle, making the evaluation results more in line with reality and more accurate. The construction model is as follows: Suppose there are n decision-making units, and their input and output matrices are as follows:

$$\sigma t = \frac{\sqrt{(1/n) \sum_{i=1}^{n} \left(\text{FI}_{it} - \text{FI}_{it}\right)^2}}{\text{FI}_{it}},$$

$$u_{(j|i)} = w_{ij} A_i, \quad (6)$$

$$s_j = \sum_i c_{ij} u_{(j|i)}.$$

The coding adopts a binary coding method, assigning a value of 1 to the selected subset and assigning a value of 0 to the unselected subset, then any problem solution can be represented by a set of binary codes, that is, a queue. This coding method is also convenient for the later selection, crossover, and mutation operations to search for solutions to problems, among them$c$is the weight variable:

$$\ln\left(\frac{\text{FI}_{it}}{\text{FI}_{it} - 1}\right) = \alpha + \beta \ln \text{FI}_{it} - 1 + v_i + \mathfrak{I}_t, \quad (7)$$

$$c_{ij} = \frac{e^{b_{ij}}}{\sum_k e^{b_{ik}}}.$$

3. Design of Manufacturing Innovation Network Evolution Model

3.1. Network Evolution Model. The main body of simulation in this paper is divided into three categories: evolutionary network, manufacturing (cluster), and innovation evolution systems. When using the fuzzy analytic hierarchy process, the data is collected by issuing questionnaires to company leaders with innovative management experience and comparing and scoring the influencing factors of various indicators according to the 0.1–0.9 scale method. In addition, for asset input in the following year, the total assets of the manufacturing industry at the end of the previous fiscal year are selected, and the total number of personnel in the manufacturing industry at the end of the previous fiscal year is selected as personnel—input for the next year. The output of the second stage uses the indicator of total manufacturing exports. Factors that influence the evolution of research are innovation resources, innovation opportunities, innovation desires, innovation pressures, the strength of relationships, network size, network scope, and network differences.

3.2. Network Evolution Model Construction and Evaluation

3.2.1. Model Construction. The DEA method can establish performance benchmarks by evaluating the efficiency of decision-making units and help decision-makers find shortcomings that affect performance improvement, which is conducive to improving and enhancing the performance of decision-making units. Judging from the efficiency measurement of the existing DEA methods, the traditional DEA treats the decision-making unit as a whole and only measures its operational efficiency through input and output data. It does not fully consider the internal operation process of the decision-making unit, so it is difficult to comprehensively and systematically analyze the innovation activity process of the decision-making unit. Based on the multistage and nonlinear characteristics of advanced manufacturing R&D innovation and export transformation activities, this paper intends to use a two-stage dynamic intertemporal DEA model to analyze the manufacturing industry's R&D innovation, export transformation, and overall efficiency. In the construction of the two-stage DEA model, it is further extended to a dynamic model. That is, the periods are linked together by cyclic activities, which is called the dynamic interperiod DEA model. This paper adopts the dynamic intertemporal two-stage comprehensive model proposed by Xiong et al. to construct the analysis framework. This article assumes that the first stage (R&D and innovation stage) and the second stage (export conversion stage) are of equal importance, so the weights are set to 1/2 in advance. That is, the overall efficiency is defined as the weighted average sum of the efficiencies of the two substages:

$$\theta_0^t = \min \frac{1}{2} \theta_{10}^t + \frac{1}{2} \theta_{20}^t,$$

$$c_{ij} = \frac{e^{b_{ij}}}{\sum_k e^{b_{ik}}}.$$

(8)

Advanced manufacturing is an important carrier for regional innovation activities, but the traditional two-stage DEA model is a single-period static model and cannot measure interperiod dynamic changes. From the perspective of manufacturing R&D innovation and export transformation activities, it has the characteristics of dynamic intertemporal.

3.2.2. Carryover Variable Indicators. Since the innovation value chain process is a dynamic interactive process, the back-end activities of this period will also have an impact on the front-end activities of the next period, so this article considers adding carryover variables. The carryover variable in the first stage is the stock of patent knowledge. The reason for adopting this carryover variable is that the patents generated in the current year will be included in the knowledge stock at a certain depreciation rate and will affect the knowledge production activities in the next year. On the one hand, patents will form knowledge accumulation over time, which will act as a knowledge pool for the production of new knowledge in the following year. On the other hand, new knowledge will continue to be produced. New knowledge produced in the past will gradually be depreciated. We need to consider the depreciation of knowledge. Drawing on the experience of previous studies, the depreciation rate of knowledge is calculated using a depreciation rate of 15%. In the selection of carryover variables in the second stage, this article uses the indicator of total manufacturing exports multiplied by a fixed ratio. The reason for adopting this carryover variable is that, on the one hand, the company will use part of the total export value of the current year for the following year's export trade expenditures and export conversion incentives. On the other hand, the company will invest part of the total export value according to the export situation. The first phase of export transformation forms a virtuous circle of export transformation. Therefore, this stage adopts the carryover variable of total exports multiplied by a fixed ratio (10%).

3.2.3. Selection of Econometric Regression Indicators. To analyze the relevant factors affecting the R&D innovation, export transformation, and overall efficiency of advanced manufacturing from the perspective of innovation-driven, this paper selects relevant control variable indicators from the three perspectives of the manufacturing external environment, internal conditions, and innovation value chain. The external environment includes four indicators: city technical level, city economic level, city openness, and geographic distance. The city's technology level (S&T) is measured by dividing the city's annual science and technology expenditure by the city's annual fiscal expenditure, the city's economic level (Eco) is measured by the city's per capita GDP, and the city's openness is measured by dividing the city's annual foreign direct investment by the city's current GDP measured, geographic distance (Dist) is measured by the straight-line distance of each city from the nearest coastline, and this indicator is obtained using Google Maps. The internal conditions of the manufacturing industry

include two indicators: human capital and debt financing. Human capital (Hr) is measured by the number of employees with a college degree or above in each manufacturing industry, and debt financing (Df) is measured by dividing the year-end liabilities of the previous year by the year-end assets. The innovation value chain index selects the efficiency value (E2) in the R&D and innovation stage and uses this indicator to return the efficiency value in the export transformation stage. This is also a key indicator to analyze the impact of R&D and innovation on export transformation from an innovation-driven perspective.

4. Influencing Factors on Evolution of Advanced Manufacturing Innovation Network

4.1. Evolution Factors of Multiagent Networks. To grasp the law of innovation evolution system confrontation from the perspective of multiagent simulation, the evolution evaluation index is based on the overall emergence in the simulation process, rather than the simple correlation between the cycle length of each loop and the evolution result. In the overall evolution process, the information advantage is reflected in the amount of target information and the average acquisition time; the determination effect is reflected in the accurate determination of the target threat information and the average determination time, and the decision advantage is reflected in the accuracy of the decision and the average decision response time, and action advantage is reflected in the number of effective strikes completed and the average strike time. Since this model does not set legal targets and does not distinguish between general frequency bands, special frequency bands and procedures, and visual manufacturing targets for flight control, it does not involve the index analysis of decision-making accuracy.

As shown in Figure 1, political factors include political requirements and social responsibilities. The former refers to the state and government's rigid requirements for the implementation of relevant policies and spirit of enterprises, while the latter refers to the social obligations undertaken by enterprises that are higher than their own goals. The former is passive, while the latter emphasizes proactive behavior. Both help companies maintain relationships with stakeholders such as the government and partners and further help companies obtain innovation resource support, thereby promoting platform innovation. For example, most of the decisions in the development of Wanda can be combined with the latest party and government policies. Only by knowing what your country needs can you guide your company in that direction (political requirements ⟶ platform innovation).

As shown in Table 1, dynamic capability is the ability of an enterprise to adapt to a rapidly changing complex environment. It also emphasizes that enterprises can grasp the development opportunities brought about by environmental changes through the reconfiguration of resources and skills. It includes four dimensions: integration capability, technical capability, absorptive capacity, and organizational forgetting. Here, organizational forgetting is used as an example to illustrate the impact of platform innovation. At the same
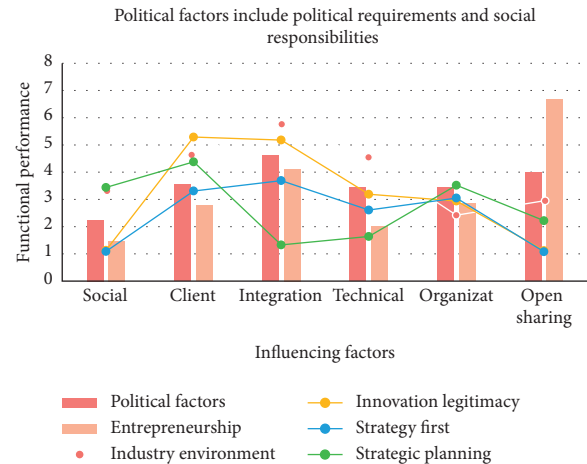
FIGURE 1: Political factors include political requirements and social responsibilities.

time, according to the calculation results, the average manufacturing conversion efficiency (0.523) is significantly lower than the average R&D innovation efficiency (0.725), which to a certain extent indicates that the manufacturing industry still has weak links in the export conversion stage at the back end of the innovation value chain. Internal enterprises may have problems such as low ability to transform scientific and technological achievements and insufficient export competitiveness of high-tech products, which to a large extent affects and restricts the improvement of manufacturing, export, transformation efficiency.

As shown in Figure 2, the industry environment includes policy orientation, environmental changes, and the degree of competition. To illustrate the impact of platform innovation, we will only take environmental changes as an example. Environmental changes are the most active and uncontrollable factor, and corporate strategies must be continuously adjusted to environmental changes. As shown in Table 2, this change will prompt enterprises to carry out reforms and innovations. For example, the continuous change of the economic and financial landscape and the large changes in the economic situation will prompt CCB to carry out platform innovation and transformation.

As shown in Figure 3, market demand includes customer needs and social pain points. The former is based on a microperspective, while the latter has an impact on platform innovation from a macro level. The "demand leads to innovation" theory believes that the stronger the customer demand, it will drive the enterprise to innovate and promote the growth of the enterprise. For example, Haier's "big enterprise disease" blocked customer demand and made enterprise production and user demand farther and farther away, while the innovation of the "Rendanheyi" platform made "the enterprise borderless" and narrowed the distance between the enterprise and the customer.

The corporate strategy includes three dimensions: strategic advancement, strategic planning, and strategic flexibility. Here, only strategic precedents are used to illustrate the impact of platform innovation. As shown in Figure 4, the advanced strategy will enable companies to

TABLE 1: Dynamic capability is the enterprise adapting to rapid changes.

Item	Industry environment	Political factors	Entrepreneurship	Innovation legitimacy	Strategy first	Strategic planning
Social	3.31	2.25	1.48	1.13	1.09	3.44
Client	4.67	3.56	2.77	5.29	3.31	4.38
Integration	5.78	4.61	4.12	5.18	3.69	1.33
Technical	4.54	3.45	2	3.19	2.61	1.64
Organizat	2.42	3.45	2.84	2.94	3.05	3.52
Sharing	2.95	4	6.67	1.12	1.08	2.22
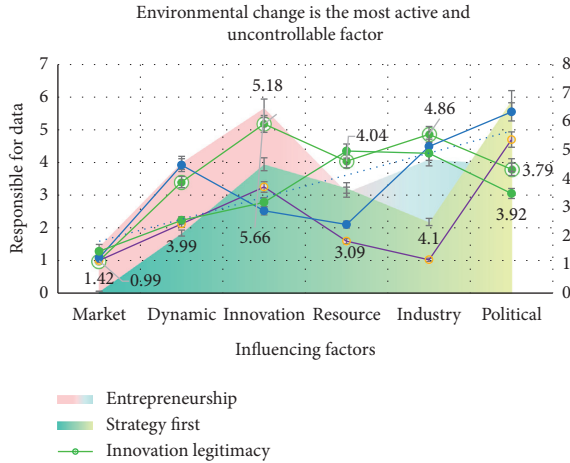
FIGURE 2: Environmental change is the most active and uncontrollable factor.

establish long-term development visions and innovation plans and promote companies to carry out innovative practices. Platform innovation is strategically oriented and requires the guidance and support of advanced strategies.

Innovation culture includes three dimensions: active collaboration, open sharing, and innovative atmosphere. As shown in Table 3, we only take the innovation atmosphere as an example to illustrate the impact of platform innovation. An innovative atmosphere refers to the common perception of innovation-related factors in the work environment among employees within an enterprise. When employees feel that the enterprise supports platform innovation more strongly, their enthusiasm and innovative behavior increase, and the enterprise's platform innovation capability becomes stronger. The case companies have a good atmosphere for innovation. In interviews, CCB frequently holds creative salons and maker contests to collect ideas for different products from employees, providing mentors and long-term tracking for good creative incubation. Three ideas related to the "Three Strategies" incubate new products and market them. Another example is that Haier's innovative atmosphere is very strong. "Everyone can become a CEO" has inspired many entrepreneurs who lack resources and relationships to start their own business on the Haier platform.

Entrepreneurship factors are shown in Figure 5. Entrepreneurship is an innovative behavior. This study divides it into three dimensions, namely, the discovery of opportunities, courage to change, and belief and confidence. Here, we only use the discovery of opportunities as an example to illustrate the impact of platform innovation. As Meituan

Wang Xing said, "Entrepreneurship is the willingness to discover and pursue opportunities." Successful discovery and conversion of opportunities into practice will promote the development of enterprise platform innovation.

4.2. Sensitivity Analysis of Manufacturing Innovation Network Evolution. To further analyze the model, this paper uses MATLAB numerical simulation to determine the sensitivity of the number of users to changes in platform profit, to determine the factors that affect the platform profit the most, and to adjust the factors in conjunction with the pricing model to maximize platform profit. Suppose the simulation conditions are shown in Table 4.

As shown in Figure 6, in terms of output in the R&D and innovation stage, although patents are used as a proxy variable for R&D activities, there are certain shortcomings, but patents are an important content of knowledge and an important indicator of innovation output. In the relevant empirical analysis of R&D activities, scholars use the number of patent applications as the proxy variable of R&D output. At the same time, in view of the fact that invention patents have the highest gold content in patents and can better reflect innovation and knowledge, this paper selects the index of invention patent applications as a measure of R&D output. In terms of investment in the second stage, the export transformation stage, on the basis of the main case, continues to compare and analyze the follow-up cases to make the conclusions more comprehensive and objective.

Platform innovation is a destructive business model innovation. If you do not actively discard outdated thinking and inherent traditions, the reform will not be thorough and the innovation will not be effective. As shown in Figure 7, when analyzing the network evolution model in this study, the simulation curve basically reached theoretical saturation, and no new aspects appeared. We tested our conclusions using the following cases and finally found that the categorical code obtained in this study had good theoretical saturation. After revising and integrating the conceptual categories obtained from the analysis of all case data, the final result is obtained, as shown in Table 5.

As shown in Figure 8, when innovation resources are insufficient, the motivation for enterprise platform innovation will decrease. This research divides resource adequacy into three dimensions: human capital, social network, and performance basis. Here, the social network is used as an example to illustrate the impact of platform innovation. Social network refers to the formal or informal relationship link between an enterprise and related external institutions. As shown in Table 6, the social network relationship formed

TABLE 2: The economic and financial landscape is constantly changing.

Item	Entrepreneurship	Innovation legitimacy	Strategy first	Strategic planning	Social pain points	Client needs
Market	1.42	0.99	0.06	1	1.08	1.28
Dynamic	3.99	3.4	2.1	2.12	3.92	2.23
Innovation	5.66	5.18	4.51	3.25	2.52	2.78
Resource	3.09	4.04	3.68	1.59	2.1	4.35
Industry	4.1	4.86	2.49	1.02	4.49	4.28
Political	3.92	3.79	6.75	4.7	5.55	3.05
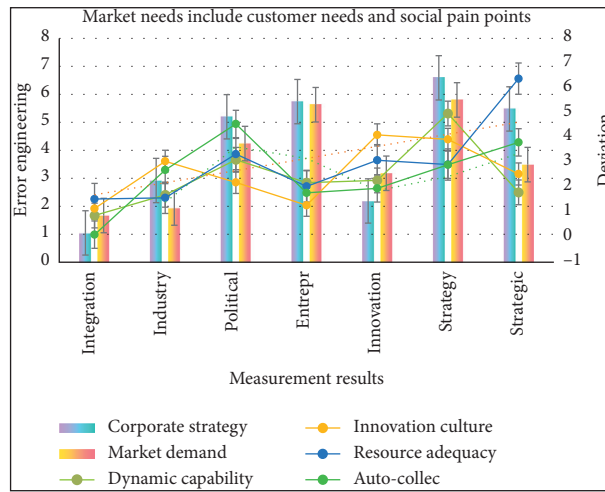
FIGURE 3: Market needs include customer needs and social pain points.
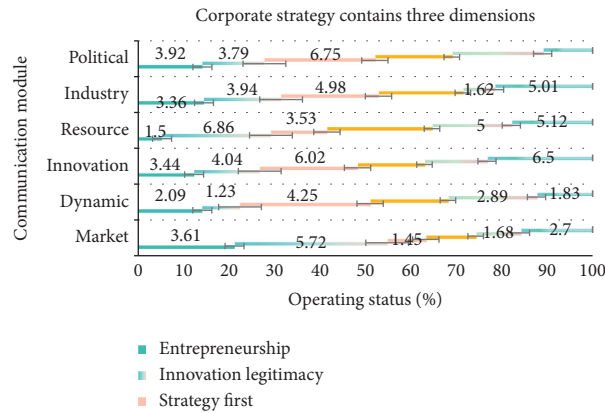
FIGURE 4: Corporate strategy contains three dimensions.

TABLE 3: Take innovation atmosphere as an example to illustrate the impact on platform innovation.

Item	Corporate strategy	Market demand	Dynamic capability	Innovation culture	Resource adequacy	Autocollect
Integration	1.05	1.67	0.88	1.16	1.54	0.11
Industry	2.92	1.94	1.71	3.06	1.59	2.71
Political	5.2	4.24	3.12	2.21	3.35	4.56
Entrepreneurship	5.74	5.63	2.2	1.29	2.05	1.79
Innovation	2.19	3.18	2.29	4.12	3.1	1.97
Strategy	6.59	5.8	4.98	3.94	2.93	2.92
Strategic	5.48	3.49	1.81	2.55	6.38	3.82
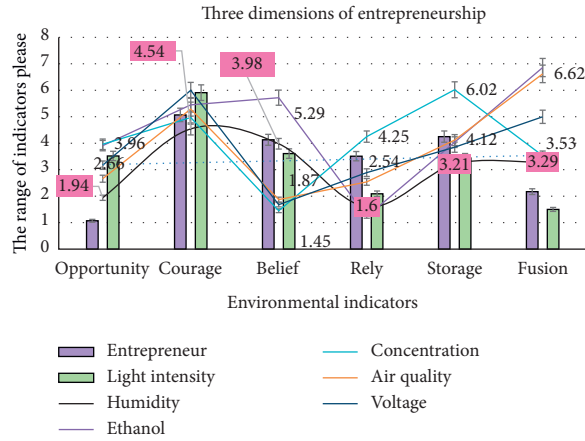
Figure 5: Three dimensions of entrepreneurship.

Table 4: Matlab assumes the simulation conditions.

Item	Entrepreneur	Humidity	Light intensity	Ethanol	Concentration	Air quality	Voltage
Opportunity	1.07	1.94	3.52	3.91	3.96	2.66	3.17
Courage	5.07	4.54	5.91	5.45	4.97	5.29	6
Belief	4.13	3.98	3.61	5.72	1.45	1.87	1.68
Rely	3.51	1.6	2.09	1.23	4.25	2.54	2.89
Storage	4.25	3.21	3.44	4.04	6.02	4.12	3.85
Fusion	2.17	3.29	1.5	6.86	3.53	6.62	5
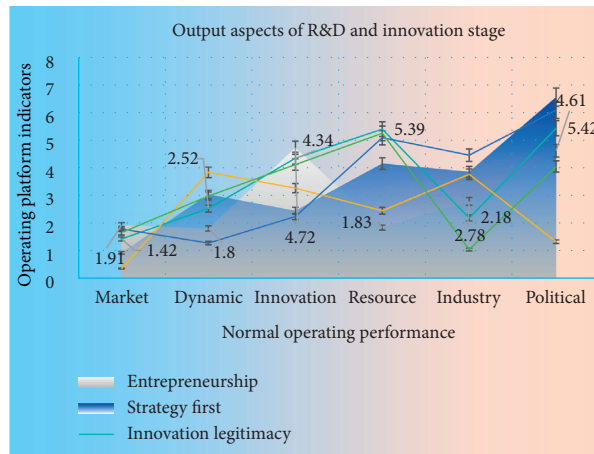
Figure 6: Output aspects of R&D and innovation stage.
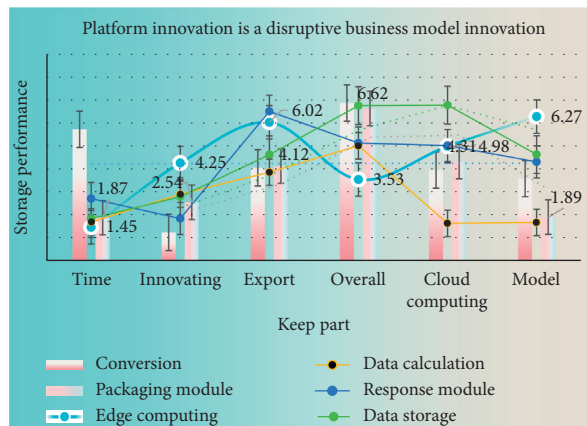
Figure 7: Platform innovation is a disruptive business model innovation.

TABLE 5: Revise the concept category obtained from data analysis.

Item	Conversion	Edge computing	Packaging module	Data calculation	Response module	Data storage
Time	5.72	1.45	1.87	1.68	2.7	1.83
Innovating	1.23	4.25	2.54	2.89	1.83	2.78
Export	4.04	6.02	4.12	3.85	6.5	4.61
Overall	6.86	3.53	6.62	5	5.12	6.75
Cloud	3.94	4.98	4.31	1.62	5.01	6.77
Model	3.57	6.27	1.89	1.66	4.3	4.62
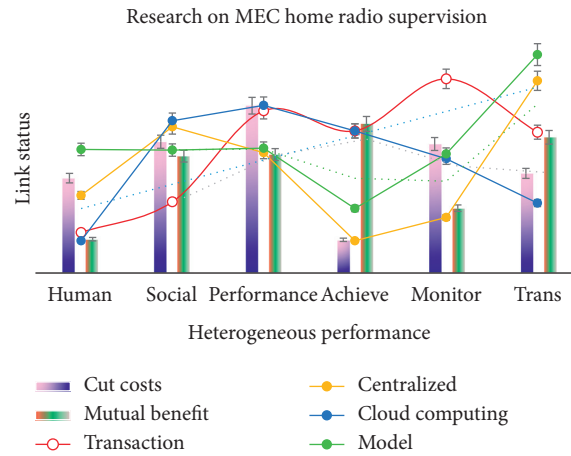
FIGURE 8: Motivation of enterprise platform innovation and innovation resources.

TABLE 6: Social network relationships formed by the interaction between external organizations.

Item	Transaction	Cut costs	Mutual benefit	Centralized	Cloud computing	Model
Human capital	4.89	3.35	2.02	1.06	1.12	1.72
Social network	3.34	3.26	6.32	2.48	3.18	4.58
Performance	3.14	4.81	4.22	1.28	6.21	3.13
Achieve	6.13	5.11	2.96	5.7	5.52	5.4
Monitor	4.75	4.34	3.24	4.54	2.42	1.52
Trans	2.74	2.12	2.9	3.47	4.69	3.54

by the interaction between enterprises and external organizations such as upstream and downstream suppliers and customers is conducive to the acquisition of knowledge and resources, thereby promoting platform innovation. For example, CCB has 6 million corporate client resources and integrates these resources together to build a matching platform, allowing customers to generate transactions, reduce costs, and benefit each other through the platform, and finally stick these customers through the platform.

As shown in Figure 9, although the main case collects a large amount of primary and secondary data, the secondary case uses only secondary data as analysis data, which has certain reliability and validity limitations and may have a certain impact on the final model. This article selects only a small number of research cases and the number of samples collected is limited. The selected cases are all well-known domestic companies, and they are companies with successful platform innovations. They lack universality. If more on-site interviews and surveys
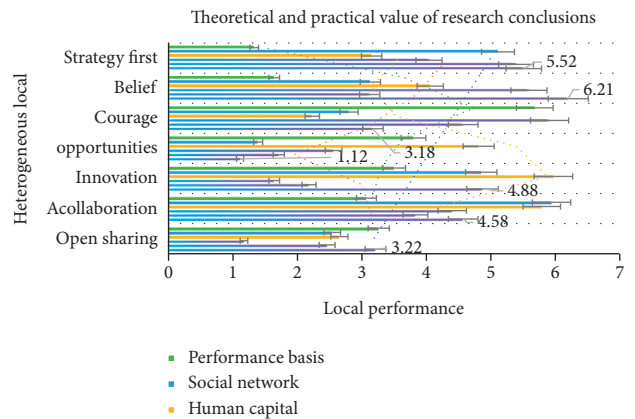
FIGURE 9: Theoretical and practical value of research conclusions.

can be used, a number of small and medium-sized interviews on companies' platform innovations will enhance the theoretical and practical value of research conclusions.

5. Conclusions

The cities with double high manufacturing industries are coastal cities and provincial capital cities. The two-stage efficiency of manufacturing in these cities is higher than the national average. The reason may be that, on the one hand, these cities have a better educational foundation and more R&D resources, which can attract more high-tech enterprises to settle in and acquire more R&D and innovation resources, which will help them improve the efficiency of R&D and innovation. On the other hand, these cities are located in coastal areas. The proportion of export industries in the manufacturing industry is relatively high, and they have a good industrial foundation. They have formed a relatively complete industrial infrastructure and related industrial supporting facilities. The market economy is relatively more active. Export transformation of scientific and technological achievements of manufacturing companies provides a good environment and foundation. Cities that are twice as low in manufacturing are in the Midwest or Northeast. The cities where these manufacturing industries are located are relatively weak in R&D and innovation. It is difficult to provide strong R&D resources for manufacturing R&D and innovation activities, and it is difficult to attract them. Enough R&D talents carry out the corresponding R&D and innovation activities, resulting in relatively low R&D and innovation efficiency.

At the same time, these manufacturing cities have weak economic foundations, insufficient market economy development, a relatively low proportion of export industries, and inadequate industrial infrastructure facilities, poor innovation awareness and atmosphere, and a low degree of openness. It is not conducive to the export transformation of R&D achievements, resulting in low efficiency in the export transformation of scientific and technological achievements of manufacturing industries in these cities. From the regression results, the urban economic development level and manufacturing human capital have a significant positive impact on the efficiency of manufacturing R&D innovation, indicating that a high level of urban economic development can provide a good economic foundation for manufacturing R&D innovation. The improvement of human capital can provide a large number of R&D and innovative talents for manufacturing R&D and innovation and promote the improvement of manufacturing R&D and innovation efficiency. The city's technological level has a positive impact on the efficiency of manufacturing R&D innovation, but it is not significant. The reason may be that there is an obvious "fence" between the city's investment in technological innovation and the R&D and innovation activities of the manufacturing industry. Although the city's investment in technological innovation can promote local technological innovation activities, it interacts with the manufacturing industry. Insufficiently, it has not been able to significantly promote the improvement of manufacturing R&D and innovation efficiency.

From the perspective of export conversion efficiency, the degree of urban openness, debt financing, and the efficiency of R&D innovation have had a significant positive impact on it. The reason may be that the increase in the degree of urban openness can promote the exchange and cooperation between the manufacturing industry and foreign countries and improve the efficiency of export conversion. At the same time, the export of high-tech products often has higher production quality and requirements and requires more investment. Therefore, the manufacturing industry can improve the export conversion efficiency of products through debt financing. From an innovation-driven perspective, R&D innovation efficiency has a significant positive impact on export conversion efficiency. The manufacturing industry continues to improve the technological content of export products through the development of R&D and innovation activities. While improving the efficiency of R&D and innovation, it can significantly promote the improvement of export transformation efficiency. This also further shows that by continuously improving the quality and efficiency of R&D and innovation, the high-quality development of manufacturing export trade will continue to be promoted, and it also confirms the inference that R&D and innovation efficiency will have a significant positive impact on export conversion efficiency. Geographical distance has a significant negative impact on export conversion efficiency, indicating that cities closer to the coastline, especially coastal cities, have higher export conversion efficiency. From the perspective of the influencing factors of overall efficiency, the level of urban economic development and debt financing has had a significant positive impact on it.

Data Availability

The data underlying the results presented in the study are available within the manuscript.

Conflicts of Interest

The authors declare that they have no conflicts of interest.

Acknowledgments

References

[1] N. Bui and J. Widmer, "Data-driven evaluation of anticipatory networking in LTE networks," *IEEE Transactions on Mobile Computing*, vol. 17, no. 10, pp. 2252–2265, 2018.

[2] D. Suh, S. Jang, S. Han et al., "Toward highly available and scalable software defined networks for service providers," *IEEE Communications Magazine*, vol. 55, no. 4, pp. 100–107, 2017.

[3] N. Benzaoui, J. M. Estarán, E. Dutisseuil et al., "CBOSS: bringing traffic engineering inside data center networks," *IEEE/OSA Journal of Optical Communications & Networking*, vol. 10, no. 7, pp. 117–125, 2018.

[4] R. Mohammadi, R. Javidan, M. Keshtgari, and R. Akbari, "A novel multicast traffic engineering technique in SDN using

TLBO algorithm," *Telecommunication Systems*, vol. 68, no. 3, pp. 583–592, 2018.

[5] M. Dayarathna, Y. Wen, and R. Fan, "Data center energy consumption modeling: a survey," *IEEE Communications Surveys & Tutorials*, vol. 18, no. 1, pp. 732–794, 2019.

[6] M. Armbrust, A. Fox, R. Griffith et al., "A view of cloud computing," *Communications of the ACM*, vol. 53, no. 4, pp. 50–58, 2020.

[7] J. Sanderson, "Risk, uncertainty and governance in megaprojects: a critical discussion of alternative explanations," *International Journal of Project Management*, vol. 30, no. 4, pp. 432–443, 2019.

[8] C. Oliver, "Determinants of interorganizational relationships: integration and future directions," *Academy of Management Review*, vol. 15, no. 2, pp. 241–265, 2019.

[9] S. Danwitz, "Managing inter-firm projects: a systematic review and directions for future research," *International Journal of Project Management*, vol. 36, no. 3, pp. 525–541, 2018.

[10] V. Ward, A. House, and S. Hamer, "Developing a framework for transferring knowledge into action: a thematic analysis of the literature," *Journal of Health Services Research & Policy*, vol. 14, no. 3, pp. 156–164, 2019.

[11] M. Lin and N. Li, "Scale-free network provides an optimal pattern for knowledge transfer," *Physica A: Statistical Mechanics and Its Applications*, vol. 389, no. 3, pp. 473–480, 2020.

[12] A. C. Inkpen and E. W. K. Tsang, "Social capital, networks, and knowledge transfer," *Academy of Management Review*, vol. 30, no. 1, pp. 146–165, 2019.

[13] A. L. Barabási and R. Albert, "Emergence of scaling in random networks," *Science*, vol. 286, no. 5439, pp. 509–512, 2018.

[14] G. Charness and M. Rabin, "Understanding social preferences with simple tests," *The Quarterly Journal of Economics*, vol. 117, no. 3, pp. 817–869, 2019.

[15] W. Zeng, M. Li, and F. Chen, "Cooperation in the evolutionary iterated prisoner's dilemma game with risk attitude adaptation," *Applied Soft Computing*, vol. 44, no. 7, pp. 238–254, 2016.

[16] H. A. Simon, "Theories of bounded rationality," *Decision and Organization*, vol. 1, no. 1, pp. 161–176, 2019.

[17] C. F. Camerer, "Progress in behavioral game theory," *Journal of Economic Perspectives*, vol. 11, no. 4, pp. 167–188, 2020.

[18] R. Fan, J. Lin, and K. Zhu, "Study of game models and the complex dynamics of a low-carbon supply chain with an altruistic retailer under consumers' low-carbon preference," *Physica A: Statistical Mechanics and Its Applications*, vol. 52, no. 8, pp. 451–460, 2019.

[19] K. Fichter, "Innovation communities: the role of networks of promotors in open innovation," *R&D Management*, vol. 39, no. 4, pp. 357–371, 2019.

[20] J. Y. Lee and C. H. Jin, "How collective intelligence fosters incremental innovation," *Journal of Open Innovation: Technology, Market, and Complexity*, vol. 5, no. 3, pp. 53–70, 2019.

[21] S. Ransbotham and G. Kane, "Membership turnover and collaboration success in online communities: explaining rises and falls from grace in wikipedia," *MIS Quarterly-Management Information Systems*, vol. 35, no. 3, pp. 613–627, 2019.

[22] C. M. Chiu, M. H. Hsu, and E. T. Wang, "Understanding knowledge sharing in virtual communities: an integration of social capital and social cognitive theories," *Decision Support Systems*, vol. 42, no. 3, pp. 1872–1888, 2016.

[23] Y. S. Hau and Y. G. Kim, "Why would online gamers share their innovation-conducive knowledge in the online game user community? Integrating individual motivations and social capital perspectives," *Computers in Human Behavior*, vol. 27, no. 2, pp. 956–970, 2020.

[24] C. Lettl, C. Herstatt, and H. G. Gemuenden, "Users' contributions to radical innovation: evidence from four cases in the field of medical equipment technology," *R&D Management*, vol. 36, no. 3, pp. 251–272, 2016.

[25] W. M. Cohen and D. A. Levinthal, "Absorptive capacity: a new perspective on learning and innovation," *Administrative Science Quarterly*, vol. 35, no. 1, pp. 128–152, 2019.

Research Article

Step-Counting Function of Adolescent Physical Training APP Based on Artificial Intelligence

Cong Du (ID)

College of Physical Education, Xuchang University, Xuchang 461000, Henan, China

Correspondence should be addressed to Cong Du; 12018001@xcu.edu.cn

With the rapid development of the information age, Internet and other technologies have been making progress, people's fitness awareness has been gradually enhanced, and sports fitness app has emerged as the times require. This paper mainly studies the step-counting function of physical training app for teenagers based on artificial intelligence. This paper uses the modular development method to achieve the functional requirements of the system as the goal, respectively, for parameter management, website configuration, system log, interface security settings, SMS configuration, WeChat template message and several functional modules to achieve system configuration. In this paper, three types of sensors are used to analyze the data changes in the process of walking through three types of data, and different weights are given as the results of step-counting. When the peak value of sensor data is measured, only the peak value of the primary axial data of each sensor is analyzed, which should be determined according to the actual axial value of the sensor. In this paper, the users' evaluation indexes of sports fitness app are divided into two groups: importance and satisfaction, so the obtained data are directly divided into two groups: importance and satisfaction of user experience indexes of sports fitness app, and the two groups of data are matched with the sample t test to ensure the scientific conclusion. Finally, the advantages and disadvantages of the user experience of college students' sports fitness app are analyzed through IPA analysis. Heuristic evaluation is carried out on the step app to score the second-level usability index of the app. The first-level usability index score and the total usability score of the step app are obtained by calculation. There is not much difference between male and female students who use sports apps. Among them, 288 are male students, accounting for 58.2% of the total and 16.4% are female students. The results show that the use of artificial intelligence technology can reduce the overall energy consumption of step-counting algorithm, so as to achieve an energy-saving step-counting algorithm.

1. Introduction

With the increase of the strength of the youth physical confrontation, in order to have a place in the world basketball, it is necessary to make the overall ability of the team outstanding, and the basis of each ability is the good physical quality of the players. Therefore, for teenagers, scientific fitness and reasonable avoidance of competitive risk events are particularly important for the participation, development, and breakthrough of competitive sports.

The virtual technology used by cloud computing technology isolates system resources, allowing users to perform artificial intelligence model training operations in their own unique virtualized systems, so that they can be adjusted for virtual environments with low resource utilization. It can

avoid the unavailability of the system environment due to human factors.

Artificial intelligence technology can improve resource utilization. Din et al. believe that, due to the existence of various pollutants produced by human, agricultural, and industrial activities, the quality of surface water has decreased. Therefore, plot the concentration of different surface water quality parameters. He tried to develop an artificial intelligence modeling method for drawing concentration maps of optical and nonoptical SWQP. For the first time, he developed a remote sensing framework based on a back-propagation neural network to quantify the concentration of different SWQP in Landsat8 satellite images. Compared with other methods (such as support vector machine), the developed Landsat8-based BPNN model is

used to obtain an important measurement coefficient between Landsat8 surface reflectivity and SWQP concentration. Although his research is innovative, it lacks certain experimental data [1]. Kulkarni and Padmanabham used the extended waterfall and agile models to model the entire process of software (SW) development. They integrate AI activities such as intelligent decision making, ML, Turing test, search, and optimization into the agile model. They evaluated two indicators in five independent software projects, such as the usability target achievement indicator and the integration index. Once the SW project is developed using these models, feedback queries will be formally collected, and the collected data will be extensively analyzed to identify the various characteristics of the product, thereby determining the product's related behavior in terms of models and indicators. Although their research is relatively comprehensive, the test content is not accurate enough [2]. Goyache et al. developed a method to use artificial intelligence to improve the design and implementation of linear morphological systems for beef cattle. The process they proposed involves an iterative mechanism, in which knowledge engineering methods are used to continuously define and calculate type features, scored by a group of well-trained human experts, and finally performed by four famous machine learning algorithms' analysis. The results obtained in this way can be used as feedback for the next iteration to improve the accuracy and effectiveness of the proposed evaluation system. Although his research sample is relatively complete, it is not innovative enough [3].

In this paper, user demands were obtained through user interviews and analysis of competing products. Then, questionnaire survey was adopted to determine the importance of teenagers' demands for mobile health applications. Then, the weight of demands was calculated through data analysis. In view of the difference in use motivation caused by gender, the users are classified by gender and age from the beginning of registration, and different user groups are pushed with different content of exercise knowledge. Combined with APP, this paper carries out professional evaluation on the exercise ability of users before exercise, quantifies and grades the evaluation results, gives scientific and reasonable exercise suggestions, promotes the formation of exercise habits, and provides a reference for sports and fitness enthusiasts to reasonably choose their own exercise projects.

2. Youth Physical Training

2.1. Artificial Intelligence Technology.
The classic sigmoid-based ESN state update equation is composed of N storage pool units, K input layer units, and L output layer units.

$$x\,(n+1) = f\left(Wx(n) + W^{\text{in}}u\,(n+1) + W^{fb}y(n)\right). \quad (1)$$

Among them, $x(n)$ is an N-dimensional reserve pool [4].
The output result obtained from the extended system can be expressed as

$$y\,(n) = g\left(W^{\text{out}}z\,(n)\right). \quad (2)$$

Among them, g is the activation function of an output layer.
The expression of the hidden layer is as follows:

$$\begin{aligned}
v_i(t) &= \begin{cases} u_r(t), & i \in A, \\ x_c(t), & i \in B, \end{cases} \\
\omega^i(t) &= \begin{cases} \omega^2, & i \in A, \\ \omega^3, & i \in B, \end{cases} \\
\text{net}_n(t+1) &= \sum_{i \in A \cup B} \omega^i(t)v_i(t), \\
x_n(t+1) &= f\left(\text{net}_n(t+1)\right).
\end{aligned} \quad (3)$$

Normally, the form of the GARCH model is as follows:

$$\begin{aligned}
r_t &= \phi_0 + \sum_{i=1}^{R} \phi_i r_{t-i} + \sum_{i=1}^{M} \varphi_i \varepsilon_{t-i} + \varepsilon_t, \\
\varepsilon_t &= u_t\sqrt{h_t}, \\
h_t &= k + \sum_{i=1}^{p} A_i \varepsilon_{t-i}^2 + \sum_{i=1}^{q} G_i h_{t-i}.
\end{aligned} \quad (4)$$

When the actual output of the network model is inconsistent with the expected output, an output error E will be generated. The expression is as follows:

$$E = \frac{1}{2}(d-O)^2 = \frac{1}{2}\sum_{k=1}^{l}(d_k - o_k)^2. \quad (5)$$

Expand the error to the hidden layer; there are

$$E = \frac{1}{2}\sum_{k=1}^{l}\left[d_k - f\,(\text{net}_k)\right]^2 = \frac{1}{2}\sum_{k=1}^{l}\left[d_k - f\left(\sum_{j=1}^{m} w_{jk}y_j\right)\right]^2. \quad (6)$$

When the weight and threshold iterations corresponding to the neurons in each layer are over, the learning and training phase of the neural network enters the forward propagation link again [5, 6].

$$\begin{aligned}
P(T(X(t)) = X(t+1)) &= P\{X(t+1) = X'|X(t) = X\} \\
&= \prod_{i=1}^{n} P\{X_i(t+1) = x_i(t+1)|X_i(t) = x_i(t)\}.
\end{aligned} \quad (7)$$

As a basic platform, in order to overcome the occurrence of the above situation, it must have basic isolation to ensure the independence of the service execution environment and hardware resources of each user. Containerized virtualization technology can provide system isolation for the platform, from the operating system to the software services, which are all defined by users, so as to provide users with a more flexible service execution environment [7]. Since the nodes in the cluster sometimes stop for various reasons, the cluster management tool usually automatically migrates all the containers running on this node to other nodes in the cluster. However, if some containers use local data volumes,

data loss will occur when the containers are migrated. Using network storage disks or distributed storage disks will be a viable choice [8].

The calculation formula of the autocorrelation coefficient of the current period and the previous period data is as follows:

$$p_k = \sum_{i=1}^{n} \frac{1}{n} \left(\frac{\widetilde{a}_i^k - \widetilde{u}_k}{\widetilde{\sigma}_k} \right) \left(\frac{\widetilde{a}_i^{k+1} - \widetilde{u}_{k+1}}{\widetilde{\sigma}_{k+1}} \right). \tag{8}$$

The FFT calculation formula is as follows:

$$X(k) = \sum_{n=0}^{N-1} \omega(n) (W_N)^{nk},$$
$$W_N = e^{-j(2\pi/N)}. \tag{9}$$

Based on the above analysis, it can be seen that compared with the step-counting algorithm in the frequency domain and the time domain, the calculation cost of the former is obviously higher than that of the latter. Although the step-counting algorithm in the frequency domain has a higher computational cost, compared with most step-counting algorithms in the time domain, the step-counting algorithm in the frequency domain usually achieves higher step-counting accuracy [9, 10].

2.2. Physical Training. Between functional physical training and traditional physical training, they are interrelated and complement each other. Specialization and integrity are the most prominent features of the former. But in the traditional physical training, it can not achieve these two points. In the physical training system, the traditional physical training is the most important foundation. At the beginning, the traditional physical training can be carried out first, and then the functional training can lay a good foundation for the body, so as to prevent the defects of strength training from causing unnecessary sports injury [11]. Functional physical training is not unitary. It needs to integrate and improve the advantages of traditional physical training. We can not ignore the traditional physical training, nor can we just carry out a kind of functional physical training. The two complement each other and complement each other, so as to make a special targeted and integrated training arrangement, so as to improve the athletes' special technical level and ability [12].

Physical fitness itself is an organic whole, not the mechanical or simple addition of various parts. We should understand physical fitness with the help of system theory. Systematic method has become an important method for people to understand and analyze things in modern science. The core idea of systematic view is the overall concept of system [13]. In general, in order to improve the basic shape of sports, improve the system initiative of athletes' organs, and give full play to the best mode of sports mechanism and effect, the physical fitness index system is taken as an important reference standard in the process of training. It belongs to the basic index of technical training and tactical training and has a positive impact on the technology, tactics,

load training, physical condition, and sports life of special sports. The establishment of a reasonable physical fitness index system can be used as a powerful carrier for the selection mechanism of athletes in reality [14].

Physical fitness is the foundation of young athletes and provides strong support for their technical level. Ordinary teenagers are mostly in the system of compulsory education or secondary and higher education, and their training purposes and means are different from those of young athletes. As far as the means of physical training are concerned, athletes will be better than ordinary teenagers in terms of selection, training, competition, and other aspects, but from the perspective of physiological development characteristics, they are in the second peak of development. The stimulation of training means will have a more obvious effect on athletes' training, which can provide training support for ordinary teenagers [15]. This will make the competition time longer and test the physical fitness of athletes. If one side's physical condition is not strong, there will be calf muscle cramps, or even acute sports injury. On the court, long-term muscle contraction and ball extension, such as fast movement, kicking, swinging, and wrist strength, are different from the periodic endurance of other sports. Athletes must have special endurance quality, special strength quality, special speed quality, etc. that change with the change of competition intensity [16].

2.3. Pedometer APP. The primary task of the pedometer algorithm is to obtain the original three-axis acceleration data based on the sensor module and then perform data analysis and algorithm design based on the entire waveform. The actual test shows that there are many interference clutters in the acceleration signal generated by the human body when counting steps in various scenes. Therefore, it is very important to preprocess the original data before formally analyzing the motion waveform [17].

The data collection function of the pedometer is realized by the main controller reading data from the sensor, and its core is the acceleration sensor. The use of analog signal sensors requires additional analog-to-digital converters, which will increase the complexity of the circuit and the space utilization rate; the use of digital signal sensors avoids this problem while using high-precision sensors to ensure the reliability of data. In addition, it is necessary to ensure a higher speed data interface, a certain processing capacity, and lower power consumption in the selection of the main controller and the sensor [18].

The overall architecture of pedometer is shown in Figure 1. According to the function requirement analysis, the acceleration and angular velocity data selected collection of six-axis accelerometer and gyroscope inertial sensor MPU6050, master controller selects 16 ultra-low power consumption microprocessor MSP430G2553. Data transmission can use serial port transmission or wireless module transmission, and the programming of the main controller can be realized through online programmable function [19].

The energy-saving pedometer mainly processes the acceleration sensor data collected by the smart phone using the
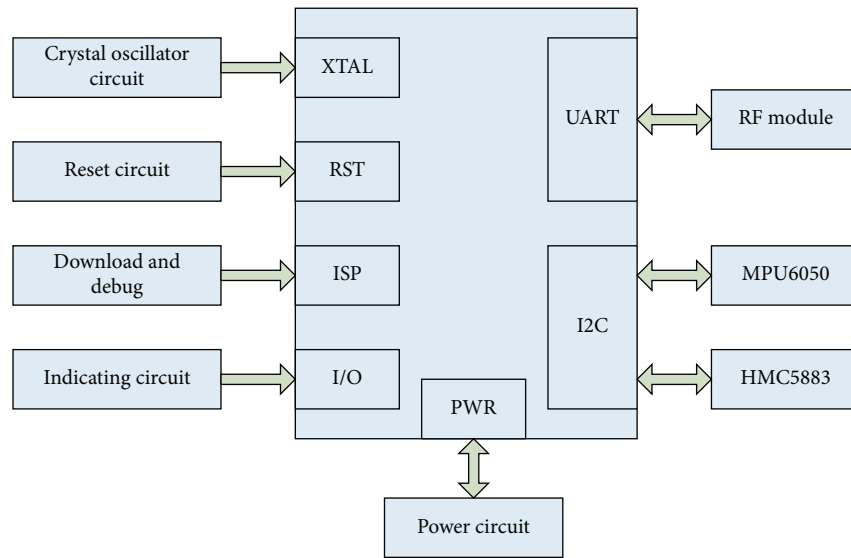
FIGURE 1: The overall architecture of the pedometer.

energy-saving pedometer algorithm to realize the pedometer function, which is also the core function of the pedometer. In addition, on the premise of meeting the step-counting function, it is also necessary to update the pedestrian walking steps in real time. In addition, in order to reduce the energy consumption of the pedometer, it is also necessary to perform the screen-out operation during pedestrian walking, so at this time, it is necessary to introduce services to realize that the pedometer program can run in the background, so as to ensure that even if the user does not interact with the front end of the pedometer for a long time or the program is switched to the background, it can still run successfully [20].

3. Physical Fitness Training APP Step-Counting Function Experiment

3.1. Operating Environment Configuration. This article adopts a modular development method to achieve the functional requirements of the system as the goal, based on the principle of science and practicality, and implements the system with several functional modules including parameter management, website configuration, system logs, interface security settings, SMS configuration, and WeChat template messages. Configuration: this system uses PHP dynamic development language, Php5.0–7.0 to build the system framework, MYSQL database management, LINUX, WINDOWS and other mainstream platform operating systems, HTML, CSS, JS, JQUERY, and other technologies to build front-end pages [21]. The experimental equipment parameters are shown in Table 1.

3.2. Establishment of the Human Motion Model. When the human body is walking normally, the arm swing can be regarded as a simple pendulum movement. According to the characteristics of pendulum, the acceleration changes sinusoidally. Although there are differences in the swing of human walking, the characteristic of sinusoidal

variation of acceleration is not affected [22]. A periodic sinusoidal waveform corresponds to a pair of peaks and troughs, and the number of sine waves detected is equivalent to the number of peaks detected. Therefore, the actual step-counting algorithm detects the number of steps through the wave peak of acceleration signal, and a wave peak represents a further advance. Because the human body has a certain rhythm when walking, that is, complete a stepping action as a cycle for circular motion. By calculating the peak or trough formed by the acceleration of gravity, the number of human steps can be detected and the step-counting function of mobile phone can be realized [23].

3.3. Step-Counting Rules. This article uses three types of sensors to analyze the data changes during walking through three types of data and assigns different weights as the result of step-counting. There is a maximum and minimum acceleration and a minimum and maximum angular velocity in a step cycle. The acceleration is set to $0.2\,g\sim2\,g$, and the angular velocity is set to $20°/s–200°/s$. When the data exceeds, it is considered as an invalid step. When measuring the peak value of sensor data, only the primary axial data of each sensor is analyzed for peak value, which needs to be determined according to the axial direction of the actual wearing sensor [24].

3.4. Model Evaluation Indicators. First of all, the BPNN model does not need to make any assumptions about the functional relationship between lagged returns and future returns. Secondly, by orthogonalizing the input space, the possible multicollinearity is eliminated and the uniqueness of hidden nodes is guaranteed. Again, the step-by-step selection process selects the most streamlined model to ensure that the training data will not be overfitted. Finally, it reduces the computational cost required to find the best model structure. Among the methods to achieve this goal, the

TABLE 1: Experimental equipment parameters.

Phone name	CPU model	CPU frequency (GHz)	RAM capacity (GB)	Battery capacity (mAh)
Google Nexus 5	Qualcomm Snapdragon 800	2.3	2	2300
Google Nexus 6	Qualcomm Snapdragon 805	2.7	3	3220

cross-validation method can avoid the occurrence of overfitting and ensure the stability of model performance by controlling the variance of model performance [25].

3.5. Pedometer APP Interface Test. The test of APP system is to correct the interface, check whether the interface is complete enough, whether there is content omission, whether the text in the interface is accurate, whether the format is beautiful, whether the interface style is consistent with the requirements, and whether the pictures and instructions are confused in the most intuitive way. In this paper, the users' evaluation indexes of sports fitness app are divided into two groups: importance and satisfaction, so the obtained data are directly divided into two groups: importance and satisfaction of user experience indexes of sports fitness app, and the two groups of data are matched with sample *t* test to ensure the scientific conclusion. Finally, the advantages and disadvantages of the user experience of college students' sports fitness app in the emerging stage are analyzed through IPA analysis method [26].

3.6. Pedometer APP Usability Evaluation. First, the APP user demand expansion table is listed on the left wall of the house of quality, and then the APP usability index expansion table is included on the ceiling of the house of quality, and the APP usability evaluation quality house is established. The second-level index weight is calculated by the percentage within the second-level index and the first-level index weight. Carry out heuristic evaluation of step-counting APP, score the second-level index of APP usability, and obtain the first-level index score of step-counting APP usability and the total usability score through calculation [27].

4. Experimental Results of Step-Counting Function

4.1. Physical Training Results. With the growth of age, degenerative changes of body function and aging appear. Women's aging rate is faster than men's; participating in sports can improve the degenerative changes caused by age, improve immunity, and delay aging. Women put forward higher requirements for their own health. Sports app has relatively perfect guidance on sports content and sports mode, which meets the needs of women to participate in sports. The results of reliability analysis are shown in Table 2. The reliability of each dimension of the questionnaire is greater than 0.70, so the internal consistency of the data measured in the questionnaire is high and the reliability is high.

Figure 2 shows the degree of college students' understanding of the pedometer APP. As can be seen from the figure, those who know very well account for 13.37% of the

total; those who know basics account for 57.90% of the total; those who are unclear account for 12.09% of the total; those who do not know well account for 9.67% of the total; those who do not understand at all account for 6.97% of the total. According to the sample data, less than 10% of college students still do not understand sports fitness APP at all. It can be seen that, on the one hand, the current sports fitness APP has a high degree of recognition among college students and has a certain social influence. Sports fitness APP has not only received the attention of the public, but also received extensive attention from college students. On the other hand, it can be seen that the publicity of sports and fitness apps for college students is still lacking. In a group that accepts emerging things so quickly, there are still many college students who do not understand sports and fitness apps at all. This should cause sports and fitness apps. The attention of managers and publicity still need to be strengthened.

The gender differences in the use of step app by adolescents are shown in Figure 3. According to the data, there is no significant difference in the proportion of male and female college students using sports app, of which 288 are male students, accounting for 58.2% of the total number, and 16.4% are more than female students. There are three possible reasons for this situation: first, boys' interest in sports far exceeds girls' and their curiosity about sports app far exceeds girls' level; second, boys are better than girls in sports talent and physiological function due to differences in body structure at both the student stage and the adult stage; third, boys should be more determined to exercise.

The number of strength trainings for teenagers is shown in Table 3. In the process of strength training, 26 people can train according to the coach's arrangement, accounting for 27.08% of the total number of people; in the process of strength training, 31 people can adjust the training content and intensity according to their own actual situation, accounting for 32.29%; in the process of strength training, 21 people can adjust the training content and intensity according to their own wishes. Accounting for 21.88% of the total number of people, 18 people did not know how to carry out strength training, accounting for 18.75% of the total number. Combined with the data in the table, the results of the male and female subjects in the control group before and after the experiment were tested, and the P values were 0.003 and 0.002, respectively, both <0.01, showing a very significant difference. In the mode of upper limb strength as the basis of basic quality training, dynamic training can ensure the athletes to complete the required actions within the specified time and limit the time to a certain range. It can effectively cultivate the rapid contraction and relaxation ability of athletes' body muscles, adapt to the basic requirements of competitive sports, and assist with flexibility

TABLE 2: Reliability analysis results.

	Cronbach's alpha coefficient	Number of items
Overall data	0.940	23
Health anxiety	0.899	6
Leisure and entertainment	0.830	6
Social needs	0.867	7
Emotional catharsis	0.807	4
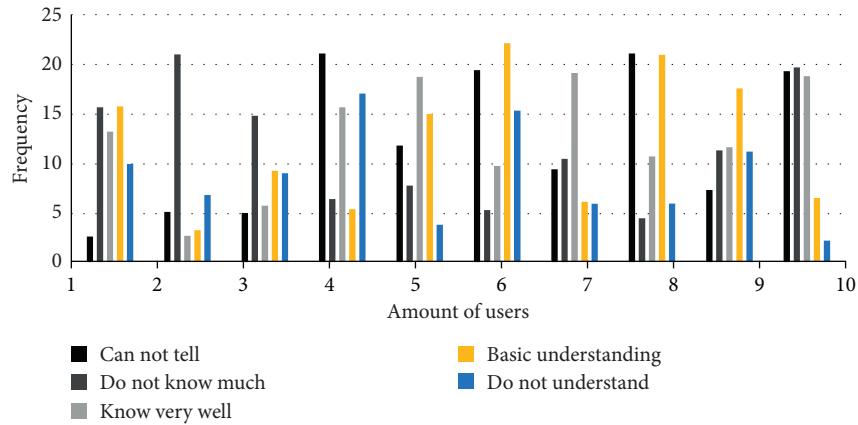
FIGURE 2: Undergraduates' understanding of step-counting APP.
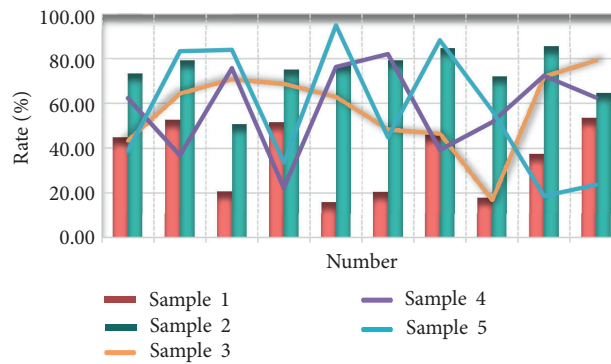
FIGURE 3: Gender differences between men and women of teenagers using pedometer apps.

TABLE 3: Number of strength trainings performed by adolescents.

Frequency	Coach		Athlete	
	Number of people	Proportion	Number of people	Proportion (%)
1 time	2	6.67	13	13.54
2 times	24	80	75	78.13
3 times	2	6.67	3	3.13
4 times and above	2	6.67	5	5.21

relaxation training. This can improve the elasticity and extensibility of individual energy parts of the body.

With the continuous improvement of the competitive level of athletes in specialized training, due to the competitive characteristics of competitive sports that explore the limits of the human body, the imbalance of the body caused by specialized training has become more serious. Managers from sports training should establish the concept of rehabilitation physical

training and consider the stages of athletes' training for many years when designing strategic goals. The comparison of pedometer's step accuracy is shown in Figure 4. The accuracies of energy-saving pedometer and autocorrelation pedometer are very similar, and they are better than that of crest detection pedometer. However, under the latter two walking modes, the step-counting accuracy of the three pedometers changed significantly, which may be caused by the obvious changes in the
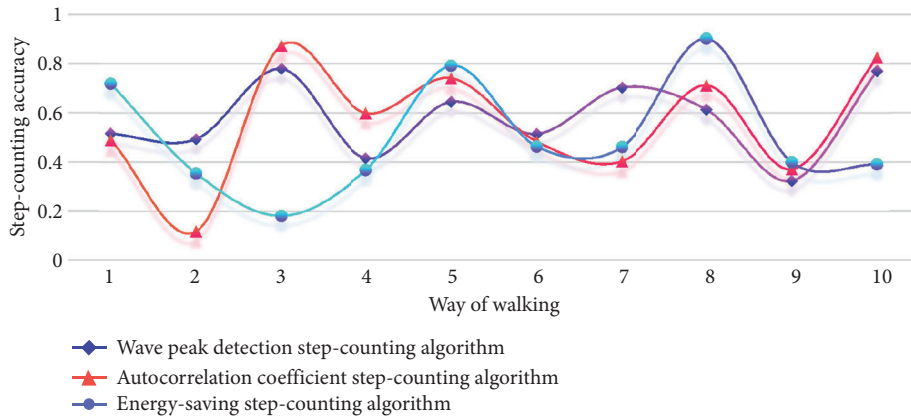
Figure 4: Comparison of step-counting accuracy of pedometer.

walking amplitude of the experimenters during the upstairs process. The experimental results show that the average accuracies of the crest detection step-counting algorithm, the autocorrelation coefficient step-counting algorithm, and the energy-saving step-counting algorithm are 92.4%, 94.4%, and 93.9%, respectively, and the standard deviations of the overall step-counting accuracy of the three step-counting algorithms are 0.045, 0.053, and 0.058, respectively. Through the above experimental results, the average step-accuracy of the three step-counting algorithms can be obtained as 92.7%, 94.7%, and 94.1%, and the average standard deviation of the overall step accuracy is 0.04, 0.045, and 0.055. This result is sufficient to show that the step-counting performance of the energy-saving step-counting algorithm proposed in this paper is approximately the same as the autocorrelation coefficient step-counting algorithm and is better than the step-counting performance of the crest detection step-counting algorithm.

4.2. Analysis of Physical Characteristics.

For athletes, in most cases, physical training is to place people in a more difficult environment for high-intensity, long-term, heavy-load continuous training. The survey results of coaches' awareness of youth physical training are shown in Table 4. 96.7% of the coaches believe that young athletes should be physically trained by age, and they have also considered age characteristics and energy expenditure characteristics.

Figure 5 shows the comparison of the sitting position before and after bending. The data well supports the theory of the sensitive period for the development of flexibility. 6–13 years of age is the best period for children and adolescents to develop flexibility. The high starting point of the pretest data illustrates this point, but there is room for improvement between the experimental group and the control group. The comparison shows that scientific and continuous physical training can accelerate the development of flexibility, but a thorough warm-up should be carried out before the development of flexibility. The experimental group $t = 5.11$, $P = 0 < 0.001$, the difference between the test variables is extremely significant. In the control group, $t = 0.36$, $P = 0.72 > 0.05$, there was no significant difference between the test variables. Analyze the data of the

Table 4: Survey results.

Problem	Yes	Percentage (%)	No	Percentage (%)
1	118	96.7	4	3.3
2	118	96.7	4	3.3
3	4	3.3	118	96.7
4	108	88.5	14	11.5
5	31	25.4	91	74.6
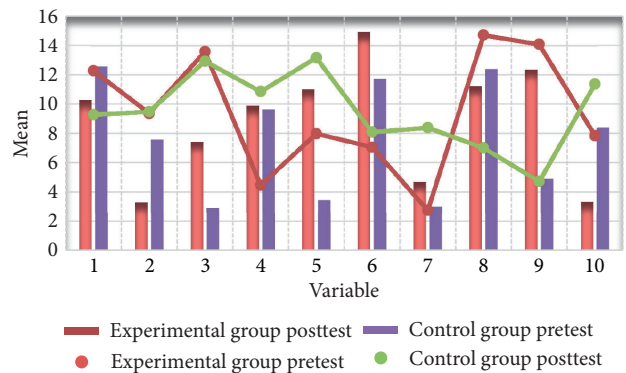
Figure 5: Comparison of sitting position before and after bending.

experimental group and the control group. Although the experimental group has a significant increase in the measured data before and after, the improvement is not large, and the control group data has not improved at all. Not much, but physical training also has a direct impact on the improvement of strength quality.

The score of the first-level index of youth special physical training is shown in Figure 6. The K-S values of each sports quality index are 0.781, 0.344, 0.391, 0.912, 0.135, 0.935, 0.169, 0.914, 0.517, 0.352, 0.807, and 0.694, which are all greater than 0.05. The index data obey the normal distribution, and the standard percentage method can be used to establish a single score table. Through the first-level index score and comprehensive score, we can easily determine the score of any one of the 30 young male badminton players at all levels. However, this has not yet achieved the purpose of comprehensive evaluation. If we do not establish the first-
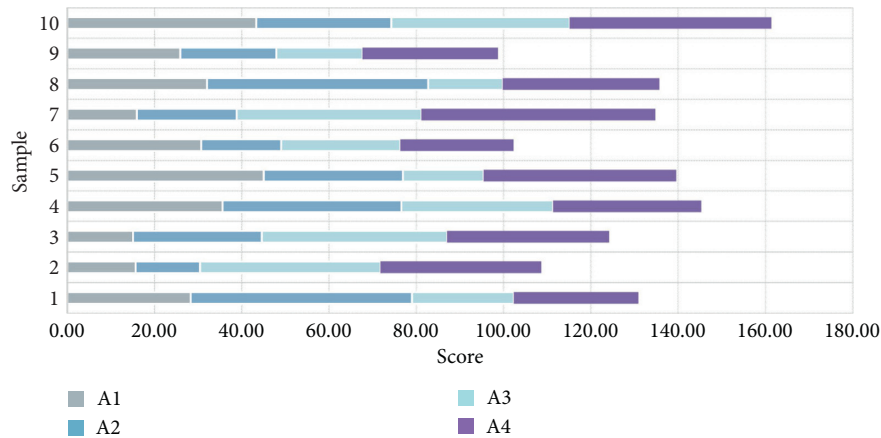
FIGURE 6: The first-level index scores of youth special physical training.

level index and comprehensive quality evaluation standard of athletes, we can not scientifically judge the level and level of athletes in the first-level index and comprehensive quality.

The comparison of FMS test results is shown in Figure 7. This is because the two-point movement is easy to complete, and it can reach the standard in the initial test. The three-point movement is difficult, and only one guard can complete it in the posttest. The three-point movement requires the athletes to complete the balance movement under the condition of the same knee support, which is very difficult for the basketball players with high average height. The average score of the third test is 2.86 higher than that of the first test, and the total score of the three tests shows a very significant difference ($P < 0.01$), which indicates that the formulation and implementation of the plan for the athletes' action mode and prerehabilitation training are successful.

4.3. Impact of Artificial Intelligence Technology. The results of the core group endurance test for adolescents are shown in Figure 8. The average duration of the whole team's plate support is 103 s, and the duration of the back bridge is 108.14 s. Compared with the two events, the duration of the back bridge is shorter. This is because the force environment of the back bridge is obviously better than that of the plate support no matter from the force arm or the strength of the active muscle. Theoretically, there should be a large gap between the maximum duration of the two movements. Through training, the gluteal muscle activation was higher, and the ability of back bridge was also greatly improved. There was a very significant difference between the results of the first back bridge test and that of the first back bridge test ($P < 0.01$). In basketball, the completion of technical action is mostly in the form of explosive force, so the explosive force directly affects the technical effect of athletes. Especially for young athletes, under the premise of lack of muscle and absolute strength, giving priority to the development of explosive force is the key to this stage of training.

The growth and development of adolescents are characterized by persistence and stages. Body shape and motor function are the two dimensions of physical fitness. The characteristics of adolescents aged 13 to 15 are the basis for

the construction of physical training content. The physical activity characteristics of children, adolescents, and adults are also reflected in these two aspects. For example, the height and weight of training equipment should be reduced for teenagers before their height suddenly increases, so as to adapt to the adaptability of their training. The sensitivity of different types of strength quality of adolescents is shown in Figure 9. Through the results, we can see that, in the process of describing each strength, its weight and proportion are also different. In this way, in the process of evaluation, we can classify and analyze different strength elements and qualities according to different types, which is also helpful for us to grasp the core index connotation in the training process, and avoid blindness and ineffectiveness in training.

The experimental results of the pedometer method are shown in Table 5. It can be seen from the table that even though the proposed method does not always perform the best for each walking activity considered, its accuracy is close to the optimal, with an average accuracy of 95.74%, which is at least 3.81% higher than the commonly used algorithm, which is at least 3.39% higher than the comparative step-counting software. From the maximum and minimum values, it can be known that the accuracy of this method is in the range of 77.97%–100%. Compared with other methods and step-counting software in the table, the difference between the maximum and minimum value of this method is the smallest, which indicates that the performance of FG method is relatively stable. This method is less affected by personal factors, and there is no case that the step-counting method has a high accuracy rate for one volunteer, but the other is very poor. Through observation, it can be found that, for RBF neural network, the more the number of hidden layer nodes, the higher the prediction accuracy. For the four models with hard ridge penalty, when the number of hidden layer nodes is reduced from 50 to 16, they also have the highest prediction accuracy; that is, the optimal hidden layer node is 16.

5. Conclusions

This article first selects NFS files and CEPH files as the object of the system performance test, selects the distributed file system as the basic storage, selects the CEPH file system as
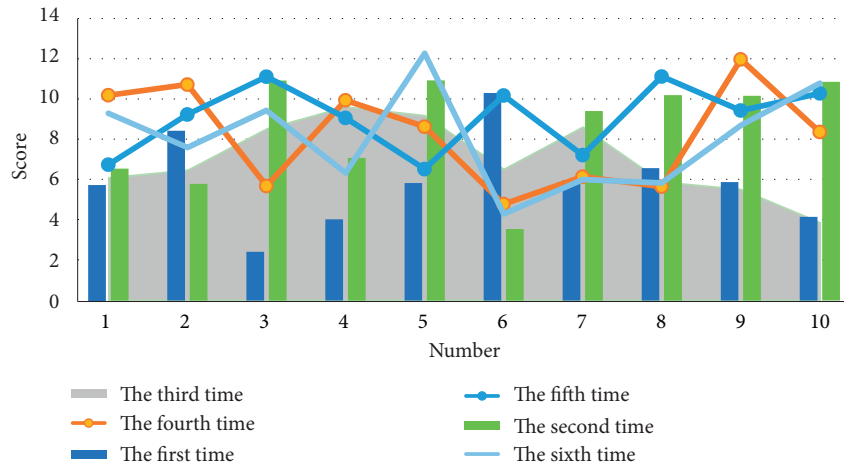
Figure 7: Comparison of FMS test results.
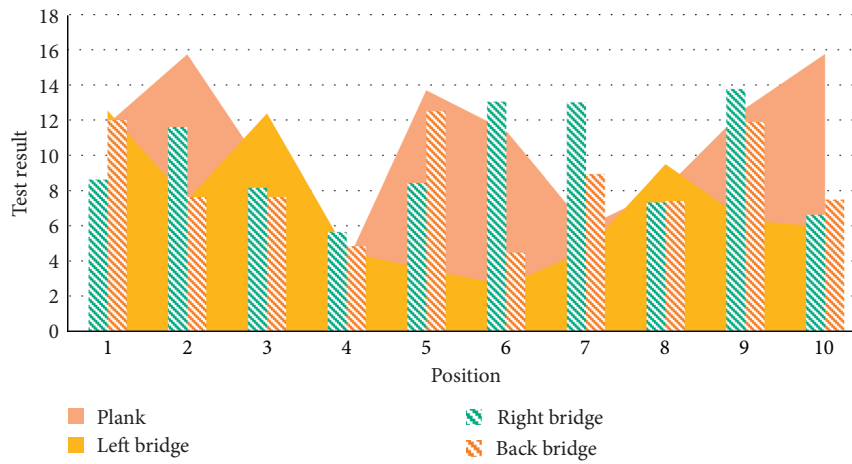
Figure 8: Endurance test results of adolescent core muscles.
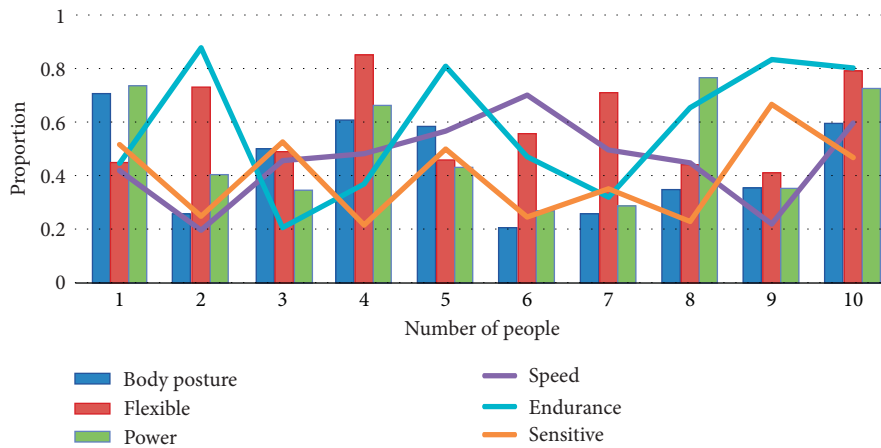
Figure 9: The sensitivity of adolescents to different types of strength qualities.

TABLE 5: Experimental results of step-counting method.

Method		J A (%)	K A (%)	L A (%)	M A (%)	N A (%)	O A (%)
FG	Minimum	96.54	91.55	93.42	90.35	87.32	77.97
	Max	100	98	99.57	99.57	100	100
	Average	98.55	95.83	96.47	96.76	94.9	91.95
FA	Minimum	87.67	67.83	58.55	67.37	89.83	47.46
	Max	98.5	98	98.25	98.22	98.59	80
	Average	93.49	86.67	86.47	86.15	95.86	69.32
AC	Minimum	89.43	82.63	90.83	72.73	54.24	47.46
	Max	100	97.39	98.7	99.58	96.72	88.14
	Average	95.83	88.84	95.55	88.06	78.76	70.2

the storage medium, and selects files based on the network layer. The traditional analysis method based on correlation coefficient can no longer deal with the relationship between dependent variables and multiple groups of independent variables, but the data mining algorithm can find the independent variables with strong correlation with the dependent variables from the massive data, so as to take them as the input set of the model.

Pedometers can not only play a certain medical role in aging and obesity patients, but also are increasingly used in people's daily exercise and fitness. It is accepted by the public and pays attention to the health of today's fast social life. It will be beneficial to the improvement of the overall health of the society and the development of pedometer design. The step-counting method uses peak detection method to obtain the fusion result of step-counting by taking different weights for different and quality data.

Through actual measurement and evaluation, the data shows that the pedometer designed in this paper has a step accuracy of 95%, stable performance, and strong anti-interference ability. Different from other mobile phone step-counting algorithms that only use acceleration sensor data, this paper combines acceleration and distance sensor data to realize step-counting, using acceleration sensor data for gait feature analysis, using distance sensor data to determine the location of the mobile phone, and improving the accuracy of human hand-held mobile phone step-counting, especially when walking without swinging arms.

Data Availability

No data were used to support this study.

Conflicts of Interest

The author declares that there are no conflicts of interest regarding the publication of this paper.

References

[1] E. S. E. Din, Y. Zhang, and A. Suliman, "Mapping concentrations of surface water quality parameters using a novel remote sensing and artificial intelligence framework," *International Journal of Remote Sensing*, vol. 38, no. 4, pp. 1023–1042, 2017.

[2] R. H. Kulkarni and P. Padmanabham, "Integration of artificial intelligence activities in software development processes and measuring effectiveness of integration," *IET Software*, vol. 11, no. 1, pp. 18–26, 2017.

[3] F. Goyache, J. J. Del Coz, J. R. Quevedo et al., "Using artificial intelligence to design and implement a morphological assessment system in beef cattle," *Animal Science*, vol. 73, no. 1, pp. 49–60, 2016.

[4] D. Norman, "Design, business models, and human-technology teamwork as automation and artificial intelligence technologies develop, we need to think less about human-machine interfaces and more about human-machine teamwork," *Research-Technology Management*, vol. 60, no. 1, pp. 26–30, 2017.

[5] B. K. Bose, "Artificial intelligence techniques in smart grid and renewable energy systems-some example applications," *Proceedings of the IEEE*, vol. 105, no. 11, pp. 2262–2273, 2017.

[6] A. Ema, N. Akiya, H. Osawa et al., "Future relations between humans and artificial intelligence: a stakeholder opinion survey in Japan," *IEEE Technology and Society Magazine*, vol. 35, no. 4, pp. 68–75, 2016.

[7] M. Nasr, A. E. D. Mahmoud, M. Fawzy, and A. Radwan, "Artificial intelligence modeling of cadmium(II) biosorption using rice straw," *Applied Water Science*, vol. 7, no. 2, pp. 823–831, 2017.

[8] A. H. Mazinan and A. R. Khalaji, "A comparative study on applications of artificial intelligence-based multiple models predictive control schemes to a class of industrial complicated systems," *Energy Systems*, vol. 7, no. 2, pp. 237–269, 2016.

[9] I. I. Baskin, T. I. Madzhidov, I. S. Antipin, and A. A. Varnek, "Artificial intelligence in synthetic chemistry: achievements and prospects," *Russian Chemical Reviews*, vol. 86, no. 11, pp. 1127–1156, 2017.

[10] M. A. Ali, "Artificial intelligence and natural language processing: the Arabic corpora in online translation software," *International Journal of Advanced and Applied Sciences*, vol. 3, no. 9, pp. 59–66, 2016.

[11] S. Narita, N. Ohtani, C. Waga, M. Ohta, J. Ishigooka, and K. Iwahashi, "A pet-type robot Artificial Intelligence Robot-assisted therapy for a patient with schizophrenia," *Asia-Pacific Psychiatry*, vol. 8, no. 4, pp. 312-313, 2016.

[12] M. Taheri, M. R. A. Moghaddam, and M. Arami, "Improvement of the/Taguchi/design optimization using artificial intelligence in three acid azo dyes removal by electro-coagulation," *Environmental Progress & Sustainable Energy*, vol. 34, no. 6, pp. 1568–1575, 2016.

[13] S. Tkatek, S. Bahti, and J. Abouchabaka, "Artificial intelligence for improving the optimization of NP-hard problems: a review," *International Journal of Advanced Trends in Computer Science and Engineering*, vol. 9, no. 5, pp. 7411–7420, 2020.

[14] R. C. Adams and B. Rashidieh, "Can computers conceive the complexity of cancer to cure it? Using artificial intelligence technology in cancer modelling and drug discovery," *Mathematical Biosciences and Engineering*, vol. 17, no. 6, pp. 6515–6530, 2020.

[15] M. Y. Zub, "Transformation of labor market infrastructure under the influence of artificial intelligence," *Business Inform*, vol. 8, no. 511, pp. 146–153, 2020.

[16] L. Hudasi and L. Ady, "Artificial intelligence usage opportunities in smart city data management," *Interdisciplinary Description of Complex Systems*, vol. 18, no. 3, pp. 391–397, 2020.

[17] S. Jha and E. J. Topol, "Adapting to artificial intelligence: radiologists and pathologists as information specialists," *JAMA*, vol. 316, no. 22, pp. 2353-2354, 2016.

[18] L. D. Raedt, K. Kersting, S. Natarajan, and D. Poole, "Statistical relational artificial intelligence: logic, probability, and computation," *Synthesis Lectures on Artificial Intelligence and Machine Learning*, vol. 10, no. 2, pp. 1–189, 2016.

[19] R. Liu, B. Yang, E. Zio, and X. Chen, "Artificial intelligence for fault diagnosis of rotating machinery: a review," *Mechanical Systems and Signal Processing*, vol. 108, no. 8, pp. 33–47, 2018.

[20] J. H. Thrall, X. Li, Q. Li et al., "Artificial intelligence and machine learning in radiology: opportunities, challenges, pitfalls, and criteria for success," *Journal of the American College of Radiology*, vol. 15, no. 3, pp. 504–508, 2018.

[21] P. Glauner, J. A. Meira, P. Valtchev, R. State, and F. Bettinger, "The challenge of non-technical loss detection using artificial intelligence: a survey," *International Journal of Computational Intelligence Systems*, vol. 10, no. 1, pp. 760–775, 2017.

[22] M. Seyedmahmoudian, B. Horan, T. K. Soon et al., "State of the art artificial intelligence-based MPPT techniques for mitigating partial shading effects on PV systems—a review," *Renewable and Sustainable Energy Reviews*, vol. 64, no. 10, pp. 435–455, 2016.

[23] R. Barzegar, J. Adamowski, and A. A. Moghaddam, "Application of wavelet-artificial intelligence hybrid models for water quality prediction: a case study in Aji-Chay river, Iran," *Stochastic Environmental Research and Risk Assessment*, vol. 30, no. 7, pp. 1797–1819, 2016.

[24] Z. Wang and R. S. Srinivasan, "A review of artificial intelligence based building energy use prediction: contrasting the capabilities of single and ensemble prediction models," *Renewable and Sustainable Energy Reviews*, vol. 75, no. 8, pp. 796–808, 2016.

[25] L. Caviglione, M. Gaggero, J. F. Lalande et al., "Seeing the unseen: revealing mobile malware hidden communications via energy consumption and artificial intelligence," *IEEE Transactions on Information Forensics & Security*, vol. 11, no. 4, pp. 799–810, 2017.

[26] T. Yang, A. A. Asanjan, E. Welles, X. Gao, S. Sorooshian, and X. Liu, "Developing reservoir monthly inflow forecasts using artificial intelligence and climate phenomenon information," *Water Resources Research*, vol. 53, no. 4, pp. 2786–2812, 2017.

[27] C. Modongo, J. G. Pasipanodya, B. T. Magazi et al., "Artificial intelligence and amikacin exposures predictive of outcomes in multidrug-resistant tuberculosis patients," *Antimicrobial Agents and Chemotherapy*, vol. 60, no. 10, pp. 5928–5932, 2016.

Research Article

Image Processing Technology Based on Internet of Things in Intelligent Pig Breeding

Shan Hua [iD]**, Kaiyuan Han, Zhifu Xu, Minjie Xu, Hongbao Ye, and Cheng Quan Zhou**

Key Laboratory of Creative Agriculture, Ministry of Agriculture and Rural Affairs, Institute of Agricultural Equipment, Zhejiang Academy of Agricultural Sciences, Hangzhou 310021, Zhejiang, China

Correspondence should be addressed to Shan Hua; huashan@zaas.ac.cn

In recent years, with the continuous innovation of the Internet of Things technology, the image processing technology in the Internet of Things technology has become more and more mature. Automated pig raising will become the mainstream pig raising technology, making the research of image processing technology in the intelligent pig breeding face a change. It has become more and more important. The traditional pig raising model cannot provide a suitable growth and development environment for the pigs. The pigs are disturbed by diseases and environmental discomforts during the growth process, which increases the mortality of the pig breeding process and cannot provide consumers with a guarantee. In order to solve the problem of unfavorable factors during the growth of live pigs, this article uses image processing technology to analyze data through images obtained through automated monitoring and management, uses the system to conduct intelligent, digitized, and standardized management of pig breeding data, and reports to the corresponding. The control module issues instructions to improve the corresponding environmental information and realize the intelligent management of pig breeding. This article will use image processing technology to monitor the growth of pigs in intelligent pig breeding. Studies have shown that the use of image processing technology to realize the intelligent management of pig breeding can help pig farms to carry out manual management to improve production efficiency and management efficiency. The management mode of the pig industry has changed from fuzzy to refined. The breeding cost of pig farms and a lot of manpower and material resources should be reduced, reducing the probability of pigs getting sick and the impact of the environment, reducing the mortality of pigs, improving their economic benefits, and providing consumers with a strong guarantee.

1. Introduction

tWith the continuous advancement of science and technology, intelligent breeding will become the main method of pig raising innovation. Strong productivity is the basic way of national economic growth, using the latest scientific and technological means and scientific methods to increase production, achieve the purpose of improving production efficiency, and effectively ensure people's daily demand for pork. Pork is the main meat product in China. As the number of pigs raised continues to increase, a lot of manpower and material resources need to be spent to ensure the living environment of the pigs and the prevention and control of diseases. At this time, the way of intelligent pig breeding should be timely. As a result, compared with

traditional breeding methods, intelligent breeding greatly reduces the risk of breeding.

With the development of computers and the development of intelligent control theory, control and management automation technology continues to improve, and it has been developed rapidly in the world [1]. At present, the indoor facilities of modern foreign farms have developed to a relatively complete level, and some standards have been set. Augspurger et al. and others invented the fully automatic breeding pig production performance measurement system FIFR, which measures the weight and diet of sows and selects ideal breeding pigs from it [2]. Wu et al. proposed that the information of sows can be used for scientific feeding of sows at each stage of feeding and at the same time for estrus detection, as well as individual sows for different breeding

conditions and litter [3]. Jiao et al. proposed that the characteristics of pig farm environmental monitoring and management are to maintain the pig farm environment and regulate the temperature, humidity, and air condition of the pig farm [4].

China's research on smart pig breeding is relatively late. At present, there is still a certain gap between China's technological level and the ability to adjust the self-developed measurement and control system and developed countries. The research on my country's overall environmental measurement and control technology has just begun, and some domestic experts and researchers have also developed some equipment and management systems. Izmailov proposed that the traceability of pigs should be converted from the traceability of central farm information to the traceability of decentralized breeding information, thereby expanding the scope of the traceability system [5]. Njock et al. proposed that, through the wireless network transmission in the data center, users can use their surrounding computers or mobile terminals to remotely manage the data center [6], so that the breeding environment information of poultry can be monitored in real time, and the breeding environment can be optimized according to the monitoring data [7].

In order to solve the problems of pig growth environment, health, diet, and other aspects, this paper uses image processing technology to obtain data such as pig growth environment and then judges through the system and then sends instructions to the corresponding control module to take corresponding measures. For example, the pig house is too dirty, and the system calls the cleaning pig house module to improve the pig house environment. In this paper, the establishment method of comparative reference method is used to establish an experimental group and a control group with 10 cubs in each group. The experimental group adopts intelligent breeding and the control group adopts the most primitive breeding method. The results showed that the weight gain of pigs in the experimental group was significantly faster than that of the control group, and the probability of infection was significantly lower than that of the control group. The main contributions of this article are comprehensive monitoring and management of pig breeding, breeding, breeding, slaughter, and other links to ensure consumer rights. Respond promptly, respond to major epidemics in time, and provide effective guarantee for the quality and safety of live pigs. Greatly reduce the labor cost and workload of employees, and improve data collection efficiency and data accuracy.

2. Image Processing Technology Based on Internet of Things in Intelligent Pig Breeding

2.1. Internet of Things. The system of the Internet of Things is very complex. It includes various applications such as electronics, communications, computers, and agronomy. By using IoT technology for data collection and reception, reliable transmission, intelligent processing, and automatic control, various production and transmission links can be established. Wait for the complete follow-up [8, 9].

However, if the network environment is different, its communication protocol may not be fully compatible [10]. Traditional wireless networks include mobile networks and LAN wireless networks. These network communication plans are aimed at point-to-point or multipoint-to-point transmission and have higher communication goals and measures.

2.1.1. IoT Architecture. The current IoT system model is not universal and lacks a complete system structure. When building an IoT system, you must consider network performance, such as scalability, reusability, and security. It is necessary to summarize the research results of the Internet of Things architecture and related theories and models of the wireless network architecture model. The main basis for designing and verifying the structure of the Internet of Things is still to simulate the actual scenarios of the Internet of Things, which should be combined with the existing examples of Internet of Things applications for summary and improvement. Understand the development direction of the Internet of Things. Finally, for different types of terminal equipment, it is necessary to consider related parameters, application technologies, and related standard specifications [11, 12], and a specific plan for the needs of users and the implementation of their functions is required. According to most research results at home and abroad, the Internet of Things system is divided into perception layer, network layer, and application layer, as shown in Figure 1.

(1) Perception Layer. The perception layer is the lowest structure of the Internet of Things. At the sensory level, a large number of sensory nodes are distributed in the environment where the development of pigs and other areas should be monitored. They are used for data collection, such as temperature and humidity, light intensity, and CO_2 concentration. At the same time, it analyzes, processes, and automatically manages the nodes and sends the sent data to the heterogeneous network [13, 14]. Most of the information changes in the environment are continuous and simulated; although the information on the network is completely different, different types of sensor devices are required to process the types of information obtained [15]. In order to be able to locate and retrieve information, provide strong support for production and guidance [16].

(2) Transport Layer. The IoT layer acts as a bridge between the perception level and the application level. The relevant information collected from the perception level is wirelessly transmitted to the terminal device. Commonly used are IEEE802.3-based Ethernet transmission technology, IEEE802.11-based WiFi transmission technology, IEEE802.15.1x Foundation-based Bluetooth transmission technology, IEEE802.15.4-based ZigBee transmission technology, 6Lan multitransmission technology and 6Low transmission technology mobile Transmission technology, such as GSM, GPRS, and 3G technology, based on IEEE802.16, and Mi MAX transmission technology. Both 802.3-based Ethernet and 802.11-based wifi are IP-based network communication
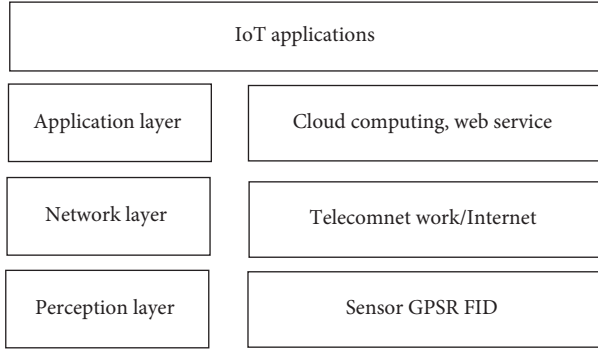
FIGURE 1: Internet of Things system composition diagram.

protocols, and 802.3-based Ethernet is the most widely used communication technology and multilayer structure in the IP protocol architecture. It can be achieved through other communication protocols and can also be applied to the Internet of Things architecture [17, 18].

(3) Application Layer. Process the data transmitted by the network layer and send the results obtained after algorithm analysis to different systems [19], which facilitates the operation and use of end users, including production, management, and maintenance. Business activities, such as raw pork monitoring, production pork processing, traceability management, logistics management, disease detection, and other systems will increase raw pork production and reduce production costs.

2.2. Image Processing Technology

2.2.1. Digital Image Processing Technology. The displacement measurement method based on digital image processing is a noncontact displacement tracking method, and its cost is lower than the displacement meter, GPS, electronic total station, and laser interferometer [20]. The existing displacement tracking methods based on digital image processing are mainly divided into two categories, namely, digital image correlation methods and specific target tracking methods.

(1) Digital Image Correlation. The digital image correlation method, also known as the digital position correlation method, is an important method for monitoring distortion in the field of digital image processing. The basic principle is to take point images before and after the structure is deformed and divide the point images before the deformation into smaller subregions. When the subarea is small, each subarea can be regarded as rigid motion. Next, for each subregion, by selecting a specific correlation function for calculation, find the region in the distorted image with the highest correlation coefficient with the subregion and treat it as the new position of the subregion after deformation, and then perform shift. The number of partitions can be achieved [21, 22]. If you need to calculate the displacement of the entire field, you can calculate the correlation of all subregions. The performance of the correlation function will directly affect the search accuracy and calculation speed of the digital image correlation method:

$$C_{\text{ZNCC}} = \sum_{i=-M}^{M} \sum_{j=-M}^{M} \left[\frac{\{f(x_i, y_i) - f_m\}\{g(x_i, y_i) - g_m\}}{\Delta f \Delta g} \right],$$

$$C_{\text{ZNSSD}} = \sum_{i=-M}^{M} \sum_{j=-M}^{M} \left[\frac{f(x_i, y_i) - f_m}{\Delta f} - \frac{g(x_i, y_i) - g_m}{\Delta g} \right]^2,$$

(1)

where $f()$ and $g()$, respectively, represent the gray value of each pixel position before and after distortion, and f_m, g_m, Δf, and Δg are concepts and mathematical formulas:

$$f_m = \frac{1}{(2M+1)^2} \sum_{i=-M}^{M} \sum_{j=-M}^{M} f(x_i, y_i),$$

$$g_m = \frac{1}{(2M+1)^2} \sum_{i=-M}^{M} \sum_{j=-M}^{M} g(x_i, y_i),$$

$$\Delta f = \sqrt{\sum_{i=-M}^{M} \sum_{j=-M}^{M} \left[f(x_i, y_i) - f_m \right]^2},$$

$$\Delta g = \sqrt{\sum_{i=-M}^{M} \sum_{j=-M}^{M} \left[g(x_i, y_i) - g_m \right]^2}.$$

(2)

The advantages of the digital image correlation method are the algorithm is simple and easy to implement, the field of view is wide, the noncontact distortion tracking method is adopted, and the tracking accuracy is high.

The disadvantage of the digital image correlation method is the essence of the method is to perform a large number of iterative calculations, and the calculation complexity is very high, especially when the image pixels are large, and the image correlation calculation amount will be abnormally large and cannot meet the requirements of tracking speed.

(2) Specific Target Tracking. As the name suggests, target tracking is to locate a specific target in each frame of an image to create a target trajectory. Place the calibration board on the target to be measured to compensate for the offset. After sampling the displacement of the calibration plate with a digital camera, you can know the displacement at this time. This is the method of tracking displacement through target tracking [23, 24].

Compared with digital imaging technology, this target tracking technology is more suitable for tracking structure migration. The current weakness of this technology is mainly reflected in the unreasonable setting of monitoring targets. Some researchers use lasers and other light sources as monitoring targets [25], which not only has high requirements for the monitoring environment but also has a greater impact on the environment.

2.2.2. Analog Image Processing. Analog image processing includes optical lens processing, photography, and TV production, which are all real-time processing. Its processing

speed is fast and can work in parallel. In theory, the speed of analog image processing can reach the speed of light. The disadvantages are low precision, control flexibility, almost no crisis function, and nonlinear processing function [26, 27].

2.3. Artificial Intelligence.
Relying on deep learning and big data, the development of artificial intelligence has entered a new era. The reason why the achievements of artificial intelligence are "panicked" is that they have trained their own experience models through a large amount of sample data research and completed further in-depth learning of self-play and self-communication on this basis. In order to train himself to obtain more precise reaction and processing capabilities, he reached a higher level of evolutionary system upgrade [28].

2.3.1. Main Characteristics of Artificial Intelligence.
It is people-oriented, serving the people. Artificial intelligence is actually a system based on computer hardware and programs written by humans and works according to specific logic and algorithms [29]. Artificial intelligence is designed and manufactured by humans and must serve humans.

According to human design, it can recognize the environment and produce corresponding emergency behaviors and can interact with people. The design of an artificial intelligence system must be able to perceive, perceive, smell, touch, and test the five human touch senses through language, words, expressions, and actions.

It has adaptability, learning ability, evolutionary repetition, and connection expansion. Artificial intelligence systems must have the ability to adapt to the environment and the ability to learn independently. It has the ability to adjust corresponding parameters, data, and tasks in real time according to environmental changes.

2.3.2. Existing Artificial Intelligence Technology.
The main research technologies of artificial intelligence are expert systems, natural language understanding, machine learning, distributed artificial intelligence, machine learning, and pattern recognition. In recent years, the rapid development of computer hardware technology has led to a significant increase in computer performance. The global popularity of the Internet has provided large databases of big data technology and deep learning technology, which has led to the further development of two technologies. Artificial intelligence happened. It has rapid development and is widely used in family life, medicine and health, transportation, and other fields; various industries are actively exploring how to use artificial intelligence technology to solve industry problems, and education is no exception [30].

2.4. Intelligent Breeding.
The system mainly collects basic information about pigs in the pig industry. Complete the identification of individual piglets in the herd, and obtain accurate information about individual piglets and relevant data about the piglet's diet, including the number of ear tags, feeding frequency, and feeding speed.

In the decision analysis part, the feed intake curve and the pig growth model curve are drawn based on the basic information collected from the pigs. The system determines the feed intake of piglets, the type of feed consumed, and the proportion of each category according to the model curve. Control the growth curve of piglets more scientifically [31, 32]. The automatic decision-making system of live pigs will automatically identify the piglets they may need to eat, feed them automatically, and urge breeders to take the next step and take the next step.

The pig raising monitor and control unit monitors the pig raising environment in detail and creates a false alarm mechanism. The piglets that may be suffering from diseases can be controlled in time, which will benefit the growth and development of other piglets. Through this mechanism, the traditional method of capturing Chinese captives can be changed, and the semirandom method of piglets can be completed through the integrated monitoring system. This can not only improve the quality of young pork but also control the living environment of melon young [33]. This will also help us to improve the efficiency of pig raising more effectively. At the same time, real-time monitoring of the environment of the pig farm can provide a good growth environment for the growth and development of piglets.

2.5. Information Management.
Information management must reflect the progress and dynamics of the project in the fastest and most flexible way, and record the occurrences and problems in a timely manner. Information is only effective when it is delivered to people who need it and have a strong topicality. Therefore, it is necessary to provide useful information to relevant departments and personnel in the fastest and most effective way, which becomes the basis for decision-making, management, and control. In order to ensure the accuracy of the information, the original information must be reliable [34]. Only reliable original information can process accurate information. When collecting and sorting out original data, information workers must adopt an attitude of seeking truth from facts, transcending subjective arbitrariness, and carefully verifying the original data so that it can accurately reflect the true situation. In this research, images are collected by monitoring equipment, transmitted to the system, and then processed from the system communication database, and then the corresponding control units are instructed to change their respective living environments.

Database management technology is used to manage animal information in a specific environment. In actual production, information system management can be completed by analyzing data and formulating a logical production plan [35]. In the process of raising pigs, it is important to preserve better feed and pollution, feed pigs automatically, save manpower and material resources, and use individual differences to manage the galaxy. At the same time, the production data of each group of animals and poultry used to select seeds can be recorded and stored. In

the past, American researchers created the FeedLogic system to feed and produce pigs. The system can monitor the production status of pigs, dynamically adjust the feed supply of pigs, and use remote computers to control the feeding of pigs, thereby improving the feed conversion efficiency and nutritional level [36].

3. Experimental Research on Image Processing Technology Based on Internet of Things in Intelligent Pig Breeding

3.1. Test Subject. This study mainly selected *X* pig farms, two pig houses with similar environments, and 20 healthy piglets of the same breed into two groups. They are the experimental group and the control group. The experimental group adopts advanced intelligent breeding technology, and the control group adopts original artificial breeding technology. The weight and health status of pigs are collected every 3 days for later data comparison and analysis. Among them, the experimental group needs to check the monitoring equipment, feeding equipment, and sprinkler equipment, regularly to prevent equipment damage from affecting the experimental results, and tries to ensure the survival of the piglets as much as possible. The control group arranges staff to raise regularly and clean regularly. To ensure the validity of the data and the accuracy and reliability of the experiment, the live pig is the main source of the data. Through this experiment, you can explore the advantages and disadvantages of intelligent farming over artificial farming, and you can also see what role image recognition technology plays in intelligent farming.

3.2. RBPMF-EPCA Algorithm Experiment. In order to verify the robustness of the RBPMF-EPCA algorithm under different attack strengths and different attack types, the experiment selected the filling scale 3% and 5% and the attack scale 1%, 2%, 5%, 8%, 10%, and 15%; the attack type is average attack, random attack, and fuzzy attack as the attack overview. In order to verify the robustness of the algorithm, make the experiment more convincing and better explain the effect of the experiment; this paper chooses three more classic robust recommendation algorithms as the comparison experiment, as follows MMF: based on *M* estimation matrix factorization algorithm, LTSMF: matrix factorization algorithm based on minimum truncated squares, and VarSelect SVD: robust collaborative recommendation algorithm. Good recommendation accuracy has always been the primary goal pursued by the recommendation system. This article will first analyze and compare the recommendation accuracy of each algorithm. This paper chooses RMSE as the index to evaluate the accuracy of the recommendation system.

3.3. Experimental Data Collection. In the intelligent pig breeding system, the basic information of pigs from slaughter to slaughter to slaughter is stored, relevant data are grouped according to user needs, and relevant query, data entry, and modification interfaces are provided according to

the logical structure of the system. This article uses Mysql database technology, and the following are the advantages and functions of Mysql database:

(1) Mysql database is an open-source relational data management system. When transaction processing is not required, Mysql is the best choice for information management.

(2) There is no limit to the number of people accessing the database at the same time.

(3) High security, providing users with multiple authentication methods to connect to the data system, while providing encryption procedures. Users can encrypt data files without modifying the host development program to meet basic data security requirements.

(4) Compared with other databases, the amount of database information that can be stored is more, and the maximum amount of information that can be stored can reach 50 million.

(5) It has good running speed and is currently the fastest database system on the market.

(6) Good portability, simple, and effective user power adjustment.

(7) Compared with other large databases, debugging, management, and optimization are relatively simple. Because the design of Mysql database is consistent with the design of Pig management system database, this system chooses Mysql database as the development of Pig information management database.

3.4. Gather Data. During the experiment, data were collected regularly on the weight of all pigs in the experimental group and the control group, the environment of the pig house, and the health of the pigs every 3 days. Table 1 is a comparison of the 27-day average weight of pigs in the experimental group and the control group (health and environment: 1 means good and 0 means bad).

In this way, we have a more intuitive, comprehensive, and in-depth understanding of the status quo of all aspects of intelligent farming, combined with relevant literature and information, and put forward some targeted related suggestions and countermeasures based on the actual situation.

4. Research and Analysis of Image Processing Technology Based on Internet of Things in Intelligent Pig Breeding

4.1. Analysis Based on the Average Weight Gain of Pigs in 27 Days. The contrast and positioning accuracy of the image are enhanced, and the difficulty of image processing is reduced. The method of extracting the S value from the HSL model is used to realize the image gray-scale processing. The image is divided into blocks to detect the feature points, and the threshold is automatically selected in each block. The obtained feature point area is controllable, the number is controllable, and the overall distribution is uniform. Collect

TABLE 1: Basic information and environmental information sheet for pigs.

	Time	10.8	10.11	10.14	10.17	10.20	10.23	10.26	10.29	11.1	11.4
Test group	Weight	39.8	42.5	45.3	48.1	50.8	53.6	56.3	59	61.8	64.7
	Health	1	1	1	1	1	1	1	1	1	1
	Surroundings	1	1	1	1	1	1	1	1	1	1
Control group	Weight	40.1	42.3	44.4	46.7	48.9	51.1	53.3	55.4	57.6	59.7
	Health	1	1	1	1	0	0	1	1	1	1
	Surroundings	1	1	1	0	0	1	1	1	1	1

data on the body weight of pigs every 3 days and find the average value, as shown in Figure 2.

It can be seen intuitively from Figure 2 that the experimental group grew from 39.8 kg through the intelligent pig image processing system to 64.7 kg, and the control group grew from 40.1 kg through the traditional artificial breeding method to 59.7 kg, which can be seen intuitively The growth rate of the experimental group was significantly better than that of the control group. The image processing technology based on the Internet of Things has achieved certain success in the research of intelligent pig breeding. It can also be seen that the growth of pigs raised by intelligent breeding technology is significantly better than artificial breeding. With the increasing maturity of technology, the intelligent pig image processing system can greatly reduce labor costs and personnel workload and improve data collection efficiency and data accuracy.

4.2. Analysis of the Impact of Live Pig's Living Environment on Health.

In the analysis and design of the intelligent pig raising management system, we have learned a lot of important information through interviews with pig farmers. By systematically analyzing and judging the information provided by pig farmers, we have come to the main requirements and main design points of the system.

Plot the relationship between health and living environment data collected in 27 days, as shown in Figure 3. It can be objectively seen that health and living environment are closely related. When the living environment declines, live pigs gradually become infected with diseases. It can be concluded that intelligent breeding can greatly reduce the probability of pigs being infected with diseases.

4.3. Analysis Based on the Accuracy of the Information Obtained by Image Recognition

4.3.1. Image Recognition Technology for Accuracy Analysis of Feed Information.

The monitoring equipment of the experimental group collects the information about insufficient feed and sends it to the system. The system calls the database gallery to judge the insufficient feed and calls the feeding function. Here, we analyze the accuracy of image recognition technology. Since there will be workers checking the feeding equipment on a regular basis, here is a random sample of one day, and the feeding equipment is checked every two hours to obtain a data plot, as shown in Figure 4.

The system performs database comparison, and the image recognition technology has an accuracy of 95% for feed information. As long as the feed is bottomed out and the monitoring equipment collects the data, the system compares the data, that is, calls the feeding function. There is no need to worry about the feed. Pigs will naturally eat when they are hungry. The remaining deviation is caused by imperfect data collected by the monitoring system. This aspect is also an area that can be improved. For example, the data collected by two monitoring devices are used for double judgment.

4.3.2. Image Recognition Technology for Accuracy Analysis of Living Environment Information.

The monitoring equipment of the experimental group collected information on the presence or absence of pig excrement on the ground and passed it into the system. The system called the database library to judge whether there was any pig excrement and called the cleaning function. Here, we analyze the accuracy of image recognition technology. As the experimental group will have workers regularly check the cleanliness of the pig house floor, here is a random sampling of one day, every two hours to check the cleanliness of the pig house floor and at the same time compare the plot with the control group (cleanliness score 1–10: 0 is the best and 10 is the worst), as shown in Figure 5.

The system performs database comparisons, and the accuracy of image recognition technology for living environment information has reached 99%. As long as there is excrement monitoring equipment on the ground of the pig house to collect data, the system compares the data and calls the cleaning function. It can be seen that the image recognition technology has reached a high standard for the accuracy of living environment information and can basically ensure the cleanliness of the pig house.

4.3.3. Analysis of Experimental Group and Control Group.

We collect and draw data on the manpower, material resources, and cost issues of the experimental group and the control group, as shown in Table 2.

It can be seen from Table 2 that the experimental group spends less manpower and material resources, but it needs to spend a lot of money to install monitoring equipment and systems and this is a once-and-for-all method, just pay attention to regular maintenance, and the control group spends more manpower and material resources. The cost is not much. In terms of the benefits
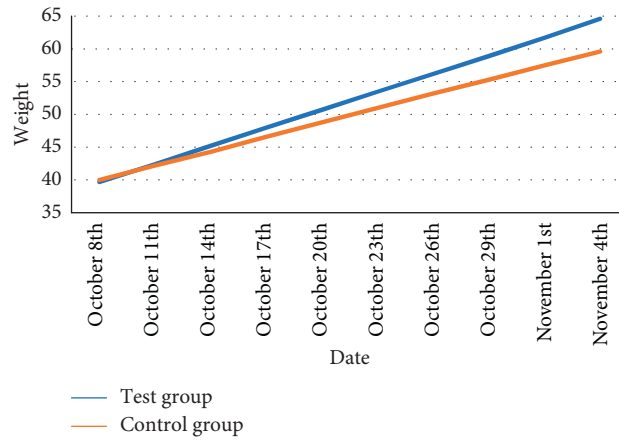
Figure 2: The weight of pigs in the experimental group and the control group changing over time.
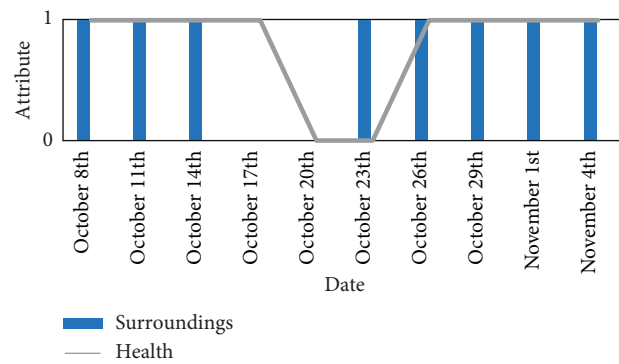
Figure 3: Relationship between health and living environment.
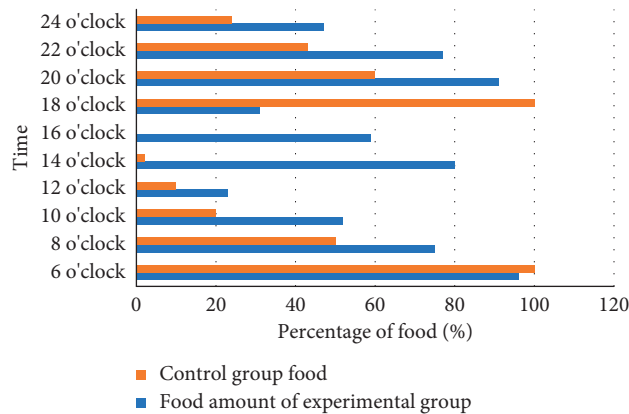
Figure 4: Feed ratio chart.

obtained, the experimental group is higher than the control group. At the same time, as far as China's current development concept is concerned, it is necessary to take a long-term perspective. On the one hand, the traditional pig raising model cannot provide a suitable growth and development environment for the pigs, which are disturbed by diseases and environmental discomforts during the growth process, which increases the mortality of the pig breeding process, and there is no valid pig resume record for each pig. This also illustrates the important role of image processing technology in intelligent pig breeding from the side.
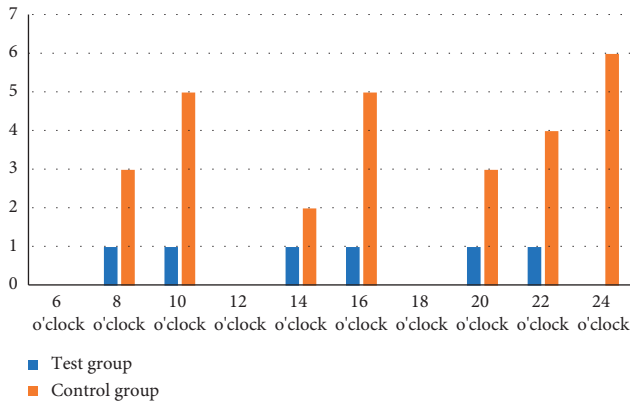
FIGURE 5: Comparison chart of living environment scores of pigs.

TABLE 2: The labor, material, and cost issues of the experimental group and control group.

	Human and material resources	Cost	Profit
Test group	Less	High	High
Control group	High	Less	Less

5. Conclusions

The pig raising environment has a vital influence on the growth and development of pigs. The pig farm has been collected and adapted to the environment to achieve the best pig raising environment and improve animal welfare. At the same time, the basic conditions for live pigs from slaughter and feed vaccine entry and exit to exit are calculated and converted into electronic files to provide data support for pork safety and report healthy pig breeds. According to the actual needs of the pig farm, a high-definition network camera was selected to monitor the living conditions of the pigs in the pig farm, and an online monitoring platform was created so that the administrator can check the situation of the pig farm at any time. The growth of pigs raised through intelligent breeding technology is significantly better than artificial breeding. As the technology matures, the intelligent pig image processing system can greatly reduce labor costs and personnel workload and improve data collection efficiency and data accuracy.

The design is only based on the preliminary exploration of the intelligent pig breeding management system. Although some results have been achieved, there is still a big gap between the goals of fully intelligent replication. With the development of environmental information nodes for pig farms and breeding pigs, the general humidity should be relatively high and node humidity should be increased to improve the stability and lifespan of the nodes. In the complex environment of pig farms, other environments need to be studied and more accurate environmental information parameters are needed to raise pigs. This article is just a simple statistic about the total number and consumption of pigs. It can also be used for each pig. It can measure the daily consumption of pigs so that big data analysis can be used to simulate the daily consumption of pigs, achieve more precise catering goals, and improve economic efficiency.

This article uses image recognition technology to study the role of intelligent breeding and closely monitor and manage pig reproduction, reproduction, reproduction, and slaughter. Through this system, relevant production companies and health management departments can track the source and production process of live pigs to determine the purchase process and the development process of live pigs. At the same time, the system provides comprehensive and relevant data and information from breeding pigs to slaughter pigs, thereby improving worker management and consumer confidence, providing rapid response and timely treatment of major epidemics, and providing quality and quality an effective guarantee. Safe pig raising: improving pig breeding information and quality not only improves the efficiency of the intelligent management system but also contributes to the formation of animal husbandry information.

Data Availability

No data were used to support this study.

Conflicts of Interest

The authors declare that they have no conflicts of interest.

Acknowledgments

References

[1] C. D. Saudek, "Data source automation: new technology for the management of patient-generated test results," *Diabetic Medicine A Journal of the British Diabetic Association*, vol. 6, no. 5, pp. 394–399, 1989.

[2] N. R. Augspurger, M. Ellis, D. N. Hamilton et al., "The effect of sire line on the feeding patterns of grow-finish pigs," *Applied Animal Behaviour Science*, vol. 75, no. 2, pp. 103–114, 2002.

[3] H. X. Wu, H. R. Hallingbäck, and L. Sánchez, "Performance of seven tree breeding strategies under conditions of inbreeding depression," *G3 Genesgenetics*, vol. 6, no. 3, pp. 529–540, 2016.

[4] J. Jiao, H. Ma, Y. Qiao, Y. Du, W. Kong, and Z. Wu, "Design of farm environmental monitoring system based on the Internet of Things," *Advance Journal of Food Science and Technology*, vol. 6, no. 3, pp. 368–373, 2014.

[5] A. Y. Izmailov, "Intelligent technologies and robotic means in agricultural production," *Herald of the Russian Academy of Sciences*, vol. 89, no. 2, pp. 209-210, 2019.

[6] P. G. A. Njock, S. L. Shen, A. Zhou et al., "Evaluation of soil liquefaction using AI technology incorporating a coupled ENN/t-SNE model," *Soil Dynamics and Earthquake Engineering*, vol. 130, p. 105988, 2020.

[7] C. S. S. Bernardo, H. Lloyd, F. Olmos, L. F. Cancian, and M. Galetti, "Using post-release monitoring data to optimize avian reintroduction programs: a 2-year case study from the Brazilian Atlantic Rainforest," *Animal Conservation*, vol. 14, no. 6, pp. 676–686, 2011.

[8] S. Li, L. D. Xu, and S. Zhao, "The Internet of Things: a survey," *Information Systems Frontiers*, vol. 17, no. 2, pp. 243–259, 2014.

[9] A. Al-Fuqaha, M. Guizani, M. Mohammadi, M. Aledhari, and M. Ayyash, "Internet of Things: a survey on enabling technologies, protocols, and applications," *IEEE Communications Surveys & Tutorials*, vol. 17, no. 4, pp. 2347–2376, 2015.

[10] F. Massion, "Intelligent terminology," *Multilingual Computing & Technology*, vol. 30, no. 5, pp. 30–34, 2019.

[11] N. N. Sirdesai, A. Singh, L. K. Sharma, R. Singh, and T. N. Singh, "Determination of thermal damage in rock specimen using intelligent techniques," *Engineering Geology*, vol. 239, no. 9, pp. 179–194, 2018.

[12] S. Sicari, A. Rizzardi, L. A. Grieco, and A. Coen-Porisini, "Security, privacy and trust in Internet of Things: the road ahead," *Computer Networks*, vol. 76, pp. 146–164, 2015.

[13] J. Wu, J. Liu, Z. Huang et al., "Intelligent network selection for data offloading in 5G multi-radio heterogeneous networks," *China Communications*, vol. 12, no. 1, pp. 132–139, 2015.

[14] J. Mahmoudi, M. A. Arjomand, M. Rezaei, and M. Mohammadi, "Predicting the earthquake magnitude using the multi layer perception neural network with two hidden layers," *Civil Engineering Journal*, vol. 2, no. 1, pp. 1–12, 2016.

[15] G. Loureiro and A. G. Taboada, "Do improvements in the information environment enhance insiders' ability to learn from outsiders?" *Journal of Accounting Research*, vol. 53, no. 4, pp. 863–905, 2015.

[16] B. Sharma and D. Koundal, "Cattle health monitoring system using wireless sensor network: a survey from innovation perspective," *IET Wireless Sensor Systems*, vol. 8, no. 4, pp. 143–151, 2018.

[17] D. Li, J. Cui, H. Zhang, H. Li, M. Wang, and Y. Shen, "Effect of hole transport layer in planar inverted perovskite solar cells," *Chemistry Letters*, vol. 45, no. 1, pp. 89–91, 2015.

[18] M. Yuan, O. Voznyy, D. Zhitomirsky, P. Kanjanaboos, and E. H. Sargent, "Synergistic doping of fullerene electron transport layer and colloidal quantum dot solids enhances solar cell performance," *Advanced Materials*, vol. 27, no. 5, pp. 917–921, 2015.

[19] M. Mitsumura, H. Masuyama, S. Kasahara, and Y. Takahashi, "Effect of application-layer rate-control mechanism on video quality for streaming services," *Journal of Industrial and Management Optimization*, vol. 8, no. 4, pp. 807–819, 2012.

[20] L. Ma, "Research on distance education image correction based on digital image processing technology," *EURASIP Journal on Image and Video Processing*, vol. 2019, no. 1, Article ID 18, 9 pages, 2019.

[21] D. Corr, M. Accardi, L. Graham-Brady, and S. P. Shah, "Digital image correlation analysis of interfacial debonding properties and fracture behavior in concrete," *Engineering Fracture Mechanics*, vol. 74, no. 1-2, pp. 109–121, 2007.

[22] Y. Gao, T. Cheng, Y. Su, X. Xu, Y. Zhang, and Q. Zhang, "High-efficiency and high-accuracy digital image correlation for three-dimensional measurement," *Optics and Lasers in Engineering*, vol. 65, pp. 73–80, 2015.

[23] C. Jiang, X. Zhu, C. Li, and G. Chen, "A robust tracking with low-dimensional target-specific feature extraction," *IEICE Transactions on Information and Systems*, vol. E102.D, no. 7, pp. 1349–1361, 2019.

[24] V. P. Jilkov and J. Wu, "Efficient GPU-accelerated implementation of particle and particle flow filters for target tracking," *Journal of Advances in Information Fusion*, vol. 10, no. 1, pp. 73–88, 2015.

[25] M. Z. A. Bhuiyan, G. Wang, and A. V. Vasilakos, "Local area prediction-based mobile target tracking in wireless sensor networks," *IEEE Transactions on Computers*, vol. 64, no. 7, pp. 1968–1982, 2015.

[26] M. Parodi, M. Storace, and C. Regazzoni, "Circuit realization of Markov random fields for analog image processing," *International Journal of Circuit Theory and Applications*, vol. 26, no. 5, pp. 477–498, 1998.

[27] Y. Tang, C.-W. Ten, C. Wang, and G. Parker, "Extraction of energy information from analog meters using image processing," *IEEE Transactions on Smart Grid*, vol. 6, no. 4, pp. 2032–2040, 2015.

[28] H. Lu, Y. Li, M. Chen, H. Kim, and S. Serikawa, "Brain intelligence: go beyond artificial intelligence," *Mobile Networks and Applications*, vol. 23, no. 2, pp. 368–375, 2017.

[29] V. D. Daygon, S. Prakash, M. Calingacion et al., "Understanding the Jasmine phenotype of rice through metabolite profiling and sensory evaluation," *Metabolomics*, vol. 12, no. 4, pp. 1–15, 2016.

[30] M. Q. Raza and A. Khosravi, "A review on artificial intelligence based load demand forecasting techniques for smart grid and buildings," *Renewable and Sustainable Energy Reviews*, vol. 50, pp. 1352–1372, 2015.

[31] P. Sengottuvelan and N. Prasath, "BAFSA: breeding artificial fish swarm algorithm for optimal cluster head selection in wireless sensor networks," *Wireless Personal Communications*, vol. 94, no. 4, pp. 1979–1991, 2017.

[32] M. Merdan, W. Lepuschitz, G. Koppensteiner, and R. Balogh, *Robotics in Education*, Springer Verlag, New York, NY, USA, 2017.

[33] V. Mascardi, D. Weyns, A. Ricci et al., "Engineering multiagent systems," *ACM SIGSOFT Software Engineering Notes*, vol. 44, no. 1, pp. 18–28, 2019.

[34] B. Hazeltine, "A framework of information technology supported intelligent learning environment," *Computing Reviews*, vol. 57, no. 8, pp. 510-511, 2016.

[35] K. Lv, "Study on pharmaceutical database management based on data mining technology," *Journal of Information and Computational Science*, vol. 12, no. 8, pp. 2979–2986, 2015.

[36] C. C. Hedji, F. M. Houndonougbo, U. P. Tougan, M. R. B. Houinato, and D. E. Fiogbe, "Technological, sensorial and nutritional meat quality traits from pig fed with conventional and unconventional diets," *Food and Nutrition Sciences*, vol. 6, no. 16, pp. 1514–1521, 2015.

Research Article

Assistant Training System of Teenagers' Physical Ability Based on Artificial Intelligence

Cong Du (ID)

College of Physical Education, Xuchang University, Xuchang 461000, Henan, China

Correspondence should be addressed to Cong Du; 12018001@xcu.edu.cn

The rapid development of artificial intelligence technology makes it widely used in various fields. In order to more scientifically assist teenagers in physical training, this paper develops a set of teenagers' physical training system based on artificial intelligence technology. Firstly, the experimental platform is built, and the sensor nodes are connected with the test host through the serial port to collect data to the experimental platform. The system consists of target detection module, data analysis module, and human posture estimation module. The background modeling method based on vibe model is used to form the target detection module, and the canny edge detection algorithm is used to form the data analysis module. Finally, the posture auxiliary index is established to estimate the human posture. This paper makes a systematic application test on a youth sports team. The experimental group was trained with artificial intelligence-based physical training system, while the control group was trained with traditional training methods. Before the experiment, the physical fitness of the two groups of subjects were evaluated, including standing long jump, 50 meters sprint, 30 s single swing rope skipping, pull-up, and squat 1RM. After 3 and 6 weeks of training, the physical fitness was evaluated again. The experimental results show that the intelligent assistant system established in this paper can accurately show that the physiological load of the athlete is in line with the law of physiological function change. After six weeks of training, the standing long jump of the experimental group has been improved by 20.97 cm, the 50 meters dash has been accelerated by 1.21 s, the 30 second single swing rope has been increased by 13.76, the pull-up has been increased by 1.41, and the squat 1RM has been increased by 15.16. This shows that the auxiliary training system based on artificial intelligence can help young athletes improve their physical quality and enhance their sports skills.

1. Introduction

1.1. Background Significance. Although China's sports industry has been more rapid development, the athletes' physical training is always not satisfactory. Improper physical training methods and schemes will not only lead to the training to not reach the expected effect and athletes not able to play their true level in the competition but also may cause harm to the athletes' body [1]. Especially, for the athletes in their youth, their physical functions and skills are in the stage of development [2]. A scientific physical training system will undoubtedly provide solutions to these problems. In this paper, based on artificial intelligence technology, the construction of intelligent physical assistant training system is of great significance to strengthen the effect of physical training for teenagers.

1.2. Related Work. Physical training has become an integral part of the European education system because it brings knowledge and insights centered on the principles and concepts of learning skills in the 21st century. Roliak A O analyzed the structure, content, and goal of basic sports in Danish professional teacher training system [3]. Taking mountaineering training as an example, Chen *h* introduced the development and design of virtual reality technology in sports training courses [4]. First, he described the overall design of the mountaineering training system based on

virtual reality technology and then introduced the implementation process of each part. On this basis, he put forward the autonomous learning training mode of the system and, finally, carried out the control experiment to verify the effectiveness of the system.

With the development of computer technology, artificial intelligence technology is widely used in the evaluation system. Decision support system is a computer-based information system. The development of sports evaluation decision system can provide scientific support for sports training. Xie puts forward a method to optimize the analysis of physical education teaching evaluation system and the design of intelligent evaluation system. The system has multiple teaching management modules, which can realize dynamic physical education evaluation and reasonably arrange students' daily training plan [5]. The traditional training system based on case teaching is to carry out strength training for aerobics special movements according to the analysis of previous competitions and training cases. The training results cannot be evaluated intelligently and accurately, and the performance of dynamic analysis is poor. In view of this problem, Jia designed the core training system of aerobics special strength quality based on artificial intelligence to realize the intelligent training of aerobics special strength quality [6]. Through the research of fuzzy normal form system, the intelligent functions of optimization and decision-making of intelligent fuzzy network are realized. He uses FIR filter to deal with the phase distortion in the process of signal transmission and realizes the information management of trainees and statistical query of training results through the information management module. His research provides a technical reference for the construction of the experimental platform in this paper.

1.3. Innovative Points in This Paper. In order to improve the quality of physical assistive training for teenagers and cultivate higher quality young athletes for Chinese sports, this paper studies the physical assistive training system for teenagers based on artificial intelligence technology. The innovations of this paper are as follows: (1) the experimental platform is successfully built. The sensor nodes are connected with the test host through the serial port, and the data can be transmitted to the experimental platform after collecting. (2) The function template of the designed intelligent system includes three modules: target detection module, data analysis module, and human posture estimation module. (3) Through the comparison of training experimental data, the intelligent auxiliary training system constructed in this paper can improve the physical quality level of young athletes and help them improve their sports skills.

2. Artificial Intelligence Technology and Auxiliary Training Method of Physical Fitness

2.1. Motion Recognition Algorithm

2.1.1. Bone Data Filtering. The basic data of motion recognition is the joint data provided by the bone tracking

system, but most of the joint data returned by the bone tracking system will have some noise. So, it is necessary to denoise and filter the data. Bone data belongs to time series data, there will be a certain time interval between each frame data, and the joint position data will have a jump change [7]. There will be noise and peak tip in time series, so the filtering method is needed to smooth the data.

The data filter of joint position can eliminate unnecessary noise and jitter, obtain smooth and accurate joint position data, and avoid the phenomenon of data delay. If the difference between the input data and the output data of the filter is less than the threshold, the filtered output is equivalent to the input [8]. Otherwise, the output change will be limited. The jitter filter variant of exponential filter can be used to suppress the input change, as shown in

$$\widehat{X}_n = \begin{cases} X_n, & |X_n - \widehat{X}_{n-1}| < z, \\ \omega X_n + (1-\omega)\widehat{X}_{n-1}, & |X_n - \widehat{X}_{n-1}| \geq z, \end{cases} \quad (1)$$

where z is the threshold. In addition, the median filter can eliminate the peak, and the median can limit the change of input, as shown in

$$\widehat{X}_n = \begin{cases} X_n, & |X_n - X_m| < z, \\ X_m, & |X_n - X_m| < z, \end{cases} \quad (2)$$

where X_m is the median value of the last n input data. The data filtered by jitter clearing can be processed by using double exponential smoothing filter. The double exponential smoothing filter, as shown in (3) and (4), respectively, corresponds to the trend of input data and the filtered smoothing output:

$$Q: a_n = \lambda\left(\widehat{X}_n - \widehat{X}_{n-1}\right) + (1-\lambda)a_{n-1}, \quad (3)$$

$$S: \widehat{X}_n = \eta X_n + (1-\eta)\left(\widehat{X}_{n-1} + a_{n-1}\right), \quad (4)$$

where λ and η are parameters that control the weight of input data. Bone data will become smoother after filtering peak tip and noise, and the data will be more accurate in describing bone features.

2.1.2. Finite State Machine Based on Bone Spatial Features. In the past, the traditional analytic geometry method was always used to calculate the angle of three-dimensional space, but this method needs to consider the boundary conditions, so the calculation is very complex. The space vector rule does not need to consider the boundary conditions, first maps the space coordinate system to the conventional mathematical coordinate system, and uses the vector method [9]. The coordinates of PQ two points are (x, y, z) and $(x\prime, y\prime, z\prime)$ respectively, so the transformation of vector is shown in

$$\overrightarrow{PQ} = (x\prime - x, y\prime - y, z\prime - z). \quad (5)$$

The vectors between the joints of the human body can be transformed in the above way. By calculating the angle between the two vectors, the angle between the joints can be

obtained. Using the space vector method, we can extract the spatial features of bones and use them as the state description of creating the finite state machine, which can achieve more accurate and complete motion recognition [10].

The function of FSM is to describe the state sequence of the target in the period and the influence of external events on the state sequence. The main characteristics of FSM are the discreteness and finiteness of states, which are widely used in modeling. The components of FSM include state, transition, detector, and event [11]. When the transition condition is satisfied, the state will change, and the detector will detect the state transition condition in real time.

2.1.3. Dynamic Time Warping. Based on the idea of dynamic programming, dynamic time warping (DTW) measures the similarity of two discrete time series to find the minimum matching path [12]. The reference templates of two time series are given as follows:

$$X = \{X(1), X(2)...X(i)...X(I)\}, \tag{6}$$

$$Y = \{Y(1), Y(2)...Y(j)...Y(J)\}, \tag{7}$$

where ij represents the timing label of the reference template X and the timing label of the test template Y, respectively. The distance between the corresponding points of two sequences can be calculated by Euclidean distance, as shown in

$$d(a,b) = (X_a - Y_b)^2. \tag{8}$$

Dynamic programming is based on the local optimal path to achieve the global optimal path. The nth element of regular path is defined as follows:

$$W_n = (i, j)_n. \tag{9}$$

Regular paths need to satisfy the constraints of boundary conditions, monotonicity, and continuity. When the constraint conditions are satisfied, the path with the least cost of regularization is selected, and the calculation is shown in

$$DTW = (X, Y) = \min \left\{ \frac{\sqrt{\sum_{r=1}^{R} W_r}}{R} \right\}. \tag{10}$$

According to the set R value, from the matching similarity of the current node and the maximum similarity of the direct cumulative similarity, the formula of the regular path is as follows:

$$D(a_i, b_j) = d[X(i), Y(j)] \\ + \min \left(D(a_i, b_{j+1}), D(a_{i+1}, b_j), D(a_{i+1}, b_{j+1}) \right). \tag{11}$$

2.2. Human Pose Estimation Algorithm

2.2.1. Human Pose Estimation Based on Model. In the model-based human pose estimation method, the joint tree or other complex model of the human object is established first, and then, the parameters of human activity are obtained to realize the estimation of human pose. The preparation stage of model-based human pose estimation is to build a human model based on prior knowledge, so as to effectively constrain the feature change space, improve the computational efficiency, and further narrow the search range of matching [13]. The skeleton model is the simplest one in the human body structure model. The joints are represented by points and the bones are represented by line segments, as shown in Figure 1.

In the observation phase of model-based human pose estimation, it is necessary to project the three-dimensional human model to the image plane and then find the optimal human pose parameters. Generally, image features such as color, contour, and edge are used in the observation process. The prediction stage is to reduce the feasible and searching space of attitude. Low-dimensional subspace is used to represent the constraints in the process of human motion, and various dimensionality reduction methods are used to reduce the dimension of attitude vector.

The accuracy of human pose estimation based on the model is high, and it can also solve the problems of occlusion and self-occlusion. However, the human pose parameters need to be searched and matched in high-dimensional pose space, so the optimization is slow and time-consuming. Moreover, with the increase of search time, the noise and error will increase, which may lead to the failure of attitude estimation.

2.2.2. Model-Free Human Pose Estimation. Model-free human pose estimation generally uses the mapping relationship between human features in image observation space and human pose space to transform pose estimation problem into pattern recognition problem [14]. There are two types of estimation methods: learning based and sample based.

Learning-based human pose estimation method needs to use a large number of training samples to test the linear regression model, which is based on the learning of big data samples. It has the advantages of no specific initialization operation, low storage cost, and high execution efficiency. However, the results are easily affected by the size of training samples, resulting in bias [15]. It is difficult to build a multidimensional feature model, and it takes a long time to adjust the parameters.

The human pose estimation method based on matching firstly extracts the corresponding features in the image and then compares them with the features in the sample template library. Therefore, to use this method, we must first obtain a large number of known human posture training samples to establish the sample template library. It is difficult to build sample template library, and this method is only suitable for the pose in sample set. If it is a relatively complex motion, it is easy to produce deviation.

2.2.3. Human Pose Estimation Based on Contour Edge Features. Canny edge detection algorithm is generally used to extract human contour edge [16]. Firstly, the Gaussian
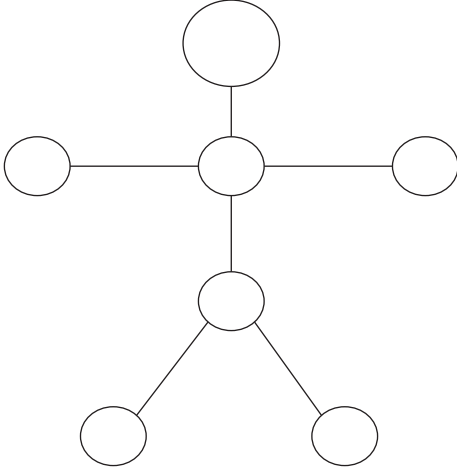
Figure 1: Skeleton model diagram.

filter is used to smooth the image and suppress the noise. Gaussian filtering can be realized by one-dimensional Gaussian kernel function and two-dimensional Gaussian kernel function, as shown in formulas (12) and (13), respectively:

$$K = \frac{1}{\sqrt{2\pi}\sigma} n^{(x*x/2\sigma*\sigma)}, \tag{12}$$

$$K = \frac{1}{\sqrt{2\pi}\sigma * \sigma} n^{(x*x+y*y/2\sigma*\sigma)}. \tag{13}$$

The matrix of partial derivatives of image in x and y directions is calculated by first-order partial derivative difference. The expression of gray value gradient of image is shown in

$$J_1 = \begin{vmatrix} -1 & -1 \\ 1 & 1 \end{vmatrix}, J_2 = \begin{vmatrix} 1 & -1 \\ 1 & -1 \end{vmatrix}, \tag{14}$$

$$\phi_1(a,b) = f(a,b) * J_1(x,y), \tag{15}$$

$$\phi_2(a,b) = f(a,b) * J_2(x,y), \tag{16}$$

$$\phi(a,b) = \sqrt{\phi_1^2(a,b) + \phi_2^2(a,b)}, \tag{17}$$

$$\theta_\phi = \tan^{-1} \frac{\phi_2(a,b)}{\phi_1(a,b)}, \tag{18}$$

where J_1 and J_2 represent convolution operator and ϕ and θ represent amplitude and direction of edge gradient, respectively.

According to the global gradient alone cannot accurately locate the edge position, so it is necessary to suppress the gradient amplitude to highlight the edge. At the same time, the double threshold method can be used to reduce the number of false edges. Double threshold needs to select high threshold and low threshold to get different threshold images [17]. After obtaining the contour edge, it is further processed to obtain the corresponding human joint data.

Joint points of the head and foot are extracted by horizontal line scanning algorithm, joint points of the knee, hip, neck, and chest are extracted by length proportion constraint, and joint points of the hand, elbow, and shoulder are extracted by vertical scanning algorithm [18, 19].

2.3. Digital-Assisted Physical Training

2.3.1. Content System of Physical Training. Physical training is a systematic project with certain structural characteristics and process. A complete physical training content structure system needs to integrate isolated elements and follow a reasonable training process. The internal structure of physical training includes body shape, body function, sports quality, and health level [20].

The process of physical training generally consists of five steps: test, evaluation, target determination, plan making, and plan implementation [21]. Generally speaking, the goal of physical training is to improve competitive ability and obtain excellent results. In the guidance stage, we need to divide the training time and the specific tasks of each section to ensure that the athletes present the best competitive state in the competition. Therefore, it is necessary to arrange the periodic training reasonably in the guidance stage. In the implementation stage, we should determine the specific training methods and consider the athletes' load and fatigue recovery degree. Training methods should be combined with sports characteristics, personal ability, and external conditions. The load is generally measured by the percentage of the maximum load of an individual. Fatigue recovery plays an important role in the prevention of injury and physical maintenance. The control stage is an accurate and comprehensive evaluation of the whole training process, including goals and implementation, which is conducive to timely understanding of athletes.

2.3.2. Scientific Physical Training System. Functional training theory, periodic training theory, systematic training theory, and plate structure theory are the theoretical basis of scientific physical training. Functional training theory emphasizes the frequency and load intensity of training and thinks that physical training can enhance athletes' anaerobic and aerobic ability and make muscles more developed, but ignores the cultivation of flexibility [22]. The purpose of functional training theory is to eliminate the gap between the physical training and the physical ability required by the competition. The training strategy has the characteristics of specialization and individuation, and the performance in the competition reflects the training effect.

Periodic training theory divides the training process of athletes into preparation period, competition period, and transition period. Different periods have different training tasks, objectives, and load arrangements. According to the change law of athletes' competitive ability and the periodic characteristics of competition, the periodic training is arranged. It is necessary to consider the changes of training intensity and time when athletes appear in the best competitive state during training and combine practical training

according to different cycles [23]. And, the adjacent cycles should be gradual and moderate convergence.

According to the theory of systematic training, if we want to achieve the ideal training effect, we need continuous and systematic training because the competitive ability is unstable. If there is no continuous training, the competitive ability will gradually degenerate [24]. According to the theory of plate structure, more concentrated short-term training can bring greater load stimulation, meet the intensity requirements of athletes, and achieve better training effect. Under the theory of plate structure, the competition can be arranged in each training stage.

2.3.3. The Demand of Intelligent Physical Assistant Training. With the development of artificial intelligence technology, physical training also began to use scientific and technological means to assist. At present, there are some problems in physical training, such as unscientific teaching methods, unclear selection criteria, frequent sports injuries, and lack of digital sports resources [25].

Physical training is relatively boring, and it is difficult to master the main points of movements in high-tech training. Traditional physical training teaching has some problems in theory explanation and action demonstration, so it is difficult for learners to have a deep understanding of it. Intelligent training and teaching can help learners understand better from multiple sensory aspects. The inaccuracy of the selection criteria is reflected in the fact that the selection of athletes only depends on the performance of the competition. Some athletes with strong plasticity may find it difficult to perform well because of their irregular technical movements.

Unreasonable training methods and load will lead to sports injury. Although sports injury cannot be completely avoided, it can be prevented through the physical assistant training system to reduce the possibility of injury. Physical training and modern teaching technology have not been closely combined, leading to the lack of digital sports resources. Intelligent physical assistant training can quantify the training situation of athletes as parameters, analyze the advantages and disadvantages, and make personalized training programs.

3. Experiment on the Construction of the Intelligence System of Teenagers' Physical Ability Assistant Training

3.1. System Experiment Platform. In this paper, the intelligent system of physical assistant training is designed for young athletes and coaches to improve the efficiency of young physical training. The structure of the specific experimental platform is shown in Figure 2. Sensor nodes are connected to the test host through serial port, and data is collected and transmitted to the experimental platform.

3.2. System Components

3.2.1. Target Detection Module. The first step of the system is to extract human targets and their features effectively, which
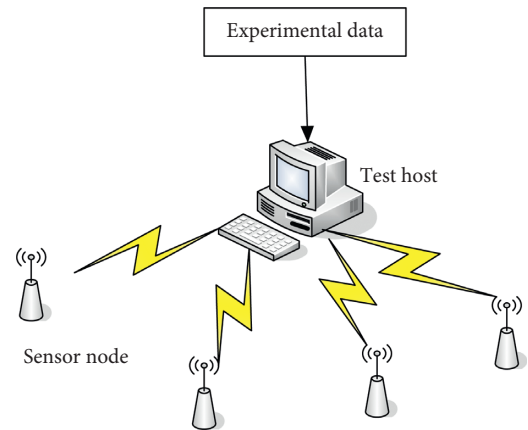
FIGURE 2: Structure of experimental platform.

is also the basic step of the auxiliary training system. The background modeling method based on the vibe model is adopted. Firstly, the pixel background model is initialized, then the target segmentation is performed on the subsequent image sequence, and finally the background model is updated according to the neighborhood update method.

3.2.2. Data Analysis Module. Canny edge detection algorithm is used to process the data detected by the target detection module, including bone filtering and smoothing, contour extraction, and edge thinning. Then, the processed data are analyzed, and the parameters of athletes in the training process are calculated, which are displayed in the system interface in the form of a chart. Athletes can log in to the mobile client to view their training data. The client login page is shown in Figure 3.

3.2.3. Human Pose Estimation Module. In this paper, the most important part of the intelligent system of physical training is to estimate the human body posture, obtain the human body posture information through the data analysis module, and establish the posture auxiliary index. This link can help athletes correct the nonstandard posture in the process of training, predict the next action of athletes, and give corresponding instructions.

3.3. System Application Test. This paper makes a systematic application test on a youth sports team. Fourteen boys in a youth sports team were randomly divided into two groups. The experimental group adopted the AI-based physical training system for physical training, while the control group adopted the traditional physical training method. Before the experiment, the physical fitness of the two groups of subjects were evaluated, including standing long jump, 50 meters sprint, 30s single swing rope skipping, pull-up, and squat 1RM. After 3 and 6 weeks of training, the physical fitness was evaluated again.

Figure 3: Client login page.

4. Discussion on the Performance and Effect of the System

4.1. System Performance. Firstly, an athlete in the youth sports team is randomly selected as the object of the system monitoring, and the physiological load monitoring performance of the physical fitness assistant training system based on artificial intelligence is tested. The results are as follows.

As shown in Figure 4, when the athlete carries out a complete single training, the intelligent assistant system created in this paper can accurately show that the physiological load of the athlete is in line with the law of physiological function change. The OA stage is the mobilization stage, the AB stage is the stable stage, the BD stage is the fatigue stage, and the DF stage is recovery stage.

4.2. Changes of Physical Fitness

4.2.1. Pretest Results. Before the beginning of the experiment, the physical fitness of the experimental group and the control group were tested.

As shown in Table 1, by comparing the results of the physical fitness test conducted between the two groups before the experiment, it can be seen that there was no significant difference in the physical fitness indexes between the experimental group and the control group before the experiment began. The results of standing long jump and squat 1RM of the experimental group were slightly better than those of the control group. The results of 50 m sprint, 30 s rope skipping, and pull-up of the control group were slightly better than those of the experimental group.

As shown in Figure 5, there is no significant difference between the experimental group and the control group in the test results of standing long jump, 50m sprint, 30s single swing rope skipping, pull-up, and squat 1RM. The smallest difference of all was in the pull-up test. There were 6.84 in the experimental group and 6.91 in the control group, a difference of 0.07 between the two groups.

4.2.2. The Measured Results in the Experiment. Three weeks after the beginning of the experiment, the physical fitness of the experimental group and the control group were tested.

As shown in Table 2, after three weeks of training, the experimental group performed slightly better than the control group in the standing long jump, the 50-meters dash, the single-swing rope jump for 30s, the pull-up, and the squat 1RM.

As shown in Figure 6, the biggest difference between the experimental group and the control group is the test results of standing long jump, the experimental group is 178.23 ± 11.05 cm, the control group is 174.34 ± 11.78 cm, the difference between the two groups is 3.89 cm. The second is the test result of squat 1RM, the experimental group is 107.67 ± 8.21, the control group is 106.35 ± 7.64, and the difference between the two groups is 1.32.

4.2.3. Post-Test Results. Six weeks after the beginning of the experiment, that is, at the end of the experiment, the physical fitness of the experimental group and the control group were tested.

As shown in Table 3, after six weeks of training, the test results of the experimental group and the control group were significantly different. The standing long jump scores of the two groups were 193.64 ± 9.38 cm and 179.39 ± 12.35 cm, respectively. The results of 50 meters dash were 7.14 ± 1.03 s and 7.59 ± 1.07 s, respectively. The results of rope skipping in 30 s were 67.34 ± 5.24 and 61.25 ± 6.13, respectively. The results of the chin up were $8.25 + 0.84$ and $7.42 + 1.27$, respectively. The results of 1 RM squat were 120.66 ± 5.31 and 111.39 ± 7.35, respectively.

As shown in Figure 7, the biggest difference between the experimental group and the control group is the test results of standing long jump and the difference between the two groups is 14.25 cm. The second is the test result of squat 1RM; the difference between the two groups is 9.27. 30 s single jump rope skipping results in two groups of 6.15; the difference between the chin up performance is 0.83, and 50 m sprint results' difference is 0.45 s.

4.2.4. Longitudinal Comparison of Two Groups of Test Results. The longitudinal comparison results of each item in the experimental group and the control group are shown in Table 4.

As shown in Table 4, the scores of the experimental group and the control group were improved in the three tests. However, the experimental group's performance of various indicators improved significantly faster than the control group. In the first test, the scores of the two groups were almost the same, and the scores of the control group were even better than the experimental group in some items. In the second test, the results of the experimental group have begun to be slightly better than the control group. In the third test, the results of the experimental group have been significantly better than that of the control group. The results
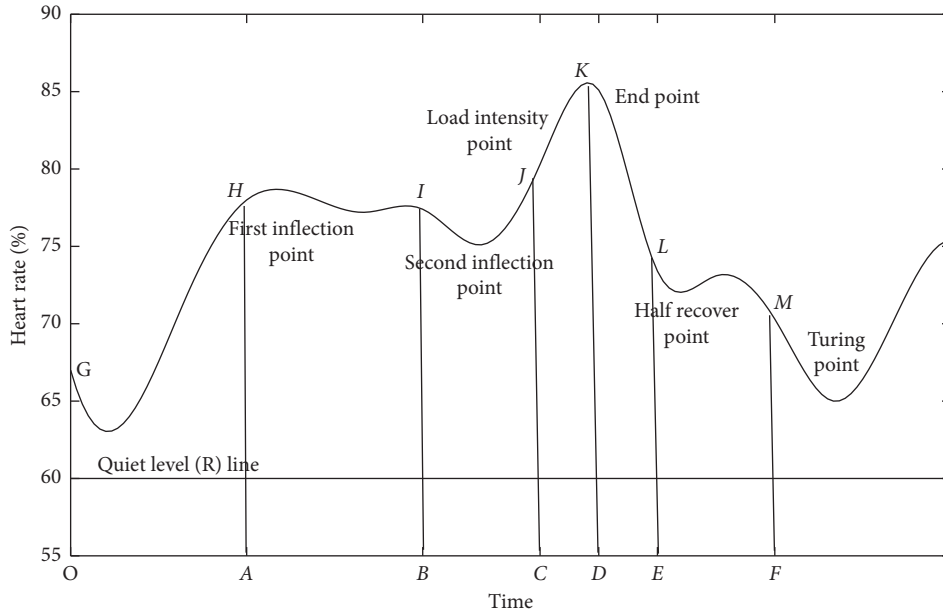
FIGURE 4: Physiological load response curve.

TABLE 1: Physical fitness test results of two groups of athletes before the experiment.

Project	Experience group	Control group
Standing long jump (cm)	172.67 ± 10.15	169.94 ± 11.72
50 meters dash (s)	8.35 ± 1.14	8.24 ± 1.21
30 s single swing rope skipping	53.58 ± 5.74	56.24 ± 6.15
Pull up	6.84 ± 1.03	6.91 ± 1.09
Squat 1RM	105.5 ± 8.34	104.8 ± 7.85
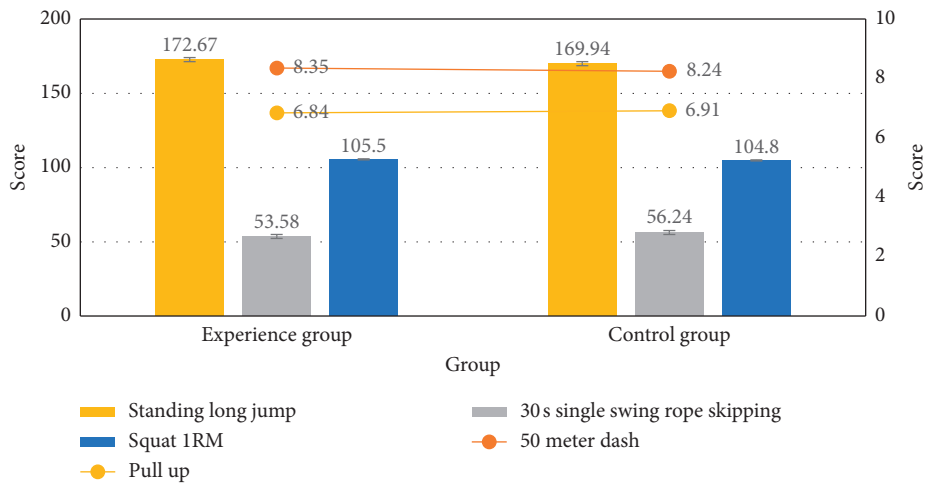
FIGURE 5: Results of pretest.

of the three tests in the experimental group are shown in Figure 8.

As shown in Figure 8, after six weeks of training of the physical assistance training intelligent system, the experimental group's standing long jump improved 20.97 cm, 50 m sprint accelerated 1.21 s, 30 s single shake rope jump increased 13.76, pull-up increased 1.41, and squat 1RM increased 15.16.

The results of the three tests in the control group are shown in Figure 9.

As shown in Figure 9, after six weeks of training with the intelligent system of physical assistant training, the standing

TABLE 2: Physical fitness test results of two groups of athletes after three weeks of training.

Project	Experience group	Control group
Standing long jump (cm)	178.23 ± 11.05	174.34 ± 11.78
50 meters dash (s)	8.21 ± 1.08	8.22 ± 1.17
30s single swing rope skipping	58.84 ± 6.01	58.25 ± 6.17
Pull up	7.36 ± 1.13	7.21 ± 1.13
Squat 1RM	107.67 ± 8.21	106.35 ± 7.64
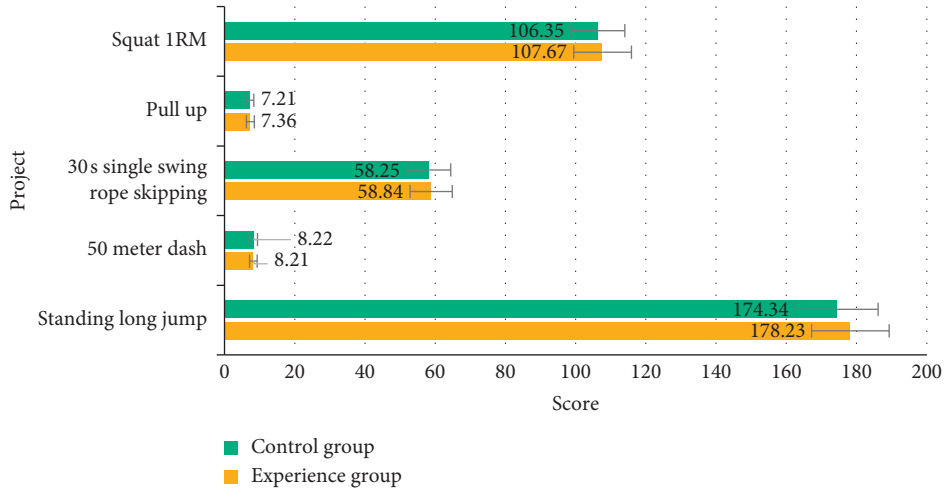
FIGURE 6: Intermediate test results.

TABLE 3: Physical fitness test results of two groups of athletes after six weeks of training.

Project	Experience group	Control group
Standing long jump (cm)	193.64 ± 9.38	179.39 ± 12.35
50 meters dash (s)	7.14 ± 1.03	7.59 ± 1.07
30s single swing rope skipping	67.34 ± 5.24	61.25 ± 6.13
Pull up	8.25 ± 0.84	7.42 ± 1.27
Squat 1RM	120.66 ± 5.31	111.39 ± 7.35
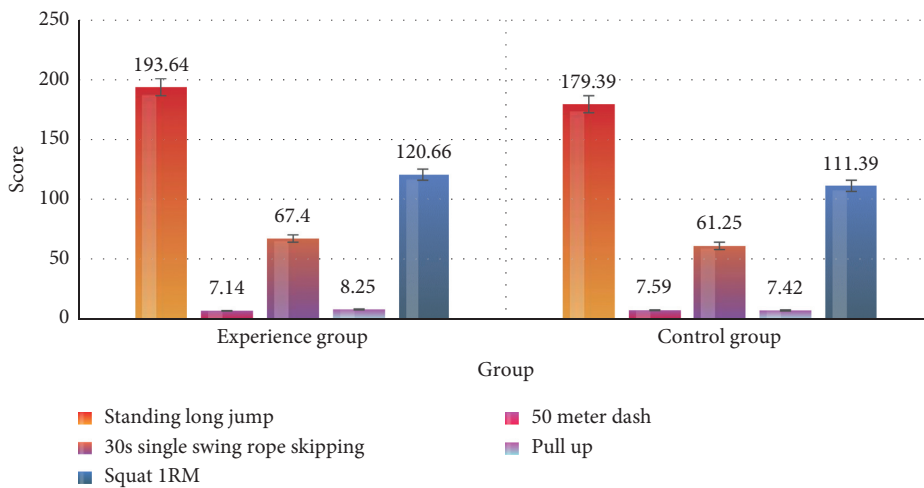
FIGURE 7: Post-test results.

TABLE 4: Longitudinal comparison of test results between the two groups.

Times	Standing long jump	50 meters dash	30 s single swing rope skipping	Pull up	Squat 1RM
E1	172.67	8.35	53.58	6.84	105.5
E2	178.23	8.21	58.84	7.36	107.67
E3	193.64	7.14	67.34	8.25	120.66
C1	169.94	8.24	56.24	6.91	104.8
C2	174.34	8.22	58.25	7.21	106.35
C3	179.39	7.59	61.25	7.42	111.39
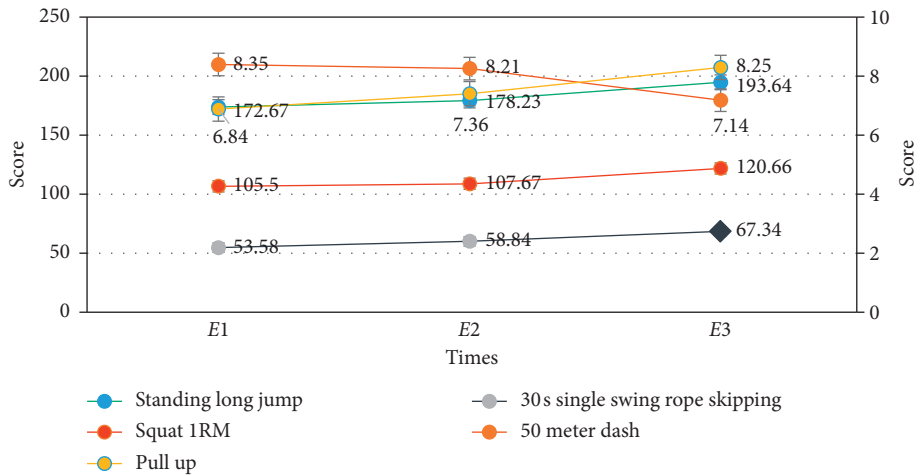
FIGURE 8: Changes of test results of the experimental group for three times.
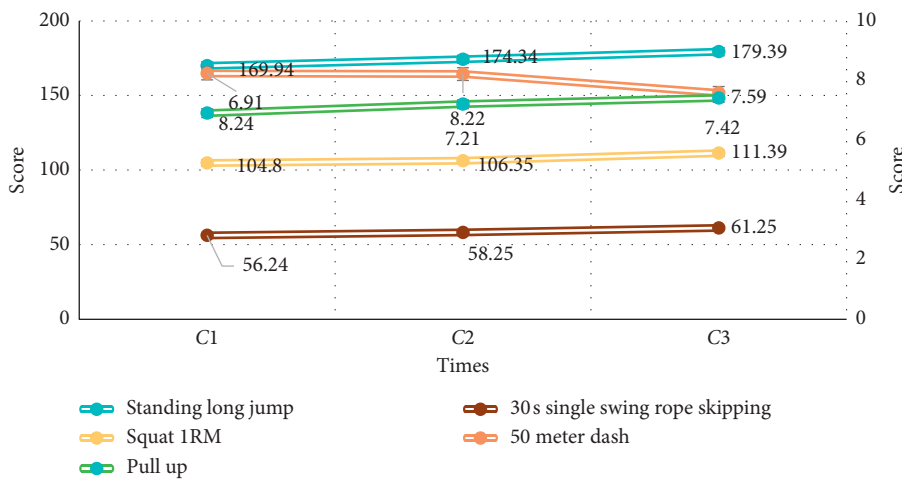
FIGURE 9: Results of three tests in the control group.

long jump of the control group has been improved by 9.45 cm, the 50 meters dash has been accelerated by 0.65 s, the 30 second single swing rope jumping has increased by 5.01, the pull-up has increased by 0.51, and the squat 1RM has increased by 6.59.

5. Conclusions

Physical training is a systematic project with certain structural characteristics and process. A complete physical training content structure system needs to integrate isolated elements and follow a reasonable training process. At present, there are some problems in physical training, such as unscientific teaching methods, unclear selection criteria, frequent sports injuries, and lack of digital sports resources. Therefore, with the development of artificial intelligence technology, physical training also began to use scientific and technological means to assist.

First of all, it is necessary to extract the human body target and its features effectively, which is also the basic step

of the auxiliary training system. Canny edge detection algorithm is used to process the data detected by the target detection module, including bone filtering and smoothing, contour extraction, and edge thinning. Then, the processed data is analyzed, and the module obtains the human posture information and establishes the posture auxiliary index.

Through the comparison of the three stages of physical fitness test data, the artificial intelligence-based adolescent physical training system can help adolescent athletes improve their physical quality and enhance their mastery of sports skills. However, due to the limited time and knowledge, this paper did not investigate the feedback of the system in the end. In the future research work, we should communicate with athletes and coaches, get feedback information, and optimize and improve the system.

Data Availability

No data were used to support this study.

Conflicts of Interest

The authors declare that they have no conflicts of interest.

References

[1] L. Aneta, L. Awomir, K. Anna et al., "Influence of protein deficient diet, vitamin B2 supplementation and physical training on serum composition of polyunsaturated fatty acids (PUFAs) in rats," *The Annals of Agricultural and Environmental Medicine*, vol. 24, no. 2, pp. 185–189, 2017.

[2] J.-N. Yen, H.-C. Hung, H.-C. Hsu, and Y.-C. Lee, "Systematic design an intelligent simulation training system: from learn-memorize perspective," *Microsystem Technologies*, vol. 24, no. 10, pp. 4137–4147, 2018.

[3] A. O. Roliak, "Professional education of teachers in physical training and health: the experience of Denmark," *Pedagogy of Physical Culture and Sports*, vol. 24, no. 3, pp. 143–150, 2020.

[4] H. Chen and M. Liu, "Development and design of Virtual reality technology in physical training course," *Agro Food Industry Hi Tech*, vol. 28, no. 1, pp. 3134–3137, 2017.

[5] X. Xie, "An optimization method for physical education teaching evaluation system analysis and intelligent assessment system design," *Boletin Tecnico/Technical Bulletin*, vol. 55, no. 16, pp. 62–67, 2017.

[6] L. Jia and L. Li, "Research on core strength training of aerobics based on artificial intelligence and sensor network," *EURASIP Journal on Wireless Communications and Networking*, vol. 2020, no. 1, 16 pages, 2020.

[7] W. Han, B. Zhang, Q. Wang, J. Luo, W. Ran, and Y. Xu, "A multi-agent based intelligent training system for unmanned surface vehicles," *Applied Sciences*, vol. 9, no. 6, p. 1089, 2019.

[8] X. Yaxu, J. Zhaojie, X. Kui et al., "Multiple sensors based hand motion recognition using adaptive directed acyclic graph," *Applied Sciences*, vol. 7, no. 4, p. 358, 2017.

[9] M. Xing, J. Hu, Z. Feng et al., "Dynamic hand gesture recognition using motion pattern and shape descriptors," *Multimedia Tools and Applications*, vol. 78, no. 8, pp. 1–24, 2018.

[10] Ł. Okruszek, M. Wordecha, M. Jarkiewicz, B. Kossowski, J. Lee, and A. Marchewka, "Brain correlates of recognition of communicative interactions from biological motion in schizophrenia," *Psychological Medicine*, vol. 48, no. 11, pp. 1862–1871, 2018.

[11] А. ц. ЕвГений and А. Г. Алексей, "Theoretical aspects of professionally applied physical training of rescuers of the Ministry of Emergencies of Belarus," *Journal of Civil Protection*, vol. 4, no. 4, pp. 442–449, 2020.

[12] L.-D. BeaulieuM.-H. Milot et al., "Changes in transcranial magnetic stimulation outcome measures in response to upper-limb physical training in stroke: a systematic review of randomized controlled trials," *Annals of Physical And Rehabilitation Medicine*, vol. 61, no. 4, pp. 224–234, 2018.

[13] M. L. Sbardelotto, G. S. Pedroso, F. T. Pereira et al., "The effects of physical training are varied and occur in an exercise type-dependent manner in elderly men," *Aging and Disease*, vol. 8, no. 6, p. 887, 2017.

[14] A. Baghban and M. Adelizadeh, "Physical training in patients with chronic heart failure: an elaboration of the statements from the Committee on Cardiac Rehabilitation of The Netherlands Society of Cardiology and The Netherlands Heart Foundation and review of studies on physical training in chronic heart failure," *Fuel*, vol. 230, no. 6, pp. 344–354, 2018.

[15] Y. Park, "The social context of collective physical training among Chinese elderly: an anthropological case study in a park in beijing," *Anthropology & Aging*, vol. 38, no. 1, pp. 30–43, 2017.

[16] S. U. Oh, S.-H. Park, and H. Park, "Effects of twisting training on middle-aged normal weight obese women," *Journal of The Korean Society of Living Environmental System*, vol. 25, no. 6, pp. 827–838, 2018.

[17] C. Nanthakumar, "Yoga for anxiety and depression - a literature review," *The Journal of Mental Health Training, Education and Practice*, vol. 15, no. 3, pp. 157–169, 2020.

[18] J. B. Justesen, K. Søgaard, T. Dalager, J. R. Christensen, and G. Sjøgaard, "The effect of intelligent physical exercise training on sickness presenteeism and absenteeism among office workers," *Journal of Occupational & Environmental Medicine*, vol. 59, no. 10, p. 942, 2017.

[19] M. H. Smaili, J. Breeman, T. J. J. Lombaerts et al., "Intelligent flight control systems evaluation for loss-of-control recovery and prevention," *Journal of Guidance Control Dynamics*, vol. 40, no. 4, pp. 1–15, 2017.

[20] W. Jin, Y. Liu, Y. Jin, M. Jia, and L. Xue, "The construction of builder safety supervision system based on CPS," *Wireless Communications and Mobile Computing*, vol. 2020, no. 1, 11 pages, Article ID 8856831, 2020.

[21] R. Liu, B. Yang, E. Zio, and X. Chen, "Artificial intelligence for fault diagnosis of rotating machinery: a review," *Mechanical Systems and Signal Processing*, vol. 108, pp. 33–47, 2018.

[22] J. H. Thrall, X. Li, Q. Li et al., "Artificial intelligence and machine learning in radiology: opportunities, challenges, pitfalls, and criteria for success," *Journal of the American College of Radiology*, vol. 15, no. 3, pp. 504–508, 2018.

[23] F. E. Staff, "An interview with Dr. Raj Reddy on artificial intelligence," *Frontiers of Information Technology & Electronic Engineering*, vol. 19, no. 1, pp. 3–5, 2018.

[24] P. Stano, Y. Kuruma, and L. Damiano, "Synthetic biology and (embodied) artificial intelligence: opportunities and challenges," *Adaptive Behavior*, vol. 26, no. 1, pp. 41–44, 2018.

[25] C. Qi, A. Fourie, Q. Chen, and Q. Zhang, "A strength prediction model using artificial intelligence for recycling waste tailings as cemented paste backfill," *Journal of Cleaner Production*, vol. 183, pp. 566–578, 2018.

Research Article

The Scoring Mechanism of Players after Game Based on Cluster Regression Analysis Model

Jin Xu[1] and Chao Yi [iD] [2]

[1]*School of Sports, Hunan City University, Yiyang 413000, Hunan, China*
[2]*College of General Education, Fujian Chuanzheng Communications College, Fuzhou 350007, Fujian, China*

Correspondence should be addressed to Chao Yi; fjczjtyc@163.com

Cluster regression analysis model is an effective theory for a reasonable and fair player scoring game. It can roughly predict and evaluate the performance of athletes after the game with limited data and provide scientific predictions for the performance of athletes. The purpose of this research is to achieve the player's postmatch scoring through the cluster regression model. Through the research and analysis of past ball games, the comparison and experiment of multiple objects based on different regression analysis theories, the following conclusions are drawn. Different regression models have different standard errors, but if the data in other model categories are put into the centroid model expression, the standard error and the error of the original model are within 0.3, which can replace other models for calculation. In the player's postmatch scoring, although the expert's prediction of the result is very accurate, within the error range of 1 copy, the player's postmatch scoring mechanism based on the cluster regression analysis model is more accurate, and the error formula is in the 0.5 range. It is best to switch the data of the regression model twice to compare the scoring mechanism using different regression experiments.

1. Introduction

With the development of computer technology, especially the development of artificial intelligence technology in recent years, computer technology is increasingly used in people's study, work, and life [1]. Using machine learning to study the performance of basketball players is an interdisciplinary subject that combines comprehensive evaluation and machine learning. In real life and work, we often encounter the problem of evaluating or scoring various things or problems. Generally speaking, all types of scoring and evaluation problems are called comprehensive evaluation problems. In basketball, postgame scoring is always an essential part. Scoring can play a role in many aspects, such as promotion, team management, and competition prediction. Therefore, the postcompetition scoring system has great commercial value and can guarantee the fairness of the competition.

A clustering algorithm based on fast search and density peak discovery is to quickly find the cluster center. Its accuracy is excessively dependent on the threshold, and no effective method is given to select the appropriate threshold. It is recommended to estimate the threshold based on experience. Li et al. proposed a new method to extract the threshold automatically by using the potential entropy of the original data field. For any dataset to be clustered, the threshold value can be calculated objectively from the dataset, rather than empirical estimation [2]. Although the existence of correlation in clusters (the tendency of similar response of items in clusters) is generally regarded as an obstacle to good reasoning, the complex structure of cluster data provides significant analysis advantages over independent data, but the focus is regression analysis of cluster data. A key advantage is the ability to separate effects at the individual (or project specific) and group (or cluster specific) levels. Begg and Parides reviewed different ways to separate the effects of individual level and cluster levels on response, their proper interpretation, and gave suggestions for model fitting according to the intention of data analysts. Different from many previous papers on this topic, Begg and Parides

emphasized the explanation of cluster level covariate effect. The main idea is to analyze the relationship between birth weight and IQ through the data of brothers and sisters in a large birth cohort study [3]. When exposure variables are expensive or difficult to measure, two-stage design is a well-known and cost-effective method for biomedical research. Recent research advances further allow one or two phases of a two-phase design to depend on a continuous result variable. The sampling characteristics related to the results further improve the efficiency of parameter estimation and research the overall cost reduction. Among them, the research and design of cancer biomarkers include sampling of specimens and analysis of results. A semiparametric mixed effects regression model of two-stage design data was established. Xu's method can explain the cluster or central effect of research objects [4].

This research is an experimental analysis based on mathematical theory and cluster regression analysis method. The research process uses mathematical formulas, interview methods, control experiments, and other methods. There is a fierce discussion on the scoring mechanism of NBA and CBA. Based on the regression model, this study puts forward some ideas that can be improved, including the combination of clustering and regression. The experimental results also show that the combination of clustering and regression has the best effect. Finally, the idea of using expert scores after the game to predict the results of the game is proposed. Using the expert scores to compare with the method based on the cluster regression analysis model, you can judge whether the method is based on the theoretical model by looking at the error between the result and the actual is reference.

2. Cluster Regression Analysis Model

2.1. Cluster Analysis Method. Machine learning can be divided into two categories: supervised learning and unsupervised learning [5]. When all input and output variables in the learning situation are fully observed, we define the learning process as supervised learning [4]. In other words, in supervised learning problems, there are no missing or potential variables in the database. Therefore, supervised learning is more direct [6]. For some learning problems, in addition to being able to fully observe all variables, if we can fully observe the structure of the data production process, supervised learning can be regarded as a parameter evaluation problem. Like the maximum probability or least square estimation, if you do not know the data creation process, you must select a suitable model from many models to complete the learning problem [7].

Because the model is not boundless and complex, for example, AIC, BIC, or cross-validation can find a "possibly correct" model to describe the data production process, which is Occam theory or PAC learning. In general, we do not know the process of data creation, but we also lack variables. When the output variable is lost, the learning problem becomes unsupervised [8, 9]. For unsupervised learning, the direct execution of AIC or BIC cannot reveal the distribution of potential variables and the information contained in potential variables. We must try to separate potential variables from the original data and evaluate them [10]. If the potential variables and other variables are independent of each other, the absence of such "offshore" variables will not have a great impact on the estimation. If the potential variable depends on other observed variables, we can use other observable variables to estimate the distribution or summary statistics of potential variables. In general, before evaluating potential variables, we need to determine the type of distribution, whether absolute or continuous [11]. In the case of continuous distribution, the best method is usually factor analysis or factor modeling, using all other variables to construct a new continuous distribution variable [12].

Assuming that the potential variable is a polynomial, we can construct a Gaussian mixture model [13]. The above techniques are called cluster analysis. Cluster analysis collects infinite information in some limited set variables and uses these set variables to group the observed objects. In short, set analysis is a data processing method to classify a group of observation objects reasonably [14]. It is an important part of experimental machine learning and a common technology for analyzing statistical data. System analysis in machine learning is a part of unsupervised learning. Unlike supervised learning, the data in the dataset has no class label and is segmented by the similarity of feature data [15].

2.2. Cluster Regression Analysis Method. Clustering analysis is the process of dividing a group of physical or abstract objects into similar object classes. According to the survey object and purpose, regression analysis determines which is the independent variable (explanatory variable) and which is the dependent variable (explanatory variable), through the establishment of a regression model and control independent variables to evaluate and predict the dependence between research variables. For example, through correlation analysis, we can know that some variables are closely related, but which parts are the most important, and the degree of their interaction must be selected through cluster regression analysis [16, 17].

Quantitative analysis is a method to determine the mathematical model based on statistical data and use the mathematical model to calculate the index and the value of the analysis object [18, 19]. It not only keeps the dependence on observation experiments and the collection of empirical data but also retains the characteristics of dependence on logical thinking and reasoning [20]. The application of the example combines the observation experiment method with the mathematical form [21]. Therefore, quantitative analysis often emphasizes the objectivity and observability of real objects, as well as the relationship and causality between phenomena and variables [10].

Clustering refers to finding out the common characteristics of a group of objects in the database and classifying them into different categories according to different ways. Its purpose is to match the data elements in the database with the given category through the classification model [11]. It can be

applied to application classification and trend prediction, and data groups can be divided into different categories according to the similarity and difference of data. The data belonging to the same category are very similar, but the data similarity between different categories is very small, and the data correlation between categories is very low [22].

Regression analysis should reflect the characteristics of database eigenvalues, and use a function to express the relationship of data mapping to find the dependency between attribute values. It can be applied to the research of data series prediction and correlation. Let the dependent variable y and the independent variables $x1, X_2, X_K$ be related to

$$
\begin{aligned}
v &= b_0 + b_1 x_1 + \cdots + b_k b_k + e, \\
e &\sim N\left(0, \sigma^2\right).
\end{aligned}
\tag{1}
$$

Through sampling, n groups of observation data are obtained:

$$
\begin{aligned}
&(y_1; x_{11}, x_{21}, \cdots, x_{k1}), \\
&(y_2; x_{2n}, x_{2n}, \cdots, x_{kn}), \\
&\cdots \\
&(y_n; x_{1n}, x_{2n}, \cdots, x_{kn}),
\end{aligned}
\tag{2}
$$

where x_{ij} is the jth observation value of the independent variable xi and yj is the jth value of the dependent variable y, substituting the above formula to get the data structure of the model:

$$
\begin{aligned}
y_1 &= b_0 + b_1 x_{11} + b_2 x_{12} + \cdots + b_k x_{k1} + e_1, \\
y_2 &= b_0 + b_1 x_{12} + b_2 x_{12} + \cdots + b_k x_{k2} + e_n, \\
&\cdots \\
y_n &= b_0 + b_1 x_{1n} + b_2 x_{1n} + \cdots + b_k x_{kn} + e_n.
\end{aligned}
\tag{3}
$$

The above equation is a k-element normal linear regression model, in which b0, b1,...,bk and $\sigma2$ are unknown parameters to be estimated and $\varepsilon_1, \varepsilon_2, \ldots, \varepsilon_n$ are independent identically distributed $N(0, \sigma^2)$.

2.3. Fitting of the Multiple Regression Model.
From the perspective of correlation analysis, studying the linear correlation between one variable and multiple variables is called complex correlation analysis [23, 24]. There is no difference between dependent variables and independent variables in complex correlation, but in practical applications, complex correlation analysis is often associated with multiple linear regression analysis. Therefore, complex correlation analysis generally refers to the dependent variable y and k independent variables $x_1, x_2, \ldots, x_k$.

Multivariate linear regression model is required to meet the Gauss hypothesis of multivariate regression. The least square method is used to estimate the regression coefficients $b_0, b_1, \ldots, b_k$.

$$
\begin{aligned}
l_{11} b_1 + l_{12} b_2 + \cdots + l_{1k} b_k &= L_{1y}, \\
l_{21} b_1 + l_{22} b_2 + \cdots + l_{2k} b_k &= L_{2y}, \\
&\cdots \\
l_{k1} b_1 + l_{k2} b_2 + \cdots + l_{kk} b_k &= L_{ky}, \\
b_0 &= \overline{y} - b_1 \overline{x} + b_2 \overline{x}_2 + \cdots + b_k x_k.
\end{aligned}
\tag{4}
$$

Calculate the distance between all known stations, use the calculus knowledge to solve the above equation group, and skip the random term to get the multiple linear regression equation. The residual analysis uses the outlier test, and the standard residuals of the test points fall in the space $(-2, 2)$.

2.4. The Dilemma between Bias and Error.
In any statistical model, the model error includes two parts: variance error and deviation error (frequency scientists believe that the error comes from the change sample, and Bayes believes that the change of parameters will also cause errors) [25]. If we use all data to estimate, the bias error will be very high; if the model contains very few features, compared to the rich functions, the variance error will be very large. This is the so-called "dilemma between bias and variance" [26].

Look at this from another perspective: if too many variables are added to the model, it is almost certain that some non-existent possibilities will be added. It is also called overfitting, because the model contains not only the real possibilities, but also some unnecessary possibilities. If we collect data outside the sample and use the overload model to predict, the prediction error will be very large. On the contrary, insufficient fitting means that the model contains only part of the required information, not all of it [27]. In the underfitting model, using the data outside the sample to predict will also cause a lot of prediction errors.

Overfitting and underfitting are just like the dilemma of bias and variance. If we match "nearly fair" data, it means that we find a good balance between "the dilemma of bias and variance." Therefore, the following work mainly involves the minimization of "test error." Ideally, we can collect more "out-of-sample" data as "test data." However, as an ideal solution, we can collect more data samples and test some models in some fantasy scenarios.

In most cases, data cannot be collected outside the sample for various reasons. As a pseudo solution, we divide the sample into two parts: one for evaluation, called "training sample," and the other for testing, called "test sample." The advantage of using this trick is that we can minimize "false errors" to ensure that the model has a good description of the data [28], to achieve the best balance between bias and variance.

3. Experimental Design and Analysis

3.1. Dataset.
The research object is 10 games of CBA playoffs semifinals and 4 games of finals in 2018-2019 season, 5 games of NBA Playoffs Southwest finals, 6 games of

Northwest finals, and 5 games of finals. Among them, the CBA semifinal team includes Liaoning team, Sichuan team, Guangdong team, and Xinjiang team; the CBA final team includes Liaoning team and Guangdong team; the NBA semifinal team includes San Antonio Spurs, Memphis Grizzlies, Dallas Mavericks, and Denver Nuggets; the NBA final team includes Memphis Grizzlies and Dallas Mavericks.

3.2. Experiment Process

3.2.1. Data Collection. Collect the player's personal information, team information, and game videos, and learn about the game situation and other relevant information in recent years through the official websites of NBA and CBA. The interview outline is built around the relevant education elements of basketball players' actual combat ability. It should be interviewed and negotiated with relevant experts and trainers, and the interview process and content should be organized. The specific interview content includes the scoring rules, mechanism, and system of competition. Provide accurate data support for the training of basketball team players and the scoring mechanism of this study, as shown in Table 1.

3.2.2. Experimental Steps. This paper introduces a system analysis method based on cluster regression analysis model. The process of calculating this algorithm is completely automatic. The analyst should only set a precision limit T according to the needs of the actual work, and the algorithm divides the objects whose distance is less than the limit into the same category. When performing the algorithm, T is also defined as the set centroid stop threshold of the model set. That is, when $R > T$ sets the radius, the center of the model stops changing. Algorithm 1 is described as follows.

3.3. Mathematical Statistics.
Input the collected competition information into the algorithm model, see the difference between the actual results and the results obtained by the algorithm model, collect the collected data for classification, and analyze, summarize, and sort out the statistical data by using Excel 2015 software. Exploratory and confirmatory factor analysis was used to test the validity of the scale, and reliability analysis was used to test the reliability of the scale. After the competition, single factor analysis and multiple comparative analysis were used to evaluate the accuracy of the system. The correlation analysis method was used to discuss the correlation of the scoring mechanism, and the multiple linear regression analysis method was used to explore the internal correlation of the rating mechanism.

4. Research on the Cluster Regression Analysis Model

4.1. Regression Standard Error of Each Model. Regression analysis is only an estimate of players' score after the game. There is a way out between it and the actual value, but the error is within a reasonable range. The errors between different models are different. Discuss and analyze the differences between different models, as shown in Figure 1.

Four different types of regression models are tested and compared with their centroid models. As can be seen from the figure, there is not a big way out between the data. If the first mock exam is the first mock exam, the model error is not the same as the original model, which means that, in the same model category, the centroid model can better represent other models in the model. Therefore, in the first mock exam of the same model category, it is not necessary to build regression models one by one. Only selecting the centroid model of this model type can represent this kind of class very well, greatly reducing the modeling work and improving modeling efficiency.

4.2. Dataset of the Quadratic Switching Regression Model. If the dataset of quadratic polynomial regression is adopted, the parameters are taken from Table 1, the quadratic switching regression model is $y = \beta_{i1} + \beta_{i2}x + \beta_{i3}x^2$, and the distribution of the experimental dataset of quadratic switching is shown in Table 2.

From the data in the table, it can be seen that the four different regression models present different results and shapes due to different constant values. As shown in Figure 2, it is the secondary switching regression model presented by the dataset A.

The graph of the dataset A is two kinds of symmetric quadratic function graphs. Line 1 is opened downward, and the peak value is 11 when the independent variable x is 15. The opening of line 2 is upward, and the minimum value is 5.5 when the independent variable x is 15. The intersection of the two lines is 9.5 and 23.5, and the dependent variable values are 8 and 7, respectively.

4.3. Players' Postgame Score Prediction. The construction of the scoring model is also the main work of scoring players after the game. A good scoring model can improve the accuracy and reliability of scoring, to improve the application value of scoring. To build the model, this study proposes a regression algorithm-based model. The model uses the statistical data of athletes in the competition to match the scores of experts in the competition. After the model is built, the player statistics in the test set are used for testing and compared with the expert scoring data in the test set, as shown in Figure 3.

The experimental results show that although the error of expert scoring is very small, the scoring mechanism based on cluster regression analysis model is more accurate, the error range is within 0.5 points, and the error range of expert scoring is within 1 point. Expert score and regression analysis model score can well predict the ball game score.

4.4. Experimental Results of Different Regression Methods. The third-party library of *Python*, scikit learn, contains a large number of commonly used regression methods. It only needs simple calls and parameter settings to test the effect of different regression methods. Therefore, using the regression

TABLE 1: Information gathering.

Category	Information
Personal information	Name, height, weight, competition position
Member information	Team profile, full-year game data
Personal statistics	Player's field average ranking and full-year competition data
Team profile	Team field average data ranking
Team statistics	The team's performance ranking in recent years
Performance statistics	Video of 10 games in the team's rematch and final

(1) For $i = 1, 2,...,N$, repeat the following steps (2)–(8);
(2) Select any model from the model set A and record it as M_i;
(3) If $i = 1$, separate Mi into one category, and make $A = A - M$, and then perform step (2); otherwise, directly perform step (4);
(4) Calculate the distance between M_i and the centroids of each clustering model set, select the model set with the minimum distance from M_i, and record the model set as A_j, and the distance between the two as D_{ij}, and perform step (5);
(5) If $D_{ij} < T$, classify M_i as model set A_j and make $A = A-M_i$; perform step (6); otherwise, perform step (8);
(6) If the mass center of A_j is not fixed, adjust the mass center and radius of A_j, record the new radius as $R(A_j)$, and carry out step (7). Otherwise, perform step (2).
(7) If $R(A_j) > T$, fix the A_j center of mass and carry out step (2). Otherwise, perform step (2) directly.
(8) Separate M_i into one group and make $A = A-M$. Perform step (2);
(9) Finally, the centroid of each model set is readjusted;
(10) The algorithm ends.

ALGORITHM 1: For the set of multiple linear regression models $A = (M_1, M_2, \ldots, M_N)$, the accuracy of clustering is limited to T.
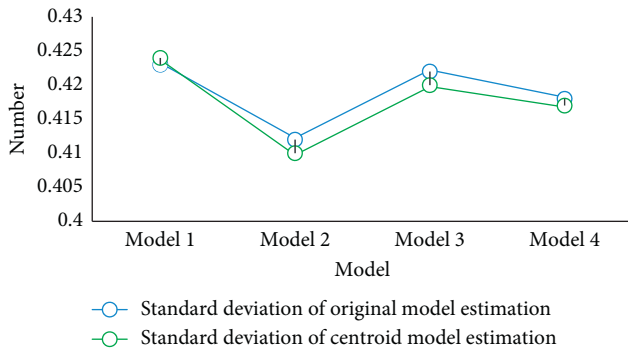
FIGURE 1: Regression standard error of various models.
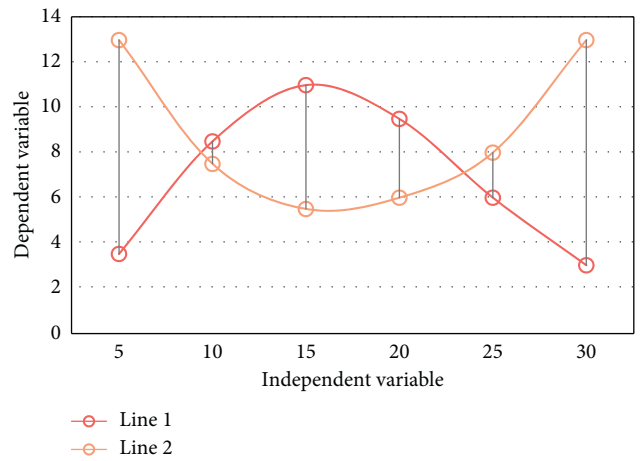
FIGURE 2: Quadratic switching regression model.

TABLE 2: Experimental dataset.

Dataset	n	X value interval	β_1	β_2
A	42	[25, 29]	(20, −1, 0.0625)	(−4, 2, −0.0625)
B	31	[7, 22]	(20, −2, 0.0625)	(−3, 1, −0.0625)
C	28	[7, 11]	(16, −2, 0.03125)	(−1, 1, −0.03125)
D	44	[9, 19]	(165, −23, 1)	(278, −42, 2)

method package provided by scikit learn, we try to call a lot of different regression methods to replace the BP neural network in the basic scoring model and carry out training and testing. The experimental effect of some regression methods is not ideal, so this study does not show and analyze the regression methods with poor effect; only three methods with better experimental results are screened for comparative analysis with BP neural network: linearSVR, RFR, and ridge, as shown in Figure 4.

Through the analysis, we can see that the relationship between the input and output data tends to be linear, so the linear regression method is better. Among other things, ridge is particularly good at the accuracy of the game prediction results, but the performance of the test set is that generally there is a state of fitting. If we can get all the data of OPTA and increase the amount of data in the training set, we should be able to get better results. In many linear regressions, RFR is the best. Therefore, other improved methods in
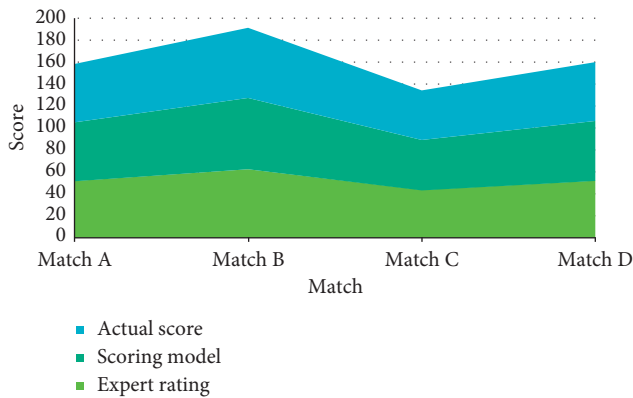
Figure 3: Players' postmatch scoring prediction.
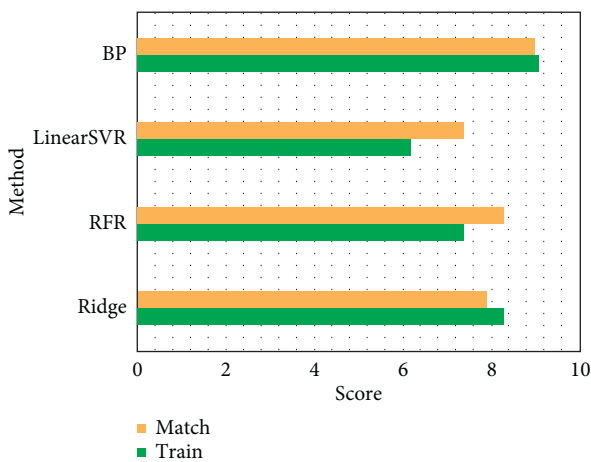
Figure 4: Experimental results of different regression methods.

the future choose RFR regression as the training method in the model. The least deviation is BP regression method, the deviation range is 0.1, the more obvious deviation is RFR and linearSVR, and the deviation value is about 1.

5. Conclusions

This research focuses on the scoring of basketball players, combined with different machine learning algorithms, in three aspects of data collection, model design and optimization, and the application of ratings. This research first introduces the research background, research status, and problems encountered. After that, data preparation was carried out for these problems, and experiments and results analysis were carried out on these problems. A regression-based ball scoring model is proposed, which uses player statistics to match expert data. Experimental results show that the degree of influence of this model is higher than the accuracy of expert ratings.

Although many different data are used in the comparative experiment, in this study, there is a certain deviation between the experimental conclusion and the actual situation, because there are only a few 30 games as the reference object because of the less value of the game parameter.

Moreover, the data characteristics are not rich enough, just for the study of the ball scoring mechanism of basketball; ball includes not only basketball, but also football and table tennis, and so on. Among them, for the polynomial form of the switching regression model, in this form, there is a linear relationship between the characteristics of the strain and the independent variable; therefore, for the nonlinear data space, we can find a transformation to divide the nonlinear space into some combination of linear subspaces, so that the polynomial regression exchange model can be applied to the nonlinear data set, and expand the scope of application of the model.

Cluster analysis and regression analysis are the main methods in this study, and the common methods of system analysis should be summarized. When the data creation process is unknown and the variables are lost, to realize the distribution of latent variables and the information contained in the latent variables, it is necessary to try to separate and evaluate the latent variables from the original data. Clustering analysis is generally understood as clustering data. It is pointed out that both Gaussian mixture model and factor analysis model are the application of the maximum entropy principle, but only make different assumptions about the distribution of potential variables. The collected data is closer to the actual data production process than any classification. This is actually a preparation for the later grouping algorithm. On the whole, they all provide a good theoretical basis for the scoring mechanism after competition. With the development of information technology, increasingly advanced and complex mechanical learning methods have been put forward. How to learn from and use the advanced methods in other fields and optimize and improve the characteristics of ball games is the focus of the next work.

Data Availability

No data were used to support this study.

Conflicts of Interest

The authors declare that they have no conflicts of interest.

Acknowledgments

References

[1] Q. Wang and P. Lu, "Research on application of artificial intelligence in computer network technology," *International Journal of Pattern Recognition and Artificial Intelligence*, vol. 33, no. 5, Article ID 1959015, 2019.

[2] C. Li, G. Ding, D. Wang et al., "Clustering by fast search and find of density peaks with data field," *Chinese Journal of Electronics*, vol. 25, no. 3, pp. 397–402, 2016.

[3] M. D. Begg and M. K. Parides, "Separation of individual-level and cluster-level covariate effects in regression analysis of correlated data," *Statistics in Medicine*, vol. 22, no. 16, pp. 2591–2602, 2003.

[4] S. Zhao, T. Hu, L. Ma, P. Wang, and J. Sun, "Regression analysis of interval-censored failure time data with the additive hazards model in the presence of informative censoring," *Statistics and Its Interface*, vol. 8, no. 3, pp. 367–377, 2015.

[5] Z. Lv, L. Qiao, Q. Wang, and F. Piccialli, "Advanced machine-learning methods for brain-computer interfacing," *IEEE/ACM Transactions on Computational Biology and Bioinformatics*, 2020.

[6] H. Wang, Y. Li, and J. Sun, "Focused and model average estimation for regression analysis of panel count data," *Scandinavian Journal of Statistics*, vol. 42, no. 3, pp. 732–745, 2015.

[7] Y. Feng, L. Ma, and J. Sun, "Regression analysis of current status data under the additive hazards model with auxiliary covariates," *Scandinavian Journal of Statistics*, vol. 42, no. 1, pp. 118–136, 2015.

[8] F.-É. Racicot, W. F. Rentz, and A. L. Kahl, "Rolling regression analysis of the pástor-stambaugh model: evidence from robust instrumental variables," *International Advances in Economic Research*, vol. 23, no. 1, pp. 75–90, 2017.

[9] L. Bo and Y. Fang, "Portfolio selection model based on fuzzy regression analysis," *Xitong Gongcheng Lilun Yu Shijian/System Engineering Theory and Practice*, vol. 35, no. 7, pp. 1770–1776, 2015.

[10] P. Mistry, G. Bora, and G. Bora, "Development of yield forecast model using multiple regression analysis and impact of climatic parameters on spring wheat," *International Journal of Agricultural and Biological Engineering*, vol. 12, no. 4, pp. 110–115, 2019.

[11] N. Krishnaraj, M. Elhoseny, E. L. Lydia, K. Shankar, and O. ALDabbas, "An efficient radix trie-based semantic visual indexing model for large-scale image retrieval in cloud environment," *Software Practice and Experience*, 2020, in Press.

[12] B. Li, M. Lu, Y. Zhang, and J. Huang, "A weekend load forecasting model based on semi-parametric regression analysis considering weather and load interaction," *Energies*, vol. 12, no. 20, p. 3820, 2019.

[13] G. Xiao, Q. Cheng, and C. Zhang, "Detecting travel modes using rule-based classification system and Gaussian process classifier," *IEEE Access*, vol. 7, pp. 116741–116752, 2019.

[14] Y. Zhao, X. Wang, Y. Wang, and Z. Zhu, "Logistic regression analysis and a risk prediction model of pneumothorax after CT-guided needle biopsy," *Journal of Thoracic Disease*, vol. 9, no. 11, pp. 4750–4757, 2017.

[15] X. U. Peng, Q. I. Lu, X. Jian et al., "A regression analysis model of ordinal variable to psychological data," *Acta Psychologica Sinica*, vol. 47, no. 12, p. 1520, 2015.

[16] G. Yu, L. Zhu, J. Sun, and L. L. Robison, "Regression analysis of incomplete data from event history studies with the proportional rates model," *Statistics and its Interface*, vol. 11, no. 1, pp. 91–97, 2018.

[17] S. Bhandari and A. J. Johnson-Syder, "A generic model of predicting probability of success-distress of an organization: a logistic regression analysis," *Journal of Applied Business Research (JABR)*, vol. 34, no. 1, pp. 169–182, 2018.

[18] M. K. Al Mesfer, M. Danish, and M. M. Alam, "Optimization of performance model of ethyl acetate saponification using multiple regression analysis," *Russian Journal of Applied Chemistry*, vol. 91, no. 11, pp. 1895–1904, 2018.

[19] L. Yin, X. Li, L. Gao, C. Lu, and Z. Zhang, "A novel mathematical model and multi-objective method for the low-carbon flexible job shop scheduling problem," *Sustainable Computing: Informatics and Systems*, vol. 13, no. 3, pp. 15–30, 2017.

[20] M. A. Mondal, D. H. Stefaan, and J. K. Ladha, "Multivariate regression analysis method for two-variance model," *Journal of Mechanical Engineering Research & Developments*, vol. 37, no. 2, pp. 19–26, 2015.

[21] S. Bouzebda, C. Papamichail, and N. Limnios, "Regression analysis of stochastic fatigue crack growth model in a martingale difference framework," *Journal of Statistical Theory and Practice*, vol. 14, no. 2, pp. 1–41, 2020.

[22] J. Rice, "Scoring with uniquely geometrical packaging," *Packaging World*, vol. 23, no. 7, p. 44, 2016.

[23] C.-Y. Chou and P.-H. Lin, "Promoting discussion in peer instruction: discussion partner assignment and accountability scoring mechanisms," *British Journal of Educational Technology*, vol. 46, no. 4, pp. 839–847, 2015.

[24] R. Zellweger, D. Dalcher, K. Mutreja et al., "Rad51-mediated replication fork reversal is a global response to genotoxic treatments in human cells," *Journal of Cell Biology*, vol. 208, no. 5, pp. 563–579, 2015.

[25] Q. Xue, Y. Zhu, and J. Wang, "Joint distribution estimation and naïve Bayes classification under local differential privacy," *IEEE Transactions on Emerging Topics in Computing*, vol. 1, p. 1, 2020.

[26] C. Martel, V. Zhurov, M. Navarro et al., "Tomato whole genome transcriptional response to tetranychus urticae identifies divergence of spider mite-induced responses between tomato and arabidopsis," *Molecular Plant-Microbe Interactions*, vol. 28, no. 3, pp. 343–361, 2015.

[27] Y. Sheng, Z. Honghong, G. Leilei et al., "Deep sequencing and bioinformatic analysis of lesioned sciatic nerves after crush injury," *PLoS One*, vol. 10, no. 12, Article ID e0143491, 2015.

[28] V. Puri, S. Jha, R. Kumar et al., "A hybrid artificial intelligence and internet of things model for generation of renewable resource of energy," *IEEE Access*, vol. 7, pp. 111181–111191, 2019.

[29] W. Xu and H. Zhou, "Mixed effect regression analysis for a cluster-based two-stage outcome-auxiliary-dependent sampling design with a continuous outcome," *Biostatistics*, vol. 13, no. 4, pp. 650–664, 2012.

Research Article

Improved Particle Swarm Optimization Algorithm in Power System Network Reconfiguration

Yanmin Wu [ID] [1,2] **and Qipeng Song**[3]

[1]*College of Electric Engineering, Naval University of Engineering, Wuhan 430033, Hubei, China*
[2]*School of Building Environment Engineering, Zhengzhou University of Light Industry, Zhengzhou 450002, Henan, China*
[3]*China Electric Power Research Institute, Beijing 100192, China*

Correspondence should be addressed to Yanmin Wu; 2006121@zzuli.edu.cn

With the rapid development of the social economy, the rapid development of all social circles places higher demands on the electricity industry. As a fundamental industry supporting the salvation of the national economy, society, and human life, the electricity industry will face a significant improvement and the restructuring of the network as an important part of the power system should also be optimised. This paper first introduces the development history of swarm intelligence algorithm and related research work at home and abroad. Secondly, it puts forward the importance of particle swarm optimization algorithm for power system network reconfiguration and expounds the basic principle, essential characteristics, and basic model of the particle swarm optimization algorithm. This paper completes the work of improving PSO through the common improved methods of PSO and the introduction of mutation operation and tent mapping. In the experimental simulation part, the improved particle swarm optimization algorithm is used to simulate the 10-machine 39-bus simulation system in IEEE, and the experimental data are compared with the chaos genetic algorithm and particle swarm optimization discrete algorithm. Through the experimental data, we can know that the improved particle swarm optimization algorithm has the least number of actions in switching times, only 4 times, and the chaos genetic algorithm and discrete particle swarm optimization algorithm are 5 times; compared with the other two algorithms, the improved particle swarm optimization algorithm has the fastest convergence speed and the highest convergence accuracy. The improved particle swarm optimization algorithm proposed in this paper provides an excellent solution for power system network reconfiguration and has important research significance for power system subsequent optimization and particle swarm optimization algorithm improvement.

1. Introduction

Electricity is the main energy base of a country, related to saving the national economy. The development of modern electricity has entered a period of multiple services, which is linked to global resources, environmental protection, and sustainable development. At present, with the development of economy and the improvement of people's living standards, the requirements of consumers for electric energy are constantly improving. The requirements of "safety, reliability, economy, high quality, and environmental protection" in the power supply are also constantly improving, and the power system is developing in the direction of automation, optimization, adaptation, intelligence, coordination, and regionalization. For the time being, China has entered the stage of integrated electricity generation. In energy production, rational planning of production, transmission, distribution, and transformation not only improves the reliability of the electricity network, but it also improves the economy of the electricity network, saving human and economic resources.

However, the power system has nonlinear, multiconstrained, unconventional, and high-dimensional optimization problems. However, the traditional heuristic algorithm is not a strict optimization method and cannot deal with the interaction between various objective functions. The

mathematical optimization method is very difficult to calculate the optimization problem, which is easy to cause dimension disaster. The swarm intelligence algorithm includes genetic algorithm, simulated annealing algorithm, tabu algorithm, ant colony algorithm, fish swarm algorithm, and particle swarm optimization. Among them, the particle swarm optimization algorithm has the advantages of fast convergence speed, multiparticle parallel processing, and easy application, which can solve the optimization problem of the power system.

The concept of swarm intelligence was first proposed by American scholars Hackwood and Beni in the molecular automation system. Inspired by the collective behavior of natural groups, the swarm intelligence algorithm has been widely used in life [1]. Cheng is based on the combination of the swarm intelligence algorithm and data mining, so that big data problems can be better understood and analyzed [2]. American scholars Eberhart and Kennedy studied the foraging behavior of birds and proposed particle swarm optimization (PSO). The main theoretical basis of the algorithm is artificial life and evolutionary information theory, and its basic idea is to find the best solution through the cooperation between individuals. Since the particle swarm optimization was proposed, in order to improve the performance of the algorithm, a large number of researchers at home and abroad have improved it. These improved algorithms mainly have the following ideas: improving the inertia weight of its own parameters, improving its own parameter learning factor, and combining with other algorithms. Mahi introduced the 3-opt algorithm into the particle swarm optimization algorithm to optimize the performance of the algorithm to improve the defects of the local solution of the particle swarm optimization algorithm [3]. Gong proposed a new particle swarm optimization algorithm called the genetic particle swarm optimization algorithm, which uses genetic evolution technology to cultivate the particle swarm optimization algorithm [4].

The optimization algorithm adopted in this article is based on the classical particle speed optimization algorithm, which accelerates the rate of convergence and improves the accuracy of convergence. Calculation results have little chance, good stability, and a strong global search capability. This article is mainly concerned with improving the PSO learning method and the optimization algorithm. The model of analysis of convergence theory and the improved particle optimization algorithm shall be used to study the reformulation of the power grid. The main purpose of this work is to propose a more appropriate and valuable algorithm for the restructuring of the power grid.

2. Basic Model and Improved Method of Particle Swarm Optimization

2.1. Basic Principle of Particle Swarm Optimization Algorithm.
Since Kennedy and Eberhart first proposed the particle cluster optimization algorithm, more and more attention has been drawn to and research by domestic and foreign researchers and has proposed various improved versions and applications from one angle [5]. Particle swarm optimization

is an evolutionary algorithm based on population, and its ideological source is the theory of artificial life and evolutionary computing [6]. According to Reynolds' research on bird flight, a single bird only needs to track a limited number of birds around it, but the final result is that the whole flock seems to fly orderly under an invisible control. In other words, the complex and elegant global behavior is generated by the simplest rule interaction, which is the essence of swarm intelligence. Particle swarm optimization is derived from the study of foraging behavior of birds: a group of birds are looking for food randomly. If there is only one piece of food in this area, then the simplest and most effective search strategy is to find food in the nearest place to the food. Particle swarm optimization is inspired from this mode and further used to solve optimization problems [7, 8]. In addition, people usually make decisions based on their own and others' experience, which is also in line with the basic idea of particle swarm optimization: when particle swarm optimization is used to solve optimization problems, the solution of the problem corresponds to the position of a bird (particle) in the search space. The particle not only has its own position and velocity but also has a suitable value determined by the objective function. Each particle remembers and follows the current optimal particle and searches the solution space: each search (iteration) contains some random factors, but these factors are not completely random. If a better solution is found, the next good solution can be found on this basis. Specifically, the particle swarm optimization starts with a random initial particle. In each iteration, the particle updates its position by tracking two "extreme points": one is the best solution found by the particle itself (i.e., individual extreme point, pbest) and the other is the extreme point (gbest) of the whole particle swarm or the extreme point of the whole neighborhood (lbest). On the basis of the original inertia, particles adjust the flight direction and speed according to these two extrema to maintain the overall optimum [9, 10].

2.2. Essence and Characteristics of Particle Swarm Optimization.

(1) Particle swarm optimization is a new swarm intelligence optimization technology, which is the simulation of group society. After much research and practice by the PSO, the substance of the PSO can be summed up as "random" and "leadership." Random is the blood of particle optimization. Particulate optimization is based on the Monte Carlo algorithm of the previous generation, which fully inherits the characteristics of random number resolution. Leadership is the evolution of the particle swarm optimization algorithm. It simulates the phenomenon of mutual cooperation in a group society. Individuals have the ability to learn, and the group has the ability to cooperate with each other. According to the guidance of leader particles, the whole population will converge to the global optimal solution [11, 12]. Therefore, the advantages and disadvantages of PSO are easy to understand. Due to the randomness of

PSO, it has advantages in solving nonconvex, discontinuous, high-dimensional, nonlinear, and nondifferentiable optimization problems. Similarly, due to the randomness, its calculation results may be randomness. If the leadership is enhanced, the randomness of the calculation results of the algorithm will be reduced; due to the strong leadership of the PSO, the PSO may easily fall into If the randomness is increased, the algorithm may jump out of the local optimum and find the global optimal [13, 14].The essence of particle swarm optimization "random" and "leader" have the characteristics of "spear" and "shield," which need a kind of thought of trade-off to balance.

2.3. Basic Model of Algorithm. Particle optimization is a smart algorithm based on repetitive function. His basic idea is to randomly prepare a particle group with memory but without volume and mass. Each particle represents a feasible solution to the optimization problem and determines a moderate value through the measurement function. Good and bad particle count is judged by the appropriate value [15]. Each particle has the ability of memory and can adjust its own motion trajectory according to its current position, information sharing between peers, and the best position experienced in memory. After iteration, the particle keeps approaching the best position and finally reaches the optimal position [16].

The mathematical description of the basic particle swarm optimization algorithm is as follows.

Assuming that the population size of a particle is n, the position information of the ith particle ($i = 1, 2, \ldots, n$) in d-dimensional space is represented by

$$x_i = (x_{i1}, x_{i2}, \ldots, x_{id}, \ldots, x_{iD}), \tag{1}$$

and the velocity of the ith particle is expressed by v_i

$$v_i = (v_{i1}, v_{i2}, \ldots, v_{id}, \ldots, v_{iD}). \tag{2}$$

Thus, at time $t + 1$ ($t = 1, 2, \ldots, T_{\max})T_{\max}$, the flight velocity v_{id} of the ith particle in the d-dimensional ($d = 1, 2, \ldots, d$) subspace is adjusted according to the following formula:

$$\begin{aligned} v_{id}(t+1) = {} & v_{id}(t) + c_1 r_1(t)\left(p_{id}(t) - x_{id}(t)\right) \\ & + c_2 r_2(t)\left(P_{gd} - x_{id}(t)\right). \end{aligned} \tag{3}$$

In formula (3), p_{id} represents the historical optimal position of the current particle, p_{gd} represents the global historical optimal position of the particle, and c_1 and c_2 are nonnegative acceleration constants, also known as convergence factors. The convergence factor c_1 is called cognitive constant, which represents the characteristics of particles learning from their own optimal state. r_1 and r_2 are a random number distributed in the interval [0,1]. It can be seen from the formula that the first the flying speed of a particle is mainly determined by the following three parts: the first part is the speed of the particle at time t, which represents the particle's trust in the flight speed at

time t and makes inertial motion according to its own speed at time t; the second part is the cognitive part of the particle itself, which represents the particle's thinking about its position, thinking about the position before the particle itself, so as to determine the next step. The third part is the "social" part of particles, which represents the information exchange and cooperation between particles and their peers. In the process of searching, particles synthesize their own previous flight experience and the experience of their companions and finally determine their own flight speed according to formula (3).

Weight of inertia W: the global search capability of the main population is controlled by global search speed and inertia. If w gets a fixed higher value, the algorithm convergence speed will be too slow and the final accuracy of the solution is also very low. This is because the position of particles changes greatly each time, and it is very easy to miss the optimal value region, which leads to the algorithm is difficult to determine the existence area of the optimal value and does not have the local fine search ability; if the fixed small value of W is taken, the algorithm can detect the local region. Because the search step size is small and the particle position changes little after each update, it is difficult to traverse the whole search space, so it is difficult to locate the region where the optimal value exists. Therefore, the algorithm is prone to premature convergence and premature in this case. In addition, it is found that the inertia weight setting value of PSO is too high. It is the best to decrease between 0.9 and 0.4, because the population has a large inertia weight at the beginning of evolution and can traverse a wider range, which is helpful to find the region where the optimal solution may exist. In the later stage of population evolution, the inertia weight is small, and the algorithm has strong local search ability, which is helpful to find the best solution in the field where the optimal solution exists [17, 18].

Convergence factors c_1 and c_2: these two parameters represent the acceleration weights of particles approaching individual and global extremum, respectively. The size of c_1 determines the cognitive ability of particles, that is, the ability of particles to learn from themselves. In extreme cases, when $c_1 = 0$, particles have no cognitive ability and are only affected by the "social part." At this time, the population has the maximum ability to traverse the whole feasible solution space, and the convergence speed is fast. However, when solving the complex multipeak problems, it is very easy to find the local optimal problem. The size of c_2 determines the social information sharing ability of particles, that is, the ability of particles to advance toward the current global optimal value. In extreme cases, $c_2 = 0$, particles in the population will not share information. The algorithm only has the "cognitive" model. Since there is no information interaction between particles, it is very unlikely that the algorithm can get the optimal solution.

2.4. Algorithm Flow. Particle swarm optimization can be summarized as the following steps:

(1) The position and velocity of all particles (population size n) and the basic parameters of the algorithm are initialized.

(2) Taking the initial position of each particle as individual extremum, the initial fitness value of each particle in the population is calculated, and the optimal position of the current population is obtained.

(3) Update the speed and position of each particle.

(4) Compare the current fitness value with the historical optimal value. If the current fitness value is superior to the historical optimal value, the historical optimal value of the particle is set to the current fitness value, and the particle position is updated.

(5) If the current fitness value is better than the historical population optimal value, the historical population optimal value is set as the current fitness value to update the global optimal solution of the population.

(6) Check the end conditions. If the optimization results meet the conditions for the iteration stop, the optimal solution is obtained and the iteration is terminated. Otherwise, turn back to step 4 and continue the optimization until the iteration stop condition is met.

2.5. Several Common Improved Particle Swarm Optimization Algorithms

2.5.1. Particle Swarm Optimization Model with Inertia Weight. Shi and Eberhart add the inertia weight parameter to the speed update formula of the basic particle swarm optimization algorithm, which is multiplied by the particle velocity at t time. This method makes the algorithm achieve the effective balance between global search and local search by adjusting the value of inertia weight and improves the search ability of the algorithm. The main purpose of introducing inertia weight parameters is to better balance the global detection and local search capabilities of particle swarm optimization [19]. The results show that when w is set larger, it is beneficial to global breadth search; conversely, it is beneficial to local depth search. This improvement is achieved by adding an inertia coefficient w to the speed update formula; that is, the new speed update formula is as follows:

$$v_{id} = wv_{id}(t-1) + c_1 \text{rand}\left[pbest_{id}(t-1) - p_{id}(t-1)\right]$$
$$+ c_2 \text{rand}()\left[gbest_d(t-1) - p_{id}(t-1)\right], \tag{4}$$

where W is called inertia weight.

2.5.2. Adding Convergence Factor. Clerc adds a convergence factor χ to the speed update formula of the basic particle swarm optimization algorithm to ensure the convergence of the algorithm. This method is actually v_i reselection of parameters w, c_1, and c_2. By properly selecting these controllable parameters, the value of a does not have to be limited in $[-v_{\max}, v_{\max}]$. In this case, the corresponding algorithm speed update formula can be expressed as follows:

$$v_{id}(t) = \chi\left[v_{id}(t-1) + c_1 \text{rand}()\left(pbest_{id}(t-1) - p_{id}(t-1)\right)\right.$$
$$\left. + c_2 \text{rand}()\left(gbest_d(t-1) - p_{id}(t-1)\right)\right]. \tag{5}$$

In the experiment, $\chi = (2/|2 - \varphi - \sqrt{\varphi^2 - 4\varphi}|)$, $\varphi = c_1 + c_2 > 4$, φ is usually taken as 4.1 (at this time, $c_1 = c_2 = 2.05$, i.e., $\chi = 0.729$), which is equivalent to $w = 0.729$, $c_1 = c_2 = 1.1494$ in formula (5), which is called the particle swarm optimization algorithm with convergence factor. Experimental data show that the particle swarm optimization with convergence factor effectively overcomes the shortage of linear decreasing weight and has its unique effect compared with the inertia weight of other formats. Therefore, this technology has been paid attention to in the design of the particle swarm optimization algorithm [20].

2.5.3. Differentiation Algorithm. The basic idea of the differential evolution algorithm is to take the differential carrier of two randomly selected individuals in the population as a source of random change of the third person, i.e., to create the mutant person, and then the new person is created by the crossover function between the mutant person and the target person. If the value and the suitability of the new person are better than those of the target person, the target person will be informed as a new person to enter the next generation. Otherwise, the target person will be preserved in the next generation [21,22].

The implementation process of differentiation algorithm is as follows:

(1) Generating initial population

M individuals are randomly generated in n-dimensional space:

$$x_{ij}(0) = x_{ij}^L + \text{rand}(0,1)\left(x_{ij}^U - x_{ij}^L\right), \tag{6}$$

where rand $(0, 1)$ is a random number between [0, 1].

(2) Mutation operation

The key step of differential evolution is mutation operation, which randomly selects three individuals x_{p1}, x_{p2}, x_{p3} and $p1 \neq p2 \neq p3 \neq i$ from the feasible solutions:

$$h_{ij}(g) = x_{p1j} + F\left(x_{p2j} - x_{p3j}\right). \tag{7}$$

(3) Cross operation

The main purpose of cross operation is to increase the diversity of feasible solutions:

$$v_{ij}(g+1) = \begin{cases} h_{ij}(g), & \text{if } r \text{ and } (0,1) \leq \text{CR or } j = \text{rand}(1,n), \\ x_{ij}(g), & \text{if } r \text{ and } (0,1) > \text{CR or } j \neq \text{rand}(1,n), \end{cases} \tag{8}$$

where Cr is the crossover probability, $CR \in [0, 1]$, and rand $(1, n)$ is a random integer between $[1, n]$.

(4) Select action

In order to update the template individuals, vector $v_{ij}(g+1)$ and vector $x_i(g)$ were compared:

$$x_i(g+1) = \begin{cases} v_i(g+1), & \text{if } f(v_i(g+1)) < f(x_i(g)), \\ x_i(g), & \text{if } f(v_i(g+1)) \geq f(x_i(g)). \end{cases} \tag{9}$$

The mutation operation is repeated until the required convergence precision is reached or the maximum evolution algebra is reached.

2.6. Discrete Mode of Particle Swarm Optimization.

Power system network reconfiguration is a discrete multiobjective combinatorial optimization problem. The final result of the reconfiguration is a group of switching action combinations. For the power grid model used in this paper, the reconstruction result can be regarded as a 20-dimensional vector. Therefore, in order to make the particle swarm optimization algorithm solve the problem of this topic, it must be discretized chemical treatment.

At first, particle swarm optimization (PSO) can only be directly used to solve the continuous optimization problem. The discrete binary particle swarm optimization (dbpso) mainly adjusts the speed update mode of particle swarm optimization and introduces the probability function:

$$\begin{cases} v_{id}^{k+1} = v_{id}^k + c_1 r_1 (i_{id} - x_{id}) + c_2 r_2 (P_{gd} - x_{id}), \\ x_{id}^{k+1} = \begin{cases} 1, & \text{rand} < S(v_{id}^{k+1}), \\ 0, & \text{rand} \geq S(v_{id}^{k+1}). \end{cases} \end{cases} \tag{10}$$

In the formula, () Rand is the random number of [0, 1]; the function s represents v_{id} probability function in the interval [0, 1] determined by the velocity a. The closer the s is to 1, the more likely it is to take 1; otherwise, the more likely it is to take 0. Generally, the fuzzy function sigmoid is used as the probability function. The sigmoid function is as follows:

$$\text{Sigmoid}(v_{id}^{k+1}) \begin{cases} 0, & v_{id}^{k+1} < V_{\min}, \\ [1 + \exp(-v_{id}^{k+1})], & V_{\min} \leq v_{id}^{k+1} < V_{\max}, \\ 0.99, & v_{id}^{k+1} > V_{\max}. \end{cases} \tag{11}$$

3. Improved Particle Swarm Optimization Algorithm

In order to make the improved particle swarm optimization algorithm more suitable for power system network reconfiguration, this paper introduces a variety of algorithms based on the abovementioned improved particle swarm optimization algorithm and uses the self-made parameters of the experimental simulation system to verify the performance of the improved particle swarm optimization algorithm.

3.1. Definition of Population Diversity.

In general, the more concentrated the particles are in the search space, the lower the population diversity. The more dispersed the particle distribution, the higher the diversity of the population [23]. This paper adopts the definition of diversity in the following formula:

$$\text{diversity}(S) = \frac{1}{|S||L|} \bullet \sum_{i=1}^{|S|} \sqrt{\sum_{j=1}^{\text{Dim}} (p_{ij} - \overline{p_j})^2}. \tag{12}$$

In the formula, p_{ij} is the j-th variable of the ith particle, $\overline{p_j}$ is the average value of the j-th variable of all particles, $|s|$ is the population size, $|L|$ is the longest radius of the search space, and dim is the dimension of the solution space. The diversity (s) value reflects the average distance between all particles in the population and the center of the search space and reflects the density of particles. The smaller the diversity (s), the more concentrated the particles in the population, and the larger the diversity (s), the more dispersed the particles in the population.

3.2. Introducing Mutation Operation.

The rapid decrease of population diversity will lead to premature convergence of PSO, which is the biggest defect of PSO. Therefore, the mutation operation is introduced into the algorithm to adjust the population diversity attenuation process of particle swarm optimization: in this paper, ρ_0 mutation operator similar to the genetic algorithm is introduced in the mutation operation of the improved particle swarm optimization algorithm. The specific operation is as follows: set the mutation rate a and the mutation random quantity ρ_j on the particle position component, where $J = 1, 2, \ldots, \text{dim}$ and ρ_j is the interval [0, 1]. For the position component in the j-th dimension of a particle, if $\rho_j < \rho_0$, the position component ρ_j of a particle in this dimension will be replaced by the position component of its adjacent position particle in the memory library, and it will change to the particle dimension component with higher fitness value at the approximate rate and change to the particle dimension position component with smaller fitness value with a smaller probability [24, 25].

3.3. Initialization of Improved Particle Swarm Optimization Algorithm Based on Tent Mapping.

Speed is an important objective of the restructuring of the power grid. A better initialization formula can improve the speed of convergence of the algorithm to the best solution. The traditional form of random initialization does not favour convergence of the algorithm, and the likelihood of finding the best solution is also greatly reduced.

At present, most experts use chaos rules based on logistic map to initialize population. Chaotic motion has the characteristics of regularity, ergodicity, and randomness. Chaos initialization is proposed based on this characteristic. Chaos initialization can improve the quality of the initial solution and enhance the diversity of the initial population, which is conducive to the population traversing the whole feasible solution region in the early evolution stage.

However, different chaotic maps have different effects on the chaotic optimization process. The ergodic uniformity and search efficiency of tent map are better than the logistic map. Therefore, this paper considers using tent map to initialize population particles. The iterative formula of the tent chaotic mapping operator is as follows:

$$r_{k+1} = \begin{cases} 2r_k, & r_k \in [0, 0.5], \\ 2(1 - x_k), & r_k \in (0.5, 1], \end{cases} \quad (13)$$

where $k = 12, 3, m_o$. Let the initial value of r_{k+1} take the random number in the interval [0, 1]. Through the iterative calculation of the above formula, the random number between M can be obtained. Using the above model to generate chaotic variables, map them to the interval of decision variables $[x \min, x \max]$ and get the initial particle swarm optimization population.

3.4. Specific Steps of Power System Network Reconfiguration Simulation Based on Improved Particle Swarm Optimization Algorithm. The use of the improved particle swarm optimization algorithm to reconfigure the power grid is usually divided into the following steps, and the specific process is shown in Figure 1:

(1) Code the primary and secondary load with 0, 1, and 2 codes, 0 represents that the standby path switch is open, 1 represents that the normal path switch is closed, and 2 represents the standby path switch is closed; for the third-level load, 0 is for the switch is open, and 1 is for the switch to remain closed.

(2) The initial population size, initial mutation rate ρ_0, and initial inertia weight W are set.

(3) The fitness value of each particle is calculated, and the current position information of the particle is recorded in the memory database to update the individual history optimal and population global optimal.

(4) Update the position and velocity of population particles.

(5) The diversity value of the current population was calculated.

(6) Update inertia weight W and variation rate ρ_0.

(7) Mutate the particles.

(8) Check whether the maximum number of iterations is reached. If the maximum number of iterations is reached, the best fitness value and its location information are output. Otherwise, return to step 3 to continue iteration.

4. Network Reconfiguration Simulation Experiment Based on Improved Particle Swarm Optimization Algorithm

4.1. Experimental Simulation of Improved Particle Swarm Optimization Algorithm. In this paper, the IEEE 10-machine 39-bus simulation system is used to carry out the simulation experiment, and the existing fault occurs in 22 and 32 nodes.
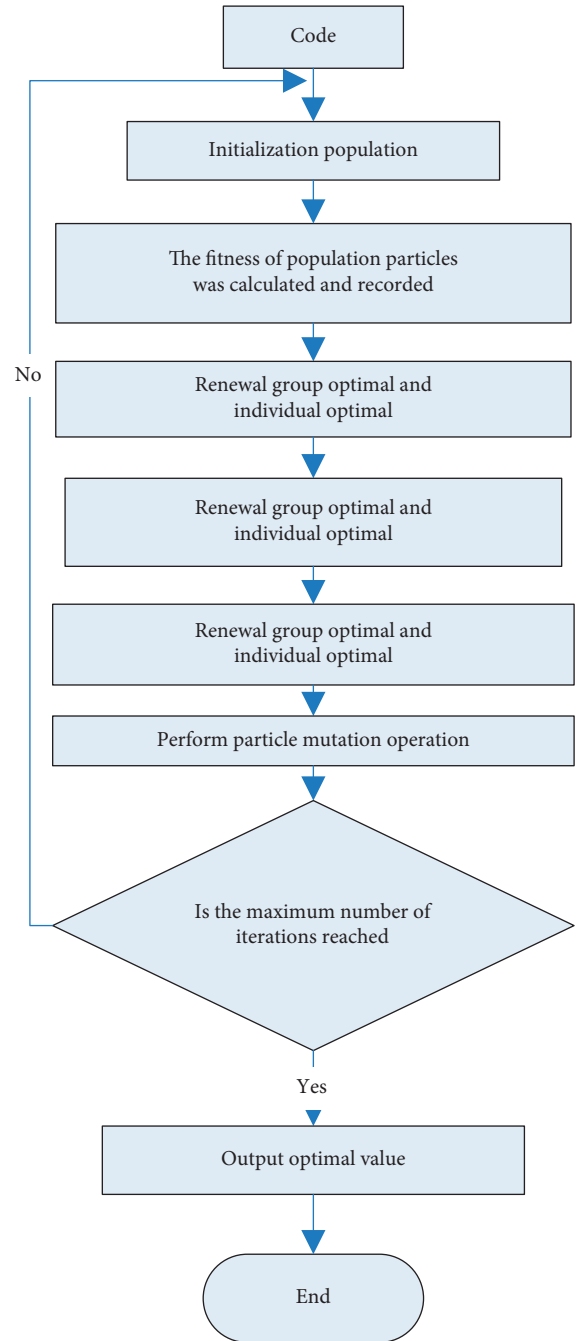
FIGURE 1: Power system network reconfiguration process.

The simulation experiment parameters are set as follows: population size $M = 50$, population dimension dim = 10, maximum iteration times $t = 50$, acceleration factor $c_1 = c_2 = 2$, initial inertia weight $W = 0.8$, and initial value of variation rate is 0.1.

It can be seen from Table 1 and Figure 2 that the number of switches decreases with the iteration of the algorithm, from the first generation of 10 times of global optimal solution switching times to the fifth generation of four times, and it remains stable in the subsequent iterations. Table 2 and Figure 2 reflect the change of the global optimal adaptive speed with the algorithm iteration. It can be seen that the

Table 1: Optimal particle switching times.

Number of iterations/k	1	2	3	4	5–50
Optimal particle switching times	10	8	7	5	4
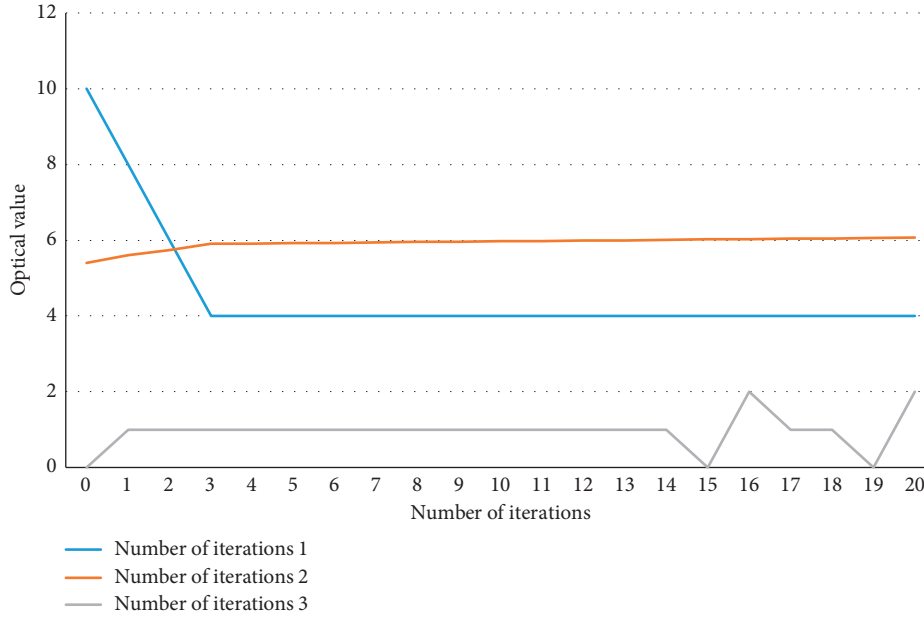
Figure 2: Iterative results.

Table 2: Optimal particle fitness change.

Number of iterations/k	1	2	3	4	5	6–50
Optimal fitness/w	5.76	5.80	5.83	5.85	5.88	5.90

optimal fitness value reaches the maximum when the algorithm is iterated to the sixth generation, and the drag racing is stable. The last graph in Figure 2 shows the optimal particle coding after 50 iterations.

All the final schemes of power network reconfiguration are that branches 14 and 19 are unloaded and branches 15 and 20 use standby power supply. This method can solve the fault problem safely, effectively, and quickly, so the improved particle swarm optimization algorithm used in this paper is feasible.

4.2. Comparison of Improved Particle Swarm Optimization Algorithm with Chaos Genetic Algorithm and Discrete Particle Swarm Optimization Algorithm. In order to prove the performance of the improved particle swarm optimization algorithm, the chaos genetic algorithm and discrete particle swarm optimization algorithm are used to simulate the same fault, and the experimental results of the two algorithms are compared with the experimental results of the improved particle swarm optimization algorithm.

In this experiment, the New England 10-machine 39-bus simulation system is still used in the experiment. The fault of the experiment is set as 6 and 21 nodes, and the three algorithms are iterated 40 times each.

It can be seen from Table 3 and Figure 3 that the maximum switching times of the global optimal solution of the chaos genetic algorithm are 12, the minimum switching times are 5, and the minimum number of switching times is 28; the maximum switching times of the discrete particle swarm optimization algorithm are 20, the minimum switching times are 5, and the minimum number of switching times is only 22; the maximum switching times of the improved particle swarm optimization algorithm are 10, the minimum number of switching times is only 4 among the three algorithms, and the minimum number of switching times is 38 times in the three algorithms.

Table 4 and Figure 4 record the global optimal fitness values of the three algorithms with the iteration of the algorithm. The minimum value of the global optimal fitness of the chaos genetic algorithm is 5.49, the maximum value is 5.65, and the maximum number of times is 26; the minimum value of discrete particle swarm optimization algorithm is 5.27, the maximum value is 5.64, and the maximum number of times is 21; the improved particle swarm optimization algorithm is the best among the three algorithms, with the maximum value of 5.72, the minimum value of 5.53, and the maximum occurrence times of up to 38 times.

Figure 5 shows the optimal particle code obtained by the three algorithms through iteration. From the optimal particle code of the three algorithms, we can get the corresponding reconstruction scheme: the reconstruction scheme of the chaotic genetic algorithm and discrete particle swarm optimization algorithm is the same, branch 5 and 9 are

TABLE 3: Comparison of switching times.

Optimal particle switching times	Maximum	Minimum	Minimum number of times
CGA's optimal particles	12	5	28
DPSO's optimal particles	20	5	22
IPSO's optimal particles	10	4	38
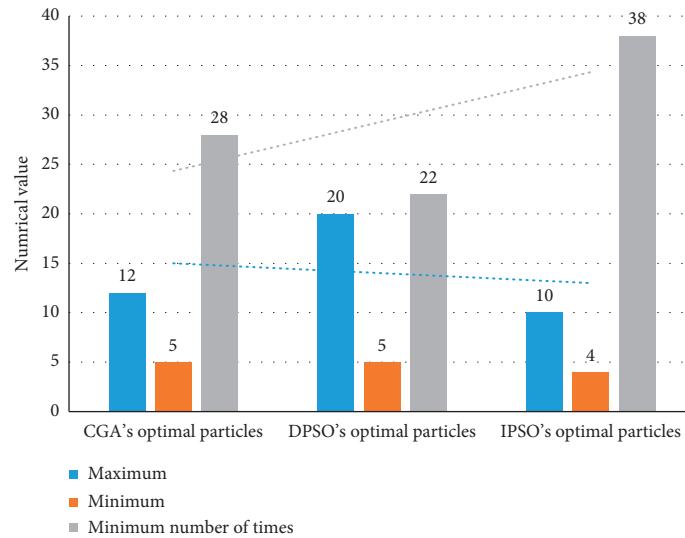
FIGURE 3: Comparison of switching times.

TABLE 4: Fitness comparison of optimal particles.

Fitness of optimal particles	Maximum	Minimum	Maximum number of times
CGA's optimal particles	5.65	5.49	26
DPSO's optimal particles	5.64	5.27	21
IPSO's optimal particles	5.72	5.53	38
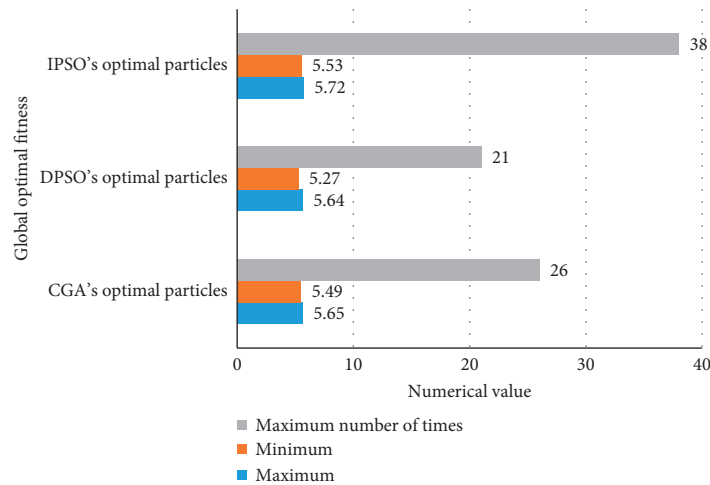
FIGURE 4: Fitness comparison of optimal particles.

restored by the backup path, and the branches 4, 13, and 17 are unloaded. The improved particle swarm optimization algorithm is that the power supply of branch 5 and 9 is restored by the standby path, and branches 13 and 17 are unloaded.

By sorting out the results, we can know that in terms of switching operation times, the improved particle swarm optimization algorithm has the least number of actions, only 4 times, and the other two algorithms are 5 times; in terms of the earliest convergence algebra, the improved particle
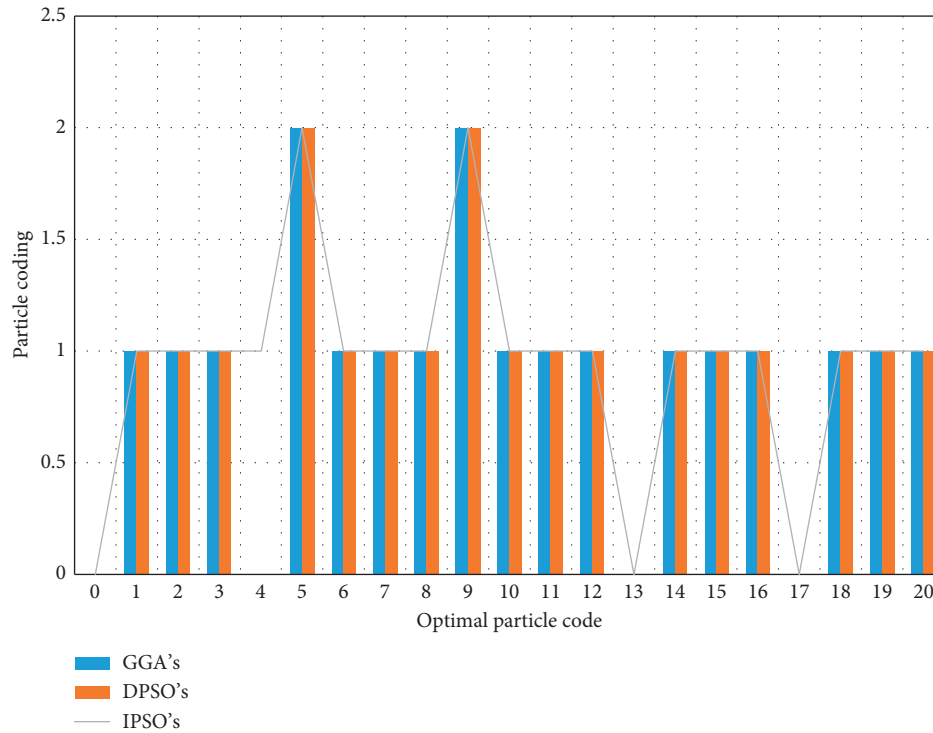
FIGURE 5: Three algorithm load ordinals.

swarm optimization algorithm is the first to converge to the global optimum, and the chaos inheritance algorithm and discrete particle swarm optimization algorithm need a lot of iterations to achieve the global optimal; in the restorability, the improved particle swarm optimization algorithm can achieve the global optimization. In the aspect of energy, it is obvious that the restoration scheme provided by the improved particle swarm optimization algorithm can meet the requirements of maximum recovery of load power supply, and the convergence accuracy is the highest.

Through the above comparison, it can be seen that the improved particle swarm optimization algorithm has a certain degree of improvement in the number of iterations and the solution accuracy. The recovery scheme obtained is better than other algorithms, the switching operation cost is also low, and the convergence performance is also improved, which can ensure that a better recovery scheme can be finally obtained.

5. Conclusions

Under the background of the continuous expansion of the scale and complexity of the power system, how to ensure the realization of the operation control objectives of the power system and how to construct and solve various optimization problems in the power system under the constraints of many complex and uncertain conditions are always the important issues faced by power engineers. Power system network reconfiguration is an important part of modern power system intelligent management and an important guarantee for stable and reliable operation of power grid. Once a large-scale blackout occurs, if there is

no predetermined recovery plan, it will cause great economic losses. Therefore, it is very necessary to study the topic of power system network reconfiguration, which is of great theoretical and practical significance for reducing power system failure and outage losses and ensuring safe, rapid and intelligent restoration of power supply after accidents.

In this paper, based on the basic principle and model of particle swarm optimization, mutation operation and tent mapping are introduced, and an improved particle swarm optimization algorithm for power system network reconfiguration is proposed. The algorithm combines the definition of population diversity, discrete particle swarm optimization, inertia weight, and convergence factor selection and dynamic update to improve and optimize the classical particle swarm optimization algorithm. The improved particle swarm optimization (PSO) algorithm is used to simulate the power network system reconfiguration, and the experimental results are compared with the other two algorithms.

The experimental results show that the improved particle swarm optimization algorithm has faster calculation speed, better convergence speed, and convergence accuracy in power system network reconfiguration; the calculation results have small randomness and good stability and have excellent performance compared with the other two algorithms. The improved particle swarm optimization algorithm can provide solutions for power system network reconfiguration and better solve the problems in power system network reconfiguration, which provides ideas and evidence for the next research in this field.

Data Availability

The data that support the findings of this study are available from the corresponding author upon reasonable request.

Conflicts of Interest

The authors declare that they have no conflicts of interest.

References

[1] Y. Tan and K. Ding, "A survey on GPU-based implementation of swarm intelligence algorithms," *Annals of Thoracic and Cardiovascular Surgery: Official Journal of the Association of Thoracic and Cardiovascular Surgeons of Asia*, vol. 11, no. 9, pp. 391–396, 2015.

[2] S. Cheng, Q. Zhang, and Q. Qin, "Big data analytics with swarm intelligence," *Industrial Management & Data Systems*, vol. 116, no. 4, pp. 646–666, 2016.

[3] M. Mahi, Ö. K. Baykan, and H. Kodaz, "A new hybrid method based on particle swarm optimization, ant colony optimization and 3-opt algorithms for traveling salesman problem," *Applied Soft Computing*, vol. 30, pp. 484–490, 2015.

[4] Y. J. Gong, J. J. Li, Y. Zhou et al., "Genetic learning particle swarm optimization," *IEEE Transactions on Cybernetics*, vol. 46, no. 10, pp. 2277–2290, 2017.

[5] N. K. Jain, U. Nangia, and J. Jain, "A review of particle swarm optimization," *Journal of the Institution of Engineers*, vol. 99, no. 4, pp. 1–5, 2018.

[6] M. Schmitt and R. Wanka, "Particle swarm optimization almost surely finds local optima," *Theoretical Computer Science*, vol. 561, pp. 57–72, 2015.

[7] R. Y. Harold and M. Rajaram, "Energy-aware multipath routing scheme based on particle swarm optimization in mobile ad hoc networks," *The Scientific World Journal*, vol. 2015, Article ID 284276, 9 pages, 2015.

[8] B. Yao, B. Yu, P. Hu, J. Gao, and M. Zhang, "An improved particle swarm optimization for carton heterogeneous vehicle routing problem with a collection depot," *Annals of Operations Research*, vol. 242, no. 2, pp. 303–320, 2016.

[9] X. Liang, W. Li, Y. Zhang, and M. Zhou, "An adaptive particle swarm optimization method based on clustering," *Soft Computing*, vol. 19, no. 1, pp. 431–448, 2015.

[10] F. Marini and B. Walczak, "Particle swarm optimization (PSO). a tutorial," *Chemometrics and Intelligent Laboratory Systems*, vol. 149, pp. 153–165, 2015.

[11] M. Chih, "Self-adaptive check and repair operator-based particle swarm optimization for the multidimensional knapsack problem," *Applied Soft Computing*, vol. 26, pp. 378–389, 2015.

[12] M. R. Bonyadi and Z. Michalewicz, "Particle swarm optimization for single objective continuous space problems: a review," *Evolutionary Computation*, vol. 25, no. 1, pp. 1–54, 2017.

[13] Y. Li, X. Bai, L. Jiao, and Y. Xue, "Partitioned-cooperative quantum-behaved particle swarm optimization based on multilevel thresholding applied to medical image segmentation," *Applied Soft Computing*, vol. 56, pp. 345–356, 2017.

[14] L. Wang, H. Geng, P. Liu et al., "Particle swarm optimization based dictionary learning for remote sensing big data," *Knowledge-Based Systems*, vol. 79, pp. 43–50, 2015.

[15] S. Chatterjee, S. Sarkar, S. Hore, N. Dey, A. S. Ashour, and V. E. Balas, "Particle swarm optimization trained neural network for structural failure prediction of multistoried RC buildings," *Neural Computing and Applications*, vol. 28, no. 8, pp. 2005–2016, 2017.

[16] F. Shabbir and P. Omenzetter, "Particle swarm optimization with sequential niche technique for dynamic finite element model updating," *Computer-Aided Civil and Infrastructure Engineering*, vol. 30, no. 5, pp. 359–375, 2015.

[17] Z. Beheshti and S. M. Shamsuddin, "Non-parametric particle swarm optimization for global optimization," *Applied Soft Computing*, vol. 28, pp. 345–359, 2015.

[18] Z. Beheshti, S. M. Shamsuddin, and S. Hasan, "Memetic binary particle swarm optimization for discrete optimization problems," *Information Sciences*, vol. 299, pp. 58–84, 2015.

[19] R. P. Singh, V. Mukherjee, and S. P. Ghoshal, "Particle swarm optimization with an aging leader and challengers algorithm for the solution of optimal power flow problem," *Applied Soft Computing*, vol. 40, pp. 161–177, 2016.

[20] Z. Chen, R. Xiong, and J. Cao, "Particle swarm optimization-based optimal power management of plug-in hybrid electric vehicles considering uncertain driving conditions," *Energy*, vol. 96, pp. 197–208, 2016.

[21] F. Kuang, S. Zhang, Z. Jin, and W. Xu, "A novel SVM by combining kernel principal component analysis and improved chaotic particle swarm optimization for intrusion detection," *Soft Computing*, vol. 19, no. 5, pp. 1187–1199, 2015.

[22] J. Rada-Vilela, M. Johnston, and M. Zhang, "Population statistics for particle swarm optimization: single-evaluation methods in noisy optimization problems," *Soft Computing*, vol. 19, no. 9, pp. 2691–2716, 2015.

[23] S. Guelcue and H. Kodaz, "A novel parallel multi-swarm algorithm based on comprehensive learning particle swarm optimization," *Engineering Applications of Artificial Intelligence*, vol. 45, pp. 33–45, 2015.

[24] H. Banka and S. Dara, "A Hamming distance based binary particle swarm optimization (HDBPSO) algorithm for high dimensional feature selection, classification and validation," *Pattern Recognition Letters*, vol. 52, pp. 94–100, 2015.

[25] J. J. Kim and J. J. Lee, "Trajectory optimization with particle swarm optimization for manipulator motion planning," *IEEE Transactions on Industrial Informatics*, vol. 11, no. 3, pp. 620–631, 2017.

Research Article

Research and Application of Combined Algorithm Based on Sustainable Computing and Artificial Intelligence

Bo Hu (iD)

Science and Technology College, Jiangxi Normal University, Nanchang, Jiangxi 330027, China

Correspondence should be addressed to Bo Hu; 002869@jxnu.edu.cn

The Internet is a popular form of information technology development in the new century, and it organizes and analyzes big data by taking effective measures to find useful information. With manpower, it is obviously not enough to be in such a huge information system, so the emergence of sustainable computing and artificial intelligence has become the core of large-scale data processing at this stage. This paper studies the application of the combined algorithm based on sustainable computing and artificial intelligence. In this paper, a new combined intelligent search algorithm is proposed by combining sustainable computing with artificial intelligence. The combination algorithm firstly analyzes the value from the aspects of ecological environment and economic benefits and studies the overall evaluation of sustainable development ability. Secondly, the energy analysis method is used to establish a reasonable comprehensive ecosystem and evaluate its impact on the sustainable development of environment and economy. Finally, the impact of resource consumption, wind speed detection, waste discharge, and utilization of renewable resources in a certain area is analyzed by simulation. Through the experimental results, on the one hand, it is proved that the data obtained by the combined algorithm are more accurate than the single algorithm; on the other hand, the combined algorithm can be further sublimated and widely used for other data detection. The combination algorithm proposed in this paper can effectively detect the required data and has high applicability.

1. Introduction

In recent years, due to the continuous development of information technology and the continuous expansion of the network field, a large number of offline software and online applications came into being, playing a corresponding role in various fields [1]. The background of these applications is mainly data driven, and users can also generate a large amount of data by using the application [2]. Diversified data can not only facilitate users to quickly find the information they want to know in an acceptable time and understand the world without leaving home but also help enterprises combine online and offline business to expand business scope. Online commerce [3] has become the mainstream. At the same time, the government can also work efficiently through municipal data information, solve problems in time, and carry out more convenient service projects [4]. The emergence and existence of data promote the growth and

progress of various industries and public utilities. However, most of the time, people tend to pay too much attention to new data and conduct a lot of research on new data. However, a large number of previously generated data are generally stored in the database and can only be taken out as a reference when necessary. But we all know that the analysis of new things is often based on the past things, using the corresponding method to find the relationship between the old and the new, so as to get the development law of new things. Therefore, in the face of new data, how to extract and mine more useful information from massive data and generate more commercial value and social value has become a hot issue at this stage.

In view of the rapid growth of data, detection data has become an effective way to make full use of data. Data detection [5] means that the tester can judge and speculate the future results of the tested object with high precision by mastering the existing information, using certain scientific

knowledge, laws, and detection methods, so as to understand the development direction of things conveniently. The detection should not only consider the past characteristics and possible laws of the detected object but also consider various uncertain factors of the detected object at present or in the future. The test is similar to the budget before the start of a business activity. Before the start of the event, the organizer will plan and estimate the activity based on previous experience and preliminary preparation and make a financial forecast for the implementation of the activity, so as to prevent accidents. Similarly, detection is also based on historical data to establish a model and find out the law, through the detection model to outline the data development curve, so as to get the possible results in the future. Taking the power system as an example, power producers or power departments conduct short-term or long-term detection based on the electricity consumption in the past few weeks, months, or even years [6].

Intelligent search [7] is an important branch of artificial intelligence. The fundamental purpose of the intelligent search is to derive the required target state according to the initial state of the system, that is, the operation rules of each member in the system. Because of its great practical significance, it has attracted the praise of numerous famous scientists. Since artificial intelligence was formally put forward [8], intelligent search has made great progress over the years and has become an extensive interdisciplinary and frontier science. Generally speaking, the purpose of the intelligent search is to make computers think like people. After the advent of computers, human beings began to have tools to simulate human thinking. Computers play a role for human beings with their high speed and accuracy.

Because the data is more or less affected by external factors and there is noise in the data, the combined algorithm mode can be used for data processing to remove the noise in the original data and reduce the adverse effects. At the same time, the combined algorithm mode can absorb the advantages of the first simulation and discard its disadvantages [9], so that we can learn from each other to make up for the disadvantages. In order to better determine the proportion of several single methods in the combination method, the artificial intelligence optimization algorithm is used to dynamically adjust the corresponding weight of each method to fully improve the detection effect. Based on the above characteristics, this paper studies the combined detection model based on sustainable computing and artificial intelligence optimization, in order to make the detection results with high accuracy and small error and ensure the wide applicability of the detection method. In this paper, the data validation of the ecosystem in a certain place not only proves that the combined method is more effective than the single method and other similar combination methods but also proves that the method is widely applicable and can be applied to many other aspects. In addition, in order to show that the sustainable calculation and energy analysis method are helpful to improve the detection accuracy, this paper also compares the data errors detected by the combined method

model and further proves the good detection effect of the proposed method.

2. Establishment of Combined Algorithm Model Based on Sustainable Computing and Artificial Intelligence

2.1. Overview of Sustainable Computing.
The concept of sustainable computing [10] is characterized by the integration of economy, resources, environment, and society. The essence of sustainable development is to realize the unity of economic and ecological benefits. The economic benefits are mainly reflected in the profit level of production activities and the tax revenue created the remuneration paid to the workers, while the ecological benefits are mainly reflected in improving the ecological environment and reducing the consumption of natural resources directly or indirectly [11, 12]. In the face of the rapid development of human industrial production activities, a series of questions about the real value of resources, environment and industrial production activities, the impact of industrial production activities on resources and environment, and how to quantitatively analyze and systematically evaluate the sustainable product production process need to be answered.

2.2. Definition of Artificial Intelligence.
The development of artificial intelligence [13] is based on hardware and software. Its development has experienced a long process of development. Long ago, people began to study the formation of their own thinking. Aristotle took the early steps of developing artificial intelligence as early as a year B.C., when he began to explain and annotate deductive reasoning, which he called syllogism. It can be regarded as the original knowledge expression standard.

Artificial intelligence is a frontier interdisciplinary subject in the world, but like many emerging disciplines, artificial intelligence does not have a unified definition [14]. Artificial intelligence is difficult to define precisely. Many human activities, such as solving problems, guessing, discussing, making plans, writing computer programs, and even driving cars and bicycles [15], require "intelligence." If the machine can complete this task, it can be considered that the machine has some kind of "artificial intelligence."

2.3. Types of Detection Models.
Before the detection, once the appropriate method is selected, in order to complete the detection more accurately, it is necessary to establish a specific detection model. According to the first mock exam method, the number of models is single. Since most of the previous detection is based on the linear relationship between data, we use the known historical data to find the corresponding regular curve and calculate the next data according to the linear equation of the regular curve. However, the data in practical application are very complex. In addition to a small amount of data, there are a large number of data with a certain nonlinear relationship. In order to solve the problem of nonlinear detection effectively,

the first simulated test is generated step by step. Therefore, the first mock exam can be further divided into traditional methods based on theoretical statistics and artificial intelligence methods that can effectively solve the data diversity characteristics [16].

(1) The first mock exam of a single model is usually a single detection model [17]. According to the different characteristics of data samples and the further study of theoretical methods, the models can be roughly divided into the following two categories: on the basis of traditional data models, the future value can be detected directly based on mathematical models. This method has the characteristics of simple method and small sample data. It mainly includes the following methods: empirical detection method, trend extrapolation method, regression detection method, time series detection method, and grey detection method. The method of artificial intelligence was proposed by Dartmouth University society in 1956. It belongs to a kind of computer science, which is formed by the combination and penetration of various disciplines. Its goal is to research and develop intelligent entities. Artificial intelligence methods mainly include artificial neural network technology, swarm intelligence, and support vector machine [18].

(2) Combined detection model [19]: although the traditional detection methods and artificial intelligence methods can achieve better detection results in some fields, the detection accuracy cannot be further improved due to the single method. For example, the traditional detection method can effectively deal with the detection of linear data, and the artificial intelligence method can well deal with the detection of nonlinear data [20]. However, most of the data at this stage contain both linear and nonlinear parts. Only by combining the advantages of the two can we solve the problem better. At the same time, the first simulated test model can be applied to different fields more widely. The combination model can dynamically adjust the weight of each method according to different data, which has achieved good results in many fields. The main idea of the first mock exam is to create a new detection method based on different characteristics of data and using their respective advantages to dynamically combine different single models.

2.4. Test and Evaluation Standards.
Because detection is an estimation of the possible trend, there must be a gap between the detection and the actual value, and this gap is inevitable. The quality of the model is determined by the error value to a great extent. In order to evaluate the detection model objectively and accurately, the following six evaluation indexes are generally used: absolute, relative, average, root mean square, and standard error.

2.5. Energy Analysis.
Energy [21] is a new scientific concept put forward by famous American ecologists. It is defined as the amount of another energy contained in a flowing or stored energy, called the energy value of energy. Because all kinds of resources, products, or services come from solar energy directly or indirectly in the formation process, in practical application, the energy value of different types of energy is measured with solar energy as the benchmark and solar Joule as the unit [22].

Energy analysis theory [23] is the latest system analysis method in the development of system ecology and ecological economics. This method inherits the idea of whole life cycle system analysis. Based on solar energy value, different types of noncomparable energy in ecosystem or eco economic system are transformed into the same standard energy field for measurement and analysis. Energy analysis can deeply understand the structure and function characteristics of ecosystem by calculating various input energy values and constructing evaluation indexes and ecological economic benefits.

The energy analysis method makes different energy and materials get the same comparison standard [24]. It can objectively evaluate the actual contribution of various forms of noncomparable energy, such as economic input. After inspection and verification, it is determined that the revised content is consistent with the original intention of the author. System analysis method [25] is a new analysis method for developing traditional energy, but it is still imperfect, the application of the industrial system is still in the initial stage, the systematic energy index system needs to be improved, and the comprehensive evaluation index system of sustainable development is still lacking.

As shown in Table 1, we compare the above methods of system analysis. It is found that the energy analysis method is very suitable for the establishment of the combined algorithm detection system proposed in this paper. Energy analysis is based on energy analysis. It converts all kinds of energy, nonenergy material flow, and capital flow into the same standard energy for data processing and system analysis.

2.6. Establishment of Combined Algorithm Model.
In this paper, the model of the combined algorithm based on sustainable computing and artificial intelligence is divided into three parts: the prior processing part, the independent detection part, and the weight adjustment part. These parts are adjusted as follows:

(1) Priority processing part before inspection: due to the influence of various uncertain factors on time series data, there will be missing or unavailable "dirty" data in the original data, resulting in relatively poor detection results and being unable to achieve the expected purpose. In order to eliminate the interference caused by noise data, the data is processed before the simulation experiment. Wavelet denoising [26] is used to analyze the original data. By setting the minimum value, the data whose noise is

TABLE 1: Simple comparison of various system methods.

	Net energy analysis	Exergy analysis	Analysis of accumulated effective energy	Energy analysis
Comparison content	Energy	Energy	Energy	Energy
Company	J	J	J	scj
Energy quality	No	Yes	Yes	Yes
Evaluating indicator	Energy production input ratio	Effective energy efficiency	Minimum recovery work and regeneration factor	Energy comprehensive index system

less than the value is eliminated, and the remaining data are reorganized accordingly to obtain the data with no noise or less noise.

(2) Separate detection part: because the data has been processed prior to inspection, the separate detection part is to redistribute the priority processed data. After wavelet denoising, the weight of each part is calculated by evaluating the error between the detected value and the actual value, and the weight is obtained by considering the detection accuracy of each part.

(3) In the weight adjustment module [27], the dynamic weight selection of a single method can make the whole detection model fully absorb the advantages and disadvantages of a single method in detection and further improve the detection accuracy. Secondly, the weight dynamic selection can be dynamically adjusted according to the different data processed, which is suitable for many fields. Particle swarm optimization algorithm is used to adjust the weight [28]. Particle swarm optimization algorithm has a certain storage capacity in the process of parameter adjustment. It can approach the local optimal and global optimal step by step. It can quickly find the optimal solution and allocate the weights of three independent methods in the proposed combined algorithm, so as to obtain the final detection results.

Because the ecological data [29] is inevitably affected by various factors and contains noise, if the original data is directly used for detection, the detection error will increase, which will directly affect the effectiveness of the detection model. Therefore, before detection, the noise of one-dimensional time series is decomposed by wavelet. Generally speaking, there is no perfect and effective method for the selection of decomposition level, which can only rely on experience. Assuming that the first mock exam is composed of these two single models, the process of obtaining the combined algorithm of sustainable computing and AI is as follows:

(1) Firstly, the combination algorithm model is used to predict the time series in the prediction interval.

(2) Secondly, by evaluating the error between the predicted value and the actual value, the corresponding weight of each model is calculated, and the detection accuracy of each model is considered.

(3) Finally, the weighted prediction is combined. Here, depending on the structure of the model, the inputs to the model may be the same or different. However, we found that they prefer to use the same input data by reading the existing literature. Generally speaking, the input data is a time series of past wind speeds; however, in some cases, other meteorological conditions such as wind direction, temperature, air pressure, and air humidity may improve the accuracy of the detection model.

2.7. Comparison of Different Combination Algorithms. The weighted combination algorithm and the combination algorithm with preprocessing are very suitable for long-term difficult detection. This kind of detection usually requires power system dispatching, optimal unit startup and shutdown, load tracking, and other operations [30]. The weighted composite algorithm can also be used for long-term projects such as the maintenance of wind turbines or conventional power plants. In addition, the combination algorithm is mainly used in ecological benefits and marketing, including parameter selection and data optimization methods, to improve the occasion of high-precision detection. However, the method combined with error processing only gives reasonable results in the case of systematic error, so it is not aimed at a certain field. Finally, it is worth mentioning that some combination algorithms do not necessarily improve the detection performance of a single model and even lead to worse results in some cases.

3. Application of Combined Algorithm Based on Sustainable Computing and Artificial Intelligence

3.1. Application of Combined Algorithm in Integrated Ecosystem. The combined algorithm uses the detection to get comprehensive ecosystem data and explores different ecosystem survival modes, such as ecological agriculture, forestry and fruit industry, aquaculture, construction land, and leisure and entertainment modes [31]. The combined algorithm model can effectively track the status of the ecosystem and give the evaluation system of ecological restoration benefits, which can maintain and supervise the stability of the environment and resources that need to be repaired. It will also make an effective feedback mechanism

to the economic standards and ecosystem service functions, to the restored places, and to contribute to the sustainable development of ecological restoration of the ecosystem [32].

The ecological restoration model is an effective way to reprocess the detected data and transform the negative effects into positive ones [33]. The economic benefits of the restored ecosystem have been greatly improved. Other restoration modes include the following:

(1) Ecological botanical garden restoration mode: clean up the cliffs where plants are difficult to grow. We always adhere to the concept of sustainable development, through the combined algorithm of land area detection, and the land can be planted for reasonable allocation, planting easy-to-grow flowers and plants.

(2) Sustainable ecological ranching model: the construction of pasture requires a large area of land support and sufficient water and electricity. Detect the wind speed in a certain area through the group and algorithm, and use renewable resources to build wind farms to solve the problem of large-scale land irrigation.

3.2. Application of Combination Algorithm

(1) The first major achievement in combinatorial algorithms is the development of chess programs that can solve complex problems, such as chess. Some techniques used in chess programs, such as looking forward to several steps and decomposing difficult problems into easier subproblems, have developed into search and problem simplification. Today's computer programs can play checkers, Gobang, and chess at various tournament levels. Some programs can even use the experience to improve their performance.

(2) Logical reasoning [34] is one of the most persistent branches of combinatorial algorithms. It is particularly important to try to focus only on relevant facts in large databases, pay attention to credible evidence, and correct them when new information appears. It is indeed an intellectual task to find a proof or reverse proof for a conjecture theorem in mathematics. This requires not only the ability to reason based on assumptions but also some intuitive skills.

(3) Natural language processing (NLP) [35] is one of the research fields in the combinatorial algorithm. It has written programs that can answer internal database questions in English. These programs can translate sentences from one language to another by reading text materials and building internal databases, execute instructions given in English, and acquire knowledge. Some programs can even translate the oral instructions of the microphone to a certain extent, rather than from the keyboard to the computer. At present, the main theme of language processing research is to pay attention to the importance of a large number of general knowledge, world knowledge, and expected function based on the theme and dialogue situation in sentence translation. The combinatorial algorithm has made great achievements in language translation and speech comprehension and has become a new concept of human natural language processing.

(4) Automatic programming [36] is developed to write computer programs for various purposes, such as input-output, high-level language description, and even English description algorithm [37]. Progress in this area is limited to a few recognized examples. The research on automatic programming can not only promote the development of semiautomatic software development systems but also develop artificial intelligence systems that learn by modifying their own numbers, that is, modifying their performance [38]. The task of automatically compiling a program to obtain a specified result is closely related to the task of proving that a given program will get the specified result. The latter is called program verification [39].

(5) One of the great achievements in combinatorial algorithms is the development of chess programs that can solve difficult problems. Some techniques used in chess programs, such as looking forward to several steps and decomposing difficult problems into easy subproblems, have developed into intelligent search techniques such as search and problem simplification. Today's computer programs can play checkers, Gobang, and chess at various tournament levels. Some programs can even use the experience to improve their performance. Among the many achievements made by computers, it is very important to extract their common features from their solutions and find out the general ideas to solve them.

3.3. Shortcomings of Combined Algorithm.

Because the first simulation has different performance and fitting ability for nonlinear data under different data sets and detection ranges [39], the first mock exam method takes advantage of the different single models. The first mock exam method can improve the performance of the final detection and has many advantages over the single model. In the first simulation test, the most important thing is that the application field of the combination model is more extensive. The first mock exam is better than a single model. It is necessary to select the most suitable model through testing. When the first mock exam is difficult to determine, the combination model can overcome the shortcomings of the above single model. However, the definition and structure of the combination model are still controversial in the existing literature. However, the commonly accepted combination model structure in the existing literature is to assign a weight
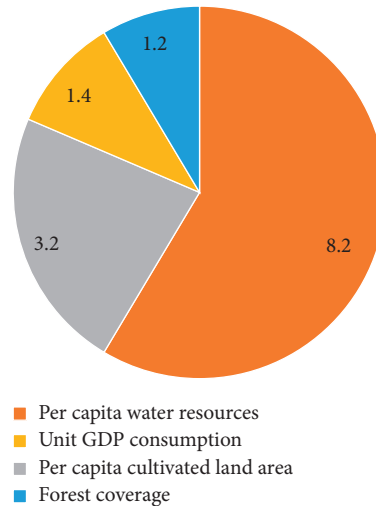
FIGURE 1: Detection of resource consumption error results.
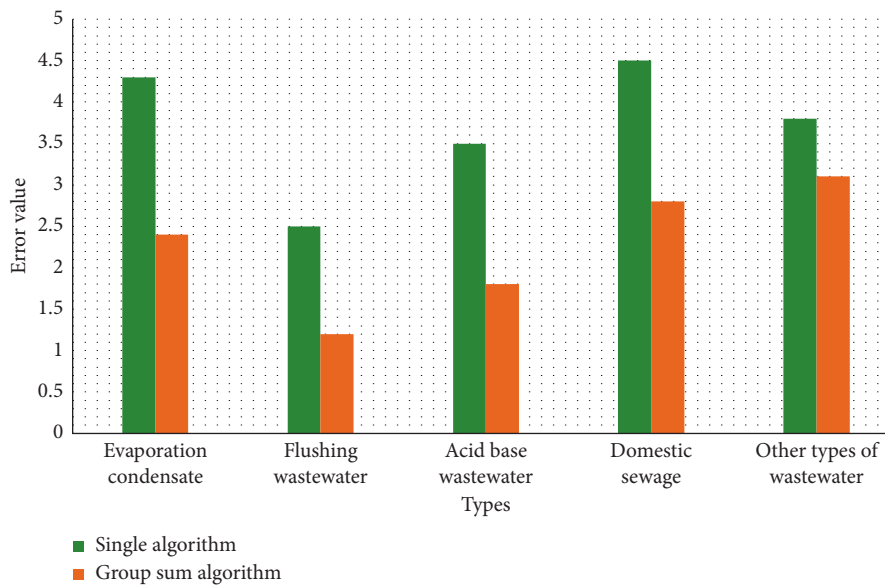
FIGURE 2: Test results of wastewater discharge.

coefficient to each model corresponding to its detection performance. In addition, other wind speed forecasting models with different methods are also called combined models.

4. Results and Discussion

4.1. Error Analysis of Combined Algorithm Detection Resource Consumption. As shown in Figure 1, we use the combined algorithm model to analyze the data of resource consumption, which shows that the error of per capita water resources is the largest, reaching 8.2%. Secondly, the average cultivated land area data analysis error is 3.2%. Then, the data analysis results of unit GDP consumption and forest coverage rate show that the error is relatively small. Through the error comparison, we can see that the most accurate way

to detect resource consumption is the calculation of forest coverage rate, and the error is only 1.2%.

4.2. Comparison of Error Results of Different Algorithms for Wastewater Discharge Detection. As shown in Figure 2, in order to compare the effectiveness of the combined algorithm detection, we compare the results of the two algorithms to detect the wastewater discharge. According to the record, the single algorithm has obvious disadvantages compared with the combined algorithm. Mainly from the evaporation of condensate water, flushing wastewater, acid-base wastewater, domestic sewage, and other types of wastewater, the most significant error reduction is evaporation condensate, acid-base wastewater, and domestic sewage. With the help of the combined algorithm, the
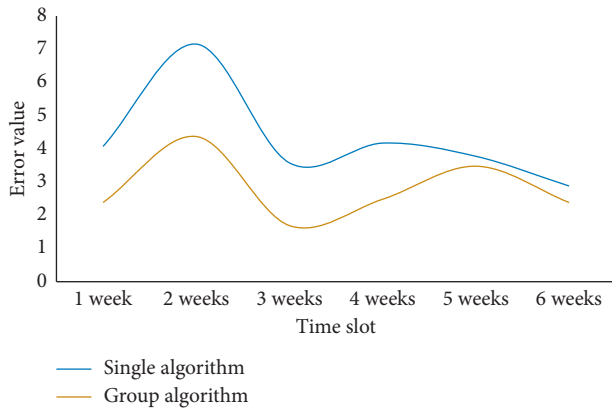
Figure 3: Error comparison of wind speed detection by different noise reduction algorithms.
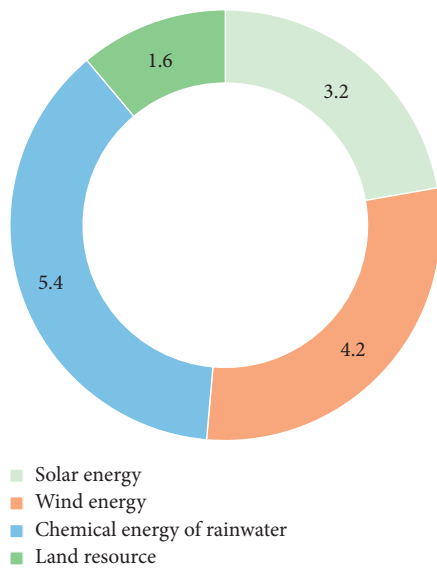
Figure 4: Error comparison of group sum algorithm for renewable resources utilization.

calculation of wastewater discharge is more accurate, which greatly reduces the shortcomings of single algorithm and reduces the risk of error.

4.3. Influence of Noise Reduction Degree of Different Algorithms on Wind Speed Detection Error.
As shown in Figure 3, we carry out a series of tests on different levels of noise reduction data and study the detection accuracy of single algorithm and combined algorithm by detecting 0%, 25%, 50%, 75%, and 100% noise reduction modes. The results show that 75% noise reduction has a great improvement on the detection accuracy of the combined algorithm. Compared with the single algorithm, there is no significant change in the detection of different noise levels. We carry out wind speed detection for 6 weeks. The error of single

algorithm is higher than that of combined algorithm in these six weeks, while the minimum error of combined algorithm is as low as 1.8% in the third week.

4.4. Error of Combined Algorithm for Renewable Resource Utilization Detection.
A shown in Figure 4, we detect the renewable resources systematically. Compared with the previous detection system, the detection error of the combined algorithm is slightly improved. Particularly in the detection of land resources, the result error is only 1.1%. The second is the test results of the chemical energy of rainwater, with an error of 2.2%. The detection error of solar energy resources is large, which may be due to the inaccurate data measurement, resulting in more uncertain factors in the calculation of the combined algorithm, so the error is large. But in other aspects, the detection error rate has a very obvious downward trend.

5. Conclusion

Under the situation of rapid economic growth, severe environmental conditions, and relative scarcity of resources, it is an important strategic choice to realize the coordinated development of economy, society, and environment and develop circular economy. The whole world is making great efforts to realize the sustainable development strategy, and the whole country is exploring the renewable situation of economic value, ecological environment, and resources. Based on the above strategic objectives, this paper proposes a new combination algorithm based on sustainable computing and artificial intelligence. Firstly, the combined algorithm proposed in this paper is used to detect the resource consumption and the utilization of visible resources. It is found that the error of detecting forest coverage is only 1.2%. The detection of land resources is particularly significant, and the error is only 1.1%. It can be seen that the detection effect of the combined algorithm for large area resource reuse and consumption is particularly prominent. Secondly, the single algorithm and the combination algorithm are analyzed and compared; the main content is the impact of wastewater discharge detection and noise reduction degree on wind speed detection. The comparison shows that the error rate of the combined algorithm is lower than that of the single algorithm. It is found that the detection error of the combined algorithm with 75% noise reduction is the minimum, which is as low as 1.8%. Finally, it is found that the advantages of the combined algorithm are that it can detect accurate data, process and analyze the data more carefully, and play a low error data detection under 75% noise reduction environment, which is further on the road to sustainable development.

Data Availability

The data that support the findings of this study are available from the corresponding author upon reasonable request.

Conflicts of Interest

The authors declare that they have no conflicts of interest.

References

[1] Z. Xiang, V. P. Magnini, and D. R. Fesenmaier, "Information technology and consumer behavior in travel and tourism: insights from travel planning using the internet," *Journal of Retailing and Consumer Services*, vol. 22, no. jan, pp. 244–249, 2015.

[2] H. Tao, W. Zhao, R. Liu, and M. Kadoch, "Space-air-ground IoT network and related key technologies," *IEEE Wireless Communications*, vol. 27, 2019.

[3] K. Vikas and P. Prasann, "Reputation management through online feedbacks in e-business environment," *International Journal of Enterprise Information Systems*, vol. 12, no. 1, pp. 21–37, 2016.

[4] W. Wu, Y. Liu, C. H. Wu, and S. B. Tsai, "An empirical study on government direct environmental regulation and heterogeneous innovation investment," *Journal of Cleaner Production*, vol. 254, Article ID 120079, 2020.

[5] B. Wang, L. Dai, T. Mir, and Z. Wang, "Joint user activity and data detection based on structured compressive sensing for noma," *IEEE Communications Letters*, vol. 20, no. 7, pp. 1473–1476, 2016.

[6] C. Li, H. J. Yang, F. Sun, J. M. Cioffi, and L. Yang, "Multiuser overhearing for cooperative two-way multiantenna relays," *IEEE Transactions on Vehicular Technology*, vol. 65, no. 5, pp. 3796–3802, 2016.

[7] Y. Xing, Y.-Z. Gong, Y.-W. Wang, and X.-Z. Zhang, "A hybrid intelligent search algorithm for automatic test data generation," *Mathematical Problems in Engineering*, vol. 2015, no. 16, pp. 1–15, 2015.

[8] Q. Wang and P. Lu, "Research on application of artificial intelligence in computer network technology," *International Journal of Pattern Recognition and Artificial Intelligence*, vol. 33, no. 5, Article ID 1959015, 2019.

[9] Y. Tang and M. Elhoseny, "Computer network security evaluation simulation model based on neural network," *Journal of Intelligent & Fuzzy Systems*, vol. 37, no. 3, p. 3197, 2019.

[10] L. Laurent and J. M. Pierson, "Introduction to special issue on sustainable computing for ultrascale computing," *Sustainable Computing: Informatics and Systems*, vol. 17, no. mar, pp. 25-26, 2018.

[11] H. Shiyan, Y. Bei, and Y. Huafeng, "Ieee transactions on sustainable computing: guest editorial on special issue on sustainable cyber-physical systems," *IEEE Transactions on Sustainable Computing*, vol. 3, no. 2, pp. 58-59, 2018.

[12] Z. Lv and L. Qiao, "Optimization of collaborative resource allocation for mobile edge computing," *Computer Communications*, vol. 161, pp. 19–27, 2020.

[13] H. Lu, Y. Li, M. Chen, H. Kim, and S. Serikawa, "Brain intelligence: go beyond artificial intelligence," *Mobile Networks and Applications*, vol. 23, no. 2, pp. 368–375, 2017.

[14] E. D. Crawford, J. T. Batuello, P. Snow et al., "The use of artificial intelligence technology to predict lymph node spread in men with clinically localized prostate carcinoma," *Cancer*, vol. 88, no. 9, pp. 2105–2109, 2015.

[15] Z. Lv, L. Qiao, K. Cai, and Q. Wang, "Big data analysis technology for electric vehicle networks in smart cities," *IEEE Transactions on Intelligent Transportation Systems*, vol. 22, 2020.

[16] Z. Lv, H. A. N. Yang, K. S. Amit, M. Gunasekaran, and l. Haibin, "Trustworthiness in industrial IoT systems based on artificial intelligence," *IEEE Transactions on Industrial Informatics*, vol. 17, 2020.

[17] W. Kim, S. Suh, and J.-J. Han, "Face liveness detection from a single image via diffusion speed model," *IEEE Transactions on Image Processing*, vol. 24, no. 8, pp. 2456–2465, 2015.

[18] Z. Lv, S. Zhang, and W. Xiu, "Solving the security problem of intelligent transportation system with deep learning," *IEEE Transactions on Intelligent Transportation Systems*, 2020.

[19] L. Zhao, X. Dong, W. Chen, L. Jiang, and X. Dong, "The combined cloud model for edge detection," *Multimedia Tools and Applications*, vol. 76, no. 13, pp. 15007–15026, 2017.

[20] S. Xiao, S. Liu, F. Jiang, M. Song, and S. Cheng, "Nonlinear dynamic response of reciprocating compressor system with rub-impact fault caused by subsidence," *Journal of Vibration and Control*, vol. 25, no. 11, pp. 1737–1751, 2019.

[21] N. Duan, X. D. Liu, J. Dai et al., "Evaluating the environmental impacts of an urban wetland park based on emergy accounting and life cycle assessment: a case study in beijing," *Ecological Modelling*, vol. 222, no. 2, pp. 351–359, 2017.

[22] V. Puri, S. Jha, R. kumar et al.,"A hybrid artificial intelligence and internet of things model for generation of renewable resource of energy," *IEEE Access*, vol. 7, pp. 111181–111191, 2019.

[23] H. H. Lou, M. A. Kulkarni, A. Singh, and Y. L. Huang, "A game theory based approach for emergy analysis of industrial ecosystem under uncertainty," *Clean Technologies & Environmental Policy*, vol. 6, no. 3, pp. 156–161, 2004.

[24] X.-S. Gao, X.-J. Luo, L.-J. Deng, and M. Zeng, "Analysis of material metabolism of eco-economic system in chongqing based on the emergy theory," *Low Carbon Economy*, vol. 2, no. 1, pp. 32–40, 2011.

[25] S. An, J. Lee, S. Kim, and J. Kim, "A review of the systemic analysis method on dental sedation for children," *The Journal of the Korean Academy of Pedtatric Dentistry*, vol. 42, no. 4, pp. 331–339, 2015.

[26] Y. Ding and I. W. Selesnick, "Artifact-free wavelet denoising: non-convex sparse regularization, convex optimization," *IEEE Signal Processing Letters*, vol. 22, no. 9, pp. 1364–1368, 2015.

[27] Y. Wu, Y. Ke, C. Xu, and L. Li, "An integrated decision-making model for sustainable photovoltaic module supplier selection based on combined weight and cumulative prospect theory," *Energy*, vol. 181, no. AUG.15, pp. 1235–1251, 2019.

[28] M. A. El Aziz, A. M. Hemdan, A. A. Ewees et al., "Prediction of biochar yield using adaptive neuro-fuzzy inference system with particle swarm optimization," in *Proceedings of the 2017 IEEE PES PowerAfrica Conference*, pp. 115–120, Accra, Ghana, June 2017.

[29] E. P. Smith, "Randomization methods and the analysis of multivariate ecological data," *Environmetrics*, vol. 9, no. 1, pp. 37–51, 2015.

[30] M. Elhoseny, "Multi-object detection and tracking (MODT) machine learning model for real-time video surveillance systems," *Circuits, Systems, and Signal Processing*, vol. 39, no. 2, pp. 611–630, 2019.

[31] W. Yun, G. Shenglian, X. Lihua, L. Pan, and L. Dedi, "Daily runoff forecasting model based on ann and data preprocessing techniques," *Water*, vol. 2015, no. 7, pp. 4144–4160, 2015.

[32] H. Tsukimoto, "Pattern reasoning: logical reasoning of neural networks," *Systems & Computers in Japan*, vol. 32, no. 2, pp. 1–10, 2015.

[33] Y. Chen, W. Zheng, W. Li, and Y. Huang, "The robustness and sustainability of port logistics systems for emergency supplies from overseas," *Journal of Advanced Transportation*, vol. 2020, Article ID 8868533, 10 pages, 2020.

[34] S. Meystre and P. J. Haug, "Natural language processing to extract medical problems from electronic clinical documents: performance evaluation," *Journal of Biomedical Informatics*, vol. 39, no. 6, pp. 589–599, 2015.

[35] D. Kim, Y. Kwon, P. Liu et al., "Apex: automatic programming assignment error explanation," *ACM SIGPLAN Notices*, vol. 51, no. 10, pp. 311–327, 2016.

[36] B. J. Harding, J. J. Makela, C. R. Englert, K. D. Marr, and T. J. Immel, "The mighti wind retrieval algorithm: description and verification," *Space Ence Reviews*, vol. 212, no. 4, pp. 1–16, 2017.

[37] H. Zhou, Y. Chang, X. Wu, D. Yang, and X. Qiu, "Horseradish peroxidase modification of sulfomethylated wheat straw alkali lignin to improve its dispersion performance," *ACS Sustainable Chemistry & Engineering*, vol. 3, no. 3, pp. 518–523, 2015.

[38] R. W. Lo, K. N. Levitt, and R. A. Olsson, "Validation of array accesses: integration of flow analysis and program verification techniques," *Software Testing Verification and Reliability*, vol. 7, no. 4, pp. 201–227, 2015.

[39] C.-L. Lai, J.-S. Lee, and J.-C. Chen, "A curve fitting approach using ann for converting ct number to linear attenuation coefficient for ct-based pet attenuation correction," *IEEE Transactions on Nuclear Science*, vol. 62, no. 1, pp. 164–170, 2015.

Research Article

Virtual Reality Technology of Multi UAVEarthquake Disaster Path Optimization

Yi Wang[1,2] and Ensheng Liu [ID][3,4]

[1]*Anhui Earthquake Agency, Hefei, Anhui 230031, China*
[2]*Anhui Mengcheng National Geophysical Observatory, Mengcheng 233500, Anhui, China*
[3]*College of Building Engineering, Jing Gang Shan University, Jian, Jiangxi 343009, China*
[4]*College of Surveying and Geo-Informatics, Tongji University, Shanghai 200092, China*

Correspondence should be addressed to Ensheng Liu; 1410893@tongji.edu.cn

China is a country with frequent earthquake disasters. After the occurrence of earthquake disasters, the key to disaster monitoring and rescue is to quickly obtain images of postdisaster areas. Unmanned aerial vehicle (UAV) path planning is the core of multi-UAV cooperative control. With the increasing popularity of UAVs, people with more complex living environments contact with UAVs more frequently, which also poses a challenge to the overall control of UAVs, making single UAV and even multi-UAV cooperative path planning become a hot research issue in recent years. The complexity of communication between aircraft in three-dimensional flight space and multidegree of freedom navigation makes multi-UAV cooperation more challenging. According to the research results at home and abroad, this paper takes multitarget tracking algorithm, ant colony algorithm, and hybrid particle swarm optimization algorithm as research methods. Based on virtual reality technology, by comparing the advantages and disadvantages of several algorithms, the research model of path optimization is established, and a multitarget detection method based on virtual reality technology is established. Through the analysis and improvement of multitarget tracking algorithm, ant colony algorithm, and hybrid particle swarm optimization algorithm, the path optimization problem of UAV after an earthquake based on virtual reality technology is studied. The results show that, compared with the previous research models, the overall optimization efficiency of UAV route is improved by 15%, which is more practical.

1. Introduction

With the continuous development of artificial intelligence technology, unmanned aerial vehicle (UAV) autonomous flight technology has been widely concerned and studied by the academic community. Path planning is an important basic guarantee for UAVS to realize automatic flight. The main purpose of UAV path planning is to plan the path that meets the constraints of UAV according to the UAV target. The actual flight environment of UAV is high-dimensional space. If the time limit is considered, the scale will be increased to four dimensions, which will cause the problem of "scale disaster" in the planning process. Therefore, how to choose an appropriate algorithm to develop an optimal path planning system for multiple UAVs is the main problem in the field of UAV research.

Path planning of three-dimensional UAV is an important part of UAV autonomous control system. To solve the complex path optimization problem of rotor vertical takeoff and landing (VTOL) aircraft, Chen proposed an improved center force optimization method. Chen used the linear difference equation method to analyze the convergence of the whole modified central force optimization (MCFO) method [1]. Taking a six-degree-of-freedom four-rotor helicopter control system as an example, Chen proposed a new path planning method. Finally, the six algorithms of Chen were compared and simulated, and the problem of angle of arrival tracking using multiple UAVs in three-dimensional space was studied [2]. Xu proposed a distributed 3D AOA target tracking method which is composed of a distributed estimator and multi-UAV path optimization algorithm and a new 3D distributed pseudolinear Kalman filter (DPLKF) to

improve the stability of the solution of the extended Kalman filter. DPLKF consists of two coupled filters; Dogancay proposed a method to reduce the deviation and a distributed path optimization algorithm constrained by communication distance and no-fly zone [3]. The algorithm uses gradient descent optimization in *XY* plane and grid search along *z*-axis to calculate UAV waypoints. To improve the tracking performance, the tracking error covariance matrix is minimized [4]. UAV relay technology is an important means to realize remote wireless communication. Li proposed a broadcast communication system based on fixed-wing UAV as the relay platform between the base station and mobile mission UAV cluster. To improve the system performance, especially to ensure the quality of service (QoS) of UAV in high priority mission, the route optimization method of relay UAV is investigated. Firstly, the system model and signal model of UAV relay broadcasting communication system are given, and the approximate expression of single link traversal capacity is derived. Then, according to the different requirements of mission UAV, Li proposed a path optimization method for relay UAV based on the weighted and ergodic capacity maximization criteria [5]. On this basis, the exact outage probability and closed-form ergodic capacity of relay links are derived to quantify the system performance. Finally, the optimal path of the relay UAV in the two simulation scenarios is given.

Recently, UAV is considered as a means to provide enhanced coverage or relay services for mobile users in wireless systems with limited or no infrastructure [6]. Jeong has studied a mobile cloud computing system based on UAV [7]. The system gives computing power to the mobile UAV and provides computing offloading opportunities for system with limited local processing capacity. Liu proposed a particle swarm optimization method for UAV path planning based on the potential odor intensity grid. The odor intensity is created to color the highest probability region where candidate particles may be located in the search space [8]. Based on different odor intensity levels, Duan designed a potential grid building operator. Potential grid construction operators generate two potential location grids with the highest odor intensity [9]. Then the intermediate point is regarded as the final position in the current particle dimension, and the global optimal solution is solved as the average value.

In this paper, based on the research results at home and abroad, multitarget tracking algorithm, ant colony algorithm, and hybrid particle swarm optimization algorithm are used as research methods. Based on virtual reality technology, the research model is established. Through the comparative analysis of several algorithms, the experimental simulation and system research on the UAV path optimization problem are carried out. The main innovations of this paper are as follows: The threat distribution model of various obstacles is designed, and the concept of comprehensive threat field of virtual reality model is defined. This paper extends the traditional method of single threat source and improves some threat distribution models. The smoothing algorithm is used to smooth the initial path, and based on the characteristics of smooth trajectory, a cooperative criterion

based on interval distance is proposed, which defines when UAVs can cooperate with each other and how UAVs will cooperate. As the core content of this paper, based on the above points, a set of "environment modeling, initial path planning, and path smoothing collaborative planning" process is established, and the simulation experiment is implemented.

2. Path Optimization Method for Multiple UAVs under Earthquake Disaster

2.1. Optimization of Earthquake Disaster Path. Path planning is carried out in the configuration space. Firstly, the concept of configuration space is introduced. Path planning problems usually need to know four parts in advance.

(1) The geometric description of UAV.

(2) The description of the planning environment of UAV which is also called the workspace.

(3) The degree-of-freedom description of UAV.

(4) Planning task, through which the configuration space (C space) of UAV can be compiled. These three configuration spaces can be described by several parameters. For example, the configuration space of two UAVs moving in 3D space can be described by three parameters *x*, *y*, and *z*. N-dimensional vector can be used to describe the minimum number of parameters required to describe the configuration space and porthole position of UAVS [10, 11].

The vector set corresponding to all positions of UAV is the configuration space of UAV. Due to the limitation of various conditions, the area that UAV cannot reach (such as the area where the obstacles are located) is weighed as the forbidden configuration in *C* space, and its set is represented by *Cx*, the remaining area that UAV can reach is called the free configuration, and its set is represented by *CR*. There is no intersection between available configurations and available configurations, and the two sets together constitute the configuration space; that is, $C = CX \cap CR = 0$.

Path planning is one of the key technologies of multi-UAV formation flight, which mainly includes formation assembly route plan, formation maintenance route plan, and formation reconstruction route plan [12,13]. Among them, formation assembly path planning is the process of formation generation of multiple UAVs. The purpose is to make a group of UAVs start from different starting points and reach the corresponding positions in the designated formation assembly area at the same time, to achieve the required formation. Formation maintenance path planning is to plan an optimal reference path, which can safely reach the target destination of UAV formation flying in a specific formation; the formation reconfiguration plan is to plan a set of optimal paths for each UAV, so that each UAV can quickly transfer from the current formation to the new formation. The main constraints considered in the planning process are safety, flight capability, and other constraints: path safety means that the planned path can avoid the threat of obstacles in the flight area and environment, and there will

be no collisions between aircraft. Path flightability means that the planned path can meet the kinematic constraints of each UAV, such as the minimum turning radius constraint, path curvature continuity constraint, and maximum climbing angle constraint [14,15]. Other constraints include time coordination constraint and maximum path length constraint.

2.2. Ant Colony Algorithm.

The flight altitude of UAV is constant in cruising time because frequent altitude changes will consume a lot of fuel and increase engine loss. In the process of flight, the aircraft should not be too high or too low [16,17]. The too high flight will increase the risk of being detected by the enemy's radar and be attacked by the enemy's defense system. To avoid the attack of local defense systems and radar, flying too low will lead to bumping into natural obstacles such as mountains. Considering the above concerns, the aircraft needs to keep the altitude within a certain range during the flight process, and the UAV needs to keep the flight altitude no higher than Hmax and no less than Hmin when performing tasks. The formal language description is as follows, where IH represents the real-time flight altitude of each trajectory.

$$T_{ij}(0) = \text{const}, \tag{1}$$

where $T_{ij}(0)$ is the pheromone concentration between city I and city J at the initial time; const is a constant, usually 0. When the classical ant colony algorithm is not running, the pheromone concentration on all paths is 0.

To avoid falling into local optimization easily in the process of solving the optimization problem, domestic scholars proposed an improved ant colony algorithm based on information entropy in 2005 [18]. The information entropy is used to determine the next transfer city, and random disturbance is introduced to realize the dynamic adjustment of the algorithm. When the value of information entropy rises to the maximum threshold set by the algorithm, the execution of the algorithm ends. According to the value of information entropy, the next step transition probability is obtained. The calculation formula of information entropy and pheromone updating is as follows:

$$P_i = \frac{\tau_i(t)}{\sum_{ies} \tau_i(t)}, \tag{2}$$

$$S = -ki \sum_{i=1}^{n} p_i \ln p_i, \tag{3}$$

$$\tau(t) = (1 - \rho)\tau(t - 1) + \rho\Delta\tau(t), \tag{4}$$

where P_i is the ratio of the amount of information on the edge i of the path to the total information; that is, $P_i \geq 0$. In the initial stage of the algorithm, the pheromone of each path is the same, and the entropy is the global maximum [19, 20]. After a period of time, the information concentration of some path edges increases, and the entropy becomes smaller and smaller. If we do not pay attention to the adjustment, the

entropy may drop to 0; that is to say, in the later stage of the algorithm, only one path has the highest pheromone, which will lead to premature.

2.3. Hybrid Particle Swarm Optimization Algorithm.

The intelligent optimization method is a model that uses biological characteristics to solve practical problems, and the PSO algorithm is a typical swarm intelligence random search optimization algorithm [21]. In PSO, the search space of the problem is similar to the flight space of a group of birds, and each bird is one of them. Each bird is reduced to particles of negligible weight and size, representing a viable solution to the problem. The optimization process of the algorithm is similar to the process of species searching for food and finally finding the most abundant food, which is equivalent to obtaining the optimal solution of a complex optimization problem [22, 23].

The selection mechanism of the hybrid PSO algorithm is similar to that of the genetic algorithm [24]. In the hybrid PSO algorithm, we design the fitness degree of each individual's current position and rank it. Then we replace the position and speed of the weak adaptive individual with the position and speed of the weak adaptive individual and keep the best position of each individual. Therefore, the scope of group search is concentrated in relatively good areas, but it is still affected by the best location of previous individuals. Each particle in the particle swarm is set manually to the propagation probability [25]. In each iteration, a certain number of particles are randomly selected from the population according to the propagation probability to generate the same number of new particles [26, 27]. To keep the number of particles in the population constant, we use the generated new particles to completely replace the original particles. The new particle's position and velocity update formula is as follows:

$$X_{\text{child}-i} = \mu x_i(t) + (1 - \mu)X_j(t), \tag{5}$$

$$v_{\text{child}-j} = \left(v_i(t) + v_j(t)\right) \cdot \frac{|v_i(t)|}{|v_i(t) + v_j(t)|}, \tag{6}$$

where μ [0,1], X_i, and X_j are the position vectors of the random particles $V_{\text{child}-i}$ and $V_{\text{child}-j}$ and are the corresponding velocity vectors of each primitive particle $V_{\text{child}-i}$, and $V_{\text{child}-j}$ and $V_{\text{child}-j}$ are new particles. The hybrid particle swarm optimization algorithm has higher search accuracy and faster speed. It can achieve satisfactory results in solving a class of nonlinear optimization problems. The flight speed of particles has a great impact on the performance of the algorithm [26]. When the flight speed is too fast, particles can quickly reach the target area, but when approaching the target value, too fast speed will easily cause the particles to cross the target value and fly to other regions, thus reducing the convergence speed of particles [27]. The algorithm cannot even converge; when the particle flying speed is too slow, the particle can quickly approach the target area, although it can ensure a local fine search, it directly leads to the reduction of the overall detection ability of the algorithm.

Therefore, to balance the overall development ability of the algorithm, measures must be taken to control the flight speed of particles [28].

3. Simulation Research and Design of Multi-UAV Path Optimization for Rapid Assessment after Earthquake Disaster

Global path planning is the first step to realize collision avoidance in the autonomous path planning system, and it is the basis of subsequent path planning (such as local path planning and renavigation). According to the research results of some scholars and the general steps of global path planning, the global path planning of UAV is realized: firstly, the autonomous navigation environment model of UAV is established [2], then the initial path planning is carried out by using Dijkstra algorithm, and finally, the initial path is optimized by hybrid particle swarm optimization algorithm, to find the global shortest path.

(1) Environment modeling: according to the distribution and size of obstacles in the electronic chart, the corresponding convex surface is defined, and the autonomous navigation environment model of the unmanned ship is established by link graph method and network topology diagram (link graph) [29].

(2) Initial path planning: use the Dijkstra algorithm to search the link graph from the starting point to the destination, and prepare the initial optimal path by the punctuation method, which is used for the path optimization of hybrid particle swarm optimization algorithm [30].

(3) Path optimization: based on the initial path, the hybrid particle swarm optimization algorithm is used to optimize the path to find the best path.

Different from the ant colony algorithm, when using a hybrid particle swarm optimization algorithm, the priority of each target is fixed, which makes the system more predictable. Therefore, it is more appropriate to use the hybrid particle swarm optimization algorithm to design the target priority of the simulation system. However, the result of target priority division is not absolute, so it cannot be designed according to the hybrid particle swarm optimization algorithm in practical application [31], because the hybrid particle swarm optimization algorithm is based on a series of assumptions, and all the targets in the target set must be periodic objectives.

(1) The setting time and period of each goal are equal

(2) Each target is independent of each other, and the operation of each target is not associated with other targets

(3) The use time of the target remains unchanged in each cycle

(4) Ignore the target plan and target replacement time

Model the third-party software, set the scene material, so that the model can get the real mapping, and finally initialize the virtual reality system [32]. To model the real scene, first of all, we must accurately collect the real building data, measure the actual length, width, and height with a ruler, and then take photos of the real objects. After obtaining the front data, the scene is modeled with 3ds Max referring to digital photos. To ensure fidelity, the material and texture of the scene are essential. Our goal is to refer to the real model for material setting and mapping, to restore its authenticity as much as possible and make the performance as close to reality as possible.

4. Simulation Results Analysis of Multi-UAV Path Optimization Based on Virtual Reality for Rapid Evaluation after Earthquake Disaster

4.1. Simulation Analysis of Multi-UAV Path Optimization in Virtual Environment. As shown in Table 1, in addition to the obstacles with known motion law and unknown motion law, there is also a kind of obstacle whose motion information is partially known; that is, the movement trend of the obstacle is known, but the actual position cannot be determined. These obstacles can be divided into two categories: one is the obstacle with a known trajectory and moving speed within a certain range [33]; the other is obstacles. The speed of the object is known, but the other direction is unknown. To verify the superiority of the improved hybrid particle swarm optimization algorithm, ant colony algorithm and improved hybrid particle swarm optimization algorithm with artificial potential field are used to simulate and compare the path planning environment of UAV, and the number of sampling points is less. In the simulation, 400 sampling points are used, and four kinds of obstacles are set up in the environment, and the risk degree of obstacles ranges from 1 to 10.

It can be seen from the table that the larger the radius of the obstacle, the higher the risk score. When the radius of obstacle 3 is 68, the risk degree score is the highest, reaching 8 points, which shows that the theoretical accuracy of the target location can be significantly improved by using multipath information effectively. The fact that the detection probability is 1 is considered in the theoretical calculation. The detection probability of the outbound base station equivalent to the multipath effect is less than 1. As the observation angle increases, the observation and measurement information will increase, and the accuracy of target estimation will be improved.

As shown in Figure 1, in order to verify the effectiveness of the proposed hybrid particle swarm optimization algorithm in probability graphs with different scales, the environment in the graph is simulated with 100, 200, 300, and 400 sampling points. From the comparison of iterative curves, it can be seen that the algorithm can quickly converge to the final result in the case of different sampling points. With the increase of the number of sampling points, the planning environment described by the probability graph becomes more and more detailed, and the shortest path length calculated is becoming shorter and shorter.

In a word, the update of particle speed takes into account the current velocity and the particle's own optimization. The

Table 1: Obstacle distribution information.

Obstacle source	Obstacle 1	Obstacle 2	Obstacle 3	Obstacle 4
Central coordinates	164,247	133,165	246,214	184,269
Radius	50	39	68	42
Risk level	6	4	8	5
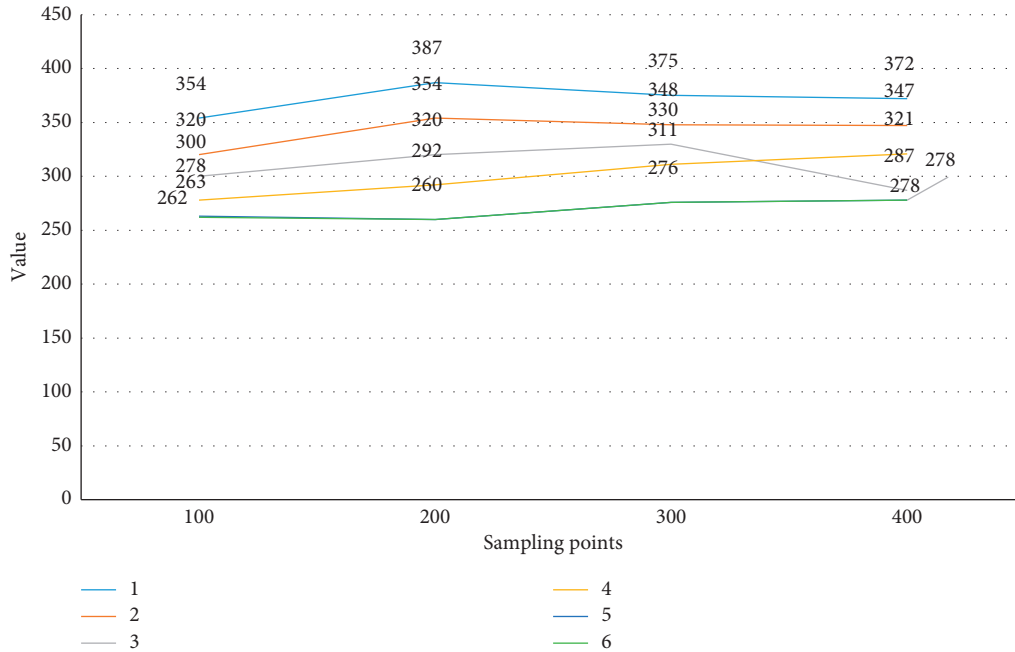
Figure 1: The iterative curve of path length with a different number of sampling points.

position and optimal position of the particle swarm optimization algorithm are calculated by the weighted sum of the three. Therefore, the method is an efficient algorithm with strong global search ability and fast convergence speed in practical application. In addition, this algorithm is also a kind of intelligent algorithm with good generality, which can be widely used in a variety of optimization. At the same time, it has good scalability and is easy to combine with other traditional and intelligent algorithms. The advantages of this algorithm complement each other, providing more ideas and methods for solving practical problems.

As shown in Figure 2, the verification of the periodic task scheduling strategy can be carried out by calculating the running frequency of each periodic task. If every periodic task can run periodically according to the set frequency, the design of the periodic task scheduling strategy is correct. In the simulation example, the operation frequency of each cycle task is calculated in a specific cycle second from the start of UAV taxiing to takeoff [34]. From the verification results, the running frequency of periodic tasks is consistent with the set frequency, and the scheduling strategy of periodic tasks meets the system requirements.

4.2. Schedulability Analysis of UAV Path Planning in Virtual Environment.
From the path of hybrid particle swarm optimization, it can be seen that the path planned by the algorithm is close to the boundary of obstacles or passes through the vertices of obstacles to meet the requirements of the shortest path. Although the obstacle model has been extended to a certain extent, due to the interference of wind, wave, and currents in the actual navigation process, UAVs may collide with obstacles when navigating according to the global path, resulting in damage or mission failure of UAVs. Through the analysis of the schedulability verification method of simulation research, it can be seen that the maximum schedulability utilization calculation method of the hybrid particle swarm optimization algorithm requires that the task set is periodic [35].

As shown in Figure 3, to verify the effectiveness of the algorithm under different sampling time, four obstacle environments are used to simulate the path search under different sampling times. Finally, compare the different results between the primary and secondary plans based on the time of the obstacle. The comparison of the four groups of data in the figure shows that the time required for the second plan is less than that for the first plan when the number of sampling points is different, and the calculation time increases with the increase of sampling time. The growth of the primary plan is faster than that of the secondary plan. This is due to the expansion of all feasible locations in the planning environment in the initial plan. With the increase of sampling time, the number of path points in the search tree increases, and the collision
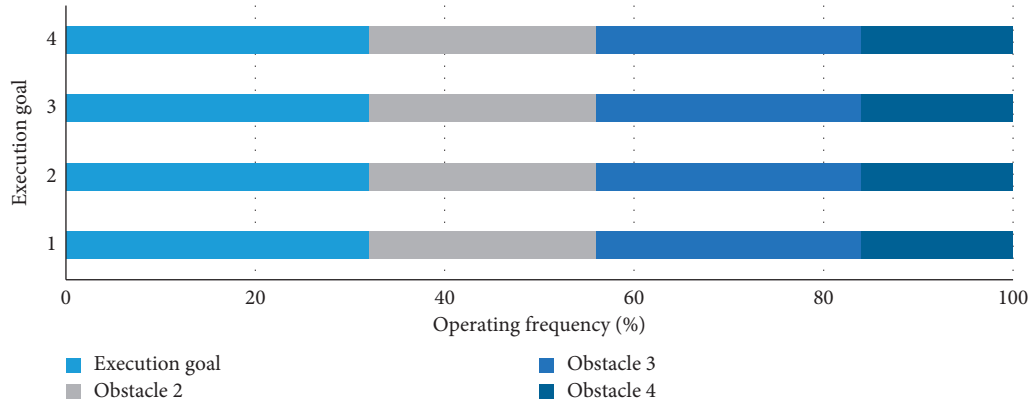
FIGURE 2: System target operating frequency test results.
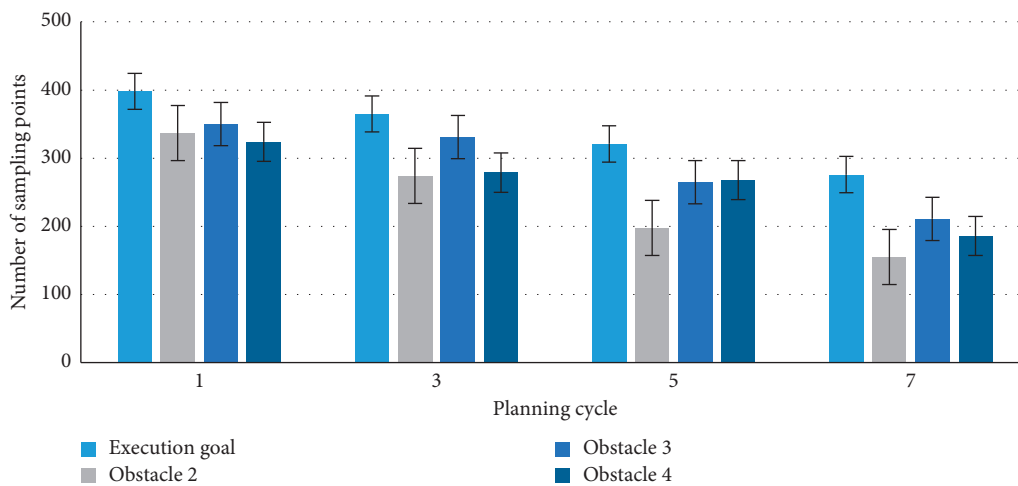
FIGURE 3: Planning cycle comparison results.

detection time increases rapidly. However, due to the introduction of a sorting mechanism in the secondary plan, the number of conflict detections will not increase significantly with the increase of the number of nodes [36].

4.3. UAV Planning Path Assessment in Virtual Environment. For different sampling times, the path length obtained by the algorithm is compared. Because the UAV flies at a constant speed, the arrival time of the target point can directly reflect the information of the path length.

The results of multiple evaluations under the same conditions are different. The first assessment of Route 2 failed and the others succeeded. However, for the second assessment, the assessment of Route 1 and Route 3 failed and the assessment of other routes was successful. The two assessments provide a correct assessment of each route. However, for the second assessment, there was no significant difference in the output values corresponding to "medium" and "good" in Route 1 assessment results. According to the principle that the evaluation result is the maximum weight, the evaluation grade of Route 3 is "poor," while the actual route level is good, so the

evaluation result is wrong. Routes 1 and 2 have similar disadvantages. In the first assessment, due to the above reasons, there will be assessment errors.

Figure 4 shows the simulation results of path arrival time obtained by primary planning and secondary planning. The results show that, with the increase of sampling time, the arrival time becomes smaller and shorter, which indicates that the path length is shorter and shorter.

When the number of samples increases to 400, the change trend of path length becomes slower. This is because the system has completed most of the planned space coverage, and the search results are close to the best path. The arrival time of the initial plan is shorter than that of the secondary plan. This is because, after a sudden threat, the path obtained through the initial plan is no longer feasible. To avoid a sudden threat, it needs to take a longer path, and the arrival time increases accordingly. The simulation results show that although there are some differences between the two evaluation results, both of them have made a correct evaluation of the advantages and disadvantages of the route. The figure shows that the output value of the path level is significantly higher than that of other levels, and the path level can be judged intuitively and accurately from the
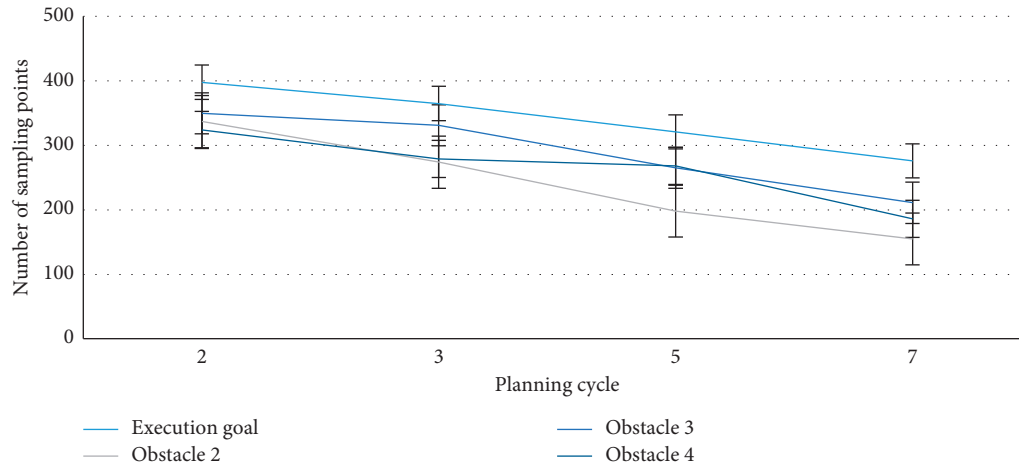
FIGURE 4: Trend of sampling path length change.

diagram. The experimental results show that firstly, the initial weight and threshold are optimized, and then the accuracy of routing evaluation can be significantly improved by network training, which is an effective evaluation method. The fuzzy comprehensive evaluation method is based on the experience of relevant experts to comprehensively evaluate the route [37], judge the advantages and disadvantages of the route, carry out a quantitative evaluation on the route, give the corresponding score, and make a more detailed evaluation. If it is necessary to make a fine evaluation on the route evaluation of the BP neural network, the samples and evaluation values of the fuzzy comprehensive evaluation method can be used as the training samples of the BP neural network trained by the network, and the score value can be used as the expected output of training samples. Not only can the test samples be used to test the advantages and disadvantages of the route, but also the route score can obtain volume value.

5. Conclusion

In geological disaster emergency response, UAV image acquisition provides a scientific and reasonable decision-making basis for rescue and disaster assessment. The efficiency and effect of unmanned path planning directly affect the whole emergency process. Autonomous optimal path planning is one of the main functions of UAV, which reflects the intelligence level of UAV. It mainly includes overall path planning and partial path planning. Among them, the overall path planning is the basic guarantee for the normal and safe driving of UAV and is also the basis of partial path planning, which has a certain value for the research of UAV optimal path planning. However, at present, most of the global optimal path planning algorithms at home and abroad are easy to fall into the local optimal solution and the convergence speed is slow, and most of them only consider the single target of the shortest path, which leads to the problem that the corner is too large and the distance is too close, and the actual navigation of obstacles and unmanned aircraft is inconsistent.

To solve these problems, based on the research results at home and abroad, this paper takes multitarget tracking algorithm, ant colony algorithm, and hybrid particle swarm optimization algorithm as research methods; based on virtual reality technology, through the comparative analysis of the advantages and disadvantages of several algorithms, the research model of path optimization method for multiple UAVs based on virtual reality technology is established. The path optimization method of UAV after an earthquake based on virtual reality technology is studied. The results show that the hybrid particle swarm optimization algorithm based on virtual reality technology is necessary and advanced for UAV global path planning. This paper analyzes the basic particle swarm optimization algorithm and hybrid particle swarm optimization algorithm based on virtual reality technology. This paper introduces the formal definition of UAV path planning and the kinematic constraints of various UAVs. It focuses on several commonly used path planning algorithms in this field, some of which focus on environmental modeling, and some focus on path search. Generally speaking, intelligent methods are the future trend.

At present, the development of multi-UAV cooperative path planning is still a hot issue. Due to the author's limited experience, the research on some problems in this paper is not comprehensive enough. In the future, UAV collaborative planning, UAV task allocation, and path planning can be combined, and the communication between UAVs can be considered. The individual to master intelligence makes the whole system more flexible.

Data Availability

The data that support the findings of this study are available from the corresponding author upon reasonable request.

Conflicts of Interest

The authors declare that they have no conflicts of interest.

References

[1] Y. Chen, J. Yu, Y. Mei, Y. Wang, and X. Su, "Modified central force optimization (MCFO) algorithm for 3D UAV path planning," *Neurocomputing*, vol. 171, pp. 878–888, 2016.

[2] Z. Lv, L. Qiao, M. Shamim Hossain, and B. J. Choi, *Analysis of Using Blockchain to Protect the Privacy of Drone Big Data*, IEEE Network, New York, NY, USA, 2020.

[3] S. Xu, K. Doğançay, and H. Hmam, "Distributed pseudolinear estimation and UAV path optimization for 3D AOA target tracking," *Signal Processing*, vol. 133, pp. 64–78, 2017.

[4] W. Xu, S. Qu, L. Zhao, and H. Zhang, "An improved adaptive sliding mode observer for middle- and high-speed rotor tracking," *IEEE Transactions on Power Electronics*, vol. 36, no. 1, p. 1043, 2021.

[5] D. Li, C. Li, and H. Liu, "Path-optimization method for UAV-aided relay broadcast communication system," *Physical Communication*, vol. 31, pp. 40–48, 2018.

[6] S. Jeong, O. Simeone, and J. Kang, "Mobile edge computing via a UAV-mounted cloudlet: optimization of bit allocation and path planning," *IEEE Transactions on Vehicular Technology*, vol. 67, no. 3, pp. 2049–2063, 2018.

[7] Y. Liu, X. Zhang, X. Guan, and D. Delahaye, "Potential odor intensity grid based UAV path planning algorithm with particle swarm optimization approach," *Mathematical Problems in Engineering*, vol. 2016, Article ID 7802798, 16 pages, 2016.

[8] H. Duan, P. Li, Y. Shi, X. Zhang, and C. Sun, "Interactive learning environment for bio-inspired optimization algorithms for UAV path planning," *IEEE Transactions on Education*, vol. 58, no. 4, pp. 276–281, 2015.

[9] Q. Yang, Z. Yang, T. Zhang, and G. Hu, "A random chemical reaction optimization algorithm based on dual containers strategy for multi-rotor UAV path planning in transmission line inspection," *Concurrency and Computation: Practice and Experience*, vol. 31, no. 12, pp. e4658.1–e4658.13, 2019.

[10] D. Zhang and H. Duan, "Social-class pigeon-inspired optimization and time stamp segmentation for multi-UAV cooperative path planning," *Neurocomputing*, vol. 313, pp. 229–246, 2018.

[11] Z. Xiangyin, L. Xingyang, J. Songmin et al., "A novel phase angle-encoded fruit fly optimization algorithm with mutation adaptation mechanism applied to UAV path planning," *Applied Soft Computing*, vol. 70, pp. 371–388, 2018.

[12] W. Li, S. Sun, J. Li et al., "UAV dynamic path planning algorithm based on segmented optimization RRT[J]," *Xi Tong Gong Cheng Yu Dian Zi Ji Shu/Systems Engineering and Electronics*, vol. 40, no. 8, pp. 1786–1793, 2018.

[13] Z. Shao, F. Yan, Z. Zhou, and X. Zhu, "Path planning for multi-UAV formation rendezvous based on distributed cooperative particle swarm optimization," *Applied Sciences*, vol. 9, no. 13, p. 2621, 2019.

[14] 2-OptACO, "An improvement of ant colony optimization for UAV path in disaster rescue," *Journal of Information Ence and Engineering*, vol. 34, no. 4, pp. 1063–1077, 2018.

[15] M. Ben Ghorbel, D. Rodriguez-Duarte, H. Ghazzai et al., "Joint position and travel path optimization for energy efficient wireless data gathering using unmanned aerial vehicles," *IEEE Transactions on Vehicular Technology*, no. 3, p. 1, 2019.

[16] J. J. Park, S. C. Chen, and K. K. Raymond Choo, "3D UAV flying path optimization method based on the douglas-peucker algorithm," *Multimedia And Ubiquitous Engineering*, vol. 448, pp. 56–60, 2017.

[17] Y. Chen, J. Yu, X. Su, and G. Luo, "Path planning for multi-UAV formation," *Journal of Intelligent & Robotic Systems*, vol. 77, no. 1, pp. 229–246, 2015.

[18] E. Rudnick-Cohen, J. W. Herrmann, and S. Azarm, "Risk-based path planning optimization methods for unmanned aerial vehicles over inhabited areas," *Journal of Computing and Information Ence in Engineering*, vol. 16, no. 2, pp. 021004.1–021004.7, 2016.

[19] M. Zhang, J. Song, L. Huang et al., "Distributed cooperative search with collision avoidance for a team of unmanned aerial vehicles using gradient optimization," *Journal of Aerospace Engineering*, vol. 30, no. 1, pp. 04016064.1–04016064.11, 2017.

[20] Y. Chen, Y. Tan, L. Cheng et al., "Path planning for a heterogeneous aerial-ground robot system with neighbourhood constraints," *Jiqiren/Robot*, vol. 39, no. 1, pp. 1–7, 2017.

[21] L. Blasi, S. Barbato, and E. D'Amato, "A mixed probabilistic-geometric strategy for UAV optimum flight path identification based on bit-coded basic manoeuvres," *Aerospace Science and Technology*, vol. 71, pp. 1–11, 2017.

[22] P. Kumar, S. Garg, A. Singh, S. Batra, N. Kumar, and I. You, "MVO-based 2-D path planning scheme for providing quality of service in UAV environment," *IEEE Internet of Things Journal*, vol. 5, no. 3, pp. 1698–1707, 2018.

[23] A. Abraham, P. K. Muhuri, A. K. Muda et al., "Multi-UAV path planning with multi colony ant optimization," *Advances in Intelligent Systems and Computing*, vol. 736, pp. 407–417, 2018.

[24] M. Elhoseny, X. Yuan, H. K. El-Minir, and A. M. Riad, "Extending self-organizing network availability using genetic algorithm," in *Proceedings of the Fifth International Conference on Computing, Communications and Networking Technologies (ICCCNT)*, Hefei, China, 2014.

[25] M. A. El Aziz, A. M. Hemdan, A. A. Ewees et al., "Prediction of biochar yield using adaptive neuro-fuzzy inference system with particle swarm optimization," in *Proceedings of the 2017 IEEE PES PowerAfrica*, pp. 115–120, IEEE, Accra, Ghana, June 2017.

[26] D. Popescu, F. Stoican, and L. Ichim, "Control and optimization of UAV trajectory for aerial coverage in photogrammetry applications," *Advances in Electrical and Computer Engineering*, vol. 16, no. 3, pp. 99–106, 2016.

[27] L. He, L. Zhengzheng, Z. Moning et al., "Integrated optimization of unmanned aerial vehicle task allocation and path planning under steady wind," *PLoS One*, vol. 13, no. 3, Article ID e0194690, 2018.

[28] Q. Zhang, R. Wang, J. Yang, K. Ding, Y. Li, and J. Hu, "Modified collective decision optimization algorithm with application in trajectory planning of UAV," *Applied Intelligence*, vol. 48, no. 8, pp. 2328–2354, 2018.

[29] S. Wan, "Topology hiding routing based on learning with errors," *Concurrency and Computation: Practice and Experience*, no. 6, p. 5740, 2020.

[30] M. Elhoseny, A. Shehab, and X. Yuan, "Optimizing robot path in dynamic environments using genetic algorithm and bezier curve," *Journal of Intelligent & Fuzzy Systems*, vol. 33, no. 4, pp. 2305–2316, 2017.

[31] K. Guo, "Research on location selection model of distribution network with constrained line constraints based on genetic algorithm," *Neural Computing and Applications*, vol. 32, no. 6, pp. 1679–1689, 2019.

[32] Z. Lv, D. Chen, R. Lou, and H. Song, "Industrial security solution for virtual reality," *IEEE Internet of Things Journal*, no. 99, p. 1, 2020.

[33] H. Zhang, S. Qu, H. Li, J. Luo, and W. Xu, "A moving shadow elimination method based on fusion of multi-feature," *IEEE Access*, vol. 8, pp. 63971–63982, 2020.

[34] Z. Lv, "The security of Internet of drones," *Computer Communications*, vol. 148, pp. 208–214, 2019.

[35] Y. Chen, W. Zheng, W. Li, and Y. Huang, "Large group Activity security risk assessment and risk early warning based on random forest algorithm," *Pattern Recognition Letters*, vol. 144, no. 4, 2021.

[36] Z. Lv and H. Song, "Mobile internet of things under data physical fusion technology," *IEEE Internet of Things Journal*, no. 99, p. 1, 2019.

[37] Y. Tang and M. Elhoseny, "Computer network security evaluation simulation model based on neural network," *Journal of Intelligent & Fuzzy Systems*, vol. 37, no. 3, p. 3197, 2019.

Research Article

AI Based Gravity Compensation Algorithm and Simulation of Load End of Robotic Arm Wrist Force

Liang Chen [ID],[1] **Hanxu Sun,**[1] **Wei Zhao,**[2] **and Tao Yu**[3]

[1]*School of Automation, Beijing University of Posts and Telecommunications, Beijing 10876, China*
[2]*School of Information Engineering, Beijing Institute of Graphic Communications, Beijing, China*
[3]*College of Mechanical Engineering and Automation, Liaoning University of Technology, Jinzhou, Liaoning, China*

Correspondence should be addressed to Liang Chen; chenliang968@bupt.edu.cn

With the rapid development of mechatronics and robotics technology, the application of robots has been extended from the industrial field to daily life and has become an indispensable part of work and daily life. The accuracy and flexibility of the operator determine the operating efficiency of the robot. Although the level of development of the operator is constantly improving, the traditional operator has a simple structure and generally adopts parallel movement or tightening. The holding structure has poor flexibility and stability, making it difficult to achieve precise position capture and control and cannot meet the requirements of delicate tasks. In this paper, a basic force analysis of the manipulator is carried out, and the change trend of the force and driving force of each joint when the manipulator is grasping objects is obtained, so as to determine that the manipulator can grasp the object stably; then, in the strength analysis of the manipulator, it is determined that the material meets the strength requirements. This paper conducts an output voltage experiment on the static performance and coupling error of the mechanical arm wrist force sensor. Secondly, in order to study the influence of the temperature change in the space environment on the zero-point output of the mechanical arm sensor, a high and low temperature test box are used to simulate the temperature brought by the temperature change to the sensor. Experiments show that the maximum coupling error of the sensor is 1.81%, which is less than 2% of the design index. This indicates that the operator sensor is used to detect the force and torque that the space operator's edge operator experiences when it interacts with the external environment and provides the necessary power sensing information for power control and compatible operator motion control, completing some complex; the Fine project is an important prerequisite for realizing the intelligence of space operators.

1. Introduction

As the requirements for refinement and intelligence of operation tasks continue to increase, mechanical arms that lack force perception will not be able to meet the requirements of operation tasks. Increasing the force-sensing ability on the robotic arm is an important functional requirement and development trend of the robotic arm. Manipulator wrist force sensor is one of the most important multidimensional power sensors for robots. It is a power sensor with two ends connected to the robot wrist and claws. When the robot arm tightens the workpiece for operation, it can measure the robot arm and the external environment. According to the concept and characteristics of supply chain

integration, the relevant factors that influence the methods of evaluation and evaluation of business performance determine the supply chain integration and the indicators of measuring the performance of companies and define relevant models. This document uses the existing data from listed companies in the software services and information technology industry to separate supply chain integration into customer integration and supplier integration, exploring the relationship between customer integration, vendor integration, and corporate performance.

Relying on its advanced software and hardware platforms, computer vision technology, and motion control technology, foreign countries have always been in a leading position in the field of wrist force sensor research. In recent

years, dozens of wrist force sensor products or prototypes have been developed. Sprowl analyzed the relationship between the influence of the gravity level disturbance on the inertial navigation system and the maneuvering mode of the carrier. The gravity level disturbance signal caused by the vertical deviation is a distance-related signal. The maneuvering mode of the carrier determines the distance-related signal to time elated signal conversion method [1]. Ahlin et al. quantitatively analyzed the influence of vertical deviation on inertial navigation based on the single-channel error covariance model of inertial navigation [2]. Cuervo proposed that the attitude error and velocity error caused by the vertical deviation in the Schuler ring have different frequency domain characteristics, and the grid resolution required for the compensation attitude calculation and velocity calculation is different [3]. Farman et al. discussed the influence of the measurement error of the gravity gradiometer on the gravity gradient/inertial integrated navigation system [4].

At present, our country has mastered the kinematics and trajectory planning technology of manipulators, as well as the software and hardware design technology of control system. But on the whole, there is a certain gap between the domestic research level and foreign ones, and the accuracy and reliability are worse than foreign ones. Ekaputra et al. believed that even if inertial sensors, navigation algorithms, and navigation computers are ideal, there will still be errors in inertial navigation. The source of the errors is the error of Earth's gravity field information used in inertial navigation [5]. Jawale et al. proposed using gravity gradient for matching and positioning. Five independent components in the gravity gradient tensor constitute the matching feature. The gravity gradient measurement can better isolate the influence of carrier acceleration, which is conducive to the realization of dynamic measurement [6]. Noort et al. used the stiffness coefficient to adjust the stiffness of the geometric transformation to be solved, which can better cope with the changes of inertial navigation error and speed error [7]. Kim used cloud atomization technology to convert different levels of physical nodes into virtual machine nodes through the research of fog computing framework [8].

Aiming at the correction of the six-dimensional force/torque sensor in the space environment, this paper proposes a method for online calibration of the six-dimensional force/torque sensor based on the space manipulator joint torque sensor and exerts a series of different effects on each joint through the control commands of the manipulator force, making the mechanical arm in a state of internal force balance. Finally, with the introduction of the wrist force sensor gravity compensation model, in combination with the kinematic equations of the robot arm, the wrist force sensor end gravity compensation algorithm is deduced, the reading is corrected, and the force solution method is adjusted. The robot arm and the tip of the robot arm are obtained accurately. The contact force is finally verified by a simulation to verify the correctness of the gravity compensation algorithm at the load end of the arm mechanical force sensor.

2. Gravity Compensation Algorithm and Simulation of Load End of Manipulator Wrist Force Sensor

2.1. Calibration Method of Manipulator Wrist Force Sensor Based on Neural Network. Due to the design and manufacturing of the sensor, there is a mutual coupling between the output signal of the sensor and the actual six-dimensional component force. This interference is very complicated and difficult to accurately describe in theory. It restricts the measurement accuracy of the multidimensional wrist force sensor. One of the main factors [9, 10] is to adopt signal processing methods to eliminate or suppress the coupling between sensor dimensions. This method can not only reduce the requirements on the sensor manufacturing process but also obtain more accurate measurement results. In factor analysis, the weight of each main factor is not determined, but is determined by the relevant variables that affect the changes of these factors.

2.1.1. Linear Calibration of Manipulator Wrist Force Sensor Based on Least Square Method. With certain performance improvements, there are new requirements for general adaptability and specific adaptability. The main problem with basketball gymnastics in Japan is that there are too many regular gymnastics, special gymnastics are not covered, and the obtained physical condition cannot be used for special gymnastics. Suppose F is the input force vector, V is the output voltage vector, and H is the coupling matrix [11, 12], for the mechanical arm wrist force sensor:

$$V = HF. \tag{1}$$

The following transformation is made to the formula:

$$H^T V = \left(H^T H\right) F. \tag{2}$$

We get

$$F = \left(H^T H\right)^{-1} H^T V. \tag{3}$$

Then, we do the following:

$$C = \left(H^T H\right)^{-1} H^T. \tag{4}$$

We call C the calibration matrix. So there are

$$F = CV. \tag{5}$$

When the calibration matrix C is known, for the direct output type manipulator wrist force sensor, the expression is

$$\begin{bmatrix} F_x \\ F_y \\ F_z \end{bmatrix} = \begin{bmatrix} c_{11} & c_{12} & c_{13} \\ c_{21} & c_{22} & c_{23} \\ c_{31} & c_{32} & c_{33} \end{bmatrix} \begin{bmatrix} V_1 \\ V_2 \\ V_3 \end{bmatrix}. \tag{6}$$

In the calculation process of (5), the interdimensional decoupling of the mechanical arm wrist force sensor is also completed. It can be seen that the key to the calibration of the entire sensor is to obtain the calibration matrix C.

Human motion tracking based on template matching currently primarily uses error metrics between two matching pixel blocks. There are three main error metrics based on block matching. An error metric is based on a cross-correlation function and a normalized mean square. When the number of force vectors is equal to the number of output channels, the transfer coefficient matrix can be obtained as [13, 14]

$$C = FV^{-1},$$
$$C = FV^T\left(VV^T\right)^{-1}. \tag{7}$$

2.1.2. Nonlinear Calibration of Manipulator Wrist Force Sensor Based on BP Neural Network.
(1) Artificial Neural Networks. Artificial neuron is the simplification and simulation of biological neuron, and it is the basic processing unit of neural network system. The input and output relationship can be described as

$$y_i = f\left(\sum_{j=1}^n w_{ij} u_j - \theta_i\right). \tag{8}$$

We make

$$x_i = \sum_{j=1}^n \left(w_{ij}\theta_j - \theta_i\right). \tag{9}$$

Then, there are

$$y_i = f\left(x_i\right). \tag{10}$$

Different types of activation functions can be selected to obtain different types of neuron models. If $-\theta_i$ is regarded as the weight corresponding to the input quantity u_0 which is always equal to 1, then (8) can be written as

$$y_i = f\left(x_i\right) = f\left(\sum_{j=0}^n w_{ij} u_j\right). \tag{11}$$

Among them, $w_{i0} = -\theta_i$, $u_0 = 1$. The output performance of the artificial neuron and even the neural network model is related to the form of the activation function. Therefore, when constructing the neural network model to solve different problems, you should choose the appropriate activation function [15, 16], as shown in (12) and (13). We have the following:

$$f\left(x\right) = \tanh\left(x\right) = \frac{1}{1 + \exp\left(-\beta x\right)}, \quad \beta > 0, \tag{12}$$

$$f\left(x\right) = \tanh\left(x\right) = \frac{1 - \exp\left(-\beta x\right)}{1 + \exp\left(-\beta x\right)}, \quad \beta > 0. \tag{13}$$

The maximum communication delay that the user can tolerate under the cloud and fog architecture is guaranteed, and the user's request is processed within the acceptable communication delay. Therefore, in order to judge whether the manipulator is singular, it is first necessary to determine the Jacobian matrix of the manipulator and then judge whether it is a singular state according to the Jacobian matrix [17].

(2). BP Neural Network. Therefore, it is of theoretical and practical importance for the application of the particle swarm algorithm to generate the initial particle swarm in an appropriate manner. The single-particle tree structure coding design emphasizes the connection between upstream and downstream in the supply chain network. Each node in the network has a unique neuron structure, and its activation function usually uses a sigmoid function, but there is also a linear activation function at the output level [18, 19]. Its structure is shown in Figure 1.

Suppose that in a given sample pair of group L, the sample input u_p and output d_p of group p are

$$u_p = \left(u_{1p}, u_{2p}, \ldots, u_{np}\right), d_p = \left(d_{1p}, d_{2p}, \ldots, d_{np}\right),$$
$$p = 1, 2, \ldots, L. \tag{14}$$

The output of node i when inputting p sample is

$$y_{ip}\left(t\right) = f\left[u_{ip}\left(t\right)\right] = f\left[\sum_j w_{ij}\left(t\right) I_{jp}\right]. \tag{15}$$

Among them, I_{jp} represents the j input of node i when the p sample is input; $f\left(\cdot\right)$ represents the differentiable S type activation function. According to (15), starting from the input layer and deducing layer by layer, the output of the nodes of the network output layer can be obtained. Suppose E_p is the objective function of the network when the p sample is input and the L_2 norm is taken; then

$$E_p\left(w, t\right) = \frac{1}{2}\left\|d_p - y_p\left(t\right)\right\|_2^2 = \frac{1}{2}\sum_k \left[d_{kp} - y_{kp}\left(t\right)\right]^2,$$
$$= \frac{1}{2}\sum_k e_{kp}^2\left(t\right). \tag{16}$$

where $y_{kp}\left(t\right)$ represents the output of the k node in the output layer when the p group of samples are input after the t weight adjustment; $e_{kp}\left(t\right)$ represents the error between the output of the k node of the output layer and the expected output when the p group of samples are input after t weight adjustments. Therefore, the overall objective function of the network is

$$J\left(w, t\right) = \sum_p E_p\left(w, t\right), \tag{17}$$

if

$$J\left(w, t\right) \leq \varepsilon. \tag{18}$$

Then, the network training ends; otherwise, taking formula (17) as the objective function, the $t + 1$ adjustment formula of the connection weight of neuron j to neuron i can be obtained by the gradient descent method:
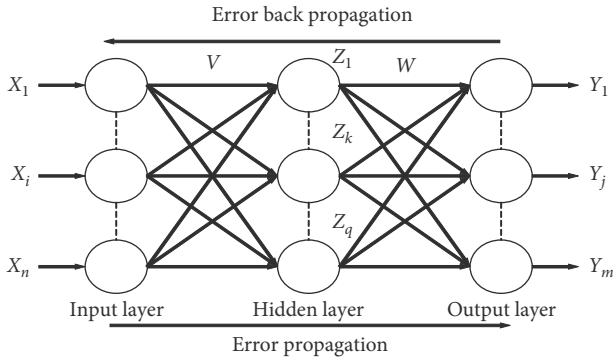
FIGURE 1: Neural network structure model based on BP algorithm.

$$w_{ij}(t+1) = w_{ij}(t) + \Delta w_{ij}(t),$$

$$\Delta w_{ij} = -\eta \sum_{P} \frac{\partial E_p(w,t)}{\partial w_{ij}(t)}. \tag{19}$$

Here, η is the step size factor, which is called the learning operator here.

2.2. Load Balancing Algorithm

2.2.1. Load Balancing Technology. Load balancing technology uses different methods and technical means to make the equipment in the system more fully function, improve data processing capacity and throughput, and build a network with better flexibility and wider availability. When the load is small, the significance of load balancing is not great. As the load increases, the role of load balancing technology will be clearly seen [20, 21]. Load balancing technology effectively solves the problem of network congestion, improves node utilization, network server response speed, and maintainability, avoids point-to-point network failures, significantly accelerates user access speed and efficiency, and improves system performance.

2.2.2. Load Balancing Technology Classification. The economic environment is the most basic environment. It is the basis for the survival of the financial system and determines the degree of development of the financial system. The financial system was created after economic growth reached a certain level and developed simultaneously with economic growth. The operation of the software must consume part of the system resources, and as the processing load increases, the software itself consumes a large amount of system resources [22, 23]. Global load balancing can achieve geographic independence and schedule tasks on server groups with different network structures. It is used to locate the nearest server through the user's IP address and can also be used for uniform resource allocation. This method can effectively prevent server point failures and network congestion and improve user access efficiency.

2.2.3. Common Load Balancing Algorithms. The law must be able to effectively protect the interests of investors and creditors, to contribute to the establishment and maintenance of good economic order, and thus to ensure the smooth and efficient operation of the financial system. A well-developed credit system can not only effectively reduce the cost of information collection but also reduce the negative choice and moral hazard caused by information asymmetry and reduce the occurrence of financial gaps and financial crises. Servers with different performance have different weights, so that servers with better performance can get more user requests. This algorithm can perform task scheduling according to the processing capacity of the server and reduce the uneven load distribution caused by the difference in the processing capacity of the server [24, 25]. Each load balancing algorithm has certain advantages and disadvantages. Some are suitable for specific scenarios, some are simple to implement, and some have good load balancing effects but higher system overhead and higher cost. By proposing some improvements to existing load balancing algorithms, better load balancing effects can often be achieved.

3. Experimental Design of Gravity Compensation Algorithm for Load End of Manipulator Wrist Force Sensor

3.1. Simulation Platform Construction. After the model is imported into the Adams software, the quality and material parameters of each part need to be set to keep the parameters consistent with the real robot arm. The coordinate system where the center point of the robot arm base is located is the base coordinate system, and the robot arm base is fixed on the ground with a fixed pair. The six joints of the robotic arm are all connected by rotating joints, and other mechanisms are connected by fixed pairs. In this way, the constraint relationship between every two parts of the robotic arm is defined to ensure the correct movement of the robotic arm.

3.2. Data Sources. There are many factors that cause the zero drift of the sensor, mainly two factors, time and temperature. In order to measure the impact of time on the zero point of the sensor, it can be expressed by stability or zero-point drift. Zero-point drift refers to the sensor zero-point drift caused by time. This article first conducts an output voltage experiment on the static performance and coupling error of the mechanical arm wrist force sensor and, secondly, in order to study the influence of temperature changes in the space environment on the zero-point output of the mechanical arm sensor. A high- and low-temperature test box was used to simulate the temperature drift caused by temperature changes to the sensor, and these experimental data were collected for subsequent experimental analysis.

3.3. Experimental Method. The torque information detected by the hinge torque sensor is used as standard force/torque information, which is then converted to the standard power load applied to the six-dimensional force/torque sensor via

TABLE 1: Data sheet of evaluation index system for index reliability testing.

	Very clear	Clear	General	Not clear	Chaotic	Alpha
Poisson ratio	0.317	0.358	0.174	0.093	0.058	0.9064
Elastic limit	0.294	0.261	0.203	0.166	0.096	0.8433
Yield strength	0.254	0.284	0.189	0.177	0.086	0.8169
Tensile strength	0.242	0.266	0.192	0.174	0.126	0.7672
Linear expansion coefficient	0.237	0.218	0.214	0.194	0.137	0.7394

the Jacobian force. In addition, the voltage signal of the six-dimensional power/torque sensor is collected simultaneously with the output information, and then the minimum quadratic method can be used to perform the electronic calibration of the six-dimensional power/torque sensor. The hinge torque can be used as the standard power sensor, so the hinge torque sensor can be considered to be used to calibrate the robotic arm's six-dimensional force/torque sensor on the web.

3.4. Statistical Data Processing Method. SPSS23.0 software was used for data processing, and count data was expressed as percentage (%), k is the number of data in this experiment, σ^2 is the variance of all survey results, and $P < 0.05$ indicates that the difference is statistically significant. The formula for calculating reliability is shown in the following:

$$a = \frac{k}{k-1}\left(1 - \frac{\sum \sigma_i^2}{\sigma^2}\right). \tag{20}$$

4. Gravity Compensation Algorithm for Load End of Manipulator Wrist Force Sensor

4.1. Index Reliability Test and Patient Condition Analysis. The α coefficient above 0.8 indicates that the effect of index setting is very good, and that above 0.7 is also acceptable. Here, we analyze the reliability of each type of object, and the reliability index we choose for each type of object is slightly different. The results are shown in Table 1.

It can be seen from Figure 2 that the data obtained from Poisson's ratio, elastic limit, yield strength, tensile strength, and linear expansion coefficient of the material has an acceptable impact on this experiment ($\alpha > 0.7$). From this, it can be seen that the properties of the materials used in the robotic arm are sufficient to meet the needs of this experiment and provide a basis for subsequent experiments.

4.2. Based on the Static Performance and Coupling Error of the Sensor

4.2.1. Analysis of Various Static Performance Indicators Based on Sensors. Through the processing of the experimental data of loading and unloading in each direction of the sensor, and using the least square method to decouple the sensor, the static performance indicators of the sensor are analyzed here (Table 2).

It can be seen from Figure 3 that the linearity of the sensor is less than 2%, the maximum linearity is 1.93% in the Mx direction, the minimum linearity is 0.45% in the Fx direction, the maximum repeatability error is 1.43% in the Fz direction, the smallest the repeatability error is 0.94% in the Fx direction, the stability of the sensor is good, the maximum stability error is 0.93% in the My direction, the maximum hysteresis characteristic of the sensor is 1.09% in the Fz direction, and the smallest hysteresis characteristic is 0.56 in the My direction %.

4.2.2. Analysis Based on the Coupling Error of the Sensor. Through the processing of the experimental data of loading and unloading in each direction of the sensor, and using the least square method to decouple the sensor, the coupling error of the sensor is analyzed here, and the results are shown in Table 3.

It can be seen from Figure 4 that the maximum coupling error in the Fx direction is 0.93%, the maximum coupling error in the Fy direction is 0.71%, the maximum coupling error in the Fz direction is 1.81%, the maximum coupling error in the Mx direction is 0.76%, the maximum coupling error in the My direction the error is 1.31%, the maximum coupling error in the Mz direction is 1.33%, and the maximum coupling error of the sensor is 1.81%, which is less than 2% of the design index, so it meets the requirements.

4.3. Temperature Drift Characteristics of Wrist Force Sensor Based on Manipulator

4.3.1. Sensor Temperature Drift Experiment. Assume that the sensor's zero-point drifts due to temperature changes, and the phenomenon that causes the sensor to have a force output is the temperature drift of the sensor. In this paper, the false output force output by the sensor zero-point change caused by temperature drift is defined as temperature drift force, and the results are shown in Table 4.

The collected output voltage signal vector of each sampling point of the sensor caused by temperature change is compared and analyzed, and the temperature drift force can be obtained by using the sensor calibration matrix obtained by static calibration. It is found that the temperature changes will have a great impact on the sensor, among which Fy and Fz have the greatest impact. The specific situation is shown in Figure 5. When the number of partners is small, the degree of new and old model in relation to the optimal solution is not obvious. When the number of partners is large, the new model's model optimization effect is slightly reduced. As the number of partners gradually increased, the degree of optimization of the new model compared to the old model became more and more evident ($P < 0.05$).
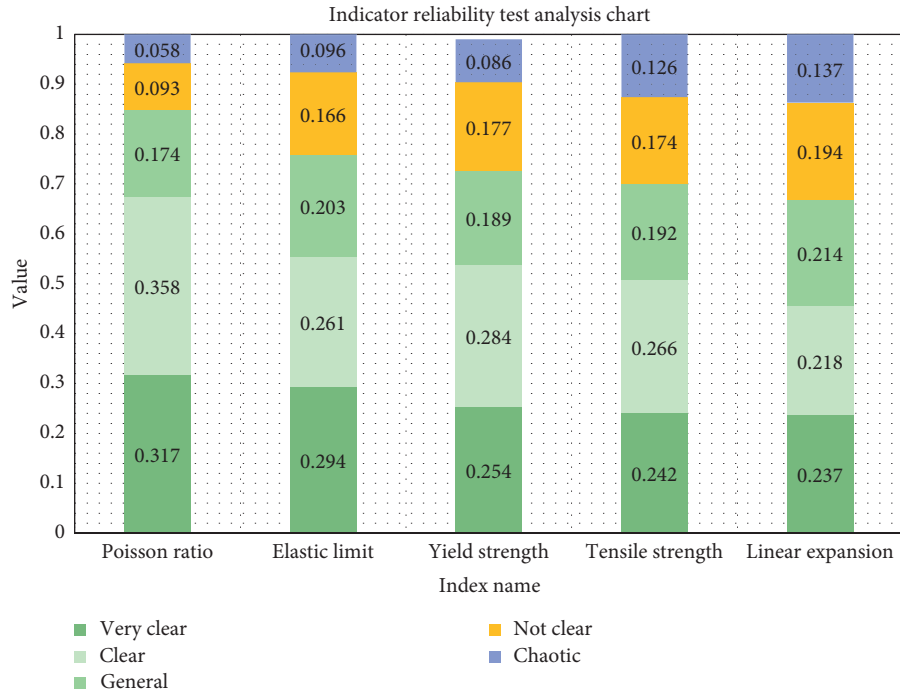
Figure 2: Indicator reliability test analysis chart.

Table 2: The static performance of F/T sensor.

Index	Fx (%)	Fy (%)	Fz (%)	Mx (%)	My (%)	Mz (%)
Linearity	0.45	0.56	0.57	1.93	0.82	1.53
Repeatability	0.94	1.01	1.43	1.32	1.39	1.18
Stability	0.63	0.77	0.79	0.81	0.93	0.68
Hysteresis	0.71	0.61	0.84	1.09	0.56	0.84
Accuracy	1.27	0.82	1.57	1.33	1.36	1.54
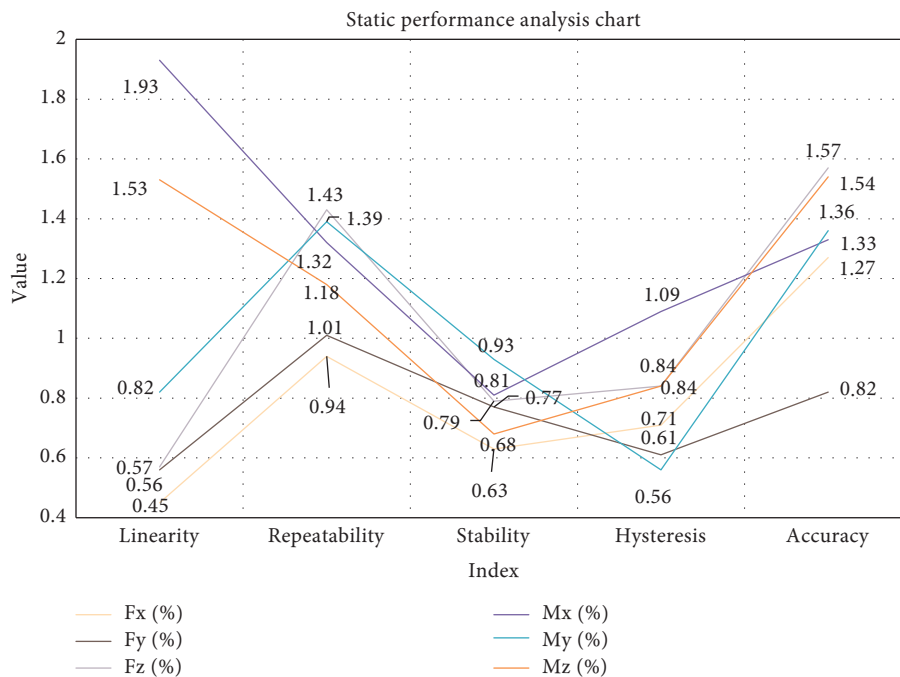
Figure 3: The static performance analysis chart of the sensor.

TABLE 3: The coupling error of F/T sensor.

Applied force/moment	Fx (%)	Fy (%)	Fz (%)	Mx (%)	My (%)	Mz (%)
Fx	0.75	0.19	1.43	0.23	0.75	1.04
Fy	0.93	0.75	1.81	0.32	0.12	1.33
Fz	0.86	0.43	0.75	0.76	0.74	0.29
Mx	0.73	0.22	1.51	0.75	1.31	0.14
My	0.18	0.27	0.81	0.16	0.75	0.36
Mz	0.61	0.71	0.63	0.57	0.72	0.75
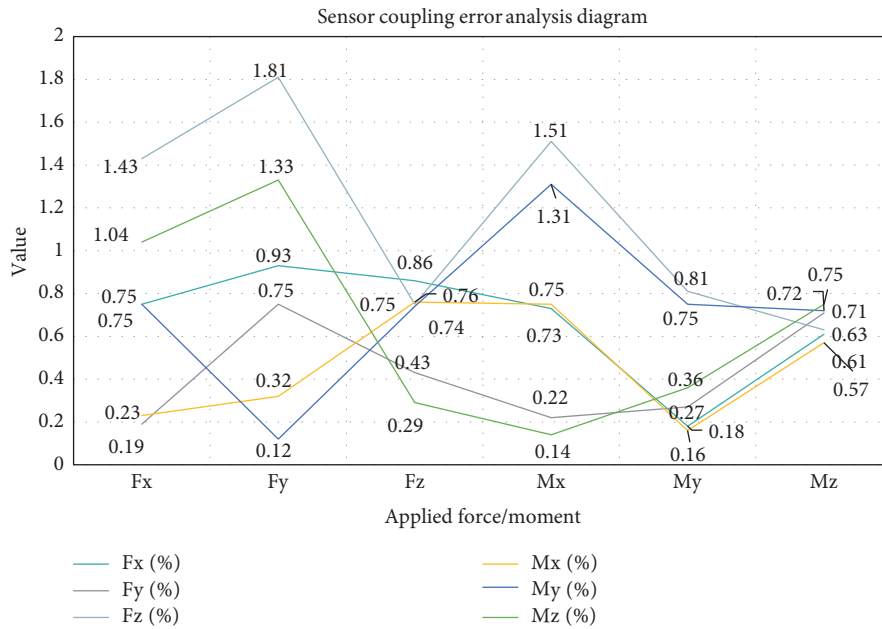
FIGURE 4: Sensor coupling error analysis diagram.

TABLE 4: The force caused by temperature drift in each sample.

Temperature (°C)	Fx	Fy	Fz	Mx	My	Mz
−20	1.01	1.68	1.73	2.18	2.47	2.57
−10	1.44	1.50	1.65	2.14	2.48	2.42
0	1.27	1.62	1.97	1.78	2.09	2.65
10	1.30	1.30	1.82	2.15	2.18	2.70
20	1.20	1.34	1.99	2.29	2.33	2.71
30	1.23	1.32	1.75	2.24	2.48	2.83
40	1.11	1.58	1.67	2.22	2.31	2.62
50	1.10	1.36	1.51	2.02	2.08	2.81

4.3.2. Research on Sensor Temperature Drift Compensation Based on Least Square Method. In order to quantify the influence of temperature drift on the force or torque in each direction of the sensor, the author defines the temperature drift error, which can be expressed as the force or torque caused by temperature divided by the rated force or torque of each dimension, and the results are shown in Table 5. Show.

As the temperature increases, the temperature drift error of Fx remains basically unchanged, and the temperature drift error of Fy and Mx gradually decreases from a positive value to zero and then changes to a negative value. The temperature drift errors of Fz, My, and Mz gradually increase from a negative value to zero and then continue to increase to a positive value. It shows that the effect of temperature drift on Fx is almost negligible, and the effect of temperature drift on Mx and Mz is similar, except that the positive and negative characteristics are opposite. The maximum temperature drift errors of Fx, Mx, and Mz are all less than 2%. The maximum temperature drift errors of My, Fy, and Fz are all greater than 2%, as shown in Figure 6.
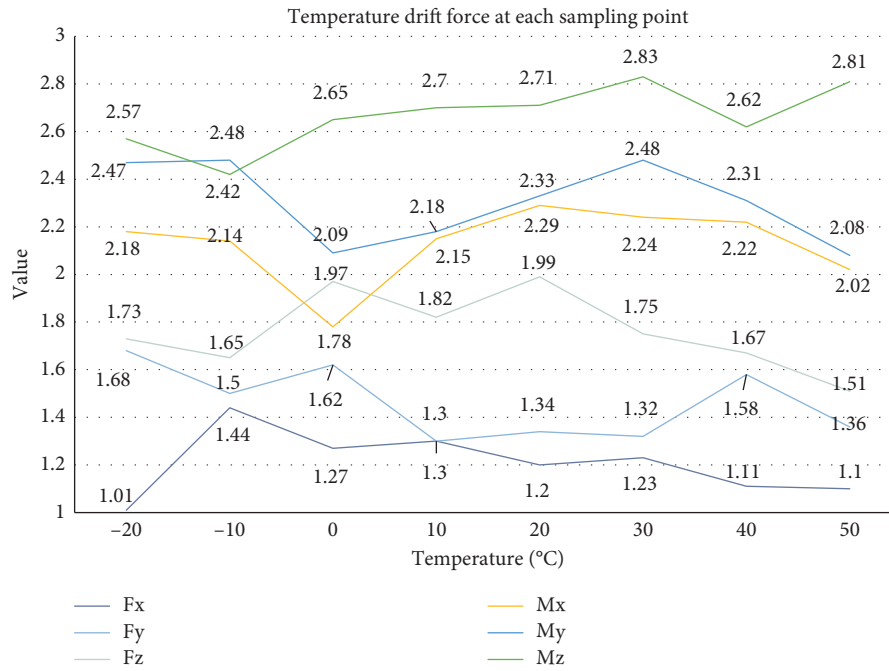
FIGURE 5: Analysis graph of temperature drift force at each sampling point.

TABLE 5: The temperature drift error in each sample.

Temperature (°C)	Fx	Fy	Fz	Mx	My	Mz
−20	0.3	8.7	−16.9	2.3	−6.7	−3.7
−10	−0.3	6.4	−11.6	1.8	−4.4	−3.1
0	0.1	4.6	−8.4	1.3	−3.2	−2.5
10	0.3	3.5	−3.7	0.8	−2.6	−2.1
20	0.3	0.7	0.4	0.3	−0.9	−0.8
30	0.4	−1.9	4.6	−0.2	0.5	0.2
40	0.6	−4.3	8.1	−0.7	1.6	1.1
50	0.8	−6.2	10.3	−1.1	2.5	1.9
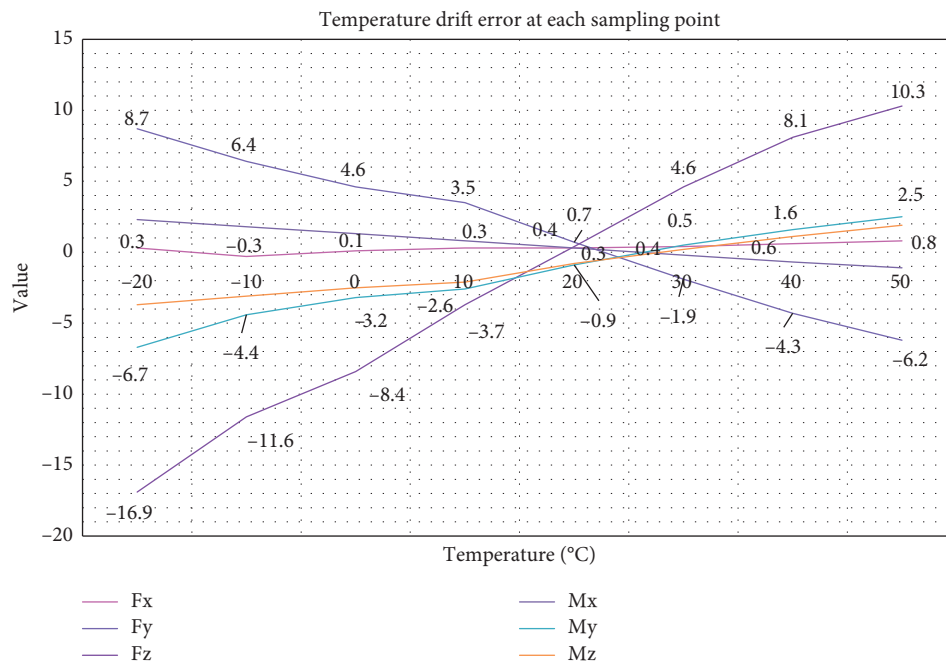
FIGURE 6: Analysis graph of temperature drift error at each sampling point.

TABLE 6: The temperature drift error compensated by RBF neural network.

Temperature (°C)	Fx	Fy	Fz	Mx	My	Mz
−20	1.21	1.62	1.57	2.26	2.04	2.41
−10	1.36	1.69	1.97	2.24	2.12	2.9
0	1.24	1.61	1.73	1.93	2.37	2.68
10	1.11	1.32	1.90	1.93	2.50	2.64
20	1.37	1.35	1.92	1.88	2.42	2.61
30	1.46	1.41	1.53	2.06	2.05	2.68
40	1.45	1.49	1.68	2.26	2.05	2.59
50	1.02	1.46	1.79	1.90	2.32	2.64
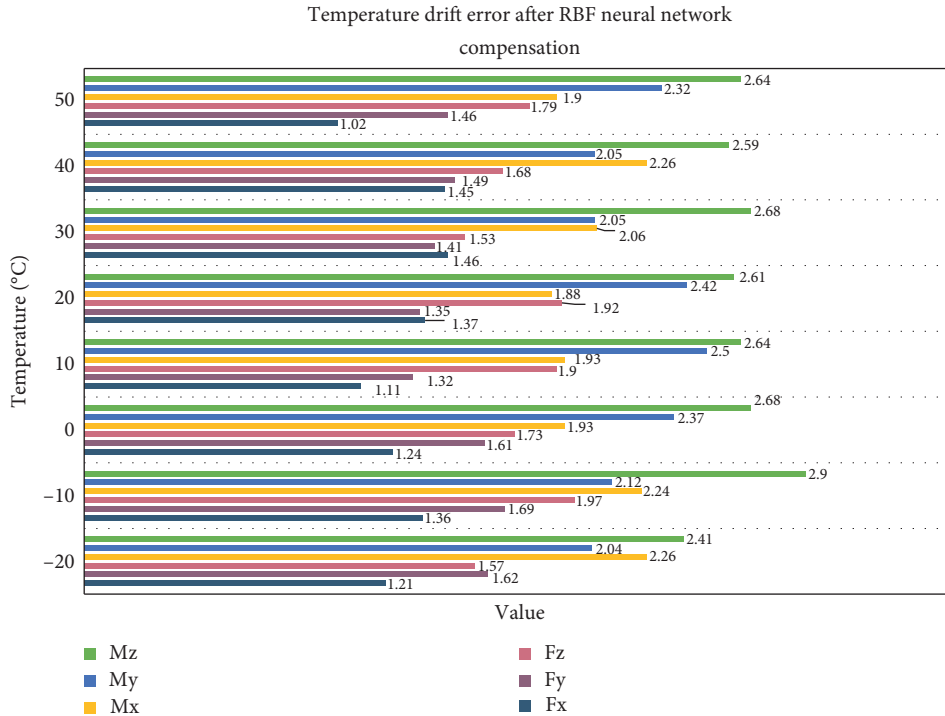
FIGURE 7: Analysis of temperature drift error after RBF neural network compensation.

4.3.3. Analysis Based on Initial Indicators. The temperature drift error of the sensor after temperature compensation through the RBF network is shown in Table 6.

After compensation, the temperature drift error of Fx is greater than 0.08% and less than 0.5%; the temperature drift error of Fy is greater than 0.1% and less than 0.25%; the temperature drift error of Fz is greater than 0.25% and less than 0.6%; the temperature drift error of Mx is greater than 0.25% and less than 0.5%; the temperature drift error of My is greater than 0.1% and less than 0.5%; the temperature drift error of Mz is greater than 0.1% and less than 0.25%, as shown in Figure 7.

5. Conclusions

The influence of the behavior change of the operator terminal load on the zero value of the six-dimensional force sensor and the gravity and center of gravity position of the operator terminal load can be obtained through experimental methods. The wrist force gravity tip load algorithm and the operator's end force calculation method create a model of the wrist force sensor gravity compensation system. When reading the six-dimensional force sensor on the wrist, this method solves the effect of excessive gravity on the load end of the robotic arm. When the operator is in a variable stop motion with low angular acceleration, in principle, the inertia during the motion can be ignored, and the influence of gravity on the load end of the power sensor can be eliminated. The simulation proves the effectiveness of this method and can be widely used based on power feedback and other heavy industrial robots in similar operating environments.

Due to the very complex structure of the six-dimensional force/torque sensor's sensitive components, it is impossible to obtain accurate theoretical expressions. Although the results of finite element analysis are more accurate, the amount of calculation is very large, and the sensor model with the best performance is often not available. Regarding the disadvantages, the sensor is used to detect the force and moment that the end manipulator of the space manipulator

bears when interacting with the external environment and provides necessary force sensing information for the force control and compliant motion control of the manipulator, so as to complete some complex and delicate tasks. It is an important condition to realize the intelligentization of the space manipulator. In this article, the author proposes a response surface method to obtain an approximate mathematical model of the sensor's sensitive components and then, based on the fitted response surface model, use the minimum condition number of the sensor strain compliance matrix as the optimization goal.

In order to obtain the static characteristics of the arm wrist mechanical force sensor, a calibration system based on the pulley weight is designed and the calibration system error is analyzed. The calibration matrix of the arm mechanical strength sensor is obtained with the minimum square method, and various static performance indicators and sensor connection errors are obtained through loading and unloading experiments. In order to change the sensor temperature, a compensation method is proposed based on optimizing the particle velocity optimization based on a square support carrier machine. A basic mechanical analysis was performed on the operator and the operator's tendency to change the driving force and the constant variation of the force of each joint when the operator was held was determined. The power of the operator was analyzed, and the material was determined to meet the strength requirements.

Data Availability

No data were used to support this study.

Conflicts of Interest

The authors declare that they have no conflicts of interest.

References

[1] B. Sprowl, "AI robotic arm gets experience cooking fried chicken and tater tots," *Unmanned Systems*, vol. 36, no. 8, p. 52, 2018.

[2] K. Ahlin, B. Joffe, A.-P. Hu, G. McMurray, and N. Sadegh, "Autonomous leaf picking using deep learning and visual-servoing," *IFAC-PapersOnLine*, vol. 49, no. 16, pp. 177–183, 2016.

[3] M. C. Cuervo, "Joint amplitude MEMS based measurement platform for low cost and high accessibility telerehabilitation: elbow case study," *Journal of Bodyward Movement Therapies*, vol. 21, no. 3, pp. 574–581, 2017.

[4] M. Farman, M. Al-Shaibah, Z. Aoraiath, and F. Jarrar, "Design of a three degrees of freedom robotic arm," *International Journal of Computer Applications*, vol. 179, no. 37, pp. 12–17, 2018.

[5] I. M. Ekaputra, J. D. Setiawan, and J. Setiawan, "Pengembangan wearable robotic arm input dan virtual instrument untuk pengendalian dan pemantauan lengan robot," *Jurnal Rekayasa Mesin*, vol. 8, no. 2, pp. 109–119, 2017.

[6] H. P. Jawale, A. Jaiswal, and K. N. Bhasme, "Design and analysis of three-axis cantilever type force sensor," *World Journal of Engineering*, vol. 16, no. 4, pp. 497–508, 2019.

[7] J. C. V. D. Noort, R. Verhagen, K. J. V. Dijk et al., "Quantification of hand motor symptoms in Parkinson's disease: a proof-of-principle study using inertial and force sensors," *Annals of Biomedical Engineering*, vol. 45, no. 10, pp. 2423–2436, 2017.

[8] G.-S. Kim, "Development of a wrist bending rehabilitation robot with a three-axis force sensor," *Journal of Sensor Science and Technology*, vol. 25, no. 1, pp. 27–34, 2016.

[9] C. Bals, "Toward a supply chain finance (SCF) ecosystem - proposing a framework and agenda for future research," *Journal of Purchasing and Supply Management*, vol. 25, no. 2, pp. 105–117, 2019.

[10] Y. Du and Q. Zhu, "Decentralized adaptive force/position control of reconfigurable manipulator based on soft sensors," *Proceedings of the Institution of Mechanical Engineers, Part I: Journal of Systems and Control Engineering*, vol. 232, no. 9, pp. 1260–1271, 2018.

[11] R. Azzi, R. K. Chamoun, and M. Sokhn, "The power of a blockchain-based supply chain," *Computers & Industrial Engineering*, vol. 135, no. SEP, pp. 582–592, 2019.

[12] S. Fldi, T. Horváth, F. Zieger et al., "A novel non-invasive blood pressure waveform measuring system compared to Millar applanation tonometry," *Journal of Clinical Monitoring and Computing*, vol. 32, no. 4, pp. 717–727, 2018.

[13] J. Wang, G. Zuo, J. Zhang et al., "Research on assist-as-needed control strategy of wrist function-rehabilitation robot," *Journal of Biomedical Engineering*, vol. 37, no. 1, pp. 129–135, 2020.

[14] A. Mancisidor, A. Zubizarreta, I. Cabanes, P. Bengoa, and J. H. Jung, "Kinematical and dynamical modeling of a multipurpose upper limbs rehabilitation robot," *Robotics and Computer-Integrated Manufacturing*, vol. 49, no. feb, pp. 374–387, 2018.

[15] S. Zhang, S. Guo, B. Gao et al., "Muscle strength assessment system using sEMG-based force prediction method for wrist joint," *Journal of Medical and Biological Engineering*, vol. 36, no. 1, pp. 121–131, 2016.

[16] G. I. Zamora-Gómez, A. Zavala-Río, D. J. López-Araujo, E. Nuño, and E. Cruz-Zavala, "An output-feedback global continuous control scheme with desired gravity compensation for the finite-time and exponential regulation of bounded-input robotic systems," *IFAC-PapersOnLine*, vol. 51, no. 22, pp. 108–114, 2018.

[17] Q. H. Wang, S. C. Wu, J. W. Liu, and J. R. Li, "Design of a 6-DOF force device for virtual assembly (FDVA-6) of mechanical parts," *Mechanics Based Design of Structures and Machines*, vol. 46, no. 5, pp. 567–577, 2018.

[18] G. Feng, Q. ChenKun, A Y Ren, and X. Zhao, "Hardware-in-the-loop simulation for the contact dynamic process of flying objects in space," *Science China Technological Sciences*, vol. 59, no. 8, pp. 1167–1175, 2016.

[19] Y. He, F. Zhang, M. Yang et al., "Design of tracking suspension gravity compensation system for satellite antenna deployable manipulator," *Jiqiren/Robot*, vol. 40, no. 3, pp. 377–384, 2018.

[20] Z. Zhu, J. Yuan, J. Song, and R. Cui, "An improving method for micro-G simulation with magnetism-buoyancy hybrid system," *Advances in Space Research*, vol. 57, no. 12, pp. 2548–2558, 2016.

[21] D. Lee, S. Lee, J. Park, and T. Seo, "Novel gravity compensation mechanism by using wire-winding," *Journal of Institute of Control, Robotics and Systems*, vol. 22, no. 9, pp. 733–737, 2016.

[22] P. Ni, W. Zhang, X. Zhu et al., "Learning an end-to-end spatial grasp generation and refinement algorithm from simulation," *Machine Vision and Applications*, vol. 32, no. 1, pp. 1–12, 2021.

[23] S. M. Farzam and A. A. Khan, "A novel Local Time Stepping algorithm for shallow water flow simulation in the discontinuous Galerkin framework - ScienceDirect," *Applied Mathematical Modelling*, vol. 40, no. 1, pp. 70–84, 2016.

[24] N. Tajbakhsh, J. Y. Shin, S. R. Gurudu et al., "Convolutional neural networks for medical image analysis: full training or fine tuning?" *IEEE Transactions on Medical Imaging*, vol. 35, no. 5, pp. 1299–1312, 2016.

[25] Z. Z. Quancong, Z. Wu, Z. Cao, Q. Jiang, and Z. Hua, "Simulation and heat exchanger network designs for a novel single-column cryogenic air separation process," *Chinese Journal of Chemical Engineering*, vol. 27, no. 07, pp. 47–58, 2019.

Research Article

Blended Teaching Design of College Students' Mental Health Education Course Based on Artificial Intelligence Flipped Class

Shan Shan[1] **and Yu Liu** [2]

[1]*College of Teacher Education, Harbin University, Harbin 150086, Heilongjiang, China*
[2]*School of Control Engineering, Chengdu University of Information Technology, Chengdu 610000, Sichuan, China*

Correspondence should be addressed to Yu Liu; liuyu123@cuit.edu.cn

The current education methods are mostly based on test-oriented education and rarely really care about the content of students' concerns, and flipped psychological education methods have appeared in some areas. The main purpose of this thesis is to combine artificial intelligence and flipped classroom psychology. This article mainly introduces the characteristics of artificial intelligence and the definition of flipped classroom. What are the advantages of the intelligent teaching platform compared to traditional teaching? This article selects key 1 class, key 2 class, key 3 class, and key 4 class from the students of our school. Groups A1 and B1 conduct a semester of artificial intelligence combined with the concept of flipped classroom psychology. Groups A2 and B2 teach students in accordance with traditional teaching. The experimental results show that the proportion of groups A1 and B1 increased by 8.2% and 8.14%. The midterm and final average scores of groups A1 and B1 are 10.87, 7.2, 14.13, and 12.2 points higher than those of groups A2 and B2, and their scores have increased by 10.3% and 7.02%, 12.4%, and 11.9%. The mental health education course effect of artificial intelligence and flipped classroom psychology can more stimulate students' interest and promote the improvement of students' performance through autonomous learning.

1. Introduction

Teachers can understand students' psychological state through their performance in class and after class and give them some psychological guidance, which is helpful to the improvement of students' academic performance. The curriculum of the talent training program complements each other. However, in actual teaching, teaching information between different courses is rarely interoperable, and the awareness of curriculum group construction is weak and superficial, resulting in loose curriculum relations. At the same time, students' knowledge transfer ability is not good; the possibility of independent integration of courses and forming a good three-dimensional cognitive structure is low. Therefore, it is necessary to integrate the curriculum, gradually break through the curriculum barriers, build a bridge between the previously separate courses and courses, and use more scientific

teaching models to guide and assist students to effectively build a professional thinking system.

Lu et al. not only developed the next generation of artificial intelligence technology but also developed a new concept of general intelligent cognitive technology beyond AI. Specifically, we plan to develop an intelligent learning model called brain intelligence (BI), which can generate new ideas without experiencing events by using artificial life with imaginative functions. We will also show the developed Bi intelligent learning mode in the fields of automatic driving, precision medical treatment, and industrial robot [1, 2]. Raza and Khosravi make a comprehensive and systematic literature review on the short-term load forecasting technology based on artificial intelligence. The main purpose of this study is to review, identify, evaluate, and analyze the performance and research gaps of load forecasting model based on artificial intelligence (AI). The accuracy of the neural network prediction model depends on the number of parameters such as

the structure of the prediction model, input combination, network activation function, training algorithm, and other exogenous variables that affect the input of the prediction model [3]. Xiao proposed a new multisensor data fusion method based on evidence-based confidence measurement and confidence entropy. He designed a new Belief Jensen-Shannon divergence to measure the ddifference and the degree of conflict between the evidence, and then through the obtained credibility, the reliability of evidence is indicated [4]. The array consists of quartz crystal microbalances (qcms), each of which is coated with different polymeric materials. The first method uses the decision tree classification algorithm to determine the minimum number of features needed to correctly classify training data. The second method uses the hill-climbing search algorithm to search the optimal minimum feature set in the feature space, so as to maximize the performance of neural network classifier. In order to reduce computation time, we also study the value of simple statistical processes that can be integrated into search algorithms [5]. The advantages and limitations of the two methods are discussed. Flexible pressure sensors based on organic materials combine the unique advantages of flexibility and low cost and have broad application prospects in artificial intelligence systems and wearable medical devices [6]. Zang et al. focus on the basic principles of flexible pressure sensors and then explore several key concepts of functional materials and optimized sensing devices to achieve practical applications. In addition, this study also discusses the development direction of self driving, transparent and implantable pressure sensing devices [7].

Elhoseny et al. produced four online video clips on endometrial hyperplasia, cervical dysplasia, adnexal mass assessment, and ovarian cancer, instructing students to watch these videos before active learning in class [8]. This study uses the open classroom learning management system to establish an open classroom learning activity management platform. Students are satisfied with both aspects of the flipped course. In addition, we also compared the National Board of Medical Examination (NBME) lectures on gynecological oncology before and after the implementation of the course and students' comprehensive performance on gynecological oncology problems [9]. Flipped classroom is a learner centered teaching method. Gilboy explains how to implement the flipped classroom and describes students' views on two undergraduate nutrition courses. The process described in the report has been successful for both teachers and students [10]. Peterson shows cumulative test scores and student evaluation data for two parts of my recent statistics course: a traditional lecture ($n = 19$) and a flipped classroom ($n = 24$). Independent sample t test shows that students in flipped classroom scored one letter higher than their classmates in the final exam [11]. Tsai et al. used a simulation method to examine the relationship between benchmark tests and OKP, and how the knowledge inertia in benchmark tests affects OKP in different network structures. Their results show that fast benchmarking (low knowledge inertia) and moderate mutual learning can produce higher short-term OKP; slow benchmarking (high knowledge inertia) and moderate mutual learning can achieve higher long-term OKP [12]. The main outcome indicators are the final course performance and satisfaction with the course [13].

This paper mainly introduces the characteristics of artificial intelligence and the definition of flipped classroom. Based on artificial intelligence and flipped classroom, the hybrid teaching design of mental health education course can be realized through intelligent teaching platform. What advantages does intelligent teaching platform have compared with traditional teaching? Most of the students' interest in learning has improved in the entertainment classroom, which shows that the research method of this article is effective. For the study of other subjects, you can get experience from this article.

2. Artificial Intelligence and Flipped Classroom

2.1. Artificial Intelligence. Artificial intelligence is the research and development of the theory, technology, and application system for simulating, expanding, and expanding human intelligence. It is a new technology science with different understanding and definition in different fields. The basic definition of artificial intelligence is to study how to use computer to simulate the human brain's reasoning, identification, understanding, participation, learning, thinking, and problem-solving thinking activities [14]. These unique thinking activities are in the past, only human beings can do it, and its core idea is to make the computer performance more perfect and comprehensive development [15].

Since the introduction of artificial intelligence, people's traditional concepts have been gradually changed, and the level of human knowledge and humanistic education has been improved. In the history of education development, the elimination of the old and the introduction of new technologies often provide a powerful driving force for educational reform, making teaching more convenient and efficient and making education more fair and popular. The teaching software with artificial intelligence can look, listen, speak, and learn like human beings and even understand and feed back the user's emotions or emotions, so that users can communicate with the computer naturally and fluently through language, text, and other ways, so as to realize human-computer interaction [16].

As a computer technology simulating human intelligence, artificial intelligence has the following characteristics:

(1) Artificial intelligence has the ability of learning. It is also an important symbol to judge whether a machine has intelligence. This feature can make intelligence automatically acquire new knowledge, improve practical ability, and adapt to the changing environment. Human beings are some machine learning methods developed according to their own learning ability.

(2) Artificial intelligence needs to have the ability of perception. This kind of intelligent machine perception requires the perception ability similar to human beings [17], that is, to transmit information to the outside world through the senses of vision, hearing, touch, and smell. Its main purpose is to

improve the perception ability of intelligent machine and realize human-computer interaction.

(3) Artificial intelligence has a certain thinking ability. The artificial intelligence system can record the external information sensed by the sense organs and store the information by itself. In the process of perceiving information, it involves its own basic skills, such as knowledge expression and reasoning. Simulating the human thinking process is the way of intelligent thinking.

(4) Artificial intelligence needs behavioral ability because the perception of the artificial intelligence system is used as the input function module; then the behavior ability of the artificial intelligence system is taken as the output function module. For example, intelligent control is the combination of artificial intelligence technology and traditional automatic control technology, which is unnecessary. In the case of artificial intervention, all have artificial intelligence. The system can be completed independently.

2.2. Flipped Classroom. Flipped classroom originated from Woodland Park High School in the United States. Colorado is located in a remote area. Due to the limitation of living conditions, local students often cannot get to school on time or even miss classes for a long time. In order to help students finish their studies on time, two teachers of the school first thought of uploading teaching videos to the Internet so that students can watch the learning process by themselves and help them master the teaching progress in time [18].

At present, the flipped classroom mode is further defined, which is teachers making video courseware in advance [19], students study at home before class, teachers and students communicate on the problems in the video in class, and complete a variety of effective classroom practice teaching forms. In the flipped classroom teaching mode, teachers are no longer bound by textbooks and courseware and have more energy and time to know the teaching progress, explain, and learn specific problems. The flipped classroom teaching mode does not give the learning task to students but emphasizes the dominant position of teachers. The teaching process of flipped classroom is inseparable from teachers. Teachers are always ready to help students answer questions. Compared with traditional teaching mode, the flipped classroom model has four characteristics:

(1) The change of the roles of teachers and students: under the flipped classroom teaching mode, the teacher transforms from the knowledge transmitter to the student's learning instructor and promoter. Students, as "listeners" and passive receivers of teachers' explanation in class, are transformed into autonomous learners. Flipped classroom mode is a teaching process in which students are the main body of learning.

(2) Teaching process: the flipped classroom teaching process is that students learn content in advance and finish their homework in class. In other words, in the flipped classroom teaching mode, the absorption and understanding of knowledge is completed by students watching the teaching video before class, and the digestion of knowledge is completed through the discussion [12].

(3) Teaching environment: the flipped classroom teaching mode provides a good learning environment for students; they no longer rely on teachers to give lectures in class, but through the teaching video, teaching media and other courseware provided by teachers for autonomous learning before class [15]. For the weak learning ability of students, they can read the content of this class in advance before class, and then the class can follow the teacher's explanation. For students with strong learning ability, when teachers explain what they have understood, they can learn more about what they do not understand. For these two types of learning, you can adjust your learning progress according to your own learning situation.

(4) Teaching resources: the flipped classroom teaching model is that all teachers unite and adopt unified teaching to formulate teaching plans, study, discuss, and record video together and realize the sharing of educational resources for the whole grade. For a specific topic, the teaching video is usually about 10–20 minutes. Through the collective lesson preparation, we can strengthen the communication and communication between teachers and make the recorded course content, difficulty, and class type design more perfect. Teaching resources are open to all teachers and students.

2.3. Hybrid Teaching of Artificial Intelligence and Flipped Classroom. Artificial intelligence itself can not have an impact on teaching, but it can be transformed into a medium or tool used by teachers to play a role in education and teaching. The artificial intelligence teaching platform uses big data, cloud computing, and other technologies to realize the comprehensive docking function of teachers, students, and parents [20].

With the advent of Internet plus era and the rapid development of artificial intelligence, many open and intelligent teaching platforms such as Tencent classroom have emerged. Most of the functions of these platforms include video recording, teacher-student interaction, precise teaching, after-school testing, and other functions [21, 22]. In order to promote the progress of teaching mode and teaching means and improve the teaching quality, more and more intelligent teaching platforms are used by teachers, which solves the problems of poor communication and low interaction in the classroom and is recognized by teachers, students, and parents [23]. The intelligent teaching platform has the following characteristics.

2.3.1. Accuracy. With the continuous increase of multimedia demand in schools and the rapid development of learning

analysis technology, adaptive learning technology has developed into a mature and effective learning technology. It can automatically adapt to the learning situation of different students [24, 25]. Based on the theory of knowledge space, it decomposes knowledge points and "scores". That is, the simple content of learning, the degree of suffering, and the degree of differentiation predict the learning ability of students, matche learning resources, reduce the repetition rate of students, and accelerate the progress of education [26, 27].

2.3.2. Based on Data.
The intelligent education platform uses deep network technology to realize students' efficient learning, continuously collects various data during the students' learning process, and records every progress. In the communication, the intelligent education platform will record one by one and automatically generate a data analysis chart based on the recorded data. Through the intelligent teaching platform, students can browse the records of the interactive process, discover their own shortcomings, and view insufficient knowledge points [28, 29]. Teachers can analyze the habits of users through the data recorded by the intelligent education platform and then help students make learning plans suitable for students, thereby improving students' academic performance [30].

2.3.3. Sharing.
Through cloud computing, the intelligent teaching platform can share teachers' lesson preparation resources, recorded teaching videos, and students' learning

materials in the cloud. Students can obtain the materials and teaching videos that they do no't know through the intelligent teaching platform and carry out independent learning. The data generated in the learning process of students in the intelligent teaching platform are saved in the cloud, which can be guaranteed to watch at any time. Teachers can view the data of students' learning process and analyze students' learning habits in the intelligent teaching platform [31, 32].

2.4. University Student Model in Artificial Intelligence Teaching

2.4.1. Student Learning Interest Model.
This article will use the vector space model to represent the learning interest model. In this representation model, students' interest is modeled by recording the learning resources corresponding to student browsing, learning, testing, and other behaviors, and the form of learning resources is defined by feature vectors:

$$Q = \{(u_1, v_1, w_1), (u_2, v_2, w_2), (u_n, v_n, w_n)\}, \tag{1}$$

where u_i is a feature item that can represent learning resources; v_i is the weight of the feature item u_i in Q; and w_i is the category of the feature item. Taking into account the difference in the length of interest, the feature vector is improved, the construction of the learning interest model is defined as

$$\text{Lif} = \left\{ \left(u_1, V_1^S, V_1^L, t_1, t y_1, \text{parent}_1 \right), \ldots, \left(u_n, V_n^S, V_n^L, t_n, t y_n, \text{parent}_n \right) \right\}, \tag{2}$$

where V_1^S represents the short-term interest weight of the feature item; V_1^L represents the long-term interest weight of the feature item; t_i is the update time of the long-term interest weight; $t y_i$ is the category to which the feature item belongs; and parent_1 is the parent feature item of the feature item.

Short-term interest represents students' interest in a relatively short period of time, and its calculation formula is shown in the following formula:

$$V_1^S = \frac{1}{N} \sum_{j=1}^{N} \frac{1}{S} \sum_{k=1}^{S_j} v(u_i, p_k), \tag{3}$$

where N is the statistical time size; S_j is the number of students browsing system pages on the jth day; $v(u_i, p_k)$ is the weight of the feature item in the current page feature vector p_k, and the calculation formula is as follows:

$$v(u_i, p_k) = \frac{f(u_i, p_k) \times \log((m/mu_i) + 0.01)}{\sqrt{\sum_{p_k}^{u_i} u f(u_i, p_k) \times \log((m/mu_i) + 0.01)}} \times \text{const}(p_k). \tag{4}$$

where mu_i is the number of web pages where the feature item appears, and $\text{const}(p_k)$ is an additional parameter of

learners' behavior in p_k. The value formula ofconst(p_k) is obtained from the acquisition of learning interest information as shown in the following formula:

$$\text{const}(p_k) = \begin{cases} 0, & \frac{\text{timep}_k}{\text{wnp}_k} < \text{TH}, \\ 1, & \frac{\text{timep}_k}{\text{wnp}_k} \geq \text{TH}, \\ 2, & \text{save, download, print, mark.} \end{cases} \tag{5}$$

Among them, timep_k is the time spent by learners to browse the page; wnp_k is the total number of words on the page or the length of the page content; TH is the threshold; saving, downloading, printing, and collecting are regarded as one type of behavior; and any one of them is taken only once, without stacking.

Long-term interest is a student's learning interest over a long period of time and generally does not change easily, so it is also the main data source for estimating students' learning interest. However, the interest of students is not permanent. It will change and forget with the passage of time and different levels of students' knowledge. Of course, new

long-term learning interests will also appear as a short-term interest continues to increase [33, 34]. When assessing long-term interests, time and short-term interests must be integrated, as shown in the following formula:

$$V_i^l = V_i^{l-\text{pre}} \times e^{-(\ln 2/h \times l^{\text{cur}})(d-d_i)+V_i^S}, \tag{6}$$

where -pre is the weight of the learner's long-term learning interest before the update and $e^{-(\ln 2/h \times l^{\text{cur}})(d-d_i)}$ is the forgetting factor that indicates that the learning interest gradually weakens with time.

2.4.2. Student Cognitive Ability Model. The input of students' relevant information and their behavior and performance during the test are the key information sources in the CoFSM modeling process of the cognitive ability model [35, 36].

(1) Vector Calculation Self-Built Test Results. There are N types of test questions for each knowledge item. When multiple knowledge points are examined, a set of simulated exercises will be formed using the unitized knowledge domain triple random automatic question-building algorithm [37]. After the student has tested a certain type of question multiple times, it will be recorded in the test result table. Suppose that after the student has tested the mental health type question multiple times, the given mental health question cognitive vector is

$$AB_i = \{ab(1), ab(2), ab(3), ab(4), ab(5), ab(6)\}. \tag{7}$$

Then, the correct usage rate of knowledge point ID = 1 in mental health questions is R (a1):

$$R(p1) = \frac{R1(1)}{(R1(1) + R1(-1))}. \tag{8}$$

The obtained cognitive ability vector is QNi:

$$ANi = R(p1) * \text{Abi}. \tag{9}$$

Considering N types of questions, the student's cognitive ability mastery vector AN can be obtained when the test knowledge point ID = 1:

$$AN = \{AN1, AN2, \ldots, ANn\}. \tag{10}$$

Add the weights set by various question types to comprehensively calculate the students' cognitive ability V for this knowledge point:

$$V = WT * AN. \tag{11}$$

Among them, WT is the weight vector of various question types.

(2) Vector Recording Expert Test Result. Suppose the student tests the multiple choice question type, and calculate the correct rate of the six cognitive abilities of the student in the multiple choice question type according to the recorded vector table and defines it as vector i.

It is the correct rate of a certain cognitive ability, calculated as

$$p_i = \frac{R_{ij}(1)}{R_{ij}(1) + R_{ij}(-1)}, \tag{12}$$

where the number of single-choice questions in the p_i test and $R_{ij}(1)$ is the total number of correct answers to the t-th cognitive ability during this test; on the contrary, $R_{ij}(-1)$ is the total number of incorrect answers.

When testing knowledge points in mental health subjects, the general question types include multiple choice questions, true or false questions, fill-in-the-blank questions, translation questions, and writing questions. Various questions are obtained for each question type combined with the abovementioned computational cognitive ability method [38, 39]. The matrix G of various cognitive abilities:

$$G = \begin{pmatrix} p_{11} & \cdots & p_{16} \\ \cdots & \cdots & \cdots \\ p_{51} & \cdots & p_{56} \end{pmatrix}. \tag{13}$$

Add the weight vector B of each question type test and calculate the final cognitive ability evaluation result obtained by the student after the test as V:

$$V = C * G = (V_1, V_2, V_3, V_4, V_5, V_6). \tag{14}$$

Calculate the comprehensive cognitive ability M obtained by the students during this test:

$$M = \sum_{i=1}^{6} V_i * A_i. \tag{15}$$

(3) Comprehensive Calculation of Cognitive Ability. Students choose the form of self-built question bank in unit study to get cognitive ability V and test in expert question bank to get cognitive ability M. Finally, the cognitive ability vector W of this knowledge point is

$$W = \lambda_1 * V + \lambda_2 * M, \tag{16}$$

where λ_1 and λ_2 are self-built question bank and expert question bank test to obtain the weight coefficient of cognitive ability in the final cognitive ability.

3. Experimental Design

3.1. Experimental Data Collection. This paper selects key 1 class, key 2 class, key 3 class, and key 4 class from the students of our school. The size of these 4 classes is 53–55. The test scores of these classes are similar, which has certain comparative significance. Divide key 1 class, key 2 class, key 3 class, and key 4 into 2 groups randomly, and divide into artificial intelligence and flipped classroom group (key 1 class and key 3 class) and general teaching group (key 2 class and key 4 class)). In order to facilitate identification, the key group 1 and key group 3 are marked as groups A1 and A2. Key 2 class and key 3 class are marked as B1 and B2 groups.

3.2. Experimental Steps. The steps of the course design are as follows:

(1) First explain the mixed teaching concept of artificial intelligence and flipped classroom psychology with groups A1 and B1, so that students are fully prepared to accept the new hybrid teaching.

(2) The teacher prepares the mental health education textbook, then records the teaching video for 10–20 minutes, uploads it to the intelligent teaching platform, and explains clearly how to log in to the intelligent teaching platform and find the teaching video for learning.

(3) The recorded teaching video will be equipped with a test about the content of teaching video, and the test questions are about 5. The test can make students understand the content of the teaching video deeply and can also detect whether the students have watched the teaching video carefully.

(4) In order to reflect the students' problems in watching the teaching video, the last question of the test is that is there anything you do not understand? Then, the teacher summarizes the content of the last question and answers the students' questions while giving a lecture on the other day. Increasing the interaction between students and teachers can stimulate students' interest and promote their learning.

(5) According to the students' learning process records and students' performance in the classroom, teachers can analyze students' learning behavior and make better learning plans for students.

(6) In a certain period of time, teachers upload a big test on the intelligent teaching platform to test the students' learning and mastering situation in this period of time, analyze the students' academic achievements, and make the next stage of learning curriculum design for students. For students with poor learning ability, teachers should be more targeted to guide students, to prevent students from falling behind in the learning process. Students can also stage the line of the test, to adjust their learning plan in time, for their own bad knowledge to review and promote students' autonomous learning; general education group: according to the previous teaching method.

4. Analysis of Experimental Results

4.1. Comparison of Mental Health Education Learning Attitude. The likes of each group in the study are shown in Figure 1.

It can be seen from the figure that, after this experiment, the acceptance in each group has been improved. The combination has increased the fun of the classroom and further enhancing students' acceptance, which not only improves the quality of education but also enhances the culture. Communication brings positive meaning.

4.2. Comparison of Mental Health Education Course Scores of 24 Classes in Midterm Examination. The midterm

examination results of groups A1 and A2, B1 and B2 are shown in Table 1.

As shown in Table 1 and Figure 2, the curriculum reform takes school-enterprise cooperation as the motive force and real projects as the link and integrates mental health education course in the integrated curriculum group. The project-related knowledge points and skill points are organized in an orderly manner according to the development process, and we combined teachers' macro-thinking advantages, the experience of the company's personnel, the technical advantages, and the support of the company's equipment escort the project, fully linking both inside and outside of class and mobilizing the students' subjective initiative, so that students can gradually understand and adapt to the business operation mode and experience the industry during the project practice. Let students have more professional knowledge, cultivate their professional thinking ability, and lay a solid foundation for their career.

4.3. Comparison of Mental Health Education Course Scores in Final Examination of 4 Classes. The final examination results of groups A1 and A2, B1 and B2 are shown in Table 2.

As shown in Figure 3, the industry applicability of graduates is maximized through the improvement of artificial intelligence talent training programs, the construction of internal and external training bases, and the reformation and deepening of curriculum teaching. Content settings that are out of touch with industry development will only make the training of applicable talents more effective. The best way to obtain local industry development information is for teachers to go deep into the local area.

4.4. Evaluation of Mental Health Education Course Learning Effect. Although the final examination scores can show the learning effect of most students at a certain stage, it is only because a single test score is not scientific in determining a person's long-term academic performance. Artificial intelligence and flipped classroom psychology concept is a form of teaching; it does not want to judge a student's cultivation according to the examination results of a student. Instead, it should pay attention to the performance of students in each learning link, rather than in the final examination with partial generality.

In this paper, five people were randomly selected from group A1 and group B1 for evaluation. The evaluation scheme was divided into four stages. While retaining the final part is to cater to the school's unified final assessment system, the students can have a good review and summary of the previous learning content at the end of the semester. Record the students' three learning activities: classroom performance, extracurricular performance, and each integral item of intelligent teaching platform, as shown in Figure 4.

As can be seen from Figure 4, the score of student J's three learning activities is the highest among 10 students. At the same time, from the beginning of school to the end of the semester, student J made the most progress. J thinks he has made full use of the teacher's resources and will watch the
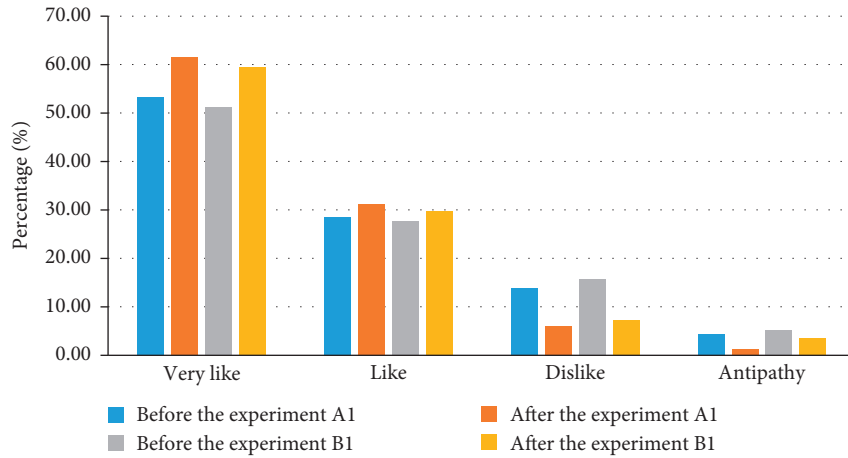
FIGURE 1: Comparison of cultural acceptance of key groups.

TABLE 1: Midterm examination results of 4 classes.

Group	Class size	Number of people					Average
		Above 130 points	110–130 points	100–110 points	90–100 points	Less than 90 points	
A1	55	10	20	15	7	3	115.65
A2	54	6	15	16	11	6	104.78
B1	54	9	19	12	10	4	109.65
B2	55	5	15	21	10	5	102.45
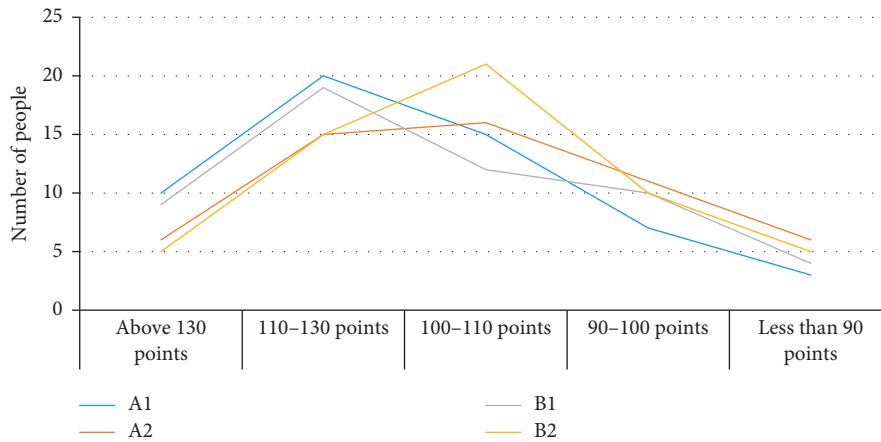
FIGURE 2: The number of students in different classes in different sections.

TABLE 2: The final mental health education course scores of 4 classes.

Group	Class size	Number of people					Average
		Above 130 points	110–130 points	100–110 points	90–100 points	Less than 90 points	
A1	55	12	20	17	5	1	118.78
A2	54	7	14	18	11	4	104.65
B1	54	11	19	15	7	2	116.65
B2	55	5	15	20	10	5	102.45

learning videos repeatedly. She also asked that the course resources and videos after the teacher's lecture could also be put on the intelligent teaching platform, so that she could learn the rest of the courses during the holiday. Student *A* ranked second in the class in all academic achievements. She believes that she has made great progress in mental health
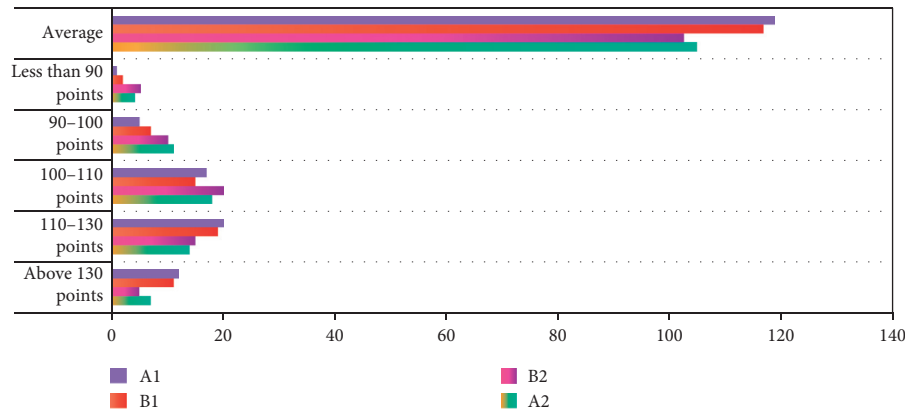
FIGURE 3: The final mental health education course scores of 4 classes.
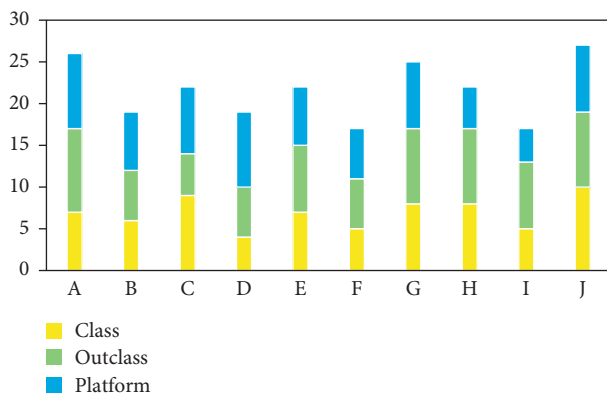
FIGURE 4: Student's points in three learning activities.

education course this semester, and she would like to continue the mixed teaching with the concept of artificial intelligence and flipped classroom psychology in the next semester. It is worth mentioning that, although J and A are the top two students in the class, J did well in the final exam, but A did not. The test results are not the only standard to measure the learning effect. The test results are one-sided and cannot detect all the learning situations. This is especially true for language learning, which requires a comprehensive assessment scheme.

After a semester of artificial intelligence and flipped classroom psychology concept, the artificial intelligence and flipped classroom psychology concept can stimulate students' interest in learning mental health education course more than traditional teaching.

5. Conclusion

Artificial intelligence is a sign of the maturity of innovation and entrepreneurship education. In the process of the development of innovation and entrepreneurship practice, each laboratory, instructor team, and student organization have established and formed their own innovation and entrepreneurship practice resources. On this basis, in the college, according to the relevant national policies and regulations, the existing resources are integrated to form an integrated innovation and entrepreneurship practice

platform structure system. The key to the implementation of the technological innovation-driven development strategy lies in talents. Innovative development puts forward new and higher requirements for the cultivation of talents in higher education. The Ministry of Education has continuously issued a series of requirements and measures to strengthen the construction of the innovation and entrepreneurship education curriculum system, extensively carry out innovation and entrepreneurship practice activities, improve the quality standards of talent training, cultivate the spirit and ability of innovation and entrepreneurship, and strengthen the practical ability.

This paper mainly introduces the characteristics of artificial intelligence and the definition of flipped classroom. Based on artificial intelligence and flipped classroom, the hybrid teaching design of mental health education course can be realized through intelligent teaching platform. What advantages does intelligent teaching platform have compared with traditional teaching? The fundamental purpose of the innovation and entrepreneurship practice platform is to cultivate and improve students' engineering practice ability, innovative thinking, and entrepreneurial ability. It should be an innovative, open, collaborative and shared innovation and entrepreneurship project incubation platform.

Colleges and universities are the base for constructing innovation and entrepreneurship education for college students, as well as the main place to deepen education reform, innovate curriculum system, and strengthen practical education. The results of the mixed teaching of artificial intelligence and flipped classroom psychology may have some limitations.

Data Availability

The data that support the findings of this study are available from the corresponding author upon reasonable request.

Conflicts of Interest

The authors declare that they have no conflicts of interest regarding the publication of the research article.

Acknowledgments

References

[1] H. Lu, Y. Li, M. Chen, H. Kim, and S. Serikawa, "Brain intelligence: go beyond artificial intelligence," *Mobile Networks and Applications*, vol. 23, no. 2, pp. 368–375, 2017.

[2] S. Wan, Z. Gu, and Q. Ni, "Cognitive computing and wireless communications on the edge for healthcare service robots," *Computer Communications*, vol. 149, 2020.

[3] M. Q. Raza and A. Khosravi, "A review on artificial intelligence based load demand forecasting techniques for smart grid and buildings," *Renewable and Sustainable Energy Reviews*, vol. 50, pp. 1352–1372, 2015.

[4] F. Xiao, "Multi-sensor data fusion based on the belief divergence measure of evidences and the belief entropy," *Information Fusion*, vol. 46, pp. 23–32, 2019.

[5] Y. Chen, W. Zheng, W. Li, and Y. Huang, "Large group Activity security risk assessment and risk early warning based on random forest algorithm," *Pattern Recognition Letters*, vol. 144, 2021.

[6] Z. Lv, A. Halawani, S. Feng, R. Shafiq Ur, and H. Li, "Touchless interactive augmented reality game on vision-based wearable device," *Personal and Ubiquitous Computing*, vol. 19, no. 3-4, pp. 551–567, 2015.

[7] Y. Zang, F. Zhang, C. A. Di et al., "Advances of flexible pressure sensors toward artificial intelligence and health care applications," *Materials Horizons*, vol. 2, no. 2, pp. 25–59, 2015.

[8] M. Elhoseny, G.-B. Bian, S. K. Lakshmanaprabu, K. Shankar, A. K. Singh, and W. Wu, "Effective features to classify ovarian cancer data in internet of medical things," *Computer Networks*, vol. 159, pp. 147–156, 2019.

[9] H. Morgan, K. Mclean, C. Chapman, J. Fitzgerald, A. Yousuf, and M. Hammoud, "The flipped classroom for medical students," *The Clinical Teacher*, vol. 12, no. 3, pp. 155–160, 2015.

[10] M. B. Gilboy, S. Heinerichs, and G. Pazzaglia, "Enhancing student engagement using the flipped classroom," *Journal of Nutrition Education and Behavior*, vol. 47, no. 1, pp. 109–114, 2015.

[11] D. J. Peterson, "The flipped classroom improves student achievement and course satisfaction in a statistics course," *Teaching of Psychology*, vol. 43, no. 1, pp. 10–15, 2015.

[12] S. B. Tsai, W. Wu, S. Ma, C. H. Wu, and B. Zhou, "Benchmarking, knowledge inertia, and knowledge performance in different network structures," *Enterprise Information Systems*, vol. 14, 2019.

[13] S. Whillier and R. P. Lystad, "No differences in grades or level of satisfaction in a flipped classroom for neuroanatomy," *Journal of Chiropractic Education*, vol. 29, no. 2, pp. 127–133, 2015.

[14] Z. Lv, H. A. N. Yang, K. S. Amit, m. Gunasekaran, and l. haibin, "Trustworthiness in industrial IoT systems based on artificial intelligence," *IEEE Transactions on Industrial Informatics*, vol. 16, 2020.

[15] N. N. Hurrah, S. A. Parah, N. A. Loan, J. A. Sheikh, M. Elhoseny, and K. Muhammad, "Dual watermarking framework for privacy protection and content authentication of multimedia," *Future Generation Computer Systems*, vol. 94, pp. 654–673, 2019.

[16] Z. Lv, "Virtual reality in the context of internet of things," *Neural Computing and Applications*, vol. 32, pp. 1–10, 2019.

[17] J. Yang, C. Wang, B. Jiang, H. Song, and Q. Meng, "Visual perception enabled industry intelligence: state of the art, challenges and prospects," *IEEE Transactions on Industrial Informatics*, vol. 17, no. 3, p. 2204, 2021.

[18] X. Yuan, D. Li, D. Mohapatra, and M. Elhoseny, "Automatic removal of complex shadows from indoor videos using transfer learning and dynamic thresholding," *Computers & Electrical Engineering*, vol. 70, pp. 813–825, 2018.

[19] S. Ding, S. Qu, Y. Xi, and S. Wan, "A long video caption generation algorithm for big video data retrieval," *Future Generation Computer Systems*, vol. 93, pp. 583–595, 2019.

[20] X. Li, H. Jianmin, B. Hou, and P. Zhang, "Exploring the innovation modes and evolution of the cloud-based service using the activity theory on the basis of big data," *Cluster Computing*, vol. 21, no. 1, pp. 907–922, 2018.

[21] Q. Wang and P. Lu, "Research on application of artificial intelligence in computer network technology," *International Journal of Pattern Recognition and Artificial Intelligence*, vol. 33, no. 5, p. 1959015, 2019.

[22] R. Polikar, R. Shinar, L. Udpa et al., "Artificial intelligence methods for selection of an optimized sensor array for identification of volatile organic compounds," *Sensors & Actuators B Chemical*, vol. 80, no. 3, pp. 243–254, 2015.

[23] N. Nandhakumar and J. K. Aggarwal, "The artificial intelligence approach to pattern recognition—a perspective and an overview," *Pattern Recognition*, vol. 18, no. 6, pp. 383–389, 2015.

[24] P. Yeaton, R. J. Sears, T. Ledent et al., "Discrimination between chronic pancreatitis and pancreatic adenocarcinoma using artificial intelligence-related algorithms based on image cytometry-generated variables," *Cytometry*, vol. 32, no. 4, pp. 309–316, 2015.

[25] S. Makridakis, "The forthcoming Artificial Intelligence (AI) revolution: its impact on society and firms," *Futures*, vol. 90, pp. 46–60, 2017.

[26] F. Goyache, J. J. Del Coz, J. R. Quevedo et al., "Using artificial intelligence to design and implement a morphological assessment system in beef cattle," *Animal Science*, vol. 73, no. 1, pp. 49–60, 2016.

[27] J. Hill, W. Randolph Ford, and I. G. Farreras, "Real conversations with artificial intelligence: a comparison between human-human online conversations and human-chatbot conversations," *Computers in Human Behavior*, vol. 49, pp. 245–250, 2015.

[28] J. J. Ye, "Artificial intelligence for pathologists is not near- it is here: description of a prototype that can transform how we practice pathology tomorrow," *Archives of Pathology & Laboratory Medicine*, vol. 139, no. 7, pp. 929–935, 2015.

[29] S. Khokhar, A. A. B. Mohd Zin, A. S. B. Mokhtar, and M. Pesaran, "A comprehensive overview on signal processing and artificial intelligence techniques applications in classification of power quality disturbances," *Renewable and Sustainable Energy Reviews*, vol. 51, pp. 1650–1663, 2015.

[30] R. Liu, B. Yang, E. Zio, and X. Chen, "Artificial intelligence for fault diagnosis of rotating machinery: a review," *Mechanical Systems and Signal Processing*, vol. 108, pp. 33–47, 2018.

[31] A. F. Chen, A. C. Zoga, and A. R. Vaccaro, "Point/counterpoint: artificial intelligence in healthcare," *Healthcare Transformation*, vol. 2, no. 2, pp. 84–92, 2017.

[32] S. A. Harrington, M. V. Bosch, N. Schoofs, C. Beel-Bates, and K. Anderson, "Quantitative outcomes for nursing students in a flipped classroom," *Nursing Education Perspectives*, vol. 36, no. 3, pp. 179–181, 2015.

[33] N. T. T. Thai, B. De Wever, and M. Valcke, "The impact of a flipped classroom design on learning performance in higher education: looking for the best "blend" of lectures and guiding questions with feedback," *Computers & Education*, vol. 107, pp. 113–126, 2017.

[34] M. Eaton, "The flipped classroom," *The Clinical Teacher*, vol. 14, no. 4, pp. 301-302, 2017.

[35] E. Blair, C. Maharaj, and S. Primus, "Performance and perception in the flipped classroom," *Education and Information Technologies*, vol. 21, no. 6, pp. 1465–1482, 2016.

[36] S. E. Park and T. H. Howell, "Implementation of a flipped classroom educational model in a predoctoral dental course," *Journal of Dental Education*, vol. 79, no. 5, pp. 563–570, 2015.

[37] X. Li, "The construction of intelligent English teaching model based on artificial intelligence," *International Journal of Emerging Technologies in Learning (iJET)*, vol. 12, no. 12, p. 35, 2017.

[38] X. Research, "On the intelligent English multimedia teaching resources based on the data mining," *International English Education Research: English Version*, vol. 2019, no. 2, pp. 50–52, 2019.

[39] Y. Yu, F. Li, S. Zhao et al., "Virtual experiment method for MOOC to solve teaching practice skills and difficult points," *Control & Intelligent Systems*, vol. 47, no. 2, pp. 77–82, 2019.

Research Article

Robotic Arm Control System Based on AI Wearable Acceleration Sensor

Liang Chen (iD),[1] **Hanxu Sun,**[1] **Wei Zhao,**[2] **and Tao Yu**[3]

[1]*School of Automation, Beijing University of Posts and Telecommunications, Beijing 100876, China*
[2]*School of Information Engineering, Beijing Institute of Graphic Communications, Beijing, China*
[3]*College of Mechanical Engineering and Automation, Liaoning University of Technology, Jinzhou, Liaoning, China*

Correspondence should be addressed to Liang Chen; chenliang968@bupt.edu.cn

The position of mechanical arm in people's life is getting higher and higher. It replaces the function of human arm, moving and moving in space. Generally, the structure is composed of mechanical body, controller, servo mechanism, and sensor, and some specified actions are set to complete according to the actual production requirements. The manipulator has flexible operation, good stability, and high safety, so it is widely used in industrial automation production line. With the development of science and technology, many practical production requirements for the function of the manipulator are more and more refined, especially in the high-end research field. For example, medical devices, automobile manufacturing, deep-sea submarines, and space station maintenance put forward higher requirements for it. In terms of miniaturization and precision, it can meet the needs of scientific research and actual production. But these are inseparable from the motion control system technology. This paper mainly introduces the research of manipulator control system based on AI wearable acceleration sensor, aiming to provide some ideas and directions for the research of wearable manipulator. This paper presents the research method of manipulator control system based on AI wearable acceleration sensor, including the establishment of manipulator kinematics model, common filtering algorithm, and PI algorithm of speed control system. It is used for the research and experiment of manipulator control system based on AI wearable acceleration sensor. The experimental results show that the average matching rate of the manipulator control system based on AI wearable acceleration sensor is as high as 88.89%, and the stability of the feature descriptor is high.

1. Introduction

With the upgrading of modern sensors and microprocessors, robotics has developed rapidly. In the context of the era of artificial intelligence and the Internet of things, more intelligent robots have more room for development and have more applications in aviation exploration, deep-sea operations, medical assistance, smart homes, and automated factories. In the "Made in China 2025" strategic document, robotics is listed as one of the ten major development areas, which is enough to reflect the importance of the development of robotics in current life and production. As the most intuitive operation unit in the robot system, the robotic arm has become one of the most concerned research directions in the robotics research field under the increasingly stringent automation standards. How to make the control method of the robotic arm more effective and convenient is currently the research hotspot. At present, most manipulators are roughly divided into two types according to the control method. The first is a dedicated manipulator that can complete preprogrammed processing actions by itself. Most of these control methods are industrial manipulators, which are often used in assembly lines in factories. It can be used to handle a lot of repetitive work; the second is a general-purpose manipulator that uses real-time command input manually to obtain the feedback action of the manipulator. The manipulator using this control method has high flexibility and can be used in tasks with complex environments.

The robotic arm is one of the most widely used automation devices in the field of robotics science and technology. At present, the traditional manipulator control methods are mostly completed by preprogramming

processing or command input from external devices. Such control methods are usually complicated and cumbersome and require operators to familiarize themselves with specific programming methods or according to different types of manipulators control instruction. With the advent of accelerometers, a brand-new noncontact somatosensory technology has been rapidly developed, showing a broad application prospect in the field of intelligent robots. In order to realize a more convenient and flexible manipulator control method, this paper designs a manipulator control system based on AI wearable acceleration sensor. The design of the robotic arm system better recognizes and senses changes in the human body, so as to achieve noncontact control.

Jarrahi's research found that artificial intelligence has penetrated into many organizational processes, leading to growing concerns that intelligent machines will soon replace humans in making decisions. In order to provide a more positive and pragmatic perspective, Jarrahi's research emphasizes the complementarity of humans and artificial intelligence and explores how to play their respective advantages in the organizational decision-making process, which is usually uncertain, complex, and ambiguous. Artificial intelligence has greater computational information processing capabilities and analysis methods, which can expand human cognition when dealing with complex problems, and humans can still provide a more comprehensive solution when dealing with uncertainties and ambiguities in organizational decisions intuitive method. This premise reflects the idea of intelligent enhancement, that is, the design of artificial intelligence systems should focus on enhancing rather than replacing human contributions. This research is theoretically strong, but lacks practical examples [1]. Choi and Kang proposed a software architecture of a wearable vital sign measurement device based on real-time user behavior recognition. Using wearable devices to measure vital signs helps users measure their health status related to their behavior, because wearable devices can be worn in daily life. Especially when the user is running or sleeping, blood oxygen saturation and heart rate are used to diagnose respiratory problems. However, in the measurement of vital signs, the traditional continuous measurement method is unreasonable because motion artifacts can reduce the accuracy of the vital signs. Moreover, due to the limited resources of wearable devices, in order to repair the distortion, Choi and Kang proposed a wearable device software architecture, which uses a simple filter and acceleration sensor to identify the user's behavior and measures accurately through the behavior state vital signs. This research lacks experimental data support and is not very scientific [2]. Navarro-Alarcon et al. proposed a feedback method that uses a manipulator to automatically servo control the three-dimensional shape of a soft object. Due to its potential applications in the food industry, household robots, medical robots, and manufacturing industries, the problem of soft object manipulation has attracted widespread attention from robotics researchers in recent years. A major complication in automatically controlling the shape of an object is the estimation of its deformation characteristics, which determines how the motion of the manipulator is actively transformed into deformation. In order to solve this problem, Navarro-Alarcon et al. have developed a new algorithm for real-time calculation of soft object deformation parameters, which provides valuable adaptive behavior for deformation controllers, which cannot be achieved by traditional fixed model methods. In order to verify the proposed adaptive controller, a detailed experimental study of the robot was carried out. This research is not practical and not suitable for popularization in practice [3].

The innovations of this paper are as follows: (1) the commonly used filter processing algorithm is proposed for the research of the robotic arm control system based on the AI wearable acceleration sensor; (2) the PI algorithm of the speed control system is proposed for the AI wearable acceleration sensor; (3) based on the research on the arm control system, a wearable robotic arm that can be grasped collaboratively is designed.

2. Method of Robotic Arm Control System Based on AI Wearable Acceleration Sensor

2.1. Establishment of Kinematic Model of Robotic Arm. The size of the working space of the robotic arm reflects the kinematics of the robotic arm, and the kinematics of the robotic arm is the basis for the study of the working space of the robotic arm [4]. In order to accurately control the robot arm to complete the command action in the follow-up somatosensory control experiment, it is necessary to analyze the kinematics and workspace of the robot arm used in the experiment [5].

The D-H method is a robot attitude representation method described by Denavit and Hartenberg in the calculation of robot motion parameters. By establishing the corresponding coordinate system on each joint link and using the homogeneous transformation of the matrix, the position and posture relationship between adjacent links can be determined, and a series of coordinate systems can be transformed by matrix, so as to establish the robot arm kinematic model [6]. Use the DH method to determine the motion model of the robotic arm, where a_i is the length of the link, θ_i is the angle between two adjacent joint axes, d_i is the spatial distance between two adjacent links, and β_i is the spatial angle of two adjacent links [7].

In order to determine the posture state of the operating end of the manipulator, the movement of each joint can be recursively step by step through the adjacent links [8]. The movement transfer process has the following matrix transformation formula:

$$
{}_{i}^{i-1}T = \begin{bmatrix} c\beta_i & -s\beta_i & 0 & a_{i-1} \\ s\beta_i c\theta_{i-1} & c\beta_i c\theta_{i-1} & -s\theta_{i-1} & -d_i s\theta_{i-1} \\ s\beta_i s\theta_{i-1} & c\beta_i s\theta_{i-1} & c\theta_{i-1} & d_i c\theta_{i-1} \\ 0 & 0 & 0 & 1 \end{bmatrix}.
\tag{1}
$$

The transformation matrix between adjacent units is as follows:

$$
{}^0_1T = \begin{bmatrix} c\beta_1 & -s\beta_1 & 0 & 0 \\ s\beta_1 & c\beta_1 & 0 & 0 \\ 0 & 0 & 1 & 0 \\ 0 & 0 & 0 & 1 \end{bmatrix}, \tag{2}
$$

$$
{}^1_2T = \begin{bmatrix} c\beta_2 & -s\beta_2 & 0 & 0 \\ 0 & 0 & 1 & d_2 \\ -s\beta_2 & -c\beta_2 & 0 & 0 \\ 0 & 0 & 0 & 1 \end{bmatrix}, \tag{3}
$$

$$
{}^2_3T = \begin{bmatrix} c\beta_3 & -s\beta_3 & 0 & a_2 \\ s\beta_3 & c\beta_3 & 0 & 0 \\ 0 & 0 & 1 & 0 \\ 0 & 0 & 0 & 1 \end{bmatrix}. \tag{4}
$$

In order to manipulate the position vector between the end coordinate system reference and the base origin coordinate system, the following formula exists:

$$
P = \begin{bmatrix} a_3c_{23}c_1 - d_2s_1 + a_2c_1c_2 - d_1s_{234}c_1 \\ d_5\left(c_4\left(c_2s_1s_3 + c_3s_1s_2\right) - s_4\left(s_1s_2s_3 - c_2c_3s_1\right)\right) - a_3\left(s_1s_2s_3 - c_2c_3s_1\right) + a_2c_1s_1 \\ -a_3s_{23} - a_2s_2 - d_5c_{234} \end{bmatrix}. \tag{5}
$$

2.2. Common Filter Processing Algorithms.

Digital filtering methods are very commonly used in processing data noise. According to the different requirements of data processing in actual projects, the corresponding digital filtering methods can be selected [8, 9]. The different use characteristics of digital filtering can be divided into two categories: digital filtering methods that deal with occasional large interference and digital filtering methods that deal with small fluctuations in high frequency [10].

2.2.1. Digital Filtering Method to Deal with Occasional Large Interference.

During data acquisition, due to the unstable influence of the instrument, random and large interference sometimes occurs. This kind of data interference occurs at a low frequency, but it causes a great disturbance to the data analysis. For this kind of interference, limit filtering methods and median filtering methods can be used [11].

(1) Limiting Filtering Method. The principle of the limiting filtering method is to set a deviation threshold T based on actual projects and empirical judgments. When the detected two adjacent data exceed this threshold, the current measurement value is discarded and the previous measurement data is selected to replace [12, 13]. This filtering method can effectively remove random interference caused by accidental factors, but it cannot be used in data smoothness processing [14]. Its expression is

$$
\begin{cases} \left|Y(t_2) - Y(t_1)\right| \le T, Y(t_2) = Y(t_2), \\ \left|Y(t_2) - Y(t_1)\right| > T, Y(t_2) = Y(t_1). \end{cases} \tag{6}
$$

(2) Median Filtering Method. The median filter is a typical low-pass filter proposed by Yüzer et al. [15]. This technology can usually overcome the blurring of some details in the image generated by the linear filter under certain conditions and can eliminate the interference pulse well and at the same time can form a certain degree of protection for the edge of the target image [16].

The basic principle of median filtering is to establish a sliding window, which contains many pixels, and take the median value of all these pixels and use it as the new value of the center point of the window [17]. The specific process is to first determine a square (circular, diamond, linear, etc.) area with a certain pixel as the center. This neighborhood is generally called a window. Secondly, the gray values of all pixels in the window are sorted, and after sorting is completed, the median value in the arrangement is taken as the new value of the gray value of the center pixel of this window [18]. It should be noted here that if the number of pixels is odd, then the median value is the middle value after sorting by size; if the number of pixels is even, then the gray values of the middle two pixels after sorting are averaged as the middle value [19]. In the image denoising process, the image signal can be regarded as a two-dimensional signal, so the output of the median filter in the two-dimensional case can be expressed as

$$
g(x, y) = \text{median}\{f(x - i, y - j)\}, \quad (i, j) \in W, \tag{7}
$$

where $g(x, y)$ represents the gray value of the output pixel, $f(x - i, y - j)$ represents the input gray value, and W is the template window [20].

2.2.2. Digital Filtering Method to Deal with Small Fluctuations in High Frequency.

For high-frequency and small-amplitude data fluctuations, the average filtering method is often used, which is characterized by the ability to suppress continuous small noise and high signal smoothness [21].

(1) Arithmetic Average Filtering Method. Arithmetic average filtering is to find the average value after summing the data of N consecutive samples. The following formula exists:

$$y = \frac{1}{N} \sum_{i=1}^{n} X_i. \tag{8}$$

It can be seen that as N increases, the result is more accurate, and the smoothness of the data after the solution increases, but the calculation time increases and the sensitivity decreases [22]. In actual engineering, the value of N is usually selected according to specific requirements to obtain the required filtering effect [23].

(2) Moving Average Filtering Method. Arithmetic average filtering needs to collect N continuous data when determining the sampling value. This method has a slower detection time and is not suitable for high-frequency data input [24]. Moving average filtering is suitable for high-frequency input systems. First determine the window size. When there are new data, discard the first data in the window, fill the new data to the end of the window, and perform arithmetic average calculation on several fixed data in the window [25]. The following formula exists:

$$y(n) = \frac{1}{\text{windowSize}} (x(n) + x(n-1) + \cdots + x(n-(\text{windowSize}-1))). \tag{9}$$

(3) Limiting Moving Average Filtering Method. When there is the influence of large pulse interference, only using the average filtering method will average the larger pulse error into the filtering result, which will distort the filtered data [26]. The limited moving average filtering method can remove random large-scale interference on the basis of ensuring the smoothness of the processed data and make the filtered data highly fit the authenticity of the original data [27].

2.3. PI Algorithm for Speed Control System.

The PI algorithm is the most commonly used control algorithm applied to the speed control system. It is composed of two parts: the proportional regulator P and the integral regulator I [28]. The speed control system needs a fast and stable control effect, so the regulator P plays a role of rapid adjustment, and the integral regulator I plays a role of steady-state error-free, thus meeting the fast and stable requirements of the speed control system [29].

The PI regulator expression is

$$u(t) = k_p \left(\text{error}(t) + \frac{1}{T_1} \int_0^t \text{error}(t) \mathrm{d}t \right). \tag{10}$$

Discrete processing is carried out:

$$u(k) = K_p \times \text{error}(k) + K_I \times \sum_{i=1}^{k} \text{error}(i). \tag{11}$$

The incremental expression of the digital PI regulator is

$$\Delta u(k) = K_p \times [\text{error}(k) - \text{error}(k-1)] + K_I \times \text{error}(k). \tag{12}$$

Incremental PI uses the deviation between the current error and the last error to obtain the output increment, so that there will be no cumulative error problem. The output formula is

$$u(k) = u(k-1) + \Delta u(k). \tag{13}$$

The method part of this paper uses the abovementioned method to study the robotic arm control system based on AI

wearable acceleration sensor. The specific process is shown in Figure 1.

3. Experiment of Robotic Arm Control System Based on AI Wearable Acceleration Sensor

3.1. Structure Design of Test Platform Control System

3.1.1. Servo Control System Component Design

(1) Sensor Fixture. Before designing the sensor fixture, we must first understand the sensor size and the structure of the indexing table disc. In order to facilitate the installation of 32 MEMS acceleration sensors on the VRNC-210 indexing table, corresponding sensor fixtures need to be designed. This project has designed an expansion disc and 32 L-shaped sensor fixtures to realize the installation of 32 sensors.

The expansion disc is connected to the VRNC-210 indexing table with M8 screws at 4 positioning holes, and the U-line card slot is designed according to the specific shape of the indexing table and 32 MEMS acceleration sensors of 20 mm × 20 mm × 20 mm. Then, use 3D CAD design software to model and design VRNC-210 indexing table, expansion disc, and L-shaped sensor fixture. Firstly, the model of VRNC-210 is established, and the model effect is that 32 L-shaped clamps are fixed on the expansion disk through 4 M2.5 screws, and the sensors are connected through 3 positioning holes at different positions on the L-shaped clamp, with a design diameter of 283 mm. The expansion disk can be placed at the same time to place 32 sensors to realize the static acceleration test of *X*, *Y*, and *Z* axes.

(2) Development of Interface Cables. The entire test process must be carried out under standard environmental conditions, and a single temperature change can be maintained to record the impact of the external environment on the test results. The temperature performance test of the sensor needs to be carried out in the high- and low-temperature box. The acceleration sensor on the fixture is driven by the rotating shaft to operate in the high- and low-temperature box, and the temperature change in the high- and low-temperature box is set. Through continuous recording and analysis of the sensor in the set, different temperature
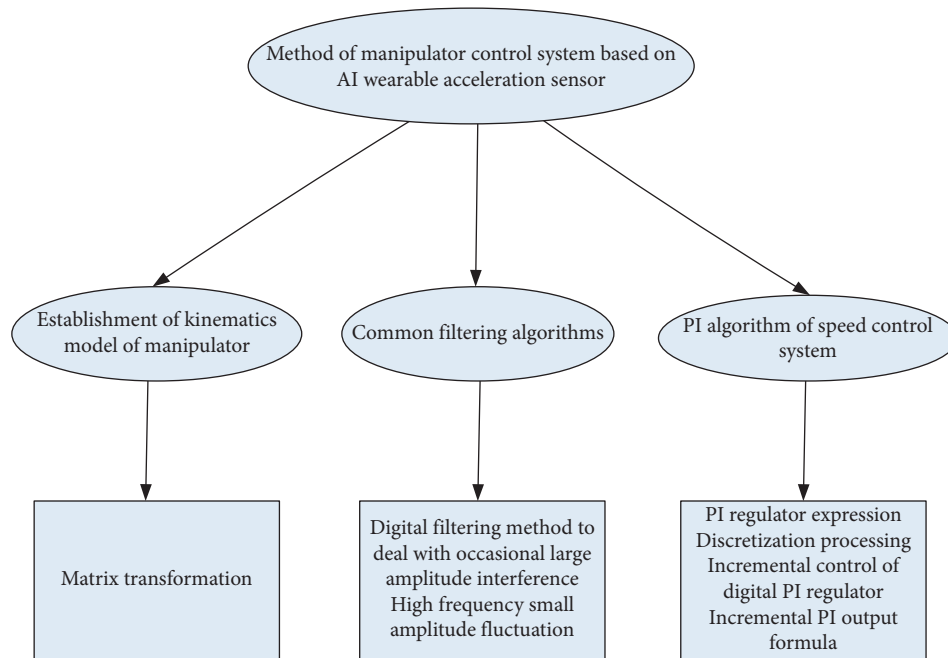
FIGURE 1: Part of the technical process of this method.

environments lower the output to get the relevant temperature performance index of the acceleration sensor. In the case of unexpected power failures in the servo control system, the motion control card must be combined with the RS-422 interface cable to ensure high-precision return to origin.

The high- and low-temperature box and the servo drive are respectively provided with RS-485 interface and RS-422 interface. First, the PCI slot of the industrial control computer can be installed with a model interface converter to expand a RS-485 and RS-422 hardware interface, respectively. General PCI interface conversion cards have built-in protection devices to suppress transient voltage to protect the transient overvoltage and surge voltage generated on the line for various reasons and use very small interelectrode capacitance to reliably ensure serial communication high-speed transmission.

3.1.2. Control Platform Collection Box

(1) Shell Design of Data Acquisition Chassis. Multichannel acquisition equipment needs to complete the acquisition of 32 analog channels and 32 digital channels. The acquisition equipment is mainly composed of analog signal acquisition subsystem, digital signal acquisition subsystem, power supply subsystem, and peripherals such as interfaces and indicators on the panel. The chassis is designed as a rectangular parallelepiped. In order to facilitate stacking with a 19-inch industrial computer (test control and data acquisition and processing computer), the width of the chassis is designed to be 429 mm.

(2) Design of Power Supply Subsystem and Program-Controlled Power Supply. Use Altium Designer 9.0 software to complete the development of the power supply board. First, select the appropriate components in the component library of the software and place them in an accurate position. After naming them, set the packaging, etc., and use the components in the schematic area. The meaningful lines and symbols are connected to form a complete circuit schematic diagram. The schematic diagram should be easy to understand and clear. In order to prevent coupling during wiring, the input and output signal lines should be wired as much as possible, and the wires should be less bent, the width of the wires and the distance between the wires should be appropriately larger, and then you can design and generate the netlist to complete the error check and circuit modification to produce a qualified circuit board.

3.2. Cooperative Grasping Design of Wearable Robotic Arm.
The wearable robotic arm system designed in this research, wearable control gloves, can remotely grasp the identified objects, which has a good application prospect in production, life, industrial medical treatment, etc.

3.2.1. Collaborative Grabbing Action Design.
In different scenes, facing different objects, the robotic arm can take different grasping actions to reduce the load of its steering gear and make the grasping objects more stable. Therefore, in view of the actual situation, this research carried out the registration of multiple actions on the robotic arm, so that the robotic arm can adapt to various situations. The entire grasping action is burned on the robotic arm control board through graphical software, so that the subsequent wearable control gloves can call the control information.

The software represents the six degrees of freedom of the robotic arm from different parts. Controlling different

freedoms to complete different actions can form a grasping action group. Adjust the PWM value of each degree of freedom to make the robotic arm complete different actions.

3.2.2. Glove Coordinated Control.
First, write the control program on the Arduino control board that controls the gloves, and then send the control commands to the actuator end of the robotic arm through the wireless communication module, so that the robotic arm executes different action groups to complete the grasping task. First, connect the control glove Arduino circuit board to the computer through the CH340 serial cable, then open the Arduino programming software, and select the corresponding development version model and COM port model; the port model here can be managed in the computer equipment after connecting the control glove to the computer. After setting the port number, you need to calibrate the wearable control gloves before entering the coordinated action.

Calibration requires two steps to complete: first, open the control glove upper computer software, which can realize data reception and data transmission. When the control glove is calibrated, its data receiving function is mainly used; then, wear the control glove and turn on the data glove ON button. If the indicator light is on, it is the working state. After pressing the calibration button on the circuit board, hold the five fingers and spread the five fingers in the opposite direction. Repeat this action several times to maximize the grip and stretch range of the ADXL345 tilt sensor. When subsequent commands for controlling the robotic arm are issued, different action groups can be accurately called for grabbing.

3.2.3. Judgment of the Suitability of the Object's Cooperative Grasping Temperature.
Sometimes, the temperature determination of the object to be grasped is also very important. Whether the temperature of the object is suitable for grasping is the problem to be solved. Under certain conditions, the temperature of the object to be grasped is too high or too low to damage the end jaws of the robotic arm. Therefore, judging the temperature of the object to be grasped is also a task to protect the wearable robotic arm system. In this study, a DS18B20 patch temperature sensor is placed at the end of a six-degree-of-freedom gripper to complete this task.

DS18B20 is a temperature sensor with a single bus interface. It only needs one I/O interface to communicate with the microprocessor, and it has the characteristics of small size, strong anti-interference ability, wide measurement range, and high accuracy. Its temperature measurement range is $-55°$ to $+125°$, and the accuracy is very high in the range of $-10°$ to $+85°$. In this study, a patch type DS18B20 sensor was used to solve the task, and the sensor module was encapsulated in a silicone wire.

Stick the DS18B20 probe on the sensitive area of the gripper end of the robotic arm to feel the temperature of the object being grasped. When the gripper at the end of the robotic arm grips the object, the patch temperature sensor DS18B20 will touch the temperature measurement object.

When the temperature of the object to be grasped exceeds $60°$, the temperature sensor transmits the signal to the STM32 single-chip microcomputer of the robot arm base, which is remotely transmitted to the control terminal through the wireless module. If there is a high temperature pop-up prompt, the operator should consider whether to continue grasping. If the grabbing temperature is normal, there is no other prompt, and the subsequent grabbing task can be performed.

3.2.4. Judgment of Pressure Threshold for Object Collaborative Grabbing.
Since the wearable robotic arm system grabs objects remotely, when the gripper of the actuator of the robotic arm grabs the object, it can be judged whether the grasped object is clamped according to the size of the force used. It is a remote control clamp. Take the key issues facing you. This research uses RFP602 chip piezoresistive pressure sensor and conversion module to solve this problem. Put the mechanical arm patch type piezoresistive pressure sensor on the jaw end of the actuator to solve the problem of measuring the pressure required to grasp different objects. When the external force acts on the sensing point, its resistance will become regular with the external force. When there is no pressure, the resistance value of the resistance is large and the maximum value. As the pressure value continues to increase, its resistance is continuously decreasing, which is inversely proportional to the pressure value. Connect the sensor to the voltage conversion module and connect it to the STM32 microcontroller to obtain the collected voltage. The pressure information is obtained through the resistance-pressure relationship conversion formula. Finally, the wireless module is fed back to the control terminal serial port, and the serial port feedback control end host.

This part of the experiment proposes the abovementioned steps for the research experiment of the robotic arm control system based on the AI wearable acceleration sensor. The specific process is shown in Table 1.

4. Robotic Arm Control System Based on AI Wearable Acceleration Sensor

4.1. Experimental Correlation Analysis

(1) The first is the functional experiment of the gesture recognition manipulator. On the MEMS gesture sensing sensor, the hand makes a prescribed action, records the coordinate values related to the five gestures in processing, and observes whether the manipulator is set determined actions. In the process of gesture control, it is necessary to ensure that all dynamic actions should be within the designed working range, so that the steering gear can rotate in a matched manner. If the movement exceeds the range, the steering gear will lose the corresponding control. The data corresponding to different gesture controls are shown in Table 2 and Figure 2.

TABLE 1: Experimental steps in this article.

Research and experiment of manipulator control system based on AI wearable acceleration sensor	3.1	Structure design of test platform control system	1	Component design of servo control system
			2	Control platform collection box
	3.2	Cooperative grasping design of wearable manipulator	1	Cooperative grasping action design
			2	Cooperative control of gloves
			3	Determination of temperature suitability for object cooperative grasping
			4	Determination of pressure threshold for cooperative grasping of objects

TABLE 2: Corresponding data of gesture control experiment.

Steering gear angle (°)	hand_x	hand_y	hand_z	hand_α	hand_β	hand_θ
Initial state (a)	90	90	90	45	45	45
X axis, 20 cm (b)	96	84	112	86	107	94
Y Axis, 20 cm (c)	89	97	82	95	86	83
Z axis, 20 cm (d)	102	96	126	81	92	79
Wrist clockwise, 90° (e)	84	91	87	90	114	81
Open hand, 6 cm (f)	81	92	90	87	85	73
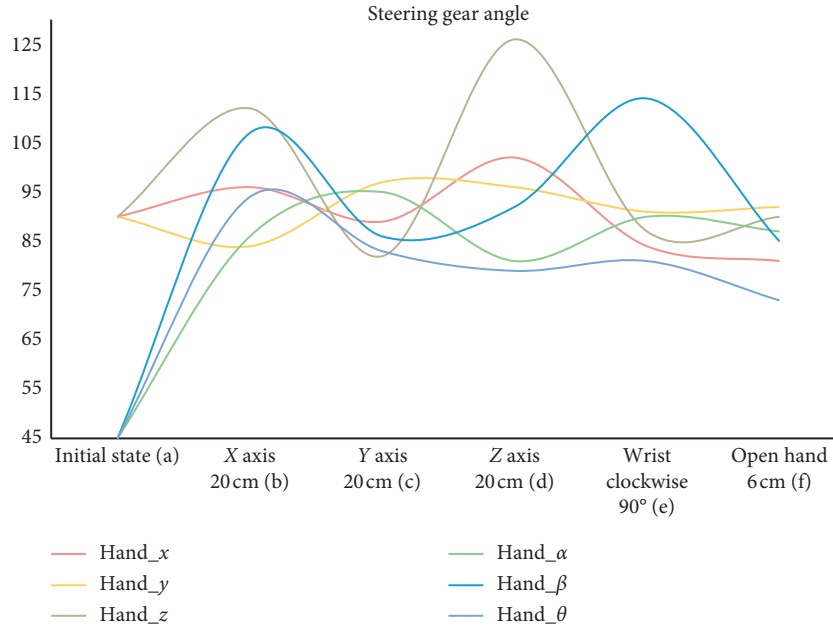
FIGURE 2: Corresponding data of gesture control experiment.

From the above experimental process and results, it can be seen that the functional verification experiments of dynamic gesture recognition and control of the five joints of the robotic arm can be successfully completed.

(2) This paper uses a two-segment rigid chain simulation model to verify the joint parameter estimation method based on joint constraints. A virtual measurement coordinate system is established at any position on the surface of rigid body A and rigid body B to simulate the measurement data of the inertial measurement unit. The rigid body A makes free rotation, and the rigid body B rotates around the rigid body A with two degrees of freedom. In order to verify the influence of linear acceleration measurement error on the estimation algorithm, noise was added to the signal. In the simulation data, 15 sets of data are randomly selected as the measurement data. When the system is noise-free, the estimated data are completely consistent with the preset parameters. The estimated error percentages of joint parameters under different linear acceleration measurement noises are shown in Table 3 and Figure 3.

It can be seen from the graph that when the linear acceleration measurement signal-to-noise ratio increases from 10 dB to 60 dB, the estimation error of the joint parameters drops from 5.37% to 0.81%.

TABLE 3: Error percentage of joint parameter estimation under different acceleration measurement noise.

SNR (dB)	Joint parameters (A)			Joint parameters (B)		
	X (%)	Y (%)	Z (%)	X (%)	Y (%)	Z (%)
10	3.26	4.32	5.37	4.12	3.94	4.26
20	2.75	3.25	4.82	3.69	2.81	3.49
30	1.89	2.06	3.26	2.57	1.46	2.81
40	1.23	1.14	2.48	1.26	0.97	1.87
50	0.64	0.72	1.23	0.87	0.58	0.89
60	0.51	0.64	0.81	0.62	0.46	0.57
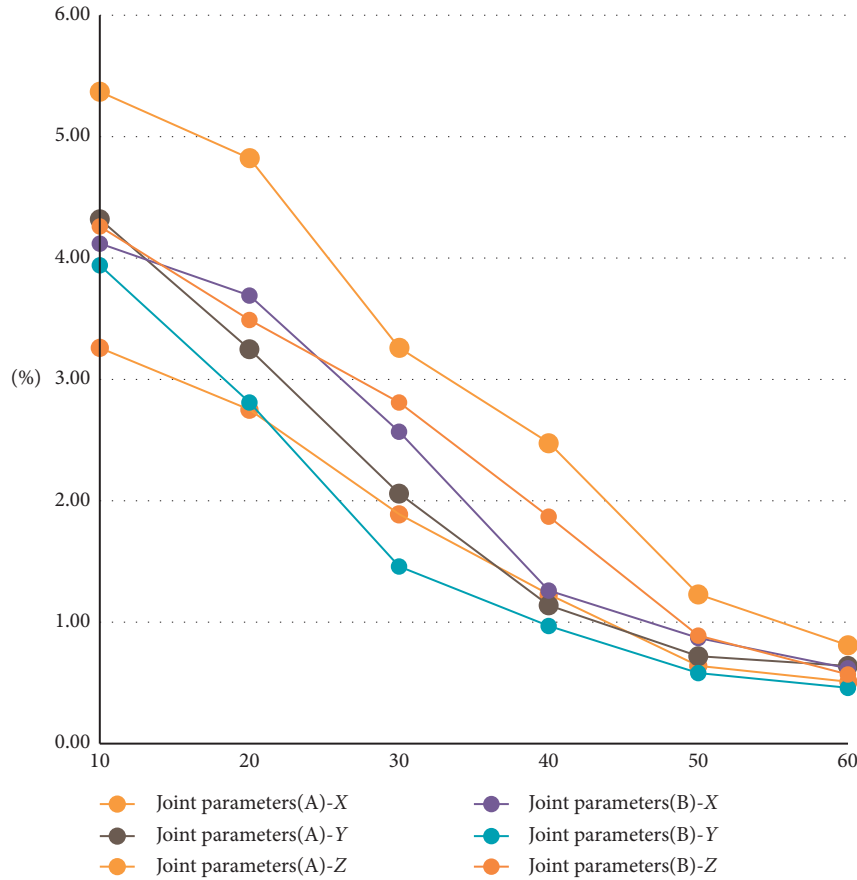
FIGURE 3: Error percentage of joint parameter estimation under different acceleration measurement noise.

4.2. System Performance Analysis

(1) When the system is running, the action feature as a representation has an obvious recognition effect in the JHMDB and MPII datasets. However, in the gesture sensing process, the complex background pixels affect the feature acquisition effect, thereby reducing the recognition efficiency, and 3D-SIFT is used. Representing static information improves the sensing effect. This paper selects the recognition rates of arms, elbows, wrists, and fingers to extract RGB features and SIFT features for comparison. The different feature recognition effects extracted from different body regions are shown in Table 4 and Figure 4.

From the recognition rates obtained by different methods, it can be seen that the action recognition

TABLE 4: Different feature recognition effects extracted from different arm regions.

	RGB	SIFT
Arms	8.9	10.4
Elbows	10.9	13.1
Wrists	11.3	12.6
Fingers	7.6	8.7

rate after using the elbow and wrist to propose features is relatively close. When the entire arm area is combined, the recognition rate is the highest, and compared with the direct recognition of the entire arm area, the recognition rate of the combination of various parts of the human body is the lowest.
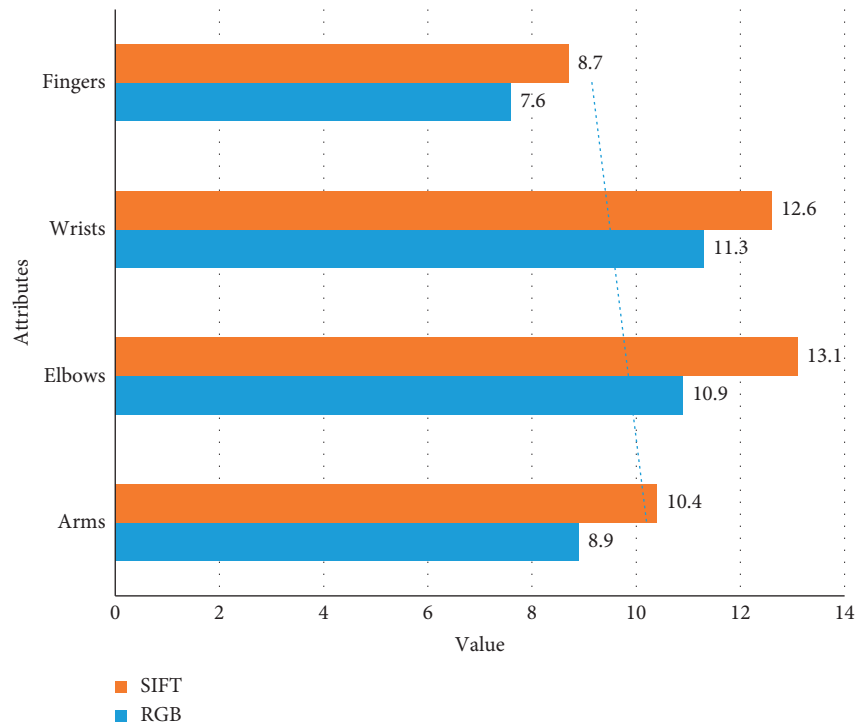
FIGURE 4: Different feature recognition effects extracted from different arm regions.

(2) The movement speed of different actions of the sports car body during the remote grasping task is also an index that cannot be ignored. By setting different values for PWM in the Arduino program, the rotation speed of the motor is different, but the PWM value is too high, the circuit current is large, and the burden on the circuit is also large, so in the test, set the PWM, PWM range is 0~255. In the open space in the laboratory, the speed of the vehicle body during various walking methods in omnidirectional motion was tested. The specific data are shown in Table 5 and Figure 5.

It can be seen from the abovementioned test data that the various speeds of the omnidirectional sports car body meet the actual requirements.

(3) In order to evaluate the proposed SIFT hardware architecture design, it is compared with other studies from the three perspectives of the stability of feature descriptors, the consumption of hardware resources, and the speed of hardware execution. Perform stability detection on the extracted feature descriptors, select an original image a, perform scale change, rotation, blur, and illumination on a to generate image b, and extract the feature descriptors of a and b for matching. The matching method is violent matching library functions provided by Opencv. Select 18 best matching point pairs from the

matching results. The matching rate is expressed by the ratio of the number of correct matching point pairs to 18. The higher the matching rate, the higher the stability of the feature descriptor. The results of the stability detection of the feature descriptor of the image rotating counterclockwise are shown in Table 6 and Figure 6.

From the calculation of the data in the chart, it can be concluded that the average matching rate after scale change processing is as high as 88.89%, and the feature descriptor stability is high. The rotated image feature descriptor is matched with the reference image feature descriptor. As the degree of rotation increases, the matching rate shows a downward trend.

(4) For the target recognition time, the system pure software target recognition time is about 10.81 seconds. The time for SIFT feature extraction is about 9.23 seconds. Draw the specific situation into a chart, as shown in Table 7 and Figure 7.

After using FPGA acceleration, the time for SIFT feature extraction is about 0.91 seconds, which is 8.32 seconds less than the pure software implementation. Therefore, after using FPGA acceleration, the target recognition time is reduced to 2.49 seconds, and the real-time performance is significantly improved.

TABLE 5: Movement speed test data.

How to move	Distance or angle (m)	PWM settings	Time (s)	Speed (m/s)
Forward and backward	6	110	14.1	0.43
Left and right	6	115	11.7	0.51
Diagonally	6	125	9.8	0.61
Rotate	6	135	8.7	0.69
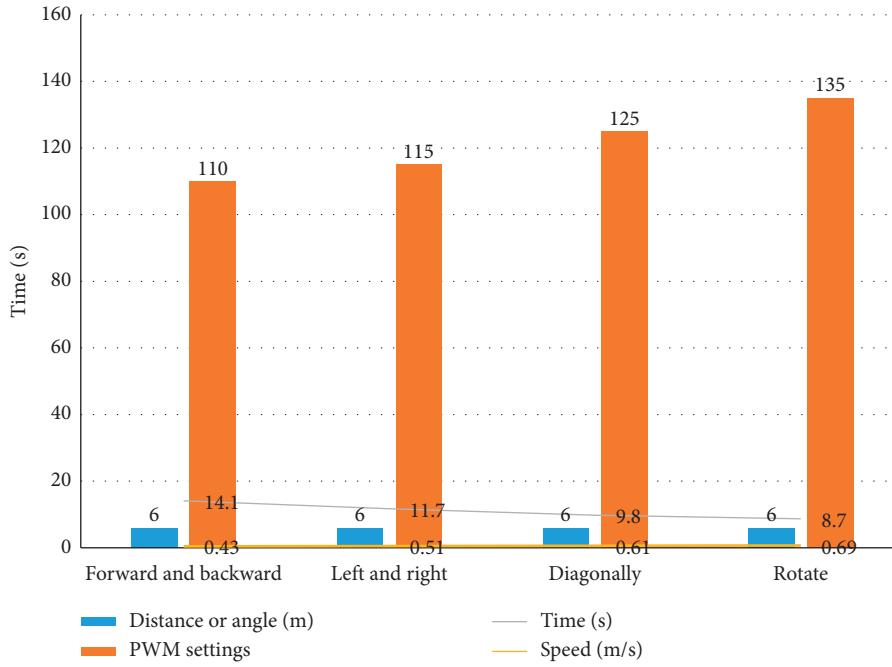
FIGURE 5: Movement speed test data.

TABLE 6: Rotation change feature descriptor stability detection.

Degree of rotation (°)	Match rate before processing (%)	Match rate after processing (%)
5	81.42	86.49
10	67.31	83.26
15	72.43	89.17
20	76.12	91.09
25	67.26	94.14
30	75.45	84.56
Rotating change average match rate	73.33	88.12
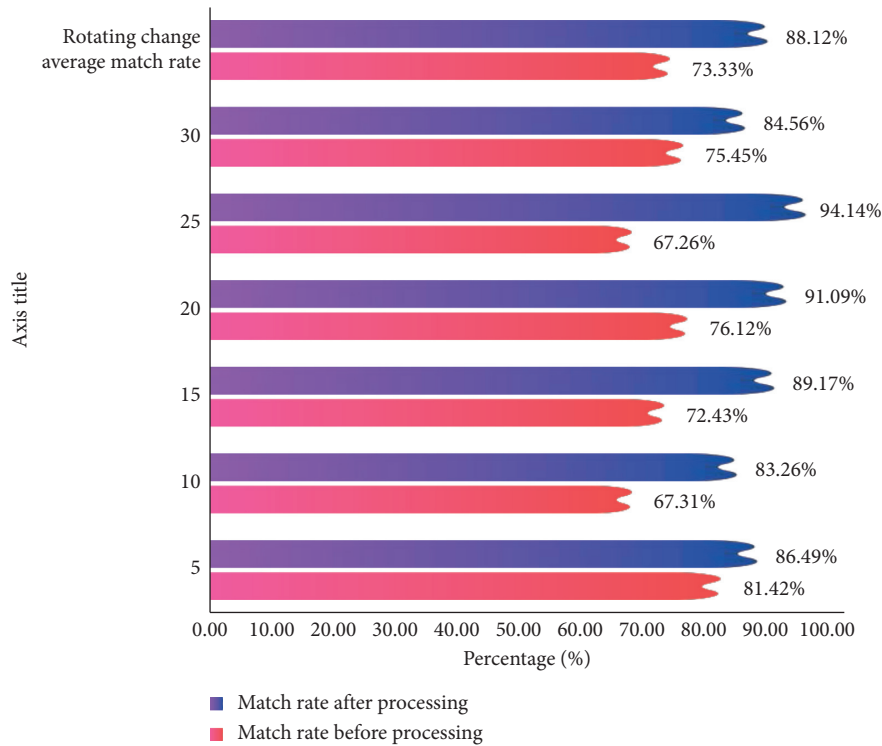
Figure 6: Stability detection of rotation change feature descriptor.

Table 7: Comparison of target recognition time before and after acceleration.

Target recognition	Pure software running time (s)	Running time after acceleration (s)
Get an image and correct it	0.31	0.31
Solving depth information by stereo matching	0.46	0.46
SIFT feature extraction	9.23	0.91
Feature matching	0.59	0.59
Mean shift clustering	0.22	0.22
Total	10.81	2.49
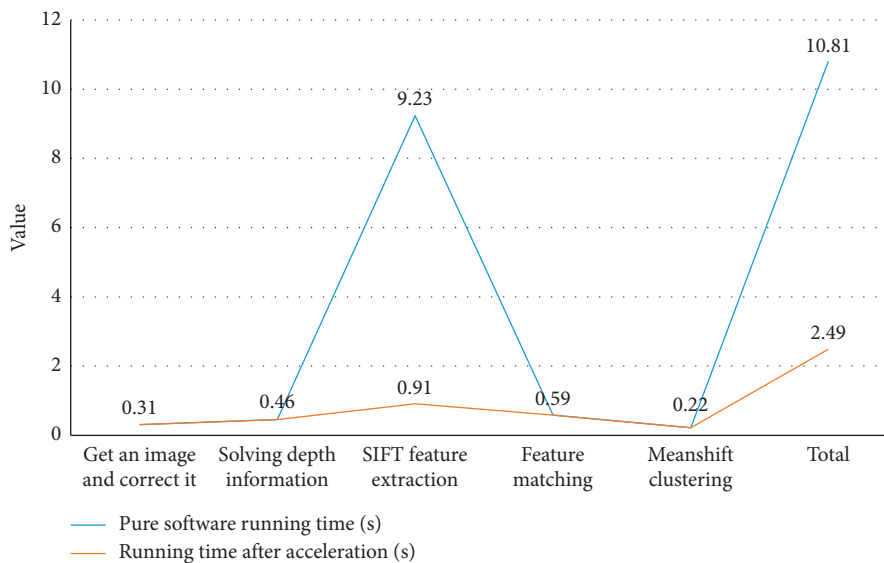
Figure 7: Comparison of target recognition time before and after acceleration.

5. Conclusions

With the development of computer technology, robotics technology has also matured. It combines technologies from computers, electronics, machinery, sensors, and control and is widely used in military, industry, agriculture, medicine, education, scientific research, and other fields. It basically covers all aspects of people's lives. As a powerful productivity tool, robots play a huge role in improving production efficiency, optimizing production methods, and broadening the production environment.

As a practical type of robot, the manipulator has extremely high work efficiency, stable repeatability, and powerful functions, so it is widely used in transportation services, product processing, and other fields. On the assembly line of high-tech manufacturing industry, various types of robotic arms can complete many different tasks, such as handling die-cast or stamped parts or components, laser cutting, and assembling mobile phone parts and painting them.

In this paper, the robot arm control system of the AI wearable acceleration sensor is designed to realize the remote grasping operation, which requires the whole body movement. The structure of the system is designed according to its functional requirements, and the main hardware is designed at the same time. First, select the model, aiming at the six-degree-of-freedom manipulator structure in this system, a sensor gesture recognition model is established based on the feature value extraction technology in the DH method; all software development environments used in this system are introduced in detail. In the design process of the robotic arm control system based on the AI wearable acceleration sensor, due to the limitations of experimental conditions and our professional level, there are still many shortcomings, such as the remote control distance being too short and the number of dynamic interactive gestures being insufficient. In the process of wireless data transmission, data security and anti-interference ability are not considered. This will be the focus and research direction of future work.

Data Availability

No data were used to support this study.

Conflicts of Interest

The authors declare that they have no conflicts of interest.

References

[1] M. H. Jarrahi, "Artificial intelligence and the future of work: human-AI symbiosis in organizational decision making," *Business Horizons*, vol. 61, no. 4, pp. 577–586, 2018.

[2] D.-J. Choi and S.-J. Kang, "Software architecture of a wearable device to measure user's vital signal depending on the behavior recognition," *The Journal of Korean Institute of Communications and Information Sciences*, vol. 41, no. 3, pp. 347–358, 2016.

[3] D. Navarro-Alarcon, H. M. Yip, Z. Wang et al., "Automatic 3-D manipulation of soft objects by robotic arms with an adaptive deformation model," *IEEE Transactions on Robotics*, vol. 32, no. 2, pp. 1–13, 2016.

[4] D. Hassabis, D. Kumaran, C. Summerfield, and M. Botvinick, "Neuroscience-inspired artificial intelligence," *Neuron*, vol. 95, no. 2, pp. 245–258, 2017.

[5] H. Lu, Y. Li, M. Chen et al., "Brain intelligence: go beyond artificial intelligence," *Mobile Networks and Applications*, vol. 23, no. 7553, pp. 368–375, 2017.

[6] R. J. Spiro, B. C. Bruce, and W. F. Brewer, "Theoretical issues in reading comprehension: perspectives from cognitive psychology, linguistics, artificial intelligence, and education," *Reading Teacher*, vol. 3, pp. 368–373, 2017.

[7] F.-Y. Wang, "Artificial intelligence and intelligent transportation: driving into the 3rd axial age with ITS," *IEEE Intelligent Transportation Systems Magazine*, vol. 9, no. 4, pp. 6–9, 2017.

[8] N. N. Darren, Z. Alexey, S. Yasushi et al., "Synthetic biology routes to bio-artificial intelligence," *Essays in Biochemistry*, vol. 60, no. 4, pp. 381–391, 2016.

[9] S. Jha and E. J. Topol, "Information and artificial intelligence," *Journal of the American College of Radiology*, vol. 15, no. 3, pp. 509–511, 2018.

[10] A. Sarwar, J. Suri, M. Ali, and V. Sharma, "Novel benchmark database of digitized and calibrated cervical cells for artificial intelligence based screening of cervical cancer," *Journal of Ambient Intelligence & Humanized Computing*, vol. 12652, no. 16, pp. 353–358, 2016.

[11] W. A. Marie, L. Yong, K. R. Regner et al., "Artificial intelligence, physiological genomics, and precision medicine," *Physiological Genomics*, vol. 50, no. 4, pp. 237–243, 2018.

[12] D. Dai, "Human intelligence needs artificial intelligence," *Sensors*, vol. 5855, no. 3, pp. 95–99, 2018.

[13] A. Bouzekri, T. Allaoui, M. Denai et al., "Artificial intelligence-based fault tolerant control strategy in wind turbine systems," *International Journal of Renewable Energy Research*, vol. 7, no. 2, pp. 652–659, 2017.

[14] W. K. Lin, S. J. Lin, and T. N. Yang, "Integrated business prestige and artificial intelligence for corporate decision making in dynamic environments," *Cybernetics and Systems*, vol. 48, no. 4, pp. 1–22, 2017.

[15] A. H. Yüzer, H. Sümbül, and K. Polat, "A novel wearable real-time sleep apnea detection system based on the acceleration sensor," *IRBM*, vol. 41, no. 1, pp. 39–47, 2020.

[16] S. Lee, S. Gandla, M. Naqi et al., "All-day mobile healthcare monitoring system based on heterogeneous stretchable sensors for medical emergency," *IEEE Transactions on Industrial Electronics*, vol. 67, no. 10, pp. 8808–8816, 2020.

[17] F. Tan, X. Xie, and L. Li, "Taekwondo motion state recognition system based on the wearable computing," *Journal of Mines Metals & Fuels*, vol. 65, no. 2, pp. 75–79, 2017.

[18] M. Davide, B. Leonardo, C. Michele et al., "Profiling the propagation of error from PPG to HRV features in a wearable physiological-monitoring device," *Healthcare Technology Letters*, vol. 5, no. 2, pp. 59–64, 2018.

[19] S. Li, P. Zhou, W. Xiao et al., "A wearable system for cervical spondylosis prevention based on artificial intelligence," *Zhongguo Yi Liao Qi Xie Za Zhi = Chinese Journal of Medical Instrumentation*, vol. 44, no. 1, pp. 33–37, 2020.

[20] L. C. Wu, V. Nangia, K. Bui et al., "In vivo evaluation of wearable head impact sensors," *Annals of Biomedical Engineering*, vol. 44, no. 4, pp. 1234–1245, 2016.

[21] N. Dawar, S. Ostadabbas, and N. Kehtarnavaz, "Data augmentation in deep learning-based fusion of depth and inertial sensing for action recognition," *IEEE Sensors Letters*, vol. 3, no. 1, pp. 1–4, 2019.

[22] A. S. Jamaludin, M. N. Razali, N. Jasman, A. N. Ghafar, and M. A. Hadi, "Design of spline surface vacuum gripper for pick and place robotic arms," *Journal of Modern Manufacturing Systems and Technology*, vol. 4, no. 2, pp. 48–55, 2020.

[23] V. L. Nguyen, C. H. Kuo, and C. Y. Lin, "Gravity compensation design of planar articulated robotic arms using the gear-spring modules," *Journal of Mechanisms and Robotics*, vol. 12, no. 3, pp. 1–35, 2019.

[24] M. U. Farooq and S. Y. Ko, "An automated extracorporeal knot-tying system using two concentric tube robotic arms for deployment through a 3-mm port," *International Journal of Control, Automation and Systems*, vol. 18, no. 1, pp. 1–9, 2020.

[25] S. Wong and C. Gui, "Brain controlled robotic arms—advancements in prosthetic technology," *University of Western Ontario Medical Journal*, vol. 87, no. 2, pp. 59–61, 2019.

[26] M. Alikhani, B. Khalid, R. Shome, C. Mitash, K. Bekris, and M. Stone, "That and there: judging the intent of pointing actions with robotic arms," *Proceedings of the AAAI Conference on Artificial Intelligence*, vol. 34, no. 6, pp. 10343–10351, 2020.

[27] M. Falconi, "IEEE, control systems society, and women in engineering in Ecuador [member activities]," *IEEE Control Systems*, vol. 38, no. 4, pp. 15-16, 2018.

[28] L. Mönch, O. Rose, R. Sturm et al., "A simulation framework for the performance assessment of shop-floor control systems," *Simulation*, vol. 79, no. 3, pp. 163–170, 2003.

[29] Q. Li, J. Chen, N. P. Minton et al., "CRISPR-based genome editing and expression control systems in *Clostridium acetobutylicum* and *Clostridium beijerinckii*," *Biotechnology Journal*, vol. 11, no. 7, pp. 961–972, 2016.

Research Article

Tone Recognition Database of Electronic Pipe Organ Based on Artificial Intelligence

Shuyi Zhao [iD]

College of Music, Shenyang Normal University, Shenyang 110034, Liaoning, China

Correspondence should be addressed to Shuyi Zhao; zhaoshuyi0716@synu.edu.cn

In the past few decades, artificial intelligence technology has experienced rapid development, and its application in modern industrial systems has grown rapidly. This research mainly discusses the construction of a database of electronic pipe organ tone recognition based on artificial intelligence. The timbre synthesis module realizes the timbre synthesis of the electronic pipe organ according to the current timbre parameters. The audio time domain information (that is, the audio data obtained by file analysis) is framed and windowed, and fast Fourier transform (FFT) is performed on each frame to obtain the frequency domain information of each frame. The harmonic peak method based on improved confidence is used to identify the pitch, obtain the fundamental tone of the tone, and calculate its multiplier. Based on the timbre parameters obtained in the timbre parameter editing interface, calculate the frequency domain information of the synthesized timbre of each frame, and then perform the inverse Fourier transform to obtain the time domain waveform of each frame; connect the time domain waveforms of different frames by the cross-average method to obtain the time-domain waveform of the synthesized tone (that is, the audio data of the synthesized tone). After collecting the sound of the electronic pipe organ, the audio needs to be denoised, and the imported audio file needs to be parsed to obtain the audio data information. Then, the audio data are frequency-converted and the timbre characteristic information is analyzed; the timbre parameters are obtained through the human-computer interaction interface based on artificial intelligence, and the timbre of the electronic pipe organ is generated. If the timbre effect is not satisfactory, you can re-edit the timbre parameters through the human-computer interaction interface to generate timbre. During the experiment, the overall recognition rate of 3762 notes and 286 beats was 88.6%. The model designed in this study can flexibly generate electronic pipe organ sound libraries of different qualities to meet the requirements of sound authenticity.

1. Introduction

With the rapid popularization of the Internet in today's society, the accelerated merger of computers, communications and consumer electronics, the development trend of electronic product specialization and miniaturization [1], with the technological development of software and hardware equipment, the capabilities and superiority of artificial intelligence have quickly penetrated into life. Of course, various fields in the music technology field have become the hottest words in the field of music technology.

We know that the promotion of music is actually based on technological changes. Without the invention of tools, there would be no musical instruments; without the emergence of electronic technology, there would be no electronic music. Therefore, how much change the major technology of artificial intelligence can bring to music is also one of the motivations for me to write this article. The generation of artificial intelligence arrangement is an interdisciplinary field. It requires researchers to master a lot of interdisciplinary knowledge, including music production, music technology, artificial intelligence, and automatic accompaniment. Because it is an emerging field, domestic research is still relatively poor.

Artificial intelligence (AI) has brought the frontier of development to the fields of power electronics and power engineering. Bose believes that these technologies provide powerful tools for modern smart grid (SG) control. His applications include the automation design of modern wind power generation systems and their operating status monitoring under operating conditions, the failure mode recognition of SG subsystems, and the SG control based on real-time simulators. Although the concept of these application examples he

proposed can be extended to develop many other applications, there is still a lack of specific data [2]. Raedt et al. studied uncertainty in probability theory and graphical models and studied relations logically. He focused on two detailed representations: Markov logic network (an expansion of the relationship between undirected graphical models and weighted first-order predicate calculus formulas) and Problog (probability expansion of logic programs), which can also be regarded as Turing complete expansion of the relational Bayesian network. His research discusses Markov logic networks but still lacks theory [3, 4]. Din et al. believes that due to the existence of various pollutants produced by human, agricultural, and industrial activities, the quality of surface water has decreased. Traditionally, the concentration of SWQP is measured through intensive field work. His research attempts to develop an artificial intelligence modeling method to plot the concentration of optical and nonoptical SWQP. Although his research can retrieve different SWQP concentrations from Landsat8 images, it still lacks logic [5]. Hashemi et al. believes that process-based models have been widely used for storm surge prediction. He used the high-resolution wave and surge modeling system on the East Coast of the United States to numerically simulate 1,050 tropical tropical storms. His research provides an unprecedented data set. Although his research can be used to train artificial intelligence models for surge prediction in those areas, the accuracy is not high [6].

The timbre synthesis module realizes the timbre synthesis of the electronic pipe organ according to the current timbre parameters. The audio time domain information (that is, the audio data obtained by file analysis) is framed and windowed, and fast Fourier transform (FFT) is performed on each frame to obtain the frequency domain information of each frame. The harmonic peak method based on improved confidence is used to identify the pitch, obtain the fundamental tone of the tone, and calculate its multiplier. Based on the timbre parameters obtained in the timbre parameter editing interface, calculate the frequency domain information of the synthesized timbre of each frame, and then perform the inverse Fourier transform to obtain the time domain waveform of each frame; connect the time domain waveforms of different frames by the cross-average method to obtain the time-domain waveform of the synthesized tone (that is, the audio data of the synthesized tone). After collecting the sound of the electronic pipe organ, the audio needs to be denoised, and the imported audio file needs to be parsed to obtain the audio data information [7]. Then, the audio data are frequency-converted and the timbre characteristic information is analyzed; the timbre parameters are obtained through the human-computer interaction interface based on artificial intelligence, and the timbre of the electronic pipe organ is generated.

2. Analysis of Experimental Results of Construction of Electronic Tube Wind and Sound Recognition Database

2.1. Artificial Intelligence.
Artificial intelligence replaces human physical and mental power [8], to a certain extent, reduces the number of repetitive jobs required for the development of cultural industries, in the planning, creation, and production of cultural products. At the same time, higher requirements are put forward for the talent structure, and the input of creative jobs and high-end scientific and technological talents has increased, so that the cultural industry has great development potential and vitality [9, 10]. Artificial intelligence is the most powerful new engine to promote the efficiency of cultural industry production and operation and will help the cultural industry enter a new height [11]. It can be seen that various voice technologies of artificial intelligence make it possible to customize sound and improve the level of audio production. It has broad application prospects in the field of cultural industry and is expected to become indispensable in the production of video and song dubbing and soundtrack production technology [12, 13].

2.2. Electronic Pipe Organ Playing Game Music.
Like game design and other popular cultures, video game music has also had its place in the mainstream industry [14]. Nowadays, an internationally renowned symphony orchestra will perform a soundtrack for a game [15, 16]. With the continuous improvement of game development technology, the field of game music is also gradually growing. The electronic pipe organ is also gradually designing the field of game music, its timbre is rich and changeable, it can simulate the performance of a variety of musical instruments, and it can also be played by overlapping multiple timbres [17]. Now is the age of electronic music, the performance of popular music in the electronic organ is very important, and the simulation requirements for various popular emerging electronic musical instruments are also quite high [18, 19]. For example, the electronic pipe organ has the timbre of the jazz organ, and through the setting of the timbre parameters, it can create the ever-changing jazz organ timbre and play colorful jazz music [20]. Therefore, performers must have high performance skills and master the performance characteristics of modern electronic musical instruments [21, 22]. The electronic pipe organ has the function of simulating other musical instruments. To find how to simulate the timbre of other musical instruments more vividly, we must first master the playing skills of the electronic pipe organ [23]. The diversification of musical instruments and the variability of music have created diversified requirements for the touch method of the electronic pipe organ [24, 25].

2.3. Tone.
From the perspective of the filter bank, the STFT of the signal is

$$X^{\mathrm{STFT}}_{(k,n)} = \sum_{j=n}^{n+N-1} x(\mathrm{jw})(j-k)\exp\left(-i2\pi\frac{j}{N}\right). \qquad (1)$$

Among them, jw is a continuous window function [26]. The kth component of the CQT spectrum of the nth frame signal is

$$X_{(k,n)}^{CQT} = \sum_{j=n-[N_k/2]}^{n+[N_k/2]} x(j)a_k\left(j - n + \frac{N_k}{2}\right). \tag{2}$$

Among them, k represents the frequency subscript of CQT [27, 28]:

$$K = \left\lceil B \cdot \log_2\left(\frac{f_{max}}{f_{min}}\right) \right\rceil, \tag{3}$$

where B represents the number of subscripts per octave [29]:

$$a_k^n = \frac{1}{N_k} w\left(\frac{n}{N_k}\right) \exp\left[-i2\pi n \frac{f_k}{f_s}\right], \tag{4}$$

where f_s represents the sampling frequency. The center frequency f_k corresponding to the subscript k is

$$f_k = f_{min} 2^{(k-1)/B}, \tag{5}$$

$$Q = \left(2^{1/B} - 1\right)^{-1}. \tag{6}$$

Among them, Q represents the quality factor. The window length N_k corresponding to the frequency subscript k is

$$N_k = \left\lceil Q \frac{f_s}{f_k} \right\rceil, \tag{7}$$

$$0 < H_k \le \frac{1}{2}N_k, \tag{8}$$

where H_k represents the frame jump range that can be selected.

2.4. Tone Synthesis. The sound library generation software needs to complete audio file reading and writing, audio collection, audio file analysis, tone analysis, tone parameter acquisition, tone synthesis, and other functions. Considering the applicability of the software and the convenience of operation, the C# language is used to develop Windows in Visual Studio Express 2013. Use the Form application to facilitate user interface design and software system development.

The audio information analysis module is used to analyze audio information, complete audio denoising preprocessing, note extraction, FFTAFFT pitch recognition, octave extraction, audio information display, and other functions; the timbre parameter acquisition module edits and acquires timbre parameters through the human-computer interaction interface. The timbre synthesis module is used to synthesize timbre files, supports the batch synthesis of multiple timbres, and displays the synthesis progress in real time; the analog performance module is used to simulate the timbre or music [30, 31]. The timbre synthesis model is shown in Figure 1.

The additive synthesis method emphasizes the role of the fundamental and overtone series in the sound. Based on the Fourier principle, the signals of different frequencies are superimposed to form a new sound, as follows [32, 33]:

$$x_{f1}(t) = \sum_f A_f \sin(2\pi ft + \phi_f). \tag{9}$$

According to the principle of additive synthesis, this paper synthesizes electronic pipe organ timbre, adopts Fourier transform algorithm, and uses the directly measured original signal to calculate the frequency, amplitude, and phase of different sine wave signals in the signal by accumulation. After a lot of analysis and experiments, the immutable features in the model are determined. The specific model is expressed as follows:

$$x_{f_1}(t) = \sum_{k=1}^{K} \sum_{f \in D_k} s_f v_k A_f \sin(2\pi ft + \phi_f) + \sum_{f \in D_k} A_f \sin(2\pi ft + \phi_f). \tag{10}$$

In the formula, $x_{f_1}(t)$ represents the sound of the electronic pipe organ when the pitch frequency is f_1. Variable frequency range D meets

$$D = \bigcup_{k}^{K} D_k = D_1 \cup D_2 \cup \ldots \cup D_k \cup \ldots \cup D_K, \quad k = 1, 2, \ldots K, \frac{x - \mu}{\sigma}. \tag{11}$$

Variable frequency range of section k is

$$f_k - \partial f_1 \le D_k \le f_k + \partial f_1. \tag{12}$$

Among them, f_1 is the pitch frequency. The multiplier of the sound is

$$f_k = kf_1 (k = 1, 2, 3, \ldots, K). \tag{13}$$

The timbre synthesis uses the timbre synthesis model proposed in this article to synthesize timbre to verify the effect of synthetic timbre. The steps for synthesizing tones are as follows:

(1) Framing and windowing the actual electronic pipe organ timbre, and fast Fourier transform (FFT) for each frame to obtain the frequency domain information of each frame.

(2) Use the harmonic peak method based on improved confidence to recognize the pitch, obtain the fundamental tone f, and calculate the multiplier $f = k$.

(3) According to the audio synthesis model of the editable tone, select the appropriate tone parameters (maximum multiplier K, amplitude modification coefficient Dk, synthesis parameter 2, linear s) to form the frequency domain information of each frame of synthesized tone.

(4) Perform inverse Fourier transform of the frequency domain information of each frame of the synthesized tone to obtain the time domain waveform of each frame and then use the cross-average method to connect the time domain waveforms of different frames to obtain the time domain waveform diagram of the synthesized tone.
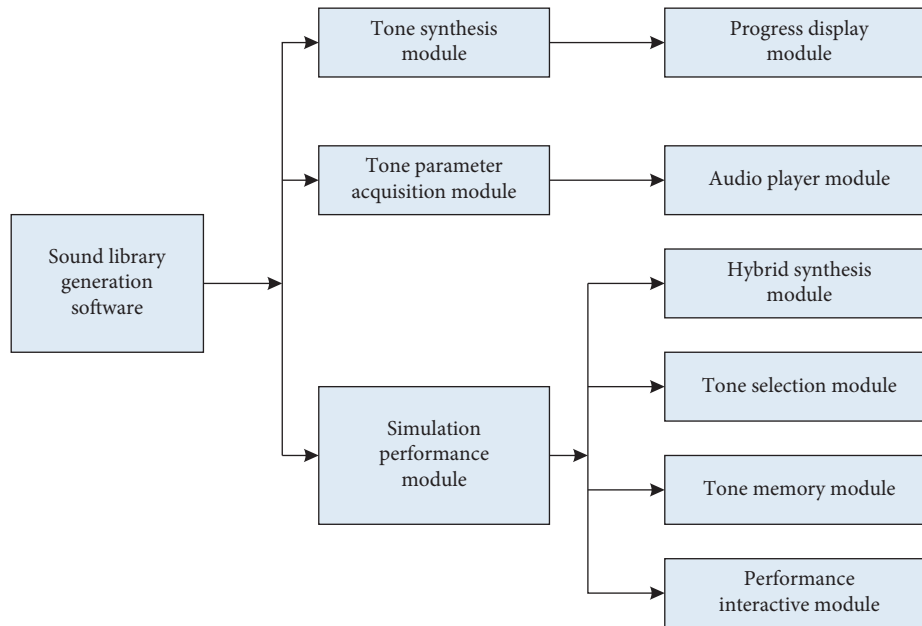
FIGURE 1: Tone synthesis model.

3. Experiment of Constructing Electronic Pipe Organ Tone Recognition Database

3.1. Overall Architecture of Sound Library Generation Software. The electronic pipe organ sound library first needs to input the first frequency, and the software supports 2 first input methods: electronic pipe organ sound collection and the import of existing audio files. After collecting the electronic pipe organ sound, the audio needs to be denoised, and the imported audio file needs to be audio. File analysis was done to obtain audio data information. Then, the audio data are frequency-converted and the timbre characteristic information is analyzed; the timbre parameters are obtained through the human-computer interaction interface based on artificial intelligence, and the timbre of the electronic pipe organ is generated. The timbre generated by analog playback can be saved as an audio file if the timbre effect is satisfactory or directly generate and save the electronic pipe organ sound library in batches; if the timbre effect is not satisfactory, the timbre parameters can be re-edited through the human-computer interaction interface to generate timbre. The overall structure of the sound library generation software is shown in Figure 2.

3.2. Tone Library Generation Process

3.2.1. Audio File Reading and Writing Module. The audio file reading and writing module of the software is used to complete audio file input, audio file analysis, audio file writing, and other functions.

(1) Audio File Import. Click the audio import in the menu file, the open file window will pop up, select an audio file in the ".wav" format to open, and the system will analyze the
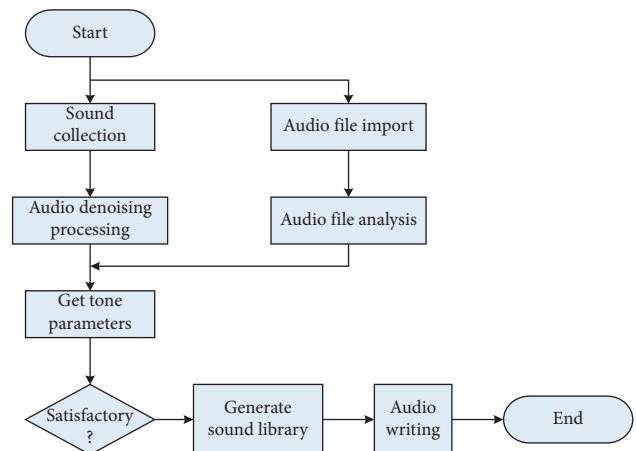
FIGURE 2: Overall architecture of sound library generation software.

audio file. After the analysis is completed, the audio information will be analyzed and displayed.

The structure of a WAV file includes a "RIFF" block, a "fmt" sub-block and a "data" sub-block. The "fmt" sub-block contains the number of channels, sampling rate, number of bits, etc. Perform audio file analysis according to the data format of WAV file, define class WavReader, and complete the analysis and writing function of WAV file. Class WavReader defines read function ReadWAVFile() and write function buildwav() and various variable packaging functions getNumChannels(), getdsize0, getwavdata(), and getwavdata20, variable type conversion, and other auxiliary functions.

(2) Sound Signal Collection. The collection of sound signals is completed through an interactive interface. The upper part of the interface is the audio waveform display

area. When the acquisition is completed, the system analyzes the buffered recording and automatically displays the time-domain waveform of the recording; there are five buttons at the bottom of the interface, and the "collection start" and "collection end" buttons are used to control the sound collection. The module starts or stops sound collection; the "Play" button realizes the playback of the buffered recording; the "Clear" button is used to clear the buffered recording and at the same time clear the audio waveform in the upper area of the interface; click the "Save" button to pop up the save file dialog box to realize the buffer recording preservation.

Under the file menu list, there are three items of "audio import," "audio capture," and "save as." Audio import realizes the audio file import function and supports commonly used WAV format audio files; audio capture through the microphone and sound card of the sound capture module realizes the collection and preservation of sound; save as it is used to realize the writing of audio files.

3.2.2. Audio Information Analysis Module. Audio information analysis module is used for audio information processing and analysis, including denoising preprocessing module, note extraction module, FFTIFFT module, pitch recognition module, octave extraction module, and audio information display module. The pitch extraction module uses the harmonic analysis method with improved confidence proposed in this paper to extract the pitch.

3.3. Tone Parameter Acquisition Module. The timbre parameter module is used to obtain timbre parameters through the interactive page of timbre parameter editing. The top of the tone parameter editing interface is the menu bar, the upper left is the currently open file list, the upper right is the audio waveform display area, the lower part is the tone parameter editing area, and the bottom is the six control buttons. The tone color parameter editing area displays the pitch frequency of the audio. It supports the modification of generation parameters, three types of correction line types, and fourteen spectral coefficients. The generation parameters default to 0.3, the correction line type defaults to linear, and the fourteen spectral coefficients default to 1. The "Reset" button is used to reset the parameters with one key. The "Play" and "Stop" buttons control the playback and stop of the audio. The "Generate Tone Source" button synthesizes the tone based on the current tone parameters and refreshes the audio waveform display. In the area, the "Save" button is used to save the current sound. Click the "Generate Sound Library" button to enter the sound library generation interface and perform batch synthesis of sounds.

3.4. Tone Synthesis Module. The timbre synthesis module realizes the timbre synthesis of the electronic pipe organ according to the current timbre parameters. In order to facilitate the generation of electronic pipe organ sound library, the software supports batch synthesis of multiple tones. The specific steps are as follows:

(1) Obtain the file number n and file name in the audio source path.

(2) Open the first electronic organ tone file under the sound source path, and perform file analysis to obtain audio data.

(3) The audio time domain information (that is, the audio data obtained by file analysis) is divided into frames and windows, and fast Fourier transform (FFT) is performed on each frame to obtain the frequency domain information of each frame.

(4) Use the harmonic peak method based on improved confidence to recognize the pitch, obtain the fundamental tone of the tone, and calculate its multiplier.

(5) Based on the timbre parameters obtained in the timbre parameter editing interface, calculate the frequency domain information of the synthesized timbre of each frame, and then perform inverse Fourier transform to obtain the time domain waveform of each frame; the time domain waveforms of different frames are processed by the cross-average method. Connect to obtain the time-domain waveform of the synthesized tone (i.e., the audio data of the synthesized tone).

(6) Write the audio data of the synthesized tone into an audio file with the same name and save it in the save path. The current progress displays +1.

(7) Open the next tube organ tone file in the sound source path for analysis, and repeat steps 3–7 until all n files are completed.

3.5. Simulation Performance Module. The simulation performance module is used to perform electronic pipe organ performance. It can perform real-time timbre synthesis and switching according to performance needs. It supports mixed performance of multiple timbres, which is equivalent to an upgraded version of intelligent electronic pipe organ. The simulation performance module includes a tone storage module, a performance interaction module, a tone selection module, a hybrid synthesis module, and an audio playback module.

The tone storage module is used to store the tone library of different levels for each instrument and is provided to the tone selection module and the hybrid synthesis module; the performance interaction module is used for performance interaction, including setting the tone performance mode, performing the simulation performance of the instrument, and according to the automatic performance. The score takes the score information; the timbre selection module judges according to the feedback information and the score information provided by the performance interaction module, determines whether timbre synthesis is needed, and gives synthesis instructions; the hybrid synthesis module uses the timbre storage module after receiving the synthesis instructions The feedback information and score information provided by the timbre library and interactive module synthesize mixed timbre; the audio playback module performs audio playback.

The simulation method includes the following steps:

(1) Use the interactive unit to perform performance interaction and obtain feedback information, and obtain score information according to the score.

(2) The timbre generation unit judges based on the feedback information and score information provided by the interactive unit and selects the timbre in the timbre storage unit for playback or gives synthesis instructions.

(3) After receiving the synthesis instruction from the tone generating unit, the mixing synthesis unit uses the tone library in the tone storage unit and the feedback information and score information provided by the interactive unit to synthesize and play the mixed tone.

3.6. Audio Pitch Shift and Real-Time Harmony. In sound recording and playback, real-time recording of performance music segments can be stored in the cache, and subsequent changes can be played. However, if the "pf~" technology of the "gizmo" object can be used to realize real-time audio processing, it will be possible to form a harmony group with the audio real-time pitch shift and the original sound. FFT is an efficient DFT algorithm, namely, fast Fourier transform (FastFourierTransform), and the "pft~" object can perform fast Fourier transform on the input waveform to obtain each harmonic component and perform various analysis and processing before performing inverse fast Fourier transform (IFFT), thus getting the output result. The "gizmo~" object that works with the "pfft~" technology can be adjusted in the frequency domain. Based on the FFT algorithm, the speed can meet the real-time requirements.

4. Electronic Pipe Organ Tone Recognition Database

4.1. Tone Effect Analysis. The timbre test effect is shown in Table 1. From the auditory timbre effect, judge whether it is a tube organ audio. In Table 1, the electronic pipe organ timbre discrimination refers to the number of five actual electronic pipe organs judged by the testee as the number of electronic pipe organs, and the synthetic timbre discrimination refers to the number of five synthetic timbres judged by the testee as the number of electronic pipe organs. The data "10 × 5" mean that each of 10 people judged 5 tones as a tube organ, and the data 9 × 5 + 1 × 4 mean that 9 of 10 people judged 5 tones as a tube organ, and one judged 4 tones as a tube organ. In the results of the auditory discrimination test, among the 30 testees' judgments on the 5 synthesized tones, 10 testees who did not receive formal music education (hereinafter referred to as Type A test subjects) judged that all 5 synthesized tones were electronic pipe organ tone, 10 testees who have learned instrument performance for more than 2 years (hereinafter referred to as Type B test subjects) judged that all 5 synthesized tones are electronic pipe organ sounds, and 10 test subjects who have learned electronic pipe organ performance for more than 2 years (hereinafter referred to as among the category C test subjects), 9 people judged that all 5 synthesized tones are electronic pipe organ sounds, one person thinks that 4 are electronic pipe organ

sounds, and one is not electronic pipe organ sounds. In the A and B test subjects, the matching degree of the synthetic tone is 100%, and in the C test subjects, the synthetic matching degree is 98%. In summary, the test match is close to 100%, and it can be concluded that the synthetic tone and the actual electronic pipe organ tone cannot be distinguished by human hearing. From the theoretical comparison experiments and auditory discrimination experiments, the following conclusions can be drawn: the synthetic timbre belongs to the electronic pipe organ timbre, which meets the authenticity and high quality requirements of the electronic pipe organ sound library generation.

The time-domain waveform of the synthesized timbre is shown in Figure 3. In the figure, the abscissa represents the sampling point, and the abscissa divided by the sampling frequency 44100 is the time (in seconds); the ordinate represents the amplitude of each sampling point. The specific tone synthesis model and experimental size are shown in Figure 4. The frequency domain waveform of the synthesized tone is shown in Figure 4. In Figure 4, the abscissa represents the frequency, the unit is 1 Hz, and the range is from 1 Hz to 220S0 Hz; the ordinate represents the amplitude of each frequency.

Comparing the synthesized timbre with the actual electronic pipe organ timbre, the time-domain waveform comparison of the two is shown in Figure 5. In Figure 5, the top is the synthetic tone, and the bottom is the actual tone. The abscissa represents the sampling point. The abscissa divided by the sampling frequency of 44100 is the time (in seconds); the ordinate represents the amplitude of each sampling point. The frequency domain waveform comparison between the two is shown in Figure 6. In Figure 6, the upper is the synthetic tone, and the lower is the actual tone. The abscissa represents the frequency, the interval is 1 Hz, and the range is from 1 Hz to 22050 Hz; the ordinate represents the amplitude of each frequency. From the comparison of the time-domain waveforms of the synthesized timbre and the actual electronic pipe organ timbre in Figure 5, it can be seen that the time-domain waveforms of the two are roughly the same, with only very subtle details different. Therefore, it can be judged that the two are very different from the volume and waveform changes. Similarly, the real-time domain envelope is approximately the same; from the frequency domain waveform comparison of the synthetic tone and the actual electronic pipe organ tone, it can be seen that the frequency domain waveform characteristics of the two are roughly the same, the frequency distribution is clean and clear, and both are at the frequency of the multiplier. The amplitude is larger, and there are more frequency components with smaller amplitude in the low frequency range. This part of the frequency forms the tap sound of the electronic pipe organ at the moment of pressing; that is, the frequency domain distribution of the two is approximately the same. Therefore, according to the timbre is jointly determined by the frequency domain (frequency composition and amount) and time domain, it can be basically judged that the timbre of the two is similar, and both belong to the timbre of the electronic pipe organ. The frequency of the electronic pipe organ is shown in Table 2. The beat of the electronic pipe organ is shown in Table 3.

TABLE 1: Tone test results.

Subject	Piano tone judgment	Synthetic tone discrimination	Suitability (%)
No formal music education (10 people)	10×5	10×5	100
Play musical instruments more than 2 years (10 people)	10×5	10×5	100
Learn piano for more than 2 years (10 people)	10×5	$9 \times 5 + 1 \times 4$	98
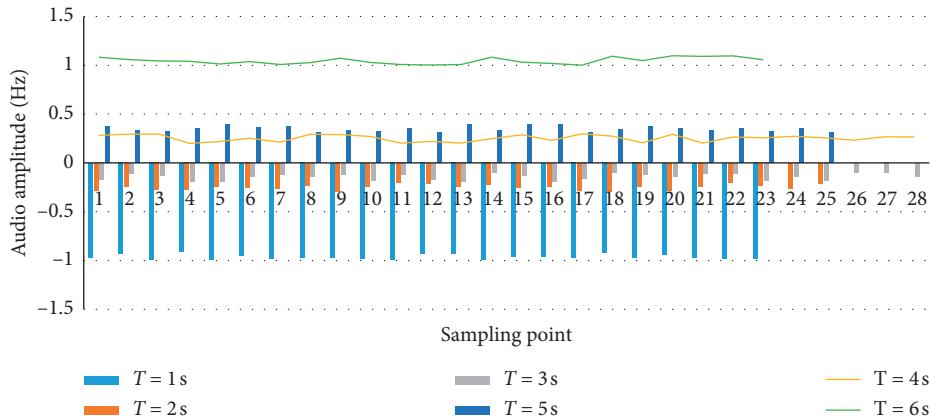
FIGURE 3: Time-domain waveform of the synthesized voice.
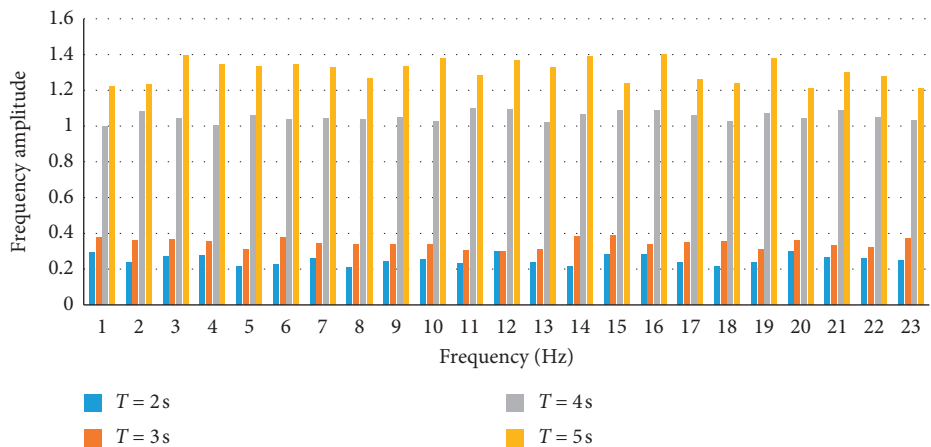
FIGURE 4: The frequency domain waveform of the synthesized tone.

4.2. Recognition Effect of Chords. Choose three different styles of songs. The chord recognition results are shown in Table 4. Through the analysis of the recognition results, it is found that most of the errors occur in empty chords, especially in some fast-paced time periods. Since the analysis window is definite, if the input is a fast-paced segment, it means that the window will span more notes, and a frame of data is likely to contain more than one type of chords, which confuses the system. The beat synchronization analysis algorithm will effectively avoid this problem, because not only is usually the speed of chord changes slower than the speed of beat changes, but also empty chords rarely appear in a beat. In addition to some sporadic errors, some errors are concentrated on the minor a seventh chord and the major C triad. The minor A seventh chord is composed of four pure tones A, C, E, and G, of which C, E, and G are major C triads. The three pure tones included. As mentioned earlier,

because this article regards the minor A triad and minor A seventh chord as the same type, in the presence of pure tone G, the system is likely to mistake the minor A seventh chord as a major C triad. Therefore, we hope that the system can effectively avoid such confusion when increasing the type set of chords to include seventh chords in the system chord classification.

The relative frequencies used when extracting the base collar are shown in Table 5. There are 86 wav files used to test the recognition rate of the system, including typical music of foreign nationalities, classical music, and popular classics. Under this definition, the overall recognition rate of 3762 notes and 286 beats is 88.6%. The accuracy of recognition is still quite high. It must be noted that, in order to facilitate the following comparison, in the abovementioned method of extracting the pitch time value, the difference between two
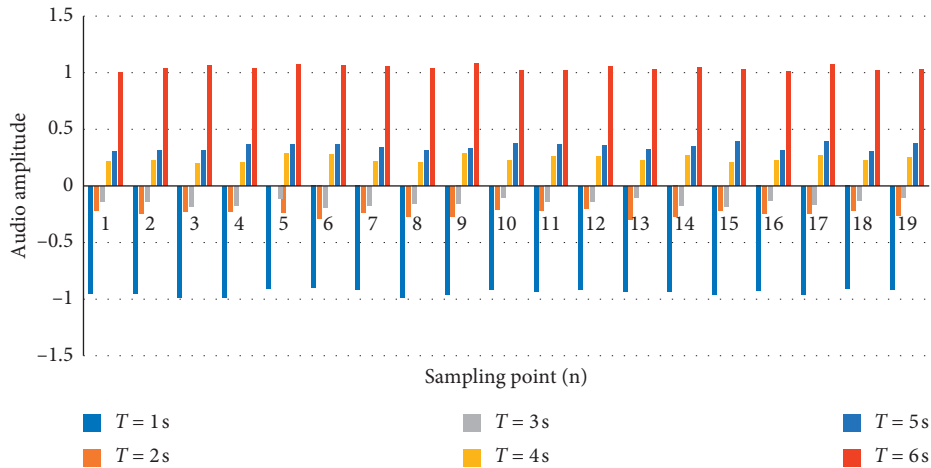
FIGURE 5: Comparison of synthesized sound and actual electronic pipe organ sound.
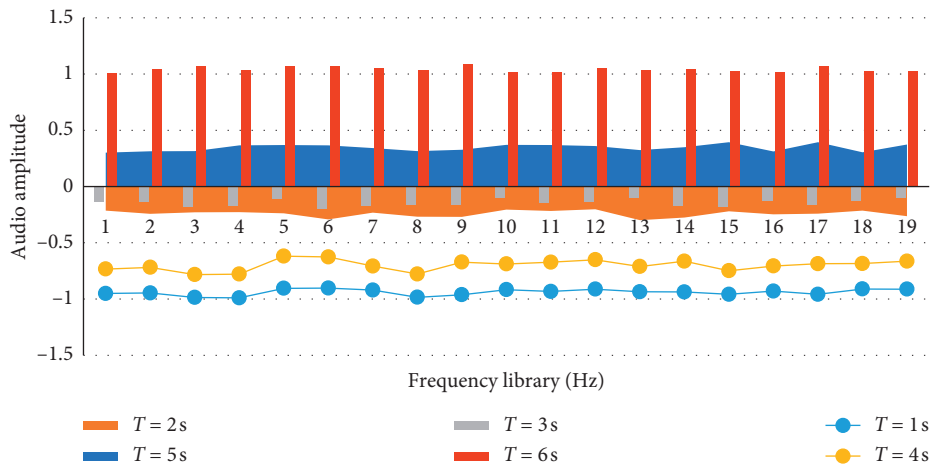
FIGURE 6: Frequency domain waveform comparison between the two.

TABLE 2: Frequency of electronic pipe organ.

Note	5	5	6	2	1	1	6	2
Frequency (Hz)	523.25	523.25	587.33	392	349.23	349.23	293.66	39.2

TABLE 3: Tube organ beat.

Note	5	5	6	2	1	1	6	2
Time (s)	0.5	0.25	0.25	1	0.5	0.25	0.25	39.2

consecutively repeated sounds and a continuous sound of equal duration is not distinguished, that is, in the extraction and normalization. In the process of transformation, for example, two types of sounds are considered equal. It can be seen that the experimental results and theoretical values have a good approximation. Here, the normalized way is to use the smallest time unit in the music (such as quarter beat, etc.) as the metric for the duration of each note played and take its proportional value.

The research result of the dual-tone pitch time value extraction module is shown in Figure 7. The experimental data are still derived from the performance of learners of electronic pipe organ performance. However, the data used in the module test are the basic two-tone chords in music and will not change after triggering the vibration; that is, it is stable on two notes. To test the performance of this module, 100 two-tone chords with different ranges, different spans, and different degrees of harmony were selected. The dual-tone pitch time value extraction module accurately reflects

TABLE 4: Recognition results of chords.

Test data	Length	Recognition rate (%)
Fragments of piano music	8.26 seconds/44 frames	81.1 8
Song please, please me	125 seconds/662 frames	78.70
Song yesterday	121 seconds/644 frames	74.53

TABLE 5: Relevant frequencies used when extracting base collar.

Musical alphabet	Calculated frequency (Hz)	Normalized starting frequency (Hz)	Normalized stop frequency (Hz)	Program use pitch (Hz)
#a	220	213	235	220
cl	233.08	226	239	233
#c1	246. 94	240	253	217
t1	261.63	254	268	262
#d1	277.18	269	281	277
e1	293. 66	285	301	294
f1	311.13	302	319	311
#f1	329. 63	320	338	330
g1	349.23	339	358	349
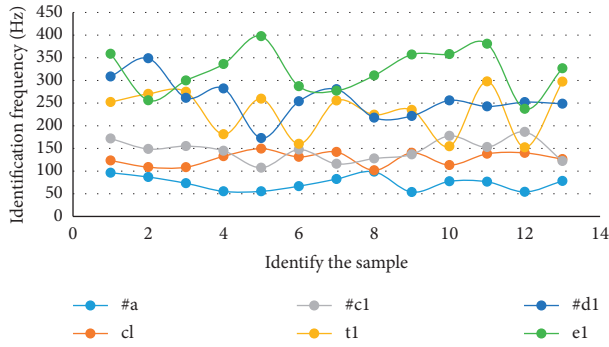
FIGURE 7: Research results of the dual-tone pitch time value extraction module.

the chord time value and pitch information. The data input to the module in.wav format is also output as a time-event graph. In the figure, two straight horizontal lines distinguish the time distribution of the central *c* and central *g*. Through this module, the corresponding height and vibration time of the dual-tone chord can be analyzed. We tested on 100 experimental samples, 82 samples with recognition rate above 95%, 1 sample with recognition rate lower than 50%, and 6 samples lower than 70%. Observing the experimental results, it is found that such experimental samples are samples of absolute concord chords in music, and the two-tone interval is more than 13 degrees apart; that is to say, this module has a low resolution of the absolute consonant interval of the polytone, which is due to its frequency spectrum caused by aliasing. This module has a low resolution effect on dual-tone experimental data with frequent changes in pitch and a relatively high computational

complexity. This is a place that can be further improved in future work.

4.3. Basic Function Analysis. The basic function test result is shown in Figure 8. The electronic keyboard product will enter the main interface of the auxiliary system about 30 seconds after powering on. The main interface defaults to the first big button in the upper left corner. Clicking the big button will switch the bottom panel between tone selection and tone attribute compilation. When the bottom panel has multiple pages, you can turn pages, and you can also turn pages. Each control can be adjusted normally. The default value of the slide bar is generally 63, which can be adjusted between 0 and 127 with the button or the scroll wheel, and there is no border crossing. Press any one of a group of rhythm keys on the keyboard, the bottom panel of the main interface will become the rhythm selection panel, and press it again to become the rhythm attribute editing panel of the corresponding group. Pressing the exit key when any interface is in an idle state will return to the main interface. If you do not change the main interface parameters through the keyboard physical keys, the main interface will remain the same as when you left it the last time. The pop-up edit box shows the selected file, and the suffix name is hidden in the edit box. In the state of renaming, the cursor in the edit box can be moved and characters can be deleted or inserted in the corresponding position, which can realize the input of English and number punctuation. And the system has a sound processing method for a variety of naming accidents. The overall function test is shown in Table 6. The test data of the file management module are shown in Table 7. The electronic pipe organ is shown in Figure 9.
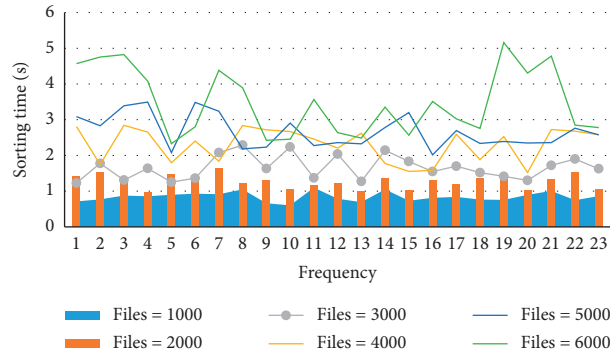
Figure 8: Basic function test results.

Table 6: Overall functional test.

Frequency	Start time (s)	Key response (ms)	File transfer	Record audio (M)
1	15.6	20	1.7 M/s	6
2	16.2	30	1.6 M/s	7
3	15.9	20	1.6 M/s	8
4	17.1	25	1.8 M/s	7
5	16.4	25	1.9 M/s	8

Table 7: File management module test data.

Frequency	Number of files	File layers	Positioning time (s)	Sort time	Copy rate	Average download speed
1	1000	2	1.2	2.0 s	1.8 M/s	504 K/s
2	2000	3	1.5	2. 4 s	1.8 M/s	485 K/s
3	3000	4	1.6	3.2 s	1.8 M/s	512 K/s
4	4000	5	1.9	3.6 s	1.8 M/s	492 K/s
5	5000	3	2.3	4.3 s	1.8 M/s	497 K/s
6	6000	2	2.0	3.5 s	1.9 M/s	502 K/s

Figure 9: The electronic pipe organ (from http://alturl.com/qsobx).

5. Conclusion

The electronic pipe organ sound library first needs to input the first frequency, and the software supports 2 first input methods: electronic pipe organ sound collection and the import of existing audio files. After collecting the electronic pipe organ sound, the audio needs to be denoised, and the imported audio file needs to be audio. File analysis was done to obtain audio data information. Then, the audio data are frequency-converted and the timbre characteristic

information is analyzed; the timbre parameters are obtained through the human-computer interaction interface based on artificial intelligence, and the timbre of the electronic pipe organ is generated. The timbre generated by analog playback can be saved as an audio file if the timbre effect is satisfactory or directly generate and save the electronic pipe organ sound library in batches; if the timbre effect is not satisfactory, the timbre parameters can be re-edited through the human-computer interaction interface to generate timbre.

The simulation performance module includes a tone storage module, a performance interaction module, a tone selection module, a hybrid synthesis module, and an audio playback module. The tone storage module is used to store the tone library of different levels for each instrument and is provided to the tone selection module and the hybrid synthesis module; the performance interaction module is used for performance interaction, including setting the tone performance mode, performing the simulation performance of the instrument, and according to the automatic performance. The score takes the score information; the timbre selection module judges according to the feedback information and the score information provided by the performance interaction module, determines whether timbre synthesis is needed, and gives synthesis instructions; the hybrid synthesis module uses the timbre storage module

after receiving the synthesis instructions, synthesizing mixed sounds from feedback information and score information provided by the sound library and interactive module.

The audio playback module performs audio playback. Use the interactive unit to perform performance interaction and obtain feedback information, and obtain score information according to the score; the timbre generation unit judges according to the feedback information and score information provided by the interaction unit, selects the timbre in the timbre storage unit for playback, or gives synthesis instructions; mix after the synthesis unit receives the synthesis instruction from the timbre generation unit, and it uses the timbre library in the timbre storage unit and the feedback information and score information provided by the interaction unit to synthesize and play the mixed timbre.

Data Availability

The data that support the findings of this study are available from the corresponding author upon reasonable request.

Conflicts of Interest

The authors declare that they have no conflicts of interest.

Acknowledgments

References

[1] Z. Lv, A. Halawani, S. Feng, H. Li, and S. U. Réhman, "Multimodal hand and foot gesture interaction for handheld devices," *ACM Transactions on Multimedia Computing, Communications, and Applications*, vol. 11, no. 1, pp. 1–19, 2014.

[2] B. K. Bose, "Artificial intelligence techniques in smart grid and renewable energy systems-some example applications," in *Proceedings of the IEEE*, vol. 105, no. 11, pp. 2262–2273, 2017.

[3] L. D. Raedt, K. Kersting, S. Natarajan, and D. Poole, "Statistical relational artificial intelligence: logic, probability, and computation," *Synthesis Lectures on Artificial Intelligence and Machine Learning*, vol. 10, no. 2, pp. 1–189, 2016.

[4] B. Wang, J. Cheng, and X. Zhou, "A multiple hierarchical structure strategy to quantized control of Markovian switching systems," *Applied Mathematics and Computation*, vol. 373, Article ID 125037, 2020.

[5] E. S. E. Din, Y. Zhang, and A. Suliman, "Mapping concentrations of surface water quality parameters using a novel remote sensing and artificial intelligence framework," *International Journal of Remote Sensing*, vol. 38, no. 4, pp. 1023–1042, 2017.

[6] M. R. Hashemi, M. L. Spaulding, A. Shaw, H. Farhadi, and M. Lewis, "An efficient artificial intelligence model for prediction of tropical storm surge," *Natural Hazards*, vol. 82, no. 1, pp. 471–491, 2016.

[7] H. Song and M. Brandt-Pearce, "A 2-D discrete-time model of physical impairments in wavelength-division multiplexing systems," *Journal of Lightwave Technology*, vol. 30, no. 5, pp. 713–726, 2012.

[8] Q. Wang and P. Lu, "Research on application of artificial intelligence in computer network technology," *International Journal of Pattern Recognition and Artificial Intelligence*, vol. 33, no. 5, Article ID 1959015, 2019.

[9] H. Lu, Y. Li, and M. Chen, "Brain intelligence: go beyond artificial intelligence," *Mobile Networks and Applications*, vol. 23, no. 7553, pp. 368–375, 2017.

[10] S. Jha and E. J. Topol, "Adapting to artificial intelligence," *JAMA*, vol. 316, no. 22, pp. 2353-2354, 2016.

[11] D. Hassabis, "Artificial intelligence: chess match of the century," *Nature*, vol. 544, no. 7651, pp. 413-414, 2017.

[12] D. Yan, Q. Zhou, and J. Wang, "Bayesian regularisation neural network based on artificial intelligence optimisation," *International Journal of Production Research*, vol. 55, no. 7-8, pp. 2266–2287, 2016.

[13] A. Ema, N. Akiya, H. Osawa et al., "Future relations between humans and artificial intelligence: a stakeholder opinion survey in Japan," *IEEE Technology and Society Magazine*, vol. 35, no. 4, pp. 68–75, 2016.

[14] T. R. Besold, "On cognitive aspects of human-level artificial intelligence," *Ki Künstliche Intelligenz*, vol. 30, no. 3-4, pp. 343–346, 2016.

[15] Y. Feng, N. Cui, Q. Zhang, L. Zhao, and D. Gong, "Comparison of artificial intelligence and empirical models for estimation of daily diffuse solar radiation in North China Plain," *International Journal of Hydrogen Energy*, vol. 42, no. 21, pp. 14418–14428, 2017.

[16] R. H. Kulkarni and P. Padmanabham, "Integration of artificial intelligence activities in software development processes and measuring effectiveness of integration," *Iet Software*, vol. 11, no. 1, pp. 18–26, 2017.

[17] D. Norman, "Design, business models, and human-technology teamwork," *Research-Technology Management*, vol. 60, no. 1, pp. 26–30, 2017.

[18] F. Liu, Y. Shi, and Y. Liu, "Intelligence quotient and intelligence grade of artificial intelligence," *Annals of Data Science*, vol. 4, no. 2, pp. 179–191, 2017.

[19] S. Abid, S. Jyotsna, A. Mehbob, and S. Vinod, "Novel benchmark database of digitized and calibrated cervical cells for artificial intelligence based screening of cervical cancer," *Journal of Ambient Intelligence & Humanized Computing*, vol. 12652, no. 16, pp. 353–358, 2016.

[20] N. Dudhwala, K. Jadhav, and P. Gabda, "Prediction of stock market using data mining and artificial intelligence," *International Journal of Computer Applications*, vol. 134, no. 12, pp. 9–11, 2016.

[21] A. H. Mazinan and A. R. Khalaji, "A comparative study on applications of artificial intelligence-based multiple models predictive control schemes to a class of industrial complicated systems," *Energy Systems*, vol. 7, no. 2, pp. 237–269, 2016.

[22] J. Davies, "Program good ethics into artificial intelligence," *Nature*, vol. 538, no. 7625, p. 291, 2016.

[23] M. O'Neill, R. F. E. Sutcliffe, and C. Ryan, "Artificial intelligence and cognitive science," *Applied Artificial Intelligence*, vol. 5, no. 2, pp. 153–162, 2016.

[24] J. Luther, "Discovery in an age of artificial intelligence," *Learned Publishing*, vol. 29, no. 2, pp. 75-76, 2016.

[25] T. M. Massaro, H. L. Norton, and M. E. Kaminski, "SIRI-OUSLY 2.0: what artificial intelligence reveals about the first amendment," *Social Science Electronic Publishing*, vol. 101, no. 6, pp. 2481–2525, 2017.

[26] D. S. Manu and A. K. Thalla, "Artificial intelligence models for predicting the performance of biological wastewater treatment plant in the removal of Kjeldahl Nitrogen from wastewater," *Applied Water Science*, vol. 7, no. 7, pp. 1–9, 2017.

[27] R. J. Spiro, B. C. Bruce, and W. F. Brewer, "Theoretical issues in reading comprehension: perspectives from cognitive psychology, linguistics, artificial intelligence, and education," *Reading Teacher*, vol. 3, pp. 368–373, 2017.

[28] M. A. Ali, "Artificial intelligence and natural language processing: the Arabic corpora in online translation software," *International Journal of Advanced and Applied Sciences*, vol. 3, no. 9, pp. 59–66, 2016.

[29] M. Taheri, M. R. A. Moghaddam, and M. Arami, "Improvement of the/Taguchi/design optimization using artificial intelligence in three acid azo dyes removal by electrocoagulation," *Environmental Progress & Sustainable Energy*, vol. 34, no. 6, pp. 1568–1575, 2016.

[30] E. Sinagra, M. Badalamenti, M. Maida et al., "Use of artificial intelligence in improving adenoma detection rate during colonoscopy: might both endoscopists and pathologists be further helped," *World Journal of Gastroenterology*, vol. 26, no. 39, pp. 5911–5918, 2020.

[31] M. Y. Zub, "Transformation of labor market infrastructure under the influence of artificial intelligence," *Business Inform*, vol. 8, no. 511, pp. 146–153, 2020.

[32] M. Ehteram, A. Ferdowsi, M. Faramarzpour et al., "Hybridization of artificial intelligence models with nature inspired optimization algorithms for lake water level prediction and uncertainty analysis," *Alexandria Engineering Journal*, vol. 60, no. 2, pp. 2193–2208, 2021.

[33] T. K. Ng, "New interpretation of extracurricular activities via social networking sites: a case study of artificial intelligence learning at a secondary school in Hong Kong," *Journal of Education and Training Studies*, vol. 9, no. 1, pp. 49–60, 2021.

Research Article

Sports Big Data Analysis Based on Cloud Platform and Its Impact on Sports Economy

Ye Cheng[1] and Yan Song [iD][2]

[1]*Department of Physical Education, Hebei University of Economics and Business, Shijiazhuang 050061, Hebei, China*
[2]*College of Physical Education, Kunsan National University, Kunsan 54150, Jeonro-do, Republic of Korea*

Correspondence should be addressed to Yan Song; 1920034@office365.kunsan.ac.kr

The service information system is constantly transforming to a networked information model, and domestic hardware equipment is constantly updated. Independent controllability has also become the basic requirement of the new information age. With the development of the information age and the new era of independent control, more and more services and applications will also be deployed on autonomous and controllable cloud platforms. With the rapid development of Internet technology in the information age and the resulting changes in productivity, people can record, store, and transmit more and more information. When information becomes recordable, storage, and easy to transmit, information becomes modern meaning nowadays, an era of information explosion characterized by massive, volatile, timely transmission, and diverse forms has truly come, forming what is now called the "big data era". This article mainly introduces the analysis of sports big data based on the cloud platform and the research on the impact on the sports economy and intends to provide ideas and directions for the analysis of sports big data and the research on the impact on the sports economy. This paper proposes a cloud platform-based sports big data analysis and research methods for its impact on the sports economy, including the use of Hadoop cloud platform big data processing systems and support vector regression algorithms for cloud platform-based sports big data analysis and sports economy. The experimental results of this paper show that the average correlation between sports big data analysis and sports economic development is 0.5155, and appropriate cloud platform-based sports big data analysis plays a positive role in promoting sports economic development.

1. Introduction

Today's world is an era of data explosion. IDC report shows that the global digital volume was about 130 EB in 2005, and it will reach 40000 EB by 2020. There is no doubt that human society has entered the era of big data. Big data has penetrated into all walks of life and is an important part of the global economy. Without big data, it will be difficult for modern economy to have more innovation and vitality. The development and application of big data have become important sources to enhance the competitiveness of the country and enterprises.

In the 21st century, with the rapid development of science and technology and the gradual improvement of people's material and cultural level, people gradually realize the importance of physical health. In recent years, people have begun to pay attention to the healthy development of the body. A series of fitness methods such as fitness, yoga, and marathon have become the icon of the new century. This shows that the overall healthy development of the body is inseparable from sports. The development of sports has received more and more attention from the government and the masses, and the economic development of the sports industry has made great progress. With the normalization of my country's economy, the development of the sports industry has gradually entered normalization. The "Thirteenth Five-Year Plan" for the Development of Sports Industry issued by the State Sports General Administration clearly pointed out the main tasks in expanding social supply, requiring the active promotion of "Internet + sports". The State

Sports General Administration further emphasized the importance of the Internet for the development of sports, and the development of sports economy should keep up with the times and meet the needs of the masses. At the national level, enterprises and individuals are also encouraged to jointly provide the supply of sports public service information, and the development and utilization of mobile APP and other software are encouraged. Under the background of big data, the analysis of sports big data based on cloud platform and the research of its impact on sports economy is imminent.

Zhong et al. believe that, with the development of the Internet, recommendation systems are playing an increasingly important role in the field of big data processing such as e-commerce. Aiming at the big data processing problem in the recommendation system, Zhong et al. proposed a cloud platform collaborative filtering algorithm based on clustering and correlation. The algorithm uses k-medoids clustering and related multitree data structure to solve traditional the user-based collaborative filtering algorithm has been improved. First, the user-based cloud platform collaborative filtering technology is analyzed. On this basis, k-medoids clustering is used to propose a cloud platform collaborative filtering algorithm based on k-medoids, which can effectively solve the problem of data sparseness. Aiming at the problem of reduced recommendation accuracy caused by clustering technology, Zhong et al. propose a data structure of associative multitrees, which associates user information with neighbor information. It can be used to calculate the extended user project scores, making full use of the correlation between data on the cloud platform. This research is expensive and not suitable for popularization in practice [1]. Liu et al. conducted a lot of experiments on the Ali data set on the Hadoop cloud platform and found that the virtual opportunities on the cloud platform are affected by various factors, which can cause performance degradation and downtime, thereby affecting the reliability of the cloud platform. Traditional cloud platform anomaly detection algorithms and strategies have defects in detection accuracy, detection speed, and adaptability. Liu et al. proposed an SOM-based dynamic adaptive virtual machine anomaly detection algorithm and proposed an SOM-based unified modeling method for machine performance in the detection area, which avoided the cost of modeling a single virtual machine and improved the cloud platform the detection speed and reliability of large-scale virtual machines. In the process of SOM modeling, the important parameters that affect the modeling speed are optimized, which significantly improves the accuracy of SOM modeling, thereby improving the accuracy of virtual machine anomaly detection. The practicality of this research is weak [2]. Tang et al. believe that data-intensive analysis is the main challenge in smart cities due to the deployment of various sensors everywhere. The natural features of geographic distribution require a new computing paradigm to provide location awareness and delay-sensitive monitoring and intelligent control. Fog computing extends computing to the edge of the network to meet this demand. In the study, Tang et al. introduced a hierarchical distributed fog computing architecture to support the integration of a large number of infrastructure components and services in future smart cities; a case study was analyzed using a smart pipeline monitoring system based on optical fiber sensors and sequential learning algorithms. To detect events that threaten pipeline security, a working prototype was constructed to evaluate the event detection performance of 12 different events through experimental evaluation. This research lacks experimental data support [3].

The innovations of this paper are as follows: (1) it proposes to use Hadoop-based sports big data analysis cloud platform to conduct experiments; (2) it proposes the establishment of sports economic data under the background of big data; (3) it conducts sports big data analysis cloud platform module design.

2. Sports Big Data Analysis Based on Cloud Platform and Research Method of Its Impact on Sports Economy

2.1. Hadoop-Based Sports Big Data Analysis Cloud Platform

2.1.1. Hadoop System. The Hadoop system is a top open-source software project under the name of the Apache open source organization. It evolved from Google's GFS distributed file system and MapReduce parallel computing framework. It is committed to creating an open source, scalable, and distributed large data processing platform. The infrastructure is given in [4]. Hadoop can be deployed on one to thousands of ordinary computer nodes, using distributed file systems to provide large amounts of data storage and using parallel programming models to process and analyze large amounts of data stored in distributed file systems [5]. Each node in the Hadoop cluster provides local storage and local computing, and the local storage and local computing of all nodes are unified to form a larger and more efficient storage and computing cluster. In many companies, such as Facebook and Yahoo, Hadoop clusters with a scale of thousands of nodes are deployed to integrate and streamline the large amounts of data generated by the company every day [6].

2.1.2. Overview of Hadoop. As the originator of big data processing, Hadoop has formed a complete ecological chain. Hadoop is mainly composed of two parts, namely, HDFS and MapReduce. HDFS is a distributed file system implemented by Hadoop, and MapReduce is a distributed parallel computing framework implemented by Hadoop [7, 8]. The Hadoop ecosystem also includes the following commonly used software: Hbase, Hive, Pig, Mahout, Zookeeper, Flume, and Sqoop.

Hbase is a distributed database based on HDFS that evolved from Google's BigTable. It provides real-time access to big data. It retrieves data through the primary keys Key and Range, which are more suitable for storing loose data [7].

Hive is a data warehousing tool for Hadoop. It provides complete Sql query operation commands. At the same time, MapReduce tasks can be executed with Sql statements,

which greatly reduce the cost of programmers running MapReduce tasks. MapReduce tasks can be executed through Sql-like statements to further improve the scalability of the Hadoop system [9].

Pig is the scripting language of Hadoop, which can query and process the data structure in the program. Pig has two operating modes: local mode and MapReduce mode. In MapReduce mode, Pig can automatically optimize the MapReduce program to improve the efficiency of program operation [10].

2.1.3. HDFS Reads Files

(1) The client initiates an RPC request to read data to the remote NameNode by obtaining an instance of DistributeFileSystem [11].

(2) The NameNode responds to the request and returns file block information related to the file. The file block information is mainly the address of the data node where the file block is located [12].

(3) The client obtains an FSDataInputStream instance, starting from the first data block, and calls its read() method to read the file block data in the nearest data node [5].

(4) After the client finishes reading the data of the current file block, it closes the connection with this data node, and, at the same time, searches for the data node address corresponding to the next file block and starts the data reading process of the file block [13].

(5) After the client finishes reading all the file block data contained in the target file, it calls the close() method in the FSDataInputStream instance to complete the file reading process [14].

2.2. Support Vector Regression

2.2.1. Support Vector Machine. Suppose there is a training set $h = \geq \{(x_1, y_1), (x_2, y_2), \ldots, (x_n, y_n)\}, \quad x \in R^n, y \in$

$(-1, +1)$, y is a class label, and x is a vector with n attributes [15]. There is a general form of linear discriminant function in two-dimensional linear space:

$$f(x) = \langle \omega, x \rangle + b. \tag{1}$$

The normalized form of the equation of the optimal classification line L is

$$\langle \omega, x \rangle + b = 0. \tag{2}$$

If you want to make the points in the training set as far as possible from the classifier, find an optimal classifier to maximize the blank area on both sides of it [16]. Then, the optimal classifier should satisfy the following formula:

$$y_i (\langle \omega, x_i \rangle + b) \geq 1, \quad i = 1, 2, \ldots, n.$$
$$\min J(\omega) = \frac{\|\omega\|^2}{2}. \tag{3}$$

Find by Lagrangian function:

$$L(w, b, a) = \frac{1}{2}\|\omega\|^2 - \sum_{i=1}^{n} a_i (y_i (\omega x_i + b) - 1)a_i. \tag{4}$$

Among them, a_i is the Lagrange multiplier, and its partial derivative is taken to be zero. The following formula exists:

$$\frac{\partial L}{\partial \omega} = 0 \longrightarrow w = \sum_{i=1}^{n} a_i y_i x_i,$$
$$\frac{\partial L}{\partial b} = 0 \longrightarrow \sum_{i=1}^{n} a_i y_i = 0. \tag{5}$$

According to the KKT condition and duality principle, solving the maximum interval can be transformed into an optimization problem of finding the following function:

$$W(a)_{\min} = \frac{1}{2}\sum_{i=1}^{n}\sum_{i=1}^{n} y_i y_j a_i a_j (x_i x_j) - \sum_{j=1}^{n} a_j,$$

$$\text{subject to} \begin{cases} a_i \geq 0, \quad i = 1, 2, \ldots, n \\ \sum_{i=1}^{n} a_i y_i = 0 \end{cases}. \tag{6}$$

Get the optimal solution $a' = (a'_1, a'_2, \ldots, a'_i)^h$, then the modulus of the optimal classifier ω' has the following formula:

$$\|\omega'\|^2 = 2\omega(a') = \sum_{SV} a'_i a'_j (x_i x_j) y_i y_j. \tag{7}$$

The finally obtained classification function has the following expression:

$$f(x) = \text{sgn}\left(\sum_{SV}^{n} y_i a'_i (x_i x) + b\right). \tag{8}$$

2.2.2. Support Vector Regression Algorithm. The idea of support vector regression is very similar to classification; only the loss function is introduced. The goal is to find a function $f(x)$ whose error with the objective function y_i in all training sets is at most θ, while ensuring that θ is as small as possible [17, 18]. The following formula exists:

$$f(x) = \langle w, x \rangle + b, \quad w \in X, b \in \theta. \tag{9}$$

Minimize experience risk:

$$\text{minmize} \frac{1}{2} \|\omega\|^2, \text{subject to} \left\{ \begin{array}{l} y_i - \langle \omega, x \rangle - b \leq \theta \\ \langle \omega, x \rangle + b - y_i \leq \theta \end{array} \right\}. \tag{10}$$

The kernel function is introduced to solve nonlinear problems. The simplest way is to map the data to a higher-dimensional space to make the data linearly separable and then use linear regression to solve the problem in the new high-dimensional space [19]. In fact, the kernel function is a kind of mapping. For different kernel functions, the data set will be mapped to different data spaces, which means different transformation functions, thereby improving the performance of various kernel function methods [20]. Under normal circumstances, there are mainly the following kernel functions:

The linear kernel function is expressed as

$$K(x_i, x_j) = (x_i x_j). \tag{11}$$

The polynomial kernel function is expressed as

$$K(x_i, x_j) = (x_i x_j + c)^d, \quad d > 0. \tag{12}$$

The Gaussian kernel function is expressed as

$$K(x_i, x_j) = e^{\gamma \|x_i - y_i\|^2}, \quad \gamma > 0. \tag{13}$$

Among them, because the feature space corresponding to the Gaussian kernel function is infinite dimensional, a limited sample set must be linearly segmented in the feature space, so the Gaussian kernel function is the most widely used kernel function in support vector regression [21].

The method part of this article uses the above method to analyze the sports big data based on the cloud platform and study the impact on the sports economy. The specific process is shown in Figure 1.

3. Sports Big Data Analysis Based on Cloud Platform and Research Experiment on Its Influence of Sports Economy

3.1. Establish a Sports Economic Database

3.1.1. Data Needs and Sources. Raw data needs: relevant information and data of local sports economic parks; China map data; statistics of various provinces; data of the level of sports development of various provinces [22].

Data analysis software requires Excel 2016, ArcGIS 10.2, and SPSS 24.0.

Sources of data acquisition: National Sports General Administration; National Bureau of Statistics; local sports

bureaus; local statistical bureaus; National Basic Geographic Center; National Geographic Surveying Information Bureau, etc. [23].

3.1.2. Data Collection and Processing. Taking the sports economic parks in 31 provinces, autonomous regions, and municipalities directly under the Central Government (excluding Hong Kong, Macao, and Taiwan) as the survey object, the relevant information and data of local sports economic parks are collected through the State Sports General Administration, and the addresses, names, approval year, leading sports industry category, and other information are sorted into Excel 2020 software [24, 25]. 1 : 4 million map spatial data of China are obtained through the National Basic Geographic Center. Use the Baidu picking coordinate system tool to collect the specific latitude and longitude of the local sports economic park and sort it into the Excel 2020 software. The statistical data of various provinces, municipalities, and autonomous regions are obtained from the official website of the National Bureau of Statistics [26].

3.2. Design of Cloud Platform Module for Sports Big Data Analysis

3.2.1. Design of Experimental Cluster Management Module

(1). Cluster Virtual Network Design. Use Hadoop's Neutron component to design the cluster network required for the experiment. The normal configuration of big data components when the cluster is created requires a specific virtualized network to support, and the cluster operation also requires a correct network environment. If the network is not designed in advance, users need to learn the steps of using the Hadoop virtualized network before deploying the cluster and create a corresponding network for their own experimental cluster, which will increase the cost of learning Hadoop, which is not beneficial to the experiment. Therefore, the predesign of the virtual network can pave the way for the rapid acquisition of experimental clusters in the experiment. When monitoring virtual machines and user experiment behaviors at the same time, it is also necessary to obtain data through the virtual network.

(2). Cluster One-Click Deployment Design. The user experiment is carried out on a virtualized big data cluster. Therefore, the deployment of the cluster is an essential part of the experiment. The experimental cluster management module starts with the quick response and convenient operation to complete the cluster one-click deployment design, thereby simplifying user operations and shortening the time for users to deploy experimental clusters.

The general steps for native deployment of big data clusters on Hadoop are upload image ⟶ register image ⟶ create node group template ⟶ create cluster template ⟶ deploy cluster. Uploading the image uses the Glance component of Hadoop, and the last four steps are completed by the Sahara component. From uploading a mirror image to
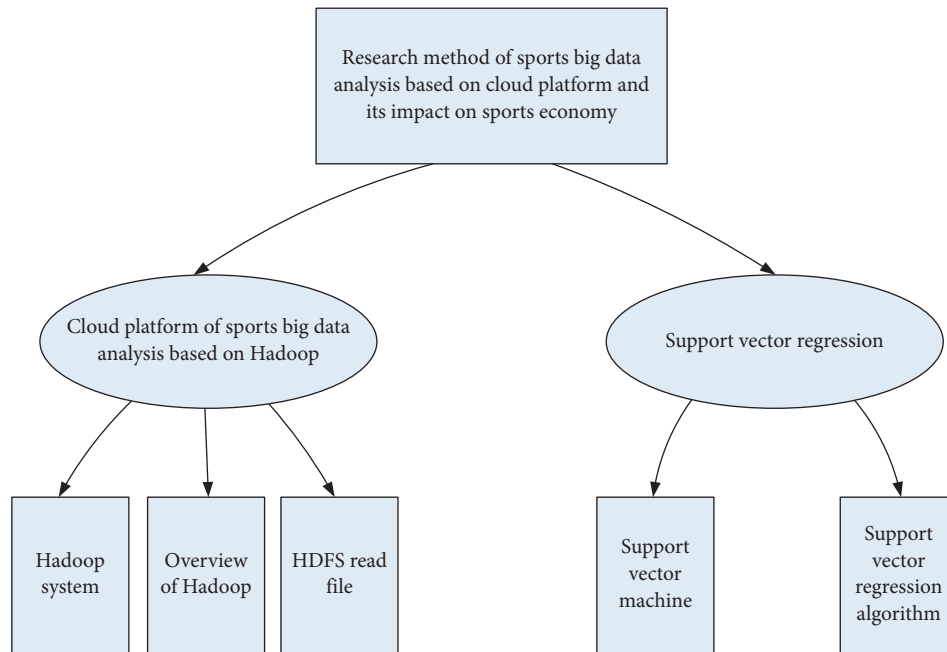
FIGURE 1: Part of the technical flow chart of this method.

creating a cluster template, it can be designed in advance based on the experimental content and provide a reusable template.

(3). Import of Experimental Tools. Prepare the tools and data sets that may be needed during the experiment in advance and save them to the server. Provide a one-click import button to remotely transfer from the server to the virtual machine.

(4) Cluster Changes. After the user successfully applies for the cluster, the cluster information and virtual machine information are displayed to the user, and operations for adding, deleting, modifying, and checking are provided. Including increasing or decreasing the number of nodes in the cluster can query cluster information through cluster naming or status, verify cluster status, and delete clusters owned by users.

3.2.2. Platform Monitoring Module Design. The granularity of Hadoop monitoring only reaches the resource usage allocated by the physical server, so it is necessary to design a fine-grained monitoring module for the user level including physical resource monitoring submodule, virtual machine resource monitoring submodule, and user experiment behavior monitoring submodule. The following three points need to be achieved: one is to refine the monitoring granularity and monitor from the three aspects of physical machines, virtual machines, and user experimental behaviors. The second is monitoring information processing. The resource monitoring information can be saved to the database, and historical warning records can be saved. Behavior monitoring, after categorizing users, is saved as a log file. The third is to isolate the monitoring information between users and show them to users.

For multinode physical server resource monitoring, the monitoring service is written as a script and automatically added to the Linux system service of each server. When the monitoring service transfers the information obtained by the query to the control node, it will bring its own host information, sort it according to the host name, and store it in the MySQL database. The control node will filter the information occupied by physical resources, filter out the time points when the resource occupancy rate exceeds the threshold, and store the resource shortage information in the historical warning file. Finally, the information occupied by physical resources is only displayed to the administrator on the interface after passing the authority judgment.

For virtual machine resource monitoring, a virtual machine information collector on the control node is used to query all virtual machines on all nodes. The information of all virtual machines is stored in the database of the control node. The computing node has no database to store the virtual machine information. If the virtual machine information collector is deployed in each computing node, the computing node also needs to obtain the virtual machine from the database of the control node. Machine information is used in order to collect resources. In order to reduce the number of remote database connections, a virtual machine information collector is deployed on the control node to complete the acquisition of all virtual machine information.

3.3. Performance Testing. After setting up the local cluster, perform the ParaView drawing test. First, perform a single-node test, and then perform a multinode test to compare the performance of cluster drawing. The tested data are VTK three-dimensional scalar data with sizes of 18.5 M, 291.8 M, 1425 M, and 8748 M, and the four sets of data are numbered data1-data4 in sequence.

3.3.1. Single-Node Test. This test uses a piece of test code written in Python to test. The measured parameters are the number of data points of the data to be tested, the number of data points drawn per second, and the total drawing time. To perform a single-node test, first start the ParaView server on node 1, then start the ParaView client on node 1, and connect to the server just started, and then you can run the test code to test the data.

3.3.2. Two-Node Data Test. To perform a two-node test, first start the ParaView server on node 1 and node 2 in MPI parallel mode, then start the ParaView client on node 1, connect to the ParaView server that has just been started, and run the test code to test the two-node data. Respectively draw data1-data4 just drawn on a single node on the ParaView client on node 1.

3.3.3. Four-Node Data Test. Finally, a four-node drawing test is performed. Start the four nodes of node 1 to 4 at the same time, then use MPI to run ParaView server in parallel, then start ParaView client on node 1 to connect to the server started, and run the test code to test the four nodes.

This part of the experiment proposes that the above steps are used for cloud platform-based sports big data analysis and research experiments on the impact on sports economy. The specific process is shown in Table 1.

4. Sports Big Data Based on Cloud Platform and Its Impact on Sports Economy

4.1. Development of Sports Economy Industrial Park

4.1.1. Time Development Characteristics. In 2006, the national sports industry base system was established; in 2011, under the guidance of the "Guiding Opinions of the General Office of the State Council on Accelerating the Development of the Sports Industry," the State Sports General Administration issued the "National Sports Industry Base Management Measures (Trial)" to further clarify the national sports industry. The concept and type of the base standardize the management of the base; in 2014, the "Several Opinions of the State Council on Accelerating the Development of the Sports Industry and Promoting Sports Consumption" was formally promulgated, clearly proposing to "create a group of sports industries that conform to market laws and have market competitiveness." In 2016, the State Sports General Administration issued a notice on further strengthening the construction of the national sports industry base and the "Thirteenth Five-Year Plan for Sports Development" put forward programmatic requirements and higher goals for the development of the sports industry base. In view of the national sports industry base's leading role in the development of the regional sports industry and the policy needs of the development of the regional sports industry, various localities have begun to actively initiate the construction of local sports economic parks. The development of China's local sports economic parks is drawn into a chart, as shown in Table 2 and Figure 2.

As can be seen from the chart, China was approved as the first batch of local sports economic parks in 2011. As of 2017, there were a total of 143 local sports economic parks. After that, it developed to 166 sports economic parks in 2018 and 176 in 2019 (a sports economic park). The growth rate generally showed a development trend of first increasing and then decreasing. The growth of local sports economic parks was mainly concentrated in 2016, 2017, and 2018.

4.1.2. Type Structure of Sports Economic Park. In the classification of the leading industries of local sports economic parks, we mainly refer to the National Sports Industry Statistical Classification issued by the National Bureau of Statistics in 2015. The National Sports Industry Statistical Classification defines the scope of the sports industry as sports management activities, sports competition performance activities, sports fitness, and leisure. There are eleven categories: activities, stadium services, sports intermediary services, sports training and education, sports media and information services, other sports-related services, sports goods and related product manufacturing, sports goods and related product sales, trade agency and rental, sports facilities construction. Statistics and sorting out the development types of national and local sports economic parks are shown in Table 3 and Figure 3.

It can be seen from the chart that the number of local sports economic parks belonging to the categories of sports management activities, sports competition performance activities, and sports fitness and leisure activities is the largest, with 95, 91, and 90 respectively, accounting for 11.85%, 11.35%, and 11.22 of the total (%); there are 86 sports venue services, accounting for 10.72% of the total; 68 sports intermediary services, accounting for 8.48% of the total; 63 sports training and education, accounting for 7.86% of the total; 64 sports media and information services, accounting for 7.98% of the total; other sports-related services, sports goods and related product manufacturing, sports goods and related product sales, trade agency and rental, and sports facilities construction accounted for 6.86%, 7.48%, 6.36%, and 5.74% of the total, respectively, 4.11%.

4.2. Sports Big Data Analysis Based on Cloud Platform and Its Impact on Sports Economic Development.
(1) On the whole, the change trend of the total scale of national sports industry construction is basically consistent with that of the total scale under construction, both of which have basically maintained a rising trend. The specific situation is shown in Table 4 and Figure 4.

It can be seen from this that the development of the sports industry has always been on the rise during the period from 2012 to 2019, the sports economy is developing well, and the people are paying more and more attention to the importance of physical exercise and physical fitness.

(2) In 2008, the United States first broke out the subprime mortgage crisis and spread to the world. Affected by it, the vitality of my country's real economy began to decline. The crisis also affected the development of the tertiary industry. At that time, the scale of the sports industry was

TABLE 1: Experimental steps in this article.

Sports big data analysis based on cloud platform and research experiment on its influence on sports economy	3.1	Establish a sports economic database	1	Data needs and sources
			2	Data collection and processing
	3.2	Design of cloud platform module for sports big data analysis	1	Design of experimental cluster management module
			2	Platform monitoring module design
	3.3	Performance testing	1	Single-node test
			2	Two-node data test
			3	Four-node data test

TABLE 2: Development of sports economic park.

Year of approval	Number of sports economic industrial parks	Growth	Growth rate
2011	9	9	
2012	9	0	
2013	15	6	66.67
2014	24	9	60.00
2015	40	16	66.67
2016	70	30	75.00
2017	143	73	104.29
2018	166	23	16.08
2019	176	10	6.02
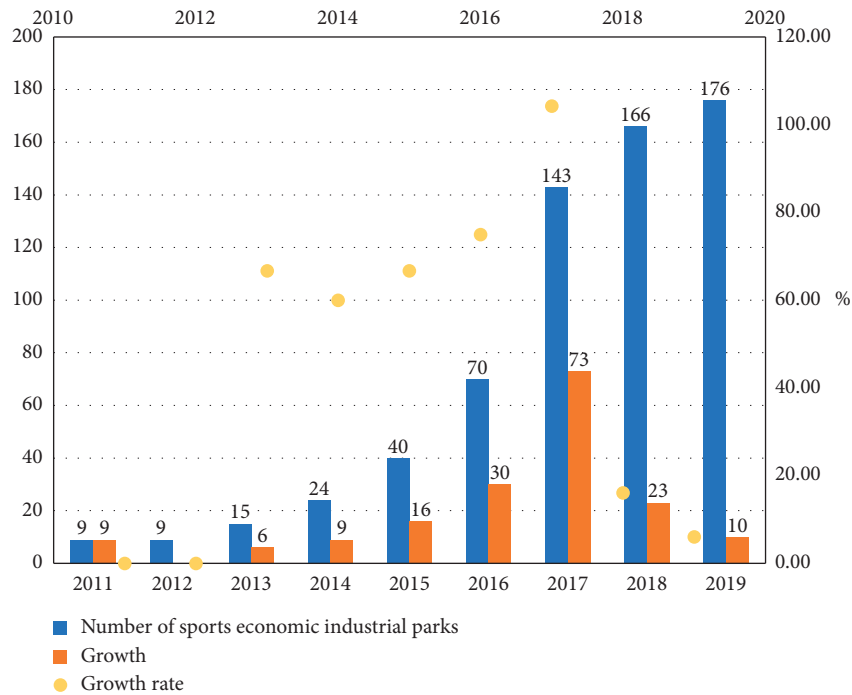
FIGURE 2: Development of sports economic park.

TABLE 3: Types of development of sports economic parks.

Type		Number of parks	Percentage (%)
1	Sports management activities	95	11.85
2	Sports competition performance activities	91	11.35
3	Sports fitness and leisure activities	90	11.22
4	Stadium services	86	10.72
5	Sports intermediary services	68	8.48
6	Sports training and education	63	7.86
7	Sports media and information services	64	7.98

TABLE 3: Continued.

Type		Number of parks	Percentage (%)
8	Other sports-related services	55	6.86
9	Sports goods and related product manufacturing	60	7.48
10	Sports goods and related products sales	51	6.36
11	Trade agency and rental	46	5.74
12	Sports venues and facilities construction	33	4.11
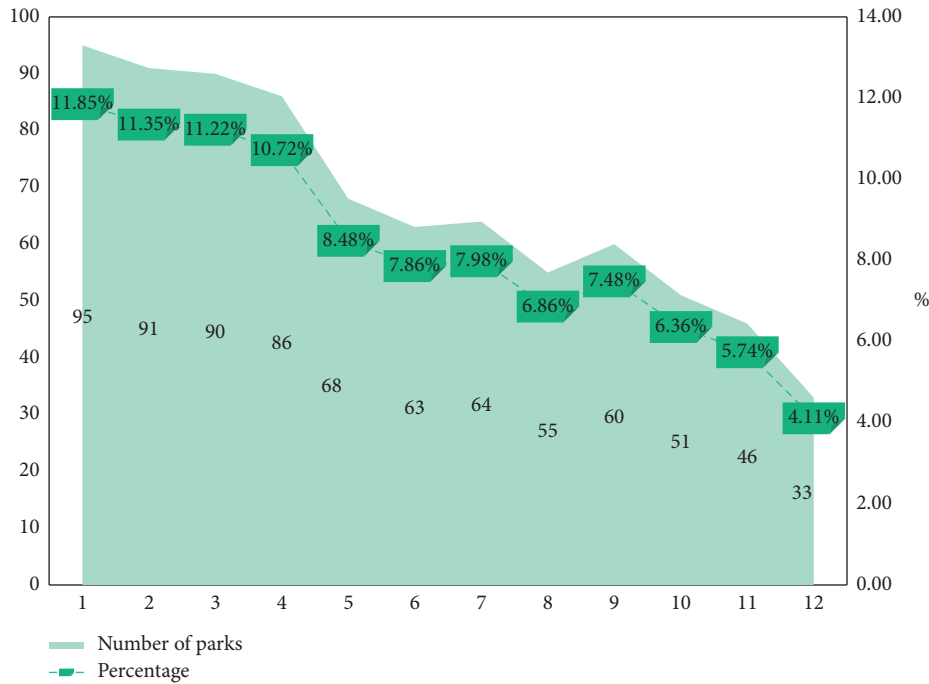
FIGURE 3: Development types of sports economic parks.

TABLE 4: Development scale of sports industry in recent years (unit: 100 million yuan).

Years	Sports industry scale under construction	Sports industry scale has been built
2012	2132.6	2791.7
2013	2167.4	2839.8
2014	2230.1	2978.4
2015	2287.5	3010.2
2016	2311.4	3233.4
2017	2379.6	3310.6
2018	2412.5	3419.1
2019	2420.7	3526.3

affected. In 2009, in order to stimulate the economic recovery and manage the economic crisis, the Chinese government launched a "4 trillion" large-scale stimulus policy. Driven by this, the vitality of sports-related companies has increased, and the total number of booths has rebounded sharply. Since then, it has basically maintained an upward trend. The specific situation is shown in Table 5 and Figure 5.

In 2019, the total number of booths in the sports industry-related commodity trading market reached 42,053, an increase of 1.05% compared with 41,611 in 2018. From the perspective of the total number of booths in the sports economy the upward trend is basically maintained, but the increase is relatively small.

(3) The number of employees is also the most sensitive indicator reflecting the scale of the development of an industry or industry. This article uses the number of employees in the retail industry above the quota for sports goods and retail equipment to represent the number of employees in the sports industry, as shown in Table 6 and Figure 6.
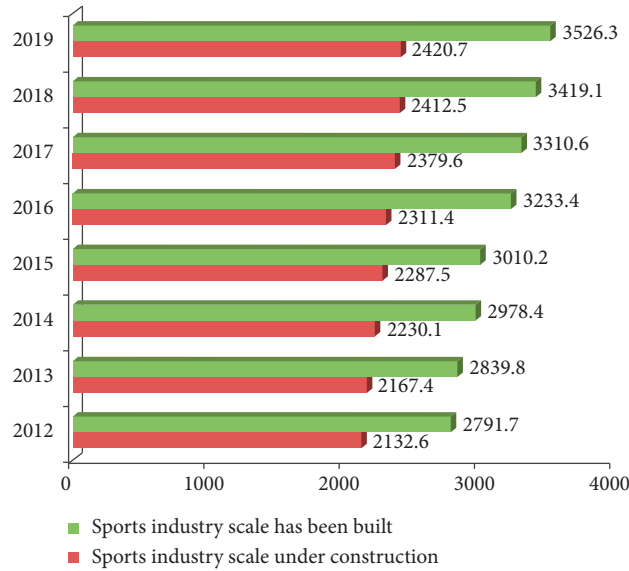
Figure 4: Development scale of sports industry in recent years (unit: 100 million yuan).

Table 5: Total number of stalls in the sports-related industry commodity trading market with a value of more than 100 million yuan in recent years.

Years	Total number of sporting goods booths	Total number of sports and entertainment booths	Total number of fitness exercise booths	Total number of booths for sports media and information services	Total number of booths for sports training and education	Total number of sports intermediary booths
2014	8411	8384	8124	6542	4589	5427
2015	8670	8706	8019	6431	4487	5306
2016	8331	8675	7941	6327	4931	5297
2017	8572	8531	7724	6540	4527	5441
2018	8431	8842	7609	6601	4761	5367
2019	8643	8967	7864	6527	4531	5521

It can be seen from Table 6 that from the retail perspective, the number of employees in the sports industry in my country has continued to increase, reaching 31,987 in 2019, an increase of 9.79% over the previous year; however, the annual growth rate of sports employees has fluctuated. Among them, the number of employees in 2014 has increased significantly, from 16,729 in 2013 to 19,947, an increase of 16.13%.

(4) According to the support vector machine regression algorithm described in the method section above, the original data are initialized through the calculation formula of the initial point zero image. The purpose of the initial value processing is to make each data correspond to the curve has a common point of intersection to facilitate comparison and analysis between various factors. Obtain the correlation between sports output value, sports consumption, number of sports industry employment, and sports big

data analysis, and the absolute correlation between sports big data analysis and sports economic development can be obtained, as shown in Table 7, Figure 7.

From the numerical calculation of the correlation degree in Table 7, the average correlation degree between sports big data analysis and sports economic development is 0.5155, which is relatively high. Appropriate sports big data analysis based on cloud platform plays a positive role in promoting the development of sports economy.

Based on the above statistical analysis on the scale of the sports industry, the scale of the national sports industry has been expanding, and the construction scale and the total scale under construction have shown a continuous expansion trend. The total number of stalls in the commodity trading market over 100 million yuan has also continued to rise. The number of employees in the retail
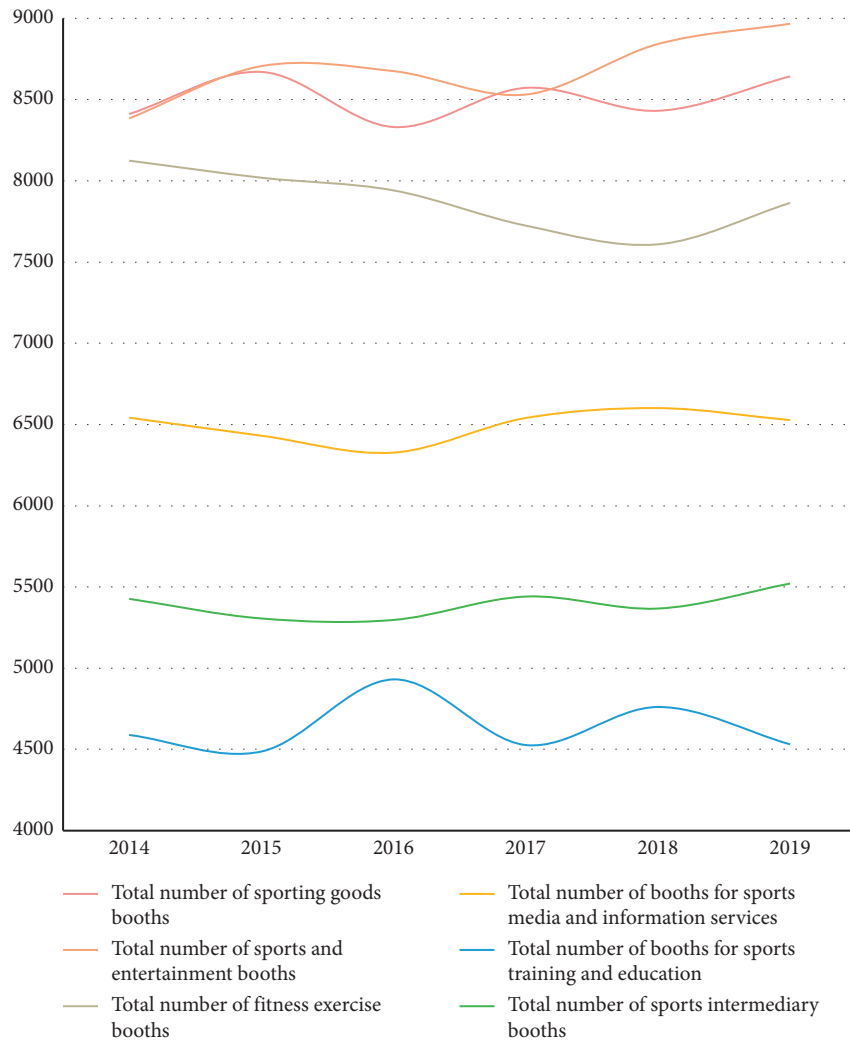
FIGURE 5: Total number of stalls in the sports-related industry commodity trading market with a value of more than 100 million yuan in recent years.

TABLE 6: The number of employees in retail industry above designated size for sporting goods and retail equipment in recent years.

Years	Number of employees	Growth rate (%)
2013	16729	11.17
2014	19947	16.13
2015	22021	9.42
2016	24437	10.97
2017	26014	6.06
2018	29135	12.00
2019	31987	9.79

industry above the designated size of retail equipment continues to increase. This shows that, with the development of the big data era, big data analysis has gradually been applied to the development of the sports economy. Through big data analysis, the current development situation, existing problems, and future development directions of the industry can be better grasped, which is conducive to making more suitable. Decisions related to the development of sports economy promote the development of the sports economy industry and can also provide more employment opportunities and promote social development.
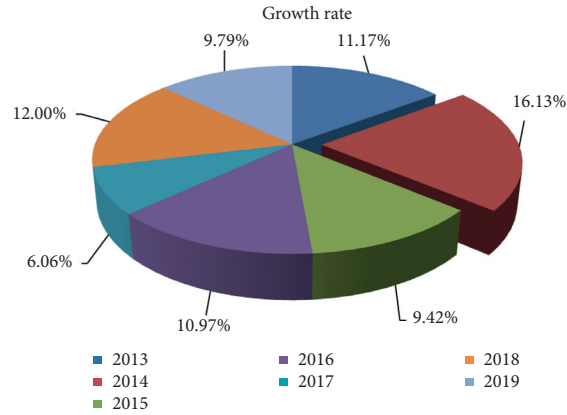
FIGURE 6: The number of employees in retail industry above designated size for sporting goods and retail equipment in recent years.
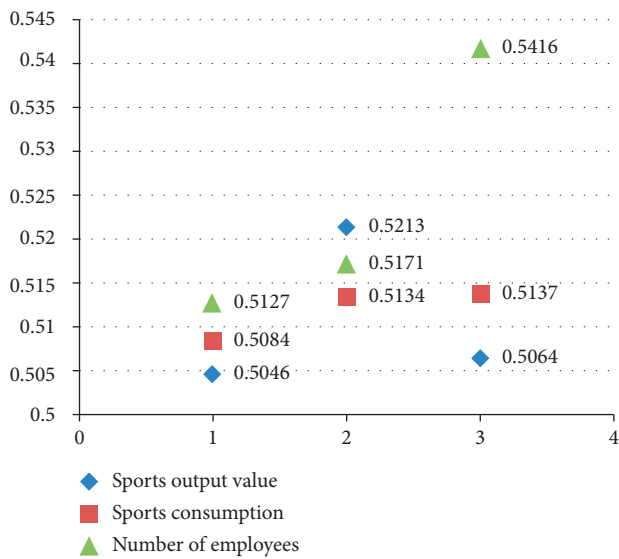
FIGURE 7: The absolute correlation between sports big data analysis and sports economic development.

TABLE 7: The absolute correlation between sports big data analysis and sports economic development.

	Total GDP of sports economy	Per capita GDP of sports economy	Per capita consumption expenditure of urban residents
Sports output value	0.5046	0.5213	0.5064
Sports consumption	0.5084	0.5134	0.5137
Number of employees	0.5127	0.5171	0.5416

5. Conclusions

Through the elaboration and comparison of data, information, big data and statistics research scope, characteristics, and analysis ideas, we believe that big data is information, but big data has given more meanings related to change. It is the whole process of collecting, processing, converting, storing, transmitting, analyzing, algorithm, and application of data (all types of data) and even productization and industrialization. This whole process not only changes the traditional data analysis, but also even will change people's work attributes and lifestyle. The basic purpose of data is to provide a basis for the collection and processing of information. The value of data is equivalent to the value of information. Big data has all the attributes of information. The key to data analysis is to discover new information from the complex data, thereby enhancing the understanding of things and making scientific and reasonable decisions.

With the rapid development of computer technology today, as computer hardware technology matures and the amount of information stored continues to increase, it becomes more difficult to screen, mine, and efficiently use large amounts of information. In the field of sports, with the rapid development of sports, the big data analysis of sports in my country is also facing the same problem. Big data analysis is conducive to discovering the potential connections and laws hidden in the massive data and is conducive to the deeper analysis of data, so as to play a certain role in guiding, predicting, and analyzing the development of sports economy.

Although of the thesis has conducted relevant research and analysis on the impact of sports big data analysis in the development of sports economy; these studies only consider the impact of relevant factors at the surface level and do not consider these methods in sports economic development statistics. Therefore, how to improve the coefficients in the models or formulas in these methods to make them more universal? This is also one of the contents worth studying in the future.

Data Availability

No data were used to support this study.

Conflicts of Interest

The authors declare that they have no conflicts of interest.

References

[1] X. Zhong, G. Yang, L. Li et al., "Clustering and correlation based collaborative filtering algorithm for cloud platform," *Iaeng International Journal of Computer Ence*, vol. 43, no. 1, pp. 108–114, 2016.

[2] J. Liu, S. Chen, Z. Zhou, and T. Wu, "An anomaly detection algorithm of cloud platform based on self-organizing maps," *Mathematical Problems in Engineering*, vol. 2016, Article ID 3570305, 9 pages, 2016.

[3] B. Tang, Z. Chen, G. Hefferman et al., "Incorporating intelligence in fog computing for big data analysis in smart cities," *IEEE Transactions on Industrial Informatics*, vol. 13, no. 5, pp. 2140–2150, 2017.

[4] S. Liu, J. Tang, C. Wang, Q. Wang, and J.-L. Gaudiot, "A unified cloud platform for autonomous driving," *Computer*, vol. 50, no. 12, pp. 42–49, 2017.

[5] J. Yang, H. Wang, Z. Lv et al., "Multimedia recommendation and transmission system based on cloud platform," *Future Generation Computer Systems*, vol. 70, pp. 94–103, 2016.

[6] C. Cao, F. Cui, and L. Xu, "Research on intelligent traffic control model and simulation based on the Internet of things and cloud platform," *Journal of Computational and Theoretical Nanoscience*, vol. 13, no. 12, pp. 9886–9892, 2016.

[7] W. J. Huang and H. L. Yi, "Advances in the application of cloud platform in diagnosis and treatment of OSA," *Lin Chuang Er Bi Yan Hou Ke Za Zhi=Journal of Clinical Otorhinolaryngology*, vol. 33, no. 4, pp. 310–312, 2019.

[8] T. S. Priyeshkumar and D. Devaka, "A scalable and highly available distributed architecture for e-governance applications on private cloud platform," *International Journal of Computer Sciences and Engineering*, vol. 7, no. 3, pp. 811–814, 2019.

[9] X. Lu and S. Tan, "Cloud platform curriculum model design for nursing education under the integration of vocational education alliance background," *Boletin Tecnico/Technical Bulletin*, vol. 55, no. 8, pp. 239–248, 2017.

[10] R. Xu, "Design of a bionic corn seed threshing machine based on rough sets under a cloud platform," *Agro Food Industry Hi Tech*, vol. 28, no. 1, pp. 2057–2061, 2017.

[11] J. Wan, X. Yang, Z. Ren, and Z. Ye, "Performance evaluation and modeling method research based on IaaS cloud platform," *International Journal of Grid and Distributed Computing*, vol. 9, no. 10, pp. 141–152, 2016.

[12] C.-m. Jiang, Y.-b. Li, and L. Zhi-Cong, "Review of the research on the optimization of the energy consumption of the cloud platform," *International Journal of Smart Home*, vol. 10, no. 8, pp. 241–250, 2016.

[13] W. Yuan, P. Deng, T. Taleb, J. Wan, and C. Bi, "An unlicensed taxi identification model based on big data analysis," *IEEE Transactions on Intelligent Transportation Systems*, vol. 17, no. 6, pp. 1703–1713, 2016.

[14] Z. Liu, K. K. R. Choo, and M. Zhao, "Practical-oriented protocols for privacy-preserving outsourced big data analysis: challenges and future research directions," *Computers & Security*, vol. 69, pp. 97–113, 2016.

[15] H. A. Mahdiraji, E. Kazimieras Zavadskas, A. Kazeminia, and A. Abbasi Kamardi, "Marketing strategies evaluation based on big data analysis: a CLUSTERING-MCDM approach," *Economic Research-Ekonomska Istraživanja*, vol. 32, no. 1, pp. 2882–2898, 2019.

[16] A. Ganesh, K. Vijiyakumar, K. Vijiyakumar, K. Premkumar, and P. Mathivanan, "To improve the accuracy in identifying breast cancer using various techniques of big data analysis," *International Journal of Advanced Research*, vol. 7, no. 10, pp. 491–498, 2019.

[17] A. M. Abdelaziz, K. K. A. Ghany, T. H. A. Soliman, and A. A. E. M. Sewisy, "A parallel multi-objective swarm intelligence framework for big data analysis," *International Journal of Computer Applications in Technology*, vol. 63, no. 3, pp. 200–212, 2020.

[18] C.-W. Yang, "A study on detecting the linked accounts by using big-data analysis," *Korean Journal of Financial Studies*, vol. 48, no. 1, pp. 73–103, 2019.

[19] Y. Jiang, T. Wang, H. Zhao et al., "Big data analysis applied in agricultural planting layout optimization," *Applied Engineering in Agriculture*, vol. 35, no. 2, pp. 147–162, 2019.

[20] Y. Liu, L. Pang, and X. Lu, "Click-through rate prediction based on mobile computing and big data analysis," *Ingénierie des systèmes d information*, vol. 24, no. 3, pp. 313–319, 2019.

[21] H. Li, "Estimation of stadium construction schedule based on big data analysis," *International Journal of Computers & Applications*, vol. 41, no. 3-4, pp. 268–275, 2019.

[22] J. D. Yu, I. S. Lee, and I. S. Lee, "A prediction of stock price through the big-data analysis," *Journal of Society of Korea Industrial and Systems Engineering*, vol. 41, no. 3, pp. 154–161, 2018.

[23] H. E. Naess, "Investment ethics and the global economy of sports: the Norwegian oil fund, Formula 1 and the 2014 Russian grand prix," *Journal of Business Ethics*, vol. 158, no. 2, pp. 535–546, 2019.

[24] S.-H. Kim and E.-J. Jeong, "A study on the economic impacts of sports activities expenditure," *Korean Journal of Sport Management*, vol. 22, no. 5, pp. 1–13, 2017.

[25] A. Gvercn, "The factors that affect the development of sports industry as an economy," *International Journal of Ence Culture and Sport*, vol. 4, no. 18, p. 515, 2016.

[26] D. Cumming and S. Johan, "Venture's economic impact in Australia," *The Journal of Technology Transfer*, vol. 41, no. 1, pp. 25–59, 2016.

Research Article

New Retail Marketing Strategy Combining Virtual Reality and 5G Mobile Communication

Xing Zhang [ID]

Zhejiang Technical Institute of Economics, Hangzhou 310018, Zhejiang, China

Correspondence should be addressed to Xing Zhang; zx@zjtie.edu.cn

At present, China's retail industry has been completely opened to the outside world, and it is exactly the same. The retail industry has become one of China's most market-oriented and competitive industries. At the same time, the changes in consumer demand are becoming more and *more* diversified. In order to meet the diversified and personalized needs of consumers, retail companies must continue to increase investment in services, management, marketing, and branding. This paper combines virtual technology and 5G mobile communication technology to design and realize a set of 3D virtual fitting system. According to people's fitting needs, the research is carried out from two aspects: clothing style and body type matching degree and clothing fabric drape. In the comparison of body shape test results with conventional body shape judgment experience, the correct rate of the virtual fitting system's body shape judgment was 86%, and the error rate was 14%. In the comparison of online shopping data of consumers on different communication networks, it was found that the speed of different networks is different. The shopping experience has a relatively large impact. As a newly developed network mobile communication technology, 5G's ultra-high speed advantage has a great impact on the consumer experience; in the analysis and comparison of the traditional operation mode and the combination of online and offline operation modes, it is concluded that the traditional marketing model is far from meeting people's current life needs, and new retail is catering to the consumer needs of people in the new era.

1. Introduction

1.1. Background Meaning. The continuous development of information technology has enabled the telecommunications industry to develop rapidly and extensively [1]. While continuing to promote social development, it has had a huge impact on people's life and work styles and has become a pillar industry for world economic development. Mobile communication, satellite communication, and optical fiber communication are important components of modern communication networks for integrated services, and it is said that they are three new communication methods [2]. In particular, with the success of the recent development of mobile Internet and Internet of things services, mobile communication technologies continue to develop and develop [3]. In such a huge environment, 5G mobile communication technology has become a new hot spot to promote the development of communication technology, providing prospects for various applications.

1.2. Related Work. With the development of communication technology, people have entered the 5G era, and the demand for communication technology is increasing, and at the same time, it has brought great convenience to people. Tang analyzed and discussed the characteristics of 5G mobile communication, its development trend, and several technologies of 5G mobile communication [4]. Pan conducted an in-depth study on the future development trend of transmission under 5G mobile communication technology, hoping to provide help for the rapid development of mobile communication technology [5]. Zhang and Ma deeply explored the marketing of the mobile communication industry and proposed a suitable marketing strategy for mobile communication enterprises in the new era [6]. Liu et al. proposed a mobile VR network solution, which further analyzes the expansion effect introduced in application activation and aims to provide a reference and promote mobile VR applications in 5G networks demonstration effect of application development of 5G ecosystem [7, 8]. Zhao

et al. analyzed the current status of virtual reality equipment based on VR technology and a complete set of supporting exoskeleton structures and pioneered the creation of a virtual reality system with multiple senses and multiple synergistic devices as virtual real world provides new ideas [9]. Wang proposed the multidimensional impact of 5G on mainstream media integration. To correct the development direction of mainstream media, mainstream media needs to have an objective and profound understanding of the specific impacts of 5G on the ecology and pattern of media integration [10, 11]. In summary, judging from the current status of 5G technology research in the past, most of them are stating the future development trend of 5G, a few of them describe the application of 5G to a certain field, and few mention the use of virtual reality and 5G mobile communication technology.

1.3. Innovations in This Article. (1) Virtual technology and 5G mobile technology are combined to design and implement a 3D virtual fitting system. (2) The 3D modeling technology in the clothing CAD field is used to show the 3D visual dressing effect. (3) The clothing model of the 3D virtual fitting system is created by Maya three-dimensional modeling.

2. Overview of Related Theories Such as Virtual Reality and 5G Mobile Communication

2.1. Virtual Reality. Virtual reality refers to an artificial media space created by a computer [12]. It is a kind of virtual reality that can produce a sense of immersion when using a device to enter a virtual environment. With the rapid development of computer software and hardware technology, computer graphics applications have also been rapidly developed in various industries. Virtual reality, scientific visualization, computer animation, and computer graphics are the three main research directions [13, 14]. This kind of virtual environment can be created by a computer and can simulate the real world or the virtual world.

2.2. 5G Mobile Communication System. The 5G cellular network is a digital cellular network, an updated version of the previous 4G. In the 5G network, the coverage area covered by the supplier is divided into many small cell geographical areas [15]. The analog signal of the mobile phone is digitized by an analog-digital converter and then converted into a bit stream. All 5G radios in the cell use radio waves to communicate with the local antenna array and low-power automatic transceivers in the cell [16]. The transceiver allocates channels from the public rating pool, and these channels can be reused in geographically separated units. The local antenna is connected to the telephone network and the Internet through a high-bandwidth optical fiber or wireless backhaul connection. Just like existing mobile phones, mobile devices will automatically switch to the antenna of the new cell when switching from one cell to another cell [17]. The main advantage of the 5G network is that the data transmission

rate is much faster than the previous 4G network, up to 10 Gbps, which is faster than the current wired Internet and the previous 4G network nearly 100 times faster than talking. Another advantage is that compared with 4G's 30–70 milliseconds, the network delay is less than 1 millisecond.

2.2.1. Features of 5G Mobile Communication

(1) Good System Performance. As the number of antennas, points, users, and communities in 5G networks continues to grow, the focus of technology applications is on networks with antennas and coordination between users and communities [18]. This improves the performance of all aspects of the system. In the communication business process, indoor business has become the center of existing business methods. The 5G system takes indoor business as the business premise, continuously expands three new business areas, and gradually expands the area coverage. The wireless network has completely covered [19].

(2) Using Hyperspectral. Through in-depth research and development of 5G communication technology, the use rate of high-frequency radio waves is very high, so that light professional wireless network technology, broadband wireless technology, and wireless technology are effectively combined [20]. The use of radio frequency spectrum ensures the stable development of 5G mobile communication technology [21].

(3) Low Price and Low Energy Consumption. When researching cellular network technology, affected employees are worried about reducing costs and using electricity. With the deepening of research, designing software configuration has become an important part of the research. After a comprehensive market analysis, operators can understand business development and traffic requirements, continuously optimize network resources, and further reduce system costs and power consumption [22].

2.3. Overview of New Retail. New retail is that companies that rely on the Internet are using advanced technologies such as big data and artificial intelligence to improve and change the production, distribution, and sales processes of their products [23]. This will improve the new business structure distribution model and redesign the offline experience of online services in the ecosystem and tightly integrate the latest logistics [24].

2.3.1. Characteristics of New Retail. Now, "new retail" is a conceptual representation of a new retail format that is different from existing retail stores. It is dominated by information technology (big data, Internet, artificial intelligence, etc.), which can improve customer experience (shopping scenarios that meet the different needs of consumers). A new business form is produced by refactoring three elements: online and offline people, products,

and disciplines [25, 26]. People correspond to consumer portraits and data, products correspond to supply chain organizational relationships and brand relationships, and markets correspond to shopping malls. The market is the shape of the front end of the new retail store, and people and goods are the main changes in the back end. For example, "Hema Xiansheng" opened by Alibaba is a combination of "fresh supermarket + e-commerce experience + catering + logistics distribution" and other business functions, creating a "supply chain-store-warehousing-distribution" and other business functions [27, 28].

From a human perspective, online e-commerce platforms have multiple ways to obtain traffic, and offline physical stores are also actively implementing traffic data, so that customer portraits can be more and more accurate, and demand analysis is fully explored [29, 30].

From a product perspective, the era of big data and artificial intelligence has fundamentally changed the traditional retail industry's reliance on past experience in purchasing and management models [31, 32]. For example, Hippo Fresh uses big data from consumer terminals to digitize various application scenarios from front end to back end, accurately record consumer needs, and provide customers with targeted products and services to quickly integrate into the business community [33].

In specific locations, the gradual maturity of technologies such as image recognition, artificial intelligence, and intelligent manufacturing, as well as the rapid popularization of mobile payments, not only make the consumption scene more diversified but also greatly improve the comfort level [34–36].

2.4. Commonly Used Wireless Propagation Models.
In the mobile network environment, the complex and changeable wireless propagation environment directly determines the loss of signal propagation and affects the quality of wireless signal transmission [37]. In order to simulate the attenuation of wireless signals in the actual environment, it is necessary to summarize and establish propagation models based on different environments according to theoretical research and measured data and to correct the models according to the needs of the actual scene, so that it can more accurately fit the actual situation wireless communication environment. Currently, the frequently used wireless propagation models include Okumura–Hata model, COST-231 Hata model, and LEE model [38].

2.4.1. Okumura–Hata Model.
The Okumura–Hata model is an empirical formula based on the statistical analysis of a large number of wireless propagation loss test data in the city. It is mainly suitable for macrocellular systems with a cell radius of 1 km~20 km. Other applicable conditions include frequency between 150 and 1500 MHz, base station effective antenna height is between 30 and 200 m, and the effective antenna height of the mobile station is between 1 and 10 m. The empirical formula of Okumura–Hata model path loss is

$$L_{\text{Okumura–Hata}} \text{(dB)} = 69.55 + 26.16 lg\, f_c - 13.82 lg\, h_{\text{te}}$$
$$- \alpha(h_{\text{re}}) + (44.9 - 6.55 lg\, h_{\text{te}}) lg\, d + C_{\text{cell}}. \tag{1}$$

In the formula, L is the path loss between the base station and the mobile station, in dB; f_c is the operating frequency, in MH$_z$; h_{te} is the effective height of the base station antenna, in m; h_{re} is the effective height of the mobile station antenna, in m; d is the horizontal distance between the base station antenna and the mobile station antenna, in m; $\alpha(h_{\text{re}})$ is the effective antenna correction factor; and C_{cell} is the cell type correction factor.

2.4.2. COST-231 Hata Model.
The COST-231 Hata model is an extended version of the Hata model proposed by the European Research Council. It is mainly suitable for macrocellular systems with a cell radius of 1 km~20 km. Other applicable conditions include the following: the application frequency is between 1500 and 2300 MHz, and the effective transmitting antenna height is 30. Between ~200 m, the effective receiving antenna height is between 1 and 10 m. The empirical formula for calculating the path loss of the COST-231Hata model is

$$L_{\text{COST–231Hata}} \text{(dB)} = 46.3 + 33.9 lg\, f_c - 13.82 lg\, h_{\text{te}} - \alpha(h_{\text{re}})$$
$$+ (44.9 - 6.55 lg\, h_{\text{te}}) lg\, d + C_{\text{cell}} + C_M. \tag{2}$$

In the formula, L is the path loss between the base station and the mobile station, the unit is dB; f_c is the operating frequency, the unit is MH$_z$; h_{te} is the effective height of the base station antenna, the unit is m; h_{re} is the effective height of the mobile station antenna, the unit is m; D is the horizontal distance between the base station antenna and the mobile station antenna, the unit is m; $\alpha(h_{\text{re}})$ is the effective antenna correction factor; C_{cell} is the cell type correction factor; and C_M is the correction factor for the metropolitan center.

2.4.3. Improved LEE Propagation Model.
This article improves the traditional LEE propagation model and proposes a propagation environment correction factor G_{AREA} to accurately describe the comprehensive impact of different test areas and different geographic attributes. The improved LEE propagation model is shown in the following formula:

$$P_r = P_{r_1} + (-\gamma) \cdot \lg \frac{d}{d_0} + \alpha_0 - n \lg \frac{f}{f_0} + G_{\text{AREA}}. \tag{3}$$

In the formula, P_r is the received power; d is the horizontal distance between the transmitting and receiving antennas; γ is the distance attenuation factor; P_{r_1} is the received power at 1 km of the base station antenna used in the actual measurement in a specific city under the normal transmitting state; G_{AREA} is the propagation environment correction factor, which locally corrects the propagation loss according to the geographical attributes in the test area; and α_0 is the correction factor for sending and receiving. In

actual use, when the base station antenna is different from the standard antenna, it is corrected. The calculation formula of α_0 is shown in the following formula:

$$\alpha_0 = \left(\frac{h_t}{h_{t_{\mathrm{REF}}}}\right)^2 \frac{P_1}{P_{t_{\mathrm{REF}}}} 10^{G_t - G_{t_{\mathrm{REF}}}/P_{t_{\mathrm{REF}}}}. \tag{4}$$

In the formula, h_t, P_t, G_t are the actual base station antenna height, base station transmitting power, and base station antenna gain, respectively; $h_{t_{\mathrm{REF}}}$, $P_{t_{\mathrm{REF}}}$, $G_{t_{\mathrm{REF}}}$ are the base station antenna height, base station transmitting power, and base station antenna gain when measuring P_{r_1} and γ, respectively.

In the improved LEE model, d_0 takes 1 km, f_0 takes 850 MH$_z$, and n is determined by f and f_0, as shown in the following formula:

$$n = \begin{cases} 20, & f < f_0, \\ 30, & f < f_0. \end{cases} \tag{5}$$

2.5. Cluster Head Selection Algorithm Based on Fuzzy Logic in Wireless Sensor Networks

2.5.1. Trust Management Plan.
Suppose the evaluation node and the evaluated node are node i and node j, respectively. Direct trust calculation is based on the direct observation of node i to node j, using node α_{ij} to represent the number of normal behaviors of node j and β_{ij} to represent the number of abnormal behaviors of node j. The trust value DT_{ij} of node i to node j can be calculated from the mathematical expectation of the *Beta* distribution.

$$\mathrm{DT}_{ij} = \frac{\alpha_{ij} + 1}{\alpha_{ij} + \beta_{ij} + 2}. \tag{6}$$

More interaction between nodes will improve the accuracy of trust calculations; however, some different situations will lead to the same direct trust value. Therefore, Conf is introduced to reflect the reliability of direct trust:

$$\mathrm{Conf} = \frac{\int_{D_{ij}-\varepsilon}^{D_{ij}+\varepsilon} p^{\alpha_{ij}-1} (1-p)^{\beta_{ij}-1} dp}{\int_0^1 p^{\alpha_{ij}-1} (1-p)^{\beta_{ij}-1} dp}. \tag{7}$$

Among them, ε is the error level, assuming that p is the threshold of Conf, when Conf $\geq p$; it means that the direct trust is sufficiently reliable, and the total trust value $T_{ij} = \mathrm{DT}_{ij}$; otherwise, indirect trust calculation is required.

In indirect trust calculation, it is necessary to collect the suggested values of the common neighbor nodes of node i and node j, and these common neighbor nodes are called suggested nodes. First, calculate the direct trust DT_{ik} of node i and node k according to the above formula. Taking γ as the threshold, when $\mathrm{DT}_{ik} < \gamma$, it means that node i does not trust node k, and node i will ignore the suggestions from node k. If $\mathrm{DT}_{ik} \geq \gamma$, it means that node k can be trusted. ω_k represents the weight of different suggestions, calculated as

$$\omega_k = \frac{\mathrm{DT}_{ik}}{\sum_{m=1}^n \mathrm{DT}_{im}}, \quad k = 1, 2, \ldots, n, \tag{8}$$

where n represents the number of trusted suggestion nodes, and highly reliable trusted nodes have a higher weight. Assuming that α_{ij} and β_{ij} are the recommended information about node j, the indirect trust value IT_{ij} can be expressed as

$$\mathrm{IT}_{ij} = \frac{\sum_{k=1}^n \omega_k * \alpha_{kj} + 1}{\sum_{k=1}^n \omega_k * \alpha_{kj} + \sum_{k=1}^n \omega_k * \beta_{kj} + 2}. \tag{9}$$

In the formula, α_{kj} and β_{kj} represent the number of normal and abnormal behaviors of node i observed by the proposed node.

In order to improve the adaptability, the trust value is updated with the period π. Because the trust value and the interactive behavior are bright, the evaluation node $T + \pi$ updates the historical record at all times:

$$\begin{aligned} \alpha^{t+\pi} &= (1 - \theta) * \alpha^t + \theta * \Delta\alpha, \\ \beta^{t+\pi} &= (1 - \theta) * \beta^t + \theta * \Delta\beta. \end{aligned} \tag{10}$$

Among them, $\Delta\alpha$, $\Delta\beta$ represent the behavior record in the period π, and the parameter θ is the forgetting factor, which reflects the weight of the historical record. The forgetting factor can change dynamically during the update process:

$$\theta = \begin{cases} \theta_h, & \text{if } \Delta\alpha < \Delta\beta, \\ \theta_i, & \text{if } \Delta\alpha \geq \Delta\beta. \end{cases} \tag{11}$$

Among them, $0 < \theta_i < \theta_h < 1$ means that if the evaluated node performs badly in the period π, its abnormal behavior will be severely punished. When the node performs well in the period π, its influence on the current trust evaluation becomes smaller. This is to prevent the node from pretending to improve its trust value.

Finally, the overall trust value T_{ij} of node i to node j is obtained:

$$T_{ij} = \mu * \mathrm{DT}_{ij} + (1 - \mu) * \mathrm{IT}_{ij}. \tag{12}$$

Among them, μ is a weighting factor reflecting the importance of direct trust, which can be selected according to different application scenarios.

2.5.2. Fuzzy Logic Cluster Head Selection.
When selecting cluster heads, the fuzzy logic system requires three input variables: trust value T, energy parameter E, and parameter D, reflecting the density of nodes:

$$\begin{aligned} E &= \frac{E_r}{E_0}, \\ D &= \frac{n}{N}, \end{aligned} \tag{13}$$

where E_r represents the remaining energy of the node and E_0 represents the initial energy; N represents the number of neighbors of the node, and N represents the total number of nodes.

After the current cluster head works for a period of time or when its remaining energy is lower than a preset value, the cluster head broadcasts a new election message. Once new election information is received, each node will automatically generate a random number between 0 and 1. If the random number is less than the threshold $T(n)$, then the node becomes a candidate cluster head. The calculation formula of the threshold $T(n)$ is as follows:

$$T(n) = \begin{cases} \dfrac{P}{1 - P \times [r \bmod (1/P)]}, & n = G, \\ \\ 0, & \text{otherwise,} \end{cases} \quad (14)$$

where P is the percentage of cluster heads and r is the current round number and G represents the set of nodes that have no cluster heads in the last $r \bmod (1/P)$ round.

Fuzzy processing of variables:

$$\text{priority} = \frac{\int x \cdot \mu(x) \mathrm{d}x}{\int x \mathrm{d}x}, \quad (15)$$

where $u(x)$ is the membership function of the fuzzy set $priority$. Ordinary nodes select the highest priority node from the trusted candidates as the cluster head and then send a $join-in$ message. After receiving the $join-in$ message from the member node, the cluster head rejects the request of the node with low trust value to isolate the malicious node.

3. Design of a 3D Virtual Fitting System Based on the Combination of Virtual Reality Technology and 5G Mobile Communication Technology

At present, China's retail model has been transformed into a physical retail model closely integrated with e-commerce. However, in the field of clothing, more and more traditional methods of buying clothing must be seen first and the display methods of current online shopping platforms are increasingly used. For example, the unique text introduction of clothing and 2D product photos can no longer meet the needs of this person. Therefore, 3D virtual personalization technology has emerged. As a 3D virtual technology, it provides real-time interaction, visual display, and the advantages of meeting the psychological needs of consumers.

3.1. 3D Virtual Fitting System Architecture Construction

3.1.1. Layered Architecture Design. At present, the software architecture model widely used in the software field has adopted several layered architectures of virtual switchgear system architecture. The characteristics of multilayer design are to simplify the design and keep the system structure clear, accurate, and loosely coupled. At the same time, it recognizes that the user interface layer, business logic layer, and data access layer are separated from each other, and it improves flexibility and scalability.

3.1.2. System Model Architecture Design. The virtual fitting system can be designed and described with a simple three-tier architecture under the B/S mode. In the three-tier architecture design used by the virtual fitting system, the presentation layer is located at the outermost layer of the entire architecture and is the layer directly contacted by the user. The data used to determine the body shape in the virtual fitting system is entered by the user at this layer and display the body shape judgment result directly based on the relevant judgment data. Between the presentation layer and the data access layer is the business logic layer, which is in a very important link in the overall architecture relationship. Mainly check the business logic relationship of the whole system, test the effect of fitting, and provide the mutual interface with other layers.

3.1.3. System Flow Design. The process design of this system is mainly to display the operation procedures of clothing browsing, clothing, and body type matching effect. The user name and password entered by the user at the front desk of the system are used to determine their identity. For the system administrator, it is also necessary through the identification of the foreground to obtain the authority of the background operation.

3.1.4. System Module Design. The user can enter the homepage of the fitting system after obtaining the identity recognition. Through the registered user identity recognition, they can enter body data, obtain body type judgments, browse clothing styles, view clothing wearing effects, etc., and the system administrator can pass through the system homepage. After identification, you can enter the system background through the link entry on the homepage. After the administrator is in the system background, the administrator can modify the user name and password of the administrator, add or delete clothing styles, manage body types, and perform clothing and body types. The system design adopts modular design, which makes it easier to build, maintain, and modify the system. Modular design also has the characteristics of easy maintenance and clear thinking of system design. Divide the function of the entire system into several small problems, analyze, and design their functions one by one. Through the connection and combination between modules, the overall functions of the system are realized, so that the whole system can realize the functions of the system set at the beginning of the design. The main functions are as follows:

(1) Body Shape Judgment Module. In order to achieve the effect of fitting, it is first necessary to obtain the user's body characteristics. The design of this module completes the judgment of the user's body characteristics through the input of the user's body shape data, which is the leading link for the subsequent virtual fitting.

(2) Clothing Browsing Module. The design of this module is based on the characteristics of clothing styles in the clothing sales businesses, adding the model diagrams of the clothing

styles in the store to the background management system. In the clothing browsing module, the user can view the styles of clothing that the store owns, then make a choice and decide whether to try it on.

(3) Virtual Fitting Module. Consumers' demand for fitting is to see the effect of different styles of clothing on themselves as a basis for judging whether to buy clothing. The design of this module mainly realizes the effect of virtual try-on. According to the body shape judged by the previous module, combined with the clothing style selected by the user to browse the clothing, a clothing effect diagram is given (providing a multiangle display effect), so that the user can get an immersive try-on experience.

(4) Administrator Login Module. This module is one of the main modules of the system and the basic module of the system. Users with administrator rights can enter the background interface of the Metropolitan System through this module. The setting of this module ensures the effectiveness and safety of the front-end release system to prevent ordinary users from arbitrarily changing the management of clothing style models and body type classification management.

(5) Clothing Management Module. The function of this module is to add, modify, delete, and do other operations on the clothing model diagram. The clothing in the clothing store needs to be updated from time to time according to seasonal changes and sales conditions. The virtual fitting environment also needs to be adjusted accordingly. The design of this module can be added and deleted in time according to the change of clothing styles to ensure the effectiveness of the fitting environment.

(6) Body Type Module. The current research and design of the system are only at the preliminary stage, and the classification of human body types is relatively preliminary. In order to improve the satisfaction of the try-on effect, it is necessary to continue to subdivide according to the characteristics of the human body to improve the effectiveness of the try-on clothing.

(7) Display Graph Management Module. The system needs to make timely adjustments to the clothing model according to the style changes in the clothing store and wear the new virtual clothing on the virtual model. This process requires the help of an experienced 3D expert to complete it. The setting of this module is designed to ensure the rationality of the clothing try-on effect.

(8) Administrator Module. This module is mainly designed according to the changes of staff in the store. According to the actual situation, the staff in the store may be replaced. For the use of the system, different employees can set their own login names and passwords to improve the feasibility of system maintenance and application.

3.1.5. System Design Goals. In the design of the overall system framework, according to the actual needs of the

virtual fitting project, the system is divided into multiple functional modules to achieve different functional requirements, and the functions of each individual module are designed separately to make the entire fitting system. The function is realized. Each module is provided with its own function, and an external interface is set between one function module and the other function module, and the modules are assembled according to the overall framework of the design, so that they can realize different functions.

The ultimate goal of system design is to clarify the specific role of each module; let them play their respective functions, determine how to implement the program function implementation, and make the design of the entire system as simple and clear as possible, easy to learn, and easy to operate for users.

Through the program management in the background, the system administrator can clearly manage clothing information, body shape information, etc., and add or delete clothing styles, body subdivision styles, etc., and can also manage the details of clothing wearing effects to enable front-end users to operate more timely and clear. After logging into the homepage of the system through registration, the user can obtain the body shape judgment through the input of his body shape data; after browsing the various clothing styles provided by the store, he can choose his favorite clothing and check the effect that the clothing is wearing a similar body shape on the model. Any piece of clothing content of the clothing style management function can be deleted, and new clothing styles can be added according to the fashion trend and the purchase situation in the store.

Figure 1 is the flow chart of the fitting system. When a user logs in, his identity is verified to determine whether he is a front-end user or a system administrator. When you are an administrator user, you can manage the addition and deletion of clothing style models according to the new synchronization of the store's clothing styles and manage the renderings of different virtual body types wearing corresponding styles of clothing models; if it is a general user, enter the clothing style browsing and style selection, body shape data input, and body shape judgment operation process. The fitting process is shown in Figure 1:

3.2. System Database Design. The database is developed on the basis of the file management system. It is a data collection that can realize the unified management of large-scale data. It is the core and foundation of the digital system. The database enables the information system to obtain the required information accurately, conveniently, and timely.

3.2.1. Database Security

(1) The Security of Information in the Database. In order to ensure the security of the information in the database, system administrators must pass identity verification before they can enter the system background for operation. Each legal administrator needs to enter a user name, and each legal administrator user only corresponds to a password. This kind of identity verification operation can prevent
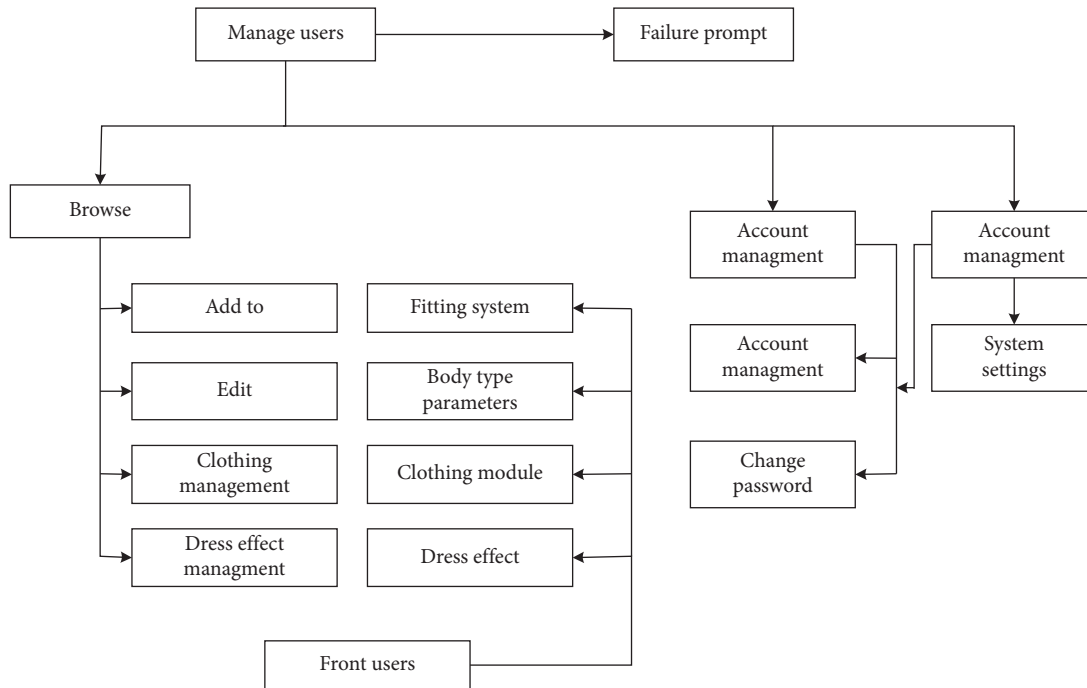
FIGURE 1: Fitting system process.

nonadministrators from entering, so that the data in the database can be adjusted and changed at will.

(2) Data Security. In the process of data setting, in order to ensure data security, the system isolates the database layer from the client layer, so that the data in the database will not be arbitrarily destroyed, and data cannot be added or modified.

(3) Consistency of the Database. When setting the clothing style information and clothing dress display settings, it is ensured that when the clothing style information is deleted, the corresponding clothing dress effect is also deleted, ensuring the consistency of the database.

3.2.2. Database Design. Database design is mainly used to solve the input method and implementation method of the entire system design, how to map the model to a specific software system structure, and how to divide modules to determine each function of each module and the relationship between them. When performing system design work, designers must use multiple design methods based on the analysis methods used in the analysis phase. Data express abstract things in the form of data and analyze and obtain the real world. There are internal connections in the specified application environment, and designers can effectively process data according to user information requirements and data processing requirements.

3.3. 3D Clothing Model Creation

3.3.1. 3D Modeling Technology in the Field of Clothing CAD. With the continuous update of computer technology, the clothing industry has higher requirements for the three-dimensional and real sense of clothing in computers, which promotes the development of clothing CAD to three-dimensional technology. Garment CAD 3D technology not only overcomes the defects of virtual imaging in 2D but also makes it possible to network the production and purchase of garments. Garment CAD technology operates in accordance with the traditional garment design and production process. First, the designer's conceived garment image is drawn into a plane dressing effect drawing and a style structure plan, and then it is input into the 3D module for virtual stitching; you can see the 3D visualization of the dressing effect. At present, the transformation from a structural plan of a clothing style to a two-dimensional clothing piece is still an artificial conversion process, which requires professional cutting knowledge to complete.

At present, the geometric modeling technology of clothing still focuses on how to express the glossiness, reflection and absorption of light, fold texture, and other effects of clothing fabrics. For the soft nature of clothing fabrics, the performance of fabric tension and tensile strength needs to be more in-depth research and discussion. The current 3D modeling technology only uses all kinds of fabrics as deformable geometric objects and uses B-spline surfaces, Bezier surfaces, and INURBS surfaces to express the surface modeling of clothing.

3.3.2. Physical Modeling. The physical modeling of clothing is to imitate the physical characteristics of clothing, such as the refraction and reflection of light and the reflection of gravity, through computer graphics technology; to create it visually, this kind of method can be more realistic. The physical model creation method analyzes the physical data embodied by the fabric through mathematical models and

algorithms, so as to realize the reproduction of the specific physical object form in the virtual environment. In clothing physical modeling, it is usually divided into energy method and force method according to different calculation methods. Among them, the energy method is usually used to simulate the static drape fabric, and the force law is mostly used for the dynamic drape fabric simulation.

3.3.3. Photographic Method to Obtain Clothing Model. The most commonly used in the field of photography modeling is the IBMR technology. The use of IBMR technology to model is faster and more convenient, and the technology of building a 3D model on the basis of 2D images can make the model feel like a photo. It is a modeling method that generates a three-dimensional model according to the contour line of the captured object image, in which determining the position of the camera is an essential and important step. In this step, it is not only necessary to determine the orientation of the camera but also the parameter settings during shooting will become reference values. This camera calibration process can be achieved by using a specific device to set the position of the subject to be fixed and change the position of the shooting camera; it can also use a controllable mechanical turntable to rotate the subject while the camera position is fixed. This type of calibration can ensure the accuracy of the 3D model.

3.3.4. Creation of Clothing Model in the Fitting System. In this virtual fitting system, the aesthetic difference between the circumference change and the clothing wearing is solved first, and the clothing fitting effect suitable for the weight of the user is provided. Consumers' body types are preliminarily divided into four basic body types: "thin body type," "standard body type," "fat body type," and "fat body type." In order to provide users with the effect of wearing the same clothing with different body shapes, clothing models are created based on the obtained human body shapes to show users the visual display effect of corresponding body shapes wearing the same clothing.

3.3.5. Establishment of 3D Clothing Model. Due to the limitation of technology and equipment, the creation of clothing model in this system is obtained by Maya three-dimensional modeling. The clothing model creation first locks the total length of the clothing and creates it according to the height of 165 mm. In order to retain the style characteristics of the clothing in the try-on renderings, it is first necessary to determine several key points and key line parameters of the clothing. For example, clothing length, waistline height, neckline width, neckline depth, shoulder width, sleeve length, hem size, and other dimensions are all obtained from the measurement of clothing products, combined with the effect of wearing clothing on a model with a standard body shape of 165 mm. For example, the lower edge of the neckline is at the reference position of the clavicle of the model, the shoulder width is at the corresponding position of the shoulder point, and the size of the

sleeve is lower than the relative position of the armpit; the clothing model is created based on the measurement positions of the standard body model wearing the clothing.

3.3.6. Stakeout Display of Clothing Model. The key lines set in the clothing model play a great role in the clothing stakeout link. According to the clothing model standard and the key girth in clothing cutting, the difference between different body types (only the difference between body weight and thinness is considered as the body type judgment standard in the first stage of the system creation) on the key line data is used as the basis. Use the difference in the key line circumference setting of the clothing model to obtain the lofting effect of different models of clothing.

4. 3D Virtual Fitting System Test and Analysis

4.1. Body Shape Judgment Test. In order to test whether the fitting system's body shape judgment is reasonable and to experience whether the virtual fitting system can achieve the aesthetic needs of clothing styles, the body shape data of some potential users are selected for body shape judgment testing. This experiment selects the body type data and age of 20 potential users. See Table 1 and Figure 2 for specific data information.

It can be seen from Table 1 and Figure 2 that according to the comparison of the body shape test results with the conventional body shape judgment experience, the correct rate of the virtual fitting system is 86% and the error rate is 14%. Among them, the improper body shape judgment of data no. 009 is caused by the difference of body shape. The body shape of the tested object of 009 is obviously a body shape, and the test result shows "fat" because its hip circumference parameter is obviously larger than the standard parameter, and the waist circumference parameter slightly larger than the standard parameters are caused by the fact that the hip bones are wider and the hip circumference parameters are larger, which makes the result of the virtual fitting system judged by the actual body shape gap. The 003 data and the 011 data are judged to be "fat" by the system, but in fact, the skeletons of the two measured objects are large skeletons, and the circumference parameters of the bones themselves are relatively large, and the actual body type is thin. From the results of the above tests, the system can basically meet the body shape judgment of young and middle-aged women during virtual try-on, and the accuracy rate is high.

4.2. Comparison of Online Shopping Data of Consumers on Different Communication Networks. This experiment is mainly to test the impact of different mobile communication networks on online shopping. Twenty people (divided into 4 groups, 5 people in each group) were randomly selected to use 2G, 3G, 4G, and 5G networks on an e-commerce platform to limit the time to one-hour online shopping; the main test data are total online shopping time, average purchase time per item, purchase quantity, purchase type, and online shopping satisfaction (standard:

TABLE 1: Body type test data.

Serial number	Height	Bust	Waistline	Hips	Age	Test body shape
1	155	83	83	97	38	Bust+
2	162	69	69	97	30	Bust+
3	164	66.5	66.5	93	29	Fat
4	167	73	73	91	27	Waistline+
5	170	84.5	84.5	98	48	Waistline+
6	165	68	68	98	25	Fat
7	181	81	81	97	58	Waistline+
8	160	75	75	98	36	Normal
9	160	68	68	95	19	Fat
10	160	77	77	104	19	Bust+
11	170	61	61	91	19	Normal
12	163	68	68	89	19	Normal
13	168	71	71	96	19	Fat
14	160	63	63	87	19	Normal
15	168	70	70	95	19	Fat
16	160	67	67	91	19	Fat
17	165	64	64	91	19	Normal
18	162	71	71	93	19	Bust+
19	162	72	72	91	19	Bust+
20	170	65	65	92	19	Slightly fat
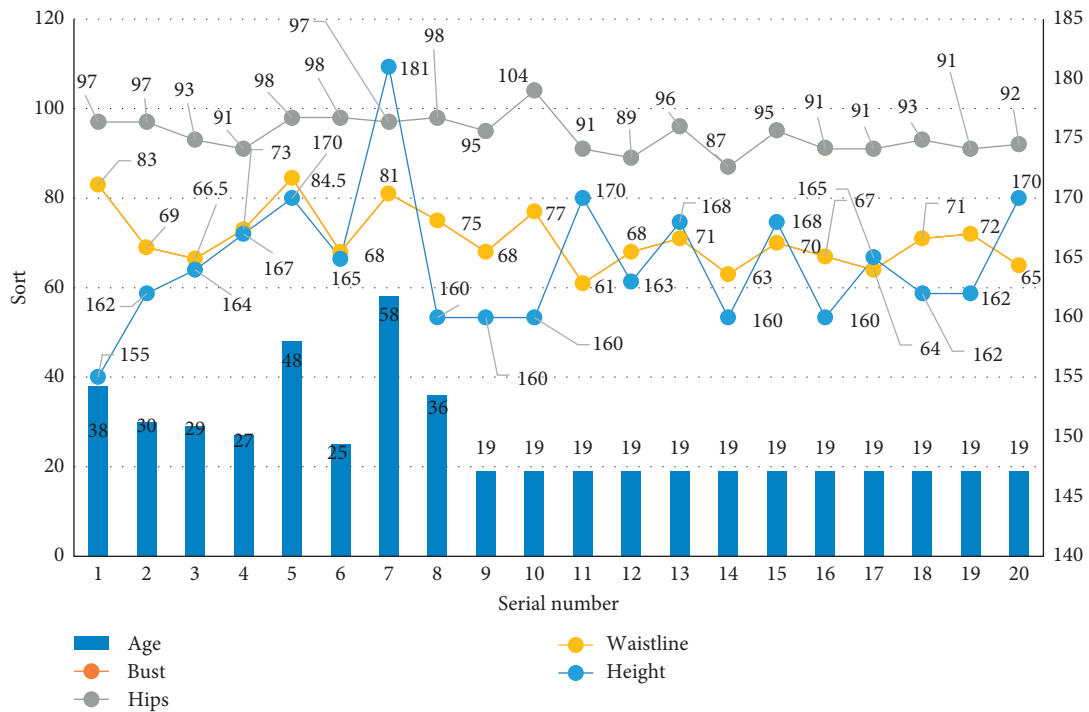
FIGURE 2: Body type test data.

1–10 points). See Table 2 and Figure 3 for specific data information.

It can be seen from Table 2 and Figure 3 that in this online shopping, the users in the 2G group had a total purchase time of 55 minutes. They purchased 3 products and 3 types of products. The average shopping time per item was 18.33 minutes, and the satisfaction was only 1 point. In this online shopping, users in the 3G group had a total purchase time of 43 minutes. They purchased a total of 6 products and 5 types of products. The average shopping time per item was 7.17 minutes, and the satisfaction score was 2 points. In this online shopping, users in the 4G group had a total purchase time of 31 minutes. They purchased a total of 11 products and 9 types of products. The average shopping time per item was 2.82 minutes, and the satisfaction score was 7 points. In this online shopping, users in the 5G group had a total purchase time of 16 minutes. They purchased 18 products and 15 types of products.

TABLE 2: Comparison of online shopping data of different networks.

	Total online shopping time	Average use time	Purchase quantity	Type of purchase	Satisfaction
2G	55	18.33	3	3	1
3G	43	7.17	6	5	2
4G	31	2.82	11	9	7
5G	16	0.88	18	15	8
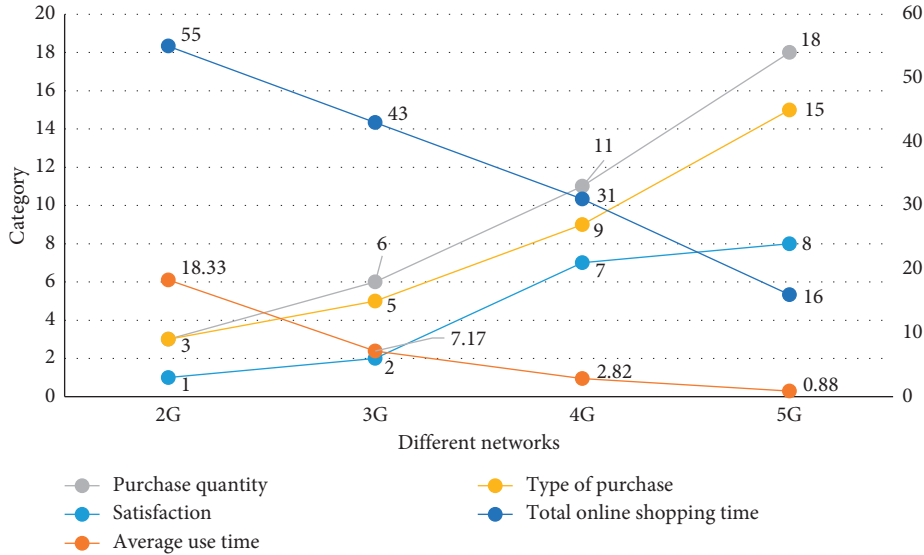
FIGURE 3: Comparison of online shopping data of different networks.

The average shopping time per item was 0.88 minutes, and the satisfaction score was 8 points. Among them, the longest time spent on online shopping is 55 minutes for the 2G user group, while the time required for the 5G user group is 16 minutes, and the time spent by the 2G user group is 3.44 times that of the 5G user group; the length of time spent on online shopping order is 2G, 3G, 4G, and 5G. The online shopping experience of 2G user group, 3G user group, and 4G user group and 5G user group is very polarized, and the ranking of satisfaction is 5G, 4G, 3G, and 2G. In summary, in the online shopping experience, the speed of different networks has a greater impact on the shopping experience. As a newly developed network mobile communication technology, 5G has a great impact on the consumer experience due to its ultra-high speed advantage.

4.3. Comparison of Traditional Operation Mode and Combination of Online and Offline Operation Mode

4.3.1. One-Week Revenue Comparison. In order to further compare the difference between the traditional marketing operation model and the new retail operation model, this experiment uses a combination of online and offline operations of a Hui supermarket (A1) and an ordinary traditional supermarket (A2) to compare the weekly revenue. Both in a superior geographical location, the tested data include total traffic, daily average traffic, purchase times,

replenishment times, total revenue, and weekend revenue. See Table 3 and Figure 4 for details.

From Table 3 and Figure 4, it can be seen that A1 has 136,657 people in a week, with an average of 1042 people per day, 17 times of restocking, 11 times of replenishment, weekend revenue of 176,300 yuan, online revenue of 131,800 yuan, and total revenue of 419,700 yuan. A2 has 153,364 people in a week, with an average of 1283 people per day, 13 times of restocking and 5 times of replenishment, weekend revenue of 152,200 yuan, online revenue of only 34,400 yuan, and total revenue of 335,600 yuan. It can be seen from the above data that although A1 has relatively less total traffic and daily average traffic than A2, the ratio of weekend revenue and online revenue is much higher than that of A2, of which online revenue is equivalent 5.1 times of A2, the number of replenishments is 2.2 times of A2. A1 revenue under the new retail model is higher than A2 revenue under the traditional model. Generally speaking, with the improvement of people's consumption level and the change of consumption concept, the traditional marketing model is far from being able to meet the needs of people nowadays, and new retail is catering to the consumption needs of people in the new era.

4.3.2. Comparison of Revenue Structure. In the above data analysis, the comparison between A1 and A2 is the comparison between total revenue, which shows that the new marketing model is more suitable for people's consumption

TABLE 3: Comparison of supermarket data of different models in a week.

	Total traffic	Average traffic	Number of purchases	Replenishment times	Weekend revenue (ten thousand)	Online revenue (ten thousand)	Total revenue (ten thousand)
A1	136657	1042	17	11	17.63	13.18	41.97
A2	153364	1283	13	5	15.22	3.44	33.56
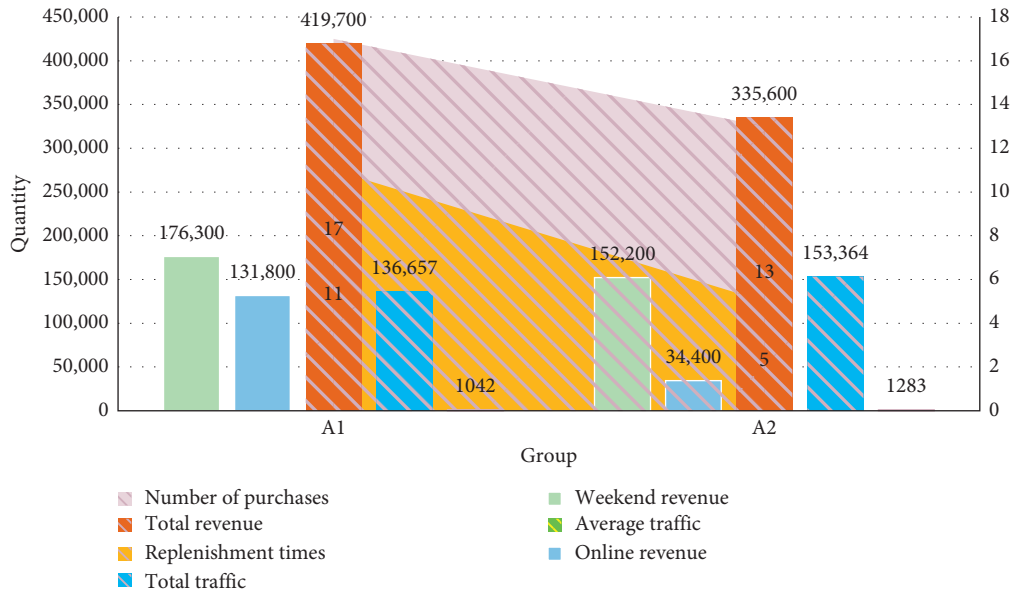
FIGURE 4: Comparison of supermarket data of different models in a week.

needs. In order to further understand the revenue structure of the new retail marketing model and the differences between it and the traditional model, the weekly revenue of the two models is divided in detail. See Table 4 and Figure 5 for details.

From Table 4 and Figure 5, it can be seen that A1's total revenue is 419,700 yuan, of which online revenue is 131,800 yuan, accounting for 31.4% of total revenue; offline revenue is 287,900 yuan, accounting for 68.6% of total revenue; and weekend revenue is 176,300 Yuan, accounting for 42% of total revenue. A2's total revenue is 335,600 yuan, of which online revenue is 34,400 yuan, accounting for 10.3% of total revenue; offline revenue is 301,200 yuan, accounting for 89.7% of total revenue; and weekend revenue is 152,200 yuan, accounting for 45.3% of total revenue. It can be seen that A1's revenue structure is relatively balanced, with online revenue, offline revenue, and weekend revenue, accounting for 31.4%, 68.6%, and 42% of total revenue, respectively. However, A2's revenue structure is uneven, with online revenue accounting for only 10.3%, but offline revenue accounting for 89.7%, basically focusing on offline. Through the above analysis and comparison, the revenue structure of the new retail model is different from that of the traditional model. The main business income under the new retail model no longer focuses on offline revenue, but is

TABLE 4: Comparison of weekly revenue structure (unit: ten thousand).

	Total revenue	Average revenue	Online revenue	Offline revenue	Weekend revenue
A1	41.97	5.99	13.18	28.79	17.63
A2	33.56	4.8	3.44	30.12	15.22

more evenly distributed to online and weekend promotions. In terms of revenue, the main business revenue under the traditional model still focuses on offline revenue. Online revenue is minimal, and the revenue structure is uneven and needs to be optimized.

4.4. Mobile APP Usage of 5G Users. This chapter is mainly to explore users' preferences for online shopping. For this purpose, 50 5G mobile phone users are investigated for mobile APP usage. See Table 5 and Figure 6 for details.

From Table 5 and Figure 6, it can be seen that, first of all, from the perspective of user selection, the total number of selections reached 943, with an average of nearly 7 selections per capita. This shows that users have higher and higher demand for APP, and APP use is very active; then, judging from the frequent use of apps by users, WeChat and QQ
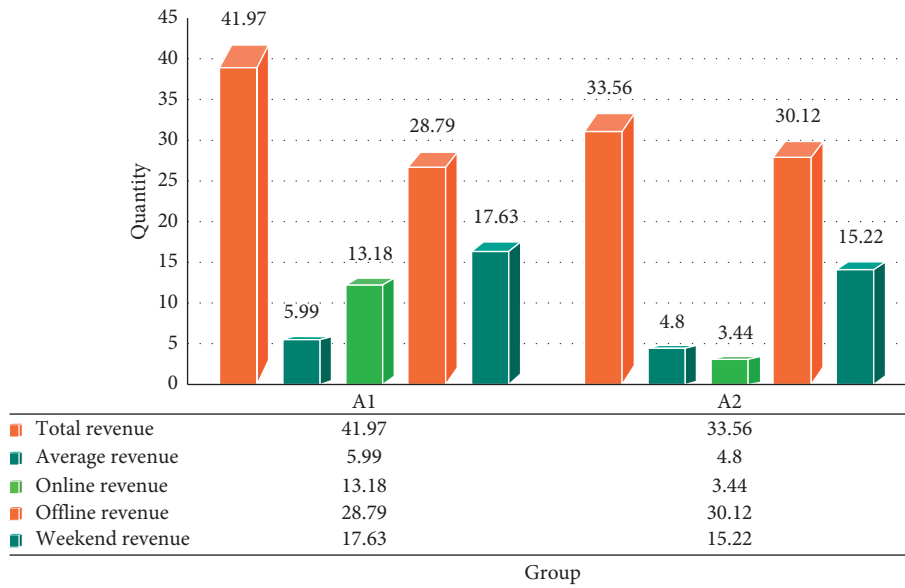
Figure 5: Comparison of weekly revenue structure (unit: ten thousand).

Table 5: 5G users' mobile APP usage.

APP	Frequency	Percentage	APP	Frequency	Percentage
QQ	152	16.1	Meitu Xiuxiu	25	2.7
WeChat	165	17.5	QQ Music	54	5.7
Meituan	58	6.2	QQ mailbox	23	2.4
Tencent Video	74	7.8	Weibo	29	3.1
Public comment	10	1.1	Landlord	25	2.7
Taobao	98	10.4	Xiao Xiao Le	32	3.4
Ink weather	23	2.4	Alipay	54	5.7
Vipshop	24	2.5	Ctrip Travel	10	1.1
Flight Butler	15	1.6	IQIYI	57	6.0
Where to travel	15	1.6	Total	943	100
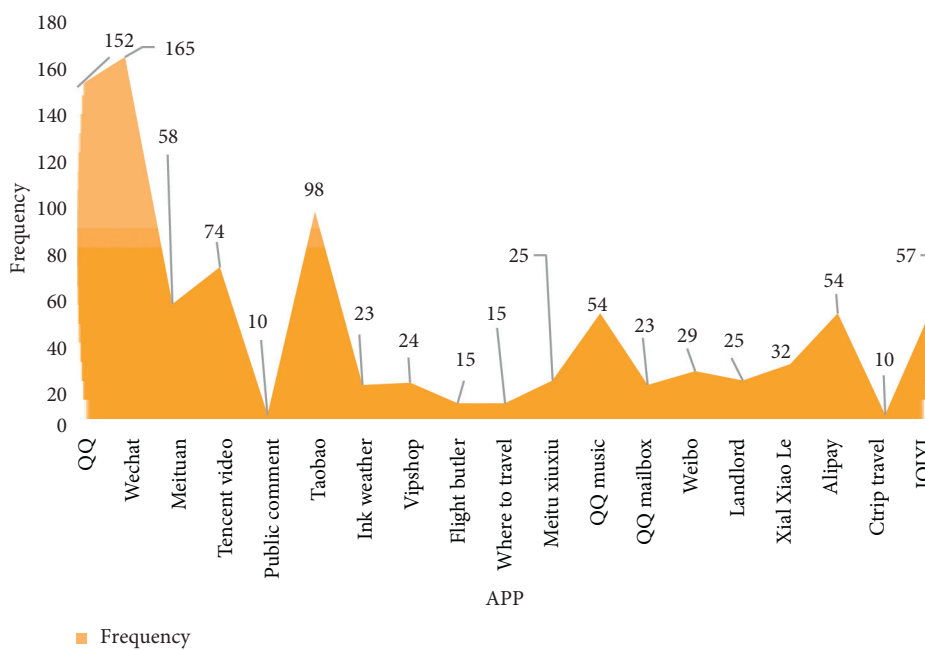
Figure 6: Commonly used apps by users.

accounted for 17.5% and 16.1%, respectively, indicating that customers have strong demand for instant messaging software, followed by mobile phone Taobao, which accounted for 10.4%, indicating that customers use mobile phones. Shopping demand is strong; once again Tencent Video accounted for 7.8%, and then functional apps, such as Meituan, QQ Music, and Alipay, accounted for 6.2%, 5.7%, and 5.7%, respectively. In summary, the main user needs instant messaging and life service apps. Therefore, the marketing strategy of the new retail model also needs to focus on the development and research of shopping apps on the mobile phone, which is not only in line with the consumer's already-developed "buy without leaving home." The consumption habits of the required items can also promote the growth of total revenue under the new retail model through online marketing.

5. Conclusion

Under the technology of digital network, people's life style has undergone earth-shaking changes. The expensive and large digital devices such as desktop computers and digital cameras are gradually being replaced by smart phones in their pockets, and the areas where people rely on smart phones are gradually expanding, and e-commerce platforms are also shifting to smart phones. It is an inevitable trend for virtual fittings to gradually shift to the convenient platform of smart phones to make more efficient use of people's fragmented time.

This paper proposes a new network fitting concept, which divides people into several body types according to their body characteristics, calls the corresponding human body model according to the data parameters input by the user, and displays the user's selected clothing according to the body shape characteristics of the human body model. Finally, the clothing wearing effect of the characteristic body shape is displayed on the interface of the mobile terminal. This idea not only conforms to the actual situation of current mobile data traffic but also can display the clothing style on the three-dimensional human body model to meet the user's requirements for the matching degree of the clothing style and the body type.

With the rapid development of Internet technology, more new application scenarios have emerged in the retail industry. Retailers have changed a lot in this regard. Together with existing offline retailers, online retailers' improved customer experience is at the core of the retail transformation that combines today's online and offline retailers. Only with the help of advanced technology and various sales channels to enhance the user's willingness to buy by improving the satisfaction and viscosity of the customer experience can the company's work efficiency be effectively improved. Therefore, retailers must adopt extensive experimental marketing strategies to enhance consumers' purchasing motivation and enhance their competitiveness in the market.

Data Availability

No data were used to support this study.

Conflicts of Interest

The author declares no conflicts of interest.

References

[1] A. M. Al-Momani, M. A. Mahmoud, and M. S. Ahmad, "Factors that influence the acceptance of Internet of things services by customers of telecommunication companies in Jordan," *Journal of Organizational and End User Computing*, vol. 30, no. 4, pp. 51–63, 2018.

[2] Z. Lv, R. Lou, and A. K. Singh, "AI empowered communication systems for intelligent transportation systems," *IEEE Transactions on Intelligent Transportation Systems*, no. 99, pp. 1–9, 2020.

[3] M. Zhou, Y. Wang, Z. Tian, Y. Lian, Y. Wang, and B. Wang, "Calibrated data simplification for energy-efficient location sensing in Internet of things," *IEEE Internet of Things Journal*, vol. 6, no. 4, pp. 6125–6133, 2019.

[4] Z. Tang, "Analysis on the development trend of 5G mobile communication and discussion on some key technologies," *China New Telecommunications*, vol. 18, no. 20, pp. 6-7, 2016.

[5] F. Pan, "Explore the future development trend of transmission under 5G mobile communication technology," *Information and Computer*, vol. 400, no. 6, pp. 143-144+147, 2018.

[6] F. Zhang and S. Ma, "On the marketing strategy of mobile communication enterprises in the new era," *Operator*, vol. 34, no. 3, pp. 108–112, 2020.

[7] J. Liu, Q. Wang, and Y. Lin, "Mobile VR application in 5G network," *Telecommunications Science*, vol. 34, no. 10, pp. 149–155, 2018.

[8] Z. Lv, L. Qiao, and Q. Wang, "Cognitive robotics on 5G networks," *ACM Transactions on Internet Technology (TOIT)*, 2020.

[9] X. Zhao, H. Wen, L. Zhao et al., "Comprehensive sensory application of virtual reality based on 5G technology and exoskeleton," *Technology and Market*, vol. 27, no. 6, pp. 68-69, 2020.

[10] X. Wang, "How to promote re-integration of mainstream media in the 5G era," *Youth Reporter*, vol. 667, no. 11, pp. 41-42, 2020.

[11] N. N. Hurrah, S. A. Parah, N. A. Loan, J. A. Sheikh, M. Elhoseny, and K. Muhammad, "Dual watermarking framework for privacy protection and content authentication of multimedia," *Future Generation Computer Systems*, vol. 94, pp. 654–673, 2019.

[12] Z. Lv, D. Chen, R. Lou, and H. Song, "Industrial security solution for virtual reality," *IEEE Internet of Things Journal*, no. 99, p. 1, 2020.

[13] J. Yuan, "The prospects and ethical dilemmas of virtual reality news in the 5G era," *Communication Research*, vol. 3, no. 27, p. 42, 2019.

[14] J. Li, "Analysis of the impact of virtual reality technology on news dissemination in the 5G era," *Communication Research*, vol. 3, no. 36, p. 290, 2019.

[15] Du Jin, "The exploration and practice of hybrid teaching mode under the background of 5G network era," *Industry and Technology Forum*, vol. 19, no. 7, pp. 208-209, 2020.

[16] N. Zhang, N. Cheng, A. T. Gamage, K. Zhang, J. W. Mark, and X. Shen, "Cloud assisted HetNets toward 5G wireless networks," *IEEE Communications Magazine*, vol. 53, no. 6, pp. 59–65, 2015.

[17] Z. Huo and Y. Zhang, "5G communication technology and its application in coal mines," *Industry and Mine Automation*, vol. 46, no. 3, pp. 1–5, 2020.

[18] L. Wu, Q. Zhang, C.-H. Chen, K. Guo, and D. Wang, "Deep learning techniques for community detection in social networks," *IEEE Access*, vol. 8, pp. 96016–96026, 2020.

[19] X. Zhang, "The 5G era is coming and the ten application scenarios of cross-age technology description," *Big Data Era*, vol. 25, no. 4, pp. 62–78, 2019.

[20] B. Zhu, S. Ma, R. Xie, J. Chevallier, and Y.-M. Wei, "Hilbert spectra and empirical mode decomposition: a multiscale event analysis method to detect the impact of economic crises on the European carbon market," *Computational Economics*, vol. 52, no. 1, pp. 105–121, 2018.

[21] L. Yang and Y. Ning, "Implementation of 5G mobile network slicing technology," *China New Telecommunications*, vol. 21, no. 9, pp. 15–17, 2019.

[22] J. Liu, Y. Wu, and J. Guo, "Application of VR interactive technology in the display of scientific and technological achievements," *Qinghai Science and Technology*, vol. 27, no. 3, pp. 104–106, 2020.

[23] Y. Sun, H. Song, A. J. Jara, and R. Bie, "Internet of things and big data analytics for smart and connected communities," *IEEE Access*, vol. 4, pp. 766–773, 2016.

[24] T. Fu, "Opportunities and challenges for the development of the "virtual reality technology + social platform" model under 5G technology," *News Research Guide*, vol. 11, no. 3, pp. 53-54, 2020.

[25] H. Chen, "Features and applications of 5G mobile communication," *Communication World*, vol. 331, no. 24, pp. 102-103, 2017.

[26] D. Wang, M. Hou, and B. Zhang, "Research on the actual combat of experimental training based on 5G technology," *Electronics World*, vol. 580, no. 22, pp. 128-129+132, 2019.

[27] Y. Liao, "The development and application trend of 5G mobile communication technology," *Communication Power Technology*, vol. 35, no. 9, pp. 187-188, 2018.

[28] Y. Chen, W. Zheng, W. Li, and Y. Huang, "The robustness and sustainability of port logistics systems for emergency supplies from overseas," *Journal of Advanced Transportation*, vol. 2020, Article ID 8868533, 1 page, 2020.

[29] P. Lu, J. Li, and W. Zhao, "Application of 5G in vertical industries," *ZTE Technology*, vol. 219, no. 25, pp. 67–74.

[30] W. Guo and Y. Liu, "Teaching research on the design of cultural and creative products based on virtual reality," *Digital Design*, vol. 8, no. 17, pp. 55-56, 2019.

[31] Z. Lv, "5G business marketing strategy based on 4P supplemented by 4C," *China New Telecommunications*, vol. 22, no. 2, p. 30, 2020.

[32] C. Zhao, "Innovative exploration of marketing strategies for SMEs in the 5G era," *China SMEs*, vol. 286, no. 9, pp. 149–151, 2019.

[33] X. Du, "The impact of 5G mobile communication on broadcast and television and countermeasures," *Digital Communication World*, vol. 181, no. 1, pp. 158-159, 2020.

[34] Q. He, "Intelligent marketing in the 5G era," *Digital World*, vol. 176, no. 6, p. 43, 2020.

[35] B. Chen and Q. Zeng, "Precision marketing and collaborative marketing for carriers' stock customer retention in the 5G era," *Communication World*, vol. 26, no. 9, pp. 62-63, 2019.

[36] Z. Lv, L. Qiao, and S. Verma, "AI-enabled IoT-edge data analytics for connected living," *ACM Transactions on Internet Technology (TOIT)*, 2020.

[37] Q. Wang, Y. Li, and X. Liu, "Analysis of feature fatigue EEG signals based on wavelet entropy," *International Journal of Pattern Recognition and Artificial Intelligence*, vol. 32, no. 8, Article ID 1854023, 2018.

[38] W. Zeng, "The Internet of Things era under 5G mobile communication technology," *China Strategic Emerging Industries*, vol. 156, no. 24, pp. 85–87, 2018.

Research Article

Basketball Technology Simulation Application Based on Virtual Reality

Yushuai Song (ORCID)

Physical Training College, Beijing Sport University, Beijing 100084, China

Correspondence should be addressed to Yushuai Song; huanxiang82@bsu.edu.cn

The combination of virtual reality (VR) technology and basketball technology simulation can make the players have a real experience and experience, so as to effectively improve the quality of basketball training. It can also, according to the individual needs of different players, promote their physical and mental health development and improve the enthusiasm of basketball training, so as to improve the level of basketball technology. Immersive feeling and interest of human-computer interaction are the essential characteristics of virtual reality. The real conception of space-time environment, that is, the process of enlightening thinking and obtaining basketball technology simulation information, is the ultimate goal of virtual reality. In this experiment, five high-level basketball players in our city were selected and numbered from no. 1 to no. 5. Before the experiment, it is necessary to make the players warm up fully before the experiment and then test the forward turning technical movements of basketball. The test variables are based on different angles and distances. After that, standardized selection of basketball technical statistical indicators includes shooting hit rate, two-point hit rate, three-point hit rate, and free throw hit rate. According to the results of the experiment, it took the most time for the curve technique to lower the buffer stage, and it took up 29% of the total time of the entire precursor shot and turned back and the aerial shot stage is 23% and 22%, respectively. There is 20% time in the takeoff phase and 6% time in the brake phase. It has a great influence on the results of the game.

1. Introduction

1.1. Background and Significance.

As science and technology continues to develop, more and more advanced facilities have been introduced into athletic activities. To improve the training quality and training effectiveness of athletes, different training techniques are used to change training methods [1]. Sue needs new skills and equipment to make training more difficult. Due to the increase in training time and practice, the athlete's mind and body fatigue rapidly increases and the athletes' skill learning and performance are affected, lowering performance and even impeding exercise. Virtual reality technology is developed in recent years. It is a technology that uses computer simulation to create a three-dimensional virtual world. It provides users with visual, auditory, tactile, and other sensory simulation, so that users can feel themselves in the scene [2]. In a three-dimensional space, the participants can experience and interact with the virtual world through appropriate devices.

1.2. Related Work.

The objective is to explore the effect of virtual reality technology (VRT) combined with rehabilitation robot training on motor function and event-related potential (ERR) in patients with hemiplegia after cerebral infarction. From December 2012 to December 2013, Maples-Keller used the random number table method. All patients had unilateral lower limb hemiplegia. The patients were divided into the control group ($n = 40$) and the intervention group ($n = 40$). Both groups were given routine rehabilitation training. The control group was trained by robots, and the intervention group was trained by virtual reality technology combined with rehabilitation robot training. The FMA and Berg Balance Scale were used to evaluate the efficacy of the two groups before and 8 weeks after treatment [3]. Donghui focuses on selecting the exact placement model suitable for psychological evaluation, psychological resilience training, and psychological intervention needs by combining historical development trends and features of virtual reality. We need to study more deeply to improve

research methods, control development costs, and strengthen process experiences and interactions [4].

In order to observe the effect of whey protein powder on the hematological indexes of professional athletes in basketball training, Koeva randomly divided the athletes into the control group and nutrition group. Athletes completed 30-minute quantitative exercise with bicycle before and one month after the experiment. Blood was drawn immediately after exercise, heparin was extracted, and hematological indexes such as hemoglobin, erythrocyte count, hematocrit, and mean corpuscular volume were measured [5]. Chen compared the changes of spinal curvature between young male basketball players and the nontraining control group in 2 years. The study included 10 basketball players and 11 untrained men. At the beginning of the study, all participants were 13 years old; at baseline and in the first and second years of the study, they measured the anterior and posterior curvature of the spine at baseline and at the first and second year of the study [6].

1.3. Innovation. Virtual reality technology can simulate basketball technology, observe a true three-dimensional basketball court from different induction angles, and create different scenes through change to make the final basketball technology effective. It can provide an effective basis for building mockups; the environment for adapting to computers has changed; initially, people always communicated with computers when dealing with everyday environmental problems. It is now more intuitive and transparent to find the best basketball technology simulation information through similar sensing devices [7].

2. Simulation Application of Basketball Technology Based on Virtual Reality

2.1. 3D Modeling. The traditional method for 3D modeling of a real shape is based on a figure or a geometric plane view and is a simulation of the light interaction process of an object in a real situation [8]. When reconstructing, the modeling system is used to determine the geometric model of the scene, and then the material and pattern of the object are specified to check the position and intensity of the light source in the scene. It calculates the brightness of all visible points, identifies the properties of shape elements such as points, lines, faces, and bodies with a computer, and then realizes them through computer design and display [9, 10]. In fact, these two stages are inseparable in the implementation process. In order to facilitate the description, the process is shown as two stages of modeling and drawing. The expression from natural shape to the computer 3D geometric model is called modeling. The establishment of the virtual scene model is the basis of the whole real-time roaming system, and the quality of the model directly affects the performance and accuracy of the scene [11]. For complex large-scale scenes, the establishment and optimization of the model is very important [12].

The integrity of the virtual reality science education model is reflected in the process of learning activities,

learning experience, and learning objectives. When establishing the model, we must conduct a comprehensive evaluation, understand the different stages of the learning process, clarify the learning activities and learning objectives, and analyze the implementation process of virtual reality science education, which fully reflects the integrity of the model [13]. In the construction of the geometric object model, it is necessary to study the virtual coordinate system and the original and organization structure. The mass center of the observed object can choose the coordinate system composed of the main inertial axis and the orthogonal direction. The origin of coordinates can also be selected as the observation point, but because there are many observation points, the model stores a lot of information. The front end contains the preview of face primitive and volume primitive. The connection between front ends can be displayed by using the matrix sum tree or network. The structural expression of objects includes surface/boundary representation, generalized cone method, and volume representation method. An object with an edge interface or edge line is called a surface/boundary representation [14]. According to the space curve, the scanning object composed of two-dimensional parts is called the cone method [15]. The object of the primitive representation of the actual connected volume is the object generated by the Boolean operation of the volume representation and the set of primitives (block, cylinder, cone, and sphere). The complex shape model is used in hierarchical structure, and the object is divided into several subordinate objects. The geometric model is represented by the lower object model and its connection: the human model is composed of head and body; the left and right arm models are composed of two layers of arm and arm. In the hierarchical structure, the change of the direction and position of the lower target can generate different posture actions [16].

Virtual reality (VR) technology in the simulation technology, sensor technology, display technology, and immersion interaction [17], while all teaching changes can rely on technology, can fully meet the requirements of athletes' understanding, experience, and mutual learning. This sense of engagement cannot be achieved with existing teaching techniques. With the blessing of virtual reality technology, athletes can eliminate cognitive barriers caused by time and space and let them immerse themselves in the imaginary simulation scene [18]. Compared with the performance characteristics of knowledge in traditional training, the performance of VR teaching is three-dimensional, which helps athletes deepen their impression of knowledge. The combination of VR and basketball technology simulation can play a strong value in the field of training [19].

2.2. Construction of Basketball Player's Character Model. First of all, the success or failure of the 3D character model construction depends on the accuracy and appropriateness of the character model. Therefore, modeling is the core of making the model. As Maya has powerful modeling and animation performance functions, the software environment is used to create the skeleton and skin of basketball

players [20]. In the construction of the skeleton, the connection between the human body model and the bone will be affected by the relevant bones and the weight of the model, which is directly related to the deformation of the model surface in the bone movement [21]. Here, we need to adjust the weight of the human body to improve the above problems. At the same time, using UV texture mapping, merging organization models, simplifying the number of models, and realizing optimization model can ensure the effect of reducing file size and the fluency of virtual interactive environment [22].

The motion path collected by the motion capture system is the data points of human joints, which should be able to drive the character model according to the trajectory movement [23]. When binding bones, in order to ensure the physical coordination of model motion, we should pay attention to the influence of data point weight of each node in the model [23]. The specific procedure is as follows. First, the initial data collected from the movement capture system are input to the computer software and the basic structure of the movement image model is set to 0 so that the shape of the human body adapts to the initial movement, which is the basic skeletal posture. The characteristics of the 23 data volume nodes are the areas that form the basic structure, and then the raw data were collected using motion and magnification tools in a situation where the skeleton model is not in motion; then, the proportion and angle of the initial motion are kept unchanged, and the raw data are compared with the key nodes of the human skeletal model. The data are captured, driven, and archived [24]. Finally, the binding and debugging of moving bones are completed. The new character data model can be inserted into the computer software. The movement of the data model can be driven by character control tools, and the 3D animation of basketball players can be realized by using motion capture technology.

2.3. Special Physical Training.

Special physical training is connected with the latest scientific and technological achievements in many fields, such as scientific education, sports physiology, scientific life, industry, and computer science, and has become an important way to improve the technical level of modern basketball [25]. Sports is a basic science with strong direction and structure. In some countries, it is specially studied as a learning direction of university. Every NBA team has more than one sports coach, and everyone has conducted in-depth research on some aspect of basketball technology. However, so far, in the specific basketball specific physical training, there is no complete set of the special physical training system. Training theory, concept confusion, and physical exercise specific characteristics are not obvious, and training methods continue to use track and field events, not targeted and practical [26]. On the one hand, due to the lack of experts in this field, most of the physical fitness coaches of some sports teams come from the field of track and field, and not every team has a coach. On the other hand, in the minds of many coaches, special physical training is still a narrow or vague concept. Due to the lack of detailed and systematic research on the characteristics of their own sports and the required physical education teaching, training has been caused to practice blindly mechanically and copy other training methods [27].

Modern sports has a wide range of concepts and rich colors, including body shape, body function, and sports quality. Each part has many goals, such as the quality of sports, speed, endurance, sensitivity, flexibility, coordination, and flexibility. The speed of basketball players is divided into starting speed, turning speed, and braking speed. At the same time, there are differences between general physical fitness and special physical fitness, and each of which must be guided in detail by the coach [28]. The most important thing is how to scientifically combine physical training with special skills and routine training and really apply it to actual combat. It will become a special strength and a special ability and eventually evolve into a wonderful moment for basketball players to snatch, block, lay up, take off, and dunk. This is the need to take many complex and delicate methods and steps, and long-term research and continuous exploration of sports coaches are needed.

2.4. Application of Virtual Reality Technology in Basketball Technology

2.4.1. Breaking through the Limitation of Time and Space and Enhancing the Immersion of Basketball Teaching.

Virtual reality technology can meet people's needs by using a computer to simulate various real scene environments. When VR sports technology is used to display 3D images on virtual reality devices through computers, athletes can learn through simulated sports scenes and make up for the defects in teaching conditions [29]. In the virtual reality scene, we can complete the skill movement which has a certain degree of danger in the basketball teaching method and let the players complete the basketball skills which are difficult to complete in reality and can avoid the occurrence of dangerous injuries and so on. With the help of VR technology, we can also simulate the scene of the basketball game, so that all players can experience the fierce atmosphere of the basketball game. At the same time, we can boldly use the skills we have learned to make the players more immersed in the simulated basketball practice scene and enhance their learning fun.

2.4.2. Breaking the Traditional Physical Education Teaching Mode and Enhancing the Diversity of Basketball Teaching.

Traditional basketball teaching mainly focuses on learning the basic skills of basketball, for example, learning basketball dribble, catch, shoot, and three-point shot, teaching content is cliche, the teaching method is single, and subjective learning intention of athletes is not strong. In addition, in the teaching process, most coaches cannot focus on the needs of athletes in the new era. However, with the blessing of virtual technology, not only can the virtual scene be simulated, but also their favorite basketball stars can show basketball skills and provide supplementary courses to meet the curiosity of athletes and the pursuit of advanced technology [30]. This will greatly enhance the enthusiasm of

athletes in learning and improve the quality of teaching. Due to the limitation of physical quality and basic knowledge of basketball in traditional basketball teaching, many players do not experience the pressure, stimulation, excitement, enjoyment, and satisfaction brought by basketball competition. Therefore, after introducing virtual reality technology, they can simulate the game scene and let the players voluntarily use various basketball skills and tactics to participate in the intense and fierce basketball competition, so that the players have always maintained in a high atmosphere [31].

2.4.3. Breaking the Limitation of Teaching Supervision and Enhancing the Timeliness of Learning. Basketball education should not only rely on course learning and practice but also need continuous training and practice after class, which can improve the athletes' sports quality and the sensitivity of ball games such as basketball skills. Although in basketball class, coaches can provide guidance and help to athletes directly, it is not easy to supervise after class. The introduction of virtual reality technology can play a role of supervision, provide accurate guidance to athletes, and clearly record the completion status of athletes' technical movements, so as to check the accuracy and standardization of their actions, and it can evaluate the behavior of athletes, point out the shortcomings, and put forward suggestions for improvement, which can improve the learning effect. In the process of practice, the coach can analyze the specific learning situation of all the athletes by a computer [32] and provide performance feedback to the athletes and coaches, so that the coach can easily master and supervise the overall learning situation of the athletes and make appropriate learning plans for all athletes.

3. Basketball Technology Simulation Application Experiment Research Based on Virtual Reality

3.1. Research Object. Five high-level basketball players in our city are selected as the experimental objects. They are all professional basketball players who have practiced for more than ten years, they have relatively stable technical movements, and they are also used more frequently in basketball technology. They are familiar with the rules of the basketball game and train hard every day. Therefore, the percentage of shooting percentage is relatively high. In these five high-level athletes, each person uses the right hand to realize the shooting movement.

3.2. Experimental Steps. The virtual reality technology equipment uses HTC Vive equipment, the software selects VR Sports software [33], VR Sports is a VR sports software including basketball, table tennis, badminton, and other seven sports items. Basketball can be used to exercise fixed-point shooting in this software, and the position of players will automatically change, with different degrees of difficulty to choose.

Before the motion data acquisition, in order to prevent computer hardware errors, it is necessary to select a working environment that is not disturbed by the earth's magnetic field. Athletes need to wear special clothes to complete the cable connection between inertial sensors. At the same time, it is necessary to check the correct position of all inertial sensors and reasonably correct the position of sensors and the corresponding human body. In addition, it is necessary to ensure that there are no metal objects on the surface and near the space of the model body [34]; otherwise, the electromagnetic field will be distorted and the accuracy will be affected. Then, the athletes are guided to perform some routine actions, such as stop, walk, run, and jump, and calibrate the actions before the action capture function to make the motion data more accurate.

The number of athletes participating in the experiment is 1–5 before the experiment, and the athlete must complete the exercises such as warming up, limb stretching, and shooting to activate the athlete sufficiently. Predicting and practicing forward and backward movements is necessary to secure the range of roles. After loosening, direction is changed before starting the test. The test subject takes six turns and shoots before receiving the ball. Completing the point, the angle is 0°, the distance is 2 m, the angle is 45°, the distance is 4 m, the angle is 90°, and the distance is 2 m, 4 meters away from a 90-degree angle. The accuracy of the movement must be ensured by performing three movements each time. Statistical standards for basketball include shooting accuracy, two-point hit ratio, three-point hit ratio, and free throw hit ratio.

3.3. Correlation Analysis Theory. Related analysis is a statistical method that is often used to study the accessibility of variables. Correlation is a universal correlation that refers to the relationship between two objects. That is, when one variable X obtains a specific value, the other Y variable cannot take one value according to a specific function. Related relationships can be divided into linear and nonlinear relationships. Linear correlation analysis studies the degree and direction of the linear relationship between two variables. Correlation coefficient is a statistical value describing the strength and direction of this linear relationship, usually expressed by r. The correlation factor r has no unit, and its value varies between −1 and 1. The sample observation values (X, Yi) of n groups of random variables X and Y and the correlation coefficient between $i = 1, 2, \ldots, n$, variables X and Y were calculated by Pearson product moment correlation formula:

$$r = \frac{\sum_{i=1}^{n} (X_i - \overline{X})(Y_i - Y)}{\sqrt{\sum_{i=1}^{n} (X_i - \overline{X})^2} \sqrt{\sum_{i=1}^{n} (Y_i - \overline{Y})^2}}. \quad (1)$$

In the above formula, $\overline{X}$ and $\overline{Y}$ are the mean values of variables X and Y, respectively. Xi and Yi are the ith sample values of variables X and Y, respectively.

4. Basketball Technology Simulation Application Experiment Analysis Based on Virtual Reality

4.1. Forward Turn Shooting Technique. In order to study the movement technique carefully, we must study from the time characteristic, the space characteristic, the speed characteristic, the angle characteristic, the angular velocity characteristic, the acceleration characteristic, and many aspects, and this experiment to the front turn shot technical movement research analysis mainly from the three aspects such as time characteristic, the angle characteristic, and the acceleration characteristic. Through the research of athletes, it is found that most of them take their right hand as the shooting hand, and they are used to take the right foot as the central foot and the left foot as the rotating foot. According to the video shooting and related research, in order to refine the technical action, the technical action of front turning is roughly divided into the following five stages: turning stage, braking stage, kicking off stage, taking off stage, and landing buffer stage. The sequence is "body center of gravity drops slightly and the left foot drives the left knee and left hip to rotate clockwise," "the left foot lands and feet touch the ground to cushion," "feet push the body off the ground," "body soars to complete the hand," and "body gravity drops and feet touch the ground and double knees cushion" [35].

In order to make a more detailed analysis of the technical movements of the five athletes, the experiment divided them into five stages: the turning stage, the braking stage, the kicking off stage, the air release stage, and the falling buffer stage. The time spent in each stage was statistically analyzed, as shown in Table 1.

The data in the table allow each athlete to accurately record the specific time consumption in step 5. The time difference between athletes in the same exercise step is very small, but the time difference in different movement steps is even more. As can be seen in Figure 1, the descent buffer stage occupies the longest time and 29% of the total shooting time. The turn and air fire stages then account for 23% and 22%, respectively, followed by 20% of the landing and takeoff phases and finally 6% of the braking phase.

In the turning stage, the heel of the rotating foot starts to leave the ground, and then the forefoot gradually leaves the ground and starts to rotate towards the toe. The body changes from the original two-foot support to the single support stage with the central foot as the support point. With the rotation of the rotating leg, the hip joint expands outward, and the body rotates with the direction of the toe rotation until the rotating foot begins to contact the ground, which is the beginning and end of this stage. In this stage, the turning action needs to obtain a certain horizontal force, which is the result of the force from the support foot, the swing leg, and the waist and abdomen. The turning effect is the reasonable combination of the horizontal force and the rotation speed.

TABLE 1: Time consuming in different stages.

Number	Twist	Breaking	Take off	Free hand	Buffer
1	0.28	0.12	0.3	0.28	0.38
2	0.29	0.1	0.28	0.24	0.34
3	0.27	0.1	0.26	0.26	0.36
4	0.29	0.09	0.25	0.24	0.38
5	0.28	0.11	0.27	0.25	0.36
Average value	0.282	0.104	0.272	0.254	0.364
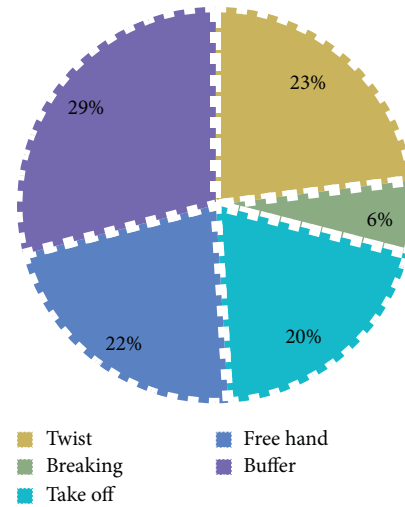
FIGURE 1: Time structure chart of each stage of forward turn shooting.

4.2. Analysis of Angle Characteristics at the Beginning Stage of Rotation. In the process of rotation, the movement form of the transfer leg mainly depends on the swing of the rotating foot, and the swing of the knee joint drives the force of the hip joint. With the different body shapes in the turning process, in order to maintain the body posture, the hip angle, knee angle, and ankle angle in the rotation leg present different angles, and with the turning stage going on, the hip angle, knee angle, and ankle angle show different angles. The angles of the three joints of the rotating leg also change continuously, as shown in Figure 2.

As can be seen in Figure 2, the average hip angle of the athlete's leg rotation is 172.8° and the range of hip angle is 158.2° to 186.3° according to the statistical data. The average knee angle of the rotating leg is 139.6°, and the range of the knee angle in the rotating leg is 128.6° to 157.3°. The average ankle angle of rotation leg is 122.7°, and the range of ankle angle is 105.7° to 150.8°. Through the comparison of hip angle, knee angle, and ankle angle, we found that hip angle > knee angle > ankle angle.

The average hip angle of the supporting leg was 148.7° in the rotation stage, and the hip angle ranged from 139.2° to 155.8°. The average knee angle of the supporting leg is 153.2°, and the range of knee angle is 142.6° to 159.2°. The average
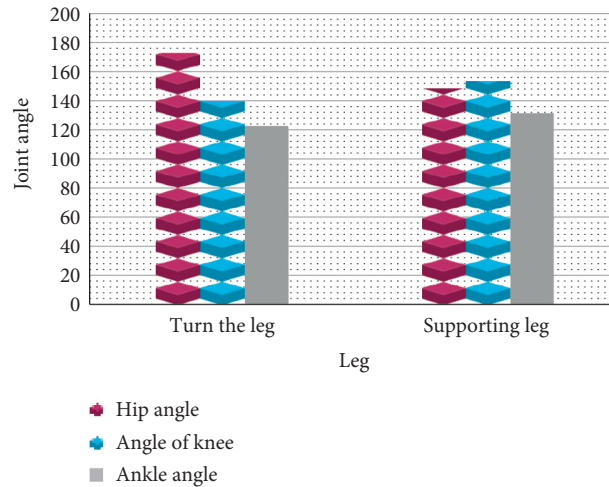
Figure 2: Joint angles of the rotation leg and supporting leg.

ankle angle of the supporting leg is 131.5°, and the range of ankle angle is 112.8° to 158.7° in the supporting leg.

4.3. Correlation Analysis between Score Ratio and Other Technical Statistical Ratios. In accordance with the rules of the basketball game, the basketball game is scored. In the game, the goal of the team's tactical combination and player skill management is scoring. It is necessary to analyze the correlation between the score rate and the descriptive statistics index on the basis of comparing the ratio of descriptive statistics in order to study the factors of the game match in basketball. Factors and tactical features can be analyzed.

In order to analyze the technical statistic index factors of winning basketball match, the linear correlation between score ratio and technical statistics data ratio is measured by correlation analysis theory. The greater the Pearson correlation coefficient between the ratio of technical index data and the ratio of competition score indicates that there is a big difference between opponents in the technical statistics and the greater the influence on the victory and defeat of the competition, the smaller the Pearson correlation coefficient, the smaller the difference of the technical statistical data, and the smaller the impact on the victory or defeat of the competition. After the correlation analysis of score ratio, the analysis results are shown in Figure 3.

From the above data, we can know that the correlation coefficient between the score and the shooting percentage is 0.52, the correlation coefficient with the three-point shot shooting times is 0.347, the correlation coefficient between the free throw shooting rate and the free throw shooting rate is 0.582, and the correlation coefficient with the three-point

shot number is 0.135. Through the correlation analysis theory, the probability p value of their correlation coefficient test is close to 0. Therefore, it is considered that there is a strong linear relationship between them and scores, which has a greater impact on the outcome of the game, while other technical indicators have no significant impact on the outcome of the game.

4.4. Difference Test of Each Index. Comparing the data of the experimental group before and after the experiment, except for the shooting percentage under fatigue state [36], the p values of the test indexes reflecting ankle joint strength and stability and basketball technical level are all less than 0.05, as shown in Figure 4. It shows that there are significant differences between the experimental data after the experiment and those before the experiment.

Before and after the experiment, there were significant differences and significant progress in the test results of ankle strength and stability and basketball technical level in the experimental group. The first reason is that the normal footwork training and basic basketball skill training have improved the human body's sports ability, and the basketball technical level has been significantly improved. The targeted training improves the stability ability and habitual posture in the movement process, thus promoting the strength transmission and cohesion of each link in human movement, and greatly improves the work efficiency of each link. The second reason is that the training of ankle strength and stability can strengthen the strength and stability of ankle muscle group, provide the last fulcrum to stabilize the human body when the lower limbs do movements, and improve and stabilize the efficiency of energy transfer of lower limb work.

Figure 3: Results of correlation analysis between score ratio and other technical statistical ratios.
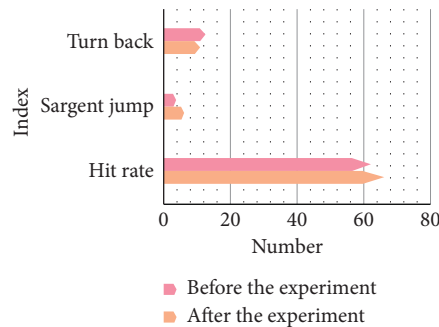
Figure 4: The difference test of each index before and after the experiment.

5. Conclusions

Virtual reality technology has the characteristics of immersion, interactivity, multiple perception, and imagination. It can create and experience the virtual world generated by the computer. The "world" here refers to a sense of reality. From a three-dimensional perspective, it can be a real representation of a specific real world, or a planned world. Experts can carry out specific stage activities or virtual reality technology simulation communication through sensory perception. This technology will become a necessary means of college physical education in the future. The combination of virtual reality technology and school physical education can subvert the traditional teaching methods, provide athletes with real scenes for different teaching needs, strengthen and deepen the experience of athletes, and help athletes master, integrate, and understand sports skills.

Incorporating virtual reality technology into college basketball education can break old educational models. The coach provides nondiscriminatory training for the entire class, allowing all players to experience the true scene in a virtual education environment and feel the pleasure of successfully practicing basketball skills and even tactics. The application of virtual reality technology can provide athletes with a higher level of basketball skill demonstrations and can demonstrate and assist with their favorite basketball stars with action demonstrations. Because the professional difference between the two and the basketball skill level does not match, the basketball skill movement is not normative, beautiful, and even wrong presentation. By using virtual reality technology to reduce the stress of the coach, the coach can catch the wrong movements.

Basketball skill movements are natural, lively, and represent an infinite 3D animation format, and athletes are complete and intuitive by observing the details and key points of the skill movements in each direction and at any distance. It helps to create human movements. Interaction between humans and computers stimulates the excitement of athletes to imitate training, improves self-learning skills, and can enhance the effectiveness of educational training. The working principle of the Moventraphic collection system is that when collecting 3D basketball technical data, the coach will often integrate and use teaching resources and establish and update the project database in real time to meet the needs of teaching. By conducting scientific teaching studies using exercise parameter data collected in physical

education, the exercise rules of exercise technology are analyzed to make the course more intuitive and smart. Of course, data can be monitored and used effectively. In the course of doing this, they made higher demands on computer training for physical education instructors.

Data Availability

No data were used to support this study.

Conflicts of Interest

The authors declare that they have no conflicts of interest.

References

[1] Y. Zhao, H. Li, S. Wan et al., "Knowledge-aided convolutional neural network for small organ segmentation," *IEEE Journal of Biomedical and Health Informatics*, vol. 23, no. 4, pp. 1363–1373, 2019.

[2] Z. Yan and Z. Lv, "The influence of immersive virtual reality systems on online social application," *Applied Sciences*, vol. 10, no. 15, p. 5058, 2020.

[3] J. L. Maples-Keller, B. E. Bunnell, S.-J. Kim, and B. O. Rothbaum, "The use of virtual reality technology in the treatment of anxiety and other psychiatric disorders," *Harvard Review of Psychiatry*, vol. 25, no. 3, pp. 103–113, 2017.

[4] C. Donghui, L. Guanfa, Z. Wensheng et al., "Virtual reality technology applied in digitalization of cultural heritage," *Cluster Computing*, vol. 22, no. 4, pp. 1–12, 2017.

[5] M. Koeva, M. Luleva, and P. Maldjanski, "Integrating spherical panoramas and maps for visualization of cultural heritage objects using virtual reality technology," *Sensors*, vol. 17, no. 4, p. 829, 2017.

[6] H. Chen, "Research of virtools virtual reality technology to landscape designing," *The Open Construction and Building Technology Journal*, vol. 9, no. 1, pp. 164–169, 2015.

[7] M. Zhou, Y. Wang, Z. Tian, Y. Lian, Y. Wang, and B. Wang, "Calibrated data simplification for energy-efficient location sensing in internet of things," *IEEE Internet of Things Journal*, vol. 6, no. 4, pp. 6125–6133, 2019.

[8] T. Sarıtaş, "Chemistry teacher candidates acceptance and opinions about virtual reality technology for molecular geometry," *Educational Research & Reviews*, vol. 10, no. 20, pp. 2745–2757, 2015.

[9] Y. Sang, Y. Zhu, H. Zhao, and M. Tang, "Study on an interactive truck crane simulation platform based on virtual reality technology," *International Journal of Distance Education Technologies*, vol. 14, no. 2, pp. 64–78, 2016.

[10] Z. Liang and R. Shuang, "Research on the value identification and protection of traditional village based on virtual reality technology," *Boletin Tecnico/Technical Bulletin*, vol. 55, no. 4, pp. 592–600, 2017.

[11] H. Zhang and H. Zheng, "Research on interior design based on virtual reality technology," *Boletin Tecnico/Technical Bulletin*, vol. 55, no. 6, pp. 380–385, 2017.

[12] S. Namasudra and P. Roy, "PpBAC," *Journal of Organizational and End User Computing*, vol. 30, no. 4, pp. 14–31, 2018.

[13] J. Yao, L. Wang, J. Zhao, and H. Yuan, "A modeling method for gas station simulation system based on virtual reality technology," *Journal of Computational Information Systems*, vol. 11, no. 9, pp. 3165–3171, 2015.

[14] T. N. Chen, X. T. Yin, and X. G. Li, "Application of 3D virtual reality technology with multi-modality fusion in resection of glioma located in Central Sulcus region," *Zhonghua Yi Xue Za Zhi*, vol. 98, no. 17, pp. 1302–1305, 2018.

[15] S. Yingying, H. Lianjuan, W. Jianan, and W. Huimin, "Quantum-behaved RS-PSO-LSSVM method for quality prediction in parts production processes," *Concurrency and Computation: Practice and Experience*, p. e5522, 2019.

[16] H. Li, "Design of multimedia teaching platform for Chinese folk art performance based on virtual reality technology," *International Journal of Emerging Technologies in Learning (IJET)*, vol. 12, no. 9, p. 28, 2017.

[17] Z. Lv, X. Li, and W. Li, "Virtual reality geographical interactive scene semantics research for immersive geography learning," *Neurocomputing*, vol. 254, pp. 71–78, 2017.

[18] L. Zeming, "Design and implementation of a Korean language teaching system based on virtual reality technology," *Agro Food Industry Hi Tech*, vol. 28, no. 1, pp. 2156–2159, 2017.

[19] Y. Sang, Y. Han, Y. Dai, and F. Li, "The development of an interactive automatic tool changer system based on virtual reality technology," *International Journal of Multimedia and Ubiquitous Engineering*, vol. 9, no. 9, pp. 329–342, 2016.

[20] G.. Han, "Application of virtual reality technology in swimming teaching," *Applied Mechanics & Materials*, vol. 475-476, no. 11, pp. 1230–1234, 2016.

[21] S. Wang, J. Ying, L. Wei, S. Li, and J. Jing, "Effects of parasagittal meningiomas on intracranial venous circulation assessed by the virtual reality technology," *Int J Clin Exp Med*, vol. 8, no. 8, pp. 12706–12715, 2015.

[22] R. S. Bhadoria and N. S. Chaudhari, "Pragmatic sensory data semantics with service-oriented computing," *Journal of Organizational and End User Computing*, vol. 31, no. 2, pp. 22–36, 2019.

[23] S. Ronghui, "The reasearch on the anti-fatigue effect of whey protein powder in basketball training," *The Open Biomedical Engineering Journal*, vol. 9, no. 1, pp. 330–334, 2015.

[24] F. M. Clemente, "Small-sided and conditioned games in basketball training," *Strength and Conditioning Journal*, vol. 38, no. 3, pp. 49–58, 2016.

[25] M. Grabara, "Sagittal spinal curvatures in adolescent male basketball players and non-training individuals-a two-year study," *Science & Sports*, vol. 31, no. 5, pp. e147–e153, 2016.

[26] W. Qin, "Application analysis of basketball training system based on personalized recommendation systems," *Boletin Tecnico/Technical Bulletin*, vol. 55, no. 16, pp. 124–133, 2017.

[27] I. G. B. Arias, W. A. Chasipanta, A. B. Cano, and E. E. A. Zambonino, "Programa básico de entrenamiento de baloncesto con deportistas de la categoría inferior/basic basketball training program with athletes of the lower category," *Apunts. Educacion Fisica Y Deportes*, vol. 21, no. 225, pp. 1–10, 2017.

[28] Z. Guo, "Chinese women's basketball team player to attack based on goal programming technology and method of exploration," *Journal of Computational and Theoretical Nanoscience*, vol. 13, no. 12, pp. 10072–10075, 2016.

[29] A.-C. Macquet and K. Kragba, "What makes basketball players continue with the planned play or change it? a case study of the relationships between sense-making and decision-making," *Cognition, Technology & Work*, vol. 17, no. 3, pp. 345–353, 2015.

[30] S. Liao, M. Wang, and H. Yang, "Research on tracking technology in basketball video," *International Journal of Multimedia and Ubiquitous Engineering*, vol. 11, no. 1, pp. 55–66, 2016.

[31] S. Weibing, "Application of video analysis technology on basketball tactics," *Agro Food Industry Hi Tech*, vol. 28, no. 1, pp. 395–399, 2017.

[32] N. N. Hurrah, S. A. Parah, N. A. Loan, J. A. Sheikh, M. Elhoseny, and K. Muhammad, "Dual watermarking framework for privacy protection and content authentication of multimedia," *Future Generation Computer Systems*, vol. 94, pp. 654–673, 2019.

[33] Z. Lv and N. Kumar, "Software defined solutions for sensors in 6 G/IoE," *Computer Communications*, vol. 153, pp. 42–47, 2020.

[34] N. Gao and Y. Zhang, "A low frequency underwater meta-structure composed by helix metal and viscoelastic damping rubber," *Journal of Vibration and Control*, vol. 25, no. 3, pp. 538–548, 2019.

[35] S. Wang, J. Ying, L. Wei, S Li, and J Jing, "Effects of para-sagittal meningiomas on intracranial venous circulation assessed by the virtual reality technology," *International Journal of Clinical and Experimental Medicine*, vol. 8, no. 8, in press, Article ID 12706, 2015.

[36] Q. Wang, Y. Li, and X. Liu, "Analysis of feature fatigue EEG signals based on wavelet entropy," *International Journal of Pattern Recognition and Artificial Intelligence*, vol. 32, no. 8, Article ID 1854023, 2018.

Research Article

Comprehensive Management and Coordination Mechanism of Marine Economy

Jinzhao Tian [iD],[1,2] **Qiqi Xia,**[2] **and Peinan Wang**[2]

[1]*School of Mechanical, Aerospace and Civil Engineering, The University of Manchester, Oxford Rd, M13 9PL, Manchester, UK*
[2]*School of Engineering, The University of Melbourne, Grattan ST, Parkville 3010, Victoria, Australia*

Correspondence should be addressed to Jinzhao Tian; tianjinzhaoricky@163.com

With the rapid development of economy and society and the continuous progress of science and technology, the public demand for marine products and services is increasing, and the marine economic and social benefits are rising. It is very important to improve the management level of marine economy. The purpose of this study is to analyze the comprehensive management and coordination mechanism of China's marine economy. This study selects Lianyungang City as the research object and takes the marine economic data from 2010 to 2019 as the research data. This study establishes three evaluation index systems of marine economic development. Then, according to the influence of the marine industry development, social development, population, marine resources and environment, regional scientific and technological innovation ability, government comprehensive management, and other factors on the regional marine economic management, this paper puts forward a set of marine economy comprehensive coordination management system and method and evaluates the current situation of marine economic development in Lianyungang City. The results show that, in the 10 years from 2010 to 2019, the comprehensive management evaluation value of China's marine economy has increased from 0.20 to 0.33, with an average annual increase of 6.57 percentage points. The system level has been upgraded from the initial "poor" to "average," achieving rapid growth. It is concluded that the index system evaluation of this study well reflects the change of the management level of China's marine economy and has a promoting effect on the development of China's marine economy, making contributions to China's economic management.

1. Introduction

The ocean is the broadest natural geographical area on the Earth, which contains huge marine resources. However, with the vigorous development of China's marine economy, there are also many problems uncoordinated with economic development. In the process of marine economic development, there are still some problems, such as lack of systematic theoretical guidance, lack of coordinated development and scientific planning, imperfect system, and obvious contradiction of industrial structure. There are widespread problems of the traditional marine industry and ecological environment deterioration, low economic efficiency and sustainable development, and how to evaluate the sustainable development of marine economy. If these problems cannot be solved scientifically and timely, it will have a serious impact on the sustainable development of China's marine economy.

From the perspective of national economic development and world environment, the development of national economy and society is inseparable from the marine industry. The world's maritime powers continue to rely on marine management to strengthen their comprehensive competitiveness. China said that regardless of changes in domestic demand and external environment, the ocean plays an important role in the country's total output, highlighting the basic role of marine management systems in marine sustainable development. A sound integrated ocean management system can not only promote the development of marine economy and the sustainability of marine ecology but also protect the marine rights and sovereignty of a country.

In the study of integrated management and coordination mechanism of marine economy, Caiishi S proposed a new method to quantify the vulnerability of marine economy in Bohai rim area. His data envelopment analysis (DEA) is an analysis method combining the relative efficiency and performance of multi-input and multioutput decision-making units, which has been widely used in many fields. On the basis of understanding the vulnerability of marine economy, he combined the pressure state response model (P-S-R) and the exposure sensitivity adaptability model and established the evaluation index system of marine economic vulnerability from three aspects of pressure, sensitivity, and adaptability. His method uses the weighted loose econometric model to measure the marine economic vulnerability of 17 coastal cities in the Bohai Rim region. He used the kernel density estimation method to analyze the dynamic evolution of marine economic vulnerability in the Bohai Rim region. His method is not stable [1]. Li et al. think that the traditional grey relational model directly describes the behavior characteristics of the system based on the connection of sample points because a few grey relational models can measure the dynamic periodic fluctuation law of objects, which leads to the instability of association results. He used the transformation function to fit the system behavior curve, redefined the area difference between the curves, and established the grey correlation model based on discrete Fourier transform (dftgra), applied dftgra to verify its effectiveness, feasibility, and superiority, and studied the correlation between macroeconomic growth and marine economic growth in China's coastal areas. His method is not practical enough [2]. Jing et al.'s research uses the neural network, genetic algorithm, multistage principle, and Monte Carlo simulation to propose a process control and operation planning system based on integrated simulation. By using different time scales and computing scales, the process control can be well realized. The hourly process control strategy forwards the results to the business planning module, where long-term arrangements can be further evaluated. He took marine wastewater management as an example to verify the effectiveness of the method. Six different treatment criteria were examined within 20 days, and the 20 gauge standard seemed to be the most economical option with an average net cost of $18 per day. The accuracy of his method is very low [3].

This study first introduces the meaning and characteristics of marine economy and then describes three marine economic management modes in detail: relatively centralized, decentralized, and centralized. This study also describes the coordination mechanism of marine economy and the relative operation rules. The algorithm of this study is mainly to distinguish the types of marine economic coordinated development. In this study, Lianyungang City is taken as the research object, and the marine economic data in recent ten years are selected for analysis. Three evaluation methods of regional marine economic coordinated development and comprehensive management evaluation index system are also put forward. Based on the experimental results, this paper analyzes the fund demand, development status, comprehensive evaluation, and management of marine economic development. The current situation of marine economic development in China is obtained, and corresponding coordination measures are made.

2. Comprehensive Management and Coordination Mechanism of Marine Economy

2.1. Meaning and Characteristics of Marine Economy

2.1.1. The Meaning of Marine Economy

(1) In a narrow sense, marine economy refers to the economy formed by the development and utilization of marine waters and marine space [4].

(2) In a broad sense, marine economy refers to the economic activities that provide conditions for marine development and utilization, such as industries at the upper and lower boundaries of the narrow marine economy and the manufacturing of land and sea general equipment.

(3) The generalized marine economy refers to the land industry of the island, the land industry of the coastal zone, and the inland river economy of the river ocean system [5, 6].

2.1.2. Characteristics of Marine Economy

(1) Integrity: due to the continuity of marine waters, coastal areas, sea areas, and continental shelf at sea are connected together, and the exploitation and utilization of marine resources are interdependent. This can be illustrated by the mobility of marine living resources and the expansion of marine pollution.

(2) Publicity: marine resources are public resources, and the marine economy for the development and utilization of marine resources is also a public economy [7, 8].

(3) High tech: in order to develop marine resources for production activities, we must rely on special technical equipment, which will increase the technical requirements and high technical dependence on marine economic activities. At the same time, with the help of modern materials and equipment and science and technology, human beings can effectively develop and utilize marine resources, resulting in an independent marine economy [9].

2.2. Marine Economic Coordination Mechanism.
One is cooperation, division of labor, and cooperation that can get the most benefits. The use of sea contains many different themes. It is necessary to implement division of labor and adjustment. The second is adjustment. In China, it is very necessary to resolve conflicts and disputes that have occurred. In order to effectively solve the contradiction of marine economic development, we need corresponding laws, deliberative organs, rules, and mechanisms. The third is harmony. Harmony is embodied in the change of development concept and the realization of sustainable development of marine economy [10, 11].

The characteristics of the adjustment mechanism including institutional factors: all relevant personnel must

abide by the fact that the mechanism is a systematic and theoretical method based on various effective methods and methods. Mechanisms generally depend on many methods. All kinds of methods and methods work. The mechanism is an effective and relatively fixed method in practice [12].

2.3. Management Mode of Marine Economy

(1) Relatively centralized type: there is no full-time marine management functional department, there is a national higher marine economic business adjustment organization, the limitation system of marine law is basically sound, and there is a maritime law enforcement department. It will be more flexible and efficient to adjust and implement the change in the system. The contradiction of marine economic management can only be handled passively and cannot be avoided actively through system integration [13, 14].

(2) Decentralized: there is no centralized marine management department, most of them have comprehensive marine economic adjustment institutions such as special committees, and there is no unified maritime law enforcement team. Industry management is more professional, and with a wide range of marine industry characteristics and strong professional awareness, it is difficult to concentrate on one department. If the function of subdividing, repeating, and dispersing these operations is not clear, it will easily cause inefficiency. Level adjustment and comprehensive management are not strong [15].

(3) Centralized: the higher the efficiency of management and coordination, the more conducive to the implementation of a comprehensive marine policy, and the higher the status of the department, the more helpful it is to improve people's marine awareness. It is difficult to achieve complete centralization, and it is easy to cause functional conflicts between new and old departments, and the system change cost is relatively high.

2.4. Operation Rules of Comprehensive Management and Coordination Mechanism of Marine Economy

(1) It is necessary to cut off the meaning of all the subjects to participate in the administrative decision. In the past, the main themes of marine economic management were marine departments and coastal local autonomous bodies. Now, the number of marine enterprises and citizen groups participating in the management and supervision of marine economy is increasing, and the scope of decision-making themes is far beyond the original administrative departments. Range: as a result, representatives of enterprises and citizens have also been incorporated into the design of members of the above-mentioned Marine Economic Commission. Within the scope of extensive participation in decision-making, all maritime institutions can provide the opportunity to resolve disputes; represent the opinions and suggestions of governments, industrial departments, enterprises, and ordinary citizens in different administrative regions; and reflect them in the final adjustment decision-making [16, 17].

(2) It is necessary to improve the decision-making process, deepen the understanding of the sea, and improve the scientific nature of decision-making. The sea is still the least understood area. The traditional detailed management of maritime industry artificially creates barriers to marine information. Lack of knowledge and information will affect the science and rationality of decision-making. Therefore, in the decision-making process of comprehensive management and adjustment mechanism of marine economy, the government as the "leader" must increase investment, strengthen marine research, learn more knowledge, and share with other topics. It must break the information barriers of various maritime industries, share marine economic data and research results, and make scientific and reasonable adjustment decisions based on sufficient information [18].

(3) It is necessary to change the idea of decision-making and make decisions based on the sustainable development of national marine economy. In order to realize scientific and reasonable decision-making, it is necessary to change the thinking of decision-makers into the practical decision-making thought with the highest interests of regions and departments and establish the decision-making idea of taking economic development as the priority and taking sustainable development as the goal in order to maximize the limited aquatic resources. It not only meets the needs of current economic development but also provides the possibility of foreseeable sustainable development in the future, so as to generate the maximum benefits [19, 20]. Sustainable development is the basic basis and principle of adjusting the interests of various departments and the ultimate goal of making scientific decisions. Therefore, government departments must carry out extensive publicity and education among different themes, strengthen the overall image of each theme, and create a good ideological environment for the implementation of coordinated decision-making [21, 22].

2.5. Criteria for Judging the Types of Coordinated Development of Marine Economy.
Through the analysis and verification of the interaction stress relationship among the three subsystems of the marine eco-economic system, it can be seen that there are objectively various dynamic stress and constraint interaction relationships among the subsystems of China's marine eco-economic system [23, 24]. With the help of system science theory, a dynamic coupling model is established to measure the coordination of the marine ecological-economic systems, and the development of 11 coastal and urban marine ecological-economic systems

under the pressure of systems is discussed quantitatively. The basic derivation process of the model formula is as follows [25].

The interaction stress and evolution process of any two subsystems of the marine eco-economic system can be regarded as a nonlinear process, and its evolution equation can be expressed as follows:

$$\frac{dx(t)}{dt} = f(x_1, x_2, \ldots, x_n); \quad i = 1, 2, \ldots, n. \quad (1)$$

F is a nonlinear function of x_i.

The motion adjustment of a nonlinear system depends on the property of the characteristic root of the first-order approximate system. Therefore, on the premise of practical use of the adjustment, the approximate expression of the above evolution equation can be obtained by using the Taylor series expansion near the origin and omitting the higher-order term $e(x_1, x_2, \ldots, x_n)$:

$$\frac{dx(t)}{dt} = \sum_{i=1}^{n} a_i x_i; \quad i = 1, 2, \ldots, n. \quad (2)$$

According to this formula, the marine eco-economic system can establish the representation function of the development of any two subsystems:

$$f(G) = \sum_{k=1}^{n} b_k g_k; \quad k = 1, 2, \ldots, m,$$
$$f(H) = \sum_{j=1}^{n} c_j h_j; \quad j = 1, 2, \ldots, l. \quad (3)$$

Among them, G and H are the evaluation indexes of the development status of the two subsystems, and B and C are the weight of each index.

Considering the interaction pressure relationship among the subsystems of the marine eco-economic system, it can be regarded as a composite system. Obviously, $f(G)$ and $f(H)$ can reflect the development and evolution of any two composite systems, regardless of the influence of the third subsystem. According to the general system theory, the evolution equation of the interaction stress relationship between the two subsystems expressed by the adjustment degree can be obtained:

$$A = \frac{df(G)}{dt} = \alpha_1 f(G) + \alpha_2 f(H),$$
$$V_A = \frac{dA}{dt},$$
$$B = \frac{df(H)}{dt} = \beta_1 f(G) + \beta_2 f(H), \quad (4)$$
$$V_B = \frac{dB}{dt},$$
$$\alpha = \arctan\left(\frac{V_A}{V_B}\right),$$

where A and B denote the evolution states of any two given systems of the marine eco-economic system affected by itself and another system, and V_A, V_B are the evolution speeds of

two subsystems affected by itself and other systems. In the marine environmental economic system, A and B interact with each other. If you modify a subsystem, the entire composite system will be modified, and the third subsystem will be retained. In the subsystem, the evolution speed V of the two subsystems can be regarded as a function of V_A, V_B; that is, $V = f(V_A, V_B)$. By analyzing the change value of V, we can investigate the adjustment of the two subsystems.

3. Marine Economic Management Index System

3.1. Subjects.
In this survey, from 2010 to 2019, the marine economic data of Lianyungang City were selected as the survey data. According to the factors of marine industry development and social development in Lianyungang City, a series of evaluation index methods are put forward to evaluate the influence of sustainable development of regional marine economy on marine economy, and the development status of marine economy in Lianyungang City is evaluated.

3.2. Evaluation of Coordinated Development of Regional Marine Economy

3.2.1. Index Analysis.
The index of the evaluation object is selected as the base number, the remaining index of the evaluation object is calculated as a percentage, the weight of each index is determined, and the included indexes are calculated and sorted. The index analysis method is easy to calculate and the evaluation result is intuitive. However, this method requires a subjective determination of the reference object. From this, we can get the evaluation result of subjective mediation. In addition, in the distribution of weights, the differences in the influence of indicators on the ability of scientific and technological innovation are not considered. Basically, the primary and secondary relations of factors cannot be highlighted, and the differences that can not truly reflect the importance of the overall indicators of the scientific and technological innovation system can be adopted.

3.2.2. Factor Analysis.
Firstly, the original index is standardized to exclude the influence of size on the evaluation results, and the calculation principle is based on the principle that the characteristic root is greater than 1. In order to make the main factors have a clear meaning, the factor load matrix is rotated orthogonally, and the load of each primary variable of the main factor is divided into 0 and 1. The relationship between the factors and the original variables and the scores of various common factors were calculated, and the total score was calculated. The comprehensive score is based on the weighted sum of the scores of the main reasons. Here, the weighting is determined by the ratio of the contribution rate of the main factors in the cumulative contribution rate.

3.2.3. Fuzzy Mathematics Analysis.
Using correct mathematical language can explain the ambiguity that traditional mathematics cannot explain. Among them, fuzzy comprehensive evaluation can integrate various factors of nature to

correctly evaluate the objective things. The fuzzy comprehensive evaluation method is suitable for linear and nonlinear problems.

3.3. Establishment of Evaluation Index System for Comprehensive Management of Marine Economy

3.3.1. Marine Ecosystem Subsystem. Marine biological community and marine abiotic inorganic environment are natural organic whole which are connected by energy flow and material circulation, which are interdependent and interactive and have an automatic regulation mechanism.

3.3.2. Marine Economic Subsystem. Marine economy takes the ocean as the labor object and the development of marine resources as the core. Marine resources refer to marine organisms, minerals, chemistry, cosmos, energy, and so forth, which exist in the marine ecosystem and can be used by human beings now or in the future. All resources and marine economy are industrial activities and output processes to develop or redevelop marine resources, which are available in the ocean and its space.

3.3.3. Marine Society Subsystem. Marine social system refers to the social groups that gather in specific coastal areas, mainly engaged in marine production and operation activities and related activities, or rely on marine economic products and ecological services. According to specific restrictions, it depends on the corresponding marine ecological environment and economic basis. All artificial organic system combined with the system. Specifically speaking, the marine social system is human-centered, which is composed of people who rely on the sea for production and life and have unique marine thinking.

4. Comprehensive Management Effect of Marine Economy

4.1. Financial Demand for Marine Economic Development. The analysis of the financial correlation rate in 11 coastal and 11 cities shows that the relatively small indicators, such as deposit and loan data, are used to measure financial assets and to clarify the level of financial development in coastal areas. There are two main reasons for choosing deposits and loans as indicators. One is that there are no special financial assets statistics in various regions of China, so data collection is limited, and the other is one of the most important factors in the current financial development process. As more than 90% of the social financing methods are carried out through bank loans, the main financial assets are concentrated in banks, and the most important assets for banks are deposits and loans. Table 1 shows financial assets in coastal areas and across the country.

From Table 1 to 2019, the financial assets in China's coastal areas will increase year by year. Before 2003, the proportion of coastal financial assets in national financial assets continued to increase, reaching the highest value of 58.92% in 2013. After 2014, although the proportion of financial assets of coastal areas in national financial assets decreased as a whole, there was no change, basically about 57% every year. Through the implementation of China's regional economic coordinated development strategy, we can see that the growth of financial assets in the central and western regions is accelerating. However, the proportion of about 57% fully shows that coastal areas are still the main collection areas of domestic financial assets. Figure 1 shows the GDP of coastal areas and its proportion in the whole country.

It can be seen from Figure 1 that after China's entry into WTO, the development of coastal areas has made great progress. From 2011 to 2019, the GDP of coastal areas basically accounts for 60% of annual GDP, especially 62.32% in 2016, which fully shows the economic growth of China's coastal areas. The development speed is faster than the national average speed, and the development gap between inland and coastal areas tends to expand continuously. In 2017 and 2018, mainly affected by the US financial crisis, the proportion decreased. The financial crisis has had a greater impact on coastal areas than inland areas.

4.2. Current Situation of Marine Economic Development in Lianyungang City. The total area of Lianyungang sea area is more than 670 square meters. It has a total land area of 5194 square kilometers and a population of 35.44 million, accounting for 70% and 75.6% of the city, respectively. In 2016, Leon marine economy realized 26 billion yuan of total output value and 10 billion yuan of added value. The added value of the marine industry is equivalent to 19.1% of the total output of the city in the same period, and the added value of the marine industry increases steadily year by year. Figure 2 shows the change of the added value of marine industry.

From Figure 2, we can see the changes of various marine industries in Lianyungang.

4.2.1. Marine Fishery and Related Industries. Due to the rapid development of Marine Fisheries and tidal plain agriculture, forestry, and animal husbandry in Lianyungang City, the adjustment of marine fishery structure has been accelerated, and the marine fishery has gradually expanded to the outer ocean and sea area, and the area and species structure of marine aquaculture have been continuously optimized. The proportion of aquaculture in marine fishery is increasing year by year. The production capacity has been steadily improved, significant achievements have been made in the adjustment of fishery structure, and the income level of fishermen has continued to rise. From 2012 to 2018, the city completed a total of 18.73 million tons of aquatic products, with a total fishery output value of 17.67 billion yuan. This is an increase of 32% compared with 2003. In 2018, the average net income of fishermen in the city was 18160 yuan, 4.6 times the average net income of farmers in the city.

TABLE 1: Financial assets of coastal areas and the whole country.

Particular year	Coastal financial assets	National financial assets	Coastal area/national (%)
2011	140068.75	255933.87	54.82
2012	170517.38	302217.35	56.51
2013	216270.33	367053.83	57.85
2014	243496.01	419623.15	58.12
2015	277343.82	481858.97	57.65
2016	319662.44	560717.36	57.23
2017	367082.15	651062.14	56.42
2018	432867.94	769598.84	56.16
2019	558791.69	1197453.62	55.98
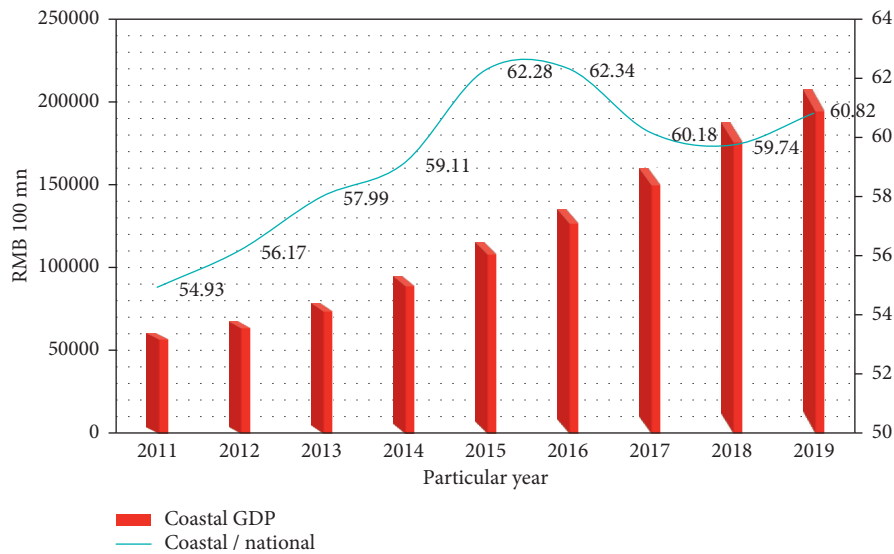
FIGURE 1: Coastal GDP and its proportion in China.

4.2.2. Marine Industry. In 2018, the city's marine industry realized an industrial output value of 8.9 billion yuan, with an added value of 2.4 billion yuan. The output value and added value of marine industry are 2.44 times and 3.77 times those of 2012. The operation capacity of major enterprises has been strengthened, and the support capacity for economic development has been further strengthened. The production of salt industry has developed steadily, and its output has increased from 180 million yuan in 2012 to 260 million yuan in 2018. With the rapid development of marine chemicals, the continuous acceleration of technological change of marine industrial enterprises and the further enhancement of research and development capacity, the production volume increased from 2.43 billion yuan in 2012 to 4 billion yuan in 2018.

4.2.3. Port Construction and Marine Transportation. Lianyungang port infrastructure construction increased significantly, with a total investment of 1.76 billion yuan, 3 new production bases, 1 berth's expansion, 3 berths' upgrading, 11 berths' upgrading, and 70000-ton berths entering the port. The new capacity of this channel is 7.98 million tons. With the goal of developing a 100-million-ton port, Lianyungang has built the first 100000-ton deep-sea

terminal and the largest container terminal in Lianyungang. There are now more than 10000 tons of 30 berths, as well as infrastructure such as railways and highways supporting port 13. Construction has been continuously improved, and a three-dimensional ocean, land, and air transport network centered on the port has initially taken shape. The port transport capacity has continued to increase, and new European routes to Rotterdam, the Netherlands, Hamburg, and Germany have been opened successively, and the sea transportation routes to the west coast of the United States have been opened. The production of the maritime transportation industry increased from 840 million yuan in 2012 to 1180 million yuan in 2018. The added value increased from 240 million yuan to 455 million yuan.

4.3. Comprehensive Evaluation of Marine Economic Development Status. As shown in Figure 3, the sustainable development state index of each subsystem.

It can be seen from Figure 3 that from 2015 to 2019, the sustainable development index value of the regional economic marine industry development subsystem has steadily increased from 0.593 to 0.863, and the corresponding sustainable development level has also transferred from the medium level sustainable development state to the strong
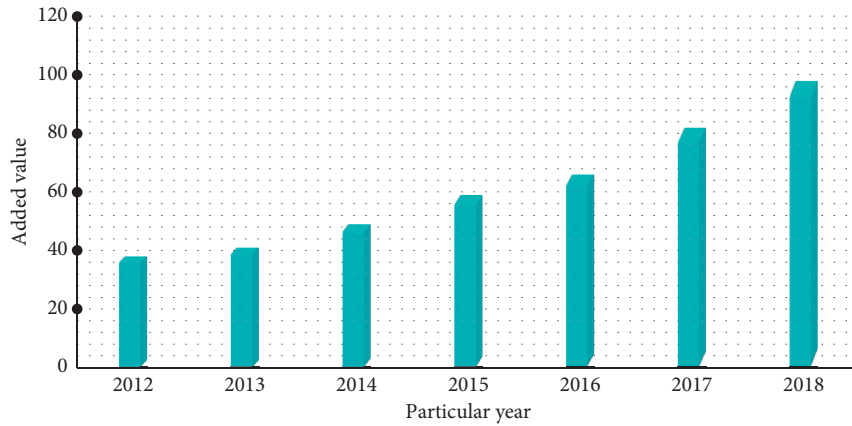
FIGURE 2: Change of the added value of marine industry.

sustainable development state. The state of continuous development: the sustainable development index value of the social development subsystem increased steadily from 0.63 to 0.714. The sustainable development index value of population, marine resources, and environment subsystem changes first increases, then decreases, and after that slowly increases. In 2018, it will fall into a low sustainable development state, and in 2019, it will enter a development state with medium sustainability. However, the current sustainability index has not exceeded its peak in 2017. The sustainable development index value of the government integrated management subsystem changes. At first, it drops to the bottom, then increases, and after that decreases slightly. However, in the state of sustainable development, even the bottom can maintain a strong level of sustainable development. The subsystem index also exceeded the key value of 0.75 sustainable level.

4.4. Evaluation of Integrated Management of Marine Economy.

The development of China's marine resources is gradually booming, maintaining the momentum of rapid progress. With the large-scale development of marine resources, especially the rapid rise of secondary marine industry with high investment, high consumption, and high emission, the marine ecological environment in coastal areas is deteriorating. Figure 4 shows the comprehensive evaluation value of the marine economic system.

As can be seen from Figure 4, in the 10 years from 2010 to 2019, the evaluation value of China's marine economic system has increased from 0.20 to 0.33, with an average annual increase of 6.57 percentage points, and the system level has upgraded from "bad" at the initial stage to "average." Rapid growth: at the same time, the evaluation value of the marine social subsystem increased from 0.13 to 0.47, with an average annual growth of 26.11%. In addition, the system level has been upgraded from "poor" to "ordinary," and the development momentum is good.

However, China's marine economic subsystem and social subsystem are developed on the basis of large-scale utilization of marine resources and the environment at the cost of the large consumption of nonrenewable resources.
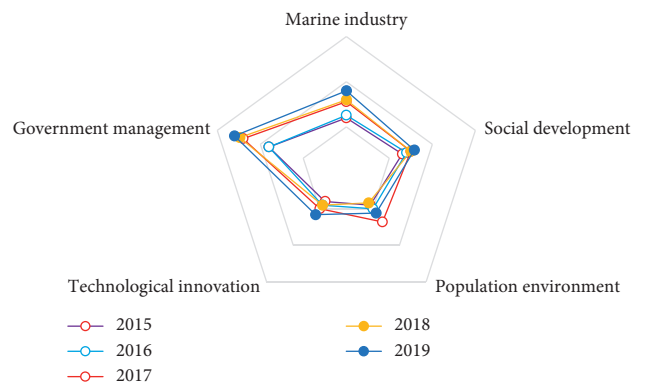
FIGURE 3: Sustainable development state index of each subsystem.
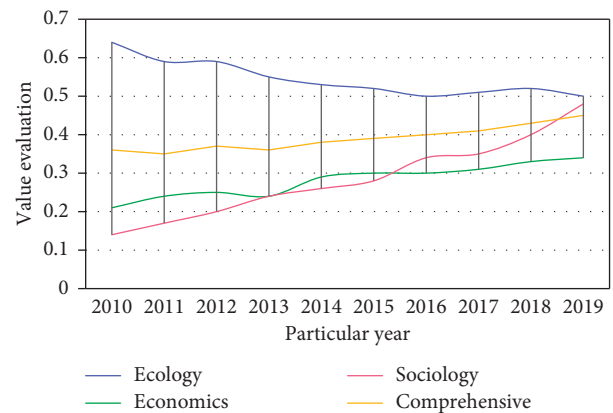
FIGURE 4: Comprehensive evaluation value of the marine eco-economic system.

Although the two subsystems grow rapidly in a short period of time, they have achieved rapid growth in the long term. From this point of view, the potential crisis of the overall degradation of marine ecosystem subsystems has been recognized. The "sustainable development" of China's marine ecosystem has declined from "good" to "normal" from 10.51% in the initial assessment, and the "sustainable development" of China's marine ecosystem has declined from 10.51% in the first year. However, the comprehensive

assessment value of China's marine eco-economic system increased from 0.35 in 2010 to 0.44 in 2019, with an average annual increase. Although it is 2.70 percentage points, the development speed is relatively slow.

5. Conclusion

The theme of the comprehensive management and coordination mechanism of China's marine economy mainly includes all levels of government, scientific research institutions, marine enterprises, and ordinary citizens. The relationship between the themes is the object of the adjustment mechanism. According to the governance theory, through the application of the cooperation network, we can form a good interaction between the main bodies, adjust the plans and objectives of the main bodies, and achieve the development and management objectives of the overall adjustment of the marine economy. The adjustment mechanism in the form of a committee should be established in the organizational model, and the Marine Economic Commission should be set up at all levels. The application rules are formulated from the perspectives of decision-making, negotiation, profit adjustment, and dispute resolution. From the perspective of system protection, it is suggested to establish a complete conference adjustment system, information sharing system, and temporary meeting adjustment system. Adjust the institution establishment system, supervision and evaluation system, and so forth.

The marine economic system is a special composite system with a specific structure and function formed by the interaction, interweaving, and mutual penetration of the marine ecosystem and marine social system. Its coordinated development makes the subsystems influence each other, which means that the functions of marine ecological structure, marine economic structure, and marine social structure can be integrated after feedback and cooperation. This makes it possible to maintain an effective dynamic balance between the fixed structure and the orderly function.

In order to manage the ocean thoroughly and effectively and realize the economic and cultural value of the ocean, China needs to further improve the integrated ocean management system, refine the division of the functions of the integrated ocean management, standardize the establishment of the marine management organs, and improve the construction of the system of the law of the sea. In order to establish a characteristic marine integrated management system in line with China's basic national situation, this paper proposes to improve China's comprehensive marine management system; promote the rapid, healthy, and sustainable development of marine economy; protect marine life, resources, and sovereign rights and interests; safeguard marine ecological culture; protect the Ming Dynasty; optimize the environment; and finally build a socialist maritime power with Chinese characteristics.

Data Availability

The data that support the findings of this study are available from the corresponding author upon reasonable request.

Conflicts of Interest

The authors declare that they have no conflicts of interest.

References

[1] S. Caizhi, Q. Xionghe, L. Bo et al., "Assessment of marine economy vulnerability of coastal cities in Bohai sea ring area based on WSBM model," *Entia Geographica Sinica*, vol. 36, no. 5, pp. 705–714, 2016.

[2] X. Li, Y. Zhang, and K. Yin, "A new grey relational model based on discrete Fourier transform and its application on Chinese marine economic," *Marine Economics and Management*, vol. 1, no. 1, pp. 79–100, 2018.

[3] L. Jing, B. Chen, B. Y. Zhang et al., "An integrated simulation-based process control and operation planning (IS-PCOP) system for marine oily wastewater management," *Journal of Environmental Informatics*, vol. 28, no. 2, pp. 126–134, 2016.

[4] K. Nazir, M. Yongtong, K. Hussain et al., "A study on the assessment of fisheries resources in Pakistan and its potential to support marine economy," *Indian Journal of Geo-Marine Sciences*, vol. 45, no. 9, pp. 1181–1187, 2016.

[5] D. I. Qianbin and D. Shaoyu, "Symbiotic state of Chinese land-marine economy," *Chinese Geographical Ence*, vol. 27, no. 2, pp. 176–187, 2017.

[6] J. L. Gan, X. L. Gu, L. D. Li et al., "Oil pollution and its relation to marine economy along Guangdong province coast of China during 2001–2010 based on oyster as a bio-indicator," *Journal of Ecology and Rural Environment*, vol. 34, no. 10, pp. 897–902, 2018.

[7] Z. Li, "Impact of educational expenditure on the development of regional marine economy: evidence from Chinese coastal provinces," *Journal of Human Resource and Sustainability Studies*, vol. 6, no. 1, pp. 108–117, 2018.

[8] M. Cavallo, Á. Borja, M. Elliott, V. Quintino, and J. Touza, "Impediments to achieving integrated marine management across borders: the case of the EU marine strategy framework directive," *Marine Policy*, vol. 103, no. 5, pp. 68–73, 2019.

[9] P. Burbridge, "Commentary 7 to the Manifesto for the marine social sciences: integrated coastal zone management," *Maritime Studies*, vol. 19, no. 2, pp. 139-140, 2020.

[10] X. Liu, W. Shi, S. Yuan et al., "Integrated management strategies analysis of marine disaster risk in China," *International Journal of Offshore and Polar Engineering*, vol. 26, no. 2, pp. 192–198, 2016.

[11] A. Lara-Lopez, T. Moltmann, and R. Proctor, "Australia's integrated marine observing system (IMOS): data impacts and lessons learned," *Marine Technology Society Journal*, vol. 50, no. 3, pp. 23–33, 2016.

[12] J. I. Ulrikke, "Integrated Ocean management in the arctic: comparative analyses of the implementation and use of marine protected areas in Canada and Norway," *Ocean Yearbook*, vol. 32, no. 1, pp. 206–238, 2018.

[13] W. L. Balthis, J. L. Hyland, C. Cooksey et al., "Sediment quality benchmarks for assessing oil-related impacts to the deep-sea benthos," *Integrated Environmental Assessment & Management*, vol. 13, no. 5, pp. 1–15, 2017.

[14] T. A. Palmer, P. A. Montagna, R. H. Chamberlain et al., "Determining the effects of freshwater inflow on benthic macrofauna in the Caloosahatchee Estuary, Florida," *Integrated Environmental Assessment and Management*, vol. 12, no. 3, pp. 529–539, 2016.

[15] G. Mancinelli, P. Chainho, L. Cilenti et al., "The Atlantic blue crab *Callinectes sapidus* in southern European coastal waters:

distribution, impact and prospective invasion management strategies," *Marine Pollution Bulletin*, vol. 119, no. 1, pp. 5–11, 2017.

[16] M. Mateo, L. Pawlowski, and M. Robert, "Highly mixed fisheries: fine-scale spatial patterns in retained catches of French fisheries in the Celtic Sea," *ICES Journal of Marine Science*, vol. 74, no. 1, pp. 91–101, 2017.

[17] N. V. Shadrin, "The alternative saline lake ecosystem states and adaptive environmental management," *Journal of Oceanology and Limnology*, vol. 36, no. 6, pp. 2010–2017, 2018.

[18] B. Paterson, B. Neis, and R. L. Stephenson, "A social-ecological study of stock structure and fleet dynamics in the Newfoundland herring fishery," *ICES Journal of Marine Science*, vol. 75, no. 1, pp. 257–269, 2018.

[19] D. J. Packer, C. T. H. Miners, and N. D. Ungson, "Benefiting from diversity: how groups' coordinating mechanisms affect leadership opportunities for marginalized individuals," *Journal of Social Issues*, vol. 74, no. 1, pp. 56–74, 2018.

[20] M. Drosou, F. Kamatsos, and C. A. Mitsopoulou, "Recent advances in the mechanisms of the hydrogen evolution reaction by non-innocent sulfur-coordinating metal complexes," *Inorganic Chemistry Frontiers*, vol. 7, no. 1, pp. 37–71, 2020.

[21] D. Zissis, G. Ioannou, and A. Burnetas, "Coordinating lot sizing decisions under bilateral information asymmetry," *Production and Operations Management*, vol. 29, no. 2, pp. 371–387, 2020.

[22] Q. F. Li, J. Lu, J. W. Yu et al., "Advances in molecular mechanisms of brassinosteroid-abscisic acid crosstalk coordinating plant growth and stress tolerances," *Zhiwu Shengli Xuebao/Plant Physiology Journal*, vol. 54, no. 3, pp. 370–378, 2018.

[23] J.-M. Li, Y.-H. Wang, Y. Yu, R.-B. Wu, J. Weng, and G. Lu, "Copper-catalyzed remote C-H functionalizations of naphthylamides through a coordinating activation strategy and single-electron-transfer (SET) mechanism," *ACS Catalysis*, vol. 7, no. 4, pp. 2661–2667, 2017.

[24] R. U. Osarogiagbon, H. P. Rodriguez, D. Hicks et al., "Deploying team science principles to optimize interdisciplinary lung cancer care delivery: avoiding the long and winding road to optimal care," *Journal of Oncology Practice*, vol. 12, no. 11, pp. 983–991, 2016.

[25] A. Lindberg, N. Berente, J. Gaskin, and K. Lyytinen, "Coordinating interdependencies in online communities: a study of an open source software project," *Information Systems Research*, vol. 27, no. 4, pp. 751–772, 2016.

Research Article

Intelligent Recommendation System Based on Mathematical Modeling in Personalized Data Mining

Yimin Cui (iD)

School of Information Engineering, Xi'an University, Xi'an 710065, Shaanxi, China

Correspondence should be addressed to Yimin Cui; cuiyimin@xawl.edu.cn

With the advent of the era of big data, data mining has become one of the key technologies in the field of research and business. In order to improve the efficiency of data mining, this paper studies data mining based on the intelligent recommendation system. Firstly, this paper makes mathematical modeling of the intelligent recommendation system based on association rules. After analyzing the requirements of the intelligent recommendation system, Java 2 Platform, Enterprise Edition, technology is used to divide the system architecture into the presentation layer, business logic layer, and data layer. Recommendation module is divided into three substages: data representation, model learning, and recommendation engine. Then, the fuzzy clustering algorithm is used to optimize the system. After the system is built, the performance of the system is evaluated, and the evaluation indexes include accuracy, coverage, and response time. Finally, the system is put into a trial operation of an e-commerce platform. The click-through rate and purchase conversion rate of recommended products before and after the operation are compared, and a questionnaire survey is randomly launched to the platform users to analyze the user satisfaction. The experimental data show that the MAE of this system is the lowest, maintained at about 0.73, and its accuracy is the highest; before the recommended threshold exceeds 0.5, the average coverage rate of this system is the highest: 0.75; in $Q1$–$Q5$ subsets, the shortest response time of the system is 0.2 s. Before and after the operation of the system, the average click-through rate increased by 11.04%, and the average purchase rate increased by 9.35%. Among the 1216 users, 43% of the users were satisfied with 4 and 9% with 1. This shows that the system algorithm convergence speed is fast; it can recommend products more in line with user needs and interests and promote higher click-through rate and purchase rate, but user satisfaction can be further improved.

1. Introduction

1.1. Background Significance. The information of our times is expanding unprecedentedly, and all kinds of information are dazzling. Faced with various problems brought about by huge information, personalized intelligent recommendation system came into being. The core of recommendation system is recommendation algorithm, which determines the effect of recommendation [1]. Data mining integrates the theory and technology of many fields and has been widely used in various industries [2]. All kinds of massive data from the Internet pose new challenges to data mining technology [3]. The application of intelligent recommendation system to data mining technology is of innovative and practical significance, which can provide more targeted and intelligent information for people.

1.2. Related Work. Intelligent recommendation system is widely used in video websites and e-commerce platform, so the relevant research results are also relatively more [4]. Li proposed a new model, which uses social network and mining user preference information expressed in microblog to evaluate the similarity between online movies and TV dramas [5] and uses a series of data mining methods and social computing model [6]. Yang proposed a solution based on hybrid recommendation algorithm, including content-based recommendation algorithm, item-based collaborative filtering recommendation algorithm, and demography-based recommendation algorithm [7]. In order to expand the recommendation dimension, he uses classification clustering algorithm to mine the historical data of items and users. Lu trains the network to achieve the required accuracy. Then, redundant connections in the network are

removed by network pruning algorithm, the activation value of hidden units in the network is analyzed, and classification rules are generated according to the analysis results [8]. Angeli elaborated and explained some key issues of data mining in educational technology classroom research, investigated students' learning behavior and experience in computer supported classroom activities, and used fuzzy representation to summarize questionnaire data [9]. His research provides data support for the application of data mining technology in the field of education, but the number of training samples used in his experiment is too small, which will have a certain impact on the mining effect.

1.3. Innovative Points in This Paper. In order to improve the efficiency of information processing and the quality of data mining, more personalized information recommendation services should be provided for people. Based on the related algorithms of mathematical modeling intelligent recommendation system, this paper makes an in-depth study on personalized data mining. The innovations of this study are as follows: (1) based on J2EE technology and association rule algorithm, an intelligent recommendation system is constructed. The system architecture includes the presentation layer, business logic layer, and data layer. The system recommendation module includes three substages: data expression, model learning, and recommendation engine. (2) The fuzzy clustering algorithm is used to optimize the recommendation system and improve the confidence degree of the fuzzy clustering algorithm. Then the fuzzy clustering of items and users is established, respectively. (3) The prediction accuracy, coverage, and response time of the system are tested. The data show that the system has high accuracy and coverage and short response time. (4) After the system is put into operation, it can recommend products that are more in line with the needs and interests of users by comparing the click-through rate and purchase conversion rate before and after the operation.

2. Intelligent Recommendation System of Mathematical Modeling and Personalized Data Mining

2.1. Composition and Structure of the Intelligent Recommendation System

2.1.1. Common Methods of the Intelligent Recommendation System. The recommendation system based on demography is easy to implement. It can discover the correlation between users according to the demographic characteristics so as to predict the interests and preferences of users and recommend resources with similar preferences to the target users. The method will not involve the historical data of current users' preference for resources, nor will it involve the information of resources themselves. However, it has the disadvantage of too coarse recommendation granularity, and the collected information may be false, which will affect the prediction results.

The content-based recommendation system obtains the user's interest preference by analyzing the user's use or viewing history and then compares the similarity between the user's interest description and the resource content and sorts the resources to recommend [10]. The system also adjusts and optimizes the user's interest description according to the user's feedback on the recommended resources.

The recommendation methods based on collaborative filtering can be divided into two types: user-based and project-based. Based on the user's needs, the data expression is used to deal with the modeling problem between the user and the resource, and then the neighbor users are calculated based on the similarity of the user's behavior. Finally, the resource with the highest evaluation is found from the neighbor users and recommended to the current user [11]. The project-based type is to use the matrix of analyzing users and resources to calculate the relationship between resources, so as to generate recommendations. The recommendation method of collaborative filtering faces the problems of cold start of new users, the neglect of new project resources, and data sparsity.

2.1.2. Composition of the Intelligent Recommendation System. The intelligent recommendation system consists of three modules: input, recommendation, and output. The input module is mainly responsible for collecting, sorting, and updating user information. The information content includes user's personal information, implicit browsing information, rating information, search keyword information, purchase history information, and expert information [12].

The recommendation module uses the appropriate recommendation algorithm to process and analyze the input information and finally produces the recommendation results. This module directly determines the recommendation quality of the first mock exam system. Therefore, different algorithms will be adopted in different actual situations, and specific problems should be analyzed.

The output module will sort the recommended content according to the user's interest, and the final output will be provided to the user. There are different forms of output. The common output methods are product list, user evaluation and rating, e-mail, and expert introduction. Different output modes will reflect different emphasis.

2.1.3. Evaluation Criteria of the Intelligent Recommendation System. The accuracy of recommendation system is different in different types of systems. For example, in a product recommendation system, accuracy is the ratio of the number of products recommended and purchased by the system to the total number of products in the recommendation set [13], as shown in the following formula:

$$P = \frac{|B \cap R|}{|R|}, \tag{1}$$

where R and B represent the recommendation set and purchase set, respectively. The calculation formula of the

coverage rate of the commodity recommendation system is as follows:

$$C = \frac{|B \cap R|}{|B|}. \tag{2}$$

The accuracy rate can describe the accuracy of the recommendation set of the system recommendation engine, while the coverage rate shows the ability of the recommendation engine to be purchased by users.

The diversity of the recommendation system is calculated by the similarity of the recommended resources obtained by users. The greater the similarity, the worse the diversity of the system. Let R_a be the recommendation set provided to user a; then, the definition of R_a diversity is shown in the following formula:

$$\text{Diversity}(R_a) = \frac{\sum_{j,k \in R_a} (1 - \text{sim}(j,k))}{(1/2)L(L-1)}, \tag{3}$$

where $\text{sim}(j,k)$ is the similarity of resource j, k and $L = |R_a|$ is the length of recommendation list. Therefore, the definition of diversity of the whole recommendation system is shown in the following formula:

$$\text{Diversity} = \frac{1}{|a|} \sum_{a \in A} \text{Diversity}(R_a). \tag{4}$$

2.2. Intelligent Recommendation Algorithm

2.2.1. Association Rule Algorithm.
The most classic association rule mining algorithm is Apriori algorithm, which adopts a cyclic method of hierarchical order search [14]. Then strong association rules are generated from frequent itemsets to find the confidence threshold that meets the user's requirements. The confidence level of rule $X \Rightarrow Y$ in the project set is recorded as follows:

$$\text{confidence}(X \Rightarrow Y) = \frac{\text{support}(X \cup Y)}{\text{support}(X)}. \tag{5}$$

The confidence degree is used to measure the credibility of association rules. The high confidence degree proves that it is easier to attract users' interest to change association rules.

The implementation of Apriori algorithm is very simple, but it needs to scan the database whenever a candidate set with different number of itemsets is generated. When the size of the candidate set is too large, the algorithm takes a long time. In addition, due to the increasing data in the transaction database, each time the data is added, the two tasks of generating association rules from the frequent itemsets calculated by the algorithm need to restart the database after the new data is added, which is not conducive to the effective discovery of relevant rules [15]. This algorithm is suitable for single-dimensional transaction databases but is not suitable for storing multidimensional datasets.

2.2.2. Collaborative Filtering Algorithm.
Collaborative filtering algorithm based on articles is often used in e-commerce recommendation system. The algorithm needs to calculate the similarity between items and generate recommendation list by using user's purchase records [16]. An important step in item-based collaborative filtering algorithm is to find other items with high similarity to one item. There needs to be an appropriate method for measuring the similarity between items. The column vector of evaluation matrix is usually used to calculate the similarity between items. The common similarity measurement methods include vector cosine, Pearson correlation, and corrected vector cosine.

Set the threshold t; when the similarity between an item and item i exceeds the threshold, the article is put into the nearest neighbor set $Z(i)$ of article i, as shown in the following formula:

$$Z(i) = \{j \in I | \text{sim}(i,j) > t\}. \tag{6}$$

Once the nearest neighbor set is confirmed, the weighted sum of user h's scores on these nearest neighbor items can be calculated to obtain the predicted score of user h on item i, as shown in the following formula:

$$p(h,i) = \frac{\sum_{j \in Z(i)} \text{sim}(i,j) \times k_{hj}}{\sum_{j \in Z(i)} |\text{sim}(i,j)|}. \tag{7}$$

The collaborative filtering algorithm based on articles can deal with the situation that the number of users is greater than the number of items in e-commerce websites and shows good recommendation quality. When the number of items is small, offline mode can be used to reduce the workload [17]. However, collaborative filtering algorithm also has some shortcomings, such as cold start problem in the face of new users and being unable to recommend; the other is the problem of data sparsity, which will directly affect the accuracy of nearest neighbor set construction.

2.2.3. Fuzzy Clustering Algorithm.
The basic steps of fuzzy clustering include data standardization, establishing similarity matrix, and fuzzy clustering [18]. Data standardization will map the data to the interval $[0, 1]$, which is transformed by variance method or standard deviation. The establishment of fuzzy similarity matrix is commonly used in Euclidean distance, Manhattan distance, Mahalanobis distance, and angle cosine [19].

Euclidean distance is derived from the calculation of the distance between two points in geometry, and its calculation is shown in the following formula:

$$d = \sqrt{\sum_{k=1}^{n} (x_k - y_k)^2}. \tag{8}$$

Manhattan distance is not a straight line but a broken line distance in the plane. Its calculation is shown in the following formula:

$$d = \sum_{k=1}^{n} |x_k - y_k|. \tag{9}$$

The Mahalanobis distance has nothing to do with the dimension, so the correlation interference between variables can be eliminated. The calculation is shown in the following formula:

$$d = \sqrt{(x - y)^T S^{-1} (x - y)}. \tag{10}$$

The calculation of included angle cosine is shown in the following formula:

$$d = \frac{\sum_{k=1}^{n} x_k y_k}{\sqrt{\sum_{k=1}^{n} x_k^2} \sqrt{\sum_{k=1}^{n} y_k^2}}. \tag{11}$$

In the whole universe X, n samples are divided into several disjoint subsets, and the subsets satisfy the following formula:

$$\begin{aligned} X_1 \cup X_2 \cup \cdots \cup X_e &= X, \\ X_a \cap X_b &= \varnothing, \end{aligned} \tag{12}$$

where $1 \le a \ne b \le e$. The membership relationship of any sample x_k to any subset X_a is shown in the following formula:

$$\omega_{X_a}(x_k) = \omega_{ak} = \begin{cases} 1, & x_k \in X_a, \\ 0, & x_k \notin X_a. \end{cases} \tag{13}$$

Fuzzy clustering divides the sample set X into e fuzzy subsets and extends the membership of samples to the interval $[0, 1]$ from the binary form of 0 or 1. For such a sample x_k, its membership must satisfy the following formula:

$$\sum_{a=1}^{e} \omega_{ak} = 1, \quad \forall k. \tag{14}$$

This kind of clustering is called fuzzy clustering.

2.3. Personalized Data Mining

2.3.1. Data Mining Function. The essence of data mining is to mine predictive knowledge in large-scale data, including generalized knowledge, association knowledge, classification and clustering knowledge, predictive knowledge, and bias knowledge [20]. The main functions of data mining include concept description, association analysis, classification analysis, clustering analysis, outlier analysis, and time series analysis [21].

The concept description can summarize and compare the data and give the overall description. It is commonly used in statistical database business data, including mean and variance. Association analysis is carried out in massive data, and the association relationship behind the data can be found out, and then more advanced prediction can be carried out. Classification analysis classifies and models the whole data, while cluster analysis gathers things with the same similarity.

Outlier analysis is used to analyze outlier data that are different from conventional data. Although the number of isolated points is small, the information they carry is very important and cannot be ignored. The data of time series analysis include fixed interval value and dynamic interval value [22, 23]. Its main functions include similarity search, pattern mining, and trend analysis.

2.3.2. Data Mining Process. Data mining is an iterative process of human-computer interaction, which is mainly divided into four parts: problem definition, data sorting, data mining implementation, and interpretation and evaluation of mining results [24]. The purpose of problem definition is to have a clear understanding and definition of mining target.

Data consolidation includes data selection, preprocessing, and reduction. Data selection needs to select samples or data according to the defined problem requirements to determine the target data. Data preprocessing includes checking the integrity and consistency of data and eliminating data noise. If data redundancy occurs, it is necessary to clear and fill in missing data. Data reduction is to reduce the amount of data through projection or other operations and filter out task-related datasets.

The implementation of data mining requires the use of data mining technology and algorithms, mining in the dataset, and finding out useful related information and expressing it. Finally, it is necessary to explain the rationality and evaluate the value of the information. If the information is redundant or less relevant, it should be eliminated.

2.3.3. Technology of Data Mining. The common methods of classification mining include Bayesian classification, decision tree, and support vector machine [25]. Bayesian network is an important technology in data mining, which can easily use graphical patterns to display the causal relationship of time and can also be used for predictive analysis [26]. The conditional probability, joint probability, and total probability formula will be used in the use of Bayesian networks, as shown in the following formulas:

$$P(Y|X) = \frac{P(XY)}{P(X)}, \tag{15}$$

$$P(XY) = P(X)P(Y|X), \tag{16}$$

$$P(X) = \sum_{i=1}^{n} P(Yi)P(X|Yi), \tag{17}$$

where X, Y are all events and $P(Yi) > 0$, $i = 1, 2, \ldots, n$. According to the above three formulas, Bayesian formula can be deduced, as shown in the following formula:

$$P(Yi|X) = \frac{P(X|Yi)P(Yi)}{\sum_{j=1}^{n} P(X|Yj)P(Yj)}. \tag{18}$$

Bayesian formula is the basis of Bayesian network learning and prediction.

Clustering technology includes traditional pattern recognition methods and mathematical taxonomy, while clustering analysis of data mining includes system clustering, decomposition, addition, and fuzzy clustering [27]. Even for the same record set, different clustering methods will produce different clustering results.

3. Experiments on Construction and Application of Mathematical Modeling Intelligent Recommendation System

3.1. Modeling of the Intelligent Recommendation System Based on Association Rules

3.1.1. Demand Analysis. In practical application, intelligent recommendation system must be able to provide users with real-time, dynamic, and accurate services. Real-time service requires that recommendation algorithm has speed advantage in data mining. Especially in the case of large datasets, online recommendation generation has high requirements for system method running memory. Dynamic service is to ensure that the collection of recommendations can not only reflect the latest needs of users but also pay attention to real time, and if the time interval of recommendation to users is too short, the speed of online recommendation will decline. Accurate service requires that the system can accurately predict the needs of users. In the actual situation, sometimes accurate service will be sacrificed for real-time service, so the improvement of accuracy depends on the improvement of algorithm. This paper takes the intelligent recommendation system of e-commerce as an example to analyze the data mining.

3.1.2. Technology Choice. Using Java 2 Platform, Enterprise Edition (J2EE), technology, the system is divided into customer layer, presentation layer, business logic layer, and data layer. The core design is business logic layer, which is implemented by Enterprise Java Bean (EJB) component. Java Server-Side Page (JSP) technology provides powerful built-in components, which can simplify the program design, and its access to the database can also ensure the portability of the program. Therefore, J2EE architecture has the advantages of high execution, easy-to-use script language, ability to deal with a large number of concurrent users, logic of managing complex things, easy division of development projects, simple component deployment, and maintenance of client applications.

3.1.3. System Design. Combined with J2EE technology, the structure of e-commerce intelligent recommendation system can be divided into three parts: presentation layer, business logic layer, and data layer. The recommendation module of the system is divided into three substages: data representation, model learning, and recommendation engine. The module framework is shown in Figure 1.

3.2. System Improvement Based on Fuzzy Clustering Algorithm

3.2.1. Improved Clustering Algorithm. The membership degree of the traditional fuzzy clustering algorithm is improved. The element x_r, whose nearest cluster is s, has the largest membership degree in s, and its value is u_{sr}. The second nearest cluster is z and the membership degree is u_{zr}. Then, the membership degree of x_r element to clusters s and z is calculated as shown in the following formulas:

$$u_{sr} = u_{sr} + (1 - \alpha)u_{zr}, \tag{19}$$

$$u_{zr} = \alpha u_{zr}. \tag{20}$$

Among them, α is an attractive inhibitory factor.

In the improved algorithm, we can adjust the size of α to control the size of inhibition and then control the convergence speed of the calculation.

3.2.2. Establishing Fuzzy Clustering. The improved fuzzy clustering algorithm is used for all the data, and the fuzzy clustering of users and items is established, respectively. After successful establishment, the nearest neighbor user set can be constructed by using other users in the target user-based clustering. The higher the membership degree is, the more similar the user is to the target user.

3.3. System Test and Operation

3.3.1. Selection of Test Data. This paper selects the historical data of an e-commerce platform in the database for nearly two years and then takes them as test data after effective screening and filtering. The dataset contains the basic information of 500 users, 2000 shopping records, 800 e-commerce stores, and 3000 pieces of shopping evaluation information.

The dataset is randomly divided into five similar subsets, and cross validation method is used to compare the intelligent recommendation system constructed in this paper with the traditional content-based recommendation system, traditional association rule recommendation system, and collaborative filtering recommendation system, and the performance of the system is analyzed.

3.3.2. Test and Evaluation Index. Firstly, the prediction accuracy is selected as the evaluation index of the test method in this paper. The difference between the target user's scoring system of the commodity and the real score in the test dataset is the absolute average error (MAE). The smaller the value, the more accurate the prediction of the system.

The average coverage of different recommendation systems is compared, and the coverage is calculated by formula (2) in Section 2. The last test parameter is the response time of the system, that is, the running time required for the recommendation system to generate the recommended result set.
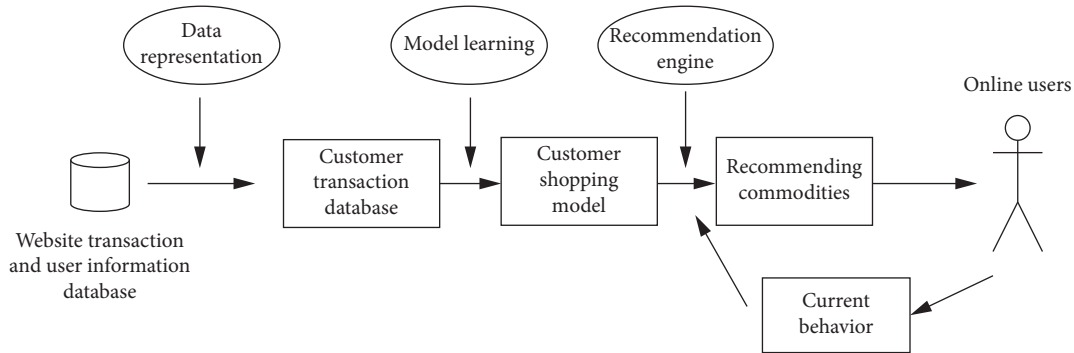
Figure 1: Module framework of the intelligent recommendation system.

3.3.3. Actual Operation. The intelligent recommendation system is tested in an e-commerce shopping platform, and its application effect in personalized data mining is analyzed. The final result is the change of click-through rate and purchase rate of recommended products. At the same time, an online questionnaire survey was launched to attract users of the platform to participate with shopping vouchers as gifts to ensure the participation rate. The content of the questionnaire survey mainly includes users' satisfaction with the products recommended by the improved platform.

4. Discussion on Application Effect in Personalized Data Mining

4.1. Evaluation Results of the Recommendation System. The test dataset is randomly divided into five subsets, named Q1–Q5. Then, the intelligent recommendation system and the traditional content-based recommendation system, traditional association rule recommendation system, and collaborative filtering recommendation system are used to run the five subsets, and the performance test is carried out. In order to facilitate the recording and sorting of data, the above four systems are named A, B, C, and D, respectively.

4.1.1. Prediction Accuracy of Different Recommendation Systems. The prediction accuracies of the intelligent recommendation system (A), the traditional content-based recommendation system (B), the traditional association rule recommendation system (C), and the collaborative filtering recommendation system (D) for Q1-Q5 datasets are compared, and the difference of absolute average error (MAE) is analyzed.

As shown in Table 1, different precision will appear in the same recommendation system in different subsets. In the same subset, different recommendation systems show different precision. The accuracy of each recommendation system in different subsets is analyzed.

As shown in Figure 2, the most accurate is the intelligent recommendation system created in this paper, and its MAE value always remains between 0.72 and 0.74. The same subsystem was compared with different prediction accuracies.

As shown in Figure 3, the highest MAE is that of the traditional content-based recommendation system, which is

Table 1: Comparison of prediction accuracies of different recommendation systems.

System type	Q1	Q2	Q3	Q4	Q5
A	0.73	0.74	0.72	0.74	0.72
B	0.83	0.85	0.84	0.84	0.85
C	0.78	0.8	0.79	0.78	0.79
D	0.75	0.78	0.77	0.76	0.77

maintained at about 0.84, so the accuracy is lower. The lowest MAE is that of the intelligent recommendation system, which is maintained at about 0.73, with the highest accuracy.

4.1.2. Coverage of Different Recommendation Systems. The average coverage of four recommendation systems in five data subsets was calculated, and their changes under different thresholds (0.1, 0.2, 0.5, 0.7, and 0.8) were compared.

As shown in Table 2, with the increase of the recommendation threshold, the coverage rate of each recommendation system decreases. In particular, when the recommended threshold value is 0.8, the coverage rate of the intelligent recommendation system reduces to the lowest, which is 0.26. The change trend is shown with more intuitive graphics and analyzed.

As shown in Figure 4, before the recommendation threshold exceeds 0.5, the average coverage of the intelligent recommendation system created in this paper is always the highest, which is 0.75, 0.71, and 0.68, respectively. However, after the recommendation threshold exceeds 0.5, the average coverage of the intelligent recommendation system created in this paper has decreased significantly. However, the traditional content-based recommendation system with low coverage has the highest coverage rate of 0.35 when the threshold value is 0.8.

4.1.3. Response Time of Different Recommendation Systems. Record the running time of the recommendation system to generate the recommended result set in each subset, and test its response time.

Figure 2: System prediction accuracy in different subsets.
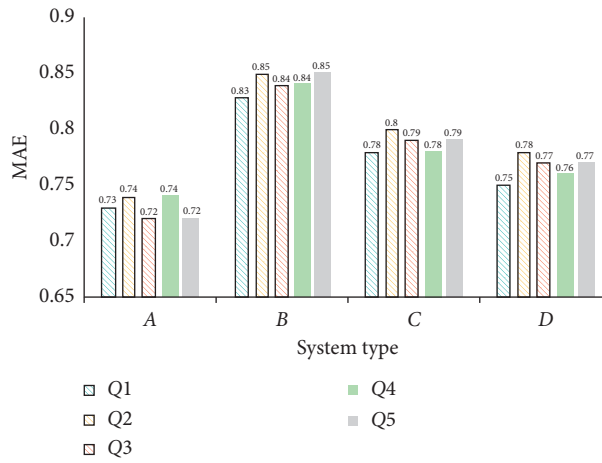
Figure 3: Prediction accuracy of different systems in the same subset.

Table 2: Average coverage changes under different recommended thresholds.

System type	0.1	0.2	0.5	0.7	0.8
A	0.75	0.71	0.68	0.37	0.26
B	0.63	0.55	0.49	0.41	0.35
C	0.61	0.54	0.41	0.36	0.29
D	0.65	0.57	0.51	0.42	0.3

As shown in Table 3, the same recommendation system has different response times in different data subsets. In the same data subset, the response time of different recommendation systems is more different. Furthermore, the response time of each recommendation system in different subsets is analyzed.

As shown in Figure 5, in Q1-Q5 subsets, the response time of the intelligent recommendation system created in this paper is always the shortest, which is 0.24 s, 0.21 s, 0.24 s, 0.2 s, and 0.23 s, respectively. The longest response time of the traditional content-based recommendation system in the Q3 subset is 0.45 s. This shows that the algorithm of the intelligent recommendation system established in this paper has fast convergence speed and short response time.

4.2. Operation Results. After testing, the intelligent recommendation system is tested in an e-commerce shopping platform, and its application effect in personalized data mining is analyzed. This paper analyzes the click-through rate and purchase rate of the recommended products in a week before and after use.

As shown in Table 4, before the system runs, the average click-through rate is 78.87%, and the average purchase rate is 13.91%. One week after the system was running, the average click-through rate was 89.91%, and the average purchase rate was 23.26%. The system before and after the operation of the commodity click rate is used for a detailed comparison.

As shown in Figure 6, a week before the intelligent recommendation system runs, the click-through rate of commodities shows a relatively stable fluctuation. The highest hit rate was 81.24%, and the lowest was 75.51%. In the week after the system was running, the click-through rate first showed an increasing trend and gradually stabilized after the fifth day, and the highest was 93.94% on the seventh day. This shows that the intelligent recommendation system can create a higher click-through rate of products, so that more users can see the products. Figure 6 makes a detailed comparison of the commodity click through rate before and after the system operation.
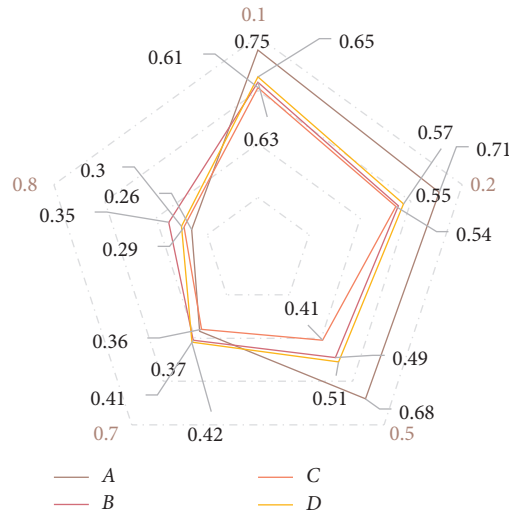
FIGURE 4: Average system coverage under different recommended thresholds.

TABLE 3: Comparison of response time predicted by different recommendation systems (s).

System type	Q1	Q2	Q3	Q4	Q5
A	0.24	0.21	0.24	0.2	0.23
B	0.41	0.4	0.45	0.39	0.36
C	0.32	0.31	0.37	0.33	0.29
D	0.28	0.25	0.29	0.27	0.26
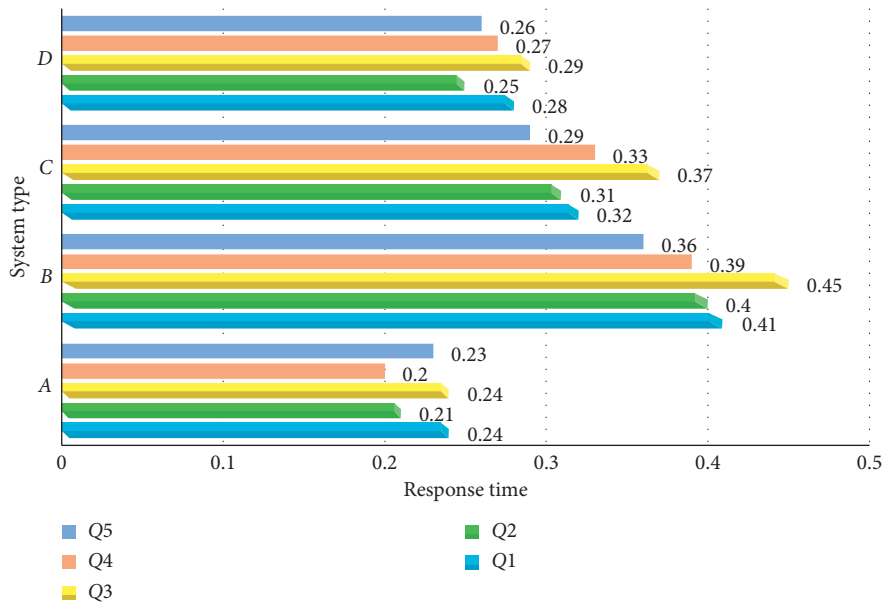
FIGURE 5: Response time predicted by different recommendation systems.

As shown in Figure 7, the purchase rate of goods also showed a relatively stable fluctuation in a week before the system was running, with the highest purchase rate on the 6th day, 14.85%, and the lowest on the 7th day, 13.17%. In the week after the system operation, the purchase rate took the lead in the trend of increase and gradually stabilized after the fifth day, with the highest of 25.81% on the 7th day. This shows that the intelligent recommendation system can recommend products that meet the needs and interests of users and promote higher purchase rate.

4.3. Survey of User Satisfaction. After one week of operation, online questionnaire survey was launched randomly for users of the platform, which mainly investigated the

TABLE 4: Click-through rate and purchase rate of products before and after system operation.

Time (d)	Before operation		After operation	
	Click-through rate (%)	Purchase rate (%)	Click-through rate (%)	Purchase rate (%)
1	78.46	13.75	82.46	19.15
2	75.51	13.97	87.34	20.91
3	79.24	14.13	88.86	22.19
4	80.11	14.15	90.04	23.84
5	79.56	13.34	93.14	25.37
6	81.24	14.85	93.59	25.55
7	77.96	13.17	93.94	25.81
Average value	78.87	13.91	89.91	23.26
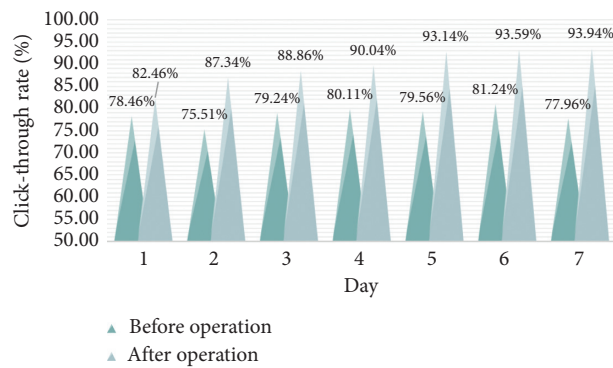
FIGURE 6: Comparison of click-through rate of products before and after system operation.
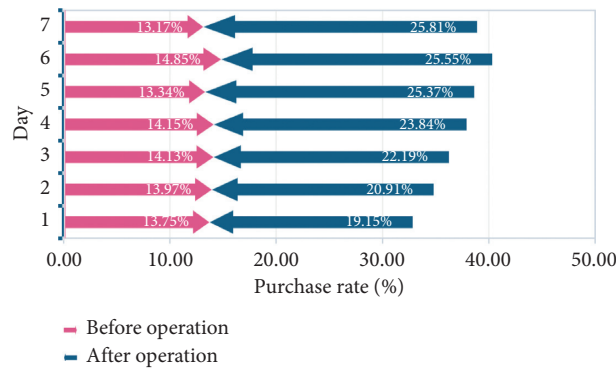
FIGURE 7: Comparison of commodity purchase rate before and after the system operation.

satisfaction of users with the recommended products of the improved platform. The questionnaire lasted for five days, and the total number of users involved was 1216. The users are divided into 1–5 grades by age; the larger the number, the higher the satisfaction.

As shown in Table 5, among the users who participated in the survey, 411 users were between 20 and 25 years of age, and 39 users were over 45 years of age. The satisfaction of different age groups was analyzed.

As shown in Figure 8, the number of users below 35 years of age with satisfaction of 4 is the largest, accounting for 94.9% of all users with satisfaction of 4. Among the users over 35 years of age, the number with satisfaction of 5 is the most, accounting for 41.9% of all users with satisfaction of 5. Leaving aside the condition of age, this paper analyzes the satisfaction distribution of all users.

As shown in Figure 9, of the 1216 users, 43% of the users are satisfied with 4, 19% are satisfied with 5 and 3, and 9% and 10%

TABLE 5: Survey of user satisfaction.

	1	2	3	4	5	Total
<20	21	10	29	88	14	162
20–25	29	36	76	209	61	411
26–30	36	40	89	154	45	364
31–35	12	15	13	49	16	105
36–40	5	9	9	10	51	84
41–45	3	3	7	9	29	51
>45	2	6	5	8	18	39
Total	108	119	228	527	234	1216
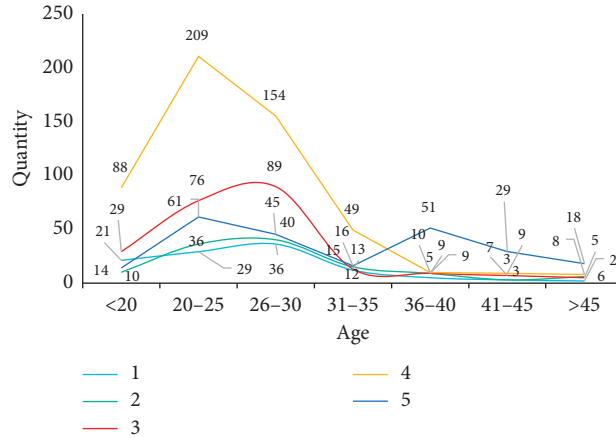
FIGURE 8: User satisfaction of different age groups.
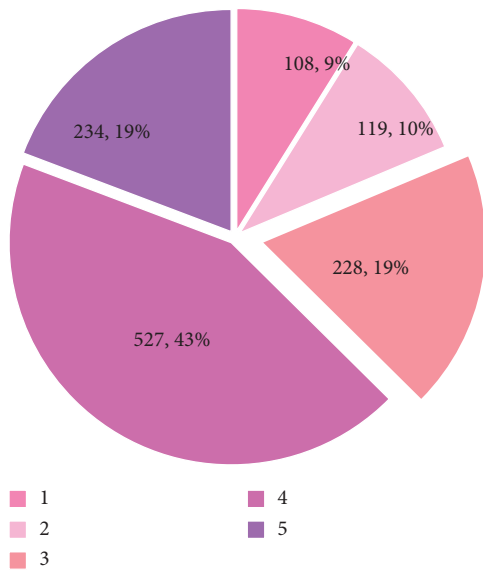
FIGURE 9: Distribution of satisfaction.

are satisfied with 1 and 2. This shows that although the user satisfaction of the system is high, it can be further improved.

5. Conclusions

There are three kinds of recommendation systems: demographic-based, content-based, and collaborative filtering-based. The intelligent recommendation system consists of three modules: input, recommendation, and output. Common recommendation algorithms include association rules, collaborative filtering, and fuzzy clustering. Data mining is an iterative human-computer interaction process, mainly including problem definition, data collation, data mining implementation, and interpretation and evaluation of mining results.

This paper constructs an intelligent recommendation system based on J2EE technology and association rules algorithm. The fuzzy clustering algorithm is used to optimize the recommendation system and improve the confidence degree of the fuzzy clustering algorithm. Then the fuzzy clustering of items and users is established, respectively. The prediction accuracy, coverage, and response time of the system are tested. The click-through rate and purchase conversion rate are compared before and after the system running. The results show that the system algorithm has fast convergence speed and high accuracy and coverage. It can recommend products that meet the needs and interests of users and promote higher click-through rate and purchase rate.

The experimental results show that the user satisfaction of this system is still insufficient, which can be further improved. Therefore, in the following research work, we should take improving user satisfaction as the main goal. In addition, during the trial operation, the user survey should be carried out many times to make the data more representative. We also need to analyze the reasons for the lack of customer satisfaction in detail and get specific feedback from users.

Data Availability

The data underlying the results presented in the study are available within the manuscript.

Conflicts of Interest

The author declares that there are no conflicts of interest.

References

[1] B. Faqihi, N. Daoudi, I. Hilal, and R. Ajhoun, "Pedagogical resources indexation based on ontology in intelligent recommendation system for contents production in d-learning environment," *Journal of Computer Science*, vol. 16, no. 7, pp. 936–949, 2020.

[2] E. L. Sachi Nandan Mohanty Lydia, M. Elhoseny, M. Majid, G. Al Otaibi, and K. Shankar, "Deep learning with LSTM based distributed data mining model for energy efficient wireless sensor networks," *Physical Communication*, vol. 40, 2020.

[3] S. R. Joseph, H. Hlomani, and K. Letsholo, "Data mining algorithms: an overview," *Neuroence*, vol. 12, no. 3, pp. 719–743, 2016.

[4] H. Kim, "Investigating the mediating role of social networking service usage on the big five personality traits and on the job satisfaction of Korean workers," *Journal of Organizational and End User Computing*, vol. 31, no. 1, pp. 110–123, 2019.

[5] C. H. Wu, Z. Yan, S. B. Tsai, W. Wang, B. Cao, and X. Li, "An empirical study on sales performance effect and pricing strategy for E-commerce: from the perspective of mobile information," *Mobile Information Systems*, vol. 2020, Article ID 7561807, 8 pages, 2020.

[6] H. Li, J. Cui, B. Shen, and J. Ma, "An intelligent movie recommendation system through group-level sentiment analysis in microblogs," *Neurocomputing*, vol. 210, no. 19, pp. 164–173, 2016.

[7] F. Yang, "A hybrid recommendation algorithm-based intelligent business recommendation system," *Journal of Discrete Mathematical Sciences and Cryptography*, vol. 21, no. 6, pp. 1317–1322, 2018.

[8] H. Lu, R. Setiono, and H. Liu, "Effective data mining using neural networks," *Knowledge & Data Engineering IEEE Transactions on*, vol. 8, no. 6, pp. 957–961, 2016.

[9] C. Angeli, S. K. Howard, J. Ma, J. Yang, and P. A. Kirschner, "Data mining in educational technology classroom research: can it make a contribution?" *Computers & Education*, vol. 113, pp. 226–242, 2017.

[10] W. Jiang, J. Chen, Y. Jiang et al., "A new time-aware collaborative filtering intelligent recommendation system," *Computers, Materials & Continua*, vol. 61, no. 2, pp. 849–859, 2019.

[11] S. Jaiswal, S. Virmani, V. Sethi et al., "An intelligent recommendation system using gaze and emotion detection," *Multimedia Tools and Applications*, vol. 78, no. 11, pp. 1–20, 2018.

[12] V. Subramaniyaswamy, R. Logesh, and V. Indragandhi, "Intelligent sports commentary recommendation system for individual cricket players," *International Journal of Advanced Intelligence Paradigms*, vol. 10, no. 1-2, pp. 103–117, 2018.

[13] M. Qingqing, D. Aihua, M. Qingying et al., "Intelligent costume recommendation system based on expert system," *Journal of Shanghai Jiaotong University*, vol. 23, no. 002, pp. 227–234, 2018.

[14] N. Zhu, J. Cao, K. Shen, X. Chen, and S. Zhu, "A decision support system with intelligent recommendation for multi-disciplinary medical treatment," *ACM Transactions on Multimedia Computing, Communications, and Applications*, vol. 16, no. 1, pp. 1–23, 2020.

[15] M. Badami, F. Tafazzoli, and O. Nasraoui, "A case study for intelligent event recommendation," *International Journal of Data Ence & Analytics*, vol. 5, no. 4, pp. 1–20, 2018.

[16] Y. Li, "Design and implementation of intelligent travel recommendation system based on internet of things," *Ingénierie des systèmes d'information*, vol. 23, no. 5, pp. 159–173, 2018.

[17] R. Kazmi, I. S. Bajwa, B. Ramzan et al., "An intelligent data analytics based model driven recommendation system," *Journal of Universal Computer Science*, vol. 25, no. 10, pp. 1353–1371, 2019.

[18] F. Kong, J. Li, and Z. Lv, "Construction of intelligent traffic information recommendation system based on long short-term memory," *Journal of Computational Science*, vol. 26, pp. 78–86, 2018.

[19] M. Abid, S. Umar, and S. M. Shahzad, "A recommendation system for cloud services selection based on intelligent agents," *Indian Journal of Science & Technology*, vol. 11, no. 9, pp. 1–6, 2018.

[20] C. Helma, T. Cramer, S. Kramer et al., "Data mining and machine learning techniques for the identification of mutagenicity inducing substructures and structure activity relationships of noncongeneric compounds," *J Chem Inf Comput*, vol. 35, no. 4, pp. 1402–1411, 2018.

[21] S. Sorour, K. Goda, and T. Mine, "Comment data mining to estimate student performance considering consecutive lessons," *Educational Technology & Society*, vol. 20, no. 1, pp. 73–86, 2017.

[22] G. Asa, C. Nimrod, K. Ale et al., "Agricultural soil spectral response and properties assessment: effects of measurement protocol and data mining technique," *Remote Sensing*, vol. 9, no. 10, p. 1078, 2017.

[23] H. Vathsala and S. G. Koolagudi, "Prediction model for peninsular Indian summer monsoon rainfall using data mining and statistical approaches," *Computers & Geosciences*, vol. 98, pp. 55–63, 2017.

[24] Atta-ur-Rahman and S. Dash, "Data mining for student's trends analysis using Apriori algorithm," *International Journal of Control Theory and Applications*, vol. 10, no. 18, pp. 107–115, 2017.

[25] R. J. Oskouei, N. M. Kor, and S. A. Maleki, "Data mining and medical world: breast cancers' diagnosis, treatment, prognosis and challenges," *American Journal of Cancer Research*, vol. 7, no. 3, pp. 610–627, 2017.

[26] B. K. Blaylock, J. D. Horel, and S. T. Liston, "Cloud archiving and data mining of High-Resolution Rapid Refresh forecast model output," *Computers & Geosciences*, vol. 109, pp. 43–50, 2017.

[27] Atta-ur-Rahman and S. Dash, "Big data analysis for teacher recommendation using data mining techniques," *International Journal of Control Theory and Applications*, vol. 10, no. 18, pp. 95–105, 2017.

Research Article

Application of Virtual Reality Technology in Analysis of the Three-Dimensional Evaluation System of Rural Landscape Planning

Jing Li ⬤ and Tao Hou

New Rural Construction Research Center, College of Art and Design, Wuhan University of Science and Technology, Wuhan 430000, Hubei, China

Correspondence should be addressed to Jing Li; lijing@wust.edu.cn

From the construction of "new socialist countryside" to the proposal of "full coverage of village planning," rural construction has gradually been pushed to a climax. However, the current situation of rural landscape construction in China is not optimistic. On the one hand, the rural landscape deviates from its rural and regional characteristics due to deliberately seeking novelty and differences. Based on these two extreme development trends, this article uses virtual reality technology to construct a rural landscape virtual-roaming system, and randomly select 25 people, each group of 5 people, a total of 3 groups, enter the system in batches with a real reduction degree of 30%, 45%, 60%, 75%, and 80% for experimentation and score the system after the experience. The true reduction degree of the first group is 30%; the true reduction degree of the second group is 45%; the true reduction degree of the third group is 60%; the true reduction degree of the fourth group is 75%; and the true reduction degree of the fifth group is 80%. After analyzing the experimental data, it is concluded that when the true reduction degree of the system goes from low to high, people's satisfaction is higher; when the true reduction degree is as high as 80%, the satisfaction is as high as 9 points; when the true reduction degree of the system goes from low to high, people's sense of immersion is getting deeper and deeper. When the true reduction degree is 30%, the lowest score for immersion is 1 point; when the true reduction degree is 80%, the lowest score for immersion is 7.5 points; the true reduction of the system decreases from high to low; when it is high, people's interaction degree becomes stronger and stronger. When the true reduction degree is 30%, the lowest interaction degree score is 2 points; when the true reduction degree is 80%, the lowest interaction degree score is 9 points; it can be seen from this that, with the increase in the degree of realism of the rural landscape virtual-roaming system, it is extremely difficult for people to find whether they are in the virtual or the reality, and their immersion in virtual reality is getting deeper and deeper. This test also confirmed the superiority of the virtual roaming system in rural landscapes, and the experience is extremely effective.

1. Introduction

1.1. Background Meaning. People's lives have been completely changed with the rapid development of the society. Every family built a new house. In order to improve the living environment, the villagers not only built many modern reinforced concrete buildings across the country but also demolished old buildings and built new ones. The taller the building, the more various shapes are spread across the country [1]. With the development of the economy, modern people pay little attention to rural planning, and rural landscape planning has long been ignored by people and cannot be evaluated. Therefore, the use of virtual reality technology has a very practical impact on the orderly planning of rural landscapes.

1.2. Related Work. Although our country's research on rural landscapes started relatively late, relevant scientists have conducted a lot of research studies on our situation, continued to carry out theoretical summaries and practices, and have achieved fruitful results. Ding started with the concept

of the pastoral complex, analyzed the characteristics of the current rural landscape and its existing advantages, and proposed an industrial modernization strategy to encourage the transition to the traditional second and third agribusiness. Through the organic integration of cross-industry and multifunctional spatial units, people can regain the rural landscape, while enabling urban residents and knowledge flow to obtain land and promote the development of the rural economy [2]. Tian discussed the protection of the natural ecological environment and the pursuit of sustainable development, while considering the cultural characteristics of the area and analyzing various types of rural landscapes, such as "rural settlement landscape, rural ecological landscape, and rural production landscape." In the end, he suggested respecting the traditional rural structure, establishing a warm housing model, creating comfortable rural living spaces, and enhancing the characteristics of rural areas. The landscape must respond to the suggestions of other rural landscape plans, which provide a theoretical basis for economic and civil isolation and the actual rural landscape [3]. Huang et al. after visiting and exploring 30 beautiful villages in Changzhi City, Shanxi, Shaanxi, determined that the rural landscape planning and design needs to be changed urgently, with the disappearance of local characteristics, lack of environmental protection, lack of public participation and scientific control, and other issues. To this end, four planning and design principles regarding integrity, regional characteristics, environmental protection, and sustainability are proposed, as well as three planning strategies for rural, productive, and natural ecological landscapes. For example, in Gucheng Village, Xin'anquan Town, Lucheng City, he conducted planning and design analysis and put forward rural landscape planning and design suggestions related to creating beautiful landscapes [4]. Zhao et al. conducted a field survey on the current planning status of Miyun District in Beijing, explained resource conservation and its application in rural landscape planning, and provided references for future rural landscape planning [5]. Wang et al. Taking Yongji Village, Mingshui County, Heilongjiang Province as an example, in order to solve the important problems existing in the current landscape use, relevant investigations were carried out from four aspects: residential building landscape, public facilities landscape, streetscape, and water resources [6]. Finding and proposing reasonable solutions, problem strategies, and insights are of reference significance for building beautiful towns in the region. In summary, judging from the current status of rural landscape research in the past, most of them have proposed various methods and strategies to plan rural landscapes and rarely mentioned the application of virtual technology to rural landscape planning [7].

1.3. Innovations in This Article. The innovations of this paper are mainly reflected in the following aspects. (1) Using virtual technology to construct a rural landscape roaming landscape system for rural landscape planning. (2) This paper selects the SURF algorithm which is superior to the SIFT algorithm in extracting feature points.

(3) This article is based on the Lumion platform and integrates the results of digital technology applications and research in various stages of rural landscapes. In a gradual process, a low-cost, high-efficiency comprehensive digital virtual reality construction of rural landscapes can be realized.

2. Related Theories of Virtual Reality Technology

Virtual reality (VR for short) refers to the artificial media space created by computers. It is virtual but also realistic. It allows people to enter a virtual environment through multimedia sensor interaction devices and produces an immersive feeling. With the rapid development of computer software and hardware technology, the application of computer graphics in various industries has also developed rapidly. Virtual reality, scientific visualization, and computer animation have become the three major research directions of computer graphics in recent years [8]. This kind of virtual environment is an environment that can be generated by a computer. It can be either a simulation of the real world or a conceived world. Virtual reality has three most prominent features. The first feature is interactivity, through the use of virtual interactive equipment to achieve natural interaction and operation between participants and virtual environment objects; the second feature is immersion, which allows participants to be physically present the real feeling of the environment; the third feature is conception. Participants can get perceptual and rational knowledge through the virtual environment, thereby deepening the concept and germinating new ideas. Virtual reality is a new practical technology involving many disciplines. It integrates advanced computer, sensing and measurement, simulation, and microelectronics technology. It began with the needs of the military field and played a very important role in simulation and training in the military and aerospace fields. In computer technology, it is particularly dependent on computer graphics, artificial intelligence, network technology, man-machine interface technology, and computer simulation technology [9, 10].

2.1. Application of Virtual Technology in Various Fields. The advancement of virtual reality technology has been widely used in education, medicine, entertainment, technology, industry, manufacturing, construction, and commerce. See Figure 1 for details.

2.2. Overview of Virtual 3D Modeling Technology. Virtual reality technology is a brand-new human-computer interaction technology that can truly simulate vision, hearing, motion, and other human behaviors in the natural environment. The ultimate goal is to place the user in a computer-generated virtual environment. Virtual environment modeling is one of the core technologies of virtual reality technology and the basis for creating virtual reality systems [5].
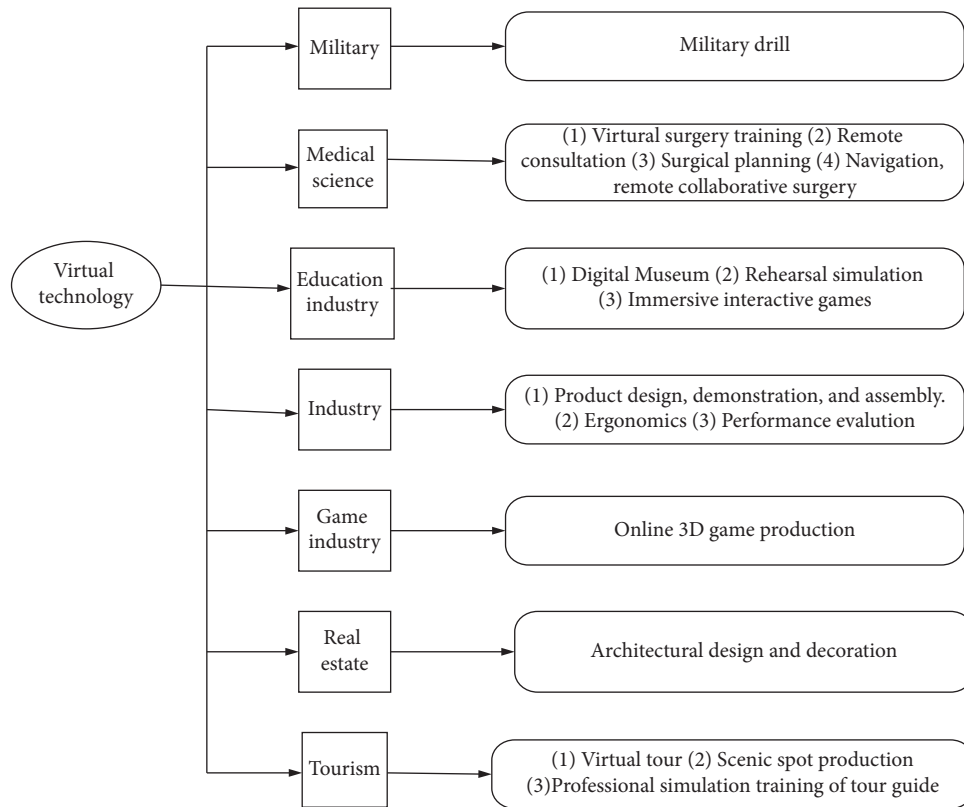
FIGURE 1: Application of virtual technology in various fields.

2.2.1. Main Technical Indicators of Virtual Reality Modeling. The quality of model construction directly affects the quality of the entire virtual reality system. Therefore, it is necessary to build a good virtual environment to understand the key technical parameters of modeling in more detail [11, 12].

The main technical indicators for evaluating virtual environment modeling are as follows:

① *Display Speed.* Many applications have large display time limits. Interactive applications want the response time as short as possible. Too long response time can have a significant impact on system availability.

② *Accuracy*It is a measure of the accuracy of the model representation of actual objects and is one of the key elements to express the reliability of the scene.

③ *Ease of Use.* Building an effective model is a very complex task. Modelers need to represent the shape and behavior of objects as accurately as possible. Through modeling technology, the design and development of excellent models are as simple as possible.

④ *Real-Time Display.*In the virtual environment, the display of the model must be above a certain frame rate limit, which often requires fast display algorithms and model simplification algorithms.

⑤ *Manipulation Efficiency.* In practical applications, in a virtual environment with multiple moving objects, model display, motion model movement, and collision detection are very common tasks that must be effectively implemented.

⑥ *Extensive* The breadth of modeling technology refers to the range of objects that can be represented. Good modeling technology can provide various geometric, physical, and behavioral object models [13, 14].

2.2.2. Features of Virtual Reality Modeling Technology. The virtual reality system emphasizes immersion and realism. In other words, it requires a high degree of authenticity, emphasizes natural interaction, and meets the requirements of real-time interaction. Generally, it can produce an immersive feeling in a realistic environment and can meet the needs of real-time and interactivity. Real-time and reality are the basic criteria for evaluating many computer graphics' algorithms. In the process of VR modeling, authenticity, real time, and interactivity are the basic principles of the distinctive features of virtual reality modeling.

2.2.3. Basic Content of Virtual Reality Modeling. Virtual reality 3D modeling can be divided into data modeling and process modeling. Data modeling includes continuous modeling and discrete modeling. Process modeling includes fractal modeling, image modeling, graphic modeling, geometric modeling, and hybrid modeling. Virtual reality modeling has mainly experienced the development process from geometric modeling to physical modeling and behavior modeling. The modeling of the virtual environment is the basis of the entire virtual reality system, including visual 3D modeling and audible 3D modeling [15].

2.3. Instantiation Technology. When a three-dimensional composite model has multiple objects with the same geometric shapes and attributes but different positions, instantiation technology can be used. Instantiation is an algorithm used in graphics, which can save computer operating costs [16]. If you create multiple objects with the same shape and attributes, the normal copy method will double the number of polygons for each other object. However, the instantiation technology can increase the number of similar objects without increasing the number of polygons. Instancing can greatly reduce the number of polygons in the scene and save a lot of memory. Using this technology in distributed simulation can greatly reduce the workload of data transmission [17, 18].

The main processing method of instantiation technology is matrix transformation. It sacrificed time for memory space. The geometric transformation matrix of the object in the three-dimensional space can be expressed by T_{3D}, and the translation, rotation, and scaling can be expressed as a unified matrix multiplication form. The expression is as follows:

$$T_{3D} = \begin{bmatrix} a_{11} & a_{12} & a_{13} & a_{14} \\ a_{21} & a_{22} & a_{23} & a_{24} \\ a_{31} & a_{32} & a_{33} & a_{34} \\ a_{41} & a_{42} & a_{43} & a_{44} \end{bmatrix}. \quad (1)$$

The unified matrix can be derived for each transformation matrix:

2.3.1. Translation Transformation. If the object position is a point $P(x, y, z)$ and the target translates T_x, T_y, and T_z positions in the three axis directions, the translation transformation matrix is as follows:

$$\begin{bmatrix} x' & y' & z' & 1 \end{bmatrix} = \begin{bmatrix} x & y & z & 1 \end{bmatrix} \begin{bmatrix} 1 & 0 & 0 & 0 \\ 0 & 1 & 0 & 0 \\ 0 & 0 & 1 & 0 \\ T_x & T_y & T_z & 1 \end{bmatrix} \quad (2)$$
$$= \begin{vmatrix} x + T_y & z + T_z & 1 \end{vmatrix}.$$

2.3.2. Scale Conversion. If the scaling ratio is (S_x, S_y, S_z), then the reference point of the scale transformation is (Xf, Yf, Zf), and the matrix is as follows:

$$\begin{bmatrix} x' & y' & z' & 1 \end{bmatrix} = \begin{bmatrix} x & y & z & 1 \end{bmatrix} = \begin{bmatrix} S_x & 0 & 0 & 0 \\ 0 & S_y & 0 & 0 \\ 0 & 0 & S_z & 0 \\ 0 & 0 & 0 & 1 \end{bmatrix}. \quad (3)$$

The process of making ratio $F(Xf, Yf, Zf)$ and rotating transformation relative to the reference point is divided into three steps:

(1) Move the coordinate origin to the reference point F

(2) Proportion and rotation transformation are made relative to the origin in the new coordinate system

(3) Move the coordinate system back to the origin

2.3.3. Rotation Transformation around the Coordinate Axis. In the right-hand coordinate system, the transformation formula for rotating angle A relative to the origin of the coordinate system around the coordinate axis is as follows.

Rotation around the θ axis is follows:

$$\begin{bmatrix} x' & y' & z' & 1 \end{bmatrix} = \begin{bmatrix} x & y & z & 1 \end{bmatrix} \begin{bmatrix} 1 & 0 & 0 & 0 \\ 0 & \cos\theta & \sin\theta & 0 \\ 0 & -\sin\theta & \cos\theta & 0 \\ 0 & 0 & 0 & 1 \end{bmatrix}. \quad (4)$$

Rotation around the y axis:

$$\begin{bmatrix} x' & y' & z' & 1 \end{bmatrix} = \begin{bmatrix} x & y & z & 1 \end{bmatrix} \begin{bmatrix} \cos\theta & 0 & -\sin\theta & 0 \\ 0 & 1 & 0 & 0 \\ \sin\theta & 0 & \cos\theta & 0 \\ 0 & 0 & 0 & 1 \end{bmatrix}. \quad (5)$$

Rotation around the Z axis:

$$\begin{bmatrix} x' & y' & z' & 1 \end{bmatrix} = \begin{bmatrix} x & y & z & 1 \end{bmatrix} \begin{bmatrix} \cos\theta & \sin\theta & 0 & 0 \\ -\sin\theta & \cos\theta & 0 & 0 \\ 0 & 0 & 1 & 0 \\ 0 & 0 & 0 & 1 \end{bmatrix}. \quad (6)$$

The instantiation technology is mainly used to save storage space. In this sense, it takes up less memory and is faster to view. At the same time, the geometric position of the object must be determined by geometric transformation so that the system increases with the number of instance objects. The calculation is clear. Other calculations will slow down the system and affect the real-time performance of the system. Therefore, when using the instantiation technology, the number of instance objects and geometric transformation must be carefully considered, so as not to affect the real-time performance of the system [19, 20].

2.4. Three-Dimensional Panoramic Technology. Based on the various characteristics of 3D panoramic images, 3D panoramic images have a very wide range of applications. It has been applied to many fields such as virtual campus construction, tourism landscape display, commercial product display, real-estate display, hotel display, and automobile display [21, 22].

2.4.1. Camera Imaging and Transformation Model between Images. Before studying the panoramic image generation technology, it is necessary to theoretically understand the transformation relationship model between camera imaging

and images. The camera is placed in the objective three-dimensional world in a certain posture. Usually, the universal coordinate system and the camera coordinate system do not completely overlap, but have a rotation and parallel relationship. In the secondary coordinates, the meaning of these relationships is represented by a 4×4 matrix:

$$\begin{pmatrix} x_c \\ Y_c \\ Z_c \\ 1 \end{pmatrix} = \begin{pmatrix} R & T \\ 0 & 1 \end{pmatrix} \begin{pmatrix} X_w \\ Y_w \\ Z_w \\ 1 \end{pmatrix} = M \begin{pmatrix} X_w \\ Y_w \\ Z_w \\ 1 \end{pmatrix}. \tag{7}$$

In the formula, C is the camera coordinate system coordinates, W is the world coordinate system coordinates, T is a 3×1 translation vector, R is a 3×3 rotation vector, and 0 is a 1×3 vector with all 0 elements.

The camera perspective photography formula is expressed as follows:

$$Z_c = \begin{pmatrix} x_c \\ y_c \\ 1 \end{pmatrix} = \begin{pmatrix} f & 0 & 0 & 0 \\ 0 & f & 0 & 0 \\ 0 & 0 & 1 & 0 \end{pmatrix} \begin{pmatrix} X_c \\ Y_c \\ Z_c \\ 1 \end{pmatrix}. \tag{8}$$

The computer uses a two-dimensional matrix to represent an image pixel by pixel, where one point corresponds to one pixel. Usually, the lower-left corner of the plane is the origin, and the coordinates (u, v) of each pixel are the number of columns and rows of pixels in the image. Therefore, in order to facilitate computer processing, the image plane needs to be set to represent pixels in physical size units. The two-formula conversion formulas are as follows:

$$\begin{pmatrix} u \\ v \\ 1 \end{pmatrix} = \begin{pmatrix} \dfrac{1}{d_x} & 0 & u_0 \\ 0 & \dfrac{1}{d_y} & v_0 \\ 0 & 0 & 1 \end{pmatrix} \begin{pmatrix} x_c \\ y_c \\ 1 \end{pmatrix}. \tag{9}$$

In the formula, (u_0, v_0) is the coordinates of point O in the coordinate system $o - uv$ and d_x and d_y represent the width and height of each pixel (in physical dimensions).

Combining the above three equations, the relationship between the image plane coordinate system and the world coordinate system can be obtained:

$$Z_c = \begin{pmatrix} \dfrac{1}{d_x} & 0 & u_0 \\ 0 & \dfrac{1}{d_y} & v_0 \\ 0 & 0 & 1 \end{pmatrix} \begin{pmatrix} f & 0 & 0 & 0 \\ 0 & f & 0 & 0 \\ 0 & 0 & 1 & 0 \end{pmatrix} \begin{pmatrix} R & T \\ 0 & 1 \end{pmatrix} \begin{pmatrix} X_w \\ Y_w \\ Z_w \\ 1 \end{pmatrix},$$

$$= \begin{pmatrix} \dfrac{f}{d_x} & o & u_0 & 0 \\ 0 & \dfrac{f}{d_y} & v_0 & 0 \\ 0 & 0 & 1 & 0 \end{pmatrix} \begin{pmatrix} R & T \\ 0 & 1 \end{pmatrix} \begin{pmatrix} X_w \\ Y_w \\ Z_w \\ 1 \end{pmatrix} = K \begin{pmatrix} R & T \\ 0 & 1 \end{pmatrix} \begin{pmatrix} X_w \\ Y_w \\ Z_w \\ 1 \end{pmatrix} = P \begin{pmatrix} X_w \\ Y_w \\ Z_w \\ 1 \end{pmatrix}. \tag{10}$$

In the formula, the matrix P is called the projective row and column; the matrix P only corresponds to the camera's internal parameters $(f, d_x, d_y, u_0, \text{and } v_0)$, which in turn correspond to the focal length of the camera, the aspect ratio of the lens, and the average coordinates of the image. The T vector and R vector are determined by the position and direction of the camera relative to the coordinate system, which are called external camera parameters. If the internal and external parameters of the camera are known, the coordinates of the image plane of a point in the three-dimensional space are determined according to the formula, and vice versa.

2.4.2. Image Transformation Model. Commonly used graph transformation models include parallel motion transformation, rotation transformation, rigid body transformation, similarity transformation, affine transformation, and perspective transformation. The rigid transformation keeps the size of the object unchanged, the similar transformation keeps the angle between the lines unchanged, and the affine transformation keeps the parallel relationship of parallel lines [23].

The image transformation model describes the coordinate transformation relationship between two three-dimensional images. The image conversion model is the key

technology for 3D panoramic image generation. Before the panoramic image is generated, an appropriate image transformation model must be selected. In homogeneous coordinates, it is usually expressed by a 3×3 matrix. Assuming that a point $P(x, y)$ on the original image is transformed to a point $P'(x', y')$ using a certain image transformation model M, their relationship is as follows:

$$
\begin{pmatrix} x' \\ y' \\ 1 \end{pmatrix} = M \begin{pmatrix} x \\ y \\ 1 \end{pmatrix} = \begin{pmatrix} m_{11} & m_{12} & m_{13} \\ m_{21} & m_{22} & m_{33} \\ m_{31} & m_{32} & m_{33} \end{pmatrix} \begin{pmatrix} x \\ y \\ 1 \end{pmatrix},
$$

$$
= \begin{pmatrix} h_{11} & h_{12} & h_{13} \\ h_{21} & h_{22} & h_{23} \\ h_{31} & h_{32} & h_{33} \end{pmatrix} \begin{pmatrix} x \\ y \\ 1 \end{pmatrix} = \begin{pmatrix} R & T \\ C & 1 \end{pmatrix} \begin{pmatrix} x \\ y \\ 1 \end{pmatrix}. \tag{11}
$$

In the formula, the matrix R formed by h_{11}, h_{12}, h_{21}, and h_{22} describes the rotation and scale changes between images; the vector T formed by h_{13} and h_{23} describes the translation between images, h_{13} is the displacement in the horizontal direction, and h_{23} is the displacement in the vertical direction; The vector C composed of h_{31} and h_{32} describes the keystone distortion of the perspective transformation between images, that is, the amount of deformation in the horizontal and vertical directions.

2.5. Commonly Used Feature Point Extraction Techniques.
Image features are points that have recognizable features in the image. Properties such as brightness, color, curvature, and texture are usually different from adjacent points, for example, corner points, straight-line intersections, discontinuous points, points with maximum curvature on the contour, etc. Feature point extraction technology includes identifying and describing points in an image that have different attributes from neighboring points. The selected feature points should be clear, easy to extract, and well distributed in the image. In order to uniquely identify each feature point and the requirements of the next feature point adaptation module, usually a smaller neighborhood around the feature point is selected, and a feature-point descriptor vector is generated according to a specific measurement method [17, 24].

The ideal feature point extraction technology should meet the criteria of repeatability, precise positioning, locality, moderate quantity, high efficiency, and robustness. Commonly used feature point extraction techniques include SUSAN, Harris, and SIFT, which are all feature point extraction algorithms based on brightness [25].

2.5.1. SIFT Algorithm.
The SIFT algorithm recognizes and describes the local feature points of the image. These local feature points are invariant to the transformation, rotation, scaling, and affine transformation in the scaling space. The basic idea of the SIFT algorithm is as follows: first, detect the end point in the scale space, determine the scale and position of the end point, then use the main tilt direction of the small neighborhood where the end point is located as the direction

feature of the target, and finally use the extreme point neighborhood gradient information. Generate feature-point descriptors with 128 dimensions. The SIFT algorithm generally has the following four main steps:

Step 1. Detect extreme points in the scale space.

In order to make feature points have scale invariance, the scale space is introduced. The scale space is an analysis method that convolves the original image with the function $G(x, y, \sigma)$ of different scales to map the original image to the scale space. The small scale can show the detailed features of the original image, and the large scale describes the general features of the original image [26, 27].

The scale space of a two-dimensional gray image is as follows:

$$
L(x, y, \sigma) = G(x, y, \sigma) * I(x, y),
$$

$$
G(x, y, \sigma) = \frac{1}{2\pi\sigma^2} e^{-\left((x^2+y^2)/2\sigma^2\right)}. \tag{12}
$$

$G(x, y, \sigma)$ is the scale-variable Gaussian function, $I(x, y)$ is the grayscale image of the original image, the symbol $*$ represents the convolution operation, (x, y) represents the position of the pixel in the image, and σ represents the scale space factor. The smaller the σ value, the smaller the corresponding scale, the more image details are retained. As σ gradually increases, the image is smoothed more and more, leaving only the overview of the image.

In order to efficiently detect stable feature points in the scale space, it is necessary to use the Gaussian difference function to project the source image into the difference scale space. The difference function is the difference between two kernels of different scales, defined as follows:

$$
D(x, y, \sigma) = (G(x, y, k\sigma) - G(x, y, \sigma)) * I(x, y),
$$

$$
= L(x, y, k\sigma) - L(x, y, \sigma). \tag{13}
$$

In the formula, k is a constant. In actual implementation, the subtraction of two adjacent scale images in the scale space $L(x, y, \sigma)$ is used to obtain the differential scale space $D(x, y, \sigma)$ because the subtraction operation greatly reduces the calculation amount.

Step 2. Screen and accurately locate feature points.

The detection in the previous step obtained a set of candidate feature points with scale invariance. However, these candidate feature points include some unstable feature points, such as points on the edges of low-contrast points, which are extremely susceptible to noise. Therefore, in this step, candidate feature points need to be screened to eliminate unstable feature points.

First, apply a quadratic function that accurately estimates the location and proportion of feature points based on the data around the candidate feature points and then is affected by noise such as "apply some simple points." For example, points with low contrast and curved edges are excluded from the threshold. Improve regulation stability and noise suppression.

To delete low-contrast candidate feature points, first fit a quadratic function according to the data around the candidate feature points to accurately estimate the position and proportion of the feature points:

$$D(X) = D + \frac{\partial D^T}{\partial X}X + \frac{1}{2}X^T\frac{\partial^2 D}{\partial X^2}X,$$

$$\hat{X} = -\frac{\partial^2 D^{-1}}{\partial X^2}\frac{\partial D}{\partial X}.$$

(14)

In the formula, $X = (x, y, \sigma)^T$ represents the offset of the original sample point.

Delete candidate feature points on the edge. Edge points usually have these characteristics. The curvature in one direction along the edge is small, and the curvature in the direction perpendicular to the edge increases. Therefore, if the principal curvature ratio is too large, edge points can be removed because the eigenvalues of the Hessian matrix are proportional to the principal curvature. Therefore, the principal curvature is calculated by the Hessian matrix. The complex matrix eigenvalues cannot be analyzed to improve the calculation efficiency, but the ratio matrix is calculated:

$$H = \begin{bmatrix} D_{xx} & D_{xy} \\ D_{xy} & D_{yy} \end{bmatrix},$$

$$\mathrm{Tr}(H) = D_{xx} + D_{yy} = \alpha + \beta,$$

$$\mathrm{Det}(H) = D_{xx}D_{yy} - (D_{xy})^2 = \alpha\beta,$$

$$\mathrm{ratio} = \frac{\mathrm{Tr}(H)^2}{\mathrm{Det}(H)} = \frac{(\alpha+\beta)^2}{(\alpha\beta)} = \frac{(\gamma\beta+\beta)^2}{\gamma\beta^2} = \frac{(\gamma+1)^2}{\gamma}.$$

(15)

The value of the ratio only depends on r and has nothing to do with the size of α and β. When $r = 1$ ($\alpha = \beta$), the ratio takes the minimum value; as r increases, the ratio also increases. Therefore, the edge points can be eliminated by ratio calculation.

Step 3. Specify the direction of feature points.

Due to the rotation invariance of the feature point descriptor, the main tilt direction of the pixel in the small local neighbor where the feature point is located is called the directional feature of the feature point. The small communities in this area are concentrated on the characteristic points, and the 1.5σ perimeter is a circle with a radius. Use the formula to find the gradient coefficient $m(x, y)$ and direction $\theta(x, y)$ of each pixel in the smaller local neighborhood:

$$m(x, y) = \sqrt{(L(x+1, y) - L(x-1, y))^2 + (L(x, y+1) - L(x, y-1))^2},$$

$$\theta(x, y) = \arctan\left(\frac{(L(x, y+1) - L(x, y-1))}{(L(x+1, y) - L(x-1, y))}\right).$$

(16)

In the formula, L is the scale space image of the feature point (scale is σ), and (x, y) is its coordinates.

Step 4. Generate local feature point descriptors.

A 16×16 rectangular area centered on the feature point and the feature point direction: use a function (which is a measure of variance feature points) to weight the gradient coefficient values of all pixels in the rectangular area, and divide a 16×16 area into 16 4×4 subareas. For each partition, you can use the same as in step 3..

2.5.2. SURF Algorithm. The SURF is a fast and powerful method for identifying and describing local invariant feature points. The overall thinking process of the SURF algorithm is similar to that of the SIFT algorithm, but the feature-point detection module uses a box filter to approximate the function and uses the integral image to speed up the convolution and calculation speed; in the feature point direction module, the radius is represented by 6σ (σ is the scale of the image where the feature point is located). The extreme value of the wavelet response of the Haar in the circle represents the direction of the feature point; in the feature-point description module, the sum of the horizontal and vertical Haar wavelet responses is relative to the feature point direction and the response. The sum of absolute values constitutes the descriptor vector [28].

The integral image is defined as follows:

$$I_{\Sigma}(x, y) = \sum_{i=0}^{i \leq x}\sum_{j=0}^{j \leq y} I(x, y).$$

(17)

In the formula, $I(x, y)$ is the original grayscale image and $I_{\Sigma}(x, y)$ represents the sum of all pixels in the matrix area with the image origin and point (x, y) as the diagonal vertices.

2.6. Three-Dimensional Modeling Technology. Virtual technology is realized by modeling in a virtual environment. Modeling is actually the real environment of simulation. Before modeling, use conventional radiation or laser scanning, take photos and other methods to obtain 3D data required for modeling, align them, and bring the aligned data into appropriate 3D modeling software to create virtual scene models [29].

2.7. Real Rendering Technology. In a virtual reality system, a certain sense of reality must be given to the virtual scene so that users can experience immersion. Therefore, the main task of photorealism reception is to simulate the visual characteristics of real objects, such as the optical properties, texture, smoothness, and other characteristics of the object surface, in order to maximize the final image effect of the real scene.

2.8. Human-Computer Interaction Technology. Virtual simulation technology can use input or output devices (such as helmet display technology, data globe, and data clothing) to obtain a free world for interacting with virtual objects, just like they are in the real world, but this is not very good. It can also interact with the body and limbs, including hands, ears, and knees, which is a natural interaction technology in a virtual environment. In recent years, some scientists are continuing to improve their existing interactive hardware and software to improve people's natural interaction in the virtual environment and, at the same time, strengthen research with new interactive methods. Gesture recognition, speech recognition, gaze tracking, and other interactive technologies have been widely used in virtual reality, and they are more common and convenient-focused interactive technologies.

3. Practical Application of Virtual Reality Technology in Rural Landscape Planning

This chapter is based on the Lumion platform and integrates the results of digital technology applications and research in various stages of rural landscapes. In a gradual process, a low-cost, high-efficiency, comprehensive digital virtual reality construction of rural landscapes can be realized. This method is not only the integration of the previous results but also the overall improvement of the protection of the rural landscape. Realization through the virtual reality platform cannot only better serve rural tourism and publicity but also improve the accuracy of rural protective planning and design, thereby effectively improving the implementation effect of protection projects.

3.1. Collection of 3D Information of Rural Landscape Architecture in a Certain Place

3.1.1. Surveying and Mapping Three-Dimensional Data. The measurement of data on the doors, windows, beams, etc., of rural buildings has two functions. One is to make postmodels, but to prepare for the digitalization of subsequent buildings. At this stage, the focus is on various data such as the plan, elevation, and section of the rural building, and even the high-definition digital camera is used to photograph the building, the surrounding environment, and some details, so as to have a reference when making the building model and scenery. According to the basis, in addition, some building structural components should be sketched by hand in order to better understand and refer to it later. In the measurement, we should not only pay attention to the rural building itself but also carry out some measurement work on the surrounding environment of the building. For example, do some understanding and related data work on the entire topography, landform of the village, and the greening situation around the village houses to pursue the artistic beauty of the rural landscape. In order to measure accuracy, expensive high-end measuring instruments, and advanced technical means must be used. For example, 3D laser scanning technology can be used to complete the acquisition of spatial information of historical buildings.

3.1.2. Photo Shooting of the Rural Landscape. The work at this stage is of great significance to the restoration of the later ancient buildings because the on-site photos can clearly and intuitively reflect any changes in the building and can also be used as basic materials for later restoration at any time, such as the compilation inside and the compilation of doors and windows. In addition, these photos can also be used as a reference for future building restoration. Through comparison, we found that the building can be restored to its original appearance through many details; therefore, in the shooting process, not only high-definition angle shooting, but also classified shooting; not only to distinguish the long-term view and the close-up view of the building, but also to pay attention to the exterior wall, structural form, etc. After shooting, number the photos in the texture map accordingly and even the detailed texture and plane CAD of brick structure, stone structure, ceramic tile, wood structure, etc. The graphs match, so the model will not cause confusion. At the same time, try to avoid obstacles blocking details, such as a surface that needs to be used as a texture. After completing this model, this is the only way to ensure the quality of texture photos and the difficulty and workload of processing textures.

3.1.3. Classifying and Summarizing the Information. This stage is mainly to sort and organize the data and pictures collected in the previous stages. First, classify the photos. The compilation objects include the following: historical pictures, architectural panoramas and landscapes, all building facades, individual building components, and inspection nodes are numbered according to certain rules. The next step is the surveying and mapping data. The principle of data sorting is to ensure that it is simple and clear, so as to prevent the production staff from seeing flowers. AutoCAD software can be used for drawing to accurately record the various data of the entity. Data classification also helps to improve the efficiency of team development and collaboration which is very useful for engineers after model making.

3.2. Establishment of a Three-Dimensional Model of the Rural Landscape. In the preliminary investigation stage of the thesis, we carried out detailed on-site surveying and mapping work, completed the field survey of the rural landscape, and obtained accurate plane and elevation data. Based on the CAD plan drawing, three-dimensional modeling can be developed. The author mainly uses Sketch Up and 3DSMAX 3D software for modeling and also uses Rhino software sparingly. Based on Sketch Up and 3DSMAX-based modeling methods and focusing on the characteristics of the two software, there are focused choices. Let us take the SketchUp modeling method as an example. The generated model is mainly surface. The advantage is that the file size is small and must meet a large number of models. The disadvantage is that the model is not very accurate, and the model is easy to cut and overlap lines. The model created using the 3DSMAX example is mainly based on points and lines, and the surface is optimized using points and lines. The model perfectly represents a high level of accuracy and detail. The disadvantage is that the model is large in size and occupies a lot of memory, which increases the computational pressure of computer hardware equipment. At the same time, the accuracy of CAD drawings is high during the modeling process. If there are heavy lines and nonclosed line segments in the drawings, it will cause the model to appear broken. At the same time, the commonly used modeling software is Rhino, which has high accuracy in the arc of the model and is often used in the modeling of industrial products. Rural buildings rarely have curved shapes, so they are not often used in architectural modeling.

3.2.1. Establishment of a Three-Dimensional Model of Traditional Houses Based on SketchUP. In the process of functional design and development, SketchUp modeling software considered the rapid modeling requirements of 3D software and introduced the concept of virtual reality development. According to the development of modeling functions, SketchUp software simplifies the details and accuracy of model processing in the modeling phase and emphasizes the speed and ease of use of modeling. Simple user interface and powerful function settings can significantly improve modeling efficiency and reduce the amount of computer calculations. The requirements for CAD drawings are also greatly reduced, so there is no need to provide a full set of drawings. In the actual operation, a rapid modeling and preliminary restoration plan is created according to the local conditions of the rural landscape and residential buildings; at the same time, in the process of coordinating the restoration, the communication opinions between the designer and the expert can also be directly used in the model creation and space modification, which greatly improves the work efficiency and realizes the rapid effect preview. In the development of virtual reality-based functions, SketchUp software provides powerful 3D visualization functions, which greatly enriches the visual presentation of the space and realizes timely preview of effects. At the same time, the functional architecture of virtual reality is also combined with the Internet platform, which can smoothly import files into the platform to establish a virtual display of models and real scenes, which greatly

improves the visual experience and establishes an intuitive effect display. It is very suitable for reuse when the country is fully digitalized to establish a virtual reality scene.

On the basis of the completion of the modeling work, the scale and structure of the model were adjusted many times, and the structural relationship of the model was explained as clearly as possible, and the connection method of the building construction was restored. Comparing the real-life photos in the original appearance of the countryside, attach the material to the white film to restore the authenticity of the houses.

3.2.2. Establishment of a Three-Dimensional Model of Traditional Houses Based on 3DSMAX. For the more complete protection of traditional dwellings and ancient building systems with the high historical value, the follow-up protection work should be done to maintain or optimize the current status quo as much as possible. After the implementation of physical protection measures, digital protection should also be carried out. To protect the residences of great significance, a thorough site survey and detailed data surveying and mapping are carried out to provide accurate data and reference systems for the later digital 3D modeling. Through the modeling of three-dimensional software, the later material rendering, effect debugging, the virtual imaging, and the restoration of the physical space are realized. Taking 3DSMAX modeling as an example, the model is more sleek, more segmented (the surface enclosed by points and lines can be automatically optimized), the model is highly accurate, the rendered image quality is excellent, and the picture is realistic. It meets the needs of high-quality modeling and is often used to make high-value digital 3D models of traditional houses.

In the process of creating the 3DSMAX model, relying on its fine segmentation and accurate data, the various modules of the object are restored one by one, and it is often used in the field of high-precision modeling. Through the comparison chart, it can be concluded that the 3DSMAX model, through the adjustment of the material and the simulation of the lighting environment, has clear picture quality and excellent effects, which vividly restore the original appearance of the countryside. Through the post-beautification processing of the image processing software Photoshop, a realistic real-life simulation is achieved. The rendered renderings are of practical significance for the guidance in the transformation process.

3.3. Establishment of Rural Virtual Reality Based on Lumion Technology. Lumion is a real-time 3D visualization tool for making movies or photos. Related disciplines include architecture, planning, and design. We can also provide live demonstrations. The advantage of Lumion lies in its ability to provide excellent images. It combines a fast and efficient workflow to save time, energy, and money, and people can create virtual reality on the computer. Lumion reduces production time by rendering high-resolution movies faster than ever, and the video shows how to create visualizations of amazing structures in seconds. In addition, you can

directly import, edit, and use files compatible with SketchUp and 3DSMAX files. In short, it provides ease of use, speed, low cost, and various functions that are very suitable for virtual roaming in the countryside.

3.3.1. Virtual Reality Scene Production.

SketchUp files are compatible with Lumion software. Act-3D adds more than 330 new objects, such as furniture, flags, and new cars. The existing character set has also been expanded to include multiple high-quality 3D animated characters, and the number of postprocessing effects, such as weather and artistic painting effects, has greatly increased. Through rapid rendering technology, even if you add more buildings, vegetation, mountains, and other landscape elements will not affect its fluency. As the principle of gradual progress, it strives to realize the comprehensive digitization of ancient villages at a lower cost, and it has huge technical advantages in terms of establishing the final operation platform of virtual reality scenes.

3.3.2. Importing the Overall Model into the Virtual Reality Platform.

Put the overall model established in Sketch Up software into proper order, save the dac format, and import it into Lumion software. There are many scenes on the Lumion platform that can be selected as the background, mainly the following typical scenes: valleys, rivers, hills and plains, nature, seascapes, etc. We can choose according to the needs of the object, such as the building scene in the countryside above us to choose a natural and idyllic plain and mountains as the background, and the "sky box" in virtual reality is very similar to this kind of scene.

3.3.3. Scene Optimization.

The postoptimization function of the Lumion software is relatively powerful. It can re-optimize the terrain scene imported in the early stage. For example, the terrain surface can be adjusted through the stretching function to make it rougher or smoother, or it can be made according to the nature of the terrain. The texture generates a scene close to the real geographical environment, which can be optimized to generate terraces that simulate rock walls or the terrain of villages surrounded by lakes.

3.4. Virtual Reality Scene Application.

Lumion is more flexible in operability and practical functions. Through the operation and editing of various functions in the virtual scene, we can feel more real in the digital virtual experience of the rural landscape. During the interaction, we can walk freely or take a certain means of transportation. The digital dynamic simulation of the rural landscape can be realized through repeated editing, and static or dynamic images can be generated.

3.4.1. Editing and Touring Based on Virtual Reality.

Lumion can completely inherit the materials contained in the SketchUp platform, their display effects are the same, and they can be optimized and edited repeatedly; in order to

distinguish objects, we can also import different solid color blocks in the SketchUp software, such as red, yellow, and blue so that it is clear at a glance. After completing the above steps, use the Lumion software to paste the material on the object. Since the calculation logic of the Lumion software platform is based on the same material as the basic selection unit for editing, it is necessary to distinguish objects of different materials in SketchUp. If the final effect after the material is pasted is quite different from the previous design, it can be optimized and modified on the Lumion platform.

After inserting the materials, there are two ways to obtain these plants, one of which comes from Lumion's own plant library. This plant library contains various buildings, cars, people, animals, streets, street decorations, soil, stones, etc., dynamic and static, with various shapes and colors, which can meet the needs of various scenes. Another way is to make it directly from SpeedTree. The advantage of this method is that it is more flexible and can satisfy some rare or unique plants, making the botanical library more abundant. These colorful botanical libraries bring great convenience to the later scene configuration and also assist the designer in the green design of the site. The scene is configured, and then, you can modify and adjust the model. There are two ways to choose. The first is to directly import the model components into the virtual reality scene, and the second is to modify the SketchUp scene model. The former method is restricted by the Lumion software and can only be placed in a scene that does not require high size, while the latter is relatively complicated, it must be operated under the logic of the SketchUp software and can be placed in some more precise sizes. Above, the two methods have their own advantages and disadvantages. These two methods cooperate with each other to achieve a perfect dynamic simulation of rural landscape renovation. For example, adding some landscape sketches to a certain scene can choose the first type, which is convenient and easy to implement; for example, the second method can be used to demolish privately constructed buildings, which can be accurately presented and can facilitate analysis and research. Through the use of virtual reality technology, the real scene of the rural landscape can be greatly restored, and through this interactive control process, a tour of the detailed scene of the rural landscape and the overall environment can be realized.

3.4.2. Static Image Rendering and Animation Production Based on Virtual Reality.

Compared with other 3D software, Lumion has a faster rendering speed, and the rendering time under the same conditions is ten times faster than other software, which greatly improves work efficiency. It also has a night-vision rendering system that can turn into a beautiful night sky scene with dim moonlight and sky. Another function of the rendering engine is to improve the sound mapping and light occlusion in the screen area. The Act 3D demo scene looks good.

3.4.3. Experimental Experience Detection Stage.

When the virtual roaming system is installed by default, users should be able to test the entire system based on experimental

experience, such as swelling detection. The user's actions and the movement of objects in the virtual environment will cause frequent expansion between objects, and the corresponding collision response will be calculated, and the screen result can be updated. Otherwise, an intrusion will occur between objects. When problems occur, timely feedback and corrections are required to ensure the authenticity of the final roaming environment.

4. Application Analysis of Virtual Reality Technology in the Analysis of the Three-Dimensional Assessment System of Zural Landscape Planning

4.1. Performance Comparison of Feature Point Extraction Algorithms. In order to find a universal feature point extraction algorithm, this experiment will compare the SIFT algorithm and the SURF algorithm from three aspects: the number of feature points extracted by the algorithm, the time required for the algorithm, and the number of correct matching point pairs. The images used in the experiment are all extracted from the video taken by the camera. The video is captured by the camera in indoor and outdoor environments. In order to make the data comparable, the same feature point matching algorithm is used to match the feature points extracted by the SIFT and SURF in the experiment. For details, see Tables 1 and 2 and Figures 1 and 2.

It can be seen from Table 1 and Figure 2 that, in the SHIFT algorithm, the number of correct matching points in the first group is 114, the second group has 55 matching points, and the third group has 13 correct matching points. The longest time for the second group B was 1.187 seconds, and the shortest time was 0.5 second for the third group A. In summary, the number of feature points extracted by the SIFT algorithm and the number of correct matching points are large, but it takes longer.

It can be seen from Table 2 and Figure 3 that, in the SURF algorithm, there are 62 correct matching points in the first group, 28 matching points in the second group, and 4 correct matching points in the third group. The longest time for the second group and the first group was 0.203 seconds, and the shortest time was 0.109 seconds for the third group A. All in all, the number of feature points and correct matching points extracted by the SURF algorithm is not large, but they do not take time.

In order to compare and analyze more intuitively, which of the SURF algorithm and the SIFT algorithm runs faster, compare the correct matching points and the required time of the two algorithms, respectively, as shown in Figure 4.

The comparative analysis shows that the SURF runs faster than the SIFT algorithm, and in the panorama image generation process, when the image quality is good, the number of effective feature points it can detect can meet the requirements of estimating model parameters. Therefore, the SURF can be used as a feature point detection method.

4.2. Experience Test Analysis of the Virtual Roaming System in Rural Landscape

4.2.1. Basic Situation of the Tester. In order to carry out the experience test analysis of the virtual roaming system in rural landscape, 25 people were randomly selected as experimental subjects in a certain village, and 5 of them were 0–18 years old (including 3 males and 2 females); 3 males 5 the age group is 18–28 years old (including 2 males and 3 females);5 of them were 18–28 years old (including 2 males and 3 females); 5-person age group is 38–48 years old (including 3 males and 2 females), and 5 people are over 48 years old (including 4 males and 1 female), see Table 3 and Figure 5.

4.2.2. The Tester's Experience of the Rural Landscape Virtual Roaming System. This experiment is based on the rural landscape virtual-roaming system of a village, randomly selecting 25 people (divided into 5 groups of 5 people) in batches to enter the system with a real reduction degree of 30%, 45%, 60%, 75%, and 80% for the testing experiment. The true reduction degree of the first group is 30%; the true reduction degree of the second group is 45%; the true reduction degree of the third group is 60%; the true reduction degree of the fourth group is 75%; the true reduction degree of the fifth group is 80%. Test the average stay time of 20 people in the system, the number of people who found the penetration phenomenon, and the number of people who returned to the origin. The test data is shown in Table 4.

It can be seen from Table 4 that the average stay time of the first group was 2 minutes, and 5 people were found to have penetrated the system, and 1 person returned to the original point; the average stay time of the second group was 3.5 minutes, and 3 people were found to have penetrated the system. 1 person returned to the origin; the average stay time of the third group was 5 minutes, and 2 persons were found to have penetrated the system, and 2 persons returned to the origin; the average stay time of the fourth group was 8 minutes, and 1 person was found to have found the penetration phenomenon, and 3 persons returned to the origin; the average stay time of the fifth group was 8 minutes, and 1 person was found to have penetrated the system, and 4 people returned to the original point.

It can be seen from Table 4 and Figure 6 that when the real reduction degree of the system goes from low to high, the average stay time of people is longer. When the real reduction degree is as high as 80%, the average residence time is 8 minutes;the real reduction degree of the system at that time increased from low to high, the number of people who found penetration in the system gradually decreased. When the true reduction degree was as high as 75%, the number of people who found the penetration phenomenon was 1; when the true reduction degree of the system went from low to high, the number of people returning to the original point gradually increased; when the true reduction degree is as high as 80%, there are 4 people returning to the original point. In summary, with the increase in the degree of realism in the rural landscape virtual-roaming system, it is

TABLE 1: The effect of the SIFT on extracting feature points.

		Number of feature points	Time required (s)	Number of correct matches
No. 1	A	556	1.094	114
	B	472	0.969	
No. 2	A	724	1.187	55
	B	437	0.828	
No. 3	A	206	0.500	13
	B	257	0.578	

TABLE 2: The effect of SURF on extracting feature points.

		Number of feature points	Time required (s)	Number of correct matches
No. 1	A	226	0.203	62
	B	263	0.203	
No. 2	A	158	0.141	28
	B	146	0.140	
No. 3	A	95	0.109	4
	B	120	0.125	
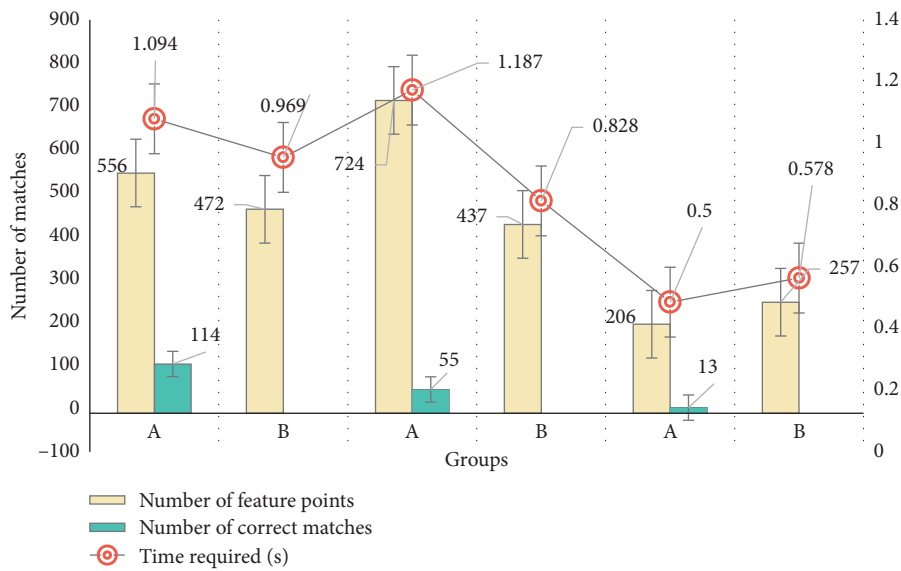
FIGURE 2: The effect of the SIFT on extracting feature points.
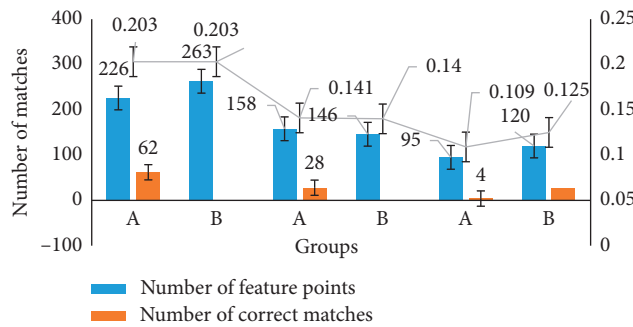
FIGURE 3: The effect of the SURF on extracting feature points.
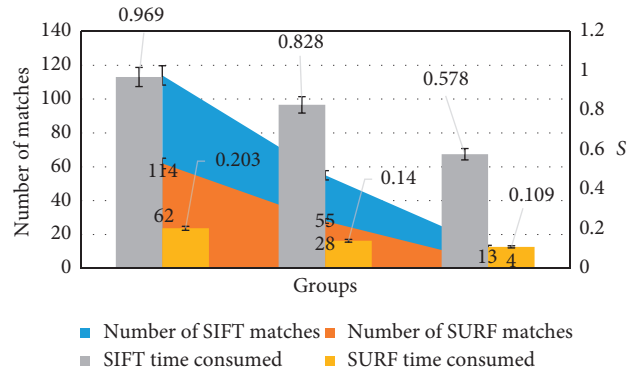
Figure 4: Comparison of the SIFT algorithm and SURF algorithm.

Table 3: Age group of testers.

	0–18 years old	18–28 years old	28–38 years old	38–48 years old	Over 48 years old
Male	3	2	1	3	4
Female	2	3	4	2	1
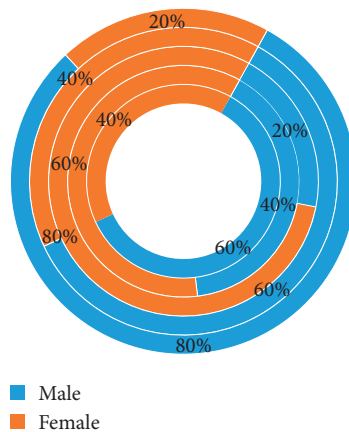
Figure 5: Age group of testers.

Table 4: Experience analysis of the virtual roaming system in rural landscape.

	Average residence time	Found penetration	Back to the start
No. 1	2	5	1
No. 2	3.5	3	1
No. 3	5	2	2
No. 4	8	2	3
No. 5	8.5	1	4

extremely difficult for people to find out whether they are in virtual or reality, and their immersion in virtual reality is getting deeper and deeper. This test also confirmed the superiority of the virtual roaming system in rural landscapes, and the experience is extremely effective.

4.2.3. Survey of Satisfaction of Testers on Experience of the Virtual Roaming System in Rural Landscape. In order to further understand the tester's satisfaction with the experience of the virtual roaming system in rural landscape, 25 people who were tested were divided into groups to conduct a questionnaire survey and scored at the true reduction degree of 30%, 45%, 60%, 75%, and 80%. The score includes authenticity, interaction, immersion, functionality, usage, expansion, and satisfaction (the lowest score for each item is 0 point, and the highest score is 10 points). See Table 5 and Figure 7 for details.
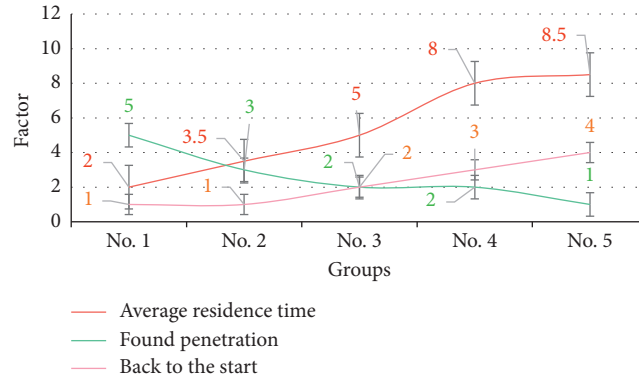
Figure 6: Experience analysis of the virtual roaming system in rural landscape.

Table 5: Testers' satisfaction with system experience.

	Trueness	Interaction	Immersion	Functionality	Usage	Expansion	Satisfaction
No. 1 (30%)	1	2	1	1	0	0	1
No. 2 (45%)	2	2	1	1	1	1	2
No. 3 (60%)	5	4	3	3	5	3	5
No. 4 (75%)	7	6.5	5.5	5	7	6	6
No. 5 (80%)	8.5	9	7.5	6	7	8	9
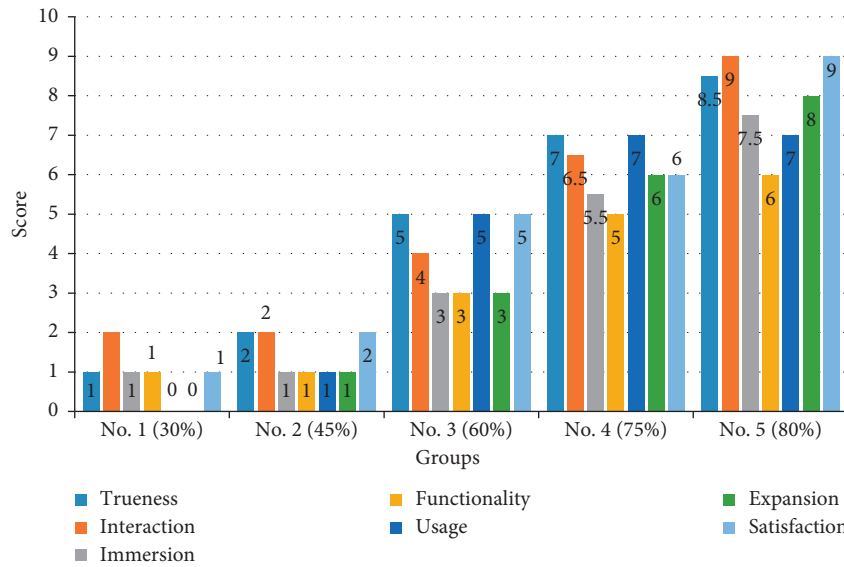
Figure 7: Testers' satisfaction with system experience.

From Table 5, it can be concluded that when the true reduction degree is 30%, the tester scores 1 point for authenticity, 1 point for interaction, 1 point for immersion, 1 point for functionality, and 1 point for functionality. The expansion score is 0 points, and the satisfaction score is 1 point; when the true reduction degree is 45%, the tester scores 2 points for authenticity, 2 points for interaction, and 1 point for immersion. The function score is 1 point, the function score is 2 points, the expansion score is 2 points, and the satisfaction score is 2 points; when the true reduction degree is 60%, the tester's authenticity score is 5 points, the degree of interaction score is 4, the immersion

score is 3, the functional score is 3, the functional score is 5, the expansion score is 3, and the satisfaction score is 5; when the true reduction is 75%, the test participants rated authenticity as 7 points, interaction score as 6.5 points, immersion score as 5.5 points, function score as 5 points, function score as 7 points, expansion score as 7 points, and satisfaction score as 7 points; when the true reduction degree is 80%, the tester's authenticity score is 8.5 points, the interaction score is 9 points, the immersion score is 7.5 points, the function score is 6 points, the function score is 7 points, the degree of expansion score is 8 points, and the satisfaction score is 9 points.

It can be seen from Table 5 and Figure 7 that when the true reduction degree of the system goes from low to high, people's satisfaction is higher. When the true reduction degree is as high as 80%, the satisfaction level is as high as 9 points; when the true reduction degree of the system goes from low to high, people's sense of immersion is getting deeper and deeper. When the true reduction degree is 30%, the lowest score for immersion is 1 point; when the true reduction degree is 80%, the lowest score for immersion is 7.5 points; the true reduction degree of the system decreases to low when it reaches high levels, and people's interaction becomes stronger and stronger. When the true reduction degree is 30%, the lowest score for interaction is 2 points; when the true reduction degree is 80%, the lowest score for interaction is 9 points; the survey shows that with the increase in the degree of true restoration of the rural landscape virtual-roaming system, people's ratings of the system also increase. At the same time, it has once again confirmed that the system has a very obvious effect on rural landscape planning.

5. Conclusion

In terms of the landscape design, virtual reality technology has a great future. Although current examples of the application of virtual reality technology are not common, the core ideas of the landscape project design are clarified, the characteristics of virtual reality technology are better utilized, and landscape design is actively constructed. After the platform and in-depth exploration of the simulated landscape design, it can promote the process of combining virtual reality technology with the landscape design, making this technology more comprehensive for the landscape design work.

Based on the Lumion platform, this paper has developed a rural landscape planning three-dimensional evaluation system by integrating virtual and three-dimensional panoramic technologies. In the process of gradual application research, a low-cost, high-efficiency rural landscape comprehensive digital virtual reality construction has been realized.

Landscape planning has a strong demand for visualization technology, and virtual reality technology has a huge application space in both urban planning and rural planning. The unique immersion and interactivity of virtual reality technology can enable planning departments, developers, technicians, designers, and ordinary people observe the results of future plans from all angles, allowing users to better grasp the scale and scope of urban planning and also allow customers to better understand design intent and design ideas and modify the unsatisfactory nodes in the design and planning in the environment. It is useful for planning and managing large projects. Designers and managers are also encouraged to modify the design plan and add it to the design in the future to detect design errors and avoid design risks.

Data Availability

No data were used to support this study.

Conflicts of Interest

The authors declare that they have no conflicts of interest.

Authors' Contributions

Both authors contributed equally to this work.

References

[1] Y. Tang, W. Feng, W. Feng, J. Chen, D. Bao, and L. Li, "Compressive properties of rubber-modified recycled aggregate concrete subjected to elevated temperatures," *Construction and Building Materials*, vol. 268, Article ID 121181, 2021.

[2] X. Ding, "A new development model of rural landscape planning and design for pastoral complex," *Modern Decoration (Theory)*, vol. 392, no. 5, pp. 80–93, 2016.

[3] Y. Z. Tian, "Analysis of rural landscape planning under the background of beautiful rural construction," *China Agricultural Resources and Regional Planning*, vol. 37, no. 9, pp. 229–232, 2016.

[4] Z. J. Huang, D. Xue, and J. P. Guo, "Rural landscape planning and design under the background of beautiful rural construction," *Forestry Investigation and Planning*, vol. 43, no. 222, pp. 135–140, 2018.

[5] Q. P. Zhao, B. Zhou, and J. Li, "Research progress of virtual reality technology," *Science & Technology Review*, vol. 34, no. 14, pp. 71–75, 2016.

[6] P. Wang, T. Yao, Z. Li et al., "A superhydrophobic/electrothermal synergistically anti-icing strategy based on graphene composite," *Composites Science and Technology*, vol. 198, Article ID 108307, 2020.

[7] Z. Yan and Z. Lv, "The influence of immersive virtual reality systems on online social application," *Applied Sciences*, vol. 10, no. 15, p. 5058, 2020.

[8] Y. Xiao, X. L. Xu, and Y. Zhai, "Design of hand function rehabilitation evaluation training system based on virtual reality technology," *Chinese Rehabilitation Theory and Practice*, vol. 22, no. 3, pp. 341–344, 2016.

[9] D. D. Zhang, S. Q. Gao, and Y. X. Li, "Research on the three-dimensional digital landscape roaming of campus—taking Northeast Forestry University as an example," *Heilongjiang Science*, vol. 9, no. 9, pp. 72-73, 2018.

[10] J. L. Ding, "Application of virtual reality technology in landscape design," *Information and Computer*, vol. 31, no. 21, pp. 13–16, 2019.

[11] D. W. Zhang and N. N. Yao, "Research on application of virtual reality technology in environmental art design," *Art Technology*, vol. 30, no. 10, p. 292, 2017.

[12] R. H. Wang, "On the application of virtual reality technology in environmental art design," *Art Education*, vol. 282, no. 2, pp. 212-213, 2016.

[13] Z. Y. Ding, "Statistical analysis of virtual reality technology landscape design application papers," *Journal of Ezhou University*, vol. 23, no. 3, pp. 100–102, 2016.

[14] J. F. Lu, Z. P. Wang, and H. J. Jin, "The application of 3D laser scanning and virtual reality technology in urban landscape," *Laser Magazine*, vol. 40, no. 7, pp. 174–178, 2019.

[15] T. Q. Sun, "Research on the combination of landscape design and virtual reality technology," *Satellite TV and Broadband Multimedia*, vol. 503, no. 22, pp. 23-24, 2019.

[16] L. B. He, Y. Feng, and Y. L. Xu, "Application of virtual reality technology in the teaching of landscape architecture

engineering course," *Abstracts of Chinese Horticulture*, vol. 32, no. 7, pp. 218–220, 2016.

[17] M. Zhu and J. J. Zhang, "The impact of virtual reality technology (VR) on the field of landscape design," *Beauty and Times (Part 1)*, vol. 712, no. 8, pp. 80-81, 2017.

[18] M. Elhoseny and K. Shankar, "Reliable data transmission model for mobile Ad Hoc network using signcryption technique," *IEEE Transactions on Reliability*, vol. 69, no. 3, p. 1077, 2020.

[19] S. Y. Wang and D. Z. Wu, "Application of virtual reality technology in the teaching of landscape architecture design," *China Forestry Education*, vol. 37, no. 3, pp. 51–55, 2019.

[20] J. Tian, "Application of virtual reality technology in architectural landscape design," *Journal of Shandong Institute of Agricultural Engineering*, vol. 37, no. 205, pp. 17–19, 2020.

[21] L. Q. Song, "Application scenarios and functional requirements analysis of landscape design based on virtual reality technology," *West China Leather*, vol. 41, no. 463, p. 55, 2019.

[22] L. Tao, "Application of virtual reality technology to architectural landscape design," *China Housing Facilities*, vol. 186, no. 11, pp. 97-98, 2018.

[23] L. Gao and Q. Shi, "Analysis of environmental art design based on virtual reality technology," *Architecture Science*, vol. 36, no. 270, p. 154, 2020.

[24] B. W. Liu and L. Lin, "Analysis on the application of ecological concepts in rural landscape planning: taking Beizhuang town, Miyun district, Beijing as an example," *Art Science and Technology*, vol. 33, no. 12, pp. 83–86, 2020.

[25] G. Y. Niu, L. N. Sun, and A. J. Dong, "Research on the theory and practice of rural landscape planning and design," *Chinese Agricultural Science Bulletin*, vol. 33, no. 24, pp. 129–136, 2017.

[26] H. B. Chen, J. Zheng, and R. Y. Fei, "Typical applications of virtual reality technology in power systems," *Power System and Clean Energy*, vol. 32, no. 2, pp. 25–30, 2016.

[27] X. Liu, "Rural landscape planning and design methods under the background of beautiful rural construction," *Journal of Shandong Institute of Agricultural Engineering*, vol. 33, no. 6, pp. 136-137, 2016.

[28] L. Zheng and G. Y. Li, "Research on rural landscape planning from the perspective of regional culture—taking Chengdu bamboo art village as an example," *Sichuan Agricultural Science and Technology*, vol. 379, no. 4, pp. 63–65, 2019.

[29] Z. Liu, "The relationship between rural landscape planning and new rural construction," *Agricultural Engineering*, vol. 7, no. 4, pp. 75-76, 2017.

Research Article

Athlete's Physical Fitness Prediction Model Algorithm and Index Optimization Analysis under the Environment of AI

Liqiu Zhao,[1] Yuexi Zhao,[2] and Xiaodong Wang [ID][3]

[1]*Ministry of Quality Education, Jiangsu Vocational College of Electronics and Information, Huai'an 223003, Jiangsu, China*
[2]*School of Economics, Minzu University of China, Beijing 100000, China*
[3]*Shool of Physical Education, Shaoguan University, Shaoguan 512000, Guangdong, China*

Correspondence should be addressed to Xiaodong Wang; wangxiaodong@sgu.edu.cn

With the rapid progress of network technology and computers, the Internet of Things has slowly entered people's lives and work. The Internet of Things can bring a lot of convenience to people's lives and work. People have been living in a networked era, and communications, computers, and network technologies are changing the entire human race and society. The extensive application of databases and computer networks, coupled with the use of advanced automatic data collection tools, has dramatically increased the amount of data that people have. There are many important information hidden behind the surge of data, and people hope to conduct higher-level analysis on it in order to make better use of these data. This article mainly introduces the prediction model algorithm and index optimization analysis of athletes' physical fitness under the Internet of things environment. This paper proposes an algorithm and index optimization method for the athletes' physical fitness prediction model in the Internet of Things environment, which is used to conduct athletes' fitness prediction model algorithm and index optimization experiments in the Internet of Things environment, and designs steps for athletes' physical fitness prediction in the Internet of Things environment to lay a solid foundation for related applications of athlete index optimization. The experimental results in this article show that the prediction accuracy rate of the professional group with the athlete's physical fitness prediction model and index optimization under the Internet of Things environment is higher than that of the control group, with a difference $p < 0.001$.

1. Introduction

The Internet of Things is an emerging global Internet-based information service architecture. It is a communication protocol based on international standards. It is the development trend of modern networks and the integration of future networks. It is a global dynamic network facility with self-configuration capabilities. People use terminals to seamlessly access the human-computer interaction interface of the Internet of Things, thereby achieving the goal of resource sharing.

As early as 2010, it was proposed that the Internet of Things is based on the sensor network as the underlying infrastructure. According to the Internet of Things protocol family specified by the International Organization for Standardization, each item in the access network is connected to the network for information communication and resource sharing. Realize a highly intelligent network system, and the Internet of Things is an extension and expansion of the existing Internet. The Internet of Things generally uses wireless networks to achieve communication. According to the survey, there are thousands of Internet of Things devices around each person. The Internet of Things may contain five to one trillion items. The Internet of Things uses electronic tags under radio frequency identification technology to number real objects one by one. From a book to a car, as long as they are connected to the Internet, their specific location and related information can be found on the Internet of Things.

Gerpott's research attempted to provide a basis for evaluating the effectiveness of IoT-enhanced forecasting in the context of existing forecasting models. Currently, many

experts consider merging IoT components to achieve forecasting advantages, thereby revising or expanding its scope and algorithm portfolio. However, unsystematic automatic connection of sensors and actuators in existing models does not necessarily lead to predictive success. Gerpott's approach is to determine the different roles that IoT components can play in predictive models. It can be achieved by combining models and algorithms with IoT components to clarify the development goals of IoT predictive models and report case examples. These examples help to highlight how to achieve the development goals of predictive models through IoT components fulfilling specific roles. Gerpott believes that when IoT components are integrated into predictive models, there may be three different functions. The functional distinction is essential to understand how IoT corrections can help relevant personnel to achieve predictive model development goals. The starting point and foothold of this research are good and sufficient, but it lacks examples to support [1]. Burg believed that wireless sensors and actuators connected through the Internet of Things are crucial to the design of athletes' fitness prediction models. In this complex heterogeneous system, the transmission link must meet stringent requirements for data throughput, delay, and range, while also complying with strict energy budgets and providing a high level of security. Burg first summarized the principle of wireless communication from the perspective of the Internet of Things and the predicted connection needs of athletes. Based on these principles, the most relevant wireless communication standards will be reviewed before focusing on the key security issues and functions of such systems. In particular, Burg pointed out the gap between the security functions in the communication standards used in the Internet of Things and athlete fitness prediction models and their actual vulnerabilities through examples and emphasized the need for more in-depth research on security issues at all protocol layers, including logical layer security and physical layer security. Although this method provides examples for proof, the examples are not typical enough [2]. Yang introduced some audit programs through investigation and research to ensure the completeness and validity of athletes' physical fitness prediction data and analyzed the program and found some safety flaws. First of all, individual models cannot retain the privacy of shared data in cloud storage; in addition, analysis shows that the data in the predictive model are vulnerable to integrity forgery attacks, and malicious cloud servers can perform the forgery attacks, even if there is no correct data storage. A malicious cloud server can forge seemingly valid prediction data for any prediction instruction. Then, Yang determined that the main reason for insecurity was that the linear combination of randomly sampled data was not properly shielded; finally, Yang proposed an improvement to the audit program while retaining data privacy and perfect index optimization, while bringing the best prediction results and calculation overhead. This research data support is relatively sufficient, but the use cost is high, which is not conducive to popularization [3].

The innovations of this article are as follows: (1) research methods for the athletes' physical fitness prediction model in the Internet of Things environment, including literature retrieval, expert survey, logical analysis, and mathematical statistics, are proposed (2) clustering algorithms for the athletes' fitness prediction model are proposed; and (3) fuzzy support vector regression is proposed.

2. Athlete's Physical Fitness Prediction Model Algorithm and Index Optimization Method in the Internet of Things Environment

2.1. Method of Athlete's Physical Fitness Prediction Model in Internet of Things

2.1.1. Document Retrieval Method. A large number of documents are searched and sorted through related academic websites such as CNKI, master and doctoral dissertation database, Baidu Academic, and Springer. The keywords are Internet of Things, athletes, physical fitness, specific physical fitness, index optimization, prediction models, and so on, and focus on collecting information relevant literature data on physical fitness prediction models provides forward-looking primary material for related research in this article [4].

2.1.2. Expert Investigation Method. On the basis of consulting the relevant literature and summarizing it, using the expert survey method, by issuing questionnaires to relevant experts, the framework of the athlete's specific physical fitness test model is initially constructed [5]. The final result of this article is to collect data from three rounds of expert questionnaires and combine expert opinions to scientifically and reasonably construct an athlete prediction model under the Internet of Things environment [1]. The main selected experts are national coaches and national referees who have been engaged in sports training and practice for a long time and professors who have been doing research in the field of competitive sports [6]. After the questionnaire is distributed to the expert group, the first round of collected questionnaires is counted and analyzed, and then the second round of questionnaires is formulated for distribution, and then the third round of questionnaires is distributed. Finally, the three rounds of questionnaires are sorted and analyzed. Our experience screens out reasonable prediction model algorithms and determines the type of physical fitness test required for fitness prediction [7].

2.1.3. Logic Analysis Method. Through the analysis of sports items, refer to the existing literature and related materials, carry out creative thinking, formulate indicators that meet the specific physical fitness of competitive athletes, and use logical analysis methods such as summary, induction, and synthesis to provide feedback from experts to construct athletes, and analyze, organize, and draw relevant conclusions and suggestions based on the physical fitness prediction model [8].

2.1.4. Mathematical Statistics. Mathematical statistics is divided into factor analysis and structural equation model analysis. Factor analysis is to use a certain amount of partial

factors to reflect most of the information content of the raw materials in order to achieve the basic structure of the factor and simplify the data [9]. Through factor analysis, common factors can be extracted from highly correlated observed variables, and the number of common factors also represents the basic structure of scale [10]. In order to verify the structure of various indicators of the expert survey method, this paper uses the principal component analysis method to make up for the subjective deficiencies of the expert survey method [11]. In scientific research, variables that do not have direct measurement operability are called latent variables. However, latent variables can be reflected indirectly by finding some objective variables [12]. Traditional statistical analysis and statistical results will always be interfered by the measurement errors of independent variables. Although traditional statistical methods can also handle measurement errors, they cannot accurately explain the relationship between variables [13]. Structural equation models can deal with errors and structural relationships between latent variables. This paper uses SPSS22.0 software to perform relevant statistical analysis on different items in the test and the collected data [14].

2.2. Athlete's Physical Fitness Prediction Model Clustering Algorithm.

Predicting physical fitness of athletes is also a kind of data collection and mining. The clustering algorithm divides objects in the database into multiple classes or clusters and finds useful information from them [15]. Data clustering makes the data objects in the same cluster as similar as possible, and the data objects in different clusters are as different as possible. Data clustering has very important applications in many fields, such as pattern recognition, information retrieval, e-commerce, marketing, and document classification [16]. In many applications, the data objects in a cluster can be treated as a whole [17]. Through clustering, it is possible to identify dense and sparse regions, thus discovering global distribution patterns and interesting correlations between data attributes [18]. In the field of data mining, research work has focused on finding appropriate methods for effective and practical cluster analysis of large databases, and the research topic has focused on the scalability of clustering methods [19]. The effectiveness of the method for clustering complex shapes and types of data, high-dimensional clustering analysis techniques, and clustering methods for mixed numerical and categorical data in large databases is focused [20]. The general method of clustering is to first define the distance between objects and then use an appropriate algorithm to cluster according to the calculated distance between objects. It can be roughly divided into division method, hierarchical method, density-based method, and grid-based method. It can be roughly divided into division method, hierarchical method, density-based method, grid-based method, and model-based methods [21, 22]. The most commonly used distance measurement methods include Euclidean distance, Manchester distance, and Mincos distance. The formulas are expressed as follows:

$$
\begin{aligned}
d(i, j) &= \sqrt{\left|x_{i_1} - x_{j_1}\right|^2 + \left|x_{i_2} - x_{j_2}\right|^2 + \Lambda + \left|x_{i_p} - x_{j_p}\right|^2}, \\
d(i, j) &= \sqrt{\left|x_{i_1} - x_{j_1}\right| + \left|x_{i_2} - x_{j_2}\right| + \Lambda + \left|x_{i_p} - x_{j_p}\right|}, \\
d(i, j) &= \sqrt{\left|x_{i_1} - x_{j_1}\right|^q + \left|x_{i_2} - x_{j_2}\right|^q + \Lambda + \left|x_{i_p} - x_{j_p}\right|^{1/q}}.
\end{aligned}
\tag{1}
$$

If each variable is assigned a weight ω_i according to its importance, then the weighted distance has the following calculation relationship:

$$
d(i, j) = \sqrt{\omega_1\left|x_{i_1} - x_{j_1}\right|^2 + \omega_2\left|x_{i_2} - x_{j_2}\right|^2 + \Lambda + \omega_p\left|x_{i_p} - x_{j_p}\right|^2}.
\tag{2}
$$

2.3. Fuzzy Support Vector Regression.

Given a training sample $A = \{(x_1, y_1), (x_2, y_2), \ldots, (x_m, y_m)\}, y_i \in \{-1, 1\}$, where x_i is the feature vector of the i-th sample and y_i is the sample label. In the sample space, the classification hyperplane can be expressed by the following formula:

$$
W^T x + b = 0.
\tag{3}
$$

In this formula, W is the normal vector that determines the direction of the hyperplane and b is the displacement term that determines the distance between the hyperplane and the origin. To determine a classified hyperplane is to determine W and b [23]. In order to correctly classify all samples and have the classification interval, the following relationship needs to be satisfied:

$$
y_i \lfloor W^T x_i + b \rfloor \geq 1, \quad i = 1, 2, \ldots, m.
\tag{4}
$$

The optimal classification hyperplane is to maximize the sum of this distance, so the problem of finding the optimal hyperplane is transformed into the following:

$$
\begin{aligned}
&\min_w \frac{1}{2}\|W\|^2, \\
&\text{s.t. } y_i\left[W^T x_i + b\right] \geq 1, \quad i = 1, 2, \ldots, m.
\end{aligned}
\tag{5}
$$

In order to avoid the influence of abnormal points on the classification hyperplane and also to avoid over-fitting of the model, with the help of the idea of soft interval, slack variables are introduced to complete, and the range of errors is controlled by the regularization constant C [24, 25]. Then, $\min_w (1/2)\|W\|^2$ has the following relationship:

$$
\min_w \frac{1}{2}\|W\|^2 + C \sum_{i=1}^{m} \xi_i, \xi > 0.
\tag{6}
$$

In the traditional support vector machine, because each sample point has the same impact on the classification hyperplane, the accuracy of the model is greatly reduced when facing noise points [26]. Fuzzy support vector machine combines the idea of membership in fuzzy set with support

vector regression and gives each sample point a membership S_i through the membership function [27]. Due to the different degree of membership, each sample point has a different slack variable, so the problem of noise point interference is solved to a certain extent, and the predictive ability of the model is improved. Lagrange coefficient is introduced. At this time, the following relationship exists:

$$f(x) = \sum_{i=1}^{m} (\alpha_i^*) k(x, x_i) + b. \tag{7}$$

The degree of membership can be expressed as a function of time:

$$S_i = f(t_i). \tag{8}$$

In the research process of this paper, it is hoped that the data closer to the prediction point will play a more important role in the regression prediction process. The membership function can be expressed in the form of a quadratic function. The formula is as follows:

$$S_i = (1 - \phi)\left(\frac{t_i - t_1}{t_1 - t_2}\right) + \phi. \tag{9}$$

For the evaluation of prediction results, two main conditions should be considered: one is that the observation value should fall into the prediction interval as much as possible; the other is that the range of the prediction interval should be as small as possible [28, 29]. According to these two conditions, two evaluation indicators can be defined: coverage (Coverage) and interval width (width). The relationship is expressed as follows:

$$\text{Coverage} = \frac{1}{n} \sum_{i=1}^{n} \text{count}_i,$$

$$\text{count}_i = \left\{ \begin{array}{ll} 1, & \widehat{x}_i^{\text{low}} < x_i < \widehat{x}_i^{\text{up}} \\ 0, & \widehat{x}_i^{\text{low}} > x_i \text{ or } \widehat{x}_i^{\text{up}} < x_i \end{array} \right\}, \tag{10}$$

$$\text{width} = \frac{1}{n} \sum_{i=1}^{n} \sqrt{\left(\widehat{x}_i^{\text{low}} - x_i\right)^2 + \left(\widehat{x}_i^{\text{up}} - x_i\right)^2}.$$

For the method part of this article, the above methods are used to study the algorithm and index optimization of the athlete's physical fitness prediction model under the Internet of Things environment. The research is carried out according to the Internet of Things, physical fitness prediction, prediction model, index optimization, and so on. The technical process is shown in Figure 1.

3. Athlete's Physical Fitness Prediction Model Algorithm and Index Optimization Experiment in the Internet of Things Environment

3.1. Design the Steps of Athlete's Physical Fitness Prediction in the Internet of Things Environment

3.1.1. Selection of Physical Fitness Evaluation Indicators. The design of the index system must have the function of reflecting the evaluation goal. In a scientific attitude, we

must follow the basic design principles, directional principles, objectivity, feasibility, independence, and comprehensiveness principles in the indicator design process, and the principle of consistency. And, the design of the evaluation index system is carried out in accordance with the following procedures: clarify the evaluation object; determine the evaluation target; propose preliminary indicators; screen the preliminary indicators; assign index weights; prepare evaluation standards; constitute an indicator system; conduct trial evaluations; and modify and improve the system.

3.1.2. Classification of Physical Fitness Test. According to the expert survey method in the previous method, the specific physical fitness test categories for athletes determined after interviews with experts include BMI, fitness percentage, Quetelet index, weight, forearm tight circumference, forearm relaxed circumference, waist circumference, chest circumference, height, hand length, foot length, leg length, arm span, heart rate, vital capacity, maximum oxygen uptake, 30 squats in 30 seconds, step test, 50-meter run, select reaction time, rapid tapping with both hands, rapid footing in sitting posture, grip strength, 1 min sit-ups, standing long jump, vertical jump, push-ups, pull-ups, flexion arm hang, parallel bars flexion and extension, 2000-meter run, 15-second standing ups, cross quadrant jump, cross change running, repeated side steps, and round trip running 20 meters × 4, sitting forward bending, standing forward bending, front and rear splitting, left and right splitting, shoulder turning, standing experiment, horizontal stepping on wood, stepping with closed eyes, and dynamic balance (walking in a straight line) and are organized into tables according to related categories, as shown in Table 1.

3.1.3. Screening of Physical Fitness Evaluation Indicators. The number of evaluation indicators initially proposed is generally large. Because of the fear of missing important factors, the indicators are confusing and cannot reflect the essential characteristics of the evaluation object. Indicators that contain contradictions and causality should be combined and classified, and they should be selected, to retain those indicators that meet the design principles and reflect the essential characteristics of the evaluation. The expert survey method is used to screen indicators. According to the principle of indicator screening, experts can select, delete, and supplement the primary indicators based on reasonable operations. A large number of indicators will also complicate testing and calculations, which is not conducive to programmatic operations. In order to select physical index characteristics that are as independent, feasible, and consistent as athletes and can accurately represent the specific physical signs of athletes, 30 sports experts were surveyed this time. They are engaged in the research of athletes' physical function and training experts, experts in the field of physical fitness and many college physical education teachers and coaches. The feedback results of various experts to sort out the indicators to ensure the rationality of indicator selection are combined. The Likert scoring method is
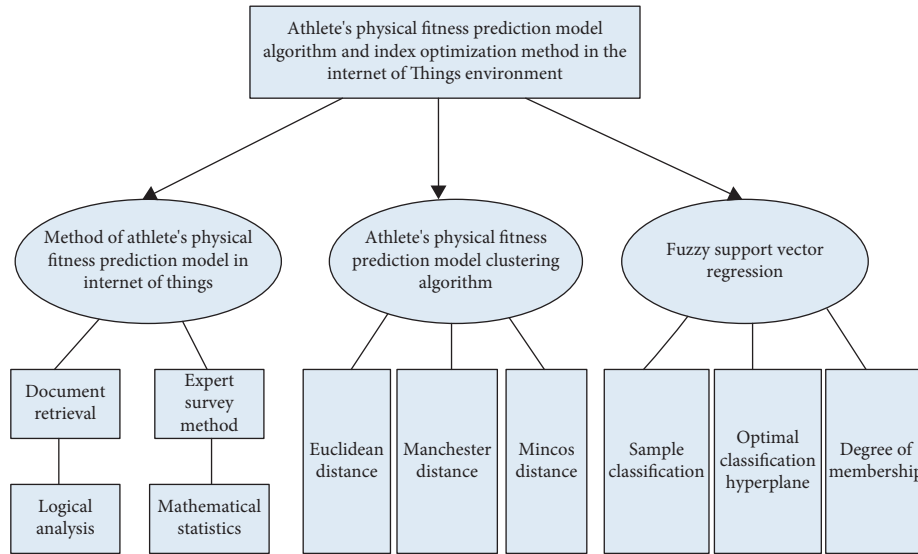
Figure 1: Part of the technical flow chart of this method.

Table 1: Classification of the physical fitness test.

Body shape	Body function	Athleticism
BMI Physique percentage Quetelet index Body weight Forearm tension Forearm relaxation Waist circumference Bust Height Hand length Foot length Leg length Arm span	Heart rate Vital capacity Maximal oxygen uptake 30 s 30 squats	50 m run Select reaction time Tap quickly with both hands Sitting fast Power grip 1 min sit-ups Standing long jump Vertical jump push-ups Pull-ups Arm hang Parallel bar arm extension 2000 m run 15 s standing up cross quadrant jump Cross run Repeated side steps Round trip 20 meters × 4 Sitting forward bending Standing forward bending Cheating Split left and right Turn shoulders Outstanding experiment Horizontal wood Keep your eyes closed Dynamic balance (walking in a straight line)

used to allow experts to evaluate the importance of indicators.

3.2. Carry Out Related Applications of Athlete Index Optimization under the Internet of Things Environment

3.2.1. System Development Environment.
The system development environment is divided into hardware environment and software environment. The hardware environment includes Intranet network environment, Sq1Server2000 database server, Windows NT server; software environment includes Windows 2000, Advanced Server, Delphi 6.0, Sqlserver2000.

3.2.2. Implementation of Index Optimization Algorithm.
First, the transaction database is converted into a relational data table, which has three columns of attributes: transaction identifier, item identifier, and cumulative count. The cumulative count is used in the construction of the schema base table later. For any given indicator, there are multiple rows in the

relationship table representing multiple items in the transaction. In addition, a relational table must be designed to store optimized data. It can be seen from the construction process of the second relational table that for any frequent item, all possible frequent patterns included can be obtained along its node chain. In addition, in the physical fitness test phase, for any frequent item, its conditional pattern base is composed of the prefix path set that appears simultaneously with it. Therefore, a list of attributes is required to reflect the set of prefix paths that appear at the same time. Since mining the relevant indicators in the second relational table is a recursive process and the table needs to be reused, it is also necessary to design a list of attributes to distinguish between different recursive processes and use this column to record the pattern before growth. The first stage of the construction of the relational table is completed, and then the frequent pattern growth method is used to mine frequent patterns from the table. For each frequent item, construct its condition pattern base table and condition pattern tree table. Then, the function can generate the conditional pattern tree. When the generated conditional pattern tree contains only a single path, the frequent pattern is generated by combining the index data and each node in the path; otherwise, it is recursively mined; when the table contains the nodes that do not repeat each other and the values in the fields are not equal, the conditional pattern tree at this time contains only a single path, and frequent patterns can be generated; if the nodes in the table are repeated or the values in the fields are equal, recursion is performed of mining.

3.2.3. Preprocessing of Physical Fitness Prediction Data. The collected analysis data are aimed at the athlete's physical fitness index record. Physical fitness indicators are all numerical, and data association rules mine Boolean data. Therefore, we must preprocess the numerical data and convert it into Boolean data before mining. The central problem of numerical association rule mining technology is the discretization of continuous attributes. After the discretization of continuous attributes is completed, the numerical association rule mining problem can be mapped to the Boolean association rule mining problem. The mapping of numeric attributes and category attributes to Boolean attributes can be completed by the following two methods: one is to map each attribute value to a Boolean attribute for category attributes or numerical attributes with fewer values; for numeric attributes, first divide its attribute value into multiple subintervals and then map each subinterval to a Boolean attribute.

4. Athlete's Physical Fitness Prediction Model Algorithm and Index Optimization Analysis under the Environment of Internet of Things

4.1. Experimental Data Sources. (1) Basic Situation of the Expert Group

This article conducts interviews and surveys with 30 experts in the sports industry in order to get more professional and accurate opinions and suggestions. The basic

situation of the expert group is shown in Table 2 and Figure 2.

It can be seen from the chart that the 30 experts selected in the survey are all engaged in sports coaching. Among them, the number of basketball coaches is the largest, with 8 people, and the number of sprint coaches is the least, with 3 people; and the expert group has basically a long experience with the most years of experience. The longest PE teaching experience is 15 years, and the least is 7 years. Experts are professional and experienced enough, and their relevant opinions are more persuasive, which is conducive to the conduct of research.

(2) The experiment selected 30 sports athletes as the professional group and 30 ordinary college students with no professional sports experience as the control group. Among them, athletes were recruited from sports colleges, with the level of national second-level athletes and above, and often participated in sports events above the city level having four years or more of professional sports experience; the students selected in the control group have not undergone professional training in ball games, track, and field, except for general physical education, and have watched related sports games frequently or occasionally. The specific situation is shown in Table 3. All athletes and students selected in the experiment are in good health, have no mental illness, and have normal vision or corrected vision. They are all right-handed. A certain amount of remuneration will be given after the experiment.

The training years and training frequency of the professional group into graphs for more intuitive analysis are drawn, as shown in Figure 3.

It can be seen from the figure that the training years, weekly training frequency, and daily training frequency of the selected athletes in the professional group are relatively average. In this case, the physical fitness test is relatively representative.

4.2. Analysis of Athlete's Body Circumference Index. According to the physical fitness test items set in the experimental part, the athlete's body circumference index is collected and sorted out and drawn into a chart, as shown in Table 4 and Figure 4.

The hip/waist circumference reflects the central obesity of the athlete's body. In sports training, the hip/waist index is appropriate, and the small hip circumference indicates that the athlete's hip muscles are lifted and tightened. This is conducive to the athletes in the exercise of jumping and other difficult movements. On the one hand, the appropriate hip-to-waist ratio index is derived from genetics. On the other hand, sports training also plays an important role in improving this index. Athletes have a good level on this index, indicating that athletes' physical condition adapts to sports in training. The bust/waist circumference reflects the upper body shape of the athlete. From the data, it can be seen that the shape of the male and female athletes indicates that the upper body of the athlete is relatively well-proportioned and has better chest muscles. The athlete needs to complete the relevant actions. Athletes have better strength to ensure

TABLE 2: Basic situation of the expert group.

Profession	Working time (unit: year)	Number of people
Long-distance running coach	8.5	4
Sprint coach	12	3
Swimming coach	9	6
Skating coach	7	5
Basketball coach	11	8
Table tennis coach	15	4

FIGURE 2: Basic situation of the expert group.
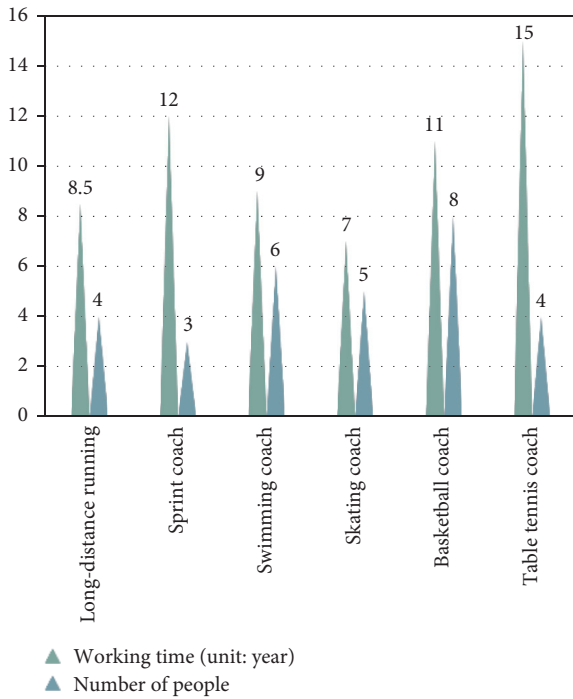
FIGURE 3: Training situation of the professional group.

TABLE 3: Basic situation of subjects.

	Professional group	Control group
Number of people	30	30
Sex	15 men, 15 women	15 men, 15 women
Age	20 ± 3	20 ± 3
Training years	8.12 ± 2.25	—
Training frequency (hours/day)	5.15 ± 2.36	—
Training frequency (day/week)	5 ± 1	—

the completion of the action and can maintain a better body shape when completing the action. The width of the medulla/shoulder width is an index of the ratio of the athlete's torso. In terms of lower limb circumference, male athletes have slightly more indicators of thigh circumference and calf circumference than female athletes, but the test value of male athletes is slightly higher. Male athletes have good performance in lower limb muscle strength, but they still need to strengthen lower limb strength training.

4.3. Experimental Manipulation Effect Analysis. Before the formal analysis, we must first determine whether there is a speed-accuracy trade-off between the subjects before and after the test and compare whether there is a significant difference between the subjects' response before and after the test, and it turns out that there is no significant change in the subjects' response time before and after the test. In addition, it is necessary to confirm the validity of the choice of the expert group and the control group. The independent sample t-test was used to compare the difference in the correctness of the action prediction between the two groups in the pretest. It was found that the correct rate of the professional group was significantly higher than that of the control. Group $p < 0.001$, which is consistent with previous studies. This result proves the professional advantages of athletes in predicting specific actions in physical fitness, which means that the grouping of subjects in this experiment is effective. Finally, in order to confirm the randomness of the intervention grouping and whether there are differences in the action responses of different groups of subjects, this article, respectively, carried out an analysis of variance on the correct rates of the pretested responses of the professional group and the control group. The results meet the requirements of the experimental design. The main effect of the intervention conditions and the interaction between the two are not significant (professional group: main effect $p_s \geq 0.270$, interaction $p = 0.857$; control group: $p_s \geq 0.563$, interaction $p = 0.728$), as shown in Table 5 and Figure 5. The above results ensure the validity of analysis and experimental design.

With correctness as the dependent variable, repeated measures analysis of variance was performed on the professional group and the control group. The results showed that the main effects of test time, intervention and test bias,

TABLE 4: Athletes' body circumference index.

		Hip/waist	Bust/waist	Hip width/shoulder width	Thigh circumference	Calf circumference
Men	15	119.12 ± 5.71	121.42 ± 4.83	71.58 ± 5.46	53.31 ± 2.17	36.45 ± 3.17
Women	15	117.35 ± 5.52	119.42 ± 4.91	69.87 ± 5.13	51.46 ± 2.56	34.67 ± 3.24
p		0.537	0.413	0.765	0.379	0.798
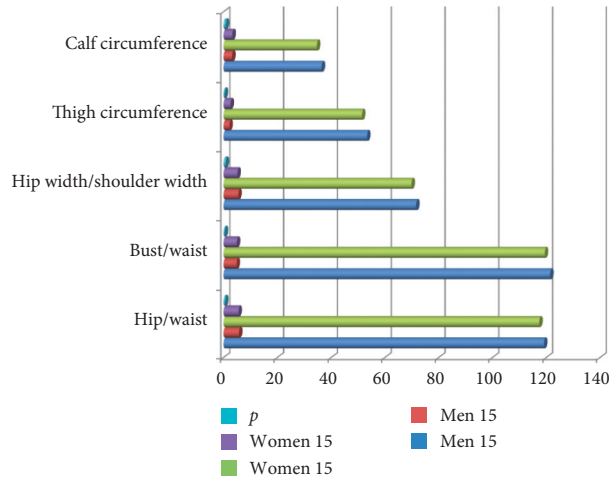
FIGURE 4: Athlete's body circumference index situation.

TABLE 5: Descriptive statistical results of the correct rate of the two groups of subjects.

		Test biased		Test unbiased	
Professional group	Intervention biased group	0.671	0.643	0.647	0.621
	Intervention unbiased group	0.735	0.681	0.612	0.615
Control group	Intervention biased group	0.603	0.732	0.711	0.693
	Intervention unbiased group	0.637	0.717	0.738	0.675
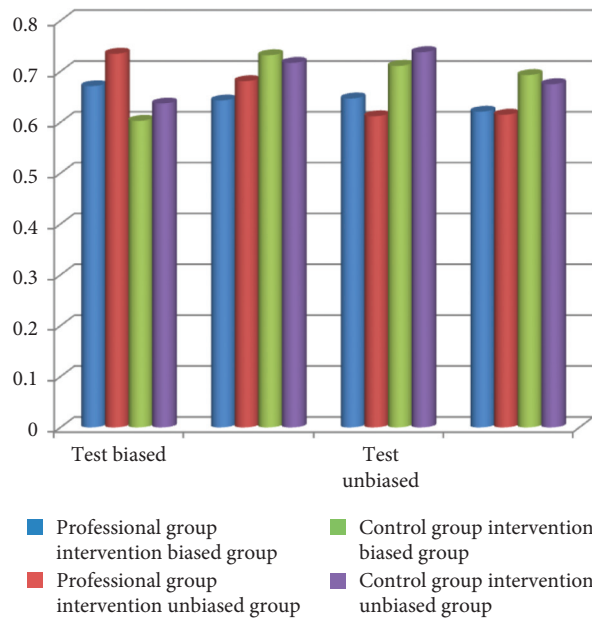
FIGURE 5: Descriptive statistics of the correct rate of the two groups of subjects.

TABLE 6: Descriptive statistical results of response time of the two groups of subjects.

		Test biased		Test unbiased	
Professional group	Intervention biased group	436.352	415.873	398.325	371.652
	Intervention unbiased group	441.173	420.365	413.268	379.254
Control group	Intervention biased group	447.254	426.358	442.731	455.214
	Intervention unbiased group	393.651	435.367	452.161	435.287
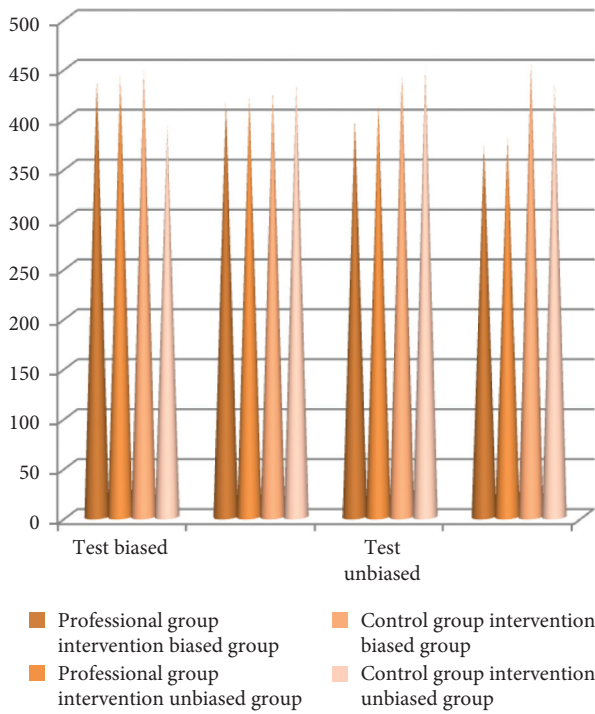
FIGURE 6: Descriptive statistics of the response time of the two groups of subjects.

and interaction effects were not significant in the professional group (main effects: $p_s \geq 0.083$; interaction effects: $p_s \geq 0.180$). However, the control group found that the main effect of test bias was significant, the interaction of intervention × test bias was significant, the interaction of test time × intervention was significant, and the edge of the third-order interaction of test time × intervention × test bias was significant. The simple effect analysis results of the third-order interaction found that whether the intervention conditions and test biases affect the prediction level of the control group participants. When the intervention is biased/test unbiased, compared with the pretest, the control group is tested after the scores of students dropped significantly ($p = 0.001$), and the scores did not change significantly under other conditions ($p_s \geq 0.513$), as shown in Table 6, Figure 6.

Combining the above statistical results, it can be inferred that the professional group is more inclined to use a reasonable and professional method for physical fitness prediction, while the control group lacks relevant professional experience and relies more on personal judgment for physical fitness prediction, which leads to conflicts between professional training methods and innate self-mobilization time, and the forecast performance dropped significantly.

5. Conclusions

After index optimization, the use of neural network technology to evaluate and predict athletes' physical functions will be more targeted, which will greatly help to improve the accuracy of neural network evaluation and prediction of athletes' physical functions in the future. After index optimization, each training site can only provide optimized index detection records, thereby improving data integrity. For an indicator of individual missing data, use the level of the indicator value that is correlated with the indicator to predict it and fill in the missing data value with the predicted value.

In the early stage of the research, this paper summarized the research methods of the athletes' physical fitness prediction model in the Internet of Things environment, including literature retrieval, expert survey, logical analysis, and mathematical statistics. It also proposed the application of the clustering algorithm to the athlete's fitness prediction model, including European Giridian distance, Manhatan distance, Mincos distance, and other formulas and proposed the fuzzy support vector regression algorithm, including classification samples, membership function, coverage, interval width. Subsequent experiments on the algorithm and index optimization of athletes' fitness prediction models in the Internet of Things environment were carried out, and the steps for athletes' fitness prediction in the Internet of Things environment were designed, such as the selection of physical fitness evaluation indicators, the classification of physical fitness tests, and the selection of fitness evaluation indicators; the Internet of Things realizes the preprocessing of physical health prediction data, the main way is through related programs optimized by athletes and index optimization algorithms.

This article combines the athlete's form, function characteristics, and competitive sports characteristics in the selection of physical training methods to strengthen the pertinence of physical training. On the basis of regular training, special physical training is strengthened, and combined training methods and functions are used in complete training. Targeted training methods such as reserve improve the athletes' completion of the complete set of competition training. The combined training method, functional reserve, and other targeted training methods are used, and the method of predicting the athlete's physical fitness improves the accuracy of the athlete's completion of the game.

Data Availability

The data used to support the findings of this study are available from the corresponding author upon reasonable request.

Conflicts of Interest

The authors declare that they have no conflicts of interest.

References

[1] T. J. Gerpott and S. May, "Integration of Internet of Things components into a firm's offering portfolio-a business development framework," *Info*, vol. 18, no. 2, pp. 53–63, 2016.

[2] A. Burg, A. Chattopadhyay, and K. Y. Lam, "Wireless communication and security issues for cyber–physical systems and the internet-of-things," *Proceedings of the IEEE*, vol. 106, no. 1, pp. 38–60, 2017.

[3] T. Yang, B. Yu, H. Wang, J. Li, and Z. Lv, "Cryptanalysis and improvement of Panda-public auditing for shared data in cloud and Internet of Things," *Multimedia Tools and Applications*, vol. 76, no. 19, pp. 19411–19428, 2017.

[4] S. Mayer, J. Hodges, D. Yu, M. Kritzler, and F. Michahelles, "An open semantic framework for the industrial Internet of Things," *IEEE Intelligent Systems*, vol. 32, no. 1, pp. 96–101, 2017.

[5] T. Andreas, "The Internet of Things," *International Paper Board Industry*, vol. 60, no. 2, pp. 40–42, 2017.

[6] T. Xu and I. Darwazeh, "Non-orthogonal narrowband Internet of Things: a design for saving bandwidth and doubling the number of connected devices," *IEEE Internet of Things Journal*, vol. 5, no. 3, pp. 2120–2129, 2018.

[7] L. Du, Y. Du, Y. Li et al., "A reconfigurable streaming deep convolutional neural network accelerator for Internet of Things," *IEEE Transactions on Circuits and Systems I: Regular Papers*, vol. 65, no. 1, pp. 198–208, 2018.

[8] X. Liu, S. Zhao, A. Liu et al., "Knowledge-aware proactive nodes selection approach for energy management in Internet of Things," *Future Generation Computer Systems*, vol. 92, pp. 1142–1156, 2017.

[9] F. H. Bijarbooneh, W. Du, C. H. Ngai et al., "Cloud-assisted data fusion and sensor selection for internet-of-things," *IEEE Internet of Things Journal*, vol. 3, no. 3, pp. 257–268, 2017.

[10] I. Joe and M. Shin, "Energy management algorithm for solar-powered energy harvesting wireless sensor node for Internet of Things," *Iet Communications*, vol. 10, no. 12, pp. 1508–1521, 2016.

[11] Z. Liu, K.-K. R. Choo, and J. Grossschadl, "Securing edge devices in the post-quantum Internet of Things using lattice-based cryptography," *IEEE Communications Magazine*, vol. 56, no. 2, pp. 158–162, 2018.

[12] M. Xia, T. Li, Y. Zhang, and C. W. de Silva, "Closed-loop design evolution of engineering system using condition monitoring through Internet of Things and cloud computing," *Computer Networks*, vol. 101, pp. 5–18, 2016.

[13] M. Voegler, J. M. Schleicher, C. Inzinger et al., "Ahab: a cloud-based distributed big data analytics framework for the Internet of Things," *Software: Practice and Experience*, vol. 47, no. 3, pp. 443–454, 2017.

[14] M. Ge, J. B. Hong, W. Guttmann, and D. S. Kim, "A framework for automating security analysis of the Internet of Things," *Journal of Network and Computer Applications*, vol. 83, pp. 12–27, 2017.

[15] S. A. Aljawarneh, R. Vangipuram, V. K. Puligadda, and J. Vinjamuri, "G-SPAMINE: an approach to discover temporal association patterns and trends in Internet of Things," *Future Generation Computer Systems*, vol. 74, pp. 430–443, 2017.

[16] R. Malhotra and M. Khanna, "Dynamic selection of fitness function for software change prediction using particle swarm optimization," *Information and Software Technology*, vol. 112, pp. 51–67, 2019.

[17] R. Arena, C. Ozemek, D. Laddu-Patel, and J. Myers, "Refining the risk prediction of cardiorespiratory fitness with network analysis," *Circulation Research*, vol. 122, no. 6, pp. 804–806, 2018.

[18] A. B. M. Fuermaier, D. Piersma, D. D. Waard et al., "Assessing fitness to drive—a validation study on patients with mild cognitive impairment," *Traffic Injury Prevention*, vol. 18, no. 2, pp. 145–149, 2016.

[19] Y. Ma, S. Wang, P. C. K. Hung et al., "A highly accurate prediction algorithm for unknown web service QoS values," *IEEE Transactions on Services Computing*, vol. 9, no. 4, pp. 511–523, 2017.

[20] B. D. Dancila, R. Botez, and D. Labour, "Fuel burn prediction algorithm for cruise, constant speed and level flight segments," *The Aeronautical Journal*, vol. 117, no. 1191, pp. 491–504, 2016.

[21] H. Nazaktabar, K. Badie, and M. N. Ahmadabadi, "RLSP: a signal prediction algorithm for energy conservation in wireless sensor networks," *Wireless Networks*, vol. 23, no. 3, pp. 919–933, 2017.

[22] W. Yi and M.-J. Liao, "Efficient inter-prediction depth coding algorithm based on depth map segmentation for 3D-HEVC," *Multimedia Tools and Applications*, vol. 78, no. 8, pp. 10181–10205, 2019.

[23] J. D. J. Rubio, I. Elias, D. R. Cruz, J. Pacheco, G. J. Gutierrez, and A. Zacarias, "A fuzzy algorithm for the prediction of future data," *IEEE Latin America Transactions*, vol. 15, no. 8, pp. 1361–1367, 2017.

[24] S. C. Hsia, W. K. Wong, and Y. H. Shih, "Fast-efficient algorithm of high-profile intra prediction for H.264 encoding system," *Iet Image Processing*, vol. 12, no. 3, pp. 329–336, 2018.

[25] A. Martchenko and G. Deng, "Fast algorithm for least-squares based image prediction," *Iet Image Processing*, vol. 10, no. 8, pp. 582–589, 2016.

[26] M. Zhu, H. Qu, and J. Zhao, "Instance expansion algorithm for micro-service with prediction," *Electronics Letters*, vol. 54, no. 6, pp. 356-357, 2018.

[27] H. konno and H. Watanabe, "Bond portfolio optimization problems and their applications to index tracking: a partial optimization approach," *Journal of the Operations Research Society of Japan*, vol. 39, no. 3, pp. 295–306, 2017.

[28] X. Zhu, W. Hong, H. Xu, L. Yu, and Y. Zhao, "Spatial quality index based rate perceptual-distortion optimization for video coding," *Journal of Visual Communication and Image Representation*, vol. 38, pp. 423–432, 2016.

[29] H. M. Dubey, M. Pandit, and B. K. Panigrahi, "Hydro-thermal-wind scheduling employing novel ant lion optimization technique with composite ranking index," *Renewable Energy*, vol. 99, pp. 18–34, 2016.

Research Article

Supply Chain Inventory Collaborative Management and Information Sharing Mechanism Based on Cloud Computing and 5G Internet of Things

Fuan Zhang [1] **and Zhenzhi Gong**[2]

[1]*School of Information Engineering, Yangzhou University, Yangzhou 225009, China*
[2]*Industrial Economics Research Institute, Yangzhou University, Yangzhou 225009, China*

Correspondence should be addressed to Fuan Zhang; fazhang@yzu.edu.cn

With the development of economic globalization, the competition among enterprises is increasingly fierce. Therefore, companies need close information sharing to realize the integration of supply chain. This article aims to study the collaborative management and information sharing mechanism of supply chain inventory based on cloud computing and 5G Internet of Things. This article first introduces the theory and methods of collaborative supply chain management and the information exchange mechanism and then discusses the problem of information sharing in the supply chain, that is, the bullwhip phenomenon, and then from the demand forecast, supply chain structure, time lag, and shortage game, six aspects are analyzed. The cause of the bullwhip phenomenon is analyzed. Secondly, this article proposes a quantitative analysis of the bullwhip effect, establishes a mathematical model of the bullwhip effect in the supply chain, and uses quantitative analysis to analyze the value of information sharing in the supply chain. Finally, this article uses cloud computing technology to build a supply chain information collaboration system architecture and uses EPC Internet of Things to build a supply chain information sharing model and describes the entire operation process of the supply chain. The experimental results of this paper show that the application of cloud computing technology to supply chain management establishes a system platform for supply chain information sharing, improves the overall operational efficiency of supply chain management, and realizes supply chain information sharing and business collaboration. In addition, the operating costs and risks of each node enterprise in the supply chain are reduced by 12% compared with the nonsharing situation, which also shows that the overall benefits of the supply chain have been correspondingly improved and market competitiveness has been enhanced.

1. Introduction

With the advent of economic globalization, integration, and the era of knowledge economy, competition among enterprises has intensified. Traditional enterprise management and operation management models can no longer be used in the new market environment. More and more companies are beginning to know how to use supply chain management ideas to achieve synergy between the internal and external environments of the enterprise and conduct integrated management [1]. In this way, customers' satisfaction with the company can be improved,

and the core competitiveness of the company in such an environment can be improved.

Use modern information technology to integrate the business processes of each node enterprise in the supply chain, covering the entire process from upstream enterprise suppliers to end customers [1], establishing partnerships between enterprises, and bringing together the information of each enterprise's independent operation and management in order to finally share the market together. Therefore, the effective operation of the supply chain and the effective sharing of information are of great significance for reducing the bullwhip effect in the supply chain.

Successful precision engineering companies need to master process innovation and supply chain solutions. In these types of businesses, the implementation of innovative collaboration solutions has become a necessary strategy for enhancing the decision-making capabilities of SMEs and improving overall business competitiveness. The purpose of Hernandez research is to introduce how to guide and support SME organizations through online-based cooperation so that it is possible to participate in improved co-operative alliances and how well-designed SMEs can benefit and enhance their capabilities. However, there are certain errors in this study [2]. Mitchell discussed a way for maritime transportation service organizations to improve information sharing in supply chain operations. An action study case study method uses design for six sigma (DFSS) methods to design an information technology solution that can effectively transport information about material movement through inland barges between all levels of the supply chain. However, this sharing method has certain risks [3]. The purpose of this study by Kim MG is to remove the barriers that hinder the adoption/proliferation of radio frequency identification (RFID) in the industry and to help companies develop effective supply chain management (SCM) using RFID by clarifying the specific mechanisms by which RFID affects supply chain performance practice (SCP) [4]. Based on the technology-organization-environment framework, his research studies the technical characteristics and actual environment of RFID in our theoretical model. He studied how the use of RFID can contribute to supply chain information sharing (SCIS) and, conversely, how SCIS affects SCP. However, this research is not practical [5].

The innovation of this paper is as follows. (1) Based on the previous research on the information sharing model, a new core enterprise trustee information sharing model based on active information services is proposed, and an information sharing platform between node enterprises is established. (2) Cloud computing technology to supply chain management is applied [6], a system platform for supply chain information sharing is established, the overall operational efficiency of supply chain management is improved, and supply chain information sharing and business collaboration are realized. At the same time, the mechanism of high-level data coordination and information sharing under this system is studied, and methods and measures to realize information sharing in supply chain management are proposed.

2. Collaborative Management and Information Sharing Method of Supply Chain Inventory Based on Cloud Computing and 5G Internet of Things

2.1. Internet of Things Technology.
RFID technology is the core part of the Internet of Things and the source of information for the entire Internet of Things system [5]. Data information in the Internet of Things is collected in advance through RFID radio frequency technology and then processed through processing [7]. The complete IoT system

mainly consists of the following parts: electronic tags (Tag), readers (Reader), EPC middleware, object name resolution service (ONS), and EPC information service (EPC IS) [8, 9]. Its structure and function flow chart is shown in Figure 1:

In the IoT system, each product has a unique EPC code, which stores the relevant information of the product. First, the reader reads the product EPC code in the electronic tag and then transmits it to the EPC middleware. After sorting and filtering, the information is stored on the corresponding EPC information server. The EPC information service stores the dynamic and static information of the product. It provides guarantee for supply chain information sharing [10]. Similarly, users (any company) can send EPC codes to the object analysis server through the information platform for inquiries. After receiving the request, ONS queries the matching address information, feeds back the information, and guides the EPC middleware to access and store the product information in EPC information server, and EPC information service sends product information to the middleware to feedback to the user so that the user can obtain the relevant information of the product [11, 12].

2.2. Bullwhip Effect in the Supply Chain.
Suppose a simple supply chain with only one manufacturer and retailer is established (the supply chain can also be a four-tier supply chain with suppliers, manufacturers, wholesalers, and retailers). In the t period, the manufacturer predicts the retailer's order quantity in the $t+1$ period based on the retailer's order quantity historical data [13]. In this supply chain, the manufacturer only faces the retailer for sales and assumes that only one product is sold. Since the retailer is closest to the market, he directly controls the demand information of the end customer, and he can predict the demand information [14]. Assume that the variable d_T represents the demand of the end customer, and this demand is random:

$$d_T = \mu d_{T-1} + \theta_T. \tag{1}$$

In formula 1, μ is a constant and greater than zero; λ refers to the correlation coefficient between demand variables in two adjacent periods, referred to as autocorrelation coefficient, and satisfies $-1 < \lambda < 1$; and θ_T refers to demand the variation error of the variable, and the error is independent in each period [15].

From formula 1, it can be known that this demand variable will change with time [16].

$$e(d_T) = \frac{\mu}{(1-\lambda)},$$

$$\mathrm{var}(d_T) = \frac{\partial^2}{(1-\lambda^2)}. \tag{2}$$

Assuming that there is an order lead time L when a retailer places an order from an upstream supplier in the supply chain, the retailer receives the goods ordered from the supplier at the end of the t period every time at the $t+L$ period [17]. It is also assumed that the retailer adopts an (S, s)

inventory strategy to ensure that the product is maintained at a certain level. Suppose order point y_T has the following function at any time t:

$$y_T = l\overline{d_T} + \phi\sqrt{ls_T}. \tag{3}$$

According to the normal distribution function, when $\phi = 1, 3$, there are 84.1% and 99.8% supply rates in L time.

Suppose the retailer adopts the moving average method to predict the market demand and standard deviation [18]. Using d_I to express the customer demand in period I, there is the following formula:

$$\overline{d}_T = \sum_{I-T-N}^{T-1} \frac{d_I}{N},$$

$$S_T^2 = \sum_{I-T-N}^{T-1} \frac{\left(d_I - \overline{d_T}\right)^2}{(N-1)}. \tag{4}$$

In formula 4, n represents the number of observation periods selected in the moving average method. The larger the value of n, the more historical data observed and the smoother the processing results [19].

Assume that the variable q_T is the quantity of goods ordered by the retailer from the upstream manufacturer, which satisfies the following formula:

$$q_T = Y_T - Y_{T-1} + d_{T-1}. \tag{5}$$

In formula 5, if the order quantity q_T appears negative, it is stipulated that the supplier allows the retailer to return the excess order quantity without cost. Then, substituting formulas 3–(5), respectively, after sorting, we get the following:

$$q_T = \left(\frac{1+l}{n}\right)d_{T-1} - \left(\frac{l}{N}\right)d_{T-N-1} + \phi\sqrt{l}\left(s_T - s_{t-1}\right). \tag{6}$$

For the order quantity q_T in formula 6, take its variance and get the following:

$$\mathrm{var}\left(q_T\right) = \left[1 + \left(\frac{2l}{N} + \frac{2l^2}{n^2}\right)\left(1 - \lambda^n\right)\right]\mathrm{var}\left(d_T\right) + \phi^2 l\,\mathrm{var}\left(s_T - s_{t-1}\right). \tag{7}$$

It can be seen from equation (7) that the second term at the right end is a non-negative number. Divide it by $\mathrm{var}(d_T)$ in equation (2) to get a value and get equation (8). And, this value represents the ratio of the variance of the order quantity received by the manufacturer to the variance of the quantity received by the retailer from the customer. Therefore, this formula can be used as the quantitative formula be of the bullwhip effect.

$$\mathrm{be} = \frac{\mathrm{var}\left(q_T\right)}{\mathrm{var}\left(d_T\right)} \geq 1 + 2\left(1 - \lambda^N\right)\frac{l(l+N)}{N^2}. \tag{8}$$

From the above analysis of applying the moving average method to forecast, it is also applicable to other forecasting methods. The following uses the exponential smoothing method for predictive analysis. From the results discussed above with the moving average method, we can derive the quantitative formula be of bullwhip effect under the exponential smoothing method in the same way, which has the following formula:

$$\mathrm{be} = \frac{\mathrm{var}\left(q_T\right)}{\mathrm{var}\left(d_T\right)} \geq 1 + \left(\frac{2l\,\partial + 2l^2\partial^2}{2 - \partial}\right)\left[\frac{(1 - \partial)}{(1 - \lambda\beta)}\right]. \tag{9}$$

In equations 8 and 9, we can clearly see that the demand information becomes larger after being transmitted from the retailer to the manufacturer in the supply chain, which produces the bullwhip effect [20, 21]. Although the above two forecasting methods can more accurately verify that the demand information in the supply chain has been distorted and increased and can give the results of quantitative analysis, they cannot provide a detailed positioning and description of the process of information increase, and it is impossible to know how to affect it [22].

In a supply chain that adopts information sharing, relevant information such as demand information, forecasting methods, and inventory decision models can be shared so that each level of the supply chain can obtain the demand forecast information of the first-level member retailer and then make corresponding decisions based on shared information [23].

Assuming that the supply chain implements information sharing, the downstream member retailers will pass the end customer demand information they have to the members at all levels through information sharing [24]. In this way, each level member has the actual demand information of the end customer. Assuming that each level member in the supply chain uses the moving average method to predict and analyze the average demand of the next level based on n observation values of demand, then

$$\overline{U_T} = \sum_{I=1}^{N} \frac{d_{t-1}}{N}. \tag{10}$$

Equation (10) means that in unit time, the predicted demand of each level member uses the same estimated value. Assuming that every member of the supply chain adopts the same inventory strategy, the order points are as follows:

$$Y_T^K = l_K \cdot \overline{U_T^K} + \phi\sqrt{l_K s_T^K}. \tag{11}$$

Combining equations 5 and 7 to derive, it is concluded that in the case of information sharing, the ratio of variance between q_T^K in the supply chain and d_T of end customer demand is as follows:

$$\frac{\mathrm{var}\left(q_T^K\right)}{\mathrm{var}\left(d_T^K\right)} \geq 1 + 2\sum_{I-1}^{K-1}\frac{l_T}{N} + 2\sum_{I-1}^{K-1}\frac{l_T^2}{N^2}. \tag{12}$$

The premise of formula 12 is that the supply chain needs to realize information sharing, the demand information mastered by each level member needs to be shared in the supply chain, and the forecasting method and inventory strategy adopted by each level member need to be consistent [25].
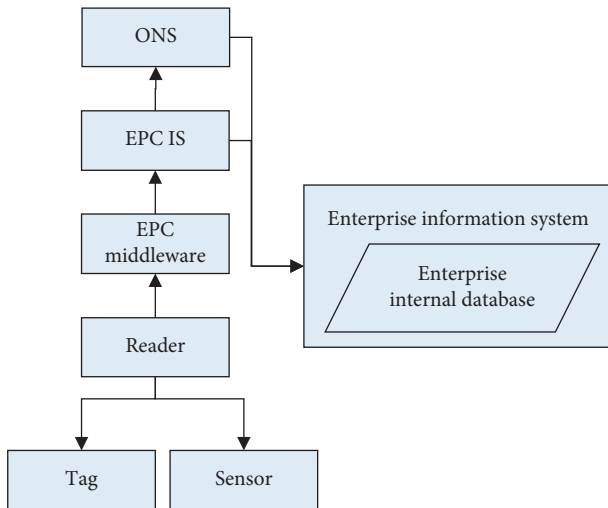
Figure 1: The structure and functions of the Internet of Things.

2.3. Supply Chain Information Sharing Mechanism.
The importance and value of information sharing in supply chain cooperation are obvious. However, the above analysis limits the application of information sharing to a certain extent. Therefore, it is necessary to establish an effective information exchange mechanism to encourage member companies to participate in information exchange and maximize the level of information exchange.

This paper has conducted some research on the information sharing mechanism [25]. In the process of studying the value of common information, researchers found that although the implementation of information exchange can improve the overall performance of the supply chain and reduce the overall cost, the problem is that the distribution of new profits has not been resolved. When determining the value of demand information, Lee et al. pointed out that retailers did not directly benefit from information exchange. If there is no proper mechanism to coordinate interests, it may generate disproportionate benefits and investment, and some member companies are reluctant to participate in information exchange. Therefore, it is necessary to establish an incentive mechanism to encourage all parties to achieve a win-win situation [26]. The incentive mechanism is an agreement or rule issued by the authorized commissioner to the representative according to the main agency relationship so that the representative's behavior conforms to the wishes of the authorized official. In the supply chain relationship, suppliers, manufacturers, and distributors will form different principal-agent relationships as needed. At present, when investigating information exchange in the supply chain, most of them first establish a specific agency relationship and then propose a mechanism to encourage information exchange. The design of this mechanism is based on the neutral risk assumption of the main factors [27]. However, the members of the supply chain are not a simple principal-agent relationship, but in this kind of cooperative relationship, you and the members have different attitudes towards risk. In the actual management of the supply chain, information exchange is two-way, and each member country

should cooperate in information exchange and share the benefits of information exchange; it should be allocated to members reasonably [14].

2.4. Supply Chain Collaborative Management Methods.
Generally speaking, supply chain coordination management includes seven aspects: specific content strategy coordination, information coordination, information coordination, trust coordination, cultural coordination, business coordination, form coordination, and distribution coordination. The research center of this paper is trust and information cooperation [28].

2.4.1. Trust Collaboration.
The cooperative relationship between supply chain node enterprises is based on trust. Only by establishing a perfect trust mechanism can the efficiency and long-term competitive advantage of the entire supply chain be guaranteed [29]. Strengthening mutual trust can intensify cooperation between business nodes and improve the flexibility of production and service and the ability to respond to emergencies. Newcomer coordination reduces unnecessary frictions and conflicts and reduces the resulting consumption of people, money, materials, and time.

2.4.2. Information Collaboration.
This is a key factor for the success of supply chain management [30]. In order to ensure the best operation of the entire supply chain, each node company in the supply chain has formed such a relationship, division of labor, cooperation, independence, and integration. The basis of this division of labor, cooperation, and independent integration is the relationship between supply chain nodes, which is easy to transmit and exchange information dynamically. Only when each node in the supply chain has good information exchange, the supply chain can become an organic network organization, which is truly guided by the needs of end users and ensures that the transmission of customer demand information will not be distorted or delay, thereby effectively reducing the negative impact of the bullwhip effect [9].

3. Cooperative Management and Information Sharing Experiment of Supply Chain Inventory Based on Cloud Computing and 5G Internet of Things

3.1. Supply Chain Model Design.
The content of this article is not to prove the existence of the "bullwhip effect" but to study the value of information sharing in the supply chain system and help companies in the supply chain to more intuitively understand the supply chain implementation of information sharing through the advantages of simulation software. Therefore, in this article, only a simple single-chain five-tier structure including customers is considered.

In this supply chain process, there are the following 4 links, which are analyzed as follows:

(1) *Purchasing Products.* This link occurs between the customer and the retailer, and the retailer meets customer needs in a timely manner and quickly processes customer orders.

(2) *Replenishing Inventory.* This link occurs between retailers and wholesalers and between wholesalers and manufacturers. This link is similar to the previous link, except that this time the customer has become a retailer or wholesaler. The purpose of replenishing inventory is to enable retailers or wholesalers to provide products to downstream members in a timely manner to avoid losses due to shortages. The order completion process in this link is the same as the customer order completion process, but the object is different. However, there is a big difference, that is, there is a big gap between the order quantities of the two orders, and the supplementary inventory orders of retailers or wholesalers are much larger than customer orders.

(3) *Product Production.* This link occurs between wholesalers and manufacturers, and it is triggered by customer orders and retailer or wholesaler replenishment of inventory orders. The wholesaler compares the demand forecast with the inventory level it owns, formulates a corresponding ordering strategy, replenishes the inventory, and then transmits the order to the manufacturer. Manufacturers make plans for production based on their own supply level and downstream demand analysis.

(4) *Raw Material Acquisition.* This link occurs between the manufacturer and the supplier, which is similar to the relationship between the retailer and the wholesaler, but there is one difference, that is, the retailer uses the uncertain demand of the end customer to increase. It is ordered by wholesalers, and when the manufacturer obtains raw materials from upstream suppliers, the demand is accurately calculated according to the production plan.

3.2. Cloud Computing-Based Supply Chain Information Collaboration System Architecture. The structure of the supply chain information cooperation platform should include four overall levels. The first layer is the level of infrastructure, including computer servers, network equipment, cloud servers, and cloud storage devices. It is the foundation of all application functions, providing parallel computers and large-capacity storage and other required cloud IaaS infrastructure services. The second layer is the cloud system service layer, which provides interfaces and software operating environment for system development and provides system service functions such as user management, manages access codes, management permissions, management records, and traffic statistics. It is a business cooperation cloud computing and information exchange system service platform [31]. The third layer is the cloud computing application service layer, that is, the cloud computing application virtualization service platform layer, which provides SaaS online software services, including order information, production and inventory information, and various functional units, such as sales services, distribution services, return services, and settlement. Information is the main work area of information exchange and supply chain cooperation. The fourth level is the access level of users who use personal computers, portable phones, and other terminal devices to transmit, process, and receive information and respond quickly to information. The above four levels constitute a complete "cloud computing" supply chain business collaboration and information sharing platform architecture.

3.3. Construction of Supply Chain Information Sharing Mode of EPC Internet of Things. The Chinese name of EPC is an electronic product code, which is a set of numbers, consisting of a question number and three other data parts (domain name management, object classification, and serial number). It is a set of numbers for each physical item (including retail product units, unique identifiers for containers, and cargo packaging). EPC solves the problem of identifying and monitoring individual products and establishes a global open label standard for each product. The EPC system is a physical Internet, which can automatically identify and exchange information in real time on a global scale and is constructed from the computer Internet using technologies such as RFID and wireless data communication.

On the physical Internet consisting of EPC tags, card readers, medium-sized EPC software, Internet, ONS server, EPC information Service (EPC IS) and many databases, the EPC read card reader is just an information report (index); this information refers to finding the IP address and receiving relevant information stored in the address and using distributed EPC media software to process a group of EPC information read by the card reader. Since there is only one EPC code on the label, the computer should know other information that matches the EPC. This requires the National Bureau of Statistics to provide automated network database services. The medium-sized EPC software transmits the EPC code to ONS, and ONS orders the medium-sized EPC software to search the server (EPC IS) that stores the product files. The file can be copied from the media EPC software so that the product information in the file can be transferred to the supply chain. The workflow of the EPC system is shown in Figure 2.

4. Supply Chain Inventory Coordination Management and Information Sharing Mechanism

4.1. Effect of Collaborative Management and Control of Supply Chain Inventory. Through data analysis of orders, it is found that there is an average value for commodity prices, wholesaler inventories, retailer inventories, and manufacturer inventories. The actual values fluctuate up and down on the average value. There are few extreme cases in the value. Preliminary research shows that the standard is positive state distribution.
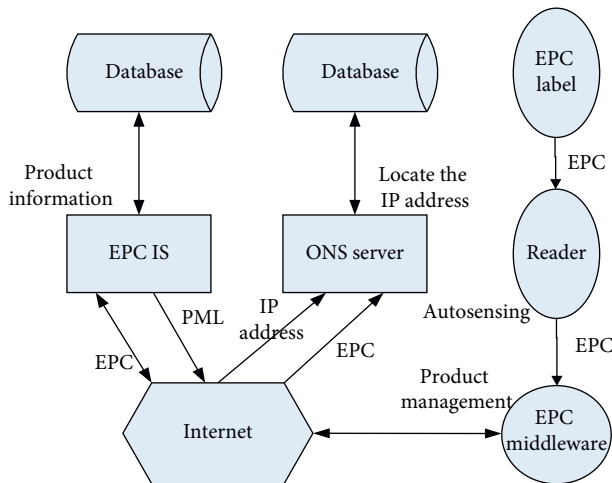
Figure 2: The workflow of the EPC system.

The demand forecast and the sensitivity analysis of each inventory are done. The analysis results are shown in Table 1 and Figure 3.

From Figure 3, we can find that the demand forecast and each inventory are significantly affected by the parameters, indicating that the model is reasonable and more in line with the actual operation of the system.

To further reflect the degree of influence of various variables on the overall supply chain inventory management under the condition of collaborative management, a further scenario analysis was made.

4.1.1. The Degree of Influence of Price on Each Inventory.
The reference price of the collaborative platform is modified to increase by 10% compared with the original. The simulation results are shown in Table 2 and Figure 4.

The data in the figure reflect that price changes have a relatively large impact on changes in consumer demand and inventory at various nodes in the supply chain. The trend of change has changed, but the general trend has not changed. The reason is that this order, as a fast-moving consumer product, has a large price elasticity coefficient. The increase in price causes a decrease in demand. The transmission of demand information through the collaborative platform obviously leads to a decrease in inventory at each node of the supply chain.

4.1.2. The Impact of Consumer Demand on Each Inventory and Price in the Previous Period.
Increase consumer demand by 10% in the previous period and conduct a simulated comparative analysis to check the changes in each inventory and price. The result is shown in Figure 5.

The data in the figure reflect that after the last period of consumer demand increased by 10%, the inventory and price did not change too much, and the trend of the change was also the same as before, indicating that the increase in consumer demand in the last period had an impact on the overall the degree of influence is not high and the price fluctuation is weaker. The reason is that after consumer

demand in the previous period increases, the collaborative platform can make timely predictions for the next period for data prediction, which increases inventory consumption while increasing inventory incoming volume so that the final inventory does not change too much. Scenario analysis is carried out on other variables in the model, and the study finds that price has a greater impact on supply chain collaborative inventory management, indicating that supply chain collaborative inventory management needs to focus on recording and analyzing prices in the actual operation process [1].

4.2. Value Analysis of Information Sharing in the Supply Chain

4.2.1. Comparative Analysis of Bullwhip Effect under Non-sharing and Sharing.
In traditional supply chain management, the order information issued by upstream companies and downstream companies is used as the basis for demand forecasting, and the predicted results are often larger than the actual demand. Therefore, the most effective way to reduce the bullwhip effect is to realize information sharing in the supply chain, not only sharing customer demand information with each level member of the supply chain but also sharing the information of each member in the supply chain. Integrate all information to forecast demand instead of relying on the only order information from downstream to make forecasts. In order to further illustrate the value of information sharing in the supply chain, the following uses the moving average prediction method to quantitatively analyze the bullwhip effect in the supply chain with or without information sharing and compares them.

According to the above formula, set BE as the ordinate and the number of observation periods n as the abscissa. The number of observation periods is $k = 1, 4$, and 6, respectively. The results are shown in Table 3 and Figure 6.

The above results are the bullwhip effect of supply chain information in the case of nonsharing and sharing. According to the data analysis in the figure, it can be seen that when $k = 1$, that is, the first-level member retailer in the supply chain, the retailer directly faces the needs of end customers, regardless of whether the information in the supply chain is shared, and the result is the same Yes, both have the same bullwhip effect pattern. When $k = 4$ or 6, the bullwhip effect in the case of information sharing is significantly lower than that in the case of no information sharing.

4.2.2. Inventory Comparison of Retailers and Wholesalers under Nonsharing and Sharing.
Since the retailer of the first-level member of the supply chain always faces the needs of end customers and the needs of end customers are the same in the case of supply chain implementation and nonimplementation of information sharing, the retailer is in order to meet customer needs in a timely manner. The inventory level maintained should also be the same in the case of information sharing and nonsharing; retailers will share the actual demand information of end customers so that upstream companies in the supply chain

TABLE 1: Sensitivity analysis table.

Time (week)	1	8	15	22	29	36	43	50
Consumer demand forecast	0	0	0	0	72.15	657.57	345.45	489.80
Retailer inventory	0	0	0	0	54.24	1384.87	-680.10	3.40
Wholesaler inventory	17.65	14.24	11.11	4.32	-2.34	-962.63	-711.34	-165.45
Manufacturer inventory	17.65	14.22	11.23	-9.23	-721.87	22.85	-478.36	-503.89
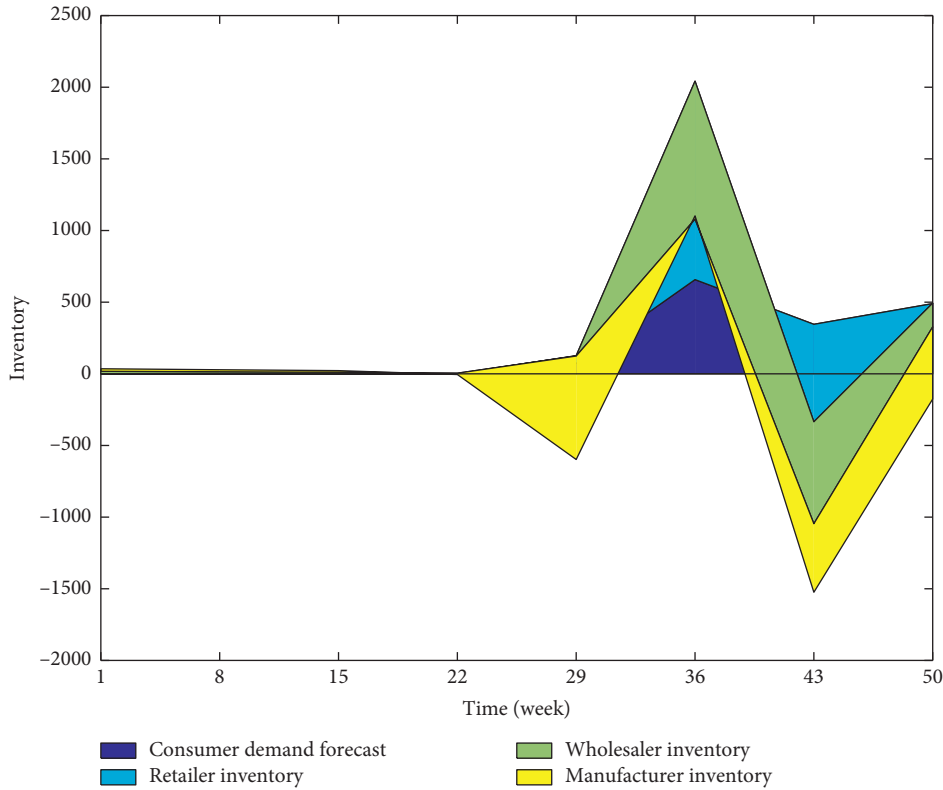
FIGURE 3: Sensitivity analysis.

TABLE 2: The impact of price on each inventory.

Time(week)	1	4	7	10	13	16	19	22	25	28
Consumer demand forecast-current	1	1	0	1	3	25	13	10	5	3
Consumer demand forecast-change	1	1	0	0	1	6	2	1.5	0.5	0
Retailer inventory-current	10	13	8	10	10	30	60	-17	-6	2
Retailer inventory-change	10	13	8	10	10	13	11	0	4	6
Wholesaler inventory-current	11	11	8	11	11	11	11	-24	-8	11
Wholesaler inventory-change	11	11	8	11	11	11	7	5	9	3
Manufacturer inventory-current	20	18	19	19.5	19	14	-23	20	-4	14
Manufacturer inventory-change	20	18	19	19.5	19	17	14	19.5	15	19

can grasp the information of downstream companies in a timely manner to formulate relevant information. Upstream companies in the supply chain can formulate inventory plans based on corresponding order information or production plans to meet the needs of downstream companies, so they do not have to worry about inventory issues. Compared with the case of nonshared information, the inventory is much lower. The results are shown in Table 4 and Figure 7.

4.2.3. Comparative Analysis of Manufacturers' Inventory under Nonsharing and Sharing. The farther the bullwhip effect is from the customer, the greater the demand fluctuation will be. In the case of nonsharing, the manufacturer produces according to the order information of the subordinate members, and the information is transmitted and modified at the first level of the supply chain, which finally causes the demand information to be distorted and enlarged, causing the manufacturer to produce too many products and
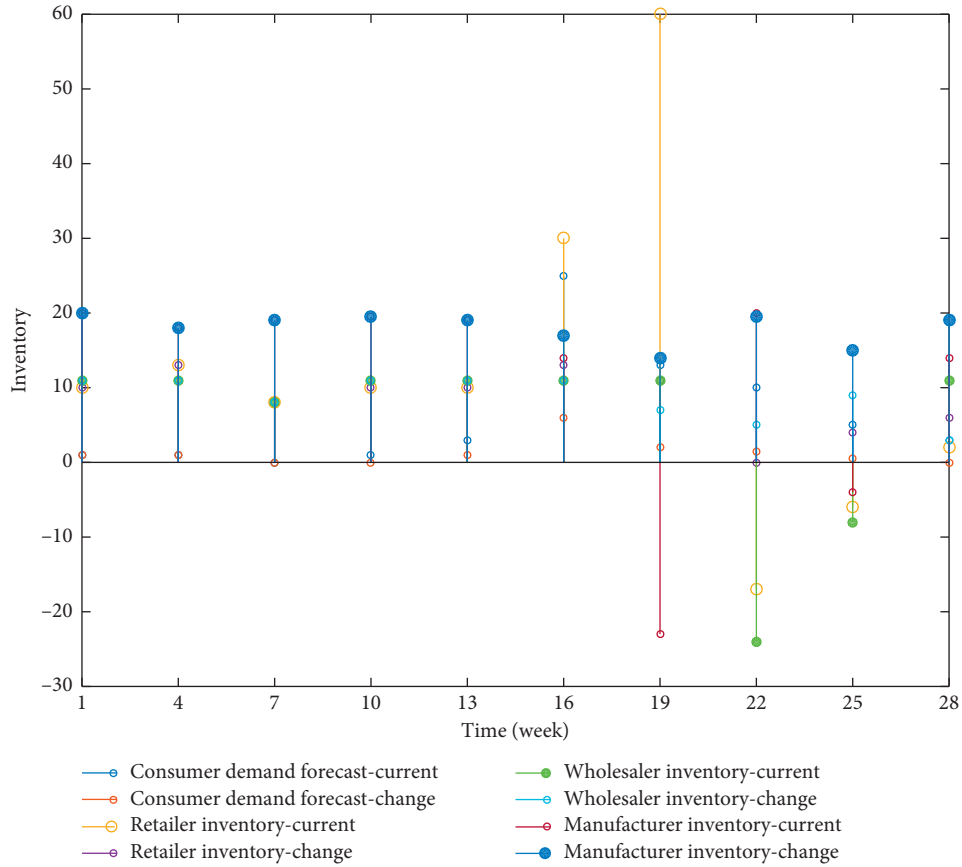
Figure 4: Degree of influence of price on each inventory.
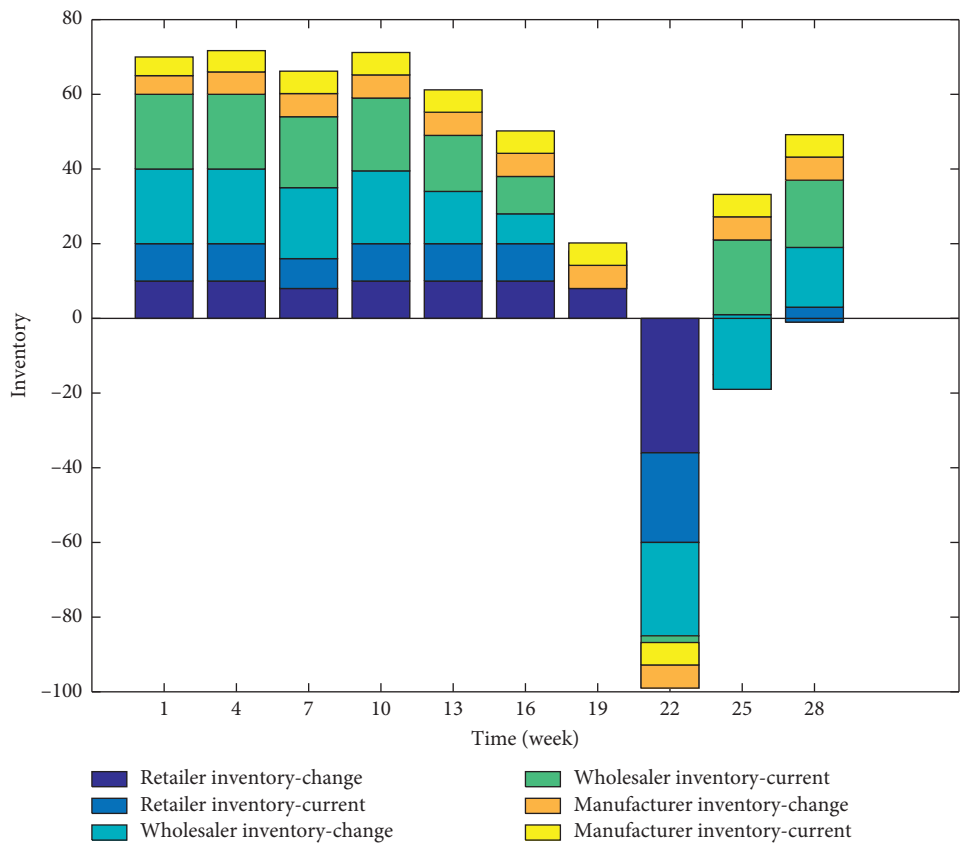
Figure 5: The degree of influence of consumer demand on each inventory and price in the first period.

TABLE 3: Comparison of the bullwhip effect with or without information sharing in the supply chain.

Information sharing	Unshared $k = 1$	Unshared $k = 4$	Unshared $k = 6$	Shared $k = 1$	Shared $k = 4$	Shared $k = 6$
1	1	7	24	1	5	10
2	1	4	6	1	3	4.7
3	1	3	4	1	3	4.1
4	1	2.5	3	1	2.5	3.2
5	1	2	2	1	2	2.3
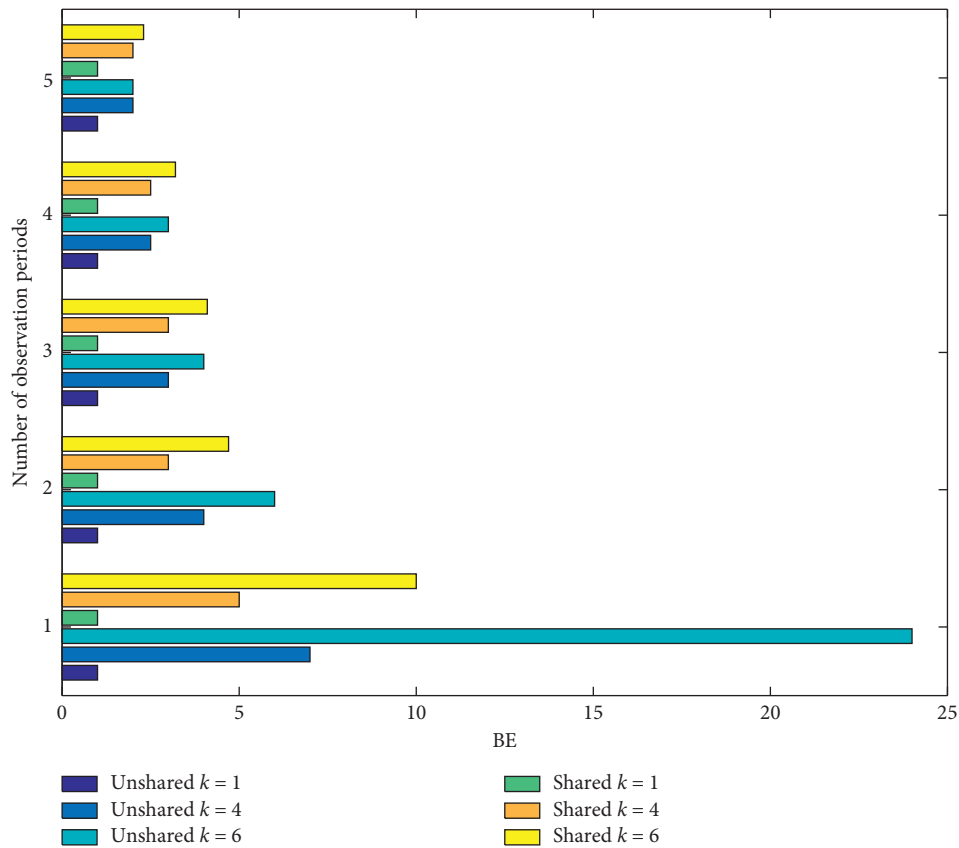
FIGURE 6: Comparison of bullwhip effect with or without information sharing in the supply chain.

TABLE 4: Inventory comparison of retailers and wholesalers under nonsharing and sharing.

Simulation value point	1	2	3	4	5	6	7	8
Nonshared-retailer inventory	0	100	48	73	25	1	0	0
Share-retailer inventory	0	98	46	73	22	2	1	0
Nonshared-batch distributor inventory	0	150	30	0	17	0	19	0
Sharebatch distributor inventory	0	170	60	11	10	11	16	0

a large backlog of inventory; under sharing, the manufacturer obtains the shared information and directly grasps the terminal customer demand information and then makes predictions and formulates the production plan based on this. As shown in Figure 8, the inventory level of producers under nonsharing is significantly greater than that under sharing.

To sum up, we can learn from the above analysis of the results that when the supply chain implements information sharing, the operating costs and risks of each node enterprise
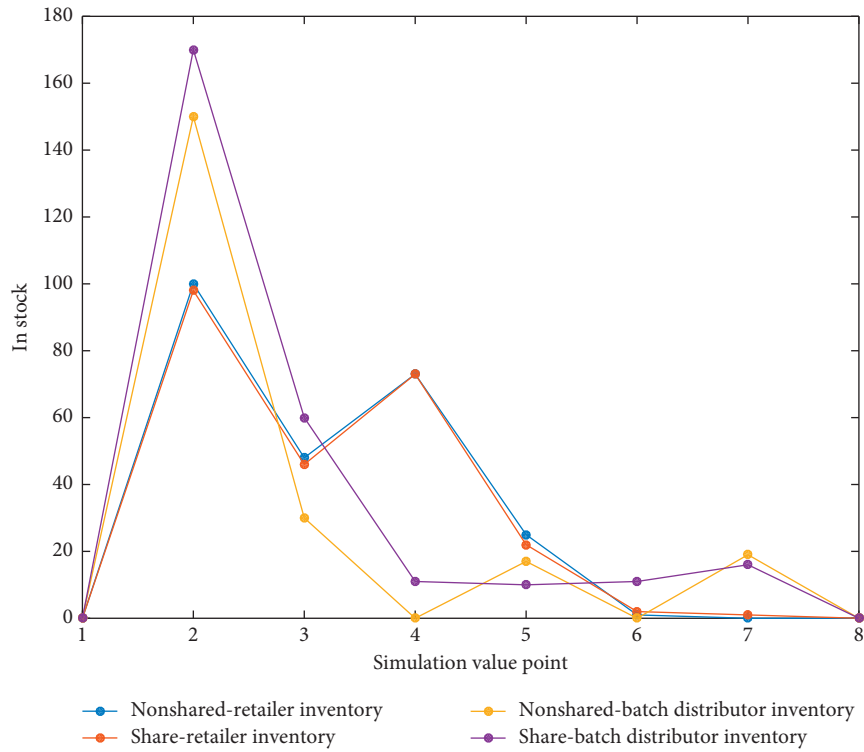
Figure 7: Inventory comparison of retailers and wholesalers under nonsharing and sharing.
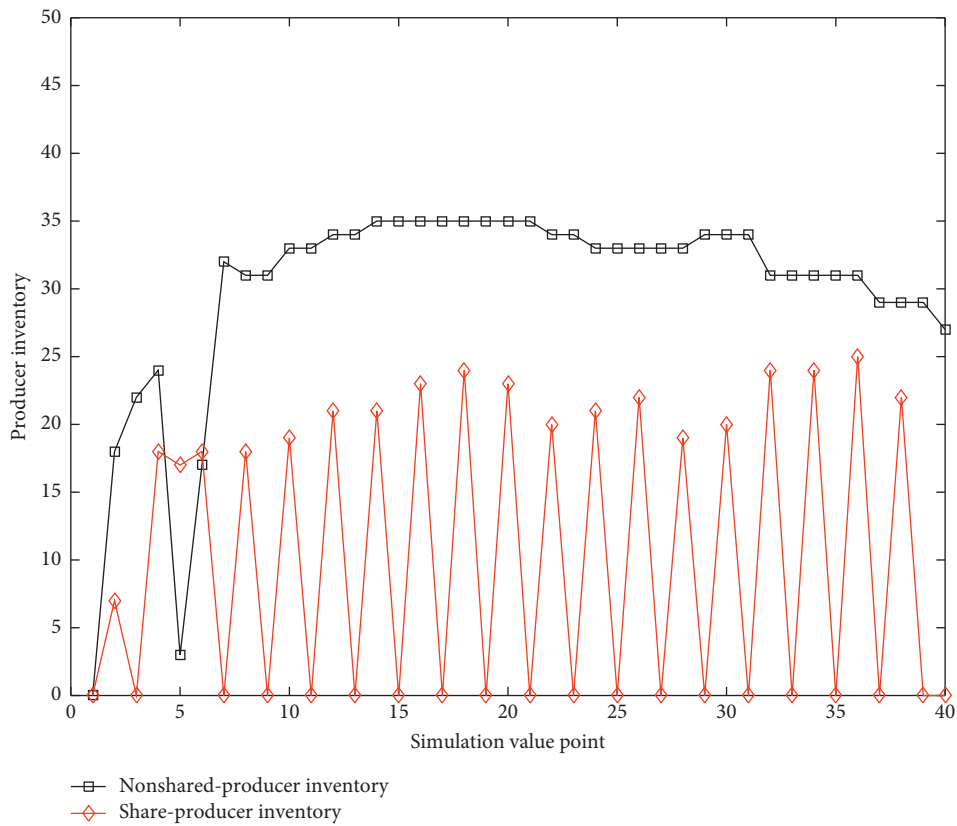
Figure 8: Comparison of manufacturer inventory under nonsharing and sharing.

in the supply chain are lower than those in the case of nonsharing [32], and it also illustrates the overall supply chain benefits are correspondingly improved, and market competitiveness is enhanced. The simulation results have good guidance and reference significance for the operation of enterprises in reality.

5. Conclusions

This article proposes an inventory management information platform framework that adapts to the environment of the Internet of Things, that is, the Internet of Things inventory management information platform. Through this information platform, the inventory information or other operational information of each node company can be provided to other companies in the supply chain through the service interface so as to achieve the role of information sharing and transmission, effectively reducing the uncertainty of the supply chain and reducing the impact of the bullwhip effect.

The supply chain is a complex system that requires members to share information to reduce the bullwhip effect, achieve synchronization of decision-making, reduce inventory, and improve market response. Therefore, information sharing is an important content of supply chain research. In the research of information exchange, most of the researchers put forward the incentive mechanism to promote information exchange on the basis of specific relationship and the lack of research on the information exchange mechanism in supply chain management. On this basis, this article focuses on this issue and discusses the relationship between the benefits, costs, risks, and the relationship between the supply chains in the information exchange implementation mechanism.

Due to time constraints and lack of experience, this information platform still has some shortcomings. (1) The interface design of the information platform is not perfect. Enterprise informatization will become an indispensable part of the future development of the enterprise. The inventory information of the Internet of Things is not very clear about the integration of enterprise resources and management systems. (2) The functionality of the system is not good enough. Although the asynchronous technology used in the system reduces the transmission of data and improves the user's operating experience, due to the shortcomings of the system itself and the degree of support of the browser, the system is in the human-machine interface, operation method and the response time cannot meet the demand well.

Data Availability

No data were used to support this study.

Conflicts of Interest

The authors declare that they have no conflicts of interest.

References

[1] S.-B. Tsai, Y.-M. Wei, K.-Y. Chen, L. Xu, P. Du, and H.-C. Lee, "Evaluating green suppliers from a green environmental perspective," *Environment and Planning B: Planning and Design*, vol. 43, no. 5, pp. 941–959, 2016.

[2] J. E. Hernández, A. C. Lyons, and K. Stamatopoulos, "A DSS-based framework for enhancing collaborative web-based operations management in manufacturing SME supply chains," *Group Decision and Negotiation*, vol. 25, no. 6, pp. 1237–1259, 2016.

[3] E. M. Mitchell and J. V. Kovach, "Improving supply chain information sharing using Design for Six Sigma," *European Research on Management and Business Economics*, vol. 22, no. 3, pp. 147–154, 2016.

[4] R. Parada, J. Melià-Seguí, and R. Pous, "Anomaly detection using rfid-based information management in an Iot context," *Journal of Organizational and End User Computing*, vol. 30, no. 3, pp. 1–23, 2018.

[5] M. G. Kim, Y. M. Hwang, and J. J. Rho, "The impact of RFID utilization and supply chain information sharing on supply chain performance: focusing on the moderating role of supply chain culture," *Maritime Economics & Logistics*, vol. 18, no. 1, pp. 78–100, 2016.

[6] Z. Lv and W. Xiu, "Interaction of edge-cloud computing based on SDN and NFV for next generation IoT," *IEEE Internet of Things Journal*, no. 99, p. 1, 2019.

[7] Z. Xia, X. Wang, L. Zhang et al., "A privacy-preserving and copy-deterrence content-based image retrieval scheme in cloud computing," *IEEE Transactions on Information Forensics & Security*, vol. 11, no. 11, pp. 2594–2608, 2017.

[8] W. Hua, Y. Xun, B. Elisa et al., "Protecting outsourced data in cloud computing through access management," *Concurrency & Computation Practice & Experience*, vol. 28, no. 3, pp. 600–615, 2016.

[9] M. Masdari, S. Valikardan, Z. Shahi, and S. I. Azar, "Towards workflow scheduling in cloud computing: a comprehensive analysis," *Journal of Network and Computer Applications*, vol. 66, pp. 64–82, 2016.

[10] X. Azar, L. Jiao, W. Li, and X. Fu, "Efficient multi-user computation offloading for mobile-edge cloud computing," *IEEE/ACM Transactions on Networking*, vol. 24, no. 5, pp. 2795–2808, 2016.

[11] F. Fu, O. Ibrahim, and N. Ithnin, "Factors influencing cloud computing adoption for e-government implementation in developing countries," *Journal of Systems and Information Technology*, vol. 18, no. 3, pp. 297–327, 2016.

[12] R. C. Shah and Y. Wang, "Cloud Things Construction - the integration of Internet of things and cloud computing," *Future Generation Computer Systems*, vol. 56, pp. 684–700, 2016.

[13] M. Mesbahi and A. M. Rahmani, "Load balancing in cloud computing: a state of the art survey," *International Journal of Modern Education and Computer Science*, vol. 8, no. 3, pp. 64–78, 2016.

[14] P. D. Masoud Rahmani, V. Papakonstantinou, and I. Kamara, "The cloud computing standard ISO/IEC 27018 through the lens of the EU legislation on data protection," *Computer Law & Security Review*, vol. 32, no. 1, pp. 16–30, 2016.

[15] D. Jiang, L. Shi, P. Zhang et al., "QoS constraints-based energy-efficient model in cloud computing networks for

multimedia clinical issues," *Multimedia Tools and Applications*, vol. 75, no. 22, pp. 1–22, 2016.

[16] K. Chandran, V. Shanmugasudaram, and K. Subramani, "Designing a fuzzy-logic based trust and reputation model for secure resource allocation in cloud computing," *International Arab Journal of Information Technology*, vol. 13, no. 1, pp. 30–37, 2016.

[17] A. Choudhary, S. Rana, and K. J. Matahai, "A critical analysis of energy efficient virtual machine placement techniques and its optimization in a cloud computing environment," *Procedia Computer Science*, vol. 78, pp. 132–138, 2016.

[18] F. A. Silva, G. Zaicaner, E. Quesado, M. Dornelas, B. Silva, and P. Maciel, "Benchmark applications used in mobile cloud computing research: a systematic mapping study," *The Journal of Supercomputing*, vol. 72, no. 4, pp. 1431–1452, 2016.

[19] M. M. Dornelas, A. S. Ibrahim, and M. E. Wahed, "Translation from Arabic speech to Arabic sign language based on cloud computing," *Egyptian Informatics Journal*, vol. 17, no. 3, pp. 295–303, 2016.

[20] F. Koch, M. D. Assunção, C. Cardonha, and M. A. S. Netto, "Optimising resource costs of cloud computing for education," *Future Generation Computer Systems*, vol. 55, pp. 473–479, 2016.

[21] R. Netto, N. Kumar, and S. Zeadally, "Network service chaining in fog and cloud computing for the 5G environment: data management and security challenges. IEEE communications magazine," *Enterprise Information Systems*, vol. 11, no. 1–5, pp. 105–121, 2017.

[22] K. Li, C. Liu, K. Li, and A. Y. Zomaya, "A framework of price bidding configurations for resource usage in cloud computing," *IEEE Transactions on Parallel and Distributed Systems*, vol. 27, no. 8, pp. 2168–2181, 2016.

[23] J. Zomaya, P. S. Thenkabail, M. K. Gumma et al., "Automated cropland mapping of continental Africa using Google Earth Engine cloud computing," *ISPRS Journal of Photogrammetry and Remote Sensing*, vol. 126, no. 12, pp. 225–244, 2017.

[24] L. Teluguntla, D. Jiang, and Z. Lv, "Modeling network traffic for traffic matrix estimation and anomaly detection based on Bayesian network in cloud computing networks," *Annals of Telecommunications*, vol. 72, no. 5-6, pp. 1–9, 2017.

[25] B. Feng, X. Ma, C. Guo et al., "An efficient protocol with bidirectional verification for storage security in cloud computing," *IEEE Access*, vol. 4, no. 99, pp. 7899–7911, 2017.

[26] T. Adhikary, A. K. Das, M. A. Razzaque, A. Almogren, M. Alrubaian, and M. M. Hassan, "Quality of service aware reliable task scheduling in vehicular cloud computing," *Mobile Networks and Applications*, vol. 21, no. 3, pp. 482–493, 2016.

[27] M. Almogren, "A survey of machine learning applications for energy-efficient resource management in cloud computing environments," in *Proceedings of the 2015 IEEE 14th International conference on machine learning and applications (ICMLA)*, Miami, FL, USA, December 2016.

[28] M. R. Palattella, M. Dohler, A. Grieco et al., "Internet of things in the 5G era: enablers, architecture, and business models," *IEEE Journal on Selected Areas in Communications*, vol. 34, no. 3, pp. 510–527, 2016.

[29] Z. Rizzo and H. Song, "Trust mechanism of multimedia network," in *Proceedings of the ACM Transactions on Multimedia Computing, Communications, and Applications (TOMM)*, New York; NY, USA, June 2020.

[30] D. Owunwanne and R. Goel, "Radio frequency identification (RFID) technology: gaining a competitive value through cloud computing," *International Journal of Management & Information Systems*, vol. 14, no. 5, pp. 157–164, 2016.

[31] S. Namasudra and P. Roy, "PpBAC," *Journal of Organizational and End User Computing*, vol. 30, no. 4, pp. 14–31, 2018.

[32] Y. Xu, W. Zheng, W. Li, and Y. Huang, "Large group Activity security risk assessment and risk early warning based on random forest algorithm," *Pattern Recognition Letters*, vol. 144, p. 1, 2021.

Research Article

To Improve the Real-Time Performance of Airborne Data Link Communication System

Gang Yao (ID)

School of Automation, Northwestern Polytechnical University, Xi'an 710072, Shaanxi, China

Correspondence should be addressed to Gang Yao; yao_gang@mail.nwpu.edu.cn

Ground-to-air data link communication has the advantages of fast transmission rate, strong anti-interference ability, and large data communication volume and has been widely used in the field of civil aviation. This article mainly studies the measures to improve the real-time performance of the airborne data link communication system. The design of the hardware platform of the jamming environment simulator needs to comprehensively consider the implementation complexity of the jamming environment model and the real-time simulation method adopted by the UAV data link system. This paper uses the multicore and multithread in the Linux operating system to simulate the functions of the original data link communication system and uses the TFT screen to display the data communication process in the multicore and multithread design scheme. When evaluating and scoring the evaluation indicators, it must be carried out in accordance with certain standards. However, most of the indicators cannot be directly assessed quantitatively only through certain specific values. This article mainly uses the AHP method to analyze the weight of indicators. In the simulation, user information is generated by a random code generator and then distributed to each branch through serial-to-parallel conversion (S/P), and the spreading process is completed by long-code spreading on each branch, respectively, by BPSK. It is modulated on different carriers to form a transmission signal; the signal passes through a Gaussian white noise channel, and a certain frequency offset noise is added at the same time to reach the receiving end; the receiving end uses correlated demodulation, and after despreading, the error rate is counted. The data shows that under different distances, the frame loss rate of the data link is different. The frame loss rate in the 500 m range is about 1%, and the frame loss rate in the 2 km range is about 2.3%. The results show that the real-time performance of the data link communication system in this paper has been greatly improved.

1. Introduction

With the popularization and application of information theory, data link technology has evolved from traditional combat support to main combat weapons and has been proved in many wars since the 1990s. Compared with traditional wireless communication, there are many scenarios in which a wireless communication base station is used [1]. It can not only realize real-time communication in closed buildings such as rooms and parking lots but also realize real-time communication in the streets with high-rise buildings. This is of great significance for the development of wireless communication base stations.

UAV downlink data link not only solves the problems of long time [2], low timeliness, and instability of traditional

relay communication but also ensures the accuracy and integrity of the received information to the greatest extent due to its mobility and flexibility and further improves the processing capacity of the whole system for docking and receiving information. Whether the communication can be carried out at high speed, timely, correctly, and safely is the key factor affecting the success of the task. Therefore, the simulation research of UAV airborne communication system has great military practical significance [3].

For wireless communication in an open space, it is bound to be subject to various interferences from the open space. Long et al. reexamined the channel characteristics of indoor visible light communication systems. His purpose is to evaluate channel frequency selectivity, in other words, to evaluate the importance of intersymbol interference (ISI) at

the receiver and the need for channel equalization to restore the transmitted data. He focused on the effect of indoor channels by assuming that there is no bandwidth limitation on light-emitting diodes and considering a simple intensity modulation technique (not including discrete multitone modulation). First, he simulated the channel impulse response (CIR) using an iterative site-based method. Then, he studied the conventional indicators used to evaluate channel frequency selectivity, namely, root mean square delay spread and channel frequency response. Although his algorithm is necessary, it lacks accuracy [4]. Rahmani Hosseinabadi et al. proposed an efficient partial transmission sequence technology based on genetic algorithm and peak optimization algorithm (gapoa) to reduce the peak-to-average power ratio (PAPR) in the visible light communication system based on orthogonal frequency division multiplexing (vlc-ofdm). By analyzing the advantages and disadvantages of the mountain climbing algorithm [5], he proposed a kind of Poa with excellent local searchability, which can further process the signal whose PAPR still exceeds the threshold after being processed by genetic algorithm (GA). He evaluated the PAPR performance and bit error rate (BER) performance, compared them with ga-pts and genetic-based PTS, and compared them with gh-pts and sflahc-pts [6]. Although his research performance is better, the factors considered are not comprehensive [7]. Thakur P believes that, recently, due to the explosive growth of application requirements for bandwidth, the demand for the radio spectrum of the next-generation communication system continues to increase, which has caused the problem of spectrum scarcity. Among the proposed solutions to this problem, he uses the well-researched cognitive radio (CR) technology and the recently introduced nonorthogonal multiple access (NOMA) technology. Both technologies are used to effectively use the spectrum and ensure a significant increase in spectrum efficiency [8]. He introduced the framework for implementing NOMA on CR and the feasibility of the proposed framework. In addition, he discussed the differences between the proposed CR-NOMA and the conventional CR framework. Finally, he discussed potential issues regarding CR-NOMA's implementation. Although his research has certain feasibility, it lacks necessary data [9]. Kaddoum considers that the decrease of data rate and energy efficiency caused by the transmission of an equal reference signal and data carrier signal constitutes the main disadvantage of the DCSK system. In order to overcome this main shortcoming, he proposed a short reference DCSK system (SR-DCSK). To construct the transmitted data signal, P tandem copies of R are used to extend the data. This operation improves data rates and energy efficiency without adding complexity to the system architecture. He uses the receiver's knowledge of integers R and P to recover data. He analyzed the proposed system and calculated the enhanced data rate and bit energy saving percentage. Although his research enhanced the data rate, it was not accurate enough [10].

In this paper, the Turbo code is selected as the error-correcting code for the airborne data chain in consideration of hardware resources, feasibility, anti-interference ability, and other aspects, the Turbo code scheme is improved, and finally, FPGA implementation is implemented. It plays a very important role in the communication system. The research on the information coding technology of airborne data link lays a certain foundation for the design of the message frame format, transmission mode, and signal processing method of the new airborne data link and verifies its effectiveness through the computer simulation, which provides a reference basis and technical support for the formulation of the message standard of the new airborne data link.

2. Airborne Data Link Communication System

2.1. Airborne Data Link. The terminal of the wireless data link, no matter it is a source or a host, is equivalent to a microcomputer, which has the ability to process information independently and can complete the modulation and demodulation function of transmitting the information. Moreover, according to the specified communication protocol, the demodulated information can be processed by group frames, and the true meaning of information transmission can be read out to achieve the purpose of communication [11]. On the other hand, the terminal equipment can also modulate the information to be expressed according to the communication protocol and then transmit it in the channel to complete the information feedback. As for the transmission channel of wireless data link, it covers a wider range, including not only transmission media but also some other devices, such as antenna [12]. In the data link communication system of a small unmanned helicopter [13], when the information load between UAV and ground station is too large, the throughput of the network will decrease, resulting in congestion. The expression of congestion detection function is as follows:

$$\rho = \frac{\left(\eta \times l_{\text{before}} + (1 - \eta) \times l_{\text{now}} \right)}{q}. \tag{1}$$

In the formula, q is the queue space. The formula for calculating the received power P_r of the receiving node is

$$\text{Pr} = P_0 + A_m + H_b + H_m + K_T. \tag{2}$$

In the automatic power control strategy, it is assumed that the energy consumption parameter α is

$$\alpha = \frac{e_r(k)}{e_0(k)}. \tag{3}$$

In general, when $k > 1$, the equivalent radius of the Earth is larger than the actual radius. For the same antenna and aircraft height, atmospheric refraction means that the communication distance of the data link increases, and the equivalent radius coefficient K of standard refraction is 1.333. The limit distance of line-of-sight propagation is

$$d_{(Km)} = 4.12 \left(\sqrt{h_{1(m)}} + \sqrt{h_{2(m)}} \right). \tag{4}$$

During the flight, the distance between the aircraft and the ground control station is constantly changing, and it may appear at any point within the line-of-sight range.

Compared with the receiver, the received signal will only be very close when it is very close to the signal source [14]. On the contrary, the farther the distance is, the worse the signal will be, and this change is not a simple linear change. When it exceeds a certain distance, the signal strength will drop sharply [15, 16]. The form of the uplink modulation signal is

$$S_{\text{up}}(t) = \sqrt{2P_{\text{Iup}}}d_{\text{TCup}}\cos(2\pi f_{\text{up}}t) - \sqrt{2P_{\text{Qup}}}d_{\text{IMGup}}(t)c_{\text{IMGup}}\sin(2\pi f_{\text{up}}t). \tag{5}$$

In the formula, $c_{\text{IMGup}}(t)$ represents the pseudocode of the uplink communication branch, and f_{up} represents the uplink carrier frequency.

The downlink modulation signal form is

$$S_{\text{dn}}(t) = \sqrt{2P_{\text{TMdn}}}d_{\text{TM}}(t)c_{\text{TMdn}}\cos(2\pi f_{\text{dn}}t) - \sqrt{2P_{\text{MIMGdn}}}d_{\text{MIMGdn}}(t)\sin[2\pi(f_{\text{dn}} \pm \Delta f_1)t]. \tag{6}$$

In the formula, Δf_1 is the frequency difference between the target image branch and the telemetry branch [17, 18].

Assuming that the coordinates of the ground station are (x_0, y_0, z_0) and the coordinates of the aircraft are (x_i, y_i, z_i), then

$$\begin{aligned}(D^2 - h^2)\cos^2\theta &= (x_i - x_0)^2, \\ (D^2 - h^2)\sin^2\theta &= (y_i - y_0)^2.\end{aligned} \tag{7}$$

Then the aircraft coordinates can be obtained:

$$\begin{aligned}x_i &= x_0 + \sqrt{(D^2 - h^2)}\cos\theta, \\ y_i &= y_0 + \sqrt{(D^2 - h^2)}\sin\theta, \\ z_i &= z_0 + h.\end{aligned} \tag{8}$$

At present, the M sequence is obtained through large-scale search and detailed calculation. Using the form of feedback function, the M sequence can be expressed as

$$f(x_1, x_2, \ldots, x_k) = x_1 + f_1(x_1, x_2, \ldots, x_k). \tag{9}$$

The autocorrelation function of the commonly used Barker code can be expressed as

$$\rho(t) = \sum_{k=1}^{n-t} x_k x_{k+t} = \begin{cases} n, & t = 0, \\ 0 \text{ or } \pm 1, & 0 < t < n, \\ 0, & t \geq n.\end{cases} \tag{10}$$

In the AWGN channel, the receiving sequence is

$$r(n) = s(n)e^{j2\pi f_e nT + j\theta} + w(n). \tag{11}$$

Among them, $w(n)$ is additive white Gaussian noise, and T is the symbol interval. Then, the ML probability is

$$\Lambda(f_e) = -\sum_{n=0}^{N-1}\left|r(n) - s(n)e^{j2\pi f_e nT + j\theta}\right|^2. \tag{12}$$

The carrier insertion method system is shown in Figure 1. At the receiving end of the communication system, the carrier frequency transmitted by the system can be filtered out by using a narrow-band filter. Here, it is necessary to ensure that the center frequency of the narrow-band filter is the same as the inserted carrier frequency. At the same time, due to the orthogonal effect, the phase shift $\pi/2$ operation is also required [19]. In a word, the key of the carrier insertion method is a narrow-band filter with the same carrier frequency, which is usually completed by PLL, and its hardware implementation is [20–22].

2.2. Communication System. In order to improve the confidentiality and security of the data link communication process, it is necessary to deeply study the confidentiality of various communication systems [23]. In order to suppress the adjacent channel interference generated by the transmitting end, a filter with a high Q value is adopted before the power amplifier rear stage of the transmitting end to filter the stray signals from the orthogonal modulation circuit and prevent the interference to the receiving end caused by amplifier amplification [24]. At the same time, in order to realize full-duplex work, a pair of a machine is designed to isolate the transmitting signal and the receiving signal, so as to prevent the large signal of the transmitting end from interfering with the receiving end [25]. Cooperative engagement capability data link with other data chain's biggest difference is the cooperative engagement capability, and conventional data link is only in view of the target track, speed grades, and tracking accuracy of information processing [26].

2.3. System Real Time. If the transmission rate is too fast, it is easy to affect the communication performance. Therefore, in order to study the relationship between transmission rate and bit error rate, the relationship between transmission rate and signal-to-noise ratio is established by taking the signal-to-noise ratio as a bridge, so as to evaluate the link bit error performance [27]. The data to be transmitted is sent to the fountain code encoder to code the transmitted data, then the pilot sequence is added according to the specified data frame structure, and the information is grouped. The grouped data is modulated by QPSK. Before transmission, the data is
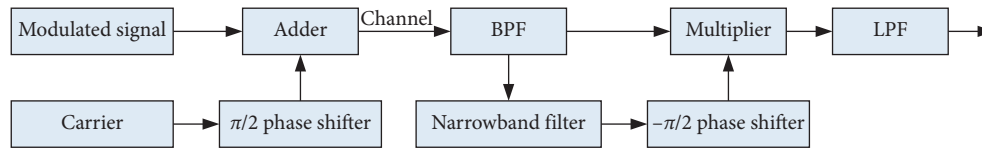
FIGURE 1: Carrier insertion method system.

baseband shaped by a baseband shaping filter. At the same time, to achieve the transmission purpose of no intersymbol interference, a matching filter is added at the receiving end [28]. The receiver sends the received data into the matched filter and uses the matched filtered data for frame synchronization. The frame synchronization information is divided into two parts. The training sequence pilot head is used to complete channel estimation. The data segment and the output of the channel estimation module are used to realize channel equalization. The output data of the equalizer is demodulated and decoded by fountain code multiuser likelihood ratio iterative detection, and finally, the received data can be obtained [29, 30].

3. System Test

3.1. System Indicators. The performance index of the UAV data link jamming environment simulator is shown in Table 1. The hardware platform design of the jamming environment simulator needs to comprehensively consider the interference environment model adopted by the UAV data link system and the implementation complexity of the real-time simulation method [31]. In the dynamic flight scene and human interference coexistence environment, the simulator should not only simulate the aviation wireless channel in different scenarios, mainly including path loss, shadow fading, multipath fading, and channel noise, but also simulate different interference patterns in real time [32–34].

3.2. Signal Acquisition. This paper simulates the functions in the original data link communication system through the multicore and multithreading in the Linux operating system and uses the TFT screen to display the data communication process in the multicore and multithreading design scheme [35]. In order to ensure that the communication data transmitted by the operating system through the serial port can be displayed on the TFT screen in real time without delay, it is necessary to test the maximum refresh rate of the TFT screen to determine whether TFT flat can be used as a display of the real-time communication process [36]. The UAV adopts downlink operation mode to transmit telemetry information such as attitude and orientation and response information of the aircraft down. The Earth station adopts the uplink operation mode to upload the inquiry control information of the Earth station; the repeater station adopts the relay operation mode to forward the downtransmitted information of the UAV to the ground station and the uploaded information of the ground station to the UAV [37].

3.3. Data Link Risk Assessment Model. When evaluating and scoring the evaluation indicators, it must be carried out in accordance with certain standards. However, most of the indicators cannot be directly assessed quantitatively only through certain specific values. This article mainly uses the AHP method to analyze the weight of the index [38].

3.4. Data Link Transceiver Equipment Test. The ground test is to select the open view conditions, assemble the airborne terminal on the UAV, fix the UAV on the off-road vehicle, and keep it connected to the flight control system. In addition, in order to observe the status of the drone, a monitoring cable is drawn from the flight control system to the computer for on-site monitoring [39]. The purpose of this operation is to simulate the working condition of the data link during the flight movement of the UAV. It is verified by a system-level simulation platform [40].

3.5. Interference Performance Test. Based on FPGA platform characteristics and clock source frequency setting, each hop differential frequency-hopping signal is processed by FFT 5 times. In the simulation, the user information is generated by the random code generator and then distributed to each branch through the serial-to-parallel conversion (S/P). The spread spectrum processing is completed in each branch through the long-code spread spectrum method and is modulated to different carriers in the way of BPSK to form the transmission signal. The signal passes through the Gaussian white noise channel and adds a certain frequency offset noise to reach the receiving end; the receiver adopts correlation demodulation, and after despreading, the BER is counted [40].

4. System Test Results

4.1. Real-Time Analysis. When the arrival rate and service time of input traffic are different, comparative experiments are carried out from four aspects: bandwidth, loss rate, queue length per unit time, and queue delay. The queue loss rate is shown in Table 2. The performance of the algorithm is shown in Figure 2. In terms of bandwidth allocation, the bandwidth of this algorithm is close to the actual bandwidth, which can well meet the output requirements of each queue. The rationality of bandwidth allocation is close to the WRR algorithm and far better than RR and SP algorithms. In terms of queue loss rate, this algorithm has the lowest queue loss rate. When the RR algorithm is used, the loss rate of queue 4 is 12.09%, and that of queue 3 is higher than 5%. When the SP algorithm is used, the loss rate of queue 4 is 23.93%. When the WRR algorithm is used, all queues are

TABLE 1: Performance indicators of UAV data link interference environment simulator.

Performance parameter	Technical index
Data link signal to be tested	Carrier frequency 70 MHz; bandwidth 10 MHz
External interference source input	Carrier frequency 70 MHz; bandwidth 10 MHz
Dry letter ratio	−20 dB~20 dB
Resolution	2 dB
Built-in noise source type	Gauss
Signal-to-noise ratio	−20 dB~40 dB; resolution 0.1 dB
Channel type	No fading, Rayleigh, rice
Channel status update rate	2 ms, 10 ms, 50 ms, 200 ms
Path loss	0~84 dB; resolution 1 dB

TABLE 2: Queue loss rate.

Loss rate (%)	Queue 1	Queue 2	Queue 3	Queue 4
RR	0	0.11	5.75	12.09
SP	0	0.49	2.21	23.93
WRR	0.99	1.85	1.81	2.88
This article	0.03	0.49	0.56	0.7

lost, but they are controlled within 3%. With this algorithm, the loss rate of each queue is controlled within 1%. As far as the queue length is concerned, both the WRR algorithm and this algorithm can control each queue to maintain a relatively equal length, while other algorithms have different queue lengths, which can easily cause some queue data to lose data due to timeout or overlength. As for queue delay, the WRR algorithm and this algorithm have more fair-queue delay, while the RR algorithm and SP algorithm have a lower delay with higher priority, and lower priority has a higher delay.

Considering that in the airborne data link system, there will inevitably be a lot of noise and various interferences during information transmission, so there is no need to consider the problem of wrong leveling. Therefore, this article mainly studies and simulates the PCCC-type Turbo code. For the data requirements in the data chain, the 1/3 code rate is adopted in the realization scheme. At the same time, considering that the block interleaver is easy to implement in hardware, in order to reduce the complexity in iterative decoding, this paper uses block interleaving as the inner interleaving of Turbo codes. The influence of the change in the number of carriers on system performance is shown in Figure 3. In the absence of frequency offset, when the number of carriers increases, the bit error rate will increase slightly. This is because when the number of carriers increases, the ISI of other carriers on each subcarrier will increase, but because the receiver works in an ideal state, its impact on the bit error rate is not too obvious. It can be seen from the figure that when there is a frequency offset, the bit error rate of the system has been significantly improved. But in the vicinity of 10db, the bit error rate can still reach 10^{-4}. With the increase of RS code redundancy, the coding efficiency is decreasing, and its realization becomes more complicated, and for any real-time communication, the bandwidth must be expanded. That is to say, the improvement of error correction performance comes at the cost of increasing bandwidth.

The comparison results of acquisition time of serial sliding correlation and variable step synchronous acquisition method under 31 symbol offsets are shown in Table 3. The time for the two methods to complete a sliding calculation is basically the same, and the variable step length takes longer time in the decision module than the sliding correlation method. Because the average sliding times are less than the sliding correlation method, the synchronous acquisition time of the variable step method is less than that of the sliding correlation method. With the increase of the number of symbol offsets, the total step size gradually decreases, which can verify the correctness of the variable step size decision method. When the number of symbol offsets between the local signal and the received signal is small, the acquisition time of serial sliding correlation is less than that of variable step size, which is mainly due to the fact that the two methods occupy too much time to the decision module; when the symbol offset of local signal and received signal is greater than 7, the acquisition time of variable step length is less than that of serial sliding correlation. This is mainly due to the large difference in the number of sliding times, and the impact of the module decision time on the overall acquisition time is small, and with the increase of the number of symbol offsets, the synchronous acquisition method with variable step size has better performance.

The synthetic test simulation result of differential frequency-hopping signal is shown as in Figure 4. It can be seen from the figure that the differential frequency-hopping signal generation module is driven by a clock with a sampling frequency of 100 MHz. When the reset signal is invalid, the residence time of each hop of the generated signal is 200 μs, which verifies the hopping of the differential frequency-hopping signal. The speed is 5000 hop/S, which also shows that the generated differential frequency-hopping signal is correct. In the designed differential frequency-hopping bandwidth, it can be clearly seen that it is a differential frequency-hopping signal with 16 frequency points, with a carrier center frequency of 6 MHz and a bandwidth of 2.4 MHz, thus verifying the correctness of the differential frequency-hopping signal.

4.2. Antijamming Performance Analysis. In the range of SNR 15 and the number of transmit and receive antennas from 1 to 10, this paper compares the average decoding time performance of MIMO-OFDM spherical equalization
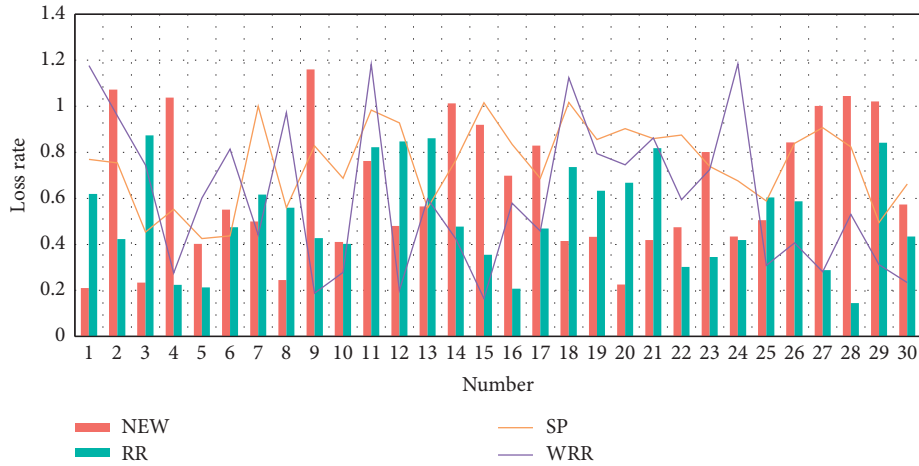
FIGURE 2: Algorithm performance.
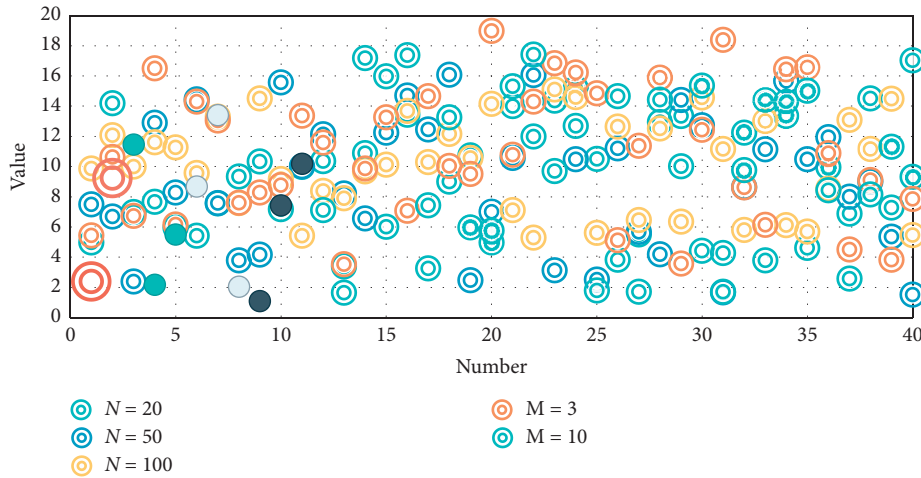
FIGURE 3: The impact of changes in the number of carriers on system performance.

TABLE 3: Comparison of capture time.

	Calculation (s)	Verdict (s)	Once (s)	All (s)
Variable step size	0.000319	0.000878	0.000929	0.010526
Sliding related	0.000107	0.000595	0.000594	0.018308

technology after external joint optimization and that of MIMO-OFDM spherical equalization technology after internal collaborative optimization. Each technology is cycled 10 times, and the performance curve of the simulation experiment is shown in Figure 5. It can be seen from the figure that the average decoding time of the two technologies increases linearly with the increase of the number of transmit and receive antennas, and the average single decoding time of MIMO-OFDM spherical equalization technology after external joint optimization is approximately 1/2 of that of the MIMO-OFDM spherical equalization technology after internal cooptimization. Due to the introduction of microcomputing and GA, the MIMO-OFDM spherical equalization technology after external joint

optimization can maintain the optimal BER performance of MIMO-OFDM spherical equalization technology after internal collaborative optimization, enhance the robustness, reduce the computational complexity, and greatly reduce the average decoding time.

The TU-6 fading channel model is shown in Table 4. The average BER of the two technologies shows a parabolic downward trend with the increase of SNR, and the low-complexity SC-FDESC-CPM technology has basically reached a BER of 0 when the SNR is about 19. The innovative equalization technology route combining SC-FDE technology and SC-CPM technology enables the UAV wireless image transmission data link system to greatly enhance the ability to resist multipath interference while fully improving bandwidth resource utilization. In order to ensure better spurious performance, a narrower bandwidth must be selected. And we choose the DDS output frequency reasonably to avoid the high spurious frequency points, so as to get better spurious performance.

The performance of the Nakagami Fading channel is shown in Figure 6. When other conditions are the same, the performance of convolutional codes in fading channels is
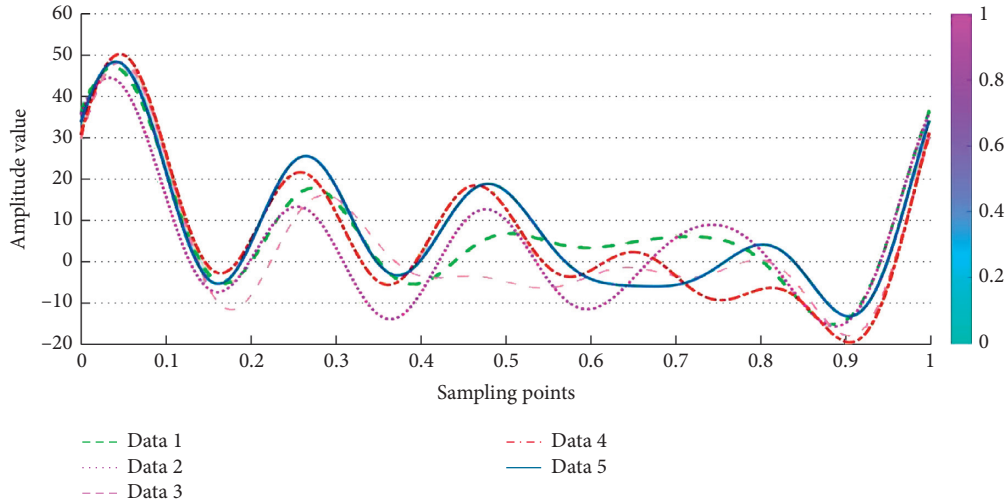
Figure 4: Comprehensive test simulation results generated by differential frequency-hopping signal.
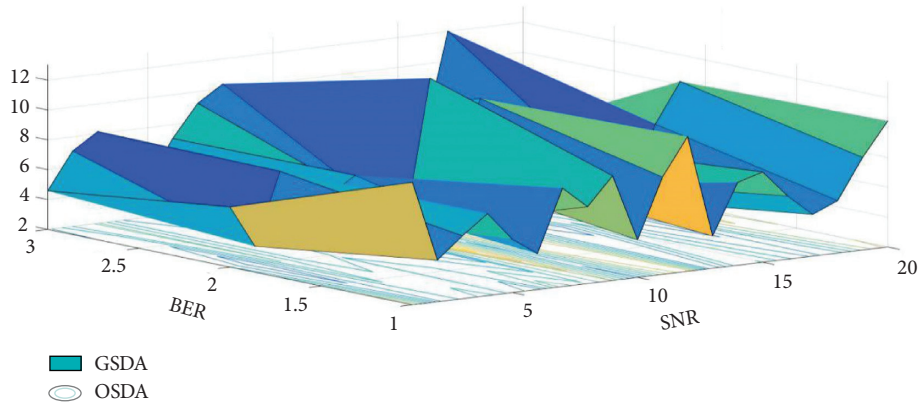
Figure 5: Simulation experiment results.

Table 4: TU-6 fading channel model.

Channel delay	Normalized power
0	0.189
1	0.379
2	0.255
8	0.090
12	0.055
25	0.032

worse than that in Gaussian white channels under the same SNR, and the smaller the m value, the worse the performance of convolutional codes. Compared with RS code, convolutional code has stronger anti-interference ability, and its encoder and decoder have a simple structure, short decoding delay, and strong random error correction ability. Therefore, the CDL and TCDL tactical common data link use convolutional code to encode the information channel, so as to improve the antijamming ability of information transmission. The message delay in the system is directly proportional to the number of messages generated per unit time and also directly related to the rationality of slot allocation. When the number of instantaneous messages exceeds the capacity of

network transmission, the message delay will be greatly increased, and the instantaneous number of messages is directly related to the simulation scenario. When the capacity of a single network cannot meet the delay requirements of the system, the number of stack networks can be increased by stacking to improve the overall capacity of the system and reduce the delay index.

4.3. Sensitivity Test Results. In the experiment, 6000 packets are tested at different distances, and a point is taken for every 20 packets. The total delay of the system is shown in Figure 7. When the distance between the UAV and base station is 200 m, the average value of total system delay is 37.5 ms. When the distance between the UAV and base station is 400 m, the average value of total system delay is about 39 ms. When the distance between the UAV and base station is 1 km, the average value of total system delay is about 43 ms. For an unmanned helicopter system, as long as the system delay is less than 80 ms under manual control, it can meet the control requirements. At different distances, the frame loss rate of the data link is different. The frame loss rate is about 1% in the range of 500 m, 2.3% in the range of 2 km,
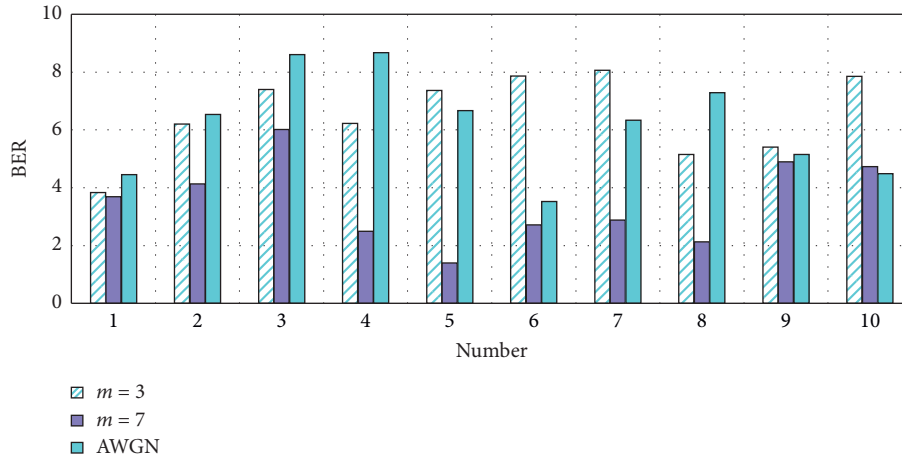
Figure 6: Nakagami fading channel performance.
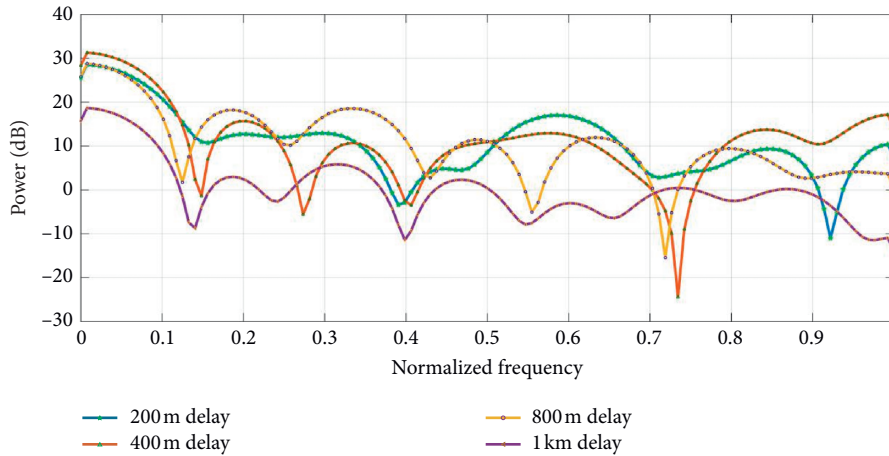
Figure 7: Delay curves at different distances.

and 4.5% in the range of 4 km. In the actual system, the uplink frequency is 30 Hz; for real-time remote control, the frame loss rate less than 10% has no effect.

Different frequency offset signal capture and tracking test results are shown in Figure 8. For the uplink measurement and control receiving channel, it is necessary to comprehensively verify its capture and tracking performance. The first is to capture and test different Doppler frequency offsets. It is necessary to constantly adjust the carrier frequency emitted by the vector signal source to simulate possible frequency offset values. The offset needs to cover the set carrier search range. The second is to test the tracking effect. When the receiver is in a stable tracking state, we adjust the carrier frequency emitted by the signal source to simulate the external dynamic stress and observe whether the Doppler value output by the carrier tracking loop can track the change of the signal. When adjusting the carrier frequency of the signal source, the value of one adjustment cannot be too large; usually, the value of each adjustment is below 1 kHz. When the signal is tracked stably, the output data of channel I and channel Q are basically noise, which can be seen from the magnitude of the correlation value; the frequency error and phase error of the phase detector change

within a small range, and the phase error should generally be kept at within ±15°; that is, if the modulus is less than 0.26, the Doppler value can track the change of the external signal. When the actual measured external signal changes at 2 KHz/s, the tracking loop can still operate normally. Simulation tests and comprehensive results show that at a global clock frequency of 40 MHz, it takes about 0.14248 ms to complete the equalization processing of every 1024 received data, and the ideal peak throughput rate can reach 115 Mbits/s. The maximum clock is 343.595 MHz, which takes fewer resources.

TCM-4CPM demodulation hardware implementation resource occupancy is shown in Table 5. From the output spurious test results of the power amplifier, it can be concluded that the output spurious of each power amplifier unit is less than −50 dBm, the spurious suppression of each power amplifier is better than −50 dBc, and the spurious suppression of the power amplifier unit can meet the design index requirements.

The simulation results of the model are shown in Figure 9. When the nodes in the network send fewer packets and the bus model runs at low load, the delay data in the network is small. When the data is transmitted according to the exponential
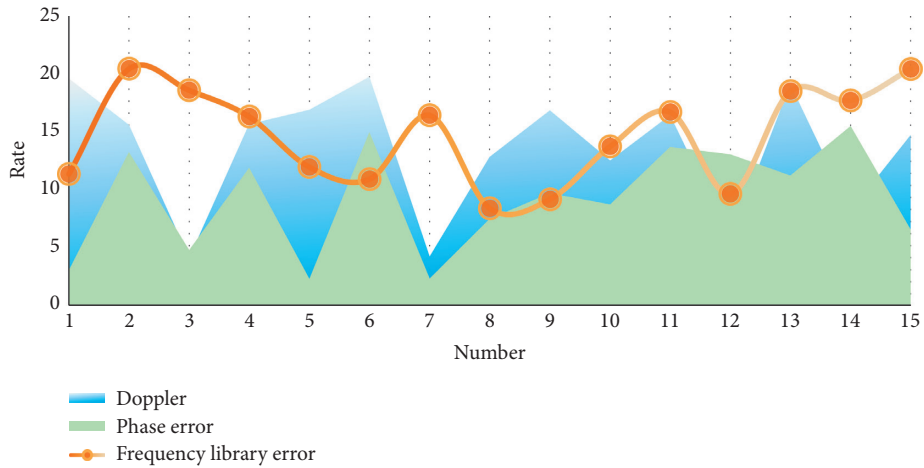
FIGURE 8: Different frequency offset signal capture and tracking test results.

TABLE 5: TCM-4CPM demodulation hardware implementation resource occupation.

Logic	Used	Available	Rate%
Registers	4737	106400	4
LUT	10911	53200	20
BLOCKRAM/FIFO	1	140	1
BUFG/BUFGCTRLs	1	32	3
DSP48 Es	3	220	1
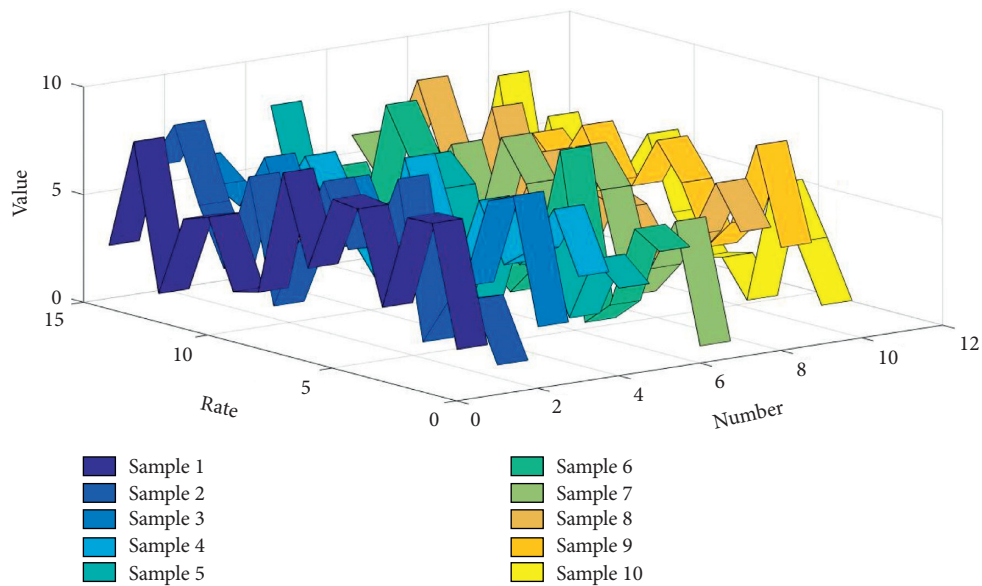
FIGURE 9: Model simulation results.

interval type, the change of network delay is not obvious, the change is not obvious, and it is maintained in a certain range. It can be seen that the real-time performance of the simulation can bus is particularly good when the network is running with low load, which meets the real-time requirements of fieldwork. Since the network is of broadcast bus type, according to the proportion of total data to the total work nodes, and considering the arbitration queue delay caused by different priorities and other factors, the received data of each work node remains stable, which indicates that all nodes have the ability to obtain data equally, and it can be seen that the influence of network arbitration delay is small.

5. Conclusions

With the rapid development of communication technology and the increasing complexity of communication systems, a data link is widely used in the military field. Therefore, it is

more and more important to carry out modeling and simulation work on communication systems and further research on system performance evaluation. This paper mainly studies the measures to improve the real-time performance of airborne data link communication systems. From the technical model and simulation model of the communication data link system, the basic working principle is understood, the modularization analysis is carried out on the communication data link system, the functions of each module and its simulation model are sorted out, and the corresponding simulation work is carried out. It provides a solid theoretical basis for the system performance evaluation model and software design. Through the establishment of the airborne ACARS platform, the accuracy, reliability, real time, and other requirements of the system in sending downlink messages and receiving uplink messages were verified, and relevant tests were conducted under actual conditions. The results show that the system has a good message transceiving function.

Due to the difference of information processing steps on different channels, it will be out of synchronization in time, and the time delayer can ensure that the information after coding is matched in time. The combat mode gradually develops from independent operation to joint operation. Therefore, the communication capacity, transmission distance, and type of transmission information are constantly expanding. In the airborne data link, due to the wide range of aircraft activities, sometimes close to the ionosphere, it is extremely easy to cause the signal to have multiple propagation paths, resulting in a multipath effect. At the same time, due to the fast-moving speed of the combat aircraft, the relative positions of the communication parties will change at a high speed, which will cause the Doppler effect.

With the development of military data communication systems against interference, the requirement of anti-interception performance is gradually improved, and the high-performance error correction algorithm is becoming more and more important in the whole system. Through the analysis of volume pick-up real-time control system request, the volume is obtained by a machine to control the system I/O response time, and the requirement of the minimum sampling period to calculate the hybrid control system of a total spool of pick-up, the I/O response time, the minimum sampling period, and the constructed hybrid bus are analyzed from the angle of real-time control system used for the feasibility of the control volume pick-up.

Data Availability

No data were used to support this study.

Conflicts of Interest

The authors declare that they have no conflicts of interest.

Acknowledgments

References

[1] S. Wan, Z. Gu, and Q. Ni, "Cognitive computing and wireless communications on the edge for healthcare service robots," *Computer Communications*, vol. 149, pp. 99–106, 2019.

[2] Z. Lv, "The security of internet of drones," *Computer Communications*, vol. 148, pp. 208–214, 2019.

[3] S. N. Mohanty, E. L. Lydia, M. Elhoseny, M. Majid, G. Al Otaibi, and K. Shankar, "Deep learning with LSTM based distributed data mining model for energy efficient wireless sensor networks," *Physical Communication*, vol 40, 2020 In press, Article ID 101097.

[4] S. Long, M. A. Khalighi, M. Wolf, S. Bourennane, and Z. Ghassemlooy, "Investigating channel frequency selectivity in indoor visible-light communication systems," *IET Optoelectronics*, vol. 10, no. 3, pp. 80–88, 2016.

[5] A. A. Rahmani Hosseinabadi, J. Vahidi, B. Saemi, A. Kumar Sangaiah, and M. Elhoseny, "Extended genetic algorithm for solving open-shop scheduling problem," *Soft Computing*, vol. 23, no. 13, pp. 5099–5116, 2018.

[6] Y. Liu, H. Deng, S. Ren et al., "Peak-to-average power ratio reduction in orthogonal frequency division multiplexing-based visible light communication systems using a modified partial transmit sequence technique," *Optical Engineering*, vol. 57, no. 1, pp. 016108.1–016108.10, 2018.

[7] P. Thakur, A. Kumar, S. Pandit, G. Singh, and S. N. Satashia, "Frameworks of non-orthogonal multiple access techniques in cognitive radio communication systems," *China Communications*, vol. 16, no. 6, pp. 129–149, 2019.

[8] C. Li, P. Liu, C. Zou, F. Sun, J. M. Cioffi, and L. Yang, "Spectral-efficient cellular communications with coexistent one-and two-hop transmissions," *IEEE Transactions on Vehicular Technology*, vol. 65, no. 8, pp. 6765–6772, 2015.

[9] G. Kaddoum, E. Soujeri, and Y. Nijsure, "Design of a short reference noncoherent chaos-based communication systems," *IEEE Transactions on Communications*, vol. 64, no. 2, pp. 680–689, 2016.

[10] Y. Kyeongseok, B. Hoki, P. Kyungmi et al., "Priority based medium access control and load balancing scheme for shared situational awareness in airborne tactical data link," *The Journal of Korean Institute of Communications and Information Ences*, vol. 41, no. 10, pp. 1210–1220, 2016.

[11] Y. Sun, D. W. K. Ng, J. Zhu, and R. Schober, "Multi-objective optimization for robust power efficient and secure full-duplex wireless communication systems," *IEEE Transactions on Wireless Communications*, vol. 15, no. 8, pp. 5511–5526, 2016.

[12] C. X. Wang, A. Ghazal, B. Ai et al., "Channel measurements and models for high-speed train communication systems: a survey," *IEEE Communications Surveys & Tutorials*, vol. 18, no. 2, pp. 974–987, 2017.

[13] Z. Lv, R. Lou, and K. S. Amit, "AI empowered communication systems for intelligent transportation systems," *IEEE Transactions on Intelligent Transportation Systems*, no. 99, pp. 1–9, 2020.

[14] Q. Wang, Y. Li, and X. Liu, "Analysis of feature fatigue EEG signals based on wavelet entropy," *International Journal of Pattern Recognition and Artificial Intelligence*, vol. 32, no. 08, Article ID 1854023, 2018.

[15] J. Zou, C. Liu, E. José, and A. Schutt, "Development of a wide-tuning-range two-parallel-plate tunable capacitor for integrated wireless communication systems," *International*

Journal of Rf & Microwave Computer-aided Engineering, vol. 11, no. 5, pp. 322–329, 2016.

[16] N. Haridas and E. Elias, "Reconfigurable farrow structure-based FRM filters for wireless communication systems," *Circuits Systems & Signal Processing*, vol. 36, no. 1, pp. 1–24, 2016.

[17] K. Foster and D. Colombi, "Thermal response of tissue to RF exposure from canonical dipoles at frequencies for future mobile communication systems," *Electronics Letters*, vol. 53, no. 5, pp. 360–362, 2017.

[18] R. Bhatia, A. K. Sharma, and J. Saxena, "Improved analysis of four wave mixing with sub-plank higher-order dispersion parameters in optical communication systems," *Optik*, vol. 127, no. 20, pp. 9474–9478, 2016.

[19] Z. Yu, Z. Jian, Z. Yan-Yu et al., "Weight threshold check coding for dimmable indoor visible light communication systems," *IEEE Photonics Journal*, vol. 10, no. 3, pp. 1–11, 2018.

[20] O. S. Badarneh, "Performance evaluation of wireless communication systems over composite α-μ/Gamma fading channels," *Wireless Personal Communications*, vol. 97, no. 4, pp. 1–15, 2017.

[21] B. Das, M. F. L. Abdullah, B. S. Chowdhry et al., "A novel signal regeneration technique for high speed DPSK communication systems," *Wireless Personal Communications*, vol. 96, no. 11, pp. 3249–3273, 2017.

[22] M. Elhoseny and K. Shankar, "Optimal bilateral filter and convolutional neural network based denoising method of medical image measurements," *Measurement*, vol. 143, pp. 125–135, 2019.

[23] Y. Lu, X. Wang, M. D. Higgins, A. Noel, N. Neophytou, and M. S. Leeson, "Energy requirements of error correction codes in diffusion-based molecular communication systems," *Nano Communication Networks*, vol. 11, no. 3, pp. 24–35, 2017.

[24] B. Arif, H. Bahadir, T. Hasan et al., "Optimum transmission distance for relay-assisted free-space optical communication systems," *Optik*, vol. 127, no. 16, pp. 6490–6497, 2016.

[25] L. Wang, W. Chen, Z. Ding, W. Guo, and M. Peng, "Practical framework for ultra-fair dynamic interference coordination in mobile communication systems," *IET Communications*, vol. 10, no. 4, pp. 372–380, 2016.

[26] S. Navaratnarajah, C. Han, M. Dianati, and M. A. Imran, "Adaptive stochastic radio access selection scheme for cellular-WLAN heterogeneous communication systems," *IET Communications*, vol. 10, no. 15, pp. 1986–1994, 2016.

[27] Y. Morag, N. Tal, M. Nazarathy, and Y. Levron, "Thermodynamic signal-to-noise and channel capacity limits of magnetic induction sensors and communication systems," *IEEE Sensors Journal*, vol. 16, no. 6, pp. 1575–1585, 2016.

[28] S. Zhao, "A serial concatenation-based coding scheme for dimmable visible light communication systems," *IEEE Communications Letters*, vol. 20, no. 10, pp. 1951–1954, 2016.

[29] S. P. Karthi and K. Kavitha, "A survey on various reconfigurable architectures for wireless communication systems," *International Journal of Pure and Applied Mathematics*, vol. 119, no. 12, pp. 1427–1433, 2018.

[30] G. Kaddoum, Y. Nijsure, and H. Tran, "Generalized code index modulation technique for high-data-rate communication systems," *IEEE Transactions on Vehicular Technology*, vol. 65, no. 9, pp. 7000–7009, 2016.

[31] I. F. Akyildiz, P. Wang, and S.-C. Lin, "SoftWater: software-defined networking for next-generation underwater communication systems," *Ad Hoc Networks*, vol. 46, no. 8, pp. 1–11, 2016.

[32] C. C. Zarakovitis, Q. Ni, and J. Spiliotis, "Energy-efficient green wireless communication systems with imperfect CSI and data outage," *IEEE Journal on Selected Areas in Communications*, vol. 34, no. 12, pp. 3108–3126, 2016.

[33] S. Chen, S. Sun, Q. Gao et al., "Adaptive beamforming in TDD-based mobile communication systems: state of the art and 5G research directions," *IEEE Wireless Communications*, vol. 23, no. 6, pp. 81–87, 2017.

[34] C. Yang, Z. Yang, and Z. Deng, "Robust weighted state fusion Kalman estimators for networked systems with mixed uncertainties," *Information Fusion*, vol. 45, pp. 246–265, 2019.

[35] Y. Fang, G. Han, P. Chen et al., "A survey on DCSK-based communication systems and their application to UWB scenarios," *IEEE Communications Surveys & Tutorials*, vol. 18, no. 3, pp. 1804–1837, 2017.

[36] A. Masmoudi and T. Le-Ngoc, "Channel estimation and self-interference cancelation in full-duplex communication systems," *IEEE Transactions on Vehicular Technology*, vol. 66, no. 1, pp. 321–334, 2017.

[37] Z. Lv, L. Qiao, M. Shamim Hossain, and B. J. Choi, "Analysis of using blockchain to protect the privacy of drone big data," *IEEE Network*, vol. 35, no. 1, 2020.

[38] A. E. Abdelkareem, B. S. Sharif, and C. C. Tsimenidis, "Adaptive time varying Doppler shift compensation algorithm for OFDM-based underwater acoustic communication systems," *Ad Hoc Networks*, vol. 45, no. 7, pp. 104–119, 2016.

[39] Z. Lv, B. Hu, and H. Lv, "Infrastructure monitoring and operation for smart cities based on IoT system," *IEEE Transactions on Industrial Informatics*, vol. 16, no. 3, pp. 1957–1962, 2020.

[40] Y. Yang, Z. Zeng, J. Cheng, and C. Guo, "An enhanced DCO-OFDM scheme for dimming control in visible light communication systems," *IEEE Photonics Journal*, vol. 8, no. 3, pp. 1–13, 2016.

Research Article

Personalized Movie Recommendation Method Based on Deep Learning

Jingdong Liu [ID],[1] **Won-Ho Choi,**[2] **and Jun Liu**[3]

[1]*China and South Korea Institute of New Media, Zhongnan University of Economics and Law, Wuhan 430073, Hubei, China*
[2]*Division of Digital Contents Dongseo University, 47, Jurye-ro, Sasang-gu, Busan 617-716, Republic of Korea*
[3]*Academy of Arts and Media, China University of Geosciences, Wuhan 430074, Hubei, China*

Correspondence should be addressed to Jingdong Liu; liujingdong@zuel.edu.cn

With the rapid development of network technology and entertainment creation, the types of movies have become more and more diverse, which makes users wonder how to choose the type of movies. In order to improve the selection efficiency, recommend Algorithm came into being. Deep learning is a research field that has received extensive attention from scholars in recent years. Due to the characteristics of its deep architecture, deep learning models can learn more complex structures. Therefore, deep learning algorithms in speech recognition, machine translation, image recognition, and other fields have achieved impressive results. This article mainly introduces the research of personalized movie recommendation methods based on deep learning and intends to provide ideas and directions for the research of personalized movie recommendation under deep learning. This paper proposes a research method of personalized movie recommendation methods based on deep learning, including an overview of personalized recommendation and collaborative filtering recommendation algorithms, which are used to conduct research experiments on personalized movie recommendation methods based on deep learning. The experimental results in this paper show that the accuracy of the training set of the Seq2Seq model based on the LSTM recurrent neural network reaches 96.27% and the accuracy of the test set reaches 95.89%, which can be better for personalized movie recommendation.

1. Introduction

In recent years, with the improvement of people's living standards and the rapid spread of mobile Internet, more and more information is flooding the Internet [1]. Because different users have different hobbies, areas of interest, personal experience, etc., it is difficult for users to filter the information they are interested in from the massive information. How to use the big data that has emerged with the rise of mobile Internet and social media to serve users and carry out personality Chemical recommendation has become the focus of research [2]. Recommendation algorithm is a type of machine learning algorithm that is very closely related to real life. It refers to a type of algorithm that does not require users to provide clear needs but models users' interests by analyzing their historical behaviors, so as to actively recommend products to users that can meet their

interests and needs. Among the various recommendation algorithms, the collaborative filtering algorithm is the most widely used and representative algorithm. The basic idea is to use the preferences of a group with similar interests and common experience to recommend what users are interested in. Individuals give a considerable degree of response (such as scoring) to the information through a cooperative mechanism and record it to achieve the purpose of filtering and help users filter information [3]. The response is not necessarily limited to those of particular interest, and the record of particularly uninteresting information is also very important.

Traditional user interest modeling methods are difficult to express the essential information of the data and require manual extraction of features, so that researchers need to spend a lot of time and energy on data labeling, processing, and feature extraction, and different data need to be

different. Feature extraction and the extracted features are not necessarily effective. The effect of feature extraction often determines the performance of the algorithm. In recent years, deep learning has been favored by researchers [4]. It can accurately express more necessary data information through multilayer nonlinear computing units and effectively reduce the difficulty of model training through unsupervised learning.

Chen found that classification is one of the most popular topics in hyperspectral remote sensing [5]. In the past two decades, experts have proposed many methods to deal with the classification of hyperspectral data, but most of them did not extract hierarchically. Chen introduced the concept of deep learning to the classification of hyperspectral data for the first time, first by following the classification based on classical spectral information to verify the qualifications of stacked autoencoders; secondly, they proposed a new method of spatially dominant information classification; A novel deep learning framework is proposed to integrate these two functions, from which the highest classification accuracy can be obtained. The framework is a mixture of principal component analysis, deep learning architecture, and logistic regression. Specifically, as a deep learning architecture, stacked autoencoders are designed to obtain useful advanced features. This research lacks experimental data support [6]. Alhamid believes that context-aware recommendation offers the potential to use social content and use relevant tags and rating information to personalize content searches in a given context. Recommendation systems solve the problem of trying to identify relevant resources from a large number of online available choices. As a result, Alhamid proposed a new recommendation model that can personalize recommendations and improve the user experience by analyzing the context when users wish to access multimedia content; empirical analysis is performed on the data set to prove use of potential preferences to rank items in a given context; use optimization functions to maximize the average average accuracy of result recommendations. This method is not very innovative [7]. Barman found that search engines have become an indispensable part of people's daily lives. They can help users find specific information from a large amount of data stored on the Internet. The query recommendation function of search engines can respond to users' original queries and provide users with Recommend multiple alternative queries. For different users from a specific geographic area, these suggestions remain basically the same, but the acceptability of these alternative queries often varies from person to person [8]. In this work, Barman D proposed a personalized recommendation system based on genetic algorithms [9] and used the search logs of commercial search engines to evaluate the proposed method. This research is not practical and not suitable for popularization in practice [10].

The innovations of this paper are as follows: (1) propose a collaborative filtering personalized movie recommendation algorithm; (2) construct a user interest model based on Seq2Seq; (3) design a personalized movie recommendation system based on deep learning.

2. Methods of Personalized Movie Recommendation Methods Based on Deep Learning

2.1. Personalized Recommendation. Through personalized recommendation by extracting the user's historical information features, it is convenient and accurate for the user to mine the things he may like from the large database and make personalized recommendation for each user [11]. For example, in the e-commerce market [12], personalized recommendation algorithms can stimulate users' potential purchase desires and reduce the time for users to select products, thereby facilitating users' shopping methods; in the news or video fields, personalized recommendation algorithms can provide users with recommendations. The information of his "appetite" improves the user's reading efficiency, reduces the time for users to select product content, and can also attract users' interest in the product [13]. Nowadays, recommended websites can obtain user behaviors such as length of stay, favorite links, and number of likes. These behaviors are roughly divided into explicit feedback behaviors and implicit feedback behaviors. Explicit feedback behaviors can directly present user preferences. Commonly it is the user's rating of the item [14].

The implicit feedback behavior cannot clarify the user's preferences [15]. A common implicit feedback behavior is the user's web browsing record. The user may not be interested in the item when browsing the web but may click and browse the item out of curiosity or unintentionally [16]. Although the record does not clearly know the user's preferences, the implicit data obtained by the general website account for a large proportion. Therefore, based on the use of explicit feedback data, it is necessary to dig out the implicit feedback data value meaning content, so as to achieve personalized recommendation [17].

According to the different data types, the algorithms needed for personalized recommendation are mainly composed of two types: the first is a recommendation algorithm based on content, and the second is a recommendation algorithm based on collaborative filtering. The main idea of the content-based recommendation algorithm is to recommend to users the information with the greatest similarity in the content of the items they like and the information they have followed; the personalized recommendation system basically uses a collaborative filtering algorithm [18], and its core recommendation idea is as follows: the user has other users with similar preferences and then recommends to the user items that other users have purchased but this user has not purchased [19].

2.2. Collaborative Filtering Recommendation Algorithm

2.2.1. Similarity Calculation. The measure of similarity between users is generally compared by the method of vector calculation. Among these comparison methods, Pearson similarity and cosine similarity are the most commonly used [20].

The calculation formula of cosine similarity is as follows, where $\text{sim}(x, y)$ represents the similarity between users x and y and $N(x)$ and $N(y)$ represent the collection of ratings of users x and y, respectively:

$$\text{sim}(x, y) = \frac{|N(x) \times N(y)|}{\sqrt{|N(x)||N(y)|}}. \quad (1)$$

The calculation formula of Pearson's correlation coefficient is as follows:

$$\text{sim}(x, y) = \frac{\sum_{i \in N(x) \cap N(b)} (R_{xi} - \overline{R}_x) * (R_{yi} - \overline{R}_y)}{\sqrt{\sum_{i \in N(x) \cap N(b)} (R_{xi} - \overline{R}_x) * (R_{ki} - \overline{R}_k)^2} * \sqrt{\sum_{i \in N(x) \cap N(b)} (R_{xi} - \overline{R}_x) * (R_{yi} - \overline{R}_y)}}. \quad (2)$$

When recommending the target user x, similarity calculation is also needed to find the n movies most similar to movie m [21]. Here, it is represented by the set $S(m, n)$; the user x's interest in movie m can be calculated by the following formula:

$$X(x, n) = \sum_{j \in S(m,n) \cap N(x)} \text{sim}(n, j) p_{xj}. \quad (3)$$

where $N(x)$ represents the set of movies that user x likes and p_{xj} represents the degree of user x's preference for movie j.

2.2.2. Matrix Decomposition Recommendation Algorithm.
The basic principle of the matrix decomposition recommendation algorithm is as follows: analyze the user's historical information and construct a rating matrix, which is composed of user ID, item ID, and rating [22]. Then, the user item rating matrix is decomposed into two low-dimensional feature matrices through matrix decomposition algorithm. Finally, these two low-dimensional matrices are used to estimate items that users have not commented on [23]. The initial user-item rating matrix $R^{n \times m}$ is decomposed, and the user vector representation and the item vector representation are obtained, respectively, and then two feature matrices are obtained [24], namely, user feature matrix $U^{k \times n}$ and item feature matrix $V^{k \times n}$, where n is the number of users, m is the number of items, and k is the dimension of the hidden vector feature space [25, 26]. Multiplying the two matrices obtained by decomposition is the predicted score:

$$R^* = U^T V. \quad (4)$$

The algorithm trains the model by optimizing the difference between the predicted score R and the real score R^*, that is, optimizing the objective function:

$$E = I(R - U^T V)^2 = \sum_{i=1}^{N} \sum_{j=1}^{M} I_{ij} (R_{ij} - U_i^T V_j)^2. \quad (5)$$

To prevent overfitting, redefine the objective function:

$$E = \sum_{i=1}^{N} \sum_{j=1}^{M} (R_{ij} - U_i^T V_j)^2 + \lambda (\|U_i\|^2 + \|V_i\|^2). \quad (6)$$

Use the stochastic gradient descent method to solve the matrices U and V [27]. Then, the partial derivatives of E with respect to U and V are expressed as the following formulas:

$$\frac{\partial E}{\partial U} = -2V + 2\lambda U,$$

$$\frac{\partial E}{\partial U} = -2U + 2\lambda V. \quad (7)$$

Get updated U and V, where α is the learning rate:

$$U = U + \alpha(V - \lambda U),$$

$$V = V + \alpha(U - \lambda V). \quad (8)$$

2.2.3. Probability Matrix Factorization.
Probabilistic matrix decomposition is to introduce a probability model on the basis of matrix decomposition to optimize. The introduction of the probability model has greatly improved the performance of matrix factorization and further improved the accuracy of the matrix factorization model [28]. Probability matrix decomposition has two leading assumptions: one is that the difference between the overall rating matrix R of the user and the inner product R of the eigenvectors of the user and the movie obeys the Gaussian distribution of variance [29]; the second is that the eigenvector matrix U of the user and the movie's elements of the eigenvector matrix V, respectively, obey the Gaussian distribution with the mean value being 0 and the variance being ϕ_u and ϕ_v [30,31].

According to hypothesis one, the probability density function of R can be obtained, where I_{ij} is an indicative function representing whether user i has made an evaluation for movie j; if the evaluation has been made, its value is 1; otherwise, it is 0:

$$p(R|U, V, \phi^2) = \prod_{i=1}^{N} \prod_{j=1}^{M} \left[N\left(\frac{R_{ij}}{U_i^T V_j}\right), \phi^2 \right]^{I_{ij}}. \quad (9)$$

According to hypothesis two, U and V probability density functions can be obtained:

$$p(U, \phi_U^2) = \prod_{i=1}^{N} N\left(\frac{U_i}{0}\right), \quad \phi_U I, p(V, \phi_V^2) = \prod_{j=1}^{M} N\left(\frac{V_j}{0}\right), \quad \phi_V I. \quad (10)$$

The stochastic gradient descent method is used to solve the matrices U and V [32]. Then, the partial derivatives of E with respect to U and V are expressed as the following formulas:

$$\frac{\partial E}{\partial U} = -V + \lambda_u U,$$

$$\frac{\partial E}{\partial V} = -U + \lambda_V V. \tag{11}$$

Get updated U and V, where α is the learning rate:

$$U = U + \alpha \left(V - \lambda_u U \right),$$

$$V = V + \alpha \left(U - \lambda_v V \right). \tag{12}$$

The method part of this article uses the above method for the research of personalized movie recommendation algorithm based on deep learning. The specific process is shown in Figure 1.

3. Experiment on Personalized Movie Recommendation Method Based on Deep Learning

3.1. Based on Seq2seq User Interest Model Construction. The personalization of personalized search is reflected in the different search results obtained by different users. First, obtain user interests through related algorithms and express and describe the user's personalized information. Secondly, the personalized information is integrated into the search algorithm or related operations such as expanding the query sentence during the query process and dynamically adjusting the search results [33]. The Seq2Seq model in deep learning is used to characterize the user's interest, and then it is integrated into the sorting algorithm of the search engine. The coding end of the Seq2Seq model is based on the LSTM recurrent neural network, which has a longer memory capacity than RNN. The decoder also uses LSTM recurrent neural network [34].

First, classify the movie titles according to the authors, put together the movie titles of the same director, and construct them into short texts. All authors in the data set are made into short text data sets; secondly, the data are input into the Seq2Seq model, and the input and output are both It is the same data for training until the loss converges and stabilizes. This process is to adjust the weight parameters of the neural network through training, and let the model capture the input semantic information; again input the relevant short text of each director into the trained code In the device, the output result at the last time step is the interest feature vector of the current audience, and it is saved for subsequent use [35]. Finally, each movie title of the search result must be input into the encoder, the generated vector and the interest vector of the audience currently using the system are calculated for similarity, and the calculation result is merged into the Lucene sorting algorithm, and then the search result is reproduced. Sort to achieve personalized search results [36].

3.1.1. Model Structure. This article uses the Seq2Seq model to express user interests. The whole model constructed in this paper is mainly divided into four levels. The first level is the data embedding layer, which embeds the text data in a vectorized manner. This paper chooses the word embedding method instead of the one-hot method. The second layer is the coding layer, which is based on the LSTM neural network and encodes text data. The third layer is the attention layer. Through the attention layer, the decoder can use a different intermediate vector at each time step. The fourth layer is the decoding layer, and the decoding layer also uses LSTM recurrent neural network to decode and output according to the intermediate vector [37, 38].

3.1.2. Data Preprocessing Vocabulary Construction. The original data need to be processed by removing the stop words, and the stop word list used is the stop word list for English text processing in the natural language processing toolkit (NLTK) related to python. Before the vocabulary is built, punctuation marks in the text are eliminated, which helps to reduce the number of unregistered words. In the process of constructing the vocabulary, the case of words is distinguished, which helps to understand semantics and enhance the expression effect. Construct the vocabulary according to the word frequency and arrange it according to the size of the word frequency. After that, the word is represented by a unique ID, that is, its sorted position in the word frequency database. The word ID is built into a batch and sent to the network, and the network performs word embedding into embedded computing that it is used for subsequent network training [39].

3.1.3. Embedding Processing Layer. The Embedding layer uses the training skip-gram model to construct word vectors. First, the movie title corpus data are counted on word frequency and sorted according to word frequency, and a fixed position is determined for each word. Next, perform one-hot encoding. Finally, a word vector matrix is generated through neural network training, where the row vector corresponding to each position is the distributed word vector of the current word [40].

3.1.4. Attention Layer Construction. It is the introduction the attention mechanism into the model. The basic idea of the attention mechanism is to break the limitation that the traditional encoder-decoder depends on a fixed vector output at the last time step of the encoding stage when decoding. Attention mechanism is realized by saving the intermediate output results generated by the encoder according to the input sequence and then training a model to selectively learn these inputs and associate the output sequence with it when the model is output [41].

3.2. Design a Personalized Movie Recommendation System Based on Deep Learning

3.2.1. Demand Analysis

(1) User Needs. The functions that users can use generally include account management, movie search, user ratings, user reviews, personalized movie recommendations, movie
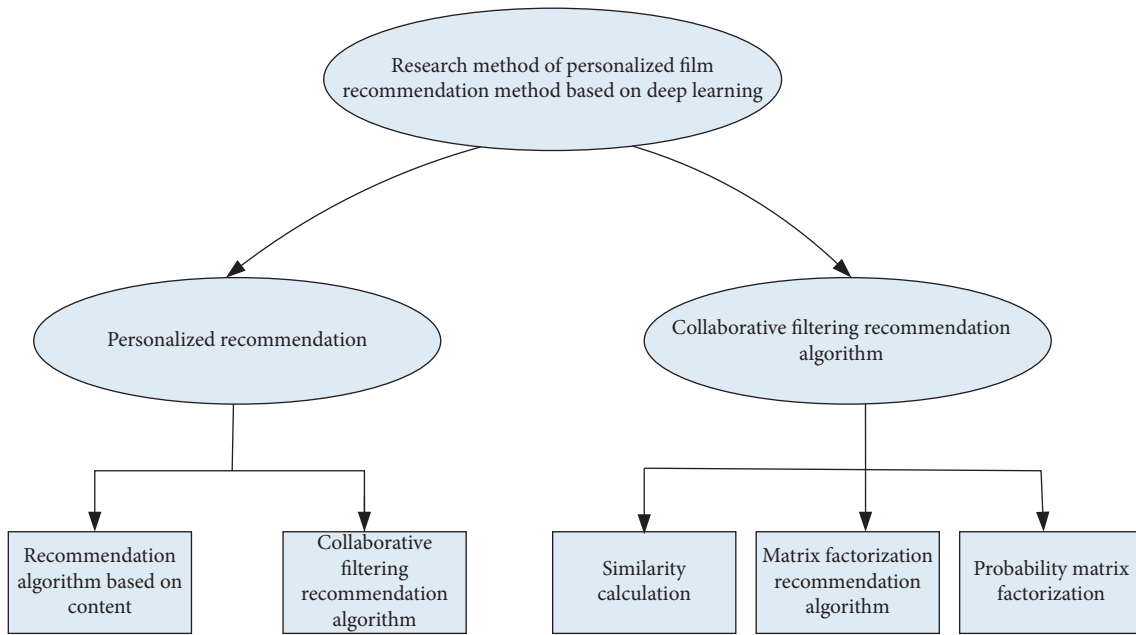
FIGURE 1: Part of the technical process of this method.

nonpersonalized recommendations, and user information management. Account management includes account login, account logout, and account registration; movie search includes movie search and movie playback sources; user information management includes user nickname modification and user password modification.

(2) Administrator Requirements. In addition to the user rights, the system administrator needs to undertake the operation and maintenance tasks of the entire movie recommendation system to ensure the normal and stable operation of the system. These include user information management, website traffic statistics, and website information maintenance. User information management includes banning users and modifying user information and website traffic statistics; website information maintenance includes adding movies, deleting movies, updating movie information, deleting comments, and viewing comments.

(3) Performance Requirements. Ensuring system performance, high availability, and scalability.

3.2.2. System Structure. This system adopts the B/S architecture, uses the MVC development model as the system's microsolution, and uses the microservice architecture as the system's macrosolution to design and develop a large-scale Web system. The development of the whole system takes MVC development model as the development model for designing and creating Web applications and chooses SpringMVC as the framework of MVC development model for development.

The interface layer is dominated by html pages, which are implemented through technologies such as JavaScript, SpringMVC, and Json. Among them, it mainly communicates with the server through the Http network communication protocol, and the users of the system interact with the system by browsing the web.

The business logic layer is mainly implemented by SpringMVC, based on the controller in the MVC development model, connecting the interface layer and the data access layer. Through the business logic layer, the data access layer can write data to the interface layer, and the data access layer can also send data back to the interface layer.

The data access layer mainly uses the Hibernate framework to complete object-relational mapping. First, it encapsulates JDBC lightly and establishes a mapping relationship between the model in the MVC development model and the database table to complete data persistence and other operations.

3.2.3. Database Design

Relational Database. The recommendation system needs a lot of data to support when updating the recommendation model, and there is a certain relationship between data and data, and the relational database is based on the relational model, so the commonly used relational database Mysql is used Store system information.

(1) Nonrelational Database. This type of data requires a performance-oriented database system. Redis is a nonrelational database, which is based on memory key-value storage, which is more efficient in storage. For example, after logging in to the movie recommendation system, I regret storing the logged-in user's Session information in Redis. The storage form of the user's Session information in Redis is as follows: Key = User ID; Value = Session Information.

3.2.4. Core Module Design

(1) Login Module. This module is mainly responsible for the user's identity verification when using the system and grants different module access permissions based on the user's identity and the access control list provided by Spring Security.

(2) Movie search Module. This module is responsible for searching out the movie corresponding to the user when the user searches for a movie and providing the playback source of the movie to the user.

(3) Offline Calculation Module. By clustering the user's ratings of all movies and the category of the movie, a part of the movies that users are most likely to be interested in are selected as a list of candidate movies, and then a deep network structure model is used to the candidate movie list to recommend and sort, which is based on deep learning.

(4) Online Recommendation Module. Sort and recommend the movie candidate list obtained by the offline module by using an improved movie recommendation algorithm based on deep learning.

(5) Information Management Module. The system administrator can add, delete, and update information on the movie resources of the system, check the comments of each movie, and delete false comments.

(6) Website Traffic Statistics. It is responsible for statistics of various traffic on the website, which is convenient for administrators to do operation and maintenance management.

(7) User Information Feedback Module. Support users to give feedback on recommended movie information in the system, including user ratings and user comments.

This experiment part proposes the above steps to be used in the research experiment of personalized movie recommendation method based on deep learning. The specific process is shown in Table 1.

4. Personalized Movie Recommendation Method Based on Deep Learning

4.1. Development Status of Intelligent Recommendation System. Nowadays, the recommendation system as a kind of intelligent information service has been applied in all walks of life, for example, the well-known e-commerce product recommendation, hot topic recommendation of news websites, high-quality content recommendation of video and music, keyword recommendation of search engines, and recommendation of similar documents in academic websites. This article counts the well-known apps on the market that contain smart recommendations, as shown in Table 2.

The recommendation system uses the user's historical behavior information to infer the user's interests and preferences, so as to provide recommendations for them. The personalized recommendation system can not only make recommendations based on users' preferences but can also recommend new items that users might like when the users are not clear about their preferences. This is called the novelty of recommendation.

4.2. Personalized Movie Recommendation User Analysis

(1) Count the average usage time of the application platform with movie personalized recommendation function in the daily life of each user layer, and draw it into a chart, as shown in Table 3 and Figure 2.

It can be seen from the chart that Saturday and Sunday are the two days when users spend the most time online. The platform can set the number of personalized recommendations on Saturdays and Sundays to be more frequent, and there are more types of pushes; users online use time on weekdays after Monday. Relatively short, the platform can be set to accurately push according to users' likes.

(2) Calculate the time period that users use the application platform with the personalized recommendation function of movies and draw them into charts, as shown in Table 4 and Figure 3.

It can be seen from the graph that users often use application platforms with personalized movie recommendation functions during commuting hours, lunch time, dinner time, etc. It should be adapted to the current conditions, and more personalized movie recommendations for users during these time periods will surely achieve a better recommendation effect.

4.3. Experimental Results

(1) This paper calculates the similarity algorithm for the collaborative filtering algorithm based on personalized recommendation and the Seq2Seq model, fuses the similarity through the fusion algorithm, and finally completes the movie recommendation. The recommendation is the Top-N method. Analyze and compare relevant experimental results. Through the fusion algorithm, the similarity between the movie similarity obtained by the item-based collaborative filtering recommendation algorithm (Item-CF) and the movie based on the Seq2Seq model is fused and statistically sorted out. Draw a chart, as shown in Table 5 and Figure 4.

It can be seen from the chart that the similar fusion ratio of Item-CF and Seq2Seq is $1:0$, which means the index result is obtained by the Item-CF algorithm. It can be seen from various evaluation indicators that when the Seq2Seq fusion ratio is relatively high, the coverage rate is significantly higher than that of the traditional collaborative filtering algorithm. As the proportion of Seq2Seq fusion decreases, the accuracy, recall, and novelty are all improved, while the coverage rate gradually decreases.

TABLE 1: Experimental steps in this article.

Research experiment on personalized movie recommendation method based on deep learning	3.1. Based on Seq2Seq user interest model construction	1. Model structure 2. Data preprocessing vocabulary construction 3. Embedding processing layer 4. Attention layer construction
	3.2. Design a personalized movie recommendation system based on deep learning	1. Demand analysis 2. System structure 3. Database design 4. Core module design

TABLE 2: App with smart recommendations.

Application field	App	Uses
E-commerce	Taobao, Jingdong, Buy together, Amazon	Online shopping
Film and television	Youtube, Youku, Tencent video, Bilibili, Aiqiyi, Douban	Watching TV and movies
Music software	NetEase Cloud Music, Kugou music, Kuwo music, QQ music, Xiami Music	Listen to the music
Radio station	Lychee fm, Radio Himalayan	Listen to the radio
News and information	Toutiao, Zite	News browsing
Life service	Meituan, Eleme	Eating, lodging, traveling
Social contact	QQ, Weibo, Wechat	Exchange, make friends
Search engines	Baidu, Google	Search for things you want to know

TABLE 3: Average user usage time (unit: minute).

User	Monday	Tuesday	Wednesday	Thursday	Friday	Saturday	Sunday
Primary and secondary school students	112.3	106.4	101.2	110.1	116.4	134.8	141.2
College students	164.1	171.3	164.6	175.3	154.9	212.3	230.6
Office worker	108.6	92.7	95.6	100.5	124.6	176.7	200.4
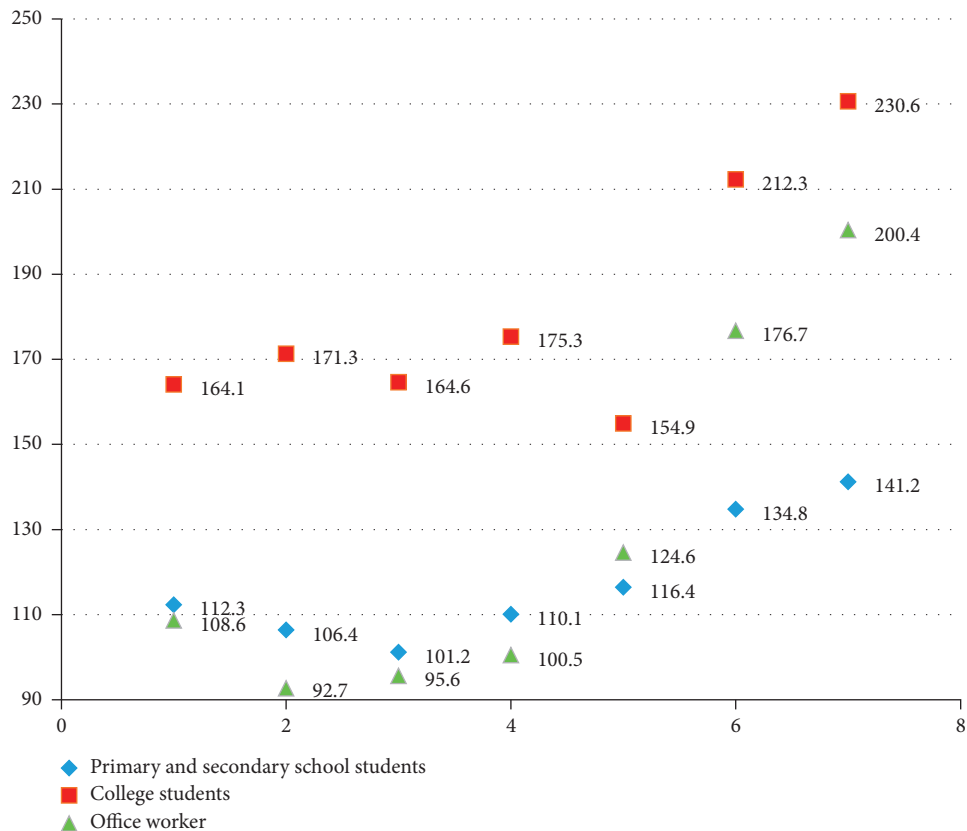
FIGURE 2: Average user usage time (unit: minute).

TABLE 4: User viewing time period.

Period	Percentage (%)
0:00–6:00	3.62
6:00–9:00	6.23
9:00–12:00	13.91
12:00–15:00	20.34
15:00–18:00	19.12
18:00–21:00	23.67
21:00–24:00	13.11
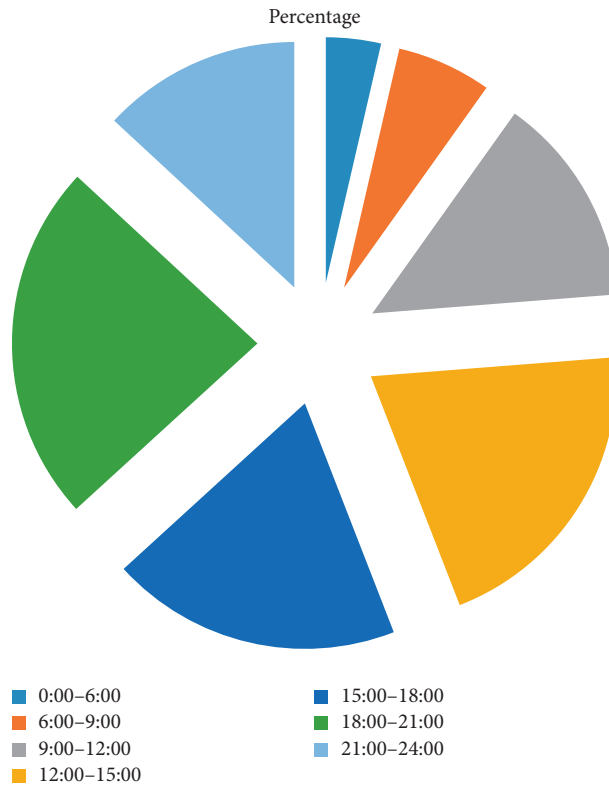
FIGURE 3: User viewing time period.

TABLE 5: Item-CF and Seq2Seq fusion results in different proportions.

Number	Similar fusion ratio of Item-CF and Seq2seq	Accuracy (%)	Recall rate (%)	Coverage (%)	Novelty
1	1:0	39.81	4.21	29.61	4.31
2	1:1	42.31	4.67	32.33	4.26
3	1:2	37.42	3.94	36.07	4.54
4	7:1	35.67	4.56	41.20	4.62
5	14:1	42.33	5.08	39.26	4.70
6	19:1	46.24	4.78	36.44	3.96
7	20:6	48.09	5.12	32.52	4.33
8	48:1	39.21	4.83	29.07	4.27
9	50:4	36.52	3.64	26.43	4.39
10	67:2	37.43	3.27	23.67	4.51
11	92:1	41.66	2.98	29.11	4.63
12	100:1	49.57	2.51	30.27	4.71

(2) The data set used in the experiment is the MovieLens data set collected by the GroupLens team of the University of Minnesota in the United States. It records users' ratings of movies and is a standard data set for personalized recommendation algorithm evaluation. The MovieLens dataset used in this article includes MovieLens-100k dataset and MovieLens-1M dataset. Based on the MovieLens-100k data set and MovieLens-
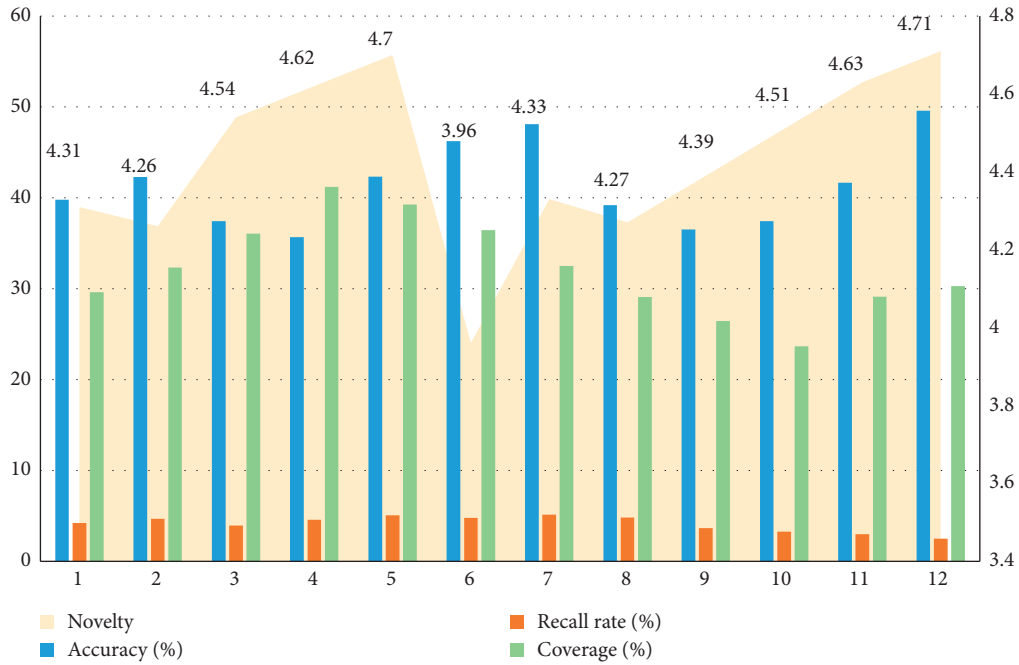
FIGURE 4: Item-based collaborative filtering recommendation algorithm and Seq2Seq fusion results in different proportions.

TABLE 6: Comparative experimental results.

User activity	MovieLens-100k			MovieLens-1M		
	HR	NDCG	ILS	HR	NDCG	ILS
0.2	0.6481	0.3421	0.4568	0.7126	0.5027	0.4613
0.3	0.6527	0.3519	0.4631	0.7217	0.5112	0.4717
0.4	0.6582	0.3607	0.4724	0.7305	0.5204	0.4806
0.5	0.6643	0.3687	0.4811	0.7396	0.5293	0.4912
0.6	0.6709	0.3724	0.4901	0.7421	0.5348	0.5071

1M data set, starting from three aspects, the output size of the hidden layer is 8. Regarding the models GMF, MLP, NeuMF, and Seq2Seq, the accuracy and diversity of the two data sets are compared Experiment to verify the superiority of the Seq2Seq model is proposed in this chapter. The specific results are shown in Table 6 and Figure 5.

It can be seen from the graph that, as the user activity increases, the accuracy fluctuates slightly and the diversity rises slightly; the increase in activity indicates that the proportion of user activity obtained by clustering gradually increases, compared to pure. The diversity characteristics of the activity derived from the number of times the project is evaluated are more obvious and bring more gains.

(3) A three-layer LSTM network model is built, the number of LSTM neurons is set to 131, the learning is 0.002, the dropout value is 0.2, the number of training rounds Epoch is 27, the batch size Batch_size is 35, Adam is the model optimizer, and Sigmoid function is used as the activation function. When the model is stable, the setting is that the LSTM layer contains 131 neurons and the batch_size of each batch of data is 70.
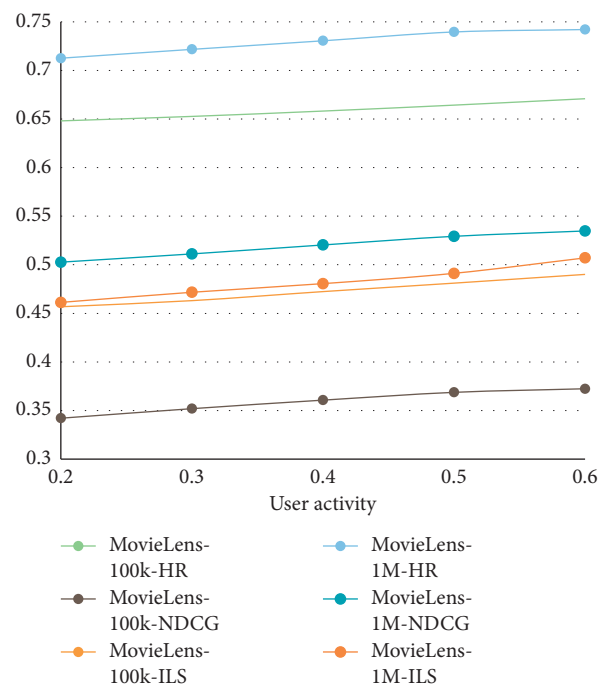
FIGURE 5: Comparison of experimental results.

TABLE 7: Loss function and accuracy rate changes.

Epoch	Loss training	Loss test	Accuracy training (%)	Accuracy test (%)
0~3	0.0152	0.0146	71.24	64.14
4~6	0.0131	0.0137	79.56	75.63
7~9	0.0127	0.0121	82.31	80.41
10~12	0.0114	0.0117	85.47	82.67
13~15	0.0097	0.0106	90.26	89.17
16~18	0.0086	0.0095	92.51	93.67
19~21	0.0082	0.0089	93.38	94.59
22~24	0.0078	0.0074	95.46	95.21
25~27	0.0073	0.0069	96.27	95.89
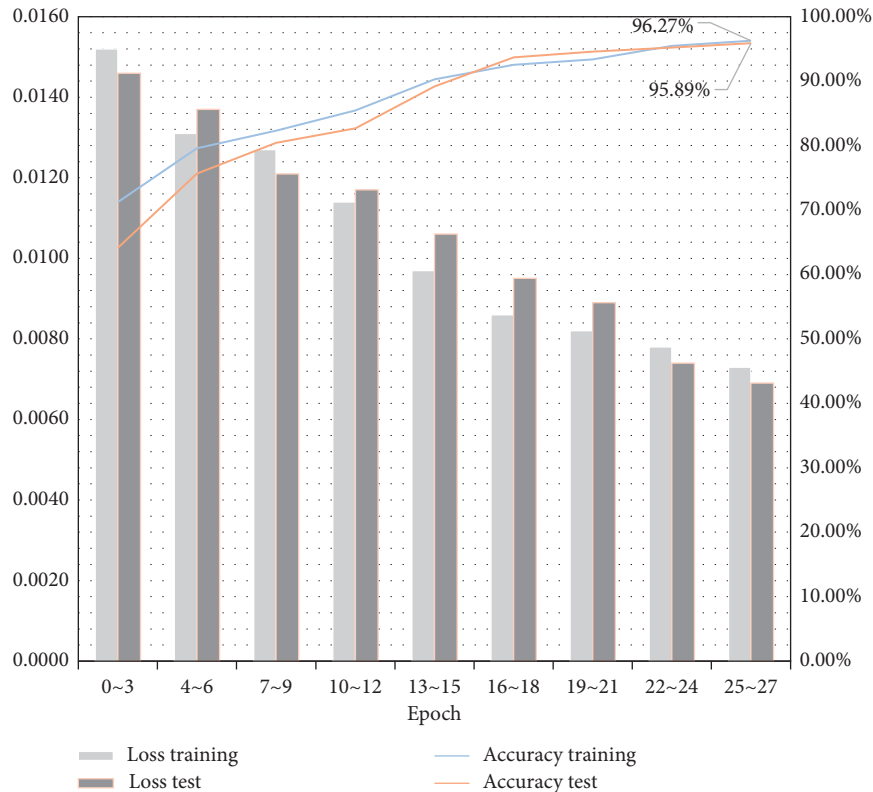
FIGURE 6: Loss function and accuracy rate changes.

After 27 iterations, the model achieves better results. The dropout value is 0.23, and Adam as a model optimizer, the sigmoid function is used as the final activation function of the model. The specific conditions of the model's loss function and accuracy rate change trend on the test set and training set are shown in Table 7 and Figure 6.

It can be seen from the graph that the loss function and accuracy of the model gradually stabilized after the epoch reached 15, and the loss function remained around 0.0080. The accuracy of the final model training set reached 96.27%, and the accuracy rate of the test set reached 95.89%. Convergence speed and model accuracy are better than traditional RNN models. Compared with traditional RNN models, processing performance has been greatly improved.

5. Conclusions

In recent years, with the rapid development of information technology and the Internet, watching movies through the Internet has become a habit of many people. However, because people cannot quickly obtain their favorite movie content from the massive movie resources, this makes the overload of movie information more and more serious. As one of the important means to alleviate the problem of information overload, the recommendation system can help users quickly find favorite movie content and bring users a good experience. Therefore, it is widely used in well-known movie and video websites at home and abroad and has great commercial value.

The advent of the 5 G era has put forward higher requirements for Internet technology. As one of the important areas, the recommendation system has been deeply applied to all aspects of the Internet. It helps people provide

solutions from massive information retrieval and changes the original passive search method. To take the initiative and bring certain economic benefits to related enterprises, it has been widely recognized by the industry. At the same time, deep learning technology has shined in the field of classification and prediction in recent years, but in the field of recommendation, the application of this technology is still in a period of rapid growth. How to combine the two more effectively is an important direction of current research.

This article begins by focusing on the research background and significance of the thesis. Through the research and judgment of the current research status in this field, combined with the development and application of algorithm technology, it analyzes and summarizes the common problems in the algorithm. Then, the related theories and technologies needed in this article are researched and organized, several basic algorithms of recommendation systems and the current popular social network-based recommendation algorithms are theoretically studied, and then the foundation of deep learning algorithms is explained. This article has conducted certain research on the movie recommendation system and its combination with deep learning, but there are still many shortcomings, which require continuous learning and hard work. The data set used in the model test in this paper is very small compared with the calculation required for actual application, and there is still a certain gap in the amount of data.

Data Availability

No data were used to support this study.

Disclosure

The content of the manuscript has not been published or submitted for publication elsewhere.

Conflicts of Interest

The authors declare that there are no conflicts of interest.

Authors' Contributions

All the authors have seen the manuscript and approved the submission of the article.

References

[1] S. Wan, X. Li, Y. Xue, W. Lin, and X. Xu, "Efficient computation offloading for Internet of Vehicles in edge computing-assisted 5G networks," *The Journal of Supercomputing*, vol. 76, pp. 2518–2547, 2020.

[2] L. M. T. Pham, L. T. T. Tran, P. Thipwong, and W. T. Huang, "Dynamic capability and organizational performance," *Journal of Organizational and End User Computing*, vol. 31, no. 2, pp. 1–21, 2019.

[3] X. Li, Y. Zhu, and J. Wang, "Highly efficient privacy preserving location-based services with enhanced one-round blind filter," *IEEE Transactions on Emerging Topics in Computing*, vol. 1, p. 1, 2019.

[4] L. Wu, Q. Zhang, C.-H. Chen, K. Guo, and D. Wang, "Deep learning techniques for community detection in social networks," *IEEE Access*, vol. 8, pp. 96016–96026, 2020.

[5] G. Wang, Y. Yao, Z. Chen, and P. Hu, "Thermodynamic and optical analyses of a hybrid solar CPV/T system with high solar concentrating uniformity based on spectral beam splitting technology," *Energy*, vol. 166, pp. 256–266, 2019.

[6] Y. Chen, Z. Lin, X. Zhao et al., "Deep learning-based classification of hyperspectral data," *IEEE Journal of Selected Topics in Applied Earth Observations & Remote Sensing*, vol. 7, no. 6, pp. 2094–2107, 2017.

[7] M. F. Alhamid, M. Rawashdeh, H. Dong et al., "Exploring latent preferences for context-aware personalized recommendation systems," *IEEE Transactions on Human-Machine Systems*, vol. 46, no. 4, pp. 1–9, 2017.

[8] Z. Lv, X. Li, and W. Li, "Virtual reality geographical interactive scene semantics research for immersive geography learning," *Neurocomputing*, vol. 254, pp. 71–78, 2017.

[9] N. Metawa, M. Elhoseny, M. Kabir Hassan, and A. E. Hassanien, "Loan portfolio optimization using genetic algorithm: a case of credit constraints," in *Proceedings of 12th International Computer Engineering Conference, ICENCO*, pp. 59–64, Cairo, Egypt, December 2016.

[10] D. Barman, R. Sarkar, A. Tudu, and N. Chowdhury, "Personalized query recommendation system: a genetic algorithm approach," *Journal of Interdisciplinary Mathematics*, vol. 23, no. 2, pp. 523–535, 2020.

[11] X. Chowdhury, G. Zhang, and S. Ma, "Deep learning," *International Journal of Semantic Computing*, vol. 10, no. 3, pp. 417–439, 2016.

[12] C.-H. Wu and S.-B. Tsai, "Using DEMATEL-based ANP model to measure the successful factors of E-commerce," *Journal of Global Information Management*, vol. 26, no. 1, pp. 120–135, 2018.

[13] G. Litjens, T. Kooi, B. E. Bejnordi et al., "A survey on deep learning in medical image analysis," *Medical Image Analysis*, vol. 42, no. 9, pp. 60–88, 2017.

[14] S. Setio, P. Pastor, A. Krizhevsky et al., "Learning hand-eye coordination for robotic grasping with deep learning and large-scale data collection," *International Journal of Robotics Research*, vol. 37, no. 4-5, pp. 421–436, 2016.

[15] L. Fabisiak, "Web service usability analysis based on user preferences," *Journal of Organizational and End User Computing*, vol. 30, no. 4, pp. 1–13, 2018.

[16] Y. J. Cha, W. Choi, G. Suh, S. Mahmoudkhani, and O. Büyüköztürk, "Autonomous structural visual inspection using region-based deep learning for detecting multiple damage types," *Computer Aided Civil and Infrastructure Engineering*, vol. 33, no. 9, pp. 731–747, 2018.

[17] X. Zhang and D. Wang, "Deep learning based binaural speech separation in reverberant environments," *IEEE/ACM Transactions on Audio, Speech, and Language Processing*, vol. 25, no. 5, pp. 1075–1084, 2017.

[18] Z. Lv and L. Qiao, "Optimization of collaborative resource allocation for mobile edge computing," *Computer Communications*, vol. 161, pp. 19–27, 2020.

[19] W. Li, H. Fu, L. Yu et al., "Stacked Autoencoder-based deep learning for remote-sensing image classification: a case study of African land-cover mapping," *International Journal of Remote Sensing*, vol. 37, no. 23-24, pp. 5632–5646, 2016.

[20] Q.-S. Zhang and S.-C. Zhu, "Visual interpretability for deep learning: a survey," *Frontiers of Information Technology & Electronic Engineering*, vol. 19, no. 1, pp. 27–39, 2018.

[21] I. Y. Choi, H. S. Moon, and J. K. Kim, "Assessing personalized recommendation services using expectancy disconfirmation theory," *Asia Pacific Journal of Information Systems*, vol. 29, no. 2, pp. 203–216, 2019.

[22] M. Kim, Y. Fang, H. Xie, J. Chong, and M. Meng, "User click prediction for personalized job recommendation," *World Wide Web*, vol. 22, no. 1, pp. 325–345, 2019.

[23] J. Zhang, "Personalised product recommendation model based on user interest," *Computer Systems Science and Engineering*, vol. 34, no. 4, pp. 231–236, 2019.

[24] M. Gan and R. Jiang, "FLOWER: fusing global and local associations towards personalized social recommendation," *Future Generation Computer Systems*, vol. 78, no. 1, pp. 462–473, 2017.

[25] W. Gu, S. Dong, and M. Chen, "Personalized news recommendation based on articles chain building," *Neural Computing and Applications*, vol. 27, no. 5, pp. 1263–1272, 2016.

[26] C. Tan, H. Li, and X. Wu, "Context-aware personalized recommendation for mobile users," *IPPTA: Quarterly Journal of Indian Pulp and Paper Technical Association*, vol. 30, no. 2, pp. 146–151, 2018.

[27] Y. Lv, "Personalized recommendation model based on incremental learning with continuous discrete attribute optimization," *Revista de la Facultad de Ingenieria*, vol. 32, no. 2, pp. 842–849, 2017.

[28] S. Lee and T. Ha, "Item-network-based collaborative filtering: a personalized recommendation method based on a users item network," *Information Processing & Management: libraries and Information Retrieval Systems and Communication Networks: An International Journal*, vol. 53, no. 5, pp. 1171–1184, 2017.

[29] G. Xiao, Q. Cheng, and C. Zhang, "Detecting travel modes using rule-based classification system and Gaussian process classifier," *IEEE Access*, vol. 7, pp. 116741–116752, 2019.

[30] C. Shi, Z. Zhang, Y. Ji, W. Wang, P. S. Yu, and Z. Shi, "SemRec: a personalized semantic recommendation method based on weighted heterogeneous information networks," *World Wide Web*, vol. 22, no. 1, pp. 153–184, 2019.

[31] J. Zhang, Y. Wang, Z. Yuan, and Q. Jin, "Personalized real-time movie recommendation system: practical prototype and evaluation," *Tsinghua Science and Technology*, vol. 25, no. 2, pp. 180–191, 2020.

[32] J. Grith, C. O. Riordan, J. Griffith et al., "Collaborative filtering," *Computer Science*, vol. 57, no. 4, p. 189, 2017.

[33] Y. Yao, H. Tong, G. Yan et al., "Dual-regularized one-class collaborative filtering with implicit feedback," *World Wide Web*, vol. 22, no. 3, pp. 1099–1129, 2019.

[34] A. Boutet, D. Frey, R. Guerraoui, A. Jégou, and A.-M. Kermarrec, "Privacy-preserving distributed collaborative filtering," *Computing*, vol. 98, no. 8, pp. 827–846, 2016.

[35] N. Polatidis and C. K. Georgiadis, "A multi-level collaborative filtering method that improves recommendations," *Expert Systems with Applications*, vol. 48, pp. 100–110, 2016.

[36] D. Zhang, T. He, Y. Liu et al., "A carpooling recommendation system for taxicab services," *IEEE Transactions on Emerging Topics in Computing*, vol. 2, no. 3, pp. 254–266, 2017.

[37] J. D. West, I. Wesley-Smith, and C. T. Bergstrom, "A recommendation system based on hierarchical clustering of an article-level citation network," *IEEE Transactions on Big Data*, vol. 2, no. 2, pp. 113–123, 2016.

[38] Z. Tian, T. Jung, Y. Wang et al., "Real-time charging station recommendation system for electric-vehicle taxis," *IEEE Transactions on Intelligent Transportation Systems*, vol. 17, no. 11, pp. 3098–3109, 2016.

[39] H. C. Zhang and Y. L. Chang, "PKR: a personalized knowledge recommendation system for virtual research communities," *Data Processor for Better Business Education*, vol. 48, no. 1, pp. 31–41, 2016.

[40] E. N. Cinicioglu and P. P. Shenoy, "A new heuristic for learning Bayesian networks from limited datasets: a real-time recommendation system application with RFID systems in grocery stores," *Annals of Operations Research*, vol. 244, no. 2, pp. 385–405, 2016.

[41] A. S. Koshiyama, N. Firoozye, and P. Treleaven, "A derivatives trading recommendation system: the mid-curve calendar spread case," *Intelligent Systems in Accounting, Finance and Management*, vol. 26, no. 2, pp. 83–103, 2019.

Research Article

Research on College Physical Education and Sports Training Based on Virtual Reality Technology

Dan Li,[1,2] **Chao Yi** [iD],[3] **and Yue Gu**[2,4]

[1]*School of Physical Education, Shaoyang University, Shaoyang 422000, Hunan, China*
[2]*School of Graduate, Adamson University, Hermita 1000, Manila, Philippines*
[3]*College of General Education, Fujian Chuanzheng Communications College, Fuzhou 350007, Fujian, China*
[4]*School of Physical Education, Hunan International Economics University, Changsha 410205, China*

Correspondence should be addressed to Chao Yi; fjczjtyc@163.com

With the continuous development of society and the rapid development of science and technology, virtual reality technology is also developing rapidly. It has been widely used in all walks of life and is playing an irreplaceable role. Modern education has also begun to integrate with science. Sports are also constantly deepening the application of information technology. In order to make students have a new understanding of college physical education and sports training and improve the technical level and training quality of college sports athletes, this paper studies the application of virtual reality technology in physical education and sports training. In this paper, the semisupervised framework is used to implement motion input and interactive virtual scene algorithms. First, based on Q statistics, virtual simulation and differential selection algorithms are used to select athletic students with strong autonomous learning ability and then use the classifier's neighbor confidence. The formula selects the student with the highest learning level and marks it. Experimental results show that this method can effectively assist physical education activities and improve students' learning efficiency. Students' efficiency in sports has increased by 30%. At the same time, 2/3 of people believe that their interest in sports training has increased 80% and another 90% of college coaches believe that the use of virtual reality technology in physical education is very necessary, which can improve the technical level and training quality of college sports athletes and contribute to the reserve of Chinese competitive sports talents.

1. Introduction

Virtual reality technology can improve the basic conditions of physical education teaching, so that sports information can be effectively exchanged, and fully meet the actual needs of students' autonomous learning of sports knowledge. It is beneficial to improve the level of students' motor skills; interesting ways can also stimulate students' interest in learning and improve the efficiency of students' training. By satisfying the students' enthusiasm for physical education, the technical level of physical exercise, and the adequacy of physical education, it is of great value for realizing personal physical exercise. The combination of virtual reality technology in traditional physical education not only improves the effectiveness of physical education but also breaks the time and space limitations of physical education and sports training and encourages students to more deeply understand the problems encountered in education and training. Virtual reality technology can improve students' physical learning ability and promote students' independent thinking ability and the application value of high-quality physical exercise. Teachers can also effectively guide students' understanding of virtual reality technology and strengthen the relationship between teachers and students. Through interaction, teachers can better grasp the status of students' sports training and guide the smooth development of classroom teaching.

In the era of rapid development of information technology and continuous improvement of university network construction, the combination of virtual reality technology

and physical education training has become an important means of physical training. While using virtual reality technology, students can also enjoy professional teaching to obtain a large amount of educational knowledge and sports training skills knowledge and information. They can also learn about sports competitions, sports health, psychological and physiological information, traditional physical education, and sports. The training method can no longer be satisfied with the physical education in colleges and universities today.

Ding proposed that physical education in colleges and universities is an important part of the higher education system and the national health plan. Promoting the scientific and modern construction of the college physical education system is conducive to improving the scientific nature and effectiveness of higher education. Aiming at the problems of single teaching method and insufficient remote teaching ability in the current college physical education process, based on virtual reality technology, a virtual reality system for college physical education based on the Internet is designed and proposed: Internet of things, cloud platform, and mobile client. The system collects relevant data from the Internet of things, interacts with virtual reality scenes in real time, renders the scenes through the cloud, and experiences virtual reality through mobile terminals. The system has good application and promotion effects and provides a scientific reference for deepening the reform of college physical education, but it does not take into account the problems of cost and actual implementation [1]. Baiyu Zhou indicated that with the development of information technology, multimedia teaching has become the main trend of university teaching. At the same time, cloud computing can dynamically allocate computing resources based on the number of users and the complexity of applications. This article analyzes the application of cloud computing-based multimedia network teaching platform in college physical education. Through the questionnaire survey, the utilization rate of multimedia teaching in physical education is 75.6%. Multimedia technology has a positive impact on physical education, especially in terms of teaching philosophy (47.56%), teaching environment (39.02%), and teaching content (50%) and innovative methods (63.41%). Therefore, the innovation of college physical education models is the general trend, but the experiment did not point out the feasibility of the plan [2]. According to Ahmadi et al., sports analysis technology has been widely used to monitor potential injuries and improve athlete performance. However, most of these techniques are expensive, can only be used in a laboratory environment, and can only check a few trials of each movement. They proposed a new type of dynamic motion analysis framework that uses wearable inertial sensors to accurately assess all activities of athletes in a real training environment. They first proposed a system that uses discrete wavelet transform (DWT) together with a random forest classifier to automatically classify various training activities. The system has too high environmental requirements and it is almost impossible to gain popularity [3]. Their research results provide theoretical and experimental reference for this study.

The innovation of this paper is to realize the application of virtual reality technology in physical education and sports training by constructing a VR sports teaching model with a semisupervised framework and, at the same time, determine the implementation method through the QSCSA algorithm. Based on virtual reality technology and KINECT, a set of teaching and training system is studied. Therefore, the combination of college physical education and sports training with virtual reality technology can make students have a new understanding of college physical education and sports training and regard sports as an interesting activity and enhance the fun of training, save training venues, and improve training efficiency, which indirectly illustrates the necessity of virtual reality technology in physical education and sports training [4].

2. Research Methods for the Application of Virtual Reality Technology

Virtual reality technology (VR) has become a new term for advanced man-machine interface technology in the computer industry. It is dedicated to establishing network interaction, immersion, and imagination. At present, it has achieved success, enabling users to obtain a truly immersive high-end experience. It uses a variety of high-quality technologies, such as computer network technology, artificial intelligence, multisensor technology, and computer graphics. Virtual education in sports is considered to be a revolutionary development of educational technology. It creates a completely different learning environment, changes traditional teaching methods, and promotes interest in new ways of learning knowledge and skills. Interaction provides students with a transformation of learning. Most of the scenes of virtual sports equipment created by virtual information technology are virtual, and the training content can be constantly updated according to the needs of new equipment at any time, so that education can keep pace with the times [5]. At the same time, virtual reality technology has a strong interactivity; students can play freely in the virtual environment, wholeheartedly. It can improve students' skills in a very safe environment. In the virtual learning system, students can practice repeatedly until they learn.

In this article, in order to express the real performance of sports, virtual reality technology based on semisupervised training for athlete identification and prevention is introduced, and the application method is first determined by the QSCSA algorithm. Virtual reality technology can be used to find unmarked sports athletes, and then the classifier member committee calculates the trust of the nearest neighbors, so that unmarked sports trainees with high confidence can be included in the marked sports training [6]. This can effectively improve the generalization of the entire model. In the end, the virtual reality technology obtained after a series of screening and extrapolation is merged to make decision output.

2.1. VR Sports Teaching Modeling Method Using Semisupervised Framework

2.1.1. Selection Algorithm Based on Statistic Q.
The difference in virtual reality technology is defined as the error tendency of athletes' data to be distinguished by different classifiers. For example, f_i and f_j respectively represent two different virtual reality technologies. This article uses Q statistics to measure the difference between virtual reality technologies. The process is expressed as follows:

$$Q_{ij}\left(f_i, f_j\right) = \frac{N_{11}N_{00} - N_{01}N_{10}}{N_{11}N_{00} + N_{01}N_{10}}. \tag{1}$$

In the formula, N_{11} refers to the number of physical education students who can be correctly graded by f_i and f_j, N_{10} refers to the number of correctly graded f_j but the number of unqualified f_i, N_{01} refers to the correct grade of f_i and incorrect FJ, and N_{00} means f_i and f_j. The QSCSA algorithm strikes a balance between the number of people whose sorting is incorrect [7].

2.2. VRT Method.
The nearest neighbor confidence formula for participating in the virtual reality technology of sports athletes is evaluated, and the BL_M member classifier set is expressed as

$$H_M = \left\{BL_1, BL_2, \ldots, BL_{M-1} \mid BL_M \in H\right\}. \tag{2}$$

In the formula, H_M represents a classifier other than BL_M. If it is necessary to classify nonsporting athletes, the following basic assumptions must be met:

(1) The data comes from different universities;

(2) If the physical education students come from the same university, they are likely to be the same according to the category [8]. They can not achieve the results of our research; based on the above two assumptions, we can roughly know the confidence level of unmarked athletes.

Assuming there are two physical education students X_M and X_N, the measure of cosine similarity can be expressed by the following formula:

$$S\left(X_M, X_N\right) = \frac{X_M \cdot X_M}{\|X_M\|\|X_N\|}. \tag{3}$$

The H_M classifier can highlight a part of the unlabeled athletes added to the L_M training set of the BL_M member classifier [9]. At this time, for a certain type of confidence level, the following formula can be used to express the consistency of x_i^u and its neighbors marked as k, $\text{Conf}\left(x_i^u\right)$, as follows:

$$\text{Conf}\left(x_i^u\right) = \sum_{\substack{q=1 \\ q \neq m}}^{M-1} \sum_{j}^{k} S\left(x_i^u, x_j^l\right) \times \text{consistency}\left(BL_q\left(x_i^u\right), y_{x_j^l}\right). \tag{4}$$

Among them,

$$\text{consistency}\left(BL_q\left(x_i^u\right), y_{x_j^l}\right) = \begin{cases} -1, BL_M\left(x_i^u\right) = y_{x_j^l} \\ 1, BL_M\left(x_i^u\right) = y_{x_j^l} \end{cases}, \quad \left(x_j^l\right) \in \varphi_i^l. \tag{5}$$

It can vote according to the member classifier set H_M to get x_i^u mark:

$$\widehat{y}_u = \arg \max H_m\left(x_u\right)_{1 \leq c \leq C}. \tag{6}$$

3. VR Physical Education Training Simulation Experiment

On the basis of virtual reality technology and KINECT, a teaching and training system is being developed. The system uses virtual reality technology and 3D SMAX tools for the virtual model of the training field and uses CryEngine engine technology to convert the training field. Identify these actions and changes in the user's position through the virtual environment, and then transmit the results observed in the experiment to the VR glasses through the Bluetooth module, so that the virtual environment in the VR glasses can change the image and sound accordingly, so that user needs can be achieved. [10]. The motion recognition subsystem of the system is developed on the basis of KINECT. In the process of motion recognition, the influence caused by the user's height and body factors should be reduced, so the human bone tissue and ligament data are used through the motion recognition subsystem. The general idea of motion recognition algorithm is as follows: firstly, the position change between joints is described by bone function. According to the time series, the limited state and standard flow data of the whole motion joint position are collected and used as the reference standard. Finally, according to the DTW standard, combined with the real-time data collection and reporting standards, the movement is evaluated. The influence of individual differences on action recognition can be avoided. The specific steps are as follows:

Data collection: use the KINECT V2 bone tissue detection function to obtain the joint position data of the test athletes. Usually, the public part data is a real-time data stream, which is composed of three parts: bone tissue data stream, depth data stream, and color image stream [11], where the bone tissue data stream is used to determine human movement, and the in-depth data stream is used to change the user's position accordingly; the color image stream is used to build a virtual environment.

Bone tissue data stream processing: the newly acquired bone tissue data stream cannot be directly used to identify actions and must be deleted from the movement; after movement is processed, the next step is to standardize the data. Finally, the joint angle feature uses the interface method to extract data from the bone tissue data stream.

Recognition of training actions: according to the standard actions of various sports courses, the common angle characteristics of each action are deleted, the limited action modes are opened, and the DTW standard matching algorithm is used to compare the action data collected by users in real education.

3.1. Filtering Experiment of Joint Position Data. The bone tissue tracking mode of the Ultra High Dynamics V2 tool can be used to receive the joint position of the test subject in the experiment. These joint position data will be used as initial data. After obtaining the preliminary test data and reducing the noise, the data should be processed to filter unnecessary noise and improve the accuracy of data recognition [12]. The common position noise filter passed by the tracking function is based on the time series data and the bone tissue data of 30 data frames between each frame of data collection, with a time interval of 30 mm. At this time, the bone data will jump and mutate because of the different speed of action, resulting in noise and continuous peak. Therefore, it is necessary to standardize the data collected by the filter.

3.2. Motion Recognition Experiment. When evaluating the similarity between joint motion characteristics and reference patterns, we generally use DTW. If the similarity of each action is higher than the predetermined standard value, it indicates that the action taken by the tester conforms to the standard. The identification process is as follows:

Selection of motion actions: link to the corresponding conditions according to the technical actions previously selected by the tester. At the same time, the motion collection database has been initialized [13].

Matching feature attributes: firstly, the movement of the athlete tester is decomposed, and the bone spatial angle features are subtracted from the time series to form a matrix. Then, DTW algorithm is used to compare the detected data with the reference standard. If they are similar, we can judge whether the decomposition satisfies the condition.

Appropriate fine movement: match and detect the bone tissue and joint characteristics of all time nodes of the technical movement, and after completing all the tests, judge the integrity of the overall movement based on all the test results.

Motion finite state machine matching: match and detect bone and joint features at all time nodes of technical motion. When all the tests are completed, the integrity of the entire operation of the tester will be judged based on all the test results [14].

3.3. Implementing Survey Experiments. After the success of the experiment, 30 volunteers were selected to experience virtual reality technology in sports training, and a feedback survey was conducted on their feelings and views of virtual reality technology in sports training by using questionnaire survey.

4. Application Analysis of Virtual Reality Technology in Sports Training

4.1. Feedback and Analysis of College Volunteers on Virtual Reality

4.1.1. The Influence of Virtual Reality on the Interest of College Sports Training. 15 volunteers thought that virtual reality technology made them very interested in sports training; 5 volunteers thought they were interested; 7 volunteers said they were not clear and could not determine whether it was helpful or not; 2 volunteers thought that virtual reality technology is not good for their own training; another volunteer thinks that virtual reality is very bad for their interest in learning [15]. On the whole, most college volunteers believe that the use of virtual reality technology in physical education training is beneficial to their interest in learning, as shown in Figure 1.

4.1.2. The Impact of Virtual Reality Technology on Sports Training Effects and Self-Confidence. 15 students think that virtual reality technology is very effective to improve the effect of sports training, 9 students think it is effective, 2 students are uncertain, 3 students think it is invalid, and only 1 student thinks that virtual reality technology is very unfavorable to improve the effect of sports training. Volunteers who think that it is beneficial say that virtual reality is a very interesting training experience, and training in a virtual environment is a very exciting process, which greatly improves training efficiency [16]. Students who think that they are disadvantaged said that there is a big gap between the practice in the virtual environment and the real training, and the training in the virtual environment cannot help them improve in actual shots; the students who think that it is very disadvantageous think that wearing VR glasses made them lose. The sense of direction and security becomes intimidating and unable to train normally. The above shows that although there are still various problems, the improvement in training effect brought by virtual reality is significant. There are 18 volunteers who think that virtual reality is very beneficial to their sports self-confidence; 3 students think it is good; 5 students are not sure; 1 student said that virtual reality is not conducive to their self-confidence in sports; the other 2 students said that virtual reality has no effect on their self-confidence in sports. The trainees said it was very unfavorable to them, as shown in Figure 2. Most of the students who think it is beneficial said that in the virtual environment, they can play freely and do not care about others' eyes. Even if they make a mistake, they will not be ridiculed. On the contrary, the students who think that virtual reality is not good for their self-confidence in sports said they feel that putting on the VR eyepieces may seem strange, and they are even more worried that the eyepieces falling during exercise will be laughed at by other students. However, judging from the overall statistics, virtual reality technology has a positive effect on students' confidence in sports [17].

4.2. Analysis of the Necessity of Implementation

4.2.1. Avoiding Accidents in Sports Training. For many highly antagonistic sports, such as taekwondo and boxing, it is often impossible to avoid injury accidents when training in reality. This also makes many colleges and universities abandon the curriculum of these programs. If students can use computer virtual technology to practice these dangerous sports items in the physical education class, they can avoid excessive injuries during training. In this nonreal simulation environment,
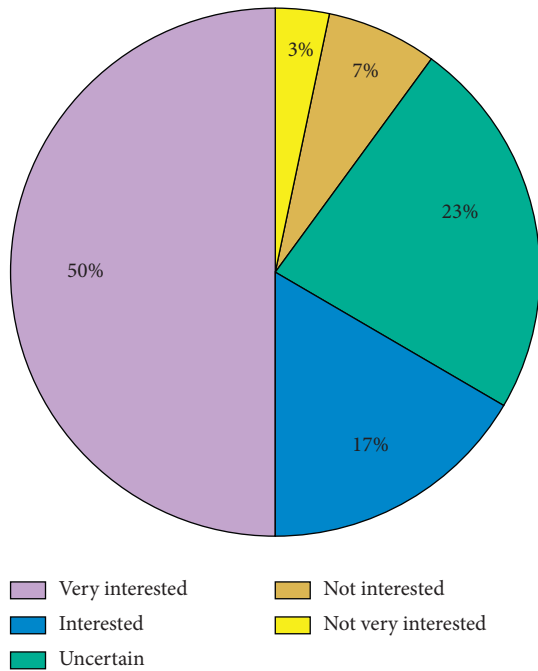
FIGURE 1: The impact of virtual reality technology on sports training interest.
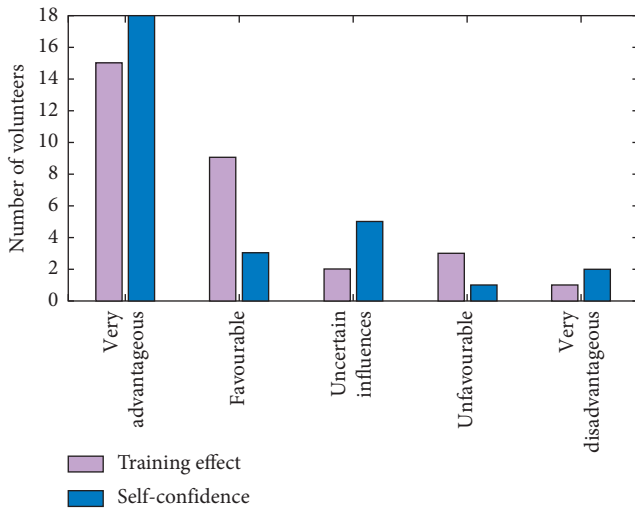
FIGURE 2: The impact of virtual reality technology on the self-confidence and effectiveness of sports training.

students can let go of their hands and feet to train the application of virtual reality technology in various fields of sports, without worrying about possible accidents on their hands or other. Not only that the computer virtual environment can evaluate the students' movements it can also correct the students' deficiencies in the training process in time and improve the quality and efficiency of training [18].

4.2.2. Avoiding Sports Injuries Caused by Difficult Actions.
In recent years, sports technology has continued to develop, and the technical difficulty in various antagonistic sports projects has become increasingly difficult. This means that

many academics will be injured due to the difficulty of training these projects, and facts have proved this is true in real sports training. The use of computer virtual technology can circumvent this very well. The use of virtual reality technology for virtual action experiments can completely avoid the sports injuries caused by difficult and complex technical actions to students [19]. Participants can safely do various difficult movements in the virtual experimental environment.

4.2.3. Changing the Defects of Insufficient Material Conditions. In actual physical training and teaching, due to material conditions that cannot fully meet the needs of sports training, schools have to purchase equipment to build training grounds when funds permit. Since then, many sports trainings have to be cancelled due to funding problems. The use of computer virtualization technology can change this situation well. Students can perform sports training through computers and get rich sensory enjoyment, without is actually setting up a huge training venue.

4.3. Application Analysis of Virtual Reality Technology.
The virtual reality system is mainly constructed by two parts: a human-machine interface device and a virtual reality engine. As the carrier of the virtual assembly process, it provides a large number of function libraries, so that users can easily construct virtual scenes and process various scenes [20]. This chapter briefly introduces the composition of the virtual reality system and the working principle and scene structure of the typical virtual reality development software WTK.

4.3.1. The Composition of the Virtual Reality System.
Generally speaking, a complete virtual reality system mainly consists of the following parts: (1) virtual reality environment platform, mainly WTK, MultiGen, and other virtual reality development platforms; (2) virtual environment generation equipment, mainly some high-performance computing virtual machines, mainly computer equipment; (3) perception devices, mainly virtual peripherals such as data gloves, helmet displays, three-dimensional mice, and joysticks; (4) pose tracking devices, such as tracking locators. The typical composition of the virtual reality system is shown in Figure 3. Among them, the three-dimensional reconstruction technology is a direct technical means to obtain the participant's motion posture and construct the landscape in the pseudoenvironment [21]. Image-based 3D reconstruction technology passively captures scene information (including participants themselves) within the field of view by arranging a camera with a certain topology structure. Then, by analyzing the passive cues such as brightness, shadow, focal length, texture, and parallax in the image, three-dimensional reconstruction is carried out, which has less restrictions on the scale and position of the modeled scene.

4.3.2. Virtual Reality Development Software WTK. WTK is a cross-platform 3D image development toolkit, which is mainly used for the development of virtual reality
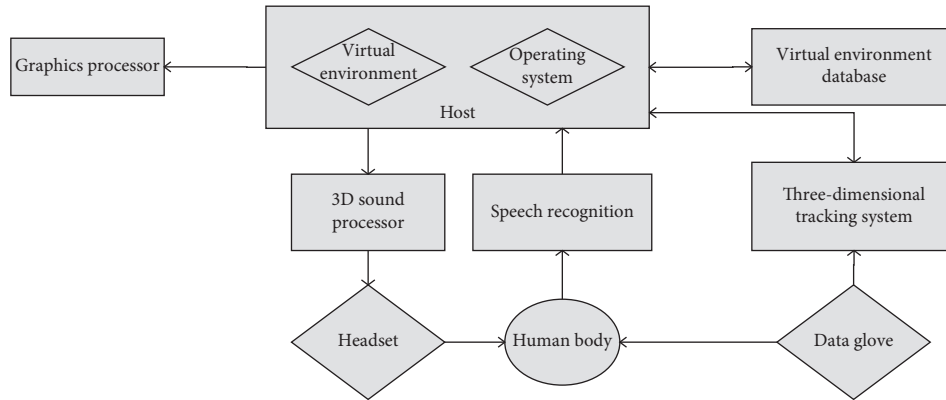
FIGURE 3: Typical composition of a virtual reality system.

simulation applications. The WTK function library contains a large number of C language function libraries, and users can programmatically call the functions in the library to construct virtual scenes. In terms of scene construction, WTK uses a hierarchical scene structure (called scene graph) to organize. WTK scene is composed of geometric model, light source model, pose model, and smoke model [22]. Some geometric models and light source models are created outside WTK, and some are created dynamically within WTK. The pose is used to describe the position and posture of the geometric model and the light source model. The smoke model is mainly used to model the effects of smoke, fog, etc. in the real environment. Using virtual reality technology to build a physical education and sports training system can use virtual reality development software WTK to more quickly apply virtual reality technology to college physical education, so that college physical education can develop rapidly, and students can experience the latest teaching mode, increase interest in sports training, and increase the efficiency of sports training.

4.4. Analysis of the Basic Situation of the Application

4.4.1. Cognition of Virtual Reality Training System by College Sports Teams. Due to the relatively large degree of difficulty of computer virtual reality technology in sports training, many aspects of virtual reality software have not been developed in the more complex sports virtual training [23]. Only a small number of sports research institutes have established virtual reality environments for sports training, and most sports academies' computer virtual reality is still at the theoretical stage. At present, except for the national trampoline team, national diving team, and national gymnastics team, computer virtual reality technology is used in daily training; most sports teams have not used it. This also leads to computer virtual

reality technology not being well applied to actual sports training. Through the investigation of the actual situation of coaches and athletes, the results of the questionnaire of computer virtual reality technology cognition are obtained. Most people know about the application of virtual reality technology in sports training, as shown in Table 1.

4.5. Application Analysis of VR Sports Teaching Based on Semisupervised Framework. The semisupervised framework of VR physical education is mainly based on the research of virtual reality technology and proposes an innovative method of physical education. The realization of this method is based on the semisupervised training framework. In the method proposed in this paper, the choice of virtual reality technology is achieved through the selection method based on Q statistics. When the feature and feature combination are different, the semisupervised training method proposed in the article and the supervised training method are compared and analyzed. The above results can be concluded that the proposed method performs well under the three standards, as listed in Table 2. Under different feature datasets, the accuracy of virtual reality technology is affected by unmarked sports students and marked sports students, as shown in Figure 4. It can be concluded from Figure 4 that in the process of physical education teaching, coaches are required to determine the best state of students' physical performance and the reasons for not achieving the best results, which is very important [24].

In the process of physical education, virtual reality technology can be used to find unmarked physical education students. Then, the effective evaluation of the sports level of sports students can be achieved through the setting of the neighbor confidence. The research results show that the integration of virtual reality technology into college physical education is one of the ways to reform and innovate college physical education.

TABLE 1: Computer virtual reality technology cognition questionnaire.

Occupation	Understanding the percentage of virtual reality training (%)	Percentages who think virtual reality training is important (%)	Percentages trained in virtual reality (%)	Percentages who think virtual reality training is helpful to them (%)
Coach	98	60	20	50
Training unit leaders	99	40	10	40
Junior athlete	95	80	5	80
Senior athlete	95	30	20	10

TABLE 2: Recognition accuracy under supervised training and semisupervised training strategies.

Feature descriptor	Precision		Recall		F-measure	
	Labeled	Art	Labeled	Art	Labeled	Art
JPCD + SRD	0.62	0.94	0.62	0.93	0.63	0.95
SRD	0.63	0.99	0.61	0.95	0.62	0.97
JPCD	0.81	0.98	0.82	0.96	0.71	0.97
Avg	0.71	0.95	0.73	0.98	0.63	0.96
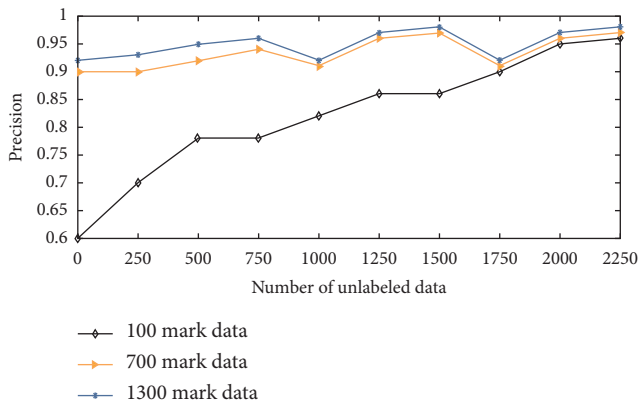
FIGURE 4: The impact of different numbers of unmarked sports students on VTR.

5. Conclusions

Media technology is developing rapidly. Virtual reality technology is its main development trend. It is also an innovation and important development. People pursue reality and humanized media technology and desire speed, convenience, and intuitive information exchange, which violates the reality. The constraints of physical, physiological, and social conditions still have to overcome the constraints of time and space, and significant progress has been made in the field of two-dimensional virtualization. As a medium, virtual reality technology has various advantages of multimedia communication, overcomes the material limitations of traditional media, and provides people with an unprecedented immersive and amazing experience.

Nowadays, colleges and universities have begun to establish a university network in order to accelerate the development of education, but for more teachers, this is a severe challenge, for the continuous development of information technology, the arrival of the computer age, and the rapid development of sports modernization.

Information-based classrooms will gradually enter major universities. Through the above analysis, it can be seen that virtual reality technology will be further developed in the field of sports. The management of sports activities in the field of office automation through information technology will be used to establish a simulation laboratory to drive sports to a higher development direction [25]. Virtual reality technology can be used in sports skills, guidance, and management. The most effective way is to use multimedia technology for sports activities, which can improve the effectiveness of physical exercise.

Virtual reality technology is a bright jewel in the development of media technology. It has unique advantages in many fields. It hides huge research value and commercial market. It is in the new field of communication that virtual reality technology will bring to us. We must understand its development law, correctly guide its development direction, serve mankind, benefit society, and make people's spiritual world more complete. Finally, combining the fictional virtual world with the real world can realize the real value of virtual reality technology and make human society progress.

Data Availability

No data were used to support this study.

Conflicts of Interest

The authors declare that they have no conflicts of interest.

Acknowledgments

References

[1] Y. Ding, Y. Li, and L. Cheng, "Application of Internet of Things and virtual reality technology in college physical education," *IEEE Access*, vol. 8, pp. 96065–96074, 2020.

[2] B. Zhou, "Smart classroom and multimedia network teaching platform application in college physical education teaching," *International Journal of Smart Home*, vol. 10, no. 10, pp. 145–156, 2016.

[3] A. Ahmadi, E. Mitchell, C. Richter et al., "Toward automatic activity classification and movement assessment during a sports training session," *IEEE Internet of Things Journal*, vol. 2, no. 1, pp. 23–32, 2017.

[4] J. Q. Coburn, I. J. Freeman, and J. L. Salmon, "A review of the capabilities of current low-cost virtual reality technology and its potential to enhance the design process," *Journal of Computing & Information Ence in Engineering*, vol. 17, no. 3, pp. 31013.1–31013.15, 2017.

[5] J. L. Maples-Keller, B. E. Bunnell, S.-J. Kim, and B. O. Rothbaum, "The use of virtual reality technology in the treatment of anxiety and other psychiatric disorders," *Harvard Review of Psychiatry*, vol. 25, no. 3, pp. 103–113, 2017.

[6] Y. Zhang, X. L. Ma, and X.-L. Ma, "Research on image digital watermarking optimization algorithm under virtual reality technology," *Discrete & Continuous Dynamical Systems*, vol. 12, no. 4-5, pp. 1427–1440, 2019.

[7] M. Koeva, M. Luleva, and P. Maldjanski, "Integrating spherical panoramas and maps for visualization of cultural heritage objects using virtual reality technology," *Sensors*, vol. 17, no. 4, p. 829, 2017.

[8] C. Donghui, L. Guanfa, Z. Wensheng et al., "Virtual reality technology applied in digitalization of cultural heritage," *Cluster Computing*, vol. 22, no. 4, pp. 1–12, 2017.

[9] Y. Sang, Y. Zhu, H. Zhao, and M. Tang, "Study on an interactive truck crane simulation platform based on virtual reality technology," *International Journal of Distance Education Technologies*, vol. 14, no. 2, pp. 64–78, 2016.

[10] Z. Liang and R. Shuang, "Research on the value identification and protection of traditional village based on virtual reality technology," *Boletin Tecnico/technical Bulletin*, vol. 55, no. 4, pp. 592–600, 2017.

[11] S. Xiang and L. C. Wang, "VGLS: a virtual geophysical laboratory system based on C# and viustools and its application for geophysical education," *Computer Applications in Engineering Education*, vol. 25, no. 3, pp. 335–344, 2017.

[12] J. Liu, R. Shangguan, X. D. Keating, J. Leitner, and Y. Wu, "A conceptual physical education course and college freshmen's health-related fitness," *Health Education*, vol. 117, no. 1, pp. 53–68, 2017.

[13] P. Di and L. Hongye, "Research and application of multimedia teaching in college physical education," *Agro Food Industry Hi Tech*, vol. 28, no. 1, pp. 339–342, 2017.

[14] W. Lin, "Human resources management of track and field web course in college physical education," *International Journal of Emerging Technologies in Learning (iJET)*, vol. 11, no. 04, p. 95, 2016.

[15] S. Q. Saeed, M. F. Khalifa, and M. H. Noaman, "Screening of obesity blood pressure and blood glucose among female students athletes at college physical education and sport sciences in university of baghdad," *Indian Journal of Public Health Research and Development*, vol. 10, no. 6, 2019.

[16] K. Petri, P. Emmermacher, and S. Masik, "Comparison of response quality and attack recognition in karate kumite between reality and virtual reality–a pilot study," *International Journal of Physical Education, Fitness and Sports*, vol. 8, no. 4, pp. 55–63, 2019.

[17] M. Jelii, O. Uljevi, and N. Zeni, "Pulmonary function in prepubescent boys: the influence of passive smoking and sports training," *Montenegrin Journal of Sports Ence & Medicine*, vol. 6, no. 1, pp. 65–72, 2017.

[18] J. W. L. Keogh and P. W. Winwood, "The epidemiology of injuries across the weight-training sports," *Sports Medicine*, vol. 47, no. 3, pp. 1–23, 2016.

[19] L. Zhang, G. Brunnett, K. Petri et al., "KaraKter: an autonomously interacting Karate Kumite character for VR-based training and research," *Computers & Graphics*, vol. 72, no. MAY, pp. 59–69, 2018.

[20] C. Wang, X. Zhang, and L. Liu, "The framework of simulation teaching system for sports dance based on virtual reality technology," *Revista De La Facultad De Ingenieria*, vol. 32, no. 15, pp. 530–536, 2017.

[21] K. Ahir, K. Govani, R. Gajera et al., "Application on virtual reality for enhanced education learning, military training and sports," *Augmented Human Research*, vol. 5, no. 1, p. 7, 2020.

[22] B. K. Wiederhold, "Living in fragments: the necessity of cloud computing and virtual reality," *Cyberpsychology, Behavior, and Social Networking*, vol. 20, no. 7, pp. 405-406, 2017.

[23] J. G. . Galán, "Learning historical and chronological time: practical applications," *European Journal of Science & Theology*, vol. 12, no. 1, pp. 5–16, 2018.

[24] D. Fortmeier, A. Mastmeyer, J. Schroder et al., "A virtual reality system for PTCD simulation using direct visuo-haptic rendering of partially segmented image data," *IEEE Journal of Biomedical & Health Informatics*, vol. 20, no. 1, pp. 355–366, 2017.

[25] A. K. Faulhaber, A. Dittmer, F. Blind et al., "Human decisions in moral dilemmas are largely described by utilitarianism: virtual car driving study provides guidelines for autonomous driving vehicles," *Science and Engineering Ethics*, vol. 25, no. 2, pp. 399–418, 2019.

Research Article

Immersive 5G Virtual Reality Visualization Display System Based on Big-Data Digital City Technology

Fei Tian (ID)

School of Environmental Art Design, Hubei Institute of Fine Arts, Wuhan 430000, Hubei, China

Correspondence should be addressed to Fei Tian; tianfei@hifa.edu.cn

The virtual reality visual display system creates a realistic virtual product display system, allowing users to swim in a three-dimensional virtual environment and perform interactive operations, fully simulating the process of shopping selection and payment in reality, so that users have an immersive feeling. The purpose of this article is to realize the design of an immersive 5G virtual reality visual display system through big-data digital city technology. This paper uses big-data digital city technology to design and implement an immersive virtual reality visualization system from the three-dimensional display mode of vision, hearing, and touch, creating a real and interactive three-dimensional visualization environment for users to have a more intuitive visual experience. The experimental results of this paper show that the smoothness of the virtual reality visualization system test can reach 60FPS, the excellent rate reaches nearly 33%, and the model scene-realistic feedback excellent rate is about 62.5%.

1. Introduction

With the rapid rise and development of the Internet, virtual reality technology has slowly entered people's lives and has also begun to be applied to people's lives and work. By creating and representing virtual spaces and virtual objects, information can be transmitted more intuitively and efficiently. Among them, the application of virtual reality technology in e-commerce is an important new development direction. Since the Internet used by e-commerce is a link between merchants and customers, this makes commodity trade no longer restricted by time and space for the traditional transaction process. Creating a virtual system to project products with a sense of reality, users can swim in a three-dimensional virtual environment and perform interactive functions. By fully simulating the purchase and payment process in reality, users can feel immersive.

Virtual reality technology is a computer system that can create and experience virtual environments, as well as an advanced interface technology. In fact, human auditory behavior is simulated in a real machine environment. Its advantage is beyond reality, and it is a new computer technology developed with the development of multimedia

technology. Virtual reality technology uses a computer to create a more realistic virtual environment, combined with the auxiliary functions of different detection equipment, so that the user is completely immersed in the generated virtual environment, and then interacts with the virtual environment through the man-machine interface, so that the user will have a kind of illusion like the illusion that the user is in the real world.

Flores proposed a case study of a Brazilian city. The purpose of his research is to analyze Twitter information to contribute to a strategic digital city. He then analyzed Twitter and evaluated the information based on its characteristics, sources, nature, quality, intelligence, and organizational level. However, due to the high complexity of the numbers, the results obtained are not very accurate [1]. Gonzalez-Franco M studied how auditory visual cues regulate this selective listening. He achieves this by combining immersive virtual reality technology with spatial audio. By allowing 32 participants to participate in the lecturer's information masking task at the same time, it was found that there were significantly more errors in the decision-making process triggered by asynchronous audiovisual voice prompts. However, due to the small number of people in the

experiment, the data obtained by the result analysis is not very accurate [2]. Huda M has explored and proposed framework models in the past ten years as a way for teachers to adapt to big data to help their teaching performance. His research will help to enhance teaching performance in the application guidelines in the era of big data, to support multiple channels for evaluating knowledge, and to extract new value insights in exploring adaptive teaching capabilities. However, because the proposed framework is too long, people do not agree with other frameworks [3]. Li H proposed that the Internet of Things (IoT) and big data are the two technological themes that have received the most attention in recent years, and there is a close relationship between them, that is, billions of "things" connected to the Internet will generate a lot of data. And, openness creates many opportunities in our lives. He predicts that the Internet of Things and big data may completely change the entire telecommunications industry [4]. However, these have not undergone large-scale market research, so the conclusions are not very theoretical [5].

Starting from the current appearance of products on the Internet, this article analyzes the advantages of virtual reality technology and tries to apply traditional concepts using virtual reality technology, computer technology, and network technology to design screens in network-based virtual screen systems.

1.1. Design of Interaction and Database Technology.

In order to create a network-based virtual display system for digital shopping malls, a new three-dimensional product display method was created. The system aims to make up for the shortcomings of existing product launch methods, such as time and space constraints and poor product interaction on the Internet, to provide users with more free, genuine, and comprehensive services. The innovation of this article lies in the use of virtual reality technology to develop a digital shopping mall prototype with interactive functions. The system will be published on the Internet and will give full play to the advantages of high-speed and rapid Internet communication and perfectly combine two-dimensional with three-dimensional to create a system with good originality and an interactive commercial website.

2. Virtual Reality Visualization Method

2.1. Multiprojection Plane-Transformation Matrix Algorithm.

Projection can turn a cone into a typical cube. In the left coordinate system of the camera space, if upward, downward, left, and right are projected onto the near-tangent plane of the camera point, the distance of these points is t, b, l, and r, and and r is the far-and-near tangent plane to the camera. If the distance of the viewing angle is (Z_f, Z_n), then the P matrix is expressed as follows:

$$P = \begin{bmatrix} \dfrac{2Z_n}{r-l} & 0 & 0 & 0 \\[2ex] 0 & \dfrac{2Z_n}{t-b} & 0 & 0 \\[2ex] \dfrac{r+l}{r-l} & \dfrac{t+b}{t-b} & \dfrac{Z_f}{Z_n-Z_f} & -1 \\[2ex] 0 & 0 & \dfrac{Z_n \cdot Z_f}{Z_n-Z_f} & 0 \end{bmatrix}. \tag{1}$$

In order to calculate the camera parameters quickly and conveniently, the camera space-distance parameters are converted to the CAVE coordinate system space for calculation. The parameters from the angle of view to the close-up level (t, b, l, r, and Z_n) in the camera space are proportional to the parameters from the angle of view to the viewing level (t, b, l, r, and Z_n) in the camera space. CAVE projection, namely,

$$\frac{t}{T} = \frac{b}{B} = \frac{l}{L} = \frac{r}{R} = \frac{Z_n}{Z_n'}. \tag{2}$$

Replace the calculation of the projection transformation matrix with the parameters of the CAVE projection space, then the front view is expressed as follows:

$$L_1 = -\frac{W_1}{2} - X, \tag{3}$$

$$R_1 = \frac{W_1}{2} - X, \tag{4}$$

$$B_1 = \frac{H}{2} - Y, \tag{5}$$

$$T_1 = \frac{H}{2} - Y, \tag{6}$$

$$Z_{n1} = \frac{W_2}{2} - Z. \tag{7}$$

Substituting formula (3) to formula (7) into formula (1) to obtain the front projection transformation matrix P_t:

$$P_t = \begin{bmatrix} \dfrac{W_2 + 2Z}{W_1} & 0 & 0 & 0 \\[2ex] 0 & \dfrac{W_2 + 2Z}{H} & 0 & 0 \\[2ex] \dfrac{-2X}{W_1} & \dfrac{-2Y}{H} & \dfrac{Z_f}{Z_n - Z_f} & -1 \\[2ex] 0 & 0 & \dfrac{Z_n \cdot Z_f}{Z_n - Z_f} & 0 \end{bmatrix}. \qquad (8)$$

Using the above method, the fast calculation type of the other three channels is obtained. This method is very helpful for the user to calculate the projection matrix in real time according to the visual position [6].

2.2. Virtual Reality Technology Algorithm. If the origin and main axis are determined, the position represented by the point should be determined. The subject determines a direction and the number of directions, and the subject also represents the difference between two points. In the three-dimensional space, we also use (x, y, z) to represent a vector. According to the context, we can understand whether it represents a point or a vector [7].

A vector contains a quantity (the coefficient or length of the vector) and a direction. In computer graphics, we are more interested in the direction of vectors. An interesting and important point is to use three x, y, and z scales to indicate that a carrier has a lot of unnecessary information [8]. In fact, only two quantities are necessary. The space formed by all possible directions in the three-dimensional space is actually a two-dimensional space. The reason is that when we define a direction, we only need to look at the normalized vector (because the length of the vector is the key to independence). For any standardized entity (x, y, z), there are

$$x^2 + y^2 + z^2 = 1. \qquad (9)$$

If you want to express the coordinates of a point in a three-dimensional space, you can assume that P is (x, y, z), and the distance between the origin O and P is $r = \sqrt{x^2 + y^2 + z^2}$. The vertical projection of the point P on the XY plane is represented by Q [9]. The angle b is used as the included angle between X axis and OQ, and the angle a is used as the included angle between Z axis and OP. According to the hypothesis, it can be known that if the angle $a = \Delta OPQ$, then OQ = asin r can be obtained.

Therefore, it is easy to use these types to calculate the corresponding Cartesian coordinates (x, y, z) according to the spherical coordinates (r, a, b). The reverse ratio can also be derived from the following formula:

$$a = a \cos \frac{z}{r}, \qquad (10)$$

$$b = b \tan \frac{y}{x}. \qquad (11)$$

The above derivation inspired us to express a vector in one direction in another way: use a set of angles to set a point in the unit sphere. It gives a unit symbol, the vector v is connected to it, and the intersection point is P. Starting from the point P, make the vertical direction of the XY level equal to the level and Q. The direction of the vector v can be determined by two XOQ = and ZOP = v [10]. According to this, it can be concluded that the sum of all direction vectors can be reproduced in the two-dimensional space, as shown in the following:

$$\Omega = \left\{ (u, v) \mid 0 \le u < 2\pi, -\frac{\pi}{2} \le v \le \frac{\pi}{2} \right\}. \qquad (12)$$

Assuming that the area surrounding the point P on the sphere is A, the solid angle of A is defined as follows:

$$\Gamma = \frac{A}{r^2}. \qquad (13)$$

In equation (13), r is the radius of the sphere. The unit of measurement becomes a solid radius. The entire sphere contains a three-dimensional radius $\hat{r}2$. The calculation of the solid angle is similar to the normal angle, which is equal to the ratio of the length of the area around the radius of the circle.

The differential fixed angle is the fixed angle corresponding to the "differential area." The small area on the surface of the sphere that tends to zero is the differential area. Usually, dw is used to represent the differential region. Here, we have given a formula to find the two angles u and v corresponding to the direction or point of the ball, from which we can see the relationship between the above concepts.

2.3. Method of Establishing Water Surface Grid. In the specific process of graphic simulation, one is to establish a mesh model, and the other is to simulate the movement of the vertices of the water surface. From the camera's perspective, the output of the object grid in the scene is very large, which limits the user's perspective. This will cause a waste of efficiency and resources and easily lead to low real-time efficiency [11]. The amount of water surface simulation calculations is reduced to ensure real-time performance of water production.

The projection grid is actually a grid projected into the space. This is not a grid created in the world space, but placed in the camera space. Like the LOD technology, according to the user's close observation of high-detail objects and low-detail objects, the waste of performance resources in the remote project of the LOD network is reduced to ensure the

real-time effect of performance. The projection process is analyzed through four spaces: object space, global space, view space, and projection space [12].

In the 3D simulation program, the object in the screen space is transformed into an image through three matrix transformations, namely, M_{world}, M_{view}, and $M_{\text{projector}}$, which transforms the object into the global space according to the global transformation table, and the projection table transforms the space projection in the object coordinate space from the global transformation table. Finally, the transformation of the coordinate object in the projection space is mapped through the projection matrix. The viewing area corresponds to the screen space, and a viewing grid is created in the final screen space. The conversion is as follows:

$$P_{\text{projector}} = M_{\text{view}} * M_{\text{project}} * P_{\text{world}}, \qquad (14)$$

where $P_{\text{projector}}$ is the display space position and P_{world} is the global space object position. After this type of inverse transformation, the position of the grid can be obtained in the global space. The initial type can be displayed at the top of the grid in the screen space, and the reverse conversion is as follows:

$$P_{\text{world}} = \left[M_{\text{view}} * M_{\text{project}} \right]^{-1} * P_{\text{projector}}. \qquad (15)$$

The first step of the grid algorithm is to create a direction where the grid level is perpendicular to the camera. The second step is to calculate the grid level. Calculated by the conversion equation (15), each peak position in the world space is calculated by the wave-making algorithm. Yes, the top of the grid is compensated vertically, the final matrix function (14) is converted, and the rendered water surface can be brought to the screen space [13].

3. Virtual Reality Visualization Display System Experiment

3.1. Data Collection.
For data collection, this paper obtains real-time data, normal information data, and stable data in the big data of the power grid. Real-time information and regular information data mainly come from our company's engineering production management system. This paper proposes an operating method for seamless access of PMS data based on the GIS system in order to obtain real-time data and enhance the maximum display effect [14]. The application programming interface (API) requires access to the PMS database for data updates, such as power transmission and conversion monitoring status, grid line power consumption, and distribution. The correction data of images, soils, and substations in our region are mainly completed through early aerial photography and modeling. After entering the data into the system, they remain unchanged for a long time [15].

3.2. Visualization System Software and Hardware Integration.
The software and hardware of the system are integrated with the following description. Integrate the big data of the power supply network through the GIS back-end system, and then,

distribute the corrected image to it. Based on the front-end image fusion engine, the spliced corrected image is divided into multiple projection signals, which are finally displayed on the website screen by the headlights. At the same time, users can control 3D GIS performance scenes, lighting, and real-time sound effects through an interactive system [16].

Among them, the virtual reality GIS, as the main component of the system software, effectively integrates various data, is responsible for the sorting and management of big data and belongs to the image fusion correction of virtual reality scenes performed on the system graphics workstation. The material of the system is mainly composed of four parts: interactive system, central control system, CAVE system, and lighting and sound system, which communicate with each other through Wi-Fi connection. The central control computer is a system interface that connects the interactive system, GIS system, and main tunnel control system and directly controls external audio and lighting systems. The interactive system includes a touch screen, a mobile terminal, and a three-dimensional mouse, which integrates external devices and systems. The communication link can improve the practicability and ease of use of the system. The main CAVE control system has a complex structure and is the main component of the system. A data visualization screen is composed of a stereo projection system and a graphic combination system [17, 18].

3.3. Function Design of the Visualization System.
The overall goal of this system is to establish a data center virtual reality visualization display system based on B/S architecture. The system is a practical solution to various problems encountered in the display of a large amount of information generated by the daily operation of the data center computer room [19]. The visual information display system of the data center is designed from different angles:

(1) The system will handle the creation of the data center computer room, the conversion of required equipment models and model forms, how to introduce virtual reality scenes, and how to standardize the entire process.

(2) Be able to browse the overall environment of the data center computer room from all angles. The system provides users with a three-dimensional view of the data center computer room. Users can click to enter and monitor the current status of the computer room from all angles.

(3) Different virtual reality methods are used to provide data information in the data center computer room; the computer management and data management center of the computer room are convenient. The system uses different three-dimensional display methods to display computer room data information on virtual reality scenes, visually and emotionally analyze and process computer room functions, and improve the management efficiency of computer room managers. Managers can also observe the operating conditions of the computer space from

different angles and can quickly make decisions about the operating conditions of the equipment in the computer room and deal with the damage on time [20].

According to different system functions, the system is divided into three main units: virtual reality scene projection function module, data-visualization information display function module, and database information query module, as shown in Figure 1. The computer room function virtual reality scene-display unit mainly includes the virtual reality display in the computer room, stage tour, and rapid placement. The functional unit of visual display of data information should specifically include three methods to change the color and texture of materials; the database query module mainly includes the query of room equipment data information [21, 22]. The system uses a tree display, with the data center computer room as the root node for display. Each node contains a virtual reality computer room view, scene roaming (you can browse the entire computer room environment), quickly place and change the color or texture mode of the material, and use the progress line mode and the moving text mode to display data information. Computer room operators can learn about the use of equipment in the data center computer room by requesting relevant information from the database. The specific functions of the system will be described in detail below.

4. Analysis of Results of the Virtual Reality Visualization Display System

4.1. Experience Analysis of the Virtual Reality Visualization System. In order to test and analyze whether the demand analysis and immersion experience of the system meet the standards, a questionnaire is designed around various indicators of the system. The question content of the questionnaire design includes system UI beauty, system stability, system ease of use, system interaction, and system emulation [23]. By providing VR system experience to 40 volunteers, the PC-side workstation configuration is shown in Table 1, and finally, the experience is counted and fed back. The calculation and analysis results are shown in Figure 2.

The results show that the overall experience of users after using the visualization system is still very good. Among them, the immersive experience of the system is the best, and 18 of them are very satisfied with it, accounting for almost 50% of the total. The stability of the system is also not bad, and 15 people commented very satisfied with this. Users are satisfied and very satisfied with the other performance of the system, and only a few people think the system is good, accounting for about 5% [24].

From the analysis of the results, it can be concluded that comprehensive, rigorous, and standardized tests have been conducted in the user's site environment in terms of function, performance, environment, reliability, and user interface. At the same time, the design system, test plan, and tests related to fluency and immersion were also investigated. According to the displayed results, it is determined that the system's functional use cases and nonfunctional
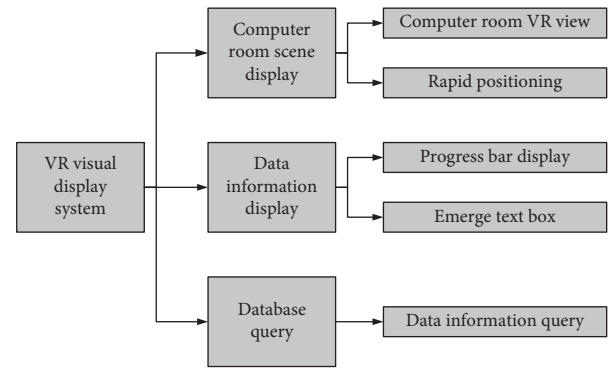
Figure 1: Visualization system function diagram.

goals are completed to the expected requirements of the software, meets the relevant design requirements, and has the following characteristics. (1) The system structure is reasonable and concise, and the system structure is clear, which can meet the target needs of the subject. (2) The function is more comprehensive. The system is composed of the interactive operation input system, scene management control module, scene model library, collision detection and terrain detection, visual rendering module, sports camera module, etc., covering business functions such as tree visualization, realistic rendering, and immersive roaming experience. Tree visualization and immersive virtual scene experience achieve a high sense of reality and immersion. (3) The security of the system is better. The Unity PlayerPrefs technology and offline mode are used to safely store local data to ensure real-time operation of visual rendering. There is no drastic change of screen connection in the system, and the fluency is high, which can effectively alleviate the dizziness caused by wearing a virtual helmet. (4) The system is flexible to use. The system implements six-degree-of-freedom roaming and collision detection in compliance with physical rules, and users can perform panoramic and flexible roaming and observation experiences. After the initial adjustment and adaptation of virtual helmet-related hardware devices, the default connection mode is adopted, that is, the system can be automatically connected and run at any time. (5) The system has high reliability. For the user to restart the device after power off or forcibly shut down, you can continue to re-run the system according to the default method to experience [25].

4.2. Algorithm Analysis of the Virtual Reality Visualization System. This paper compares and evaluates the proposed HCDDSL algorithm and the existing heterogeneous system algorithms, such as HEFT, CPOP, and HCNF. Use SLR and acceleration value to evaluate the performance of this algorithm and previous methods. The scheduling length ratio (SLR) is the ratio of the scheduling length to the scheduling length of the critical path task weights on the fastest processor. The task scheduling algorithm that gives the lowest SLR value of the graph is the best performing algorithm [26]. The average SLR pair of each algorithm is shown in Table 2.

The acceleration value speedup of the algorithm is calculated by dividing all the calculation time executed

TABLE 1: PC-side workstation configuration.

CPU		RAM	System type	GPU		USB
Intel (R)	Xeon (R)	32 GB	Windows7	NVDIA	Quadro	Four USB3.0
E5-2620v32.4 GHz		SP1 (64 bit)	K2200		USB2.0	

sequentially to the completion time of the algorithm. Sequential execution time is calculated by assigning tasks to the single processor with the smallest cumulative communication cost. The task scheduling algorithm that gives the highest acceleration value of the graph is the algorithm with the best performance. In order to compare the scheduling algorithms, this paper made a random task graph generator, which can generate a large number of DAGs with different characteristics by inputting several parameters.

This paper compares and evaluates the proposed HCDDSL algorithm and the current heterogeneous system algorithms, such as HEFT, CPOP, and HCNF [27]. Figure 3 shows the performance of the algorithm for 5 different CCR values (average SLR and average acceleration value), and Figure 4 shows the performance of the algorithm for 5 different size tasks. From these figures, it can be concluded that the average SLR value of the HCDDSL algorithm is better than the HEFT by 15.34%, CPOP algorithm by 16.24%, and HCNF algorithm by 9.16% for all generated graphs; the average acceleration value of the HCDDSL is better than the HEFT algorithm by 14.48%, CPOP algorithm by 18.17%, and HCNF algorithm by 5.88%. The efficiency of HCDDSL algorithm task scheduling has been greatly improved [28].

According to the data in the figure, it can be seen that a new algorithm called the HCDDSL is finally proposed, which is used for the scheduling of multicore heterogeneous processor-system program graphs, so as to solve the high computational complexity of stereo image matching. The algorithm optimizes the DAG topology by using clustering and locates the task position in the DAG topology in the classification stage. Through this method, all key nodes in DAG have high priority [29]. In order to reduce the scheduling length and reduce the task span time, the insertion interval and task replication are considered in the task allocation stage. Experiments are carried out by using a large number of randomly generated task graphs with different characteristics to verify the performance of the algorithm. Simulation results show that the HCDDSL algorithm is significantly better than other existing algorithms, such as the HEFT, CPOP, and HCNF. With the increase of the number of tasks and processor cores, the advantages of the new algorithm become more obvious [30].

4.3. Analysis of Virtual Reality Roaming Function.
Collision detection can also be called contact detection, which is a common phenomenon in real life: two impenetrable objects cannot share the same area of space. Collision detection is a very important part of the 3D visualization system. Its main task is to judge between object models, models and scenes, judge whether they collide, and give information such as the location of the collision [31].
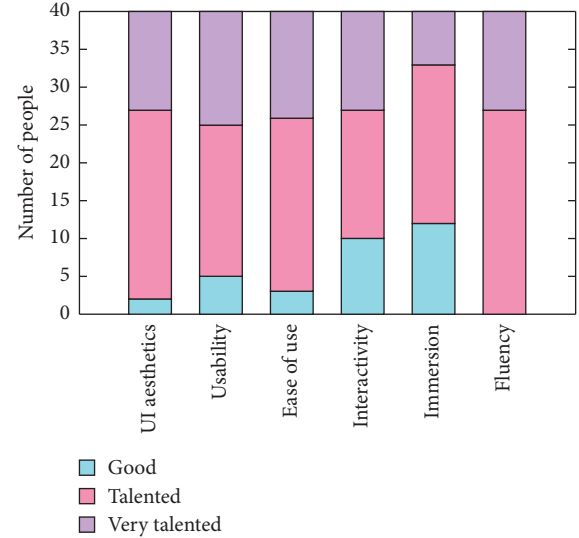
FIGURE 2: Visualized system experience results.

TABLE 2: Average SLR value of each algorithm.

CCR	HEFT	CPOP	HCNF	HCDDSL
0.1	1.6	1.5	1.3	1.5
0.5	1.8	1.7	1.5	1.6
1	2.2	2.1	1.9	1.8
5	4.5	4.4	4.2	4.1
10	5.4	5.3	5.0	4.7
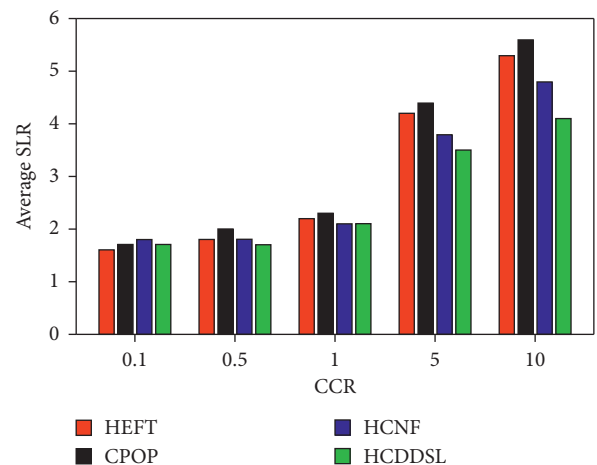
FIGURE 3: Average SLR comparison of algorithms.

Collision detection is an important part of building a 3D visualization system, which allows users to interact with 3D scenes in a more natural way. During the movement, the physical model in the three-dimensional scene is likely to
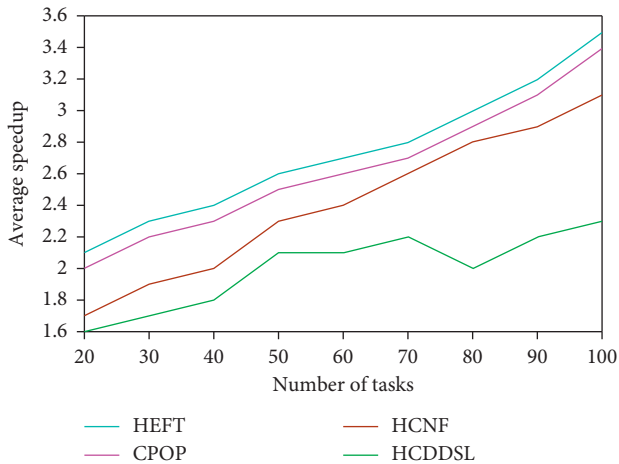
Figure 4: Comparison of average speedup values of algorithms.
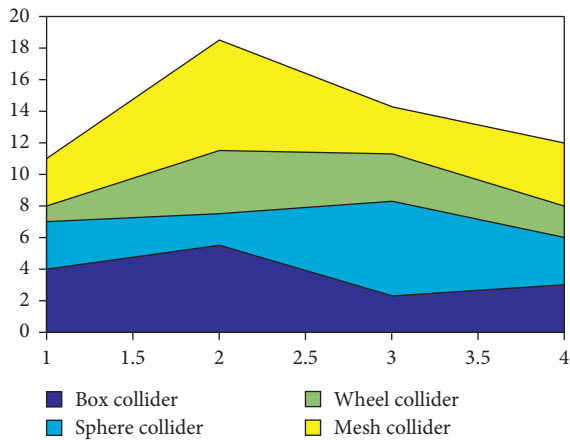
Figure 5: Cube objects use different bounding box areas.

collide, contact, and involve in other forms of interaction. A three-dimensional scene based on a physical model must be able to detect this interaction between objects and respond accordingly; otherwise, unreal phenomena such as mutual penetration or overlap between objects may occur. What needs attention in scene driving is collision detection. Whether it is the walking mode or free view mode, the physical properties of the object must be set so as not to "pass through the wall." With the continuous development of virtual reality technology, collision detection algorithms have also been continuously improved. Current collision detection algorithms are roughly divided into image space-collision detection algorithms and object space-based collision detection algorithms. Unity3d's own physics engine can complete the collision detection algorithm based on the bounding box [32].

The primary problem in realizing a 3D scene is to realize the collision detection between the physical model and the ground to avoid the physical model from crossing the ground. The Unity3d engine provides developers with several space-based hierarchical bounding boxes, namely, BoxCollider, SphereCollider, WheelCollider, and

MeshCollider. The size of the area is used to determine the effect of collision with the ground, as shown in Figure 5. By adding different types of bounding boxes to the model, different degrees of collision detection can be achieved [33]. When implementing the scene roaming function, the first-person view object adds the SphereCollider bounding box, which can realize the collision effect with the ground, thereby avoiding "passing through the ground" [34].

5. Conclusions

This article applies the design of the imaging system and divides it into three functional units: Visual unit, information query unit, and functional connection unit, and database query and equipment characteristic information: the connection method of the database and Unity3d query function. This system uses three different three-dimensional data display methods to display the characteristic information of the center, that is, the three-dimensional method should further study the occurrence to obtain more data appearance forms. It will be reviewed in future investigations. Other forms such as oil meter, thermometer, and linear meter are used to display data information; in addition, the next step should consider the operation of data transmission and reception.

This article uses a visualized virtual reality system combined with physical equipment to solve the problems of virtual reality technology, but it has more complex and time-consuming problems for visualization. In the future work, the author will further explore how to produce more efficient and better reconstruction methods. At the same time, when building a virtual reality system, study the frame rate to avoid dizziness and bring users a better virtual reality stimulation experience.

This article provides a reference for virtual reality imaging technology, but the next virtual reality of the cabin environment should be more real, and the functions of the system need to be further improved. When the user uses the system to monitor the data center, the system should issue an alarm in real time. It may be related to the actual control system. The system detects abnormal conditions in the computer room. The control system can process the equipment in the computer room in real time. For example, it can receive different types of alarm messages in real time and use sounds, images, etc. For protrusions, ensure the normal operation of the equipment compartment.

Data Availability

No data were used to support this study.

Conflicts of Interest

The author declares that there are no conflicts of interest.

References

[1] C. C. Flores and D. A. Rezende, "Twitter information for contributing to the strategic digital city: towards citizens as

co-managers," *Telematics and Informatics*, vol. 35, no. 5, pp. 1082–1096, 2018.

[2] M. Gonzalez-Franco, A. Maselli, D. Florencio et al., "Concurrent talking in immersive virtual reality: on the dominance of visual speech cues," *Entific Reports*, vol. 7, no. 1, p. 3817, 2017.

[3] M. Huda, Z. Haron, M. N. Ripin et al., "Exploring innovative learning environment (ILE): big data era," *International Journal of Applied Engineering Research*, vol. 12, no. 17, pp. 6678–6685, 2017.

[4] H. Hamidi and M. Jahanshahifard, "The role of the Internet of things in the improvement and expansion of business," *Journal of Organizational And End User Computing*, vol. 30, no. 3, pp. 24–44, 2018.

[5] H. Li, R. Lu, and J. Misic, "Guest editorial big security challenges in big data era," *IEEE Internet of Things Journal*, vol. 4, no. 2, pp. 521–523, 2017.

[6] B. Shen, T.-M. Choi, and H.-L. Chan, "Selling green first or not? A Bayesian analysis with service levels and environmental impact considerations in the Big Data Era," *Technological Forecasting and Social Change*, vol. 144, no. JUL, pp. 412–420, 2019.

[7] R. Aljawahiri and E. Milne, "Resources available for autism research in the big data era: a systematic review," *PeerJ*, vol. 5, no. 8, Article ID e2880, 2017.

[8] G. J. D. Smith, L. Bennett Moses, and J. Chan, "The challenges of doing criminology in the big data era: towards a digital and data-driven approach," *The British Journal of Criminology*, vol. 57, no. 2, pp. 259–274, 2017.

[9] A. Cocciolo, "Community archives in the digital era: a case from the lgbt community," *Preservation, Digital Technology and Culture*, vol. 45, no. 4, pp. 157–165, 2017.

[10] A. A. Genlott, A. Groenlund, and O. Viberg, "Disseminating digital innovation in school – leading second-order educational change," *Education and Information Technologies*, vol. 24, no. 5, pp. 3021–3039, 2019.

[11] E. Parteka and D. Alcides Rezende, "Digital planning of the city of Barcelona and its relations with the strategic digital city," *Journal of Technology Management and Innovation*, vol. 13, no. 4, pp. 54–60, 2018.

[12] M. Huda, A. Maseleno, M. Shahrill, K. A. Jasmi, I. Mustari, and B. Basiron, "Exploring adaptive teaching competencies in big data era," *International Journal of Emerging Technologies in Learning (iJET)*, vol. 12, no. 03, pp. 68–83, 2017.

[13] C. Ekstrand, A. Jamal, R. Nguyen, A. Kudryk, J. Mann, and I. Mendez, "Immersive and interactive virtual reality to improve learning and retention of neuroanatomy in medical students: a randomized controlled study," *Cmaj Open*, vol. 6, no. 1, pp. E103–E109, 2018.

[14] S. S. Gill, I. Chana, and R. Buyya, "IoT based agriculture as a cloud and big data service," *Journal of Organizational and End User Computing*, vol. 29, no. 4, pp. 1–23, 2017.

[15] Y. Jing, Y. Bian, Z. Hu et al., "Deep learning for drug design: an artificial intelligence paradigm for drug discovery in the big data era," *Aaps Journal*, vol. 20, no. 3, p. 58, 2018.

[16] K. Chamilothori, J. Wienold, and M. Andersen, "Adequacy of immersive virtual reality for the perception of daylit spaces: comparison of real and virtual environments," *Leukos the Journal of the Illuminating Engineering Society of North America*, vol. 15, no. 1-4, pp. 203–226, 2018.

[17] A. P. Anderson, M. D. Mayer, A. M. Fellows, D. R. Cowan, M. T. Hegel, and J. C. Buckey, "Relaxation with immersive natural scenes presented using virtual reality," *Aerospace Medicine and Human Performance*, vol. 88, no. 6, pp. 520–526, 2017.

[18] S. Rouhani, A. Ashrafi, A. Z. Ravasan, and S. Afshari, "Business intelligence systems adoption model: an empirical investigation," *Journal of Organizational and End User Computing*, vol. 30, no. 2, pp. 43–70, 2018.

[19] Z. Lai, Y. C. Hu, Y. Cui, L. Sun, N. Dai, and H.-S. Lee, "Furion: engineering high-quality immersive virtual reality on today's mobile devices," *IEEE Transactions on Mobile Computing*, vol. 19, no. 7, pp. 1586–1602, 2020.

[20] D. Dong, L. K. F. Wong, and Z. Luo, "A novel approach for assessing prospective memory using immersive virtual reality task," *Psychology*, vol. 07, no. 10, pp. 1315–1325, 2017.

[21] P. K. Roos, V. Wim, C. Jacqueline et al., "Anxiety partially mediates cybersickness symptoms in immersive virtual reality environments," *Cyberpsychology, Behavior, and Social Networking*, vol. 21, no. 3, pp. 187–193, 2018.

[22] R. S. Bhadoria, N. S. Chaudhari, and N. S. Chaudhari, "Pragmatic sensory data semantics with service-oriented computing," *Journal of Organizational and End User Computing*, vol. 31, no. 2, pp. 22–36, 2019.

[23] C. Gagliardi, A. C. Turconi, E. Biffi et al., "Immersive virtual reality to improve walking abilities in cerebral palsy: a pilot study," *Annals of Biomedical Engineering*, vol. 46, no. 571–576, pp. 1376–1384, 2018.

[24] B. Chau, I. Phelan, P. Ta et al., "Immersive virtual reality therapy with myoelectric control for treatment-resistant phantom limb pain: case report," *Innovations in Clinical Neuroence*, vol. 14, no. 7-8, p. 3, 2017.

[25] I. Sudiartha and I. C. Bawa, "Bandwidth optimization on design of visual display information system based networking at politeknik negeri bali," *Journal of Physics Conference Series*, vol. 953, no. 1, Article ID 012050, 2018.

[26] N. Ochiai and H. Kondo, "Color functionality used in visual display for occupational and environmental safety and managing color vision deficiency," *Journal of Uoeh*, vol. 39, no. 1, p. 35, 2017.

[27] S. Barathi, G. Loganathan, and V. R. Rajan, "Knowledge management," *Advances in Computational Ences and Technology*, vol. 10, no. 5, pp. 1479–1486, 2017.

[28] R. K. K. V. Giri and V. R. Mandla, "Study and evaluation of carbon sequestration using remote sensing and GIS: a review on various techniques," *International Journal of Civil Engineering and Technology*, vol. 8, no. 4, pp. 287–300, 2017.

[29] H. Pavan, M. Shettar, and M. C. Gowrishankar, "Investigation of mechanical properties of glass fiber – chicken feather hybrid composite," *International Journal of Technology*, vol. 8, no. 3, p. 408, 2017.

[30] V. R. Isaksson, N. Kristin, L. Heewon et al., "A qualitative study of barriers to genetic counseling and potential for mobile technology education among women with ovarian cancer," *Hereditary Cancer in Clinical Practice*, vol. 16, no. 1, p. 13, 2018.

[31] P. A. Beata, A. E. Jeffers, and V. R. Kamat, "Real-time fire monitoring and visualization for the post-ignition fire state in a building," *Fire Technology*, vol. 54, no. 4, pp. 995–1027, 2018.

[32] B. B. Rao, V. R. Raju, and B. B. V. L. Deepak, "Estimation and optimization of heat transfer and overall pressure drop for a shell and tube heat exchanger," *Journal of Mechanical Science and Technology*, vol. 31, no. 1, pp. 375–383, 2017.

[33] S.-Y. Lin, V. R. Parasuraman, S. L. Mekuria, S. Peng, H.-C. Tsai, and G.-H. Hsiue, "Plasma initiated graft polymerization of 2-methacryloyloxyethyl phosphorylcholine on silicone elastomer surfaces to enhance bio(hemo)

compatibility," *Surface and Coatings Technology*, vol. 315, no. Complete, pp. 342–349, 2017.

[34] V. R. Anderson, N. Nepal, S. D. Johnson et al., "Plasma-assisted atomic layer epitaxial growth of aluminum nitride studied with real time grazing angle small angle x-ray scattering," *Journal of Vacuum Ence and Technology A Vacuum Surfaces & Films*, vol. 35, no. 3, Article ID 031508, 2017.

Research Article

Knowledge Graph Question and Answer System for Mechanical Intelligent Manufacturing Based on Deep Learning

Miaoyuan Shi (ID)

R & D Department, Suzhou AI Speech Co., Ltd., Suzhou 215009, Jiangsu, China

Correspondence should be addressed to Miaoyuan Shi; goldbook@163.com

With the development of deep learning and its wide application in the field of natural language, the question and answer research of knowledge graph based on deep learning has gradually become the focus of attention. After that, the natural language query is converted into a structured query sentence to identify the entities and attributes in the user's natural language query and the specified entities and attributes are used to retrieve answers to the knowledge graph. Using the advantage of deep learning in capturing sentence information, it incorporates the attention mechanism to obtain the semantic vector of the relevant attributes in the query and uses the parameter sharing mechanism to insert candidate attributes into the triple in the same model to obtain the semantic vector of typical candidates. The experiment measured that under the 100,000 RDF dataset, the single entity query of the MIQE model does not exceed 3 seconds, and the connection query does not exceed 5 seconds. Under the one-million RDF dataset, the single entity query of the MIQE model does not exceed 8 seconds, and the connection query will not be more than 10 seconds. Experimental data show that the system of knowledge-answering questions of engineering of intelligent construction based on deep learning has good horizontal scalability.

1. Introduction

1.1. Background and Significance. With the rapid development of Internet information technology and the rapid growth of information volume, storing and retrieving massive amounts of data are a difficult task. Using search engines to find the information people need from massive amounts of data has been a research in the field of information retrieval. However, the search engine still has its limitations. It cannot understand the real needs of the user and returns an accurate answer to the user, but only checks and sorts the information about the user. Designing a knowledge-based answering system for intelligent engineering based on deep learning is a very popular research direction in the field of natural language processing. It is an information retrieval system that covers many areas of technology, such as language processing, machine learning, and data mining.

The question understanding method of answering system based on knowledge graph is divided into three levels: article, entity, and relationship. Sort question sentences from the sentence level to get the user's intention or answer category. From this, you can better understand the questions in this article and conduct the next survey. From the entity level and relationship level, the natural language question entity performance is correctly linked to the explanatory diagram to determine the relationship of the corresponding question and use the explanatory diagram to appropriately answer the user's question, which can be answered faster and correctly [1, 2].

1.2. Related Work. With the rise of artificial intelligence, question answering systems have been fully studied. Zeng proposed the definition of random variables and integration. He combined deep learning algorithms and

proposed a new unified definition of mutual information, which defines the joint distribution of two random variables by considering the marginal probability [3]. An integrated cause-effect graph is also proposed, which has the process knowledge extracted from the text and can be used to determine visual answers based on information retrieval techniques [4]. However, his selected literature is limited, and the theory is not systematically mature enough. Sawant et al. believe that in web search, queries that seek entities often trigger special question answering (QA) systems. It can use a parser to interpret the problem as a structured query, execute it on a knowledge graph (KG), and then return a direct entity response. QA systems based on precise parsing are often very fragile: subtle changes in grammar can greatly change the response. In addition, the coverage of the query is fragmented. At the other extreme, a large corpus can provide wider coverage, but the form is irregular and unreliable. They introduced AQQUCN, a quality inspection system that cleverly combines KG and corpus evidence. AQQUCN accepts a wide range of query syntax, including correctly formatted questions and short telegram keyword sequences. Faced with the inherent query ambiguity, AQQUCN aggregates the signals from KG and large corpora to directly rank KG entities, rather than perform a semantic interpretation of the query. AQQUCN models ideal interpretations as unobservable or latent variables [5]. Hu et al. found that RDF questions/answers (Q/A) in the research allow users to ask questions in natural language on the knowledge base represented by RDF. In order to answer natural language questions, the existing work uses a two-stage approach: problem understanding and query evaluation. Their focus is on understanding the problem to solve the ambiguity of natural language phrases. The most common technique is joint disambiguation, which has an exponential search space. He proposed a systematic framework for answering natural language questions on the RDF repository (RDF Q/A) from a graphical data-driven perspective. A semantic query graph is also proposed to model the query intent of natural language problems in a structured way, and on this basis, RDF Q/A is simplified to the subgraph matching problem. More importantly, when a query match is found, the ambiguity of the natural language problem is solved. If no match is found, the cost of disambiguation will be saved [6].

1.3. Innovation in This Article. The main innovations of this paper include the following aspects: (1) this paper proposes a deep learning-based intelligent manufacturing knowledge graph problem generation model, introduces the details of the model in detail, and compares it with the template-based model. (2) Using the idea of conflicting genetic networks, a semisupervised educational framework is designed that combines the creation of knowledge graph problems and the matching of questions and answers. When the number of educational data is small, the results of both tasks are achieved.

2. Deep Learning-Based Knowledge Question Answering System for Mechanical Intelligent Manufacturing

2.1. Deep Learning. Deep learning is a popular research direction in the computer field in the recent years. A deep network structure based on multiple hidden layers is formed by combining low-level features to form more abstract high-level features [7, 8]. Traditional machine learning is difficult to directly process the original data, because it is usually extracted manually when extracting features. At this time, professional knowledge needs to be used to design a feature extraction that can convert the original data into a feature representation for the machine learning system [9, 10]. Deep learning is a method that uses raw data to automatically discover internal feature expressions. Deep learning is a method that uses raw data to automatically discover internal expressions of features. It converts raw data into higher-level and more abstract feature expressions through a large number of nonlinear transformation combinations, so that deep neural networks can learn very complex operation. The idea of deep learning is to directly extract features from the original data without using artificial features to extract features [11].

Convolutional neural network is a well-known deep learning framework inspired by the mechanism of natural visual perception. It is a multilevel deep feedforward artificial neural network composed of multiple two-dimensional planes [12, 13]. Its neurons can respond to some surrounding units within the coverage area and have achieved very good results in image processing problems. Due to its characteristics, it is widely used in image recognition and image classification tasks [14, 15]. Thus, the framework of the convolutional neural network model was established, and a multilayer artificial neural network for recognizing handwritten digits was designed [16]. The network can effectively represent image features, and at that time, it directly recognized visual patterns from original pixels. This makes image visual recognition possible and also provides help for subsequent image recognition research [17, 18].

The repetitive neural network is a typical model of machine learning supervision. It contains loops that change over time and is a simple ring connection simulation. In RNN, the output of a sequence at the current time is not only related to the current time state but also related to the output of the previous time. Specifically, when calculating the output of the current time, the RNN will apply the previously memorized information to the current calculation [19, 20].

2.2. Characteristics of Mechanical Intelligent Manufacturing. Mechanical intelligent manufacturing is a comprehensive application of AI (artificial intelligence), an intelligent system integrating man and machine, and a manifestation of knowledge and intelligence. Knowledge is the basis of intelligence and intelligence is the ability to apply knowledge [21, 22]. Intelligent manufacturing is a technology and system that enables the entire manufacturing system to have self-awareness, self-diagnosis, adaptation, self-learning, self-

cooperation, and self-organization capabilities. It is a man-machine integrated intelligent system built by smart equipment and industry experts. In the manufacturing process, let the manufacturing system have independent thinking and be able to carry out intelligent activities such as analysis, reasoning, judgment, conception, and decision-making [23, 24]. From the background of manufacturing, today's excess capacity is a common problem in manufacturing, and the new market model has transformed manufacturing into a service industry. The original model can no longer meet the increasingly personalized needs and service experience. The final argument can provide a more personalized and considerate service, who can win the market [25, 26]. From the perspective of the national government, many manufacturing countries have formulated a number of advanced manufacturing development strategies and plans such as adjusting the industrial structure, such as the United States' advanced manufacturing partnership program, Germany's Industry 4.0, and the European Union's digital Europe. They promote industrial transformation, provide listings for companies, provide financial support, and promote the improvement of enterprise informationization. Now is the right time for manufacturing to build intelligent manufacturing [27, 28].

Mechanical intelligent manufacturing includes intelligent manufacturing technology (IMT) and intelligent manufacturing system (IMS). From a microperspective, as an advanced manufacturing technology, intelligent manufacturing technology mainly realizes intelligent control of product design and production, packaging and distribution, inspection and transportation, information feedback, and other processes through the intelligent control of computer and other hardware information equipment. The production process reduces a large number of manpower operations, extends the brain wisdom of experts, and realizes the integration of man and machine [29]. From a macroeconomic point of view, the intelligent manufacturing system is a systematic and integrated application of various intelligent manufacturing technologies at various stages and modules of product production, so that the manufacturing industry is an integrated and interconnected fully automated production system. Intelligent manufacturing is based on the combination of a new generation of information physics system and advanced manufacturing technology. It can implement perceptual analysis, self-decision, and self-execution of the entire process of data and information and realize a new type of manufacturing mode with the most optimized benefits. Compared with the traditional manufacturing model, the core content of the smart manufacturing model at this stage includes smart production, smart products, smart factories, and smart logistics. The specific model is shown in Figure 1.

According to the abovementioned definition of mechanical intelligent manufacturing, it can be seen that mechanical intelligent manufacturing is a product of the combination of information technology and manufacturing technology in the 21st century, and its realization must be based on the improvement of information technology. Under the requirements and
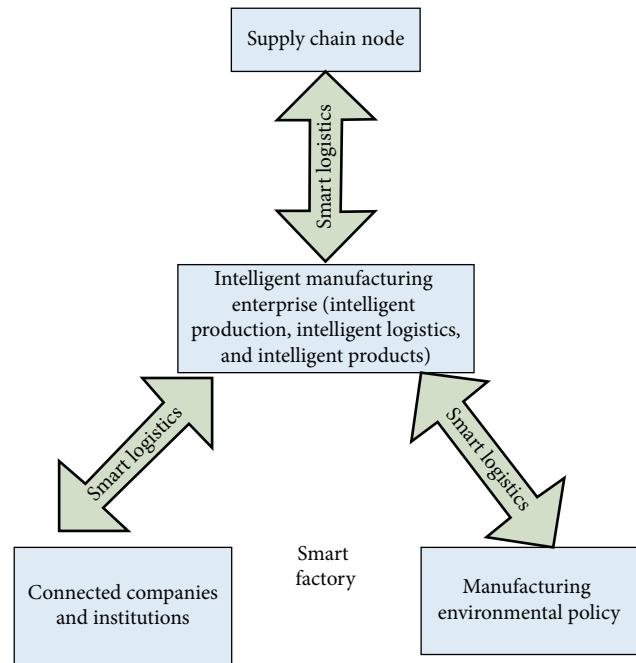
FIGURE 1: The core content model of intelligent manufacturing.

guidance of the "Made in China 2025" strategy, smart equipment manufacturers use smart equipment, production, products, management, operation, and maintenance as a starting point and use emerging information, networks, and information to improve their core competitiveness.

2.3. Knowledge Graph Question and Answer System Based on Deep Learning.

Knowledge Graph A graph-based structured knowledge database describes the concepts and their relationships in the real world in the form of symbols. Its nodes represent entities or concepts, corresponding to the semantic ontology in the real world, and edges represent the mutual relationship between entities and concepts, connecting different types of entities. Triples in the form of {entity, relationship, entity} ({subject, relation, object}) facts are the basic unit of the knowledge graph, and the knowledge graph also contains the attribute description of the entity and its basic structure, as shown in Figure 2.

The knowledge-based question and answer system is the way to answer questions according to the questions asked by users. There are currently two main types: one is to realize the structured representation of problems through semantic analysis. Methods based on query templates, problem templates, and dependency relationships are typical methods. Starting from the questions raised by users, the user questions are converted into a structured representation of the relationship path, and the fuzzy relationship matching method based on the statistical model is used to understand the question. The question answering system based on knowledge graph is to preclassify and analyze the problem first and then convert the problem into the form of problem triplet to understand the problem. One
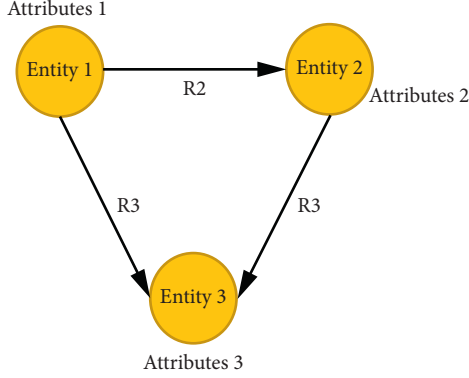
FIGURE 2: Schematic diagram of the basic components of the knowledge graph.

is to structure the problem through vector representation. First, the unstructured user question is converted into a structured knowledge graph query problem. By using two trained neural networks, the appropriate result is found for the query problem.

Most existing KBQA in-depth learning methods follow a coder comparison framework. Use deep learning to pick answers to a survey and open a project. To implement a simple question and answer based on a convergent neural network, first use the n-gram query text to search the knowledge base to create a set of KB candidate items, and then map the query and KB items. The answer to the question is obtained by calculating the correlation between the similarity of the two embedded vectors and the facts in the knowledge base. First of all, the representation learning method of word vectors is used for question and answer based on knowledge graphs. From the analysis of the structure of data stored in the knowledge base, the structure of the triples stored in the knowledge base is always <subject, relation, object>. Looking for the answer to the question becomes the process of finding the most relevant triples in the knowledge base. Through natural language processing methods such as entity recognition (NER), the model is divided into two modules: entity recognition and relationship recognition. The high accuracy of the two recognition modules improves the accuracy of question answering.

2.4. Back Propagation Algorithm.
In deep learning, the convergent neural network optimization algorithm is generally a stochastic slope descent (SSD). SSD requires the partial derivative of the loss function C in relation to each weight parameter W and b, but the network model has many weights and compensations. Therefore, the reverse propagation algorithm is proposed for the most efficient calculation of the partial derivative. The process of calculating the reverse propagation algorithm will be explained as follows:

Assume that the loss function of the network is

$$C = \frac{1}{2n}\sum \left\| y(x) - a^L(x) \right\|^2. \tag{1}$$

In formula (1), $y(x)$ is the expected output value, n is the total number of training samples, $aL(x)$ is the output vector of the network, and L is the number of layers of the network. Hypothesis 1: the total loss function can be expressed by averaging the single loss functions:

$$C = \frac{1}{n}\sum C_x,$$
$$C_x = \frac{1}{2}\left\| y - a^L \right\|. \tag{2}$$

Hypothesis 2: the loss function can be expressed as the network output function, so the loss function of a single sample can be expressed as follows:

$$C_x = \frac{1}{2}\left\| y - a^L \right\|^2 = \frac{1}{2}\sum_j \left(y_j - a_j^L \right)^2. \tag{3}$$

Error equation of output layer:

$$\delta_j^L = \frac{\partial C}{\partial Z_j^L} = \frac{\partial C}{\partial a_j^L}\frac{\partial a_j^L}{\partial Z_j^L} = \frac{\partial C}{\partial a_j^L}\sigma'\left(Z_j^L\right). \tag{4}$$

In formula (4), δ_j^L represents the error of the jth unit of the Lth layer. $\partial C/\partial Z_j^L$ measures the speed of the change of the loss function with the output of the network. $\sigma'\left(L_j^L\right)_c$ measures the speed of the change of the output of the activation function with Z_j^L. When $\sigma'\left(Z_j^L\right) \approx 0$, regardless of how big the value of $\partial C/\partial Z_j^L$ is, the value of δ_j^L will be about 0. At this time, the output neuron enters the saturation region and the network stops learning. Error transfer equation:

$$\delta^L = \left(\left(W^{L+1}\right)^T \delta^{L+1}\right)\Theta\sigma'\left(Z^L\right). \tag{5}$$

Equation (5) shows that the error δ' of the Lth layer can be obtained by calculating the error δ^{L+1} of the $L+1$ layer, and the error of any layer can be calculated by combining equations (4) and (5).

3. Knowledge Graph Question and Answer System Design

3.1. Main Framework of Q&A Knowledge Graph.
The corpus mainly includes question and answer pairs, entity annotation corpus, and attribute annotation corpus. The question-answer corpus consists of question and answer triples <question, (entity, attribute, answer)>, and the entity tagging corpus consists of <question, entity>, which is mainly used for training of deep learning entity recognition models; attribute tagging. The corpus is composed of <questions, attributes> and is mainly used for the training of attribute classification models. Question entity recognition refers to the identification of entity references from input questions. First, the semantic representation of the question needs to be processed, and then the entity references in the question are extracted through the entity recognition model; the knowledge retrieval needs to link the identified entities go to the knowledge base entity, search the entity in the knowledge

graph through the knowledge graph index, and return the entity-related triples; attribute classification first performs joint semantic characterization of the question and attribute, question and answer, and then choose from the candidate ternary. In the group, the triple with the highest score is selected as the answer according to the attribute model.

3.2. Knowledge Graph Question and Answer System Processing Flow. After creating the knowledge graph of this system using a convergent neural network, users can gain knowledge of the graph through front-end interaction. The front-end application uses html, javascript and CSS technologies. Through the @Controller annotation of the spring-boot box, the URL and html are correlated at the controller level. Intelligent machine building technology is used to classify the query, and to a specific template, it will correspond to a query sentence. For the entire knowledge graph answering system, the processing flow is as follows:

(1) Entity identification and entity correction:

First of all, we need to perform word segmentation and entity recognition to facilitate the semantic understanding later. The purpose of named entity recognition is to recognize the pointed objects of natural language questions. At present, named entity recognition mostly adopts algorithms such as conditional random field, hidden Markov, and long and short memory network LSTM.

(2) Vectorization of sentences:

A template-based question and answer is used. In the naive Bayes method, the bag of words model is used to express the question, each sentence is converted into a vector, and then the naive Bayes algorithm is used to classify the question.

(3) Problem understanding based on naive Bayes:

Naive Bayes algorithm can be divided into three stages: preparation stage, classifier training stage, and application stage. For this system, the three stages are as follows: (1) the preparation stage. Design the question template manually and use the template as training data. (2) Training phase. Read the template file and use the bag of words model to represent each sentence of the template. (3) Application phase. First, perform word segmentation and named entity recognition.

(4) Knowledge base query

The form that this system can understand is named "entity + template label"; the named entity corresponds to the entity of knowledge base, and template label corresponds to the attribute or relationship of query.

3.3. Knowledge Graph Data. This article uses freebase as the basic knowledge graph. There are 18 relationship categories and 42 named entity categories in this dataset, including 362,000 sentences in the training set and 256,000 triples and 143,000 sentences in the test set and 5372 triples. The label in most sentences is NA.

4. Data Analysis of Knowledge Graph Question Answering System

4.1. Question Classification Experiment Results. In order to evaluate the stability and applicability of the method in this paper, the experiment was conducted by randomly dividing both datasets into 10 subsets with different sizes. These sets contain a subset of 500, 1000, 1500, 2000, 2500, 3000, 3500, 4000, 4500, and 5000 questions, respectively. After that, the question classification model (Cap-net) proposed in this paper is run on each subdataset. In order to prevent the overfitting problem and obtain the best error estimate, this paper chooses ten-fold cross-validation to train these models. Use of the macroprecision to measure the experimental results is shown in Figure 3.

From the results, when the query total is increased from 500 to 3000, the classification macroaccuracy of both query datasets is significantly improved, indicating that in the case of fewer datasets, increasing the dataset size will have a significant effect on the classification results. As the dataset continues to grow, although the accuracy of the classification macros decreases slightly in some cases, the overall trend increases. This shows that the question classification model in this paper can better fit the data and complete the question classification task under a larger dataset. In view of the characteristics of questions, this paper combines two-way LSTM and attention mechanism and then adds a capsule network to complete the question classification task. In order to prove the effectiveness of the model, the model is ablated (that is, a certain part of the model is removed) to verify the validity of the combination of the question classification model in this paper. First, the attention mechanism is removed, and the output of the bidirectional LSTM layer is directly used as the input of the capsule layer as a comparative ablation experiment. Then, the capsule layer is removed, and the result of the combination of the two-way LSTM and the attention mechanism is directly connected to the output layer as a comparative ablation experiment. The experimental results are shown in Table 1, and the specific images are shown in Figure 4.

It can be seen that when the model removes the capsule layer, the classification effect is greatly reduced, which shows that adding a capsule layer to the model in this paper can effectively improve the question classification results. When the model removes the attention mechanism, although it can produce better classification results than removing the capsule layer, it still fails to achieve the results of the complete model in this article. This proves that adding attention mechanism can better complete the classification task. By comparing with two ablation experiments, it is further proved that the question classification model in this paper combines bidirectional LSTM with attention mechanism and then adding a capsule network is a reasonable and feasible improvement.
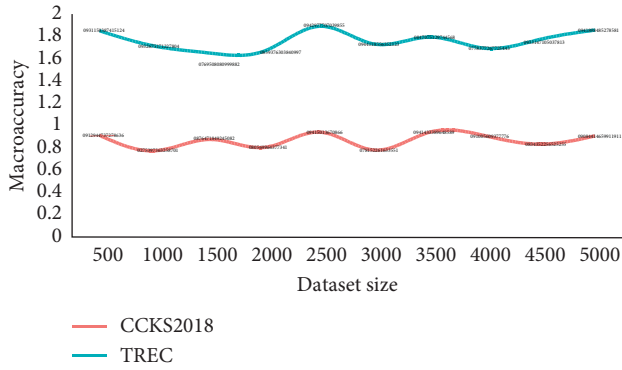
FIGURE 3: The effect of different dataset sizes on the accuracy of question classification macros.

TABLE 1: Ablation experiment of question classification model.

Experimental model	Remove the capsule layer	Remove the attention mechanism	Cap-net
CCKS2018	0.645	0.689	0.732
TREC	0.667	0.712	0.752
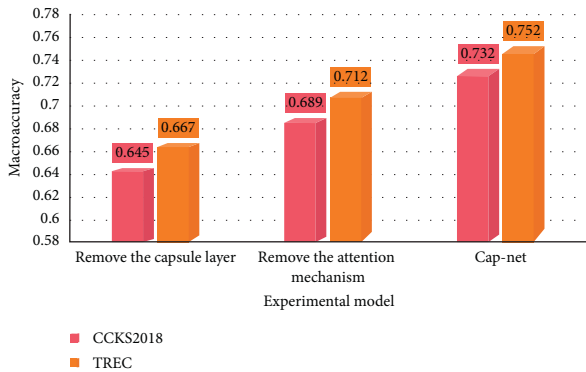
FIGURE 4: Ablation experiment of question classification model.

4.2. Query Performance Comparison of Knowledge Graph Question Answering System. In this paper, the query performance of the query engine MIQE using memory iteration technology and the query engine IIQE and Franke query model using inverted index technology are compared. This section is based on the standard LUBM dataset under the 100,000 RDF dataset and the million RDF dataset to perform single entity query and connection query performance experiments, in which a single entity query uses commonly used one query condition and two query condition queries. The connection query uses commonly known queries between two entities and three entities. Since the data loading module and SPARQL statement parsing module of the knowledge graph storage access system have been implemented above, the query performance experiments for the two models directly use

SPARQL statements for querying. In order to ensure the accuracy of the experimental results, each experiment in this paper conducted ten queries corresponding to the same query conditions but different query contents and the average query time were taken at the end. The experimental results are shown in Tables 2 and 3, and the specific images are shown in Figures 5 and 6.

It can be seen from the abovementioned two tables that under each RDF dataset, the query time of the MIQE model of each query mode is significantly longer than the query time of the Franke query model and the IIQE model. The query time of MIQE model under single entity query and connection query are both in minutes. The research found that the reason for the longer query time of the MIQE model is the Spark initialization time. Since MIQE in this article needs to load all the data in HBase in advance, and the time to load the data is calculated in the actual query time, the query time of MIQE is longer and as the amount of data increases, as MIQE loads more data, the query time will also increase. Excluding the time to load the data, the experiment measured that under the 100,000 RDF dataset, the single entity query of the MIQE model does not exceed 3 seconds, and the connection query does not exceed 5 seconds. Under the one million RDF dataset, the single entity query of the MIQE model will be not more than 8 seconds, not more than 10 seconds for connection query; the performance is weaker than the Franke query model and IIQE model. The query performance of the IIQE model is generally better than the Franke query model and the MIQE model. The query time of the IIQE model under a query condition and a single entity query of two query conditions does not exceed 5 seconds. The query time of the query does not exceed 8 seconds. The query performance of the Franke model is better than the query performance of the MIQE model, but compared with the IIQE model, although the query performance of a single entity query under two query conditions and the connected entity query between two entities are close, but based on querying a single entity under one query condition, the query performance of IIQE is significantly better than the Franke query model; when three entities are queried at the same time, the query performance of the connection query between the IIQE models is about twice that of the Franke query model. In a single entity query, the query time based on the Franke query model and the IIQE model under two query conditions is faster than the query time based on one query condition. The reason is that multiple query conditions will limit the number of query results. The query conditions will increase the query time due to the large number of results that will cause multiple data transmissions over the network. In summary, the knowledge graph storage access system based on how distributed aggregates are stored and the distributed parallel query mechanism has good horizontal scalability, and the IIQE model is more suitable for quickly searching large-scale knowledge graphs than the other two question models. Compared to IIQE, MIQE is simpler to implement and supports more integrated features. If query time is not high and you want to support more query features, the MIQE model is a good choice.

TABLE 2: Query time results for one hundred thousand RDF dataset.

	Single entity query		Connect query	
	A query condition	Two query conditions	Two entities	Three entities
Franke	775	575	794	332
MIQE	830	759	322	368
HIQE	520	420	494	876

TABLE 3: Query time results for one million RDF dataset.

	Single entity query		Connect query	
	A query condition	Two query conditions	Two entities	Three entities
Franke	786	324	836	643
MIQE	922	607	857	712
HIQE	565	567	431	552
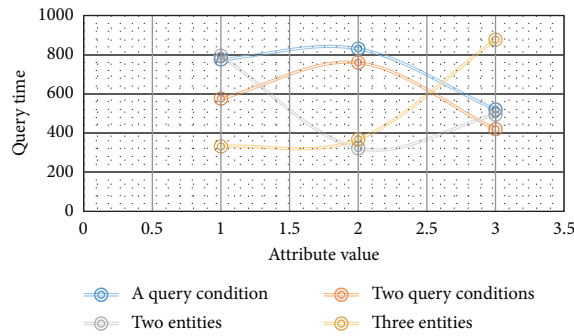
FIGURE 5: Query time results for one hundred thousand RDF dataset.
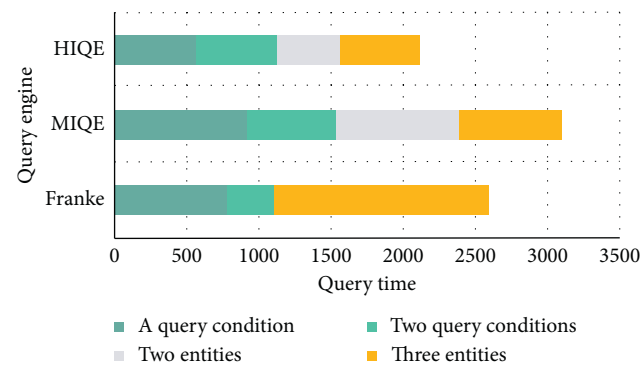
FIGURE 6: Query time results for one million RDF dataset.

5. Conclusions

In this study, we explain how to transform the human intention recognition problem into a classification problem and then explain the mathematical model based on the knowledge base in two steps: the first is to use the established knowledge correlation graph to adjust the weight of the entity words given the problem and use the contribution value and contribution multiplier to calculate the weight of the entity words. Then, it introduces the Bayesian model and how the Bayesian model is applied to the classification problem. Finally, the Bayesian model and the weight of entity words are combined to establish a weighted Bayesian algorithm. This algorithm believes that the weight of words will also affect the final accuracy rate.

In this study, through the analysis of the biological entities, the experimental entities, combining entities and other special entities contained in the biological entities, were found. By studying the principles of the R-WMD model and optimizing it for the semantic matching of biology entities, the optimization content includes resetting the weight coefficient of the normalized word bag model through richer semantic information, and introducing length-related parameters K, allows longer entities to return first. Finally, the experiment verifies that the algorithm has the best effect on entity semantic matching compared with other text similarity algorithms.

This work designs and implements a design of knowledge question answering systems for intelligent engineering based on deep learning. The system is divided into three main sections: data loading section, SPARQL sentence analysis section, and data query section. The knowledge graph is first uploaded to HBase via the data upload module. During the query, the SPARQL query statement obtains the query structure through the parser module and then creates a query tree in the data module to execute a query based on the HBase query method according to the query structure obtained. The experiments verify that the query rendering of the IIQE query engine is superior to the MIQE query engine. The knowledge graph storage access system implemented in this document can not only store knowledge graphs efficiently with a load-balanced balance but also ensure the query performance of knowledge graphs.

Data Availability

No data were used to support this study.

Conflicts of Interest

The author declares no conflicts of interest.

Acknowledgments

References

[1] T. R. Goodwin and S. M. Harabagiu, "Knowledge representations and inference techniques for medical question answering," *ACM Transactions on Intelligent Systems & Technology,* vol. 9, no. 2, pp. 1–26, 2017.

[2] T. R. Goodwin and S. M. Harabagiu, "Knowledge representations and inference techniques for medical question answering," *ACM Transactions on Intelligent Systems,* vol. 9, no. 2, pp. 14.1–14.26, 2018.

[3] G. Zeng, "A unified definition of mutual information with applications in machine learning," *Mathematical Problems In Engineering*, vol. 2015, Article ID 201874, 12 pages, 2015.

[4] C. Pechsiri and R. Piriyakul, "Developing a why-how question answering system on community web boards with a causality graph including procedural knowledge," *Information Processing in Agriculture*, vol. 3, no. 1, pp. 36–53, 2016.

[5] U. Sawant, S. Garg, S. Chakrabarti et al., "Neural architecture for question answering using a knowledge graph and web corpus," *Information Retrieval*, vol. 22, no. 3-4, pp. 324–349, 2019.

[6] S. Hu, L. Zou, J. X. Yu et al., "Answering natural language questions by subgraph matching over knowledge graphs," *IEEE Transactions on Knowledge and Data Engineering*, vol. 30, no. 99, pp. 824–837, 2018.

[7] S. Shin, X. Jin, J. Jung, and K.-H. Lee, "Predicate constraints based question answering over knowledge graph," *Information Processing & Management*, vol. 56, no. 3, pp. 445–462, 2019.

[8] A. Chandiok and D. K. Chaturvedi, "Cognitive functionality based question answering system," *International Journal of Computer Applications*, vol. 179, no. 20, pp. 1–6, 2018.

[9] H. Vasudevan, V. K. N. Kottur, and A. A. Raina, "Effect of process parameters while machining using abrasive jet machine (AJM)," in *Proceedings of International Conference on Intelligent Manufacturing and Automation (ICIMA 2018)*, pp. 575–581, Lecture Notes in Mechanical Engineering (Chapter 53), Chengdu, China, July 2018.

[10] M. C. Rumpf, R. G. Lockie, J. B. Cronin, and F. Jalilvand, "Effect of different sprint training methods on sprint performance over various distances: a brief review," *Journal of Strength and Conditioning Research*, vol. 30, no. 6, pp. 1767–1785, 2016.

[11] X. Niu, S. Singh, A. Garg et al., "Review of materials used in laser-aided additive manufacturing processes to produce metallic products," *Frontiers of Mechanical Engineering*, vol. 14, no. 3, pp. 282–298, 2019.

[12] R. H. Laird, D. J. Elmer, M. D. Barberio, L. P. Salom, K. A. Lee, and D. D. Pascoe, "Evaluation of performance improvements after either resistance training or sprint interval-based concurrent training," *Journal of Strength and Conditioning Research*, vol. 30, no. 11, pp. 3057–3065, 2016.

[13] X. Hao, G. Zhang, and S. Ma, "Deep learning," *International Journal of Semantic Computing*, vol. 10, no. 03, pp. 417–439, 2016.

[14] Y. Chen, Z. Lin, X. Zhao et al., "Deep learning-based classification of hyperspectral data," *IEEE Journal of Selected Topics in Applied Earth Observations & Remote Sensing*, vol. 7, no. 6, pp. 2094–2107, 2017.

[15] S. Levine, P. Pastor, A. Krizhevsky, and D. Quillen, "Learning hand-eye coordination for robotic grasping with deep learning and large-scale data collection," *International Journal of Robotics Research*, vol. 37, no. 4-5, pp. 421–436, 2016.

[16] X. Lu, X. Duan, X. Mao, Y. Li, and X. Zhang, "Feature extraction and fusion using deep convolutional neural networks for face detection," *Mathematical Problems in Engineering*, vol. 2017, Article ID 1376726, 9 pages, 2017.

[17] L. Zhang, L. Zhang, and B. Du, "Deep learning for remote sensing data: a technical tutorial on the state of the art," *IEEE Geoscience and Remote Sensing Magazine*, vol. 4, no. 2, pp. 22–40, 2016.

[18] T. Oshea and J. Hoydis, "An introduction to deep learning for the physical layer," *IEEE Transactions on Cognitive Communications & Networking*, vol. 3, no. 4, pp. 563–575, 2017.

[19] X. Wang, L. Gao, S. Mao, and S. Pandey, "CSI-based fingerprinting for indoor localization: a deep learning approach," *IEEE Transactions on Vehicular Technology*, vol. 66, no. 1, pp. 763–776, 2017.

[20] S. Albarqouni, C. Baur, F. Achilles, V. Belagiannis, S. Demirci, and N. Navab, "AggNet: deep learning from crowds for mitosis detection in breast cancer histology images," *IEEE Transactions on Medical Imaging*, vol. 35, no. 5, pp. 1313–1321, 2016.

[21] D. Ravi, C. Wong, F. Deligianni et al., "Deep learning for health informatics," *IEEE Journal of Biomedical and Health Informatics*, vol. 21, no. 1, pp. 4–21, 2017.

[22] X. X. Zhu, D. Tuia, L. Mou et al., "Deep learning in remote sensing: a comprehensive review and list of resources," *IEEE Geoence & Remote Sensing Magazine*, vol. 5, no. 4, pp. 8–36, 2018.

[23] D. Marmanis, M. Datcu, T. Esch, and U. Stilla, "Deep learning earth observation classification using ImageNet pretrained networks," *IEEE Geoscience and Remote Sensing Letters*, vol. 13, no. 1, pp. 105–109, 2016.

[24] W. Zhao and S. Du, "Spectral–spatial feature extraction for hyperspectral image classification: a dimension reduction and deep learning approach," *IEEE Transactions on Geoscience and Remote Sensing*, vol. 54, no. 8, pp. 4544–4554, 2016.

[25] L. De Oliveira, M. Kagan, L. Mackey et al., "Jet-images-deep learning edition," *Journal of High Energy Physics*, vol. 2016, no. 7, pp. 1–32, 2016.

[26] N. Tajbakhsh, J. Y. Shin, S. R. Gurudu et al., "Convolutional neural networks for medical image analysis: full training or fine tuning?" *IEEE Transactions on Medical Imaging*, vol. 35, no. 5, pp. 1299–1312, 2016.

[27] F. Milletari, S.-A. Ahmadi, C. Kroll et al., "Hough-CNN: deep learning for segmentation of deep brain regions in MRI and ultrasound," *Computer Vision and Image Understanding*, vol. 164, pp. 92–102, 2017.

[28] X. Wang, L. Gao, and S. Mao, "CSI phase fingerprinting for indoor localization with a deep learning approach," *IEEE Internet of Things Journal*, vol. 3, no. 6, pp. 1113–1123, 2017.

[29] S. Wang, C. Huang, J. Li, Y. Yuan, and F.-Y. Wang, "Decentralized construction of knowledge graphs for deep recommender systems based on blockchain-powered smart contracts," *IEEE Access*, vol. 7, no. 99, pp. 136951–136961, 2019.

Research Article

Music Intelligent Push Play and Data Analysis System Based on 5G Internet of Things

Cheng Chen,[1] **Tien-Shou Huang,**[2] **Jui-Chan Huang** ⓘ**,**[1] **Chi-Hung Shih** ⓘ**,**[2] **and Yun Du**[1]

[1]*Yango University, Fuzhou 350015, China*
[2]*Department of Intelligent Commerce, National Kaohsiung University of Science and Technology, Kaohsiung City 80778, Taiwan*

Correspondence should be addressed to Chi-Hung Shih; i108159110@nkust.edu.tw

With the rapid development of information science today, multifunctional and intelligent applications have gradually become the focus of attention. In the data management system, the first consideration is the reliability of the data source, followed by the intelligent processing after the data are collected. Due to the upgrade of the Internet to the Internet of Things, the way of network information transmission has also become a problem that people need to think about. The transmission mode of network information services will be converted from the passive transmission of information by traditional servers to the form of actively pushing information. The application of intelligent push technology in the field of the Internet of Things is a prominent and important direction in the development of the Internet of Things. This article mainly introduces the research on the intelligent music push and data analysis system based on the 5G Internet of Things, with the intention of providing some ideas and directions for the research of the music intelligent push and play and data analysis system. This paper proposes a research method for music intelligent push playback and data analysis system based on 5G Internet of Things, including current intelligent push related technologies, music evaluation matrix, user dissimilarity matrix, and music feature similarity calculation. The experimental results in this paper show that with the increase in the number of users, the accuracy of the recommended results of the system under the Hadoop framework gradually stabilizes, eventually reaching 91.2%.

1. Introduction

With the development of information science and technology, rapid mining of required information has become a research hotspot. Recommendation systems have emerged from this, and information mining in a big data environment has become a research hotspot. Existing recommendations are often calculated offline, and the recommendation results are updated regularly. The real-time performance is not enough, and the recommendation system generally has cold-start and data-sparse problems. In the era of rapid development of information, how to quickly and accurately respond to user needs is a problem that needs to be solved urgently. The stand-alone mode requires a lot of time to iteratively calculate the recommendation algorithm, which is difficult to meet today's business needs.

In reality, due to the variability of music platform user interest preferences and the timeliness of information [1], it is necessary to use user behavior records to make timely recommendations to users, that is, online processing of streaming data is a necessary condition for real-time music recommendation systems. For this reason, most of the recommended algorithms use parallel computing solutions. At present, distributed computing frameworks are emerging endlessly, and computing models are also diverse, each with its own advantages [2]. The most widely used frameworks are Hadoop and Spark. Big data computing modes are mainly divided into batch computing, streaming computing, interactive computing, and graph computing. The two big data processing methods are suitable for different application scenarios [3].

El-Latif A has studied the basic communication technology used by 5G networks to connect objects in the Internet of Things environment. With the development of 5G-IoT and the development of innovative technologies, it will surely bring new huge security and privacy challenges. El-Latif A uses the characteristics of quantum roaming to

construct a new *S*-box method, which plays an important role in the block cipher technology of 5G-IoT technology. As an application of the proposed *S*-box mechanism and controlled alternate quantum walk (CAQW) for 5G-IoT technology, a new robust video encryption mechanism is proposed. In addition to meeting the encryption requirements of various files in 5G-IoT, El-Latif A also uses the function of quantum roaming to design a novel encryption technology for the secure transmission of sensitive files in the 5G-IoT paradigm. The analysis and results of the cryptographic system show that, in terms of cryptographic performance, it has better security and effectiveness. The high cost of this research is not conducive to popularization [4]. Palattella believes that the Internet of Things is expected to be based on the seamless interaction between a large number of 5G devices, through a large number of new services to completely change the way people live and work. After decades of the creation of the Internet of Things concept, various communication technologies have gradually emerged in recent years, reflecting the diversity of application fields and communication requirements [5]. With the popularization of connection technologies and the emergence of 5G cellular systems, this technology become a potential key driver of the yet-to-be-emerging global Internet of Things. In the research, Palattella analyzed in detail the potential of 5G technology in the Internet of Things by considering technology and standardization, reviewed the current IoT connection pattern and the main 5G support factors of IoT, and explained the possibility of a close connection between the Internet of Things and 5G Huge business changes caused in the operator and supplier ecosystem. This research method lacks experimental data support [6]. Akpakwu believes that the Internet of Things (IoT) is a promising technology that tends to completely change and connect the global world through seamless connections based on heterogeneous smart devices [7]. The current demand for machine-type communication has led to multiple communication technologies with multiple service requirements to realize the modern IoT vision. The latest cellular standards such as long-term evolution have been introduced for mobile devices, but they are not suitable for low power consumption and low data rate devices such as IoT devices. Akpakwu found that the fifth-generation (5G) mobile network is expected to solve the limitations of previous cellular network standards and become a potential key enabler of the future Internet of Things. Akpakwu investigated the latest IoT application requirements and related communication technologies and discussed in detail a cellular-based low-power wide-area (LPWA) solution based on the Third Generation Partnership Project (3GPP) to support and enable targeted new service requirements for key IoT use cases for large-scale IoT, including an expanded global mobile communication system for the Internet of Things (EC-GSM-IoT), enhanced machine type communication (eMTC) and narrowband Internet of Things (NB-IoT). Akpakwu presented a comprehensive overview related to emerging technologies and enabling technologies, mainly focusing on 5G mobile networks, aiming to support the realization of IoT-based intelligent push systems. This study lacks examples to prove that, it is not practical [8].

The innovations of this paper are (1) proposed a music evaluation matrix; (2) proposed a user dissimilarity matrix; (3) proposed a music feature similarity calculation; (4) designed a music intelligence based on 5G Internet of Things push playback and data analysis system.

2. Method of Music Intelligent Push Playback and Data Analysis System Based on 5G Internet of Things

2.1. Related Technology

2.1.1. Hadoop Framework. The Hadoop framework is an open-source distributed basic framework developed by Apache. The two core designs are the distributed programming model MapReduce and the distributed file system HDFS (Hadoop distributed file system) [9]. The main advantage of Hadoop is its high efficiency. Hadoop's parallel working method can speed up data processing, can complete the processing of large amounts of data in an acceptable time, and has strong scalability. It is proportional; simplicity, for the use of Hadoop, can be realized by writing Map interface and Reduce interface, so that it can realize distributed operation without knowing the specific implementation details of the underlying layer, reliability, flexibility, and Hadoop. There is no mandatory requirement for data format, unlike relational databases, which require very strict data format; economical [10, 11].

2.1.2. MapReduce. MapReduce is a programming model of a distributed system. Users can complete simple distributed calculations without understanding the basic implementation of the underlying, which reduces the difficulty of distributed calculations [12]. A task generally consists of two parts: the Map phase and the Reduce phase. Among them, the main task of the Map phase is to split the input data file to generate a series of (key and value) key-value pairs, and then, the Reduce phase will merge the key-value pairs of the same key to form the final. As a result (key, final_(value)), the whole process is connected by setting the key value [13]. During the execution of MapReduce, multiple Map phases can be included, and multiple Reduce phases can also be included.

2.1.3. HDFS. The architecture of the HDFS system adopts a master-slave structure, which is generally composed of three parts, namely, a client, a name node, and multiple data nodes. Among them, the name node is the HDFS system administrator, mainly responsible for the meta information of directories and files. For a folder, the information it contains is mainly modification and access time, block size, access permission, and the constituent blocks of a file; for a directory, the main information is access permission, quota metadata, and modification time [14]. The data node is the file storage unit of HDFS. It mainly manages the verification

information and content information in the data block. When the data node is added to the cluster, the name node will establish a block mapping relationship based on the data block list generated by the data node. When the data node is running, the information in its own data block will be reported to the name node regularly to ensure that the block mapping is up-to-date. The client accesses HDFS by communicating with name node and data node to realize file operations [15].

2.1.4. JSON.
JSON is a format for data exchange. Data are stored and transmitted in JSON format, which makes it easier for developers to read and encode [16].

2.2. Music Evaluation Matrix.
In general, users will only appreciate a small part of the music in the website according to their personal preferences, so the music evaluation matrix R is a sparse matrix [17]. A large amount of sparse data will cause serious distortion of the mining results. Generally, discrete wavelet transform (DWT), principal component analysis, and other methods are used to reduce dimensionality, and representative data are extracted for mining processing [18, 19]. Compared with wavelet transform, the principal component analysis method can better deal with sparse data, while wavelet transform is more suitable for processing high-dimensional data. Principal component analysis is also called statistical-based principal component analysis. A method of dimensionality reduction processing. This method searches for KN-dimensional orthogonal vectors $K \leq N$ that best represent the data and projects the original data into a smaller vector space so that the data can be dimensionally reduced [20]. The calculation process is as follows:

Calculate the correlation coefficient matrix $R_{n \times n}$ of user evaluation matrix A for music according to the following formula:

$$r_{ij} = \frac{\sum_{k=1}^{n} (X_{ki} - \overline{X}_i)(X_{kj} - \overline{X}_j)}{\sqrt{\sum_{k=1}^{n} (X_{ki} - \overline{X}_i)^2 \sum_{k=1}^{n} (X_{kj} - \overline{X}_j)^2}}. \quad (1)$$

Calculate the contribution rate of principal components as follows:

$$Z_i = \frac{\lambda_i}{\sum_{k=1}^{p} \lambda_k}, \quad i = 1, 2, 3, \ldots, p. \quad (2)$$

Cumulative contribution rate is calculated as follows:

$$\frac{\sum_{k=1}^{m} \lambda_k}{\sum_{k=1}^{p} \lambda_k}. \quad (3)$$

Calculate the principal component loading as follows:

$$p(Z_k, x_i) = \sqrt{\lambda_i} e_{ij} (i, j = 1, 2, 3, \ldots, p). \quad (4)$$

2.3. User Dissimilarity Matrix.
The user dissimilarity matrix $S = (s_{ij})_{m \times m}$ is generated from the evaluation matrix R. There are four methods for calculating the user dissimilarity as follows:

2.3.1. Euclidean Distance.
Euclidean distance is used to calculate the distance between points $x = (x_1, x_2, \ldots, x_n)$ and $y = (y_1, y_2, \ldots, y_n)$ in space [21]. Here, the following formula is used to calculate the degree of dissimilarity between data:

$$dist(x, y) = \sqrt{\sum_{i=1}^{n} (x_i - y_i)^2}. \quad (5)$$

2.3.2. Manhattan Distance.

$$dist(i, j) = \left| x_{i_1} - x_{j_1} \right| + \left| x_{i_2} - x_{j_2} \right| + \cdots + \left| x_{i_n} - x_{j_n} \right|. \quad (6)$$

2.3.3. Pearson Correlation Coefficient.

$$sim(x, y) = \frac{COV(x, y)}{\sigma_x \times \sigma_y}. \quad (7)$$

2.3.4. Cosine Similarity.

$$sim(x, y) = \frac{|(x, y)|}{\|x\|_2 \|y\|_2}. \quad (8)$$

2.4. Music Feature Similarity Calculation.
Extract the features between music and perform feature similarity calculation [22]. Calculate the similarity between two variables and the formula is as follows:

$$p(x, y) = \frac{\sum x_i y_i - n\overline{xy}}{(n-1)SxSy} = \frac{n \sum x_i y_i - \sum x_i \sum y_i}{\sqrt{n \sum x_i^2 - (\sum x_i)^2} \sqrt{n \sum y_i^2 - (\sum y_i)^2}}. \quad (9)$$

Use Cosine coefficient to calculate document similarity and the formula is as follows:

$$T(x, y) = \frac{x \cdot y}{\|x\|^2 \times \|y\|^2} = \frac{\sum x_i y_i}{\sqrt{\sum x_i^2} \sqrt{\sum y_i^2}}. \quad (10)$$

Use Jaccard coefficient (expansion of Cosine coefficient) to calculate document similarity, and the formula is as follows:

$$T(x, y) = \frac{x \cdot y}{\|x\|^2 \times \|y\|^2 - x \cdot y} = \frac{\sum x_i y_i}{\sqrt{\sum x_i^2} \sqrt{\sum y_i^2} - \sum x_i y_i}. \quad (11)$$

The Euclidean distance between any two points x and y in n-dimensional airborne is as follows:

$$d(x, y) = \sqrt{\sum (x_i - y_i)^2}. \tag{12}$$

When $n = 2$, the space becomes a plane, and the Euclidean distance degenerates to the length of the line segment formed by two points on the plane [23]. In practical applications, the curve function formula is usually used for conversion: distance is inversely proportional to similarity, and the following formula exists:

$$sim(x, y) = \frac{1}{1 + d(x, y)}. \tag{13}$$

The method part of this article uses the above three algorithms to study the design method of the 5G Internet of Things-based music intelligent push playback and data analysis system. The specific process is shown in Figure 1.

3. Design of Music Intelligent Push Playback and Data Analysis System Based on 5G Internet of Things

3.1. Overall System Structure

3.1.1. System Structure. The system design adopts a multilayer structure; on the basis of the software architecture, each system forms a unified information platform of the Internet of Things information push system through the interactive connection between the servers, and at the same time reflects the user's operation information records and statistical data to the background management system [24].

(1) Basic Environment. The information push system provides the hardware environment and system software platform for system operation, including essential system software such as operating systems, servers, and databases [25].

(2) Data Layer. The data layer is located between the user service layer and the basic environment. It consists of a user push system, a background management system, and a statistical system data interaction platform. Among them, the application data of the back-end management system and the statistical system use relational databases. User behavior system: using text storage data [26, 27].

(3) Data Exchange Platform. It realizes the connection of information exchange and application integration of various application systems.

(4) Service Layer. It is composed of system basic components and provides standardized modules for the system [28].

(5) Application Layer. Adopting an integrated mechanism and customizing into a user behavior system, a background management system, a statistical analysis system, and a push

information system through user operations and administrators' operational requirements.

(6) Presentation Layer. It constitutes user login and information push and provides service system interface for system administrators and users.

(7) Security System. Security is an important principle of push system and website construction [29].

3.1.2. Overall System Design. The information push system is composed of four parts: user behavior system, background management system, statistical system, and information push system under the overall design framework [30].

(1) User Behavior System. The user behavior system provides a unified service window for users, provides an environment for user information registration and music playback and purchase so that all users provide a platform for music information viewing and music purchase.

(2) Backstage Management System. It is provided for the administrator to edit music information and audit users, edit with management authority, and provide advertising functions for the user behavior system [31].

(3) Statistical System. The system design adopts the model of document database and relational database, and the business system adopts relational database. The function of statistics based on the number of times the user plays music and the number of times purchased music. By recording the user's operation behavior on music information, each behavior will be recorded in a log, and then, the basic data in the log will be extracted with a shell script analysis and storage. Finally, the basic data are counted twice through the storage process and finally used as the basis for information push [32].

(4) System Push System. It provides users with information subscriptions, and administrators can send and query music information for specific user subscriptions. It also provides regular sending functions.

The overall process of the system is that the user's identity needs to be verified when the user logs in. If it is a task submitter, the task is submitted through the front desk according to the needs of the task, and the task type and task-related information are selected at the same time, such as: the user characteristics required for this task, the geographic location of the task trigger, and other information [33, 34]. After the task is submitted successfully, the scheduling system will maintain the smooth operation of the entire system and will select suitable tasks for triggering according to the set scheduling strategy. In the process of screening users, the black and white list will be activated and special personnel will be given a special deal. After the task is executed, the blacklist will be updated, and the task execution result will be fed back through the mail module. Finally, push messages to the screened personnel through push channels [35].

3.2. Feature Build Design. The construction of features mainly completes data cleaning, data merging, and data feature structuring.

3.2.1. Data Cleaning. Data cleaning is mainly to complete the wrong user information in the data, such as the user does not conform to the set structure and stores the wrong information. There is a large amount of user behavior information in the user's historical log information, but some of this information is deliberately modified by the user's own information through illegal means. This information does not meet the requirements of the push task, because for this type of information, even if the user characteristics excavated are very suitable for being a user because the user's identity is wrong, the push task to the user cannot be completed normally, so it is necessary to refresh the data. First, complete the cleaning of user data based on regular expressions. Secondly, it is also necessary to clean the historical log information that contains few information storage errors in the historical data.

3.2.2. Data Consolidation. The data after data cleaning are the redundancy of data information. The same user may exist in different log files, which is inconvenient for the development of data feature mining work. Therefore, data merging work needs to be completed. Data consolidation refers to the integration of the same user's information in the same file. First, integrate the user's basic information, retrieval information, and behavior information into the same file according to the user's identity and then integrate the user's push information and the user's feedback information after the push into the same file according to the push.

3.2.3. Structured Data Characteristics. After the data are merged, the data need to be structured. The process of structuring user information requires data fusion. For the data of the push content, the keywords of the text are found by segmenting the push text. For the keyword obtained by word segmentation, if the user clicks on the push message, it indicates that the user is more interested in the keyword; if the user does not click, it indicates that the user is not interested in the keyword. At the same time, a time factor is added to determine the changes in user interest. After obtaining the individual characteristics of the user, the individual characteristics are merged, and after the overall characteristics are obtained, the characteristics are judged offline by AUC. If the influence weight of the characteristic is less, the characteristic is deleted and the change of AUC is observed. For online, A/B test can be used for small flow tests to check the model effect.

3.3. Accurate Push. Precision push is divided into two parts, one is push based on the matching of basic user characteristics, and the other is push based on the logistic regression training model. The push based on the user's basic characteristics matching mainly judges the pushed user based on some basic information of the user. When the user does not meet any of the conditions, the user does not meet the requirements of the push, and the user is abandoned. Because users of the Android and IOS operating systems need to be pushed separately, when the users are screened, the respective users need to be counted accordingly. The number of users that the task may require is the total number of Android and IOS users or the number of Android and IOS users. At the same time, the number of new users can be specified in the task. However, because the keyset by MapReduce is the user's identity account, and because the Android and IOS identity accounts have their own connectivity, when the Reduce hash output is performed, users of the same operating system are likely to be assigned to the same The output is performed in Reduce, so that when the operating system is distinguished between users when the number of user requirements is small, the filtered users will belong to the same operating system, which is contrary to the actual proportion of real users. The obtained results are scrambled, so as to avoid the selected users are all Android or IOS, resulting in an imbalance of users.

In order to solve the user "cold start" problem, in the early stage, for each user, there is no corresponding training data, choose to push the message based on the user's basic characteristics, when the data have accumulated to a certain extent, you can use the existing data for training. An LR model, so that in the end, users will be interested in this push score. In theory, users with a score greater than 0.6 points can be considered interested in this push task, and finally, the user will be evaluated based on the user score sort and then take out topN users to push this task.

This part of the experiment proposes that the above steps are used for the design of a 5G IoT-based music intelligent push playback and data analysis system. The specific process is shown in Table 1.

4. Music Intelligent Push Play and Data Analysis System Based on 5G Internet of Things

4.1. Music Intelligent Push and Play Platform. The Internet has become the most important way to spread music today. The competition among major online music companies in my country is fierce. Most companies have been established for more than 10 years, have a certain number of customers, and have formed their own service characteristics. In today's increasingly fierce competition in the online music market, companies are scrambling to find innovative business points to breakthrough business growth bottlenecks. The main online music platforms in my country are shown in Table 2 and Figure 2.

Observing the chart, we can see that NetEase Cloud Music, which was released the latest, has become the largest online music platform for users due to its intelligent push, personalized
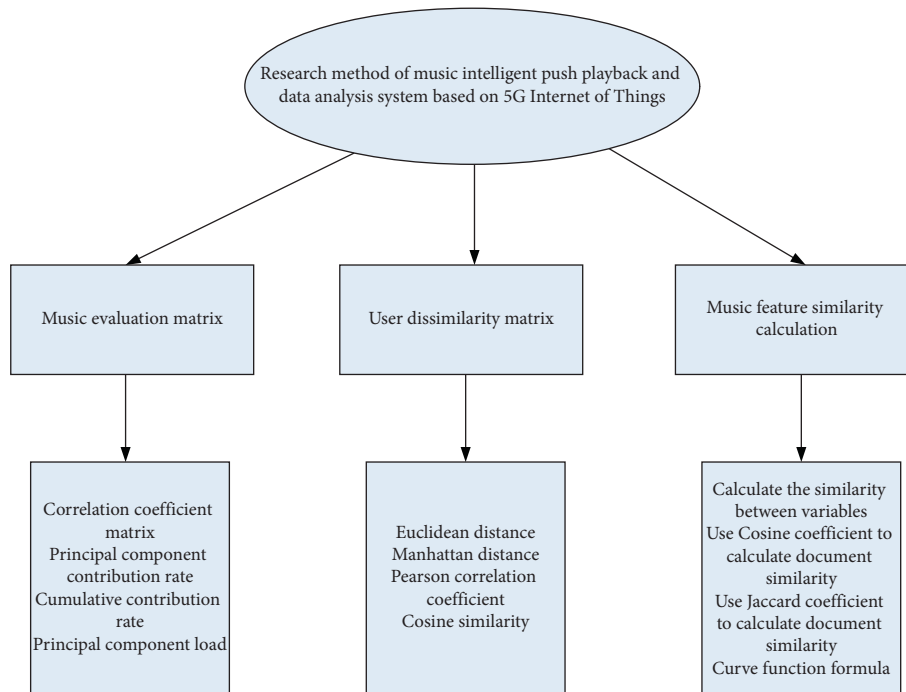
Figure 1: Part of the technical flow chart of this algorithm.

Table 1: The experimental procedure of this article.

Design of music intelligent push playback and data analysis system based on 5G Internet of Things	1	Overall system structure	1	Architecture
			2	Overall system design
	2	Feature build design	1	Data cleaning
			2	Data consolidation
			3	Structured data characteristics
	3	Accurate push	1	Push based on the matching of basic user characteristics
			2	Push based on logistic regression training model

interface, and other advantages. Mos companies tend to attract users through special services, seize users, and occupy the market. How to develop characteristic products and attract users has become the most difficult problem in finding new business breakthroughs. Using 5G Internet of Things technology to realize the intelligent push of music will help the platform attract more users, increase daily activity, and further achieve profit growth.

4.2. User Analysis of Music Smart Push Platform

4.2.1. User Distribution. Through the CLIQUE algorithm, the clustering of enterprise users is realized, and then, based on the cluster, the important knowledge is obtained through the association rule algorithm to guide the decision-making level to implement different marketing strategies for different customer groups. Use the five attributes of music style, sound quality, song price, user occupation, user location, and language type to cluster and obtain relevant data for a certain period of time on the platform after preprocessing, as shown in Table 3.

The system should intelligently push high-quality music and focus on pure music and popular music, which can attract more users and they are willing to consume high-quality music. Young students and freelancers have basically maintained their preference for music, and their peers have basically maintained similar hobbies focused on popular music in various languages.

4.2.2. Online Usage of Users

(1) Count the length of time users have used the online music platform and draw a chart, as shown in Table 4 and Figure 3.

It can be seen from the chart that Saturday and Sunday are the two days where users spend the most time online. The platform can set the number of smart pushes on Saturdays and Sundays to be more frequent and there are more types of pushes; the online use time of users on weekdays after Monday is relatively shorter, the platform can be set to accurately push according to users' likes.

TABLE 2: Major online music platforms in China.

Platform name	Release time (year)	User scale	Advantages
NetEase Cloud Music	2013	Over 800 million users	Social functions, smart push, and beautiful design
Kugou music	2006	Over 500 million users	The earliest digital music service and interactive platform
Kuwo music	2005	Over 100 million users	Many kinds of music
QQ music	2005	Over 400 million users	China's largest wireless music sales platform
Xiami music	2008	Over 500 million users	Rich in funds
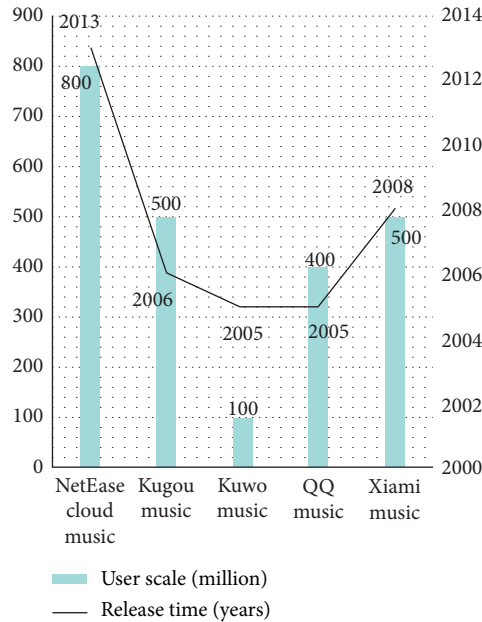
FIGURE 2: Major online music platforms in China.

TABLE 3: User distribution.

User	Favorite music style	Music language	Sound quality	Paid music budget (RMB)
Primary and secondary school students	Electronic music and pop music	Mandarin, English, Japanese, and Korean	Hi-Fi	10
College students	Pop music, rock music, and rap	Mandarin, English, Japanese, Korean, and Cantonese	Hi-Fi	15
Office worker	Lyric music, pure music, and pop music	Mandarin, English, and Cantonese	Hi-Fi	25
People engaged in art	Pure music and classical music	Mandarin, English, and Japanese	Hi-Fi	30

(2) Calculate the time period that users use the online music platform and draw a chart, as shown in Table 5 and Figure 4.

It can be seen from the chart that users often use online music platforms during commuting hours, lunch hours, and dinner hours. If you intelligently push related music to users during these time periods, you will be able to achieve a better push effect.

4.3. Comparative Experimental Analysis of Different Data Sets. In order to confirm the improvement effect of the improved method in the frequent set mining experiment, consider applying the improved method to different music data sets

and compare the improvement effect. Draw the specific situation into a chart, as shown in Table 6 and Figure 5.

As shown in the figure, the experimental results of the improved frequent itemset mining method under different data sets are recorded. Under the same support threshold, the frequent set mining effects of different data sets are basically similar. However, since users with fewer historical records are excluded in the process of selecting the data set, the number of frequent itemsets is increased to a certain extent.

4.4. Intelligent Push Accuracy Analysis. Count the related records of users' play, favorites, and purchases and draw them into a table, as shown in Table 7. Each row contains seven fields: user ID, song ID, number of listening times,

TABLE 4: User online usage time (unit: minute).

User	Monday	Tuesday	Wednesday	Thursday	Friday	Saturday	Sunday
Primary and secondary school students	45	39	41	44	43	121	109
College students	67	56	55	53	59	134	112
Office worker	59	55	47	62	66	197	201
People engaged in art	83	78	81	77	84	182	197
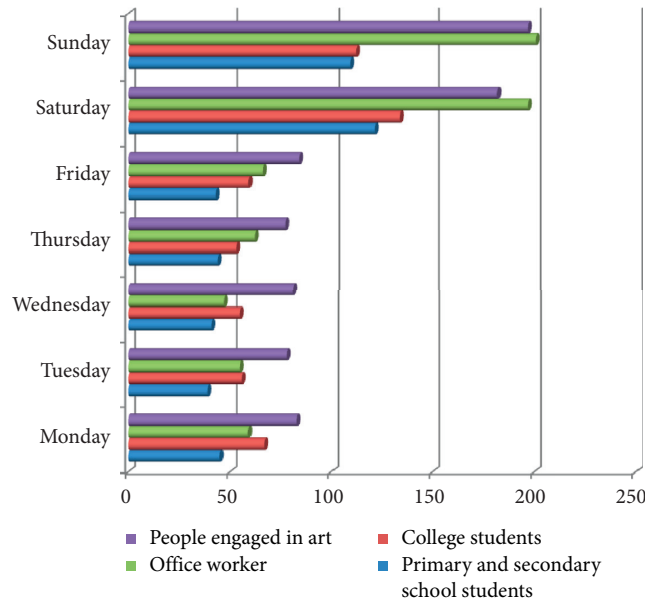
FIGURE 3: User online usage time (unit: minute).

TABLE 5: User play time period.

Period	Percentage (%)
0 : 00–6 : 00	4.7
6 : 00–9 : 00	7.3
9 : 00–12 : 00	14.6
12 : 00–15 : 00	19.4
15 : 00–18 : 00	18.7
18 : 00–21 : 00	25.1
21 : 00–24 : 00	10.2

switching times, favorites or purchases, timeline, and comments.

To test the processing performance of the method proposed in this paper, it takes a certain amount of time to prepare and start the platform under the Hadoop framework, and at the same time, the distributed computing itself also brings certain computational overhead. At this stage, five hundred users are tested and tested according to different algorithms, and the results are plotted as a graph, as shown in Figure 6.

According to the results in the figure, the recommendation method proposed in this paper has obvious advantages in comparing the accuracy of the recommendation results. When the user data reaches a certain level, the accuracy is usually higher than that of the traditional method. This method draws on and combines the recommendation ideas of the two basic methods, so regardless of the number of users, the performance is better than the traditional method. At the same time, with the increase in the number of users, the accuracy of the recommendation results of the
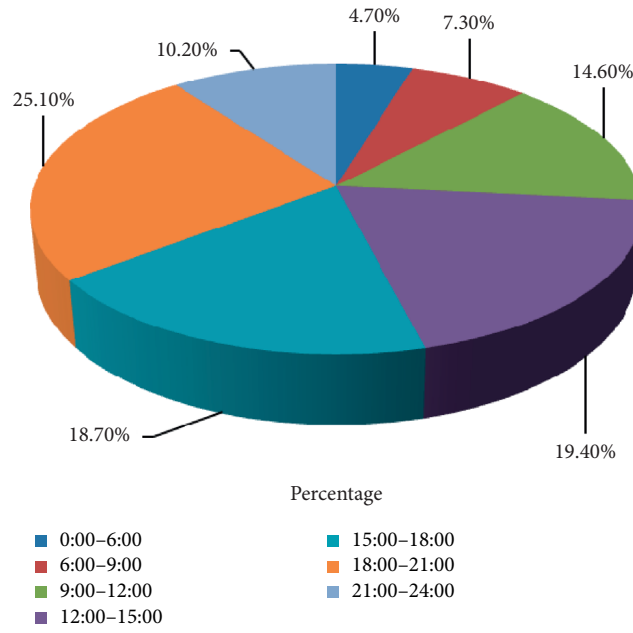
FIGURE 4: User play time period.

TABLE 6: Frequent set mining results under different data sets.

Data set		Support threshold			
		0.01	0.03	0.05	0.07
us0	us0_Gender	108	36	22	7
	us0_Language	194	64	36	21
	us0_Releasedate	121	57	57	43
	user_songs_0	246	82	53	37
us2	us2_Gender	147	49	67	56
	us2_Language	363	121	63	49
	us2_Releasedate	246	147	132	114
	user_songs_2	337	113	101	81
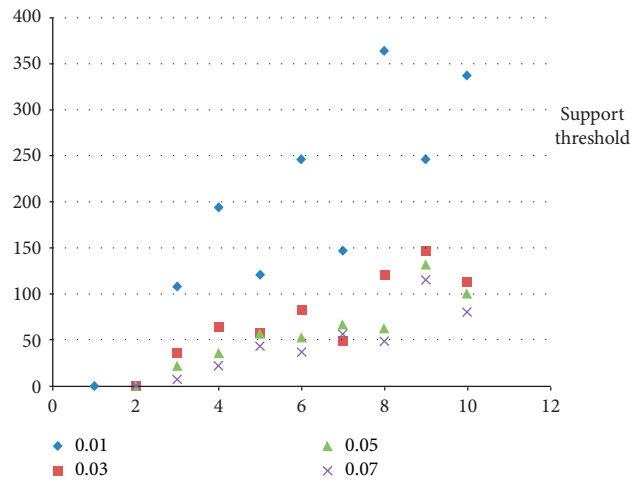
FIGURE 5: Frequent set mining results under different data sets.

TABLE 7: User behavior-contextual data display.

User id	Song id	L-times	C-times	Collect & buy	Timeline	Comment
A	37	7	1	YES	15:00–18:00	Like
B	41	4	2	YES	18:00–21:00	Like
C	132	6	1	YES	9:00–12:00	Like
D	47	8	3	NO	18:00–21:00	Dislike
E	58	5	3	NO	21:00–24:00	Dislike
F	61	6	2	YES	12:00–15:00	Like
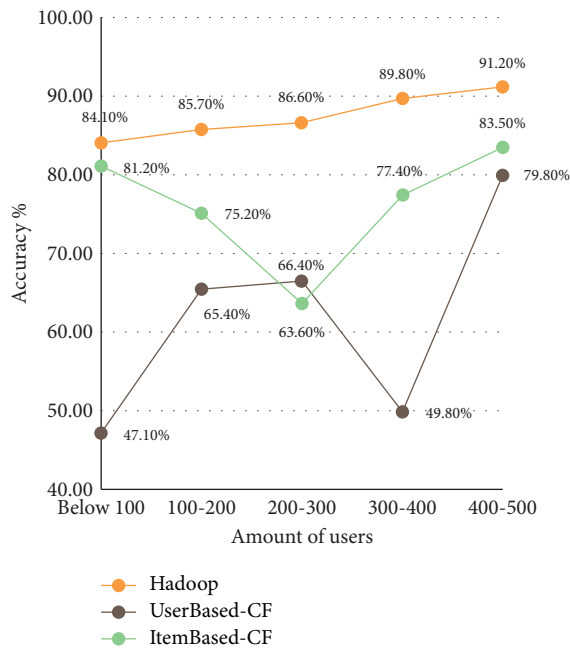
FIGURE 6: Test results of different algorithms.

system under the Hadoop framework gradually stabilized, eventually reaching 91.2%.

5. Conclusions

The Internet of Things technology is a comprehensive technology that connects objects to the Internet through communication equipment, sensors, data collection and processing systems, positioning systems, and other equipment according to a certain communication protocol. The intelligent monitoring, positioning, and management of objects can be realized through the Internet of Things. In recent years, due to a large amount of human and material resources investment, application systems based on the Internet of Things technology have also been continuously developed and improved. The use of the Internet of Things technology to achieve intelligent music push and play and data analysis systems has become a new technology.

This article mainly uses user data, music work data, user behavior data and behavior context data to mine user preferences, and complete the recommendation process. However, there are actually a lot of data that can be added to the calculation of the recommendation process. Typically, there are tag data. Tag data are used by users to mark their feelings and experiences of musical works, so tags can associate users with musical works. These data should be focused on in follow-up research.

In this paper, the optimization and experimentation of the recommended method, system design, and system realization process are all completed in an experimental environment. However, in practical industrial applications, the number of user data and music works is massive, which requires personalized services with extremely high performance and efficiency. However, the fundamental of the music intelligent push system is economic benefits. In addition, it is also necessary to consider whether the method in this article can meet the requirements of the push system and produce satisfactory economic benefits.

Data Availability

No data were used to support this study.

Conflicts of Interest

The authors declare that they have no conflicts of interest.

References

[1] Y. T. Chen, C. H. Chen, S. Wu, and C. C. Lo, "A two-step approach for classifying music genre on the strength of AHP weighted musical features," *Mathematics*, vol. 7, no. 1, p. 19, Article ID 19, 2019.

[2] A. Francis Saviour Devaraj, M. Elhoseny, S. Dhanasekaran, E. Laxmi Lydia, and K. Shankar, "Hybridization of firefly and improved multi-objective particle swarm optimization algorithm for energy efficient load balancing in Cloud computing environments," *Journal of Parallel and Distributed Computing*, 2020, In Press.

[3] Z. Lv, H. Song, P. Basanta-Val, A. Steed, and M. Jo, "Next-generation big data analytics: state of the art, challenges, and future research topics," *IEEE Transactions on Industrial Informatics*, vol. 13, no. 4, pp. 1891–1899, 2017.

[4] A. A. A. El-Latif, B. Abd-El-Atty, W. Mazurczyk et al., "Secure data encryption based on quantum walks for 5G Internet of Things scenario," *IEEE Transactions on Network and Service Management*, vol. 17, no. 99, pp. 118–131, 2020.

[5] Z. Yushu, H. Qi, C. Guo, Z. Xinpeng, and X. Yong, "A low-overhead, confidentiality-assured, and authenticated data acquisition framework for IoT," *IEEE Transactions on Industrial Informatics*, vol. 16, no. 12, pp. 7566–7578, 2020.

[6] M. R. Palattella, L. Ladid, and A. Grieco, "Internet of Things in the 5G era: enablers, architecture, and business models," *IEEE Journal on Selected Areas in Communications*, vol. 34, no. 3, pp. 510–527, 2016.

[7] M. Zhou, Y. Wang, Z. Tian, Y. Lian, Y. Wang, and B. Wang, "Calibrated data simplification for energy-efficient location sensing in Internet of Things," *IEEE Internet of Things Journal*, vol. 6, no. 4, pp. 6125–6133, 2019.

[8] J. Lu, J. Wang, and Y. Chen, "UAV-aided MIMO communications for 5G Internet of Things," *IEEE Internet of Things Journal*, vol. 6, no. 2, pp. 1731–1740, 2019.

[9] A. M. Abu-Mahfouz, B. Silva, and G. P. Hancke, "A survey on 5G networks for the Internet of Things: communication technologies and challenges," *IEEE Access*, vol. 6, no. 12, pp. 3619–3647, 2018.

[10] G. Li, J. Hua, and J. Li, "Stock forecasting model FS-LSTM based on the 5G Internet of things," *Wireless Communications and Mobile Computing*, vol. 2020, no. 6, 7 pages, Article ID 7681209, 2020.

[11] B. S. Awoyemi, A. S. Alfa, and B. T. J. Maharaj, "Resource optimisation in 5G and internet-of-things networking," *Wireless Personal Communications*, vol. 111, no. 4, pp. 2671–2702, 2020.

[12] K. Tyagi, "Setting standards for a competitive economy: in the era of 5G, Internet of Things and the blockchain technology," *IIMS Journal of Management Science*, vol. 10, no. 1-2, pp. 82–97, 2019.

[13] R. Khdhir, "5G LTE-A cognitive multiclass scheduling scheme for Internet of Things," *International Journal of Advanced Trends in Computer Science and Engineering*, vol. 8, no. 5, pp. 2485–2491, 2019.

[14] F. Xu, X. Fu, and Z. Yang, "Radar-assisted UAV detection and identification based on 5G in the Internet of Things," *Wireless Communications and Mobile Computing*, vol. 2019, no. 4, 12 pages, Article ID 2850263, 2019.

[15] N. N. Dao, M. Park, J. Kim et al., "Resource-aware relay selection for inter-cell interference avoidance in 5G heterogeneous network for Internet of Things systems," *Future Generation Computer Systems*, vol. 93, no. APR, pp. 877–887, 2018.

[16] J.-H. Lee, G.-S. Hong, Y.-W. Lee, C.-K. Kim, N. Park, and B.-G. Kim, "Design of efficient key video frame protection scheme for multimedia Internet of Things (IoT) in converged 5G network," *Mobile Networks and Applications*, vol. 24, no. 1, pp. 208–220, 2018.

[17] D. Kissinger, "Wireless technologies for 5G and the Internet of Things [from the guest editor's desk]," *IEEE Microwave Magazine*, vol. 18, no. 7, pp. 24-25, 2017.

[18] S. Rho, A. Ahmad, and A. Paul, "MGR: multi-parameter green reliable communication for internet of things in 5G network," *Journal of Parallel and Distributed Computing*, vol. 118, no. 1, pp. 34–45, 2018.

[19] J. M. Lopez-Soler, S. Sendra, and P. Ameigeiras, "Integration of LoRaWAN and 4G/5G for the industrial Internet of Things," *IEEE Communications Magazine*, vol. 56, no. 2, pp. 60–67, 2018.

[20] S. Chen, M. Peng, and G. Shou, "Toward edge intelligence: multiaccess edge computing for 5G and Internet of Things," *IEEE Internet of Things Journal*, vol. 7, no. 8, pp. 6722–6747, 2020.

[21] Y. Zhang, Y. Zhu, and S. Maharjan, "Edge intelligence and blockchain empowered 5G beyond for the industrial Internet of Things," *IEEE Network*, vol. 33, no. 5, pp. 12–19, 2019.

[22] Su and B. Hu, "Nonorthogonal interleave-grid multiple access scheme for industrial Internet of Things in 5G network," *IEEE Transactions on Industrial Informatics*, vol. 14, no. 12, pp. 5436–5446, 2018.

[23] M. Ejaz and M. Ibnkahla, "Multiband spectrum sensing and resource allocation for IoT in cognitive 5G networks," *IEEE Internet of Things Journal*, vol. 5, no. 1, pp. 150–163, 2018.

[24] I. B. F. D. Almeida, L. L. Mendes, J. J. P. C. Rodrigues et al., "5G waveforms for IoT applications," *IEEE Communications Surveys & Tutorials*, vol. 21, no. 3, pp. 2554–2567, 2019.

[25] M. S. Omar, S. A. Hassan, H. Pervaiz et al., "Multiobjective optimization in 5G hybrid networks," *IEEE Internet of Things Journal*, vol. 5, no. 3, pp. 1588–1597, 2018.

[26] H. Kim, A. Roy, and B. J. R. Sahu, "Efficient IoT gateway over 5G wireless: a new design with prototype and implementation results," *IEEE Communications Magazine*, vol. 55, no. 2, pp. 97–105, 2017.

[27] X. Chen, "Surveying the music playback experience of museum audiences based on perceived quality and perceived value," *The Electronic Library*, vol. 37, no. 5, pp. 878–892, 2019.

[28] Jérémie, Voix, Franois et al., "Design and validation of a bone conduction music playback for bike helmet," *Canadian Acoustics*, vol. 44, no. 1, pp. 9–15, 2016.

[29] S. Gouda, A. Abdelhaleim, and S. Eskander, "Design of a smart push pull inverter coupled with photovoltaic system," *Bulletin of the Faculty of Engineering. Mansoura University*, vol. 41, no. 2, pp. 11–19, 2020.

[30] I. Yeom, H. Woo, and C. Lee, "Quality measurement of push services for smart devices," *Wireless Personal Communications*, vol. 88, no. 2, pp. 319–336, 2016.

[31] K. V. Lyncker and R. Thoennessen, "Regional club convergence in the EU: evidence from a panel data analysis," *Empirical Economics*, vol. 52, no. 2, pp. 525–553, 2017.

[32] E. Rasoulinezhad and G. S. Kang, "A panel data analysis of South Korea's trade with OPEC member countries: the gravity model approach," *Iranian Economic Review (IER)*, vol. 20, no. 2, pp. 203–224, 2016.

[33] S. Ghazanfar, A. J. Bisogni, J. T. Ormerod et al., "Integrated single cell data analysis reveals cell specific networks and novel coactivation markers," *BMC Systems Biology*, vol. 10, no. S5, pp. 11–24, 2016.

[34] F. Ieva, A. M. Paganoni, and N. Tarabelloni, "Covariance-based clustering in multivariate and functional data analysis," *Journal of Machine Learning Research*, vol. 17, no. 1, pp. 1–21, 2016.

[35] P. José Manuel, B. Alexandra, C. Hugo et al., "Treatment of intracranial aneurysms with the SILK embolization device in a multicenter study," *A Retrospective Data Analysis. Neurosurgery*, vol. 81, no. 4, pp. 595–601, 2017.

Research Article

Intelligent Decision Support System of Emergency Language Based on Fog Computing

Li Wang ⓘD

School of Literature and Law, North China Institute of Science and Technology, Sanhe 065201, Hebei, China

Correspondence should be addressed to Li Wang; wangli@ncist.edu.cn

In recent years, various emergencies have frequently occurred worldwide, which has forced relevant service departments to pay more attention to decision-making and emergency management. Since emergency events are characterized by complex environments, unstable events, and time constraints, events usually involve multiple factors and promptly correct errors in the decision-making process. In fact, in many cases, emergency decision-making needs to select an optimal one from multiple alternatives for execution. The fog algorithm decision-making method can solve the problem of optimal solution selection, and it has been widely used in many fields. This article evaluates the emergencies that have occurred in the past 10 years. The evaluation indicators include direct economic loss, indirect reputation loss, ecological environment indicators, and healthy living indicators. The first two are cost-based indicators. The index value of direct economic loss and indirect reputation loss is as small as possible, while the index value of ecological environment index and healthy living index is the larger the better. Among the many selected emergencies, only the index evaluation scores of fires are reliable ($P < 0.01$), and the evaluation scores of other emergencies belonging to natural disasters are a bit wrong ($P > 0.05$). The reason for this may be that the direct economic losses caused by natural disasters are not well counted, and the families involved and the environment are too wide. Therefore, the emergency language intelligent decision support system based on fog computing has a good development prospect.

1. Introduction

With the advent of the information age, the development of computers and the Internet has greatly changed people's lives. New forms of entertainment and education using various information and image technologies have emerged one after another. The emergence of children's learning games is undoubtedly a milestone in the history of the development of children's education. It has brought great freedom and fun to children's learning. How to systematically formulate emergency decision-making methods after emergencies is the goal and urgent task faced by emergency experts and scholars in various countries in the field of emergency decision-making. Accurate and efficient emergency decision-making can not only deal with the emergencies that occur at this time and minimize the loss of life and property but also be used as a historical reference to provide effective suggestions

for the handling of similar emergencies in the future. The problem of emergency decision-making in emergencies is actually a multiobjective decision-making problem, that is, using a variety of reasonable and effective evaluation indicators or evaluation targets to measure the pros and cons of multiple emergency alternatives and finally making decisions based on the comprehensive performance of each alternative [1].

As a federal country with a vast territory and frequent natural disasters, the United States has unified management of more than 100 emergency management agencies across the country and established the United States federal emergency management agency to respond to various natural disasters and emergencies and coordinate various departments of the federal government. European and American countries have established emergency management systems and emergency management information platform systems that are in line with their own actual

conditions to achieve efficient and orderly development of emergency management [2]. Lu conducted research on public health emergencies of acute epidemic diseases and pointed out that it is necessary to strengthen the coordination and cooperation of emergency departments and strengthen management accountability, so as to improve the ability to respond to such emergencies [3]. Darren analyzed the changing trends and patterns of dynamic natural risks, man-made risks, and disaster vulnerabilities and, on this basis, studied emergency policies and emergency plans [4]. Marie analyzed the indicators of railway emergency management statistics, constructed an emergency management evaluation index system, and established an emergency management evaluation model with an improved factor analysis method [5].

Our country is at the extreme starting point of socialist construction. During the period of rapid social and economic development, natural disasters and mass emergencies occur frequently, especially the occurrence of SARS and the 2008 snow disaster, which greatly touched our country's fragile emergency management system. The research and development of the emergency management and command system for emergencies in our country is relatively late, but after unremitting efforts, most of the existing emergency management and command systems can collect, transmit, and share information resources and realize multiple communications. Bouzekri A built an emergency response model based on a conventional manpower model and developed a multiagent model of emergency response organization behavior [6]. Test simulations were conducted through actual drill scenarios. And put forward some suggestions for the current emergency system [7]. Lin designed the planning form of hierarchical network planning and used this method to study the terrorist attack incidents [8]. Manu and Thalla comprehensively studied the emergency group decision-making technology of railway emergencies and, combined with the characteristics of railway emergency decision-making, proposed the realization method of this technology [9].

In this article, emergencies are subdivided and organized according to the idea of secondary events, and the fog algorithm decision-making method is extended to apply to secondary events. Taking into account the state changes of secondary events derived from primary emergencies, it gets closer in the actual application background, the concept of "possibility" containing interval numbers that can be compared with each other is given, and the schemes with possible degrees are sorted to ensure the scientificity and rationality of the final decision result. In the emergency decision-making model constructed in this article, full consideration is given to the realistic background and the ambiguity of information that accompany the occurrence of secondary emergencies during emergencies, ensuring the scientificity and rationality of the decision-making process

and making the decision-making results more reliable and correct.

2. Intelligent Decision Support System of Emergency Language Based on Fog Computing

2.1. Multiobjective Decision

2.1.1. Connotation of Multiobjective Decision-Making. Multiobjective decision-making is a new research field of decision-making that integrates several disciplines such as operations research, economics, and psychology. Decision analysis is the process of selecting the best solution from multiple alternatives to solve the problems that may arise in the system design, design, and construction phases now or in the future. However, many of the socioeconomic decision-making issues we are currently facing, even the smaller practical issues in daily life, are usually multiobjective rather than personal. Interactions and contradictions between multiple goals in decision-making problems often make it difficult for decision-makers to make decisions easily. In an image with constantly changing gray values, if there is a point that is very different from the gray values of adjacent pixels, the point is likely to be noise. This solution was replaced by a satisfactory solution. Therefore, multiobjective decision-making means that the problem to be decided involves multiple goals or multiple indicators. Decision-makers need to continuously coordinate multiple goals or multiple indicators in decision-making under the constraints of various resource conditions to choose a relatively satisfactory solution [10] so that the program can make all relevant decision-making target values reach the decision-making process in a satisfactory state considered by the decision-makers.

2.1.2. Features and Advantages of Multiobjective Decision-Making. (1) Characteristics of Multiobjective Decision. The wireless network control system is composed of a wireless communication network, controller, and controlled objects [11]. Most of the objects controlled are continuous systems, while the controllers in network control systems are discrete systems, which makes it difficult for decision-makers. Directly use the same measurement unit and measurement standard to measure and compare multiple decision-making goals; decision-making goals are often mutually exclusive and contradictory; that is, an alternative plan usually cannot achieve the optimal value of a goal. Ensure that other decision-making goals are in the most satisfactory state or make one goal the most satisfactory but make another decision-making goal worse; There are both quantitative indicators and qualitative indicators. The former is described by data, while the latter is described by words, that is,

qualitative and quantitative indicators coexist in multi-objective decision-making. For those qualitative indicators, they need to be quantified, so as to facilitate decision-makers to consider alternatives according to the decision rules.

(2) Advantages of Multiobjective Decision-Making. The role of decision-makers in the decision-making process is strengthened; the alternatives obtained in the decision-making process are more abundant and involve a wider range of fields; the model of the decision-making problems and the intuition of decision-making problems will be more realistic.

2.1.3. Multiobjective Decision-Making Process. It can improve system reliability and other benefits. The cost of transmitting information for remote control and remote operation is very low. Instead of using analog signals, digital signals are used for transmission on a digital network. At this stage, the decision-maker and analysis will convert the general goals proposed in the initial stage into detailed and specific decision goals. In addition, the elements, restrictions, and constraints in the entire system must also be clearly defined. Finally, all the requirements must be given. Alternatives for feasibility conditions for decision-making: at this stage, decision-makers and analysts mainly clarify the relationship between decision goals and various alternatives, determine the key variables in the system, and establish models. These models usually include mental models, graphical models, and physical models. Models, mathematical models, and so forth: in addition, decision-makers and analysts also need to estimate various parameters that will be used in the model. The main work of decision-makers and analysts at this stage is divided into three parts. The first is to use the model of the previous stage to generate alternatives. The second is to use relevant decision rules to rank the pros and cons of various alternatives. The third is to select satisfaction. Executable program: put the satisfactory plan selected in the previous stage into practice and conduct real-time tracking and evaluation of the implementation effect of the satisfactory plan. The multiobjective decision-making process is shown in Figure 1.

2.2. Common Resource Scheduling Algorithms in Fog Computing

2.2.1. Algorithms Adapted to User Mobility. Let μ_0 represent the computing power of the mobile edge, $D(\lambda_t)$ represent the computing delay requirements, $\overline{C}(\mu_0)$ represent the average system cost, and μ_t represent the computing power of the cloud resources leased in the t time interval, and μ_t^* represent the cloud resources used in each time interval. For a given edge configuration μ_0, the optimal solution is

$$\mu_t^*(\mu_0) = \begin{cases} 0, & \mu_0 \geq \lambda_t + \dfrac{1}{D(\lambda_t)}, \\[2em] f_t^u(\mu_0), & 0 < \mu_0 < \lambda_t + \dfrac{1}{D(\lambda_t)}, \\[2em] \lambda_t + \dfrac{1}{D(\lambda_t) - d}, & \mu_0 = 0. \end{cases} \quad (1)$$

The formula for calculating the average system cost gradient is as follows:

$$\left[\overline{C}(\mu_0)\right]' = \frac{c_P}{T} \sum_{i=j}^{T} \left[f_{v(i)}^u(\mu_0)\right]' + c_0 \theta \mu_0^{\theta-1}. \quad (2)$$

The formula for solving the best computing power of the mobile edge is

$$\mu_0^* = \arg\min\left\{\overline{C}(\mu_0) \mid \mu_0 \in \left\{\mu_0^1, \ldots, \mu_0^{T+1}\right\}\right\}. \quad (3)$$

2.2.2. Algorithm to Balance Task Completion Time and Price. In order to fully understand the effect of time delay on the control system, we select a simple control object, analyze the step response curve of the system under different time delay conditions, and analyze the effect of time delay on the control system. Suppose the state space expression of the controlled system is

$$\min = \sum_{i=1}^{m} d_i^2,$$

$$\begin{cases} y_j^* = \begin{cases} \max y_{ij}, & j \text{ is the benefit index,} \\ \min y_{ij}, & j \text{ is the benefit index,} \end{cases} \\ d_i^2 = \sum_{j=1}^{n} \left(y_{ij}\lambda_j - y_j^*\lambda_j\right)^2, & i = 1, 2, \ldots, m, \end{cases} \quad (4)$$

$$\begin{cases} \text{s.t.,} & \sum_{j=1}^{n} \lambda_j = 1, \\ \lambda_j > 0, & j = 1, 2, \ldots, n. \end{cases}$$

According to the comprehensive weight calculation formula,

$$\omega_j = \frac{\lambda_j \mu_j}{\sum_{j=1}^{n} \lambda_j \mu_j}, \quad 1 \leq j \leq n,$$

$$Z = (z_{ij})_{m \times n} = (\omega_j y_{ij})_{m \times n}. \quad (5)$$

According to the weighted standardized matrix, the ideal solution and the negative ideal solution are obtained:
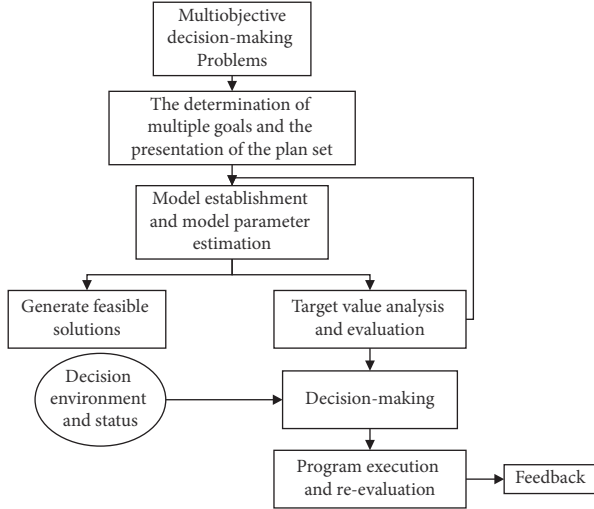
FIGURE 1: Multiobjective decision flow chart.

$$z_j^+ = \begin{cases} \max z_{ij}, & j \text{ is the benefit index,} \\ \min z_{ij}, & j \text{ is the benefit index,} \end{cases}$$
$$z_j^- = \begin{cases} \max z_{ij}, & j \text{ is the benefit index,} \\ \min z_{ij}, & j \text{ is the benefit index.} \end{cases} \tag{6}$$

The distance from the alternatives to the ideal solution and the negative ideal solution:

$$S_i^+ = \sqrt{\sum_{j=1}^{n} \left(z_j - z_j^+\right)^2}, \quad i = 1, 2, \ldots, m,$$
$$S_i^- = \sqrt{\sum_{j=1}^{n} \left(z_j - z_j^-\right)^2}, \quad i = 1, 2, \ldots, m. \tag{7}$$

In the above formula, S_i^+ is the distance from the i scheme to the ideal solution; S_i^- is the distance from the i scheme to the negative ideal solution. The relative closeness of the alternatives:

$$C_i = \frac{S_i^-}{S_i^+ + S_i^-}, \quad i = 1, 2, \ldots, m. \tag{8}$$

2.2.3. Algorithms to Reduce Task Completion Time. S_j represents the fog computing embedded system storage system of server $(j \in J)$, and S_t represents the image size of task $t \in T$:

$$x_{ij} = \begin{cases} 1, & \text{if the task image } t \in T \text{ is stored in server } j \in J, \\ 0, & \text{otherwise,} \end{cases}$$
$$\sum_{j \in J} x_{ij} = \Omega, \quad \forall t \in T. \tag{9}$$

q_{til} represents the probability that the I/O request of a task $t \in T$ will be delivered from the client $i \in I$ to the storage server $j \in J$. The introduction of τ_d represents the maximum I/O time of all tasks. The problem of minimizing the maximum I/O time can be described as

$$\text{MINLP} - \text{IO:}$$
$$\min : \tau_d. \tag{10}$$

According to the types of the minimum and maximum input/output time problems, the minimum and maximum calculation time problems can be reduced to linear programming problems by converting the minimum-maximum problem to the maximum-minimum problem. Introducing $\overline{\tau}_c = 1/\tau_c$, the problem is described as

$$\text{LP} - \text{Comp:}$$
$$\max : \overline{\tau}_c. \tag{11}$$

The workload and I/O request or job processing on one server can be freely transferred to another server. Therefore, consider the mapping between the first and second stage server protocol and the final solution:

$$m_{hh'} = \begin{cases} 1, & \text{If } h' \text{ is mapped to server } h, \\ 0, & \text{otherwise.} \end{cases} \tag{12}$$

2.3. Emergency Decision-Making Algorithm Based on Improved Group Decision-Making Method. The way the computer feeds the calculation results to the individual is a way of exchanging information that performs communication between the individual and the computer. The human-computer interaction function of the computer operating system is an important indicator of whether the computer system is advanced. When dealing with emergency situations, if there is no scientific and systematic emergency decision-making method, emergency rescue operations cannot be carried out in time. If relevant departments can make quick and effective decisions based on the development and changes of emergencies, this will play a decisive role in the effectiveness of the emergency response.

2.3.1. Traditional Gray System. Because part of the information in the gray system is unknown, people often explore and solve problems by mining and using the value of the known information. Group decision-making always follows the principle of "the minority obeys the majority." Using the expert's decision matrix to determine the consistency of the expert is the key to solving the expert's weight. In the process of determining and adjusting the weight of experts, the information is often incomplete and uncertain, so, at this time, the gray system theory has become the first choice to deal with such problems. In actual operation, it is necessary to first calculate the individual expert decision matrix and aggregate the individual expert decision matrix into the group decision result.

2.3.2. Deficiencies in Determining the Weight of Experts Based on Gray Relational Analysis

(1) Principle of "the Minority Obeys the Majority." Group decision-making always follows the principle of "the minority obeys the majority." According to this principle, the expert's decision-making power is reflected in the consistency of the decision-making results of the expert and the decision-making group. When he is consistent with the decision-making results of the group decision-making, he has more large decision-making power; otherwise, its decision-making power will be reduced. However, the principle of "the minority obeys the majority" is not always correct. We cannot rule out the special case of a minority making correct decisions and a majority making wrong decisions. At this time, if the traditional group decision-making method is used to simply eliminate individual subjective differences and reflect the will of the group, then the decision-making group will make wrong decisions.

(2) Blindness in Selecting Experts. Suppose that when dealing with emergencies, the relevant department has an expert database, and each time, a part of the experts are randomly selected from the expert database to complete group decision-making. As the experts of the decision-making group come from different fields and different industries, professional barriers and blind spots may cause them to make mistakes in decision-making in areas that they are not good at. At this time, the credibility of their decision-making results is very low. This is traditional group decision-making. Factors not considered by the law.

(3) Does Not Consider the Performance of Experts in Historical Decision-Making Events. Traditional group decision-making hardly readjusts the weight of experts based on the decision-making results after the decision, nor does it take it as consideration into the process of adjusting the weight of experts in the next emergency, that is to say, traditional group decision-making. The process is to consider each emergency as a separate event. But in fact, the development of things will not be unrelated. The past decision-making results can measure the decision-making level of the experts in the expert group and examine the decision-making effects of all relevant decisions of these experts in recent years.

2.3.3. Ideas for Improving Expert Weight Adjustment Algorithm

(1) Fully Consider the Correct Rate of Experts' Historical Decisions. Before the expert team makes emergency decisions, due to the constraints of objective conditions, the possible implementation effects of each plan are also unknown. However, after the implementation of the program is over, the expert group can evaluate and score the performance of the program. In order to ensure the objectivity of the evaluation results of the expert group, a completely different group of experts can be selected in the expert database to score the plan implementation effect after the emergency decision is over. From the emergency decision-

making cases handled in the past, we can dig out a lot of valuable information for the current case. The correct rate of the experts' historical decision-making is one of the most valuable research cases.

(2) Use Event Type as a Consideration When Drawing Experts. Suppose the decision-making group makes a decision by randomly selecting an expert group from the expert database, but due to the limitations of each expert's knowledge and expertise, it may be easy for them to make correct decisions in their areas of expertise, and easy to make in areas that they are not good at the wrong decision. In order to improve the accuracy of decision-making, the type of emergency can be considered as a factor.

(3) Prioritize Recent Historical Emergencies. Things are constantly evolving and changing. The expert may have a low rate of correct decision-making for a certain type of event, but with the accumulation of experience and the addition of knowledge, his decision-making accuracy rate will change, it may become higher and higher, or it may become lower. But it cannot be set in stone. We need to look at the problem from a developmental perspective. When calculating the correct rate of the expert's historical decision, we must give priority to the correct rate of decision-making at the most recent time point. The closer to the time point of decision-making behavior, the greater the role and value it plays. When an expert's case base is small, the advantages of this approach may not be obvious, but when an expert's case base is large and he has made many similar decisions, the advantage of this approach will be as follows: it is obvious that it is too much to aggregate all the historical decision-making accuracy rates of experts, which not only brings operational difficulties but also leads to the low credibility of the final aggregated historical decision-making accuracy rates.

3. Intelligent Decision Support System of Emergency Language Based on Fog Computing

3.1. System Architecture Design. The system structure should include three aspects: application layer, service layer, and data layer. The main task of the emergency decision-making system based on fog computing is to make inference decisions about emergencies and establish and maintain a case library. The service layer is mainly to realize the service functions of the system, including system case reasoning, case management, and system help services. The establishment of the service layer is realized by the development tools of Visual Basic 6.0. The data layer includes the rule library and the case library, and the case library is that in order to store cases, the rule base is used to implement certain functions of case reasoning and management. The establishment of the data layer is implemented by SQL 2008 database. The architecture of the system is shown in Figure 2.

3.2. Test Subject. The core algorithm of the emergency language intelligent decision support system designed in this paper uses fog computing. Before the experiment, the system
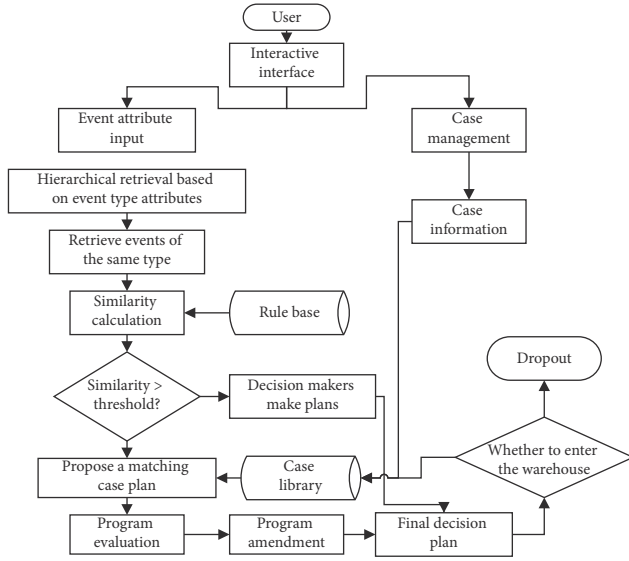
FIGURE 2: Workflow chart of emergency decision-making system for emergencies.

is trained for events. Six types of emergencies include earthquakes, typhoons, tsunamis, floods, and a total of 4000 incidents of landslides and fires, and these training data were entered into the database. Then, evaluate the emergencies that have occurred in the past 10 years. The evaluation indicators include direct economic loss, indirect reputation loss, ecological environment indicators, and healthy living indicators. The index value of direct economic loss and indirect reputation loss is as small as possible, while the index value of ecological environment index and healthy living index is the larger the better. At the same time, five emergency options are obtained for emergency events. After multiple rounds of rapid discussions, five emergency options are given, and the estimated values under each evaluation indicator perform data analysis.

3.3. Experimental Method.

There are many data standard processing methods, but different data standardization methods will have a certain impact on the evaluation results of the system. For the positive indicator standardization method,

$$y_{ij} = \frac{x_{ij} - \min\{x_{ij}\}}{\max\{x_{ij}\} - \min\{x_{ij}\}}. \tag{13}$$

For the negative index standardization method,

$$y_{ij} = \frac{\max\{x_{ij}\} - x_{ij}}{\max\{x_{ij}\} - \min\{x_{ij}\}}. \tag{14}$$

3.4. Statistical Data Processing Method.

SPSS23.0 software was used for data processing, the count data was expressed in percentage (%), k is the number of data in this experiment, σ^2 is the variance of all survey results, and $P < 0.05$ indicates

that the difference is statistically significant. The formula for calculating reliability is shown in

$$a = \frac{k}{k-1}\left(1 - \frac{\sum \sigma_i^2}{\sigma^2}\right). \tag{15}$$

4. Emergency Language Intelligent Decision Support System Based on Fog Computing

4.1. Evaluation Index System Based on Index Reliability Testing.

Reliability refers to the stability and reliability of the questionnaire. This article adopts the α coefficient method created by Cronbach. The α coefficient can be obtained by Reliability Analysis in SPSS software. It is generally believed that the α coefficient above 0.8 indicates that the effect of the index setting is very good, and above 0.7 is also acceptable. Here, we analyze the reliability of each type of object, and the reliability index we choose for each type of object is slightly different. The results are shown in Table 1.

It can be seen from Table 1 that the direct economic loss, indirect reputation loss, ecological environment indicators, and healthy living indicators have an acceptable impact on this experiment ($\alpha > 0.7$), and the environmental, social and economic impacts are within acceptable limits and meet the prerequisites for starting the experiment.

4.2. Emergencies in the past 10 Years

4.2.1. Number of Emergencies in the past 10 Years.

We first analyze the number of earthquakes, typhoons, tsunamis, floods, landslides, and fires that have occurred in the past 10 years. The first five emergencies are natural disasters, and the last one includes natural disasters and urban disasters. The results are shown in Table 2; we make a line chart based on this result, as shown in Figure 3.

Figure 3 shows the vigorous development of water conservancy projects in my country since ancient times, and modern flood disasters are becoming less and less, unless continuous heavy rains will cause sudden events like floods; natural emergencies like earthquakes, typhoons, and tsunamis are not for humans. There are no rules to control, and fires include natural disasters and urban disasters. The number of accidents per year has fluctuated. But on the whole, the annual number of fire accidents in our country has shown a continuous increase momentum.

4.2.2. Emergency Level.

According to the nature, controllability, severity, and scope of different types of emergencies, natural disasters, accidents, and public health events are divided into four levels: particularly serious, serious, large, and general. At the same time, according to the emergency degree, harm degree, and development trend caused by emergencies, their early warning levels are divided into four levels. The results are shown in Table 3. We make a doughnut chart based on this result, as shown in Figure 4.

It can be seen from Figure 4 that sudden events such as earthquakes are natural disasters. There are countless large

TABLE 1: Summary table of reliability test results.

Category	Index combination	Alpha coefficient (α)
Earthquake	Direct economic loss Indirect reputation loss Ecological environment indicators Healthy living index	0.7691
Typhoon	Direct economic loss Indirect reputation loss Ecological environment indicators Healthy living index	0.8332
Tsunami	Direct economic loss Indirect reputation loss Ecological environment indicators Healthy living index	0.7871
Landslide	Direct economic loss Indirect reputation loss Ecological environment indicators Healthy living index	0.7614

TABLE 2: The number of emergencies in the past 10 years.

Year	Earthquake	Typhoon	Tsunami	Flood	Landslide	Fire
2011	46	7	3	3	23	96
2012	21	9	5	1	27	91
2013	27	8	4	2	31	88
2014	40	13	6	0	29	107
2015	41	7	6	1	19	87
2016	40	11	6	1	22	112
2017	42	17	3	1	17	79
2018	78	9	3	0	27	104
2019	68	10	4	1	42	94
2020	42	8	2	2	25	88

and small earthquakes every year. In particular, major earthquakes are rare. And sudden events such as typhoons, tsunamis, and floods are particularly serious once they occur. Incidents of the general level rarely occur. Natural disasters such as landslides are the same as earthquakes. There are many occurrences every year, causing very few particularly significant impacts. Fires, including natural disasters and urban disasters, are more common. Natural disasters are considered special. Major emergencies, if it is an urban disaster, will cause a more general impact.

It can be seen from Figure 5 that, in order to minimize the losses caused by the frequent occurrence of emergencies, relevant decision-makers should quickly make effective emergency decisions to ensure the safety of people's lives and property. Therefore, emergency decision-making has become the key core issue of emergency management. In life practice, people have long recognized that prevention, prediction, and preplanning are effective ways to reduce or eliminate various emergencies, especially for major

emergencies. The correctness of emergency decisions is a key factor in the success of their actions. With the progress of mankind and the rapid development of the social economy, decision-making issues have become more and more complex. Emergency decision-making, as one of the important decisions, has become particularly important.

4.2.3. Assessment Index for Emergencies in the past 10 Years. Evaluate the emergencies that have occurred in the past 10 years. The evaluation indicators include direct economic loss, indirect reputation loss, ecological environment indicators, and healthy living indicators. Direct economic loss and indirect reputation loss are used as cost indicators, the smaller the index value, the better. Ecological environment index and healthy life index are good indicators, and the larger the index value, the better. The evaluation index of the event is analyzed, and the results are shown in Table 4. We make a line graph based on this result, as shown in Figure 6.

It can be seen from Figure 6 that, among so many selected emergencies, only the index evaluation scores of fires are reliable ($P < 0.01$), and the index evaluation scores of other emergencies belonging to natural disasters are a bit wrong ($P > 0.05$). The reason for this may be that the direct economic losses caused by natural disasters are not good for statistics, and the families involved are too extensive in environmental aspects. There is no reputation loss. The ecological environment indicators can be compared by the comprehensive score of the postdisaster environment today accurately. Healthy living can also be comprehensively scored according to the victim's subsequent living conditions and physical condition, which is also more accurate.

4.3. Decision-Making on Selection of Wind Farm Emergency Plan. In order to minimize the economic losses and casualties caused by the sudden accident, reduce the negative social impact, and maintain social stability in a wind farm sudden power equipment accident, the wind farm insisted on unified leadership, division of labor, strengthened linkage, and rapid in response, two experts in the industry and two senior staff were invited to conduct a comprehensive evaluation of the emergency incident based on the four indicators of the nature, severity, controllability, and scope of the incident. From three emergency plans, choose the most suitable plan among the results, and the experimental results are shown in Tables 5 and 6. We make an area map based on this result, as shown in Figure 7.

It can be seen from Figure 7 that the weight of experts and senior actors adjusted according to the traditional group decision-making method based on gray relational theory is $\lambda_{1n}^* > \lambda_{2n}^* > \lambda_{3n}^* > \lambda_{4n}^*$. It proves that it is necessary to consider the correct rate of historical decision-making as a consideration in adjusting the weight of experts and senior staff. As the concentration of salt and pepper noise increases, the average Gaussian filter and filter are less capable of handling salt and pepper noise. Medium filtering still does not perform well in terms of edge noise. The medium filter based on partial differential has the best effect on the noise of salt and
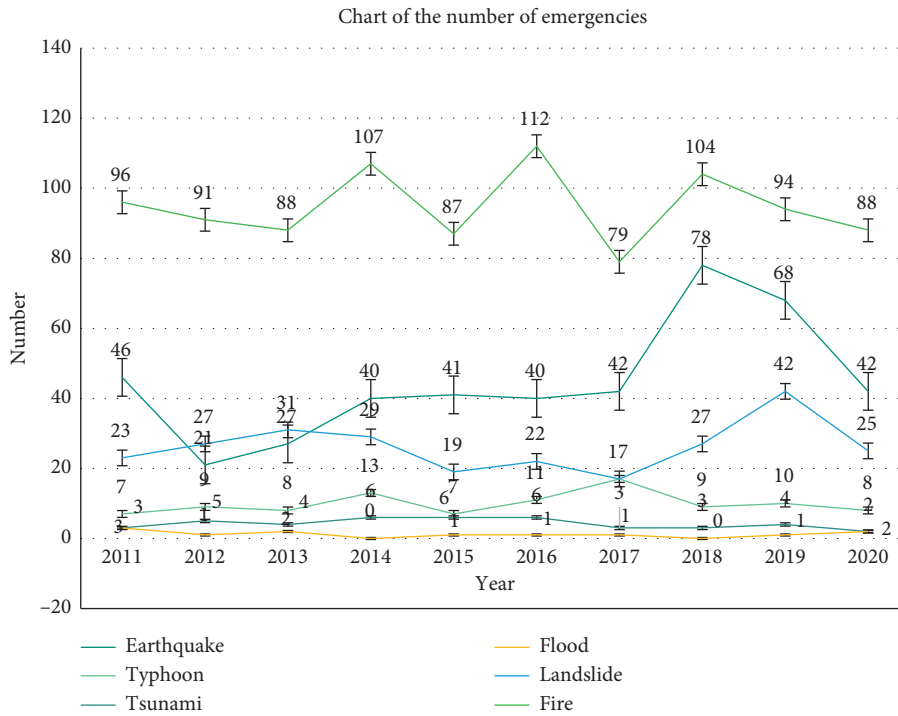
Figure 3: Chart of the number of emergencies in the past 10 years.

Table 3: Emergency rating table.

Level	Earthquake	Typhoon	Tsunami	Flood	Landslide	Fire
Particularly significant	7	73	31	8	8	42
Major	14	12	5	2	18	19
Larger	19	8	4	1	32	28
General	402	6	2	1	204	857
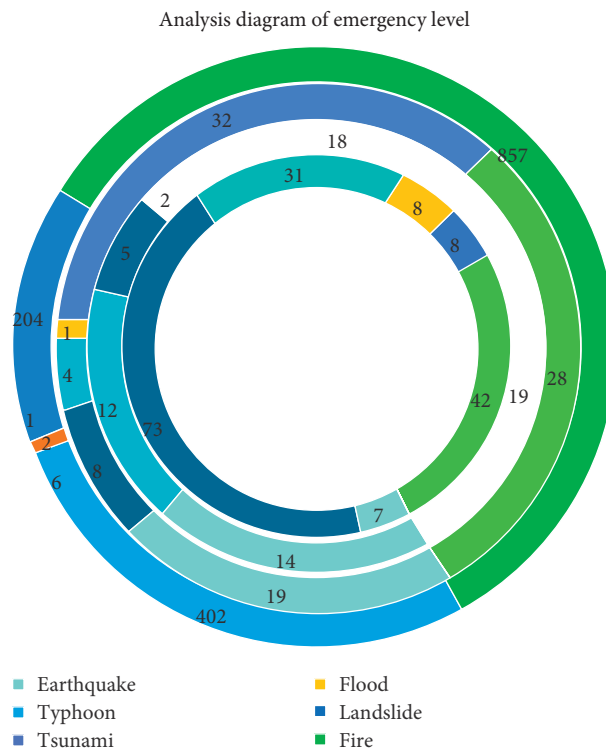
Figure 4: Analysis diagram of the emergency level.
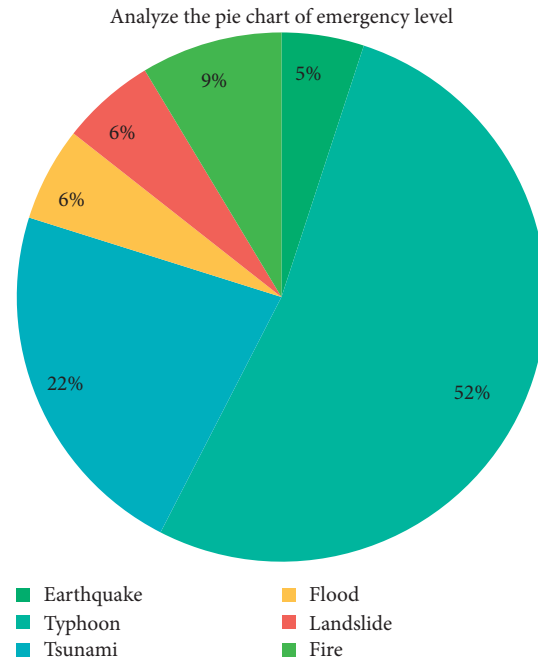
FIGURE 5: Analyze the pie chart of the emergency level.

TABLE 4: Depression data analysis table.

Evaluation index	Earthquake	Typhoon	Tsunami	Flood	Landslide	Fire
Direct economic loss	1	0.5	2	2	0.67	0.1
Indirect reputation loss	2	1	3	3	1	0.1
Ecological environment indicators	0.5	0.33	1	1	0.67	1
Healthy living index	0.5	0.33	1	1	0.67	3
P	0.2630	0.4547	0.1411	0.1411	0.8792	0.0001
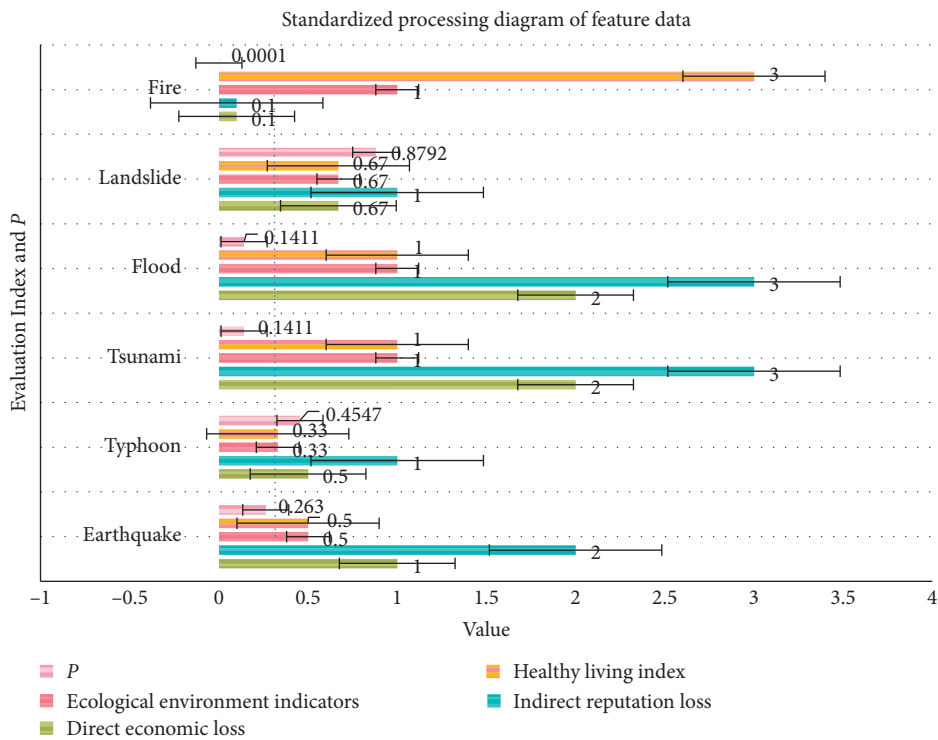
FIGURE 6: Standardized processing diagram of feature data.

TABLE 5: Two experts' feedback weight and similarity table.

Expert A	λ_{1n}^*	0.411	0.423	0.119	0.168	0.147	0.232	0.742	0.449
	ρ_n	0.4	0.5	0.8	0.2	0.2	0.8	0.4	0.5
Expert B	λ_{2n}^*	0.094	0.041	0.128	0.247	0.355	0.387	0.654	0.754
	ρ_n	0.2	0.3	0.2	0.3	0.5	0.7	0.8	0.4

TABLE 6: Feedback weight and similarity table of two senior staffs.

Senior staff A	λ_{3n}^*	0.115	0.407	0.205	0.334	0.524	0.571	0.197	0.127
	ρ_n	0.3	0.4	0.6	0.3	0.2	0.2	0.4	0.5
Senior staff B	λ_{4n}^*	0.224	0.347	0.039	0.017	0.576	0.344	0.241	0.357
	ρ_n	0.5	0.5	0.3	0.3	0.5	0.7	0.2	0.5
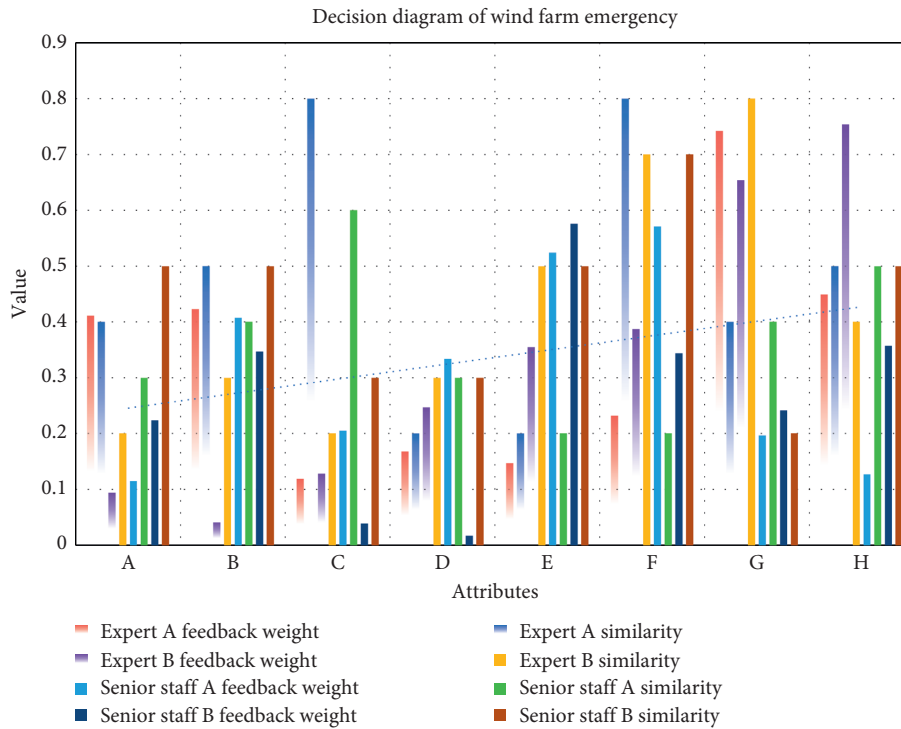
FIGURE 7: Decision diagram of wind farm emergency plan selection.

pepper. Eye movement data can also show this view. Children in the experimental group, the number of focus points of the main content, and the focus points of the content outside the main body are much higher than those of the control group, with the attention rate reaching more than 95%.

5. Conclusions

Based on the existing research on group decision-making, this paper analyzes the shortcomings of the expert weight determination method in the traditional gray-relational group decision-making method and proposes suggestions for improvement. Then, based on the improved group decision-making method, construct an emergency decision model. A group decision-making expert weight adjustment algorithm based on the gray system theory is proposed, and

three shortcomings are proposed in the implementation stage. It is recommended to improve the design response. Based on this, combined with the information provided after the implementation of the emergency plan, the correct rate of historical decision-making is considered to be a factor in adjusting the weight of experts. An expert weight adjustment algorithm based on feedback weight is proposed, and the application of the improved weight adjustment algorithm in emergency decision-making experts is explained in detail. The improved emergency decision-making model is applied to the evaluation and selection of emergency plans for wind farms. Compare the rankings and scores of the group decision plan before and after improvement, and compare the weights of experts and the scores of the projects before and before improvement. It explains the reason for the difference, proves the necessity of using the expert's historical accuracy rate as a checking factor to adjust the weight of the

expert, and, at the same time, proves the convenience and practicability of this method.

Aiming at the current problems in emergency decision-making for emergencies and combining the characteristics of fog computing, this paper applies fog computing to emergency decision-making, proposes an emergency-emergency decision-making method based on fog computing, and carries out its key technologies. Research, on the basis of method research, constructed an emergency-emergency decision-making system based on fog computing, which provides a reference for the research work of emergency-emergency decision-making. The retrieval method of emergency cases and the generation method of the emergency plan are studied. In order to improve retrieval efficiency and make retrieval results in line with actual conditions, this paper adopts a dual retrieval mechanism of layered retrieval and the nearest neighbor retrieval. The calculation of attribute similarity should consider the problem of attribute weight. This paper analyzes the advantages and disadvantages of the current commonly used weighting methods and uses the method of combining expert scores and cloud models to weight each attribute. Finally, the generation method and steps of the emergency plan are researched and discussed and verified by case analysis.

For preschool children, parents are the only objects they attach to and trust at this stage. The special physical and psychological characteristics of this stage make them vulnerable to injury. Only under the care of parents can they thrive in physical, mental, and physical aspects. For parents, because of the many difficulties in life and work, it has been a long-term pain in their hearts that they cannot accompany and care for their children well. Analyze the interaction among disaster carriers, risk factors, and vulnerable environments from the perspective of disasters. However, because catastrophe science does not take human factors into consideration, the event will be controlled by human intervention during the development process. If the relevant departments do not carry out the correct emergency response, the situation will develop in a positive direction, and on the contrary, it will move in a negative direction. Therefore, this article analyzes the scenario evolution mechanism through system dynamics and adds elements of human intervention to make the evolution mechanism of environmental emergencies more scientific and realistic. According to the system dynamics method, this article analyzes the three subsystems of environment, event, and intervention. Carry out causality analysis, and obtain the influence of energy input and output in each subsystem on the evolution of disaster scenarios.

Data Availability

No data were used to support this study.

Conflicts of Interest

The authors declare that they have no conflicts of interest.

Acknowledgments

References

[1] R. S. Bhadoria and N. S. Chaudhari, "Pragmatic sensory data semantics with service-oriented computing," *Journal of Organizational and End User Computing*, vol. 31, no. 2, pp. 22–36, 2019.

[2] H. Hamidi and M. Jahanshahifard, "The role of the Internet of things in the improvement and expansion of business," *Journal of Organizational and End User Computing*, vol. 30, no. 3, pp. 24–44, 2018.

[3] H. Lu, Y. Li, M. Chen, H. Kim, and S. Serikawa, "Brain intelligence: go beyond artificial intelligence," *Mobile Networks and Applications*, vol. 23, no. 2, pp. 368–375, 2017.

[4] N. N. Darren, Z. Alexey, S. Yasushi et al., "Synthetic biology routes to bio-artificial intelligence," *Essays in Biochemistry*, vol. 60, no. 4, pp. 381–391, 2016.

[5] W. A. Marie, L. Yong, K. R. Regner et al., "Artificial intelligence, physiological genomics, and precision medicine," *Physiological Genomics*, vol. 50, no. 4, pp. 237–243, 2018.

[6] T. Grubljesic, P. S. Coelho, and J. Jaklic, "The shift to socio-organizational drivers of business intelligence and analytics acceptance," *Journal of Organizational and End User Computing*, vol. 31, no. 2, pp. 37–64, 2019.

[7] A. Bouzekri, T. Allaoui, M. Denai et al., "Artificial intelligence-based fault tolerant control strategy in wind turbine systems," *International Journal of Renewable Energy Research*, vol. 7, no. 2, pp. 652–659, 2017.

[8] W. K. Lin, S. J. Lin, and T. N. Yang, "Integrated business prestige and artificial intelligence for corporate decision making in dynamic environments," *Cybernetics and Systems*, vol. 48, no. 4, pp. 1–22, 2017.

[9] D. S. Manu and A. K. Thalla, "Artificial intelligence models for predicting the performance of biological wastewater treatment plant in the removal of kjeldahl nitrogen from wastewater," *Applied Water Ence*, vol. 7, no. 7, pp. 1–9, 2017.

[10] L. Fabisiak, "Web service usability analysis based on user preferences," *Journal of Organizational and End User Computing*, vol. 30, no. 4, pp. 1–13, 2018.

[11] Y. Chen, W. Zheng, W. Li, and Y. Huang, "The robustness and sustainability of port logistics systems for emergency supplies from overseas," *Journal of Advanced Transportation*, vol. 2020, Article ID 8868533, 10 pages, 2020.

Research Article

Organization Evolution of Fuzzy System Based on Financial Risk Degree of Commercial Banks

Chao Liu ⓘ

Faculty of Management and Economics, Kunming University of Science and Technology, Kunming 650093, Yunnan, China

Correspondence should be addressed to Chao Liu; luck@stu.kust.edu.cn

After the market-oriented reform of China's financial industry, there have been some problems in financial risk assessment. In recent years, commercial bank finance has made rapid development, but on the whole, the financial risk assessment of commercial banks is still the weakest link in the Chinese financial system. This experiment selects data from state-owned commercial banks and foreign-funded commercial banks. Through the analysis and deconstruction of the macroenvironment, participants, and business models, this paper systematically combines the factors influencing the financial risk of commercial banks, which can identify the main sources of financial risk in this complex way of financing and clarify the effects of the transfer of financial risk between different participants. Based on this, the paper studies the differences between the assets and liabilities between banks on the risk-taking of banks and the reform of the organizational evolution of fuzzy system. According to the application scenarios and actual needs of commercial banks' financial risks, the entropy weight analysis method is used to reflect the weight of indicators by the difference degree of observed index values. The information quantity of indicators is measured to ensure that the established indicators can reflect most of the initial information. The experimental results show that, compared with state-owned banks, the proportion of foreign banks' assets in 2018 is very small. The highest value of public debt assets is 9.2 billion yuan, followed by financial institutions with 2.58 billion yuan, and deposit institutions with 280 million yuan. The central bank has no debt amount.

1. Introduction

1.1. Background and Significance. The financial risk assessment of commercial banks is the focus and difficulty of financial reform in China. How to achieve a fundamental breakthrough in the accuracy of assessment is an urgent problem and a difficult problem to solve. For a long time, information asymmetry and other factors, lack of effective collateral and high service costs, have restricted the effective provision of financial services. It is a difficult problem that basic financial services should be popularized to all people like medical, educational, postal, and other basic public services. The construction of bank financing channels plays an important role in the daily operation of banks and service points are the most basic channels for the execution of different businesses. Discussing the spatial organization of large commercial banks and the factors that influence them can optimize the layout of the system, increase the provision of financial risk services, and promote economic integration.

1.2. Related Work. In order to analyze whether personal financial risk propensity changes with family financial status and timing of individual and subjective portfolio risk, Lee derived risk propensity data from six different self-assessment aspects collected from the DNB family survey, which covers 1995–2015. Risk propensity is usually higher in the period of economic growth but lower in the period of economic recession. However, in the issue of safety investment, the risk tendency is not affected, and the risk tendency index is in a higher state in the positive return period of the stock market or the subjective risk period of the past investment. However, there are errors in the process of his investigation and research, resulting in inaccurate results [1]. Su and Furman analyzed the bilateral exchange rate returns of the Swiss Franc under the asset pricing framework to evaluate the risk aversion characteristics of the Swiss franc. Whether at average or during a crisis, a "safe haven" currency is a currency that provides a hedge against global

risk. In order to explore these problems, Su and Furman estimated the relationship between exchange rate returns and risk factors in the expanded UIP regression using the recently developed econometric method to explain the possibility that the regression coefficient may change over time. However, the method and process they studied are complicated and not very practical [2]. The way the government chooses to subsidize health interventions will affect the acceptance of health interventions and then affect the degree of medical benefits. In addition to medical benefits, some policies, such as public finance, can also provide insurance against catastrophic medical expenses. Robinson used an extended cost-benefit analysis to assess the health benefits and financial risk protection of nine interventions (including many others) that the government of Ethiopia aims to popularize. The nine interventions include measles vaccination, rotavirus vaccination, pneumococcal conjugate vaccination, diarrhea treatment, malaria treatment, pneumonia treatment, cesarean section, hypertension treatment, and *tuberculosis* treatment. However, his research is not very targeted, just a rough proof [3].

Computational modeling of organizational processes is an important method for system organization operation. For this reason, Wong A. analyzed the dynamic evolution of an organization in a system organization and took individual behavior modeling as a task-oriented self-organization process. Taking a real system organization as an example, Wong A. analyzed the organizational process and studied the organizational structure, task flow, and information flow in the process. This method provides a method to understand the dynamic organization evolution process and shows its potential application in system organization [4]. Chiu and Carducci discussed the key methods that have emerged in recent years in the study of tissue evolution, including the increasing use of coevolutionary methods, with particular emphasis on the definition of rational analysis units. Then, Chiu and Carducci introduced the extensive, multiround, and reasonable review process [5]. In order to achieve the goal of expanding the knowledge spiral to the level of interorganizational epistemology, information technology tools and virtual communities can establish effective interaction to exchange knowledge and make banks develop harmoniously. Hsu and Chen took the platform developed by the European research project "BIVEE (Business Innovation in Virtual Enterprise Environment)" as an example. The selected research method was participatory action research (PAR). Two researchers conducted par in real-time, and the other two researchers also participated in the study. This study found that the virtual evolution of banks can lead SECI model to a cross-organizational level. In addition, learning history describes how all stages of SECI process, even socialization stage, occur or get support in virtual space [6].

1.3. Innovation

(1) Through the analysis of the practical problems encountered by commercial banks in China, the countermeasures of financial risks of commercial banks in China need to be controlled and prevented from the aspects of macroeconomy and microeconomy. From the macroeconomic perspective, we should not only strengthen the financial supervision of commercial banks' risks but also pay attention to information leakage. This requires the introduction of an exit mechanism and the strengthening of the restraint mechanism for commercial banks. First, based on the original financial derivatives, this paper puts forward the methods of using credit derivatives to prevent financial risks.

(2) For the prevention of financial risks, put forward specific constructive suggestions and the establishment of China's financial risk quantitative analysis system.

(3) Analyzing the historical situation of Chinese commercial banks and the existing asset and liability gap, this paper presents the idea of establishing a financial risk assessment system according to the characteristics of commercial banks.

2. Organization Evolution of Fuzzy System Based on the Financial Risk Degree of Commercial Banks

2.1. Evolution Stage of Fuzzy System Organization of Financial Risk Degree of Commercial Banks. The evolution of fuzzy system organization of financial risk degree of commercial banks refers to the system that needs to be guided by risk assessment strategy under external conditions. Risk assessment organization and coordination organization should coordinate the allocation of system resources, appropriate operation, and reasonable incentive and evaluate financial risk and service development [7]. According to the theory of business development, business is not only a social and economic organization but also a life organization. The financial risk system of commercial banks is a subsystem of commercial banks. It follows the general business life cycle model and can be divided into four different periods: embryonic period, developmental period, maturity period, and fusion reduction period.

2.1.1. Embryonic Stage. In the embryonic stage of the development of fuzzy system of financial risk degree of commercial banks, banks mainly introduce financial risk assessment, that is, to improve the accuracy of risk assessment of banks by analyzing various large-scale financial cases in the past. In the early stage of development, banks were not even responsible for risk assessment because China's banking industry was monopolistic and could not assess risks. Although the overall economic situation of the society was poor, the basic resources for investment were very small [8]. The environment has changed and the improvement of competition makes commercial banks realize the necessity of risk assessment, start implementing the relevant financial risk assessment system, and organize relevant departments, which make the financial risk system of commercial banks unclear to be shaped.

2.1.2. *Growth Period.* The formal establishment of the financial risk rating system of China's commercial banks has made the emerging financial products and services in the market receive extensive attention from major risk assessment institutions of banks [9]. However, due to the need to continue to improve the assessment ability, the assessment results mainly focus on the relatively simple assessment of existing financial products and services. Finally, according to the actual situation, the deviation caused by the degree of financial risk is analyzed and evaluated [10]. The vague system of the degree of financial risk of commercial banks has evolved from scattered and unstable hierarchical management to systematization and perfection, which shows that the financial risk assessment process is gradually standardized and information system design and information processing developed gradually. At present, banks have to invest a lot of human, financial, and material resources to shape the banks' rating. Moreover, the level of financial risk of China's commercial banks is basically defined at the moment.

2.1.3. *Mature Stage.* When the fuzzy system of financial risk degree of commercial banks reaches the maturity stage, the infrastructure of the system has been gradually completed, and the culture of risk assessment has penetrated into various departments of the bank. In this period of time, the bank evaluation system has gradually developed into a system based on financial risk assessment, followed by the continuous enhancement of evaluation ability [11]. However, the external demand of customers is constantly changing, the financial market and competitors' financial products are also constantly fluctuating, and the methods and capabilities of risk control have been mature.

2.1.4. *Convergence Recession.* In view of the development of information processing technology and the change of market demand and environment, the rapid change of financial industry is always full of opportunities and challenges. The establishment of fuzzy system of financial risk degree of any commercial bank cannot be done once and for all, and the financial risk rating system begins to enter the fusion recession period [12]. This includes two trends: first, further strengthening the system of unclear financial risk level of commercial banks. The result of accumulation and diffusion is accompanied by the continuous improvement of the value of customers' products and services, which makes the risk assessment system of commercial banks continue to grow and shrink. This means that there is a competitive relationship between peers and nonpeers, the volatility of the financial market, and regulatory policies. The arrangement of policies will eventually lead to the failure of commercial banks to adapt to customer demand and market environment in a timely manner, resulting in stagnation [13].

2.2. *Characteristics and Types of Financial Risks.* Risk is a commonly used but fuzzy concept. Financial risk refers to the uncertainty or possibility of economic entities suffering losses in financial activities. The characteristics of financial risk are as follows:

(1) Financial risk is related to loss, and financial risk is specific to the possible loss. For a specific financial activity, as long as there is a possible loss, it shows that it has financial risk. When an investment has multiple potential returns, the possible lower return is the relative loss compared with the higher return [14].

(2) Financial risk is the inherent characteristic of financial activities. If there are financial activities, there must be economic risks and financial risks, and financial activities are inseparable [15]. The uncertainty of financial activities is the source of financial risk. The greater the uncertainty of financial activities, the greater the financial risk.

2.3. *Entropy Weight Analysis Method.* Entropy weight analysis method is based on entropy to calculate the weight of each index. Its basic principle is to use the difference degree of observation indicators to reflect the weight of indicators. The entropy weight analysis method is an objective weighting method, which uses the information provided by the entropy value of each index to determine the weight of the index [14, 16]. Entropy weight analysis method is to use entropy weight method to determine the weight of indicators, which can avoid the interference of human factors on the weight of each index and make the evaluation index and evaluation results more in line with reality [17]. By calculating the entropy value of each index, the index information can be measured to ensure that the established indicators can reflect most of the initial information [18]. Proceed as follows:

(1) If there are m objects to be evaluated and n evaluation indexes to establish decision matrix, then the value of the ith evaluation object to the jth index is $x_{i,j}$ $(i = 1, 2, \ldots, m; j = 1, 2, \ldots, n)$ and the corresponding decision matrix X is

$$\begin{bmatrix} x_{11} & x_{12} & \ldots & x_{1n} \\ x_{21} & x_{22} & \ldots & x_{2n} \\ x_{31} & x_{32} & \ldots & x_{3n} \\ x_{m1} & x_{m2} & \ldots & x_{mn} \end{bmatrix}. \quad (1)$$

(2) Normalization of decision matrix

In order to ignore the different decision effects brought by different dimensions of indicators, it is necessary to standardize the X decision matrix by creating a normalized matrix $Y = (y_{ij})_{m*n}$. There are two ways to normalize the X decision matrix [19].

First, the benefit index is too large, so the following standardized format should be adopted:

$$y_{ij} = \frac{x_{ij} - \min(x_j)}{\max(x_j) - \min(x_j)}. \quad (2)$$

Second, the smaller better index, that is, the cost index, adopts the following standardized form:

$$y_{ij} = \frac{\max(x_{ij}) - x_{ij}}{\max(x_j) - \min(x_j)}, \tag{3}$$

where y_{ij} is the normalized value of x_{ij}; $\max(x_j)$ and $\min(x_j)$ are the maximum and minimum values of the jth index, respectively. It can be found that, after standardization, $0 \leq y_{ij} \leq 1$.

2.4. Fuzzy System Algorithm.

The fuzzy system algorithm is not limited to fuzzy control and fuzzy systems theory but includes a wide range of research topics. For this reason, some people divide the fuzzy systems algorithm into four branches:

(1) Vague logic and artificial intelligence, which introduce approximate reasoning into classical logic and develop a special system based on fuzzy information and approximate reasoning [20]

(2) Fuzzy system, which includes fuzzy control and fuzzy method in signal processing and communication

(3) Security decision, which uses soft constraints to consider optimization problems [21, 22]

(4) In fuzzy mathematics, vague sets, which are used instead of classical sets to extend the concept to classical mathematics

Of course, from a practical point of view, these four branches are not completely independent but are interdependent and closely linked. The fuzzy algorithm in practice based on theory has yielded fruitful results, but the vague theory is still new. Although the application of fuzzy theory in control system has become more and more clear, efforts still need to be made to improve its accuracy and control speed, especially in other fields. Most methods and analyses are rare [23, 24].

3. Experimental Evolution of Fuzzy System Organization Based on the Financial Risk Degree of Commercial Banks

3.1. Sample Data Selection and Statistical Description.

In this experiment, the data of state-owned commercial banks and foreign-funded commercial banks are selected for analysis. The main reason for choosing these two types of banks is that the banks have a relatively long listing period and large asset scale and have strong typicality. The selected time range is 2013–2019, a total of 7 years of annual data. Data sources are the Internet, financial statements released by commercial banks, and the official website of the National Bureau of statistics.

3.2. Main Contents of the Study

3.2.1. Bank Asset Level.

Relatively large banks are not easy to go bankrupt for the following reasons: the financing channels and business scope of banks are relatively large.

Therefore, once the risk occurs, the risk management channel of the bank can deal with and solve the risk better than the ordinary bank. Secondly, if the bank's asset scale is relatively large when the bank has problems, it will have a greater impact on the financial market and economic growth. Regulatory authorities need to take strong supervision, which reduces the possibility of bankruptcy and other risks of commercial banks but also limits the blind expansion of the scope of assets.

3.2.2. GDP Growth Rate.

The characteristics of the GDP growth rate of commercial banks determine that the development of commercial banks is cyclical. The development of the banking industry is closely related to the development of the whole economic environment and financial market. Therefore, in the analysis of this experiment, the GDP growth rate is introduced as the overall analysis index of the macro environment.

3.3. Benchmark Model.

Combined with a large amount of research data, banking risk is not short term but sustained. Therefore, this experiment constructs a potential model to study the impact of interbank business on risk-taking. At the same time, we will study the differences between the assets and liabilities between banks and build a reference model as follows:

$$\text{Inrisk}_{it} = \alpha_0 + \alpha_1 \text{Inrisk}_{it-1} + \alpha_2 \text{Inibasset}_{it} + \alpha_3 \text{Policy}. \tag{4}$$

In the model, the risk_{it} level of bank i in year t is taken into account, the lag phase of risk_{it} is included in the model to investigate the persistent impact of risk, ibasset_{it} is the interbank asset variable, and policy_{it} is the policy dummy variable.

4. Experimental Fuzzy System Organization Evolution Based on the Financial Risk Degree of Commercial Banks

4.1. Assets and Liabilities of Commercial Banks.

After China's accession to the world trade organization, the transition period will soon end, the financial industry will further open to the outside world, and the state-owned commercial banks will face more severe market competition. In accordance with China's WTO commitments, the regulatory authorities will remove the regional and customer restrictions on RMB business of foreign banks and encourage foreign banks to set up or transform their existing branches into corporate banks registered locally in China. In addition, corporate banks and branches of foreign banks that have not been transformed will be treated differently according to the principle of prudential supervision. Foreign bank branches will be more restricted than corporate banks in absorbing retail deposits and other RMB retail businesses of Chinese residents. Local branches of foreign banks registered in China will fully implement the principle of national treatment and allow them to operate comprehensive foreign exchange business

and RMB business, including RMB wholesale business and retail business. The branches of foreign banks can continue to do RMB wholesale business, but small retail businesses will be restricted to a certain extent and can only absorb fixed deposits of residents above the limit. In the experimental stage, our experimental object is the artistic visual form of ceramic murals and the data source is the questionnaire that was issued and retrieved. Here, we publish questionnaires by age group to reduce significant differences.

As shown in Table 1, from 2018 to 2019, the assets of the Central Bank of China's state-owned commercial banks decreased by 6.6% and the creditor's rights of deposit institutions and financial institutions decreased by 31.78% and 4%, respectively. The assets of these three kinds of projects have declined, only the government's creditor's rights have increased, and the increase rate has more than tripled.

According to the latest statistics of the network survey, before 2019, there were 26 wholly foreign-owned and Sino foreign joint venture legal person banking institutions registered in China, with 13 branches and subsidiaries; 105 foreign-funded banks from 31 countries and regions established 278 branches and 93 subbranches in 29 cities in China; 207 foreign-funded banks from 48 countries and regions set up 306 representative offices in 29 cities in China; the total deposits of foreign banks in China reached 58.9 billion US dollars, and the loan balance was 74.3 billion US dollars. There are 30 cities in China that have opened RMB business to foreign banks, of which 9 cities have opened up ahead of time. There are more than 200 types of businesses operated by foreign banks, and 172 foreign-funded banking institutions are allowed to operate RMB business. The RMB business of foreign banks has developed rapidly.

As shown in Figure 1, compared with state-owned banks, foreign banks have a small proportion of assets. The highest value of government debt assets is 9.2 billion yuan, followed by financial institutions with 2.58 billion yuan, and deposit institutions with 280 million yuan. The central bank has no debt amount. It can be seen that the government's assistance to foreign banks is great.

4.2. Deterioration of Economic Environment.

According to the China Bureau of Economic Analysis, the inflow of foreign capital began to exceed the historical period and increased rapidly since 2015. The massive inflow of international capital creates a positive atmosphere for China's domestic market, which generally flows into the stock market and the real estate market, raising the price of these assets and causing huge financial bubbles. However, the speed of growth of the domestic real economy and the speed of adjustment of the economic structure can not afford a huge amount of capital. There is an increasingly acute imbalance between the virtual economy and the real economy, leading to the deterioration of the economic environment.

The real estate price index is used as the virtual asset price index, and the real GDP is used as the real economy index. In order to describe the departure relationship between the virtual economy and the real economy, it can be

Table 1: Balance sheet of state-owned commercial banks (unit: 100 million yuan).

Project	2018	2019
Central bank	2513	2347
Deposit institutions	258	176
Financial institution	5716	5489
Government claims	2174	6482
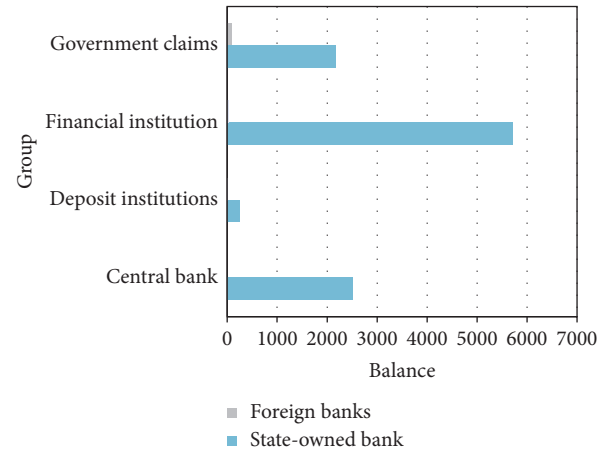
Figure 1: Assets and liabilities of state-owned banks and foreign banks in 2018.

seen from Figure 2 that the growth capacity of the virtual asset price out of the real economy began to accelerate after 2015–2018, and the nonequilibrium state of the deviation will continue with time and finally reach the peak of deviation at the end of 2017. By the occurrence of accidental events, the expected changes, and asset prices falling, the virtual economy began to return to the real economy. Therefore, it can be concluded that the virtual economy is the most sensitive when it deviates from the real economy to the maximum regional critical state, and the financial crisis may break out at any time.

As shown in Figure 2, the development rhythm of China's economy in the past four years is a true portrayal. With the collapse of the Internet bubble, China's economy has entered a recession. In order to stimulate economic growth, the rate of interest reduction in the first few years has reached its lowest level in 31 years in 2017. Due to the loose policy of long-term low-interest rate and the conditions of loan, the money flowing into the real estate market has greatly led to the rise in real estate prices. On the other hand, China's real economy is short of new economic growth points. It can only maintain a low growth rate. Finally, the expansion of the virtual economy is ultimately constrained by the development scale and absorptive capacity of the real economy to the critical point, the real estate bubble bursted, and the financial crisis is triggered at any moment.

4.3. Global Liquidity Flooding and World Economic Imbalance.

At the same time, the situation of global liquidity flooding and economic imbalance is becoming
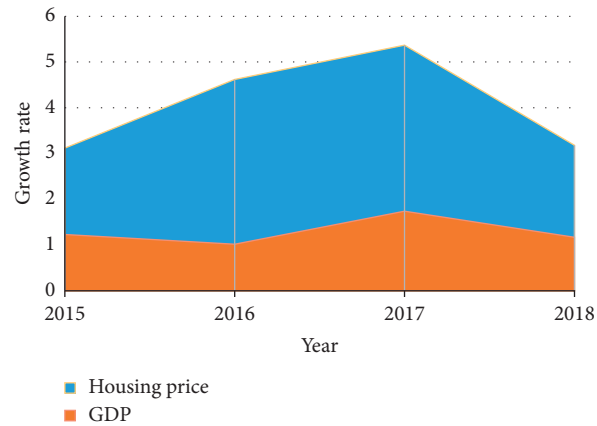
FIGURE 2: The relationship between virtual economy and real economy.

more and more serious. All these are inseparable from the current international monetary system in which the dollar is the dominant currency. After the cold war, China has become the world's number one hegemon. China's comprehensive strength determines the leading position of the US dollar in the international monetary system. However, this is a US dollar–based international monetary system that has become a deeper world economic factor for the outbreak of the subprime mortgage crisis. The global liquidity flooding and global economic imbalance brought about the foreshadowing of Chinese subprime debt crisis.

Loose monetary policy has led to global liquidity. Along with the breakdown of the NASDAQ technology bubble, China's domestic economic growth rate has dropped rapidly. As shown in Figure 3, the change of GDP growth rate between China and the United States from 2013 to 2018 is described. We can see that the GDP growth rate of both countries exceeded 3% from 2014 to 2015, but the situation turned sharply in 2016, and the GDP growth rate dropped to less than 1%. In response to China's loose monetary policy to stimulate the economy, countries around the world also keep interest rates at a low level.

4.4. Current Account Revenue and Expenditure and Government Expenditure. The global economic imbalance is mainly manifested in China's current account deficit and fiscal deficit, while the emerging market countries represented by the United States maintain a long-term trade surplus with China. This increasing imbalance is not conducive to the coordinated development of the world economy and is also the underlying cause of the outbreak of the subprime mortgage crisis. On the one hand, as a big consumer country, China has long implemented the way of expanding domestic demand to stimulate economic growth and employment, which has led to a serious shortage of private and government savings, especially the use of the special function of financial innovation tools to encourage early consumption. In the modern

financial crisis early warning system, the current account deficit/GDP has become an important assessment index. If the deficit level can be controlled within a certain scale, it is generally 4%, which is meaningful to promote domestic consumption capacity and introduce advanced technology. If the deficit continues to expand, the equilibrium state of economic development will be affected. According to the economic operation data of China before the subprime debt crisis released by the world bank, since 2015, China's current account revenue and expenditure has been in a deficit state and has deteriorated year by year. By the end of 2017, the ratio of current account deficit to GDP has reached −4.8%, and the fiscal expenditure deficit has also been −1.8%, as shown in Figure 4.

On the other hand, due to the relatively backward economic development and lack of capital in Asia, an industrial system dominated by the manufacturing industry has been formed in the international division of labor system, which determines that Asia has been pursuing export-oriented policies for a long time to drive domestic economic development. With the continuous increase of trade surplus, a large amount of foreign exchange reserves has been accumulated. In order to reduce the shrinking of foreign exchange reserves caused by the devaluation of RMB, the countermeasures adopted by developing countries are to invest the foreign exchange reserves back to China in the form of purchasing China's treasury bonds so as to make up for the current account deficit by capital account inflow and maintain the stability of RMB exchange rate. It is such a positive feedback mechanism that enables China's current account to be supported by the capital account for a long time, and thus the debt consumption pattern of China is also supported.

For a long time, China has maintained its consumption and investment through external debt. The financial derivatives related to subprime mortgage have brought this debt growth mode to the extreme. With the outbreak of the subprime mortgage crisis, it is also indicated that the mode of promoting domestic economic growth through huge fiscal deficit, trade deficit, and large amount of international capital inflow is unsustainable.
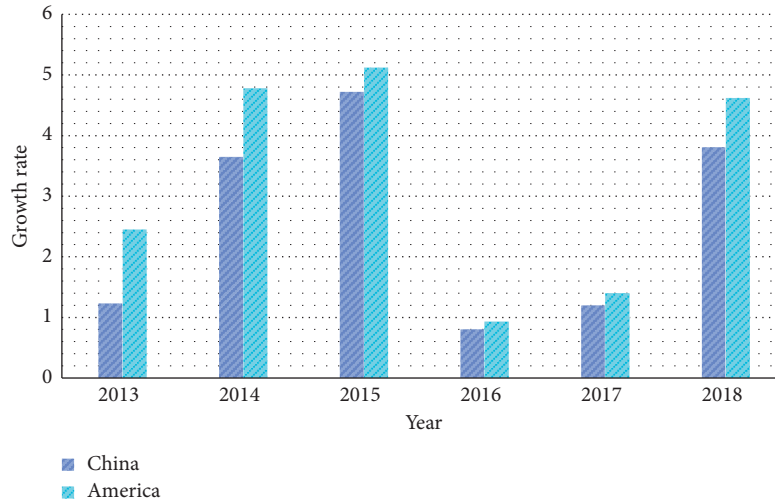
FIGURE 3: Change of GDP growth rate from 2013 to 2018.
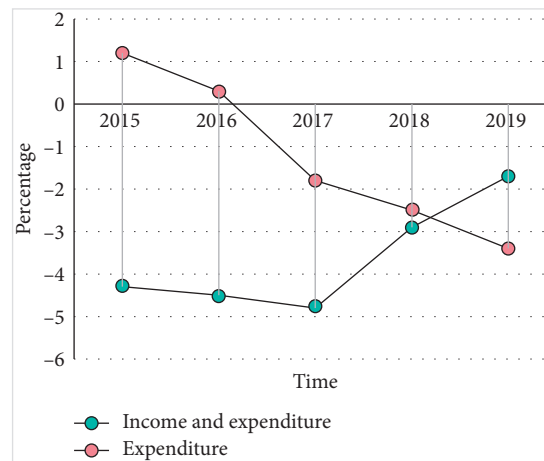
FIGURE 4: Current account revenue and expenditure and government expenditure in China.

5. Conclusions

With the rapid development of China's economy, the financial industry plays an increasingly important role in the national economy. Commercial banks account for nearly 92% of the total assets of China's financial industry. They are responsible for the implementation of macrocontrol of the national economy and the rational allocation and flow of social resources. On the one hand, they will also play a particularly critical role. However, due to historical reasons and its own problems, coupled with economic globalization, China's economic activities are more and more affected by international financial activities. Therefore, China's commercial banks are facing a variety of financial risks. The biggest risks faced by commercial banks include credit risk, market risk, and operational risk. Financial risk management is based on different technologies and methods. Therefore, appropriate methods and strategies should be adopted to manage and evaluate financial risks so as to ensure financial security, maintain finance in a relatively safe and stable environment, improve economic efficiency, and ensure that commercial banks can better serve the economy and society.

Convention is a key concept in the theory of evolutionary economics. A contract is a company's ability to be sensitive to the external environment and to anticipate changes in the external environment. Its application is "procedural" and usually automatic. It is the basis for companies or other types of organizations to engage in financial activities and to de0termine their behavior in a particular activity. The performance of a business or institution should be determined in accordance with its own practices and the practices of other institutions and financial sectors. The self-organization of the evolution of the vague system of the degree of financial risk of commercial banks is also based on contracts; the innovation strategy and the implementation of various innovation policies, management procedures, incentive policies, and corporate culture are the financial banking system contracts.

In the evolution process of complex system, the structure of the system as a whole is always adjusted under the influence of internal and external fluctuations. However, when the internal and external fluctuations represented by microfluctuations are formed, they are related to integrity

and initiative. According to the cross-action and mutual correlation, it violates the overall limitation of the initial structure of the system. When it changes greatly, it promotes the instability of the initial structure of the system and inevitably leads to the qualitative change of the overall structure of the system. In this process of frequent mutation, it may be caused by an incentive caused by internal fluctuations, or it may be caused by an invasion caused by external fluctuations. In the process of transformation, the reasons for the quantitative and qualitative changes of the system are also ambiguous.

Data Availability

No data were used to support this study.

Conflicts of Interest

The authors declare that they have no conflicts of interest.

References

[1] D. J. Lee, P. Recabal, D. D. Sjoberg et al., "Comparative effectiveness of targeted prostate biopsy using magnetic resonance imaging ultrasound fusion software and visual targeting: a prospective study," *Journal of Urology*, vol. 196, no. 3, pp. 697–702, 2016.

[2] J. Su and E. Furman, "A form of multivariate Pareto distribution with applications to financial risk measurement," *Astin Bulletin*, vol. 47, no. 1, pp. 331–357, 2015.

[3] G. K. Robinson, "Practical computing for finite moment log-stable distributions to model financial risk," *Statistics and Computing*, vol. 25, no. 6, pp. 1233–1246, 2015.

[4] A. Wong and B. Carducci, "Do sensation seeking, control orientation, ambiguity, and dishonesty traits affect financial risk tolerance?" *Managerial Finance*, vol. 42, no. 1, pp. 34–41, 2016.

[5] W.-C. Chiu, J. I. Peña, and C.-W. Wang, "Industry characteristics and financial risk contagion," *Journal of Banking & Finance*, vol. 50, pp. 411–427, 2015.

[6] F. J. Hsu and Y.-C. Chen, "Is a firm's financial risk associated with corporate social responsibility?" *Management Decision*, vol. 53, no. 9, pp. 2175–2199, 2015.

[7] J. S.-H. Li, A. C. Y. Ng, and W.-S. Chan, "Managing financial risk in Chinese stock markets: option pricing and modeling under a multivariate threshold autoregression," *International Review of Economics & Finance*, vol. 40, pp. 217–230, 2015.

[8] H. Al-Tamimi, H. Miniaoui, and W. Elkelish, "Financial risk and islamic banks' performance in the gulf cooperation council countries," *The International Journal of Business and Finance Research*, vol. 9, no. 5, pp. 103–112, 2015.

[9] M. C. Rumpf, R. G. Lockie, J. B. Cronin, and F. Jalilvand, "Effect of different sprint training methods on sprint performance over various distances," *Journal of Strength and Conditioning Research*, vol. 30, no. 6, pp. 1767–1785, 2016.

[10] E. Y. Chan and N. U. Saqib, "Online social networking increases financial risk-taking," *Computers in Human Behavior*, vol. 51, no. OCT, pp. 224–231, 2015.

[11] S. H. Hwang, D. U. Park, and C. S. Yoon, "Levels of airborne biological agents and related factors in indoor environments of fish toxicity laboratory," *Human and Ecological Risk Assessment: An International Journal*, vol. 23, no. 7, pp. 1553–1563, 2017.

[12] M. Kannadhasan, S. Aramvalarthan, S. K. Mitra, and V. Goyal, "Relationship between biopsychosocial factors and financial risk tolerance: an empirical study," *Vikalpa: The Journal for Decision Makers*, vol. 41, no. 2, pp. 117–131, 2016.

[13] J. Prades, B. Varghese, C. Reano et al., "Multi-tenant virtual GPUs for optimising performance of a financial risk application," *Journal of Parallel & Distributed Computing*, vol. 108, pp. 28–44, 2016.

[14] Y. V. Bodyanskiy, O. K. Tyshchenko, and D. S. Kopaliani, "Adaptive learning of an evolving cascade neo-fuzzy system in data stream mining tasks," *Evolving Systems*, vol. 7, no. 2, pp. 107–116, 2016.

[15] S. D. Nguyen, Q. H. Nguyen, and S.-B. Choi, "Hybrid clustering based fuzzy structure for vibration control - Part 1: a novel algorithm for building neuro-fuzzy system," *Mechanical Systems and Signal Processing*, vol. 50-51, pp. 510–525, 2015.

[16] K. Zhang, B. Jiang, P. Shi, and J. Xu, "Analysis and design of robust," *Institute of Electrical and Electronics Engineers Transactions on Cybernetics*, vol. 45, no. 7, pp. 1225–1235, 2015.

[17] X. Li, L. Chen, and J. Wang, "Fuzzy system and Improved APIT (FIAPIT) combined range-free localization method for WSN," *Ksii Transactions on Internet & Information Systems*, vol. 9, no. 7, pp. 2414–2434, 2015.

[18] K. Wu and Q. Nan, "Information characteristics, processes, and mechanisms of self-organization evolution," *Complexity*, vol. 2019, no. 2, pp. 1–9, 2019.

[19] J. Barbosa, P. Leitão, E. Adam, and D. Trentesaux, "Dynamic self-organization in holonic multi-agent manufacturing systems: the ADACOR evolution," *Computers in Industry*, vol. 66, no. C, pp. 99–111, 2015.

[20] S. Gundry, J. Zou, M. U. Uyar, C. S. Sahin, and J. Kusyk, "Differential evolution-based autonomous and disruption tolerant vehicular self-organization in MANETs," *Ad Hoc Networks*, vol. 25, pp. 454–471, 2015.

[21] Mills and Kevin, "Public vs. Private ownership:commercial bank subprime lending in the years prior to the 2007-2008 financial crisis," *Advances in Applied Mathematics & Mechanics*, vol. 1, no. 1, pp. 140–150, 2015.

[22] J. R. Booth, L. C. Booth, R. T. Hurst, C. B. Kendall, M. B. Gotway, and J. Liang, "insurance and specialization in commercial bank lending," *Review of Financial Economics*, vol. 13, no. 1, pp. 165–177, 2016.

[23] N. Tajbakhsh, J. Y. Shin, S. R. Gurudu et al., "Convolutional neural networks for medical image analysis: full training or fine tuning?" *IEEE Transactions on Medical Imaging*, vol. 35, no. 5, pp. 1299–1312, 2016.

[24] T. B. Bell, "Neural nets or the logit model? A comparison of each model's ability to predict commercial bank failures," *Intelligent Systems in Accounting Finance & Management*, vol. 6, no. 3, pp. 249–264, 2015.

Research Article

Factors Influencing the Allocation of Regional Sci-Tech Financial Resources Based on the Multiple Regression Model

Chengcheng Zhang (ID)

Business School, Wuxi Taihu University, Wuxi 214064, Jiangsu, China

Correspondence should be addressed to Chengcheng Zhang; zhangcc@wxu.edu.cn

This article uses a multiple regression model to evaluate the extent to which financial resources in various regions can be put into the most appropriate direction through the financial system or financial market. This paper uses the Tobit model to conduct empirical analysis on the input and output data of technology finance in multiple provinces and cities and explores the impact of various factors on technology finance efficiency from the perspective of three technology finance entities: high-tech enterprises, governments, and venture capital companies. Based on the DEA model and Malmquist index model in the data envelopment analysis method, this paper uses deap software to calculate the efficiency of agricultural science and technology resource allocation in Gansu Province and the efficiency of agricultural science and technology operation in many provinces in the western region. This paper divides the allocation of scientific and technological innovation resources into the ability to allocate scientific and technological innovation resources and the allocation efficiency of scientific and technological innovation resources. By constructing a performance evaluation system for the allocation of scientific and technological innovation resources, it is found that there are obvious differences in the ability and efficiency of scientific and technological innovation resource allocation in various regions. This paper proposes the selected efficiency evaluation method, the multiple regression model, which uses the data from 2012 to 2018 to evaluate the efficiency of the allocation of scientific and technological financial resources in my country, calculates the efficiency value of each region, and conducts a comparative analysis of provinces and regions. Research shows that, through multiple regression model analysis, the total technical efficiency of technology finance in Northeast China rose from 0.759 fluctuations in 2012 to 0.922 in 2018, gradually reducing the difference with the eastern and western regions. The overall promotion plays a significant role. The innovation of this article lies in the use of multiple regression models to analyze the factors affecting the allocation of regional scientific and technological financial resources, aiming to improve the efficiency of financial resource allocation.

1. Introduction

The research in this article aims to improve the efficiency of the allocation of scientific and technological financial resources and to provide suggestions for the efficient development of technological innovation, financial innovation, and the combination of technology and finance in my country. The science and technology financial system is a complex whole, and the input and output indicators have a large correlation effect. Increasing financial investment in science and technology can effectively promote the development of science and technology. But, as a developing country, how to improve the efficiency of scientific and technological financial output is the primary issue considered by governments at all levels. Therefore, this article explores the impact of various factors on the efficiency of science and technology finance from the perspectives of three technological finance entities, high-tech enterprises, governments, and venture capital companies, and studies how to use the least investment in science and technology to obtain the largest transformation of scientific and technological achievements, which is important for further improving China's science and technology. The allocation of financial resources has great practical significance.

On the macrolevel, foreign scholars are mainly concerned with the guiding role of scientific and technological policy support in the allocation of scientific and technological resources. In the horizontal and vertical directions, the current situation and effects of the allocation of scientific and technological resources have been explained in detail. Through empirical comparative analysis, Lashkari pointed out that the differences in technology policies and technological evolution between Italy and Germany are the main factors that cause the differences in the allocation of scientific and technological resources and the different scientific and technological systems between the two countries [1]. Mia found through research that factors such as per capita GDP and financial market development are in direct proportion to the country's investment in science and technology. From a micro point of view, it mainly takes enterprises as the research object and discusses the factors that affect the allocation of scientific and technological resources of enterprises from multiple angles [2]. Cyril built a multilevel decision-making model on the basis of the problem of R&D resource allocation for hierarchical organization in 1981. The essence is to provide a theoretical basis, so that enterprises can better analyze the strategy of scientific and technological resource allocation [3].

At present, the production cost of agricultural production is on the rise. Therefore, agricultural technology can help reduce the cost of agricultural development. Agricultural enterprises, colleges and universities, and agricultural scientific research institutions are the three main subjects of agricultural scientific and technological innovation in China, and they are also the main research objects for the allocation of agricultural scientific and technological resources. Gao used the BCC model of the DEA method to measure the allocation efficiency of agricultural science and technology resources in 31 provinces and cities and analyzed its comprehensive efficiency, technical efficiency, and scale efficiency [4]. Xu used the superefficiency DEA model and the Malmquist index method to calculate and analyze the allocation efficiency of agricultural science and technology resources in 12 western provinces (cities), including Ningxia, from 2008 to 2013. The ratio analysis method is the ratio of input to output. It is generally used for the efficiency of single-output and single-input systems. It is not applicable to the study of multiple inputs and multiple outputs [5]. Li people use statistical analysis to measure the efficiency of resource allocation using parameter methods, including cluster analysis and principal component analysis, mainly for the efficiency of multiple inputs and multiple outputs, and standardize the weights of various indicators to compensate for the ratio analysis the lack of law [6].

Based on the relevant theories and literature reviews of technology finance, this paper selects various input indicators and output indicators that reflect the level of local technology finance. Before the DEA model test, the SPSS software principal component analysis method is used to analyze the various input indicators and output indicators. Correlation analysis of indicators ensures the validity of the data used for DEA efficiency evaluation. A comprehensive performance evaluation system for the allocation of

scientific and technological innovation resources has been constructed. Domestic evaluations on the allocation of scientific and technological innovation resources mostly focus on "quantity" or "efficiency". A few studies use empirical methods to combine the two for comparative analysis and objectively reflect the specific differences between regions.

2. Influencing Factors of Regional Technology and Financial Resource Allocation Based on Multiple Regression Models

2.1. Multiple Regression Models in the Allocation of Regional Technology and Financial Resources

2.1.1. DEA Basic Model. Linear programming is the basic idea of the DEA method. By determining the input and output of the selected decision-making unit, the optimization variable is determined as the weight of each input and output, and finally, the efficiency frontier including all the decision-making units is established. Decision-making units that are on the frontier of efficiency are called DEA effective decision-making units. Decision-making units that do not fall on the frontier of efficiency are called decision-making units that are not DEA effective or DEA ineffective. You can adjust input and output by adding slack variables. Out, the decision-making unit DEA is reimplemented to be effective [7, 8].

The DEA method has no special requirements on the input-output function form and decision-making unit and does not need to know the functional relationship between the input and output in advance. It can avoid the deviation of evaluation due to the wrong function setting and is suitable for decision-making units with more complicated relationships. Efficiency evaluation: at the same time, the DEA method is not affected by different data units and is more convenient in data processing. Therefore, this paper uses the DEA method to evaluate the efficiency of technology finance [9, 10]. The DEA basic model includes the CCR model and BCC model, and then, this article will briefly introduce them.

(1) BCC Model. The abovementioned CCR model is realized under the assumption that the return to scale of the decision-making unit is unchanged, and in real life, the decision-making unit is more in the production state of the change of scale return. Assuming that the return to scale of the production unit is variable, it is called the BCC model. Because the change of production scale always affects the important premise of return to scale, the three scholars have continuously optimized the assumptions of the CCR model. Based on the variability of return to scale, the BCC model was established and the function Shepherd was introduced for the first time to divide the technical efficiency. For pure technical efficiency and scale efficiency, it successfully avoided the evaluation result of return to scale on technical efficiency [11, 12]. The efficiency value obtained under the CCR model is divided by the efficiency value under the BCC model to obtain the scale efficiency value. It is explored

whether the return to scale of each production unit is increasing, decreasing, or fixed.

Common BCC model functions are as follows:

$$\left\{ \sum_{j=1}^{n} \lambda_j Y_j \geq Y_0, \sum_{j=1}^{n} \lambda_j = 1, \sum_{j=1}^{n} \lambda_j Y_j \leq \theta X_0, \quad j = 1, 2, \ldots, n, \right.$$

$$(1)$$

where X_0 represents the input items of the decision-making unit and Y_0 represents the output items of the decision-making unit. λ represents the ratio of the newly constructed effective decision-making unit to the original decision-making unit. In this linear programming model, θ represents the efficiency value of the decision-making unit, that is, the effective value of X input items relative to Y output items in the production unit, the degree of utilization [13, 14].

(2) Construction of an Index System. The composition of scientific and technological finance efficiency indicators studied in this paper is divided into input indicators and output indicators. Combined with the actual problems of the study, the following indicators are selected after screening: The selection of scientific and technological financial input indicators considers the input of human, financial, and material resources. In terms of human input elements, it mainly examines the input of personnel engaged in R&D activities. This article selects the indicator R&D personnel full-time equivalent; the financial input elements mainly include government support, enterprise R&D input, and other research funding input, considering the availability and authority of data. This article selects the indicators of local fiscal expenditures on science and technology; the material input element mainly refers to the investment of enterprises in fixed assets, so this article selects the indicator of new fixed assets in high-tech industries.

Compared with the selection of input elements, the definition of scientific and technological achievements output indicators is more controversial. This article draws on the research of previous scholars and proposes to consider both direct output and indirect output [15, 16]. Direct output refers to the direct technical output and the contract value of the market for the selected index technology; indirect output refers to the output through the transformation of technological achievements, the main business income of the index high-tech industry, the sales income of new products, and the gross domestic product.

2.1.2. Tobit Regression Model. The Tobit regression model is a kind of dependent variable restricted model, based on the assumption of normal distribution. Its characteristic is that the dependent variable is restricted, and some values cannot be obtained or are fragmented values. The scientific and technological financial efficiency value obtained by DEA analysis is between 0 and 1. If the ordinary least square method (OLS) is used for regression, then the parameter estimate will be biased towards 0, and the Tobit model can solve this problem well [17, 18]. Therefore, in this paper, the total technical efficiency value of science and technology

finance is used as the explained variable, a standard Tobit model is established, and the intercept point at the left end is set to 0. The formula is as follows:

$$Y_t^* = a_t + \sum_{j=1}^{r} \beta_j X_{tj} + \varepsilon_t \quad t = 1, 2, \ldots, n; \; j = 1, 2, \ldots, r,$$

$$Y_t^* = \begin{cases} Y_t^*, & \text{if } Y_t^* \geq 0, \\ 0, & \text{if } Y_t^* \leq 0. \end{cases}$$

$$(2)$$

Among them, Y_t^* is the efficiency of science and technology finance, n is the number of regions, and r is the number of factors affecting the efficiency of science and technology finance.

2.1.3. Malmquist Index Model. The Malmquist (TFP) index was established to examine the changes in productivity in the two periods. The Malmquist index can analyze multi-input and multioutput panel data [19, 20]. When the return to scale is variable, the technical efficiency change index can be further decomposed into a pure technical efficiency index and a scale efficiency index. Thus, the Malmquist index (TPP) can be decomposed into a technical progress change index, a pure technical efficiency change index, and a scale efficiency index 3 part, namely,

$$\text{TFP} = \text{Tech} \times \text{Pech} \times \text{Sech}. \quad (3)$$

When the Malmquist index TFP >1, it means that total factor productivity is on the rise; when TFP = 1, it means that total factor productivity remains unchanged; and when TFP <1, it means that total factor productivity is on the decline.

2.2. Fiscal Decentralization and Technological Innovation Resources. Government financial investment in science and technology can stimulate the enthusiasm of enterprises in the allocation of scientific and technological innovation resources and has a positive role in promoting technological innovation.

2.2.1. Analysis of the Impact Mechanism of Fiscal Decentralization on Scientific and Technological Resources. Under the current fiscal decentralization system, local governments are agents of the central government in the localities, and they assume most of the rights and obligations within their jurisdictions. With this kind of principal-agent relationship, on the one hand, the local government can be regarded as a community of interests, pursuing more financial power and power, and the degree of fiscal decentralization tends to expand; on the other hand, local government behavior is dominated by local officials and officials under the existing decentralization system; this behavior is affected by the promotion mechanism of officials [21, 22]. It can be said that the existing promotion mechanism largely influences the behavior of local governments. Based on existing theories and literature research, the influence of local governments on scientific and technological

innovation resources stems from two factors: fiscal decentralization and the promotion mechanism of officials. These two systems have different concepts but influence each other.

(1) Fiscal decentralization affects government behavior. When local governments have a high degree of fiscal decentralization, the marginal cost of increased fiscal decentralization is huge. At the same time, competition among local governments forces local governments to improve government behavior and increase the supply of public products, strengthening the resources of scientific and technological innovation. Investment in turn leads to the improvement of the ability of local scientific and technological innovation resource allocation [23, 24]. The low level of fiscal decentralization of local government, local governments in pursuit of more financial power and the executive power, pays more attention to short-term interests, while ignoring the supply of public goods. The degree of fiscal decentralization can be measured by constructing a fiscal decentralization index based on data.

(2) The promotion mechanism of officials will affect the behavior of local governments. When the promotion mechanism uses "GDP" as the evaluation standard, local government officials have to abandon the goal of equalization of public services and instead invest more resources in the region into economic construction and participate in the "GDP evaluation" competition. When the promotion mechanism pays more attention to the provision of technological innovation resources, local government officials will pay more attention to technological innovation, adjust government behavior, and adapt to the central strategic goals. Similar local officials' efforts for promotion can be approximated by the proportion of foreign direct investment in GDP.

(3) Official promotion mechanism and fiscal decentralization affect each other. When one factor exceeds another, it will produce a substitution effect. When regions compete with GDP as the core, fiscal decentralization will have a negative effect on the allocation of scientific and technological innovation resources.

2.2.2. The Relationship between the Local Government and Each Subject of Regional Technological Innovation

(1) The Relationship between Local Governments and Technological Innovation Enterprises. Under the conditions of a socialist market economy, enterprises and governments are both the main economic and social activities, and the two are distinguished from each other and related to each other, especially in the field of technological innovation. In the field of taxation, the enterprises in the jurisdiction are the main taxpayers, and any changes in the fiscal and taxation policies of the local government will affect the operation of the enterprises; in the market field, the relationship between the supervision and the supervision of the enterprises and the government in the jurisdiction is as in [25]. As the main body of scientific and technological innovation activities, enterprises themselves have spillover effects and the influence of R&D uncertainty and require government policy support and financial support.

In the factor analysis model, science and technology innovation enterprises and the government exist as the second principal component, and the explanation strength of the regional science and technology innovation resource allocation ability is more than 40%. In the specific factor loading matrix, the correlation between science and technology innovation enterprises and the government reaches more than 70%. At the same time, the government has taken the initiative to improve the supply of public products and public services, build Internet-type infrastructure, and introduce foreign direct investment to build a good macro-environment for the technological innovation of enterprises [26]. In addition, the government builds a technology market, introduces market competition mechanisms into the technology market, improves the resource allocation capabilities of technological innovation enterprises, and reduces transaction costs.

(1) The relationship between local government and scientific research institutions and universities: scientific research institutions and universities, as the first main component to measure the ability of regional scientific and technological innovation resource allocation, are also affected by local governments. First of all, local governments are important providers of R&D funds and talent fosterers for scientific research institutions and universities. According to research, among the executive bodies of local government investment in science and technology, scientific research institutions and high implementation funds reach 50%, and local governments are also the main providers of educational resources. Second, the local government is the builder of the industry-university-research system, effectively reducing the information asymmetry between research universities and the market. Finally, local governments are also major investors in industrial projects and have a guiding role for enterprises, scientific research institutions, and universities.

2.3. Factors Affecting the Efficiency of Regional Financial Resource Allocation

2.3.1. Economic Basis. The economic foundation is the material carrier and service object of the financial configuration subject. The basic function of finance is to act as an intermediary between the surplus party and the demander through products and services. The emergence and development of financial institutions are inseparable from the needs of financial communication in the real economy. The economic foundation determines the mode, scope, and

activity of the financial market. The economic foundation generally includes two parts: economic scale and economic structure. Economic scale represents the output capacity of all enterprises in the economy and reflects the overall economic strength of all economic sectors in the region. In regions with strong overall economic strength, the internal operating efficiency of each economic sector is relatively high, and the sustained profitability is better. To ensure a good repayment ability, the moral hazard is relatively low, and the increase in the scale and strength of the economy is conducive to curbing the generation of nonperforming assets.

2.3.2. Degree of Financial Marketization. Financial marketization can reduce the excessive control imposed on financial activities and make the behavior of financial resource allocation subjects more autonomous. Financial institutions will engage in financial activities in accordance with market-based operating mechanisms. In order to meet welfare needs to the greatest extent, each entity can make highly sensitive and efficient allocation decisions based on their own rational behaviors, which will gradually attract investment and financing. Channels refine the division of labor in the financial market and meet the needs of financiers' financial resources in a variety of ways, while fully mobilizing investors' financial resources, reducing capital costs, and improving the efficiency of financial resource utilization.

3. Influencing Factors of Regional Scientific and Technological Financial Resource Allocation Based on the Multiple Regression Model

3.1. Evaluation Methods and Data Collection for the Allocation Efficiency of Scientific and Technological Innovation Resources. As the current mainstream efficiency evaluation method, DEA can incorporate multiple inputs and multiple outputs into the evaluation system while effectively avoiding the influence of dimensions. However, its shortcomings are also very obvious. It can only evaluate the relative efficiency in the current system. The evaluated efficiency value is greatly affected by the number of input and output items. In addition, the effective efficiency value cannot be effectively distinguished. Based on this, this paper uses the data on the allocation of scientific and technological resources in 29 provinces and cities and builds the Malmquist index based on the DEA analysis method, which decomposes total factor productivity into a comprehensive efficiency change index and a technical efficiency change index. Using provincial data, the Malmquist index is constructed based on the DEA-CCR model to analyze the changes in the efficiency of provincial scientific and technological resource allocation and influencing factors.

Based on learning and reference, this paper constructs an evaluation system for the allocation efficiency of scientific and technological innovation resources. The M index based on DEA can have a more horizontal and vertical comparison of the allocation of regional scientific and technological resources, and Malmquist can also reflect changes in the internal structure.

3.2. Index System of the Allocation Efficiency of Scientific and Technological Innovation Resources. "Efficiency" refers to the effective use of resources under given constraints (time, space, structure, etc.). The allocation efficiency of scientific and technological innovation resources is also within its scope. It is an expression of the input-output ratio, which can be understood as a cross-sectional efficiency, which has very important practical significance for optimizing the stock structure and effectively increasing the increment. It is the evaluation of the input-output ratio. When constructing the local scientific and technological resource allocation efficiency index, the common methods of economics are still used and the requirements of objectiveness, availability, comparability, science, and system are combined.

3.3. Research Methods. This paper uses the vector autoregressive model to empirically analyze the relationship between my country's fiscal decentralization and the allocation of scientific and technological innovation resources, so as to locate the financial and administrative powers of local governments when dealing with technological innovation. The process of using the VAR model is to first perform a unit root test on the original data, which is a stationarity test, establish the vector autoregressive model and Granger causality test, and analyze the impulse response and variance decomposition analysis of each variable in the model. The relationship between fiscal decentralization and the efficiency of scientific and technological resource allocation is obtained.

4. Experimental Research and Analysis of Factors Affecting the Allocation of Regional Scientific and Technological Financial Resources Based on Multiple Regression Models

4.1. Analysis of the Total Technical Efficiency of Regional Technology Finance Based on the Multiple Regression Model. To facilitate analysis, this paper divides the 24 provinces and cities in the data sample into eastern, central, western, and northeastern regions. The eastern region includes Beijing, Tianjin, Shanghai, Hebei, Shandong, Jiangsu, Zhejiang, Fujian, and Guangdong, the central region includes Shanxi, Henan, Hubei, Anhui, Hunan, and Jiangxi Provinces, the western region includes Inner Mongolia Autonomous Region, Shaanxi Province, Chongqing City, Sichuan Province, Guizhou Province, Yunnan Province, and the northeast region includes Heilongjiang Province, Jilin Province, and Liaoning Province.

It can be found from Table 1 and Figure 1 that, in 2018, the total technical efficiency of science and technology finance in various regions of China was between 0.85 and 0.98, and the total technical efficiency of eastern and western regions was the same, maintaining a high efficiency level of

TABLE 1: The total technical efficiency (TE) of my country's sub-regional technology finance from 2012 to 2018.

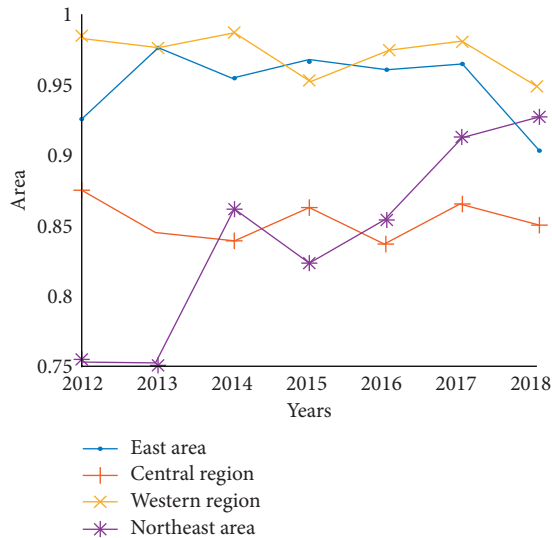|	2012	2013	2014	2015	2016	2017	2018
East area	0.925	0.975	0.954	0.966	0.960	0.964	0.902
Central region	0.875	0.846	0.837	0.863	0.836	0.864	0.850
Western region	0.983	0.976	0.986	0.951	0.973	0.981	0.949
Northeast area	0.753	0.752	0.861	0.823	0.855	0.912	0.926

FIGURE 1: From 2012 to 2018, my country's subregional technology finance total technical efficiency trend (TE).

0.95; the total technical efficiency of the central region declined first and then increased. It declined slightly from 2012 to 2018 and rose slowly from 2015 to 2018. The overall efficiency level fluctuated around 0.85; the most outstanding performance was the total technical efficiency of technology and finance in Northeast China. The fluctuation increased from 0.759 in 2012 to 0.922 in 2018, gradually reducing the difference with the eastern and western regions, which played a significant role in the overall improvement of the overall technical efficiency of China's technology finance.

4.2. Analysis of the Average Malmquist Index in Each Region.
According to my country's current economic region classification method, the average Malmquist index of each region can be shown as in Figure 2.

Figure 2 shows that the eastern region has the highest allocation efficiency of scientific and technological innovation resources, and its ability to allocate scientific and technological resources is also at the forefront of the echelon. The northeastern region is China's traditional old industrial base. Due to the transfer of the national strategic center, its ability to allocate innovative resources is affected by "genetic genes," but it has shown a good overall ability in the allocation efficiency of scientific and technological innovation resources. The high-quality flow and stock that transform this efficiency can be used to revitalize the northeast and supply-side reforms and lay a foundation; the central and
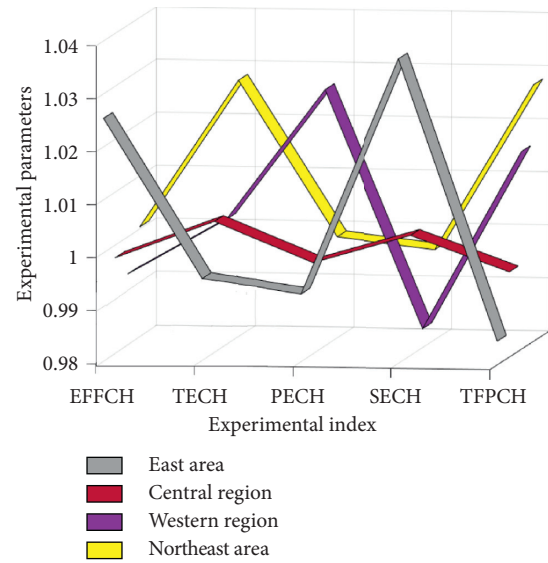
FIGURE 2: Average Malmquist index by region.

western regions have little difference in the efficiency of the allocation of scientific and technological innovation resources. At the same time, due to the small number of provinces in the central region, this averaging form of expression conceals the inadequacy of the efficiency of allocation of scientific and technological innovation resources in individual regions.

4.3. DEA Super Efficiency Analysis.
As explained in the previous article, the traditional DEA model method can divide all DMUs into two groups. One group is at the frontier of efficiency with an efficiency value of 1; the other group is relatively inefficient with an efficiency value of less than 1. This method cannot compare effective decision-making units, and the SDEA superefficiency model can make up for the shortcomings. This article will use EMS measurement software to evaluate the superefficiency of regional financial resource allocation in my country from 2015 to 2017. For the inefficient DMU, its efficiency value is the same as the traditional DEA calculation result, so this article will not repeat it. For the effective DMU under the DEA model, its superefficiency value is different from the DEA model. The superefficiency of the relatively better decision-making unit is greater. After excluding the inefficient areas, the superefficiency calculation results are shown in Figure 3.

Beijing, Tianjin, Shanghai, and Zhejiang have been at the forefront of efficiency in all or some of the years during the inspection period. These four regions are basically the regions with the richest financial resources and relatively high degree of financial marketization in China. With the continuous deepening of economic system reform and the continuous improvement of the financial system, some positive changes have occurred in various regions. Among them, Beijing and Zhejiang have been the most efficient regions in the allocation of financial resources in the three years from 2015 to 2017. The efficiency values of Tianjin and
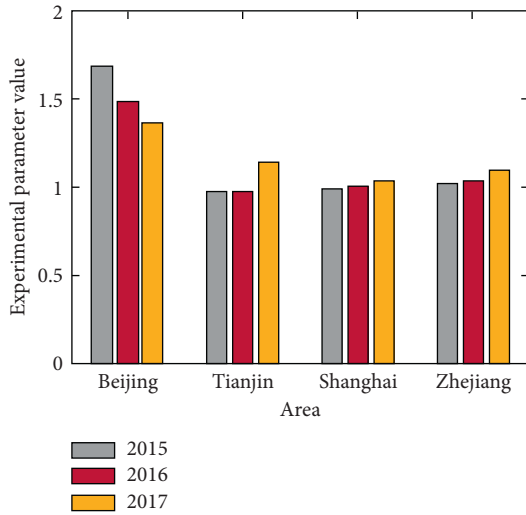
Figure 3: Regional superefficiency values from 2015 to 2017.

Shanghai have increased year by year from about 0.98 in 2015, and they are ultimately at the forefront of efficiency. Tianjin's efficiency value improved most significantly in 2017. This may be related to the State Council's promotion of the development and opening up of the Binhai New Area. Tianjin has made beneficial attempts in financial business, financial market, and financial opening reforms. Beijing has the highest allocation efficiency in three years. The efficiency value in 2017 was 1.3699, which means that even if the investment is increased by 37%, Beijing can still remain relatively effective in all regions. In the same way, other regions can also increase the corresponding amount of input to obtain the development of the financial sector and the national economy, while maintaining a higher efficiency of resource allocation.

4.4. Evaluation of the Allocation Efficiency of Agricultural Science and Technology Resources in Gansu Province under the Constant Return to Scale. The analysis in Figure 4 shows that, from 2011 to 2016, the total factor productivity of agricultural science and technology operations in Gansu Province dropped by an average of 9.5%. The main reason was the decline in the technological progress index because the technological progress index dropped by 5% and its comprehensive the average efficiency has increased by 7.1%. The experimental results are shown in Figure 4.

As can be seen from Figure 4, judging from the changes in the Malmquist index, during the six years from 2011 to 2016, Gansu Province's total factor productivity increased for three years, namely, 2011-2012, and the total factor productivity of Gansu's agricultural science and technology resource allocation increased by 22.3 from 2015 to 2016%; the increase was caused by the simultaneous increase of the
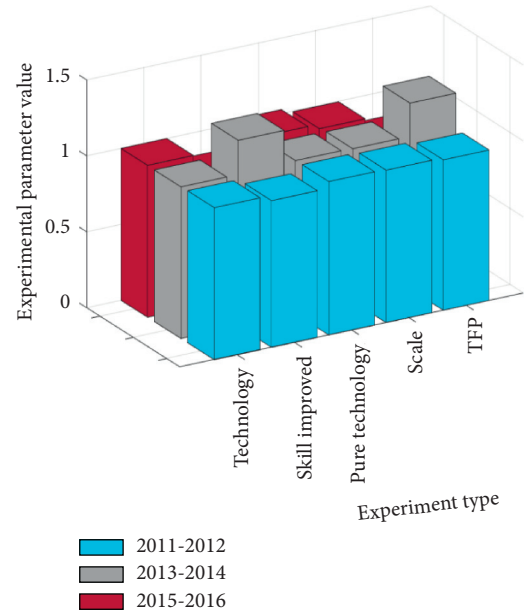
Figure 4: Changes in total factor productivity of agricultural science and technology in Gansu Province from 2022 to 2016.

technical efficiency and technical progress index. Its technical efficiency was 1, and the technical progress index increased by 22.3%, mainly due to the increase of the technical progress index.

5. Conclusions

In the construction of the evaluation system for the allocation efficiency of scientific and technological innovation resources, this paper finds that the "leading" position of the eastern region's scientific and technological innovation resource allocation ability and efficiency is stable; although the central region has a strong ability to allocate scientific and technological innovation resources, its pure technical efficiency index (PECH) is less than 1, there is no such capacity and incremental capacity to convert into efficiency, and there is a waste of scientific and technological innovation resources. The ability to allocate scientific and technological innovation resources in the western and northeastern regions is not reflected in the stock. In the scientific and technological innovation resource allocation efficiency evaluation system, the pure technical efficiency index (PECH) of the two regions is relatively high and the "catch-up effect" is obvious.

From 2011 to 2016, my country's overall technological and financial development level has steadily increased, but the distribution among regions is extremely uneven. The technological and financial development level of the eastern region is much higher than that of the central, western, and northeastern regions. From the perspective of the input and

output level of technology finance, China's technology finance investment is growing rapidly in total, but there is still a big gap between the input speed of technology finance and the speed of social and economic development. The conversion situation is not satisfactory. From the perspective of the development of high-tech industries, the scale of my country's high-tech industries continues to expand and R&D funding and personnel inputs continue to increase, but the transformation of scientific and technological achievements is not optimistic. Generally speaking, my country has a vast territory, and the development of technology and finance still has problems such as unbalanced resource distribution, unbalanced industry distribution, and mismatched input and output. The developed eastern coastal areas have good economic levels, developed high-tech industries, and high-tech financial development, while the economically underdeveloped areas such as the central and western regions have relatively slow development of scientific and technological finance, and the conversion rate of scientific and technological achievements is low.

This paper uses the Malmquist index model to calculate the total factor productivity of agricultural science and technology resource allocation in Gansu Province from 2011 to 2016 and analyzes its decomposition value. Under the condition of constant returns to scale, from 2011 to 2016, from the overall analysis, the total factor productivity of agricultural science and technology resource allocation in Gansu Province was in a state of decline, down by 9.5%. This was caused by the decline in the technological progress index because its the technical progress index dropped by an average of 5%, while the average comprehensive technical efficiency increased by 7.1%. With constant returns to scale, the main reason for the decline in total factor productivity of agricultural science and technology operations in Gansu Province is the decline in the technological progress index. Therefore, in general, the low efficiency of agricultural science and technology resources in Gansu Province is mainly caused by the low level of agricultural science and technology in the province. The innovation of this article lies in the use of multiple regression models to analyze the factors affecting the allocation of regional scientific and technological financial resources, aiming to improve the efficiency of financial resource allocation.

There are still shortcomings in the research of this paper. Due to the limitations of funds and materials, the coverage of the research data in this paper is not wide enough and the representativeness of the data is not strong enough. Future research can also analyze the factors affecting technology finance from different fields such as agriculture, industry, and manufacturing.

Data Availability

No data were used to support this study.

Conflicts of Interest

The authors declare that they have no conflicts of interest.

References

[1] M. Lashkari, "Designing a financial resource allocation model fo board of trustees medical centers using goal programming approach: case study of Afzalipour medical centers 2011–2014," *Journal of Technology Management & Innovation*, vol. 1, no. 4, pp. 10–21, 2006.

[2] M. A. Mia, S. Nasrin, and Z. Cheng, "Quality, quantity and financial sustainability of microfinance: does resource allocation matter?" *Quality & Quantity*, vol. 50, no. 3, pp. 1285–1298, 2016.

[3] C. Tomkins, "Corporate resource allocation: financial, strategic and organizational perspectives," *British Journal of Psychiatry the Journal of Mental Ence*, vol. 203, no. 2, pp. 126–131, 1991.

[4] J. Gao, J. Campbell, and C. A. K. Lovell, "Equitable resource allocation and operational efficiency evaluation," *International Journal of Healthcare Technology and Management*, vol. 7, no. 1/2, pp. 143–167, 2006.

[5] Y. Xu, J. Zhang, and M. Pinedo, "Budget allocations in operational risk management," *Probability in the Engineering and Informational Sciences*, vol. 32, no. 3, pp. 434–459, 2018.

[6] L. X. Chen, "A study on financial resources allocative efficiency in the context of Internet finance-based on long tail theory," *Business & Globalization*, vol. 03, no. 4, pp. 75–80, 2015.

[7] C. A. Maritan and G. K. Lee, "Resource allocation and strategy," *Journal of Management*, vol. 43, no. 8, pp. 2411–2420, 2017.

[8] M. Nirmala, J. Cindhamani, P. Naguboyina et al., "Effective resource allocation in cloud computing using virtualization technique," *International Journal of Pharmacy and Technology*, vol. 8, no. 4, pp. 25938–25943, 2016.

[9] H. G. Villasanti and K. M. Passino, "Feedback controllers as financial advisors for low-income individuals," *IEEE Transactions on Control Systems Technology*, vol. 25, no. 6, pp. 2194–2201, 2017.

[10] B. Z. Khan, "The impact of war on resource allocation: "creative destruction", patenting, and the American civil war," *The Journal of Interdisciplinary History*, vol. 46, no. 3, pp. 315–353, 2015.

[11] J. L. Bower, "Managing resource allocation: personal reflections from a managerial perspective," *Journal of Management*, vol. 43, no. 8, pp. 2421–2429, 2017.

[12] S.-J. Kim and I. Kwon, "On a focusing-balancing dilemma in SMEs," *Academy of Management Proceedings*, vol. 2017, no. 1, p. 17630, 2017.

[13] G. Sanjeev and V. Adrien, "Attack, defence, and contagion in networks," *Review of Economic Studies*, vol. 81, no. 4, pp. 1518–1542, 2015.

[14] A. W. Ng, W. M. Wang, B. C. F. Cheung, R. Ma, and Y. Y. Or, "Cluster-based performance measurement system for emerging technology-based ventures," *International Journal of Entrepreneurship and Innovation Management*, vol. 21, no. 6, pp. 485–508, 2017.

[15] K. L. Ross, Y. A. Zereyesus, A. Shanoyan et al., "The health effects of women empowerment: recent evidence from northern Ghana," *International Food & Agribusiness Management Review*, vol. 18, no. 1, pp. 127–144, 2015.

[16] C. Mayer, R. Felkel, and K. Peterson, "Best practice on automated passenger flow measurement solutions," *Journal of Airport Management*, vol. 9, no. 2, pp. 144–153, 2015.

[17] M. Dabbagh, B. Hamdaoui, M. Guizani, and A. Rayes, "Toward energy-efficient cloud computing: prediction,

consolidation, and overcommitment," *IEEE Network*, vol. 29, no. 2, pp. 56–61, 2015.

[18] U. Ana, S. Leonidas, and D. Valerijonas, "Financial resource allocation in higher education," *Informatics in Education*, vol. 16, no. 2, pp. 289–300, 2017.

[19] K. Palanisami, S. Kumar, R. P. S. Malik et al., "Managing water management research analysis of four decades of research and outreach programmes in India," *Economic and Political Weekly*, vol. 26 & 27, no. 26, pp. 33–43, 2015.

[20] W. Du, "Research on levying of extending VAT tax of transportation industry based on fuzzy TOPSIS," *The Open Construction and Building Technology Journal*, vol. 9, no. 1, pp. 87–91, 2015.

[21] A. Toyin, A. Timothy, and A. Oladayo, "Explaining poverty and inequality changes in rural Nigeria," *Asian Journal of Agricultural Extension, Economics & Sociology*, vol. 5, no. 4, pp. 227–237, 2015.

[22] Y.-Y. Hong, Y.-M. Lai, Y.-R. Chang, Y.-D. Lee, and P.-W. Liu, "Optimizing capacities of distributed generation and energy storage in a small autonomous power system considering uncertainty in renewables," *Energies*, vol. 8, no. 4, pp. 2473–2492, 2015.

[23] Z. Y. Lee, G. T. R. Lin, and S. J. Lee, "Measuring dynamic operation efficiency for universal top 10 TFT-LCDs by improved data envelopment analysis," *Journal of Entific and Industrial Research*, vol. 77, no. 8, pp. 447–450, 2018.

[24] S. Polykarpou, M. Barrett, E. Oborn, T. O. Salge, D. Antons, and R. Kohli, "Justifying health IT investments: a process model of framing practices and reputational value," *Information and Organization*, vol. 28, no. 4, pp. 153–169, 2018.

[25] R. A. Layton, "Formation, growth, and adaptive change in marketing systems," *Journal of Macromarketing*, vol. 35, no. 3, pp. 302–319, 2015.

[26] M. S. Elsayed and A. H. Ali, "Performance evaluation of applying fuzzy multiple regression model to TLS in the geodetic coordinate transformation," *American Scientific Research Journal for Engineering, Technology, and Sciences*, vol. 25, no. 1, pp. 36–50, 2016.

Research Article

Application of Artificial Intelligence to Social Governance Capabilities under Public Health Emergencies

Yafang Wu [ID] [1,2] **and Shaonan Shan** [3,4]

[1] *School of Business Administration, Southwestern University of Finance and Economics, Chengdu, Sichuan 611130, China*
[2] *ICN Grande Ecole, ICN Business School, CS 70148, Nancy, 54003 Lorraine, France*
[3] *School of Urban Economics and Public Administration, Capital University of Economics & Business, Beijing 100070, China*
[4] *School of Business Management, Liaoning Vocation Technical College of Modern Service, Shenyang, Liaoning 110000, China*

Correspondence should be addressed to Yafang Wu; 217120202026@smail.swufe.edu.cn

Due to the high complexity, high destructive power, and comprehensive governance characteristics of public health emergencies, the ability of social governance has been distorted and alienated under intensive pressure, and the subjects of social governance have become lazy, professional, and politicized. There are obvious problems, such as system information leakage and information asymmetry. Based on the above background, the purpose of this article is to study the application of artificial intelligence to social governance capabilities under public health emergencies. This article focuses on the relevant concepts and content of emergency management of public health emergencies and in-depth analysis of the actual application of big data technology in epidemic traceability and prediction, medical diagnosis and vaccine research and development, people's livelihood services, and government advice and suggestions, combined with investigations. The questionnaire analysis sorted out the problems in the social emergency management of public health emergencies in China. The results showed that 87.7% of the people simply sorted out laws and regulations and higher-level documents or even repeated content and lacked summary and reflection on emergency response experience, which led to the operability of emergency plans being generally even poor. In response to the shortcomings, countermeasures and suggestions were put forward, including establishing a standard data collection mechanism, establishing a data sharing mechanism, establishing a personal privacy security protection mechanism, and promoting the breadth and depth of big data applications.

1. Introduction

Since the beginning of the 21st century, the unification of the world economy is inevitable, and all countries in the world are facing the test of frequent public emergencies. During the period of social change in China, various emergencies have occurred. The major public emergencies involve social disputes, government rule, natural disasters, environmental protection, public ethics, production safety, and other fields [1]. Emergencies are diversified, intensive, and diffuse, with significant influence and destructive power. Some major emergencies have caused severe losses to people's life and property safety and social and economic development. At this stage, China has completed a comprehensive social transformation,

and the political system, financial system, and social values have also been adjusted and changed as the reform and opening up further deepen. In the process of this great change, the accidental emergency under certain circumstances may be simply converted into frequent events, and its impact will be doubled. Ability will put forward higher requirements. This is also a very critical standard for testing the comprehensive ability and quality of leading cadres under the new historical conditions.

An effective public health emergency preparedness and response system is essential to reduce the impact of all hazardous emergencies on population health [2]. Many public health agencies seek to improve their ability to respond to large-scale events such as influenza pandemics. Quality improvement (QI) is a structured method of

improving performance, which has not been widely used in the public health field [3]. Bayleyegn et al. developed and tested a pilot QI collaboration to explore whether QI can help public health departments improve their pandemic preparedness [4]. In order to meet the needs of public health emergencies, it is suggested to strengthen the construction of emergency response teams for public health emergencies to make them professional and standardized. Hadi and Fleshler adopted advanced and mature communication technology and adopted a modular combination method to ensure the smooth flow of the communication system under public health emergencies [5]. According to the needs of public health emergencies, provincial health institutions should be equipped with emergency mobile command communication platforms, formulate standard technical protocols, ensure the interoperability of public health emergencies, and provide communication support for emergency response plans [6, 7]. Kirsch et al. analyzed the types and characteristics of public health emergencies, as well as the advantages of military hospitals in responding to public health emergencies, from strengthening military–civilian cooperation, strengthening military–civilian collaboration, and strengthening military hospitals' ability to respond to public health emergencies. It discusses and provides a reference for establishing the army's emergency response mechanism in the future [8].

Society is essentially an open, evolving, adaptive, and complex network system with coupling functions [9]. Social governance is a large and complex system project. Based on the social background of social governance innovation, Zailani et al. pointed out that the research of social sports organizations presents basic theoretical research, condition analysis, and trends in the development of social sports organizations, the model construction and mechanism analysis of social sports organizations' participation in social governance, and society in the new context, the function, status, and role of sports organizations [10]. Samra et al. proposed that the country's NGOs can serve as effective media for government assistance, supplementation of public interests, and social control to contribute to social stability and development. However, NGOs are not a panacea; they have their own troubles. An effective strategy is to take necessary measures to improve the external environment and deepen internal cultivation [11]. The development of a public welfare society is not only a sign of the modernization of national governance, but also an important carrier of social mechanisms. From the perspective of social governance innovation, there are problems such as the increase in the number of public welfare social organizations, the increase in space, and the low transparency, as well as the imbalance of coverage in the social field, and the problems of survival and development [12]. In response to existing questions, Mascarenhas et al. build a government cooperation platform, performance evaluation methods, public welfare social organizations, and management systems to ensure the healthy and orderly development of social organizations [13–15].

The main innovations of this article are as follows:

(1) We studied the components of the emergency management system, the optimization principle of the emergency management system, the control elements, and the operating model of the management system.

(2) Through questionnaire analysis, we sorted out the existing problems in the social emergency management of public health emergencies in China. We explored and optimized the emergency management system of public emergencies suitable for local governments to promote economic development.

2. Public Emergencies and Artificial Intelligence

2.1. Public Emergencies

2.1.1. Characteristics of Public Emergencies. Public emergencies have the characteristics of suddenness, publicity, harmfulness, and uncertainty.

(1) Suddenness. The so-called suddenness represents a sudden accident that cannot be expected, and this is the most basic feature [16]. If there are no apparent signs and symptoms in advance, or there are some signs, but it is challenging to complete the early warning, there will be an emergency. This function usually fails to be dealt with and dealt with by the public sector and government departments in a short period of time, resulting in specific material damage and casualties [17, 18]. What happens suddenly is caused by specific reasons and opportunities. It is a leap process from the quantity change of internal contradiction to the qualitative difference. These factors and opportunities are accidental and hidden. Therefore, it is difficult to fully predict the specific emergency situation, actual scale, specific situation, and impact depth.

(2) Publicity. The public emergency's influence and subject matter are disclosed, especially for the crisis within the scope of public management. Firstly, it may endanger public life and property; secondly, it will damage public interests and public facilities [19]; and thirdly, it will violate the influence of public order and good customs [20]. Of course, the public emergencies directly involved are not necessarily in the public domain, but attract public attention. The incidents rapidly expand and become public hot spots, causing public losses, large-scale psychological panic, and social chaos. Emergencies may occur in other places, but in an open and dynamic response social system, the perceived intense stimulation will make the masses physically and mentally nervous. They are anxious about the situation, prompting the government to mobilize considerable public resources, and orderly public organizations and coordination can be properly solved [21, 22].

(3) Harmfulness. No matter what the nature and scale of public emergencies are, they will inevitably bring political and economic losses to the country, as well as various degrees of losses to people's lives, property, and spirit [23]. The

emergency situation may completely expose the original contradictions and play a specific role in promoting social progress. However, from the analysis of social chaos, economic recession and order imbalance caused by the emergency, the negative impact is greater than the positive impact [24, 25]. On the other hand, due to the destruction of the original order and the lack of adequate countermeasures, the original order cannot be restored. The blow and collapse can also not be tolerated, resulting in social chaos and psychological uneasiness. These events have caused huge economic and life losses.

(4) Uncertainty. The sudden nature of an emergency determines that such an event is often unexpected with great uncertainty. This kind of uncertainty is not only reflected in the unpredictability of its occurrence time, location, type, and scale, but also in its development and change. The speed, direction, influence scope, and harmful results of its evolution are uncertain [26]. Therefore, if not handled properly, the incident will simply escalate and may form a serious crisis and chain reaction. The method of dealing with the uncertainty of emergency is one of the keys to the study of emergency [27, 28]. The important factor to be clear in emergency is the influence of uncertainty and the necessity of countermeasures against uncertainty [29].

2.1.2. Classification of Public Emergencies. According to the occurrence process, nature, and mechanism of public emergencies, public emergencies can be divided into the following four categories:

(1) *Natural Disasters.* They mainly include flood, drought, meteorological disaster, earthquake disaster, geological disaster, marine disaster, biological disaster, and forest and grassland fire [30].

(2) *Accident Disasters.* They mainly include safety accidents, traffic accidents, public facilities and equipment accidents, and environmental pollution and ecological damage accidents of various enterprises such as industry, mining, and commerce.

(3) *Public Health Events.* They mainly include the prevalence of infectious diseases, unexplained collective diseases, food safety and labor disasters, animal epidemics, and other events that seriously affect public health and life safety.

(4) *Social Security Incidents* [31]. They mainly include terrorist attacks, economic security incidents, and foreign-related emergencies. According to the nature, severity, controllability, and influence scope, all kinds of public emergencies can be generally divided into four levels: particularly significant, major, large, and general.

2.1.3. Emergency Management of Public Emergencies. Emergency management can be divided into peacetime and wartime, peacetime preparation and wartime correspondence. However, wartime is the core and peacetime work

needs to be carried out following wartime needs [32, 33]. The preparation work in peacetime has been done well. Only when all the work has been done well can we deal with it calmly in wartime, and all corresponding work can be carried out in an orderly and effective manner [34]. Therefore, emergency management is not only a response to public emergencies but also a large-scale, more fundamental work in peacetime, which is to make full preparations.

Due to the limited time, they have to deal with the potential danger. Otherwise, the impact of the event and the loss will tend to expand. In order to cope with these needs, various resources need to be rapidly prepared. Emergency treatment should be realized when resources are used. Various demand issues, such as resource layout and effective resource scheduling, must be considered in resource management [35, 36]. Therefore, resource management is an integral part of emergency management. Resource layout is an effective way to deal with emergencies [37]. It can arrange the appropriate resources and types of resources in the right place in advance, and the effective layout helps to schedule resources. In resource scheduling, resource adjustment must be considered. The resources needed for emergency management may come from many fields, so the arrangement and adjustment of these resources are very important. Organizational quality and adjustment in various aspects will affect the efficiency of resource utilization and the success of emergency management [38].

Emergency management has several main processes, such as early warning of emergency, plan management, and event handling. Among them, early warning is a vital link [39]. The early warning is to collect, sort out, and analyze the relevant information of the emergency situation according to the characteristics of the emergency, implement the equipment and plan according to the analysis results, and issue an alarm. The purpose of early warning is to detect and deal with the possible events as soon as possible, to avoid some of the events, and to minimize the losses and losses caused by urgent circumstances. The processing flow is shown in Figure 1.

Various public health emergencies and other emergencies are one of the main factors affecting the health of all citizens and social stability, which is also a fact fully proved by historical experience and lessons. Public health emergencies usually endanger the health and safety of people's lives and property, disrupt people's regular social order, seriously threaten public social security, and even seriously hinder the normal operation of state power institutions. Social development will be thus hindered.

2.2. Artificial Intelligence

2.2.1. Strong Artificial Intelligence and Weak Artificial Intelligence

(1) Weak artificial intelligence (top-down NAI) refers to the use of programs designed to simulate the logical thinking of animals and humans. Therefore, although the action of the agent is similar to that of the human, the agent has no ideological understanding.
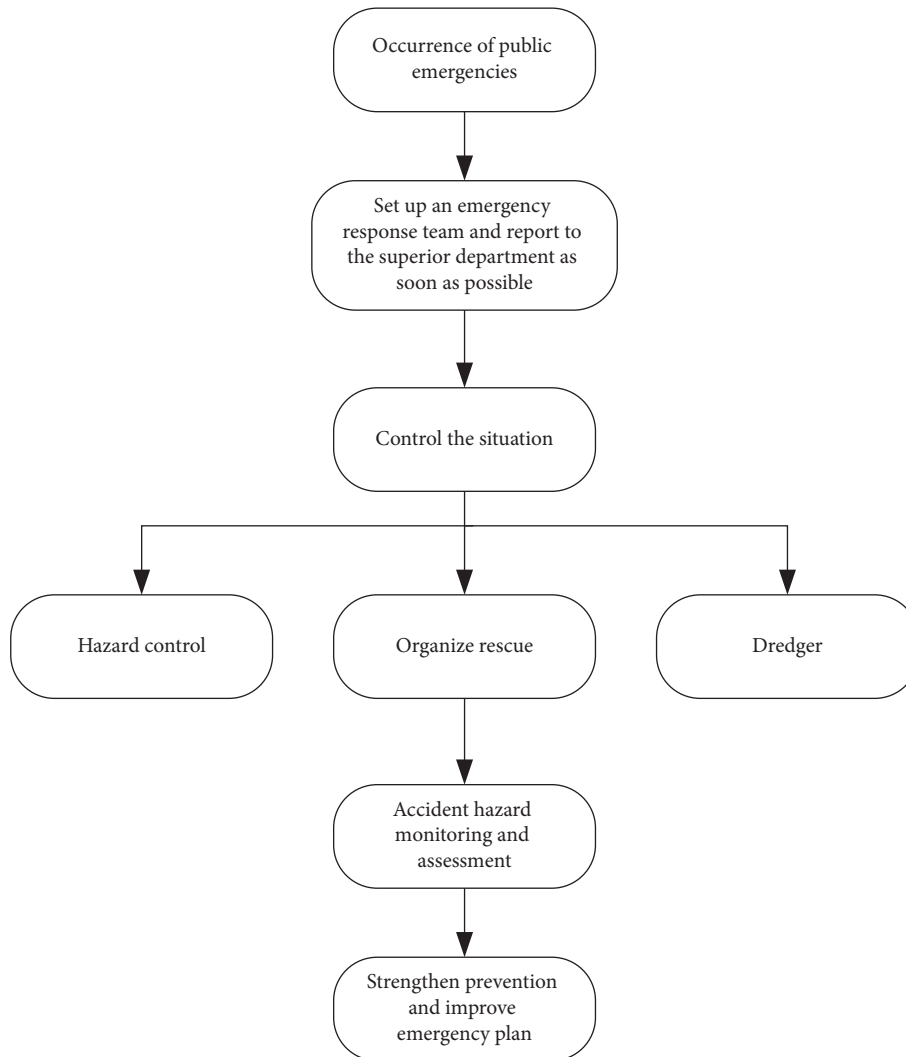
Figure 1: Emergency handling process.

Scholars who view weak AI believe that it is impossible to build an intelligent machine that can truly infer and solve problems. At present, many electronic products have a certain degree of intelligence. When the external data input changes, the corresponding program will be run to get different results, replacing people to complete repeated simple tasks. Weak artificial intelligence can be seen everywhere. Now, washing machines, televisions, and microwave ovens all have the functions of weighing, sensing, timing, and temperature sensing. However, the application of weak artificial intelligence is only limited to imitate primary human behaviors.

(2) Strong artificial intelligence (bottom-up AI) belongs to a higher level of artificial intelligence. Strong artificial intelligence believes that it is possible to create intelligent machines with real ideological consciousness, thinking ability and emotion, and can solve problems and reasoning. For strong artificial intelligence, computers can not only study consciousness. In other words, the computer will have certain cognitive ability after corresponding

programming. From this point of view, to understand the computer is also conscious.

2.2.2. Application of Artificial Intelligence Technology

(1) Expert System. The so-called expert system is actually a kind of program system. From the function, it can be defined as "a program system with expert level ladder ability in a certain field." It can work like a domain expert and can use the work experience and expertise accumulated by experts for many years to get high-level answers to problems in a concise period.

(2) Machine Learning. Machine learning, also known as knowledge acquisition, is the intelligent behavior of machines imitating human learning. Machine learning is a method by which an engine generates a specific model (a detailed description of experience) based on the existing data (i.e., the origin of experience) and uses this model to predict the unknown number (i.e., the use of experience). Ideally, machine learning hopes to provide the machine with

autonomous learning functions to achieve specific skills that cannot be input. Currently, machine learning is a process of learning models from known data and then using models to predict.

(3) Natural Language Understanding. Natural language understanding is also known as natural language processing. Language is a meaningful way to exchange information. Natural language understanding mainly studies how to let machines understand human language and realize natural language interaction between people and machines. In fact, the process of natural language understanding is a mapping process, and some expressions will be transformed into other expressions. Natural language understanding includes text understanding and phonetic understanding. The generation of natural language is more complicated than that of written language. The difficulty of natural language understanding is the expression and application of knowledge. It is much more difficult for a machine to understand the speech information sent out by humans than to understand the natural language sent out by the machine.

(4) Artificial Neural Network. Artificial neural network is a mathematical model that imitates a biological neural network. It can be used to simulate the structure and function of human neural system. Artificial neural network is an intelligent organization with its learning and organization. It uses a large number of artificial neurons to calculate, where each neuron represents a specific output function, and then connects many "neurons" to form a network.

(5) Big Data. Big data technology can handle a lot of data. It is a new data service model and organization structure, including functions such as data collection, transmission, processing, regeneration, and reuse. However, it is different from the traditional data processing technology in data collection and processing speed. The demand is faster, the amount of data is more extensive, and the data structure is more and more complex.

3. Social Emergency Management Capability Experiment

3.1. Experimental Research Methods

3.1.1. Literature Analysis. This paper consults and investigates many books, articles, journals, and other literature related to crisis management and emergency management at home and abroad, studies and understands the latest trends in relevant scientific research fields, investigates the emergency response management systems and institutions of domestic and foreign governments, summarizes advanced experience and practice, and sorts out, analyzes, and summarizes the weaknesses and shortcomings of government response.

3.1.2. Case Analysis. Sorting out and investigating the representative emergency management cases in recent years, taking the specific case analysis as the starting point,

understand the problems existing in the government's response to major emergencies and further analyze the causes, find out the problems, and research countermeasures.

3.1.3. Comparative Analysis. Based on the investigation of relevant information of emergency management theory at home and abroad, taking the successful experience and practice of some developed countries as examples, this paper compares the differences of emergency management mechanism and system construction at home and abroad and puts forward feasible countermeasures and suggestions for the gap and defects.

3.2. Investigation of Experimental Data.
To fully understand the problems existing in China's emergency management system, the author adopts the method of questionnaire 67 to collect and summarize the feedback opinions of some industry emergency management departments and relevant scientific research institutions. A total of 127 questionnaires were collected, of which 122 were valid.

The main items of this questionnaire survey are timeliness and transparency of information release, problems related to the construction of emergency plan, setting and responsibility division of emergency management organization, emergency support, emergency laws and regulations, relevant issues, and countermeasures.

3.3. Construction of Experimental Emergency Management Ability Evaluation

3.3.1. Target Analysis. The target analysis method needs to determine the system objectives first, then start from the system objectives, and then establish the system comprehensive evaluation index system by decomposing the purposes. The specific steps are as follows:

(1) Establish system objectives

(2) The system objective is decomposed continuously until the target can be measured quantitatively or qualitatively

(3) According to the target system, the evaluation index system is established

3.3.2. Output Analysis. The output analysis method is suitable for establishing the evaluation index of the system when the content and structure of the system are not known or need more knowledge. Based on the output characteristics of the system, a comprehensive system evaluation index system is constructed from the aspects of technology, economy, society, ecological environment, and risk. For example, if the output analysis method is used to establish the evaluation index system of enterprise information system, the economic aspect can be measured by the indexes such as benefit, cost, and capital flow rate, and the technical part can be determined by the comprehensive realization function and other indicators. The measurement of ecological environment is reflected by environmental pollution

and other indicators. These indicators can reflect the overall situation of the enterprise.

3.4. Artificial Intelligence Application Experiment.

The effective governance of society is inseparable from the support of improving the public service system. In the era of artificial intelligence, the construction of big data should be centered on the standards and strategies of data governance, mainly from the following aspects: first, the construction of big data should start with the structure of information databases to achieve various types of information interconnection in various fields. Share data resources of all levels and types to lay a data foundation for the information system; secondly, actively build a technological innovation platform. Pay attention to the production, education, and research of key technologies of big data, form a complete technical support system with independent intellectual property rights, and promote national technological innovation; finally, as far as possible to expand the coverage of big data public service platforms.

4. Result Analysis of Social Emergency Response Capability

4.1. Analysis of Questionnaire Survey Results of Social Emergency Management

4.1.1. Emergency Information Release.

Through the questionnaire survey, this paper found that most of the respondents knew that the information of public health emergencies was through microblog, WeChat, and other network platforms, accounting for about 60.7% (as shown in Figure 2); in terms of transparency and timeliness of government information disclosure in emergency response, 48.4% chose better and 39.3% chose general, indicating that after the "SARS" incident, the information disclosure of government information was better. The government's information disclosure work has been significantly improved; however, there is still a lot of room for improvement in the news release mechanism. In addition, 66.4% of the respondents affirmed the government's performance in emergency rescue and response, believing that the emergency rescue was timelier and more effective.

4.1.2. Emergency Plan Construction.

The respondents' choice of "relevant legal provisions" and "government related documents" for emergency plan preparation was as high as 87.7%, as shown in Figure 3. It shows that most of the compilers of the emergency plan only simply sort out the laws and regulations and superior documents, or even repeat the contents, and lack the summary and reflection on the emergency response experience, which leads to the general or even poor operability of the emergency plan.

4.1.3. Emergency Organization and Responsibilities.

About 40.2% of respondents chose "have the right to have the responsibility, and the power and responsibility are unified." 41.8% of respondents think that the power is
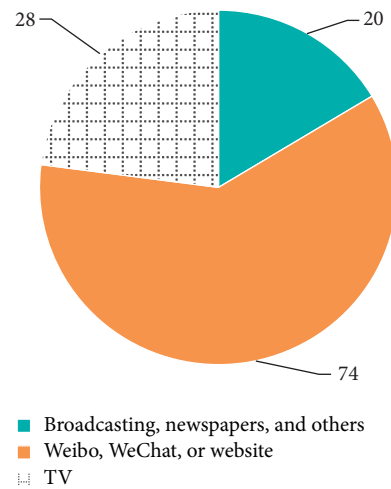
Figure 2: Questionnaire results of ways to obtain public health emergencies.
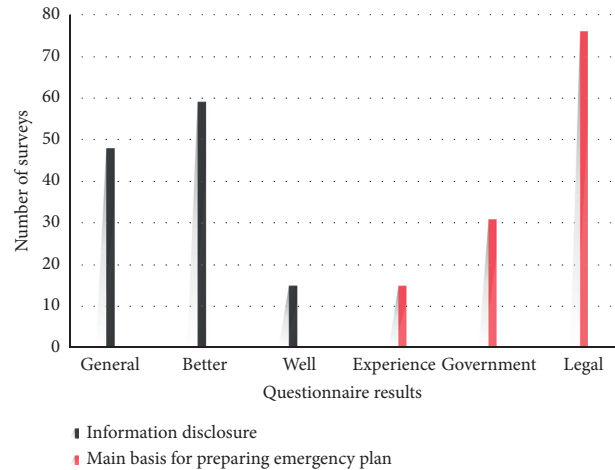
Figure 3: Information disclosure situation and emergency plan preparation are mainly based on the results of the questionnaire.

light and the responsibility is heavy, even with wrong duties. This shows that there are some deficiencies in the matching of authority and responsibility, as shown in Figure 4. Although "territorial management" is a principle that we have repeatedly emphasized in the process of emergency management, the practice of high-level coordination by high-level administrative organs is still the mainstream in the practical operation level, "territorial management" has not been fully implemented. The emergency power still needs to be adjusted appropriately, and the local response and disposal power should be increased to improve the emergency response efficiency truly.

4.1.4. Emergency Supplies and Human Resources Guarantee.

In the aspect of emergency material support, 50.8% of respondents think that it is "insufficient under special circumstances," and 36% of respondents believe it is "relatively lacking," as shown in Table 1. The technical performance of

FIGURE 4: The results of the questionnaire on major shortcomings of emergency management laws.

emergency materials and personnel, as well as emergency equipment, determines the effect of emergency rescue to a great extent, and the safeguard measures of emergency materials need to be further guaranteed and implemented.

4.1.5. Emergency Laws and Regulations. The main deficiency of emergency management laws and regulations is that most people's choices are relatively balanced, as shown in Figure 5. There is a lot of room for further improvement in the setting of emergency agencies, the guarantee of emergency forces, the standardization of emergency management process, the cultivation of crisis awareness, and the training of emergency ability.

4.1.6. Great Problems in the Field of Emergency Management. More than half of the respondents believe that "limited financial input" and "backward technical equipment" are prominent problems in the field of emergency management at this stage. Besides, "imperfect legal system" and "imperfect organizational structure" are also more choices. This reflects the basic situation in the field of emergency management. The key lies in the lack of clear and robust legal provisions on emergency preparedness measures. At the same time, the lack of law enforcement basis in the process of emergency management and even the confusion of law enforcement subjects have become the main reasons for reducing the response effect of emergencies and hindering the improvement of emergency management ability. The most fundamental way to improve the ability of emergency management is to improve the system of laws and regulations and clearly define the scope of responsibility of emergency management organization system.

4.2. Analysis of the Social Governance Mode of Artificial Intelligence Innovation. First of all, artificial intelligence promotes the synergistic effect of social governance. Artificial intelligence based on big data can change the problem of information asymmetry between the government and the public in the past and build an information exchange platform between the theme and purpose of social governance. As a weak humanization, artificial intelligence can effectively avoid the "deviation" of social governance caused by the inherent nature of human beings. This reflects the self-discipline and rationalization of social governance in the process of modernization. The theme of social governance is to further improve the fairness, interaction, and scientificity, strengthen the political identity and unity of social governance, and facilitate timely, reasonable, and social participation in political life.

Second, artificial intelligence promotes efficient social governance. As a phased achievement of the development of science and technology, artificial intelligence has penetrated into all aspects of social life. People enjoy the convenience brought by artificial intelligence in many fields such as life, education, transportation, etc. Artificial intelligence provides new technical support for social governance. For example, the intelligent early warning system established by artificial intelligence technology can simulate the track and future trend of natural disasters such as typhoons and earthquakes, so as to minimize the social harm caused by natural disasters. Moreover, artificial intelligence technologies such as 3D printing isolated housing, disinfection robot, and intelligent distribution robot also show great social value when they are popular, reducing the risk of people facing public health emergencies and improving the efficiency of epidemic control and social governance.

Third, artificial intelligence promotes the wisdom of social governance. The government is the regulator of economic development, the regulator of market operation, the provider of public services, and the "brain" of society. The "intelligence" level of the government directly determines the "intelligence" level of the whole community, society, even the country. On the other hand, with the development of society, the problems of modern government become more and more complex, and the traditional government cannot respond to people's expectations of social governance ability. Therefore, in order to build an "intelligent government," the powerful data collection and analysis function of artificial intelligence are very excellent.

TABLE 1: Questionnaire results of emergency supplies and capital reserves.

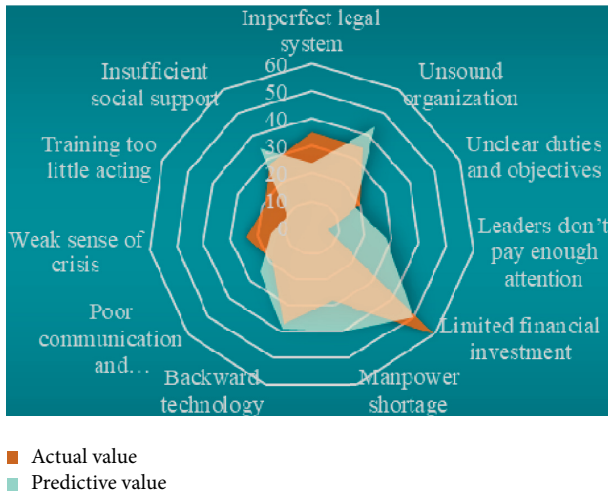|	Relatively lack, severely insufficient under special circumstances	Insufficient under special circumstances	Relatively sufficient
Emergency supplies guarantee	44	62	16
Human resources guarantee	41	58	23

FIGURE 5: Questionnaire results of outstanding issues in the field of emergency management.

On the other hand, through the participation of artificial intelligence in social governance, it can provide technical support and platforms such as government infrastructure construction, government services, multiagent interaction, etc. The social platform in the direction of intelligence and modernization can further promote the development of business activities. At the same time, artificial intelligence promotes the transformation of government functions and promotes the development of government's public service.

5. Conclusion

Responding to public health emergencies and coping is a process that needs to encounter, discover, analyze, and solve practical problems continuously. The reconstruction of social governance function not only needs to stop the internal improvement and overall promotion of high-level design, but also needs to grasp the opportunity of external stimulation improvement of public health emergencies, so as to improve the prevention and response-ability of public health emergencies. The social governance function should be reformed from many aspects to promote the modernization of the national governance system and governance function.

This research would comprehensively use academic knowledge and investigation methods to introduce the current situation, related concepts, and theoretical basis of emergency management at home and abroad and conduct a questionnaire survey on the emergency management capabilities of the Chinese government to respond to related issues and analyze China's current emergency management situation. In recent years, the investigation of public health emergencies has summarized the unresolved problems in China's public emergencies management. We have proposed a method to improve the management of public emergencies in China by combining the successful experience of developed countries with the situation of specific countries in our country.

The research and development of artificial intelligence technology in China are at the forefront of the world. The social science research on artificial intelligence focuses on the normative and predictive analysis of its social risk. There is no consistent research result because there is no empirical material support. This paper describes the development logic of artificial intelligence technology, explores the internal connection between intelligent social governance and artificial intelligence technology, analyzes the innovation and implementation path of social governance mechanism driven by artificial intelligence, and provides inspiration and reference for a new era construction of intelligent social governance.

Data Availability

No data were used to support this study.

Conflicts of Interest

The authors declare that they have no conflicts of interest regarding the publication of this paper.

Acknowledgments

References

[1] W. Wu, Y. Liu, C. H. Wu, and S. B. Tsai, "An empirical study on government direct environmental regulation and heterogeneous innovation investment," *Journal of Cleaner Production*, vol. 254, Article ID 120079, 2020.

[2] H. Chen, G. Zhang, D. Fan, L. Fang, and L. Huang, "Nonlinear Lamb wave analysis for microdefect identification in mechanical structural health assessment," *Measurement*, vol. 164, Article ID 108026, 2020.

[3] Y.-H. Yuan, S.-H. Tsao, J.-T. Chyou, and S.-B. Tsai, "An empirical study on effects of electronic word-of-mouth and Internet risk avoidance on purchase intention: from the perspective of big data," *Soft Computing*, vol. 24, no. 8, pp. 5713–5728, 2020.

[4] T. M. Bayleyegn, A. H. Schnall, S. G. Ballou et al., "Use of community assessments for public health emergency response (CASPERs) to rapidly assess public health issues—United States, 2003-2012," *Prehospital & Disaster Medicine*, vol. 30, no. 4, pp. 1–381, 2015.

[5] B. Wang, X. Zhang, and X. Dong, "Novel secure communication based on chaos synchronization," *IEICE Transactions on Fundamentals of Electronics, Communications and Computer Sciences*, vol. E101.A, no. 7, pp. 1132–1135, 2018.

[6] T. A. Hadi and K. Fleshler, "Integrating social media monitoring into public health emergency response operations," *Disaster Medicine and Public Health Preparedness*, vol. 10, no. 5, pp. 775–780, 2016.

[7] C. Li, P. Liu, C. Zou, F. Sun, J. M. Cioffi, and L. Yang, "Spectral-efficient cellular communications with coexistent one-and two-hop transmissions," *IEEE Transactions on Vehicular Technology*, vol. 65, no. 8, pp. 6765–6772, 2015.

[8] K. R. Kirsch, B. A. Feldt, D. F. Zane, T. Haywood, R. W. Jones, and J. A. Horney, "Longitudinal community assessment for public health emergency response to wildfire, Bastrop County, Texas," *Health Security*, vol. 14, no. 2, pp. 93–104, 2016.

[9] K. Shi, J. Wang, S. Zhong, Y. Tang, and J. Cheng, "Hybrid-driven finite-time H∞ sampling synchronization control for coupling memory complex networks with stochastic cyber attacks," *Neurocomputing*, vol. 387, pp. 241–254, 2020.

[10] S. Zailani, A. A. Aziz, and A. Rashidi, "Lean public emergency department efficiency evaluation by slack-based measure data envelopment analysis," *Malaysian Journal of Medicine and Health Ences*, vol. 16, no. 2, pp. 105–111, 2020.

[11] S. Samra, E. Pelayo, M. Richman, M. McCollough, and B. R. Taira, "Barriers to the right to health among patients of a public emergency department after implementation of the affordable care act," *Health Equity*, vol. 3, no. 1, pp. 186–192, 2019.

[12] M. D. M. Mascarenhas, R. M. C. V. Souto, D. C. Malta, M. M. A. D. Silva, C. M. D. Lima, and M. D. M. S. Montenegro, "Características de motociclistas envolvidos em acidentes de transporte atendidos em serviços públicos de urgência e emergência," *Ciência & Saúde Coletiva*, vol. 21, no. 12, pp. 3661–3671, 2016.

[13] S. Kurani, E. Theel, and A. Greenberg-Worisek, "Diagnostic testing for zika: observing rapid translation during a public health emergency," *Clinical and Translational Science*, vol. 11, no. 2, pp. 103–105, 2018.

[14] J. Peng, J. Quan, and L. Peng, "It application maturity, management institutional capability and process management capability," *Journal of Organizational and End User Computing*, vol. 31, no. 1, pp. 61–85, 2019.

[15] S. B. Tsai, W. Wu, S. Ma, C. H. Wu, and B. Zhou, "Benchmarking, knowledge inertia, and knowledge performance in different network structures," *Enterprise Information Systems*, vol. 14, no. 1, pp. 1–20, 2019.

[16] D. Xiuquan, L. Zhu, Y. Xinmiao, Q. Zhao, D. Gao, and B. Bai, "Formation mechanism and coping strategy of public emergency for urban sustainability: a perspective of risk propagation in the sociotechnical system," *Sustainability*, vol. 10, no. 2, pp. 386–400, 2018.

[17] Y. Kegao, R. Binbin, and A. Qingqing, "Establishing a social governance model based on collaboration, participation, and common interests: value, structure and roadmap," *Contemporary Social Sciences*, vol. 15, no. 1, pp. 77–90, 2019.

[18] B. Yang, Y. He, and W. Long, "Alienation of civic engagement in China? Case studies on social governance in Hangzhou," *Voluntas International Journal of Voluntary & Nonprofit Organizations*, vol. 27, no. 5, pp. 2150–2172, 2016.

[19] Z. Lv, B. Hu, and H. Lv, "Infrastructure monitoring and operation for smart cities based on IoT system," *IEEE Transactions on Industrial Informatics*, vol. 16, no. 3, pp. 1957–1962, 2020.

[20] Z. Jun-Hong, C. Kai-Huang, L. U. Xiao-Ling et al., "A study on incubating rural social organizations in the perspective of social governance innovation–a case study of the incubating base of rural social organizations in chonghua, guangzhou," *Journal of Guangdong Youth Vocational College*, vol. 106, no. 3, pp. 183–186, 2015.

[21] E. D. Crawford, J. T. Batuello, P. Snow et al., "The use of artificial intelligence technology to predict lymph node spread in men with clinically localized prostate carcinoma," *Cancer*, vol. 88, no. 9, pp. 2105–2109, 2000.

[22] E. S. Rigas, S. D. Ramchurn, and N. Bassiliades, "Managing electric vehicles in the smart grid using artificial intelligence: a survey," *IEEE Transactions on Intelligent Transportation Systems*, vol. 16, no. 4, pp. 1619–1635, 2015.

[23] P. Yeaton, R. J. Sears, T. Ledent, I. Salmon, R. Kiss, and C. Decaestecker, "Discrimination between chronic pancreatitis and pancreatic adenocarcinoma using artificial intelligence-related algorithms based on image cytometry-generated variables," *Cytometry*, vol. 32, no. 4, pp. 309–316, 1998.

[24] R. Polikar, R. Shinar, L. Udpa et al., "Artificial intelligence methods for selection of an optimized sensor array for identification of volatile organic compounds," *Sensors & Actuators B Chemical*, vol. 80, no. 3, pp. 243–254, 2015.

[25] M. Seyedmahmoudian, B. Horan, T. K. Soon et al., "State of the art artificial intelligence-based MPPT techniques for mitigating partial shading effects on PV systems-a review," *Renewable and Sustainable Energy Reviews*, vol. 64, no. 10, pp. 435–455, 2016.

[26] R. Barzegar, J. Adamowski, and A. A. Moghaddam, "Application of wavelet-artificial intelligence hybrid models for water quality prediction: a case study in Aji-Chay River, Iran," *Stochastic Environmental Research and Risk Assessment*, vol. 30, no. 7, pp. 1797–1819, 2016.

[27] L. Caviglione, M. Gaggero, J. F. Lalande, M. Urbański, and W. Mazurczyk, "Seeing the unseen: revealing mobile malware hidden communications via energy consumption and artificial intelligence," *IEEE Transactions on Information Forensics & Security*, vol. 11, no. 4, pp. 799–810, 2017.

[28] Z. Wang and R. S. Srinivasan, "A review of artificial intelligence based building energy use prediction: contrasting the capabilities of single and ensemble prediction models," *Renewable and Sustainable Energy Reviews*, vol. 75, no. 8, pp. 796–808, 2016.

[29] C. Yang, Z. Yang, and Z. Deng, "Robust weighted state fusion Kalman estimators for networked systems with mixed uncertainties," *Information Fusion*, vol. 45, pp. 246–265, 2019.

[30] X. Z. Lyu, Z. H. Zhao, X. J. Wang, and W. M. Wang, "Study on the permeability of weakly cemented sandstones," *Geofluids*, vol. 2019, Article ID 8310128, 14 pages, 2019.

[31] L. Gang and Z. Hanwen, "An ontology constructing technology oriented on massive social security policy documents," *Cognitive Systems Research*, vol. 60, pp. 97–105, 2020.

[32] A. Lymer, "Second international meeting on artificial intelligence in accounting, finance and tax, Punta Umbria, Spain, 27–28 September 1996," *Intelligent Systems in Accounting Finance & Management*, vol. 6, no. 3, pp. 265–267, 1997.

[33] J. Lemley, S. Bazrafkan, and P. Corcoran, "Deep learning for consumer devices and services: pushing the limits for machine learning, artificial intelligence, and computer vision," *IEEE Consumer Electronics Magazine*, vol. 6, no. 2, pp. 48–56, 2017.

[34] C. Modongo, J. G. Pasipanodya, B. T. Magazi et al., "Artificial intelligence and amikacin exposures predictive of outcomes in multidrug-resistant tuberculosis patients," *Antimicrobial Agents and Chemotherapy*, vol. 60, no. 10, pp. 5928–5932, 2016.

[35] R. Chatila, K. Firth-Butterflied, J. C. Havens, and K. Karachalios, "The IEEE global initiative for ethical considerations in artificial intelligence and autonomous systems [standards]," *IEEE Robotics & Automation Magazine*, vol. 24, no. 1, p. 110, 2017.

[36] M. Polina, O. Lucy, Y. Yury et al., "Converging blockchain and next-generation artificial intelligence technologies to decentralize and accelerate biomedical research and healthcare," *Oncotarget*, vol. 9, no. 5, pp. 5665–5690, 2018.

[37] Z. Lv and L. Qiao, "Optimization of collaborative resource allocation for mobile edge computing," *Computer Communications*, vol. 161, pp. 19–27, 2020.

[38] H. Lee, F. M. Troschel, S. Tajmir et al., "Pixel-level deep segmentation: artificial intelligence quantifies muscle on computed tomography for body morphometric analysis," *Journal of Digital Imaging*, vol. 30, no. 4, pp. 487–498, 2017.

[39] Y. Sun, H. Song, A. J. Jara, and R. Bie, "Internet of things and big data analytics for smart and connected communities," *IEEE Access*, vol. 4, pp. 766–773, 2016.

Research Article

Research and Implementation of Electronic Commerce Intelligent Recommendation System Based on the Fuzzy Rough Set and Improved Cellular Algorithm

Bo Peng ⬤

College of E-Commerce, Zhejiang Business College, Hangzhou 310053, Zhejiang, China

Correspondence should be addressed to Bo Peng; 00231@zjbc.edu.cn

With the continuous development of e-commerce, our society has transitioned from a mechanical era to an intelligent era. There have been many things that have subverted people's traditional concepts, and they have also completely changed the way of life of modern people. Due to the development of e-commerce, people can enjoy the scenery and food from all over the world at home. Online shopping and online ticket purchase have greatly facilitated people's lives and given people more choices. However, due to the excessive selection of things, there is also a phenomenon of information overload. Sometimes, it is difficult for people to find a product or content that they are very satisfied with. So, how to analyze people's browsing behavior and predict what kind of content people want and how to push products on major websites have become a major issue facing major online companies. Based on this, this paper proposes an e-commerce intelligent recommendation technology based on the fuzzy rough set and improved cellular algorithm. It provides personalized recommendations for users based on their browsing history and purchase history. The research of this article is mainly divided into four parts. The first part is to analyze the status quo of technical research in this field. By analyzing the shortcomings of the existing technology, the concept of this article is proposed. The second part introduces the classic intelligent recommendation algorithm, including the principle and process of the fuzzy rough set and improved honeycomb algorithm, and analyzes the difference of various recommendation algorithms to illustrate the adaptability of each algorithm in practical applications and their respective advantages and disadvantages. The third part introduces an intelligent recommendation system based on fuzzy clustering, comprehensively analyzes the characteristics of users and commodities, makes full use of users' evaluation information of commodities, and realizes intelligent recommendation based on content and collaborative filtering. At the end of the article, through comparative analysis experiments, the superiority of the intelligent recommendation system for electronic commerce based on the fuzzy rough set and improved cellular algorithm is further proved, and the accuracy of intelligent recommendation is improved.

1. Introduction

Electronic business generally refers to a wide range of business and trade activities all over the world. Realizing consumers' online shopping, online transactions between merchants, online electronic payments and various business activities, trade activities, financial activities, and other related activities is a new business model of comprehensive service activities [1]. Shopping centers, consumers, products, and logistics are the four major elements of e-commerce. Entering the 21st century, with the diversification of consumer information, it has become a habit of consumers to

understand the product information of local shopping malls through Baidu WeChat, Taobao, JD, and other network channels, thus enjoying the fun of on-site shopping [2].

Rough set is a practical subject. Although it only has a history of more than ten years, it has made great achievements in the fields of approximate reasoning, digital logic analysis and simplification, prediction model construction, decision support, control algorithm acquisition, machine learning algorithm, pattern recognition, and other fields [3]. Rough set can effectively deal with the following problems: uncertain or imprecise expression of knowledge; learning from experience and obtaining knowledge from experience;

analysis of inconsistent information; reasoning based on uncertain and incomplete knowledge; simplifying data without retaining information; and determining and evaluating the dependence between data [4]. The feature of automatic extraction of control rules from rough set provides a new method to solve this problem. A new control strategy, fuzzy rough control, is quietly rising and becoming an attractive development direction. Some people apply this control method to the classical control problem of "trolley inverted pendulum system" and the process control problem of cement kiln. Some representative states in the control process and the control strategies adopted by operators in these states are recorded, and good control effect is achieved. Then, the rough set theory is used to process the data, and the control strategies adopted by the operators under what conditions are analyzed, and a series of control rules are summarized. As a scientific research of intelligent computing, rough set theory has made great progress in theory and practice, showing a broad development prospect [5]. It not only provides new scientific logic and research methods for information science and cognitive science, but also provides effective processing technology for intelligent information processing. With the rapid growth of the number of communication equipment and the diversification of service requirements in wireless network, the contradiction between the limited spectrum resources and the growing wireless spectrum demand is increasingly prominent and intensified. At present, the field of wireless communication is facing the challenges of intelligence, broadband, diversification, integration, and so on. Wireless network environment is becoming more and more complex, diversified, and dynamic [6]. In addition, green network resource management, intelligent network management, and other new concepts are also developing. Therefore, how to optimize spectrum utilization and manage spectrum resources effectively is an urgent problem to be solved.

At present, the mainstream solutions are clustering algorithm, neural network, and genetic algorithm, but there are some technical problems in the actual effect. Therefore, this paper proposes a recommendation scheme of e-commerce intelligent system based on fuzzy rough set and improved cellular algorithm in order to improve the recommendation accuracy of intelligent recommendation system.

This paper describes the e-commerce intelligent system based on fuzzy rough set and improved cellular algorithm, introduces the application of neural network algorithm in the field of intelligent recommendation, and points out the disadvantages of using only neural network technology. On the basis of previous research, this paper introduces fuzzy rough set theory as optimization algorithm, combines fuzzy rough set with improved cellular algorithm, and applies it to intelligent recommendation of online enterprises. The low precision problem of traditional algorithm is improved by fuzzy neural network algorithm, and the advantages of fuzzy theory and neural network are combined. In order to verify the actual effect of this algorithm, this paper establishes a comparative experiment between content-based recommendation and original website method. Through a number

of comparative experiments, it proves that the algorithm based on fuzzy rough set and improved cellular algorithm has more accurate characteristics in intelligent recommendation of online enterprises.

The content of this paper is arranged as follows. In the second part of this paper, the relevant contributions of predecessors are introduced, and the main problems are found out, and the optimization model in this paper is put forward. The third section introduces the basic theory of e-commerce intelligent system based on fuzzy rough set and improved cellular algorithm. In the fourth section, according to the shortcomings of previous algorithms, an e-commerce intelligent system method based on the fuzzy rough set and improved cellular algorithm is proposed, which makes online enterprises have more accurate intelligent recommendation, so that users can find the desired items when browsing the content. In the fifth section, through the experimental part, the simulation experiment is carried out to show the advantages of the proposed method. The sixth section summarizes the advantages of the algorithm and the significance of this study.

2. Related Works

Intelligent recommendation is to recommend information and products that users are interested in based on the user's interest characteristics and purchasing behavior, helping customers decide how to purchase products, and how to use e-commerce systems to help customers purchase products. With the continuous expansion of the scale of e-commerce and the rapid growth of the number and types of goods, consumers need to spend a lot of time to find the goods they want to buy.

In the research of recommendation result evaluation interpretation model, general e-commerce websites only use simple methods, such as directly using the store's sales ranking or other users' praise of the product to explain recommendations to users. For example, Felfernig et al. designed the Koba4MS system. If the customer cannot choose the correct solution in the system, they will guide the customer to choose the correct solution in the system [7]. In order to persuade customers to use the recommendation system or provide recommendations, e-commerce sites need to explain the reasons for the recommendations to users. At present, the website of the e-commerce intelligent recommendation system can only meet the needs of one website and the limited centralized recommendation system, which is far from meeting the large-scale needs, especially the intelligent recommendation requirements of distributed e-commerce websites. Han Peng and others studied distributed collaborative filtering algorithm, a distributed filtering algorithm, analyzed how to implement the algorithm on distributed hash table under P2P structure, and finally proposed a distributed collaborative filtering intelligence based on P2P structure Push system [8]. This article adopts e-commerce intelligent recommendation based on fuzzy rough set and improved cellular algorithm, which can make up for the defects of previous online websites and achieve individuality in various aspects such as activity

recommendation, new product recommendation, ranking recommendation, hot-selling recommendation, evaluation recommendation, and praise recommendation.

3. Basic Theory and Core Concepts

3.1. Commonly Used Smart Recommendation System Methods. More machine learning methods are needed to describe the content characteristics from the case capture user's interest information. In a content-based recommendation system, an item or object is defined by attributes of related characteristics. According to the characteristics of the user's evaluation object, the system understands the user's interests and hobbies and verifies the matching degree of the user's information with the items to be predicted. Content-based user profiles are historical data of users, and the user profile model changes with user preferences. The biggest advantage of content-based prediction is that it can provide users with content that they are interested in, and they can also see why they are recommended [9].

The biggest advantage of collaborative filtering is that it has no special requirements for recommended objects and can handle complex unstructured objects, such as music and movies.

The recommendation based on association rules has the purchased goods as the rule header and the rule body as the recommended object. The management rules calculate the proportion of group x goods and group y goods in the transaction database, which can directly reflect the user's purchase tendency for other commodities when purchasing a certain commodity. For example, many people buy bread as well as milk [10]. Therefore, the utility model of the system depends on the utility model to a great extent [11]. Therefore, user information can be any knowledge structure that supports reasoning, can be a standardized query of users, or a more detailed representation of user requirements [12].

3.2. Introduction to Rough Set Theory. Rough set theory is an ideal algorithm to deal with big data, incomplete data, and inconsistent data. Rough set theory introduces the concept of knowledge granularity, which makes it more accurate. The accuracy of knowledge granularity description is the main index to judge whether a concept is accurate. Rough set theory is mainly to preprocess the original data, through a series of data preprocessing to mine the data, which can meet the needs, summarize the data, reduce the relationship between data feature dimensions, and put it into the corresponding database. Rough set theory does not need any additional prior information, only the dataset of related problems. Therefore, the theories that need some prior knowledge have strong complementarity when dealing with inaccuracies and inconsistencies. Rough set theory cannot deal with the data of continuous attributes but can solve the problem of discretization of continuous attributes. In addition, it can process incomplete data through data integrity operation and deal with incompatible data under the premise of allowing certain error processing.

The definition of the fuzzy rough set is as follows: let U be a nonempty finite, R be U a fuzzy relation on, that is, $R \in F(U \times U)$, called (U, R), that is, it is a fuzzy approximation space. For any $A \in F(U), (U, R)$ of A is the upper $\overline{R}(A)$, and lower approximations $\overline{R}(A)$ are defined as follows: for any $x \in$ U [13],

$$\begin{cases} \overline{R}(A)(x) = \vee(R(x,u) \wedge A(u)), \\ \underline{R}(A)(x) = \vee(1 - R(x,u) \wedge A(u)). \end{cases} \quad (1)$$

Definition 1. Set up a knowledge representation system:

$$KS = (U, At, \{Va|a \in At\}), \{Ia \in At\}. \quad (2)$$

At is knowledge of U in the domain of discourse. For a subset on a mine X, X is the positive domain of is defined as [14]

$$POS_R(X) = R(X). \quad (3)$$

For X is a subset of U, the boundary domain of X is defined as

$$BND_R(X) = \overline{R}(X) - \underline{R}(X). \quad (4)$$

For X is a subset of U, the negative field of X is defined as

$$NEG_R(X) = U - \underline{R}(X). \quad (5)$$

Knowledge domain $K = (U, At\{Va|a \in At\}, \{Ia|a \in At\})$ is defined as knowledge representation in system, and At is knowledge in the domain of U discourse. For X subsets of U, the approximation precision of X is defined as [15]

$$a(X) = \frac{|\overline{R}(X)|}{|\underline{R}(X)|}. \quad (6)$$

The roughness of X is defined as

$$P(X) = 1 - a(X) = 1 - \frac{|\overline{R}(X)|}{|\underline{R}(X)|}. \quad (7)$$

In this case, $|\bullet|$ denotes its cardinal number. The degree of certainty of X is approximate precision expression for the middle set knowledge of a knowledge representation system, and the uncertainty degree of X is rough degree expression for the knowledge of middle set of a knowledge representation system, $0 \le a(X) \le 1$, $0 \le P(X) \le 1$.

3.3. Introduction to Improved Cellular Algorithm. Cellular algorithm is mainly aimed at the multiobjective optimization problem of resource allocation, but the effect of common cellular algorithm on resource allocation is not very good. Therefore, this paper proposes an improved cellular network algorithm. The gradient descent method is used to train the weights of DNN to complete the reverse training process of the algorithm. The simulation results show that the algorithm can set the deviation degree of resource allocation scheme independently, and the convergence speed is fast. The algorithm is superior to other algorithms in

transmission rate optimization and system energy consumption optimization.

4. Intelligent Recommendation System Based on the Fuzzy Rough Set and Cellular Algorithm

As a scientific research of intelligent computing, rough set theory has made great progress in both theoretical research and practical application, showing a broad application prospect. The improved rough set is applied to the data mining of association rules in cellular algorithm. The improvement of cellular algorithm can optimize the data mining scheme and effectively improve the recommendation efficiency of e-commerce intelligent recommendation system based on rough set theory. This section first introduces e-commerce personalized service recommendation system and then proposes an association rule mining model based on rough set. Then, according to the recommendation set of user page and the user's browsing volume recommendation engine, the data recommendation set is generated, and the generated data recommendation set is added to the user's latest request page and finally transmitted to the user's browser to realize personalized service. After the user completes the e-commerce behavior, the relevant data source is modified to realize dynamic recommendation adjustment, so as to facilitate the next page browsing recommend new content and improve the accuracy of the recommendation.

4.1. Data Preprocessing. The requirement of rough set theory to data must be discrete and complete data, and it usually needs to deal with the relevant knowledge of data. The data mining method based on rough set is used to organize and solve the content of data table. Rough set theory is a good tool to deal with discrete attributes, but it does not deal with continuous attributes directly. Discretization of continuous attributes is an important issue in data preprocessing. In people's daily life, a large number of data are continuous. The diversity of data also leads to the diversity of data types. However, not all types of data can be used as processing objects in data mining. Some data are not suitable for data mining due to the continuity of data, and some data are not suitable for data mining due to incomplete factors such as insufficient data. Therefore, data completion is an indispensable step in data mining.

After preprocessing the experimental data, the data table is shown in Table 1.

4.2. Reduction Algorithm of the Fuzzy Rough Set. Reduction algorithm is based on the discernibility matrix [16].

Enter the decision table:

$$U = \{X1, X2, K, Xm\},$$
$$R = \{C1, K, Cn, d1, K, dk\}, \tag{8}$$
$$T = \{U, R, V, f\}.$$

The output is the simplified discernibility matrix $D(T)'$.

We use the difference matrix $D(T)'$ obtained after simplification and then judge $D(T)'$. There is a row with all 0 or no 0 in it; if it exists, delete the row and judge whether there are duplicates at the same time; if there are any, delete the duplicate data. Finally, output the matrix.

$$M_{m \times n} = (cij)_{n \times n} = \begin{cases} \alpha \in C \mid f(x,a) \neq f(y,a), ([X]_c \neq [Y]_c \boxplus [X]_D \neq [Y]_D) \\ 0, ([X]_c \neq [Y]_c \boxplus [X]_D \neq [Y]_D) \end{cases} \tag{9}$$

Among them, C and D are the condition attribute set and the decision attribute set, respectively.

It can be seen from formula (6) that the discernibility matrix is a symmetric matrix, so only the upper triangle or the lower triangle can be calculated. The difference of the discernibility matrix is generated by comparing the differences between two objects. Therefore, when deleting an attribute, it is necessary to calculate whether there is only one attribute distinguishing two objects. If there is only one, it cannot be deleted.

The main idea is to calculate the discernibility matrix, find the core, then combine all the attributes containing the core, and finally judge whether the reduction condition is satisfied, so as to obtain the attribute reduction. The method improves the attribute reduction method based on discernibility matrix, increases the importance of attributes, greatly reduces the amount of calculation, and improves performance efficiency.

4.3. Improved Cellular Algorithm for Data Analysis of Association Rules. Association rule mining can find high-frequency frequent item sets in transaction databases with large transaction volume according to the minimum support and then generate association rules according to the minimum confidence level of the found high-frequency sets [17]. The first step is a key and complex step. The superiority of the algorithm directly determines the complexity and efficiency of the step. The second step is relatively simple. Based on the first step of generating frequent item sets, the method of subset generation is used to generate association rules.

The original cellular operator model is used for the assignment of multiobjective communication problem [18]. The personalized interface recommended in this paper can also be applied to the assignment of multiobjective problem. The algorithm flow of this experiment is [19]. For the multiobjective optimization problem in the system model,

TABLE 1: Teachers' data after preprocessing.

Attribute	Gender	Major	Political outlook	First degree	Highest education	Graduated school	Current job title	Assess age	Educational changes	Teaching skills	Research ability	Growing up
1	0	2	4	4	4	2	1	3	1	3	3	3
2	1	2	3	2	2	2	1	2	1	3	3	2
3	1	2	2	3	3	2	1	3	1	2	2	1
...	...	...	...	...	...	...	...	...	...	...	...	...
123	1	1	2	2	3	2	3	1	1	2	2	1
124	0	2	1	3	2	2	2	3	1	3	3	2

the resource allocation algorithm based on deep reinforcement learning is mainly divided into forward transfer process and reverse training process. In the training process, the energy efficiency is the goal, the maximum error in the training process is the goal, and the minimum TD is the reverse training DNN.

The problem of transmission rate constrained optimization is transformed into unconstrained optimization problem by using augmented Lagrange multiplier method.

$$\varphi\left(D_{m,n}^{K}, P_{m,n}^{K}, u_m, \eta\right) = -R + \frac{1}{2\eta} \sum_{m=1}^{M} \left\{ \left[\max\left(0, u_m - \eta \left(P_m^{\max} - \sum_{n=1}^{N} \sum_{k=1}^{K} L_{m,n} D_{m,n}^{K} P_{m,n}^{K} \right) \right) \right] \right\}. \tag{10}$$

The partial derivatives of $D_{m,n}^{K}$ and $P_{m,n}^{K}$ are obtained, and the Lagrange multiplier iterative equation is obtained, thus forming the digital flow. Then, the neural network is constructed according to the iterative data stream, including input layer, multiplier layer, and output layer. The depth depends on the number of iterations. Then, using the constructed neural network, the user information is used as input to output each spectrum allocation scheme to find the best allocation resource. In reverse training, error function should be constructed to minimize the value of loss function.

5. Comparison of Experimental Results and Analysis

5.1. Comparison and Analysis of Fuzzy Rough Set Performance. Compared with traditional algorithms and content-based algorithms, the fuzzy rough set algorithm performed in this experiment has greatly improved the prediction accuracy. This experiment first performs data preprocessing and deletes all zeros or all nonzeros. Then, the fuzzy rough set algorithm is performed to greatly improve the prediction accuracy of the system, and the recommended products and content can better meet the needs of users.

From the data in Figure 1 and Table 2, it can be seen that the recommendation accuracy based on fuzzy rough set algorithm on major online websites is the highest. On the first online website, the accuracy based on fuzzy rough set is higher than that based on content. The recommendation algorithm and the original website algorithm are 0.14 higher, but on the third APP, the algorithm based on fuzzy rough set is only 0.07 higher than the content-based recommendation algorithm and the original website algorithm. On the fourth APP, the algorithm based on fuzzy rough set is only 0.15

higher than the recommendation algorithm based on content and the algorithm of the original website. According to Figure 1, the original algorithm of the website has the lowest accuracy. Since accuracy is the most important content of this article, to improve the accuracy of users' online browsing content and give personalized intelligent recommendations, the use of fuzzy rough set-based algorithms is the best.

In the experiment, we should not only improve the accuracy of smart recommendations when users browse, but also improve the real-time performance of smart recommendations when users browse data. The faster the recommendation time, the users can find what they want in the fastest time. Browse the content and purchase the items you want, so you cannot ignore the real-time nature while intelligently recommending the content.

As shown in Figure 2 and Table 3, the response time of the fuzzy rough set-based algorithm on APP1 is 0.21 s, and the response time of the content-based recommendation algorithm on APP1 is 0.33 s. The response time of the fuzzy rough set-based algorithm on APP3 is 0.2 s, and the response time of the content-based recommendation algorithm on APP1 is 0.3 s. The response time of the fuzzy rough set-based algorithm on APP4 is 0.23 s, and the response time of the content-based recommendation algorithm on APP4 is 0.23 s. The fuzzy rough set algorithm increases the attraction between the element and the nearest cluster center, enhances the attraction between the element and the nearest cluster center, enhances the attraction between the element and the winner, and reduces the attraction between the element and the winner. The attraction speeds up the convergence speed of the algorithm. This greatly improves the response time of the system.
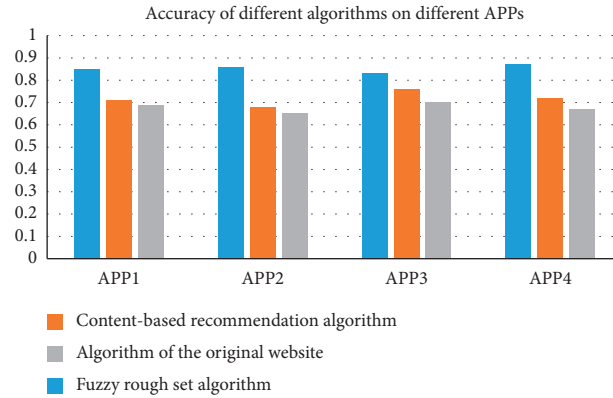
FIGURE 1: Accuracy of different algorithms on different APPs.

TABLE 2: Accuracy of different algorithms on different APPs.

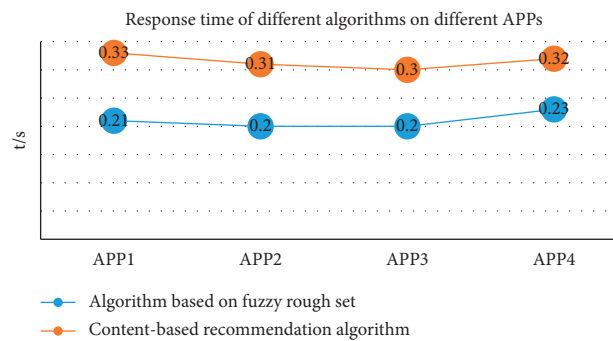| Precision	Based on fuzzy rough set algorithm	Content-based recommendation algorithm	Algorithm of the original website
APP1	0.85	0.71	0.69
APP2	0.86	0.68	0.65
APP3	0.83	0.76	0.7
APP4	0.87	0.72	0.67

FIGURE 2: Response time of different algorithms on different APPs.

TABLE 3: Response time of different algorithms on different APPs.

Time	Algorithm based on the fuzzy rough set	Content-based recommendation algorithm
APP1	0.21	0.33
APP2	0.2	0.31
APP3	0.2	0.3
APP4	0.23	0.32

5.2. Proportion of Personalized Intelligent Recommendation. Different people have different browsing habits, and the content of browsing is the same, so the personalized recommendation of intelligent recommendation is very important. This paper adopts e-commerce intelligent recommendation based on fuzzy rough set and improved cellular algorithm. The content recommended by intelligent recommendation is different for everyone, and the content recommended by intelligent recommendation makes people very satisfied, and the precision of recommended content is also very high. In this paper, the experimental group adopts e-commerce intelligent recommendation based on fuzzy rough set and improved cellular algorithm, while the control group adopts the comparison of content-based recommendation algorithm. The comparison results are shown in Figure 3.

In the data in Figure 3, the data on the left are the accuracy of the content-based recommendation algorithm used in the control group, and the data on the right are the e-commerce smart recommendation based on the fuzzy rough set and improved cellular algorithm used in this experiment. From the data in Figure 3, one can be seen that the accuracy of e-commerce intelligent recommendation based on fuzzy rough set and improved cellular algorithm is 86%, and the accuracy of algorithm based on content recommendation is 70%. It can be seen from the above that the e-commerce intelligent

Accuracy ratio of two groups

- Experience group effective
- Experience group invalid
- Control group effective
- Control group invalid
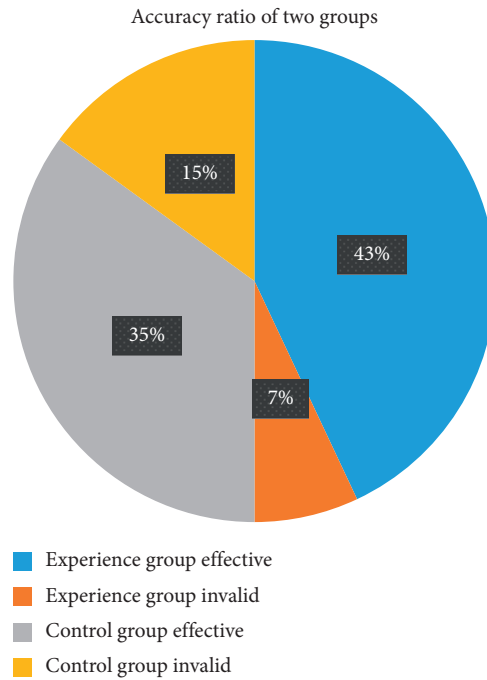
FIGURE 3: Accuracy ratio of two groups.

Online website survey of satisfaction
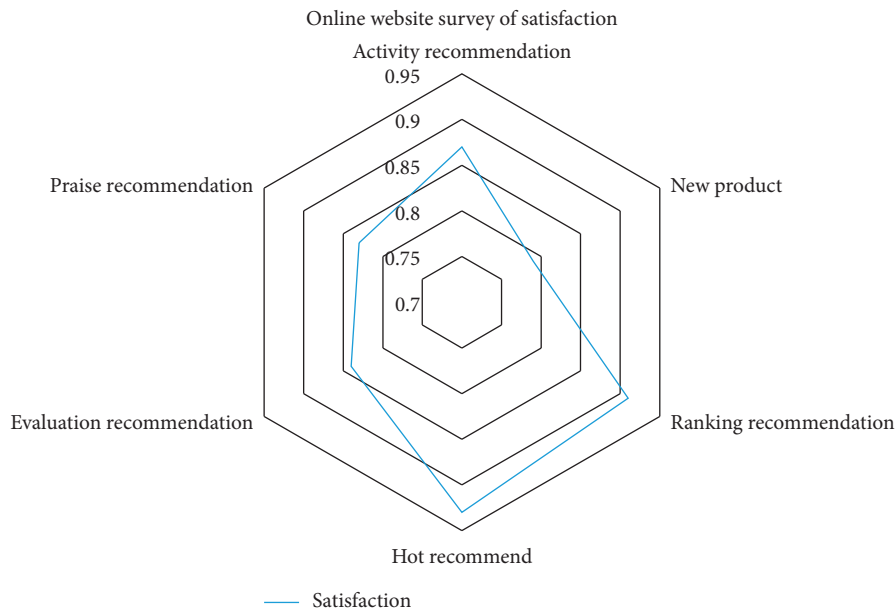
—— Satisfaction

FIGURE 4: Online website survey of satisfaction.

recommendation based on fuzzy rough set and improved cellular algorithm used in this experiment has higher accuracy than the algorithm based on content recommendation and can be applied to major online websites.

At the end, we applied the algorithm used in this experiment to some online websites and found a lot of people to test it and conducted a survey on activity recommendation, new product recommendation, ranking recommendation, hot recommendation, evaluation recommendation, and favorable recommendation. The results of the survey are shown in Figure 4.

It can be seen from the data in Figure 4 that the e-commerce smart recommendation based on fuzzy rough set and improved cellular algorithm used in this experiment has the highest satisfaction in content ranking recommendation and hot recommendation, accounting for 0.91 and 0.93, respectively. Satisfaction is relatively low in new product recommendation and high praise recommendation, with satisfaction levels of 0.79 and 0.83, respectively. It shows that there are still some difficulties in the new product recommendation. In the intelligent personalized recommendation, the new product recommendation is not very

effective. In this experiment, we are quite satisfied with the results of satisfaction, and the overall satisfaction is relatively high. In future algorithms, we will also improve the effect of new product recommendation to make it more satisfying for everyone during online surveys.

6. Conclusions

In electronic business, intelligent recommendation is a popular recommendation technology. In this experiment, the precision of e-commerce intelligent recommendation based on fuzzy rough set and improved cellular algorithm is higher than the traditional intelligent recommendation. In this paper, the experimental data are preprocessed, the repeated and incomplete data are deleted, and the perfect data are processed by fuzzy rough set and improved cellular operator neural network. According to the experimental results, we can see that in the comparative analysis of fuzzy rough set performance, the original website algorithm has the lowest accuracy. The fuzzy rough set algorithm increases the attraction between the elements and the nearest cluster center, accelerates the convergence speed of the algorithm, greatly improves the response time of the system, and makes the waiting time of users become shorter and shorter when browsing the online website pages. Finally, we tested the usability of the system, and got very satisfactory results on activity recommendation, new product recommendation, ranking recommendation, hot sale recommendation, evaluation recommendation, and praise recommendation. Among them, our algorithm will recommend more popular content for customers. In this paper, the e-commerce intelligent recommendation based on fuzzy rough set and improved cellular algorithm is better than the previous algorithm. We also believe that the online website recommendation system will make people more and more satisfied.

Data Availability

No data were used to support this study.

Conflicts of Interest

The author declares no conflicts of interest.

References

[1] Di. Tian, "Research on E-commerce intelligent recommendation system based on rough sets," *Advances in Intelligent and Soft Computing,Advances in Future Computer and Control Systems*, vol. 46, no. 9, pp. 096–129, 2016.

[2] B. Yang, *Research and implementation of e-commerce recommendation and visualization based on rough set*, Beijing University of Posts and Telecommunications, vol. 34, no. 046, , pp. 106–138, Beijing, China, 2015.

[3] J. Zhang and P. Shao, "E-commerce Intelligent Recommender System Based on Rough Set," *Information System Association China Branch Symposium*, 2016.

[4] S. Zheng, "Research and simulation of mathematical classification model based on improved fuzzy rough sets," *Bulletin of Science and Technology*, vol. 31, no. 9, pp. 196–199, 2015.

[5] K. Zhang, Z. Yuan, and L. Fan, "Research on fault line selection device based on improved algorithm based on rough set theory," *Power System Protection and Control*, vol. 61, no. 04, pp. 15–20, 2010.

[6] L. Zheng, H. Wang, and L. Liu, "Research and implementation of text classification system based on rough set and fuzzy clustering theory," *Journal of the China Railway Society*, vol. 29, no. 1, pp. 45–49, 2017.

[7] S. Liu, "Case retrieval algorithm based on domain ontology in e-commerce intelligent recommendation system," *Journal of Computer Applications*, vol. 36, no. 5, pp. 1304–1308, 2018.

[8] H. Haitao and Y. Ma, "Research on E-commerce commodity recommendation system based on weighted association rules mining algorithm," *Modern Electronic Technology*, vol. 39, no. 15, pp. 133–136, 2018.

[9] H. Wang, Y. Zhang, F. Qian et al., "Probabilistic rough set recommendation algorithm for solving EM optimal parameters," *Journal of Computer Science and Exploration*, vol. 10, no. 002, pp. 285–292.

[10] D. Ailin, Z. Yangyong, S. Baile et al., "A collaborative filtering recommendation algorithm based on item rating prediction," *Journal of Software*, vol. 14, no. 9, pp. 1621–1628, 2015.

[11] J. Peng, "Research and application of latent factor Algorithm based on MapReduce in recommender system," *Bulletin of Science and Technology*, vol. 23, no. 12, pp. 124–126, 2017.

[12] J. J. Yin, B. K. Zhang, and D. Gao, "Research and implementation of customization MES with improved scheduling based on RFID," *International Conference on Robots & Intelligent System (ICRIS)*, vol. 54, no. 49, pp. 21–28, 2018.

[13] W. Hui-Jiao and Y. Xiaoyong, "Research and implementation of an intelligent traffic monitoring system based on IOCP mechanism," *Mining & Processing Equipment*, vol. 38, no. 21, pp. 7410–7421, 2010.

[14] C. H. E. N. Chen, X. Chen, Yu Wang et al., "Research and implementation of authority control framework in EIS based on improved RBAC model. Research and implementation of an EIS authority management framework based on improved RBAC model∗," *Application Research of Computers*, vol. 27, no. 10, pp. 3855–3858, 2015.

[15] K. Hashimoto, A. M. Suzuki, A. Dos Santos et al., "CAGE profiling of ncRNAs in hepatocellular carcinoma reveals widespread activation of retroviral LTR promoters in virus-induced tumors," *Genome Research*, vol. 25, no. 12, pp. 1812–1824, 2015.

[16] Z. Hua-Mei, Z. Hua-An, L. I. Duan-Feng et al., "Research and implementation of tunnel lighting intelligent control system based on ZigBee wireless technology," *Measurement & Control Technology*, vol. 64, no. 37, pp. 61–68, 2019.

[17] X. Xiujuan, L. Xiangju, C. Fengping et al., "Research and implementation of e-learning teaching assistant system based on improved C4.5," *Journal of Jiamusi University (Natural Science Edition)*, vol. 36, no. 1, pp. 64–67, 2018.

[18] P. T. Gregory Reychler and P. T. Coralie Colbrant, "Effect of three-drug delivery modalities on olfactory function in chronic sinusitis," *The Laryngoscope*, vol. 54, no. 94, pp. 81–88, 2015.

[19] C. Ping, W. Jinshuang, P. Lin et al., "Research and implementation of SQL injection prevention method based on ISR. 2016 2nd IEEE International Conference on Computer and Communications (ICCC)," *IEEE*, vol. 14, no. 9, pp. 21–28, 2016.

Research Article

Parameter Detection of an On-Chip Embedded Debugging System of Wireless Sensor Internet Based on LEACH Algorithm

Ling-Ao Zhou (ORCID)

School of Electronic Engineering, Changzhou College of Information Technology, Changzhou 213164, Jiangsu, China

Correspondence should be addressed to Ling-Ao Zhou; zhoulingao@czcit.edu.cn

With the rapid development and maturity of unconnected communication technology, effector technology, embedded computing technology, and distributed information processing technology, as well as the rapid advancement of digital processing and computing capabilities, unconnected effector Internet has received more and more attention. It is a new type of self-organizing unconnected multihop Internet. With the development and progress of technology and society, the development of unconnected effector Internet is also advancing by leaps and bounds, and it has a wide range of applications in many fields such as military, civil, environmental, medical, and industrial. At present, the research on unconnected effector Internet mainly focuses on the communication protocol, but there is almost no research on input review of unconnected effector Internet. Due to the limited energy of the effector and the limitation of the transmission signal bandwidth, the use of limited resources for input review research in effector Internet is of great significance to the development of unconnected effector Internet. Therefore, this paper studies the input review of unconnected effector Internet based on the L-A model on the on-chip embedded tune system. Because the classic low-power adaptive cluster layering protocol (LEACH) has the problems of unbalanced energy consumption and short node life cycle, this paper uses the embedded tune technology based on the L-A model and analyzes the remaining energy and location of the unconnected effector Internet node. Parameters are tested and studied. Through the research on the input review of unconnected effector Internet, the simulation results obtained show that the research in this paper is feasible and reasonable.

1. Introduction

With the rapid development of digital links, the field of nanocommunications has become a hot spot and focus of current research [1]. The development and integration of unconnected communication technology, effector technology, and distributed information processing technology has accelerated the emergence and development of the unconnected effector Internet, which is very important for semiconductors [2]. It has been extensively and profoundly developed in many areas of the society. As a product of the combination of multiple disciplines, unconnected effector Internet has shown strong practicability and advantages in various applications. Many experts and scholars in related fields have expressed great interest and concern, and regard it as one of the most influential new technologies in the new century.

Since the birth of unconnected effector Internet, people have conducted research on them. In order to reduce the energy consumption of unconnected effector Internet and improve the Internet survival time, Qingxi et al. proposed an unconnected effector Internet cluster routing protocol based on chicken flock optimization algorithm. On the basis of the LEACH protocol, they improved and perfected the selection of cluster points and cluster heads through the chicken group optimization algorithm and updated the positions of the chickens that fell into the local optimum through Levy flight and enhanced the population diversity to ensure the algorithm's global search capabilities. The new protocol uses the Internet nodes in a balanced way, avoids the crashes of intensively used local nodes, and improves the survival time of unconnected effector Internet [3]. Sedighimanesh et al. pointed out that unconnected effector Internet can be used in the military and medical fields, but for these, the Internet

uses hundreds of low-power and low-energy effector nodes to perform large-scale tasks, which is a limitation and may lead to inefficiency or cost effectiveness. They believe that it can assist in load balancing between effector nodes, increase scalability, and improve energy consumption [4], thereby extending the life of the Internet, clustering effector nodes, and placing appropriate cluster heads in all clusters. Choosing the correct cluster head can greatly reduce the energy consumption of the Internet and prolong the life of the Internet [5]. In their research, Bhola et al. have shown that the unconnected effector Internet (WSN) often contains a large number of effector nodes, which can collect numbers in different situations. WSN discovery applications are mainly used to collect information from remote locations, such as environmental monitoring, military, and transportation security [6]. In order to use the lifetime of effector nodes to improve energy efficiency, they proposed an energy-saving routing protocol, low-energy adaptive clustering hierarchy (LEACH), and optimization algorithm genetic algorithm (GA) [7]. Due to the diversification of the application environment of unconnected effector Internet and different design requirements and goals of each environment, the routing algorithms used in each Internet are also considered to be changed, and as the application environment changes and improves, routing algorithm also becomes diversified [8, 9]. Based on this, this paper adopts the classic L-A model and adds the remaining energy and position parameters of the nodes to carry out research on the input review of unconnected effector Internet.

The digital transmission of unconnected effector Internet is inseparable from the routing protocol [10]. A good routing protocol will greatly improve the overall performance of the Internet. At present, many international scientific research institutions are also carrying out research on unconnected effector Internet protocols, and some suitable routing protocols are being proposed [8]. Among them, LEACH is a relatively mature clustering routing algorithm. Many clustering routing protocols such as TEEN and PEGASIS have been developed on the basis of it [11, 12], so this article first analyzes and studies the L-A model. Then, the on-chip embedded tune system is introduced and applied the on-chip tune technology of the embedded system to detect the parameters of unconnected effector Internet. Unconnected effector Internet nodes are generally powered by batteries, and the longer the communication distance between nodes, the greater the energy consumption [13]. In view of this, this paper optimizes the distribution of nodes and adopts a strategy that the greater the remaining energy of the node, the greater the probability of being elected as the cluster head. Finally, through MATLAB simulation experiments [14], it is verified that the research in this paper balances the energy consumption of the Internet nodes and prolongs the life cycle of unconnected effector Internet, which is feasible and reasonable.

2. Proposed Method

2.1. LEACH Algorithm.
As a basic hierarchical routing algorithm, L-A has limited applicability in different

environments [15, 16]. For specific application scenarios, the L-A algorithm can be optimized and improved according to network requirements [17]. The JC-LA routing algorithm can make certain improvements on the basis of the traditional LA protocol according to the characteristics of the home environment and divide it according to the characteristics of different rooms, making it more suitable for the actual application environment. It divides the partitions according to the relationship between the node's communication range and energy consumption balance [18, 19]. The selection of internal cluster heads is restricted to achieve the purpose of reducing power consumption. The establishment of clusters and the first round of cluster head elections are WSN for outdoor environments [20]. The limited area division method cannot meet the actual needs. The network is adjusted according to the load situation and the cluster head level. The area is divided, and the WSN network is now divided into 16 areas. Each area represents a clustered area. The cluster head level is set from far to near according to the location of the base station, and the cluster heads in areas 1 to 4 are regarded as level A, the cluster heads in areas 5 to 8 are regarded as level B, and so on.

2.1.1. Cluster Head Selection.
The selection of cluster heads in the L-A model is carried out randomly, and there are two main determinants of cluster heads: quantity rounds that the current algorithm runs and the percentage of quantity cluster head nodes to the total number of nodes [21]. There is no master node in the whole clustering process, and each node is based on the algorithm, independently decides, and joins the corresponding cluster [22]. At the beginning of the cluster establishment, all effector nodes in the Internet will randomly generate a random number with a range of [0, 1], and then, the random number is compared with the threshold T(n); if it is less than the threshold T(n), then the effector node corresponding to the random number will be elected as a cluster head of the round, and then, a broadcast message is sent to inform other effector nodes that if the random number is greater than the threshold T(n) [23, 24], then it will not be elected as the cluster head [25, 26]. If the selected cluster head node has been elected as a cluster head, then the value of T(n) is changed to 0, so as to avoid the same node continuously acting as the cluster head, resulting in excessive energy consumption of the node [27]. The calculation formula of the threshold T(n) is expressed as follows:

$$T(n) = \begin{cases} \dfrac{p}{1 - p * (r \bmod (1/p))}, & \text{if } n \in G. \\ \\ 0, & n \notin G. \end{cases} \tag{1}$$

Among them, p is the percentage of cluster heads in all nodes, r is quantity election rounds, $r \bmod (1/p)$ represents the quantity nodes that have been elected cluster heads in this round, and G represents the quantity nodes that have not been elected in this round [28]. The set of nodes have been elected cluster heads.

It can be seen from the abovementioned formula that, with the continuous advancement of the algorithm cycle, quantity nodes that have been appointed as cluster heads will continue to increase, that is, the value of rmod $(1/p)$ will continue to increase, so that the value of $T(n)$ will follow. Then, the probability that a node that has not served as a cluster head will be selected as a cluster head will increase. When there is only one node that has not been selected as a cluster head, $T(n) = 1$; in addition, when $r = 0$ and when $r = 1/p$, the value of $T(n)$ is the same, when $r = 1$ and $r = 1/p+1$, the result of $T(n)$ is also the same, and then, when the algorithm is executed for $(1/p)$ cycles, the effector nodes in the Internet will change back to the situation where cluster heads are selected with equal probability, and the cycle is repeated. The L-A model makes all nodes in the Internet have only one chance to be elected as a cluster head within $(1/p)$ cycles, and they will have a chance to be elected as a cluster head again after $(1/p)$ cycles; thus, $T(n)$ also indicates the average probability of a node that has not served as a cluster head in the rth round of being elected as a cluster head [29, 30].

It is supposed that there are N nodes in the effector Internet, and each time you want to select k cluster heads, $P = N/k$. The probability of a node becoming a cluster head in the $r + 1$ cycle is represented by $T(n)$, and then, the probability of being a cluster head in the $r+1$ cycle is

$$E = \sum_{t=1}^{N} T(t) * 1 = k. \qquad (2)$$

After the rth round, quantity nodes that have not yet become cluster heads in the current $1/p$ round are $N - k * (r \bmod N/k)$. If the node is not selected as the cluster head after the r round, then the abovementioned formula can be obtained, and the average probability of the node becoming the cluster head in the $r + 1$ round is

$$\frac{p}{(1 - p * (r \bmod 1/p))}. \qquad (3)$$

Substituting $p = N/k$ into the average probability of the abovementioned formula,

$$\frac{k}{(N - k * (r \bmod N/k))}. \qquad (4)$$

From the abovementioed derivation, the following formula can be obtained:

$$E = \sum_{t=1}^{N} T(t) * 1 = \left(N - k * \left(r \bmod \frac{N}{k}\right)\right) \frac{k}{(N - k * (r \bmod N/k))} = k. \qquad (5)$$

2.1.2. Intracluster Routing.
After the node selects it as the cluster head, a notification message will be sent to notify other nodes that it is the new cluster head. The noncluster head button selects the cluster to be merged based on the distance between the cluster and the cluster head and informs the cluster head. After receiving all cluster head merge information, it will generate TDMA timing messages and notify all nodes in the cluster [31, 32]. In order to avoid interference from neighboring clusters, the cluster head can check the CDMA codes used by all nodes in the cluster. The CDMA code at the current stage is sent with TDMA timing. When a node in the cluster receives this message, it will send digital at this interval. After the digital transmission period, the cluster head node collects the digital sent from the nodes in the cluster, processes the digital by running digital-intensive algorithms, and sends the results directly to the receiver node [33–35].

2.2. Key Technologies of Connected Effector Internet

2.2.1. Topological Structure Control.
The research premise of unconnected effector Internet topology control is to control the power supply and select the corresponding backbone Internet node copper cables to meet the the Internet coverage and connection conditions [35]. Time eliminates those unimportant communication paths in the nodes, enabling it to form a structured and efficient digital transmission network topology. Using such an excellent network topology control algorithm, not only can the efficiency of routing protocols and MAC protocols be improved but also digital aggregation and time synchronization can be effectively supported. Node energy is saved to improve the Internet life cycle when positioning targets. It can be seen that topology control technology is very important in low-power unconnected effector Internet [36].

2.2.2. Internet Protocol.
The task implementation of the Internet protocol of unconnected effector Internet enables each node to form a multihop digital transmission Internet [37]. Under the premise of efficiently using the Internet energy and improving the Internet life cycle, the purpose is to achieve effective use of the Internet bandwidth and ensure service quality.

2.2.3. Data Fusion.
Data aggregation technology is a process of processing more data as a single data more efficiently when users need it. However, because effector nodes are vulnerable to attacks, Internet effectors still need data synthesis technology to comprehensively process large amounts of data to improve the accuracy of information. According to the content of the information, data consolidation can be divided into two categories: reversible consolidation and loss consolidation. Lossless matching means saving all details and eliminating duplicate information. The loss combination saves storage space and energy by skipping some details and reducing data quality. Data synthesis technology can be used in multiple protocol layers that are not connected to the Internet. Traditional data aggregation technology has been widely used in the field of target tracking and automatic identification. Application-oriented data aggregation methods are usually the most effective for designing effects that are not connected to the Internet [22].

2.2.4. Time Synchronization and Positioning. Time is a key mechanism of synergy not connected to the Internet producing systems. Since then, however, a reason for the Internet business or to adopt Mac-sensitive time-division multiplexing protocol according to the clocks of the nodes must be synchronized. The writer receives the clock synergy to make light of it to the Internet protocol. There are three basic synergies to the time of the machinations of the author and the finisher. This local node includes its current position and situation of the external targets, the accuracy and efficacy of the positioning of the collected data, the effects of limitations nodes, and the positioning mechanism to satisfy the sap self-order and energy efficiency in Internet nodes. Usually the lymph nodes are divided into a network, according to the work in [38]. A kind of art was placed in its proper place accurate information with the unknown; the ship was able to obtain the node at the sight of a knot to which it is being appointed, in the night, and it adopts algorithms that make use of a triangulation, trilateration, and augue node to determine a maximum price location.

2.3. Embedded Tune Technology. Integration with football is enhanced, with more powerful functions and the growth in demand embedded software development, and tune embedded continuous progress in technology is promoted. During the tune embedded system development, a variety of techniques are used for tune revoked. There are obvious differences between different technologies for tune based on the principles and implementation. Most commonly, having been held chip and tune of life analyses, during SOC popularization of technology, on-chip tune began to embed systems. The technology chip tune embedded control module is involved in the process. When certain conditions are met within a certain process, recipes will be in a specific state. In this state, it is possible to run on the server software tune interface outside through a specific process (the port module has access to various resources, and secured tune memory is written in order). The basic idea is to add an additional processor within a module of Brabant tune hardware and software tune command for resource access and processing operation for the tune module. There are many different implementations of chip tune technology. Currently, on-chip tune technologies are using BDM (dackground characteristic) and GATJ (Eds Test Action Group). For users, the two technologies to provide tune functions are similar, but there are many other great tune standards and principles of implementation [22]. The following tune standards are described.

After the preliminary debugging, it is necessary to verify the rationality, implementation, and rhythm of the configuration. For robots that may be interfered, it is necessary to confirm whether there is interference between robots through linkage operation, and when the speed is affected, reconfiguration will lead to duplication of work and change of welding process card. In the case of more welding positions, in order to obtain the best welding path, it usually takes more profiling time and verification time. On-site teaching operation is simple and direct, but it is difficult to

realize complex motion trajectories using that. The programmer's experience directly affects the programming quality, and the programming efficiency is low. Compared with online programming, offline programming uses simulation software to precomplete the welding path of the robot before the on-site debugging of the production line, while verifying the beat, avoiding the interference area, and obtaining the optimal welding path, which overcomes various shortcomings of online programming. Now, we can easily use roboguide simulation software to program each robot offline and get the offline program. However, there must be some deviation between the position of the field robot and other related equipment and its position in the simulation environment. How to reduce it is the focus of discussion to correct this deviation and ensure the accuracy that meets the requirements after the offline program is imported. From the sources of deviations in the process of selecting reference points and drawing lines on the production line, due to the limitations of the on-site environment, the accuracy of equipment and instruments, and the errors of manual operation, it is inevitable that there are small deviations between the actual environment and the simulation environment. These deviations are mainly reflected in the following aspects: the deviation of the tooling installation of the production line, the level of the robot base is not good, and the parallelism of the robot installation is not good. In the car body production line, the position of the fixture determines the position of the product. We are concerned about the relative deviation between the robot and the fixture, that is, it can be assumed that the position of the fixture is absolutely accurate, and all deviations are considered to be caused by insufficient robot installation accuracy. Online programming is to use the teach pendant to teach the robot welding trajectory on site. The entire robot system includes the robot body, the robot control cabinet, and the welding controller. Before online programming, the communication between the robot and the control cabinet and the controller and the robot must be completed. According to signal transmission, robot welding gun configuration, and then, the welding point distribution on the welding process, teaching the welding trajectory online programming has the following characteristics, for some inconvenient solder joints, such as solder joints on the floor. In the teaching process, the welding torch is easily interferes with the parts or even deforms the parts. Before profiling, sometimes, it is not possible to accurately determine the process welding point.

3. Experiments

3.1. Data Sources. In order to better evaluate whether the performance of research in the field effectors is not appropriate, experiments related to the method of producing the Internet are conducted in this paper. According to experimental data in the trial, as the results are more accurate and objective, this paper sets the size of the area as ten thousand square meters; the model does not pertain to the Internet, and 30 nodes are distributed in this area. The geographic location of the lymph random, undoubtedly, is

randomly generated. Fifty trials are performed here, and the average data for the final result are obtained.

3.2. Experimental Evaluation Standards.

Because unconnected effector Internet nodes have the characteristics of limited energy, the length of their life cycle will be directly affected by the energy of the node. When judging that the performance of the research method is higher and more in line with the the Internet requirements, there are several hard standards that can be different research methods used for evaluation, mainly including the following:

(1) The length of time that the connection point is blocked by the firewall

The research of this article will judge the remaining time of synaesthesia from three aspects: the connection point type, user, and environment.

(2) Utilization of energy

This article will record the total energy consumption of Internet nodes in real time and determine whether the corresponding research methods are suitable for the Internet.

(3) Energy use opportunities

In load matching based on single-point sampling, only the load data of a single point is compared with historical load data for similarity, so when calculating the Euclidean distance between two points, there is no problem of phase shift of the waveform. After adopting the dynamic load description, the load pattern is represented by multiple forms of sampling points. These continuous sampling points with sequential characteristics can be regarded as the process of load change. Although the collected data are discrete points, these sample point sequences still have some characteristics of the waveform, such as period, peak value, and frequency.

(4) Remaining nodes

In order to describe the load more accurately, this article focuses on the dynamic change characteristics of the load, based on the idea of multiple sampling, collects multiple performance data during the observation period, and uses these continuous performance slices to describe the dynamic change of the load.

(5) The amount of information received by the base station

Obviously, the greater the amount of information received by the base station, the more beneficial the information received by the observer, thereby improving the accuracy of the data.

3.3. Link Data.

The iterative data of the response sensing area are shown in Table 1.

Table 1: Experimental parameter settings.

Parameter name	Unit	Set parameter value
Junction	\	30
WSN response	m^2	$100 * 100$
Transmission data length	k	4000
Magnetic induction expansion	$pJ/(bit \cdot m^4)$	10
Initial energy of the node	J	0.5

4. Results

First, based on the classic L-A model, the magnetic induction of the unconnected effector is simulated, and the data obtained are recorded. Then, based on the L-A model, the remaining power and connection point location parameters are added to optimize the connection point allocation and strategy. The higher the remaining wattage of the connection point, the greater the possibility. The experimental results can be obtained by detecting the parameters of the unconnected effector on the secondary development management of the carrier. The comparison of the quantity of surviving nodes between the unconnected effector Internet using the classic L-A model and the unconnected effector Internet using the research method in this paper is shown in Figure 1, and the comparison of the remaining energy of the nodes is shown in Figure 2.

As shown in Table 2, J-LEACH and the improved algorithm select only one cluster head as the transmission hub of the network structure hierarchy in the divided sixteen-grid area. However, the cluster head data transmission path of the two is different. J-LEACH uses the cluster head and base station to directly transmit. As shown in Table 3, the SR-LEACH algorithm classifies the cluster heads. The data are transmitted from the A-level cluster heads in turn, and finally, the D-level cluster heads forward the final data to the base station.

5. Discussion

The numerical simulation selects a steel box girder to model separately. The model is established based on the ANSYS platform and is simulated by the orthotropic shell element Shell63. The established steel box girder model maintains the characteristics of the actual space box structure: the structure of the top plate, bottom plate, web, cross beam, U-shaped rib, small longitudinal beam, etc. The simulation is not simplified and accurately reflects the actual stiffness and mass distribution. In addition, the boom and support are simulated by the spring unit Combin14, and the stiffness of the spring unit is obtained by converting the design parameters. From the data in Figure 2, it is more reasonable to use the ratio between the current residual energy and the current maximum energy as a parameter in this paper. When the parameter is between 0 and 1, the energy consumption of the Internet node will not follow.

From the node death situation and the remaining energy consumption of the node in the unconnected effector Internet, it is reasonable to improve the location of the synergy
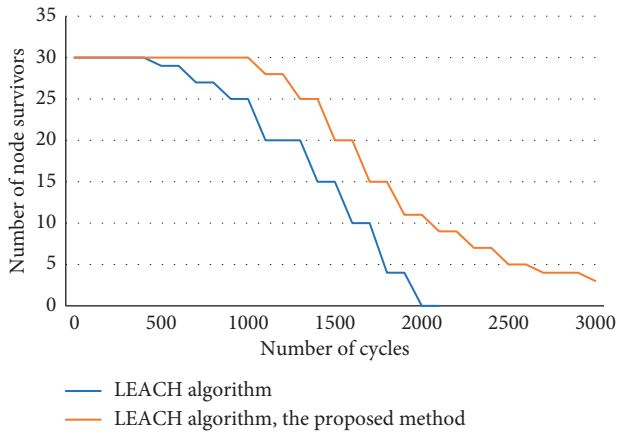
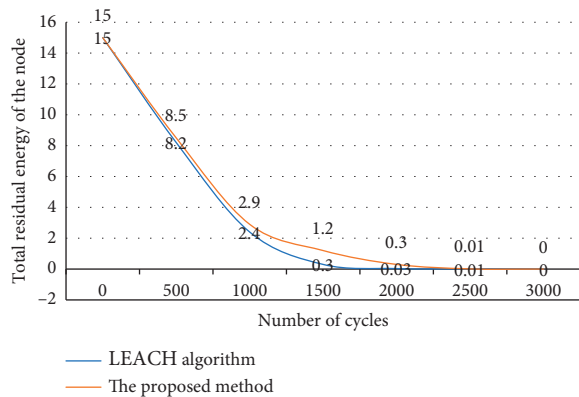Figure 1: Comparison of the quantity of surviving nodes.

Figure 2: Node residual energy comparison chart.

Table 2: Comparison of node deaths.

Experiment	1st node death	15th node death	15th node death
L-A model	585	1093	1892
Method of this paper	910	1687	2673

Table 3: Comparison of node energy consumption.

Experiment	Consume 34%	Consume 65%	Exhaust
L-A model	346	709	1894
Method of this paper	384	781	2532

node and find the node with the shortest distance from other nodes. In this case, we use the node as the distribution area The SINK node is in the middle. Improving node power parameters is the realization of a strategy that makes nodes with higher remaining power more likely to become cluster heads. In this way, the parameter distribution of each election is more balanced, and the parameter is always less than or equal to 1. According to the data in Table 1 and Table 2 mentioned above, the superiority of the method

proposed in this paper is well verified. It greatly reduces the mortality of the Internet nodes and prolongs the life of the Internet.

6. Conclusions

In the engineering structure modal test, the sensor configuration is the decisive factor of the modal resolution. Due to the limited number of sensors available in the dynamic test, they must be optimally arranged to make more reasonable use of sensor resources. However, in the practice of modal testing for large civil engineering structures, it is usually printed in a sensor configuration method in which the sensors are uniformly distributed along the main dimension of the structure. This process lacks effective optimization. It is impossible to obtain high-resolution calculations of modal test results. In response to this problem, the genetic algorithm, an optimization algorithm derived from life sciences, was introduced into the optimal configuration of large-scale civil engineering structure modal testing sensors. Through research, it can be known that the best advantage of generalized genetic algorithm in searching is that the results are stable and reliable and the convergence speed is fast. However, taking the largest nondiagonal element of the modal confidence matrix as the objective function, a genetic algorithm with binary structure coding is proposed, and a more satisfactory optimization result is obtained, which proves that the sensor optimization method based on the genetic algorithm is better than the sequence method. A genetic algorithm based on the minimum modal confidence criterion is also used to optimize a wharf structure. On the sensor configuration, the research found that the optimization method adopted is efficient and reliable. Taking a high-rise building as the engineering background, the generalized genetic algorithm is used to optimize the structure. Finally, using the classic rich algorithm proposed in this paper, through simulation experiments, the effectiveness and practicability of this research method are verified. The research results show that using the L-A model, the quantity of the Internet nodes in the unconnected effector Internet is balanced, which greatly reduces the mortality of the Internet nodes and extends the life of the unconnected effector Internet..

Data Availability

No data were used to support this study.

Conflicts of Interest

The author declares no conflicts of interest.

Acknowledgments

References

[1] Q. Feng, Y. Li, N. Wang et al., "A Biomimetic Nanogenerator of Reactive Nitrogen Species Based on Battlefield Transfer Strategy for Enhanced Immunotherapy," *Small*, vol. 16, no. 25, Article ID e2002138, 2020.

[2] B. Gao, N. Xu, and P. Xing, "Shock wave induced nanocrystallization during the high current pulsed electron beam process and its effect on mechanical properties," *Materials Letters*, vol. 237, no. 15, pp. 180–184, 2019.

[3] Qingxi, Wang, Lihua et al., "Optimization of wireless sensor networks based on chicken swarm optimization algorithm," *AIP Conference Proceedings*, vol. 1839, no. 1, pp. 1–5, 2017.

[4] S.-B. Tsai, "Using grey models for forecasting China's growth trends in renewable energy consumption," *Clean Technologies and Environmental Policy*, vol. 18, no. 2, pp. 563–571, 2016.

[5] M. Sedighimanesh, H. Z. Hesami, and A. Sedighimanesh, "Routing algorithm based on clustering for increasing the lifetime of sensor networks by using meta-heuristic bee algorithms," *International Journal of Sensors, Wireless Communications and Control*, vol. 10, no. 1, pp. 25–36, 2020.

[6] Z. Lv, S. Zhang, and W. Xiu, "Solving the security problem of intelligent transportation system with deep learning," *IEEE Transactions on Intelligent Transportation Systems*, no. 99, pp. 1–10, 2020.

[7] J. Bhola, S. Soni, and G. K. Cheema, "Genetic algorithm based optimized leach protocol for energy efficient wireless sensor networks," *Journal of Ambient Intelligence and Humanized Computing*, vol. 11, no. 3, pp. 1281–1288, 2020.

[8] D. Jiang, X. Ying, Y. Han, and Z. Lv, "Collaborative multi-hop routing in cognitive wireless networks," *Wireless Personal Communications*, vol. 86, no. 2, pp. 901–923, 2016.

[9] W. Song, H. Chen, Q. Zhang, B. Zhang, H. Wang, and H. Xu, "On-chip embedded debugging system based on leach algorithm parameter on detection of wireless sensor networks," *Mathematical Problems in Engineering*, vol. 2020, Article ID 7249674, 7 pages, 2020.

[10] M. Elhoseny and K. Shankar, "Reliable data transmission model for mobile adhoc network using signcryption technique," *IEEE Transactions on Reliability*, vol. 69, no. 3, pp. 1077–1086. In Press, 2020.

[11] M. Hamilton, "New directions in wireless embedded networked sensing of natural and agricultural ecosystems," *Gerodontology*, vol. 29, no. 1, pp. 48–53, 2004.

[12] D. Jin, Communication Protocols for Wireless Ad-Hoc and Sensor Networks, 2006.

[13] Y. Tang and M. Elhoseny, "Computer network security evaluation simulation model based on neural network," *Journal of Intelligent and Fuzzy Systems*, vol. 37, no. 3, pp. 3197–3204, 2019.

[14] S.-B. Tsai, J. Yu, L. Ma et al., "A study on solving the production process problems of the photovoltaic cell industry," *Renewable and Sustainable Energy Reviews*, vol. 82, pp. 3546–3553, 2018.

[15] Wuhan University of Technology, *Improvement and Simulation of Wireless Sensor Network LEACH Routing Protocol*, Wuhan University of Technology, Wuhan, China, 2010.

[16] M. Hu and Y. X. Wang, "Two-level linear clustering protocol based on wireless sensor networks," *Journal of Electronic Science and Technology*, vol. 14, no. 03, pp. 67–71, 2016.

[17] M. Qiu, W. Gao, M. Chen, J.-W. Niu, and L. Zhang, "Energy efficient security algorithm for power grid wide area monitoring system," *IEEE Transactions on Smart Grid*, vol. 2, no. 4, pp. 715–723, 2011.

[18] S. Zahmati F. Amir et al., "A hybrid spectrum sensing method for cognitive sensor networks," *Wireless Personal Communications*, vol. 74, no. 2, pp. 953–968, 2014.

[19] Nanjing University of Posts and Telecommunications, *Research on Routing Protocol of Wireless Sensor Network*, Nanjing University of Posts and Telecommunications, Nanjing, China, 2014.

[20] A. I. Douglas and J. K. Peter, "Learning-by-Doing Spillovers in the Semiconductor Industry," *Journal of Political Economy*, vol. 102, no. 6, pp. 1200–1227, 1994.

[21] M. Xie, *Research and Implementation of Network Protocol Stack of Wireless Sensor Network Node Operating System*, Zhejiang University, Hangzhou, China, 2008.

[22] A. K. Dutta, M. Elhoseny, V. Dahiya, and K. Shankar, "An Efficient Hierarchical Clustering Protocol for Multihop Internet of Vehicles Communication," *Transactions on Emerging Telecommunications Technologies*, vol. 35, no. 1, 2019.

[23] F. Li, M. Xiong, L. Wang, H. Peng, J. Hua, and X. Liu, "A novel energy-balanced routing algorithm in energy harvesting sensor networks," *Physical Communication*, vol. 27, no. APR, pp. 181–187, 2018.

[24] Y. Wu, B. Rong, K. Salehian, and G. Gagnon, "Cloud transmission: a new spectrum-reuse friendly digital terrestrial broadcasting transmission system," *IEEE Transactions on Broadcasting*, vol. 58, no. 3, pp. 329–337, 2012.

[25] J. q. Xu, J. l. Wang, h. Zhao et al., "Research and implementation of wireless sensor network node based on MSP430," *Miniature Microcomputer System*, vol. 29, no. 9, pp. 1652–1656, 2008.

[26] PLA information engineering university, *IEEE802.15.4 MAC Protocol Research*, PLA information engineering university, Zhengzhou, China, 2007.

[27] F. Teng and F. Zou, "Application of sensor technology in electromechanical automation control," *Urban Construction Theory Research: Electronic Edition*, no. 17, p. 116, 2015.

[28] K. Shankar and M. Elhoseny, "Trust based cluster head election of secure message transmission in MANET using multi secure protocol with TDES," *Journal of Universal Computer Science*, vol. 25, no. 10, pp. 1221–1239, 2019.

[29] H. Cai, X. Meng, D. Sun et al., "Design of a miniaturized wireless sensor network," *Aerospace Measurement Technology*, vol. 37, no. 3, pp. 60–65, 2017.

[30] M. Saidu, E. N. Onwuka, E. N. Onwuka, M. Okwori, and A. Umar, "An enhanced LEACH routing algorithm for energy conservation in A wireless sensor network," *International Journal of Wireless and Microwave Technologies*, vol. 6, no. 4, pp. 59–71, 2016.

[31] Y. Zhang, "Cluster head spacing adaptive hda-leach algorithm for wireless sensor networks," *Computer Engineering and Application*, vol. 43, no. 30, pp. 124–127, 2007.

[32] Shandong University, *Research on Energy-Saving Routing Protocol for Wireless Sensor Networks*, Shandong University, Jinan, China, 2010.

[33] Beijing Jiaotong University, *Research and Implementation of Clustering Routing Protocol for Wireless Sensor Networks*, Beijing Jiaotong University, Beijing, China, 2012.

[34] *Journal of Northeastern University (Natural Science Edition)*, vol. 31, no. 10, pp. 1385–1388, 2010.

[35] E. Laxmi Lydia, J. Samuel Raj, R. Pandi Selvam, M. Elhoseny, and K. Shankar, "Application of discrete transforms with selective coefficients for blind image watermarking," *Transactions on Emerging Telecommunications Technologies*, no. 8, 2019, In press.

[36] Y. Chen, W. Zheng, W. Li, and Y. Huang, "The robustness and sustainability of port logistics systems for emergency supplies from overseas," *Journal of Advanced Transportation*, vol. 2020, Article ID 8868533, 10 pages, 2020.

[37] Beijing University of Posts and Telecommunications, *Research on Energy Management and Energy Consumption Optimization of Wireless Sensor Networks*, Beijing University of Posts and Telecommunications, Beijing, China, 2009.

[38] Y. Z. Wang, Q. G. Chen, L. S. Wei et al., "Improvement of LEACH algorithm for wireless sensor networks," *Journal of Yanshan University*, vol. 38, no. 2, pp. 152–155, 2014.

Research Article

Efficient Object Detection Algorithm in Kitchen Appliance Scene Images Based on Deep Learning

Manhuai Lu [iD][1] **and Liqin Chen** [iD][2]

[1]*College of Mechanical and Electrical Engineering, University of Electronic Science and Technology of China, Zhongshan Institute, Zhongshan 528400, China*
[2]*School of Mechanical and Electrical Engineering, University of Electronic Science and Technology of China, Chengdu 610000, China*

Correspondence should be addressed to Liqin Chen; chenliqin_mail@163.com

The accuracy of object detection based on kitchen appliance scene images can suffer severely from external disturbances such as various levels of specular reflection, uneven lighting, and spurious lighting, as well as internal scene-related disturbances such as invalid edges and pattern information unrelated to the object of interest. The present study addresses these unique challenges by proposing an object detection method based on improved faster R-CNN algorithm. The improved method can identify object regions scattered in various areas of complex appliance scenes quickly and automatically. In this paper, we put forward a feature enhancement framework, named deeper region proposal network (D-RPN). In D-RPN, a feature enhancement module is designed to more effectively extract feature information of an object on kitchen appliance scene. Then, we reconstruct a U-shaped network structure using a series of feature enhancement modules. We have evaluated the proposed D-RPN on the dataset we created. It includes all kinds of kitchen appliance control panels captured in nature scene by image collector. In our experiments, the best-performing object detection method obtained a mean average precision mAP value of 89.84% in the testing dataset. The test results show that the proposed improved algorithm achieves higher detecting accuracy than state-of-the-art object detection methods. Finally, our proposed detection method can further be used in text recognition.

1. Introduction

Object detection is a fundamental issue in the field of computer vision and image processing and has been a hotspot of theoretical and applied research in recent years, with a wide range of applications. The main goal of object detection is to precisely predict the class and location information of various targets in an image or image sequence. The traditional target detection algorithm relies more on manually designed features. However, because of using a sliding window to select candidate bounding boxes, it has serious window redundancy problems and its feature extraction method has poor generalization performance. Moreover, twiddly steps of the traditional target detection algorithm will cause slow detection speed and poor real-time performance. With the rapid development of deep learning, deep learning-based target detection algorithms have proposed solutions to extract image features by using convolution neural networks. Therefore, both the detection accuracy and the detection speed have been greatly improved.

Object detection based on kitchen appliance scene not only attaches great importance to the natural scene object recognition that cannot be ignored, but it is also one of the most essential factors in the internet of things [1–5]. Object detection based on kitchen appliance scene images often faces different types and degrees of uncertainty interference, which seriously affects the accuracy of object detection. On the one hand, the scene itself has some internal interference such as invalid edges and pattern information unrelated to the object

of interest. Specifically, these disturbances may be boundary boxes or intuitive patterns that express functional meaning. On the other hand, the scene is also subject to serious external interference, such as various levels of specular reflection, uneven lighting, and spurious lighting. In addition, kitchen appliance scenes as a typical application also need to complete the task of detecting arbitrary symbols, such as Chinese texts and rectilinear symbols, which are positioned in the form of arrays on two-dimensional surfaces. Moreover, the position spacing and aspect ratio between different object regions is not a fixed value. The proposed improved object detection methods aim to identify object regions scattered in various areas of complex appliance scenes with uncertain position spacing and aspect ratio quickly and automatically.

Inspired by some state-of-the-art object detection algorithms, we designed a text location algorithm based on improved faster R-CNN, which considers all line patterns as potential targets and specifically considers three categories of line patterns, including text instances (text), the plus symbol "+" (add), and the minus symbol "−" (sub), as illustrated in Figure 1.

In this paper, we improve the RPN in faster R-CNN. We call it D-RPN. The main contributions of D-RPN are two-folded: (1) feature enhancement module. We design a multiscale convolution network structure for feature extraction and reinforcement, which addresses the limitation of feature extraction capability of the RPN that used single-scale convolution. Concretely, the feature enhancement module adopts convolution kernel at different scales to the feature map and extracts features at different scales. Then, it fuses and concatenates these features on the channel dimension, ultimately strengthening the expression of features. (2) The design of U-shaped network reconstruction. Using those multiscale convolution network structures, we construct a U-shaped network by max pooling layers and upsampling. The U-shaped network introduces the idea of UNet's [6] network architecture design. We replace the original RPN structure by concatenating multiple feature enhancement module in a U-shaped network structure. In this way, it not only deepens the depth of the network, extracts deeper features, but also learns more parameters.

However, we note that the field of target detection based on deep learning is presently well developed with numerous approaches, including R-CNN-based object detection methods, SSD-based object detection methods, and YOLO-based object detection methods. Therefore, we must first discuss these previous methods before outlining the presently proposed object detection method. Accordingly, related work is presented in Section 2, the proposed method is presented in Section 3, the results of experiments using kitchen appliance scene datasets are presented in Section 4, the expanded applications are presented in in Section 5, and the paper is concluded in Section 6.

2. Related Work

All object detection methods must address the inherent uncertainties associated with the size, direction, and structure of targets located within natural scene images.

Numerous conventional methods have been developed for object detection in natural image scenes in the past, such as Viola Jones detectors [7, 8], histogram of oriented gradients (HOD) detector [9], and deformable part-based model (DPM) [10]. These methods mainly employ object features extracted manually for establishing the parameters of the algorithm. However, the rapid advancement of deep learning in recent years has led to the development of numerous object detection methods based on this advanced technology [11–22]. These methods have a demonstrated capability of accurately locating object regions within natural image scenes by appropriately training their network structures. These object detection methods can be divided into three categories: R-CNN-based object detection methods, SSD-based object detection methods, and YOLO-based object detection methods.

2.1. R-CNN-Based Object Detection Methods. R-CNN-based object detection methods are two-stage target detection methods. The first stage generates bounding boxes and the second stage identifies the bounding boxes to which the category belongs. R-CNN [11], as a precursor of a deep convolutional neural network target detection framework, obtained 0.66 mAP on experimental data from the PASCAL VOC2007 test set. However, the detection process is particularly time-consuming because it performs a ConvNet for about 2000 object proposal without sharing computation. Fast R-CNN [12] made improvements on R-CNN. It organically combines the two problems of target classification and border regression, using softmax classifiers instead of support vector machines. It allows multiple object proposals to share the output features of the previous layer network. Ren et al. [13] proposed an improved version of faster R-CNN based on the fast R-CNN model. It uses the region proposal network (RPN), which solves the inefficient selection problem of proposal regions in target detection tasks. In addition, some distinguished researchers [14, 15] proposed improved algorithms for the faster R-CNN. For example, feature pyramid networks (FPN) [14], compared to regular feature pyramids, proposed a feature pyramid structure which enables independent prediction in each level of pyramid. The architecture of FPN exhibits significant advantages as a generic feature extractor in several applications. However, R-CNN-based object detection methods have room to improve the precision in generating suggestion boxes.

2.2. SSD-Based Object Detection Methods. SSD-based object detection algorithm is a one-stage target detection algorithm trained on an improved VGG16 [23] network. It is not only close to the faster R-CNN algorithm in terms of accuracy but also comparable to YOLO in terms of detection speed. Single-shot multibox detection (SSD) [16] introduced feature pyramid structure, but it takes high-level and low-level feature of the ConvNet into account. It also allows further improvements in target detection accuracy, especially for small objects. However, it is not strong enough to characterize the feature map extracted at low-level feature. Therefore, Shen et al. [17]

Input (locality)   Results of object detection
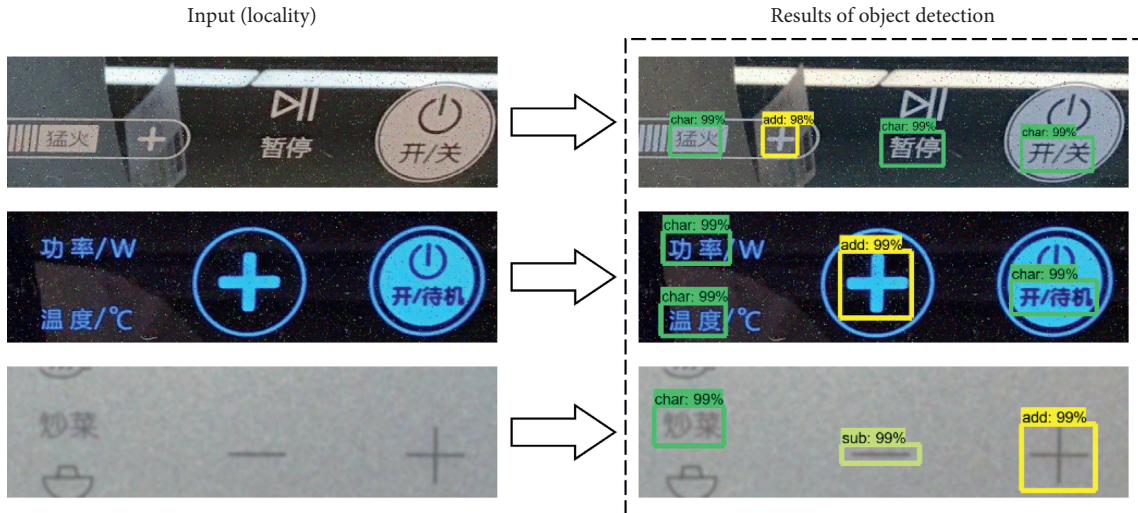

FIGURE 1: Examples of the three categories of line patterns employed during the proposed method.

proposed deeply supervised object detectors (DSOD) based on SSD network structure. It puts forward an efficient network framework and a set of principles to learn object detectors without using pretrained models on ImageNet. In terms of detection accuracy and parameter number, DSOD outperforms some state-of-the-art detectors such as SSD and Faster R-CNN. Moreover, deconvolutional single-shot detector (DSSD) [18] combines ResNet-101 [24] with SSD and uses deconvolution instead of up-sampling, which obtained 81.5% mAP on VOC2007 test and 80% mAP on VOC2012 test. But these methods are blank in the study of feature pyramids using multiple convolutional kernels on the same feature maps.

2.3. YOLO-Based Object Detection Methods. YOLO [19] first proposed an end-to-end training model transforming object detection to a regression problem of bounding boxes and associated class probabilities. However, because each grid cell only predicts two boxes and can only have one class, it causes the detection to be not very accurate. To address these issues, YOLOv2 [20] improved the performance by adding batch normalization layers on all of the convolutional layers and a new bounding box regression method by removing the fully connected layers from YOLO. Inspired by the FPN, YOLOv3 [21] predicted a score for each bounding box by using logistic regression and set more candidate boxes. Therefore, multiscale prediction and multilabel classification both can be realized. In 2020, based on the original YOLOv3 object detection architecture, YOLOv4 [22] algorithm proposed a new backbone network, named CSPDarknet-53, using Mish activation function and puts forward mosaic data augmentation method in data processing. These all enable the model to reach the best match in terms of detection speed and accuracy so far. However, YOLO-based methods have not yet been applied to the field of target detection in the kitchen appliance scene.

3. Proposed Method

In this section, the proposed method consists of three main parts: (1) data augmentation based on gamma corrections,

adding salt-and-pepper noises, and Gaussian blur; (2) feature enhancement module with multiscale convolution kernel for target feature reinforcement; (3) design of deeper feature extraction structure based on the typical encoder and decoder network of UNet [6], exerting a series of feature enhancement module.

3.1. Data Augmentation. In our experiments, the kitchen appliance control panel dataset we used is from an image collector. The dataset consists of control panel images of 28 different kitchen appliances without uniform plane size. Moreover, each of the images includes at least 15–20 object regions which scattered in various areas of complex appliance scenes with uncertain position spacing and aspect ratio.

In order to simulate both light and dark shooting environments, we first use gamma correction which is detailed as follows:

$$s = cr^{\gamma}. \tag{1}$$

Here, c is a zoom coefficient. r and s are the grayscale values of the input and output after normalization, respectively. When $\gamma < 1.0$, the gamma corrections can increase the overall brightness of the image; while $\gamma > 1.0$, the gamma correction will reduce the overall brightness, making the image darker. Thus, in our experiments, we set $\gamma = 0.7$ and $\gamma = 1.3$ to simulate both light and dark environments, respectively.

Second, we also add 1% salt-and-pepper noise to our dataset, which randomly generates some pixel positions within the image based on the signal-to-noise ratio (SNR) of the image and randomly assigns these pixels a value of 0 or 255.

Third, we use Gaussian blur to simulate a lens out of focus, which is detailed as follows:

$$f(x) = \frac{1}{\sqrt{2\pi}\sigma} \exp\left(-\frac{(x-\mu)^2}{2\sigma^2}\right), \tag{2}$$

where μ is the mean and σ is the variance. In OpenCV (Open Source Computer Vision Library), σ is calculated according to the following formula:

$$\sigma = 0.3 \times ((k\,\text{size} - 1) \times 0.5 - 1) + 0.8, \qquad (3)$$

where $k\,\text{size}$ is Gaussian kernel size. In our work, we set $\mu = 0$, $k\,\text{size} = 15$ ($\sigma = 2.6$). A three-dimensional view of the Gaussian function is shown in Figure 2(a).

Through three data augmentation methods, gamma correction, adding pretzel noise, and Gaussian blur, our data were augmented from the original 28 images to 336 images. This yielded a total of 5040–6720 object regions. Figures 2(b)–2(f) show some of the results of this data augmentation.

3.2. Overall Network Architecture.
The overall framework we proposed is shown in Figure 3. In this subsection, we will briefly describe our overall framework and it is divided into the following four components.

3.2.1. Feature Extraction Network.
This network consists of multiple convolution and pooling layers and is used to obtain feature information pertaining to appliance control panel images. First, the deep-layer features are perceived through a sliding window of the size of the convolution kernel. Next, the fine edge features of the panel are extracted initially, and redundant information is removed. Then, further dimensionality reduction and feature selection are conducted by the pooling operation. Commonly used feature extraction networks are VGG16 [23], ResNet-50 [24], and ResNet-101 [24]. In our work, we use VGG16 as our backbone feature extraction network.

3.2.2. D-RPN.
This section is a central part of our overall framework. Feature enhancement module with multiscale convolution kernel and design of deeper feature extraction structure based on UNet are proposed in D-RPN. But both will be detailed in Sections 3.3 and 3.4, respectively. Functionally, D-RPN in this paper is similar to RPN in faster R-CNN. The D-RPN is used to generate region proposals from the image and accordingly generates nine anchors of three different sizes and three different aspect ratios on each pixel of the extracted feature map. A number of candidate object regions are obtained through a one-to-one mapping of the anchors on the original image. These candidate regions contain a wide variety of information, such as entire object regions, partial object regions, and strictly background regions. Therefore, confidence levels are calculated for each anchor box reflecting the level of certainty regarding whether the anchor box contains object regions requiring detection. The object regions within anchor boxes with high confidence levels are then placed within bounding boxes, and regression adjustment of the bounding box parameters is applied. Finally, a method based on NMS is used to filter out bounding boxes that have a relatively large number of intersections.

3.2.3. ROI Pooling Layer.
The proposed regions are mapped onto the feature map in the ROI pooling layer, and the map is cropped accordingly. Then, the cropped region is divided into 7×7 segments of the same size by bilinear interpolation. Finally, maximum pooling is performed with a convolution kernel size of two to obtain the final feature map of each proposed region. As such, the process allows different region proposals to be output in the same dimension.

3.2.4. Classification Layers.
The classification layer is composed of fully connected layers and a softmax layer, which is used to classify each region proposal as either object or not-object and to output a confidence level. In addition, regression is performed to determine whether a bounding box includes an object region and to minimize deviations between the bounding boxes and the ground truth bounding boxes.

3.3. Feature Enhancement Module.
In our main work, we propose the feature enhancement module, which network framework is shown in Figure 4.

The module is divided into four parts. First, the results of previous layer input a 1×1 convolution layer to adjust the number of channels. Then, it is divided into three branches and each of them is a convolution layer with kernel size of 3×3, 5×5, and 7×7, respectively. Whereupon it uses convolution layers with different kernel size to extract features from the feature map. In this part, we set the stride of the convolution to 1, using the padding mode and rectified linear unit (Relu) activation functions. This ensures that the output of each branch has the same height, width, and number of channels for stacking. Next, we stack the features extracted from the previous part and integrate the information from different scales to strengthen the features. Finally, the results of concatenation were input to a 1×1 convolution layer again to squeeze the number of channels.

By using a convolution layer with different kernel size, respectively, the module is structured as a feature pyramid which increases not only the thickness of the network but also its adaptability to scale. Small convolution kernels such as 3×3 are sensitive to microfeatures that tend to be less semantic and more noisy, while large convolution kernels such as 7×7 are sensitive to macroscopic features that have stronger semantic information and are insensitive to noise. Therefore, we use convolution kernels with different scales, including 3×3, 5×5, and 7×7 pixels, to acquire features from different spaces on the feature map, and then these features are fused and further enhanced. This structure can increase the depth of the network and improve performance.

But if using multiscale convolution alone is prone to overfitting. The solution of easy overfitting in GoogLeNet [25] is to reduce the number of parameters by adding a layer of 1×1 convolution following each different scale convolution layer. However, in the feature enhancement module proposed in this paper, we stack the results of each scale convolution before connecting a 1×1 convolution layer. Thus, in the experimental part, a contrast experiment adding a layer of 1×1 convolution after 3×3, 5×5, and 7×7
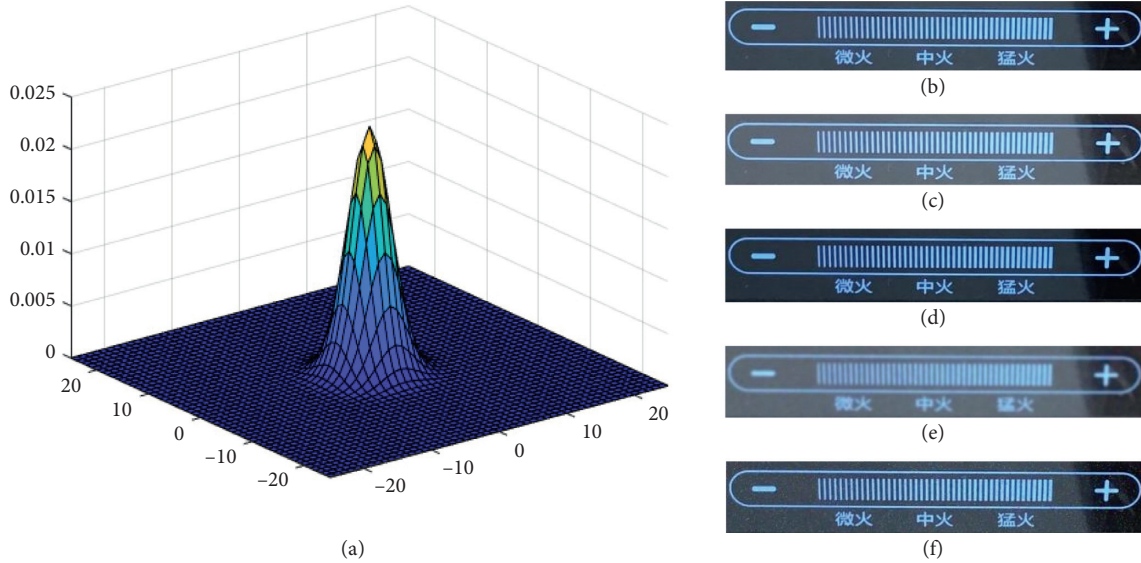
FIGURE 2: Data augmentation: (a) 3D view of the Gaussian function. (b) Original image. (c) Gamma correction ($\gamma = 0.7$) of (b). (d) Gamma correction ($\gamma = 1.3$) of (b). (e) Gaussian blur of (b). (f) 1% salt-and-pepper noise of (b).

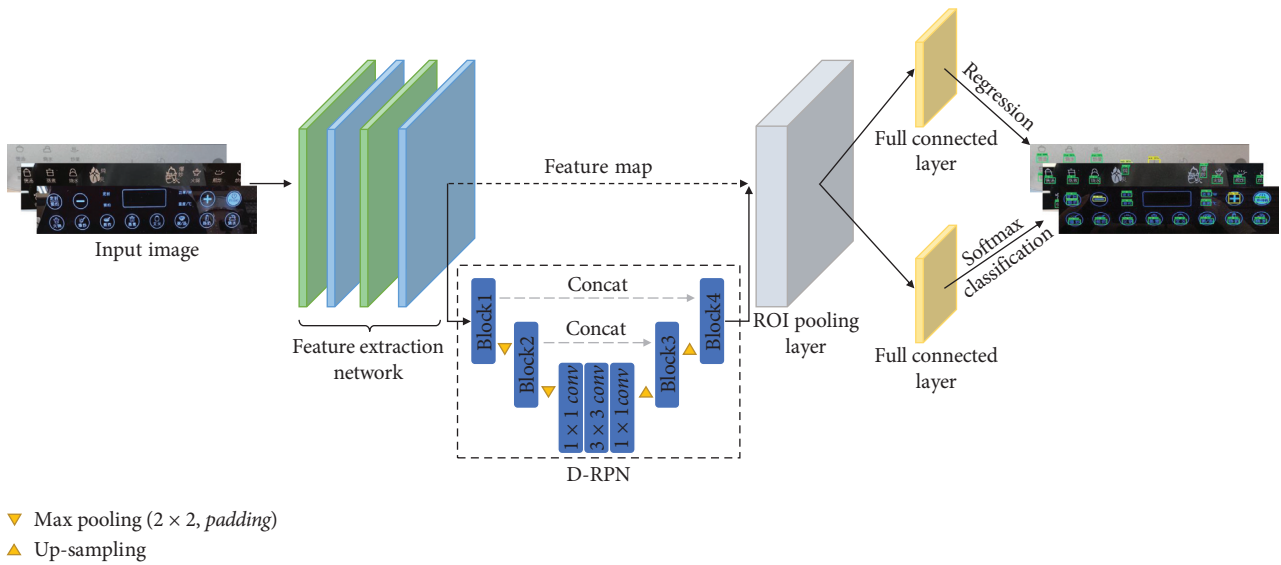▼ Max pooling (2×2, *padding*)
▲ Up-sampling

FIGURE 3: Overall framework of our proposed method based on faster R-CNN structure. It mainly consists of feature extraction network, D-RPN, ROI pooling layer, and classification layers.

convolution layers, respectively, will be designed to prove the effectiveness of the feature enhancement module proposed. In this contrast experiment, our approach is more accurate, and the corresponding comparative results will be presented in the experimental section.

3.4. The Design of U-Shaped Network Reconstruction.

In this section, we design a deeper feature extraction structure followed the typical encoder and decoder design of UNet [6]. It replaces the original RPN structure by concatenating multiple feature enhancement module in a U-shaped network structure. The overall network architecture we proposed is shown in Figure 5.

As shown in Figure 5, the left side of the structure is the encoder, which consists of two blocks in total. Each block consists of feature enhancement module, Relu activation function, and max pooling layer, and the three parameters below the feature enhancement module correspond to the number of channels C1, C2, and C3 in Figure 4, respectively. The result after feature enhancement module is activated with the Relu function. Finally, a max pooling of 2×2 is applied and output to the next block; the bottom of the structure consists of three ordinary convolution layers (their convolution kernel sizes are 1×1, 3×3, and 1×1, and the number of channels is 128); the right side of the structure is the decoder, which also consists of two blocks. In each of the blocks, the input feature map will be up-sampled in order to
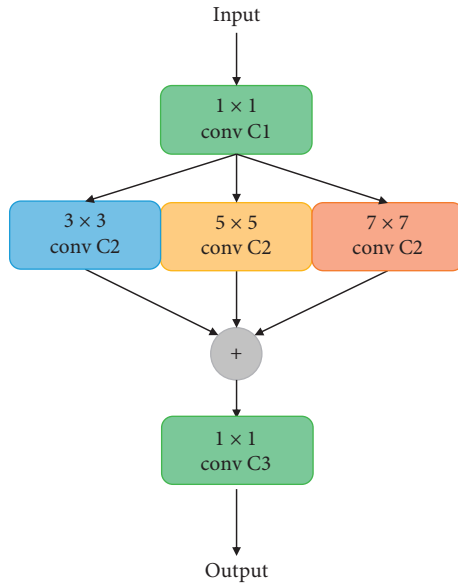
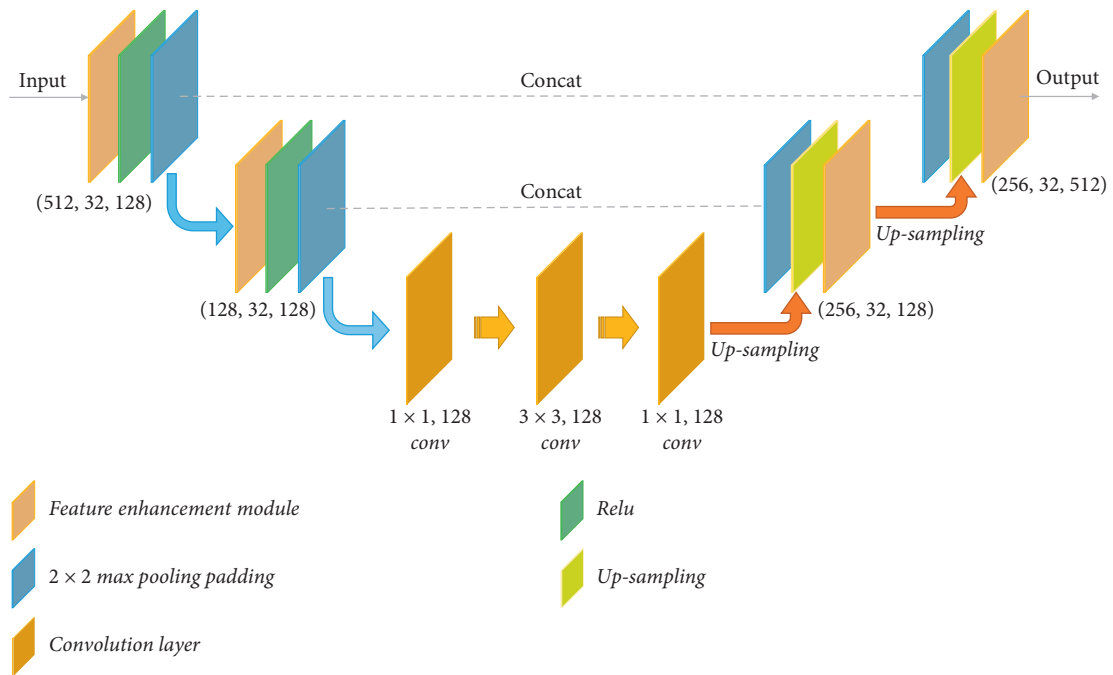FIGURE 4: Framework of feature enhancement module.

FIGURE 5: A deeper feature extraction structure we propose is composed of five components: feature enhancement module, Relu activation function, max pooling layer, ordinary convolution layer, and up-sampling.

ensure the up-sampled size is the same as that of the corresponding encoder. Then, by concatenation, the two are stacked on top of each other in the channel number dimension. It then goes through a feature enhancement module and finally outputs.

We introduce the idea of encoder and decoder in UNet into our structure. In our deeper feature extraction structure, the left side is the down-sampling layer and the right side is the up-sampling layer. During the down-sampling process, the receptive field expands step by step, which is equivalent to the meanings that the image will be compressed and the

region per unit area perceived will become larger. In this way, the low-frequency information of the image is detected more frequently. Besides, up-sampling was added to the decoder process, from which the information and size of the feature map is recovered and that ensures the most critical operations (feature fusion by concatenating) can proceed successfully. In addition, a concatenation feature fusion approach will be used in our deeper feature extraction structure. The feature map obtained at each down-sampling layer of the network is concatenated to the corresponding up-sampling layer, which creates a thicker feature map. In

other words, the feature fusion approach facilitates the integration of the information of the various stages of the down-sampling in the up-sampling process. That is, the structural information of each layer is combined during the up-sampling process.

4. Experiments and Results

4.1. Implementation and Evaluation Methods. The proposed improved model was implemented in TensorFlow with one NVIDIA GTX 1650 GPU. Our dataset first randomly selects 80% of the data for training and the remaining 20% is used as a testing dataset. Furthermore, the training data is divided into a training dataset and a validation dataset in the proportion $7:3$. For training, the learning rate was initialized to 0.001 and a weight decay of 0.0001, and the stochastic gradient descent (SGD) with momentum is set to 0.9. Training iterations are set to 20,000.

During training, the cross-entropy loss function was used for the classification task and the Smooth_{L1} loss function [12] was used for the regression task. For RPN training, we set up nine anchor boxes with three different aspect ratios and sizes. The process of mapping these boxes to the original images generated about 20,000 anchors, which were then filtered according to the confidence levels calculated using NMS with a threshold of 0.7. The proportion of overlap between an anchor and a ground truth object was calculated according to the intersection over union (IOU), and all anchors with $\text{IOU} \leq 0.7$ were designated as positive samples containing a text region, while those with $\text{IOU} \leq 0.3$ were designated as negative samples containing no text region. Then, in these anchors, 128 positive samples and 128 negative samples were selected respectively for training. The loss of the RPN is mainly composed of a classification prediction loss L_{class} based on the probability pi of predicting the i-th anchor as a target according to the i-th ground truth label p_i^*, which is set to 1 for a positive sample and set to 0 otherwise, and a regression prediction loss $L_{\text{regressioin}}$ based on the four coordinate parameters $t_i = \{t_x, t_y, t_w, t_h\}$ of the i-th predicted bounding box, where the subscripts refer to the x and y center coordinates and the width w and height h of the bounding box, and the four coordinate parameters $t_i^* = \{t_x^*, t_y^*, t_w^*, t_h^*\}$ of the i-th ground truth box. Accordingly, the loss function is defined as follows:

$$L(\{p_i\}, \{t_i\}) = L_{\text{class}}(p_i, p_i^*) + L_{\text{regression}}(t_i, t_i^*),$$

$$L_{\text{class}}(p_i, p_i^*) = \frac{1}{N_{\text{cls}}} \sum_i -\log[p_i^* p_i + (1 - p_i^*)(1 - p_i)],$$

$$L_{\text{regression}}(t_i, t_i^*) = \lambda \frac{1}{N_{\text{reg}}} \sum_i p_i^* \text{Smooth}_{L1}(t_i - t_i^*),$$

$$\text{Smooth}_{L1}(x) = \begin{cases} 0.5(|x|)^2, & \text{if} |x| < 1, \\ |x| - 0.5, & \text{otherwise}. \end{cases}$$

$$(4)$$

Here, N_{cls} is the minimum number of each input batch of predicted bounding boxes, λ is a balancing parameter that both N_{cls} and N_{reg} terms are approximately equally weighted. We set it to the default value of 10, and N_{reg} is the number of anchor boxes. Furthermore, the elements of t_i and t_i^* are subject to the following special definitions:

$$
\begin{aligned}
t_x &= \frac{(x - x_a)}{w_a}, \\
t_y &= \frac{(y - y_a)}{h_a}, \\
t_w &= \log\left(\frac{w}{w_a}\right), \\
t_h &= \log\left(\frac{h}{h_a}\right), \\
t_x^* &= \frac{(x^* - x_a)}{w_a}, \\
t_y^* &= \frac{(y^* - y_a)}{h_a}, \\
t_w^* &= \log\left(\frac{w^*}{w_a}\right), \\
t_h^* &= \log\left(\frac{h^*}{h_a}\right).
\end{aligned}
$$

$$(5)$$

Here, all terms with the subscript a represent the standard parameters of an anchor box. Minimizing the loss function yields predicted bounding box parameters that are arbitrarily close to ground truth box parameters.

In this paper, we use mean average precision (mAP) to evaluate the performance of the model. It contains two very important evaluation measures: precision and recall. They are defined as follows:

$$
\begin{aligned}
\text{Precision} &= \frac{\text{TP}}{\text{TP} + \text{FP}}, \\
\text{Recall} &= \frac{\text{TP}}{\text{TP} + \text{FN}},
\end{aligned}
$$

$$(6)$$

where TP, FP, and FN are true positive, false positive, and false negative, respectively. With precision and recall, $P - R$ curve for a category is plotted and then we calculate the area under the curve to get the average precision (AP) value for that category. The mAP is a measure of the detection accuracy of the model by calculating the mean AP of all classifications. It is defined as follows:

$$\text{mAP} = \frac{1}{m} \sum_{i=1}^{m} \text{AP}(i),$$

$$(7)$$

where m is the number of categories in the dataset. The higher the mAP value, the better the overall performance of

the model and the more accurate the prediction for each class will be.

4.2. Comparison of Different Networks.

First of all, we evaluated the predication performance of different networks: faster R-CNN with VGG16 [23], SSD, YOLOv3, and YOLOv4, and all these networks were trained with same dataset segmentation strategy. Table 1 shows the performance of different networks under the same evaluation criteria. We can observe that our proposed improved network significantly outperforms the other networks in detecting categories, add and sub. Although the AP value is slightly lower than that of the SSD model when detecting category, text, the mAP value of our method is higher. This indicates the overall better performance of our model.

To validate the advantages of our proposed feature enhancement module and design of deeper feature extraction structure, the comparison of the visualized detection results based on the same testing dataset between our improved method and the unimproved method (faster R-CNN) is shown in Figure 6. The results demonstrate that the unimproved method also has the phenomenon of omission inspection and erroneous inspection, such as undetected text object and treating patterns as text in the image. But our improved algorithm gains better performance. Therefore, our study is of relevance.

4.3. Effect of Feature Enhancement Module.

Our module is essentially a multiscale detection method. So, we further explored the effect of our proposed multiscale module. We compare five variants: our proposed feature enhancement module, module only using 3×3 convolution layer, module only using 5×5 convolution layer, module only using 7×7 convolution layer, and our proposed multiscale module which adds 1×1 convolution layers following 3×3 convolution layer, 5×5 convolution layer, and 7×7 convolution layer, respectively.

All these variants were trained under the same conditions. In Table 2, it can be learned that our proposed multiscale module is superior to other structures. This illustrates that multiscale convolution is more effective for the network to extract feature information at different scales, and the fusion of this feature information can play the role of feature enhancement.

5. Expanded Applications

Based on the high-precision detection effect of our proposed method, our detection results can also be applied to text recognition. So, in this article, we give some extended experiments on text recognition. The experiment consists of a total of two stages, character segmentation, and character recognition, each of which is described as follows.

5.1. Character Segmentation.

The character segmentation stage applies a projection-based text character segmentation method to segment the extracted text instances into independent character instances. As illustrated in Figure 8, projection-based character segmentation obtains pixel distribution information in the vertical or horizontal direction by projecting a binary image vertically or horizontally and segments characters in the detected text region based on the characteristic peaks and valleys in the pixel distribution. Here, the Otsu [26] binarization method is applied to the text region in Figure 8(a) detected in the previous step to generate the binary image in Figure 8(b), which assigns background pixels a value of 0 and foreground pixels representing text a value of 1. The vertical projection of Figure 8(b) is shown in Figure 8(c), from which a statistical pixel distribution map is obtained. The peaks and valleys in the pixel distribution map are then employed to obtain the character segmentation shown in Figure 8(d).

5.2. Character Recognition.

The character recognition stage applies a deep CNN to recognize the character instances extracted in the previous stage. Each of the abovementioned character segments obtained in the previous step is then classified using a D-CNN with the structural framework illustrated in Figure 9. Here, convolution and pooling are again employed for feature extraction, and a softmax layer is applied for calculating the probability for each category outcome, and the corresponding categories are output according to the established probabilities.

In prepossessing, we specifically prepare the dataset for character recognition. It consisted of screenshots of characters in the open source Chinese character dataset collected from natural scene images and four Chinese typeface font libraries (Arial, msyhl, msyh, and STLITI). All images were enhanced according to the same process applied to the dataset in the object detection stage. The training time of the D-CNN was streamlined by selecting 57 categories of Chinese characters during the training phase and converting all images to normalized grayscale images composed strictly of 32×32 pixels, which yielded a total of 21463 images.

In training, dataset in character recognition was randomly shuffled, and 60% of the characters in the dataset were employed for the training dataset, while the remaining 40% were evenly divided among the validation dataset and testing dataset. The learning rate was initially set to 0.0001 and the number of training iterations was limited to 500. Taking into account the computing power available during D-CNN training, a tensor of 64 images was input at each iteration. In addition, a multiclass cross-entropy function (as shown in

TABLE 1: Detection performance of different networks trained for the three target categories, including text symbols (text), the plus symbol "+" (add), and the minus symbol "−" (sub), based on the average precision (AP) obtained for the testing dataset.

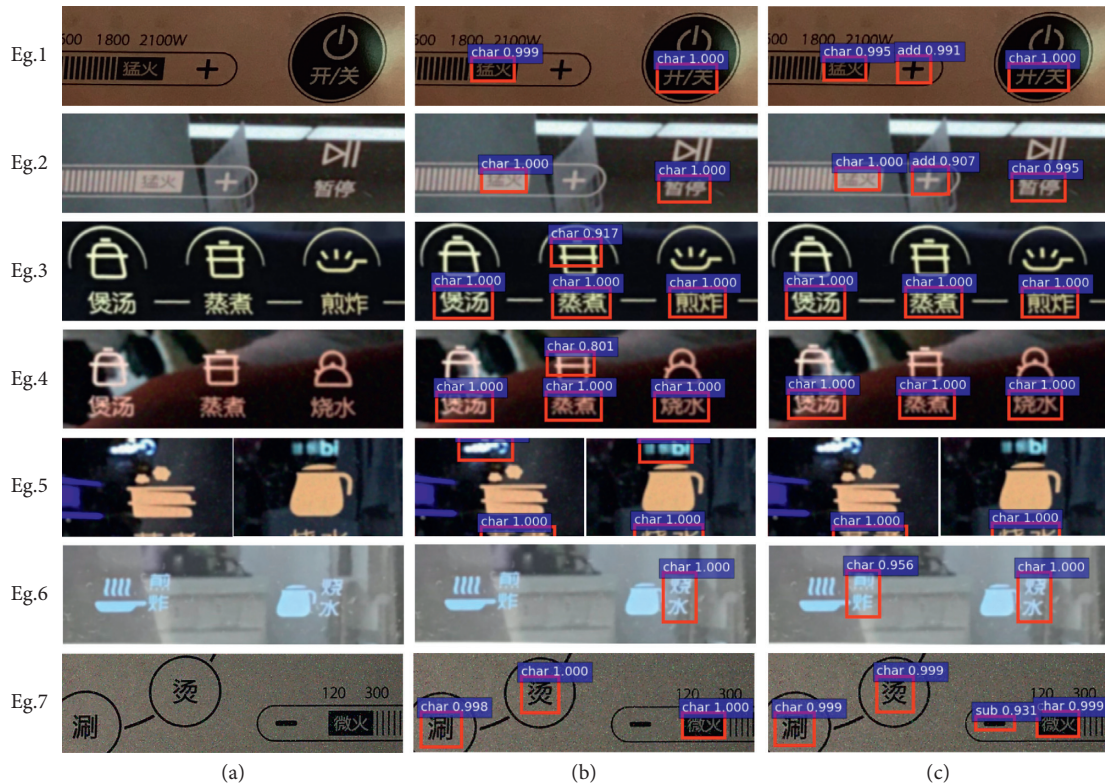| Networks	Class (AP)			
	Text	Add	Sub	mAP
Faster R-CNN	0.9091	0.9131	0.7597	0.8606
SSD	0.8449	0.9432	0.6295	0.8059
YOLOv3	0.9923	0.7907	0.6503	0.8111
YOLOv4	0.8565	0.6743	0.6257	0.7188
Our	0.9085	0.9986	0.7882	0.8984

FIGURE 6: Visualized detection results between our improved method and the unimproved method (faster R-CNN). (a) Original images. (b) The results of the unimproved method. (c) The results of our improved method.

TABLE 2: The results of all variants which were trained under the same conditions. The respective AP values for categories Text, Add, and Sub are used as indicators for evaluating each model.

Networks	Only $3*3$	Only $5*5$	Only $7*7$	Adding $1*1$	Our
Frame diagram	Figure 7(a)	Figure 7(b)	Figure 7(c)	Figure 7(d)	Figure 3
Text (AP)	0.9090	0.9091	0.9071	0.9081	**0.9085**
Add (AP)	0.9147	0.9920	0.9970	0.9923	**0.9986**
Sub (AP)	0.7759	0.7642	0.7394	0.7042	**0.7882**

equation (8)) was employed owing to the multiclass classification task involved. Finally, we adopted Adam optimization [27] during training, which can adaptively adjust the learning rate of each parameter, using estimations of the first moment and second moment of the gradient, to allow for relatively stable variations in the parameters.

$$\text{Loss} = \frac{1}{N} \left\{ \sum_i \left[-\sum_i^M y_{ic} \log(p_{ic}) \right] \right\}. \tag{8}$$

The loss obtained by the proposed character classifier from equation (8) during training and validation and its accuracy values obtained during training, validation, and testing are, respectively, presented in Figures 10(a) and 10(b) with respect to the number of iterations. We note from Figure 10(a) that the loss of our character classifier decreases very rapidly to nearly 0 after only about 100 iterations for both the training and validation datasets. Correspondingly, we also note from Figure 10(b) that the accuracy values rapidly approach 99.89%, 96.30%, and 97.99% with

increasing iterations for the training dataset, validation dataset, and testing dataset, respectively, where values are presented in the latter case only for every 5th iteration.

6. Summary

This paper addressed the unique challenges associated with the application of object detection for kitchen appliance scene images by proposing an improved network based on faster R-CNN. We put forward D-RPN structure that improved RPN in the faster R-CNN. It consists of a series of feature enhancement modules and these modules reconstructed a U-shaped network structure. Proposed feature enhancement modules use the multi-scale feature reinforcement method that fuses features extracted from 3×3, 5×5, and 7×7 convolution layers, respectively. The multiscale feature enhancement module outperforms the other module using single-scale such as only 3×3, 5×5, and 7×7 convolution layers. In addition, experiments show that our D-RPN structure
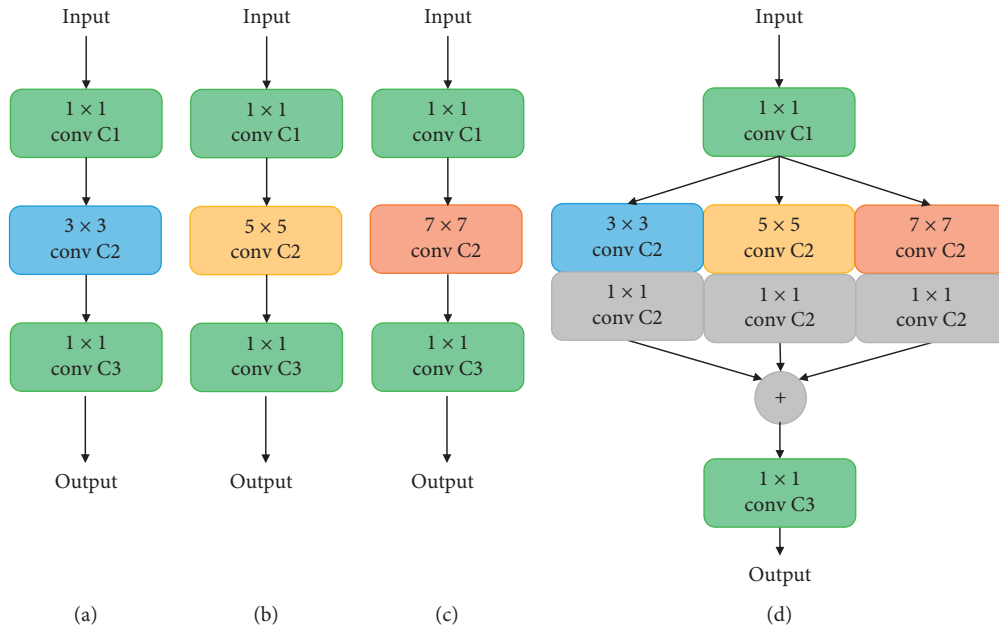
FIGURE 7: Structural diagram of four variants we set: (a) module only using 3×3 convolution layer; (b) module only using 5×5 convolution layer; (c) module only using 7×7 convolution layer; (d) our proposed multiscale module which adds 1×1 convolution layers following 3×3 convolution layer, 5×5 convolution layer, and 7×7 convolution layer.

FIGURE 8: Projection-based character segmentation: (a) object region detected in the previous object localization step; (b) binary image of (a); (c) pixel distribution map obtained from the vertical projection of (b); (d) character segmentation obtained according to the peaks and valleys in the pixel distribution map in (c).
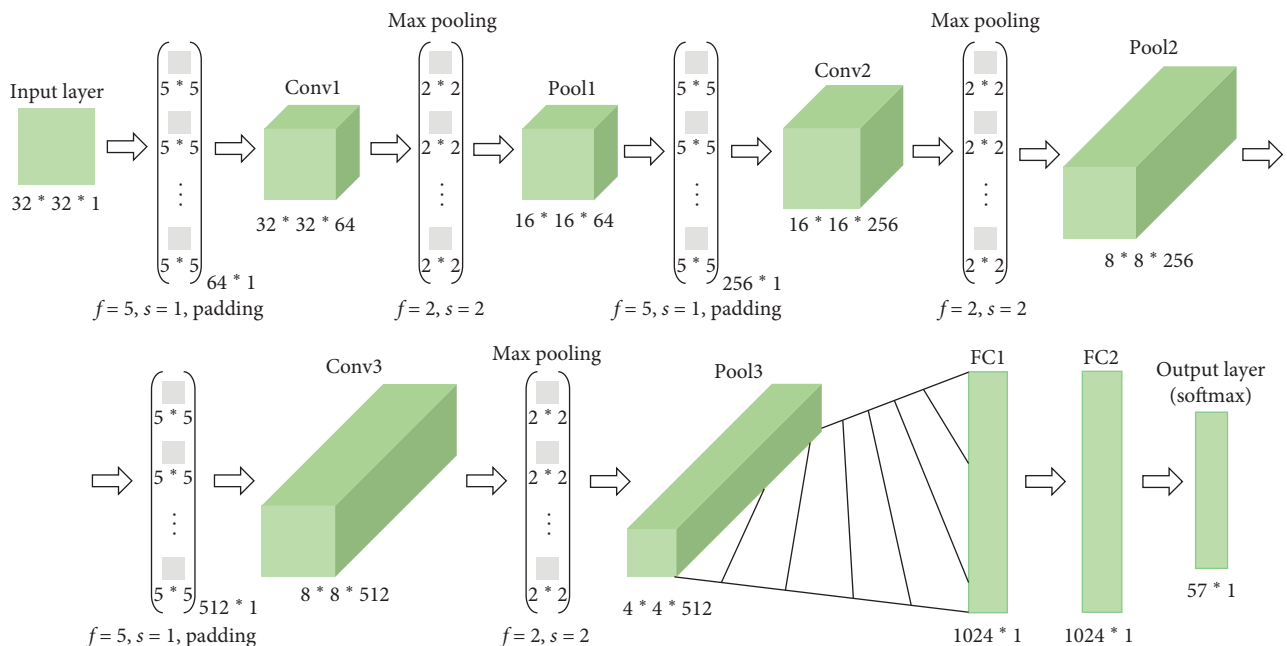

FIGURE 9: Structural framework of the D-CNN employed for classifying the character segments obtained during the previous character segmentation step.
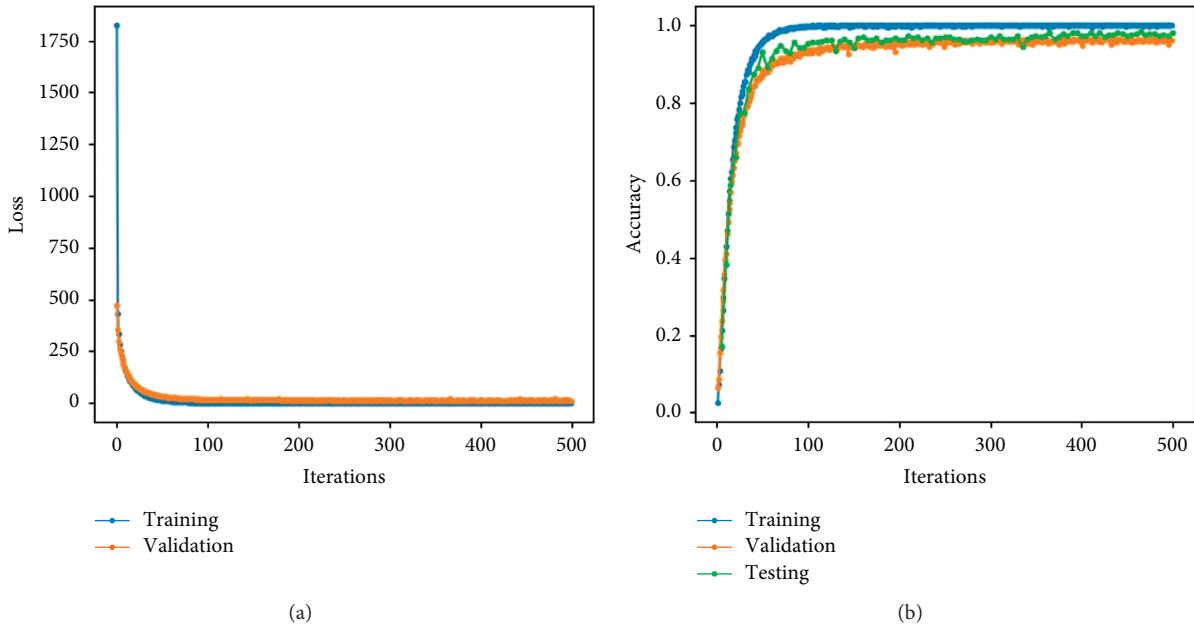
(a)

(b)

FIGURE 10: Loss values (a) obtained by the proposed character classifier from equation (8) during training and validation, and its accuracy values (b) obtained during training, validation, and testing.

acquires 0.8984 mAP value and performs better compared to other state-of-the-art object detection methods such as faster R-CNN, SSD, YOLOv3, and YOLOv4. Ultimately, our high-precision target detection method can also be applied to text recognition, also with good results.

Although we have achieved satisfactory results with our proposed approach, there are a lot of works to be done. In terms of dataset, we need more data of kitchen appliance control panel to improve the generalizability of the model and reduce the risk of overfitting. In terms of feature extraction, VGG16 is not necessarily the best backbone feature extraction network. Therefore, we need to research the influence of other backbone feature extraction networks on the accuracy of the model, for example, ResNet-50 and ResNet-101. Finally, there is a data imbalance problem in our dataset. For instance, the text symbols (text) always have much more than the plus symbols (add) and minus symbols (sub). However, we tried to use the focal loss function but did not get the results we expected, so we still need to study the data imbalance problem in our future work.

Data Availability

The data used to support the findings of this study are available from the corresponding author upon request.

Conflicts of Interest

This manuscript has not been submitted to, nor is under review at, another journal or other publishing venue. The authors have no affiliation with any organization with a direct or indirect financial interest in the subject matter discussed in the manuscript.

Acknowledgments

References

[1] A. M. Al-Momani, M. A. Mahmoud, and M. S. Ahmad, "Factors that influence the acceptance of internet of things services by customers of telecommunication companies in Jordan," *Journal of Organizational and End User Computing*, vol. 30, no. 4, pp. 51–63, 2018.

[2] I. Kitouni, D. Benmerzoug, and F. Lezzar, "Smart agricultural enterprise system based on integration of internet of things and agent technology," *Journal of Organizational and End User Computing*, vol. 30, no. 4, pp. 64–82, 2018.

[3] K. Srinivasa, B. Sowmya, A. Shikhar, R. Utkarsha, and A. Singh, "Data analytics assisted internet of things towards building intelligent healthcare monitoring systems: iot for healthcare," *Journal of Organizational and End User Computing (JOEUC)*, vol. 30, pp. 83–103, 2018.

[4] S. K. Biswas, D. Devi, and M. Chakraborty, "A hybrid case based reasoning model for classification in internet of things (iot) environment," *Journal of Organizational and End User Computing*, vol. 30, no. 4, pp. 104–122, 2018.

[5] M. R. Reddy, K. G. Srinivasa, and B. E. Reddy, "Smart vehicular system based on the internet of things," *Journal of Organizational and End User Computing*, vol. 30, no. 3, pp. 45–62, 2018.

[6] O. Ronneberger, P. Fischer, and T. Brox, "U-net: convolutional networks for biomedical image segmentation," in *Proceedings of the International Conference on Medical Image Computing and Computer-Assisted Intervention*, pp. 234–241, Lima, Peru, October 20.

[7] P. Viola and M. Jones, "Rapid object detection using a boosted cascade of simple features," in *Proceedings Of The 2001 Ieee*

Computer Society Conference On Computer Vision And Pattern Recognition, Kauai, HI USA, December 2001.

[8] P. Viola and M. J. Jones, "Robust real-time face detection," *International Journal of Computer Vision*, vol. 57, no. 2, pp. 137–154, 2004.

[9] N. Dalal and B. Triggs, "Histograms of oriented gradients for human detection," in *Proceedings of the 2005 IEEE computer society conference on computer vision and pattern recognition (CVPR'05)*, pp. 886–893, San Diego, CA, USA, September 2005.

[10] E. Hsiao, P. Felzenszwalb, D. McAllester, and D. Ramanan, "A discriminatively trained, multiscale, deformable part model," in *Proceedings of the 2008 IEEE Conference on Computer Vision and Pattern Recognition*, Anchorage, AK, USA, June 2008.

[11] R. Girshick, J. Donahue, T. Darrell, and J. Malik, "Rich feature hierarchies for accurate object detection and semantic segmentation," in *Proceedings of the IEEE Conference on Computer Vision and Pattern Recognition*, pp. 580–587, Seattle, WA, USA, June 2014.

[12] R. Girshick, "Fast r-cnn," in *Proceedings of the IEEE International Conference on Computer Vision*, pp. 1440–1448, Santiago, CL, USA, December 2015.

[13] S. Ren, K. He, R. Girshick, and J. Sun, "Faster r-cnn: towards real-time object detection with region proposal networks," in *Proceedings of the Advances in Neural Information Processing Systems*, pp. 91–99, Montreal, Canada, December 2015.

[14] T.-Y. Lin and P. Dollr, Feature pyramid networks for object detection," in *Proceedings of the IEEE Conference on Computer Vision and Pattern Recognition*, pp. 2117–2125, Seattle, WA, USA, June 2017.

[15] Z. Liu, Y. Lyu, L. Wang, and Z. Han, "Detection approach based on an improved faster rcnn for brace sleeve screws in high-speed railways," *IEEE Transactions on Instrumentation and Measurement*, vol. 69, 2019.

[16] W. Liu, D. Anguelov, D. Erhan et al., "Ssd: single shot multibox detector," in *Proceedings of the European Conference on Computer Vision*, pp. 21–37, Glasgow, UK, August 2016.

[17] Z. Shen, Z. Liu, J. Li, Y.-G. Jiang, Y. Chen, and X. Xue, "Dsod: learning deeply supervised object detectors from scratch," in *Proceedings of the IEEE International Conference on Computer Vision*, pp. 1919–1927, Venice, Italy, October 2017.

[18] C.-Y. Fu, W. Liu, A. Ranga, A. Tyagi, and A. C. Berg, "Dssd: Deconvolutional Single Shot Detector," 2017, http://arxiv.org/abs/1701.06659.

[19] J. Redmon, S. Divvala, R. Girshick, and A. Farhadi, "You only look once: unified, real-time object detection," in *Proceedings of the IEEE Conference on Computer Vision and Pattern Recognition*, pp. 779–788, Seattle, WA, USA, June 2016.

[20] J. Redmon and A. Farhadi, "Yolo9000: better, faster, stronger," in *Proceedings of the IEEE Conference on Computer Vision and Pattern Recognition*, pp. 7263–7271, Seattle, WA, USA, June 2017.

[21] J. Redmon and A. Farhadi, "Yolov3: an incremental improvement," 2018, http://arxiv.org/abs/1804.02767.

[22] A. Bochkovskiy, C.-Y. Wang, and H.-Y. M. Liao, "Yolov4: optimal speed and accuracy of object detection," 2020, http://arxiv.org/abs/2004.10934.

[23] K. Simonyan and A. Zisserman, "Very deep convolutional networks for large-scale image recognition," 2014, http://arxiv.org/abs/1409.1556.

[24] K. He, X. Zhang, S. Ren, and J. Sun, "Deep residual learning for image recognition," in *Proceedings of the IEEE Conference on Computer Vision and Pattern Recognition*, pp. 770–778, Seattle, WA, USA, June 2016.

[25] C. Szegedy, W. Liu, Y. Jia et al., "Going deeper with convolutions," in *Proceedings of the IEEE Conference on Computer Vision and Pattern Recognition*, pp. 1–9, Seattle, WA, USA, June 2015.

[26] N. Otsu, "A threshold selection method from gray-level histograms," *IEEE Transactions on Systems, Man, and Cybernetics*, vol. 9, no. 1, pp. 62–66, 1979.

[27] D. P. Kingma and J. Ba, "Adam: a method for stochastic optimization," 2014, http://arxiv.org/abs/1412.6980.

Research Article

Agricultural Productive Service System Based on the Block Chain and Edge Computing

Yuqing Wang and Xueping Han [ID]

College of Economics and Management, Northeast Agricultural University, Harbin 150030, Heilongjiang, China

Correspondence should be addressed to Xueping Han; mkck1112@126.com

With the rapid development of the service sector in economic growth, productive service industry has become a growing field of people's attention. Agricultural productive services are a supporting point to promote the development of modern agriculture, and at the same time, they also point out the direction for promoting the transformation of the agricultural development mode, which has very important strategic significance. In order to analyze and improve the rural productive service system and solve the "three rural" issues, this article designs an agricultural productive service analysis framework from the perspective of farmers, statistics of the investment in agricultural productive services in a certain region from 2015 to 2019, the expenditure of agricultural productive services in agriculture, forestry, fishery, and animal husbandry, and per capita wage income and operating income of farmers in the area under agricultural productive services, and in the process of agricultural production, farmers need agricultural productive services from the perspective of the whole process, land preparation, seeding, pest control, fertilization, and harvesting risks. The data in this experiment are stored in a distributed manner through the block chain, and the data are stored in the corresponding part in the chronological order; the data are transmitted to the edge server of the experimental network in the way of point-to-point transmission, and then edge computing technology is used to calculate and analyze the data collected in the experiment. The final result shows that, in this region, the input of the main agricultural producer service industry is growing very fast, the scale of productive services is expanding, and more and more attention is paid to the producer services in the process of agricultural production, but the internal composition of agricultural producer services is unbalanced. With the continuous improvement of the scale of agricultural productive services, the per capita income of farmers and the per capita income of management are also increasing year by year. When the scale of agricultural productive services reaches 0.09 in 2019, the per capita wage income of farmers has reached 3900 yuan, and the per capita income of farmers has reached 3750 yuan. And in the perspective of various risks in agricultural production, the higher the risk coefficient, the stronger the risk preference of farmers and the higher the risk investment in agricultural production services.

1. Introduction

1.1. Background Meaning. The producer service industry is an important part of modern agriculture, and it plays a very important role in the external effects of agriculture, broadening the income channel, and adjusting the structure of the agricultural industry [1]. With the development of agricultural modernization, farmers' demand for agricultural productive services has become more and more urgent. In recent years, the state has attached great importance to the development of agricultural productive services and has

continuously introduced encouraging policies. The development of modern agriculture requires a more complete and professional agricultural production process, which provides opportunities for the development of agricultural productive services. The coordinated development of agricultural productive services and the comprehensive development of the first, second, and tertiary industries in rural areas are objective requirements for realizing medium-scale agricultural operations, improving agricultural efficiency, and increasing farmers' incomes and are important measures to realize the transformation from small to large [2]. The

continuous advancement of our country's urbanization has released rural labor and increased the nonagricultural income of the peasants, and professional agricultural productive service organizations have developed rapidly. In order to analyze the economic benefits brought by the agricultural productive service system to the rural areas and farmers, we conducted research on the agricultural productive service system based on the block chain and edge computing. In addition, the computing edge of the edge server is closer to the terminal device, and the performance of the service device is relatively low. However, this server supports multiple communication protocols and provides distributed computing functions, which effectively improves the efficiency of the experiment and saves the time for calculating data.

The tertiary industry, that is, the service industry, plays an increasingly important role in economic development, and the agricultural productive service industry is an important part of the entire service industry. The development of the agricultural productive service industry has allowed breakthroughs in the traditional, primary, and tertiary industries, allowing the integration and penetration of agriculture and the service industry to achieve common development. Promoting the development of agricultural productive services will help improve the efficiency of agricultural production, increase the income of farmers, and promote the optimization and upgrading of the agricultural industry structure. Agricultural production services based on agricultural professional cooperatives can solve various problems in the development of modern agriculture in terms of capita, technology, and management.

1.2. Related Work. At present, many scholars have conducted relevant research on the agricultural productive service system. Jia-Ni researched the development of agricultural productive services in Suqian from five aspects and provided references for the further development of agriculture [3], but the experimental data of the research were incorrect, and the experimental results were inaccurate. Ming et al. used the tobit model to analyze the impact of agricultural production service segmentation on agricultural production efficiency [4], but the experimental model of this method has errors, and the experimental results are unreliable. Yingming et al. used the ordinary least-squares stepwise regression method to analyze the correlation between the farmland scale and agricultural production services [5], but the data calculation process of this method is too complicated. Tian et al. used the entropy method and the degree of coordination to measure the degree of coordination between agricultural productive services and the first, second, and tertiary industries of agriculture and studied the geographical distribution characteristics of the degree of coordination between the two [6], but the experimental study of data too jumbled. Zhu et al. constructed a measurement index system for the producer service industry and used the coupling coordination model to measure the extension of the agricultural industry chain and the coupling coordination between the producer service industry and

rural education [7], but the experimental procedures of this study are too complicated and not easy to operate. Wu and Chen analyzed the demand factors of the agricultural productive service industry and evaluated them [8], but the experimental subjects selected in this study were too one-sided, and the analysis of the experimental results was not comprehensive enough. Zhang and Sun analyzed the status quo of the development of agricultural productive services in our country, deeply analyzed the root causes of the backward development of agricultural productive services, and proposed a systematic optimization process from the perspective of system reform [9], but the research only has theoretical analysis, and there is a lack of data to prove the reliability of the results. Gao and Zhang compared the evaluation of the supply and demand status of agricultural productive services by three types of farmers and the farmers' demand for productive services [10], but the experimental objects and data in this study were too few to provide a strong proof for the experimental results. The above studies have certain flaws. Based on this, we have made certain improvements to the above studies and studied the agricultural productive service system of block chain and edge computing.

1.3. Innovation of this Article. This article counts the input and expenditure of agricultural productive services in a certain area, the income of farmers under agricultural productive services, and farmers' demand for agricultural productive services; from the perspective of farmers, research the agricultural productive service system based on block chain and edge algorithms. The innovations of this article are reflected in the following aspects: (1) use block-chain technology as a method of data storage to ensure data stability and security; (2) use edge computing technology to carry out related techniques and analysis of experimental data, which saves the calculation time of experimental data, improves the efficiency of the experiment, and has certain advantages in data security and privacy protection; (3) from the perspective of farmers, the analysis of agricultural productive services is in line with the development of the current national conditions, which is of great significance to promote the development of rural economy and realize a well-off society in an all-round way.

2. Related Technologies for Research on the Agricultural Productive Service System

2.1. Block Chain. Block chain is a data chain structure similar to the distributed ledger; it stores the data in the corresponding blocks in a chronological order and connects all the blocks and uses cryptography principles to realize encryption protection to ensure that economic data are not tampered with. As a distributed ledger, the block chain is usually managed by a peer-to-peer network that complies with internode communication and verification of new block protocols. Block chain enables us to have a distributed peer-to-peer network in which nontrusted members can interact with each other in a verifiable manner without a

trusted intermediary [11]. The block chain is mainly used to store data, and data can be written and stored here, so the block chain is a database. Chain block chains are classified as public, private, and union chain strands, in which three types have their own characteristics but also overlap each other in place, users can choose different types of blockchains according to their needs. The basic framework of the block chain is composed of the data layer, network layer, consensus layer, incentive layer group, contract layer, and consensus layer. Economic incentive strategies and smart contracts based on the time chain link structure, distributed node consensus mechanism, and consensus concept are the most representative innovations in block chain technology. Data layer, network layer, and basic layer are a consensus architecture block chain, and the absence of any portion of block chains cannot be called complete; the incentive layer, contract layer, and application layer are mainly used to build decentralized applications and are not a necessary part of block chain design.

The block chain does not have a central node, and every node in it is equal, and no node can handle or control other nodes. It is a series of data blocks containing information for a digital document timestamp which cannot be tampered with once it is labeled. Block chain is an open, distributed ledger that can record transactions securely, permanently, and very efficiently [12, 13]. In block chain technology, data are permanently stored in partitions, generated in a chronological order, and linked to the chain. Each chain records all transaction information generated during its creation. Each data block contains data, the hash value of the current block, and a hash value of the previous block of three parts, stored in the block depending on the type of section. Block chain represents a novel application of cryptography and information technology in the old problems of financial record keeping [14, 15]. After the block chain uses the peer-to-peer network, everyone can join; when someone enters the network, the person will get a copy of the entire block chain, and this person can verify the legality of all of the block chains, and constant verification is successful; each block will add a new block in their chain, so everyone reaches a "consensus." Block chain is a new type of information technology, which combines many existing technologies to achieve unique functions and has important applications in the future [16].

2.2. Edge Computing. Edge computing is a new type of distributed computer architecture that performs computing functions at the edge of the network. In order to ensure the quality of service while processing large amounts of data for cloud computing, edge computing has been developed [17]. Edge computing technology can effectively help smart terminals improve their computing capabilities and participate in the consensus algorithm of the block chain. Edge computing technology is considered to be one of the key technologies to realize the vision of the future Internet of Things and the fifth-generation communication technology (5G). Its purpose is to provide a networked environment with large-scale connections, high access speeds, and low latency. Integrating edge computing technology into the framework of the block chain can effectively enhance the computing power of smart terminals, thereby helping to solve the problem of proof of work. It combines computing edge nodes with the network to form a "device terminal-device edge cloud" architecture. Each level can provide the required resources and services for the application, and the application can choose the best configuration according to the needs. The architecture of edge computing is based on location-based mobility requirements, which improve system performance and service quality. It integrates independent scattered resources adjacent to users in the space or distance between networks and provides computing, storage, and network services for applications. This decentralized architecture can bring data analysis closer to users, process huge amounts of data more efficiently, and provide users with good service quality.

Edge computing can provide the user terminal equipment storage and computing and network services; cloud computing is extended at the edge of the network, and because of its unique performance advantages, it has been duly noted by scholars and technicians. Edge computing has the characteristics of solving response time requirements, battery life limitations, saving bandwidth costs, and data security and privacy [18–21]. The computing and storage nodes of edge computing are located at the edge of the internet, close to mobile devices or sensors [22]. It can deploy servers at the edge of the network and can share and upload some simple services requested by users to various local edge servers, the task calculation and data storage functions are completed through the edge server, and it is no longer necessary to upload to the cloud data center through the core network for processing. Consider uploading to the cloud data center for processing for relatively large data or data with relatively complex calculations. These operations reduce the bandwidth pressure of the cloud data center, reduce the possibility of data link congestion and failure, and improve the link capacity, which can improve the computing power of mobile devices while saving battery power [23]. And the edge server in the edge computing is closer to the terminal device and has unique advantages in data security and privacy protection.

2.3. Agricultural Productive Services. Agricultural productive services involve the entire agricultural production process, directly or indirectly providing nonpublic welfare services to all agricultural products in various production and management links before, during, and after production. Agricultural production of the service is the "separation of powers" product stage, and it belongs to large-scale operation services; agriculture is one of the methods of scale operations. The main feature of the agricultural productive service industry is based on intermediate inputs, which involve the exchange of knowledge and capita and provide customized services for participants [24]. Agricultural productive service is a typical model in practice, with regional characteristics, and the main body of its service is farmers' professional cooperatives. The development of our

country's agricultural regions is not balanced, and there are differences in the degree of development of productive services in different regions and different agricultural production sectors. The agricultural productive service industry is the support point to promote the development of modern agriculture, and it also points out the direction for promoting the transformation of the agricultural development mode. Different from the consumer goods service industry, the producer service industry is a service provided by enterprises, nonprofit organizations, and the government to provide products and labor in the production process, rather than providing end-to-end services to the final consumer. Some people think that agricultural productive services are equivalent to agricultural socialized services [25], which can increase agricultural labor productivity. Although the agricultural productive service industry does not directly involve production activities or material conversion processes, every production link in agriculture is inseparable from the productive service industry.

With the development of agricultural production today, the demand for productive services in agricultural production is becoming increasingly diversified and multilayered [26]. With the rapid development of the agricultural productive service industry, various agricultural organizations are moving towards the new service mode step by step by means of market inspection and innovation and gradually become diversified, systematic, and specialized. At the same time of rapid development, the development of agricultural productive services has also ushered in a new situation, which has begun to show diversified network nodes and become more and more mature, providing more service subjects for agricultural activities [27]. Under the guidance of the government's incentive, diversified service organizations have been widely extended to agricultural production, integrating the resources in the process of agricultural production, and various services have been continuously extended, have been learned from each other, and have constantly promoted their own improvement and progress. The development of the operation model of our country's agricultural producer service industry continues to mature, and it mainly includes the public agricultural service model led by the government agricultural department, the socialized service model based on agricultural cooperatives and industry associations, a service model with leading enterprises as the backbone, the operation model represented by the service model with the agricultural market as an important platform, and the innovative development model of the traditional agricultural productive service industry.

2.4. Three Rural Issues.

"Three rural" is a collective term for "rural, agriculture, and farmers," and the main problems of "three rural" refer to the problems that exist in the overall composition of these three. "Agriculture, rural areas, and farmers" is the top priority of the party's labor agenda, and it is related to the overall status of socialist modernization with Chinese characteristics [28]. The issue of "agriculture, rural areas, and farmers" accompanied the progress of China's revolutionary construction and reform and received great attention from successive leaders. It is closely related to the overall quality of the people and economic stability and is directly related to social development. Strengthening the research on the "three rural" issues is the basis for realizing rural stability and rural economic development. We must pay attention to major issues in real life and go deep into the forefront of agricultural production governance [29]. The current development of "agriculture, rural areas, and farmers" faces many problems: the development of agriculture affects the simultaneous development of the four modernizations, rural areas have a great influence on the construction of a well-off society, and the uncoordinated development of towns and villages makes it very difficult to alleviate poverty. In the current national conditions, China is still a country with a large population, and the peasants are the most populous group in our country. Our country attaches great importance to the development of agriculture, but our country's agricultural production fluctuates greatly, the development of agricultural science and technology is not fast enough, the competitiveness of agriculture is not strong enough, the development of rural economy is backward, and the gap between urban and rural areas is still very large. In order to achieve the coordinated development of urbanization and new rural construction, we must attach great importance to the "three rural" issues [30]. Only by comprehensively solving the "three rural" issues can we build a more complete and prosperous society that benefits all farmers.

3. Agricultural Production Service-Related Experiments

3.1. Data Collection.
This experiment is based on the statistics of agricultural production service capita investment in a certain area from 2015 to 2019, analyzes the development of agricultural productive services in the region, such as the expenditure on agricultural productive services and the per capita income of farmers in the region under agricultural productive services, and analyzes farmers' demand for agricultural productive services from the risk perspective of the whole process, land preparation, sowing, pest control, fertilization, and harvesting.

3.2. Agricultural Productive Service Analysis Framework.
In agriculture-related research, the production function is generally defined as $F(K, T)$, where K is the capita element and T is the labor factor; in this experiment, for the convenience of analysis, the capita input S used to purchase agricultural productive services is separated from the capita element. The capita investment used to purchase agricultural productive services is $S(\alpha)$, the production function becomes $F(K, T, S(\alpha))$, the farmer's utility function $R(\pi, q)$ also becomes the expected utility function $E[R(\omega + \pi), q]$, ω is the initial wealth of the farmer, π is the profit of the farmer's agricultural production, and q is the characteristic variable of the farmer's family. The expected utility function of farmers in this experiment is,

$$E[R(\omega + \pi), q] = E[R(\omega + PQ - W), q]. \quad (1)$$

In the above formula, π is the profit, P is the product price, Q is the product quality, and W is the input cost of

each element. Substituting the production function into formula (1), it can be changed to solve the problem of maximizing farmers' utility:

$$\text{Max } E[R(\pi), q] = \text{Max } E\{[R(\omega + PF(K, T, S(\alpha)) - (X_1 K + X_2 T + X_3 S(\alpha))], q\}. \quad (2)$$

X_1, X_2, and X_3 are the unit prices of capita, labor, and productive services, respectively. Find the partial derivative of formula (2):

$$\begin{cases} \dfrac{\partial R}{\partial K} = \dfrac{\partial \pi}{\partial K} * \dfrac{\partial R}{\partial \pi} = \dfrac{\partial R}{\partial \pi}(PF_1 - X_1), \\[3mm] \dfrac{\partial R}{\partial T} = \dfrac{\partial \pi}{\partial T} * \dfrac{\partial R}{\partial \pi} = \dfrac{\partial R}{\partial \pi}(PF_2 - X_2), \\[3mm] \dfrac{\partial R}{\partial S(\alpha)} = \dfrac{\partial \pi}{\partial S(\alpha)} * \dfrac{\partial R}{\partial \pi} = \dfrac{\partial R}{\partial \pi}(PF_3 - X_3). \end{cases} \quad (3)$$

To obtain the optimal solution to formula (3), the demand function of farmers for agricultural productive services can be obtained:

$$Y_3 = Y(X_1, X_2, X_3, P, R, \alpha). \quad (4)$$

According to the above formula to analyze the farmers' input demand for agricultural productive services, according to formula (4), we can know that when $Y_3 = Y$, the farmers' input demand for agricultural productive services has an optimal solution.

4. Development of Agricultural Productive Services

4.1. Investment in Agricultural Productive Services. In order to study the development of agricultural productive services, this study analyzes the development of agricultural productive services in a certain area from the three perspectives of structure, overall, and space. The experimental data includes statistics on agricultural investment in the region's main productive service industries from 2014 to 2019, and the percentage of the region's agricultural, forestry, fishery, and animal husbandry production service expenditures in total expenditures. Table 1 shows the statistics of the main industries of productive services invested in agriculture in the region from 2014 to 2019.

According to the data in Table 1, we can see that, during the period 2014–2019, the main industries of productive services in the region increased in agriculture. By 2019, the investment in the logistics industry reached 128.61 billion yuan, retail investment reached 13.86 billion yuan, financial investment reached 127910 million yuan, scientific and technological investment reached 56.55 billion yuan, and the information service input was relatively small, only 13.36 billion yuan. In order to observe the investment of agricultural productive services in the region more intuitively,

we calculated the data in the table and obtained the annual investment situation compared with the last year as shown in Figure 1.

According to the data in Figure 1, we can see that the logistics industry's investment in agricultural productive services in 2017 increased by 49.13 billion yuan over the previous year; in 2018, the retail and financial industries invested 43.19 billion yuan and 44.33 billion yuan in agricultural productive services. The logistics, retail, and financial industries invest more in agricultural productive services, while other industries invest less in agricultural productive services. It can be seen that the investment in the main industries of agricultural productive services in this area has grown very fast, but the internal composition of the agricultural productive service industries is not balanced.

4.2. Expenditure of Agricultural Productive Services in Agriculture, Forestry, Fishery, and Animal Husbandry. This study analyzes the expenditure of agricultural productive services in the region from the agriculture, forestry, fishery, and animal husbandry. Statistics of expenditure on agriculture, forestry, fishery, and livestock production services in the region from 2015 to 2019, and the results are shown in Figure 2.

According to the data in Figure 2, we can see that the area's expenditure on agricultural, forestry, fishery, and animal husbandry in 2015 accounted for 10.72% of the total expenditure on agriculture, forestry, fishery, and animal husbandry; expenditure in 2016 accounted for 10.91%, an increase of 0.19% over the previous year; expenditure in 2017 accounted for 12.15%, an increase of 1.24% over the previous year; expenditure in 2018 accounted for 14.59%, an increase of 2.44% over the previous year; and expenditure in 2019 accounted for 15.17%, an increase of 0.58% over the previous year. It can be seen that the scale of agricultural productive services in the region is constantly expanding, and the importance of productive services in the agricultural production process is increasing.

4.3. Per Capita Income of Farmers under Agricultural Productive Services. In recent years, the strong growth of agricultural productive services has promoted the development of the rural economy. The agricultural productive service system is increasingly integrated. The agricultural productive service field has been expanded to preproduction and postproduction services, and agricultural foreign investment has increased significantly. This study counts the farmer's per capita wage income, farmer's per

TABLE 1: Statistics on the input of agricultural productive services in a certain place from 2015 to 2019 (unit: billion).

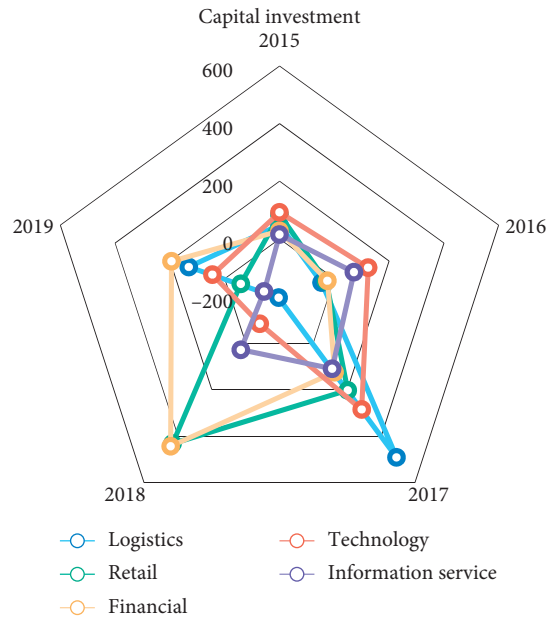| Year	Logistics	Retail	Financial	Technology	Information service
2014	814.3	697.4	413.8	142.5	50.9
2015	903.9	781.9	441.4	234.5	65.7
2016	857.9	752.3	416.3	358.1	137.7
2017	1349.2	955.2	541.5	643.8	248.3
2018	1154.8	1387.1	984.8	561	277.4
2019	1286.1	1328.6	1179.1	605.5	133.6

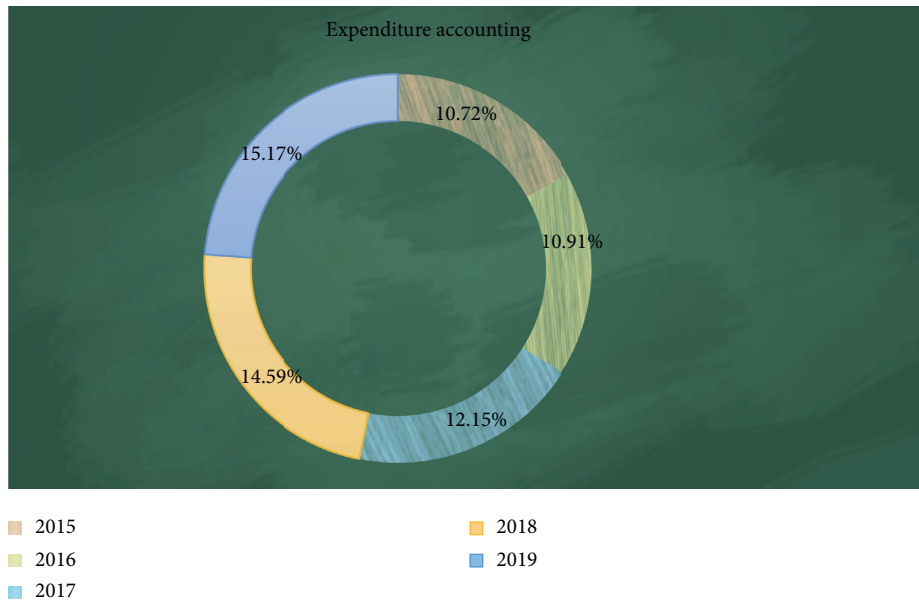FIGURE 1: The input of agricultural productive services.

FIGURE 2: Agricultural, forestry, fishery, and animal husbandry production service expenditures.

capita operating income, and the scale of agricultural productive services in the region from 2015 to 2019. The specific situation is shown in Figure 3 (unit: yuan).

According to the data in Figure 3, we can see that, from 2015 to 2019, as the scale of agricultural productive services continues to expand, the per capita income of farmers' wages
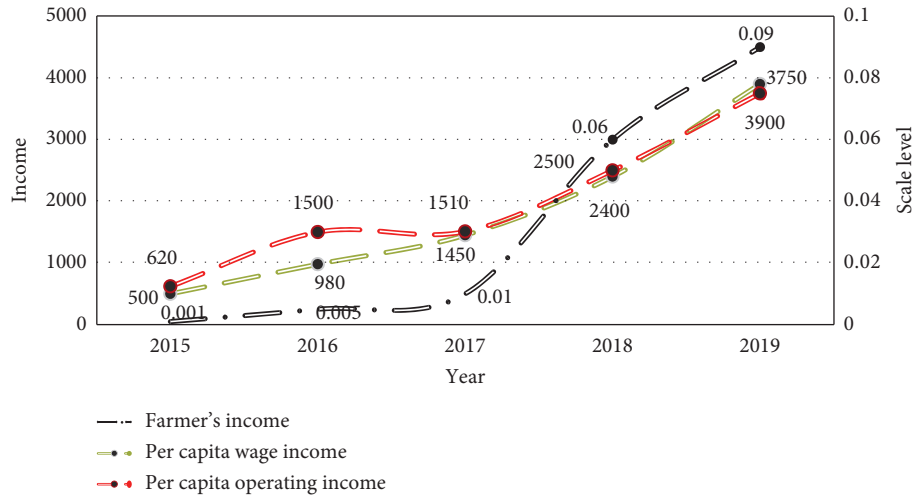
FIGURE 3: The income of farmers and the scale of agricultural productive services.
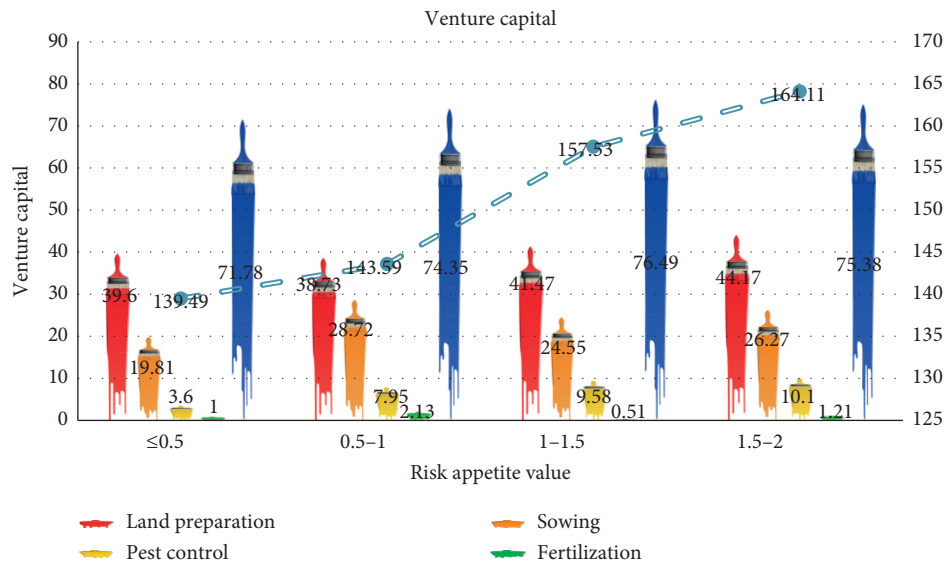

FIGURE 4: Farmers' demand for agricultural productive services from the perspective of risk.

and per capita income of operators have also increased year by year. When the scale of agricultural productive services reached 0.09 in 2019, the per capita wage income of farmers had reached 3900 yuan, and the per capita income of farmers had reached 3750 yuan.

4.4. Farmers' Demand for Agricultural Productive Services from the Perspective of Risk. Set the interval of the farmers' risk preference index to [0, 2]; among them, the closer the risk preference characteristic index is to 2, it means that the more risky and willing the farmers are to make venture capita. On the contrary, it means that farmers tend to avoid risks. Analyze the risk appetite investment of farmers in the whole area of agricultural production, land preparation, seeding, pest control, fertilization, and harvesting for every 0.5 risk preference interval. The statistical risk investment data are shown in Figure 4 (unit: yuan/mu).

According to the data in Figure 4, we can see that, as the risk appetite index increases, the more farmers prefer risk and the more venture capita they invest in agricultural productive services. In the case of different links, farmers' risk investment in harvesting is the most, which is more than 703 yuan/mu, and the total investment is 2983 yuan/mu, and the risk investment in fertilization is the least, basically less than 3 yuan/mu, and the total investment is 4.853 yuan/mu.

5. Conclusions

Agricultural production services for modern agriculture are very important; after years of development, coupled with the support of relevant government policies, the development of agricultural production of various types of services has achieved remarkable results. The differentiation of farmers has led to the diversification of the main body of agricultural production in our country, and the requirements for

agricultural productive services have gradually increased. At the same time, it is necessary to realize that there is still an imbalance between the supply and demand of agricultural productive services, and the construction of the agricultural productive service system is still a long-term process.

In this study, the input of agricultural productive services in a certain region, the expenditure of agricultural productive services in agriculture, forestry, animal husbandry, and fishery, the farmers' per capita wage income and per capita operating income under the agricultural productive services, and the farmers' demand for agricultural productive services from the perspective of various risks in the process of agricultural production analyze the impact of agricultural productive services on the economic benefits of the region and the development of agricultural productive services in the region. Finally, according to the experimental results, the region's investment in agricultural productive services is growing very fast, and the scale of agricultural productive services is getting higher and higher, but the internal composition of the agricultural productive service industry is imbalanced. With the increase in the scale of agricultural productive services, the per capita wage income and per capita operating income of farmers in this area are also increasing, and from the perspective of risk, the higher the risk index, the stronger the preference of farmers for the risk, the greater the demand for agricultural productive services, and the greater the risk investment in agricultural productive services.

This research on agricultural productive services based on block chain and edge computing is fairly successful, but this research still has shortcomings in some aspects and needs later improvements: (1) in this study, only productive agriculture of service in the time direction of a particular area is analyzed; posttest services for agricultural production will be the number of areas of comparative analysis in the spatial direction; (2) in this study, the analysis of the agricultural production of the services is not comprehensive enough, and in later experiments, one can perform analysis from other productive agricultural service indicators; and (3) this study is lacking in consideration of endogenous issues, and later experiments can use a larger sample of panel data for analysis.

Data Availability

The data that support the findings of this study are available from the corresponding author upon reasonable request.

Conflicts of Interest

The authors declare that they have no conflicts of interest regarding the publication of the research article.

References

[1] S. Zhang and Q. Tang, "Research on the development strategy of hengyang agricultural productive service industry based on SWOT analysis," *Journal of Hunan Institute of Industry and Technology*, vol. 19, no. 4, pp. 43–46, 2019.

[2] Y. Xue, S. Xiuyi, L. I. Yuqin et al., "Coupling coordination degree and spatial distribution of agricultural productive service and the convergence development of rural Primary,Secondary and tertiary industries in heilongjiang," *Northern Horticulture*, vol. 1, no. 16, pp. 35-36, 2019.

[3] Z. Jia-Ni, "Problems and countermeasures in development of agricultural productive service industry in suqian city," *Modern Agricultural Ence and Technology*, vol. 9, no. 9, pp. 78-79, 2019.

[4] L. Ming, W. Ruibo, and S. Weilin, "Effects of agricultural productive service industry on agricultural production efficiency-a case study in Shandong province," *Chinese Journal of Agricultural Resources and Regional Planning*, vol. 39, no. 5, pp. 11-12, 2018.

[5] L. Yingming, W. Xu, and L. Yang, "Effect of agricultural productive service on farmland operation scale," *Chinese Agricultural Ence Bulletin*, vol. 31, no. 35, pp. 45–49, 2015.

[6] Q. Tian, J. Peng, and Z. Deng, "Research on the development differences and driving factors of China's regional agricultural productive service industry," *Industrial Economic Review*, vol. 29, no. 6, pp. 65–77, 2018.

[7] X. Zhu, D. Zhang, and J. Chen, "Coupling and coordination of agricultural industry chain extension, producer service industry and rural education-based on the perspective of industrial convergence in shandong province," *Journal of Qingdao University (Natural Science Edition)*, vol. 33, no. 1, pp. 62–68, 2020.

[8] H. Wu and Z. Chen, "Evaluation and development path of agricultural productive service industry supply and demand in northern anhui," *Modern Trade Industry*, vol. 37, no. 28, pp. 8-9, 2016.

[9] P. Zhang and W. Sun, "The realistic problems and optimal paths of the development of my country's rural producer service industry," *Seeking Truth*, vol. 42, no. 2, pp. 61–67, 2015.

[10] J. Gao and J. Zhang, "Will the development of agricultural productive service industry narrow the income gap between urban and rural residents-an empirical test based on spatial spillover and threshold characteristics," *Western Forum*, vol. 29, no. 1, pp. 45–54, 2019.

[11] K. Christidis and M. Devetsikiotis, "Blockchains and smart contracts for the internet of things," *IEEE Access*, vol. 4, no. 1, pp. 2292–2303, 2016.

[12] S. Namasudra and P. Roy, "PpBAC," *Journal of Organizational and End User Computing*, vol. 30, no. 4, pp. 14–31, 2018.

[13] M. Iansiti and K. R. Lakhani, "The truth about blockchain," *Harvard Business Review*, vol. 95, no. 1, pp. 118–127, 2017.

[14] T. Grubljesic, P. S. Coelho, and J. Jaklic, "The shift to socio-organizational drivers of business intelligence and analytics acceptance," *Journal of Organizational and End User Computing*, vol. 31, no. 2, pp. 37–64, 2019.

[15] D. Yermack, "Corporate governance and blockchains," *Social Ence Electronic Publishing*, vol. 21, no. 1, pp. 7–31, 2015.

[16] M. Swan, "Blockchain thinking: the brain as a decentralized autonomous corporation [commentary]," *IEEE Technology and Society Magazine*, vol. 34, no. 4, pp. 41–52, 2015.

[17] W. Shi and X. Zhang, "Edge computing: state-of-the-art and future directions," *Journal of Computer Research and Development*, vol. 56, no. 1, pp. 69–89, 2019.

[18] J. Cao, Q. Zhang, W. Shi et al., "Edge computing: vision and challenges," *Internet of Things Journal, IEEE*, vol. 3, no. 5, pp. 637–646, 2016.

[19] M. R. Reddy, K. G. Srinivasa, and B. E. Reddy, "Smart vehicular system based on the internet of things," *Journal of Organizational and End User Computing*, vol. 30, no. 3, pp. 45–62, 2018.

[20] H. Hamidi and M. Jahanshahifard, "The role of the internet of things in the improvement and expansion of business,"

Journal of Organizational and End User Computing, vol. 30, no. 3, pp. 24–44, 2018.

[21] P. Singh and R. Agrawal, "A customer centric best connected channel model for heterogeneous and IOT networks," *Journal of Organizational and End User Computing*, vol. 30, no. 4, pp. 32–50, 2018.

[22] M. Satyanarayanan, "The emergence of edge computing," *Computer*, vol. 50, no. 1, pp. 30–39, 2017.

[23] S. Sardellitti, G. Scutari, and S. Barbarossa, "Joint optimization of radio and computational resources for multicell mobile-edge computing," *IEEE Transactions on Signal and Information Processing Over Networks*, vol. 1, no. 2, pp. 89–103, 2015.

[24] I. Carreno and W. Ma, "Agricultural productive public space: "an alternative for increasing ecological services, social development and urban sustainability"" *Current Urban Studies*, vol. 7, no. 4, pp. 493–516, 2019.

[25] M. Shi, G. Hou, and R. Xu, "Research on large growers' demand satisfaction of agricultural services," *Jiangsu Ence & Technology Information*, vol. 6, no. 18, pp. 33–37, 2016.

[26] D. Janiszewska, "Spatial differentiation of agricultural productive inputs in zachodniopomorskie voivodeship," *Journal of Agribusiness and Rural Development*, vol. 16, no. 4, pp. 763–770, 2017.

[27] Z. Cao, Y. Cai, and P. Liu, "Discussion on countermeasures for accelerating the development of agricultural productive service industry," *Zhejiang Agricultural Sciences*, vol. 1, no. 12, pp. 1690–1693, 2013.

[28] X. U. Tian, S. U. Zhi-Hong, S. O. Marxism et al., "Three-dimensional analysis of xi jinping's strategic thinking on "three rural issues" in the new era," *Truth Seeking*, vol. 5, no. 5, pp. 45-46, 2018.

[29] C. Mengshan, "Understanding and thinking on the survey and research of the "three rural issues" policy," *Issues in Agricultural Economy*, vol. 1, no. 7, pp. 8–10, 2019.

[30] W. Fu-Qiang and M. A. Hong-Wei, "On urban-rural integration and three rural issues," *Journal of Tangshan Vocational & Technical College*, vol. 13, no. 2, pp. 196-197, 2015.

Research Article

Knowledge Graph Construction and Application of Power Grid Equipment

Haichao Huang,[1] Zhouzhenyan Hong,[2] Huiming Zhou,[3] Jiaxian Wu,[4] and Ning Jin [4]

[1]*Information and Communication Branch, State Grid Zhejiang Electric Power Co., Ltd., 219 Shimin Street,*
 Hangzhou 310016, China
[2]*International Campus, Zhejiang University, Hangzhou 314400, China*
[3]*Zhejiang Huayun Information Technology Co., Ltd., Hangzhou 310012, China*
[4]*Key Laboratory of Electromagnetic Wave Information Technology and Metrology of Zhejiang Province,*
 College of Information Engineering, China Jiliang University, Hangzhou 310018, China

Correspondence should be addressed to Ning Jin; jinning1117@cjlu.edu.cn

Recent development of artificial intelligence (AI) technology enquires the traditional power grid system involving additional information and connectivity of all devices for the smooth transit to the next generation of smart grid system. In an AI-enhanced power grid system, each device has its unique name, function, property, location, and many more. A large number of power grid devices can form a complex power grid knowledge graph through serial and parallel connection relationships. The scale of power grid equipment is usually extremely large, with thousands and millions of power devices. Finding the proper way of understanding and operating these devices is difficult. Furthermore, the collection, analysis, and management of power grid equipment become major problems in power grid management. With the development of AI technology, the combination of labeling technology and knowledge graph technology provides a new solution understanding the internal structure of a power grid. As a result, this study focuses on knowledge graph construction techniques for large scale power grid located in China. A semiautomatic knowledge graph construction technology is proposed and applied to the power grid equipment system. Through a series of experimental simulations, we show that the efficiency of daily operations, maintenance, and management of the power grid can be largely improved.

1. Introduction

In the era of big data and artificial intelligence (AI), a large number of data from various sources are constantly generated from different perspectives of human lives [1–3]. Various AI powered service technologies are proposed utilizing the existing big data to facilitate the current sustainable smart city design, e.g., the development of smart grid [4], smart building [5], smart communication systems [6], and many more [7–9]. Such kinds of AI powered service technologies include Internet of Things (IoT) [10], cloud computing [11], edge computing [12], the fifth-generation (5G) mobile communication network [13], sensing networks

[14], social networks [15, 16], big data recommendation systems [17], etc. Research on data characteristics and correlations is demanded for deep analysis to make a more comprehensive and accurate judgment [16, 17].

The power grid system is usually a very complex and huge system, especially for large countries, such as China and the United States (USA). There are thousands of different types of basic devices existing in the current power grid system [18, 19]. In China, the state grid power system carried out data center construction since 2016, transforming the existing power grid towards the next generation smart grid system. As of January 2018, the total number of equipment devices in operation in a provincial power grid is

as follows: 2.17 million main network, 25.68 million distribution network, and 11.53 million low-voltage equipment devices, a total of 29.83 million sets. The total data storage capacity is 560.48 TB, including 209.5 TB of structured data, 254.86 TB of unstructured data, 72.02 TB of real-time measurement data, and 24.1 TB of online application data. In the current condition with such a huge data volume, a development of data visualization using knowledge graph is highly demanded.

Based on the grid equipment database provided by the State Grid China, this paper uses the AI-enhanced labeling system to construct a knowledge graph model for facilitating the grid management and search functions. The model construction process can be generally divided into data collection, labeling, analysis, and application phases. The whole construction process is semi-automated with the help of Neo4j [20]. The proposed knowledge graph construction model has the following contributions to both fields of computer science and smart grid development.

The developed knowledge graph system is greatly helpful enhancing the stability and reliability of the existing power grid system, the smart maintenance system, and sharing the grid equipment utilization information to a broad range of user groups.

The knowledge construction process is semiautomatic using the emerging data management tool named Neo4j. The entire construction process therefore is more transparent and easier for implementation compared to the traditional knowledge graph construction approaches.

A graphic processor unit (GPU) optimized breath-first searching algorithm is designed to output the internal connection between any two nodes existing in the knowledge graph. The proposed searching algorithm is optimized in terms of searching efficiency. According to the experimental results, the proposed search algorithm is two to three times faster than existing algorithms.

2. Labeling Technology and Knowledge Graph

A labeling system refers to a summary of existing features of a specific group of objects, where in the current context it is referring to the grid equipment devices. In general, business entities are labeled reflecting the business entities' properties from multiple perspectives. Particularly, the description of the power grid equipment includes the perspectives of type, voltage level, area, line, daily operation status, etc. Since the description of a specific object from various perspectives is difficult, a multilabeling system is proposed for grouping the devices with similar properties.

Knowledge graph is a huge knowledge system built on the semantic network. The knowledge graph itself refers to an emerging technology for large-scale knowledge management and intelligent services in the era of big data [21]. The knowledge graph captures and presents the intricate relationship between domain concepts and connects the fragmented knowledge, which plays a vital role in applications such

as information retrieval, question answering, and visualization [22, 23]. Ji et al. [24] introduced an adaptive sparse transfer matrix for knowledge graph entity relationship linkages. The proposed "TranSparse" knowledge graph outperforms most existing knowledge graph approaches. Song et al. [25] studied a graph summarization framework to accelerate the knowledge graph information search. Zheng et al. [26] proposed a meta path-based knowledge graph, which extends entities using entity set expansions (ESEs). Another famous example of knowledge graph technique raised by Google is knowledge expressing in documents [27]. The knowledge graph is constructed based on wiki-data and freebase databases as well as public databases [28]. Various sources of semantic search information are utilized to enhance the effectiveness of search engines [29].

The equipment devices existing in the current power grid lie in forms of network structures, which are easily interpreted using the knowledge graph. As a result, the knowledge graph is constantly evolving and it has become an efficient management tool for grid data. The visualized knowledge graph helps people understand massive information much easier. In the knowledge graph, knowledge exists in the form of entity-relationship-entity triplets, and the relationship between entities and entities is presented in the form of nodes and edges. The knowledge graph provides an ideal technical means for solving the problem of knowledge islands in the power grid and improving the service quality of the grid data center.

3. Constructing Power Grid Equipment Portrait System

3.1. Constructing the Labeling System. The labeling system of the power grid equipment devices is constructed based on the main business system of the power grid in China. Corresponding to the profile of each power grid equipment device, the labeling system is designed based on the historical and current operating status of the equipment, the possible future position of each device, the inspection, management and maintenance status, and the operational quality of various manufacturers. The hierarchical relationship of the grid equipment labeling system is shown in Figure 1.

From Figure 1, for each data piece collected from the power grid, three levels of the labels can be assigned, namely, the fact label, the model label, and the decision label. The fact label is the lowest level label, which most of the data pieces should have. The fact label is a fundamental fact that can be easily extracted from the data. The model label indicates the most appropriate decision model for the data piece generating the decision label. Not all data pieces have the model labels and decision labels. The basic rules of generating the labeling system include the following:

Standard rule: The standard for generating labels for each level must be consistent between different data pieces.

Connection rule: The total number of the children is equivalent to the total number of parents; otherwise, the division is incomplete or there are more children.
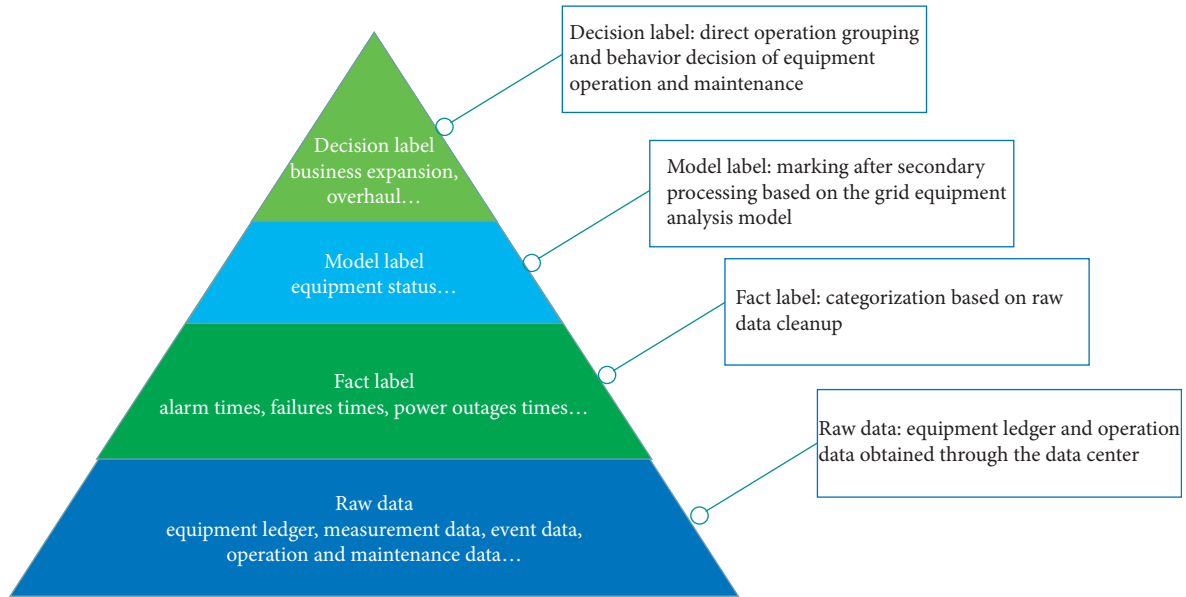
FIGURE 1: The hierarchical relationship of the grid equipment labeling system.

Division rule: The divided concepts cannot be compatible, and the genus concepts cannot be parallel.

Based on the above three basic rules of the labeling system, the ultimate labels are determined based on the extraction sources, data association relationships, and extraction logics. The difficulty and complexity of generating rules increase gradually with the labeling level increment.

There are four updating strategies for the labeling system:

(1) Updating strategy: The updating cycles for different labels are different. In general, an updating cycle for a particular label can be real-time, monthly, or three-monthly depending on the label type.

(2) Updating conditions: This strategy establishes the label updating trigger mechanisms based on the properties of data pieces. For each label, the label update is triggered under various situations.

(3) Updating authority strategy: The authority strategy determines the label updating authorization priority sequence based on the classification levels of the original data.

(4) Recycling strategy: There is also a label elimination mechanism to delete useless labels to avoid wasting resources.

The knowledge graph construction process labels each piece of power grid data following the above four strategies. For data pieces that have multiple labels or conflicting labels, the above four rules are re-visited to determine the highest priority label for that particular data piece.

3.2. Data Preprocessing.
The construction of power grid equipment portraits involves connectivity information among the huge number of equipment devices. A robust and efficient data processing framework/technique is demanded to support data storage, analysis, and knowledge graph construction. In this study, a three-layer data preprocessing framework is proposed consisting of the data layer, the preprocessing layer, and the analysis layer, as shown in Figure 2.

3.2.1. The Data Layer.
The basic data required for the power grid equipment portrait consists of two parts, namely, the power grid system data and the third-party data, according to the types of sources. Among them, the grid data mainly includes equipment account data, equipment operation data, and equipment management data. The equipment account data consists of the type, voltage level, name, information of the storage grid equipment, etc. Device operating data is the voltage, current, active power, reactive power, and events of the storage device during the operations. The equipment management data stores work operation tickets, inspection reports, and maintenance reports related to equipment operation and maintenance. In order to further expand and label the power grid equipment data, the relationships between grid energy production, consumption, and environment data, as well as data from the third-party entities, e.g., the national economic data or the national meteorological environment data, are considered externally wherever necessary. In this study, both grid data and third-party data consist of structured data, semi-structured data, and unstructured data.

3.2.2. The Preprocessing Layer.
Above the data layer is the data preprocessing layer. The preprocessing steps for power grid equipment data include collection, cleaning, integration, reduction, and feature extraction.

Data collection refers to the unified accesses of grid equipment and operation, operation and maintenance data
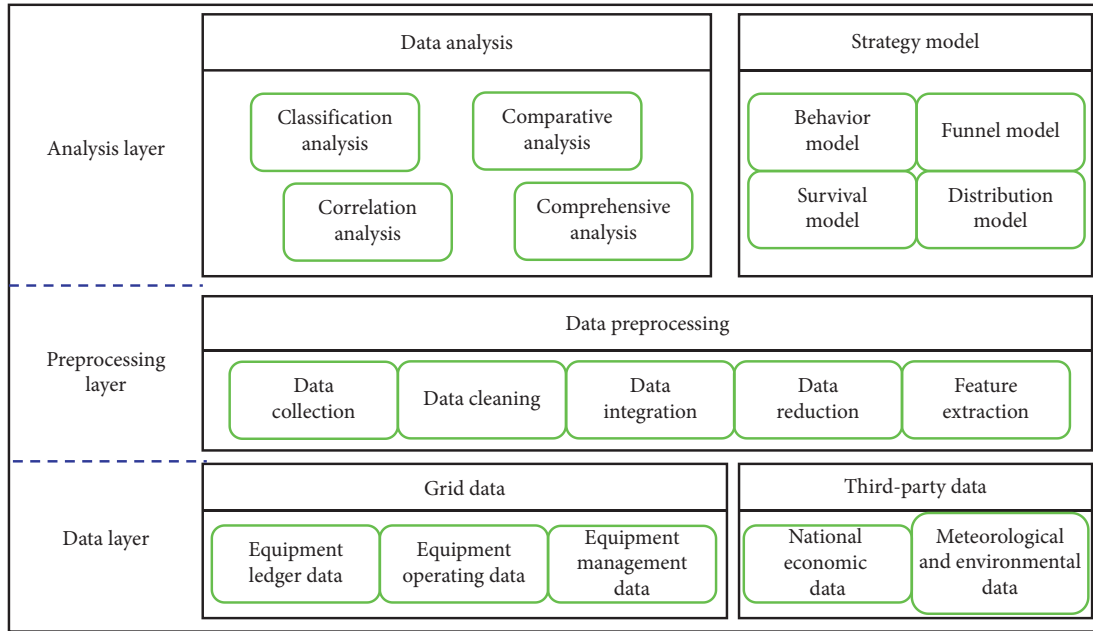
FIGURE 2: Hierarchical relationship of power system equipment label system.

of the supervisory control and data acquisition (SCADA) center, energy management system, user acquisition system, distribution automation system, property management system (PMS), etc.

Data cleaning performs tasks such as omission filling, anomaly elimination, noise smoothing, and correction of inconsistent data in the aggregated data.

Data integration carries out pattern integration, data entity identification, and splicing processing on data from multiple systems and summarizes, aggregates, generalizes, and normalizes data.

Data reduction balances the efficiency and value of data processing in the case of large-scale grid data analysis of complex content data that requires a lot of time and computer resources. The specific data analysis tools include cubic aggregation, dimensionality reduction, data compression, data block reduction, and other processing.

The data feature extraction process utilizes two basic AI techniques, i.e., the principal component analysis (PCA) method [30] and the linear discriminant analysis (LDA) method [31]. The PCA method projects the original data into higher dimension to reduce the data dimension using matrix multiplication. The reduced datasets are further processed using LDA with the label information. LDA is a supervised data reduction method and can be greatly helpful for data retrieval and data management for the constructed knowledge graph. The ultimate purposed of data reduction is to improve the data retrieval efficiency in the data management level.

3.2.3. The Analysis Layer.
The analysis layer is the core layer for realizing the knowledge graph of the power grid equipment. It can be divided into two major blocks, namely, the strategy models block and the data analysis block. The

strategy models include behavior model, funnel model, survival model, and distribution model. The data analysis block includes classification analysis, comparative analysis, association analysis, and comprehensive analysis. A database management system called Neo4j is employed to build the analysis layer for the power grid equipment devices. The Neo4j graphic platform is originally introduced by Webber in 2012 [32]. We extend the current Neo4j platform implementing both strategy models' block and the data analysis block for the power grid equipment management system.

3.3. Visualization of the Power Grid Equipment Connections Using the Knowledge Graph.
Considering the current database has a large amount of unstructured data, this study employs the Data-Driven Documents (D^3) to visualize the knowledge graph for the power grid equipment devices. D^3 is a function library written in JavaScript, which was proposed by Bostock et al. in 2011 [33]. The D^3 technique is nowadays widely adopted handling unstructured data for data visualization.

Since the number of power grid equipment devices is huge, and the scale of the corresponding power grid equipment knowledge graph is large, we only show part of the documented knowledge graph in Figure 3. The nodes and edges represent the equipment and the relationship between power grid equipment devices, respectively. Each node contains detailed information about the equipment, such as equipment type, equipment status, equipment name, voltage level, and commissioning time. The knowledge graph of power grid equipment displays the connection between the equipment devices in the form of a graphical network and provides equipment specific information. Users can browse the knowledge graph interactively and
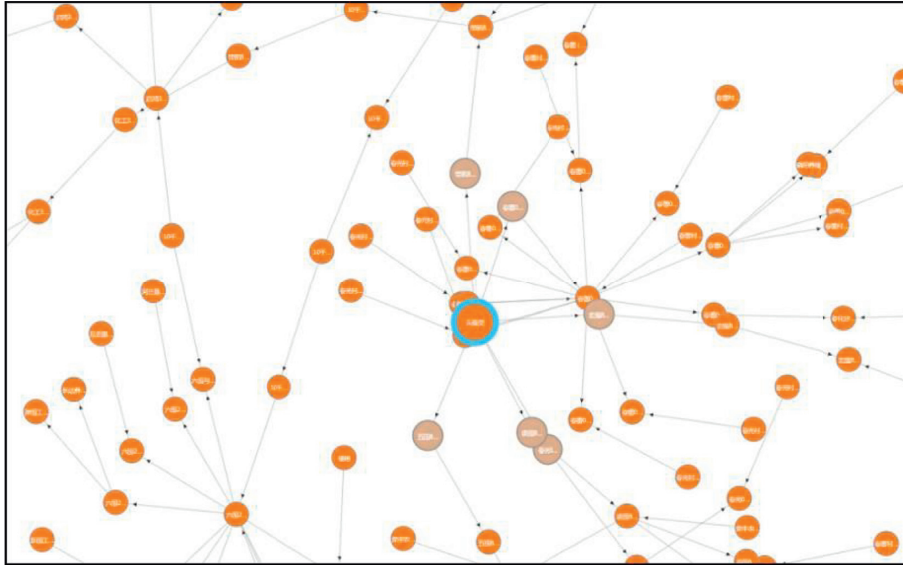
FIGURE 3: Knowledge graph of power grid (partially).

select one of the devices to further explore the information or construct queries. The relationship between equipment and equipment in the knowledge graph is intricate. These relationships are difficult to discover by observing database tables. It helps staff solve the knowledge island problem of the relationship between equipment devices and enhance the connectivity of knowledge resources of power grid equipment. At the same time, it can also help staff browse the knowledge of power grid equipment at the conceptual level and discover the potential connections between different types of equipment, so as to better understand the complexity of the power network. The graphic user interface of Neo4j allows us to visualize the devices and connections with a connectivity graph. Several examples of the proposed knowledge graph construction are shown in Figures 3 and 4.

The knowledge graph supports querying the details, which can be viewed by selecting the device you want to know. This paper takes selecting a substation type node as an example. The knowledge graph can also be clicked on the device node to continuously extend the display outwards, as shown in Figure 4. Due to data confidentiality requirements, some details in the figure are treated anonymously. For example, "Substation X" is a substation type node. The enlarged part of Figure 4 shows some equipment nodes related to " Substation X", including transmission lines, line switches, high-voltage fuses, capacitors, and capacitor grounding blades device.

3.4. Search and Recommendation System Design for Power Grid Knowledge Graph.

The knowledge graph enables users by entering search conditions according to their needs. When a device failure occurs, the search page can automatically bring out the relevant fault information of the current device. Furthermore, decision recommendations are sent to the users for possible actions to solve the device failure instance.

The power network is huge and complex in structure, and the speed of query operation using the traditional database technology is extremely slow and poor. Knowledge graph can significantly improve the efficiency of knowledge retrieval and make the search results more comprehensive and accurate. It can systematically understand the user's query intent and directly return accurate answers instead of a large number of search results. In this paper, a grid knowledge intelligent retrieval system is developed based on the grid knowledge map. For example, in the power grid system, if you want to know whether a device failure will affect a certain key device, the traditional relational database searches for the relationship path between the two devices in advance, making the whole query process slow and difficult to edit.

In the proposed knowledge graph construction framework, an optimized breadth-first search strategy based on graphic processor unit (GPU) programming is proposed to search through the Neo4j database. The time complexity of the data network traversal is only O (n). The proposed breadth-first search algorithm returns the shortest path from the starting vertex V_s to the target vertex V_t. The detailed algorithm is listed in Algorithm 1; and the flowchart of Algorithm 1 is depicted in Figure 5.

This paper takes the query of two substation nodes that are adequately separated as an example. The returned path is shown in Figure 6. The knowledge graph retrieval system can quickly and accurately return the relationship path between two devices. The blue nodes in the path represent transmission lines, the green nodes represent substations, and the orange nodes represent distribution lines.

4. Experimental Results

For the purposes of reflecting the efficiency and effectiveness of the proposed knowledge graph construction technique for the knowledge retrieval tasks in the power grid system, a
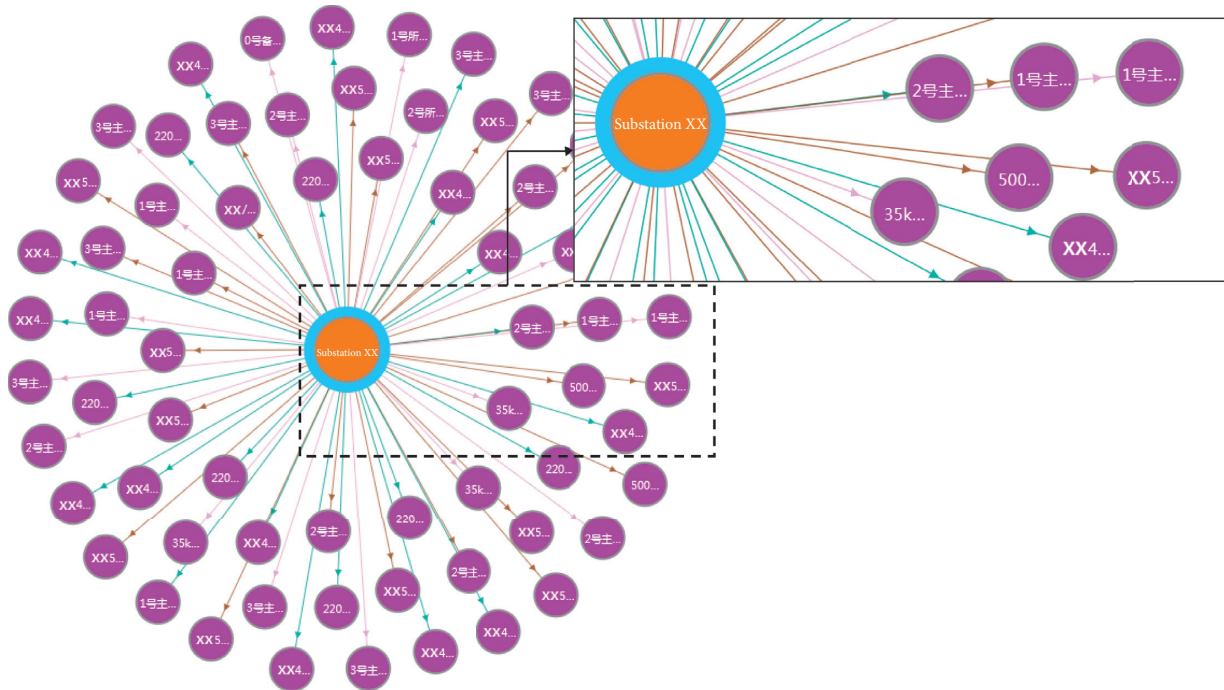
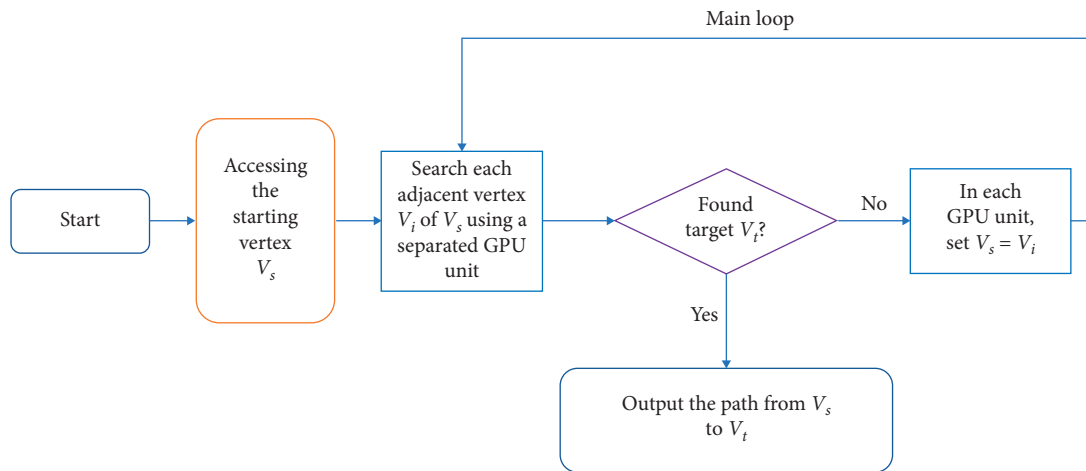FIGURE 4: A substation node and some of its subequipment devices.

FIGURE 5: An optimized breadth-first search algorithm based on GPU programming.

series of experiments were carried out in this section. We implemented the proposed knowledge graph technology on the grid system and performed knowledge retrieval tasks with relational databases. It is noted that it is a completely different scenario for knowledge retrieval tasks to be handled using the knowledge graph compared to the relational database. More complex data routines are stored in the relational networks in Neo4j with much more connectivity information compared to the traditional relational database management system. The searching engine is also optimized using GPU, which retrieves data relational paths more efficiently and accurately. In Table 1, we show the performance comparison using a set of the same knowledge retrieval tasks using the knowledge graph and relational database. The total time consumed by both methods and the numbers of

returned paths are listed. The column of "Performance improvement" shows the percentage of time/output advances of the proposed knowledge gra ph data management method over the traditional relational database management method.

From Table 1, it is evident that, for all knowledge retrieval tasks, the time required of the knowledge graph is always shorter than that of the traditional relational database. In some tasks, the number of searching records (calculated outputs) of knowledge graph is more than that of relational database. For more complex tasks, which cannot be accomplished by relational database, it is still possible for the knowledge graph to find out the paths, since the underlying data structures of the knowledge graph are more advanced using Neo4j. The underline implementation of the knowledge graph stored in Neo4j is a high-
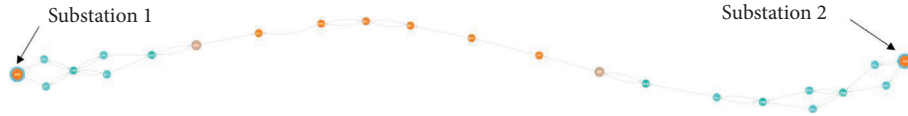
FIGURE 6: Equipment relationship path between two substations.

Input: Database D; Input vertex V_s; Target vertex V_t
Output: The path between V_s and V_t
(1) From the V_s, look for the adjacent vertices V_i;
(2) For each V_i:
(3)   A separated GPU unit and a distributed memory unit are assigned to V_i
(4)   if (V_i is V_t)
(5)   return path;
(6)   end if
(7)   Look for the adjacent vertices of V_i
(8) end for

ALGORITHM 1: GPU-based breath-first search algorithm.

TABLE 1: The performance comparison between relational database and knowledge graph for different knowledge retrieval tasks.

Knowledge retrieval task	Relational database		Knowledge graph		Performance improvement
	Time consumption (ms)	Number of records	Time consumption (ms)	Number of records	
Path from substation A to substation B	353	1	135	1	61.76%
Path from substation B to substation A	288	1	45	1	84.38%
All on-column transformers in a substation	1072	28	205	66	80.88%
All transmission operation towers under a substation	381	17	198	17	48.03%
Substation to which a contact belongs	81	1	78	1	3.70%
Path from substation C to substation D	Cannot achieve	—	5420	16	—
Path from substation D to substation C	Cannot achieve	—	774	2	—
Distribution station under a substation	Cannot achieve	—	156	314	—
Substation connected to a distribution switch station	Cannot achieve	—	238	11	—

performance graphic engine with GPU. It stores structured data using the relational networks instead of using simple tables. It overcomes the fact that traditional relational databases are not efficient at dealing with relational networks. For those relationships between the searched device nodes, which are too complex or where the searched path is too long, searching failure messages are returned from the relational database management system. The results listed in Table 1 show that, for the same searching result, the proposed knowledge graph database management system is more efficient. And for the more complex searching problems, which the traditional relational database management system cannot handle, the knowledge graph system returns more accurate (exact) paths. The averaged performance improvement is around 56%.

While the number of provincial power grid equipment devices reaches 100 million, the efficiency and timeliness of data migration is another important indicator of the evaluation model. In the process of implementing the knowledge map of the power grid, we recorded the time consumptions of data analysis using the traditional LOAD-CSV method and the Neo4j-Import method proposed in this paper with randomized orders of nodes. LOAD-CSV and Neo4j-Import are two data analysis methods provided by Neo4j, suitable for different application scenarios. The comparison results of the two methods are shown in Figure 7, where Figure 7(a) shows the time comparisons between the traditional LOAD-CSV method and the Neo4j method and Figure 7(b) shows the actual differences.

From Figure 7(a), it is evident that when the number of nodes increases, the required data analysis time of the LOAD-CSV method increases from 1.579 s to 534.505 s, while the time requirements of the Neo4j-Import method only increase from 1.582 s to 15.463 s. The efficiency of Neo4j-Import method is significantly higher than that of LOAD-CSV in the data import and analysis stage. From Figure 7(b), the data analysis between the two methods is positively correlated with the amount of data increments. The time requirement differences increased from the initial −0.003 s to 5519.042 s, where −0.003 s is considered the program testing error. It is noted that, for actual power grid equipment data, the size of power grid equipment data is exponentially larger than that adopted in the experiment,
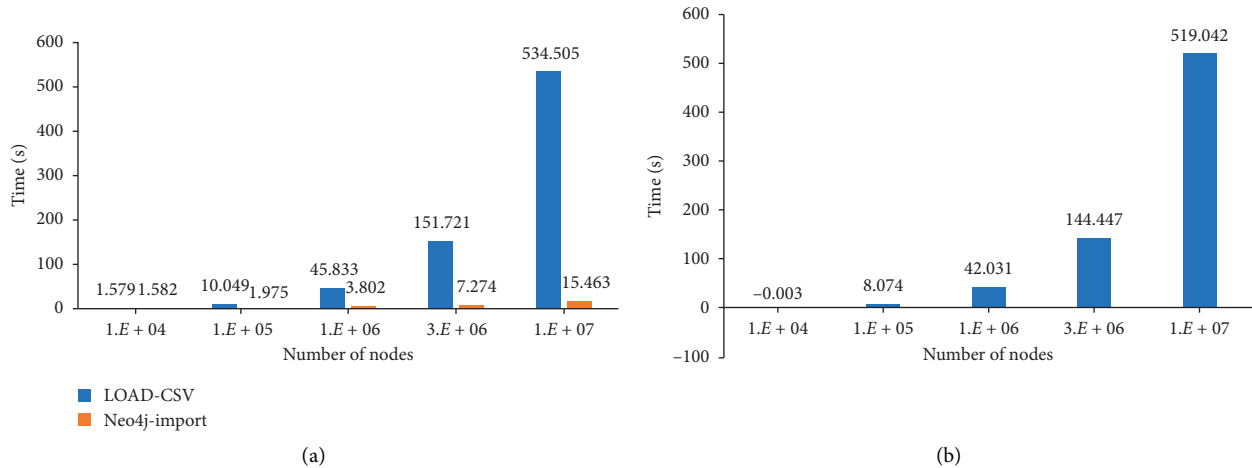
FIGURE 7: (a) Time required for LOAD-CSV and Neo4j-Import; (b) time difference between LOAD-CSV and Neo4j-Import.

with much more complex relationships between the nodes. Hence, the data analysis efficiency improvement using the Neo4j-Import is extremely important. The whole power grid knowledge graph construction process can be realized as a semiautomatic process, which saves tremendous amount of human resources, time, and financial costs.

5. Conclusion

In power grid management, the number of power grid equipment devices can be huge in appliance level, with enormous amount of information generated every day. The traditional data management systems and approaches are not only inefficient but also inaccurate, causing serious flaws in knowledge retrieval and data analysis for the next-generation smart grid implementation. The storage, query, and management of power grid equipment information became an emerging issue for the smart grid system development, especially for developing countries. This paper proposed to realize the functions of power grid equipment devices and power grid equipment information by constructing a next-generation power grid knowledge graph integrating AI technologies and GPU programming.

The proposed knowledge graph construction process is generally divided into three steps. First, the raw grid equipment information is preprocessed using data analysis tools, generating multiple relationship tables. Next, a data migration model is proposed to transfer the grid equipment information from the relational table to the Neo4j graph database in a semiautomatic way. Finally, based on the Neo4j database, the functions of power grid equipment information visualization and power grid equipment information search are revealed using the constructed knowledge graph. In the process of data migration, this article uses the Neo4j-Import method, which is significantly faster than the LOAD-CSV method when the amount of data is large. In the field of data visualization, this method facilitates the grid staff to view the equipment information more clearly. The parameters and operation status of each equipment in the substation

are also displayed, which is beneficial for the data management.

The experimental results show that the proposed knowledge graph searches more records in a shorter time than the traditional relational database. In addition, the search path can be visually displayed, which enhances the stability and reliability of the power system, which can be greatly useful in sharing, utilizing, and analyzing the power grid equipment information.

The main limitation of the proposed work is that the current study (including the experimental simulation) is only restricted in the area of power grid knowledge graph construction. The usage of the proposed algorithm in other knowledge/data management areas is not justified. As one of the future works, the proposed knowledge graph construction algorithm will be extended to the research field, such as molecular modeling [34, 35], healthcare engineering [36, 37], and business applications [38]. In addition, the topology analysis function development of the power grid subtasks is another future task for power grid appliances flow calculation, state estimation, line loss calculation, etc., targeting more efficient analysis tools for the operating states and faults of the power grid. The topology analysis function improves the safety performance of the power grid system and brings higher economic benefits of the power grid.

Data Availability

The data are confidential.

Conflicts of Interest

The authors declare no conflicts of interest.

Authors' Contributions

H.H. and N.J. contributed to conceptualization; H.H. and H.Z. contributed to methodology; J.W. contributed to software, data curation, and visualization; Z.H. contributed to validation; H.Z. contributed to formal analysis; N.J. contributed to investigation, writing, review, and editing,

References

[1] X. Zhou, W. Liang, K. I.-K. Wang, R. Huang, and Q. Jin, "Academic influence aware and multidimensional network analysis for research collaboration navigation based on scholarly big data," *IEEE Transactions on Emerging Topics in Computing*, p. 1, 2018.

[2] L. Amoore and V. Piotukh, "Life beyond big data: governing with little analytics," *Economy and Society*, vol. 44, no. 3, pp. 341–366, 2015.

[3] X. Zhou, W. Liang, I. Kevin et al., "Deep learning enhanced human activity recognition for internet of healthcare things," *IEEE Internet of Things Journal*, vol. 7, no. 7, pp. 6429–6438, 2020.

[4] W. Wang, B. Lou, X. Li, X. Lou, N. Jin, and K. Yan, "Intelligent maintenance frameworks of large-scale grid using genetic algorithm and k-mediods clustering methods," *World Wide Web*, vol. 23, no. 2, pp. 1177–1195, 2020.

[5] C. Zhong, K. Yan, Y. Dai, N. Jin, and B. Lou, "Energy efficiency solutions for buildings: automated fault diagnosis of air handling units using generative adversarial networks," *Energies*, vol. 12, no. 3, p. 527, 2019.

[6] A. M. Al-Momani, M. A. Mahmoud, and M. S. Ahmad, "Factors that influence the acceptance of internet of things services by customers of telecommunication companies in Jordan," *Journal of Organizational and End User Computing*, vol. 30, no. 4, pp. 51–63, 2018.

[7] S. J. Pittman, L. D. Rodwell, R. J. Shellock et al., "Marine parks for coastal cities: a concept for enhanced community well-being, prosperity and sustainable city living," *Marine Policy*, vol. 103, pp. 160–171, 2019.

[8] W. Zhong, X. Yin, X. Zhang et al., "Multi-dimensional quality-driven service recommendation with privacy-preservation in mobile edge environment," *Computer Communications*, vol. 157, pp. 116–123, 2020.

[9] T. Grublješič, P. S. Coelho, and J. Jaklič, "The shift to socio-organizational drivers of business intelligence and analytics acceptance," *Journal of Organizational and End User Computing (JOEUC)*, vol. 31, no. 2, pp. 37–64, 2019.

[10] Y. Chen, N. Zhang, Y. Zhang, X. Chen, W. Wu, and X. S. Shen, "Energy efficient dynamic offloading in mobile edge computing for Internet of Things," *IEEE Transactions on Cloud Computing*, p. 1, 2019.

[11] Y. Hao, Y. Miao, L. Hu, M. S. Hossain, G. Muhammad, and S. U. Amin, "Smart-Edge-CoCaCo: AI-enabled smart edge with joint computation, caching, and communication in heterogeneous IoT," *IEEE Network*, vol. 33, no. 2, pp. 58–64, 2019.

[12] X. Xu, C. He, Z. Xu, L. Qi, S. Wan, and M. Z. A. Bhuiyan, "Joint optimization of offloading utility and privacy for edge computing enabled IoT," *IEEE Internet of Things Journal*, vol. 7, no. 4, pp. 2622–2629, 2019.

[13] X. Xu, X. Zhang, X. Liu, J. Jiang, L. Qi, and M. Z. A. Bhuiyan, "Adaptive computation offloading with edge for 5G-envisioned internet of connected vehicles," *IEEE Transactions on Intelligent Transportation Systems*, pp. 1–10, 2020.

[14] L. Qi, X. Wang, X. Xu, W. Dou, and S. Li, "Privacy-aware cross-platform service recommendation based on enhanced locality-sensitive hashing," *IEEE Transactions on Network Science and Engineering*, p. 1, 2020.

[15] J. Li, T. Cai, K. Deng, X. Wang, T. Sellis, and F. Xia, "Community-diversified influence maximization in social networks," *Information Systems*, vol. 92, Article ID 101522, 2020.

[16] X. Zhou, B. Wu, and Q. Jin, "Analysis of user network and correlation for community discovery based on topic-aware similarity and behavioral influence," *IEEE Transactions on Human-Machine Systems*, vol. 48, no. 6, pp. 559–571, 2017.

[17] X. Zhou, W. Liang, K. I.-K. Kevin, K. Wang, and L. T. Yang, "Deep correlation mining based on hierarchical hybrid networks for heterogeneous big data recommendations," *IEEE Transactions on Computational Social Systems*, pp. 1–8, 2020.

[18] W. Chen, M. Yang, S. Zhang, P. Andrews-Speed, and W. Li, "What accounts for the China-US difference in solar PV electricity output? An LMDI analysis," *Journal of Cleaner Production*, vol. 231, pp. 161–170, 2019.

[19] J. Yan, Y. Yang, P. Elia Campana, and J. He, "City-level analysis of subsidy-free solar photovoltaic electricity price, profits and grid parity in China," *Nature Energy*, vol. 4, no. 8, pp. 709–717, 2019.

[20] Z. Zhu, X. Zhou, and K. Shao, "A novel approach based on Neo4j for multi-constrained flexible job shop scheduling problem," *Computers & Industrial Engineering*, vol. 130, pp. 671–686, 2019.

[21] W. Ma, M. Zhang, Y. Cao, W. Jin, C. Wang, Y. Liu et al., "Jointly learning explainable rules for recommendation with knowledge graph," in *Proceedings of the World Wide Web Conference*, pp. 1210–1221, San Francisco, CA, USA, May 2019.

[22] B. Nie and S. Sun, "Knowledge graph embedding via reasoning over entities, relations, and text," *Future Generation Computer Systems*, vol. 91, pp. 426–433, 2019.

[23] H. Wang, Z. Wang, S. Hu, X. Xu, S. Chen, and Z. Tu, "DUSKG: a fine-grained knowledge graph for effective personalized service recommendation," *Future Generation Computer Systems*, vol. 100, pp. 600–617, 2019.

[24] G. Ji, K. Liu, S. He, and J. Zhao, "Knowledge graph completion with adaptive sparse transfer matrix," in *Proceedings of the Thirtieth AAAI Conference on Artificial Intelligence*, Phoenix, Arizona, USA, February 2016.

[25] Q. Song, Y. Wu, P. Lin, L. X. Dong, and H. Sun, "Mining summaries for knowledge graph search," *IEEE Transactions on Knowledge and Data Engineering*, vol. 30, no. 10, pp. 1887–1900, 2018.

[26] Y. Zheng, C. Shi, X. Cao, X. Li, and B. Wu, "A meta path based method for entity set expansion in knowledge graph," *IEEE Transactions on Big Data*, 2018.

[27] G. Ercan, S. Elbassuoni, and K. Hose, "Retrieving textual evidence for knowledge graph facts," in *Proceedings of the 16th International European Semantic Web Conference, ESWC 2019*, pp. 52–67, Portorož, Slovenia, June 2019.

[28] T. Xia and Y. Gu, "Building terrorist knowledge graph from global terrorism database and wikipedia," in *Proceedings of the 2019 IEEE International Conference on Intelligence and Security Informatics (ISI)*, pp. 194–196, Shenzhen, China, 2019 July.

[29] R. Lu, C. Fei, C. Wang et al., "HAPE: a programmable big knowledge graph platform," *Information Sciences*, vol. 509, pp. 87–103, 2020.

[30] A. A. M. H. A. Asbahi, F. Z. Gang, W. Iqbal, Q. Abass, M. Mohsin, and R. Iram, "Novel approach of principal component analysis method to assess the national energy performance via energy trilemma index," *Energy Reports*, vol. 5, pp. 704–713, 2019.

[31] V. L. Skrobot, E. V. R. Castro, R. C. C. Pereira, V. M. D. Pasa, and I. C. P. Fortes, "Use of principal component analysis (PCA) and linear discriminant analysis (LDA) in gas chromatographic (GC) data in the investigation of gasoline adulteration," *Energy & Fuels*, vol. 21, no. 6, pp. 3394–3400, 2007.

[32] J. Webber, "A programmatic introduction to Neo4j," in *Proceedings of the 3rd Annual Conference on Systems, Programming, and Applications: Software for Humanity (SPLASH '12)*, pp. 217-218, Tucson, AZ, USA, 2012 October.

[33] M. Bostock, V. Ogievetsky, and J. Heer, "D³ data-driven documents," *IEEE Transactions on Visualization and Computer Graphics*, vol. 17, no. 12, pp. 2301–2309, 2011.

[34] B. A. Eckman and P. G. Brown, "Graph data management for molecular and cell biology," *IBM Journal of Research and Development*, vol. 50, no. 6, pp. 545–560, 2006.

[35] K. Yan, B. Wang, H. Cheng, Z. Ji, J. Huang, and Z. Gao, "Molecular skin surface-based transformation visualization between biological macromolecules," *Journal of Healthcare Engineering*, vol. 2017, Article ID 4818604, 12 pages, 2017.

[36] T. Yu, J. Li, Q. Yu et al., "Knowledge graph for TCM health preservation: design, construction, and applications," *Artificial Intelligence in Medicine*, vol. 77, pp. 48–52, 2017.

[37] X. Zhou, Y. Li, and W. Liang, "CNN-RNN based intelligent recommendation for online medical pre-diagnosis support," *IEEE/ACM Transactions on Computational Biology and Bioinformatics*, 2020.

[38] F. Färber, S. K. Cha, J. Primsch, C. Bornhövd, S. Sigg, and W. Lehner, "SAP HANA database," *ACM Sigmod Record*, vol. 40, no. 4, pp. 45–51, 2012.

Research Article

Fault Diagnosis and Identification of Power Capacitor Based on Edge Cloud Computing and Deep Learning

Xiangbing Zhao, Xulong Zhang , **and Peihua Ren**

School of Computer and Network Engineering, Shanxi Datong University, Datong 037009, China

Correspondence should be addressed to Xulong Zhang; zxllongge2018@sxdtdx.edu.cn

Nowadays, power electronic technology is widely affecting people's daily work and life. However, there are still many problems in the current power supply research. When the fault information of power transformer is not complete or there is some ambiguity or even the information is lost, it will largely lead to the conclusion and correct conclusion of fault diagnosis. In this case, the fuzzy theory is applied to the fault diagnosis of shunt capacitor, and the fuzzy fault diagnosis system of shunt capacitor is studied. At the same time, a map-based fault diagnosis system is proposed. In this paper, the cloud computing technology is introduced into the deep learning and compared with SVM and DBN algorithm. The research results of this paper show that the accuracy of fuzzy diagnosis results is 94%, 84%, 90%, 80%, 83%, and 70%, respectively, which shows that the model diagnosis reliability is relatively high. Among the three algorithms, MR-DBN overall detection rate is higher and the time-consuming is lower than the other two methods. The diagnostic accuracy and misjudgment rate of DBN are as follows: 96.33% and 3.90%. The diagnosis accuracy and misjudgment rate of SVM are as follows: 96.40% and 3.83%. The diagnostic accuracy and misjudgment rate of MR-DBN are, respectively, 99.52% and 0.57%. Compared with the other two methods, MR-DBN has the highest diagnostic accuracy and the lowest error rate, which to a large extent indicates that MR-DBN algorithm has higher diagnostic accuracy and has greater advantages and reliability in power supply diagnosis and identification. It not only improves the accuracy of power capacitor fault diagnosis and identification but also provides a new method for the application of power capacitor fault research and development.

1. Introduction

With the rapid development of science and technology, fault diagnosis has been paid more and more attention. Reactive power compensation and voltage support have become a decisive factor for the safe and stable operation of power grid. Power capacitor is the basic component of reactive power compensation device in power system. By changing the reactive flow in power system, the power can be greatly improved. The voltage level in the power system can reduce the related power loss and improve the related state performance of the power system; therefore, the normal operation of the power capacitor is related to the stability and economy of the power system operation.

At present, based on the continuous and rapid growth of power demand and the rapid development of smart grid, the relevant capacity of power system network is also becoming larger and larger and gradually developing towards the direction of high voltage and ultrahigh voltage; however, with the continuous development of power system, the impact and loss caused by the relevant faults of power system equipment are more and more; therefore, high precision is proposed. The method of power capacitor fault diagnosis and identification based on degree is very important.

Wang et al. put forward a kind of capacitor dielectric loss factor identification algorithm based on deep learning, trained a feedforward multilayer artificial neural network with online sampling period, identified the dielectric loss angle from the new monitoring data with resolution of 0.001%, put forward the calculation method of dielectric loss factor identification signal D δ (T), and verified that the

amplitude of D δ (T) is dielectric loss angle, and the waveform shape includes the interference of the monitoring device. Although the dielectric loss factor identification algorithm has accuracy, it still lacks a certain economy [1]. Chen et al. proposed a correlation model for fault diagnosis and prediction of thermal power units based on deep learning and multimedia system, which greatly improved the balance between power systems. The research results of Chen et al. show that this method is reliable. Although this method has stability and reliability, it still lacks certain practicability [2]. Based on the deep learning algorithm, Jian et al. constructed a layered automatic coding network. By introducing sparse constraints to compress and reduce the input data, the network can accurately extract the fault characteristics of the input data and improve the fault identification ability of the network by introducing random noise. Although the stack automatic coding network has accuracy, it lacks certain stability [3].

In this paper, the fuzzy theory is applied to the fault diagnosis of shunt capacitor, and on this basis, a fuzzy fault diagnosis system of shunt capacitor is studied, which can accurately diagnose what kind of fault happened to capacitor and its related severity to a great extent; at the same time, a distributed DBN based on Map Reduce is used in this paper. It introduces deep learning and this is compared with SVM and DBN, which highlights the advantages and reliability of MR-DBN algorithm, provides related services for fault diagnosis and identification of capacitors, improves the accuracy of fault diagnosis and identification of capacitors, and provides some theoretical experience for the research and application of capacitor faults.

2. Edge Calculation and Power Capacitor

2.1. Edge Computing

2.1.1. Concept of Edge Computing. Edge computing belongs to a distributed open platform, which integrates core functions such as network, computing, storage, and application on the edge of the network. It provides relevant edge intelligence services nearby, so as to meet the requirements of agile connection, real-time business, data optimization, application intelligence, security, and privacy protection to a large extent. Edge computing can not only connect the related physical and digital worlds but also be used in intelligent assets, intelligent gateways, and intelligent systems, as well as intelligent services that provide some effective information [4].

2.1.2. Edge Computing Advantages. There will be an open interface about the model in each layer of the edge computing reference architecture, so as to fully open the architecture. The related reference architecture of the edge computing can realize the whole business process and the whole life cycle intelligent service interface through vertical management services and security services to a large extent; compared with the traditional cloud computing model, the edge computing model can play an important role in the network to a large extent and can better support the

application of the Internet of things. Its advantages mainly lie in the following two aspects:

(1) Relieve the Pressure of Network Bandwidth and Data Center. The typical feature of Internet of things data is high redundancy, most of which are temporary data. Edge computing can make scientific and effective use of this function to process a large number of temporary data at the edge of the network, so as to reduce its adverse impact on the network bandwidth and data center [5].

(2) High Data Security. In the relevant mode of cloud computing, all the data are concentrated in the data center, which makes it difficult for users to control the access and use of relevant data. However, edge computing can store and use the data in the network edge device closer to the user, thus greatly improving the security of data [6].

2.2. Power Capacitor

2.2.1. Power Capacitor. Power capacitor refers to a kind of nondynamic reactive power compensation device. Its main function is to provide reactive power for the power system, so as to improve the relevant power factor to a large extent. Using local reactive power compensation can not only greatly reduce the transmission current of transmission line but also greatly reduce the related loss of line energy and improve the equipment benefit utilization which plays an important role [7]. In addition, capacitors play a very important role in improving the power quality of power system, which is an important means to ensure the economic and safe operation of power system. Its safe operation and fault handling are very important. In the long-term operation, due to the influence of operation environment, human factors, design problems, and other related factors, the phenomenon of fault is common, which to a large extent has a bad impact on the safe operation of the power system.

2.2.2. Structural Advantage. Modern high-voltage shunt capacitor elements mainly use oil-immersed polypropylene film as the medium between electrodes and aluminum foil as the plate. One end of the plate extends out of the medium and the other end folds and sinks into the medium [8]; the structural advantages of this plate are as follows:

(1) The electric field distribution at the edge of the plate is improved

(2) The PD performance is improved obviously

(3) The related resistance and loss of the electrode plate are greatly reduced, the speed of temperature rise is also reduced, and the thermal stability is also improved

(4) The protruding plate can be used to connect components, thus greatly simplifying the structure and manufacturing process and saving related labor time [9]

In many related engineering practices, it is necessary to make a detailed analysis of the electric field distribution law of the weakest part of the board edge insulation and the relative strength between the largest electric fields, so as to ensure the safety and reliability to a large extent. In general, it is enough to make a general analysis and understanding of the electric field distribution law of the rest parts, and it is not necessary to accurately calculate the board. It is not necessary to accurately calculate the electric field intensity of each point in the edge area of the plate so that the simplified calculation method can be carried out and the calculation time can be saved [10].

2.2.3. Related Relationship.

With the continuous increase of the average electric field strength of the capacitor, the maximum electric field strength at the edge of the board increases synchronously. The voltage of the capacitor unit is the product of the number of element strings and the voltage of the element. Increasing the element voltage can reduce the number of element strings to a large extent, which makes the relevant structure and manufacturing of the capacitor more and more simplified without increasing the average field. Under the premise of strong, the related consumption of aluminum foil can be saved, and the related cost can be reduced to a large extent [11]. However, the continuous increase of the working voltage of the module will increase the film thickness between the two poles, so as to increase the correlation coefficient of electric field distortion and the maximum field strength at the edge of the plate [12].

It can be said that the maximum field strength at the edge of the capacitor plate is one of the most fundamental and influential factors restricting the development of power capacitor technology. Generally, the choice of the working field strength of the capacitor is concerned, that is, the average field strength. On the premise of ensuring reliability, the higher the average field strength is, the lower the volume and weight cost of the corresponding capacitor is and the higher the level of the capacitor is; conversely, in order to ensure the safety and reliability of the capacitor, there is a method that requires strict control of the average field strength not greater than a certain value. This method only focuses on the impact of the average field strength and ignores the impact of the maximum field strength at the edge of the plate [13].

2.3. Fault Diagnosis and Maintenance of Power Capacitor

2.3.1. Power Capacitor Leakage Oil.

The leakage of oil is mainly caused by loose seal or insecure seal. The capacitor is a completely sealed equipment. If the seal is not tight, air, moisture, and impurities may enter the oil tank, which will cause certain damage to the insulation layer, resulting in serious damage. Therefore, the capacitor is not allowed to leak oil. In fact, the leaking parts are mainly at the welds and casings of the oil tank, which indicates that the welding process of these parts is poor, and the manufacturer has not carried out strict requirements for the sealing test, instead of conducting the leakage test one by one. According to the

general standard, it should be heated to 75°C and kept for 2 hours to carry out the test. When purchasing, the manufacturer should be strictly required to carry out the test. In fact, the leaking part of the casing pipe is mainly the root, cover, bolt, and other welded joints. The causes of the leakage mainly include processing technology problems, structural design problems, and human factors. The mechanical strength of the welding used for the bolt and cover is very poor. If the tightening force is slightly large, the screw will be removed for welding. Therefore, when the temperature changes, the bolt will be applied with a certain degree of pressure. It is easy to open the screw welded joint; in addition, the sleeve is lifted directly during the transportation process, so careless treatment will also make the weld crack. In view of the above reasons, corresponding measures should be taken to strengthen the management of production enterprises and operation and maintenance personnel, so as to solve the relevant leakage problems to a certain extent [14].

2.3.2. Poor Insulation.

This kind of phenomenon is found in the preventive test; basically, there are two situations as follows:

(1) In the long-term heating and voltage life test, the change of capacitance value is very small. If the capacitance value suddenly increases, it can only be regarded as the breakdown and short circuit of some capacitor elements. Because the capacitor is composed of multiple components in series, the capacitance will increase only when the number of series segments is reduced, and the capacitance value will decrease if some elements are disconnected.

(2) The second part of the poorly insulated capacitor is that the dielectric loss angle exceeds a certain range, which will slightly increase the dielectric loss angle of the capacitor during long-term operation, and the multiple increase is abnormal, because only when partial discharge and partial overheating occur, the dielectric loss angle will exceed a certain range, so it can only be replaced. The insulation strength of the welding electrode to the oil tank is usually very high, but due to the defects in the welding process, such that the insulating cardboard between the parts and the oil tank is burnt out, the wire is not insulated, the oil is insufficient, the short tail sleeve is used, the insulation distance is insufficient, and the quality of the porcelain sleeve is poor, during the relevant test process, the discharge and burst of the sleeve may occur. Therefore, patrol inspection should be strengthened, hidden dangers should be found in time, and corresponding treatment should be carried out [15].

(3) Capacitor case bulge: in case of large expansion of the capacitor shell, it is caused by excessive internal pressure. The internal pressure is too high due to the gas produced by the internal free medium or the gas produced by breakdown, discharge, and other

phenomena. The generated gas will increase the internal pressure of the capacitor and cause the phenomenon of shell expansion [16]. When the above phenomenon occurs, it should be handled in time.

(4) Capacitor explosion: when a capacitor breaks down or discharges between poles due to a sharp increase of internal energy, the capacitor will explode. This usually happens in a capacitor without internal fuse. Many low-voltage capacitors are equipped with protection fuses, so low-voltage capacitors rarely explode. The short-circuit breakdown characteristics of paper film capacitors and full film capacitors are different, so they are released by the authority after electricity, and the insulating paper will be carbonized under high temperature, thus forming the capacitor element of full film and paper film composite dielectric. Because the separation of carbonized paper will keep discharging for a period of time, a large amount of gas will be generated at this time. If there is no fuse protection, the oil tank will break. After discharging, the film of full film capacitor will be affected by high temperature, and melting will make two-electrode short-circuit contact without arc discharge or gas explosion, so full film capacitor shall be used for explosion proof [17].

(5) Capacitor heating: when there are harmonics in the system, the harmonic current will damage the capacitor to a certain extent, which will aggravate the related loss of the insulation medium of the capacitor, so it is easy to make the insulation layer age rapidly; sometimes, it may bring the related risk of thermal breakdown, which will have a bad impact on the safe operation of the capacitor to a large extent, in the case of harmonics, the electrode of the capacitor. The voltage between them may reach a large value, which may cause the risk of internal discharge of the capacitor and threaten the insulation of the power container, which may easily cause the capacitor to heat [18].

(6) Environmental temperature problems: there is a certain range of temperature around the capacitor, which should not be too high or too low. If the ambient temperature exceeds a certain safety range, the heat generated by the capacitor during operation cannot be eliminated; if the ambient temperature is lower than a certain range, the oil in the capacitor may freeze and be easily broken by electricity [19].

(7) Maintenance of power capacitor: the power capacitor bank in operation shall be subject to routine patrol inspection, relevant maintenance and repair, and regular power outage inspection [20].

  (1) The capacitor shall be equipped with relevant personnel on duty, and the operation of the equipment shall be recorded.
  (2) The working capacitor bank shall be subject to certain appearance inspection every day according to the regulations. If the expansion of the shell is noticed, it shall be stopped to avoid damage.
  (3) Check the load of each phase of capacitor bank with ammeter.
  (4) When the capacitor bank is put into use, the ambient temperature under normal conditions shall not be lower than −4°C, the ambient temperature during operation shall not be higher than +40°C, and the average ambient temperature during operation shall not be higher than +30°C [21].
  (5) After connecting the capacitors, it will cause the grid voltage to rise, especially in light load; in this case, some or all capacitors shall be disconnected from the grid [22].
  (6) The surface of capacitor and supporting insulator shall be cleaned regularly to ensure that no damage or discharge trace is found. At the same time, the shell of capacitor shall also be cleaned to ensure that there is no deformation and oil leakage, and the capacitor and iron frame shall not be covered with dust and other pollutants.
  (7) It is necessary to pay attention to the reliability of all contacts on the circuit connected to the capacitor bank (current bank, ground wire, circuit breaker, fuse, switch, etc.), as long as there is a contact fault in the circuit, even if the nut is loose, the capacitor may be damaged prematurely and the whole equipment will be damaged.
  (8) If the capacitor needs to pass the withstand voltage test for a period of time, the relevant test shall be carried out according to the specified value.

2.4. Common Troubleshooting and Preventive Measures

  (1) In case of fire such as discharge and explosion of capacitor, cut off the power supply first, and then put out the fire.

  (2) When the corresponding circuit breaker of the capacitor trips, first discharge the capacitor completely, and then check the condition of the relevant equipment. If there is no abnormality in the inspection, it may be caused by the fluctuation of the grid voltage. If the operation is abnormal, it may be caused by the internal fault of the capacitor. Check and test each capacitor until the relevant cause of the fault is found [23].

  (3) When the fuse is damaged, the capacitor shall be discharged completely first, then the fuse shall be replaced, and the corresponding equipment can be put into use only after no other abnormal phenomenon is found. If the trial operation is not successful, each capacitor shall be inspected and tested after power failure.

(4) Control the working temperature correctly; do not work at a temperature higher than 60°C. If the temperature rises, pay attention to ventilation. If it is not caused by ventilation problems, quickly find out the causes and deal with the abnormalities, and do not operate at high temperature for a long time [24].

(5) In the process of capacitor installation, the method of series reactor can prevent the harm of harmonic to a large extent and plays a crucial role in the overall operation [25].

3. Deep Learning

3.1. Deep Learning. Deep learning technology is the latest achievement in machine learning research. Deep learning model is a breakthrough of the original neural network model, which imitates the abstract reflection of human brain to objective things. The difference between the deep learning model and the neural network model is that the deep learning model can largely solve the overfitting problem when training the multilayer neural network. The depth model is composed of multilayer neural network. There is no mutual connection between nodes in the same layer of neural network. It uses greedy algorithm to train each layer of network. When the layer of network reaches the accuracy requirements, it begins to train the next layer. Each layer is an abstract expression of different sides of the original data. For example, an image is composed of many pixels, many pixels form part of the image, and some regional images form the whole image; for example, statements are composed of a single character, multiple characters form words, multiple words form sentences with meaning similarly, network data packets are composed of multiple binary bits, multiple binary bits form each protocol field, and protocol fields form a protocol.

Because the depth model is layer-by-layer learning, learning a higher-level representation of the previous layer, that is, the simulation of the previous layer in different dimensions, so given the sample data, the process of depth learning is the process of approaching the distribution or function of the sample data. The deep learning model is mainly composed of input-output layer and multiple hidden layers. The data is input from input layer and output from output layer through the transformation of each hidden layer. The purpose of training model is to make the information of output layer consistent with the total information of input layer. However, in the actual process, the multilayer transmission of information will always be weakened, so it is impossible to achieve exactly the same in the actual training. The training model parameters within the preset error range are considered to have achieved the training goal.

3.2. DBN Model

3.2.1. Overview of DBN. The deep trust network (DBN) is a deep structure composed of several restricted Boltzmann machines (RBM) and BP neural network. Its training process mainly includes the following two aspects: one is to use

i-strong-m structure training to filter the relevant data feature information; the other is to connect each layer of RBM, establish BP neural network in the last layer, and use the output of RBM as BP neural network. Compared with the traditional neural network, DBN has the advantages of long training time, easy to fall into local optimum, and slow processing speed of big data.

3.2.2. RBM Algorithm. If V_i is the node value of visible layer, H_J is the node value of hidden layer, A_i and B_j are their offsets, and W_{ij} is the weight between nodes, then

$$P\left(h_j = 1\right) = \frac{1}{1 + \exp\left(-a_j - \sum_i v_i w_{ij}\right)}. \tag{1}$$

Since the hidden layer and the visible layer can represent each other, there are

$$P\left(v_i = 1\right) = \frac{1}{1 + \exp\left(-b_i - \sum_j h_j w_{ji}\right)}. \tag{2}$$

Then train the CD (Contrastive Divergence) criterion of RBM and propose the update formula of weight vector $\theta(a, b, w)$ as

$$\theta_{i+1} = \theta_i + u \frac{\partial \log_p (v, h)}{\partial \theta} \theta_i. \tag{3}$$

4. Discussion on Experimental Methods and Results

4.1. Experiment

4.1.1. Experimental Method

(1) Fuzzy Theory. In this paper, the fuzzy theory is applied to the fault diagnosis of shunt capacitor, and people's long-term experience of fault diagnosis is expressed mathematically. On this basis, a kind of fuzzy fault diagnosis system of shunt capacitor is studied, which can accurately diagnose what kind of fault happened to the capacitor and its severity.

(2) Map Reduce-Based Distributed DBN. In this paper, the fault diagnosis and identification method of power capacitor based on Map Reduce distributed DBN is adopted, and the cloud computing-related technology is integrated into the deep learning. At the same time, some comparative analysis is made with SVM and DBN, so as to highlight the relevant advantages of MR-DBN algorithm in power capacitor fault diagnosis to a large extent.

4.1.2. Correlative Design of Fuzzy Diagnosis Systems

(1) Fuzzy Algorithm. There are four common algorithm models of fuzzy operator m (·, +). In order to consider the influence of all factors and keep all the information of single factor evaluation, the following algorithm is selected:

$$M(\cdot, +) = \sum_{i=1}^{m} x_i y_{ij}, \qquad (4)$$

where $j = 1, 2, ..., n$.

4.1.3. Overall Framework of the System.
The overall frame structure is shown in Figure 1.

It can be seen from Figure 1 that the overall framework includes a main control operation module and four functional modules for data acquisition, and the four functional modules for data acquisition include signal analysis, feature extraction, fault diagnosis, and database.

4.1.4. Map Reduce Model Process

(1) *Input.* Read the relevant data in the distributed file system and divide the relevant data into certain data pieces. Each map function in the Map Reduce framework can allocate a data piece.

(2) *Map.* Data slicing is considered as a set of key-value pairs. According to the relevant program logic of the mapping function, the relevant key-value pairs allocated by Map Reduce framework are processed, and a new intermediate key-value pair is generated.

(3) *Shuffle.* In this stage, the intermediate key-value pair is transferred from the mapping node to the reduction node, and the same intermediate key-value pair is merged at the same time to form the intermediate key chain and key-value sorting.

(4) *Reduce.* Execute the reduce function.

(5) *Output.* Output the processing result of reduce function, and save the result in the specified distributed file system.

4.1.5. Evaluation Index

(1) The accuracy of power capacitor fault judgment is as follows:

$$\text{accuracy} = \frac{a}{b} \times 100\%. \qquad (5)$$

(2) The error rate of power capacitor fault judgment is

$$\text{False}_{ij} = \frac{c}{a} \times 100\%. \qquad (6)$$

4.2. Analysis of Experimental Results

4.2.1. Analysis of Fuzzy Diagnosis Results of Capacitor Fault Diagnosis.
According to the symptoms of capacitor fault, combined with a large number of data related to the system in actual operation and the related data in parallel capacitors, according to the relevant membership method, carry out the relevant fuzzy diagnosis for the fault diagnosis of parallel capacitors; the specific situation is shown in Table 1.

It can be seen from Table 1 that the value of fuzzy diagnosis matrix reflects the close relationship between symptoms and fault causes, which is the quantification of 0-1 fuzzy relationship between symptoms and faults in the process of fuzzy reasoning; in the initialization process of R value, there is inevitably subjective component, which may lead to wrong judgment. After a long time of operation, the performance and characteristic parameters of parallel capacitors will occur. In order to make the diagnosis conclusion more practical, it is necessary to modify R continuously during the operation of shunt capacitor.

4.2.2. Analysis of Fault Data Diagnosis Results Based on Fuzzy Theory.
The diagnosis results of 60 groups of parallel capacitors using this system are shown in Table 2.

According to Table 2, the accuracy of the diagnosis results is 94%, 84%, 90%, 80%, 83%, and 70%, respectively; when the accuracy of the diagnosis results is greater than 90%, it means that the reliability of the model diagnosis is very high; when the accuracy of the diagnosis results is greater than 75%, it means that the reliability of the model diagnosis is relatively high; when the accuracy of the diagnosis results is less than 75%, it means that the reliability of the model diagnosis is not to a large extent. In order to improve the reliability of model diagnosis, it is necessary to improve the fuzzy diagnosis matrix R.

4.2.3. Comparative Analysis of MR-DBN and Other Methods in Detection Rate and Detection Time.
The comparison of detection rate and detection time between MR-DBN and other methods is shown in Figure 2.

It can be seen from Figure 2 that the detection rates of three methods, SVM, DBN, and MR-DBN, are 96.43, 97.52, and 98.48, respectively. The RW detection rates of SVM, DBN, and MR-DBN were 3.42, 2.45, and 2.31, respectively. The detection rates of SVM, DBN, and MR-DBN were 8.13, 7.52, and 7.54, respectively. The detection time of SVM, DBN, and MR-DBN was 20.31, 19.22, and 18.41, respectively. It can be seen that, among the three methods, the detection rate of MR-DBN is higher than that of the other two.

4.2.4. Analysis of Accuracy, Parameters, and MR-DBN Diagnosis Results of Different Algorithms.
In order to verify the reliability and practicability of the fault diagnosis algorithm used in this paper, this paper compares the MR-DBN algorithm with the related support vector machine and DBN algorithm. The accuracy and parameters of different algorithms are shown in Figure 3, and the MR-DBN diagnosis results are shown in Figure 4.

It can be seen from Figures 3 and 4 that the diagnostic accuracy and misjudgment rate of DBN are, respectively, 96.33% and 3.90%. The diagnosis accuracy and misjudgment rate of SVM are as follows: 96.40% and 3.83%. The diagnostic accuracy and misjudgment rate of MR-DBN are as follows: 99.52% and 0.57%. Therefore, compared with the other two methods, MR-DBN has the highest diagnostic accuracy and
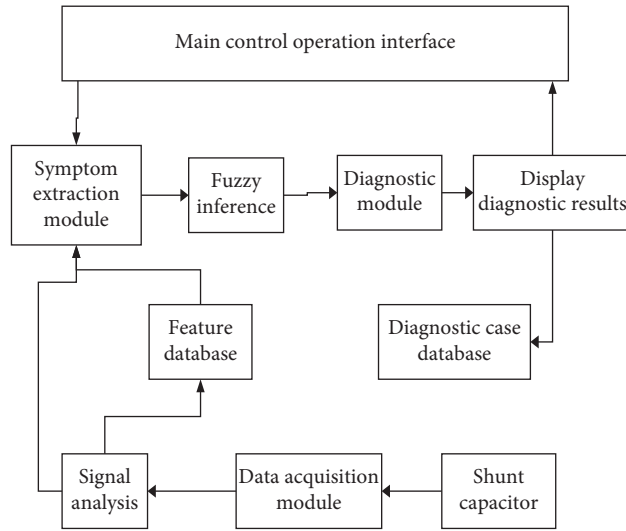
FIGURE 1: Overall structure of the system.

TABLE 1: Fault diagnosis matrix of shunt capacitor.

Fault symptoms	Cause of failure				
	$Y1$	$Y2$	$Y3$	$Y4$	$Y5$
$X1$	0.95	0.83	0.02	0.02	0.01
$X2$	0	0.01	0.02	0.58	0.86
$X3$	0.1	0	0.1	0.5	0.1

TABLE 2: Summary of diagnosis results.

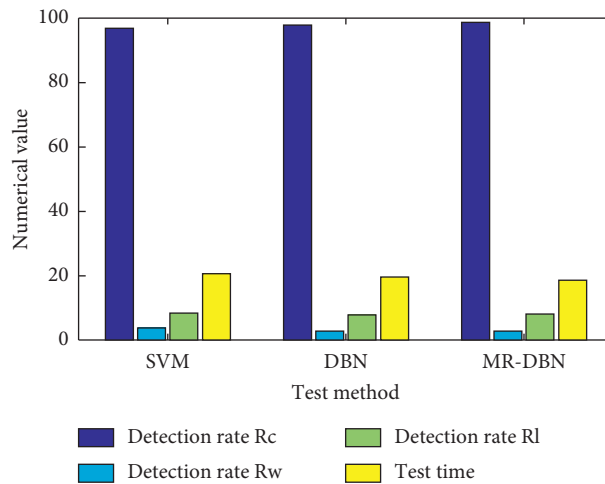| Fault type	Group number	Diagnostic accuracy (%)
Shell deformation	18	94
Oil leakage	24	84
Overtemperature	5	90
Fuse blown	6	80
Splashing sparks and fire	3	83
Poor insulation	4	70

FIGURE 2: Comparison of detection rate and detection time between MR-DBN and other methods.
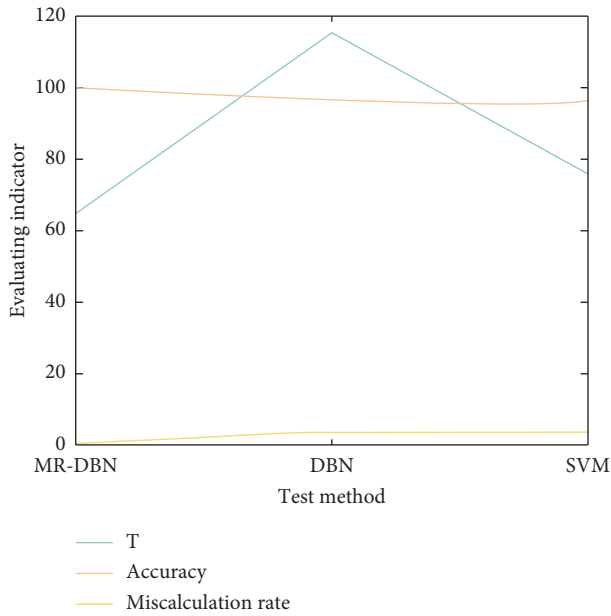
FIGURE 3: Accuracy and parameters of different algorithms.

FIGURE 5: Comparison of diagnosis results.

related aspects of power capacitor fault diagnosis and identification. It not only improves the accuracy of power capacitor fault diagnosis and identification but also improves the stability of capacitor fault diagnosis and identification and provides a new method for the research and application of power container fault diagnosis and identification.
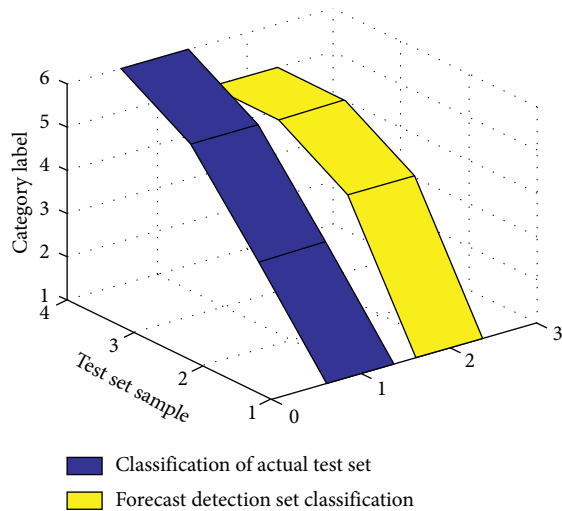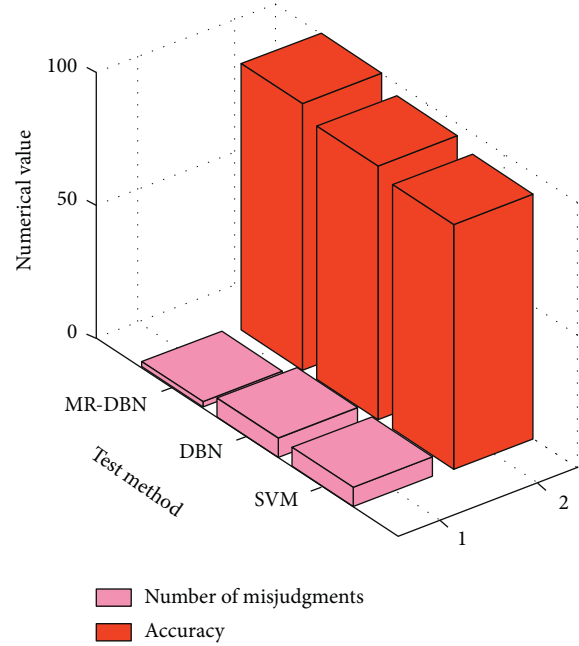
5. Conclusions

FIGURE 4: MR-DBN diagnosis results.

the lowest misjudgment rate; in the diagnosis results of MR-DBN, the actual detection set is the same as the difference between the prediction detection sets is small.

4.2.5. Comparative Analysis of Diagnosis Results of Three Algorithms. The diagnosis results of the three algorithms are shown in Figure 5.

It can be seen from Figure 5 that the fault accuracy of the algorithm MR-DBN is 99.52%, the number of misjudgments is 2, the fault accuracy of DBN is 94.83%, the number of misjudgments is 7, the fault accuracy of SVM is 91.43%, and the number of misjudgments is 8. By comparing the fault diagnosis accuracy of different methods and the number of wrong judgments, we can see that the MR-DBN algorithm has a high diagnosis rate and plays an important role in the

In this paper, the fuzzy diagnosis is applied to the fault diagnosis of shunt capacitor. Based on the operation experience of shunt capacitor, the fuzzy diagnosis matrix is established, the fuzzy algorithm and diagnosis principle are determined, and the fuzzy fault diagnosis system is designed. The results of this paper show that the fuzzy diagnosis method is effective in the fault diagnosis of parallel capacitors. In addition, in view of the related defects of traditional methods in the fault diagnosis of power capacitors, such as low accuracy, large error, and poor real-time performance, this paper also introduces the cloud computing technology into the deep learning and proposes a power capacitor fault diagnosis and solution based on map. In comparison with DBN and SVM, it is found that the diagnosis accuracy of the algorithm is relatively high.

The research of this paper shows that the accuracy of fuzzy diagnosis results is 94%, 84%, 90%, 80%, 83%, and 70%, respectively. When the accuracy of diagnosis results is greater than 90%, it means that the reliability of model diagnosis is very high. When the accuracy of diagnosis results is greater than 75%, it means that the reliability of model diagnosis is relatively high. When the accuracy of diagnosis results is less than 75%, it means that the reliability of model diagnosis is not very good. In order to improve the reliability of model diagnosis, it is necessary to improve the

fuzzy diagnosis matrix. Among the three methods, the diagnostic accuracy and misjudgment rate of DBN are 96.33% and 3.90%, respectively, the diagnostic accuracy and misjudgment rate of SVM are 96.40% and 3.83%, respectively, and the diagnostic accuracy and misjudgment rate of MR-DBN are 99.52% and 0.57%, respectively. Therefore, compared with the other two methods, the diagnostic accuracy and misjudgment rate of MR-DBN are the highest and the lowest, which to a large extent shows that the accuracy and misjudgment rate adopted in this paper are the lowest; the MR-DBN algorithm used in this paper has high accuracy in correlation diagnosis. It plays an important role in power capacitor fault diagnosis. It not only improves the correlation accuracy of capacitor fault diagnosis and identification but also provides a new method for related application research and analysis.

In the related power distribution system, capacitors play a very important role in the power system, but there are still some deficiencies in the corresponding fault analysis and research work. With the continuous improvement of the design level and manufacturing process of power equipment, the quality of capacitors will be further improved. At present, the integrated capacitor is slowly replacing the traditional capacitor bank, but new equipment and technology will also bring a series of problems. It is a very important but long-term task to analyze and deal with the related problems of capacitor.

Data Availability

No data were used to support this study.

Conflicts of Interest

The authors declare that they have no conflicts of interest.

Acknowledgments

References

[1] X. Wang, Y. Zhu, and Y. Wang, "Online identification method of power capacitor dielectric loss angle based on deep learning," *Diangong Jishu Xuebao/Transactions of China Electrotechnical Society*, vol. 32, no. 15, pp. 145–152, 2017.

[2] F. Chen, L. Z. Fu, and L. Zhen, "Thermal power generation fault diagnosis and prediction model based on deep learning and multimedia systems," *Multimedia Tools & Applications*, vol. 78, no. 4, pp. 4673–4692, 2019.

[3] Y. Jian, X. Qing, and L. He, "Fault diagnosis of motor bearing based on deep learning," *Advances in Mechanical Engineering*, vol. 11, no. 9, 2019.

[4] G. Zhang, W. Bao, and X. Zhu, "A server consolidation method with integrated deep learning predictor in local storage based clouds," *Concurrency, Practice and Experience*, vol. 30, no. 23, pp. e4503.1–e4503.16, 2018.

[5] X. Hou and G. Zhao, "Resource scheduling and load balancing fusion algorithm with deep learning based on cloud computing," *International Journal of Information Technology and Web Engineering*, vol. 13, no. 3, pp. 54–72, 2018.

[6] W. Gao and Y. Zhu, "A cloud computing fault detection method based on deep learning," *Journal of Computer & Communications*, vol. 05, no. 12, pp. 24–34, 2017.

[7] J. Tang, D. Sun, and S. Liu, "Enabling deep learning on IoT devices," *Computer*, vol. 50, no. 10, pp. 92–96, 2017.

[8] M. U. Yaseen, A. Anjum, and M. Farid, "Cloud-based video analytics using convolutional neural networks," *Software Practice & Experience*, vol. 49, no. 4, pp. 565–583, 2019.

[9] J. Li, G. Luo, and N. Cheng, "An end-to-end load balancer based on deep learning for vehicular network traffic control," *IEEE Internet of Things Journal*, vol. 6, no. 1, pp. 953–966, 2019.

[10] S. Li, Y. Nie, and J. Li, "Condition monitoring and diagnosis of power equipment: review and prospective," *High Voltage*, vol. 2, no. 2, pp. 82–91, 2017.

[11] A. A. Elserougi, A. M. Massoud, and S. Ahmed, "Arrester-less DC fault current limiter based on pre-charged external capacitors for half-bridge modular multilevel converters," *Generation, Transmission & Distribution, IET*, vol. 11, no. 1, pp. 93–101, 2017.

[12] J. Amini and M. Moallem, "A fault-diagnosis and fault-tolerant control scheme for flying capacitor multilevel inverters," *Industrial Electronics, IEEE Transactions on*, vol. 64, no. 3, pp. 1818–1826, 2017.

[13] J. Liu, Q. Li, and W. Chen, "A discrete hidden Markov model fault diagnosis strategy based on K-means clustering dedicated to PEM fuel cell systems of tramways," *International Journal of Hydrogen Energy*, vol. 43, no. 27, pp. 12428–12441, 2018.

[14] J. H. Jung, H. K. Ku, and Y. D. Son, "Open-switch fault diagnosis algorithm and tolerant control method of the three-phase three-level NPC active rectifier," *Energies*, vol. 12, no. 13, p. 2495, 2019.

[15] H. Givi, E. Farjah, and T. Ghanbari, "Switch fault diagnosis and capacitor lifetime monitoring technique for DC–DC converters using a single sensor," *Science, Measurement & Technology, IET*, vol. 10, no. 5, pp. 513–527, 2016.

[16] E. Farjah, H. Givi, and T. Ghanbari, "Application of an efficient rogowski coil sensor for switch fault diagnosis and capacitor ESR monitoring in nonisolated single-switch DC–DC converters," *IEEE Transactions on Power Electronics*, vol. 32, no. 2, pp. 1442–1456, 2017.

[17] F. Naseri, E. Farjah, and M. Allahbakhshi, "Online condition monitoring and fault detection of large supercapacitor banks in electric vehicle applications," *Electrical Systems in Transportation, IET*, vol. 7, no. 4, pp. 318–326, 2017.

[18] J. Hannonen, J. Honkanen, and J. P. Strm, "Capacitor aging detection in a DC–DC converter output stage," *IEEE Transactions on Industry Applications*, vol. 52, no. 4, pp. 3224–3233, 2016.

[19] W. Chen and A. M. Bazzi, "Logic-based methods for intelligent fault diagnosis and recovery in power electronics," *IEEE Transactions on Power Electronics*, vol. 32, no. 7, pp. 5573–5589, 2017.

[20] S. H. A. Niaki, S. M. Hosseini, and A. A. Abdoos, "Fault detection of HVDC cable in multi-terminal offshore wind farms using transient sheath voltage," *Renewable Power Generation, IET*, vol. 11, no. 13, pp. 1707–1713, 2017.

[21] K. Yao, C. Cao, and S. Yang, "Noninvasive online condition monitoring of output capacitor's ESR and C for a flyback converter," *Instrumentation & Measurement IEEE Transactions on*, vol. 66, no. 12, pp. 3190–3199, 2017.

[22] H. Jouybari-Moghaddam, T. S. Sidhu, and M. R. D. Zadeh, "Shunt capacitor banks online monitoring using a superimposed reactance method," *Smart Grid IEEE Transactions on*, vol. 9, no. 6, pp. 5554–5563, 2018.

[23] L. Liao, H. Gao, and Y. He, "Fault diagnosis of capacitance aging in DC link capacitors of voltage source inverters using evidence reasoning rule," *Mathematical Problems in Engineering*, vol. 2020, no. 9, pp. 1–12, 2020.

[24] K. Bi, Q. An, and J. Duan, "Fast diagnostic method of open circuit fault for modular multilevel DC/DC converter applied in energy storage system," *IEEE Transactions on Power Electronics*, vol. 32, no. 5, pp. 3292–3296, 2017.

[25] W. C. Santos, F. V. Lopes, and N. S. D. Brito, "High-impedance fault identification on distribution networks," *Power Delivery IEEE Transactions on*, vol. 32, no. 1, pp. 23–32, 2017.

Research Article

A Multilevel Optimization Framework for Computation Offloading in Mobile Edge Computing

Nanliang Shan [iD], Yu Li [iD], and Xiaolong Cui [iD]

College of Information Engineering, Engineering University of PAP, Xi'an 710086, China

Correspondence should be addressed to Xiaolong Cui; shannanliang@126.com

Mobile edge computing is a new computing paradigm that can extend cloud computing capabilities to the edge network, supporting computation-intensive applications such as face recognition, natural language processing, and augmented reality. Notably, computation offloading is a key technology of mobile edge computing to improve mobile devices' performance and users' experience by offloading local tasks to edge servers. In this paper, the problem of computation offloading under multiuser, multiserver, and multichannel scenarios is researched, and a computation offloading framework is proposed that considering the quality of service (QoS) of users, server resources, and channel interference. This framework consists of three levels. (1) In the offloading decision stage, the offloading decision is made based on the beneficial degree of computation offloading, which is measured by the total cost of the local computing of mobile devices in comparison with the edge-side server. (2) In the edge server selection stage, the candidate is comprehensively evaluated and selected by a multiobjective decision based on the Analytic Hierarchy Process based on Covariance (Cov-AHP) for computation offloading. (3) In the channel selection stage, a multiuser and multichannel distributed computation offloading strategy based on the potential game is proposed by considering the influence of channel interference on the user's overall overhead. The corresponding multiuser and multichannel task scheduling algorithm is designed to maximize the overall benefit by finding the Nash equilibrium point of the potential game. Amounts of experimental results show that the proposed framework can greatly increase the number of beneficial computation offloading users and effectively reduce the energy consumption and time delay.

1. Introduction

With the development of artificial intelligence and Internet of Things (IoT) technology, a large number of computation-intensive and time-sensitive mobile applications have appeared on mobile terminals, such as face recognition, natural language processing, and augmented reality. However, the limited computing capability and energy storage of mobile terminals cannot provide intensive computing and complete high-energy tasks. A large number of applications training process must be deployed on the cloud service platform, so that a large amount of training data generated on the mobile terminal need to be transmitted to the cloud through the core network, resulting in a sharp increase in the already congested core network load. Application transmission delay and transmission energy consumption will

also increase greatly, which will cause service request failure and QoS of the user to decline.

Currently, mobile edge computing (MEC) [1–3] has become an important solution to the above contradictions. However, in the MEC scheme based on the public cloud [3–5], accessing the mobile cloud service through the wireless channel results in a large channel blocking rate and delay. Meanwhile, the MEC scheme based on the cloudlet [6] can only connect to cloud services via WiFi, which has a large space limitation.

In response to the above limitations, an edge server-based MEC solution has been proposed and widely used. As shown in Figure 1, the edge server is deployed on the wireless LAN side in the edge server-based MEC solution, which shortens the distance between servers and the users. This solution can use computing offload to expand the service

capabilities of mobile devices, provide localized computing and storage resources for mobile devices nearby, reduce data transmission costs, and meet the needs of the fast and interactive response. Among them, mobile devices and users are collectively referred to as mobile edge nodes, and the combination of wireless base stations and edge servers is referred to as edge server nodes. The edge server nodes can further offload the preprocessing results to the remote cloud service center through the mobile core network. Therefore, the key technology of the MEC solution based on the edge server is computing offloading. How to formulate a reasonable and efficient computing offloading framework will be an issue that we urgently need to solve. When many users offload computing tasks to the same edge server through the same channel at the same time, it will cause congestion and greater delay. The evaluation indicators for computing offload include energy consumption and service delay.

In order to minimize the energy consumption and service delay of mobile users, the main contributions of this paper are listed as follows:

(1) The concept of beneficial computation offloading is proposed. The overall cost of the mobile edge computing system is defined as the weighted sum of energy consumption, the corresponding transmission delay of computation offloading, and the task processing of all edge nodes. When the total cost of computation offloading is less than the total cost of the local computing, beneficial computation offloading is obtained. Beneficial computation offloading is a prerequisite for users to make computation offloading decisions.

(2) A Cov-AHP strategy for multiobjective servers offloading decision is proposed. Considering the transmission time, energy consumption, and server residual resources, the server to be selected for undertaking offloading is comprehensively evaluated by the covariance judgment matrix. The experimental results show that the Cov-AHP algorithm is objective and can effectively realize load balancing.

(3) A multiuser multichannel distributed computation offloading algorithm based on the potential game is proposed. The computation offloading optimization of multiuser in a multichannel wireless interference scenario is an NP-Hard problem. According to the number of beneficial computation offloading users and the total system cost, the efficiency of the Nash equilibrium is quantified. Users can formulate an interaction mechanism based on the group strategy to achieve the maximum benefit and the highest resource utilization. The algorithm can optimize its computation offloading performance as the size of the user increases.

The remainder of this paper is organized as follows. Section 2 reviews the related studies. Section 3 introduces the system model and describes the problem statement and solution. In Sections 4, 5, and 6, a three-level strategy for the computation offloading framework is illustrated in detail.

The experiment and result analysis are discussed in Section 7. The final section summarizes the paper and discusses future work.

2. Related Studies

Researches on computation offloading can be divided into three types. In the mode of single-user single-available edge server, a dynamic computation migration algorithm (LODCO) based on Lyapunov optimization [7] is proposed to optimize the execution delay of the application. In [8], the optimization of mobile device energy is defined as a constrained Markov decision process. Then, a computational migration decision algorithm is proposed to equalize the execution delay and the energy consumption of the mobile terminal. The literature [9] defined the computational migration decision problem as a nonconvex quadratic constrained programming and proposed a semicustom random heuristic algorithm to significantly reduce the overall cost of the system. In order to balance the energy consumption and delay during the migration process, the literature [10] adopted cost function to measure the migration request aggregation and proposed an online algorithm considering both energy consumption and QoS. A deep learning model based on network packet information to evaluate the quality of experience (QoE) of users and servers was proposed in [11].

In the mode of multiuser single-available edge server, an offloading algorithm based on distributed deep learning is proposed [5], which can provide approximate optimal offloading decisions for multiple mobile device users and single edge servers in MEC. A classification-based energy-saving computation migration algorithm (EECO) is proposed in [3, 12], which can save about 15% energy consumption in comparison. A three-step algorithm is proposed to design the semideterministic relaxation (SDR), alternating optimization (AO), and sequential adjustment (SA) strategies [13] to achieve a joint optimization scheme of computing resources and communication resources. A novel approach to formulate cost-efficient fault tolerance strategies for multitenant service-based systems is proposed in [14].

In the mode of multiuser multiavailable edge servers, the linear relaxation method and the semidetermined relaxation (SDR) method are used to minimize the total task execution delay and energy consumption in the MEC with the multiedge servers [15]. The best computation distribution between multiple edge servers is given in [16]. In order to maximize the long-term utility, a model-free reinforcement learning offloading mechanism (Q-learning) is proposed in [17]. An adaptive computation offloading method with both macrobase stations (MABSs) in 5G and roadside units (RSUs) in Internet of Connected Vehicles (IoCV) to optimize the task execution delay and energy consumption of the edge system is proposed in [18]. A two-phase computation offloading optimization method to maximize the resource utilization of ECUs, minimize the execution time, and balance the privacy preservation and execution performance is proposed in [19]. A blockchain-enabled computation offloading method to achieve tradeoffs among minimizing
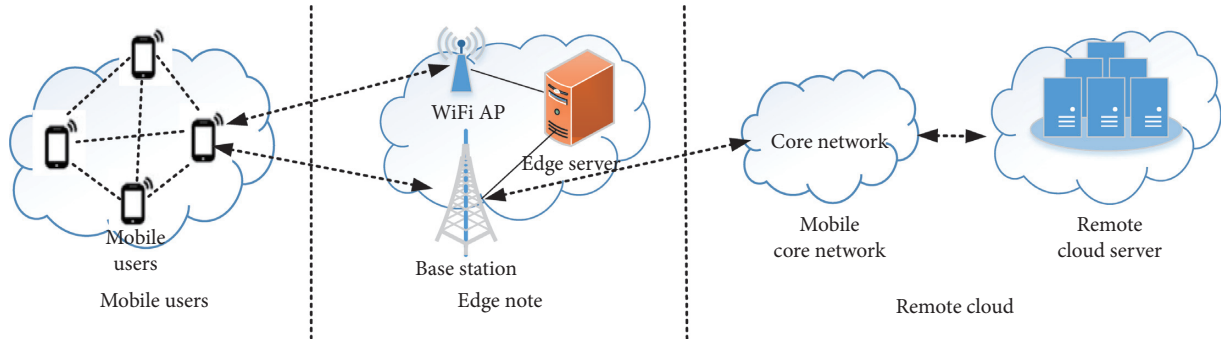
FIGURE 1: Mobile edge computing (MEC) architecture

ECDs' task offloading time, optimizing energy consumption, and maintaining load balance for IoT is devised in [20]. An optimal approach to solve the dynamic QoS edge user allocation (EUS) problem and a heuristic approach for quickly finding suboptimal solutions to large-scale instances of the dynamic QoS EUS problem are proposed in [21].

Additionally, multichannel radio interference has aroused much attention. The literature [3] utilizes game theory to realize efficient distributed channel allocation and computation offloading in multichannel wireless interference environments. A two-layer optimization method based on orthogonal frequency division multiplexing (OFDM) is proposed in [22, 23] to solve the problem of subcarrier allocation and task offloading of multiuser access multi-available edge servers. A theorem method to describe edge user allocation (EUA) problem as potential games and a novel decentralized algorithm that can solve EUA problem effectively are proposed in [24]. An optimal method to deal with EUA problem is proposed in [25]. The EUA problem is modelled as a bin packing problem, and the Lexicographic Goal Programming technique is adopted. An metric that can measure the community-diversified influence is proposed in [26]. Three novel QoS-aware service selection approaches for composing multitenant SBSs that achieve three different multitenancy maturity levels is presented in [27]. A novel strategy CFT4MTS (Criticality-Based Fault Tolerance for Multi-Tenant SBSs) that formulates cost-effective fault tolerance for multitenant SBSs by providing redundancy for the critical component services is proposed in [14]. A novel Web API recommendation method called keywords-based and compatibility-aware API recommendation based on weighted API correlation graph is proposed in [28]. A multidimensional quality ensemble-driven recommendation method based on the Locality-Sensitive Hashing technique and Order Preference by Similarity to Ideal Solution technique is proposed in [29]. The original stochastic problem is transformed to the determinist optimization problem by adopting stochastic optimization techniques, and an energy efficient dynamic offloading algorithm is proposed in [30]. A blockchain-based computation offloading method for edge computing in 5G networks is proposed in [31].

In summary, single-user scenarios are an idealized abstraction of computation offloading. While the multiuser, multiserver, and multichannel scenarios are so complicated that involve multiusers' offloading decisions, computing resource requirements, edge server selection, and multiple channel interferences. This paper focuses on the problem of computation offloading under multiuser, multiserver, and multichannel scenarios and proposes a computation offloading framework considering the QoS of users, server resources, and channel interference. This framework consists of three stages: (1) offloading decision stage; (2) server selection stage; (3) channel selection stage. In the corresponding stage, the corresponding solution model is proposed to optimize the user's decision.

3. System Model and Problem Statement

In the Mobile Edge Cloud Service model, we consider setting up N mobile users and K edges server nodes, where each user has a computation-intensive task [32] and each edge server node is composed of a base station and an edge server. Mobile users can offload computing tasks to edge servers through the base station. We also consider setting M wireless channels between mobile users and each edge server node. Table 1 lists the parameters used in this paper. Computing tasks that are offloaded to the same edge server node will be transmitted over different channels. The mobile users evaluate the computing task characteristics, energy reserve, computing capability, and network communication quality to make computation offloading decisions, which are divided into local computing and edge server-side computing. In the edge server-side computing mode, mobile users search for a suitable edge server, for which computing tasks offloading decisions is beneficial [33]. We call this beneficial computation offloading, which can reduce the energy consumption, shorten the delay, and guarantee the QoS of users. Then, we search a channel with high bandwidth and low interference to the selected edge server. The computation task is offloaded to the edge server, and the result is returned to the edge user through the channel. Among them, communication and computation are the two most important components of the Mobile Edge Cloud Service model. And, the model is described as follows.

In order to effectively represent different scenarios in the edge server-based MEC scheme, this paper proposes a Mobile Edge Cloud Service model, including the communication model and computation model.

TABLE 1: Parameter description.

Parameter	Description
M	Number of channels
k	Number of the edge servers
k'	Number of wireless base-stations
B_n	Size of computation task
D_n	Number of CPU cycles required to the computation task
f_n^l	Computing speed of user CPU
f_n^v	Computing speed of single VM CPU
f_n^c	Computing speed of edge server CPU
γ_n^l	Consumed energy per CPU cycle
λ_n^t	Weight of computational time
λ_n^e	Weight of energy consumption
β	Distance between users and the base station
α	Channel loss factor
g_n	Channel gain
q_n	Transmission power
σ	Background noise power
K	Channel bandwidth

3.1. Mobile Edge Cloud Service Communication Model.
Each edge-end user can process tasks locally or offload computing tasks to the edge server over a wireless channel. Assume that the number of edge-end users that may perform computational offloading is N and there are M wireless channels between the edge-end user and the edge server node. User n's computational offload strategy a_n is defined as

$$a_n = \begin{cases} 0, & \text{User } n \text{ processes tasks locally,} \\ 1, & \text{User } n \text{ unloads the task to the edge server.} \end{cases} \tag{1}$$

Then, $a_N = (a_1, a_2, \ldots, a_n)$ is the set of computation offloading decisions for all users. According to the Shannon spectrum formula, the edge user offloads the computing task to the edge server, and the uplink transmission rate is given as

$$C_n(a_N) = K log_2 \left(1 + \frac{S_n}{N_i}\right), \tag{2}$$

where $S_n = q_n g_n$, q_n and g_n are the transmission energy and channel gain of the user n communicating with the base station, K is the channel bandwidth of the wireless transmission process, and $N_i = \sigma + \sum_{i \in \{N\}: a_i = a_n} q_i g_i$, in which σ is the background white noise interference and $\sum_{i \in \{N\}: a_i = a_n} q_i g_i$ is the communication interference of other channels. The channel capacity calculated by Shannon theorem is the maximum available data transmission rate. Usually, the actual data transmission rate is less than the channel capacity. Using Shannon theorem to evaluate the achievable data transmission rate, the minimum delay of data transmission can be obtained. This minimum delay value can be used as a threshold for offloading decisions.

3.2. Mobile Edge Cloud Service Computation Model.
The computation model includes local computing and edge server-side computing. The compute-intensive tasks for edge

users are defined as $I_n \triangleq (B_n, D_n)$, where B_n is the data amount that the user needs to complete the task [34] and D_n is the number of CPU clock cycles required to complete the task [35].

3.2.1. Local Computing.
When the edge user's decision is local computing, the edge user n executes the computation task I_n locally. Assume f_n^l is the computing capability of the edge user (the clock frequency unit of the edge user CPU runs is HZ). γ_n^l is the energy consumption of each CPU cycle, which can be obtained by the measurement method in [36]. So, we can get the execution time and energy consumption of the local computing task I_n as

$$t_n^l = \frac{D_n}{f_n^l}, \tag{3}$$

$$e_n^l = \gamma_n^l D_n.$$

For the total cost of the local computing task, we have that

$$K_n^l = \lambda_n^t t_n^l + \lambda_n^e e_n^l. \tag{4}$$

Among them, $\lambda_n^t, \lambda_n^e \in (0, 1)$ indicates the weights of the computation time and energy consumption given by the edge user n in the decision-making, respectively. The user can flexibly set the two weights according to the requirements of the energy consumption and sensitivity of the delay in the scenario, thereby dynamically adjusting the overall cost of the system.

3.2.2. Edge Server Side Computing.
When the edge-side user's decision is the edge server-side computing, the edge-side user n offloads the computation-intensive task to the edge server through the wireless channel, and the time and energy consumption overhead of the offload transmission process is defined as

$$t_{n,\text{up}}^c(a_N) = \frac{B_n}{c_n(a_N)}, \tag{5}$$

$$e_{n,\text{up}}^c(a_N) = \frac{q_n B_n}{c_n(a_N)} + T_n. \tag{6}$$

Among them, T_n is the tailing energy generated in wireless transmission. On the edge server-side, the computing capability of the edge server is the clock frequency f_n^c, then the time of computing tasks I_n performs on the edge server node can be given as

$$t_{n,\text{exe}}^c = \frac{D_n}{f_n^c}. \tag{7}$$

According to (5), (6), and (7), we can compute the total cost of edge server-side computations as

$$K_n^c(a_N) = \lambda_n^t \left(t_{n,\text{up}}^c(a_N) + t_{n,\text{exe}}^c\right) + \lambda_n^e e_{n,\text{up}}^c(a_N). \tag{8}$$

Among them, $\lambda_n^t, \lambda_n^e \in (0, 1)$, the time and energy cost of sending computation results back to the edge node from the

edge server node [22] is ignored. Because for many intensive computing applications that need to be offloaded (e.g., face recognition and virtual reality), the size of the data set that is fed back to the user is often several orders of magnitude smaller than the size of the input data set.

3.3. Problem Statement and Solution.

Therefore, the computation offloading of the Mobile Edge Cloud Service model involves three problems:

(1) How to decide whether the computing task is completed locally or offloaded to the edge server?

(2) How to determine the appropriate edge server for computation offloading?

(3) How to choose the right channel to achieve the highest wireless transmission efficiency?

In order to solve the above problems, the computation offloading optimization framework proposed in this paper consists of three levels.

3.3.1. Offloading Decision Stage.

In this level, we propose a beneficial computation offloading decision strategy. And, according to the strategy, the overall cost of edge user local computing and edge server-side computing is compared. Then, the computing mode is determined based on the beneficial degree of computation offloading.

3.3.2. Edge Server Selection Stage.

After the edge user makes the decision to computation offloading, we propose a server selection strategy, which considers the transmission time, transmission energy consumption, and remaining CPU resources of the edge server. Then, we use the Cov-AHP multiobjective decision method to evaluate and select the offload table edge server according to the final weight.

3.3.3. Channel Selection Stage.

To solve the problem of signal interference caused by multiple users simultaneously selecting the same edge server for computation offloading, we propose a multiuser multichannel distributed computation offloading strategy based on the potential game. In detail, the Nash equilibrium point is defined as the optimal solution for the combined optimization problem of channel selection and beneficial computation offloading.

4. Offloading Decision Stage

At this level, we present the beneficial computation offloading decision strategy. The weighted sum of the energy consumption of the edge user to offload and process the computing task and the corresponding transmission and processing delay is defined as the total cost of the system for the edge node to complete the task. We propose a beneficial computation offloading decision strategy, which minimizes the overall cost of the system by optimizing the task offloading decision a_n.

Definition 1. Beneficial computation offloading: if and only if the overall cost of edge server-side computing is less than the total cost of local computing, we call such computing offloading beneficial to the user, i.e.,

$$K_n^e(a_N) < K_n^l. \tag{9}$$

Here, we construct an indicator function $I_{\{A\}}$. When event A is true, then $I_{\{A\}} = 1$; otherwise, $I_{\{A\}} = 0$. The edge-user offloading decision $a_n = 1$ if and only if the computing task satisfies a beneficial offload.

In summary, the beneficial computation offloading problem boils down to maximizing the number of users performing beneficial edge computation and minimizing the overall cost of performing all computational tasks, so the objective function and constraints are defined as

$$\begin{cases} \max \sum_{n \in N} I_{\{a_n=1\}}, \\ K_n^c(a_N) < K_n^l, \\ \min_{\{a_n\}} \sum_{n=1}^{N} \left(K_n^l(1 - a_n) + K_n^c(a_N)a_n\right), \\ a_n \in \{0, 1\}, \quad n \in N. \end{cases} \tag{10}$$

5. Edge Server Selection Stage

At this level, we present the Cov-AHP- (Analytic Hierarchy Process Based on Covariance-) based server selection strategy. When the task satisfies the beneficial computation offloading, we consider the transmission energy consumption, the transmission delay, and the remaining resources of the edge server to select the server that meets the computation offloading condition. The novelty of the Cov-AHP-based method is that the feasibility of its evaluation scheme no longer depends on the experience of experts but on the relationship between the scheme itself and the target layer to judge. This approach can greatly reduce the subjectivity, and at the same time objectively evaluate the connection between various schemes and goals.

Firstly, we need to address the evaluation of server selection. In order to overcome the influence of human subjective judgment, this paper builds a judgment matrix based on covariance and the Cov-AHP-based server selection strategy [37] whose calculation results and sorting are unique. The strategy includes four steps.

5.1. Establishing a Hierarchical Structure.

The Cov-AHP-based server selection strategy is established according to the progressive order of the target layer, the criteria layer, and the scheme layer. The Cov-AHP-based server selection strategy is shown in Figure 2.

The target layer is the ultimate goal that the strategy will ultimately achieve. In this paper, our ultimate goal is to choose the most suitable server for computing offload. The criteria layer is the element that depends on the evaluation of the server. We select three elements: transmission delay, transmission energy consumption, and remaining CPU
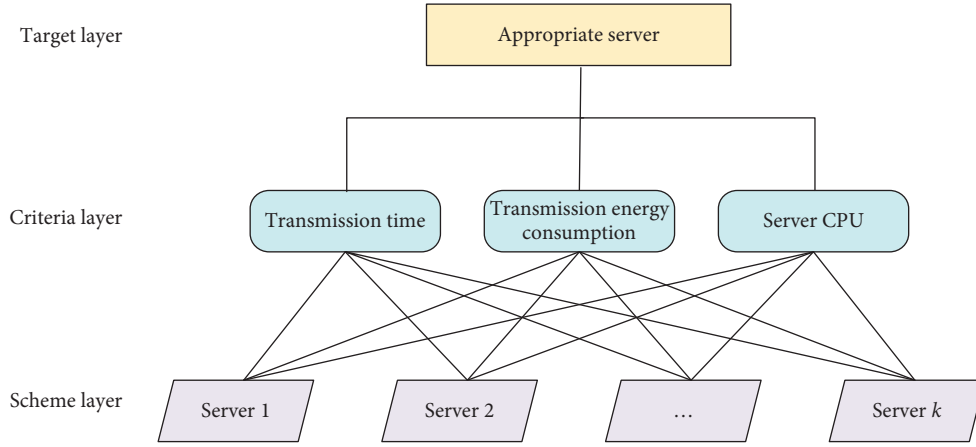
FIGURE 2: Cov-AHP-based server selection strategy.

resources of the server. The scheme layer is the servers that can be used for computing offload.

5.2. Constructing Judgment Matrix.

For a system that has k alternatives, there is a certain objective relationship between its constituent elements, which can be expressed by covariance. The basic idea of Cov-AHP is to construct a judgment matrix reflecting the relative importance of each element. Then, based on the covariance matrix, we can obtain the weight of the relative importance of quantitative indicators between the relative layers during the analytic hierarchy process.

Suppose that the value of scheme 1 corresponding to element a is x_1 and the value of scheme 2 corresponding to element a is x_2, then the covariance of x_1 and x_2 is c_{12} and we have $c_{ij} = c_{ji}$. The covariance matrix A of element a is expressed as

$$A = \begin{pmatrix} c_{11} & \cdots & c_{1k} \\ \vdots & \ddots & \vdots \\ c_{k1} & \cdots & c_{kk} \end{pmatrix}. \tag{11}$$

Using the covariance c_{ij} of each column divide covariance c_{ii} and then taking the transformation of the product of all paired elements into one, i.e., $b_{ij} = a_{ij}/\sqrt{a_{ij} \times a_{ji}}$, finally, the judgment matrix B is constructed as

$$B = \begin{pmatrix} 1 & \cdots & b_{1k} \\ \vdots & \ddots & \vdots \\ b_{k1} & \cdots & 1 \end{pmatrix}. \tag{12}$$

Then, use the judgment matrix to calculate the weight of each element. The principle of the analytic hierarchy process shows that the eigenvector corresponding to the largest eigenvalue of the judgment matrix B is the weight vector of each element. The square root method is used to solve the feature vector as follows:

(i) Calculate the product of each row element of the judgment matrix B: $M_i = \prod_{j=1}^{k} b_{ij}$

(ii) Calculate the k-th root of each line M_i: $\omega_i = \sqrt[k]{M_i}$

(iii) Normalize and then get the weight of each element: $\omega_\alpha = \omega_i / \sum_{i=1}^{k} \omega_i$

Then, the weight vector of the B matrix can be obtained as $\omega_a = (\omega_1, \omega_2, \ldots, \omega_k)'$.

5.3. Consistency Test.

Multiply the judgment matrix B by the weight vector $\omega_a = (\omega_1, \omega_2, \ldots, \omega_k)'$ of B matrix to obtain a k-order column vector BW, and then, according to the formula, $\lambda_{\max} = (1/k) \sum_{i=1}^{k} ((BW)_i / \omega_i)$, we can get the largest eigenvalue $\lambda_{\max}$ of the judgment matrix B. Among them, $(BW)_i$ represents the i-th component of the column vector BW.

The indicator CI that measures the deviation of the judgment matrix B is calculated as

$$CI = \frac{\lambda_{\max} - k}{k - 1}. \tag{13}$$

The random consistency ratio CR is calculated as

$$CR = \frac{CI}{RI}. \tag{14}$$

Among them, CR is a random consistency standard (Table 2).

When CR < 0.10, it is generally considered that the judgment matrix B has satisfactory consistency; otherwise, the judgment value needs to be adjusted until the consistency check is passed.

5.4. Weight Integration and Server Selection.

Suppose the weights of the elements of the criteria layer for the target layer are usually set according to the user needs of the edge user, the weight of each scheme relative to each element of the criteria layer is $\omega_a = (\omega_{1a}, \omega_{2a}, \ldots, \omega_{ka})'$, $\omega_b = (\omega_{1b}, \omega_{2b}, \ldots, \omega_{kb})'$, and $\omega_c = (\omega_{1c}, \omega_{2c}, \ldots, \omega_{kc})'$. The weight of each scheme relative to the target layer is

Table 2: Random consistency standard.

k	1	2	3	4	5	6	7	8	9	10
RI	0.00	0.00	0.58	0.90	1.12	1.24	1.32	1.41	1.45	1.49

$$\begin{bmatrix} W_1 \\ W_2 \\ \vdots \\ W_k \end{bmatrix} = \begin{bmatrix} \omega_{1a} & \omega_{1b} & \omega_{1c} \\ \omega_{2a} & \omega_{2b} & \omega_{2c} \\ \vdots & \vdots & \vdots \\ \omega_{kn} & \omega_{kb} & \omega_{kc} \end{bmatrix} [m_a, m_b, m_c]. \tag{15}$$

As can be seen from the above formula, $\max(W_1, W_2, \ldots, W_k)$ will be the most preferred offload server solution.

6. Channel Selection Stage

At this level, we present the channel selection stage strategy. After completing the edge server selection, it is necessary to solve how to select the appropriate wireless channel for computation offloading, assuming that there is a set of available wireless channels $M = \{1, 2, \ldots, m\}$ between the edge user and the edge server node. Then, the user decision is $a_{n,m}$. Multiple users simultaneously selecting the same wireless channel for beneficial computation offloading can cause severe signal interference.

Defining the total cost of user n as Z_n, the objective function of the multiuser multichannel computing offload decision problem is defined as

$$\min_{a_{n,m} \in \{0,1\}} \sum_{n \in N} Z_n. \tag{16}$$

Using the potential game [38] analyses the multiuser multichannel distributed computation offloading decision problem, the potential function is constructed to prove that the multiuser multichannel distributed computation offloading decision problem satisfies the potential game condition, and there is a Nash equilibrium point. Among them, the Nash equilibrium point [38] is defined as the optimal solution to the NP-hard [39] problem of the multiuser multichannel distributed computing offload.

6.1. Game Analysis of Multiuser Multichannel Distributed Computation Offloading.
In the distributed computing offload decision, the set of computation offloading decisions for all users except the edge-side user n is $a_{N-n} = (a_{1,m}, \ldots, a_{n-1,m}, a_{n+1,m}, \ldots, a_{N,m}), \forall m \in M$. Whether the user n chooses local computing or edge server-side computing to reduce their overall overhead, i.e., is given as

$$\min_{a_{n,m} \in \{0,1\}} Z_n(a_{n,m}, a_{N-n}), \quad \forall n \in N, m \in M. \tag{17}$$

According to equations (4) and (8), the mathematical expression of the overall cost of user n can be derived as

$$Z_n(a_{n,m}, a_{N-n}) = \begin{cases} K_n^l, & a_{n,m} = 0, \\ K_n^c(a_N), & a_{n,m} = 1. \end{cases} \tag{18}$$

Then, we express the above problem as a strategic game $\Gamma_{\mathrm{MCC}} = (N, \{a_{n,m}\}_{mN,m,M,M}, \{Z_n\}_{neN})$; the edge user strategy set conforming to Nash Equilibrium is $a_N = (a_{1,m}, a_{2,m}, \ldots, a_{n,m})$. Then, according to the definition of Nash Equilibrium, if the multiuser system is in equilibrium, no user can change the strategy unilaterally to further reduce the overhead. i.e.,

$$Z_n(a_{n,m}, a_{N-n}) \leq Z_n(a_{n,m}^*, a_{N-n}), a_{n,m} \in \{0, 1\}, \\ n \in N, m \in M. \tag{19}$$

In this formula, $a_{n,m}^*$ denotes the decision after the edge user changes.

6.2. Proof of the Existence of Multiuser Multichannel Distributed Computation Offloading Nash Equilibrium Points.
The potential game is a subset of the strategy game. Each subject will continually approach the optimal objective function after a finite iteration to find the optimal solution of the objective function, and each potential game obeys a potential function. Here, we need to construct a potential function to prove that the target problem is a potential game problem, and then there is a Nash equilibrium point. From (4), (8), and (10), we can get $K_n^c(a_N) \leq K_n^l$ equivalent to

$$\Rightarrow \lambda_n^t (t_{n,\mathrm{up}}^c(a_N) + t_{n,\mathrm{exe}}^c) + \lambda_n^e e_{n,\mathrm{up}}^c(a_N) \leq \lambda_n^t t_n^l + \lambda_n^e e_n^l$$

$$\Rightarrow \lambda_n^t \left(\frac{B_n}{C_n(a_N)} + t_{n,\mathrm{exe}}^c \right) + \lambda_n^e \left(\frac{q_n B_n}{C_n(a_N)} + T_n \right) \leq \lambda_n^t t_n^l + \lambda_n^e e_n^l$$

$$\Rightarrow \frac{B_n(\lambda_n^t + \lambda_n^e q_n)}{C_n(a_N)} + \lambda_n^t t_{n,\mathrm{exe}}^c + \lambda_n^e T_n \leq \lambda_n^t t_n^l + \lambda_n^e e_n^l$$

$$\Rightarrow C_n(a_N) \geq \frac{B_n(\lambda_n^t + \lambda_n^e q_n)}{\lambda_n^t t_n^l + \lambda_n^e e_n^l - \lambda_n^t t_{n,\mathrm{exe}}^c - \lambda_n^e T_n}. \tag{20}$$

According to (2), we then have that the interference μ_n in the wireless channel has an extremum TH_n when the edge-side user n implements the beneficial computation offloading:

$$\mu_n = \sum_{i \in \{N\}: a_i = a_n} q_i g_i \leq \frac{q_n g_n}{\left(B_n(\lambda_n^t + \lambda_n^e q_n)/2^{K\left(\lambda_n^t t_n^l + \lambda_n^* e_n^- \lambda_n^t r_{n,\mathrm{sec}} - \lambda_n^e T_n\right)} \right) - 1} - \sigma, \tag{21}$$

$$\mathrm{TH}_n = \frac{q_n g_n}{\left(B_n(\lambda_n^t + \lambda_n^e q_n)/2^{K\left(\lambda_n^t t_n^l + \lambda_n^e e_n^l - \lambda_n^t t_{n,\mathrm{exe}}^c - \lambda_n^e T_n\right)} \right) - 1} - \sigma. \tag{22}$$

It can be seen that when the wireless channel interference is sufficiently low, it is beneficial for the user to adopt the edge server-side computation mode. Otherwise, the user should perform the computation task locally. Based on the above results, we can know that channel interference has an extreme value, which satisfies the potential game condition. And, the following potential function is constructed to prove that the multiuser

multichannel computation offloading satisfies the potential game:

$$\phi(a_N) = \frac{1}{2}\sum_{i=1}^{N}\sum_{j\neq i}q_i g_i q_j g_j I_{\{a_i=a_j\}}I_{\{a_i=1\}} + \sum_{i=1}^{N}q_i g_i TH_i I_{\{q=0\}}.$$

(23)

The potential game has a finite increment property (FIP) [38]; its incremental path length is limited, and the game subject can reach the Nash equilibrium after a finite number of iterations. Any edge user updates its current decision $a_{k,m}, m \in M$ for $a^*_{k,\widetilde{m}}, \widetilde{m} \in M, k \in N$; when in Nash equilibrium, it will lead to an increase in overall overhead, i.e.,

$$Z_k(a_{k,m}, a_{N-k}) < Z_k(a^*_{k,\widetilde{m}}, a_{N-k}), a_k \in \{0,1\}, \quad k \in N, m, \widetilde{m} \in M.$$

(24)

The objective function is proved to be a potential function in three cases.

Case 1 ($a_{k,m} = 1, a^*_{k,\widetilde{m}} = 1$). The user overhead $Z_k(a_{k,m}, a_{N-k})$ is inversely proportional to data uplink rate $C_k(a_N)$, according to (2), that is, proportional to channel interference. This implies that

$$\sum_{j\in N\setminus\{k\}: a_j=a_k}q_j g_j < \sum_{j\in N\setminus\{k\}: a_j=a^*_k}q_j g_j.$$

(25)

Since $a_{k,m} = 1, a^*_{k,\widetilde{m}} = 1$, according to (22), (23), and (24), it is obvious that

$$\phi(a_{k,m}) < \phi(a^*_{k,\widetilde{m}})$$

$$= \frac{1}{2}\sum_{k=1}^{N}\sum_{j\neq k}q_k g_k q_j g_j I_{\{a_j=a_k\}} - \frac{1}{2}\sum_{k=1}^{N}\sum_{j\neq k}q_k g_k q_j g_j I_{\{a_j=a^*_k\}}$$

$$= \frac{1}{2}q_k g_k \sum_{j\neq k}q_j g_j I_{\{a_j=a_k\}} + \frac{1}{2}q_j g_j \sum_{j\neq k}q_k g_k I_{\{a_k=a_j\}}$$

$$- \frac{1}{2}q_k g_k \sum_{j\neq k}q_j g_j I_{\{a_j=a^*_k\}} - \frac{1}{2}q_j g_j \sum_{j\neq k}q_k g_k I_{\{a^*_k=a_j\}}$$

$$= q_k g_k \sum_{j\neq k}q_j g_j I_{\{a_j=a_k\}} - q_k g_k \sum_{j\neq k}q_j g_j I_{\{a_j=a^*_k\}} < 0.$$

(26)

Case 2 ($a_{k,m} = 0, a^*_{k,\widetilde{m}} = 1$). Since $a_{k,m} = 0, a^*_{k,\widetilde{m}} = 1$, and $Z_k(a_{k,m}, a_{N-k}) < Z_k(a^*_{k,\widetilde{m}}, a_{N-k})$, when the user changes his local computing decision to the mobile edge computing decision process, the overall overhead increases, that is, the channel interference is greater than the maximum extreme value of the beneficial mobile edge computing interference:

$$\sum_{j\in N\setminus\{k\}: a_j=a_k}q_j g_j > TH_k,$$

(27)

$$\phi(a_{k,m}) < \phi(a^*_{k,\widetilde{m}})$$

$$= \sum_{j=1}^{N}q_j g_j TH_k - \frac{1}{2}\sum_{k=1}^{N}\sum_{j\neq k}q_k g_k q_j g_j I_{\{a_j=a^*_k\}}$$

$$= q_k g_k TH_k - \frac{1}{2}q_k g_k \sum_{j\neq k}q_j g_j I_{\{a_j=a^*_k\}}$$

$$- \frac{1}{2}q_j g_j \sum_{k\neq j}q_k g_k I_{\{a^*_k=a_j\}}$$

$$= q_k g_k TH_k - q_k g_k \sum_{j\neq k}q_j g_j I_{\{a_j=a^*_k\}} < 0.$$

(28)

Case 3 ($a_{k,m} = 1, a^*_{k,\widetilde{m}} = 0$). By a similar argument in the second case, since $a_{k,m} = 1, a^*_{k,\widetilde{m}} = 0$, and $Z_k(a_{k,m}, a_{N-k}) < Z_k(a^*_{k,\widetilde{m}}, a_{N-k})$, $\phi(a_{k,m}) < \phi(a^*_{k,\widetilde{m}})$.

For the above three cases, both the definitions of the potential game are satisfied. Then, we can get $\phi(a_{k,m}) < \phi(a^*_{k,\widetilde{m}})$ from $Z_k(a_{k,m}, a_{N-k}) < Z_k(a^*_{k,\widetilde{m}}, a_{N-k})$.

Combined with the above proof, it can be known that the target problem (multiuser multichannel computation offloading problem in the Mobile Edge Cloud Service strategy) is a potential game problem, and there is a Nash equilibrium point. The Nash equilibrium point can be used as the optimal value for multiuser multichannel mobile edge computing task offloading.

6.3. Multiuser Multichannel Task Scheduling Algorithm

6.3.1. Algorithm Design. We design the multiuser multichannel task scheduling algorithm according to the finite increment property of the potential game and ensure that any asynchronous response update process reaches Nash equilibrium within a finite number of iterations. Algorithm 1 of the whole auction flow is described as follows:

Step 1: initialization
Step 2: all computing tasks are done locally, i.e. $a_n(0) = 0$
Step 3: **end initialization**
Step 4: **repeat** for each user n and server node in each decision slot t
Step 5: **transmit** the pilot signal on the chosen channel m to the mobile cloud server base-stations
Step 6: **receive** the information of the received powers on all channels from each mobile edge user n
Step 7: **compute** the best response set $\Delta_n(t)$ in the base-stations
Step 8: **if** $\Delta_n(t) \neq \phi$ **then**
Step 9: **send** RTU message to the cloud for contending for the decision update opportunity
Step 10: **if receive** the UP message from the cloud then
Step 11: **choose** the decision $a_{n,\widetilde{m}}(t+1) \in \Delta_n(t)$ for next slot
Step 12: **else** choose the original decision $a_{n,m}(t+1) \in a_{n,m}(t)$ for next slot
Step 13: **end if**
Step 14: **else choose** the original decision $a_{n,m}(t+1) \in a_{n,m}(t)$ for next slot
Step 15: **end if**
Step 16: **until** END message is received from the mobile cloud server base-stations

ALGORITHM 1: Multiuser multichannel task scheduling algorithm.

Specifically, the user synchronizes with the clock signal from the wireless base station, and the time slot used to update the computation offloading decision is called a decision period, and each decision period includes two phases:

Radio interference measurement phase: at this stage, we measure interference on different channels to select the appropriate channel for access. In the current decision slot, each edge node user who selects mobile edge computation offloading mode (i.e. $a_{n,m}(t) = 1$) will transmit the pilot signal on its selected channel m and then measure the total received power $\rho_m(a_N(t)) \triangleq \sum_{i \in N: a_i(t)=1} q_i g_i$ of each channel $m \in M$ on the radio base station. And, the power information received on all channels will be fed back to the edge node user. Therefore, each user n can grasp the interference on its channel $m \in M$ from other users as

$$\mu_n e(m, a_{-n}(t)) = \begin{cases} \rho_m(a_N(t)) - q_n g_n, & a_{n,m}(t) = 1, \\ \rho_m(a_N(t)), & a_{n,k}(t) = 1, k \neq m. \end{cases} \tag{29}$$

The interference received on the channel m currently selected by the edge user is equal to the measured total power minus the signal power. For other channels that do not transmit the pilot signal, the interference received is equal to the measured total power.

Offloading decision update phase: at this stage, we motivate the multiuser computing offload's finite incremental properties by having an edge node user perform a decision update. Based on interference information measured on different channels $\mu_n(m, a_{-n}(t)), m \in M$, each edge node user first calculates its best response update set as

$$\Delta_n(t) \triangleq \left\{ \begin{array}{l} \widetilde{m}: \widetilde{m} = arg \min_{m \in M} \mu_n(m, a_{-n}(t)) \\ \mu_n(\widetilde{m}, a_{-n}(t)) < \mu_n(m, a_{-n}(t)) \end{array} \right\}. \tag{30}$$

Then, in case $\Delta_n(t) \neq \phi$ (i.e., user n can improve its offload decision), user n will send a request-to-update (RTU) message to the edge server node to indicate that it wants to

contend for the decision update opportunity. Otherwise, user n will not compete for updates in the next decision slot and keep their current offloading decisions unchanged (i.e. $a_{n,m}(t+1) = a_{n,m}(t)$). The edge server node will select the user with the highest priority from the user who has sent the RTU and send an update-permission (UP) command to update the decision $a_{n,\widetilde{m}}(t+1) \in \Delta_n(t)$ in the next time slot. For users who do not receive the UP command, they will not update their decision in the next time slot (i.e. $a_{n,m}(t+1) = a_{n,m}(t)$).

6.3.2. Analysis of Convergence and Solvability. From the finite increment attribute (FIP) of the potential game, the algorithm will converge to the Nash equilibrium of the multiuser multichannel computation offloading game in a limited number of decision slots. In the simulation experiment, when the edge server does not receive any RTU message of the edge user in any decision time slot, that is, the game has reached the Nash equilibrium. Then, the edge server broadcasts the end message to all edge users, indicating that the updating process of the computation offloading decision is terminated. We analyze the convergence and solvability of the distributed computation offloading algorithm by calculating the extreme value of the number of required decision slots for the computation offloading algorithm.

In each decision slot, each edge user will execute steps 3–10 in Algorithm 1 in parallel. Since most operations involve only some basic arithmetic computations, the main part is to calculate the optimal response set in step 5, which involves the computation and sequence of m-channels measurement data, usually with the computational complexity of $O(mlogm)$. So, the computational complexity in each decision slot is $O(mlogm)$. Assuming that it requires C decision slots to terminate the algorithm, the total computational complexity of the distributed computation offloading algorithm is $O(Cmlogm)$. Let

$$\begin{cases} \text{TH}_{\max} \triangleq \max_{n \in N}\{\text{TH}_n\}, \\ Q_n \triangleq q_n g_{n,m}, \\ Q_{\max} \triangleq \max_{n \in N}\{Q_n\}, \\ Q_{\min} \triangleq \min_{n \in N}\{Q_n\}, \end{cases} \tag{31}$$

where TH_n, q_n, and $g_{n,m}$ are the channel interference extremum, transmission power, and channel gain, respectively. Because we need C decision slots to converge, we have the following inference.

When TH_n and Q_n are nonnegative integers for any $n \in N$, the distributed computation offloading algorithm will terminate within at most $(Q_{\max}/2Q_{\min})N^2 + (TH_{\max}Q_{\max}/Q_{\min})N$ decision slot, i.e.,

$$C \le \frac{Q_{\max}}{2Q_{\min}}N^2 + \frac{TH_{\max}Q_{\max}}{Q_{\min}}N. \tag{32}$$

Proof. According to (23),

$$0 \le \phi(a_N) \le \frac{1}{2}\sum_{i=1}^{N}\sum_{j \ne i} Q_{\max}^2 + \sum_{i=1}^{N} Q_{\max}TH_{\max}$$

$$\Rightarrow 0 \le \phi(a_N) \le \frac{1}{2}Q_{\max}^2 N^2 + Q_{\max}TH_{\max}N. \tag{33}$$

In a decision slot, assume that an edge user $k \in N$ updates its current decision $a_{k,m}, m \in M$ to $a^*_{k,\widetilde{m}}, \widetilde{m} \in M$. And, this decision leads to a reduction in the overall cost of the user, i.e., $Z_k(a_{k,m}, a_{N-k}) > Z_k(a^*_{k,\widetilde{m}}, a_{N-k})$. According to the definition of the potential function, it can be seen that the potential function will also be reduced by at least $Q_{\min}$, i.e.,

$$\phi_k(a_{k,m}) \ge \phi_k(a^*_{k,\widetilde{m}}) + Q_{\min}. \tag{34}$$

We will consider three situations: (a) $a_{k,m} = 1, a^*_{k,\widetilde{m}} = 1$; (b) $a_{k,m} = 0, a^*_{k,\widetilde{m}} = 1$; (c) $a_{k,m} = 1, a^*_{k,\widetilde{m}} = 0$.

While $a_{k,m} = 1, a^*_{k,\widetilde{m}} = 1$, we can see from equation (26) that

$$\phi(a_{k,m}) - \phi(a^*_{k,\widetilde{m}}) = Q_k\left(\sum_{j \ne k} Q_j I_{\{a_j = a_k\}} - \sum_{j \ne k} Q_j I_{\{a_j = a_k^*\}}\right) > 0. \tag{35}$$

Since Q_j are integers for any $j \in N$, then

$$\sum_{j \ne k} Q_j I_{\{a_j = a_k\}} \ge \sum_{j \ne k} Q_j I_{\{a_j = a_k^*\}} + 1. \tag{36}$$

According to the above formula,

$$\phi(a_{k,m}) \ge \phi(a^*_{k,\widetilde{m}}) + Q_k \ge \phi(a^*_{k,\widetilde{m}}) + Q_{\min}. \tag{37}$$

While $a_{k,m} = 0, a^*_{k,\widetilde{m}} = 1$, we can get by formula (28) that

$$\phi(a_{k,m}) - \phi(a^*_{k,\widetilde{m}}) = Q_k\left(TH_k - \sum_{j \ne k} Q_j I_{\{a_j = a_k^*\}}\right) > 0. \tag{38}$$

Since Q_k is the integer for any $j \in N$,

$$\text{TH}_k \ge \sum_{j \ne k} Q_j I^I_{[a_j = a_k^*]} + 1. \tag{39}$$

According to the above formula,

$$\phi(a_{k,m}) \ge \phi(a^*_{k,\widetilde{m}}) + Q_k \ge \phi(a^*_{k,\widetilde{m}}) + Q_{\min}. \tag{40}$$

While $a_{k,m} = 1$ and $a^*_{k,\widetilde{m}} = 0$, through a similar argument to the second case, we get

$$\phi(a_{k,m}) \ge \phi(a^*_{k,\widetilde{m}}) + Q_k \ge \phi(a^*_{k,\widetilde{m}}) + Q_{\min}. \tag{41}$$

Therefore, according to (33)–(41), we know that the algorithm will terminate by driving the potential function $\phi_k(a_N)$ to a minimum point within at most decision slots:

$$C \le \frac{\phi_{\max}(a_N)}{Q_{\min}} = \frac{Q_{\max}}{2Q_{\min}}N^2 + \frac{TH_{\max}Q_{\max}}{Q_{\min}}N. \tag{42}$$

For the general case, the numerical results of the previous section indicate that the distributed computation offloading algorithm can also converge quickly, and the number of convergence decision slots increases linearly (almost) as the number of users N increases. The inferences in this section further indicate that the distributed computation offloading algorithm can converge quickly under normal conditions and has a quadratic convergence time $C_{\max}$ (i.e., an upper bound). Note that in the simulation experiment, the transmission power and channel gain are nonnegative (i.e., $q_n, g_{n,m} \ge 0$), so we know that $Q_n = \{q_n g_{n,m}\} \ge 0$. The nonnegative condition $\text{TH}_n \ge 0$ ensures that each user has the opportunity to implement a beneficial computing offload (otherwise, the user can only choose the local computing all the time). Therefore, the algorithm makes sense only when Q_n and TH_n are nonnegative integers. $\text{TH}_{\max}$, $Q_{\max}$, and $Q_{\min}$ can be obtained from known conditions, and then the algorithm can be solved. $\square$

7. Simulation and Analysis

7.1. Experiment Settings. In this experiment, the face recognition algorithm [40] has been used as a computation task. MATLAB is used to simulate the computation offloading framework proposed in this paper. We will set up 5 edge server nodes in each experimental scenario, including 5 wireless base stations and 5 edge servers, running 30 virtual machines on each edge server, and the computing power of each virtual machine is set to 10GH [40]. The coverage of the base station is 100 meters [27], and edge users are randomly distributed in coverage [27]. Each task is executed by a single virtual machine. The various data parameters [3, 33, 41–44] in the simulation experiment are shown in Table 3.

7.2. Analysis of Simulation Results. In this section, we analyze the simulation results and discuss the performance of the framework proposed.

TABLE 3: Various data parameter tables in the simulation experiment.

Parameter	Values	Parameter	Values
M	5	λ_n^t	0.5
k	5	λ_n^e	0.5
$k\prime$	5	β	$0\sim100\,\text{m}$
B_n	5 MB	α	4
D_n	1000 M cycles	g_n	$\beta^{-\alpha}$
f_n^l	1 GHz	q_n	100 mW
f_n^v	10 GHz	σ	-100 dBm
f_n^c	$200\sim300\,\text{GHz}$	K	5 MHz
γ_n^l	1 mW		

7.2.1. Performance Analysis of Beneficial Computation Offloading Decision Strategy.

We consider the two indicators of beneficial computation offloading users and real-time system overhead. The two indicators of the beneficial computation offloading decision strategy used in this paper are evaluated. Experiments are set up for analysis: (1) the change of the number of beneficial computation offloading users with the change of the decision time slot among the 50 users who perform the computation offloading is measured; (2) the change of the real-time system overhead of the user with the change of the decision time slot among the 50 users who perform the computation offloading is measured; (3) the comparison of the number of beneficial computation offloading users with the change of the user number of different computation offloading decision strategies (random computation offloading decision, beneficial computation offloading decision, and full computation offloading decision). All test data in this paper are the average of 100 trials.

From Figure 3, we can see the dynamic process of the number of beneficial computation offloading users under the beneficial computation offloading decision strategy. It shows that the strategy can increase the number of beneficial computation offloading users in the system and converge to a balance. From Figure 4, we can see the dynamic process of the overall cost of the mobile device user system under the beneficial computing offload decision strategy. It shows that the strategy can also keep the total overhead of the mobile device user system in the process of computation offloading from decreasing and eventually converging to an equilibrium. Figure 5 shows that, under the condition that each edge service node has sufficient computing resources in the mobile edge network, the number of beneficial computation offloading users will increase with the number of users. The performance of the computation offloading decision strategy used in this paper compared with the other two strategies is improved by 30%.

7.2.2. Performance Analysis of Cov-AHP Based Server Selection Strategy.

We focus on the stability evaluation of the Cov-AHP-based server selection strategy used in this paper. Two experiments are set up: (1) compare the server weight of different server selection strategies in the same region [45] with the change of the task execution time; (2) compare the server weight of the server selection strategy used in this paper with the change of the task execution time in different
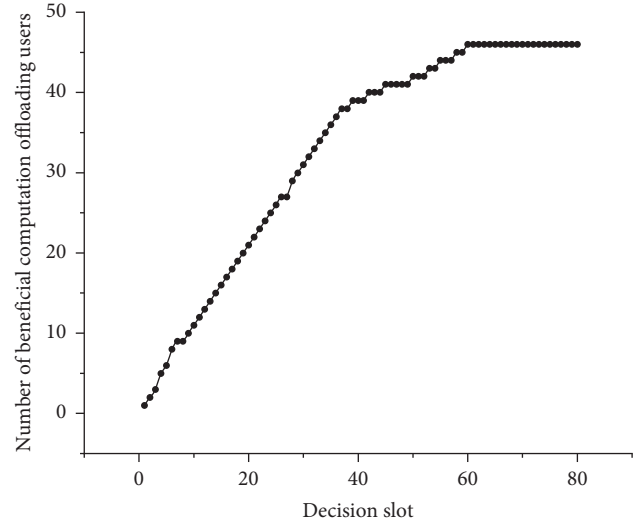

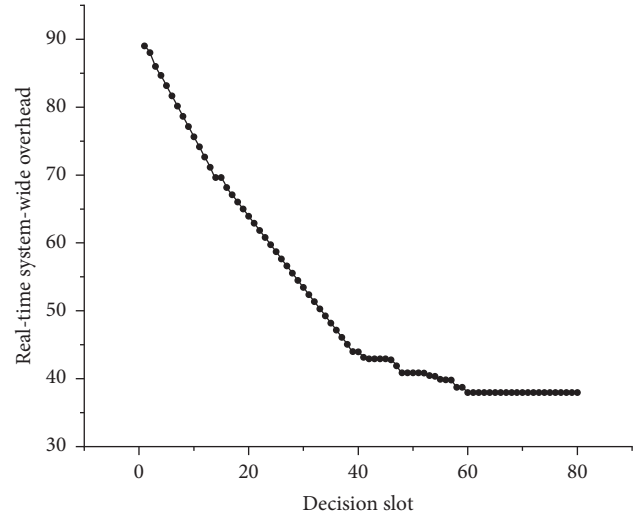FIGURE 3: Dynamic beneficial computation offloading users.

FIGURE 4: Real-time computing offload system overhead.

regions. In this experiment, we set the performance parameters of the server to be more realistic, and the performance of the server has advantages and disadvantages. The specific parameters are shown in Table 4.

The server weights based on different server selection strategies fluctuate with the task execution time in the same area (Figure 6). The server selection strategy based on Cov-AHP can reduce the weight fluctuation of each server in the same area effectively, and so that the user offloading decision is relatively stable. It also achieves load balancing between servers in the same area effectively.

The server weight based on the server selection strategy adopted in this paper varies with the task execution time in different regions (Figure 7). These regions depend on where the users are. The server selection strategy based on Cov-AHP can maintain the weight of each server in different regions effectively, so that the server weight fluctuation is small in the same region, which indicates that the server selection strategy based on Cov-AHP can efficiently achieve
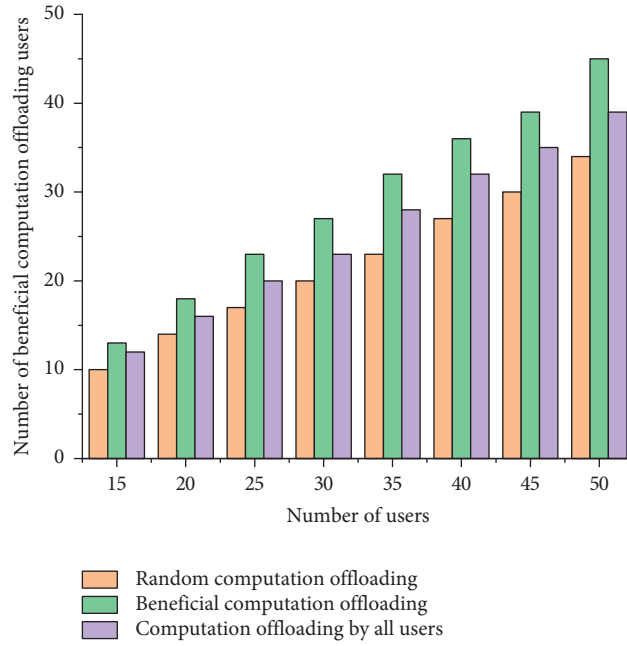
Figure 5: The number of beneficial computation offloading users for different computing offload decision strategies under different user numbers.

Table 4: Server performance parameters.

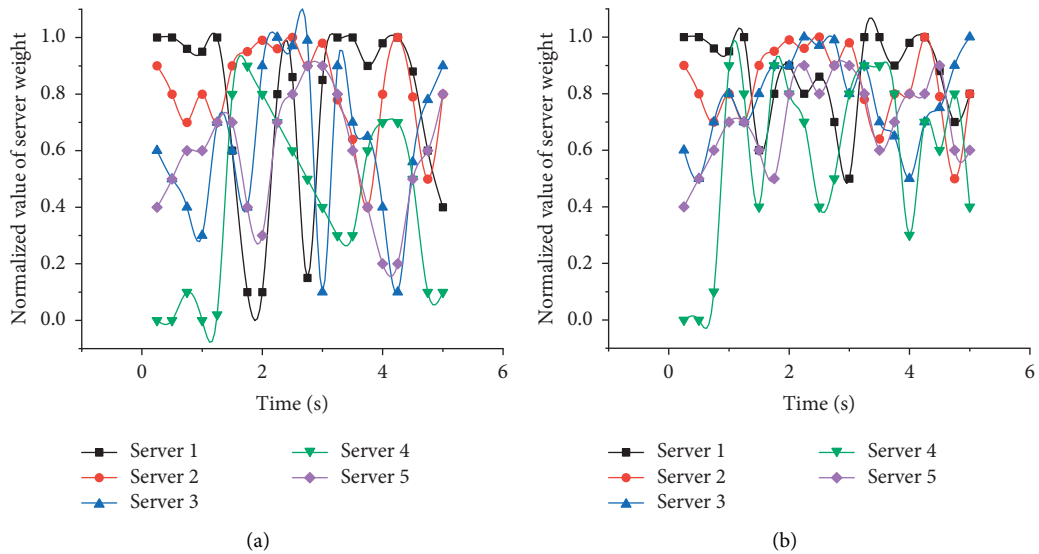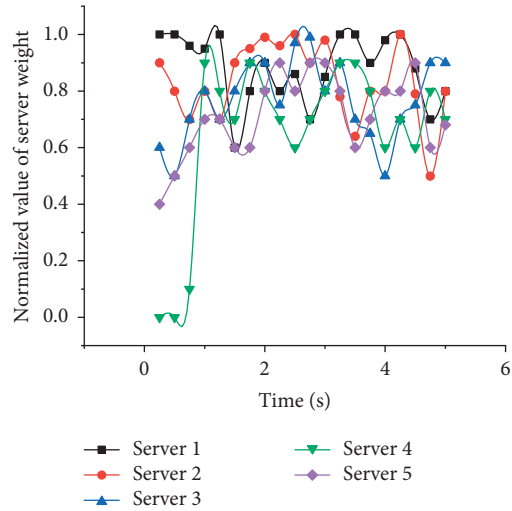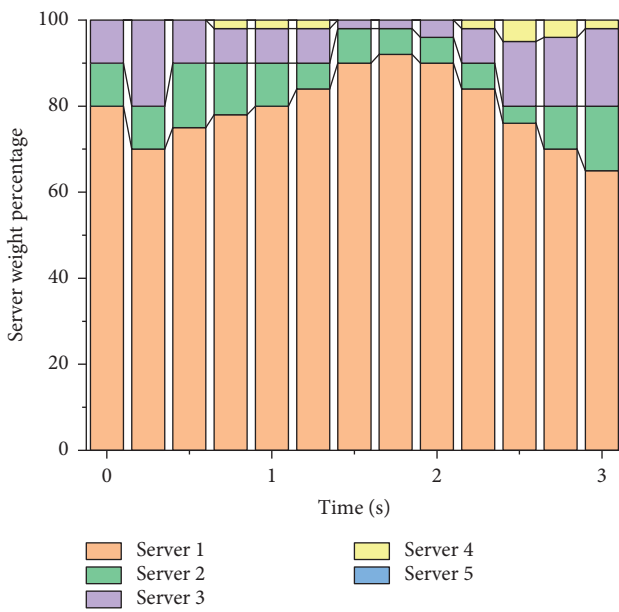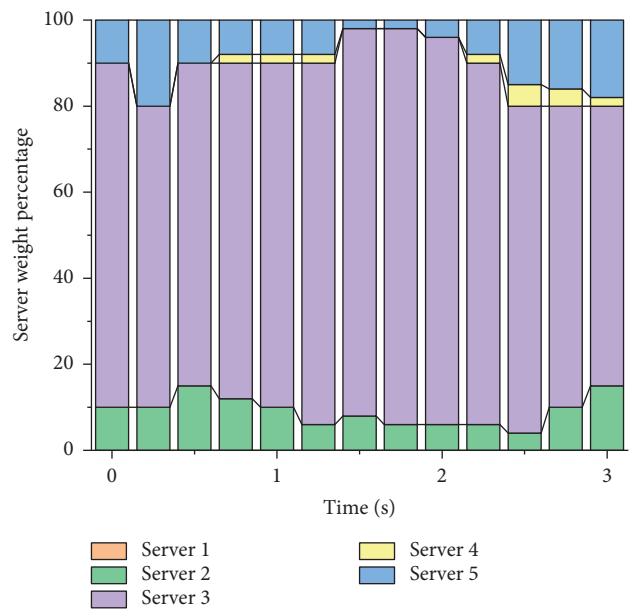|	Bandwidth (M)	Number of VM	VM CPU computing speed (GHz)	Server CPU computing speed (GHz)
Server 1	5	40	8	320
Server 2	6	30	10	300
Server 3	7	20	14	280
Server 4	4	30	10	300
Server 5	6	30	9	270

(a)

(b)

Figure 6: Continued.

(c)

FIGURE 6: Server weight fluctuation based on (a) a random server selection strategy, (b) the polling server selection strategy, and (c) the Cov-AHP server selection strategy.

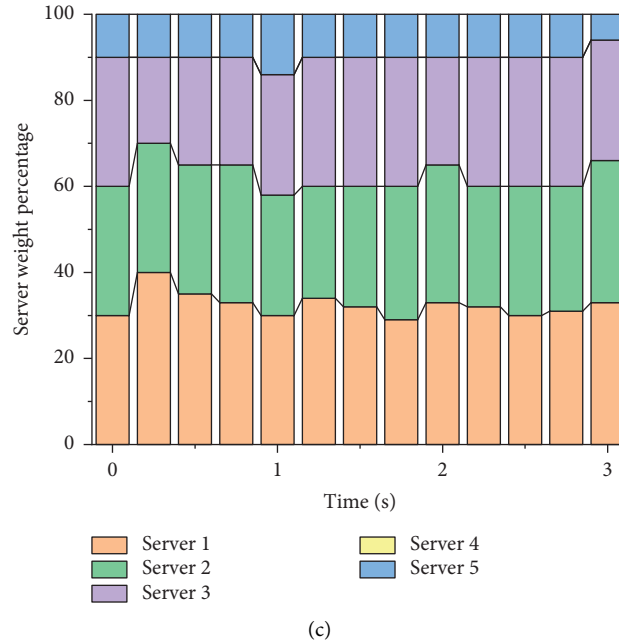(a)

(b)

FIGURE 7: Continued.

(c)

FIGURE 7: Server load fluctuations in different regions based on the Cov-AHP server selection strategy. (a) Region 1. (b) Region 2. (c) Region 3.
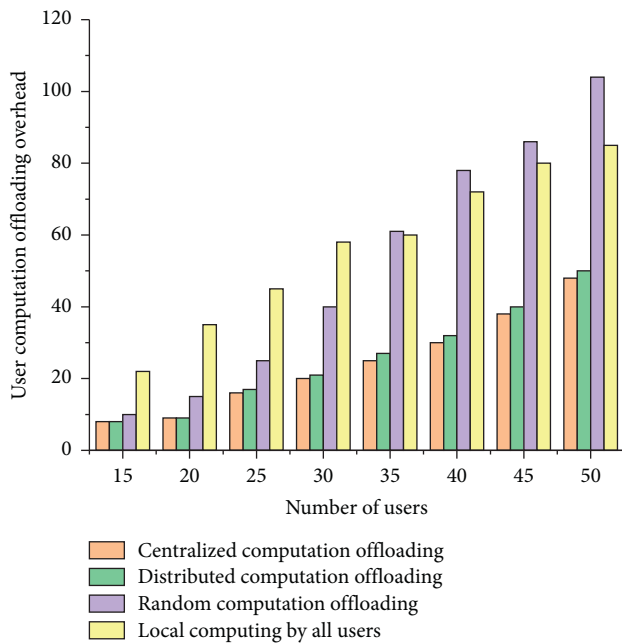

FIGURE 8: User overhead of different channel selection models.

FIGURE 9: Task completion time of different channel selection models.

load balancing between servers in different areas within the coverage of the base station.

7.2.3. Performance Analysis of Multiuser Multichannel Distributed Computation Offloading Strategy Based on Potential Game. In this section, we focus on two important indicators of the user's computation offloading overhead and task completion time in the process of making channel selection
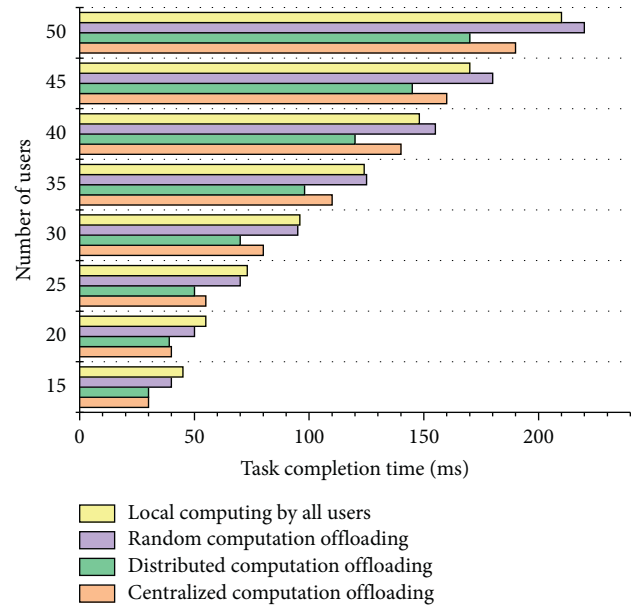
decisions and completing the computation offloading. We evaluate two indicators of the multiuser multichannel distribution computation offloading strategies based on potential games is used in this paper. And, two experiments are set up separately: (1) compare the total user overhead of different channel selection strategies [2] in the process of computation offloading; (2) compare the time of different channel selection strategies [2] to complete the computation task. Among them, the centralized computation offloading algorithm uses the global optimization method to calculate

the overall cost of centralized computation offloading and requires the edge server to continuously interact with the edge users. It has been proved to be able to effectively find the approximate optimal solution of the complex combinatorial optimization problem.

The variation of the total user overhead of different channel selection strategies to complete the computation offloading process with the increase of the number of users is shown in Figure 8. The multiuser multichannel distributed computation offloading strategy based on the potential game has a larger advantage relative to the random computation offloading and the full local computing, which saves twice as much on average. The centralized computation offloading strategy is almost consistent or even slightly superior to the user overhead of the strategy in this paper, but it pays a large price in terms of delay. The task completion time of different channel selection strategies increases with the increase in the number of users (Figure 9). The multiuser multichannel distributed computation offloading strategy based on potential game used in this paper will greatly reduce the completion time of tasks compared with other strategies. This is because the strategy in this paper makes the most suitable decision for each user based on their own combined channel conditions. The centralized offloading decision needs to collect all users' information for centralized analysis, which will greatly increase the additional delay and affect the QoS of the users.

8. Conclusions

This paper proposes a multilevel computation offloading optimization framework suitable for multiuser multichannel multiserver scenarios in MEC to meet the needs of computing-intensive applications on mobile devices. From the perspective of edge users, delay and energy consumption are used as the basis for computation offloading decision, and then the concept of beneficial computation offloading is proposed. Through the Cov-AHP strategy for multiobjective decision-making, we make a comprehensive evaluation of the optional edge server and select the appropriate server to perform computation offloading. It is proved that the multiuser multichannel distributed computation offloading accords with the potential game condition, and it indicates that there is always a Nash equilibrium point in the potential game. Then, a distributed computation offloading algorithm is designed, which can realize Nash equilibrium. The simulation results show that the proposed offloading framework has higher stability than the similar methods, which can effectively reduce the delay and the overall cost of energy consumption of the edge client and improve the execution speed of the computation offloading and the standby time of the mobile device.

In future work, we will consider how edge devices optimize computation offloading in ad hoc networks, which will make it possible for users to share computing resources in more urgent situations.

Data Availability

No data were used to support this study.

Conflicts of Interest

The authors declare that there are no conflicts of interest regarding the publication of this paper.

Acknowledgments

References

[1] Y. C. Hu, M. Patel, D. Sabella, N. Sprecher, and V. Young, "Mobile edge computing—a key technology towards 5G," *ETSI White Paper*, vol. 11, pp. 1–16, 2015.

[2] C. Dong and W. Wen, "Joint optimization for task offloading in edge computing: an evolutionary game approach," *Sensors*, vol. 19, no. 4, p. 740, 2019.

[3] X. Chen, L. Jiao, W. Li, and X. Fu, "Efficient multi-user computation offloading for mobile-edge cloud computing," *IEEE/ACM Transactions on Networking*, vol. 24, no. 4, pp. 2795–2808, 2015.

[4] K. Ren, C. Wang, and Q. Wang, "Security challenges for the public cloud," *IEEE Internet Computing*, vol. 16, no. 3, pp. 69–73, 2012.

[5] L. Huang, X. Feng, L. Zhang, L. Qian, and Y. Wu, "Multi-server multi-user multi-task computation offloading for mobile edge computing networks," *Sensors*, vol. 19, no. 1, p. 1446, 2019.

[6] M. Satyanarayanan, P. Bahl, R. Caceres, and N. Davies, "The case for VM-based cloudlets in mobile computing," *IEEE Pervasive Computing*, vol. 8, no. 4, pp. 14–23, 2009.

[7] Y. Mao, J. Zhang, and K. B. Letaief, "Dynamic computation offloading for mobile-edge computing with energy harvesting devices," *IEEE Journal on Selected Areas in Communications*, vol. 34, no. 4, pp. 3590–3605, 2016.

[8] M. Kamoun, W. Labidi, and M. Sarkiss, "Joint resource allocation and offloading strategies in cloud enabled cellular networks," in *Proceedings of the IEEE International Conference on Communications (ICC)*, pp. 5529–5534, London, UK, 2015.

[9] M. H. Chen, B. Liang, and M. Dong, "A semidefinite relaxation approach to mobile cloud offloading with computing access point," in *Proceedings of the IEEE 16th International Workshop on Signal Processing Advances in Wireless Communications (SPAWC)*, pp. 186–190, Stockholm, Sweden, June 2015.

[10] A. Sehati and M. Ghaderi, "Energy-delay tradeoff for request bundling on smartphones," in *Proceedings of the INFOCOM IEEE Conference on Computer Communications*, pp. 1–9, Atlanta, GA, USA, May 2017.

[11] M. Lopez-Martin, B. Carro, J. Lloret, S. Egea, and A. Sanchez-Esguevillas, "Deep learning model for multimedia quality of experience prediction based on network flow packets," *IEEE Communications Magazine*, vol. 56, no. 9, pp. 110–117, 2018.

[12] K. Zhang, Y. Mao, S. Leng et al., "Energy-efficient offloading for mobile edge computing in 5G heterogeneous networks," *IEEE Access*, vol. 4, no. 12, pp. 5896–5907, 2016.

[13] M. H. Chen, B. Liang, and M. Dong, "Joint offloading and resource allocation for computation and communication in mobile cloud with computing access point," in *Proceedings of*

the IEEE INFOCOM IEEE Conference on Computer Communications, pp. 1–9, Atlanta, GA, USA, May 2017.

[14] Y. Wang, Q. He, D. Ye, and Y. Yang, "Formulating criticality-based cost-effective fault tolerance strategies for multi-tenant service-based systems," *IEEE Transactions on Software Engineering*, vol. 44, no. 3, pp. 291–307, 2018.

[15] T. Q. Dinh, J. Tang, Q. D. La, and T. Q. Quek, "Offloading in mobile edge computing: task allocation and computational frequency scaling," *IEEE Transactions on Communications*, vol. 65, no. 2, pp. 3571–3584, 2017.

[16] Y. Wang, M. Sheng, X. Wang, L. Wang, and J. Li, "Mobile-edge computing: partial computation offloading using dynamic voltage scaling," *IEEE Transactions on Communications*, vol. 64, no. 10, pp. 4268–4282, 2016.

[17] T. Q. Dinh, Q. D. La, T. Q. Quek, and H. Shin, "Learning for computation offloading in mobile edge computing," *IEEE Transactions on Communications*, vol. 66, no. 4, pp. 6353–6367, 2018.

[18] X. L. Xu, X. Zhang, X. H. Liu, J. Jiang, L. Qi, and M. Z. A. Bhuiyan, "Adaptive computation offloading with edge for 5G-envisioned Internet of connected vehicles," *IEEE Transactions on Intelligent Transportation Systems*, vol. 1, no. 1, pp. 1–10, 2020.

[19] X. L. Xu, C. X. He, Z. Y. Xu, L. Qi, S. Wan, and M. Z. A. Bhuiyan, "Joint optimization of offloading utility and privacy for edge computing enabled IoT," *IEEE Internet of Things Journal*, vol. 7, no. 4, pp. 2622–2629, 2019.

[20] X. L. Xu, X. Y. Zhang, H. H. Gao, Y. Xue, L. Qi, and W. Dou, "BeCome: blockchain-enabled computation offloading for IoT in mobile edge computing," *IEEE Transactions on Industrial Informatics*, vol. 16, no. 6, pp. 4187–4195, 2019.

[21] P. Lai, Q. He, G. Cui, X. Y. Xia et al., "Edge user allocation with dynamic quality of service," in *Proceedings of the 17th International Conference on Service-Oriented Computing (ICSOC2019)*, Toulouse, France, October 2019.

[22] K. Cheng, Y. Teng, W. Sun, A. Liu, and X. Wang, "Energy-efficient joint offloading and wireless resource allocation strategy in multi-MEC server systems,," in *Proceedings of IEEE International Conference on Communications (ICC)*, pp. 1–6, Kansas City, MO, USA, May 2018.

[23] C. Shi, K. Habak, P. Pandurangan et al., "Cosmos: computation offloading as a service for mobile devices," in *Proceedings of the 15th ACM International Symposium on Mobile Ad Hoc Networking and Computing*, pp. 287–296, Philadelphia, PA, USA, August 2018.

[24] Q. He, G. Cui, X. Zhang et al., "A game-theoretical approach for user allocation in edge computing environment," *IEEE Transactions on Parallel and Distributed Systems*, vol. 31, no. 3, pp. 515–529, 2020.

[25] P. Lai, Q. He, M. Abdelrazek et al., "Optimal edge user allocation in edge computing with variable sized vector bin packing," in *Proceedings of the 16th International Conference on Service-Oriented Computing (ICSOC2018)*, pp. 230–245, Hangzhou, China, November 2018.

[26] J. Li, T. Cai, K. Deng et al., "Community-diversified influence maximization in social networks," *Information Systems*, vol. 92, pp. 1–12, 2020.

[27] Q. He, J. Han, F. Chen et al., "QoS-aware service selection for customisable multi-tenant service-based systems: maturity and approaches," in *Proceedings of the International Conference on Cloud Computing (CLOUD2015)*, pp. 237–244, New York, USA, July 2015.

[28] L. Qi, Q. He, F. Chen et al., "Finding all you need: web APIs recommendation in web of things through keywords search,"

[29] W. Zhong, X. Yin, X. Zhang et al., "Multi-dimensional quality-driven service recommendation with privacy-preservation in mobile edge environment," *Computer Communications*, vol. 157, pp. 116–123, 2020.

[30] Y. Chen, N. Zhang, Y. Zhang, X. Chen, W. Wu, and X. Shen, "Energy efficient dynamic offloading in mobile edge computing for internet of things," *IEEE Transactions on Cloud Computing*, vol. 109, no. 10, pp. 1–11, 2019.

[31] X. Xu, Y. Chen, X. Zhang, Q. Liu, X. Liu, and L. Qi, "A blockchain-based computation offloading method for edge computing in 5G networks," *Software: Practice and Experience*, pp. 1–18, 2019.

[32] P. J. Darwen, "Computationally intensive and noisy tasks: co-evolutionary learning and temporal difference learning on backgammon," in *Proceedings of the 2000 Congress on Evolutionary Computation*, vol. 2, pp. 872–879, La Jolla, CA, USA, July 2000.

[33] K. Liu, J. Peng, H. Li, X. Zhang, and W. Liu, "Multi-device task offloading with time-constraints for energy efficiency in mobile cloud computing," *Future Generation Computer Systems*, vol. 64, no. 3, pp. 1–14, 2016.

[34] E. Cuervo, A. Balasubramanian, D. K. Cho et al., "MAUI: making smartphones last longer with code offload," in *Proceedings of the 8th International Conference on Mobile Systems, Applications, and Services*, pp. 49–62, San Francisco, CA, USA, June, 2010.

[35] L. Yang, J. Cao, Y. Yuan, T. Li, A. Han, and A. Chan, "A framework for partitioning and execution of data stream applications in mobile cloud computing," *Acm Sigmetrics Performance Evaluation Review*, vol. 40, no. 5, pp. 23–32, 2013.

[36] Y. Wen, W. Zhang, and H. Luo, "Energy-optimal mobile application execution: taming resource-poor mobile devices with cloud clones," in *Proceedings of the IEEE INFOCOM*, pp. 2716–2720, Orlando, FL, USA, March 2012.

[37] Z. Xie, "Cov-AHP: An improvement of analytic hierarchy process method," *Journal of Quantitative & Technical Economics*, vol. 8, pp. 137–148, 2015.

[38] O. Candogan, A. Ozdaglar, and P. A. Parrilo, "Dynamics in near-potential games," *Games and Economic Behavior*, vol. 82, no. 4, pp. 66–90, 2013.

[39] K. H. Loh, B. Golden, and E. Wasil, "Solving the maximum mardinality bin packing problem with a weight annealing-based algorithm," in *Operations Research and Cyber-Infrastructure*, pp. 147–164, Springer Science & Business Media, Berlin, Germany, 2009.

[40] T. Soyata, R. Muraleedharan, C. Funai, M. Kwon, and W. Heinzelman, "Cloud-vision: real-time face recognition using a mobile-cloudlet-cloud acceleration architecture," in *Proceedings of the IEEE Symposium on Computers and Communications (ISCC)*, pp. 000059–000066, Cappadocia, Turkey, July 2012.

[41] T. S. Rappaport, *Wireless Communications: Principles and Practice*, Prentice Hall PTR, Upper Saddle River, NJ, USA, 1996.

[42] M. Xiao, N. B. Shroff, and E. K. P. Chong, "A utility-based power-control scheme in wireless cellular systems," *IEEE/ACM Transactions on Networking*, vol. 11, no. 2, pp. 210–221, 2003.

[43] M. Chiang, P. Hande, T. Lan, and C. W. Tan, "Power control in wireless cellular networks power control in wireless cellular

networks mung chiang," *Foundations & Trends in Networking*, vol. 2, pp. 381–533, 2008.

[44] J. Wallenius, P. C. Fishburn, S. Zionts et al., "Multiple criteria decision making, multiattribute utility theory: recent accomplishments and what lies ahead," *Management Science*, vol. 54, no. 1, pp. 1336–1349, 2008.

[45] J. Sheng, J. Hu, X. Teng, B. Wang, and X. Pan, "Computation offloading strategy in mobile edge computing," *Information*, vol. 10, no. 4, p. 191, 2019.